Principles of Physical Chemistry

• PURI • SHARMA • PATHANIA

PRINCIPLES OF
PHYSICAL CHEMISTRY

Comprehensively Covering the B.Sc. and M.Sc. Syllabi Prescribed by the UGC

Also catering to the needs of students appearing in various competitive examinations

Late B.R. PURI
M.Sc., Ph.D., F.R.I.C., F.N.A.,
Professor of Physical Chemistry,
Panjab University, Chandigarh

L.R. SHARMA
M.Sc., Ph.D., F.R.I.C. (London),
Formerly, Professor of Physical Chemistry,
Department of Chemical Engineering & Technology,
Panjab University, Chandigarh

MADAN S. PATHANIA
M.Sc., Ph.D. (West Virginia University, U.S.A.),
Formerly, Professor of Physical Chemistry,
Panjab University, Chandigarh

VISHAL PUBLISHING CO.

Published by :
VISHAL PUBLISHING CO.
Adm. cum Head Office :
BOOKS MARKET, OLD RAILWAY ROAD,
JALANDHAR-144 008 (PB.) INDIA
Ph.: (0181) (O) 6450403, 5005403-05 (R) 5005401, 5005402 • Telefax : (0181) 5005406
• E-mail : vishalpubco@rediffmail.com, support@vishalpubco.com • Website : www.vishalpubco.com

Sales Office :
4271/XI, 3-Ansari Road,
Daryaganj, Delhi - 110 002
Ph. 011-23260206

First published : July, 1962

Price : ₹ **550/-** (for Pb., Haryana, H.P., J&K and Delhi)
₹ **560/-** (for other states)
₹ **850/-** (Library & International Edition)

ISBN : 81-88646-74-1

Printed at
Instant Printers
Jalandhar

PREFACE TO THE 46th EDITION

This is the Golden Jubilee Year of the publication of *the Principles of Physical Chemistry* and the occasion calls for some kind of celebration. It is a matter of immense pleasure and satisfaction that this text has successfully retained its prestigious position for five decades (the first edition of the book appeared in 1962). This has been due to the fact that we have been revising the book almost every year to highlight modern topics. At several places the text has been thoroughly revised.

Physical chemistry is traditionally divided into three parts—structure, equilibrium, change—and usually taught in that sequence though certain topics cannot be neatly accommodated in this scheme. The syllabus suggested by the UGC broadly conforms to this pattern and we have produced a text which deals with the subject in a rigorous and comprehensive way to cater to the needs of the graduate and post-graduate students of physical chemistry in the Indian universities and colleges.

The significant feature of this edition is that two new chapters have been added : Quantum mechanics is dealt with in three chapters, instead of the earlier two, and statistical thermodynamics is spread over two chapters. Some material has been shifted at several places within the chapters to maintain continuity and impart lucidity and simplicity to the treatment. Structure dominates science and chemistry is no exception. And quantum mechanics and spectroscopy are the chemist's tools to deal adequately with structure. Complete quantum mechanical treatment of the hydrogen atom, with special emphasis on the detailed solution of the Schrödinger equation, has been given. The radial equation and the spherical harmonics have at last received the emphasis they really deserved. Also, the approximate methods for the wave mechanical treatment of many-electron atoms have been updated. The perturbation theory—both non-degenerate and degenerate—has been adequately dealt with and applied to the first excited state of hydrogen atom. Several other modern topics which were earlier written as Appendices or *Further information* have been shifted to where they properly belong in the text. The treatment of angular momentum and atomic spectra is fairly comprehensive; the inessential details have been avoided. Several solved examples have been added.

The partition function dominates statistical thermodynamics even as the wavefunction is of paramount importance in quantum mechanics. The chapter on statistical thermodynamics centres around the partition function derived from quantum mechanics. The new chapter on classical statistical mechanics builds on the concepts of phase space and Gibbsian ensembles and rederives results already known from conventional thermodynamics.

We have deliberately highlighted the new material to show where physical chemistry is going. It has benefited from developments in physics and mathematics.

Physical chemistry has, in fact, become chemical physics. The quantum revolution of the 1920s has drastically changed the face of all science from physics, chemistry and the life sciences to pharmaceutical sciences. The impact of physical chemistry is felt on biology, engineering, materials science, nanoscience, astronomy and technology. There is no denying the fact that physical chemistry is a magnificent edifice whose range is truly interdisciplinary.

We make no claim for originality of treatment. Original books are written by excellent teachers and eminent researchers; we have all the regard for their excellence and eminence. (These qualities are unfortunately conspicuous in us by their absence. However, we are very enthusiastic about chemistry). We have attempted to build on their legacy by incorporating about nine hundred solved examples in all the chapters. These examples illustrate and illuminate theoretical concepts and are, indeed, the distinguishing feature of this book. The reader is urged to master them to have an adequate understanding of the subject. It goes without saying that without the available goldmine of definitive information listed in the bibliography it would not have been possible to write this book. The bibliography is fairly representative and lists some of the best and modern books for further reading. Great books fascinate us for they are a perennial source of entertainment, instruction and edification. The chapter-end material is limited to review questions and simple problems.

Several teachers and students have over the years been sending their valuable suggestions for the improvement of the text to keep it upto date. Their feedback has tremendously helped us in introducing novel innovations in the book. We take this opportunity to thank them and hope that they would judge our efforts indulgently and continue obliging us with their constructive criticism in future also. We take pleasure in recording our sincerest thanks to M/s Vishal Publishing Co., our efficient publishers, for their courtesy, full cooperation and determination to go with us to any length in publishing the book to our entire satisfaction.

August, 2012

AUTHORS

L.R. Sharma, 88/17, Panchkula (Haryana)
Ph. 0172-2560892

M.S. Pathania, 362/4, Panchkula (Haryana)
Ph. 0172-2582081

CONTENTS

CHAPTER 0

MATHEMATICAL CONCEPTS

We summarize here key concepts of mathematics often encountered in physical chemistry. It is mathematics which makes science a fascinating, frustrating and magnificent edifice.

CURVE SKETCHING, LINEAR GRAPHS AND SLOPES

Inclination of a Line and the Slope of a Line

The angle which a line makes with the positive direction of x-axis, measured in the anti-clockwise direction, is called its **inclination** (or angle of inclination), usually denoted by θ (Fig. 1). It may be mentioned that *(a)* the inclination of a line parallel to x-axis or the x-axis itself is $0°$ and *(b)* the inclination of a line parallel to the y-axis or the y-axis itself is $90°$.

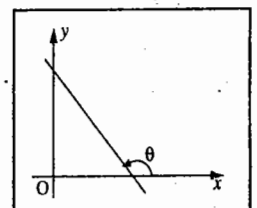

Fig. 1. Inclination of a straight line.

If $\theta (\neq 90°)$ is the inclination of a line, then $\tan\theta$ is called its **slope** (or gradient), usually denoted by m : $m = \tan\theta$.

Scientific data, obtained through painstaking research, can be best appreciated and understood by plotting graphs. Linear graphs are described by the appropriate equation of a straight line. There are several equations of a straight line, all of them first degree in x and y.

Equtions of a Straight Line

1. ***General equation of a straight line*** **is**

$$ax + by + c = 0 \qquad ...(i)$$

where both a and b are not equal to 0 and a, b, c are real numbers.

2. ***Slope–Intercept form*** **:** $y = mx + b$ ...(2)

where m is the slope of the line and b is the intercept on the y-axis.

3. ***Slope–Point form*** **:** The equation of a line with slope m and passing through a point (x_1, y_1) is

$$y - y_1 = m(x - x_1) \qquad ...(3)$$

4. ***Two–Point form*** **:** The equation of a line passing through two points (x_1, y_1) and (x_2, y_2) is

$$y - y_1 = \frac{y_2 - y_1}{x_2 - x_1}(x - x_1) \; ; \quad x_2 \neq x_1 \qquad ...(4)$$

5. ***Intercept form*** **:** $\dfrac{x}{a} + \dfrac{y}{b} = 1$ ...(5)

where x-intercept of the line is a and y-intercept is b.

The slope, m, of a line is the ratio of the change in y compared with the change in x. Thus,

$$m = \frac{\text{Change in } y}{\text{Change in } x} = \frac{dy}{dx} \qquad ...(6)$$

where dy is the infinitesimal change in y corresponding to infinitesimal change in x, dx. If (x_1, y_1) and (x_2, y_2) are two points on a line and m is the slope of the line, then

$$m = \frac{y_2 - y_1}{x_2 - x_1}; \; x_1 \neq x_2 \qquad ...(7)$$

Parallel and Perpendicular Lines : Two **non-vertical** lines are parallel if and only if the slopes of the two lines are equal, *i.e.*,

$$m_1 = m_2 \qquad ...(8)$$

Two non-vertical lines are perpendicular if and only if the product of their slopes is -1, *i.e.*,

$$m_1 m_2 = -1 \qquad ...(9)$$

Curve Sketching. In the study of motion of a particle, the displacement–time graphs and the velocity—time graphs are among the simplest graphs. The shortest distance between the initial and the final positions of an object (or a particle) is called its *displacement*, $\vec{S}$. Velocity is the rate of change of displacement : $\vec{v} = d\vec{S}/dt$. Acceleration is the rate of change of velocity : $\vec{a} = d\vec{v}/dt$.

Fig. 2 shows the commonly encountered displacement *versus* time graphs.

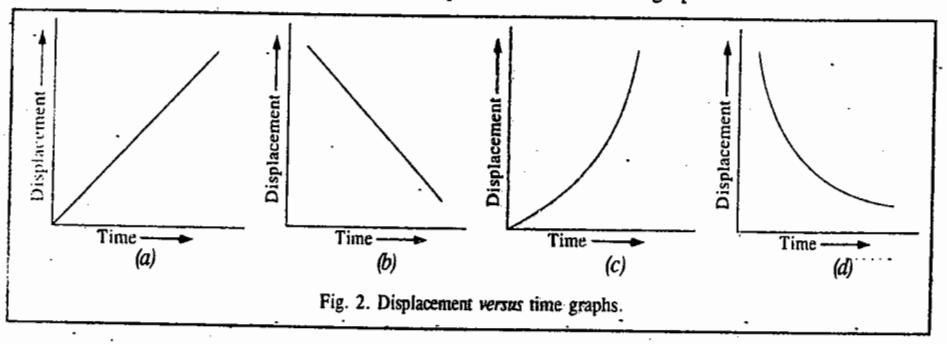

Fig. 2. Displacement *versus* time graphs.

Fig. 2*(a)* shows uniform positive velocity. Fig. 2*(b)* shows uniform negative velocity. Fig. 2*(c)* shows variable positive velocity whereas Fig. 2*(d)* shows negative variable velocity.

Functions of a Real Variable. A variable y is said to be a function of another variable x, written as $y = f(x)$, if there is a rule which relates one value of y with value of x in its range of values. For instance, if $f(x) = x^2 + 5x$, then $f(1) = 6$. That is, there is only one value of y corresponding to a single value of x. Such a function $f(x)$ is called a *single-valued function*. The variable y whose value depends on the chosen value of x is called the *dependent variable* while x is called the *independent variable*. A function $f(x)$ may have more than one value associated with it corresponding to a single value of x. Such a function is called a *multivalued function*, *e.g.*, if $y^2 = x - 5$ then $y = \pm(x-5)^{1/2}$ which indicates that corresponding to a single value of x, the function $y = f(x)$ is a double-valued function. The range (interval) of the independent variable is called the *domain* of the function. Some frequently encountered elementary functions are :

1. ***Polynomial.*** A polynomial is a function

$$f(x) = a_0 + a_1 x + a_2 x^2 + \ldots\ldots + a_n x^n \qquad ...(10)$$

where a_i are *constants* and the exponent n, which is a positive integer, is called the *degree* of the polynomial. If $f(x) = 0$, then the equation has exactly n equal roots. Thus, $x^3 - 6x^2 + 12x - 8 = 0$, *i.e.*, $(x-2)^3 = 0$ has three equal roots.

2. ***Exponential functions,*** $f(x) = e^x$ where $e = 2{\cdot}7182818\ldots\ldots$ The algebraic operations with respect to exponential functions are

$$e^x \times e^y = e^{x+y}; \quad e^x/e^y = e^{x-y}; \quad \frac{1}{e^x} = \ln x \qquad ...(11)$$

The inverse of e^x is called the **natural logarithm** of x, $\ln x$ and e is called the *base* of the logarithm. When e is replaced by 10, then $1/10^x = \log x$. This is called the **common logarithm** of x. The $\ln x$ and $\log x$ are related by $\ln x = 2{\cdot}303 \log x$. The fundamental relations satisfied by the natural (and also by the common) logarithm are

$$\ln(xy) = \ln x + \ln y \qquad \text{(Product formula)} \; ...(12)$$

$$\ln(x/y) = \ln x - \ln y \qquad \text{(Quotient formula)} \; ...(13)$$

$$\ln x^n = n \ln x \qquad \text{(Power formula)} \; ...(14)$$

3. ***Trigonometric functions*** such as $f(x) = \sin x$, $\cos x$, $\tan x$, $\cot x$, $\sec x$ and $\operatorname{cosec} x$ are *periodic*, *i.e.*, they satisfy the relation

$$f(x + k) = f(x) \qquad ...(15)$$

where k in radians is the *period* for all the periodic functions. For example, $\sin x$ and $\cos x$ have the period 2π. Note that $\sin(-x) = -\sin x$ and $\cos(-x) = \cos x$. Hence, $\sin x$ is called an *odd function* and $\cos x$ is an *even function*. Some fundamental relations among trigonometric functions are mentioned below :

(a) $\sin^2 x + \cos^2 x = 1$; $\sec^2 x = 1 + \tan^2 x$; $\operatorname{cosec}^2 x = 1 + \cot^2 x$

(b) $\sin(x \pm y) = \sin x \cos y \pm \cos x \sin y$

(c) $\cos(x \pm y) = \cos x \cos y \pm \sin x \sin y$

(d) $\tan(x \pm y) = (\tan x \pm \tan y) / (1 \pm \tan x \tan y)$

(e) $\cos 2x = \cos^2 x - \sin^2 x$; $\sin 2x = 2 \sin x \cos x = \dfrac{2 \tan x}{1 + \tan^2 x}$

(f) $\sin^2 x = \frac{1}{2}(1 - \cos 2x)$; $\cos^2 x = \frac{1}{2}(1 + \cos 2x)$

(g) $\sin 3x = 3 \sin x - 4 \sin^3 x$; $\cos 3x = 4 \cos^3 x - 3 \cos x$

(h) $\sin x + \sin y = 2 \sin \dfrac{x+y}{2} \cos \dfrac{x-y}{2}$; $\sin x - \sin y = 2 \cos \dfrac{x+y}{2} \sin \dfrac{x-y}{2}$

(i) $\cos x + \cos y = 2 \cos \dfrac{x+y}{2} \cos \dfrac{x-y}{2}$

(j) $\cos x - \cos y = 2 \sin \dfrac{x+y}{2} \sin \dfrac{y-x}{2} = -2 \sin\left(\dfrac{x+y}{2}\right) \sin\left(\dfrac{x-y}{2}\right)$

4. ***Inverse trigonometric functions*** such as $f(x) = \sin^{-1} x$, $\cos^{-1} x$, $\tan^{-1} x$, etc., are the inverse of the corresponding trigonometric functions. For example, if $x = \sin y$, then

$$y = (-1)^n \sin^{-1}(x + n\pi), \; n = 0, 1, 2, \ldots\ldots \text{ and } -\pi/2 \leq \sin^{-1} x \leq \pi/2 \qquad ...(16)$$

When $n = 0$, $y = \sin^{-1} x$ is the *principal value* of the angle y.

5. ***Hyperbolic functions*** are defined in terms of the exponential functions as

$$\sinh x = \tfrac{1}{2}(e^x - e^{-x}); \qquad \cosh x = \tfrac{1}{2}(e^x + e^{-x}) \qquad ...(17)$$

$$\tanh x = \frac{e^x - e^{-x}}{e^x + e^{-x}}; \qquad \coth x = \frac{e^x + e^{-x}}{e^x - e^{-x}} \qquad ...(18)$$

DIFFERENTIATION

Derivative of a Function. The derivative of a function $y = f(x)$ at a point x is defined as

$$f'(x) = \lim_{h\to 0} \frac{f(x+h)-f(x)}{h} = \lim_{\Delta x\to 0} \frac{\Delta y}{\Delta x} = \frac{dy}{dx} \quad \ldots(19)$$

where $\Delta x = h$ and $\Delta y = f(x + h) - f(x)$ are the increments in the variables x and y, respectively. The derivative of $f(x)$ is denoted by dy/dx provided the limit exists, *i.e.*,

$$\frac{dy}{dx} = \lim_{h\to 0} \frac{f(x+h)-f(x)}{h} \quad \ldots(20)$$

and may be interpreted as the rate of change of y w.r.t. x. The process of finding the derivative is called *differentiation*. The derivative of the function $f(x)$ at a given point represents a slope of the tangent drawn to the curve of $y = f(x)$ at the point where the function is defined. The derivative is also called *differential coefficient (d.c.)*.

Differentiation Formulas. We give below a few differentiation formulas which the reader should memorize. In these formulas it is assumed that u and v are differentiable functions of x and c, n are arbitrary constants :

1. $\frac{d}{dx}(c) = 0$

2. $\frac{d}{dx}(u+v) = \frac{du}{dx} + \frac{dv}{dx}$

3. $\frac{d}{dx}(cx) = c\frac{du}{dx}$ [The constant multiple rule]

4. $\frac{d(uv)}{dx} = u\frac{dv}{dx} + v\frac{du}{dx}$ [The product rule]

5. $\frac{d}{dx}(u/v) = \frac{v\frac{du}{dx} - u\frac{dv}{dx}}{v^2}, \; v \neq 0$ [The quotient rule]

6. $\frac{dx^n}{dx} = nx^{n-1}$ [The power rule for positive and negative integers]

7. $\frac{de^x}{dx} = e^x$

8. $\frac{da^x}{dx} = a^x \log a$

9. $\frac{d}{dx}(\log x) = \frac{1}{x}$

10. $\frac{d}{dx}(\sin x) = \cos x$

11. $\frac{d}{dx}(\cos x) = -\sin x$

12. $\frac{d}{dx}(\tan x) = \sec^2 x$

13. $\frac{d}{dx}(\cot x) = -\operatorname{cosec}^2 x$

14. $\frac{d}{dx}(\sec x) = \sec x \times \tan x$

15. $\frac{d}{dx}(\operatorname{cosec} x) = -\operatorname{cosec} x \times \cot x$

16. $\frac{d}{dx}(\sin^{-1} x) = \frac{1}{\sqrt{1-x^2}}$

17. $\frac{d}{dx}(\cos^{-1} x) = -\frac{1}{\sqrt{1-x^2}}$

18. $\frac{d}{dx}(\tan^{-1} x) = \frac{1}{1+x^2}$

19. $\frac{d}{dx}(\cot^{-1} x) = -\frac{1}{1+x^2}$

20. $\frac{d}{dx}(\sec^{-1} x) = \frac{1}{x\sqrt{x^2-1}}$

21. $\frac{d}{dx}(\operatorname{cosec}^{-1} x) = -\frac{1}{x\sqrt{x^2-1}}$

The Chain Rule. It states that the derivative of the composite of two differentiable functions is the product of their derivatives evaluated at appropriate points. Thus,

$$\frac{dy}{dx} = \frac{dy}{du} \times \frac{du}{dx} \quad \ldots(21)$$

Example 1. Differentiate x^x w.r.t. x

Solution : Let $y = x^x$

Taking logs, $\log y = x \log x$ [Note this step]

Differentiating w.r.t. x, $\frac{1}{y}\frac{dy}{dx} = x\left(\frac{1}{x}\right) + \log x(1) = 1 + \log x$

$\therefore$ $dy/dx = y(1 + \log x) = x^x(1 + \log x)$

Maxima and Minima. Graphs of functions show maxima and/or minima and in some cases the functions are merely increasing or decreasing. The first derivative $f'(x)$ and the second derivative $f''(x)$ of a function $f(x)$ play a key role here.

A function $f(x)$ is said to have a *maximum* for $x = a$ if $f(x) - f(a)$ is negative for all x when $|x-a| < \varepsilon$, where ε is a small positive number. A function $f(x)$ is said to have a *minimum* for $x = a$ if $f(x) - f(a)$ is positive for all x when $|x - a| < \varepsilon$, where ε is a small positive number.

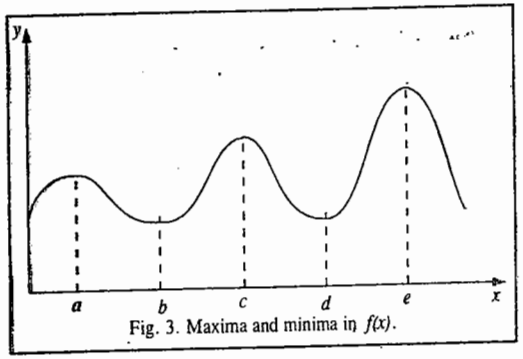

Fig. 3. Maxima and minima in $f(x)$.

Fig. 3 shows a plot of $f(x)$ versus x showing several maxima and minima. We see from the figure that a, c and e are the maxima and b and d are the minima. It should be pointed out that the maximum value of $f(x)$ at a point is not necessarily its greatest value and similarly, the minimum value of the function at a point is not necessarily its smallest value. The following points should be noted :

(*i*) At least one maximum or one minimum lies between two equal values of a function.

(*ii*) Maxima and minima must occur alternately.

(*iii*) A function may have several maxima and minima.

(*iv*) A function $y = f(x)$ is maximum at $x = a$ if dy/dx changes its sign from +ve to -ve as x passes through a.

(*v*) A function $y = f(x)$ is minimum at $x = a$ if dy/dx changes its sign from -ve to +ve as x passes through a.

(*vi*) If the sign of dy/dx does not change while x passes through a, then the function $y=f(x)$ is neither maximum nor minimum at $x = a$.

(*vii*) A function $f(x)$ is said to be *monotonically increasing* if $f'(x) > 0$.

(*viii*) A function $f(x)$ is said to be *monotonically decreasing* if $f'(x) < 0$.

Rules for finding Maxima-Minima

(*i*) Find $f'(x)$.

(*ii*) Solve $f'(x) = 0$. Each value of x so obtained is a candidate for a maximum or a minimum. Let $x = c$ be one of its points.

(*iii*) Find $f''(x)$. (*a*) If $f''(c) > 0$, then $x = c$ is a point of minima. (*b*) If $f''(c) < 0$, then $x = c$ is a point of maxima.

Maxima or Minima in an Interval :

Let $f(x)$ be a function defined in an interval $[a, b]$. Let $x = c$ be a candidate for a maximum. Then, max. $\{f(a), f(b), f(c)\}$ is the maximum value of the function. Similarly, let $x = d$ be a point of a minimum. Then, min. $\{f(a), f(b), f(d)\}$ is the minimum value of the function.

Example 2. Determine the interval in which

(i) $f(x) = x^3 + 3x^2 - 105x + 5$ is decreasing.

(ii) $f(x) = 2x^3 - 15x^2 + 36x + 7$ is increasing.

Solution : *(i)* $f'(x) = 3x^2 + 6x - 105 = 3(x - 5)(x + 7)$. Clearly, $f'(x) < 0$ when $-7 < x < 5$. Hence, $f(x)$ is decreasing in the interval $]-7, 5[$

(ii) $$f'(x) = 6x^2 - 30x + 36 = 6(x - 3)(x - 2)$$

Clearly, $f'(x) > 0$ when $x < 2$ and also when $x > 3$. Hence $f(x)$ is increasing in the interval $]-\infty, 2[\cup]3, \infty[$.

Example 3. Determine the interval in which

(i) $f(x) = x^4 - 2x^2$ is decreasing

(ii) $f(x) = x^3 + 2x^2 - 3$ is increasing.

Solution : *(i)* $f'(x) = 4x^3 - 4x = 4x(x - 1)(x + 1)$

Clearly, $f'(x) < 0$ when $x < -1$ and also when $x > 1$. Hence, $f(x)$ is decreasing in the interval $]-\infty, -1[\cup]1, \infty[$

(ii) $$f'(x) = 3x^2 + 4x = 3x\left(x + \frac{4}{3}\right)$$

Clearly, $f'(x) > 0$ when $x < -\frac{4}{3}$ and also when $x > 0$. Hence, $f(x)$ is increasing in the interval $]-\infty, -\frac{4}{3}[\cup]0, \infty[$

Example 4. When x is positive, what is the maximum value of $(1/x)^x$?

Solution : Let $$y = (1/x)^x = x^{-x}$$

Taking logs, $$\log y = -x \log x$$

Differentiating, $$\frac{1}{y}\frac{dy}{dx} = -x \times \frac{1}{x} - \log x \times 1 = -(1 + \log x)$$

$$\therefore \quad \frac{dy}{dx} = -x^{-x}(1 + \log x)$$

$$\frac{d^2y}{dx^2} = x^{-x}(1 + \log x)^2 - x^{-x} \times \frac{1}{x}$$

$$= x^{-x}(1 + \log x)^2 - x^{-x-1}$$

Now, $dy/dx = 0$ implies that $(1 + \log x) = 0$

or $$\log x = -1 = \log (1/e) \text{ so that } x = 1/e.$$

$$\therefore \quad \left[\frac{d^2y}{dx^2}\right]_{x=1/e} = -\left(\frac{1}{e}\right)^{-\frac{1}{e}-1} < 0$$

Hence, $x = 1/e$ is a point of maxima.

$$\therefore \quad \text{Maximum value} = e^{1/e}$$

Example 5. Show that the function $y = x^5 - 5x^4 + 5x^3 - 10$ has a maximum for $x = 1$, a minimum for $x = 3$ and neither a maximum nor a minimum for $x = 0$. (The point $x = 0$ is called an inflection point).

Solution. $$y = x^5 - 5x^4 + 5x^3 - 10$$

$$dy/dx = 5x^4 - 20x^3 + 15x^2 = 5x^2(x^2 - 4x + 3)$$

For the given function to have a maximum or a minimum, $dy/dx = 0$ so that

$$5x^2(x^2 - 4x + 3) = 0 \text{ ; whence } x = 0, 1, 3$$

Now, $$d^2y/dx^2 = 20x^3 - 60x^2 + 30x$$

$$\left[\frac{d^2y}{dx^2}\right]_{x=1} = 20(1)^3 - 60(1)^2 + 30(1) = -10 < 0.$$

Hence, $x = 1$ is a point of maximum.

Again, $$\left[\frac{d^2y}{dx^2}\right]_{x=3} = 20(3)^3 - 60(3)^2 + 30(3) = 90 > 0.$$

Hence, $x = 3$ is a point of minimum.

Now, $$\left[\frac{d^2y}{dx^2}\right]_{x=0} = 0 \text{ and } d^3y/dx^3 = 60x^2 - 120x + 30$$

$$\left[\frac{d^3y}{dx^3}\right]_{x=0} = 30 \neq 0$$

Hence, there is neither a maximum nor a minimum at $x = 0$. This is called a ***point of inflection.***

Partial Differentiation

We can extend the concept of differentiation of a function of one variable to that of a function of two or more variables. Let $z = f(x, y)$ be a function of two independent variables (x, y). The *partial derivatives* of $f(x, y)$ with respect to x and y are defined by

$$\frac{\partial z}{\partial x} = \frac{\partial f}{\partial x} = \lim_{\Delta x \to 0} \frac{f(x + \Delta x, y) - f(x, y)}{\Delta x} \qquad \ldots(22)$$

$$\frac{\partial z}{\partial y} = \frac{\partial f}{\partial y} = \lim_{\Delta y \to 0} \frac{f(x, y + \Delta y) - f(x, y)}{\Delta y} \qquad \ldots(23)$$

provided the limits exist. For the partial derivative $\partial f/\partial x$, y is held constant and x is considered as a variable. Similarly, for the partial derivative $\partial f/\partial y$, x is held constant and y is considered as a variable.

The differentiation of $\partial f/\partial x$ w.r.t. x or y yields second-order derivatives :

$$\frac{\partial}{\partial x}\left(\frac{\partial f}{\partial x}\right) = \frac{\partial^2 f}{\partial x^2} \text{ and } \frac{\partial}{\partial y}\left(\frac{\partial f}{\partial x}\right) = \frac{\partial^2 f}{\partial y \partial x} \qquad \ldots(24)$$

Similarly, $$\frac{\partial}{\partial x}\left(\frac{\partial f}{\partial y}\right) = \frac{\partial^2 f}{\partial y \partial x}, \text{ and } \frac{\partial}{\partial y}\left(\frac{\partial f}{\partial y}\right) = \frac{\partial^2 f}{\partial y^2} \qquad \ldots(25)$$

If $f(x, y)$ and its partial derivatives (also called *partial differential coefficients*) are continuous, then the order of differentiation is immaterial, *i.e.*,

$$\partial^2 f/\partial x \partial y = \partial^2 f/\partial y \partial x \quad i.e., \quad f_{xy} = f_{yx} \qquad \ldots(26)$$

The **total differential** df of the function $f(x, y)$ is defined as

$$df = \left(\frac{\partial f}{\partial x}\right) dx + \left(\frac{\partial f}{\partial y}\right) dy \qquad \ldots(27)$$

Euler Reciprocal (Reciprocity) Relation

Let $z = f(x, y)$ be the state function of the two independent variables x and y. A state function depends upon the initial and the final states of a system and is independent of the path via which the state is reached. The differential of z, called an *exact or total differential*, is given by

$$dz = \left(\frac{\partial z}{\partial x}\right)_y dx + \left(\frac{\partial z}{\partial y}\right)_x dy \qquad \ldots(28)$$

$$= M(x, y)\,dx + N(x, y)\,dy \qquad ...(29)$$

where $$M(x, y) = (\partial z/x)_y \text{ and } N(x, y) = (\partial z/\partial y)_x \qquad ...(30)$$

Since $M(x, y)$ and $N(x, y)$ are assumed to have continuous partial derivatives,

$$\frac{\partial^2 z}{\partial x \partial y} = \frac{\partial^2 z}{\partial y \partial x} \qquad ...(31)$$

Taking mixed second derivatives of Eq. 30, we have

$$\left(\frac{\partial M}{\partial y}\right)_x = \frac{\partial^2 z}{\partial y \partial x}; \quad \text{and} \quad \left(\frac{\partial N}{\partial x}\right)_y = \frac{\partial^2 z}{\partial x \partial y} \qquad ...(32)$$

From Eqs. 31 and 32, we obtain

$$\left(\frac{\partial M}{\partial y}\right)_x = \left(\frac{\partial N}{\partial x}\right)_y \qquad ...(33)$$

Eq. 33 is called the *Euler reciprocity relation*. It corresponds to an *exact differential*.

Euler Chain Relation (Cyclic Rule). From Eq. 28 we see that if the change occurs at constant z, then $dz = 0$ so that

$$0 = \left(\frac{\partial z}{\partial x}\right)_y dx + \left(\frac{\partial z}{\partial y}\right)_x dy \qquad ...(34)$$

Hence, $$\left(\frac{\partial x}{\partial y}\right)_z = -\frac{(\partial z/\partial y)_x}{(\partial z/\partial x)_y} \qquad ...(35)$$

or $$\left(\frac{\partial z}{\partial x}\right)_y \left(\frac{\partial x}{\partial y}\right)_z \left(\frac{\partial y}{\partial z}\right)_x = -1 \qquad ...(36)$$

Eq. 36 is called the *Euler chain relation* (or the cyclic rule), applicable only for state functions.

Leonhard Euler (1707-1783), the Swiss mathematician, was the most prolific mathematician of all time, who made important contributions to mathematical analysis, algebra and hydrodynamics.

INTEGRATION

If $f(x) = dy/dx$ on a certain interval of the x-axis, then y is called the *antiderivative* or *indefinite integral* of x and is denoted by

$$y = \int f(x)dx = \int \frac{dy}{dx}dx \qquad ...(37)$$

The indefinite integral of a given function is note unique. It differs by an integration constant, c. The *definite integral* of $f(x)$ with respect to x between the interval $a \le x \le b$ is defined as

$$\int_a^b f(x)dx = \lim_{h\to 0} h[f(a) + f(a + h) + f(a + 2h) + \cdots\cdots + f(a + (n - 1)h] \qquad ...(38)$$

provided the limit exists. The quantities a and b are called the *lower* and the *upper* limits of the integral. Eq. 38 can be written symbolically as

$$\int_a^b f(x)dx = \lim_{h\to 0} h \sum_{k=0}^{k=n-1} f(a + kh) \qquad ...(39)$$

If $f(x)$ is continuous over the interval $a \le x \le b$, then the definite integral 39 represents the area under the curve $y = f(x)$ bounded by x-axis and the coordinates at $x = a$ and $x = b$. The process of finding integrals is called *integration*. Below are given some important theorems for both the definite and the indefinite integrals :

(i) If $g(x) = \int_a^b f(x)\,dx$, then $\frac{dg(x)}{dx} = f(x)$ ...(40)

(ii) If $f(x) = \frac{dg(x)}{dx}$ is continuous in the interval $a \le x \le b$, then

$$\int_a^b f(x)\,dx = g(x)\Big|_a^b = g(b) - g(a) \qquad ...(41)$$

Methods of Integration. For the discussion of methods of integration, the reader should refer to books on calculus.

Integration Formulas. Below are listed some integration formulas for both the indefinite and the definite integrals, the arbitrary constants of integration have been omitted (these constants must be included for indefinite integrals). These formulas have been derived in standard text books of calculus.

a. Indefinite Integrals

1. $\int \frac{df(x)}{dx}dx = f(x)$
2. $\int [f(x) \pm g(x)]\,dx = \int f(x)dx \pm \int g(x)dx$
3. $\int c\,f(x)\,dx = c\int f(x)\,dx$
4. $\int x^n\,dx = \frac{x^{n+1}}{n+1}; \; n \ne -1$
5. $\int \sin x\,dx = -\cos x$
6. $\int \cos x\,dx = \sin x$
7. $\int \tan x\,dx = \log_e(\sec x)$
8. $\int \cot x\,dx = \log_e(\sin x)$
9. $\int \sec x\,dx = \log_e(\sec x + \tan x)$
10. $\int \operatorname{cosec} x\,dx = \log_e(\operatorname{cosec} x - \cot x)$
11. $\int \sec^2 x\,dx = \tan x$
12. $\int \operatorname{cosec}^2 x\,dx = -\cot x$
13. $\int e^x\,dx = e^x$
14. $\int \frac{dx}{x} = \log_e x$
15. $\int e^{ax}\sin bx\,dx = \frac{e^{ax}(a\sin bx - b\cos bx)}{a^2 + b^2}$
16. $\int e^{ax}\cos bx\,dx = \frac{e^{ax}(a\cos bx + b\sin bx)}{a^2 + b^2}$
17. $\int \frac{dx}{\sqrt{a^2 - x^2}} = \sin^{-1}\frac{x}{a}$
18. $\int \frac{dx}{\sqrt{a^2 + x^2}} = \tan^{-1}\frac{x}{a}$
19. $\int \sinh x\,dx = \cosh x$
20. $\int \cosh x\,dx = \sinh x$

b. Definite Integrals

21. $\int_0^\infty e^{-ax^2}dx = \frac{1}{2}\left(\frac{\pi}{a}\right)^{\frac{1}{2}}$
22. $\int_0^\infty x^n e^{-ax}\,dx = \frac{n!}{a^{n+1}}$
23. $\int_0^\infty x^{2n} e^{-ax^2}dx = \frac{(1)(3)(5)\ldots(2n-1)}{2^{n+1}a^n}\left(\frac{\pi}{a}\right)^{1/2}$

24. $\int_0^\infty x\,e^{-ax^2}dx = \frac{1}{2a}$ 25. $\int_0^a f(x)\,dx = \int_0^a f(x-a)\,dx$

26. $\int_{-a}^{a} f(x)\,dx = \begin{cases} 0, \text{when } f(x) \text{ is odd} \\ 2\int_0^a f(x)dx, \text{when } f(x) \text{ is even} \end{cases}$

Example 6. Evaluate the following integrals :

(i) $\int_0^{\pi/2} \sin^2 x\,dx$ *(ii)* $\int_0^{\pi/2} \cos^2 x\,dx$

Solution :

(i) $\int_0^{\pi/2} \sin^2 x\,dx = \int_0^{\pi/2} \frac{1-\cos 2x}{2}dx = \frac{1}{2}\left[x - \frac{\sin 2x}{2}\right]_0^{\pi/2} = \frac{\pi}{4}$

(ii) $\int_0^{\pi/2} \cos^2 x\,dx = \int_0^{\pi/2} \frac{1+\cos 2x}{2}dx = \frac{1}{2}\left[x + \frac{\sin 2x}{2}\right]_0^{\pi/2} = \frac{\pi}{4}$

Example 7. Evaluate the following integrals :

(i) $\int \tan^2 x\,dx$ *(ii)* $\int e^{-\log x}\,dx$

Solution : *(i)* $\int \tan^2 x\,dx = \int (\sec^2 x - 1)\,dx = \int \sec^2 x\,dx - \int 1\,dx$

$= \tan x - x + c$, where c is the constant of integration

(ii) $\int e^{-\log x}\,dx = \int e^{\log(x^{-1})}\,dx = \int x^{-1}\,dx = \int \frac{dx}{x} = \log|x| + c$,

where c is the constant of integration.

Example 8. Evaluate the integral $\int_{-\infty}^{\infty} x e^{-ax^2}dx$

Solution : $\int_{-\infty}^{\infty} x e^{-ax^2}dx = \int_{-\infty}^{0} x e^{-ax^2}dx + \int_0^{\infty} x e^{-ax^2}dx = -\int_0^{\infty} x e^{-ax^2}dx + \int_0^{\infty} x e^{-ax^2}dx$

$= 0$ [since xe^{-ax^2} is an odd function]

Example 9. Show that $\int u\,dv = uv - \int v\,du$

Solution : Since $d(uv) = u\,dv + v\,du$, we have

$\int d(uv) = \int u\,dv + \int v\,du$ or $uv = \int u\,dv + \int v\,du$

Hence, $\int u\,dv = uv - \int v\,du$

Example 10. Evaluate $\int \log x\,dx$

Solution : $\int \log x\,dx = \int 1 \times \log x\,dx = (\log x)x - \int \frac{1}{x} x\,dx + c$,

$= x \log x - x + c = x(\log x - 1) + c$,

where c is an arbitrary constant.

Factorial Notation. The factorial $n!$ of a natural number n is defined as the product of the first n natural numbers :

$n! = n(n-1)(n-2)\cdots\cdots(2)(1)$ ...(42)

Thus, $4! = (4)(3)(2)(1) = 24$

Also, $n! = n(n-1)!$ and $0! = 1$, *i.e.*, zero factorial = 1 ...(43)

PERMUTATIONS AND COMBINATIONS

Permutations mean arrangements whereas combinations mean selections (or forming groups). We shall summarize some basic concepts here.

1. Fundamental Theorem. If there are m ways of doing a thing and for each of these m ways there are associated n ways of doing a second thing, then the total number of ways of doing both the things is $m \times n$.

2. Permutations

(i) The number of permutations of n dissimilar things taken r at a time is given by

$${}^nP_r = \frac{n!}{(n-r)!} = n(n-1)(n-2)\cdots\cdots(n-r+1) \quad ...(44)$$

(ii) Number of permutations of n dissimilar things, taken all at a time is ${}^nP_n = n!$

(iii) Number of circular permutations of n different things taken all at a time is $(n-1)!$.

(iv) Number of permutations of n things, taken all at a time, when p_1 are alike of one kind, p_2 are alike of second kind,....., p_r are alike of rth kind, is given by

$$\frac{n!}{(p_1!)(p_2!)\ldots(p_r!)} \quad ...(45)$$

3. Combinations

(i) Number of combinations of n different things, taken r at a time, is given by

$${}^nC_r = \frac{n!}{(n-r)!(r!)} = \frac{{}^nP_r}{r!} \quad ...(46)$$

(ii) ${}^nC_o = 1, {}^nC_n = 1$ ...(47)

(iii) ${}^nC_p = {}^nC_q \Rightarrow p + q = n$ or $p = q$ ...(48)

(iv) ${}^nC_r = {}^nC_{n-r}$ ...(49)

(v) ${}^nC_{r-1} + {}^nC_r = {}^{n+1}C_r$ ...(50)

(vi) Number of combinations of n different things, taken r at a time when p particular things always occur is given by

$$= {}^{n-p}C_{r-p} \quad ...(51)$$

(vii) Number of combinations of n different things taken r at a time when p particular things never occur is given by

$${}^{n-p}C_r \quad ...(52)$$

Example 11. In how many ways can 4 letters be mailed if there are 3 boxes available ?

Solution : Each of the 4 letters may be mailed in any of the 3 mail boxes. Hence, the required number of ways is

$(3)(3)(3)(3) = 3^4 = 81$

Example 12. If ${}^4P_r = 3024$ **and** ${}^nC_r = 126$, **find** r.

Solution : ${}^nP_r = r!\,({}^nC_r)$ [From Eq. 46]

$\therefore \quad r! = \frac{{}^nP_r}{{}^nC_r} = \frac{3024}{126} = 24$

$\therefore \quad r = 4$

Example 13. How many diagonals are there in a polygon of n sides ?

Solution : A polygon having n sides has n vertices. On joining any two vertices at a time, we obtain either a side or a diagonal. Thus, the number of all such line sigments is ${}^nC_2$. These contain n sides.

Hence, number of diagonals $= {}^nC_2 - n = \frac{n(n-1)}{2} - n = \frac{1}{2}n(n-3)$

Example 14. What is the number of diagonals in a decagon ?

Solution : Number of diagonals $= \frac{1}{2}n(n-3) = \frac{1}{2}(10)(10-3) = 35$

PROBABILITY

Let us consider an experiment which involves random drawing of one card from a well-shuffled pack of 52 playing cards. Each drawing of a card is called an *event*. There will be 52 events if we draw one card at a time from a pack of 52 cards. These events are designated as E_1, E_2,....., E_{52}. Other examples of events include throwing a dice and tossing a coin. The result of a single performance of the experiment is called the *outcome* of the event.

1. Random Experiment. If in each trial of an experiment conducted under identified conditions, the *outcome* is not always the same but may be any of the possible outcomes, then that experiment is called a *random experiment*. Thus, tossing a fair coin, rolling an unbiased dice, drawing a card from a well-shuffled pack of cards are all examples of random experiment.

2. Sample space. The set of all possible outcomes in a random experiment is called a *sample space* S . Let us consider the following examples :

(i) In tossing a fair coin we have

$$S = \{H, T\}, \quad i.e., \{head, tail\}$$

where the head H and tail T are enclosed in braces.

(ii) In a throw of a dice, we have

$$S = \{1, 2, 3, 4, 5, 6\}$$

(iii) When two coins are tossed together,

$$S = \{HH, HT, TH, TT\}$$

(iv) When two dices are thrown together,

$$\begin{aligned} S = \{&(1,1), (1,2), (1,3), (1,4), (1,5), (1,6)\\ &(2,1), (2,2), (2,3), (2,4), (2,5), (2,6),\\ &(3,1), (3,2), (3,3), (3,4), (3,5), (3,6),\\ &(4,1), (4,2), (4,3), (4,4), (4,5), (4,6),\\ &(5,1), (5,2), (5,3), (5,4), (5,5), (5,6),\\ &(6,1), (6,2), (6,3), (6,4), (6,5), (6,6)\} \end{aligned}$$

4. Simple Event. Each outcome of an experiment is called a *simple event.*

5. Event. Any combination of simple events is called an *event* denoted by the upper case letter E. (Other uppercase letters such as A, B, C, etc., can also be used to denote an event.) Thus, for example, when a die is thrown, then each one of 1, 2, 3, 4, 5, 6 is a simple event. However, getting a prime number is an event : $E = \{2, 3, 5\}$.

6. Mutually Exclusive Event. A set of events is called *mutually exclusive* if the happening of one event excludes the happening of the other. Thus, E_1 and E_2 are mutually exclusive if

$$E_1 \cap E_2 = \phi \text{ where } \phi \text{ is an empty set.}$$

If $E_1 \cap E_2 \neq \phi$, then E_1 and E_2 are called *compatible events.*

Let us consider throwing a dice ; we have

$$S = \{1, 2, 3, 4, 5, 6\}$$

Let E_1 be the event of getting a number less than 3; clearly, $E_1 = \{1, 2\}$. Also, let E_2 be the event of getting a number greater than 4. Clearly, $E_2 = \{5, 6\}$. We see that $E_1 \cap E_2 = \phi$.

7. Exhaustive Events. The events E_1, E_2,.....,E_k such that $E_1 \cup E_2 \cup ..... \cup E_k = S$ are called *exhaustive events.*

8. Equally Likely Events. Events are said to be equally likely if none of them is expected to occur in preference to the other. Thus, drawing a card from a pack of well-shuffled cards results in 52 *equally likely events.*

9. Probability. In a random experiment let S be the sample space and let E be a subset of S, *i.e.*, $E \subseteq S$. Then E is an event. Then

$$P(E) = \frac{\text{Number of distinct elements in } E}{\text{Number of distinct elements in } S} = \frac{n(E)}{n(S)} \quad ...(53)$$

$$= \frac{\text{Number of outcomes favourable to } E}{\text{Number of all possible outcomes}} \quad ...(54)$$

10. Odds in favour of an Event and Odds Against it. If m is the number of ways an event can occur and n is the number of ways in which it does not occur, then

(i) Odds in favour of the event $= m/n$ ...(55)

(ii) Odds against the event $= n/m$ ...(56)

11. Complementary Event. Let S be the sample space and let $E \subseteq S$. Then, E is an event. Also, $E^c \subseteq S$. Hence, E^c is also an event, called the *complementary event,* sometimes denoted by $\bar{E}$ or E'.

12. Addition Theorem :

$$P(E_1 \cup E_2) = P(E_1) + P(E_2) - P(E_1 \cap E_2) \quad ...(57)$$

Note that if $E_1 \cap E_2 = \phi$ (*i.e.*, an empty set), then

$$P(E_1 \cup E_2) = P(E_1) + P(E_2) \quad ...(58)$$

13. Independent Events. Two events are said to be *independent* if the occurrence of one does not depend on the occurrence of the other. For example, suppose two coins are tossed. Let E_1 be the event of getting a head on the first coin and let E_2 be the event of getting a head on the second coin. Evidently, the occurrence of head on the second coin does not depend on the occurrence of head on the first coin. Thus, E_1 and E_2 are *independent events.*

14. Multiplication Theorem. If E_1 and E_2 are independent events, then

$$P(E_1 \cap E_2) = P(E_1) \cdot P(E_2) \quad ...(59)$$

15. Conditional Probability. The probability of the occurrence of an event E_1 when an event E_2 has already occurred, is called the *conditional probability,* $P(E_1/E_2)$. It can be shown that

(i) $$P(E_1/E_2) = \frac{P(E_1 \cap E_2)}{P(E_2)} \quad ...(60)$$

(ii) $$P(E_2/E_1) = \frac{P(E_1 \cap E_2)}{P(E_1)} \quad ...(61)$$

16. Binomial Theorem of Probability. Let there be n independent trials of an experiment with p as the probability of success and $q = (1 - p)$ as the probability of failure. Then,

$$P(r \text{ successes}) = {}^nC_r\, p^r\, q^{n-r} \quad ...(62)$$

17. Mathematical Expectation. If x is a random variable having values $x_1, x_2, x_3, \ldots\ldots, x_n$ with corresponding probabilities $p_1, p_2, p_3, \ldots\ldots, p_n$, then the mathematical expectation of x is defined as

$$E(x) = x_1p_1 + x_2p_2 + \ldots\ldots + x_np_n = \sum_{i=1}^{n} x_ip_i \qquad \ldots(63)$$

Example 15. A fair coin is tossed twice. Calculate the probability of getting heads in both trials.

Solution : $S = \{HH, HT, TH, TT\}$; $E = \{HH\}$

$$\therefore \quad P(\text{both heads}) = \frac{n(E)}{n(S)} = \frac{1}{4} \qquad \text{[Eq. 53]}$$

Example 16. A card is drawn from a well shuffled pack of 52 cards. What is the probability of getting a king of heart or a queen of club ?

Solution : Total number of ways = 52

Since there is one king of heart and one queen of club, therefore, number of favourable ways = 1 + 1 = 2

$$\therefore \quad \text{The required probability} = \frac{2}{52} = \frac{1}{26}.$$

Example 17. What is the probability that a card drawn from a well-shuffled pack of 52 playing cards is a black card or an ace ?

Solution : Total number of ways = 52.

There are 26 black cards and 4 aces but two aces are black.

$$\therefore \quad \text{Number of favourable ways} = 26 + 4 - 2 = 28$$

$$\therefore \quad \text{The required probability} = \frac{28}{52} = \frac{7}{13}$$

Example 18. What is the probability that a card drawn at random from a well-shuffled pack of 52 playing cards will be a diamond or a king ?

Solution : There are 13 cards of diamond and 4 kings but one of them is a king of diamond.

Number of favourable ways = 13 + 4 - 1 = 16. The required probability $= \frac{16}{52} = \frac{4}{13}$.

Example 19. A pair of dice is thrown. What is the probability of getting a total of 7 ?

Solution : Total number of possible outcomes = $6 \times 6 = 36$

Let E be the event of getting a total of 7. Then,

$$E = \{(1, 6), (2, 5), (3, 4), (4, 3), (5, 2), (6, 1)\}$$

$$\therefore \quad P \text{ (a total of 7)} = \frac{n(E)}{n(S)} = \frac{6}{36} = \frac{1}{6}$$

OTHER MATHEMATICAL RELATIONS

We summarize other concepts in mathematics which are needed to understand wave mechanics and statistical mechanics. No details will be given here.

1. Vectors. A vector in three-dimensional space can be represented in terms of the unit vectors $\hat{i}, \hat{j}, \hat{k}$ in the x, y and z directions :

$$A = A_x\hat{i} + A_y\hat{j} + A_z\hat{k}$$

where A_x, A_y and A_z are the projections on the x, y and z axes. Using the Pythagorus theorem, the length of A is given by

$$|A| = A = (A_x^2 + A_y^2 + A_z^2)^{1/2}$$

The **dot product** (scalar product) $A.B$ of two vectors is defined by

$$A.B = |A||B| \cos\theta = B.A$$

where θ is the angle between the vectors. The dot product is a scalar. In terms of the components,

$$A.B = A_xB_x + A_yB_y + A_zB_z$$

The cross product (vector product) is a vector with the magnitude

$$|A \times B| = |A||B| \sin\theta$$

pointed perpendicular to the plane defined by A and B in the direction such that A, B and $A \times B$ form a right-handed system. The vector product can be conveniently expressed in terms of the components of the individual vectors in the determinantal form :

$$A \times B = \begin{vmatrix} \hat{i} & \hat{j} & \hat{k} \\ A_x & A_y & A_z \\ B_x & B_y & B_z \end{vmatrix}$$

In terms of the components, we have

$$A \times B = (A_yB_z - A_zB_y)\,\hat{i} + (A_zB_x - A_xB_z)\,\hat{j} + (A_xB_y - A_yB_x)\,\hat{k}$$

2. Matrices. A matrix is an array of numbers. If a matrix has m rows and n columns it may be represented as

$$A = \begin{vmatrix} a_{11} & a_{12} & a_{13} & \ldots. & a_{1n} \\ a_{21} & a_{22} & a_{23} & \ldots. & a_{2n} \\ \vdots & \vdots & \vdots & \vdots & \vdots \\ a_{m_1} & a_{m_2} & a_{m_3} & & a_{mn} \end{vmatrix}$$

The sum of two matrices is defined by

$$C = A + B$$

where $c_{ij} = a_{ij} + b_{ij}$ for every i and j.

The product of a scalar c and a matrix is defined by

$$B = cA$$

where $b_{ij} = ca_{ij}$ for every i and j.

The product of two matrices is similar to the scalar product of two vectors :

$$C = AB \text{ where}$$

$$c_{ij} = \sum_{k=1}^{n} a_{ik}\, b_{kj}$$

where n is the number of columns in A.

If we want to multiply B by A, then B must have as many rows as A has columns. For example,

$$AB = \begin{bmatrix} a_{11} & a_{12} \\ a_{21} & a_{22} \\ a_{31} & a_{32} \end{bmatrix} \begin{bmatrix} b_{11} & b_{12} \\ b_{21} & b_{22} \end{bmatrix} = \begin{bmatrix} a_{11}b_{11} + a_{12}b_{21} & a_{11}b_{12} + a_{12}b_{22} \\ a_{21}b_{11} + a_{22}b_{21} & a_{21}b_{12} + a_{22}b_{22} \\ a_{31}b_{11} + a_{32}b_{21} & a_{31}b_{12} + a_{32}b_{22} \end{bmatrix}$$

Matrix multiplication is not *commutative* ; for example, let

$$A = \begin{bmatrix} 2 & 1 \\ 3 & -2 \end{bmatrix} \text{ and } B = \begin{bmatrix} 1 & 4 \\ 0 & 2 \end{bmatrix}$$

Then,

$$AB = \begin{bmatrix} 2 & 1 \\ 3 & -2 \end{bmatrix} \begin{bmatrix} 1 & 4 \\ 0 & 2 \end{bmatrix} = \begin{bmatrix} 2\times1+1\times0 & 2\times4+1\times2 \\ 3\times1-2\times0 & 3\times4-2\times2 \end{bmatrix} = \begin{bmatrix} 2 & 10 \\ 3 & 8 \end{bmatrix}$$

$$BA = \begin{bmatrix} 1 & 4 \\ 0 & 2 \end{bmatrix}\begin{bmatrix} 2 & 1 \\ 3 & -2 \end{bmatrix} = \begin{bmatrix} 1\times 2 + 4\times 3 & 1\times 1 - 4\times 2 \\ 0\times 2 + 2\times 3 & 0\times 1 - 2\times 2 \end{bmatrix} = \begin{bmatrix} 14 & -7 \\ 6 & -4 \end{bmatrix}$$

We see that since $AB \neq BA$, the two matrices A and B do not commute.

One of the best applications of matrices is in the solution of the simultaneous linear equations. For example, consider the set of simultaneous linear equations :

$$a_{11}x_1 + a_{12}x_2 + a_{13}x_3 = c_1$$
$$a_{21}x_1 + a_{22}x_2 + a_{23}x_3 = c_2$$
$$a_{31}x_1 + a_{32}x_2 + a_{33}x_3 = c_3$$

These equations can be written in the matrix notation as

$$\begin{bmatrix} a_{11} & a_{12} & a_{13} \\ a_{21} & a_{22} & a_{23} \\ a_{31} & a_{32} & a_{33} \end{bmatrix}\begin{bmatrix} x_1 \\ x_2 \\ x_3 \end{bmatrix} = \begin{bmatrix} c_1 \\ c_2 \\ c_3 \end{bmatrix}$$

or $$AX = C$$

The inverse of a matrix A^{-1} is defined such that

$$A^{-1}A = AA^{-1} = E$$

where E is the identity matrix :

$$E = \begin{bmatrix} 1 & 0 & 0 & .... & 0 \\ 0 & 1 & 0 & .... & 0 \\ 0 & 0 & 1 & .... & 0 \\ 0 & 0 & 0 & & 1 \end{bmatrix}$$

Multiplying both sides of $AX = C$ by A^{-1}, we obtain

$$A^{-1}AX = X = A^{-1}C$$

Thus, the solution X of the simultaneous equations is obtained by multiplying C by the inverse of A. Small matrices may be *inverted* by hand by the Gaussian elimination and large matrices may be inverted with a computer to obtain the solution of the simultaneous linear equations.

3. Determinants. A determinant is a *square array* of numbers. Its value is defined as a certain sum of products of sub sets of elements. If the determinant has n rows and columns, each term in the sum has n factors in it. For a determinant of order 2,

$$\begin{vmatrix} a_1 & b_1 \\ a_2 & b_2 \end{vmatrix} = a_1b_2 - a_2b_1$$

The value of a large determinant can be obtained by expanding by *minors*. For a determinant of order 3,

$$\begin{vmatrix} a_1 & b_1 & c_1 \\ a_2 & b_2 & c_2 \\ a_3 & b_3 & c_3 \end{vmatrix} = a_1\begin{vmatrix} b_2 & c_2 \\ b_3 & c_3 \end{vmatrix} - b_1\begin{vmatrix} a_2 & c_2 \\ a_3 & c_3 \end{vmatrix} + c_1\begin{vmatrix} a_2 & b_2 \\ a_3 & b_3 \end{vmatrix}$$

Determinants of higher order are defined by an analogous row (or column) expansion.

4. Complex Numbers. A complex number z can be written as

$$z = x + iy$$

where $i = \sqrt{-1}$, and x and y are *real* numbers. A complex number can be represented as a point in

the **Argand diagram** in the complex plane (Fig. 4).

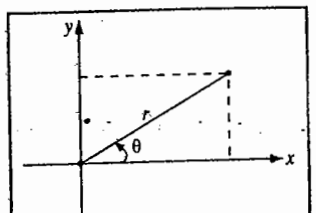

Fig. 4. The Argand diagram for a complex number.

The real part of z is plotted on the horizontal axis and the imaginary part on the vertical axis. The distance r is called the absolute value or **modulus** of z :

$$|z| = r = (x^2 + y^2)^{1/2}$$

Since $$x = r\cos\theta \text{ and } y = r\sin\theta,$$
$$z = r\cos\theta + ir\sin\theta = re^{i\theta}$$

where the last relation is obtained using

$$e^{i\theta} = \cos\theta + i\sin\theta$$

The **complex conjugate** of z is defined by

$$z^* = x - iy = re^{-i\theta}$$

The product of z and its complex conjugate z^* is

$$zz^* = x^2 + y^2 = r^2 = |z|^2$$

which is a real number.

5. Series. Some commonly used series are :

$$(i) \quad e^x = 1 + x + \frac{x^2}{2!} + \frac{x^3}{3!} + ... \qquad [\text{for all } x]$$

$$(ii) \quad \ln(1+x) = x - \frac{x^2}{2} + \frac{x^3}{3} - \frac{x^4}{4} + ... \qquad [x^2 < 1]$$

$$(iii) \quad (1+x)^{-1} = 1 - x + x^2 - x^3 + ... \qquad [x^2 < 1]$$

$$(iv) \quad (1-x)^{-1} = 1 + x + x^2 + x^3 + ... \qquad [x^2 < 1]$$

$$(v) \quad (1-x)^{-2} = 1 + 2x + 3x^2 + 4x^3 + ... \qquad [x^2 < 1]$$

$$(vi) \quad \sin x = x - \frac{x^3}{3!} + \frac{x^5}{5!} - ....$$

$$(viii) \quad \cos x = 1 - \frac{x^2}{2!} + \frac{x^4}{4!} - ....$$

6. Stirling Approximation. We know that

$$\int_1^n \ln x\,dx = [x\ln x - x]_1^n = n\ln n - n + 1 \qquad ...(i)$$

If we plot the curve $y = \ln x$ versus x (Fig. 5) and draw ordinates to it for $x = 2, 3, 4, ... n-1, n$, then the sum of the areas of the strips is approximately equal to

$$\ln 2 + \ln 3 + \ln 4 + ... + \ln n = \ln(1\times 2\times 3\times ..... n) = \ln n! \qquad ...(ii)$$

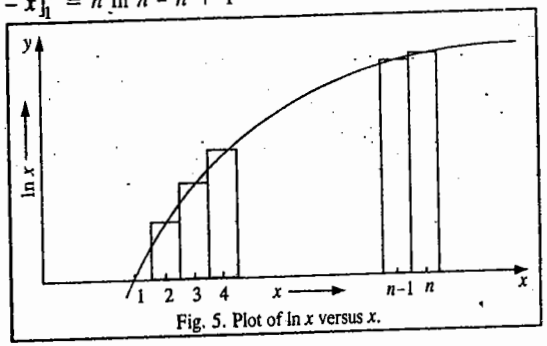

Fig. 5. Plot of $\ln x$ versus x.

For large n, the error incurred in regarding the strips as rectangles is regligible so that the sum of the areas of the reactangles given by Eq. *(ii)* can be equated to the area of the curve [Eq. *(i)*] Thus,

$$\ln n! \simeq n\ln n - n$$

or $$n! = (n/e)^n \qquad ...(iii)$$

where 1 on the right hand side of Eq. *(i)* has been neglected in comparison with n. Eq. *(iii)* is the Stirling approximation in its simple form.

Example 20. Test the Stirling approximation that $\ln n ! = n \ln n - n$, for $n = 5$, 10 and 15 by comparing its predictions with the exact values. Repeat the comparison for the more exact form of the approximation :

$$\ln n ! = \left(n + \tfrac{1}{2}\right) \ln n - n + \tfrac{1}{2} \ln 2\pi$$

Solution. The exact and approximate values are as follows :

n	5	10	15
$\ln n !$	4·7875	15·1044	27·8993
Approximation 1	3·0472	13·0259	25·6208
Approximation 2	4·7708	15·0961	27·8937

We see that for the largest value of $n(=15)$, the second approximation gives a very good agreement with the exact value.

7. Evaluation of Integrals of the Type $\int_0^\infty x^n e^{-ax^2} dx$

***(i)* Reduction of the Integrals.** Integration by parts, using the expression

$$\int u\,dv = uv - \int v\,du$$

can be carried out with

$$dv = x\,e^{-ax^2} dx \text{ and thus } v = -\frac{1}{2a} e^{-ax^2}$$

and

$$u = x^{n-1} \text{ and thus } du = (n-1)x^{n-2}\,dx$$

Using these substitutions, integration by parts gives

$$\int_0^\infty x^n e^{-ax^2} dx = \frac{x^{n-1}}{2a} e^{-ax^2} \Big]_0^\infty - \int_0^\infty \left[-\frac{1}{2a}(n-1)x^{n-2} e^{-ax^2}\right] dx$$

$$= 0 + \frac{n-1}{2a} \int_0^\infty x^{n-2} e^{-ax^2} dx$$

In this way integrals of the general type can be reduced either to one involving the integrand $x\,e^{-ax^2}$ or to one involving the integrand e^{-ax^2}.

***(ii)* For n odd.** In this case the method used in *(i)* leads to the integral $\int_0^\infty x\,e^{-ax^2} dx$ which can be integrated directly to give

$$-\frac{1}{2a} e^{-ax^2} \Big]_0^\infty = \frac{1}{2a}.$$

***(iii)* For n even.** Here, the method used in *(i)* leads to the integral $\int_0^\infty e^{-ax^2} dx$.

Evaluation of this integral is accomplished by writing the product of two such integrals based on two independent coordinates x and y which can be pictured as being cartesian coordinates. We thus investigate

$$\int_0^\infty e^{-ax^2} dx \int_0^\infty e^{-ay^2} dy = \int_0^\infty \int_0^\infty e^{-a(x^2+y^2)}\,dx\,dy$$

The coordinates x and y can now be related to two new coordinates r and θ by the relations which associate cartesian coordinates with *polar coordinates* :

$$x^2 + y^2 = r^2 \text{ and } dx\,dy = r\,dr\,d\theta$$

Again, since in the xy coordinate system the integration is over the first quadrant, the corresponding limits of integration involving r and θ are 0 to ∞ and 0 to $\pi/2$. We thus have the problem, in r and θ, of the double integral $\int_0^{\pi/2} \int_0^\infty e^{-ar^2}\,r\,dr\,d\theta$

The two integrations can be performed to give $(\pi/2)[1/(2a)]$, and thus the original integral is evaluated as

$$\int_0^\infty e^{-ax^2} dx = \frac{1}{2}\left(\frac{\pi}{2}\right)^{1/2}$$

***(iv)* Even and odd character and the limits of integration.** Functions of the type $x^n e^{-ax^2}$ are *even* if n is even and *odd* if n is odd. Integration from $-\infty$ to $+\infty$ will, therefore, give zero for n odd and will give twice the value of the integral from 0 to ∞ for n even.

***(v)* Values of the most often used integrals :**

$$\int_{-\infty}^\infty e^{-ax^2} dx = \left(\frac{\pi}{2}\right)^{1/2} \qquad \int_0^\infty x e^{-ax^2} dx = \frac{1}{2a} \qquad \int_{-\infty}^\infty x^2 e^{-ax^2} dx = \frac{1}{2a}\left(\frac{\pi}{a}\right)^{1/2}$$

$$\int_0^\infty x^3 e^{-ax^2} dx = \frac{1}{2a^2} \qquad \int_{-\infty}^\infty x^4 e^{-ax^2} dx = \frac{3}{4a^2}\left(\frac{\pi}{a}\right)^{1/2}$$

MEMORABILIA PHYSICO-MATHEMATICA

Nature, and Nature's laws, lay hid in night,
God said, Let Newton be, and all was light. *–Alexander Pope*

Maxwell could say, when he was finished with his discovery, *"Let there be electricity and magnetism, and there is light".* *–Richard P. Feynman*

Experiments are the only means of knowledge at our disposal. The rest is poetry, imagination. *–Max Planck*

It seems that if one is working from the point of view of getting beauty in one's equations, and if one has a really sound insight, one is on a sure line of progress. *–P.A.M. Dirac*

Number rules the universe. *–Pythagorus*

God ever geometrizes. *–Plato*

God ever arithmetizes. *–Jacobi*

In questions of science the authority of a thousand is not worth the humble reasonings of a single individual. *–Galileo*

It is remarkable to what extent Indian mathematics enters into the science of our time. Both the form and the spirit of arithmetic and algebra of modern times are essentially Indian and not Grecian. *–F. Cajori*

The greatest mathematicians Archimedes, Newton and Gauss always united theory and applications in equal measure. *–Felix Klein*

There is an astonishing imagination even in the science of mathematics... We repeat, there was far more imagination in the head of Archimedes than in that of Homer. *–Voltaire*

Mathematicians are like Frenchmen : whatever you say to them they translate into their own language and forthwith it is something entirely different. *–Goethe*

An old French geometer used to say that a mathematical theory was never to be considered complete till you had made it so clear that you could explain it to the first man you met in the street. *-H.J.S. Smith*

Everybody praises the incomparable power of the mathematical method, but so is everybody aware of its incomparable unpopularity. *-J. Rosanes*

Archimedes who combined a genius for mathematics with a physical insight, must rank with Newton, who lived nearly two thousand years later, as one of the founders of mathematical physics... The day (when having discovered his famous principle of hydrostatics he ran through the streets shouting Eureka ! Eureka !) ought to be celebrated as the birthday of mathematical physics ; the science came of age when Newton sat in his orchard. *-A.N. Whitehead*

Euler could repeat the Aeneid from the beginning to the end, and he could even tell the first and last lines in every page of the edition which he used. In one of his works there is a learned memoir on a question in mechanics, of which, as he himself informs us, a verse of the Aeneid gave him the first idea. *-David Brewster*

All the results of nature are only mathematical results of a small number of immutable laws. *-Laplace*

As the sun eclipses the stars by his brilliancy, so the man of knowledge will eclipse the fame of others in assemblies of people if he proposes algebraic problems, and still more if he solves them. *-Brahmagupta*

Mathematics is the queen of science, and arithmetic the queen of mathematics. *-Gauss*

The infinite ! No other question has ever moved so profoundly the spirit of man. *-David Hilbert*

A monument to Newton ! A monument to Shakespeare ! Look up to the Heaven, look into the human heart. Till the planets and the passions, the affections and the fixed stars, are extinguished their names cannot die. *-John Wilson*

Newton was the greatest genius that ever lived, and the most fortunate, for we cannot find more than once a system of the world to establish. *-Lagrange*

The aim of research is the discovery of the equations which subsist between the elements of phenomena. *-Ernst Mach*

If my theory of relativity is proven successful, Germany will claim me as a German and France will declare that I am a citizen of the world. Should my theory prove untrue, France will say that I am a German and Germany will declare that I am a Jew. *-Einstein*

Dirac to whom in my opinion we owe the most logical presentation of quantum mechanics..... *-Einstein*

One may be a mathematician of the first rank without being able to compute. It is possible to be a great computer without having the slightest idea of mathematics. *-Novalis*

There is a largeness about mathematics that transcends race and time... The greatest mathematics has the simplicity and inevitableness of supreme poetry and music, standing on the borderland of all that is wonderful in Science and all that is beautiful in Art. Mathematics transfigures the fortuitous concourse of atoms into the tracery of the finger of God. *-H.W. Turnbull*

He [Ramanujan] had an extraordinary memory. He could remember the idiosyncracies of numbers in an almost uncanny way. It was Mr. Littlewood (I believe) who remarked that "every positive integer was one of his personal friends." I remember once going to see him when he was lying ill... I had ridden a taxi-cab number 1729, and remarked that the number seemed to be rather a dull one, and that I hoped it was not an unfavorable omen. "No," he replied, "It is a very interesting number ; it is the smallest number expressible as a sum of two cubes in two different ways." *-G.H. Hardy*

Symmetry, as wide or as narrow as you may define it, is one idea by which man, through the ages has tried to comprehend order, beauty, and perfection. *-Hermann Weyl*

But elements of symmetry are either present or absent ; no intermediate case is possible. *-L.D. Landau*

Fermi's aversion to mathematical technicalities is well known. Even when a mathematical argument had played a role in his initial thinking of a problem, he was careful to erase all its traces from his final account. I was once to talk to a seminar and when I expressed my doubts as to what I should talk about, he advised, "If I were you, I would not be technical," And I asked, "Do you mean, if I were you or you were me ?" This baffled him ; it was the only occasion I got the better of him. *-S. Chandrasekhar*

If a book is to be published at a time T and if it is supposed to be up-to-date to a time $T - t$, then it will certainly be out-of-date at the time $T + t$. *-Freeman J. Dyson*

QUANTUM MECHANICS–I. WAVE MECHANICAL TREATMENT OF SIMPLE SYSTEMS

Electron and the Old Quantum Theory (1900–1926)

John Dalton (1766-1844), the great British propounder of atomic theory, regarded the atom as a hard, dense and smallest indivisible particle of matter. However, the emission of negatively and positively charged particles from radioactive elements as well as from gases on the passage of electricity through them at very low pressures convinced the scientists that atom is not indivisible but consists of much smaller fundamental particles. Thus, if electric discharge from a high potential source is passed through a discharge tube evacuated to pressures around 0·01 mm or less, rays are emitted from the cathode. These are called **cathode rays.** These rays travel in straight lines at right angles to the cathode surface. They produce mechanical motion in a small paddle wheel placed in their path indicating that they are material particles. These particles are deflected from their path by electric and magnetic fields showing that they are electrically charged. The direction of deflection indicates that they are negatively charged. These particles are called **electrons.** The British physicist J.J.Thomson (1856–1940) determined the **ratio e/m of electron** by subjecting the beam of electrons produced in a discharge tube to magnetic as well as electric fields. The magnetic field is applied at right angles to the direction of the beam. Under the influence of magnetic force which is equal to Beu (where B is the strength of the magnetic field, e is the charge on electron and u is its velocity), the electron starts moving in a circular path of radius r. The centrifugal force mu^2/r arising from this circular motion is equal and opposite to the magnetic force. *i.e.*, .

$$Beu = mu^2/r \quad \text{or} \quad e/m = u/rB; \quad \text{where } m \text{ is the electron mass.} \qquad ...(1)$$

Now suppose an electric field of strength E is also applied to the electron beam. The electrical force experienced by each electron is given by Ee. The magnetic and electric fields are so adjusted as to produce equal and opposite effects in such a way that there is no deflection of the electron beam from its original position. Thus,

$$Beu = Ee \quad \text{or} \quad u = E/B \qquad ...(2)$$

Substituting the above value of u in Eq. 1, we have

$$e/m = E/rB^2 \qquad ...(3)$$

The value of r is obtained from the deflection of a spot of light on a fluorescent screen when magnetic field alone is applied. Knowing the strengths of electric and magnetic fields (E and B) for no deflection, the value of e/m can be easily calculated. Thomson found the value of e/m to be the same ($=1{\cdot}75875 \times 10^{11}$ C kg^{-1}) irrespective of the nature of the gas taken in the cathode ray tube or the material constituting the cathode. J.J. Thomson was awarded the Physics Nobel Prize in 1906 for his work on the conduction of electricity by gases.

Robert Millikan determined the charge on electron by using his famous **oil drop technique.** In this technique, an oil spray consisting of microscopic droplets of an oil produced by an atomizer is injected into a chamber containing air at a controlled pressure. The air is ionized by exposing to X-rays. The

electrons produced as a result of ionization of air get attached to oil droplets. The charged oil droplets move down under the action of gravity and acquire a constant velocity u_1 when the force of gravity ($= Mg$) is balanced by the viscous resistance of air. The droplets moving with uniform velocity u_1 enter a region in between two parallel plates held at a suitable distance from each other. These plates can act as electrodes. An electric field of strength E is then applied through the two metal plates in such a way that it acts against the action of gravity. The total force which acts on the falling droplet would thus be $(Mg - Ee)$ where M is the mass and e is the charge on the droplet. If the rate of fall of the droplet is now u_2, then

$$u_1/u_2 = Mg/(Mg - Ee) \qquad ...(4)$$

The velocities u_1 and u_2 are determined by means of a travelling microscope.

When the droplets move only under the action of gravity, their velocity (u_1) is also given by Stokes' law, that is,

$$u_1 = 2gr^2 \rho/9\eta \qquad ...(5)$$

where r, ρ and η are, respectively, the radius of the droplet, the density of the droplet and the coefficient of viscosity of air. Assuming that the particle is spherical, its mass $M=(4/3)\pi r^3\rho$. The radius r is determined with the help of Eq. 5, assuming that density of the droplet is the same as the density of the oil. Thus, knowing the mass of the droplet, M, the charge on the droplet, e, can be easily calculated with the help of Eq. 4.

Millikan carried out a number of experiments by varying the value of E and found that charge e was always equal to a simple multiple of $1{\cdot}6022\times10^{-19}$ coulomb. This indicates that oil droplet had captured one, two, three or more electrons, each carrying a charge equal to $1{\cdot}6022\times10^{-19}$ C. The American physicist Robert Millikan (1868–1953) was awarded the Physics Nobel Prize in 1923 for determining the charge on electron.

In recent years, the viscosity of air has been redetermined more accurately and the charge on electron is taken as $1{\cdot}60206\times10^{-19}$ C.

Since $e = 1{\cdot}60206\times10^{-19}$ C and $e/m = 1{\cdot}75875\times10^{11}$ C kg^{-1}, hence

$$\text{mass of electron} = \frac{e}{e/m} = \frac{1{\cdot}60206\times10^{-19}\ \text{C}}{1{\cdot}75875\times10^{11}\ \text{C kg}^{-1}} = 9{\cdot}109\times10^{-31}\ \text{kg}. \qquad ...(6)$$

This is called the rest mass of the electron, *i.e., the mass which it possesses when it is moving with a speed much smaller than that of light.* The rest mass of electron is now taken as $9{\cdot}1095\times10^{-31}$ kg. On the atomic mass scale, the rest mass of electron=0·0005486 u, where u. is the atomic mass unit. At high speeds, the mass of a particle, according to Einstein's theory of relativity, is given by

$$m = \frac{m_0}{(1-u^2/c^2)^{1/2}} \qquad ...(7)$$

where m is the mass of the particle moving with velocity u, c is the speed of light and m_0 is the *rest mass* of the particle. Evidently, as u approaches c, m becomes infinity.

Careful experiments with discharge tubes containing perforated cathode reveal the emission of another type of radiations which start from the side of the anode and pass through the holes of the cathode. These radiations, which carry positive charge, are called **positive rays** or **anode rays.** Further studies reveal that these rays consist of **positively charged particles** whose e/m ratio varies with the nature of the gas taken in the discharge tube. The positive particles are, in fact, the positive residues of the gas left when one or more electrons are knocked out of the atoms of the gas. The smallest positive

particle given out by the lightest element hydrogen is called the **proton.** It is another fundamental particle whose charge has been found to be equal in magnitude but opposite in sign to that of electron. Its mass is $1{\cdot}6726\times10^{-27}$ kg or 1·00722 u. The charge on an electron or a proton is the smallest charge of electricity. It is usual to speak of the charge on an electron as **unit negative charge** and the charge on a proton as **unit positive charge.**

The Rutherford's Scattering Experiments. In 1911, the British physicist Ernest Rutherford (1871–1937) and the two eminent experimenters Geiger and Marsden directed a narrow beam of alpha particles obtained from polonium at an extremely thin sheet of a metal like silver and gold. After passing through the metal sheet, the alpha particles were made to strike a fluorescent screen. These experiments suggested that

1. Most of the alpha particles pass through the metallic sheet without suffering any change in their path showing that the atom consists predominantly of empty space.

2. An extremely small number of alpha particles get deflected through wider angles or even backwards showing the presence of a heavy positively charged body in each atom and that the volume of this body is only a minute fraction of the total volume of the atom.

The Rutherford's Atomic Model. Based on his scattering experiments, Rutherford suggested that an atom consists of :

1. A minute positively charged body located at the centre, called the *nucleus,* in which almost the entire mass of the atom is concentrated. Since the mass of an atom is almost entirely due to protons, all the protons are present in the nucleus.

2. An equal number of extremely small negatively charged electrons distributed around the nucleus to balance its positive charge.

In order to explain why the electrons do not fall into the nucleus on account of the mutual electrostatic attraction, Rutherford proposed that the electrons are revolving round the nucleus at extremely high speeds at great distances from the nucleus. The centrifugal force arising from this motion balances the force of electrostatic attraction. The electrons, therefore, do not fall into the nucleus. The Rutherford's **nuclear atomic model** was fully confirmed in 1913 by further experiments performed by Geiger and Marsden. Rutherford was awarded the 1908 Chemistry Nobel Prize for contributions to the chemistry of radioactive substances.

James Chadwick (1891—1974), the British physicist, discovered in 1932 that when beryllium or boron is bombarded by alpha particles, new particles which carry no charge but have mass almost equal to that of a proton, are emitted. These particles are called **neutrons.** Chadwick won the Physics Nobel Prize in 1935 for the discovery of neutron.

All the neutrons are present in the nucleus alongwith protons. Because of the presence of protons, the nucleus carries a positive charge, as mentioned above. The number of unit positive charges carried by the nucleus of an atom is called the **atomic number** of the element. In other words, atomic number is equal to the number of protons present in the nucleus of the atom. The sum of the number of protons and neutrons present in the nucleus of an atom is called the **mass number** of the element.

It was pointed out by Niels Bohr (1885–1962), the Danish physicist, that Rutherford's atom should be highly unstable. J.C.Maxwell (1831–1879), the great Scottish mathematical physicist, the pioneer of electromagnetic theory, had shown that whenever an electric charge is subjected to acceleration, it emits radiation and loses energy. Bohr argued, therefore, that if an electron (a charged particle) moves round the nucleus in an orbit, as in Rutherford's model, it should be subjected to acceleration The electron should, therefore, continuously emit radiation and lose energy. Thus, its orbit should become smaller and smaller and finally it should drop into the nucleus. This, however, does not happen. Bohr

solved this problem on the basis of the quantum theory of radiation put forth by the German physicist Max Planck (1858-1947) in 1900 to explain the observed distribution of energy in the spectrum of the heat radiations emitted by a hot body. The *energy density, i.e.,* the amount of energy radiated per unit volume, by a black body depends upon the temperature. However, the energy radiated at a particular temperature is not of a single frequency (or wave length). The correlation between energy density and wave length at different temperatures is depicted in Fig. (1). These curves have the following characteristics:

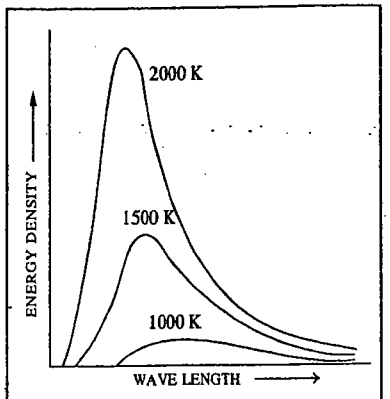

Fig. 1. Emission of radiation from a black body at different temperatures.

1. For each temperature, there is a particular wave length at which the energy radiated is the maximum.

2. The position of the maximum shifts towards lower wave lengths with increase in temperature.

3. The higher the temperature, the more pronounced is the maximum.

These curves are referred to as the black body radiation curves. A **black body** is defined as an object that absorbs all the radiations falling on it. A perfect absorber is also a perfect emitter of radiation. Thus, of all bodies heated to a given temperature, maximum energy is radiated by a black body.

According to **Wien's displacement law**, $\lambda_m T = b$, where λ_m is the wave length corresponding to the maximum in the curve. The Wien constant $b = 0{\cdot}0029$ m K. Wilhelm Wien (1864—1928), the German physicist, was awarded the 1911 Physics Nobel Prize for his discoveries concerning the laws governing the heat radiations.

Quantum Theory of Radiation. The energy distribution in black body radiations could not be explained by the application of classical physics. The correct expression was derived by Planck on the basis of the quantum theory of radiation. According to this theory,

1. Radiant energy is emitted or absorbed discontinuously in the form of tiny bundles of energy known as **quanta.**

2. Each quantum is associated with a definite amount of energy $E(=h\nu)$ where E is the energy in joules, ν is the frequency of radiation in reciprocal seconds (s^{-1}) and h is a fundamental constant known as **Planck's constant**. The numerical value of h is $6{\cdot}626\times10^{-34}$ J s.

The value of a quantum of energy is also given by $hc\bar{\nu}$ where $\bar{\nu}$ is the **wave number** defined as the reciprocal of wave length *i.e.,* $\bar{\nu} = (1/\lambda)$. Evidently, $\nu = c/\lambda = c\bar{\nu}$ and $E = hc\bar{\nu}$.

3. A body can emit or absorb energy only in whole number multiples of quantum, *i.e.,* $1h\nu$, $2h\nu$, $3h\nu$....., $nh\nu$. Energy in fractions of a quantum cannot be lost or absorbed. This is known as **quantization of energy**.

Based on his theory, Planck obtained the following expression for energy density of black body radiation :

$$E(\nu)d\nu = \frac{8\pi h\nu^3}{c^3} \times \frac{d\nu}{\exp(h\nu/kT)-1} \qquad ...(8)$$

Eq. 8 adequately accounts for the black body radiation curves at all wave lengths obtained at different temperatures, as shown in Fig. 1. Planck was awarded the Physics Nobel Prize in 1918 for propounding the quantum theory of radiation.

Photoelectric Effect. J.J. Thomson, in some of his famous experiments, observed that when light of a *certain frequency* strikes the surface of a metal, electrons are ejected from the metal. This phenomenon is known as the photoelectric effect. A few metals show this effect under the action of

visible light but many more show it under the action of more energetic ultraviolet light. Cesium, which amongst the alkali metals has the lowest ionisation energy, is also the metal from which electrons are ejected most easily by light. This metal is, therefore, used largely in **photoelectric cells.**

After making careful studies of photoelectric effect under different conditions, the following observations were made :

1. For each metal, a certain minimum frequency of incident light is needed to eject electrons. This is known as **threshold frequency,** ν_0. A light of smaller frequency than this cannot eject electrons no matter how long it falls on the metal surface or how high is its intensity. The threshold frequency is different for different metals.

2. The kinetic energy of ejected electrons is independent of the intensity of the incident light but varies linearly with its frequency.

3. The number of ejected electrons from the metal surface depends upon the intensity of the incident radiation. The greater the intensity, the larger is the number of ejected electrons.

The photoelectric effect cannot be explained on the basis of the classical wave theory of light. According to this theory, energy of light depends on its *intensity.* If this view is correct, then light of *any frequency,* if made sufficiently intense, can cause ejection of electrons. But this does not happen. The quantum theory of radiation affords an easy explanation for the photoelectric effect. According to this theory, light consists of bundles of energy called **photons,** the energy of each photon being equal to $h\nu$ where ν is the frequency of the light. When a photon of light of frequency ν_0 (threshold frequency) strikes an electron in a metal, it imparts its entire energy ($= h\nu_0$) to the electron. This energy enables the electron to break away from the atom by overcoming the attractive influence of the nucleus. Thus, each photon can eject one electron. If the frequency of the light is less than ν_0, there will be no ejection of electron. Now suppose the frequency of the light falling on a metal surface is higher than the threshold frequency. Let it be ν. When photon of this light strikes a metal surface, some of its energy (which is equal to the energy binding the electron with the nucleus) is consumed to separate the electron from the metal and the remaining energy will be imparted to the ejected electron to give it certain velocity u (*i.e.,* kinetic energy $= \frac{1}{2}mu^2$). Einstein, applying quantum theory, showed that

$$h\nu = \phi + \tfrac{1}{2}mu^2 \qquad ...(9)$$

where ϕ is the threshold energy (or the **work function**) of the metal and $\frac{1}{2}m_e u^2$ is the kinetic energy imparted to the ejected electron. Evidently,

$$\phi = h\nu_0 \qquad ...(10)$$

Substituting the above value of ϕ in Eq. 9 and rearranging, we have

$$\tfrac{1}{2}mu^2 = h(\nu - \nu_0) \qquad ...(11)$$

Eq. 11 is the **Einstein photoelectric equation.** Albert Einstein (1879–1955), the German physicist, won the Physics Nobel Prize in 1921 for explaining the photoelectric effect and other contributions to mathematical physics. It may be mentioned that Einstein's contributions to the Theory of Relativity, considered controversial in those days, were not mentioned in the Nobel Prize citation.

Eq. 11 was tested by Robert Millikan. The kinetic energies of the emitted electrons for various frequencies of light were determined by finding the opposing potential required to stop the photoelectric current. Knowing kinetic energy corresponding to a given incident light of frequency ν and also knowing ν_0, *i.e.,* the threshold frequency required just to cause ejection of electrons, the value of h was calculated. It was found to be $6{\cdot}570\times10^{-34}$ J s. This is in excellent agreement with the value $6{\cdot}626\times10^{-34}$ J s obtained from experiments on black body radiations.

It is evident from the above discussion that photoelectric effect can be explained only on the basis of the corpuscular or particle theory of light. But certain phenomena, such as diffraction, interference and polarisation of light, can be explained only on the basis of the classical wave theory of light. Thus, light is considered to have a **dual character.** It behaves as a *particle* and also as a *wave.*

Example 1. A photon of wave length 4000 Å strikes a metal surface, the work function of the metal being 2·13 eV. Calculate *(i)* the energy of the photon in eV *(ii)* the kinetic energy of the emitted photo-electron and *(iii)* the velocity of the photo-electron. Mass of electron = $9{\cdot}109\times10^{-31}$ kg.

Solution : *(i)* Energy of the photon :

$$\nu = c/\lambda = 3\times10^{8}\ \text{m s}^{-1}/4000\times10^{-10}\ \text{m} = 7{\cdot}5\times10^{14}\ \text{s}^{-1}$$

$$E = h\nu = (6{\cdot}626\times10^{-34}\ \text{J s})\ (7{\cdot}5\times10^{14}\ \text{s}^{-1}) = 4{\cdot}97\times10^{-19}\ \text{J}$$

Since $1\ \text{eV} = 1{\cdot}602\times10^{-19}\ \text{J}$

$$\therefore \quad E = 4{\cdot}97\times10^{-19}\ \text{J}/1{\cdot}602\times10^{-19}\ \text{J/eV} = 3{\cdot}10\ \text{eV}$$

***(ii)* Kinetic energy of emitted photo-electron :**

$\phi = 2{\cdot}13$ eV. Hence, from Eq. 9,

$$\text{K.E.} = h\nu - \phi = 3{\cdot}10\ \text{eV} - 2{\cdot}13\ \text{eV} = 0{\cdot}97\ \text{eV}$$

***(iii)* Velocity of photo-electron :**

$$\text{K.E.} = \tfrac{1}{2}m_e u^2 = 0{\cdot}97\ \text{eV} = 0{\cdot}97\times1{\cdot}602\times10^{-19}\ \text{J}$$

$$\therefore \quad u = \left[\frac{2\times0{\cdot}97\times1{\cdot}602\times10^{-19}\ \text{J}}{9{\cdot}109\times10^{-31}\ \text{kg}}\right]^{1/2} = 5{\cdot}85\times10^{5}\ \text{m s}^{-1} \qquad (\text{J} = \text{kg m}^2\ \text{s}^{-2})$$

The Bohr's Model of the Atom

Niels Bohr, a Danish physicist, proposed his model of the atom in 1913. He retained Rutherford's model of a very small positively charged nucleus at the centre which contains all the protons and neutrons present in an atom. Bohr also agreed that the negatively charged electrons are revolving round the nucleus in the same way as the planets are revolving round the sun. But he took a bold step forward by applying Planck's quantum theory to the electron revolving round the nucleus. The important postulates of Bohr's theory are :

1. The electrons in an atom revolve around the nucleus only in certain selected circular orbits. As long as the electron remains in a particular orbit, it neither loses nor gains energy. In other words, the energy of an electron remains constant in a particular orbit. This leads to the idea that each orbit is associated with a definite energy, *i.e.*, with a definite whole number of quanta of energy. The orbits, therefore, are also known as energy levels or energy shells. Bohr gave numbers 1, 2, 3, 4, etc., (starting from the nucleus) to these energy levels. These numbers are now termed as principal quantum numbers. The various energy levels are also designated by letters *K, L, M, N,* etc. The farther the energy level from the nucleus, the greater is the energy associated with it.

2. The energy of an electron cannot change continuously. It changes only abruptly as the electron jumps from one energy level to another. The same idea has been expressed by the statement that for a change of electronic energy, the electron has to jump and not to 'flow' from one energy level to another.

3. The angular momentum of an electron moving round the nucleus is quantised. An electron, like any other body moving in a circular orbit, has an angular momentum given by *mur* where *m* is the mass, *u* is the linear velocity of the electron and *r* is the radius of the orbit. Bohr postulated that the angular momentum of an electron in an atom can have only definite or discrete values given by the expression

$$\text{Angular momentum} = mur = n(h/2\pi)$$

where *n* is any integer (1, 2, 3, etc.) Thus, the angular momentum of an electron may be $h/2\pi$ or a simple whole number multiple of $h/2\pi$ such as $2h/2\pi$, $3h/2\pi$,.....nh/π. This principle is known as quantisation of angular momentum.

Bohr Equation for the Energy of Electron in Hydrogen and Hydrogen-like Atoms. Working on the above postulates, Bohr was able to calculate the energy of the electron moving in different orbits round the nucleus in hydrogen or hydrogen-like atoms such as He^+, Li^{2+}, etc. He assumed, as had been

suggested by Rutherford, that the electron remains in its orbit because the electrostatic force of attraction exerted by the nucleus is exactly balanced by the centrifugal force arising from its circular motion.

Let the charge on the nucleus be $+Ze$. For hydrogen atom, $Z=1$ and for hydrogen-like atoms such as He^+ and Li^{2+}, $Z=2$ and 3, respectively. A hydrogen atom, having one proton in the nucleus and one electron outside the nucleus, is represented in Fig. 2. The electron with charge $-e$ revolves round the nucleus in an orbit of radius *r*. Let *u* be the tangential velocity and *m* be the mass of the electron.

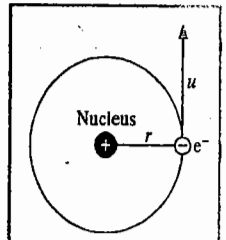

Fig. 2. Bohr's hydrogen atom.

According to the laws of classical mechanics, the centripetal force acting on the electron in a hydrogen-like atom, given by $Ze\times e/r^2$, tends to pull the electron towards the nucleus. However, the centrifugal force acting on the electron, given by mu^2/r tends to take it away from its orbit. Under the influence of these two opposing forces, the electron keeps on revolving in its orbit. When the two force balance,

$$Ze^2/r^2 = mu^2/r$$

Hence, $$u^2 = Ze^2/mr \qquad ...(12)$$

According to Bohr's postulate, the angular momentum, *mur*, is an integral multiple of $h/2\pi$, *i.e.*,

$$mur = n(h/2\pi)$$

or $$u = nh/2\pi mr \qquad ...(13)$$

Squaring Eq. 13, $$u^2 = n^2h^2 / 4\pi^2m^2r^2 \qquad ...(14)$$

Eliminating u^2 from Eqs. 12 and 14, we have

$$Ze^2/mr = n^2h^2 / (4\pi^2m^2r^2)$$

or $$Ze^2 = n^2h^2 / (4\pi^2mr) \qquad ...(15)$$

From Eq. 15, the radius *r* of the orbit is given by

$$r \equiv r_n = \frac{n^2h^2}{4\pi^2Zme^2} \qquad ...(16)$$

Since, for hydrogen atom, $Z=1$, hence,

$$r \equiv r_n = \frac{n^2h^2}{4\pi^2me^2} \qquad ...(17)$$

For hydrogen atom in the ground state ($n=1$), the radius of the orbit (r_1) is designated as the **Bohr radius**, a_0. Thus,

$$r_1 \equiv a_0 = \frac{h^2}{4\pi^2me^2} \qquad ...(18)$$

The total energy *E* of electron revolving in the *n*th orbit is equal to the sum of the kinetic energy ($= 1/2\ mu^2$) and the potential energy ($= -Ze^2/r_n$). Accordingly,

$$E = 1/2\ mu^2 - Ze^2/r_n \qquad ...(19)$$

From Eq. 12, $$mu^2 = Ze^2/r_n$$

Substituting the above value of mu^2 in Eq. 19, we have

$$E = \frac{Ze^2}{2r_n} - \frac{Ze^2}{r_n} = -\frac{Ze^2}{2r_n} \qquad ...(20)$$

Substituting the value of r_n from Eq. 16 in Eq. 20, we get

$$E = -\frac{Ze^2}{2} \times \frac{4\pi^2Zme^2}{n^2h^2} \qquad ...(21)$$

Thus, the **energy of electron in the *n*th orbit,** which we may designate as E_n, is given by

$$E_n = -\frac{2\pi^2 Z^2 me^4}{n^2h^2} \qquad ...(22)$$

This is the famous **Bohr equation** applicable to hydrogen and hydrogen-like atoms.

Niels Bohr (1885-1962), was awarded the 1922 Physics Nobel Prize for his investigations on the structure of the atom.

In **SI system,** Eqs. 16 and 22 take the forms

$$r_n = \frac{(4\pi\varepsilon_0)n^2h^2}{4\pi^2 Zme^2} \qquad ...(23)$$

$$E_n = -\frac{2\pi^2 Z^2 me^4}{(4\pi\varepsilon_0)^2 n^2h^2} \qquad ...(24)$$

The factor $4\pi\varepsilon_0$ is called the **permittivity factor,** its numerical value being $1{\cdot}11264\times10^{-10}$ C^2 N^{-1} m^{-2}.

Bohr Radius. According to Eq. 23, the Bohr radius of hydrogen atom (a_0) is given by

$$a_0 \equiv r_1 = \frac{(4\pi\varepsilon_0)h^2}{4\pi^2 me^2} = \frac{(1{\cdot}11264\times10^{-10}\,C^2\,N^{-1}\,m^{-2})(6{\cdot}626\times10^{-34}\,J\,s)^2}{4\pi^2(9{\cdot}109\times10^{-31}\,kg)(1{\cdot}602\times10^{-19}\,C)^2}$$

$$= 0{\cdot}529\times10^{-10}\ m$$

Velocity of Electron. According to Eq. 13, the velocity of electron, in the *first orbit* of hydrogen atom, is given by

$$u_1 = \frac{nh}{2\pi mr} = \frac{(1)(6{\cdot}626\times10^{-34}\,J\,s)}{2\pi(9{\cdot}109\times10^{-31}\,kg)(0{\cdot}529\times10^{-10}\,m)} = 2{\cdot}186\times10^{6}\ m\,s^{-1}$$

It may be noted that this velocity is about (1/150)th of the velocity of light.

The energy of electron in hydrogen atom ($Z=1$) in ground state, *i.e.*, when it is revolving in the first orbit ($n=1$), is easily obtained from Eq. 24. Thus,

$$E_1 = -\frac{(2\pi^2)(1)^2(9{\cdot}109\times10^{-31}\,kg)(1{\cdot}602\times10^{-19}\,C)^4}{(1{\cdot}11264\times10^{-10}\,C^2\,N^{-1}\,m^{-2})^2(1)^2(6{\cdot}626\times10^{-34}\,J\,s)^2} \qquad (J = kg\,m^2\,s^{-2})$$

$$= -2{\cdot}179\times10^{-18}\,J\ (\text{per atom}) = -1312{\cdot}19\ kJ\ mol^{-1}$$

$$= -\frac{2{\cdot}179\times10^{-18}\,J}{1{\cdot}602\times10^{-19}\,J/eV} = -13{\cdot}6\ eV\ (\text{per atom})$$

The energy of electron in excited states can be obtained by putting n = 2, 3, 4, etc., in Eq. 24.

Evidence for the Bohr quantization came from the celebrated **Franck-Hertz experiment** involving the impact of an electron on an atom. The German physicists James Franck (1882-1964) and Gustav Hertz (1887-1975) were awarded the 1926 Physics Nobel Prize for this work.

Bohr's Theory and the Origin of Hydrogen Spectrum. Hydrogen atom contains only one electron. But its spectrum consists of a large number of lines. Bohr supplied the reason. A given sample of hydrogen contains a very large number of atoms, of the order of several millions. Suppose energy is supplied to this sample of the gas. Now different atoms will absorb different amounts of energy. The

solitary electron in different atoms will, therefore, shift to different energy levels depending upon the energy absorbed by the atoms. Some of the hydrogen atoms, for example, may absorb sufficient energy to shift their electrons to the second energy level only while some others may absorb more energy and may be able to shift their electrons to third or even to one of the higher energy levels. The electrons then tend to fall back, almost immediately, to one or other of the lower energy levels. The various possibilities by which the electrons fall back from various excited state energy levels to lower energy levels (called electronic transitions), are depicted in Fig. 3. During each transition, energy is released which appears in the form of radiation of specific frequency and hence of specific wave length.

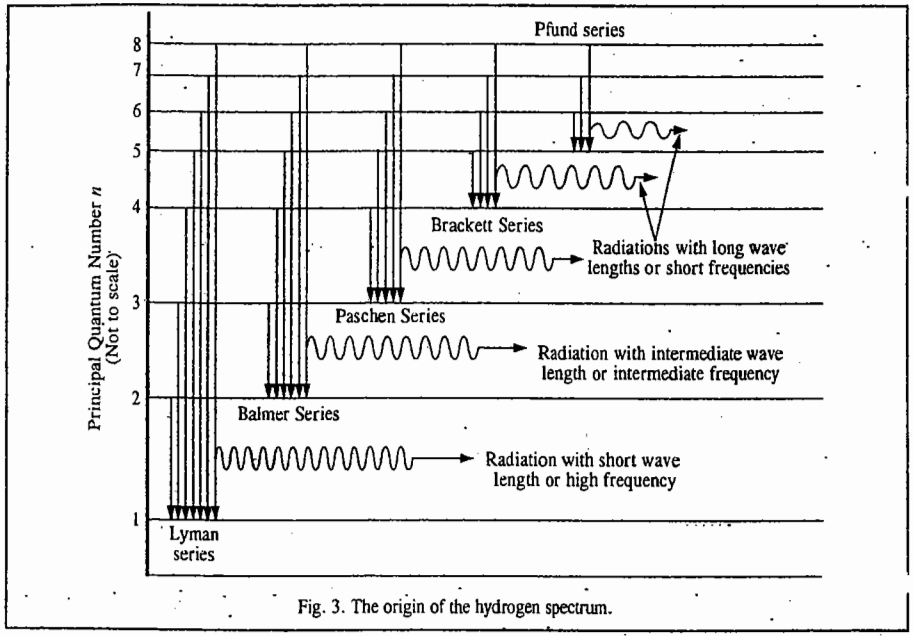

Fig. 3. The origin of the hydrogen spectrum.

Suppose an electron lying in energy level n_2 where its energy is E_2, jumps to a lower energy level n_1 where its energy is E_1. The energies in these two states, are

$$E_2 = -\frac{2\pi^2 me^4}{(4\pi\varepsilon_0)^2 n_2^2h^2} \quad \text{and} \quad E_1 = -\frac{2\pi^2 me^4}{(4\pi\varepsilon_0)^2 n_1^2h^2}$$

The difference in energy, $\Delta E = E_2 - E_1$, would be emitted in the form of radiation of a specific frequency and hence of a specific wave length. The emission spectrum of hydrogen would thus show a line at the frequency of the emitted radiation. If ν is the frequency of the spectral line, then

$$\Delta E = E_2 - E_1 = -\frac{2\pi^2 me^4}{(4\pi\varepsilon_0)^2 n_2^2h^2} + \frac{2\pi^2 me^4}{(4\pi\varepsilon_0)^2 n_1^2h^2} = h\nu \qquad ...(25)$$

or $$\nu = \frac{\Delta E}{h} = \frac{2\pi^2 me^4}{(4\pi\varepsilon_0)^2 h^3}\left(\frac{1}{n_1^2} - \frac{1}{n_2^2}\right)$$

or $$\bar{\nu} = \frac{1}{\lambda} = \frac{\nu}{c} = \frac{2\pi^2 me^4}{(4\pi\varepsilon_0)^2 h^3 c}\left(\frac{1}{n_1^2} - \frac{1}{n_2^2}\right) \qquad ...(26)$$

$$= R_H\left(\frac{1}{n_1^2} - \frac{1}{n_2^2}\right) \qquad ...(27)$$

where R_H is called the **Rydberg constant of the hydrogen atom**. Thus,

$$R_H = \frac{2\pi^2 me^4}{(4\pi\varepsilon_0)^2 h^3 c}\ \text{cm}^{-1} = \frac{2\pi^2 me^4}{(4\pi\varepsilon_0)^2 h^2}\ \text{J} \qquad ...(28)$$

(Frequency in cm^{-1} is multiplied by hc to get energy in joules)

Numerical value of $R_H = 109690{\cdot}8\ \text{cm}^{-1} = 21{\cdot}79 \times 10^{-19}\ \text{J} = 13{\cdot}6\ \text{eV}$

The appearance of various series of spectral lines in the emission spectrum of hydrogen can be easily explained with the help of Eq. 27. The **Lyman** series are produced when the electron jumps from the second, third, fourth or a higher energy level to the first energy level. The frequencies of the various spectral lines of this series can thus be obtained by substituting $n_1 = 1$ and $n_2 = 2, 3, 4$, etc., in Eq. 27. The Balmer series result when the electron jumps from third, fourth, fifth, etc., energy levels to the second energy level. The frequencies of the various spectral lines of the Balmer series can, thus, be obtained by substituting $n_1 = 2$ and $n_2 = 3, 4, 5, 6$, etc. In the same way, the Paschen series originate from the electronic jumps from the fourth, fifth, sixth, etc., energy levels to the third energy level. The frequencies of these spectral lines can be obtained by substituting $n_1 = 3$ and $n_2 = 4, 5, 6$, etc., in Eq. 28, and so on.

The frequencies (in wave numbers m^{-1}) of the spectral lines of the three series calculated from Eq. 27 and those determined experimentally, are given in Table 1.

TABLE 1

Frequencies in Wave Numbers (m^{-1}) of Various Lines of Hydrogen Spectrum

Lyman Series		Balmer Series		Paschen Series	
Experimental	**Calculated**	**Experimental**	**Calculated**	**Experimental**	**Calculated**
$82{\cdot}2 \times 10^5$	$82{\cdot}2 \times 10^5$	$15{\cdot}2 \times 10^5$	$15{\cdot}21 \times 10^5$	$5{\cdot}3 \times 10^5$	$5{\cdot}30 \times 10^5$
97·5	97·6	20·6	20·60	7·8	7·80
102·8	102·7	23·0	23·05	9·1	9·12
105·2	105·2	24·3	24·35	9·2	9·25
106·3	106·2	25·2	25·18	10·5	10·45
107·2	107·1	25·7	25·55		
108·0	107·9				

The agreement between the experimental and the calculated values is excellent. This offered a very strong support to Bohr's theory of the hydrogen atom.

Combining Eqs. 24 and 28, we get

$$E_n = -R_H Z^2/n^2 \qquad ...(29)$$

Example 2. Calculate the value of the Rydberg constant of hydrogen atom in eV.

Solution : $$R_H = \frac{1}{(4\pi\varepsilon_0)^2}\frac{2\pi^2 me^4}{ch^3}$$

Substituting the various values and remembering that $1\text{eV} = 8{\cdot}0655 \times 10^5\ \text{m}^{-1}$, we have

$$R_H = \frac{2(3{\cdot}14)^2(9{\cdot}1\times10^{-31}\text{kg})(1{\cdot}6\times10^{-19}\text{C})^4}{(1{\cdot}11265\times10^{-10}\text{N}^{-1}\text{C}^2\text{m}^{-2})^2(3\times10^8\text{ms}^{-1})(6{\cdot}626\times10^{-34}\text{Js})^3(8{\cdot}0655\times10^5\text{m}^{-1}/\text{eV})}$$

$(\text{J} = \text{kg m}^2\text{s}^{-2})$

$$= 13{\cdot}59\ \text{eV} \approx 13{\cdot}60\ \text{eV}$$

Example 3. Calculate the ground state energies of the electron (in eV) in the case of *(i)* H *(ii)* He^+ *(iii)* Li^{2+} (iv) Be^{3+} species, assuming that their Rydberg constants are equal.

Solution : From Eq. 29, $E_n = -R_H Z^2/n^2$. For ground state ($n = 1$), $R_H = 13{\cdot}60$ eV (from example 2)

(i) For H $(Z = 1)$: $E_1 = -13{\cdot}60$ **eV**

(ii) For H^+ $(Z = 2)$: $E_1 = -(13{\cdot}60)\,(2)^2 = -54{\cdot}40$ **eV**

(iii) For Li^{2+} $(Z = 3)$: $E_1 = -(13{\cdot}60)\,(3)^2 = -122{\cdot}40$ **eV**

(iv) For Be^{3+} $(Z = 4)$: $E_1 = -(13{\cdot}60)\,(4)^2 = -217{\cdot}60$ **eV**

Example 4. Show that the ground state energy of electron in hydrogen atom is equal to the first excited state energy of electron in He^+ ion, assuming that their Rydberg constants are equal.

Solution : $E_n = -R_H Z^2/n^2$; $(n = 1, 2, 3, \ldots.) = -13{\cdot}60\ Z^2/n^2$ eV (from Example 2)

For hydrogen atom in ground state, $Z = 1$, $n = 1$, $\therefore E_1 = -13{\cdot}60$ **eV**

For He^+ ion in first excited state, $Z = 2$, $n = 2$, $\therefore E_2 = -13{\cdot}60$ **eV**

Hence the result.

Example 5. Calculate the short and the long wave length limits of Lyman series in the spectrum of hydrogen. Given $R_H = 109{,}691\ \text{cm}^{-1}$.

Solution : From Eqs. 26 and 27,

$$\bar{\nu} = \frac{1}{\lambda} = R_H\left[\frac{1}{n_1^2} - \frac{1}{n_2^2}\right]$$

For short wave length limit, $\lambda = \lambda_s$, $n_1 = 1$ $n_2 = \infty$. Hence, we find that $\lambda_s = 91{\cdot}16$ **nm**

For long wave length limit, $\lambda = \lambda_l$, $n_1 = 1$ $n_l = 2$. Hence, we find that $\lambda_l = 0{\cdot}1215$ **nm**

Example 6. Calculate the value of the Bohr radius.

Solution : The Bohr radius, *i.e.*, radius of the electron in the first orbit of hydrogen atom, is given by

$$a_0 = \frac{(4\pi\varepsilon_0)h^2}{4\pi^2 me^2} = \frac{1{\cdot}11265\times10^{-10}\,\text{N}^{-1}\text{C}^2\text{m}^{-2}\left(6{\cdot}626\times10^{-34}\ \text{Js}\right)^2}{(4)(3{\cdot}14)^2\,(9{\cdot}1\times10^{-31}\,\text{kg})(1{\cdot}6\times10^{-19}\,\text{C})^2}$$

$$= 5{\cdot}29\times10^{-11}\ \text{m} = 52{\cdot}9\ \text{pm}$$

Example 7. Calculate the radii of the second, third and fourth orbits of hydrogen atom ($a_0 = 0{\cdot}53$Å).

Solution : The radius of the *nth* orbit is given by

$$r_n = n^2 a_0\ ;\ n = 1, 2, 3.....$$

(1) $n = 2$, $r_2 = 2^2\,(0{\cdot}53\ \text{Å}) = 2{\cdot}12\ \text{Å} = 212$ **pm**

(2) $n = 3$, $r_3 = 3^2\,(0{\cdot}53\ \text{Å}) = 4{\cdot}77\ \text{Å} = 477$ **pm**

(3) $n = 4$, $r_4 = 4^2\,(0{\cdot}53\ \text{Å}) = 8{\cdot}48\ \text{Å} = 848$ **pm**

Example 8. Which state of the triply ionized beryllium (Be^{3+}) has the same orbital radius as that of the ground state of hydrogen atom ?

Solution : For hydrogen atom, $r_1 = (4\pi\varepsilon_0)h^2/(4\pi^2 me^2)$ ...*(i)*

For hydrogen-like atom, $r_n' = (4\pi\varepsilon_0)\,n^2h^2/(4\pi^2 mZe^2)$ ...*(ii)*

Dividing Eq. *(ii)* by Eq. *(i)*, we get $r_n'/r_1 = n^2/Z = n^2/4$ $(\because Z = 4$ for $Be^{3+})$

Since $r_n' = r_1$, hence $n = 2$

Thus, the second energy level of Be^{3+} ion has the same radius as that of the ground state of hydrogen atom.

Sommerfeld's Extension of the Bohr Theory

Bohr theory of hydrogen atom enabled calculation of radii and energies associated with the permissible orbits in the hydrogen atom. The calculated values were found to be in good agreement with the experimental values. This theory could also explain successfully the positions of various series of spectral lines in the hydrogen spectrum. The theory was, therefore, largely accepted. However, a few

years later, the use of spectroscopes of high resolving powers revealed the presence of *fine structures* (*i.e.*, groups of closely spaced spectral lines) in the spectrum of hydrogen. Bohr's theory could not explain the occurrence of groups of these closely spaced spectral lines. The theory was, therefore, extended by Arnold Sommerfeld (1868–1951), the German mathematical physicist, by putting forward the idea of *elliptical orbits*.

According to Sommerfeld, an electron revolving around a central positively charged nucleus is so influenced by the nuclear charge that it is set into motion in elliptical orbits with the nucleus situated at one of the foci (Fig. 4). Thus, while according to Bohr's theory, electrons move in circular orbits, according to Sommerfeld's modification, electrons move in elliptical orbits. In the latter case, there will be a major axis and a minor axis having different lengths. As the orbit broadens, the lengths of the two axes become closer and they become equal when the orbit becomes circular, as shown in Fig. 4. Thus, the circular orbit is only a special case of elliptical orbits.

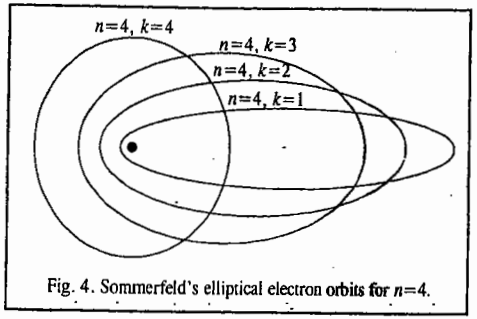

Fig. 4. Sommerfeld's elliptical electron orbits for $n=4$.

The electron travelling in an elliptical orbit will have its angular momentum. The momentum, according to the quantum theory, must also be quantised and thus can have only a limited number of values given by the factor $kh/2\pi$ where k is an integer known as the *azimuthal quantum number*. It can be shown that n, the principal quantum number, used by Bohr and k, the azimuthal quantum number used by Sommerfeld, are related to one another as

$$\frac{n}{k} = \frac{\text{length of major axis}}{\text{length of minor axis}} \qquad ...(30)$$

Thus, for any given value of n (except 1), k can have more than a single value. When $k=n$, the orbit must be circular. But, as k becomes smaller, the orbits become elliptical with greater and greater eccentricity (Fig. 4). It may be noted that k cannot be zero because in that case minor axis would be zero which would imply linear motion of the electron passing through the nucleus. The number of possible values of k is equal to the principal quantum number n. Thus, if n is 4, k can have four values; *viz.*, 4, 3, 2 and 1. When n is 1, k can have only one value.

According to Sommerfeld's extension of Bohr theory, also referred to as the **Bohr–Sommerfeld model,** the energy depends not only on n, the principal quantum number, but also, on the azimuthal quantum number, k. Hence, the transition of an electron from one energy level n_2 to another energy level n_1 will be different as it would also depend upon the various possible values of k in the two states. This explains the occurrence of groups of very closely spaced spectral lines observed in the hydrogen spectrum by using highly refined spectroscopes. The frequencies of some of these spectral lines were found to be in agreement with the frequencies calculated from the Bohr–Sommerfeld model.

Alternative Explanation for the Emission of Fine Hydrogen Spectrum. The emission of fine structure hydrogen spectrum referred to above can be explained more satisfactorily by taking into consideration the role of angular momentum of the electron, as discussed below.

Electron moving around the nucleus in a particular orbit will have a particular angular momentum called the *orbital angular momentum*. A portion of the energy of the electron will be associated with its angular momentum which is described by the quantum number l, called the **orbital angular momentum quantum number.** This is related to the principal quantum number n as $l = n - 1$. Electrons in an atom are thus grouped together not only into major energy shells given by n but also into energy subshells given by l.

Since $l=n-1$, hence the value of l will be 0, 1, 2, 3 ... according as the value of n = 1, 2, 3, ... respectively. The subshells corresponding to $l=0$, 1, 2, 3 ... are designated as *s, p, d, f,* ... subshells, respectively

If $n=1$, l will have only one value, *i.e.*, 0. There will, therefore, be only one subshell, *viz.*, *s* subshell. Thus, the first major shell will have only one subshell.

If $n=2$, l will have two values, *i.e.*, 0 and 1. Thus, the second energy shell will have two subshells, *viz.*, *s* and *p* subshells.

If $n=3$, l will have three values, *i.e.*, 0, 1 and 2. There would thus be three subshells, *viz.*, *s, p* and *d* subshells according as the value of $l=0$, 1 and 2, respectively. Thus, the third energy shell will have three subshells.

Similarly, the fourth energy shell will have four subshells, *s, p, d* and *f* and so on.

Suppose in a spectral study, on excitation of hydrogen atoms, the solitary electrons move to the fourth energy shell. The fourth major energy shell will have four subshells, *viz., s, p, d* and *f* subshells. The electrons will thus be present in the *s, p, d* and *f* subshells of the fourth energy shell. Electronic transitions would thus take place from these four subshells to the lower levels. The energies released during these transitions would appear in the form of a group of four spectral lines differing only slightly in their frequencies because the energies of the *s, p, d* and *f* subshells differ only slightly from one another. This explains the occurrence of a group of four closely spaced lines in the spectrum of hydrogen. If, however, the spectroscope is not powerful enough to resolve these frequencies, the electronic transitions would appear in the form of a single spectral line of a composite frequency as was observed by Bohr.

According to the **Heisenberg uncertainty principle**, (discussed later in details), it is impossible to determine simultaneously the exact position and velocity (momentum) of a minute moving particle like an electron. Therefore, the postulate of Bohr theory that electrons revolve round the nucleus in *well defined orbits* with *will defined velocities* is untenable.

In order to overcome this shortcoming, the use of the term orbit in electronic motion has been dispensed with. In its place, we make use of the term **energy level** or **energy shell** only. This is because energy of an electron can be known with certainty but *not* its position.

Wave-Particle Duality of Electron. Einstein had suggested, in 1905, that light has a *dual character ; as wave* and also as '*particle*'. The French physicist Louis de Broglie (1892–1987) proposed that *matter also has a dual character;* as wave and as particle. The name *wavicle* was suggested for such a particle. de Broglie was awarded the Physics Nobel Prize in 1929.

In Bohr's theory, electron is treated as a particle. But, de Broglie's theory suggested that matter and, therefore, electron also, has a dual character, both as a material particle and as a wave. He derived an expression for calculating the wave length λ of a particle of mass m moving with velocity u according to which

$$\lambda = h/mu \qquad ...(31)$$

Eq. 31 is known as the **de Broglie equation.**

The de Broglie equation can be easily derived by using the Einstein's mass-energy relationship, *viz.*, $E=mc^2$.

Equating this energy with the energy of a photon associated with frequency ν, we have

$$h\nu = mc^2 \qquad ...(32)$$

Since $\nu=c/\lambda$, hence $hc/\lambda = mc^2$ so that

$$\lambda = h/mc \qquad ...(33)$$

Replacing c by the velocity of the electron, u, we have

$$\lambda = h/mu = h/p \qquad ...(34)$$

where p is the linear momentum of the particle.

Example 9. Calculate the de Broglie wave length of electron moving with a velocity of $1{\cdot}20\times10^5$ m s^{-1}.

Solution : $\lambda = \dfrac{h}{m_e u} = \dfrac{(6{\cdot}626\times10^{-34}\ \text{J s})}{(9{\cdot}1\times10^{-31}\ \text{kg})(1{\cdot}20\times10^5\ \text{m s}^{-1})} = 6{\cdot}068\times10^{-9}$ m. $\quad (\text{J} = \text{kg m}^2\ \text{s}^{-2})$

Example 10. Calculate the de Broglie wave length of a body of mass 1 kg moving with a velocity of 2000 m s^{-1}.

Solution : $\lambda = \dfrac{h}{mu} = \dfrac{6{\cdot}626\times10^{-34}\ \text{J s}}{(1\ \text{kg})(2000\ \text{m s}^{-1})} = 3{\cdot}313\times10^{-37}$ m $\quad (\text{J} = \text{kg m}^2\ \text{s}^{-2})$

It may be noted that the above wave length is too small to be measured by any conceivable technique.

Distinction between matter waves and electromagnetic waves. It should be carefully noted that matter waves are distinctly different from electromagnetic waves. The speed of these waves is not the same as that of light ; it is, understandably, much less. These waves cannot be radiated in empty space. They are certainly not emitted by the particle under consideration ; they are simply associated with it. The wave lengths of matter waves are generally very small as compared to the wave lengths of electromagnetic waves.

Derivation of the Bohr Angular Momentum Postulate from de Broglie's Relation. Consider an electron moving in a circular orbit of radius r around a nucleus. The wave train would be as shown in Fig. 5. Evidently, if the wave is to remain continually in phase (Fig. 5 *a*), the circumference of the circular orbit must be an integral multiple of wave length λ, that is,

$$2\pi r = n\lambda = nh/mu \qquad ...(35)$$

Thus, the angular momentum,

$$L = mur = nh/2\pi \qquad ...(36)$$

This is the Bohr postulate.

Evidently, if the circumference is bigger or smaller than the value $nh/2\pi$ given in Eq. 36, the wave will no longer remain in phase (Fig. 5 *b*).

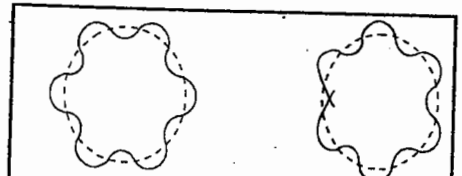

(a) Wave continually in phase *(b)* Wave not in phase

Fig. 5. The wave trains of an electron moving in a circular path around a nucleus.

Experimental verification of de Broglie's equation. The verification of de Broglie's equation is possible only by deriving from it certain consequences which may then be tested experimentally.

Let an electron of charge e be accelerated by a potential $\Delta\phi$. Then its kinetic energy is $e\Delta\phi$. The kinetic energy is also equal to $\frac{1}{2}mu^2$ where u is velocity of the electron. Thus,

$$\tfrac{1}{2}mu^2 = e\Delta\phi \quad \text{or} \quad u = (2e\Delta\phi/m)^{1/2} \qquad ...(37)$$

Substituting this value of u into de Broglie's equation, we have

$$\lambda = h/(2me\Delta\phi)^{1/2} \qquad ...(38)$$

Incorporating the numerical values of various quantities, we have

$$\lambda = \frac{6{\cdot}626\times10^{-34}\ \text{J s}}{[(2)(1{\cdot}602\times10^{-19}\ \text{C})(9{\cdot}109\times10^{-31}\ \text{kg})(\Delta\phi\ \text{volt})]^{1/2}}$$

$$= 12{\cdot}26\times10^{-10}\,\Delta\phi^{-1/2}\ \text{m} \qquad ...(39)$$

where $\Delta\phi$ is the numerical value of potential in volts.

If an electron is accelerated through a potential of 100 volts, its wave length should be $1{\cdot}226\times10^{-10}$ m. If potentials are varied between 10 and 10,000 volts, λ should vary between $3{\cdot}877\times10^{-10}$ m and $0{\cdot}1226\times10^{-11}$ m. It is well known that X-rays have wave lengths of this order. It is also well known that crystalline solids can act as diffraction gratings for X-rays having wavelengths

of the above order. Therefore, if de Broglie's view regarding wave-particle duality of electron is correct, the crystalline solids should act as diffraction gratings for a beam of electrons as well. This has been verified experimentally.

Davisson-Germer Experiment. The de Broglie hypothesis regarding wave character of electron received first experimental support from C.J. Davisson and L.H. Germer. In their experiment, electrons were emitted from a hot filament and were accelerated by a potential ranging between 40 and 68 volts before striking a nickel plate, as shown in Fig. 6.

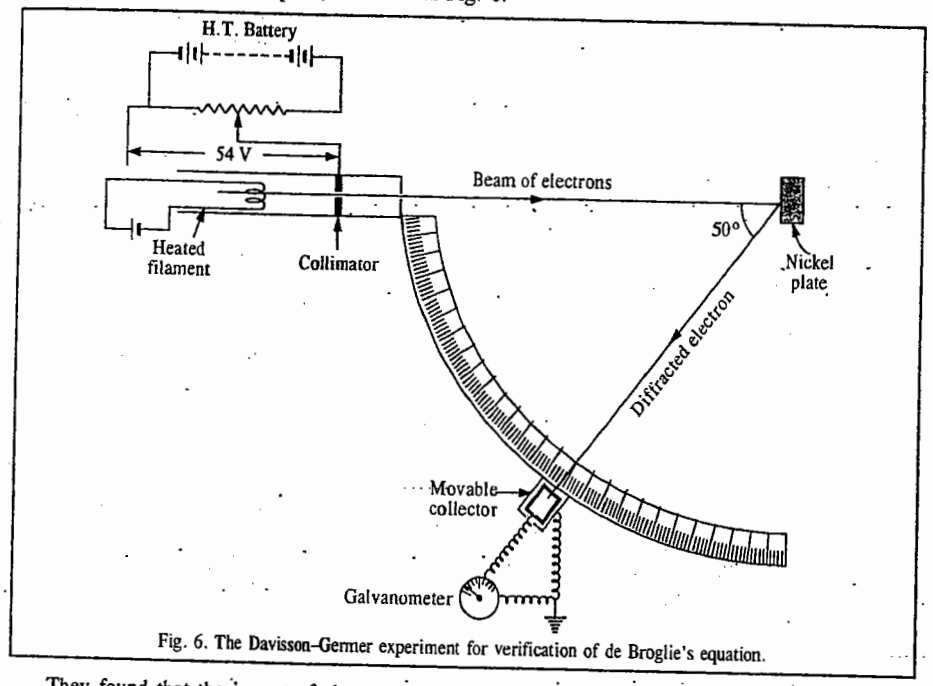

Fig. 6. The Davisson–Germer experiment for verification of de Broglie's equation.

They found that the impact of electrons resulted in the production of diffraction patterns which were similar to those given by X-rays under similar conditions. Since X-rays possess wave character, the experiment gave direct evidence for wave character of electron as well.

The intensities of electron waves scattered by the nickel plate at different angles were measured. It was found that the reflection was most intense and took place at an angle of 50° when electrons were accelerated through 54 volts. Substituting the value of $\Delta\phi$ as 54 V in Eq. 39, it can be shown that the value of λ, the wave length of the electron wave, comes out to be 1·668 Å. This wave length also lies in the range of X-rays. This is another point of similarity between electron waves and X-rays. It should be possible, therefore, to apply the Bragg equation derived for X-ray diffraction, to electron diffraction as well. According to this equation

$$2d\sin\theta = n\lambda \qquad ...(40)$$

when n is a whole number (1, 2, 3, etc.) of wave length λ for a reflection of maximum intensity, d is the distance between successive lattice planes of the crystal (nickel crystal in the present case) and θ is the grazing angle of the waves. This provided an independent experimental method for determining wave length of electron waves. Davisson and Germer found the value of λ to be very close to that obtained by de Broglie's equation. The Davisson–Germer experiment thus offered full support to de Broglie's views and his equation. The American physicist C.J. Davisson (1881–1958) shared the 1937 Physics Nobel Prize with the British physicist G.P. Thomson (1892–1975) for the investigation of electron diffraction by crystals. It has been remarked that J.J. Thomson was awarded the Nobel

Prize for showing that the electron is a *particle* and G.P. Thomson, his son, was awarded the Nobel Prize for showing that the electron is a *wave*.

Heisenberg's Uncertainty Principle. It states that *it is not possible to determine precisely both the position and the momentum (velocity) of a small moving particle.*

Consider a photon incident on a particle. If the particle is of reasonable size, its position or velocity will not be altered by the impact of light photons. Hence it will be possible to know exactly both the position and velocity of the particle. But, this cannot be so when the particle is extremely minute, such as an electron. It will suffer a change in its velocity and path due to the impact of even a single photon of light used to observe it. The path and velocity of an electron, after the impact of light photons, may be quite different from the original path and velocity. For an electron moving in x-direction, the Heisenberg uncertainty principle is expressed mathematically as

$$(\Delta x)(\Delta p_x) \geq h/4\pi \qquad \ldots(41)$$

where Δx is uncertainty with regard to its position and Δp_x is the corresponding uncertainty with regard to its momentum. Evidently, if Δx is very small, *i.e.*, the position of a particle is known more or less exactly, Δp would be large, *i.e.*, uncertainty with regard to momentum will be large. Similarly, if an attempt is made to measure exactly the momentum of the particle, the uncertainty with regard to position will become large. Werner Heisenberg (1900–1976), the German physicist, won the Physics Nobel Prize in 1932.

Example 11. A microscope using suitable photons is employed to locate an electron in an atom within a distance of 0·1 Å. What is the uncertainty involved in the measurement of its velocity ? Mass of electron = $9{\cdot}1\times10^{-31}$ kg.

Solution : From Eq. 41,

$$\Delta x \times \Delta p_x \geq h/4\pi \quad \text{or} \quad \Delta x \times m\Delta u_x \geq h/4\pi$$

$$\therefore \quad 0{\cdot}1\times10^{-10}\ \text{m}\times9{\cdot}1\times10^{-31}\ \text{kg}\times\Delta u_x = 6{\cdot}626\times10^{-34}\ \text{J s}/4\pi$$

$$\Delta u_x = 0{\cdot}579\times10^{7}\ \text{m s}^{-1} \qquad (\text{J} = \text{kg m}^2\ \text{s}^{-2})$$

Example 12. A cricket ball weighing 100 g is to be located within 0·1 Å. What is the uncertainty in its velocity ? Comment on your result.

Solution : From Eq. 41,

$$\Delta x \times \Delta p_x \geq h/4\pi \quad \text{or} \quad \Delta p_x \geq h/4\pi\Delta x$$

$$\therefore \quad \Delta u_x = \Delta p_x/m = h/4\pi\Delta x m = 6{\cdot}626\times10^{-34}/4\pi(10^{-11}\ \text{m})\ (0{\cdot}1\ \text{kg}) = 0{\cdot}527\times10^{-22}\ \text{m s}^{-1}$$

Comparing this value with the typical velocity of a cricket ball, we find that this uncertainty in velocity is completely negligible. This means that we can disregard the uncertainty principle for the motion of *macroscopic bodies*. We can thus say that for such cases, both the position and velocity can be determined to a reasonable degree of precision.

Compton Effect. Arthur Compton found that if monochromatic X-rays (*i.e.*, X-rays having one particular wave length) are allowed to fall on carbon or some other light element, the scattered X-rays have wave lengths larger than the incident rays. In other words, the scattered X-rays have lower frequency, *i.e.*, lower energy than the incident X-rays. Since scattering is caused by electrons, it is evident that some interaction between X-rays and electrons has taken place and this has resulted in decrease in energy of the former. This decrease in energy or increase in wave length of X-rays after scattering from the surface of an object is known as the **Compton effect.**

By applying the law of conservation of energy and the law of conservation of momentum and assuming X-rays to consist of photons, each possessing energy equal to $h\nu$, Compton showed that

$$\Delta\lambda = (2h/mc)\sin^2(\theta/2) \qquad \ldots(42)$$

where $\Delta\lambda$ is the increase in the wave length (termed as **Compton shift**) produced as a result of the collision, m is the rest mass of the electron, c is the velocity of light and θ is the angle between the incident and the scattered X-rays.

According to this equation, Compton shift should be independent of the wavelength of the incident X-rays. This has been found to be so experimentally. Further, the values of Compton shift, as obtained from the above equation, by substituting the known values of h, c, m and θ, have been found to be in close agreement with the experimental values. Arthur Compton (1892–1962), the American physicist, shared the 1927 Physics Nobel Prize with C.T.R. Wilson (1869-1959).

Compton effect provides a good illustration of the uncertainty principle. Suppose X-rays are used to determine the position and momentum of an electron. As a result of mutual interaction of X-rays and the electron, the wave length of X-rays increases, *i.e.*, the frequency or energy of the X-rays decreases. This energy must have been transferred to the electron and, therefore, the momentum of the electron must have changed during the process. Consequently, the momentum of the electron cannot be determined with certainty. Compton effect also provides evidence for the corpuscular or photon nature of radiation. The Compton equation (42) can also be written as

$$\Delta\lambda = \lambda' - \lambda = \frac{h}{mc}(1 - \cos\theta) \qquad \ldots(43)$$

We see that the wave length λ' of scattered X-rays is always greater than the wave length λ of incident X-rays. The wave length shift is independent of the nature of the substance and the wave length of incident X-rays. It depends only on the scattering angle θ. The following three cases may be considered :

Case 1. $\theta = 0°$, *i.e.*, the scattered radiation is parallel to the incident radiation. In this case, $\cos\theta = 1$ so that $\Delta\lambda = 0$, *i.e.*, there is no wave length shift.

Case 2. $\theta = 90°$, *i.e.*, the scattered radiation is perpendicular to the incident radiation. In this case, $\cos\theta = 0$ so that

$$\Delta\lambda = h/mc = 6{\cdot}626\times10^{-34}\ \text{J s}/(9{\cdot}109\times10^{-31}\ \text{kg})(3\times10^{8}\ \text{m s}^{-1})$$
$$= 0{\cdot}02422\times10^{-10}\ \text{m}$$

In the present case, $\Delta\lambda$ is referred to as the **Compton wave length.**

Case 3. $\theta = 180°$, *i.e.*, the radiation is scattered in a direction opposite to the incident radiation. In this case, $\cos\theta = -1$ so that

$$\Delta\lambda = 2h/mc = 0{\cdot}0484\times10^{-10}\ \text{m}$$

This is twice the value of the Compton wave length.

QUANTUM MECHANICS (WAVE MECHANICS)

Introduction to Quantum Mechanics. Classical mechanics, as formulated by Sir Isaac Newton (1642—1727) in the seventeenth century, is obeyed by *macroscopic* 'particles' such as planets and rigid bodies. However, since the *microscopic* particles such as electrons, protons, atoms and molecules show wave-particle duality, they do not obey Newtonian dynamics. They, however, obey **quantum mechanics** (or **wave mechanics**) a key feature of which is the quantization of energy and angular momentum. The laws of quantum mechanics were formulated in 1925 by the German physicists M. Born, W. Heisenberg and P. Jordan (in the formulation known as **matrix mechanics**) and in 1926 by the Austrian physicist E. Schrödinger. The Schrödinger formulation of quantum mechanics is more familiar to chemists than the Born–Heisenberg–Jordan formulation of matrix mechanics, though both the forms are equivalent. We shall not discuss matrix mechanics in this book. In 1928, P.A.M. Dirac, the British physicist, formulated his celebrated **relativistic quantum mechanics** and showed that the electron spin emerges as a natural consequence of his theory whereas in the Schrödinger non-relativistic quantum mechanics, it has to be imposed later. Again, we shall not discuss the Dirac theory though it has become indispensable in the physics of elementary particles whose velocities approach that of light when accelerated in a cyclotron and other high energy accelerators.

Now we shall dwell on the reason why the Heisenberg uncertainty principle forces us to abandon Newtonian mechanics. We know that the motion of a one-particle, one-dimensional classical system

is governed by Newton's second law of motion, *i.e.*, $F = ma = md^2x/dt^2$. In order to obtain the position x as a function of time, this differential equation is to be integrated twice with respect to time. The first integration yields dx/dt and the second integration gives x. Each integration, however, introduces an arbitrary integration constant. Hence, the integration of $F=ma$ gives an equation for x that contains two unknown constants c_1 and c_2. We thus have

$$x = f(t, c_1, c_2) \qquad ...(44)$$

where f is some function. To evaluate c_1 and c_2 we require two pieces of information about the system. If we know that at a certain time t_0, the particle is at the position x_0 and has speed u_0, then c_1 and c_2 can be calculated from the equations

$$x_0 = f(t_0, c_1, c_2) \quad \text{and} \quad u_0 = f'(t_0, c_1, c_2), \qquad ...(45)$$

where f' is the derivative of f with respect to t. Thus, if we know the force F and the initial position and velocity (or linear momentum) of the particle, we can use Newton's second law of motion to predict the position of the particle at any future time. The same argument holds for a three-dimensional, many-particle system.

In classical mechanics, the *state of a system* is defined by specifying all the forces acting and all the positions and velocities (or momenta) of the particles. Thus, as stated above, a knowledge of the present state of a classical mechnical system allows its future state to be predicted with certainty. It is at this stage that the Heisenberg uncertainty (or indeterminacy) principle comes into the picture. It shows that simultaneous specification of position and momentum is impossible for a microscopic particle. The state of a quantum mechanical system necessarily involves less knowledge about the system than in classical mechanics. In other words, the *certainties* of classical mechanics shall have to be abandoned in favour of the *uncertainties* of quantum mechanics. Classical mechanics is a deterministic theory in that it allows us to predict the exact paths (or trajectories) taken by the particles of the system and tells us where they will be at a future time. In contrast, quantum mechanics gives only the probabilities of finding the particles at various locations in space. Besides Newton, contributions to classical mechanics were made by the great French mathematicians Pierre-Simon Laplace (1749–1827) and Joseph L. Lagrange (1736–1813) and by the Irish mathematician William Rowan Hamilton (1805–1865).

As we shall see shortly, in quantum mechanics, the state of a system is defined by the state function or wavefunction ψ which is a function of the coordinates of the particles of the system and is also a function of time (since the state may change with time). Thus, for a two-particle system, the wavefunction can be written as

$$\psi = f(x_1, y_1, z_1, x_2, y_2, z_2, t) \qquad ...(46)$$

where x_1, y_1, z_1 are the coordinates of particle 1, etc. For an n-particle system, the equation governing the time-dependence of ψ is given by

$$\sum_{i=1}^{n} -\frac{\hbar^2}{2m_i}\left(\frac{\partial^2\psi}{\partial x_i^2}+\frac{\partial^2\psi}{\partial y_i^2}+\frac{\partial^2\psi}{\partial z_i^2}\right) + V(x_i, y_i, z_i, t)\psi = i\hbar\frac{\partial\psi}{\partial t} \qquad ...(47)$$

where m_i is the mass and V is the potential energy of the particle.

The above equation is the celebrated *time-dependent second-order differential equation*, known as the Schrödinger wave equation. Notice that this equation contains the first derivative of ψ with respect to time. Therefore, a single integration with respect to time gives us ψ. Integration of this equation thus introduces only one integration constant which can be evaluated if ψ is known at the initial time t_0. Thus, knowing the initial quantum mechanical state, we can use this equation to predict the future quantum mechanical state. The time-dependent Schrödinger wave equation is the quantum mechanical analogue of Newton's second law which allows the future state of a classical mechanical system to be predicted from its present state. However, the knowledge of the state in quantum mechanics usually involves a knowledge of only *probabilities* rather than *certainties*.

We may ask, "what is the relation between quantum mechanics and classical mechanics ?" It is known experimentally that when $v \ll c$, *i.e., the velocity v of a macroscopic body is far less than the velocity of light c*, relativistic mechanics gives the same results as Newton's classical mechanics. Similarly, it was shown by P. Ehrenfest that in the classical limit of taking $h \to 0$ (where h is the Planck's constant), the time-dependent Schrödinger wave equation reduces to Newton's second law. This is a very remarkable result. Also, the Bohr correspondence principle (also called the principle of complementarity) states that classical mechanics and quantum mechanics tend to give the same results when systems are in highly excited quantum states.

It is interesting to point out that the probabilistic nature of quantum mechanics disturbed many physicists, including Schrödinger, de Broglie and Einstein. In 1926, Einstein wrote : "Quantum mechanics says a lot but does not really bring us closer to the secret of God. I, at any rate, am convinced that He does not throw dice." These and many other scientists believed that quantum mechanics does not furnish a complete description of physical reality. However, all attempts to replace quantum mechanics by an underlying causal deterministic theory, have failed. There appears to be some fundamental randomness at the microscopic level. As S. Hawking said, "Quantum mechanics allows us in principle to predict nearly everything around us, within the limits set by the uncertainty principle."

Postulates of Quantum Mechanics. The formulation of quantum mechanics or wave mechanics for the wave mechanical treatment of the structure of atom rests upon a few postulates which, for a system moving in one dimension, say, along the x-coordinate, are given below.

First Postulate. The physical state of a system at time t is described by the wavefunction $\psi(x, t)$.

Second Postulate. The wavefunction $\psi(x, t)$ and its first and second derivatives $\partial\psi(x,t)/\partial x$ and $\partial^2\psi(x,t)/\partial x^2$ are continuous, finite and single valued for all values of x. Also, the wavefunction $\psi(x, t)$ is *normalized, i.e.*,

$$\int_{-\infty}^{\infty} \psi^*(x,t)\,\psi(x,t)dx = 1 \qquad ...(48)$$

where ψ^* is the *complex conjugate* of ψ formed by replacing i with $-i$ wherever it occurs in the function $\psi(i = \sqrt{-1})$.

Third Postulate. A physically observable quantity can be represented by a *Hermitian operator.* An operator $\hat{A}$ is said to be Hermitian if it satisfies the following condition :

$$\int \psi_i^* \hat{A}\psi_j\,dx = \int \psi_j\,(\hat{A}\psi_i)^*\,dx \qquad ...(49)$$

where ψ_i and ψ_j are the wavefunctions representing the physical states of the quantum system, such as a particle, an atom or a molecule.

Fourth Postulate. The allowed values of an observable A are the eigenvalues, a_i, in the operator equation

$$\hat{A}\,\psi_i = a_i\psi_i \qquad ...(50)$$

Eq. 50 is known as an **eigenvalue equation.** Here $\hat{A}$ is the operator for the observable (physical quantity) and ψ_i is an eigenfunction of $\hat{A}$ with eigenvalue a_i. In other words, measurement of the observable A yields the eigenvalue a_i.

Fifth Postulate. The average value (or, the expectation value), $< A >$, of an observable A, corresponding to the operator $\hat{A}$, is obtained from the relation

$$< A > = \int_{-\infty}^{\infty} \psi^* \hat{A}\,\psi\,dx \qquad ...(51)$$

where the function ψ is assumed to be normalized in accordance with Eq. 48. Thus, the average value

of, say, the x-coordinate is given by

$$< x > = \int_{-\infty}^{\infty} \psi^* \hat{x} \psi \, dx \qquad ...(52)$$

Sixth Postulate. The quantum mechanical operators corresponding to the observables are constructed by writing the classical expressions in terms of the variables and converting the expressions to the operators, as shown in Table 2.

TABLE 2

Wave Mechanical Operators for Evaluating Various Classical Variables

Classical variable	Quantum mechanical operator	Operator	Operation
x	$\hat{x}$	x	Multiplication by x
p_x	$\hat{p}_x$	$-i\hbar\frac{\partial}{\partial x}$	Taking derivative with respect to x and multiplying by $-i\hbar$
x^2	$\hat{x}^2$	x^2	Multiplication by x^2
p_x^2	$\hat{p}_x^2$	$-\hbar^2\frac{\partial^2}{\partial x^2}$	Taking second derivative with respect to x and multiplying by $-\hbar^2$
t	$\hat{t}$	$\hat{t}$	Multiplying by t
E	$\hat{E}$	$i\hbar\frac{\partial}{\partial t}$	Taking derivative with respect to t and multiplying by $i\hbar$

Seventh Postulate. The wave function $\psi(x,t)$ is a solution of the time-dependent Schrödinger equation

$$\hat{H}\psi(x,t) = i\hbar\frac{\partial\psi(x,t)}{\partial t} \qquad ...(53)$$

where $\hat{H}$ is the Hamiltonian operator of the system.

The Schrödinger Wave Equation

Erwin Schrödinger, in 1926, gave a wave equation to describe the behaviour of electron waves in atoms and molecules. In Schrödinger's wave model of an atom, the discrete energy levels or orbits proposed by Bohr are replaced by mathematical functions, ψ, which are related to the probability of finding electrons at various places around the nucleus.

Consider a simple wave motion as that of the vibration of a stretched string. Let y be the amplitude of this vibration at any point whose coordinate is x at time t. The equation for such a wave motion may be expressed

$$\frac{\partial^2 y}{\partial x^2} = \frac{1}{u^2}\times\frac{\partial^2 y}{\partial t^2} \qquad ...(54)$$

where u is the velocity with which the wave is propagating. There are two variables, x and t, in the above differential equation, *i.e.*, the amplitude y depends upon two variables x and t.

In order to solve the above differential equation, it is necessary to separate the two variables. Thus, y may be expressed as

$$y = f(x)\, g(t) \qquad ...(55)$$

where $f(x)$ is a function of the coordinate x only and $g(t)$ is a function of the time t only. For stationary waves, such as occur in a stretched string, the function $g(t)$ is represented by the expression

$$g(t) = A \sin(2\pi\nu t) \qquad ...(56)$$

where ν is the vibrational frequency and A is a constant known as the maximum amplitude. Hence, for

stationary waves, the equation for y may be written as

$$y = f(x)\, A \sin(2\pi\nu t) \qquad ...(57)$$

Hence,
$$\frac{\partial^2 y}{\partial t^2} = -f(x)\, 4\pi^2\nu^2 A \sin(2\pi\nu t) \qquad ...(58)$$

$$= -4\pi^2\nu^2 f(x)\, g(t) \qquad ...(59)$$

Similarly, it follows from Eq. 57 that

$$\frac{\partial^2 y}{dx^2} = \frac{\partial^2 f(x)}{\partial x^2} g(t) \qquad ...(60)$$

Combining Eqs. 54, 59 and 60, we have

$$\frac{\partial^2 f(x)}{\partial x^2} = -\frac{4\pi^2\nu^2}{\nu^2} f(x) \qquad ...(61)$$

As is well known, the frequency of the vibrations ν is related to the velocity u by the expression $u=\nu\lambda$, where λ is the corresponding wave length. Hence, from Eq. 61, we have

$$\frac{\partial^2 f(x)}{\partial x^2} = -\frac{4\pi^2}{\lambda^2} f(x) \qquad ...(62)$$

Eq. 62 is valid for the wave motion in one dimension only. We may now extend it to three dimensions represented by the coordinates x, y and z. Evidently, $f(x)$ will then be replaced by the amplitude function for the three coordinates, say, $\psi(x, y, z)$. For the sake of simplicity, it may be put merely as ψ. Hence, Eq. 62 takes the form

$$\frac{\partial^2\psi}{\partial x^2}+\frac{\partial^2\psi}{\partial y^2}+\frac{\partial^2\psi}{\partial z^2} = -\frac{4\pi^2}{\lambda^2}\psi \qquad ...(63)$$

Following de Broglie's ideas, Schrödinger, the Austrian physicist, applied the above treatment to material waves associated with all particles including electrons, atoms and molecules.

Incorporating de Broglie's relationship, *viz.*, $\lambda = h/mu$, in Eq. 63, we have

$$\frac{\partial^2\psi}{\partial x^2}+\frac{\partial^2\psi}{\partial y^2}+\frac{\partial^2\psi}{\partial z^2} = -\frac{4\pi^2 m^2 u^2}{h^2}\psi \qquad ...(64)$$

where m is the mass and u is the velocity of the particle.

The kinetic energy of the particle given by $\frac{1}{2}mu^2$, is equal to the total energy E *minus* the potential energy V of the particle, *i.e.*,

$$K.E. = \tfrac{1}{2}mu^2 = E - V \quad \text{or} \quad mu^2 = 2(E - V) \qquad ...(65)$$

Combining this result with Eq. 64, we get

$$\frac{\partial^2\psi}{\partial x^2}+\frac{\partial^2\psi}{\partial y^2}+\frac{\partial^2\psi}{\partial z^2}+\frac{8\pi^2 m(E-V)}{h^2}\psi = 0 \qquad ...(66)$$

Eq. 66 is the well-known **Schrödinger wave equation** proposed by him in 1926. It is the most celebrated equation in wave mechanics. It is customarily written in the following form:

$$\left[-\frac{\hbar^2}{2m}\left(\frac{\partial^2}{\partial x^2}+\frac{\partial^2}{\partial y^2}+\frac{\partial^2}{\partial z^2}\right)+V\right] = E\psi \qquad ...(67)$$

or
$$\left[-\frac{\hbar^2}{2m}\nabla^2 + V\right]\psi = E\psi \qquad (\hbar = h/2\pi) \qquad ...(68)$$

where ∇^2 (read as 'del squared') is the **Laplacian operator,** defined as

$$\nabla^2 = \frac{\partial^2}{\partial x^2} + \frac{\partial^2}{\partial y^2} + \frac{\partial^2}{\partial z^2} \quad ...(69)$$

Defining the **Hamiltonian operator** $\hat{H}$ as

$$\hat{H} = \frac{-\hbar^2}{2m}\nabla^2 + V, \quad ...(70)$$

the **time-independent Schrödinger equation** (Eq. 68) becomes

$$\hat{H}\psi = E\psi \quad ...(71)$$

It may be noted that Eq. 71 can also be derived from Eq. 53.

E. Schrödinger (1887-1961) shared the 1933 Physics Nobel Prize with P.A.M. Dirac (1902-1984) for the discovery of new productive forms of atomic theory.

The Schrödinger equation can have several solutions, not all of which correspond to any physical or chemical reality. Such solutions or wave functions are, therefore, not acceptable. The acceptable wave functions must satisfy the following conditions :

1. The wave function ψ is *single-valued, i.e.,* for each value of the variables x, y, z, there is only one value of ψ. Suppose one of the variables is an angle θ. Then, single-valuedness of ψ requires that $\psi(\theta) = \psi(\theta + 2n\pi)$ where n is an integer.

2. The wave function ψ and its first derivative with respect to its variables must be *continuous, i.e.,* there must not be any sudden change in ψ when its variables are changed.

3. For bound states, ψ must vanish at infinity. If ψ is a complex function, then $\psi^*\psi$ must vanish at infinity (ψ^* is the complex conjugate of ψ).

Satisfying the above conditions, the Schrödinger equation yields *significant solutions for certain definite values of the total energy E.* These values are called eigenvalues. Eq. 71 is, thus, an eigenvalue equation and we can write it as

$$\hat{H}\psi_n = E_n\psi_n \qquad (n = 1, 2, 3, ...) \quad ...(72)$$

where n is the quantum number. We express Eq. 72 by saying that ψ_n are the eigenfunctions and E_n are the eigenvalues. For an atom, these eigenvalues correspond to discrete sets of energy values postulated by Bohr.

4. The eigenfunctions are said to form an **orthonormal set** if

$$\int \psi_n^* \psi_m \, d\tau = \begin{cases} 0, & n \neq m \\ 1, & n = m \end{cases} = \delta_{nm} \text{ (called the Kronecker delta)} \quad ...(73)$$

They are **orthogonal** when $\int \psi_n^* \psi_m \, d\tau = 0$ ...(74)

and **normalized** when $\int \psi_n^* \psi_m \, d\tau = 1$ ...(75)

It is possible to identify regions of space around the nucleus where there is *high probability* of locating an electron associated with a specific energy. This space is called an atomic orbital. An **atomic orbital,** thus, represents a definite region in three-dimensional space around the nucleus where there is high probability of finding an electron of a specific energy E.

Statistical interpretation of ψ. It was Max Born (1882–1970), the German physicist, who gave statistical interpretation of the function ψ, calling it the **probability amplitude function.** Born won the 1954 Physics Nobel Prize for this interpretation. If $\psi(x)$ is the wavefunction of a particle, then, the probability of finding the particle within the range from x to $x+dx$ is given by

$$P(x)dx = \psi^*\psi \, dx = |\psi|^2 dx \quad ...(76)$$

where ψ^* is the **complex conjugate** of ψ. Note that $P(x)dx$ is the **probability** and $P(x)$ is the **probability density.**

We know that in the case of light waves, the intensity of the electromagnetic field is proportional to the square of the amplitude of the wave at that point. Likewise, in the case of a particle, the probability of its being found between the region x and $(x+dx)$ is proportional to the square of the wavefunction, *i.e.,* the square of the probability amplitude function at that point. Since the total probability of locating the particle must be unity, we have

$$\int_{-\infty}^{\infty} P(x)dx = \int_{-\infty}^{\infty} \psi^*\psi \, dx = \int_{-\infty}^{\infty} |\psi|^2 dx = 1 \quad ...(77)$$

For motion in three dimensions,

$$\int P(\vec{r})d^3r = \int |\psi(\vec{r})|^2 d^3r = 1 \quad ...(78)$$

where the integration is carried over the three-dimensional volume element $d^3r = dx\,dy\,dz$.

It may be noted that in Bohr's theory, the electron associated with a definite energy is considered to be located at a definite distance from the nucleus. In wave mechanics, the equation for calculating the *exact energy* of the electron has been derived but there is a considerable uncertainty with regard to its exact location. This is in conformity with the Heisenberg uncertainty principle.

Operators in Quantum Mechanics

The concept of operators is very important in wave mechanics. We have already listed a few operators in the sixth postulate of quantum mechanics. Here we shall briefly deal with the algebra of operators. If $\hat{A}$ and $\hat{B}$ are two operators and f is a function upon which they operate, then

$$(\hat{A} + \hat{B})f = \hat{A}f + \hat{B}f \quad ...(79)$$

and $$(\hat{A} - \hat{B})f = \hat{A}f - \hat{B}f \quad ...(80)$$

Thus, we can generate new operators $\hat{A}+\hat{B}$ and $\hat{A}-\hat{B}$ by adding and subtracting $\hat{A}$ and $\hat{B}$. Also,

$$\hat{A} + \hat{B} = \hat{B} + \hat{A} \quad ...(81)$$

$$\hat{A} - \hat{B} = -\hat{B} + \hat{A} \quad ...(82)$$

The multiplication of operators can be carried out by doing successive operations with two or more operators on a function. If $\hat{A}$ and $\hat{B}$ are two operators and f is their **operand,** then we can obtain the quantity $\hat{A}\hat{B}f$ as follows : We first operate on f with $\hat{B}$ to obtain f', that is, $\hat{B}f = f'$. Then, f' is operated upon by $\hat{A}$ to obtain f'', that is, $\hat{A}f' = f''$. Thus, we have

$$\hat{A}\hat{B}f = f'' \quad ...(83)$$

It should be remembered that the order of application of operators is always from right to left as they are written. Application of the same operator several times in succession is written with a power. Thus, we have

$$\hat{A}\hat{A}f = \hat{A}^2 f \quad ...(84)$$

Commutation of Operators. The algebra of operators should be distinguished from the algebra of ordinary numbers. If a and b are two numbers, then we know that

$$a \times b = b \times a \quad ...(85)$$

However, if $\hat{A}$ and $\hat{B}$ are two operators, then their product $\hat{A}\hat{B}$ may or may not be equal to $\hat{B}\hat{A}$.

If $\hat{A}\hat{B} = \hat{B}\hat{A}$, then the **commutator** of the two operators is defined as

$$[\hat{A}, \hat{B}] = \hat{A}\hat{B} - \hat{B}\hat{A} = 0 \qquad ...(86)$$

Example 13. Show that

(a) $[\hat{A}, \hat{B}] = -[\hat{B}, \hat{A}]$ *(b)* $[\hat{A}^2, \hat{B}] = \hat{A}[\hat{A}, \hat{B}] + [\hat{A}, \hat{B}]\hat{A}$

Solution : *(a)* $[\hat{A}, \hat{B}] = (\hat{A}\hat{B} - \hat{B}\hat{A}) = -(\hat{B}\hat{A} - \hat{A}\hat{B}) = -[\hat{B}, \hat{A}]$

(b) R.H.S. $= \hat{A}[\hat{A}, \hat{B}] + [\hat{A}, \hat{B}]\hat{A} = \hat{A}(\hat{A}\hat{B} - \hat{B}\hat{A}) + (\hat{A}\hat{B} - \hat{B}\hat{A})\hat{A}$

$= \hat{A}^2\hat{B} - \hat{A}\hat{B}\hat{A} + \hat{A}\hat{B}\hat{A} - \hat{B}\hat{A}^2 = \hat{A}^2\hat{B} - \hat{B}\hat{A}^2 = [\hat{A}^2, \hat{B}]$ = L.H.S.

Expressions for Operators. Expressions for operators can be obtained by operating with the operators on an operand and removing the operand at the end of the operation.

Example 14. Find expressions for the following operators :

(a) $\left(\frac{d}{dx} + x\right)^2$ *(b)* $\left(\frac{d}{dx} + x\right)\left(\frac{d}{dx} - x\right)$ *(c)* $\left(\frac{d}{dx} - x\right)\left(\frac{d}{dx} + x\right)$

Solution : Let $\psi(x)$ be the operand.

(a) $\left(\frac{d}{dx} + x\right)^2 \psi(x) = \left(\frac{d}{dx} + x\right)\left(\frac{d}{dx} + x\right)\psi(x) = \left(\frac{d}{dx} + x\right)\left(\frac{d\psi}{dx} + x\psi\right)$

$= \frac{d^2\psi}{dx^2} + 2x\frac{d\psi}{dx} + x^2\psi + \psi = \left(\frac{d^2}{dx^2} + 2x\frac{d}{dx} + x^2 + 1\right)\psi$

Removing ψ from both sides of this equation, we have

$$\left(\frac{d}{dx} + x\right)^2 = \frac{d^2}{dx^2} + 2x\frac{d}{dx} + x^2 + 1$$

(b) $\left(\frac{d}{dx} + x\right)\left(\frac{d}{dx} - x\right)\psi(x) = \left(\frac{d}{dx} + x\right)\left(\frac{d\psi}{dx} - x\psi\right)$

$= \frac{d^2\psi}{dx^2} - \frac{d}{dx}(x\psi) + x\frac{d\psi}{dx} - x^2\psi = \frac{d^2\psi}{dx^2} - \left(x\frac{d\psi}{dx} + \psi\frac{dx}{dx}\right) + x\frac{d\psi}{dx} - x^2\psi$

$= \frac{d^2\psi}{dx^2} - \psi - x^2\psi = \left(\frac{d^2}{dx^2} - 1 - x^2\right)\psi$ $\qquad (\because\ dx/dx = 1)$

Removing ψ from both sides of the equation, we have

$$\left(\frac{d}{dx} + x\right)\left(\frac{d}{dx} - x\right) = \frac{d^2}{dx^2} - 1 - x^2$$

(c) $\left(\frac{d}{dx} - x\right)\left(\frac{d}{dx} + x\right)\psi(x) = \left(\frac{d}{dx} - x\right)\left(\frac{d\psi}{dx} + x\psi\right) = \frac{d^2\psi}{dx^2} + \frac{d}{dx}(x\psi) - x\frac{d\psi}{dx} - x^2\psi$

$= \frac{d^2\psi}{dx^2} + \left(x\frac{d\psi}{dx} + \psi\frac{dx}{dx}\right) - x\frac{d\psi}{dx} - x^2\psi$

$= \frac{d^2\psi}{dx^2} + \psi - x^2\psi = \left(\frac{d^2}{dx^2} + 1 - x^2\right)\psi$

Removing ψ from both sides of the equation, we have

$$\left(\frac{d}{dx} - x\right)\left(\frac{d}{dx} + x\right) = \frac{d^2}{dx^2} + 1 - x^2$$

Example 15. If $\hat{A}$ and $\hat{B}$ are two operators such that $[\hat{A}, \hat{B}] = 1$, show that $[\hat{A}, \hat{B}^2] = 2\hat{B}$.

Solution : $[\hat{A}, \hat{B}] = \hat{A}\hat{B} - \hat{B}\hat{A} = 1$

$[\hat{A}, \hat{B}^2] = \hat{A}\hat{B}^2 - \hat{B}^2\hat{A} + \hat{B}\hat{A}\hat{B} - \hat{B}\hat{A}\hat{B} = (\hat{A}\hat{B}^2 - \hat{B}\hat{A}\hat{B}) + (\hat{B}\hat{A}\hat{B} - \hat{B}^2\hat{A})$

$= (\hat{A}\hat{B} - \hat{B}\hat{A})\hat{B} + \hat{B}(\hat{A}\hat{B} - \hat{B}\hat{A}) = (1)\hat{B} + \hat{B}(1) = 2\hat{B}$

Example 16. Show that the commutator $\left[x, \frac{d}{dx}\right] = -1$.

Solution : By definition, $\left[x, \frac{d}{dx}\right] = x\frac{d}{dx} - \frac{d}{dx}x$

Let $\psi(x)$ be the operand, then operating on $\psi(x)$ by the right-hand side expression, we have

$$\left(x\frac{d}{dx} - \frac{d}{dx}x\right)\psi = x\frac{d\psi}{dx} - \frac{d}{dx}(x\psi) = x\frac{d\psi}{dx} - x\frac{d\psi}{dx} - \psi\frac{dx}{dx} = -\psi \qquad (\because\ dx/dx = 1)$$

Removing ψ from both sides of this equation, we have

$$\left[x, \frac{d}{dx}\right] = -1.$$

Example 17. Show that the commutator $[\hat{x}^n, \hat{p}_x] = i\hbar n x^{n-1}$ where n is a positive integer.

Solution : The operators for the x-coordinate and the x-component of the linear momentum, p_x are :

$$\hat{x} \to x \quad \text{and} \quad \hat{p}_x \to -i\hbar\frac{d}{dx}$$

$$[\hat{x}^n, \hat{p}_x] = x^n\left(-i\hbar\frac{d}{dx}\right) - \left(-i\hbar\frac{d}{dx}\right)x^n = -i\hbar x^n\frac{d}{dx} + i\hbar\frac{d}{dx}x^n$$

Operating on the arbitrary operand $\psi(x)$ by this operator, we have

$$-i\hbar x^n\frac{d\psi}{dx} + i\hbar\frac{d}{dx}(x^n\psi) = -i\hbar x^n\frac{d\psi}{dx} + i\hbar x^n\frac{d\psi}{dx} + i\hbar n x^{n-1}\psi = i\hbar n x^{n-1}\psi$$

Hence, $[\hat{x}^n, \hat{p}_x] = i\hbar n x^{n-1}$ [Removing ψ from both sides of this equation]

Solution of the Schrödinger Wave Equation for Some Simple Systems

The Schrödinger wave equation can be solved exactly for the following simple systems :

1. Particle in a One-Dimensional Box.
2. Particle in a Three-Dimensional Box.
3. One-Dimensional Simple Harmonic Oscillator (S.H.O.)
4. The Rigid Rotor (or Rotator).
5. The Hydrogen Atom.

Note that since the solutions of the Schrödinger equation, subject to boundary conditions, yield quantized (integral) energy eigenvalues and eigenfunctions, wave mechanics is also called quantum mechanics.

1. Particle in a One-Dimensional Box. This is the simplest quantum mechanical problem which represents **translational motion.** Here a particle of mass m is confined to move in a one-dimensional box of width a, having infinitely high walls (Fig. 7). It is assumed, for the sake of simplicity, that the potential energy of the particle is zero everywhere inside the box, that is

$$V(x) = 0 \qquad ...(87)$$

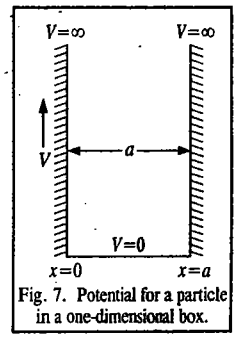

Fig. 7. Potential for a particle in a one-dimensional box.

Thus, inside the box the Schrödinger equation, *viz.*,

$$\left[-\frac{\hbar^2}{2m}(d^2/dx^2)+V(x)\right]\psi(x) = E\psi(x) \quad ...(88)$$

takes the form $$-\frac{\hbar^2}{2m}(d^2\psi/dx^2) = E\psi(x) \quad ...(89)$$

Our problem is to solve this equation for energy E and the wave function $\psi(x)$.

Mathematically, Eq. 89 may be rewritten as

$$\frac{d^2\psi}{dx^2}+(2mE/\hbar^2)\psi = 0 \quad ...(90)$$

or as $$\frac{d^2\psi}{dx^2}+k^2\psi = 0 \quad ...(91)$$

where k^2 $(= 2mE/\hbar^2)$ is a constant, independent of x.

Eq. 91 is an ordinary second-order differential equation which has solution of the form

$$\psi = A\cos kx + B\sin kx \quad ...(92)$$

where A and B are constants. Before we proceed further, it should be pointed out that *outside* the box where $V(x) = \infty$, the Schrödinger equation (88) is

$$\left[-\frac{\hbar^2}{2m}(d^2/dx^2)+\infty\right]\psi(x) = E\psi(x) \quad ...(93)$$

or $$\frac{d^2\psi}{dx^2}+\frac{2m}{\hbar^2}(E-\infty)\psi = 0 \quad ...(94)$$

This equation is satisfied if ψ is zero everywhere *outside* the box. This is another way of saying that the particle cannot be found outside the box ; it is confined within the box. This implies that ψ must be zero at the walls of the box, *i.e.*, at $x=0$ and at $x=a$. Since the postulate of quantum mechanics requires that ψ must be a continuous function of x, we are forced to conclude that in Eq. 92, A must be zero. Thus, the solution of Eq. 91 is of the form

$$\psi = B\sin kx \quad ...(95)$$

Since $\psi = 0$ at $x = 0$ and at $x = a$, we have

$$B\sin ka = 0 \text{ or } \sin ka = 0 \text{ or } ka = n\pi \text{ so that } k = n\pi/a \quad ...(96)$$

where $n(=0, 1, 2, 3, 4.....,)$ is the quantum number. Hence, the allowed solutions of Eq. 91 are

$$\psi \equiv \psi_n = B\sin(n\pi x/a) ; \quad (n = 1, 2, 3, ...) \quad ...(97)$$

Notice that the $n=0$ value of the quantum number, though allowed, is not *acceptable* since it implies that the wave function ψ is zero everywhere inside the box. This is not correct since the particle is taken to be inside the box, to begin with. From Eqs. 91 and 96, we have

$$(2mE/\hbar^2) = n^2\pi^2/a^2 \quad ...(98)$$

or $$E \equiv E_n = n^2\hbar^2\pi^2/2ma^2 = n^2h^2/8ma^2 ; \quad n = 1, 2, 3,.....\text{and } \hbar = h/2\pi \quad ...(99)$$

Note that $\hbar$ is called **reduced Planck's constant** and also **Dirac's constant.**

Eq. 99 gives the expression for the energy of the particle in a one-dimensional box. Since energy depends upon the quantum number n, the energy levels are quantized. Let us determine the coefficient B in the wavefunction given by Eq. 97. This can be done by normalizing the wave function.

Normalization of ψ. Since the total probability of finding the particle within the box is 1,

$$\int_0^a \psi_n^2\,dx = 1 \text{ [Born's interpretation of wave function]} \quad ...(100)$$

$$\int_0^a (B\sin n\pi x/a)^2\,dx = 1 \text{ [Using } \psi_n \text{ from Eq. 97]} \quad ...(101)$$

... or $$B^2\int_0^a \sin^2(n\pi x/a)\,dx = 1 \quad ...(102)$$

Since $\sin^2\theta = \frac{1}{2}(1-\cos 2\theta)$, hence from Eqs. 100 and 102, we have

$$\int_0^a \psi_n^2\,dx = B^2\left[\frac{1}{2}\int_0^a dx - \frac{1}{2}\int_0^a \cos\left(\frac{2n\pi x}{a}\right)dx\right] \quad ...(103)$$

$$= B^2[a/2 - 0] = 1 \quad ...(104)$$

Hence, $B = (2/a)^{1/2}$ ...(105)

Thus, the normalized wave functions for the particle are :

$$\psi_n(x) = (2/a)^{1/2}\sin(n\pi x/a) ; \quad n = 1, 2, 3, ... \quad ...(106)$$

Note that the quantization arises naturally from the boundary conditions. We have gone beyond the stage of Planck and Bohr where quantum numbers are introduced in an *ad hoc* manner.

A few normalized wave functions and the corresponding probability functions for a particle in a box are given in Fig. 8. The most probable position for a particle in the $n = 1$ energy level is the centre of the box. Note that $\psi_n(x)$ are waves with wave length $\lambda_n = 2a/n$. This means that ψ_n is zero at values of x equal to an integral number of $\lambda_n/2$. These zeros are called nodes of the wave function. In one-dimensional problems, the more nodes in an eigenfunction, the higher its eigenvalue of energy. For this problem, the number of nodes is $n - 1$.

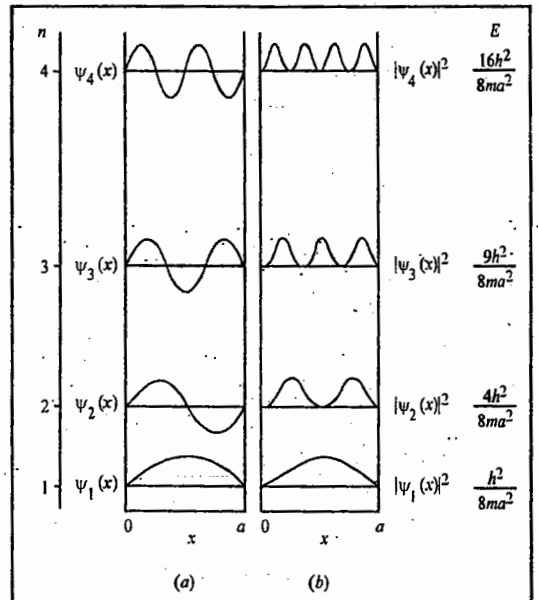

Fig. 8. The energy levels, wavefunctions (*a*) and (*b*) probability densities for the particle in a one-dimensional box.

Example 18. Calculate the energies (in eV) of an electron constrained to move in a one-dimensional box of width 1 Å and exhibit them on an energy level diagram.

Solution :

$$E_n = \frac{n^2(6{\cdot}626\times10^{-34}\text{ J s})^2}{(8)(9{\cdot}109\times10^{-31}\text{ kg})(10^{-10}\text{ m})^2(1{\cdot}602\times10^{-19}\text{ J/eV})}$$

$$= 37{\cdot}6n^2\text{ eV} \approx 38n^2\text{ eV}$$

Energies of the electron corresponding to different values of n are :

$n = 1, \quad E_1 = 38$ eV
$n = 2, \quad E_2 = 38\,(2)^2 = 152$ eV
$n = 3, \quad E_3 = 38\,(3)^2 = 342$ eV
$n = 4, \quad E_4 = 38\,(4)^2 = 608$ eV, and so on.

The above energies are shown in the form of an energy level diagram in Fig. 9. Notice that the energy levels are sufficiently far apart; their quantization is thus distinctly evident.

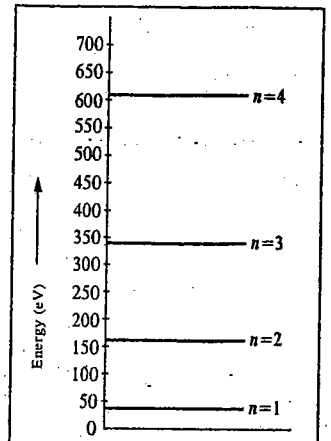

Fig. 9. Energies of an electron moving in a one-dimensional box.

Notice that as a gets large, the energy levels get closer together. In the limit of a very large box (or a very heavy particle), the energy levels are so close together that the quantization may be unnoticeable. In the limit that a becomes very large, all energies become allowed (*i.e.*, the allowed energies get very close together so that any energy is an eigenvalue), so the perfectly free particle can have any energy.

Example 19. An electron is confined in a one-dimensional box of length 1 Å. Calculate its ground state energy in electron volts (eV). Is quantization of energy levels observable ?

Solution : From Eq. 99, the ground state energy of the electron is

$$E_1 = \frac{n^2h^2}{8ma^2} = \frac{(1)^2(6{\cdot}626\times10^{-34}\text{ J s})^2}{(8)(9{\cdot}109\times10^{-31}\text{ kg})(10^{-10}\text{ m})^2(1{\cdot}602\times10^{-19}\text{ J/eV})}$$
$$= 37{\cdot}6 \text{ eV}$$

Let us calculate the energy of the first excited state with $n=2$.

$$E_2 = \frac{(2)^2(6{\cdot}626\times10^{-34}\text{ J s})^2}{(8)(9{\cdot}109\times10^{-31}\text{ kg})(10^{-10}\text{ m})^2(1{\cdot}602\times10^{-19}\text{ J/eV})} = 150{\cdot}4 \text{ eV}$$

Therefore, $\Delta E = E_2 - E_1 = 150{\cdot}4 - 37{\cdot}6 = 112{\cdot}8$ eV

This energy corresponds to that of a quantum of X-rays which can be readily observed. Thus, we conclude that it is possible to observe quantization in the energy levels of microscopic systems.

Example 20. A ball of mass 1 g, confined to a one-dimensional box of length 0·1 m, moves with a velocity of 0·01 m s^{-1}. Calculate the quantum number n. Is it possible to observe the quantization of energy levels of the ball ?

Solution : The kinetic energy of the ball equals the total energy. In the ground state, $n=1$.

$$\therefore \quad E_1 = \tfrac{1}{2}mu_x^2 = \tfrac{1}{2}(0{\cdot}001\text{ kg})\,(0{\cdot}01\text{ m s}^{-1})^2 = 5\times10^{-8}\text{ J} \quad [\text{since } V_{(x)}=0] \quad (\text{J}=\text{kg m}^2\text{ s}^{-2})$$

Since from Eq. 99, $E_n = n^2h^2/8ma^2$, hence, $n^2 = 8ma^2E_n/h^2$

$$\therefore \quad n = [8ma^2E_n/h^2]^{1/2} = (8mE_n)^{1/2}a/h$$

Substituting the various values, we have

$$n = [8(0{\cdot}001\text{ kg})\,(5\times10^{-8}\text{ J})]^{1/2}\left[\frac{0{\cdot}1\text{ m}}{6{\cdot}626\times10^{-34}\text{ J s}}\right] = 3\times10^{27}$$

Notice the fantastically high value of the quantum number n.

Let us calculate ΔE between energy levels characterized by the quantum numbers n and $n+1$:

$$\Delta E = E_{n+1} - E_n = [(n+1)^2 - n^2]\,h^2/(8ma)^2 = (2n+1)\,E_0$$

where $E_0 = h^2/8ma^2 = (6{\cdot}626\times10^{-34})^2/8ma^2 = 5{\cdot}48\times10^{-68}/ma^2$ J

Since, $n = 3\times10^{27}$, $n+1 = 3\times10^{27}+1 = 3\times10^{27}$

(We can safely neglect 1 in comparison with 3×10^{27})

$$\therefore \quad \Delta E = (2n+1)\,E_0 = [2(3\times10^{27})+1]\,\frac{5{\cdot}48\times10^{-68}}{(0{\cdot}001\text{ kg})(0{\cdot}1\text{ m})^2}\text{ J} = 3{\cdot}3\times10^{-35}\text{ J}$$

This implies that $E_1 = 5\times10^{-8}$ J and $E_2 = 5\times10^{-8}\text{ J} + 3{\cdot}3\times10^{-35}\text{ J} \approx 5\times10^{-8}$ J

Since E_1 and E_2 are practically the same, it is not possible to observe quantization in the energy levels of macroscopic systems like the ball.

Example 21. Calculate the expectation (average) value of the energy of a particle of mass m confined to move in a one-dimensional box of width a and infinite height with potential energy zero inside the box. The normalized wavefunction of the particle is $\psi_n(x)=(2/a)^{1/2}\sin(n\pi x/a)$ where $n=1, 2, 3,\ldots$

Solution : Total energy E of a particle is the sum of kinetic energy T and potential energy V. Since the potential energy inside the box is zero, *i.e.*, $V=0$, hence,

$$E = T$$
$$T = \tfrac{1}{2}mu^2 = m^2u_x^2/2m = p_x^2/2m$$

As shown in Table 1, the operator of p_x^2 is $-\hbar^2\,\partial^2/\partial x^2$, hence

$$\hat{H} = -(\hbar^2/2m)\,d^2/dx^2$$

$$\therefore \langle E \rangle = \int_0^a \psi_n(x)\hat{H}\psi_n(x)dx$$

$$= -\frac{\hbar^2}{2m}\int_0^a\left(\frac{2}{a}\right)^{1/2}\sin\left(\frac{n\pi x}{a}\right)\frac{d^2}{dx^2}\left[\left(\frac{2}{a}\right)^{1/2}\sin\left(\frac{n\pi x}{a}\right)\right]dx$$

$$= -\frac{\hbar^2}{ma}\int_0^a\sin\left(\frac{n\pi x}{a}\right)\left[\frac{-n^2\pi^2}{a^2}\sin\left(\frac{n\pi x}{a}\right)\right]dx = \frac{n^2h^2}{4ma^3}\int_0^a\sin^2\left(\frac{n\pi x}{a}\right)dx \qquad (\because \hbar = h/2\pi)$$

$$= \frac{n^2h^2}{4ma^3}\int_0^a\frac{1-\cos(2n\pi x/a)}{2}dx = \frac{n^2h^2}{8ma^3}\left\{[x]_0^a - \frac{a}{2n\pi}\left[\sin\left(\frac{2n\pi x}{a}\right)\right]_0^a\right\}$$

$$= \frac{n^2h^2}{8ma^3}(a-0) = n^2h^2/8ma^2$$

Note that this is also the value obtained by solving the Schrödinger equation for this system.

Example 22. Verify that the wavefunctions of a particle in a one-dimensional box of width a and infinite height are orthogonal.

Solution : $\psi_n(x) = \left(\frac{2}{a}\right)^{1/2}\sin\left(\frac{n\pi x}{a}\right)$; $n = 1, 2, 3.....$

The orthogonality condition requires that $\int_0^a \psi_m^*(x)\psi_n(x)dx = 0$ (cf. Eq. 74)

Since the wavefunctions are real,

$$\psi_m^*(x) = \psi_m(x) = (2/a)^{1/2}\sin(m\pi x/a)$$

Hence, $$\int_0^a\psi_m^*\psi_n dx = \int_0^a\left(\frac{2}{a}\right)^{1/2}\sin\left(\frac{m\pi x}{a}\right)\left(\frac{2}{a}\right)^{1/2}\sin\left(\frac{n\pi x}{a}\right)dx$$

$$= \left(\frac{2}{a}\right)\int_0^a\sin\left(\frac{m\pi x}{a}\right)\sin\left(\frac{n\pi x}{a}\right)dx \qquad \ldots(i)$$

Since $\sin A \sin B = \frac{1}{2}[\cos(A-B) - \cos(A+B)]$,

Eq. *(i)* can be written as

$$\int_0^a\psi_m^*\psi_n\,dx = \frac{1}{a}\int_0^a\left(\cos(m-n)\frac{\pi x}{a} - \cos(m+n)\frac{\pi x}{a}\right)dx$$

$$= \frac{1}{a}\left\{\frac{a}{(m-n)\pi}\sin\left[(m-n)\frac{\pi x}{a}\right]_0^a - \frac{a}{(m+n)\pi}\sin\left[(m+n)\pi\frac{x}{a}\right]_0^a\right\} = 0$$

Hence the result. ($\because$ m and n are integers)

Example 23. Calculate the average values of x, x^2, p_x and p_x^2 for a particle in a one-dimensional box of width a and infinite height and verify that $\Delta p_x \Delta x = \hbar/2$, where Δx is the uncertainty in the positional coordinate x and Δp_x is the uncertainty in the linear momentum along the x-coordinate.

Solution : We know that for the given system, the normalized wavefunctions are

$$\psi_n(x) = \left(\frac{2}{a}\right)^{1/2}\sin\left(\frac{n\pi x}{a}\right);\ n = 1,2,3,..... \qquad \text{(Eq. 106)}$$

and $$< x > = \int_0^a \psi_n \hat{x}\, \psi_n dx \qquad \text{(From Eq. 52)}$$

$$= \int_0^a \left(\frac{2}{a}\right)^{1/2}\sin\left(\frac{n\pi x}{a}\right) x \left(\frac{2}{a}\right)^{1/2}\sin\left(\frac{n\pi x}{a}\right)dx$$

$$= \frac{2}{a}\int_0^a x\sin^2\left(\frac{n\pi x}{a}\right)dx = \frac{2}{a}\int_0^a x\left[\frac{1-\cos(2n\pi x/a)}{2}\right]dx = (2/a)(a^2/4) = a/2$$

$$< x^2 > = \frac{2}{a}\int_0^a x^2\sin^2\left(\frac{n\pi x}{a}\right)dx = \frac{2}{a}\int_0^a x^2\left[\frac{1-\cos(2n\pi x/a)}{2}\right]dx$$

$$= \frac{1}{a}\left[\int_0^a x^2 dx - \int_0^a x^2\cos\left(\frac{2n\pi x}{a}\right)dx\right] = \frac{1}{a}\left[\frac{a^3}{3} - \frac{a^3}{2n^2\pi^2}\right] = \frac{a^2}{3} - \frac{a^2}{2n^2\pi^2}$$

Since the operator of p_x is $-i\hbar d/dx$ (Table 1), hence,

$$< p_x > = \int_0^a \psi_n\left[\left(-i\hbar\frac{d}{dx}\right)^2\right]\psi_n dx = -\hbar^2\int_0^a\left(\frac{2}{a}\right)^{1/2}\sin\left(\frac{n\pi x}{a}\right)\frac{d^2}{dx^2}\left[\left(\frac{2}{a}\right)^{1/2}\sin\left(\frac{n\pi x}{a}\right)\right]dx$$

$$= -(i\hbar)\left(\frac{2}{a}\right)\left(\frac{n\pi}{a}\right)\int_0^a \sin\left(\frac{n\pi x}{a}\right)\cos\left(\frac{n\pi x}{a}\right)dx = 0$$

$$<p_x^2> = \int_0^a \psi_n\left[\left(-i\hbar\frac{d}{dx}\right)^2\right]\psi_n dx = -\hbar^2\int_0^a\left(\frac{2}{a}\right)^{1/2}\sin\left(\frac{n\pi x}{a}\right)\frac{d^2}{dx^2}\left[\left(\frac{2}{a}\right)^{1/2}\sin\left(\frac{n\pi x}{a}\right)\right]dx$$

$$= \hbar^2\left(\frac{n\pi}{a}\right)^2\int_0^a\left(\frac{2}{a}\right)\sin^2\left(\frac{n\pi x}{a}\right)dx \qquad ...(i)$$

The integral on the R.H.S. of Eq. *(i)* equals E_n, the energy of the particle so that

$$<p_x^2> = \hbar^2\,(n\pi/a)^2 E_n = n^2h^2/4a^2 = 2mE_n \text{ where } E_n = n^2h^2/8ma^2$$

We know that $$(\Delta p_x)^2 = <p_x^2> - <p_x>^2 = <p_x^2> = n^2h^2/4a^2 \qquad (\because < p_x >^2 = 0)$$

Again, $$(\Delta x)^2 = <x^2> - <x>^2 = \frac{a^2}{3} - \frac{a^2}{2n^2\pi^2} - \left(\frac{a}{2}\right)^2 = \frac{a^2}{12} - \frac{a^2}{2n^2\pi^2}$$

Hence, $$(\Delta p_x)^2(\Delta x)^2 = \left(\frac{n^2h^2}{4a^2}\right)\left(\frac{a^2}{12} - \frac{a^2}{2n^2\pi^2}\right) = \frac{n^2h^2}{4}\left(\frac{1}{12} - \frac{1}{2n^2\pi^2}\right) = \frac{\hbar^2}{4}\left(\frac{n^2\pi^2}{3} - 2\right)$$

$$\therefore \quad \Delta p_x \Delta x = (\hbar/2)\,[(n^2\pi^2/3) - 2]^{1/2}$$

or $$\Delta p_x\,\Delta x > \hbar/2 \qquad (\because n^2\pi^2/3 \text{ is always gteater than 2})$$

The reader will recognize that here we have **verified the Heisenberg uncertainty principle** for the particle in a one-dimensional box.

Example 24. What will happen if the walls of the one-dimensional box are suddenly removed ?

Solution : When the walls for the particle in a one-dimensional box are suddenly removed, it becomes free to move without any restriction on the value of the potential energy. If the potential energy is taken to be zero, then the solution of Schrödinger equation (94) is given by Eq. 96. However, the arbitrary constants A or B and k in Eq. 96 can have any values which may be assigned to them. Thus, the energy eigenvalues given by $E = k^2h^2/8\pi^2m$ are not quantized. Hence we conclude that a freely moving particle (which may be an electron) without any restriction has *continuous energy spectrum.*

Example 25. What is the zero-point energy of a particle in a one-dimensional box of infinite height ? Is the occurrence of zero-point energy in accordance with the Heisenberg uncertainty principle ?

Solution : Since $E_n = n^2h^2/8ma^2$, the energy corresponding to $n=1$, *viz.*, $E_1 = h^2/8ma^2$, is called the zero-point energy (Z.P.E.) of the particle. Since Z.P.E. is finite (and not equal to zero) it means that the particle inside the box is not at rest even at 0 K. This being so, the position of the particle cannot be precisely known. Again, since only the expectation (and not exact) value of the kinetic energy $<\frac{1}{2}mu^2>$ is known, the linear momentum of the particle is also not precisely known. Thus, occurrence of Z.P.E. implies uncertainty in the position, Δx and also uncertainty in the x-component of the linear momentum Δp_x. This means that the occurrence of Z.P.E. is in keeping with the Heisenberg uncertainty principle.

Example 26. Set up and solve the Schrödinger wave equation for a particle of mass m moving in a one-diminsional potential with rigid walls, *i.e.*,

$$V(x) = \begin{bmatrix} 0, & -a<x<a \\ \infty, & |x|>a \end{bmatrix}$$

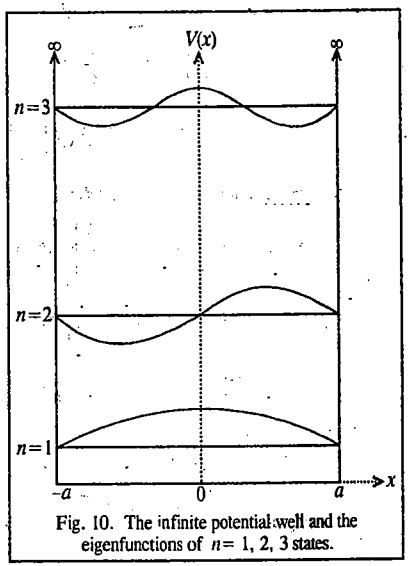

Fig. 10. The infinite potential well and the eigenfunctions of $n = 1, 2, 3$ states.

Solution : See Fig.10 below for the infinite potential well.

The time-independent Schrödinger wave equation for the particle in the region $|x| < a$ is

$$\frac{d^2\psi}{dx^2} + k^2\psi = 0, \qquad \text{where } k^2 = 2mE/\hbar^2 \qquad ...(i)$$

whose solution is

$$\psi(x) = A\sin kx + B\cos kx \qquad ...(ii)$$

Since $V(x) = \infty$ at $x = \pm a$, $\psi(\pm a) = 0$. Using this boundary condition we have

$$A\sin ka + B\cos ka = 0$$

and $$-A\sin ka + B\cos ka = 0$$

From these two equations we find that $B\cos ka = 0$, and $A\sin ka = 0$. Now the solution $A = 0$, $B = 0$ leads to the physically unacceptable solution $\psi = 0$. The other possible cases are $A = 0$, $B \neq 0$ and $A \neq 0$, $B = 0$. The first condition gives,

$$\cos ka = 0, \qquad ka = n\pi/2, \qquad n = 1, 3, 5, ...$$

Thus, $$k^2 = \frac{2mE}{\hbar^2} = \frac{n^2\pi}{4}$$

or, $$E_n = \frac{k^2\hbar^2}{2m} = \frac{\pi^2h^2n^2}{8ma^2}, \quad n = 1, 3, 5, ... \qquad ...(iii)$$

The eigenfunction corresponding to this energy eigenvalue is

or, $$\psi_n(x) = B\cos\frac{n\pi x}{2a}, \quad n = 1, 3, 5, ... \qquad ...(iv)$$

The second condition leads to

$$E_n = \frac{\pi^2\hbar^2 n^2}{8ma^2}, \quad n = 2, 4, 6, \ldots \qquad \ldots(v)$$

with the eigenfunction

$$\psi_n(x) = A\sin\frac{n\pi x}{2a}, \quad n = 2, 4, 6, \ldots \qquad \ldots(vi)$$

Note that quantum number $n = 0$ is not included as it corresponds to a trivial solution $\psi(x) = 0$. In normalization of the wavefunctions gives $A = B = 1/\sqrt{a}$. Thus, the confinement of the particle in the infinite potential well with rigid walls leads to the quantization of energy given by

$$E_n = \frac{\pi^2\hbar^2 n^2}{8ma^2}, \quad n = 1, 2, 3, \ldots \qquad \ldots(vii)$$

The complete set of normalized eigenfunctions are

$$\psi_n(x) = \begin{cases} \frac{1}{\sqrt{a}}\sin\frac{n\pi x}{2a}, & n = 2, 4, 6, \ldots \\ \frac{1}{\sqrt{a}}\cos\frac{n\pi x}{2a}, & n = 1, 3, 5, \ldots \end{cases} \qquad \ldots(viii)$$

These eigenfunctions for the first three states are shown in Fig. 10. From Eq. (*viii*) we see that the wavefunctions corresponding to odd quantum numbers are symmetric with respect to the operation $x \to -x$ (*i.e.*, they are *even functions*), whereas those for even quantum numbers are antisymmetric (*i.e.*, *odd functions*). The energy and the wavefunction of the ground state are

$$E_1 = \frac{\pi^2\hbar^2}{8ma^2} \quad \text{and} \quad \psi_1(x) = \frac{1}{\sqrt{a}}\cos\frac{\pi x}{2a} \qquad \ldots(ix)$$

We see that the particle confined in the box has a certain minimum energy, called the **zero-point energy**, which is a manifestation of the Heisenberg uncertainty principle. This is understandable since an uncertainty, Δx, of order a in position implies an uncertainty, Δp_x, of order $\hbar/2a$ in momentum, which, in turn, gives a minimum kinetic energy of $\hbar^2/(8ma^2)$.

2. Particle in a Three-Dimensional Cubical Box. Let us now consider the motion of a particle of mass m confined to a three-dimensional cubical box with edges of length a and volume equal to a^3. The potential is zero within the box and is infinite outside the box and at its boundaries. The time-independent Schrödinger equation for the particle is

$$\left[-\frac{\hbar^2}{2m}\left(\frac{\partial^2}{\partial x^2} + \frac{\partial}{\partial y^2} + \frac{\partial^2}{\partial z^2}\right)\right]\psi(x, y, z) = E\psi(x, y, z) \qquad \ldots(107)$$

Eq. 107 may be rewritten as

$$\frac{\partial^2\psi}{\partial x^2} + \frac{\partial^2\psi}{\partial y^2} + \frac{\partial^2\psi}{\partial z^2} + \left(\frac{2mE}{\hbar^2}\right)\psi = 0 \qquad \ldots(108)$$

Assuming that the wavefunction ψ is a product of three parts which separately depend on x, y and z, we have

$$\psi(x, y, z) = X(x)\, Y(y)\, Z(z) \qquad \ldots(109)$$

Hence,

$$\frac{\partial^2\psi}{\partial x^2} = YZ\frac{\partial^2 X}{\partial x^2} \qquad \ldots(110)$$

$$\frac{\partial^2\psi}{\partial y^2} = XZ\frac{\partial^2 Y}{\partial y^2} \qquad \ldots(111)$$

$$\frac{\partial^2\psi}{\partial z^2} = XY\frac{\partial^2 Z}{\partial z^2} \qquad \ldots(112)$$

Substituting Eqs. 110–112 in Eq. 108 and dividing throughout by $(2m/\hbar^2)XYZ$, we have

$$\frac{\hbar^2}{2m}\left[\frac{1}{X}\frac{\partial^2 X}{\partial x^2} + \frac{1}{Y}\frac{\partial^2 Y}{\partial y^2} + \frac{1}{Z}\frac{\partial^2 Z}{\partial z^2}\right] + E = 0 \qquad \ldots(113)$$

We notice that the first term is a function of x only and is independent of y and z; the second term is a function of y only and is independent of x and z and the third term is a function of z only and is independent of x and y. The fourth term E is a constant. If energy E is written as the sum of three contributions associated with the three coordinates, then Eq. 113 can be separated into three equations. Thus, for instance, for motion along the X-axis (where X varies while Y and Z remain constant), the second and third terms on the left-hand side of Eq. 113 remain constant. Let this constant be E_x. Accordingly, we can write

$$-\frac{\hbar^2}{2m}\left(\frac{1}{X}\frac{\partial^2 X}{\partial x^2}\right) = E_x \qquad \ldots(114)$$

$$-\frac{\hbar^2}{2m}\left(\frac{1}{Y}\frac{\partial^2 Y}{\partial y^2}\right) = E_y \qquad \ldots(115)$$

$$-\frac{\hbar^2}{2m}\left(\frac{1}{Z}\frac{\partial^2 Z}{\partial z^2}\right) = E_z \qquad \ldots(116)$$

where $E = E_x + E_y + E_z$. $\ldots(117)$

We see that each of the Eqs. 114—116 is of the form of Eq. 89, the solution of which is given by Eq. 106, *i.e.*, we have

$$X(x) = (2/a)^{1/2}\sin(n_x\pi x/a); \quad n_x = 1, 2, 3\ldots. \qquad \ldots(118)$$

and $$E_x = n_x^2\hbar^2/8ma^2 \qquad \ldots(119)$$

Similar solutions exist for $Y(y)$ and $Z(z)$. Hence,

$$\psi(x, y, z) = X(x)\, Y(y)\, Z(z) = (8/a^3)^{1/2}\sin(n_x\pi x/a)\sin(n_y\pi y/a)\sin(n_z\pi z/a) \qquad \ldots(120)$$

and $$E = E_x + E_y + E_z = \frac{(n_x^2 + n_y^2 + n_z^2)h^2}{8ma^2} \qquad \ldots(121)$$

where $n_x, n_y, n_z = 1, 2, 3, 4, \ldots$.

Degeneracy. It is seen from Eq. 121 that the total energy depends upon the sum of the squares of three quantum numbers. It is evident that groups of different states, each specified by a unique set of quantum numbers, can have the *same* energy. In such a case, the energy level and the corresponding independent states are said to be **degenerate.** Consider the energy level having energy $= 14h^2/8ma^2$. There are six combinations of n_x, n_y and n_z which can give this value of energy :

n_x	1	1	2	3	2	3
n_y	2	3	1	1	3	2
n_z	3	2	3	2	1	1

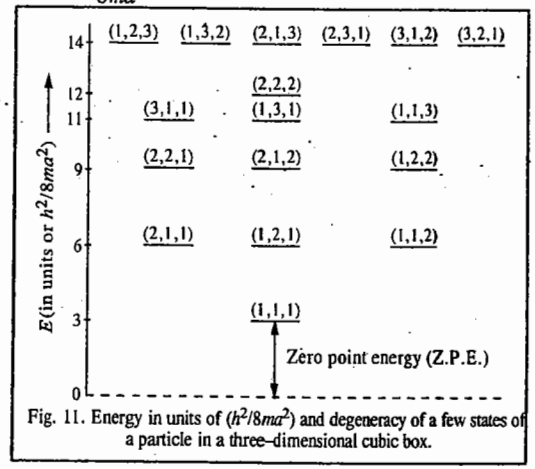

Fig. 11. Energy in units of $(h^2/8ma^2)$ and degeneracy of a few states of a particle in a three-dimensional cubic box.

This energy level is, therefore, 6-*fold degenerate, i.e.,* its degeneracy is equal to 6. Proceeding in this manner we can calculate degeneracy of the energy levels of a particle in a three-dimensional cubical box. The results are shown in Fig. 11.

3. One-Dimensional Simple Harmonic Oscillator. A diatomic vibrating molecule is an example of the so-called simple harmonic oscillator. (S.H.O.). This system represents **vibrational motion.**

According to Hooke's law, the force acting on the molecule is given by $f = -kx$, where x is the displacement from the equilibrium position and k is a constant called the **force constant.** The **Hooke's law potential energy** $V(x)$ of this molecule is given by

$$V(x) = -\int_0^x f dx = \int_0^x kx\,dx = \frac{1}{2}kx^2 \qquad ...(122)$$

Eq. 122 is the equation of a parabola. Thus, if we plot potential energy of a particle executing simple harmonic oscillations as a function of displacement from the equilibrium position, we get a curve as shown in Fig. 12.

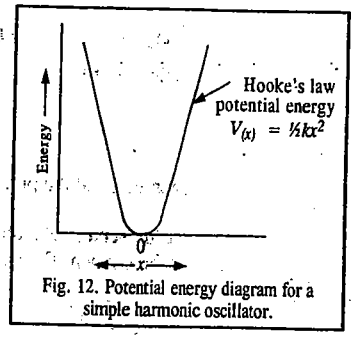

Fig. 12. Potential energy diagram for a simple harmonic oscillator.

The vibrational frequency of the oscillator of mass m is given by

$$\nu = \frac{1}{2\pi}\left(\frac{k}{m}\right)^{1/2} \qquad ...(123)$$

It is more accurate to define the vibrational frequency as

$$\nu = \frac{1}{2\pi}\left(\frac{k}{\mu}\right)^{1/2} \qquad ...(124)$$

where μ is the reduced mass of the diatomic molecule defined as

$$\frac{1}{\mu} = \frac{1}{m_1} + \frac{1}{m_2} \qquad ...(125)$$

where m_1 and m_2 are the atomic masses of the two atoms.

Using the potential energy given by Eq. 122, for one-dimensional S.H.O., the Schrödinger equation (Eq. 67) is represented as

$$\left[-\frac{\hbar^2}{2m}\left(\frac{d^2}{dx^2}\right) + \frac{1}{2}kx^2\right]\psi(x) = E\psi(x) \qquad ...(126)$$

Mathematically, Eq. 126 may be written as

$$\frac{d^2\psi}{dx^2} + \frac{2m}{\hbar^2}\left(E - \frac{1}{2}kx^2\right)\psi = 0 \qquad ...(127)$$

It is convenient to use the mass, rather than the reduced mass, of the S.H.O. in the following discussion ; also bear in mind that the force constant k of the oscillator is given by $k = m\omega^2$, where $\omega(=2\pi\nu)$ is the angular frequency. Thus, Eq. 127 is written as

$$\frac{d^2\psi}{dx^2} + \frac{2m}{\hbar^2}\left(E - \frac{1}{2}m\omega^2x^2\right)\psi = 0 \qquad ...(128)$$

Defining a new variable ξ and a new parameter λ by

$$\xi = (m\omega/\hbar)^{1/2}x \text{ and } \lambda = 2E/\hbar\omega \qquad ...(129)$$

Eq. 128 may be written as

$$\frac{d^2\psi}{d\xi^2} + \left(\lambda - \xi^2\right)\psi = 0 \qquad ...(130)$$

We shall now investigate the **asymptotic solution** of Eq. 130, *i.e.,* to find ψ when $\xi \to \infty$. When ξ is very large, $\lambda - \xi^2 \cong -\xi^2$ so that Eq. 130 becomes

$$\frac{d^2\psi}{d\xi^2} - \xi^2\psi = 0 \qquad ...(131)$$

Its asymptotic solutions are

$$\psi(x) = \exp\left(\pm\xi^2/2\right) \qquad ...(132)$$

since substitution of Eq. 132 in Eq. 131 gives

$$\frac{d^2\psi}{d\xi^2} = \left(\xi^2 + 1\right)\exp\left(\pm\xi^2/2\right) \cong \xi^2\psi$$

Out of the two asymptotic solutions, $\exp\left(\xi^2/2\right)$ is not acceptable since it diverges when $|\xi| \to \infty$. The exact solution of Eq. 130 may thus be written as

$$\psi(x) = e^{-\xi^2/2}H(\xi) \qquad ...(133)$$

where $H(\xi)$ is a function of ξ and the product $e^{-\xi^2/2}H(\xi)$ tends to zero as $|\xi| \to \infty$.

We next carry out the **series solution.** Substituting Eq. 133 into Eq. 131, we obtain the **Hermite equation** (named after the eminent French mathematician Charles Hermite (1822-1901)) :

$$\frac{d^2H(\xi)}{d\xi^2} - 2\xi\frac{dH(\xi)}{d\xi} + (\lambda - 1)H(\xi) = 0 \qquad ...(134)$$

We look for the function $H(\xi)$ as a series solution of the type

$$H(\xi) = \sum_{n=0}^{\infty} a_n\xi^n \qquad ...(135)$$

Substitution of Eq. 135 in Eq. 134 gives

$$\sum_{k=0}^{\infty}\left[(k+1)(k+2)a_{k+2} - (2k + 1 - \lambda)a_k\right]\xi^k = 0 \qquad ...(136)$$

In order that this equation be valid it is essential that the coefficient of each power of ξ must vanish separately. When the coefficient of ξ^k is equated to zero we obtain the so-called **recurrence relation :**

$$a_{k+2} = \frac{2k + 1 - \lambda}{(k+1)(k+2)}a_k \qquad ...(137)$$

This relation allows the calculation of all even coefficients in terms of a_0 and the odd coefficients in terms of a_1. Eq. 135 will have only odd coefficients if $a_0 = 0$ and even coefficients if $a_1 = 0$. Thus, we have two independent solutions of Eq. 135 and the linear combination of the two will give the most general solution. The two solutions are :

$$H_e(\xi) = a_0 + a_2\xi^2 + a_4\xi^4 + ... \qquad ...(138)$$

and

$$H_o(\xi) = \xi(a_1 + a_3\xi^2 + a_5\xi^4 + ...) \qquad ...(139)$$

We now proceed to determine the **energy eigenvalues :**

When $k \to \infty$ in Eq. 137, we obtain

$$\frac{a_{k+2}}{a_k} = \frac{2}{k} \qquad ...(140)$$

Let us consider the Taylor series expansion of exp (ξ^2) :

$$\exp(\xi^2) = \sum_{0,2,4} \frac{1}{(k/2)!}\xi^k \qquad ...(141)$$

The ratio of the coefficients of the successive terms in Eq. 141 is

$$\frac{a_{k+2}}{a_k} = \frac{(k/2)!}{[(k/2)+1]!} = \frac{1}{[(k/2)+1]} \cong \frac{2}{k} \qquad ...(142)$$

where k is large. Thus, for large values of k, $\psi = \exp(-\xi^2/2)\, H(\xi)$ tends to behave like $\exp(-\xi^2/2)$ if the series is even, and $\xi \exp(-\xi^2/2)$ if the series is odd, which is not acceptable. This unrealistic solution can be avoided if the series in Eq. 135 terminates after a finite number of terms. In such a situation, $\psi(\xi) \to 0$ as $\xi \to \infty$ because of the factor $\exp(-\xi^2/2)$. The series can be terminated by choosing λ in such a way that $(2k+1-\lambda)$ vanishes for $k = n$. Thus, one of the series becomes a polynomial and the other can be eliminated by setting the first coefficient equal to zero. Substitution of the value of λ gives

$$2n + 1 - 2E/(\hbar\omega) = 0$$

or,
$$E_n = \left(n + \frac{1}{2}\right)\hbar\omega, \qquad n = 0, 1, 2, \ldots \qquad ...(143)$$

The energy of the S.H.O. , using the old quantum theory, is

$$E_n = n\hbar\omega \qquad n = 0, 1, 2, \ldots \qquad ...(144)$$

From Eqs. 143 and 144 we see that the quantum mechanical energy value (obtained by solving the Schrödinger equation for the oscillator) is higher than the old quantum theory value by $\frac{1}{2}\hbar\omega$, which is the energy possessed by the linear oscillator in the lowest vibrational state ($n = 0$). The oscillator possesses this energy, $\frac{1}{2}\hbar\omega$, called the **zero-point energy**, even at absolute zero of temperature. The occurence of zero-point energy is a manifestation of the Heisenberg uncertainty principle. Note that $E = 0$ implies that both position and the momentum associated with it are well defined, which violates the uncertainty (indeterminacy) principle. We can, in fact, prove that the minimum energy of the oscillator without violating the uncertainty principle is $\frac{1}{2}\hbar\omega$.

We shall now determine the **energy eigenfunctions** of the S.H.O. When the parameter $\lambda = 2n+1$, Eq. 134 reduces to

$$\frac{d^2H_n(\xi)}{d\xi^2} - 2\xi\frac{dH_n(\xi)}{d\xi} + 2nH_n(\xi) = 0 \qquad ...(145)$$

The solutions of Eq. 145 are the **Hermite polynomials.**

The Hermite polynomial of degree n is defined as

$$H_n(\xi) = (-1)^n e^{\xi^2}\left\{\frac{\partial^n(e^{-\xi^2})}{\partial\xi^n}\right\} \qquad ...(146)$$

A few Hermite polynomials are given below :

$$H_0(\xi) = 1 \qquad H_3(\xi) = 8\xi^3 - 12\xi$$
$$H_1(\xi) = 2\xi \qquad H_4(\xi) = 16\xi^4 - 48\xi^2 + 12 \qquad ...(147)$$
$$H_2(\xi) = 4\xi^2 - 2$$

The unnormalized wave functions of the one-dimensional S.H.O. are then written as

$$\psi_n(\xi) = N_n H_n(\xi)\exp\left(-\xi^2/2\right), \quad \xi^2 = (m\omega/\hbar)x^2 \qquad ...(148)$$

The normalization condition leads to

$$|N_n|^2\left(\frac{\hbar}{m\omega}\right)^{1/2}\int_{-\infty}^{\infty} H_n^2(\xi)\exp\left(-\xi^2\right)d\xi = 1 \qquad \text{or} \qquad |N_n|^2\left(\frac{\hbar}{m\omega}\right)^{1/2}\pi^{1/2}2^n(n!) = 1$$

or
$$N_n = \left[\left(\frac{m\omega}{\hbar\pi}\right)^{1/2}\frac{1}{2^n(n!)}\right]^{1/2}$$

The normalized eigenfunctions and the ground state eigenfunction are given by

$$\psi_n(\xi) = \left[\left(\frac{m\omega}{\hbar\pi}\right)^{1/2}\frac{1}{2^n(n!)}\right]^{1/2} H_n(\xi)\exp\left(\frac{-\xi^2}{2}\right) \qquad ...(149)$$

The ground-state ($n = 0$) eigenfunction is

$$\psi_n(x) = \left(\frac{m\omega}{\hbar\pi}\right)^{1/4}\exp\left(-\frac{m\omega x^2}{2\hbar}\right) \qquad ...(150)$$

The wave functions $\psi_n(x)$ and the probability density $|\psi_n(x)|^2$ of the lowest three states are also illustrated in Fig. 13.

We note from Fig.13 that the linear oscillator eigenfunctions are even for even values of the vibrational quantum number n and odd for odd values of n. This is understandable as $\exp(-\xi^2/2)$, which is the Gaussian function, is always even and the Hermite polynomials $H_n(\xi)$ are even or odd according as n is even or odd. We may also note that the quantum oscillator can be *outside* the parabolic Hooke's law potential barrier since the wave function ψ does not vanish at the classical turning points. This implies that the particle can penetrate the barrier to some extent. This barrier penetration, called **quantum mechanical tunnelling,** is a significant feature of quantum mechanics ; classical mechanics does not permit it. A final point to note is the nature of the probability distribution of classical and quantal (quantum

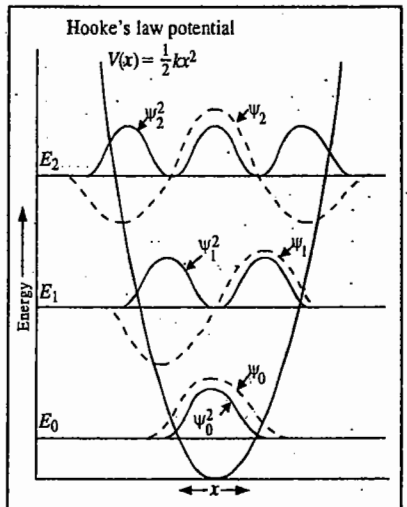

Fig. 13. The wavefunctions, the probability density functions and the energy levels of the three lowest states of a simple harmonic oscillator.

mechanical) oscillators. Classically, the probability of finding an oscillator at a given point is inversely proportional to its velocity at that point. The total energy of the oscillator is

$$E = \text{K.E.} + \text{P.E.} = \tfrac{1}{2}mv^2 + \tfrac{1}{2}kx^2, \text{ or } v = [(2E - kx^2)/m]^{1/2} \quad ...(151)$$

Hence, the classical probability

$$P_c \propto [m/(2E - kx^2)]^{1/2} \quad ...(152)$$

This probability is minimum at the mean position ($x = 0$) and maximum at the extreme positions. For the quantum case, for $n = 0$, the probability is maximum at $x = 0$ and as the quantum number increases the maximum probability moves towards the extreme positions.

Fig. 14 shows the probability density $|\psi_{10}|^2$ and the classical probability distribution (dotted line) for the same energy. Though the two distributions become more and more similar for high quantum numbers, the rapid oscillations of $|\psi_n|^2$ is still a discrepancy. The energy for $n = 0$ is called the **zero point energy** of the oscillator. Classical mechanics predicts that the zero-point energy of the oscillator is zero whereas quantum mechanics predicts that the zero-point energy is non-zero. *The occurrence of the zero-point energy is consistent with the Heisenberg uncertainty principle.*

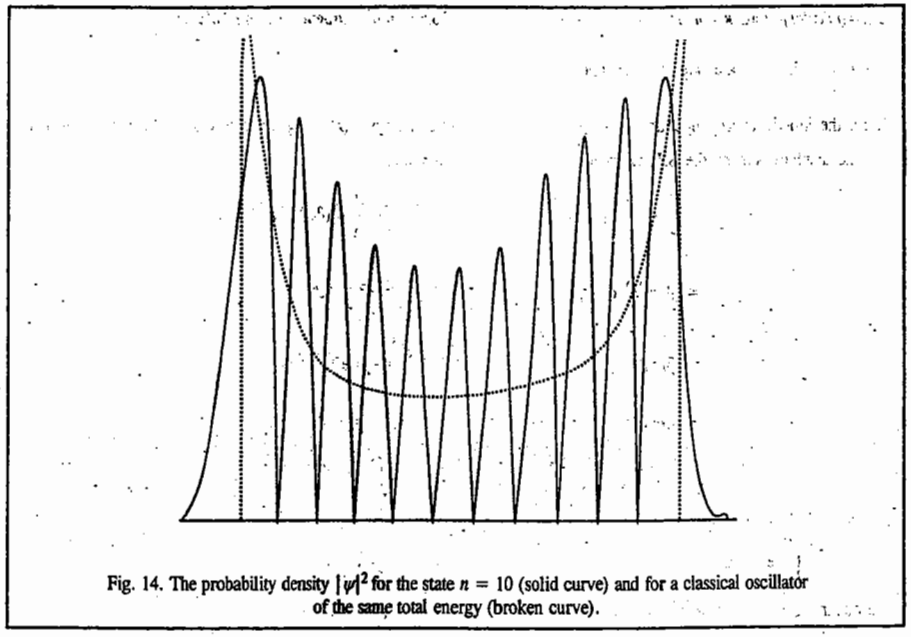

Fig. 14. The probability density $|\psi|^2$ for the state $n = 10$ (solid curve) and for a classical oscillator of the same total energy (broken curve).

It may be mentioned here that the solutions of the time-independent Schrödinger equation are called stationary state wave functions. An atom or a molecule can be in any of the stationary energy states, say, the nth, represented by its own eigenfunction ψ_n with energy, E_n.

Example 27. What is the restriction on α/β if the $n=1$ wave function of a one-dimensional S.H.O. has to satisfy the wave equation $d^2\psi_1/d\xi^2 + (\alpha/\beta - \xi^2)\psi_1 = 0$? Given that $\psi_1 = N\xi\exp(-\xi^2/2)$ where N is a constant.

Solution : $\psi_1 = N\xi e^{-\xi^2/2}$

$$\frac{d\psi_1}{d\xi} = N\xi(-\xi)e^{-\xi^2/2} + Ne^{-\xi^2/2} = -N\xi^2e^{-\xi^2/2} + Ne^{-\xi^2/2}$$

$$\frac{d^2\psi_1}{d\xi^2} = -N\xi^2(-\xi)e^{-\xi^2/2} - 2N\xi e^{-\xi^2/2} - N\xi e^{-\xi^2/2} = N\xi^3e^{-\xi^2/2} - 3N\xi e^{-\xi^2/2}$$

$\frac{d^2\psi_1}{d\xi^2} + \left(\frac{\alpha}{\beta} - \xi^2\right)\psi_1$ will be equal to zero

if $N\xi^3e^{-\xi^2/2} - 3N\xi e^{-\xi^2/2} + \frac{\alpha}{\beta}N\xi e^{-\xi^2/2} - N\xi^3e^{-\xi^2/2} = 0$

or if $-3N\xi e^{-\xi^2/2} + (\alpha/\beta)N\xi e^{-\xi^2/2} = 0$

or if $\alpha/\beta = 3$

which is the **desired restriction.**

Example 28. "According to the virial theorem for a diatomic S.H.O., the expectation (average) value of the kinetic energy, $< T >$, is equal to the expectation value of the potential energy, $< V >$". Verify this statement for the ground state of the S.H.O., given that the ground state wavefunction is

$$\psi_0(x) = (\beta/\pi)^{1/4}\exp(-\beta x^2/2)$$

where $\beta = (mk)^{1/2}/\hbar$ and $k = m\omega^2$; $\omega = 2\pi\nu$ where ν is the vibrational frequency of the S.H.O.

Solution : Let us calculate $<\hat{T}>$ and $<\hat{V}>$.

Here, the kinetic energy operator is $-\frac{\hbar^2}{2m}\frac{\partial^2}{\partial x^2}$ and potential energy $V(x) = \frac{1}{2}kx^2$ where k is the force constant and x is the displacement of the S.H.O. from the equilibrium position.

$$<\hat{T}> = \int_{-\infty}^{\infty}\psi_0^*\hat{T}\psi_0 dx = \int_{-\infty}^{\infty}(\beta/\pi)^{1/4}e^{-\beta x^2/2}\left(-\frac{\hbar^2}{2m}\frac{d^2}{dx^2}\right)(\beta/\pi)^{1/4}e^{-\beta x^2/2}dx$$

$$= (\beta/\pi)^{1/2}\left(-\hbar^2/2m\right)\int_{-\infty}^{\infty}e^{-\beta x^2/2}\left(\frac{d^2}{dx^2}\right)e^{-\beta x^2/2}dx$$

$$= (\beta/\pi)^{1/2}\left(-\hbar^2/2m\right)\int_{-\infty}^{\infty}e^{-\beta x^2/2}\left(\frac{d}{dx}\right)(-\beta x e^{-\beta x^2/2})dx$$

$$= (\beta/\pi)^{1/2}\left(-\hbar^2/2m\right)(-\beta)\int_{-\infty}^{\infty}e^{-\beta x^2/2}[1-\beta x^2]e^{-\beta x^2/2})dx$$

$$= (\beta/\pi)^{1/2}(\hbar^2/2m)\left[\beta\int_{-\infty}^{\infty}e^{-\beta x^2}dx - \beta^2\int_{-\infty}^{\infty}x^2e^{-\beta x^2}dx\right]$$

Using the standard integrals

$$\int_{-\infty}^{\infty}e^{-ax^2}dx = (\pi/a)^{1/2} \quad \text{and} \quad \int_{-\infty}^{\infty}x^2e^{-ax^2}dx = \frac{1}{2a}(\pi/a)^{1/2},$$

we obtain $<\hat{T}> = (\beta/\pi)^{1/2}(\hbar^2/2m)[(\beta)(\pi/\beta)^{1/2} - (\beta^2)(1/2\beta)(\pi/\beta)^{1/2}]$

$$= \frac{\beta\hbar^2}{2m} - \frac{\beta\hbar^2}{4m} = \frac{\beta\hbar^2}{4m} = \frac{\hbar\omega}{4} = \frac{h\nu}{4} \quad (\text{since } \beta = (mk)^{1/2}/\hbar \text{ ; } k = m\omega^2 \text{ and } \omega = 2\pi\nu) \quad ...(i)$$

Again,

$$<\hat{V}> = \int_{-\infty}^{\infty}\psi_0^*\hat{V}\psi_0 dx = \int_{-\infty}^{\infty}(\beta/\pi)^{1/4}e^{-\beta x^2/2}\left(\frac{1}{2}kx^2\right)(\beta/\pi)^{1/4}e^{-\beta x^2/2}dx$$

$$= (\beta/\pi)^{1/2}\left(\frac{1}{2}k\right)\int_{-\infty}^{\infty}x^2e^{-\beta x^2}dx = (\beta/\pi)^{1/2}(k/2)\left(\frac{1}{2\beta}\right)(\pi/\beta)^{1/2}$$

$$= \frac{k}{4\beta} = \frac{m\omega^2}{4(mk)^{1/2}/\hbar} = \frac{m\omega^2\hbar}{4m\omega} = \frac{\hbar\omega}{4} = \frac{h\nu}{4} \qquad ...(ii)$$

From Eqs. *(i)* and *(ii)*, we see that

$$< \hat{T} > = < \hat{V} >, \text{ which is the virial theorem.}$$

Example 29. Verify the Heisenberg uncertainty principle for the ground state of a one-dimensional S.H.O.

Solution : We know that $\Delta x = [< x^2 > - < x >^2]^{1/2}$

$$(\Delta p_x) = [< p_x^2 > - < p_x >^2]^{1/2}$$

For an S.H.O.: $\psi_0(x) = (\beta/\pi)^{1/4} e^{-\beta x^2/2}$

Now, $$< x > = \int_{-\infty}^{\infty} \psi_0^* \hat{x} \, dx = \int_{-\infty}^{\infty} (\beta/\pi)^{1/4} e^{-\beta x^2/2} \hat{x} (\beta/\pi)^{1/4} e^{-\beta x^2/2} dx$$

$$= (\beta/\pi)^{1/2} \int_{-\infty}^{\infty} x e^{-\beta x^2} dx = 0 \text{ (since the integrand is odd)} \qquad ...(i)$$

Again, $$< x^2 > = \int_{-\infty}^{\infty} \psi_0^* \hat{x}^2 \psi_0 dx$$

Proceeding as in Example 28, we find that

$$< x^2 > = 1/2\ \beta \qquad ...(ii)$$

$$< \hat{p}_x > = \int_{-\infty}^{\infty} \psi_0^* (-i\hbar d/dx) \psi_0 \, dx = (\beta/\pi)^{1/2} (-i\hbar) \int_{-\infty}^{\infty} e^{\beta x^2/2} [-\beta x e^{-\beta x^2/2}] dx$$

$$= (\beta/\pi)^{1/2} (-i\hbar)(-\beta) \int_{-\infty}^{\infty} x e^{-\beta x^2} dx$$

$$= 0 \text{ (because the integrand is odd)} \qquad ...(iii)$$

Again, $$< p_x^2 > = \int_{-\infty}^{\infty} \psi_0^* (-\hbar^2 d^2/dx^2) \psi_0 dx = (-\hbar^2)(\beta/\pi)^{1/2} \int_{-\infty}^{\infty} e^{-\beta x^2/2} (d^2/dx^2) e^{-\beta x^2/2} dx$$

Proceeding as in Example 28, where we have evaluated $< \hat{T} >$, we find that

$$< p_x^2 > = \beta\hbar^2/2 \qquad ...(iv)$$

From Eqs. *(i)*, *(ii)*, *(iii)* and *(iv)*, we find on simplification that

$$\Delta x . \Delta p_x = \hbar/2,$$

which is the **Heisenberg uncertainty principle**. A rigorous mathematical derivation gives the inequality

$$\Delta x . \Delta p_x \geq \hbar/2$$

Example 30. For a one-dimensional simple harmonic oscillator in the ground vibrational state,

(*a*) Where is the probability density maximum ?

(*b*) Determine the value of the maximum probability density.

Solution : (*a*) $$\psi_0(x) = \left(\frac{m\omega}{\hbar\pi}\right)^{1/4} \exp\left(-\frac{m\omega x^2}{2\hbar}\right)$$

The probability density is $$P(x) = \psi_0^*(x)\psi_0(x) = \left(\frac{m\omega}{\hbar\pi}\right)^{1/2} \exp\left(-\frac{m\omega x^2}{\hbar}\right)$$

The probability will be a maximum where $dP(x)/dx = 0$

Thus, $$\left(\frac{m\omega}{\hbar\pi}\right)^{1/2} \left(-\frac{m\omega}{\hbar}\right) 2x \exp\left(-\frac{m\omega x^2}{\hbar}\right) = 0$$

which implies that $x = 0$, *i.e.*, the probability is maximum at $x = 0$

(*b*) The maximum probability at $x = 0$ is

$$P(0) = \left(\frac{m\omega}{\hbar\pi}\right)^{1/2}$$

Example 31. Show that the Z.P.E. (zero-point energy), ($\frac{1}{2}\hbar\omega$), of a one-dimensional S.H.O. is a manifestation of the Heisenberg uncertainty principle.

Solution : As we have shown in Example 31, the average position, $<x>$, and average momentum, $<p>$, of an S.H.O., bound to the origin, is zero. Hence,

$$(\Delta x)^2 = \langle x^2 \rangle - \langle x \rangle^2 = \langle x^2 \rangle \quad \text{and} \quad (\Delta p)^2 = \langle p^2 \rangle - \langle p \rangle^2 = \langle p^2 \rangle$$

For the total energy E,

$$<E> = \frac{1}{2m}\langle p^2 \rangle + \frac{1}{2}k\langle x^2 \rangle, \qquad \text{(where } k = m\omega^2\text{)}$$

[where ω is the angular frequency of the oscillator].

or $$<E> = \frac{1}{2m}(\Delta p)^2 + \frac{1}{2}k(\Delta x)^2$$

Replacing $(\Delta p)^2$ with the help of the relation $(\Delta p)^2(\Delta x)^2 \geq \frac{\hbar^2}{4}$ [using the uncertainty principle]

we get $$<E> \geq \frac{\hbar^2}{8m(\Delta x)^2} + \frac{1}{2}k(\Delta x)^2$$

For the right-hand side to be minimum, the differential of $<E>$ with respect to $(\Delta x)^2$ must be zero :

$$\frac{-\hbar^2}{8m(\Delta x)^4_{\min}} + \frac{1}{2}k = 0, \quad \text{or} \quad (\Delta x)^2_{\min} = \frac{\hbar}{2m\omega}$$

and $$<E>_{\min} = \frac{\hbar^2}{8m}\frac{2m\omega}{\hbar} + \frac{1}{2}m\omega^2\frac{\hbar}{2m\omega} = \frac{1}{2}\hbar\omega.$$ Hence proved.

[Note : (Δx) is also called **standard deviation**, and $(\Delta x)^2$ is the **variance**, σ_x^2, which measures the spread around the mean value of the observable x.]

Example 32. Show that the probability density of the linear (simple) harmonic oscillator, S.H.O., in an arbitrary superposition state is periodic with the period equal to the period of the oscillator.

Solution : The time-dependent wave function of the S.H.O. in a superposition state is

$$\psi(x,t) = \sum_n c_n \psi_n(x) \exp\left(-\frac{iE_n t}{\hbar}\right)$$

where $\psi_n(x)$ is the time-independent wave function of the harmonic oscillator in the nth state. Now, the probability density

$$P(x,t)=|\Psi(x,t)|^2 = \sum_m\sum_n c_m^* c_n \psi_m^* \psi_n \exp\left[\frac{i(E_m-E_n)t}{\hbar}\right]$$

It is obvious that $P(x, t)$ is dependent on time. Let us investigate what happens to $P(x, t)$ if t is replaced by $t + (2\pi/\omega)$. We see that

$$\exp\left[\frac{i(E_m-E_n)}{\hbar}\left(t+\frac{2\pi}{\omega}\right)\right] = \exp\left[\frac{i(E_m-E_n)t}{\hbar}\right]\exp\left[\frac{i(E_m-E_n)}{\hbar}\frac{2\pi}{\omega}\right]$$

$$= \exp\left[\frac{i(E_m-E_n)t}{\hbar}\right]$$

as $(E_m - E_n)$ is an integral multiple of $\hbar\omega$. That is, $P(x, t)$ is periodic with period $2\pi/\omega$, the period of the linear harmonic oscillator.

Example 33. Solve the time-independent Schrödinger equation for a three-dimensional harmonic oscillator whose potential energy is

$$V(x, y, z) = \frac{1}{2}\left(k_1x^2+k_2y^2+k_3z^2\right)$$

Solution : The theory developed for a linear harmonic oscillator can easily be extended to the case of three-dimensional oscillator. The Schrödinger equation for the system is

$$\frac{-\hbar}{2m}\nabla^2\psi(x,y,z)+V\psi(x,y,z) = E\psi(x,y,z)$$

This equation can be separated into three equations by writing the wave funciton

$$\psi(x,y,z) = X(x)\,Y(y)\,Z(z)$$

The Schrödinger equation now separates into three equations of the form

$$\frac{d^2X(x)}{dx^2}+\frac{2m}{\hbar}\left(E_x-\frac{1}{2}m\omega_x^2x^2\right)X(x) = 0$$

$$\frac{d^2Y(y)}{dy^2}+\frac{2m}{\hbar}\left(E_y-\frac{1}{2}m\omega_y^2y^2\right)Y(y) = 0$$

$$\frac{d^2Z(z)}{dz^2}+\frac{2m}{\hbar}\left(E_z-\frac{1}{2}m\omega_z^2z^2\right)Y(z) = 0$$

where $E_x + E_y + E_z = E$, the total energy of the system, and

$$\omega_x=\sqrt{\frac{k_1}{m}}, \qquad \omega_y=\sqrt{\frac{k_2}{m}}, \qquad \omega_z=\sqrt{\frac{k_3}{m}}$$

Using the results of the one-dimensional S.H.O.,

$$E_x = \left(n_x+\frac{1}{2}\right)\hbar\omega_x, \qquad n_x = 0, 1, 2, ...$$

$$E_y = \left(n_y+\frac{1}{2}\right)\hbar\omega_y, \qquad n_y = 0, 1, 2, ...$$

$$E_z = \left(n_z+\frac{1}{2}\right)\hbar\omega_z, \qquad n_z = 0, 1, 2, ...$$

The eigenfunctions are given by

$$\psi_{n_xn_yn_z} = NH_{n_x}(\xi x)H_{n_y}(\eta y)H_{n_z}(\zeta z)\exp\left[-\frac{1}{2}\left(\xi^2x^2+\eta^2y^2+\zeta^2z^2\right)\right]$$

where N is the normalization constant and

$$\xi=\left(\frac{m\omega_x}{\hbar}\right)^{1/2}, \qquad \eta=\left(\frac{m\omega_y}{\hbar}\right)^{1/2}, \qquad \zeta=\left(\frac{m\omega_z}{\hbar}\right)^{1/2},$$

The normalization constant is given by

$$N = \frac{\xi^{1/2}\eta^{1/2}\zeta^{1/2}}{\pi^{3/4}\left(2^{n_x+n_y+n_z}n_x!n_y!n_z!\right)^{1/2}}$$

4. Rigid Rotor (or Rotator). A diatomic molecule rotating about an axis perpendicular to the internuclear axis and passing through the centre of gravity of the molecule, constitutes an example of a rigid rotor, it being assumed that the internuclear distance does not change during rotation. This system represents **rotational motion.** The kinetic energy (K.E.) of the molecule is given by

$$\text{K.E.} \equiv T = \tfrac{1}{2}I\omega^2 = L^2/2I \qquad ...(153)$$

where ω is the angular velocity and I is the moment of inertia of the rotating molecule. The angular momentum $L=I\omega$. If no force acts on the rotor, we can set the potential energy $V=0$. Hence, the Hamiltonian is expressed as

$$H = T + V = L^2/2I \qquad ...(154)$$

The expression for L^2 in spherical polar coordinates (r, θ, ϕ) is given by

$$L^2 = -\hbar^2\left[\frac{1}{\sin\theta}\frac{\partial}{\partial\theta}\left(\sin\theta\frac{\partial}{\partial\theta}\right)+\frac{1}{\sin^2\theta}\frac{\partial^2}{\partial\phi^2}\right] \qquad ...(155)$$

The Schrödinger equation $\hat{H}\psi = E\psi$ may thus be written as

$$\frac{1}{2I}\left[-\hbar^2\left\{\frac{1}{\sin\theta}\frac{\partial}{\partial\theta}\left(\sin\theta\frac{\partial\psi}{\partial\theta}\right)+\frac{1}{\sin^2\theta}\frac{\partial^2\psi}{\partial\phi^2}\right\}\right] = E\psi \qquad ...(156)$$

The above equation may be written as

$$\frac{1}{\sin\theta}\frac{\partial}{\partial\theta}\left(\sin\theta\frac{\partial\psi}{\partial\theta}\right)+\frac{1}{\sin^2\theta}\frac{\partial^2\psi}{\partial\phi^2}+\frac{8\pi^2I}{h^2}E\psi = 0 \qquad ...(157)$$

Eq. 157 contains two angular variables θ and ϕ. It can be solved by the method of separation of variables, *i.e.*, we look for a solution of the form

$$\psi(\theta,\phi) = \Theta(\theta)\,\Phi(\phi) \qquad ...(158)$$

Substituting Eq. 158 into Eq. 157, we obtain

$$\frac{\sin\theta}{\Theta}\frac{\partial}{\partial\theta}\left(\sin\theta\frac{\partial\Theta}{\partial\theta}\right)+\frac{8\pi^2IE}{h^2}\sin^2\theta=-\frac{1}{\Phi}\frac{\partial^2\Phi}{\partial\phi^2} \qquad ...(159)$$

We can set both sides of Eq. 159 equal to a constant, say m^2, thereby obtaining two differential equations each in one variable. These equations are :

$$\frac{\partial^2\Phi}{\partial\phi^2}+m^2\Phi=0 \text{ and} \qquad ...(160)$$

$$\frac{1}{\sin\theta}\frac{\partial}{\partial\theta}\left(\sin\theta\frac{\partial\Theta}{\partial\theta}\right)+\left(\lambda-\frac{m^2}{\sin^2\theta}\right)\Theta=0 \qquad (\text{where } \lambda=8\pi^2IE/h^2) \qquad ...(161)$$

Eq. 160 has the solution

$$\Phi(\phi)=N\exp(\pm im\phi), \qquad i=\sqrt{-1} \qquad ...(162)$$

where N is the normalization constant. This wavefunction is acceptable provided m is an integer. This condition arises because Φ must be single-valued. Thus,

$$\Phi(\phi)=\Phi(\phi+2\pi) \qquad ...(163)$$

Hence, $\exp(2\pi im)=1$ ...(164)

Since $e^x=\cos x+i\sin x$ **(Euler's relation)** ...(165)

$\therefore$ $\cos 2\pi m+i\sin 2\pi m=1$ ...(166)

This can be true only if $m=0, \pm 1, \pm 2, \pm 3, \ldots$, etc. Let us now normalize the wave function $\Phi(\phi)$ to determine the normalization constant N.

$$\int_0^{2\pi}\Phi^*\Phi\,d\phi=1 \quad (0\le\phi\le 2\pi) \qquad ...(167)$$

or $$N^2\int_0^{2\pi}e^{im\phi}\times e^{-im\phi}d\phi=1 \qquad ...(168)$$

or $N^2\int_0^{2\pi}d\phi=1$, *i.e.*, $N^2(2\pi)=1$ so that $N=(2\pi)^{-1/2}$ ...(169)

Hence, the normalized wave functions become

$$\Phi_{\pm m}(\phi)=(2\pi)^{-1/2}\exp(\pm im\phi)\,;\ m=0,1,2,3,\ldots \qquad ...(170)$$

We shall not attempt to give a complete solution of Eq. 161 (which also occurs in the hydrogen atom problem) but will merely state that if $\lambda=l(l+1)$ where l is the **rotational quantum number,** then this equation becomes a standard mathematical equation whose solutions are known to be **associated Legendre polynomials** $P_l^{|m|}(\cos\theta)$ where l is either zero or a positive integer and $l>|m|$. The normalized solutions are given by

$$\Theta(\theta)=\Theta_{l,\pm m}(\theta)=\left[\frac{2l+1}{2}\times\frac{(l-|m|)!}{(l+|m|)!}\right]^{1/2}P_l^{|m|}\cos\theta \qquad ...(171)$$

The eigenfunctions of the rigid rotor are the **spherical harmonics,** obtained by the product of the angular functions :

$$Y_{l,m}(\theta,\phi)=\Theta_{l,m}(\theta)\,\Phi_m(\phi)\equiv Y_l^m(\theta,\phi) \qquad ...(172)$$

The energy eigenvalues of the rigid rotor are obtained as follows :

$$\lambda=8\pi^2IE/h^2=l(l+1) \qquad ...(173)$$

Thus, $$E=\frac{l(l+1)h^2}{8\pi^2I};\ l=0,1,2,3,\ldots \qquad ...(174a)$$

In spectroscopy it is customary to use the symbol J rather than l for the rotational quantum number so that the rotational energy levels are given by the expression,

$$E_J=\frac{J(J+1)h^2}{8\pi^2I};\ J=0,1,2,3,\ldots \qquad ...(174b)$$

5. The Schrödinger Equation for Hydrogen Atom. Hydrogen atom is the simplest of all atoms. It is a three-dimensional system and the Schrödinger equation for this system is

$$\hat{H}\psi=E\psi \qquad ...(175)$$

where $$\hat{H}=-\frac{\hbar^2}{2m}\nabla^2+V(x,y,z) \qquad ...(176)$$

and where the Laplacian operator in Cartesian coordinates is given by

$$\nabla^2=\frac{\partial^2}{\partial x^2}+\frac{\partial^2}{\partial y^2}+\frac{\partial^2}{\partial z^2} \qquad ...(177)$$

The potential energy of interaction between the electron and the nucleus is given by

$$V(r)=-Ze^2/4\pi\varepsilon_0 r \qquad ...(178)$$

Since this attractive potential has spherical symmetry depending only upon r, it is convenient to express the Schrödinger equation in terms of polar coordinates (r,θ,ϕ), rather than Cartesian coordinates (x, y, z). The Cartesian coordinates are related to polar coordinates (see Fig. 15) as follows :

$$x=r\sin\theta\cos\phi$$

$$y=r\sin\theta\sin\phi$$

$$z=r\cos\theta$$

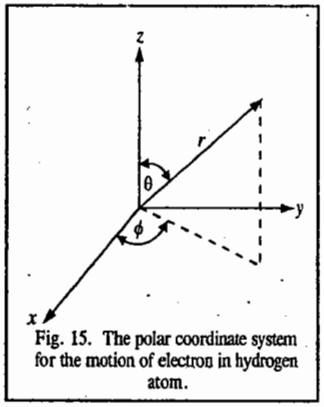

Fig. 15. The polar coordinate system for the motion of electron in hydrogen atom.

The Schrödinger equation for hydrogen atom in terms of polar coordinates becomes

$$\frac{1}{r^2}\frac{\partial}{\partial r}\left(\frac{r^2\partial\psi}{\partial r}\right)+\frac{1}{r^2\sin\theta}\frac{\partial}{\partial\theta}\left(\sin\theta\frac{\partial\psi}{\partial\theta}\right)+\frac{1}{r^2\sin^2\theta}\frac{\partial^2\psi}{\partial\phi^2}+\frac{2\mu}{\hbar}(E-V(r))\,\psi=0 \qquad ...(179)$$

where μ is the reduced mass of the electron and the nucleus, that is, $\mu=m_em_n/(m_n+m_e)$. Assuming that $V(r)$ is a function of r only, the above wave equation can be solved by separating the variables :

$$\psi(r,\theta,\phi)=R(r)\,\Theta(\theta)\,\Phi(\phi) \qquad ...(180)$$

where $R(r)$ is the **radial function** which is a function of r only, and $\Theta(\theta)$ and $\Phi(\phi)$ are **angular functions.**

Substituting Eq. 180 in Eq. 179 and multiplying by $r^2\sin^2\theta/R\Theta\Phi$, we have

$$\frac{\sin^2\theta}{R}\frac{d}{dr}\left(r^2\frac{dR}{dr}\right)+\frac{\sin\theta}{\Theta}\frac{d}{d\theta}\left(\sin\theta\frac{d\Theta}{d\theta}\right)+\frac{2\mu}{\hbar^2}[E-V(r)]r^2\sin^2\theta=-\frac{1}{\Phi}\frac{d^2\Phi}{d\phi^2} \qquad ...(181)$$

The left-hand side of Eq. 181 is a function of r and θ and the right side is a function of ϕ alone. This is possible only when each side is a constant, say m^2. Thus, we can write

$$\frac{d^2\Phi(\phi)}{d\phi^2} = -m^2\Phi(\phi) \qquad ...(182)$$

and

$$\frac{\sin^2\theta}{R}\frac{d}{dr}\left(r^2\frac{dR}{dr}\right)+\frac{\sin\theta}{\Theta}\frac{d}{d\theta}\left(\sin\theta\,\frac{d\Theta}{d\theta}\right)+\frac{2\mu}{\hbar^2}[E-V(r)]r^2\sin^2\theta=m^2 \qquad ...(183)$$

Dividing both sides of Eq. (183) by $\sin^2\theta$ and rearranging, we get

$$\frac{1}{R}\frac{d}{dr}\left(r^2\frac{dR}{dr}\right)+\frac{2\mu}{\hbar^2}(E-V)r^2=-\frac{1}{\Theta\sin\theta}\frac{d}{d\theta}\left(\sin\theta\frac{d\Theta}{d\theta}\right)+\frac{m^2}{\sin^2\theta}$$

This is possible when both sides are equal to a constant, say λ. Consequently, we get the Θ-equation and the radial equation :

$$\frac{1}{\sin\theta}\frac{d}{d\theta}\left(\sin\theta\frac{d\Theta}{d\theta}\right)+\left(\lambda-\frac{m^2}{\sin^2\theta}\right)\Theta = 0 \qquad ...(184)$$

and

$$\frac{1}{r^2}\frac{d}{dr}\left(r^2\frac{dR}{dr}\right)+\frac{2\mu}{\hbar^2}[E-V(r)]R-\frac{\lambda}{r^2}R = 0 \qquad ...(185)$$

We see that the three-dimensional Schrödinger wave equation in spherical polar coordinates (Eq. 179) has been separated into three one-dimensional equations (182, 184 and 185). These are called, respectively, the Φ-equation, the Θ-equation and the R-equation.

Solution of the Φ-equation : This equation also occurs in the Schrödinger equation for the rigid rotator and has already been solved (see Eq. 170), which we rewrite as

$$\Phi_m(\phi) = \frac{1}{\sqrt{2\pi}}e^{im\phi}, \quad m = 0, \pm1, \pm2, ... \qquad ...(186)$$

A few of the normalized $\Phi_{\pm m}(\phi)$ are given in Table 1. Since $\sin(|m|\phi)$ and $\cos(|m|\phi)$ are also solutions of Eq. 182, the real forms of the solutions are also given in this Table 1.

Table 1. The First-few Normalized $\Phi(\phi)$ functions

$\lvert m\rvert$	Complex form	Real form
0	$\Phi_0 = \frac{1}{\sqrt{2\pi}}$	$\Phi_0 = \frac{1}{\sqrt{2\pi}}$
1	$\Phi_1 = \frac{1}{\sqrt{2\pi}}e^{i\phi}$	$\Phi_{1\cos} = \frac{1}{\sqrt{\pi}}\cos\phi$
	$\Phi_{-1} = \frac{1}{\sqrt{2\pi}}e^{-i\phi}$	$\Phi_{1\sin} = \frac{1}{\sqrt{\pi}}\sin\phi$
2	$\Phi_2 = \frac{1}{\sqrt{2\pi}}e^{i2\phi}$	$\Phi_{2\cos} = \frac{1}{\sqrt{\pi}}\cos(2\phi)$
	$\Phi_{-2} = \frac{1}{\sqrt{2\pi}}e^{-i2\phi}$	$\Phi_{2\sin} = \frac{1}{\sqrt{\pi}}\sin(2\phi)$

Solution of the Θ-equation. We define a new variable $z = \cos\theta$, so that $dz = -\sin\theta d\theta$. We can also write

$$\frac{d}{d\theta} = -\sin\theta\frac{d}{dz} = -\left(1-z^2\right)^{1/2}\frac{d}{dz}$$

In terms of z, Eq. 184 becomes

$$\frac{d}{dz}\left[\left(1-z^2\right)\frac{d\Theta(z)}{dz}\right]+\left(\lambda-\frac{m^2}{1-z^2}\right)\Theta(z) = 0 \qquad ...(187)$$

which is **associated Legendre equation** (in honour of the French mathematician A.M. Legendre (1752-1833)). Equation (187) has poles at $z = \pm1$. For physically acceptable solution,

$$\lambda = l(l+1), \qquad l = 0, 1, 2, ... \qquad m = 0, \pm1, \pm2, ..., \pm l$$

The solution of Eq. (187) is the **Legendre polynomial** $P_l(z)$ for $m = 0$ and the **associated Legendre polynomials** $P_l^{|m|}(z)$ for $m \neq 0$. The normalized solution is then

$$\Theta(\theta) = N_{lm}P_l^{|m|}(z) \qquad ...(188)$$

where N_{lm} is the normalization constant. The normalization condition is

$$|N_{lm}|^2\int_{-1}^{+1}P_k^{|m|}(z)P_l^{|m|}(z)dz = 1$$

The orthogonality relation for the associated Ligendre polynomials

$$\int_{-1}^{+1}P_k^{|m|}(z)P_l^{|m|}(z)dz = \frac{2}{(2l+1)}\frac{(l+|m|!)}{(l-|m|!)}\delta_{lk} \qquad ...(189)$$

leads to

$$\Theta_l^m(\theta) = \varepsilon\sqrt{\frac{(2l+1)(l-|m|)!}{2(l+|m|)!}}P_l^m(\cos\theta) \quad \text{(see Eq. 171)} \qquad ...(190)$$

where $\varepsilon = (-1)^m$ for $m > 0$ and $\varepsilon = 1$ for $m \leq 0$ as per the established phase convention.

Spherical Harmonics : The solution of the angular part of the equation, called the *spherical harmonics*, is independent of the energy, E, and the potential energy, $V(r)$. Combining the expressions for $\Phi_m(\phi)$ (Eq. 186) and $\Theta_l^m(\theta)$ (Eq. 190), the normalized expression for the spherical harmonics is

$$Y_{l,m}(\theta,\phi) = \varepsilon\sqrt{\frac{(2l+1)(l-|m|)!}{4\pi(l+|m|)!}}P_l^m(\cos\theta)e^{im\phi} \qquad ...(191)$$

where $l = 0, 1, 2, ...$ $m = 0, \pm1, \pm2, ..., \pm l$ ...(192)

The spherical harmonics are mutually orthogonal and the first-few of them are given in Table 2.

Table 2. The First few Spherical Harmonics

Complex form	Real form
$Y_{0,0} = \frac{1}{(4\pi)^{1/2}}$	$Y_{0,0} = \frac{1}{(4\pi)^{1/2}}$
$Y_{1,0} = \left(\frac{3}{4\pi}\right)^{1/2} \cos\theta$	$Y_{1,0} = \left(\frac{3}{4\pi}\right)^{1/2} \cos\theta = \left(\frac{3}{4\pi}\right)^{1/2} \frac{z}{r}$
$Y_{1,1} = \left(\frac{3}{8\pi}\right)^{1/2} (\sin\theta) e^{i\phi}$	$Y_{1,1\cos} = \left(\frac{3}{4\pi}\right)^{1/2} \sin\theta\cos\phi = \left(\frac{3}{4\pi}\right)^{1/2} \frac{x}{r}$
$Y_{1,-1} = \left(\frac{3}{8\pi}\right)^{1/2} (\sin\theta) e^{-i\phi}$	$Y_{1,1\sin} = \left(\frac{3}{4\pi}\right)^{1/2} \sin\theta\cos\phi = \left(\frac{3}{4\pi}\right)^{1/2} \frac{y}{r}$
$Y_{2,0} = \left(\frac{5}{16\pi}\right)^{1/2} (3\cos^2\theta - 1)$	$Y_{2,0} = \left(\frac{5}{16\pi}\right)^{1/2} (3\cos^2\theta - 1) = \left(\frac{5}{16\pi}\right)^{1/2} \left(\frac{3z^2}{r^2} - 1\right)$
$Y_{2,1} = -\left(\frac{15}{8\pi}\right)^{1/2} (\sin\theta\cos\theta) e^{i\phi}$	$Y_{2,1\cos} = \left(\frac{15}{4\pi}\right)^{1/2} \sin\theta\cos\theta\cos\phi = \left(\frac{15}{4\pi}\right)^{1/2} \frac{xz}{r^2}$
$Y_{2,-1} = \left(\frac{15}{8\pi}\right)^{1/2} (\sin\theta\cos\theta) e^{-i\phi}$	$Y_{2,1\sin} = \left(\frac{15}{4\pi}\right)^{1/2} \sin\theta\cos\theta\sin\phi = \left(\frac{15}{4\pi}\right)^{1/2} \frac{yz}{r^2}$
$Y_{2,2} = \left(\frac{15}{32\pi}\right)^{1/2} (\sin^2\theta) e^{2i\phi}$	$Y_{2,2\cos} = \left(\frac{15}{16\pi}\right)^{1/2} \sin^2\theta\cos(2\phi) = \left(\frac{15}{16\pi}\right)^{1/2} \frac{x^2 - y^2}{r^2}$
$Y_{2,-2} = \left(\frac{15}{32\pi}\right)^{1/2} (\sin^2\theta) e^{-2i\phi}$	$Y_{2,2\sin} = \left(\frac{15}{16\pi}\right)^{1/2} \sin^2\theta\sin(2\phi) = \left(\frac{15}{16\pi}\right)^{1/2} \frac{xy}{r^2}$

It may be noted that the presence of the $\exp(im\phi)$ factor makes the spherical harmonics complex, in general. It is, in fact, advantageous to work with the real form. We know that a linear combination of degenerate eigenfunctions of a degenerate energy level is also an eigenfunction with the same eigenvalue. Thus, for example, we can express $Y_{1\,1}$ and $Y_{1,-1}$ in the real form by taking a suitable linear combination of them. Similar linear combinations can also be taken for other spherical harmonics. The real forms of the first few spherical harmonics are listed in Table 2.

The evaluation of the spherical harmonics listed in Table 2 can be carried out as shown below :

The spherical harmonics of a point A (x, y, z) in the Cartesian coordinate system are defined as

$$Y_n^{m_A} = \Theta_{n,m_A} \Phi_{m_A} \qquad ...(193)$$

where

$$\Theta_{n,m_A} = \sqrt{\frac{(2n+1)}{2} \frac{|n-|m_A|}{|n+|m_A|}} P_n^{m_A}(\cos\theta) \qquad ...(194)$$

and

$$\Phi_{m_A} = \frac{1}{\sqrt{2\pi}} e^{im_A\phi} \qquad ...(195)$$

Here, $P_n^{m_A}$ is the associated Legendre polynomial function and both Θ_{n,m_A} and Φ_{m_A} are normalised. The general form of associated Legendre polynomial $P_n^{m_A}(x)$ is

$$P_n^{m_A}(x) = (1-x^2)^{|m_A|/2} \frac{d^{m_a} P_n(x)}{d_x^{m_a}} \qquad ...(196)$$

where $P_n(x)$ is Legendre polynomial which is given by

$$P_n(x) = \frac{1}{2^n n!} \frac{d^n (x^2-1)^n}{d^n} \qquad ...(197)$$

In Eq. 193 for spherical harmonics we do not assign any specific meaning to n and m_A. These are simply numbers. It is evident from Eq. 194 that the maximum value of $|m_A|$ can be n. In other words, $|m_A|$ can have values $= \pm n, \pm (n-1), \pm (n-2)$ .....0 only.

In order to evaluate the spherical harmonics of point A for different sets of n and $|m_A|$, we need the values of $P(x)$, and $P_n^{m_A}(x)$. Eq. 197 for $P(x)$ yields the following results :

$$P_0(x) = 1 \quad \therefore \quad P_0(\cos\theta) = 1$$

$$P_1(x) = x \quad \therefore \quad P_1(\cos\theta) = \cos\theta$$

$$P_2(x) = \tfrac{1}{2}(3x^2 - 1) \quad \therefore \quad P_2(\cos\theta) = \tfrac{1}{2}(3\cos^2\theta - 1)$$

$$P_3(x) = \tfrac{1}{2}(5x^3 - 3x) \quad \therefore \quad P_3(\cos\theta) = \tfrac{1}{2}(5\cos^3\theta - 3\cos\theta)$$

$$P_4(x) = \tfrac{1}{8}(35x^4 - 30x^2 + 3) \quad \therefore \quad P_4(\cos\theta) = \tfrac{1}{8}(35\cos^4\theta - 30\cos^2\theta + 3)$$

Similarly, Eq. 196 for $P_n^{|m_A|}(x)$ yields the following results :

$$P_0^0(x) = 1 \quad \therefore \quad P_0^0(\cos\theta) = 1$$

$$P_1^0(x) = x \quad \therefore \quad P_1^0(\cos\theta) = \cos\theta$$

$$P_1^{|1|}(x), \textit{ i.e., } P_1^{\pm1}(x) = (1-x^2)^{1/2} \quad \therefore \quad P_1^{\pm1}(\cos\theta) = \sin\theta$$

$$P_2^0(x) = \tfrac{1}{2}(3x^2 - 1) \quad \therefore \quad P_2^0(\cos\theta) = \tfrac{1}{2}(3\cos^2\theta - 1)$$

$$P_2^{|1|}(x), \textit{ i.e., } P_2^{\pm1}(x) = 3x(1-x^2)^{1/2} \quad \therefore \quad P_2^{\pm1}(\cos\theta) = 3\cos\theta\sin\theta$$

$$P_2^{|2|}(x), \textit{ i.e., } P_2^{\pm2}(x) = 3(1-x^2) \quad \therefore \quad P_2^{\pm2}(\cos\theta) = 3\sin^2\theta$$

$$P_3^0(x) = \tfrac{1}{2}(5x^2 - 3)x \quad \therefore \quad P_3^0(\cos\theta) = \tfrac{1}{2}\cos\theta(5\cos^2\theta - 3)$$

$$P_3^{|1|}(x), \textit{ i.e., } P_3^{\pm1}(x) = \tfrac{3}{2}(1-x^2)^{1/2}(5x^2 - 1) \quad \therefore \quad P_3^{\pm1}(\cos\theta) = \tfrac{3}{2}\sin\theta(5\cos^2\theta - 1)$$

$$P_3^{|2|}(x), \textit{ i.e., } P_3^{\pm2}(x) = 15x(1-x^2) \quad \therefore \quad P_3^{\pm2}(\cos\theta) = 15\cos\theta\sin^2\theta$$

$$P_3^{|3|}(x), \textit{ i.e., } P_3^{\pm3}(x) = 15x(1-x^2)^{3/2} \quad \therefore \quad P_3^{\pm3}(\cos\theta) = 15\sin^3\theta$$

$$P_4^0(x) = \tfrac{1}{8}(35x^4 - 30x^2 + 3) \quad \therefore \quad P_4^0(\cos\theta) = \tfrac{1}{8}(35\cos^4\theta - 30\cos^2\theta + 3)$$

$P_4^{|1|}(x)$, *i.e.*, $P_4^{\pm1}(x) = (1-x^2)^{1/2}(7x^3-3x)\frac{5}{2} \therefore P_4^{\pm1}(\cos\theta) = \frac{5}{2}\sin\theta\cos\theta(7\cos^2\theta-3)$

$P_4^{|2|}(x)$, *i.e.*, $P_4^{\pm2}(x) = (1-x^2)(7x^2-1)\frac{15}{2} \therefore P_4^{\pm2}(\cos\theta) = \frac{15}{2}\sin^2\theta(7\cos^2\theta-1)$

$P_4^{|3|}(x)$, *i.e.*, $P_4^{\pm3}(x) = 105\,x(1-x^2)^{3/2} \therefore P_4^{\pm3}(\cos\theta) = 105\sin^3\theta\cos\theta$

$P_4^{|4|}(x)$, *i.e.*, $P_4^{\pm4}(x) = (1-x^2)^2 \times 105 \therefore P_4^{\pm4}(\cos\theta) = 105\sin^4\theta$

With the help of the results reported above and making use of Eqs. 193—195, we can easily arrive at the following values for spherical harmonics, $Y_n^{m_A}$:

$\Theta_{0,0} = \frac{1}{\sqrt{2}}$	$Y_0^0 = \frac{1}{2\sqrt{\pi}}$
$\Theta_{1,0} = \sqrt{\frac{3}{2}}\cos\theta$	$Y_1^0 = \sqrt{\frac{3}{2}}\frac{1}{\sqrt{2\pi}}\cos\theta$
$\Theta_{0,\pm1} = \sqrt{\frac{3}{4}}\sin\theta$	$Y_1^{\pm1} = \sqrt{\frac{3}{4}}\sin\theta\frac{1}{\sqrt{2\pi}}e^{\pm i\phi}$
$\Theta_{2,0} = \sqrt{\frac{5}{8}}(3\cos^2\theta-1)$	$Y_2^0 = \sqrt{\frac{5}{8}}(3\cos^2\theta-1)\frac{1}{\sqrt{2\pi}}$
$\Theta_{2,\pm1} = \sqrt{\frac{15}{4}}\sin\theta\cos\theta$	$Y_2^{\pm1} = \sqrt{\frac{15}{4}}\sin\theta\cos\theta\frac{1}{\sqrt{2\pi}}e^{\pm i\phi}$
$\Theta_{2,\pm2} = \sqrt{\frac{15}{16}}\sin^2\theta$	$Y_2^{\pm2} = \sqrt{\frac{15}{16}}\sin^2\theta\frac{1}{\sqrt{2\pi}}e^{\pm i2\phi}$
$\Theta_{3,0} = \sqrt{\frac{7}{8}}\cos\theta(5\cos^2\theta-3)$	$Y_3^0 = \sqrt{\frac{7}{8}}\cos\theta(5\cos^2\theta-3)\frac{1}{\sqrt{2\pi}}$
$\Theta_{3,\pm1} = \sqrt{\frac{21}{32}}\sin\theta(5\cos^2\theta-1)$	$Y_3^{\pm1} = \sqrt{\frac{21}{32}}\sin\theta(5\cos^2\theta-1)\frac{1}{\sqrt{2\pi}}e^{\pm i\phi}$
$\Theta_{3,\pm2} = \sqrt{\frac{105}{16}}\sin^2\theta\cos\theta$	$Y_3^{\pm2} = \sqrt{\frac{105}{16}}\sin^2\theta\cos\theta\frac{1}{\sqrt{2\pi}}e^{\pm i2\phi}$
$\Theta_{3,\pm3} = \sqrt{\frac{35}{32}}\sin^3\theta$	$Y_3^{\pm3} = \sqrt{\frac{35}{32}}\sin^3\theta\frac{1}{\sqrt{2\pi}}e^{\pm i3\phi}$
$\Theta_{4,0} = \sqrt{\frac{9}{128}}(35\cos^4\theta-30\cos^2\theta+3)$	$Y_4^0 = \sqrt{\frac{9}{128}}(35\cos^4\theta-30\cos^2\theta+3)\frac{1}{\sqrt{2\pi}}$
$\Theta_{4,\pm1} = \sqrt{\frac{45}{32}}\sin\theta\cos\theta(7\cos^2\theta-3)$	$Y_4^{\pm1} = \sqrt{\frac{45}{32}}\sin\theta\cos\theta(7\cos^2\theta-3)\frac{1}{\sqrt{2\pi}}e^{\pm i\phi}$
$\Theta_{4,\pm2} = \sqrt{\frac{45}{64}}\sin^2\theta(7\cos^2\theta-1)$	$Y_4^{\pm2} = \sqrt{\frac{45}{64}}\sin^2\theta(7\cos^2\theta-1)\frac{1}{\sqrt{2\pi}}e^{\pm i2\phi}$
$\Theta_{4,\pm3} = \sqrt{\frac{315}{32}}\sin^3\theta\cos\theta$	$Y_4^{\pm3} = \sqrt{\frac{315}{32}}\sin^3\theta\cos\theta\frac{1}{\sqrt{2\pi}}e^{\pm i3\phi}$
$\Theta_{4,\pm4} = \sqrt{\frac{315}{256}}\sin^4\theta$	$Y_4^{\pm4} = \sqrt{\frac{315}{256}}\sin^4\theta\frac{1}{\sqrt{2\pi}}e^{\pm i4\phi}$

While expressing angular wave functions of hydrogen-like systems in terms of spherical harmonics, we use symbols l and m in place of n and m_A, respectively, in Eqs. 193—195. Accordingly, we write :

$$Y_l^m = \Theta_{l,m}\Phi_m \quad ...(198)$$

$$\Theta_{l,m} = \sqrt{\frac{(2l+1)}{2}\frac{|l-|m|}{|l+|m|}}P_l^m\cos\theta \quad ...(199)$$

$$\Phi_m = \frac{1}{\sqrt{2\pi}}e^{im\phi} \quad ...(200)$$

The symbols l and m used for hydrogen-like systems are referred to as orbital angular momentum quantum number and magnetic quantum number, respectively. As already mentioned, while the radial wavefunction gives the size of the orbitals, the spherical harmonics give both the size and the shape of the orbitals. We must emphasize that the spherical harmonics are wavefunctions for specific states of orbital angular momentum. More specifically, they are orthogonal functions of the angular coordinates θ and ϕ. These functions are polynomials in sin θ and cos θ. The spherical harmonics are the angular factors in centrosymmetric atomic orbitals ; they are angular momentum eigenfunctions; they are also the eigenfunctions of the rigid diatomic rotor.

Complete Wavefunctions and Shapes of Orbitals. Let us write complete wavefunctions for some of the orbitals and deduce their shapes.

Complete wavefunctions for *s* orbitals and their shapes. For an *s* orbital, $l = 0$, therefore, $m = 0$. The complete wave function is, therefore, written as

$$R_{n,0}(r)Y_0^0 = R_{n,0}(r)\frac{1}{\sqrt{2}}\times\frac{1}{\sqrt{2\pi}} = R_{n,0}(r)\frac{1}{2\sqrt{\pi}} \quad ...(201)$$

Since the complete wavefunction in this case is independent of the angles θ and ϕ, therefore, the orbital is *symmetrical* along all directions for a particular r, *i.e.*, it has a **spherical shape**. The 1*s* orbital has no radial node whereas 2*s* and 3*s* orbitals have one and two radial nodes, respectively, as shown in Fig. 16.

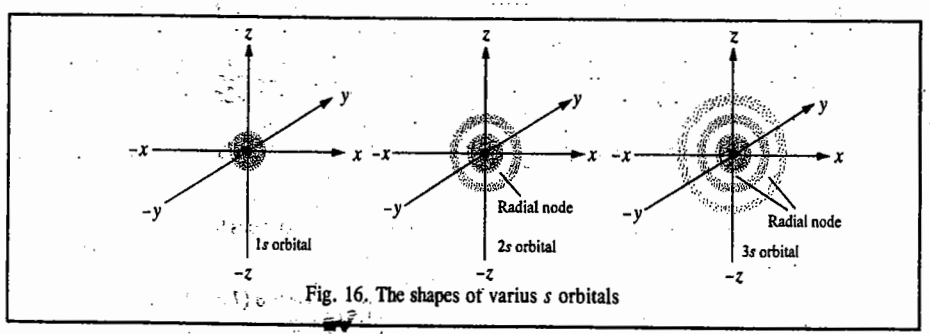

Fig. 16. The shapes of varius *s* orbitals

Complete wavefunctions for *p* orbitals and their shapes. For *p* orbitals, $l=1$. Therefore, $m = 0, +1, -1$. The corresponding complete wave functions are written as (0), (+1) and (-1), respectively. The sets of single electronic wave functions having the same l and the same m but different m_s are written as (m_1), (m_2), etc. Thus,

$$(0) = R_{n,1}(r)\,Y_1^0 = R_{n,1}(r)\sqrt{3/2}\cos\theta\times1/\sqrt{2\pi} = R_{n,1}(r)\sqrt{3/4\pi}\cos\theta \quad ...(202)$$

$$(+1) = R_{n,1}(r)\, Y_1^{+1} = R_{n,1}(r)\sqrt{3/4}\sin\theta \times 1/\sqrt{2\pi}\, e^{+i\phi} \quad ...(203)$$

$$(-1) = R_{n,1}(r)\, Y_1^{-1} = R_{n,1}(r)\sqrt{3/4}\sin\theta \times 1/\sqrt{2\theta}\, e^{-i\phi} \quad ...(204)$$

While the wavefunction represented by Eq. 202 is real, the wavefunctions represented by Eqs. 203 and 204 are not real as they contain the imaginary quantity i and as such cannot be visualised. An acceptable solution of wave equation is that which yields a real wavefunction. In order to obtain real wavefunctions for p orbitals, two linear combinations of angular wavefunctions represented by Eqs. 203 and 204 are taken into consideration. The two normalised linear combinations thus obtained are :

$1/\sqrt{2}\,[(+1) + (-1)]$, *i.e.*, $1/\sqrt{2}\, R_{n,1}(r)(\Theta_{1,+1}\Phi_{+1} + \Theta_{1,-1}\Phi_{-1})$ and

$1/\sqrt{2}\,[(+1) - (-1)]$, *i.e.*, $1/\sqrt{2}R_{n,1}(r)\,(\Theta_{1,+1}\Phi_{+1} - \Theta_{1,-1}\Phi_{-1})$.

These wavefunctions yield the following results :

Combination $1/\sqrt{2}\,[(+1) + (-1)]$ for real p wavefunction $= R_{n,1}(r)\sqrt{3/4\pi}\sin\theta\cos\phi$ ...(205)

Combination $1/\sqrt{2}\,[(+1) - (-1)]$ for real p wavefunction $= R_{n,1}(r)\sqrt{3/4\pi}\sin\theta\sin\phi$ ...(206)

Thus, Eqs. 202, 205 and 206 now represent a set of *real* wave functions for p orbitals.

Let us now investigate the **shapes of the 2p orbitals** represented by the real wavefunctions as given by Eqs. 202, 205 and 206. Expressing these functions in terms of the Cartesian coordinates, the real p wave function, as given by Eq. 202, is

$$(0) = R_{2,1}(r)\sqrt{3/4\pi}\cos\theta \quad ...(207)$$

$$= R_{2,1}(r)\sqrt{3/4\pi}\times z/r \;[\because z = r\cos\theta \text{ (Fig. 15)}] \quad ...(208)$$

This is, evidently, a function of z and is, therefore, known as p_z wavefunction. The wavefunction p_z when plotted in three-dimensional space yields a dumb-bell shaped curve along the z-axis, as shown in Fig. 17.

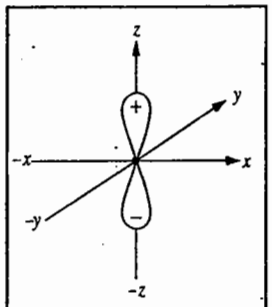

Fig. 17. The shape of p_z orbital

It can be seen from Eq. 208 that the function p_z will be positive when z is positive and negative when z is negative. It may be noted that + and – signs are geometric signs of the plotted wavefunctions only and should not be confused with positive or negative charges.

Let us now consider the real wavefunction given by Eq. 205. Expressing it in terms of Cartesian coordinates, we get

$$1/\sqrt{2}\,[(+1) + (-1)] = R_{2,1}(r)\sqrt{3/4\pi}\,\sin\theta\cos\phi$$

$$= R_{2,1}(r)\,\sqrt{3/4\pi}\times x/r \;[\because \sin\theta\cos\phi = x/r \text{ (Fig. 17)}] \quad ...(209)$$

Evidently, the p wavefunction given by Eq. 209 varies with x only. It is, therefore, referred to as p_x wave function. A plot of p_x wave function in three-dimensional space gives a dumb-bell shaped curve along the x-axis, as shown in Fig. 18.

It can be easily seen from Eq. 209 that the function p_x would be positive when x is positive and negative when x is negative.

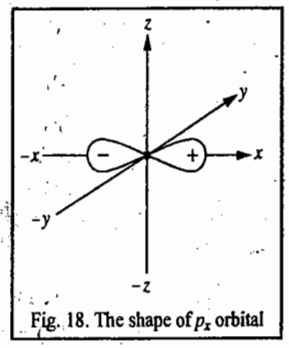

Fig. 18. The shape of p_x orbital

Similarly, the real wave function as given by Eq. 206, when expressed in terms of Cartesian coordinates, yields Eq. 211. Thus,

$$1/\sqrt{2}\,[(+1) - (-1)] = R_{2,1}(r)\sqrt{3/4\pi}\,\sin\theta\sin\phi \quad ...(210)$$

$$= R_{2,1}(r)\sqrt{3/4\pi}\times y/r \;[\because \sin\theta\sin\phi = y/r \text{ (Fig. 15)}] \quad ...(211)$$

Thus, the p wavefunction in this case varies with y only. It is, therefore, called p_y wavefunction.

A plot of p_y wavefunction in three-dimensional space gives a dumb-bell shaped curve along the y-axis, as shown in Fig. 19.

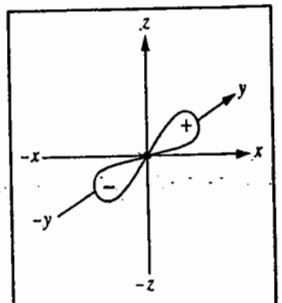

Fig. 19. The shape of p_y orbital

The complete wavefunctions of $2p$, $3p$, $4p$ orbitals would give rise to dumb-bell shaped curves except for the fact that the $4p$ orbital would occupy more space than $3p$ orbital and $3p$ orbital would occupy more space than $2p$ orbital (Fig. 18).

Also, the $4p$ orbital would have *two radial nodes*, the $3p$ orbital would have *one radial node* and $2p$ orbital would have *no radial node* (the number of radial nodes is given by $n - l - 1$).

The shapes of $2p_x$, $3p_x$ and $4p_x$ orbitals with radial nodes are shown in Fig. 20.

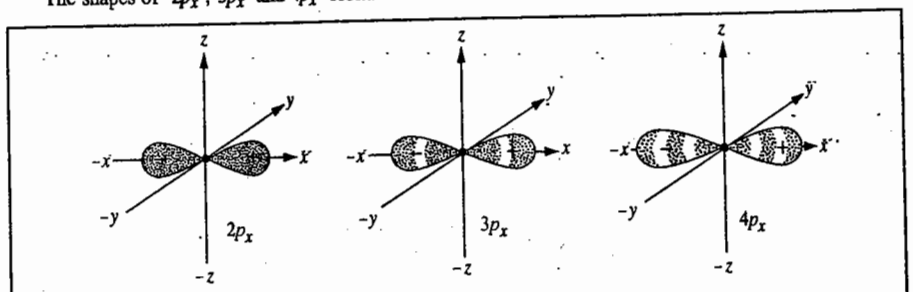

Fig. 20. The shapes of $2p_x$, $3p_x$ and $4p_x$ orbitals.

Complete wave functions for d orbitals and their shapes. For d orbitals, $l = 2$ so that $m = 0, +1, +2, -1, -2$. The complete wave functions for the d orbitals may be written as follows :

$$(0) = R_{n,2}(r)\, Y_2^0 = R_{n,2}(r)\sqrt{5/16\pi}\,(3\cos^2\pi - 1) \quad ...(212)$$

$$(+1) = R_{n,2}(r)\, Y_2^{+1} = R_{n,2}(r)\sqrt{15/8\pi}\,(\sin\theta\cos\theta)e^{i\phi} \quad ...(213)$$

$$(+2) = R_{n,2}(r)\, Y_2^{2+} = R_{n,2}(r)\sqrt{15/32\pi}\,(\sin^2\theta)\,e^{i2\phi} \quad ...(214)$$

$$(-1) = R_{n,2}(r)\, Y_2^{-1} = R_{n,2}(r)\sqrt{15/8\pi}\,(\sin\theta\cos\theta)e^{-i\phi} \quad ...(215)$$

$$(-2) = R_{n,2}(r)\, Y_2^{-2} = R_{n,2}(r)\sqrt{15/32\pi}\,(\sin^2\pi)\,e^{-i2\phi} \quad ...(216)$$

Of the above five wave functions, only one wave function given by Eq. 212 is real. All other wave functions contain the imaginary quantity i for d orbitals. We obtain real d orbital wave functions by the procedure similar to the one we adopted for obtaining p orbital wave functions. The real d orbital wave functions obtained from linear combination of Eqs. 213 and 215 are : (*i*) $1/\sqrt{2}\,[(+1) + (-1)]$, *i.e.*, $1/\sqrt{2}\,R_{n,2}(r)\,(\Theta_{2,1}\Phi_1 + \Theta_{2,-1}\Phi_{-1})$ and (*ii*) $1/\sqrt{2}\,[(+1) - (-1)]$, *i.e.*, $1/\sqrt{2}R_{n,2}(r)(\Theta_{2,1}\Phi_1 - \Theta_{2,-1}\Phi_{-1})$ and the d orbital wave functions obtained from linear combination of Eqs. 214 and 216 are :

(*i*) $1/\sqrt{2}\,[(+2) + (-2)]$, *i.e.*, $1/\sqrt{2}R_{n,2}(r)(\Theta_{2,2}\Phi_2 - \Theta_{2,-2}\Phi_{-2})$ and (*ii*) $1/\sqrt{2}\,[(+2) - (-2)]$, *i.e.*, $1/\sqrt{2}\,R_{n,2}(r)\,(\Theta_{2,2}\,\Phi_2 - \Theta_{2,-2}\Phi_{-2})$.

From these wavefunctions, the five real d orbital wavefunctions obtained are as follows :

$$\text{Real } d \text{ wavefunction (0)} = R_{n,2}(r)\ \sqrt{5/16\pi}\ (3\cos^2\theta - 1) \quad ...(217)$$

$$\text{Real } d \text{ wavefunction } 1/\sqrt{2}\ [(+1) + (-1)] = R_{n,2}(r)\ \sqrt{15/4\pi}\ \sin\theta\cos\theta\cos\phi \quad ...(218)$$

$$\text{Real } d \text{ wavefunction } 1/\sqrt{2}\ [(+1) - (-1)] = R_{n,2}(r)\ \sqrt{15/4\pi}\ \sin\theta\cos\theta\sin\phi \quad ...(219)$$

$$\text{Real } d \text{ wavefunction } 1/\sqrt{2}\ [(+2) + (-2)] = R_{n,2}(r)\ \sqrt{15/16\pi}\ \sin^2\theta\cos 2\phi \quad ...(220)$$

$$\text{Real } d \text{ wavefunction } 1/\sqrt{2}\ [(+2) - (-2)] = R_{n,2}(r)\sqrt{15/16\,\pi}\ \sin^2\theta\sin 2\phi \quad ...(221)$$

Expressing the above wavefunctions in terms of Cartesian co-ordinates, we get

(*i*)
$$(0) = R_{n,2}(r)\sqrt{15/16\,\pi}\ (3\cos^2\theta - 1)$$

$$= R_{n,2}(r)\sqrt{15/16\,\pi}\ (3z^2 - r^2)\times 1/r^2 \quad ....(222)$$

As can be seen, the above d wavefunction *varies as* z^2. Hence, it is called d_z^2 wavefunction.

(*ii*)
$$1/\sqrt{2}\ [(+1) + (-1)] = R_{n,2}(r)\sqrt{15/4\pi}\ \sin\theta\cos\theta\cos\phi$$

$$= R_{n,2}(r)\sqrt{15/4\pi}\times xz/r^2 \quad ...(223)$$

Since the d wavefunction *varies as* xz, it is called d_{xz} wavefunction.

(*iii*)
$$1/\sqrt{2}\ [(+1) - (-1)] = R_{n,2}(r)\sqrt{15/4\,\pi}\ \sin\theta\cos\theta\sin\phi$$

$$= R_{n,2}(r)\sqrt{15/4\,\pi}\times yz/r^2 \quad ...(224)$$

Since the d wavefunction *varies as* yz, it is called d_{yz} wavefunction.

(*iv*)
$$1/\sqrt{2}\ [(+2) + (-2)] = R_{n,2}(r)\sqrt{15/16\pi}\ \sin^2\theta\cos 2\phi$$

$$= R_{n,2}(r)\sqrt{15/16\pi}\sin^2\theta(\cos^2\phi - \sin^2\phi)$$

$$= R_{n,2}(r)\sqrt{15/16\pi}\,(\sin^2\theta\cos^2\phi - \sin^2\theta\sin^2\phi)$$

$$= R_{n,2}(r)\sqrt{15/16\pi}\,(x^2 - y^2)/r^2 \quad ...(225)$$

Since the d wavefunction *varies as* $x^2 - y^2$, it is called $d_{x^2-y^2}$ wavefunction.

(*v*)
$$1/\sqrt{2}\ [(+2) - (-2)] = R_{n,2}(r)\sqrt{15/16\pi}\ \sin^2\theta\sin 2\phi$$

$$= R_{n,2}(r)\sqrt{15/16\,\pi}\sin^2\theta\,2\sin\phi\cos\phi$$

$$= R_{n,2}(r)\sqrt{15/4\pi}\ \sin\theta\sin\phi\sin\theta\cos\phi$$

$$= R_{n,2}(r)\sqrt{15/4\pi}\ xy/r^2 \quad ...(226)$$

Since the d wavefunction *varies as* xy, it is called d_{xy} wavefunction.

Thus, the five real wavefunctions of d orbitals are d_{z^2}, d_{xz}, d_{yz}, $d_{x^2-y^2}$ and d_{xy}. These wavefunctions when plotted in three-dimensional space yield curves as shown in Fig. 21. It may be remembered that all these are solid curves, *i.e., these are three-dimensional* because of their dependence on $r\,(=\sqrt{x^2+y^2+z^2})$.

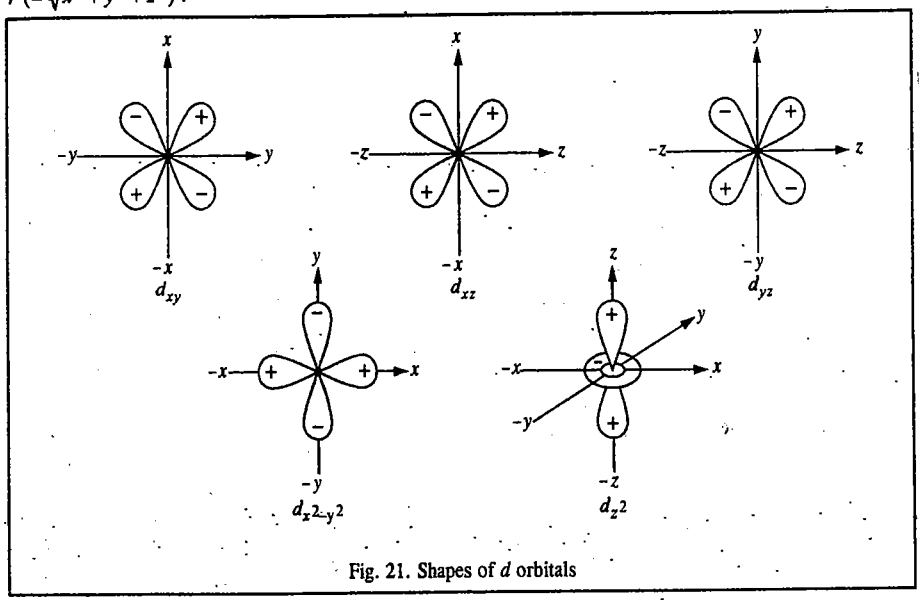

Fig. 21. Shapes of d orbitals

The orbital d_{z^2} has a dumb-bell shaped curve symmetric about the z-axis, having a ring-like collar in xy plane. The dumb-bell shaped part of the curve has a *positive geometric sign* (because whatever be the sign of z, positive or negative, its square is always positive) whereas the collar in the xy plane has a *negative geometric sign.*

The orbital d_{xy} has a double dumb-bell shape. The quantity xy will be positive when both x and y are positive or when both are negative. However, xy will be negative when either of x or y is negative. Thus, the sign of the curve is positive in first and third quadrants while it is negative in second and fourth quadrants. The shapes of d_{xz}, d_{yz} orbitals can be explained in a similar manner.

The orbital $d_{x^2-y^2}$ is also double dumb-bell shaped but its lobes lie on x and y axes. The signs of the lobes on x axis will always be positive (because whatever be the sign of x, x^2 will always be positive) whereas the signs of the lobes on y axis will always be negative (because whatever be the sign of y, $-y^2$ will always be negative). The *exact shapes* of d orbitals are obtained by taking into consideration the total wave function. Accordingly, $3d_{x^2-y^2}$ orbital would be similar in shape to $4d_{x^2-y^2}$ orbital or $5d_{x^2-y^2}$ orbital except for the fact that

1. A $5d$ orbital would have *two*, a $4d$ orbital would have *one* and a $3d$ orbital would have *no* radial node.

2. A $5d$ orbital would occupy more space than a $4d$ orbital and a $4d$ orbital would occupy more space than a $3d$ orbital, as shown in Fig. 22.

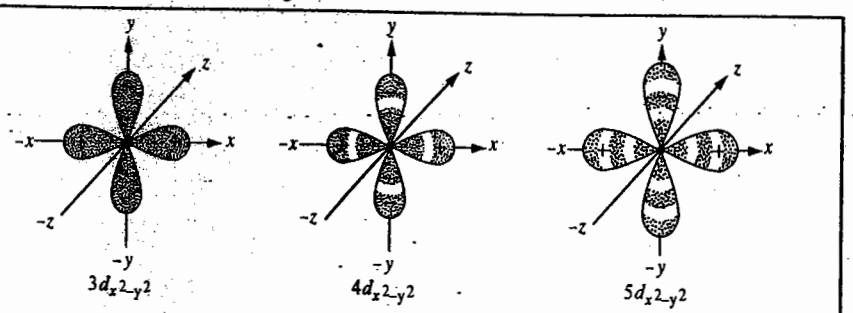

Fig. 22. Curves for $3d_{x^2-y^2}$, $4d_{x^2-y^2}$ and $5d_{x^2-y^2}$ orbitals in three-dimensional space. The curves for the other $3d$, $4d$, $5d$ orbitals can be drawn on similar lines.

In a similar manner, we can determine the shapes of f orbitals

The set of complete wave functions for f orbitals is given below :

$$(0) = R_{n,3}(r)\,Y_3^0$$

$$(\pm 1) = R_{n,3}(r)\,Y_3^{\pm 1}$$

$$(\pm 2) = R_{n,3}(r)\,Y_3^{\pm 2}$$

$$(\pm 3) = R_{n,3}(r)\,Y_3^{\pm 3}$$

The spherical harmonics for the f orbital wave functions have been given earlier. In the set given above, only (0) is real. The rest of the six f orbital wave functions are imaginary. We can derive the real set of f orbital wave functions by following the same procedure as was adopted by obtaining sets of real p and d orbital wave functions. The real f orbital wave functions thus obtained would be desinated as follows :

$f_{z(x^2-y^2)}$, $f_{y(z^2-x^2)}$, $f_{x(y^2-z^2)}$, $f_{z(5z^2-3r^2)}$, $f_{x(5x^2-3r^2)}$, $f_{y(5y^2-3r^2)}$ and $f_{(x,y,z)}$

Solution of the Radial Equation (the R-equation). To solve Eq. 185 we need the explicit form of the potential energy $V(r)$. However, before we attempt the solution, we shall show how the concept of orbital angular momentum arises from this equation. Eq. 185 can be expressed in the form of a one-dimensional equation by writing

$$R(r) = \frac{\chi(r)}{r} \qquad ...(227)$$

The radial equation now reduces to

$$\frac{d^2\chi}{dr^2} + \frac{2\mu}{\hbar^2}\left(E - V(r) - \frac{l(l+1)\hbar^2}{2\mu r^2}\right)\chi = 0 \qquad ...(228)$$

This has the form of a one-dimensional Schrödinger equation of a particle of mass μ moving in the direction of r in a field of effective potential

$$V_{\text{eff}} = V(r) + \frac{l(l+1)\hbar^2}{2\mu r^2} \qquad ...(229)$$

The additional potential energy term $\frac{l(l+1)\hbar^2}{2\mu r^2}$ is a rapulsive one and corresponds to a force $\frac{l(l+1)\hbar^2}{\mu r^3}$. The *centrifugal force* $\mu r\omega^2$ can be written in terms of the orbital angular momentum L as

$$\mu r\omega^2 = \frac{\left(\mu r^2\omega\right)^2}{\mu r^3} = \frac{L^2}{\mu r^3} \qquad ...(230)$$

This form of the centrifugal force and the force corresponding to the additional potential suggests that the square of the orbital angualr momentum, L^2, can be taken as

$$L^2 = l(l+1)\hbar^2 \qquad ...(231)$$

where l is called the orbital angular momentum quantum number. Though orbital angular momentum is equal to $l\hbar$, its exact value is $\left[l(l+1)\right]^{1/2}\hbar$. If $V(r)$, the central field potential, is Coulombic $(-Ze^2/r)$, the additional potential is negligible at large distances. However, this becomes the dominant term at small distances. Fig. 23 shows a plot of the *effective potential*, V_{eff} as a function of r for a Coulombic potential.

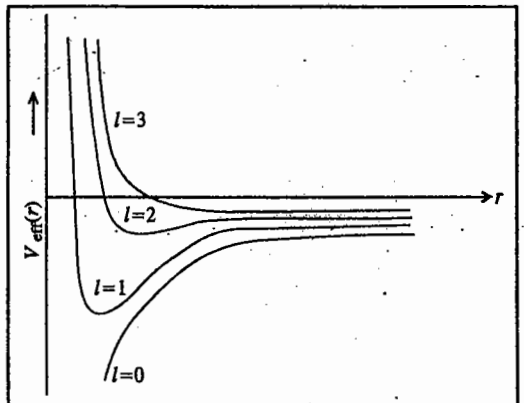

Fig. 23. The effective potential V_{eff} verses r for a Coulomb potential.

We now return to the solution of the radial equation (Eq. 185), which we rewrite as

$$\frac{1}{r^2}\frac{d}{dr}\left(r^2\frac{dR}{dr}\right) + \frac{2\mu}{\hbar^2}\left[E - \frac{l(l+1)\hbar^2}{2\mu r^2} + \frac{Ze^2}{r}\right]R = 0 \qquad ...(232)$$

To solve Eq. (232), let us introduce a variable ρ and a constant λ defined by

$$\rho = \sqrt{\frac{-8\mu E}{\hbar^2}}\,r, \qquad \lambda = \frac{Ze^2}{\hbar}\sqrt{\frac{\mu}{-2E}} \qquad ...(233)$$

As E is negative for bound states, ρ and λ are real quantities. In terms of the new variable, Eq. (232) becomes

$$\frac{d^2R}{d\rho^2} + \frac{2}{\rho}\frac{dR}{d\rho} + \left[-\frac{1}{4} - \frac{l(l+1)}{\rho^2} + \frac{\lambda}{\rho}\right]R = 0 \qquad ...(234)$$

Let us first investigate its asymptotic solution. When $\rho \to \infty$, Eq. 234 reduces to

$$\frac{d^2R}{d\rho^2} - \frac{1}{4}R = 0 \qquad ...(235)$$

Its solutions are $R = \exp(-\rho/2)$ and $\exp(\rho/2)$. out of these only $\exp(-\rho/2)$ is acceptable since $\exp(\rho/2) \to \infty$ as $\rho \to \infty$. The exact solution of Eq. 234 is

$$R(\rho) = e^{-\rho/2}F(\rho) \qquad ...(236)$$

Substitution of Eq. (236) in Eq. (235) gives the differential equation satisfied by $F(\rho)$ as

$$\rho^2\frac{d^2F}{d\rho^2}+\rho(2-\rho)\frac{dF}{d\rho}+\left[\rho\lambda-l(l+1)-\rho\right]F(\rho)=0 \qquad ...(237)$$

When $\rho = 0$, we get

$$l(l+1)\,F(0)=0 \quad \text{or} \quad F(0)=0,\ l\neq 0 \qquad ...(238)$$

Therefore if we try a power series solution for $F(\rho)$ it must not contain a constant term. Hence,

$$F(\rho)=\sum_{k=0}^{\infty}a_k\rho^{c+k} \qquad ...(239)$$

With this value of $F(\rho)$, Eq. (237) reduces to

$$\sum_k a_k(\lambda-1-c-k)\rho^{c+k+1}+\sum_k a_k(c^2+2ck+k^2+c+k-l^2-l)\rho^{c+k}=0 \qquad ...(240)$$

Eq. 240 is valid for all values of ρ only if the coefficient of each power of ρ vanishes separately. Equating the coefficient of ρ^c to zero, we have

$$a_0\left(c^2+c-l^2-l\right)=0$$

or
$$c^2+c-l^2-l=0 \qquad (\text{since } a_0\neq 0)$$

or
$$(c-l)(c+l+1)=0$$

Hence,
$$c=l \quad \text{or} \quad c=-(l+1) \qquad ...(241)$$

If $c = -(l + 1)$, the first term in $F(\rho)$ would be a_0/ρ^{l+1} which tends to infinity as $\rho \to 0$. Hence, $c = l$ is the only acceptable value. Setting the coefficient of ρ^{l+k+1} in Eq. 240 to zero, we obtain

$$a_{k+1}=\frac{l+k+1-\lambda}{(k+1)(k+2l+2)}a_k \qquad ...(242)$$

This recursion relation allows us to determine the coefficients $a_1, a_2, a_3, \ldots$ in terms of a_0 which is quite arbitrary. For large values of k, we get from Eq. (242)

$$\frac{a_{k+1}}{a_k}=\frac{1}{k}$$

In the expansion

$$e^{\rho}=\sum_{k=0}^{\infty}\frac{1}{k!}\rho^k=\sum_{k=0}^{\infty}A_k\rho^k$$

$$\frac{A_{k+1}}{A_k}=\frac{k!}{(k+1)!}=\frac{1}{k+1}\xrightarrow[k\to\infty]{}\frac{1}{k}$$

Hence as $k \to \infty$, the series for $F(\rho)$ behaves like $\rho^l e^{\rho}$ and

$$R(\rho)=e^{-\rho/2}\rho^l e^{\rho}=\rho^l e^{\rho/2}$$

This value of $R(\rho)$ is not acceptable and therefore the series must break off after a certain value of k, say n'. For this to happen $a_{n'+1}$ must be zero. Then, from Eq. 242,

$$l+n'+1-\lambda=0, \qquad n'=0,1,2,\ldots \qquad ...(243)$$

Energy eigenvalues : Defining a new quantum number n by

$$n=l+n'+1=\lambda=\frac{Ze^2}{\hbar}\left(\frac{\mu}{-2E}\right)^{1/2}$$

we have
$$E_n=-\frac{\mu Z^2e^4}{2\hbar^2n^2}, \qquad n=1,2,3,\ldots \qquad ...(244)$$

Since n' and l are integers including zero,

$$n=1,2,3,\ldots \qquad ...(245)$$

As $n \geq l + 1$, the highest possible value of l is $(n - 1)$. Thus,

$$l=0,1,2,\ldots,(n-1) \qquad ...(246)$$

The new quantum number n is called the **principal quantum number** which determines the energy. For hydrogen the atomic number $Z = 1$ and the reduced mass $\mu \approx m$, the mass of the electron.

The energy expression (244) can be written as

$$E_n=-\frac{R_HZ^2}{n^2} \qquad ...(247)$$

where $R_H\left(=\mu e^4/2\hbar^2\right)$ is the Rydberg constant of the hydrogen atom. In atomic units (a.u.) often employed in quantum mechanics, we arbitrarily set $e = \mu = \hbar = a_0 = 1$, so that for the ground state $(n = 1)$, $E_1 = -\frac{1}{2}$(a.u.); the negative sign implies that the electron is attracted to the nucleus.

We note that the energy expression for E_n is the same as the one obtained in the Bohr theory of hydrogen atom, (Eq. 22), the major difference being the occurrence of the concept of **stationary states** and quantization of energy as a consequence of the solution of the Schrödinger wave equation.

Radial wavefunctions : The quantization restriction on energy converts the series for $F(\rho)$ into a polynomial. Writing

$$F(\rho)=\rho^l L(\rho) \qquad ...(248)$$

Eq. 237 reduces to

$$\rho\frac{d^2L(\rho)}{d\rho^2}+(2l+2-\rho)\frac{dL(\rho)}{d\rho}+(n-l-1)L(\rho)=0 \qquad ...(249)$$

The **associated Laguerre polynomial** of order p and degree $(q-p)$, denoted as $L_q^p(\rho)$, satisfies the equation

$$\rho\frac{d^2L_q^p}{d\rho^2}+(p+1-\rho)\frac{dL_q^p}{d\rho}+(q-p)L_q^p(\rho)=0 \qquad ...(250)$$

(The Laguerre polynomials are named after the French mathematician Edmond Laguerre (1834-1886)).

Eqs. (249) and (250) are identical if $L(\rho)$ is taken as $L_{n+l}^{2l+1}(\rho)$. Hence,

$$R_{nl}(r)=Ne^{-\rho/2}\rho^l L_{n+l}^{2l+1}(\rho) \qquad ...(251)$$

The normalization integral

$$\int_0^\infty R_{nl}^2(r)r^2dr=1$$

allows the determination of the normalization constant N. Hence,

$$\frac{n^3\hbar^6}{8\mu^3Z^3e^6}|N|^2\int_0^\infty e^{-\rho}\rho^{2l}\left(L_{n+l}^{2l+1}\right)^2\rho^2d\rho=1$$

Using the orthogonal properties of associated Laguerre polynomials,

$$\frac{n^3\hbar^6}{8\mu^3Z^3e^6}|N|^2\frac{2n[(n+l)!]^3}{(n-l-1)!}=1$$

or

$$|N|=\pm\left\{\left(\frac{2Z\mu e^2}{n\hbar^2}\right)\frac{(n-l-1)!}{2n[(n+l)!]^3}\right\}^{1/2} \qquad ...(252)$$

Thus, the normalized radial wavefunctions are

$$R_{nl}(r)=-\left\{\left(\frac{2Z}{na_H}\right)^3\frac{(n-l-1)!}{2n[(n+l)!]^3}\right\}^{1/2}e^{-\rho/2}\rho^l L_{n+l}^{2l+1}(\rho) \qquad ...(253)$$

where

$$a_H=\frac{\hbar^2}{\mu e^2} \qquad ...(254)$$

The negative sign is selected to make R_{10} positive. As μ is approximately equal to the electron mass, $a_H \approx a_0$, the Bohr radius. Some of the radial wavefunctions are given in Table 3. It may be noted that at the origin the wavefunctions R_{10}, R_{20}, R_{30} are finite whereas R_{21}, R_{31}, R_{32} are zero.

Table 3. The First six Radial Wavefunctions of a Hydrogenic Atom

n	l	$R_{nl}(r)$
1	0	$2\left(\frac{Z}{a_0}\right)^{3/2}e^{-Zr/(a_0)}$
2	0	$\left(\frac{Z}{2a_0}\right)^{3/2}\left(2-\frac{Zr}{a_0}\right)e^{-Zr/(2a_0)}$
	1	$\frac{1}{\sqrt{3}}\left(\frac{Z}{2a_0}\right)^{3/2}\frac{Zr}{a_0}e^{-Zr/(2a_0)}$
3	0	$\frac{2}{27}\left(\frac{Z}{3a_0}\right)^{3/2}\left(27-18\frac{Zr}{a_0}+\frac{2Z^2r^2}{a_0^2}\right)e^{-Zr/(3a_0)}$
	1	$\frac{4\sqrt{2}}{54}\left(\frac{Z}{3a_0}\right)^{3/2}\frac{Zr}{a_0}\left(6-\frac{Zr}{a_0}\right)e^{-Zr/(3a_0)}$
	2	$\frac{4}{27\sqrt{10}}\left(\frac{Z}{3a_0}\right)^{3/2}\left(\frac{Zr}{a_0}\right)^2e^{-Zr/(3a_0)}$

All the radial wavefunctions represent an exponential "decay", and for $n = 2$ the decay is slower than for $n = 1$. We see that radial functions decay as $\exp(-Zr/na_0)$.

Wavefunctions of the hydrogenic atom

The complete wavefunctions for a hydrogen-like atom are given by

$$\psi_{nlm}(r,\theta,\phi)=R_{nl}(r)Y_{lm}(\theta,\phi) \qquad ...(255)$$

where $n = 1, 2, 3, \ldots$, $l = 0, 1, 2, 3, \ldots, (n-1)$, $m = 0, \pm1, \pm2, \ldots, \pm l$

The explicit forms of the wavefunctions for a few states are

$$\psi_{100}=\frac{1}{\pi^{1/2}}\left(\frac{Z}{a_0}\right)^{3/2}e^{-Zr/a_0} \qquad ...(256a)$$

$$\psi_{200}=\frac{1}{\pi^{1/2}}\left(\frac{Z}{2a_0}\right)^{3/2}\left(1-\frac{Zr}{2a_0}\right)e^{-Zr/(2a_0)} \qquad ...(256b)$$

$$\psi_{210}=\frac{1}{\pi^{1/2}}\left(\frac{Z}{2a_0}\right)^{5/2}re^{-Zr/(2a_0)}\cos\theta \qquad ...(256c)$$

$$\psi_{21,\pm1}=\frac{1}{8\pi^{1/2}}\left(\frac{Z}{a_0}\right)^{5/2}re^{-Zr/(2a_0)}(\sin\theta)e^{\pm i\theta} \qquad ...(256d)$$

It may be noted that the expressions for the $l = 1$ state contain the factor r^1. The $l=2$ states will have the factor r^2, and so on. The presence of the factor r^l makes the wavefunction zero at $r = 0$ except for the s-states.

Radial probability density : For the state specified by the wavefunction $\psi_{nlm} \equiv |nlm\rangle$, the probability of finding the electron in a volume element $d\tau$ is

$$|\psi_{nlm}|^2 d\tau = |R_{nl}|^2 |Y_{lm}|^2 r^2 \sin\theta\, dr\, d\theta d\phi$$

The probability of finding the electron in a thin spherical shell bounded by radii r and $(r + dr)$ is then

$$P(r)\, dr = |R_{nl}|^2 r^2 dr \int_0^{\pi} \int_0^{2\pi} |Y_{lm}|^2 \sin\theta\, d\theta d\phi$$

Since the spherical harmonics are normalized to unity

$$P_{nl}(r)\, dr = |R_{nl}|^2 r^2 dr \qquad ...(257)$$

The *radial probability density* $P_{nl}(r)$ is defined as the probability of finding the electron of the hydrogen atom at a distance r from the nucleus. Then

$$P_{nl}(r) = r^2 |R_{nl}|^2 \qquad ...(258)$$

Plots of radial probability density for some of the states are illustrated in Fig. 24.

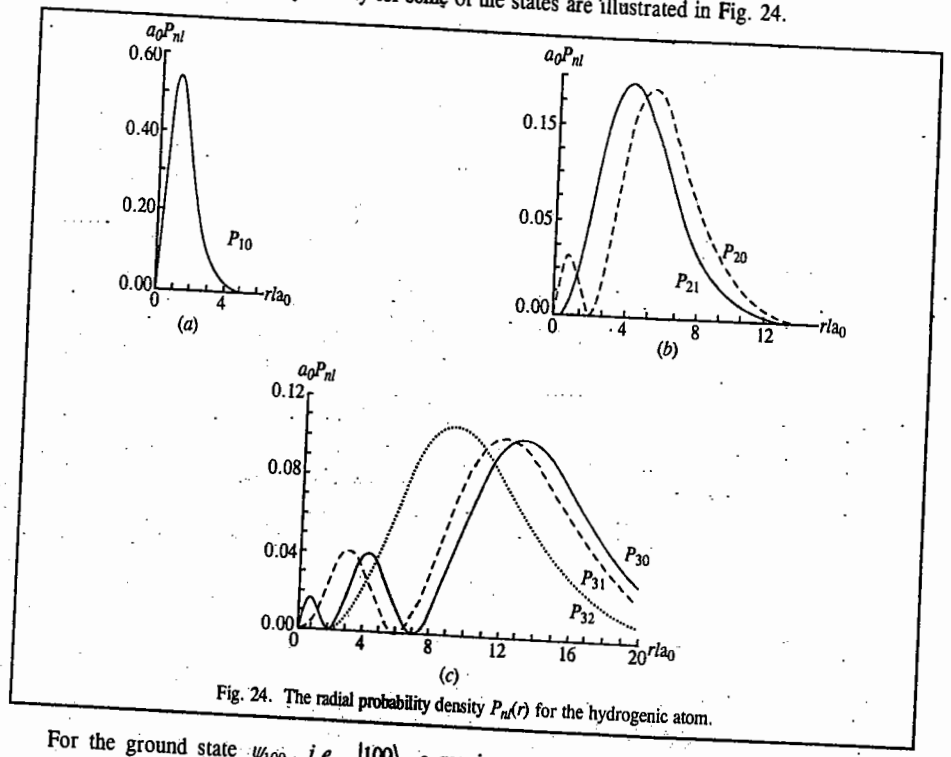

Fig. 24. The radial probability density $P_{nl}(r)$ for the hydrogenic atom.

For the ground state ψ_{100}, *i.e.*, $|100\rangle$, a maximum probability density P_{10} exists at a radial position given by

$$\frac{dP_{10}}{dr} = 0, \quad \text{or} \quad \left(2r - \frac{2r^2}{a_0}\right) e^{-2r/a_0} = 0, \quad \text{or} \quad r = a_0$$

The maximum occurs at a distance equal to the Bohr radius from the origin. Thus, the radial probability density for hydrogen atom in the ground state is maximum at the Bohr radius.

This view of the probability density consists in considering an atom to be composed of "layers" much like an onion and examining the probability of finding the electron in the "layer" which extends from r to $r+dr$ (Fig. 25). The volume of the thin shell may be considered to be dV. Since the volume of the sphere is $V=(4/3)\pi r^3$, $dV=4\pi r^2 dr$, so that $R_{nl}^2 dV = 4\pi r^2 R_{nl}^2 dr$. The essential features of the probability function are that (*i*) at $r = 0$, $4\pi r^2 R_{nl}^2 = 0$; hence the value of the function at the nucleus must be zero; (*ii*) at large values of r, $R_{nl} \to 0$ rapidly and hence $4\pi r^2 R_{nl}^2$ must $\to 0$. Note that although the radial function for the 2s orbital is both positive $(r < 2a_0/Z)$ and negative $(r > 2a_0/Z)$, the probability function is everywhere *positive* (as, of course, it must be to have any physical meaning) as a result of the squaring operation.

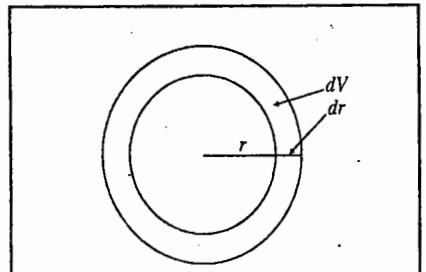

Fig. 25. Volume of a shell of thickness dr.

We may mention here that the presence of a node in the wavefunction indicates a point in space at which the probability of finding the electron has become zero. This raises the interesting question, "How does the electron get from one side of the node to the other if it can never be found exactly at the node?" This is not a valid question as posed, since it presupposes our macroscopically prejudiced view that the electron is a particle. If we consider the electron to exhibit wave-particle duality (as it does according to the de Broglie hypothesis), then the electron behaves as a standing wave, and no problem arises because it simultaneously exists on both sides of the node. We can even imagine that the electron "leaks" or "tunnels" through the node.

The presence of one or more nodes and maxima may have some effect on chemical bonding. Thus, since covalent bonding depends upon the overlap of atomic orbitals on adjacent atoms, it is evident that if one atom had a maximum in its radial wavefunction overlapping with a region with a node (minimum) in the wavefunction of a second atom, the overlap (as determined by the overlap integral $\int \psi_A \psi_B d\tau$ of the two atoms A and B) would be poor. However, accurate quantum mechanical calculations have shown that the nodes lie too close to the nucleus to affect the bonding appreciably. The presence of nodes and small "subnodal maxima" does have a profound effect on the *energy* of electrons in different orbitals. Electrons in an orbital with these subnodal maxima (particularly *s* orbitals with higher values of n) are said to be *penetrating*, *i.e.*, they have considerable electron density in the region of the nucleus. This is the reason for the ordering of the energy levels in polyelectronic atoms : 1s, 2s, 2p, 3s, 3p, etc. We may finally note that the number of radial nodes in a hydrogenic wavefunction is $n - l - 1$; the number of angular nodes (nodal planes) is l. Thus, the total number of nodes is $n - 1$. We see that *n*s orbitals have $n - 1$ radial nodes, *n*p orbitals have $n - 2$ radial nodes, etc.

Quantum Numbers. As discussed earlier, the solution of the Schrödinger wave equation for hydrogen atom yields three quantum numbers n, l and m. Amongst these, n, the principal quantum number, determines, to a large extent, the energy of the electron. It also determines the average distance of an electron from the nucleus. As the value of n increases, the electron gets farther away from the nucleus and its energy increases.

A portion of this energy is, however, associated with the orbital motion of the electron around the nucleus. This orbital motion is described by the angular momentum of the electron which is characterised by the angular momentum quantum number or the azimuthal quantum number, l. This quantum number accounts for the appearance of a group of closely spaced lines in the hydrogen spectra. But *the energy*

associated with the angular momentum of an electron must be well within its total energy determined by n. Thus, the electrons in atoms are grouped not only into main energy levels given by n but also into energy sub-levels given by l. The value of l gives the subshell in which the electron is located. *It also determines the shape of the orbital* in which the electron is located. The number of subshells within a principal shell are determined by the value of n for that principal energy level. Thus, l may have all possible whole number values from 0 to $n-1$. The various sublevels are designated as *s, p, d, f...* according as the value of l=0, 1, 2, 3, respectively.

Since an electron has an angular momentum, its motion may be likened to the flow of an electric current through a loop. Such a flow of current, as is well known, creates a magnetic field. This field can interact with an external magnetic or electric field. As a result of this interaction, *the electrons in a given energy sublevel orient themselves in certain specific regions of space around the nucleus.* These regions of space are called orbitals. The number of orbitals in a given energy sublevel within a principal energy level is given by the magnetic quantum number, m. The number of values allowed to m depends on the values of l. It is known from theory as well as experiment that the possible values of m range from $-l$ through 0 to $+l$, thus, making a total of $2l+1$ values.

The fourth quantum number, *viz.*, the **spin quantum number** does not follow from the wave mechanical treatment. The electron possesses an intrinsic angular momentum or spin, specified by the quantum number $s=\frac{1}{2}$. By analogy with the relation between the angular momentum quantum number l and the orbital angular momentum L (*viz.*, $L=[l(l+1)]^{1/2}\hbar$), the spin angular momentum has a magnitude

$$S = [s(s+1)]^{1/2}\hbar = \left(\sqrt{3}/2\right)\hbar \cdot \text{since } s = \tfrac{1}{2} \qquad ...(259)$$

The components of S in the direction of the magnetic field B are specified by the quantum number m_s, where $m_s=+\frac{1}{2}$ or $-\frac{1}{2}$. The $m_s=+\frac{1}{2}$ component has an upward orientation ($\uparrow$) and the $m_s=-\frac{1}{2}$ component has a downward orientation ($\downarrow$) (Fig. 26).

The spinning electron behaves like a tiny bar magnet. This fact was beautifully demonstrated by the celebrated **Stern–Gerlach experiment.** In alkali metal atoms, the outermost electrons are in an s orbital and the inner electrons are in a closed shell with an inert-gas configuration. The outermost electron has spin-magnetic properties similar to those of an isolated electron. In their experiment, Stern and Gerlach passed a beam of the atoms of an alkali metal through a strong inhomogeneous magnetic field. They found that the beam was split into two separate beams. The field divided the atoms into two beams corresponding to $m_s=+\frac{1}{2}$ and $m_s=-\frac{1}{2}$ for the valence electron. Otto Stern (1888–1969), the American physicist, was awarded the 1943 Physics Nobel Prize for his discovery of the magnetic moment of proton. The electron spin had been postulated in the early 1920s by G. Uhlenbeck and S. Goudsmit. The 1944 Physics Nobel Laureate I.I. Rabi (1898–1988) remarked that it would always remain a mystery why these physicists never won the Nobel prize. The electron spin emerges beautifully from the solution of Dirac's relativistic wave equation for the electron, but this topic is beyond the scope of this book.

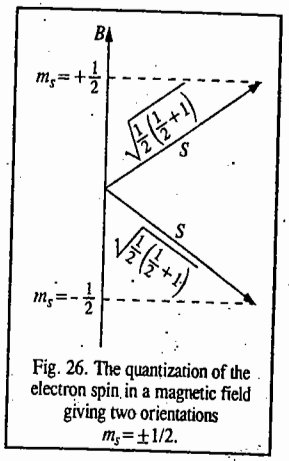

Fig. 26. The quantization of the electron spin in a magnetic field giving two orientations $m_s=\pm 1/2$.

Zeeman Effect. Zeeman, in 1896, found that when a strong magnetic field is applied to a system whose spectrum is being recorded, *each spectral line gets split up into a number of separate lines.* This phenomenon is known as the **Zeeman effect.**

As already stated, there are $(2l+1)$ components of orbital angular momentum vector along any chosen direction, say, the z-direction. The magnitudes of these components are given by $mh/2\pi$. Since the magnetic field generated due to the motion of electron in an orbital has also $(2l+1)$ orientations of

orbital angular momentum vector and since the magnetic field generated depends upon the magnitude of orbital angular momentum, it will also have $(2l+1)$ components along the z-axis whose magnitudes depend on the magnitudes of the z-components of the orbital angular momentum (*i.e.*, $mh/2\pi$).

In the absence of any external magnetic field, all the orientations of the orbital angular momentum (and hence of the magnetic field generated due to the motion of the electron in the orbital) have equal probability to occur. But, if an external magnetic field is applied along the z-axis, the orientation with maximum positive value of m will have maximum magnetic field component *parallel* to the direction of the external field applied. Such an orientation of orbital angular momentum will, therefore, be of lowest energy. Similarly, the orientation with maximum negative value of m will have maximum magnetic field component *antiparallel* to the direction of the external magnetic field applied. Such an orientation will, therefore, be of highest energy. Likewise, the energies of all other orientations of orbital angular momenta having different values of m will be different, ranging between the two extremes mentioned above, in the presence of external magnetic field.

Let us consider the example of a d orbital whose orbital angular momentum is $\sqrt{2(2+1)}\,h/2\pi$. It has five orientations of different energies in the presence of external magnetic field. Each orientation has a different z-component whose value ranges from $+2h/2\pi$ to $-2h/2\pi$, as shown in Fig. 27. Thus, a spectral line obtained in the absence of external magnetic field due to the shift of electron from a higher to a lower d orbital of an atom will be split up into five lines in the presence of the external magnetic field.

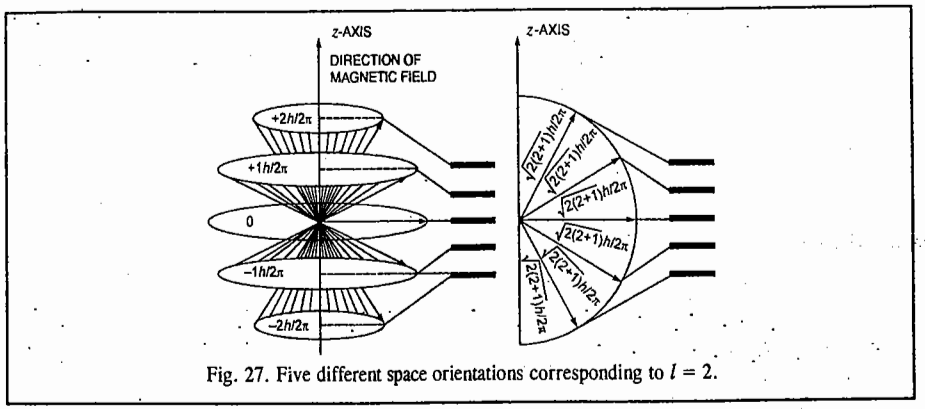

Fig. 27. Five different space orientations corresponding to $l = 2$.

Pauli's Exclusion Principle

This is an important generalisation put forth by Wolfgang Pauli, in 1925, which determines the maximum number of electrons that an energy level can accommodate. Pauli's exclusion principle states that *it is impossible for any two electrons in the same atom to have all the four quantum numbers identical.* Wolfgang Pauli (1900-1958), the Austrian physicist, was awarded the 1945 Physics Nobel Prize for the discovery of the exclusion principle. Thus, in the same atom, any two electrons may have three quantum numbers identical but not the fourth which must be different. This principle is very useful *in determining the maximum number of electrons that can occur in any quantum group.* For K shell, for instance, since $n=1$, l can have only one value (*viz.*, 0) and m can also have only one value (*viz.*, 0). Hence, m_s can be either $+1/2$ or $-1/2$. Thus, there are two combinations of the quantum numbers, as shown:

$$n=1 \quad l=0 \quad m=0 \quad m_s = +1/2$$
$$n=1 \quad l=0 \quad m=0 \quad m_s = -1/2$$

This shows that in the K shell, there is only one subshell $l=0$ and in this only two electrons of opposite spins can be accommodated.

For L shell, since $n = 2$, l can have two values (0 and 1), m can have only one value for $l = 0$ and three values for $l = 1$, *viz.*, -1, 0 and $+1$ and m_s can have two values, *viz.*, $+1/2$ and $-1/2$, for each value of m. These possibilities would give rise to eight combinations of the four quantum numbers, keeping in view the *exclusion principle*. Thus, L shell can accommodate 8 electrons, 2 in the $l = 0$ subshell (s subshell) and 6 in the $l = 1$ subshell (p subshell). Similarly, it can be shown that the M shell can have 18 electrons, 2 in the $l = 0$ subshell (s subshell), 6 in the $l = 1$ subshell (p subshell) and 10 in the $l = 2$ subshell (d subshell) and so on. The *maximum number* of electrons that can be accommodated in the first four principal energy shells as distributed in the various subshells (l values) are given in Table 4.

TABLE 4

Distribution of Electrons in Various Energy Shells and Subshells

Principal energy shell (n)	Subshells (l)	Orbitals (m)	Number of electrons in : Subshell	Number of electrons in : Principal energy shell
1	0 (1s subshell)	0 (one orbital)	2	2
2	0 (2s subshell)	0 (one orbital)	2	8
	1 (2p subshell)	−1, 0, +1 (three orbitals)	6	
3	0 (3s subshell)	0 (one orbital)	2	18
	1 (3p subshell)	−1, 0, +1 (three orbitals)	6	
	2 (3d subshell)	−2, −1, 0, +1, +2 (five orbitals)	10	
4	0 (4s subshell)	0 (one orbital)	2	32
	1 (4p subshell)	−1, 0, +1 (three orbitals)	6	
	2 (4d subshell)	−2, −1, 0, +1, +2 (five orbitals)	10	
	3 (4f subshell)	−3, −2, −1, 0, +1, +2, +3 (seven orbitals)	14	

Physical Interpretation of the Hydrogenic Atomic Orbitals. According to the Bohr theory, the angular momentum L of an electron in an orbital is given by

$$L = n\hbar ; \qquad n = 1, 2, 3,... \qquad ...(260)$$

However, according to wave mechanics, the value of L is given by

$$L = [l(l + 1)]^{1/2}\hbar \qquad ...(261)$$

Thus, while according to the Bohr theory the ground state angular momentum is equal to $\hbar$ since $n=1$ (*i.e.*, it is finite), according to wave mechanics its value is zero (since $l=0$).

It can be shown that, other things being equal, an electron in an orbital of high angular momentum tends to stay farther from the nucleus than an electron in a state of lower angular momentum. Fig. 28 shows the radial parts of the hydrogenic wave functions for the principal quantum number $n = 3$. We see that the higher the value of l, the less likely it is to be found near the nucleus. Thus, for a given value of n, the size of the orbit increases with increase in the azimuthal quantum number, l.

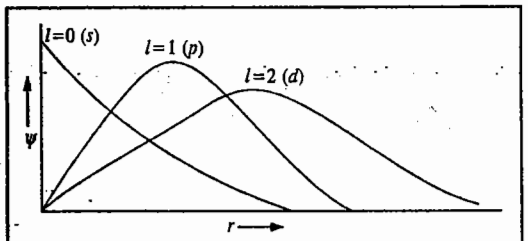

Fig. 28. Radial parts of the hydrogenic wave functions for the principal quantum number n–3.

The increasing order of energy of various orbitals, in general, is as follows :

1s, 2s, 2p, 3s, 3p, 4s, 3d, 4p, 5s, 4d, 5p, 6s, 4f, 5d, 6p, 7s, 5f, 6d.....

Filling of Orbitals. The filling of orbitals in the ground state of an atom is determined by the following rules :

1. The electrons are added one by one to various orbitals as we move from one element to the next in the order of increasing atomic numbers.

2. The electrons enter the various orbitals in the order of increasing energy. This is known as the **aufbau principle**.

3. Electron-pairing in any orbital is not possible until all the available orbitals of a given subshell contain one electron each. This is known as **Hund's rule.**

4. An orbital cannot contain more than two electrons. This is based on Pauli's exclusion principle.

5. Electrons prefer to enter those subshells which, thereby, get either *completely filled* or *just half-filled.*

Electronic configurations of all the known elements based on the above rules are given in the Periodic Table annexed at the beginning of the book.

Fine Structure in the Hydrogen Atomic Spectrum. We have seen that in the Bohr theory of hydrogen atom, the electronic transitions observed in the form of the various spectral series such as Lyman, Balmer, Paschen series, are governed by the selection rule that $\Delta n = 1, 2, 3,....$ *i.e.*, the principal quantum number, n, may change by any integral value. However, observation of the spectrum under conditions of high resolution reveals many additional spectral lines. Bohr's theory cannot explain these additional lines. Schrödinger's quantum mechanics has successfully accounted for these extra lines in the spectrum of hydrogen. It is found that the spectral transitions are governed by the selection rules :

(i) Δn = any integer, *i.e.*, 1, 2, 3,....

(ii) $\Delta l = \pm 1,$

Transitions which obey these selection rules are called **allowed transitions** and transitions which do not obey (or violate) these selection rules are known as **forbidden transitions.**

Angular Momentum in Quantum Mechanics

In quantum mechanics we come across several examples of angular momentum. Thus, angular momentum may be possessed by *(i)* a rotating molecule *(ii)* an electron orbiting around an atom *(iii)* the spinning electrons and *(iv)* certain spinning nuclei. We shall confine ourselves to only a general discussion of angular momentum. For a particle of mass m revolving around a point at a distance r, the

angular momentum L is given by

$$L = mur = mr^2\omega = I\omega \quad ...(262)$$

where u is the linear velocity, ω is the angular velocity ($\omega = u/r$) and I ($=mr^2$) is the moment of inertia of the particle. The particle has kinetic energy E_k given by

$$E_k = \tfrac{1}{2}mu^2 = \tfrac{1}{2}mr^2\omega^2 = \tfrac{1}{2}I\omega^2 \quad ...(263)$$

From Eqs. 262 and 263, kinetic energy can be written in terms of the angular momentum as

$$E_k = L^2/2I \quad ...(264)$$

In three dimensions the angular momentum is represented by a vector, $\vec{L}$. Consider a mass m rotating about a fixed point P with a linear velocity $\vec{u}$. Then, $\vec{L}$ is given by

$$\vec{L} = \vec{r} \times m\vec{u} = \vec{r} \times \vec{p} \quad ...(265)$$

where $\vec{r}$ is the vector from the fixed point P to the mass point and $\vec{p}$ is the linear momentum vector. The vector $\vec{L}$ is perpendicular to the plane defined by $\vec{r}$ and $\vec{p}$. From classical mechanics, the components of the classical angular momentum vector are given by

$$L_x = yp_z - zp_y \quad ...(266)$$

$$L_y = zp_x - xp_z \quad ...(267)$$

$$L_z = xp_y - yp_x \quad ...(268)$$

The square of the angular momentum is given by the scalar product of $\vec{L}$ with itself. Thus,

$$L^2 = \vec{L}.\vec{L} = L_x^2 + L_y^2 + L_z^2 \quad ...(269)$$

The square of the angular momentum is a scalar. If no torque is acting on the particle, its angular momentum remains constant in classical mechanics. Classical mechanics permits all possible values of L.

In quantum mechanics the angular momentum is represented by an operator. The quantum mechanical operators for the components of angular momentum are obtained by replacing the quantities in Eqs. 266, 267 and 268 with their corresponding quantum mechanical operators.

Thus, $\hat{p}_x = -i\hbar\partial/\partial x$, and so on. Hence,

$$\hat{L}_x = -i\hbar\left(y\frac{\partial}{\partial z} - z\frac{\partial}{\partial y}\right) \quad ...(270)$$

$$\hat{L}_y = -i\hbar\left(z\frac{\partial}{\partial x} - x\frac{\partial}{\partial z}\right) \quad ...(271)$$

$$\hat{L}_z = -i\hbar\left(x\frac{\partial}{\partial y} - y\frac{\partial}{\partial x}\right) \quad ...(272)$$

The operator for the square of the momentum is given by

$$\hat{L}^2 = |\vec{L}|^2 = \vec{L}.\vec{L} = \hat{L}_x^2 + \hat{L}_y^2 + \hat{L}_z^2 \quad ...(273)$$

One may now ask if we can measure the angular momentum L and its components L_x, L_y and L_z

simultaneously. It is found from quantum mechanics that, according to Heisenberg's uncertainty principle, only the square of the angular momentum, L^2 and only one of its components can be measured simultaneously, *i.e.*, L^2 and L_x or L^2 and L_y or L^2 and L_z can be simultaneously measured. This fact is expressed by saying that L^2 commutes with one of its components, *i.e.*,

$$[\hat{L}^2, \hat{L}_x] = [\hat{L}^2, \hat{L}_y] = [\hat{L}^2, \hat{L}_z] = 0 \quad ...(274)$$

On the Other hand, $\hat{L}_x$, $\hat{L}_y$; $\hat{L}_y$, $\hat{L}_z$ and $\hat{L}_z$, $\hat{L}_x$ *cannot be simultaneously measured.* In quantum mechanical language, these operators *do not commute with each other, i.e.,*

$$[\hat{L}_x, \hat{L}_y] \neq 0; \quad [\hat{L}_y, \hat{L}_z] \neq 0; \quad [\hat{L}_z, \hat{L}_x] \neq 0 \quad ...(275)$$

Angular momentum is discussed in detail in Chapter 2 ; Eq. 275 is derived there.

Again, in the time-independent Schrödinger equation $\hat{H}\psi = E\psi$, we know that ψ is the eigenfunction and E is the eigenvalue of the Hamiltonian operator, $\hat{H}$. Naturally we want to know the eigenfunctions and eigenvalues of the angular momentum operators. There is another important quantum mechanical result according to which *if two operators commute with each other, they have the same eigenfunctions.* Thus, according to Eq. 274, L^2 and $\hat{L}_z$ (or $\hat{L}^2$ and $\hat{L}_x$, etc.) have the same eigenfunctions, which are spherical harmonics. Keeping in view the above considerations, it can be easily shown that the eigenvalues of $\hat{L}^2$ and $\hat{L}_z$ are

$$|\vec{L}^2| = [l(l+1)]\hbar^2; \quad l = 0, 1\ 2, 3 \quad ...(276)$$

$$|\vec{L}_z| = m_l\hbar; \quad m_l = -l, -l+1, \ldots l-1, l \quad ...(277)$$

where m_l is the component of l along a suitable axis, ; in this case, the z-axis. From Eq. 276,

$$|\vec{L}| = [l(l+1)]^{1/2}\hbar \quad ...(278)$$

Solved Examples in Quantum Mechanics

Example 34. Calculate the magnitude of the angular momentum of an electron that occupies the following atomic orbitals : *(a)* 1*s* *(b)* 3*s* *(c)* 2*p* *(d)* 3*d* *(e)* 3*p*.

Solution : $\vec{L} = [l(l+1)^{1/2}\hbar$; $l = 0,1,2,3$ ($\hbar = 1{\cdot}055 \times 10^{-34}$ J s)

(a) For 1*s* electron : $l = 0$; $|\vec{L}| = 0$

(b) For 3*s* electron : $l = 0$; $|\vec{L}| = 0$

(c) For 2*p* electron : $l = 1$; $|\vec{L}| = [1(1+1)]^{1/2}\hbar = 1{\cdot}414\ \hbar = 1{\cdot}49 \times 10^{-34}$ J s

(d) For 3*d* electron : $l = 2$; $|\vec{L}| = [2(2+1)]^{1/2}\hbar = \sqrt{6}\ \hbar = 2{\cdot}58 \times 10^{-34}$ J s

(e) For 3*p* electron : $l = 1$; $|\vec{L}| = 1{\cdot}414\ \hbar = 1{\cdot}49 \times 10^{-34}$ J s

Example 35. Calculate the angular momentum of a rigid diatomic rotating molecule (say, HCl) in the second rotational energy level. Compare it with the angular momentum of an electron in the 2*p* atomic orbital.

Solution : For a rigid diatomic rotating molecule,

$$|\vec{L}| = [J(J+1)]^{1/2}\ \hbar\ ;\ J = 0,\ 1,\ 2,\ 3....$$

where J is the rotational quantum number. For the second rotational state, $J=1$.

$$\therefore \quad |\vec{L}| = \sqrt{2}\hbar = \sqrt{2}(1{\cdot}055 \times 10^{-34}\ \text{J s}) = 1{\cdot}49 \times 10^{-34}\ \text{J s}.$$

Again, for an electron in an atomic orbital,

$$|\vec{L}| = [l(+1)]^{1/2}\hbar \; ; \; l = 0, 1, 2, 3, \ldots.$$

For the 2*p*-electron, $l = 1$

$$\therefore \quad |\vec{L}| = \sqrt{2}\,\hbar = 1{\cdot}49\times10^{-34} \text{ J s}$$

We see that the two values are the same.

Example 36. The unnormalized angular function, which is a solution of the Φ-equation, is $\Phi(\phi) = N \exp(im\phi)$. Normalize it.

Solution : The wave function is normalized if

$$< \Phi(\phi) \; |\Phi(\phi)> \; = \int_0^{2\pi} \Phi^* \Phi \, d\phi = 1$$

Substituting the value of $\Phi(\phi)$, we have

$$N^2 \int_0^{2\pi} e^{im\phi} e^{-im\phi} d\phi \; = N^2 \int_0^{2\pi} d\phi = N^2(2\pi) = 1$$

$$\therefore \quad N = (1/2\pi)^{1/2}$$

Hence, the normalized angular function is

$$\Phi(\phi) = \frac{1}{\sqrt{2\pi}} . \exp(im\phi)$$

Example 37. Obtain the real functions from the angular functions defined by

$$\Phi_{\pm m}(\phi) = (1/2\pi)^{1/2} \exp(\pm im\phi), \text{ for } m = 1.$$

Solution : $\Phi_{+1}(\phi) = \frac{1}{\sqrt{2\pi}} e^{i\phi}$; $\Phi_{-1}(\phi) = \frac{1}{\sqrt{2\pi}} e^{-i\phi}$

Taking the linear combinations of these functions, we have

$$\Phi_+ = \frac{1}{\sqrt{2\pi}} (e^{i\phi} + e^{-i\phi}) = \frac{1}{\sqrt{2\pi}} (2 \cos \phi)$$

$$\Phi_- = \frac{1}{\sqrt{2\pi}} \left(\frac{e^{i\phi} - e^{-i\phi}}{i} \right) = \frac{1}{\sqrt{2\pi}} (2 \sin \phi)$$

If Φ_+ and Φ_- are further normalized, the normalization constant is found to be $1/\sqrt{2}$. Hence, we have

$$\Phi_+ = \frac{1}{\sqrt{\pi}} \cos \phi \text{ and } \Phi_- = \frac{1}{\sqrt{\pi}} \sin \phi$$

Note : In this problem we have made use of Euler's formula, according to which $e^{\pm i\phi} = \cos \phi \pm i \sin \phi$

Example 38. Determine the radial functions $R_{n,l}(r)$ for *(a)* the 1*s* orbital *(b)* 2*p* orbital.

Solution : *(a)* For the 1*s*-orbital, $n = 1$, $l = 0$. Hence, the associated Laguerre polynomial is

$$L_1^1(\rho) = \frac{d}{d\rho} \left[e^{\rho} \frac{d}{d\rho} (\rho e^{-\rho}) \right] = \frac{d}{d\rho} (1 - \rho) = -1$$

Hence,

$$R_{1,0}(r) = -\left(\frac{2Z}{a_0}\right)^{3/2} \left[\frac{0!}{2(1!)^3} \right]^{1/2} e^{-\rho/2} \rho^0 (-1) = 2\left(\frac{Z}{a_0}\right)^{3/2} e^{-\rho/2} = 2\left(\frac{Z}{a_0}\right)^{3/2} e^{-Zr/a_0}$$

(b) For the 2*p*-orbital, $n = 2$, $l = 1$. Hence, the associated Laguerre polynomial is

$$L_3^3(\rho) = \frac{d^3}{d\rho^3} \left[e^{\rho} \frac{d^3}{d\rho^3} (\rho^3 e^{-\rho}) \right]$$

Now, $\frac{d^3}{d\rho^3} (\rho^3 e^{-\rho}) = \frac{d^2}{d\rho^2} [(3\rho^2 - \rho^3) e^{-\rho}] = (6 - 18\rho + 9\rho^2 - \rho^3) e^{-\rho}$

Hence, we obtain

$$L_3^3(\rho) = \frac{d^3}{d\rho^3} \left[e^{\rho} (6 - 18\rho + 9\rho^2 - \rho^3) e^{-\rho} \right] = \frac{d^3}{d\rho^3} (6 - 18\rho - 9\rho^2 - \rho^3) = -6$$

Hence,

$$R_{2,1}(r) = -\left(\frac{Z}{a_0}\right)^{3/2} \left[\frac{(2-1-1)!}{2\times2[(2+1)!]^2} \right]^{1/2} e^{-\rho/2} \rho(-6) = \left(\frac{Z}{a_0}\right)^{3/2} \frac{1}{2\sqrt{6}} \rho e^{-\rho/2}$$

$$= \frac{1}{2\sqrt{6}} \left(\frac{Z}{a_0}\right)^{5/2} r e^{-Zr/2a_0} \qquad (\because \rho = 2Zr/a_0)$$

Example 39. Show that the 1*s* wavefunction of hydrogen atom given by

$$\psi_{1s} \equiv \psi_{1,0,0} = \frac{1}{\sqrt{\pi}\, a_0^{3/2}} \exp(-r/a_0), \text{ is normalized ; } a_0 \text{ is the Bohr radius.}$$

Solution : For the wavefunction to be normalized the following condition holds :

$$\int \psi_{1s}^* \psi_{1s} d\tau = 1$$

In polar coordinates (r, θ, ϕ), the volume element $d\tau = r^2 \, dr \sin \theta \, d\theta \, d\phi$. Using this expression for $d\tau$ and integrating between appropriate limits, we have

$$\int \psi_{1s}^* \psi_{1s} d\tau \; = \frac{1}{\pi a_0^3} \int_0^{\infty} r^2 e^{-2r/a_0} dr \int_0^{\pi} \sin\theta \, d\theta \int_0^{2\pi} d\phi$$

Each of these integrals can be evaluated separately as follows :

$$\int_0^{2\pi} d\phi \; = 2\pi \text{ and } \int_0^{\pi} \sin\theta \, d\theta = [-\cos\theta]_0^{\pi} \; = -(-1) - (-1) = 2$$

The first integral is evaluated by using the result

$$\int_0^{\infty} x^n e^{-ax} dx = \frac{n!}{a^{n+1}}, \; n \text{ is a positive integer ; } a > 0.$$

Thus, $\int r^2 e^{-2r/a_0} dr \; = \frac{2}{(2/a_0)^3} = \frac{a_0^3}{4}$

$$\therefore \quad \int \psi_{1s}^* \psi_{1s} d\tau = 1$$

Hence, ψ_{1s} is normalized.

Example 40. The un-normalized 1*s* wavefunction for hydrogen atom is given by

$$\psi_{1s} \equiv \psi_{1,0,0} = N \exp(-r/a_0), \text{ where } a_0 \text{ is the Bohr radius.}$$

Determine the normalized wavefunction.

Solution : Here we have to determine the normalization constant, N. For the wavefunction to be normalized, the following condition holds :

$$\int \psi_{1s}^* \psi_{1s} d\tau \; = 1 \qquad \text{(since } \psi_{1s} \text{ is real, } \psi_{1s}^* \text{ is equal to } \psi_{1s})$$

In polar coordinates (r, θ, ϕ), the volume element $d\tau = r^2 \, dr \sin\theta d\theta d\phi$. Using this expression for $d\tau$ and integrating between appropriate limits, we have

$$\int \psi_{1s}^* \psi_{1s} d\tau \; = N^2 \int e^{-2r/a_0} d\tau = N^2 \int_0^{\infty} r^2 e^{-2r/a_0} dr \int_0^{\pi} \sin\theta \, d\theta \int_0^{2\pi} d\phi = 1$$

Each of these integrals can be evaluated separately as follows :

$$\int_0^{2\pi} d\phi \; = 2\pi \text{ and } \int_0^{\pi} \sin\theta \, d\theta = [-\cos\theta]_0^{\pi} \; = -(-1) - (-1) = 2$$

Using the result

$$\int_0^\infty x^n e^{-\alpha x} dx = \frac{n!}{a^{n+1}} \; ; \; n \text{ is a positive integer} \; ; \; a > 0, \text{ we obtain}$$

$$\int_0^\infty r^2 e^{-2r/a_0} dr = \frac{2!}{(2/a_0)^3} = \frac{a_0^3}{4}$$

Hence, $N^2 \, (a_0^3/4) \, (2) \, (2\pi) = 1$

$$\therefore \quad N = 1/\sqrt{\pi} a_0^{3/2}$$

Hence, the normalized ground-state wavefunction is

$$\psi_{1s} = 1/\sqrt{\pi} a_0^{3/2} \exp(-r/a_0)$$

Note : This example is the reverse of the last example.

Example. 41. Show that the 1s and 2s wavefunctions of hydrogen atom, given by

$\psi_{1s} \equiv \psi_{1,0,0} = \dfrac{1}{\sqrt{\pi} a_0^{3/2}} \exp(-r/a_0)$ **and** $\psi_{2s} \equiv \psi_{2,0,0} = \dfrac{1}{4\sqrt{2\pi} \, a_0^{3/2}} \left(2 - \dfrac{r}{a_0}\right) \exp(-r/2a_0)$ **are orthogonal to each other.**

Solution : For the given wavefunctions to be orthogonal, they should satisfy the following condition :

$$\int \psi_{1s} \psi_{2s} \, d\tau = 0$$

Since in polar coordinates, $d\tau = r^2 \, dr \sin\theta \, d\theta \, d\phi$, we have, after integrating between appropriate limits,

$$\int \psi_{1s} \psi_{2s} \, d\tau = \frac{1}{4\sqrt{2\pi} a_0^3} \left[2 \int_0^\infty r^2 e^{-3r/2a_0} dr - \frac{1}{a_0} \int_0^\infty r^3 e^{-3r/2a_0} dr \right] \int_0^\pi \sin\theta \, d\theta \int_0^{2\pi} d\phi$$

Now, $\int_0^\infty \sin\theta \, d\theta \left[-\cos\theta\right]_0^\pi = -(-1) - (-1) = 2$ and $\int_0^{2\pi} d\phi = 2\pi$

Using the standard result $\int_0^\infty x^n e^{-\alpha x} dx = \dfrac{n!}{a^{n+1}}$, we have

$$\int_0^\infty r^2 e^{-3r/2a} a_0 \, dr = \frac{2!}{(3/2a_0)^3} = \frac{16 a_0^3}{27} \text{ and } \int_0^\infty r^3 e^{-3r/2a_0} dr = \frac{3!}{(3/2a_0)^4} = \frac{32 a_0^4}{27}$$

Using the above values of the various integrals we find that

$$\int \psi_{1s} \psi_{2s} \, d\tau = 0$$

Hence, the 1s and 2s wavefunctions of hydrogen atom are orthogonal.

Example 42. Using the normalized wavefunction,

$$\psi_{1s} = (1/\pi a_0^3)^{1/2} \exp(-r/a_0)$$

for the ground state of hydrogen atom, calculate the probability for the electron to be confined in a sphere of radius $r = a_0$, the Bohr radius.

Solution : We know from Born's interpretation of the wave function, the probability is given by

$$P(r) \, dr = \psi^* \, \psi \, d\tau$$

$\therefore$ Integrating, we obtain

$$\int P(r) dr = \int \psi^* \psi d\tau, \quad \text{where } d\tau = r^2 dr \sin\theta \, d\theta \, d\phi$$

or

$$P = \frac{1}{\pi a_0^3} \int_0^{a_0} r^2 e^{-2r} dr \int_0^\pi \sin\theta d\theta \int_0^{2\pi} d\phi = \frac{4}{a_0^3} \int_0^{a_0} r^2 e^{-2r} dr$$

Carrying out integration by parts, we obtain

$$P = \frac{4}{a_0^3} \left\{ \left[\frac{a_0}{2} r^2 e^{-2r/a_0} \right]_0^{a_0} + \left[-\frac{a_0^2}{2} r e^{-2r/a_0} \right]_0^{a_0} + \left[-\frac{a_0^3}{4} e^{-2r/a_0} \right]_0^{a_0} \right\}$$

$$= 5e^{-2} + 1 = \mathbf{0{\cdot}323}$$

Example 43. Calculate the most probable distance, r_{mp}, of the electron from the nucleus in the ground state of hydrogen atom, given that the normalized ground state wavefunction is

$$\psi_{1s} = \frac{1}{\sqrt{\pi} a_0^{3/2}} \exp(-r/a_0)$$

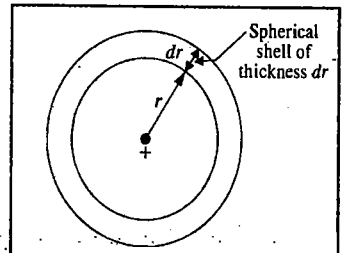

Fig. 29. Spherical shell of thickness dr at a distance r from the nucleus.

Solution : Quantum mechanically, the probability of finding the electron in a spherical shell of thickness dr at a distance r from the nucleus (Fig. 29) is given by

$$P(r)dr = 4\pi \, |\psi_{1s}|^2 \, r^2 dr$$

$$= 4\pi r^2 \, (1/\pi a_0^3) e^{-2r/a_0} \, dr$$

For the probability to be a maximum,

$dP(r)/dr = 0$. Thus,

$$\frac{dP(r)}{dr} = \frac{4}{a_0^3} \left(-\frac{2r^2}{a_0} + 2r \right) e^{-2r/a_0} = 0$$

Since the Bohr radius $a_0 \neq 0$ and the exponential is also $\neq 0$, hence

$$-\frac{2r^2}{a_0} + 2r = 0 \qquad \therefore \; r = r_{mp} = a_0$$

Example 44. Calculate the average distance of the electron from the nucleus in the ground state of hydrogen atom ; given that the normalized ground state wave function is $\psi_{1s} = \dfrac{1}{\sqrt{\pi} a_0^{3/2}} \exp(-r/a_0)$.

Solution : In quantum mechanics, the average (or expectation) value of dynamical variable r is given by

$$< r > = \int \psi_n^* r \psi_n \, d\tau$$

In the present case, the average distance of the electron from the nucleus is given by

$$< r > = \int \psi_{1s}^* r \psi_{1s} \, d\tau$$

Since $d\tau = r^2 \, dr \sin\theta \, d\theta \, d\phi$, hence, integrating between appropriate limits, we get

$$< r > = \frac{1}{\pi a_0^3} \int_0^\infty r^3 e^{-2r/a_0} dr \int_0^\pi \sin\theta \, d\theta \int_0^{2\pi} d\phi = \frac{1}{\pi a_0^3} \left(\frac{3!}{(2/a_0)^4} (2)(2\pi) \right)$$

Note : The results of the last two examples are quite instructive. According to Bohr's theory of hydrogen atom, the distance of the electron from the nucleus in the ground state is exactly equal to a_0, the Bohr radius. But, according to Heisenberg's uncertainty principle, the electron cannot be exactly located in its orbit. Hence, quantum mechanically, while the most probable distance is a_0, the average distance is $3a_0/2$ *i.e.*, the average distance is 50% greater than the Bohr theory result ! The inescapable conclusion we draw from this is that we really do not know where the electron is located in its orbit at a given moment.

Example 45. Show that the average value of $1/r$ for an electron in the 1s-orbital of hydrogen atom is $1/a_0$, where a_0 is the Bohr radius ; given that

$$\psi_{1s} = \frac{1}{\sqrt{\pi} a_0^{3/2}} \exp(-r/a_0)$$

Solution : $< 1/r > = \int \psi_{1s}^* (1/r) \psi_{1s} \, d\tau$

Since $d\tau = r^2\, dr \sin\theta\, d\theta\, d\phi$, hence, integrating between appropriate limits,

$$< 1/r > = \frac{1}{\pi a_0^3}\int_0^\infty r e^{-2r/a_0} dr \int_0^\pi \sin\theta\, d\theta \int_0^{2\pi} d\phi = \frac{1}{\pi a_0^3}\left(\frac{1}{(2/a_0)^2}(2)(2\pi)\right) = \frac{1}{a_0}$$

Example 46. X-rays with λ = 1.0 Å are scattered from a metal block. The scattered radiation is viewed at 90° to the incident radiation. Evaluate the Compton shift.

Solution : Compton shift is $\Delta\lambda = \dfrac{h}{m_e c}(1-\cos\theta)$

or $$\Delta\lambda = \left(\frac{(6.626\times10^{-34}\ \text{Js})(1-\cos 90°)}{(9.109\times10^{-31}\ \text{kg})\,(3\times10^{8}\ \text{m s}^{-1})}\right) = 2.42\times10^{-12}\ \text{m} = 0.024\ \text{Å} \quad [\cos 90° = 0]$$

Example 47. Indicate which of the following functions are acceptable as wave functions :

(*a*) $\psi = x$, (*b*) $\psi = x^2$, (*c*) $\psi = \sin x$, (*d*) $\psi = e^x$, (*e*) $\psi = e^{-x}$,

(*f*) $\psi = e^{-x^2}$, (*g*) $\psi = \tan x$

Solution : (*a*) Not acceptable, as $\psi \to \infty$ as $x \to \infty$;

(*b*) not acceptable,

(*c*) acceptable,

(*d*) not acceptable, as $\psi \to \infty$ as $x \to \infty$;

(*e*) not acceptable, as $\psi \to \infty$ as $x \to -\infty$

(*f*) acceptable, as $\psi \to 0$ as $x \to \pm\infty$;

(*g*) not acceptable, as $\psi \to \infty$ as $x = \pi/2$.

Example 48. Show that the function $\psi(x) = A\exp(ikx)$ represents a de Broglie wave.

Solution : As x changes to $x + \lambda$ (where λ is the wavelength of the de Broglie wave),

$$\psi(x+\lambda) = A\exp(ik(x+\lambda)) = A\exp(ikx).\exp(ik\lambda)$$

$$= A\exp(ikx).\exp(ikh/p) = A\exp(ikx)\exp(2\pi i) \qquad [\because p = k\hbar/2\pi]$$

$$= A\exp(ikx)(\cos 2\pi + i\sin 2\pi) = A\exp(ikx) = \psi$$

Thus, the function $\psi(x)$ repeats after an interval of λ; hence it represents a de Broglie wave.

Example 49. Find the eigenfunctions and eigenvalues of linear momentum operator $\hat{p}_x$. Show that in the absence of any restriction there is a continuous series of eigenvalues of $\hat{p}_x$.

Solution : $\hat{p}_x\psi = \lambda\psi$ [the eigenvalue equation]

Since $\hat{p}_x \to -i\hbar\ (\mathrm{d}/\mathrm{d}x)$, $-i\hbar\dfrac{d\psi}{dx} = \lambda\psi$ where λ is the eigenvalue ψ, or $d\psi/dx = ik\psi$ (where $k = \lambda/\hbar$), whose solution is $\psi = A\exp(ikx)$, which is the required eigenfunction with eigenvalue $\lambda = k\hbar$. If there is no restriction on k there will be no restriction on λ provided ψ is finite, single-valued and continuous for all values of x.

Example 50. What is the Schmidt orthogonalization procedure ?

Solution : We know that eigenfunctions of a Hermitian operator corresponding to different eigenvalues are orthogonal. However, if the eigenfunctions ψ_1 and ψ_2 are degenerate (*i.e.*, they have the same eighnvalues ($\lambda_1 = \lambda_2$), then ψ_1 and ψ_2 may not be orthogonal. However, we can always construct an orthogonal pair ϕ_1 and ϕ_2 by taking suitable linear combinations of ψ_1 and ψ_2 as shown below.

Let ψ_1 and ψ_2 be the two linearly independent degenerate eigenfunctions which are normalized but not orthogonal. Let $\phi_1 = \psi_1$ and $\phi_2 = a_1\psi_1 + a_2\psi_2$. Let $\int\psi_1\psi_2\, d\tau = S$. We have now to determine the coefficients a_1 and a_2 such that

$$\int\phi_1\phi_2\, d\tau = 0 \ ; \text{ and } \int\phi_2\phi_2\, d\tau = 1 \qquad (i)$$

Using the above conditions,

$$\int\psi_1(a_1\psi_1 + a_2\psi_2)\, d\tau = 0 \qquad (ii)$$

or $$a_1\int\psi_1^2\, d\tau + a_2\int\psi_1\psi_2\, d\tau = 0 \ ; \quad \text{or} \quad a_1 + a_2 S = 0 \ ; \text{ or } a_1 = -a_2 S \qquad (iii)$$

Again, $$\int(a_1\psi_1 + a_2\psi_2)^2\, d\tau = 1 \qquad (iv)$$

$$a_1^2\int\psi_1^2\, d\tau + a_2^2\int\psi_2^2\, d\tau + 2a_1a_2\int\psi_1\psi_2\, d\tau = 1 \qquad (v)$$

or $$a_1^2 + a_2^2 + 2a_1a_2 S = 1 \qquad (vi)$$

or $$a_2^2 S^2 + a_2^2 - 2a_2^2 S^2 = 1 \qquad (\because a_1 = -a_2 S \text{ from Eq. (iii)}) \qquad (vii)$$

or $a_2 = (1-S^2)^{-1/2}$, so that $a_1 = -S(1-S^2)^{-1/2}$ (viii)

Hence, the desired orthogonal pair is

$$\phi_1 = \psi_1 ;$$

$$\phi_2 = a_1\psi_1 + a_2\psi_2 = -S(1-S^2)^{-1/2}\psi_1 + (1-S^2)^{-1/2}\psi_2 = (1-S^2)^{-1/2}(\psi_2 - \psi_1 S)$$

This is called the "Schmidt orthogonalization" procedure.

Example 51. Derive the expression for the linear momentum operator of a particle moving in the *x*-direction.

Solution : Consider a particle wave, whose wave function can be represented by the wave function,

$$\psi(x) = A\exp(\pm 2\pi i\, x/\lambda).$$ where λ is the wave length.

Differentiating with respect to x,

$$\frac{d\psi}{dx} = \pm\frac{2\pi i}{\lambda}(A\exp(\pm 2\pi i x/\lambda)) = \pm\frac{2\pi i}{\lambda}\psi \quad (\because \lambda = h/p_x, \text{ by de Broglie's relation})$$

or $$\hat{p}_x\psi = \pm\frac{h}{2\pi i}\frac{d\psi}{dx} = \pm\frac{\hbar}{i}\frac{d\psi}{dx}$$

Removing ψ from both sides, we have

$$\hat{p}_x = \pm(\hbar/i)(d/dx)$$

[+ and − signs refer to positive and negative x-directions, respectively.]

Example 52. Examine if d^2/dx^2 is a Hermitian operator.

Solution : For an operator to satisfy the Hermitian condition we say that if an operator $\hat{A}$ has two eigenfunctions ψ and ϕ, and if

$$\int\psi(\hat{A}\phi)\, d\tau = \int(\hat{A}\psi).\phi\, d\tau \qquad (\psi \text{ and } \phi \text{ are real})$$

or $$\int\psi^*(\hat{A}\phi)\, d\tau = \int(\hat{A}\psi)^*.\phi\, d\tau \qquad (\psi \text{ and } \phi \text{ are complex})$$

then $\hat{A}$ is called the Hermitian operator.

Let $\psi = e^{ix}$, and $\phi = \sin x$ be the two acceptable eigenfunctions. Then,

$$\int\psi(\hat{A}\phi)\, d\tau = \int e^{-ix}\frac{d^2}{dx^2}(\sin x)\, dx = -\int e^{-ix}\sin x\, dx$$

$$\int\phi(\hat{A}\psi)^*\, d\tau = \int\sin x\left[\frac{d^2}{dx^2}(e^{ix})^*\right] dx = \int\sin x\left(i^2 e^{ix}\right)^* dx$$

$$= -\int\sin x\, e^{-ix}\, dx$$

Since the two integrals are the same, d^2/dx^2 is Hermitian.

Example 53. Show that the operator $\hat{p}_x$ for linear momentum is Hermitian.

Solution : It is required to prove that

$$\int_{-\infty}^{\infty} \psi^* \left(-i\hbar \frac{d}{dx}\right) \phi \, dx = \int_{-\infty}^{\infty} \phi \left(-i\hbar \frac{d}{dx}\right)^* \psi^* \, dx$$

Integrating by parts, the left-hand-side is equal to

$$-i\hbar \left[\psi^* \phi\right]_{-\infty}^{\infty} - (-i\hbar) \int_{-\infty}^{\infty} \phi \frac{d\psi^*}{dx} dx = 0 + \int_{-\infty}^{\infty} \phi \left(i\hbar \frac{d}{dx}\right) \psi^* \, dx = \int_{-\infty}^{\infty} \phi \left(-i\hbar \frac{d}{dx}\right)^* \psi^* \, dx = \text{R.H.S.}$$

Hence $\hat{p}_x$ is a Hermitian operator.

Example 54. Show that the Hamiltonian operator for the total energy of a system is Hermitian provided that the eigenfunction is well-behaved.

Solution : $\hat{H} = -\left(\hbar^2/2m\right)\left(d^2/dx^2\right) + \hat{V}(x)$ (in the x-direction)

Assuming the eigenfunctions to be real, it is required to prove that

$$\int_{-\infty}^{\infty} \psi \hat{H} \phi \, dx = \int_{-\infty}^{\infty} \phi \hat{H} \psi \, dx$$

For the potential energy part, we have

$$\int_{-\infty}^{\infty} \psi \hat{V}(x) \phi \, dx = \int_{-\infty}^{\infty} \phi \hat{V}(x) \psi \, dx \qquad (\because \; V(x) \text{ is just a multiplier})$$

For the kinetic energy part,

$$\int_{-\infty}^{\infty} \psi \frac{d^2}{dx^2} \phi \, dx = \left[\psi \frac{d\phi}{dx}\right]_{-\infty}^{\infty} - \int_{-\infty}^{\infty} \frac{d\phi}{dx} \cdot \frac{d\psi}{dx} dx \qquad \text{[integrating by parts]}$$

Also,

$$\int_{-\infty}^{\infty} \phi \frac{d^2}{dx^2} \psi \, dx = \left[\phi \frac{d\psi}{dx}\right]_{-\infty}^{\infty} - \int_{-\infty}^{\infty} \frac{d\psi}{dx} \cdot \frac{d\phi}{dx} dx$$

If the wave functions ψ and ϕ are well-behaved then ψ, $d\psi/dx$, ϕ, $d\phi/dx$ must vanish at infinity, making the first term in each integral zero; the second terms in both the integrals are identical since they differ only in the order of multiplication of $d\psi/dx$ and $d\phi/dx$. Thus, both the potential energy $V(x)$ and the kinetic energy part d^2/dx^2 are Hermitian, while $-(\hbar^2/2m)$ is just a constant factor. Hence proved.

Example 55. Show that if two operators $\hat{A}$ and $\hat{B}$ are Hermitian, then their product $(\hat{A}\hat{B})$ is also Hermitian if and only if $\hat{A}$ and $\hat{B}$ commute.

Solution : Since $\hat{A}\hat{B} = \hat{B}\hat{A}$ (Given),

$$\int \psi^* (\hat{A}\hat{B}) \phi \, d\tau = \int \psi^* (\hat{B}\hat{A}) \phi \, d\tau = \int \psi^* \hat{B} (\hat{A}\phi) \, d\tau$$

Since $\hat{B}$ is Hermitian, the integral is equal to

$$\int (\hat{A}\phi)(\hat{B}\psi)^* \, d\tau = \int (\hat{B}\psi)^* (\hat{A}\phi) \, d\tau = \int \phi \hat{A}^* (B\psi)^* \, d\tau$$

$$= \int \phi (\hat{A}\hat{B})^* \psi^* \, d\tau \qquad (\because \; \hat{A} \text{ is also Hermitian})$$

Hence, $\hat{A}\hat{B}$ is also Hermitian.

Example 56. Calculate the probability that a particle in a one-dimensional box of length a is found to be between 0 and $a/2$.

Solution : The probability that the particle will be found between 0 and $a/2$ is

$$P(0 \le x \le a/2) = \int_0^{a/2} \psi_n^*(x) \psi_n(x) \, dx = \frac{2}{a} \int_0^{a/2} \sin^2 \frac{n\pi x}{a} \, dx$$

Let $n\pi x/a = z$, so that

$$P(0 \le x \le a/2) = \frac{2}{n\pi} \int_0^{n\pi/2} \sin^2 z \, dz = \frac{2}{n\pi} \left| \frac{z}{2} - \frac{\sin 2z}{4} \right|_0^{n\pi/2}$$

$$= \frac{2}{n\pi} \left(\frac{n\pi}{4} - \frac{\sin n\pi}{4}\right) = \frac{1}{2} \quad \text{(for all } n\text{)}$$

Thus, the probability that the particle lies in one-half of the interval $0 \le x \le a/2$ is $\frac{1}{2}$.

Example 57. Assume that a particle of mass m is confined to a cubic box and its energy is 101 $\hbar^2/8ma^2$. What is the degeneracy of this level ?

Solution :

$$E_{n_x, n_y, n_z} = \left(h^2/8ma^2\right)\left(n_x^2 + n_y^2 + n_z^2\right) = \frac{h^2\left(n_x^2 + n_y^2 + n_z^2\right)}{8mV^{2/3}}$$

where V is the volume of the cube. The solution to this problem is to find the sets of quantum numbers that will generate the number 101. By trial and error these are :

10,1,0 ; 10,0,1; 1,10,0; 1,0,10; 0,1,10; 0,10,1; 9,4,2; 9,2,4; 2,9,4; 2,4,9; 4,2,9; 4,9 2; 8,6,1; 8,1,6; 1, 8, 6; 1,6,8; 6,8,1; 6,1,8; 7,6,4; 7,4,6; 6,4,7; 6,7,4; 4,7,6; and 4,6,7. There are thus 24 states in this energy level, so that its degeneracy is **24.**

Example 58. Determine the number of energy states less than $E = 3/2\,kT$ (the translational kinetic energy of an ideal gas molecule) at $T = 298$ K for an N_2 (g) molecule in a container with volume $V = 24{\cdot}8$ dm^3.

Solution : The number of states is given by $N = (\pi V/6h^3)\,(8mE)^{3/2}$. Substituting the data for $N_2(g)$, we have

$$N = \frac{(\pi)(24{\cdot}8\,\text{L})(10^{-3}\,\text{m}^3\,\text{dm}^{-3})}{(6)(6{\cdot}26\times10^{-34}\,\text{J s})^3} \left[(8)\frac{28{\cdot}0\times10^3\,\text{kg mol}^{-1}}{6{\cdot}022\times10^{23}\,\text{mol}^{-1}}\left(\frac{3}{2}\right)(1{\cdot}381\times10^{-23}\,\text{J K}^{-1})(1\,\text{kg m}^2\,\text{s}^{-2}/1\text{J})(298\,\text{K})\right]^{3/2} = 4{\cdot}91\times10^{30}$$

Comment. Notice that the number of energy states is fantastically large! That is why we say that the translational energy is *not* quantized.

Example 59. Show that for a conjugated organic molecule, using the free-electron molecular orbital (FEMO) theory envisaging the particle in a one-dimensional box model, the electronic transition 1→2 is allowed and the transition 1→3 is forbidden.

Solution : An selection rule for an electronic transition states that for allowed transitions the transition moment integral $\langle \psi_n | \mu | \psi_m \rangle \equiv \langle n | \mu | m \rangle \neq 0$, and is zero for forbidden transitions, Now the transition dipole moment $\mu = e\,x$ for motion along the x direction. Using the eigenfunctions $\psi_n(x) = (2/a)^{1/2} \sin(n\pi x/a)$, where a is the width of the box, for1→ 2 transition, $\langle 2|\mu|1\rangle = e \int \psi_2 x \psi_1 \, dx$

$$= \frac{2}{a} e \int \sin\left(\frac{2\pi x}{a}\right) x \sin\left(\frac{\pi x}{a}\right) dx \qquad (i)$$

Recalling that $\sin A \sin B = \frac{1}{2}\cos(A-B) - \frac{1}{2}\cos(A+B)$, we find that

$$\langle 2|\mu|1\rangle \propto \int x \left[\cos(\pi x/a) - \cos(3\pi x/a)\right] dx \qquad (ii)$$

and $$\langle 3|\mu|1\rangle \propto \int \sin\left(\frac{3\pi x}{a}\right) x \sin\left(\frac{\pi x}{a}\right) dx \propto \int x\left[\cos(2\pi x/a) - \cos(4\pi x/a)\right] dx \qquad (iii)$$

Both the integrals (*ii*) and (*iii*) can be evaluated using the standard form

$$\int x(\cos A\,x)\,dx = (1/A^2)\cos Ax + (x/A)\sin A\,x$$

$$\int_0^a x\cos(\pi x/a)\,dx = \frac{1}{(\pi/a)^2}\cos(\pi x/a)\Big|_0^a + \frac{x}{(\pi/a)}\sin(\pi x/a)\Big|_0^a = -2(a/\pi)^2 \neq 0$$

$$\int_0^x x\cos(3\pi x/a)\,dx = \frac{1}{(3\pi/a)^2}\cos(3\pi x/a)\Big|_0^a + \frac{x}{(3\pi/a)}\sin(3\pi x/a)\Big|_0^a = -2(a/3\pi)^2 \neq 0$$

Hence, $<2|\mu|1> \equiv \mu_{21} \neq 0$, so that $1 \rightarrow 2$ electronic transition is allowed. Similarly, $<3|\mu|1> \equiv \mu_{31} = 0$ so that $1 \rightarrow 3$ electronic transition is forbidden.

Example 60. An electron of mass m_e is constrained to move along a circular ring on which the potential energy is constant. Set up and solve the Schrödinger wave equation for this system.

Solution : The Schrödinger equation (assuming that potential energy V is zero) can be written as

$$\frac{d^2\psi}{dx^2} + k^2\psi = 0, \qquad k^2 = 2mE/\hbar^2 \tag{i}$$

The general solution of this equation is

$$\psi = A\cos kx + B\sin kx \tag{ii}$$

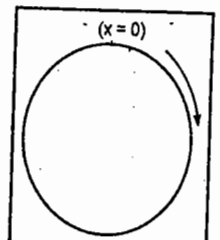

Fig. 30. Electron moving in a ring of constant potential energy.

(See Fig. 30 for the motion of the electron.) In this Figure, an arbitrary point on the ring is chosen as origin (*i.e*, $x = 0$) and the coordinate x varies around the circular ring the length of whose circumference is C. Since the wave functions must be single-valued, we have

$$\psi(x) = \psi(x + C) \tag{iii}$$

The boundary conditions are different from those of a one-dimensional box. From Eq. (*iii*), $\psi(0) = \psi(C)$, so that

$$A = A\cos kC + B\sin kC \tag{iv}$$

Recall that with the particle in a one-dimensional box there was discontinuity in $d\psi/dx$ at the walls of the box because at those points there was a discontinuity in the potential energy. This implied that while ψ was continuous, $d\psi/dx$ was not.

However, in the present case where there is no discontinuity in V, both ψ and $d\psi/dx$ must be continuous. Hence, we have here another condition,

$$\left(\frac{d\psi}{dx}\right)_{x=0} = \left(\frac{d\psi}{dx}\right)_{x=C} \tag{v}$$

This leads to the following equation :

$$Bk = Bk\cos kC - Ak\sin kC \tag{vi}$$

Multiplying Eq. (*iv*) with Ak and Eq. (*vi*) with B and adding, we obtain

$$\cos kC = 1, \text{ or } kC = 2n\pi\,,\ n = 0, \pm1, \pm2, \ldots \quad \text{(because } \cos(-\theta) = \cos\theta) \tag{vii}$$

Hence, the energy levels are given by

$$E_n = \frac{n^2h^2}{2mC^2} \tag{viii}$$

which follows from Eq. (*vii*) and the fact that $k^2 = 2mE/\hbar^2$.

A comparison of these results with those of the electron in a one-dimensional box shows that in the present case the quantum number n can have values of zero, positive or negative integers so that each energy level, except for $n = 0$, is doubly degenerate. The unnormalized wave functions may be written as

$$\psi_n(x) = A\cos(2n\pi x/C) + B\sin(2n\pi x/C) \tag{ix}$$

which follows from Eqs. (*ii*) and (*vii*). For a state with $n = 0$ for which $E = 0$, the wave function is given by

$$\psi_0 = A = \text{constant} \tag{x}$$

Thus, in the ground state the wave function does not vary around the ring. Therefore, the zero point energy is not encountered when the potential energy does not change around the circular ring. This, of course, does not violate the Heisenberg uncertainty principle because the electron can be found anywhere on the ring with equal probability and therefore the uncertainty in its position in infinite.

The relationship between constants A and B can be obtained from the normalization of the eigenfunctions :

$$\int_0^C [A\cos(2n\pi x/C) + B\sin(2n\pi x/C)]^2\,dx$$

$$= A^2\int_0^C \cos^2(2n\pi x/C)\,dx + B^2\int_0^C \sin^2(2n\pi x/C)\,dx + 2AB\int_0^C \cos(2n\pi x/C)\sin(2n\pi x/C)\,dx = 1$$

or $$(A^2 + B^2)C/2 = 1$$

or $$A^2 + B^2 = 2/C \tag{xi}$$

from which it follows that A and B can be written as

$$A = (2/C)^{1/2}\sin\alpha, \qquad B = (2/C)^{1/2}\cos\alpha \tag{xii}$$

where α can have any value. Hence the normalized wave functions are

$$\psi_n(x) = (2/C)^{1/2}\sin\alpha\cos(2n\pi x/C) + (2/C)^{1/2}\cos\alpha\sin(2n\pi x/C)$$

$$= (2/C)^{1/2}\sin((2n\pi x/C) + \alpha) \tag{xiii}$$

Example 61. Confirm that a Gaussian function of the form $\exp(-\beta x^2)$ is an asymptotic solution of the Schrödinger wave equation for the ground state of a one-dimensional S.H.O., and find the expression for β in terms of mass and force constant of the oscillator.

Solution : $-\frac{\hbar^2}{2m}\frac{d^2\psi}{dx^2} + \frac{1}{2}kx^2 = E\psi$ . . [Schrödinger equation for S.H.O.]

In an asymptotic solution the wave function $\psi(x) \rightarrow 0$ as $x \rightarrow \infty$.

$$\psi = e^{-\beta x^2}\,, \text{ so } d\psi/dx = -2\beta x e^{-\beta x^2}$$

$$d^2\psi/dx^2 = -2\beta e^{-\beta x^2} + 4\beta^2x^2e^{-\beta x^2} = -2\beta\psi + 4\beta^2x^2\psi$$

Substituting in the Schrödinger equation, we obtain

$$\left(\frac{\hbar^2\beta}{m}\right)\psi - \left(\frac{2\hbar^2\beta^2}{m}\right)x^2\psi + \frac{1}{2}kx^2\psi = E\psi \quad \text{(where } k \text{ is the force constant)}$$

or, $$\left[\left(\frac{\hbar^2\beta}{m}\right) - E\right]\psi + \left(\frac{1}{2}k - \frac{2\hbar^2\beta^2}{m}\right)x^2\psi = 0$$

The equation is satisfied (since $\psi \neq 0$ for this will imply a trivial solution) if

$$E = \frac{\hbar^2\beta}{m} \text{ and } 2\hbar^2\beta^2 = \frac{1}{2}mk \text{ or } \beta = \frac{1}{2}\left(\frac{mk}{\hbar^2}\right)^{1/2}$$

Therefore, $$E = \frac{1}{2}\hbar\left(\frac{k}{m}\right)^{1/2} = \frac{1}{2}\hbar\omega \quad \text{where } \omega = (k/m)^{1/2} \text{ is the angular fraquency of the oscillator.}$$

Example 62. State and verify Bohr's Correspondence Principle.

Solution : The Bohr correspondence principle states that quantum mechanics reduces to classical mechanics in the limit of large quantum numbers. This can be illustrated by an example Bohr chose from the line spectrum of a hydrogenic atom. Classically, during the periodic motion of an electron in a stationary atom, the frequency of light emitted by the atom is equal to its frequency of revolution, ν_r. Now, from the Bohr theory of hydrogen atom,

$$\nu_r = \frac{v_n}{2\pi r_n} = \frac{me^4}{2\pi n^3 h^3} \quad \text{(in c.g.s. units)}$$

(where v_n is the velocity of the electron in the nth orbit of radius r_n.) For the transition $(n+1) \to n$, the frequency of the emitted radiation is given by

$$\nu = \frac{2\pi^2 me^4}{h^3}\left[\frac{1}{n^2} - \frac{1}{(n+1)^2}\right] = \frac{2\pi^2 me^4}{h^3}\left[\frac{2n+1}{n^2(n+1)^2}\right] \quad \text{(in c.g.s. units)}$$

We see that $\nu \to \nu_r$ when $n \to \infty$, as required by the correspondence principle.

Example 63. Show that the average distance of the electron from the nucleus in hydrogen atom is $6a_0$ in the 2s-state and $5a_0$ in the $2p_z$ state, where a_0 is the Bohr radius.

Solution :

$$\psi_{2s} = \frac{1}{4\sqrt{2\pi}}\left(\frac{Z}{a_0}\right)^{3/2}\left(2 - \frac{Zr}{a_0}\right)\exp(-Zr/a_0) \qquad (Z=1)$$

$$\langle r_{2s}\rangle = \int \psi_{2s}^* r\, \psi_{2s}\, d\tau = \frac{1}{32\pi a_0^3}\int_0^\infty \left(2 - \frac{r}{a_0}\right)^2 \exp(-r/a_0)\, r.r^2\, dr \int_0^\pi \sin\theta \int_0^{2\pi} d\phi$$

$$= \frac{1}{8a_0^3}\int_0^\infty \left(4r^3 - \frac{4r^4}{a_0} + \frac{r^5}{a_0^2}\right)^2 \exp(-r/a_0)\, dr \qquad [d\tau = r^2 dr \sin\theta\, d\theta\, d\phi]$$

$$= \frac{1}{8a_0^3}\left[\frac{4\times 3!}{\left(\frac{1}{a_0}\right)^4} - \frac{4\times 4!}{a_0\left(\frac{1}{a_0}\right)^5} + \frac{5!}{a_0^2\left(\frac{1}{a_0}\right)^6}\right] = 6a_0 \qquad \text{(using standard integrals)}$$

Again,

$$\psi_{2p_z} = \frac{1}{\sqrt{32\pi}}\left(\frac{Z}{a_0}\right)^{5/2}(r)\exp(-Zr/2a_0)\cos\theta \qquad (Z=1)$$

$$\langle r_{2p_z}\rangle = \int \psi^*_{2p_z}\, r\, \psi_{2p_z}\, d\tau = \frac{1}{32\pi a_0^5}\int_0^\infty (r\exp(-r/2a_0))^2\, r.r^2 dr \int_0^\pi \sin\theta\, \cos\theta\, d\theta \int_0^{2\pi} d\phi$$

$$= \frac{1}{32\pi a_0^5}\int_0^\infty r^5 \exp(-r/a_0)\, dr \int_0^\pi \frac{\sin 2\theta}{2} d\theta \int_0^{2\pi} d\phi$$

$$= \frac{1}{24 a_0^5}\frac{5!}{\left(\frac{1}{a_0}\right)^6} = 5a_0$$

Example 64. Show by explicit integration that hydrogenic $2p_x$ and $2p_y$ orbitals are mutually orthogonal.

Given

$$\psi_{2p_x} = \frac{1}{4\sqrt{2\pi}}\left(\frac{Z}{a_o}\right)^{3/2} \rho\, e^{-\rho/2} \sin\theta\cos\phi$$

$$\psi_{2p_y} = \frac{1}{4\sqrt{2\pi}}\left(\frac{Z}{a_0}\right)^{3/2} \rho e^{-\rho/2} \sin\theta\sin\phi; \quad \rho = Zr/a_0$$

Solution : $\psi_{2p_x} = f(r)\sin\theta\cos\phi$; $\psi_{2p_y} = f(r)\sin\theta\sin\phi$

$$\therefore \int_{\text{all space}} \psi_{2p_x}\psi_{2p_z}\, d\tau = \int_{\text{all space}} \psi_{2p_x}\psi_{2p_y} r^2 dr \sin\theta\, d\theta\, d\phi$$

$$= \int_0^\infty f(r)^2 r^2\, dr \int_0^\pi \sin^2\theta\, d\theta \int_0^{2\pi} \cos\phi\, \sin\phi\, d\phi$$

The first factor is non-zero since the radial functions are normalized. The second factor is $\pi/2$. The third factor is zero. Hence, the product of the three integrals is zero and the given wavefunctions are **orthogonal.**

Note : We can also solve the problem by recalling that $p_x \propto x/r$, and $p_y \propto y/r$. Thus,

$$\int_{\text{all space}} p_x p_y\, dx\, dy\, dz = \int_{-\infty}^{\infty}\int_{-\infty}^{\infty}\int_{-\infty}^{\infty} (xy/r^2)\, dx\, dy\, dz$$

This is an integral of an odd function of x and y over the entire range of variables from $-\infty$ to $+\infty$. Therefore, the integral is zero.

Example 65. Show that the three $2p$-eigenfunctions of hydrogen atom are orthogonal to each other.

Solution : The three $2p$-eigenfunctions of hydrogen atom are

$$\psi_{200} = \frac{1}{\pi^{1/2}}\left(\frac{Z}{2a_0}\right)^{3/2}(1 - Zr/2a_0)\exp(-Zr/2a_0)$$

$$\psi_{210} = \frac{1}{\pi^{1/2}}\left(\frac{Z}{2a_0}\right)^{5/2} r\exp(-Zr/2a_0)\cos\theta = c_1 r\exp(-r/2a_0)\cos\theta$$

$$\psi_{21\pm1} = \frac{1}{8\pi^{1/2}}\left(\frac{Z}{a_0}\right)^{5/2} r\exp(-Zr/2a_0)\sin\theta\exp(\pm i\phi) = c_2 r\exp(-r/2a_0)\sin\theta\exp(\pm i\phi)$$

where c_1 and c_2 are constants and $Z=1$. The ϕ-dependent part of $\psi^*_{21,1}\psi_{21,-1}$ gives $\exp(-2i\phi)$. The corresponding ϕ-integral becomes

$$\int_0^{2\pi} e^{-2i\phi}\, d\phi = \frac{1}{-2i}\left[e^{-2i\phi}\right]_0^{2\pi} = 0$$

The ϕ-integral of $\int \psi^*_{210}\int \psi_{211}\, d\tau = \int_0^{2\pi} e^{i\phi}\, d\phi = 0$

The ϕ-integral of $\int \psi^*_{210}\, \psi_{21,-1}\, d\tau = \int_0^{2\pi} e^{-i\phi}\, d\phi = 0$

Thus, the three $2p$-eigenfunctions of hydrogen atom are orthogonal to each other. Note that we did not carry out the r-integration and θ-integration, because the ϕ-integration vanishes, so the product of the three integrations vanishes.

Example 66. Prove that $1s$, $2p$ and $3d$ orbitals of a hydrogen-like atom show a single maximum in the radial probability curves. Obtain the values at which these maxima occur.

Solution : The radial probability density $P_{nl} = r^2|R_{nl}|^2$ where

$$R_{10} = (\text{constant})\exp(Zr/a_0)$$

$$R_{21} = (\text{constant})\, r\exp(-Zr/2a_0); \quad R_{32} = (\text{constant})\, r\exp(-Zr/3a_0)$$

P_{nl} will be a maximum when $dP_{nl}/dr = 0$. Therefore,

$$\frac{dP_{10}}{dr} = 0 = (\text{constant})\left(2r - 2Zr^2/a_0\right)\exp(-2Zr/a_0) \text{ or } r = a_0/Z$$

$$\frac{dP_{21}}{dr} = 0 = \text{(constant)}\ (4r^3 - Zr^4/a_0)\exp(-Zr/a_0) \quad \text{or} \quad r = 4a_0/Z$$

Similarly $\frac{dP_{32}}{dr} = 0$ gives $r = 9\ a_0/Z$

In general, $r_{max} = n^2\ a_0/Z$

Comment. The result $r_{max} = a_0/Z$ suggests that the 1*s*- orbital of atoms shrinks in proportion to the increase in *Z*.

Example 67. State the virial theorem and apply it to (*a*) an S.H.O; and (*b*) hydrogen atom.

Solution : Virial theorem states that if the potential energy $V(x)$ of a quantum system moving in the *x*-direction is of the form, $V(x) \propto x^s$, where *s* is constant, then the expectation (mean) value of kinetic energy, $\langle \hat{T} \rangle$, and the expectation value of the potential energy, $\langle \hat{V} \rangle$, are related by

$$\langle \hat{T} \rangle = \frac{1}{2} s \langle \hat{V} \rangle$$

(*a*) S.H.O : $V(x) = \frac{1}{2}kx^2$, where *k* is force constant, so here $s = 2$. Hence, $\langle \hat{T} \rangle = \frac{1}{2}(2)\langle \hat{V} \rangle$, *i.e.*, $\langle \hat{T} \rangle = \langle \hat{V} \rangle$.

(*b*) Hydrogen atom : $V(r) = \frac{-Ze^2}{4\pi\varepsilon_0 r}$; here $x \to r$; $s = -1$

$$\therefore \quad \langle \hat{T} \rangle = \frac{1}{2}(-1)\langle \hat{V} \rangle = -\frac{1}{2}\langle \hat{V} \rangle$$

Example 68. Confirm that function $\psi = \cos ax \cos by \cos cz$ is an eigenfunction of the Laplacian operator ∇^2 and determine its eigenvalue.

Solution : In cartesian coordinates (x,y,z) the Laplacian operator is

$$\nabla^2 = \frac{\partial^2}{\partial x^2} + \frac{\partial^2}{\partial y^2} + \frac{\partial^2}{\partial z^2}$$

Now, $\frac{\partial^2 \psi}{\partial x^2} = \frac{\partial^2 (\cos ax \cos by \cos cz)}{\partial x^2} = -a^2 \cos ax \cos by \cos cz = -a^2\psi$

Similarly, $\frac{\partial^2 \psi}{\partial y^2} = -b^2\psi$; $\frac{\partial^2 \psi}{\partial z^2} = -c^2\psi$

Thus, $\nabla^2\psi = -(a^2 + b^2 + c^2)\ \psi$

We see that ψ is an eigenfunction of ∇^2 with the eigenvalue $-(a^2+b^2+c^2)$.

Example 69. If the interelectron repulsion in helium atom is ignored, what would be its ground state energy and the wavefunction ?

Solution : He atom has two electrons. For a hydrogen-like atom we know that

$$E_1 = -13.6\,Z^2\ \text{eV}, \text{ and } \psi_{100} = \left(Z^3/\pi a_0^3\right)^{1/2} \exp(-Zr/a_0)$$

When the interelectronic repulsion energy is ignored, the energy of the system is the sum of the energies of two electrons and the wave function is the product of the two 1*s*-wave functions. Thus,

$$E = -13.6\,Z^2 - 13.6\,Z^2 = -108.8\ \text{eV} \qquad [Z = 2 \text{ for helium atom}]$$

$$\psi = \psi_1(r_1)\,\psi_2(r_2) = \frac{1}{\pi}\left(\frac{Z}{a_0}\right)^3 \exp\left[-Z(r_1 + r_2)/a_0\right]$$

where r_1 and r_2 are the radius vectors of electrons 1 and 2, respectively.

Example 70. What is the most probable distance of the electron of hydrogen atom in its 2*p*-state ? What is the radial probability at that distance ?

Solution : Radial probability density $P_{nl}(r) = r^2\ |R_{nl}|^2$, where

$$R_{21} = \left(\frac{1}{2a_0}\right)^{3/2} \frac{1}{a_0\sqrt{3}}\, r \exp\left(-r/2a_0\right)$$

$$\therefore \quad P_{21}(r) = r^2 R_{21}^2 = \frac{1}{24\,a_0^5}\, r^4 \exp(-r/a_0)$$

For $P_{21}(r)$ to be maximum

$$\frac{d\,P_{21}(r)}{dr} = \frac{1}{24\,a_0^5}\left(4r^3 - \frac{r^4}{a_0}\right)\exp\left(-r/a_0\right) = 0$$

or $r_{mp} = 4a_0$. Thus, the most probable distance is four times the Bohr radius ; and $P_{21}(4a_0) = (32/3a_0)\ \exp(-4)$.

Example 71. Calculate the "size" of a hydrogen atom in its ground state by assuming that the size of an atom is measured by the radius of a sphere that contains 90 percent of the charge density of the electrons in the outermost occupied orbital.

Solution : The hydrogen atom has only one electron which occupies the 1*s*-orbital in the ground state,

$\psi_{1s} = \frac{1}{\pi a_0^{3/2}}\ \exp(-r/a_0)$. Hence, the probability of the electron being within a sphere of radius r' is

$$P = \int_0^{r'}\int_0^{\pi}\int_0^{2\pi} \psi_{1s}^2\, r^2\, dr \sin\theta\, d\theta\, d\phi\,.$$

The integral over θ and ϕ gives a factor of 4π, so that

$$0{\cdot}90 = \frac{4}{a_0^3}\int_0^{r'} r^2\, e^{-2r/a_0}\, dr$$

The integral in the above expression is evaluated by integration by parts, giving

$$-\frac{a_0\, r^2\, e^{-2r/a_0}}{2}\Bigg|_0^{r'} + a_0\left[-\frac{a_0\, r\, e^{-2r/a_0}}{2}\Bigg|_0^{r'} + \frac{a_0}{2}\left(-\frac{a_0\, e^{-2r/a_0}}{2}\right)\Bigg|_0^{r'}\right]$$

$$= -\frac{a_0\,(r')^2\, e^{-2r'/a_0}}{2} - \frac{a_0^2\, r'}{2}\, e^{-2r'/a_0} - \frac{a_0^3}{4}\, e^{-2r'/a_0} + \frac{a_0^3}{4}$$

Multiplying by $\left(4/a_0^3\right)$ and factoring $\exp(-2r'/a_0)$, we get

$$0{\cdot}90 = \left[-2\left(\frac{r'}{a_0}\right)^2 - 2\left(\frac{r'}{a_0}\right) - 1\right] e^{-2r'/a_0} + 1$$

or $$2\left(\frac{r'}{a_0}\right)^2 + 2\left(\frac{r'}{a_0}\right) + 1 = 0{\cdot}10\ e^{-2r'/a_0}$$

This equation can be solved numerically to give $r' = 2.66\ a_0$, which is thus the "size" of the hydrogen atom in the ground state.

Example 72. The energy of atoms and molecules, as obtained by solving the Schrödinger equation, is generally expressed in units of 'hartrees' after Hartree who has done fundamental work in quantum mechanics. Verify that 1 hartree=27·2 eV.

Solution : 1 hartree $= e^2/a_0$ where a_0, the Bohr radius, is given by $a_0=\hbar^2/me^2$

$\therefore$ 1 hartree $= me^4/\hbar^2$ (in c.g.s. units)

$$= \frac{me^4}{(4\pi\varepsilon_0)^2\hbar^2} \quad \text{(in SI units)}$$

Let us solve this problem in both the units.

(i) In c.g.s. units :

$$1 \text{ hartree} = \frac{(9{\cdot}107\times10^{-23}\text{g})(4{\cdot}8\times10^{-10}\text{e.s.u.})^4}{(1{\cdot}0545\times10^{-27}\text{ergs})^2(1{\cdot}602\times10^{-12}\text{erg / eV})} = 27{\cdot}2 \text{ eV}$$

(ii) In SI units :

$$1 \text{ hartree} = \frac{(9{\cdot}107\times10^{-31}\text{kg})(1{\cdot}602\times10^{-19}\text{C})^4}{(1{\cdot}11264\times10^{-10}\text{C}^2\text{N}^{-1}\text{m}^{-2})^2(1{\cdot}0545\times10^{-34}\text{Js})^2(1{\cdot}602\times10^{-19}\text{J/eV})} = 27{\cdot}2 \text{ eV}$$

Note : 1 hartree of energy is also called the atomic unit (a.u.) of energy.

1 hartree = 27·2 eV = 2Ry where Ry = Rydberg.

Example 73. Write the Hamiltonian for the following quantum systems: *(a)* Helium atom *(b)* Lithium atom *(c)* H_2^+ *(d)* H_2 *(e)* H_2^-. Which of the terms is hardest to handle in solving the Schrödinger equation in each case ?

Solution : ***(a)* He atom :** It contains one nucleus and two electrons numbered 1 and 2 (Fig. 31). Here r_1 is the distance of electron 1 from the nucleus, r_2 is the distance of electron 2 from the nucleus and r_{12} is the interelectron distance. The charge on the electron is e while that on the nucleus is Ze (Here Z=2).

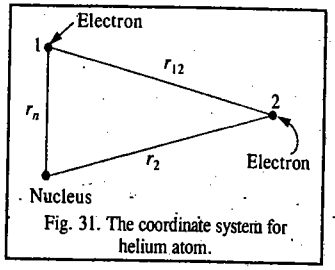

Fig. 31. The coordinate system for helium atom.

The Hamiltonian for the system is given by

$$\hat{H} = -\frac{\hbar^2}{2m}\nabla_1^2 - \frac{\hbar^2}{2m}\nabla_2^2 - \frac{2e^2}{4\pi\varepsilon_0 r_1} - \frac{2e^2}{4\pi\varepsilon_0 r_2} + \frac{e^2}{4\pi\varepsilon_0 r_{12}} \quad \ldots(i)$$

$$= -\frac{\hbar^2}{2m}(\nabla_1^2+\nabla_2^2) + \frac{2e^2}{4\pi\varepsilon_0}\left(\frac{-1}{r_1}-\frac{1}{r_2}\right) + \frac{e^2}{4\pi\varepsilon_0 r_{12}} \quad \ldots(ii)$$

In Eq. *(i)*, the first two terms are the kinetic energy (Laplacian) operators for electrons 1 and 2, respectively ; the third and fourth terms give the attraction of two electrons to the nucleus and the last term gives the repulsion between the two electrons ; it is called the inter-electron repulsion energy term.

***(b)* Lithium atom.** It contains one nucleus and three electrons 1, 2 and 3 (here Z = 3). Hence,

$$\hat{H} = -\frac{\hbar^2}{2m}(\nabla_1^2+\nabla_2^2+\nabla_3^2) + \frac{1}{4\pi\varepsilon_0}\left[-\frac{3e^2}{r_1}-\frac{3e^2}{r_2}-\frac{3e^2}{r_3}+\frac{e^2}{r_{12}}+\frac{e^2}{r_{23}}+\frac{e^2}{r_{31}}\right]$$

The interpretation of these terms is similar to that given in *(a)* above. The last three terms are interelectron repulsion energy terms.

(c) H_2^+. It contains two nuclei A and B and one electron Z = 1(Fig. 32).

The Hamiltonian is given by

$$\hat{H} = -\frac{\hbar^2}{2m}\nabla^2 + \frac{1}{4\pi\varepsilon_0}\left[-\frac{e^2}{r_A}-\frac{e^2}{r_B}+\frac{e^2}{R_{AB}}\right]$$

There is no interelectron repulsion term here because the system contains only one electron. The last term is internuclear repulsion energy term.

(d) H_2 : It contains two nuclei A and B and two electrons 1 and 2. Z=1 (Fig. 33). The Hamiltonian of the system is given by

$$\hat{H} = -\frac{\hbar^2}{2m}(\nabla_1^2+\nabla_2^2) + \frac{1}{4\pi\varepsilon_0}\left[-\frac{e^2}{r_{A_1}}-\frac{e^2}{r_{A_2}}-\frac{e^2}{r_{B_1}}-\frac{e^2}{r_{B_2}}+\frac{e^2}{r_{12}}+\frac{e^2}{R_{AB}}\right]$$

Here the term e^2/r_{12} is the interelectron repulsion term and the last term is the internuclear repulsion.

(e) H_2^-. It contains three electrons 1, 2, 3 and two nuclei A and B. Hence,

$$\hat{H} = -\frac{\hbar^2}{2m}(\nabla_1^2+\nabla_2^2+\nabla_3^2) + \frac{1}{4\pi\varepsilon_0}\left[-\frac{e^2}{r_{A_1}}-\frac{e^2}{r_{A_2}}-\frac{e^2}{r_{A_3}}-\frac{e^2}{r_{B_1}}-\frac{e^2}{r_{B_2}}-\frac{e^2}{r_{B_3}}+\frac{e^2}{r_{12}}+\frac{e^2}{r_{13}}+\frac{e^2}{r_{23}}+\frac{e^2}{R_{AB}}\right]$$

Here the interelectron repulsion terms are (e^2/r_{12}), (e^2/r_{13}) and (e^2/r_{23}) while the last term is internuclear repulsion term.

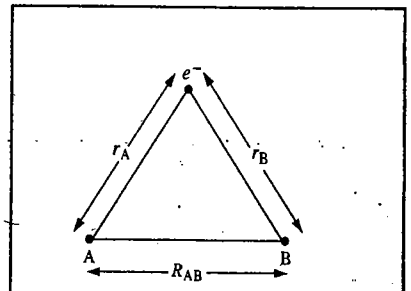

Fig. 32. The coordinate system for H_2^+.

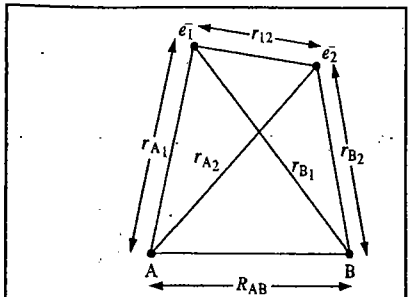

Fig. 33. The coordinate system for H_2.

In all the above cases, the interelectron repulsion term is the most difficult to handle in solving the Schrödinger equation. For molecules, the internuclear term is considered a constant since the nuclei are infinitely heavier than the electrons.

Example 74. Define the term degeneracy of an energy level. Calculate the degeneracies of the following systems : *(i)* third energy level of a particle in a one-dimensional box of infinite height *(ii)* the rigid diatomic rotor in the third rotational energy level *(iii)* the hydrogen atom in the third energy state and *(iv)* the hydrogen atom in the third excited state.

Solution : When two or more wave functions (eigenfunctions) belong to the same energy state, *i.e.*, have the same energy, the energy level is said to be degenerate, *i.e.*, it is said to possess degeneracy, g. Degeneracy is a dimensionless quantity. An energy level with g = 2 is called two-fold degenerate and an energy level with g = 3 is called three-fold degenerate, and so on.

(i) In this case, g = 1, *i.e.*, the energy level is **non-degenerate.** One-dimensional systems are always non-degenerate in all the energy levels.

(ii) For a diatomic molecule rotating as a rigid rotor, the degeneracy is given by

$$g_J = 2J+1 \; ; \; J=0, 1, 2, 3,....$$

where J is the rotational quantum number.

Here J=2 ; hence, $g_2 = 2\times2+1=5$, *i.e*, the energy level is *five-fold degenerate.*

(iii) For hydrogen atom, since the energy is given by

$$E_n = -R_H/n^2 \text{ where } n = 1, 2, 3, 4,....,$$

the degeneracy is given by $g_n = n^2$.

Here n=3, so that $g_3=(3)^2=9$, *i.e.*, the energy level is **nine-fold degenerate.**

(iv) Here n=4, so that $g_4=(4)^2=16$, *i.e.*, the energy level is **16-fold degenerate.**

Example 75. Calculate the degeneracies of a particle of mass m in a three-dimensional cubical box of width a having energies equal to *(i)* 6 *(ii)* 9 *(iii)* 12 and *(iv)* 14 in units of $(h^2/8ma^2)$.

Solution : $E_{n_x, n_y, n_z} = (n_x^2 + n_y^2 + n_z^2)(h^2/8ma^2)$, where $n_x, n_y, n_z = 1, 2, 3, \ldots$

Here we shall tabulate the various combinations of n_x, n_y and n_z which give rise to the energies given above.

(i) $n_x^2 + n_y^2 + n_z^2 = 6$:

Three different combinations of n_x, n_y and n_z, *viz.*, (2, 1, 1), (1, 2, 1) and (1, 1, 2) give energy $= 6(h^2/8ma^2)$.

Hence, $g=3$, *i.e.*, the energy level is **three-fold degenerate.**

n_x	n_y	n_z
2	1	1
1	2	1
1	1	2

(ii) $n_x^2 + n_y^2 + n_z^2 = 9$:

The combinations are (2, 2,1), (2, 1, 2) and (1, 2, 2).

Hence, $g=3$.

n_x	n_y	n_z
2	2	1
2	1	2
1	2	2

(iii) $n_x^2 + n_y^2 + n_z^2 = 12$

$g=1$ because only one combination (2, 2, 2) gives energy$=12(h^2/8ma^2)$. The energy level is **non-degenerate.**

(iv) $n_x^2 + n_y^2 + n_z^2 = 14$:

Here, six combinations, as shown, give energy$=14(h^2/8ma^2)$.

Hence, $g=6$. The energy level is thus **six-fold degenerate**

n_x	n_y	n_z
1	2	3
1	3	2
2	1	3
3	1	2
2	3	1
3	2	1

Hermitian Operators. Hermitian operators, named after the 19th century mathematician Charles Hermite, play a very important role in quantum mechanics. An operator $\hat{A}$ is said to be *Hermitian* if

$$\int \psi_1^* (\hat{A}\psi_2) d\tau = \int (\hat{A}\psi_1)^* \psi_2 d\tau \qquad \ldots(279)$$

where ψ_1 and ψ_2 are the eigenfunctions of the operator $\hat{A}$. The asterisk shown as superscript represents the complex conjugate of the quantity. We shall prove a significant result that a *Hermitian operator has real eigenvalues*. Since $\hat{A}$ is an operator it obeys the eigenvalue equation

$$\hat{A}\psi = \lambda\psi \qquad \ldots(280)$$

where ψ is the eigenfunction of $\hat{A}$ and λ is its eigenvalue. Multiplying both sides of Eq. 280 by the complex conjugate of ψ, *viz.*, ψ^* and integrating over all space, we have

$$\int \psi^* \hat{A}\psi \, d\tau = \lambda \int \psi^* \psi \, d\tau \qquad \ldots(281)$$

Taking the complex conjugate of every quantity in Eq. 280, we obtain

$$\hat{A}^* \psi^* = \lambda^* \psi^* \qquad \ldots(282)$$

Multiplying both sides with ψ and integrating over all space, we obtain

$$\int \psi A^* \psi^* \, d\tau = \lambda^* \int \psi^* \psi \, d\tau \qquad \ldots(283)$$

According to the definition of the Hermitian operator, the left hand sides of Eqs. 281 and 283 are

equal, so that

$$\lambda \int \psi^* \psi d\tau = \lambda^* \int \psi^* \psi d\tau \qquad \ldots(284)$$

i.e., $\lambda = \lambda^*$. This means that the eigenvalue λ is equal to its complex conjugate which is true only if λ is *real*. Since most of the observables (observable quantities) are represented by Hermitian operators in quantum mechanics, they have real eigenvalues.

Important Theorems of Quantum Mechanics

1. Theorem 1. Two eigenfunctions of a Hermitian operator with different eigenvalues are orthogonal.

2. Theorem 2. If two operators commute, they have the same set of eigenfunctions.

3. Theorem 3. A wavefunction which is not an eigenfunction of an operator, $\hat{A}$, can be arbitrarily expanded in a series of orthonormal functions *i.e.*, it can be written as a **linear superposition** of the orthonormal eigenfunctions of $\hat{A}$.

Proof of Theorem 1. Let $\hat{A}$ be the Hermitian operator. Then its eigenvalue equations are

$$\hat{A}\psi_1 = \lambda_1\psi_1 \qquad \ldots(285)$$

$$\hat{A}\psi_2 = \lambda_2\psi_2 \qquad \ldots(286)$$

where ψ_1 and ψ_2 are the eigenfunctions of $\hat{A}$ with λ_1 and λ_2 the corresponding eigenvalues, respectively. Taking the complex conjugate of Eq. 285 and recalling that λ_1 is real,

$$\hat{A}^*\psi_1^* = \lambda_1\psi_1^* \qquad \ldots(287)$$

Multiplying Eq. 287 on the left by ψ_2 and integrating,

$$\int \psi_2 \hat{A}\psi_1^* d\tau = \lambda_1 \int \psi_2 \psi_1^* d\tau \qquad \ldots(288)$$

Again, multiplying Eq. 286 on the left by ψ_1^* and integrating,

$$\int \psi_1^* \hat{A}\psi_2 d\tau = \lambda_2 \int \psi_1^* \psi_2 d\tau \qquad \ldots(289)$$

Since $\hat{A}$ is a Hermitian operator, the left hand sides of Eqs. 288 and 289 are equal so that

$$\lambda_1 \int \psi_2 \psi_1^* d\tau = \lambda_2 \int \psi_1^* \psi_2 d\tau \quad \text{or} \quad (\lambda_1 - \lambda_2) \int \psi_1^* \psi_2 d\tau = 0 \qquad \ldots(290)$$

Since $\lambda_1 \neq \lambda_2$, $\int \psi_1^* \psi_2 d\tau = 0$. Thus, ψ_1 and ψ_2 are orthogonal.

Proof of Theorem 2. Let $\hat{A}$ be the operator whose eigenvalue equation is

$$\hat{A}\psi_i = a_i\psi_i \qquad \ldots(291)$$

where ψ_is are the set of eigenfunctions with a_is as the corresponding eigenvalues.

Since $\hat{A}$ and $\hat{B}$ commute, hence

$$\hat{A}\hat{B} = \hat{B}\hat{A} \qquad \ldots(292)$$

Operating on ψ_i, $\hat{A}\hat{B}\psi_i = \hat{B}\hat{A}\psi_i = \hat{B}(a_i\psi_i) = a_i(\hat{B}\psi_i)$ $\ldots(293)$

This shows that $(\hat{B}\psi_i)$ is an eigenfunction of $\hat{A}$ with eigenvalue a_i. This is possible only if $(\hat{B}\psi_i)$ is a multiple of ψ_i, *i.e.*,

$$\hat{B}\psi_i = b_i\psi_i \qquad \ldots(294)$$

In other words, ψ_i is also an eigenfunction of $\hat{B}$.

Proof of Theorem 3. The proof of this theorem has not been rigorously established but it seems to be valid for Hermitian operators. This theorem states that

$$\psi = \sum_i c_i \phi_i \qquad \ldots(295)$$

where ψ is an arbitrary function and ϕ_i are orthonormal functions, *i.e.*, they are both orthogonal and normalized :

$$\left.\begin{aligned} \int \phi_i^* \phi_j \, d\tau &= 0 \quad \text{(orthogonality condition)} \\ \int \phi_i^* \phi_i \, d\tau &= 1 \quad \text{(normalization condition)} \end{aligned}\right\} \qquad \ldots(296)$$

The two conditions, or criteria, can be summed up by the relation

$$\int \phi_i^* \phi_j \, d\tau = \delta_{ij} = \begin{cases} 1, & i = j \\ 0, & i \neq j \end{cases} \qquad \ldots(297)$$

where δ_{ij} is called the **Kronecker delta** in honour of the 19th century German mathematician Leopold Kronecker (1823–1891).

4. Virial Theorem. According to the virial theorem, if the potential energy $V(x)$ of a quantum mechanical system moving in the x-direction is of the form

$$V(x) \propto x^s, \qquad \ldots(298)$$

where s is a constant, then the expectation (average) value of the kinetic energy, $\langle \hat{T} \rangle$ and the expectation value of the potential energy, $\langle \hat{V} \rangle$ are related by

$$\langle \hat{T} \rangle = \tfrac{1}{2} s \langle \hat{V} \rangle \qquad \ldots(299)$$

Virial theorem is a very important theorem in quantum mechanics and is the real test of the accuracy of the wavefunction of the quantum mechanical system (atom or molecule), obtained by the solution of the Schrödinger wave equation by the Hartree–Fock self-consistent field (SCF) method.

5. Variation Theorem. If ψ is the approximate wave function of a quantum mechanical system described by the Hamiltonian, $\hat{H}$, then the expectation value of the energy, $\langle E \rangle$ given by the integral

$$\langle E \rangle = \int \psi^* \hat{H} \psi \, d\tau \equiv \langle \psi^* | \hat{H} | \psi \rangle \qquad \ldots(300)$$

is an *upper limit* to the ground state energy, E_0, of the system, *i.e.*,

$$E \geq E_0 \qquad \ldots(301)$$

6. Koopmanns' Theorem. The ionization potential (energy) of a molecule is equal to the negative of the energy of the HOMO (highest occupied molecular orbital). This theorem was discovered by T. Koopmanns, the cowinner of the 1975 Nobel Memorial Prize in Economics.

7. Unsöld Theorem. The electron density in a completely filled atomic orbital is spherically symmetric.

8. Hellmann–Feynman Theorem. Discovered independently by H. Hellmann and R.P. Feynman, it states that the force acting on each nucleus of a molecule is exactly that calculated by classical electrostatics from the charges and positions of the other nuclei and the electrons. Since at the equilibrium configuration of a molecule the resultant force acting on each nucleus vanishes, for this

configuration the repulsion of a given nucleus by other nuclei is just balanced by its attraction by the electrons. This important theorem gives deeper insight into molecular electronic structure and has inspired considerable theoretical research activity.

9. Kramers Theorem. It states that in the absence of the external magnetic field, the electronic states of any molecule or ion having an odd number of electrons are at least doubly degenerate. If follows that all complicated interactions (spin–spin interaction, spin–orbit interaction and ligand–field splitting) in transition metal ions cannot remove the degeneracy of a state with total electron spin $S = \frac{1}{2}, \frac{3}{2}, \frac{5}{2}$, etc. (Note that $(2S+1)$ is the **multiplicity** of a state so that the states with $S = \frac{1}{2}, \frac{3}{2}, \frac{5}{2}$, etc. are doublet, quartet and sextet states, respectively.) The spin degeneracy of systems containing odd number of electrons is called **Kramers' degeneracy**. The spin-levels are split even in the absence of the magnetic field, the splitting being referred to as **zero-field splitting** (ZFS).

10. Jahn-Teller Theorem. According to this theorem a non-linear molecule in an electronically degenerate state always distorts itself into a less symmetric but more stable configuration in which the electronic degeneracy has been removed.

11. Bohr's Correspondence (or Complementarity) Principle. It states that classical mechanics and quantum mechanics tend to give the same result when systems are in highly excited quantum states.

Since science is an intellectual edifice based on theories, which must ultimately be tested by experiment, and theories imply the existence of theorems, important theorems such as those mentioned above are a part of the scientist's arsenal and must be on his/her fingertips.

I. Review Questions

1. Describe Planck's quantum theory of radiation. State and explain Einstein's photoelectric equation.
2. Using the Bohr postulates derive the equation for the energy of hydrogen atom.
3. Derive the Brogile relation. How was it verified ?
4. Set up and solve the Schrödinger wave equation for a particle in an infinite one-dimensional box, with potential energy zero inside the box. Normalize the wavefunctions.
5. Show that $\exp(ikx)$ is an eigenfunction of the operator d/dx. Also show that $\exp(kx^2)$ is not an eigenfunction of d/dx.
6. Determine which of the following functions are eigenfunctions of the operator d^2/dx^2 : *(a)* $\exp(ikx)$, *(b)* $\cos kx$, *(c)* $\exp(-\alpha x^2)$? Determine the eigenvalue where appropriate. **[Ans. *(a)*, *(b)*]**
7. Show that for a particle in a one-dimensional box of width a,

   (i) $\langle x \rangle = a/2$ *(ii)* $\langle p_x \rangle = 0$ *(iii)* $\langle x^2 \rangle = a^2 \left[\frac{1}{3} - \frac{1}{2\pi^2 n^2} \right]$

8. Discuss the solution of Schrödinger wave equation for a particle in a three-dimensional cubic box with edges of length a assuming that the potential is zero within the box and infinite outside the box. What is meant by degeneracy of energy levels?
9. Set up the Schrödinger wave equation for a simple harmonic oscillator, and solve it for the energy eigenvalues.
10. Derive an expression for the energy of a rigid rotor using the Schrödinger wave equation.
11. Write the Schrödinger wave equation for hydrogen atom in terms of polar coordinates. Separate the resultant equation in three equations using the technique of separation of variables. How do the quantum numbers n, l and m emerge from the solution of the wave equation ?
12. Show that the following radial wavefunction of hydrogen atom is normalized :

$$R_{1,0}(r) = (2/a_0)^{3/2} \exp(-r/a_0)$$

II. Problems

1. The work function of cesium metal is 2·14 eV. Calculate the kinetic energy and the speed of electrons emitted when the metal is irradiated with light of wave length *(a)* 700 nm *(b)* 300 nm.
[Ans. *(a)* No ejection *(b)* 837 km s^{-1}]

2 Calculate the short and long wave length limits of the Lyman series in the spectrum of hydrogen atom ($R_H = 1{\cdot}09677 \times 10^8\ m^{-1}$). [Ans. λ_s = 911·6 Å, λ_l = 1215 Å]

3. In the Balmer series for hydrogen spectrum what is the wave length of the series limit ? [Ans. 364·7 μ]

4. Calculate the de Brolie wave length of a body of mass 1 mg moving with a velocity of 10 m s^{-1}
[Ans. $6{\cdot}626\times10^{-29}$ m]

5. Calculate the de Broglie wave length of electron that has been accelerated through a potential difference of 100 V. [Ans. 0·1226 nm]

6. An electron has kinetic energy $2{\cdot}8\times10^{-25}$ J. Calculate the Broglie wave length. $m_e = 9{\cdot}1\times10^{-31}$ kg.
[Ans. $\lambda = 9{\cdot}245\times10^{-7}$ m]

7. Calculate the uncertainty in the velocity of an electron if the uncertainty in its position is approximately 1 Å.
[Ans. $5{\cdot}8\times10^{-7}$ m s^{-1}]

8. An electron in a one-dimensional box of width 1 Å undergoes a transition from the ground state (n=1) to the first excited state (n=2). Calculate the transition energy in eV. [Ans. $1{\cdot}128\times10^2$ eV]

9. A proton in a one-dimensional box of width 1 Å undergoes a transition from the ground state to the first excited state. Calculate the transition energy in eV. [Ans. $6{\cdot}141\times10^{-2}$ eV]

10. Calculate the probability (P) of finding a particle between 0·49 a and 0·51 a for the states y_1 and y_2, where a is the width of the one-dimensional infinite box. [Ans. P_1 = 0·0399 ; P_2 = 0·0001]

11. Neglecting the electron spin, calculate the degeneracy, g_n, of the energy levels of hydrogen atom with the following values of the principal quantum number, n : *(a)* 1 *(b)* 2 *(c)* 3 *(d)* 4. [Ans. *(a)* 1 *(b)* 4 *(c)* 9 *(d)* 16]

12. A radio station operates at a frequency of 108·7 MHz. If the power output is 250 kW, what is the rate of emission of the quanta from the station ? [Ans. $3{\cdot}4\times10^{30}$ quanta/second]

13. Calculate the number of times the electron goes around the first Bohr orbit of hydrogen atom per second. The Bohr radius = 0·529 0 Å.

[Hint : $T = 2\pi a_0/v$, where T is the time period and v is the velocity. Also number of revolutions of the electron is $n = 1/T$]. [Ans. $6{\cdot}57\times10^{15}$ s^{-1}]

14. An atom makes a transition from an excited state with lifetime of 1 ns to the ground state by emitting a photon of wave length 600 nm. Calculate the uncertainty in the energy of the excited state. Also calculate the percentage uncertainty if the energy is measured from the ground state. [Hint : $\Delta E.\Delta t \geq h/4\pi$; Also, $E = h\nu$]
[Ans. $5{\cdot}28\times10^{-26}$ J ; $1{\cdot}6\times10^{-5}$ %]

15. Determine which of the following functions are eigenfunctions of the operator d/dx : *(a)* exp (ikx) *(b)* cos kx *(c)* kx *(d)* exp $(-ax^2)$? Determine the eigenvalue where appropriate. [Ans. *(a)*]

16. Which of the functions given in the last problem are eigenfunctions of the operator d^2/dx^2 ? Give the eigenvalue where appropriate. [Ans. *a, b*]

17. Verify that the wave function $\psi(x) = x\,e^{-ax^2}$ is an eigenfunction of the operator $d^2/dx^2 - 4a^2x^2$. What is the corresponding eigenvalue ? [Ans. $-6a$]

18. An electron in a one-dimensional box of width 10 Å undergoes a transition from the ground state to the first excited state. Calculate the wave length of the photon absorbed. [Ans. λ = 10,29999 Å]

19. Calculate the ground state energy (in kJ mol^{-1}) for an electron that is confined to a one-dimensional infinite potential well with a width of 0·2 nm. [Ans. 907 kJ mol^{-1}]

20. Calculate the degeneracies of the first six energy levels for a particle in an infinite cubical box.
[Ans. 1, 3,3, 3, 1, 6]

21. Calculate the degeneracy of the energy level with energy equal to
(i) $11(h^2/8ma^2)$ and *(ii)* $12(h^2/8ma^2)$ for a particle in a cubical box. [Ans. *(i)* 3 *(ii)* 1]

22. Calculate the probability of locating the particle in the ground state one-dimensional box between $a/4$ and $3a/4$, where a is the width of the box. [Ans. 0·83]

23. Calculate the wave lengths of the first three lines of Paschen series for hydrogen atom.

CHAPTER 2

QUANTUM MECHANICS–II. ADVANCED TOPICS AND ATOMIC SPECTRA

After discussing simple applications of quantum mechanics in Chapter 1, we shall deal with advanced topics in quantum mechanics including the solution of Schrödinger equation for quantum mechanics of many-electron atoms, approximation methods, angular momentum, atomic spectra and quantum mechanical tunneling, in this chapter.

Solution of Schrödinger Equation for Multi-Electron Atoms

The Schrödinger wave equation cannot be solved exactly for atoms beyond hydrogen atom in the periodic table. The troublesome term is the interelectron repulsion term in the Hamiltonian because of which the n–electron wave equation cannot be split into n one–electron wave equations. Hence, methods have been developed for the approximate solution of the multi–electron Schrödinger wave equation. In this book we shall deal briefly with these methods omitting mathematical details. One of these methods is based on the time-independent perturbation theory and the other, called the variation method, involves the selection of a trial wave function.

1. The Time–independent Perturbation Theory. The Schrödinger wave equation to be solved is

$$\hat{H}\psi = E\psi \qquad ...(1)$$

The Hamiltonian is decomposed into two parts as

$$\hat{H} = \hat{H}^{(0)} + \lambda\hat{H}' \qquad ...(2)$$

where $\hat{H}^{(0)}$ is the unperturbed part and $\lambda\hat{H}'$ is the **perturbation** where λ is the *perturbation parameter* which measures the deviation of the problem of interest from the unperturbed system. It is further assumed that

$$\lambda\hat{H}' << \hat{H}^{(0)} \qquad ...(3)$$

In general, λ is set equal to unity which means that perturbation is fully applied. Associated with $\hat{H}^{(0)}$ are a set of eigenvalues $E_1^{(0)}$, $E_2^{(0)}$, ..., $E_n^{(0)}$ and the corresponding eigenfunctions $\psi_1^{(0)}$, $\psi_2^{(0)}$, ... $\psi_n^{(0)}$, *i.e.*,

$$\hat{H}\psi_n^{(0)} = E_n^{(0)}\psi_n^{(0)} \qquad ...(4)$$

It is assumed that the eigenfunctions ψ_n and the energy eigenvalues E_n of the total Hamiltonian $\hat{H}$ can be expressed in the form of a power series of λ :

$$\psi_n = \psi_n^{(0)} + \lambda\psi_n^{(1)} + \lambda^2\psi_n^{(2)} + \lambda^3\psi_n^{(3)} + ... \qquad ...(5)$$

$$E_n = E_n^{(0)} + \lambda E_n^{(1)} + \lambda^2 E_n^{(2)} + \lambda^3 E_n^{(3)} + ... \qquad ...(6)$$

The first term in Eq. 5 is the zeroth–order term, the second represents the first order correction ;

the third represents the second-order correction, etc., to the unperturbed zeroth-order term. The eigenfunctions $\psi_n^{(1)}$, $\psi_n^{(2)}$,... and the eigenvalues $E_n^{(1)}, E_n^{(2)}$, ... are independent of λ and $\psi_n^{(1)}$, $\psi_n^{(2)}$, ... are so chosen that they are orthogonal to $\psi_n^{(0)}$ which is assumed to be normalized.

Substituting Eqs. 5 and 6 in Eq. 1, we get

$$\left(\hat{H}^{(0)} + \lambda \hat{H}'\right)\left(\psi_n^{(0)} + \lambda\psi_n^{(1)} + \lambda\psi_n^{(2)} + \ldots\right)$$

$$= \left(E_n^{(0)} + \lambda E_n^{(1)} + \lambda^2 E_n^{(2)} + \ldots\right)\left(\psi_n^{(0)} + \lambda\psi_n^{(1)} + \lambda^2\psi_n^{(2)} + \ldots\right)$$

or $$\left(\hat{H}^{(0)} - E_n^{(0)}\right)\psi_n^{(0)} + \lambda\left(\hat{H}'\psi_n^{(0)} + \hat{H}^{(0)}\psi_n^{(1)} - E_n^{(1)}\psi_n^{(0)} - E_n^{(0)}\psi_n^{(1)}\right) = 0 \quad \ldots(7)$$

Since the perturbation parameter λ is arbitrary, the coefficient of each power of λ must vanish separately and, therefore, we have

$$\hat{H}^{(0)}\psi_n^{(0)} = E_n^{(0)}\psi_n^{(0)} \quad \ldots(8)$$

$$\hat{H}'\psi_n^{(0)} + \hat{H}^{(0)}\psi_n^{(1)} = E_n^{(1)}\psi_n^{(0)} + E_n^{(0)}\psi_n^{(1)} \quad \ldots(9)$$

$$H'\psi_n^{(1)} + \hat{H}^{(0)}\psi_n^{(2)} = E_n^{(2)}\psi_n^{(0)} + E_n^{(1)}\psi_n^{(1)} + E_n^{(0)}\psi_n^{(2)} \quad \ldots(10)$$

We are ordinarily interested only in the terms upto second order ; we, therefore, neglect equations beyond Eq. 10. It may be noted that Eq. 8 is identical with Eq. 4 as expected since it refers to the zero-order perturbation. We shall now consider the following two cases of perturbation theory :

A. Nondegenerate Perturbation Theory

Here we shall consider perturbation on nondegenerate energy levels. It will be convenient to use the wave function itself to label the states.

1. First-order correction to the energy. Multiplying Eq. 9 from the left by $\left\langle\psi_n^{(0)}\right|$, we get

$$\left\langle\psi_n^{(0)}\middle|\hat{H}'\middle|\psi_n^{(0)}\right\rangle + \left\langle\psi_n^{(0)}\middle|\hat{H}^{(0)}\middle|\psi_n^{(1)}\right\rangle = E_n^{(1)}\left\langle\psi_n^{(0)}\middle|\psi_n^{(0)}\right\rangle + E_n^{(0)}\left\langle\psi_n^{(0)}\middle|\psi_n^{(1)}\right\rangle \quad \ldots(11)$$

Since $\hat{H}^{(0)}$ is Hermitian, the second term on the left reduces to $E_n^{(0)}\left\langle\psi_n^{(0)}\middle|\psi_n^{(1)}\right\rangle$ and Eq. 11 gives

$$E_n^{(1)} = \left\langle\psi_n^{(0)}\middle|\hat{H}'\middle|\psi_n^{(0)}\right\rangle \quad \ldots(12)$$

In simplified form, Eq. 12 can be written as

$$E_n^{(1)} = \langle n|\hat{H}'|n\rangle \quad \ldots(13)$$

which is called the **matrix element.** The first order correction to the energy is thus the expectation (average) value of the perturbation Hamiltonian over the corresponding unperturbed states of the system (atom or a molecule).

2. First order correction to the wave function. The first order correction to the wave function is written as a linear combination of the unperturbed eigenfunctions of the system :

$$\psi_n^{(1)} = \sum_{l=1}^{\infty} a_l\psi_l^{(0)} \quad \ldots(14)$$

Substitution of Eq. 14 in Eq. 9 and multiplication from the left by $\left\langle\psi_m^{(0)}\right|$, gives

$$\left\langle\psi_m^{(0)}\middle|\hat{H}'\middle|\psi_n^{(0)}\right\rangle + \sum_{l=1}^{\infty} a_l E_l^{(0)}\left\langle\psi_m^{(0)}\middle|\psi_l^{(0)}\right\rangle = E_n^{(1)}\left\langle\psi_m^{(0)}\middle|\psi_n^{(0)}\right\rangle + \sum_{l=1}^{\infty} a_l E_n^0\left\langle\psi_m^{(0)}\middle|\psi_l^{(0)}\right\rangle$$

or $$\left\langle\psi_m^{(0)}\middle|\hat{H}'\middle|\psi_n^{(0)}\right\rangle + a_m E_m^{(0)} = a_m E_n^{(0)}$$

or $$a_m = \frac{\left\langle\psi_m^{(0)}\middle|\hat{H}'\middle|\psi_n^{(0)}\right\rangle}{E_n^{(0)} - E_m^{(0)}} = \frac{\langle m|\hat{H}'|n\rangle}{E_n^{(0)} - E_m^{(0)}} \quad \ldots(15)$$

All the as except a_n in Eq. 14 can be calculated using Eq. 15. The coefficient a_n is found to be zero from the normalization condition $\langle\psi_n|\psi_n\rangle = 1$. It follows that

$$\psi_n^{(1)} = \sum_m{}' \frac{\langle m|\hat{H}'|n\rangle}{E_n^{(0)} - E_m^{(0)}}\left|\psi_m^0\right\rangle \quad \ldots(16)$$

Consequently, the energy and wave function corrected to first order are

$$E_n = E_n^{(0)} + \langle m|\hat{H}'|n\rangle \quad \ldots(17)$$

and $$\psi_n = \psi_n^{(0)} + \sum_m{}' \frac{\langle m|\hat{H}'|n\rangle}{E_n^{(0)} - E_m^{(0)}}\left|\psi_m^0\right\rangle \quad \ldots(18)$$

where the prime on the sum means that the state $m=n$ should be excluded.

3. Second-order correction to the energy. We use the same procedure to obtain the second-order correction to the energy from Eq. 10. Multiplying Eq. 10 from left by $\left\langle\psi_n^{(0)}\right|$ and using the Hermitian property of the unperturbed Hamiltonian $\hat{H}^{(0)}$, we obtain

$$\left\langle\psi_n^{(0)}\middle|\hat{H}'\middle|\psi_n^{(1)}\right\rangle = E_n^{(2)}\left\langle\psi_n^{(0)}\middle|\psi_n^{(0)}\right\rangle + E_n^{(1)}\left\langle\psi_n^{(0)}\middle|\psi_n^{(1)}\right\rangle \quad \ldots(19)$$

The form of $\psi_n^{(1)}$, Eq. 16, suggests that the second term on the right vanishes. Therefore,

$$E_n^{(2)} = \left\langle\psi_n^{(0)}\middle|\hat{H}'\middle|\psi_n^{(1)}\right\rangle \quad \ldots(20)$$

Substituting the value of $\psi_n^{(1)}$ in Eq. 20, we have

$$E_n^{(2)} = \sum_m{}' \frac{\langle \psi_m^{(0)} | \hat{H}' | \psi_n^{(0)} \rangle \langle \psi_n^{(0)} | \hat{H}' | \psi_m^{(0)} \rangle}{E_n^{(0)} - E_m^{(0)}} = \sum_m{}' \frac{\langle m|\hat{H}'|n\rangle \langle n|\hat{H}'|m\rangle}{E_n^{(0)} - E_m^{(0)}} \quad ...(21)$$

If $\hat{H}'$ is Hermitian $\langle n|\hat{H}'|m\rangle = \langle m|\hat{H}'|n\rangle^*$. Then,

$$E_n^{(2)} = \sum_m{}' \frac{|\langle m|\hat{H}'|n\rangle|^2}{E_n^{(0)} - E_m^{(0)}} \quad ...(22)$$

Since $|\langle m|\hat{H}'|n\rangle|^2$ is always positive, the sign of the correction is determined by the denominator in Eq. 22. The second-order correction to the energy level n due to energy levels for which $E_n^{(0)} > E_m^{(0)}$ is positive, whereas that due to levels for which $E_n^{(0)} < E_m^{(0)}$ is negative.

It can be further shown that

$$E_n^{(3)} = \langle \psi_n^{(0)} | \hat{H}' | \psi_n^{(2)} \rangle \quad ...(23)$$

and

$$E_n^{(n)} = \langle \psi_n^{(0)} | \hat{H}' | \psi_n^{(n-1)} \rangle \quad ...(24)$$

These equations show that the calculation of nth order energy requires a knowledge of $(n-1)$th order eigenfunctions. Since the contribution of second order, third order, etc., terms goes on successively decreasing, we are primarily interested in the first order correction. The above treatment is called the **Rayleigh-Schrödinger perturbation theory.**

4. Second-order correction to the wavefunction. The second-order correction to the wave function, $\psi_n^{(2)}$, is written as a linear combination of the unparturbed wave functions of the system :

$$\psi_n^{(2)} = \sum_k b_k \psi_k^{(0)} \quad ...(25)$$

Substitution of Eq. 25 in Eq. 10 and multiplication from left by $\langle \psi_l^0 |$, gives

$$\sum_m{}' a_m \langle l|\hat{H}'|m\rangle + \sum_k{}' b_k \langle l|\hat{H}^{(0)}|k\rangle = E_n^{(2)} \langle l|n\rangle + \sum_m{}' a_m E_n^{(1)} \langle l|m\rangle + \sum_k b_k E_n^{(0)} \langle l|k\rangle$$

The first term on the right is zero. Rearranging, we get

$$b_l \left(E_l^{(0)} - E_n^{(0)}\right) = E_n^{(1)} a_l - \sum_m{}' a_m \langle l|\hat{H}^{(0)}|m\rangle$$

Substituting the values of the as and $E_n^{(1)}$, we get

$$b_l = \frac{\langle n|\hat{H}'|n\rangle \langle l|\hat{H}'|n\rangle}{\left(E_l^{(0)} - E_n^{(0)}\right)\left(E_n^{(0)} - E_l^{(0)}\right)} - \sum_m{}' \frac{\langle n|\hat{H}'|n\rangle \langle l|\hat{H}'|m\rangle}{\left(E_n^{(0)} - E_m^{(0)}\right)\left(E_l^{(0)} - E_n^{(0)}\right)}$$

$$= \sum_m{}' \frac{\langle n|\hat{H}'|n\rangle \langle l|\hat{H}'|m\rangle}{\left(E_n^{(0)} - E_m^{(0)}\right)\left(E_n^{(0)} - E_l^{(0)}\right)} - \frac{\langle n|\hat{H}'|n\rangle \langle l|\hat{H}'|n\rangle}{\left(E_n^{(0)} - E_l^{(0)}\right)^2} \quad ...(26)$$

The normalization condition of the wave function shows that the coefficient b_n is zero. It follows that the energy and wave function of the system corrected to second order in the perturbation is

$$E_n = E_n^{(0)} + \langle n|\hat{H}'|n\rangle + \sum_m{}' \frac{|\langle n|\hat{H}'|m\rangle|^2}{E_n^{(0)} - E_m^{(0)}} \quad ...(27)$$

$$\psi_n = \psi_n^{(0)} + \sum_m{}' a_m \psi_m^{(0)} + \sum_m{}' b_l \psi_l^{(0)} \quad ...(28)$$

where the coefficients a_m and b_l are given by Eqs. 15 and 26, respectively. The prime on the summation again signifies the omission of the states $m = n$ or $l = n$, as the case may be.

Application of First-Order Perturbation Theory to Helium Atom. We shall solve the Schrödinger wave equation for the ground state of helium atom using the first-order time-independent perturbation theory.

$$\hat{H}\psi = E\psi \quad ...(29)$$

$$\hat{H} = \hat{H}^{(0)} + \hat{H}' \quad ...(30)$$

where the unperturbed Hamiltonian, $\hat{H}^{(0)}$, is given by

$$\hat{H}^{(0)} = -\frac{\hbar^2}{2\mu}(\nabla_1^2 + \nabla_2^2) - \frac{Ze^2}{4\pi\varepsilon_0}\left(\frac{1}{r_1} + \frac{1}{r_2}\right) \quad ...(31)$$

and the perturbation is the interelectron repulsion term :

$$\hat{H}' = e^2/4\pi\varepsilon_0 r_{12} \quad ...(32)$$

Here r_1 and r_2 are the distances of the two electrons from the helium nucleus of charge Ze and r_{12} is the interelectron distance. We shall use atomic units, a.u. ($\hbar = e = \mu \approx m_e = 1/4\pi\varepsilon_0 = a_0 = 1$), so that

$$\hat{H}^{(0)} = -\frac{1}{2}(\nabla_1^2 + \nabla_2^2) - \left(\frac{2}{r_1} + \frac{2}{r_2}\right) \quad (\because Z = 2 \text{ for helium}) \quad ...(33)$$

$$\hat{H}' = 1/r_{12} \quad ...(34)$$

Since $\hat{H}' << \hat{H}^{(0)}$, it is pertinent to use perturbation theory.

Since $\hat{H}^{(0)}$ is the *sum* of two one-electron Hamiltonians, the unperturbed wave function $\psi^{(0)}(r_1, r_2)$ can be written as the *product* of two hydrogenic wave functions :

$$\psi^{(0)}(r_1, r_2) = \psi^{(0)}(r_1)\, \psi^{(0)}(r_2) \quad ...(35)$$

where $\psi^{(0)}(r_i)$ is the wave function of the ith electron in a hydrogenic atom with nuclear charge = Ze. Thus,

$$\psi^{(0)}(r_1, r_2) = \left(\frac{Z^3}{\pi a_0^3}\right)^{1/2} e^{-Zr_1/a_0} \times \left(\frac{Z^3}{\pi a_0^3}\right)^{1/2} e^{-Zr_2/a_0}$$

$$= (Z^3/\pi)e^{-Z(r_1+r_2)} \quad \text{(in a.u.)} \quad ...(36)$$

The unperturbed ground state energy, $E_0^{(0)}$, is equal to the sum of the ground state energies of two hydrogenic atoms :

$$E_0^{(0)} = (-Z^2/2) + (-Z^2/2) = -Z^2 \text{ (in a.u.)} \quad ...(37)$$

The first-order correction to the groundstate energy is

$$E_0^{(1)} = \langle \psi^{(0)} | \hat{H}' | \psi^{(0)} \rangle$$

$$= \iint \psi^{*(0)}(r_1, r_2) \hat{H}' \psi^{(0)}(r_1, r_2) d\tau_1 d\tau_2 \quad ...(38)$$

Substituting the value of $\psi^{(0)}(r_1, r_2)$ from Eq. 36 into Eq. 38, we obtain

$$E_0^{(1)} = \frac{Z^6}{\pi^2} \iint e^{-2Z(r_1+r_2)} (1/r_{12}) d\tau_1 d\tau_2 \quad ...(39)$$

where the volume elements of the two electrons (in spherical polar coordinates) are

$$d\tau_1 = r_1^2 \sin\theta_1 \, dr_1 \, d\theta_1 \, d\phi_1$$
$$d\tau_2 = r_2^2 \sin\theta_2 \, dr_2 \, d\theta_2 \, d\phi_2$$

The evaluation of the interelectron repulsion integral (Eq. 39) is rather tedious ; it can be shown that it is given by

$$E_0^{(1)} = \left(\frac{5}{8}\right) Z \quad ...(40)$$

Notice that $E_0^{(1)}$ is positive, as was to be expected since the repulsion energy between two electrons is always positive.

Adding Eqs. 37 and 40, we have

$$E_0 = E_0^{(0)} + E_0^{(1)} = -Z^2 + \left(\frac{5}{8}\right) Z$$

$$= -\left(Z^2 - \frac{5}{8} Z\right) \text{ (in a.u.)} \quad ...(41a)$$

Reincorporating the original units we find that

$$E_0 = -\left(Z^2 - \frac{5}{8} Z\right) \frac{\mu e^2}{2\hbar^2} \quad \text{(for 2 electrons)} \quad ...(41b)$$

Recalling that the ground state energy of hydrogen atom is $-\frac{1}{2}$ a.u. or $-\mu e^4/2\hbar^2$ or $-13{\cdot}60$ eV, we get for helium atom

$$E_0 = -\left(Z^2 - \frac{5}{8} Z\right)(27{\cdot}2) \text{ eV} = -74{\cdot}80 \text{ eV} = -2{\cdot}75 \text{ a.u.} \quad ...(42)$$

The experimental value is $-2{\cdot}904$ a.u. or $-78{\cdot}986$ eV. The agreement between the theoretical and experimental values is not good. If the second-order and higher order contributions are included, the agreement improves but is still not very good.

Example 1. Show that the first-order Stark effect on the ground state of hydrogen atom is zero.

Solution. This is another interesting application of the perturbation theory. In the Stark effect, named after the German physicist J. Stark, who won the 1919 Physics Nobel Prize, the system, atom or molecule, is placed in an electric field. The energy levels are split by the field. Let ε be the electric field applied in the z-direction, assuming that the hydrogen atom is placed at the origin of the three-dimensional Cartesian coordinate system. Hence, the

perturbation is

$$\hat{H}' = e\varepsilon z = e\varepsilon r \cos\theta \quad \text{(in polar coordinates)} \quad ...(i)$$

$$\hat{H} = \hat{H}^{(0)} + \hat{H}' \quad ...(ii)$$

The eigenfunctions and eigenvalues of the unperturbed Hamiltonian, $\hat{H}^{(0)}$ for the ground state of hydrogen atom, are

$$E_0^{(0)} = -\frac{1}{2} \text{ (a.u.)} \quad ...(iii)$$

$$\psi_0^{(0)} = \psi_{1s}^{(0)} \equiv 1s = \frac{1}{\sqrt{\pi}} e^{-r} \text{ (in a.u.)} \quad ...(iv)$$

$$E_n = E_n^{(0)} + E_n^{(1)} + E_n^{(2)} + ... \quad \text{(assuming } \lambda = 1\text{)}$$

For the ground state, $n = 0$ so that

$$E_0 = E_0^{(0)} + E_0^{(1)} + E_0^{(2)} + ... \quad ...(v)$$

From Eq. 12, $E_0^{(1)} = \langle \psi_0^{(0)} | \hat{H}' | \psi_0^{(0)} \rangle \equiv 1s | \hat{H}' | 1s \rangle$

$$= \langle 1s | e\varepsilon r \cos\theta | 1s \rangle = e\varepsilon \langle 1s | r \cos\theta | 1s \rangle$$

$$= e\varepsilon \int \psi_{1s}^{*(0)} \, r \cos\theta \, \psi_{1s}^{(0)} \, d\tau \quad ...(vi)$$

Recalling that in spherical polar coordinates,

$$d\tau = r^2 \sin\theta \, dr \, d\theta \, d\phi, \quad ...(vii)$$

we have from Eqs. *(iv), (vi) and (vii),*

$$E_0^{(1)} = e\varepsilon (1/\pi) \int_0^\infty r^3 e^{-2r} dr \int_0^\pi \sin\theta\cos\theta \, d\theta \int_0^{2\pi} d\phi$$

$$= 2e\varepsilon \int_0^\infty r^3 e^{-2r} \, dr \int_0^\pi \sin\theta\cos\theta \, d\theta \quad ...(viii)$$

We need not evaluate the first integral in Eq. *(viii)* because the second integral is zero :

$$\int_0^\pi \sin\theta\cos\theta \, d\theta = \frac{1}{2} \int_0^\pi \sin 2\theta \, d\theta = 0 \quad ...(ix)$$

Hence, $E_0^{(1)} = 0$ ...(x)

Thus, we see that there is no first-order Stark effect on the ground state of hydrogen atom.

B. Degenerate Perturbation Theory

We must emphasize here that the unperturbed wave function $\psi_n^{(0)}$ is a unique one in the non-degenerate case. When there is a degeneracy, a linear combination of the degenerate wave functions can be taken as the unperturbed wave function. For simplicity, we shall consider a case in which the unperturbed energy level, $E_n^{(0)}$, is two-fold degenerate. Let $\psi_n^{(0)}$ and be $\psi_l^{(0)}$ be the eigenfunctions corresponding to the eigenvalues $\psi_n^{(0)}$ and be $\psi_l^{(0)}$. Thus, a linear combination of the two is

$$\phi = c_n \psi_n^{(0)} + c_l \psi_l^{(0)} \quad \text{(where } c_n \text{ and } c_l \text{ are constants)} \quad ...(43)$$

Replacing $\psi_n^{(0)}$ in Eq. 9 by ϕ, we get

$$\hat{H}'\left|\left(c_n\psi_n^{(0)}+c_l\psi_l^{(0)}\right)\right\rangle+\hat{H}^{(0)}\left|\psi_n^{(1)}\right\rangle=E_n^{(1)}\left|\left(c_n\psi_n^{(0)}+c_l\psi_l^{(0)}\right)\right\rangle+E_n^{(0)}\left|\psi_n^{(0)}\right\rangle \quad ...(44)$$

Multiplying Eq. 44 from left by $\left\langle\psi_n^{(0)}\right|$, we have

$$c_n\left\langle\psi_n^{(0)}\left|\hat{H}'\right|\psi_n^{(0)}\right\rangle+c_l\left\langle\psi_n^{(0)}\left|\hat{H}'\right|\psi_l^{(0)}\right\rangle+\left\langle\psi_n^{(0)}\left|\hat{H}^{(0)}\right|\psi_n^{(1)}\right\rangle=c_nE_n^{(1)}+E_n^{(0)}\left\langle\psi_n^{(0)}\left|\psi_n^{(1)}\right\rangle \quad ...(45)$$

Since $\hat{H}^{(0)}$ is Hermitian,

$$\left\langle\psi_n^{(0)}\left|\hat{H}^{(0)}\right|\psi_n^{(1)}\right\rangle=E_n^{(0)}\left\langle\psi_n^{(0)}\left|\psi_n^{(1)}\right\rangle$$

and Eq. 45 reduces to

$$\left(H'_{nn}-E_n^{(1)}\right)c_n+\hat{H}'_{nl}\,c_l=0 \quad ...(46)$$

Operating Eq. 44 from left by $\psi_n^{(0)}$, we have

$$H'_{lm}c_n+\left(H'_{ll}-E_n^{(1)}\right)c_l=0 \quad ...(47)$$

Eqs. 46 and 47 together form a set of simultaneous equations for the coefficients c_n and c_l. A nontrivial solution of these equations exists only if the determinant of the coefficients vanish :

$$\begin{vmatrix}H'_{nn}-E_n^{(1)} & H'_{nl}\\ H'_{ln} & H'_{ll}-E_n^{(1)}\end{vmatrix}=0 \quad ...(48)$$

This is called the secular equation and its two solutions are

$$E_{n\pm}^{(1)}=\frac{1}{2}\left(H'_{nn}+H'_{ll}\right)\pm\frac{1}{2}\left[\left(H'_{nn}+H'_{ll}\right)^2+4\left|H'_{nl}\right|\right]^{1/2} \quad ...(49)$$

Thus, the corrected energies are

$$E_n=E_n^{(0)}+E_{n+}^{(1)} \quad \text{and} \quad E_l=E_n^{(0)}+E_{n-}^{(1)} \quad ...(50)$$

Both the energies will be real since the diagonal matrix elements H'_{nn} and H'_{ll} of the Hermitian operator $\hat{H}'$ are real. If $H'_{nn}=H'_{ll}$ and $H'_{nl}=0$, $E_{n+}=E_{n-}$ and the degeneracy is not removed in the first order.

When the two roots of Eq. 48 are distinct, each (say E_{n+}) can be used to calculate the ratio c_n/c_l either from Eq. 46 or from Eq. 47. The normalization condition enables us to calculate the values of the coefficients c_n and c_l. The values of these coefficients give the desired linear combination associated with the energy level $E_n^{(0)}+E_{n+}$. Similarly, the combination associated with the energy level $E_n^{(0)}+E_{n-}$ can also be evaluated.

Stark Effect on the First Excited State of hydrogen Atom

The first excited state of hydrogen atom (with principal quantum number $n=2$) is four-fold degenerate, since it has the (l, m) values (0, 0), (1, 0), (1, 1) and (1, –1). We assume, as before, that the electric field, ε, is applied along the positive z-axis so that the perturbation Hamiltonian is $\hat{H}'=e\varepsilon z=e\varepsilon r\cos\theta$. The four degenerate states (wavefunctions) can be conveniently specified by the quantum numbers (nlm) as

$$|nlm\rangle:\ |200\rangle,\ |210\rangle,\ |211\rangle,\ |21,-1\rangle$$

Since the state is four-fold degenerate ($2s$, $2p_z$, $2p_x$, $2p_y$ being the degenerate orbitals), we have to evaluate sixteen matrix elements of $\hat{H}'$, as required by the degenerate perturbation theory. Of these, the four diagonal matrix elements are zero since they correspond to the same parity ($\hat{H}'$ is of odd parity). The off-diagonal matrix elements between states of different m values (10 in numbers) are zero since

$$\int_0^{2\pi}\exp\left[i\left(m'-m\right)\phi\right]d\phi=0 \quad \text{if } m'\neq m$$

The remaining two matrix elements $\langle 200|\hat{H}'|210\rangle$ and $\langle 210|\hat{H}'|200\rangle$ are the only nonvanishing ones. These can be evaluated using the expressions

and
$$\psi_{200}=\frac{1}{4\sqrt{2\pi}}\frac{1}{a_0^{3/2}}\left(2-\frac{r}{a_0}\right)\exp\left(-\frac{r}{2a_0}\right) \quad ...(51)$$

$$\psi_{210}=\frac{1}{4\sqrt{2\pi}}\frac{1}{a_0^{3/2}}\frac{r}{a_0}\exp\left(-\frac{r}{2a_0}\right)\cos\theta \quad ...(52)$$

Therefore

$$\langle 200|\hat{H}'|210\rangle=\frac{e\varepsilon}{32\pi a_0^4}\int_0^{2\pi}\int_0^{\pi}\int_0^{\infty}\left(2-\frac{r}{a_0}\right)r^2\exp\left(-\frac{r}{a_0}\right)\cos^2\theta\, r^2\sin\theta\, dr\, d\theta\, d\phi$$

$$=\frac{e\varepsilon}{16a_0^4}\int_0^{\pi}\cos^2\theta\sin\theta\, d\theta\int_0^{\infty}\left(2r^4-\frac{r^5}{a_0}\right)\exp\left(-\frac{r}{a_0}\right)dr$$

Using standard integrals, we have

$$\langle 200|\hat{H}'|210\rangle=-3e\varepsilon a_0 \quad ...(53)$$

Similarly,
$$\langle 210|\hat{H}'|200\rangle=-3e\varepsilon a_0 \quad ...(54)$$

The perturbation matrix is, therefore,

$$\hat{H}'=\begin{array}{c}(nlm)\\ \downarrow\\ (200)\\ (210)\\ (211)\\ (21,-1)\end{array}\begin{array}{c}\rightarrow\\ \\ \\ \\ \\ \end{array}\begin{array}{cccc}(200) & (210) & (211) & (21,-1)\\ \hline 0 & -3e\varepsilon a_0 & 0 & 0\\ -3e\varepsilon a_0 & 0 & 0 & 0\\ 0 & 0 & 0 & 0\\ 0 & 0 & 0 & 0\end{array} \quad ...(55)$$

The secular determinant is then

$$\begin{vmatrix} -E_2^{(1)} & -3e\varepsilon a_0 & 0 & 0 \\ -3e\varepsilon a_0 & -E_2^{(1)} & 0 & 0 \\ 0 & 0 & -E_2^{(1)} & 0 \\ 0 & 0 & 0 & -E_2^{(1)} \end{vmatrix} = 0 \quad ...(56)$$

The four roots of this determinantal equation are $3e\varepsilon a_0$, $-3e\varepsilon a_0$, 0 and 0; where a_0 is the Bohr radius. The states $|200\rangle$ and $|210\rangle$ are affected by the applied (external) electric field whereas the states $|211\rangle$ and $|21,-1\rangle$ are not. The four-fold degeneracy is thus lifted partially. Eigenstates (eigenfunctions) corresponding to these eigenvalues can be evaluated using Eq. 46 or Eq. 47 and the normalization condition for the coefficients. For the eigenvalue $3e\varepsilon a_0$, from Eq. 46, $c_n/c_l = -1$ and the condition $c_n^2 + c_l^2 = 1$ gives $c_n = 1/\sqrt{2}$ and $c_l = -1/\sqrt{2}$. The eigenstate corresponding to the eigenvalue $3e\varepsilon a_0$ is then $\left(1/\sqrt{2}\right)\left(|200\rangle - |210\rangle\right)$. Similarly, the eigenstate corresponding to the eigenvalue $-3e\varepsilon a_0$ is $\left(1/\sqrt{2}\right)\left(|200\rangle + |210\rangle\right)$. The energies along with the eigenstates of the $n = 2$ state of hydrogen atom in an electric field ε along the z-direction are shown in Fig. 1.

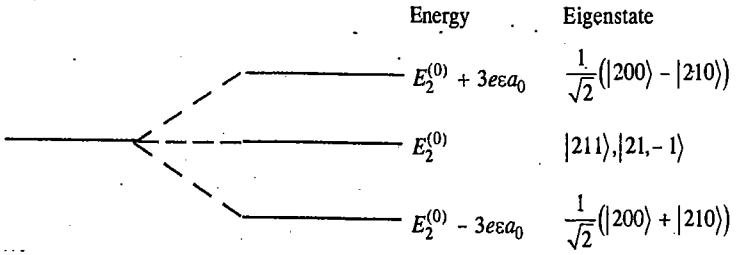

Fig. 1. Energies and wave functions of the first excited state of hydrogen atom in an electric field ε

We thus see that hydrogen atom in the first excited state passess a permanent electric dipole moment of magnitude $3ea_0$ with three different orientations—one state parallel to the external electric field, one state antiparallel to the field and two states with zero component along the field. The states $|211\rangle$ and $|21,-1\rangle$ do not possess dipole moments and, therfore, do not have a first-order interaciton with the electric field.

2. Variation Method (The Variation Theorem). According to the variation method, also called the *variation theorem*, if ψ is an approximate wave function of a quantum mechanical system, an atom or a molecule, described by the Hamiltonian $\hat{H}$, then the energy eigenvalue of the system, approximately given by the integral

$$E = \frac{\langle \psi|\hat{H}|\psi\rangle}{\langle \psi|\psi\rangle} \equiv \frac{\int \psi^* \hat{H} \psi \, d\tau}{\int \psi^* \psi \, d\tau} \quad ...(57)$$

or, if ψ is normalized (so that $\langle \psi|\psi\rangle = 1$), by the integral

$$E = \langle \psi|\hat{H}|\psi|\rangle \equiv \int \psi^* \hat{H} \psi \, d\tau \quad ...(58)$$

is an **upper bound** to the ground state energy, E_0, of the system, *i.e.*,

$$E \geq E_0 \quad ...(59)$$

If the approximate wave function, also called the **trial function**, happens to be exact (true) wave function, then

$$E = E_0 \quad ...(60)$$

However, this is seldom the case since we have no idea of the exact wave function, to begin with. The application of the variation method involves the following steps :

(i) Choose a trial wave function ψ dependent on *variable parameters*.

(ii) Evaluate the integral $\langle \psi|\hat{H}|\psi\rangle$

(iii) Minimise the above integral with respect to the variable parameters.

(iv) The function ψ with the optimum value of the parameters is the best approximation to the true wavefunction and the lowest value of $\langle \psi|\hat{H}|\psi\rangle$ is the nearest approximation to the true energy.

The proof of variation theorem is given later in this chapter.

Application of Variation Method to Helium Atom. The Hamiltonian for He atom (in atomic units) is

$$\hat{H} = -\frac{1}{2}\left(\nabla_1^2 + \nabla_2^2\right) - \left(\frac{2}{r_1} + \frac{2}{r_2}\right) + \frac{1}{r_{12}} \quad ...(61)$$

where the symbols have their usual meanings. As a result of screening, each electron (1 and 2) shields the other from the nucleus so that the two electrons do not "see" the same nuclear charge. Here it is natural to use a wave function with nuclear charge Z less than 2. That is, Z is a **variation parameter** which we shall determine from the variational calculation. It is important to remember that the Hamiltonian in Eq. 61 contains the exact value of $Z = 2$. The variational parameter appears only in the trial wave function :

$$\psi(r_1, r_2) = \left(\frac{Z^3}{\pi}\right)^{\frac{1}{2}} e^{-Zr_1} \times \left(\frac{Z^3}{\pi}\right)^{\frac{1}{2}} e^{-Zr_2} \quad ...(62)$$

$$= (Z^3/\pi) \exp\left[-Z(r_1 + r_2)\right] \quad ...(63)$$

$$E = \langle \psi|\hat{H}|\psi\rangle \quad ...(64)$$

Substituting the value of $\hat{H}$ from Eq. 61 in Eq. 64, we have

$$E = -\frac{1}{2}\langle \psi|\nabla_1^2|\psi\rangle - \frac{1}{2}\langle \psi|\nabla_2^2|\psi\rangle - 2\left\langle \psi\left|\frac{1}{r_1}\right|\psi\right\rangle - 2\left\langle \psi\left|\frac{1}{r_2}\right|\psi\right\rangle + \left\langle \psi\left|\frac{1}{r_{12}}\right|\psi\right\rangle \quad ...(65)$$

The Laplacian operator in spherical polar coordinates (r, θ, ϕ) is given by

$$\nabla^2 = \frac{1}{r^2}\frac{\partial}{\partial r}\left(r^2 \frac{\partial}{\partial r}\right) + \frac{1}{r^2 \sin\theta}\frac{\partial}{\partial \theta}\left(\sin\theta \frac{\partial}{\partial \theta}\right) + \frac{1}{r^2 \sin^2\theta}\frac{\partial^2}{\partial \phi^2} \quad ...(66)$$

Since the trial wave function (Eq. 62) does not depend upon angles θ and ϕ, differentiations with respect to θ_1, ϕ_1, θ_2 and ϕ_2 vanish so that for the first kinetic energy operator in Eq. 65, we get

$$-\frac{1}{2}\langle \psi|\nabla_1^2|\psi\rangle = \left(\frac{Z^3}{\pi}\right)^2 \int e^{-Zr_1}\left[-\frac{1}{2r_1^2}\frac{\partial}{\partial r_1}\left(r_1^2 \frac{\partial}{\partial r_1}\right)\right] e^{-Zr_1} \times r_1^2 \sin\theta_1 \, dr_1 \, d\theta_1 \, d\phi_1 \int e^{-2Zr_2} r_2^2 \sin\theta_2 \, dr_2 \, d\theta_2 \, d\phi_2 \quad ...(67)$$

The functions of r_2 are not affected by differentiation. Carrying out the integrations over all angles we obtain

$$-\frac{1}{2} < \psi |\nabla_1^2| \psi > = \left(\frac{Z^3}{\pi}\right)^2 (4\pi)^2 \int_0^\infty e^{-Zr_1}\left[-\frac{1}{2r_1^2}\frac{\partial}{\partial r_1}\left(r_1^2 \frac{\partial e^{-Zr_1}}{\partial r_1}\right)\right] r_1^2 dr_1 \times \int_0^\infty e^{-2Zr_2} \quad ...(68)$$

The second integral in Eq. 68, evaluated using the standard integral, is equal to $2!/(2Z)^3$ so that Eq. 68 becomes

$$(4Z^3)^2\left(-\frac{1}{2}\right)\frac{2!}{(2Z)^3}\int_0^\infty e^{-Zr_1}\left[\frac{\partial}{\partial r_1}(-Zr_1^2 e^{-Zr_1}\right] dr_1$$

$$= (-2Z^3)\int_0^\infty e^{-Zr_1}(-2Zr_1 + Z^2 r_1^2)e^{-Zr_1} dr_1$$

$$= (-2Z^3)\left[-2Z\int_0^\infty r_1 e^{-2Zr_1} dr_1 + Z^2\int_0^\infty r_1^2 e^{-2Zr_1} dr_1\right]$$

$$= (-2Z^3)\left[-\frac{2Z}{(2Z)^2} + \frac{Z^2 2!}{(2Z)^3}\right] = \frac{Z^2}{2} \quad ...(69)$$

Similarly, the second kinetic energy operator term in Eq. 65 gives $Z^2/2$. The third and the fourth electron–nuclear attraction energy terms can be handled easily. The third term, for instance, simplifies to

$$\left(\frac{Z^3}{\pi}\right)^2 \int e^{-Zr_1} e^{-Zr_2}\left[-\frac{2}{r_1}\right] e^{-Zr_1} e^{-Zr_2} r_1^2 \sin\theta_1 \, dr_1 \, d\theta_1 \, d\phi_1 \times r_2^2 \sin\theta_2 \, dr_2 \, d\theta_2 \, d\phi_2$$

$$= (4Z^3)^2 (-2) \int_0^\infty r_1 e^{-2Zr_1} dr_1 \int_0^\infty r_2^2 e^{-2Zr_2} dr_2$$

$$= -32Z^6 \times \frac{1}{(2Z)^2} \times \frac{2!}{(2Z)^3} = -2Z \quad ...(70)$$

Similarly, the fourth term in Eq. 65 gives $-2Z$. The fifth term, the interelectron repulsion energy integral, is somewhat more tedious. So, we will not go into details about its evaluation, merely stating that it evaluates to (5/8) Z. Combining all these contributions,

$$E = 2(Z^2/2) + 2(-2Z) + (5/8)Z = Z^2 - (27/8)Z \quad ...(71)$$

Using the variation method, we minimize the energy with respect to Z, obtaining

$$\partial E/\partial Z = 2Z - 27/8 = 0, \text{ whence } Z = 27/16 = 1{\cdot}69$$

Substituting this value of Z in Eq. 71, we obtain the ground state energy of helium atom :

$$E_0 = (27/16)^2 - (27/8)(27/16) = -2{\cdot}8476 \text{ a.u.}$$
$$= -(2{\cdot}8476)(27{\cdot}21 \text{ eV})$$
$$= -77{\cdot}48 \text{ eV} \qquad [\because 1 \text{ a.u.} = 27{\cdot}21 \text{ eV}] \quad ...(72)$$

This is much better than the first-order perturbation theory result, *viz.*, – 74·80 eV, the experimental value being – 2·904 a.u., *i.e.*, – 78·986 eV. In 1929, the Norwegian physicist E.A. Hyleraas, using a more complicated wave function and the concept of the so-called **electron correlation** which stipulates that electrons try to avoid each other, obtained a result for the ground state energy of helium which is very close to the experimental value. However, this is the realm of electronic computers and we shall not delve into the mathematical details which are beyond the scope of this book.

Example 2. Using the normalized trial wave function $\psi = (\sqrt{30}/a^{5/2})\, x(a - x)$ for a particle of mass m moving inside an infinite one-dimensional box of width a, calculate the upper bound to the ground state energy and compare with the true value $h^2/8ma^2$.

Solution. $$<E> = \int_0^a \psi^* \hat{H} \psi \, dx$$

where $$\hat{H} = (-\hbar^2/2m)\, d^2/dx^2, \quad 0 < x < a$$

Thus, $$<E> = -\frac{30\hbar^2}{2ma^5}\int_0^a (ax - x^2)\frac{d^2}{dx^2}(ax - x^2)\, dx$$

$$= -\frac{30\hbar^2}{ma^5}\int_0^a (x^2 - ax)\, dx = -\frac{30\hbar^2}{ma^5}\left|\frac{x^3}{3} - \frac{ax^2}{2}\right|_0^a = \frac{5h^2}{4\pi^2 ma^2}$$

Since the true value $E_0 = h^2/8ma^2$, we see that $< E >$ **is greater than** E_0, which is as it should be according to the variation theorem.

$$\% \text{ error} = \frac{(5/4\pi^2 - 1/8)(h^2/ma^2)}{(1/8)(h^2/ma^2)} \times 100 = 1{\cdot}3\%.$$

Comment. Though it is not a true variational calculation since it does not use a variation parameter, this example does illustrate the fact that an approximate trial function always yields an *upper bound* to the true ground state energy.

Example 3. The hydrogen atom problem has been solved quantum mechanically, the exact ground state wave function being of the form exp (– r) (in a.u.), neglecting the normalization factor ; here r is the distance of the electron from the nucleus. Introduce a variational parameter α in the exponent to get a trial wave function exp (– αr) (in a.u.). Using variation method, estimate the ground state energy of the electron in hydrogen atom.

Solution. The Schrödinger wave equation is $\hat{H}\psi = E\psi$ ...(*i*)

where $$\hat{H} = -\frac{1}{2}\nabla^2 - \frac{1}{r} \text{ (in a.u.) since in a.u., } \hbar = m_e = e = 1/4\pi\varepsilon_0 = 1 \quad ...(ii)$$

We know that the Laplacian operator ∇^2, in polar coordinates, is given by

$$\nabla^2 = \frac{1}{r^2}\frac{\partial}{\partial r}\left[r^2\frac{\partial}{\partial r}\right] + \frac{1}{r^2\sin\theta}\frac{\partial}{\partial\theta}\left[\sin\theta\frac{\partial}{\partial\theta}\right] + \frac{1}{r^2\sin^2\theta}\frac{\partial^2}{\partial\phi^2}$$

We see that the trial function $\psi(r) = e^{-\alpha r}$ is spherically symmetric since if does not depend upon coordinates θ and ϕ. Hence, the partial derivatives $\partial\psi/\partial\theta$ and $\partial^2\psi/\partial\phi^2$ vanish, giving

$$\nabla^2 = \frac{1}{r^2}\frac{\partial}{\partial r}\left(r^2\frac{\partial}{\partial r}\right) \quad ...(iii)$$

Substituting in Eq. *(ii)* $$\hat{H} = -\frac{1}{2r^2}\frac{\partial}{\partial r}\left(r^2\frac{\partial}{\partial r}\right) - \frac{1}{r} \quad ...(iv)$$

Instead of first normalizing the given trial function and then determining the energy from the relation

$$E = <\hat{H}> = \int \psi^* \hat{H}\psi \, d\tau \equiv <\psi|\hat{H}|\psi> \quad ...(v)$$

we will keep it unnormalized and determine the energy using the relation

$$E \equiv <\hat{H}> = \frac{<\psi|\hat{H}|\psi>}{<\psi|\psi>} \equiv \frac{\int \psi^* \hat{H}\psi \, d\tau}{\int \psi^*\psi \, d\tau} \quad ...(vi)$$

We recall that in spherical polar coordinates (r, θ, ϕ), the volume element $d\tau = r^2 \sin\theta \, dr d\theta d\phi$, where $0 \le r \le \infty$; $0 \le \theta \le \pi$ and $0 \le \phi \le 2\pi$.

Let us first evaluate $\hat{H}\psi$:

$$\hat{H}\psi = -\frac{1}{2r^2}\frac{\partial}{\partial r}\left(r^2\frac{\partial e^{-\alpha r}}{\partial r}\right) - \frac{1}{r}e^{-\alpha r}$$

$$\frac{\partial e^{-\alpha r}}{\partial r} = -\alpha e^{-\alpha r}$$

and $$\frac{\partial}{\partial r}(-\alpha r^2 e^{-\alpha r}) = (-\alpha)\frac{\partial}{\partial r}(r^2 e^{-\alpha r}) = (-\alpha)(2r - \alpha r^2)e^{-\alpha r} = (-2\alpha r + \alpha^2 r^2)e^{-\alpha r}$$

Thus, $$\hat{H}\psi = -\frac{1}{2r^2}(-2\alpha r + \alpha^2 r^2)e^{-\alpha r} - \frac{1}{r}e^{-\alpha r} = \left(\frac{\alpha - 1}{r} - \frac{\alpha^2}{2}\right)e^{-\alpha r}$$

Substituting in Eq. *vi*, $$E = \frac{\int_0^\infty e^{-\alpha r}\left[\frac{\alpha-1}{r} - \frac{\alpha^2}{2}\right]e^{-\alpha r} r^2 dr \int_0^\pi \sin\theta\, d\theta \int_0^{2\pi} d\phi}{\int_0^\infty e^{-\alpha r} e^{-\alpha r} r^2 dr \int_0^\pi \sin\theta\, d\theta \int_0^{2\pi} d\phi}$$

Cancelling the common factors in the numerator and the denominator and simplifying, we get

$$E = \frac{(\alpha - 1)\int_0^\infty r\, e^{-2\alpha r} dr - \frac{\alpha^2}{2}\int_0^\infty r^2 e^{-2\alpha r} dr}{\int_0^\infty r^2 e^{-2\alpha r} dr}$$

The integrals occurring in the above equation can be evaluated using the standard integral

$$\int_0^\infty x^n e^{-ax} dx = \frac{n!}{a^{n+1}}, \text{ giving } E = \frac{(\alpha - 1)\frac{1}{4\alpha^2} - \frac{\alpha^2}{2}\frac{2}{(2\alpha)^3}}{2/(2\alpha)^3}$$

$$= \frac{\frac{\alpha - 1}{4\alpha^2} - \frac{1}{8\alpha}}{1/4\alpha^3} = \frac{(2\alpha - 2 - \alpha)/8\alpha^2}{1/4\alpha^3} = \frac{1}{2}(\alpha^2 - 2\alpha) \qquad ...(vii)$$

Using the variation method, differentiating E with respect to α and setting $(\partial E/\partial\alpha)_{\alpha_0} = 0$, we have $\partial E/\partial\alpha = (1/2)(2\alpha - 2) = \alpha - 1 = 0$, whence $\alpha = 1$, as expected. Substituting this value of the variational parameter in Eq. *vii*, we have

$$E_0 = -\frac{1}{2} \text{ (a.u.)}$$

which, we recall, is the exact ground state energy of hydrogen atom corresponding to the exact ground state function $\psi = e^{-r}$ (in a.u.)

Example 4. Using the variation method estimate the ground state energy of a one-dimensional S.H.O. of mass m and anguler frequency ω using a Gaussian trial wave function.

Solution : $$\hat{H} = -\frac{\hbar^2}{2m}\frac{d^2}{dx^2} + \frac{1}{2}m\omega^2 x^2$$

and the Gaussian trial wavefunction is

$$\psi(x) = N \exp(-\alpha x^2)$$

where N is the normalization constant and α is the variation parameter. The normalization condition gives

$$1 = \int_{-\infty}^{\infty} \psi^* \psi dx = |N|^2 \int_{-\infty}^{\infty} \exp(-2\alpha x^2) dx$$

$$= |N|^2 (\pi/2\alpha)^{1/2} \qquad \text{[using the standard integral formula]}$$

so that $N^2 = (2\alpha/\pi)^{1/4}$, and the normalized wave function is

$$\psi(x) = (2\alpha/\pi)^{1/4} \exp(-\alpha x^2) \qquad (i)$$

Hence, $$E = \langle\hat{H}\rangle = \langle\psi|\hat{H}|\psi\rangle = \left\langle\psi\left|-\frac{\hbar^2}{2m}\frac{d^2}{dx^2} + \frac{1}{2}m\omega^2 x^2\right|\psi\right\rangle$$

$$= -\frac{\hbar^2}{2m}\left\langle\psi\left|\frac{d^2}{dx^2}\right|\psi\right\rangle + \frac{1}{2}m\omega^2\langle\psi|x^2|\psi\rangle \qquad (ii)$$

where $$\left\langle\psi\left|\frac{d^2}{dx^2}\right|\psi\right\rangle = -\left(\frac{2\alpha}{\pi}\right)^{1/2} 2\alpha\int_{-\infty}^{\infty}\exp(-2\alpha x^2)dx + \left(\frac{2\alpha}{\pi}\right)^{1/2} 4\alpha^2\int_{-\infty}^{\infty} x^2\exp(-2\alpha x^2)dx$$

$$= -\left(\frac{2\alpha}{\pi}\right)^{1/2} 2\alpha\left(\frac{\pi}{2\alpha}\right)^{1/2} + \left(\frac{2\alpha}{\pi}\right)^{1/2} 4\alpha^2\frac{1}{4\alpha}\left(\frac{\pi}{2\alpha}\right)^{1/2} = -\alpha \qquad (iii)$$

and $$\langle\psi|x^2|\psi\rangle = \left(\frac{2\alpha}{\pi}\right)^{1/2}\int_{-\infty}^{\infty} x^2\exp(-2\alpha x^2)dx = \frac{1}{4\alpha} \qquad (iv)$$

Thus, we have from Eqs. *ii*, *iii* and *iv*

$$E = \langle\hat{H}\rangle = \frac{\hbar^2\alpha}{2m} + \frac{1}{2}m\omega^2\frac{1}{4\alpha} = \frac{\hbar^2\alpha}{2m} + \frac{m\omega^2}{8\alpha} \qquad (v)$$

Using the variation method, differentiating E with respect of α and setting $(\partial E/\partial\alpha)_{\alpha_0} = 0$, we have

$$\partial E/\partial\alpha = \frac{\hbar^2}{2m} - \frac{m\omega^2}{8\alpha^2} = 0, \text{ whence } \alpha_0 = \frac{m\omega}{2\hbar}$$

Substituting this value of α_0 in Eq. *v*

$$E_{min} = \langle H\rangle_{min} = \frac{1}{2}\hbar\omega = \frac{1}{2}h\nu \qquad (\because\ \omega = 2\pi\nu)$$

which, we recall, is the exact ground state energy of the S.H.O. $\left[E_n = \left(n + \frac{1}{2}\right)h\nu,\ n = 0, 1, 2, \ldots\right]$. Hence, the trial wave function we have used is, in fact, the exact eigenfunction.

Example 5. An anharmonic oscillator moves under the potential energy

$$V(x) = \frac{1}{2}kx^2 + \frac{1}{6}\gamma x^3$$

Calculate the first-order correction to the harmonic oscillator energy levels.

Solution : The unperturbed eigenfunctions of the oscillator are

$$\psi_n^{(0)}(x) = \left[\frac{\beta^{1/2}}{2^n n!\sqrt{\pi}}\right]^{1/2} e^{-\beta x^2} H_n(\beta^{1/2}x); \quad \beta = (\mu k)^{1/2}/\hbar$$

Here $H_n(\beta^{1/2}x)$ are the Hermite polynomials.

The unperturbed energies are

$$E_n^{(0)} = \left(n + \frac{1}{2}\right)h\nu$$

where ν is the oscillator frequency : $\nu = (1/2\pi)(k/\mu)^{1/2}$; μ is the reduced mass and k is the force constant.

The perturbation term of the oscillator is

$$\hat{H}^{(1)} = \frac{1}{6}\gamma x^3$$

Hence,

$$E_n^{(1)} \equiv \Delta E = \left[\frac{\beta^{1/2}}{2^n n!\sqrt{\pi}}\right]\frac{\gamma}{6}\int_{-\infty}^{\infty} H_n(\beta^{1/2}x)x^3 H_n(\beta^{1/2}x)\exp(-\beta x^2)\,dx$$

This integral can be evaluated for any value of n by remembering that the Hermite polynomials are either even or odd functions. Thus, the integrand here is overall an odd function, so that the integral itself vanishes, giving $\Delta E=0$. Thus,

$$E_n = \left(n+\frac{1}{2}\right)h\nu + \text{higher order terms.}$$

There is no change in the energy upto first order. Thus, the first-order contribution to energy = 0.

Example 6. The anharmonic oscillator moves under the potential energy which includes quadratic, cubic and quartic terms *viz.*,

$$V(x) = \frac{1}{2}kx^2 + \frac{1}{6}\gamma x^3 + \frac{1}{24}bx^4$$

Calculate the first-order correction to the ground state energy of the oscillator.

Solution : In this case the perturbation is

$$\hat{H}^{(1)} = \frac{1}{6}\gamma x^3 + \frac{1}{24}bx^4$$

The ground state wave function of the harmonic oscillator is

$$\psi_0(x) = \left(\frac{\beta}{\pi}\right)^{1/4}\exp\left(-\beta x^2/2\right); \quad \beta = (\mu k)^{1/2}/\hbar$$

The first-order correction to the ground-state energy is given by

$$E_0^{(1)} \equiv \Delta E = \left(\frac{\beta}{\pi}\right)^{1/2}\int_{-\infty}^{\infty}\left(\frac{1}{6}\gamma x^3 + \frac{1}{24}bx^4\right)\exp\left(-\beta x^2\right)dx$$

The integral involving $\gamma x^3/6$ here vanishes because the integrand is odd. The remaining integral is

$$\Delta E = \frac{b}{12}\left(\frac{\beta}{\pi}\right)^{1/2}\int_0^{\infty} x^4\exp(-\beta x^2)\,dx$$

This integral is found in the tables of integrals, and is equal to $3\pi^{1/2}/8\beta^{5/2}$, and so

$$\Delta E = b/32\beta^2 = b\hbar^2/32k\mu \neq 0$$

The total ground state energy is

$$E = \frac{h\nu}{2} + \frac{b\hbar^2}{32k\mu} + \text{higher-order terms.}$$

We see that there *is* a change in energy upto first-order.

Example 7. Discuss quantum mecheanically the spin-orbit interaction in an atom.

Solution : The electron in an atom moves in a central potential energy $V(r)$ (assumed to be spherically symmetric) that is produced by the nucleus and the other electrons. The interaction between its orbital and spin magnetic moments produces a term in the energy of the system. This phenomenon is called *spin-orbit-interaction.* The spin-orbit Hamillanion $\hat{H}_{so}$ is given by

$$\hat{H}_{so} = \zeta(r)\,L.S., \text{ where } \zeta(r) = \frac{1}{2m_e^2c^2}\frac{1}{r}\frac{dV}{dr}$$

The radial average of the function $\zeta(r)\hbar^2$ is written as $hc\zeta$, where ζ is called the *spin-orbit coupling constant.* Then,

$$hc\zeta = \langle nl|\zeta|nlm\rangle\hbar^2$$

On the basis of this definition, ζ is a wave number and $hc\zeta$ is an energy. For an electron in a hydrogenic atom, the potential energy

$$V(r) = -\frac{Ze^2}{r} \quad \text{or} \quad \frac{dV}{dr} = \frac{Ze^2}{r^2} \qquad \text{(in c.g.s. units)}$$

Hence,

$$\hat{H}_{so} = \zeta(r)\,\text{L.S} = \frac{Ze^2}{2m_e^2c^2}\frac{1}{r^3}\,\text{L.S}$$

The expectation value of $1/r^3$ for the hydrogenic wave functions is

$$\left\langle nlm\left|\frac{1}{r^3}\right|nlm\right\rangle = \frac{Z^3}{n^3a_0^3l(l+\frac{1}{2})(l+1)}$$

where a_0 is the Bohr radius. The spin-orbit coupling constant for a hydrogenic atom is given by

$$hc\zeta_{nl} = \frac{Z^4e^2\hbar^2}{2m_e^2c^2a_0^3n^3l\ (l+\frac{1}{2})(l+1)}$$

It can be written as

$$\zeta_{nl} = \frac{Z^4\alpha^2R^2}{n^3l(l+\frac{1}{2})(l+1)}$$

where the *fine structure constant* $\alpha = e^2/\hbar c = 1/137$ and R is the Rydberg constant $= 2\pi^2m_ee^4/h^3c$.

Thus, we see that the spin-orbit interaction is proportional to Z^4 and is very predominant in heavy elements having large value of the atomic number Z.

After this preliminary discussion of spin-orbit interaction, we proceed to determine its effect on the energy levels. Since $\hat{H}_{so}$ is very weak compared with the energy level separations of the atom, it can be treated as a perturbation on the unperturbed Hamiltonian $\hat{H}^{(0)}$ which has degenerate eigenvalues for a given n and l. However, we can avoid working with degenerate perturbation theory by using the basis $|lsjm\rangle$ since L^2, S^2, J^2 and J_z commute. The first-order correction to the energy of the state $|lsjm\rangle$ is

$$E_{so} = \left\langle lsjm\left|\hat{H}_{so}\right|lsjm\right\rangle = \langle lsjm|\zeta(r)\,\text{L.S}|\,lsjm\rangle$$

The matrix elements of the scaler product L.S can be easily evaluated by writing

$$J^2 = L^2 + S^2 + 2\,L.S \quad \text{or} \quad L.S = \frac{1}{2}\left(J^2 - L^2 - S^2\right)$$

It follows that

$$\langle lsjm|L.S|lsjm\rangle = \frac{1}{2}\hbar^2[j(j+1) - l(l+1) - s(s+1)]$$

Hence, the interaction energy is

$$E_{so} = \frac{1}{2}hc\zeta_{nl}[j(j+1) - l(l+1) - s(s+1)$$

$$= \frac{hcZ^4\alpha^2R}{2} \frac{j(j+1)-l(l+1)-s(s+1)}{n^2l(l+\frac{1}{2})(l+1)}$$

The E_{so} is independent of m_j and, therefore, each level is (2j+1)-fold degenerate. For an s electron, the spin-orbit interaction is zero, since $l=0$ and $j=s$.

Hartree and Hartree-Fock Self-Consistent Field (SCF) Method

We have seen that the application of the above two approximate methods to the solution of the Schrödinger wave equation for helium atom, the simplest two-electron system, does not give very accurate result. For the other atoms in the periodic table, the number of inter-electron repulsion terms in the Hamiltonian will increase thereby rendering the exact solution of the wave equation even more difficult. Thus, we need more powerful methods for the calculation of the ground state energy and wave functions of many-electron atoms or ions. In 1928, the British physicist D.R. Hartree suggested that the wave function of an n-electron atom be written as the ***product*** of n one-electron wave functions :

$$\psi(1, 2, 3, ..., n) = \phi_1(1)\,\phi_2(2)\,\phi_3(3)\,.....\,\phi_n(n) \qquad ...(73)$$

where $\phi(i)$ are normalized and mutually orthogonal one-electron wave functions. Thus, $\phi_1(1)$ means that electron 1 occupies atomic orbital ϕ_1, etc. Hartree proposed the self-consistent field (SCF) method *according to which each electron is assumed to move in a spherically symmetrical potential due to the nucleus and the average potential of all the electrons except the one under consideration.* Thus, potential energy (in a.u.) of electron 1 can be written as

$$V_1 = -\frac{Z}{r_1} + \sum_{i\neq 1} \int \frac{\phi_i^2(i)}{r_{1i}} d\tau_i \qquad ...(74)$$

Similarly, for every other electron i in the atom,

$$V_i = -\frac{Z}{r_i} + \sum_{j\neq i} \int \frac{\phi_j^2(j)}{r_{ij}} d\tau_j \qquad ...(75)$$

where the first term is the attractive potential energy between the ith electron and the nucleus ; it is a negative term. *It is the second term in Eq. 75 which represents the self-consistent field* ; here r_{ij} is the distance between electrons i and j ; the integral is over all space accessible to electron j and the summation is over all j electrons except $j=i$. The quantity $\phi_i^2(i)$ is the probability distribution of electron i. Using Eq. 75 for V_i, the Schrödinger wave equation for the ith electron in an atom is

$$\left(-\frac{1}{2}\nabla_i^2 + V_i\right)\phi_i(i) = \varepsilon_i\phi_i \qquad (i = 1, 2, 3, ... n) \qquad ...(76)$$

where ε_i is the energy of the ith orbital, ϕ_i, assumed to be normalized. The n non-linear simultaneous equations cannot be solved since V_i requires a prior knowledge of all other one-electron wave functions ϕ_j. The SCF method is as follows : First, we choose an arbitrary set of AOs ϕ_j, ϕ_k, etc. The potential energy field V_i arising from all the electrons except the ith electron is calculated from this chosen set of functions and Eq. 76 is solved numerically on the computer to obtain ϕ_i. This procedure is repeated for each of the n electrons in the atom. In general, the calculated set of ϕ_is is not identical with the original chosen set. The calculations are then repeated using the calculated set of orbitals. The process of iteration is continued until the assumed set of ϕ_is and the calculated set are identical. This is expressed by saying that the set of Eq. 76 has been solved by the SCF method.

If $\phi_1'(1)$, $\phi_2'(2)$, $\phi_3'(3)$,.... are the self-consistent orbitals (one-electron wave functions) then the total wave function of the n-electron system is given by

$$\psi'(1, 2, 3, ..., n) = \phi_1'(1)\,\phi_2'(2)\,\phi_3'(3).....\phi_n'(n) \qquad ...(77)$$

The corresponding energy ε associated with this wavefunction is

$$\varepsilon = \langle \psi' | \hat{H} | \psi' \rangle$$

$$= \langle \phi_1'(1)\,\phi_2'(2)....\phi_n'(n) \left| -\frac{1}{2}\sum_i \nabla_i^2 - \sum_i \frac{Z}{r_i} + \frac{1}{2}\sum_{i\neq j}\frac{1}{r_{ij}} \right| \phi_1'(1)\,\phi_2'(2)....\phi_n'(n)\rangle$$

$$= \sum_i \langle \phi_1'(i) \left| -\frac{1}{2}\nabla_i^2 - \frac{Z}{r_i} \right| \phi_1'(i)\rangle + \frac{1}{2}\sum_i\sum_j \langle \phi_i'(i)\phi_j'(j) \left| \frac{1}{r_{ij}} \right| \phi_i'(i)\,\phi_j'(j)\rangle$$

Omitting further mathematical details, the final result is

$$\varepsilon = \sum_i \varepsilon_i' - \frac{1}{2}\sum_{\substack{i\\ i\neq j}}\sum_j \langle \phi_i'(i)\,\phi_j'(j) \left| \frac{1}{r_{ij}} \right| \phi_i'(i)\,\phi_j'(j)\rangle \qquad ...(78)$$

In 1930, the Russian physicist V. Fock proposed that since the Hartree wave function (Eq. 73) was the product of n one-electron *spatial* functions, an improved wave function should include both the spatial part and the electron spin part. This suggestion had also been made by J.C. Slater. Fock solved the many-electron Schrödinger wave equation using such a wave function and the Hartree method. This technique is called the Hartree–Fock SCF method. E. Clementi obtained the SCF wave functions for atoms of various elements in 1965. Hartree-Fock calculations give good agreement with experimental data. Because the Hartree-Fock method uses determinantal wave functions, there is some correlation between electrons with the same spin, because two electrons with the same spin cannot occupy the same orbital. Neverthless, the Hartree-Fock method is not exact, and so we define a correlation energy

$$\text{Correlation energy (CE)} = E_{\text{exact}} - E_{\text{HF}} \qquad ...(79)$$

Though correlation energies appear to be small, they are really very significant.

Slater Determinant for n-Electron Atoms

It was proposed by J.C. Slater in 1930 that for a multielectron atom the total wave function must consist of the *spatial* part and the *spin* part. He showed that the total atomic wave function, which is the product of the spatial wave function and the spin wave function, is *antisymmetric* (A) with respect to the interchange of electrons, *i.e.*,

$$\Psi_{\text{total}} = \psi_{\text{space}} \times \psi_{\text{spin}} \text{ (antisymmetric)} \qquad ...(80)$$

Thus, for helium atom with the ground state electronic configuration $1s^2$,

$$\psi_{\text{space}} = 1s(1)\,1s(2) \qquad ...(81)$$

Interchanging the two electrons,

$$\psi_{\text{space}} = 1s(2)\,1s(1) \qquad ...(82)$$

That is, ψ_{space} is symmetric (S) ; it does not change sign. If α and β are the spin wave functions for

the upward (↑) orientation and the downward (↓) orientation, respectively, then

$$\psi_{spin} = \begin{cases} \alpha(1)\alpha(2); (S) \\ \frac{1}{\sqrt{2}}[\alpha(1)\beta(2)+\alpha(2)\beta(1)]; (S) \\ \frac{1}{\sqrt{2}}[\alpha(1)\beta(2)-\alpha(2)\beta(1)]; (A) \\ \beta(1)\beta(2); (S) \end{cases} \quad ...(83)$$

We see that there are three symmetric (S) and one antisymmetric (A) spin wave functions.

Thus, $\Psi_{total} = \psi_{space} \times \psi_{spin}$

$$= 1s(1)\ 1s(2)\ ;(S) \times \begin{cases} \alpha(1)\alpha(2); (S) \\ \frac{1}{\sqrt{2}}[\alpha(1)\beta(2)+\alpha(2)\beta(1)]; (S) \\ \frac{1}{\sqrt{2}}[\alpha(1)\beta(2)-\alpha(2)\beta(1)]; (A) \\ \beta(1)\beta(2); (S) \end{cases} \quad ...(84)$$

Hence, the only combination which gives total antisymmetric wavefunction is the product of the symmetric spatial wavefunction and the antisymmetric spin function. Thus,

$$\Psi_{total} \equiv \psi(1, 2) = 1s(1)\ 1s(2) \left\{\frac{1}{\sqrt{2}}[\alpha(1)\beta(2) - \alpha(2)\beta(1)]\right\}$$

$$= \frac{1}{\sqrt{2}}\ [1s(1)\ \alpha(1)\ 1s(2)\ \beta(2) - 1s(1)\ \beta(1)\ 1s(2)\ \alpha(2)] \quad ...(85)$$

which can be written as a 2×2 determinant,

$$\Psi(1, 2) = \frac{1}{\sqrt{2!}}\begin{vmatrix} 1s(1)\alpha(1) & 1s(2)\alpha(2) \\ 1s(1)\beta(1) & 1s(2)\beta(2) \end{vmatrix} \quad ...(86)$$

This is called the **Slater determinant** for helium atom.

Interchanging electrons 1 and 2 in Eq. 333, we have

$$\Psi(2, 1) = \frac{1}{\sqrt{2!}}\begin{vmatrix} 1s(2)\alpha(2) & 1s(1)\alpha(1) \\ 1s(2)\beta(2) & 1s(1)\beta(1) \end{vmatrix} = -\Psi(1, 2) \quad ...(87)$$

This result follows from the fact that if in a determinant two rows (or columns) are interchanged, it changes sign. What is true of a two-electron system is also true of polyelectron atoms and molecules. The polyelectron wave function also satisfies the antisymmetry rule. The solution of the Schrödinger wave equation for such systems must start from the appropriate Slater determinant for a given electronic configuration. The Hartree-Fock SCF method, using Slater determinants has been successfully employed by theoretical chemists and physicists. In 1951 the American physicist C.C.J. Roothaan extended it to molecules as well.

Example 8. Write the Slater determinants for the ground states of *(a)* lithium atom ($1s^2\ 2s^1$) and *(b)* carbon atom ($1s^2\ 2s^2\ 2p^2$).

Solution. *(a)* $$\Psi(1, 2, 3) = \frac{1}{\sqrt{3!}}\begin{vmatrix} 1s(1)\alpha(1) & 1s(2)\alpha(2) & 1s(3)\alpha(3) \\ 1s(1)\beta(1) & 1s(2)\beta(2) & 1s(3)\beta(3) \\ 2s(1)\alpha(1) & 2s(2)\alpha(2) & 2s(3)\alpha(3) \end{vmatrix}$$

(b) $\Psi(1, 2, 3, 4, 5, 6) =$

$$\frac{1}{\sqrt{6!}}\begin{vmatrix} 1s(1)\alpha(1) & 1s(2)\alpha(2) & 1s(3)\alpha(3) & 1s(4)\alpha(4) & 1s(5)\alpha(5) & 1s(6)\alpha(6) \\ 1s(1)\beta(1) & 1s(2)\beta(2) & 1s(3)\beta(3) & 1s(4)\beta(4) & 1s(5)\beta(5) & 1s(6)\beta(6) \\ 2s(1)\alpha(1) & 2s(2)\alpha(2) & 2s(3)\alpha(3) & 2s(4)\alpha(4) & 2s(5)\alpha(5) & 2s(6)\alpha(6) \\ 2s(1)\beta(1) & 2s(2)\beta(2) & 2s(3)\beta(3) & 2s(4)\beta(4) & 2s(5)\beta(5) & 2s(6)\beta(6) \\ 2p_{+1}(1)\alpha(1) & 2p_{+1}(2)\alpha(2) & 2p_{+1}(3)\alpha(3) & 2p_{+1}(4)\alpha(4) & 2p_{+1}(5)\alpha(5) & 2p_{+1}(6)\alpha(6) \\ 2p_0(1)\alpha(1) & 2p_0(2)\alpha(2) & 2p_0(3)\alpha(3) & 2p_0(4)\alpha(4) & 2p_0(5)\alpha(5) & 2p_0(6)\alpha(6) \end{vmatrix}$$

We may mention here that the Slater determinant is the quantum mechanical version of the Pauli principle. Thus, for instance, the Slater determinant for the electronic configuration $1s^3$ is zero. This is in accordance with the Pauli principle according to which $1s$ orbital cannot have three electrons. Thus, Pauli's exclusion principle may be stated as follows :

The wave function for any system of electrons must be antisymmetric with respect to the interchange of any two electrons. If a system of electrons in an atom could be symmetric with respect to the interchange of any two electrons, there would be an entirely different set of elements. There is no simple expression for the energy of a many-electron atom. However, in contrast with the energy of the hydrogen atom, the energy of the polyelectronic atom can be written as

$$E_n = -\frac{2\pi^2 Z_{eff}^2\ \mu e^4}{(4\pi\varepsilon_0)^2\ n^2 h^2} \quad ...(88)$$

where n is the effective principal quantum number, μ is the reduced mass and Z_{eff} is the effective nuclear charge, defined as $Z_{eff} = Z - \sigma$ where Z is the atomic number (the true nuclear charge) and σ is the **screening constant** (or, **shielding constant**) which depends upon the quantum numbers n and l.

The American physicist J.C. Slater (1900-1976) formulated the following empirical rules (known as **Slater's rules**) for estimating σ :

1. Electrons farther away from the nucleus than the electron under consideration do not contribute to σ.

2. The electrons in the same group, *i.e.*, *ns*, *np*, *nd* or *nf*-electrons, contribute 0·35 to σ (except $1s$-electron for which σ=0·30).

3. In the case of electrons in the *ns* and *np* orbitals, all electrons in the $(n-1)$ shell contribute 0·85 each and all electrons in the $(n-2)$ shell contribute 1·0 each.

4. For electrons in the *nd* and *nf* orbitals, each electron in the lower groups contributes 1·0 to σ.

Knowing the value of σ Z_{eff} can be calculated.

Example 9. Calculate the effective nuclear charge for *(i)* the 3*s* electron in sulphur (Z=16) *(ii)* the 4*s* electron in potassium (Z=19) *(iii)* a 3*d* and a 4*s* electron in vanadium (Z=23).

Solution : *(i)* Electronic configuration of S atom is : $1s^2\ 2s^2\ 2p^6\ 3s^2\ 3p^4$

For the 3s electron, $\sigma = (5\times0{\cdot}35) + (8\times0{\cdot}85) + (2\times1{\cdot}00) = 10{\cdot}55$

$\therefore$ $Z_{eff} = Z - \sigma = 16 - 10{\cdot}55 = \mathbf{5{\cdot}45}$

(ii) Electronic configuration of K atom is : $1s^2\ 2s^2\ 2p^6\ 3s^2\ 3p^6\ 4s^1$

For the 4*s* electron, $\sigma = 8\times0{\cdot}85 + 1\times 10 = 16{\cdot}80$

$\therefore$ $Z_{eff} = Z - \sigma = 19 - 16{\cdot}80 = \mathbf{2{\cdot}20}$

(iii) Electronic configuration of V atom is : $1s^2\ 2s^2\ 2p^6\ 3s^2\ 3p^6\ 3d^3\ 4s^2$

For the 3*d* electron, $\sigma = 2\times0{\cdot}35 + 18\times1 = 18{\cdot}70$

$\therefore$ $Z_{eff} = Z - \sigma = 23 - 18{\cdot}70 = \mathbf{4{\cdot}30}$

For the 4*s* electron,

$$\sigma = 0{\cdot}35\times1 + 11\times0{\cdot}85 + 10\times1 = 0{\cdot}35 + 9{\cdot}35 + 10 = 19{\cdot}70$$

$$\therefore \quad Z_{eff} = 23 - 19{\cdot}70 = 3{\cdot}30$$

Atomic Term Symbols. (These are discussed in detail later in this chapter). In an atom the electron spin angular momentum may couple with the total angular momentum as follows :

The coupling of spin angular momenta of two electrons, known as *s–s* coupling, gives rise to a quantum number S (called **total spin number**), where

$$S = \tfrac{1}{2} + \tfrac{1}{2} \text{ or } \tfrac{1}{2} - \tfrac{1}{2} \text{ or } -\tfrac{1}{2} - \tfrac{1}{2}, \quad i.e., \ 1, 0 \text{ or } -1 \qquad ...(89)$$

Similarly, the coupling of orbital angular momenta of two electrons, known as *l–l* coupling, gives rise to a quantum number L (called **total orbital angular momentum quantum number**), where

$$L = (l_1 + l_2), (l_1 + l_2 - 1), \ldots |l_1 - l_2| \qquad ...(90)$$

The term $|l_1 - l_2|$ signifies absolute value of $l_1 - l_2$.

The coupling of L and S, known as the **Russell–Saunders coupling**, gives rise to quantum number J where

$$J = (L + S), (L + S - 1), \ldots |L - S| \qquad ...(91)$$

The terms L, S and J collectively constitute an important symbol known as **atomic term symbol** which is generally designated as ${}^{2S+1}L_J$. The superscript represents the multiplicity of the term and subscript is the value of J as given by Eq. 91. Just as $l = 0$, 1, 2, and 3 corresponds to the atomic orbitals s, p, d and f, respectively, similarly, L=0,1,2,3 correspond to *atomic states* S,P,D and F, respectively. (The state S should not be confused with the total spin quantum number S).

THE SCHRÖDINGER EQUATION FOR A FINITE POTENTIAL BARRIER : QUANTUM MECHANICAL TUNNELLING

1. Finite Potential Well

Potential energy barriers are never infinite in a real world and a box with infinitely hard walls has no physical counterpart. However, potential wells with barriers of *finite height* certainly do exist. We shall here investigate the wave functions and energy levels in such a well. Fig. 2 shows potential well with square corners that is V_0 high and a wide. It contains a particle whose *energy is less than* V_0. According to classical mechanics, when the particle strikes the sides of the well, it bounces off without entering regions I and III. In quantum mechanics, however, the particle also bounces back and forth, but now it has a *finite probability* of penetrating into regions I and III even though $E < V_0$.

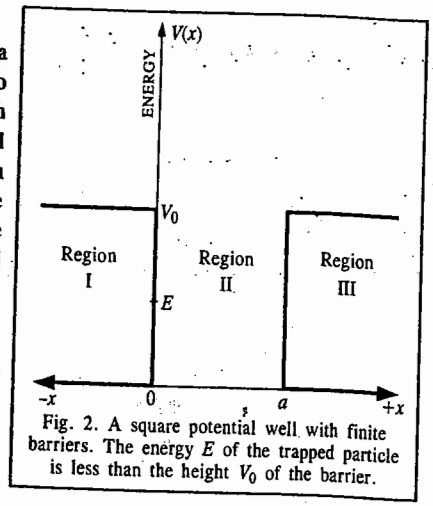

Fig. 2. A square potential well with finite barriers. The energy E of the trapped particle is less than the height V_0 of the barrier.

In regions I and III, the Schrödinger wave equation is

$$\frac{d^2\psi}{dx^2} + \frac{2m}{\hbar^2}(E - V_0)\psi = 0 \qquad ...(92)$$

or

$$\frac{d^2\psi}{dx^2} - k^2\psi = 0 \ ; \ x < 0 \text{ and } x > a \qquad ...(93)$$

where $k = [2m(V_0 - E)]^{1/2}/\hbar$.

The solutions of Eq. 92 are real exponentials, *viz.*,

$$\psi_I = Ae^{kx} + Be^{-kx} \qquad ...(94)$$

$$\psi_{III} = Ce^{kx} + De^{-kx} \qquad ...(95)$$

Both ψ_I and ψ_{III} must be finite everywhere. Since $e^{-kx} \to \infty$ as $x \to -\infty$ and $e^{kx} \to \infty$ as $x \to \infty$, the coefficients B and C must, therefore, be zero. Hence, we have

$$\psi_I = Ae^{kx} \text{ and } \psi_{III} = De^{-kx} \qquad ...(96)$$

These wave functions decrease exponentially inside the barriers at the sides of the well.

Within the well, the Schrödinger wave equation is

$$\frac{d^2\psi}{dx^2} + \frac{2mE}{\hbar^2}\psi = 0 \qquad ...(97)$$

since $V = 0$ there. The solution of Eq. 97 is

$$\psi_{II} = E\sin\frac{(2mE)^{1/2}}{\hbar}x + F\cos\frac{(2mE)^{1/2}}{\hbar}x \qquad ...(98)$$

In the case of a well with *infinitely high barriers*, it is found that $F = 0$ in order that $\psi = 0$ at x=0 and $x = a$. Here, however, $\psi_{II} = A$ at $x = 0$ and $\psi_{II} = D$ at $x = a$; so both the sine and cosine solutions of Eq. 98 are possible.

For either solution, both ψ and $d\psi/dx$ must be continuous at x=0 and x=a. The wave functions inside and outside each side of the well must not only have the same value where they join but also the same slopes so that they match perfectly. When these boundary conditions are taken into account, the result is that exact matching only occurs for certain values of energy (E_n) of the particle. The complete wave functions and their probability densities are shown in Fig. 3.

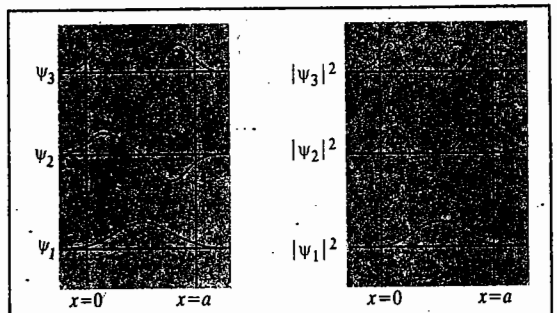

Fig. 3. Wave functions and probability densities of a particle in a finite potential well.
The particle has a certain probability of being found outside the well.

2. Quantum Mechanical Tunnelling

This phenomenon plays a central role in the Gamow-Gurney-Condon theory of the alpha decay of nuclei, the Marcus theory of electron-transfer reactions, hydrogen bonding, semiconductors, superconductors and scanning tunnelling microscopy (STM). Consider a beam of identical particles all of which have the kinetic energy E. The beam is incident from the left on a potential barrier of height V_0 and with width a (Fig. 4). Mathematically, we have

$$V(x) = \begin{cases} 0, & x < 0 \quad \text{(Region I)} \\ V_0, & 0 < x < a \quad \text{(Region II)} \\ 0, & x > a \quad \text{(Region III)} \end{cases}$$

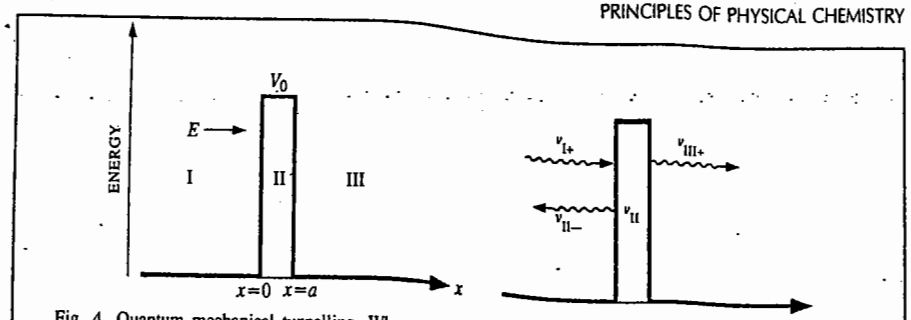

Fig. 4. Quantum mechanical tunnelling. When a particle of energy $E < V_0$ approaches a potential barrier, according to classical mechanics, the particle must be reflected. In quantum mechanics, the de Broglie waves that correspond to the particle are partly reflected and partly transmitted, which means that the particle has a finite probability of *penetrating* the barrier or *tunnelling* through the barrier.

On both sides of the barrier, $V = 0$ which means that no forces act on the particles there. In these regions the Schrödinger wave equation is

$$\frac{d^2\psi_I}{dx^2} + \frac{2mE}{\hbar^2}\psi_I = 0 \qquad ...(99)$$

$$\frac{d^2\psi_{III}}{dx^2} + \frac{2mE}{\hbar^2}\psi_{III} = 0 \qquad ...(100)$$

The solutions to these equations are

$$\psi_I = Ae^{ik_1x} + Be^{-ik_1x} \qquad ...(101)$$

$$\psi_{III} = Fe^{ik_1x} + Ge^{-ik_1x} \qquad ...(102)$$

where

$$k_1 \left(= \frac{(2mE)^{1/2}}{\hbar} = \frac{p}{\hbar} = \frac{2\pi}{\lambda} \right) \qquad ...(103)$$

is the *wave number* of de Broglie waves that represent the particles outside the potential energy barrier. Since according to Euler's formula,

$$e^{i\theta} = \cos\theta + i\sin\theta \text{ and } e^{-i\theta} = \cos\theta - i\sin\theta$$

we find that these solutions (Eqs 101 and 102) are equivalent to those of a particle inside a potential box of infinite height—the values of the coefficients are different in each case, of course—but are in a more suitable form to describe particles that are not trapped. The various terms in Eqs. 101 and 102 are easy to interpret. As shown schematically in Fig. 4, Ae^{ik_1x} is a wave of amplitude A incident from the left on the barrier. Hence, we can write, for the *incoming wave*,

$$\psi_{I+} = Ae^{ik_1x} \qquad ...(104)$$

This wave corresponds to the incident beam of particles in the sense that $|\psi_{I+}|^2$ is their probability density. If v_{1+} is the **group velocity** of the incoming wave, which equals the velocity of the particles, then

$$S = |\psi_{1+}|^2 v_{1+}$$

is the **flux** of particles (*i.e.*, number of particles per square metre per second) that arrive at the barrier.

At $x=0$, the incident wave strikes the barrier and is partially reflected. Thus, for the *reflected wave*, we have

$$\psi_1 = Be^{-ik_1x}$$

Hence,

$$\psi_I = \psi_{I+} + \psi_{I-} \qquad ...(105)$$

$$...(106)$$

On the far side of the barrier ($x > a$), there can be only one wave *viz.*, the transmitted wave,

$$\psi_{III+} = Fe^{ik_1x} \qquad ...(107)$$

travelling in the $+x$ direction at velocity v_{III+} since region III contains nothing that could reflect the wave. Hence, $G = 0$, and

$$\psi_{III} = \psi_{III+} = Fe^{ik_1x} \qquad ...(108)$$

The **transmission probability**, T, for a particle to pass through the barrier is given by

$$T = \frac{|\psi_{III+}|^2 v_{III}}{|\psi_{1+}|^2 v_1} = \frac{FF^* v_{III}}{AA^* v_1} \qquad ...(109)$$

between the flux of particles that emerges from the barrier and the flux that arrives at it. In other words, *T is the fraction of the incident particles that succeed in tunnelling through the barrier.* Classically, $T = 0$ because the particle with energy $E < V_0$ cannot exist inside the barrier. We shall now consider the quantum mechanical result.

In region II, the Schrödinger wave equation for the particles is

$$\frac{d^2\psi_{II}}{dx^2} + \frac{2m}{\hbar^2}(E - V_0)\psi_{II} = \frac{d^2\psi_{II}}{dx^2} - \frac{2m}{\hbar^2}(V_0 - E)\psi_{II} = 0 \qquad ...(110)$$

Since $V_0 > E$, the solution for the *wavefunction inside the barrier* is

$$\psi_{II} = Ce^{-k_2x} + De^{k_2x} \qquad ...(111)$$

where the *wave number inside the barrier is*

$$k_2 = [2m(V_0 - E)]^{1/2}/\hbar \qquad ...(112)$$

Since the exponents are real quantities, ψ_{II} does not oscillate and, therefore, does not represent a moving particle. However, the probability density $|\psi_{II}|^2$ is not zero, so there is a finite probability of finding a particle within the barrier. Such a particle may emerge into region III or it may return to region I.

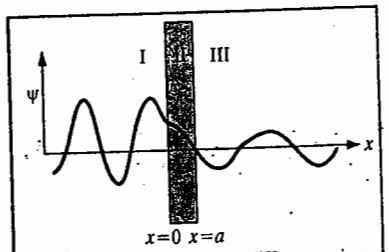

Fig. 5. The wave functions in different regions.

We shall derive the formula for the transmission probability by applying the boundary conditions to ψ_I, ψ_{II} and ψ_{III}. Fig. 5 shows the wave functions in regions I, II and III. Both ψ and its derivative $d\psi/dx$ must be continuous everywhere.

At each wall of the barrier, the wave functions inside and outside it must match up perfectly, which means that they must have the same values and same slopes there.

This implies that for a perfect fit at each side of the barrier, the wave functions inside and outside must have the same value and the same slope. However, at the left hand side of the barrier, we have

$$\left.\begin{aligned}\psi_I &= \psi_{II} \\ d\psi_I/dx &= d\psi_{II}/dx\end{aligned}\right\} \text{ (Boundary conditions at } x = 0) \qquad ...(113)$$

and at the right hand side,

$$\left.\begin{aligned}\psi_{II} &= \psi_{III} \\ d\psi_{II}/dx &= d\psi_{III}/dx\end{aligned}\right\} \text{ (Boundary conditions at } x = a) \qquad ...(114)$$

Substituting for ψ_I, ψ_{II} and ψ_{III} from Eqs. 101, 108 and 111 into the above equations,

we have in the same order

$$A + B = C + D \qquad ...(115$$

$$ik_1A - ik_1B = -k_2C + k_2D \quad ...(116)$$

$$Ce^{-k_2a} + De^{k_2a} = Fe^{ik_1a} \quad ...(117)$$

$$-k_2Ce^{-k_2a} + k_2De^{k_2a} = ik_1Fe^{ik_1a} \quad ...(118)$$

Eqs. 115 to 118 may be solved for (A/F) to give

$$\left(\frac{A}{F}\right) = \left[\frac{1}{2} + \frac{i}{4}\left(\frac{k_2}{k_1} - \frac{k_1}{k_2}\right)\right]e^{(ik_1+k_2)a} + \left[\frac{1}{2} - \frac{i}{4}\left(\frac{k_2}{k_1} - \frac{k_1}{k_2}\right)\right]e^{(ik_1-k_2)a} \quad ...(119)$$

Assume that $V_0 > E$ so that $k_2/k_1 > k_1/k_2$ and

$$\frac{k_2}{k_1} - \frac{k_1}{k_2} \approx \frac{k_2}{k_1} \quad ...(120)$$

We shall further assume that the barrier is wide enough for ψ_{II} to be severely weakened at $x=0$ and $x=a$. This means that $k_2a >> 1$ and $e^{k_2a} >> e^{-k_2a}$. With these assumptions, Eq. 119 can be approximated to

$$\left(\frac{A}{F}\right) = \left(\frac{1}{2} + \frac{ik_2}{4k_1}\right)e^{(ik_1+k_2)a} \quad ...(121)$$

In order to calculate the complex conjugate of (A/F) we replace i by $-i$ wherever it occurs in (A/F) :

$$\left(\frac{A}{F}\right)^* = \left(\frac{1}{2} + \frac{ik_2}{4k_1}\right)e^{(-ik_1+k_2)a} \quad ...(122)$$

Multiplying (A/F) by $(A/F)^*$, we have

$$\frac{AA^*}{FF^*} = \left(\frac{1}{4} + \frac{k_2^2}{16k_1^2}\right)e^{2k_2a}$$

Here $v_{III+} = v_{I+}$ so that $v_{III+}/v_{I+} = 1$ in Eq. 109, which means that the transmission probability is given by

$$T = \frac{FF^*v_{III+}}{AA^*v_{I+}} = \left(\frac{AA^*}{FF^*}\right)^{-1} = \left[\frac{16}{4 + (k_2/k_1)^2}\right]e^{-2k_2a} \quad ...(123)$$

From the definitions of k_1 (Eq. 103) and k_2 (Eq. 112), we find that

$$\left(\frac{k_2}{k_1}\right)^2 = \frac{2m(V_0 - E)/\hbar^2}{2mE/\hbar^2} = \frac{V_0}{E} - 1 \quad ...(124)$$

From this result we see that the quantity in brackets in Eq. 123 varies much less with E and V_0 than does the exponential. Furthermore, the bracketed quantity is always of the order of magnitude of 1 in value. Hence, the approximate formula for the transmission probability is

$$T \approx e^{-2k_2a} \quad ...(125)$$

Thus, we conclude in the words of R.P. Feynman that "it is possible in quantum mechanics to sneak quickly across a region which is illegal energetically."

Example 10. Electrons with energies of 1·0 eV and 2·0 eV are incident on a barrier 10·0 eV high and 0·50 nm wide. *(a)* Calculate their respective transmission probabilities *(b)* How are these affected if the barrier is doubled in width ?

Solution : *(a)* For the 1·0 eV electrons,

$$k_2 = \frac{[2m(V_0 - E)]^{1/2}}{\hbar} = \frac{[(2)(9{\cdot}1 \times 10^{-31}\,\text{kg})[(10{\cdot}0 - 1{\cdot}0)\,\text{eV}]1{\cdot}6 \times 10^{-19}\,\text{J/eV}]^{1/2}}{1{\cdot}504 \times 10^{-34}\,\text{Js}}$$

$$= 1{\cdot}6 \times 10^{10}\,\text{m}^{-1}$$

Since $a = 0{\cdot}50\,\text{nm} = 5{\cdot}0 \times 10^{-10}$ m, $2k_2a = (2)(1{\cdot}6 \times 10^{-10}\,\text{m}^{-1})(5{\cdot}0 \times 10^{-10}\,\text{m}) = 16$ and the approximate transmission probability is given by

$$T_1 \approx \exp(-2k_2a) = e^{-16} = 1{\cdot}1 \times 10^{-7}$$

Thus, we see that one 1·0 eV-electron out of 8·9 million can tunnel through the 10 eV barrier on the average. For the 2·0 eV-electrons, a similar calculation gives $T_2 \approx 2{\cdot}4 \times 10^{-7}$. These electrons are over twice as likely to tunnel through the barrier.

(b) If the barrier is doubled in width to 1·0 nm, the transmission probability becomes

$$T_1' = 1{\cdot}3 \times 10^{-14}, \quad T_2' \approx 5{\cdot}1 \times 10^{-14}$$

Evidently, T is more sensitive to the width of the barrier than to the particle energy.

SIMPLE HARMONIC OSCILLATOR : THE ALGEBRAIC METHOD

Although the Schrödinger wave equation for the simple harmonic oscillator (S.H.O.), which plays a very important role in quantum mechanics and relativistic quantum field theory, can be solved using the brute force solution, *i.e.*, the more traditional tools of differential equations, special functions and the power series method, it is more instructive to treat the S.H.O. (also called linear harmonic oscillator (L.H.O.)) as an application of the diabolically clever algebraic technique, using the so called ladder operators which exploit the commutation relations and operator identities. We shall outline here the algebraic technique.

The time-independent Schrödinger wave equation for the S.H.O. is

$$\hat{H}\psi = E\psi \quad ...(126)$$

or

$$\frac{-\hbar^2}{2m}\frac{d^2\psi}{dx^2} + \frac{1}{2}m\omega^2x^2\psi = E\psi \quad ...(127)$$

where the Hooke's law potential $V(x) = (1/2)\,kx^2 = (1/2)\,m\omega^2x^2$. Here k is the force constant $= m\omega^2$ where m is the mass of the oscillator and $\omega(= 2\pi\nu)$ is the *angular frequency* ; ν being the *frequency* of the S.H.O. Rewriting Eq. 127 in the more suggestive form :

$$\frac{1}{2m}[p^2 + (m\omega x)^2]\psi = E\psi \quad ...(128)$$

where $p = -i\hbar(d/dx)$ is the linear momentum operator. The basic idea is to *factor* the Hamiltonian,

$$H = (1/2m)\,[p^2 + (m\omega x)^2] \quad ...(129)$$

If these were *numbers*, it would be easy :

$$a^2 + b^2 = (ia + b)(-ia + b)$$

Here, however, it's not quite so simple because p and x are *operators* and operators do not, in general, commute (xp is not the same as px). Still, this does motivate us to examine the quantities

$$a_\pm \equiv \frac{1}{\sqrt{\hbar m\omega}}(\mp ip + m\omega x) \quad ...(130)$$

(The factor in front is just there to make the final results look nicer).

Let us evaluate the product a_-a_+ :

$$a_-a_+ = \frac{1}{2\hbar m\omega}(ip + m\omega x)(-ip + m\omega x)$$

$$= \frac{1}{2\hbar m\omega}[p^2 + (m\omega x)^2 - im\omega(xp - px)] \quad ...(131)$$

The extra term in Eq. 131, involving $(xp - px)$ is called the commutator of x and p, written as $[x, p] = xp - px$. Thus,

$$a_- a_+ = \frac{1}{2\hbar m\omega}[p^2 + (m\omega x)^2] - \frac{i}{2\hbar}[x, p] \quad ...(132)$$

To evaluate $[x, p]$, we operate on the test function $f(x)$:

$$[x, p] f(x) = \left[x(-i\hbar)\frac{df(x)}{dx} - (-i\hbar)\frac{d\{xf(x)\}}{dx}\right]$$

$$= -i\hbar\left(x\frac{df}{dx} - x\frac{df}{dx} - f\right) = i\hbar f(x) \quad ...(133)$$

Dropping the test function, which has served its purpose,

$$[x, p] = i\hbar \quad ...(134)$$

This lovely and ubiquitous result is known as the **canonical commutation relation.**

[Theoretical physicists feel that in a deep sense all of the mysteries of quantum mechanics can be traced to the fact that position and momentum do not commute. Eq. 134 is the quantum mechanical version of the Heisenberg uncertainty principle, Indeed, some authors take the canonical commutation relation as an *axiom* and use it to *derive* $p = -i\hbar\, d/dx$.]

Using Eq. 134, Eq. 132 becomes

$$a_- a_+ = \left(\frac{1}{\hbar\omega}\right)H + \frac{1}{2} \quad ...(135)$$

or

$$H = \hbar\omega\left(a_- a_+ - \frac{1}{2}\right) \quad ...(136)$$

Evidently, the Hamiltonian does not *factor* perfectly - there is extra - 1/2 on the right. Notice that the ordering of a_+ and a_- is important here. The same argument with a_+ on the left yields

$$a_+ a_- = \left(\frac{1}{\hbar\omega}\right)H - \frac{1}{2} \quad ...(137)$$

Now, the commutator of a_- and a_+ is

$$[a_-, a_+] = 1 \quad ...(138)$$

So, the Hamiltonian can equally well be written as

$$H = \hbar\omega\left(a_+ a_- + \frac{1}{2}\right) \quad ...(139)$$

In terms of $a_\pm$, the Schrödinger equation for the S.H.O. takes the form

$$\hbar\omega\left(a_\pm a_\mp \pm \frac{1}{2}\right)\psi = E\psi \quad ...(140)$$

(In Eq. 140 we read the upper signs all the way across, or else the lower signs).

Now we proceed to prove the crucial result which states that *if ψ satisfies the Schrödinger equation with energy E (i.e., $H\psi = E\psi$), then $a_+\psi$ satisfies the Schrödinger equation with energy $(E + \hbar\omega)$ i.e., $H(a_+\psi) = (E + \hbar\omega)(a_+\psi)$*. Thus,

$$H(a_+\psi) = \hbar\omega\left(a_+ a_- + \frac{1}{2}\right)(a_+\psi) = \hbar\omega\left(a_+ a_- a_+ + \frac{1}{2}a_+\right)\psi$$

$$= \hbar\omega a_+\left(a_- a_+ + \frac{1}{2}\right)\psi = a_+\left[\hbar\omega\left(a_+ a_- + 1 + \frac{1}{2}\right)\psi\right]$$

$$= a_+(H + \hbar\omega)\psi = a_+(E + \hbar\omega)\psi = (E + \hbar\omega)(a_+\psi)$$

Here we have used Eq. 138 to replace $a_- a_+$ by $(a_+ a_- + 1)$ in the second line. Notice that whereas the ordering of a_+ and a_- *does* matter, the ordering of $a_\pm$ and any *constants*—such as $\hbar$, ω and E—does *not* ; an operator commutes with any constant. Similarly, we can show that $a_-\psi$ is a solution with energy $(E - \hbar\omega)$:

$$H(a_-\psi) = \hbar\omega\left(a_- a_+ - \frac{1}{2}\right)(a_-\psi) = \hbar\omega a_-\left(a_+ a_- - \frac{1}{2}\right)\psi$$

$$= a_-\left[\hbar\omega\left(a_- a_+ - 1 - \frac{1}{2}\right)\psi\right]$$

$$= a_-(H - \hbar\omega)\psi = a_-(E - \hbar\omega)\psi$$

$$= (E - \hbar\omega)(a_-\psi)$$

Here, then, is the wonderful machine for generating new solutions, with higher and lower energies if we could just find *one* solution to get started ! We call $a_\pm$ **ladder operators** because they allow us to climb up and down in energy ; a_+ is the raising operator and a_- is the lowering operator. The ladder of states is illustrated in Fig. 6.

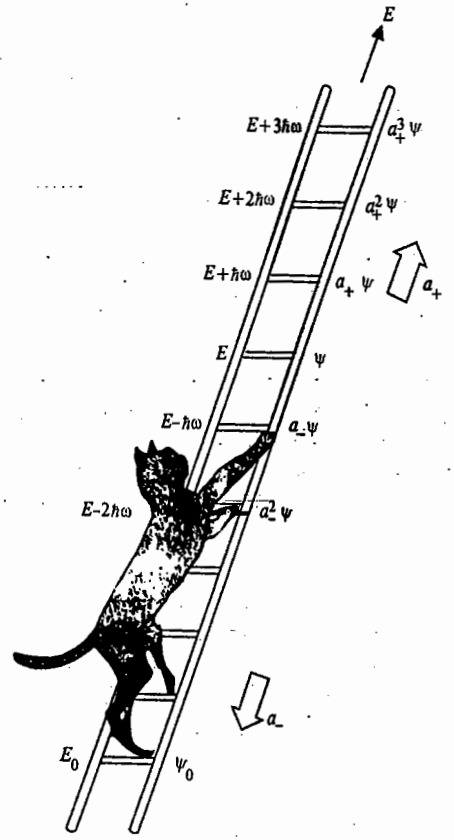

Fig. 6. The "ladder" of states for the harmonic oscillator.

If, however, we apply the lowering operator repeatedly, we eventually reach a state with energy less than zero which does not exist ! At some point the machine must fail. We know that $a_-\psi$ is a new solution to the Schrödinger equation and there occurs a lower rung (call it ψ_0) such that

$$a_-\psi_0 = 0 \qquad ...(141)$$

We can use this to determine $\psi_0(x)$:

$$\frac{1}{\sqrt{2\hbar m\omega}}\left(\hbar\frac{d}{dx} + m\omega x\right)\psi_0 = 0$$

or, $$\frac{d\psi_0}{dx} = -\frac{m\omega}{\hbar}x\psi_0 \qquad ...(142)$$

This differential equation can be solved easily :

$$\int\frac{d\psi_0}{\psi_0} = -\frac{m\omega}{\hbar}\int x\,dx \;;\text{ or } \ln\psi_0 = -\frac{m\omega}{2\hbar}x^2 + \text{constant} \qquad ...(143)$$

so that $$\psi_0(x) = N\exp\left(-\frac{m\omega}{2\hbar}x^2\right) \qquad ...(144)$$

which can be normalized easily :

$$N^2\int_{-\infty}^{\infty}\exp\left(-\frac{m\omega x^2}{\hbar}\right)dx = N^2\left(\frac{\pi\hbar}{m\omega}\right)^{\frac{1}{2}} = 1 \qquad ...(145)$$

so that $$N^2 = (m\omega/\pi\hbar)^{\frac{1}{2}} \qquad ...(146)$$

Hence, $$\psi_0(x) = \left(\frac{m\omega}{\pi\hbar}\right)^{\frac{1}{4}}\exp\left(-\frac{m\omega x^2}{2\hbar}\right) \qquad ...(147)$$

To determine the energy of this state we substitute it into the Schrödinger equation (in the form of Eq. 140), $\hbar\omega\left(a_+a_- + \frac{1}{2}\right)\psi_0 = E_0\psi_0$ and exploit the fact that $a_-\psi_0 = 0$. Accordingly,

$$E_0 = \frac{1}{2}\hbar\omega \qquad ...(148)$$

This is the zero point energy (Z.P.E.) of the S.H.O. With our foot now firmly planted on the bottom rung (the ground state of the S.H.O), we simply apply the raising operator (repeatedly) to generate the excited states, increasing the energy by $\hbar\omega$ with each step :

$$\psi_n(x) = N_n(a_+)^n\psi_0(x), \text{ with } E_n = \left(n + \frac{1}{2}\right)\hbar\omega \qquad ...(149)$$

where N_n is the normalitzation constant and n is the vibrational quantum number. By applying the raising operator (repeatedly) to ψ_0, we can (in principle) construct all the stationary states of the S.H.O. Meanwhile, without even doing that explicitly, we have determined the allowed energies. We can even get N_n algebraically, but it takes some fancy footwork. So we stop here.

ANGULAR MOMENTUM OPERATORS, COMMUTATION RELATIONS, LADDER OPERATORS, EIGENFUNCTIONS AND EIGENVALUES

1. Angular Momentum Operators. The Cartesian components of the angular momentum operators are given by

$$\hat{L}_x = -i\hbar\left[y\frac{\partial}{\partial z} - z\frac{\partial}{\partial y}\right] \qquad ...(150a)$$

$$\hat{L}_y = -i\hbar\left[z\frac{\partial}{\partial x} - x\frac{\partial}{\partial z}\right] \qquad ...(150b)$$

$$\hat{L}_z = -i\hbar\left[x\frac{\partial}{\partial y} - y\frac{\partial}{\partial x}\right] \qquad ...(150c)$$

In order to determine whether L_x, L_y and L_z can be precisely specified simultaneously, we must determine whether each of the pairs of the corresponding operators commute. Let us evaluate the commutator $[\hat{L}_x, \hat{L}_y]$.

$$[\hat{L}_x, \hat{L}_y] = \hat{L}_x\hat{L}_y - \hat{L}_y\hat{L}_x$$

$$\hat{L}_x\hat{L}_y = -i\hbar\left[y\frac{\partial}{\partial z} - z\frac{\partial}{\partial y}\right](-i\hbar)\left[z\frac{\partial}{\partial x} - x\frac{\partial}{\partial z}\right]$$

$$= -\hbar^2\left[y\frac{\partial}{\partial z}\times z\frac{\partial}{\partial x} - y\frac{\partial}{\partial z}x\frac{\partial}{\partial z} - z\frac{\partial}{\partial y}z\frac{\partial}{\partial x} + z\frac{\partial}{\partial y}x\frac{\partial}{\partial z}\right]$$

$$= -\hbar^2\left[y\frac{\partial}{\partial x} + yz\frac{\partial^2}{\partial z\partial x} - yx\frac{\partial^2}{\partial z^2} - z^2\frac{\partial^2}{\partial y\partial x} + zx\frac{\partial^2}{\partial y\partial z}\right]$$

(because terms like $\partial z/\partial x = 0$ and $\partial z/\partial z = 1$)

Again, $$\hat{L}_y\hat{L}_x = -\hbar^2\left[z\frac{\partial}{\partial x} - x\frac{\partial}{\partial z}\right]\left[y\frac{\partial}{\partial z} - z\frac{\partial}{\partial y}\right]$$

$$= -\hbar^2\left[z\frac{\partial}{\partial x}y\frac{\partial}{\partial z} - z\frac{\partial}{\partial x}z\frac{\partial}{\partial y} - x\frac{\partial}{\partial z}y\frac{\partial}{\partial z} + x\frac{\partial}{\partial z}z\frac{\partial}{\partial y}\right]$$

$$= -\hbar^2\left[zy\frac{\partial^2}{\partial x\partial z} - z^2\frac{\partial^2}{\partial x\partial y} - xy\frac{\partial^2}{\partial z^2} + x\frac{\partial}{\partial y} + xz\frac{\partial^2}{\partial z\partial y}\right]$$

Hence, $$\hat{L}_x\hat{L}_y - \hat{L}_y\hat{L}_x = -\hbar^2\left[y\frac{\partial}{\partial x} - x\frac{\partial}{\partial y}\right] = i\hbar\left[i\hbar\left(y\frac{\partial}{\partial x} - x\frac{\partial}{\partial y}\right)\right]$$

$$= i\hbar\left[-i\hbar\left(x\frac{\partial}{\partial y} - y\frac{\partial}{\partial x}\right)\right] = i\hbar\hat{L}_z \text{ (using Eq. 150c)} \qquad ...(151)$$

Thus, $$[\hat{L}_x, \hat{L}_y] = i\hbar\hat{L}_z \qquad ...(152)$$

Similarly, we can show that

$$[\hat{L}_y, \hat{L}_z] = i\hbar\hat{L}_x \text{ and } [\hat{L}_z, \hat{L}_x] = i\hbar\hat{L}_y \qquad ...(153)$$

None of the relations in Eqs. 152 and 153 is zero, which means that the three components L_x, L_y, L_z of angular momentum cannot be specified simultaneously. If we specify one component, the other two become uncertain. By convention, the component L_z is chosen to have a specific value so that L_x and L_y cannot have specific values. However, the z-axis itself is chosen arbitrarily. But when the atom or molecule is placed in a magnetic or electric field, the direction of the field is chosen as the z-axis.

Next we are intersested in knowing whether L (the angular momentum itself) and L_z (its z-component) can be specificed simultaneously or not. To find it out, we recall that L is given by

$$L = (L_x^2 + L_y^2 + L_z^2)^{1/2}$$

This means that the operator $\hat{L}$ has to be defined as the square root of another operator. Ignoring the meaning of the square root of an operator, let us find out whether the operators $\hat{L}^2$ and $\hat{L}_z$ commute.

$$\begin{aligned}[\hat{L}^2, \hat{L}_z] &= [\hat{L}_x^2 + \hat{L}_y^2 + \hat{L}_z^2, \hat{L}_z] \\ &= \hat{L}_x^2\hat{L}_z + \hat{L}_y^2\hat{L}_z + \hat{L}_z^2\hat{L}_z - \hat{L}_z\hat{L}_x^2 - \hat{L}_z\hat{L}_y^2 - \hat{L}_z\hat{L}_z^2 \\ &= (\hat{L}_x^2\hat{L}_z - \hat{L}_z\hat{L}_x^2) + (\hat{L}_y^2\hat{L}_z - \hat{L}_z^2\hat{L}_y) + (\hat{L}_z^2\hat{L}_z - \hat{L}_z\hat{L}_z^2) \\ &= [\hat{L}_x^2, \hat{L}_z] + [\hat{L}_y^2, \hat{L}_z] + [\hat{L}_z^2, \hat{L}_z] \qquad \ldots(154)\end{aligned}$$

The first term in Eq. 154, *viz.*,

$$\begin{aligned}[\hat{L}_x^2, \hat{L}_z] &= \hat{L}_x\hat{L}_x\hat{L}_z - \hat{L}_z\hat{L}_x\hat{L}_x \\ &= \hat{L}_x\hat{L}_x\hat{L}_z - \hat{L}_x\hat{L}_z\hat{L}_x + \hat{L}_x\hat{L}_z\hat{L}_x - \hat{L}_z\hat{L}_x\hat{L}_x \\ &= \hat{L}_x(\hat{L}_x\hat{L}_z - \hat{L}_z\hat{L}_x) + (\hat{L}_x\hat{L}_z - \hat{L}_z\hat{L}_x)\hat{L}_x \\ &= \hat{L}_x[\hat{L}_x, \hat{L}_z] + [\hat{L}_x, \hat{L}_z]\hat{L}_x \\ &= -i\hbar\hat{L}_x\hat{L}_y - i\hbar\hat{L}_y\hat{L}_x \qquad (\because [\hat{L}_x, \hat{L}_z] = -[\hat{L}_z, \hat{L}_x]) \\ &= -i\hbar(\hat{L}_x\hat{L}_y + \hat{L}_y\hat{L}_x) \qquad \ldots(155)\end{aligned}$$

Similarly, it can be shown that

$$[\hat{L}_y^2, \hat{L}_z] = i\hbar(\hat{L}_x\hat{L}_y + \hat{L}_y\hat{L}_x) \qquad \ldots(156)$$

and

$$[\hat{L}_z^2, \hat{L}_z] = 0 \qquad \ldots(157)$$

Adding Eqs. 155, 156 and 157, we have

$$[\hat{L}^2, \hat{L}_z] = 0 \qquad \ldots(158)$$

which means that the square of the angular momentum and its z-component can be specified simultaneously. We can similarly show that $\hat{L}^2$ commutes with $\hat{L}_x$ and $\hat{L}_y$.

Commutation relations (Eqs. 152, 153 and 158) mean that the angular momentum L of a relating particle can be represented by a vector of precise length L with one and only one of its components (conventionally L_z) precisely defined. Since the other two components (L_x and L_y) are uncertain, the vector may lie anywhere on the surface of a cone whose axis coincides with the z-axis. In the classical sense, it corresponds to the vector L precessing around z-axis (Fig. 7).

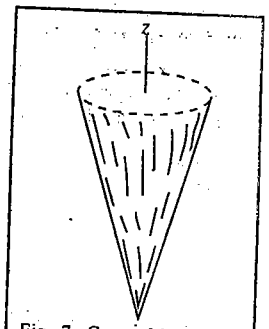

Fig. 7. Cone of location of angular momentum vector.

The relations 152, 153 and 158 constitute the quantum mechanical definition of angular momentum. In fact, any vector J may be called **generalized angular momentum** if it satisfies the following relations:

$$[\hat{J}_x, \hat{J}_y] = i\hbar\hat{J}_z; [\hat{J}_y, \hat{J}_z] = i\hbar\hat{J}_x; [\hat{J}_z, \hat{J}_x] = i\hbar\hat{J}_y \qquad \ldots(159)$$

$$[\hat{J}^2, \hat{J}_k] = 0, \text{ where } k = x, y, z \qquad \ldots(160)$$

and

$$J^2 = (\hat{J}_x^2 + \hat{J}_y^2 + \hat{J}_z^2)^{\frac{1}{2}} \qquad \ldots(161)$$

A rotating system is thus characterized by two operators $\hat{J}^2$ and $\hat{J}_z$ and their eigenvalues. Before we proceed to find the eigenvalues and eigenfunctions, we shall introduce two new operators $\hat{J}_+$ and $\hat{J}_-$, called the **ladder operators** (or **step-up** and **step-down operators, shift operators** and, sometimes, **raising** and **lowering operators**) and examine some of their commutation properties.

2. Ladder Operators. These operators are defined as

$$\left.\begin{aligned}\hat{J}_+ &= \hat{J}_x + i\hat{J}_y \\ \hat{J}_- &= \hat{J}_x - i\hat{J}_y\end{aligned}\right\} \qquad \ldots(162)$$

They are so called because, as we shall see later, they have the effect of raising and lowering eigenvalues, respectively. These operators commute with $\hat{J}^2$ but not with $\hat{J}_z$; they also do not commute between themselves as described below :

$$\begin{aligned}[\hat{J}^2, \hat{J}_+] &= [\hat{J}^2, (\hat{J}_x + i\hat{J}_y)] = \hat{J}^2(\hat{J}_x + i\hat{J}_y) - (\hat{J}_x + i\hat{J}_y)\hat{J}^2 \\ &= \hat{J}^2\hat{J}_x + i\hat{J}^2\hat{J}_y - \hat{J}_x\hat{J}^2 - i\hat{J}_y\hat{J}^2 = (\hat{J}^2\hat{J}_x - \hat{J}_x\hat{J}^2) + i(\hat{J}^2\hat{J}_y - \hat{J}_y\hat{J}^2) \\ &= [\hat{J}^2, \hat{J}_x] + i[\hat{J}^2, \hat{J}_y] = 0 + 0 = 0 \qquad \ldots(163)\end{aligned}$$

Similarly,

$$[\hat{J}^2, \hat{J}_-] = 0 \qquad \ldots(164)$$

Again,

$$[\hat{J}_+, \hat{J}_z] = [(\hat{J}_x + i\hat{J}_y), \hat{J}_z] = (\hat{J}_x + i\hat{J}_y)\hat{J}_z - \hat{J}_z(\hat{J}_x + i\hat{J}_y)$$

$$= \hat{J}_x \hat{J}_z + i \hat{J}_y \hat{J}_z - \hat{J}_z \hat{J}_x - i \hat{J}_z \hat{J}_y$$

$$= (\hat{J}_x \hat{J}_z - \hat{J}_z \hat{J}_x) + i(\hat{J}_y \hat{J}_z - \hat{J}_z \hat{J}_y)$$

$$= [\hat{J}_x, \hat{J}_z] + i[\hat{J}_y, \hat{J}_z] = -i\hbar \hat{J}_y - \hbar \hat{J}_x$$

$$= -\hbar(\hat{J}_x + i \hat{J}_y) = -\hbar \hat{J}_+ \quad ...(165)$$

Similarly, we can show that

$$[\hat{J}_-, \hat{J}_z] = -\hbar \hat{J}_- \quad ...(166)$$

and

$$[\hat{J}_+, \hat{J}_-] = -2\hbar \hat{J}_z \quad ...(167)$$

3. Eigenfunctions and Eigenvalues of $\hat{J}^2$ and $\hat{J}_z$. The commutation relations provide an elegant means of arriving at the eigenvalues of the angular momentum operators $\hat{J}^2$ and $\hat{J}_z$. Since $\hat{J}^2$ and $\hat{J}_z$ commute, they have a common set of eigenfunctions. Denoting these eigenfunctions as $\psi_{j,m}$ (or, in the Dirac notation, as $|j, m>$), the two eigenvalue equations are

$$\hat{J}^2 \mid j,m > = k_j \mid j, m > \quad ...(168)$$

$$\hat{J}_z \mid j,m > = k_m \mid j, m > \quad ...(169)$$

where j and m are the quantum numbers which specify the eigenvalues k_j and k_m, respectively. Operating on both sides of Eq. 169 by $\hat{J}_z$, we obtain

$$\hat{J}_z^2 \mid j,m > = \hat{J}_z(k_m \mid j,m >) = k_m(\hat{J}_z \mid j,m >) = k_m^2 \mid j,m > \quad ...(170)$$

Subtracting Eq. 170 from Eq. 168, we get

$$(\hat{J}^2 - \hat{J}_z) \mid j,m > = (k_j - k_m^2) \mid j,m > \quad ...(171)$$

or

$$(\hat{J}_x^2 + \hat{J}_y^2) \mid j,m > = (k_j - k_m^2) \mid j,m > \quad ...(172)$$

(because $\hat{J}^2 = \hat{J}_x^2 + \hat{J}_y^2 + \hat{J}_z^2$)

Now, $(\hat{J}_x^2 + \hat{J}_y^2)$ is the operator for the physical quantity $(J_x^2 + J_y^2)$ which can never be negative; hence, the eigenvalue $(k_j - k_m^2)$ in Eq. 172 must always be positive, that is,

$$k_j \geq k_m^2 \text{ for any value of } k_m \quad ...(173)$$

Let us now consider the effect of the ladder operators and to know why they are called by this name. We shall first consider the effect of $\hat{J}_+$ on the eigenvalue of $\hat{J}^2$. Since $\hat{J}^2$ commutes with $\hat{J}_+$ (Eq. 163), we have

$$\hat{J}^2 \hat{J}_+ \mid j,m > = \hat{J}_+ \hat{J}^2 \mid j\,m > = \hat{J}_+(k_j \mid j,m >) = k_j(\hat{J}_+ \mid j,m >) \quad ...(174)$$

(in view of Eq. 168)

This means that $\hat{J}_+ \mid j,m >$ is also an eigenfunction of $\hat{J}^2$ with the same eigenvalue (k_j), that is, there is no effect of J_+ on the eigenvalue of $\hat{J}^2$.

Let us now consider the effect on k_m. By adding and subtracting $\hat{J}_+ \hat{J}_z$, we obtain

$$\hat{J}_z \hat{J}_+ \mid j,m > = (\hat{J}_+ \hat{J}_z + \hat{J}_z \hat{J}_+ - \hat{J}_+ \hat{J}_z) \mid j,m > = \{\hat{J}_+ \hat{J}_z + [\hat{J}_z, \hat{J}_+]\} \mid j,m >$$

$$= \{\hat{J}_+ \hat{J}_z \mid j,m > + [\hat{J}_z \hat{J}_+] \mid j,m >\}$$

$$= \hat{J}_+ k_m \mid j,m > + \hbar \hat{J}_+ \mid j,m > = \hat{J}_+(k_m + \hbar) \mid j,m >$$

$$= (k_m + \hbar) \hat{J}_+ \mid j,m > \quad ...(175)$$

(by Eqs. 169 and 165, and from the fact that $[\hat{J}_z, \hat{J}_+] = -[\hat{J}_+, \hat{J}_z]$)

This means that $\hat{J}_+ \mid j,m >$ is also an eigenfunction of $\hat{J}_z$ but its eigenvalue is raised from k_m to $(k_m + \hbar)$, *i.e.*, by one atomic unit. The clue to this derivation is that $\hat{J}_+$ does not commute with $\hat{J}_z$.

Similarly, it can be shown that $\hat{J}_-$ lowers the eigenvalue of $\hat{J}_z$ from k_m to $(k_m - \hbar)$, *i.e.*, by one atomic unit but keeps that of $\hat{J}^2$ unaltered, that is,

$$\hat{J}^2(\hat{J}_- \mid j,m >) = k_j(\hat{J}_- \mid j,m >) \quad ...(176)$$

$$\hat{J}_z(\hat{J}_- \mid j,m >) = (k_m - \hbar)(\hat{J}_- \mid j,m >) \quad ...(177)$$

It is now easy to show that

$$\hat{J}_\pm(\hat{J}_\pm \mid j;m >),\ \hat{J}_\pm[\hat{J}_\pm(\hat{J}_\pm \mid j,m >)],\ldots \quad ...(178)$$

are all eigenfunctions of $\hat{J}_z$ with altered eigenvalues and also of $\hat{J}^2$ with unaltered eigenvalues. Successive applications of the operators $\hat{J}_\pm$ will, therefore, generate a series of eigenfunctions of $\hat{J}_z$ whose eigenvalues constitute the series

$$k_m', k_m' + \hbar, k_m' + 2\hbar, \ldots, k_m'' - 2\hbar, k_m'' - \hbar, k_m''$$

or $k_m', k_m' + 1, k_m' + 2, \ldots, k_m'' - 2, k_m'' - 1, k_m''$ (in atomic units) ...(179)

(recall that in quantum mechanics, we set $e = \hbar = m_e = 1$ arbitrarily, using atomic units)

where for a given value of k_j, k_m' is the lowest and k_m'' is the highest eigenvalue. The lowest and the highest values of k_m are governed by the condition contained in Eq. 173, *viz.*, $k_m^2 \leq k_j$. It also follows that the maximum and minimum values are related as

$$k_n'' = k_m' + n\hbar$$

or

$$k_n'' = k_m' + n \text{ (in a.u.)}$$

where n is a positive integer.

For the maximum value of k_m, *i.e.* k_m'', let $| j'', m'' >$ be the eigenfunctions; then we have the eigenvalue equation

$$\hat{J}_z | j'', m'' > = k_m'' | j'', m'' > \quad ...(180)$$

Since k_m'' is the upper limit of the eigenvalue, further application of the operator will yield zero as the eigenvalue, *i.e.*, $\hat{J}_+ | j'', m'' > = 0$.

Operating with $\hat{J}_-$, we get

$$\hat{J}_- \hat{J}_+ | j'', m'' > = 0$$

or $$(\hat{J}_x - i\hat{J}_y)(\hat{J}_x + i\hat{J}_y) | j'', m'' > = 0$$

or $$(\hat{J}_x^2 + \hat{J}_y^2 + i\hat{J}_x\hat{J}_y - i\hat{J}_y\hat{J}_x) | j'', m'' > = 0$$

or $$(\hat{J}^2 - \hat{J}_z^2 + i^2\hbar\hat{J}_z) | j'', m'' > = 0$$

or $$(k_j - k_m''^2 - \hbar k_m'') | j'', m'' > = 0 \quad \text{(because } k_j'' = k_j\text{)} \quad ...(181)$$

since $| j'', m'' > \neq 0$, $k_j = k_m''(k_m'' + \hbar)$

Similarly, we can show that

$$k_j = k_m'(k_m' - \hbar) \quad ...(182)$$

From Eqs. 181 and 182, we get

$$k_j = k_m''(k_m'' + \hbar) = k_m'(k_m' - \hbar) \quad ...(183)$$

and from Eq. 180,

$$(k_m' + n\hbar)[k_m' + (n+1)\hbar] = k_m'(k_m' - \hbar)$$

or $$2(n+1)\hbar k_m' + n(n+1)\hbar^2 = 0$$

or $$k_m' = -n\hbar/2 = -j\hbar \text{ (where } j = n/2) \quad ...(184)$$

Similarly, $$k_m'' = +n\hbar/2 = +j\hbar \quad ...(185)$$

Eqs. 184 and 185 show that j must be either an integer or a half-integer. Hence, Eq. 183 gives

$$k_j = j(j+1)\hbar^2 \text{ or } j(j+1) \text{ (in a.u.)} \quad ...(186)$$

and $$k_m = m\hbar \text{ or } m \text{ (in a.u.)} \quad ...(187)$$

where for a given value of j, m can take any of the values in the series

$$j, j-1, j-2, \ldots, 0, \ldots -(j-2), -(j-1), -j \quad ...(188)$$

making a total of $2j+1$ values for m.

Eqs. 168 and 169 may, thus, be written as

$$\hat{J}^2 | j, m > = [j(j+1)\hbar^2] | j, m > \quad ...(189)$$

$$\hat{J}_z | j, m > = m\hbar | j, m > \quad ...(190)$$

where m takes any value in the series (Eq. 188). Thus, for $j = 2$, $m = +2, +1, 0, -1$ or -2, and for $j = (3/2)$ m can be $3/2$, $1/2$, $-1/2$ or $-3/2$.

The physical interpretation is that the behaviour of the angular momentum vector J is governed by Eqs. 189 and 190, *i.e.*, the magnitude of J is quantized and given by $[j(j+1)]^{1/2}\hbar$, where j is the angular momentum quantum number. The vector is oriented in space in such a manner that its z-component has the value $m\hbar$, where m is the quantum number corresponding to the z-component of J (Fig. 8.)

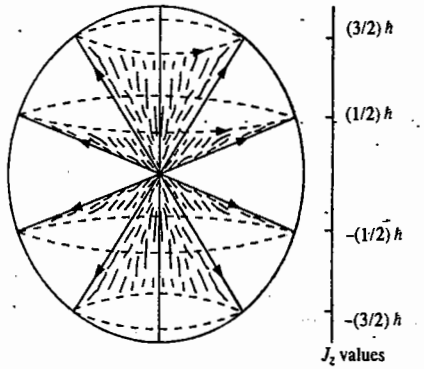

Fig. 8. Quantization of the angular momentum vector J for which $j = 3/2$

4. Orbital and Spin Angular Momentum Operators : Their Eigenfunctions and Eigenvalues.

The electrons (and other elementary particles) execute two types of rotational motion, *viz.*, the motion around the orbit called the *orbital motion*, and the rotation about its own axis, called the *spinning motion*. The corresponding angular momenta are designated L and S, respectively. They obey the same commutation rules and have similar eigenvalue equations. The angular momentum operators for the orbital motion are designed by $\hat{L}^2$ and $\hat{L}_z$ and those for the spinning motion by $\hat{S}^2$ and $\hat{S}_z$. The two quantum numbers needed to characterize the eigenfunctions are denoted as l and m_l for the orbital motion and s and m_s for the spinning motion.

The eigenfunctions of the orbital angular momentum operators are the **spherical harmonics** $Y_{l,m_l}(\theta, \phi)$, written in the Dirac notation as $|l, m_l >$; and the eigenfunctions for the spin angular momentum operators are $| \alpha >$ and $| \beta >$, where $| \alpha > \equiv | \frac{1}{2}, \frac{1}{2} >$ and $| \beta > \equiv | \frac{1}{2}, -\frac{1}{2} >$, *i.e.*, $| s, m_s >$, where for $s = \frac{1}{2}$, $m_s = +\frac{1}{2}$ or $-\frac{1}{2}$.

The eigenvalue equations are

$$\left.\begin{aligned} \hat{L}^2 | l, m_l > &= l(l+1)\hbar^2 | l, m_l > \\ \hat{L}_z | l, m_l > &= m_l\hbar | l, m_l > \end{aligned}\right\} \quad ...(191)$$

and
$$\left.\begin{aligned}\hat{S}^2 \mid s, m_s > &= s(s+1)\hbar^2 \mid s, m_s > \\ \hat{S}_z \mid s, m_s > &= m_s\hbar \mid s, m_s >\end{aligned}\right\} \quad ...(192)$$

Eqs. 192 can be written as

$$\left.\begin{aligned}\hat{S}^2 \mid \alpha > &= \tfrac{3}{4}\hbar^2 \mid \alpha >;\ \hat{S}^2 \mid \beta > = \tfrac{3}{4}\hbar^2 \mid \beta > \\ \hat{S}_z \mid \alpha > &= \tfrac{1}{2}\hbar \mid \alpha >;\ \hat{S}_z \mid \beta > = -\tfrac{1}{2}\hbar \mid \beta >\end{aligned}\right\} \quad ...(193)$$

Physically, the magnitude of the vector S is $(\sqrt{3}/2)\hbar$ and it is oriented only in any of such directions that its z-component is either $\hbar/2$ or $-\hbar/2$ (Fig. 9).

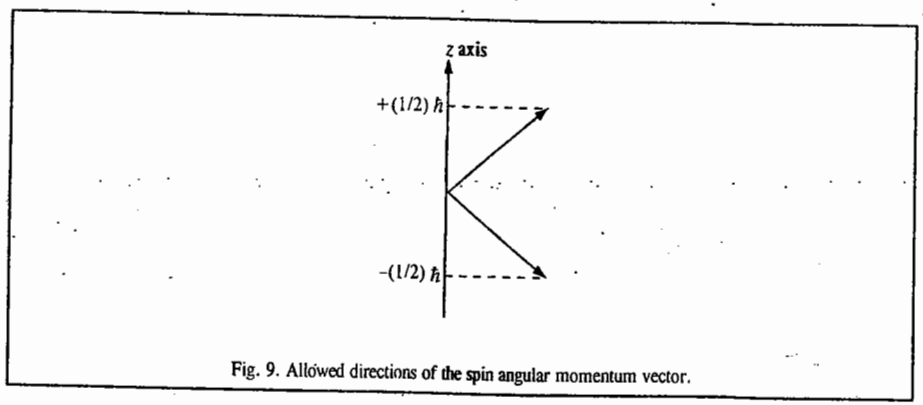

Fig. 9. Allowed directions of the spin angular momentum vector.

Note : Here $\mid \alpha >$ refers to upward ($\uparrow$) spin orientation and $\mid \beta >$ refers to downward ($\downarrow$) spin orientation.
For a detailed treatment of angular momentum see the last section of this chapter.

Derivation of the Variation Theorem

Suppose ψ is an approximate wave function of a quantum system. Then, the energy of the system is given by **Rayleigh ratio**

$$E = \frac{\int \psi^* \hat{H} \psi \, d\tau}{\int \psi^* \psi \, d\tau} = \frac{< \psi \mid \hat{H} \mid \psi >}{< \psi \mid \psi >} \quad ...(194)$$

Let ϕ_n denote the exact set of orthonormal eigenfunctions of the Hamiltonian, $\hat{H}$:

$$\hat{H}\phi_n = E_n\phi_n ;\ (n = 0, 1, 2, 3.....) \quad ...(195)$$

The wave function ψ can be expanded in terms of the eigenfunctions, ϕ_n, of $\hat{H}$:

$$\psi = \sum_n c_n\phi_n \quad ...(196)$$

Substituting for ψ from Eq. 196 into Eq. 194, we get

$$E = \frac{\int (\sum_n c_n^* \phi_n^*) \hat{H} (\sum_m c_m\phi_m) d\tau}{\int (\sum_n c_n^* \phi_n^*)(\sum_m c_m\phi_m) d\tau} \quad ...(197)$$

Using Eq. 195, we obtain

$$E = \frac{\sum_n \sum_m c_n^* \, c_m E_m \int \phi_n^* \, \phi_m \, d\tau}{\sum_n \sum_m c_n^* \, c_m \int \phi_n^* \, \phi_m \, d\tau} = \frac{\sum_n c_n^* c_n E_n}{\sum_n c_n^* c_n} = \frac{\sum_n |c_n|^2 E_n}{\sum_n |c_n|^2} \quad ...(198)$$

Substracting E_0, the ground state energy, from both sides of Eq. 198, we have

$$E - E_0 = \frac{\sum_n |c_n|^2 (E_n - E_0)}{\sum_n |c_n|^2} \quad ...(199)$$

since $\int \phi_n^* \phi_m^* \, d\tau = < \phi_n \phi_m > = \delta_{nm} = \begin{cases} 1, n = m \\ 0, n \neq m \end{cases}$

Further, $E_n \geq E_0$ since, by definition, E_0 is the ground state energy. Again, since $|c_n|^2 \geq 0$ for all n, it follows that

$$E - E_0 \geq 0 \quad \text{or} \quad E \geq E_0 \quad ...(200)$$

This important inequality called **Eckart's inequality** shows that *the approximate energy E, corresponding to the approximate wave function ψ, is always greater than the true energy, E_0.* This is the statement of the **variation theorem.** Using the inequality 200 one can obtain an **upper bound** to the ground state energy E_0. The procedure is to construct a 'trial' wave function which depends upon a set of variation parameters $\{\alpha_i\}$. Thus, we can write

$$\psi = \psi(\alpha_1, \alpha_2, ... \alpha_n) \quad ...(201)$$

The parameters $\{\alpha_i\}$ may, for instance, enter the trial function as exponential factors.

Using this trial function in Eq. 194, the energy E is calculated. We then choose $\{\alpha_i\}$ so as to minimize E, that is,

$$\partial E/\partial \alpha_i = 0 \text{ for } i = 1, 2, 3, ... n \quad ...(202)$$

The minimum energy thus obtained provides an upper bound to E_0 which will be closer to the exact value if the trial function approximates the ground state wave function ϕ_0.

It may be remarked that in Eckart's inequality reside both the power and the weakness of the variation method for seeking approximate solutions to Schrödinger's equation. The power lies in the fact that it is possible to choose the 'best' wave function from several functions on the basis of the lowest energy. The weakness, on the other hand, is that the energy does not turn out to be a sensitive criterion with respect to the 'best' wave function for other physical properties of the quantum system.

ATOMIC STATES AND TERM SYMBOLS

As we have remarked in the discussion of angular momentum of many-electron atoms, as a result of the *spin-orbit interaction*, the term symbol in the Russell-Saunders coupling scheme is designated by the symbol $^{2S+1}L_J$. The term symbol for the ground state of hydrogen atom is $^2S_{1/2}$ whereas the term symbol for the ground state of helium atom is $^1S_0$. For an atom such as boron atom whose electronic configuration is $1s^2\,2s^2 2p^1$, we can make use of the fact that all *closed shells and subshells contribute nothing to the term symbol.* Hence, both $1s^2$ and $2s^2$ electrons give $L = S = J = 0$. The $2p^1$ electron has $L=1$, $S=1/2$ and $J=1 \pm 1/2$, yielding the term symbols $^2P_{1/2}$ and $^2P_{3/2}$. For carbon atom whose electronic configuration is $1s^2\,2s^2 2p^2$, there are two p electrons. The spins may be paired or unpaired, so $L = 2, 1, 0$; $S = 1, 0$; and $J = 3, 2, 1, 0$. To work out the appropriate states for this atom, we require a systematic approach which we shall outline here.

Term Symbols for p^2 Configuration. For determining the term symbols for p^2 configuration we proceed as follows :

1. *Determine the possible values of M_L and M_S.* For the p^2 configuration, L can have a maximum value of 2 and M_L can have values of -2, -1, 0, +1, +2. The electrons can be paired (M_S=0) or parallel (M_S = +1, - 1).

2. *Determine the electronic configurations that are allowed by the Pauli exclusion principle.* The easiest way to do this is to draw up a number of sets of p orbitals as in Fig. 10 (each vertical column represents a set of three p orbitals) and fill in electrons until all possible arrangements have been formed. The M_L value for each arrangement can be found by summing m_l and M_S is evaluated from the sum of m_s (spin-up electrons have arbitrarily been assigned m_s = +1/2). Each microstate consists of one combination of M_L and M_S.

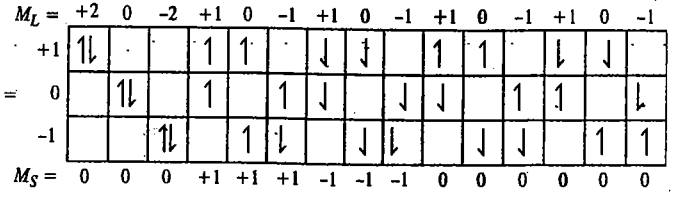

Fig. 10. The fifteen microstates and resultant values of M_L and M_S for the $1s^2 2s^2 2p^2$ electronic configuration of carbon.

3. *Set up a chart of microstates.* For example, the microstate corresponding to the first vertical column in Fig. 1 has M_L = +2 and M_S = 0. It is then entered into the table below under those values. The fifteen microstates of p^2 yield :

		M_S		
		+1	0	-1
	-2		x	
	-1	x	xx	x
M_L	0	x	xxx	x
	+1	x	xx	x
	+2		x	

4. *Resolve the chart of microstates into appropriate atomic states.* An atomic state forms an array of microstates consisting of $2S+1$ columns and $2L+1$ rows. Thus, for instance, a ^{1}D state requires a single column of 5 and a ^{5}D state requires a 5×5 array, etc. Looking at the array of microstates, it is easy to spot the unique third microstate at M_L=0 and M_S= 0 ; this must be a ^1S. A central column of M_S=0 provides a ^{1}D. Removing these two states from the table, one is left with an obvious 3×3 array of a ^{3}P state :

		M_S		
		+1	0	-1
	-2			
	-1	x	x	x
M_L	0	x	x	x
	+1	x	x	x
	+2			

The atomic states of carbon atom are, therefore, ^{1}S, ^{1}D and ^{3}P. The ^{3}P state is further split by differing J values to the terms $^3P_0$, $^3P_1$ and $^3P_2$. The relative magnitudes of splitting are shown in Fig. 11.

It is possible to predict the ground term of an atom by using three empirical rules, known as **Hund's rules.** According to **Hund's first rule**, for a given ground configuration, the term with the greatest multiplicity ($2S+1$) lies lowest in energy. **Hund's second rule** states that for a term of given multiplicity, the greater the value of L, the lower the energy.

Hund's third rule states that for levels with the same S and L, the one with the lowest energy depends on the extent to which the subshell is filled :

(a) If the subshell is less than half-filled, the state with the smallest value of J is most stable.

(b) If the subshell is more than half-filled, the state with the largest value of J is the most stable.

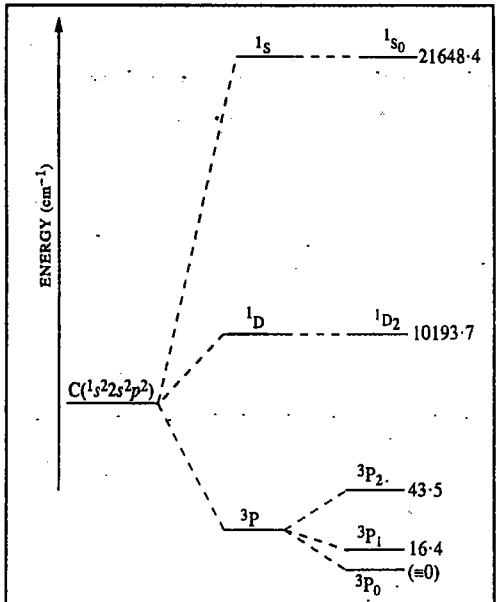

Fig. 11. Term splitting in the ground state ($1s^2 2s^2 2p^2$) configuration of carbon. All energies are in cm^{-1}. The ^{3}P, ^{1}D and ^{1}S terms are split as a result of electron-electron repulsion. The ^{3}P term is further split with J= 0, 1, 2 as a result of spin-orbit coupling. The scale of the latter is exaggerated.

Thus, of the three terms of carbon atom derived above, ^{3}P is the ground state term (from Hund's first rule) because such a system having a maximum number of parallel spins will be stabilized by **exchange energy** resulting from their more favourable spatial distribution compared with that of paired electrons. Using the Hund's second rule, ^{1}D lies lower in energy than ^1S. This is explained by saying that when L is high, each electron can stay clear of its partner and hence have a lower coulombic interaction with it because (in a classical picture of the atom) the electrons are then orbiting in the same direction. If L is low, the electrons are orbiting in the opposite direction and meet more often (and hence repel each other more strongly.

We shall conclude this discussion by briefly mentioning the so-called **Racah parameters.** The different terms of a configuration have different energies on account of the coulombic repulsion between electrons. These inter-electron repulsion energies are given by complicated integrals over the orbitals occupied by the electrons. In the 1940s, Giulio Racah, the Italian physicist, developed theoretical expressions for inter-electron repulsion energies in terms of three combinations of integrals A, B, C, called the Racah parameters. The Racah parameters can, in fact, be treated as empirical quantities obtained from spectroscopy. All the three Racah parameters are positive (they represent inter-electron repulsions); they summarize the energies of all the terms that may arise from a single configuration. The parameters are the quantitative expression of the ideas in Hund's rules and are more powerful than the rules alone since they also account for deviations from them.

Example 11. The term symbol for the ground state of sodium is $3^2S_{1/2}$ and that of the first excited state is $3^2P_{1/2}$. List the possible quantum numbers n, l, j and m_j of the outer electron in each case.

Solution : The electronic configuration of Na atom is $1s^2\ 2s^2\ 2p^6\ 3s^1$. Recall that all closed shells and subshells

do not contribute to the term symbol. Now $2S+1 = 2$ so that $S = 1/2$. Hence,

$$3^2S_{1/2}: \quad n = 3, \quad l = 0 \quad j = \frac{1}{2} \quad m_j = \pm\frac{1}{2} \qquad [J = L \pm S]$$

$$3^2P_{1/2}: \quad n = 3, \quad l = 1 \quad j = \frac{3}{2} \quad m_j = \pm\frac{1}{2}, \pm\frac{3}{2}$$

$$n = 3, \quad l = 1 \quad j = \frac{1}{2} \quad m_j = \pm\frac{1}{2}$$

Example 12. Why is it impossible for a $2^2P_{5/2}$ state to exist ?

Solution : $2S + 1 = 2$, so that $S = 1/2$. A P state has $L = 1$

and $J = L \pm S = 1 \pm \frac{1}{2}$, hence $J = \frac{5}{2}$ is impossible.

Example 13. What is the ground term for the electronic configurations (a) $3d^5$ of Mn^{2+} and (b) $3d^3$ of Cr^{3+} ?

Solution : (*a*) Mn^{2+} (d^5)

↑	↑	↑	↑	↑

$L=2$; $M_L=$ 2 +1 0 -1 -2

We see that $S = 5\times1/2 = 5/2$, and multiplicity $2S+1 = 6$

Also, $M_L = +2+1+0-1-2 = 0$; so $L=0$, an S term.

Hence, the term is a sextet : ^6S

(*b*) Cr^{3+} ($3d^3$)

↑	↑	↑		

$L = 2$; $M_L=$ + 2 + 1 0 - 1 - 2

We see that $S = 3\times1/2 = 3/2$ and multiplicity $2S+1 = 4$

Also, $M_L = 2 + 1 + 0 = 3$; so $L = 3$, an F term.

Hence, the term is a quartet : ^4F

Note : The ground state term symbol can be derived (as illustrated here) by using a method that does not require writing all the permitted microstates.

Example 14. The term symbol for the ground state of N atom is $^4S_{3/2}$. Determine the electronic configuration for this element.

Solution. $2S+1 = 4$. Hence, $S = M_S = 3/2$, implying that there are three unpaired electrons. The S term gives $L = M_L = 0$, which agrees with one electron in each of the p orbitals.

$$M_L = (+ 1) + (0) + (- 1) = 0$$

∴ The configuration is $1s^2\,2s^2\,2p^3$ or $1s^2\,2s^2\,2p_x^1\,2p_y^1\,2p_z^1$

Example 15. The term symbol for the ground state of Nb is $^6D_{1/2}$. Does this agree with the predicted outer electronic configuration of $5s^2\,4d^3$?

Solution : Recall that closed shells or subshells do not contribute to the term symbol; so the d^3 configuration gives

$$M_L = L = (+ 2) + (+ 1) + (0) = + 3; \quad M_S = S = \left(+\frac{1}{2}\right)+\left(+\frac{1}{2}\right)+\left(+\frac{1}{2}\right) = \frac{3}{2}$$

which leads to the incorrect term symbol ^4F. The outer electronic configuration of $5s^1\,4d^4$ gives

$$M_L = L = (0) + (+ 2) + (+ 1) + (0) + (- 1) = + 2$$

$$M_S = S = \left(+\frac{1}{2}\right)+\left(+\frac{1}{2}\right)+\left(+\frac{1}{2}\right)+\left(+\frac{1}{2}\right)+\left(+\frac{1}{2}\right) = \frac{5}{2}$$

which leads to the correct term symbol of ^6D.

Example 16. Determine the term symbol for the ground state of Ni which has the outer electronic configuration $3d^8$.

Solution :

(*a*) Ni $3d^8$

↑↓	↑↓	↑↓	↑	↑

$L = 2$; $M_L =$ +2 +1 0 -1 -2

$$M_L = (+ 2) + (+ 1) + (0) + (- 1) + (- 2) + (+ 2) + (+ 1) + (0) = 3$$

$$M_S = \left(+\frac{1}{2}\right)+\left(+\frac{1}{2}\right)+\left(+\frac{1}{2}\right)+\left(+\frac{1}{2}\right)+\left(+\frac{1}{2}\right)+\left(-\frac{1}{2}\right)+\left(-\frac{1}{2}\right)+\left(-\frac{1}{2}\right) = 1$$

These values are assumed to be L and S, respectively, giving the term ^3F. The values of $L = 3$ and $S = 1$ correspond to $J = 4$, 3 and 2. Choosing the greatest value for J because the subshell is more than half-filled gives $^3F_4$.

The Russell-Saunders coupling (also called LS coupling) which we have used to determine the atomic term symbols, works for lighter atoms with atomic number Z < 30. In heavier atoms (Z > 30), this hierarchy breaks down and the **spin-orbit coupling** eventually becomes stronger than the LS coupling. In this limit a different coupling scheme, the ***jj* coupling** is used in which individual electrons acquire total angular momentum $j_i = l_i + s_i$. The total angular momentum is then given by $J=\Sigma j_i$. In atoms of intermediate Z, neither approximation is valid and the situation is very complicated but the eigenfunction of the Hamiltonian is still an eigenfunction of J^2. However, for heavier atoms it is still convenient to use the Russell-Saunders coupling scheme to determine the term symbols. The complexity of determining the appropriate terms increases with increase in the number of electrons. States for various electronic configurations are shown in Table 1.

TABLE 1

Term Symbols for Various Electronic Configurations

Configurations	Term Symbols for Equivalent Electrons
s^2, p^6 and d^{10}	^1S
p and p^5	^2P
p^2 and p^4	^3P, ^1D, ^1S
p^3	^4S, ^2D, ^2P
d and d^9	^2D
d^2 and d^8	^3F, ^3P, ^1G, ^1D, ^1S
d^3 and d^7	^4F, ^4P, ^2H, ^2G, ^3F, ^2F, ^2D, ^2D, ^2P
d^4 and d^6	^5D, ^3H, ^3G, ^3F, ^3F, ^3D, ^3P, ^3P, ^1I, ^1G, ^1G, ^1F, ^1D, ^1D, ^1S, ^1S
d^5	^6S, ^4G, ^4F, ^4D, ^4P, ^2I, ^2H, ^2G, ^2G, ^2F, ^2F, ^2D, ^2D, ^2D, ^2P, ^2S
	Term Symbols for Nonequivalent Electrons
$s\,s$	^1S, ^3S
$s\,p$	^1P, ^3P
$s\,d$	^1D, ^3D
$p\,p$	^3D, ^1D, ^3P, ^1P, ^3S, ^1S
$p\,d$	^3F, ^1F, ^3D, ^1D, ^3P, ^1P
$d\,d$	^3G, ^1G, ^3F, ^1F, ^3D, ^1D, ^3P, ^1P, ^3S, ^1S
$s\,s\,s$	^4S, ^2S, ^2S
$s\,s\,p$	^4P, ^2P, ^2P
$s\,p\,p$	^4D, ^2D, ^2D, ^4P, ^2P, ^2P, ^2P, ^4S, ^2S, ^2S
$s\,p\,d$	^4F, ^2F, ^2F, ^4D, ^2D, ^2D, ^4P, ^2P, ^2P

Example 17. An atom with orbital angular momentum L and spin angular momentum S often has a term in its Hamiltonian of the form $\lambda L.S$, called the spin-orbit coupling term. Since the angular momentum $J = L + S$ commutes with the Hamiltonian, the states of this atom can be labelled with the eigenvalues of J^2, J_z, L^2 and S_z. Notice that $L.S = (1/2)\ (J^2 - L^2 - S^2)$ so that the eigenvalue of $L.S$ is $(1/2)\ [J\ (J+1) - L\ (L+1) - S\ (S+1)]$. This can lead to observable energy level splittings. Thus, for example, the excited states of an alkali atom with the outermost electron excited from the s to the next higher p orbital will have $L = 1$ and $S = 1/2$. This leads to two possible J values : 3/2 and 1/2. Calculate the energy level splitting due to spin-orbital coupling.

Solution. The energy term due to $\lambda L.S$ will be

$$\lambda\left[J(J+1) - 1(1+1) - \frac{1}{2}\left(\frac{1}{2}+1\right)\right] = A\left[J(J+1) - \frac{11}{4}\right]$$

For $J = 3/2$, the energy term equals λ; for $J = 1/2$ it equals $-2A$, giving a splitting of 3λ.

In Na atom, the observed splitting of the intense yellow fluorescent lines is 17 cm^{-1}. Thus, . $\lambda = 5{\cdot}7\ cm^{-1}$, as shown in Fig. 12. λ is called spin-orbit coupling constant.

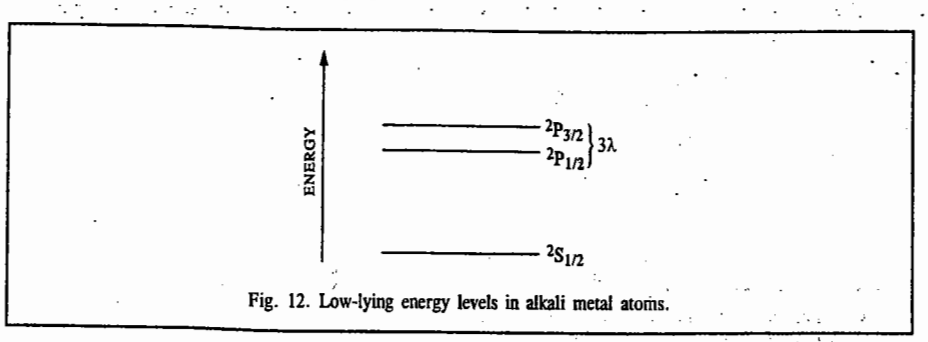

Fig. 12. Low-lying energy levels in alkali metal atoms.

ATOMIC SPECTRA

The spectrum of hydrogen atom is the simplest of all spectra. This spectrum is governed by the selection rule :

$$\Delta n = \text{anything},\quad \Delta l = \pm 1,\quad \Delta m = \pm 1, 0 \qquad ...(203)$$

We may mention here that most intense spectroscopic transitions involve the interaction of the electric vector of the electromagnetic radiation with instantaneous electric dipole moment induced in the atom or molecule. These are called **electric dipole transitions.** Electric dipole transitions are due to the oscillating electric field component of the radiation and **magnetic dipole transitions** are due to oscillating magnetic field component of radiation. Magnetic dipole transitions are generally about 10^5 times weaker (*i.e.*, less probable) than electric dipole transitions.

From the selection rule given in Eq. 203, we see that an electron in the ground state ($1s$ orbital) can undergo a transition to any p state :

$$1s \longrightarrow np\ (n \geq 2)$$

while a $2p$ electron can undergo transitions to either an s state or a d state :

$$2p \longrightarrow ns \text{ or } nd$$

Since s and d orbitals are here degenerate, the energies of both these transitions will be identical. These transitions are shown in Fig. 13. A diagram of the type shown in Fig. 13 which summarises the energies of the atomic states and the transitions between them is called **Grotrian diagram.**

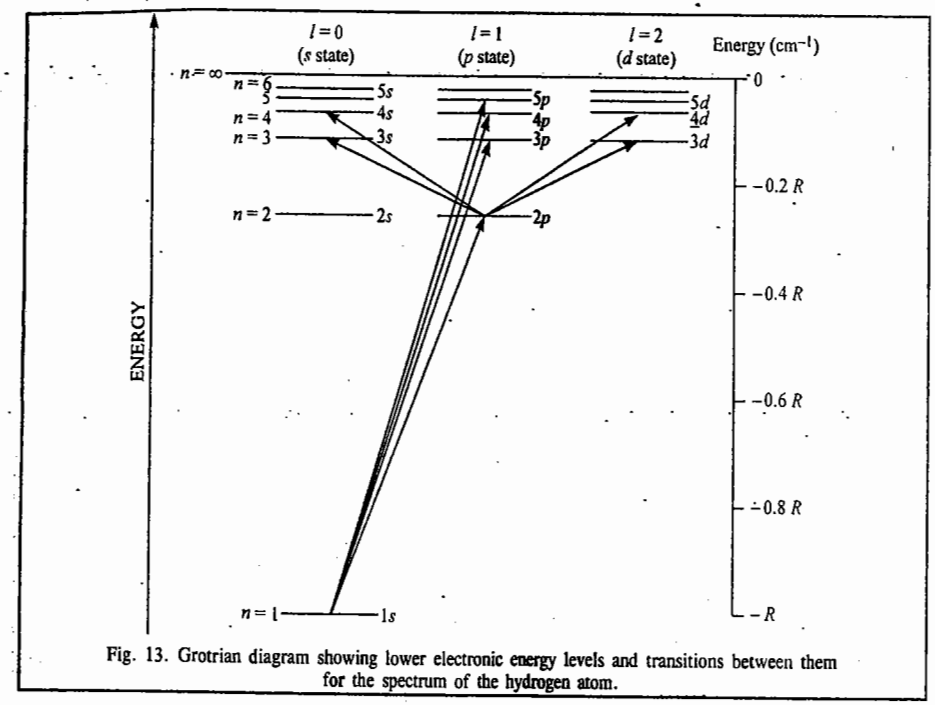

Fig. 13. Grotrian diagram showing lower electronic energy levels and transitions between them for the spectrum of the hydrogen atom.

We shall deal briefly with *(i)* fine structure *(ii)* the Zeeman effect *(iii)* the Stark effect and *(iv)* hyperfine structure in atomic spectra.

A. Fine Structure

This structure arises from **spin-orbit interaction**, *i.e.*, coupling of orbital and spin angular momenta of electrons ; thus,

$$j = l + s \qquad ...(204)$$

where $j = |l + s|, |l + s - 1|, \ldots, |l - s|$

Due to the coupling between the spin angular momentum, s, and the orbital angular momentum, l, to give the total angular momentum j, most of the energy levels shown in Fig. 13 are split into doublets. For example, for the $2p$ case we have $l = 1$, and $s = 1/2$, and hence $j = 3/2$ and $1/2$. These states are labelled by the term symbols $^{2s+1}L_j$, so that we have $^2P_{3/2}$ and $^2P_{1/2}$. On the other hand, the $1s$ orbital remains a singlet since $l = 0$; thus the ground state term symbol for hydrogen atom is $^2S_{1/2}$. The selection rules for n and l are the same as before :

$$\Delta n = \text{anything} ; \Delta l = \pm 1 \text{ only} \qquad ...(205)$$

but there is an additional solution rule for j :

$$\Delta j = 0, \pm 1, \qquad ...(206)$$

Thus, the $1s \rightarrow 2p$ transition in hydrogen atom will give rise to a doublet, *i.e.*, two lines. In other words, the transitions are allowed between any S level and any P level (Fig. 14) :

$$^2S_{1/2} \longrightarrow {}^2P_{1/2}\ (\Delta j = 0)$$

$$^2S_{1/2} \longrightarrow {}^2P_{3/2}\ (\Delta j = +1)$$

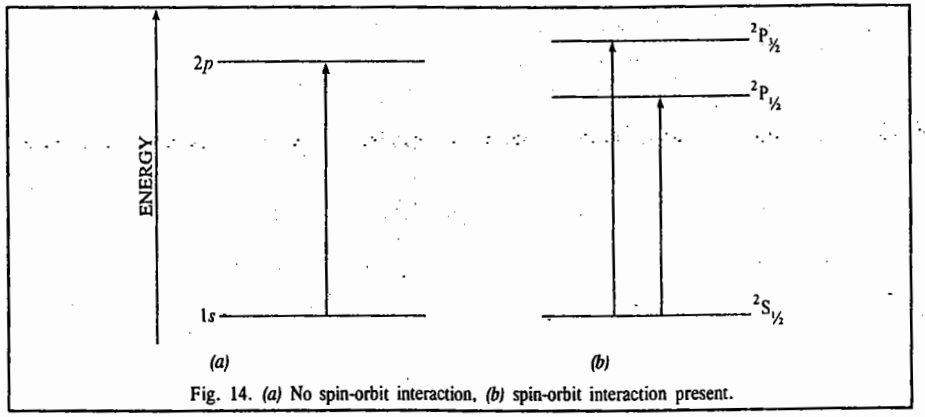

Fig. 14. *(a)* No spin-orbit interaction, *(b)* spin-orbit interaction present.

This coupling is very weak for hydrogen atom and the first few hydrogenic ions. Fig. 15 shows a few lower energy levels of hydrogen atom, showing the *j*-splitting and some transitions. This spectrum showing $^2S_{1/2} \longrightarrow {}^2P_{1/2,3/2}$ gives a simple doublet. However, the spectrum (Fig. 16) showing $^2P \longrightarrow {}^2D$ transition gives the following three allowed transitions :

$$^2P_{3/2} \longrightarrow {}^2D_{3/2} \ (\Delta j = 0)$$

$$^2P_{3/2} \longrightarrow {}^2D_{5/2} \ (\Delta j = +1)$$

$$^2P_{1/2} \longrightarrow {}^2D_{3/2} \ (\Delta j = +1)$$

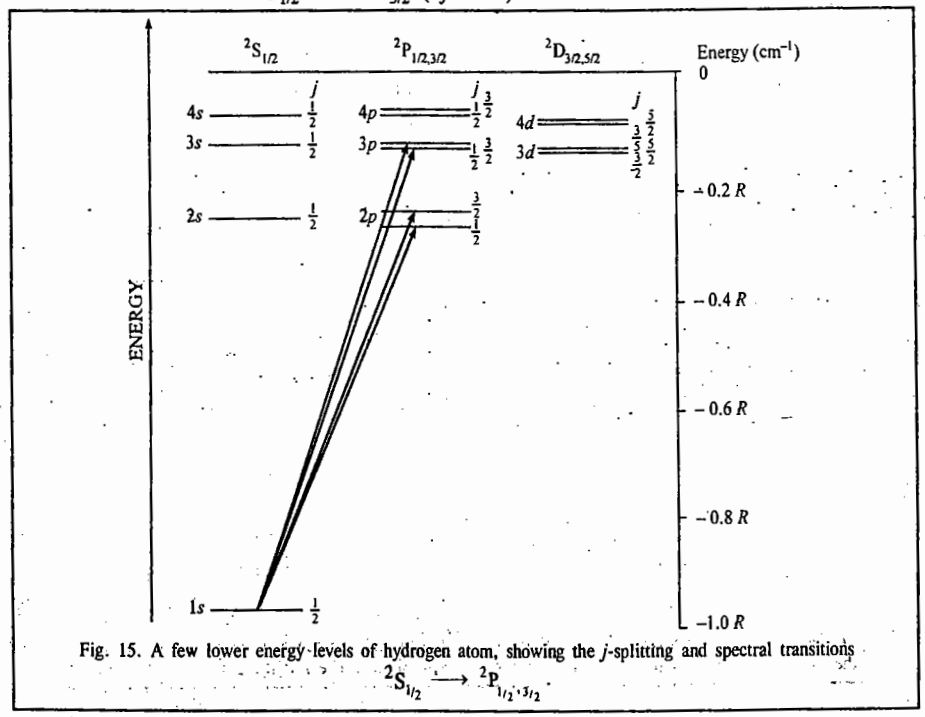

Fig. 15. A few lower energy levels of hydrogen atom, showing the *j*-splitting and spectral transitions $^2S_{1/2} \longrightarrow {}^2P_{1/2,3/2}$.

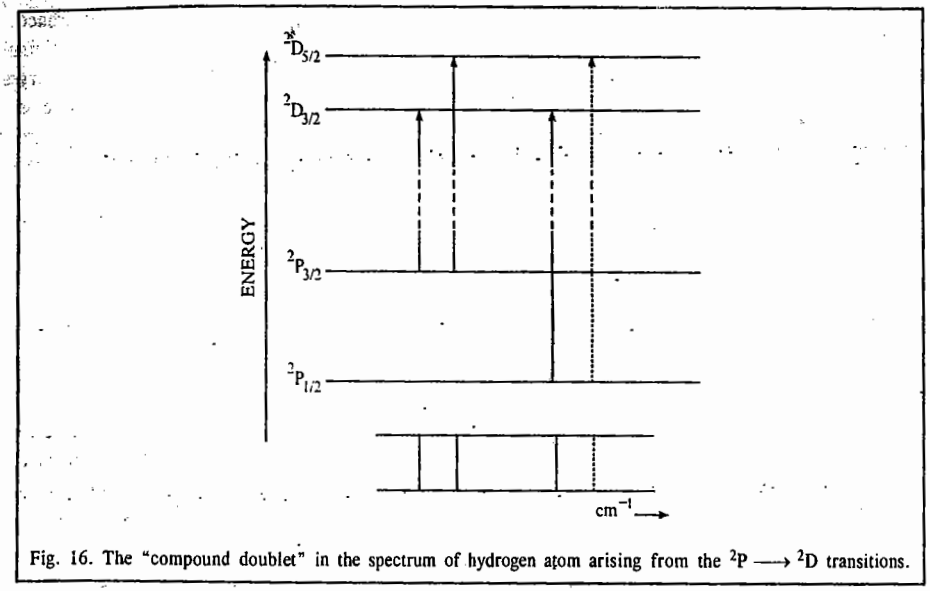

Fig. 16. The "compound doublet" in the spectrum of hydrogen atom arising from the $^2P \longrightarrow {}^2D$ transitions.

Note that the fourth transition (shown dotted), $^2P_{1/2} \longrightarrow {}^2D_{5/2}$, is forbidden for it corresponds it $\Delta j = +2$.

We next consider the spectrum of lithium atom. Fig. 17 shows the energy levels of lithium.

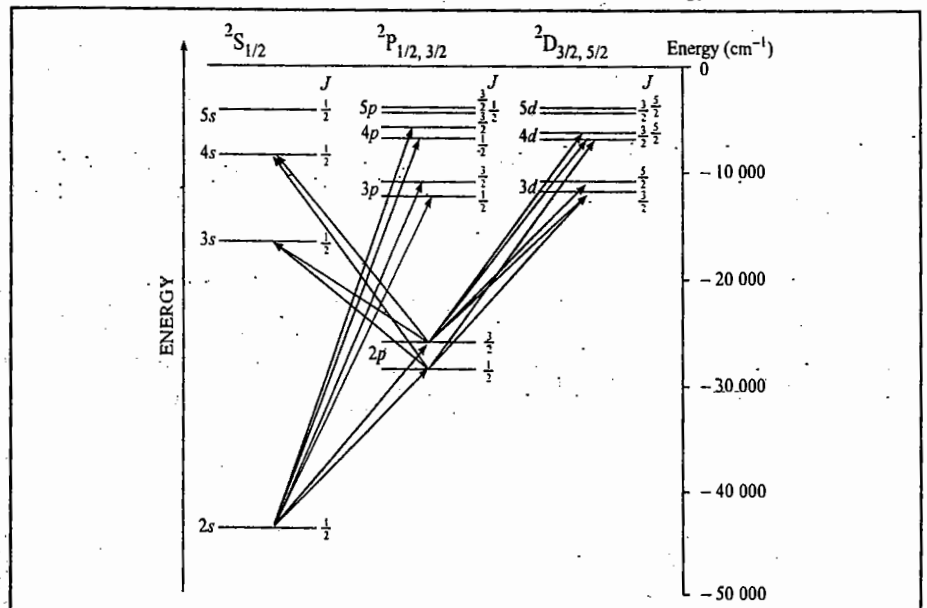

Fig. 17. A few lower energy levels of the lithium atom, showing the difference in energy of *s*, *p*, and *d* states with the same value of *n*. Some allowed transitions are also shown. The *j*-splitting is greatly exaggerated.

Notice that this diagram is similar to that for hydrogen atom (Fig. 3) except for the difference between the *s*, *p* and *d* orbitals of a given *n* in the case of lithium atom and the fact that, for the lithium atom, the 1*s* state is filled with electrons which do not take part in spectral transitions under ordinary conditions. The selection rules for lithium metal (and of course, other Group I metals) are the same as for hydrogen atom, *viz*; Δn = anything, $\Delta l = \pm 1$, $\Delta j = 0, +1$, with the result that the spectra are similar. Contrary to the hydrogen atom case, the fine structure in the spectra of alkali metals can be easily resolved (Fig. 17).

When, however, there is more than one electron, the addition of spin and orbital angular momenta is governed by *(a)* the **Russell-Saunders coupling scheme** (for atoms with $Z \leq 30$) and *(b)* by ***jj*-coupling scheme** (for heavier atoms with $Z > 30$). This we have already discussed while determining the term symbols of many-electron atoms. For many-electron atoms the relevant selection rules are

$$\Delta S = 0,\ \Delta L = \pm 1 \text{ and } \Delta J = 0, \pm 1 \qquad ...(207)$$

Let us consider the spectrum of helium atom. Russell-Saunders coupling scheme shows that the terms of helium are a series of singlets ($^1S_0$, $^1P_1$, $^1D_1$) and a series of triplets ($^3S_1$; $^3P_{2,1,0}$, $^3D_{3,2,1}$). Using the selection rule (1), the spectral transitions in the helium atom spectrum are shown in Fig. 18. Note that transitions between the singlet and the triplet energy levels are forbidden.

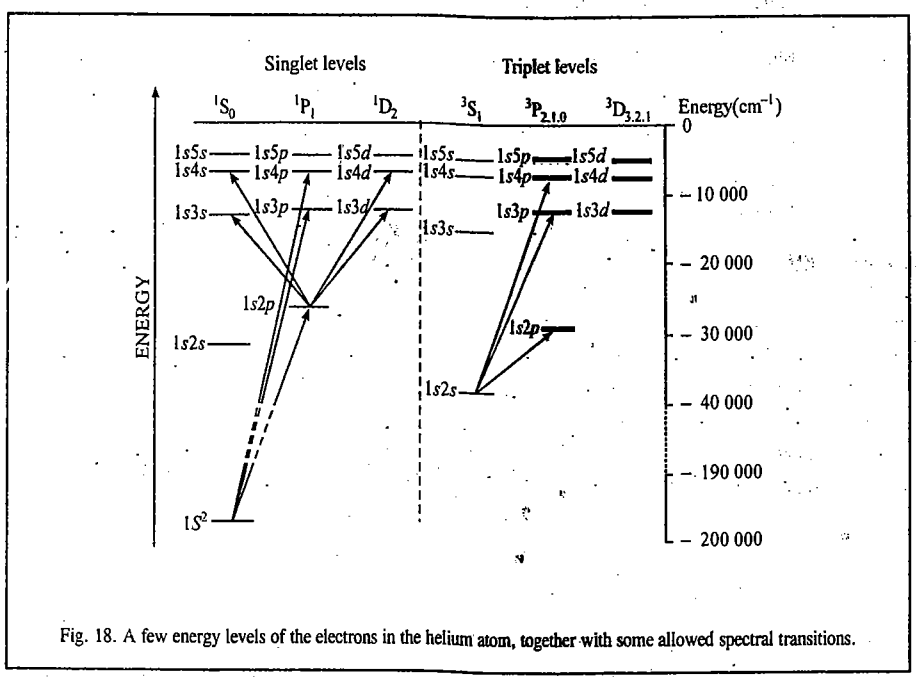

Fig. 18. A few energy levels of the electrons in the helium atom, together with some allowed spectral transitions.

Fig. 19 shows a transition between ^3P and ^3D states ; we see that the spectrum (shown at the foot of the figure) consists of six lines. This spectrum is ordinarily not resolved since the spacing is very close; only three lines are observed ; hence, the spectrum is referred to as a **compound triplet.**

Other atoms containing two outer electrons — as, for instance, alkaline earths, beryllium, magnesium, calcium, etc. — exhibit spectra similar to helium atom.

Example 18. State and prove Lande's interval rule.

Solution : According to the Lande's interval rule the separation between the two *J* levels of a Russell-Saunders term, brought about by spin-orbit interaction, is proportional to the larger *J* value of the pair.

$$J = L + S$$

$$J^2 = J^2 + S^2 + 2L.S$$

whence, the spin-orbit interaction, $L.S$ is

$$L.S = \frac{1}{2}(J^2 - L^2 - S^2)$$

We know that the eigenvalues of the various angular momenta are

$$J^2 = J(J+1)\hbar^2;\ L^2 = L(L+1)\hbar^2;\ S^2 = S(S+1)\hbar^2$$

Hence, the energy of the level characterized by the quantum number J, as a result of the spin-orbit interaction, is

$$E_J = \frac{1}{2}[J(J+1) - L(L+1) - S(S+1)]\hbar^2$$

For a term with the same L and S but with $J = J - 1$, we get

$$E_{J-1} = \frac{1}{2}[J-1)J - L(L+1) - S(S+1)]\hbar^2$$

Thus, $\Delta E = E_J - E_{J-1} = J\hbar^2$

which is **Lande's interval rule.**

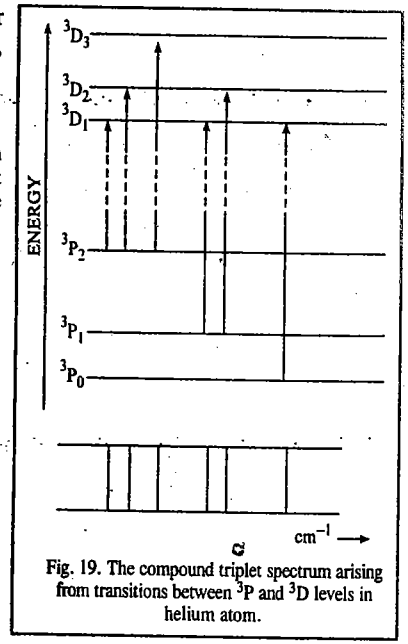

Fig. 19. The compound triplet spectrum arising from transitions between ^3P and ^3D levels in helium atom.

B. Zeeman Effect

The splitting of spectral lines in the presence of an applied magnetic field B (called the magnetic flux density) is called the Zeeman effect, first observed by P. Zeeman in 1896. This effect arises as a result of the interaction between B and the magnetic moment, μ, associated with the electron spin and orbital motion ; thus,

$$E_{int} = -\mu.B \qquad ...(208)$$

The applied magnetic field B splits a term with a given J value into $2J + 1$ sub-levels, characterized by the quantum number M_J, which is the component of J along the direction of the magnetic field (usually chosen as the *z*-axis) ; thus,

$$E(M_J) = g_J \mu_B B_z M_J \qquad ...(209)$$

where g_J is the **Lande' *g*-factor**, defined as

$$g_J = 1 + \frac{J(J+1) + S(S+1) - L(L+1)}{2J(J+1)} \qquad ...(210)$$

μ_B is the Bohr magneton ($= 9{\cdot}273 \times 10^{-24}$ JT^{-1}). The selection rule for the Zeeman effect is $\Delta M_J = 0, \pm 1$. Note that the Zeeman transitions between the singlet terms are referred to as the **normal Zeeman effect** and the Zeeman transitions between terms of higher multiplicity (between, for instance, the doublet terms, or the triplet terms, etc.) are called the **anomalous Zeeman effect**. In fact, the anomalous Zeeman effect, in which the original line splits into more than three components, is much

more common than the normal Zeeman effect, in which the original line splits into three components.

We shall illustrate the Zeeman effect by a few solved examples.

Example 19. Work out the Zeeman pattern for a $^1P_1 \longleftrightarrow {}^1D_2$ transition in atomic spectra.

Solution : The Lande g-factor is

$$g_J = 1 + \frac{J(J+1) + S(S+1) - L(L+1)}{2J(J+1)} \quad \text{[Eq. 210]}$$

Note : 0 divided by 0 in the second term is treated not as indeterminate but as equal to 0.

For the $^1P_1$ and $^1D_2$ terms $J = L$ because $= 0$. Substituting in the expression for g_J, gives $g = 1$, for both the singlet terms. Hence, the $^1P_1$ and $^1D_2$ levels will be split into equally spaced sub-levels. Using the selection rule $\Delta M_J = 0, \pm 1$, we get nine transitions (Fig. 20) but only three lines, each being triply degenerate.

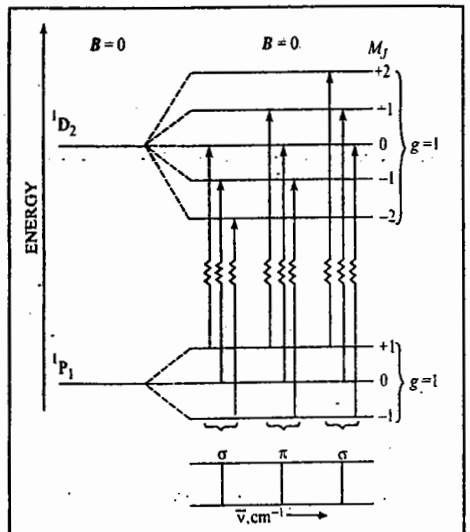

Fig. 20. The Zeeman pattern for a $^1P_1 \longleftrightarrow {}^1D_2$ transition.

It is customary to call the outer components of a Zeeman pattern the σ-components and the inner ones the π-components. In drawing the Zeeman pattern we have ignored the relative intensity of the σ- and π-components, all the components having been drawn equally intense.

Example 20. Work out the Zeeman pattern for a $^1S_0 \longleftrightarrow {}^1P_1$ transition in atomic spectra.

Solution : As shown in the previous example, for the $^1S_0$ and $^1P_1$ terms $J = L$ because $S = 0$. Substituting in the expression for the Lande g-factor g_J gives $g = 1$ for both the singlet terms. The number of states that each term splits into is given by the M_J quantum number. There are $2J + 1$ values of M_J. For the $^1S_0$ term, $M_J = 0$ and no splitting occurs. For $^1P_1$ state, the $2(1) + 1 = 3$ values of M_J are +1, 0 and −1. Using the selection rule $\Delta M_J = 0, \pm 1$, we get three transitions (Fig. 21).

Example 21. Work out the Zeeman pattern for the $^2P_{1/2,3/2} \longleftrightarrow {}^2S_{1/2}$ transition in sodium atom. (This transition corresponds to the 3p ⟷ 3s transition in sodium, which results in the D-lines in the sodium atom spectrum).

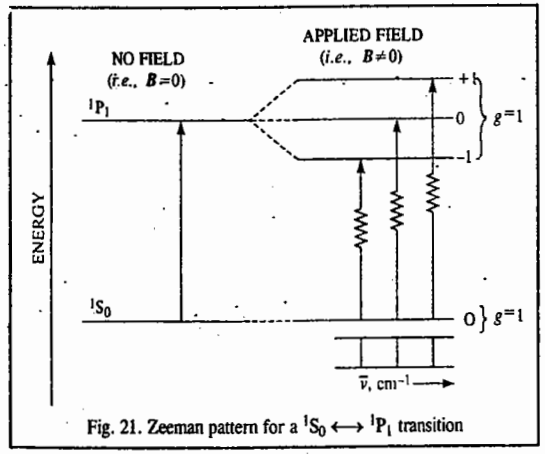

Fig. 21. Zeeman pattern for a $^1S_0 \longleftrightarrow {}^1P_1$ transition

Solution : For the $^2S_{1/2}$ level, $S = \frac{1}{2}$. $L = 0$, $J = \frac{1}{2}$ Hence, $g_J = 2$. For the $^2P_{1/2}$ level, $S = \frac{1}{2}$, $L = 1$, $J = \frac{1}{2}$. Hence, $g_J = 2/3$. Again, for the $^2P_{3/2}$ level, $S = \frac{1}{2}$, $L = 1$, $J = 3/2$; so that $g_J = 4/3$. The Zeeman field splits the $^2P_{3/2}$ level into four equally spaced sub-levels corresponding to $M_J = +3/2, +1/2, -1/2, -3/2$. From the values of g_J we see that the $^2S_{1/2}$, $^2P_{1/2}$ and $^2P_{3/2}$ levels are split by the Zeeman field in the ratio of 3 : 1 : 2. The selection rules for the transitions are

$$\begin{aligned} \Delta S &= 0 \\ \Delta L &= 0, \pm 1 \text{ (but } L = 0 \not\longleftrightarrow L = 0) \\ \Delta J &= 0, \pm 1 \text{ (but } J = 0 \not\longleftrightarrow J = 0) \\ \Delta M_J &= 0, \pm 1 \end{aligned} \quad \ldots(211)$$

Using these selection rules, the energy level diagram and the transitions between the energy levels are shown in Fig. 22. (The resulting spectrum is also shown under the corresponding spectral transitions).

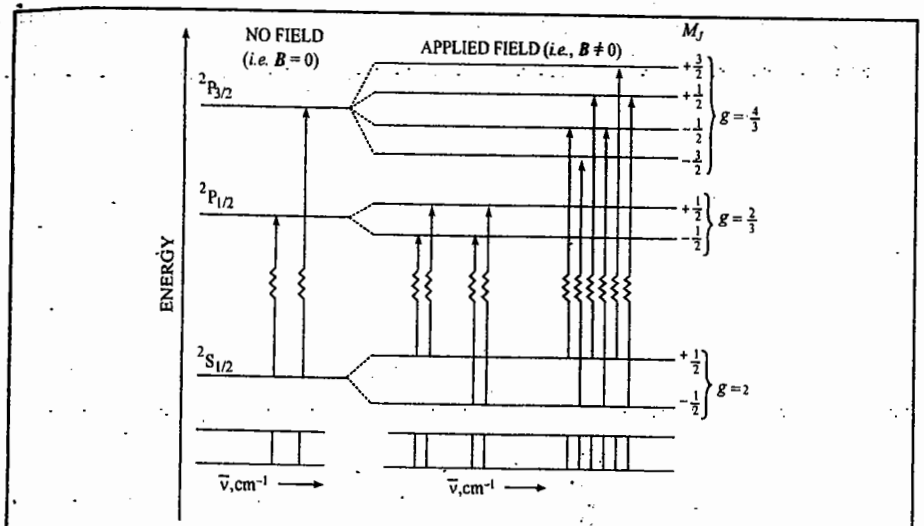

Fig. 22. The Zeeman pattern for a $^2S_{1/2} \longleftrightarrow {}^2P_{1/2,3/2}$ transition.

Example 22. Work out the Zeeman pattern for a $^3S \longleftrightarrow {}^3P$ transition in atomic spectra.

Solution : Proceeding as in Example 21, the Zeeman pattern, showing the energy level diagram and the transitions between them, is drawn in Fig. 23, along with the resulting spectrum.

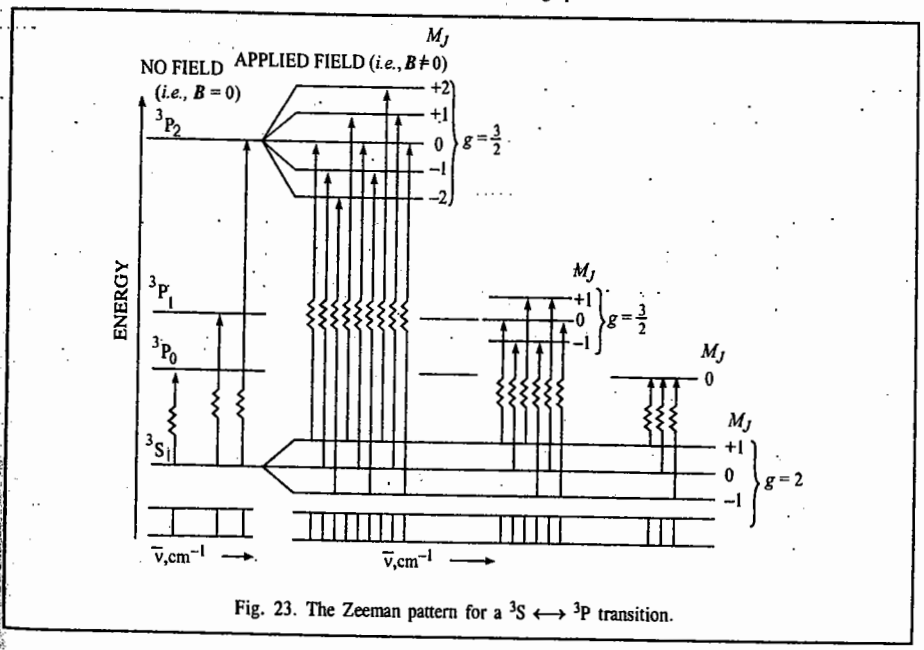

Fig. 23. The Zeeman pattern for a $^3S \longleftrightarrow {}^3P$ transition.

We may conclude this discussion of Zeeman effect by referring to the **Paschen-Back Effect**. This effect arises when the strength of the applied magnetic field becomes greater than the multiplet splittings. In this region the orbital and the spin angular momenta are no longer coupled to each other but are coupled separately to the magnetic field. In this case only the normal Zeeman effect is observed even when doublet or higher spin states are present.

C. Stark Effect

The splitting of spectral lines in the presence of an applied electric field, E is called the Stark effect, first observed by the German physicist J. Stark in 1913. This effect arises as a result of the interaction between E and the induced electric dipole moment, μ, as a result of electron polarization. The energy of interaction is given by

$$E_{int} = -\mu . E \qquad ...(212)$$

Since, however, μ is proportional to E, the splitting of the energy levels is proportional to E^2. The differences between the Zeeman and the Stark effects are that in the latter case the splitting pattern is not symmetric about the original line, and the energy values depend on $M_J^2 E^2$.

D. Hyperfine structure

The hyperfine interaction arises as a result of the interaction of the electron spin with the nuclear spin. Recall that fine structure arises from the interaction of the electron spin with the electron orbital motion. The nuclear spin, I, may be zero, integral or half-integral, depending on the nature of the nucleus. The nuclear spin angular momentum is given by

$$I = \sqrt{I(I+1)}\,\hbar \qquad ...(213)$$

The total angular angular momentum (electronic + nuclear) of an atom is defined by

$$F = \sqrt{F(F+1)}\,\hbar \qquad ...(214)$$

where F is the total momentum quantum number. If J is the total electronic angular momentum quantum number ($J = L + S$) then,

$$F = J + I, J + I - 1, \ldots . \mid J - I \mid \qquad ...(215)$$

thus giving $2J + 1$ or $2I + 1$ different energy states whichever is less. The hyperfine structure splitting is always far less than fine structure splitting.

Example 23. Show that the hyperfine structure (HFS) is smaller than the fine structure (FS) by approximately the ratio $m_e/(m_p Z)$.

Solution : Rigorously speaking, FS is the result of the interaction between the magnetic moment, μ_e of the electron and the Coulumb field, E, of the nucleus. Thus, the fine structure energy is given by

$$E_{FS} = \mu_e . S = g_e \mu_B E \qquad ...(i)$$

(where g_e is the electron g-factor and μ_B is the Bohr magneton). HFS, on the other hand, is due to the interaction between the magnetic moment, μ_n, of the nucleus and the magnetic field B, produced at the nucleus by the orbital motion of the electron. The hyperfine interaction energy is

$$E_{HFS} = \mu_n . B = g_N \mu_N B \qquad ...(ii)$$

(where g_N is the nuclear g-factor and μ_N is the nuclear magneton). We see from Eqs. *(i)* and *(ii)* that

$$E_{FS} \propto 1/m_e \text{ ; and } E_{HFS} \propto 1/m_p$$

However, E_{FS} also increases with increasing nuclear charge, Z, so that $E_{FS} \propto Z$. Hence, $E_{FS} \propto Z/m_e$.

We thus see that

$$E_{HFS}/E_{FS} = m_e/m_p Z \qquad ...(iii)$$

THOMAS-FERMI MODEL OF THE ATOM

Thomas–Fermi model of the atom is a statistical one in which the electrons are treated as a gas obeying Fermi-Dirac statistics. In this model, the central potential $V(r)$ is assumed to be slowly varying, slow enough to have number of electrons in an electron wavelength. In other words, many electrons are localized within a volume over which the potential is almost a constant. As the electrons are treated as a gas of fermions, one can apply the concept of cells in phase space to the states of individual electrons.

The volume of phase space occupied by electrons which have momenta less than p and are in the volume dV is $(4/3)\pi p^3\, dV$. The number of cells (states) corresponding to this volume is $2(4/3)\pi p^3\, dV$, the factor of 2 being included to account for the two possible spin states. Assuming that all these states are occupied, the number of electrons per unit volume $n(r)$ whose kinetic energy does not exceed $p^2/2m$ is given by

$$n(r) = \frac{8\pi p^3}{3h^3} = \frac{p^3}{3\pi^2 \hbar^3} \qquad ...(216)$$

For the electrons not to escape from the nucleus, the maximum allowed kinetic energy at any distance r from the nucleus is $-V(r)$. That is,

$$p^2/2m = -V(r) \qquad ...(217)$$

From Eqs. 216 and 217,

$$n(r) = \frac{[-2m\,V(r)]^{3/2}}{3\pi^2 \hbar^3} \qquad ...(218)$$

The electrostatic potential $-V(r)/e$ and the charge density $-en(r)$ obey the Poisson equation

$$-\frac{1}{e}\nabla^2 V(r) = -4\pi e n(r) \qquad ...(219)$$

The potential is spherically symmetric since the nucleus is at the origin and, therefore,

$$\nabla^2 V(r) = \frac{1}{r^2}\frac{d}{dr}\left(r^2 \frac{dV}{dr}\right) \qquad ...(220)$$

With this value of $\nabla^2 V(r)$, Eq. (219) becomes

$$\frac{1}{r^2}\frac{d}{dr}\left(r^2 \frac{dV}{dr}\right) = -4\pi e^2 n(r) \qquad ...(221)$$

Substituting the value of $n(r)$ from Eq. 218 in Eq. 221, we have

$$\frac{1}{r^2}\frac{d}{dr}\left(r^2 \frac{dV}{dr}\right) = -\frac{4e^2}{3\pi \hbar^3}[-2m\,V(r)]^{3/2} \qquad ...(222)$$

When $r \to 0$, the leading term in the potential is due to the nucleus so that $V(r) \to -Ze^2/r$. Hence, it

is convenient to introduce the function $\chi(r)$ defined by

$$V(r) = -\frac{Ze^2\,\chi(r)}{r} \qquad ...(223)$$

Substituting this value of $V(r)$ in Eq. 222, we have

$$\frac{d^2\chi}{dr^2} = \frac{4e^3(2m)^{3/2}Z^{1/2}}{3\pi\hbar^3}\frac{\chi^{3/2}}{r^{1/2}} \qquad ...(224)$$

Eq. 224 can be written in a dimensionless form by writing

$$r = bx \qquad ...(225)$$

The parameter b will be defined shortly. In terms of the new variable, Eq. 224 reduces to

$$\frac{d^2\chi}{dx^2} = b^{3/2}\frac{4e^3(2m)^{3/2}Z^{1/2}}{3\pi\hbar^3}\frac{\chi^{3/2}}{x^{1/2}} \qquad ...(226)$$

We select the value of the parameter b in such a way that the coefficient of $\chi^{3/2}/x^{1/2}$ is unity. This gives

$$b = \frac{1}{2}\left(\frac{3\pi}{4}\right)^{2/3}\frac{\hbar^2}{me^2}\frac{1}{Z^{1/3}} = \frac{0.8853a_0}{Z^{1/3}} \qquad ...(227)$$

where a_0 is the Bohr radius. With this substitution, Eq. 227 becomes

$$\frac{d^2\chi}{dx^2} = \frac{\chi^{3/2}}{x^{1/2}} \qquad ...(228)$$

Eq. 228 is called the **dimensionless Thomas-Fermi equation**. As $V(r) \to -Ze^2/r$ when $r \to 0$, by virtue of Eq. 223, $\chi(0) = 1$. As $r \to \infty$, there will not be any net charge inside the sphere of radius r so that $V(r)$ falls off more rapidly than $1/r$ and $rV(r) \to 0$. Hence, $\chi(\infty) = 0$.

Solution of Eq. 228 subject to these boundary conditions was first carried out by Bush and Caldwell in 1931. A knowledge of $\chi(x)$ allows the determination of charge distribution in the atom and the r-dependence of the potential $V(r)$ in Eq. 223. The Thomas-Fermi model being a statistical model, we can expect better results as atomic number Z increases.

Enrico Fermi (1901-1954), the great Italian physicist, was probably the only 20th century physicist who was equally at home in theory and experiment. He never considered himself a theorist, though theoretical physics has been enriched by several terms associated with his name—Fermi-Dirac statistics, Thomas-Fermi atom, Fermi energy, Fermi level, Fermi sea, Fermi surface, Fermi sphere, Fermi temperature, Fermions, Fermi's theory of beta-secay, Fermi liquid, Fermi's golden rule, Fermi resonance, Fermi contact interaction and last but not least, Fermi-type calculation. He was awarded the 1938 Physics Nobel Prize for his contributions to the existence of new radioactive elements produced by neutron-irradiation, and related nuclear reactions. A staunch opponent of Fascism, Nazism and totalitarianism, he escaped to the U.S.A. in the 1930s with the help of his American admirers, thereby evading the Italian dictator Mussolini who had intended to have him assassinated. He was an outstanding teacher, among his students were the great Chinese-American theorists C.N. Yang and T.D. Lee, the winners of the 1957 Physics Nobel Prize. He along with Edward Teller was associated with the Manhattan Project (under the supervision of physicist J.R. Oppenheimer) which built the first atomic bomb that brought about the horrible devastation of Hiroshima and Nagasaki in August, 1945, thereby ending the Second World War. At the University of Chicago his distinguished colleague was the famous Indian astrophysicist, S. Chandrasekhar, with whom he coauthored a research paper in astronomy. The Enrico Fermi Institute in the University of Chicago has been established in his memory.

ANGULAR MOMENTUM REVISITED

1. Angular Momentum Matrices

The states $|jm>$ form a complete orthonormal set and they can be used as a basis for the matrix representation of angular momentum. In this representation a function F of the angular momentum components can be represented by a matrix with matrix elements $\langle j'm'|\ F\ |jm\rangle$. The rows of the matrix will be labelled by j' and m' values and the columns by the j, m values.

a. Matrices for J^2 and J_z. Since J^2 commutes with J_z the matrices for J^2 and J_z will be diagonal. In that representation J_x and J_y will not be diagonal since J_z does not commute with J_x and J_y. We have already obtained the following eigenvalue equations for J^2 and J_z :

$$J^2\ |\ jm\ \rangle = j\,(j+1)\,\hbar^2\ |\ jm\ \rangle \qquad ...(229)$$

and

$$J_z\ |\ jm\ \rangle = m\hbar\ |\ jm\ \rangle \qquad ...(230)$$

Multiplication of Eqs. 1 and 2 from left by $\langle\ j'\ m'\ |$ gives

$$\langle\ j'\ m'\ |\ J^2\ |\ jm\ \rangle = j\,(j+1)\ \hbar^2\ \delta_{jj'}\ \delta_{mm'} \qquad ...(231)$$

and

$$\langle j'm'\ |\ J_z\ |\ jm\ \rangle = m\hbar\ \delta_{jj'}\ \delta_{mm'} \qquad ...(232)$$

The presence of the Kronecker deltas $\delta_{jj'}$ and $\delta_{mm'}$ indicates that the matrices are diagonal, as expected. The explicit form of J^2 and J_z matrices are given in Tables 1 and 2; they are of infinite dimensions.

TABLE 1

Matrix for J^2 : $\langle j'\ m'\ |\ J^2\ |\ jm\rangle = j\,(j+1)\ \hbar^2\ \delta_{jj'}\ \delta_{mm'}$

j'	m'	j / m : 0 / 0	1/2 / 1/2 −1/2	1 / 1 0 −1	...
0	0	0	(0)	(0)	...
1/2	1/2	(0)	$\begin{bmatrix} 3\hbar^2/4 & 0 \\ 0 & 3\hbar^2/4 \end{bmatrix}$	(0)	...
	−1/2				
1	1	(0)	(0)	$\begin{bmatrix} 2\hbar^2 & 0 & 0 \\ 0 & 2\hbar^2 & 0 \\ 0 & 0 & 2\hbar^2 \end{bmatrix}$	...
	0				
	−1				
⋮	⋮	⋮	⋮	⋮	

TABLE 2

Matrix for J_z : $\langle j' m' \mid J_z \mid jm \rangle = m\hbar\ \delta_{jj'}\ \delta_{mm'}$

j'	m'	j / m : 0 / 0	1/2 / 1/2 −1/2	1 / 1 0 −1	...
0	0	0	(0)	(0)	...
1/2	1/2	(0)	$\begin{bmatrix} \hbar/2 & 0 \\ 0 & -\hbar/2 \end{bmatrix}$	(0)	...
	−1/2				
1	1	(0)	(0)	$\begin{bmatrix} 1\hbar & 0 & 0 \\ 0 & 0 & 0 \\ 0 & 0 & -1\hbar \end{bmatrix}$	...
	0				
	−1				
⋮	⋮	⋮	⋮	⋮	

b. Matrices for J_+, J_-, J_x and J_y : We have already shown that

$$J_z J_+ \mid jm \rangle = (m+1)\hbar\ J_+ \mid jm \rangle \qquad \ldots(233)$$

This implies that $J_+ \mid jm \rangle$ is an eigenket (eigenfunction) of J_z with eigenvalue $(m+1)\hbar$. The eigenvalue equation for J_z with eigenvalue $(m+1)\hbar$ can also be written as

$$J_z \mid j, m+1 \rangle = (m+1)\ \hbar \mid j, m+1 \rangle \qquad \ldots(234)$$

Since the eigen values of J_z (Eqs. 233 and 234) are equal, the eigenvectors can differ at most by a multiplicative constant, say a_m.

$$J_+ \mid jm \rangle = a_m \mid j, m+1 \rangle \qquad \ldots(235)$$

Similarly, we get

$$J_- \mid jm \rangle = b_m \mid j, m-1 \rangle \qquad \ldots(236)$$

where $$a_m = \langle j, m+1 \mid J_+ \mid jm \rangle \quad \text{or} \quad a_m^* = \langle jm \mid J_- \mid j, m+1 \rangle \qquad \ldots(237)$$

$$b_m = \langle j, m-1 \mid J_- \mid jm \rangle \quad \text{or} \quad b_{m+1} = \langle jm \mid J_- \mid j, m+1 \rangle \qquad \ldots(238)$$

Comparison of Eqs. 237 and 238 gives

$$a_m^* = b_{m+1} \qquad \ldots(239)$$

Operating on Eq. 235 from the left by J_- gives

$$J_- J_+ \mid jm \rangle = a_m J_- \mid j, m+1 \rangle \qquad \ldots(240)$$

It can be shown that

$$J_- J_+ = J^2 - J_z^2 - \hbar J_z \qquad \ldots(241)$$

Using this result and Eq. 236 we obtain

$$(J^2 - J_z^2 - \hbar J_z) \mid jm \rangle = a_m\, b_{m+1} \mid jm \rangle \qquad \ldots(242)$$

or $$[j(j+1) - m^2 - m]\ \hbar^2 \mid jm \rangle = \mid a_m \mid^2 \mid jm \rangle \qquad \ldots(243)$$

or $$a_m = [j(j+1) - m(m+1)]^{1/2}\hbar \qquad \ldots(244)$$

With this value of a_m

$$J_+ \mid jm \rangle = [j(j+1) - m(m+1)]^{1/2}\ \hbar \mid jm \rangle \qquad \ldots(245)$$

or $$\langle j' m' \mid J_+ \mid jm \rangle = [j(j+1) - m(m+1)^{1/2}\ \hbar\ \delta_{jj'}\ \delta_{m', m+1} \qquad \ldots(246)$$

Similarly,

$$\langle j' m' \mid J_- \mid jm \rangle = [j(j+1) - m(m-1)^{1/2}\ \hbar\ \delta_{jj'}\ \delta_{m', m-1} \qquad \ldots(247)$$

Eqs. 246 and 247 give the matrix elements for J_+ and J_-. They are infinite-dimensional matrices like J^2 and J_z matrices. The nature of the Kronecker deltas in Eqs. 246 and 247 indicates that all non-vanishing elements occur in blocks along the diagonal corresponding to $j' = j$. The block matrices corresponding to $j = 0$, 1/2 and 1 are given below. The rows are labelled by the value of m' and the columns by the value of m. The non-vanishing matrices for J_x and J_y are evaluated using the relation

$$J_x = \frac{1}{2}(J_+ + J_-) \qquad \text{and} \qquad J_y = \frac{1}{2i}(J_+ - J_-) \qquad \ldots(248)$$

For $j = 0$, $J_+ = 0$, $J_- = 0$, $J_x = 0$, $J_y = 0$ $\qquad \ldots(249)$

For $j = 1/2$,

$$J_+ = \hbar\begin{pmatrix} 0 & 1 \\ 0 & 0 \end{pmatrix}, \qquad J_- = \hbar\begin{pmatrix} 0 & 0 \\ 1 & 0 \end{pmatrix}$$

$$J_x = \frac{1}{2}\hbar\begin{pmatrix} 0 & 1 \\ 1 & 0 \end{pmatrix}, \quad J_y = \frac{1}{2}\hbar\begin{pmatrix} 0 & -i \\ i & 0 \end{pmatrix} \qquad \ldots(250)$$

For $j = 1$,

$$J_+ = \hbar\begin{pmatrix} 0 & \sqrt{2} & 0 \\ 0 & 0 & \sqrt{2} \\ 0 & 0 & 0 \end{pmatrix}, \quad J_- = \hbar\begin{pmatrix} 0 & 0 & 0 \\ \sqrt{2} & 0 & 0 \\ 0 & \sqrt{2} & 0 \end{pmatrix}$$

$$J_x = \frac{1}{\sqrt{2}}\hbar\begin{pmatrix} 0 & 1 & 0 \\ 1 & 0 & 1 \\ 0 & 1 & 0 \end{pmatrix}, \quad J_y = \frac{1}{\sqrt{2}}\hbar\begin{pmatrix} 0 & -i & 0 \\ i & 0 & -i \\ 0 & i & 0 \end{pmatrix} \qquad \ldots(251)$$

Our discussion would be incomplete without a word about the eigen function (eigenvector). The eigen vector with respect to the $\mid jm \rangle$ basis would be a column vector of infinite extent. The appropriate part of this infinite column vector would be used for the particular cases : j=0, j=1/2, j=1, ...

2. Spin Angular Momentum and Pauli Spin Matrices

It may be recalled that space quantization of spin angular momentum had been demonstrated by the great Stern-Gerlach experiment in 1921. Also, to account for the multiplicity of atomic states Uhlenbeck and Goudsmit had proposed in 1925 that an electron in an atom possesses an *intrinsic* (or *internal*) angular momentum, called the spin angular momentum, in addition to orbital angular momentum. This spin angular momentum S, as we have said above, has $S_z = m_s\hbar$, where $m_s = \pm\ 1/2$, on the z-axis.

Associated with S is an intrinsic (spin) magnetic moment, μ_S, given by

$$\mu_S = -(e/m_e)\, S \qquad ...(252)$$

Assuming that all stable and unstable particles have spin angular momentum S, we expect its components S_x, S_y and S_z to obey the general commutation relations

$$[\hat{S}_x, \hat{S}_y] = i\hbar S_z, \quad [\hat{S}_y, \hat{S}_z] = i\hbar \hat{S}_x, \quad [\hat{S}_z, \hat{S}_x] = i\hbar \hat{S}_y \qquad ...(253)$$

and $\hat{S}^2$ and $\hat{S}_z$ to have eigenvalues $s(s+1)\hbar^2$ and $m_s\hbar$, where $m_s = -s, -s+1, \ldots\ldots\ldots, s$, respectively.

For most of the spin-1/2 systems (such as stable elementary particles like electrons, protons, neutrons, etc.) the matrices representing S_x, S_y and S_z are obtained directly from the J_x, J_y and J_z matrices by taking the part corresponding to $j = 1/2$. Hence,

$$S_x = \frac{1}{2}\hbar\begin{pmatrix}0 & 1\\ 1 & 0\end{pmatrix}; \quad S_y = \frac{1}{2}\hbar\begin{pmatrix}0 & -i\\ i & 0\end{pmatrix}; \quad S_z = \frac{1}{2}\hbar\begin{pmatrix}1 & 0\\ 0 & -1\end{pmatrix} \qquad ...(254)$$

Often it is convenient to work with a matrix σ defined by

$$S = \frac{1}{2}\hbar\sigma \qquad ...(255)$$

where

$$\sigma_x = \begin{pmatrix}0 & 1\\ 1 & 0\end{pmatrix}; \quad \sigma_y = \begin{pmatrix}0 & -i\\ i & 0\end{pmatrix}; \quad \sigma_z = \begin{pmatrix}1 & 0\\ 0 & -1\end{pmatrix} \qquad ...(256)$$

The σ_x, σ_y and σ_z matrices are called the **Pauli spin matrices**. From the definition, it is obvious that their eigenvalues are ± 1. These matrices satisfy the relations

$$\sigma_x^2 = \sigma_y^2 = \sigma_z^2 = 1 \qquad ...(257)$$

$$\sigma_x\sigma_y = i\sigma_z, \quad \sigma_y\sigma_z = i\sigma_x, \quad \sigma_z\sigma_x = i\sigma_y \qquad ...(258)$$

$$\sigma_x\sigma_y + \sigma_y\sigma_x = \sigma_y\sigma_z + \sigma_z\sigma_y = \sigma_z\sigma_x + \sigma_x\sigma_z = 0 \qquad ...(259)$$

Pauli was the first to recognize the necessity of two-component state vectors to explain certain observed features of atomic spectra.

3. Spin Vectors for Spin-1/2 System

If we include the spin, then the spin-1/2 system such as an electron has four degrees of freedom, *viz.*, the three position coordinates (x, y, z) and another observable pertaining to spin. Taking the z-component S_z as the fourth variable, the electron wave function can be written as $\psi(r, S_z)$ or $\psi(r, m_s)$; the coordinate m_s takes the values $+1/2$ or $-1/2$. When the interaction between the spin and space parts is negligible, the wave function can be written as the product function :

$$\psi(r, m_s) = \phi(r)\,\chi(m_s) \qquad ...(260)$$

where $\phi(r)$ represents the part that depends on the space coordinates and $\chi(m_s)$, the part that depends on the spin coordinates. The eigenvectors of the spin matrices S_x, S_y and S_z can easily be obtained by writing the eigenvalue equation. Since the matrices are 2×2, the eigenvectors must be column vectors with two components. The eigenvalue equation for S_z with eigenvalue $\hbar/2$ is

$$\frac{1}{2}\hbar\begin{pmatrix}1 & 0\\ 0 & -1\end{pmatrix}\begin{pmatrix}a_1\\ a_2\end{pmatrix} = \frac{1}{2}\hbar\begin{pmatrix}a_1\\ a_2\end{pmatrix} \quad \text{or} \quad \begin{pmatrix}a_1\\ -a_2\end{pmatrix} = \begin{pmatrix}a_1\\ a_2\end{pmatrix}$$

It is evident that $a_2 = 0$. The normalization condition gives

$$|a_1|^2 = 1 \text{ or } a_1 = 1$$

The eigenvector of the matrix S_z corresponding to the eigenvalue $\hbar/2$ is then $\begin{pmatrix}1\\ 0\end{pmatrix}$.

Proceeding on similar lines, the eigenvector for the eigenvalue $-\hbar/2$ is $\begin{pmatrix}0\\ 1\end{pmatrix}$.

These eigenvectors are denoted by α and β and are usually called the *spin-up* and *spin-down* states respectively :

$$\alpha = \begin{pmatrix}1\\ 0\end{pmatrix}, \qquad \beta = \begin{pmatrix}0\\ 1\end{pmatrix} \qquad ...(261)$$

The two-component eigenvectors of spin-(1/2) particles are sometimes called **spinors.** Eigenvectors of S_x and S_y can also be found in the same way. The spin matrices of a spin-(1/2) system along with their eigenvalues and eigenvectors are tabulated in Table 3.

TABLE 3

Spin Matrices S_x, S_y and S_z of a Spin-(1/2) System with Their Eigenvalues and Eigenvectors

Spin component	Spin matrix	Eigenvalue	Eigenvectors
S_x	$\frac{\hbar}{2}\begin{pmatrix}0 & 1\\ 1 & 0\end{pmatrix}$	$\frac{\hbar}{2}$ $-\frac{\hbar}{2}$	$\frac{1}{\sqrt{2}}\begin{pmatrix}1\\ 1\end{pmatrix}$ $\frac{1}{\sqrt{2}}\begin{pmatrix}1\\ -1\end{pmatrix}$
S_y	$\frac{\hbar}{2}\begin{pmatrix}0 & -i\\ i & 0\end{pmatrix}$	$\frac{\hbar}{2}$ $-\frac{\hbar}{2}$	$\frac{1}{\sqrt{2}}\begin{pmatrix}1\\ i\end{pmatrix}$ $\frac{1}{\sqrt{2}}\begin{pmatrix}1\\ -i\end{pmatrix}$
S_z	$\frac{\hbar}{2}\begin{pmatrix}1 & 0\\ 0 & -1\end{pmatrix}$	$\frac{\hbar}{2}$ $-\frac{\hbar}{2}$	$\begin{pmatrix}1\\ 0\end{pmatrix}$ $\begin{pmatrix}0\\ 1\end{pmatrix}$

4. Addition of Angular Momenta

Addition of angular momenta is very important in the study of atomic spectra and nuclear structure. We shall consider here the general problem of the addition of two angular momenta. We consider two non-interacting systems having angular momenta J_1 and J_2 and eigenkets $|j_1m_1\rangle$ and $|j_2m_2\rangle$, respectively. Thus,

$$J_1^2 |j_1m_1\rangle = j_1(j_1+1)\hbar^2 |j_1m_1\rangle \qquad ...(262)$$

$$J_{1z} |j_1m_1\rangle = m_1\hbar |j_1m_1\rangle \qquad ...(263)$$

and

$$J_2^2 |j_2m_2\rangle = j_2(j_2+1)\hbar^2 |j_2m_2\rangle \qquad ...(264)$$

$$J_{2z} |j_2m_2\rangle = m_2\hbar |j_2m_2\rangle \qquad ...(265)$$

where $m_1 = j_1, j_1 - 1, \ldots\ldots, -j_1$; $m_2 = j_2, j_2 - 1, \ldots\ldots, -j_2$

(Clebsch-Gordon series)

Since the two systems are non-interacting

$$[J_1, J_2] = 0 \quad \text{and} \quad [J_1^2, J_2^2] = 0 \qquad \ldots(266)$$

and therefore the operators $J_1^2, J_{1z}, J_2^2, J_{2z}$ form a complete set with simultaneous eigenkets $|\, j_1 m_1, j_2 m_2\rangle$, which is a product of $|\, j_1 m_1\rangle$ and $|\, j_2 m_2\rangle$. For given values of j_1 and j_2

$$|\, j_1 m_1, j_2 m_2\rangle = |\, j_1 m_1\rangle\, |\, j_2 m_2\rangle = |\, m_1 m_2\rangle \qquad \ldots(267)$$

Since m_1 and m_2 can respectively have $(2j_1 + 1)$ and $(2j_2 + 1)$ orientations, the subspace with definite values of j_1 and j_2 will have $(2j_1 + 1)\,(2j_2 + 1)$ dimensions.

Clebsch-Gordon Coefficients. For the total angular momentum vector

$$J = J_1 + J_2$$

$$J \times J = i\,\hbar\, J \qquad \ldots(268)$$

Also, it follows that

$$[J^2, J_z] = 0, \quad [J^2, J_1^2] = [J^2, J_2^2] = 0 \qquad \ldots(269)$$

The orthonormal eigenkets of J^2 and J_z will be $|\, jm\rangle$. Since J^2 commutes with J_z, J_1^2 and J_2^2, they form another complete set and their simultaneous eigenkets will be $|\, j_1 j_2 jm\rangle$. For given values of j_1 and j_2, $|j_1 j_2\, jm\rangle = |jm\rangle$. The completeness of the known kets $|\, m_1 m_2\rangle$ allows us to express the unknown kets $|jm\rangle$ as a linear combination of $|m_1 m_2\rangle$:

$$|jm\rangle = \sum_{m_1, m_2} C_{jmm_1m_2}\, |m_1 m_2\rangle \qquad \ldots(270)$$

The coefficients of this linear combination are called **Clebsch-Gordon coefficients** or **Wigner coefficients** or **vector coupling coefficients**. Multiplying Eq. 270 with the bra $\langle m_1 m_2|$, we get

$$\langle m_1 m_2 \mid jm\rangle = C_{jmm_1m_2} \qquad \ldots(271)$$

Substituting this value of the coefficient in Eq. 270, we have

$$|\, jm\rangle = \sum_{m_1, m_2} |\, m_1 m_2\rangle \langle m_1 m_2 \mid jm\rangle \qquad \ldots(272)$$

As the coefficients $\langle m_1 m_2 |\, jm\rangle$ relate two orthonormal bases, $|j, m\rangle$ and $|m_1, m_2\rangle$ they form a unitary matrix. In the matrix formed by these elements, m_1, m_2 label the rows and j, m label the columns. The parameters j_1 and j_2 are not appearing explicitly in the coefficients as we are working for definite values of j_1 and j_2. In the strict sense the coefficients would be $\langle j_1 m_1, j_2 m_2 \mid j_1 j_2\, jm\rangle$. The inverse of Eq. 272 is given by

$$|\, m_1 m_2\rangle = \sum_{j, m} \langle jm \mid m_1 m_2\rangle \mid jm\rangle \qquad \ldots(273)$$

where the summation over m is from $-j$ to j and j is from $|\, j_1 - j_2 \,|$ to $j_1 + j_2$. The unitary character of Clebsh-Gordon coefficients is expressed by the equations.

$$\sum_{j, m} \langle m_1 m_2 \mid jm\rangle \langle jm \mid m_1' m_2'\rangle = \langle m_1 m_2 \mid m_1' m_2'\rangle = \delta m_1 m_1' \delta m_2 m_2' \qquad \ldots(274a)$$

and $$\sum_{j, m} \langle jm \mid m_1 m_2\rangle \langle m_1 m_2 \mid j'm'\rangle = \langle jm \mid j'm'\rangle = \delta jj'\, \delta mm' \qquad \ldots(274b)$$

where $$\langle jm \mid m_1 m_2\rangle = \langle\, m_1 m_2 \mid jm\,\rangle^* \qquad \ldots(274c)$$

Omitting details which are found in advanced books, we can obtain the recursion relations connecting the Clebsch-Gordon coefficients which enable us in determining the Clebsch-Gordon coefficients. The results are shown in Tables.4 and 5.

TABLE 4.

Clebsch-Gordon Coefficients for $|\, m_1 m_2\,\rangle = |\, j_1, j_2 - 1\rangle$ and $|\, j_1 - 1, j_2\,\rangle$

m_1	m_2	$\mid jm\,\rangle$	
		$\mid j_1 + j_2, j_1 + j_2 - 1\rangle$	$\mid j_1 + j_2 - 1, j_1 + j_2 - 1\rangle$
j_1	$j_2 - 1$	$\left(\frac{j_2}{j_1 + j_2}\right)^{1/2}$	$\left(\frac{j_1}{j_1 + j_2}\right)^{1/2}$
$j_1 - 1$	j_2	$\left(\frac{j_1}{j_1 + j_2}\right)^{1/2}$	$-\left(\frac{j_2}{j_1 + j_2}\right)^{1/2}$

TABLE 5.

Clebsch-Gordon Coefficients for $|\, m_1 m_2\rangle = |\, j_1, j_2 - 2\rangle$, $|\, j_1 - 1, j_2 - 1\rangle$ and $|\, j_1 - 2, j_2\rangle$

m_1	m_2	$\mid jm\,\rangle$		
		$\mid j_1 + j_2, j_1 + j_2 - 2\rangle$	$\mid j_1 + j_2 - 1, j_1 + j_2 - 2\rangle$	$\mid j_1 + j_2 - 2, j_1 + j_2 - 2\rangle$
j_1	$j_2 - 2$	$\left[\frac{j_2(2j_2 - 1)}{(j_1 + j_2)A}\right]^{1/2}$	$\left[\frac{j_1(2j_2 - 1)}{(j_1 + j_2)B}\right]^{1/2}$	$\left[\frac{j_1(2j_1 - 1)}{AB}\right]^{1/2}$
$j_1 - 1$	$j_2 - 1$	$\left[\frac{4j_1 j_2}{(j_1 + j_2)A}\right]^{1/2}$	$\frac{j_1 - j_2}{[(j_1 + j_2)B]^{1/2}}$	$-\left[\frac{(2j_1 - 1)(2j_2 - 1)}{AB}\right]^{1/2}$
$j_1 - 2$	j_2	$\left[\frac{j_2(2j_1 - 1)}{(j_1 + j_2)A}\right]^{1/2}$	$-\left[\frac{j_2(2j_1 - 1)}{(j_1 + j_2)B}\right]^{1/2}$	$\left[\frac{j_2(2j_2 - 1)}{AB}\right]^{1/2}$

where $A = 2j_1 + 2j_2 - 1$ and $B = j_1 + j_2 - 1$.

Note : The standard treatise on this subject is E.U. Condon and G.H. Shortley, *The Theory of Atomic Spectra*, Cambridge, 1935. Angular momentum has fascinated the finest theorists of 20th century physics, among them G. Racah, J.C. Slater, J.S. Schwinger, and, of course, E.P. Wigner. Their papers have been reprinted in L.C. Biedenharn and H. van Dam (eds.), *Quantum Theory of Angular Momentum*, Academic Press, 1965. The reader is encouraged to study this monumental volume. This is the stuff dream research is made of. Here imagination and creativity have gone hand-in-hand. The depth of mathematical treatment is astounding. It is pertinent to mention here that Charlotte E. Moore (1898-1990), the great American spectroscopist, produced and critically analyzed a very complete compilation of spectral data and atomic energy levels. The result of her effort, *Atomic Energy Levels*, is a classic work that provides data for 485 atomic species in a uniform clear format with standardized notation.

I. Review Questions

1. Using the first-order time-independent perturbation theory solve the Schrödinger wave equation for the ground state energy of helium atom.
2. Using the variation method solve the Schrödinger wave equation for the ground state energy of helium atom.
3. State and prove variation theorem.
4. Outline the salient features of the Hartree-Fock self-consistent field (SCF) theory for solving the Schrödinger wave equation for a many-electron atom.
5. Construct the angular momentum matrices for J^2 and J_z.
6. Write a short note on spin angular momentum and Pauli spin matrices.

II. Problems

1. Use the variational principle to istimate the ground state energy of a linear harmonic oscillator using the trial function $\psi(x) = 1/(1 + \beta x^2)$, where β, is variational parameter. [Ans. $E_{min} = 0.707\,\hbar\,(k/\mu)^{1/2}$]
2. Use the trial function of the form $\exp(-\alpha r)$ to calculate the ground state energy of hydrogen atom. [Ans. $E_{min} = -1/2$ (a.u)]
3. Use the first-order perturbation theory to calculate the energy of a particle in a one-dimensional box from $x = 0$ to $x = a$ with a slanted bottom, such that $V(x) = V_0 x/a$, $0 \le x \le a$ [V_0 is a constant]

$$\left[\text{Ans. } E = \frac{n^2\hbar^2}{8ma^2} + \frac{V_0}{2} + O\left(V_0^2\right),\ n = 1,2,3\ldots\right]$$

4. Using the Gaussian trial wavefunction $e^{-\alpha r^2}$ for the ground state of hydrogen atom show that the ground-state energy is given by $E(\alpha) = \frac{3\hbar^2\alpha}{2m_e} = \frac{e^2\alpha^{1/2}}{2^{1/2}\varepsilon_0\pi^{3/2}}$ and that $E_{min} = -\frac{4}{3\pi}\frac{m_e e^4}{16\pi^2\varepsilon_0^2\hbar^2}$. Use the Hamiltonian

$$\hat{H} = -\frac{\hbar^2}{2m_e r^2}\frac{d}{dr}\left(r^2\frac{d}{dr}\right) - \frac{e^2}{4\pi\varepsilon_0 r}$$

5. Tabulate the number of angular, radial and total nodes for the following hydrogenic wavefunctions :
(*a*) 1s, (*b*) 2s, (*c*) 2p, (*d*) 3p, and (*e*) 3d.
[Ans. The number of angular nodes is l ; the number of radial nodes is $n - l - 1$; the total number of nodes is $n - 1$]

	1s	2s	2p	3p	3d
n	1	2	2	3	3
l	0	0	1	1	2
Angular	0	0	1	1	2
Radial	0	1	0	1	0
Total	0	1	1	2	2

CHAPTER 3

CHEMICAL BONDING : MOLECULAR QUANTUM MECHANICS

After the discovery of wave (quantum) mechanics by E. Schrödinger in 1926, matrix mechanics by W. Heisenberg in 1925 (which was later modified by M. Born, P. Jordan and Heisenberg) and the relativistic quantum mechanics by P. Dirac in 1927, the new mechanics was applied to determine atomic and molecular structure. The idea of chemical bonding between two atoms based on sharing of electrons was given by G.N. Lewis in 1916. The Lewis picture of bonding is still relevant today but the quantum mechanical formulation, incorporating de Broglie's wave particle duality, Pauli's exclusion principle and Heisenberg's uncertainty principle, gave a deeper insight into the nature of the chemical bond.

The attack on the chemical bonding proceeded along two lines : **The valence bond theory (VBT)** and the conceptually simpler and popular **molecular orbital theory (MOT).** VBT was pioneered by W. Heitler and F. London (in 1928) and later by J.C. Slater and L. Pauling. During the same period (1927–1932), molecular orbital theory was developed by F. Hund, R.S. Mulliken and J.E. Lennard-Jones, though it is Mulliken who is credited with the real formulation of MOT. During this period, E. Hückel formulated the molecular orbital theory of conjugated systems. It was modified as EHT (**extended Hückel theory**) in 1963 by R. Hoffmann. Quantum theory of organic reactivity was proposed during 1951–1965 by K. Fukui, R. Woodward and R. Hoffmann in the form of **conservation of orbital symmetry.** R. Marcus applied quantum theory and activated complex theory to the understanding of electron transfer reactions. The formidable difficulties encountered in solving the Schrödinger wave equation for large molecules were partially surmounted by J. Pople. Again, in 1964, W. Kohn formulated **density functional theory (DFT)** which bypasses Schrödinger's wave equation and is an alternative approach to comprehend the subtleties of chemical bonding. The major theme that runs through chemistry and chemical physics is summed up in the Japanese word **BONSAI** meaning '*Bonding Structure and Interactions*'. The following scientists have been awarded Nobel Prizes in chemistry for applying quantum mechanics to various aspects of chemical bonding : Pauling (1954) for VBT, Mulliken (1966) for MOT, Fukui and Hoffmann (1981) for conservation of orbital symmetry in pericyclic reactions ; Marcus (1992) for electron-transfer reactions, and Pople who shared the 1998 Nobel Prize with Kohn.

Broadly speaking, there are two types of bonds between atoms :

1. **Ionic bond** in which electrons are transferred between atoms and the bond arises from the coulombic interactions between the resulting ions.
2. **Covalent bond** in which electron pairs are shared more or less equally between neighbouring atoms. The idea of a **dative bond** or **covalent-coordinate bond,** in which one partner donates both the electrons of the shared pair, symbolized by $B \rightarrow A$, is now obsolete and the term 'covalent bond' signifies that a bond has been formed by electron-sharing irrespective of the donor of the electron pair.

A covalent bond may be further classified as polar or non-polar. A **polar covalent bond** is a covalent bond in which the electron pair is shared unequally between the two atoms, with the result that the two atoms carry partial electric charges. A **non-polar covalent bond** is a covalent bond in which the electron pair is shared equally between the two atoms. Covalent bonds are also classified as single, double or triple. A single bond consists of one shared pair of electrons; a double bond consists of two shared pairs of electrons and a triple bond consists of three shared pairs of electrons. Quadruple bonds containing four shared pairs of electrons are rarely encountered though they occur quite frequently in the transition metal clusters. Modern theories of chemical bonding have largely dispensed with the distinction between the various types of bonds. They consider bonding as a consequence of the lowering of energy that occurs when electrons occupy molecular orbitals that spread over all the atoms in the molecule. The bonding influence of an electron pair, according to MOT, may be distributed over many atoms. In fact, an electron-pair is not essential to bond formation but merely represents the maximum number of electrons that can occupy a given orbital thereby contributing to bonding.

MOLECULAR ORBITAL THEORY (MOT)

Just as the atomic orbitals are the solutions of the time-independent Schrodinger wave equation for atoms, molecular orbitals are the corresponding solutions for molecules. Molecular orbital theory is very simple to treat mathematically and is a landmark in molecular quantum mechanics. The electrons in atoms occupy atomic orbitals (AOs) that are represented as the regions around the nuclei where there is a high probability of finding the electrons. In the so-called **LCAO (linear combination of atomic orbitals)** approach, as pioneered by Hund and Mulliken, when AOs come close together, they *overlap* forming MOs (molecular orbitals). Two AOs can overlap to form two MOs, one of which lies at a lower energy level than the overlapping AOs and is called a **bonding molecular orbital (BMO)** and the other lies at a higher energy level and is called an **antibonding molecular orbital (ABMO)**. Each MO can hold one or two electrons in accordance with Pauli's exclusion principle. MOT can explain the paramagnetism of molecules such as O_2 and NO and other spectral features. The ordering of the molecular energy levels can be verified experimentally by photoelectron spectroscopy (PES). The Hartree–Fock Self-Consistent-Field (SCF) theory can be extended to molecules in which case it is called Hartree–Fock–Roothaan theory. Its relativistic version is called Dirac–Hartree–Fock–Roothaan (DHFR) theory.

Of great importance to molecular quantum mechanics is the **Born–Oppenheimer approximation,** according to which it is supposed that the nuclei, being so much heavier than the electron, move relatively slowly. Thus, nuclei can be treated as stationary so that the electrons move relative to them. Treating the nuclei as being fixed at an arbitrary distance, the Schrödinger wave equation can be solved for the electronic wave functions. This approximation holds good for the ground state of molecules and may break down for the excited states.

The mathematical treatment of the Born-Oppenheimer Approximation is discussed later in this chapter.

We shall deal with the molecular orbital theory of a homonuclear diatomic, H_2, molecule. In the LCAO–MO method, the MO ψ can be written as

$$\psi = c_1\phi_1 + c_2\phi_2 \qquad \ldots(1)$$

where the ϕs are the AOs (in this case, the two 1*s* orbitals) centered on hydrogen atoms, 1 and 2 and c_1, c_2 are the coefficients of these AOs. (The atomic orbitals such as *s, p, d,* etc., are called the *basis sets*). The energy E of the MO can be obtained by solving the Schrödinger wave equation

$$\hat{H}\psi = E\psi \qquad \ldots(2)$$

where $\hat{H}$ is the Hamiltonian operator.

Since the MOs are unnormalized, the energy E is given by

$$E = \int \psi^* \hat{H} \psi d\tau \Big/ \int \psi^* \psi d\tau \qquad \ldots(3)$$

If ψs are real, then $\psi^* = \psi$.

Substituting Eq. 1 into Eq. 3, we have

$$E = \frac{\int (c_1\phi_1 + c_2\phi_2)\hat{H}(c_1\phi_1 + c_2\phi_2)d\tau}{\int (c_1\phi_1 + c_2\phi_2)^2 d\tau}$$

$$= \frac{\int (c_1\phi_1\hat{H}c_1\phi_1 + c_1\phi_1\hat{H}c_2\phi_2 + c_2\phi_2\hat{H}c_1\phi_1 + c_2\phi_2\hat{H}c_2\phi_2)d\tau}{\int (c_1^2\phi_1^2 + 2c_1c_2\phi_1\phi_2 + c_2^2\phi_2^2)d\tau} \qquad \ldots(4)$$

Let $\quad H_{11} = \int \phi_1 \hat{H} \phi_1 d\tau$

$$H_{12} = H_{21} = \int \phi_1 \hat{H} \phi_2 d\tau = \int \phi_2 \hat{H} \phi_1 d\tau ; H_{22} = \int \phi_2 \hat{H} \phi_2 d\tau$$

$$S_{11} = \int \phi_1^2 d\tau ; S_{22} = \int \phi_2^2 d\tau ; S_{12} = S_{21} = \int \phi_1\phi_2 d\tau$$

In the above notation, H_{11}, H_{12}, H_{22}, etc., are called **matrix elements**. Using this notation, Eq. 4 can be written in a simplified form as

$$E = \frac{c_1^2H_{11} + 2c_1c_2H_{12} + c_2^2H_{22}}{c_1^2S_{11} + 2c_1c_2S_{12} + c_2^2S_{22}} \qquad \ldots(5)$$

The energy obtained above gives always the **upper bound**. The ground state energy is obtained by using the *variation theorem;* this is done by carrying out the differentiation $(\partial E/\partial c_i)$, *i.e.,* by differentiating with respect to each coefficient (i = 1, 2) independently and setting the derivative equal to zero; $\partial E/\partial c_i = 0$. Thus, we have

$$\frac{\partial E}{\partial c_1} = \frac{(c_1^2S_{11} + 2c_1c_2S_{12} + c_2^2S_{22})(2c_1H_{11} + 2c_2H_{12})}{(c_1^2S_{11} + 2c_1c_2S_{12} + c_2^2S_{22})^2}$$

$$- \frac{(c_1^2H_{11} + 2c_1c_2H_{12} + c_2^2H_{22})(2c_1S_{11} + 2c_2S_{12})}{(c_1^2S_{11} + 2c_1c_2S_{12} + c_2^2S_{22})^2} = 0 \qquad \ldots(6)$$

Hence, $\quad c_1H_{11} + c_2H_{12} = \dfrac{(c_1^2H_{11} + 2c_1c_2H_{12} + c_2^2H_{22})(c_1S_{11} + c_2S_{12})}{c_1^2S_{11} + 2c_1c_2S_{12} + c_2^2S_{22}} \qquad \ldots(7)$

From Eqs. 5 and 7, we obtain

$$c_1H_{11} + c_2H_{12} = E(c_1S_{11} + c_2S_{12})$$

or $\quad c_1(H_{11} - ES_{11}) + c_2(H_{12} - ES_{12}) = 0 \qquad \ldots(8)$

Similarly, minimizing E with respect to c_2, by requiring that $\partial E/\partial c_2 = 0$, we have

$$c_1(H_{21} - ES_{21}) + c_2(H_{22} - ES_{22}) = 0 \qquad \ldots(9)$$

Eqs. 8 and 9 form a system of two simultaneous linear equations in the two unknowns c_1 and c_2. According to the principle of linear algebra, the essential condition for these equations to have a **non-trivial solution** is that the determinant of the coefficients of c_1 and c_2 should vanish, *i.e.*,

$$\begin{vmatrix} H_{11} - ES_{11} & H_{12} - ES_{12} \\ H_{21} - ES_{21} & H_{22} - ES_{22} \end{vmatrix} = 0 \qquad ...(10)$$

Eq. 10 is called the 2×2 **secular equation** and the left-hand side of this equation is called the **secular determinant.**

Generalizing this result to a MO of the form

$$\psi_i = \sum_{j=1}^{n} c_{ij}\phi_j \qquad (i = 1, 2, 3, \ldots\ldots, n) \qquad ...(11)$$

where ϕs are the AOs, we obtain an $n \times n$ secular determinantal equation :

$$\begin{vmatrix} H_{11} - S_{11}E & H_{12} - S_{12}E & H_{13} - S_{13}E & \ldots & \ldots & H_{1n} - S_{1n}E \\ H_{21} - S_{21}E & H_{22} - S_{22}E & H_{23} - S_{23}E & \ldots & \ldots & H_{2n} - S_{2n}E \\ H_{31} - S_{31}E & H_{32} - S_{32}E & H_{33} - S_{33}E & \ldots & \ldots & H_{3n} - S_{3n}E \\ \ldots\ldots & \ldots\ldots & \ldots\ldots & \ldots & \ldots & \ldots\ldots \\ \ldots\ldots & \ldots\ldots & \ldots\ldots & \ldots & \ldots & \ldots\ldots \\ \ldots\ldots & \ldots\ldots & \ldots\ldots & \ldots & \ldots & \ldots\ldots \\ H_{n1} - S_{n1}E & H_{n2} - S_{n2}E & H_{n3} - S_{n3}E & \ldots & \ldots & H_{nn} - S_{nn}E \end{vmatrix} = 0 \qquad ...(12)$$

The secular equation (12) is a very important feature of both MOT and VBT. It consists of three kinds of integrals, *viz.*, Coulomb integral, the exchange integral and the overlap integral.

(i) Coulomb integral $H_{ii} = \int \phi_i H \phi_i \, d\tau$. It represents the energy of the electron in the AO centred on atom i

(ii) Exchange integral $H_{ij} = \int \phi_i H \phi_j \, d\tau$. It represents the energy of interaction of electrons in the atoms i and j.

(iii) Overlap integral $S_{ij} = \int \phi_i \phi_j \, d\tau$. It represents the overlap of the orbitals centered on atoms i and j. If $i=j$, then $S_{ii} = \int \phi_i \phi_i \, d\tau = 1$ (for normalized AOs).

The solution of Eq. 12 on the computer gives the values of energy levels of the MOs of an n-electron molecule. For diatomic molecules, the secular Eq. 10 is solved to obtain the energies of the MOs.

The theoretical treatment outlined in Eqs. 1 through 10 applies both to H_2^+ and H_2. To determine the coefficients c_1 and c_2, we proceed as follows : Consider H_2^+. If we label the two nuclei as a and b rather than 1 and 2 (for the sake of notational convenience), then (Fig. 1) the electronic Hamiltonian in the Born-Oppenheimer approximation is written as

$$\hat{H} = -\frac{\hbar^2}{2m_e}\nabla^2 - \frac{e^2}{4\pi\varepsilon_0}\left(\frac{1}{r_a} + \frac{1}{r_b} - \frac{1}{R}\right) \qquad ...(13)$$

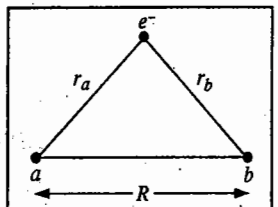

Fig. 1. The coordinates of H_2^+.

where m_e is the mass of the electron, r_a, r_b and R are the distances between the electron and the nucleus a,

between the electron and the nucleus b and the internuclear distance, respectively. It is customary to use atomic units in quantum chemistry : $e = m_e = \hbar = 1/4\pi\varepsilon_0 = 1$ (Note that these quantities are not really equal but they are arbitrarily set equal to unity). Then,

$$\hat{H} = -\frac{1}{2}\nabla^2 - \frac{1}{r_a} - \frac{1}{r_b} + \frac{1}{R} \qquad ...(14)$$

The secular equation (10) is rewritten as

$$\begin{vmatrix} H_{aa} - E & H_{ab} - SE \\ H_{ab} - SE & H_{bb} - E \end{vmatrix} = 0 \qquad ...(15)$$

Expansion of Eq. 15 gives a quadratic equation which has two solutions E_g and E_u :

$$E_g = (H_{aa} + H_{ab})/(1 + S) \qquad ...(16)$$

$$E_u = (H_{aa} - H_{ab})/(1 - S) \qquad ...(17)$$

Substitution of Eq. 16 or 17 into Eq. 8, which is rewritten as

$$c_1(H_{aa} - E) + c_2(H_{ab} - SE) = 0 \qquad ...(18)$$

yields

$$c_1 = c_2 \quad \text{or} \quad c_1 = -c_2 \qquad ...(19)$$

Substitution of Eq. 19 into Eq. 1 gives, after normalization,

$$\psi_g = \frac{1}{[2(1+S)]^{1/2}}(\phi_a + \phi_b) \qquad ...(20)$$

$$\psi_u = \frac{1}{[2(1-S)]^{1/2}}(\phi_a - \phi_b) \qquad ...(21)$$

where $\phi_a \equiv 1s_a$, $\phi_b \equiv 1s_b$, ψ_g is BMO and ψ_u is ABMO.

When a molecule (such as H_2^+ or H_2) has a centre of symmetry, the wave function may or may not change sign when it is inverted through the centre of symmetry. If, for instance, $\psi(x,y,z) = \psi(-x, -y, -z)$, the wave function is said to have *even parity* and is designated by the subscript g for *gerade* (German for even). If $\psi(x, y, z) = -\psi(-x, -y, -z)$, the wave function is said to have *odd parity* and is designated with a subscript u for *ungerade* (German for odd). ψ_g is called BMO because the electron density ψ_g^2 is increased midway between the nuclei and ψ_u is called ABMO because ψ_u^2 is zero midway between the nuclei (Fig. 2). Another way of expressing it is that the BMO arises from the constructive interference of the neighbouring AOs and the ABMO arises from their destructive interference. The BMO has no node and the ABMO has a node between the atoms.

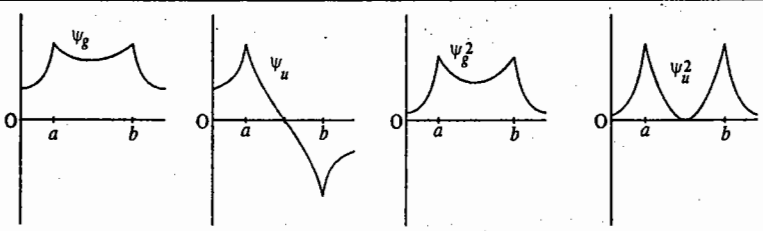

Fig. 2. MOs ψ_g and ψ_u for H_2^+ ion and the corresponding electron densities ψ_g^2 and ψ_u^2 along the internuclear axis.

Example 1. Write the Hamiltonian opertar for He_2^+ molecule-ion.

Solution : The complte Hamiltonian operator is given by

$$\hat{H} = \frac{-\hbar^2}{2}\sum_{\alpha}^{\text{all nuclei}}\frac{1}{m_\alpha}\nabla^2 + \frac{-\hbar^2}{2m_e}\sum_{i}^{\text{all electrons}}\nabla_i^2 + \sum_{\beta}\sum_{\alpha<\beta}\frac{Z_\alpha Z_\beta e^2}{4\pi\varepsilon_0 r_{\alpha\beta}} - \sum_{i}\sum_{\alpha}\frac{Z_\alpha e^2}{4\pi\varepsilon_0 r_{i\alpha}} + \sum_{j}\sum_{i<j}\frac{e^2}{4\pi\varepsilon_0 r_{ij}} \quad \ldots (i)$$

The *Born-Oppenheimer approximation* allows neglecting the ∇_α^2 terms and treating the $r_{\alpha\beta}^{-1}$ terms as constants at a given time. For the three electrons in He_2^+, (Eqn. (*i*) gives

$$\hat{H} = \frac{\hbar^2}{2m_e}(\nabla_1^2 + \nabla_2^2 + \nabla_3^2) + \frac{e^2}{4\pi\varepsilon_0}\left(\frac{4}{r_{ab}} - \frac{2}{r_{1a}} - \frac{2}{r_{2a}} - \frac{2}{r_{3a}} - \frac{2}{r_{1b}} - \frac{2}{r_{2b}} - \frac{2}{r_{3b}} + \frac{1}{r_{12}} + \frac{1}{r_{13}} + \frac{1}{r_{23}}\right) \quad \ldots (ii)$$

where $Z_a = Z_b = 2$.

Example 2. Write the Hamiltonian operator for the K_2 molecule.

Solution : The electrons in this molecule can be classified into two types : the core electrons around each atom that do not contribute to the bonding and the two valence electrons that provide the bonding. Using the *valence-electron approximation* Eq. (*i*) in example 1, gives

$$1\hat{H} = \frac{-\hbar^2}{2m_e}(\nabla_1^2 + \nabla_2^2) + \frac{e^2}{4\pi\varepsilon_0}\left(\frac{1}{r_{ab}} - \frac{1}{r_{1a}} - \frac{1}{r_{2a}} - \frac{1}{r_{1b}} - \frac{1}{r_{2b}} + \frac{1}{r_{12}}\right)$$

where the effective nuclear charge of 1 was used.

Example 3. Write the expression for a trial wave function for the He_2^+ system.

Solution : The wave function ϕ can be written as the product of wavefunctions for the individual electrons.

$$\phi = \phi_1\phi_2\phi_3 \ldots \quad \ldots (i)$$

where the $\phi_{(i)}$ are produced by taking linear combinations of hydrogenic atomic orbitals (LCAO) :

$$\phi_i = c_{ia}\psi_a(i) + c_{ib}\psi_b(i) + \ldots \quad \ldots (ii)$$

The $a_{i\alpha}$ terms are constants, and ψ_α (*i*) denotes a hydrogenic atomic wavefunction describing electrion *i* in terms of position with respect to nucleus α. In this case, using Eqs (*i*) and (*ii*) gives

$$\phi = \phi_1\phi_2\phi_3$$
$$\phi_1 = c_1\psi_a(1) + c_2\psi_b(1)$$
$$\phi_2 = c_3\psi_a(2) + c_4\psi_b(2)$$
$$\phi_3 = c_5\psi_a(3) + c_6\psi_b(3)$$

where ψ_a and ψ_b would be the 1s wavefunction for H.

Example 4. Write the expression for a trial wave function for the K_2 molecules.

Solution : Assuming the valence-electron approximation, using (*i*) and (*ii*) gives

$$\phi = \phi_1\phi_2$$
$$\phi_1 = c_1\psi_a(1) + c_2\psi_b(1)$$
$$\phi_2 = c_3\psi_a(2) + c_4\psi_b(1)$$

where ψ_a and ψ_b would be the 4s wavefunction for H.

Example 5. Write the expression for a trial wave function describing the HF molecule.

Solution : Assuming the valence-electron approximation, using Eqs., (*i*) and (*ii*) in examples 3 gives

$$\phi = \phi_1\phi_2$$

$$\phi_1 = c_1\psi_a(1) + c_2\psi_b(1)$$
$$\phi_2 = c_3\psi_a(2) + c_4\psi_b(1)$$

where ψ_a would be the 1*s* wavefunction for H and ψ_b would be the 2*p* wavefunction for F.

Example 6. Identify the ionic and covalent terms in the expression for ϕ determined in examples 5.

Solution : The complete trial wavefunction for HF is

$$\phi = \phi_1\phi_2 = [c_1\psi_a(1) + c_2\psi_n(1)]\,[c_3\psi_a(2) + c_4\psi_b(2)]$$
$$= c_1c_2\psi_a(1)\,\psi_a(2) + c_2c_3\psi_b(1)\,\psi_a(2) + c_1c_2\psi_a(1)\,\psi_a(2) + c_2c_4\psi_b(1)\,\psi_b(2)$$

The first and fourth terms in this expression for ϕ each indicate that both electrons are araound the same nucleus and are the ionic terms. The second and third terms each indicate that the electrons are around different nuclei and are the covalent terms.

Example 7. Because He_2^+ is a homonuclear diatomic system, assume that the $c_{i\alpha}$ are all equal to *c* and that identical normalized hydrogenlike wave functions are chosen. Determine the value of *c* in terms of *S* where $S_{aa} = S_{bb} = 1$ and $S_{ab} = S_{ba} = S$ is the overlap integral.

Solution : The overlap integral is

$$\int \phi^*\phi d\tau = \int (\phi_1\phi_2\phi_3)^*(\phi_1\phi_2\phi_3)\,d\tau_1\,d\tau_2 d\tau_3 = \int \phi_1^*\phi_2^*\phi_1\phi_2 d\tau_1 d\tau_2 \int \phi_3^*\phi_3 d\tau_3$$

$$= \int \phi_1^*\phi_1 d\tau_1 \int \phi_2^*\phi_2 d\tau_2 \int \phi_3^*\phi_3 d\tau_3 = \left(\int \phi_1^*\phi_1 d\tau_1\right)^3$$

Substituting $\psi_1 = a\psi_a(1) + a\psi_b)(1)$ gives

$$\int \phi_1^*\phi_1 d\tau_1 = \int [c\psi_a(1) + c\psi_b(1)]^*\,[c\psi_a(1) + c\psi_b(1)]\,d\tau_1$$

$$= c^2\left(\int [\psi_a^*(1)\,\psi_a(1) + \psi_a^*(1)\,\psi_b(1) + \psi_b^*(1)\psi_a(1) + \psi_b^*(1)\,\psi_a(1)]\,d\tau\right)$$

$$= c^2(S_{aa} + S_{ab} + S_{ba} + S_{bb}) = c^2(1 + S + S + 1) = c^2(2 + 2S)$$

The overlap integral becomes

$$\int \phi^*\phi d\tau = [c^2(2 + 2S)]^3 = 1$$

Solving $c = (2 + 2S)^{-1/2}$.

Example 8. Determine the energy of the He_2^+ molecule-ion in terms of H_{aa}, H_{ab} and *S* using the variation method.

Solution : The secular determinant for the system is given by

$$\begin{vmatrix} H_{aa} - ES_{aa} & H_{ab} - ES_{ab} \\ H_{ba} - ES_{ba} & H_{bb} - ES_{bb} \end{vmatrix} = 0$$

in this case $H_{aa} = H_{bb}$, $S_{ab} = S_{ba} = S$, and $S_{aa} = S_{bb} = 1$, giving

$$\begin{vmatrix} H_{aa} - E & H_{ab} - ES \\ H_{ab} - ES & H_{aa} - E \end{vmatrix} = 0$$

Expanding gives

$$(H_{aa} - E)^2 - (H_{ab} - ES)^2 = 0$$
$$[(H_{aa} - E) + (H_{ab} - ES)]\,[(H_{aa} - E) - (H_{ab} - ES)] = 0$$

The two roots are $$E_1 = \frac{H_{aa} + H_{ab}}{1 + S} \quad \ldots (i)$$

and $$E_2 = \frac{H_{aa} - H_{ab}}{1 - S} \quad \ldots (ii)$$

Example 9. For the He_2^+ molecular ion described by the wave function

$$\phi = \phi_1 = a_1\psi_a(1) + a_2\psi_b(1) \quad \ldots (iii)$$

it can be shown that $$H_{aa} = E(\mathrm{H}) + J \quad \ldots (iv)$$

$$H_{ab} = E(\mathrm{H})S + J \quad \ldots (v)$$

where $E(\mathrm{H})$ is the ground-state energy of the hydrogen atom ($-13{\cdot}60eV = 2{\cdot}179 \times 10^{-18}J$), the *Coulomb integral* is given by

$$J = \frac{-e^2}{4\pi\varepsilon_0} \int \psi_a^*(1) \frac{1}{r_{ib}} \psi_a(1)\, d\tau$$

the *exchange* (or *resonance*) *integral* is given by

$$K = \frac{-e^2}{4\pi\varepsilon_0} \int \psi_b^*(1) \frac{1}{r_{ib}} \psi_a(1)\, d\tau$$

and the *overlap integral* is given by

$$S = \int \psi_a^*(1)\, \psi_a(1)\, d\tau$$

Rewrite the expressions for energy given by Eqs. (*i*) and (*ii*) in example 8 in terms of these integrals.

Solution : Substituting Eqs. (*iv*) and (*v*) into Eqs. (*i*) and (*ii*) gives

$$E_1 = \frac{[E(\mathrm{H}) + J] + [E(\mathrm{H})S + K]}{1 + S} = E(\mathrm{H}) + \frac{J + K}{1 + S}$$

$$E_2 = \frac{[E(\mathrm{H}) + J] + [E(\mathrm{H})S + K]}{1 - S} = E(\mathrm{H}) + \frac{J - K}{1 - S}$$

Example 10. The observed internuclear distance in H_2^+ is 0·1057 nm. Calculate the total energy of the system at this value of r_{ab} assuming that ψ_α (*i*) is given by 1s hydrogenlike orbitals.

Solution : If the $\psi_\alpha(i)$ are hydrogenlike 1*s* atomic orbitals, the various integrals are given by

$$S = e^{-\rho}\left(1 + \rho + \frac{\rho^2}{3}\right) \quad \ldots (i)$$

$$J = \frac{e^2}{4\pi\varepsilon_0 a_0}\left[\frac{-1}{\rho} + e^{-2\rho}\left(1 + \frac{1}{\rho}\right)\right] \quad \ldots (ii)$$

$$K = \frac{-e^2}{4\pi\varepsilon_0 a_0} e^{-\rho}(1 + \rho) \quad \ldots (iii)$$

where $$\rho = r_{ab}/a_0 \quad \ldots (iv)$$

and $a_0 = 0{\cdot}0529$ nm. Substituting $r_{ab} = 0{\cdot}1057$ nm into Eq. (*iv*) gives

$$\rho = \frac{0{\cdot}1057 \text{ nm}}{0{\cdot}0529 \text{ nm}} = 1{\cdot}997$$

Substitution of this value of ρ into Es. (*i*), (*ii*) and (*iii*) gives

$$S = e^{-1{\cdot}997}\left(1 + 1{\cdot}997 + \frac{(1{\cdot}997)^2}{3}\right) = 0{\cdot}5873$$

$$J = \left[\frac{(1{\cdot}602 \times 10^{-19}\mathrm{C})^2\,[1 \text{ kg m s}^{-2})/(1\mathrm{N})\,[(1\mathrm{J})/(1 \text{ kg m}^2\,\mathrm{s}^{-2})]}{(1{\cdot}112 \times 10^{-10}\,\mathrm{C}^2\,\mathrm{N}^{-1}\,\mathrm{m}^{-2})\,(5{\cdot}292 \times 10^{-11}\,\mathrm{m})}\right]\left[\frac{-1}{1{\cdot}997} + e^{-2\,(1{\cdot}997)}\left(1 + \frac{1}{1{\cdot}997}\right)\right]$$

$$= (4{\cdot}360 \times 10^{-18}\,\mathrm{J})\,(-0{\cdot}4731) = -2{\cdot}063 \times 10^{-18}\,\mathrm{J}$$

$$= (-4{\cdot}360 \times 10^{-18}\,\mathrm{J})\,e^{-1{\cdot}997}(1 + 1{\cdot}997) = -1{\cdot}774 \times 10^{-18}\,\mathrm{J}$$

Substitution of these values of S, J and K into the expressions for E_1 and E_2 in example 9 gives

$$E_1 = -2{\cdot}179 \times 10^{-18}\mathrm{J} + \frac{-2{\cdot}063 \times 10^{-18}\,\mathrm{J} + (-1{\cdot}774 \times 10^{-18}\mathrm{J})}{1 + 0{\cdot}5873} = -4{\cdot}596 \times 10^{-18}\,\mathrm{J}$$

$$E_2 = -2{\cdot}179 \times 10^{-18}\mathrm{J} + \frac{-2{\cdot}063 \times 10^{-18}\,\mathrm{J} - (-1{\cdot}774 \times 10^{-18}\mathrm{J})}{1 - 0{\cdot}5873} = -2{\cdot}879 \times 10^{-18}\,\mathrm{J}$$

The total energy (E') is found by adding the nuclear repulsion term that was treated as a constant in Eq. (*i*) in example 1 by the Born-Oppenheimer approximation :

$$E_1' = E_1 + \frac{e^2}{4\pi\varepsilon_0 r_{ab}} = -4{\cdot}596 \times 10^{-18}\,\mathrm{J} + \frac{(1{\cdot}602 \times 10^{-19})^2}{(1{\cdot}112 \times 10^{-10})\,(1{\cdot}057 \times 10^{-10})}$$

$$= -2{\cdot}413 \times 10^{-18}\,\mathrm{J}$$

$$E_2' = -2{\cdot}879 \times 10^{-18} + 2{\cdot}183 \times 10^{-18} = -0{\cdot}696 \times 10^{-18}\,\mathrm{J}$$

The results of similar calculations are plotted in Fig. 3.

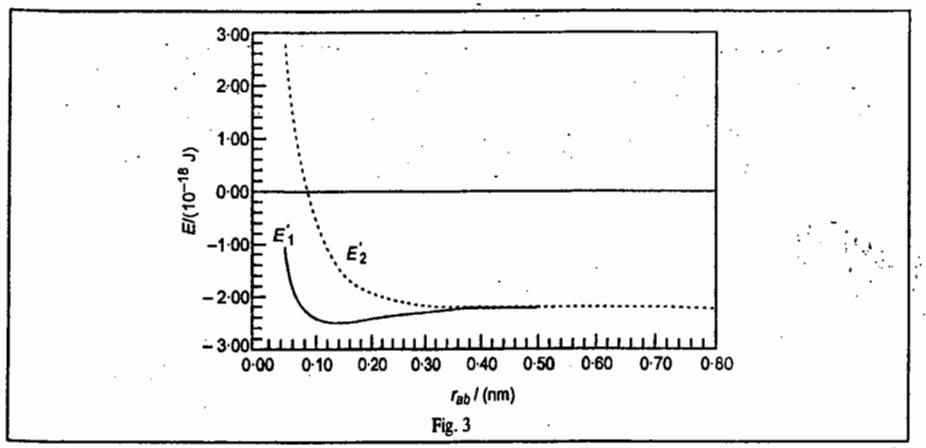

Fig. 3

Example 11. What is the limit of the total energy for H_2^+ as $r_{ab} \to \infty$?

Solution : Taking the limits of Eqs. (*i*), (*ii*) and (*iii*) in example 10, and the nuclear repulsion term as r_{ab} or $\rho \to \infty$ gives

$$\lim_{\rho\to\infty}(S) = \lim_{\rho\to\infty}\left(\frac{1+\frac{2}{3}\rho}{-e^{-\rho}}\right) = \lim_{\rho\to\infty}\left(\frac{\frac{2}{3}}{e^{-\rho}}\right) = 0\ ; \quad \lim_{\rho\to\infty}(J) = 0$$

$$\lim_{\rho\to\infty}(K) = \frac{-e^2}{4\pi\varepsilon_0 a_0}\lim_{\rho\to\infty}\left(\frac{1}{-e^{-\rho}}\right) = 0;\ \lim_{\rho\to\infty}\left(\frac{e^2}{4\pi\varepsilon_0 r_{ab}}\right) = 0$$

The limiting values of total energy are

$$E_1' = E(\mathrm{H}) + \frac{0+0}{1+0} + 0 = E(\mathrm{H}) = -2{\cdot}179 \times 10^{-18}\ J$$

$$E_2' = E(\mathrm{H}) + \frac{0-0}{1-0} + 0 = E(\mathrm{H})$$

Example 12. Using Fig. 3, predict the equilibrium value of r_{ab} and the dissociation energy for the H_2^+ molecule-ion.

Solution : The minimum value of E_1' in Fig. 3 appears at $r_{ab} = 0{\cdot}132$ nm and $-2{\cdot}46 \times 10^{-18}$ J. The predicted equilibrium value of r_{ab} is 0·132 nm, which is 1·24 times greater than the observed value of 0·1057 nm. In example 11, the limiting value of E_1' was determined to be $-2{\cdot}179 \times 10^{-18}$ J as $r_{ab} \to \infty$. The difference gives the predicted value of the dissociation energy(D_e) as

$$D_e = (-2{\cdot}179 \times 10^{-18}\mathrm{J}) - (-2{\cdot}46 \times 10^{-18}\mathrm{J}) = 0{\cdot}28 \times 10^{-18}\mathrm{J}$$

which is considerably less than the observed value of $0{\cdot}4472 \times 10^{-18}$ J.

Example 13. Assuming the H_2^+ molecule-ion to be described by the wavefunction $\phi = \phi_1 = c_1\psi_a(1) + c_2\psi_b(1)$, determine the relation between c_1 and c_2.

Soluton : For this system the secular equation (Eq. 15) simplifies to

$$c_1(H_{aa} - E) + c_2(H_{ab} - ES) = 0$$

Substituting the expression for E_1 in Example 8 gives

$$c_1\left(H_{aa} - \frac{H_{aa}+H_{ab}}{1+S}\right) + c_2\left(H_{ab} - \frac{H_{aa}+H_{ab}}{1+S}\right) = 0$$

$$c_1[(1+S)H_{aa} - H_{aa} - H_{ab}] + c_2[(1+S)H_{ab} - SH_{aa} - SH_{ab}] = 0$$

$$c_1(SH_{aa} - H_{ab}) + c_2(H_{ab} - SH_{aa}) = 0$$

$$c_1 = c_2$$

for E_1. Likewise, substituting the expresion for E_2 in example 8, gives $c_1 = -c_2$ for E_2.

Example 14. Evaluate c_1 and c_2 in the wave function given in Example 13.

Solution : For E_1, it was shown in Example 13 that $c_1 = c_2$. The wavefunction becomes

$$\phi = c_1\psi_a(1) + c_1\psi_b(1) = c_1[\psi_a(1) + \psi_b(1)]$$

Using the normalization requirement, we have

$$\int \phi^*\phi\, d\tau = \int c_1[\psi_a(1) + \psi_b(1)]^*\, c_1[\psi_a(1) + \psi_b(1)]\, d\tau$$

$$= c_1^2\left(\int \psi_a^*(1)\,\psi_a(1)\,d\tau + \int \psi_a^*(1)\,\psi_b(1)\,d\tau\right) + \int \psi_a^*(1)\,\psi_a(1)\,d\tau + \int \psi_b^*(1)\,\psi_b(1)\,d\tau\Big)$$

$$= c_1^2(S_{aa} + S_{ab} + S_{ba} + S_{bb}) = c_1^2(1+S+S+1) = c_1^2(2+2S) = 1 \qquad \ldots (i)$$

$$c_1 = (2+2S)^{-1/2}$$

where $S_{aa} = S_{bb} = 1$ and $S_{ab} = S_{ba} = S$. The wave function corresponding to E_1 is given by

$$\phi_1 = (2+2s)^{-1/2}[\psi_a(1) + \psi_b(1)] \qquad \ldots(ii)$$

Likewise for E_2, $c_1 = (2-2S)^{-1/2}$, giving

$$\phi_2 = (2-2S)^{-1/2}[\psi_a(1) - \psi_b(1)] \qquad \ldots (iii)$$

Example 15. Prepare a plot of $\phi^*\phi$ for the wavefunctions give in Example 14, along the internuclear axis using $r_{ab} = 0{\cdot}1057$ nm.

Solution : The hydrogenic 1s wavefunction is

$$\psi_{1s} = \left(\frac{Z}{a_0}\right)^{3/2}\frac{1}{\pi^{1/2}}e^{-Zr/a_0} = \frac{e^{-r/a_0}}{a_0^{3/2}\pi^{1/2}}$$

At $r_{ab} = 0{\cdot}1057$ nm, $S = 0{\cdot}5873$ (see Example 10). Substituting (eq. (*ii*)) gives

$$\phi_1 = \frac{e^{-r_a/a_0} + e^{-r_b/a_0}}{[2+2(0{\cdot}5873)]^{1/2}\,a_0^{3/2}\pi^{1/2}} = \frac{e^{-r_a/a_0} + e^{-r_b/a_0}}{1{\cdot}216\times10^{-15}\mathrm{m}^{3/2}} \qquad \ldots (iv)$$

Likewise,

$$\phi_2 = \frac{e^{-r_a/a_0} + e^{-r_b/a_0}}{[2-2(0{\cdot}5873)]^{1/2}a_0^{3/2}\pi^{1/2}} = \frac{e^{-r_a/a_0} + e^{-r_b/a_0}}{6{\cdot}199\times10^{-16}\mathrm{m}^{3/2}} \qquad \ldots (v)$$

Because these wave functions consist of only real terms, $\phi^*\phi = \phi_i^2$. As a sample calculation, consider a point along the bonding axis that is 0·0500 nm from nucleus *a*. If nucleus *a* is placed at $r_{ab} = 0$ and nucleus *b* is placed at $r_{ab} = 0{\cdot}1057$ nm, the values of r_a and r_b used in Eqs. (*iv*) and (*v*) will be

$$r_a = |\,r\,| = 0{\cdot}0500 \text{ nm}$$

$$r_b = |\,r - 0{\cdot}1057 \text{ nm}\,| = |0.0500\text{nm} - 0{\cdot}1057 \text{ nm}\,| = 0{\cdot}0557 \text{ nm}$$

giving

$$\phi_1^*\phi_1 = \left[\frac{e^{-(0{\cdot}0500\text{ nm})(0.0529\text{nm})} + e^{-(0{\cdot}0557\text{ nm})/(0{\cdot}0529\text{ nm})}}{1{\cdot}216\times10^{-15}\mathrm{m}^{3/2}}\right]^2 = 3{\cdot}68\times10^{29}\ \mathrm{m}^{-3}$$

$$\phi_2^*\phi_2 = \left[\frac{e^{-(0{\cdot}0500)/(0{\cdot}0529)} - e^{-(0{\cdot}0557)/(0{\cdot}0529)}}{6{\cdot}199\times10^{-16}\mathrm{m}^{3/2}}\right]^2 = 4{\cdot}24\times10^{27}\ \mathrm{m}^{-3}$$

This plot is shown in Fig. 4.

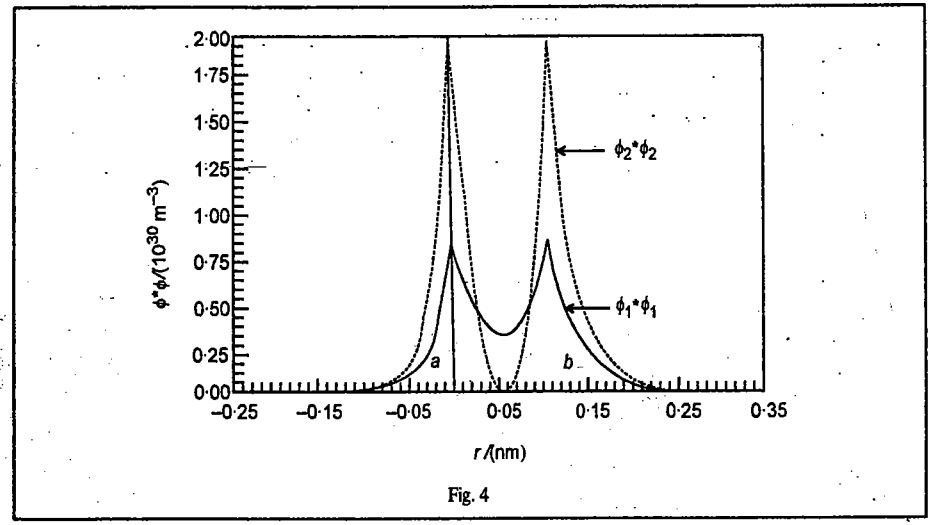

Fig. 4

Example 16. Calculate the probability of finding the electron in a small volume element of 1 pm^3 located along the bonding axis in H_2^+ at r = 0·0500 nm. Assume that the nuclei are separated at a distance of 0·1057 nm.

Solution : The probability is given by $P = \phi^*\phi\, d\tau$, where the values of $\phi^*\phi$ were determined in Example 15 for this system. The respective probabilities are

$$P_1 = (3{\cdot}68 \times 10^{29}\text{m}^{-3})\ (1 \times 10^{-12}\ \text{m})^3 = 3{\cdot}68 \times 10^{-7}$$

$$P_2 = (4{\cdot}24 \times 10^{27})\ (1 \times 10^{-12})^3 = 4{\cdot}24 \times 10^{-9}$$

Example 17. Repeat the calculations of example 16 for the volume element located at r = 0·0500 nm from nucleus a and at a distance of 0·0200 nm off the bonding axis.

Solution : The values of r_a and r_b to be used in Es. (*iv*) and (*v*) in eqample 15 can be determined using the

$$r_a = [(0{\cdot}0500\ \text{nm}) + (0{\cdot}0200\ \text{nm})^2]^{1/2} = 0{\cdot}0539\ \text{nm}$$

$$r_b = [(0{\cdot}1057\ \text{nm} - 0{\cdot}0500\ \text{nm})^2 + (0{\cdot}0200\ \text{nm})^2]^{1/2} = 0{\cdot}0592\ \text{nm}$$

Substituting into Eq. (*iv*) in example 15 gives

$$\phi_1 = \frac{e^{-(0{\cdot}0539\ \text{nm})/(0{\cdot}0529\ \text{nm})} + e^{-(0{\cdot}0532\ \text{nm})/(0{\cdot}0592\ \text{nm})}}{1{\cdot}216 \times 10^{-15}\text{m}^{3/2}} = 5{\cdot}65 \times 10^{14}\ \text{m}^{-3/2}$$

Likewise, $\phi_2 = 5{\cdot}55 \times 10^{13}\ \text{m}^{-3/2}$. The respective probabilities are

$$P_1 = (5{\cdot}65 \times 10^{-14}\ \text{m}^{-3/2})^2 \cdot (1 \times 10^{-12}\ \text{m})^3 = 3{\cdot}19 \times 10^{-7}$$

$$P_2 = (5{\cdot}55 \times 10^{-13})^2\ (1 \times 10^{-12})^3 = 3{\cdot}08 \times 10^{-9}$$

Term Symbols for a Diatomic Molecule

The hydrogen molecule (and other diatomic molecules) have a large number of excited electronic states which are designated by ***molecular term symbols.*** As in an atom, in diatomic molecules the orbital angular momenta of electrons couple to give a resultant orbital angular momentum L and the electron spin momenta couple to give a resultant spin angular momentum S. The component of the orbital angular momentum along the axis of the molecule is given by

$$M_L = m_1 + m_2 + \cdots\cdots\cdots$$

where $m_i = 0$ for a σ orbital and $m_i = \pm 1$ for a π orbital, and so on. The quantum number Λ is defined as the absolute value of M_L and is represented by the code letters

Λ =	0	1	2	3
Symbol =	Σ	Π	Δ	Φ

in analogy to atomic term symbols. The multiplicity of an electronic state of a diatomic molecule is given by $2S+1$ where S is the sum of the spins of the electrons in the molecule. The term symbol of a molecule is represented by $^{2S+1}\Lambda$.

For Σ terms, a superscript of plus or minus is added according to the behaviour of the wave function upon reflection in the plane containing the internuclear axis. A plus sign indicates that the wave function is invariant under this operation and a negative sign indicates that the wave function changes sign on reflection in this plane. If a diatomic molecule, such as a homonuclear diatomic, has a centre of symmetry, a right subscript of g or u is attached to the term symbol to denote the *parity* of the orbital. The parity of an orbital is determined by observing the *inversion* symmetry. When a point on an orbital is inverted an equal distance through the centre of the molecule, the orbital is said to be *gerade* (g) if it has the same sign at the two points; otherwise it is said to be *ungerade* (u); The reader can convince himself of the fact that in an atom an s orbital is g, a p orbital is u, a d orbital is g, and an f orbital is u. The parity of a multielectron molecule is obtained by noting g or u for every orbital and forming products, using the relations :

$$g \times g = g,\ g \times u = u,\ u \times u = g$$

Example 18. Show that the ground state term symbol of H_2 is $^1\Sigma_g^+$.

Solution : The H_2 molecule has the electronic configuration $(\sigma_g, 1s)^2$, *i.e.*, both the electrons are in the σ_g

orbital. For the σ electrons, $m_1 = 0$, $m_2 = 0$ so that $M_L = 0$. Since $s = |M_L|$, hence, Λ = 0. This means that the term symbol is Σ. Since $S_1 = 1/2$ and $S_2 = -1/2$, hence, $S = S_1 + S_2 = 0$ so that multiplicity $2S + 1 = 1$ which corresponds to a singlet state. Since the σ orbital is invariant under reflection in the plane containing the internuclear axis, we use the superscript of plus (+). Again, since the orbital is gerade (g), we use the subscript g. Thus, the complete term symbol for H_2 is $^1\Sigma_g^+$.

Symmetry of Molecular Orbitals. Some of the possible combinations of atomic orbitals in the LCAO–MO scheme are shown in Fig. 5. Those orbitals which are cylindrically symmetrical about the

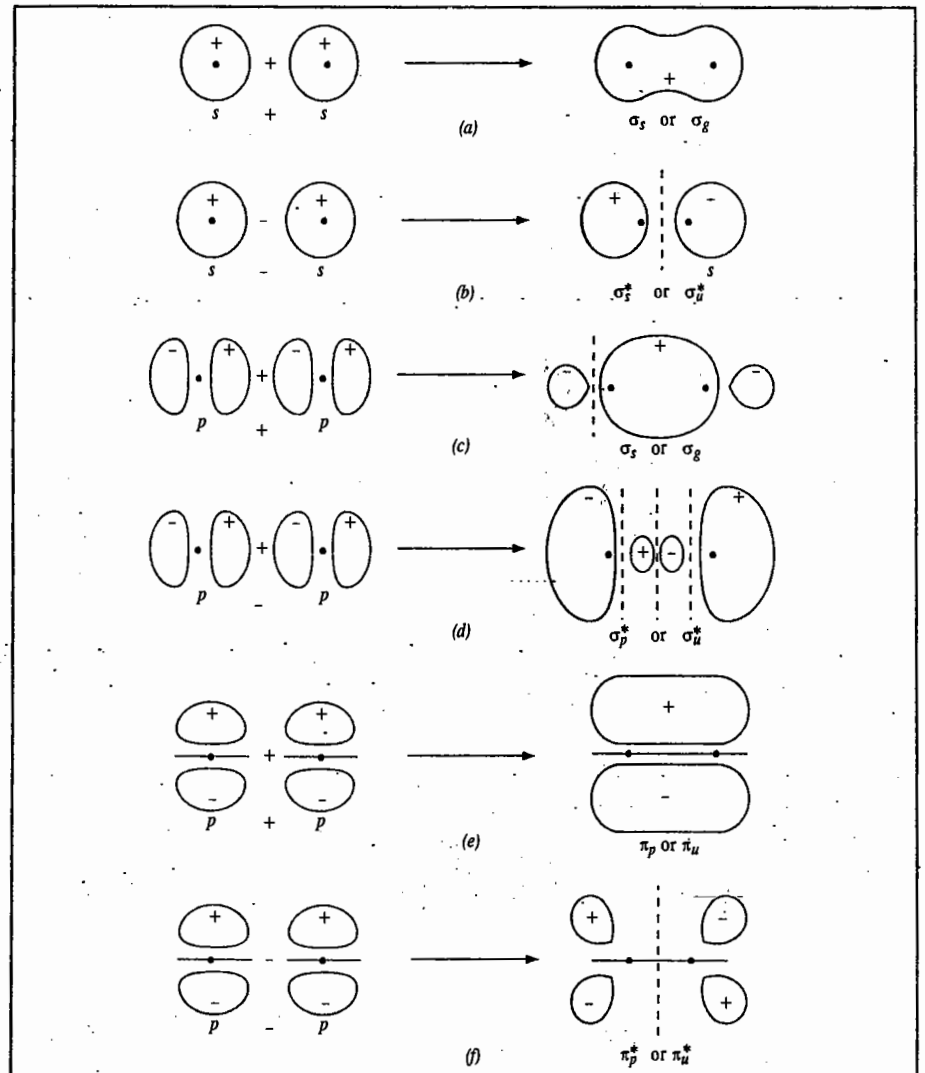

Fig. 5. Combinations of s, s and p, p atomic orbitals to form molecular orbitals of different symmetries. The figure displays the contours of the atomic and molecular orbitals. The traditional shapes of s and p orbitals arise from the projection of the contours on the respective axes.

internuclear axis are called σ orbitals, analogous to an *s* orbital of the highest symmetry. If the internuclear axis lies in the nodal plane, a π bond is formed. In δ bonds (encountered in the metal-metal quadruple bond in transition-metal chemistry), the internuclear axis lies in two mutually perpendicular nodal planes. All antibonding orbitals, identified with an *, possess an additional nodal plane perpendicular to the internuclear axis and lying between the nuclei. Also the MOs may or may not have a centre of symmetry. Thus, π_{p-p} orbitals are ungerade and π^*_{p-p} orbitals are gerade.

MOs for Homonuclear Diatomic Molecules

The simplest molecules are those containing two atoms of the same element ; these are called homonuclear diatomics. We shall now consider the LCAO-MO approximation for such molecules using the basis functions of the two atoms, such as the AOs 1*s*, 2*s*, 2*p*, 3*s*, etc. The two criteria that must be satisfied for the formation of BMOs are *(i)* the overlap between the AOs must be positive, the energies of the AOs must be approximately the same in order that there is effective interaction between the AOs of different atoms.

The molecules are built up by adding electrons to MOs in the same way as the atoms are built up by adding electrons to AOs. The principles involved in both cases are the same. The basic principles can be summed up as follows :

1. The MO with the lowest energy is filled first.
2. The maximum number of electrons in a MO cannot exceed two and the two electrons must be of opposite sign.
3. If there are two degenerate MOs, pairing of electrons will occur only after each degenerate MO has one electron.

It is useful to define the term **bond order** that is roughly proportional to the strength of bonding. This is equal to one-half the difference between the number of bonding electrons and the number of antibonding electrons. Thus,

$$\text{Bond order} = \tfrac{1}{2}(N_b - N_a) \qquad \ldots(22)$$

Bond orders of 1, 2 and 3 signify single, double and triple bonds. Bond order of zero means that no bond is formed. The bond order of a molecule is directly proportional to its bond dissociation energy. This means that the higher the bond order, the larger the bond dissociation energy and the smaller the bond length.

We shall now consider the homonuclear diatomic molecules of the first and second row elements of the Periodic table.

1. $H_2 : \sigma(1s)^2$; bond order $= \frac{1}{2}(2 - 0) = 1$. The molecule has a single bond.

The bond dissociation energy of H_2 molecule has been found to be 458 kJ mol^{-1} and bond length equal to 0·74 Å.

2. Hydrogen molecule ion, H_2^+. This molecule has been detected spectroscopically when electric discharge is passed through hydrogen gas under reduced pressure. The molecule has only one electron and its electronic configuration is

$$H_2^+ : (\sigma(1s)^1 \quad \text{and its bond order} = \tfrac{1}{2}(1 - 0) = \tfrac{1}{2}$$

The positive value of bond order indicates that the bond is formed and the molecule is stable. However, the bond in H_2^+ ion is weaker than that in H_2 molecule. The bond dissociation energy of H_2^+ ion (269 kJ mol^{-1}) is less than that of H_2 molecule (458 kJ mol^{-1}). The bond length in H_2^+ ion (1·04 Å) is larger than that in H_2 molecule (0·74 Å). These observations support the fact that the bond in H_2^+ ion is weaker than the bond in H_2 molecule.

3. He_2. The electronic configuration of hypothetical He_2 molecule is

$$He_2 : \sigma(1s)^2\, \sigma^*(1s^2) \quad \text{and its bond order} = \tfrac{1}{2}(2 - 2) = 0.$$

The zero bond order indicates that the molecule does not exist. Calculations have shown that the antibonding effect of an antibonding MO is stronger than the bonding effect of a bonding MO. Consequently, there is no possibility whatsoever for the existence of He_2 molecule.

Diatomic Molecules of the Second Row Elements. In these elements, the 1*s* orbitals are completely filled. In the formation of molecular orbitals, the electrons in the inner shells (*i.e.*, 1*s* electrons) of each atom remain essentially unperturbed in their respective atomic orbitals and may be kept out of consideration. In the formulation of electronic configurations of these molecules, the letters *KK* are generally used for denoting the fully filled inner shells (*K* shells) in the two atoms.

4. Li_2. The electronic configuration of lithium atom ($Z = 3$) is $1s^2\, 2s^1$. There are six electrons to be accommodated in lithium molecule. The four electrons are present in *K* sheils and there are only two electrons to be accommodated in molecular orbitals. These two electrons go into σ(2*s*) BMO which has lower energy and σ*(2*s*) ABMO remains empty. The electronic configuration of Li_2 molecule is thus represented as

$$Li_2 : KK\, \sigma(2s)^2 \quad \text{and its bond order} = \tfrac{1}{2}(2 - 0) = 1$$

Thus, there is one Li - Li sigma bond. The bond dissociation energy of the molecule is quite low, being about 105 kJ mol^{-1}. The bond length is 2·67 Å.

5. Be_2. The elecronic configuration of Be_2 molecule is

$Be_2 : KK\sigma(2s)^2\, \sigma^*(2s)^2$ and its bond order $= \frac{1}{2}(2 - 2) = 0$

The zero bond order suggests that the existence of stable Be_2 molecule is not possible.

6. B_2. The electronic configuration of B_2 molecule is

$B_2 : KK\, \sigma(2s)^2\, \sigma^*(2s^2)\, \pi(2p_x)^1\, \pi(2p_y)^1$ and its bond order $= \frac{1}{2}(4 - 2) = 1$

The molecule has only one B—B sigma bond. The bond dissociation energy is 289 kJ mol^{-1} and bond length is equal to 1·59 Å.

7. C_2. The electronic configuration of C_2 molecule is

$C_2 : KK\, \sigma(2s)^2\, \sigma^*(2s^2)\, \pi(2p_x)^2\, \pi(2p_y)^2$ and its bond order $= \frac{1}{2}(6 - 2) = 2$

Since C_2 molecule does not have any unpaired electron, it is diamagnetic, as observed experimentally. The bond dissociation energy of C_2 molecule is 627·9 kJ mol^{-1} and bond length equal to 1·31 Å.

8. N_2. The electronic configuration of nitrogen molecule is

$N_2 : KK\, \sigma(2s)^2\, \sigma^*(2s)^2\, \pi(2p_x)^2\, \pi(2p_y)^2\, \sigma(2p_z)^2$ and its bond order $= \frac{1}{2}(8 - 2) = 3$.

Thus, nitrogen molecule contains a triple bond.

It is evident that in the formation of N_2 molecule, only one ABMO is involved, the remaining four being all BMOs. Hence, the nitrogen molecule is highly stable. This is confirmed by its high bond dissociation energy, *viz.*, 945·6 kJ mol^{-1} and small bond length equal to 1·10 Å. Also since there are no unpaired electrons in any orbital, N_2 molecule is diamagnetic.

9. O_2. The electronic configuration of O_2 molecule is

$$O_2 : KK\, \sigma(2s)^2\, \sigma^*(2s)^2\, \sigma(2p_z)^2\, \pi(2p_x)^2\, \pi(2p_y)^2\, \pi^*(2p_x)^1\, \pi^*(2p_y)^1$$

Since it contains two unpaired electrons, the oxygen molecule is paramagnetic.

Bond order $= \frac{1}{2}(8 - 4) = 2$. O_2 moelcule, thus, contains a double bond.

Because of the presence of 4 electrons in ABMOs, O_2 molecule is less stable than N_2 molecule. Its bond dissociation energy is much less, being 494·6 kJ mol^{-1} and bond length is larger, being 1·21 Å.

10. F_2. The electronic configuration of fluorine molecule is

$$F_2 : KK\, \sigma(2s)^2\, \sigma^*(2s)^2\, \sigma(2p_z)^2\, \pi(2p_x)^2\, \pi(2p_y)^2\, \pi^*(2p_x)^2\, \pi^*(2p_y)^2$$

Bond order is $\frac{1}{2}(8 - 6) = 1$. The F_2 molecule, thus, contains a single bond. Because of the presence of as many as 6 electrons in the ABMOs, the bonding in F_2 is weaker than that in O_2. Therefore, bond dissociation energy of F_2 is very low, being 155 kJ mol^{-1} and bond length is 1·42 Å.

Since there are no unpaired electrons, the molecule is diamagnetic.

11. Ne_2. The electronic configuration of the hypothetical neon molecule is

$$Ne_2 : KK\ \sigma(2s)^2\ \sigma^*(2s)^2\ \sigma(2p_z)^2\ \pi(2p_x)^2\ \pi(2p_y)^2\ \pi^*(2p_x)^2\ \pi^*(2p_y)^2\sigma^*(2p_z)^2$$

Bond order is equal to $\frac{1}{2}(8 - 8) = 0$. Since ABMOs slightly dominate over BMOs, Ne_2 molecule would be incapable of existence.

Molecular Orbital Energy Level Diagrams of Heteronuclear Diatomic Molecules

The cases of heteronuclear diatomic molecules, in which the two atoms constituting a molecule are different, may now be considered. The principles involved in the distribution of electrons are the same as discussed before. However, the molecular orbital diagrams will not be symmetrical.

Let us discuss the electronic configurations and molecular orbital diagrams for some common heteronuclear diatomic molecules.

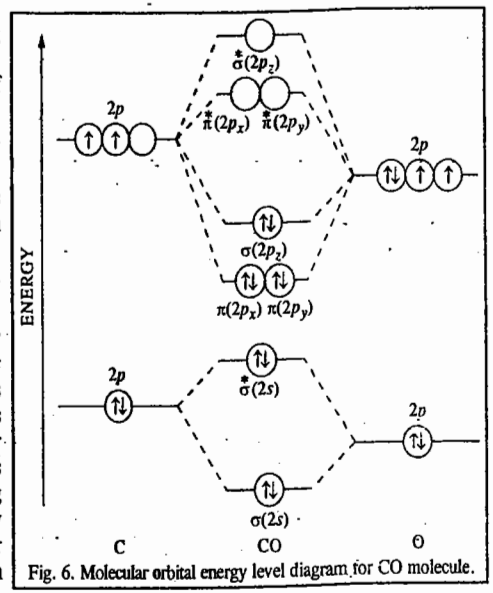

Fig. 6. Molecular orbital energy level diagram for CO molecule.

1. CO. The electronic configurations of C and O atoms are $1s^2 2s^2 p^2$ and $1s^2 2s^2 p^4$, respectively. There are 4 electrons in the outer shell of carbon and 6 electrons in the outer shell of oxygen. Thus, a total of 10 outer electrons are to be accommodated in the molecular orbitals of CO molecule. Because of higher electronegativity of oxygen, its atomic orbitals would be of lower energy than the corresponding atomic orbitals of carbon. Due to this energy difference, the bonding and antibonding molecular orbitals will receive different contributions from atomic orbitals of carbon and oxygen. The bonding molecular orbitals will receive more contribution from atomic orbitals of lower energy, *i.e.*, the atomic orbitals of oxygen and would be closer to it in energy than the antibonding molecular orbitals which would be closer to carbon in energy, as shown in Fig. 6. The bonding molecular orbitals would have more characteristics of atomic orbitals of oxygen and antibonding molecular orbitals would have more characteristics of carbon.

The electronic configuration of CO molecule is

$$CO : KK\ \sigma(2s)^2\ \sigma^*(2s)^2\ \pi(2p_x)^2\ \pi(2p_y)^2\ \sigma(2p_z)^2$$

Bond order is $\frac{1}{2}(8 - 2) = 3$. Thus, CO contains a triple bond. Its bond dissociation energy is 1067 kJ mol^{-1} and bond length is equal to 1·14 Å.

2. NO. The electronic configurations of N and O atoms are $1s^2 2s^2 p^3$ and $1s^2 2s^2 p^4$, respectively. There are 5 electrons in the outer shell of nitrogen and 6 electrons in the outer shell of oxygen. Thus, a total of 11 outer electrons are to be accommodated in the molecular orbitals of NO molecule.

The electronic configuration of NO molecule is, thus,

$$NO : KK\ \sigma(2s)^2\ \sigma^*(2s)^2\ \sigma(2p_z)^2\ \pi(2p_x)^2\ \pi(2p_y)^2\ \pi^*(2p_x)^1$$

The bond order is $\frac{1}{2}(8 - 3) = 2\frac{1}{2}$. This represents one σ bond and two π bonds less the anti-bonding

effect of one unpaired electron in the $\pi^*(2p_x)$ molecular orbital. The presence of this anti-bonding electron makes the NO molecule less stable than the N_2 molecule. This is confirmed by the fact that the bond dissociation energy of nitric oxide, *viz.*, 667·8 kJ mol^{-1}, is less than that of nitrogen which is 945·6 kJ mol^{-1}. Since NO contains an unpaired electron, it is paramagnetic.

As in the case of CO molecule, the bonding molecular orbitals would have greater characteristics of atomic orbitals of oxygen and the antibonding molecular orbitals would have greater characteristics of atomic orbitals of nitrogen.

3. HF. The electronic configurations of hydrogen and fluorine are $1s^1$ and $1s^2 2s^2 p^5$, respectively. In the formation of HF molecule, only the 2*p* electrons of fluorine atom would combine effectively with the solitary electron of hydrogen atom. As has been already explained, only a p_z orbital is able to combine with an *s* orbital. The combination of a p_x or p_y orbital with an *s* orbital is ruled out on symmetry considerations. The $2p_z$ orbital of fluorine gives a highly effective overlap with the *s* orbital of hydrogen to form $\sigma(sp)$ BMO and $\sigma^*(sp)$ ABMO.

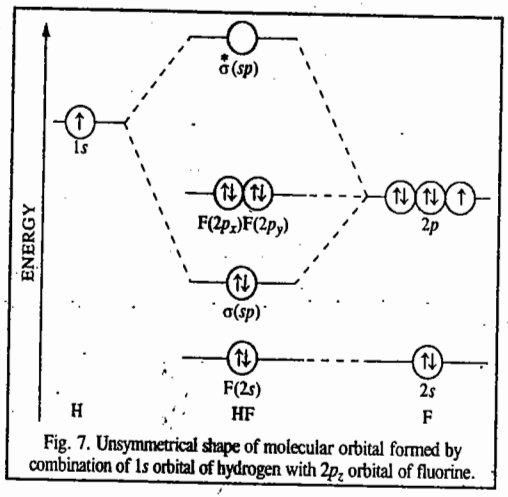

Fig. 7. Unsymmetrical shape of molecular orbital formed by combination of 1*s* orbital of hydrogen with $2p_z$ orbital of fluorine.

The bonding molecular orbital is fully filled with 2 electrons. The rest of the electrons remain in their atomic orbitals. The MO formed in the case of HF molecule will not be symmetrical. The asymmetry occurs because the energies of H(1*s*) and F($2p_z$) atomic orbitals are not the same. The MO diagram for HF molecule is shown in Fig. 7.

As can be seen, the bonding MO has an energy which lies closer to that of $2p_z$ orbital of fluorine than to that of higher energy 1*s* orbital of hydrogen.

4. HCl. The electronic configurations of H and Cl atoms are $1s^1$ and $1s^2 2s^2 p^6 3s^2 p^5$, respectively. In this case also, there is only one bonding MO and one anti-bonding MO formed by the combination of 1*s* orbital of hydrogen with $3p_z$ orbital of chlorine. The rest of the electrons of the chlorine atom remain in their respective AOs.

The electronic configuration of HCl may thus be represented as

$$HCl : KL\ (3s)^2\ \sigma(sp)^2\ (3p_x)^2\ (3p_y)^2$$

Here, too, the MO formed will not be symmetrical. The MO energy level diagram of HCl molecule will be exactly similar to the one shown in Fig. 7 for HF molecule.

Example 19. Write the electronic configurations of H_2, H_2^+ and the hypothetical species H_2^- in terms of molecular orbital theory.

Solution : H_2, H_2^- and H_2^+ have 2, 1 and 3 electrons, respectively. Hence, their electronic configurations are :

$$H_2 : \sigma(1s)^2$$

$$H_2^+ : \sigma(1s)^1$$

$$H_2^- : \sigma(1s)^2\ \sigma^*(1s)^1$$

Example 20. Why does He_2^+ exist whereas He_2 does not ?

Solution : Electronic configuration of He_2 is : $\sigma(1s)^2\sigma^*(1s)^2$

$$\therefore \quad \text{Bond order} = \frac{1}{2}(2 - 2) = 0$$

Electronic configuration of He_2^+ is = $\sigma(1s)^2\sigma^*(1s)^1$

$$\therefore \quad \text{Bond order} = \tfrac{1}{2}(2-1) = \tfrac{1}{2}$$

Thus, while the bond order of He_2 is zero, that of He_2^+ is 1/2. Hence, He_2^+ exists while He_2 does not.

Example 21. Of the species O_2, O_2^+, O_2^- and O_2^{2-}, which would have the maximum bond strength ?

Solution : Higher bond orders are associated with shorter bond lengths and higher bond strengths. We will first calculate the bond orders for the various species from their electronic configurations :

O_2 : $KK\ \sigma(2s)^2\ \sigma^*(2s^2)\ \sigma(2p_z)^2\ \pi(2p_x)^2\pi(2p_y)^2\pi^*(2p_x)^1\pi^*(2p_y)^1$

$$\text{Bond order} = \tfrac{1}{2}(8-4) = 2$$

O_2^+ : One electron is removed from the antibondng $\pi^*(2p_y)$ MO.

$$\text{Bond order} = \tfrac{1}{2}(8-3) = 2\tfrac{1}{2}$$

O_2^- : One electron is added to the antibonding $\pi^*(2p_x)$ MO.

$$\text{Bond order} = \tfrac{1}{2}(8-5) = 1\tfrac{1}{2}$$

O_2^{2-} : Two electrons are added to the outermost antibonding MOs.

$$\text{Bond order} = \tfrac{1}{2}(8-6) = 1$$

Since O_2^+ has the highest bond order, it has the shortest bond length and hence the **maximum bond strength.**

Example 22. Of the following species, which has the shortest bond length : NO, NO^+, NO^{2+}, NO^- ?

Solution : We shall first calculate the bond orders for the given species from their electronic configurations.

NO : $KK\ \sigma(2s)^2\ \sigma^*(2s)^2\sigma(2p_z)^2\ \pi(2p_x)^2\pi(2p_y)^2\pi^*(2p_x)^1$

$$\text{Bond order} = \tfrac{1}{2}(8-3) = 2\tfrac{1}{2}$$

NO^+ : One electron is removed from the antibonding $\pi^*(2p_x)$ MO.

$$\text{Bond order} = \tfrac{1}{2}(8-2) = 3$$

NO^{2+} : One electron is removed from the antibonding $\pi^*(2p_x)$ MO and the other electron is removed from the bonding $\pi(2p_y)$ MO.

$$\text{Bond order} = \tfrac{1}{2}(7-2) = 2\tfrac{1}{2}$$

NO^- : One electron is added to the antibonding $\pi^*(2p_x)$ MO.

$$\text{Bond order} = \tfrac{1}{2}(8-4) = 2$$

Evidently, the species NO^+ has the highest bond order and thus has the **shortest bond length.**

Example 23. Compare the bond energy, bond length and magnetic character of CN and CN^- species with the help of molecular orbital theory.

Solution : We shall first calculate bond orders for these species from their electronic configurations.

CN has 13 electrons and its electronic configuration is

$$CN : KK\ \sigma(2s)^2\ \sigma^*(2s)^2\ \pi(2p_x)^2\ \pi(2p_y)^2\ \sigma(2p_z)^1$$

$$\text{Bond order} = \tfrac{1}{2}(7-2) = 2\tfrac{1}{2}$$

CN^- : In this case, one electron is added to $\sigma(2p_z)$ MO so that its electronic configuration is

$$CN^- : KK\ \sigma(2s)^2\ \sigma^*(2s)^2\ \pi(2p_x)^2\ \pi(2p_y)^2\ \sigma(2p_z)^2$$

$$\text{Bond order} = \tfrac{1}{2}(8-2) = 3$$

Since CN^- has a higher bond order, it has larger bond energy and smaller bond length than CN. Further, since there is one unpaired electron in $\sigma(2p_z)$ MO of CN, it is paramagnetic. CN^- is evidently diamagnetic.

Example 24. Construct a molecular orbital wave function for the bond between H and Cl in HCl assuming that the bond is formed from the 1s electron of H atom and a 3p electron of Cl atom.

Solution : Let H atom be designated by A and Cl atom by B. Let the 1s electron of H atom be labelled as electron 1 and 3p electron of Cl atom be labelled as electron 2.

For notational convenience, we shall use the symbol ψ for MO and the symbol ϕ for AO.

$$\psi_{MO} = \psi_1\psi_2 \cdot \text{ where}$$

$$\psi_1 = c_1\phi_A(1) + c_2\phi_B(1)$$

and $$\psi_2 = c_1\phi_A(2) + c_2\phi_B(2)$$

$$\therefore \quad \psi_{MO} = \psi_1\psi_2 = [c_1\phi_A(1) + c_2\phi_B(1)]\,[c_1\phi_A(2) + c_2\phi_B(2)]$$

$$= c_1^2[\phi_A(1)\phi_A(2)] + c_1c_2[\phi_A(1)\,\phi_B(2) + \phi_A(2)\phi_B(1)] + c_2^2[\phi_B(1)\phi_B(2)]$$

As can be seen, the first and the last terms are *ionic* whereas the middle terms are *covalent.* Also the covalent terms have *equal weight* but the ionic terms have *different weights* from the covalent terms and also from each other.

Example 25. Write down the molecular orbital wave function for H_2^- molecule anion.

Solution : H_2^- molecule anion contains three electrons which may be labelled as 1, 2 and 3. It contains two nuclei which may be designated as A and B.

$$\psi_{MO} = \psi_1\psi_2\psi_3$$

where

$$\psi_1 = c_1\phi_A(1) + c_2\phi_B(1)$$

$$\psi_2 = c_3\phi_A(2) + c_4\phi_B(2)$$

$$\psi_3 = c_5\phi_A(3) + c_6\phi_B(3)$$

Example 26. Using the LCAO for the wave function for H_2^+, obtain the normalised wave function for the BMO and the ABMO.

Solution : Using the LCAO-MO approximation, the wave function for H_2^+ is written as

$$\psi = N(c_1\phi_A + c_2\phi_B) \qquad \ldots(i)$$

where N is the normalisation constant.

According to the normalization condition, for real ψ (using Dirac's 'bra' and 'ket' notation),

$$\psi^2 d\tau \equiv <\psi|\psi> = 1 \qquad \ldots(ii)$$

Incorporating the value of ψ from Eq. *(i)* in Eq. *(ii)*, we have

$$N^2 <(c_1\phi_A + c_2\phi_B)\,|\,(c_1\phi_A + c_2\phi_B)> = 1$$

or $$c_1^2[<\phi_A|\phi_A>] + c_2^2.[<\phi_B|\phi_B>] + 2c_1c_2\,[<\phi_A|\phi_B>] = 1/N^2 \qquad \ldots(iii)$$

Assuming that ψ_A and ψ_B are normalised, *i.e.*,

$$<\phi_A|\psi_A> \equiv \int\phi_A^2 d\tau = 1 \text{ and } <\phi_B|\phi_B> \equiv \int\phi_B^2 d\tau = 1,$$

we have $c_1^2 + c_2^2 + 2c_1c_2S = 1/N^2$ where S is the overlap integral defined as $\qquad \ldots(iv)$

$$S = <\phi_A|\phi_B> \equiv \int\phi_A\phi_B d\tau \qquad \ldots(v)$$

so that $$N = (c_1^2 + c_2^2 + 2c_1c_2S)^{-1/2} \qquad \ldots(vi)$$

Hence, from Eq. *(i)*, $$\psi = (c_1^2 + c_2^2 + 2c_1c_2S)^{-1/2}(c_1\phi_A + c_2\phi_B) \qquad \ldots(vii)$$

We know that for BMO, $c_1 = c_2$ and for ABMO, $c_1 = -c_2$

Hence, from Eq. *(vii)*, $$\psi_{BMO} = \frac{1}{\sqrt{2(1+S)}}(\phi_A + \phi_B)$$

and $$\psi_{ABMO} = \frac{1}{\sqrt{2(1-S)}}(\phi_A - \phi_B)$$

Example 27. Write down the wavefunction for the BMO for a heteronuclear diatomic molecule AB assuming that the electron on an average spends 90% of its time on nucleus *A* and 10% of its time on nucleus B.

Solution : In the LCAO-MO scheme, $\psi_{MO} = c_A\phi_A + c_B\phi_B$

where the coefficients c_A and c_B are such that $[c_A]^2$ and $[c_B]^2$ determine the probability of finding the electron in the AOs ϕ_A and ϕ_B, respectively. Then, clearly,

$$[c_A]^2 = 90\% = 0{\cdot}9 \text{ and}$$

$$[c_B]^2 = 10\% = 0{\cdot}1$$

Hence, $c_A = \pm\sqrt{0.9} = \pm 0.95$ and

$c_B = \pm\sqrt{0.1} = \pm 0.32$

Thus, $\psi_{MO} = 0.95\phi_A + 0.32\phi_B$

Table 1 gives the ground state electronic configurations of homonuclear diatomics (along with other relevant data) in a slightly different notation.

TABLE 1

Ground State Electronic Configurations of Homonuclear Diatomics

Molecule	Number of Electrons	Electronic Configuration	Term Symbol	Bond Order	R_e (pm)	D_e(eV)	D_e (kJ mol^{-1})
H_2^+	1	$(1\sigma_g)^1$	$^2\Sigma$	$\frac{1}{2}$	106·0	2·79	269·5
H_2	2	$(1\sigma_g)^2$	$^1\Sigma$	1	74·12	4·75	458·1
He_2^+	3	$(1\sigma_g)^2(1\sigma_u)$	$^2\Sigma$	$\frac{1}{2}$	108·0	2·5	238·0
He_2	4	$(1\sigma_g)^2(1\sigma_u)^2$	$^1\Sigma$	—	—	—	—
Li_2	6	$[He_2](2\sigma_g)^2$	$^1\Sigma$	1	267·3	1·14	110·0
Be_2	8	$[He_2](2\sigma_g)^2(2\sigma_u)^2$	$^1\Sigma$	0	—	—	—
B_2	10	$[Be_2](1\pi_u)^2$	$^3\Sigma$	1	158·9	~3·0	~290
C_2	12	$[Be_2](1\pi_u)^4$	$^1\Sigma$	2	124·2	6·36	613·8
N_2	14	$[Be_2](1\pi_u)^4(3\sigma_g)^2$	$^1\Sigma$	3	109·4	9·90	955·4
O_2^+	15	$[N_2](1\pi_g)^2$	$^2\Pi$	$2\frac{1}{2}$	112·27	6·7	653·1
O_2	16	$[N_2](1\pi_g)^2$	$^3\Sigma$	2	120·74	5·21	502·9
F_2	18	$[N_2](1\pi_g)^4$	$^1\Sigma$	1	143·5	1·34	118·8
Ne_2	20	$[N_2](1\pi_g)^4(3\sigma_u)^2$	$^1\Sigma$	0	—	—	—

VALENCE BOND THEORY (VBT)

This theory was the first quantum mechanical theory of the chemical bond proposed by Heitler and London in 1927 and subsequently developed by Slater and Pauling in the 1930s. It is collectively referred to as the Heitler–London–Slater–Pauling (HLSP) theory and was fully formulated by Pauling during 1940–1960.

VBT draws heavily on the Lewis concept of a covalent bond as a shared pair of electrons. The theory makes the **perfect pairing approximation** in which it is assumed that structures with electrons paired in all possible ways dominate the wave function of the molecule. The overall wave function is a superposition of all possible perfectly paired canonical structures, with those of the lowest energy making the main contribution.

Let us determine the normalized valence bond eigenfunction of H_2 molecule which has only one perfectly paired canonical structure, the one corresponding to the Lewis structure H—H. Let the two electrons of H_2 be designated 1 and 2 and the two nuclei a and b (Fig. 8). The valence bond wave function can be written as

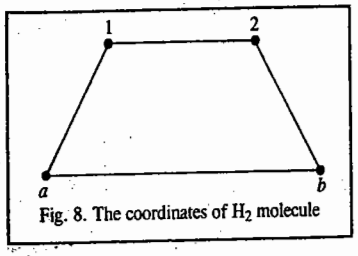

Fig. 8. The coordinates of H_2 molecule

$$\psi_{AB} = c_1\psi_1 + c_2\psi_2 \qquad ...(23)$$

where c_1 and c_2 are the coefficients and ψ_1 and ψ_2 can be written as

$$\psi_1 = \phi_a(1)\,\phi_b(2) \qquad ...(24a)$$

$$\psi_2 = \phi_b(1)\,\phi_a(2) \qquad ...(24b)$$

where the ϕs are the 1s atomic orbitals (AOs) of the two hydrogen atoms. (Here we have neglected the spins of the two electrons for the sake of simplicity). ψ_1 is the wave function corresponding to the situation where electron 1 is on the AO ϕ_a, centred on the nucleus a and electron 2 is on the AO ϕ_b, centred on the nucleus b. Since H_2 is a homonuclear diatomic molecule, it is evident that $c_1 = \pm c_2$. Substituting Eqs. 24 a and b in Eq. 23 we obtain the following Heitler–London wave functions for H_2 :

$$\psi_+ = N_+[\phi_a(1)\,\phi_b(2) + \phi_b(1)\,\phi_a(2)] \qquad ...(25a)$$

$$\psi_- = N_-[\phi_a(1)\,\phi_b(2) - \phi_b(1)\,\phi_a(2)] \qquad ...(25b)$$

where N_+ and N_- are the corresponding normalization constants. According to the normalization condition (embodied in the Born interpretation of the wave function)

$$\int_{-\infty}^{\infty} \psi_\pm^* \psi_\pm \, d\tau \equiv \langle \psi_\pm | \psi_\pm \rangle = 1$$

Let us normalize ψ_+. Assuming that the wave functions are real,

$$\int \psi_+^2 \, d\tau \equiv \langle \psi_+ \mid \psi_+ \rangle = N_+^2\left[\int \phi_a^2(1)\phi_b^2(2)\,d\tau + 2\int \phi_a(1)\phi_b(1)\phi_a(2)\phi_b(2)\,d\tau + \int \phi_b^2(1)\phi_a^2(2)\,d\tau\right] = 1$$

or $N_+^2\left[\int \phi_a^2(1)\,d\tau_1 \int \phi_b^2(2)\,d\tau_2 + 2\int \phi_a(1)\phi_b(1)\,d\tau_1 \times \int \phi_a(2)\phi_b(2)\,d\tau_2 + \int \phi_b^2(1)\,d\tau_1 \times \int \phi_a^2(2)\,d\tau_2\right] = 1$ ($\because d\tau = d\tau_1\, d\tau_2$)

Since the ϕs are normalized,

$$\int \phi_a^2(1)\,d\tau_1 = \int \phi_b^2(2)\,d\tau_2 = \int \phi_b^2(1)\,d\tau_1 = \int \phi_a^2(2)\,d\tau_2 = 1$$

and $$= \int \phi_a(1)\phi_b(1)\,d\tau_1 = \int \phi_a(2)\phi_b(2)\,d\tau_2 = S$$

where S is the overlap integral. Hence,

$$N_+^2[(1)(1) + 2(S)(S) + (1)(1)] = 1$$

or $$N_+^2[2(1 + S^2)] = 1 \text{ whence } N_+ = 2/(1 + S^2)^{\frac{1}{2}}$$

Substituting in Eq. 25a, the normalized VB wave function is

$$\psi_+ = \frac{1}{\sqrt{2(1 + S^2)}}\,[\phi_a(1)\,\phi_b(2) + \phi_b(1)\,\phi_a(2)] \qquad ...(26a)$$

Similarly, we can show that

$$\psi_- = \frac{1}{\sqrt{2(1 - S^2)}}\,[\phi_a(1)\,\phi_b(2) - \phi_b(1)\,\phi_a(2)] \qquad ...(26b)$$

Since $0 < S < 1$ and, in general, $S << 1$. We can write

$$\psi_+ = \frac{1}{\sqrt{2}}[\phi_a(1)\phi_b(2) + \phi_b(1)\phi_a(2)] \qquad ...(27a)$$

$$\psi_- = \frac{1}{\sqrt{2}}[\phi_a(1)\phi_b(2) - \phi_b(1)\phi_a(2)] \qquad ...(27b)$$

Let us now consider the role of the ionic structures in VBT. For H_2 molecule the ionic structures are those in which the electrons 1 and 2 are located on nucleus a or on b giving rise to structures $H_a^+H_b^-$ and $H_a^-H_b^+$. A little reflection shows that these structures are unlikely since there is no electronegativity

difference between the two hydrogen atoms. However, such structures become important in heteronuclear diatomics. Thus, the valence bond wave function can be written as composed of a covalent part and an ionic part.

$$\psi_{VB} = \psi_{covalent} + \lambda\psi_{ionic} \quad ...(28)$$

or, equivalently, as $$\psi_{VB} = (1 - \lambda)\,\psi_{covalent} + \lambda\psi_{ionic} \quad ...(29)$$

The second form is generally preferred. Here λ is a parameter whose value determines the polar character **(ionicity)** of the bond.

Example 28. Write down the valence bond wave function for the HF molecule (assuming that it is formed from 1*s* orbital of H and $2p_z$ orbital of F) in the following three cases : *(a)* HF is purely covalent *(b)* HF is purely ionic and *(c)* HF is 80% covalent and 20% ionic.

Solution : Let the H atom be represented by A and F atom by B. Let the electron numbered 1 be the 1*s* electron of H atom and the electron numbered 2 be the p_z electron of F atom.

(a) For purely covalent structure of HF, the wave function is written as

$$\psi_{covalent} = \phi_A(1)\phi_B(2) + \phi_A(2)\phi_B(1)$$

(b) For purely ionic structure H^+F^-, both the electrons are on the F atom so that

$$\psi_{ionic} = \phi_B(1)\phi_B(2)$$

(c) HF is a resonance hybrid shown as

$$H{-}F \longleftrightarrow H^+F^-$$

$$\therefore \quad \psi = c_1\psi_{covalent} + c_2\psi_{ionic} \quad \text{with} \quad c_1^2 + c_2^2 = 1$$

Since $c_1^2 = 0{\cdot}80$ and $c_2^2 = 0{\cdot}20$ (given), hence,

$$c_1 = \sqrt{0{\cdot}80} = 0{\cdot}89$$

and $$c_2 = \sqrt{0{\cdot}20} = 0{\cdot}45$$

$$\therefore \quad \psi = 0{\cdot}89\,[\phi_A(1)\phi_B(2) + \phi_A(2)\phi_B(1)] + 0{\cdot}45\,[\phi_B(1)\,\phi_B(2)].$$

Example 29. Assuming that the ionic character in H—Br bond is 11%, calculate the fraction of the contribution of ionic character to the valence bond wave function.

Solution : According to Eq. 28, $\psi_{AB} = \psi_{covalent} + \lambda\psi_{ionic}$

The % ionic character is given by $\dfrac{\lambda^2}{1+\lambda^2} \times 100$

$$\therefore \quad 11 = 100\lambda^2/(1 + \lambda^2)$$

or $$\lambda^2 = 11/89$$

Hence, $$\lambda = \sqrt{11/89} = 0 \cdot 35$$

Thus, the fraction of contribution of ionic character to ψ_{AB} is **0·35.**

Example 30. Write down the normalised VB wave function and MO wave function for H_2 molecule and comment on the expressions obtained.

Solution : H_2 molecule contains two electrons labelled 1 and 2 and two hydrogen nuclei labelled A and B. The pairing of electrons leads to the formation of a covalent bond. In the VB approach, if electron 1 is on nucleus A, then electron 2 would be on nucleus B and vice-versa. Since, however, the two electrons are indistinguishable, therefore, the VB wave function for H_2 molecule can be written as

$$\psi_{AB} = (1/\sqrt{2})\,[\phi_A(1)\,\phi_B(2) + \phi_A(2)\,\phi_B(1)] \quad ...(i)$$

where $1/\sqrt{2}$ is the normalization constant obtained by normalizing ψ_{VB}.

In the MO theory, the MO wave function for H_2 molecule is given by

$$\psi_{MO} = \psi_1\psi_2 \quad ...(ii)$$

where ψ_1 and ψ_2 are the normalised wave functions for MOs of H_2 given by

$$\psi_1 = (1/\sqrt{2})[\phi_A(1) + \phi_B(1)] \quad ...(iii)$$

$$\psi_2 = (1/\sqrt{2})[\phi_A(2) + \phi_B(2)] \quad ...(iv)$$

Multiplying ψ_1 and ψ_2, we get the ψ_{MO} as

$$\psi_{MO} = \phi_1\phi_2\,[\phi_A\,(1) + \phi_B\,(1)]\,[\phi_A\,(2) + \phi_B\,(2)] \quad ...(v)$$

$$= \tfrac{1}{2}\,[\phi_A(1)\,\phi_A(2) + \phi_B(1)\,\phi_B(2)] + 1/2\,[\phi_A(1)\,\phi_B(2) + \phi_B(1)\,\phi_A(2)] \quad ...(vi)$$

In Eq. *(vi)*, the first two terms represent the probability of finding both the electrons on the same atom at the same time. In other words, these terms represent the ionic structures of H_2 molecule which may be written as

$$\overset{+}{H}_A\overset{-}{H}_B \quad \text{and} \quad \overset{-}{H}_A\overset{+}{H}_B.$$

The last two terms in Eq. *(vi)* represent the covalent structure of the H_2 molecule.

Comparing ψ_{VB} and ψ_{MO}, we observe that while the wave function in VBT does not give any weightage to ionic structures, the MOT gives equal weightage to covalent and ionic structures.

Example 31. Determine the energy of H_2 molecule at infinite internuclear separation using the Heitler-London (valence bond) normalized wave functions

$$\phi = \frac{1}{2^{1/2}}\,[\psi_a(1)\,\psi_b(2) \pm \psi_a(2)\,\psi_b(1)] \quad ...(i)$$

where ψ_α is the hydrogenic 1s wavefunction.

Solution : The Hamiltonian operator for this system is given by

$$\hat{H} = \frac{-\hbar^2}{2m_e}(\nabla_1^2 + \nabla_2^2) + \frac{e^2}{4\pi\varepsilon_0}\left(\frac{1}{r_{ab}} - \frac{1}{r_{1a}} - \frac{1}{r_{2a}} - \frac{1}{r_{1b}} - \frac{1}{r_{2b}} + \frac{1}{r_{12}}\right)$$

At infinite separation of the nuclei, the Hamiltonian reduces to

$$\hat{H} = \frac{-\hbar^2}{2m_e}(\nabla_1^2 + \nabla_2^2) + \frac{e^2}{4\pi\varepsilon_0}\left(-\frac{1}{r_{1a}} - \frac{1}{r_{2b}}\right) \quad ...(ii)$$

Hence, the expectation value of energy is

$$< E > = \int \phi^* \left[\frac{-\hbar^2}{2m_e}\left(\nabla_1^2 + \nabla_2^2\right) - \frac{e^2}{4\pi\varepsilon_0}\left(\frac{1}{r_{1a}} + \frac{1}{r_{2b}}\right)\right]\phi\, d\tau$$

$$= \int \phi^* \left[\frac{-\hbar^2}{2m_e}\nabla_1^2 - \frac{e^2}{4\pi\varepsilon_0}\left(\frac{1}{r_{1a}}\right)\right]\phi\, d\tau$$

$$+ \int \phi^* \left[\frac{-\hbar^2}{2m_e}\nabla_2^2 - \frac{e^2}{4\pi\varepsilon_0}\left(\frac{1}{r_{2b}}\right)\right]\phi\, d\tau = 2\int \phi^* \hat{H}(\mathrm{H})\,\phi\, d\tau$$

where $\hat{H}$ (H) is the Hamiltonian operator for a hydrogen atom. Substituting Eq. *(i)* gives

$$< E > = 2\int \frac{1}{2^{1/2}}\,\psi_a(1)\,\psi_b(2) \pm \psi_a(2)\,\psi_b(1)]^*\,\hat{H}(\mathrm{H})\,\frac{1}{2^{1/2}}[\psi_a(1)\,\psi_b(2) \pm \psi_a\,(2)\,\psi_b(1)]\,d\tau$$

$$= \int \psi_a^*(1)\, \psi_b^*(2)\, \hat{H}(H)\, \psi_b(2)\, d\tau \pm \int \psi_a^*(2)\, \psi_b^*(1)\, \hat{H}(H)\, \psi_a(1)\, \psi_b(2)\, d\tau$$

$$\pm \int \psi_a^*(1)\, \psi_b^*(2)\, \hat{H}(H)\, \psi_a(2)\, \psi_b(1)\, d\tau + \int \psi_a^*(2)\, \psi_b^*(1)\, \hat{H}(H)\, \psi_a(2)\, \psi_b(1)\, d\tau$$

At infinite separation of the nuclei, the second and third integrals are equal to zero, giving

$$< E > = \int \psi_a^*(1)\, \hat{H}(H) \psi_a(1)\, d\tau \int \psi_b^*(2)\, \psi_b(2)\, d\tau$$

$$\pm 0 \pm 0 + \int \psi_b^*(1)\, \hat{H}(H)\, \psi_b(1)\, d\tau \int \psi_a^*(2)\, \psi_a(2)\, d\tau$$

$$= E(H)\, S_{bb} + E(H)\, S_{aa} = 2E(H)$$

where $S_{aa} = S_{bb} = 1$ and $E(H)$ is the energy of the hydrogen atom.

Example 32. Write the complete normalized wave functions in VBT for H_2 molecule, including the spin wave functions.

Solution : The wave function with the positive sign is symmetric with respect to the exchange of electrons :

$$\hat{P}(1, 2)\, \phi_+ = \hat{P}(1, 2) \frac{1}{2^{1/2}} [\psi_a(1)\, \psi_b(2) + \psi_a(2)\, \psi_b(1)]$$

$$= \frac{1}{2^{1/2}} [\psi_a(2)\, \psi_b(1) + \psi_a(1)\, \psi_b(2)] = \phi_+$$

According to the Pauli exclusion principle, an antisymmetric spin wave function must be used. Thus, using antisymmetric spin wave function, we obtain

$$\phi_1 = \frac{1}{2^{1/2}} [\psi_a(1)\, \psi_b(2) + \psi_a(2)\, \psi_b(1)] \frac{2^{1/2}}{2} [\alpha(1)\, \beta(2) - \beta(1)\, \alpha(2)]$$

$$= \frac{1}{2} [\psi_a(1)\, \psi_b(2) + \psi_a(2)\, \psi_b(1)][\alpha(1)\, \beta(2) - \beta(1)\, \alpha(2)]$$

Likewise, the wave function with the negative sign can be shown to be antisymmetric, and the symmetric spin wave functions are used, giving

$$\phi_2 = \frac{1}{2^{1/2}} [\psi_a(1)\, \psi_b(2) - \psi_a(2)\, \psi_b(1)]\alpha(1)\, \beta(2)]$$

$$\phi_3 = \frac{1}{2^{1/2}} [\psi_a(1)\, \psi_b(2) - \psi_a(2)\, \psi_b(1)]\beta(1)\, \beta(2)$$

$$\phi_4 = \frac{1}{2} [\psi_a(1)\, \psi_b(2) - \psi_a(2)\, \psi_b(1)][\alpha(1)\, \beta(2) + \beta(1)\, \alpha(2)]$$

When VBT is applied to polyatomics, each canonical structure is formed by pairing all the available electrons. Thus, each canonical structure corresponds to a possible Lewis structure of the molecule, and each has its characteristic energy. Consider, for instance, CO_2 molecule which is a resonance hybrid of three canonical structures :

$$\underset{\text{I}}{O{=}C{=}O} \quad \longleftrightarrow \quad \underset{\text{II}}{\overset{+}{O} \equiv C - \overset{-}{O}} \quad \longleftrightarrow \quad \underset{\text{III}}{\overset{-}{O} - C \equiv \overset{+}{O}}$$

The wave function of CO_2 can be written as a linear combination of the wave functions corresponding to the three structures :

$$\psi = c_I \psi_I + c_{II} \psi_{II} + c_{III} \psi_{III} \qquad ...(30)$$

Since ionic structures II and III are equivalent, $c_{II} = c_{III}$, so that

$$\psi = c_I \psi_I + c_{II}(\psi_{II} + \psi_{III}) \qquad ...(31)$$

Again, consider C_6H_6 which is a resonance hybrid of two Kekule structures (I and II) and three 'long bond' structures, the so-called Dewar structures (III, IV and V) :

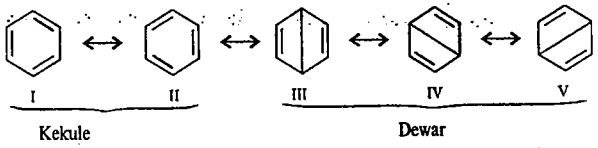

The corresponding valence bond wave function is

$$\psi = c_I \psi_I + c_{II} \psi_{II} + c_{III} \psi_{III} + c_{IV} \psi_{IV} + c_V \psi_V \qquad ...(32)$$

Since the two Kekule structures and the three Dewar structures are equivalent, their coefficients must be the same, *i.e.*,

$$c_I = c_{II} = c_1 \text{ (say)}$$

$$c_{III} = c_{IV} = c_V = c_2 \text{ (say)}$$

Hence, $$\psi = c(\psi_I + \psi_{II}) + c_2(\psi_{III} + \psi_{IV} + \psi_V) \qquad ...(33)$$

The number of canonical structures to be included in the wave function increases dramatically with increase in the number of atoms in the molecule. Thus, for naphthalene and anthracene the number of canonical structures are 42 and 429, respectively and for coronene the number is more than 10^5. Naturally the theorist feels rather uneasy with VBT for the solution of the Schrödinger wave equation for even a moderately large molecule.

American chemical physicists Linus Pauling (1901–1994) and Robert S.Mulliken (1896–1986) are the pioneers of VBT and MOT, respectively. Pauling's work cuts across the frontiers of chemistry, physics and molecular biology. He is the only scientist who has won two Nobel prizes : for chemistry (1954) and for peace (1963); both prizes were *unshared.* He is generally considered to be the greatest 20th century chemist. However, Mulliken's MOT is, as said above, conceptually simpler than Pauling's VBT; but *we need both the theories.* In the words of the eminent inorganic chemist J.E. Huheey, "the chemist who does not become thoroughly familiar with both the theories is like the carpenter who refuses to carry a saw because he already has a hammer ! Both are severely limiting their skills by limiting their tools."

HYBRIDIZATION

Beryllium, boron and carbon (Atomic Nos. 4, 5 and 6) furnish interesting cases of compound formation. According to the ground state electronic configurations of the atoms of these elements, Be ($1s^2 2s^2$), with *no* half-filled orbital, should be *zero-valent* ; B($1s^2 2s^2 2p_z^1$), with *one* half-filled orbital, should be *monovalent* and C ($1s^2 2s^2 p_z^1 p_x^1$), with *two* half-filled orbitals should be *bivalent*. But actually, Be is bivalent, B is trivalent and C is tetravalent. In order to explain these anomalies, Pauling introduced the concept called **hybridization.** This concept is extremely helpful. We shall elucidate this concept by referring to the formation of beryllium fluoride.

For Be atom the promotion of a $2s$ electron to a $2p$ orbital results in an excited state configuration of Be, *viz.*, $1s^2 2s^1 p^1$ which has two half-filled orbitals. Thus, Be atom in its excited state is capable of showing a covalency of 2. The energy required for the promotion of $2s$ electrons is the energy that is released when Be atom and, say, F atoms combine to form BeF_2 molecule. If the energy supplied to Be atom for the promotion of the electron from $2s$ to $2p$ orbital is less than the energy released due to the formation of the two covalent bonds in BeF_2, the formation of BeF_2 would be energetically feasible.

This offers a plausible explanation for the existence of stable compounds of beryllium such as BeF_2, BeH_2, etc.

Since 2*s* and 2*p* orbitals have different energies, hence the two bonds in BeF_2 should have different strengths. This is because one Be—F bond will be formed by the overlapping of 2*s* orbital of beryllium and 2*p* orbital of fluorine while the second Be—F bond will be formed by the overlapping of 2*p* orbital of beryllium and 2*p* orbital of fluorine. But, actually both the bonds are of equal strength. This is explained by postulating that the *s* and *p* orbitals of beryllium mix, *i.e.*, hybridise to give two identical orbitals, *i.e.*, orbitals of equivalent energy. The redistribution of energy by mixing different orbitals of an atom to give new orbitals of equivalent energy is called hybridization. The new orbitals thus formed are called hybrid orbitals. The bonds formed by such orbitals are called hybrid bonds. Since in the formation of bivalent compounds of beryllium, one *s* and one *p* orbital is involved in hybridisation, it is called *sp hybridization* and the two identical orbitals which result from this process are known as *sp* hybrid orbitals.

The amount of energy released $(B.E.)_1$ due to the formation of sigma bonds between Be and X atoms involving hybrid orbitals is greater than the energy released $(B.E.)_2$ in case the sigma bonds had involved the pure *s* and *p* orbitals. This is illustrated in Fig. 9. It is evident from Fig. 9 that some additional energy is released due to the involvement of the *sp* hybrid orbitals in bond formation. Because of this additional decrease of energy, the sigma bonds formed by hybrid orbitals of Be are stronger than the bonds formed by pure *s* and *p* orbitals.

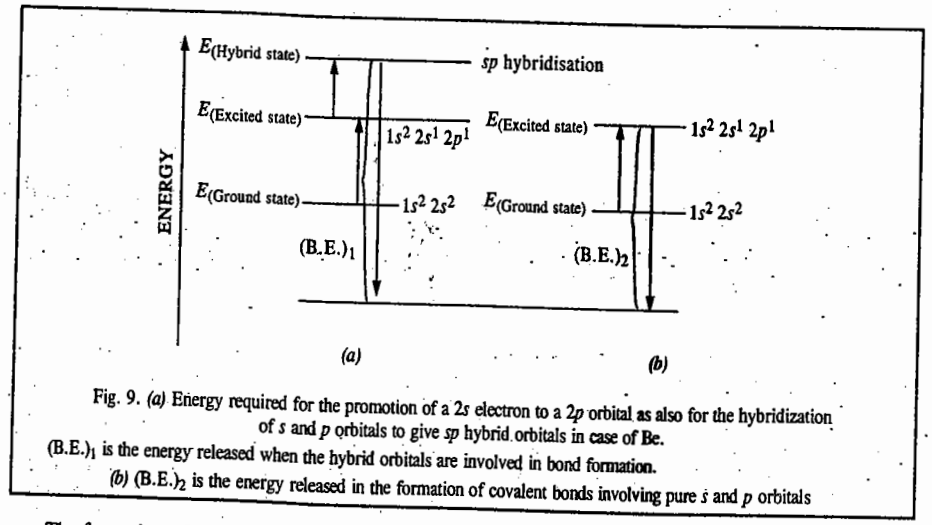

Fig. 9. *(a)* Energy required for the promotion of a 2*s* electron to a 2*p* orbital as also for the hybridization of *s* and *p* orbitals to give *sp* hybrid orbitals in case of Be.
$(B.E.)_1$ is the energy released when the hybrid orbitals are involved in bond formation.
(b) $(B.E.)_2$ is the energy released in the formation of covalent bonds involving pure *s* and *p* orbitals

The formation of *sp* hybrid orbitals is shown pictorially in Fig. 10.

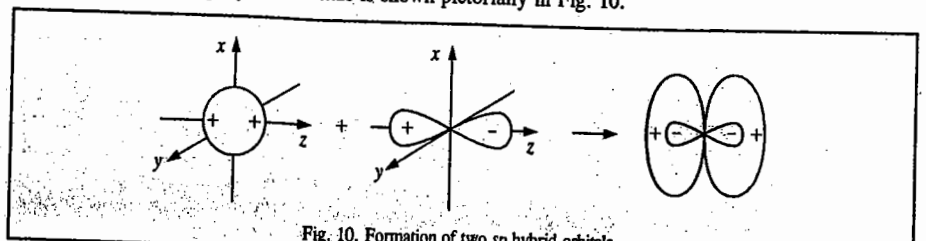

Fig. 10. Formation of two *sp* hybrid orbitals.

In the formation of BeF_2, the half-filled *p* orbital of each fluorine atom overlaps with each of the two half-filled *sp* hybrid orbitals of Be atom. We next consider the sp^2 hybridization.

In the case of boron (ground state configuration $1s^2 2s^2 p^1$), for instance, the promotion of one of the 2*s* electrons into one of the vacant 2*p* orbitals gives rise to an excited state configuration, *viz.*, $1s^2 2s^1 p_z^1 p_x^1$. There are, thus, three half-filled orbitals which account for tri-covalency of boron. The three orbitals, *viz.*, one 2*s* and two 2*p*, hybridise to give three sp^2 hybrid orbitals of equivalent energy. The formation of three sp^2 hybrid orbitals is shown in Fig. 11.

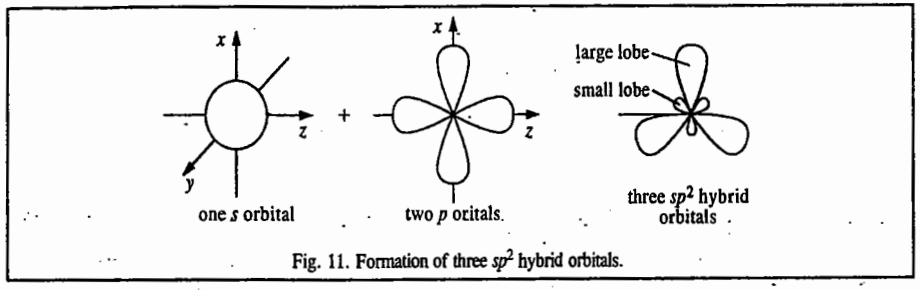

Fig. 11. Formation of three sp^2 hybrid orbitals.

In the formation of boron trifluoride, BF_3, molecule, the half-filled *p* orbital of each fluorine atom overlaps with each of the three half-filled sp^2 hybrid orbitals of the boron atom.

In the case of carbon (ground state configuration $1s^2 2s^2 p_z^1 p_x^1$), the promotion of one of the 2*s* electrons into the vacant $2p_y$ orbital yields an excited state configuration, *viz.*, $1s^2\ 2s^1 p_z^1 p_x^1 p_y^1$. There are now four half-filled orbitals which account for the tetracovalency of carbon. These four orbitals, *i.e.*, one *s* and three *p* orbitals hybridise to give four sp^3 hybrid orbitals of equivalent energy. The formation of four sp^3 hybrid orbitals is shown in Fig. 12.

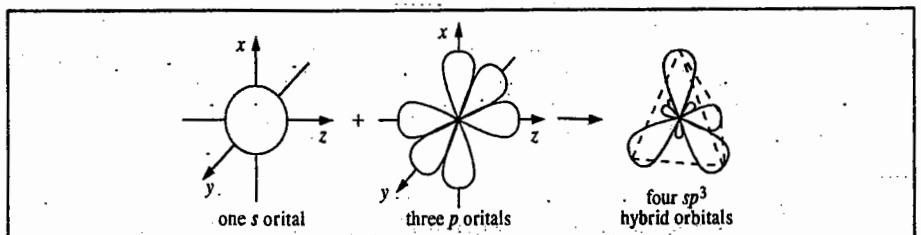

Fig. 12. Formation of four sp^3 hybrid orbitals by overlapping of one *s* and three *p* orbitals.

In the formation of methane, CH_4, molecule, the half-filled 1*s* orbital of each hydrogen atom overlaps with each of the four half-filled sp^3 hybrid orbitals of the carbon atom. Similarly, we can explain the sp^3d hybridisation in PCl_5 and sp^3d^2 hybridization in SF_6.

The salient features of hybridization may be summed up as follows :

1. One of the electrons from an orbital in the ground state configuration of the atom gets promoted to the next available orbital of higher energy (as, for example, from 2*s* to 2*p* orbital in case of second row elements and from n(*s*) to (n–1)*d* orbital in case of transition elements), resulting in an excited state configuration with appropriate number of half-filled orbitals. This process would require sufficient amount of energy. The orbitals in the excited state undergo hybridization giving hybrid orbitals of equivalent energy. The process of hybridization, *i.e.*, mixing of orbitals, requires some additional amount of energy. The entire input of energy is, however, more than recovered when the hybrid orbitals undergo covalent bond formation with other atoms accompanied by the release of energy.

2. The number of hybrid orbitals formed is equal to the number of pure atomic orbitals which undergo hybridisation.

3. The energy released during sigma bond formation involving hybrid orbitals is much more than the energy released if sigma bond formation involves pure atomic orbitals. Therefore, the sigma bonds formed with hybrid orbitals are more stable than those formed with pure orbitals.

4. Hybridization invariably involves atomic orbitals of the same atom.

5. Effective hybridization occurs only when the orbitals undergoing hybridisation are of similar energy.

6. The electronic charge in hybrid orbitals is concentrated more in one direction. This leads to a better overlap with orbitals of the other atoms.

7. Hybrid orbitals generally form either sigma bonds or contain lone pairs of electrons. They do not form pi bonds.

8. The hybrid orbitals are associated with higher energy than the parent pure orbitals. The stability of bonds formed by the hybrid orbitals is due to excessive overlapping of orbitals provided by them.

Calculation of the Coefficients of AOs used in Hybridization

The wavefunctions for the hybrid orbitals are obtained by taking linear combination of the angular wave functions of the appropriate AOs. Many organic molecules involve hybrid orbitals which are formed from the linear combination of s and p AOs. The wave function for the ith hybrid orbital formed from the s and p AOs is given by

$$\phi_i = a_i s + b_i p_x + c_i p_y + d_i p_z \qquad \ldots(34)$$

The coefficients a_i, b_i, c_i, d_i can be determined from the following rules :

1. Each wavefunction is normalized, *i.e.*,

$$a_i^2 + b_i^2 + c_i^2 + d_i^2 = 1 \qquad \ldots(35)$$

2. Each hybrid orbital in the set of hybrid orbitals must be orthogonal to the other hybrids, *i.e.*,

$$a_i a_j + b_i b_j + c_i c_j + d_i d_j = 0 \qquad \ldots(36)$$

3. The squares of the coefficients of any component atomic function summed over all the hybrids in which it participates must be equal to unity, *i.e.*,

$$\sum_i a_i^2 = 1 \qquad \ldots(37)$$

With the help of the above rules the following procedure is employed to generate the equivalent hybrid orbitals:

1. Choose a cartesian coordinate system and place one of the ith hybrid orbitals along one of the coordinate axes and as many of the other orbitals as possible in the plane containing this axis and other coordinate axes.

2. Since the s orbital has a spherical symmetry, each equivalent hybrid orbital of a set contains $1/n$ of the total of the unit s orbital distributed in n hybrid orbitals. Hence, the coefficient in each hybrid orbital is $1/\sqrt{n}$.

Example 33. Construct the wavefunctions for the sp hybrid orbitals.

Solution : We shall take the example of BeH_2. The two sp hybrid orbitals are :

$$\psi_{sp(1)} = a_1 2s + b_1 2p_x \qquad \ldots(i)$$

$$\psi_{sp(2)} = a_2 2s + b_2 2p_x \qquad \ldots(ii)$$

Since the s orbital is equally distributed between the two hybrid orbitals, hence,

$$a_1^2 = a_2^2 = 1/2$$

$$\therefore \quad a_1 = a_2 = 1/\sqrt{2}$$

Since $\psi_{sp(1)}$ is normalized, hence

$$\int \psi_{sp(1)}^2 d\tau = \int (a_1 2s + b_1 2p_x)^2 d\tau$$

$$= a_1^2 \int (2s)^2 d\tau + b_1^2 \int (2p_x)^2 d\tau + 2a_1 b_1 \int (2s)(2p_x) d\tau = 1$$

Since the AOs are individually normalized and orthogonal, hence

$$\int \psi_{sp(1)}^2 d\tau = a_1^2(1) + b_1^2(1) + 2a_1 b_1(0) = a_1^2 + b_1^2 = 1$$

Since $a_1 = 1/\sqrt{2}$, hence $b_1 = 1/\sqrt{2}$

Again, since $\psi_{sp(1)}$ and $\psi_{sp(2)}$ are orthogonal, we have

$$a_1 a_2 + b_1 b_2 = 0$$

Substituting for a_1, a_2 and b_1, we have

$(1/\sqrt{2})(1/\sqrt{2}) + (1/\sqrt{2}) b_2 = 0$, whence

$$b_2 = -1/\sqrt{2}$$

Hence, the two hybrid orbital wavefunctions are

$$\psi_{sp(1)} = 1/\sqrt{2}\,(2s + 2p_x) \qquad \ldots(iii)$$

$$\psi_{sp(2)} = 1/\sqrt{2}\,(2s - 2p_x) \qquad \ldots(iv)$$

Example 34. Construct the wavefunctions for the sp^2 hybrid orbitals.

Solution : We shall take the example of BH_3. The wavefunctions for the three sp^2 hybrid orbitals are :

$$\psi_{sp^2(1)} = a_1 2s + b_1 2p_x + c_1 2p_y \qquad \ldots(i)$$

$$\psi_{sp^2(2)} = a_2 2s + b_2 2p_x + c_2 2p_y \qquad \ldots(ii)$$

$$\psi_{sp^2(3)} = a_3 2s + b_3 2p_x + c_3 2p_y \qquad \ldots(iii)$$

Since the s orbital is equally distributed among the three hybrid orbitals, we have

$a_1^2 = a_2^2 = a_3^2 = 1$ so that

$$a_1 = a_2 = a_3 = 1/\sqrt{3}$$

Assume that $\psi_{sp^2(1)}$ points towards the x-axis. Hence, this hybrid orbital will have contribution from $2s$ and $2p_x$ orbitals only. The contribution of the $2p_y$ orbital will be zero so that $c_1 = 0$.

Since $\psi_{sp^2(1)}$ is normalized,

$$a_1^2 + b_1^2 + c_1^2 = 1 \quad \text{or} \quad a_1^2 + b_1^2 = 1$$

Since $a_1 = 1/\sqrt{3}$, hence $b_1 = \sqrt{(2/3)}$

Since $\psi_{sp^2(1)}$ and $\psi_{sp^2(2)}$ are orthogonal (as also are $\psi_{sp^2(1)}$ and $\psi_{sp^2(3)}$), hence

$$a_1 a_2 + b_1 b_2 = 0$$

$$a_1 a_3 + b_1 b_3 = 0$$

Hence

$$b_2 = -\frac{a_1 a_2}{b_1} = -\frac{\left(\frac{1}{\sqrt{3}} \cdot \frac{1}{\sqrt{3}}\right)}{\sqrt{\frac{2}{3}}} = -\frac{1}{\sqrt{6}}$$

$$b_3 = -\frac{a_1 a_3}{b_1} = -\frac{\left(\frac{1}{\sqrt{3}} \cdot \frac{1}{\sqrt{3}}\right)}{\sqrt{\frac{2}{3}}} = -\frac{1}{\sqrt{6}}$$

Again, since $\psi_{sp^2}(2)$ is normalized,

$$a_2^2 + b_2^2 + c_2^2 = 1$$

Hence, $$c_2^2 = 1 - (a_2^2 + b_2^2) = 1 - (1/3 + 1/6) = 1/2$$

Thus, $$c_2 = \pm 1/\sqrt{2}$$

Further, since $\psi_{sp^2(3)}$ is normalized,

$$a_3^2 + b_3^2 + c_3^2 = 1$$

Hence, $$c_3^2 = 1 - (a_3^2 + b_3^2) = 1 - (1/3 + 1/6) = 1/2$$

Thus, $$c_3 = \pm 1/\sqrt{2}$$

Let c_2 have a positive value ; then, the value for c_3 will have to be negative, so that $\psi_{sp^2(2)}$ and $\psi_{sp^2(3)}$ fulfil the requirement of orthogonality, *i.e.*, $a_2a_3 + b_2b_3 + c_2c_3 = 0$. Thus,

if $$c_2 = +1/\sqrt{2} \text{ and } c_3 = -1/\sqrt{2}$$

Hence, the three sp^2 hybrid orbital wavefunctions are :

$$\psi_{sp^2(1)} = \left(1/\sqrt{3}\right) 2s + \left(\sqrt{2/3}\right) 2p_x \quad \ldots(iv)$$

$$\psi_{sp^2(2)} = \left(1/\sqrt{3}\right) 2s - \left(1/\sqrt{6}\right) 2p_x + \left(1/\sqrt{2}\right) 2p_y \quad \ldots(v)$$

$$\psi_{sp^3(3)} = \left(1/\sqrt{3}\right) 2s - \left(1/\sqrt{6}\right) 2p_x - \left(1/\sqrt{2}\right) 2p_y \quad \ldots(vi)$$

Example 35. Construct the wavefunctions for the sp^3 hybrid orbitals.

Solution : We shall consider the case of the hybrid orbitals of CH_4. The wave functions for the four sp^3 hybrid orbitals are :

$$\psi_{sp^3(1)} = a_1 2s + b_1 2p_x + c_1 2p_y + d_1 2p_z \quad \ldots(i)$$

$$\psi_{sp^3(2)} = a_2 2s + b_2 2p_x + c_2 2p_y + d_2 2p_z \quad \ldots(ii)$$

$$\psi_{sp^3(3)} = a_3 2s + b_3 2p_x + c_3 2p_y + d_3 2p_z \quad \ldots(iii)$$

$$\psi_{sp^3(4)} = a_4 2s + b_4 2p_x + c_4 2p_y + d_4 2p_z \quad \ldots(iv)$$

Since the s orbital is equally distributed among the four hybrid orbitals, we have

$$a_1^2 = a_2^2 = a_3^2 = a_4^2 = 1/4$$

Hence, $$a_1 = a_2 = a_3 = a_4 = 1/\sqrt{4} = 1/2$$

Assuming that $\psi_{sp^3(1)}$ is developed along the x-axis, this hybrid will have contributions from $2s$ and $2p_x$ orbitals only so that the contributions of $2p_y$ and $2p_z$ orbitals will vanish, with the result that

$$c_1 = d_1 = 0$$

Since $\psi_{sp^3(1)}$ is normalized, hence,

$$a_1^2 + b_1^2 + c_1^2 + d_1^2 = 1$$

or $$a_1^2 + b_1^2 = 1 \qquad (\because c_1 = d_1 = 0)$$

Hence, $$b = \sqrt{1 - a_1^2} = \sqrt{1 - 1/4} = \sqrt{3}/2$$

The orthogonality conditions for $\psi_{sp^3(1)}$ and $\psi_{sp^3(2)}$, $\psi_{sp^3(1)}$ and $\psi_{sp^3(3)}$ and $\psi_{sp^3(1)}$ and $\psi_{sp^3(4)}$ are

$$a_1a_2 + b_1b_2 = 0$$

$$a_1a_3 + b_1b_3 = 0$$

$$a_1a_4 + b_1b_4 = 0$$

Hence, $$b_2 = b_3 = b_4 = -a_1a_2/b_1 = -a_1a_3/b_1 = -a_1a_4/b_1$$

$$= -\frac{(1/2)(1/2)}{\sqrt{3}/2} = -\frac{1}{2\sqrt{3}}$$

Assuming that $\psi_{sp^3(2)}$ lies in the xz-plane, the hybrid orbital will have contributions from $2s$, $2p_x$ and $2p_z$ orbitals and the contribution of $2p_y$ to $\psi_{sp^3(2)}$ will vanish, so that

$$c_2 = 0$$

The normalization condition for $\psi_{sp^3(2)}$ gives

$$a_2^2 + b_2^2 + c_2^2 + d_2^2 = 1$$

or, $$a_2^2 + b_2^2 + d_2^2 = 1 \quad (\because c_2 = 0)$$

Hence, $$d_2^2 = 1 - (a_2^2 + b_2^2) = 1 - (1/4 + 1/12) = 2/3$$

Thus, $$d_2 = \sqrt{2/3}$$

The requirement of orthogonality conditions for $\psi_{sp^3(2)}$ and $\psi_{sp^3(3)}$, and for $\psi_{sp^3(2)}$ and $\psi_{sp^3(4)}$ gives

$$a_2a_3 + b_2b_3 + d_2d_3 = 0$$

$$a_2a_4 + b_2b_4 + d_2d_4 = 0$$

Hence, $$d_3 = d_4 = -(a_2a_3 + b_2b_3)/d_2$$

or, $$-\frac{a_2a_4 + b_2b_4}{d_2} = -\frac{(1/4 + 1/12)}{\sqrt{2/3}} = -\frac{1}{\sqrt{6}}$$

The normalization requirement for $\psi_{sp^3(3)}$ gives

$$a_3^2 + b_3^2 + c_3^2 + d_3^2 = 1$$

$$c_3^2 = 1 - (a_3^2 + b_3^2 + d_3^2)$$

$$= 1 - \left(\frac{1}{4} + \frac{1}{12} + \frac{1}{6}\right) = \frac{1}{2}$$

$$\therefore \quad c_3 = 1/\sqrt{2}$$

Proceeding in this way, the normalization requirement for $\psi_{sp^3(4)}$ and the orthogonality condition between $\psi_{sp^3(3)}$ and $\psi_{sp^3(4)}$ gives

$$c_4 = -1/\sqrt{2}$$

Hence, the four sp^3 hybrid wave functions are

$$\psi_{sp^3(1)} = (1/2)2s + \left(\sqrt{3}/2\right)2p \quad \ldots(v)$$

$$\psi_{sp^3(2)} = (1/2)2s - (1/2)2p_x + \left(\sqrt{2/3}\right)2p_z \quad \ldots(vi)$$

$$\psi_{sp^3(3)} = (1/2)2s - \left(1/2\sqrt{3}\right)2p_x + \left(1/\sqrt{2}\right)2p_y - \left(1/\sqrt{6}\right)2p_z \quad \ldots(vii)$$

$$\psi_{sp^3(4)} = (1/2)2s - \left(1/2\sqrt{3}\right)2p_x + \left(1/\sqrt{2}\right)2p_y - \left(1/\sqrt{6}\right)2p_z \quad \ldots(viii)$$

Conjugated Molecules

The linear conjugated dienes and polyenes can be treated quantum mechanically by the so-called **free-electron molecular orbital (FEMO) theory.** It is assumed that the p electrons which form pi bonds in compounds such as 1,3-butadiene and 1,3, hexatriene

$CH_2=CH-CH=CH_2$ (1,3-butadiene) $\qquad$ $CH_2=CH-CH=CH-CH=CH_2$ (1,3-hexatriene)

move freely in a constant potential along the molecular skeleton. This treatment is, then, analogous to the motion of a particle in a one-dimensional box of infinite height for which the energy levels are given by

$$E_n = n^2h^2/8m_ea^2\ ;\ n = 1, 2, 3,..... \qquad ...(38)$$

In Eq. 38, a is the length of the linear conjugated chain, m_e is the mass of the electron. The electrons in the pi MOs are filled in accordance with the Pauli exclusion principle and Hund's rules. If N is the number of π orbitals (formed from the overlap of Np atomic orbitals) then only $N/2\pi$ orbitals are filled in the ground state since each orbital can accommodate two electrons with spins paired. The longest wave length transition involves the HOMO → LUMO transition, *i.e.*, excitation of the electron from the $N/2$ highest occupied molecular orbital (HOMO) to the $(N/2)+1$ (lowest unoccupied molecular orbital LUMO). Thus, for the HOMO → LUMO transition,

$$\Delta E = E_2 - E_1 \equiv E_{(N/2)+1} - E_{N/2} = h\nu \qquad ...(39)$$

so that the excitation frequency is given by

$$\nu = \Delta E/h$$

$$= \frac{h}{8m_ea^2}\left[(N/2+1)^2 - (N/2)^2\right] = \frac{(N+1)h}{8m_ea^2} \qquad ...(40)$$

Since $\nu = c/\lambda = \bar{\nu}$ (where $\bar{\nu} = 1/\lambda$), hence,

$$\bar{\nu} = \frac{(N+1)h}{8m_ea^2c} \qquad ...(41)$$

Before we can use Eq. 41, we must estimate a, the length of the conjugated chain. This quantity is generally considered as equal to the number of actual bonds between N carbon atoms $+2$. If l is the length of the C—C bond in a delocalized conjugated system, then

$$a = (N-1+2)\,l = (N+1)\,l \qquad ...(42)$$

where l=139 pm. In arriving at Eq. 42, we assume that the π MO can extend one bond length beyond the end carbon atom. Substituting for a in Eq. 41, we have

$$\bar{\nu} = \frac{(N+1)h}{8m_ec(N+1)^2l^2} = \frac{h}{8m_ec(N+1)l^2} \qquad ...(43)$$

Using the values of h, m_e, c and l, we obtain for the HOMO ⟶ LUMO transition,

$$\bar{\nu} = 148{,}137\cdot6/(N+1)\ \text{cm}^{-1} \qquad ...(44)$$

Better agreement with experiment is obtained if the π electrons are assumed to move along the skeletal frame work in a sinusoidal potential with a minimum at the centre of each double bond. In that case, Eq. 44 is modified to

$$\bar{\nu} = \frac{153{,}000\,\text{cm}^{-1}}{N+1} + (16{,}000\,\text{cm}^{-1})\left(1-\frac{1}{N}\right) \qquad ...(45)$$

Example 36. Using the FEMO theory, calculate the frequency (in cm^{-1}) of the HOMO ⟶ LUMO transition in 1, 3, 5-hexatriene molecule. The observed frequency is 37,313·4 cm^{-1}.

Solution : In 1,3,5-hexatriene, $CH_2=CH-CH=CH-CH=CH_2$, $N = 6$ so that, using Eq. 40,

$$\bar{\nu} = \frac{148{,}137\cdot6}{N+1}\ \text{cm}^{-1} = 21{,}162\cdot5\ \text{cm}^{-1}.$$

The agreement with the observed frequency is very poor. However, if we use the modified Eq. 41, then,

$$\bar{\nu} = \frac{153{,}000\ \text{cm}^{-1}}{7} + (16{,}000\ \text{cm}^{-1})(1-1/6) = \mathbf{34{,}495\cdot3\ cm^{-1}}$$

We see that the agreement with the observed value is now satisfactory.

Hückel Molecular Orbital (HMO) Theory of Conjugated Systems

The conjugated linear polyenes such as 1,3-butadiene and 1,3,5-hexatriene and cyclic polyenes such as benzene, naphthalene, etc., were investigated by E. Hückel in 1931. His treatment was extended by C. Coulson, H.C. Longuet-Higgins and R. Hoffmann. In a conjugated unsaturated hydrocarbon with alternate single and double bonds, the molecule is generally planar. In an n-carbon system, each carbon atom is sp^2 hybridized and has a $2p_z$ orbital centred on it. The electrons in the sp^2 hybrid orbitals, called the σ electrons, are contained in the molecular plane. Each $2p_z$ orbital which is perpendicular to the molecular plane contains one π electron. According to the LCAO-MO approximation, the molecular orbital is written as

$$\psi_i = \sum_{j=1}^{n} c_{ij}\,\phi_j \quad (i = 1, 2, 3,.....n) \qquad ...(46)$$

where ϕ_j is the $2p_z$ orbital centered on carbon atom j. The ϕs are called the *basis set*. The n π MOs are formed by the overlap of n $2p_z$ AOs. The HMO theory is similar to the MOT of homonuclear diatomics. In the HMO theory the basis functions are $2p_z$ AOs whereas in the case of H_2 the basis functions are the $1s$ AOs. Proceeding as before, we obtain the secular equation (12). Hückel made the following asumptions about the three kinds of integrals, Coulomb integral, exchange (resonance) integral and overlap integral, to simplify this secular equation :

1. All overlap integrals are zero, *i.e.*, $S_{ij} = 0$.
2. Coulomb integral H_{ii}, which refers to the energy of an electron in the $2p_z$ orbital on the ith carbon atom, is denoted by the symbol α.
3. The exchange integrals $H_{ij}=H_{ji}=0$ unless the ith and jth orbitals are on adjacent carbon atoms in which case they are designated as β.

The neglect of the overlap integrals on adjacent carbon atoms in a conjugated molecule is the severest assumption of the HMO theory and is not really justified. However, despite this assumption this theory gives a good description of bonding and qualitative agreement between theory and experiment.

The Hückel secular equation can now be written as

$$\begin{vmatrix} \alpha-E & \beta & 0 & 0 & .... & 0 & .... \\ \beta & \alpha-E & \beta & 0 & .... & 0 & .... \\ 0 & \beta & \alpha-E & \beta & .... & 0 & .... \\ 0 & 0 & \beta & \alpha-E & & \beta & .... \\ .... & .... & .... & .... & .... & .... & .... \\ .... & .... & .... & .... & .... & .... & .... \\ .... & .... & .... & .... & .... & .... & .... \end{vmatrix} = 0 \qquad ...(47)$$

Defining a dimensionless parameter x as $x = (\alpha - E)/\beta$, Eq. 47 becomes :

$$\begin{vmatrix} x & 1 & 0 & 0 & .... & 0 & .... \\ 1 & x & 1 & 0 & .... & 0 & .... \\ 0 & 1 & x & 1 & .... & 0 & .... \\ 0 & 0 & 1 & x & & 1 & .... \\ .... & .... & .... & .... & .... & .... & .... \\ .... & .... & .... & .... & .... & .... & .... \\ .... & .... & .... & .... & .... & .... & .... \end{vmatrix} = 0 \qquad ...(48)$$

Expansion of this $n \times n$ determinant yields a polynomial equation which has n real roots ; thus, the conjugated polymer has n energy levels and n MOs. The energy of the kth MO is given by

$$E_k = \alpha + x_k \beta \qquad ...(49)$$

where x_k is the kth root of the polynomial. Since the Coulomb integral α and the resonance integral β are both negative, a positive value of x_k represents an energy level which is more negative and, hence, more stable than the energy of an electron in a carbon $2p_z$ orbital. This energy level is called a BMO. Similarly, a negative value of x_k corresponds to an ABMO.

We shall now briefly consider the application of HMO theory to ethylene, 1,3–butadiene and benzene. The application to ethylene, though a good starting point, is not of much interest since it is not a conjugated system.

Ethylene. (Fig. 13). The Hückel secular equation is

$$\begin{vmatrix} x & 1 \\ 1 & x \end{vmatrix} = 0; \quad (\text{where } x = (\alpha - E)/\beta) \qquad ...(50)$$

which, upon expansion, gives

$$x^2 - 1 = 0, \quad \text{or} \quad x = \pm 1$$

For $x = -1$, $E_1 = \alpha + \beta$ (BMO) ...(51)

For $x = +1$, $E_2 = \alpha - \beta$ (ABMO) ...(52)

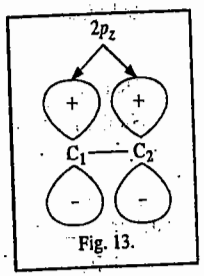

Fig. 13.

The two π electrons of ethylene occupy the BMO (Fig. 14) in the ground state in accordance with the Pauli exclusion principle.

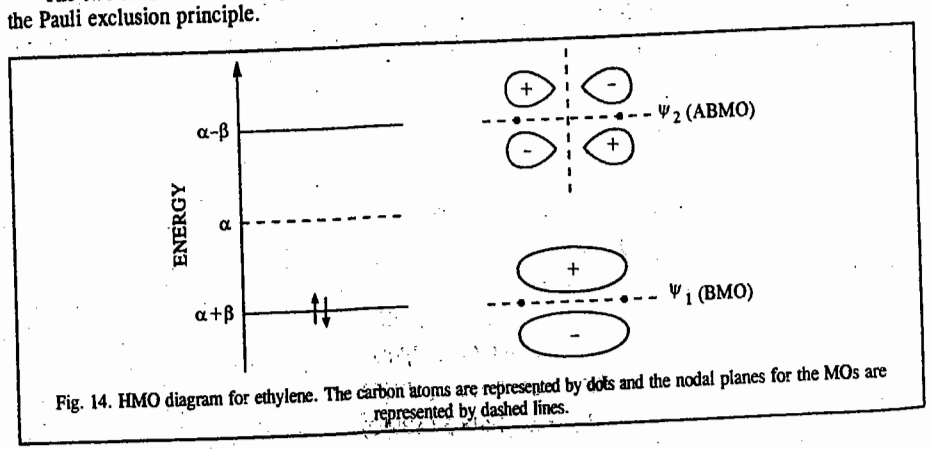

Fig. 14. HMO diagram for ethylene. The carbon atoms are represented by dots and the nodal planes for the MOs are represented by dashed lines.

The total π–electron energy, E_π, is equal to $2(\alpha + \beta)$. Since the energy of the two electrons in the isolated carbon $2p_z$ orbital is equal to 2α, the π–bond energy in ethylene is equal to $[2(\alpha + \beta) - 2\alpha]$, *i.e.*, 2β.

To determine the BMO ψ_1 and the ABMO ψ_2, we proceed as follows : The secular equation corresponds to the two simulataneous linear equations

$$c_1 x + c_2 = 0 \text{ and } c_1 + c_2 x = 0 \qquad ...(53)$$

For the BMO ψ_1, $x = -1$ so that substitution gives

$$-c_1 + c_2 = 0 \text{ and } c_1 - c_2 = 0, \textit{ i.e.}, c_1 = c_2 \text{ (in each case).}$$

Since ψ_1 must be normalized, *i.e.*, $\int \psi_1 \psi_1 \, d\tau = 1$, we have

$$\int (c_1\phi_1 + c_2\phi_2)(c_1\phi_1 + c_2\phi_2) d\tau = 1 \qquad ...(54)$$

or $c_1^2 \int \phi_1\phi_1 \, d\tau + c_2^2 \int \phi_2\phi_2 \, d\tau + 2c_1c_2 \int \phi_1\phi_2 \, d\tau = 1 \qquad ...(55)$

Again, ϕs form an orthonormal set, *i.e.*,

$$\int \phi_i \phi_j \, d\tau = \delta_{ij} = \begin{cases} 1, & i = j \\ 0, & i \neq 1 \end{cases} \qquad ...(56)$$

where δ_{ij} is called the Kronecker delta.

In the present case, it implies that

$$\int \phi_1\phi_1 \, d\tau = \int \phi_2\phi_2 \, d\tau = 1 \quad \text{and} \quad \int \phi_1\phi_2 \, d\tau = 0 \qquad ...(57)$$

Substitution in Eq. 55 gives

$$c_1^2 + c_2^2 = 1 \text{ or } c_1 = 1/\sqrt{2} \; (\because c_1 = c_2) \qquad ...(58)$$

Hence, $\psi_1 = (\phi_1 + \phi_2)/\sqrt{2}$ ...(59)

Similarly, for $x = 1$, proceeding as above, we can show that

$$\psi_2 = (\phi_1 - \phi_2)/\sqrt{2} \qquad ...(60)$$

Note that nodes (and the nodal planes) are the regions in which the probability of finding the π electrons is zero.

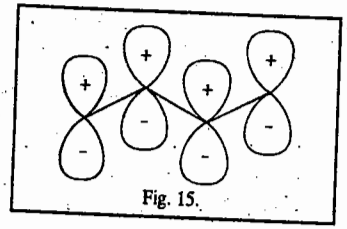

Fig. 15.

1, 3–Butadiene. This system consists of four carbon $2p_z$ orbitals and four π electrons. (Fig. 15) The Hückel secular equation is

$$\begin{vmatrix} x & 1 & 0 & 0 \\ 1 & x & 1 & 0 \\ 0 & 1 & x & 1 \\ 0 & 0 & 1 & x \end{vmatrix} = 0 \text{ (where } x = (\alpha - E)/\beta) \qquad ...(61)$$

which, upon expansion, gives the polynomial equation

$$x^4 - 3x^2 + 1 = 0$$

which has the roots $x = \pm 1{\cdot}618, \pm 0{\cdot}618$ ...(62)

We obtain the following four energy levels : ...(63)

$E_1 = \alpha + 1{\cdot}618\,\beta$ (BMO) ...(64)

$E_2 = \alpha + 0{\cdot}618\,\beta$ (BMO) ...(65)

$E_3 = \alpha - 0{\cdot}618\,\beta$ (ABMO) ...(66)

$E_4 = \alpha - 1{\cdot}618\,\beta$ (ABMO) ...(67)

The four π electrons of 1,3-butadiene occupy the two BMOs ψ_1 and ψ_2 (Fig. 16) in the ground state of the molecule in accodance with Pauli exclusion principle.

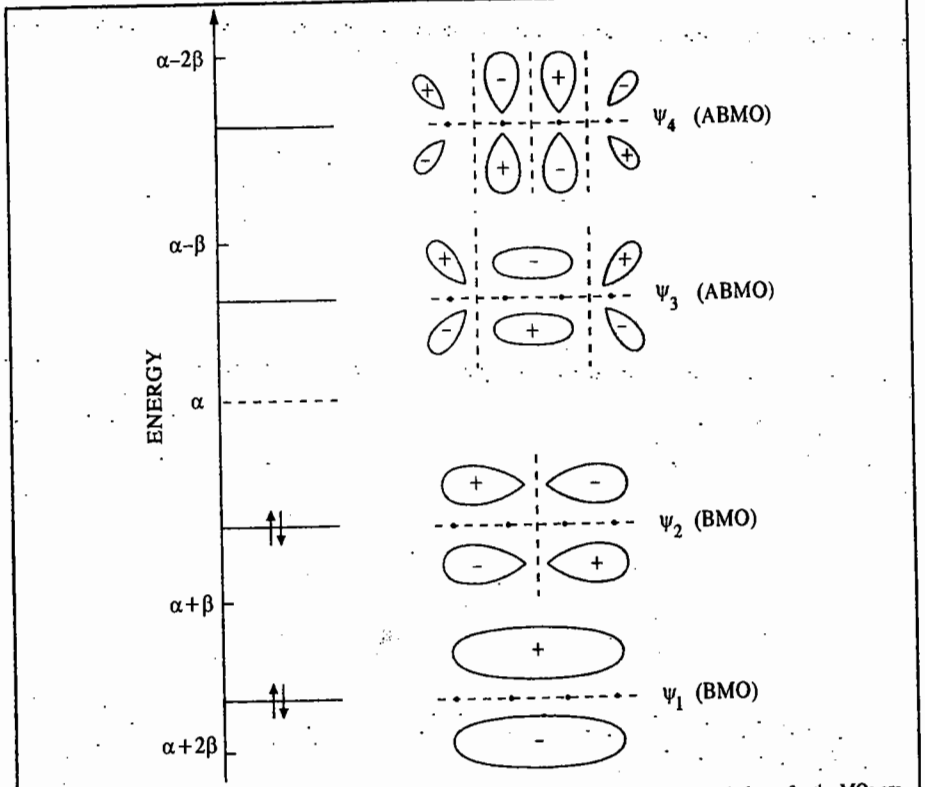

Fig. 16. HMO diagram for 1,3-butadiene. The carbon atoms are represented by dots and the nodal planes for the MOs are represented by dashed lines.

The four MOs (two BMOs and two ABMOs) can be obtained using a procedure employed in the case of ethylene molecule. It is found that

$$\psi_1 = 0{\cdot}3755\,(\phi_1 + \phi_4) + 0{\cdot}6070\,(\phi_2 + \phi_3) \quad ...(68)$$

$$\psi_2 = 0{\cdot}6070\,(\phi_1 - \phi_4) + 0{\cdot}3755\,(\phi_2 - \phi_3) \quad ...(69)$$

$$\psi_3 = 0{\cdot}6070\,(\phi_1 + \phi_4) - 0{\cdot}3755\,(\phi_2 + \phi_3) \quad ...(70)$$

$$\psi_4 = 0{\cdot}3755\,(\phi_1 - \phi_4) - 0{\cdot}6070\,(\phi_2 - \phi_3) \quad ...(71)$$

These HMOs are sketched in Fig. 16.

As remarked earlier, nodes (and nodal planes) are regions where the probability of finding the electrons is zero. Ground state has no node. The number of nodes in an MO increases with increase in energy. Thus, ψ_2 has one node, ψ_3 has two nodes and ψ_4 has three nodes.

The total π electron energy, E_π, is equal to $[2(\alpha+1{\cdot}618\,\beta) + 2\,(\alpha + 0{\cdot}618\,\beta)]$, *i.e.*, $4\alpha + 4{\cdot}472\,\beta$. As proved earlier, the energy of two π electrons in ethylene is $2(\alpha+\beta)$. The delocalization energy (*DE*), also called the resonance energy (RE), is defined as the difference in energy of π electrons in a molecule and sum of the energies of *isolated* double bonds present in the classical structure of the same

molecule. Thus, for 1,3-butadiene, DE (or RE) = $4\alpha+4{\cdot}472\,\beta - 2(2\alpha+2\beta) = 0{\cdot}472\,\beta$. Since DE is a measure of the stability of the molecule, hence 1,3-butadiene is more stable than two ethylene molecules by an energy of $0{\cdot}472\,\beta$.

Example 37. Set up the Hückel secular equation for cyclobutadiene, calculate the energies of the π orbitals and determine the DE (delocalization energy).

Solution : See Fig. 17.

The Hückel secular equation is

$$\begin{vmatrix} x & 1 & 0 & 1 \\ 1 & x & 1 & 0 \\ 0 & 1 & x & 1 \\ 1 & 0 & 1 & x \end{vmatrix} = 0, \text{ (where } x = (\alpha - E)/\beta) \quad ...(72)$$

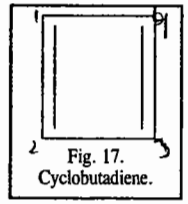

Fig. 17. Cyclobutadiene.

which upon expansion gives the polynomial equation

$$x^4 - 4x^2 = 0 \quad \text{or} \quad x = 0 \text{ (twice)} ; \pm 2 \quad ...(73)$$

Hence, the energy levels are

$$x = -2 \; : \; E = \alpha + 2\beta \text{ (BMO)} \quad ...(74)$$

$$x = 0 \; : \; E_2 = E_3 = \alpha \text{ (degenerate pair); (NBMO)} \quad ...(75a)$$

$$x = 2 \; : \; E_4 = \alpha - 2\beta \text{ (ABMO)} \quad ...(75b)$$

The molecular diagram for cyclobutadiene is shown in Fig. 18.

The four π electrons occupying the MOs, in accordance with the Pauli exclusion principle and Hund's rule, are shown in Fig. 18. Two π electrons occupy the lowest orbital (of energy $\alpha+2\beta$) and two occupy the doubly degenerate orbitals (of energy α); Thus, E_π is equal to $[2(\alpha+2\beta)+2\alpha)]$, *i.e.*, $4\alpha + 4\beta$. Hence, DE = $4\alpha+2\beta - 4(\alpha+\beta) = 0$. We see that HMO theory predicts that cyclobutadiene is unstable because its DE=0. Bayer's theory had earlier ascribed the instability of the four-membered cyclic ring to the tremendous ring strain. The Hückel theory gives a better explanation for this instability.

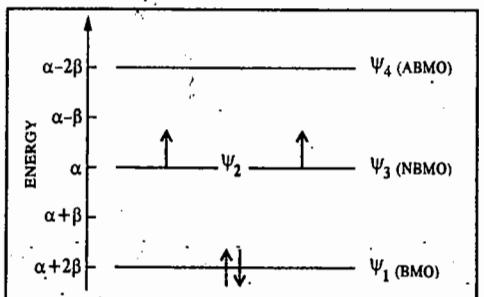

Fig. 18. HMO diagram for cyclobutadiene.

Benzene. (Fig. 19) The Hückel secular equation is

$$\begin{vmatrix} x & 1 & 0 & 0 & 0 & 1 \\ 1 & x & 1 & 0 & 0 & 0 \\ 0 & 1 & x & 1 & 0 & 0 \\ 0 & 0 & 1 & x & 1 & 0 \\ 0 & 0 & 0 & 1 & x & 1 \\ 1 & 0 & 0 & 0 & 1 & x \end{vmatrix} = 0 \text{ (where } x = (\alpha - E)/\beta) \quad ...(76)$$

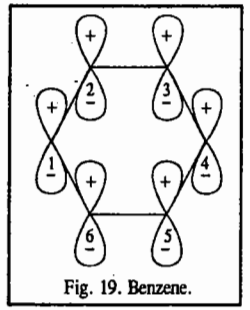

Fig. 19. Benzene.

which on expansion gives the polynomial equation

$$x^6 - 6x^4 + 9x^2 - 4 = 0 \quad ...(77)$$

with roots $x = -2 ; -1$ (twice) ; $+1$ (twice); 2 ...(78)

(These roots can be found by the inspection of the polynomial).

Hence, the energy levels are

$$x = -2 \;:\; E_1 = \alpha + 2\beta \qquad \text{(BMO)} \qquad ...(79)$$

$$x = -1 \;:\; E_2 = E_3 = \alpha + \beta \qquad \text{(degenerate pair, BMO)} \qquad ...(80)$$

$$x = +1 \;:\; E_4 = E_5 = \alpha - \beta \qquad \text{(degenerate pair, ABMO)} \qquad ...(81)$$

$$x = +2 \;:\; E_6 = \alpha - 2\beta \qquad \text{(ABMO)} \qquad ...(82)$$

The molecular diagram for benzene is shown in Fig. 20.

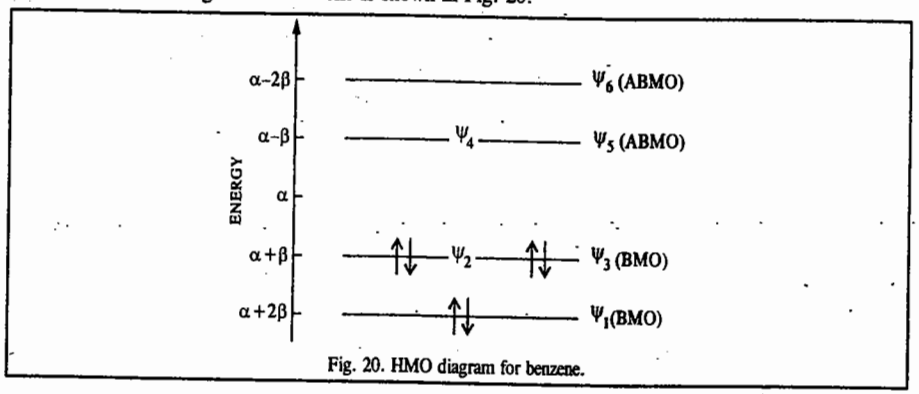

Fig. 20. HMO diagram for benzene.

The occupancy of the six π electrons in the three BMOs is shown in Fig. 20.

$$E_\pi = 2(\alpha + 2\beta) + 4(\alpha + \beta) = 6\alpha + 8\beta \qquad ...(83)$$

$$\text{DE} = 6\alpha + 8\beta - 6(\alpha + \beta) = -2\beta \qquad ...(84)$$

The six normalized HMOs are found to be

$$\psi_1 = \frac{1}{\sqrt{6}}(\phi_1 + \phi_2 + \phi_3 + \phi_4 + \phi_5 + \phi_6) \qquad ...(85)$$

$$\psi_2 = \frac{1}{2}(\phi_1 + \phi_2 - \phi_4 - \phi_5) \qquad ...(86)$$

$$\psi_3 = \frac{1}{\sqrt{12}}(\phi_1 - \phi_2 - 2\phi_3 - \phi_4 + \phi_5 + 2\phi_6) \qquad ...(87)$$

$$\psi_4 = \frac{1}{2}(\phi_1 - \phi_2 + \phi_4 - \phi_5) \qquad ...(88)$$

$$\psi_5 = \frac{1}{\sqrt{12}}(\phi_1 + \phi_2 - 2\phi_3 + \phi_4 + \phi_5 - 2\phi_6) \qquad ...(89)$$

$$\psi_6 = \frac{1}{\sqrt{6}}(\phi_1 - \phi_2 + \phi_3 - \phi_4 + \phi_5 - \phi_6) \qquad ...(90)$$

It may be noted that benzene is a classic example of delocalization conferring extra stability. This molecule is often represented in the languages of both VBT and MOT, VBT being used for its σ-framework (where each carbon atom is sp^2 hybridized) and MOT being used to describe the π electrons. Since the resonance integral $\beta \approx 75$ kJ mol^{-1}, hence DE for benzene $\approx -2\beta \approx -150$ kJ mol^{-1}. The strong aromatic stability of benzene arises from two contributions. First, the shape of the regular hexagon is ideal for forming a strong and relaxed σ bond frame work. Second, the three HMOs which accommodate the six π electrons are all BMOs.

Hückel's $4n+2$ Rule of Aromaticity (Aromatic Character)

An important result of HMO theory is the celebrated *Hückel rule*, according to which an aromatic molecule must contain cyclic clouds of delocalized π electrons above and below the plane of the

molecule; furthermore, the π electron clouds must contain $(4n+2)$ π electrons, *i.e.*,

$$N_\pi = (4n + 2) \text{ where } n = 0, 1, 2, 3, 4, ... \qquad ...(91)$$

Thus, for systems containing π electrons, $N_\pi = 2, 6, 10, 14, 18...$ are aromatic.

Example 38. Using the Hückel rule, determine which of the following molecules are aromatic or non-aromatic :

(a) benzene (b) cyclopentadienyl cation (c) cycloheptadienly radical (d) cyclopentadienyl anion (e) cycloheptatrienyl cation (tropylium cation) (f) cycloheptatrienyl radical (g) cycloheptatrienyl anion (h) cyclooctatetraene (i) cyclooctatetraenyl dianion (j) cyclopropenyl cation (k) cyclopropenyl radical (l) cyclopropenyl anion (m) cyclooctadecanonaene.

Solution : $N_\pi = 4n+2$, $n = 0, 1, 2, 3, ...$ (Hückel Rule),

(a)  $N_\pi = 6$ (aromatic)

(b) 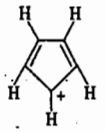 $N_\pi = 4$ (non-aromatic)

(c) 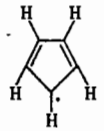 $N_\pi = 5$ (non-aromatic)

(d) 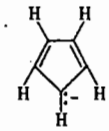 $N_\pi = 6$ (aromatic)

(e) 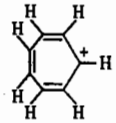 $N_\pi = 6$ (aromatic)

(f) 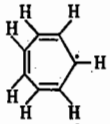 $N_\pi = 7$ (non-aromatic)

(g) 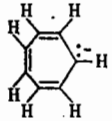 $N_\pi = 8$ (non-aromatic)

(h) Cyclooctatetraene $N_\pi = 8$ (non-aromatic)

(i) cyclooctatetraenyl dianion $N_\pi = 10$ (aromatic)

(j) cyclopropenyl cation $N_\pi = 2$ (aromatic)

(k) cyclopropenyl radical $N_\pi = 3$ (non-aromatic)

(l) cyclopropenyl anion $N_\pi = 4$ (aromatic)

(m) cyclooctadecanonaene $N_\pi = 18$ (aromatic)

Example 39. Using HMO theory set up and solve the Hückel secular determinantal equation for the allyl system which consists of the allyl radical and the related cation and the anion. Calculate the resonance energy, also known as the delocalization energy (DE) for the three species and construct molecular diagrams for each species.

Solution : Labelling the carbon atoms of the skeletal framework as 1, 2, 3 as shown below Fig. 21, the wavefunction (MO) for the π-electron in the LCAO-MO approximation is

$$\psi_j = \sum_{i=1}^{3} c_{ij}\,\phi_i \;;\; (j = 1, 2, 3) \qquad ...(92a)$$

Using only one subscript for the coefficients,

$$\psi = \sum_{i=1}^{3} c_i\,\phi_i = c_1\phi_1 + c_2\phi_2 + c_3\phi_3 \qquad ...(92b)$$

where the c_i's are the coefficients to be determined and ϕ_i's are the $2p_z$ AOs of the basis set, centred on the three carbon atoms.

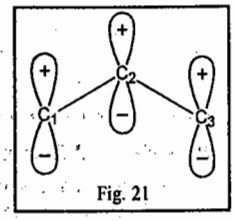

Fig. 21

Using the rules for setting up the Hückel secular determinant, we get

$$\begin{vmatrix} & \phi_1 & \phi_2 & \phi_3 \\ \phi_1 & x & 1 & 0 \\ \phi_2 & 1 & x & 1 \\ \phi_3 & 0 & 1 & x \end{vmatrix} = 0 \qquad ...(93)$$

where $x = (\alpha - E)/\beta$.

This determinant, upon expansion, gives the cubic equation

$$x^3 - 2x = 0$$
$$x(x^2 - 2) = 0$$
$$x(x + \sqrt{2})(x - \sqrt{2}) = 0$$

Thus, the roots are $x = 0, \pm\sqrt{2}$

Hence, the energy levels are :

$$\left.\begin{aligned} x = -\sqrt{2}:\ E_1 &= \alpha + \sqrt{2}\beta \quad \text{(BMO)} \\ x = 0:\ E_2 &= \alpha \quad \text{(NBMO)} \\ x = +\sqrt{2}:\ E_3 &= \alpha - \sqrt{2}\beta \quad \text{(ABMO)} \end{aligned}\right\} \qquad ...(94)$$

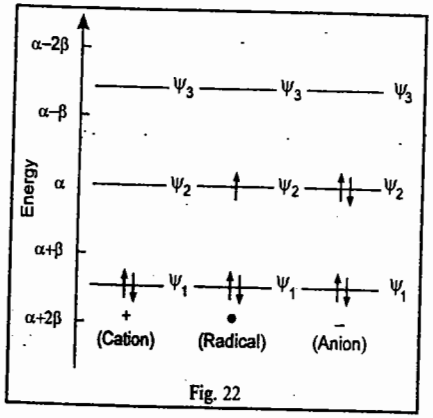

Fig. 22

Now, in the allyl system the cation has two electrons, the radical three electrons and the anion four electrons. Recalling that the resonance integral β is a negative quantity we can construct the energy level diagram for the allyl system as shown in Fig. 22.

In accordance with the Pauli exclusion principle the filling up of the orbitals in the three subsystems is shown in Fig. 22. The two π-electrons in the allyl carbonium ion, $C_3H_5^+$, are placed in the bonding molecular orbital (BMO), ψ_1, having total π-electron energy

$$E_\pi^{\oplus} = 2(\alpha + \sqrt{2}\ \beta) = 2\alpha + 2\sqrt{2}\ \beta \qquad ...(95)$$

Of the three π-electrons in the allyl radical, $C_3H_5^{\bullet}$, the first two go in ψ_1 and the third in the non-bonding molecular orbital (NBMO), ψ_2 having total π-electron energy

$$E_\pi^{\odot} = 2(\alpha + \sqrt{2}\ \beta) + \alpha = 3\alpha + 2\sqrt{2}\ \beta \qquad ...(96)$$

The four π-electrons of the allyl anion, $C_3H_5^-$ are accommodated in ψ_1 BMO and the ψ_2 NBMO. Thus,

$$E_\pi^{\ominus} = 2(\alpha + \sqrt{2}\ \beta) + 2\alpha = 4\alpha + 2\sqrt{2}\ \beta \qquad ...(97)$$

Calculation of the Delocalization Energy (*DE*)

(1) $C_3H_5^+$. The cation resonates between the following structures :

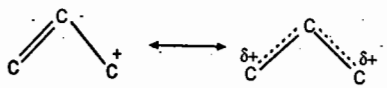

(*i*) (*ii*)

In structure (*i*), the π-electrons are localized in the double bond and the molecule has no resonance stabilization. In structure (*ii*), the electrons are delocalized over the entire molecular framework. The resonance energy, also called the delocalization energy DE, is defined as the energy difference between the energy of the localized structure, $(E_\pi)_{loc}$ and the energy of the actual molecule, E_π. The localized structure (*i*) has two π-electrons in the ethylenic linkage with energy $2(\alpha + \beta)$, *viz.*, the same energy as that of an isolated ethylene molecule, whereas the actual energy of the carbonium ion, from Eq. 95 is $2(\alpha + \sqrt{2}\ \beta)$. Hence, the π-electron delocalization energy of the cation is

$$DE \equiv (E_\pi^+)_{deloc} = 2(\alpha + \beta) - 2(\alpha + \sqrt{2}\ \beta) = -0{\cdot}828\ \beta \qquad ...(98)$$

(2) $C_3H_5^{\bullet}$. The free radical resonates between the following structures :

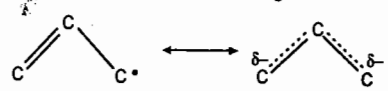

$$(E_\pi^{\bullet})_{deloc} = 2(\alpha + \beta) - (3\alpha + 2\sqrt{2}\ \beta) = -0{\cdot}828\beta \qquad ...(99)$$

(3) $C_3H_5^-$. Similarly, for the anion resonating between the following structures,

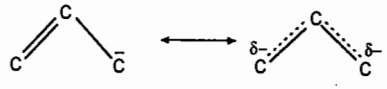

$$E_\pi^- = [2\ (\alpha + \beta) + 2\alpha] - [2(2\alpha + \sqrt{2}\ \beta)] = -0{\cdot}828\ \beta \qquad ...(100)$$

From Eqs. 98, 99 and 100 we see that the allyl cation, radical and anion have the same DE. This is understandable since while in the localized structures (going in the sequence cation ⟶ radical ⟶ anion), we put electrons in the $2p_z$ orbitals of the isolated atom having energy α, in the actual molecule, electrons are fed into the NBMO having the same energy α. Thus, DE remains the same.

Determination of the MOs

The requirement of normalization stipulates that for each MO

$$\sum_{i=1}^{3} c_i^2 = 1 \qquad ...(101)$$

If we reincorporate coefficients c_1, c_2, c_3 into the secular determinantal equation, (93), we obtain

$$\begin{vmatrix} c_1x & c_2 & 0 \\ c_1 & c_2x & c_3 \\ 0 & c_2 & c_3x \end{vmatrix} = 0 \qquad ...(102)$$

which corresponds to a system of the following three simultaneous linear homogenous equations in three unknown coefficients c_1, c_2, c_3 :

$$\left.\begin{aligned} c_1x + c_2 &= 0 \\ c_1 + c_2x + c_3 &= 0 \\ c_2 + c_3x &= 0 \end{aligned}\right\} \qquad ...(103)$$

For the BMO ψ_1, $x = -\sqrt{2}$

Substituting this value of x in Eq. 103, we get

$$\left.\begin{aligned} -\sqrt{2}c_1 + c_2 &= 0 \\ c_1 - \sqrt{2}c_2 + c_3 &= 0 \\ c_2 - \sqrt{2}c_3 &= 0 \end{aligned}\right\} \qquad ...(104)$$

From the first of Eqs. 104, $c_2 = \sqrt{2}\ c_1$

From the third of Eqs. 104, $c_2 = \sqrt{2}\ c_3$

Hence, $c_1 = c_3$

Since $c_1^2 + c_2^2 + c_3^2 = 1$ (from Eq. 101)

$c_1^2 + 2c_1^2 + c_1^2 = 1$ or $c_1 = c_3 = \frac{1}{2}$ and $c_2 = \frac{1}{\sqrt{2}}$

Hence, $\psi_1 = \frac{1}{2}\phi_1 + \frac{1}{\sqrt{2}}\phi_2 + \frac{1}{2}\phi_3$

$$= \frac{1}{2}(\phi_1 + \sqrt{2}\phi_2 + \phi_3) \qquad ...(105)$$

Again, for the NBMO ψ_2, $x = 0$.

Substituting the value of x in Eq. 103, we get

$$\left.\begin{aligned} c_2 &= 0 \\ c_1 + c_3 &= 0 \\ c_2 &= 0 \end{aligned}\right\} \quad ...(106)$$

Hence, $c_1 = -c_3$; $c_2 = 0$

Since $c_1^2 + c_2^2 + c_3^2 = 1$ (from Eq. 101)

$\therefore$ $c_1^2 + c_1^2 = 1$ or $c_1 = \frac{1}{\sqrt{2}}$ and $c_3 = -\frac{1}{\sqrt{2}}$

Hence, $\psi_2 = \frac{1}{\sqrt{2}}(\phi_1 - \phi_3)$ ...(107)

For the ABMO ψ_3, $x = \sqrt{2}$

Substituting this value of x in Eq. 103, we have

$$\left.\begin{aligned} \sqrt{2}c_1 + c_2 &= 0 \\ c_1 + \sqrt{2}c_2 + c_3 &= 0 \\ c_2 + \sqrt{2}c_3 &= 0 \end{aligned}\right\} \quad ...(108)$$

Hence, $c_2 = -\sqrt{2}c_1 = -\sqrt{2}c_3$ so that $c_1 = c_3$

Since $c_1^2 + c_2^2 + c_3^2 = 1$ (from Eq. 101)

$\therefore$ $c_1^2 + 2c_1^2 + c_1^2 = 1$

Hence, $4c_1^2 = 1$ or $c_1 = \frac{1}{2}$

Thus, $c_3 = \frac{1}{2}$ and $c_2 = \frac{1}{\sqrt{2}}$

$\therefore$ $\psi_3 = \frac{1}{2}(\phi_1 - \sqrt{2}\phi_2 + \phi_3)$ ...(109)

To sum up, from Eqs. 105, 107 and 109, the normalized MOs for the allyl system are

$$\left.\begin{aligned} \psi_1 &= \tfrac{1}{2}(\phi_1 + \sqrt{2}\phi_2 + \phi_3) \quad \text{(BMO)} \\ \psi_2 &= \frac{1}{\sqrt{2}}(\phi_1 - \phi_3) \quad \text{(NBMO)} \\ \psi_3 &= \tfrac{1}{2}(\phi_1 - \sqrt{2}\phi_2 + \phi_3) \quad \text{(ABMO)} \end{aligned}\right\} \quad ...(110)$$

The qualitative shape of the three MOs is shown in Fig. 23.

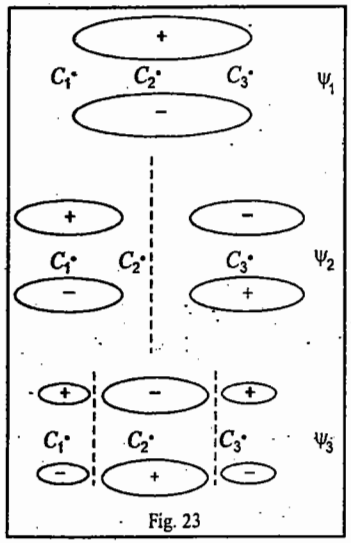

Fig. 23

We see that ψ_1 has no node, ψ_2 has one node passing through c_2 and ψ_3 has two nodes between c_1 and c_2 and between c_2 and c_3. Nodes are the points where the probability of the electron being found is zero.

Example 40. Set up and solve the Hückel secular determinantal equation for the cyclopropenyl system which consists of the cyclopropenyl radical and the related cation and anion. Calculate the delocalization energy (DE) of the system.

Solution : The MO for the cyclopropenyl system (Fig. 24), in the LCAO-MO approximation is

$$\psi_i = \sum_{i=1}^{3} c_{ij}\,\phi_i \; ; \quad (j = 1, 2, 3) \quad ...(111)$$

or $$\psi = \sum_{i=1}^{3} c_i\,\phi_i = c_1\phi_1 + c_2\phi_2 + c_3\phi_3 \quad ...(112)$$

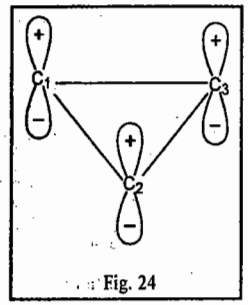

Fig. 24

The secular equation, in terms of the dimensionless variable x, is

$$\begin{vmatrix} & \phi_1 & \phi_2 & \phi_3 \\ \phi_1 & x & 1 & 1 \\ \phi_2 & 1 & x & 1 \\ \phi_3 & 1 & 1 & x \end{vmatrix} = 0 \quad ...(113)$$

where $x = (\alpha - E)/\beta$

This determinant, upon expansion, gives the polynomial equation,

$$x^3 - 3x + 2 = 0 \quad \text{or} \quad (x + 2)(x - 1)^2 = 0$$

whence $x = -2, 1, 1$

Hence, the energy levels β are

$$\left.\begin{aligned} x = -2: \quad & E_1 = \alpha + 2\beta \\ x = +1: \quad & E_2 = E_3 = \alpha - \beta \quad \text{(degenerate pair)} \end{aligned}\right\} \quad ...(114)$$

In the cyclopropenyl system, the radical has three π-electrons, the cation has two π-electrons and the anion has four π-electrons. The resonance integral β being negative, the energy level diagram for the three subsystems and the filling up of the MOs is as shown in Fig. 25.

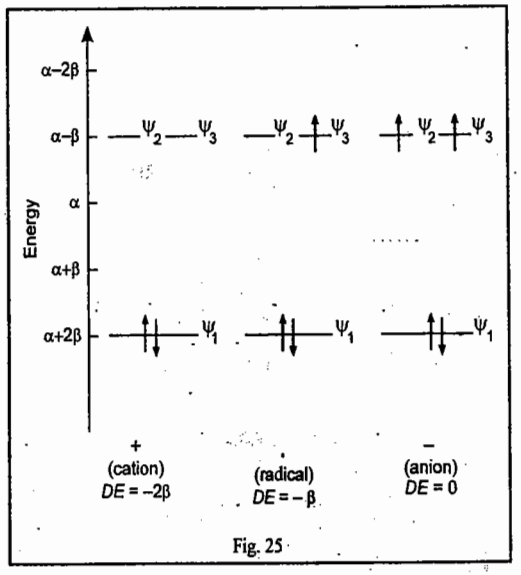

Fig. 25

The total π-electron energy is given by

$E_\pi^+ = 2(\alpha + 2\beta) = 2\alpha + 4\beta$

$E_\pi^\cdot = 2(\alpha + 2\beta) + (\alpha - \beta) = 3\alpha + 3\beta$

$E_\pi^- = 2(\alpha + 2\beta) + 2(\alpha - \beta) = 4\alpha + 2\beta$

The delocalization energy is

$(E_\pi^+)_{deloc} = 2(\alpha + \beta) - (2\alpha + 4\beta) = -2\beta$

$(E_\pi^\cdot)_{deloc} = 2(\alpha + \beta) + \alpha - (3\alpha + 3\beta) = -\beta$

$(E_\pi^-)_{deloc} = 2(\alpha + \beta) + 2\alpha - (4\alpha + 2\beta) = 0$

We see that the cation is more stable, the stability decreasing in the order :

cation > radical > anion

Determination of the MOs

Reincorporating coefficients c_1, c_2, c_3 in the secular equation (109), we get the following simultaneous linear equations :

$$\left.\begin{aligned} c_1x + c_2 + c_3 &= 0 \\ c_1 + c_2x + c_3 &= 0 \\ c_1 + c_2 + c_3x &= 0 \end{aligned}\right\} \quad ...(115)$$

For $x = -2$, we get

$$\left.\begin{aligned} -2c_1 + c_2 + c_3 &= 0 \\ c_1 - 2c_2 + c_3 &= 0 \\ c_1 + c_2 - 2c_3 &= 0 \end{aligned}\right\} \quad ...(116)$$

Subtracting the second equation from the first, $c_1 = c_2$

Subtracting the third equation from the first, $c_1 = c_3$

Since $c_1^2 + c_2^2 + c_3^2 = 1$ (from normalization condition)

$$3c_1^2 = 1$$

Thus, $$c_1 = c_2 = c_3 = \frac{1}{\sqrt{3}}$$

Hence, $$\psi_1 = \frac{1}{\sqrt{3}}(\phi_1 + \phi_2 + \phi_3)$$

It is not possible, using MO theory, to determine the coefficients of the degenerate MOs ψ_2 and ψ_3. However, according to a theorem of quantum mechanics if two eigenfunctions of a Hermitian operator have different eigenvalues, they are orthogonal. Since the Hamiltonian operator is Hermitian and ψ_2 and ψ_3 are its eigenfunctions, hence

$$\langle \psi_2 \mid \psi_3 \rangle = 0 \quad ...(117)$$

Also, $$\langle \psi_1 \mid \psi_2 \rangle = 0 \quad ...(118)$$

For $x = 1$, we obtain from Eq. 115,

$$\left.\begin{aligned} c_1 + c_2 + c_3 &= 0 \\ c_1 + c_2 + c_3 &= 0 \\ c_1 + c_2 + c_3 &= 0 \end{aligned}\right\} \quad ...(119)$$

Now, as long as the coefficients c_1, c_2, c_3 satisfy the normalization requirement,

$$c_1^2 + c_2^2 + c_3^2 = 1$$

we can choose any values for them. Let $c_2 = 0$ so that

$$c_1 = -c_3$$

$$c_1^2 + c_3^2 = 1$$

whence, $$c_1 = \frac{1}{\sqrt{2}}; \qquad c_3 = -\frac{1}{\sqrt{2}}$$

Hence, $$\psi_2 = \frac{1}{\sqrt{2}}(\phi_1 - \phi_3) \quad ...(120)$$

Let us now determine ψ_3.

Since $$\psi_3 = c_1\phi_1 + c_2\phi_2 + c_3\phi_3, \quad ...(121)$$

hence, from Eqs. 117, 120 and 121,

$$\langle \psi_2 \mid \psi_3 \rangle = \int \frac{1}{\sqrt{2}}(\phi_1 - \phi_3)(c_1\phi_1 + c_2\phi_2 + c_3\phi_3)d\tau = 0$$

or $$\frac{c_1}{\sqrt{2}}\langle \phi_1 \mid \phi_1 \rangle + \frac{c_2}{\sqrt{2}}\langle \phi_1 \mid \phi_2 \rangle + \frac{c_3}{\sqrt{2}}\langle \phi_1 \mid \phi_3 \rangle - \frac{c_1}{\sqrt{2}}\langle \phi_1 \mid \phi_3 \rangle - \frac{c_2}{\sqrt{2}}\langle \phi_2 \mid \phi_3 \rangle - \frac{c_3}{\sqrt{2}}\langle \phi_3 \mid \phi_3 \rangle = 0$$

Now, $$\langle \phi_i \mid \phi_j \rangle = \delta_{ij} = \begin{cases} 1, & i = j \\ 0, & i \neq j \end{cases}$$

Hence, all the integrals in the above expression, except the first and the last, vanish, giving

$$\frac{1}{\sqrt{2}}(c_1 - c_3) = 0 \quad \text{or} \quad c_1 = c_3$$

Also, from Eq. 119, $c_1 + c_2 + c_3 = 0$ so that $c_2 = -2c_1$

Again, $c_1^2 + c_2^2 + c_3^2 = 1$ (from normalization condition)

$$(c_1^2) + (-2c_1)^2 + (c_1)^2 = 1$$

$$6c_1^2 = 1$$

Thus, $$c_1 = c_3 = \frac{1}{\sqrt{6}}; \qquad c_2 = \frac{-2}{\sqrt{6}}$$

Hence, $$\psi_3 = \frac{1}{\sqrt{6}}(\phi_1 - 2\phi_2 + \phi_3)$$

To sum up,

$$\left.\begin{aligned} \psi_1 &= \frac{1}{\sqrt{3}}(\phi_1 + \phi_2 + \phi_3) \\ \psi_2 &= \frac{1}{\sqrt{2}}(\phi_1 - \phi_3) \\ \psi_3 &= \frac{1}{\sqrt{6}}(\phi_1 - 2\phi_2 + \phi_3) \end{aligned}\right\} \quad ...(122)$$

Example 41. A mnemonic device, called Frost-Hückel circle mnemonic, has been suggested for obtaining MO energies of cyclic conjugated systems, C_nH_n. Using this mnemonic, show diagrammatically the energy levels of C_nH_n (where n = 3, 4, 5, 6, 7, 8).

Solution : As we have noticed in Hückel calculations on the cyclic polyenes (also called polymethines), done earlier, the ground state energy level is nondegenerate but the higher energy levels are doubly degenerate except the top energy level for n even, where n is the number of conjugated carbon atoms. This result can be shown diagrammatically by means of the Frost-Hückel circle mnemonic. First, we draw a circle of radius $2|\beta|$ (where β is the resonance integral of the HMO theory). Then, we inscribe the appropriate regular polygon in the circle in such a way that one vertex is placed at the bottom of the circle. Each corner of the polygon corresponds to the carbon atom of the skeletal framework. For the cyclopropenyl system, C_3H_3, we inscribe an upside down equilateral triangle ; for cyclobutadiene, C_4H_4, a square with one vertex down; for the cyclopentadienyl system, a pentagon, for benzene, a hexagon ; for cyclohepta-trienyl, a heptagon; and for cyclooctatetraene, an octagon. Corresponding to each intersection of the polygon with the circle there exists an MO whose energy is given by the vertical placement, *i.e.*, its projection on a vertical energy scale. The centre of the circle is taken as the zero, the bottom as $+2\beta$ and the top as -2β. Using simple trigonometry the vertical placements from zero can be obtained. The circle mnemonics for C_nH_n are shown in Fig. 26. So we see that these mnemonics enable us to write the energy levels without actually solving the Hückel secular equation.

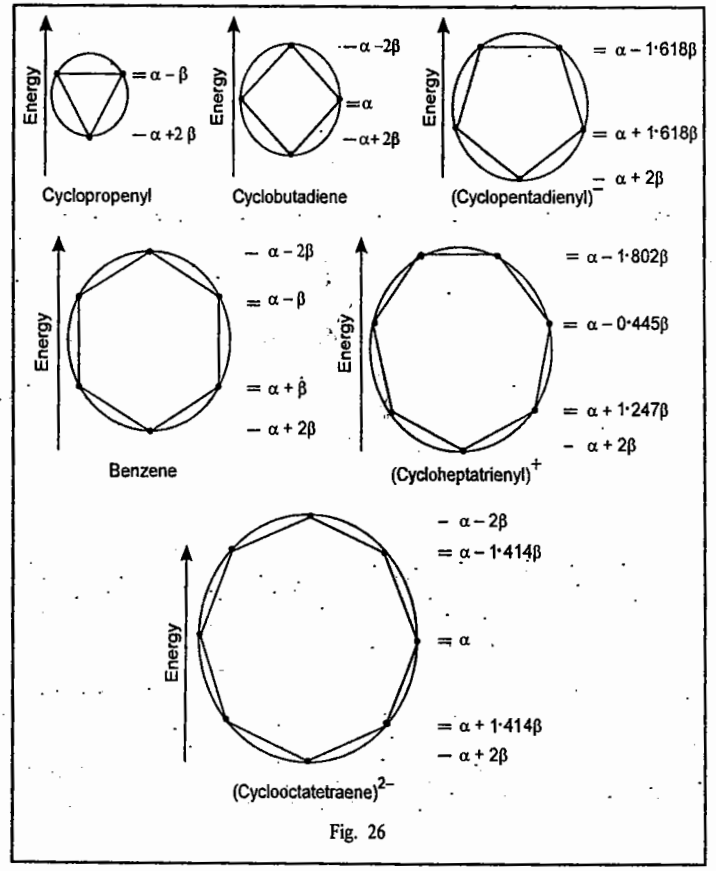

Fig. 26

Example 42. Using HMO theory determine the most stable structure of the H_3 system.

Solution. The H_3 system consists of the cation, H_3^+; the radical, H_3 and the anion H_3^-. The cation

contains two electrons, the free radical three electrons and the anion four electrons. Strictly speaking, we cannot solve this problem with the Hückel approximation since the electrons which hold the three molecular species together are not π-electrons. However, if we assume that the electrons are delocalized over the entire nuclear framework—which is a reasonable assumption—then the H_3 system is amenable to Hückel treatment. The geometrical structure can be (*a*) linear and (*b*) bent, triangular.

Case (*a*). Linear Structure $H_1 - H_2 - H_3$

The secular equation is

$$\begin{vmatrix} x & 1 & 0 \\ 1 & x & 1 \\ 0 & 1 & x \end{vmatrix} = 0 \qquad \ldots(123)$$

The determinant on expansion gives the cubic equation

$$x^3 - 2x = 0$$

$$x(x^2 - 2) = 0$$

$$x(x + \sqrt{2})(x - \sqrt{2}) = 0 \qquad \text{or,} \qquad x = -\sqrt{2}, 0, +\sqrt{2}$$

Hence, the Hückel energy levels are.

$$\left.\begin{aligned} x = -\sqrt{2}: \quad & E_1 \equiv \alpha + \sqrt{2}\beta \quad \text{(BMO)} \\ x = 0: \quad & E_2 = \alpha \quad \text{(NBMO)} \\ x = +\sqrt{2}: \quad & E_3 = \alpha - \sqrt{2}\beta \quad \text{(ABMO)} \end{aligned}\right\} \qquad \ldots(124)$$

The total Hückel energy is

$$\left.\begin{aligned} H_3^+: \quad & E = 2(\alpha + \sqrt{2}\beta) = 2\alpha + 2\sqrt{2}\beta \\ H_3: \quad & E = 2(\alpha + \sqrt{2}\beta) + \alpha = 3\alpha + 2\sqrt{2}\beta \\ H_3^-: \quad & E = 2(\alpha + \sqrt{2}\beta) + 2\alpha = 4\alpha + 2\sqrt{2}\beta \end{aligned}\right\} \qquad \ldots(125)$$

Case (*b*) : Triangular Configuration (Fig. 27)

The secular equation is

$$\begin{vmatrix} x & 1 & 1 \\ 1 & x & 1 \\ 1 & 1 & x \end{vmatrix} = 0 \qquad \ldots(126)$$

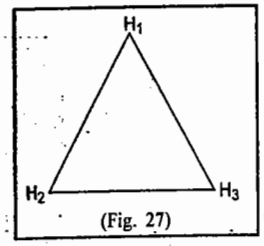

(Fig. 27)

which, on expansion, gives the polynomial

$$x^3 - 3x + 2 = 0$$

$$(x + 2)(x - 1)^2 = 0 \qquad \text{or} \qquad x = -2, 1, 1$$

Hence, the Hückel energy levels are

$$\left.\begin{aligned} x = -2: \quad & E_1 = \alpha + 2\beta \\ x = 1: \quad & E_2 = E_3 = \alpha - \beta \quad \text{(degenerate pair)} \end{aligned}\right\} \qquad \ldots(127)$$

The total Hückel energy is

$$\left.\begin{aligned} H_3^+: \quad & E = 2(\alpha + 2\beta) = 2\alpha + 4\beta \\ H_3: \quad & E = 2(\alpha + 2\beta) + (\alpha - \beta) = 3\alpha + 3\beta \\ H_3^-: \quad & E = 2(\alpha + 2\beta) + 2(\alpha - \beta) = 4\alpha + 2\beta \end{aligned}\right\} \qquad \ldots(128)$$

In may be recalled that the resonance integral β is a negative quantity. The criterion for the stability of a molecule in a given configuration is that it should have lower energy in the ground state. From Eqs. 125 and 128 we conclude that

H_3^+ : Triangular configuration is more stable
H_3 : Both configurations are about equally stable
H_3^- : Linear configuration is more stable.

Example 43. Calculate the Hückel energies of pyridine. Compare the energy level diagram of this molecule with that of benzene.

[Hint : In contrast to pyrrole, the N-atom in pyridine supplies only one *p*-electron to the ring. The secular equation for pyridine is exactly analogous to that for benzene. As in the case of pyrrole, the α and β integrals have to be adjusted. If N atom is numbered as 1, the following substitutions are made :

$$\alpha_1 = \alpha_N = \alpha + k\beta, \quad k = 0.2$$
$$\alpha_2 = \alpha_6 = \alpha + l\beta, \quad l = k/8$$
$$\beta_{12} = \beta_{16} = m\beta, \quad m = l$$

(The values of k, l and m have been recommended from more elaborate calculations). Hence, the secular equation for pyridine is

$$\begin{vmatrix} (\alpha+k\beta)-E & m\beta & 0 & 0 & 0 & m\beta \\ m\beta & (\alpha+l\beta)-E & \beta & 0 & 0 & 0 \\ 0 & \beta & \alpha-E & \beta & 0 & 0 \\ 0 & 0 & \beta & \alpha-E & \beta & 0 \\ 0 & 0 & 0 & \beta & \alpha-E & \beta \\ m\beta & 0 & 0 & 0 & \beta & (\alpha+l\beta)-E \end{vmatrix} = 0 \qquad \ldots(129)$$

The solution of the secular equation gives the energy level diagram shown in Fig. 28, where the energy level diagram for benzene is also shown for comparison.

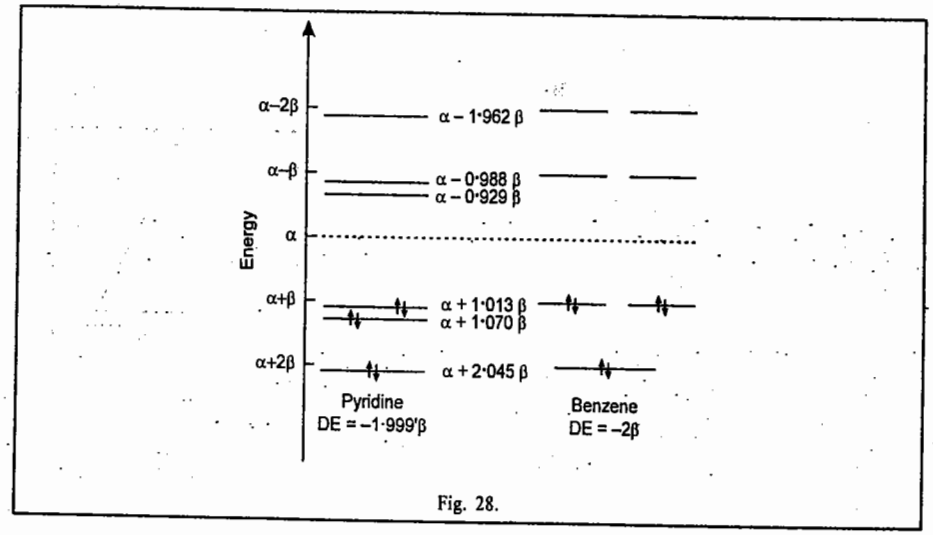

Fig. 28.

The charge densities ρ_μ and the bond order $p_{\mu\nu}$ are

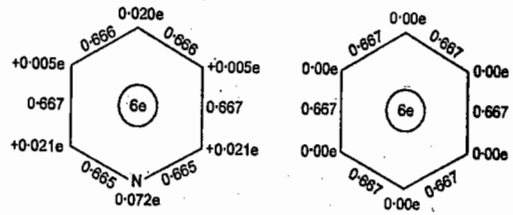

Example 44. In the various problems dealt with earlier on HMO theory, the delocalization energy (*DE*) has been expressed in terms of the resonance integral, β. The next task, therefore, is to evaluate β. Outline methods which lead to the determination of β.

Solution : Three experimental methods have been used to determine β. They are : (*a*) Measurement of ionization potentials (*b*) Electronic spectral data and (*c*) Measurement of DE.

(*a*) **Measurement of Ionization Potentials.** In a molecule where each MO is doubly occupied in accordance with the requirements of the Pauli principle, the total energy is given by

$$E = 2\sum_m E_m \qquad ...(130)$$

where the summation is over the occupied MO*s*. When the molecule absorbs sufficient energy to remove the electron from the highest occupied molecular orbital (HOMO), the topmost orbital, say, ψ_n, is singly occupied. Hence, the total π-electron energy of the ion is

$$E\ (\text{ion}) = 2\sum_m E_m + E_n (m \neq n) \qquad ...(131)$$

Ionization potential, *I*, is the difference in energy between the molecule and the ion. It is the energy required to ionize the molecule. From Eqs. 129 and 130,

$$I = E\ (\text{ion}) - E = -E_n \qquad ...(132)$$

From Eq. 129 we see that the ionization potential is equal to minus the energy of HOMO. This statement is known as Koopmans' theorem.

Experimental measurement of the ionization potential enables us to determine both the Coulomb integral, α and the resonance integral, β. For graphite the value of I = 4·3 eV. Since for graphite the highest orbital has an energy equal to α, therefore, α = − 4·3 eV. Once α is known from measurements on graphite, β can be determined from the ionization potentials and the orbital energies of a series of related molecules. The data for the polyacene series is tabulated below :

Polyacene	Ionization Potential, eV	E_n
C_6H_6	9·57	α + β
$C_{10}H_8$	8·68	α + 0·618 β
$C_{14}H_{10}$	8·20	α + 0·414 β
$C_{18}H_{12}$	7·71	α + 0·295 β

A plot of I versus $-E_n$ gives β ≈ −2·4 eV = 230 kJ mol^{-1}.

(*b*) **Electronic Spectra :** When an electron in a conjugated system occupying the orbital ψ_m with energy $E_m = \alpha + x_m \beta$, undergoes a transition to the orbital ψ_n with energy $E_n = \alpha + x_n \beta$, the energy of transition, ΔE, which lies in the ultraviolet region, is given by

$$\Delta E = E_n - E_m = (\alpha + x_n\beta) - (\alpha + x_m\beta) = (x_n - x_m)\ \beta$$

The frequency of transition, in cm^{-1}, is

$$\bar{\nu} = \Delta E/hc$$

Thus, if $\bar{\nu}$ is known for a series of conjugated compounds from the u.v. spectra, it can be correlated with the results of HMO theory, leading to the determination of β.

(*c*) **Measurement of the DE :** Taking the example of benzene, the actual heat of formation is determined from thermochemical measurements. The energy of a hypothetical moleeule having a Kekule structure is then estimated by using the energies for the C–C, C=C and C–H bonds found in molecules such as ethane and ethylene. The difference between the two energies gives the resonance energy which is the same as the DE of the HMO theory. Thus,

$$3(D_{C\text{–}C}) + 3(D_{C=C}) + 6(D_{C\text{–}H}) = 4{,}184 \text{ kJ mol}^{-1}$$

The observed heat of formation is 4,347 kJ mol^{-1}. Since

$$DE = -2\beta$$

Therefore,

$$|\ \beta\ | = \frac{1}{2}(DE) = \frac{1}{2}(4{,}347 - 4{,}184) = 84 \text{ kJ mol}^{-1}.$$

The β-values for other members of the polyacene series, *viz.*, naphthalene, anthracene, naphthacene, etc., are also found to be in the same range.

Alternatively, β can be evaluated as follows. The heat of hydrogenation of benzene to cyclohexane is found

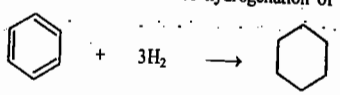

to be −208.4 kJ mol^{-1}. The heat of hydrogenation of cyclohexene to cyclohexane is found to be −119.6 kJ mol^{-1}.

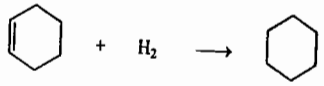

The DE of benzene is the difference between three times the heat of hydrogenation of cyclohexene and the heat of hydrogenation of benzene :

$$DE = 3(-119{\cdot}6) - (-208{\cdot}4) = -150{\cdot}4 \text{ kJ mol}^{-1}.$$

Thus,

$$|\ \beta\ | = \frac{1}{2}\ DE = 75 \text{ kJ mol}^{-1}.$$

The measurement of DE is the most accurate method of determining β. The ionization potential method, outlined in (a) above, gives very high values of β and is not reliable. The consistency of the β values obtained from various molecules provides a measure of the validity of the HMO theory.

Example 45. Since in a conjugated system the π-electrons are delocalized over the entire molecule and even the single bonds partake of the double bond character, it is natural to speak of "electron density" at a given atom, the "bond-order" between a pair of atoms, and the residual valence at each atom. Such concepts have, indeed, been introduced into HMO theory. Calculate (*i*) the π-electron charge density, (*ii*) the charge density, (*iii*) the π-electron bond order (also called mobile bond order), and (*iv*) free-valence index in the following molecules :

a. **the allyl system** ***b.*** **the butadiene [butadiene]$^+$ and [butadiene]$^-$ systems and** ***c.*** **benzene.**

Solution : The total π-electron charge density q_μ at an atom μ is defined as

$$q_\mu = \sum_{\nu\ \text{occ.}} n_\nu\, c_{\mu\nu}^2 \qquad ...(133)$$

where n_ν is the number of electrons in the νth MO and the summation is over all the occupied MOs. Since according to Pauli's principle n_ν = 2,

hence

$$q_\mu = 2\sum_{\nu\ \text{occ.}} c_{\mu\nu}^2 \qquad ...(134)$$

The quantity $c_{\mu\nu}^2$ is the partial electron density at atom μ due to the electron in the MO ψ_ν.

Originally, there was one π-electron at each carbon atom. Since this electron is delocalized over the entire molecular framework, the charge density at atom μ is defined as

$$\rho_\mu = 1 - q_\mu \qquad ...(135)$$

The partial mobile π-bond order is defined for the μν bond in the λth MO as

$$p_{\mu\nu}^{\lambda} = c_{\mu\lambda}\, c_{\nu\lambda} \qquad ...(136)$$

Hence, the total π-electron bond order $p_{\mu\nu}$ between μ and ν is

$$p_{\mu\nu} = \sum_{\text{all electrons}} p_{\mu\nu}^{\lambda} = \sum_{\lambda\ \text{occ.}} n_\lambda c_{\mu\lambda}\, c_{\nu\mu} = 2\sum_{\lambda\ \text{occ.}} c_{\mu\lambda}\, c_{\nu\lambda} \qquad ...(137)$$

The free valence index F_μ at an atom μ is defined as

$$F_\mu = 4{\cdot}732 - \sum_{\text{bond}} p_{\mu\lambda} \qquad ...(138)$$

where 4·732 is the maximum possible bonding power of the μth atom. The last term in Eq. 138 is the sum of

the bond orders of all bonds to the μth atom, including the σ-bonds of the skeletal framework. In this definition the σ-bonds have the order of 1.

a. **Allyl System**

1. Cation (carbonium ion). The two π-electrons occupy MO ψ_1.

$$\psi_1 = \frac{1}{2}(\phi_1 + \sqrt{2}\,\phi_2 + \phi_3)$$

(*i*) $q_1 = q_3 = 2\left(\frac{1}{2}\right)^2 = 0.5$ (using Eq. 134)

$$q_2 = 2\left(\frac{\sqrt{2}}{2}\right)^2 = 1.00$$

(*ii*) $\rho_1 = \rho_3 = 1 - .5 = 0.5$ (using Eq. 135)

$\rho_2 = 1 - 1.00 = 0.00$

(*iii*) $p_{12} = 2\left(\frac{1}{2}\right)\left(\frac{\sqrt{2}}{2}\right) = 0.707$ (using Eq. 137)

$$p_{23} = 2\left(\frac{\sqrt{2}}{2}\right)\left(\frac{1}{2}\right) = 0.707$$

Thus, $p_{12} = p_{23}$

(*iv*) The σ-bond order = 3

Thus, $F_1 = 4.732 - \Sigma p$ (using Eq. 138)

$= 4.732 - (3.00 + p_{12})$

$= 4.732 - (3.00 + .707) = 1.02$

$F_3 = 4.732 - (3.00 + p_{23}) = 1.02 = F_1$

$F_2 = 4.732 - (3.00 + p_{12} + p_{23})$

$= 4.732 - (3.00 + 0.707 + 0.707)$

$= 0.32$

The numerical results can be represented schematically as follows :

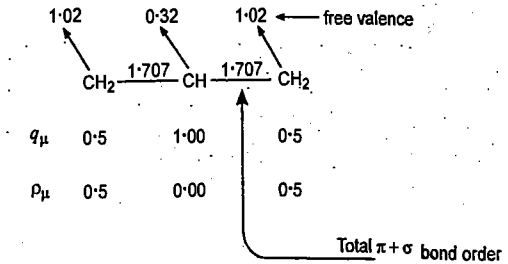

2. Radical. The three π-electrons occupy the MOs ψ_1 and ψ_2.

$$\psi_1 = \frac{1}{2}(\phi_1 + \sqrt{2}\phi_2 + \phi_3) \quad \text{and} \quad \psi_2 = \left(\frac{1}{\sqrt{2}}\right)(\phi_1 - \phi_3)$$

(*i*) $q_1 = 2\left(\frac{1}{2}\right)^2 + (1)\left(\frac{1}{\sqrt{2}}\right)^2 = \frac{1}{2} + \frac{1}{2} = 1.00$

$$q_2 = 2\left(\frac{\sqrt{2}}{2}\right)^2 + (0)^2 = 1.00$$

$$q_3 = 2\left(\frac{1}{2}\right)^2 + (1)\left(-\frac{1}{\sqrt{2}}\right)^2 = 1.00$$

(*ii*) $\rho_1 = \rho_2 = \rho_3 = 0.00$

(iii) $p_{12} = 2\left(\frac{1}{2}\right)\left(\frac{\sqrt{2}}{2}\right) + (1)\left(\frac{1}{\sqrt{2}}\right)(0) = \frac{1}{\sqrt{2}} = 0.707$

$$p_{23} = 2\left(\frac{\sqrt{2}}{2}\right)\left(\frac{1}{2}\right) + (1)(0)\left(-\frac{1}{\sqrt{2}}\right) = \left(\frac{1}{\sqrt{2}}\right) = 0.707$$

Thus, $p_{12} = p_{23}$

(*iv*) $F_1 = 4.732 - (3.00 + 0.707) = 1.02$

Similarly, $F_3 = F_1 = 1.02$

$F_2 = 4.732 - (3.00 + 0.707 + 0.707) = 0.32$

Schematically,

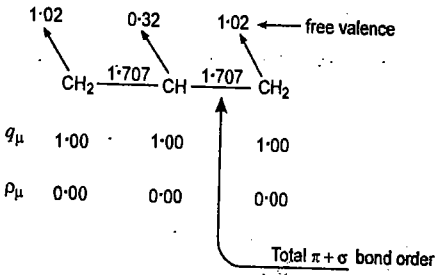

3. Anion (Carbanion). The four π-electrons occupy the MOs ψ_1 and ψ_2. The reader can verify that

(*i*) $q_1 = q_3 = 1.5$ $q_2 = 1.00$

(*ii*) $\rho_1 = \rho_3 = -0.5$ $\rho_2 = 0.00$

(*iii*) $p_{12} = p_{23} = 0.707$

(*iv*) $F_1 = F_3 = 1.02$ $F_2 = 0.32$

Schematically,

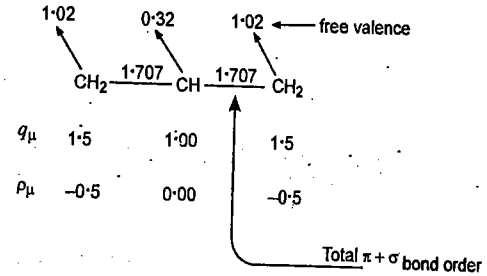

b. **Butadiene.** The four π-electrons occupy MOs ψ_1 and ψ_2 :

$\psi_1 = 0.372\,\phi_1 + 0.602\,\phi_2 + 0.602\,\phi_3 + 0.372\,\phi_4$

$\psi_2 = 0.602\,\phi_1 + 0.372\,\phi_2 - 0.372\,\phi_3 - 0.602\,\phi_4$

(*i*) $q_1 = 2(0.372)^2 + 2\,(0.602)^2 = 1$

$q_2 = 2(0.602)^2 + 2\,(0.372)^2 = 1$

$q_3 = 2(0.602)^2 + 2\,(-0.372)^2 = 1$

$q_4 = 2(0.372)^2 + 2\,(-0.602)^2 = 1$

Thus, $q_1 = q_2 = q_3 = q_4 = 1$

(*ii*) $\rho_1 = \rho_2 = \rho_3 = \rho_4 = 0.00$

(*iii*) $p_{12} = 2(0{\cdot}372)(0{\cdot}602) + 2\,(0{\cdot}602)(0{\cdot}372) = 0{\cdot}896$

$p_{23} = 2(0{\cdot}602)(0{\cdot}602) + 2\,(0{\cdot}372)(-0{\cdot}372) = 0{\cdot}448$

$p_{34} = 2(0{\cdot}602)(0{\cdot}372) + 2(-0{\cdot}372)(-0{\cdot}602) = 0{\cdot}896$

Thus, $p_{12} = p_{34} = 0{\cdot}896$

(*iv*) $F_1 = 4{\cdot}732 - \Sigma p = 4{\cdot}732 - (3{\cdot}00 + p_{12})$

$= 4{\cdot}732 - (3{\cdot}00 + 0{\cdot}896) = 0{\cdot}830$

$F_4 = 4{\cdot}732 - (3{\cdot}00 + p_{34}) = 0{\cdot}830$

Thus, $F_1 = F_4 = 0{\cdot}830$

$F_2 = 4{\cdot}732 - (3{\cdot}00 + p_{12} + p_{23})$

$= 4{\cdot}732 - (3{\cdot}00 + 0{\cdot}896 + 0{\cdot}448) = 0{\cdot}390$

$F_3 = 4{\cdot}732 - (3{\cdot}00 + p_{23} + p_{34})$

$= 4{\cdot}732 - (3{\cdot}00 + 0{\cdot}448 + 0{\cdot}896) = 0{\cdot}390$

Thus, $F_2 = F_3 = 0{\cdot}390$

Schematically,

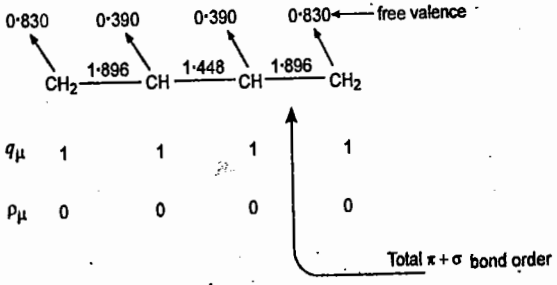

c. **Benzene.** The six π-electrons occupy the MOs ψ_1, ψ_2 and ψ_3.

$$\psi_1 = \frac{1}{\sqrt{6}}(\phi_1 + \phi_2 + \phi_3 + \phi_4 + \phi_5 + \phi_6)$$

$$\psi_2 = \frac{1}{2}(\phi_1 + \phi_2 - \phi_4 - \phi_5)$$

$$\psi_3 = \frac{1}{\sqrt{12}}(\phi_1 - \phi_2 - 2\phi_3 - \phi_4 + \phi_5 + 2\phi_6)$$

(*i*) $q_1 = 2\left(\frac{1}{\sqrt{6}}\right)^2 + 2\left(\frac{1}{2}\right)^2 + 2\left(\frac{1}{\sqrt{12}}\right)^2 = 1{\cdot}00$

$q_2 = 2\left(\frac{1}{\sqrt{6}}\right)^2 + 2\left(\frac{1}{2}\right)^2 + 2\left(-\frac{1}{\sqrt{12}}\right)^2 = 1{\cdot}00$

$q_3 = 2\left(\frac{1}{\sqrt{6}}\right)^2 + 2\,(0)^2 + 2\left(\frac{-2}{\sqrt{12}}\right)^2 = 1{\cdot}00$

$q_4 = 2\left(\frac{1}{\sqrt{6}}\right)^2 + 2\left(-\frac{1}{2}\right)^2 + 2\left(-\frac{1}{\sqrt{12}}\right)^2 = 1{\cdot}00$

$q_5 = 2\left(\frac{1}{\sqrt{6}}\right)^2 + 2\left(-\frac{1}{2}\right)^2 + 2\left(\frac{1}{\sqrt{12}}\right)^2 = 1{\cdot}00$

$$q_6 = 2\left(\frac{1}{\sqrt{6}}\right)^2 + 2\,(0)^2 + 2\left(\frac{-2}{\sqrt{12}}\right)^2 = 1{\cdot}00$$

Thus, $q_1 = q_2 = q_3 = q_4 = q_5 = q_6 = 1{\cdot}00$

(*ii*) $\rho_1 = \rho_2 = \rho_3 = \rho_4 = \rho_5 = \rho_6 = 0{\cdot}00$

(*iii*) $p_{12} = 2\left(\frac{1}{\sqrt{6}}\right)\left(\frac{1}{\sqrt{6}}\right) + 2\left(\frac{1}{2}\right)\left(\frac{1}{2}\right) + 2\left(\frac{1}{\sqrt{12}}\right)\left(-\frac{1}{\sqrt{12}}\right) = \frac{2}{3} = 0{\cdot}667$

$p_{23} = 2\left(\frac{1}{\sqrt{6}}\right)\left(-\frac{1}{\sqrt{6}}\right) + 2\left(\frac{1}{2}\right)(0) + 2\left(-\frac{1}{\sqrt{12}}\right)\left(-\frac{2}{\sqrt{12}}\right) = \frac{2}{3} = 0{\cdot}667$

Similarly, we can compute other bond-orders. The result is

$p_{12} = p_{23} = p_{34} = p_{45} = p_{56} = p_{61} = 0{\cdot}667$

(*iv*) $F_1 = 4{\cdot}732 - \Sigma p = 4{\cdot}732 - (3{\cdot}00 + p_{12} + p_{61})$

$= 4{\cdot}732 - (3{\cdot}00 + 0{\cdot}667 + 0{\cdot}667) = 0{\cdot}40$

$F_2 = 4{\cdot}732 - (3{\cdot}00 + p_{12} + p_{23}) = 0{\cdot}40$

It can be easily verified that

$F_1 = F_2 = F_3 = F_4 = F_5 = F_6 = 0{\cdot}40$

Schematically, we have

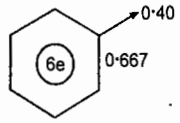

$q_\mu = 1{\cdot}00$, $\rho_\mu = 0{\cdot}00$

Walsh Diagrams. The Walsh diagram, introduced by A.D. Walsh in 1953, also known as the Mulliken-Walsh diagram, is a **correlation diagram** that portrays the variation in the orbital energies of a molecule as its shape is changed (for instance, as a bond angle is changed). By selecting the bond angle that results in the lowest total energy (which may be approximated by the sum of the orbital energies) we can predict the probable shape of the molecule from the occupation of its orbitals. Also, from a knowledge of the changes in the populations of the orbitals one can predict how the shape will change when the molecule is electronically excited.

Consider the general case of the H_2A molecule (H_2O is a particular example of this kind of molecule). The atomic orbital basis set consists of the 1*s* orbitals of the two H atoms and the four valence A *s* and A *p* orbitals of the central A atom. Their relative energies are estimated by considering how their overlap with each other varies as the bond angle is varied. Six MOs can be built from these six AOs using the LCAO-MO approximation. The plot of the energies of the MOs as the bond angle changes from 180° in the linear molecule to 90° in the angular molecule gives the Walsh diagram (Fig. 28).

The lowest orbital in 90° H_2A molecule is the one labelled 1*a*, which is constructed from the overlap of the A *s* and A p_z orbitals with one *symmetry adapted combination* of the H 1*s* orbitals. As the bond angle is changed to 180°, the two H 1*s* orbitals overlap less and hence are raised in energy. In the linear molecule, however, only the A *s* orbital contributes to the bond and the elimination of the higher-energy A *p* component of the orbital *lowers* the overall energy of the MO. When the mixing of the A orbitals is significant, the energy of the orbital falls as the molecule becomes linear.

The energy of the orbital 1 b_2 is lowered because the H 1*s* orbitals move into a better position for overlap with A p_y orbital. The biggest change occurs for the 2 a_1 orbital. In the first place, it contains

considerable A s character in the 90° molecule but is pure A p in the 180° molecule. Secondly, though it is largely AH nonbonding and slightly HH bonding in the 90° molecule, it is purely nonbonding in the 180° molecule.

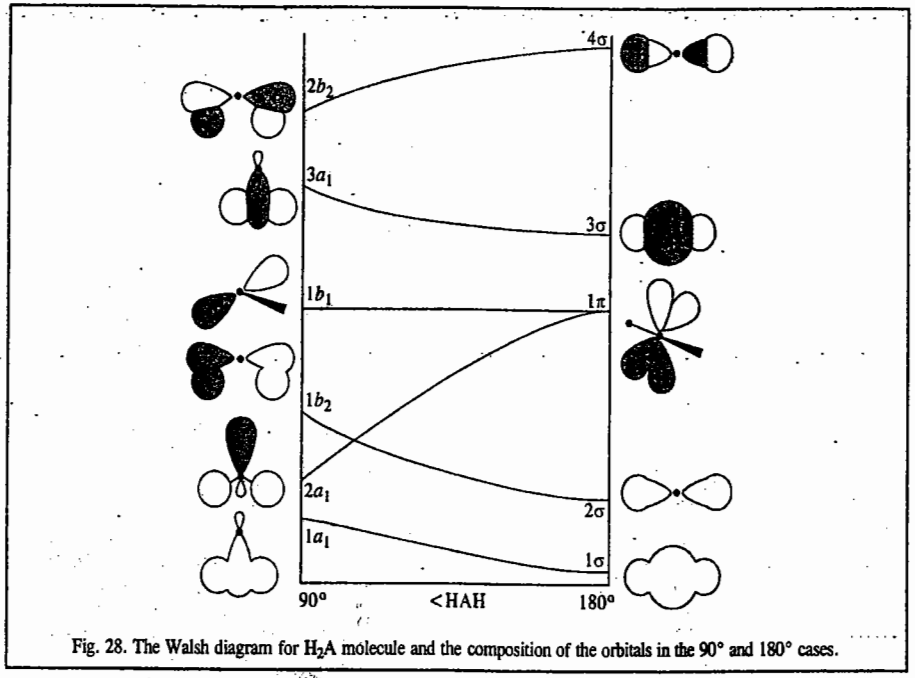

Fig. 28. The Walsh diagram for H_2A molecule and the composition of the orbitals in the 90° and 180° cases.

The $1b_1$ orbital is a nonbonding A p_x orbital perpendicular to the molecular plane in the 90° molecule and it remains nonbonding in the linear molecule. Therefore, its energy hardly changes with angle. The $3a_1$ orbital is antibonding in the 90° molecule and has both A s and A p character ; in the linear molecule it is pure A s on the central atom and possibly less antibonding. Hence, its energy decreases as the molecule becomes linear. The uppermost orbital, $2b_2$, is the antibonding partner of the $1b_2$ orbital and increases in energy as the H $1s$ orbitals achieve better overlap in the linear molecule.

The main feature which determines whether or not the H_2A molecule is bent is whether the $2a_1$ orbital is occupied. The $2a_1$ orbital has a much lower energy in the angular molecule than in the linear molecule. Hence, a lower total energy is achieved if, when it is occupied, the molecule is angular. The shape adopted by an H_2A molecule, therefore, depends on the number of electrons occupying the orbital. In H_2O, which has eight valence electrons to accommodate, the $2a_1$ orbital must be occupied ; so we predict that the molecule will be bent. On the other hand, the transient BeH_2 molecule, which has four valence electrons, is predicted to be linear since the $2a_1$ orbital is not occupied and the occupied orbitals have only a weak effect on the molecular geometry.

Molecular geometry is predicted using the two theories, *viz.*, the VSEPR (valence shell electron pair repulsion) theory and the Walsh diagrams. The former was proposed by N.V. Sidgwick and H.M. Powell in the 1930s but given a modern formulation by R. Nyholm and R.J. Gillespie. It is discussed in detail in Inorganic Chemistry books. Suffice it to state here that the generally accepted view (accepted because it works, not because it is fully understood) is that in a molecule lone pairs repel more strongly than bonding pairs; so the order of repulsions is

$$(LP, LP) > (LP, BP) > (BP, BP)$$

where LP stands for a nonbonding lone pair and BP stands for a bonding pair (or super pair). The molecule adjusts its shape so that the repulsions are minimized in the light of this ordering.

The Walsh diagram approach has an advantage over the VSEPR theory in that it is formulated in terms of the occupation of the delocalized MOs and the energies of these orbitals incorporate electron–electron and nucleus–nucleus repulsions, electron–nucleus attractions, and the kinetic energies of the electrons. Thus, the Walsh diagram approach is, in principle, richer than the VSEPR theory, for the latter is expressed entirely in terms of repulsions between localized pairs of electrons. However, in the words of P.W. Atkins, "to some extent the advantage is illusory because the VSEPR theory can be expressed in more sophisticated terms and there is some uncertainty about the precise significance of the 'orbital energy' that is plotted in a Walsh diagram". The two approaches attempt qualitatively to identify dominant bonding influences. The Walsh approach is useful for discussing the excited states of molecules, an area where the VSEPR approach is almost completely silent. It must be emphasized again that *in the Walsh model the shape of a molecule is predicted on the basis of the occupation of MOs that, in a correlation diagram, show a strong dependence on bond angle.* In general, any H_2A molecule with from five to eight valence electrons is predicted to be angular. The observed bond angles are :

BeH_2	BH_2	CH_2	NH_2	OH_2
180	131	136	103	105

These experimental observations are qualitatively in line with Walsh's approach but for detailed quantitative predictions one has to rely on detailed MO calculations.

Problem 46. Using the Walsh diagram predict the geometry of *(i)* BeH_2 *(ii)* CH_2 *(iii)* H_2O molecules.

Solution. *(i)* **BeH_2** has four valence electrons. These four electrons occupy the lowest two MOs. If the lowest energy is achieved with the molecule being angular, then that will be its shape. We can decide whether the molecule is angular by accommodating the electrons in the lowest two MOs corresponding to an arbitrary bond angle in the Walsh diagram (Fig. 28). We then note that the HOMO (highest occupied molecular orbital) decreases in energy on going to the right of the diagram and that the lowest total energy is obtained when the molecule is linear. Hence, BeH_2 is predicted to be **linear** and has the configuration $1\sigma^2 2\sigma^2$.

(ii) **CH_2** molecule has two more electrons than BeH_2; hence, three of the MOs must be occupied. Here, the lowest energy is achieved if the molecule is **angular** and has the configuration $1a_1^2 2a_1^2 1b_2^2$.

(iii) **H_2O.** Here, too, as in cases *(i)* and *(ii)*, we choose an intermediate bond angle along the horizontal axis of the Walsh diagram and accommodate the eight valence electrons. The resulting configuration is $1a_1^2 2a_1^2 1b_2^2 1b_1^2$. The $2a_1$ orbital is occupied; so we expect the molecule to be **nonlinear** since in this configuration it has lower energy than the linear molecule.

We have given a brief survey of the most important applications of quantum mechanics to atomic structure (Chapters 1 and 2) and chemical bonding (this Chapter). Physicists have used it to explain the interaction of electrons and photons, the nature of the solid state, the band theory of metals, the phenomena of superconductivity and superfluidity and theories of cosmology and gravity. Quantum mechanics ranks with the Relativity as the two most important theories in Physics in the twentieth century. Quantum Electrodynamics (QED), pioneered in the 1940s by the 1965 Physics Nobel Laureates R.P. Feynman, J.S. Schwinger and S. Tomonaga, has been called the "Jewel of Physics". Quantum mechanics is, indeed, a fascinating theory ; it has challenged the best minds. In the words of the 1963 Physics Nobel Laureate, E.P. Wigner (1902 - 1995), "The discovery of quantum mechanics was nearly a total surprise. It described the physical world in a way that was fundamentally new. It seemed to many of us a miracle". The significance of quantum mechanics was described by Dirac (the cowinner, with Schrödinger, of the 1933 Physics Nobel Prize) very boldly in the following words :

"The underlying physical laws necessary for the mathematical theory of a large part of physics and the whole of chemistry are thus completely known and the difficulty is only that the exact application of these laws leads to equations which are too complicated to be soluble."

If Dirac were alive he would be happy to know that computational quantum chemistry has, thanks to the high-speed computers, made tremendous strides in surmounting the difficulties he had anticipated, and that quantum chemistry has, indeed, a bright future ahead.

Born-Oppenheimer Approximation

For a molecule consisting of N nuclei ($\mu,\nu\ldots$) and n electrons ($i, j,\ldots$), the complete Hamiltonian operator, neglecting the spin-orbit interaction and other magnetic interactions, is given by

$$\hat{H} = -\frac{\hbar^2}{2}\sum_{\mu}^{N}\frac{1}{m_\mu}\nabla_\mu^2 - \frac{\hbar^2}{2m_e}\sum_{i}^{n}\nabla_i^2 + \sum_{\mu,\nu}\frac{Z_\mu Z_\nu e^2}{(4\pi\varepsilon_0)r_{\mu\nu}} - \sum_{i,\mu}\frac{Z_\mu e^2}{(4\pi\varepsilon_0)r_{i\mu}} + \sum_{i,j}\frac{e^2}{(4\pi\varepsilon_0)r_{ij}} \quad \ldots(139)$$

In Eq. 139, the first term represents nuclear kinetic energy; the second, electronic kinetic energy; the third, nuclear potential energy; the fourth, nuclear–electron attraction potential energy and the fifth, electronic repulsion potential energy.

The Schrödinger equation for the molecule can be written as

$$\hat{H}\psi = E\psi \quad \ldots(140)$$

where E is the total energy and ψ the total wave function. The proton being about 1840 times as heavy as the electron, the electronic motion is extremely fast compared with the nuclear motion. If we assume that the two motions are independent of each other, the total wave function can be written as a product of the electronic wave function ψ_e and the nuclear wave function, ψ_n :

$$\psi = \psi_e\psi_n \quad \ldots(141)$$

In the Born-Oppenheimer approximation, the nuclear kinetic energy is neglected while writing the Schrödinger equation for electronic motion. Thus, we have, from Eqs. 139 and 140,

$$\left[-\frac{\hbar^2}{2m_e}\sum_{i}^{n}\nabla_i^2 + \sum_{\mu,\nu}\frac{Z_\mu Z_\nu e^2}{(4\pi\varepsilon_0)r_{\mu\nu}} - \sum_{i,\mu}\frac{Z_\mu e^2}{(4\pi\varepsilon_0)r_{i\mu}} + \sum_{i,j}\frac{e^2}{(4\pi\varepsilon_0)r_{ij}}\right]\psi_e = E\psi_e \quad \ldots(142)$$

We see that for a particular fixed nuclear framework, the electronic wave function, ψ_e depends only on the coordinates of the electrons. Of course, the nuclear coordinates *do* affect ψ_e and E_e. But, if we have a fixed nuclear configuration, then the nuclear repulsion potential energy, given by the second term in Eq. 142, can be considered a constant. The electronic energy E_e is then given by

$$E_e = E - \sum_{\mu\nu}\frac{Z_\mu Z_\nu e^2}{(4\pi\varepsilon_0)r_{\mu\nu}} \quad \ldots(143)$$

Hence. Eq. 142 becomes

$$\left[\sum_i\left(-\frac{\hbar^2}{2m_e}\nabla_i^2 - \sum_{i,\mu}\frac{Z_\mu e^2}{(4\pi\varepsilon_0)r_{i\mu}}\right) + \sum_{i,j}\frac{e^2}{(4\pi\varepsilon_0)r_{ij}}\right]\psi_e = E_e\psi_e \quad \ldots(144)$$

The Schrödinger equation for nuclear motion is written as

$$\left[-\frac{\hbar^2}{2}\sum_{\mu}^{N}\frac{1}{m_\mu}\nabla_\mu^2 + E_e(r_{\mu\nu})\right]\psi_n = E_n\psi_n \quad \ldots(145)$$

The nuclear wave function ψ_n describes the rotational and vibrational motions in a potential field supplied by the *electrons*. Thus, we see from Eq. 145 that we can describe the nuclear motion by using an effective Hamiltonian in which the potential energy is the one that is provided by the electrons in the

fixed nuclei approximation. Eqs. 144 and 145 show that, as a result of the Born-Oppenheimer approximation, the electronic and nuclear motions have been separated. Eq. 144 is solved for a fixed value of internuclear separation, $r_{\mu\nu}$ (usually designated as R), thereby obtaining E_e as a function of R : $E_e = E_e(R)$. For a diatomic molecule, a plot of $E_e(R)$ versus R gives the potential energy curve shown in Fig. 29. The most stable nuclear configuration for a given electronic state corresponds to the value of R leading to a minimum in the energy. The value of E_e obtained from Eq. 144 is used as potential energy in Eq. 145. The total energy, E, of the molecule is the sum of the contributions from the electronic and the nuclear motions :

$$E = E_e + E_n$$

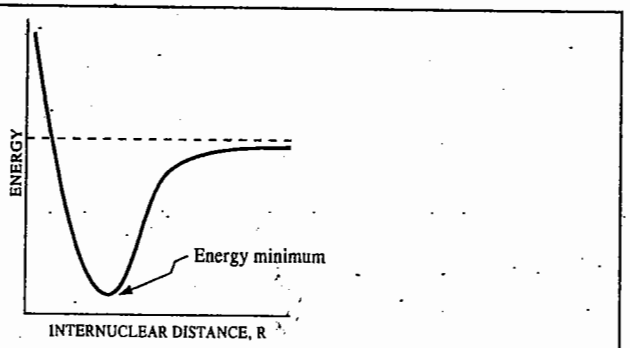

Fig. 29. Potential energy curve obtained by plotting energy *versus* internuclear distance.

Hellmann-Feynman Theorem

The concept of energy, as embodied in the Schrödinger wave equation, pervades chemical thinking of chemists, physicists and bioscientists. However, the **force concept** introduced by the German physicist H.Hellmann and, independently, by the American physicist Richard Feynman in the late 1930s, is a novel and penetrating way of gaining deeper insight into the nature of chemical bonding. The **Hellmann-Feynman electrostatic theorem** states that the effective force acting on a nucleus in a molecule can be calculated by simple electrostatics as the sum of the Coulombic forces exerted by the other nuclei and by a hypothetical electron cloud whose charge density, *viz.*, $-e\rho(x,y,z)$, is found by solving the electronic Schrödinger wave equation.

We consider a system with a time-independent Hamiltonian $\hat{H}$ that involves parameters. An obvious example is the molecular electronic Hamiltonian which depends parameterically on the nuclear coordinates. The stationary state wave functions also depend on the parameters in $\hat{H}$. We now investigate how E_n varies with each of the parameters. More specifically, let λ be one of the parameters. We are interested in evaluating $\partial E_n/\partial\lambda$, where the partial derivative is taken with all other parameters held constant. The Schrödinger wave equation is

$$\hat{H}\psi_n = E_n\psi_n \quad \ldots(146)$$

where ψ_n are the normalized stationary state eigenfunctions. Because of normalization, we have

$$E_n = \int \psi_n^*\,\hat{H}\,\psi_n\,d\tau \quad \ldots(147)$$

and

$$\frac{\partial E_n}{\partial\lambda} = \frac{\partial}{\partial\lambda}\int \psi_n^*\,\hat{H}\,\psi_n\,d\tau \quad \ldots(148)$$

The integral in Eq. 147 is a definite integral over all space and its value depends parameterically on λ since $\hat{H}$ and ψ_n depend on λ. Provided the integrand is well behaved, we can find the integral's derivative *w.r.t.* a parameter by differentiating the integral *w.r.t.* the parameter and then integrating. Thus,

$$\frac{\partial E_n}{\partial \lambda} = \int \frac{\partial}{\partial \lambda}(\psi_n^* \hat{H} \psi_n) d\tau = \int \frac{\partial \psi_n^*}{\partial \lambda} \hat{H} \psi_n \, d\tau + \int \psi_n^* \frac{\partial}{\partial \lambda}(\hat{H} \psi_n) d\tau \quad ...(149)$$

Also, we have

$$\frac{\partial}{\partial \lambda}(\hat{H} \psi_n) = \frac{\partial}{\partial \lambda}(\hat{T} \psi_n) + \frac{\partial}{\partial \lambda}(\hat{V} \psi_n) \quad ...(150)$$

The potential energy operator is simple multiplication by V so that

$$\frac{\partial}{\partial \lambda}(\hat{V} \psi_n) = \frac{\partial V}{\partial \lambda} \psi_n + V \frac{\partial \psi_n}{\partial \lambda} \quad ...(151)$$

Similarly, $$\frac{\partial}{\partial \lambda}(\hat{T} \psi_n) = \left(\frac{\partial \hat{T}}{\partial \lambda}\right) \psi_n + \hat{T}\left(\frac{\partial \psi_n}{\partial \lambda}\right) \quad ...(152)$$

where $\partial \hat{T} / \partial \lambda$ is found by differentiating $\hat{T}$ *w.r.t.* λ just as if it were a function instead of an operator. From Eqs. 151 and 152,

$$\frac{\partial}{\partial \lambda}(\hat{H} \psi_n) = \left(\frac{\partial \hat{H}}{\partial \lambda}\right) \psi_n + \hat{H}\left(\frac{\partial \psi_n}{\partial \lambda}\right) \quad ...(153)$$

Thus, Eq. 149 becomes

$$\frac{\partial E_n}{\partial \lambda} = \int \frac{\partial \psi_n^*}{\partial \lambda} \hat{H} \psi_n \, d\tau + \int \psi_n^* \frac{\partial \hat{H}}{\partial \lambda} \psi_n \, d\tau + \int \psi_n^* \hat{H} \frac{\partial \psi_n}{\partial \lambda} d\tau \quad ...(154)$$

For the first integral in Eq. 154, we have

$$\int \frac{\partial \psi_n^*}{\partial \lambda} \hat{H} \psi_n \, d\tau = E_n \int \frac{\partial \psi_n^*}{\partial \lambda} \psi_n \, d\tau \quad ...(155)$$

The Hermitian property of $\hat{H}$ and Eq. 146 give, for the last integral in Eq. 154,

$$\int \psi_n^* \hat{H} \frac{\partial \psi_n}{\partial \lambda} d\tau = \int \frac{\partial \psi_n^*}{\partial \lambda} (\hat{H} \psi_n)^* d\tau = E_n \int \psi_n^* \frac{\partial \psi_n}{\partial \lambda} d\tau \quad ...(156)$$

Hence, $$\frac{\partial E_n}{\partial \lambda} = \int \psi_n^* \frac{\partial \hat{H}}{\partial \lambda} \psi_n \, d\tau + E_n \int \frac{\partial \psi_n^*}{\partial \lambda} \psi_n \, d\tau + E_n \int \psi_n^* \frac{\partial \psi_n}{\partial \lambda} d\tau \quad ...(157)$$

Since the wavefunctions are normalized,

$$\int \psi_n^* \psi_n \, d\tau = 1 \quad \text{and} \quad \frac{\partial}{\partial \lambda} \int \psi_n^* \psi_n \, d\tau = 0$$

or $$\int \frac{\partial \psi_n^*}{\partial \lambda} \psi_n \, d\tau + \int \psi_n^* \frac{\partial \psi_n}{\partial \lambda} d\tau = 0 \quad ...(158)$$

Hence, from Eqs. 157 and 158, we obtain

$$\frac{\partial E_n}{\partial \lambda} = \int \psi_n^* \frac{\partial \hat{H}}{\partial \lambda} \psi_n \, d\tau \quad ...(159)$$

Eq. 159 is called the **generalized Hellmann-Feynman theorem.** The Hellmann-Feynman theorem, with E_n being the Hartree-Fock energy, is obtained by Hartree-Fock (as well as exact) wave functions.

It is reasonable to suppose that the Hellmann-Feynman theorem follows from the Born-Oppenheimer approximation since the rapid motion of the electrons allows the electronic wave function and probability density to adjust immediately to changes in nuclear configuration. The rapid motion of the electrons causes the sluggish nuclei to 'see' the electrons as a charge cloud rather than as discrete particles. The fact that the effective forces on the nuclei are electrostatic affirms that there are no 'mysterious quantum-mechanical forces' acting in molecules.

Application of Hellmann-Feynman Theorem to Chemical Bonding. Let us consider a diatomic molecule. We take the internuclear axis as the z-axis (Fig. 30).

By symmetry, the x and y components of the effective forces on the two nuclei are zero. For the z-component of force on nucleus a, we have (in a.u.) :

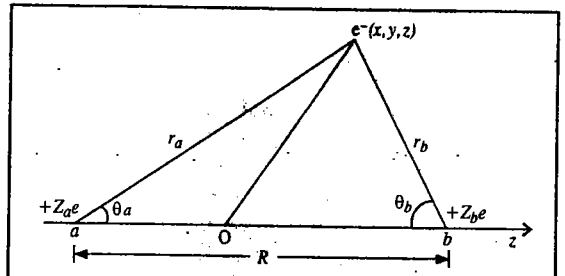

Fig.30. The coordinate system for a diatomic molecule; the origin is at O.

$$F_{z,a} = -Z_a \iiint \rho \frac{z_a - z}{r_a^3} dx\, dy\, dz - \frac{Z_a Z_b}{R^2} \quad ...(160)$$

where R is the internuclear distance, given by

$$R = [(x_a - x_b)^2 + (y_a - y_b)^2 + (z_a - z_b)^2]^{1/2}$$

From Fig. 30, we see that

$r_a \cos \theta_a = -z_a + z$ (z_a is negative). Hence,

$$F_{z,a} = Z_a \iiint \rho \frac{\cos \theta_a}{r_a^2} dx\, dy\, dz - \frac{Z_a Z_b}{R^2} \quad ...(161)$$

Similarly, we find that

$$F_{z,b} = -Z_b \iiint \rho \frac{\cos \theta_b}{r_b^2} dx\, dy\, dz + \frac{Z_a Z_b}{R^2} \quad ...(162)$$

Also, $$F_{z,a} = -\frac{dE(R)}{dz_a} = -\frac{\partial E(R)}{\partial R} \frac{\partial R}{\partial z_a} = -\frac{dE}{dR} \frac{z_a - z_b}{R}$$

$$= \frac{dE}{dR} \frac{\partial R}{\partial z_b} = -F_{z,b} \quad ...(163)$$

The effective forces on nuclei a and b are equal in magnitude and opposite in direction. From Eq. 161, the z-component of the effective force on nucleus a due to the element of electronic charge in the region about (x, y, z) is $Z_a \rho (\cos \theta_a / r_a^2) dx dy dz$. Similarly, the z-component of force on nucleus b due to this charge is $-Z_b \rho (\cos \theta_b / r_b^2)\, dx dy dz$. In these expressions the value corresponds to a force in the $+z$ direction, that is, to the right of Fig. 30. When the force on nucleus a is algebraically greater than the force on nucleus b, then the element of electronic charge tends to draw a towards b. Hence the electronic charge that is binding is located in the region where

$$Z_a \rho \frac{\cos \theta_a}{r_a^2} dx\, dy\, dz > -Z_b \rho \frac{\cos \theta_b}{r_b^2} dx\, dy\, dz \quad ...(164)$$

Since the probability density ρ is non-negative, division by ρ preserves the direction of inequality sign and the binding region of space is where

$$Z_a \frac{\cos\theta_a}{r_a^2} + Z_b \frac{\cos\theta_b}{r_b^2} > 0 \qquad \ldots(165)$$

When the force on b is algebraically greater than that on a, the electronic charge element tends to draw b away from a. The antibinding region of space is thus characterized by a negative value for the left side of Eq. 165. The surfaces for which the left side of Eq. 165 equals zero divide the space into the **binding** and **antibinding regions.** This concept of binding and antibinding regions was proposed by T. Berlin in 1951. Berlin's ideas have been extended to polyatomic molecules. Figs. 31 and 32 show the binding and antibinding regions for a homonuclear and a heteronuclear diatomic molecule.

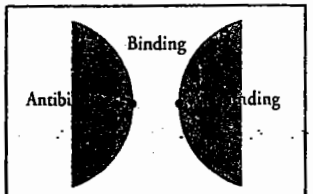

Fig. 31. Cross section of binding and antibinding regions in a homonuclear diatomic molecule. To obtain the three-dimensional regions, we rotate about the internuclear axis.

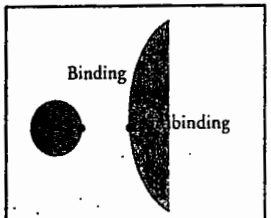

Fig. 32. Binding and antibinding regions for a heteronuclear diatomic molecule with $Z_b > Z_a$.

As might be expected, the binding region for a homonuclear diatomic molecule lies between the nuclei. Charge in this region tends to draw the nuclei together. From the basic principles of bonding we know that bonding leads to a transfer of charge probability density into the region between the nuclei because of the overlap of the bonding AOs. Fundamental work on Hellmann-Feynman theorem has been done by R.F.W. Bader and his coworkers (Henneker, P. Cade, A.K. Chandra) and B.M. Deb. For further applications of the Hellmann-Feynman theorem, one can refer to the following book :

B.M. Deb (ed.), *The Force Concept in Chemistry*, Van Nostrand Reinhold, 1981.

COMPUTATIONAL QUANTUM CHEMISTRY

Thanks to the pioneering contributions of J.A. Pople and his colleagues in the U.S.A., computational quantum chemistry has revolutionized research in theoretical chemistry since the 1960s. Much of the modern computational quantum chemistry uses Gaussian orbitals as a basis set. Pople has developed algorithms for the **ab initio calculation** of molecular properties based on Gaussian orbitals. The computer programs developed by Pople and his many collaborators have been packaged as a commonally available program called GAUSSIAN 94. This program, released in 1994, was developed at Carnegie-Mellon university in the U.S.A. In the **ab initio calculations** (which use the exact Hamiltonian), the task is greatly simplified by expressing the AOs used in the LCAO as linear combinations of Gaussian orbitals. A **Gaussian type orbital (GTO)** is a function of the form $e^{-\alpha r^2}$. However, in the **semi-empiricial calculations**, the AOs have been used as Slater-type orbitals as basis sets. A **Slater-type orbital** (STO) is a function of the form $e^{-\alpha r}$. (Hydrogenic orbitals as basis sets are not at all satisfactory.) We may recall that the set of AOs used to construct LCAO-MOs is called the **basis set.** In the case of diatomic molecules, the hydrogenic orbitals form the basis set. For example, the 1s orbitals of the two atoms constitute the basis set for the MO $\sigma_g(1s)$. For polyatomic molecules, the first basis set used in large scale computational studies consisted of STOs :

$$S_{nlm}(r, \theta, \phi) = N_n r^{n-1} e^{-\xi r} Y_{l,m}(\theta, \phi) \qquad \ldots(166)$$

where N_n is the normalization constant defined as

$$N_n = \frac{(2\xi)^{n+1/2}}{[(2n)!]^{1/2}}$$

where ξ (zeta) is the **orbital exponent,** n and l are the principal and orbital momentum (azimuthal) quantum numbers and $Y_{l,m}(\theta, \phi)$ are the angularly dependent spherical harmonics. The STOs differ from

the hydrogenic orbitals in that the STOs have no nodes and the orbital exponent is not necessarily equal to Z/n. In principle, the orbital exponents should be chosen to minimize the energy but this selection is still a formidable task even with modern computers. Slater has given a set of empirical rules for determining ξ for orbitals in free atoms. ξ increases with increasing atomic number, reflecting the contraction of the orbitals as the nuclear charge increases.

The STOs are not used directly in modern theoretical research because the integrals in the resulting secular determinants are difficult to evaluate. In particular, integrals involving more than one nuclear centre, called **multicentre integrals,** are awkward to evaluate using STOs. If we use GTOs instead of STOs, however, all the multicentre integrals are very easy to evaluate. As a matter of fact, the four-centre integrals can become two-centre integrals which can be easily computed. The use of GTOs was suggested in 1950 by S.F. Boys. The advantage of GTOs is that the product of two Gaussian functions is itself a Gaussian function that lies between the centres of the two contributing functions. The GTOs may be represented by

$$G_{nlm}(r, \theta, \phi) = N_n r^{n-1} e^{-\alpha r^2} Y_{l,m}(\theta, \phi) \qquad \ldots(167)$$

for the basis set in MO calculations.

The GTO does a reasonably good job of describing the STO for values of r greater than a_0 (the Bohr radius) but it underestimates its magnitude for values of r less than a_0. These discrepancies turn out to be very significant in molecular calculations. To overcome this difficulty quantum theorists prefer the use of curve-fit STOs to sums of Gaussian functions, the curve-fit improving with N, the number of Gaussian functions used. If, for instance, $N=3$, *i.e.*, we use a sum of three Gaussian functions to represent one STO ; such a basis set is called the **STO-3G basis set.** In the STO-3G basis set, all AOs are described by a sum of three Gaussian functions. Although this procedure leads to a proliferation of integrals to evaluate, each one is relatively easy. Thus, the overall procedure is quite efficient. However, there are some disadvantages, too, in using GTOs since many GTOs are needed to obtain for atoms the same degree of accuracy as the STOs.

It will be pertinent to define here the so-called **valence state ionization potentials.** Consider the electronic configuration of carbon atom, *viz.*, $1s^2\,\chi_1^1\,\chi_2^1\,\chi_3^1\,2p_z^1$ where χ_i (i=1, 2, 3) are the three triply hybridized orbitals in the sp^2 hybridised state, the hybrids being formed from 2s, 2p_x and 2p_y AOs. Here the carbon atom is said to be promoted to a **valence state** obtained through electronic rearrangement prior to the bond formation. This electronic configuration may be considered to be equivalent to the configuration $1s^2 2s^1 2p_x^1 2p_y^1 2p_z^1$. The valence state ionization potential of the $2p_z$ orbital in the carbon atom is given by the difference in energy between neutral carbon atom in the configuration $1s^2\,2s^1\,2p_x^1\,2p_y^1\,2p_z^1$ and the C^+ ion in the configuration $1s^2\,2s^1\,2p_x^1\,2p_y^1$. Similarly, the valence state ionization potential of the 2s orbital in carbon atom is given by the energy difference between the neutral atom configuration $1s^2\,2s^1\,2p_x^1\,2p_y^1\,2p_z^1$ and the C^+ ion in the configuration $1s^2 2p_x^1 2p_y^1 2p_z^1$. Typical values of the valence state ionization potentials are –13·60 eV (for hydrogen 1s), –21·4 eV (for carbon 2s), –11·4 eV (for carbon 2p) and – 26·0 eV (for nitrogen 2s).

A few remarks are in order for three important terms, *viz.*, correlation energy, electron correlation and configuration interaction, which are often involved in both the Hartree-Fock SCF theory of multielectron atoms and Hartree-Fock-Roothaan SCF theory of polyatomic molecules. It may be recalled that for helium atom, the use of a hydrogenic 1s orbital with variable orbital exponent gives a ground state energy of –77·5 eV, compared with the true value of –79·0 eV. The Hartree-Fock wave function for the helium ground state gives an energy of –77·9 eV which is still in error by 1·1 eV. The energy error of the Hartree-Fock wave function is called the **correlation energy** since it results from the fact that the Hartree Fock wave function neglects the instantaneous correlations in the motions of the electrons. Electrons repel one another and correlate their motions to avoid being close together; this phenomenon is called **electron correlation.**

Let us now consider **configuration interaction.** A method used to improve the Hartree-Fock wave function is configuration interaction. When a Hartree-Fock ground state wave function of an atom or a molecule is calculated, one also obtains expressions for unoccupied excited state orbitals. It is possible to show that the set of functions obtained by making all possible assignments of electrons to the available orbitals is a complete set. Hence, the true wave function of the ground state can be expressed as

$$\psi = \sum_j c_j \psi_{\text{orb}.j} \qquad \ldots(168)$$

where the $\psi_{\text{orb}.j}$s are approximate orbital functions that differ in the assignment of electrons to orbitals. Each $\psi_{\text{orb}.j}$ is a Slater determinant of spin orbitals. The functions $\psi_{\text{orb}.j}$ are called **configuration functions** (or **configurations**). One uses a variation procedure to find the values of the coefficients c_j that minimize the variational integral. This type of calculation is called **configuration interaction.**

A. Hartree-Fock-Roothaan Self-Consistent Field (SCF) Method for Polyatomic Molecules

The Hartree-Fock SCF method for atoms was extended by Roothaan in 1951 to polyatomic molecules. This SCF formulation of the MO theory is based on the many-electron Hamiltonian. (It may be recalled that the HMO theory uses an effective one-electron Hamiltonian which fails to consider electron repulsion energy term such as e^2/r_{ij} adequately). For a π-electron system, the Hamiltonian operator (in a.u.) is given by

$$\hat{H} = \sum_i^{\text{all electrons}} \hat{H}_i(\text{core}) + \frac{1}{2}\sum_{i\neq j}\frac{1}{r_{ij}} \qquad \ldots(169)$$

The first term in Eq. 169 is the attraction energy of the core for the π-electron. This is a one-electron operator since it depends on the coordinates of one electron only and is given by

$$\hat{H}_i(\text{core}) = -\frac{1}{2}\nabla_i^2 - \sum_a^{\text{all nuclei}} Z_a/r_{ia} \qquad \ldots(170)$$

where Z_a is the nuclear charge on nucleus a and r_{ia} is the distance of the ith electron from nucleus a. Each $1/r_{ij}$ term in Eq. 169 involves the coordinates of both electrons simultaneously and cannot be evaluated exactly. We can, however, approximate this term by considering, say, electron 1, subjected to the average potential field of electron 2 occupying the MO, say ψ_i. The average field is given by

$$\int \psi_i^2(2)(1/r_{12})\,d\tau_2$$

Since electrons can be exchanged among MOs, this can be taken care of by including the term

$$\int \psi_i(2)\psi_j(2)(1/r_{12})d\tau_2$$

These two terms are then summed over all the occupied MOs. Thus, the eigenvalue equation to be solved for electron 1 in MO, say, $\psi_j(1)$, is

$$\left[\sum_i^{\text{all electrons}} \hat{H}_i(\text{core}) + \sum^{\text{occupied MOs}} (2\hat{J}_i - \hat{K}_i)\right]\psi_j(1) = \varepsilon_j \psi_j(1) \qquad \ldots(171)$$

where

$$\hat{J}_i\,\psi_j(1) = \left\{\int \psi_i^2(2)(1/r_{12})\,d\tau_2\right\}\psi_j(1)$$

$$\hat{K}_i\,\psi_j(1) = \left\{\int \psi_i(2)\psi_j(2)(1/r_{12})\,d\tau_2\right\}\psi_i(1)$$

$\hat{J}$ and $\hat{K}$ are called the **Coulomb** and **exchange operators.** The Coulomb term is double since each MO is occupied by two electrons. The exchange term, on the other hand, is a single term; it vanishes unless

the MOs ψ_i and ψ_j refer to the same spin. The operator on the L.H.S. of Eq. 171 is called **effective Fock operator,** $\hat{F}$, which thus obeys the eigenvalue equation

$$\hat{F}\,\psi_i = \varepsilon_i\,\psi_i \qquad \ldots(172)$$

In the LCAO–MO approximation, the MOs are given by

$$\psi_i = \sum_j^{\text{All AOs}} c_{ij}\,\phi_j \qquad \ldots(173)$$

where ϕ_js are the AOs. Applying the variation method and minimizing the energy, we obtain the secular determinantal equation :

$$\begin{vmatrix} \alpha_{11}-\varepsilon & \beta_{12}-S_{12}\varepsilon & \beta_{13}-S_{13}\varepsilon & \ldots \\ \beta_{12}-S_{12}\varepsilon & \alpha_{22}-\varepsilon & \beta_{23}-S_{23}\varepsilon & \ldots \\ \ldots & \ldots & \ldots & \ldots \\ \ldots & \ldots & \ldots & \ldots \end{vmatrix} = 0 \qquad \ldots(174)$$

where

$$\left.\begin{aligned} \alpha_i &= F_{ii} \equiv \langle \phi_i \mid \hat{F} \mid \phi_i \rangle \\ \beta_{ij} &= F_{ij} \equiv \langle \phi_i \mid \hat{F} \mid \phi_j \rangle \\ S_{ij} &= \langle \phi_i \mid \phi_j \rangle \end{aligned}\right\} \qquad \ldots(175)$$

Evaluation of the diagonal terms, α_i and the off-diagonal terms, β_{ij}, omitting details, gives

$$\alpha_i = \alpha_i(\text{core}) + \tfrac{1}{2}q_i \langle \phi\phi_i \mid \phi\phi_i \rangle + \sum_{j\neq i} \langle \phi_i\phi_i \mid \phi_j\phi_j \rangle \qquad \ldots(176)$$

$$\beta_{ij} = \beta_{ij}(\text{core}) - \tfrac{1}{2}p_{ij} \langle \phi_i\phi_i \mid \phi_j\phi_j \rangle \qquad \ldots(177)$$

where q_i is the total π-electron density on atom i, p_{ij} is the mobile bond order if i and j are neighbouring atoms linked directly; α_i *(core)* and β_{ij} *(core)* are defined as

$$\alpha_i(\text{core}) = \langle \phi_j \left| \sum_i^{\text{all electrons}} \hat{H}_i(\text{core}) \right| \phi_j \rangle ;\ i = j \qquad \ldots(178)$$

$$\beta_{ij}(\text{core}) = \langle \phi_j \left| \sum_i^{\text{all electrons}} \hat{H}_i(\text{core}) \right| \phi_j \rangle ;\ i \neq j \qquad \ldots(179)$$

$$= 0, \text{ otherwise.} \qquad \ldots(180)$$

We shall now comment on the matrix elements (integrals) in Eqs. 176 and 177. The integral $\langle \phi_i\,\phi_i \mid \phi_i\,\phi_i \rangle$ in Eq. 176 represents electron repulsion between two electrons in the field of the same core; the integral $\langle \phi_i\,\phi_i \mid \phi_j\,\phi_j \rangle$ in Eq. 177 describes electron repulsion between electrons on the neighbouring cores.

Pariser-Parr-Pople Approximation (PPP Approximation). This appoximation, proposed independently, in 1953, by Pariser and Parr (in a joint publication) and by Pople, attempts to evaluate the matrix elements α_i (core), β_{ij} (core) and the one-centre and two-centre electron repulsion integrals of Eqs. 176 and 177. They suggested that

$$\alpha_i(\text{core}) = -I_c \qquad \ldots(181)$$

where I_c is the valence state ionization potential of carbon and that

$$< \phi_c\phi_c \mid \phi_c\phi_c > = I_c - A_c \qquad ...(182)$$

where A_c is the corresponding valence state electron affinity of carbon atom. The resonance integral β_{ij} (core) was assumed to be zero for all orbitals except those on the nearest neighbouring atoms. For the C—C bond in benzene it was estimated to be −2·39 eV. The two-centre integrals, *viz.*, $< \phi_i \phi_i \mid \phi_j \phi_j >$, which depend on the internuclear separation R_{ij}, must follow the following boundary conditions :

$$\left.\begin{aligned} \gamma_{ij} &= \gamma_{ii}, \quad R_{ij} \to 0 \text{ (one - centre integral)} \\ \gamma_{ij} &= e^2/R_{ij}, \quad R_{ij} \to \infty \end{aligned}\right\} \qquad ...(183)$$

where $\gamma_{ij} = < \phi_i \phi_i \mid \phi_j \phi_j >$

Configuration Interaction

In order to calculate molecular properties to a high degree of accuracy, one must usually go beyond the Hartree-Fock-Roothaan SCF method and include electron correlation. This can be done using the configuration interaction (CI). The steps in a CI calculation are : (1) One chooses a set of basis functions $g_1, g_2 \ldots, g_i, \ldots$ (2) Each MO ϕ_j is written as a linear combination of basis functions : $\phi_j = \sum c_i g_i$ where the expansion coefficients c_i are to be determined. This expression for the MOs is substituted into the Hartree-Fock equations $\hat{F}\phi_j = \varepsilon_j \phi_j$ and the SCF interation procedure in carried out to solve for the coefficient c_i which determine the MOs, ϕ_j. The SCF procedure gives expressions for many MOs, some occupied and some unoccupied. The unoccupied MOs are called **virtual orbitals.** The ground state SCF wave function is a Slater determinant with the lowest MO occupied. (3) The molecular wave function ψ is then expressed as a linear combination of the SCF wave functions found in step 2 and functions with one or more electrons placed in virtual orbitals : $\psi = \Sigma_j a_j \psi_{orb.j}$ and the variation method is used to find the coefficients a_j that minimize the variational integral.

If the sum $\Sigma_j\, a_j\, \psi_{orb.j}$ includes functions with all possible assignments of electrons to virtual orbitals (this is called *full* CI) and if the basis set used to expand the MOs is a complete set, then one can prove that the exact wave function will be obtained. In practice, the basis set must be limited in size (and is, therefore, incomplete), and full CI takes far too much computer time to be feasible (except for small molecules and small basis sets).

In practice, it has been formed that the Hartree-Fock-Roothaan SCF-CI calculations with small basis sets do not give highly accurate results for molecular properties and basis sets at least as large as 6-31 G* should be used in CI calculations. (The basis sets (listed in the order of increasing size) include the STO-3G, 3-21G, 3-21G*, 6-31G* and 6-31G** sets where the numbers and symbols are related to the number of basis functions on each atom. STO-3G is a minimal basis set and often gives unreliable results, so this set is essentially obsolete. The 6–31 G* basis set is not a particularly large set and many larger sets have been formed by adding functions to 6–31 G**.)

B. Semi-Empirical and Ab Initio Methods

We have already dealt briefly with the semi-empirical PPP approximation used to evaluate the multicentre integrals occurring in the Hartree-Fock-Roothaan SCF theory. Thus, in **semi-empirical methods** many of the integrals are estimated by appealing to spectroscopic data or physical properties such as ionization energies and using several rules to set certain integrals to zero. In the **ab initio methods,** an attempt is made to calculate all integrals that appear in the secular determinant explicitly and, after using the SCF procedure, to derive the MOs. It is evident that for a given size of computation, semi-empirical methods are applicable to a fairly large molecule whereas the ab initio methods apply to a small-sized molecule.

Extended Hückel Theory (EHT). We recall that in the Hückel molecular orbital (HMO) theory of 1931, the π orbitals in a conjugated π-electron system are treated separately from the σ orbitals and the latter form a rigid framework that determines the shape of the molecule. This assumption is called the

σ – π separability. The EHT, formulated by Hoffmann in 1963, includes both σ and π orbitals and so it is not confined to planar conjugated hydrocarbons. Also, EHT does not ignore overlap but calculates all the overlap integrals explicitly. It employs a one-electron Hamiltonian. In the LCAO-MO approximation, each MO is written as

$$\psi_i = \sum_\nu c_{i,\nu} \phi_\nu \qquad ...(184)$$

where the ϕ_νs are the nonmalized STOs (for the valence electrons) on the ν-th atom in the molecule; the subscript i refers to the MOs and ν to the AOs. On each centre, except hydrogen atom, there is more than one AO. Thus, STOs are the basis set in EHT. Application of the variation method leads to the secular determinant :

$$\begin{vmatrix} H_{11} - \varepsilon & H_{12} - S_{12}\varepsilon & H_{13} - S_{13}\varepsilon & \ldots \\ H_{12} - S_{12}\varepsilon & H_{22} - \varepsilon & H_{23} - S_{23}\varepsilon & \ldots \\ \ldots & \ldots & \ldots & \ldots \end{vmatrix} = 0 \qquad ...(185)$$

The matrix elements $H_{\mu\nu}$ are defined as

$$H_{\mu\nu} = < \phi_\mu | \hat{H} | \phi_\nu > \qquad ...(186)$$

The diagonal matrix elements $H_{\mu\mu}$ (or α_μ) are set equal to the negative of the valence state ionization potential of the appropriate AO. The off-diagonal elements $H_{\mu\nu}$ (corresponding to β and 0 in the HMO theory) are assumed to be proportional to the overlap integral, $S_{\mu\nu}$. A typical expression, proposed by Ballhausen and Gray in 1962, is

$$H_{\mu\nu} = 0{\cdot}5\, [H_{\mu\mu} + H_{\nu\nu}]\, S_{\mu\nu} K \text{ with } K = 1{\cdot}75 \qquad ...(187)$$

The integrals $S_{\mu\nu}$ are calculated using the STOs and the secular determinant (Eq. 20) is then solved for the orbital energies and the coefficients. The total energy is calculated by summing the energies of the occupied MOs by taking into consideration their occupancy numbers. For a closed shell, for instance, the total electronic energy is given by

$$E_{EHT} = 2\sum_i^{occ.} \varepsilon_i \qquad ...(188)$$

The EHT method was also independently proposed by Wolfsberg and Helmholz. The Hückel and extended Hückel methods are quite crude in that they use a very simplified Hamiltonian that contains no inter-electron repulsion terms. Several improved semi-empirical theories have been developed that include some of the electron repulsion terms in the Hamiltonian operator and that apply to both conjugated and non-conjugated molecules. The most widely used are the methods AM1 and PM3.

The AM1 (**Austin Model 1**) method (named after the University of Texas at Austin where the method was developed) was devised by M.J.S. Dewar and coworkers in 1985. AM1 treats only the valence electrons. It solves equations resembling the Hartree-Fock equations $\hat{F}\phi_i = \varepsilon_i \phi_i$ (where $\hat{F}$ is the Fock operator) to find the SCF MOs but since an approximate Hamiltonian is used and rather drastic approximations are made for many of the integrals that occur, the MOs found are only rough approximations to the Hartree-Fock-Roothaan MOs. By choosing reasonable values of the parameters, the AM1 method gives reasonable values of the heats of atomization of many compounds. PM3 (parametric method 3) is similar to AM1 except that it uses different sets of parameters. The molecular geometries and molecular dissociation energies calculated using these methods are not very accurate though they do give satisfactory bond lengths and bond angles.

Current versions of EHT are easy to implement with a computer and give useful qualitative pictures of MOs in molecules with known structures. Unfortunately, it cannot predict the correct three-dimensional structures of even simple molecules. Thus, for instance, EHT predicts that linear H_2O molecule has lower energy than angular H_2O molecule.

We shall conclude the discussion on EHT by briefly commenting on the so-called **population analysis.** For a two-atom MO of the form $\psi = c_1\phi_1 + c_2\phi_2$ (where ϕ_1 and ϕ_2 are the AOs centered on atoms 1 and 2), the probability density for an electron that occupies this orbital is given by $\psi^2 = c_1^2\phi_1^2 + c_2^2\phi_2^2 + 2c_1c_2\phi_1\phi_2$. The integral of this probability density over all space gives the total probability of finding the electron in the molecule :

$$1 = c_1^2 + c_2^2 + 2c_1c_2S_{12} \qquad ...(189)$$

This expression suggests that the total probability of finding the electron in the molecule is the sum of the probability of finding it on orbital 1 (the term c_1^2), the probability of finding it on orbital 2 (the term c_2^2) and the probability that it is in the overlap region between the two atoms (the term $2c_1c_2S_{12}$). The last term is called the **overlap population.** This kind of apportioning of the population is called the **Mulliken Population Analysis (MPA),** after R. S. Mulliken who suggested it in 1955. In general, for an MO expressed as a linear combination of AOs with coefficients c_i, the **atomic populations,** ρ_i, are given by

$$\rho_i = c_i^2 \qquad ...(190)$$

and the overlap populations are given by

$$\rho_{ij} = 2\, c_i c_j\, S_{ij} \qquad ...(191)$$

If two electrons occupy an orbital, then these contributions should be doubled. The overall populations are the sums of these quantities for all the occupied MOs in the molecule multiplied by the number of electrons in each MO. If we apportion one-half of each overlap population to the neighbouring atoms, we obtain the **gross orbital population.**

Semi-Empirical Self-Consistent-Field (SCF) Theory. The semi-empirical SCF theory makes use of the Roothaan method to obtain the SCF MOs for all valence electrons. In 1965, Pople, Santry and Segal introduced the **zero differential overlap (ZDO)** approximation, according to which if ϕ_μ and ϕ_ν are two AOs centered either on the two nuclei or on the same nucleus, then $\phi_\mu\phi_\nu = 0$ wherever they occur. Other elements of the Fock operator were determined by appeal to experimental data. The ZDO approximation is more drastic than the neglect of the overlap integral ($S_{\mu\nu}=0$). This seminal 1965 paper of Pople, inspired other semi-empirical theories such as **complete neglect of differential overlap (CNDO), intermediate neglect of differential overlap (INDO)** and **modified intermediate neglect of differential overlap (MINDO)** (as proposed by M.J.S. Dewar and coworkers). Let us illustrate CNDO by reference to the Fock matrix which has **multicentre integrals** of the form,

$$\langle \phi_a\, \phi_b \mid \phi_c\, \phi_d \rangle = \int \phi_a(1)\phi_b(1)(1/r_{12})\phi_c(2)\phi_d(2)\, d\tau_1\, d\tau_2 \qquad ...(192)$$

where ϕ_a, ϕ_b, ϕ_c and ϕ_d are AOs which, in general, are centered on different nuclei. We can appreciate that, if there are several dozen AOs used to construct the MOs, then there will be tens of thousands of integrals to evaluate. In the CNDO approximation all integrals are set equal to zero unless ϕ_a and ϕ_b are the same AOs centred on the same nucleus, and likewise for ϕ_c and ϕ_d. The surviving integrals are then adjusted until the energy levels are in good agreement with experiment. The CNDO procedure and its descendants (INDO, MINDO, etc.) are now readily available in commercial software packages and can be used with very little detailed knowledge of their mode of calculation. The packages also have sophisticated graphical output procedures which enable one to analyse the shapes of orbitals and the electric charge distribution in molecules. Commercial software packages are also available for *ab initio* calculations to evaluate as efficiently as possible thousands of integrals. Use of GTOs in *ab initio* methods plays a very important role, as already stated. We must emphasize that an *ab initio* calculations uses the true molecular Hamiltonian and does not use empirical data in the calculations. A semi-empirical method uses a simpler Hamiltonian than the true one; it also uses empirical data to assign values to some of the integrals that occur in the calculations and neglects some of the integrals.

Further Remarks on Computer Programs. As already stated, Gaussian is the most widely used program for *ab initio* and density functional theory (DFT) calculations. The first version of Gaussian,

developed by Pople and coworkers, was released in 1970. Its updated versions Gaussian 94 and Gaussian 98 were released in 1994 and 1998, respectively. Some other quantum-chemistry programs are the free program GAMESS, Q-Chem, Jaguar, SPARTAN, HyperChem, MOPAC 2000 and AMPAC. These are available on World Wide Web (www). Gaussian exists in versions for UNIX workstations and Windows personal computers. The free Windows program Arguslab does Hartree-Fock, AM1 and PM3 calculations. Computer programs such as MATHEMATICA and MAPLE are used for less demanding mathematical calculations. Most computer programs in use today can be obtained from the Quantum Chemistry Program Exchange (QCPE), Chemistry department, Indiana University, Bloomington, U.S.A. We may also mention here that though the two-electron integrals can be evaluated by a variety of procedures, one can save a great deal of labour using general formulas found in several different compilations frequently used by quantum chemists. A few of these compilations are :

Miller, J., J.M. Gerhausen and F.A. Matsen, *Quantum Chemistry Integrals and Tables*, University of Texas Press, Austin (U.S.A.), 1959.

Kotani, M., *et al*, *Tables of Molecular Integrals*, Maruzen, Tokyo (Japan), 1963.

Preuss, H., *Integraltafeln zur Quantenchemie*, 4 vols; Springer-Verlag, Berlin, 1956.

Abramowitz, M., and I.A. Stegun (ed)., *Handbook of Mathematical Functions*, Dover Publications, New York, 1963. (P.W. Atkins has remarked that this amazing book is "an ideal desert-island book for shipwrecked quantum chemists.")

C. Density-Functional Theory (DFT). In the last decade of the twentieth century, **DFT** attained great prominence in quantum chemistry research. The enthusiasts of DFT—and there are a host of them—claim that this theory will be *the* theory of chemical bonding in the twenty-first century. What is DFT ? What is so exciting about it ? Or rather, what is *not* so very exciting about it ? We shall deal briefly with this topic here.

In DFT we do not calculate the molecular wave function. Instead, we work with electron probability density $\rho(x, y, z)$. DFT is based on the **Hohenberg-Kohn theorem,** proposed in 1964 by P. Hohenberg and W. Kohn. This theorem states that *the energy and all other properties of a ground state molecule are uniquely determined by the ground state electron probability density.* This is expressed by saying that the ground state electronic energy E_{gs} is a *functional* of ρ. This is written as $E_{gs}=E_{gs}[\rho(x, y, z)]$ or simply as

$$E_{gs} = E_{gs}[\rho] \qquad ...(193)$$

where the square brackets denote a functional relation. (In mathematics a function of a function is called a **functional**.)

Kohn-Sham Method. Unfortunately, the functional $E_{gs}[\rho]$ in Eq. 28 is unknown, so the Hohenberg-Kohn theorem does not tell us *how* to calculate E_{gs} from ρ or how to find ρ without first finding the ground state molecular electronic function. In 1965, W. Kohn and L.J. Sham devised a practical method to calculate E_{gs} from ρ. Of course, the Kohn-Sham equations do contain an unknown functional, but using a combination of physical insight and guesswork, theorists have developed approximations to this functional that allow accurate calculations of molecular properties thereby turning DFT into a landmark in quantum theory.

Kohn-Sham method uses a **fictitious reference system** (usually denoted by the subscript s) that contains the same number of electrons (n) as the molecule under study, but differs from the molecule in that (a) the electrons in the reference system do not exert forces on one another, (b) each electron i ($i=1, 2, \ldots, n$) in the reference system experiences a potential energy $V_s(x_i, y_i, z_i)$, where V_s is the same function for each electron and is such as to make the electron probability density ρ_s in the reference system exactly equal to the ground state electron probability density ρ in the real molecule : $\rho=\rho_s$. The actual form of V_s is not known. (In the real molecule, the electrons experience attractions to the nuclei but these are not present in the reference system.)

Because the electrons in the reference system do not interact with one another, the Hamiltonian $\hat{H}_s$ of the reference system is the sum of the Hamiltonians of the individual electrons :

$$\hat{H}_s = -\frac{\hbar^2}{2m_e}\sum_{i=1}^{n}\nabla_i^2 + \sum_{i=1}^{n}V_s(x_i,y_i,z_i) \equiv \sum_{i=1}^{n}\hat{h}_i^{KS}$$

where $$\hat{h}_i^{KS} = -\frac{\hbar^2}{2m_e}\nabla_i^2 + V_s(x_i,y_i,z_i) \quad ...(194)$$

In Eq. 194, $\hat{h}_i^{KS}$ is the one-electron Kohn-Sham Hamiltonian. Since the reference system *s* consists of non-interacting particles, its ground state wave function, including both the spatial and spin wave functions, is a Slater determinant of spin-orbitals, one for each electron. Each spin orbital is the product of a spatial orbital θ_i^{KS} and a spin function (either α or β). The Kohn-Sham orbitals θ_i^{KS} are eigenfunctions of θ_i^{KS} :

$$\hat{h}_i^{KS}\theta_i^{KS} = \varepsilon_i^{KS}\theta_i^{KS} \quad ...(195)$$

where ε_i^{KS} is the Kohn-Sham orbital energy of θ_i^{KS}. Each Kohn-Sham orbital holds two electrons of opposite sign. By definition,

$$\rho = \rho_s = \sum_{i=1}^{n}|\theta_i^{KS}|^2 \quad ...(196)$$

Kohn-Sham Energy Expression. Next we need the energy expression for the molecule's ground state electronic energy E_e. (The reference system and the molecule have the same probability density function but they do not have the same ground-state energy.) Kohn and Sham derived the following exact equation for E_e :

$$E_e = < K_{e,s} > + < V_{Ne} > + J + V_{NN} + E_{xc}[\rho] \quad ...(197)$$

In Eq. 197, $< K_{e,s} >$ is the average electronic kinetic energy in the reference system; $< V_{Ne} >$ is the average potential energy of attractions between the electrons and nuclei in the molecule ; J is the classical energy of electrical repulsion that arises between the infinitesimal charge elements of a hypothetical smeared-out electron charge cloud whose probability density is $\rho(x, y, z)$. It can be calculated from $\rho(x, y, z)$. $< K_{es} >$ and $< V_{Ne} >$ can be calculated from the Kohn-Sham orbitals of the reference system. (We are not interested here in the explicit formulas for the calculation of these two quantities.) The internuclear repulsion potential energy, V_{NN}, is a constant that depends on the nuclear charges and the internuclear distances and is calculated from the molecular geometery at which the calculation is being made. $E_{xc}[\rho]$, called the **exchange-correlation energy functional**, is a functional of ρ that is defined as

$$E_{xc}[\rho] \equiv < K_e > - < K_{es} > + < V_{ee} > - J \quad ...(198)$$

$E_{xc}[\rho]$ is the sum of two differences : (*a*) the difference $< K_e > - < K_{es} >$ between the average electronic kinetic energy in the molecule and in the reference system and (*b*) the difference $< V_{ee} > - J$ between the average potential energy of interelectronic repulsion $< V_{ee} >$ in the molecule and the classical charge-cloud self-repulsion energy J. The values of $< K_e >$ and $< K_{es} >$ are expected to be similar to each other; also the values of $< V_{ee} >$ and J are similar. Hence, the two differences in Eq. 198 are relatively small quantities. These two differences are not zero because the Pauli exclusion principle requirement that the wave function be antisymmetric with respect to exchange, produces exchange effects on the energy and because the instantaneous correlation between the motions of the electrons produces *correlation* effects on the energy.

Eq. 197 is an exact expression for the molecular electronic energy. However, the true mathematical expression for the functional E_{xc} is not known. The terms $E_{xc}[\rho]$ can be found if we know ρ and if we know what the functional E_{xc} is. If Eq. 198 is substituted into Eq. 197, we obtain

$$E_e = < K_e > + < V_{Ne} > + < V_{ee} > + V_{NN} \quad ...(199)$$

an equation that follows from the Born-Oppenheimer approximation, *viz.*, $\hat{H}_e = \hat{K}_e + \hat{V}_{Ne} + \hat{V}_{ee} + \hat{V}_{NN}$ by taking average values of each side of this approximation.

Kohn-Sham Orbitals. As we have noted in the discussion following Eq. 197, the quantities $< K_{es} >$, $< V_{Ne} >$, J and E_{xc} can all be calculated if we know the Kohn-Sham orbitals θ_i^{KS}. V_{NN} is easily calculated from the location of the nuclei. Thus, if the Kohn-Sham orbitals are known, E_e can be calculated. Hohenberg and Kohn proved that the true ground state electron probability ρ minimizes the functional $E_e[\rho]$ for the energy. Since ρ is determined by the KS orbitals θ_i^{KS} (Eq. 196), one can vary the orbitals θ_i^{KS} so as to minimize E_e in Eq. 197.

Parr and Yang have shown that the orthonormal (*i.e.*, orthogonal and normalized) KS orbitals that minimize E_e satisfy the eigenvalue equation Eq. 195 where the one-electron KS Hamiltonian $\hat{h}_i^{KS}$ is given by the sum of the following four one-electron terms : (*a*) The one-electron energy operator $-\left(\frac{\hbar^2}{2m_e}\right)\nabla_i^{KS}$; (*b*) The potential energy $-\sum\alpha Z\alpha e^2/4\pi\varepsilon_0 r_{1\alpha}$ of attraction between electron 1 and the nuclei ; (*c*) the potential energy of repulsion between electron 1 and a hypothetical charge cloud of electron density ρ due to smeared-out electrons; (*d*) an exchange-correlation potential $V_{xc}(x_1, y_1, z_1)$ whose form is discussed below. (The sum of terms *b*, *c* and *d* equals what is called V_s in Eq. 194).

It is pertinent to mention here that the first three terms in $\hat{h}_i^{KS}$ are, in fact, identical to the first three terms in the Fock operator $\hat{F}$ of the Hartree-Fock equations $\hat{F}\phi_i = \varepsilon_i\phi_i$. The only difference between the Hartree-Fock equations for the Hartree-Fock orbitals and the Kohn-Sham equations [Eq. 195] is that the exchange operator (term *d*) of the Hartree-Fock equations is replaced by the **exchange-correlation potential,** V_{xc}. The expression for V_{xc} is found to be

$$V_{xc}(x, y, z) = \frac{\delta E_{xc}[\rho]}{\delta\rho} \quad ...(200)$$

where the notation $\delta E_{xc}/\delta\rho$ indicates the **functional derivative** of the functional E_{xc} that occurs in the energy equation 197. The fourth term (*d*) in the Fock operator $\hat{F}$ of the Hartree-Fock equations allows for the effects of electron exchange (the Pauli principle) but does not allow for electron correlation. The fourth term V_{xc} in the KS operator $\hat{h}_i^{KS}$ allows for both exchange and correlation.

DFT Calculational Procedure. If we assume that a reasonable approximation for the exchange-correlation energy functional $E_{xc}[\rho]$ exists, then we proceed as follows : We start with an initial guess for the molecule's electron density $\rho(x, y, z)$ found by superimposing calculated electron densities of the individual atoms at the nuclear geometry chosen for the calculation. From the initial ρ, we find $E_{xc}[\rho]$ and then find its functional derivative to obtain an initial estimate of V_{xc} (Eq. 200) . This V_{xc} is used in the Kohn-Sham equations (Eq. 195) to solve for initial estimates of the orbitals θ_i^{KS}. (As is done in solving the Hartree-Fock equations, we usually expand the unknown orbitals using a basis set. Many of the same basis sets used for the Hartree-Fock calculations are also used in the Kohn-Sham calculations.) The initial orbitals θ_i^{KS} are used to calculate an improved probability density ρ from Eq. 196. This improved ρ is used to find an improved $E_{xc}[\rho]$ from which an improved V_{xc} is found. The improved V_{xc}

is used in the KS equations (Eq. 195) to find improved *KS* orbitals. The iterations are continued until no further significant change is found from one cycle to the next. The molecular energy is then found from Eq. 197 using the final orbitals and ρ.

Exchange-Correlation Energy Functional $E_{xc}[\rho]$. Kohn and Sham proposed a certain form for $E_{xc}[\rho]$, called the **local (spin) density approximation (LDA or LSDA)** that theory shows to be accurate when the electron density ρ varies slowly with position. In a molecule, ρ does not vary very slowly with position. It is found that LSDA KS DFT calculations give satisfactory results for molecular geometries, dipole moments and vibrational frequencies but poor results for atomization energies.

It is convenient to split E_{xc} into an exchange part and a correlation part :

$$E_{xc}[\rho] = E_x[\rho] + E_c[\rho] \qquad ...(201)$$

This is a good approximation for $E_{xc}[\rho]$ suggested by Kohn and Sham. A better approximation used in the late 1980s was the so-called **generalized-gradient approximation (GGA)**, in which E_{xc} is expressed as an integral of a certain function of ρ and the derivatives $\partial\rho/\partial x$, $\partial\rho/\partial y$, $\partial\rho/\partial z$. (These derivatives are called the *gradient* of ρ). Another functional called a **hybrid functional** has also been used ; it is of the form $E_{xc}^{GGA} + aE_x^{HF}$ where E_x^{HF} has the form of the expression used for the exchange energy in Hartree-Fock calculations but is evaluated using the KS rather than Hartree-Fock orbitals, and a is an empirical parameter whose value was chosen to optimize the performance of E_{xc} in calculations on a series of molecules. The most widely used functional in DFT calculations done in the period 1995-2000 was the hybrid functional called B3LYP where B indicates that it includes a term for E_x^{GGA} devised by Becke, LYP indicates a term for E_c^{GGA} devised by Lee, Yang and Parr, and 3 indicates that it contains three empirical parameters whose values were chosen to optimize the performance.

The time needed to do a DFT calculation is roughly the same as the time needed to do a Hartree-Fock calculation on the same molecule with the same basis set. In practice, since the true functional $E_{xc}[\rho]$ is unknown, DFT calculations yield approximate results. The quality of the result depends on how good the E_{xc} used in the calculation is. With present-day E_{xc} functionals, DFT calculations yield substantially more accurate results than Hartree-Fock calculations. DFT calculations should not be done with basis sets smaller than 6–31*G**. Although the KS orbitals are calculated for the fictitious reference system (and not for the real molecule), one finds that these orbitals closely resemble the Hartree-Fock SCF MOs calculated for the real molecule.

Despite its many successes, DFT does have some drawbacks. DFT is basically a ground state theory. Researchers are currently working to extend it to excited states. In DFT, the performance of a given functional cannot be predicted and one must try it out on a variety of molecules and properties to assess its performance. There is no systematic way in DFT to devise better functionals. The currently available functionals do not give good accuracy when dealing with van der Waals intermolecular interactions, nor can they match the performance of very high-level *ab initio* methods. For more details on DFT and on quantum chemistry, the following books should be referred :

Parr, R.G, and W. Yang, *Density-Functional Theory of Atoms and Molecules*, Oxford, 1989.

Koch, W. and M.C. Holthausen, *A Chemist's Guide to Density Functional Theory*, Wiley-VCH, 2000.

March, N.H. and B.M. Deb (eds.), *Single-Particle Density in Physics and Chemistry*, Academic Press, 1987.

Yamaguchi, Y.,Y. Osamura, J.D. Goddard, and H.F. Schaeffer III, *A New Dimension to Quantum Chemistry*, Oxford, 1994.

TIME-DEPENDENT PERTURBATION THEORY (TDPT)

Time-dependent perturbation theory (TDPT) is of great importance in quantum mechanics. It is concerned with the solution of the time-dependent Schrödinger equation (TDSE) even as the time-independent perturbation theory (TIPT) is concerned with the approximate solution of the time-independent

Schrödinger equation (TISE). The transition probabilities between the stationary state energy levels, and thus the selection rules for spectral transitions, are derived from TDPT. When a system is isolated and the Hamiltonian is independent of time, the energy eigenstates are true stationary states. If the system initially is in a particular state ψ_n, which is an eigenstate (eigenfunction) of the unperturbed time-independent Hamiltonian $H^{(0)}$, it will stay there for all time. The time-dependence of ψ_n is of the form

$$\psi_n(t) = \psi_n(0) \exp(-iE_nt/\hbar) \qquad ...(202)$$

where E_n is the energy of the state n. If however, the Hamiltonian is time-dependent, the energy is no longer a constant of motion. In that case, the knowledge of the behaviour of the system is obtained by solving the TDSE

$$i\hbar\frac{\partial}{\partial t}\psi = \hat{H}\psi \qquad ...(203)$$

We assume that the Hamiltonian of the system can be divided into two parts :

$$\hat{H} = \hat{H}^{(0)}(r) + \hat{V}(r,t) \qquad ...(204)$$

where $\hat{H}^{(0)}$ is the unperturbed time-independent Hamiltonian whose wave functions describe the stationary states of the unperturbed system ; $\hat{V}(r,t)$ is a very small perturbation that depends on both space and time variables such that

$$|H^{(0)}(r)| >> |\hat{V}(r,t)| \qquad ...(205)$$

Since the total Hamiltonian $\hat{H}(r,t)$ is time-dependent, the energy cannot be conserved, so that there are no stationary states. Let ψ_n denote the set of eigenfunctions (eigenkets) of $\hat{H}^{(0)}$:

$$\hat{H}^{(0)}\psi_n = E_n\psi_n = \hbar\omega\psi_n \qquad ...(206)$$

where E_n ($= \hbar\omega_n$) represents the corresponding energy eigenvalues. The wave function corresponding to the actual state $\Psi(t)$ can be expanded in terms of ψ_n :

$$\Psi(t) = \sum_n b_n(t)\psi_n(r) \qquad ...(207)$$

where $|b_n(t)|^2$ can be interpreted as the probability of finding the system in the state n at time t. For the sake of convenience, we write

$$b_n(t) = a_n(t)e^{-i\omega_n t}$$

so that

$$\Psi(t) = \sum_n a_n(t)\,e^{-i\omega_n t}\psi_n(r) \qquad ...(208)$$

Obviously, $|a_n(t)|^2$ will also represent the probability of finding the system in the state n at time t. Our objective is to develop a perturbation theory for the calculation of $a_n(t)$ for a given $V(t)$. (We shall write $V(r, t)$ as $V(t)$ and $H^{(0)}(r)$ as $\hat{H}^{(0)}$ for the sake of convenience).

From Eqs. 203, 204 and 208, we have

$$i\hbar\frac{\partial}{\partial t}\Psi(t) = (\hat{H}^{(0)} + \hat{V}(t))\Psi(t)$$

$$= (\hat{H}^{(0)} + \hat{V}(t))\sum_n a_n(t)e^{-i\omega_n t}\psi_n(r) = \sum_n (E_n + V)a_n(t)\psi_n(r)e^{-i\omega_n t} \qquad ...(209)$$

where in the last step we have used Eq. 208. Using Eq. 209, the left-hand side of Eq. 209 becomes

$$i\hbar\frac{\partial}{\partial t}\Psi(t) = i\hbar\frac{\partial}{\partial t}\sum_n a_n(t)\,e^{-i\omega_n t}\psi_n = i\hbar\sum_n[\dot{a}_n - i\omega_n a_n]e^{-i\omega_n t}\psi_n \quad ...(210)$$

where the dot over a refers to differentiation with respect to time, t.

Thus, we have

$$i\hbar\sum_n[\dot{a}_n - i\omega_n a_n]e^{-i\omega_n t}\psi_n = \sum_n(E_n + V)a_n(t)\,e^{-i\omega_n t}\psi_n \quad ...(211)$$

where the second term on the left hand side cancels the first term on the right hand side. Multiplying the left hand side by ψ_m^* and remembering the orthonormality relation

$$\int\psi_m^*\psi_n d\tau = <m|n> = \delta_{mn} \quad ...(212)$$

where δ_{mn} is the Kronecker delta, we get

$$i\hbar\frac{da_m}{dt} = \sum_n a_n(t)V_{mn}(t)\exp(i\omega_{mn}t) \quad ...(213)$$

where

$$\omega_{mn} = \omega_m - \omega_n = (E_m - E_n)/\hbar \quad ...(214)$$

$$V_{mn}(t) = \int\psi_m^* V(t)\psi_n d\tau = <m|V|n> \quad ...(215)$$

Assume that at time t, the amplitudes have not changed very much from their values at $t = 0$, *i.e.*, we replace $a_n(t)$ by $a_n(0)$ on the right hand side of Eq. 213. We can then integrate Eq. 213 to give

$$i\hbar\,[a_m(t) - a_m(0) = \sum_n a_n(0)\int_0^t V_{mn}\exp(i\omega_{mn}t)dt \quad ...(216)$$

We can apply this to the case where we know that the system is in a particular state i at $t = 0$. Thus,

$$a_m(0) = 1 \text{ for } m = i \quad ...(217)$$
$$= 0 \qquad \text{for } m \neq i$$

so that

$$a_f(t) = \frac{1}{i\hbar}\int_i^t V_{fi}(t)\exp(i\omega_{fi}t)dt \quad (f \neq i) \quad ...(218)$$

Eq. 218 gives the probability amplitudes at later times of states other than the initial one.

Let us now suppose that at $t = 0$, the perturbation is switched on and for $t > 0$, is independent of time; then,

$$a_f(t) = \frac{1}{i\hbar}V_{fi}\int_0^t\exp(i\omega_{fi}t)dt = -V_{fi}\frac{\exp(i\omega_{fi}t)-1}{\hbar\omega_{fi}} \quad ...(219)$$

Thus, the probability for reaching the state f (at time t) is given by

$$P_f(t) = |a_f(t)|^2 = |V_{fi}|^2\frac{1}{\hbar^2}\frac{\sin^2(\omega_{fi}t/2)}{(\omega_{fi}/2)^2} \quad ...(220)$$

We rewrite Eq. 220 in terms of E_f and E_i :

$$P_f(t) = |V_{fi}|^2\left[\frac{\sin(E_f - E_i)t/2\hbar}{(E_f - E_i)/2}\right]^2 \quad ...(221)$$

Fig. 33 shows the behaviour of $P_f(t)$ as a function of E_f.

We note the following :

(i) The perturbation theory result, *viz.* Eq. 221, is valid only when $P_f(t) << 1$.

(ii) As long as t is small enough such that

$$(E_f - E_i)(t/2\hbar) << 1 \quad ...(222)$$

the quantity $P_f(t)$ is proportional to t^2 for all values of E_f. In fact

$$P_f(t) \approx |V_{fi}|^2(t^2/\hbar^2) \quad ...(223)$$

(iii) $\lim_{E_f \to E_i} P_f(t) = |V_{fi}|^2(t^2/\hbar^2)$ ...(224)

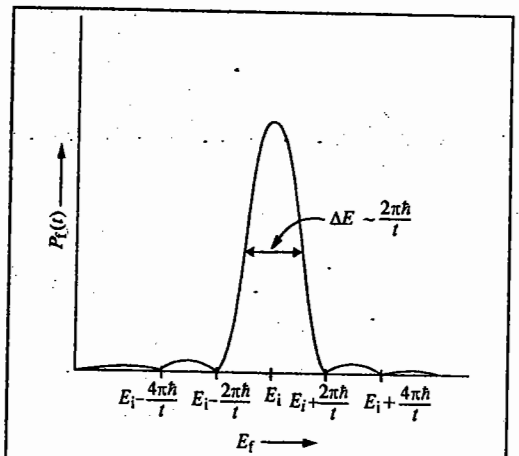

Fig. 33. The variation of $P_f(t)$ [$= |V_{fi}|^2 \sin(E_f - E_i)t/2\hbar \div \{(E_f - E_i)/2\}^2$] as a function of E_f.
Notice that the function is peaked at $E_f = E_i$ with a width $\Delta E \sim \hbar/t$.

Eq. 221 represents the probability of transition to one particular state ψ_f. We are, in fact, interested in transitions to a group of closely spaced states. Thus, the probability of transition to any one of the states is given by

$$w = \int P_f(t)\rho_f(E_f)dE_f, \quad ...(225)$$

where $\rho_f(E_f)\,dE_f$ represents the number of final states in the energy interval dE_f. The **density of states (DOS)** is usually a very smoothly varying function and since $P_f(t)$ is very sharply peaked around $E_f \approx E_i$, we may write

$$w \approx \rho_f(E_i)\int_{\Delta E}P_f(t)dE_f \quad ...(226)$$

where ΔE represents the central peak. We may now replace the limits of integration by $-\infty$ and $+\infty$ to obtain

$$w \approx \rho_f(E_i)|V|^2\int_{-\infty}^{+\infty}\left[\frac{\sin(E_f - E_i)t/2\hbar}{(E_f - E_i)/2}\right]^2 dE_f \approx \rho_f(E_i)\frac{2t}{\hbar}|V|^2\int_{-\infty}^{+\infty}\frac{\sin^2\xi}{\xi^2}d\xi$$

or

$$w \approx \frac{2\pi}{\hbar}|V_{fi}|^2\rho_f(E_i)t \quad ...(227)$$

The transition probability per unit time is given by

$$\Gamma = \frac{dw}{dt} = \frac{2\pi}{\hbar}|V_{fi}|^2\rho_f(E_i) \quad ...(228)$$

which is usually referred to as **Fermi's golden rule.** We may mention here that in carrying out the integration of Eq. 227, we have assumed that t is large enough so that the function $P_f(t)$ is very sharply peaked about $E_f = E_i$ (so that ρ_f can be taken outside the integral). We shall not discuss here the applications of TDPT; these are available in standard texts on quantum mechanics.

In his marvellous book, *Quanta : A Handbook of Concepts*, 2nd edn; P.W. Atkins writes (p.2), "Scientific disciplines collect acronyms like combs collect hairs, and quantum chemistry is no exception". For an uptodate account of these acronyms and software packages for electronic structure calculations the reader is referred to P. Atkins and R. Friedman, *Molecular Quantum Machanics*, 4th edition, and to I.N. Levine, *Quantum Chemistry*, 6th edition. Here the researcher will learn why theoreticians are obsessed with molecules. Incidentally, quantum chemists affectionately refer to Mulliken, the pioneer of MOT, as "Mr. Molecule".

I. Review Questions

1. What is molecular orbital theory ? Discuss it mathematically, leading to the derivation of the secular equation.
2. Outline the solution of the Schrödinger equation for H_2^+ ion. Sketch the BMO and ABMO and the corresponding electron density on the bond axis.
3. Explain valence bond theory. How would you determine the normalized valence bond eigenfunctions of H_2 molecule?
4. What is hybridisation ? Explain showing sp, sp^2, sp^3, dsp^2 and d^2sp^3 hybridization.
5. Define the terms resonance, resonance hybrid and resonance energy.
6. What is Walsh diagram ? Illustrate giving an example.
7. Set up and solve the Hückel secular equation for the cyclopropenyl system and show the results on an M.O. diagram. Also, calculate the resonance energy.
8. Repeat the above problem for 1, 3-butadiene.
9. Repeat the above problem for benzene.
10. Outline the Hartee-Fock-Roothaan SCF theory of polyatomic molecules.
11. What is the PPP approximation in MOT ?
12. Outline the salient features of the extended Hückel theory.
13. Discuss the Kohn-Sham treatment of density functional theory (DFT). What are its limitations ?
14. Discuss the application of the Hellmann-Feynman theorem to chemical bonding.
15. Discuss the basic features of TDPT.

CHAPTER 4

GROUP THEORY–I. BASIC CONCEPTS

Symmetry is a very fascinating phenomenon in nature. It is found in geometrical figures such as a cube, a sphere, an equilateral triangle, a rectangle, a square, a regular pentagon, a regular hexagon, etc. Its importance was recognized by eminent Greek philosophers Pythagoras and Plato. However, in this chapter we shall be concerned with the symmetry found in molecules and solids. Mathematical study of symmetry is called **Group theory**. Its foundations were laid in the 19th century by the French mathematician E. Galois and the European mathematicians Jordan, Frobenius, Sylvester, Sylow, Cayley, Lie and Abel. In the 20th century, applications of group theory to physics and chemistry were pioneered by H. Weyl and E.P. Wigner, the Hungarian-American mathematical physicist. Murray Gell-Mann, the American theoretical physicist, was awarded the 1969 Physics Nobel Prize for applying symmetry to the classification of elementary particles and the postulation of quarks which are the constituents of hadrons. In the words of P.W. Atkins, "symmetry is the quantification of beauty."

Symmetry Elements and Symmetry Operations

Symmetry Element. A symmetry element is a geometrical entity such as a point, a line or a plane about which a symmetry operation is performed.

Symmetry Operation. A symmetry operation is the movement of a molecule about the symmetry element in such a manner that the resulting configuration of the molecule is indistinguishable from the original. The molecule may assume an *equivalent configuration* or an *identical configuration*.

There are five types of symmetry elements : E, C_n, σ, S_n and i. E is called the identity; C_n is the n-fold proper axis of rotation; σ is the plane of symmetry; S_n is the n-fold improper axis of rotation and i is the centre of symmetry (or the inversion centre). These symmetry elements and the corresponding symmetry operations are listed in Table 1.

TABLE 1

Symmetry Elements and Symmetry Operations

Symmetry Element	Symmetry Operation
1. Identity (E)	The operation leaves the molecule unchanged.
2. Proper axis of rotation (C_n)	Rotation by an angle $\theta = 2\pi/n$ about the axis.
3. Plane of symmetry (σ)	Reflection in the plane.
4. Improper axis of rotation or rotation-reflection axis, S_n	Rotation about the axis followed by reflection in a plane perpendicular to the axis.
5. Inversion centre or centre of symmetry (i)	Inversion of all atoms in the molecule through the inversion centre.

1. Proper Axis of Rotation (C_n). A molecule is said to possess a proper axis of rotation of order n, C_n, if rotation about the axis by an angle $\theta = 2\pi/n$ leaves the molecule in a configuration which is indistinguishable from the original one. Consider, for instance, BF_3 molecule in which there is a C_3 axis, *i.e.*, an axis of order 3, which is perpendicular to the plane containing all the atoms and passing through the boron atom (Fig. 1).

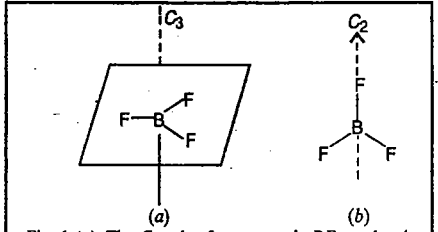

Fig. 1 (*a*) The C_3 axis of symmetry in BF_3 molecule. (*b*) The C_2 axis of symmetry is BF_3 molecule.

The BF_3 molecule also possesses three C_2 axes of symmetry in addition to the C_3 axis. One such axis is shown in Fig. 1(*b*). The C_3 axis is called the *principal axis*. In general, if a molecule possesses C_n axes of different orders, the axis of the highest order is known as the *principal axis*. An H_2O molecule has one two-fold axis C_2 whereas an NH_3 molecule has one three-fold axis C_3 (*i.e.*, rotation axis of order 3), as shown in Figs. 2 (*a*) and (*b*).

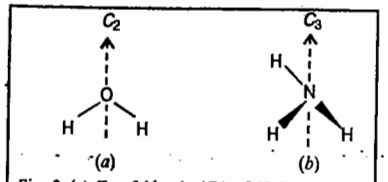

Fig. 2 (*a*) Two-fold axis (C_2) of H_2O molecule. (*b*) Three-fold axis (C_3) of NH_3 molecule

Note that there is only one two-fold rotation associated with a C_2 axis because clockwise and anticlockwise rotations are identical. However, with a three-fold axis C_3, two symmetry operations are associated, one being 120° rotation in a clockwise direction and the other 120° rotation in a counterclockwise sense.

The principal axis of benzene molecule is the six-fold axis, C_6, perpendicular to the regular hexagonal ring (Fig. 3).

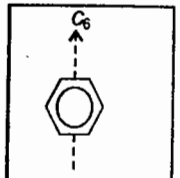

Fig. 3. The 6-fold axis C_6 in benzene.

A sphere possesses an infinite number of symmetry axes (along any diameter) of all possible integral values of *n*.

2. Plane of Symmetry (σ). A molecule possesses a plane of symmetry if reflection through the plane leaves the molecule unchanged. For instance, BF_3 molecule possesses two planes of symmetry, the *vertical plane* (σ_v) and the *horizontal plane* (σ_h). The σ_v plane contains the highest-order rotation axis, *i.e.*, the C_3 axis; σ_h is perpendicular to the C_3 axis (Fig. 4).

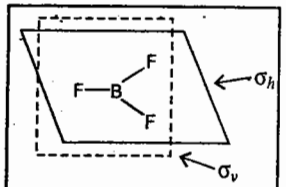

Fig. 4. The vertical and horizontal planes in BF_3 molecule.

Then there is the *dihedral plane* σ_d, which is a vertical plane that bisects the angle between the two C_2 axes.

3. Improper Axis of Rotation (S_n). A molecule is said to possess an improper axis of rotation of order *n* if rotation about the axis by $2\pi/n$ followed by reflection in a plane perpendicular to the axis leaves the molecule in an indistinguishable position. Examples are : allene which possesses an S_2 axis and the staggered form of ethane which possesses an S_6 axis (Figs. 5(*a*) and (*b*)).

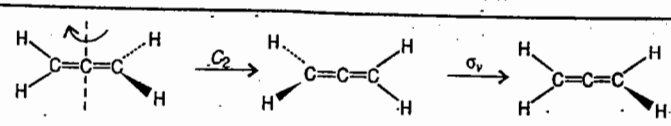

Fig. 5(*a*). Allene : S_2 axis.

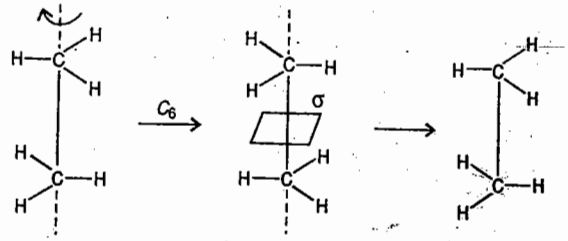

Fig. 5(*b*). Ethane (staggered form) : S_6 axis.

4. Centre of Symmetry (*i*). If in a molecule the coordinates (x, y, z) of every atom are changed into $(-x,-y,-z)$ and the molecule is left in an indistinguishable position, then the point of origin, *i.e.*, $(0, 0, 0)$, is called the centre of symmetry of the molecule. Examples are all homonuclear diatomic molecules and trans-1,2-dichloroethylene (Fig. 6).

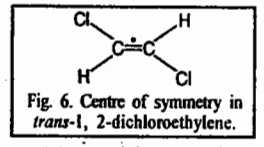

Fig. 6. Centre of symmetry in *trans*-1, 2-dichloroethylene.

5. The Identity Element (*E*). All molecules possess an identity element which does not do anything to the molecule.

Group Postulates. The complete set of operations forms a mathematical group. In order that the symmetry elements *A*,*B*,*C*,... form a mathematical group *G*, the following conditions must be satisfied :

1. Two elements *A* and *B* of a group combine to give the third element *C*, which is also an element of the group :

$$AB = C$$

It means that the application of *B* followed by *A* is equivalent to the application of *C*. If $AB = BA$, the elements *A* and *B* are said to *commute*.

2. An element combines with itself to form another element of the group.

3. The group must contain the identity element *E* which commutes with all the elements and leaves them unchanged :

$$EA = AE = A$$

$$EB = BE = B, \text{ etc.}$$

4. Every element of the group obeys the *associative law of combination* :

$$A(BC) = (AB)C$$

5. Every element *A* of a group has an inverse A^{-1} which is also an element of the group :

$$AA^{-1} = A^{-1}A = E$$

Example 1. Show that the set of rational numbers from zero to infinity forms a mathematical group.

Solution.: Let 5 and 7 be any two rational numbers. Then $5\times7 = 7\times5 = 35$. The numbers 5 and 7 are in the same group and 35 is also in the same group. Also, $1\times4 = 4\times1 = 4$. The number 4 is in the same group and the identity element *E* is 1. Again, $3\times\frac{1}{3}=\frac{1}{3}\times3=1$. $\frac{1}{3}$ is the inverse of 3. Further, $4\times(5\times6) = (4\times5)\times6$. Hence, the set of rational numbers between 0 and ∞ forms a group.

Types of Groups

1. Abelian and non-Abelian Groups. A group is said to be Abelian if all the elements commute and non-Abelian if all the symmetry elements do not commute with one another. We shall later show that H_2O molecule belongs to an Abelian group and NH_3 molucule to a non-Abelian group.

2. Cyclic Groups. A group is said to be cyclic if all its elements can be generated from one symmetry element. Thus, A, A^2, A^3,.....A^n form the elements of a cyclic group ; here $A^n = E$, the identity element. In general, the roots of the equation $x^n-1=0$ form a cyclic group. Note that *all cyclic groups are Abelian.*

Other Definitions

1. Order of a Group. The total number of elements of a group is called the order (h) of the group.

2. Subgroup. This is a group within a group. If any selection or subset of the elements of a group satisfies the definition of a group, then this subset of elements is called a subgroup. A subgroup must necessarily include the identity element E.

3. Multiplication Table. Consider a water molecule. It has four symmetry elements, *viz.*, E, $C_2(z)$, $\sigma_v(xz)$ and $\sigma_v'(yz)$ (Fig. 7).

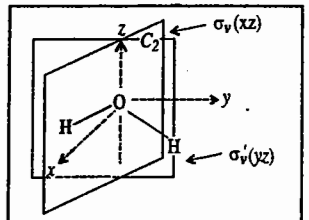

Fig. 7. The four symmetry elements of H_2O molecule.

We can easily show that the product of any two symmetry elements is one of the four elements of the group. Thus, for instance, $C_2(z)\sigma_v(xz) = \sigma_v'(yz)$. Proceeding this way the symmetry operations of H_2O molecule can be listed in a Group Multiplication Table (GMT) (Table 2).

TABLE 2

Group Multiplication Table of the Symmetry Operations of H_2O Molecule

	E	$C_2(z)$	$\sigma_v(xz)$	$\sigma_v'(yz)$
E	E	$C_2(z)$	$\sigma_v(xz)$	$\sigma_v'(yz)$
$C_2(z)$	$C_2(z)$	E	$\sigma_v'(yz)$	$\sigma_v(xz)$
$\sigma_v(xz)$	$\sigma_v(xz)$	$\sigma_v'(yz)$	E	$C_2(z)$
$\sigma_v'(yz)$	$\sigma_v'(yz)$	$\sigma_v(xz)$	$C_2(z)$	E

4. Similarity Transformation and Conjugate Elements. If A and X are two elements of a group obeying the relation

$$X^{-1}AX = B \qquad \ldots (1)$$

where B is also in the same group, then B is called the similarity transformation of A by X and A and B are said to be conjugate to each other.

5. Class. A set of elements in a group which are conjugate to one another is said to form a *class*.

Let us perform the similarity transformation of the C_2 operation of H_2O molecule with all the other operations :

$$E^{-1}\,C_2\,E = C_2 \;; \quad \sigma_v^{-1}\,C_2\,\sigma_v = C_2$$

$$(\sigma_v')^{-1}\,C_2\,\sigma_v' = C_2 \;; \quad (C_2)^{-1}\,C_2\,C_2 = C_2$$

We see that C_2 belongs to a *separate class* since the similarity transformation of C_2 with all the operations generates C_2. A symmetry operation which commutes with all the symmetry operations is in a separate class. Thus, E, σ_h and i belong to separate classes. In an Abelian group, every symmetry operation belongs to a separate class.

Point Groups. All the symmetry operations in a molecule can be combined to form a molecular group. This group is called **point group** since all the symmetry elements of the molecule intersect at a common point which remains fixed under all the symmetry operations. Crystals have very high symmetry. In fact, they have *translational symmetry* which is not found in gaseous molecules. The molecular point

groups are represented by the **Schoenflies symbols** whereas the point groups for crystals are denoted by **Hermann-Mauguin symbols**. Table 3 lists some molecular point groups which are of interest to chemists.

TABLE 3

Some Molecular Point Groups

Point Group	Symmetry Elements	Examples
C_1	E	CHFClBr
C_2	E, C_2	H_2O_2
C_3	E, C_3	C_2H_6
C_s	E, σ_v	NOCl
C_{2v}	E, C_2, $2\sigma_v$	H_2O, $CH_2{=}O$, pyridine
C_{3v}	E, C_3, $3\sigma_v$	NH_3, $CHCl_3$, PH_3
$C_{\infty v}$	E, C_∞, $\infty\sigma_v$	HCl, NO, CO
C_{2h}	E, C_2, σ_h, i	trans CHCl=CHCl
D_{2h}	E, $3C_2$, 3σ, i	$CH_2{=}CH_2$, naphthalene
D_{3h}	E, $2C_3$, $3C_2$ ($\perp$ to C_3), $3\sigma_v$, σ_h, $2S_3$	BF_3(trigonal planar)
D_{4h}	E, C_4, $4C_2$ ($\perp$ to C_4), $2\sigma_v$, $2\sigma_d$, σ_h, C_2, S_4 (coincident with C_4), i	$[PtCl_4]^{2-}$ (square planar)
D_{6h}	E, $2C_6$, $6C_2$ ($\perp$ to C_6), $3\sigma_v$, $3\sigma_d$, σ_h, C_2, $2C_3$, $2S_6$, $2S_3$, i	C_6H_6
T_d	E, $4C_3$, $3C_2$, $3S_4$ (coincident with C_2), $6\sigma_d$	CH_4
O_h	E, $3C_4$, $4C_3$, $3S_4$ and $3C_2$ (both coincident with the C_4 axes), $6C_2$, $4S_6$, $3\sigma_h$, $6\sigma_d$	SF_6

Example 2. The similarity transformation diagonalises a square matrix. Let us consider a 2×2 matrix A and the transformation matrix X, defined by

$$A = \begin{bmatrix} -7 & 6 \\ -18 & 14 \end{bmatrix}; \quad X = \begin{bmatrix} 2 & 1 \\ 3 & 2 \end{bmatrix}$$

Using the similarity transformation, diagonalise A.

Solution : In this example we assume that the reader is familiar with matrix algebra and knows how to determine the inverse of a matrix. The similarity transformation is defined as

$$X^{-1}A\,X = B$$

The inverse X^{-1} of matrix X is given by

$$X^{-1} = \text{adj}\,X/|X|$$

where adj X is the adjoint of X and $|X|$ is the determinant of X ($|X| \neq 0$).

Consider, $X = \begin{bmatrix} 2 & 1 \\ 3 & 2 \end{bmatrix}$. It can be easily shown that $X^{-1} = \begin{bmatrix} 2 & -1 \\ -3 & 2 \end{bmatrix}$.

Hence, $X^{-1}AX = \begin{bmatrix} 2 & -1 \\ -3 & 2 \end{bmatrix}\begin{bmatrix} -7 & 6 \\ -18 & 14 \end{bmatrix}\begin{bmatrix} 2 & 1 \\ 3 & 2 \end{bmatrix} = \begin{bmatrix} 2 & 0 \\ 0 & 5 \end{bmatrix}$

We see that B is a diagonal matrix. Thus, matrix A has been diagonalized.

Representations of Molecular Point Groups. The five kinds of symmetry operations, *viz.*, E, C_n, σ, S_n, i can be represented by matrices. It can be shown (we omit the derivation) that if these operations operate on a two-dimensional position vector

$$\vec{r} = x\hat{i} + y\hat{j} \qquad \ldots (2)$$

where $\hat{i}$, $\hat{j}$ are the unit vectors along the x and y axes, respectively, they generate five 2×2 matrices :

$$\begin{bmatrix} x' \\ y' \end{bmatrix} = \underbrace{\begin{bmatrix} \quad & \quad \\ \quad & \quad \end{bmatrix}}_{2\times2 \text{ matrix}} \begin{bmatrix} x \\ y \end{bmatrix} \qquad \ldots (3)$$

Here we have written the position vector as a column vector and the transformed vector as a primed column vector. The matrices are :

$$E = \begin{bmatrix} 1 & 0 \\ 1 & 0 \end{bmatrix};\ C_2 = \begin{bmatrix} \cos\theta & \sin\theta \\ -\sin\theta & \cos\theta \end{bmatrix};\ \sigma_{yz} = \begin{bmatrix} -1 & 0 \\ 0 & 1 \end{bmatrix};\ \text{etc.} \qquad \ldots(4)$$

On the other hand, if the same operations operate on a three-dimensional position vector

$$\vec{r} = x\hat{i} + y\hat{j} + z\hat{k}, \qquad \ldots(5)$$

they generate five 3×3 matrices :

$$E = \begin{bmatrix} 1 & 0 & 0 \\ 0 & 1 & 0 \\ 0 & 0 & 1 \end{bmatrix};\ C_n(z) = \begin{bmatrix} \cos\theta & \sin\theta & 0 \\ -\sin\theta & \cos\theta & 0 \\ 0 & 0 & 1 \end{bmatrix};\ \sigma_{yz} = \begin{bmatrix} -1 & 0 & 0 \\ 0 & 1 & 0 \\ 0 & 0 & 1 \end{bmatrix}; \qquad \ldots(6a)$$

$$S_n = \sigma_{xy}C_n(z) = \begin{bmatrix} \cos\theta & \sin\theta & 0 \\ -\sin\theta & \cos\theta & 0 \\ 0 & 0 & -1 \end{bmatrix};\ i = \begin{bmatrix} -1 & 0 & 0 \\ 0 & -1 & 0 \\ 0 & 0 & -1 \end{bmatrix};\ \sigma_{xy} = \begin{bmatrix} 1 & 0 & 0 \\ 0 & 1 & 0 \\ 0 & 0 & -1 \end{bmatrix};\ \text{etc.} \qquad \ldots(6b)$$

The sum of the diagonal elements of a matrix is called the **trace or character** χ of the matrix. The characters of the various matrices corresponding to the symmetry operations described above are given in Table 4.

TABLE 4
Characters of the Symmetry Operations

Symmetry operation (R)	Character of R, $\chi(R)$
E	$\chi(E) = 3$
C_n	$\chi(C_n) = 2\cos\theta + 1$
σ	$\chi(\sigma) = 1$
S_n	$\chi(S_n) = 2\cos\theta - 1$
i	$\chi(i) = -3$

We can verify the remarkable fact that these matrices combine like the symmetry operations themselves. Thus, for instance,

$$\sigma_{xz}\sigma_{yz} = \begin{bmatrix} 1 & 0 & 0 \\ 0 & -1 & 0 \\ 0 & 0 & 1 \end{bmatrix}\begin{bmatrix} -1 & 0 & 0 \\ 0 & 1 & 0 \\ 0 & 0 & 1 \end{bmatrix} = \begin{bmatrix} -1 & 0 & 0 \\ 0 & -1 & 0 \\ 0 & 0 & 1 \end{bmatrix} = C_2(z) \qquad \ldots(7)$$

The set of matrices corresponding to the symmetry operations (or the symmetry elements) of a group is called its **representation.** It must be borne in mind that this set of matrices is not a unique set. For a point group of a molecule there can be many other sets of matrices (and hence many representations) which combine in the same way as the symmetry operations themselves. We are, however, interested in the most fundamental representation from which other representations can be derived.

Representations can be classified into (*a*) **Reducible representations (reps)** and (*b*) **Irreducible representations (irreps)**, also called **symmetry species.**

Reps. Let A, B, C,.... be the matrices which form the representation of a group and let X be the similarity transformation matrix of this group such that

$$X^{-1}AX = A' \qquad \ldots(8)$$

$$X^{-1}BX = B' \qquad \ldots(9)$$

$$X^{-1}CX = C' \qquad \ldots(10)$$

Then, if X is the proper transformation matrix, we have

$$X^{-1}AX = A' = \begin{bmatrix} a_1' & & & 0 \\ & a_2' & & \\ & & a_3' & \\ 0 & & & a_4' \end{bmatrix} \qquad \ldots(11)$$

The new matrix A' is now *blocked out* along the diagonal into smaller matrices a_1', a_2', a_3', a_4', etc., with the off-diagonal elements equal to zero. Similarly, we have

$$X^{-1}BX = B' = \begin{bmatrix} b_1' & & & 0 \\ & b_2' & & \\ & & b_3' & \\ 0 & & & b_4' \end{bmatrix};\ \text{etc.} \qquad \ldots(12)$$

This is expressed by saying that the given sets of matrices form a **reducible representation (rep).**

Irreps. If it is not possible to find a similarity transformation which will reduce the matrices A, B, C,.... to block-diagonalized form, the representation is called an **irreducible representation (irrep).**

Grand/Great Orthogonality Theorem (G.O.T.)

This is the most important theorem of group theory. It concerns the matrix elements (*i.e.*, elements of the matrices) which constitute the irreps of a point group. Mathematically, it is stated as follows :

$$\sum_R \Gamma_i(R)_{mn}\Gamma_j(R)^*_{m'n'} = \frac{h}{\sqrt{l_i l_j}}\delta_{ij}\delta_{mm'}\delta_{nn'} \qquad \ldots(13)$$

Here Γ_i and Γ_j are the ith and jth irreps of a point group of order h with dimensions l_i and l_j, respectively ; $\Gamma_i(R)_{mn}$ is the mnth matrix element corresponding to the symmetry operation R belonging to the ith irrep and $\Gamma_j(R)^*_{m'n'}$ is the complex conjugate of the $m'n'$th matrix element corresponding to the symmetry operation R belonging to the jth irrep. The δs are the well known 'Kronecker deltas' which have the following property :

$$\delta_{ij} = \begin{cases} 1, & i = j \\ 0, & i \neq j \end{cases};\quad \delta_{mm'} = \begin{cases} 1, & m = m' \\ 0, & m \neq m' \end{cases};\quad \delta_{nn'} = \begin{cases} 1, & n = n' \\ 0, & n \neq n' \end{cases} \qquad \ldots(14)$$

The summation is performed over all the symmetry operations R of the molecule. If the matrix elements are *real*, then

$$\Gamma_j(R)^*_{m'n'} = \Gamma_j(R)_{m'n'} \qquad \ldots(15)$$

The following three cases arise for the G.O.T. assuming that the matrix elements are real :

1 For two different irreps, $i \neq j$, $m = m'$ and $n = n'$,

$$\sum_R \Gamma_i(R)_{mn}\Gamma_j(R)_{mn} = 0 \qquad \ldots(16)$$

2 For the same irrep $i = j$, $m \neq m'$ and $n \neq n'$,

$$\sum_R \Gamma_i(R)_{mn}\Gamma_i(R)_{m'n'} = 0 \qquad \ldots(17)$$

3 For an irrep i and for $m = m'$, $n = n'$,

$$\sum_R [\Gamma_i(R)_{mn}]^2 = h/l_i \qquad \ldots(18)$$

In practice, we do not use the G.O.T. in the form given above but in a slightly different form involving the *characters* of the irreps, as shown in the next section.

Important Properties of Irreducible Representations (Irreps)

The properties of the *irreps* can be derived from the G.O.T. Consider a point group of order h. Recall that h is the number of symmetry operations of a point group. Let the h symmetry operations be divided

into k classes. We shall denote the irreps by $\Gamma_1, \Gamma_2, \Gamma_3, \ldots \Gamma_k$ and their dimensions by $l_1, l_2, l_3, \ldots l_k$. Using the G.O.T., the following properties of the irreps can be obtained :

1. The number of irreps in a point group is equal to the number of its symmetry classes.

2. The sum of the squares of the dimensions of the irreps of a group is equal to h, the order of the group. Thus,

$$\sum_{i=1}^{k} l_i^2 = h \qquad \ldots (19)$$

3. The sum of the squares of the characters of the identity operation in the irreps is equal to h, the order of the group :

$$\sum_{i=1}^{k} \left(\chi_i(E)\right)^2 = h \qquad \ldots (20)$$

4. The characters of the symmetry operations in two different irreps satisfy the relation

$$\sum_{p=1}^{k} g_p \chi_i(R_p)\chi_j(R_p) = h\delta_{ij} \qquad \ldots (21)$$

where δ_{ij} is the Kronecker delta :

$$\delta_{ij} = \begin{cases} 1, & i = j \\ 0, & i \neq j \end{cases} \qquad \ldots (22)$$

For $i \neq j$, this relation reduces to

$$\sum_{p=1}^{k} g_p \chi_i(R_p)\chi_j(R_p) = 0 \qquad \ldots (23)$$

and for $i = j$, it becomes

$$\sum_{p=1}^{k} g_p \left(\chi_i(R_p)\right)^2 = h \qquad \ldots (24)$$

In these equations, g_p refers to the number of symmetry operations in the *pth* class ; R_p is the symmetry operation of the *pth* class and $\chi_i(R_p)$ and $\chi_j(R_p)$ are the characters of the matrix for the symmetry operation R_p in the i and j irreps, respectively.

5. The characters of all matrices belonging to the symmetry operations in the same class are identical.

Use of G.O.T. to Construct Character Tables for the Molecular Point Groups. Let us use the G.O.T. to construct the character table for the C_{3v} point group to which NH_3 belongs. This point group has three symmetry elements E, C_3 and $3\sigma_v$; the corresponding *six* symmetry operations can be divided into the following *three* classes : E, (C_3^1, C_3^2), $3\sigma_v$.

According to rule 1, the three symmetry classes give rise to three irreps. From rule 2,

$$\sum_{i=1}^{3} l_i^2 = l_1^2 + l_2^2 + l_3^2 = 6 \qquad \ldots (25)$$

where the order of the group is 6.

The only positive integral values of l_i that satisfy Eq. 25 are 1, 1 and 2. Here we state a very important property that every point group possesses a totally symmetric irrep in which all the symmetry operations have character equal to 1. From rule 3,

$$\sum_i [\chi_i(E)]^2 = [\chi_1(E)]^2 + [\chi_2(E)]^2 + [\chi_3(E)]^2 = 6 \qquad \ldots (26)$$

which is satisfied only if

$$\chi_1(E) = 1, \ \chi_2(E) = 1 \text{ and } \chi_3(E) = 2 \qquad \ldots (27)$$

We can now draw up the following table for the characters of different representations :

TABLE 5

Characters of Different Representations

Irrep	$\chi(E)$	$\chi(C_3)$	$\chi(\sigma_v)$
Γ_1	1	1	1
Γ_2	1	p	q
Γ_3	2	r	s

We have to determine the values of the unknown characters p, q, r and s in the irreps Γ_2 and Γ_3. Applying rule 4 to irreps Γ_1 and Γ_2, we have

$$\sum_{p=1}^{k} g_p \chi_i(R_p)\chi_j(R_p) = 0 \qquad \ldots (28)$$

$$\sum_{p=1}^{3} g_p \chi_1(R_p)\chi_2(R_p) = g_1\chi_1(E)\chi_2(E) + g_2\chi_1(C_3)\chi_2(C_3) + g_3\chi_1(\sigma_v)\chi_2(\sigma_v) = 0 \qquad \ldots (29)$$

From Table 5, remembering that $g_1=1$, $g_2=2$ and $g_3=3$, we obtain

$$1 + 2p + 3q = 0 \qquad \ldots (30)$$

Applying Eq. 24 to the irrep Γ_2, we obtain

$$1 + 2p^2 + 3q^2 = 6 \qquad \ldots (31)$$

Solving Eqs. 30 and 31, we obtain

$$p = 1 \text{ and } q = -1$$

Proceeding similarly, we obtain from the irreps Γ_1 and Γ_3, the following equations :

$$2 + 2r + 3s = 0 \qquad \ldots (32)$$

and

$$4 + 2r^2 + 3s^2 = 6 \qquad \ldots (33)$$

Solving Eqs. 32 and 33, we obtain

$$r = -1 \quad \text{and} \quad s = 0$$

Using the values of p, q, r and s in Table 5, we obtain the desired character table (Table 6) for C_{3v} point group.

TABLE 6

Character Table for C_{3v} Point Group

C_{3v}	E	$2C_3$	$3\sigma_v$
$\Gamma_1 \equiv A_1$	1	1	1
$\Gamma_2 \equiv A_2$	1	1	−1
$\Gamma_3 \equiv E$	2	−1	0

The symbols Γ_1, Γ_2 and Γ_3 are the **Bethe notation** for the irreps and A_1, A_2 and E are the **Mulliken notation** for the irreps.

Character Tables for Point Groups

For practical purposes, it is sufficient to know only the characters of each symmetry class of a point group to which a molecule belongs. A character table lists the characters of all the symmetry classes for all the irreps of a group. Character tables for the C_{2v} and C_{3v} point groups are given in Tables 7 and 8.

TABLE 7

Character Table for C_{2v} Point Group

C_{2v} I	E	$C_2(z)$	$\sigma_v(xz)$ II	$\sigma_v(yz)$	III	IV
A_1	1	1	1	1	z	x^2, y^2, z^2
A_2	1	1	−1	−1	R_z	xy
B_1	1	−1	1	−1	x, R_y	xz
B_2	1	−1	−1	1	y, R_x	yz

TABLE 8

Character Table for C_{3v} Point Group

C_{3v} I	E	$2C_3$ II	$3\sigma_v$	III	IV
A_1	1	1	1	z	$x^2 + y^2, z^2$
A_2	1	1	−1	R_z	
E	2	−1	0	(x,y) (R_x,R_y)	(x^2-y^2, xy) (xz,yz)

The character tables can be obtained from the properties of the irreps given above. We can explain the character table by dividing it into four sections I, II, III and IV :

Section I. In the top row, the Schoenflies symbol for the point group is given. This section also lists the Mulliken symbols for the different irreps. Symbols A and B are used to label one-dimensional irreps and E and T to label two-dimensional and three-dimensional irreps, respectively. The nomenclature E should *not* be confused with the identity operation. A is used when the character for the rotation about the *principal axis* is +1 and B when it is −1. In other words, A stands for symmetric and B for antisymmetric to such rotation. For a molecule having a centre of symmetry, the subscripts g and u are used to label the irreps that are respectively symmetric and antisymmetric to inversion through the centre of symmetry. Subscripts 1 and 2 are used to label the irreps that are respectively symmetric and antisymmetric to reflection in a vertical plane σ_v. The superscripts ′ and ″ are used it denote the irreps that are respectively symmetric and antisymmetric to reflection in a horizontal plane σ_h.

Section II. This section gives the characters for all the symmetry operations of different irreps. The characters of the identity operation for the one-dimensional, two-dimensional and three-dimensional irreps are, respectively, 1, 2 and 3.

Section III. It gives the transformation properties of the Cartesian coordinates x, y, z and rotations R_x, R_y, R_z about these axes.

Section IV. It gives the transformation properties of the binary products of Cartesian coordinates xy, yz, zx, etc. and the squares of the coordinates x^2, y^2, z^2, x^2+y^2, $x^2+y^2+z^2$, etc. The Cartesian coordinates, their squares and binary products, etc., listed in sections III and IV are referred to as the **basis functions** on which the symmetry operations operate.

Example 3. Verify that the characters given in the C_{2v} point group obey the properties of the irreps.

Solution : Refer to the Character Table 7 for the C_{2v} point group. We find that

(*i*) the number of irreps is equal to the number of classes (in this case 4) of the group.

(*ii*) All the four irreps are one-dimensional so that

$$\sum_{i=1}^{4} l_i^2 = l_1^2 + l_2^2 + l_3^2 + l_4^2 = (1)^2 + (1)^2 + (1)^2 + (1)^2 = 4$$

which is the order of the group.

(*iii*) $$\sum_{i=1}^{4}\left(\chi_i(E)\right)^2 = \left(\chi_{A_1}(E)\right)^2 + \left(\chi_{A_2}(E)\right)^2 + \left(\chi_{B_1}(E)\right)^2 + \left(\chi_{B_2}(E)\right)^2 = (1)^2 + (1)^2 + (1)^2 + (1)^2 = 4$$

(*iv*) $$\sum_{p=1}^{4} g_p \chi_i(R_p)\chi_j(R_p) = h\,\delta_{ij}$$

For the A_1 and A_2 irreps, we obtain (1)(1)(1) + (1)(1)(1) + (1)(1)(−1) + (1)(1)(−1) = 0 and for the B_1 irrep, we obtain (1)(1)^2 + (1)(−1)^2 + 1(1)^2 + 1(−1)^2 = 4 and so on. **Hence the result.**

Example 4. Verify that the characters given in the C_{3v} point group obey the properties of the irreps.

Solution : Refer to the Character Table 8 for the C_{3v} point group. We find that

(*i*) the number of irreps is equal to the number of classes (in this case 3) of the group.

(*ii*) Two irreps A_1 and A_2 are one-dimensional, *i.e.*, $l_1 = l_2 = 1$ and the third is two-dimensional, *i.e.*, $l_3 = 2$. Thus,

$$\sum_{i=1}^{3} l_i^2 = l_1^2 + l_2^2 + l_3^2 = (1)^2 + (1)^2 + (2)^2 = 6$$

which is the order of the group.

(*iii*) $$\sum_{i=1}^{3}\left(\chi_i(E)\right)^2 = \left(\chi_{A_1}(E)\right)^2 + \left(\chi_{A_2}(E)\right)^2 + \left(\chi_E(E)\right)^2 = (1)^2 + (1)^2 + (2)^2 = 6$$

(*iv*) $$\sum_{p=1}^{3} g_p \chi_1(R_p)\chi_j(R_p) = h\delta_{ij}$$

For the irreps A_2 and E (say), this relation gives (1)(1)(2) + (2)(1)(−1) + 3(−1)(0) = 0

For the irreps A_1 and A_2 (say), it gives (1)(1)(1) + (2)(1)(1) + (3) (1)(−1) = 0 and for the irrep E, it gives (1)(2)^2 + 2(−1)^2 + 3(0)^2 = 6 and so on. **Hence the result.**

It is important to recognize the point groups of some common molecules. Homonuclear diatomic molecules (H_2, N_2, O_2, Cl_2, etc.) and linear molecules with a centre of symmetry (CO_2, HC≡CH) belong to the point group $D_{\infty h}$. On the other hand, heteronuclear diatomic molecules and other linear molecules that do not have a centre of symmetry (HCl, CO, NO, OCS, NNO) belong to the point group $C_{\infty v}$. Tetrahedral (T_d) and octahedral (O_h) molecules have more than one non-collinear principal axes of symmetry. A tetrahedral molecule such as CH_4 has four non-collinear C_3 axes, one along each C–H bond. A closely related group, the icosahedral group I_h which characterises the icosahedron has non-collinear five-fold axes. The icosahedral group I_h occurs prominently in boron compounds and in fullerene (C_{60}) molecule. A regular tetrahedron has four equilateral triangles for its faces, an octahedron has eight, a dodecahedron twelve and an icosahedron has twenty faces. We may mention here that atoms, being spherical, belong to the **full rotation group** (R_3).

Table 9 lists the point groups of some common molecules along with their geometry and general formulae.

TABLE 9

Point Groups and Geometry of Some Common Molecules

Molecule/Complex ion	General Formula	Point Group	Geometry
H_2	A_2	$D_{\infty h}$	Linear with *i*
HF	AB	$C_{\infty v}$	Linear without *i*
CO_2	AB_2	$D_{\infty h}$	Linear with *i*
COS	ABC	$C_{\infty v}$	Linear without *i*
H_2O	A_2B	C_{2v}	Angular
C_2H_2	A_2B_2	$D_{\infty h}$	Linear with *i*
CH_2Cl_2	AB_2C_2	C_{2v}	Tetrahedral
$CHCl_3$	ABC_3	C_{3v}	Tetrahedral
NH_3	AB_3	C_{3v}	Pyramidal
CH_4	AB_4	T_d	Tetrahedral
PCl_5	AB_5	D_{3h}	Trigonal bipyramidal
SF_4	AB_4	C_{2v}	Angular
$[PtCl_4]^{2-}$	$[AB_4]^{2-}$	D_{4h}	Square planar
BrF_5	AB_5	C_{4v}	Square pyramidal
SF_6	AB_6	O_h	Octahedral
IF_7	AB_7	D_{5h}	Pentagonal bipyramidal
$[B_{12}H_{12}]^{2-}$	$[A_{12}B_{12}]^{2-}$	I_h	Icosahedral

Example 5. List the symmetry elements and locate as many of them as possible (in the molecule) for the following molecules :

(*a*) CH_4, (*b*) $[PtCl_4]^{2-}$, (*c*) H_2, (*d*) HF, (*e*) HCN and (*f*) C_2H_2

Solution : (*a*) CH_4 (tetrahedral). It belongs to the T_d point group. The symmetry elements are E, $4C_3$, $3C_2$, $3S_4$ and $6\sigma_d$ (Fig. 8).

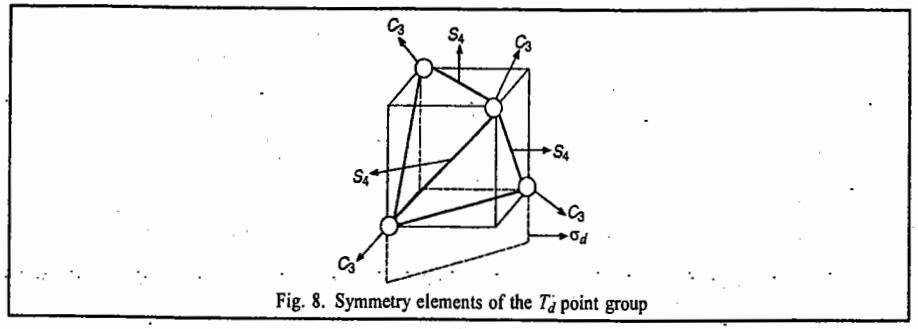

Fig. 8. Symmetry elements of the T_d point group

(*b*) $[PtCl_4]^{2-}$ (square planar). This molecule has the general formula AB_4 and belongs to the D_{4h} point group. The symmetry elements are E, C_4, S_4, $4C_2$, $4\sigma_v$, σ_h and i (Fig.9).

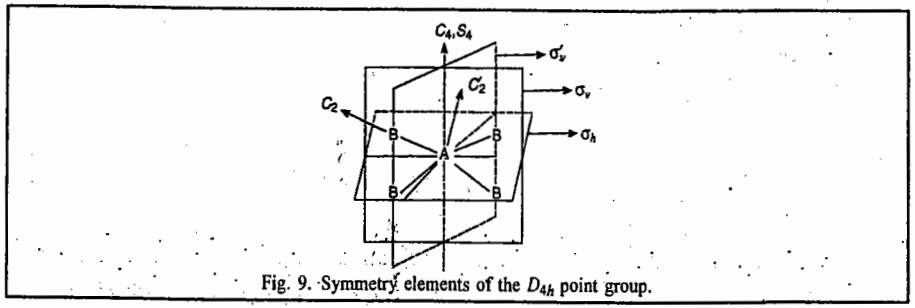

Fig. 9. Symmetry elements of the D_{4h} point group.

(*c*) H_2 (linear with a centre of symmetry, (*i*). It belongs to the $D_{\infty h}$ point group. It has the symmetry elements E, $2C_\infty$, $\infty\sigma_v$, σ_h, i, $2S_\infty$ and ∞C_2 (Fig. 10).

(*d*) HF (linear without centre of symmetry, (*i*). It belongs to the $C_{\infty v}$ point group and has the symmetry elements : E, C_∞ and $\infty\sigma_v$ (Fig. 11).

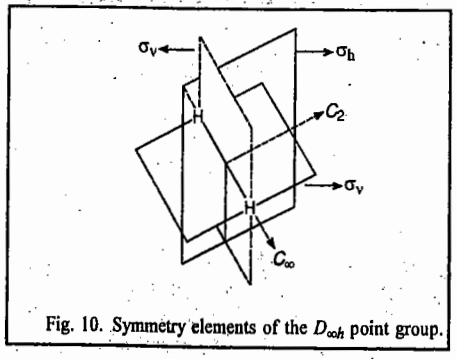

Fig. 10. Symmetry elements of the $D_{\infty h}$ point group.

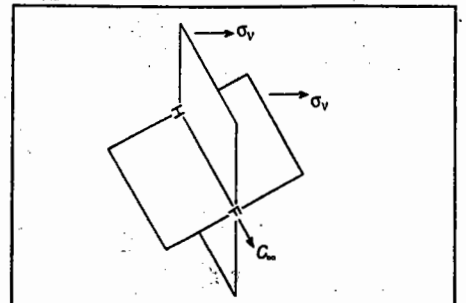

Fig. 11. Symmetry elements of the $C_{\infty v}$ point group.

(*e*) HC≡N (linear without centre of symmetry, (*i*). It belongs to $C_{\infty v}$ point group and possesses the symmetry elements : E, C_∞ and $\infty\sigma_v$ (Fig. 12).

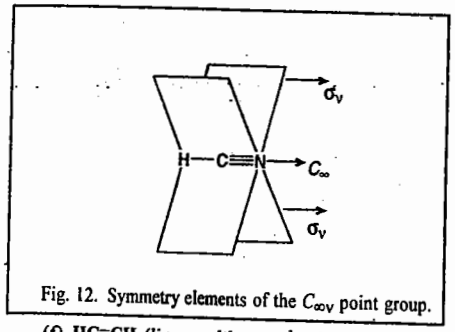

Fig. 12. Symmetry elements of the $C_{\infty v}$ point group.

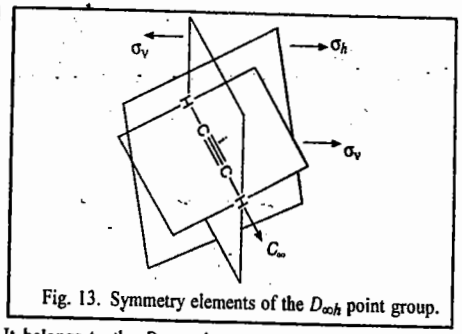

Fig. 13. Symmetry elements of the $D_{\infty h}$ point group.

(*f*) HC≡CH (linear with centre of symmetry, (*i*). It belongs to the $D_{\infty h}$ point group and has the symmetry elements : E, $2C_\infty$, $\infty\sigma_v$, σ_h, i, $2S_\infty$ and ∞C_2 (Fig. 13).

Example 6. Illustrate diagrammatically that H_2O molecule is Abelian whereas NH_3 molecule is non-Abelian.

Solution. A molecule is said to be Abelian if all the symmetry elements commute with one another and non-Abelian if they do not commute with one another.

H_2O molecule : See Fig. 14.

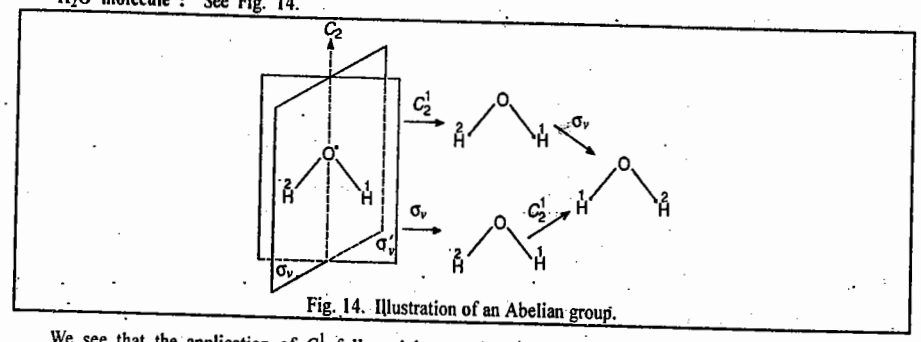

Fig. 14. Illustration of an Abelian group.

We see that the application of C_2^1 followed by σ_v gives the same configuration as the application of σ_v followed by C_2^1.

Hence, C_2^1 and σ_v commute, *i.e.*, $\sigma_v C_2^1 = C_2^1 \sigma_v$

Thus, H_2O molecule belongs to an Abelian point group (C_{2v}).

NH_3 molecule : See Fig. 15.

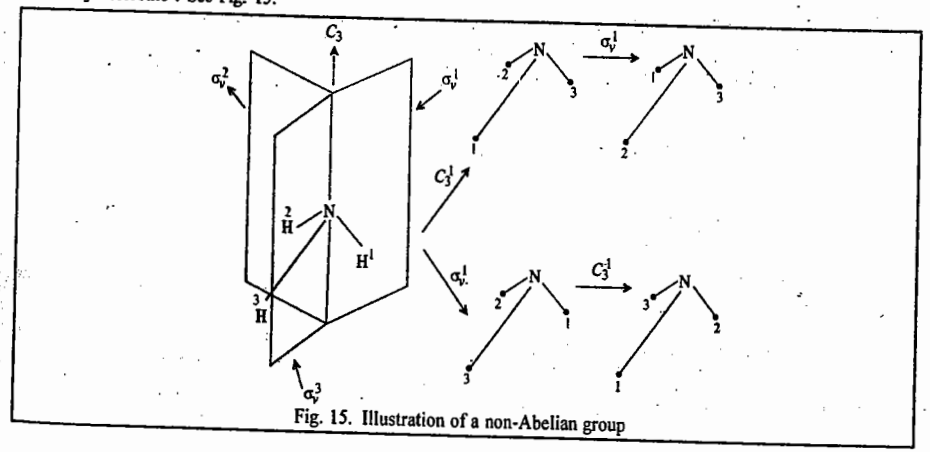

Fig. 15. Illustration of a non-Abelian group

Here we find that application of C_3^1 followed by σ_v^1 gives a different configuration of NH_3 molecule than the configuration obtained by the application of σ_v^1 followed by C_3^1, *i.e.*,

$$\sigma_v^1 C_3^1 \neq C_3^1 \sigma_v^1$$

so that the two symmetry operations do not commute. Thus, NH_3 molecule belongs to a non-Abelian point group (C_{3v}).

As an application of group theory to quantum mechanics, consider the Schrodinger equation for helium atom

$$\hat{H}\psi = E\psi \qquad \ldots (37)$$

where $\hat{H} = -\frac{1}{2}(\nabla_1^2 + \nabla_2^2) - \frac{2}{r_1} - \frac{2}{r_2} + \frac{1}{r_{12}}$ (in atomic units)

(see Fig. 16 for the description of the coordinates of the two electrons.)

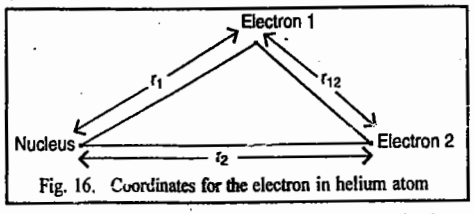

Fig. 16. Coordinates for the electron in helium atom

If we use a symmetry operation called **parity**, $\hat{P}$, which interchanges the coordinates of the two electrons, we find that $\hat{H}$ remains unchanged. This is expressed in group-theoretical language by saying that the Hamiltonian (and hence the energy E) is *invariant* under the symmetry operation $\hat{P}$. In fact, the Hamiltonian operator $\hat{H}$ is invariant under all the symmetry operations of the point group of an atom or a molecule since it commutes with them, *i.e.*,

$$[\hat{H}, \hat{P}] = \hat{H}\hat{P} - \hat{P}\hat{H} = 0 \qquad \ldots (38)$$

Applying the parity operation to both sides of Eq. 37 and using Eq. 38, we have

$$\hat{P}\hat{H}\psi = \hat{H}\hat{P}\psi \qquad \ldots (39)$$

Hence, $$\hat{H}(\hat{P}\psi) = E(\hat{P}\psi) \qquad \ldots (40)$$

This means that $\hat{P}\psi$ is also a solution of Eq. 37 with the eigenvalue E. Thus, assuming the absence of degeneracy (*i.e.*, no two wave functions have the same energy), we can say that there is no difference between $\hat{P}\psi$ and ψ.

Let us next consider the effect of parity on ψ. Consider the eigenvalue equation

$$\hat{P}\psi = \lambda\psi \qquad \ldots (41)$$

where λ is the eigenvalue of $\hat{P}$. Operating on Eq. 41 again with $\hat{P}$, we obtain

$$\hat{P}^2\psi = \hat{P}\lambda\psi \qquad \ldots (42)$$

or $$\psi = \lambda\hat{P}\psi = \lambda^2\psi \qquad \ldots (43)$$

i.e., $$\lambda^2 = 1 \qquad \ldots (44)$$

$\therefore$ $$\lambda = \pm 1$$

Substituting in Eq. 41, we find that

$$\hat{P}\psi = \pm\psi \qquad \ldots (45)$$

Eq. 45 implies that *ψ would either be symmetric (does not change sign) or antisymmetric (changes sign) to exchange of any pair of electrons.* Particles such as electrons and protons which have half-integral spin are classified as *fermions* because their wave function is *antisymmetric* to exchange of their coordinates and particles such as photons and phonons which have integral spin are classified as *bosons* since their wave function is symmetric to exchange of their coordinates. Fermions obey Fermi–Dirac statistics and bosons obey Bose–Einstein statistics.

From the above discussion we see that since ψ and $\hat{P}\psi$ both belong to the energy level E, the parity operation $\hat{P}$ transforms the eigenfunctions of E into each other. In the language of group theory this implies that we can choose the eigenfunctions of $\hat{H}$ with energy E as a basis set for the irreps of the point group.

Crystallographic Symmetry

We shall come across in the chapter on the Solid State that there are seven crystal systems, fourteen Bravais lattices, thirty two classes (or point groups) and 230 space groups. A crystallographer needs to determine to which crystal system, Bravais lattice, point group and space group a given unknown crystal belongs. This would be a very arduous task, indeed. The additional symmetry which ultimately produces space groups in crystals is a consequence of unique features not found in molecules.

It can be shown from purely geometrical considerations that a crystal can possess only 1-, 2-, 3-, 4- or 6-fold axis of symmetry but *not a 5-fold axis of symmetry*. Every crystal possesses external symmetry and internal symmetry. The former is determined by the symmetry elements and the interfacial angles of the crystal whereas the latter is determined by the arrangement of atoms in the lattice.

External Symmetry of Crystals. This symmetry is described by ten basic symmetry elements: n (where n=1, 2, 3, 4 and 6) and $\bar{n}$ (where $\bar{n} = \bar{1}, \bar{2}, \bar{3}, \bar{4}$ and $\bar{6}$). Here n is the n-fold proper axis and $\bar{n}$ is the n-fold proper axis combined with the operation of inversion through a central point on the axis. In other words, $\bar{n}$ is the n-fold *rotation-inversion axis*. On the basis of external symmetry, crystals are classified into 32 point groups which are listed in Table 10 in both the Hermann-Mauguin (HM) notation, (preferred by crystallographers) and in Schoenflies notation, reserved for molecules.

TABLE 10

The 32 Crystallographic Point Groups

Hermann-Mauguin Notation	Schoenflies Notation	Hermann-Mauguin Notation	Schoenflies Notation
n (1, 2, 3, 4, 6)	C_n(C_1, C_2, C_3, C_4, C_6)	n/m 2/m 2/m (n is even)	D_{nh} (n is even)
$\bar{n}$ ($\bar{1}$, $\bar{2}$, $\bar{3}$, $\bar{4}$, $\bar{6}$)	(C_i, C_s, S_6, S_4, S_3)	(2/m 2/m 2/m, 4/m 2/m 2/m,	
n 22 (n is even)	D_n (n is even)	6/m 2/m 2/m)	(D_{2h}, D_{4h}, D_{6h})
(222, 422, 622)	(D_2, D_4, D_6)	$\bar{6}$ 2m	D_{3h}
32	D_3	$\bar{4}$ 2m	D_{2d}
nmm (n is even)	C_{nv} (n is even)	$\bar{3}$ 2/m ($\bar{3}$ m)	D_{3d}
(2mm, 4mm, 6mm)	(C_{2v}, C_{4v}, C_{6v})	23	T
3m	C_{3v}	$\bar{4}$ 3m	T_d
n/m (n is even)	C_{nh} (n is even)	2/m $\bar{3}$	T_h
(2/m, 4/m, 6/m)	(C_{2h}, C_{4h}, C_{6h})	432	O
		4/m $\bar{3}$ 2/m	O_h

We shall now explain the rather unfamiliar Hermann-Mauguin (HM) notation for the crystallographic point groups. Crystals containing the proper axis of symmetry alone are denoted by the symbol n. The HM notation for crystals possessing the centre of symmetry alone is $\bar{1}$. The symbol $\bar{2}$ stands for the crystal having rotation-inversion axis of order 2. As shown below, $\bar{2}$ is equivalent to σ_h, the horizontal reflection plane :

$$\bar{2} = C_2^1 i = C_2^1 C_2^1 \sigma_h = E\sigma_h = \sigma_h \qquad \ldots (46)$$

The crystallographic point group having a mirror plane is denoted by the symbol m. A crystal which possesses a rotation-inversion axis of order 3 is denoted by the notation $\bar{3}$. $\bar{3}$ can be shown to be equivalent to the rotation-reflection axis of order 6 as follows :

$$\bar{3} = C_3^1 i = C_3^1 C_2^1 \sigma_h = C_6^2 C_6^3 \sigma_h = C_6^5 \sigma_h = S_6^5 \qquad \ldots (47)$$

A crystal possessing a rotation-inversion axis of order 4 is denoted by the symbol $\bar{4}$ which is equivalent to a rotation-reflection axis of order 4 :

$$\bar{4}=C_4^1 i = C_4^1 C_2^1 \sigma_h = C_4^1 C_4^2 \sigma_h = C_4^3 \sigma_h = S_4^3 \quad \ldots (48)$$

And finally, the $\bar{6}$ group has the rotation-inversion axis of order 6 :.

$$\bar{6}=C_6^1 i = C_6^1 C_2^1 \sigma_h = C_6^1 C_6^3 \sigma_h = C_6^4 \sigma_h = C_3^2 \sigma_h = S_3^5 \quad \ldots (49)$$

D_n groups are denoted by the symbol $n22$ when the principal axis is of even order; here n refers to the principal axis and 22 corresponds to two sets of C_2 axes in different classes. D_3 group is denoted by 32 which implies the presence of C_3 axis and 2-fold axes ; the 2-fold axes are in the same class.

C_{nv} groups are denoted by nmm when the principal axis n is of even order ; mm denotes two sets of vertical planes in different classes. C_{3v} group is denoted by $3m$; here 3 stands for 3-fold principal axis and m for vertical planes all of which are in the same class. C_{nh} symmetry is referred to as n/m when n is even (2, 4 or 6). The n/m point groups contain C_n axis and a horizontal plane σ_h. $\bar{6}$ is the HM notation for the C_{3h} point group.

If a crystal with D_{nh} symmetry contains a C_n axis of even order, then the HM notation is $n/m\ 2/m\ 2/m$. It denotes the presence of the C_n axis, two sets of C_2 axes in different classes and the horizontal plane. The notation $\bar{6}2m$ corresponds to D_{3h} point group. It means that the crystal has an $S_3(\bar{6})$ axis, C_2 axes and mirror planes. The $\bar{6}$ axis generates C_3 axis, σ_h and identity operation E. The HM notation for D_{2d} and D_{3d} point groups is $\bar{4}2m$ and $\bar{3}2/m$, respectively. The D_{2d} point group possesses a $\bar{4}$ axis, C_2 axes and dihedral planes, whereas the D_{3d} point group possesses the S_6 axis, C_2 axes and dihedral planes. A crystal cannot have the D_{4d} symmetry since $\bar{8}$ or S_8 axis cannot occur.

The T group is denoted by 23 which means the presence of 2-fold axes and 3-fold axes. If, in addition, i, C_2 and C_3 axes are also present, the point group obtained is T_h whose HM notation is $2/m\ \bar{3}$. T_d group is denoted by $\bar{4}3m$; it contains $\bar{4}$ axis, 3-fold axes and mirror planes. The point group O is represented by 432 ; it contains C_4, C_3 and C_2 axes whereas the HM notation for the point group O_h is $4/m\ \bar{3}2/m$; it implies the presence of C_4 axes, C_2 axes, S_6 axes and mirror planes.

Crystal Systems. It is known that the unit cell of a crystal is specified by the six unit cell parameters a, b, c, α, β and γ where a, b, c are the crystallographic axes and α, β, γ are the angles at which these axes intersect one another. The 32 point groups are grouped into seven crystal systems, *viz.*, cubic, tetragonal, hexagonal, rhombohedral (trigonal), orthorhombic, monoclinic and triclinic.

The cube which belongs to the O_h point group has the maximum symmetry and the triclinic system has the minimum symmetry. The cube and the octahedron are mutual polyhedra.

Table 11 lists the various n-fold rotation axes n and the n-fold rotation-inversion axes $\bar{n}$ possessed by the seven crystal systems :

TABLE 11

The n or $\bar{n}$-axes of the Seven Crystal Systems

Crystal System	n or $\bar{n}$-axis	Crystal System	n or $\bar{n}$-axis
Cubic	Many 3-fold or $\bar{3}$ axes	Orthorhombic	2 or many 2-fold axes
Tetragonal	4 or $\bar{4}$ axes	Monoclinic	2 or $\bar{2}$ axes
Hexagonal	6 or $\bar{6}$ axes	Triclinic	1 or $\bar{1}$ axis
Trigonal	3 or $\bar{3}$ axes		

Table 12 lists the 32 point groups corresponding to seven crystal systems :

TABLE 12

The 32 Point Groups Corresponding to the Seven Crystal Systems

System	Example	Unit Cell Parameters	Point Groups (HM Notation)
Cubic	NaCl	$a=b=c$, $\alpha=\beta=\gamma=90°$	23, $2/m\ \bar{3}$, $\bar{4}$, $3m$, 432, $4/m$, $\bar{3}\,2/m$
Tetragonal	SnO_2	$a=b\neq c$, $\alpha=\beta=\gamma=90°$	4, $\bar{4}/m$, $4mm$, $\bar{4}2m$, 422, $4/m\ 2/m\ 2/m$
Hexagonal	SiO_2	$a=b\neq c$, $\alpha=\beta=90°$, $\gamma=120°$	6, $\bar{6}$, $6/m$, $6mm$, 622, $\bar{6}2m$, $6/m\ 2/m\ 2/m$
Trigonal	$CaCO_3$	$a=b=c$, $\alpha=\beta=\gamma\neq 90°$	3, $\bar{3}$ $3m$, 32, $\bar{3}\,2/m$
Orthorhombic	KNO_3	$a\neq b\neq c$, $\alpha=\beta=\gamma=90°$	$2mm$, 222, $2/m\ 2/m\ 2/m$
Monoclinic	$CaSO_4.2H_2O$	$a\neq b\neq c$, $\alpha=\beta=90°$, $\gamma\neq 90°$	2, m, $2/m$
Triclinic	$K_2Cr_2O_7$	$a\neq b\neq c$, $\alpha\neq\beta\neq\gamma\neq 90°$	I, 1

Internal Symmetry of Crystals. On the basis of the arrangement of atoms or ions in the lattice, Auguste Bravais, the 19th century French crystallographer, determined that only fourteen space lattices, now referred to as the *Bravais Lattices*, are possible for the seven crystal systems. When combined with the symmetry operations, they generate 230 space groups (Table 13).

TABLE 13

14 Bravais Lattices and 230 Space groups

System	Number of Space Lattices*	Number of Space Groups
Cubic	3 (P, I, F)	36
Tetragonal	2 (P, I)	68
Hexagonal	1 (P)	27
Trigonal (Rhombohedral)	1 (R)	25
Orthorhombic	4 (P, F, I, C)	59
Monoclinic	2 (P, C)	13
Triclinic	1 (P)	2
	Total : 14	Total : 230

*P : Primitive ; I : Body-centered ; F : Face-centered ; C : End-centered ; R : Rhombohedral

Two types of space groups result depending upon the presence or absence of translational elements of symmetry in a crystal. It is found that the 230 space groups can be grouped into 73 space groups containing no translational elements of symmetry and 157 space groups involving translational elements of symmetry.

1. Space groups without translational elements of symmetry. The symbol for such a space group is described by mentioning the space lattice and the symmetry point group of the crystal in the Hermann-Mauguin (HM) notation.

A few examples of space groups are I 23 (in the cubic system), P 6 *mm* (in the hexagonal system), F $2/m\ 2/m\ 2/m$ (in the orthorhombic system) and C $2/m$ (in the monoclinic system). They denote, respectively, the body-centered Bravais lattice with point group 23, the primitive Bravais lattice with point group 6 *mm*, the face-centered Bravais lattice with point group $2/m\ 2/m\ 2/m$ and the side-centered Bravais lattice with point group $2/m$.

2. Space groups with translational elements of symmetry. In order to describe such space groups we must first describe what is translational symmetry. Translational symmetry is defined by two symmetry elements, *viz., the screw axis* and *the glide plane.*

Screw Axis. Let us consider a set of equivalent atoms, say, a_1, a_2, a_3, a_4, a_5, a_6 within a crystal structure. A screw axis is defined by an operation which combines a rotation corresponding to 2-, 3-, 4- or 6-fold axis with a translation parallel to the axis. Fig. 17(*a*) shows a normal 2-fold axis in which atom a_1 is related to atom a_2 by a rotation about the rotation axis through 180°. Fig. 17(*b*), on the other hand, shows a 2-fold screw axis, denoted by 2_t, in which atom a_1 is related to atom a_2 by rotation through 180° about the rotation axis followed by $t/2$ translation parallel to the axis. This is expressed by saying that a 2-fold axis generates a 2_t *screw axis*.

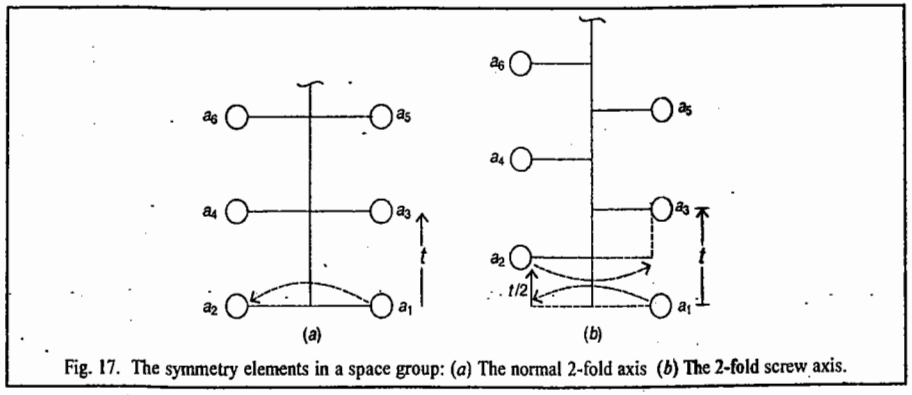

Fig. 17. The symmetry elements in a space group: (*a*) The normal 2-fold axis (*b*) The 2-fold screw axis.

Similarly, a 3-fold axis generates two screw axes : 3_1 and 3_2 ; the former corresponding to a 120° rotation about the axis followed by a translation $t/3$, and the latter corresponding to a 240° rotation about the axis followed by a translation $2t/3$. Similarly, a 4-fold axis generates three screws axes 4_1, 4_2 and 4_3 while a 6-fold axis generates 6_1, 6_2, 6_3, 6_4 and 6_5 screw axes.

Glide Planes. Consider again a set of equivalent atoms a_1, a_2, a_3, a_4, a_5, a_6, a_7, a_8 within a crystal structure. A glide plane is defined by an operation which involves a translation $t/2$ parallel to the reflection plane followed by reflection across the plane. Here t is the distance between the successive atoms. Fig. 18(*a*) shows a normal mirror plane and Fig. 18(*b*) shows the glide plane. The glide planes are further classified into three kinds, *viz., axial glides*, *diagonal glides* and *diamond glides*.

Axial glides are planes having glide component parallel to a crystallographic axis *a*, *b* or *c* and with length equal to $a/2$, $b/2$ or $c/2$. They are denoted as *a* glide, *b* glide or *c* glide. Diagonal glides, denoted by the symbol *n*, correspond to planes whose glide component is the vector sum of any of the two vectors $a/2$, $b/2$ or $c/2$. The diamond glides, denoted by the symbol *d*, correspond to planes whose glide component is the vector sum of any of the two vectors $a/4$, $b/4$ or $c/4$.

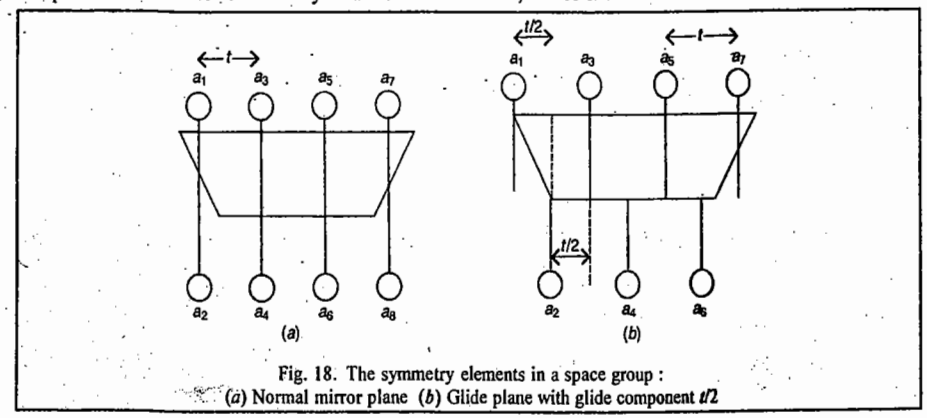

Fig. 18. The symmetry elements in a space group :
(*a*) Normal mirror plane (*b*) Glide plane with glide component $t/2$

The space group for a crystal containing translational symmetry elements is described by mentioning the Bravais lattice, the symmetry point group of the crystal in the HM notation and the translational symmetry elements. Thus, for instance, the space group $P\,2_1/b\,2_1/a\,2/m$ for an orthorhombic crystal has the following interpretation : It means that (*i*) the Bravais lattice is primitive ; (*ii*) the *a*-axis is a 2_1 screw axis having a *b*-glide plane normal to it ; (*iii*) the *b*-axis is also a 2_1 screw axis with an *a*-glide plane normal to it ; (*iv*) the *c*-axis is the ordinary 2-fold axis and (*v*) the ordinary mirror plane is normal to the 2-fold axis. All the 230 space groups have similar notation and interpretation.

Molecular Symmetry and Crystallographic Symmetry. Table 14 compares the two kinds of symmetry.

TABLE 14

Comparison between Molecular and Crystallographic Symmetry

Molecular Symmetry	Crystallographic Symmetry
1. C_n axis of order n (where n =1, 2, 3, 4,..., ∞) is present.	C_n axis of order n (n = 1, 2, 3, 4, 6) is present. Note that 5-fold axis is not present.
2. Rotation-reflection axis is present.	Rotation-inversion axis is present.
3. The number of point groups is not limited.	The number of point groups is 32.
4. Schoenflies notation is used to denote point groups.	Hermann-Mauguin (HM) notation is used to denote point groups.

Quasicrystals. Recently, quasicrystals have been prepared by metallurgists. A quasicrystal has 5-fold axis of symmetry. The best known quasicrystal is an alloy of solidified aluminium and a transition metal such as chromium, manganese or iron. It possesses the icosahedral symmetry (the icosahedral point group I_h consists of twelve 5-fold axes of symmetry). A quasicrystal occurs primarily as a metastable phase and its dimension is so small that it cannot be investigated by the conventional X-ray single crystal diffractometry. Quasicrystals can be prepared by techniques such as rapid solidification of alloys, rapid pressurization of the melt and precipitation from solid solutions. They can be studied by transmission electron microscopy. Quasicrystals having the symmetry of such polyhedra as icosahedron, pentagonal dodecahedron and triacontahedron have been prepared. They are very hard and are also very poor conductors of heat and electricity ; they are used as thermoelectric materials which convert heat into electricity. They were discovered by the Israeli scientist Daniel Shechtman who was awarded the 2011 Nobel Prize in Chemistry. Their discovery was a "shock" to crystallographers. Even Linus Pauling, the great colossus of science, had mounted a "crusade" against Shechtman, saying, "There is no such thing as quasicrystals, only quasi-scientists". However, nature has always the last laugh.

Problems

1. List the symmetry elements and the Schoenflies symbols for each of the following molecules :

(*a*) H_2S, (*b*) PCl_3 (pyramidal), (*c*) $\begin{matrix}H\\Cl\end{matrix}\!\!>\!C{=}O$, (*d*) IF_5 (square pyramidal), (*e*) B_2H_6, (*f*) p-Dichlorobenzene (*g*) Naphthalene, (*h*) Thiophene, (*i*) SiF_4, (*j*) NH_2Cl, (*k*) BF_4^-, (*l*) CO_3^{2-}(*m*) SiFClBrI, (*n*) trans-N_2F_2, (*o*) Cyclohexane, (*p*) $CHClBr(CH_3)$, (*q*) $CF_2{=}CF_2$, (*r*) 1,2-dichlorobenzene, (*s*) XeF_2(linear), (*t*) monosodium acetylide (H–C≡C–Na), (*u*) *trans*-$[CrBr_2(H_2O)_4]^+$ (ignore Hs), (*v*) gauche-CH_2Cl CH_2Cl, (*w*) Ketene ($CH_2{=}C{=}O$), (*x*) $CH_2{=}O$, (*y*) $[IO_6]^{5-}$ (octahedral), (*z*) 

[Ans. (*a*) C_{2v}, (*b*) C_{3v}, (*c*) C_s, (*d*) C_{4v}, (*e*) D_{2h}, (*f*) D_{2h}, (*g*) D_{2h}, (*h*) C_{2v}, (*i*) T_d, (*j*) C_s, (*k*) T_d, (*l*) D_{3h}, (*m*) C_1, (*n*) C_{2h}, (*o*) D_{3d}, (*p*) C_1, (*q*) D_{2h}, (*r*) C_{2v}, (*s*) $D_{\infty h}$, (*t*) $C_{\infty v}$, (*u*) D_{4h}, (*v*) C_2, (*w*) C_{2v}, (*x*) C_{2v}, (*y*) O_h, (*z*) C_{2v} **]**

2. Which of the following molecules and ions has (*i*) a centre of inversion, (*ii*) an S_4 axis, : (*a*) CO_2, (*b*) C_2H_2, (*c*) BF_3, (*d*) SO_4^{2-}? [Ans. (*i*) CO_2, C_2H_2, (*ii*) SO_4^{2-}]

3. Assuming that a molecule AB_6 belongs to O_h point group, determine the point groups that result if it is changed into (*a*) AB_5C, (*b*) trans-AB_4C_2, (*c*) *cis*-AB_4C_2 [Ans. (*a*) C_{4v}, (*b*) D_{4h}, (*c*) C_{2v}]

4. In the solid state, phosphorus(V) chloride exists as an ionic solid composed of PCl_4^+ cations and PCl_6^- anions but the vapour is molecular. To what point groups do the ionic species in the solid belong ? [Ans. T_d and O_h, respectively]

5. Draw the structures of three distinct isomers of $C_2H_2Cl_2$ and determine their point groups. Which of them is polar ?

[Ans. 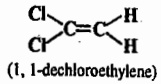 (1, 1-dechloroethylene) (C_{2v}) ; polar 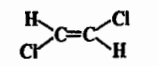 (*trans*-1, 2-dichloroethylene) (C_{2h}) ; nonpolar 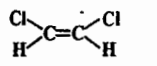 (*cis*-1, 2-dichloroethylene) (C_{2v}) ; polar]

6. There are 10 distinct isomers of dichloronaphthalene, $C_{10}H_6Cl_2$. Two of them are nonpolar. Draw the structures of these nonpolar isomers and determine the point group to which they belong.

[Ans. 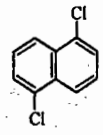 (C_{2h}) ; 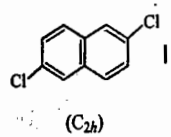 (C_{2h})]

7. Explain why a set of numbers cannot form a group by the process of division.

[Ans. The reason is that the associative law of combination is not obeyed, *i.e.*, $A/(B/C) \neq (A/B)/C$. Thus, for example, 3/(4/5) = 15/4 ; and (3/4)/5 = 3/20]

8. Explain why the set of integers between 0 and ∞ do not form a group under the process of multiplication.

[Ans. The reason is that the inverse of every element is a fraction which is not a member of the set.]

9. In some of the electronic excited states, acetylene, a linear molecule, may exist as *cis*-bent or as *trans*-bent, as shown below :

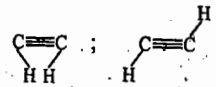
(*cis*-bent) (*trans*-bent)

Determine the point groups of these geometries. [Ans. C_{2v} and C_{2h}]

10. State G.O.T. and list the properties of the irreps.

11. Using G.O.T., derive the character table for C_{2v} point group.

12. Using G.O.T., derive the character table for C_{3v} point group.

CHAPTER 5

GROUP THEORY–II. APPLICATIONS

The basic concepts of group theory have been discussed at length in the previous chapter. The ideas of symmetry described mathematically by the group theory find wide applications which will be discussed in this chapter. These applications include ; assigning the modes of molecular vibrations to the irreducible representations of the point groups to which a molecule belongs, determining which orbitals are used for hybridisation in chemical bonding, deriving the selection rules for spectral transitions, etc. The most spectacular application of group theory is in determining the vanishing of the integrals (matrix elements) in quantum mechanical calculations.

1. Decomposing a Reducible Representation into its Irreducible Representations

We shall derive an extremely important result which allows us to determine how many times the *j*th irrep is contained in a rep (reducible representation). In general, any rep Γ can be written as a linear combination of irreps as shown below :

$$\Gamma = n_1\Gamma_1 + n_2\Gamma_2 + n_3\Gamma_3 + \ldots\ldots \qquad \ldots(1)$$

where Γ_1, Γ_2, Γ_3, ... are the irreps and n_1, n_2, n_3, ... are the number of times each irrep occurs in Γ.

Recalling that the character of a matrix is unaltered by a similarity transformation, we can write

$$\chi(R) = \Sigma n_i \chi_i(R) \qquad \ldots(2)$$

where $\chi(R)$ is the character of the matrix corresponding to an operation R in the rep and n_i refers to the number of times the block constituting the irrep repeats itself in the diagonal; $\chi_i(R)$ is the character of the matrix for the operation R in the *i*th irrep. Multiplying Eq. 2 by $\chi_j(R)$ and summing over R, we obtain

$$\sum_R \chi_j(R)\chi(R) = \sum_R \sum_i n_i\chi_j(R)\chi_i(R) = \sum_i n_i \sum_R \chi_i(R)\chi_j(R) \qquad \ldots(3)$$

Using the property of the irreps, *viz.*,

$$\sum_R \chi_i(R)\chi_j(R) = h\delta_{ij}, \qquad \ldots(4)$$

we find that Eq. 3 becomes

$$\sum_R \chi_j(R)\chi(R) = \sum_i n_i h\delta_{ij} \qquad \ldots(5)$$

The term for which $i = j$ survives in the summation so that Eq. 5 reduces to

$$\sum_R \chi_j(R)\chi(R) = n_j h \qquad \ldots(6)$$

Hence,

$$n_j = \frac{1}{h}\sum_R \chi_j(R)\chi(R) \qquad \ldots(7)$$

If g_p is the number of operations in the *p*th class of the group, then Eq. 7 becomes

$$n_j = \frac{1}{h}\sum_{R_p} g_p\chi(R_p)\chi_j(R_p) \qquad \ldots(8)$$

where R_p denotes the symmetry operation in the pth class. Eq. 7 or Eq. 8, known as **the standard reduction formula**, gives the relation which determines the number of times the jth irrep occurs in the rep.

Example 1. Suppose that the characters of a reducible representation of the C_{2v} point group are $\chi(E) = 4$, $\chi(C_2) = 2$, $\chi(\sigma_v) = 0$ and $\chi(\sigma_v') = 2$. This is usually expressed by writing $\Gamma = 4\ 2\ 0\ 2$. Determine how many times each irreducible representation of C_{2v} is contained in $\Gamma = 4\ 2\ 0\ 2$.

Solution :
$$n_j = \frac{1}{h}\sum_R \chi_j(R)\chi(R) \qquad \text{(Eq. 7)}$$

The order h of the C_{2v} point group is 4. Hence, using the character table of the C_{2v} point group and the above equation, we get

$$n_{A_1} = \frac{1}{4}[1\times 4 + 1\times 2 + 1\times 0 + 1\times 2] = 2$$
$$n_{A_2} = \frac{1}{4}[1\times 4 + 1\times 2 + (-1)\times (0) + (-1)\times 2] = 1$$
$$n_{B_1} = \frac{1}{4}[1\times 4 + (-1)\times 2 + 1\times 0 + (-1)\times 2] = 0$$
$$n_{B_2} = \frac{1}{4}[1\times 4 + (-1)\times 2 + (-1)\times 0 + 1\times 2] = 1$$

Thus, $\Gamma = 2A_1 + A_2 + B_2$

Example 2. Suppose that the characters of a reducible representation of the C_{3v} point group are expressed as $\Gamma = 3\ 0\ -1$. Determine how many times each irreducible representation of C_{3v} is contained in the above rep.

Solution :
$$n_j = \frac{1}{h}\sum_{R_p} g_p\chi(R_p)\chi_j(R_p) \qquad \text{[Eq. 8]}$$

The order h of the C_{3v} point group is 6. Hence, using the character table of the C_{3v} point group and the above equation, we get

$$n_{A_1} = \frac{1}{6}[1\times 3\times 1 + 2\times 0\times 1 + 3\times (-1)\times 1] = 0$$
$$n_{A_2} = \frac{1}{6}[1\times 3\times 1 + 2\times 0\times 1 + 3\times (-1)\times (-1)] = 1$$
$$n_E = \frac{1}{6}[1\times 3\times 2 + 2\times 0\times (-1) + 3\times (-1)\times 0] = 1$$

Thus, $\Gamma = A_2 + E$

2. Group Theory and Normal Modes of Vibrations of Polyatomic Molecules

The normal modes of vibration that set a polyatomic molecule into a periodic oscillation in which the nuclei move in phase, that is, they all pass through the mean position at the same time, are of great importance in vibrational analysis since any arbitrary vibration of the molecule can be described by a superposition of the normal modes. We shall briefly review the normal mode analysis here.

The potential energy V of a molecule can be written as a Taylor's series :

$$V = V_0 + \sum_i \left(\frac{\partial V}{\partial q_i}\right)_0 q_i + \frac{1}{2}\sum_i\sum_j \left(\frac{\partial^2 V}{\partial q_i \partial q_j}\right)_0 q_i q_j + \cdots \qquad \ldots(9)$$

where q_i, q_j, ... are the coordinates of the nuclei i, j, ..., and the subscript zero refers to the equilibrium state of the molecule. Since V_0 is the potential energy in the equilibrium state and hence, a constant, we can arbitrarily call it zero. The term $(\partial V/\partial q)_0$ corresponds to the minimum of the potential energy curve and is, therefore, also set equal to zero. Neglecting all the higher terms except one in Eq. 9, Eq. 9 reduces to

$$V = \frac{1}{2}\sum_i\sum_j \left(\frac{\partial^2 V}{\partial q_i \partial q_j}\right)_0 q_i q_j = \frac{1}{2}\sum_i\sum_j b_{ij} q_i q_j \qquad \ldots(10)$$

where $b_{ij} = \left(\dfrac{\partial^2 V}{\partial q_i \partial q_j}\right)_0$

Similarly, the kinetic energy T of the molecule can also be written in the form of a Taylor's series. Thus,

$$T = \frac{1}{2}\sum_i\sum_j a_{ij}\,\dot{q}_i\,\dot{q}_j \qquad \ldots(11)$$

where $\dot{q} = dq/dt$ and the a_{ij} are functions of the mass of atoms.

Eqs. 10 and 11 can be used to construct the Hamiltonian operator, $\hat{H}$, for the Schrödinger wave equation. (Recall that $H = T + V$.) However, the cross products of the types q_iq_j prevent the separation of variables. This problem can be solved by using the normal coordinates Q such that

$$\left.\begin{aligned} q_1 &= c_{11}Q_1 + c_{12}Q_2 + c_{13}Q_3 + \cdots\cdots \\ q_2 &= c_{21}Q_1 + c_{22}Q_2 + c_{23}Q_3 + \cdots\cdots \\ &\cdots\cdots\cdots\cdots\cdots\cdots\cdots \\ q_i &= c_{i1}Q_1 + c_{i2}Q_2 + c_{i3}Q_3 + \cdots\cdots \end{aligned}\right\} \qquad \ldots(12)$$

By a suitable choice of the coefficients c_{ij} of this linear transformation, it is possible to write T and V in terms of the new coordinates as

$$T = \frac{1}{2}(\dot{Q}_1^2 + \dot{Q}_2^2 + \cdots\cdots + \dot{Q}_{3N}^2) = \frac{1}{2}\sum_i \dot{Q}_i^2 \qquad \ldots(13)$$

and
$$V = \frac{1}{2}(\lambda_1\dot{Q}_1^2 + \lambda_2\dot{Q}_2^2 + \cdots\cdots + \lambda_N\dot{Q}_{3N}^2) = \frac{1}{2}\sum_i \lambda_i Q_i^2 \qquad \ldots(14)$$

where $\lambda_i = 4\pi^2\nu_i^2$.

We can now proceed to solve the time-independent Schrödinger wave equation for the vibrational problem. For each normal coordinate Q_i, that is, for each normal mode, we have

$$\hat{H} = \hat{T} + \hat{V} \qquad \ldots(15)$$

so that the Schrödinger wave equation is

$$-\frac{\hbar^2}{2}\frac{\partial^2\psi(Q_i)}{\partial Q_i^2} + \frac{\lambda_i Q_i^2}{2}\psi(Q_i) = E_i\psi(Q_i) \qquad \ldots(16)$$

The total vibrational energy is given by

$$E_{vib} = E_1 + E_2 + E_3 + \cdots\cdots + E_{3N-5,6} = \sum_i^{3N-5,6} E_i \qquad \ldots(17)$$

where $E_i = \left(v + \dfrac{1}{2}\right)h\nu_i$. The total wave function is given by

$$\psi_{vib} = \psi_v(Q_1)\ \psi_v(Q_2)\ \cdots\cdots\ \psi_v(Q_{3N-5,6}) = \prod_i^{3N-5,6} \psi_v(Q_i) \qquad \ldots(18)$$

where the subscript v denotes the particular vibrational level and i the particular vibrational mode.

We know that the eigenfunctions of a simple harmonic oscillator are given by

$$\psi_v(\xi) = N_v H_v(\xi)\exp(-\xi^2/2) \qquad \ldots(19)$$

where $H_v(\xi)$ are the Hermite polynomials. Writing Q_i for ξ, we have, for the ground state ($v=0$),

$$\psi_0(Q_i) = \left(\frac{1}{\alpha_i\pi}\right)^{1/2}\exp\left(-\frac{1}{2}Q_i^2/\alpha_i\right) \qquad \ldots(20)$$

and for the first excited state ($v=1$),

$$\psi_1(Q_i) = \left(\frac{1}{\alpha_i^3\pi}\right)^{1/2} Q_i\exp\left(-\frac{1}{2}Q_i^2/\alpha_i\right) \qquad \ldots(21)$$

Thus, assuming the simple harmonic model, we have broken the vibrational motion of the molecule down into $3N$–5 or $3N$–6 S.H.O.s in the normal coordinates Q_i. Assuming the vibrational transition $v=0 \rightarrow 1$, as required by the selection rule, there will be $3N - 5$ fundamental vibrational frequencies for the linear and $3N - 6$ fundamental vibrational frequencies for the nonlinear molecules. The vibrational frequency for the ith normal mode is given by

$$\nu_i = \frac{1}{2\pi}\left(\frac{k}{\mu}\right)^{1/2} \qquad ...(22)$$

where k is the force constant and μ is some complicated function of masses. It should be noted that k is no longer associated with a single bond as in the diatomic case and there is no straightforward correlation between k and the strength of the chemical bond.

3. Procedure for Determining the Irreducible Representations of the Vibrational Modes in Nonlinear Molecules. The procedure involves the following steps :

1. Determine the point group of the molecule.
2. Obtain the reducible representations (reps) for all the symmetry operations of the point group.
3. Split the rep into the irreps using the standard reduction formula.
4. The irreps Γ_{3N} thus obtained correspond to the translational, rotational and vibrational degrees of freedom. By subtracting the irreps (corresponding to the translational and rotational degrees of freedom) from Γ_{3N}, the irreps corresponding to the vibrational motion, Γ_{vib}, are obtained.

We shall apply the above procedure to three molecules, *viz.*, H_2O, NH_3 and BF_3.

a. Normal Modes of Vibration of H_2O Molecule. H_2O belongs to the C_{2v} point group whose character table is given below :

TABLE 1

Character Table of the C_{2v} Point Group

C_{2v}	E	C_2	σ_v	σ_v'	$h = 4$	
A_1	1	1	1	1	z	x^2, y^2, z^2
A_2	1	1	–1	–1	R_z	xy
B_1	1	–1	1	–1	x, R_y	xz
B_2	1	–1	–1	1	y, R_x	yz

The coordinate axis system for H_2O and the symmetry elements in H_2O molecule are shown in Fig. 1.

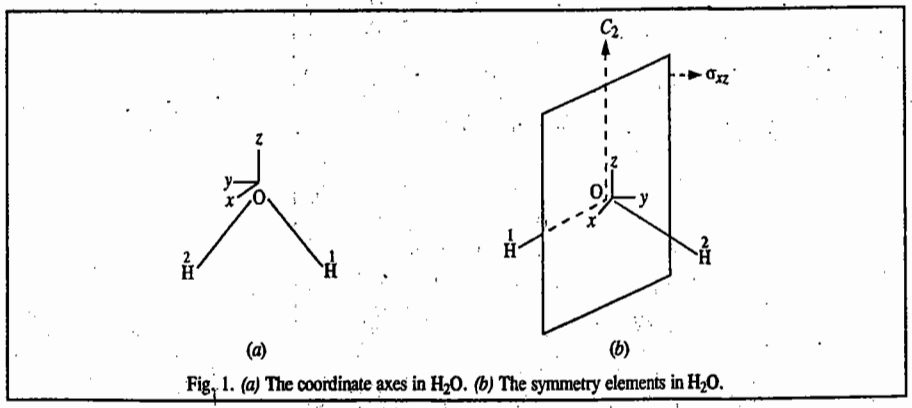

Fig. 1. *(a)* The coordinate axes in H_2O. *(b)* The symmetry elements in H_2O.

The three atoms in H_2O have 9 coordinates. Four 9×9 matrices can be constructed for the four symmetry operations (E, $C_2(z)$, $\sigma_v(x, z)$ and $\sigma_v'(y, z)$) of this molecule, as shown below :

***E* Matrix :**

$$\begin{bmatrix} x_1' \\ y_1' \\ z_1' \\ x_2' \\ y_2' \\ z_2' \\ x_3' \\ y_3' \\ z_3' \end{bmatrix} = \begin{bmatrix} 1&0&0&0&0&0&0&0&0 \\ 0&1&0&0&0&0&0&0&0 \\ 0&0&1&0&0&0&0&0&0 \\ 0&0&0&1&0&0&0&0&0 \\ 0&0&0&0&1&0&0&0&0 \\ 0&0&0&0&0&1&0&0&0 \\ 0&0&0&0&0&0&1&0&0 \\ 0&0&0&0&0&0&0&1&0 \\ 0&0&0&0&0&0&0&0&1 \end{bmatrix} \begin{bmatrix} x_1 \\ y_1 \\ z_1 \\ x_2 \\ y_2 \\ z_2 \\ x_3 \\ y_3 \\ z_3 \end{bmatrix} \qquad ...(23)$$

The character $\chi(E)$ of this matrix is equal to 9.

C_2 Matrix :

$$\begin{bmatrix} x_1' \\ y_1' \\ z_1' \\ x_2' \\ y_2' \\ z_2' \\ x_3' \\ y_3' \\ z_3' \end{bmatrix} = \begin{bmatrix} 0&0&0&-1&0&0&0&0&0 \\ 0&0&0&0&-1&0&0&0&0 \\ 0&0&0&0&0&1&0&0&0 \\ -1&0&0&0&0&0&0&0&0 \\ 0&-1&0&0&0&0&0&0&0 \\ 0&0&1&0&0&0&0&0&0 \\ 0&0&0&0&0&0&-1&0&0 \\ 0&0&0&0&0&0&0&-1&0 \\ 0&0&0&0&0&0&0&0&1 \end{bmatrix} \begin{bmatrix} x_1 \\ y_1 \\ z_1 \\ x_2 \\ y_2 \\ z_2 \\ x_3 \\ y_3 \\ z_3 \end{bmatrix} \qquad ...(24)$$

The character $\chi(C_2)$ of this matrix is equal to –1.

$\sigma_v(xz)$ Matrix :

$$\begin{bmatrix} x_1' \\ y_1' \\ z_1' \\ x_2' \\ y_2' \\ z_2' \\ x_3' \\ y_3' \\ z_3' \end{bmatrix} = \begin{bmatrix} 0&0&0&1&0&0&0&0&0 \\ 0&0&0&0&-1&0&0&0&0 \\ 0&0&0&0&0&1&0&0&0 \\ 1&0&0&0&0&0&0&0&0 \\ 0&-1&0&0&0&0&0&0&0 \\ 0&0&1&0&0&0&0&0&0 \\ 0&0&0&0&0&0&1&0&0 \\ 0&0&0&0&0&0&0&-1&0 \\ 0&0&0&0&0&0&0&0&1 \end{bmatrix} \begin{bmatrix} x_1 \\ y_1 \\ z_1 \\ x_2 \\ y_2 \\ z_2 \\ x_3 \\ y_3 \\ z_3 \end{bmatrix} \qquad ...(25)$$

The character $\chi(\sigma_v(x\,z))$ of this matrix is equal to 1.

$\sigma_v'(yz)$ Matrix :

$$\begin{bmatrix} x_1' \\ y_1' \\ z_1' \\ x_2' \\ y_2' \\ z_2' \\ x_3' \\ y_3' \\ z_3' \end{bmatrix} = \begin{bmatrix} -1&0&0&0&0&0&0&0&0 \\ 0&1&0&0&0&0&0&0&0 \\ 0&0&1&0&0&0&0&0&0 \\ 0&0&0&-1&0&0&0&0&0 \\ 0&0&0&0&1&0&0&0&0 \\ 0&0&0&0&0&1&0&0&0 \\ 0&0&0&0&0&0&-1&0&0 \\ 0&0&0&0&0&0&0&1&0 \\ 0&0&0&0&0&0&0&0&1 \end{bmatrix} \begin{bmatrix} x_1 \\ y_1 \\ z_1 \\ x_2 \\ y_2 \\ z_2 \\ x_3 \\ y_3 \\ z_3 \end{bmatrix} \qquad ...(26)$$

The character $\chi(\sigma_v(yz))$ of this matrix is equal to 3.

We thus obtain the following Γ_{3N} reducible representation (rep) for the $3N$ coordinates :

Operation	E	C_2	$\sigma_v(xz)$	$\sigma_v'(yz)$
Γ_{3N}	9	–1	1	3

A simple rule states that the character for the operation R in the rep $\chi_{xyz}(R)$ is equal to the product of the number of *unshifted* atoms, U_R and the character of the matrix for the operation R, $\chi(R)$.

Using the standard reduction formula (Eq. 8) and the character table for the C_{2v} point group, the above mentioned reducible representation is split into the various irreps as follows :

$$n_{A_1} = \frac{1}{4}[1 \times 9 \times 1 + 1 \times (-1) \times 1 + 1 \times 1 \times 1 + 1 \times 3 \times 1] = 3$$

$$n_{A_2} = \frac{1}{4}[1 \times 9 \times 1 + 1 \times (-1) \times 1 + 1 \times 1 \times (-1) + 1 \times 3 \times (-1)] = 1$$

$$n_{B_1} = \frac{1}{4}[1 \times 9 \times 1 + 1 \times (-1) \times (-1) + 1 \times 1 \times 1 + 1 \times 3 \times (-1)] = 2$$

$$n_{B_2} = \frac{1}{4}[1 \times 9 \times 1 + 1 \times (-1) \times (-1) + 1 \times 1 \times (-1) + 1 \times 3 \times 1] = 3$$

Hence, $\Gamma_{3N} = 3A_1 + A_2 + 2B_1 + 3B_2$ ...(27)

Now, Γ_{vib}, *i.e.*, the sum of the irreps of the vibrational modes, is related to Γ_{3N} by

$$\Gamma_{vib} = \Gamma_{3N} - (T_x + T_y + T_z + R_x + R_y + R_z) \quad ...(28)$$

where T_x, T_y, T_z refer to the representations of the translational degrees of freedom and R_x, R_y, R_z refer to the representations of the rotational degrees of freedom. Note that $x \to T_x$, $y \to T_y$ and $z \to T_z$ so that using the values of T_x, T_y, T_z and R_x, R_y, R_z from the section III of the C_{2v} point group, we obtain

$$\Gamma_{vib} = (3A_1 + A_2 + 2B_1 + 3B_2) - (B_1 + B_2 + A_1 + B_2 + B_1 + A_2) \quad ...(29)$$

or $\Gamma_{vib} \equiv \Gamma_{3N-6} = 2A_1 + B_2$

We thus find that the three normal modes of vibration of H_2O molecule belong to A_1 and B_2 symmetry species (irreps). The vibrations belonging to A_1 symmetry are called totally symmetric vibrations. (If a vibration is symmetric with respect to the highest-fold rotation axis, it is designated by A and if the vibration is antisymmetric about the same axis, it is designated by B. The letter E which is absent here, is for doubly degenerate vibrations).

b. Normal Modes of Vibration of NH_3 Molecule. NH_3 belongs to the C_{3v} point group whose character table is given below :

TABLE 2

Character Table of the C_{3v} Point Group

C_{3v}	E	$2C_3$	$3\sigma_v$	$h = 6$	
A_1	1	1	1	z	$x^2 + y^2, z^2$
A_2	1	1	–1	R_z	
E	2	–1	0	(x, y) (R_x, R_y)	$(x^2 - y^2, xy)$, (xz, yz)

Using the procedure given above, we obtain the following reducible representation (rep) for the NH_3 molecule (whose symmetry elements are shown in Fig. 2) :

Operation	E	$2C_3$	$3\sigma_v$
Γ_{3N}	12	0	2

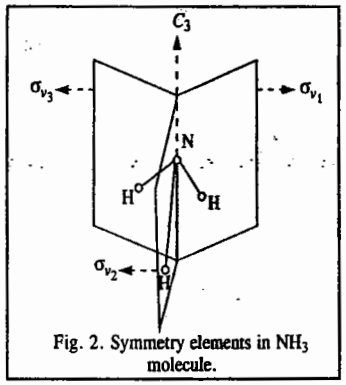

Fig. 2. Symmetry elements in NH_3 molecule.

Using the standard reduction formula (Eq. 8), this reducible representation is split into the following irreps :

$$\Gamma_{3N} = 3A_1 + A_2 + 4E \quad ...(30)$$

Now, Γ_{vib}, *i.e.*, the sum of the reps of the vibration modes, is related to Γ_{3N} by

$$\Gamma_{vib} = \Gamma_{3N} - (T_x + T_y + T_z + R_x + R_y + R_z) \quad ...(31)$$

From section III of the C_{3v} point group,

$$T_x + T_y + T_z = A_1 + E \text{ and } R_x + R_y + R_z = A_2 + E$$

Hence, $\Gamma_{vib} = (3A_1 + A_2 + 4E) - (A_1 + E + A_2 + E)$

$$= 2A_1 + 2E \quad ...(32)$$

We see that two normal modes of vibration of NH_3 molecule belong to the totally symmetric species A_1 and four modes belong to the doubly degenerate symmetry E.

c. Normal Modes of Vibration of BF_3 Molecule. BF_3 belongs to the D_{3h} point group whose character table is given below :

TABLE 3

Character Table of the D_{3h} Point Group

D_{3h}	E	$2C_3$	$3C_2$	σ_h	$2S_3$	$3\sigma_v$	$h=12$	
A_1'	1	1	1	1	1	1		$x^2 + y^2, z^2$
A_2'	1	1	–1	1	1	–1	R_z	
E'	2	–1	0	2	–1	0	(x, y)	$x^2 - y^2, xy$
A_1''	1	1	1	–1	–1	–1		
A_2''	1	1	–1	–1	–1	1	z	
E''	2	–1	0	–2	1	0	(R_x, R_y)	(xz, yz)

Using the procedure given above, we obtain the following reducible representation (rep) for the BF_3 molecule (whose symmetry elements are shown in Fig. 3) :

Operation	E	$2C_3$	$3C_2$	σ_h	$2S_3$	$3\sigma_v$
Γ_{3N}	12	0	–2	4	–2	2

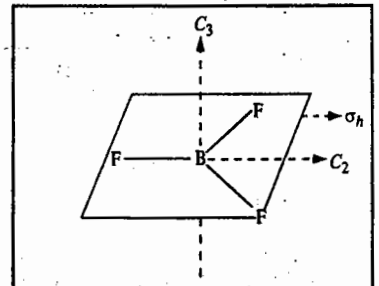

Fig. 3. The symmetry elements in BF_3 molecule

Using the standard reduction formula (Eq. 8), this reducible representation is split into the following irreps :

$$\Gamma_{3N} = A_1' + A_2' + 3E' + 2A_2'' + E'' \quad ...(33)$$

As before, $\Gamma_{vib} = \Gamma_{3N} - (T_x + T_y + T_z + R_x + R_y + R_z)$ ...(34)

From section III of the character table of the D_{3h} point group, we have

$$(T_x, T_y) = E' \text{ and } T_z = A_2'' \text{ (for translation)}$$

$$(R_x, R_y) = E'' \text{ and } R_z = A_2' \text{ (for rotations)}$$

Hence,
$$\Gamma_{vib} = (A_1' + A_2' + 3E' + 2A_2'' + E'') - (E' + A_2'' + E'' + A_2')$$
$$= A_1' + A_2'' + 2E' \quad ...(35)$$

Fig. 4 shows the normal modes of vibration of BF_3 molecule.

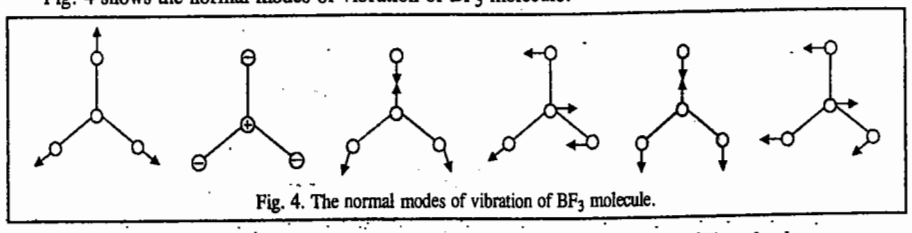

Fig. 4. The normal modes of vibration of BF_3 molecule.

Example 3. Establish the symmetry species of the normal modes of vibration of CH_4 molecule.

Solution : Refer to Fig. 5. There are $3\times5 = 15$ possible displacements, of which $3\times5 - 6 = 9$ are the normal modes of vibration.

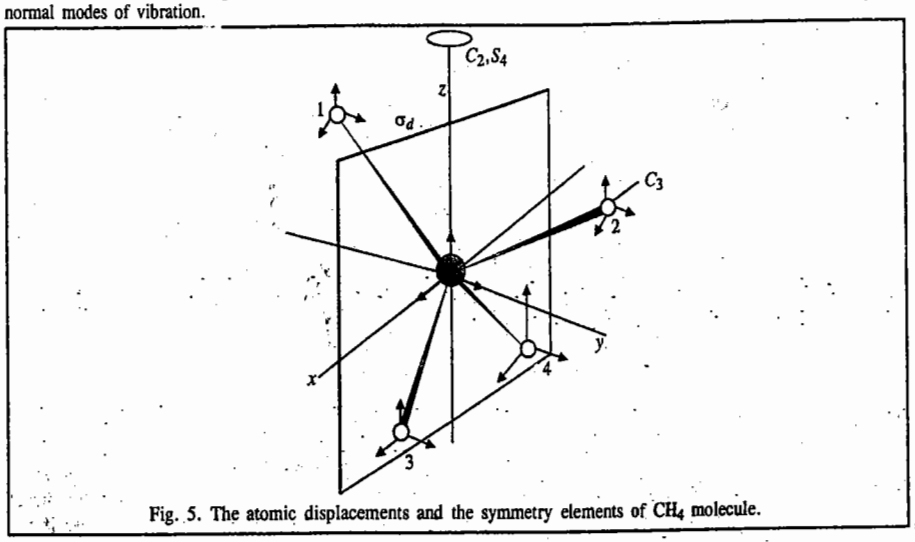

Fig. 5. The atomic displacements and the symmetry elements of CH_4 molecule.

The character table of the T_d point group to which CH_4 molecule belongs is given below :

TABLE 4

Character Table of the T_d Point Group

T_d	E	$8C_3$	$3C_2$	$6S_4$	$6\sigma_d$	$h = 24$	
A_1	1	1	1	1	1		$x^2 + y^2 + z^2$
A_2	1	1	1	-1	-1		
E	2	-1	2	0	0		$(2z^2 - x^2 - y^2, x^2 - y^2)$
T_1	3	0	-1	1	-1	(R_x, R_y, R_z)	
T_2	3	0	-1	-1	1	(x, y, z)	(xy, xz, yz)

Under the identity operation E, no displacement coordinates are changed. Hence, the character is 15. Under C_3, no. displacements are left unchanged, so the character is 0. Under a C_2 rotation, the z-displacement of the central atom is left unchanged while the x- and y-displacement components both change sign. Hence, $\chi(C_2) = 1 - 1 - 1 + 0 + 0 = -1$. Under S_4, the z-displacement of the central atom is reversed, so $S_4 = -1$. Under σ_d, the x- and z-displacements of C, H (3) and H (4) are left unchanged and the y-displacements are reversed. Hence, $\chi(\sigma_d) = 3 + 3 - 3 = 3$. Thus, we obtain the following reducible representation (rep) for the $3N$ coordinates :

Operation	E	$8C_3$	$3C_2$	$6S_4$	$6\sigma_d$
Γ_{3N}	15	0	-1	-1	3

Using the standard reduction formula (Eq. 8) and the character table for the T_d point group, we find that

$$\Gamma_{3N} = A_1 + E + T_1 + 3T_2 \quad ...(36)$$

Since the translations span T_2 and the rotations span T_1, we have

$$\Gamma_{vib} = (A_1 + E + T_1 + 3T_2) - (T_2 + T_1)$$
$$= A_1 + E + 2T_2 \quad ...(37)$$

The normal vibrational modes of CH_4, a tetrahedral molecule, are shown in Fig. 6.

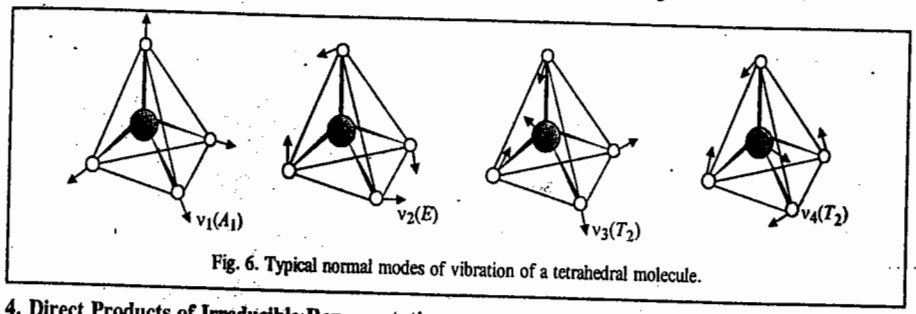

Fig. 6. Typical normal modes of vibration of a tetrahedral molecule.

4. Direct Products of Irreducible Representations

If ψ_i and ψ_j are the wave functions which form a basis for the irreps of a point group, then the product of these wave functions can also form a basis for the representation of the group. This representation is called the **direct product representation.** Let $\chi^{\mu}(R)$ and $\chi^{\nu}(R)$ denote the characters for operation R in the representations μ and ν, respectively. Then the character $\chi^{\mu\nu}(R)$ of the operation R in the direct product representation is given by

$$\chi^{\mu\nu}(R) = \chi^{\mu}(R)\, \chi^{\nu}(R) \quad ...(38)$$

An important application of this concept is that *the integral of the product of two or more functions over symmetric interval is nonzero if the direct product representation is totally symmetric.* If the direct product representation is reducible, then the integral of the product function is non-zero only if the direct product representation contains the totally symmetric species.

Let ψ_i and ψ_j be the wave functions of two energy states i and j and μ, the dipole moment vector whose components are μ_x, μ_y and μ_z is thus given by

$$\mu = \mu_x + \mu_y + \mu_z \quad ...(39)$$

Also, $\mu_x = ex$; $\mu_y = ey$ and $\mu_z = ez$ where e is the electronic charge. The transition will be allowed only if μ_{ij}, the matrix element (transition dipole moment integral) between the states i and j is nonzero :

$$\mu_{ij} = \langle \psi_i | \mu | \psi_j \rangle \equiv \int \psi_i \mu \psi_j \, d\tau \quad ...(40)$$

More specifically, the transition will be allowed if at least one of the components μ_{ij} is different from zero. Since μ_{ij} is a real physical property of the molecule, it must be invariant with respect to any

rotation, reflection or inversion about the molecular symmetry axis. In other words, a transition is allowed if the product $\psi_i \mu \psi_j$ is totally symmetric for at least one orientation of μ. That is to say, if the product $\psi_i \psi_j$ and at least one of the components of μ belongs to the same irrep (IR), the transition is allowed. This can be written as direct product of irrep (IR) as

$$\Gamma_{\psi_i} \times \Gamma_{\mu} \times \Gamma_{\psi_j} = \Gamma_1 \quad \text{or} \quad A_1 \text{ (totally symmetric)} \qquad ...(41)$$

Consider H_2O molecule which belongs to the C_{2v} point group. The irreps (IRs) of the dipole moment components are : $\mu_x = B_1$, $\mu_y = B_2$, $\mu_z = A_1$. The various other states are A_1, A_2, B_1, B_2 (which are the IRs of the C_{2v} point group). Consider the transition $A_1 \rightarrow A_1$. Now,

$$\Gamma_{\psi_i} = A_1, \quad \Gamma_{\psi j} = A_1 \qquad ...(42)$$

Thus, for the μ_x component, $A_1 \mu_x A_1 = A_1 \times B_1 \times A_1 = B_1$ ...(43)

for the μ_y component, $A_1 \mu_y A_1 = A_1 \times B_2 \times A_1 = B_2$ ...(44)

for the μ_z component, $A_1 \mu_z A_1 = A_1 \times A_1 \times A_1 = A_1$ ...(45)

As the z-component gives a symmetric irrep (IR) A_1, the transition $A_1 \rightarrow A_1$ is allowed.

Consider next the transition $A_1 \rightarrow A_2$. Then,

$$\Gamma_{\psi_i} = A_1, \Gamma_{\psi_j} = A_2 \text{ so that}$$

for the μ_x component, $A_1 \times B_1 \times A_2 = B_2$ ...(46)

for the μ_y component, $A_1 \times B_2 \times A_2 = B_1$ ...(47)

for the μ_z component, $A_1 \times A_1 \times A_2 = A_2$ ...(48)

As none of the components reduces to the symmetric irrep (*IR*) A_1, the transition $A_1 \rightarrow A_2$ is forbidden, *i.e.*, not allowed. We can similarly investigate the other transitions. (It should be noted that the acronym *IR* in the above discussion stands for irreducible representation (irrep) and not for infrared.)

Thus, we conclude that **the selection rule for infrared spectra is that a fundamental vibrational frequency will be infrared-active if the excited normal modes have the same symmetry as one of the Cartesian coordinates.**

Example 4. How do you justify that if the symmetry species of a normal mode is the same as any of the symmetry species of *x*, *y* or *z*, then the mode is infrared-active ?

Solution : Consider the transition dipole moment integral between the ground state vibrational wave function ψ_0 and the first excited state wave function ψ_1 :

$$\mu_{10} = e \int \psi_0 x \psi_1 \, d\tau \qquad ...(49)$$

for the *x*-component, with similar expressions for the two other components of the transition moment. The ground state vibrational wave function is a Gaussian function of the form e^{-x^2}, so it is symmetric in *x*. The wave function for the first excited state will give a non-vanishing integral only if it is proportional to *x*, because then the integrand is proportional to x^2 rather than to *xy* or *xz*. Consequently, the excited state wave function must have the same symmetry as the displacement *x* and hence the mode is infrared active.

Example 5. Which fundamental vibrational modes of CH_4 molecule are infrared-active ?

Solution : We have shown in Example 3 that the vibrational modes of CH_4 molecule span $A_1 + E + 2T_2$, *i.e.*,

$$\Gamma_{vib} = A_1 + E + 2T_2 \qquad \text{[Eq. 37]}$$

Referring to the character table of the T_d point group (Table 4), we find that the symmetry species (irrep) of *x*, *y* and *z* is T_2. Using the selection rule stated earlier, *viz.*, the vibrational mode is infrared-active if its symmetry species is the same as any of the symmetry species of *x*, *y*, or *z*, we conclude that only the T_2 modes are infrared-active.

Example 6. Which normal modes of H_2O molecule are infrared-active ?

Solution : The normal modes of H_2O molecule are sketched in Fig. 7.

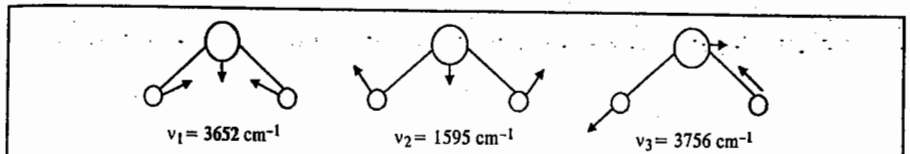

Fig. 7. The three normal modes of H_2O molecule.

The symmetric stretch and the bending mode belong to A_1 and the asymmetric stretch belongs to B_2. From the character table of C_{2v} point group to which H_2O belongs we see that *x* belongs to B_1, *y* to B_2 and *z* to A_1. Therefore, **all the three modes of H_2O molecule are infrared-active.**

Example 7. Which of the three vibrations of an AB_2 molecule are infrared or Raman-active when it is *(a)* bent *(b)* linear ?

Solution : Refer to the vibrational modes of H_2O molecule (bent) and CO_2 molecule (linear). Decide which modes correspond to *(i)* a changing electric dipole moment *(ii)* a changing polarizability and take note of the mutual exclusion rule.

(a) Nonlinear : All modes both infrared and Raman-active.

(b) Linear : The symmetric stretch is infrared-inactive but Raman-active. The antisymmetric stretch is infrared-active and (by the mutual exclusion rule) Raman-inactive. The two bending modes are infrared-active and, therefore, Raman-inactive.

Example 8. Consider the vibrational mode that corresponds to the uniform expansion of the benzene ring. Is the mode *(a)* Raman-active *(b)* infrared-active ?

Ans. The uniform expansion is as shown 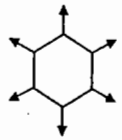

Benzene is centrosymmetic and so the mutual exclusion rule applies. The mode is infrared-inactive (symmetic breathing leaves the molecular dipole moment unchanged at zero) and, therefore, the mode may be Raman-active (and it is). In group theoretical terms, the breathing mode has symmetry A_{1g} in D_{6h} which is the point group to which benzene belongs and the quadratic terms $x^2 + y^2$ and z^2 have this symmetry (see the character table for C_{6h}, a subgroup of D_{6h}). Hence, the mode is Raman-active.

Example 9. Determine the infrared activity (active or inactive) of the normal modes of vibration of SO_3 molecule shown in Fig. 8.

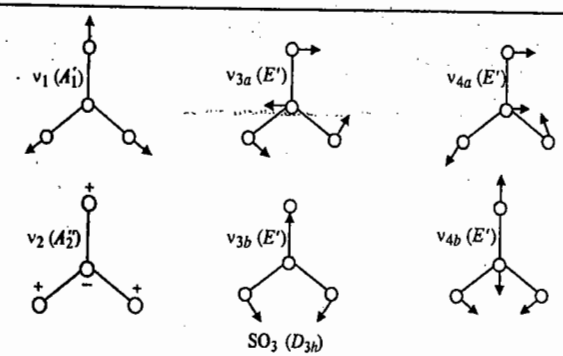

Fig. 8. The normal modes of vibration of SO_3 molecule.

Solution : SO_3 belongs to the D_{3h} point group. From its character table (Table 3), we see that x and y belong to E' and that z belongs to A_2''. Referring to the normal modes shown above we see that the ν_1 mode (which belongs to A_1') is infrared-inactive and others (which belong to A_2'' and E') are infrared-active.

We shall now state the **selection rule for vibrational Raman spectra of molecules.** A fundamental vibrational mode of a molecule will show Raman spectrum, *i.e.*, will be Raman-active if the polarizability of the molecule changes during the vibration. The transition integral in this case is

$$\int_{-\infty}^{\infty} \psi_v'' \alpha \psi_v' d\tau \qquad ...(50)$$

where α is the molecular polarizability operator which is one of the following quadratic functions of the Cartesian coordinates : x^2, y^2, z^2, xy, yz, zx, $(x^2 - y^2)$. The functions ψ_v are the vibrational wave functions, double prime ('') referring to the ground state and the single prime (') referring to the excited state. A vibration is Raman-active if it has the same irrep as one of the quadratic or binary cartesian coordinates listed above.

For **centrosymmetric molecules** (*i.e.*, molecules such as CO_2, C_2H_2, which contain a centre of symmetry) the infrared and Raman activity of fundamental vibrations is determined by the **mutual exclusion rule** which states that any vibration which is infrared-active is Raman-inactive and vice versa. This rule can be derived from group theory. The centrosymmetric molecules have point groups with two sets of irreps. The irreps which are symmetric with respect to the centre of inversion, i, are called gerade (g) representations and the irreps which are antisymmetric with respect to i are called ungerade (u) representations. Now the coordinate x, when operated upon by i, changes sign, *i.e.*, $x \rightarrow -x$; similarly, $y \rightarrow -y$ and $z = -z$ through inversion. Hence, all representations generated by the Cartesian coordinates x, y or z must belong to the u representation. However, the product of two coordinates x and y does not change sign on inversion ; thus, $(-x)(-y) = xy$. We see that the binary product xy generates a g representation. In fact, all the binary or quadratic coordinates generate the g representation. Hence, from group theory we conclude that in centrosymmetric molecules, the vibrational modes belonging to the u symmetry species (irreps) are infrared-active and those belonging to the g symmetry are Raman-active (Table 5). For H_2O and NH_3 molecules, which are non-centrosymmetric molecules, all the vibrations are both IR-active and Raman-active.

TABLE 5

Infrared and Raman Activity in Some Molecules

Molecule	Point group	Symmetry species	IR-active species	Raman-active species
CO_2	$D_{\infty h}$	A_{1g}, A_{1u}, E_{1u}	A_{1u}, E_{1u}	A_{1g}
C_2H_2	$D_{\infty h}$	$2A_{1g}, E_{1g}, E_{1u}, A_{1u}$	A_{1u}, E_{1u}	A_{1g}, E_{1g}
H_2O	C_{2V}	$2A_1, B_2$	A_1, B_2	A_1, B_2
NH_3	C_{3V}	$2A_1, 2E$	A_1, E	A_1, E
BF_3	D_{3h}	$A_1', 2E', A_2''$	A_2'', E'	A_1', E'

5. Selection Rules for Atomic Spectra

Since the intensity of a spectral line is proportional to the square of the transition (dipole) moment integral,

$$\text{Intensity} \propto |\langle \psi_n |\mu| \psi_m \rangle|^2 \qquad ...(51)$$

i.e.,

$$\text{Intensity} \propto \left| \int \psi_n \mu \psi_m d\tau \right|^2 \qquad ...(52)$$

the intensity is zero if the transition moment integral between the states ψ_n and ψ_m vanishes and is non-zero if it does not vanish. This integral determines the selection rules for all branches of spectroscopy.

The three components of the dipole moment μ are μ_x, μ_y and μ_z (in Cartesian coordinates) where $\mu_x = ex$, $\mu_y = ey$ and $\mu_z = ez$, where e is the electronic charge. A transition between the states ψ_n and ψ_m of an atom is allowed if one of the components of the transition moment integral

$$\langle \psi_n |\mu_x| \psi_m \rangle, \langle \psi_n |\mu_y| \psi_m \rangle, \langle \psi_n |\mu_z| \psi_m \rangle \qquad ...(53)$$

is non-zero, *i.e.*, does not vanish. In group theory language, the transition moment integral

$$e \int \psi_n x \psi_m d\tau \qquad ...(54)$$

will be nonzero if the direct product representation of ψ_n, x and ψ_m has even symmetry (or belongs to the totally symmetric representation). Since the Cartesian coordinates x, y and z have odd symmetry, it is evident that the direct product representation of ψ_n and ψ_m, also, should have odd symmetry. This means that if ψ_n is odd, ψ_m must be even. (Here ψ_n and ψ_m are AOs.). Now from the contours of s, p, d and f atomic orbitals in a hydrogenic atom we know that the s and d orbitals have even symmetry whereas the p and f orbitals have odd symmetry. Thus, the transition $1s \rightarrow 2p$ is allowed whereas the transition $1s \rightarrow 3d$ is forbidden in the hydrogen atom spectrum, using the above mentioned argument. This is the basis of the $\Delta l = \pm 1$ selection rule in atomic spectra. For multi-electron atoms, the selection rules for spectral transitions are more elaborate, being determined by the Russell-Saunders coupling scheme and jj coupling scheme of angular momenta.

Example 10. Using the result that the integral $\int f_1 f_2 f_3 \, d\tau$ is non-zero if the direct product representation of the integrand is symmetric, determine if the integral $\int (3d_{xy})(x)(3d_{z^2}) d\tau$ will vanish in a C_{2V} molecule.

Solution : Referring to the character table of the C_{2v} point group (Table 1) and recalling that the orbitals transform as their subscripts, we draw up the following table :

	E	C_2	$\sigma_v(xz)$	$\sigma_v'(yz)$	
$f_1 = d_{xy}$	1	1	-1	-1	A_2
$f_2 = x$	1	-1	1	-1	B_1
$f_3 = d_{z^2}$	1	1	1	1	A_1
$f_1 f_2 f_3$	1	-1	-1	1	

The characters are those of B_2. Hence, the given integral is necessarily zero.

6. Use of Group Theory for Determining the Selection Rules for the $n \rightarrow \pi^*$ and $\pi \rightarrow \pi^*$ Transitions in Formaldehyde

The electronic transitions in the carbonyl chromophore $>C=O$ of aldehydes and ketones have been investigated experimentally and theoretically. The typical energy level diagram involving the MOs σ, π, n, π^* and σ^* and the possible electronic transitions between them, *viz.*, ($\sigma \rightarrow \sigma^*$, $\pi \rightarrow \pi^*$, $n \rightarrow \pi^*$ and $n \rightarrow \sigma^*$) are shown in Fig. 9.

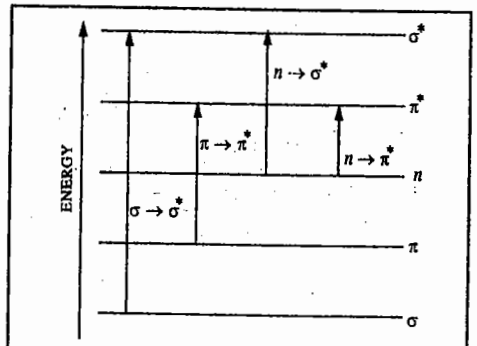

Fig. 9. Various electronic transitions in the carbonyl group.

We are primarily interested in the electronic transitions $n \rightarrow \pi^*$ and $\pi \rightarrow \pi^*$ in formaldehyde, $CH_2=O$. The MO energy level diagram for the carbonyl group in this molecule is shown in Fig. 10.

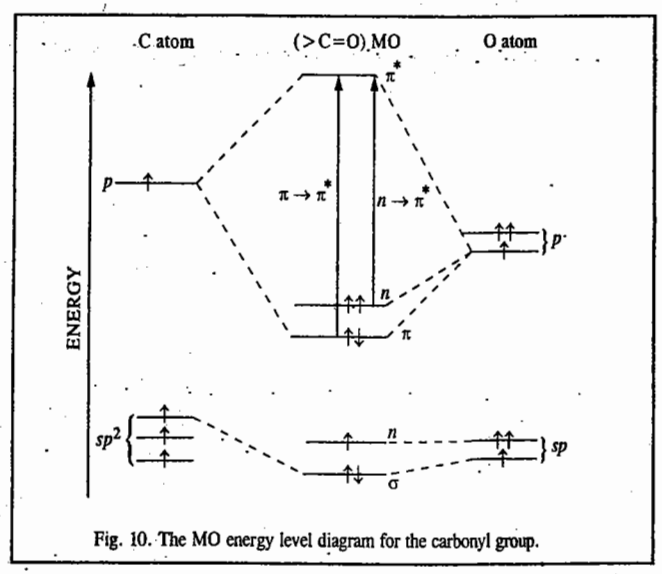

Fig. 10. The MO energy level diagram for the carbonyl group.

Fig. 11 shows the electron distribution in the relevant MOs involved in the $n \rightarrow \pi^*$ and $\pi \rightarrow \pi^*$ transitions.

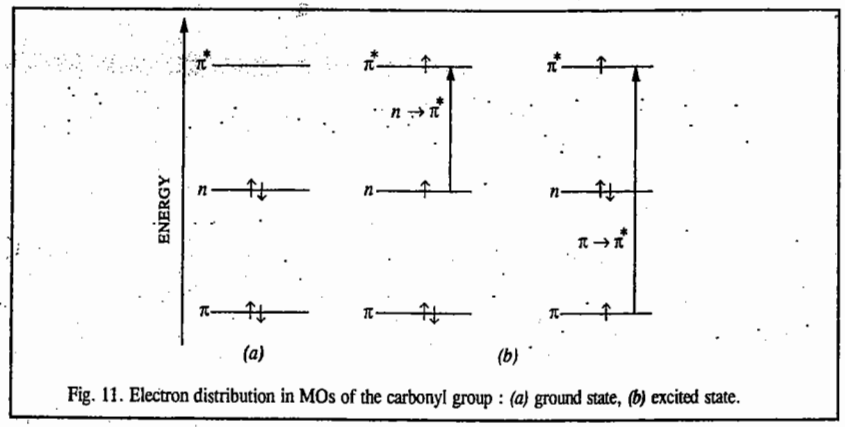

Fig. 11. Electron distribution in MOs of the carbonyl group : *(a)* ground state, *(b)* excited state.

The $n \rightarrow \pi^*$ Transition. This transition will be allowed if any one of the following three transition moment integrals, *viz.*,

$$e\int \psi_g x \psi_e \, d\tau, \quad e\int \psi_g y \psi_e \, d\tau, \quad e\int \psi_g z \psi_e \, d\tau$$

is non-zero. Here, as usual, e is the electronic charge ; x, y, z are the Cartesian coordinates and ψ_g and ψ_e are the wave functions for the ground state and excited state, respectively. The ground state wave function is given by

$$\psi_g = (\pi^2)(n^2) \qquad ...(55)$$

The excited state wave function is given by

$$\psi_e = (\pi^2)(n)(\pi^*) \qquad ...(56)$$

The coordinate system and the shapes of MOs of interest in formaldehyde are shown in Fig. 12.

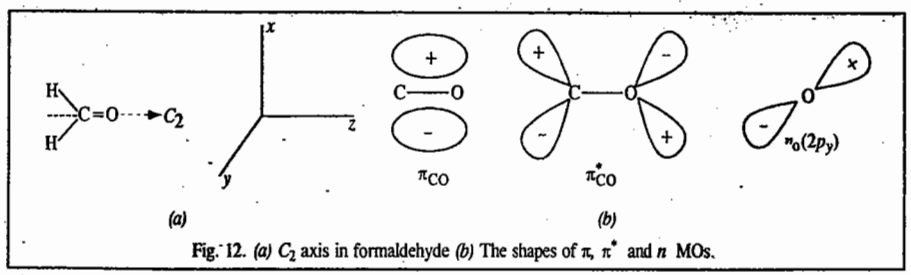

Fig. 12. *(a)* C_2 axis in formaldehyde *(b)* The shapes of π, π^* and n MOs.

Now, the $n \rightarrow \pi^*$ transition will be allowed if the direct product representation of ψ_g and ψ_e has the same symmetry as one of the Cartesian coordinates x, y or z. To determine the direct product representation of ψ_g and ψ_e we proceed as follows : The $CH_2=O$ molecule belongs to the C_{2v} point group. We perform the symmetry operations of this group on the MOs π, n and π^* to obtain the reducible representations of ψ_g and ψ_e. The representation Γ_g for the ground state wave function ψ_g is given by

$$\Gamma_g = (\Gamma_\pi^2)(\Gamma_n^2) \qquad ...(57)$$

Γ_π^2 or Γ_n^2 corresponds to A_1 since two electrons are present in the π or n MO. Thus, Γ_g is totally symmetric. The representation Γ_e for the excited state wave function ψ_e is given by

$$\Gamma_e = (\Gamma_\pi^2)\Gamma_n\Gamma_{\pi^*} = A_1\Gamma_n\Gamma_{\pi^*} \qquad ...(58)$$

Γ_n and Γ_{π^*} can be obtained by performing the symmetry operations of the C_{2v} point group on the n and π^* orbitals of the carbonyl group of $CH_2=O$. These are tabulated as follows :

	E	$C_2(z)$	$\sigma_v(xz)$	$\sigma_v'(yz)$
Γ_n	1	–1	–1	1
Γ_{π^*}	1	–1	1	–1

Referring to the character table of the C_{2v} point group (Table 1), we see that Γ_n and Γ_{π^*} correspond to the irreps B_2 and B_1, respectively. Thus, substitution of these irreps for Γ_n and Γ_{π^*} in Eq. 58, we obtain

$$\Gamma_e = A_1B_2B_1 = A_2 \qquad ...(59)$$

The direct product representation of ψ_g and ψ_e is given by

$$\Gamma_g\Gamma_e = A_1A_2 = A_2 \qquad ...(60)$$

From the character table of the C_{2v} point group (Table 1), we find that A_2 does not correspond to the representation of any one of the Cartesian coordinates. Hence, the $n \rightarrow \pi^*$ transition is not allowed in formaldehyde.

The $\pi \rightarrow \pi^*$ Transition. As we have noted above, the representation of the ground state wave function ψ_g is A_1. The excited state wave function is

$$\psi_e = (\pi)(n^2)(\pi^*) \qquad ...(61)$$

Performing the symmetry operations of the C_{2v} point group on the π orbital of the carbonyl group,

we obtain the following representation :

	E	$C_2(z)$	$\sigma_v(xz)$	$\sigma_v'(yz)$
Γ_π	1	–1	1	–1

From the character table for the C_{2v} point group we see that Γ_π corresponds to the B_1 irreducible representation. Thus, the representation of ψ_e is given by

$$\Gamma_e = \Gamma_\pi(\Gamma_{n^2})\Gamma_{\pi^*} = B_1A_1B_1 = A_1 \qquad ...(62)$$

The direct product representation of ψ_g and ψ_e is

$$\Gamma_g\Gamma_e = A_1A_1 = A_1 \qquad ...(63)$$

From the character table of the C_{2v} point group (Table 1) we find that A_1 corresponds to the symmetry species (irrep) of the z-coordinate. Hence, $\pi \rightarrow \pi^*$ transition in the carbonyl group of formaldehyde is allowed. Experimentally, it is found that the λ_{max} for $n \rightarrow \pi^*$ and $\pi \rightarrow \pi^*$ transitions is 280 nm and 160 nm, respectively. The former transition, being forbidden, is very weak whereas the latter transition, being allowed, is very strong, *i.e.*, intense.

7. Use of Group Theory in Constructing Hybrid Orbitals in Simple Molecules

Hybridisation plays a very important role in chemical bonding. We know, for instance, that the C—H bonds in CH_4 involve sp^3 hybrid orbitals and the B—F sigma bonds in BF_3 involve sp^2 hybrid orbitals. Group theory can help us in predicting the possible combinations of AOs in hybridisation. To do this, we need to know the **transformation properties** of AOs, which can be described in terms of the transformation properties of the Cartesian components. These are listed in sections III and IV of all the character tables. In fact, *an orbital transforms just as its subscripts*. Thus, in any point group, a p_x orbital transforms as the Cartesian coordinate x does and a d_{xy} orbital transforms as the function xy and so on. Since an s orbital is spherically symmetric and possesses no angular dependence, it is invariant to all the symmetry operations of a point group. This is expressed in group theory language by saying that the s orbital forms a *basis* for the totally symmetric representation of each point group. Consider, for instance, the tetrahedral CH_4 molecule. Here the s orbital belongs to the A_1 representation and the three $2p$ orbitals ($2p_x$, $2p_y$, $2p_z$) form a basis for the triply degenerate irrep T_2.

We employ the following procedure for constructing the hybrid orbitals for sigma bonds in molecules:

1. Obtain the point group to which the molecule belongs.

2. Obtain the rep as follows : Treat each sigma bond as a vector and perform the symmetry operations of the point group on each vector. *The number of unshifted vectors by each symmetry operation gives the character of the operation in the reducible representation.* The set of characters thereby obtained for all the symmetry operations of the point group constitutes the reducible representation.

3. Using the standard reduction formula (Eq. 8), reduce this representation into the set of irreps of the point group.

4. From sections III and IV of the character table, identify the coordinates and products of coordinates, or binary products of coordinates, which correspond to these irreps.

5. Identify the orbitals corresponding to these coordinates and products of coordinates.

6. The orbitals so identified are combined to form the hybrid orbitals. The s orbital should be included in the hybrid if the totally symmetric irrep occurs in the reducible representation.

We shall illustrate the above procedure for the construction of hybrid orbitals for sigma bonds in CH_4 and $[PtCl_4]^{2-}$.

Methane Molecule, CH_4

The tetrahedral CH_4 molecule belongs to the T_d point group whose character table has already been given (Table 4). We obtain the reducible representation of CH_4 by applying the symmetry operations, *viz.*, E, $8C_3$, $3C_2$, $6S_4$ and $6\sigma_d$ on the four vectors (C—H bonds). Fig. 13 *(a)* shows the molecular geometry of CH_4 while Fig. 13*(b)* shows the four vectors r_1, r_2, r_3, r_4 representing the four

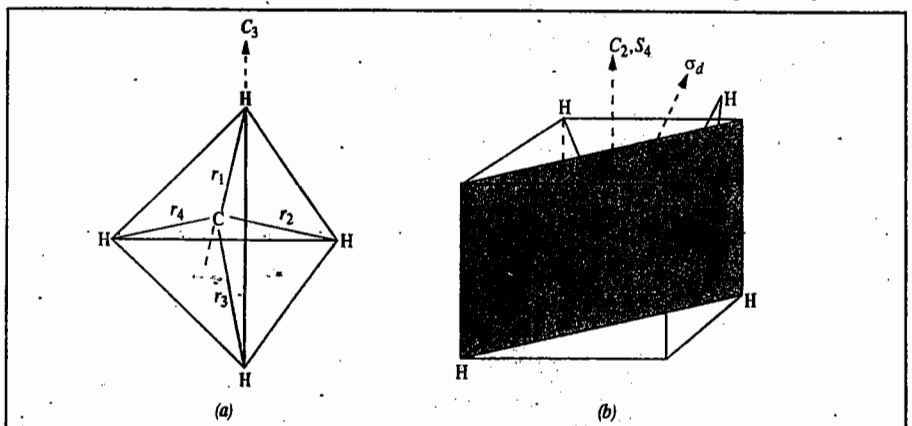

Fig. 13. *(a)* The molecular geometry of CH_4 molecule showing the four C—H sigma bonds ; *(b)* The four vectors representing the four C—H sigma bonds, along with some symmetry elements in CH_4 molecule.

C—H sigma bonds, along with some symmetry elements in CH_4. All the four vectors (C—H sigma bonds) in CH_4 remain unshifted by the identity operation, E. A rotation about the C_3 axis passing through r_1 leaves it unshifted. Symmetry operation C_2 interchanges vector r_1 with vector r_2. Similarly, vectors r_3 and r_4 are interchanged. The σ_d operation leaves vectors r_3 and r_4 unshifted. The S_4 operation shifts all the vectors. Accordingly, we obtain the reducible representation, Γ_R as follows :

Operation	E	$8C_3$	$3C_2$	$6S_4$	$6\sigma_d$
Γ_R	4	1	0	0	2

Using the standard reduction formula (Eq. 8), this rep is reduced to the sum of irreps as follows:

$$n_{A_1} = (1/24)\,[(1 \times 4 \times 1) + (8 \times 1 \times 1) + (3 \times 0 \times 1) + (6 \times 0 \times 1) + (6 \times 2 \times 1)] = 1$$

$$n_{T_2} = (1/24)\,[(1 \times 4 \times 3) + (8 \times 1 \times 0) + (3 \times 0 \times (-1)) + (6 \times 0 \times (-1)) + (6 \times 2 \times 1)] = 1$$

Similarly, we can show that

$$n_{A_2} = n_E = n_{T_1} = 0$$

Hence,
$$\Gamma_R = A_1 + T_2 \qquad ...(64)$$

Using sections III and IV of the character table for the T_d point group (Table 4), we find the possible combinations of orbitals with A_1 and T_2 symmetry as shown below :

Irreducible Representation	A_1	T_2
Coordinates or products of coordinates or binary products of coordinates	$x^2 + y^2 + z^2$	(x,y,z) ; (xy, xz, yz)
Orbitals	s	(p_x, p_y, p_z) ; (d_{xy}, d_{xz}, d_{yz})

We find that there are two possible types of hybrid orbitals with T_d symmetry, *viz.*, sp^3 and sd^3. Since, however, carbon atom does not have d orbitals, so the natural choice is sp^3 hybridisation for the four C—H sigma bonds.

Tetrachloroplatinate (II) anion, $[PtCl_4]^{2-}$

This complex anion belongs to the D_{4h} point group. It is square planar. The character table for the D_{4h} point group is given below.

TABLE 6

Character Table for the D_{4h} Point Group

D_{4h}	E	$2C_4$	C_2	$2C_2'$	$2C_2''$	i	$2S_4$	σ_h	$2\sigma_v$	$2\sigma_v'$	$h = 16$	
A_{1g}	1	1	1	1	1	1	1	1	1	1		$x^2 + y^2, z^2$
A_{2g}	1	1	1	−1	−1	1	1	1	−1	−1	R_z	
B_{1g}	1	−1	1	1	−1	1	−1	1	1	−1		$x^2 - y^2$
B_{2g}	1	−1	1	−1	1	1	−1	1	−1	1		xy
E_g	2	0	−2	0	0	2	0	−2	0	0	(R_x, R_y)	(xz, yz)
A_{1u}	1	1	1	1	1	−1	−1	−1	−1	−1		
A_{2u}	1	1	1	−1	−1	−1	−1	−1	1	1	z	
B_{1u}	1	−1	1	1	−1	−1	1	−1	−1	1		
B_{2u}	1	−1	1	−1	1	−1	1	−1	1	−1		
E_u	2	0	−2	0	0	−2	0	2	0	0	(x, y)	

The four vectors representing the Pt–Cl sigma bonds and some symmetry elements in $[PtCl_4]^{2-}$ are shown in Fig. 14.

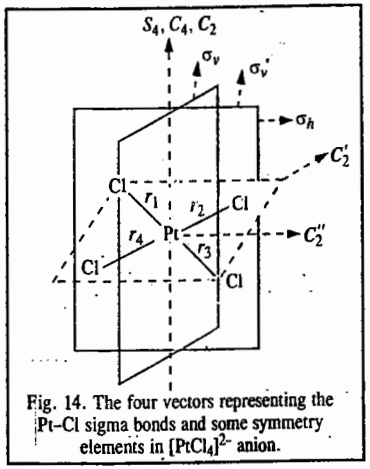

Fig. 14. The four vectors representing the Pt–Cl sigma bonds and some symmetry elements in $[PtCl_4]^{2-}$ anion.

We obtain the following reducible representation, Γ_R, by finding the number of unshifted vectors by each of the symmetry operations (E, $2C_4$, C_2, $2C_2'$, $2C_2''$, i, $2S_4$, σ_h, $2\sigma_v$ and $2\sigma_v'$) of the D_{4h} point group :

Operation	E	$2C_4$	C_2	$2C_2'$	$2C_2''$	i	$2S_4$	σ_h	$2\sigma_v$	$2\sigma_v'$
Γ_R	4	0	0	2	0	0	0	4	2	0

Using the standard reduction formula (Eq. 8), this rep is reduced to the following sum of irreps :

$$\Gamma_R = A_{1g} + B_{1g} + E_u \qquad ...(65)$$

Using sections III and IV of the character table for the D_{4h} point group, we find the possible combinations of orbitals with A_{1g}, B_{1g} and E_u symmetry as shown in the following table :

Irreducible Representation	A_{1g}	B_{1g}	E_u
Orbitals	(s, d_{z^2})	$d_{x^2-y^2}$	(p_x, p_y)

We find that there are two possible types of hybrid orbitals with D_{4h} symmetry, *viz.*, dsp^2 and d^2p^2. Since the $[PtCl_4]^{2-}$ anion is diamagnetic, the hybridisation is dsp^2.

8. Use of Group theory in Factoring the Secular Equation in MOT

In MOT we encounter the secular equation in our attempt to solve the Schrödinger wave equation for many-electron molecules. For a molecule containing π electrons in conjugated systems, for instance, the direct solution of the secular (determinantal) equation involves considerable labour and the problem can be solved speedily only on the digital computer. However, symmetry properties of such a molecule enable the reduction of the $n \times n$ determinant to a set of smaller order determinants so that the energy eigenvalues can be easily obtained without using a computer. The steps involved in this procedure are given below :

1. Determine the point group of the molecule.
2. Use the rotational subgroup of the point group to obtain the rep for the π MOs in the molecule.
3. Using the standard reduction formula, reduce this rep and obtain the symmetries of the orbitals
4. Determine the symmetry orbitals and use them to solve the secular equation of the conjug π-electron system.
5. Solve the resulting smaller order determinant and determine the energy of the π-electron syste

Let us apply these steps to two best known conjugated π-electron systems, *viz.*, *trans*-1,3-butadie and benzene.

Trans-1,3-Butadiene. In the HMO theory discussed in Chapter on Chemical Bonding we have fou nd that the secular determinant for this molecule is :

$$\begin{vmatrix} \alpha - E & \beta & 0 & 0 \\ \beta & \alpha - E & \beta & 0 \\ 0 & \beta & \alpha - E & \beta \\ 0 & 0 & \beta & \alpha - E \end{vmatrix} = 0 \qquad ...(66)$$

where α is the Coulomb integral and β is the resonance integral. We use group theory to simplify the determinant and obtain the energy values.

Steps 1 and 2. Trans-1,3-butadiene molecule belongs to the C_{2h} point group whose character table is given below (Table 7).

TABLE 7

Character Table for the C_{2h} Point Group

C_{2h}	E	C_2	i	σ_h	$h = 4$	
A_g	1	1	1	1	R_z	x^2, y^2, z^2, xy
B_g	1	−1	1	−1	R_x, R_y	xz, yz
A_u	1	1	−1	−1	z	
B_u	1	−1	−1	1	x, y	

We choose the rotational subgroup C_2 of the point group C_{2h} and perform its operations on the four $p\pi$ orbitals of the carbon atoms. The identity operation E leaves all the orbitals unshifted. The symmetry operation C_2 interchanges the atomic orbital ϕ_1 with ϕ_4 and ϕ_2 with ϕ_3. (The numbering of the atoms and the AOs of the given molecule are shown in Fig. 15).

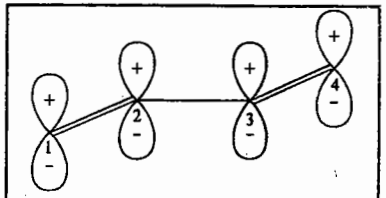

Fig. 15. The *trans*-1,3-butadiene molecule.

The following table lists these transformations :

Symmetry operation	Orbital			
	1	2	3	4
E	1	2	3	4
C_2	4	3	2	1

The character of each symmetry operation in the rep is equal to the number of orbitals unshifted by the operation so that we obtain the rep Γ_R in which $\chi(E)=4$ and $\chi(C_2)=0$. This is written schematically as

	E	C_2
Γ_R	4	0

Steps 3 and 4. Using the standard reduction formula (Eq. 8), we find out how many times each of the irreps A and B occur in Γ (which we write as Γ_π). Thus,

$$n_A = \frac{1}{2}(1\times 4 + 1\times 0) = 2$$

$$n_B = \frac{1}{2}(1\times 4 - 1\times 0) = 2$$

$$\text{This gives } \Gamma_\pi = 2A + 2B \qquad ...(67)$$

where A and B are the symmetry species (irreps) of the C_2 point group whose partial character table is as shown below :

C_2	E	C_2
A	1	1
B	1	-1

Eq. 67 means that A contains two *symmetry orbitals* ψ_1' and ψ_2' and B contains two *symmetry orbitals* ψ_3' and ψ_4'. These symmetry orbitals are obtained by using the so-called basis-generating machine procedure as follows :

We apply each symmetry operation in turn to each non-equivalent atomic orbital and multiply the atomic orbital by the character. (In fact, we are here making use of the so-called projection operators to obtain SALCs, *i.e.*, symmetry adapted linear combinations of atomic orbitals. Thus,

$$\psi_1' = \sum_R R\,\phi_j\,\chi_i(R)$$

For *trans*-1,3-butadiene we have, for the A irrep,

For ϕ_1 : $\psi_1' = E\phi_1\chi(E) + C_2\phi_1\chi(C_2) = \phi_1 + \phi_4$ ...(68)

For ϕ_2 : $\psi_2' = E\phi_2\chi(E) + C_2\phi_2\chi(C_2) = \phi_2 + \phi_3$ ...(69)

Thus, we get the following four linear combinations of atomic orbitals :

$$\phi_1 + \phi_4,\ \phi_2 + \phi_3,\ \phi_3 + \phi_2, \text{ and } \phi_4 + \phi_1$$

The two *independent* symmetry orbitals are

$$\phi_1 + \phi_4 \text{ and } \phi_2 + \phi_3$$

These orbitals correspond to the A_u irrep of the C_{2h} point group.

Similarly, for the B irrep, we have

For ϕ_1 : $\psi_3' = E\phi_1\chi(E) + C_2\phi_1\chi(C_2) = \phi_1 - \phi_4$ ...(70)

For ϕ_2 : $\psi_4' = E\phi_2\chi(E) + C_2\phi_2\chi(C_2) = \phi_2 - \phi_3$ ...(71)

These orbitals belong to the B_g irrep in the C_{2h} point group. After normalization the four symmetry orbitals are :

$$\psi'_{A_u}(1) = \left(\frac{1}{\sqrt{2}}\right)(\phi_1+\phi_4)\ ;\quad \psi'_{A_u}(2) = \left(\frac{1}{\sqrt{2}}\right)(\phi_2+\phi_3) \qquad ...(72)$$

$$\psi'_{B_g}(3) = \left(\frac{1}{\sqrt{2}}\right)(\phi_1-\phi_4)\ ;\quad \psi'_{B_g}(4) = \left(\frac{1}{\sqrt{2}}\right)(\phi_2-\phi_3) \qquad ...(73)$$

Using these four symmetry orbitals, the Hückel secular determinant for 1,3-butadiene can be written as

$$\begin{vmatrix} H^s_{11}-E & H^s_{12} & H^s_{13} & H^s_{14} \\ H^s_{12} & H^s_{22}-E & H^s_{23} & H^s_{24} \\ H^s_{13} & H^s_{23} & H^s_{33}-E & H^s_{34} \\ H^s_{14} & H^s_{24} & H^s_{34} & H^s_{44}-E \end{vmatrix} = 0 \qquad ...(74)$$

where $H^s_{ii} = \int \psi_i' \hat{H} \psi_i'\, d\tau$; $H^s_{ij} = \int \psi_i' \hat{H} \psi_j'\, d\tau$ ...(75)

We can use the direct product representation to show which matrix elements H_{ij} in Eq. 74 vanish. Recall that the integral of the product of two or more functions over symmetric interval is nonzero (*i.e.*, does not vanish) if the direct product representation is totally symmetric. Consider, for instance, the matrix element H^s_{14}.

$$H^s_{14} = \int \psi_1' \hat{H} \psi_4'\, d\tau = \int \psi'_{A_u}(1)\, \hat{H}\, \psi'_{B_g}(4) d\tau \qquad ...(76)$$

Now, the Hamiltonian operator, $\hat{H}$, belongs to the totally symmetric irrep since it is unaffected by any symmetry operation. The symmetry orbital ψ_1' belongs to the symmetry species A_u and the symmetry orbital ψ_4' belongs to the symmetry species B_g. Thus, the direct product representation of ψ_1', ψ_4' and $\hat{H}$ is not totally symmetric so that the matrix element (integral) H^s_{14} vanishes. Similarly, we can show that the matrix elements (integrals) H^s_{13}, H^s_{14}, H^s_{23} and H^s_{24} vanish, *i.e.*, are equal to zero, since the two symmetry orbitals involved in each of them do not have the same symmetry. Grouping all the orbitals of the same symmetry, we obtain the symmetry-factored secular determinant given below :

$$\left|\begin{array}{cc:cc} H^s_{11}-E & H^s_{12} & 0 & 0 \\ H^s_{12} & H^s_{22}-E & 0 & 0 \\ \hdashline 0 & 0 & H^s_{33}-E & H^s_{34} \\ 0 & 0 & H^s_{34} & H^s_{44}-E \end{array}\right| = 0 \qquad ...(77)$$

We see that the symmetry considerations of group theory enable the reduction of the 4×4 secular determinant (Eq. 66) of butadiene to two 2×2 secular determinants :

Symmetry	Determinant	
A_u	$\begin{vmatrix} H^s_{11}-E & H^s_{12} \\ H^s_{12} & H^s_{22}-E \end{vmatrix} = 0$	...(78)
B_g	$\begin{vmatrix} H^s_{33}-E & H^s_{34} \\ H^s_{34} & H^s_{44}-E \end{vmatrix} = 0$	...(79)

Step 5. The A_u and B_g secular determinants can now be solved to obtain the energy values. Let us evaluate the matrix elements H^s_{11}, H^s_{12} and H^s_{22} of the A_u determinant.

$$H^s_{11} = \int \psi'_{A_u}(1)\hat{H}\psi_{A_u}(1)d\tau = \int\left(\frac{1}{\sqrt{2}}\right)(\phi_1+\phi_4)\hat{H}\left(\frac{1}{\sqrt{2}}\right)(\phi_1+\phi_4)d\tau$$

$$= \left(\frac{1}{2}\right)\left[\int\phi_1\hat{H}\phi_1 d\tau + \int\phi_4\hat{H}\phi_1 d\tau + \int\phi_1\hat{H}\phi_4 d\tau + \int\phi_4\hat{H}\phi_4 d\tau\right]$$

$$= (1/2)\,[\alpha + 0 + 0 + \alpha] = \alpha \qquad ...(80)$$

$$H^s_{12} = \int \psi'_{A_u}(1)\hat{H}\psi_{A_u}(2)d\tau = \int\left(\frac{1}{\sqrt{2}}\right)(\phi_1+\phi_4)\hat{H}\left(\frac{1}{\sqrt{2}}\right)(\phi_2+\phi_3)d\tau$$

$$= \left(\frac{1}{2}\right)\left[\int\phi_1\hat{H}\phi_2 d\tau + \int\phi_4\hat{H}\phi_2 d\tau + \int\phi_1\hat{H}\phi_3 d\tau + \int\phi_4\hat{H}\phi_3 d\tau\right]$$

$$= (1/2)\,[\beta + 0 + 0 + \beta] = \beta \qquad ...(81)$$

We can similarly show that

$$H^s_{22} = \alpha + \beta \qquad ...(82)$$

(Here α is the Coulomb integral and β is the resonance integral of the HMO theory.)

Substituting the values of H^s_{11}, H^s_{12} and H^s_{22}, the A_u determinant becomes

$$\begin{vmatrix} \alpha - E & \beta \\ \beta & \alpha + \beta - E \end{vmatrix} = 0 \qquad ...(83)$$

Consider next the B_g determinant. Proceeding as above, we find that the matrix elements (integrals) H^s_{33}, H^s_{34} and H^s_{44} are :

$$H^s_{33} = \alpha\ ;\ H^s_{34} = \beta\ ;\ H^s_{44} = \alpha - \beta \qquad ...(84)$$

so that the B_g determinant becomes

$$\begin{vmatrix} \alpha - E & \beta \\ \beta & \alpha - \beta - E \end{vmatrix} = 0 \qquad ...(85)$$

Dividing by β and making the substitution $(\alpha - E)/\beta = x$, where x is the dimensionless parameter, the A_u determinant becomes

$$\begin{vmatrix} x & 1 \\ 1 & x+1 \end{vmatrix} = 0 \qquad ...(86)$$

which, on expansion, gives the quadratic equation $x^2 + x - 1 = 0$ whose solution is

$$x = \frac{(-1 \pm \sqrt{5})}{2} \qquad ...(87)$$

Now $(\alpha - E)/\beta = x$ so that $E = \alpha - x\beta$. Hence, the energy eigenvalues of the two A_u orbitals are

$$E_{A_u}(1) = \alpha - \frac{(-1+\sqrt{5})\beta}{2} = \alpha - 0{\cdot}618\,\beta \qquad ...(88)$$

$$E_{A_u}(2) = \alpha - \frac{(-1-\sqrt{5})\beta}{2} = \alpha + 1{\cdot}168\,\beta \qquad ...(89)$$

Similarly, the B_g determinant is modified to

$$\begin{vmatrix} x & 1 \\ 1 & x-1 \end{vmatrix} = 0 \qquad ...(90)$$

which, on expansion, gives the quadratic equation $x^2 - x - 1 = 0$ whose solution is

$$x = (1 \pm \sqrt{5})/2 \qquad ...(91)$$

Hence, the energy eigenvalues of the two B_g orbitals are

$$E_{B_g}(3) = \alpha - \frac{(1+\sqrt{5})\beta}{2} = \alpha - 1{\cdot}618\,\beta \qquad ...(92)$$

$$E_{B_g}(4) = \alpha - \frac{(1-\sqrt{5})\beta}{2} = \alpha + 0{\cdot}618\,\beta \qquad ...(93)$$

Notice that the four energy levels of 1,3-butadiene, obtained above using symmetry considerations, are the same which were obtained in the HMO theory of this molecule discussed in Chapter 3 on Chemical Bonding. These are redrawn in the HMO diagram (in Fig. 16) with the appropriate designations of the symmetry species (irreps) to which they belong. We have already shown that the delocalization energy (DE) of this molecule is equal to 0·472 β :

$$DE = (4\alpha + 4{\cdot}472\,\beta) - (4\alpha + 4\beta) = 0{\cdot}472\beta \qquad ...(94)$$

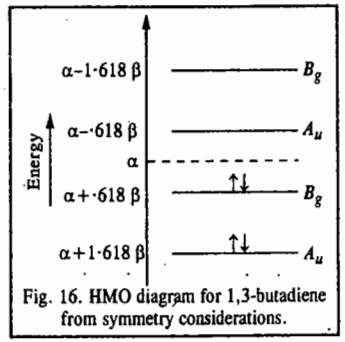

Fig. 16. HMO diagram for 1,3-butadiene from symmetry considerations.

Benzene, C_6H_6. We shall briefly summarize the symmetry classification of the MOs of benzene which belongs to D_{6h} point group. In the HMO theory discussed in Chapter 2 on Chemical Bonding, we have found that the secular determinant for benzene molecule is

$$\begin{vmatrix} \alpha-E & \beta & 0 & 0 & 0 & \beta \\ \beta & \alpha-E & \beta & 0 & 0 & 0 \\ 0 & \beta & \alpha-E & \beta & 0 & 0 \\ 0 & 0 & \beta & \alpha-E & \beta & 0 \\ 0 & 0 & 0 & \beta & \alpha-E & \beta \\ \beta & 0 & 0 & 0 & \beta & \alpha-E \end{vmatrix} = 0 \qquad ...(95)$$

where, as usual, α is the Coulomb integral and β is the resonance integral. Using group theory, this determinant can be simplified to obtain the energy levels. The character table for the D_{6h} point group is shown in Table 8.

TABLE 8

Character Table for the D_{6h} Point Group

D_{6h}	E	$2C_6$	$2C_3$	C_2	$3C'_2$	$3C''_2$	i	$2S_3$	$2S_6$	σ_h	$3\sigma_d$	$3\sigma_v$	$h = 24$	
A_{1g}	1	1	1	1	1	1	1	1	1	1	1	1		$x^2 + y^2, z^2$
A_{2g}	1	1	1	1	-1	-1	1	1	1	1	-1	-1	R_z	
B_{1g}	1	-1	1	-1	1	-1	1	-1	1	-1	1	-1		
B_{2g}	1	-1	1	-1	-1	1	1	-1	1	-1	-1	1		
E_{1g}	2	1	-1	-2	0	0	2	1	-1	-2	0	0	(R_x, R_y)	(xz, yz)
E_{2g}	2	-1	-1	2	0	0	2	-1	-1	2	0	0		$(x^2 - y^2, xy)$
A_{1u}	1	1	1	1	1	1	-1	-1	-1	-1	-1	-1		
A_{2u}	1	1	1	1	-1	-1	-1	-1	-1	-1	1	1	z	
B_{1u}	1	-1	1	-1	1	-1	-1	1	-1	1	-1	1		
B_{2u}	1	-1	1	-1	-1	1	-1	1	-1	1	1	-1		
E_{1u}	2	1	-1	-2	0	0	-2	-1	1	2	0	0	(x, y)	
E_{2u}	2	-1	-1	2	0	0	-2	1	1	-2	0	0		

We choose the rotational subgroup C_6 of the point group D_{6h} and perform its symmetry operations on the six $p\pi$ orbitals of the carbon atoms in benzene (Fig. 17).

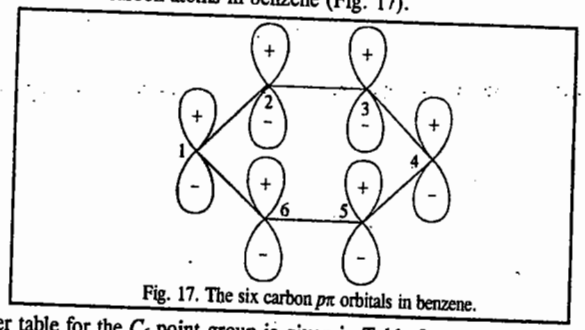

Fig. 17. The six carbon $p\pi$ orbitals in benzene.

The character table for the C_6 point group is given in Table 9.

TABLE 9

Character Table for the C_6 Point Group

C_6	E	C_6	C_3	C_2	C_3^2	C_6^5	$\epsilon = \exp(2\pi i/6)$	
A	1	1	1	1	1	1		
B	1	-1	1	-1	1	-1	z, R_z	x^2+y^2, z^2
E_1	1	ϵ	$-\epsilon^*$	-1	$-\epsilon$	ϵ^*		
	1	ϵ^*	$-\epsilon$	-1	$-\epsilon^*$	ϵ	$(x, y)\ (R_x, R_y)$	(xz, yz)
E_2	1	$-\epsilon^*$	$-\epsilon$	1	$-\epsilon^*$	$-\epsilon$		
	1	$-\epsilon$	$-\epsilon^*$	1	$-\epsilon$	$-\epsilon^*$		(x^2-y^2, xy)

The character of each symmetry operation is given by the number of unshifted $p\pi$ orbitals by the operation. The identity operation E leaves all the orbitals unshifted. Every symmetry operation of the C_6 subgroup shifts every orbital to a different place. Thus, we obtain the following rep :

	E	C_6	C_3	C_2	C_3^2	C_6^5
Γ_π	6	0	0	0	0	0

Using the standard reduction formula (Eq. 8), we find that

$$\Gamma_\pi = A + B + E_1 + E_2 \qquad \text{...(96)}$$

In the parent D_{6h} point group, this becomes

$$\Gamma_\pi = A_{2u} + B_{2g} + E_{1g} + E_{2u} \qquad \text{...(97)}$$

Thus we find that in a cyclic hydrocarbon having the general formula $(CH)_n$ there will always be n π-MOs, one belonging to each symmetry species of the subgroup C_n. It is also known from group theory that in a conjugated cyclic π-system the coefficients of the MOs in the LCAO-MO approximation are the characters of the irreps of the rotation subgroup. Thus, using the sets of the characters of the irreps of the rotation subgroup C_6, we can write the symmetry orbitals (*i.e.*, SALCs) for benzene :

$$A \to A_{2u}: \quad \phi_1 + \phi_2 + \phi_3 + \phi_4 + \phi_5 + \phi_6 \qquad \text{...(98)}$$

$$B \to B_{2g}: \quad \phi_1 - \phi_2 + \phi_3 - \phi_4 + \phi_5 - \phi_6 \qquad \text{...(99)}$$

$$E_1 \to E_{1g}\begin{cases} E'_{1g}: \phi_1 + \epsilon\phi_2 - \epsilon^*\phi_3 - \phi_4 - \epsilon\phi_5 + \epsilon^*\phi_6 \\ \epsilon^*\phi_2 - \epsilon\phi_3 - \phi_4 - \epsilon^*\phi_5 + \epsilon\phi_6 \end{cases} \qquad \text{...(100)}$$

$$E_2 \to E_{2g}\begin{cases} E^1_{2u}: \phi_1 - \epsilon^*\phi_2 - \epsilon\phi_3 + \phi_4 - \epsilon^*\phi_5 - \epsilon\phi_6 \\ E^2_{2u}: \phi_1 - \epsilon\phi_2 - \epsilon^*\phi_3 + \phi_4 - \epsilon\phi_5 - \epsilon^*\phi_6 \end{cases} \qquad \text{...(101)}$$

The normalized symmetry orbitals, *i.e.*, SALCs, belonging to the various symmetry species (irreps) can be shown to be given by

$$\psi'(A_{2u}) = (1/\sqrt{6})\ (\phi_1 + \phi_2 + \phi_3 + \phi_4 + \phi_5 + \phi_6) \qquad \text{...(102)}$$

$$\psi'(B_{2g}) = (1/\sqrt{6})\ (\phi_1 - \phi_2 + \phi_3 - \phi_4 + \phi_5 - \phi_6) \qquad \text{...(103)}$$

$$\psi'(E^1_{1g}) = (1/\sqrt{12})\ (2\phi_1 + \phi_2 - \phi_3 - 2\phi_4 - \phi_5 + \phi_6) \qquad \text{...(104)}$$

$$\psi'(E^2_{1g}) = (1/2)\ (\phi_2 + \phi_3 - \phi_5 - \phi_6) \qquad \text{...(105)}$$

$$\psi'(E^1_{2u}) = (1/\sqrt{12})\ (2\phi_1 - \phi_2 - \phi_3 + 2\phi_4 - \phi_5 - \phi_6) \qquad \text{...(106)}$$

$$\psi'(E^2_{2u}) = (1/2)\ (\phi_2 - \phi_3 + \phi_5 - \phi_6) \qquad \text{...(107)}$$

Using these symmetry orbitals, the secular determinant for benzene can be written as

A_{2u}	B_{2g}	E_{1g}		E_{2u}	
$H^s_{11}-E$	0	0	0	0	0
0	$H^s_{22}-E$	0	0	0	0
0	0	$H^s_{33}-E$	H^s_{34}	0	0
0	0	H^s_{34}	$H^s_{44}-E$	0	0
0	0	0	0	$H^s_{55}-E$	H^s_{56}
0	0	0	0	H^s_{56}	$H^s_{66}-E$

$= 0$ ...(108)

Thus, the 6×6 Hückel secular determinant is factored as follows :

Symmetry	Determinant	
A_{2u}	$H^s_{11}-E = 0$	...(109)
B_{2g}	$H^s_{22}-E = 0$	...(110)
E_{1g}	$\begin{vmatrix} H^s_{33}-E & H^s_{34} \\ H^s_{34} & H^s_{44}-E \end{vmatrix} = 0$	...(111)
E_{2u}	$\begin{vmatrix} H^s_{55}-E & H^s_{56} \\ H^s_{56} & H^s_{66}-E \end{vmatrix} = 0$	...(112)

To determine the energy of the MO belonging to the A_{2u} irrep, we have

$$H^s_{11} - E = 0$$

or

$$H^s_{11} = E \qquad \text{...(113)}$$

where

$$H^s_{11} = \int \psi'(A_{2u})\, \hat{H}\, \psi'(A_{2u})\, d\tau \qquad \text{...(114)}$$

Substituting for the symmetry orbital $\psi'(A_{2u})$ from Eq. 102, we find that

$$H^s_{11} = \frac{1}{6}\int (\phi_1+\phi_2+\phi_3+\phi_4+\phi_5+\phi_6)\,\hat{H}(\phi_1+\phi_2+\phi_3+\phi_4+\phi_5+\phi_6)\,d\tau \qquad \text{...(115)}$$

$$= \frac{1}{6}\Big[\int \phi_1\hat{H}\phi_1 d\tau + \int \phi_2\hat{H}\phi_2 d\tau + \int \phi_3\hat{H}\phi_3 d\tau + \int \phi_4\hat{H}\phi_4 d\tau + \int \phi_5\hat{H}\phi_5 d\tau + \int \phi_6\hat{H}\phi_6 d\tau$$
$$+ \int \phi_1\hat{H}\phi_2 d\tau + \int \phi_2\hat{H}\phi_1 d\tau + \int \phi_2\hat{H}\phi_3 d\tau + \int \phi_3\hat{H}\phi_2 d\tau + \int \phi_3\hat{H}\phi_4 d\tau + \int \phi_4\hat{H}\phi_3 d\tau$$
$$+ \int \phi_4\hat{H}\phi_5 d\tau + \int \phi_5\hat{H}\phi_4 d\tau + \int \phi_5\hat{H}\phi_6 d\tau + \int \phi_6\hat{H}\phi_5 d\tau + \int \phi_1\hat{H}\phi_6 d\tau + \int \phi_6\hat{H}\phi_1 d\tau\Big] \qquad \text{...(116)}$$

or $$H_{11}^s = \left(\frac{1}{6}\right)(6\alpha + 12\beta) = \alpha + 2\beta \quad \ldots(117)$$

Thus, $$E(A_{2u}) = \alpha + 2\beta \quad \ldots(118)$$

Similarly, $$E(B_{2g}) = \alpha - 2\beta \quad \ldots(119)$$

We next consider the E_{1g} and E_{2u} determinants.

$$E_{1g}: \begin{vmatrix} H_{33}^s - E & H_{34}^s \\ H_{34}^s & H_{44}^s - E \end{vmatrix} = 0; \quad E_{2u}: \begin{vmatrix} H_{55}^s - E & H_{56}^s \\ H_{56}^s & H_{66}^s - E \end{vmatrix} = 0 \quad \ldots(120)$$

Since $H_{33}^s = H_{44}^s$; $H_{55}^s = H_{66}^s$; $H_{34}^s = H_{56}^s = 0$, the E_{1g} and E_{2u} determinants become

$$E_{1g}: \begin{vmatrix} H_{33}^s - E & 0 \\ 0 & H_{33}^s - E \end{vmatrix} = 0; \quad E_{2u}: \begin{vmatrix} H_{55}^s - E & 0 \\ 0 & H_{55}^s - E \end{vmatrix} = 0 \quad \ldots(121)$$

Expansion of the determinants yields

$$\left(H_{33}^s - E\right)^2 = 0 \quad \text{and} \quad \left(H_{55}^s - E\right)^2 = 0 \quad \ldots(122)$$

The solution of these equations gives the following values of the energies of E_{1g} and E_{2u} MOs :

$E(E_{1g}) = \alpha + \beta$; $E(E_{2u}) = \alpha - \beta$ ...(123)

Notice that the energies $E(A_{2u})$, $E(B_{2g})$, $E(E_{1g})$ and $E(E_{2u})$ of benzene obtained using symmetry arguments, are the same which were obtained in the HMO theory of this molecule discussed in Chapter 3. These are redrawn in the HMO diagram (Fig. 18) with the appropriate designations of the symmetry species (irreps) to which they belong. We have already shown that the delocalization energy (DE) of benzene molecule is equal to 2β :

$$DE = (6\alpha + 8\beta) - (6\alpha + 6\beta) = 2\beta \quad \ldots(124)$$

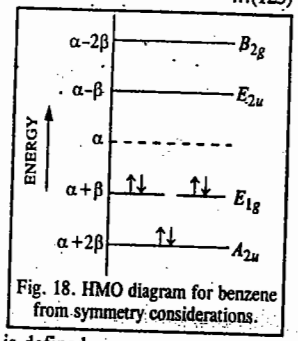

Fig. 18. HMO diagram for benzene from symmetry considerations.

9. Use of Generating Operators (Projection Operators) to Determine Linear Combinations of AOs that are Basis for Irreducible Representations

The generating operator or the projection operator for the jth irrep is defined as

$$\hat{P}_j = \frac{l_j}{h} \sum_{\hat{R}} \chi_j(\hat{R})\,\hat{R} \quad \ldots(125)$$

where l_j is the dimensionality of the jth irrep. Though Eq. 125 looks somewhat formidable, it is easy to use. In fact, we have already made use of the projection operators to determine SALCs. What follows is a slightly brief treatment.

Let us consider the *trans*-1,3-butadiene molecule which belongs to C_{2h} point group :

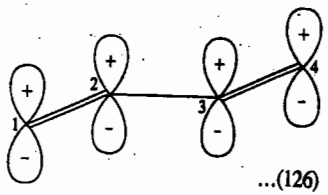

Denoting the $2p_z$ orbital on carbon atom i by ϕ_i, Eq. 125 yields

$$\hat{P}_{A_g}\phi_1 = \frac{1}{4}\sum_{\hat{R}} \chi_{A_g}(R)\,R\phi_1 \quad \ldots(126)$$

$$= \frac{1}{4}\left[(1)E\phi_1 + (1)\,C_2\phi_1 + (1)i\phi_1 + (1)\,\sigma_h\phi_1\right]$$

$$= \frac{1}{4}\left(\phi_1 + \phi_4 - \phi_4 - \phi_1\right) = 0 \quad \ldots(127)$$

$$\hat{P}_{A_g}\phi_2 = \frac{1}{4}(\phi_2 + \phi_3 - \phi_3 - \phi_2) = 0 \quad \ldots(128)$$

with similar results for ϕ_3 and ϕ_4.

Similarly, using ϕ_1 and ϕ_2, we obtain

$$\left.\begin{aligned} \hat{P}_{B_g}\phi_1 &= \frac{1}{4}(\phi_1 - \phi_4 - \phi_4 + \phi_1) \propto \phi_1 - \phi_4 \\ \hat{P}_{B_g}\phi_2 &= \frac{1}{4}(\phi_2 - \phi_3 - \phi_3 + \phi_2) \propto \phi_2 - \phi_3 \\ \hat{P}_{A_u}\phi_1 &= \frac{1}{4}(\phi_1 + \phi_4 + \phi_4 + \phi_1) \propto \phi_1 + \phi_4 \\ \hat{P}_{A_u}\phi_2 &= \frac{1}{4}(\phi_2 + \phi_3 + \phi_3 + \phi_2) \propto \phi_2 + \phi_3 \end{aligned}\right\} \quad \ldots(129)$$

$$\hat{P}_{B_u}\phi_1 = \hat{P}_{B_u}\phi_2 = 0 \quad \ldots(130)$$

Here we have ignored the numerical factors in front of the various symmetry orbitals since we are interested only in their functional form. Normalization of the orbitals can be easily carried out.

Eq. 129 gives four symmetry orbitals, two belonging to B_g symmetry species and two belonging to A_u symmetry species. Using these symmetry orbitals, the HMO theory secular determinant of 1, 3-butadiene factors into two 2×2 blocks :

$$\left|\begin{array}{cc:cc} x & 1 & 0 & 0 \\ 1 & x+1 & 0 & 0 \\ \hdashline 0 & 0 & x & 1 \\ 0 & 0 & 1 & x-1 \end{array}\right| = 0 \quad \ldots(131)$$

which, upon expansion, gives $(x^2 + x - 1)(x^2 - x - 1) = 0$, whence ...(132)

$$x = \frac{-1 \pm \sqrt{5}}{2} \quad \text{and} \quad x = \frac{1 \pm \sqrt{5}}{2} \quad \ldots(133)$$

or $x = 0{\cdot}6180$, $-1{\cdot}6180$, $1{\cdot}6180$ and $-0{\cdot}6180$. These are the same values which we obtained in the HMO treatment of butadiene.

Notice that no symmetry orbital belongs to A_g or B_u. As a matter of fact, we did not really have to apply the generating operators for A_g and B_u to learn this. Let us apply the four group operations E, C_2, i, and σ_h to the four $2p_z$ AOs. For the identity operation E, $E\phi_j = \phi_j$ for each j. This result can be written in the matrix form :

$$E\begin{bmatrix}\phi_1\\ \phi_2\\ \phi_3\\ \phi_4\end{bmatrix} = \begin{bmatrix}1&0&0&0\\0&1&0&0\\0&0&1&0\\0&0&0&1\end{bmatrix}\begin{bmatrix}\phi_1\\ \phi_2\\ \phi_3\\ \phi_4\end{bmatrix} \quad \ldots(134)$$

The character of this matrix is $\chi(E) = 4$. Similarly, $C_2\phi_1 = \phi_4$, $C_2\phi_2 = \phi_3$, $C_2\phi_3 = \phi_2$, and $C_2\phi_4 = \phi_1$, or in the matrix form :

$$C_2\begin{bmatrix}\phi_1\\ \phi_2\\ \phi_3\\ \phi_4\end{bmatrix} = \begin{bmatrix}0&0&0&1\\0&0&1&0\\0&1&0&0\\1&0&0&0\end{bmatrix}\begin{bmatrix}\phi_1\\ \phi_2\\ \phi_3\\ \phi_4\end{bmatrix} \quad \ldots(135)$$

Thus, $\chi(C_2) = 0$.

Similarly,

$$i\begin{bmatrix}\phi_1\\ \phi_2\\ \phi_3\\ \phi_4\end{bmatrix} = \begin{bmatrix}0 & 0 & 0 & -1\\ 0 & 0 & -1 & 0\\ 0 & -1 & 0 & 0\\ -1 & 0 & 0 & 0\end{bmatrix}\begin{bmatrix}\phi_1\\ \phi_2\\ \phi_3\\ \phi_4\end{bmatrix} \quad ...(136)$$

Thus, $\chi(i) = 0$.

Again,

$$\sigma_h\begin{bmatrix}\phi_1\\ \phi_2\\ \phi_3\\ \phi_4\end{bmatrix} = \begin{bmatrix}-1 & 0 & 0 & 0\\ 0 & -1 & 0 & 0\\ 0 & 0 & -1 & 0\\ 0 & 0 & 0 & -1\end{bmatrix}\begin{bmatrix}\phi_1\\ \phi_2\\ \phi_3\\ \phi_4\end{bmatrix} \quad ...(137)$$

so that $\chi(\sigma_h) = -4$. Thus, we have

	E	C_2	i	σ_h
Γ_R	4	0	0	-4

We see from these results that the four $2p_z$ AOs belong to the reducible representation Γ_R.

We can write Γ_R without writing out all the matrices. Recall that there is a 1 on a diagonal in a representation if the $2p_z$ orbital is unchanged, a -1 if it remains on the original atom but changes direction and a 0 if it is moved to another atom. The operation E leaves all four unchanged ; the operations C_2 and i move all of them to different atoms and σ_h changes the direction of all four but does not move them otherwise.

Using the standard reduction formula, the above rep can be reduced to a sum of irreps as follows :

$$n_{A_g} = \frac{1}{4}[1\times4 + 1\times0 + 1\times0 + 1\times(-4)] = 0$$

$$n_{B_g} = \frac{1}{4}[1\times4 + (-1)\times0 + 1\times0 + (-1)\times(-4)] = 2$$

$$n_{A_u} = \frac{1}{4}[1\times4 + 1\times0 + (-1)\times0 + (-1)\times(-4)] = 2$$

$$n_{B_u} = \frac{1}{4}[1\times4 + (-1)\times0 + (-1)\times0 + 1\times(-4)] = 0$$

Thus, $\Gamma_R = 2B_g + 2A_u$, in agreement with our earlier result that no symmetry orbital belongs to A_g or B_u.

MISCELLANEOUS SOLVED EXAMPLES

Example 11. List the symmetry elements of $CHCl_3$ molecule which belongs to the C_{3v} point group and locate them in the molecule.

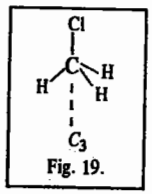

Fig. 19.

Solution : The elements, other than the identity E are a C_3 axis and three vertical mirror planes σ_v. The symmetry axis passes through the C—Cl nuclei. The mirror planes are defined by the three ClCH planes (see Figure 19).

Example 12. Which of the following molecules may be polar : *(a)* pyridine (C_{2v}) *(b)* CH_3Cl(C_{3v}) *(c)* $SnCl_4$(I_d) *(d)* gas phase $HgBr_2$(D_{4h}) *(e)* $B_3N_3H_6$(D_{3h}) *(f)* nitroethane (C_s) ?

Solution : A molecule is *nonpolar* if it has a centre of symmetry or perpendicular C_2 axes. This means that only molecules belonging to C_n, C_{nv} and C_s may be *polar*. Hence, of the listed molecules, only *(a)* pyridine *(b)* CH_3Cl and *(f)* nitroethane are polar.

Example 13. The group C_{2h} consists of the elements E, C_2, σ_h, i. Construct the group multiplication table and give an example of a molecule that belongs to the group.

Solution : See Fig. 20 showing the symmetry operation of the C_{2h} point group.

Note that $R^2 = E$ for all the operations of the group ; $ER = RE = R$ and $RR' = R'R$ for this group. Since $C_2\sigma_h = i$; $\sigma_h i = C_2$ and $iC_2 = \sigma_h$, we can draw up the following multiplication table :

	E	C_2	σ_h	i
E	E	C_2	σ_h	i
C_2	C_2	E	i	σ_h
σ_h	σ_h	i	E	C_2
i	i	σ_h	C_2	E

Hence, the trans-CHCl=CHCl molecule belongs to the C_{2h} point group.

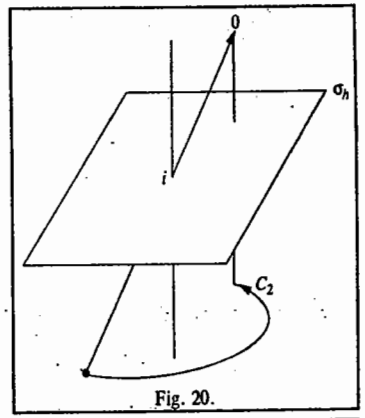

Fig. 20.

Example 14. The point group D_{2h} has a C_2 axis perpendicular to the principal axis and a horizontal mirror plane. Show that the group must, have a centre of inversion, i.

Solution : Refer to Fig. 21.

The effect of σ_h on a point P is to generate $\sigma_h P$ and the effect of C_2 on $\sigma_h P$ is to generate the point $C_2\sigma_h P$. The same point is generated from P by the inversion i so that $C_2\sigma_h P = iP$ for all points P. Hence, $C_2\sigma_h = i$ and i must be a number of the group.

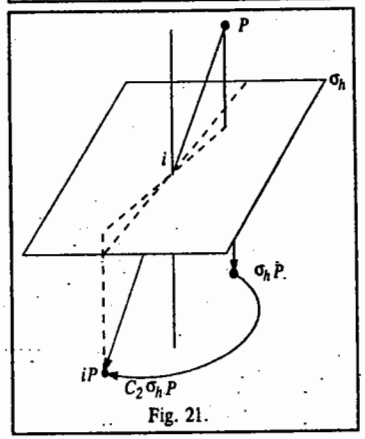

Fig. 21.

Example 15. List the symmetry elements of the following molecules and name the point groups to which they belong : *(a)* staggered ethane, *(b)* chair and boat cyclohexane, *(c)* diborane B_2H_6, *(d)* $[Co(en)_3]^{3+}$, where *en* is ethylenediamine (ignore its detailed structure), *(e)* crown-shaped S_8. Which of these molecules can be *(i)* polar *(ii)* chiral ?

Solution : *(a)* Staggered CH_3CH_3 : E, C_3, C_2, $3\sigma_d$; D_{3d}

(b) Chair C_6H_{12} : E, C_3, C_2, $3\sigma_d$; D_{3d}; Boat C_6H_{12} : E, C_2, σ_v, σ_v' ; C_{2v}

(c) B_2H_6 : E, C_2, $2C_2'$, σ_h ; D_{2h}

(d) $[Co(en)_3]^{3+}$: E, $2C_3$, $3C_2$; D_3

(e) Crown S_8 : E, C_4, C_2, $4C_2'$, $4\sigma_d$, $2S_8$; D_{4d}

Only boat C_6H_{12} may be polar since all others are D point groups. Only $[Co(en)_3]^{3+}$ belongs to a group without any improper axis of rotation ($S_1 = \sigma$), and hence is chiral.

Example 16. Molecules belonging to the point groups D_{2h}, C_{3h}, T_h and T_d cannot be chiral. Which elements of these rule out chirality ?

Solution : A molecule cannot be chiral if it has an improper rotation axis S_n of any order (look for such an axis even in a disguised form : $S_1 = \sigma$, $S_2 = i$) or a centre of inversion or a plane of symmetry. D_{2h} and T_h contain i, C_{3h} contains σ_h, T_d contains S_4. Therefore, molecules belonging to these point groups cannot be chiral.

Example 17. List the symmetry elements in the followiug molecules and name the point groups to which they belong : *(a)* naphthalene, $C_{10}H_8$, *(b)* anthracene, $C_{14}H_{10}$ and *(c)* the three dichlorobenzenes.

Solution. *(a)* Naphthalene : E, C_2, C_2', σ_h ; D_{2h}

(b) Anthracene : E, C_2, C_2', σ_h ; D_{2h}

(c) Dichlorobenzenes :

(i) 1, 2-dichlorobenzene : E, C_2, σ_v, σ_v' ; C_{2v}

(ii) 1, 3-dichlorobenzene : E, C_2, σ_v, σ_v' ; C_{2v}

(iii) 1, 4-dichlorobenzene : E, C_2, C_2', σ_h ; D_{2h}

Example 18. List the symmetry elements of the following molecules and name the point groups to which they belong : (a) NO_2 (b) N_2O (c) $CHCl_3$ (d) $CH_2=CH_2$ (e) *cis*-CHCl=CHCl (f) *trans*-CHCl=CHCl.

Solution : (a) NO_2 : E, C_2, σ_v, σ_v' ; C_{2v} (b) N_2O : E, C_∞, C_2, σ_v ; $C_{\infty v}$

(c) $CHCl_3$: E, C_3, $3\sigma_v$; C_{3v} (d) $CH_2=CH_2$: E, C_2, $2C_2'$, σ_h ; D_{2h}

(e) *cis*-CHCl=CHCl : E, C_2, σ_v, σ_v' ; C_{2v} (f) *trans*-CHCl=CHCl : E, C_2, σ_h, i ; C_{2h}

Example 19. The group C_{2v} consists of the elements E, C_2, $\sigma_v(xz)$ and $\sigma_v'(yz)$. Construct the group multiplication table for this group.

Solution : We draw up the following group multiplication table :

	E	C_2	$\sigma_v(xz)$	$\sigma_v'(yz)$
E	E	C_2	$\sigma_v(xz)$	$\sigma_v'(yz)$
C_2	C_2	E	$\sigma_v'(yz)$	$\sigma_v(xz)$
$\sigma_v(xz)$	$\sigma_v(xz)$	$\sigma_v'(yz)$	E	C_2
$\sigma_v'yz)$	$\sigma_v'(yz)$	$\sigma_v(xz)$	C_2	E

Example 20. The group C_{3v} consists of the symmetry operations E, C_3, C_3^2, $\sigma_v(1)$, $\sigma_v(2)$ and $\sigma_v(3)$. Construct the group multiplication table for this group.

Solution : We draw up the following group multiplication table :

	E	C_3	C_3^2	$\sigma_v(1)$	$\sigma_v(2)$	$\sigma_v(3)$
E	E	C_3	C_3^2	$\sigma_v(1)$	$\sigma_v(2)$	$\sigma_v(3)$
C_3	C_3	C_3^2	E	$\sigma_v(2)$	$\sigma_v(3)$	$\sigma_v(1)$
C_3^2	C_3^2	E	C_3	$\sigma_v(3)$	$\sigma_v(1)$	$\sigma_v(2)$
$\sigma_v(1)$	$\sigma_v(1)$	$\sigma_v(3)$	$\sigma_v(2)$	E	C_3^2	C_3
$\sigma_v(2)$	$\sigma_v(2)$	$\sigma_v(1)$	$\sigma_v(3)$	C_3	E	C_3^2
$\sigma_v(3)$	$\sigma_v(3)$	$\sigma_v(2)$	$\sigma_v(1)$	C_3^2	C_3	E

Example 21. Identify the point group to which the following objects belong : (a) a sphere (b) an isosceles triangle (c) an equilateral triangle (d) an unsharpened cylindrical pencil (e) a sharpened cylindrical pencil (f) a three-balanced propellor (g) a four-legged table (h) yourself approximately.

Solution : Refer to Fig. 22.

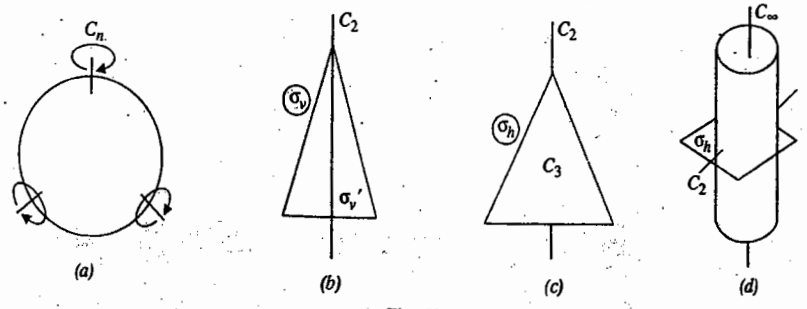

Fig. 22

(a) Sphere : An infinite number of summetry axes ; therefore, R_3.
(b) Isosceles triangle : E, C_2, σ_v, σ_v' ; therefore, C_{2v}.
(c) Equilateral triangle : E, C_3, C_2, σ_h ; therefore, D_{3h}
(d) Cylinder : E, C_∞, C_2, σ_h ; therefore, $D_{\infty h}$.

Cont.

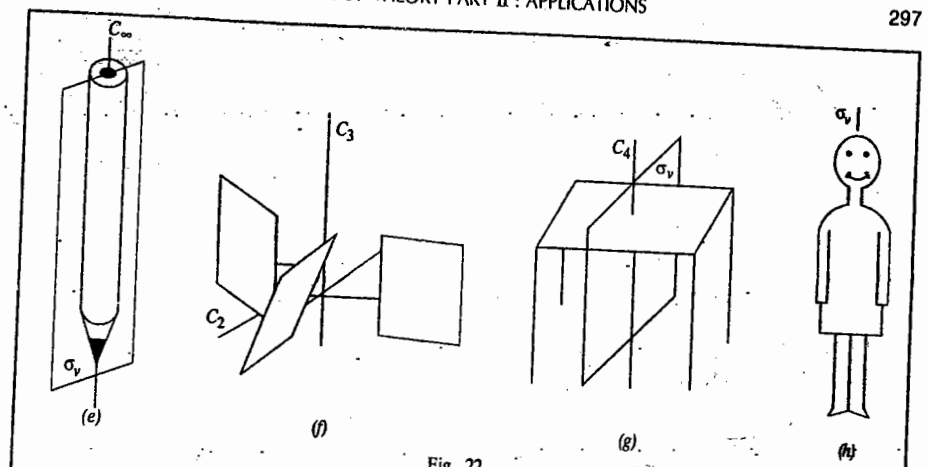

Fig. 22.

(e) Sharpened pencil : E, C_∞, σ_v ; therefore, $C_{\infty v}$
(f) Propellor : E, C_3, $3C_2$; therefore, D_3
(g) Square Table : E, C_4, $4\sigma_4$; therefore, C_{4v} ; Rectangular table : E, C_2, $2\sigma_v$; therefore, C_{2v}
(h) Person : E, σ_v (approximately) ; therefore, C_s

Example 22. Using similarity transformation show that the six elements of the C_{3v} point group (to which NH_3 molecule belongs) can be divided into three classes.

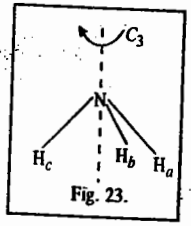

Fig. 23.

Solution : The NH_3 molecule is shown in Fig. 23.

Two elements, say, A and B, of a group are said to be conjugate if

$$A = X^{-1}BX$$

where X is another element of the same group. Such a transformation is known as similarity transformation. The six symmetry operations of NH_3 are E, C_3, C_3^2, σ_{v_a}, σ_{v_b} and σ_{v_c}. The identity E is a class by itself since for every other element of the group $X^{-1}EX = E$. We can show that C_3 and C_3^2 form a class by examining their similarity transformation with every other element of the group.

$$E^{-1}C_3E = EC_3E = C_3$$

$$C_3^{-1}C_3C_3 = C_3^2C_3C_3 = C_3^2C_3^2 = C_3$$

$$(C_3^2)^{-1}C_3C_3^2 = C_3C_3C_3^2 = C_3C_3^3 = C_3$$

$$(\sigma_{v_a}^{-1})C_3\sigma_{v_a} = \sigma_{v_a}C_3\sigma_{v_a} = \sigma_{v_a}\sigma_{v_c} = C_3^2$$

$$(\sigma_{v_b}^{-1})C_3\sigma_{v_b} = \sigma_{v_b}\sigma_{v_a} = C_3^2$$

$$(\sigma_{v_c}^{-1})C_3\sigma_{v_c} = \sigma_{v_c}\sigma_{v_b} = C_3^2$$

Similarly, we can show that the similarity transformation of C_3^2 by E, C_3 and C_3^2 gives C_3^2 and by σ_{v_a}, σ_{v_b} and σ_{v_c} gives C_3. Hence, C_3^2 and C_3 are conjugate and belong to the same class. We can similarly show that the three σ_v planes belong to a class. The three classes of the C_{3v} point group are written as

E, (C_3 and C_3^2), (σ_{v_a}, σ_{v_b}, σ_{v_c})

or, in a compact manner as E, $2C_3$, $3\sigma_v$.

Example 23. Define isomorphism in group theory.

Solution : Two groups G and G' of the same order are said to be *isomorphous* if we can establish a one-to-one correspondence between their elements such that, if the element A of the group G corresponds to the element A' of G' and B of G to B' of G', then AB corresponds to $A'B'$. Two such groups have identical properties though the actual meaning of their elements may be different.

Example 24. From the character table for the D_{6h} point group, determine the direct product $E_{1u}\times E_{1u}$. Show that its irreducible components are A_{1g}, A_{2g} and E_{2g}.

Solution : Refer to the character table of the D_{6h} point group (Table 8). The information we get is tabulated below :

	E	$2C_6$	$2C_3$	C_2	$3C_2'$	$3C_2''$	i	$2S_3$	$2S_6$	σ_h	$3\sigma_d$	$3\sigma_v$
$\chi(E_{1u}\times E_{1u})$	4	1	1	4	0	0	4	1	1	4	0	0

Using the standard reduction formula (Eq. 8), *viz.*,

$$n_j = \frac{1}{h}\sum_{R_p} g_p \chi(R_p)\chi_j(R_p)$$

and the characters of the direct product representation obtained above, we obtain

$$n_{A_{1g}} = \frac{1}{24}[1\times4\times1+2\times1\times1+2\times1\times1+1\times4\times1+3\times0\times1+3\times0\times1+1\times 4\times1+2\times1\times1+2\times1\times1+1\times4\times1+3\times0\times1+3\times0\times1] = 0$$

$$n_{A_{2g}} = \frac{1}{24}[4+2+2+4+4+2+2+4] = 1$$

$$n_{E_{2g}} = \frac{1}{24}[8-2-2+8+8-2-2+8] = 1$$

Hence, $$E_{1u}\times E_{1u} = A_{1g} + A_{2g} + E_{2g}$$

Example 25. Use symmetry properties to determine whether or not the integral $\int p_x z p_z d\tau$ is necessarily zero in a molecule with symmetry C_{4v}.

Solution : The character table for the C_{4v} point group is given below :

Table 10

Character Table for the C_{4v} Point Group

C_{4v}	E	$2C_4$	C_2	$2\sigma_v$	$2\sigma_d$	$h = 8$	
A_1	1	1	1	1	1	z	x^2+y^2, z^2
A_2	1	1	1	−1	−1	R_z	
B_1	1	−1	1	1	−1		x^2-y^2
B_2	1	−1	1	−1	1		xy
E	2	0	−2	0	0	$(x, y)(R_x, R_y)$	(xz, yz)

$$I = \int f_1 f_2 f_3 \, d\tau \quad \text{where } f_1 = p_x, \quad f_2 = z, \quad f_3 = p_z$$

For the integral to be non-zero, it is necessary that the product $f_1f_2f_3$ spans A_1. We draw up the following table of characters and their products :

	E	$2C_4$	C_2	$2\sigma_v$	$2\sigma_d$	
$f_3 = p_z$	1	1	1	1	1	A_1
$f_2 = z$	1	1	1	1	1	A_1
$f_1 = p_x$	2	0	−2	0	0	E
$f_1f_2f_3$	2	0	−2	0	0	

The number of times that A_1 appears is 0 (since 2, 0, −2, 0, 0 are the characters of E itself). Hence the integral is necessarily zero.

Example 26. Show that the transition $A_1 \rightarrow A_2$ is forbidden for electric dipole transitions in a C_{3v} molecule.

Solution : Refer to the character table of the C_{3v} point group (Table 2).

consider all the components of the electric dipole moment operator and draw up the following table :

Component of μ	x			y			z		
A_1	1	1	1	1	1	1	1	1	1
$\Gamma(\mu)$	2	−1	0	2	−1	0	1	1	1
A_2	1	1	−1	1	1	−1	1	1	−1
$A_1\Gamma(\mu)A_2$	2	−1	0	2	−1	0	1	1	−1
		E			E			A_2	

Since A_1 is not present in any product, the transition dipole moment must be zero and hence the transition $A_1 \rightarrow A_2$ is forbidden.

Example 27. Does the product xyz necessarily vanish when integrated over *(a)* a cube *(b)* a tetrahedron *(c)* a hexagonal prism each centred on the origin ?

Solution :

(a) xyz changes sign under the inversion operation (one of the symmetry operations of the cube). Hence, it does not span A_{1g} and its integral must vanish.

(b) xyz spans A_1 in T_d and so its integral need not be zero.

(c) $xyz \rightarrow -xyz$ under $z \rightarrow -z$ (the σ_h operation in D_{6h}) and so its integral must vanish.

Example 28. The ClO_2 molecule, which belongs to the C_{2v} point group, was trapped in a solid. Its ground state is known to be B_1. Light polarized parallel to the y-axis (parallel to the OO separation) excited the molecule to an upper state. What is the symmetry of that state ?

Solution : Refer to the character table for the C_{2v} point group. For the transition to occur, the direct product representation of the integrand must be A_1 or must contain A_1. Now the direct product representation is $\Gamma_f \times \Gamma(\mu) \times \Gamma_i$ (where i refers to the initial state and f refers to the final state). Then, since $\Gamma_i = B_1$, $\Gamma(\mu) = \Gamma(y) = B_2$, we can draw up the following table of characters :

	E	C_2	σ_v	σ_v'	
B_2	1	−1	−1	1	
B_1	1	−1	1	−1	
B_1B_2	1	1	−1	−1	$= A_2$

Hence, the upper state is A_2 because $A_2\times A_2 = A_1$.

Example 29. What states (irreps or symmetry species) of *(a)* benzene *(b)* naphthaleue may be reached by electric dipole transitions from their (totally symmetric) ground states ?

Solution : *(a)* Refer to the character table for D_{6h} point group to which benzene belongs. In D_{6h}, μ spans $E_{1u}(x, y)$ and $A_2(z)$ and the ground term is A_{1g}. Then using $A_{2u}\times A_{1g}=A_{2u}$, $E_{1u}\times A_{1g} = E_{1u}$; $A_{2u}\times A_{2u}=A_{1g}$ and $E_{1u}\times E_{1u}=A_{1g}+A_{2g}+E_g$, we conclude that the upper term is either E_{1u} or A_{2u}. This is in agreement with the requirement that the transition moment integral is non-zero if the direct product representation of the integrand spans the totally symmetric representation or, if reducible, contains the totally symmetric representation (A_{1g}).

(b) Refer to the character table for the D_{2h} point group to which naphthalene belongs. In D_{2h} itself the dipole moment μ components span $B_{3u}(x)$, $B_{2u}(y)$ and $B_{1u}(z)$ and the ground term is A_g. Hence, since $A_g \times \Gamma = \Gamma$ in this point group, the upper terms are B_{3u} (x-polarized), B_{2u} (y-polarized) and B_{1u} (z-polarized).

Example 30. Using symmetry arguments determine which overlap integrals in the secular determinant for the molecular orbital theory treatment of H_2O will vanish and which will not vanish.

Solution : As we have said, an integral is non-zero if the direct product representation of the integrand is symmetric. This is expressed by saying that (at least for one-dimensional irreducible representations) the overlap integral, S_{ij}, must necessarily be zero if the orbitals ϕ_i and ϕ_j belong to (or are basis of) different irreducible representations.

The coordinate system for H_2O molecule is shown in Fig. 24.

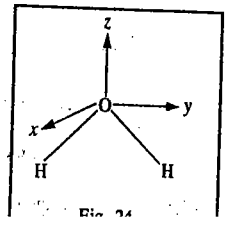

Fig. 24

H_2O molecule lies in the y—z plane. Let us evaluate S_{ij} for a $2p_x$ orbital on the oxygen atom ($2p_{xO}$) and the sum of the 1s orbitals on the hydrogen atoms ($1s_{H_A} + 1s_{H_B}$). The linear combination of 1s orbitals of H is symmetric under all operations of the C_{2v} point group and so transforms as A_1. We choose $1s_{H_A} + 1s_{H_B}$ rather than $1s_{H_A}$ or $1s_{H_B}$ individually for this reason. Referring to the character table for C_{2v} point group, we see that the $2p_x$ orbital on the oxygen atom transforms as x which transforms as (*i.e.*, belongs to) B_2. Hence, we can say that the overlap integral of $2p_{xO}$ and $1s_{H_A} + 1s_{H_B}$, *viz.*,

$$\int (2p_{x_O})(1s_{H_A} + 1s_{H_B})d\tau = 0$$

since the two orbitals belong to different irreducible representations. The same argument shows that

$$\int (2p_{y_O})(1s_{H_A} + 1s_{H_B})d\tau = 0$$

However,

$$\int (2p_{z_O})(1s_{H_A} + 1s_{H_B})d\tau \neq 0.$$

Example 31. Show that the overlap integral involving $2p_{xN}$ and $(1s_{H_A} + 1s_{H_B} + 1s_{H_C})$ in NH_3 molecule (C_{3v}) is equal to zero.

Solution. The overlap integral, S_{ij} must necessarily be zero if the orbitals ϕ_i and ϕ_j belong to (or are basis of) different irreducible representations. The linear combination $(1s_{H_A} + 1s_{H_B} + 1s_{H_C})$ belongs to the totally symmetric irreducible representation A_1 since it is symmetric under all operations of the C_{3v} point group. Referring to the character table for the C_{3v} point group, we see that the nitrogen atom orbital ($2p_{xN}$) transforms as x, which transforms as (or belongs to) E. Hence, the overlap integral

$$\int (2p_{xN})(1s_{H_A} + 1s_{H_B} + 1s_{H_C})d\tau = 0$$

Example 32. If we carry out a molecular orbital calculation on H_2O molecule using the minimal basis set atomic orbitals (AOs), $1s_{H_A}$, $1s_{H_B}$, $1s_{H_C}$, $2s_O$, $2p_{x_O}$, $2p_{y_O}$ and $2p_{z_O}$ without using group theory, we would obtain a 7×7 secular determiuant. How will this determinant look if we use group theory to generate symmetry orbitals ?

Solutiou : H_2O molecule belongs to the C_{2v} point group. We shall first determine the reducible representation of the seven AOs (as we did above for butadiene). We picture the s orbitals as spheres on each hydrogen atom and the $2p$ orbitals on the oxygen atom, like the coordinate axis system shown earlier. Clearly $\chi(E)=7$. The symmetry operation C_2 moves the $1s_H$ orbitals to different atoms, does not alter $1s_O$, $2s_O$ and $2p_{zO}$ and changes the direction of $2p_{xO}$ and $2p_{yO}$; hence, $\chi(C_2)=3-2=1$. Similarly, σ_v moves the $1s_H$ to different atoms, does not alter $1s_O$, $2s_O$, $2p_{xO}$ and $2p_{zO}$ and changes the direction of $2p_{yO}$. Therefore, $\chi(\sigma_v) = 4-1 = 3$. Finally, $\chi(\sigma_v') = 6 - 1 = 5$. Hence, the reducible representation is

Symmetry operation	E	C_2	$\sigma_v(xz)$	$\sigma_v'(yz)$
Γ	7	1	3	5

Using the standard reduction formula (Eq. 8), this rep can be reduced to sum of irreps as follows :

$$n_j = \frac{1}{h}\sum_{R_p} g_p \chi_j(R_p)\chi(R_p) \; ; \; h = 4$$

$$n_{A_1} = \frac{1}{4}[1\times 7 + 1\times 1 + 1\times 3 + 1\times 5] = 4$$

$$n_{A_2} = \frac{1}{4}[1\times 7 + 1\times 1 + (-1)\times 3 + (-1)\times 5] = 0$$

$$n_{B_1} = \frac{1}{4}[1\times 7 + (-1)\times 1 + 1\times 3 + (-1)\times 5] = 1$$

$$n_{B_2} = \frac{1}{4}[1\times 7 + (-1)\times 1 + (-1)\times 3 + 1\times 5] = 2$$

Thus, $\Gamma = 4A_1 + B_1 + 2B_2$. We see that four combinations belong to A_1, none to A_2, one to B_1 and two to B_2. The original 7×7 secular determinant blocks into a 1×1, a 2×2, and a 4×4 determinant. The energies obtained for the 1×1, 2×2, and 4×4 determinants correspond to the molecular orbitals of B_1, B_2 and A_1 symmetry, respectively. We can easily show that $1s_{H_A} + 1s_{H_B}$, $1s_O$, $2s_O$ and $2p_{z_O}$ belong to A_1 ; that $2p_{x_O}$ belongs to B_1 and that $2p_{y_O}$ and $1s_{H_A} - 1s_{H_B}$ belong to B_2.

Concluding Remarks. The 1963 Physics Nobel Laureate E.P. Wigner, whose monumental contributions to group theory have revolutionized mathematical physics, brought group theory from the realm of mathematics to physics and chemistry. Though books by Bishop, Cotton, Kettle, Ladd, Harris and Bertolucci, Tinkham and others deal with various aspects of the subject, the beginner can obtain a good insight into elements of group theory and of quantum chemistry by referring to books by K.V. Raman and A.K. Chandra, respectively. The student who intends to savour the excitement of physical chemistry and quantum chemistry will have to read the fabulous books written by the Oxford University Professor, the inimitable P.W. Atkins (there are a host of them, each different from the other). I.N. Levine's books on physical chemistry, quantum chemistry and spectroscopy are edifying, too. D.A. McQuarrie's books on quantum chemistry, statistical mechanics and physical chemistry are in the same league as those of Atkins and Levine. And finally, to delve into physics (whence physical chemistry and chemical physics are primarily derived), there are the great *Feynman Lectures on Physics*, renowned as much for their content as for Feynman's wit and wisdom. Richard Feynman (1918-1988), the 1965 Physics Nobel Laureate, who has contributed to several areas of physics, *viz.*, QED, path integral approach to quantum mechanics, theory of partons in elementary particle physics and theory of liquid helium, was an exceptionally brilliant teacher as well. The Feynman diagrams, have invaded theoretical chemistry, too! H.A.Bethe (1906-2005), the 1967 Physics Nobel Laureate was to the second half of the twentieth century what Einstein was to the first half.

Problems

1. Derive the standard reduction formula for the number of times an irrep occurs in a reducible representation.
2. Using the character table for the C_{2v} point group and the standard reduction formula, determine the symmetry species (irreps) to which the three normal modes of vibration of H_2O belong.
3. Repeat problem 2 for NH_3 molecule which belongs to the C_{3v} point group.
4. Repeat problem 2 for BF_3 molecule which belongs to D_{3h} point group.
5. Using group theory, factorise the Hückel secular equation for trans-1,3-butadiene (C_{2h} point group), and determine the SALCs for this molecule. Also, solve the Hückel secular equation for the energy levels, labelling them with the appropriate symmetry species (irresp) and draw the HMO diagram.
6. The first singlet excited state of ethylene is tested so that the two hydrogens and carbon on one side are in a plane perpendicular to the plane containing the other three atoms. To which symmetry group does it belong ? Does it have a dipole moment ? (Ans. D_{2d} ; no dipole moment)
7. Consider the three distinct isomers of dichlorobenzene. To which symmetry group does each belong ? Which can have a dipole moment ?

   (Ans. 1, 2-Dichlorobenzene, C_{2v}, dipole ; 1,3-dichlorobenzene, C_{2v}, dipole ; 1,4-dichlorobenzene, D_{2h}, no dipole)
8. Suppose the characters of a reducible representation (rep) of the C_{2v} point group are $\Gamma = 27 \; -1 \; 1 \; 5$. Determine how many times each irrep of C_{2v} is contained in the rep. Γ. (Ans. $\Gamma = 8A_1 + 5A_2 + 6B_1 + 8B_2$)
9. Suppose the characters of a reducible representation (rep) of the D_{3h} point group are $\Gamma = 12 \; 0 \; -2 \; 4 \; -2 \; 2$. Determine how many times each irrep of D_{3h} is contained in the rep. Γ. (Ans. $\Gamma = A_1' + A_2' + 3E' + 2A_2'' + E''$)
10. Consider a tetrahedral molecule xy_4 whose point group is T_d. Show that for constructing its hybrid orbitals, $\Gamma_R = 4 \; 1 \; 0 \; 0 \; 2$, which reduces to $\Gamma = A_1 + T_2$. Now argue that hybrid orbitals with T_d symmetry can be formed from an s orbital and p_x, p_y and p_z orbitals (or the d_{xy}, d_{yz} and d_{zx} orbitals) to give sp^3 (or sd^3) hybrid orbitals.

CHAPTER 6

MOLECULAR SPECTROSCOPY–I
(ROTATIONAL, VIBRATIONAL AND ELECTRONIC SPECTRA)

What is Spectroscopy ? Chemists, physicists, biochemists and other scientists are deeply interested in knowing the structure of molecules. If one could actually 'see' a molecule, there would probably be little fun in investigating it further. However, these systems are of so infinitesimal dimensions that it is not possible to see them, though some progress has of late been made in 'photographing' these species. Our knowledge about molecular structure is derived indirectly from the technique known as **spectroscopy**. *which deals with the transitions that a molecule undergoes between its energy levels upon absorption of suitable radiations determined by quantum mechanical selection rules.*

Quantum mechanics tells that the energy levels of all systems are *quantized* and are designated by appropriate quantum numbers. These energy levels are obtained by the solutions of the time-independent Schrödinger equation, the details of which are not really essential to the understanding of spectroscopy. Let us consider how a spectrum arises. Consider two molecular energy levels E_n and E_m, as shown in Fig. 1. If a photon of frequency ν falls on a molecule in the ground state and its energy $h\nu$ is exactly equal to the energy difference ΔE ($= E_m - E_n$) between the two molecular energy levels, then the molecule undergoes a **transition** from the lower energy level to the higher energy level with the *absorption* of a photon of energy $h\nu$. The spectrum thus obtained is called the **absorption spectrum**. If the molecule falls from the excited state to the ground state with the *emission* of a photon of energy $h\nu$, the spectrum obtained is called the **emission spectrum.**

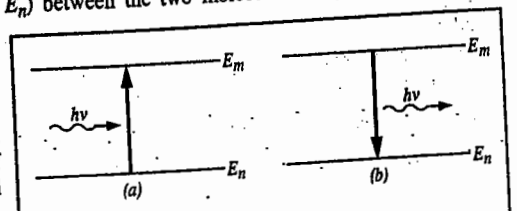

(a) Absorption spectrum *(b)* Emission spectrum.

Fig. 1. Spectroscopic transitions between molecular energy levels.

Basic Features of a Spectrometer

The schematic diagram of the spectrometer used for absorption spectroscopy is given in Fig. 2.

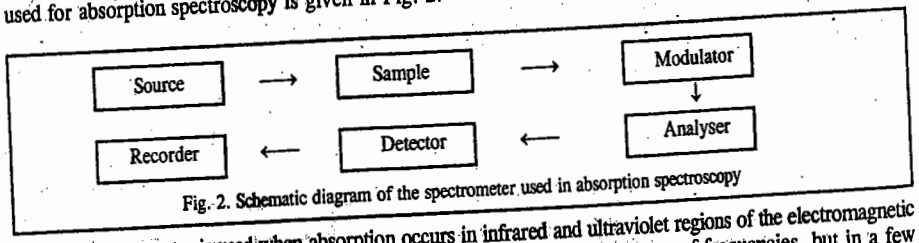

Fig. 2. Schematic diagram of the spectrometer used in absorption spectroscopy

This spectrometer is used when absorption occurs in infrared and ultraviolet regions of the electromagnetic spectrum. The source in a spectrometer produces radiation spanning a range of frequencies, but in a few cases (such as lasers), it is almost a monochromatic radiation. The radiation source in an absorption spectrometer is a heated ceramic filament coated with rare-earth oxides (a Nernst emitter or filament) for the infrared region. The source for the visible region of the spectrum is a tungsten filament which gives out intense white light ; for the ultraviolet region the source is a hydrogen discharge lamp. A

klystron (which is also used in radar installations and microwave ovens) or, more commonly, a semiconductor device called *Gunn diode*, is used to generate microwaves. The radiofrequency radiation is generated by causing an electric current to oscillate in a coil of wire.

The variation of absorption with frequency is determined, traditionally, by analyzing the spectral radiation by means of a *dispersing element* which separates different frequencies into rays that travel in different directions. The simplest dispersing element is a glass or a quartz prism but a diffraction grating is more widely used. A *diffraction grating* consists of a glass or ceramic plate into which fine grooves have been cut about 1000 nm apart (a spacing comparable to the wave length of visible light) and covered with a reflective aluminium coating. The grating causes interference between waves reflected from its surface and constructive interference occurs at specific angles that depend on the frequency of the radiation being used. Thus, each wave length of light is directed into a specific direction.

The third component of the spectrometer is the *detector*, a device that converts the spectral radiation into an electrical signal that is passed on to a recording device operating synchronously with the analyzer, thus producing either a trace on a chart recorder or a computer record of the spectrum. Common detectors are the radiation-sensitive semiconductors. The radiation is chopped by a shutter that rotates in the beam so that an alternating signal is obtained from the detector (an oscillating signal is easier to amplify than a steady signal). A modulator is introduced to convert the signal to an alternating character. This procedure enables more AC electronics to be employed in the recording stages. In the microwave region the source frequency is varied and the analyser is not necessary.

The highest resolution is obtained when the sample is gaseous and at such low pressure that collisions between molecules are infrequent. Gaseous samples are essential for microwave (pure rotational) spectroscopy since molecules can freely rotate only in the gaseous state. In order to achieve sufficient absorption, the path lengths of gaseous samples must be very long, of the order of metres. Long path lengths are achieved by multiple passage of the beam between two parallel mirrors at each end of the sample cavity. For infrared spectroscopy, the sample is typically a liquid held between windows of sodium chloride (which is transparent down to 700 cm^{-1}) or potassium bromide (down to 400 cm^{-1}). Other ways of preparing the sample include grinding it into a paste with 'Nujol', a hydrocarbon oil, or pressing it into a solid disk, with powdered potassium bromide.

Nowadays it is a common practice to use **Fourier-transform technique in spectroscopy**, particularly with infrared (IR) and nuclear magnetic resonance (NMR) spectroscopies. In Fourier-transform infrared (FTIR) spectroscopy, a Michelson-type interferometer is used to analyse the spectrum. It functions by producing an interferogram which is the superposition of a series of waves, each of which represents a component in the spectrum in terms of intensity and wave number. A Fourier transformation of the interferogram then produces a well-resolved absorption spectrum of the species, with a good signal-to-noise (S/N) ratio, also abbreviated as SNR.

The molecular spectra are governed by the so-called **selection rules** which specify the changes in the quantum numbers accompanying a particular transition. The chemist is lucky that selection rules exist which determine a spectrum. If there were no selection rules, the resulting spectrum would have been very chaotic indeed ! The selection rules are, in fact, the 'backbone' of spectroscopy and are obtained from the quantum theory of interaction of radiation with matter. Let us enumerate a few examples which would later be elucidated. For a diatomic molecule, such as H_2, NO, CO, etc., the selection rule for a pure *rotational transition* is $\Delta J = \pm 1$, where J is the rotational quantum number. The selection rule for a pure *vibrational transition* is $\Delta v = \pm 1$, where v is the vibrational quantum number.

The selection rules, however, are not always obeyed strictly. This is because certain approximations which have been used in the derivation of the selection rules are not valid strictly. The spectral transitions which obey a given selection rule are called **allowed transitions** whereas those which violate a selection rule are called **forbidden transitions.** In general, the allowed transitions are more intense (stronger) than the forbidden transitions which are weak. The selection rules for spectral transitions are derived from time-dependent perturbation theory (TDPT), discussed in Chapter 2.

The **natural linewidth** (or **life-time broadening**) of a spectral line is determined by the Heisenberg uncertainty principle, $\Delta E \Delta t \geq h/4\pi$, where ΔE is the uncertainty in the energy and Δt is the uncertainty in the life-time of the energy level. Since for a photon $E = h\nu$ so that $\Delta E = h\Delta\nu$, hence the natural linewidth, $\Delta\nu$, is given by

$$\Delta\nu \geq (4\pi\Delta t)^{-1} \qquad ...(1)$$

Width and Intensity of Spectral Lines. When we analyse the spectrum of a molecule, the first thing we wish to know is how sharp and how intense (strong) is the spectral line. In other words, we are interested in the width and intensity of a spectral line. These two quantities are common to all branches of spectroscopy. Fig. 3*(a)* shows a sharp spectral line having no width while Fig. 3*(b)* shows a spectral line having a width ΔE at half-height. The chemist would, indeed, be a happy person if the spectral lines were all very sharp and very intense. In practice, this is not so.

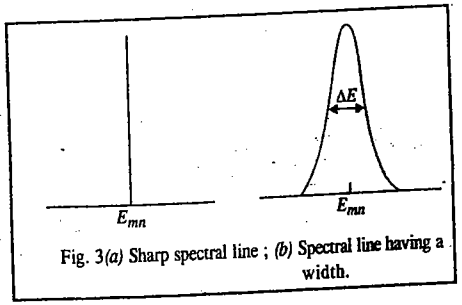

Fig. 3*(a)* Sharp spectral line ; *(b)* Spectral line having a width.

Two factors contribute to broadening of a spectral line : *(i)* The **collision broadening** and *(ii)* the **Doppler broadening**. The collision broadening is largely responsible for the width of spectral lines in the ultraviolet (UV) and visible regions. These transitions mostly take place between electrons in the outer shells in a molecule. When molecules in the gaseous or liquid phase collide with one another, they deform the charge clouds of the outer electrons thereby slightly perturbing the energy levels of these electrons. Hence, the spectral transitions between these perturbed energy levels are broadened.

Doppler broadening arises when the molecule under investigation has a velocity relative to the observer or observing instrument. This is generally the case with gaseous samples where the molecules are undergoing random motion according to the postulates of the kinetic theory of gases. If the molecule is moving *towards* the measuring instrument with velocity u, then the frequency ν' of radiation 'seen' by the molecule is given by

$$\nu' = \nu (1 + u/c) \qquad ...(2a)$$

where ν is the radiation frequency and c is the velocity of light. If, on the other hand, the molecule is moving *away* from the measuring instrument, the frequency of radiation 'seen' by the molecule is given by

$$\nu' = \nu (1 - u/c) \qquad ...(2b)$$

Rearranging Eq. 2*a*, we obtain

$$(\nu - \nu')/\nu = \Delta\nu/\nu = -u/c \qquad ...(3a)$$

Similarly, rearranging Eq. 2*b*, we obtain

$$(\nu - \nu')/\nu = \Delta\nu/\nu = u/c \qquad ...(3b)$$

The quantity $\Delta\nu$ is the *Doppler broadening*. We see that, depending upon the direction of motion of the molecule relative to the instrument, the observed frequency becomes either higher or lower than the actual radiation frequency. From the kinetic theory of gases, it can be shown that the Doppler broadening of the spectral line of a molecule of mass m is given by

$$\Delta\nu/\nu = (2/c)(2kT \ln 2/m)^{1/2} \qquad ...(4)$$

Since $\Delta\nu/\nu$ is directly proportional to $T^{1/2}$, Doppler broadening can be reduced (and spectral lines of maximum sharpness can be obtained) by working with cold gaseous samples.

We now turn to the **intensity of spectral lines.** The intensity of a spectral line is determined by

(i) the **Boltzmann population** of the energy levels and *(ii)* the **transition probability** between them.

According to Boltzmann, if, at temperature T, N_0 is the number of molecules in the ground state, then the number of molecules, N, in the excited state is given by

$$N = N_0 e^{-\Delta E/kT} \qquad ....(5)$$

where ΔE is the energy difference between the ground and excited states and k is the Boltzmann constant. The relative population at equilibrium is, thus, given by

$$N/N_0 = e^{-\Delta E/kT} \qquad ...(6)$$

Evidenty, if ΔE is large, N/N_0 is small, *i.e.*, the number of molecules in the excited state is less than that in the ground state. In fact, at room temperature, most of the molecules are in the ground state. Hence, the spectral lines originating from transitions from the ground state to a higher, say, third excited state would be more intense than those originating from transitions from the first excited state to the third excited state. The term transition probability, as the name implies, means the probability of transition between two given energy levels. We have said earlier that a molecule, upon absorption of a photon, does not just go anywhere it pleases ; it ends up in an energy level determined by the *selection rules* for that particular transition. The selection rules, in turn, determine the allowed transitions and the forbidden transitions. Clearly, the allowed transitions yield spectral lines which have greater intensity than the forbidden ones. The quantum theory of radiation was put forth by Einstein in 1916.

We may mention parenthetically that atomic spectra (discussed in Chapter 2) are the simplest spectra, consisting of sharp lines arising from electronic transitions, and are called **line spectra.** They are distinguished from molecular spectra (to be discussed in this chapter), which consist of bands arising from rotational and vibrational transitions accompanying electronic transitions ; they are called **band spectra.**

Molecular Spectra. In contrast to atomic spectra which arise from the transitions of an electron between the atomic energy levels, the molecular spectra arise from three types of transitions, *viz.*, *rotational, vibrational* and *electronic transitions*. Broadly speaking, the total energy of a molecule, according to the Born-Oppenheimer approximation, is given by

$$E = E_{tr} + E_{rot} + E_{vib} + E_{el} \qquad ...(7)$$

i.e., the energy is the sum of translational energy, E_{tr} ; rotational energy, E_{rot} ; vibrational energy, E_{vib} and electronic energy, E_{el}. The translational energy is, however, not quantized. Furthermore,

$$E_{el} >> E_{vib} >> E_{rot} >> E_{tr}$$

Since the translational energy is negligibly small, we can write the Born-Oppenheimer approximation as

$$E = E_{rot} + E_{vib} + E_{el} \qquad ...(8)$$

Let us illustrate these energies with reference to a diatomic molecule. Rotational energy arises when the molecule rotates about an axis perpendicular to the internuclear axis and passing through the centre of gravity of the molecule. Vibrational energy is associated with the to and fro motion of the nuclei of the molecule such that the centre of gravity does not change. And finally, electronic energy is associated with the transition of an electron from the ground state energy level to an excited state energy level of the molecule due to the absorption of a photon of suitable frequency.

Associated with each electronic state are a series of vibrational energy levels (designated by the vibrational quantum number v) and associated with each vibrational energy level are a series of rotational energy levels (designated by the rotational quantum number J), as shown in Fig. 4. It is customary to use a single prime superscript to designate a higher energy level and a double prime superscript to designate a lower energy level.

The rotational spectra of a molecule are observed in the microwave region ; the vibrational spectra in the infrared (IR) region and the electronic spectra in the ultraviolet (UV) and/or visible regions of the

electromagnetic spectrum.

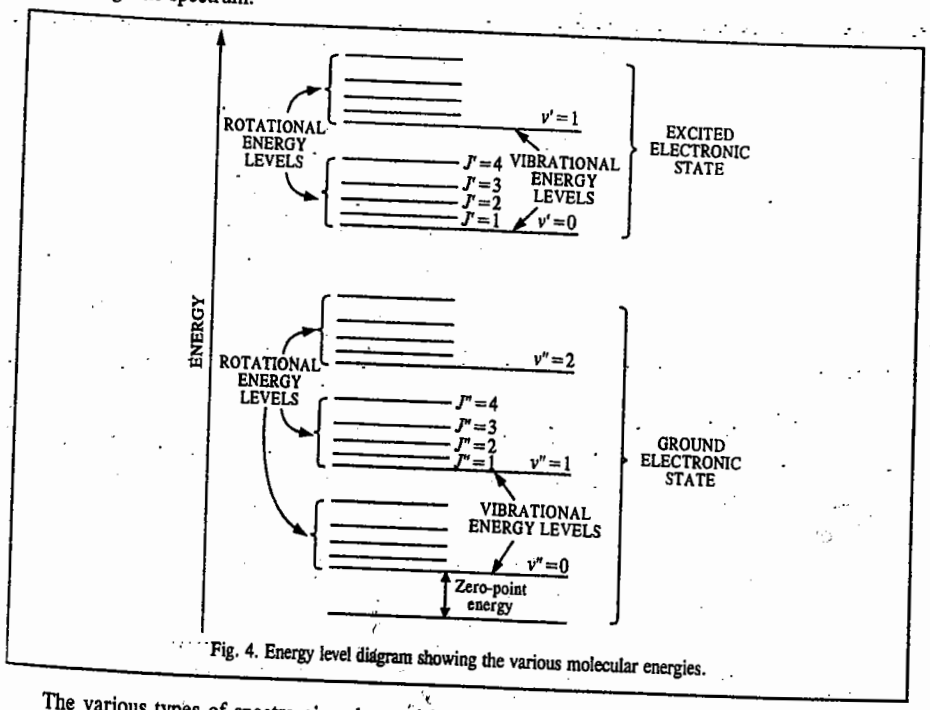

Fig. 4. Energy level diagram showing the various molecular energies.

The various types of spectra given by a molecule, the regions in which these spectra lie and the energy changes that take place in the molecule on absorption of radiation, are listed below.

1. Rotational (Microwave) Spectra. These spectra result from transitions between the rotational energy levels of a *gaseous* molecule on the absorption of radiations falling in the microwave region. These spectra are shown by molecules which *possess a permanent dipole moment, e.g.*, HCl, CO, H_2O vapour, NO, etc. Homonuclear diatomic molecules such as H_2, Cl_2, etc., and linear polyatomic molecules such as CO_2, which do not possess a dipole moment, do not show microwave spectra. Microwave spectra occur in the spectral range of 1 – 100 cm^{-1}.

2. Vibrational and Vibration-Rotation (Infrared) Spectra. These spectra originate from transitions induced between the vibrational energy levels of a molecule on the absorption of radiations belonging to the infrared region. IR spectra are shown by molecules when vibrational motion is accompanied by a *change in the dipole moment of the molecule*. These spectra occur in the spectral range of 500 – 4000 cm^{-1}.

3. Raman Spectra. Raman spectra relate to vibrational and/or rotational transitions in molecules but in a different manner. In this case, what we measure is the *scattering* and not the absorption of radiation. An intense beam of monochromatic radiation in the *visible region* is allowed to fall on a sample and the intensity of scattered light is observed at right angles to the incident beam. Most of the scattered light has the same frequency as the incident beam (this is called *Rayleigh scattering*). However, some of the scattered light has different frequencies than the incident beam. This is called *Raman scattering*. The energy differences between these weak lines and the main Rayleigh line correspond to vibrational and/or rotational transitions in the molecule under investigation. Raman spectra are observed in the visible region, *viz.*, 12,500 – 25,000 cm^{-1}.

4. Electronic Spectra. Electronic spectra arise from electronic transitions in a molecule by absorption of radiations falling in the visible and ultraviolet regions. While electronic spectra in the visible region span 12,500 – 25,000 cm^{-1}, those in the ultraviolet region span 25,000 – 70,000 cm^{-1}. Since electronic transitions in a molecule are invariably accompanied by vibrational and rotational transitions, the eletronic spectra of molecules are highly complex.

5. Photoelectron Spectra (PES). These spectra help in the determination of ionization energies of molecules. If a light photon falling on a molecule possesses very high energy, it can cause ionization of the molecule, *i.e.*, the removal of the electron from the molecule. If the energy of the incident photon is greater than the ionization energy, the ejected electron will possess excess kinetic energy. In PES, a beam of photons of known energy is allowed to fall on the sample and the kinetic energy of the ejected electrons is measured. The difference between the photon energy and the excess kinetic energy gives the **binding energy** of the electron. PES offers one of the most accurate methods for determining the ionization energies of molecules. Photoelectron spectra can be studied either using the X-ray photons or the UV photons. In the former case, they are called XPES spectra and in the latter case, the UVPES (or UPES) spectra.

6. Nuclear Magnetic Resonance (NMR) and Nuclear Quadrupole Resonance (NQR) Spectra. NMR spectra result from transitions induced between the nuclear spin energy levels of a molecule in an applied magnetic field. NQR spectra result from the transitions between the nuclear spin energy levels of a molecule arising from the interaction of the unsymmetrical charge distribution in nuclei with the electric field gradients (EFG) which arise from the bonding and non-bonding electrons in the molecule. NMR and NQR spectra span the radiofrequency regions, *viz.*, 5 – 100 MHz.

7. Electron Spin Resonance (ESR) or Electron Paramagnetic Resonance (EPR) Spectra. ESR spectra result from transitions induced between the electron spin energy levels of a molecule in an applied magnetic field. These spectra are exhibited by systems which contain odd (unpaired) electrons such as free radicals, transition metal ions and rare-earth ions. Molecules such as nitric oxide and oxygen and other paramagnetic systems also show ESR spectra. This branch of spectroscopy falls in the microwave region, *viz.*, 2 – 9·6 GHz.

8. Mössbauer Spectra (also called Nuclear Gamma Resonance Fluorescence (NRF) Spectra). Mössbauer spectra constitute a type of nuclear resonance spectra like nuclear magnetic resonance spectra. However, while NMR spectra result from absorption of low energy photons of frequency around 60 MHz, Mössbauer spectra result from absorption of high energy γ-photons of frequency around 10^{13} MHz by the nuclei. Gamma ray spectra have been used specifically for the study of compounds of iron and tin. In this case, γ-radiations from ^{57}Co source are allowed to fall on a sample in which the iron nuclei are in an environment identical with that of the source atoms. This results in resonant absorption of γ-rays. The splittings in Mössbauer lines are found to be of the same order as in NMR spectroscopy.

ROTATIONAL (MICROWAVE) SPECTRA OF DIATOMIC MOLECULES

Consider a diatomic molecule in which m_1 and m_2 are the masses of the two atoms and r is the equilibrium bond length, rotating about an axis passing through its centre of gravity, c.g. (Fig. 5).

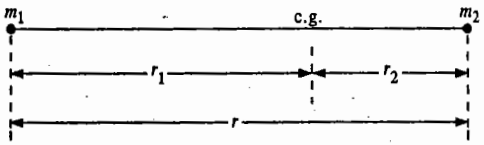

Fig. 5. Rotation of a diatomic molecule about its centre of gravity.

The centre of gravity is defined by the equality of the moments about it, *i.e.*,

$$m_1 r_1 = m_2 r_2 \qquad \ldots(9)$$

The **moment of inertia** I of a **molecule** (rotating as a rigid rotor, not subject to contrifugal forces that tend to distort the molecular geometry and change the moments of inertia) is defined as

$$I = \sum_i m_i r_i^2 \qquad ...(10)$$

where r_i is the distance of the ith particle of mass m_i from the centre of gravity. Since a diatomic molecule has two atoms, we have

$$I = m_1 r_1^2 + m_2 r_2^2 = m_2 r_2 r_1 + m_1 r_1 r_2 \quad \text{(using Eq. 9)} = r_1 r_2 (m_2 + m_1) \qquad ...(11)$$

Also, as seen from Fig. 5, $r = r_1 + r_2$ ...(12)

Therefore, from Eqs. 9 and 13, ...(13)

$$m_1 r_1 = m_2 r_2 = m_2 (r - r_1) \qquad ...(14)$$

Hence,

$$r_1 = \frac{m_2 r}{m_1 + m_2} \quad \text{and} \quad r_2 = \frac{m_1 r}{m_1 + m_2}$$

Substituting the above values of r_1 and r_2 in Eq. 11, we have

$$I = \frac{m_1 m_2^2}{(m_1 + m_2)^2} r^2 + \frac{m_1^2 m_2}{(m_1 + m_2)^2} r^2 \qquad ...(15)$$

$$= \frac{m_1 m_2 (m_1 + m_2)}{(m_1 + m_2)^2} r^2 = \frac{m_1 m_2}{m_1 + m_2} r^2 = \mu r^2 \qquad ...(16)$$

where $\mu = m_1 m_2/(m_1 + m_2)$ is called the **reduced mass** of the molecule.

Classically, the angular momentum L of a rotating molecule is given by $L = I\omega$ where ω is its angular velocity. However, the angular momentum is quantized, being given by

$$L = \sqrt{J(J+1)}\ \hbar\ ; \quad J = 0, 1, 2, ... \qquad ...(17)$$

where J is the rotational quantum number. The energy of a rotating molecule is given by $\frac{1}{2} I\omega^2$. Hence, the quantized rotational energy levels of a rigid diatomic rotor (rotating molecule) are given by

$$E_J = \tfrac{1}{2} I\omega^2 = (I\omega)^2/2I = L^2/2I \qquad ...(18)$$

Using the expression for L from Eq. 17, we have

$$E_J = J(J+1)\frac{\hbar^2}{2I}\ ; \text{ where } J = 0, 1, 2, ... \qquad ...(19)$$

Eq. 19 is also obtained by solving the Schrödinger wave equation for a rigid diatomic rotor (Chapter 1). It is customary to express the energy in cm^{-1} rather than in joules. This is done by dividing energy in joules by hc when we get

Here Total rotational energy, written as

$$F(J) = E_J/hc = J(J+1)\frac{\hbar}{4\pi cI}\ ; J = 0, 1, 2, ... \qquad ...(20)$$

$F(J)$, is called the **rotational term**. Defining the **rotational constant** B as

$$B = \frac{\hbar}{4\pi cI}\ \text{cm}^{-1}, \qquad ...(21)$$

we have

$$F(J) = BJ(J+1)\ ;\ J = 0, 1, 2, ... \qquad ...(22a)$$

and

$$E_J = hcBJ(J+1)\ ;\ J = 0, 1, 2, ... \qquad ...(22b)$$

If we want to take into account **centrifugal distortion** whose effect on the diatomic rotor is to stretch the bond and hence to increase the moment of inertia, and thereby to reduce the rotational constant and hence bring the energy levels closer than in the rigid-rotor approximation, then the energy level expression (22*a*) becomes

$$F(J) = BJ(J+1) - D_J J^2 (J+1)^2 \qquad ...(22c)$$

where D_J is the centrifugal distortion constant given by $D_J = 4B^3/\bar{\nu}^2$, where $\bar{\nu}$ is the vibrational frequency of the molecule.

Next we need a ***selection rule*** to determine the radiative transitions between the rotational energy levels. The derivation of the selection rule is a quantum-mechanical problem ; its details need not concern us here. Suffice it to mention that the rotational transitions for a rigid diatomic molecule are governed by the selection rule

$$\Delta J = \pm 1 \qquad ...(23)$$

i.e., only those transitions are allowed in which the rotational quantum number changes by unity. The + sign refers to absorption and the – sign to emission of radiation. Microwave spectra are usually observed as absorption spectra so that the operative part of the selection rule is $\Delta J = +1$. For a transition taking place from J to $J + 1$, the rotational frequency is given by

$$\nu_{(J \to J+1)} = B(J+1)(J+2) - BJ(J+1) \qquad ...(24)$$

$$= B(J^2 + 3J + 2) - B(J^2 + J) \qquad ...(25)$$

$$= 2B(J+1)\ \text{cm}^{-1} \qquad ...(26)$$

Thus, $\nu_{(0 \to 1)} = 2B$; $\nu_{(1 \to 2)} = 4B$;

$\nu_{(2 \to 3)} = 6B$; $\nu_{(3 \to 4)} = 8B$, etc.

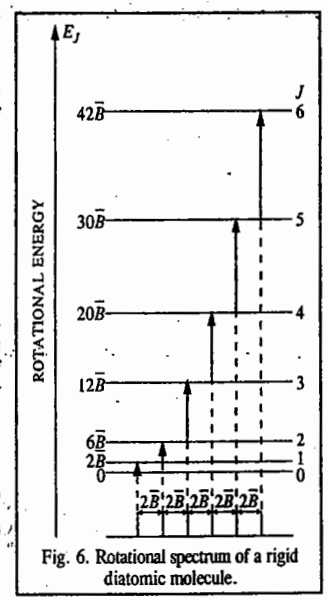

Fig. 6. Rotational spectrum of a rigid diatomic molecule.

We see that the rotational spectrum of a rigid diatomic molecule consists of a series of lines at $2B$, $4B$, $6B$, $8B$, etc. Evidently, these lines are equally spaced by an amount of $2B$ (Fig. 6) called **frequency separation.**

Example 1. The internuclear distance (*i.e.*, bond length) of carbon monoxide molecule is 1·13 Å. Calculate the energy (in joules and in eV) and angular velocity of this molecule in the first excited rotational level. The atomic masses are : $^{12}C = 1{\cdot}99 \times 10^{-26}$ kg ; $^{16}O = 2{\cdot}66 \times 10^{-26}$ kg.

Solution :

$$r = 1{\cdot}13\ \text{Å} = 1{\cdot}13 \times 10^{-8}\ \text{cm} = 1{\cdot}13 \times 10^{-10}\ \text{m}$$

$$\mu = \frac{m_1 m_2}{m_1 + m_2} = \frac{(1{\cdot}99 \times 10^{-26}\ \text{kg})(2{\cdot}66 \times 10^{-26}\ \text{kg})}{(1{\cdot}99 + 2{\cdot}66) \times 10^{-26}\ \text{kg}} = 1{\cdot}14 \times 10^{-26}\ \text{kg}$$

$$I = \mu r^2 = (1{\cdot}14 \times 10^{-26}\ \text{kg})\ (1{\cdot}13 \times 10^{-10}\ \text{m})^2 = 1{\cdot}46 \times 10^{-46}\ \text{kg m}^2$$

$$E_1 = \hbar^2/I\ \text{joule} \quad \text{[Eq. (19)]}$$

$$= \frac{(1{\cdot}054 \times 10^{-34}\ \text{Js})^2}{(1{\cdot}46 \times 10^{-46}\ \text{kg m}^2)} = 7{\cdot}61 \times 10^{-23}\ \text{joule} = \frac{7{\cdot}61 \times 10^{-23}\ \text{J}}{1{\cdot}602 \times 10^{-19}\ \text{J/eV}} = 4{\cdot}76 \times 10^{-4}\ \text{eV}$$

Since from Eq. 18, $E_1 = \frac{1}{2} I\omega^2$, where ω is the angular velocity, hence

$$\omega = \sqrt{\frac{2E_1}{I}} = \sqrt{\frac{2 \times (7{\cdot}61 \times 10^{-23}\ \text{J})}{1{\cdot}46 \times 10^{-46}\ \text{kg m}^2}} = 3{\cdot}23 \times 10^{11}\ \text{radians s}^{-1}$$

Example 2. Compare the first excited state rotational energy of CO molecule obtained in the last example with its thermal energy at room temperature and comment on the result.

Solution : Thermal energy of CO molecule at room temperature, *i.e.*, 25°C = kT

$$= \frac{1{\cdot}38\times10^{-23}\,\text{J K}^{-1}(298\,\text{K})}{1{\cdot}602\times10^{-19}\,\text{J / eV}} = 2{\cdot}6\times10^{-2}\ \text{eV}$$

Comparing it with the first excited state rotational energy of CO (*viz*, $4{\cdot}76\times10^{-4}$ eV), obtained in the last example, we find that the thermal energy is far greater. Hence, we conclude that at room temperature, all the molecules in the gaseous sample of carbon monoxide are in the excited rotational energy levels.

Example 3. The pure rotational (microwave) spectrum of the gaseous molecule CN consists of a series of equally spaced lines separated by 3·7978 cm^{-1}. Calculate the internuclear distance (*i.e.*, equilibrium bond length) of the molecule. The molar masses are : ^{12}C = 12·011 g mol^{-1} and ^{14}N = 14·007 g mol^{-1}

Solution : The spacing between the lines = $2B$ = 3·7978 cm^{-1}

$$\therefore \quad B = 3{\cdot}7978/2 = 1{\cdot}8989\ \text{cm}^{-1}$$

$$B = \frac{\hbar}{4\pi cI}\ \text{cm}^{-1} \qquad \text{(Eq. 21)}$$

$$\therefore \quad I = \frac{\hbar}{4\pi Bc} = \frac{1{\cdot}054\times10^{-34}\,\text{J s}}{(4\pi)(1{\cdot}8989\,\text{cm}^{-1})(3\times10^{10}\,\text{cm s}^{-1})}$$

$$= 1{\cdot}4742\times10^{-46}\ \text{kg m}^2 \qquad (\text{J} = \text{kg m}^2\,\text{s}^{-2})$$

The reduced mass is given by

$$\mu = \frac{(M_1/N_A)(M_2/N_A)}{(M_1/N_A)+(M_2/N_A)} = \frac{M_1M_2}{(M_1+M_2)N_A}$$

where N_A is Avogadro's number and M_1, M_2 are the molar masses of C and N, respectively. Thus,

$$\mu = \frac{(12{\cdot}011\,\text{g mol}^{-1})(14{\cdot}007\,\text{g mol}^{-1})}{(26{\cdot}018\,\text{g mol}^{-1})(6{\cdot}022\times10^{23}\,\text{mol}^{-1})} = 1{\cdot}0737\times10^{-23}\ \text{g}$$

$$= 1{\cdot}0737\times10^{-26}\ \text{kg}$$

Since $I = \mu r^2$, hence, $r = \left(\frac{I}{\mu}\right)^{1/2} = \left[\frac{1{\cdot}4742\times10^{-46}\,\text{kg m}^2}{1{\cdot}0737\times10^{-26}\,\text{kg}}\right]^{1/2} = 1{\cdot}1717\times10^{-10}\ \text{m} = \mathbf{117\ pm}$

Example 4. The pure rotational (microwave) spectrum of gaseous HCl consists of a series of equally spaced lines separated by 20·80 cm^{-1}. Calculate the internuclear distance of the molecule. The atomic masses are : ^{1}H = $1{\cdot}673\times10^{-27}$ kg : ^{35}Cl = $58{\cdot}06\times10^{-27}$ kg.

Solution : The spacing between the lines = $2B$ = 20·80 cm^{-1}

$$\therefore \quad B = 20{\cdot}80/2 = 10{\cdot}40\ \text{cm}^{-1}$$

$$B = \frac{\hbar}{4\pi cI}\ \text{cm}^{-1}$$

$$I = \frac{\hbar}{4\pi Bc} = \frac{1{\cdot}054\times10^{-34}\,\text{J s}}{(4\pi)(10{\cdot}40\,\text{cm}^{-1})(3\times10^{10}\,\text{cm s}^{-1})}$$

$$= 0{\cdot}2689\times10^{-46}\ \text{kg m}^2 \qquad (\text{J} = \text{kg m}^2\,\text{s}^{-2})$$

$$\mu = \frac{(1{\cdot}673\times10^{-27}\,\text{kg})(58{\cdot}06\times10^{-27}\,\text{kg})}{(1{\cdot}673+58{\cdot}06)\times10^{-27}\,\text{kg}} \qquad \text{(From Eq. 16)}$$

$$= \frac{(1{\cdot}673\times58{\cdot}06)10^{-27}}{59{\cdot}73}\ \text{kg} = 1{\cdot}626\times10^{-27}\ \text{kg}$$

$$\frac{(1{\cdot}673\times58{\cdot}06)10^{-27}}{59{\cdot}73}\ \text{kg} = 1{\cdot}626\times10^{-27}\ \text{kg}$$

Since $I = \mu r^2$, hence, $r = 1{\cdot}29\times10^{-10}$ m = **129 pm**

Relative Intensities of Rotational Spectral Lines. The relative intensities of spectral lines depend upon the relative populations of the energy levels. As we see from Example 2, even at room temperature many of the diatomic molecules are present in the excited state energy levels. Since the energy level population is given by the Boltzmann distribution, the intensity of rotational lines is evidently proportional to the Boltzmann distribution of molecules in the rotational energy levels, *i.e.*,

$$\text{Intensity} \propto N_J/N_0 = e^{-E_J/kT} \qquad \ldots(27)$$

Rotational energy levels are, however, degenerate, their degeneracy (g_J) for a diatomic molecule being given by

$$g_J = 2J+1 \qquad \ldots(28)$$

In other words, for a given value of J, the energy level is $(2J+1)$-fold degenerate. For $J=0$, $g_J=1$; for $J=1$, $g_J=3$; for $J=2$, $g_J=5$ and so on.

Thus, the intensity of the rotational spectral lines is determined by the product of the degeneracy factor and the Boltzmann exponential factor. Hence,

$$\text{Intensity} \propto N_J/N_0 = (2J+1)e^{-E_J/kT} \qquad \ldots(29)$$

Since $$E_J = hcF(J) \qquad \ldots(30)$$

and $$F(J) = BJ(J+1), \qquad \ldots(31)$$

hence, $$N_J/N_0 = (2J+1)\,e^{-BJ(J+1)\,hc/kT} \qquad \ldots(32)$$

The quantity N_J/N_0 is plotted versus J for a diatomic molecule at room temperature in Fig. 7.

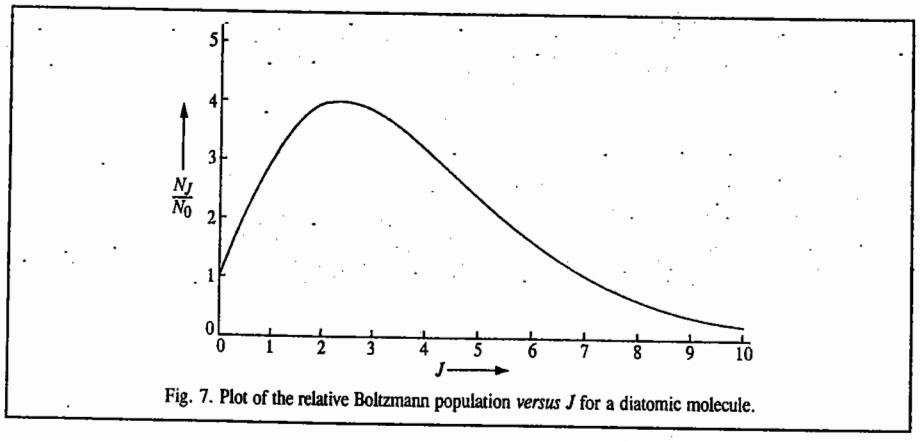

Fig. 7. Plot of the relative Boltzmann population *versus* J for a diatomic molecule.

We see that the relative intensity passes through a maximum. It can be shown that the value of J corresponding to the maximum in population is given by

$$J_{max} = \left(\frac{kT}{2hcB}\right)^{1/2} - \frac{1}{2} \qquad \ldots(33)$$

The J_{max} should be rounded off to the nearest integral value.

Example 5. Calculate J_{max} for a rigid diatomic molecule for which at 300 K, the rotational constant is 1·566 cm^{-1}.

Solution : $$J_{max} = \left(\frac{kT}{2hcB}\right)^{1/2} - \frac{1}{2} \qquad \text{(Eq. 33)}$$

$$\simeq \left[\frac{(1{\cdot}38 \times 10^{-23}\ \text{J K}^{-1})(300\ \text{K})}{2(6{\cdot}626 \times 10^{-34}\ \text{J s})(3 \times 10^{10}\ \text{cm s}^{-1})(1{\cdot}566\ \text{cm}^{-1})}\right]^{1/2} - \frac{1}{2} = 7{\cdot}56 \simeq 8$$

Application of Microwave Spectroscopy for the Determination of Bond Distances in Polyatomic Molecules. For the sake of simplicity, consider the gaseous linear triatomic molecule O=C=S for which we want to determine the two bond distances O—C and C—S. This can be done by **isotopic substitution method.** Consider first the molecule $^{16}O{=}^{12}C{=}^{32}S$ (Fig. 8).

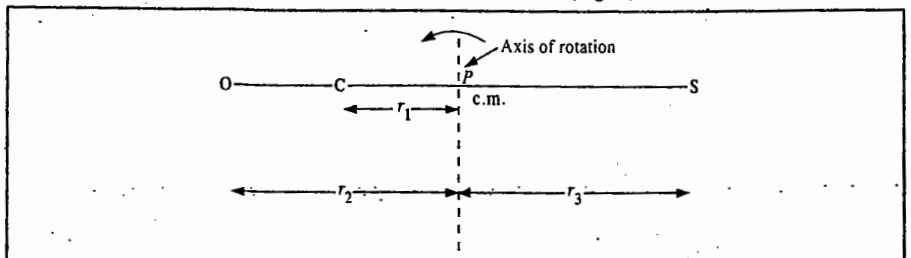

Fig. 8. The rotation of $^{16}O{=}^{12}C{=}^{32}S$ molecule about an axis of rotation passing through its centre of mass (c.m.)

Since the centre of mass is at P (from where the various distances are measured),

$$\therefore \qquad m_C r_1 + m_O r_2 = m_S r_3 \qquad \text{...(34)}$$

The moment of inertia is given by

$$I = m_C r_1^2 + m_O r_2^2 + m_S r_3^2 \qquad \text{...(35)}$$

Also, $$r_2 = r_{CO} + r_1\ ;\ r_3 = r_{CS} - r_1 \quad \text{(Fig. 8)} \qquad \text{...(36)}$$

where r_{CO} and r_{CS} are the two interatomic distances to be determined. Substituting Eq. 36 into Eq. 34, we have

$$m_C r_1 + m_O (r_{CO} + r_1) = m_S (r_{CS} - r_1) \qquad \text{...(37)}$$

or, rearranging,

$$(m_C + m_O + m_S)\, r_1 = m_S\, r_{CS} - m_O\, r_{CO} \qquad \text{...(38)}$$

Since $m_C + m_O + m_S = M$ (the mass of the O=C=S molecule), hence,

$$Mr_1 = m_S\, r_{CS} - m_O\, r_{CO}$$

$$r_1 = (m_S\, r_{CS} - m_O\, r_{CO})/M \qquad \text{...(39)}$$

Substituting Eq. 36 into Eq. 35, we have

$$I = m_C\, r_1^2 + m_O\, (r_{CO} + r_1)^2 + m_S\, (r_{CS} - r_1)^2 \qquad \text{...(40)}$$

Substituting for r_1 from Eq. 39 into Eq. 40 and simplifying, we obtain

$$I = (m_S\, r_{CS}^2 - m_O\, r_{CO}^2 + 2m_O m_S\, r_{CO}\, r_{CS} - m_S\, r_{CS}^2)/M \qquad \text{...(41)}$$

Eq. 44 contains the unknowns r_{CO} and r_{CS}.

Now we make an important assumption *that isotopic substitution does not alter the interatomic distances.* Applying this assumption to the $^{16}O{=}^{12}C{=}^{34}S$ molecule, we obtain a similar expression for the moment of intertia I' of the molecule :

$$I' = (m_S'\, r_{CS}^2 - m_O\, r_{CO}^2 + 2m_O\, m_S'\, r_{CO}\, r_{CS} - m_S'\, r_{CS}^2)/M \qquad \text{...(42)}$$

Thus, we can obtain both I and I' from the microwave spectra of $^{16}O{=}^{12}C{=}^{32}S$ and $^{16}O{=}^{12}C{=}^{34}S$ molecules and from these moments of inertia, the unknowns r_{CO} and r_{CS} can be determined.

The interatomic distances in gaseous O=C=S, using several pairs of isotopes are given in Table 1.

TABLE 1

Interatomic Distances in O=C=S Molecule

Pairs of Isotopic Molecules	r_{C-O} (in Å)	r_{C-S} (in Å)
$^{16}O{=}^{12}C{=}^{32}S$ and $^{16}O{=}^{12}C{=}^{34}S$	1·1647	1·5576
$^{16}O{=}^{12}C{=}^{32}S$ and $^{16}O{=}^{13}C{=}^{32}S$	1·1629	1·5591
$^{16}O{=}^{12}C{=}^{34}S$ and $^{16}O{=}^{13}C{=}^{34}S$	1·1625	1·5594
$^{16}O{=}^{12}C{=}^{32}S$ and $^{18}O{=}^{12}C{=}^{32}S$	1·1652	1·5653

Notice that there are small differences in bond lengths caused by changing the isotopes. These differences are due to *zero-point vibrations* whose amplitudes depend upon the masses of the atoms. Thus, measured bond lengths change upon isotopic substitution.

Microwave Oven. In recent years, the microwave oven has become a very familiar and useful cooking device in the kitchen. Its mode of operation depends upon the absorption by the food of the microwave radiation in which it is placed. The water molecules in the food absorb the microwave radiation and are thereby raised to the higher rotational states. The biological molecules in the food, on the other hand, are far too big to be able to rotate. The heating in the microwave oven is entirely *internal,* in contrast to the conventional oven where the food is cooked by *external* heating. In internal heating, the water molecules in the food are excited and the excess rotational energy is re-emitted as heat with the help of which the food gets cooked.

Unfortunately, the microwave radiation also affects the human body. Hence, the door seal of the microwave oven must be in good condition to ensure that no radiation leaks out.

ROTATIONAL SPECTRA OF POLYATOMIC MOLECULES

The rotational spectra of polyatomic molecules show features not found in the spectra of diatomic molecules. Whereas the diatomics have only one bond distance and hence only one moment of inertia, polyatomic molecules have more than one bond distance and hence several moments of inertia. In fact, in the Cartesian coordinate system (x, y, z), there are *nine* components of the moment of inertia.

However, in the so-called principal axis system (A, B, C), these components reduce to three moments of inertia, I_A, I_B, I_C, where I_A, I_B and I_C are, respectively, the principal moments of inertia about the A, B and C axes. Thus, polyatomic molecules in microwave spectroscopy are classified into different types of rotators (rotors) as shown in Table 2.

1. Linear Rotor. The energy of a linear rotor such as O=C=S is given by Eq. 22, *viz.*, the same as that for a diatomic rotor. In this case, isotopic substitution method is used to determine the bond distances, as discussed above.

TABLE 2

Classification of Polyatomic Molecules

Moment of Inertia	Type of Rotor	Examples
$I_A = I_B,\ I_C = 0$	Linear	HX, O=C=S, H—C≡N
$I_A = I_B = I_C$	Spherical top	CH_4, SF_6, UF_6
$I_A > I_B = I_C$	Prolate symmetric top	NH_3, $CHCl_3$, CH_3Cl
$I_A < I_B = I_C$	Oblate symmetric top	
$I_A \neq I_B \neq I_C$	Asymmetric top	H_2O

2. Spherical Top Molecules. Since a spherical top molecule such as CH_4 or SF_6 does not possess a permanent dipole moment, it is not microwave-active and is of only academic interest.

3. Symmetric Top Molecules. The solution of the Schrödinger wave equation for a symmetric top molecule gives the following expression for the energy levels of this rotor :

$$E_{J,K} = BJ(J+1) + (A - B)K^2 \quad ...(43)$$

where K is the component of J about the unique axis and the rotational constants A and B (in cm^{-1}) are defined as

$$A = h/(8\pi^2 I_A c) \text{ and } B = h/(8\pi^2 I_B c) \quad ...(44)$$

For every value of J, there are $2J+1$ values of K given by

$$K = 0, \pm 1, \pm 2, \cdots\cdots, \pm J \quad ...(45)$$

The selection rules for rotational transitions are

$$\Delta J = 0, \pm 1; \ \Delta K = 0 \quad ...(46)$$

4. Asymmetric Top Molecules. The solution of the Schrödinger wave equation for an asymmetric top rotor is a very difficult problem and there is no simple expression for the energy levels. We shall, therefore, not discuss this rotor here.

Stark Effect in Microwave Spectra. The splitting of molecular rotational energy levels in the presence of the external electric field E is called the **Stark effect,** after the German physicist, J. Stark (1874–1957) who was awarded the 1919 Physics Nobel Prize for his discovery of Doppler effect in canal rays and the splitting of spectral lines in electric fields. The shift of rotational frequency, $\Delta\nu$, for a linear gaseous molecule in the Stark effect is given by

$$\Delta\nu \propto (\mu E)^2 \quad ...(47)$$

where μ is the electric dipole moment of the molecule. Thus, knowing E and measuring $\Delta\nu$, μ can be determined. The Stark effect is extremely useful for determining the dipole moments of gaseous molecules.

Other Applications of Microwave Spectroscopy

The two most important applications of microwave spectroscopy are the study of internal rotation and the inversion spectrum of NH_3.

1. Internal Rotation. If a part of a molecule can rotate about a *single bond* then the internal potential energy of the molecule depends on the orientation of this part with respect to the rest of the molecule. Consider $F_3C—CH_3$ (*i.e.*, 1,1,1-trifluoroethane) molecule. The variation of the potential energy of this molecule when CF_3 group rotates about the C—C single bond, as a function of the angle θ is given by

$$V(\theta) = V_0(1 - \cos 3\theta) \quad ...(48)$$

where V_0 is the height of the potential energy barrier (Fig. 9). For low potential energy barriers, free rotation takes place. The potential energy barriers of a number of compounds have been determined using microwave spectroscopy. However, the origin of these barriers still remains obscure.

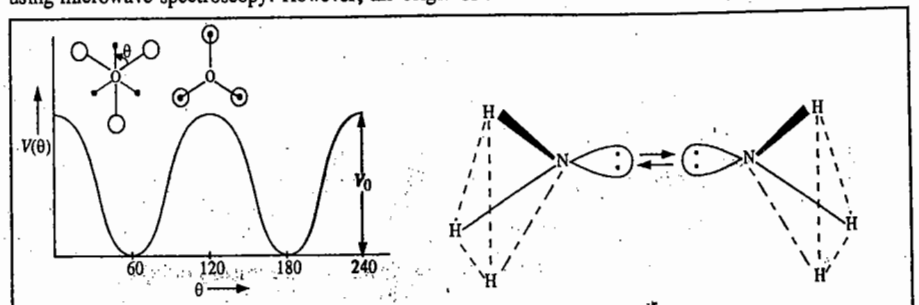

Fig. 9. Potential energy as a function of θ in internal rotation.

Fig. 10. The inversion of NH_3 molecule.

2. Inversion Spectrum of NH_3. Consider the inversion of the N atom through the plane of the three H atoms (Fig. 10).

The new configuration is the mirror image of the original configuration; it cannot be obtained by the rotation of the molecule. The two configurations have the same energy. A plot of the potential energy curve shows two minima with a hump in between (Fig. 11). The height of the hump, *i.e.*, the potential energy barrier, represents the *restriction to inversion*. Its value for NH_3 is about 25 kJ mol^{-1}.

Classically, it is impossible for the molecule to invert if it is in one of the first two vibrational levels. However, quantum mechanically it can 'tunnel' through the barrier. The inversion, in principle, is a vibrational motion. However, since it is hindered, it is observed in the microwave region. The splitting of the vibrational levels shown in Fig. 11 is a result of the *resonance interaction* between the two identical configurations. This **inversion doubling** causes the rotational lines to split.

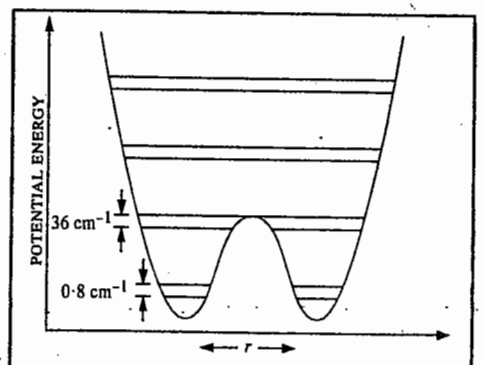

Fig. 11. A plot of the potential energy curve of NH_3 molecule.

VIBRATIONAL (INFRARED) SPECTRA OF DIATOMIC MOLECULES

A diatomic molecule with atomic masses m_1 and m_2 joined by a chemical bond vibrates as a one-dimensional simple harmonic oscillator (S.H.O.). Classically, the vibrational frequency of a mass point m connected by a spring of force constant k is given by

$$\nu = \frac{1}{2\pi}\left(\frac{k}{m}\right)^{1/2} \quad ...(49)$$

In the case of a diatomic molecule, the masses m_1 and m_2 vibrate back and forth relative to their centre of mass in opposite directions (Fig. 12).

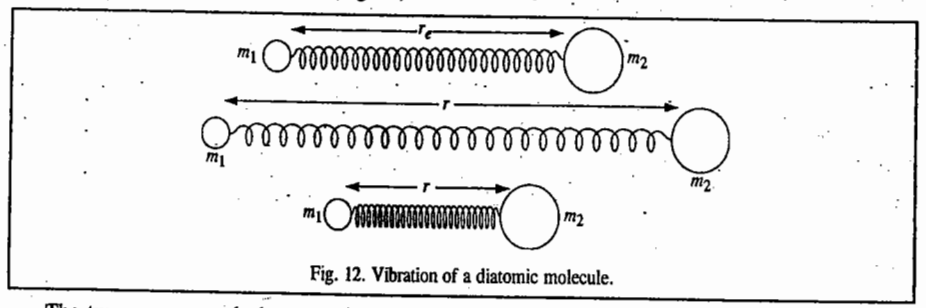

Fig. 12. Vibration of a diatomic molecule.

The two masses reach the extreme of their respective motions at the same time. The vibrational frequency of the molecule is given by a relation analogous to that of Eq. 49 with mass m replaced by the reduced mass μ :

$$\nu = \frac{1}{2\pi}\left(\frac{k}{\mu}\right)^{1/2} s^{-1} \quad ...(50)$$

To convert the frequency ν from s^{-1} (hertz) to cm^{-1}, we divide by c, the velocity of light. Thus,

$$\bar{\nu} = \frac{1}{2\pi c}\left(\frac{k}{\mu}\right)^{1/2} cm^{-1} \quad ...(51)$$

The units of the force constant are N m^{-1}. The potential energy of the simple harmonic oscillator (S.H.O.) as a function of displacement from the equilibrium configuration is given by the parabolic Hooke's law equation, *viz.*,

$$V(x) = \tfrac{1}{2}k(r - r_e)^2 = \tfrac{1}{2}kx^2 \qquad ...(52)$$

where x $(= r - r_e)$ is the displacement, r_e being the equilibrium bond length. The Hooke's law potential energy is shown in Fig. 13.

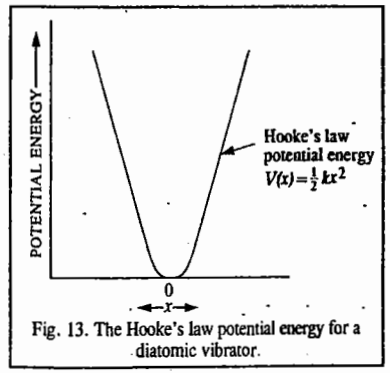

Fig. 13. The Hooke's law potential energy for a diatomic vibrator.

The solution of the Schrödinger equation for a simple harmonic oscillator gives the quantized vibrational energy levels

$$E_v = (v + \tfrac{1}{2})\,h\nu\,;\ v = 0, 1, 2, 3, \qquad .....(53)$$

where v is the **vibrational quantum number** and ν is the vibrational frequency given by Eq. 50. Notice that the energy of the lowest vibrational level of the oscillator is not zero but is equal to $\frac{1}{2}h\nu$; this is called **zero-point energy (Z.P.E.).** The energy levels of the S.H.O. are equally spaced, the spacing being equal to $h\nu$. To convert the energy from joules to cm^{-1} we divide by hc, obtaining

$$G(v) = E_v/hc = (v + \tfrac{1}{2})\,\nu/c = (v + \tfrac{1}{2})\omega_e \qquad ...(54)$$

where ω_e is the equilibrium vibrational frequency. $G(v)$ is called the **vibrational term.**

The selection rule for a vibrational transition in the simple harmonic oscillator is

$$\Delta v = \pm 1 \qquad ...(55)$$

The operative part of the selection rule for the absorption spectrum is $\Delta v = +1$, *i.e.*, the vibrational quantum number changes by unity. Using the selection rule, the frequency of the vibrational transition is given by

$$\bar{\nu} = G(v \to v+1) = (v+1+\tfrac{1}{2})\,\omega_e - (v+\tfrac{1}{2})\,\omega_e = \omega_e \qquad ...(56)$$

At room temperature, most of the molecules are in the ground vibrational state (v=0) so that the only transition of interest is that which takes place from v=0 to v=1. The vibrational frequency corresponding to this transition is called **fundamental vibrational frequency.** Diatomic molecules have only one vibrational frequency. This is a stretching vibrational frequency. Diatomic molecules do not have a bending vibrational frequency.

Vibrational spectra are observed in the infrared (IR) region. There is a very important requirement for a molecule to show an infrared spectrum. It states that the *dipole moment of the molecule must change during the vibration.* Homonuclear diatomic molecules such H_2, O_2, N_2, etc., do not have a permanent dipole moment nor does the stretching of the bond between the two atoms change the dipole moment from zero. Hence, homonuclear diatomics do not show IR spectra. On the other hand, heteronuclear diatomic molecules such as CO, NO, CN, HCl, do possess a dipole moment which changes when the bond length changes. Hence they show IR spectra. Thus, *homonuclear diatomics are IR-inactive while heteronuclear diatomics are IR-active.*

In practice, the molecule does not always vibrate as a simple harmonic oscillator ; there is present what is called **anharmonicity.** In 1929, P.M. Morse suggested an empirical expression for the potential energy of an anharmonic diatomic oscillator, given by

$$V(r) = D_e\,[1 - \exp(-a\{r - r_e\})]^2 \qquad ...(57)$$

Here a is a constant and D_e is the dissociation energy of the molecule. The **Morse potential energy** is sketched in Fig. 14.

It may be pointed out that the dissociation energy D_e in the Morse potential energy curve is measured from the bottom of the potential well. The experimentally measured dissociation energy D_0 is the one that is measured from the ground level (v = 0) to the top. Thus,

$$D_e = D_0 + h\nu/2 \qquad ...(58)$$

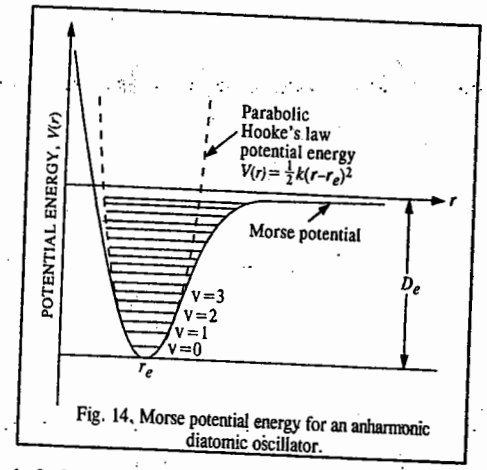

Fig. 14. Morse potential energy for an anharmonic diatomic oscillator.

When the Schrödinger equation for an *anharmonic oscillator* is solved using the Morse potential energy, the energy levels are given by

$$G(v) = (v + \tfrac{1}{2})\,\omega_e - (v + \tfrac{1}{2})^2\,\omega_e x_e\ ;\ (v = 0, 1, 2, 3,...) \qquad ...(59)$$

where $\omega_e x_e$ is called the **anharmonicity constant.** As expected, $\omega_e x_e \ll \omega_e$. The consequence of anharmonicity is that the vibrational energy levels of the S.H.O. are all slightly lowered and the spacing between them is no longer constant but goes on steadily decreasing with increase in vibrational quantum number. Also, because of anharmonicity, the rule for vibrational transitions is no longer $\Delta v = \pm 1$. Instead, transitions corresponding to $\Delta v = \pm 2, \pm 3$, etc., are also observed in the IR spectra. These are called the first overtone, the second overtone, etc., respectively. The *intensity of an overtone is dependent on the anharmonicity of the vibration.* Compared with the highly intense fundamental vibrational frequency, the overtones are very weak, *i.e.*, of considerably low intensity.

Example 6. The fundamental vibrational frequency of HCl is 2,890 cm^{-1}. Calculate the force constant of this molecule. The atomic masses are $^1H = 1{\cdot}673\times10^{-27}$ kg ; $^{35}Cl = 58{\cdot}06\times10^{-27}$ kg.

Solution. The reduced mass of HCl is given by

$$\mu = \frac{m_1 m_2}{m_1 + m_2} = \frac{(1{\cdot}673\times10^{-27}\,\text{kg})(58{\cdot}06\times10^{-27}\,\text{kg})}{(1{\cdot}673+58{\cdot}06)\times10^{-27}\,\text{kg}} = 1{\cdot}626\times10^{-27}\ \text{kg}$$

Since from Eq. 51, $\bar{\nu} = \dfrac{1}{2\pi c}\left(\dfrac{k}{\mu}\right)^{1/2}$ cm^{-1},

$$\therefore\quad k = 4\pi^2 c^2\,(\bar{\nu})^2\,\mu = 4\pi^2\,(3\times10^{10}\ \text{cm})^2\,(2890\ \text{cm}^{-1})^2\,(1{\cdot}626\times10^{-27}\ \text{kg})$$
$$= 4{\cdot}83\times10^2\ \text{kg s}^{-2} = 4{\cdot}83\times10^2\ \text{kg m s}^{-2}\times\text{m}^{-1} = 483\ \text{N m}^{-1}$$

Example 7. The force constant of CO is 1840 N m^{-1}. Calculate the vibrational frequency in cm^{-1} and the spacing between the vibrational energy levels in eV. Compare this spacing with the thermal energy at room temperature and comment on your result. The atomic masses are $^{12}C = 19{\cdot}9\times10^{-27}$ kg ; $^{16}O = 26{\cdot}6\times10^{-27}$ kg; 1 eV = 8066 cm^{-1}

Solution. The reduced mass of CO is given by

$$\mu = \frac{m_1 m_2}{m_1 + m_2} = \frac{(19{\cdot}9\times10^{-27}\,\text{kg})\times(26{\cdot}6\times10^{-27}\,\text{kg})}{(19{\cdot}9+26{\cdot}6)\times10^{-27}\,\text{kg}} = 11{\cdot}4\times10^{-27}\ \text{kg}$$

$$\bar{\nu} = \frac{1}{2\pi c}\left(\frac{k}{\mu}\right)^{1/2} = \frac{1}{2(3{\cdot}1416)(3\times10^{10}\,\text{cm s}^{-1})}\left(\frac{1840\ \text{kg s}^{-2}}{11{\cdot}4\times10^{-27}\,\text{kg}}\right) = 2140\ \text{cm}^{-1}$$

The spacing between energy levels $= \Delta E = E_{v+1} - E_v = h\nu$ joules $= h\nu/hc = \nu/c = \bar{\nu} = 2140\ \text{cm}^{-1}$

Since $1\ eV = 8066\ cm^{-1}$

$$\therefore \quad \Delta E = \frac{2140\ cm^{-1}}{8066\ cm^{-1}/eV} = 0{\cdot}265\ eV$$

$$\text{Thermal energy} = kT = \frac{(1{\cdot}38\times10^{-23}\ JK^{-1})(300\ K)}{1{\cdot}602\times10^{-19}\ J/eV} = 2{\cdot}6\times10^{-2}\ eV = 0{\cdot}026\ eV$$

We see that $kT < \Delta E$. Hence, we conclude that most of the molecules are in the ground vibrational state at room temperature. This situation is in contrast with the rotational states where $kT > \Delta E$ and consequently most of the molecules are in the excited rotational states at room temperature.

The force constant for a diatomic molecule can be calculated with the help of Eq. 51. Table 3 gives the calculated force constants for some diatomic molecules which contain triple bonds (N≡N), double bonds (O=O), single bonds (H—Cl) and ionic bonds (Na^+Cl^-).

TABLE 3

Observed Vibrational Frequencies and Calculated Force Constants for Some Diatomic Molecules

Molecules	$\bar{\nu}$ (cm^{-1})	Reduced mass μ (kg)	k ($N\ m^{-1}$)
N_2	2331	$1{\cdot}1625\times10^{-26}$	2240
CO	2141	1·1384	1860
NO	1776	1·2397	1550
O_2	1556	1·3279	1140
HF	3958	0·15658	870
H_2	4159	0·08367	510
HCl	2886	0·16272	480
F_2	892	1·5773	450
I_2	213	10·536	170
NaCl	378	2·3162	120

Example 8. For the molecule BH, $\omega_e = 2368\ cm^{-1}$ and the anharmonicity constant $\omega_e x_e = 49\ cm^{-1}$. Calculate the vibrational terms of the first four vibrational levels and determine the spacing between them.

Solution. From Eq. 59,

$$G(v) = (v + \tfrac{1}{2})\,\omega_e - (v + \tfrac{1}{2})^2\,\omega_e x_e$$

$$G(0) = (0 + \tfrac{1}{2})\times2368 - (0 + \tfrac{1}{2})^2\times49 = 1184 - 12 = 1172\ cm^{-1}$$

$$G(1) = (1 + \tfrac{1}{2})\times2368 - (1 + \tfrac{1}{2})^2\times49 = 3552 - 110 = 3442\ cm^{-1}$$

$$G(2) = (2 + \tfrac{1}{2})\times2368 - (2 + \tfrac{1}{2})\times49 = 5920 - 306 = 5614\ cm^{-1}$$

$$G(3) = (3 + \tfrac{1}{2})\times2368 - (3 + \tfrac{1}{2})\times49 = 8288 - 600 = 7688\ cm^{-1}$$

The spacings between the energy levels are :

$$G(1) - G(0) = 3442 - 1172 = 2270\ cm^{-1}$$

$$G(2) - G(1) = 5614 - 3442 = 2172\ cm^{-1}$$

$$G(3) - G(2) = 7688 - 5616 = 2074\ cm^{-1}$$

Notice that the energy levels are not equally spaced and the spacing goes on steadily decreasing with increase in the vibrational quantum number.

Example 9. The force constant of H_2 is 510 N m^{-1} and its dissociation energy is 4·5 eV. Assuming that it vibrates as a simple harmonic oscillator, calculate the vibrational quantum number corresponding to its dissociation energy.

Solution. From the given value of the force constant, the frequency of vibration can be easily calculated ; it is found to be 4159 cm^{-1}. Since vibrational levels of an S.H.O. are equally spaced, the dissociation energy of 4·5 eV (*i.e.*, $4{\cdot}5\times8066\ cm^{-1} = 36{,}297\ cm^{-1}$) corresponds to

$$\frac{36297\ cm^{-1}}{4159\ cm^{-1}} = 8{\cdot}7 = 9\text{th energy level}$$

Hence, the vibrational quantum number corresponding to the given dissociation energy is **8.**

ROTATION–VIBRATION (IR) SPECTRA OF DIATOMIC MOLECULES

Pure vibrational spectra can be observed only in liquids where interactions between molecules inhibit rotation. Since rotational energies are considerably smaller than vibrational energies, the freely moving molecules in the gaseous state are almost always rotating regardless of their vibrational state. Hence, molecules in gaseous state show rotation–vibration spectra. The rotation and vibration are, to a first approximation, independent of each other. Ignoring the effect of centrifugal distortion and taking into account the anharmonicity, the **rotation-vibration term,** S (v, J), for vibrating rotator is given by

$$S(v, J) = F(J) + G(v) \qquad \ldots(60)$$

$$= BJ(J+1) + (v + \tfrac{1}{2})\,\omega_e - (v + \tfrac{1}{2})^2\,\omega_e x_e\ cm^{-1} \qquad \ldots(61)$$

where we have used Eq. 31 for $F(J)$ and Eq. 59 for G(v).

The selection rules for combined vibrational and rotational transitions are

$$\Delta v = \pm1 \text{ and } \Delta J = \pm1 \qquad \ldots(62)$$

It is customary to designate the lower energy state by double prime and the upper energy state by a single prime. Using the energy level expression (61) and the selection rule (62), we have

$$\Delta S(v, J) = [B'J'(J'+1) + \tfrac{3}{2}\,\omega_e - \tfrac{9}{4}\,\omega_e x_e] - [B''J''(J''+1) + \tfrac{1}{2}\,\omega_e - \tfrac{1}{4}\,\omega_e x_e]$$

$$= \omega_0 + B(J' - J'')(J' + J'' + 1)\ cm^{-1}$$

where $\omega_0 = \omega_e(1 - 2x_e)$. $\qquad \ldots(63)$

Here we have assumed that the rotational constant B is the same in the upper and lower vibrational states, an assumption that is justified by the fact that rotation and vibration are, to a first approximation, independent. Since most of the molecules are in the ground vibrational state at room temperature, only the v = 0 to v = 1 transition is of interest.

(i) For the $\Delta J = +1$ transition, $J' = J''+1$, *i.e.*, $J' - J'' = +1$ so that

$$\Delta S(v, J) = \omega_0 + 2B(J''+1)\ cm^{-1};\ J'' = 0, 1, 2, 3,\ldots \qquad \ldots(64)$$

(ii) For the $\Delta J = -1$ transition, $J'' = J'+1$, *i.e.*, $J' - J'' = -1$ so that

$$\Delta S(v, J) = \omega_0 + 2B(J'+1)\ cm^{-1};\ J' = 0, 1, 2, 3,\ldots \qquad \ldots(65)$$

Combining the expressions 64 and 65,

$$\Delta S(v, J) = \bar{\nu}_{spec} = \omega_0 + 2Bm\ cm^{-1};\ m = \pm1, \pm2, \pm3,\ldots \qquad \ldots(66)$$

Notice that $m = J''+1$ in Eq. 64 and $= J'+1$ in Eq. 65 ; it is positive for $\Delta J = +1$ and negative for $\Delta J = -1$. The frequency ω_0, called the **band centre,** does not appear in the rotation–vibration spectrum which consists of equally spaced lines with spacing equal to $2B$ on each side of the band centre (Fig. 15).

The lines corresponding to $\Delta J = -1$ are called the **P branch** while those corresponding to $\Delta J = +1$ are called the **R branch.**

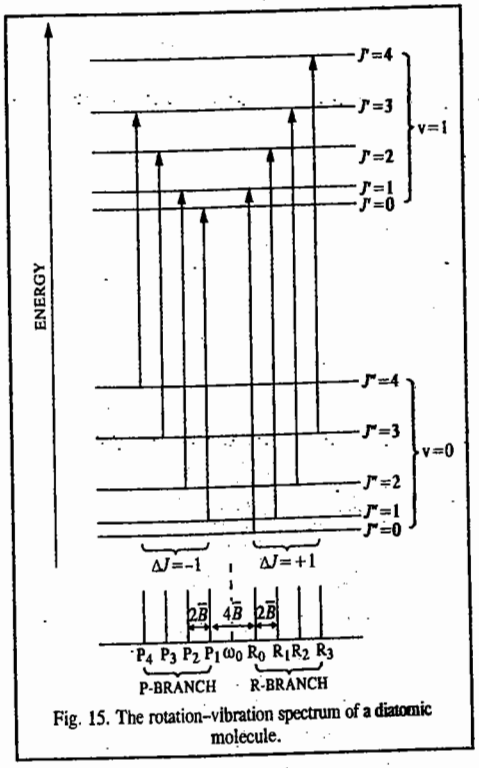

Fig. 15. The rotation–vibration spectrum of a diatomic molecule.

VIBRATIONAL SPECTRA OF POLYATOMIC MOLECULES

In order to study the vibrational spectra of polyatomic molecules, we have to investigate the vibrations of polyatomic molecules for which we start with the classical model of a molecule where the atoms (or nuclei) are represented by mathematical mass points. Each point requires three coordinates (such as x, y, z in a Cartesian coordinate system) to define its position. This is expressed by saying that there are *three* independent *degrees of freedom* in the x, y and z directions. For a molecule containing N atomic nuclei, there will be $3N$ degrees of freedom for all the nuclear masses in the molecule.

We need three coordinates to specify the centre of gravity of the molecule. Thus, the centre of gravity of the molecule has *three* independent *translational* degrees of freedom. For a non-linear molecule in its equilibrium configuration, three rotational coordinates are needed to specify the molecular orientation about the centre of gravity. These can be the three angular coordinates specifying rotation about three mutually perpendicular axes, each passing through the centre of gravity. Thus, a non-linear molecule has *three* independent *rotational* degrees of freedom. On the other hand, a linear molecule has only *two* independent *rotational* degrees of freedom about the two mutually perpendicular axes which are perpendicular to the molecular axis.

If we subtract the translational and rotational degrees of freedom from the total $3N$ degrees of freedom, we find that we are left with $3N - 6$ *internal* degrees of freedom for a non-linear molecule and $3N - 5$ *internal* degrees of freedom for a linear molecule. The $3N - 6$ internal degrees of freedom of motion of a non-linear molecule correspond to its $3N - 6$ independent *normal modes of vibration.* Similarly, the $3N - 5$ internal degrees of freedom of motion of a linear molecule correspond to its $3N - 5$ independent normal modes of vibration (or simply, normal vibrations). A **normal mode of vibration** is *defined as a molecular motion in which all the atoms in the molecule vibrate with same frequency and all the atoms pass through their equilibrium positions simultaneously.* The relative vibrational amplitudes of individual atoms may be different in magnitude and direction but the centre of gravity of the molecule does not change.

As has been stated earlier, in order for a molecule to be IR-active, *i.e.*, to show vibrational spectrum, it must either possess a permanent dipole moment μ or the dipole moment must change during a vibration, *i.e.*,

$$d\mu/dr \neq 0 \qquad ...(67)$$

The three normal modes of vibration (*i.e.*, fundamental vibrational frequencies) of H_2O molecule are shown in Fig. 16. They are all IR-active since each of them is accompanied by a change in dipole moment. The displacement vectors attached to the various nuclei in the molecule show the direction and relative amplitude of vibration of each nucleus. The symmetric stretching frequency is labelled as $\bar{\nu}_1$;

the symmetric bending frequency as $\bar{\nu}_2$ and the antisymmetric (asymmetric) stretching frequency as $\bar{\nu}_3$. The values of the three frequencies for water are $\bar{\nu}_1 = 3651{\cdot}7\ cm^{-1}$; $\bar{\nu}_2 = 1595{\cdot}0\ cm^{-1}$ and $\bar{\nu}_3 = 3755{\cdot}8\ cm^{-1}$. It is easier to bend a molecule than to stretch it. Hence, the bending frequency is generally lower than the stretching frequency. Also, it is easier to stretch a molecule symmetrically than to stretch it asymmetrically. Hence, the symmetric stretching frequency is lower than the asymmetric stretching frequency.

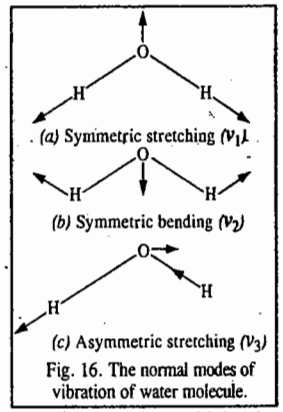

Fig. 16. The normal modes of vibration of water molecule.

The determination of the exact form of normal vibrations of a polyatomic molecule requires the solution of a system of simultaneous mathematical equations of motion (known as the **Lagrangian equations of motion**), involving the atomic masses, the bond force constants and parameters of molecular geometry. This mathematical analysis of molecular vibrations, called the **Normal Coordinate Analysis**, was carried out in 1935 by E.B. Wilson Jr., of Harvard University in the U.S.A. The best reference on the subject is E.B. Wilson, Jr., J.C. Decius, and P.C. Cross, *Molecular Vibrations*, McGraw Hill, 1955.

The linear CO_2 molecule has $3\times3 - 5 = 4$ fundamental vibrational frequencies while the linear acetylene molecule has $3\times4-5 = 7$ fundamental vibrational frequencies. These are shown in Fig. 17 and Fig.18, respectively. Of the four fundamental vibrations of CO_2 molecule two have the same frequency and are said to be *degenerate.* The symmetric stretching frequency $\bar{\nu}_1$ is not observed in the IR spectrum of CO_2 since it is not accompanied by a change in the dipole moment of the molecule with vibration.

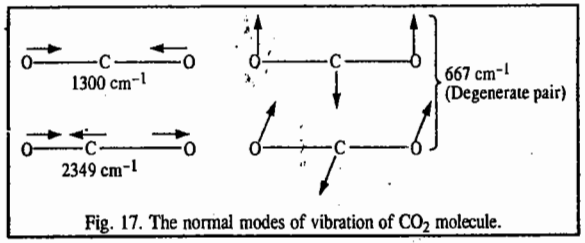

Fig. 17. The normal modes of vibration of CO_2 molecule.

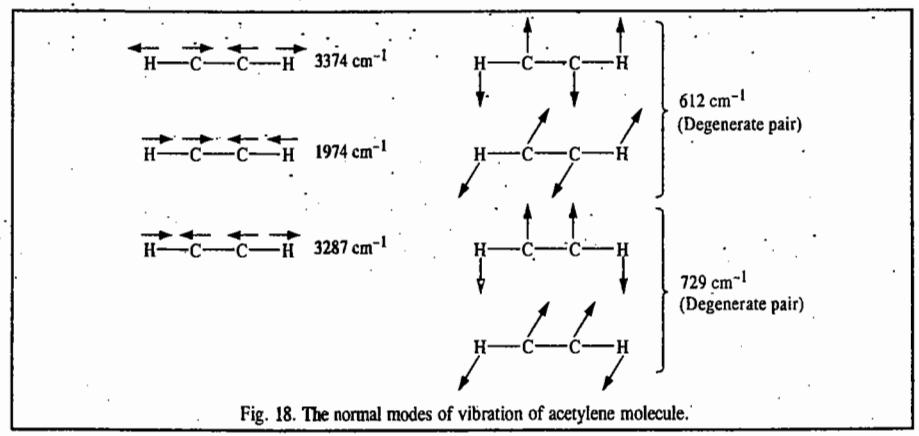

Fig. 18. The normal modes of vibration of acetylene molecule.

For acetylene, there are two degenerate pairs of frequencies at 612 cm^{-1} and 729 cm^{-1} (Fig.18). The former is not observed in IR region since it does not involve a change in dipole moment with vibration. The symmetric stretching frequencies (3374 cm^{-1} and 1974 cm^{-1}) are also IR-inactive for the same reason.

In general, a **normal mode of vibration** is an independent, synchronous motion of atoms or groups of atoms that may be excited without leading to the excitation of any other normal mode and without involving transtation or rotation of the molecule as a whole. The N_{vib} normal modes of polyatomics in general, are the key to the description of molecular vibrations. Each normal mode, q, behaves like an independent, harmonic oscillator (if anharmonicities are neglected), so each has a series of vibrational terms

$$G_q(v) = \left(v + \frac{1}{2}\right)\bar{\nu}_q, \quad \bar{\nu}_q = \frac{1}{2\pi c}\left(\frac{k_q}{m_q}\right)^{1/2}$$

where $\bar{\nu}_q$ is the wave number of the q mode and depends on the force constant k_q for the mode and on the effective mass m_q of the mode. The effective mass of the mode is a measure of the mass that is swung about by the vibration and in general is a complicated function of the masses of the atoms. For example, in the symmetric stretch of CO_2, the C atom is stationary and the effective mass depends on the masses of only O atoms. In the antisymmetric stretch and in the bends, all the three atoms move ; so all contribute to the effective mass. For the three normal modes of H_2O (Fig. 16) the predominantly bending mode (ν_2) has lower frequency than the others, which are predominantly stretching modes. It is generally the case that the frequencies of the bending motions are lower than those of the stretching modes. One point that must be appreciated is that only in special cases (such as the CO_2 molecule) are the normal modes purely stratches or purely bends. In general, a normal mode is a composite motion of simultaneous stretching and bending of bonds. Another point to note is that heavy atoms generally move less than light atoms in normal modes.

Since the nuclei in a polyatomic molecule do not always vibrate in a simple harmonic manner, there arises **anharmonicity** in molecular vibrations. The harmonic vibrations give rise to $3N-5$ (or $3N-6$) fundamental vibrational frequencies as stated above. On the other hand, the anharmonic vibrations give rise to the so called **overtones** and **combination bands.** The overtones occur as multiples of a given fundamental frequency. Thus, for H_2O molecule which has three fundamental vibrational frequencies $\bar{\nu}_1$, $\bar{\nu}_2$ and $\bar{\nu}_3$, the overtones would occur at (or near) $2\bar{\nu}_1, 3\bar{\nu}_1, \ldots, 2\bar{\nu}_2, 3\bar{\nu}_2 \ldots, 2\bar{\nu}_3, 3\bar{\nu}_3, \ldots$, etc. The first overtone of $\bar{\nu}_1$ is designated as $2\bar{\nu}_1$, the second as $3\bar{\nu}_1$, the third as $4\bar{\nu}_1$ and so on. The **combination bands** are merely the sum of two or more fundamental frequencies or overtones while the **difference bands** are the differences of two or more fundamental frequencies or overtones. Thus, combination bands are $\bar{\nu}_1 + \bar{\nu}_2$, $2\bar{\nu}_1 + \bar{\nu}_2$, $\bar{\nu}_1 + \bar{\nu}_2 + \bar{\nu}_3$, etc., while the difference bands are $\bar{\nu}_1 - \bar{\nu}_2$, $2\bar{\nu}_1 - \bar{\nu}_2$, $\bar{\nu}_1 - \bar{\nu}_2 + \bar{\nu}_3$, $\bar{\nu}_1 + \bar{\nu}_2 - \bar{\nu}_3$, etc. The overtones and combination bands have low intensity.

The complete IR spectrum of a polyatomic molecule, therefore, consists of the highly intense fundamental vibrational frequencies and the less intense overtones, combination bands and difference bands. *The overtones, combination bands and difference bands arise as a result of the violation of the selection rule for harmonic vibrations.* The analysis of the IR spectrum of water vapour is given in Table 4.

TABLE 4

IR Spectrum of H_2O Vapour

$\bar{\nu}$ (cm^{-1})	Intensity	Assignment
1595·0	Very strong	$\bar{\nu}_2$
3151·4	Medium	$2\bar{\nu}_2$
3651·6	Strong	$\bar{\nu}_1$
3755·8	Very Strong	$\bar{\nu}_3$
5332·0	Medium	$\bar{\nu}_2 + \bar{\nu}_3$
6874·0	Weak	$2\bar{\nu}_2 + \bar{\nu}_3$

Sometimes it may happen that a fundamental mode of vibration becomes *accidentally degenerate* with an overtone or a combination band. As a result, the intensity of the overtone or the combination band which is otherwise very low is enhanced by a resonance

phenomenon, known as **Fermi resonance,** after E. Fermi who first observed it. The classic example of Fermi resonance is furnished by CO_2 molecule where $\bar{\nu}_1 = 1330\ cm^{-1}$ and $2\bar{\nu}_2 = 1334\ cm^{-1}$. Quantum mechanically it can be shown that, as a result of Fermi resonance, the higher frequency is raised whereas the lower frequency is depressed. The two bands of CO_2 mentioned above are not observed in IR but they are observed in the Raman spectrum at 1285 cm^{-1} and 1385 cm^{-1}, respectively. Their mean is near 1330 cm^{-1}.

In fact, the consequence of anharmonic interactions is that the energy levels change as a result of their mixing under the perturbative anharmonic potential energy. Also, the transitions take on different intensities because wavefunctions mix and so acquire characteristics of one another. This is most striking in the case of an allowed fundamental vibration and a forbidden combination, for the latter may acquire intensity by virtue of the component of the allowed fundamental that the anharmonicity mixes into it. Fermi resonance represents the type of mode mixing in which the interaction is between a fundamental and a combination band or overtone. In fact, Fermi resonance can be viewed as the vibrational analogue of configuration interaction in molecular quantum mechanics.

We shall now consider an entirely different kind of force, known as the **Coriolis force** (which was studied by the 19th century French physicist G.G. Coriolis and has important implications for the movements of the oceans and the atmopshere resulting from earth's rotation). This force brings about a different kind of interaction between vibrational and rotational modes of a molecule. Let us consider how the Coriolis force affects a rotating molecule when its antisymmetrical vibrational mode has been excited (Fig. 19). When one of the bonds stretches, it experiences a retarding Corioils force; at the same time, the bond that is shortening experiences an accelerating Coriolis force. As a result, the molecule tends to bend. As the bonds next contract and lengthen, respectively, the Coriolis force acts in the opposite way, and the molecule is forced to bend in the opposite direction. This effect of the rotation on the antisymmetric stretch, therefore, is to induce one of the bending modes. This is expressed quantum mechanically by saying that rotation provides a perturbation that mixes the antisymmetric stretch with one of the components of the doubly degenerate pair of bending modes. As a result, the two levels move apart in energy, and the bending mode in the plane of rotation is no longer degenerate with the bending mode perpendicular to the plane. Transitions to these two levels no longer fall at the same energy and so the lines are doubled by the rotation. This effect is called *l*-**type doubling.**

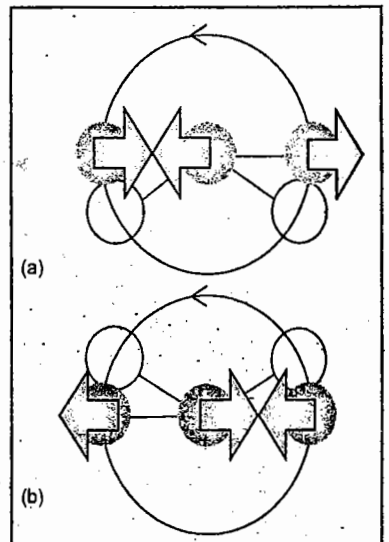

Fig. 19. Normal mode coupling in a rotating molecule : (*a*) and (*b*) show different stages of the antisymmetric stretch.

We may mention parenthetically that in the case of pyramidal molecules AB_3 (belonging to the C_{3v} point group), when the potential energy barrier is high, the inversion of the pyramid is difficult but when the barrier is low, the inversion is easy and the molecule (NH_3, for instance) can invert and take on the character of H_3N. In this case, the mixing of the wavefunctions on the left and right side of the barrier, $\psi_L \pm \psi_R$, leads to the phenomenon called **inversion doubling** of the energy levels. Details can be found in advanced books on quantum mechanics.

ROTATION-VIBRATION (*IR*) SPECTRA OF POLYATOMIC MOLECULES

1. Linear Molecules. Linear molecules such as CO_2 and HCN, whether they possess permanent electric dipole moment or not, are IR-active if some of their vibrations produce an oscillating dipole moment. Consider CO_2 molecule. It has two types of IR-active vibrations :

(i) The oscillating dipole is parallel to the molecular axis :

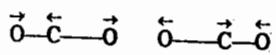

Such a vibration produces the so-called **parallel band.** The selection rules are $\Delta v = \pm 1$ and $\Delta J = \pm 1$.

(ii) The oscillating dipole is perpendicular to the molecular axis :

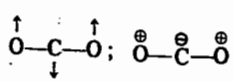

(Here $\ominus$ indicates vibration of C atom perpendicular to the plane of the paper downwards and $\oplus$ indicates vibration of O atom perpendicular to the plane of the paper upwards). Such a vibration gives rise to a **perpendicular band.** The selection rules are $\Delta v = \pm 1$ and $\Delta J = 0, \pm 1$.

2. Symmetric Top Molecules (Symmetric Rotors). Ignoring anharmonicity and centrifugal distortion, the energy levels of a symmetric top molecule such as CH_3Cl are given by

$$E_{J,K} = \left(v + \frac{1}{2}\right)\omega_e + B_v J(J+1) + (A - B)K^2$$

where A and B are defined in Eq. 44 and the values of K are given in Eq. 45. The selection rules are :

Parallel band : $\Delta J = 0, \pm 1, \Delta K = 0$

Perpendicular band : $\Delta J = 0, \pm 1, \Delta K = \pm 1$

3. Asymmetric Top Molecules (Asymmetric Rotors). Since the solution of the Schrödinger wave equation for the asymmetric top molecules is very difficult, we shall not deal with that here.

Vibrational Frequencies of Different Functional Groups

In general, the bond lengths and bond angles for given moieties of various compounds remain approximately constant. However, small changes occur in these parameters due to other species present in the molecule. These changes give rise to characteristic ranges of vibrational wave numbers and intensities for functional groups in molecules. Assignment of these wave numbers in an infrared spectrum often provides a rapid method for the identification of a compound. Some normal modes of vibration of organic molecules can be regarded as motions of individual functional groups ; others are regarded as the collective motions of the molecule as a whole. The latter are generally of low frequency and occur below about 1500 cm^{-1} in the spectrum. The resulting whole-molecule region of the absorption spectrum is called a **fingerprint region** of the spectrum since it is characteristic of the molecule. The matching of the fingerprint region with the spectrum of a known compound in a library of infrared spectra is a very powerful way of confirming the presence of a particular substance.

From studies over a range of compounds, charts have been developed that give the vibrational wave number ranges for most functional groups in different compounds. These wave numbers that occur outside the fingerprint region are very useful for the identification of an unknown compound. Table 5 lists some of

the assignments for a selection of the commoner functional groups encountered in organic chemistry. Lower frequency bending modes usually occur in the fingerprint region and so are less easily identified. The IR of a molecule can be regarded as made of several regions :

TABLE 5
Typical Vibrational Wave Numbers for Functional Groups

Group	Mode	Range (cm^{-1})	Intensity
>CH_2 $-CH_3$ >C–H	C–H(s)	3000–2850	*s*
>CH_2		2900–2880	*w*
$-CH_3$	C–H(b)	1470–1430	*m*
$-CH_3$	CH_3(sb)	1390–1370	*m*
>CH_2	CH_2(r)	700–750	*w*
$-C\equiv C-H$	CH(s)	3300	*s*
R, H, C=C, H, R	CH(s)	960–980	*s*
>C=C<	C=C(s)	1680–1620	*s*
–O–H	O–H(b)	1410–1260	*s*
–O–H	O–H(s)	3650–3590	*s*
>C–OH	C–OH(s)	1150–1050	*s*
>N–H =N–H	N–H(ss/as)	3500–3300	*m*
>C=O	C=O(s)	1780–1680	*vs*
Hydrogen bonds	O–H(s)	3570–3200	*s*

Key : s, stretch ; b, bend ; sb, symmetric bend ; r, rock ; ss, symmetric stretch ; as, asymmetric stretch ; *vs*, very strong; *s*, strong ; *m*, medium ; *w*, weak.

1. *Hydrogen stretching vibrations,* 3700–2500 cm^{-1}. These vibrations occur at higher wave numbers because of the low mass of the hydrogen atom. If H atom is replaced by D atom (*i.e.,* deuterium atom), the vibrational wave number falls by a factor of $1/\sqrt{2}$ because of the greater reduced mass of the deuterium molecule. If an –OH group is not involved in hydrogen bonding, it usually has a vibrational wave number in the vicinity of 3700–3600 cm^{-1}. Hydrogen bonding causes this wave number to drop by 300–1000 cm^{-1} or more.

2. *Triple-bond region,* 2500–2000 cm^{-1}. These bonds have high vibrational wave numbers because of the large force constants. The C ≡ C group usually causes absorption between 2300 and 2050 cm^{-1} but this absorption may be weak or absent because of the symmetry of the molecule. The C ≡ N group absorbs near 2300–2200 cm^{-1}.

3. *Double-bond region,* 2000–1600 cm^{-1}. Absorption bands of substituted aromatic compounds fall in this range and are a good indicator of the position of the substitution. Carbonyl groups of ketones, aldehydes, acids, amides and esters usually show strong absorption in the vicinity of 1700 cm^{-1}. Alkenes may show absorption in the vicinity of 1650 cm^{-1}.

4. *Single-bond stretch and bend region,* 500–1700 cm^{-1}. This region is not diagnostic for particular functional groups but it is a useful fingerprint region since it shows differences between similar molecules.

RAMAN SPECTROSCOPY

Quantum Theory of Raman Scattering. In contrast with other branches of spectroscopy, Raman spectroscopy deals with the *scattering of light* and not with its absorption. Consider a photon of frequency ν falling on a molecule. If the collision is *elastic*, then the scattered photon will have the same energy as the incident photon. If, however, the collision is *inelastic*, the scattered photon will have either a higher or a lower energy than the incident photon. If we further assume that the total kinetic energy of the photon and the molecule remains unchanged before and after the collision, then, from the law of conservation of energy,

$$h\nu + E = h\nu' + E' \qquad ...(68)$$

where $h\nu$ is the energy of the incident photon and $h\nu'$ is the energy of the scattered photon after collision; E is the energy of the molecule (rotational, vibrational and electronic) before collision and E' is the molecular energy after collision. Rearranging Eq. 68, we obtain

$$(E' - E)/h = \nu - \nu' \qquad ...(69)$$

Consider now the following cases ;

Case I : $\nu = \nu'$ so that $E = E'$

Case II*(a)* : $\nu < \nu'$ so that $E > E'$

Case II*(b)* : $\nu > \nu'$ so that $E < E'$

Case I is referred to as *Rayleigh scattering* and cases II*(a)* and II*(b)* as *Raman scattering*. Thus, in the Rayleigh scattering, the scattered photon has the same frequency (or energy) as the incident photon while in the Raman scattering, when the photon collides with the molecule, the energy is either transferred to, or taken away from, the molecule. The Rayleigh scattering and the Raman scattering are shown schematically in Fig. 20.

The Raman scattering had been predicted by the German physicist A. Smekel in 1923. It was observed by C.V. Raman and K.S. Krishnan in 1928. The Indian physicist C.V. Raman (1888 - 1970) won the Nobel Prize for Physics in 1930 for his work on the scattering of light and for the discovery of Raman effect.

When the molecule, excited to the higher unstable vibrational state, returns to the original vibrational state, we get Rayleigh scattering. If it returns to a different vibrational state, this gives rise to Raman scattering (Stokes lines). When the molecule, initially in the *first excited vibrational state*, is promoted to a higher unstable vibrational state and returns to the *ground state*, this again gives rise to Raman scattering (anti-Stokes lines). Thus, *the Raman spectrum of a molecule consists of Stokes lines and anti-Stokes lines, situated symmetrically about the Rayleigh line.*

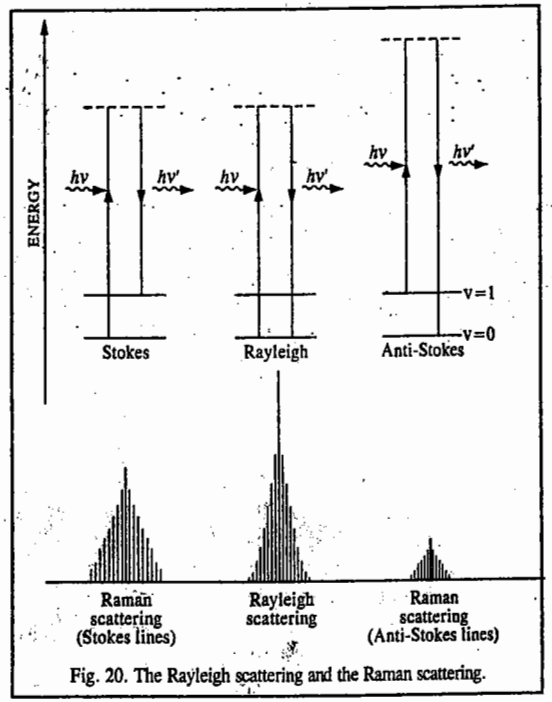

Fig. 20. The Rayleigh scattering and the Raman scattering.

The Rayleigh line is far more intense than the Stokes lines which, in turn, have greater intensity than the anti-Stokes lines. The anti-Stokes lines are very difficult to observe in the conventional Raman spectroscopy because they correspond to the return of a molecule from the unstable excited vibrational state to the ground state and initially there are very few molecules in the excited vibrational state. We can write Eq. 68 as

$$E' - E = h(\nu - \nu') = h\Delta\nu_{\text{Raman}} = hc\Delta\bar{\nu}_{\text{Raman}} \qquad ...(70)$$

The shifts in frequency $(\nu - \nu')$ are called **Raman shifts.** The Raman shifts fall in the range 100–4,000 cm^{-1} for vibrational energy changes. Their values are smaller for rotational energy changes. Since $\bar{\nu} = 1/\lambda$, we have

$$\bar{\nu}\ (\text{in cm}^{-1}) = \frac{10^8}{\lambda(\text{in Å})}$$

Hence, Raman shift (in cm^{-1}) is given by

$$\Delta\bar{\nu}_{\text{Raman}}\ (\text{in cm}^{-1}) = \frac{10^8}{\lambda_{\text{exc}}(\text{in Å})} - \frac{10^8}{\lambda_{\text{Raman}}(\text{in Å})} \qquad ...(71)$$

where λ_{exc} is the wave length corresponding to the exciting (incident) frequency.

Classical Theory of Raman Scattering. The classical theory of Raman effect, also called the polarizability theory, was developed by G. Placzek in 1934. We will discuss it briefly here. It is known from electrostatics that the electric field E associated with the electromagnetic radiation induces a dipole moment μ in the molecule, given by

$$\mu = \alpha E \qquad ...(72)$$

where α is the polarizability of the molecule. The electric field vector E itself is given by

$$E = E_0 \sin 2\pi\nu t \qquad ...(73)$$

where E_0 is the amplitude of the vibrating electric field vector and ν is the frequency of the incident light radiation. Thus, from Eqs. 72 and 73,

$$\mu = \alpha E_0 \sin 2\pi\nu t \qquad ...(74)$$

Such an oscillating dipole emits radiation of its own oscillation with a frequency ν, giving the Rayleigh scattered beam, If, however, the polarizability varies slightly with molecular vibration, we can write

$$\alpha = \alpha_0 + (\partial\alpha/\partial q)\, q \qquad ...(75)$$

where the coordinate q describes the molecular vibration. We can also write q as

$$q = q_0 \sin 2\pi\nu_m t \qquad ...(76)$$

where q_0 is the amplitude of the molecular vibration and ν_m is its frequency. From Eqs. 75 and 76, we have

$$\alpha = \alpha_0 + (\partial\alpha/\partial q)\, q_0 \sin 2\pi\nu_m t \qquad ...(77)$$

Substituting for α in Eq. 74, we have

$$\mu = \alpha_0 E_0 \sin 2\pi\nu t + (\partial\alpha/\partial q)\, q_0 E_0 \sin 2\pi\nu t \sin 2\pi\nu_m t \qquad ...(78)$$

Making use of the trigonometric relation $\sin x \sin y = \frac{1}{2}[\cos(x-y) - \cos(x+y)]$, this equation reduces to

$$\mu = \alpha_0 E_0 \sin 2\pi\nu t + \tfrac{1}{2}(\partial\alpha/\partial q)\, q_0 E_0 \cos 2\pi(\nu - \nu_m)\, t - \tfrac{1}{2}(\partial\alpha/\partial q)\, q_0 E_0 \cos 2\pi(\nu + \nu_m)t \quad ...(79)$$

$$= \alpha_0 E_0 \sin 2\pi\nu t + \tfrac{1}{2}(\partial\alpha/\partial q)\, q_0 E_0 \times [\cos 2\pi(\nu - \nu_m)\, t - \cos 2\pi(\nu + \nu_m)\, t] \quad ...(80)$$

Thus, we find that the oscillating dipole has three distinct frequency components : *(i)* the exciting frequency ν with amplitude $\alpha_0 E_0$ *(ii)* $\nu - \nu_m$ and *(iii)* $\nu + \nu_m$ with very small amplitudes = (1/2) $(\partial\alpha/\partial q)\, q_0 E_0$. Hence, the Raman spectrum of a vibrating molecule consists of a relatively intense band at the incident frequency and two very weak bands at frequencies slightly above and below that of the intense band.

If, however, the molecular vibration does not change the polarizability of the molecule, then $(\partial\alpha/\partial q) = 0$ so that the dipole oscillates only at the frequency of the incident (exciting) radiation. The same is true of the molecular rotation. We conclude that *for a molecular vibration or rotation to be active in the Raman spectrum, it must cause a change in the molecular polarizability, i.e.,*

$$\partial\alpha/\partial r \neq 0. \quad ...(81)$$

Homonuclear diatomic molecules such as H_2, N_2, O_2, which do not show IR spectra since they do not possess a permanent dipole moment, *do show Raman spectra since their vibration is accompanied by a change in polarizability of the molecule.* As a consequence of the change in polarizability, there occurs a change in the induced dipole moment at the vibrational frequency.

The selection rule for the vibrational Raman spectrum of a diatomic molecule is

$$\Delta v = \pm 1 \quad ...(82)$$

Rotational Raman Spectrum of a Diatomic Molecule

The selection rule for pure rotational Raman spectrum of a diatomic molecule is

$$\Delta J = 0, \pm 2 \quad ...(83a)$$

The operative part of the rotational selection rule is

$$\Delta J = +2 \quad ...(83b)$$

since $\Delta J = 0$ corresponds to Rayleigh scattering and $\Delta J = -2$ transition can be ignored as the rotational quantum number of the upper state must be greater than that of the lower state. Using the selection rule (Eq. 83*b*) with the energy level expression for rigid diatomic rotor, *viz.*,

$$F(J) = BJ(J+1)\ \text{cm}^{-1}\ (J = 0, 1, 2, 3...), \quad \text{(Eq. 31)}$$

we find that $\Delta F(J) = F(J+2) - F(J) = B(4J+6)\ \text{cm}^{-1}$ ...(84)

It is customary to call the $\Delta J = +2$ transitions as **S-branch lines.** Thus,

$$\Delta F(J) = B(4J+6)\ \text{cm}^{-1}\ (J = 0, 1, 2, 3,...) \quad ...(85)$$

where J is the quantum number of the *lower* rotational energy level. Hence, the Raman spectral lines appear at the wave numbers given by the following equation :

$$\bar{\nu}_S = \bar{\nu}_{exc} \pm \Delta F(J) = \bar{\nu}_{exc} \pm B(4J+6)\ \text{cm}^{-1} \quad ...(86)$$

where ν_{exc} is the exciting (incident) frequency, the negative sign refers to the Stokes lines and the positive sign to the anti-Stokes lines.

The energy level diagram and the rotational Raman spectrum for a diatomic molecule are shown in Fig. 21. We see that the first Stokes line (or the first anti-Stokes line) appears at a distance of $6B$ from the exciting Rayleigh line. This is evident from Eq. 85, where putting $J=0$ we obtain $\Delta F(J) = 6B$. The separation of the successive Raman lines is, however, $4B$, as can be easily verified by putting $J=1, 2, 3$, etc., in Eq. 86.

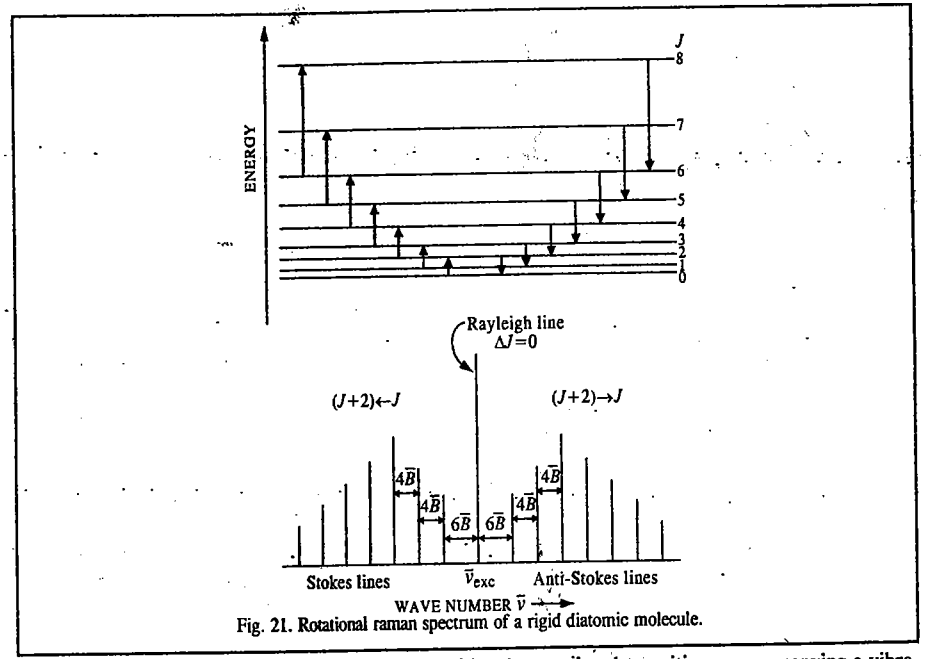

Fig. 21. Rotational raman spectrum of a rigid diatomic molecule.

Rotation–Vibration Raman Spectrum. Consider the rotational transitions accompanying a vibrational Raman transition of a diatomic molecule. The selection rules now involve the changes in both the vibrational and the rotational quantum numbers. For a diatomic molecule, the selection rules are :

$$\Delta v = +1\ ;\ \Delta J = 0, \pm 2 \quad ...(87)$$

Since at room temperature most of the molecules are in the ground vibrational state (v=0), only the vibrational transition, v=0 to v=1, is of interest. The transitions with $\Delta J = 0$ form a Q-branch ; those with $\Delta J = +2$ form an S-branch and those with $\Delta J = -2$ form an O-branch. The rotational Raman transitions accompanying a $0 \rightarrow 1$ vibrational transition are shown in Fig. 22. Here, $\Delta\bar{\nu}$ measures the displacement from the exciting mercury line. The Q-branch exhibits an intense 'narrow line' at $\bar{\nu}_{exc}$ that is usually unresolved while the S and O branches form weak wings which extend to lower and higher wave numbers, respectively, from the intense narrow line.

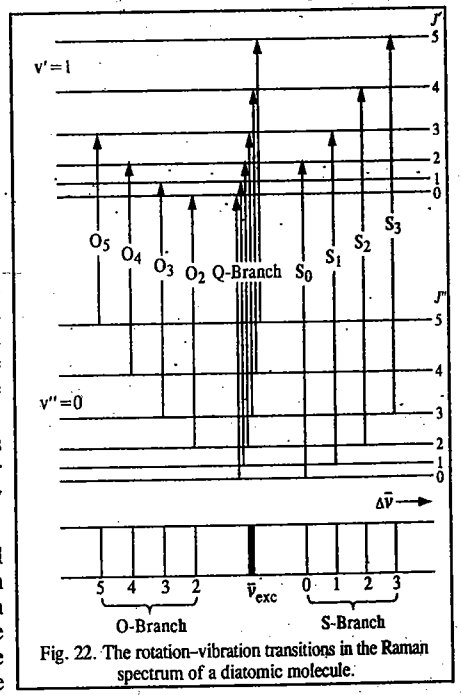

Fig. 22. The rotation–vibration transitions in the Raman spectrum of a diatomic molecule.

Experimental Raman Spectroscopy. The original experimental set-up for Raman spectroscopy is shown in Fig. 23. Intense monochromatic radiation from a source consisting of a large spiral discharge tube with mercury electrodes is allowed to fall on the cell containing a gaseous or liquid sample. When the

electric discharge passes through the tube, mercury emits lines in its spectrum the most intense of which at 4358 Å (*i.e.*, 435·8 nm) serves as the exciting line. The scattered light is observed at right angles to the direction of incident radiation. The detector is either a photographic plate or a photomultiplier. The horn shape of the cell helps in reducing the direct reflection of the source from the back of the cell.

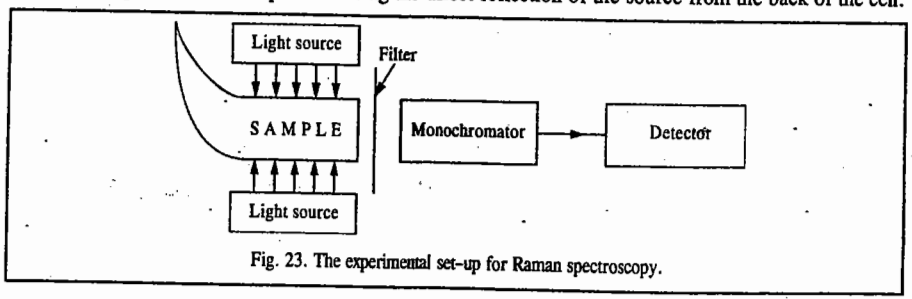

Fig. 23. The experimental set-up for Raman spectroscopy.

The Raman spectra of gases are generally weaker than those of liquids. It is necessary to use very long discharge lamps and cells, the latter containing mirrors at both ends arranged so as to increase the effective path length of the cell.

Between 1930 and 1960, Raman spectroscopy was not used for analytical work as was the case with IR spectroscopy. However, with the discovery of the 'LASER' (light amplification by stimulated emission of radiation) by Townes, Basov and Prokhorov in the late 1950s, Raman spectroscopy has become an extremely important analytical tool. The laser has replaced Hg as the source of radiation. The laser radiation is coherent and monochromatic, *i.e.*, it is a radiation of very high intensity in a narrow beam with a well-defined frequency. Thus, it can be easily focussed and collimated. The line width of the laser line is also far smaller than that of the mercury-excited line. Modern scientific laboratories are now equipped with laser Raman spectrometers. Using a laser Raman spectrometer, the spectrum of a sample can be recorded quickly.

Raman spectroscopy, despite difficulties with sensitivity, has several advantages. It gives information about molecular vibrations that are inactive in the infrared region because of molecular symmetry. According to the **'mutual exclusion rule'**, for centrosymmetric molecules (*i.e.*, molecules such as H_2, CO_2, C_2H_2, etc., that possess a centre of symmetry), the vibration which is active in IR is inactive in Raman and the vibration which is inactive in IR is active in Raman spectra. Raman spectroscopy, in fact, complements IR spectroscopy. Thus, the stretching vibrations of homonuclear diatomic molecules (such as H_2, O_2, N_2, etc.,) which are inactive in IR (since they are not accompanied by a change in dipole moment which is already zero) are observed in Raman spectra. Also, the symmetric stretching vibration of CO_2, that is inactive in IR, is active in Raman spectra. Another example is that of planar dichloroethylene, $C_2H_2Cl_2$, which consists of *cis* and *trans* configurations in equilibrium proportions. Only the *trans* configuration has a centre of symmetry. Thus, the coincident frequencies observed in IR and Raman spectra of the sample can be assigned to the *cis* configuration. In this manner the analysis of the mixture of *cis* and *trans* isomers can be carried out. Again, for CS_2, all the vibrations that are Raman-active are infrared-inactive and vice versa, whereas for N_2O, the vibrations are simultaneously Raman and infrared-active. From the spectral data we conclude that CS_2 has a centre of symmetry whereas N_2O has no centre of symmetry. Thus, the CS_2 structure is of the type S—C—S while the N_2O structure must be N—N—O rather than N—O—N.

Raman spectroscopy has another advantage in that it uses visible or ultraviolet radiation rather than infrared radiation. Hence, the walls of the sample cell and other units of the optical system can be made of glass or quartz rather than of special materials that are transparent to IR radiation. Also, the experimentalist can work very conveniently with aqueous media since water is far more transparent in the visible and UV regions than in the IR region. Thus, Raman spectroscopy can be utilized for the investigation of biological systems such as the polypeptides and the proteins in aqueous solution.

Example 10. A sample was excited by the 4358 Å line of mercury. A Raman line was observed at 4447 Å. Calculate the Raman shift in cm^{-1}.

Solution : Since the Raman line is observed at longer wave length (shorter frequency) than the exciting line, it is evidently a Stokes line in the Raman spectrum. From Eq. 71, the Raman shift is given by

$$\Delta\bar{\nu}_{\text{Raman}}\ (\text{cm}^{-1}) = \frac{10^8}{\lambda_{\text{exc}}(\text{Å})} - \frac{10^8}{\lambda_{\text{Raman}}(\text{Å})}$$

$$= \frac{10^8}{4{\cdot}358\times10^3} - \frac{10^8}{4{\cdot}447\times10^3} = (2{\cdot}295 - 2{\cdot}249)\times10^4$$

$$= 0{\cdot}046\times10^4 = \mathbf{460\ cm^{-1}}$$

Example 11. At what wave length in Å would the anti-Stokes line appear in the Raman spectrum of the sample in Example 10 ?

Solution : The anti-Stokes line will appear at a frequency 460 cm^{-1} higher than the frequency (in cm^{-1}) associated with 4358 Å Hg line used as a source of excitation. Now,

$$\bar{\nu}_{\text{exc}}\ (\text{cm}^{-1}) = \frac{10^8}{\lambda_{\text{exc}}(\text{Å})} = \frac{10^8}{4{\cdot}358\times10^3} = 2{\cdot}295\times10^4\ \text{cm}^{-1}$$

Hence, $\bar{\nu}_{\text{anti-Stokes}} = (2{\cdot}295\times10^4\ \text{cm}^{-1}) + (460\ \text{cm}^{-1}) = 2{\cdot}341\times10^4\ \text{cm}^{-1}$

$$\therefore\quad \lambda\ (\text{in Å}) = \frac{10^8}{\bar{\nu}\ (\text{cm}^{-1})} = \frac{10^8}{2{\cdot}341\times10^4} = \mathbf{4272\ Å}$$

RESONANCE RAMAN SPECTROSCOPY

Ordinarily, a Raman spectrum is excited using light of frequency that is not absorbed by the sample. (Recall that the conventional Raman technique involves the *inelastic scattering* of a radiation photon by a molecule.) The probability of absorption is very low and excitation is to a virtual excited state whose lifetime is very short and whose energy is correspondingly poorly defined. If we use light whose absorption probability is high, the effects of local heating by the laser beam are usually so great that the sample decomposes. If we can avoid this local heating, possibly by spinning the sample rapidly under the laser spot so that different parts of the sample are heated in turn, we observe stronger Raman signals as the exciting radiation is absorbed by the sample. This effect is called **resonance Raman effect**. The intensity of this effect is very high. However, in general, only a few vibrational modes are involved and often only one is detectable. It is usual to find a progression indicating significant transition probabilities to many vibrational levels of the modes concerned. The energy levels of the resonance Raman effect are shown in Fig. 24.

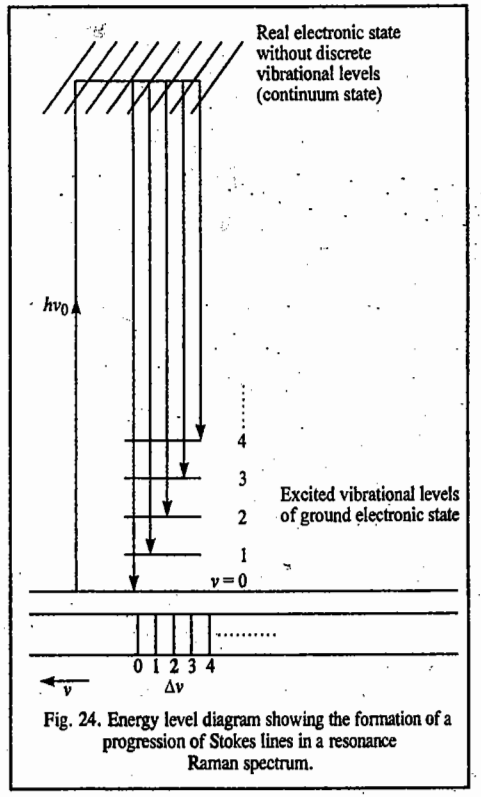

Fig. 24. Energy level diagram showing the formation of a progression of Stokes lines in a resonance Raman spectrum.

The particular vibrations excited are often found to be closely associated with the electronic transition within whose band the exciting radiation

falls and this can sometimes be useful in assigning electronic transitions. The use of a tunable laser may be helpful since the excitation profiles, which show the intensity of resonance-enhancement as a function of exciting frequency, may allow overlapping electronic bands to be distinguished from one another. In terms of vibrational spectroscopy, resonance Raman spectroscopy has the following three advantages over simple Raman spectroscopy :

1. Enhancement of intensity, enabling weakly scattering or very dilute samples to be investigated.
2. Greatly simplified spectrum, as only a few vibrations are enhanced.
3. The experimental observation of the spectrum enables the vibrational potential function (such as the Morse potential energy function) to be specified over a wide range of vibrational quantum numbers.

The resonance Raman effect can be observed with a normal Raman spectrometer and is independent of any special properties of laser excitation . The intensity enhancement relies on the electronic transition being allowed by symmetry. Thus, the vibrations whose intensities are enhanced are almost always usually symmetric.

The resonance Raman technique has enabled spectra to be obtained from the metallic cores of biological molecules such as haemoglobin and some enzymes, where the low concentration of the metal and the low solubility of the substance itself make it difficult to study vibrational spectra in any other way. The IR or normal Raman spectrum of these biological molecules, too, is very complex but the resonance Raman spectrum can be easily interpreted because of its simplicity. Fig. 25 shows the resonance Raman spectrum of the tetrahedral chromate ion present in solid potassium chromate, K_2CrO_4. A clear-cut progression of peaks due to the totally symmetric stretching mode of the anion is seen, upto the ninth or tenth member. Excitation carried out was by UV laser line within the absorption band whose low frequency wing in the blue/violet region is responsible for the yellow colour of the salt. The sample is rotated rapidly to reduce the effects of local heating for absorbed laser light. The broadening of the higher bands reflects progressively shorter lifetimes for the al highly excited vibrational states.

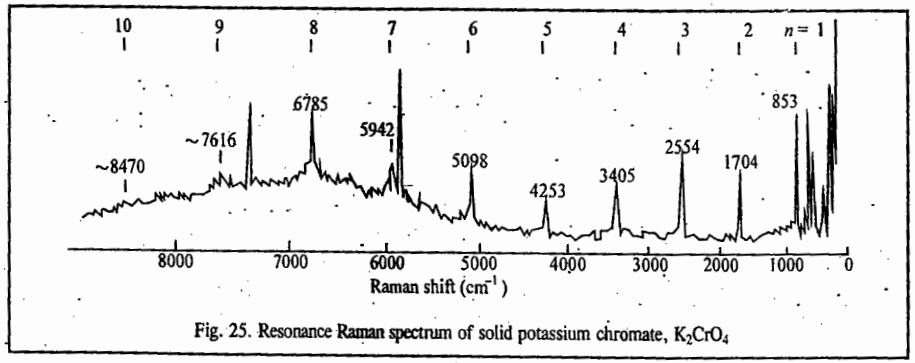

Fig. 25. Resonance Raman spectrum of solid potassium chromate, K_2CrO_4

Laser Raman Spectroscopy

The large intensity possessed by lasers leads to nonlinear polarization of the medium which is responsible for the observation of nonlinear phenomena such as nonlinear Raman spectroscoy, multiphoton spectroscopy, saturation spectroscopy, second harmonic generation (SHG), etc. Lasers are also used in **stimulated Raman spectroscopy (SRS).** In this form of spectroscopy, there is multiple scattering resulting in the emission of larger number of Stokes and anti-stockes lines. A brief description of SRS and some other forms of laser Raman spectroscopy is given here. When a laser pulse is focussed into a sample and the scattered radiation is observed along the laser beam direction at small angles to it,

it is found to consist of the incident frequency ν_0 and the Stokes and anti-Stokes lines at $\nu_0 \pm n\nu_m$, $n=1, 2, 3, \ldots$, where ν_m corresponds to Raman-active vibration of the scattering molecule. This phenomenon is called **stimulated Raman scattering (SRS).** The process involving stimulation is shown schematically in Fig.26. In SRS there is no need for population inversion of the states.

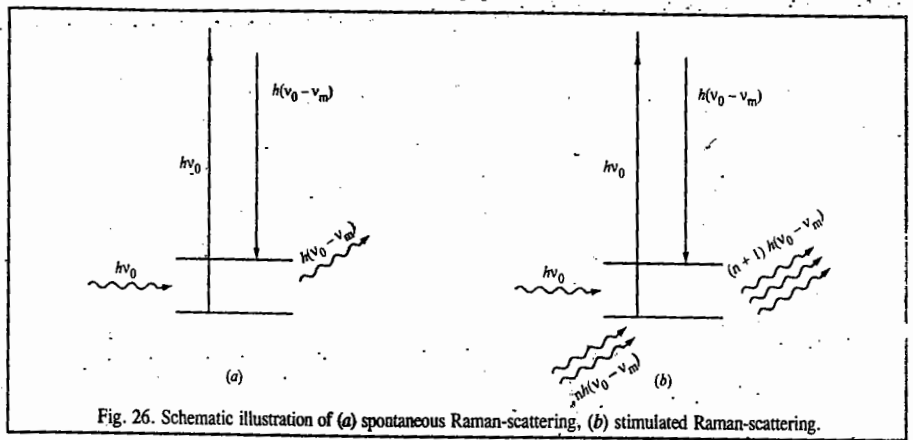

Fig. 26. Schematic illustration of (*a*) spontaneous Raman-scattering, (*b*) stimulated Raman-scattering.

The Stokes line produced by spontaneous Raman scattering at frequency $\nu_0 - \nu_m$ becomes intense enough quickly to act as powerful source to produce a Stokes line at $(\nu_0 - 2\nu_m)$. This is illustrated in Fig. 27. As this line gains in intensity, it acts as a source and so on.

Stimulated Raman scattering differs from normal Raman scattering not only in its wave number pattern and angular dependence but also on its intensity. The ν_0–ν_m line will be very intense, ν_0–$2\nu_m$ slightly less intense, and so on. At least upto n=3 or 4, the intensity will be larger than found in normal Raman scattering. The width of lines in SRS is also much less than that found in normal Raman scattering. The high conversion efficiency of SRS means that it can be used to generate intense coherent laser-like sources over a wide range of wave numbers by judicious selection of scattering material.

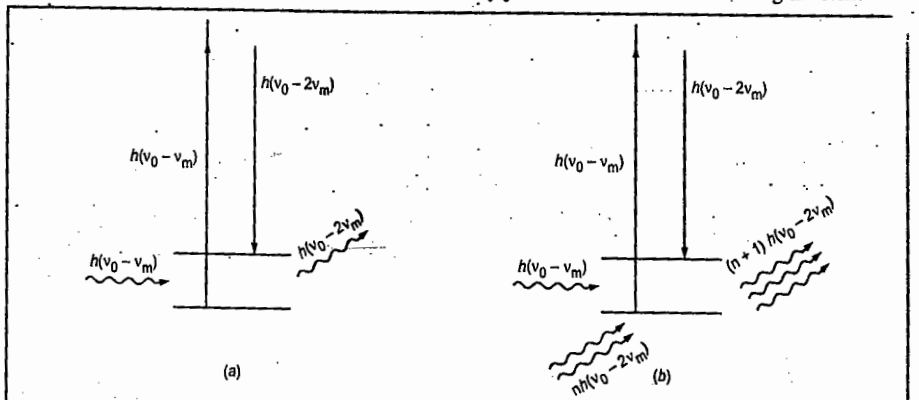

Fig. 27. Illustration of (*a*) spontaneous Raman scattering at $(\nu_0 - 2\nu_m)$, (*b*) stimulated Raman scattering at $(\nu_0 - 2\nu_m)$.

Raman scattering is inelastic scattering of photons of energy $h\nu_0$ by molecules. If the scattered photon has an energy $h(\nu_0+\nu_m)$, the incident photon gains an energy by an amount $h\nu_m$ from the molecule. The energy balance equation for this normal anti-Stokes-Raman scattering is shown in Fig. 28*a*. If this process is inverted, the scattering molecule absorbs radiation of frequency $(\nu_0+\nu_m)$,

resulting in the molecule going to a higher energy level and the emission of radiation of frequency ν_0. This phenomenon is called the inverse **anti-Stokes Raman effect** (Fig. 27*b*).

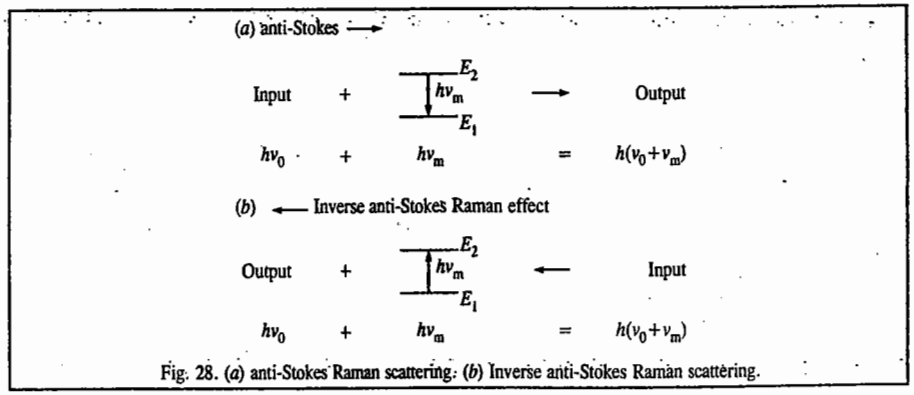

Fig. 28. (*a*) anti-Stokes Raman scattering. (*b*) Inverse anti-Stokes Raman scattering.

The absorption of radiation of frequency $\nu_0 - \nu_m$ by the molecule would result in a decrease in the energy of the scattering molecule by $h\nu_m$ and emission of radiation of energy $h\nu_0$. This is inverse anti-Stokes Raman scattering. This complementary effect requires appropriate population of the upper state. It is found that absorption at frequencies $\nu_0 \pm \nu_m$ can occur only in the presence of a very intense radiation at frequency ν_0. Thus, the essential requirements for the observation of inverse Raman scattering are the simultaneous irradiation of the sample with a giant pulse laser beam of frequency ν_0 and a strong continuum covering the Stokes and anti-Stokes regions in which absorptions are expected. With improved experimental techniques, inverse Raman spectroscopy, offers a potential method for the study of very short-lived species and the measurement of very short lifetimes.

Coherent antiStokes-Raman scattering (CARS) which combines the advantages of SRS and the general applicability of normal Raman scattering. When coherent radiation of frequency ν_1 is mixed with coherent radiation of frequency ν_2 ($\nu_1 > \nu_2$) in a molecular medium, coherent radiation of frequency $\nu_3 = 2\nu_1 - \nu_2 = \nu_1 + (\nu_1 - \nu_2)$ is generated, if the irradiances of the two frequencies are sufficiently large. Here mixing implies spatial and temporal coincidence of the two beams. If ν_1 is fixed and ν_2 is varied so that $\nu_1 - \nu_2 = \nu_m$, a Raman active vibration of the molecule under investigation, then $\nu_3 = \nu_1 + \nu_m$, which is an anti-Stokes Raman frequency. Radiation produced in this way is called CARS. Fig. 29 illustrates a typical CARS set-up where the two incident radiations are provided by the 514·5 nm argon laser line (ν_1) and a continuous wave (CW) dye laser (ν_2) pumped by the same argon laser.

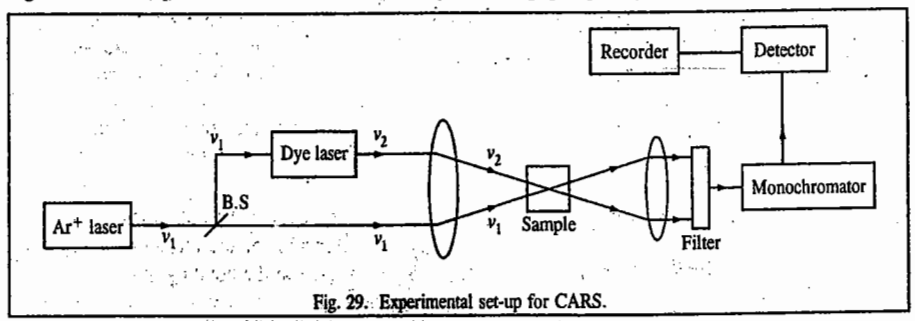

Fig. 29. Experimental set-up for CARS.

With CARS, the conversion efficiency to $\nu_3 = (\nu_1 + \nu_m)$ is several orders of magnitude greater than the conversion frequencies in the normal Raman scattering. The radiations resulting from CARS form a highly coherent collimated beam whereas normal Raman scattering is incoherent and extends over a

solid angle 4π. Since CARS is highly collimated, fluorescence and thermal radiation from hot samples can effectively be filtered by placing a screen with a hole of a few mm diameter between the detector and the sample which just passes only the CARS beam. Moreover, in principle, no dispersing medium is needed for CARS experiment. The fluorescence-free nature of CARS makes it an ideal tool for high resolution spectroscopic studies and analysis of biological samples.

ELECTRONIC SPECTRA

The electronic band spectra of molecules are generally very complex and are, investigated with considerable difficulty. They are observed in the ultraviolet and visible regions of the electromagnetic spectrum. Their complexity arises from the fact that a transition between two electronic states is almost invariably accompanied by simultaneous transitions between the vibrational and rotational energy levels as well. This is expressed by saying that electronic spectra have **vibrational fine structure and rotational fine structure.** As discussed earlier, according to the Born-Oppenheimer approximation, the total energy of a molecule in the lower (ground) state is given by

$$E'' = E''_{el} + E''_{vib} + E''_{rot} \qquad ...(88)$$

neglecting the translational energy, E''_{tr}, which is not quantized. Here, E''_{el}, E''_{vib} and E''_{rot} are, respectively, the electronic, vibrational and rotational energies. Assuming that the Born-Oppenheimer approximation is valid in the upper (excited) state as well, the excited state energy E' is given by

$$E' = E'_{el} + E'_{vib} + E'_{rot} \qquad ...(89)$$

The energy change for an electronic transition is given by

$$\Delta E = E' - E'' = (E'_{el} - E''_{el}) + (E'_{vib} - E''_{vib}) + (E'_{rot} - E''_{rot}) \qquad ...(90)$$

$$= \Delta E_{el} + \Delta E_{vib} + \Delta E_{rot} \qquad ...(91)$$

Considerable simplification of spectra results by recognizing that

$$\Delta E_{el} >> \Delta E_{vib} >> \Delta E_{rot} \qquad ...(92)$$

The frequency for the electronic transition is given by the **Bohr frequency condition,** *viz.*,

$$\bar{\nu} = \frac{\Delta E}{hc} = \frac{\Delta E_{el} + \Delta E_{vib} + \Delta E_{rot}}{hc} \text{ cm}^{-1} \qquad ...(93)$$

Eq. 93 shows how an electronic transition possesses the vibrational and rotational fine structures.

A very useful guiding principle for investigating the vibrational structure of electronic spectra is provided by the well known **Franck-Condon principle** which states that *an electronic transition takes place so rapidly that a vibrating molecule does not change its internuclear distance appreciably during the transition.* This principle is, to a first approximation, true since the electrons move so much faster than the nuclei that during the electronic transition the nuclei do not change their position. Hence, *an electronic transition may be represented by a vertical line on a plot of potential energy versus the internuclear distance.*

Let us demonstrate the Franck-Condon principle for the electronic transition of a diatomic molecule. Consider Fig. 30. where we have shown two potential energy curves for the molecule in the ground electronic state (E_0) and in the first excited electronic state (E_1). Since the bonding in the excited state is weaker than in the ground state, the minimum in the potential energy curve for the excited state occurs at a slightly greater internuclear distance than the corresponding minimum in the ground electronic state. Also, quantum mechanically it is known that the molecule is in the *centre* of the ground vibrational level of the ground electronic state. Thus, when a photon falls on the molecule, the most probable electronic transition, according to the Franck-Condon principle, takes place from $v''=0$ to

$v'=2$ (written schematically as $0 \rightarrow 2$). Transitions to other vibrational levels of the excited electronic state occur with lower probabilities so that their relative intensities are smaller than the intensity of the $0 \rightarrow 2$ transition, as shown in Fig. 31.

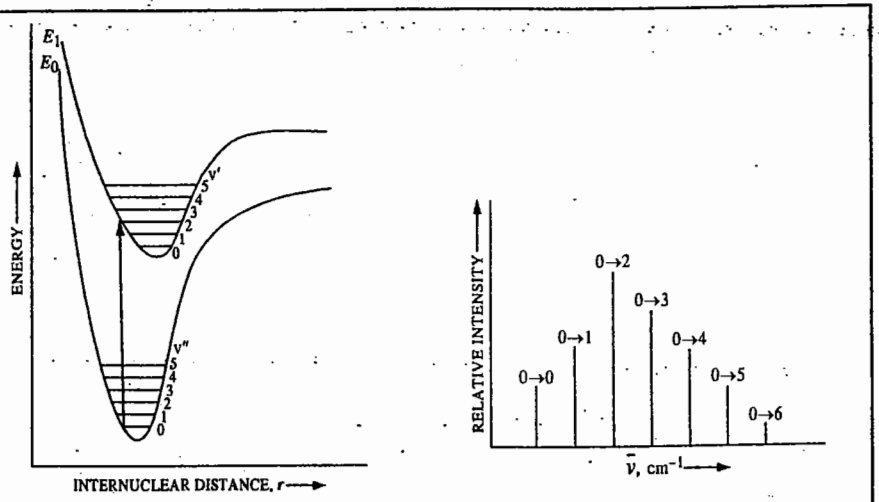

Fig. 30. Electronic transition in a diatomic molecule.

Fig. 31. Electronic spectrum of a diatomic molecule.

Consider now a slightly different case of a diatomic molecule which has a potential energy curve E_0 in ground state and two potential energy curves E_1 and E_2 in excited states. The potential energy curve E_2 does not have a minimum, as shown in Fig. 32.

The equilibrium internuclear distance is longer in E_1 than in E_0 since the bond is weaker in the excited state. The transition indicated by arrow a has, according to the Franck-Condon principle, maximum intensity. Other possible transitions are from the first excited vibrational level of the ground electronic state; they are indicated by the duplication of the vertical arrows b_1 and b_2. The transition b_1 ends in the lowest vibrational level of the first excited electronic state where the molecule is still held firmly. However, the transition b_2 promotes the molecule to a point where its energy is far above the potential energy plateau of state E_1 at large distance with the result that the molecule dissociates.

The molecule will also dissociate if it is excited to a level below the plateau in E_1 but above point c where the potential energy curves for E_1 and E_2

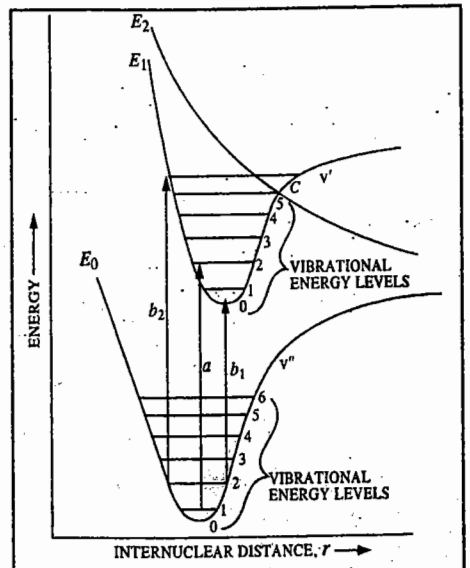

Fig. 32. Potential energy curves for the ground state and two excited states of a diatomic molecule. The curve E_2 crosses the curve E_1.

cross. At an internuclear distance corresponding to the point c, the molecule may undergo a crossover from one state to the other without energy change and continue to dissociate.

In the case of homonuclear diatomic molecules such as H_2 and N_2, the highest occupied molecular orbital (HOMO) in the ground state is a bonding molecular orbital (BMO) whereas the lowest unoccupied molecular orbital (LUMO) is an antibonding molecular orbital (ABMO). The HOMO and LUMO orbitals are collectively referred to as **frontier molecular orbitals** (FMOs). The electronic transition HOMO → LUMO takes place, *i.e.*, the electron, upon absorption of a photon, undergoes a transition from HOMO to LUMO. This lies in the short wave length side of the ultraviolet (UV) region. An exception is provided by the oxygen molecule O_2 that has two unpaired electrons in the ground state which is thus a triplet state. The electronic transition occurs from the triplet ground state to the triplet excited state (rather than to the singlet excited state). The electronic spectrum of O_2 molecule is, of course, complex.

Though the heteronuclear diatomic molecules such as CO, HCl, NO, BH, etc., have more complex structures in terms of the molecular orbitals occupied by the various electrons in them, their electronic spectra are essentially similar to those of the homonuclear diatomics, consisting of absorption bands in the near ultraviolet region.

Electronic Spectra of Polyatomic Molecules

The electronic spectra of polyatomic molecules show greater degree of complexity. The vibrational structure and the rotational fine structure of electronic spectra can only be observed in the gaseous states of small molecules. In solution, the rotational energy levels are not well defined; moreover, large molecules have very high moments of inertia. Hence, the rotational fine structure is totally wiped out in solution. Even vibrational transitions are broad, as shown by the Franck-Condon principle. Thus, the electronic spectra of molecules in solution appear as large unresolved bands rather than as sharp peaks. This is a characteristic feature of electronic spectra in condensed media and must be borne in mind. It also follows that if the rotational and vibrational structure of an electronic band can be fully resolved in the gaseous state, considerable information can be obtained from the electronic spectrum.

Organic compounds, particularly those containing groups like C=C, C=O, -N=N- and extensively conjugated systems, form a special class of polyatomic molecules whose electronic spectra are amenable to simple interpretation even though the investigation of their detailed spectral features may require knowledge of quantum mechanics and group theory. On the basis of the molecular orbital theory (MOT), the electrons can be classified as σ, π or *n*(non-bonding) depending upon the MOs they occupy. For organic carbonyl compounds, the electronic transitions involve promotion of the electrons in *n*, σ and π orbitals in the ground state to σ* and π* ABMOs in the excited state (Fig. 33). In other words, only the transitions of the type $\sigma^* \leftarrow \sigma$, $\pi^* \leftarrow \pi$ and $\pi^* \leftarrow n$ are allowed. Since electrons in the *n* orbitals are not involved in bond formation, there are no ABMOs associated with them.

The $\sigma^* \leftarrow \sigma$ transitions occurring in saturated hydrocarbons and other types of compounds in which all valence shell electrons are involved in single bonds, are found in ultraviolet region since they involve very high energy. The $\pi^* \leftarrow \pi$ and the $\pi^* \leftarrow n$ transitions, on the other hand, are found either in the UV or visible regions. The unsaturated molecules containing C=C and C=O groups (such as aldehydes and ketones) show $\pi^* \leftarrow n$ and $\pi^* \leftarrow \pi$ transitions. For aldehydes and ketones the more intense band near 1800 Å (180 nm) is due to $\pi^* \leftarrow \pi$ transition and the weaker band around 2850 Å (285 nm) is due to $\pi^* \leftarrow n$ transition. Olefinic hydrocarbons show a $\pi^* \leftarrow \pi$ transition in the wave length 160 - 170 nm. Acetylene shows an absorption near 180 nm.

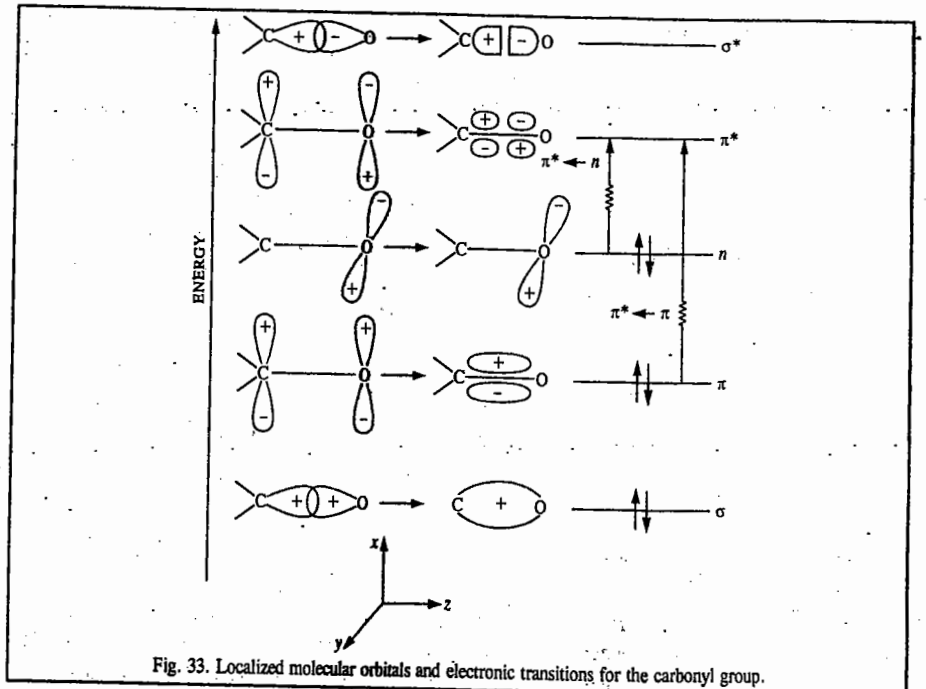

Fig. 33. Localized molecular orbitals and electronic transitions for the carbonyl group.

Functional groups such as C=C, -N=N- which absorb at wave lengths longer than 180 nm, are called **chromophores.** Other chromophores are nitro, nitroso, carbonyl, thiocarbonyl, sulphoxide groups as well as aromatic rings. Molecules such as CH_3NH_2 and CH_3I which do not contain a π orbital, show $\sigma^* \leftarrow n$ transitions.

In extensively conjugated systems, the π-electrons are delocalized over the entire skeletal framework. Such systems are treated in terms of the 'free-electron model' and it is found that *the absorption bands shift to longer wave lengths as the extent of conjugation increases.* Thus, in the compound C_6H_5–$(CH=CH)_n$–C_6H_5, the $\pi^* \leftarrow \pi$ transition lies in the UV region when $n=1$ or 2. As n increases, the electronic transition shifts to the visible region. This aspect is dealt with later in this chapter. This phenomenon is shown schematically in Fig. 34. Thus, λ_{max} is proportional to the extent of conjugation.

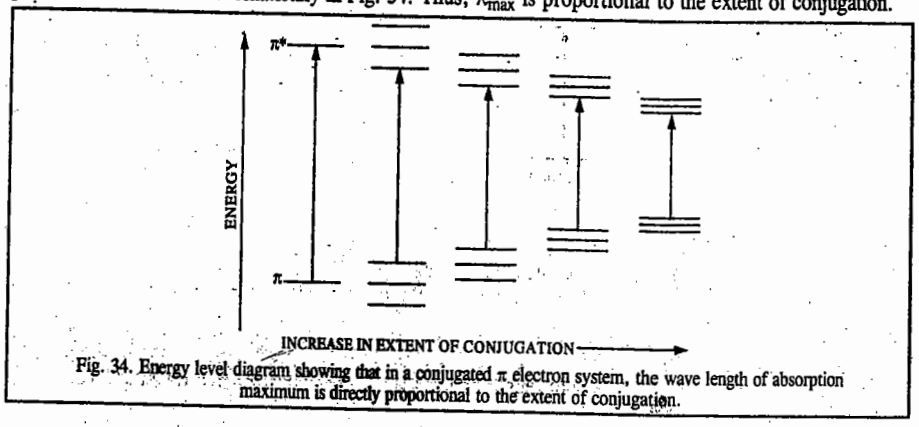

Fig. 34. Energy level diagram showing that in a conjugated π electron system, the wave length of absorption maximum is directly proportional to the extent of conjugation.

The intensity of an electronic band is determined by the extent of overlap of the wave functions in the ground and excited states. Since there is very poor overlap of wave functions of the ground and excited states in the $\pi^* \leftarrow n$ transition and there is considerable overlap of the corresponding wave functions in the $\pi^* \leftarrow \pi$ transitions, the $\pi^* \leftarrow n$ transitions are less intense (*i.e.*, weaker) than the $\pi^* \leftarrow \pi$ transitions. Also, in strongly acidic media, the $\pi^* \leftarrow n$ band disappears due to the protonation of lone pair of electrons. In fact, the protonation may increase the excitation energy to such an extent that the $\pi^* \leftarrow n$ transition may shift far out into the UV region and may not be observed.

The protonation of a functional group introduces profound changes in the spectra. Thus, the spectra in such cases are strongly dependent upon *p*H. Solvent effects, too, are useful in identifying the nature of these transitions. The $\pi^* \leftarrow n$ transitions are altered by the solvent effects in cases where the lone pair electrons in oxygen or nitrogen-containing systems interact with polar solvents. It is customary in spectroscopic literature to refer to the shifts in absorption bands and their intensity changes as follows :

1. **Bathochromic shift** (or the **red shift**) : a shift of λ_{max} to longer wave lengths.
2. **Hypsochromic shift** (or the **blue shift**) : a shift of λ_{max} to shorter wave lengths.
3. **Hyperchromic shift** : an increase in the intensity of an absorption band with reference to its molar extinction coefficient.
4. **Hypochromic shift** : a decrease in the intensity of an absorption band with reference to its molar extinction coefficient.

The term **auxochrome** refers to an atom or a group of atoms which does not give rise to an absorption band on its own but, when in conjugation with a chromophore, causes a bathochromic shift and a hyperchromic effect. For instance, $\rangle C=C\langle$ group is a chromophore in ethylene; when one of the hydrogens is replaced by a halogen atom, a bathochromic shift and a hyperchromic effect are produced. This is because the lone pair on the halogen atom conjugates with the alkene double bond. We conclude that the halogen atom acts as an auxochrome.

As said earlier, solvent effects are important in identifying $\pi^* \leftarrow \pi$ and $\pi^* \leftarrow n$ transitions. Polar solvents often stabilize the ground state of $\pi^* \leftarrow n$ transitions more than they stabilise the excited state, causing blue shifts (Fig. 35*a*). On the other hand, for $\pi^* \leftarrow \pi$ transitions, the excited state is stabilized more than the ground state, causing red shifts (Fig. 35*b*).

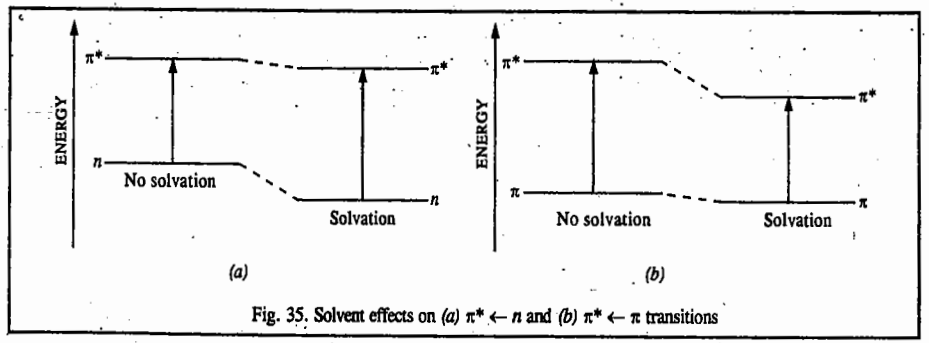

Fig. 35. Solvent effects on *(a)* $\pi^* \leftarrow n$ and *(b)* $\pi^* \leftarrow \pi$ transitions

One of the most important applications of UV spectroscopy, based on the Lambert-Beer law, is in quantitative analysis. According to the Lambert-Beer law, the absorbance A of a compound of concentration c is given by $A = \varepsilon bc$ where b is the path length and ε is the molar extinction coefficient. Consider the

equilibrium $X \rightleftarrows Y$. If X and Y have absorption bands that overlap and if at some wave length over the overlapped region both X and Y have equal absorbance, then there will be no change in the absorbance at this wave length as the ratio $[Y]/[X]$ is varied. This gives rise to the so called **isosbestic point.** When there is more than one isosbestic point present, we have

$$A_1 = b(\varepsilon_X^{(1)} c_X + \varepsilon_Y^{(1)} c_Y)$$

$$A_2 = b(\varepsilon_X^{(2)} c_X + \varepsilon_Y^{(2)} c_Y)$$

where 1 and 2 indicate the two wave lengths. Since A_1 and A_2 can be measured, the concentrations of X and Y, *viz.*, c_X and c_Y (and hence the equilibrium constant $K = [Y]/[X]$) can be calculated if the various extinction coefficients $\varepsilon_X^{(1)}, \varepsilon_X^{(2)}, \varepsilon_Y^{(1)}$ and $\varepsilon_Y^{(2)}$ are known.

Finally, we may mention that UV spectroscopy has an advantage over IR spectroscopy as far as applications to biological systems are concerned. Most biological systems have high water contents and since water absorbs strongly in the IR, its use is severely limited. On the other hand, aqueous solutions can be conveniently investigated by UV spectroscopy. UV spectra have also better resolution than IR spectra of biochemical systems.

CHARGE-TRANSFER (CT) SPECTRA

The theory of charge-transfer spectra was proposed by R.S. Mulliken who won the 1966 Chemistry Nobel Prize. The charge-transfer complexes (also called donor-acceptor complexes) are generally highly coloured. Thus, hydroquinone is colourless and quinone is yellow but quinhydrone crystals possess a highly green metallic colour. According to Mulliken, when two molecules which form loose complexes are mixed together, one of them acts as an electron-donor (D) while the other as an electron-acceptor (A) and they give rise to a donor-acceptor complex :

$$D + A \rightleftharpoons \underset{\text{Complex}}{(DA)} \overset{h\nu}{\rightleftarrows} \underset{\text{Donor-Acceptor Complex}}{(\overset{+}{D}-\overset{-}{A})}$$

Typical examples of donor-acceptor complexes are the quinhydrone, benzene/iodine solution and the compound $BF_3 \rightarrow NH_3$. The charge-transfer band for the complex formed between tetracyanoethylene and 1,2,4,5-tetramethyl benzene is shown in Fig. 36. It arises from the transition of an electron from the highest occupied molecular orbital (HOMO) of the donor molecule to the lowest unoccupied molecular orbital (LUMO) of the acceptor molecule (Fig. 37). Excitation of the electron to the higher unoccupied molecular orbitals of the acceptor gives rise to additional charge-transfer (CT) absorption bands.

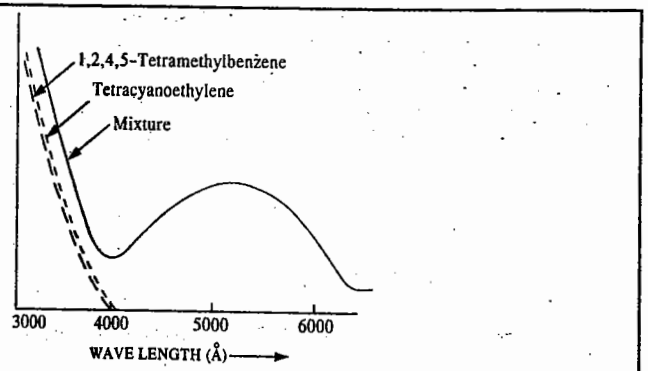

Fig. 36. The charge-transfer spectrum.

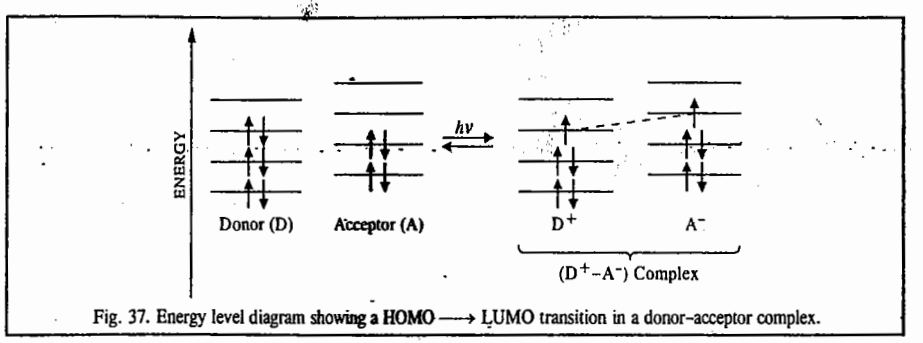

Fig. 37. Energy level diagram showing a HOMO ⟶ LUMO transition in a donor-acceptor complex.

The donor molecules are of two types : π-donors and n-donors. In the π-donors (such as aromatic hydrocarbons, alkenes, alkynes), the electron available for donation occupies the π MO of the molecule. In the n-donors (*e.g.*, alcohols, ethers, amines, etc.) the non-bonding electron is donated. The acceptor molecules are, on the other hand, of many types. The acceptor molecules are tetracyanoethylene, trinitrobenzene and other compounds containing highly electronegative substituents. The inorganic acceptors are the halogens, metal halides, etc. One of the best known CT complexes is that of benzene/iodine. It shows an absorption band at 3000 Å which has no counterpart in the spectrum of either benzene or iodine. In the quinhydrone complex, the donor and the acceptor orbitals are delocalized π molecular orbitals and the chemical bond between the two components of the complex is a delocalized bond.

The aromatic carbonyl compounds have absorption bands which can be identified as $\pi^* \leftarrow \pi$, $\pi^* \leftarrow n$ transistions and charge transfer (CT) transitions. Of these transitions, the CT transitions have the highest intensity, which means that they have the highest value of the extinction coefficient and of the oscillator strength. The **oscillator strength** of a transition is defined as the ratio of the experimental intensity to the theoretical intensity. In the complexes of the transition metal ions, intramolecular CT transitions may be observed where the electron is transferred from the ligand (L) to the metal ion (M), *i.e.*, the $L \rightarrow M$ transition can be a CT transition. The CT transitions are prominent in biological systems, too.

We must emphasize the difference between a normal electronic transition and a charge-transfer transition. In the former, the electron is promoted from the ground state to the excited state of the *same* molecule ; in the latter, the electron is promoted from the BMO of the donor (D) to the ABMO of the acceptor (A). The CT transition is determined by the ionization potential of the donor and the electron affinity of the acceptor.

ELECTRONIC SPECTRA OF TRANSITION METAL COMPLEXES*

The valence shell electrons in a transition metal complex are arbitrarily divided into : those in orbitals primarily associated with the metal, those in orbitals associated with ligands and those responsible for the metal-ligand bonding. Fig. 38 shows a simple energy level diagram for a transition metal complex. For instance, in a simple hexa-aquo ion such as $[Ni(H_2O)_6]^{2+}$, there are partly filled metal 3*d* orbitals containing eight electrons. We thus speak of this as a d^8 species. There are also electrons associated with the O–H bonds in H_2O molecules and others in BMOs formed by the overlap of lone-pair filled orbitals on oxygen atom with vacant *s*, *p* and *d* orbitals on the metal. The metal-ligand BMOs are ordinarily full, as are the bonding orbitals of the ligands themselves. There are also lone-pair orbitals not involved in metal-ligand bonding. Again, some ligands, such as organic ligands

*For detailed information, refer to the sister publication, **Principles of Inorganic Chemistry** by Puri, Sharma & Kalia.

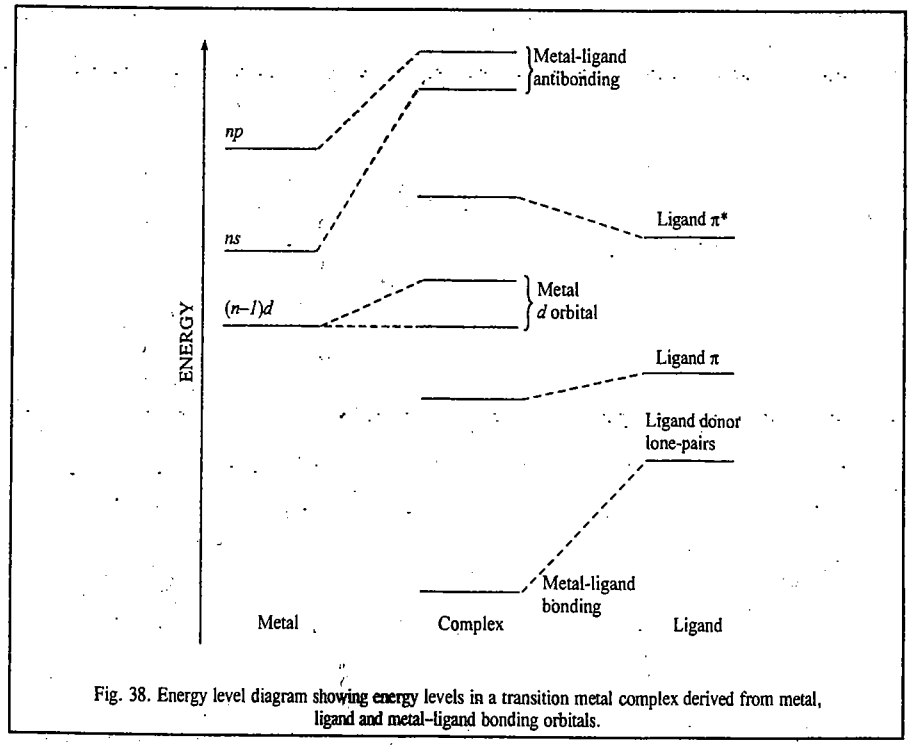

Fig. 38. Energy level diagram showing energy levels in a transition metal complex derived from metal, ligand and metal–ligand bonding orbitals.

containing π-systems, exemplified by pyridine and other aromatic amines, have low-lying empty orbitals, generally weakly antibonding in character. Since metal–ligand bonding is likely to involve the very orbitals that are the lower energy levels in such transitions, the transition energies are greatly affected by the metal centre, usually shifting to higher energy compared with those in the free ligand. More subtle effects are found to occur when we compare one complex with another. Thus, ligand–ligand transition energies will be found to vary with the nature and the charge on the central metal ion.

We shall now briefly comment on two important topics, *viz.*, 1. high-spin and low-spin states and 2. Jahn-Teller distortion.

1. High-spin and low-spin states. When a metal centre has more than enough electrons to half fill the lower set of d orbitals arising from ligand field splitting (the t_{2g} set for an octahedral complex, for instance), a complication arises through a competition between the tendency of all electrons to enter the lowest possible energy level and the tendency for as many electrons as possible to occupy different orbitals so that they may have the same spin. If the gap due to the ligand field splitting, Δ, is large, the first tendency will win and we will find as many electrons as possible in the lower set of d orbitals, even though the spins have to be paired when the electrons occupy the same orbital. This is called a **low-spin state.** If, on the other hand, the second tendency wins because the energy gap Δ is small, we will find electrons occupying some or all of the upper d orbitals (in the e_g set) as well as the lower t_{2g} set, thereby resulting in a higher total spin. This is called a **high-spin state.** This is illustrated in Fig.39 for a d^5 metal centre, such as Fe^{3+} in an octahedral environment. Here the low-spin case can be written as $t_{2g}^5 e_g^0$, with only one unpaired electron. The high-spin case is $t_{2g}^3 e_g^2$ with five unpaired electrons.

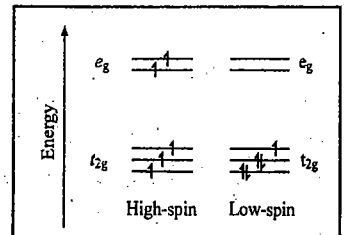

Fig. 39. High-spin and low-spin electron configurations of a d^5 metal centre in an octahedral environment.

2. Jahn-Teller Distortion. Theoretical treatment carried out in 1937 by H.A. Jahn and E. Teller and borne out experimentally shows that any complex with a degenerate (e or t) set of orbitals which is occupied unsymmetrically (*i.e.*, neither completely filled nor half filled) distorts its ligand environment spontaneously in such a way as to remove the degeneracy. For example, an octahedral d^7 ion with a filled t_{2g} (lower) set of d orbitals and a single electron in the doubly degenerate e_g upper set would distort in such a way that the e_g levels split, such as by an elongation along the z-axis, giving a tetragonal ligand arrangement as in Fig 40*(c)*. The single electron then occupies the lower orbital d_{z^2}, thereby reducing the overall energy pattern of the system. This clearly allows a new transition from the d_{z^2} to the empty $d_{x^2-y^2}$ level. As a consequence, the number of bands associated with an excitation of an electron from the t_{2g} to the e_g set of levels will increase—both sets are now split, so several extra bands will appear in the electronic spectrum.

We thus see that the high-spin/low-spin states and Jahn–Teller distortion have profound effects on the analysis of the d–d bands to which we now turn our attention.

Metal–Metal Transitions (d – d Bands)

The most characteristic transitions of transition metal complexes, known as the d–d transitions are those involving partly filled d subshells. These are formally forbidden in a strictly octahedral environment. According to the symmetry selection rules, the d levels separate into t_{2g} (lower) and e_g (upper) sets (Fig. 40) and the excitation of an electron from one set to the other is forbidden by the g → u selection rule (as well as the **Laporte rule** which prohibits transitions between levels which have the same orbital angular momentum quantum number, l ($\Delta l = \pm 1$). In a tetrahedral system, the d shell separates into e (lower) and t_2 (upper) sets (Fig. 40). Nor only is there no g/u distinction in this case, as there is no inversion centre, but even the Laporte rule can be circumvented, as the metal p subshell also has symmetry t_2, so that the upper d set can acquire some p orbital (l=1) character and the $e \rightarrow t_2$ transition becomes fully allowed. Even in truly octahedral systems, d – d transitions do occur, though only weakly, usually because of vibronic coupling involving vibrations though of low symmetry.

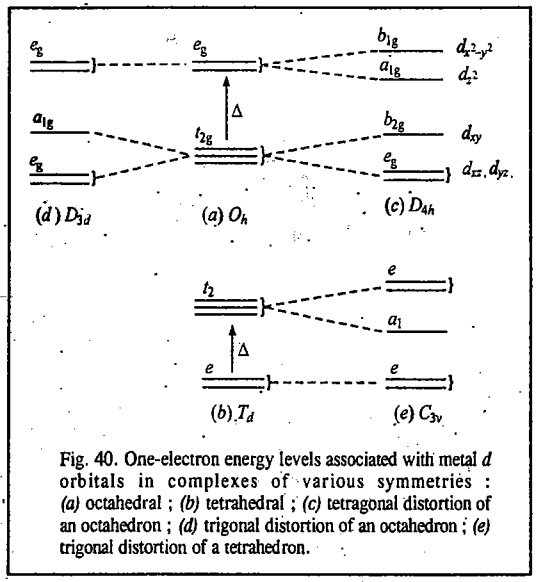

Fig. 40. One-electron energy levels associated with metal d orbitals in complexes of various symmetries : *(a)* octahedral ; *(b)* tetrahedral ; *(c)* tetragonal distortion of an octahedron ; *(d)* trigonal distortion of an octahedron ; *(e)* trigonal distortion of a tetrahedron.

For complexes with lower symmetry, the two-fold degeneracy of the e levels and/or the three-fold degeneracy of the t_2 levels is lost giving rise to more complex patterns of d levels thereby allowing more transitions to be observed. Figs. 39*(c)*, *(d)* and *(e)* show the energy level diagrams resulting from the more important distorted environments. The energy level diagrams of Fig. 40 refer strictly to the energy of a single electron, much as the energy level diagram for a hydrogen atom gives the possible energies for the single electron. For complexes with only a single d electron (such as those of Ti^{III}, V^{IV},

Cr^{V}, Mn^{VI}, etc.), such diagrams give a fairly good idea of the spectra to be expected in various complexes and Δ, the ligand field splitting parameter which gives the energy of the single transition for an octahedral or tetrahedral complex, depends on only a single parameter, *viz.*, the ligand field strength. Most transition metal complexes, however, have more than one *d* electron and the one-electron energy levels become less appropriate because of the importance of couplings between the spin and orbital angular momenta of the electrons. In this case, it is convenient to start with the electronic states (term symbols) of the free ion and then to consider the effects of the symmetry of the complex on the energy levels.

Let us, for illustrative purposes, consider the d^3 system. The lowest energy state for the free atom or ion is usually the quartet ^4F, with another quartet state, ^4P, of higher energy. In an octahedral environment, the ^4P state remains single, having symmetry $^4T_{1g}$, but the ^4F state gives rise to three levels whose energies diverge as the ligand field strength increases (Fig. 40). All the levels involved are still *g* (symmetric to the inversion centre), so all transitions are formally forbidden by both the $g \rightarrow u$ and the Laporte selection rules, but there are three possible excitations, from the lowest level to the three higher ones. These give bands in simple systems of this type, such as VCl_6^{4-} in molten $AlCl_3$. Fig. 41 is called an Orgel diagram for a d^3 system in an octahedral environment. Similar diagrams can be drawn up for any number of *d* electrons in environments of any symmetry, showing the nature and energies of the transitions expected for a given ligand field strength. L.E. Orgel was the first to introduce these diagrams in the 1950s.

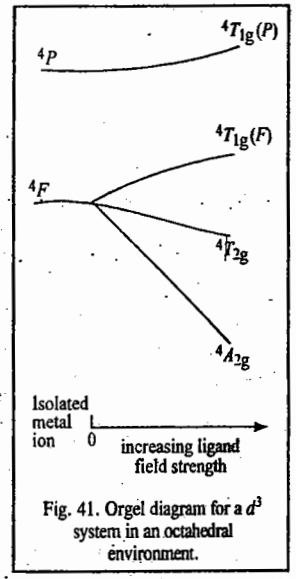

Fig. 41. Orgel diagram for a d^3 system in an octahedral environment.

The positions (energies) and intensities of the *d–d* bands can be used to infer the nature of the central metal and its surrounding ligands. We might, however, mention that although the information derived from the analysis of *d–d* band spectra is not formally 'structural' in the same sense as that derived from diffraction methods, from XPS or (indirectly) from the analysis of a vibrational spectrum, this may be all that can be obtained for a species in solution. Thus, it plays a valuable role in elucidating the structures of transition metal complexes. For an excellent treatment, see B.N. Figgis, *Introduction to Ligand Fields*, Wiley, 1966.

The Tanabe-Sugano diagrams, introduced by the two Japanese chemical physicists in 1954, give a more rigorous treatment of the electronic spectra of transition metal complexes than the Orgel diagrams. These are discussed at length in inorganic chemistry books.

Charge Transfer Bands

Because of the close approach of metal atom and ligand it is often possible for transitions to occur between a metal-based level and a ligand-based level. As these formally involve transfer of an electron from metal to ligand or from ligand to metal, they are called charge transfer (CT) transitions. These are particularly important for Second and Third row transition metal complexes where they tend to dominate the spectra so that the weak *d–d* bands and even ligand bands are obscured by the much stronger charge transfer bands. There are two kinds of charge transfer bands, *viz.*, ligand-to-metal charge transfer (LMCT) band and the metal-to-ligand charge transfer (MLCT) band. In an LMCT transition, a lone pair of the ligand is promoted into a predominantly metal orbital. Charge transfer bands in the visible region of the spectrum (and hence contributing to the intense colours of the complexes) may occur if the ligands have lone pairs of relatively high energy or if the metal has low-lying empty orbitals. In an MLCT transition, a transfer of charge from metal to ligand is observed in complexes with ligands that have low-lying π^* orbitals, especially aromatic ligands, such as bipyridine and phenanthroline.

An example of a CT band is provided by the permanganate ion. Here we formally write the ground state as $[Mn^{7+}(O^{2-})_4]$, in which case the charge transfer transition involves transferring one electron from O^{2-} ligand to Mn^{7+}, giving $[Mn^{6+}(O^{2-})_3O^-]$ as the upper state. This is an example of an LMCT and may be regarded as an *internal redox reaction*. The reverse MLCT is possible, as, for example, in organic amine complexes of low-valent metals, such as $[TiCl_3(bipy)]$, where bipy is 2,2′-bipyridine. Here the ground state is $[Ti^{3+}(Cl^-)_3bipy^0]$ and the excited state is $[Ti^{4+}(Cl^-)_3bipy^-]$. CT bands may overlap with *d – d* bands and with bands corresponding to excitation within ligands themselves, and it is often hard to make unambiguous assignments. Fig. 42 shows the electronic energy levels and CT transitions.

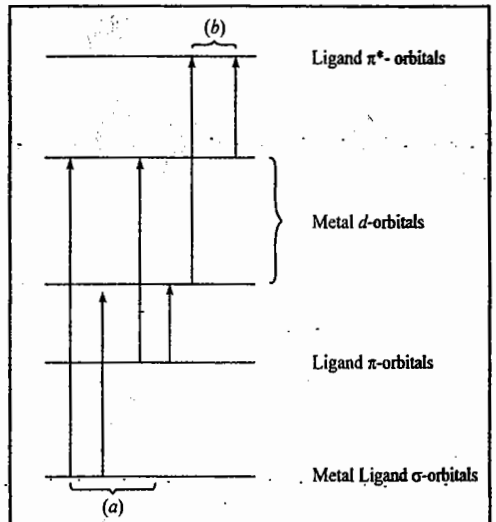

Fig. 42. Some possible LMCT transitions *(a)* and MLCT transitions *(b)*. Note that the metal-ligand σ-bond orbitals are derived primarily from ligand-based orbitals.

Electronic Spectra of Lanthanides and Actinides

The 4*f* electrons in the lanthanides and the 5*f* electrons in the actinides and their compounds are well screened from external effects by the filled shells of higher quantum numbers. This has important consequences, the first being that the *f–f* bands of such species are characteristic of the element concerned and are hardly affected by even the ligands in the immediate vicinity. All compounds of a particular ion are expected to have very similar spectra though species with different numbers of *f* electrons will have different states and hence different transitions. The lanthanide elements are generally found in the form of complexes of M^{3+} ions, each element having its own characteristic colour. The actinide elements have more varied colours since they are found in variable oxidation states. However, the spectra of actinide compounds derived from a given oxidation state are generally very similar.

The second consequence of this insulation of *f* electrons from external influences is that the *f–f* bands are sharp—in fact, much narrower than the typical *d–d* bands. They are also characteristically weak, the effects of deviations from perfect inversion symmetry (which is often found for complexes of lanthanide elements) being insufficient to relax the $g \rightarrow u$ selection rule. All *f* levels are of *u* symmetry in a centrosymmetric environment so that *f–f* transitions are forbidden. The colours of lanthanide compounds are, therefore, pale. The actinides have rather strong colours because of the effect of spin-orbit coupling which is greater for heavier atoms. Charge transfer transitions are less important for the *f*-block elements than for the *d*-block elements, mainly because they are less likely to form complexes with ligands having suitable donor orbitals. The Canadian physicist, G. Herzberg (1904-1999), known for his great monographs on spectroscopy, was awarded the 1971 Chemistry Nobel Prize for contributions to electronic structure, spectroscopy and geometry of molecules and free radicals.

ELECTRONIC SPECTRA OF CONJUGATED MOLECULES

The electronic spectra of conjugated systems using free-electron molecular orbital (FEMO) theory is based on the theory proposed in the 1930s by Pauling and, independently, by Kathleen Lonsdale and H. Kuhn, that the pi electrons are delocalized over the entire carbon skeletal framework. Thus, there is no true carbon–carbon single bond or carbon–carbon double bond and we can use the particle-in-a-one dimensional box approach for such systems. For this model, we have

$$E_n = n^2h^2/(8m_ea^2) \qquad (n = 1, 2, 3,\ldots) \qquad \ldots(94)$$

The electrons in the π MOs are filled according to the Pauli principle and Hund's rule. Thus, if N is the number of π orbitals, only $N/2$ π orbitals are filled in the ground state.

The *longest wave length* transition involves the excitation of the π electron from the $N/2$ HOMO to $(N/2)+1$ LUMO. Hence, the frequency of the electronic transition is given by

$$\nu = \frac{E_{(N/2)+1} - E_{N/2}}{h} = \frac{h}{8m_e a^2}\left[\left(\frac{N}{2}+1\right)^2 - \left(\frac{N}{2}\right)^2\right]$$

$$= h\,(N+1)/8m_e a^2 \qquad ...(95)$$

$$\therefore \quad \bar{\nu} = \nu/c = h\,(N+1)/(8m_e a^2 c) \qquad ...(96)$$

Let us now estimate the value of the chain length a of the conjugated system (*i.e.*, the width of the box). Since there is a residual free valence at each of the two terminal carbon atoms, hence

a = number of actual C—C bonds between N carbon atoms + 2

$$= (N - 1 + 2)\,l = (N + 1)\,l \qquad ...(97)$$

where l is the C—C bond length, assumed to be equal to 139 pm. Here we have made allowance for the molecular orbitals to extend one bond length l past each terminal carbon atom which is a very plausible assumption. Substituting for a in Eq. 96, we have

$$\bar{\nu}\,(\text{cm}^{-1}) = \frac{h(N+1)}{8m_e c(N+1)^2 l^2} = \frac{h}{8m_e c(N+1)l^2}$$

$$= 148{,}137{\cdot}6/(N+1) \text{ (after substituting various constants)} \qquad ...(98)$$

A more realistic approach is the use of sinusoidal form of potential energy with a minimum at the centre of the double bond considered. Eq. 98 is then modified to

$$\bar{\nu}\,(\text{cm}^{-1}) = \frac{153{,}000}{N+1} + 16{,}000\left(1 - \frac{1}{N}\right) \qquad ...(99)$$

Example 12. Using the FEMO theory, estimate the wave number of the lowest energy transition in the 1, 3, 5-hexatriene molecule.

Solution : The 1, 3, 5-hexatriene molecule is

$$CH_2=CH-CH=CH-CH=CH_2 \quad \textit{i.e.,} \quad CH_2{=}CH{=}CH{=}CH{=}CH{=}CH_2$$

Here $N = 6$. Hence,

$$\bar{\nu}(\text{cm}^{-1}) = 148{,}137{\cdot}6/(N+1) = 148{,}137{\cdot}6/7 = 21{,}162{\cdot}5 \qquad \text{[Eq. 98]}$$

Using the modified FEMO theory,

$$\bar{\nu}(\text{cm}^{-1}) = \frac{153{,}000}{N+1} + 16{,}000\left(1 - \frac{1}{N}\right) = 34{,}495{\cdot}83 \qquad \text{[Eq. 99]}$$

(The experimental value is 37,313·4 cm)

Example 13. Derive an expression for the lowest frequency (*i.e.*, highest wave length) transition from HOMO to LUMO for polymethine dyes.

Solution : The general formula of polymethine dyes is

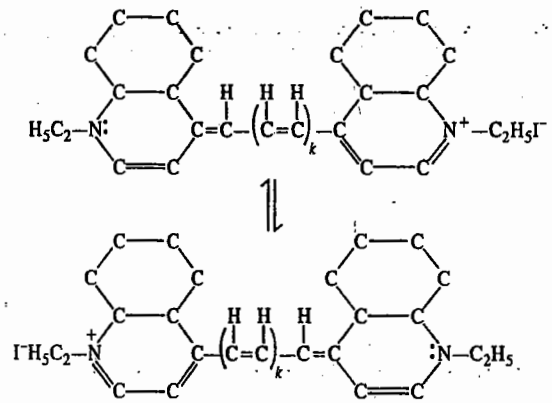

Using the FEMO theory,

$$\bar{\nu}(\text{cm}^{-1}) = \frac{h(N+1)}{8m_e a^2 c} \qquad \text{[Eq. (96)]}$$

If n_c is the number of carbon atoms in the polymethine dye, then N (the total number of π-electrons) = n_c+3. The three electrons are due to two nitrogen atoms, two due to one and one due to the other N atom. Assuming, as before, that the molecular orbitals extend by one bond length on either side and all bonds are equal

$$a = (n_c + 2 - 1 + 2)l \quad \text{or} \quad a = (n_c + 3)l \qquad ...(i)$$

Substituting the values of a and N, Eq. 96 becomes

$$\bar{\nu} = \frac{h(n_c + 3 + 1)}{8m_e c(n_c + 3)^2 l^2} = \frac{(n_c + 4) \times 1{\cdot}48 \times 10^5}{(n_c + 3)^2}\ \text{cm}^{-1} \qquad ...(ii)$$

Example 14. Assuming that $k = 1$ in the polymethine dye given above, calculate the wave number and the wave length of the lowest energy HOMO-to-LUMO electronic transition.

Solution : If $k = 1$, then $n_c = 9$.

Hence, from Eq. *(ii)* of Example 13, we obtain

$$\bar{\nu} = 1{\cdot}3361 \times 10^4\ \text{cm}^{-1} \quad \text{and} \quad \lambda = 748{\cdot}4\ \text{nm}$$

MISCELLANEOUS SOLVED EXAMPLES IN SPECTROSCOPY

Example 15. The selection rules for spectral transitions in atomic spectra are : *(i)* Δn = 1, 2, 3, 4,..., and *(ii)* $\Delta l = \pm 1$. Using these selection rules, determine which of the following transitions are allowed and which are forbidden :

(a) $1s \rightarrow 2p$ *(b)* $2s \rightarrow 3s$ *(c)* $2p \rightarrow 3s$

(d) $3d \rightarrow 4f$ *(e)* $4p \rightarrow 5f$ *(f)* $3p \rightarrow 3d$

Solution : For allowed transitions, both selection rules should be obeyed simultaneously. Accordingly,

Allowed transitions are : *(a)*, *(c)*, *(d)* and *(f)*

Forbidden transitions are : *(b)* and *(e)*.

Example 16. Obtain an expression for the natural line-width of a spectral transition. Using this expression calculate the natural line-width (in cm^{-1}) of a spectral line which results when a quantum system in an

excited state of life time 0·1 ns (nanosecond) makes a transition to the ground state.

Solution : We know from the Heisenberg uncertainty principle that

$$\Delta E \times \Delta t \approx h/4\pi \qquad \ldots(i)$$

where ΔE is the uncertainty in the energy and Δt is the uncertainty in lifetime of the quantum system—an atom or a molecule. Since for a photon of frequency ν, $E = h\nu$, hence,

$$\Delta E = h\Delta\nu \qquad \ldots(ii)$$

From Eqs. *(i)* and *(ii)*,

$$h\Delta\nu \times \Delta t = h/4\pi$$

$$\therefore \quad \Delta\nu = 1/4\pi\Delta t$$

If $\Delta t \approx \tau$, the life time, then

$$\Delta\nu = 1/4\pi\tau \qquad \ldots(iii)$$

Now $\tau = \Delta t = 0{\cdot}1 \text{ ns} = 0{\cdot}1 \times 10^{-9} \text{ s} = 1{\cdot}0 \times 10^{-10} \text{ s}$,

hence $$\Delta\nu = \frac{1}{4(3{\cdot}1416)(1{\cdot}0 \times 10^{-10}\,\text{s})} = 0{\cdot}8 \times 10^{9}\ \text{s}^{-1}$$

$$\therefore \quad \Delta\bar{\nu} = \frac{\Delta\nu}{c} = \frac{0{\cdot}8 \times 10^{9}\,\text{s}^{-1}}{3 \times 10^{10}\,\text{cm}^{-1}} = 0{\cdot}0267\ \text{cm}^{-1}$$

Example 17. Using the Heisenberg unertainty principle, estimate the lifetime of an energy state which gives rise to a line-width of *(a)* 0·1 cm *(b)* 1 cm *(c)* 60 MHz.

Solution : As shown in the last example,

$$\tau \approx 1/4\pi\Delta\nu = 1/4\pi c\Delta\bar{\nu} \qquad (\because\ \nu = c\bar{\nu})$$

(a) $$\Delta\bar{\nu} = 0{\cdot}1\ \text{cm}^{-1}\ ; \quad \tau \approx \frac{1}{(4\pi)(3 \times 10^{10}\,\text{cm s}^{-1})(0{\cdot}1\,\text{cm}^{-1})} = 2{\cdot}5 \times 10^{-11}\ \text{s}$$

(b) $$\Delta\bar{\nu} = 1{\cdot}0\ \text{cm}^{-1}\ ; \quad \tau \approx 2{\cdot}7 \times 10^{-12}\ \text{s}$$

(c) $$\Delta\bar{\nu} = 60\ \text{MHz}\ ; \quad \tau \approx \frac{1}{(4\pi)(60 \times 10^{6}\,\text{s}^{-1})} = 1{\cdot}35 \times 10^{-9}\ \text{s} = 1{\cdot}35\ \text{ns}$$

Example 18. In a certain fluxional molecule two groups that are interchanged by the conversion have vibrational absorption bands at 1650 cm^{-1} and 1655 cm^{-1}. Calculate, using the Heisenberg uncertainty principle, the minimum lifetime of the states for which the separate absorptions could be distinguished.

Solution : The absorptions are indistinguishable if the lifetimes are less than $1/4\pi\Delta\nu$, or in terms of the wave number, *less than*

$$\tau = \frac{1}{4\pi c\Delta\bar{\nu}} = \frac{1}{(4\pi)(3 \times 10^{10}\,\text{cm s}^{-1})(5\,\text{cm}^{-1})} = 0{\cdot}5 \times 10^{-12}\ \text{s} = 0{\cdot}5\ \text{ps}$$

0·5 ps is the time for the molecule to undergo about 10 oscillations in each conformation.

Example 19. Experimentally it is found that a molecule in a liquid undergoes approximately 10^{13} collisions per second. Calculate the linewidth (in cm^{-1}) of a spectral transition between a vibrationally excited state and the ground state assuming *(a)* that every collision deactivates the molecule vibrationally *(b)* that one in fifty collisions is effective in deactivating the molecule.

Solution : $\Delta\bar{\nu} = 1/(4\pi c\tau)$, where τ is the lifetime of the state.

(a) $$\tau = (1/10^{13})\ \text{s} = 10^{-13}\ \text{s}$$

$$\Delta\bar{\nu} \approx \frac{1}{(4\pi)(3 \times 10^{10}\,\text{cm s}^{-1})(10^{-13}\,\text{s})} = 25\ \text{cm}^{-1}$$

(b) $$\tau = (50/10^{13})\ \text{s} = 5 \times 10^{-12}\ \text{s}$$

$$\Delta\bar{\nu} \approx \frac{1}{(4\pi)(3 \times 10^{10}\,\text{cm s}^{-1})(5 \times 10^{-12}\,\text{s})} = 0{\cdot}5\ \text{cm}^{-1}$$

Example 20. Which of the following molecules will show a pure rotational (microwave) spectrum and why: H_2, HCl, CO, CH_3Cl, H_2O (liquid), NH_3, NH_4Cl (s) ?

Solution : Pure rotational spectra are shown by a *gaseous* molecule which possesses a permanent dipole moment, μ. Thus, the microwave-active molecules are : HCl, CO, CH_3Cl and NH_3.

Example 21. Which of the following molecules will show a vibrational infrared spectrum and why : H_2, HCl, CO, CH_3Cl, H_2O, NH_3, NH_4Cl, CH_3–CH_3, C_6H_6, CCl_4, CO_2.

Solution : Vibrational spectra are shown by a molecule when the vibrational motion is accompanied by a *change* in dipole moment *i.e.*, $d\mu/dr \neq 0$. All the molecules (except H_2) will be infrared-active. H_2 does not have a dipole moment, nor is the vibrational motion accompanied by a change in dipole moment. Again, although CO_2 is a symmetric molecule with no dipole moment, the *asymmetric* stretching motion and *bending* mode of vibration do result in a change in dipole moment.

Example 22. Which of the following molecules will show a rotational Raman spectrum and why : H_2HCl, CO, CH_4, CH_3Cl, H_2O, NH_3, C_2H_6, SF_6 ?

Solution : Rotational Raman spectra are shown by a molecule in which the rotational motion is accompanied by a *change* in the *polarizability i.e.*, $d\alpha/dr \neq 0$. Here all the molecules (except CH_4 and SF_6) will show rotational Raman spectrum.

Example 23. Which of the following molecules will show a vibrational Raman spectrum and why : H_2, HCl, CO, CH_4, CH_3Cl, H_2O, NH_3, C_2H_6, SF_6 ?

Solution : Vibrational Raman spectra are shown by a molecule in which the vibrational motion is accompanied by a *change* in the *polarizability*. Here all the molecules will show vibrational Raman spectrum.

Example 24. Give the quantum mechanical description of the Franck-Condon principle with special reference to the Franck-Condon factor and derive an expression for the relative intensity of the 0–0 vibronic transition as a function of ΔR, the change in nuclear coordinates.

Solution : Quantum mechanically, the vibronic transition (as described by the Franck-condon principle) is a vertical transition which qualitatively occurs from the ground vibrational state of the lower electronic state to the vibrational state that it most resembles in the upper electronic state. In that way, the vibrational wavefunctions undergo least change, which corresponds to the preservation of the dynamical state of the nuclei as required by the Franck–Condon principle. The vibrational state with a wavefunction that most resembles the original bell-shaped Gaussian function of the vibrational ground state is one with a peak immediately above the ground state. Thus, the wavefunction corresponds to the energy level that lies in much the same position as in the vertical transition of the classical description. It can be shown that the transition dipole moment between the ground vibronic state, $|\varepsilon\, \upsilon>$ and the upper vibronic state $|\varepsilon'\upsilon'>$ is given by

$$<\varepsilon'\upsilon'|\mu|\,\varepsilon\upsilon> = \mu_{\varepsilon'\varepsilon}\int \psi^{*}_{\upsilon'}(R)\,\psi_{\upsilon}(R)\,d\tau_N = \mu_{\varepsilon'\varepsilon}S(\upsilon',\upsilon)$$

where $$S(\upsilon',\upsilon) = \int \psi^{*}_{\upsilon'}(R)\,\psi_{\upsilon}(R)\,d\tau_N$$

is the overlap integral between the two vibrational states in their respective electronic states. Here R refers to the nuclear coordinates. The transition dipole moment is therefore largest between vibrational states that have the greatest overlap. This is the quantitative version of the previous qualitative discussion, where we looked for the upper vibrational state that had a local bell-shaped region above the gaussian function of the ground vibrational state of the lower electronic state. Here $\mu_{\varepsilon'\varepsilon}$ may be treated as a constant.

Several vibrational states have similar values of $S(\upsilon',\upsilon)$, and so transitions occur to all of them. Thus, a *progression* of transitions is stimulated and a series of lines are observed in the electronic spectrum. The relative intensities of the lines are proportinal to the square of the transition dipole moments and hence to the **Franck-Condon factors,** $|S(\upsilon',\upsilon)|^2$. The 0–0 transition refers to the transition from the ground vibrational level ($\nu = 0$) of the ground electronic state to the vibrational state with $\upsilon' = 0$ of the upper electronic state.

We need to evaluate the Franck-Condon factor $|S(0,0)|^2$. To do so we calculate the overlap integral $S(0,0)$ using harmonic oscillator wavefunctions,one centred on $x=0$ and the other on $x=\Delta R$. We shall need the following standard integral :

$$\int_{-\infty}^{\infty} e^{-ax^2}dx = \left(\frac{\pi}{a}\right)^{1/2}$$

The wavefunctions for the two states are

$$\psi_0 = \left(\frac{\alpha}{\pi}\right)^{1/4} e^{-\alpha x^2/2}, \psi_0' = \left(\frac{\alpha}{\pi}\right)^{1/4} e^{-\alpha(x-\Delta R)^2/2}$$

where $\alpha = m\omega/\hbar$ and the wavefunctions are normalized in the sense

$$\int_{-\infty}^{\infty} |\psi_0|^2 \, dx = 1$$

Hence,

$$S(0,0) = \left(\frac{\alpha}{\pi}\right)^{1/2} \int_{-\infty}^{\infty} e^{-\alpha x^2/2 - \alpha(x-\Delta R)^2/2} dx$$

$$= \left(\frac{\alpha}{\pi}\right)^{1/2} e^{-\alpha(\Delta R/2)^2} \int_{-\infty}^{\infty} e^{-\alpha(x-\Delta R/2)^2} dx = e^{-\alpha(\Delta R/2)^2}$$

The Franck-Condon factor for the transition is therefore

$$|S(0,0)|^2 = e^{-\alpha(\Delta R)^2/2}$$

This function is plotted in Fig. 43. Strong dependence of the function on ΔR is clearly evident.

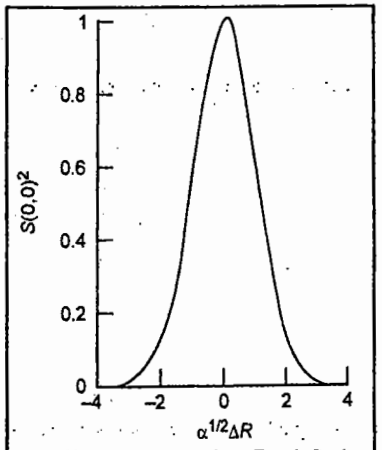

Fig. 43. The variation of the Franck-Condon factor with displacement of the minimum of the upper electronic state. Note that the factor is a maximum (1) when the two curves lie exactly over one another.

The recent references on spectroscopy and lasers are :

Gupta, R., (ed.), *Laser Spectroscopy (selected reprints)*, American Association of Physics Teachers, Pennsylvania, 1993.

van Hecke, G.R., and K.K. Karukstis, *A Guide to Lasers in Chemistry*, Jones and Bartlett, Boston, 1998.

Siegman, A.E., *Lasers*, 2nd edn., University Science Books, Sausalito, California, 1986.

Svelto, O., *Principles of Lasers*, 4th edn., Plenum, 1998.

Thorp, J.S., *Masers and Lasers*, Macmillan, London, 1969.

McHale, J.L., *Molecular Spectroscopy*, Prentice-Hall, 1999.

Scully, M.O., and M.S. Zubairy, *Quantum Optics*, Cambridge, 1997.

Struve, W., *Fundamentals of Molecular Spectroscopy*, Wiley Interscience, 1989.

Svanberg, S. *Atomic and Molecular Spectroscopy*, 3rd edn., Springer-Verlag, Berlin, 2001.

Aruldhas, G., *Molecular Structure and Spectroscopy*, 2nd edn., Prentice-Hall of India, New Delhi, 2007.

Batani, D., C.J. Joachain, S. Martelluci, and A.N. Chester (eds.), *Atoms, Solids and Plasmas in Super-Intense Laser Fields*, Kluver Academic-Plenum, 2001.

Turro, N.J., *Modern Molecular Photochemistry*, University Science Books, Sausalito, California, 1991.

Demtröder, W., *Laser Spectroscopy*, 3rd edn., Springer, Berlin, 2003.

Chu, S.I., *Advances in Atomic and Molecular Physics* 21, 197 (1985).

Faisal, F.H.M., *Theory of Multiphoton Processes*, Plenum, 1986.

I. Review Questions

1. Discuss the factors which determine the width and intensity of spectral lines.
2. Show that for a rigid diatomic rotor the moment of inertia is given by $I = \mu r^2$.
3. Using the energy level expression and the selection rules draw an energy level diagram and the spectral transitions for the microwave (pure rotational) spectrum of a rigid diatomic rotor. Also show the appearance of the spectrum. No discussion is required.

4. Using the energy level expression and the appropriate selection rules draw an energy level diagram and the spectral transitions for the rotation–vibration spectrum of a diatomic molecule. Also show the appearance of the spectrum consisting of the P and R branches. No discussion is required.
5. Discuss the quantum theory of Raman spectroscopy and show how the Stokes and anti-Stokes lines appear in the Raman spectrum of a molecule.
6. Using the energy level expression and the appropriate selection rules draw an energy level diagram and the spectral transitions for the rotational Raman spectrum of a rigid diatomic rotor. Also show the appearance of the spectrum. No discussion is required.
7. Why are the anti-Stokes lines less intense than the Stokes lines in the Raman spectrum ? How has the use of the laser source of exciting radiation helped in Raman spectroscopy ?
8. State and illustrate with suitable potential energy curves the Franck–Condon principle in the vibronic spectrum of a diatomic molecule. Discuss briefly.
9. Which factors govern the intensities of rotational spectral lines in a rigid diatomic rotor ? Illustrate using the appropriate curve.
10. What is the Stark effect in microwave spectra ?
11. How is microwave spectroscopy used in investigating (*i*) internal rotation and (*ii*) the inversion spectrum of NH_3 ?
12. What is the effect of (*i*) centrifugal distortion on the rotational energy levels of a rigid diatomic rotor and of (*ii*) anharmonicity on the vibrational energy levels of a diatomic S.H.O. ?
13. Sketch the normal modes of vibration of (*a*) H_2O and (*b*) CO_2 and determine which are IR-active/inactive and why?
14. Why do overtones and combination bands appear in IR spectra ? Also, how does the phenomenon of Fermi resonance appear in IR spectra ?
15. Discuss briefly, using an energy level diagram, the resonance Raman spectroscopy. What are its advantages over simple Raman spectroscopy ?
16. Show diagrammatically the $\sigma^* \leftarrow \sigma$, $\sigma^* \leftarrow n$, $\sigma^* \leftarrow \pi$ transitions in the electronic spectra of polyatomic molecules.
17. Discuss briefly the change-transfer (CT) spectra of molecules.
18. Discuss briefly (*a*) Jahn-Teller distortion (*b*) metal–metal transition *d–d* bands and (*c*) charge-transfer bands in the electronic spectra of transition metal complexes.
19. How is the particle-in-a-box model applied to FEMO theory of the electronic spectra of conjugated molecules ?
20. Discuss SRS, Inverse Raman scattering and CARS, emphasizing the salient features.

II. Problems

1. Calculate the energy in joules per quantum, joules per mole, and in electron-volts (eV) of photons of wave length 300 nm.
   [Ans. $6{\cdot}62\times10^{-19}$ J; $3{\cdot}98\times10^{5}$ J mol^{-1}, 4·13 eV]
2. Calculate the frequency (in cm^{-1}) and wave length (in cm) of the rotational transition ($J' = 0 \rightarrow 1$) for $D^{35}Cl$
   [Ans. 10·89 cm^{-1} ; 0·9183 cm]
3. The far infrared spectrum of HI consists of a series of equally spaced lines with spacing equal to 12·8 cm^{-1}. Calculate (*a*) the moment of inertia and (*b*) the internuclear distance.
   [Ans. (*a*) $4{\cdot}37\times10^{-47}$ kg m^2 (*b*) 0·163 nm]
4. Calculate the relative Boltzmann populations of the first five rotational levels of the ground vibrational state of $H^{35}Cl$ at 300 K. Given the rotational constant is 10·4398 cm^{-1}.
   [Ans. N_J/N_0 for J = 0, 1, 2, 3, 4, 5 = 1·00, 2·71, 3·70, 3·84, 3·31 and 2·45]
5. The force constant of HF molecule is 970 N m^{-1}. Calculate the fundamental vibrational frequency as well as the zero-point energy.
   [Ans. $1{\cdot}247\times10^{14}$ s^{-1} ; $4{\cdot}129\times10^{-20}$ J]
6. Why is it that in the excited state of a molecule, the vibrational frequency, ν, is smaller than in the ground state ?
   [Ans. The reason is that ν is proportional to force constant, k, which is smaller in the excited state.]

7. The hydrogen halides have the following fundamental vibrational frequencies : HF (4141·3 cm^{-1}), $H^{35}Cl$ (2988·9 cm^{-1}), $H^{81}Br$ (2649·7 cm^{-1}), HI (2309·5 cm^{-1}). Calculate the force constants of the hydrogen–halogen bonds.
[Ans. 967, 516, 412, 314 N m^{-1}]

8. From the data in the last problem predict the fundamental vibrational frequencies of the deuterium halides.
[Ans. 3002, 2144, 1886, 1640 cm^{-1}]

9. Calculate the relative Boltzmann population of the $v = 1$ and $v = 0$ vibrational energy levels of a diatomic molecule, at 25°C, if they are separated by 1,000 cm^{-1}. **[Ans. $N_{v=1}/N_{v=0}$ = 0·008]**

10. The anharmonicity constant for $^{35}Cl^{19}F$ is $\omega_e x_e$ = 9·9 cm^{-1} and the fundamental vibrational frequency is 793·2 cm^{-1}. Calculate the energies of the first four vibrational energy levels.
[Ans. 1167·52 cm^{-1}, 1921·13 cm^{-1}, 2654·23 cm^{-1}, and 3368·93 cm^{-1}]

11. How many fundamental vibrational frequencies (*i.e.*, fundamental vibrational degrees of freedom) are expected for the following molecules :

(a) CO_2 (linear) *(b)* H_2O (bent) *(c)* SO_2 (bent) *(d)* O_2 *(e)* CH_3Cl *(f)* $CHCl_3$ *(g)* CH_4 *(h)* C_6H_6 *(i)* trans-N_2F_2 *(j)* C_2F_2 (linear) *(k)* N_2O *(l)* NO_2 ?

[Ans. *(a)* 4, *(b)* 3, *(c)* 3, *(d)* 1, *(e)* 9, *(f)* 9, *(g)* 9, *(h)* 30, *(i)* 6, *(j)* 7, *(k)* 3, *(l)* 3]

12. The infrared and Raman spectra of a triatomic molecule of the type MX_2 show two infrared frequencies and one Raman frequency. Determine whether the molecule is linear or bent. **[Ans. linear]**

13. The triatomic molecule AB_2 shows three strong infrared absorption bands. What is the structure of molecule ?
[Ans. ABB bent or BAB bent]

14. The fundamental vibrational frequencies of SO_2 are 1151·38, 517·69, and 1361·76 cm^{-1}. Account for the absorption bands at 1875·55, 2295·88 and 2499·55 cm^{-1}. **[Ans. $\bar{\nu}_2 + \bar{\nu}_3$, $2\bar{\nu}_1$ and $\bar{\nu}_1 + \bar{\nu}_3$]**

15. If $H^{35}Cl$ is irradiated with 435·8 nm mercury line, calculate the Raman line in nm if the fundamental vibrational frequency of $H^{35}Cl$ is $8·667 \times 10^{13}$ s^{-1}. **[Ans. 498·57 nm]**

16. List all the electronic transitions possible for *(a)* CH_4 *(b)* CH_3Cl *(c)* $H_2C{=}O$.
[Ans. *(a)* $\sigma^* \leftarrow \sigma$, *(b)* $\sigma^* \leftarrow \sigma$ and $\sigma^* \leftarrow n$ (there are no π or π^* MO's),
(c) $\sigma^* \leftarrow \sigma$, $\pi^* \leftarrow \sigma$, $\sigma^* \leftarrow \pi$, $\pi^* \leftarrow n$, $\pi^* \leftarrow \pi$ and $\pi^* \leftarrow n$]

17. Identify the two geometric isomers of stilbene, $C_6H_5CH{=}CHC_6H_5$, from their λ_{max} values, 294 nm and 278 nm.
[Ans. The higher the energy *cis*-isomer has, the shorter the λ_{max}. Steric strain prevents full coplanarity of the *cis* phenyl groups and the conjugative effect is attenuated.]

18. Predict the kind of electronic transitions in *(a)* Cl_2 and *(b)* C=O group. Also give their intensity.
[Ans. *(a)* $\sigma^* \leftarrow \sigma$ (allowed transition, strong) $\sigma^* \leftarrow n$ (forbidden transition, weak)
***(b)* $\pi^* \leftarrow \pi$ and $\sigma^* \leftarrow \sigma$ (both allowed, strong) $\pi^* \leftarrow n$, and $\sigma^* \leftarrow n$ (both forbidden, weak)]**

CHAPTER 7

MOLECULAR SPECTROSCOPY–II
(NMR, ESR, NQR, NRF and PES)

MAGNETIC RESONANCE SPECTROSCOPY

Molecular spectra including rotational (microwave) spectra, vibrational and vibration-rotation (infrared) spectra, Raman spectra and electronic (visible and ultraviolet) spectra have been discussed in the last chapter. In this chapter, we shall discuss some very important spectoscopies which are of interest in structural chemistry. NMR is an indispensable tool in the hands of an organic chemist in his synthetic investigations; ESR tells us about the transience of extremely short-lived free radicals; both NQR and NRF are useful in determining the strong electric field gradients (EFGs) found in metals and alloys and PES helps us in verifying quantum mechanical calculations on atoms and molecules and in determining their ionisation potentials.

NMR SPECTROSCOPY

NMR was independently discovered in 1946 by the American physicists F. Bloch (1905–1983) of Stanford University and E.M. Purcell (1912–1997) of Harvard University ; they shared the 1952 Physics Nobel Prize. The first application of NMR to chemistry was made in 1951 when NMR spectrum of ethanol was recorded. Since then NMR technique has almost completely been monopolized by chemists, biochemists and molecular biologists, for structural elucidation, physicists being primarily interested in its theoretical aspects.

All atomic nuclei possess nuclear spin, I, which may be integral (*i.e.*, 1, 2, 3, etc.) or half-integral (*i.e.*, 1/2, 3/2, 5/2, 7/2 etc.). The proton and the neutron each has spin 1/2. Since a nucleus contains nucleons (collective term for protons and neutrons), it is evident that the spin of the nucleus may be considered as the resultant of the spins of protons and neutrons comprising it. Consider, for instance, the deuteron nucleus, ^2D, which contains one proton and one neutron. Now, depending upon whether the spins of the proton and the neutron are aligned parallel (↑↑) or antiparallel (↑↓), the deuteron is expected to have a spin of 1 or 0. It is, however, found that in the ground state, deuteron has spin of 1 which means that the proton and neutron spins are aligned parallel to each other.

It is difficult to predict the spin of a nucleus. The following rules are, however, helpful in predicting the nuclear spin :

(i) If the mass number A is odd, nuclear spin I is *half integral*. Thus, in the case of ^1H, ^{15}N, ^{19}F, ^{31}P, I = 1/2 and in the case of ^{11}B, I = 3/2.

(ii) If the mass number A and the atomic number Z are both even, the spin is *zero*. Thus, in the case of ^4_2He, $^{12}_6C$, $^{16}_8O$, $I = 0$.

(iii) If the mass number A is even but the atomic number Z is odd, the spin is *integral*. Thus, the spin of ^2_1H and $^{14}_7N$ is 1 while that of $^{10}_5B$ is 3.

Since a nucleus possesses an electric charge, *the spinning nucleus gives rise to a magnetic field whose axis coincides with the axis of spin*. Thus, each nucleus can be thought of being equivalent to a minute magnet having a magnetic moment μ. Each nucleus with $I > 0$ has magnetic moment.

However, $^{12}_{6}C$ and $^{16}_{8}O$ having $I=0$ do not possess a magnetic moment, *i.e.*, they are non-magnetic.

Nuclei possessing $I \geq 1$ have also a ***nuclear electric quadrupole moment, Q,*** which is a measure of the deviation of the nuclear charge distribution from spherical symmetry. Some common quadrupolar nuclei are $^{2}_{1}H$ (deuteron) and $^{14}_{7}N$ both of which have $I=1$. The nuclear quadrupole moment interacts with the electric field gradient (EFG) created at the nucleus by the bonding and non-bonding electrons in a molecule. The quantity e^2Qq (where e is the electronic charge and q the EFG) is known as the *nuclear quadrupole coupling constant*. Suffice it to mention here, avoiding mathematical details, that quadrupolar nuclei not only 'spoil' their own NMR spectra but also the NMR spectra of nuclei attached to them in a molecule. Thus, the NMR spectra of quadrupolar nuclei are generally very broad and not at all sharp.

When a magnetic nucleus is placed in a uniform magnetic field, the magnetic dipole associated with the magnetic moment assumes only ***a discrete set of orientations.*** This is expressed by saying that the nuclear spin (and hence the magnetic moment associated with it) is *quantized* with respect to the direction of the applied magnetic field. The magnetic nucleus assumes any one of the $2I+1$ orientations with respect to the direction of the applied magnetic field. Suppose that a nucleus with spin I is placed in an external magnetic field B_z, applied along the z-direction. Then, as a result of quantization of spin, the observable component m_I of the spin I along the direction of the field is given by

(i) $m_I = I, I-1, I-2, \ldots, 0, \ldots, -(I-2), -(I-1), -I$ *(for integral spins)*

(ii) $m_I = I, I-1, I-2, \ldots, 1/2, -1/2, -3/2, \ldots, -I$ *(for half-integral spins)*

In each case, there are $(2I+1)$ values of m_I.

A nucleus with spin has associated with it a magnetic dipole moment (or simply magnetic moment) $\vec{\mu}$ that is proportional to the angular momentum $\vec{I}$ given by $[(I(I+1)]^{1/2}\hbar$. Thus,

$$\vec{\mu} = g_N \mu_N \vec{I} \qquad \ldots(1)$$

where g_N is called the nuclear g-factor and μ_N is the nuclear megneton defined as $\mu_N = e\hbar/2m_p$, where e is the electronic charge, m_p is the mass of the proton. Substituting the various values,

$$\mu_N = \frac{(1{\cdot}602 \times 10^{-19}\text{C}) \times (1{\cdot}055 \times 10^{-34}\text{Js})}{(2) \times 1{\cdot}673 \times 10^{-27}\text{kg}} = 5{\cdot}05 \times 10^{-27}\ \text{J T}^{-1}$$

The *magnitude* of the nuclear magnetic moment is thus given by

$$\mu = g_N \mu_N [I(I+1)]^{1/2} \qquad \ldots(2)$$

Also, since the magnetic moment and the angular momentum can be parallel or antiparallel vectors, g_N can have a positive or a negative value. It may be noted that whereas the value of the electron g-factor, g_e has been very accurately calculated to be equal to 2·0023, the value of the nuclear g-factor, g_N, can only be obtained from experiment and is different for different nuclei.

Example 1. Calculate the nuclear spin angular momentum and the magnetic moment for a proton, given that $I = \frac{1}{2}$, g_N for proton is 5·585 and $\mu_N = 5{\cdot}05 \times 10^{-27}$ J T^{-1}.

Solution : The nuclear spin angular momentum

$$= [I(I+1)]^{1/2}\hbar = \left[\tfrac{1}{2}\left(\tfrac{1}{2}+1\right)\right]^{1/2} \times (1{\cdot}054 \times 10^{-34}\ \text{Js})$$

$$= 0{\cdot}866 \times 1{\cdot}055 \times 10^{-34}\ \text{J s} = 0{\cdot}914 \times 10^{-34}\ \text{Js}$$

The nuclear magnetic moment is given by

$$\mu = g_N \mu_N [I(I+1)]^{1/2}$$

$$= (5{\cdot}585) \times (5{\cdot}05 \times 10^{-27}\ \text{J T}^{-1}) \left[\tfrac{1}{2}\left(\tfrac{1}{2}+1\right)\right]^{1/2} = 2{\cdot}44 \times 10^{-26}\ \text{J T}^{-1}$$

NMR of a 'bare' proton. A 'bare' nucleus is, of course, an ideality. Actually, nuclei are parts of atoms and molecules. However, it is useful to consider the NMR of a bare proton. From quantum mechanics it is known that the energy of interaction of nuclear magnetic moment μ with an external magnetic field B_z, applied in the z-direction, is given by

$$E = -\mu B_z \qquad \ldots(3)$$

Substituting the value of $\vec{\mu}$ from Eq. 1, we find that

$$E = -g_N \mu_N B_z \vec{I} \qquad \ldots(4)$$

As already mentioned, the nuclear spin I is quantized in the presence of the magnetic field and the energy of nuclear spin is defined only by its component m_I. We may thus write :

$$E_{m_I} = -g_N \mu_N B_z m_I \qquad \ldots(5)$$

Consider a bare proton ^{1}H with $I=1/2$ so that $m_I = \pm 1/2$. Thus, for $m_I = 1/2$, the energy

$$E_{1/2} = -\tfrac{1}{2} g_N \mu_N B_z \qquad \ldots(6)$$

and for $m_I = -1/2$, the energy

$$E_{-1/2} = \tfrac{1}{2} g_N \mu_N B_z \qquad \ldots(7)$$

It should be noted that in the absence of the external magnetic field, the two components of the proton spin have the same energy (*i.e.*, they are *degenerate*). However, in the presence of the magnetic field, the components have different energies given by Eqs. 6 and 7. This is expressed by saying that *the magnetic field lifts or removes the degeneracy of the spin components*. This is called ***Zeeman splitting of energy levels.*** The energy difference is given by

$$\Delta E = E_{-1/2} - E_{1/2} = g_N \mu_N B_z \qquad \ldots(8)$$

This is illustrated in Fig. 1.

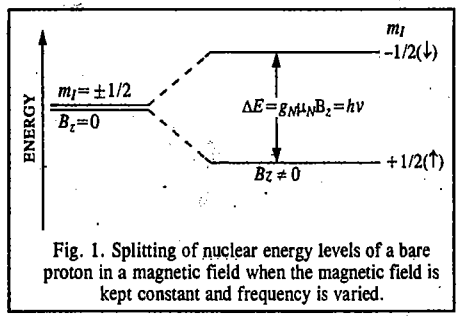

Fig. 1. Splitting of nuclear energy levels of a bare proton in a magnetic field when the magnetic field is kept constant and frequency is varied.

In order to induce transitions between the two energy levels $E_{-1/2}$ and $E_{1/2}$, *i.e.*, in order to let the nuclear spin 'flip' from the upward direction ($\uparrow$) to the downward direction ($\downarrow$), we must apply an oscillating radiofrequency field perpendicular to the direction of B_z. *The nuclear spin flips, provided the energy $h\nu$* of the radiofrequency photon of frequency ν is exactly equal to ΔE, *i.e.*,

$$\Delta E = g_N \mu_N B_z = h\nu \qquad \ldots(9)$$

This is called the **Bohr frequency condition.** Thus, the NMR frequency of a **bare proton** (or a bare nucleus with $I=1/2$) is given by

$$\nu = \frac{\Delta E}{h} = \frac{g_N \mu_N B_z}{h} \qquad \ldots(10)$$

It may be noted that g_N can be positive or negative but ν must be positive. Hence, only the absolute value of g_N should be used in calculating ν.

Eq. 10 shows that ν is directly proportional to B_z. We thus see that the NMR spectra can be recorded in two ways, *viz.*, *(i)* keeping the magnetic field B_z fixed and varying the frequency ν (Fig. 1)

or *(ii)* keeping ν fixed and varying B_z (Fig. 2). The latter mode is preferred in modern NMR spectrometers.

Example 2. Calculate the NMR frequency (in MHz) of the proton (^{1}H) in a magnetic field of intensity 1·4092 tesla, given that g_N = 5·585 and $\mu_N = 5{\cdot}05\times10^{-27}$ J T^{-1}.

Solution : From Eq. 10,

$$\nu = \frac{g_N\mu_N B_z}{h} = \frac{(5{\cdot}585)\times(5{\cdot}05\times10^{-27}\,\text{J T}^{-1})\times(1{\cdot}4092\,\text{T})}{6{\cdot}626\times10^{-34}\,\text{J s}}$$

$$= 60\times10^6\ \text{s}^{-1} = 60\times10^6\ \text{Hz} = \mathbf{60\ MHz}$$

This frequency lies in the radiofrequency region.

Example 3. Calculate the magnetic field strength required to observe the NMR frequency for fluorine (^{19}F) at 60 MHz. Given g_N for ^{19}F = 5·257 and $\mu_N = 5{\cdot}05\times10^{-27}$ J T^{-1}.

Solution. Since from Eq. 10, $\nu = g_N\mu_N B_z/\hbar$, we have

$$B_z = \frac{h\nu}{g_N\mu_N} = \frac{(6{\cdot}626\times10^{-34}\,\text{J s})(60\times10^6\ \text{s}^{-1})}{(5{\cdot}257)(5{\cdot}05\times10^{-27}\,\text{J T}^{-1})} = \mathbf{1{\cdot}4973\ T}$$

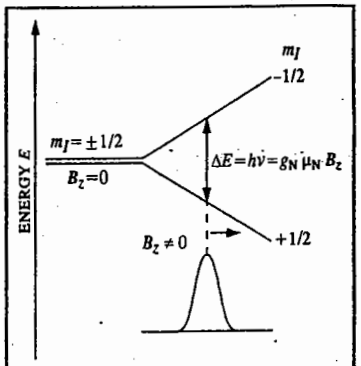

Fig. 2. Energy level diagram showing the splitting of nuclear energy levels of a bare proton in a magnetic field when the frequency is kept fixed and the magnetic field is varied.

It should be borne in mind that nuclei such as $^{12}_{6}$C and $^{14}_{6}$C have no spin (I=0) so that they have no magnetic moment ; they are called *non-magnetic* nuclei. Non-magnetic nuclei do not show NMR spectra because, their magnetic moment being zero, their energy levels do not exist. Thus, if an organic compound contains hydrogen, carbon and oxygen, only hydrogen nuclei (I=1/2) will show NMR spectra.

Some nuclear properties and NMR frequencies of a few nuclei in a magnetic field of intensity 1·4092 T are given in Table 1.

TABLE 1

Nuclear Magnetic Properties of Some Nuclei

Nucleus	% Abundance	Spin, I	g_N	NMR frequency ν in MHz at 1·4092 T
^{1}H	99·99	1/2	5·585	60·000
^{2}D	0·01	1	0·857	9·210
^{10}B	18·83	3	0·600	6·448
^{11}B	81·17	3/2	1·792	19·248
^{13}C	1·11	1/2	1·404	15·086
^{14}N	99·63	1	0·404	4·334
^{15}N	0·36	1/2	0·566	6·079
^{17}O	0·037	5/2	−0·757	8·134
^{19}F	100	1/2	5·255	56·444
^{29}Si	4·70	1/2	−1·110	11·919
^{31}P	100	1/2	2·261	24·286
^{35}Cl	75·41	3/2	0·547	5·879
^{37}Cl	24·60	3/2	0·455	4·893
^{127}I	100	5/2	1·118	12·005

Classically, the phenomenon of magnetic resonance can also be understood by invoking Larmor precession. A nucleus having a magnetic moment μ behaves as a bar magnet which spins on its axis. In the presence of the magnetic field B_z, the interaction of μ with B_z produces a torque. This torque causes μ to *precess* about B_z, as shown in Fig. 3. This phenomenon is called **Larmor precession** (in honour of the 19th century British mathematician, Joseph Larmor) and the angular frequency of precession is referred to as the **Larmor frequency,** ω_L (expressed in radians per second). Mathematically, Larmor frequency is given by

$$\omega_L = \gamma B_z \qquad \ldots(11)$$

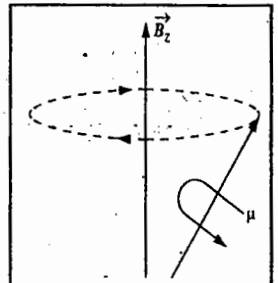

Fig. 3. Larmor precession of a nucleus in a magnetic field.

where γ is the **magnetogyric ratio** (formerly called gyromagnetic ratio) of the nucleus. It is defined as the ratio of the nuclear magnetic moment μ and the nuclear spin angular momentum $I\hbar$, *i.e.*,

$$\gamma = \frac{\mu}{I\hbar} \qquad \ldots(12)$$

It is expressed in terms of radians T^{-1} s^{-1} (or, simply as T^{-1} s^{-1}). Note that $\omega = 2\pi\nu$ where ν is the NMR frequency. It may be noted that $\gamma\hbar = g_N\mu_N$.

Positive values of g_N and μ_N denote a magnetic moment that is parallel to the spin; negative values indicate that the magnetic moment and spin are antiparallel.

Example 4. In a spectrometer operating at 1 T, the NMR frequency of ^{19}F is 40·06 MHz. Calculate the magnetogyric ratio of ^{19}F.

Solution : From Eq. 11,

$$\gamma = \frac{\omega_L}{B_z} = \frac{2\pi\nu}{B_z} = \frac{2\times(3{\cdot}1416)\times(40{\cdot}06\times10^6\,\text{s}^{-1})}{1\,\text{T}} = 2{\cdot}517\times10^8\ \text{T}^{-1}\,\text{s}^{-1}$$

Example 5. The magnetic moment of ^{31}P is equal to 1·1305 nuclear magnetons, *i.e.*, 1·1305 μ_N. Calculate its magnetogyric ratio and the *g*-factor. Given $\mu_N = 5{\cdot}05\times10^{-27}$ J T^{-1} and nuclear spin of ^{31}P is 1/2.

Solution : From Eq. 12,

$$\gamma = \frac{\mu}{I\hbar} = \frac{1{\cdot}1305\times(5{\cdot}05\times10^{-27}\,\text{J T}^{-1})\times(2\times3{\cdot}1416)}{(1/2)\times(6{\cdot}626\times10^{-34}\,\text{J s})} = 1{\cdot}083\times10^8\ \text{T}^{-1}\,\text{s}^{-1}$$

Now, from Eq. 1, $\mu = g_N\mu_N I$

For ^{31}P, $\mu = 1{\cdot}1305\,\mu_N$ and $I = \frac{1}{2}$ (given)

$\therefore$ $1{\cdot}1305\,\mu_N = \frac{1}{2}g_N\mu_N$, thus, $g_N = 2\times1{\cdot}1305 = \mathbf{2{\cdot}261}$

Experimental Technique of NMR Spectroscopy. A typical NMR spectrometer, shown in Fig. 4, consists of the following components : (1) a radiofrequency source of radiation (2) a receiver coil for the detection of the absorption of energy (3) a d.c.–magnetic field and (4) a receiver or an oscilloscope to display the NMR spectrum. The relation $\nu = g_N\mu_N B_z/h$ shows that the spectrum may be run at a fixed magnetic field by varying frequency or a fixed frequency by varying the magnetic field. In practice, it is preferable for most instruments to use a fixed frequency (which for protons is

of the order 60 MHz) supplied by a crystal-controlled radiofrequency oscillator and to vary the magnetic field applied to the sample by an electromagnet. When magnetic resonance condition is reached, the energy absorbed by the sample from the r.f. oscillator is measured electrically and displayed on the chart of a recorder or on an oscilloscope.

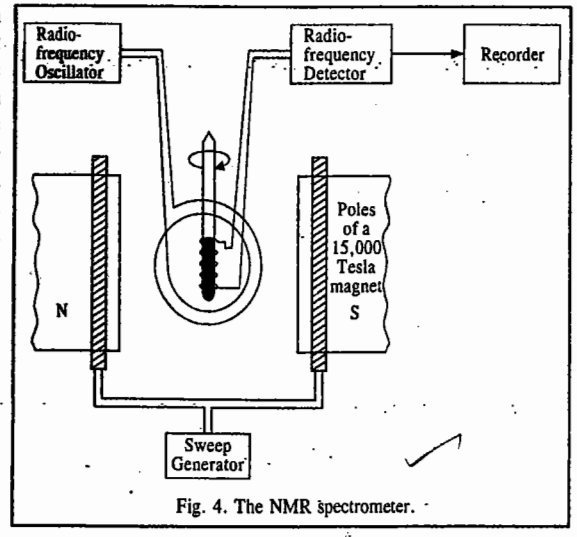

Fig. 4. The NMR spectrometer.

Chemical Shift. In practice, one does not investigate the NMR spectra of 'bare' nuclei. Nuclei are essential parts of molecules held together by the electrons of the chemical bonds. The magnetic field at which a free or 'bare' nucleus resonates is quite different from the field at which the same nucleus in a molecule resonates. It is thus clear that the electrons in a molecule affect the NMR frequency of a given nucleus in the molecule. The electrons are said to *shield* or *deshield* a nucleus from the applied magnetic field, depending upon whether the magnetic field generated by their motion opposes or reinforces the field. We shall discuss this aspect a little later in this chapter. Suffice it to mention here that the applied external magnetic field affects the motion of the electrons surrounding the nuclei thereby inducing local magnetic fields. The magnitude of the local magnetic field is determined by the electron distribution around a nucleus. The difference between the magnitudes of the magnetic field at which 'free' nuclei and molecular nuclei resonate is called **chemical shift.**

For measuring chemical shifts it is not possible to use a free nucleus as a reference. Instead, chemists use those compounds that exhibit only a *single sharp resonance line* as a reference for measuring chemical shifts. The most frequently employed reference compound is tetramethylsilane (TMS) having the formula, $Si(CH_3)_4$.

The local magnetic field B_{local} experienced by a nucleus in a molecule is related to the external magnetic field B_0 by

$$B_{local} = B_0 (1 - \sigma) \qquad ...(13)$$

where σ, a dimensionless quantity, is called the **screening constant** (or the **shielding constant**). For two nuclei A and B in a molecule, the local fields are

$$B_A = B_0 (1 - \sigma_A) \qquad ...(14)$$

$$B_B = B_0 (1 - \sigma_B) \qquad ...(15)$$

where σ_A and σ_B are the respective screening constants, Thus,

$$B_B - B_A = B_0 (1 - \sigma_B) - B_0 (1 - \sigma_A)$$

$$= B_0 (\sigma_A - \sigma_B) = B_0 \delta_{AB} \qquad ...(16)$$

where δ_{AB} (or, simply, δ) is the chemical shift of nucleus A with respect to nucleus B. In practice, we define chemical shift of a sample as

$$\delta = \frac{B_{sample} - B_{ref}}{B_0} \times 10^6 \text{ ppm} \qquad ...(17)$$

Since $B \propto \nu$, hence

$$\delta = \frac{\nu_{sample} - \nu_{TMS}}{\nu_0} \times 10^6 \text{ ppm} \qquad ...(18)$$

where the reference compound is tetramethylsilane (TMS). The chemical shift is expressed in parts per million (ppm).

The reasons for using TMS as the reference are as follows :

1. It has 12 equivalent protons ; this can be seen from its structure $Si(CH_3)_4$.

Since all the protons are in the same environment, TMS gives a single intense peak in its NMR spectrum.

2. It has a low boiling point (27°C) and thus can be easily recovered, if desired, after the spectrum is recorded.

3. It is chemically inert.

4. As will be discussed shortly in this chapter, the methyl groups in TMS are highly shielded by their electrons from the external magnetic field. Consequently, TMS shows NMR at a very high magnetic field strength compared to other protons.

It is pertinent to mention here that two chemical-shift scales, *viz.*, the δ-scale and the τ-scale are used in recording NMR signals. They are related by the expression

$$\delta + \tau = 10$$

i.e.,

$$(\tau = 10 - \delta) \qquad ...(19)$$

On the δ-scale, δ is set equal to zero at the reference peak (or signal) of TMS and it *increases downfield*. This scale has the disadvantage that a large value of δ implies that a proton undergoes a resonance at low field. Hence, it implies a low-shielding of the nucleus by the external magnetic field.

In the τ-scale, τ is set equal to 10 at the reference peak of TMS and it *decreases downfield.* Thus, a low value of τ implies that a proton undergoes a resonance at low field. Hence, it implies a low-shielding of the nucleus by the external magnetic field. It follows that a higher value of τ means a more shielded nucleus and hence a high-field resonance.

The τ-values for most organic compounds lie between 0 and 10. They are highly characteristic of the chemical environment of the magnetic nuclei. Thus, they can help in locating different kinds of protons in an organic molecule. The τ-values for some protons are given in Table 2.

TABLE 2

Typical Chemical Shifts For Protons in Different Environments

Compound	τ-Value (in ppm)	Compound	τ-Value (in ppm)
TMS	10·00	Dioxane	6·20
Cyclopropane	9·78	Water	4·80
Methane	9·77	Benzene	2·73
Tetramethylmethane	9·08	Ethylene	4·16
Ethanol :		Acetylene	7·81
methyl protons	8·83	Methyl fluoride	5·70
methylene protons	6·41	Methyl chloride	7·01
Cyclohexane	8·56	Methyl bromide	7·30
Acetone	7·91	Methyl iodide	7·81
Acetaldehyde :		Chloroform	2·30
methyl protons	7·85	Naphthalene	2·27
aldehydic protons	0·28		

Consider the proton-NMR spectrum of ethanol (Fig. 5). Each proton in the pure compound has its own electronic environment and hence a characteristic chemical shift. The liquid ethanol shows in its NMR spectrum three peaks at three values of the applied magnetic field corresponding to the **-OH** proton, the two equivalent $>CH_2$ protons and the three equivalent $-CH_3$ protons. The areas under the three absorption peaks are in the ratio of 1 : 2 : 3, respectively

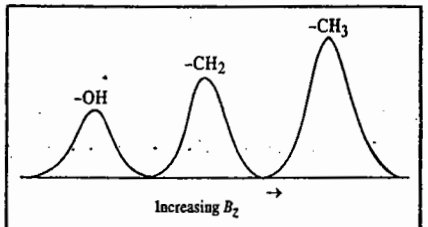

Fig. 5. Low-resolution NMR spectrum of ethanol.

Example 6. A compound shows a proton-NMR peak at 240 Hz down-field from the TMS peak in a spectrometer operating at 60 MHz. What are the values of the chemical shifts δ and τ in ppm relative to TMS ?

Solution : From Eq. 18, $\delta = \frac{\nu_{sample} - \nu_{TMS}}{\nu_0} \times 10^6$ (ppm) $= \frac{240\,s^{-1}}{60 \times 10^6\,s^{-1}} \times 10^6 = 4$ ppm ; $\tau = 10 - \delta = 6$ ppm

Shielding and Deshielding of Protons. The concept of chemical shift, introduced above, is closely linked with the shielding or deshielding of protons in a molecule. A *bare* proton, when exposed to a radiofrequency photon, 'flips' its spin from lower energy level to a higher energy level, *i.e.*, its spin changes its orientation from (↑) to (↓). However, all protons do not change or flip their spins at the same applied magnetic field because their energy depends upon the chemical environment of the protons. The magnetic field 'sensed' by a proton in a molecule is not the same as the applied magnetic field since the electrons in the bond close to the proton and the neighbouring electrons in other bonds *induce* their own magnetic field. This induced field may oppose or reinforce the applied magnetic field. The field experienced by the proton is thus the resultant of the applied and induced fields, as shown in Fig. 6. When the two fields reinforce, as in Fig. 6*(b)*, a smaller field must be applied to flip the proton. Such a proton is said to be *deshielded* and absorbs more *down-field* (*i.e.*, at lower magnetic field strength). On the other hand, when the fields oppose, as in Fig. 6*(c)*, a stronger field must be applied. The proton is now *shielded* and absorbs more *upfield* (*i.e.*, at higher magnetic field strength).

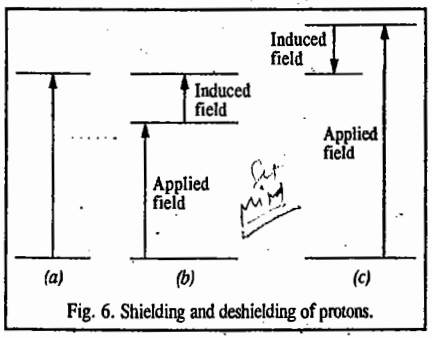

Fig. 6. Shielding and deshielding of protons.

Shielding Mechanism in NMR

The total contribution to shielding in NMR is customarily represented as

$$\sigma = \sigma(\text{local}) + \sigma(\text{molecule}) + \sigma(\text{solvent}) \quad ...(20)$$

where σ(local), the local contribution to shielding, is the sum of the positive diamagnetic contribution, σ_d and a negative paramagnetic contribution, σ_p, that is,

$$\sigma(\text{local}) = \sigma_d(\text{local}) + \sigma_p(\text{local}) \quad ...(21a)$$

The local contribution essentially comes from the electrons of the atom that contains the nucleus of interest. A magnetic field induces electronic circulation about a nucleus in a plane perpendicular to the applied magnetic field.

σ_d can be calculated from the **Lamb formula :**

$$\sigma_d = \frac{e^2\mu_0}{12\pi m_e}\left\langle\frac{1}{r}\right\rangle \quad ...(21b)$$

where μ_0 is the vacuum permeability, and r is the electron-nucleus distance.

In linear molecules such as acetylene, the total shielding which a proton experiences is a result of paramagnetic effect. Paramagnetic shielding arises from electronic circulations within molecules when they are specifically oriented with respect to the magnetic field. These electronic circulations about a nucleus produce a secondary magnetic field that is parallel to the applied magnetic field and frequently contributes to the shielding experienced by a neighbouring nucleus. *Local* paramagnetic circulations do not contribute to the shielding of protons but paramagnetic *electronic* circulations about atoms such as carbon, nitrogen and oxygen may contribute to the shielding of an adjacent or a neighbouring proton. Such is the case for acetylene molecule when it is oriented *parallel to the applied magnetic field.* The induced magnetic fields are paramagnetic at carbon but diamagnetic at the proton (Fig. 7*a*). This paramagnetic effect is important in shielding of other linear molecules. It may be noted that a proton may experience shielding effects caused by electronic circulations that originate in other parts of the molecule. Effects arising from electronic currents in other molecules will be averaged to zero by rapid thermal motion. Similarly, the currents in the same molecule will not cause shielding of a proton if such currents are averaged to zero by rapid rotation about single bonds. However, *in a relatively rigid molecule such currents can cause either shielding or deshielding of a proton.* These effects are called **anisotropic** effects since they depend on the *orientation* of the magnetic current.

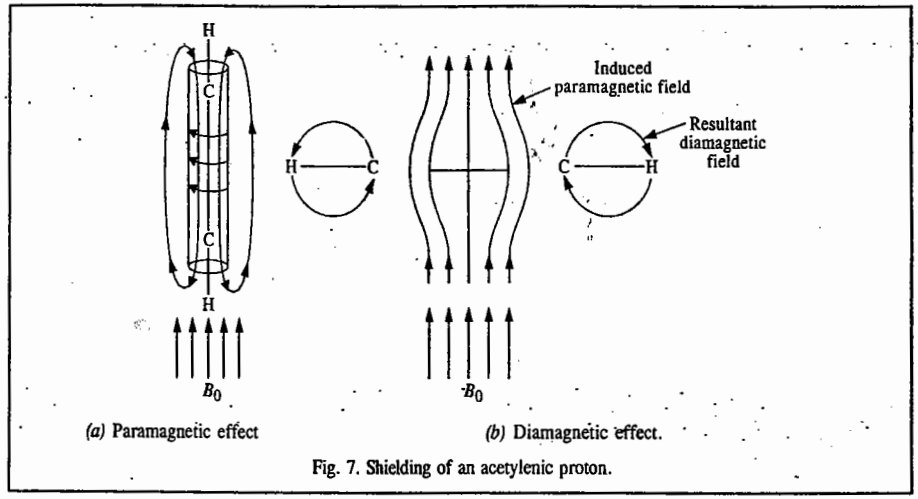

Fig. 7. Shielding of an acetylenic proton.

When acetylene molecule is oriented *perpendicular to the magnetic field* (Fig. 7*b*), a diamagnetic anisotropic effect occurs. The electronic circulations within the cylinderical pi-electron cloud induce a diamagnetic shielding at the acetylenic proton.

Let us next consider formaldehyde molecule, $CH_2=O$. When the carbonyl group is oriented such that the plane of the trigonal carbon atom is perpendicular to the field, diamagnetic circulations in the group produce anisotropic effect at the proton (Fig. 8.) that results in *deshielding*. It is probable that olefinic protons and, in fact, any group attached to the alkenic bond are *desheilded* because of diamagnetic anisotropic effects in the plane of the carbon-carbon double bond. Aromatic nuclei contain large closed loops of pi-electrons in which strong diamagnetic currents are induced by the magnetic field ; this is

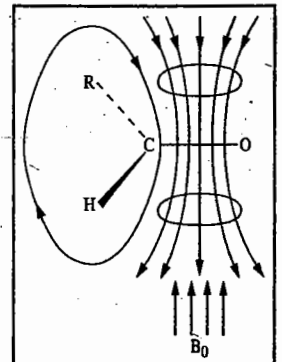

Fig. 8. Deshielding of an aldehydic proton by diamagnetic effect.

called the **ring current effect**. It causes *deshielding* of aromatic protons (Fig. 9).

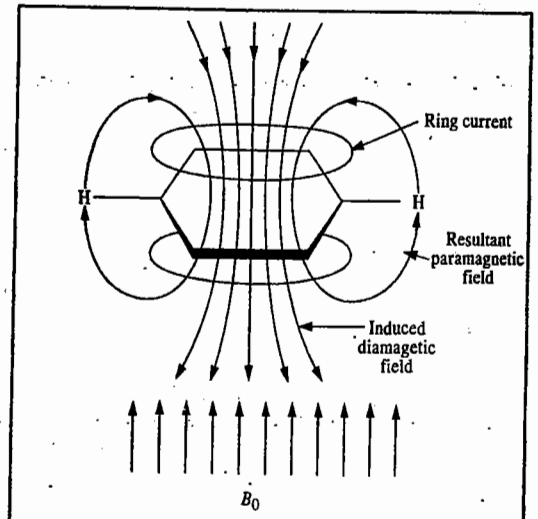

Fig. 9. Deshielding of aromatic protons due to ring current effect.

The shielding by the solvent can arise in a number of ways. Thus, the solvent polarity can affect the electron distribution near a magnetic nucleus. If a solvent is nonpolar, the polar solute can induce an electric dipole in the solvent molecules so that the polarized solvent molecules can distort the electron distribution of the solute molecule. The solute-solvent interactions such as hydrogen bonding, etc., can also lead to shielding or deshielding effects.

Nuclear Spin–Spin Interaction : Fine Structure in NMR

The NMR spectrum of ethanol, first observed in Bloch's laboratory in 1951, is of great historical importance because it demonstrated the application of NMR to structural elucidation in organic chemistry.

When the NMR spectrum of *acidified* ethanol is examined under high resolution, the peaks for CH_2 and CH_3 groups are seen to be split into multiplets, as shown in Fig. 10.

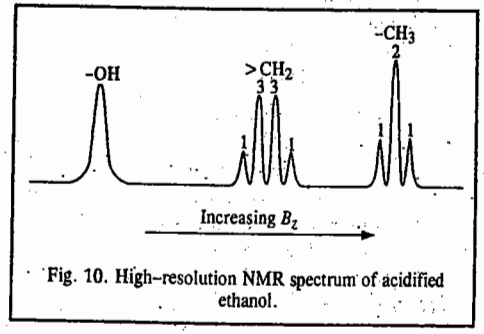

Fig. 10. High-resolution NMR spectrum of acidified ethanol.

This splitting of the lines arises as a result of **nuclear spin-spin interaction**, as illustrated below.

Relative to a given proton in the CH_3 group, the two protons of the CH_2 group can align themselves in four different ways, as shown below :

	(1)	(2)	(3)	(4)
Alignment of protons	↑↑	↑↓	↓↑	↓↓
Degeneracy	1	2		1
Σm_I	+1	0	0	-1

Since alignments (2) and (3) are energetically equivalent, the net spin combinations total *three*.

Relative to a proton in the CH_2 group, the three protons of the CH_3 group can align themselves in eight different ways, as shown below :

	(1)	(2)	(3)	(4)	(5)	(6)	(7)	(8)
Alignment of protons	↑↑↑	↑↑↓	↑↓↑	↓↑↑	↑↓↓	↓↑↓	↓↓↑	↓↓↓
Degeneracy	1	3			3			1
Σm_I	$+\frac{3}{2}$	$+\frac{1}{2}$	$+\frac{1}{2}$	$+\frac{1}{2}$	$-\frac{1}{2}$	$-\frac{1}{2}$	$-\frac{1}{2}$	$-\frac{3}{2}$

As can be easily seen, alignments (2), (3) and (4) are energetically equivalent and so are alignments (5), (6) and (7). The net spin combinations of protons in CH_3 group thus total *four*.

The three possible orientations of the CH_2 protons produce *three* different local fields at the CH_3 protons, thus splitting the CH_3 absorption peak into a *triplet, i.e.*, three lines of relative intensity ratio 1 : 2 : 1. Similarly, the *four* possible orientations of the CH_3 protons produce four different local fields at the CH_2 protons, thus splitting the CH_2 resonance into a *quartet, i.e.*, four lines of relative intensity ratio 1 : 3 : 3 : 1.

What about the influence of the OH proton on the CH_2 and the CH_3 protons of acidified ethanol? The answer is that H^+ ion of the acid catalyzes the exchange of protons between the OH groups of different molecules so that the life-time of an OH proton in any given conformation becomes too short to permit the observation of the effect of the OH proton on the CH_2 and CH_3 groups and vice versa. In other words, there is *no spin-spin interaction* between the OH proton and the other protons. Hence, the high resolution NMR spectrum of *acidified* ethanol consists of an OH singlet, a CH_2 quartet (1 : 3 : 3 : 1) and a CH_3 triplet (1 : 2 : 1), as shown in Fig. 10.

The proton NMR spectrum of *pure* ethanol is, however, different. Here because of the absence of the H^+ catalyst, the OH proton does not undergo any exchange between the OH groups of different ethanol molecules. The three different orientations of the CH_2 protons will split the OH peak into a *triplet* (1 : 2 : 1). Also, each of the lines of the CH_2 quartet would be split into a doublet as a result of two possible orientations of the OH proton which will produce two different local fields at the CH_2 protons. The NMR spectrum of pure ethanol thus consists of 3 lines for OH group, 8 lines for CH_2 group and 3 lines for CH_3 group. Since the CH_2 group in ethanol is flanked by OH and CH_3 groups, the magnitude of its splitting by the OH and CH_3 protons would be very much pronounced. However, the influence of the OH proton on the CH_3 protons will be negligible since these protons are not on adjacent carbon atoms.

The magnitude of the splitting between the lines of a given multiplet is given by the **spin-spin coupling constant** J (measured in units of Hz).

There are some general rules about spin-spin interactions which are helpful in calculating the number of lines expected in the NMR spectra. These are :

1. Protons of the same group do not interact among themselves to cause observable splitting (*e.g.*, the three protons in the CH_3 group do not interact with one another).

2. The multiplicity of the peak of a group of equivalent protons is determined by the *neighbouring* protons. In general, if n equivalent protons interact or couple with the protons on an adjacent carbon atom, the resonance peak is split into $n+1$ peaks or signals.

3. The intensities are symmetric about the mid-point of the group and the relative intensities of the $n+1$ peaks are given by the coefficients of the binomial expansion of order n, *i.e.*, $(1+x)^n$. These coefficients can be arranged in the so-called **Pascal's triangle**, as shown in Table 3.

TABLE 3

Pascal's Triangle giving Intensities of NMR Signals

Number of Protons, n	Number of NMR lines	Relative Intensities
0	1	1
1	2	1 1
2	3	1 2 1
3	4	1 3 3 1
4	5	1 4 6 4 1
5	6	1 5 10 10 5 1
6	7	1 6 15 20 15 6 1

It may be noted that the spin-spin interaction is *independent* of the applied magnetic field strength whereas the chemical shift depends on the field strength.

The proton-NMR spectrum of a molecule thus gives information about

(a) The *number of peaks* which enables us to know about the kinds of protons present in a molecule.

(b) *The positions of the peaks* which tell us about the electronic environment of each kind of proton.

(c) *The intensities of the peaks* which tell us about the number of protons of each kind that are present and

(d) *The splitting of a peak into several peaks* which tells us about the environment of a proton with respect to other nearby protons in the molecule.

Example 7. Predict the proton-NMR spectrum of ethyl acetate using the three rules mentioned earlier.

Solution : The molecule has the structure $CH_3—CO—O—CH_2—CH_3$

(a) From rule 1, there is no splitting due to spin-spin interaction of the protons in either of the two methyl groups or in the methylene group.

(b) From rule 2, the CH_2 protons split the CH_3 peak into three lines (*i.e.*, a triplet) and the CH_3 protons split the CH_2 peak into four lines (*i.e.*, a quartet).

(c) From rule 3, the intensities of the CH_3 triplet are given by the coefficients of the expansion $(1 + x)^2 = 1 + 2x + x^2$, *i.e.*, by the ratio of 1 : 2 : 1 and the intensities of the CH_3 quartet are given by the coefficients of the expansion $(1+x)^3 = 1 + 3x + 3x^2 + x^3$, *i.e.*, by the ratio of 1 : 3 : 3 : 1.

Example 8. Which of the following nuclei do not show nuclear magnetic resonance :

^1H, ^2H, ^{12}C, ^{13}C, ^{14}N, ^{15}N, ^{16}O, ^{19}F, ^{31}P, ^{32}S ?

Solution : Nuclei that contain odd number of protons and/or neutrons show NMR spectra, *i.e.*, are NMR-active since they have half-integral spin. Nuclei that have integral spin (in particular zero spin) are those which contain even numbers of protons and/or neutrons. These nuclei are NMR-inactive, *i.e.*, they do not show NMR. Thus, the NMR-inactive nuclei are ^{12}C (6p, 6n), ^{16}O (8p, 8n) and ^{32}S (16p, 16n).

Chemical Shift-Equivalent and Magnetically Equivalent Nuclei. If nuclei have exactly the same chemical shift, they are called **chemical shift-equivalent nuclei** and are designated by the same letter. Chemical shift-equivalent nuclei can be interchanged by one of the symmetry operations of a molecule. Thus, all the protons in benzene are chemical shift-equivalent since they can be interchanged by the six-fold symmetry axis of benzene.

If nuclei are coupled in exactly the same way to every other nucleus in the molecule, they are called **magnetically equivalent nuclei.** Thus, in parafluoronitrobenzene,

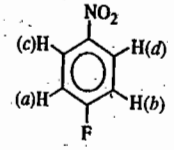

the protons *(a)* and *(b)* are chemical shift-equivalent since they are related by the mirror plane which bisects the molecule. The nuclear spin of F is $I = \frac{1}{2}$. Since F has identical bond distances and angles with respect to protons *(a)* and *(b)*, these protons are identically coupled to F. However, protons *(a)* and *(b)* are not identically coupled to protons *(c)* and *(d)*. Hence, they are not magnetically equivalent. Similarly, protons *(c)* and *(d)* are not magnetically equivalent.

Another way to decide the equivalence of two protons is by replacing each alternately by a group X. If the X derivatives are the same, the protons are equivalent. If the replacement of each H in a CH_2 gives 2 diastereomers, the protons are not equivalent.

Example 9. How many kinds of protons are there in

(i) CH_3CH_3 *(ii)* $CH_3CH_2CH_3$ *(iii)* $(CH_3)_2CHCH_2CH_3$ *(iv)* $C_6H_5CH_3$

(v) $C_6H_5NO_2$ *(vi)* $CH_2=CH_2$ *(vii)* $CH_3CH=CH_2$?

Solution : *(i)* One kind (all equivalent) : $CH_3^a\,CH_3^a$ *(ii)* 2 kinds : $CH_3^a\,CH_2^b\,CH_3^a$

(iii) 4 kinds : $(CH_3^a)_2\,CH^b\,CH_2^c\,CH_3^d$

(iv) 2 kinds : $C_6H_5^a\,CH_3^b$

Theoretically there are three kinds of aromatic protons, *viz.*, ortho, meta and para. However, the ring protons are little affected by alkyl groups and are thus nearly equivalent.

(v) 3 kinds : 2 ortho, 2 meta and one para. *(vi)* One kind (all equivalent)

(vii) 4 kinds :

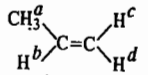

Example 10. Determine which of the following molecules will show spin-spin coupling in their NMR spectra. If the coupling or splitting is observed, give the multiplicity of each kind of proton, *i.e.*, give the number of lines arising from each proton :

(a) $ClCH_2CH_2Cl$ *(b)* $ClCH_2CH_2I$ *(c)*

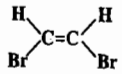

(d)

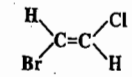

(e)

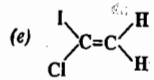

(f) $CH_3—CH=O$ *(g)*

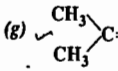

(h) $CH_3—C(Cl_2)—CH_3$

Solution : Spin-spin splitting is not observed in *(a)*, *(c)*, *(g)* and *(h)* which have only equivalent protons. The protons of the CH_2 groups in *(b)* are non-equivalent each being split into a 1 : 2 : 1 triplet. In *(d)* the two protons are not equivalent and each is split into a doublet. The vinyl protons in *(e)* are not equivalent since one is *cis* to Cl and the other is *cis* to I so that each is split into a doublet. Notice that in this case the protons undergoing spin-spin interaction are on the same carbon. In *(f)* the protons of CH_3 and the proton of the —CH=O group are not equivalent ; the CH_3 resonance is split into a doublet and the —CH=O resonance is split into a 1 : 3 : 3 : 1 quartet.

Example 11. Predict the low-resolution NMR spectrum and the high-resolution NMR spectrum of acetone.

Solution : The low-resolution NMR spectrum shows only chemical shift of NMR lines of different protons whereas the high-resolution NMR spectrum shows both the chemical shift and the spin-spin coupling. However, in the case of acetone, $CH_3\diagdown\!\!\diagup C{=}O$, since all the protons are equivalent, only one line is observed in the low-resolution NMR as well as in the high-resolution NMR spectrum.

Example 12. An organic compound C_3H_6O contains a carbonyl group $\diagdown\!\!\diagup C{=}O$. How will its NMR spectrum decide whether it is an aldehyde or a ketone ?

Solution : The two possible structures are :

$CH_3^a\,CH_2^b\,CH^c{=}O$ and $CH_3^a\diagdown\!\!\diagup C{=}O$ (CH_3^a)

(I) (II)

For aldehyde (structure I), NMR spectrum will consist of a triplet for H^a, a complex multiplet (in fact, 8 lines) for H^b and a triplet for H^c. For ketone (structure II), since all the protons are equivalent, we will get only a singlet, *i.e.*, no spin–spin splitting occurs. Thus, the NMR spectrum would readily decide whether the compound is an aldehyde or a ketone.

Example 13. Predict the NMR spectrum of the compound $CH_3COCH_2C{\equiv}CCH_3$

Solution : Since in the compound $CH_3^a-CO-CH_2^b-C{\equiv}C-CH_3^c$, the three groups of protons (*a*, *b* and *c*) are far apart, no spin–spin coupling will be observed. Only the effects of chemical shifts of the three kinds of protons will be observed. H^a, H^b and H^c each will give rise to a singlet with relative intensities of 3 : 2 : 3, respectively.

Example 14. How do you account for the fact that nuclear spin–spin splitting is observed in 2–methyl propene but not in 1–chloro–2, 2–dimethyl propane ?

Solution : In 2-methyl propene, 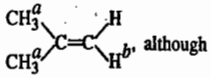 although H^a and H^b are not on adjacent carbon atoms, they undergo spin–spin splitting because the coupling is transmitted through the π-electrons. In $(CH_3^a)_3C-CH_2^bCl$, H^a and H^b do not couple because they are not on adjacent carbon atoms : they are too far away from one another.

Example 15. How can the NMR spectrum distinguish between the isomers *p*–xylene and ethyl benzene ?

Solution : The isomers are

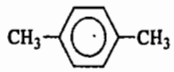 *i.e.*, $p\text{-}CH_3^a\,C_6H_4^b\,CH_3^a$

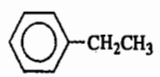 *i.e.*, $C_6H_5^a\,CH_2^b\,CH_3^c$

$p\text{-}CH_3^a\,C_6H_4^b\,CH_3^a$ has two kinds of protons and its NMR spectrum consists of two singlets. $C_6H_5^a\,CH_2^b\,CH_3^c$ has three kinds of protons and its NMR spectrum consists of a singlet for H^a, a quartet for H^b and a triplet for H^c.

Example 16. Predict the high–resolution proton–NMR spectra of CH_3CH_2Cl and CH_3CHDCl.

Solution : Deuterium(D) does not give a signal in the proton–NMR spectrum nor does it split the nearby protons. Thus, we can ignore its presence in the molecule. The NMR spectrum of $CH_3^a\,CH_2^bCl$ consists of 1 : 2 : 1 triplet for H^a and, more down–field, a 1 : 3 : 3 : 1 quartet for H^b. The NMR spectrum of $CH_3^a\,CH^bDCl$ has a doublet for H^a and, more downfield, 1 : 3 : 3 : 1 quartet for H^b.

Example 17. Predict the proton–NMR spectra of H_2, CH_4, C_2H_6 and C_6H_6.

Solution : All the four molecules contain equivalent protons which do not show spin–spin interaction. Hence, their proton–NMR spectra will consist of one signal only, *i.e.*, a *singlet*.

Example 18. Below are given the molecular formulae of some organic compounds that have only one NMR signal :

(*a*) C_5H_{12} (*b*) C_3H_6 (*c*) C_3H_4 (*d*) C_4H_6 (*e*) C_8H_{18} (*f*) C_2H_6O (*g*) $C_2H_4Br_2$

Draw structural formula for each of them.

Solution : Since there is only one NMR signal, all the protons must be equivalent.

(a) The compound is $(CH_3)_4C$ in which all 12 protons are present in 4 equivalent CH_3 groups.

(b) The compound is cyclopropane with structure, 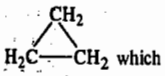 which has 3 equivalent CH_2 groups.

(c) The compound has the structure, $H_2C{=}C{=}CH_2$ (allene) which has 2 equivalent CH_2 groups and a C atom with no protons.

(d) The compound has the structure, $CH_3C{\equiv}CCH_3$ which has 2 equivalent CH_3 groups and 2 carbons with no protons.

(e) The compound has the structure. $(CH_3)_3C-C(CH_3)_3$ which has 6 equivalent CH_3 groups and 2 other carbons with no protons

(f) The compound is dimethyl ether, CH_3-O-CH_3 which has 2 equivalent CH_3 groups.

(g) The compound has the structure, $BrCH_2-CH_2Br$ which has 2 equivalent CH_2 groups.

Example 19. Below are given the molecular formulae of some organic compounds that give 2 singlets in their proton–NMR spectra :

(*a*) $C_3H_6O_2$ (*b*) $C_3H_8O_2$ (*c*) C_2H_5OCl (*d*) $C_3H_5Cl_3$ (*e*) $C_5H_{10}Cl_2$.

Draw structural formula for each of them.

Solution : Since there is no spin–spin interaction, non–equivalent protons cannot be situated on adjacent carbons.

(a) The compound has the structure, $CH_3^aCO-O-CH_3^b$.

(b) The compound has the structure, $CH_3^a\,OCH_2^b\,OCH_3^a$

(c) The compound has the structure, $ClCH_2^a\,OCH_3^b$

(d) The compound has the structure, $CH_3^a\,CCl_2\,CH_2^b\,Cl$

(e) The compound has the structure, $ClCH_2^aC(CH_3^b)_2\,CH_2^a\,Cl$

Mechanism of Nuclear Spin–Spin Interaction. In 1951, N.F. Ramsey and E.M. Purcell proposed that in liquids and gases, the interaction between two nuclear spins is transmitted through the electrons of the chemical bonds that intervene between them. This is called *indirect electron–coupled nuclear spin–spin interaction.* Suppose two nuclear spins a and b are separated by a chemical bond formed between two electrons with spins 1 and 2, as follows :

If electron with spin 1 has a finite probability of being found at the nucleus with spin a, then the electron spin tends to be aligned antiparallel to the nuclear spin a. The electron spin 1 affects the alignment of spin 2 which, in turn, affects the alignment of nuclear spin b. Thus, as a result of the electron spin 1, the magnetic field at the other nucleus b is affected. In other words, the energy levels of nucleus b depend upon the spin orientation of nucleus a. It is thus evident that the nuclear spins a and b interact through the intervention of the electron spins 1 and 2. It may be remarked that this Ramsey–Purcell mechanism of nuclear spin–spin interaction is merely an extension of the so–called **Fermi contact interaction**, proposed by E. Fermi in 1930, according to which if an *s*–electron has a finite value of its wave function at the centre of a nucleus, then the electron spin can be 'felt' by the nuclear spin. N.F. Ramsey was the cowinner (with H.G. Dehmelt and W. Paul) of the 1989 Physics Nobel Prize.

One may well ask why there is no *direct nuclear* spin–spin interaction in liquids and gases. The reason is the following : According to electrodynamics, the energy of interaction through space between two nuclear dipole moments μ_1 and μ_2 (associated with the nuclear spins) is given by

$$E \propto \mu_1\mu_2\,(3\cos^2\theta - 1)/r^3 \qquad \ldots(22)$$

where r is the distance between μ_1 and μ_2 and θ is the angle between them. In a *solid*, this direct dipole–dipole interaction energy is found to be considerable. However, in fluids (*i.e.*, liquids and gases) due to the random *tumbling motion* of the molecules, the average value of $3\cos^2\theta = 1$ so that E vanishes. Thus, we find that while the direct dipole–dipole interaction is considerable in solids, it vanishes in liquids and gases.

The magnitude of nuclear spin–spin interaction falls off with increasing number of bonds intervening between the nuclei involved. This is expected because now the nuclei are too far to interact. A double bond, however, transmits spin–spin coupling more readily than a single bond, *i.e.*, the spin–spin coupling constant J between two atoms joined by a double bond is generally greater than

that joined by a single bond. The spin–spin coupling can also be transmitted through lone pair of electrons between nuclei that are sufficiently close together although not directly bonded.

The magnitude of the coupling constant J is also intimately related to the geometrical relationship of the bonds over which the coupling is transmitted. Thus, in the system H—C—C—H, the H—H coupling constant, known as the **vicinal coupling constant**, depends upon the dihedral angle ϕ between the C—H bonds. The angle ϕ is the angle between the projections of the two C—H bonds viewed along the C—C bond axis. It is found that

$$J_{vic} = 4{\cdot}22 - 0{\cdot}5 \cos \phi + 4{\cdot}5 \cos 2\phi \quad \ldots(23)$$

This is called the **Karplus relation**, proposed by the American chemical physicist, M. Karplus.

The variation of the vicinal coupling constant, J_{vic}, with the dihedral angle ϕ between the two vicinal C—H bonds, is shown in Fig. 11.

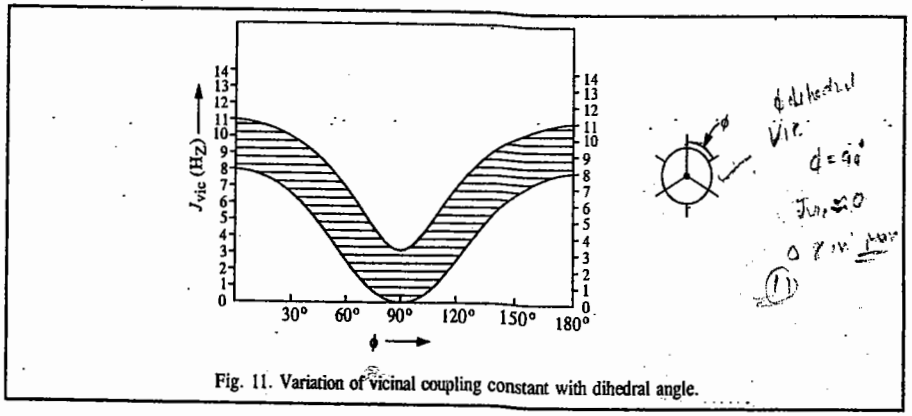

Fig. 11. Variation of vicinal coupling constant with dihedral angle.

Some typical J-values are given in Table 4.

TABLE 4

Spin–Spin Coupling Constants of Some Systems

System	J (Hz)	System	J (Hz)
H—H	276	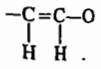	7 to 10
H—F	521		
H—C	120 - 260	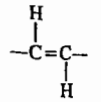	12 to 19
	- 20 to +6		
	5·5 to 7·5		ortho 6 to 9 meta 0·5 to 4 para 0 to 2·5

Largest vicinal couplings arise with the protons in the *trans* coplanar positions (ϕ=180°). Vicinal couplings for *cis* coplanar protons are almost as large (ϕ=0). Very small couplings arise between protons which are 90° to each other.

Complex NMR Spectra. The appearance of NMR spectra depends upon δ/J, *i.e.*, the ratio of the chemical shift to the spin–spin coupling constant. The spectra are called **first-order spectra** if δ/J is very large. The NMR spectrum of ethanol under high-resolution is a first-order spectrum. However, when the ratio δ/J is not large, several peaks appear resulting in a *complex* NMR spectrum.

NMR spectra are classified into AB system, AX system, ABC system, etc. If the chemical shift values of two nuclei are close together, the spin system is called an AB system. If, however, the chemical shift values of two nuclei are far apart (as in the case of hydrogen fluoride, HF) the spin system is called an AX system. Similarly, if the chemical shift values of three nuclei are close together, the system is called an ABC system. On the other hand, the spin system A_2BXY_2 has two A nuclei, one B nucleus with chemical shift close to that of the A nuclei and one X and two Y nuclei with chemical shift values close to one another but far removed from those of A and B.

Fig. 12 shows the NMR spectra of the AB spin system for J=10 Hz and δ/J values of *(a)* 5, *(b)* 4, *(c)* 3, *(d)* 2 and *(e)* 1. The inner pair of peaks has higher intensity than the outer pair. The coupling constant is obtained from the spacing between either pair of peaks. However, the differences in the values of the chemical shifts can be determined by an elaborate calculation involving the positions of all the peaks. The NMR spectra of complex nuclear systems are difficult to calculate quantum mechanically. They are *simulated* on high-speed computers.

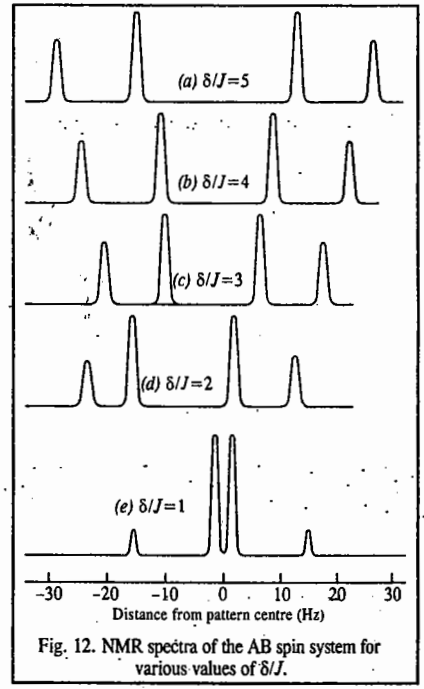

Fig. 12. NMR spectra of the AB spin system for various values of δ/J.

Complex NMR spectra can be simplified by methods which make chemical shift differences larger than spin–spin coupling constant. Since δ is *field-dependent* while J is *field-independent*, it is evident that a complex proton NMR spectrum, obtained at, say, 1·4 T (60 MHz), will be simplified if it is obtained at a higher field, say, 2·34 T (100 MHz). The NMR spectra run at 100 MHz yield chemical shifts almost twice as large as those run at 60 MHz. Spectral simplification can also be obtained by means of the so-called *shift reagents*, such as the complexes of the rare-earth metals, particularly those of europium and praseodymium. A small amount of the shift reagent added to the sample under study causes a marked increase in the chemical shift thereby reducing the distorted pattern of the spectrum.

NMR Spectra of Other Nuclei. Besides protons, other nuclei having nuclear spin $I=\frac{1}{2}$, such as ^{13}C, ^{19}F, ^{29}Si and ^{31}P, have also been investigated by NMR spectroscopy. The NMR spectra of ^{1}H and ^{19}F are most easily obtained because of their high natural abundance and large magnetogyric ratios. Spectra of other nuclei provide structural information about compounds the same way as the proton magnetic resonance spectra do. While ^{1}H-chemical shifts extend only over a small range of the order of 15 ppm, ^{31}P-chemical shifts have a span of about 400 ppm and ^{19}F-chemical shifts have a still wider span of 600 ppm. This wider range can be attributed to the greater number and mobility of extranuclear electrons which produce greater variation in diamagnetic shielding.

Nuclei such as ^{2}H, ^{10}B, ^{14}N, ^{35}Cl, etc., having nuclear spin $I > \frac{1}{2}$, do not have spherically symmetric charge distributions and, as a consequence, possess an electric quadrupole moment, eQ, where e is electric charge and Q is a measure of the deviation of the nuclear charge distribution

from spherical symmetry. Quadrupolar nuclei are quite "troublesome"; not only their own NMR lines are broadened but also those of the other nuclei in the molecule with which they undergo spin–spin interaction. Consider the two isotopically labelled ammonia molecules, $^{15}NH_3$ and $^{14}NH_3$. Whereas the NMR spectrum of the former (containing ^{15}N with $I=1/2$) is sharp, that of the latter (containing ^{14}N with $I=1$) is broad. The reason is that the electric qudrupole moment of the quadrupolar nucleus in question interacts with the fluctuating *EFG* (electric field gradient) which arises from the bonding and non-bonding electrons. This interaction effectively shortens the spin–lattice relaxation time, leading to broadening of NMR signal.

In recent years, the ^{13}C-NMR spectroscopy has emerged as a good structural tool although there is considerable difficulty in recording the ^{13}C-NMR spectra. This is due to the fact that ^{13}C has a very small natural abundance and a small value of the magnetogyric ratio.

Example 20. Predict the NMR spectrum of borohydride ion BH_4^-. The nuclear spin of ^{11}B is 3/2.

Solution : The four protons in BH_4^- are equivalent. Thus, the ^{11}B resonance splits into a quintet with the relative intensity ratio 1 : 4 : 6 : 4 : 1. Since the nuclear spin, I of ^{11}B is 3/2, in the presence of magnetic field its four components are +3/2, +1/2, –1/2 and –3/2. Thus, the proton resonance is split into a quartet by interaction with the ^{11}B nucleus, the four lines being equally intense.

Example 21. The ^{31}P-NMR spectrum of phosphonic acid gives a doublet whereas that of phosphinic acid gives a triplet. Write the structures of the two acids, justifying them.

Solution : Phosphonic acid, 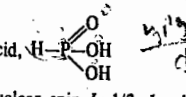 Phosphinic acid, 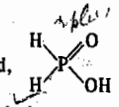

Both ^1H and ^{31}P have nuclear spin $I=1/2$. In phosphonic acid, the P atom is attached to one proton which causes its resonance to be split into a doublet. In phosphinic acid, the P atom is attached to two protons which cause its resonance to be split into a triplet in the intensity ratio 1 : 2 : 1.

Example 22. Describe the proton and deuteron-NMR spectra of HD.

Solution : For ^1H, $I=1/2$ and for ^2D, $I=1$. In the presence of magnetic field, the proton spin has two components, m_I = 1/2 and –1/2, whereas the deuteron spin has three components m_I = +1, 0 –1. Thus, the deuteron resonance is split by the proton into a doublet and the proton resonance is split by the deuteron into a triplet (1 : 2 : 1).

Example 23. Describe the proton-NMR and phosphorus-NMR spectra of phosphonium ion, PH_4^+.

Solution : Both ^1H and ^{31}P have $I=1/2$. Thus, the P atom splits the resonance of the four equivalent protons in PH_4^+ ion into a doublet and the protons split the phosphorus resonance into a quintet in the intensity ratio 1 : 4 : 6 : 4 : 1.

Example 24. Describe the proton-NMR and nitrogen-NMR spectra of the ammonium ion, NH_4^+.

Solution : ^1H has $I=1/2$ whereas ^{14}N has $I=1$. In the presence of the magnetic field, the ^{14}N-spin has three components : m_I = +1, 0, –1. Thus, the N-atom splits the resonance of the four equivalent protons in NH_4^+ ion into a 1 : 1 : 1 triplet. The protons split the nitrogen resonance into 1 : 4 : 6 : 4 : 1 quintet.

Example 25. Why is NMR spectrum of NH_3 broad whereas that of NH_4^+ ion is sharp ?

Solution : We know that ^{14}N ($I=1$) is a quadrupolar nucleus. The electric field gradient (*EFG*) at this nucleus due to the bonding electrons and the lone pair electrons on N atom interacts with the nuclear quadrupole moment of ^{14}N in NH_3, thereby broadening the NMR spectrum of ^{14}N which, in turn, broadens the spectrum of ^1H. However, in the case of NH_4^+ ion which is *spherically symmetrical*, the *EFG* vanishes (this is a result of quantum mechanics), so that there is *no* nuclear quadrupole interaction of *EFG* with the quadrupole moment of ^{14}N. Hence, the NMR spectrum of NH_4^+ ion is sharp.

FOURIER-TRANSFORM NMR SPECTROSCOPY

In 1966, R.R. Ernst and W.A. Anderson published a remarkable paper on the Fourier-Transform (FT) NMR spectroscopy. In this technique, spectra are presented in the *time-domain* as against the

conventional *continuous wave* (CW) NMR, where the spectra are presented in the *frequency domain*. In the frequency domain, the intensity of the radiation at the detector is a function of frequency, *i.e.*, $I(\nu)$, and in the time-domain, the intensity is a function of time, *i.e.*, $F(t)$. The $I(\nu)$ can be transformed by the mathematical technique known as **Fourier transform** into $F(t)$, as follows :

$$F(t) = \int_{-\infty}^{+\infty} e^{2\pi i\nu t} I(\nu)\, d\nu \qquad ...(24a)$$

Conversely, $F(t)$ can be transformed into $I(\nu)$ by the **inverse Fourier transform** :

$$I(\nu) = \int_{-\infty}^{+\infty} e^{-2\pi i\nu t} F(t)\, dt \qquad ...(24b)$$

These transforms are carried out by a computer attached to the NMR apparatus. $F(t)$ contains all the information about the NMR spectrum that $I(\nu)$ does. Now the question arises : Why do we need $F(t)$ if $I(\nu)$ can do the job ? The reason is that to measure the NMR spectrum in the frequency domain, one has to scan a very broad range of frequencies, which is time-consuming. On the other hand, to record the spectrum in the time-domain, *one can apply all the frequencies in a very short time*. Thus, a CW-NMR spectrum which takes, say, 25 minutes to scan, can be scanned in 25 seconds as FT-NMR spectrum. Clearly, FT-NMR is vastly faster than CW-NMR.

In order to excite FT-NMR, the band of frequencies required is obtained by applying a short, approximately square-wave pulse of radiofrequency power in the xy plane. Fig. 13 shows the Fourier synthesis of a square wave which is a superposition of several sinosoidal waves. Better approximation to square wave can be achieved by including more sine waves. Conversely, the analysis of $F(t)$ into its Fourier components yields a whole spectrum of different superimposed harmonic (sinosoidal) waves. In the pulsed FT-NMR spectrometer, the pulse B_1 is supplied by a radiofrequency field that has the Larmor (NMR) frequency ν_0 which is of the order of 100 MHz for ^1H-NMR. The Fourier components add to, or subtract from, this carrier frequency. Suppose the length of the pulse is t_p ($\approx$ 100 μs). The sample receives a range of frequencies of about $\nu_0 \pm 1/t_p$ which, in the present example, are 100 MHz ± 10 kHz.

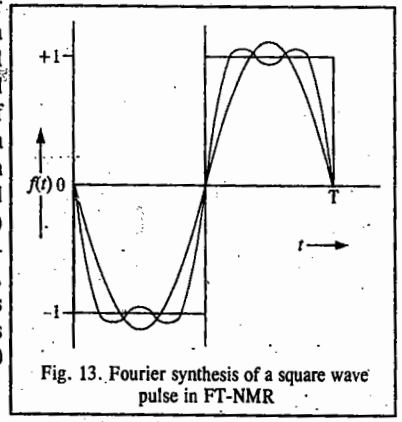

Fig. 13. Fourier synthesis of a square wave pulse in FT-NMR

As soon as the radiofrequency pulse B_1 terminates, the magnetization vector (of all the magnetic nuclei in the sample) in the xy-plane starts decaying. This important process is called **free induction decay** (FID) because the nuclei are freely precessing about the Zeeman field, B_0, in the absence of the radio frequency field B_1. Without going into details, we may remark that in order to improve the *signal-to-noise* (S/N) *ratio*, several consecutive pulses can be applied to the sample thereby considerably enhancing the intensity of the signal. The FIDs are collected in the computer and averaged before being Fourier-transformed to give the $I(\nu)$ spectrum. Most modern NMR spectrometers are based on the Fourier-transform technique. The Swiss scientist R.R. Ernst (1933 –) was awarded the 1991 Chemistry Nobel Prize for his contributions to the development of the methodology of high resolution NMR spectroscopy.

Thermal Equilibrium of Nuclear Spins and the Relaxation Processes in Magnetic Resonance

The Zeeman splitting of the nuclear or electron spins obtained by applying magnetic fields at room temperature, is very small. The relative Boltzmann population of the nuclear spins in the upper state and in the lower state is given by

$$n_{upper}/n_{lower} = \exp(-\Delta E/kT) = \exp(-g_N \mu_N B_0/kT) \qquad ...(25)$$

where n_{upper} and n_{lower} are the numbers of spins in the upper and lower energy states. At room temperature, $g_N \mu_N B_0 << kT$ so that the exponential can be approximated by a power series to give :

$$n_{upper}/n_{lower} \approx 1 - (g_N \mu_N B_0/kT) \quad ...(26)$$

The excess population in the lower state is then given by

$$\frac{n_{lower} - n_{upper}}{n_{lower} + n_{upper}} = \frac{g_N \mu_N B_0}{2kT} \quad ...(27)$$

which, for ordinary temperatures and magnetic field B_0, is very small. Now only the spins in the low energy state can absorb radiation which has to be of the right frequency to be absorbed. Since the excess population in the lower energy state is directly proportional to the magnetic flux density, B_0, the intensity of the NMR signal increases as B_0 increases. If the spin system is irradiated with too high a power, the excess spins at the lower energy will be used up so that the upper and lower energy states will become *equally populated*. No further energy can be absorbed from the field and the resonance absorption becomes *saturated*. As a result, no NMR measurement is possible. Fortunately, there is a mechanism whereby this situation is avoided. To record an NMR spectrum, there is a process known as **relaxation** *which removes the excitation energy from the upper state to restore the excess population in the ground state* so that the energy can be continuously absorbed from the radiofrequency field, B_1.

The transition from the lower to upper energy state corresponds to flipping of the nuclear magnetic moment vector from one allowed orientation to the other in the large Zeeman field B_0. In the ground state, the proton spins are aligned so that the z-components of the magnetic moment μ_z are in the direction of B_0. The radiofrequency field B_1 flips the nuclear moments to the opposite direction as the energy is absorbed. The relaxation process flips them back to the original orientation with the result that *the spin system returns to the ground state by transferring its energy of excitation to the random thermal motions in the surroundings.* In other words, the nuclear spin system becomes *cooler* and its surroundings become *warmer* as a result of the energy transfer.

If the excess number of nuclei in the lower energy level is represented by n and the initial number is n_0, the approach to the new equilibrium n_{eq} is described by

$$n - n_{eq} = (n_0 - n_{eq}) \exp(-t/T_1) \quad ...(28)$$

where t is the time and T_1 is called the **spin-lattice relaxation time**. The name *spin-lattice relaxation* originates from the fact that the first experiments were carried out on solid samples where the relaxation was brought about by the transfer of spin excitation energy to the lattice vibrations. The term spin-lattice relaxation has been retained but it refers to relaxation due to fluctuating magnetic fields arising from random motions in the surroundings of the spin system. This, in brief, is the basis of the so-called **Bloembergen-Purcell-Pound (BPP)** theory of relaxation processes in magnetic resonance, proposed in 1948. The detailed theory of the relaxation processes in magnetic resonance is very complicated, having been worked out by theorists such as Waller, van Vleck, Bloembergen, Purcell, Pound, Kubo and Tomita. It may be mentioned here that another quantity, the **transverse relaxation time**, T_2, also characterizes the relaxation process. The T_2-relaxation amounts to *loss of phase coherence of the precessing spins*. It can be considered as the characteristic time for the *transfer of entropy* from the surroundings to the spins. The most common cause of the T_1-relaxation is the magnetic dipole-dipole interaction. Paramagnetic substances, if present in the sample, *increase* the efficiency of the nuclear spin relaxation and thus *decrease* T_1. In liquids, T_1 and T_2 are almost equal. In solids, T_2 is of the order of microseconds. E.M. Purcell was the cowinner (with F. Bloch) of the 1952 Physics Nobel Prize and N. Bloembergen, the cowinner (with K. Siegbahn and A.L. Schawlow) of the 1981 Physics Nobel Prize.

Example 26. Calculate the relative Boltzmann population of the proton spins in the lower state to that in the upper state in a magnetic field of flux density 1T at room temperature. What is the excess population in the lower state ?

Solution :

$$\frac{n_{lower}}{n_{upper}} = 1 + \frac{g_N \mu_N B_0}{kT} = 1 + \frac{(5{\cdot}585)(5{\cdot}05 \times 10^{-27}\,JT^{-1})(1T)}{(1{\cdot}38 \times 10^{-23}\,JK^{-1})(298\,K)} = 1 + 6{\cdot}686 \times 10^{-6}$$

$$\frac{n_{lower} - n_{upper}}{n_{lower} + n_{upper}} = \frac{g_N \mu_N B_0}{2kT} = 3{\cdot}343 \times 10^{-6}$$

Study of Hindered Rotation by NMR Spectroscopy

When the NMR spectrum of N, N-dimethyl formamide (DMF), $HCON(CH_3)_2$, is recorded at room temperature, it consists of *two* signals, though one would expect the two CH_3 groups in magnetically equivalent environments. DMF is a resonance hybrid of the following forms which result from the conjugation between the carbonyl group and the nitrogen nonbonding pair, as a consequence of which the double-bond character of the C—N bond is increased sufficiently to cause hindered rotation at room temperature :

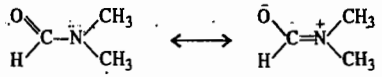

Similarly, the NMR spectrum of N,N-dimethylacetamide, consists of two NMR signals at room temperature as a result of hindered rotation about the C—N double bond :

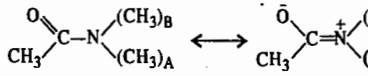

Fig. 14 shows the pmr (*i.e.*, proton-NMR) spectrum of N,N-dimethylacetamide when it is heated from 308 K to 368 K. At the lower temperature, two peaks are observed because the molecular skeleton is almost planar and the protons in the two methyl groups have different chemical shifts ν_A and ν_B. As the temperature is increased, the rate of the *cis-trans* isomerization increases so that at higher temperatures a single pmr signal is obtained since the rotation about the C—N bond is very rapid compared with the difference in the chemical shifts.

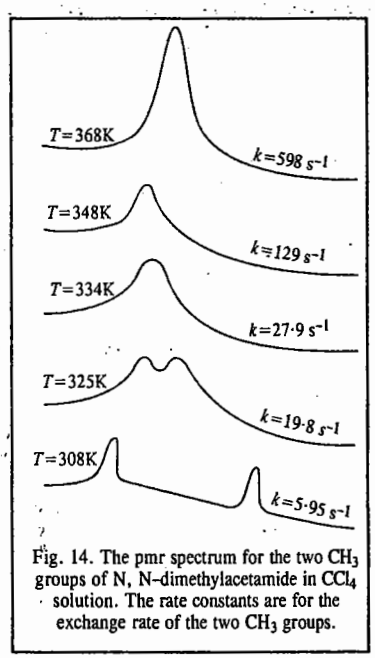

Fig. 14. The pmr spectrum for the two CH_3 groups of N, N-dimethylacetamide in CCl_4 solution. The rate constants are for the exchange rate of the two CH_3 groups.

Another example is that of 1, 2-dibromoethane ($BrCH_2CH_2Br$) whose four protons appear to be chemically indistinguishable and thus magnetically equivalent so that one would expect the NMR spectrum to show the same chemical shift for all the protons. However, the Newman projections shown in Fig. 15 show that the protons in different conformations are not in magnetically equivalent environments. Thus, the ringed proton is flanked by H and Br in the first conformer but by H and H in the second. The pmr spectrum, recorded at *low temperatures*, will enable these features to be distinguished since the molecular rotations about the C—C bond are sufficiently 'frozen'.

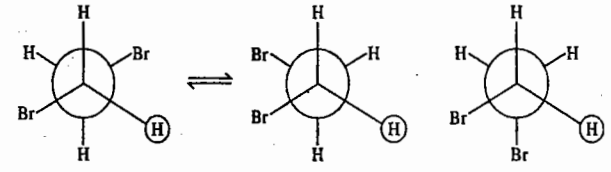

Fig. 15. Rotational isomers of 1, 2-dibromoethane.

However, at room temperature, the rotation is so rapid that each proton experiences the same time-averaged environment and only one sharp peak appears in the pmr spectrum.

Similar effects are found in *fluxional* molecules and in structures where steric effects can intervene as, for example, in the case of cyclohexane. (Fig. 16) :

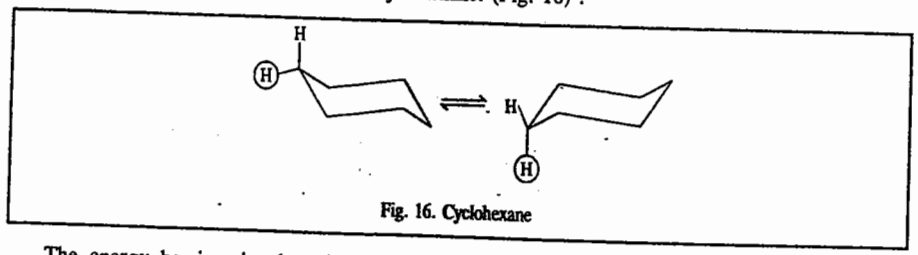

Fig. 16. Cyclohexane

The energy barriers involved in these rotational changes can be measured by NMR using a variable-temperature sample probe and noting the temperature at which the spectrum changes from that of the mixed conformers to that of a time-averaged situation. The basic theory of the exchange effects is outlined below.

For a reaction A $\rightleftarrows$ B, the mean life-time of the species A is $\tau = k_1^{-1}$ where k_1 is the first-order rate constant for the exchange. Thus, the width of the NMR peak (*i.e.*, signal) at half-height is $\delta\nu = k_1/\pi$. However, before we use this relation to calculate k_1, we must subtract the natural line width in the absence of exchange to obtain the residual broadening due only to exchange. In the other limit, at high exchange rates when the individual peaks have fused or coalesced, the line width is $\delta\nu = \pi(\nu_A - \nu_B)^2/k_1$, where ν_A and ν_B are the individual frequencies of the peaks for A and B, as determined by the measurements at low temperatures. At the temperature at which the NMR spectrum changes from that of two peaks to that of a single peak, *i.e.*, the flat-topped peak,

$$k_{1_c} = \pi\Delta\nu_0/\sqrt{2} \qquad \ldots(29)$$

where $\Delta\nu_0$ is the frequency separation between the two peaks.

Example 27. At the coalescence temperature 331 K, the frequency separation between the two NMR signals of N,N-dimethylacetamide is 10·85 Hz. Calculate the rate constant for the first-order chemical exchange of the two methyl groups.

Solution : $k_1 = \pi\,\Delta\nu_0/\sqrt{2} = \pi\,(10{\cdot}85\ s^{-1})/\sqrt{2} = 24{\cdot}1\ s^{-1}$

The Arrhenius-type plot of ln k_1 versus $1/T$ enables the evaluation of the activation energy which in this case is found to be 70 kJ mol^{-1}.

NUCLEAR MAGNETIC DOUBLE RESONANCE

Nuclear magnetic double resonance (NMDR), also called *double irradiation* or *spin decoupling*, is a technique very frequently used in the interpretation of complex NMR spectra. It is based on the principle that when one group of equivalent protons in a molecule is *irradiated* by applying very strong stationary radiofrequency field at the Larmor (resonance) frequency of the protons, it can no longer undergo spin-spin coupling with the neighbouring groups containing equivalent protons. As a result, the spectrum is simplified.

Fig. 17 shows the double resonance spectrum for pure ethanol. When protons of CH_3 group are irradiated (Fig. 17*b*), the resonance of the methylene protons collapses to a doublet because they are coupled only with the OH proton ; the coupling with CH_3 protons is destroyed. Similarly, when protons of the CH_2 group are irradiated (Fig. 17*c*), the resonances of the OH and methyl protons both collapse to singlets.

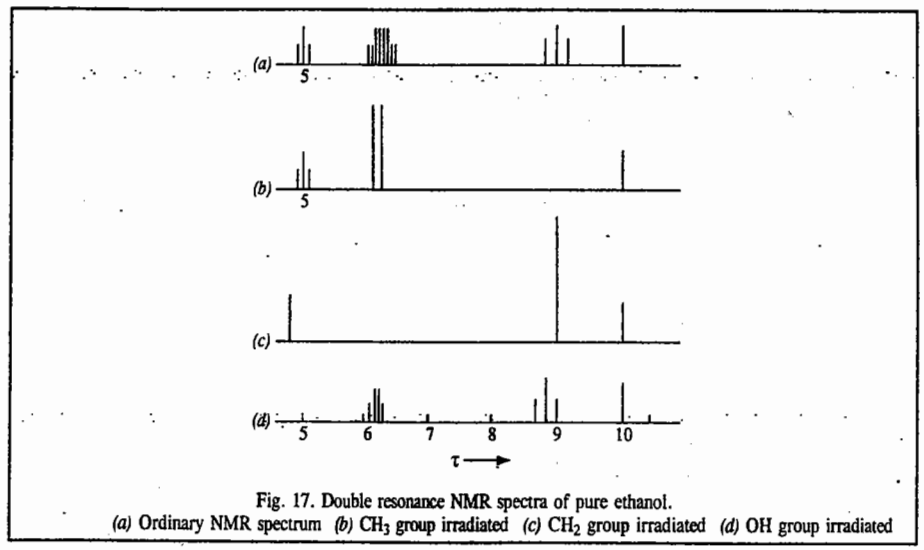

Fig. 17. Double resonance NMR spectra of pure ethanol.
(a) Ordinary NMR spectrum *(b)* CH_3 group irradiated *(c)* CH_2 group irradiated *(d)* OH group irradiated

Since an additional field is used, the experiment is called double resonance. Double irradiation always yields a simpler spectrum. For example, in an ABX spectrum, where it is difficult to extract coupling constants, irradiation of the X nucleus yields a simple AB system from which spin-spin coupling constants can be easily obtained.

SPECIAL TOPICS IN NUCLEAR MAGNETIC RESONANCE

1. Quantum Mechanical Description of the NMR Spectrum of an AB Spin System

The AB spin system is the simplest spin system. Consider a spin system of two nuclei A and B both having nuclear spin $I = 1/2$. In the presence of the Zeeman magnetic field, B_z, applied in the z-direction, the Hamiltonian for the various magnetic interactions is given by

$$\hat{H} = \hat{H}_{\text{Zeeman}} + \hat{H}_{sc} + \hat{H}_{\text{dip}} \qquad \ldots(30)$$

$\hat{H}_{\text{Zeeman}}$, which represents the interaction of the nuclei with B_z, is given by

$$\hat{H}_{\text{Zeeman}} = -g_N\mu_N I_z^A B_z(1-\sigma_A) - g_N\mu_N I_z^B B_z(1-\sigma_B) \qquad \ldots(31)$$

where I_z^A and I_z^B are the components of the nuclear spin quantum numbers of the nuclei A and B in the z-direction. $\hat{H}_{sc}$ (which represents the scalar coupling), is, in fact, the *indirect* spin-spin interaction, given by

$$\hat{H}_{sc} = J\,\boldsymbol{I}^A\cdot\boldsymbol{I}^B \qquad \ldots(32)$$

where J, the coupling constant, is a measure of the spin-spin interaction, and is given in Hz. The dipolar Hamiltonian, $\hat{H}_{\text{dip}}$, is given by

$$\hat{H}_{\text{dip}} = g_N^2\mu_N^2\left[\frac{\boldsymbol{I}^A\cdot\boldsymbol{I}^B}{r^3} - \frac{3(\boldsymbol{I}^A\cdot\boldsymbol{r})(\boldsymbol{I}^B\cdot\boldsymbol{r})}{r^5}\right] \qquad \ldots(33)$$

(Here r is the distance between the two nuclei). This Hamiltonian represents the *direct* interaction between the two nuclear spins in space. As a result of fast tumbling motion of molecules in the *liquid state*, it averages to zero. (It does not vanish in the solid state but we are here concerned with the NMR of the AB system in the liquid state.) It is convenient to work in frequency units, so Eq. 1 can be written as

$$\hat{H} = -\nu_0(1-\sigma_A)I_z^A - \nu_0(1-\sigma_B)I_z^B + JI^A \cdot I^B \quad ...(34)$$

where $$I^A \cdot I^B = I_x^A I_x^B + I_y^A I_y^B + I_z^A I_z^B \quad ...(35)$$

The Schrödinger wave equation is

$$\hat{H}\psi = E\psi \quad ...(36)$$

where ψ, the exact eigenfunction of $\hat{H}$, can be written as a linear combination of the basis set, *i.e.*, the basis spin functions ϕ_i :

$$\psi = \sum_i c_i \phi_i \quad ...(37)$$

For a two-nuclei AB system with $I = \frac{1}{2}$, there are four possible combinations of nuclear spins given by

$$\phi_1 = \alpha^A \alpha^B; \ \phi_2 = \alpha^A \beta^B \quad ...(38a)$$

$$\phi_3 = \beta^A \alpha^B; \ \phi_4 = \beta^A \beta^B \quad ...(39b)$$

Assuming that ψ is normalized, the energy E in Eq. 36 is given by

$$E = <\psi|\hat{H}|\psi> = \int \psi \hat{H} \psi \, d\tau \quad ...(39)$$

Using the variation method, the values of E are obtained by solving the secular determinant :

$$\begin{vmatrix} H_{11}-E & H_{12} & H_{13} & H_{14} \\ H_{21} & H_{22}-E & H_{23} & H_{24} \\ H_{31} & H_{32} & H_{33}-E & H_{34} \\ H_{41} & H_{42} & H_{43} & H_{44}-E \end{vmatrix} = 0 \quad ...(40)$$

We are now interested in evaluating the matrix elements H_{ij} occurring in Eq. 40. We can do this by employing the so-called *raising* and *lowering operators*, I^+ and I^-, defined by

$$I^+ = I_x + iI_y \quad ...(41a)$$

$$I^- = I_x - iI_y \quad ...(41b)$$

From the theory of angular momentum, these operators are known to have the following properties:

$$I^+|\alpha> = 0; \ I^+|\beta> = 1\alpha> \quad ...(42a)$$

$$I^-|\alpha> = \beta; \ I^-|\beta> = 0 \quad ...(42b)$$

Thus, we have $$I^{A+}I^{B-} = (I_x^A I_x^B + I_y^A I_y^B) + i(I_y^A I_x^B - I_x^A I_y^B) \quad ...(43a)$$

$$I^{A-}I^{B+} = (I_x^A I_x^B + I_y^A I_y^B) - i(I_y^A I_x^B - I_x^A I_y^B) \quad ...(43b)$$

Hence, Eq. 34 can be rewritten as

$$\hat{H} = \nu_0(1-\sigma_A)I_z^A - \nu_0(1-\sigma_B)I_z^B + J\left[I_z^A I_z^B + \tfrac{1}{2}(I^{A+}I^{B-} + I^{A-}I^{B+})\right] \quad ...(44)$$

It can be shown that if ϕ_i and ϕ_j have different values of m_I (the component of nuclear spin), then

$$\int \phi_i \hat{H} \phi_j \, d\tau = \int \phi_j \hat{H} \phi_i \, d\tau = 0 \quad ...(45)$$

The various matrix elements H_{ij} in Eq. 40 can be shown to be given by

$$H_{11} = -\frac{\nu_0}{2}(1-\sigma_A) - \frac{\nu_0}{2}(1-\sigma_B) + \frac{J}{4}$$

$$H_{22} = \frac{\nu_0}{2}(1-\sigma_A) - \frac{\nu_0}{2}(1-\sigma_B) - \frac{J}{4}$$

$$H_{33} = -\frac{\nu_0}{2}(1-\sigma_A) + \frac{\nu_0}{2}(1-\sigma_B) - \frac{J}{4}$$

$$H_{44} = \frac{\nu_0}{2}(1-\sigma_A) + \frac{\nu_0}{2}(1-\sigma_B) + \frac{J}{4}$$

$$H_{23} = H_{32} = \frac{J}{2}$$

The remaining matrix elements H_{12}, H_{21}, H_{13}, H_{31}, H_{14}, H_{41}, H_{24}, H_{42}, H_{34} and H_{43} are all zero. Eq. 40 now becomes

$$\begin{vmatrix} x_1 & 0 & 0 & 0 \\ 0 & x_2 & \frac{J}{2} & 0 \\ 0 & \frac{J}{2} & x_3 & 0 \\ 0 & 0 & 0 & x_4 \end{vmatrix} = 0 \quad ...(46)$$

where

$$x_1 = -\frac{\nu_0}{2}(1-\sigma_A) - \frac{\nu_0}{2}(1-\sigma_B) + \frac{J}{4} - E$$

$$x_2 = \frac{\nu_0}{2}(1-\sigma_A) - \frac{\nu_0}{2}(1-\sigma_B) - \frac{J}{4} - E$$

$$x_3 = -\frac{\nu_0}{2}(1-\sigma_A) + \frac{\nu_0}{2}(1-\sigma_B) - \frac{J}{4} - E$$

$$x_4 = \frac{\nu_0}{2}(1-\sigma_A) + \frac{\nu_0}{2}(1-\sigma_B) + \frac{J}{4} - E$$

The solution of the secular determinant (Eq. 46) yields

$$E_1 = \nu_0\left(-1 + \frac{\sigma_A}{2} + \frac{\sigma_B}{2}\right) + \frac{J}{4} \quad ...(47a)$$

$$E_4 = \nu_0\left(1 - \frac{\sigma_A}{2} - \frac{\sigma_B}{2}\right) + \frac{J}{4} \quad ...(47b)$$

Thus, $$E_1 = -M + \frac{J}{4}; \ E_4 = M + \frac{J}{4} \text{ where } M = \nu_0\left(1 - \frac{\sigma_A}{2} - \frac{\sigma_B}{2}\right)$$

For the other two energy values (E_2 and E_3) we have to evaluate the roots of the secular determinant

$$\begin{vmatrix} \frac{\nu_0}{2}(1-\sigma_A) - \frac{\nu_0}{2}(1-\sigma_B) - \frac{J}{4} - E & \frac{J}{2} \\ \frac{J}{2} & -\frac{\nu_0}{2}(1-\sigma_A) + \frac{\nu_0}{2}(1-\sigma_B) - \frac{J}{4} - E \end{vmatrix} = 0 \quad ...(48)$$

which yields $$E = -\frac{J}{4} \pm \left(\frac{\nu_0^2\delta^2}{4} + \frac{J^2}{4}\right)^{1/2} \quad \text{where } \delta = \sigma_A - \sigma_B$$

Thus, we have

$$E_2 = -\frac{J}{4} - \frac{1}{2}(\nu_0^2\delta^2 + J^2)^{1/2} = -\frac{J}{4} - \frac{1}{2}\nu_0\delta\left(1 + \frac{J^2}{2\nu_0^2\delta^2} + \ldots\ldots\right) \qquad \ldots(49a)$$

and $$E_3 = -\frac{J}{4} + \frac{1}{2}(\nu_0^2\delta^2 + J^2)^{1/2} = -\frac{J}{4} + \frac{1}{2}\nu_0\delta\left(1 + \frac{J^2}{2\nu_0^2\delta^2} + \ldots\ldots\right) \qquad \ldots(49b)$$

[In Eqs. (49*a*) and (49*b*), we have used the Taylor's series expansion, *viz.*,

$$(1+x)^{1/2} \approx 1 + x/2 + x^2/4 + \ldots\ldots]$$

Fig. 18 shows the energy level changes due to the various interactions.

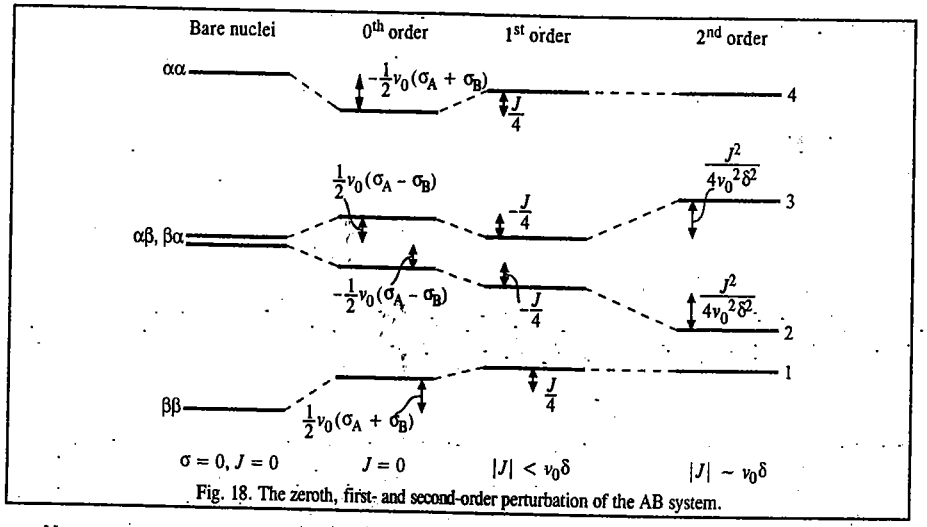

Fig. 18. The zeroth, first- and second-order perturbation of the AB system.

Next we are interested in the selection rules for the NMR transitions of the AB system. We apply the radio-field $\boldsymbol{B}_1$ to the sample to bring about transitions between nuclear sub- energy levels *m* and *n*. Experimentally $\boldsymbol{B}_1$ is applied in the *x*-direction; thus, $\boldsymbol{B}_1$ is perpendicular to the external Zeeman (magnetic) field $\boldsymbol{B}_z$. (If $\boldsymbol{B}_1$ and $\boldsymbol{B}_z$ are in the same z-direction, then the effect is merely the modulation of the Zeeman energy levels.) The interaction between $\boldsymbol{B}_1$ and the nuclear magnetic moment μ_x is given by the Hamiltonian , $\hat{H}'$:

$$\hat{H}' = \mu_x \boldsymbol{B}_1 \qquad \ldots(50)$$

where μ_x is the component of the nuclear magnetic moment in the *x*-direction. The transition probability is proportional to the square of the matrix element (or transition moment integral) $|< \psi_n |\hat{H}'| \psi_m >|^2$ or simply to $|< \psi_n |I_x| \psi_m >|^2$ since $\mu_x = I_x/\hbar\gamma$ where γ is the magnetogyric ratio of the nucleus. Omitting details, we can show that this last matrix element is zero (by substituting $I_x = (I^+ + I^-)/2$) unless the magnetic

spin quantum numbers for the two spin states *m* and *n* differ by ±1. Thus, the selection rule for the NMR transitions is $\Delta m_I = \pm 1$.

Using this selection rule, the allowed spectral transitions (in Hz) are :

$$E_2 - E_1 = -\frac{J}{2} + M - \frac{1}{2}\nu_0\delta\xi \qquad \ldots(51a)$$

$$E_3 - E_1 = -\frac{J}{2} + M + \frac{1}{2}\nu_0\delta\xi \qquad \ldots(51b)$$

$$E_4 - E_2 = \frac{J}{2} + M + \frac{1}{2}\nu_0\delta\xi \qquad \ldots(51c)$$

$$E_4 - E_3 = \frac{J}{2} + M - \frac{1}{2}\nu_0\delta\xi \qquad \ldots(51d)$$

where $$\xi = \left(1 + \frac{J^2}{2\nu_0^2\delta^2} + \ldots\ldots\right)$$

Fig. 19 shows the theoretical NMR spectra for the AB system for various values of *J* and $\nu_0\delta$.

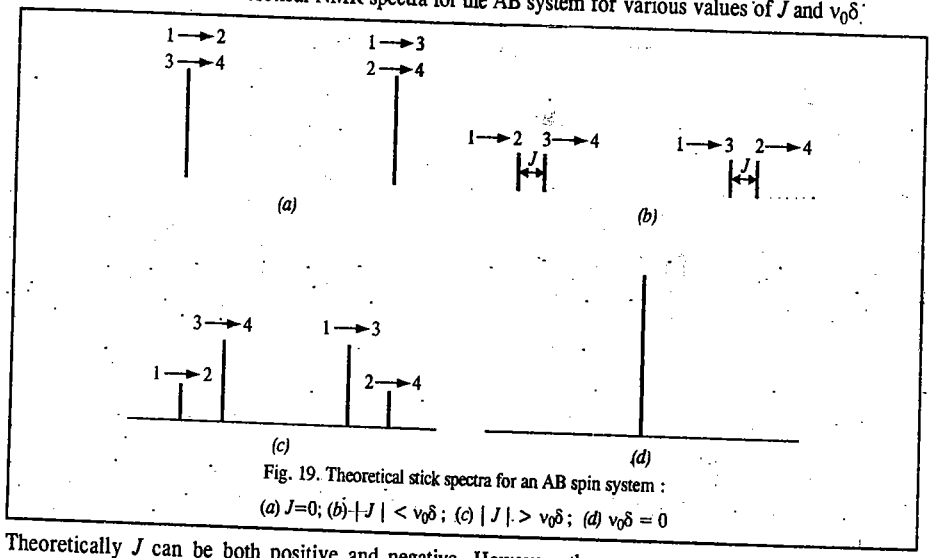

Fig. 19. Theoretical stick spectra for an AB spin system :
(*a*) *J*=0; (*b*) |*J*| < $\nu_0\delta$; (*c*) |*J*| > $\nu_0\delta$; (*d*) $\nu_0\delta$ = 0

Theoretically *J* can be both positive and negative. However, the appearance of the NMR spectrum depends only on the modulus of *J*, *i.e.*, | *J* |, the absolute magnitude.

With reference to Figs. 18 and 19, the following points may be noted :

1. In Fig. 18, the labelling of energy levels (| αα >, | αβ >, etc.) applies only to bare nuclei, zeroth- and first-order case. In the second-order perturbation case, the energy levels originally corresponding to |αβ > and |βα > are "mixed" ; they are thus really represented by linear combinations of the type (| αβ > ± | β α >).

2. In the first-order case where | *J* | < $\nu_0\delta$, the system is said to be *weakly coupled* and is usually called an AX system rather than AB system. The AB case applies only when there is a strong coupling between the nuclei, *i.e.*, | *J* | > $\nu_0\delta$.

3. Though the position and intensity of the spectral lines may change depending on the magnitude of the spin-spin interaction, the total area under the observed spectrum is the same for all cases.

4. When two nuclei have the same chemical shift, only one line is observed even though there is spin-spin interaction between them.

In practice, the analysis of an NMR spectrum is carried out by trial and error. This method consists in making intelligent guesses of Js and $\nu_0\delta s$ and constructing theoretical spectra to compare with the experimental spectrum.

2. Two-Dimensional NMR Spectroscopy

In Fig. 20, the rectangles denote radio frequency pulses applied to an NMR sample. Fig. 20(a) shows a single radio frequency pulse applied to the system followed by observation of the FID (free induction decay) as a function of time t. Fourier transformation of this function of t gives the NMR spectrum as a function of frequency ν.

This is a one-dimensional (1D) NMR spectrum. In Fig. 20(b) a pulse is applied, and after a time t_1, a second pulse is applied, and the FID is observed as a function of time t_2 upto a time $t_{2,max}$. Fourier transformation of this function of t_2 gives the NMR spectrum as a function of frequency. The spectrum's appearance will be influenced by the first pulse. We have obtained the spectrum as a function of a single variable; so this is still a 1D spectrum.

Now suppose we repeat the experiment in Fig. 20(b) except that we use a slightly longer time t_1 between the two pulses. We then repeat the experiment using successively larger values of the time interval t_1 between the two pulses. By collecting all the FIDs from the successive experiments, we get an FID that is now a function $f(t_1, t_2)$ of two variables t_1 and t_2. If we now do a Fourier transformation of $f(t_1, t_2)$ by integrating over both t_1 and t_2, we will get an NMR spectrum that will be a function of two frequencies : $f(\nu_1,\nu_2)$. This spectrum is called a **two-dimensional (2D) NMR spectrum.** The frequency ν_2 has the same meaning as the frequency in 1D NMR. The significance of the frequency ν_1 depends on the nature of the pulses used in the experiments. Over 100 different pulse patterns have been used in 2D NMR. Figs. 20(c) and 20(d) show two other pulse patterns. In Fig. 20(c), the time interval Δ remains fixed and t_1 is varied. In Fig. 20(d), the second pulse is twice as long as the first.

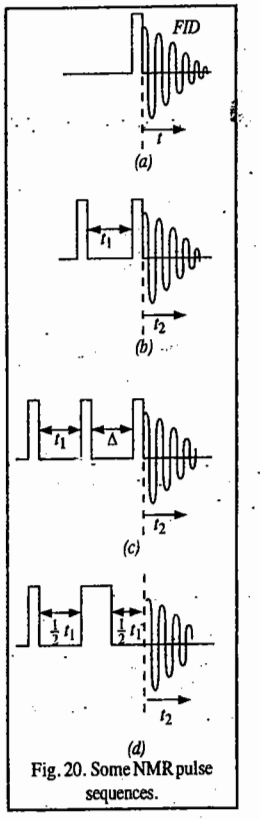

Fig. 20. Some NMR pulse sequences.

The proton NMR spectra of large molecules such as steroids, oligosaccharides, proteins, nucleic acids contain many overlapping lines and the lines that are extremely hard to assign to specific protons, even using very high field spectrometers. By using 2D NMR, we can resolve very complicated spectra and determine the structure and conformation of compounds for which the 1D spectrum is hopelessly complex. The development of 2D NMR in the 1980s has produced a revolutionary increase in the power of NMR to deduce the structures of large molecules. For further information refer to the following books :

Croasman, W.R., and R.M.K. Carlson (eds.), *Two-Dimensional NMR Spectroscopy*, VCH, 1987.

Schraml, J. and J.M. Bellama, *Two Dimensional NMR Spectroscopy*, Wiley, 1988.

3. NMR Spectra of Solids

The NMR spectra of solids, as ordinarily observed, are of little value. The first major difficulty is that dipolar couplings (the direct spin-spin interactions) which are averaged to zero by fast molecular tumblings in liquids, are not averaged to zero in solids. The long range couplings are also important. The combined effect of the many couplings in solids is to give very broad lines (resonances), often tens of kHz wide. (Changes in line widths can sometimes be used to give information about internal motions

in solids.) Secondly, the chemical shift of a nucleus depends on the orientation of the molecule with respect to the magnetic field, and in solids the effect of this chemical shift anisotropy is not averaged out by molecular tumbling and thus leads to line broadening, again of thousands of Hz. Study of this anisotropy may be helpful, but for our purposes we regard it only as something to overcome. Finally, again because of the immobility of the nuclei, the relaxation time T_1 is very long, which implies that multi-pulse methods are not very efficient. Hence, it is very difficult to get NMR spectra with good signal-to-noise ratio. Thus, solids give broad, featureless resonances with little information. However, by using special techniques, such as rapidly spinning the sample about an axis making angle θ to the magnetic field, the expression describing the line broadening due to chemical shift anisotropy includes a term $(3\cos^2\theta - 1)$. When $\theta = 54{\cdot}7°$ this term vanishes. The anisotropy effects can thus be eliminated. The spin-spin interactions are also eliminated. This technique is known as **magic angle spinning (MAS)** or **magic angle sample spinning (MASS).** We thus obtain high-resolution NMR spectra of solids. Such spectra of solids are used to study the structure and dynamics of solid polymers, biopolymers such as proteins, catalysts, molecules adsorbed on catalysts, coal, ceramics, glasses, etc. An example is of the use of ^{29}Si MAS-NMR spectra to infer the positions of Si atoms in natural and synthetic aluminosilicates.

4. Double Resonance

Though we have discussed double resonance (or double irradiation) already, we shall give further remarks on it. As we have said, in a double-resonance experiment, the sample is simultaneously exposed to rf radiation of two different frequencies, one frequency being used to observe radiation absorption and the second frequency to produce a perturbation that affects the spectrum. For instance, in observing natural-abundance ^{13}C spectra in organic compounds, in addition to applying a pulse of radio frequency radiation that covers the frequency range of ^{13}C absorptions, one also applies continuous strong rf radiation whose frequencies cover the range of proton absorption frequencies. This results in the removal of the spin-spin coupling between ^1H and ^{13}C nuclei (a process called **decoupling**). As a result, ^1H spins do not split the ^{13}C absorption lines. Since the probability that two C nuclei are both ^{13}C is very small, there is no $^{13}C - {}^{13}C$ spin-spin splitting in natural-abundance ^{13}C NMR. With no spin-spin coupling, the ^{13}C natural-abundance spectrum contains one line for each set of non equivalent carbons. In ^{13}C NMR, the reference compound is TMS and the ^{13}C chemical shifts in organic compounds usually lie in the range of δ from – 10 to 230 ppm. As with protons, the δ-value is characteristic of the kind of carbon being observed. For example, δ for C=O carbon in ketones usually between 200 and 220 ppm. The combination of proton and ^{13}C NMR is an extremely powerful method for structure determination. The convenient notation $^{13}C - \{^1H\}$ is used to identify **proton-decoupled carbon – 13 NMR spectra.** We usually double-irradiate *all* protons simultaneously while recording the ^{13}C spectrum. A decoupling signal is used that has all the ^1H frequencies spread around 80 MHz and is, therefore, a form of radio frequency noise. Spectra derived thus are ^1H-*decoupled* or *noise-decoupled.* Most ^{13}C spectra are recorded in this way.

5. The Nuclear Overhauser Effect (NOE)

Consider the following double-resonance experiment. The ^1H NMR spectrum of a molecule is recorded (using either a CW or FT spectrometer), while the sample is continuously irradiated with rf radiation of frequency ν_s, that is, the NMR absorption frequency of a specific set (which we call S) of chemically equivalent protons in the molecule. We then find that the intensities of all lines that are due to protons which are close to the set-S protons in the molecule are changed as compared with the spectrum taken without continuous radiation at ν_s. The radiation at ν_s changes the energy level population distribution of the set-S protons and the magnetic dipole-dipole interaction between the set-S protons and nearby protons changes the populations of the nearby protons, thereby changing the intensities of their NMR lines. This intensity change is the **Nuclear Overhauser Effect (NOE).** The magnitude of NOE is usually proportional to $1/r^6$ where r is the distance between the set-S protons and protons producing the line whose intensity is changed. The NOE is negligible for $r > 4$Å. The NOE can be used to help assign spectra and to find internuclear distances in a molecule.

The magnitude of NOE depends on the balance of relaxation mechanisms, and its value for an A – {X} experiment, occurring when dipole-dipole mechanisms predominate, is given by

$$NOE_{max} = 1 + \gamma_X/2\gamma_A \qquad \ldots(52)$$

where γs are the magnetogyric ratios.

Simply stated, in decoupling experiments the ratio of the total integrated double resonance intensity to single resonance intensity is called the NOE. The NOE enhancement can give a useful gain in signal-to-noise ratio. Dipolar relaxation is particularly important for spin 1/2 nuclei and as the rate is inversely proportional to the sixth power of the distance between the nuclei, it is most significant where the nucleus being irradiated is directly bonded to the one being observed. For $^{13}C - \{^1H\}$, the maximum effect is nearly 3 and enhancements close to this are normally seen for all carbons bound to hydrogen. It should also be noted that Eq. 52 leads to *negative* enhancements if γ_X or γ_A is negative. For $^{29}Si - \{^1H\}$, the maximum effect is $\sim -1{\cdot}5$ while for $^{15}N - \{^1H\}$, it is -4. But, as the minimum effect is $+1$, the actual effect may in practice be zero and expected resonances may be absent. Fig. 21 presents ^{29}Si spectra of $SiHPh_3$ showing the inversion of signals and the improvement in the signal-to-noise ratio obtained on proton decoupling.

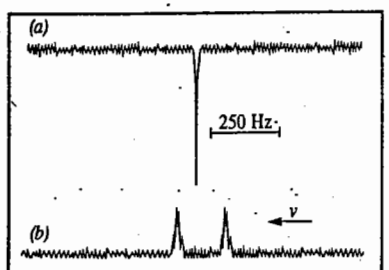

Fig. 21. Proton-decoupled (*a*) and coupled (*b*) ^{29}Si spectra of triphenylsilane.

6. Off-Resonance Proton Decoupling

Fully proton-decoupled ^{13}C NMR spectra offer a distinct advantage over fully coupled spectra (sometimes called *non-decoupled* spectra) The advantage is that the removal of coupling multiplicity makes the spectrum simpler in appearance and ensures almost no confusing overlap in adjacent signals, but there is a sensitivity bonus in addition. Thus, for example, the methyl carbon in p-hydroxyacetophenone would appear in a non-decoupled spectrum as a 1 : 3 : 3 : 1 quartet because of the three attached and coupling protons and, when this is decoupled, the whole of the signal intensity appears as a single line (of intensity 8 relative to the outside lines of the quartet). The fact that the signal is a quartet proves that it arises from a methyl group and unfortunately this valuable piece of information is lost in the fully decoupled $^{13}C - \{^1H\}$ NMR spectrum. There are several techniques which allow this information to be retained ; the simplest consists in carrying out the proton decoupling by irradiation of the sample with radiofrequency which is not quite exactly that of the protons but a few hundred hertz displaced. The consequence of this off-resonance decoupling is an incomplete collapse of the multiplicity, and vestigial quartets remain from methyl carbons, with triplets from CH_2, doublets from CH and singlets from fully substituted carbons. It is convenient to annotate signals in $^{13}C - \{^1H\}$ spectra to indicate multiplicity, with the abbreviation *q*, *t*, *d* and *s* for quartet, triplet, doublet and singlet, respectively.

7. Application of 2D NMR

There are many forms of 2D spectra. Here we shall discuss a few of them by considering the example of *s*-butylcrotonate, $CH_3CH{=}CH{-}\overset{\overset{O}{\|}}{C}{-}O{-}\overset{\overset{CH_3}{|}}{CH}{-}CH_2{-}CH_3$:

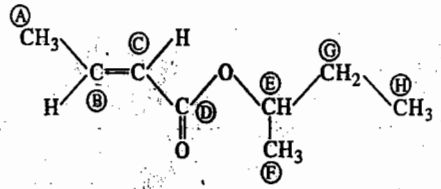

The spectrum of this compound is fairly simple and can be easily interpreted.

Fig. 22. shows a 2D spectrum as an intensity contour map. Here the frequency across the page corresponds to the ^{13}C chemical shift, while the second frequency corresponds to ^{13}C–^1H spin-spin couplings. Thus, in one spectrum all the ^{13}C resonances can be seen and each one's coupling pattern can also be recognized. There are three quartets at the low frequency end, then a triplet, three doublets and a singlet all with smaller couplings as well. The information derived from this technique is called ***heteronuclear 2D J-resolved spectroscopy.***

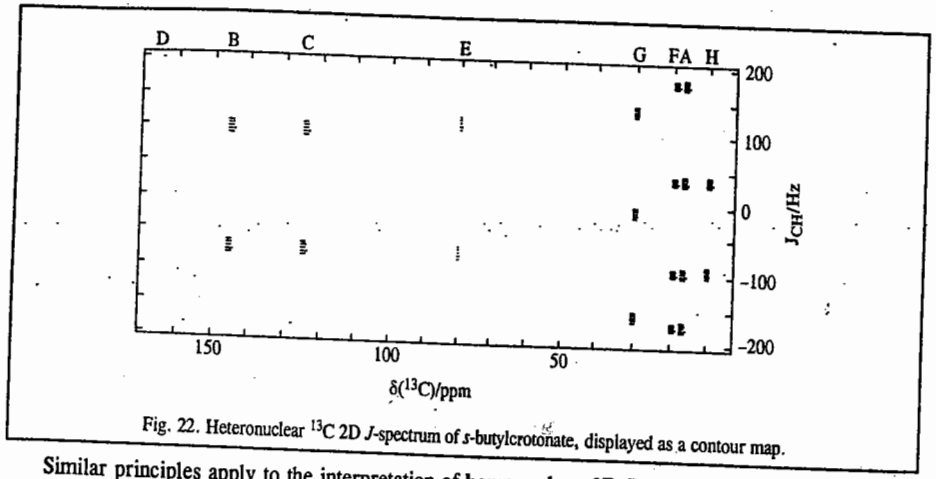

Fig. 22. Heteronuclear ^{13}C 2D *J*-spectrum of *s*-butylcrotonate, displayed as a contour map.

Similar principles apply to the interpretation of **homonuclear 2D J-resolved spectra,** although the method of obtaining them is different. Fig. 23. shows such a spectrum, again presented as an intensity contour plot. In this spectrum, one frequency scale covers ^1H chemical shifts and the other represents H—H couplings. The resonances for protons B, for instance, are clearly seen to be a doublet of quartets while those for protons A are (less clearly) a doublet of doublets. Thus, there is considerable spectral simplification, particularly for regions of the spectrum where multiplets overlap.

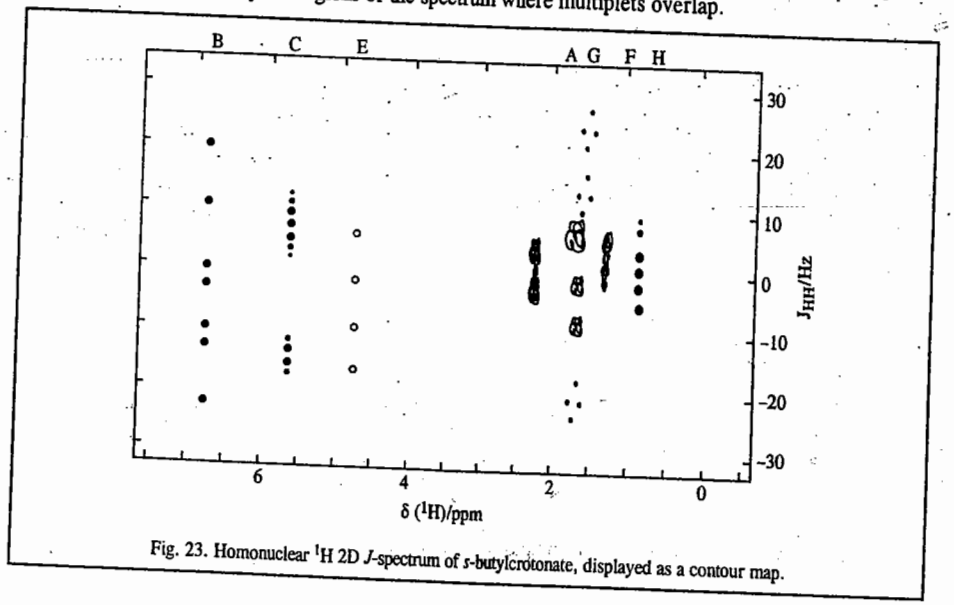

Fig. 23. Homonuclear ^1H 2D *J*-spectrum of *s*-butylcrotonate, displayed as a contour map.

Fig. 24 shows a $\delta(^{13}C) - \delta(^{1}H)$ chemical shift correlation spectrum. The correlation involves the shifts of the nuclei bonded to each other, and so in this case quaternary carbons do not appear.

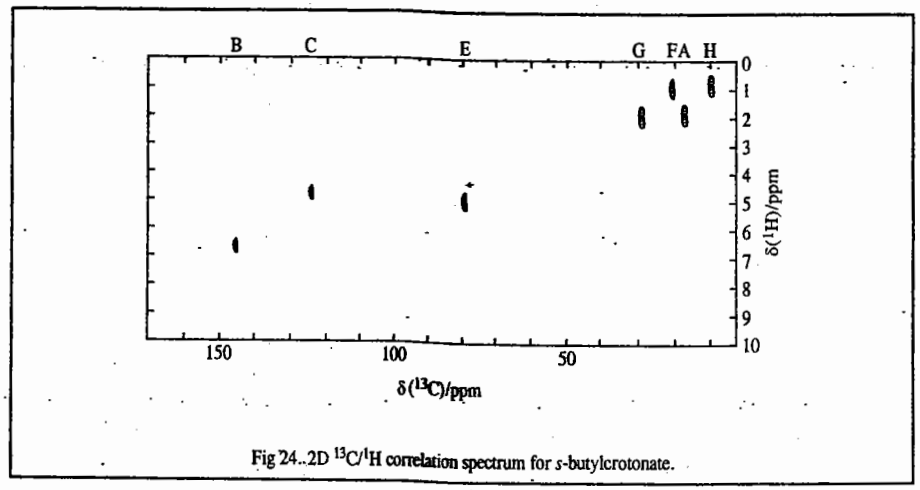

Fig 24..2D $^{13}C/^{1}H$ correlation spectrum for *s*-butylcrotonate.

It is necessary that all the one-bond coupling constants should be roughly equal. This type of spectrum offers an invaluable aid to assigning spectra. Thus, it is now clear that the higher frequency alkenic carbon resonance is associated with the higher frequency alkenic proton resonance (B), and we can also associate the methyl ^{13}C and ^{1}H resonances (A, F and H).

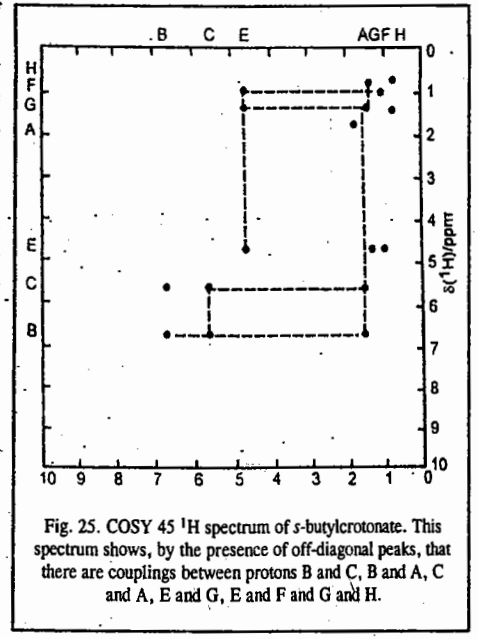

Fig. 25. COSY 45 ^{1}H spectrum of *s*-butylcrotonate. This spectrum shows, by the presence of off-diagonal peaks, that there are couplings between protons B and C, B and A, C and A, E and G, E and F and G and H.

Another 2D technique known as **correlation spectroscopy (COSY)** provides information about couplings between nuclei of a single isotope. In Fig. 25, representing COSY spectrum of *s*-butylcrotonate, both axes relate to proton chemical shifts and peaks appear on the diagonal at frequencies (the same frequency at each axis) corresponding to the resonances in the normal spectrum. The appearance of an off-diagonal peak at frequency (ν_1, ν_2) implies that there is a coupling between the nuclei resonating at ν_1 and at ν_2. Thus, it is easy to see that the two CH groups (marked as resonances B and C) couple with each other, and that one of them couples with the CH_2 group, marked A. Thus, the resonances of the crotonate group are clearly distinguished from those of the *s*-butyl group and other resonances can be made on the same basis. Other related pulse sequences include COSY 45 (actually used in Fig. 25) and NOESY (Nuclear Overhauser Effect Spectroscopy), discussed elsewhere, which depends on the local nuclear overhauser enhancements rather than couplings to give the off-diagonal peaks.

8. Internuclear Double Resonance (INDOR)

We shall now discuss INDOR, achieved through low power irradiation and Boltzmann population transfer. Consider the energy level diagram for an AX nuclear spin system (Fig. 26).

The nuclear spin wave function $|\alpha>$ refers to upwards (↑) spin orientation and the wave function $|\beta>$ refers to downward (↓) spin orientation ; they can also be called the spin quantum numbers of the A and X nuclei. At thermal equilibrium, the Boltzmann population differences are proportional to the energy differences, as these are small compared with the thermal energy k_BT. If the transition X_1 is saturated by an applied radio frequency field, the populations of the energy levels connected by this transition are equalized. As the intensities of lines A_1 and A_2 depend on the population differences of their associated energy levels, the intensity of A_2 is enhanced by irradiating X_1, while that of A_1 is diminished. In the same way, irradiation of X_2 increases the intensity of A_1 but decreases that of A_2. One way to present this information is as a plot of intensity of A_1 (or A_2) against irradiation (X) frequency, as shown in Fig. 27. This can easily be done with continuous wave NMR spectrometers simply by monitoring the chosen transition and scanning the irradiation frequency. The experiment, known as **internuclear double resonance (INDOR)**, thus provides information about the frequencies in the X-spectrum while observing only *A*. This technique, though not widely used these days, is still useful particularly if X is an insensitive nucleus for NMR or if only a proton NMR spectrometer is available. Thus, a $^{1}H - \{^{199}Hg\}$ INDOR spectrum of a compound containing SiH_3 derivatives of mercury showed a seven-line multiplet indicating that the compound had six equivalent protons, and was identified as $Hg(SiH_3)_2$ and not $HgCl(SiH_3)$.

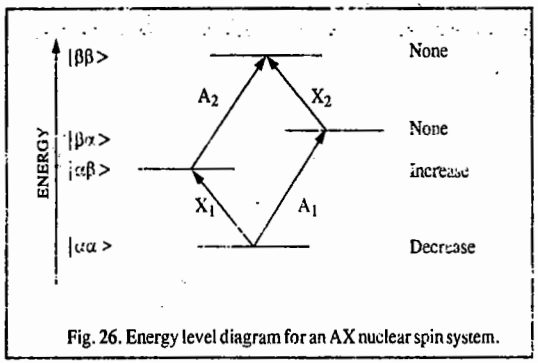

Fig. 26. Energy level diagram for an AX nuclear spin system.

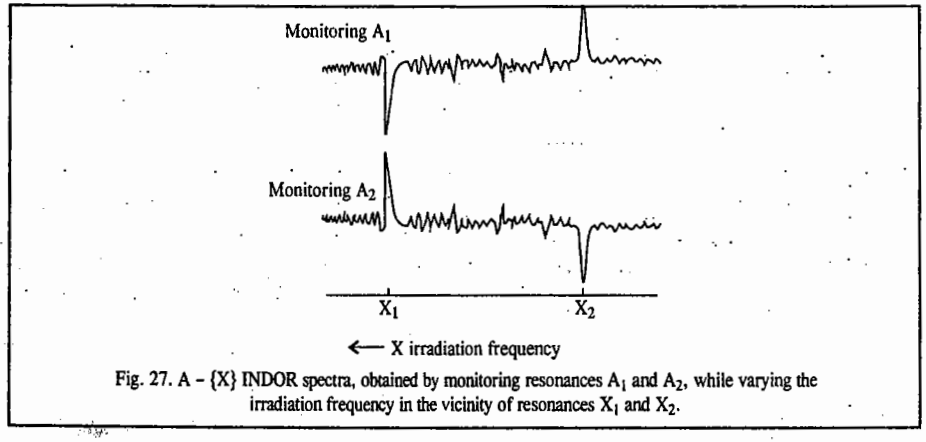

Fig. 27. A – {X} INDOR spectra, obtained by monitoring resonances A_1 and A_2, while varying the irradiation frequency in the vicinity of resonances X_1 and X_2.

9. Simplification of Complex NMR Spectra

For a non-first-order spectrum obtained at 60 MHz, three techniques are generally employed to simplify the complexity of the NMR spectrum. These are : (*a*) increased magnetic field strength, (*b*) spin decoupling (double resonance or double irradiation) and (*c*) use of chemical shift reagents.

a. Increased Field Strength. The chemical shift positions (when measured in Hz) are field-dependent whereas the spin-spin coupling constants are field-independent. Thus, a complex pmr spectrum obtained at, say, 60 MHz (1·4 T) will be simplified if it is obtained at a higher field 100 MHz (2·3T). For instance, methyl resonance in acetates appears at δ 2·0 or 2 ppm higher frequency than TMS. In a 60 MHz instrument (1·4 T), 2 ppm corresponds to 120 Hz while in a 100 MHz instrument (2·3 T), 2 ppm corresponds to 200 Hz. At 14·1T (600 MHz), 2 ppm corresponds to 1200 Hz. Thus, since the spin-spin coupling constants are field-independent, the ratio $\Delta\nu : J$ is effectively increased as the field strength is increased from 1·4 T to 14·1 T. If two coupling multiplets overlap at 1·4 T, we can pull the multiplets apart by increasing the magnetic field.

b. Double Resonance. Fig. 28 shows the double irradiation (spin decoupling) of an AX NMR spectrum of 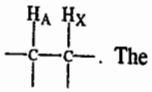 . The proton A in this figure appears as a doublet because of the two spin orientations of X. If we irradiate X with the correct rf energy, we can stimulate rapid transitions (both upwards and downwards) between the two spin states of X so that the lifetime of a nucleus in any one spin state is too short to resolve the coupling with A. If proton A 'sees' only one time-averaged view of X, then A will come to resonance only once and not twice. By the same argument, if we irradiate proton A with the correct energy to cause it to undergo rapid transitions between its two spin states, proton X will only 'see' one time-averaged view of A and appear only as a singlet. Thus, the complex NMR spectrum is simplified. To perform this operation, we require, in addition to the basic NMR instrument, a *second* tunable rf source to irradiate the proton at the necessary precession frequency while recording the remainder of the spectrum as before. Since we are making simultaneous use of two rf sources, the technique is called **double irradiation.**

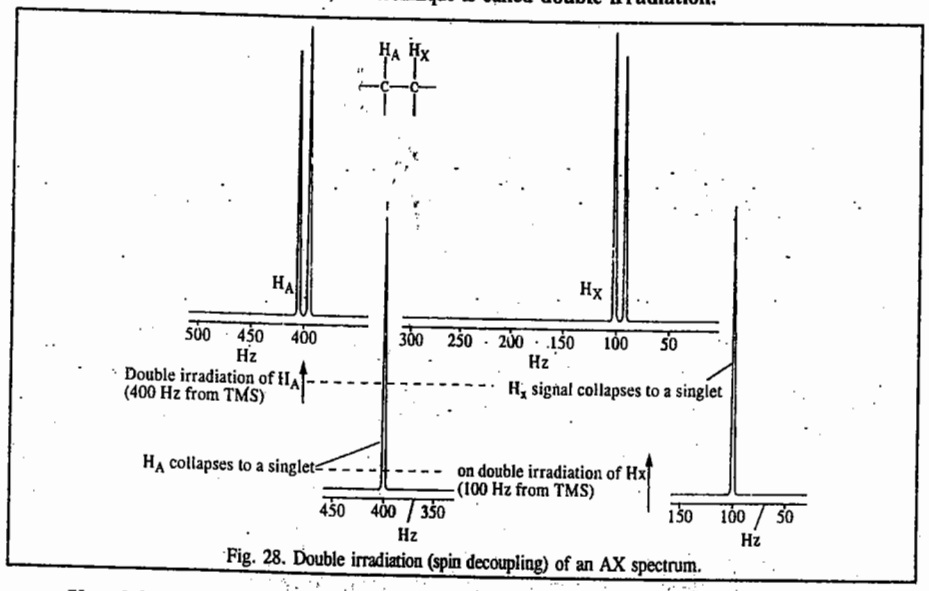

Fig. 28. Double irradiation (spin decoupling) of an AX spectrum.

c. Use of Chemical Shift Reagents (Lanthanide Shift Reagents). The addition of the paramagnetic europium (III) ion complexes to the sample under study (say, 6-methyl quinoline)—whose NMR spectrum we want to obtain —induces enormous shifts to higher frequency in the quinoline resonance. Here the shift reagent modifies the magnetic field experienced by the protons (with the consequent simplification of the spectrum). The shift reagent coordinates with electronegative atoms in the substrate and thus modifies the magnetic field experienced by neighbouring protons. In fact, the

mechanism of the shift is two-fold. Unpaired electron spin in the paramagnetic ion (*e.g.*, Eu (III)) is partially transferred *through the intervening bonds* to the protons of the organic substrate; this is called **contact shift.** The spinning paramagnetic ion also generates magnetic vectors which operate *through space,* creating secondary magnetic fields around the protons; this is called **pseudo-contact shift** and predominates in the case of lanthanide ions.

The lanthanide complex should be soluble in common NMR solvents for wide applicability. The two most commonly used shift reagents are tris-chelates of lanthanide ions with the β-diketones, 2,2,6,6,-tetramethylheptane-3,5-dione (dipivanoylmethane, abbreviated as DPM and 1,1,1,2,2,3,3-heptafluoro-7,7-dimethyloctane-4,6-dione or simply heptafluorodimethyloctanedione (abbreviated as FOD) :

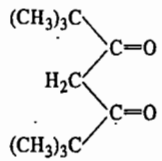
DPM

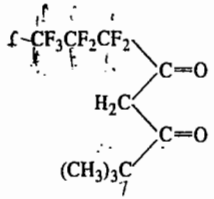
FOD

Typical lanthanide shift reagents are tris-(dipivanoylmethanato) europium and tris-1,1,1,2,2,3,3-heptafluoro-7,7-dimethyloctane-4,6-dionatoeuropium, the names of which are normally abbreviated to $Eu(dpm)_3$ and $Eu(fod)_3$, respectively :

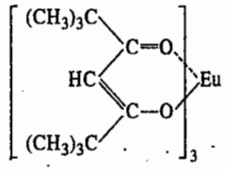
$Eu(dpm)_3$

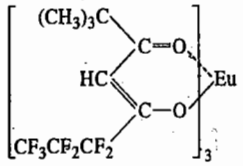
$Eu(fod)_3$

The extent of the lanthanide-induced shift is dependenent on the basicity of the functional group and on the nature, purity and concentration of the shift reagent. $Eu(fod)_3$ normally causes greater shifts as it is a stronger Lewis acid. It also has the advantage of a much higher solubility. The magnitude of the lanthanide-induced shift is considerably decreased by the presence of a small amount of water. Since many of the reagents are hygroscopic, care should be taken in their handling and storage.

10. NMR of Paramagnetic Compounds

Though paramagnetic compounds are troublesome to investigate by NMR (they are better studied by ESR), their NMR spectra do sometimes yield useful information. The two most obvious characteristics of the NMR spectra of paramagnetic materials are that the chemical shift scale is greatly expanded (for example, to more than 200 ppm for protons) and that the resonances may be broad. The signals from diamagnetic materials may also show these effects, in the presence of paramagnetic species, even in low concentrations. The broadening depends on the electronic spin-lattice relaxation time and/or the hyperfine electron-nuclear coupling.

The observed paramagnetic shifts are made up of two components. First, there is a through-space dipolar interaction between the magnetic moments of the electron and the resonating nucleus, which gives a dipolar shift, known as a **pseudo-contact shift.** This contribution may be small and is rather

difficult to calculate theoretically so that the other component, known as the **contact shift,** may be identified. The origin of the contact shift may be understood if one considers the coupling between electron and nucleus which would give a doublet in the NMR spectrum under conditions of low spin-lattice relaxation but with a coupling constant of millions of Hz ! With such a large coupling, the intensities of the two resonances are not equal so that their weighted mean position is not midway between them. Under fast relaxation conditions, the collapsed singlet may fall some thousands of Hz away from the expected position—the contact shift.

Contact shifts give a measure of the unpaired spin density of the resonating nucleus and are thus particularly useful in studying the spin distribution in organic free radicals or in ligands in organometallic compounds. We have discussed earlier the use of the paramagnetic complexes of europium as shift reagents in simplifying complex pmr spectra.

11. Chemically Induced Dynamic Nuclear Polarization (CIDNP)

When dipropionyl peroxide is thermolyzed in an NMR tube in the presence of thiophenol, ethyl radicals are produced which react with the thiophenol to form thiophenetole :

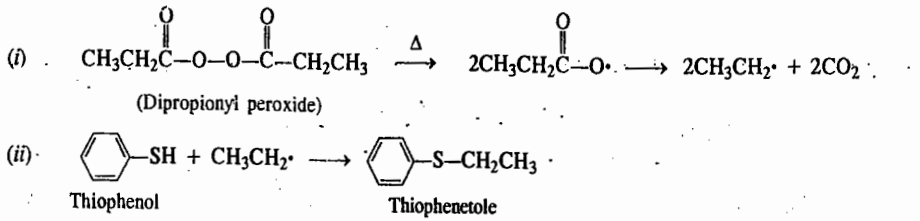

If the pmr spectrum of thiophenetole is recorded *during* the course of the reaction, the ethyl signals appear as shown in Fig. 29 (*a*). The pmr spectrum of normal thiophenetole is shown in Fig.29(*b*) for comparison. We see that some of the lines in the spectrum (*a*) have increased intensity while other lines show increased emissions. This is interpreted by saying that the nuclear spins in the product of this radical reaction (that is, the nuclear spins of thiophenetole) are undergoing *dynamic polarization* because of the chemical reaction that is producing the molecule. This phenomenon is known as **chemically induced dynamic nuclear polarization (CIDNP).** Observation of CIDNP effects during a reaction is a good evidence that, at least in part, a radical mechanism is involved.

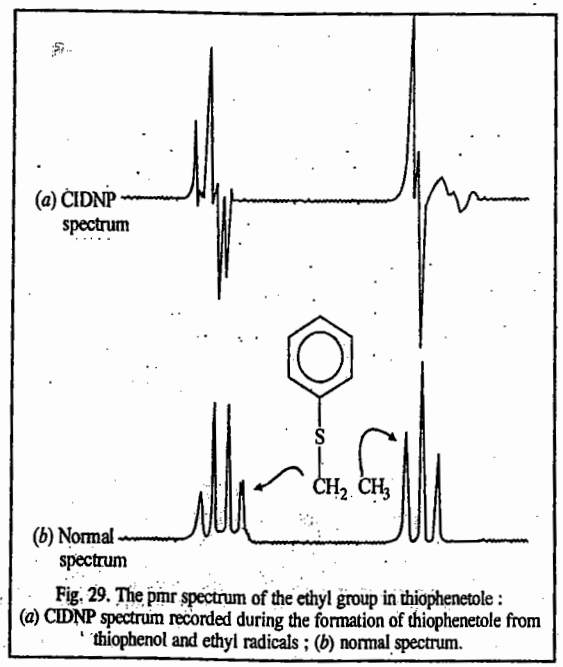

Fig. 29. The pmr spectrum of the ethyl group in thiophenetole : (*a*) CIDNP spectrum recorded during the formation of thiophenetole from thiophenol and ethyl radicals ; (*b*) normal spectrum.

The mechanism of CIDNP is complicated and the observed effect depends on the way in which particular nuclear spin states interact with the electron spins of the free radicals involved. Also, the free radicals from

a precursor molecule may follow several reaction paths, depending on whether the originally formed radical pair react together immediately or diffuse out from each other, to form other dimerization or transfer reactions. For a particular radical pair, the singlet and triplet electronic states undergo mixing processes under the influence of nearby nuclear spins ; if the resultant mixed electronic state is predominantly singlet in character, the associated nuclear spin states are enchanced in the product formed from the radical pair and the NMR of the product shows increased absorption for these spin states. If the mixed electronic state is predominantly triplet, emission will be shown for the corresponding nuclear spin states.

12. NMR of Liquid Crystals

In contrast to fluids, liquid crystals are compounds or mixtures which have one or more phases between liquid and solid, in which there is local alignment of molecules but no overall alignment. The material in these phases is thus fluid—*isotropic* in bulk but locally *anisotropic*. The liquid which is strongly anisotropic in many of its properties, produces on heating an *isotropic* liquid. These materials are referred to as **thermotropic liquid crystals** (*i.e.*, produced by melting of a solid). We have discussed in Chapter 12 the classification of liquid crystals into smectic, nematic and cholesteric crystals. In the presence of an electric or magnetic field, the fluid becomes anisotropic in bulk, as all the molecules tend to align in one particular direction, though they remain mobile. At the same time, the solute molecules also become oriented with respect to the applied field. Thus dipolar couplings are not lost by isotropic tumbling.

The NMR spectra of liquid crystals are affected dramatically because of major changes in coupling constants. Fig. 30 shows how all the couplings in $PF_2^{15}NH_2$ change and that some of the smaller ones become very large. Couplings of hundreds and thousands of Hz are normally observed. Whereas a first-order splitting J_{AX} is observed for an isotropic solution, it is replaced by

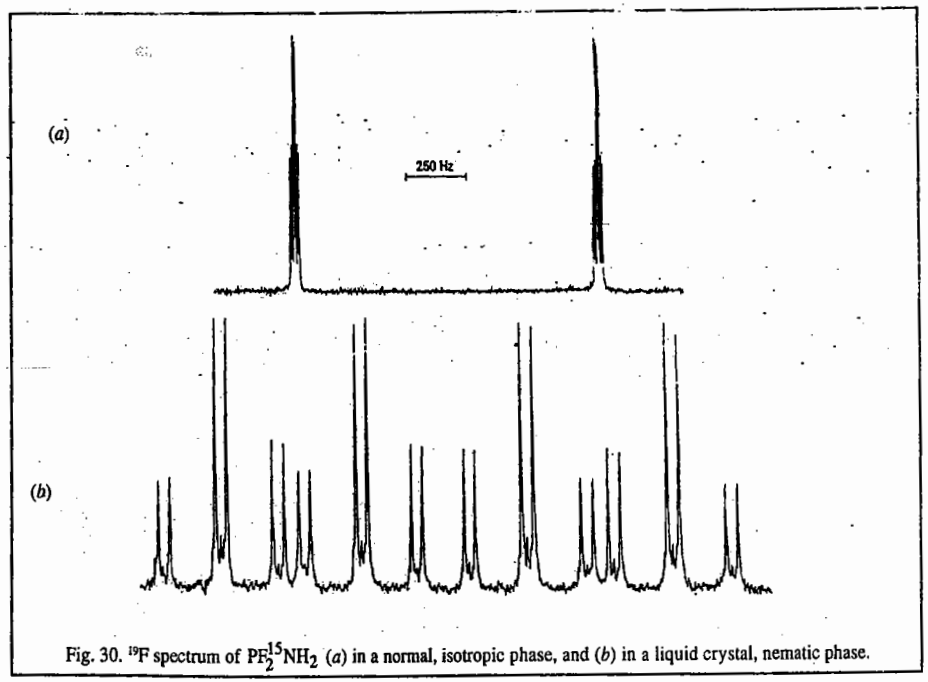

Fig. 30. ^{19}F spectrum of $PF_2^{15}NH_2$ (*a*) in a normal, isotropic phase, and (*b*) in a liquid crystal, nematic phase.

$J_{AX}+2D_{AX}$, in the case of a liquid crystal. In this way direct coupling may be determined. Also, coupling is now observed between nuclei which are chemically and magnetically equivalent. Thus, in Fig. 22 there is an extra doublet splitting corresponding to coupling between the two equivalent ^{19}F nuclei. Finally, a group of magnetically equivalent nuclei may not be fully equivalent, in that the couplings within the group (which are now observable) may not be all equal. Thus, for example, in benzene there are three different proton-proton dipolar couplings so that the ^1H spectrum is second-order. Such spectra must be analyzed in the normal way, using variants of analysis programs which take account of dipolar couplings.

Without going into details we may mention that the dipolar couplings which we assume to be measured or derived, are related to the molecular geometry and the so-called orientation parameters. These parameters describe the average orientation of the molecule with respect to the applied field. There is, of course, the problem of unknown orientation parameters, with the consequent need to make some structural assumptions. There is also a need to make allowance for the effects of vibrations on observed couplings. This involves a complete force field analysis of the molecule. There are also the problems arising from anisotropy in the indirect (J) couplings. Thus, there are many pitfalls for the unwary. However, the technique can provide useful structural data which otherwise are very difficult to obtain for molecules in solution.

MAGNETIC RESONANCE IMAGING (MRI)

The proton NMR spectroscopy can be used to form cross-sectional images of body parts in living subjects by displaying the intensity of a particular pmr transition (for example, proteins in water) as a function of the coordinates in the cross-sectional plane. This technique of **magnetic resonance imaging (MRI)** is widely used to diagnose diseases such as cancer from the signals generated from the soft tissues of the brain, eyes, spinal column, etc. The ability to scan soft tissues as, for example, of eyes, brain, spinal cord in a human skull, by MRI complements the information about the bone structure obtained from X-ray studies. This is an established medical diagnostic technique for soft tissue damage. The experimental technique has been sufficiently refined to produce not only very high resolution in detail but also a whole sequence of views of the head (see small inserts at the top of the figure) which can be presented in a sequence on a VDU (Video Display Unit) in the form of a moving picture so that the head can be "rotated" to allow all aspects to be examined.

From the basic principles of pmr we know that the protons in the head (in the water and the fat) undergo a sharp resonance at a given frequency only when the applied Zeeman magnetic field causes them to precess at their Larmor resonance frequency. At lower and higher values of the magnetic field, no pmr signal will be detected. Instead of applying a uniform magnetic field across the head, a *field gradient* is applied. At only one particular point along the field gradient (also called *phase gradient*) will the protons be in resonance and, therefore, this distance across the head can be correlated with the field gradient. The gradient is then altered and the resonance occurs at a different point, the distance of which along the gradient is again corrected. By scanning along several gradients applied across a network of axes through a slice of the head, an image of the protons present (that is, of the soft tissue present) is constructed. The complete reconstructed image is defined by repeating the process across several slices through the head.

The MRI technique is also used widely to detect physiological abnormalities and to observe metabolic processes. With **functional MRI**, blood flow in different regions of the brain can be studied and related to the mental activities of the subject. The special advantage of MRI is that it can image *soft* tissues whereas X-rays are largely used for imaging hard, bony structures and abnormally dense regions such as tumours. In fact, the invisibility of hard structures in MRI is an advantage as it allows the imaging of structures encased by bone, such as the brain and the spinal cord in the magnetic resonance imaging of human skull (Fig. 31). X-rays are known to be dangerous on account of the ionization they cause. The high magnetic fields used in MRI may also be

dangerous. However, there is no convincing evidence of their harmfulness and the technique is considered safe.

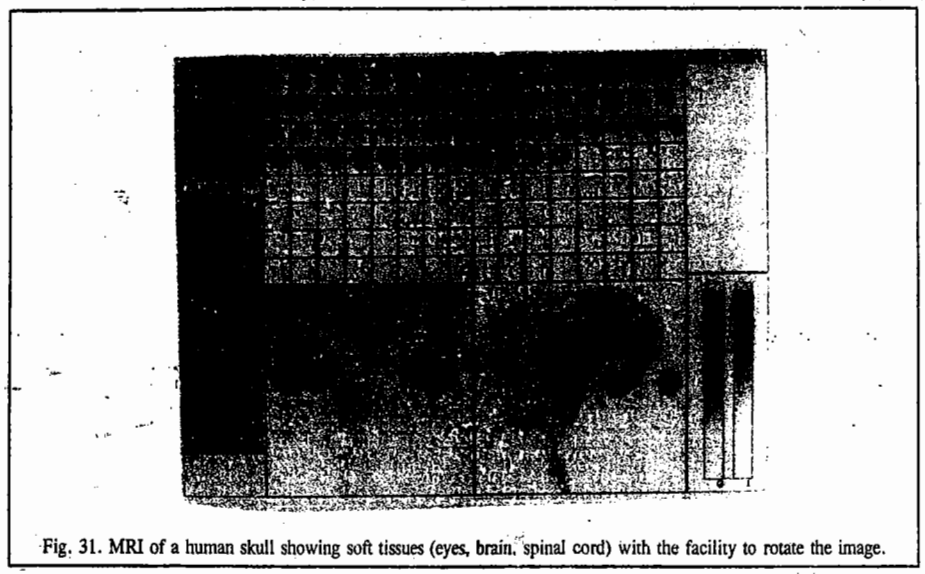

Fig. 31. MRI of a human skull showing soft tissues (eyes, brain, spinal cord) with the facility to rotate the image.

MRI is perhaps the most important non-invasive diagnostic tool in today's medicine. The 2003 Nobel Prize in Medicine/Physiology was awarded jointly to the American chemist Paul Lauterbur and the British scientist Peter Mansfield for discoveries that led to the use of "MRI for exact visualization of the various internal body structures". Lauterbur used field gradients in his investigations and Mansfield pioneered a technique in MRI, called echo planar imaging (EPI), which is an extremely rapid imaging technique using very fast gradients. MRI works by scanning essentially one line at a time. In order to make up an image, a series of such lines have to be scanned and assembled into a picture. EPI is basically a snapshot type of MRI that allows an image to be scanned all at once. This makes the process a lot quicker and renders 3D imaging feasible since a series of ten scans would generate ten 'slice' pictures. Unlike X-rays or computer-assisted tomography (CAT), MRI, as already remarked, does not use any ionizing radiation.

It must be emphasized again that MRI is particularly valuable for imaging the brain and the spinal cord. Nearly all brain disorders lead to changes in water content and even one percent difference can cause pathological change. MRI can pick up these changes. Multiple sclerosis arises from the local inflammation of the brain and the spinal cord. MRI can detect where the inflammation has occurred in the nervous system, how severe it is and the impact of treatment. Other examples are its use in treating movement disorders in Parkinson's disease and diagnosing prolonged lower back pain. Finally, it may be remarked that the 2003 Chemistry Nobel Prize awarded jointly to the U.S. medical scientists Peter Agre and Roderick McKinnon for research in the structure and chemistry of water channels and ion channels in cells, is related to MRI. While MRI is chiefly used to map the water content in cells and tissues, the work of Agre and McKinnon tells how water is transported through the cells and how signals from the cell propagate to enable the coordination of muscles and nerves. This is of utmost importance in the understanding of many diseases. A number of diseases can be attributed to the poor functioning of water and ion channels in the body. The knowledge of the structure and function of molecular channels now enables proper therapeutic intervention.

ELECTRON SPIN RESONANCE (ESR) SPECTRA

The phenomenon of **electron spin resonance (ESR)**, also called **electron paramagnetic resonance** (EPR), was discovered by the Soviet physicist Zavoisky in 1945, a year before the discovery of NMR by the American physicists Bloch and Purcell. Both NMR and ESR are collectively referred to as magnetic resonance phenomena. NMR and ESR are similar in their theoretical principles. However, while the former is observed in radiofrequency region, the latter is observed in microwave region of the electromagnetic spectrum. ESR has limited applications because it is observed primarily in systems containing unpaired electrons. Thus, the systems which can be investigated by ESR spectroscopy are organic or inorganic free radicals and ions of transition metals which contain unpaired *d* or *f* electrons. One of the most important uses of ESR technique lies in the detection of extremely short-lived (transient) free radical intermediates in chemical reactions.

ESR Spectrum of an Unpaired Electron. As is well known, an electon possesses a spin S whose value is $\frac{1}{2}$. The magnetic moment associated with this spin is given by

$$\vec{\mu} = -g_e \mu_B \vec{S} \qquad ...(53)$$

where g_e is the *Lande' g-factor* and μ_B is the Bohr magneton. The value of g_e is 2·0023. Bohr magneton, $\mu_B = e\hbar/2m_e$ where e is the electronic charge and m_e is the mass of the electron. Substituting various values, μ_B comes out to be equal to $9{\cdot}273\times10^{-24}$ J T^{-1}.

The energy associated with electron spin S in the magnetic field B_z, applied along the z-axis, is given by

$$E = -\vec{\mu}.\vec{B_z} \qquad ...(54)$$

The component of spin S along the field direction is m_s. Hence, from Eqs. 53 and 54,

$$E_{m_S} = g_e \mu_B B_z m_s \qquad ...(55)$$

Since $m_S = \pm\frac{1}{2}$, we have

$$E_{+1/2} = \frac{1}{2} g_e \mu_B B_z \qquad ...(56)$$

$$E_{-1/2} = -\frac{1}{2} g_e \mu_B B_z \qquad ...(57)$$

Here, too, as in the case of a bare proton, while in the absence of the applied magnetic field the two energy levels are degenerate, the degeneracy is removed in the presence of the magnetic field, as shown in Fig. 32

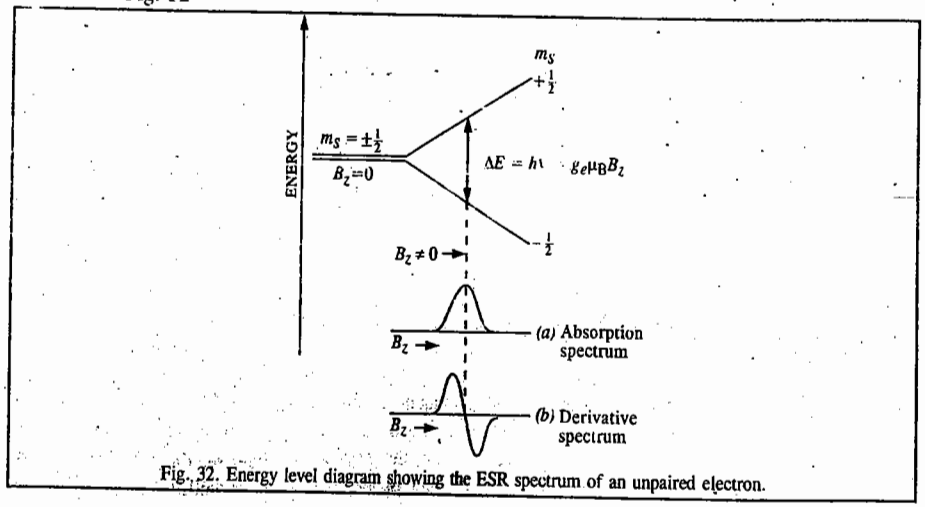

Fig. 32. Energy level diagram showing the ESR spectrum of an unpaired electron.

Application of an osciliating field perpendicular to the direction of B_z induces transitions between the two sub-energy levels provided the frequency of the oscillating field satisfies the Bohr-Einstein condition, *viz.*,

$$\Delta E = E_{1/2} - E_{-1/2} = g_e \mu_B B_z = h\nu \qquad ...(58)$$

Thus, the ESR frequency of the odd electron is given by

$$\nu = \Delta E/h = g_e \mu_B B_z/h \qquad ...(59)$$

Example 28. Calculate the ESR frequency of an unpaired electron in a magnetic field of 0·33 T, given that for the free electron, $g_e = 2$ and $\mu_B = 9{\cdot}273\times10^{-24}$ J T^{-1}.

Solution :
$$\nu = g_e \mu_B B_z/h = \frac{(2)(9{\cdot}273\times10^{-24}\text{ J T}^{-1})(0{\cdot}33\text{ T})}{6{\cdot}626\times10^{-34}\text{ J s}} \quad \text{[Eq. 59]}$$

$$= 9{,}000\times10^6\text{ s}^{-1} = 9{,}000\times10^6\text{ Hz} = 9{\cdot}00\text{ GHz}$$

Example 29. In an ESR spectrometer, the ESR frequency of the free electron is 9·5 GHz. Calculate the magnetic field at which the spectrometer is operating, $g_e = 2$ and $\mu_B = 9{\cdot}273\times10^{-24}$ J T^{-1}

Solution :
$$B_z = \frac{h\nu}{g_e\mu_B} = \frac{(6{\cdot}626\times10^{-34}\text{ J s})(9{\cdot}5\times10^9\text{ s}^{-1})}{(2)(9{\cdot}273\times10^{-24}\text{ J T}^{-1})} \quad \text{[Eq. 59]}$$

$$= 0{\cdot}339\text{ T} = 339{\cdot}0\text{ mT}$$ where mT means millitesla.

The ESR frequency falls in the microwave region. The reason why ν(ESR) falls in the microwave region whereas ν(NMR) falls in the radiofrequency region is that μ_B is about 2,000 times greater than μ_N which means that μ_e is about 660 times greater that μ_n, the nuclear magnetic moment.

In Fig. 24 is shown the ESR spectrum of the odd electron in two modes : *(a)* the absorption mode and *(b)* the derivative mode. Since the ESR spectra are generally broad (*i.e.*, not sharp), it is difficult to locate the peak in the absorption mode but it is quite easy to locate it in the derivative mode. Hence, the ESR spectra are generally recorded in the derivative mode.

Hyperfine Structure in ESR Spectra. Hyperfine structure (HFS) occurs as a result of the magnetic interaction between the electronic spin S and the nuclear spin I. The hyperfine interaction in ESR spectra is analogous to the fine structure, *i.e.*, nuclear spin-spin interaction in NMR spectra. As a result of this interaction, the ESR signals or peaks are split into several lines (HFS).

Let us consider the hyperfine interaction in the following seven cases : (1) hydrogen atom (2) methyl radical, $\cdot CH_3$ (3) the $(SO_3)_2NO^-$ radical anion (4) 1,4-benzosemiquinone radical anion (5) naphthalene negative ion (6) anthracene negative ion and (7) triphenylmethyl radical.

The selection rule for hyperfine transitions is

$$\Delta m_S = \pm 1\ ;\ \Delta m_I = 0 \qquad ...(60)$$

This selection rule may be interpreted by saying that the nuclear motion is much slower than the electronic motion so that during the time electron changes its spin orientation, the nucleus, being heavier, has no time to reorient its spin so that $\Delta m_I = 0$.

1. Hydrogen atom. It contains an unpaired electron with $S = \frac{1}{2}$ and a proton with nuclear spin $I = \frac{1}{2}$. Thus, $m_S = \pm\frac{1}{2}$ and $m_I = \pm\frac{1}{2}$. In the absence of magnetic field (B_z=0), the electron spin energy levels are degenerate, *i.e.*, have the same energy. Application of B_z removes the degeneracy between them, the $m_S = -\frac{1}{2}$ sublevel going down and the $m_s = +\frac{1}{2}$ sublevel going up (see Fig. 33). Each of these electron sublevels interacts with the nucleus giving four sublevels designated by the value of m_I. This is hyperfine interaction. Using the selection rule, two ESR lines, *i.e.*, a doublet, are observed, as shown in the experimental spectrum. They are equally intense, the spacing between them gives the **hyperfine coupling constant, *a***, expressed in units of tesla or millitesla.

2. Methyl radical, $\cdot CH_3$. It contains an unpaired electron with $S = \frac{1}{2}$ and three equivalent protons. Since for a proton, $I = \frac{1}{2}$, it is evident that for three equivalent protons, $m_I = +\frac{3}{2}, +\frac{1}{2}, -\frac{1}{2}, -\frac{3}{2}$. Also, $m_S = \pm\frac{1}{2}$. This interpretation of the ESR spectrum (Fig. 34) is similar to that of H atom given in Fig. 33. The ESR spectrum contains four equally spaced lines, *i.e.*, a quartet.

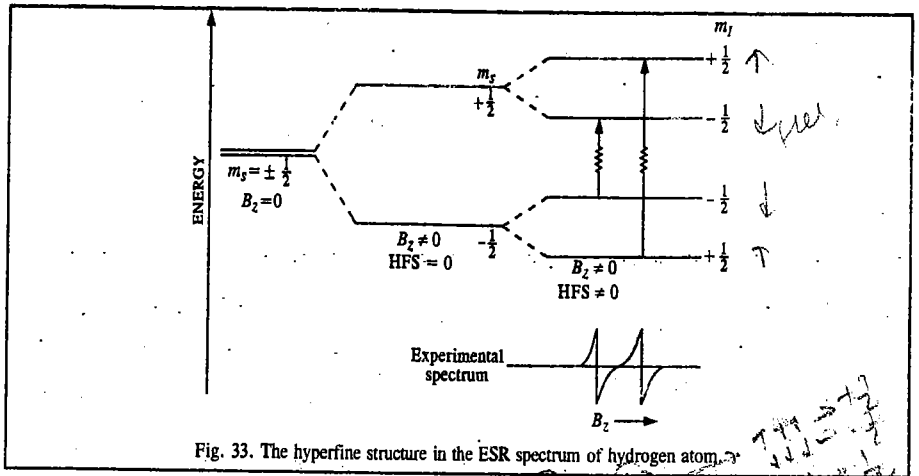

Fig. 33. The hyperfine structure in the ESR spectrum of hydrogen atom.

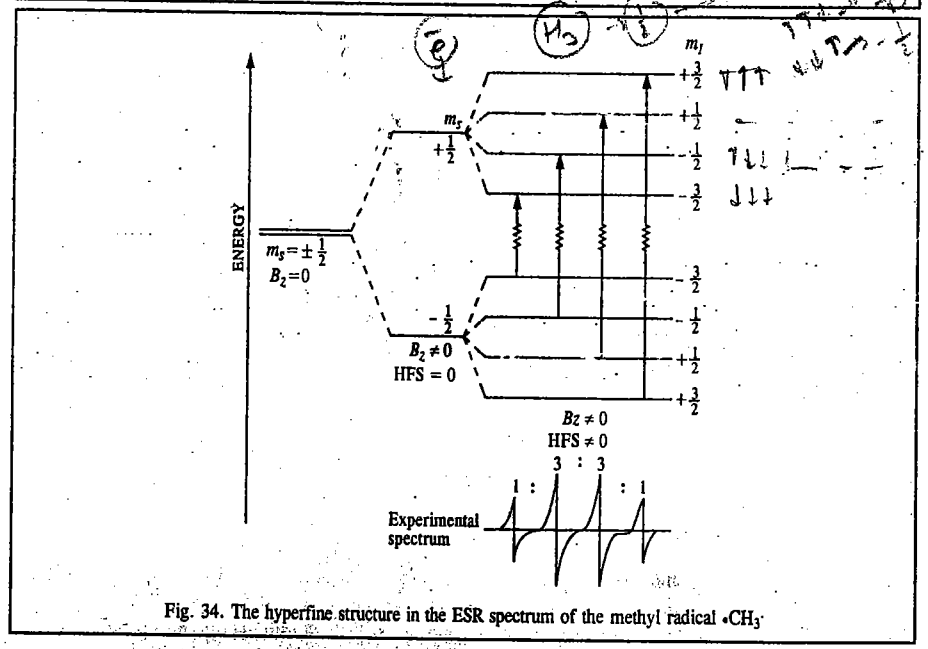

Fig. 34. The hyperfine structure in the ESR spectrum of the methyl radical $\cdot CH_3$

3. $(SO_3)_2NO^-$ anion. In this anion, the unpaired electron interacts with the nitrogen nucleus with $I=1$. Here, $m_S = \pm\frac{1}{2}$ and $m_I = +1, 0, -1$. The ESR spectrum (Fig. 35) contains three equally spaced lines, *i.e.*, a triplet.

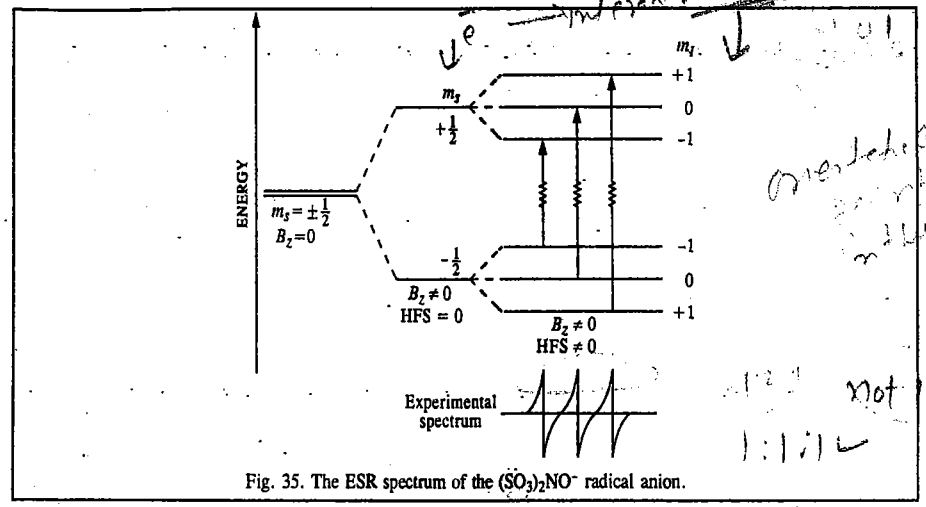

Fig. 35. The ESR spectrum of the $(SO_3)_2NO^-$ radical anion.

4. 1,4-Benzosemiquinone radical anion. This anion, having the structure 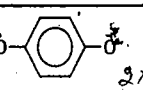 has one unpaired electron ($S = \frac{1}{2}$,) interacting with four equivalent protons. Since for a proton $I = \frac{1}{2}$, it is evident that for four equivalent protons, $m_I = +2, 1, 0, -1, -2$.

The ESR spectrum (Fig. 36) contains a quintet, *i.e.*, five equally spaced lines.

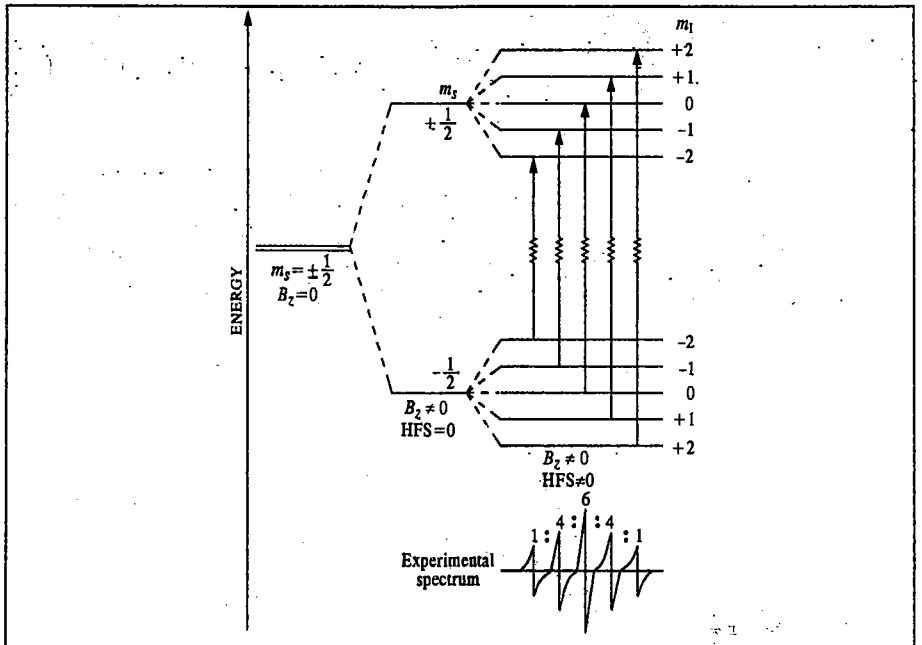

Fig. 36. The hyperfine structure in the ESR spectrum of *p*-benzosemiquinone radical anion.

5. Naphthalene negative ion,

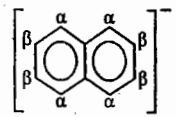

In this case, there are two sets (α and β) of four equivalent protons each. The ESR spectrum would thus show (4+1)×(4+1) = 25 lines.

6. Anthracene negative ion,

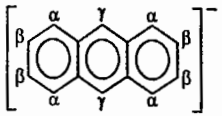

In this case, there are three sets of equivalent protons : sets α and β consist of four equivalent protons each and set γ consists of two equivalent protons. The ESR spectrum consists of (4+1) (4+1) (2+1) = 75 lines.

7. Triphenylmethyl radical, $\cdot C(C_6H_5)_3$, has the structure shown here.

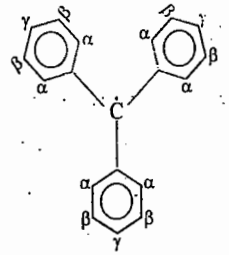

It has also three sets of equivalent protons : sets α and β consist of six equivalent protons each and set γ consists of three equivalent protons. The ESR spectrum consists of (6+1)(6+1)(3+1)=196 lines. It is a triumph of theory that all the 196 lines have been observed. One can imagine the complexity of this spectrum !

The hyperfine structure in ESR spectra of complicated organic radical ions may consist of a very large number of lines all of which can be interpreted in a manner similar to the above.

In general, the ESR spectrum of a system where the unpaired electron interacts with n equivalent protons, contains $n+1$ lines and their relative intensities are given by Pascal's triangle, discussed earlier. Thus, we have for *(i)* H atom, 2 lines (*i.e.*, a doublet) of equal intensity *(ii)* for. $\cdot CH_3$ radical, 4 lines (*i.e.*, a quartet) in the intensity ratio 1 : 3 : 3 : 1, *(iii)* for the 1, 4-benzosemiquinone anion, 5 lines (*i.e.*, a quintet) in the intensity ratio 1 : 4 : 6 : 4 : 1 and for benzene radical anion, a septet in the relative intensity ratio 1 : 6 : 15 : 20 : 15 : 6 : 1 since here the unpaired electron interacts with six equivalent protons.

For nuclei with $I > 1/2$, other rules apply. Thus, the ^{14}N nucleus in $(SO_3)_2NO^-$ anion radical, with $I = 1$, gives a hyperfine pattern of 3 lines (triplet) of equal intensity. Similarly, a ^{63}Cu nucleus ($I = \frac{3}{2}$) interacting with an odd electron gives a hyperfine pattern of four lines (quartet) of equal intensity.

The hyperfine coupling constant a in hydrogen atom is 50·68 mT. This coupling is due entirely to the **Fermi contact interaction**, being propotional to the probability density of the 1*s* electron at the nucleus. In aromatic free radicals where the unpaired electron is delocalized over the molecular orbitals extending over the entire molecule, the probability of finding the electron on a given nucleus is evidently small ; hence, the hyperfine coupling constant is also small. Thus, the ESR spectrum of benzene radical anion, $C_6H_6^-$, containing six equivalent protons, is a septet with a = 0·375 mT. For $\cdot CH_3$ radical, consisting of a quartet, a=2·3 mT.

***g*-Factor.** The *g*-factor and the hyperfine coupling constant are the most important quantites determined from the ESR spectra of odd-electron systems. From the relation, $\nu = g_e\mu_B B_z/h$, we see that $g_e = h\nu/\mu_B B_z$. Thus, the *g*-factor is essentially a measure of the ratio between frequency and magnetic field. For the free electron, g_e = 2·0023. The organic radicals such as the methyl radical, have the *g*-value very close to the free-electron g_e value. Here only the spin of the electron contributes to g_e.

The deviation of g from g_e = 2·0023 depends on the ability of the applied magnetic flux density to induce local currents in the free radical and, therefore, its value gives some information about electronic structure.

However, in the case of the transition metal ions and their complexes, there is considerable interaction between the spin and the orbital motion of the electron which prevents complete *quenching of the orbital contribution*. Hence, for such systems, the *g*-value departs from the g_e-value. In transition metal complexes containing *d* shells less than half-filled, g is less than g_e while for shells more than half-filled, g is greater than g_e. Also, the *g*-value is **anisotropic**, *i.e.*, its magnitude depends upon the direction of measurement. The anisotropy in *g*-value is shown by systems in the solid state where conditions of restricted motion exist. In systems containing axial symmetry, the *g*-values along two dimensions, say, the x and y directions, are equal while the *g*-value along the z direction is different. Consider, for instance, an octahedral complex wherein two diametrically opposed ligands are pulled or pushed symmetrically while the remaining four ligands remain undisturbed. This is a case of axial symmetry. If the magnetic field is applied along the z direction, the *g*-value is designated as $g_\parallel$. If the field is applied perpendicular to the z-axis. (*i.e.*, if it is in the xy plane), the *g*-value is designated as $g_\perp$. In solutions, because of free rotating (or tumbling) motion, the *g*-factor is **isotropic**, *i.e.*, it is the average of the three *g*-values in the x, y and z directions.

Applications of ESR. The most important application of ESR is in the determination of the structure of organic and inorganic free radicals. These radicals may be produced chemically, photochemically or by using high-energy radiation. Since the free radicals are very short-lived, they are trapped in glasses, frozen rare-gas matrices or in crystals. In order to obtain a good spectrum, the free radical must be produced in a concentration of about 10^{-13} mol dm^{-3}. The intensity of an ESR signal is directly proportional to the number of the free radicals present. Hence, using ESR we can measure relative concentrations of free radicals produced under different conditions. Hyperfine interaction in ESR spectra can provide useful information about charge distribution within a molecule. Since hyperfine structure is a characteristic property of an ion or a radical, it may be used to identify unknown ions and radicals. Free radicals produced by irradiation of polymers by means of X-rays or gamma rays have also been investigated by ESR.

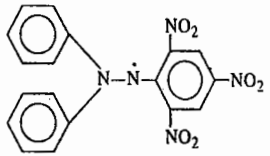

DDPH radical

One of the best known free radicals which is used for calibrating ESR spectra is DPPH (*i.e.*, α, α′-diphenylpicrylhydrazyl radical) :

It gives five extremely sharp peaks with intensity ratio 1 : 2 : 3 : 2 : 1 in the ESR spectrum.

Another application of ESR is in the investigation of molecules in the **triplet state.** A triplet state molecule has a total spin S = 1 so that its multiplicity, $2S + 1 = 3$. While a free radical with S=1/2 has an odd number of unpaired electrons, a triplet state molecule has an even number of electrons, two of them unpaired. We must carefully distinguish between a triplet state molecule and a diradical, for both contain two unpaired electrons. In a triplet state molecule, *the unpaired electrons must interact* whereas in a diradical the unpaired electrons do not interact since they are a great distance apart.

H.M. McConnell and his coworkers have found that groups with unpaired electrons can be attached to macromolecules such as proteins and membranes to obtain a great deal of information about their structure. The nitroxide molecules bound to macromolecules are called **spin labels.** These are stable molecules that possess an unpaired 2*p* electron. A commonly used nitroxide is 2,2,6, 6-tetramethyl piperidinol-N-oxyl, abbreviated TEMPOL, having the structure shown here.

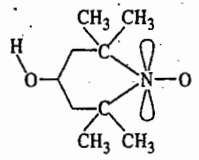

(Tempol)

The unpaired electron interacts with the ^{14}N nucleus (with I=1) giving a hyperfine ESR spectrum with three lines. Spin labels give very useful information about the molecules to which they are bound. For instance, they can tell us about the rate of motion of a macromolecule to which they are bound, or the amount of thermal motion in a membrane in which they have been inserted. It is found that the bands of the ESR spectrum are narrow when the spin label is tumbling rapidly and broad when it is immobilized. The narrowing of the ESR bands arises from the more rapid relaxation of the spin when neighbouring groups are moving rapidly with respect to the spin label.

The spin label can also give information about the polarity of its environment. The extent to which the side bands are split from the central band depends upon the dielectric constant of the medium in which the spin label is dissolved. Solvents of high dielectric constant increase the splitting by augmenting the polarity of the N—O bond. Thus, a measurement of the splitting helps in estimating the polarity of the surroundings of the spin label. One can, for instance, determine if the spin label is bound near the polar head groups or near the non-polar hydrocarbon chains of a membrane.

The hyperfine structure of an ESR spectrum is a kind of fingerprint that helps to identify the free radicals present in the sample. Again, since the magnitude of the splitting depends on the distribution of the unpaired electron near the magnetic nuclei present, the ESR spectrum can be used to map the molecular orbital occupied by the unpaired electron. This mapping is aided by the McConnell equation,

$$a = Q\rho, \text{ where } Q = 2{\cdot}25 \text{ mT} \qquad ...(61)$$

Here ρ is the unpaired electron spin density on a C atom and a is the hyperfine splitting constant observed for the H atom to which it is attached.

Example 30. The hyperfine constants in the ESR spectrum of (naphthalene)$^{-1}$ at the α and β positions are a=0·490 mT and a=0·183 mT, respectively. Map the unpaired electron spin density around the ring.

Solution : Using Eq. 61 and the given a values, we find the following mapping of the unpaired electron spin density at the α and β positions :

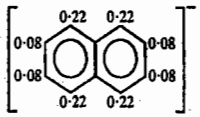

Notice that the unpaired electron spin density is greater at the α positions than at β positions because the hyperfine coupling constants at the α positions are greater than at the β positions.

Example 31. In an ESR spectrometer operating at 9·233 GHz, the centre of the spectrum of CH_3 radical occurred at 329·4 mT. Calculate the g-value of the free radical.

Solution : From Eq. 59,

$$g = \frac{h\nu}{\mu_B B} = \frac{(6{\cdot}626\times10^{-34}\text{ Js})(9{\cdot}233\times10^{9}\text{ s}^{-1})}{(9{\cdot}273\times10^{-24}\text{ JT}^{-1})(0{\cdot}3294\text{ T})} = 2{\cdot}0026$$

Example 32. The g-factor for the benzene radical anion, $C_6H_6^-$ is 2·0025. At what magnetic field intensity would you search for its ESR spectrum in a spectrometer operating at 9·302 GHz ?

Solution : Since from Eq. 59, $\nu = g\mu_B B/h$, hence, substituting various value,

$$B = \frac{h\nu}{g\mu_B} = \frac{(6{\cdot}626\times10^{-34}\text{ Js})(9{\cdot}302\times10^{9}\text{ s}^{-1})}{(2{\cdot}0025)(9{\cdot}273\times10^{-24}\text{ JT}^{-1})} = 0{\cdot}3319\text{ T} = 331{\cdot}9\text{ mT}$$

Example 33. In an ESR spectrometer operating at 9·302 GHz, the ESR spectrum of hydrogen atom gave two lines, one at 357·3 mT and the other at 306·6 mT. What is the hyperfine coupling constant of hydrogen atom ?

Solution : The spacing between the hyperfine lines in the ESR spectrum is called the *hyperfine coupling constant*; it is designated by the symbol, a. Thus,

$$a = (357{\cdot}3 - 306{\cdot}6)\text{ mT} = 50{\cdot}7\text{ mT}$$

Example 34. A free radical containing two equivalent protons gives a 1 : 2 : 1 triplet (*i.e.*, three lines) in the ESR spectrum. The lines occur at the magnetic field intensities of 330·2 mT, 332·5 mT and 334·8 mT. Calculate the hyperfine coupling constant for each proton.

Solution : Designating the ESR lines as 1, 2 and 3, and keeping in mind the fact that the protons are equivalent, we see that the hyperfine coupling constant a is given by

$$a = B(3) - B(2) = B(2) - B(1)$$
$$B(3) - B(2) = (334{\cdot}8 - 332{\cdot}5)\text{ mT} = 2{\cdot}3\text{ mT}$$
$$B(2) - B(1) = (332{\cdot}5 - 330{\cdot}2)\text{ mT} = 2{\cdot}3\text{ mT}$$
$$a = 2{\cdot}3\text{ mT}$$

Example 35. It is possible in commercial ESR spectrometers to detect the resonance from a sample containing 10^{10} spins per cm^3. Calculate the molar spin concentration corresponding to this detection limit.

Solution : Number of moles of electron spins $= \dfrac{10^{10}\text{ cm}^{-3}}{6{\cdot}022\times10^{23}\text{ mol}^{-1}} = 1{\cdot}66\times10^{-14}\text{ mol cm}^{-3}$

Thus, molar concentration (*i.e.*, the number of moles of spins per dm^3) is equal to $1{\cdot}66\times10^{-14}\text{ mol cm}^{-3}\times10^{3}\text{ cm}^{-3}/\text{dm}^3 = 1{\cdot}66\times10^{-11}\text{ mol dm}^{-3}$

The student will appreciate what an infinitesimally small molar concentration of free radical spins can be detected by ESR.

Example 36. Which valence state of copper, *i.e.*, Cu^+ ion or Cu^{2+} ion, will show an ESR spectrum and why ?

Solution : For Cu, the atomic number Z=29. Thus, Cu^+ ion contains 28 electrons and the Cu^{2+} ion 27 electrons. If we write the electronic structures of the two ions we find that Cu^+ ion is a d^{10} system containing no unpaired electron whereas Cu^{2+} ion is a d^9 system containing one unpaired d electron. Since systems containing unpaired electrons show ESR spectra, hence Cu^{2+} ion will give an ESR spectrum.

Example 37. Of the two molecules N_2 and O_2, which will show an ESR spectrum and why ?

Solution : The nitrogen molecule N_2 has fourteen electrons all of which are paired in the molecular orbitals of this molecule. However, the oxygen molecule O_2 has sixteen electrons of which there are two *unpaired* electrons in a degenerate pair of molecular orbitals. Thus, O_2 is paramagnetic and shows an ESR spectrum.

ESR OF ANISOTROPIC SYSTEMS

1. g-Factors and Hyperfine Splittings

In contrast to the ESR spectra of isotropic systems such as solutions, the chemical physicist is interested in the ESR spectra of anisotropic systems which include unstable species prepared by irradiation of crystalline materials or of substrates trapped in host matrices including frozen solutions. In such cases, the g-factors, hitherto regarded as simple scalar quantities, are treated as asymmetric tensors. A symmetric g-tensor can always be diagonalized to give the three principal g-factors, g_{xx}, g_{yy} and g_{zz}. In solution, these are averaged to give the single isotropic factor and for systems with spherical or cubic symmetry, they are equal. However, for a system with axial symmetry, one of these terms ($g_{\parallel}$) is different from the other two ($g_{\perp}$) and for lower symmetries, the three terms are all different.

Similarly, the hyperfine coupling (splitting) constants of isotropic systems must be replaced by tensors for anisotropic systems : here, too, there are two independent terms for symmetric tops and three terms for systems of lower symmetry. It is convenient to separate the hyperfine coupling constant tensor into an isotropic and an anisotropic part, as these components have different physical origins: the new anisotropic term is due to direct dipole—dipole and nucleus—electron interactions. These depend on the angle of the nucleus—electron vector to the magnetic field (that is why they are averaged to zero by tumbling) and are inversely proportional to the cube of the distance between the dipoles. Thus, the effects of anisotropy on g values and hypefine couplings in ESR spectroscopy are exactly analogous to the effects on chemical shifts and dipolar couplings in the NMR spectra of solids.

In an investigation of a single crystal by ESR, the spectra are found to depend on the orientation of the sample. Measurements taken at various angles enable us, in principle—and in several cases, in practice—to determine all the elements of the g-tensor and the hyperfine coupling tensor. Such a study yields valuable information about electron distribution. Frequently, spectral studies are made on anisotropic systems such as powders or frozen solutions which contain random mixtures aligned at all possible angles to the magnetic field. In the absence of hyperfine splitting, the resonance absorption has a distinctive envelope (Fig. 37). These envelopes have clear upper and lower cut-offs and for a system having no symmetry the envelope exhibit a well-defined maximum. Consequently,

the derivative curves have two or three peaks as shown from which the anisotropic g-values can be determined.

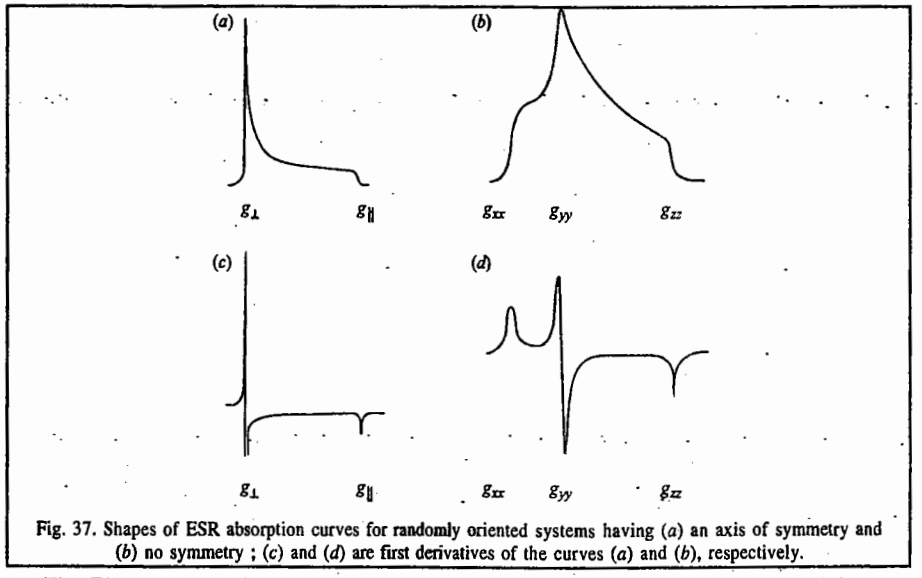

Fig. 37. Shapes of ESR absorption curves for randomly oriented systems having (a) an axis of symmetry and (b) no symmetry ; (c) and (d) are first derivatives of the curves (a) and (b), respectively.

The ESR spectra rapidly become very complex when the anisotropic hyperfine splittings are introduced. Fig. 38 shows a spectrum for the Li^+–CO_2^- ion pair, labelled with ^{13}C, in a CO_2 matrix. The patterns are basically similar to those of Fig. 29(c) with large ^{13}C and small ^7Li (I=3/2) hyperfine splittings. In this case, the spectrum is easy to analyze, though often computer fitting is necessary. In any spectral computer simulation, the spin Hamiltonian is set up ; this Hamiltonian includes terms such as quadrupolar nucleus–electron interactions, the details of which are found in standard books on the subject. In Fig. 30, parallel and perpendicular components can be seen, each showing splittings due to ^{13}C and ^7Li. The weak central lines are due to Li^+–$^{12}CO_2^-$.

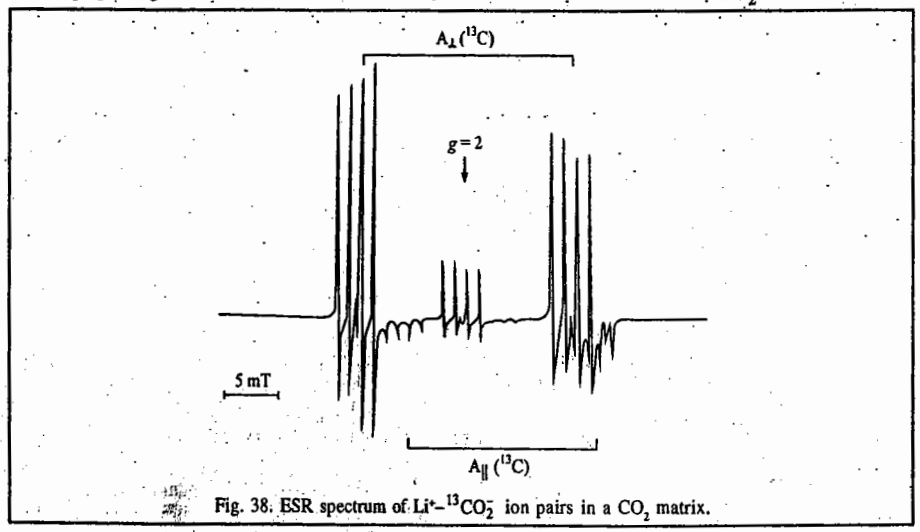

Fig. 38. ESR spectrum of Li^+–$^{13}CO_2^-$ ion pairs in a CO_2 matrix.

2. Kramers' Degeneracy and Zero-Field Splitting (ZFS)

We have so far considered ESR spectra of systems such as free radicals having just one unpaired electron. However, systems having many unpaired electrons (which involve *electron-electron interactions*) can also be investigated by ESR. There systems are, for instance, molecules having diamagnetic ground states but which possess excited triplet states (with two unpaired electrons) which have lifetimes long enough for their ESR spectra to be recorded. In the presence of a Zeeman (magnetic) field, a triplet state splits into its three components (Fig. 39), giving two possible transitions, $M_S = -1 \rightarrow 0$ and $M_S = 0 \rightarrow +1$, whose energies are identical.

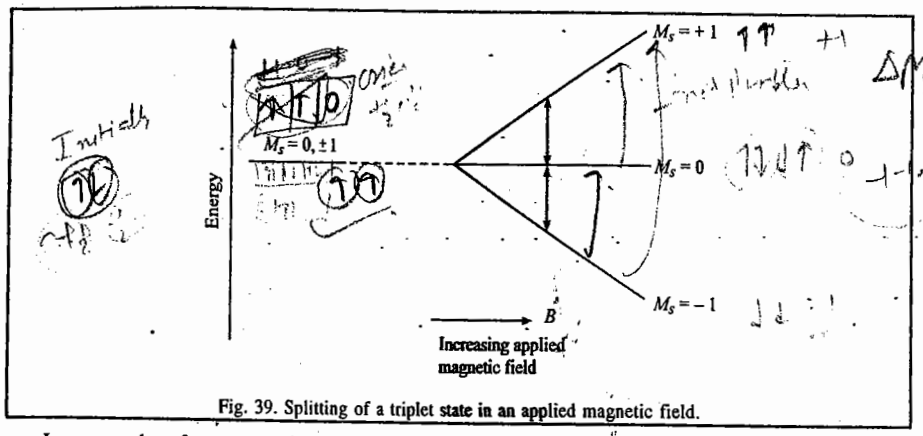

Fig. 39. Splitting of a triplet state in an applied magnetic field.

In a crystal or frozen sample, dipole-dipole interactions being anisotropic, the energy levels with $M_S = \pm1$ are shifted relative to that with $M_S = 0$ even in the absence of an applied magnetic field. Hence, when a magnetic field is applied, the two transitions no longer have the same energy (Fig. 40).

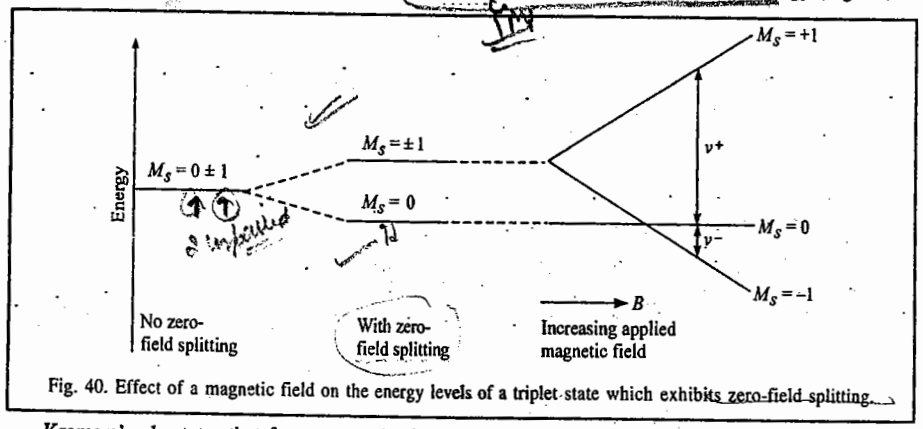

Fig. 40. Effect of a magnetic field on the energy levels of a triplet state which exhibits zero-field splitting.

Kramers' rule states that for a system having an *even* number of unpaired electron spins, the lowest energy state will be that with $M_S = 0$, as shown in Fig. 32 for a triplet state. All higher energy states in this case and *all* states for systems with an *odd* number of unpaired electron spins, will be doubly degenerate, corresponding to the two signs possible for $M_S \neq 0$. This degeneracy is known as **Kramers' degeneracy** ; it is removed by an applied magnetic (Zeeman) field, which shifts the two levels M_S=−1 and M_S=+1 in opposite directions (Fig. 40). As a consequence, the two allowed transitions (M_S=−1 → 0 and M_S=0 → +1), which are of equal energy in the absence of zero-field splitting (ZFS), are now of quite

different energy. Thus, *two* ESR signals are observed. If the ZFS is small compared with $g_{el}\mu_B B_0$, it will result in a pair of signals near $g=2{\cdot}0$, but if the splitting is large, as is often the case for transition metal ions, the apparent g-values may be very different from 2 and it may be impossible to observe the expected ESR transitions. For systems with very large splittings, the energy gap between the lowest energy level and higher ones may be so large that no crossings at all occur at magnetic fields normally used, as illustrated in Fig. 41, which shows the effect of a large ZFS on a quartet system ($S=3/2$, so that multiplicity $2S+1 = 4$). The separation induced between the $M_S = \pm 1/2$ and $M_S = \pm 3/2$ states is so large that only a single ESR signal, due to the $M_S = -1/2 \rightarrow M_S = +1/2$ transition, is observed near $g=2{\cdot}0$. The energies of the $M_S = -1/2 \rightarrow -3/2$ and $+1/2 \rightarrow +3/2$ transitions are outside the observable frequency range. In general, there is an *effective spin quantum number* which is equal to $|M_S|$ for the lowest state. This will be zero for an even number of unpaired electrons, giving no signal at all, and is often 1/2 for systems with an odd number of unpaired electrons, giving a simple spectrum in the normal frequency range.

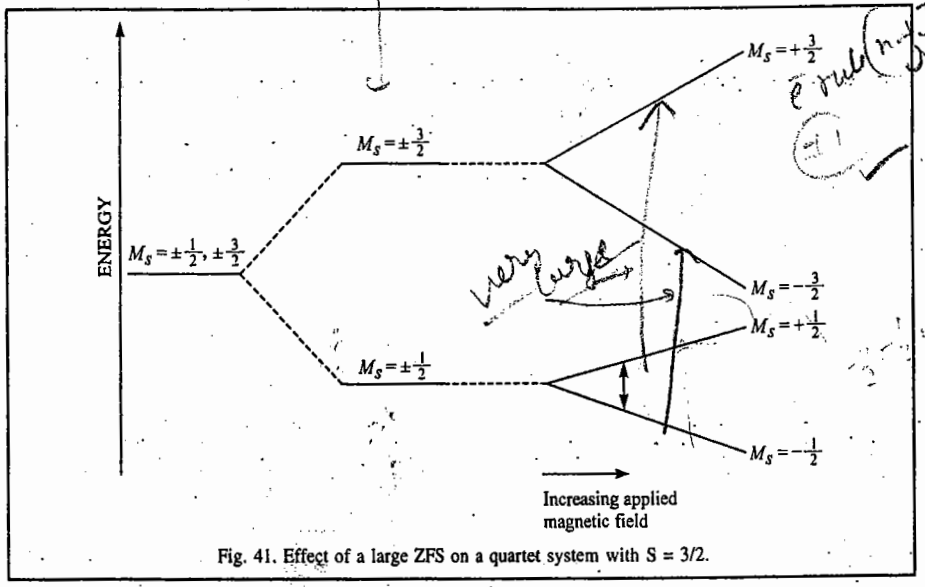

Fig. 41. Effect of a large ZFS on a quartet system with S = 3/2.

Another possible consequence of ZFS is that the $\Delta M_S = \pm 1$ selection rule for ESR transitions may break down, giving more observed transitions. Thus, the spectra, particularly for transition metal ions with several unpaired electrons, are very complicated. Also, the ZFS is anisotropic, which further complicates the ESR spectra of solids of less than cubic symmetry. No doubt, tumbling of molecules averages it to zero but in solution the spin-spin interactions cause rapid relaxation and the spectra are usually too broad to be observed. Intramolecular spin-spin interactions may similarly make spectra impossible to observe.

3. ESR Spectra of Transition Metal Complexes

The ESR spectra of transition metal ion complexes are complicated by the fact that they may have several approximately degenerate orbitals and several unpaired electrons. As a result, there may occur anisotropy in g-factors (due to orbital contribution to the magnetic moment) and also the zero-field effects, as discussed above. In an analysis of any system, we must ascertain the number of d electrons and also whether the complex is high or low spin. The consequences of Jahn-Teller distortion, which occurs to remove the degeneracy of any orbitally degenerate

ground state, and of ZFS and Kramers' degeneracy, must also be taken into consideration. Since ZFS arises primarily from spin–orbit coupling, it is much larger for heavier atoms than for lighter ones. Partly for this reason, the ESR spectra of Second and Third-row transition metal complexes are often harder to observe and interpret than those of First-row species. On the other hand, the rare-earth metal complexes for which spin-orbit coupling is small, often give clear, useful spectra. It must also be noted that if excited states lie close to the ground state, spin-lattice relaxation times will be short and spectral lines broad and the ESR spectra will be required to be observed at low temperatures.

Let us illustrate these principles by three examples :

1. d^3 system. In this system as found in Cr^{III}, the free ion ground state is ^4F and in an octahedral field, the electrons occupy the three lower (t_{2g}) orbitals giving a $^4A_2$ ground state (Fig 34). There is no Jahn-Teller distortion in this case but if there is tetragonal distortion, as in a complex with four ligands of one type and two (mutually *trans*) of another, the ground state becomes $^4B_1$. Then, there occurs ZFS and by Kramers' rule, the lowest state is degenerate and must give observable resonances. Other transitions, shown in Fig. 42 will also be observed so long as ZFS is not too large. Also, ground and excited states are well separated in energy, so spin–lattice relaxation times are long and the ESR spectral lines are narrow (sharp).

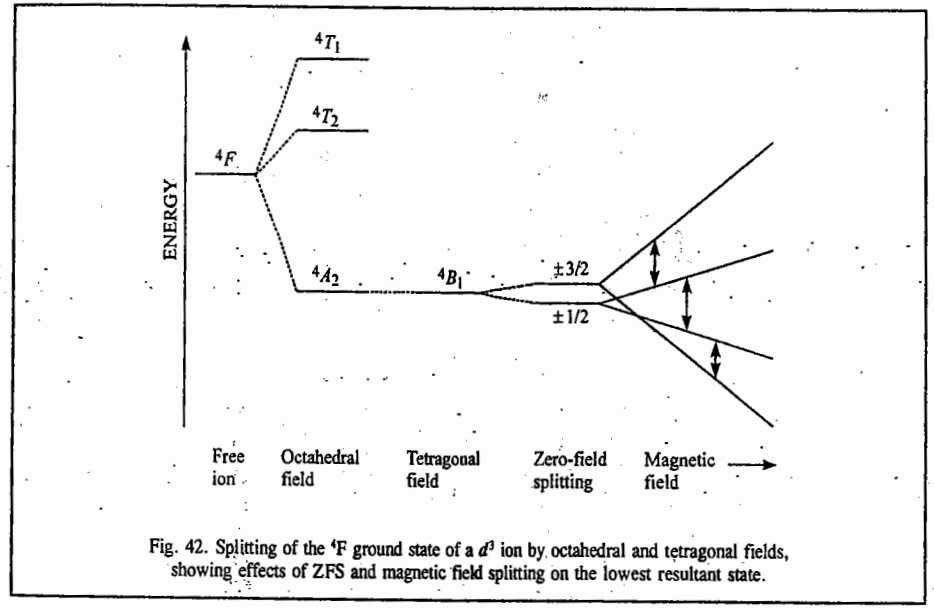

Fig. 42. Splitting of the ^4F ground state of a d^3 ion by octahedral and tetragonal fields, showing effects of ZFS and magnetic field splitting on the lowest resultant state.

2. d^6 system. Low-spin d^6 systems are diamagnetic and high-spin systems have ^5D ground states which split to give $^5T_2$ ground states in octahedral fields and $^5B_2$ states with tetragonal distortion. The ground states are connected to excited states by spin-orbit coupling giving short spin-lattice relaxation times and broad resonances and the spin-orbit coupling also gives large ZFS. The lowest level is not degenerate (Kramers' rule) and hence no resonances are observable.

3. d^9 system. For this system the ^2D ground state of the free ion becomes ^2E in an octahedral field and Jahn-Teller distortion yields a tetragonal structure whose ground state is ^2A (Fig. 35) A doublet

ground state gives ESR with no further problem. If, as is usually the case, the Jahn-Teller distortion is large, the spectral lines are narrow.

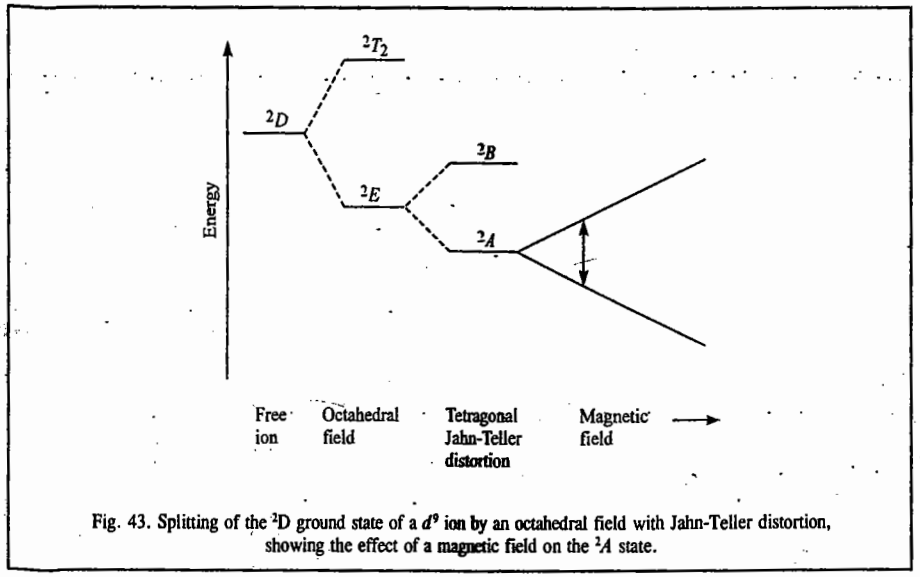

Fig. 43. Splitting of the ^2D ground state of a d^9 ion by an octahedral field with Jahn-Teller distortion, showing the effect of a magnetic field on the ^2A state.

Though the ESR spectra of transition metal ions are often very difficult to interpret, they serve as useful aids to identification, particularly using hyperfine splitting patterns ; they also serve as a means of studying the electron distribution. Values of $g_{\parallel}$ and $g_{\perp}$ can show which d orbitals are occupied and thus indicate the direction in which Jahn-Teller distortion has occurred, while hyperfine coupling constants can be used to determine the electron spin densities on various nuclei and to distinguish the components in s orbitals (isotropic) from those in p and d orbitals (anisotropic).

Example 47. *(a)*. Discuss briefly the fine structure and ZFS in ESR spectra. (*b*) Draw energy level diagrams for the values of total electron spin S = 1/2, 1, 3/2, 2, and 5/2 in the presence of applied magnetic field, showing the ESR transitions. (*c*) Draw energy level diagram for (*i*) $S = 1/2$, (*ii*) $S = 3/2$ for two different ZFS ; and (*iii*) $S = 1$ for three different ZFS.

Solution : *(a)* A species with spin S has a total of $2S+1$ energy states characterized by the quantum number M_S. In the absence of a magnetic field, all states with $M_S \neq 0$ are expected to remain doubly degenerate (*i.e.*, M_S and $-M_S$ correspond to the same energy). However, these doublets are usually separated from each other by electric fields produced by other atoms, which act *via* spin-orbit coupling. The extent of this **zero-field splitting (ZFS)** depends on the structure of the sample, the extent of spin-orbit coupling, etc. In principle, it is zero for strict cubic symmetry (Fig. 44) but, since such ideal behavior is rarely seen, ZFS is present in the vast majority of cases. The application of a magnetic field now removes the remaining degeneracy and transitions may be observed between adjacent states, following the selection rule $\Delta M_S = \pm 1$. In principle then, $2S$ transitions can occur, their separations representing the extent of ZFS (Fig. 45). The appearance of more than one line (when $S > 1/2$) is known as the **fine structure** in the spectrum. Whether or not all or any of the transitions can be observed, and what their g-values are, depends on the electron configuration and the ZFS, and, of course, on the magnetic field range of the spectrometer. We should also note that it is not entirely unknown for **forbidden lines** to appear, corresponding to $\Delta M_S = \pm 2$. It frequently happens that ZFS is very large. Under these circumstances, systems in which number n of unpaired electrons is even, may have no resonances within the observable range and those with odd n show only a single resonance corresponding to the $M_S = -\frac{1}{2}$ to $M_S = +\frac{1}{2}$ transition (Fig. 45).

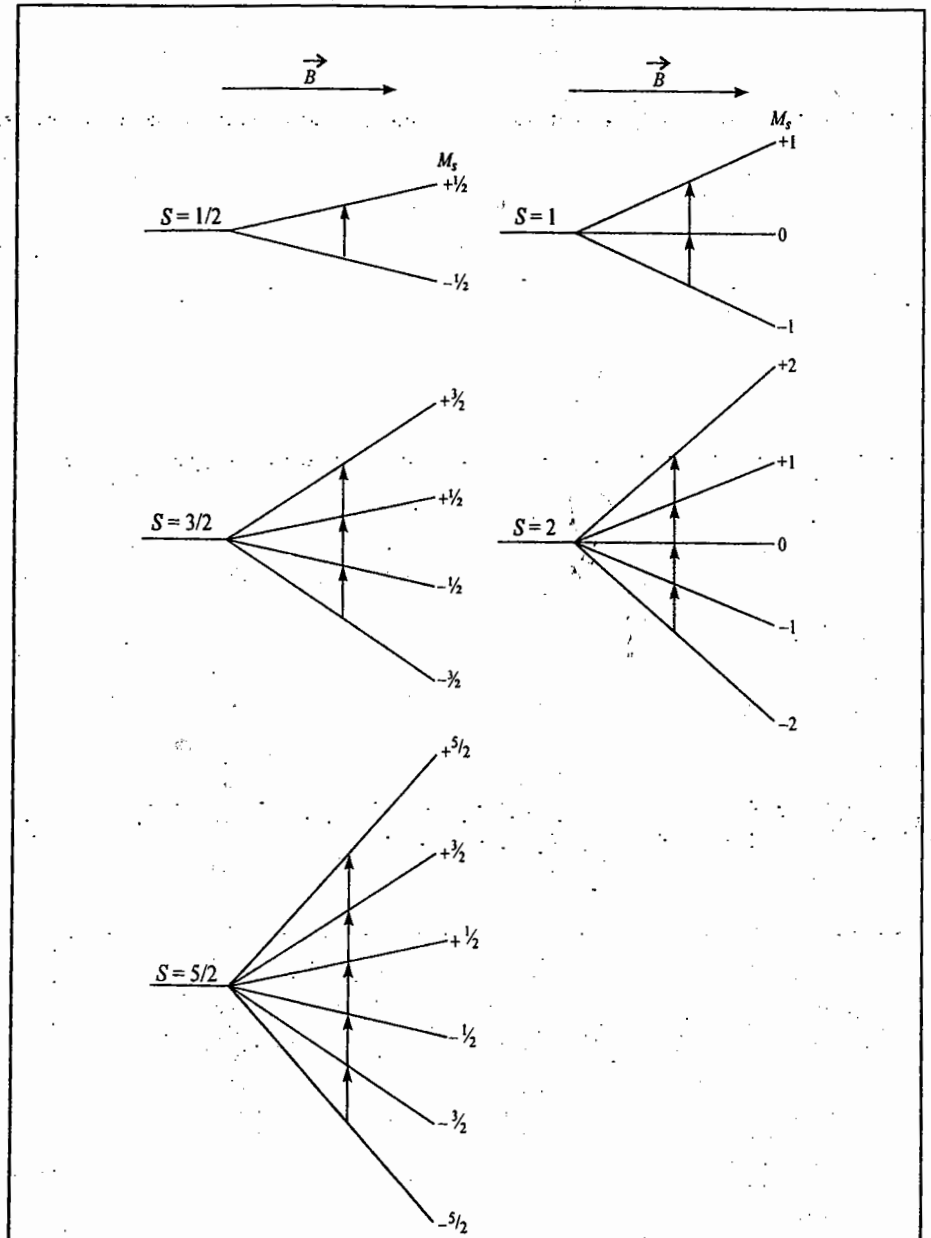

Fig. 44. Energy level diagrams for various values of S and no zero-field splitting. Note that the applied magnetic field increases from left to right and that all transitions for any one system occur at the same field-value.

(c) See Fig. 45

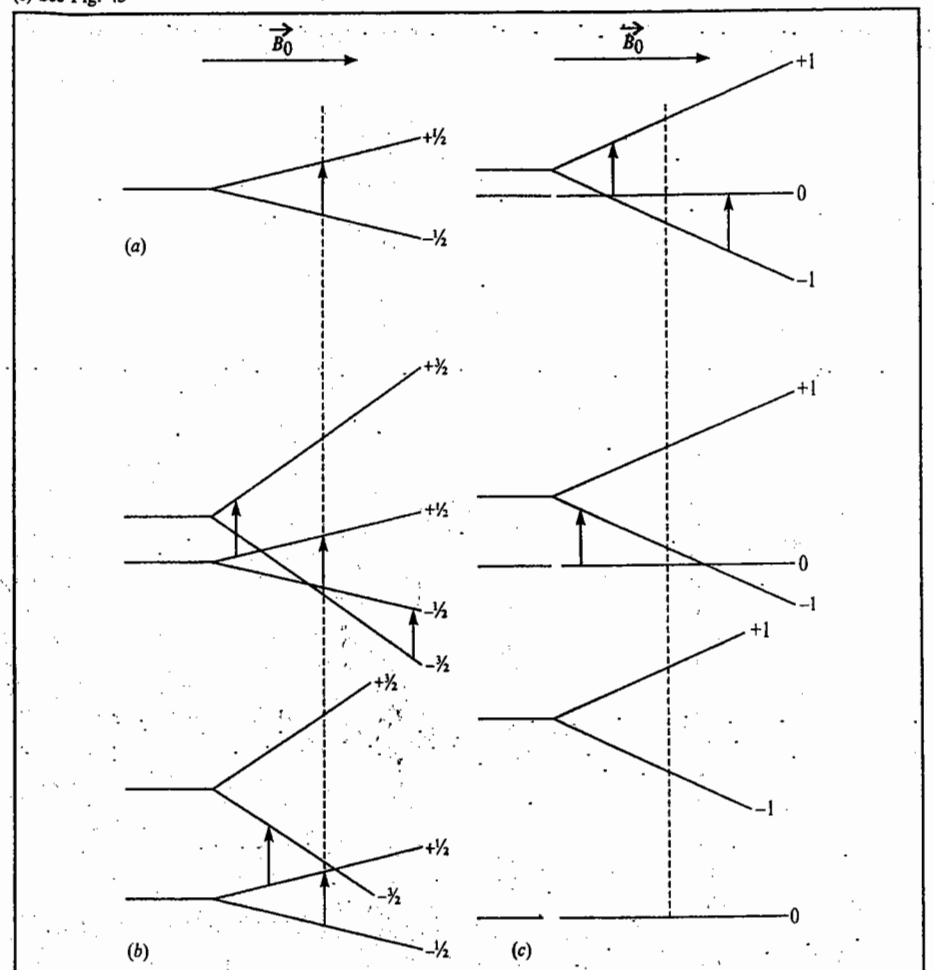

Fig. 45. Energy level diagrams : (*a*) $S=1/2$; (*b*) $S=3/2$ for two different zero-field splittings ; (*c*) $S=1$ for three different zero-field splittings. The dotted vertical lines mark the position of the (single) absorption line in the absence of zero-field splitting.

4. Multiple Resonance Techniques in ESR spectroscopy

Of the several multiple resonance techniques applied to ESR spectroscopy, two, *viz.*, **ENDOR** (electron–nuclear double resonance) and **ELDOR** (electron–electron double resonance) are of special interest. Fig. 46 shows an energy level diagram for a system which has a single electron spin and a nucleus with spin 1/2 .There are two allowed spin transitions, labelled E_1 and E_2, and the two transitions, labelled N_1 and N_2 involving the nuclear spins. These latter transitions would not normally be observed in an NMR spectrum since the resonances would be extremely broad. It may be noted that the electron–nucleus coupling constant may be comparable with or even greater than the resonance frequency of the nucleus in the absence of coupling and that the $|\alpha_e\alpha_n\rangle$ level may be lower in energy than $|\alpha_e\beta_n\rangle$.

In an ENDOR experiment, the ESR spectrum is observed while nuclear transitions are irradiated. The situation is similar to that in a nuclear INDOR experiment in that the populations of the various energy levels are perturbed and the ESR transitions change in intensity. Thus, for the system shown in Fig. 46, transition E_1 or E_2 monitored and the frequencies N_1 and N_2 are irradiated. Their frequencies depend on the magnetogyric ratio of the nucleus. One obvious application of ENDOR is in the identification of nuclei responsible for particular hyperfine splittings. Another major application is to systems for which the ESR spectrum is complex. A series of ENDOR spectra, each with as few as two lines, can greatly simplify the task of spectral assignment. Also, all double resonance methods are used for investigating relaxation processes.

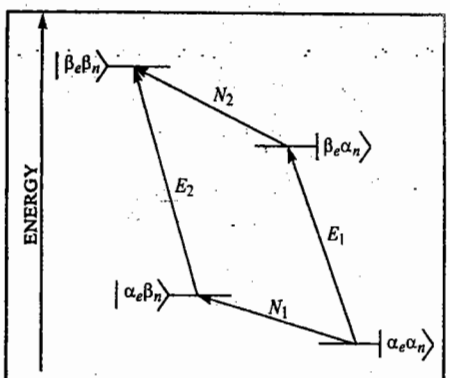

Fig. 46. Energy level diagram for a system with one unpaired electron and one nucleus with nuclear spin 1/2. The spin wave functions $|\alpha_e\ \beta_n\rangle$, etc., are designated by the spin quantum numbers of the electron and the nucleus.

An ELDOR experiment is rather different. Referring to Fig. 46, one electron spin transition is observed while the other is irradiated. As these transitions do not share energy levels, the effects of irradiation (also called *pumping*) are only seen as a result of spontaneous nuclear spin transitions. In an ELDOR spectrum, the intensity change in the monitored resonance is plotted against frequency difference, and in our example, a peak will occur at $|E_2 - E_1|$, which equals the hyperfine coupling constant. For a more complicated system, the spectrum may have several lines, each single line giving a direct measurement of a splitting constant. This is particularly useful for measuring very large splittings, or on occasion when a spectrum is complicated by numerous hyperfine splittings. ELDOR spectra also contain lines corresponding to pumping of the forbidden transitions (Fig. 46), that is $|\alpha_e\alpha_n\rangle$ to $|\beta_e\beta_n\rangle$ and $|\alpha_e\beta_n\rangle$ to $|\beta_e\alpha_n\rangle$ and these contain information about the mean nuclear frequency as well as the hyperfine coupling constant.

Example 48. Draw the energy level diagram (energy versus applied magnetic field) for a system with $S=3/2$ under the various circumstances listed below. Select a particular energy interval as corresponding to the spectrometer frequency, mark the possible ESR transition and note how their number changes [assume that the limit of applied field available is twice that corresponding to the transition in *(a)*].

***(a)* with no zero-field splitting (ZFS),**

***(b)* with small ZFS,**

***(c)* with ZFS comparable to the ESR spectrometer frequency and**

***(d)* with ZFS very much larger than the spectrometer frequency.**

Solution : See Fig. 47. Note that the $M_S = -1/2 \rightarrow +1/2$ transition is unaffected by ZFS and always appears, even though the other transitions may move out of the spectrometer range.

Example 49. Repeat the exercise of Example 48 for $S=2$.

Solution : See Fig. 48. Note the dependence of the line positions on the zero-field splitting (ZFS) and that it is possible for there to be no ESR lines at all in the spectrometer range.

Example 50. From the ESR spectrum shown in Fig. 49 estimate the *g*-value.

Solution : The centre of the line appears at about 326 mT and the reference signal at about 332 mT. Hence,

$$g = 2{\cdot}0028 \times 332/326 = 2{\cdot}04.$$

Example 51. From the ESR spectrum shown in Fig. 50, estimate the value of g and of A. Which type of spin system would give rise to this type of structure in the spectrum ?

Solution : The spectrum is a 1 : 2 : 1 triplet, centered at $B=3245$ G. The reference signal is at $B=3319$ G. Hence, $g = 2{\cdot}0028 \times 3319/3245 = 2{\cdot}048$. The hyperfine coupling constant A is the separation between the individual lines, 25 G. Such a spectrum would arise from coupling of the unpaired electron spin with two nuclei with $I=1/2$.

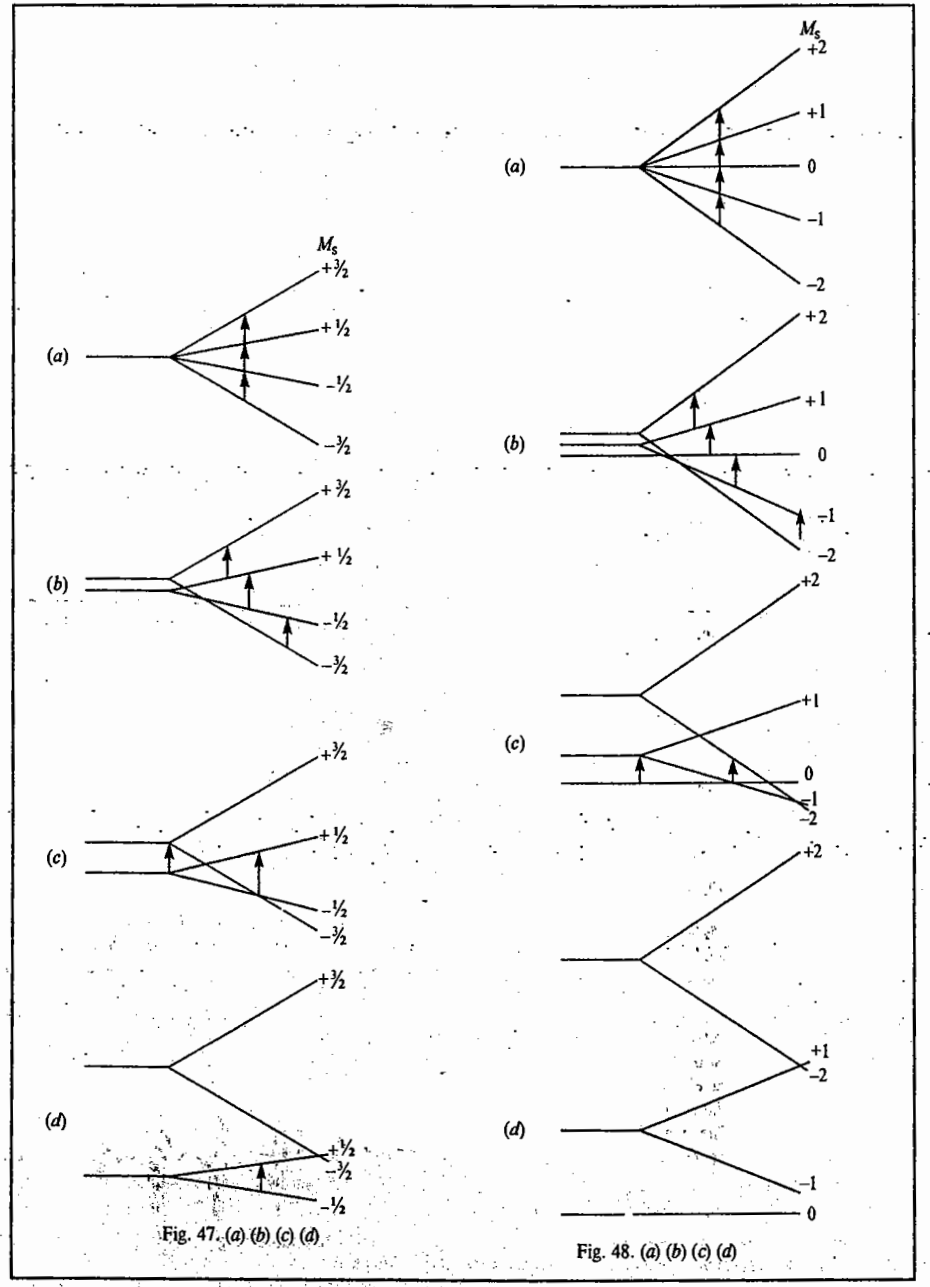

Fig. 47. (a) (b) (c) (d)

Fig. 48. (a) (b) (c) (d)

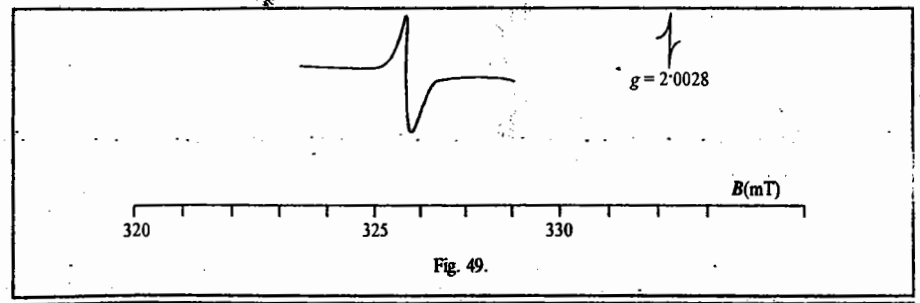

Fig. 49.

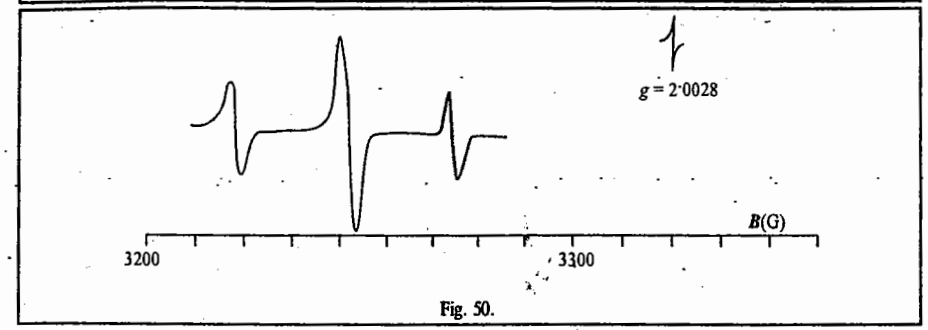

Fig. 50.

Example 52. Predict the ESR spectra expected for the following species in which M has *no* nuclear spin ($I = 0$) :

(a) $M^{\bullet}$ *(b)* $MH^{\bullet}$

(c) $MH_2^{\bullet}$ *(d)* $MH_3^{\bullet}$.

Solution : The spectra would have the following shapes :

(a) a singlet *(b)* a doublet

(c) a 1 : 2 :. 1 triplet *(d)* a 1: 3 : 3 : 1 quartet.

In *(c)* and *(d)*, the lines are equally spaced.

Example 53. The spectrum shown in Fig. 51 is for the radical anion $B_2H_6^+$, in which the boron atoms have been isotopically enriched to 98% in $^{11}B(I=3/2)$. What can be deduced about the numbers of boron and hydrogen nuclei with which the unpaired electron is interacting ? What implications does this have for the structure of the radical anion ?

Solution : The spectrum is a septet of septets. The large line-separation must be hyperfine splitting from ^{11}B. Therefore, the unpaired electron is interacting equally with both boron nuclei, *i.e.*, is delocalized equally between the two boron atoms. The small splitting must be due to the superhyperfine interaction with all six ^1H nuclei which must also be equivalent.

Diborane, B_2H_6, has an electron-deficient bridged structure containing four terminal and two bridging hydrogen atoms. The radical anion does not have this structure since the hydrogen atoms are now all equivalent. The simplest structure would be analogous to ethane, with only a single bonding electron holding the two BH_3 units together.

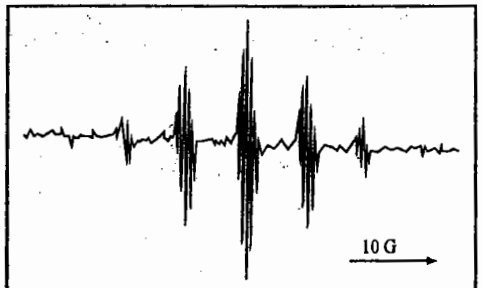

Fig. 51. The ESR spectrum of $B_2H_6^+$.

Example 54. Explain why minerals which contain iron only in oxidation state +2 do not give usually an ESR spectrum.

Solution : Most minerals contain high-spin iron (II) which has a d^6 configuration with four unpaired electrons ($S = 2$). Even-electron systems seldom give ESR spectra (see Example 49).

Example 55. Sketch the ESR spectra you would expect for

***(a)* a solution of Cu^{2+} in water and**

***(b)* The same solution after it has been frozen.**

Assume that only hyperfine coupling to Cu^{63} ($I = 3/2$) can be seen.

Solution : See Fig. 52.

(a) Solution spectra are isotropic even though the individual ions may have non-cubic symmetry. A simple quartet spectrum is, therefore, expected.

(b) When the solution is frozen, the ions are immobilized and have a random distribution of orientations. An anisotropic ESR spectrum showing $g_{\parallel}$ and $g_{\perp}$ is, therefore obtained. Since $A_{\parallel}$ is normally quite small for Cu^{2+}, A_{iso} is roughly equal to $A_{\perp}/3$, where A is the hyperfine coupling constant.

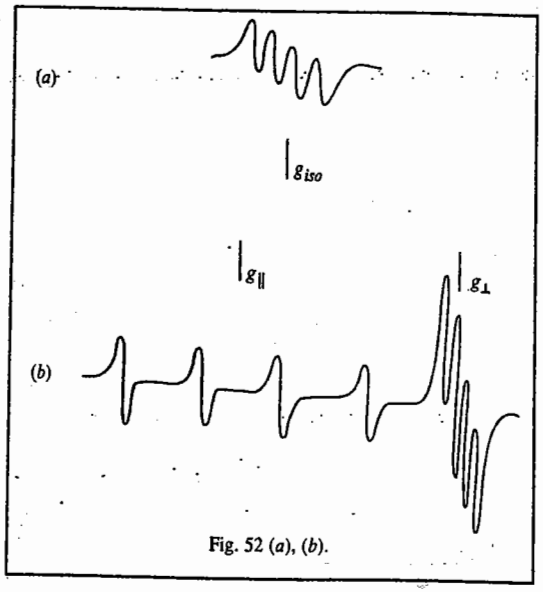

Fig. 52 (*a*), (*b*).

SPIN HAMILTONIAN

In gases and liquids, sharp magnetic resonance spectral lines occur as a result of rapid tumbling motion of molecules which average out the local fields. In solids, on the other hand, the electron finds itself in very complex environment of interacting fields. In the 1960s, Abragam and Price and later, Bleaney and Stevens, expressed the various interactions to which a paramagnetic ion is subjected, in the form of a spin Hamiltonian which is written as

$$\hat{H} = \hat{H}_{el} + \hat{H}_{cf} + \hat{H}_{L\text{-}S} + \hat{H}_{S\text{-}S} + \hat{H}_{Z} + \hat{H}_{hf} + \hat{H}_{Q} + \hat{H}_{N} + \hat{H}_{E} \qquad ...(62)$$

where the various terms, their energies given in parentheses, have the following significance :

$\hat{H}_{el}$ = Free ion or Coulomb energy (10^4 - 10^5 cm^{-1})

$\hat{H}_{cf}$ = Stark crystal field energy (10^3 - 10^4 cm^{-1})

$\hat{H}_{L\text{-}S}$ = Spin-orbit interaction (10^2 - 10^3 cm^{-1})

$\hat{H}_{S\text{-}S}$ = Electronic spin-spin interaction (0 - 1 cm^{-1})

$\hat{H}_{Z}$ = Zeeman interaction of electron with external magnetic field (0 - 1 cm^{-1})

$\hat{H}_{hf}$ = Hyperfine interaction between the electronic and magnetic moments (0 - 10^{-2} cm^{-1})

$\hat{H}_{Q}$ = Nuclear quadrupole interaction between electron and nucleus (10^{-3} cm^{-1})

$\hat{H}_{N}$ = Nuclear Zeeman interaction involving nuclear interaction with the magnetic field (10^{-4} cm^{-1})

$\hat{H}_{E}$ = Exchange interaction between two types of electrons ($< 10^{-4}$ cm^{-1}).

The energies of the nine terms in the spin Hamiltonian have been listed in the order of decreasing magnitude. The first Coulomb energy term involves the interaction of electrons with one another and with the nuclei. The second Stark term removes the $2L+1$ degeneracy of the salts of the metals of the First transition series. The Stark splittings are small in the salts of rare earths and actinides whose $4f$ and $5f$ shells, respectively, are shielded by closed electron shells.

The first three terms involve too much energy for excitation by ESR. The fourth, fifth and sixth terms are investigated in ESR since they lie in the microwave region. The last three terms are too small to be observed in the presence of $\hat{H}_Z$.

Consider Cu^{2+} ion, the $3d^9$ system with $^2D_{5/2}$ ground term. The total degeneracy of the ground electronic state is 10, being given by $(2L+1)(2S+1)$, *i.e.*, the product of the five-fold orbital degeneracy ($L=2$) and two-fold spin degeneracy $\left(S = \frac{1}{2}\right)$. In a tetragonal crystal field, the orbital degeneracy is partially removed (Fig. 53). Since the Cu^{2+} ion has an odd number of electrons, the spin degeneracy still remains, in accordance with Kramers' theorem. The spin-orbit interaction removes the orbital degeneracy completely. The Zeeman field removes the spin degeneracy. The ESR is observed between $m_s = -\frac{1}{2}$ and $m_s = +\frac{1}{2}$ levels. Since the copper nucleus has nuclear spin, $I = \frac{3}{2}$, hyperfine structure results, giving four transitions between the m_I sub-levels according to the selection rule $\Delta m_I = 0$.

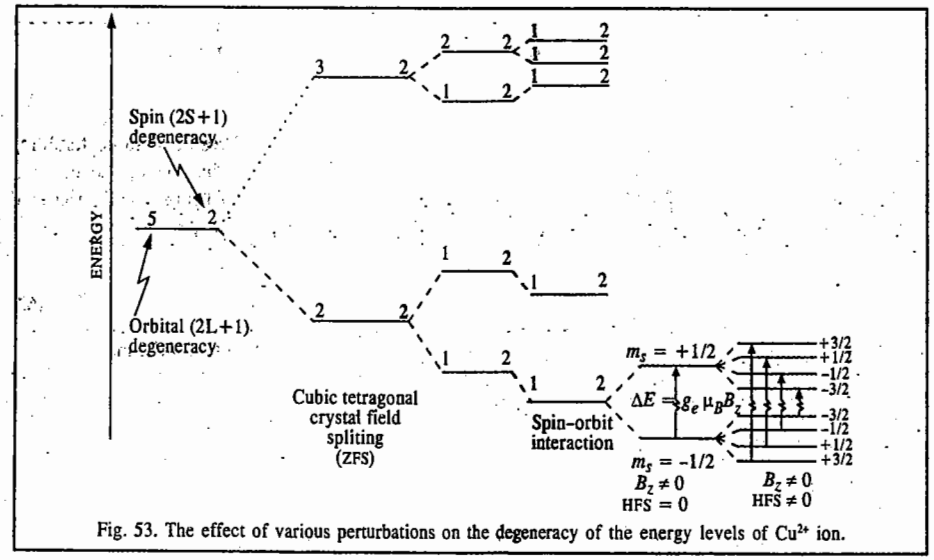

Fig. 53. The effect of various perturbations on the degeneracy of the energy levels of Cu^{2+} ion.

The spin Hamiltonian is formidable to use for computational purposes. It can, however, be used to describe the experimental results. For a trigonal or tetragonal crystal field where the magnetic field B is directed along the symmetry axis of the crystal, the spin Hamitonian can be written as

$$\hat{H} = \mu_B[g_{\perp} B_z S_z + g_{\perp}(B_x S_x + B_y S_y)] + D[S^2 - \tfrac{1}{3}S(S+1)] + E(S_x^2 - S_y^2)$$
$$+ A_z I_z S_z + A_x I_x S_x + A_y I_y S_y + Q[I_z^2 - \tfrac{1}{3}I(I+1)] - g_N \mu_N B I \qquad ...(63)$$

where the symbols have the following meaning :

S= effective electron spin; S_z = the z-component (along the magnetic field direction) of spin ;

S_x, S_y are the components along x and y-axes, respectively; I = nuclear spin and I_x, I_y, I_z are the Cartesian components ; D, E are the zero-field splitting constants, Q is the nuclear quadrupole moment and A is the hyperfine coupling constant.

The constants g, D, E, A and Q are determined empirically from experiment. The terms involving B and S denote the interaction of electronic magnetic moment with the Zeeman field; they are generally anisotropic. The terms involving D and E give rise to fine structure, resulting from the second-order effects of crystal field exerted via spin–orbit interaction. The terms involving I and S denoting hyperfine interaction are also anisotropic, resulting from dipole interactions between the nuclei and the electrons. The quadrupole interaction term (for nuclei with nuclear spin, $I \geq 1$) is also anisotropic. The last term represents the direct interaction between the nuclear magnetic moment and the Zeeman field. Though g is positive, the signs of other constants are very difficult to obtain since they have to be determined from second-order effects. Of course, not all the terms in Eq. 63 are of equal importance for a given metal ion. For instance, if an ion has no nuclear spin, the terms containing I vanish. For a free electron, on the other hand, D, E, I, A, Q are all zero so that the Hamiltonian assumes the form $H = g_e\mu_B B$, where g_e is now a scalar quantity.

By convention, S is assigned a value that makes the observed number of energy levels equal to $2S+1$. In those spin systems, where only the lower energy levels are occupied, the higher energy levels cannot be detected experimentally. Thus, the spin determined from the $2S+1$ observed levels corresponds to a fictitious state ; hence the effective spin is sometimes referred to as 'fictitious spin'.

MÖSSBAUER SPECTROSCOPY (MB SPECTROSCOPY)

The discovery of **Mössbauer effect** or Mössbauer spectroscopy (also known as the recoil-less nuclear gamma resonance fluorescence (NRF) spectroscopy) in 1958 by the German physicist Rudolf Mössbauer was hailed as a breakthrough in nuclear and solid state physics. Mössbauer shared the 1961 Physics Nobel Prize with the American nuclear physicist Robert Hofstadter (who was honoured for electron–nuclear scattering concerning the structure of the nucleons). Mössbauer spectroscopy has found wide application in elucidating the nature of the chemical bond in inorganic solid state chemistry and biological science, for instance, bonding in haemoglobin and oxyhaemoglobin.

Basic Principle of NRF Spectroscopy. Consider the original experiment performed by Mössbauer. Here ^{57}Co decays to the excited state of iron, $^{57}Fe^*$ by electron capture (EC), which further decays to the stable ^{57}Fe by the emission of delayed gamma ray (Fig. 54). This latter phenomenon is called **γ-ray fluorescence.** In the presence of a target nucleus ^{57}Fe, this gamma ray can be resonantly absorbed. Since the excited state $^{57}Fe^*$ has a finite life-time (τ), the uncertainty in the enegy of the emitted **γ-ray** is governed by the Heisenberg uncertainty principle, $\Delta E \Delta t \approx \hbar$, which can be rewritten in a slightly different notation as

$$\Gamma\tau \approx \hbar \qquad \ldots(64)$$

where Γ is the line width and τ is the life-time of the excited state. From Eq. 46 we see that since $10^{-11}\ s < \tau < 10^{-4}\ s$, $10^{-4} < \Gamma < 10^{-11}$ eV.

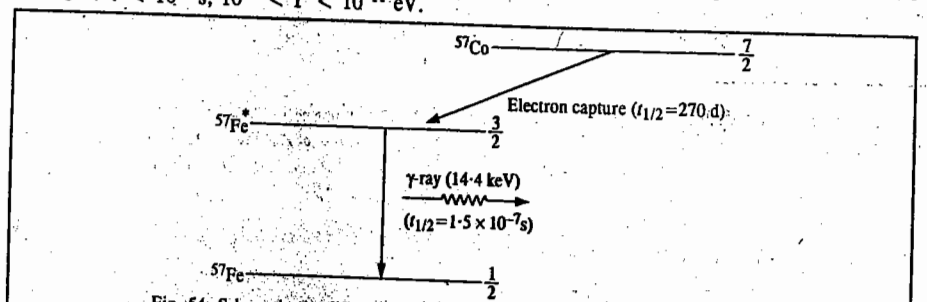

Fig. 54. Schematic simplified diagram showing the decay of the radioactive ^{57}Co to ^{57}Fe.

The momentum of the emitted γ-ray is given, according to the de Broglie relation, by

$$p = h/\lambda \qquad \ldots(65)$$

where λ is the γ-ray wave length. Since linear momentum must be conserved, the nucleus must recoil in the opposite direction, with the recoil energy R given by

$$R = p^2/2M \qquad \ldots(66)$$

where M is the mass of the recoiling nucleus. The target nucleus, too, must recoil with energy R on receiving the γ-ray, with the result that some of the energy of the γ-ray transition, E_γ, is converted into the recoil energy. Thus, for the emitting nucleus

$$E = E_\gamma - R \qquad \ldots(67)$$

and for the absorbing nucleus (absorber)

$$E = E_\gamma + R \qquad \ldots(68)$$

We see that the emission and absorption lines are centred $2R$ apart.

Since

$$E_\gamma = h\nu = hc/\lambda = pc \qquad \ldots(69)$$

we have, from Eqs. 66 and 69,

$$2R = E_\gamma^2/Mc^2 \qquad \ldots(70)$$

For the resonance absorption to occur, Γ must be greater than or equal to the loss in γ-ray energy due to recoil, *i.e.*,

$$\Gamma \approx 2R \qquad \ldots(71)$$

The plot of the number of the emitted γ-rays versus energy is given in Fig. 55.

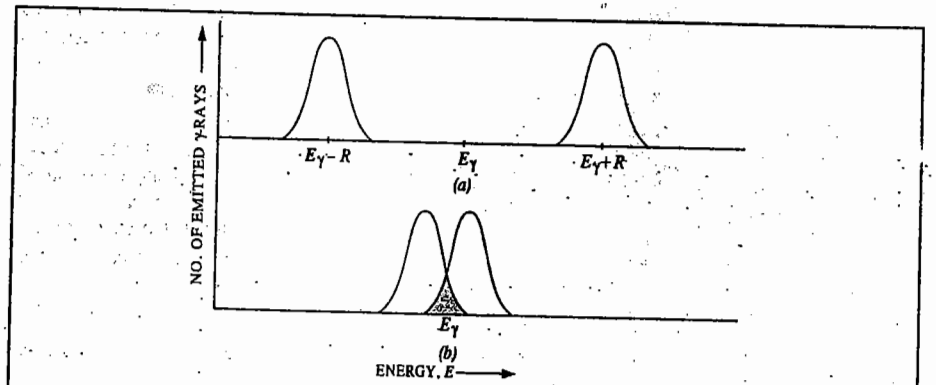

Fig. 55. *(a)* Resonance absorption and emission curves for $2R > \Gamma$.
(b) Resonance absorption and emission curves for $2R \approx \Gamma$.

Let us make an order-of-magnitude calculation. For the Mössbauer nuclide ^{57}Fe, it is found experimentally that E_γ = 14·4 keV; and $M = 1{\cdot}67 \times 10^{-27}$ kg. Hence, using Eq. 70, $R = 2 \times 10^{-3}$ eV. The life-time of the lowest excited state of ^{57}Fe is 10^{-7} s which, using Eq. 64, corresponds to Γ-value of about 5×10^{-9} eV. In other words, $R >> \Gamma$. Obviously, the resonance absorption condition, *viz.*, $\Gamma \approx 2R$ (Eq. 71) is not obtained. Mössbauer devised a very ingenious method to obtain the γ-ray resonance condition. He took the sample (containing the emitter nuclei) in the form of a solid at low temperatures. In the solid the nuclear recoil energy is dissipated among the lattice vibrations or the solid as a whole. Thus, the emitted γ-rays have the energy, E_γ. Likewise, no energy is lost to recoil

for the absorber nucleus. It should be noted that Mössbauer effect cannot be observed in liquids and gases because the recoil energy cannot be dissipated in these states of matter.

Mössbauer Experiment. The set-up that Mössbauer designed for his experiment is very simple (Fig. 56). The Doppler motion is given to the source, *i.e.*, the source is moved towards the absorber with velocity v by means of a velocity drive. The intersity of the emitted gamma rays is meausred as a function of the Doppler velocity, v. It must be remembered that the Doppler velocity given to the source relative to the absorber is necessary to bring the source and the absorber lines closer to meet the resonance absorption condition; it is *not* required to compensate the recoil energy because the recoil has already been eliminated by taking the sample in the form of a solid. When the source and the absorber move towards each other, the sign of Doppler velocity is taken to be positive. A typical Mössbauer spectrum is shown in Fig. 57.

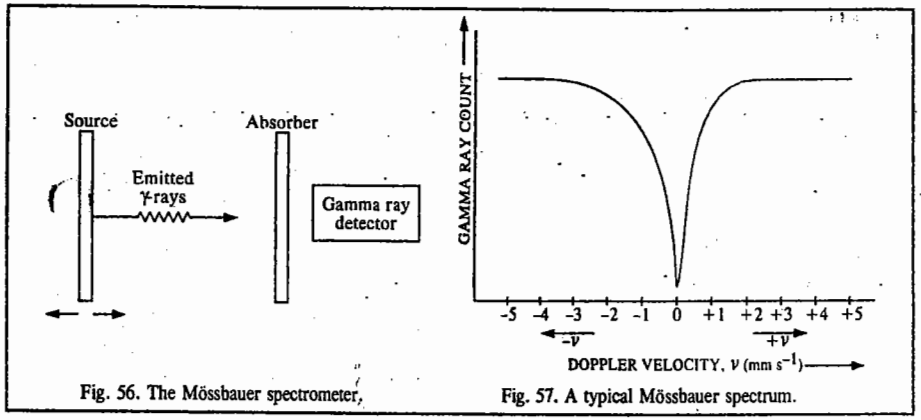

Fig. 56. The Mössbauer spectrometer.

Fig. 57. A typical Mössbauer spectrum.

More about Mössbauer Spectroscopy. Three quantities, called **hyperfine interactions**, are studied by Mössbauer spectroscopy. There are *chemical (isomer) shift* (δ); *nuclear electric quadrupole splitting* (ΔE_Q) and *nuclear Zeeman splitting*.

1. Chemical (Isomer) Shift. As a result of the electrostatic interaction between the nucleus and the electrons in a solid, the nuclear energy levels are shifted in both the source and the absorber. This shift, called the **isomer shift**, is given by

$$\delta = \frac{2\pi}{5} Ze^2 [|\psi_a(0)|^2 - |\psi_s(0)|^2](R_{ex}^2 - R_{gd}^2) \qquad ...(72)$$

where e is the electronic charge, Z the atomic number and R_{ex} and R_{gd} are the radii of the nucleus in the excited and the ground states, respectively. $|\psi_a(0)|^2$ is the electron density evaluated at the nucleus for the absorber and $|\psi_s(0)|^2$ is the corresponding quantity for the source. Since only s electrons have a finite wave function at the nucleus and the p and d electrons have vanishing wave functions at the nucleus, it is only the s electrons which are responsible for the isomer shift.

2. Nuclear Electric Quadrupole Splitting, ΔE_Q. Sometimes, as in the case of ^{57}Fe, the excited state has a nuclear spin > 1; here $I = 3/2$. If the quadrupole moment eQ of the ^{57}Fe nucleus in the absorber interacts with the *EFG* (electric field gradient) that is not spherically symmetric, the resulting interaction splits the excited state energy level into two lines, the splitting being called electric quadrupole splitting, ΔE_Q. The quantity e^2Qq is called nuclear electric quadrupole coupling constant. Fig. 58 illustrates the concepts of isomer shift and electric quadrupole splitting.

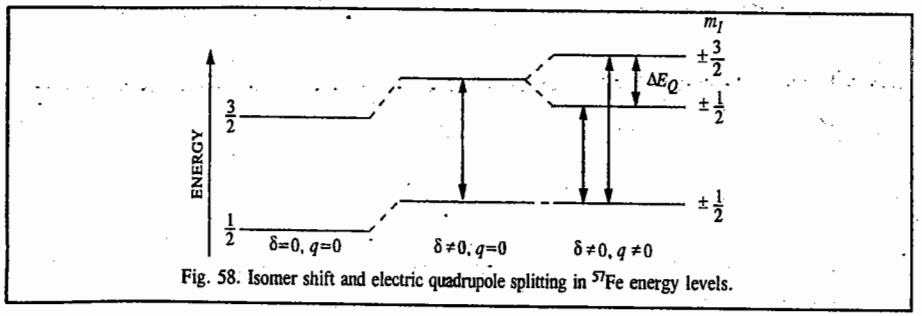

Fig. 58. Isomer shift and electric quadrupole splitting in ^{57}Fe energy levels.

Example 64. The Mössbauer spectrum of $K_4[Fe(CN)_6]$ consists of one line whereas that of $K_3[Fe(CN)_5NO]$ consists of two lines. Draw these spectra qualitatively and account for their appearance.

Solution : *(a)* $K_4[Fe(CN)_6]$. A single line Mössbauer spectrum shows only the effect of isomer shift because for the $[Fe(CN)_6]^{4-}$ anion, being spherically symmetric, $q=0$ (Fig. 59). Also, refer to Fig. 58.

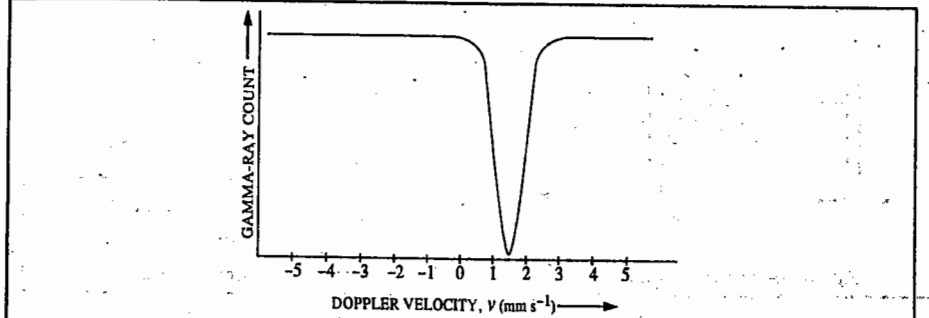

Fig. 59. The Mössbauer spectrum of $K_4[Fe(CN)_6]$. $\delta \neq 0$, $q = 0$

(b) $K_3[Fe(CN)_5NO]$. A two-line spectrum shows the effect of both the isomer shift and the quadrupole splitting because for the $[Fe(CN)_5NO]^{3-}$ anion, being not spherically symmetric, $q \neq 0$ (Fig. 60). Also, refer to Fig. 8.

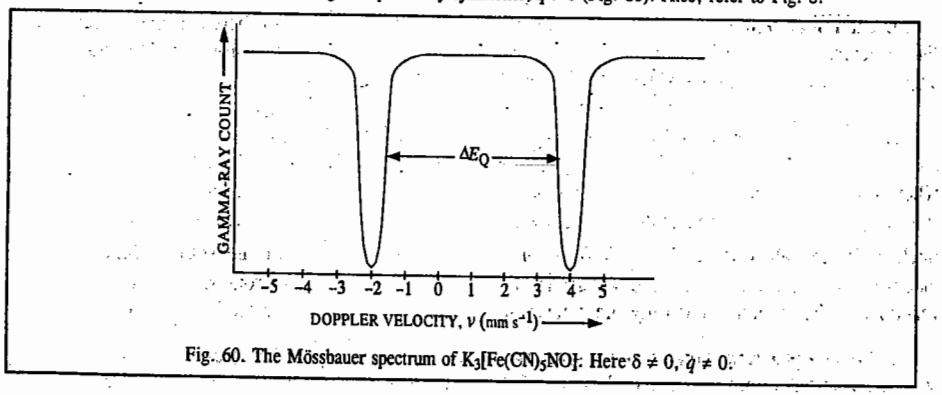

Fig. 60. The Mössbauer spectrum of $K_3[Fe(CN)_5NO]$: Here $\delta \neq 0$, $q \neq 0$.

3. Nuclear Zeeman Splitting (also called **magnetic hyperfine splitting**). The external nuclear Zeeman splitting is caused by the splitting of the nuclear energy levels by the magnetic field, B. In fact, in the metallic state of iron, very large internal magnetic field of the order of about 30 T, exists; this field, too, causes huge splitting. Fig. 61 shows the combined effect of isomer shift ($\delta \neq 0$)

and magnetic field ($\delta \neq 0$, $B \neq 0$) on the Mössbauer spectrum of ^{57}Fe. The selection rule $\Delta m_I = 0, \pm 1$ gives six lines in the spectrum.

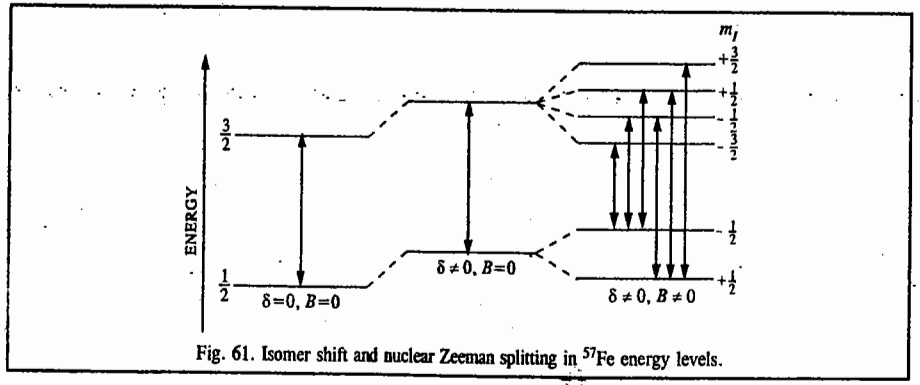

Fig. 61. Isomer shift and nuclear Zeeman splitting in ^{57}Fe energy levels.

PHOTOELECTRON SPECTROSCOPY (PES)

Photoelectron spectroscopy is a very important technique for determining the atomic and molecular energy levels and hence the ionization energies (or the binding energies) of atoms and molecules. Consider a few energy levels of an atom containing electrons with paired spins (Fig. 62). The ionization energy (IE), or preferably, the binding energy (BE) of the atom is defined as the *least* energy required to remove an electron from the highest occupied orbital. The electrons are classified as the ***valence electrons*** and the ***core electrons***. When the atom (or the molecule) is irradiated with ultraviolet (UV) radiation, photoionization occurs by the ejection of the valence electrons which carry away a certain kinetic energy (KE). On the other hand, irradiation by the highly energetic X-rays results in the ejection of the core electrons. The former technique is known as UV-PES or simply UPES and the latter as XPES. In each case, we have

$$h\nu = \text{BE} + \text{KE} \qquad \ldots(73)$$

where $h\nu$ is the photon energy. Thus,

$$\text{BE} = h\nu - \text{KE} \qquad \ldots(74)$$

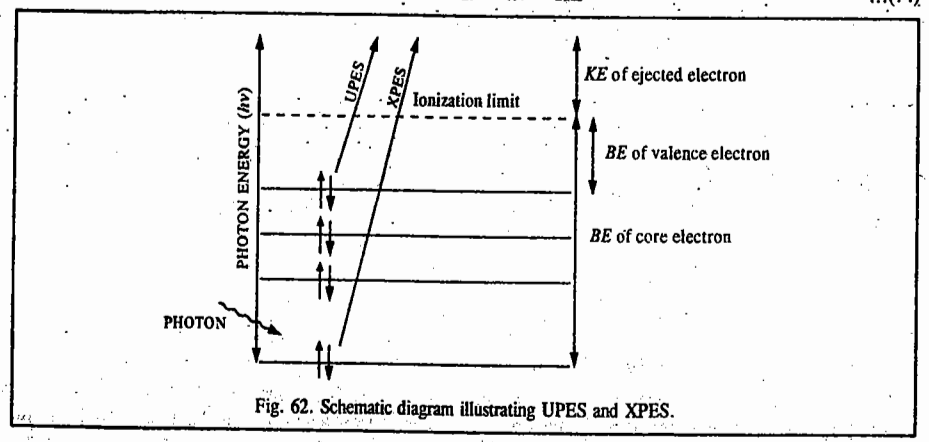

Fig. 62. Schematic diagram illustrating UPES and XPES.

It follows that knowing $h\nu$ and measuring KE, BE can be calculated. It may be mentioned that PES is the technique derived from Einstein's photoelectric effect where a beam of monochromatic

photons, incident on a metal, removes the electrons from the bulk of the metal (the metal is a "sea" of electrons), which carry away the excess kinetic energy. The work function of the metal, which is the energy required to remove the bulk electrons to the surface of the metal, is the analogue of the ionization energy of the atom (or the molecule) in PES. The Swedish physicist K. Siegbahn (1918-) pioneered the experimental and theoretical aspects of PES. He was the cowinner (with N. Bloembergen (1920-) and A.L. Schawlow (1921-)) of the 1981 Physics Nobel Prize.

In UPES, the most commonly used source of UV photons is a helium gas discharge tube; the most intense line has a wave length of 58·4 nm which corresponds to an energy of 21·22 eV. In XPES, we use an X-ray source of higher energy to ionize the inner core electrons. Here the X-ray beam is produced by electron bombardment of a metal target such as aluminium or magnesium. The K_α line for aluminium occurs at 1486·6 eV. Photoelectron spectra are interpreted in terms of **Koopmans' theorem** which states that the ionization energy, IE, is equal to the negative of the energy of the orbital (usually the HOMO) from which the electron is ejected, *i.e.*, $(\text{IE})_i = -E_i$. This very important theorem is, however, only an approximation since it ignores the fact that the remaining electrons adjust their distributions when ionization occurs.

Siegbahn's experimental technique of PES consists in measuring the kinetic energies of the photoelectrons using an electrostatic deflector which produces different deflections in the paths of the photoelectrons as they pass between charged plates. With the increase in field strength, electrons of different speeds and hence different kinetic energies, reach the detector. The photoelectron spectrum is recorded with intensity of electron flux as a function of the kinetic energy.

Atomic PES. The photoelectron spectra of inert gases argon, krypton and xenon, excited by the helium resonance radiation ($h\nu$ = 21·22 eV), are the simplest spectra. In each case, a two-line spectrum with roughly 2 : 1 intensity is obtained (Fig. 63). For argon, we have

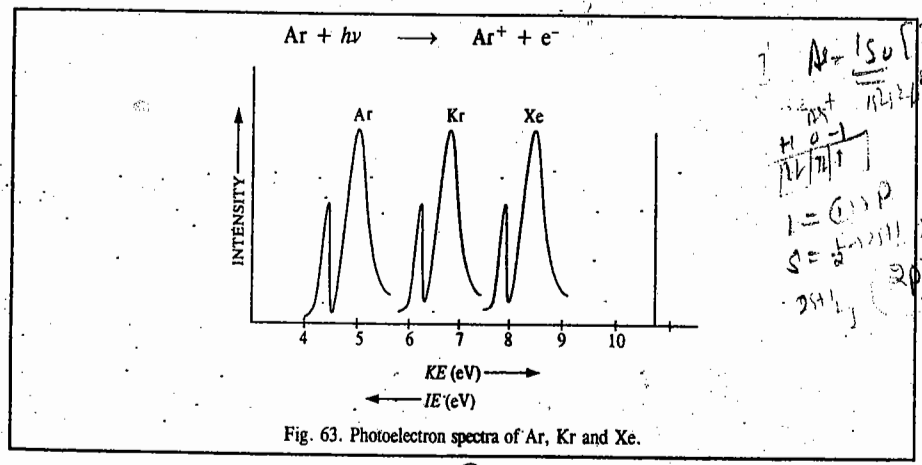

Fig. 63. Photoelectron spectra of Ar, Kr and Xe.

The term symbol of the ground state of Ar is $^1S_0$ while the term symbols of Ar^+ are $^2P_{1/2}$ and $^2P_{3/2}$. The two-line spectrum corresponds to the two transitions $^2P_{1/2} \leftarrow {}^1S_0$ and $^2P_{3/2} \leftarrow {}^1S_0$. For Argon, KE ≈ 5·40 eV (as shown in Fig. 63), so that IE = (21·22 - 5·40) eV ≈ 15·82 eV.

It may be mentioned that PES was earlier called electron spectroscopy for chemical analysis (ESCA) because it was used for research in analytical chemistry.

Applications of PES

1. Orbital Energies of Atoms. The simplest of all atoms, the hydrogen atom, using the 21·2 eV

energy photons from the helium atom, gives a kinetic energy spectrum which shows a single peak at 7·6 eV. The ion cannot have any internal energy because it has no electrons. Hence, the ionization potential of hydrogen atom is (21·2 – 7·6) = 13·6 eV, which is in agreement with values obtained by other methods.

We consider next the photoelectron spectra of the rare gas atoms, studied using the excitation energy $h\nu$ = 40·81 eV (Fig. 64).

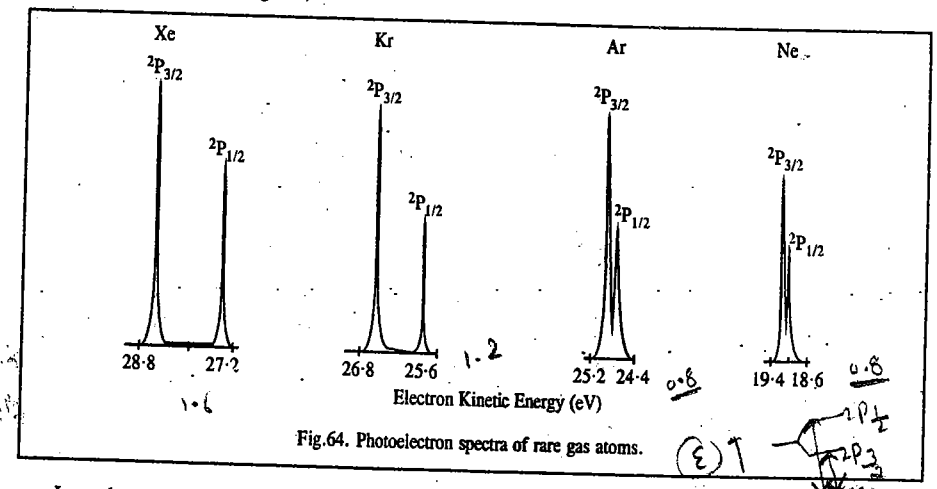

Fig.64. Photoelectron spectra of rare gas atoms.

In each case the spectrum consists of a doublet with the relative intensity in the ratio 2 : 1. The doublet is caused by the formation of two internal energy states of the ion. Argon, for instance, has the electronic configuration $1s^2\ 2s^2\ 2p^6\ 3s^2\ 3p^6$. The removal of the outermost electron gives an ion with the configuration $1s^2\ 2s^2\ 2p^6\ 3s^2\ 3p^5$ which is isoelectronic with chlorine atom. This configuration gives rise to two spin states $^2P_{3/2}$ and $^2P_{1/2}$. If the ionization leads to the lower state $^2P_{3/2}$, the ion has no internal energy and $h\nu = I + E_{el}$. If the ionization produces an upper level $^2P_{1/2}$, then $h\nu = I + E_{el} + E_{ion}$, where E_{ion} is equal to the separation between the two spin-orbit states $^2P_{3/2}$ and $^2P_{1/2}$. The relative intensities of the two peaks depend on the ratio of the degeneracies of the ionic states. Thus, we observe a doublet with the intensity ratio 2 : 1 for the photoelectron spectrum of Ar. If ionization is carried out by more energetic X-ray photons, more peaks are observed in the spectrum of Ar (Fig. 65). The

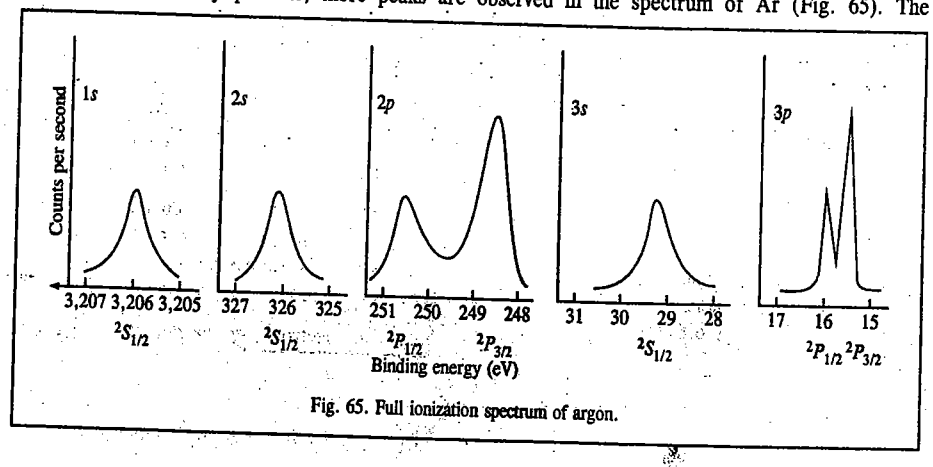

Fig. 65. Full ionization spectrum of argon.

horizontal scale gives the binding energy (BE) which is the energy required to remove the electron to form a particular state of the ion and is calculated by subtracting the photoelectron energy from the photon energy.

2. Orbital Energies of Molecules. In the case of molecules, the nature of the ionization bands produced by the emission of electrons from NBMOs, BMOs and ABMOs follows the following pattern which helps in the assignment of the ionization bands to MOs :

(*a*) If the ionized electron comes from an NBMO, the potential energy curve for the ion is almost the same as the one for the molecule, resulting in a single ionization line.

(*b*) If an electron is removed from a BMO, the bonding in the ion is expected to be weaker than that of the molecule. Hence, the potential energy curve of the ion will be shifted to the direction of longer equilibrium bonds. This gives rise to small vibrational spacing in the spectra, *i.e.*, vibrational fine structure is observed.

(*c*) If an electron is removed from a very strongly BMO or ABMO, the spectrum consists of a broad band, indicating dissociation or predissociation.

Thus, from the appearance of the spectrum and the value of the ionization potentials it is possible to deduce both the nature and the ordering of the MOs. In a high-resolution spectrum, the vibrational fine structure can often provide useful information regarding the nature of the MO involved. The most important applications of PES are in the checking of theoretical (quantum mechanical) calculations and the assignment of electronic spectra.

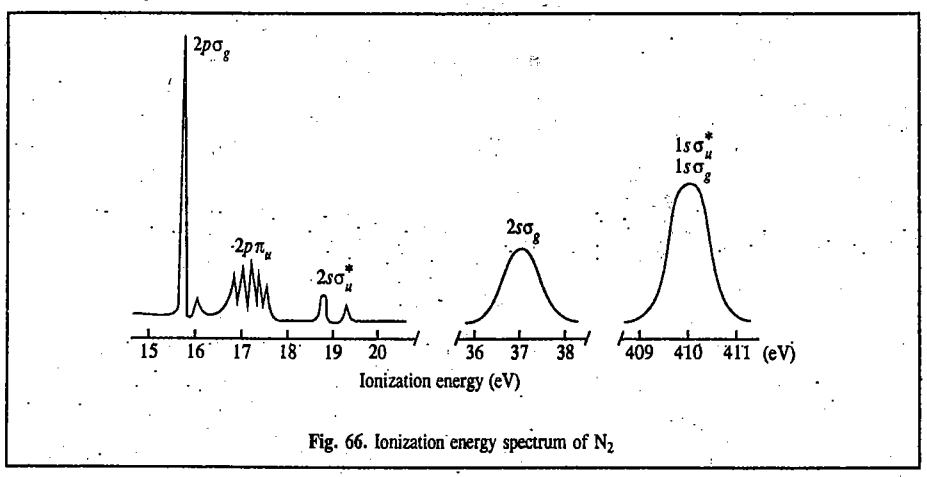

Fig. 66. Ionization energy spectrum of N_2

Fig. 66 gives the ionization energy spectrum of N_2. The molecular orbital pattern is also indicated. We may note that the $2p\sigma_g$ orbital has a lower ionization energy than the $2p\pi_u$ orbital.

3. Binding Energy of Core Electrons. The BE of core electrons varies depending on the electronic environment of the atom in the molecule. Consider the photoelectron spectrum of ethylchloroformate molecule (Fig. 67). In the molecule the electronic environment of each carbon atom is different and hence each one gives a different 1*s* ionization peak at slightly different energies. Binding energy difference of core electrons for non-equivalent atoms of the same kind in a molecule is called **chemical shift**. Chemical shifts can be obtained for the core electrons of all elements except hydrogen since the electron in a hydrogen atom is a valence electron. PES of core electrons has become a very powerful technique for structure determination.

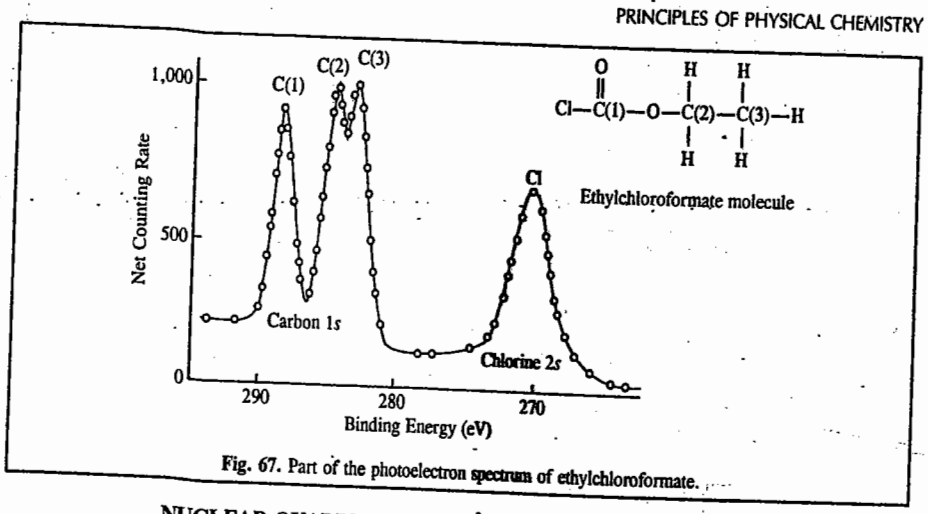

Fig. 67. Part of the photoelectron spectrum of ethylchloroformate.

NUCLEAR QUADRUPOLE RESONANCE (NQR) SPECTROSCOPY

Basic Theory. NQR spectroscopy was discovered in 1950 by physicist H.G. Dehmelt. NQR spectra, like Mössbauer spectra, are observed in the solid state. They are observed in the radiofrequency region. All nuclei having integral and half integral spins $\left(I = 1, \frac{3}{2}, 2, \frac{5}{2}, 3, \frac{7}{2}, \text{etc.}\right)$ possess nuclear electric quadrupole moments, designated as eQ (or simply as Q), where e is the electronic charge. Q is a measure of the deviation of nuclear charge from spherical symmetry. It is defined as

$$Q = \int \rho r^2 (3 \cos^2 \theta - 1)\, dr \qquad ...(75)$$

where ρ is the nuclear charge density, r is the distance from the origin to the element dr and θ is the angle between r and the spin axis. The quadrupole moment Q (or eQ) interacts with the electric field gradient (EFG), designated as q (or eq), created at the quadrupolar nucleus by the asymmetric charge distribution arising from the extranuclear electrons or the non-bonding electrons in the molecule of which the nucleus forms a part. The product of eQ and eq, *i.e.*, e^2Qq is called nuclear quadrupole coupling constant, also sometimes designated as QCC.

It is assumed that the nucleus is centred at the origin of an arbitrarily oriented coordinate system (X, Y, Z). The time-averaged electrostatic potential, V, is produced at the nucleus by all charges outside it. The electric field of all these charges is defined by

$$E = E_X \hat{i} + E_Y \hat{j} + E_Z \hat{k} \qquad ...(76)$$

where $\hat{i}$, $\hat{j}$, $\hat{k}$ are the unit vectors which specify the directions of the axes X, Y and Z, respectively. The components of the electric field are defined as

$$E_X = -(\partial V/\partial X); \quad E_Y = -(\partial V/\partial Y); \quad E_Z = -(\partial V/\partial Z)$$

The electric field gradient components are defined as

$$q_{XX} = -(\partial E_X/\partial X) = \partial^2 V/\partial X^2$$

$$q_{YY} = (\partial^2 V/\partial Y^2); \quad q_{ZZ} = (\partial^2 V/\partial Z^2)$$

Also,

$$q_{XY} = (\partial^2 V/\partial X \partial Y); \quad q_{YZ} = (\partial^2 V/\partial Y \partial Z); \text{ etc.}$$

The nine electric field gradient components may be written as a 3×3 **matrix** (or **tensor**) :

$$\begin{bmatrix} q_{XX} & q_{XY} & q_{XZ} \\ q_{YX} & q_{YY} & q_{YZ} \\ q_{ZX} & q_{ZY} & q_{ZZ} \end{bmatrix} \qquad ...(77)$$

They are found to be a *symmetric tensor* with $q_{ij} = q_{ji}$ so that

$$q_{XY} = q_{YX}; \quad q_{XZ} = q_{ZX}; \quad q_{YZ} = q_{ZY} \qquad ...(78)$$

Hence the EFG tensor given by Eq. 77 can be written as

$$\begin{bmatrix} q_{XX} & q_{XY} & q_{XZ} \\ q_{XY} & q_{YY} & q_{YZ} \\ q_{XZ} & q_{YZ} & q_{ZZ} \end{bmatrix} \qquad ...(79)$$

The diagonal components of this tensor are known to obey the **Laplace equation**

$$q_{XX} + q_{YY} + q_{ZZ} = 0 \qquad ...(80)$$

i.e., $\partial^2 V/\partial X^2 + \partial^2 V/\partial Y^2 + \partial^2 V/\partial Z^2 = 0$

or $$\nabla^2 V = 0 \qquad ...(81)$$

where $\nabla^2 = \partial^2/\partial X^2 + \partial^2/\partial Y^2 + \partial^2/\partial Z^2$ is the Laplacian operator. The four relations given by Eqs. 78 and 80 reduce the number of independent tensor components from nine to five. In general, it is convenient to choose a coordinate system (x, y, z) in which the *cross-components*, q_{ij} are zero. Such a coordinate system is called **principal axis system** and the EFG components in this system are designated as q_{xx}, q_{yy}, q_{zz}. In the principal axis system, we define

$$|q_{zz}| \geq |q_{yy}| \geq |q_{xx}| \qquad ...(82)$$

The modulus sign $|...|$ stands for the absolute value of the components. The largest EFG, q_{zz} is in the z-direction and the smallest EFG, q_{xx} is in the x-direction. From Eq. 80 the sum of the EFG components is zero. It follows, therefore, that only two parameters are needed to specify the EFG tensor. An important quantity, the **asymmetry parameter**, η, is defined as

$$\eta = (q_{xx} - q_{yy})/q_{zz} \qquad ...(83)$$

From Eqs. 80, 82 and 83, we see that the asymmetry parameter lies between 0 and 1, *i.e.*, $0 < \eta < 1$. When $\eta = 0$, we speak of a case of **axial symmetry** around the z-axis. In this case,

$$q_{xx} = q_{yy} = -\tfrac{1}{2} q_{zz} \qquad ...(84)$$

The EFG is said to be **spherical** if $q_{xx} = q_{yy} = q_{zz}$. In this case, there is no interaction of the nuclear quadrupole moment, Q, with the electronic charge distribution. The EFG is said to be nonsymmetric if $q_{xx} \neq q_{yy} \neq q_{zz}$. The following points should be borne in mind about NQR spectroscopy :

1. It is observed for nuclei with $I \geq 1$. When $I < 1$, the nuclei do not possess eQ so that there is no nuclear quadrupole interaction with eq.

2. NQR is observed in the solid state. In the gaseous and the liquid states, because of very fast molecular collisions resulting in a fast tumbling motion, the axis of rotation changes continuously so that EFG, q, averages to zero. Thus, there is no NQR interaction.

3. The quantities e^2Qq, q and η are three most important quantities in NQR spectroscopy. η is a measure of the nonsymmetry of the EFG.

With this digression on EFG, we are now ready to discuss the basic theory of NQR. The solution

of the Schrödinger wave equation for a quadrupolar nucleus having both the integral and half-integral spin ($I \geq 1$) gives the following expression for NQR energy levels :

$$E_{m_I} = \frac{e^2Qq}{4I(2I-1)}[3m_I^2 - I(I+1)]$$

$$= A(3m_I^2 - I(I+1)), \quad \text{where } A = \frac{e^2Qq}{4I(2I-1)} \qquad ...(85)$$

Here $m_I = -I, -I+1, \ldots, +I$; m_I is the component of the nuclear spin I along the axis of quantization, assumed to be the z-axis. The NQR energy level expression involves m_I^2 term; hence, the NQR energy levels are *doubly degenerate*. The selection rule for NQR transitions is $\Delta m_I = \pm 1$. Eq. 85 holds for an *axially symmetric* EFG, *i.e.*, $\eta = 0$.

We shall consider the NQR spectra of the following nuclei, assuming that $\eta = 0$: $^{14}_{7}N(I=1)$; $^{11}_{5}B\left(I=\frac{3}{2}\right)$; $^{35}_{17}Cl\left(I=\frac{3}{2}\right)$; the radioactive isotope $^{36}_{17}Cl^*(I=2)$; $^{27}_{13}Al\left(I=\frac{5}{2}\right)$; $^{132}_{55}Cs\left(I=\frac{7}{2}\right)$.

1. $^{14}_{7}\mathbf{N}$**:** ($I = 1$) so that $m_I = -1, 0, 1$. But, $m_I = -1$ and $m_I = +1$ levels are degenerate. Hence, $I \to 0, \pm 1$. Substituting these values of m_I in Eq. 85, we obtain

$E_0 = -\left(\frac{2}{4}\right)e^2Qq$, $E_{\pm 1} = \left(\frac{1}{4}\right)e^2Qq$. The selection rule $\Delta m_I = \pm 1$ gives only one NQR frequency (Fig. 68).

$$\nu\,(0 \to \pm 1) = (E_{\pm 1} - E_0)/h = \tfrac{3}{4}(e^2Qq/h) \qquad ...(86)$$

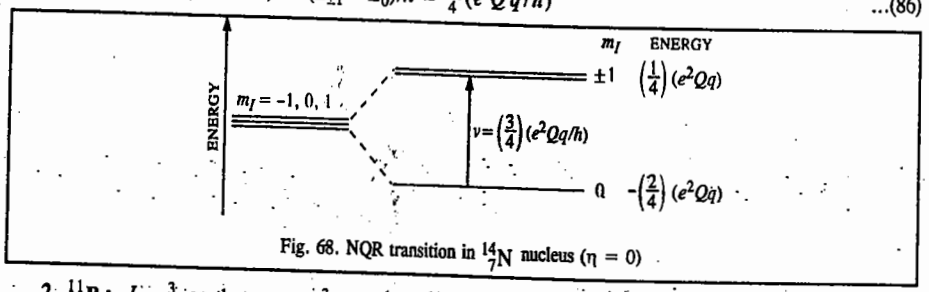

Fig. 68. NQR transition in $^{14}_{7}N$ nucleus ($\eta = 0$)

2. $^{11}_{5}\mathbf{B}$**:** $I = \frac{3}{2}$ so that $m_I = -\frac{3}{2}, -\frac{1}{2}, \frac{1}{2}, \frac{3}{2}$. Because of the m_I^2 term in the energy expression, the NQR interaction splits the $I = \frac{3}{2}$ level into two doubly-degenerate pairs of sublevels, $m_I = \pm\frac{1}{2}$ and $m_I = \pm\frac{3}{2}$. Thus, $I = \frac{3}{2} \to \pm\frac{1}{2}, \pm\frac{3}{2}$. Substituting these values of m_I in Eq. 85 we obtain $E_{\pm\frac{1}{2}} = -\left(\frac{1}{4}\right)(e^2Qq)$ and $E_{\pm\frac{3}{2}} = \left(\frac{1}{4}\right)(e^2Qq)$. The selection rule $\Delta m_I = \pm 1$ gives only one NQR frequency (Fig. 69), *viz.*,

$$\nu\left(\pm\tfrac{1}{2} \leftrightarrow \pm\tfrac{3}{2}\right) = (E_{\pm\,3/2} - E_{\pm\,1/2})/h = \left(\tfrac{1}{2}\right)(e^2Qq/h) \qquad ...(87)$$

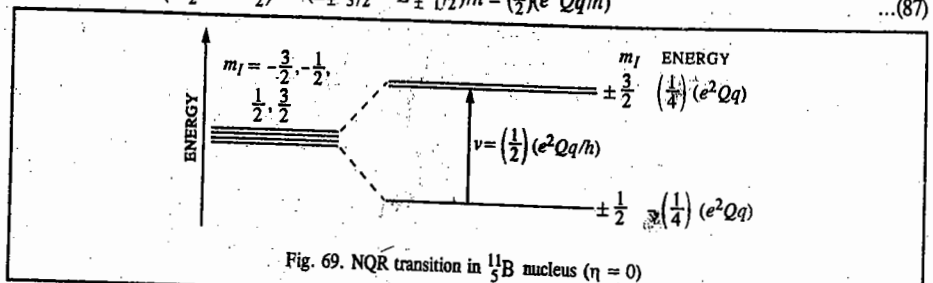

Fig. 69. NQR transition in $^{11}_{5}B$ nucleus ($\eta = 0$)

3. $^{35}_{17}\mathbf{Cl}$**:** $I = \frac{3}{2}$. The frequency is the same as in **(2)** above.

4. $^{36}_{17}\mathbf{Cl}^*$**:** $I = 2$. The NQR interaction gives the following pairs of energy sublevels : $m_I = 0$, ± 1, ± 2 (The $m_I = 0$ sublevel is non-degenerate).

$$E_0 = -\left(\tfrac{1}{4}\right)(e^2Qq); \quad E_{\pm 1} = -\left(\tfrac{1}{8}\right)(e^2Qq); \quad E_{\pm 2} = \left(\tfrac{1}{4}\right)(e^2Qq)$$

The selection rule $\Delta m_I = \pm 1$ gives two NQR frequencies (Fig. 70), *viz.*,

$$\left.\begin{aligned} \nu_1(0 \leftrightarrow \pm 1) &= (E_1 - E_0)/h = \left(\tfrac{1}{8}\right)(e^2Qq/h) \\ \nu_2(\pm 1 \leftrightarrow \pm 2) &= (E_{\pm 2} - E_{\pm 1})/h = \left(\tfrac{3}{8}\right)(e^2Qq/h) \end{aligned}\right\} \qquad ...(88)$$

We see that $\nu_1 : \nu_2 = 1 : 3$.

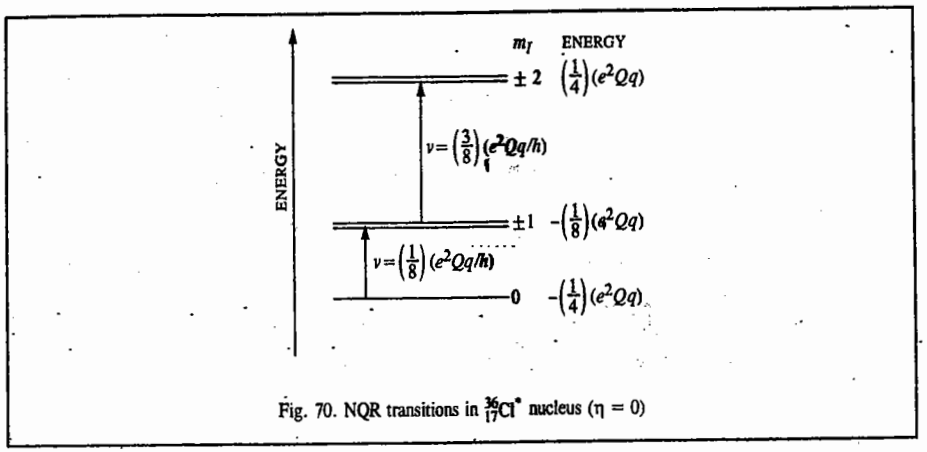

Fig. 70. NQR transitions in $^{36}_{17}Cl^*$ nucleus ($\eta = 0$)

5. $^{27}_{13}\mathbf{Al}$**:** $I = \frac{5}{2}$. The NQR interaction gives the following pairs of degenerate energy sublevels:

$$m_I = \pm\tfrac{5}{2}, \pm\tfrac{3}{2}, \pm\tfrac{1}{2}.$$

Substituting these values of m_I in Eq. 85 we obtain

$$E_{\pm\frac{1}{2}} = \left(-\tfrac{1}{5}\right)(e^2Qq); \quad E_{\pm\frac{3}{2}} = -\left(\tfrac{1}{20}\right)(e^2Qq); \quad E_{\pm\frac{5}{2}} = \left(\tfrac{1}{4}\right)(e^2Qq)$$

The selection rule $\Delta m_I = \pm 1$ gives two frequencies (Fig. 71), *viz.*,

$$\left.\begin{aligned} \nu_1\left(\pm\tfrac{1}{2} \leftrightarrow \pm\tfrac{3}{2}\right) &= \left(E_{\pm\frac{3}{2}} - E_{\pm\frac{1}{2}}\right)/h = \left(\tfrac{3}{20}\right)(e^2Qq/h) \\ \nu_2\left(\pm\tfrac{3}{2} \leftrightarrow \pm\tfrac{5}{2}\right) &= \left(E_{\pm\frac{5}{2}} - E_{\pm\frac{3}{2}}\right)/h = \left(\tfrac{6}{20}\right)(e^2Qq/h) \end{aligned}\right\} \qquad ...(89)$$

We see that $\nu_1 : \nu_2 = 1 : 2$.

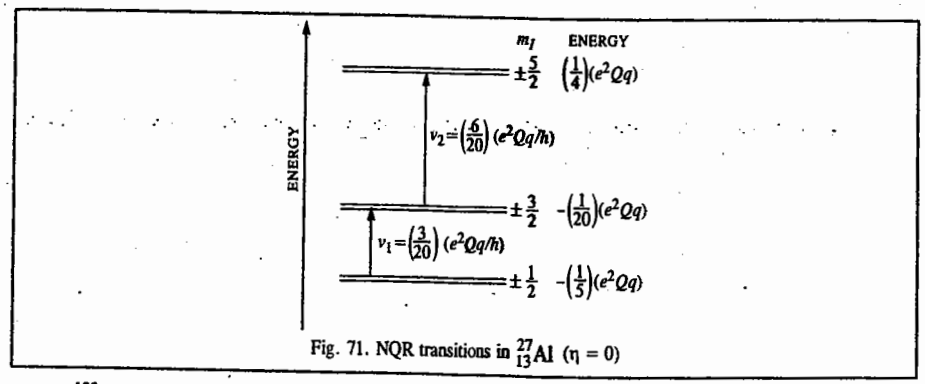

Fig. 71. NQR transitions in $^{27}_{13}Al$ ($\eta = 0$)

6. $^{133}_{55}Cs$: $I = \frac{7}{2}$. The NQR interaction gives the following pairs of degenerate energy sublevels:

$$m_I = \pm\tfrac{7}{2}, \pm\tfrac{5}{2}, \pm\tfrac{3}{2}, \pm\tfrac{1}{2}.$$

$$E_{\pm\frac{7}{2}} = \left(\tfrac{1}{4}\right)(e^2Qq) = \left(\tfrac{21}{84}\right)e^2Qq; \quad E_{\pm\frac{5}{2}} = \left(\tfrac{3}{84}\right)(e^2Qq)$$

$$E_{\pm\frac{3}{2}} = -\left(\tfrac{9}{84}\right)(e^2Qq); \quad E_{\pm\frac{1}{2}} = -\left(\tfrac{15}{84}\right)(e^2Qq)$$

The selection rule : $\Delta m_I = \pm 1$ gives three frequencies (Fig. 72), *viz.*,

$$\left.\begin{aligned}
\nu_1\left(\pm\tfrac{1}{2} \leftrightarrow \pm\tfrac{3}{2}\right) &= \left(E_{\pm\frac{3}{2}} - E_{\pm\frac{1}{2}}\right)/h = \left(\frac{6}{84}\right)(e^2Qq/h) \\
\nu_2\left(\pm\tfrac{3}{2} \leftrightarrow \pm\tfrac{5}{2}\right) &= \left(E_{\pm\frac{5}{2}} - E_{\pm\frac{3}{2}}\right)/h = \left(\frac{12}{84}\right)(e^2Qq/h) \\
\nu_3\left(\pm\tfrac{5}{2} \leftrightarrow \pm\tfrac{7}{2}\right) &= \left(E_{\pm\frac{7}{2}} - E_{\pm\frac{5}{2}}\right)/h = \left(\frac{18}{84}\right)(e^2Qq/h)
\end{aligned}\right\} \quad ...(90)$$

We see that $\nu_1 : \nu_2 : \nu_3 = 1 : 2 : 3$.

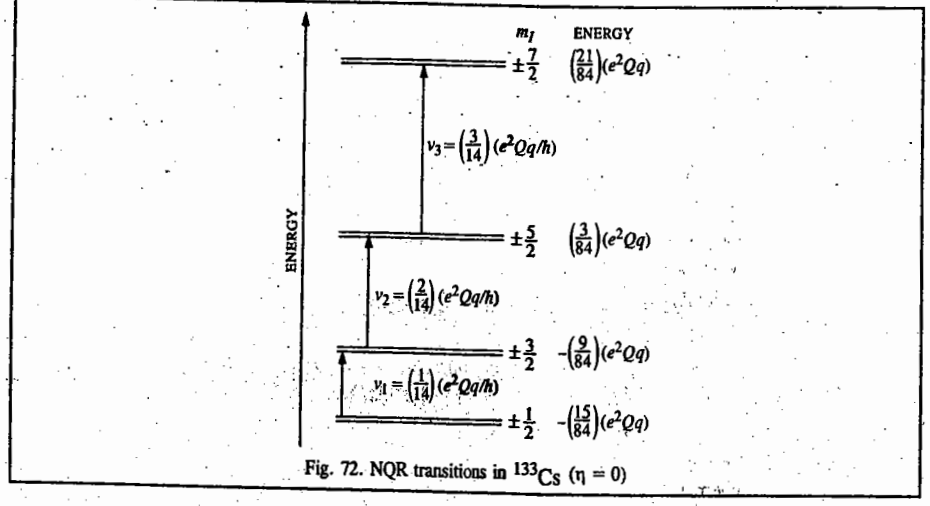

Fig. 72. NQR transitions in ^{133}Cs ($\eta = 0$)

NQR Spectra when EFG is not Axially Symmetric, *i.e.*, $\eta \neq 0$. The NQR spectra in the presence of non-axially symmetric EFG are very complex. The NQR energy level expression contains terms involving η and power of η. For instance, for $I=1$, the energy levels are given by

$$E_0 = -\tfrac{1}{2}(e^2Qq) \quad \text{and} \quad E_1 = \tfrac{1}{4}(e^2Qq)(1 \pm \eta)$$

The Bohr frequency condition and the selection rule $\Delta m_I = \pm 1$ gives the following two NQR frequencies (Fig. 73), *viz.*,

$$\left.\begin{aligned}
\nu_+(0 \rightarrow +1) &= \tfrac{3}{4}(e^2Qq/h)\left(1+\tfrac{1}{3}\eta\right) \\
\nu_-(0 \rightarrow -1) &= \tfrac{3}{4}(e^2Qq/h)\left(1-\tfrac{1}{3}\eta\right)
\end{aligned}\right\} \quad ...(91)$$

They are separated by an amount, $\Delta\nu$, given by $\Delta\nu = \frac{1}{2}(e^2Qq/h)\eta$. Thus, experimental measurement of the two frequencies yields the values of both e^2Qq and η.

For $I = \frac{3}{2}$, the two doubly degenerate energy levels are

$$E_{\pm\frac{1}{2}} = -\tfrac{1}{4}(e^2Qq)\left(1+\tfrac{1}{3}\eta^2\right)^{\frac{1}{2}}$$

$$E_{\pm\frac{3}{2}} = +\tfrac{1}{4}(e^2Qq)\left(1+\tfrac{1}{3}\eta^2\right)^{\frac{1}{2}}$$

The selection rule $\Delta m_I = \pm 1$ gives only one NQR frequency :

$$\nu\left(\pm\tfrac{1}{2} \leftrightarrow \pm\tfrac{3}{2}\right) = \tfrac{1}{2}(e^2Qq/h)\left(1+\tfrac{1}{3}\eta^2\right)^{\frac{1}{2}} \quad ...(92)$$

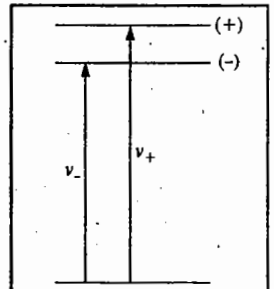

Fig. 73. NQR transitions for $I = 1$ ($\eta \neq 0$)

Since this equation contains two unknowns, e^2Qq and η, measurement of the NQR frequency does not permit them to be determined separately. If, however, from structural considerations η is known to be very small, it can be neglected and e^2Qq determined with sufficient accuracy. When $\eta > 0{\cdot}3$, the frequency expressions for $I = \frac{5}{2}, \frac{7}{2}, \frac{9}{2}$, etc., cannot be rigorously applied. Also, when $I \geq \frac{5}{2}$, we get two or more frequencies the measurement of which can yield both e^2Qq and η. When η is large, it is possible to observe some of the forbidden transitions ($\Delta m_I = \pm 2$), in addition to the strongly allowed transitions ($\Delta m_I = \pm 1$).

Zeeman Effect in NQR Spectra. The determination of both e^2Qq and η for the special case of $I = \frac{3}{2}$, which yields only one NQR frequency, can be done by using Zeeman effect. The applied magnetic (Zeeman) field removes the degeneracy of the $\pm\frac{1}{2}$ and $\pm\frac{3}{2}$ energy sublevels. It is theoretically found that whereas the $-\frac{3}{2}$ sublevel is raised in energy and the $+\frac{3}{2}$ sublevel is lowered, exactly similar splitting does not occur for the doubly degenerate sublevels $\pm\frac{1}{2}$. There occurs considerable *mixing of states* so that the $+\frac{1}{2}$ sublevel partakes some character of $-\frac{1}{2}$ sublevel and vice versa. The resulting sublevels are designated as + and –, respectively. The Zeeman splitting for the case $I = \frac{3}{2}$ is shown schematically in Fig. 74.

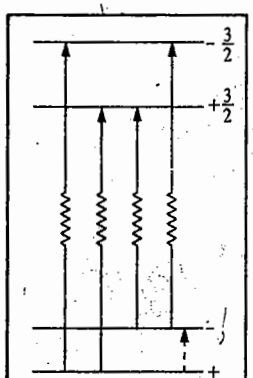

Fig. 74. Zeeman splitting for $I = \frac{3}{2}$ ($\eta \neq 0$)

The application of radiofrequency field brings about transitions between the different sublevels. The $+ \rightarrow -$ transition, shown by the dotted arrow, is of no interest since it involves a frequency much smaller than the NQR frequency. When the Zeeman field is of the order of 0·01 T, as is the case with several nuclei of chemical interest, this frequency is of the order of 0·1 MHz (or even less). This $+ \rightarrow -$ transition between the mixed states $\psi_{\pm}$ corresponds to the selection rule $\Delta|m_I| = 0$. The $\Delta|m_I| = 0$ transition, $+\frac{3}{2} \leftrightarrow -\frac{3}{2}$, not shown in Fig. 66, too, is of no interest. The $\Delta|m_I| = \pm 1$ transitions between the mixed states $\psi_{\pm}$ and the $\psi_{\pm 3/2}$ states give rise to the following four frequencies :

$$\left.\begin{aligned} \nu_\alpha \equiv \nu\left(+ \rightarrow +\tfrac{3}{2}\right);\ \nu_{\alpha'} \equiv \nu\left(- \rightarrow +\tfrac{3}{2}\right) \\ \nu_\beta \equiv \nu\left(+ \rightarrow -\tfrac{3}{2}\right);\ \nu_{\beta'} \equiv \nu\left(- \rightarrow -\tfrac{3}{2}\right) \end{aligned}\right\} \quad ...(93)$$

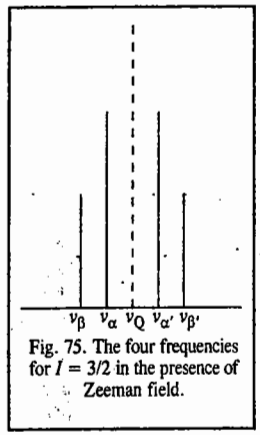

Fig. 75. The four frequencies for $I = 3/2$ in the presence of Zeeman field.

The four frequencies are symmetric about the pure NQR frequency, ν_Q. The inner pair of lines ν_α and $\nu_{\alpha'}$ has equal intensity. Likewise, the outer pair of lines ν_β and $\nu_{\beta'}$ has equal intensity. However, the α, α' pair is more intense than the β, β' pair (Fig. 75).

For a given orientation of the Zeeman field, both pairs of components α, α' and β, β' have maximum intensity when the *r.f.* field is perpendicular to the symmetry axis of the EFG tensor. Also, the intensity of the two pairs depends upon the orientation of the Zeeman field. Omitting the details of the intensity of the spectral lines, suffice it to say that from the Zeeman study, the two unknowns e^2Qq and η can be determined from the four *known* frequencies.

Townes-Dailey Theory of Nuclear Quadrupole Coupling

The nuclear quadrupole moment, Q, is known from theories of nuclear structure, but how do we calculate the EFG, q ? This problem was solved in the well, known Townes-Dailey theory proposed in 1949. These researchers suggested that in an atom, the EFG at the nucleus arises due to the electrons in various valence shells. Since closed shells, as well as the s orbitals have spherical symmetry, they do not contribute to the EFG. From the radial distribution functions in the theory of hydrogenic atoms we know that for small values of r (the distance of the electron from the nucleus), the p orbital wave function varies as r, the d orbital wave function varies as r^2, the f orbital wave function varies as r^3, etc. Thus, the probability of an electron being found at the nucleus decreases in the order $s > p > d > f$. Since quantum mechanically for an atom having one valence electron, the *EFG*, q_{atom}, is defined by

$$q_{atom} = -e\int \psi^* \left(\frac{3\cos^2\theta - 1}{r^3}\right)\psi d\tau \quad ...(94)$$

where ψ is the electronic wave function and θ is the angle between the fixed z-axis in space and the radius vector r (from the nucleus to the electron); r, θ, ϕ are the polar coordinates and the integration is over the whole range of coordinates. It follows, therefore, that contribution to q from various electrons (since it involves $<1/r^3>$ -dependence), decreases in the order $q_p >> q_d >> q_f$. As remarked above, q_s, the contribution to q from s electrons, is zero because of spherically symmetric charge distribution. Hence, we conclude that *only p electrons in an atom contribute significantly to* EFG. From Eq. 94 it can be shown theoretically that

$$q_{atom} = -\frac{2le}{2l+3} <1/r^3> \quad ...(95)$$

where l is the orbital angular momentum of the electron and $<1/r^3>$ is the expectation value (the average value) of the distance between the electron and the nucleus. The EFG gives an information about the electronic structure of an atom.

The above treatment can be extended to molecules. As in the case of atoms, in a molecule the EFG at a given nucleus due to valence electrons is given by

$$q_{mol} = -e\int \psi^* \left(\frac{3\cos^2\theta - 1}{r^3}\right)\psi d\tau \quad ...(96)$$

where ψ is now the *molecular* wave function of the electrons. Townes and Dailey used the LCAO-MO approximation for ψ :

$$\psi = \sum_i c_i \phi_i \quad ...(97)$$

where ϕ_is are the AOs and c_i the appropriate coefficients. The Townes-Dailey theory showed that the significant contribution to EFG at a nucleus in a molecule is due to the p type valence electrons involved in chemical bonding as well as the p type lone pair electrons. Contributions from the various polarization effects on the inner shells as well as other charges in the molecule are negligible.

The EFG can essentially arise from *asymmetry* in the electron distribution about the nucleus. Filled electron shells can, to a first approximation, be regarded as spherical. They can make a contribution to the EFG when they are polarized by the outer electrons or other charges (**Sternheimer effect**); this contribution can be substantial but is usually difficult to determine and is thus ignored. Non-bonding electrons in the valence shell of the atom being investigated make the biggest contribution. Thus, atoms with one, two or three lone pairs usually show very large values of the QCC. The next largest contribution arises from the electrons in the bonds to the ligands. Since these are shared with the ligand atoms, their average distance from the quadrupolar nucleus is greater than that of the non-bonding electrons. When the arrangement of bonds has symmetry less than cube, there will be a contribution to EFG. For instance, there is an EFG at the nucleus of the M atom in the molecule MAB_5 which depends upon the difference in the nature of the M–A and M–B bonds. Also, in a molecule, the electronic structure near a nucleus depends on the hybridization of the bonding orbital and the ionic character of the bond. The equation relating e^2Qq_{mol} of a halogen atom to e^2Qq is given by

$$e^2Qq_{mol} = [1 - s + d - i\,(1 - s - d)]\, e^2Qq \quad ...(98)$$

where s and d denote the amount of s and d character of the bonding orbital and i is the ionic character of the bond. If π bond is also present, then Eq. 98 is modified to

$$e^2Qq_{mol} = (1 - s + d - i - \pi)\, e^2Qq_{atom} \quad ...(99)$$

Applications of NQR Spectroscopy. As we see from Eqs. 98 and 99, a comparison of the QCCs in the atomic and the molecular state for the same nucleus gives information about the extent of hybridization and the ionic character (*i.e.*, **ionicity**) of the bond. The halogens have been extensively studied by NQR. The commonest isotopes investigated are those of chlorine and bromine, since the resonances occur in accessible regions and several halogen compounds are available. Both elements have two naturally occurring isotopes and all have I=3/2. Thus, even when all atoms occupy crystallographically identical sites, two resonances should be observed, one for each isotope. They may be recognized both from their relative intensities, 3 : 1 for ^{35}Cl : ^{37}Cl or 1 : 1 for ^{79}Br : ^{81}Br, and from their relative frequencies, 1·27 : 1 or 1·19 : 1, respectively (this is the ratio of the Qs since both must be in the same EFG). To calculate the ionicity of the interhalogen bond, for instance, we make the following reference points : (*i*) the free halogen molecule, in which the p_z-orbital of

each atom effectively contains a single electron (the p_x and p_y orbitals contain lone pairs of electrons), *(ii)* the halide ion, which is spherical and must have zero EFG. In these molecules the observed QCC is used to interpolate between the two reference values :

$$\text{Ionic character} = 1 - \frac{(e^2Qq/h)_0}{(e^2Qq/h)} \qquad \ldots(100)$$

in which $(e^2Qq/h)_0$ is the value corresponding to the halogen molecule (the halogen atom).

Table 10 gives the QCCs (quadrupole coupling constants, e^2Qq/h) of some halogen isotopes (^{35}Cl, ^{70}Br and ^{127}I) and some of their compounds.

TABLE 10

QCCs of Some Halogens and their Compounds

Molecule	e^2Qq/h (MHz)	Molecule	(e^2Qq/h) (MHz)
Cl (atomic)	109	CH_3Cl	75
Br (atomic)	769	NaBr	58
I (atomic)	2293	KBr	10·2
Br—Cl	104	CH_3Br	529
ICl	82·5	NaI	260
KCl	0·04	KI	60

NQR studies also confirm the dimeric nature of the Group III halides of the type MX_3 (which is also confirmed by X-ray diffraction). In the molecule $AlBr_3$, for instance, the basic halogen NQR spectrum consists of three resonance lines : two are closely spaced together and are far above the third. This indicates that the three halogen nuclei are not chemically equivalent. In the dimer molecule, therefore, there are two types of halogen atoms corresponding to the bridge and end positions :

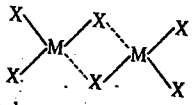

The small difference of one set of halogen resonances is presumably due to a small difference in the crystalline field around the chemically equivalent set of atoms.

Example 47. Enumerate the NQR frequencies for a nucleus with $I = 9/2$ in an axially symmetric EFG ($\eta = 0$). How do they arise ?

Solution : For $I = \frac{9}{2}$, $m_I = \pm\frac{9}{2}, \pm\frac{7}{2}, \pm\frac{5}{2}, \pm\frac{3}{2}$ and $\pm\frac{1}{2}$ because of the presence of the m_I^2 term in the energy level expression. The selection rule $\Delta m_I = \pm 1$ gives four resonances as a result of NQR interaction :

$$\nu_1\left(\pm\tfrac{1}{2} \leftrightarrow \pm\tfrac{3}{2}\right);\quad \nu_2\left(\pm\tfrac{3}{2} \leftrightarrow \pm\tfrac{5}{2}\right);\quad \nu_3\left(\pm\tfrac{5}{2} \leftrightarrow \pm\tfrac{7}{2}\right);\quad \nu_4\left(\pm\tfrac{7}{2} \leftrightarrow \pm\tfrac{9}{2}\right)$$

Example 48. The NQR frequency for a nucleus with $I = \frac{3}{2}$ in an axially symmetric EFG ($\eta = 0$) is 100 MHz. Calculate e^2Qq/h.

Solution : $\nu = \frac{1}{2}(e^2Qq/h)$. Hence, $e^2Qq/h = 2\nu = 2\ (100\ \text{MHz}) = 200\ \text{MHz}$

Example 49. A quantity of interest in NQR spectroscopy is the fraction of the unbalanced p electrons, U_p, defined as $U_p = -\frac{(e^2Qq)_{\text{observed}}}{(e^2Qq)_{\text{for one electron}}}$. At 20 K, t-butylchloride shows two NQR frequencies

at 31·195 MHz and 24·586 MHz, the former being more intense. How do you account for these results ? Also, calculate U_p for ^{35}Cl and ^{37}Cl. Given (e^2Qq/h) for atomic chlorine is −109·6 MHz.

Solution : The more intense frequency is due to the more abundant isotope ^{35}Cl and the weaker frequency is due to the less abundant isotope ^{37}Cl. Since $I = 3/2$ for both the nuclei, hence

$\nu\left(\pm\frac{1}{2} \leftrightarrow \pm\frac{3}{2}\right) = \frac{1}{2}(e^2Qq/h)$ (assuming $\eta = 0$), so that

$(e^2Qq/h) = 2\nu = 62{\cdot}39$ MHz (for ^{35}Cl) and 49·17 MHz (for ^{37}Cl). The Cl atom, $1s^2\ 2s^2\ 2p^6\ 3s^2\ 3p_x^2\ 3p_y^2\ 3p_z^1$, contains one electron in the $3p_z$ orbital and is thus said to have $U_p = 1$. The (e^2Qq/h) value for atomic chlorine is −109·6 MHz. Hence, for ^{35}Cl,

$$U_p = \frac{-62{\cdot}39}{-109{\cdot}6} = 0{\cdot}573$$

Similarly, the U_p value for ^{37}Cl can be calculated.

For details, see T.P. Das and E.L. Hahn, *Nuclear Quadrupole Resonance Spectroscopy*, Academic Press, 1958.

I. Review Questions

1. Draw the NMR spectrum of a bare proton using an energy level diagram and the appropriate selection rule.
2. Why are NMR spectra observed in the rf region and the ESR spectra in the microwave region ?
3. What is the principle of Fourier-transform NMR ?
4. Discuss the relaxation processes in magnetic resonance spectroscopy.
5. Write short notes on nuclear magnetic double resonance and NOE.
6. Discuss the use of the lanthanide shift reagents in NMR.
7. How is NMR used in studying hindered rotation in molecules ?
8. Draw the ESR spectra of

   (i) an unpaired electron, *(ii)* hydrogen atom, *(iii)* methyl radical, *(iv)* triphenylmethyl radical. How do they arise ?
9. Illustrate, using energy level diagrams, Kramers' degeneracy and ZFS.
10. Discuss the ESR spectra of transition metal complexes.
11. Illustrate diagrammaticaly the combined effects of isomer shift, Zeeman effect and hyperfine splitting in Mössbauer spectra.
12. Write notes on : *(i)* Photoelectron spectroscopy (PES), *(ii)* Nuclear Quadrupole Resonance (NQR) spectroscopy.
13. Discuss the important applications of PES.

II. Problems

1. The low resolution pmr spectrum of a compound of molecular formula C_2H_4O consists of two peaks, the intensity of one being thrice that of the other. The high resolution pmr spectrum shows that the peak with low intensity is split into four components of relative intensity 1 : 3 : 3 : 1 and the peak with high intensity is split into a doublet with relative intensity 1 : 1. Identify the structure of the compound. **[Ans. $CH_3CH{=}O$]**
2. Describe the high resolution pmr spectrum of 1,1,2-trichloroethane.

[Ans. Triplet (1 : 2 : 1 intensities) and doublet (1 : 1 intensities.]

3. A compound with the empirical formula $C_4H_{10}O$ gave a pmr spectrum consisting of two groups of peaks with relative areas 3 and 2. Another substance with the same formula gave a pmr spectrum consisting of two peaks with relative areas 9 and 1. Identify the two compounds. **[Ans. diethyl ether, and *t*-butyl alcohol]**

4. A compound $C_{10}H_{14}$ shows two 2 pmr singlets : *A* at $\delta = 8{\cdot}0$ ppm and *B* at $\delta = 1{\cdot}0$ ppm. The ratio of their intensities is $A : B = 5 : 9$. What structure is consistent with these data ?

[Ans. *A* is caused by aromatic ring Hs and *B* by alkyl Hs. The structure is $C_6H_5C(CH_3)_3$.]

5. The nmr spectrum of a compound $C_3H_5ClF_2$ has 2 noncoupled triplets. Triplet *A* is 1·5 times the intensity of the more downfield triplet *B*. Suggest a structure. **[Ans. $ClC^BH_2CF_2C^AH_3$]**

6. The pmr spectrum of liquid diketene $C_4H_4O_2$ shows two peaks of equal intensity. What is the structure of the compound ?

7. Predict which of the following species will show ESR spectrum :

(i) $\dot{C}H_3$ *(ii)* $\ddot{C}H_2$ *(iii)* CH_4 *(iv)* H_2 *(v)* O_2 *(vi)* O_2^+ *(vii)* C_6H_6 *(viii)* $C_6H_6^-$ *(ix)* $CH_3CH_2\dot{C}H_2$ *(x)* $(CH_3)_2\dot{C}H$.

[Ans. *(i), (ii), (v), (vi), (viii), (ix) (x)*]

8. The ESR spectrum of a radical having the empirical formula C_3H_7 showed 14 lines with relative intensities of 1, 1, 6, 6, 15. 15, 6, 6, 1 and 1. Identify the radical. **[Ans. isopropyl radical]**

9. Predict the ESR spectrum of benzene radical anion, $C_6H_6^-$.

[Ans. 7 lines with relative intensities of 1 : 6 : 15 : 20 : 15 : 6 : 1]

10. Predict the number of ESR lines in the spectrum of *(a)* $CH_3\dot{C}H_2$ radical *(b)* $CH_3CH_2CH_2\cdot$ radical.

[Ans. *(a)* 12, *(b)* 36]

11. The ESR spectrum of an organic radical containing two carbon atoms consisted of 12 lines having relative intensities of 1, 2, 3, 1, 6, 3, 3, 6, 1, 3, 2 and 1. Identify the radical. **[Ans. $CH_3\dot{C}H_2$]**

12. The irradiation of a crystal of ammonium perchorate by γ-rays produced a free radical whose ESR spectrum consists of 12 lines. Identify the radical $I=(N) = 1$. **[Ans. NH_3]**

13. Predict the ESR spectrum of the hypothetical $\dot{N}H$ radical. **[Ans. 5 lines with relative intensity 1:1:2:1:1]**

14. The line separations in ESR may be expressed in tesla (T) or MHz. Show how the conversion factor $1T = 2{\cdot}80 \times 10^4$ MHz is obtained.

15. An unpaired electron in the presence of two protons gives the following four-line ESR spectrum : $\Delta B/10^{-4}$ T = 0, 1, 3, 4. What are the two coupling constants in T and in MHz ?

[Ans. $a_1 = 3\times10^{-4}$ T or 8·40 MHz ; $a_2 = 1\times10^{-4}$ T or 2·80 MHz]

16. The UV spectrum of acetone shows two peaks at λ_{max}=280 nm, ε_{max}=15, and λ_{max}=190 n, ε_{max}= 100. *(a)* Identify the electronic transition for each *(b)* Which is more intense ?

[Ans. *(a)* The longer wavelength (280 nm) is associated with smaller energy ($\pi^* \leftarrow n$) transition, $\pi^* \leftarrow \pi$ transition occurs at 190 nm. *(b)* $\pi^* \leftarrow \pi$ has the larger ε_{max} and is more intense]

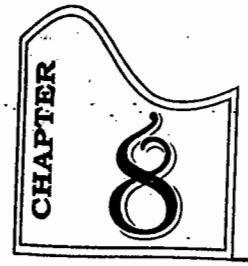

ELECTRIC AND MAGNETIC PROPERTIES OF MOLECULES

ELECTRIC PROPERTIES OF MOLECULES

Considerable structural information about a molecule can be obtained by placing it in an electrostatic field. When a molecule is placed in an electric field, the field distorts the electronic structure and changes the equilibrium positions of the nuclei giving rise to the separation of the centres of positive and negative charges. This is expressed by saying that the electric field induces a dipole moment in the molecule. The *induced dipole moment*, μ_{ind}, is directly proportional to the strength of the applied electrostatic field, *E*, *i.e.*,

$$\mu_{ind} \propto E \qquad ...(1)$$

$$= \alpha E \qquad ...(2)$$

where α, the constant of proportionality, is called the **polarizability** of the molecule. *It is a measure of the ease with which the molecule can be polarized.* From Eq. 2 we see that α is equal to the induced dipole moment generated by unit electric field strength.

The *permanent dipole moment*, μ, of a molecule having two equal charges $+q$ and $-q$, separated by a distance *r*, is defined as

$$\mu = qr \qquad ...(3)$$

The dipole moment has magnitude as well as direction. It is customary to regard it as being directed from the positively charged end towards the negatively charged end.

The dipole moment for a group of point charges q_i is given by

$$\mu = \sum_i q_i r_i \qquad ...(4)$$

where r_i is the vector distance from the origin to the charge q_i.

For a distribution of zero total charge, the dipole moment is equal to the product of the absolute charge of either the positive or the negative distribution and the vector distance *r* between the centres of the two distributions. Thus,

$$\mu = (+q)r = (-q)r \qquad ...(5)$$

Since the electronic charge $q = 1{\cdot}602\times10^{-19}$ C and $r = 10^{-10}$ m, hence,

$$\mu = (1{\cdot}602\times10^{-19}\text{ C})\times(10^{-10}\text{ m}) = 1{\cdot}602\times10^{-29}\text{ C m} = 4{\cdot}8\text{ D}$$

since 1 D (Debye) = $3{\cdot}336\times10^{-30}$ C m.

Polarization of a Molecule in an Electric Field. When a molecule is placed in an electric field, the field polarizes it in the following three ways :

1. Electronic polarization. The field distorts the electronic charge cloud of the molecule. This is called electronic polarization and the corresponding polarizability is termed electronic polarizability, α_e.

2. Atomic polarization. The nuclei, or the atoms, are distorted towards the negative end of the field. The corresponding polarizability is called **atomic polarizability**, α_a.

3. Orientation polarization. The electric field tends to align molecules having a permanent dipole moment along the direction of the field. The corresponding polarizability is called **orientation polarizability**, α_μ.

Thus, the total polarizability (α) of a molecule in an electric field is the sum of the three contributions, *i.e.*,

$$\alpha = \alpha_e + \alpha_a + \alpha_\mu \quad ...(6)$$

$$= \alpha_d + \alpha_\mu \quad ...(7)$$

where α_d ($= \alpha_e + \alpha_a$) is called the **distortion polarizability.**

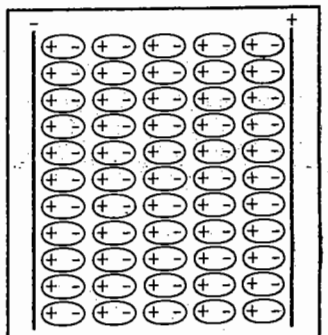

Fig. 1. Orientation of polar molecules in an electric field.

Clausius-Mosotti Equation. Suppose that several molecules of a substance in the solid, liquid or gaseous state are introduced into the space between the plates of a condenser which is charged by applying a constant electrostatic field. The substance is called a *dielectric* and is assumed to be an insulator. The charges on the condenser plates are partially compensated by the induced charges on the boundary of the dielectric (Fig. 1). The electric field strength in the dielectric is, therefore, reduced to a value E from its value E_0 in vacuum, the two quantities being related by the expression

$$E_0 = E + 4\pi P \quad ...(8)$$

where P, called the **dielectric polarization,** is the induced dipole moment per unit volume of the dielectric. Thus, $P = N\mu_{ind}$ where N is the number of molecules per unit volume of the dielectric.

From Eq. 8, $E_0/E = 1 + 4\pi(P/E) = 1 + 4\pi(N\mu_{ind}/E)$ ...(9)

or $\varepsilon_r = 1 + 4\pi N\alpha_d$ ...(10)

where the quantity ε_r ($= E_0/E$) is called the *dielectric constant* or *relative permittivity*. Here we have made use of the fact that $\alpha_d = \mu_{ind}/E$ where α_d, as already mentioned, is the distortion polarizability. The relative permittivity of the medium can be measured experimentally by using the relation.

$$\varepsilon_r = C/C_0 \quad ...(11)$$

where C and C_0 are the capacitances of the condenser with the medium and the vacuum, respectively, as the dielectric between the plates.

Suppose that one mole of a substance of molar volume V_m, density ρ and molar mass M is used as a dielectric. Then,

$$N = N_A/V_m = N_A\rho/M$$

where N_A is the Avogadro number. Hence, Eq. 10 can be written as

$$(\varepsilon_r - 1)M/\rho = 4\pi N_A\alpha_d \quad ...(12)$$

Evidently, the ratio $(\varepsilon_r - 1)/\rho$ is independent of ρ since α_d is a constant for a substance.

Eq. 12 holds for gases at very low pressures when the interaction of the dipole moments between the neighouring molecules is negligible since the molecules are far apart. However, at high pressures and for condensed phases (solids or liquids), this relation does not hold since now interactions between induced moments have to be taken into consideration. Clausius and Mosotti, taking into consideration these interactions for condensed phases, introduced the following relation :

$$P_m = \frac{\varepsilon_r - 1}{\varepsilon_r + 2} V_m = (4\pi/3)N_A\alpha_d \quad ...(13)$$

where the quantity P_m is called **molar polarization.** Eq. 13 is known as the **Clausius-Mosotti equation.**

Relative permittivity, ε_r, is also defined as $\varepsilon_r = \varepsilon/\varepsilon_0$ where ε is the permittivity of the medium and ε_0 is the permittivity of free space. In SI system, the Clausius-Mosotti equation is written as

$$P_m = \frac{\varepsilon_r - 1}{\varepsilon_r + 2} V_m = (N_A/3\varepsilon_0)\alpha_d \quad ...(14)$$

Since α_d (*viz.*, distortion polarizability) is a characteristic constant of a molecule, hence P_m, according to Eq.13, should be a constant, independent of density or temperature. This has been verified experimentally for non-polar molecules such as H_2, CO_2, CH_4, CCl_4, etc., which do not have a permanent dipole moment. The Clausius-Mosotti equation is not obeyed by polar molecules such as HCl, H_2O, NH_3, etc., which possess a permanent dipole moment.

Debye Equation. In 1912, Debye considered the behaviour of polar molecules placed between the plates of a condenser. In the absence of the electric field, as a result of thermal motion, the molecules are randomly oriented so that there is no *net* dipole moment in any direction (Fig. 2*a*). However, on the application of the electric field across the plates of the condenser, the molecules under the combined influence of the electric field and the thermal motion orient themselves as shown in Fig. 2*(b)*.

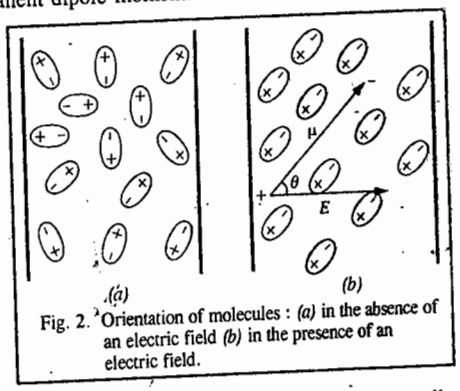

Fig. 2. Orientation of molecules : *(a)* in the absence of an electric field *(b)* in the presence of an electric field.

Debye calculated the average component of the permanent dipole moment μ of a molecule in the direction of the electric field as a function of temperature.

For a randomly oriented dipole in the absence of electric field, all orientations are equally probable. This means that the number of dipole moments directed within a solid angle $d\omega$ is $Ad\omega$, where A is a constant which depends on the number of molecules under observation.

The potential energy, U, of a polar molecule with molecular dipole moment μ oriented at an angle θ to the electric field of strength E is given by

$$U = -\mu E \cos\theta \quad ...(15)$$

According to the Boltzmann distribution, the number of molecules oriented within the solid angle $d\omega$ is given by

$$dN = A \exp(-U/kT)\, d\omega \quad ...(16)$$

$$= A \exp(\mu E \cos\theta/kT)\, d\omega \quad ...(17)$$

Hence, the average value of the dipole moment in the direction of the field is given by

$$\bar{\mu}_{ind} = \frac{\int A \exp(\mu E \cos\theta/kT)\mu\cos\theta\, d\omega}{\int A \exp(\mu E \cos\theta/kT)\, d\omega} \quad ...(18)$$

where the integrals are taken over all the possible orientations. Putting $\mu E/kT = x$ and $\cos\theta = y$ (so that $dy = \sin\theta\, d\theta$), we have

$$d\omega = 2\pi \sin\theta\, d\theta = 2\pi dy \quad ...(19)$$

Thus, Eq. 18 takes the form,

$$\frac{\bar{\mu}_{ind}}{\mu} = \frac{\int_{-1}^{+1} e^{xy} y\, dy}{\int_{-1}^{+1} e^{xy}\, dy} \quad ...(20)$$

Using the standard integrals,

$$\int_{-1}^{+1} e^{xy} dy = (e^x - e^{-x})/x \quad ...(21)$$

and $$\int_{-1}^{+1} e^{xy} y\,dy = (e^x - e^{-x})/x - (e^x - e^{-x})/x^2 \quad ...(22)$$

we find that $$\frac{\bar{\mu}_{ind}}{\mu} = \frac{e^x + e^{-x}}{e^x - e^{-x}} - \frac{1}{x} = \coth x - \frac{1}{x} \equiv L(x) \quad ...(23)$$

where $L(x)$ is called the **Langevin function.** The Langevin function is plotted in Fig. 3. At room temperature, $x << 1$ so that on expanding $L(x)$ as a power series, only the first term needs to be retained, giving $L(x) = x/3$ so that

$$\bar{\mu}_{ind} = (\mu^2/3kT)E \quad ...(24)$$

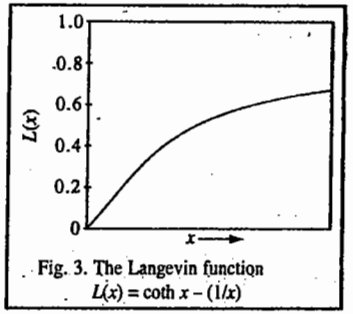

Fig. 3. The Langevin function $L(x) = \coth x - (1/x)$

Notice that $\bar{\mu}_{ind}$ decreases with increasing temperature ; also, $\bar{\mu}_{ind}$ is directly proportional to E. It must, however, be pointed out that the proportionality between $\bar{\mu}_{ind}$ and E cannot be maintained if E is large since in that case *saturation* occurs. Thus, if all the molecules are completely oriented, further increase in E will not increase $\bar{\mu}_{ind}$.

Defining the orientation polarizability α_μ as $\alpha_\mu = \bar{\mu}_{ind}/E$, we find from Eq. 24 that

$$\alpha_\mu = \mu^2/3kT \quad ...(25)$$

We see that α_μ depends upon the permanent dipole moment μ and the temperature. It decreases with increasing T. At higher temperatures, thermal motion reduces the dipole orientation in the field. Thus, from Eq. 7,

$$\alpha = \alpha_d + \mu^2/3kT \quad ...(26)$$

In Clausius-Mosotti equation, the term α_μ had been ignored. Debye, however, took into consideration both α_d and α_μ when Clausius-Mosotti equation takes the form

$$P_m = \frac{\varepsilon_r - 1}{\varepsilon_r + 2} V_m = \frac{4}{3}\pi N_A \left(\alpha_d + \frac{\mu^2}{3kT}\right) \quad ...(27)$$

In SI units, $$P_m = \frac{\varepsilon_r - 1}{\varepsilon_r + 2} V_m = \left(\frac{N_A}{3\varepsilon_0}\right)\left(\alpha_d + \frac{\mu^2}{3kT}\right) \quad ...(28)$$

Eq. 27 or 28 is called the **Debye equation.** According to this equation, P_m varies linearly with $1/T$. The slope and the intercept of the linear Debye plot are $(4/9)\pi N_A\mu^2/k$ or $(1/9\varepsilon_0)N_A\mu^2/k$ and $(4/3)\pi N_A\alpha_d$ or $(1/3\varepsilon_0)N_A\alpha_d$, respectively. From the slope and the intercept, μ and α_d of the molecule can be determined. The Dutch physicist, Peter Debye (1884–1966) was awarded the 1936 Chemistry Nobel Prize for contributions to molecular structure through his work on dipole moments.

Fig. 4 shows the linear plots for a gaseous non-polar molecule (such as CH_4 with $\mu=0$) and a gaseous polar molecule (such as HCl with $\mu \neq 0$). For a non-polar molecule, since $\mu=0$, the plot of P_m versus $1/T$ yields a straight line parallel to the $1/T$ axis.

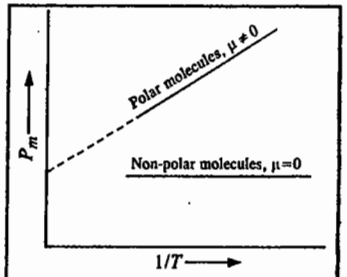

Fig. 4. Plots of P_m versus $1/T$ for gaseous polar and non-polar molecules.

Remarks on units. The units of polarizability can be deduced from Eq. 2 as follows. Since E is expressed as V m^{-1} (volt per metre) and μ_{ind} is expressed in C m, hence from dimensional analysis,

$$\alpha = \frac{\mu_{ind}}{E} = \frac{\text{C m}}{\text{V m}^{-1}} = \frac{\text{C m}}{\text{J C}^{-1}\,\text{m}^{-1}} = \text{J}^{-1}\,\text{C}^2\,\text{m}^2$$

It is customary to define **polarizaibility volume** (α') as $\alpha' = \alpha_d/4\pi\varepsilon_0$. Thus, α' has the units of volume :

$$\alpha' = \frac{\alpha_d}{4\pi\varepsilon_0} = \frac{\text{J}^{-1}\text{C}^2\,\text{m}^2}{\text{J}^{-1}\text{C}^2\,\text{m}^{-1}} = \text{m}^3$$ (The units of ε_0 are $J^{-1}\ C^2\ m^{-1}$).

The dipole moments, the polarizabilities and the polarizability volumes of some common molecules obtained from the Debye equation are given in Table 1.

TABLE 1

Dipole Moments, Polarizabilities and Polarizability Volumes of Some Common Molecules

Molecule	Dipole Moment		Polarizability	Polarizability volume
	$\mu/10^{-30}$ (C m)	μ (D)	$\alpha/10^{-40}$ ($J^{-1}\ C^2\ m^2$)	$\alpha'/10^{-30}$ (m^3)
H_2	0	0	0·91	0·82
N_2	0	0	1·97	1·77
CO_2	0	0	2·93	2·63
CO	0·39	0·12	2·20	1·98
HF	6·37	1·91	5·67	0·51
HCl	3·60	1·08	2·93	2·63
HBr	2·67	0·80	4·01	3·61
HI	1·40	0·42	6·06	5·45
H_2O	6·17	1·85	1·65	1·48
NH_3	4·90	1·47	2·47	2·22
CCl_4	0	0	11·70	10·50
$CHCl_3$	3·37	1·01	9·46	8·50
CH_2Cl_2	5·24	1·57	7·57	6·80
CH_3Cl	6·24	1·87	5·04	4·53
CH_4	0	0	2·89	2·60
C_6H_6	0	0	11·61	10·41
He	0	0	0·22	0·20
Ar	0	0	1·85	1·66

The value of α' for hydrogen atom is $0{\cdot}66\times10^{-30}$ m^3 whereas the values for alkali metals, in units of 10^{-30} m^3, are as follows : Li(12), Na(27), K(34). Notice the high polarizability volumes of the alkali metal atoms. This is due to easy distortion of valence electron density by the electric field.

Example 1. The dipole moment, μ, of HBr is 0·78 D and its dielectric constant (or relative permittivity, ε_r), at 20°C and 1 atm pressure is 1·00313. Calculate its distortion polarizability, α_d and polarizability volume, α'. Given $\varepsilon_0 = 8{\cdot}854\times10^{-12}$ $J^{-1}\ C^2\ m^{-1}$, $4\pi\varepsilon_0 = 1{\cdot}11265\times10^{-10}$ $J^{-1}\ C^2\ m^{-1}$.

Solution : From Eq. 28, $$P_m = \frac{\varepsilon_r - 1}{\varepsilon_r + 2} V_m = \frac{N_A}{3\varepsilon_0}\left(\alpha_d + \frac{\mu^2}{3kT}\right) \quad ...(i)$$

Under the given conditions of temperature and pressure, HBr behaves as an ideal gas with molar volume V_m given by $V_m = M/\rho = RT/P^0$, *i.e.*,

$$V_m = \frac{RT}{P^0} = \frac{8{\cdot}206\times10^{-5}\,\text{m}^3\,\text{atm}\,\text{mol}^{-1}\text{K}^{-1})(293\text{K})}{1\text{atm}} = 2{\cdot}40\times10^{-2}\ \text{m}^3\ \text{mol}^{-1}$$

$$\therefore \quad P_m = \frac{1{\cdot}00313 - 1}{1{\cdot}00313 + 2} \times (2{\cdot}40\times10^{-2}\ \text{m}^3\ \text{mol}^{-1}) = 0{\cdot}001\ \text{m}^3\ \text{mol}^{-1}$$

$\varepsilon_0 = 8{\cdot}854\times10^{-12}\ J^{-1}C^2m^{-1}$; $k = 1{\cdot}38\times10^{-23}\ JK^{-1}$

$$\mu = 0{\cdot}78 \text{ D} = (0{\cdot}78 \text{ D})\ (3{\cdot}336\times10^{-30} \text{ C m/D}) = 2{\cdot}60\times10^{-30} \text{ C m}$$

Substituting these values in Eq. *(i)*, we obtain

$$\alpha_d = 5{\cdot}5\times10^{-40} \text{ J}^{-1} \text{ C}^2 \text{ m}^2$$

The polarizability volume is given by

$$\alpha' = \frac{\alpha_d}{4\pi\varepsilon_0} = \frac{5{\cdot}5\times10^{-40} \text{ J}^{-1} \text{ C}^2 \text{ m}^2}{1{\cdot}11265\times10^{-10} \text{ J}^{-1} \text{ C}^2 \text{ m}^{-1}} = 4{\cdot}94\times10^{-30} \text{ m}^3$$

Dependence of Polarizability on Frequency. The treatment of polarisation discussed above is based on subjecting molecules to static electric field. When, however, the applied field is oscillating, the Debye equation is not applicable because when the frequency is very high, the permanent dipole moments of molecules cannot orient themselves sufficiently rapidly to align themselves with the ever-changing field direction. The result is that at such high frequencies the permanent dipole moment makes no contribution to the polarization of the molecules. Since a molecule requires about one pico-second (10^{-12} second) to rotate in a liquid, the dipolar contribution vanishes when the dielectric constant (or relative permittivity) is measured at frequencies above 10^{11} Hz (*i.e.*, in the microwave region). Accordingly, it is possible to measure the rate of molecular orientation in liquids by carrying out observations on the variation of polarization with frequency.

At microwave frequencies, the orientation polarization decreases with increase in frequency but thereafter the molecular distortion results in stretching and bending of the molecule by the electric field. This occurs in the infrared region (Fig. 5). When the frequency is so high that it changes more

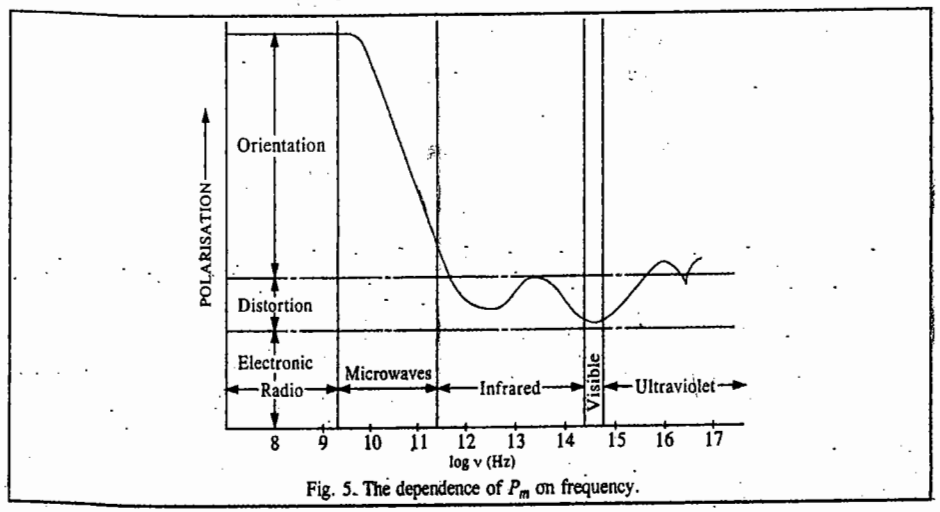

Fig. 5. The dependence of P_m on frequency.

quickly than the time required for the molecule to change its shape (which is the time required for a molecule to vibrate), *the distortion polarization makes no contribution to* P_m. Therefore, at higher frequencies falling in UV and visible regions only the *electronic contribution* to P_m remains. This is because electrons are light enough to respond to the rapidly changing direction of the applied electric field. Thus while in the infrared region, both the nuclei and the electrons follow the electric field, in UV and visible regions only electronic contribution remains.

A light wave is electromagnetic in nature, *i.e.*, it has rapidly changing electric and magnetic fields associated with it. The electric field of the light wave polarizes the medium through which it passes, pulling the electrons back and forth rapidly. Maxwell in his electromagnetic theory of light showed that at optical frequencies the dielectric constant (*i.e.*, relative permittivity) and the refractive index of the medium are related as follows :

$$\varepsilon_r \approx n_r^2 \qquad ...(29)$$

This relation, known as the **Maxwell relation,** holds only when the permanent dipole moment of a molecule does not contribute to ε_r and hence to P_m.

Thus, at optical frequencies, substitution of the Maxwell relation into the Clausius-Mosotti equation (Eq. 14) yields

$$P_m = R_m = \frac{n_r^2 - 1}{n_r^2 + 2} V_m = \frac{N_A \alpha_d}{3\varepsilon_0} \qquad ...(30)$$

where R_m is called **molar refraction.** Eq. 30 is known as the **Lorentz-Lorenz equation.** Using this equation, one can determine induced polarizations from the refractive index measurements. If these data are combined with dielectric data, the dipole moment can be determined from the Debye equation.

Eq. 30 can also be inverted to give an expression for the refractive index of a medium :

$$n_r = \left(\frac{V_m + 2R_m}{V_m - R_m}\right)^{1/2} \qquad ...(31)$$

Eq. 30 can be rearranged to yield an expression for distortion polarizability, α_d :

$$\alpha_d = 3\varepsilon_0 R_m / N_A \qquad ...(32)$$

so that the polarizability volume is given by

$$\alpha' = \alpha_d / 4\pi\varepsilon_0 = 3R_m / 4\pi N_A \qquad ...(33)$$

It may be mentioned that the Maxwell relation $\varepsilon_r \approx n_r^2$ holds only for non-polar molecules. For non-polar molecules ε_r and n_r need not be measured at the same frequency. Since in the case of non-polar molecules the orientation polarizability is absent and the nuclear distortion polarizability is negligible in comparison with the electronic distortion polarizability, it is immaterial whether ε_r and n_r are measured at the same frequency or at different frequencies. This means that the measurement of ε_r and n_r at different frequencies includes only the electronic polarization. Thus, for benzene, a non-polar molecule, $n_r = 1{\cdot}50$ and $\varepsilon_r = 2{\cdot}27$ so that $\varepsilon_r \approx n^2$. However, for water, a polar molecule, $n_r = 1{\cdot}33$ and $\varepsilon_r = 80$ so that $\varepsilon_r \neq n_r^2$. For polar molecules $\varepsilon_r \approx n_r^2$ only if both ε_r and n_r are measured *at the same frequency.*

For a molecule, R_m is additive, *i.e.*, it is equal to the sum of the molar refractions of individual atoms or of individual bonds. Table 2 lists the molar refractions of some common atoms, ions and bonds.

TABLE 2

Molar Refractions at 589 nm Wave Length

Bond	Molar Refraction R_m (cm^3 mol^{-1})	Atom or Ion	Molar Refraction R_m (cm^3 mol^{-1})
C–H	1·65	H	1·10
O–H	1·85	He	0·51
C–C	1·20	C	2·42
C=C	2·79	Li^+	0·07
C≡C	4·79	Na^+	0·46
C–O	1·41	K^+	2·12
C=O	3·34	Rb^+	3·57
C≡N	4·69	Be^{2+}	0·20
		Mg^{2+}	0·24
		Ca^{2+}	1·19

The molar refraction R_m can be calcuated from the measured value of the refractive index of the liquid or the solid. Eq. 30 can be combined with the Debye equation (Eq. 28) to obtain the following expression for the relative permittivity at low frequencies :

$$P_m = R_m + \frac{N_A \mu^2}{9\varepsilon_0 kT} \qquad ...(34)$$

i.e.,
$$\frac{\varepsilon_r - 1}{\varepsilon_r + 2} V_m = R_m + \frac{N_A \mu^2}{9\varepsilon_0 kT} \qquad ...(35)$$

In the c.g.s. system, Eq. 34 is written as

$$P_m = R_m + \frac{4\pi N_A \mu^2}{9kT} \qquad ...(36)$$

Example 2. Estimate the refractive index of water, given that the polarizability volume of water molecule at optical frequencies is $1{\cdot}5\times10^{-24}$ cm^3.

Solution : $V_m = M/\rho = 18{\cdot}02$ g mol^{-1}/1·00 g cm^{-3} = 18·02 cm^3 mol^{-1}

From Eq. 33, $R_m = \dfrac{4\pi\alpha' N_A}{3} = \dfrac{4\pi(1{\cdot}5\times10^{-24}\text{ cm}^3)\times(6{\cdot}022\times10^{23}\text{ mol}^{-1})}{3} = 3{\cdot}8$ cm^3 mol^{-1}

From Eq. 31, $n_r = \left(\dfrac{V_m + 2R_m}{V_m - R_m}\right)^{1/2} = \left\{\dfrac{(18{\cdot}02 + 2\times3{\cdot}8)\text{ cm}^3\text{ mol}^{-1}}{(18{\cdot}02 - 3{\cdot}8)\text{ cm}^3\text{ mol}^{-1}}\right\}^{1/2} = 1{\cdot}34$

Example 3. Calculate the polarizability and polarizability volume of water molecule at 20°C if at this temperature the refractive index of water is 1·3330 for a light of wave length 589 nm. Molar mass M for water = 18·015 g mol^{-1}, ρ = 0·9982 g cm^{-3} and $\varepsilon_0 = 8{\cdot}8542\times10^{-12}$ J^{-1} C^2 m^{-1}

Solution : From Eq. 32,

$$\alpha_d = \frac{3\varepsilon_0 R_m}{N_A} = \frac{3\varepsilon_0}{N_A}\left\{\frac{n_r^2 - 1}{n_r^2 + 1}\right\} V_m$$

$$= \frac{3\times(8{\cdot}8542\times10^{-12}\text{ J}^{-1}\text{C}^2\text{ m}^{-1})}{6{\cdot}022\times10^{23}\text{ mol}^{-1}} \times \left\{\frac{1{\cdot}3330^2 - 1}{1{\cdot}3330^2 + 2}\right\} \times \frac{18{\cdot}015\text{ g mol}^{-1}}{0{\cdot}9982\text{ g cm}^{-3}}$$

$$= 1{\cdot}6375\times10^{-40}\text{ J}^{-1}\text{ C}^2\text{ m}^2$$

$$\therefore \quad \alpha' = \frac{\alpha_d}{4\pi\varepsilon_0} = \frac{1{\cdot}6375\times10^{-40}\text{ J}^{-1}\text{C}^2\text{ m}^2}{4\pi\times(8{\cdot}8542\times10^{-12}\text{ J}^{-1}\text{C}^2\text{ m}^{-1}}$$

$$= 1{\cdot}4717\times10^{-24}\text{ cm}^3 = 1{\cdot}4717\times10^{-30}\text{ m}^3$$

Example 4. For a gaseous molecule AB_2 the refractive index is 1·00518 and the dielectric constant is 1·001. Determine if the molecule is linear or bent.

Solution : $n_r = 1{\cdot}00518$; $\varepsilon_r = 1{\cdot}001$. Thus, $\varepsilon_r \approx n_r^2$

Since the Maxwell relation holds for a non-polar molecule, hence the molecule AB_2 must be non-polar with dipole moment = 0. Thus, AB_2 is a linear molecule with the structure, B–A–B.

Example 5. For a gaseous hydrocarbon C_nH_{2n+2}, the refractive index at STP is 1·00138. Determine the formula of the hydrocarbon, given that the R_m values for H and C are 1·10 and 2·42 cm^3 mol^{-1}, respectively.

Solution : $R_m = \left(\dfrac{n_r^2 - 1}{n_r^2 + 2}\right)V_m = \left(\dfrac{(1{\cdot}00138)^2 - 1}{(1{\cdot}00138)^2 + 2}\right)$ (22,414 cm^3 mol^{-1}) = 20·75 cm^3 mol^{-1}

Also, since the atomic refractions are additive, hence

$R_m = nR_C + (2n+2)R_H$ so that

$20{\cdot}75$ cm^3 mol^{-1} = $[n(2{\cdot}42) + (2n+2)(1{\cdot}1)]$ cm^3 mol^{-1}

or $20{\cdot}75 = 4{\cdot}62n + 2{\cdot}2$, whence

$n = (20{\cdot}75 - 2{\cdot}2)/4{\cdot}62 = 18{\cdot}55/4{\cdot}62 = 4$

Hence, the formula of the hydrocarbon is C_4H_{10}.

Example 6. Estimate the refractive index of acetic acid for yellow sodium light (589 nm) given that at this wave length (or the corresponding frequency) the R_m values of the C—H, C—C, C—O, C=O and O—H bonds are 1·65, 1·20, 1·41, 3·34 and 1·85 cm^3 mol^{-1}, respectively. Also, for acetic acid, M = 60·05 g mol^{-1} and ρ = 1·046 g cm^{-3}.

Solution : Since the total R_m value of acetic acid molecule is the sum of the R_m values of the C—H, C—C, C—O, C=O and O—H bonds, hence

$$R_m = 3(\text{C—H}) + (\text{C—C}) + (\text{C=O}) + (\text{C—O}) + (\text{O—H})$$

$$= (3\times1{\cdot}65) + 1{\cdot}20 + 3{\cdot}34 + 1{\cdot}41 + 1{\cdot}85 = 12{\cdot}75\text{ cm}^3\text{ mol}^{-1}$$

$$V_m = M/\rho = (60{\cdot}05\text{ g mol}^{-1})/1{\cdot}046\text{ g cm}^{-3} = 57{\cdot}41\text{ cm}^3\text{ mol}^{-1}$$

Hence, from Eq. 3i,

$$n_r = \left[\frac{V_m + 2R_m}{V_m - R_m}\right]^{1/2} = \left(\frac{57{\cdot}41 + 2\times12{\cdot}75\text{cm}^3\text{ mol}^{-1}}{(57{\cdot}41 - 12{\cdot}75)\text{cm}^3\text{ mol}^{-1}}\right) = 1{\cdot}36$$

Example 7. Estimate the refractive index of steam at 100°C and 1 atm pressure, given that its polarizability volume is $1{\cdot}50\times10^{-24}$ cm^3.

Solution : As shown in the last example,

$$n_r = \left(\frac{1 + (8\pi\alpha' P/3kT}{1 - (4\pi\alpha' P/3kT}\right)^{1/2}$$

Now, $\alpha' = 1{\cdot}50\times10^{-24}\text{ cm}^3 = 1{\cdot}50\times10^{-30}\text{ m}^3$

$$4\pi\alpha' P/3kT = \frac{4\pi(1{\cdot}50\times10^{-30}\text{m}^3)(1{\cdot}01325\times10^5\text{ N m}^{-2})}{3\times[1{\cdot}38\times10^{-23}\text{ J K}^{-1})(373\text{ K})} = 1{\cdot}235\times10^{-4}$$

$$\therefore \quad n_r = \left(\frac{1 + 2{\cdot}470\times10^{-4}}{1 - 1{\cdot}235\times10^{-4}}\right)^{1/2} = 1{\cdot}00019$$

Example 8. If molar polarization of $NH_3(g)$ obeys the equation $P_m = a + b/T$ where the constants a and b have the values 5·6 and 12,000 cm^3 mol^{-1}, respectively, what is the relative permittivity of ammonia gas at S.T.P. ?

Solution : According to Eq. 27, $P_m = \left(\dfrac{\varepsilon_r - 1}{\varepsilon_r + 2}\right)V_m$,

where at STP, V_m = 22·414 dm^3 mol^{-1} = 22,414 cm^3 mol^{-1}

$$\frac{\varepsilon_r - 1}{\varepsilon_r + 2} = \frac{P_m}{V_m} = \frac{a + b/T}{V_m} = \frac{(5{\cdot}6 + 12{,}000/273)\text{ cm}^3\text{ mol}^{-1}}{22{,}414\text{ cm}^3\text{ mol}^{-1}}$$

$$= 49{\cdot}4/22{,}414 = 0{\cdot}00221$$

$$\frac{\varepsilon_r - 1}{\varepsilon_r + 2} = 0{\cdot}00221$$

$$\varepsilon_r - 1 = (\varepsilon_r + 2)(0{\cdot}00221) = 0{\cdot}00221\varepsilon_r + 0{\cdot}00442$$

$$\varepsilon_r(1 - 0{\cdot}00221) = 1{\cdot}00442$$

$$\therefore \quad \varepsilon_r = \frac{1{\cdot}00442}{0{\cdot}99779} = 1{\cdot}00664$$

Bond Moments. It is convenient to consider the permanent dipole moment of a molecule in terms of its *bond moments*. The bond moment is a vector quantity and can be associated with a chemical bond. The bond moments for some molecules are given in Table 3.

TABLE 3

Bond Moments of Some Chemical Bonds

Bond	Bond Moment (D)	Bond	Bond Moment (D)
C—H	0·4	H—I	0·4
C—F	1·4	O—H	1·6
C—Cl	1·5	N—H	1·3
C—Br	1·4	S—H	0·8
C—I	1·2	F—Cl	0·9
C—O	0·9	F—Br	1·3
C—N	0·2	Br—Cl	0·6
C=O	2·3	H—F	1·9
C—NO_2	3·5	H—Cl	1·0
		HBr	0·8

The bond moments for a given bond vary from molecule to molecule, though the variation is usually slight. For a molecule having only one bond, the bond moment is equal to the molecular dipole moment. However, for a polyatomic molecule, the molecular dipole moment is the resultant of the bond moments and can be obtained by vectorial addition of the bond moments. Thus, there is an intimate relationship between dipole moment and molecular geometry.

The molecular dipole moment can be resolved into bond moments. The *ionic character of a bond* can also be estimated from the knowledge of its bond moment. The bond moment is calculated assuming the bond to be completely ionic. This is illustrated in the following example.

Example 9. The bond angle in H_2O is 104·5° and the dipole moment is 1·85 D. Calculate the bond moment for the O—H bond. Also estimate the percent ionic character of the O—H bond, given that the O—H bond distance is 96 pm.

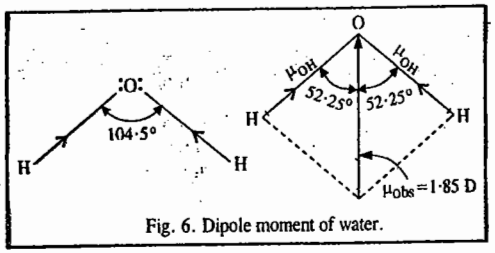

Fig. 6. Dipole moment of water.

Solution : As seen in Fig. 6, the angle between the O—H bonds in H_2O is 104·5° and the observed dipole moment is the vectorial sum of the two O—H bond moments.

Accordingly, $\mu_{observed} = 2\mu_{OH} \cos 52{\cdot}25°$

or $1{\cdot}85 \text{ D} = 2\mu_{OH} \times (0{\cdot}6129)$

$\therefore \quad \mu_{OH} = 1{\cdot}85 \text{ D}/(2 \times 0{\cdot}6129)$

$= 1{\cdot}51 \text{ D}$

$= 1{\cdot}51 \times 3{\cdot}336 \times 10^{-30} \text{ C m}$ $\quad (\because 1 \text{ D} = 3{\cdot}336 \times 10^{-30} \text{ C m})$

If the O—H bond is completely ionic, then the dipole moment

$$\mu_{ionic} = (1{\cdot}602 \times 10^{-19} \text{ C}) \times (96 \times 10^{-12} \text{ m}) = 1{\cdot}538 \times 10^{-29} \text{ C m}$$

Hence, % ionic character $= (\mu_{OH}/\mu_{ionic}) \times 100$

$$= \left(\frac{1{\cdot}51 \times 3{\cdot}336 \times 10^{-30} \text{ C m}}{1{\cdot}538 \times 10^{-29} \text{ C m}}\right) \times 100 = 24{\cdot}94$$

It should be noted that the resolution of a molecular dipole moment into bond moments is somewhat arbitrary. One could, for instance, assign a moment to the lone pair of electrons in H_2O or NH_3 as well as to the bonds.

Dipole Moments and Molecular Structure

The linear triatomic molecules of the type B—A—B (*e.g.*, CO_2) have no dipole moment, not because the individual C=O bonds are non-polar but because the two bond moments cancel being equal and opposite. Again, angular triatomic molecules (such as H_2O) and linear asymmetric molecules (such as N_2O) have dipole moments because their bond moments do not cancel. For polyatomic molecules, the

situation becomes increasingly complicated. For instance, in the case of the planar symmetrical molecule like AB_3, the three bond moments cancel to give a zero dipole moment. BF_3 belongs to this category.

On the other hand, the vector sum of bond moments of NH_3 does not cancel so that the molecule possesses a dipole moment. This indicates that the three hydrogen atoms do not lie symmetrically with respect to the nitrogen atom. The high value (1·40 D) of the dipole moment of NH_3 can be explained by assigning a triangular pyramidal structure to the molecule in which the nitrogen atom is situated at the apex of the pyramid and the three hydrogens lie at the three corners of the base.

Symmetrical polyatomic polar molecules do not show dipole moment if the vector sum of the bond moments cancels out. Examples are CH_4, CCl_4, SF_6, C_6H_6 and $[Ni(CN)_4]^{2-}$.

Dipole moments are helpful in distinguishing between the *cis* and *trans* isomers. Thus, the *cis* isomer of 1,2-dichloroethane has a dipole moment whereas the *trans* isomer does not. The zero dipole moment of the trans isomer is due to the fact that the vector sum of the bond moments of the two C—Cl bonds cancels out :

H—C—Cl ‖ H—C—Cl	H—C—Cl ‖ Cl—C—H
cis form	*trans* form
(μ = 1·86 D)	(μ = 0)

The dipole moment data can also help in the indentification of *cis* and *trans* isomers of square planar PtA_2B_2 complexes. The *trans* isomer should have a very small dipole moment whereas the *cis* isomer should possess a fairly large moment. This fact is corroborated experimentally.

It may also be noted that the experimental measurement can yield only the magnitude, not the direction, of the dipole moment. In most cases it is possible to have a fairly good idea of the direction of the dipole moment by considering the difference in electronegativities and by making comparison with similar molecules. However, in several cases, it is difficult to predict the direction of the dipole moment. A well known example is furnished by carbon monoxide, CO, which has a small value of μ=0·10 D.

Group Moments. When we want to evaluate dipole moments of benzene derivatives, we find that we need to know the *group moments* rather than the *bond moments*. For instance, the observed dipole moment of 1·68 D for chlorobenzene presumably arises from the dipole moment of the C—Cl group assuming that the C—H bonds in benzene have zero dipole moment. The group moments of some common groups are shown in Table 4.

TABLE 4

Group Moments of Some Common Groups

Group	NH_2	CH_3	H	Cl	OH	NO_2
Group moment (D)	+ 1·53	+ 0·41	0	−1·58	−1·60	−3·98

The sign of a group moment shows the direction in which the group moment operates. Thus, the negative sign implies that the group moment acts *towards* the ring whereas the positive sign implies that it acts *away* from the ring. By vectorial addition the dipole moment of a substituted benzene can be calculated.

Example 10. If in a substituted benzene, μ_1 and μ_2 are the bond moments inclined at an angle θ with respect to each other, then show that the dipole moment of the substituted benzene is given by the expression :

$$\mu = \left(\mu_1^2 + \mu_2^2 + 2\mu_1\mu_2 \cos\theta\right)^{1/2}$$

Solution : Let μ_x and μ_y be the x and y components of μ_1 and μ_2. Then,

$$\mu = \left(\mu_x^2 + \mu_y^2\right)^{1/2} \qquad \ldots(i)$$

If θ_1 and θ_2 are the angles which μ_1 and μ_2, respectively, make with the x-axis, then

$$\mu_x = \mu_{1,x} + \mu_{2,x} = \mu_1 \cos\theta_1 + \mu_2 \cos\theta_2 \quad ...(ii)$$

Similarly, $$\mu_y = \mu_{1,y} + \mu_{2,y} = \mu_1 \sin\theta_1 + \mu_2 \sin\theta_2 \quad ...(iii)$$

Substituting Eqs. *(ii)* and *(iii)* into Eq. *(i)*, we have

$$\mu = \{(\mu_1 \cos\theta_1 + \mu_2 \cos\theta_2)^2 + (\mu_1 \sin\theta_1 + \mu_2 \sin\theta_2)^2\}^{1/2}$$

$$= \{(\mu_1^2 \cos^2\theta_1 + \mu_2^2 \cos^2\theta_2 + 2\mu_1\mu_2 \cos\theta_1 \cos\theta_2) + (\mu_1^2 \sin^2\theta_1 + \mu_2^2 \sin^2\theta_2 + 2\mu_1\mu_2 \sin\theta_1 \sin\theta_2)\}^{1/2}$$

which can be rearranged to give

$$\mu = \{\mu_1^2 + \mu_2^2 + 2\mu_1\mu_2(\cos\theta_1 \cos\theta_2 + \sin\theta_1 \sin\theta_2)\}^{1/2}$$

$$= \{\mu_1^2 + \mu_2^2 + 2\mu_1\mu_2 \cos(\theta_1 - \theta_2)\}^{1/2}$$

$$= \{\mu_1^2 + \mu_2^2 + 2\mu_1\mu_2 \cos\theta\}^{1/2} \quad \text{where } \theta_1 - \theta_2 = \theta.$$

Example 11. If μ is the dipole moment of the monosubstituted benzene C_6H_5X, derive expressions for the dipole moments of 1,2-disubstituted benzene, $C_6H_4X_2$ and 1,3-disubstituted benzene, $C_6H_4X_2$.

Solution : As shown in the last example,

$$\mu = \{\mu_1^2 + \mu_2^2 + 2\mu_1\mu_2 \cos\theta\}^{1/2}$$

Now, for 1,2-$C_6H_4X_2$, $\theta = 60°$ whereas for 1,3-$C_6H_4X_2$, $\theta = 120°$

Thus, for 1,2-$C_6H_4X_2$, we have, $\mu_{total} = \{\mu_1^2 + \mu_2^2 + 2\mu_1\mu_2 \cos 60\}^{1/2}$

$$= (2\mu^2 + 2\mu^2 \cos 60)^{1/2} = (3\mu^2)^{1/2} = \sqrt{3}\mu$$

where we have made use of the fact that $\mu_1 = \mu_2 = \mu$

Similarly, for 1,3-$C_6H_4X_2$, we have,

$$\mu_{(total} = \{\mu_1^2 + \mu_2^2 + 2\mu_1\mu_2 \cos 120\}^{1/2}$$

$$= (2\mu^2 - 2\mu^2 \sin 30)^{1/2} = (2\mu^2 - \mu^2)^{1/2} = \mu$$

Example 12. The molecular dipole moment of chlorobenzene is 1·69 D. Calculate the dipole moments of *ortho*, *meta* and *para* dichlorobenzenes.

Solution : Using the expression derived in the last example, we have

for the ortho compound, $\mu = \sqrt{3}$ (1·69 D) = (1·732) (1·69 D) = 2·93 D

for the meta compound, μ = 1·69 D

and for the para compound, $\mu = 0$ since the two dipoles are directed to each other at an angle of 180°. The results agree excellently with the experimental values of 1·68 D and 0, respectively, of the meta and para disubstituted benzenes. However, there is disagreement with the experimental value (2·52 D) of the ortho compound. This is presumably due to the fact that in the ortho $C_6H_4Cl_2$, the two Cl atoms being close, there may be *repulsion* between them so that θ is greater than 60°. Also, the proximity of the two Cl atoms may alter the C–Cl bond moments.

MAGNETIC PROPERTIES OF MOLECULES

The magnetic properties of atoms and molecules are, in general, of less interest than the electrical properties dealt with above. Nevertheless, since the theory of magnetic properties is analogous in several ways to the theory of electric properties, important information about the molecular structure can be obtained by studying the magnetic behaviour of matter.

The force F acting between two magnetic dipoles of pole strengths m_1 and m_2 separated by a distance r, is given by

$$F = m_1 m_2 / \mu r^2 \quad ...(37)$$

where μ is a constant characteristic of the medium and is called **magnetic permeability** of the medium. Magnetic permeability is the magnetic counterpart of electric permittivity. Magnetic permeability

measures the tendency of the magnetic lines of force to pass through the medium, compared with their tendency to pass through vacuum for which $\mu = 1$. A substance is said to be diamagnetic when $\mu < 1$ and paramagnetic when $\mu > 1$. Thus, a diamagnetic substance is less permeable to the magnetic lines of force than a vaccum. The magnetic lines of force deflect away from a diamagnetic sample whereas they deflect towards a paramagnetic sample (Fig. 7).

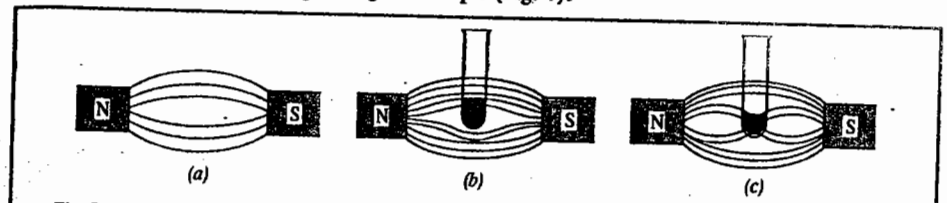

Fig. 7. Magnetic lines of force showing the effect of diamagnetic and paramagnetic substance on the magnetic field. *(a)* Vacuum *(b)* Diamagnetic *(c)* Paramagnetic.

The magnetic properties of matter are discussed in terms of the magnetic field intensity vector, H and the magnetic induction (or magnetic flux density) B. When a substance is placed in a magnetic field, the magnetization M, *i.e.*, the magnetic moment per unit volume, is related to B and H by the relation

$$B = \mu_0 (H + M) \quad ...(38)$$

where μ_0 is the permeability of vacuum.

Also, $$B = \mu H \quad ...(39)$$

From Eqs. 38 and 39, $$M = H[(\mu/\mu_0) - 1] = H(\mu_r - 1) \quad ...(40)$$

where $\mu_r = \mu/\mu_0$ is the *relative permeability* of the medium ($\mu_0 = 4\pi \times 10^{-7}$ J C^{-2} m^{-1} s^2).

A very important quantity, **magnetic susceptibility, is defined as**

$$\chi = M/H = \mu_r - 1 \quad ...(41)$$

The magnetic susceptibility is a dimensionless quantity. The *molar magnetic susceptibility* is defined as

$$\chi_m = V_m \chi \quad ...(42)$$

where V_m is the molar volume.

Magnetic susceptibility is related to magnetic permeability as follows :

$$\chi = (\mu - 1)/4\pi\rho \quad ...(43)$$

where ρ is the density in g cm^{-3}.

For *diamagnetic* solids, the relative permeability $\mu_r < 1$ so that χ is negative. Such substances are copper, graphite, antimony, bismuth, etc. For *paramagnetic* solids (such as Al, Pt, etc.,) $\mu_r > 1$ so that χ is positive. For *ferromagnetic* solids (such as Fe, Co, Ni, etc.,) μ_r and χ are very high, their values ranging between 200 and 100,000. It should be noted that for a diamagnetic substance, χ is small, negative, independent of magnetic field intensity and also independent of temperature. For a paramagnetic substance, χ is large, positive, independent of magnetic field intensity and decreases with increase in temperature. For a ferromagnetic substance, χ is very large, positive and depends upon the magnetic field intensity, the temperature and the previous history of the sample. Then, there are the so-called antiferromagnetic substances for which χ is small and positive. These substances show hysteresis effects and possess transition temperature, called the **Neel point.** The French physicist Louis Neel (1904–1999) was the cowinner (with the Swedish physicist H. Alfven (1908–1995) of the 1970 Phyiscs Nobel Prize. Neel was honoured for contributions to antiferromagnetism and ferromagnetism and Alfven was honoured for work on magnetohydrodynamics and plasma physics.

Table 5 summarizes the magnitudes, signs and origins of the various forms of magnetic behaviour.

TABLE 5

Types of Magnetic Behaviour and Their Characteristics

Type of magnetic susceptibility	Sign	Approximate magnitude	Dependence on magnetic field intensity	Origin
Diamagnetism	Negative	1×10^{-6}	Independent	Electronic charge
Paramagnetism	Positive	$0 - 10^{-4}$	Independent	Angular momentum (electron spin)
Ferromagnetism	Positive	$10^{-2} - 10^{-4}$	Dependent	↑↑ dipole exchange
Antiferromagnetism	Positive	$0 - 10^{-4}$	May depend	↑↓ dipole exchange

Molecular Interpretation of Diamagnetism and Paramagnetism

Diamagnetism. The classical theory of diamagnetism and paramagnetism was developed by P. Langevin in 1905 and the quantum theory was formulated by J.H. van Vleck in 1932. Langevin explained diamagnetism as resulting from the orbital motion of electrons of atoms or molecules. Qualitatively, it can be understood by involving Lenz's law which states that when a current flows in a coil of wire in a magnetic field, the field induces a current in the coil in a manner as to oppose the applied field. Similarly, the applied magnetic field perturbs the orbital motion of electrons, inducing a magnetic field which opposes its own direction. In atoms having more than one electron, the orbits are partially oriented at random relative to the field. The molar diamagnetic susceptibility is given by

$$\chi^d_{m,\,\text{atom}} = -\frac{ZN_A e^2}{6m_e^2}\sum_i \langle r_i^2 \rangle = -2{\cdot}832\times10^{16} \langle r_i^2 \rangle \qquad \ldots(44)$$

where $\langle r_i^2 \rangle$ is the mean square distance of ith orbit from the nucleus ; Z is the atomic number and e and m_e are, respectively, the charge and mass of electron. Notice that χ^d_m is negative and *temperature-independent*. The negative sign in Eq. 44 indicates that diamagnetic susceptibility decreases the magnetic induction through the sample and produces repulsion of the material by the magnetic field. Diamagnetism is a fundamental property of all matter irrespective of whether it possesses a permanent magnetic moment or not.

P. Pascal has shown that diamagnetism in a molecule can be estimated from contributions of atoms and bonds within the molecule. Such diamagnetic contributions of atoms and bonds in a molecule are called **Pascal's constants**. Pascal's constants for some atoms and bonds are given in Table 6.

TABLE 6

Pascal's Constants for Atoms and Bonds

Atom or Bond	Pascal's constant	Atom or Bond	Pascal's constant
H	$-2{\cdot}9\times10^{-6}$	I	−44·6
C	−6·0	Si	−13·0
N (open chain)	−5·5	S	−15·1
N (ring)	−4·6	B	−7·0
N (amines)	−1·5	C=C	5·5
O (alcohol, ether)	−4·6	C=C − C=C	10·6
O (ketones)	−1·7	N=N	1·85
O (carboxyl)	−3·3	C=N	8·2
F	−6·3	C≡N	0·8
Cl	$-20{\cdot}1\times10^{-6}$	C≡C	0·8
Br	−30·6	Benzene ring	−1·4

The results obtained with the help of Eq. 44, however, do not agree well with the experimental data. It is, therefore, necessary to treat diamagnetic susceptibilities of atoms and molecules on an empirical basis. The diamagnetic susceptibility of a molecule may be written as

$$\chi^d_{m,\,\text{molecule}} = \sum_i \chi^{d,i}_{m,\,\text{atom}} + \sum \chi_{B,j} \qquad \ldots(45)$$

where $\chi^{d,i}_{m,\text{atom}}$ is the molar atomic diamagnetic susceptibility associated with atom i and $\chi_{B,j}$ is that associated with jth bond in the molecule.

Paramagnetism. Paramagnetism can be considered as arising from the magnetic behaviour of an electron moving around the nucleus of an atom. The orbital motion of an electron corresponds to the passage of current through a coil of wire. This current produces a magnetic field perpendicular to the coil. The magnetic moment of the current loop is given by $\mu_m = iA$, where A is the area of the loop and i is the current. If the current is due to electron of mass m_e and charge e, moving with a velocity v, then $i = -ev/2\pi r$ so that

$$\mu_m = -(ev/2\pi r)\,\pi r^2 = -evr/2 \qquad \ldots(46)$$

where r is the radius of the loop.

The classical theory of paramagnetism developed by Langevin assumes that each atom or molecule is a small bar magnet having a magnetic moment μ and undergoing thermal agitation proportional to the absolute temperature. The magnetic moment may be due to either the orbital motion of an electron or to an unpaired electron spin. Assuming that the thermal agitation of the system creates a disorder in the system, the molar paramagnetic susceptibility due to the permanent magnetic moment was found to be given by

$$\chi^p_m = \frac{N_A\mu_m^2}{3kT} = \frac{C}{T} \qquad \ldots(47)$$

where C is a constant. The inverse variation of χ^p_m with temperature had been established experimentally by P. Curie prior to the development of the theory and is known as **Curie's law.** Eq. 47 holds over a limited range. Since all substances show diamagnetic behaviour, the total molar susceptibility of a substance is given by the sum of Eqs. 45 and 47. In practice, however, the diamagnetic contribution is only a small fraction of the paramagnetic contribution when the latter is present. Hence, except for accurate measurements or for large molecules it is often neglected. Eq. 47 has been derived on the assumption that the system is rigid and remains unchanged by the external field. However, the external field *does* distort (or polarize) the system so that χ^p_m is more correctly given by

$$\chi^p_m = \frac{N_A\mu_m^2}{3kT} + N_A\alpha_m \qquad \ldots(48)$$

$$= N_A\mu_0\left(\alpha_m + \frac{\mu_m^2}{3kT}\right) \qquad \ldots(49)$$

where α_m is the **magnetic polarizability** (or **magnetizability**) of the system. The magnetic moment due to electron spin is given by

$$\mu_s = g_e\mu_B\,[s\,(s+1)]^{1/2} \qquad \ldots(50)$$

where $\mu_B = e\hbar/2m_e$ is called the Bohr magneton, B.M. The value of μ_B is $9{\cdot}273\times10^{-24}$ J T^{-1} (joule per tesla). If more than one electron is present, the individual electron spins add vectorially giving

$$\mu_S = g_e\,\mu_B\,[S(S+1)]^{1/2} \qquad \ldots(51)$$

where the total spin S is given by

$$S = \sum_i s_i \qquad \ldots(52)$$

the summation being carried over the individual spins of the electrons. For an electron, $g_e = 2$.

The magnetic moment due to the orbital motion of the electrons having quantum number L is given by

$$\mu_L = \mu_B [L(L+1)]^{1/2} \qquad ...(53)$$

If μ_{eff} is the *effective magnetic moment* of an atom or a system, *i.e.*, If $\mu = \mu_{eff} = \mu_B$, then, neglecting the last term in Eq. 48, we have

$$\mu_{eff} = \left[3kT\chi_m^p / \left(N_A \mu_B^2\right)\right]^{1/2} = 2 \cdot 828 \left(\chi_m^p T\right)^{1/2} \qquad ...(54)$$

Notice that μ_{eff} can be found without neglecting $N_A\alpha_m$ if we measure χ_m^p as a function of temperature and use the slope of the resulting curve.

The orbital motions of the electrons are tied to the nuclear configuration of the atom so that they cannot orient themselves with the magnetic field. Therefore, the orbital contribution to magnetic moment given by Eq. 53 is quite small and can be neglected. According to van Vleck, this phenomenon which occurs in the ions of the metals of the First transition metal series, is called the **quenching of orbital angular momentum.** Hence,

$$\chi_m^p = \frac{N_A \mu_0 g_e^2 \mu_B^2 S(S+1)}{3kT} = \frac{6 \cdot 3001 \times S(S+1)}{T} \text{ cm}^3 \text{ mol}^{-1} \qquad ...(55)$$

From the measured value of χ_m^p, we can determine S and hence the number of unpaired electrons present. The American physicist van Vleck (1899-1980) was the cowinner {with his student P.W. Anderson and the British physicist N.F. Mott (1905–1996)} of the 1977 Physics Nobel Prize for their fundamental theoretical investigations of the electronic structure of magnetic and disordered systems.

Example 13. At 25°C, the molar magnetic susceptibility of water is $-13 \cdot 0 \times 10^{-6}$ cm^3 mol^{-1} and its density is 0·9970 g cm^{-3}. Calculate *(a)* the specific magnetic susceptibility and *(b)* the magnetic permeability of water at this temperature.

Solution : *(a)* The specific magnetic susceptibility is defined as $\chi_{sp} = \chi_m/M$.

$$\chi_{sp} = \frac{-13 \cdot 0 \times 10^{-6} \text{ cm}^3 \text{ mol}^{-1}}{18 \cdot 0 \text{ g mol}^{-1}} = -0 \cdot 722 \times 10^{-6} \text{ cm}^3 \text{ g}^{-1}$$

(b) From Eq. 43, $\chi = (\mu - 1)/4\pi\rho$; hence,

$$\mu = 4\pi\rho\chi + 1 = (4\pi)\,(0 \cdot 9970 \text{ g cm}^{-3})\,(-0 \cdot 722 \times 10^{-6} \text{ cm}^3 \text{ g}^{-1}) + 1$$
$$= -9 \cdot 0 \times 10^{-6} + 1 = 0 \cdot 99999$$

Notice that $\mu < 1$, as it should be because water is diamagnetic.

Example 14. The experimental value of molar magnetic susceptibility for benzene is $-54 \cdot 8 \times 10^{-6}$ cm^3 mol^{-1}. Compare it with the calculated value using the data given in Table 6 and comment on your result.

Solution : For benzene, we have

$$6\,C = 6\,(-6 \cdot 0 \times 10^{-6}) = -36 \cdot 0 \times 10^{-6}$$
$$6\,H = 6\,(-2 \cdot 9 \times 10^{-6}) = -17 \cdot 4 \times 10^{-6}$$
$$3\,(C=C) = 3\,(5 \cdot 5 \times 10^{-6}) = 16 \cdot 5 \times 10^{-6}$$
$$1 \text{ benzene ring} = 1\,(-1 \cdot 4 \times 10^{-6}) = -1 \cdot 40 \times 10^{-6}$$
$$\therefore \quad \chi_m = -38 \cdot 3 \times 10^{-6} \text{ cm}^3 \text{ mol}^{-1}$$

The calculated value of χ_m does not agree with the experimental value. The agreement would exist if the C=C contribution were neglected. This shows that there is no true C=C bond in the benzene molecule as is actually the case since the molecule is a resonance hybrid.

Example 15. At 25°C, a coordinate compound (M=200 g mol^{-1}) has density equal to 3·24 g cm^{-3}. If it contains three unpaired electrons, calculate the molar magnetic susceptibility and the magnetic susceptibility.

Solution : $\chi_m^p = \frac{N_A \mu_0 g_e^2 \mu_B^2 S(S+1)}{3kT} = 6 \cdot 3001 \times \frac{S(S+1)}{T}$ (Eq. 55)

For an electron, $g_e = 2$. Since the number of unpaired electrons = 3, the total spin $S = 3/2$

Hence, at 298 K,

$$\chi_m^p = \frac{(6 \cdot 3001)(3/2)(5/2)}{298} \text{ cm}^3 \text{ mol}^{-1} = 7 \cdot 9 \times 10^{-2} \text{ cm}^3 \text{ mol}^{-1}$$

The magnetic susceptibility is defined as

$$\chi = \chi_m^p / V_m = \chi_m^p \rho / M \qquad (\because V_m = M/\rho)$$

Introducing the various values, we have

$$\chi = \frac{(7 \cdot 9 \times 10^{-2} \text{ cm}^3 \text{ mol}^{-1})(3 \cdot 24 \text{ g cm}^{-3})}{200 \text{ g mol}^{-1}} = 1 \cdot 3 \times 10^{-3}$$

Measurement of Magnetic Susceptibility. The magnetic susceptibility of a substance is measured by means of the **Gouy balance** designed by the French physicist L.G. Gouy. The substance is taken in a vertical tube which is suspended vertically by means of a wire from one arm of the balance such that its lower part which contains the substance lies in the middle of the two poles of an electromagnet (Fig. 8).

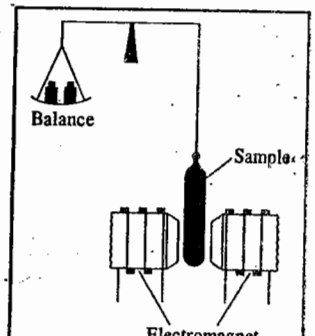

Fig. 8. Gouy's method for measurement of magnetic susceptibilities.

When the electromagnet is turned on, the sample may be attracted towards the magnetic field if it is paramagnetic or repelled by the magnetic field if it is diamagnetic. For a paramagnetic substance, the attraction is due to the alignments of the tiny magnets generated by the magnetic field. These alignments lower the potential energy of the system. For a diamagnetic substance, the potential energy is lower *outside* the magnetic field.

The modern version of the Gouy balance for the determination of magnetic susceptibility makes use of a **superconducting quantum interference device** (SQUID). A SQUID takes advantage of the quantization of magnetic flux and the property of current loops in superconductors that, as part of the circuit, include a weakly conducting link through which electrons must tunnel. The current that flows in the loop in a magnetic field depends on the value of the magnetic flux, and a SQUID can be exploited as a very sensitive magnetometer.

We are interested in calculating the force experienced by the sample as it moves in a non-homogeneous magnetic field whose value is minimum outside and maximum at the centre.

The magnetic moment of the sample within a small segment of the tube of area A and length dy (and hence the volume Ady) is given by

$$\mu_m = \chi (B/\mu_0) Ady \qquad ...(56)$$

where χ is volume magnetic susceptibility which is related to χ_m as $\chi_m = V_m\chi$, B is the strength of the magnetic field and μ_0 is the magnetic permeability of air or vacuum.

This magnetic moment acts in the direction of the magnetic field. If dB is the change in the magnetic induction over the length dy, then change in the potential energy of the sample is given by

$$dV = -\chi(B/\mu_0)(Ady)dB \qquad ...(57)$$

Since the force, dF, experienced by the sample is the negative gradient of this potential, we have

$$dF = -(dV/dy) = \frac{\chi}{\mu_0} ABdB \qquad ...(58)$$

Integration of Eq. 58 gives the total force experienced by the sample as it moves from outside the magnetic field (where the field is equal to zero) to the centre of the field (where its value is maximum).

$$F = \int_0^F dF = \int_{B=0}^{B=B_{max}} \frac{\chi}{\mu_0} ABdB \qquad ...(59)$$

$$= \frac{1}{2}\left(\frac{\chi}{\mu_0}\right) AB_{max}^2 \qquad ...(60)$$

Including the buoyancy correction, Eq. 60 can be written as

$$F = \left(\frac{1}{2}\chi_B - \chi_0\right) A(B_{max}2/\mu_0) \qquad ...(61)$$

where χ_0 is the volume magnetic susceptibility of air. In order to keep the position of the sample unshifted, the force is measured in terms of the masses that are added to or removed from the balance pan. Thus, we have

$$F = (\Delta m)g \qquad ...(62)$$

where Δm is the change in apparent mass and g is the acceleration due to gravity.

Example 16. The Gouy balance results showed that a sample of a complex ion in a tube of $1{\cdot}75\times10^{-5}$ m^2 cross-section that was partly in a magnetic flux density of 0·4 T was pushed into the field by a force equal to $2{\cdot}50\times10^{-4}$ N. Calculate the magnetic susceptibility χ. (Given $\mu_0 = 4\pi\times10^{-7}$ J C^{-2} m^{-1} s^2)

Solution : Since the sample is pushed into the field, it is *paramagnetic*, From Eq. 60,

$$\chi = 2F\mu_0/AB_{max}^2$$

$$= \frac{2(2{\cdot}50\times10^{-4}\text{ N})(4\pi\times10^{-7}\text{ J C}^{-2}\text{ m}^{-1}\text{ s}^2)}{(1{\cdot}75\times10^{-5}\text{ m}^2)(0{\cdot}4\text{ J C}^{-1}\text{ s m}^{-2})^2} = 89{\cdot}76\times10^{-6}$$

Example 17. The Gouy-balance results showed that a sample of water in a tube of 0·1 cm^2 cross-section that was partly in a magnetic flux density of 1 T was pushed out of the field by a force equal to the weight of 36 mg. Calculate the magnetic susceptibility χ and the molar magnetic susceptibility of the sample. ($\mu_0 = 4\pi\times10^{-7}$ J C^{-2} m^{-1} s^2)

Solution : $\chi = -\dfrac{2F\mu_0}{AB_{max}^2}$

$$= -\frac{2(36\times10^{-6}\text{ kg})(9{\cdot}80\text{ N kg}^{-1})(4\pi\times10^{-7}\text{ J C}^{-2}\text{ m}^{-1}\text{ s}^2)}{(0{\cdot}1\times10^{-4}\text{ m}^2)(1\text{ J C}^{-1}\text{ s m}^{-2})} \qquad (\because 1\text{ T} = \text{J C}^{-1}\text{ s m}^{-2})$$

$$= -89\times10^{-6}$$

(We have taken negative sign because the sample is *pushed out* of the field implying that it is diamagnetic.)

$$\therefore \quad \chi_m = \chi V_m = (-89\times10^{-6})\left(\frac{18\text{ g mol}^{-1}}{1{\cdot}00\text{ g cm}^{-3}}\right)$$

$$= -1{\cdot}60\times10^{-3}\text{ cm}^3\text{ mol}^{-1}$$

Ferromagnetism and Antiferromagnetism

Some paramagnetic solids at low temperatures undergo a transition to a state in which large domains of spins are aligned parallel to each other (↑↑↑↑↑↑↑↑). This cooperative alignment gives rise to very strong magnetization. The ferromagnetic transition occurs at the **Curie temperature** (in honour of P. Curie) and results in *ferromagnetism*. On the other hand, in some other solids, the cooperative effect leads to alternating spin orientations (↑↓↑↓↑↓↑↓↑↓), giving rise to low magnetization. The antiferromagnetic transition occurs at the Neel temperature and results in *antiferromagnetism*. P. Curie (1859-1906) shared the 1903 Physics Nobel Prize with his wife M. Curie (1867-1934) and H. Becquerel (1852-1908) for the discovery of spontaneous radioactivity.

I. Review Questions

1. What is meant by polarizability of a molecule ? Derive the Clausius-Mosotti equation.
2. Explain the terms : total molar polarization, induced molar polarization, orientation polarization and distortion polarization.
3. Explain how the dipole moment of a gaseous molecule can be determined the Debye equation.
4. What information regarding the structure of molecules can be obtained from the knowledge of their dipole moments ? What is meant by bond moment and group moment ?
5. Write a short note on diamagnetism, paramagnetism, ferromagnetism and antiferromagnetism.
6. What are the factors which contribute to paramagnetism in a substance ?

II. Problems

1. For $SO_2(g)$ at 0°C and 1 atm pressure, the relative permittivity is 1·00993 and the dipole moment is 1·63 D. Assuming that the gas behaves ideally, calculate *(a)* the total molar polarization *(b)* the induced molar polarization *(c)* the orientation polarization and *(d)* the distortion polarizability.
   [Ans. *(a)* $73{\cdot}95\times10^{-6}$ m^3 mol^{-1} *(b)* $14{\cdot}67\times10^{-6}$ m^3 mol^{-1} *(c)* $59{\cdot}28\times10^{-6}$ m^3 mol^{-1} *(d)* $6{\cdot}456\times10^{-40}$ J^{-1} C^2 m^2]
2. For $NH_3(g)$ at STP the dipole moment is 1·44 D and the distortion polarization is 6·0 cm^3. Calculate the relative permittivity (*i.e.*, dielectric constant) of NH_3, assuming ideality. [Ans. 1·007]
3. The refractive index of a gaseous alkane C_nH_{2n+2} is 1·38 and the density is 0·66 g cm^{-3}. If the atomic refractions of H and C are 1·1 cm^3 mol^{-1} and 2·42 cm^3 mol^{-1}, respectively, what is the molecular formula of the compound ? [Ans. C_5H_{12}]
4. The molar refractions R_m (in cm^3 mol^{-1}) of *n*-butanol, ethanol and methanol are 20·6, 12·3 and 8·3, respectively. Calculate R_m for *n*-butanol. [Ans. 22·1 cm^3 mol^{-1}]
5. The dipole moment of $NH_3(g)$ is 1·46 D. If the angle HNH is 108°, calculate the bond moment of N—H bond. [Ans. 1·458 D]
6. The bond moments of the C—H and C—Cl bonds are 0·4 D and 1·5D, respectively. Calculate the dipole moments of CH_3Cl, CH_2Cl_2 and $CHCl_3$ molecules. [Ans. 1·9D, 1·266 D, 1·902 D, respectively]
7. In a magnetic susceptibility determination experiment carried out on $[CoF_6]^{3-}$ (which contains 4 unpaired electrons). 0·1 M solution of the salt of this ion in a 1-cm diameter test tube was suspended in the Gouy balance. Calculate the change in apparent mass of the salt when the magnetic field strength was 0·5 T. [Ans. $1{\cdot}01\times10^{-5}$ kg]
8. The dipole moment of $NH_3(g)$ is 1·46 D. If the angle HNH is 108°, calculate the bond moment of N—H bond. [Ans. 1·458 D]
9. The temperature-dependence of molar polarization of water vapour is given below :

T(K)	384·3	420·1	444·7	484·1	522·0
P_m (cm^3 mol^{-1})	57·4	53·6	53·5	46·8	43·4

Using the Debye equation, calculate the dipole moment of water molecule. Assuming that the bond angle is 105°, also calculate the OH bond moment. [Ans. 1·85 D, 1·52 D]

CHAPTER 9

THE GASEOUS STATE–I IDEAL GASES

Amongst the three common states of matter, the gaseous state is the simplest. The laws of gaseous behaviour are more uniform and are better understood. The well known laws of gaseous behaviour are Boyle's law, Charles' law, Graham's law, Dalton's law and Avogadro's law. At the time of their enunciation, these laws were only empirical generalisations based on experimental observations. There was no theoretical background to justify them. In the nineteenth century, however, Kronig, Clausius, Maxwell and Boltzmann developed a theory, known as Kinetic Molecular Theory of Gases, which provided sound theoretical basis for the various gas laws. The eighteenth century Swiss mathematician, D. Bernoulli, too, had developed his ideas about the kinetic theory of gases.

Kinetic Molecular Theory of Gases. It is based on the following postulates :

1. A gas consists of a large number of minute particles, called molecules. The molecules are so small that their actual volume is a negligible fraction of the total volume (space) occupied by the gas.

2. The molecules are in a state of constant rapid motion in all possible directions, colliding in a random manner with one another and with the walls of the vessel.

3. The molecular collisions are perfectly elastic so that there is no net loss of energy when gas molecules collide with one another or against the walls of the vessel. The kinetic energy may be transferred from one molecule to another but it is not converted into any other form of energy such as heat.

4. There are no attractive forces between molecules or between molecules and the walls of the vessel in which the gas is contained. The molecules move completely independent of one another.

5. The pressure of a gas is due to the bombardment of the molecules on the walls of the containing vessel.

6. The laws of classical mechanics (in particular the Newton's second law of motion) are applicable to the motion of gaseous molecules.

It may be emphasised that the above postulates are meant for an *ideal gas only*. These are only approximately valid for a real gas.

Pressure of an Ideal Gas. From the above postulates, it is possible, by applying the laws of classical mechanics, to derive an expression for the pressure of a gas.

Let us consider N molecules of a gas, each having a mass m, enclosed in a cubical vessel of volume V, each side of the cube being l. The motion of molecules in the container, at any instant, is totally random.

Consider one molecule of the gas having a velocity c. This velocity can be resolved into three components u, v and w, along the three axes, x, y and z. The velocity components are, evidently, perpendicular to the walls of the container. It can be easily shown that

$$c^2 = u^2 + v^2 + w^2 \qquad ...(1)$$

Consider the motion of one molecule along the x-axis, striking the wall which is perpendicular to its motion. Since the collision is elastic and the wall remains stationary, on rebounding, only the sign of the velocity component changes. The resulting change of momentum in the x-direction (Δp_x) is,

therefore, given by

$$\Delta p_x = m\{u - (-u)\} = 2mu \qquad ...(2)$$

Immediately after the collision, the molecule takes time equal to l/u to collide with the opposite wall (and time equal to $2l/u$ to strike against the same wall again). Hence, the frequency of collisions on the two opposite walls is given by u/l and the change in momentum per unit time is given by

$$\Delta p_x/\Delta t = 2mu \times u/l = 2mu^2/l \qquad ...(3)$$

The total change in momentum of the single molecule per unit time arising from collisions on all the six walls is given by

$$\Delta p/\Delta t = 2mu^2/l + 2mv^2/l + 2mw^2/l = (2m/l)(u^2 + v^2 + w^2) = 2mc^2/l \qquad ...(4)$$

The total change in momentum per unit time for all the N molecules in the container is obtained by summing the contributions of all the molecules. Thus,

$$\frac{\Delta p_{\text{total}}}{\Delta t} = \sum_{i=1}^{N} \frac{2mc_i^2}{l} = \frac{2m}{l} \sum_{i=1}^{N} c_i^2 \qquad ...(5)$$

Defining mean square velocity as

$$\langle c^2 \rangle = \Sigma c_i^2/N \qquad ...(6)$$

we get,

$$\Delta p_{\text{total}}/\Delta t = \frac{2mN}{l} \langle c^2 \rangle \qquad ...(7)$$

According to Newton's second law of motion, the rate of change of momentum ($\Delta p_{\text{total}}/\Delta t$) is force ($f$) and force per unit area is pressure (P). Since the face area (A) of the cubical vessel is $6l^2$ and its volume is V, the pressure exerted by N molecules of the gas on the walls of the vessel is given by

$$P = \frac{f}{A} = \frac{2mN\langle c^2 \rangle}{l(6l^2)} = \frac{1}{3V} mN \langle c^2 \rangle \qquad ...(8)$$

Evidently, $\langle c^2 \rangle^{1/2}$ would be the **root mean square velocity** of the gaseous molecules, given by $(\Sigma c_i^2/N)^{1/2}$.

For the sake of convenience, the root mean square velocity is denoted by c. Therefore, Eq. 8, giving the pressure of the gas, is written as

$$P = (1/3V)mNc^2 \qquad ...(9)$$

Eq. 9 is generally expressed as

$$PV = (1/3)mNc^2 \qquad ...(10)$$

This is known as the **kinetic gas equation.**

Derivation of Gas Laws. All the gas laws can be easily derived from the kinetic gas equation, as shown below.

1. Boyle's Law. We know that molecular velocities increase with rise in temperature. Since kinetic energy varies as square of velocity, it is possible to define temperature in terms of kinetic energy. Thus, according to kinetic theory, the absolute temperature T of a gas is proportional to the mean kinetic energy, $\frac{1}{2}mc^2$, per molecule. It is, thus, evident that, at a constant temperature, the mean kinetic energy per molecule ($\frac{1}{2}mc^2$) of any gas remains constant.

The kinetic gas equation may be written as

$$PV = \tfrac{2}{3} \times \tfrac{1}{2} mNc^2 \qquad ...(11)$$

If a definite mass of a gas is under consideration, then the number of molecules N of the gas must also be constant. It follows, therefore, that for a given mass of a gas, at constant temperature, the quantity on the right hand side of Eq. 11 must remain constant. Hence,

$$PV = \text{constant}$$

Thus, PV is constant at constant temperature. This is **Boyle's law.**

2. Charles' Law. For a definite quantity of a gas (*i.e.*, N = constant), Eq. 11 at constant pressure may be written as

$$V \propto \tfrac{1}{2}mc^2 \qquad \ldots(12)$$

The quantity $\frac{1}{2}mc^2$, being the mean kinetic energy **per molecule**, varies as the temperature T, as discussed above. Hence,

$$V \propto T \quad \text{(at constant pressure)}$$

Thus, at constant pressure, the volume of a given **mass** of a gas varies directly as the absolute temperature. This is **Charles' law.**

3. Avogadro's Law. For any two gases, the kinetic gas **equation** may be written as

$$P_1V_1 = \tfrac{2}{3} \times \tfrac{1}{2} m_1N_1c_1^2 \quad \text{and} \quad P_2V_2 = \tfrac{2}{3} \times \tfrac{1}{2} m_2N_2c_2^2$$

When pressures and volumes of the two gases are the **same**, that is, when $P_1 = P_2$ and $V_1 = V_2$, it follows that

$$(1/2)m_1N_1c_1^2 = (1/2)m_2N_2c_2^2 \qquad \ldots(13)$$

If the two gases are also at the same temperature, **the mean** molecular kinetic energy of each gas is the same, that is,

$$(1/2)m_1c_1^2 = (1/2)m_2c_2^2 \qquad \ldots(14)$$

Dividing Eq. 13 by Eq. 14, we get

$$N_1 = N_2$$

Thus, equal volumes of all gases under the same **conditions** of temperature and pressure contain equal number of molecules. This is **Avogadro's law.**

It follows from Avogadro's law that **molar volume, *i.e.*, the** volume occupied by one mole of each substance in the gaseous state (which is numerically **equal** to 22·414 dm^3 at N.T.P.) would contain the same number of molecules. This number **is called** the **Avogadro's number**, N_A. Its numerical value is $6{\cdot}022 \times 10^{23}$ mol^{-1}. Obviously, the **quantity** n/N_A would give the number of moles, n, of the gaseous substance.

4. Ideal Gas Equation. Combining Boyle's law, **Charles' law** and Avogadro's law, we find that the volume of a gas depends on the pressure, temperature **and number** of moles, as follows :

$V \propto 1/P$ (at constant T and n) (Boyle's law)

$V \propto T$ (at constant P and n) (Charles' law)

$V \propto n$ (at constant T and P) (Avogadro's law)

Thus, V should be proportional to the product of these **three** terms, *i.e.*,

$$V \propto nT/P = R(nT/P)$$

or
$$PV = nRT \qquad \ldots(15)$$

where R, the proportionality constant, is called the **gas constant. Eq.** 15 is called the **ideal gas equation.**

Since one mole of an ideal gas occupies a volume of **22·414** dm^3 at N.T.P., we find from Eq. 15 that the ideal gas constant

$$R = \frac{PV}{nT} = \frac{(1\,\text{atm})(22{\cdot}414\,\text{dm}^3)}{(1\,\text{mol})(273{\cdot}15\,\text{K})} = 0{\cdot}08206\ \text{dm}^3\ \text{atm}\ \text{K}^{-1}\ \text{mol}^{-1}$$

In SI units, 1 atm = $1{\cdot}01325 \times 10^5$ N m^{-2} so that

$$R = \frac{PV}{nT} = \frac{(1{\cdot}03125 \times 10^5\ \text{N m}^{-2})(22{\cdot}414 \times 10^{-3}\ \text{m}^3)}{(1\,\text{mol})(273{\cdot}15\,\text{K})}$$

$$= 8{\cdot}314\ \text{N m K}^{-1}\ \text{mol}^{-1} = 8{\cdot}314\ \text{J K}^{-1}\ \text{mol}^{-1} \qquad (\text{J} = \text{N m})$$

5. Graham's Law of Diffusion. Since

$$PV = \tfrac{1}{3}mNc^2 \qquad \text{(Eq. 10)}$$

$$\therefore \quad c = \sqrt{3PV/mN} = \sqrt{3P/\rho} \qquad \ldots(16)$$

$\{\because mN/V$ = total mass of gas/volume = density of the gas $(\rho)\}$

The rate of diffusion (r) of a gas will, evidently, depend upon the mean velocity of its molecules, that is,

$$r \propto c \propto (3P/\rho)^{1/2} \propto (1/\rho)^{1/2} \quad \text{(at constant pressure)}$$

Thus, *the rate of diffusion of a gas is inversely proportional to the square root of the density of the gas at constant pressure. This is* **Graham's law of diffusion.**

6. Dalton's Law of Partial Pressures. Suppose, N_1 molecules, each of mass m_1, of a gas A, are contained in a vessel of volume V. Then, according to Eq. 9, the pressure p_a of the gas will be given by

$$p_a = m_1N_1c_1^2/3V \qquad \ldots(17)$$

where c_1 is the root mean square velocity of the molecules of the gas A.

Now, suppose, N_2 molecules, each of mass m_2, of another gas B, are contained in the same vessel at the same temperature and there is no other gas present at that time. The pressure p_b of this gas will be given by

$$p_b = m_2N_2c_2^2/3V \qquad \ldots(18)$$

where c_2 is the root mean square velocity of the molecules of the gas B.

If both the gases are present in the same vessel at the same time, the total pressure P will be given by

$$P = m_1N_1c_1^2/3V + m_2N_2c_2^2/3V = p_a + p_b$$

Similarly, if three, four or more gases are present, the total pressure will be given by

$$P = p_a + p_b + p_c + p_d + \cdots\cdots \qquad \ldots(19)$$

This is **Dalton's law** of partial pressures.

Kinetic Energy and Temperature. Suppose one mole of a gas is under consideration. The number of molecules involved will then be N_A (the Avogadro's number). The kinetic gas equation may then be written as

$$PV = \tfrac{1}{3}mN_A c^2 = \tfrac{2}{3} \times \tfrac{1}{2}mN_A c^2 = \tfrac{2}{3} \times E \qquad \ldots(20)$$

where E is the translational kinetic energy of one mole of the gas.

Since for one mole of an ideal gas, $PV = RT$,

$$\therefore \quad E = \tfrac{3}{2}RT \qquad \ldots(21)$$

Thus, *the translational kinetic energy of an ideal (perfect) gas is directly proportional to the absolute temperature.*

Further, since translational kinetic energy $\propto c^2$, it follows that

$$c^2 \propto T \quad \text{or} \quad c \propto \sqrt{T}$$

Thus, the molecular velocity of any gas is proportional to the square root of the absolute temperature. The molecular motion is, therefore, often termed as **thermal motion** of the molecules. At absolute zero (*i.e.*, T=0), kinetic energy is zero. In other words, thermal motion ceases completely at absolute zero.

It readily follows from Eq. 21 that the translational kinetic energy of a gas is independent of the volume (or pressure), the molar mass or the nature of the gas. It depends only on temperature (T). Thus, a hydrogen molecule has the same average translational kinetic energy as a molecule of nitrogen, ammonia or methane. The molecular velocity, of course, would be different in each gas.

The average translational kinetic energy of *one molecule of* an ideal gas will be given by

$$\varepsilon = E/N_A = (3/2)RT/N_A = \tfrac{3}{2}kT$$

where k ($= R/N_A$) is the **Boltzmann constant** whose numerical value = $1{\cdot}38 \times 10^{-23}$ J K^{-1}.

Example 1. Calculate the average translational kinetic energy of an ideal gas per molecule (ε) and per mole (E) at 25°C.

Solution : $\varepsilon = \frac{3}{2} kT = 3/2\ (1{\cdot}38\times10^{-23}\ \text{J K}^{-1})\ (298\ \text{K}) = 6{\cdot}17\times10^{-21}\ \text{J per molecule}$

$E = \frac{3}{2} RT = 3/2\ (8{\cdot}314\ \text{J K}^{-1}\ \text{mol}^{-1})\ (298\ \text{K}) = 3{\cdot}716\times10^{3}\ \text{J mol}^{-1}$

Maxwell Distribution of Molecular Velocities

As a result of random collisions of gaseous molecules, the molecular velocities keep on changing. Consider a gas molecule of mass m having a velocity component u. Then, the kinetic energy, ε, associated with this velocity component is $\frac{1}{2}mu^2$. The probability that this molecule has its velocity component between u and $u+du$ is given by $p(u)$. In the 19th century, Boltzmann had shown that the probability for a molecule to have an energy ε was proportional to $e^{-\varepsilon/kT}$. It is apparent that

$$p(u) \propto e^{-\varepsilon/kT} \propto e^{-mu^2/2kT} \qquad (\because\ \varepsilon = 1/2\ mu^2)$$

or
$$p(u)du = Ae^{-mu^2/2kT}du \qquad ...(22)$$

where A is the constant of proportionality. This constant can be evaluated by requiring that the total probability must be unity. Thus,

$$\int_{-\infty}^{+\infty} p(u)du = A\int_{-\infty}^{+\infty} e^{-mu^2/2kT}\,du = 1 \qquad ...(23)$$

The range of integration of velocity component u is $-\infty$ to $+\infty$ since velocity has both magnitude and direction. The integral in Eq. 23 can be easily evaluated. Setting $m/2kT=a$, it is found from calculus that

$$\int_{-\infty}^{+\infty} e^{-au^2}du = (\pi/a)^{1/2} = \left(\frac{2\pi kT}{m}\right)^{1/2} \qquad ...(24)$$

From Eqs. 23 and 24, $A(2\pi kT/m)^{1/2} = 1$ so that $A = (m/2\pi kT)^{1/2}$ ...(25)

Substituting for A in Eq. 22, we have

$$p(u)du = \left(\frac{m}{2\pi kT}\right)^{1/2} e^{-mu^2/2kT}du \qquad ...(26)$$

Eq. 26 is called the Maxwell distribution of molecular velocities in one dimension. It is easy to derive the Maxwell's distribution of molecular velocities in three dimensions by multiplying the three one-dimension distributions with one another. Thus,

$$p(u,v,w) = p(u)\,p(v)\,p(w) \qquad ...(27)$$

where v and w are the velocity components in the other two dimensions.

$$\therefore \quad p(u,v,w)du\,dv\,dw = p(u)du \times p(v)dv \times p(w)dw$$

$$= \left(\frac{m}{2\pi kT}\right)^{3/2} \exp\left[-\frac{m(u^2+v^2+w^2)}{2kT}\right]du\,dv\,dw \qquad ...(28)$$

We are, however, interested in an expression which gives the *fraction of molecules with a velocity between c and $c+dc$* ($c^2=u^2+v^2+w^2$) regardless of the direction. These are molecules whose velocity points lie within a spherical shell of thickness dc at a distance c. This shell has the volume $4\pi c^2dc$, which is the integral of $dudvdw$ in Eq. 28 over the spherical shell. Hence, we find that

$$p(c)dc = 4\pi\left(\frac{m}{2\pi kT}\right)^{3/2} c^2 \exp(-mc^2/2kT)dc \qquad ...(29)$$

This result was obtained by Maxwell in 1860 and is called the **Maxwell distribution of molecular velocities.** It is customary to write $p(c)dc$ as dN/N, where N is the total number of gas molecules. The quantity dN/N (or $p(c)dc$) gives the fraction of molecules with velocity between c and $c+dc$. The

molecular mass $m = M/N_A$ where M is the molar mass and N_A is the Avogadro's number. Accordingly, Eq. 29 may also be written as

$$p(c)dc = \frac{dN}{N} = 4\pi\left(\frac{M}{2\pi RT}\right)^{3/2} c^2 \exp\left(-\frac{Mc^2}{2RT}\right)dc \qquad ...(30)$$

The Maxwell distribution of molecular velocities is plotted in Fig. 1.

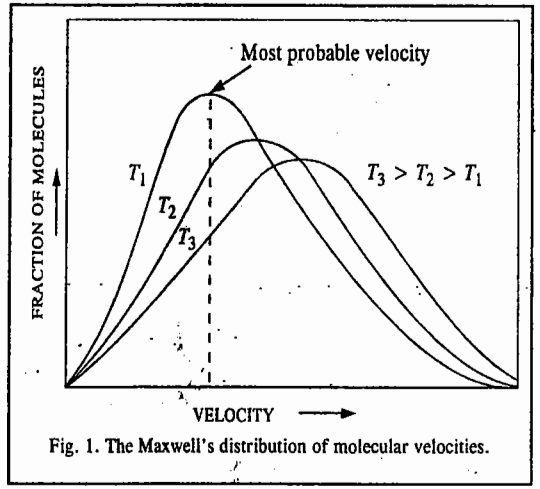

Fig. 1. The Maxwell's distribution of molecular velocities.

We see that the fraction of molecules having velocities greater than zero increases with an increase in velocity, reaches a maximum and then falls off towards zero again at higher velocities.

The important features of the curves are as follows :

1. The fraction of molecules with too low or too high velocities is very small.

2. There is a certain velocity for which the fraction of molecules is maximum. This is called the most probable velocity.

The **most probable velocity** of a gas is the velocity possessed by maximum number of molecules of the gas at a given temperature. It corresponds to the peak of the curve. Its value, at a given temperature, depends upon the volume of the gas.

Effect of Temperature on Distribution of Molecular Velocities. The most probable velocity increases with rise in temperature, as shown in Fig. 1. The entire distribution curve, in fact, shifts to the right with rise in temperature, as shown. The rise in temperature, therefore, increases the fraction of the molecules having high velocities considerably. This can readily be understood from the presence of the factor, $\exp(-mc^2/2kT)$, in Eq. 29. The exponent has a negative sign and the temperature T is in the denominator. The factor, therefore, increases markedly with increases in temperature. This factor is known as the **Boltzmann factor.**

Further, knowing that $\frac{1}{2}mc^2$ is the kinetic energy of one molecule of the gas having velocity c, the factor

$$\exp(-mc^2/2kT) = \exp(-\varepsilon/kT) \qquad ...(31)$$

where ε ($=\frac{1}{2}mc^2$) gives the kinetic energy per molecule of the gas. The greater the temperature, the greater is the value of ε. Hence, there is rapid increase of the Boltzmann factor with increase in temperature. This conclusion finds application in the theory of reaction rates also.

Maxwell Distribution of Molecular Kinetic Energies. With the help of Eq. 29 it is possible to know how the kinetic energies of translation of molecules are distributed amongst the various molecules. The fraction of molecules having kinetic energies in the range of ε and $\varepsilon+d\varepsilon$, *viz.*, dN_ε/N, can be determined as follows :

$$\varepsilon = \tfrac{1}{2}mc^2 \quad \text{or} \quad c^2 = (2\varepsilon/m)$$

$$\therefore \quad 2cdc = (2/m)(d\varepsilon) \quad \text{or} \quad cdc = d\varepsilon/m \qquad ...(32)$$

Thus,
$$c^2dc = c\frac{d\varepsilon}{m} = \left(\frac{2\varepsilon}{m}\right)^{1/2}\left(\frac{d\varepsilon}{m}\right) = \frac{\sqrt{2\varepsilon}}{(m)^{3/2}}d\varepsilon \qquad ...(33)$$

Substituting the above value of c^2dc in Eq. 29, we have

$$p(c)\,dc = \frac{dN_\varepsilon}{N} = 4\pi\left(\frac{m}{2\pi kT}\right)^{3/2}\left(\frac{\sqrt{2\varepsilon}}{m^{3/2}}\right)d\varepsilon \exp\left(-\frac{\varepsilon}{kT}\right) \quad ...(34)$$

$$= \frac{2\sqrt{\varepsilon}}{\sqrt{\pi}\,(kT)^{3/2}} \exp\left(-\frac{\varepsilon}{kT}\right)d\varepsilon \quad ...(35)$$

This is the **Maxwell distribution of molecular kinetic energies.**

Example 2. Calculate the fraction of oxygen molecules at 1 atm and 27°C whose kinetic energies lie in the range of $(\varepsilon - 0{\cdot}005\varepsilon)$ and $(\varepsilon + 0{\cdot}005\varepsilon)$.

Solution : According to the Maxwell's distribution of molecular kinetic energies,

$$\frac{dN_\varepsilon}{N} = \frac{2\sqrt{\varepsilon}}{\sqrt{\pi}\,(kT)^{3/2}} \exp\left(-\frac{\varepsilon}{kT}\right)d\varepsilon \quad \text{(Eq. 35)}$$

At 27°C, kinetic energy of the gas is given by

$$\varepsilon = 3/2\ (1{\cdot}38\times10^{-23}\ \text{J K}^{-1})\ (300\ \text{K}) = 6{\cdot}21\times10^{-21}\ \text{J}$$

$$d\varepsilon = (\varepsilon + 0{\cdot}005\varepsilon) - (\varepsilon - 0{\cdot}005\varepsilon) = 0{\cdot}01\varepsilon = 6{\cdot}21\times10^{-23}\ \text{J}$$

Substituting these values in Maxwell's equation (35), we have

$$\frac{dN_\varepsilon}{N} = \left\{\frac{2(6{\cdot}21\times10^{-21}\,\text{J})^{1/2}}{1{\cdot}77[(1{\cdot}38\times10^{-23}\,\text{JK}^{-1})(300\text{K})]^{3/2}}\right\} \times \left\{\exp\left(-\frac{6{\cdot}21\times10^{-21}\,\text{J}}{1{\cdot}38\times10^{-23}\,\text{JK}^{-1}\times300\,\text{K}}\right)(6{\cdot}21\times10^{-23}\,\text{J})\right\}$$

$$= \frac{2\times0{\cdot}788\times10^{-10}\,\text{J}^{-1}}{1{\cdot}77\times0{\cdot}266\times10^{-30}} \exp(-1{\cdot}5)\times6{\cdot}21\times10^{-23}\,\text{J}$$

$$= 4{\cdot}647\times10^{-3}$$

The Maxwell distribution of kinetic energies at two different temperatures is shown in Fig. 2 in which the factor $(1/N)\ (dN_\varepsilon/d\varepsilon)$ is plotted against ε. As can be seen, the most probable kinetic energy increases with increase in temperature as expected. The maximum in the probability function corresponds to *the most probable kinetic energy.*

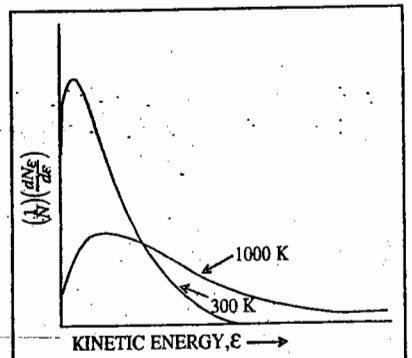

Fig. 2. Maxwell's distribution of kinetic energies at two different temperatures.

It can be easily shown with the help of Eq. 35 that *(i)* the most probable kinetic energy is given by $kT/2$ per molecule or $RT/2$ per mole of the gas and *(ii)* the average kinetic energy per mole is given by $(3/2)N_Akt=(3/2)RT$. This result is, evidently, in agreement with that obtained from the kinetic theory (Eq. 21).

Types of Molecular Velocities. Three types of molecular velocities are reckoned with in the study of gases. These are : *(i)* the most probable velocity, c_p *(ii)* the average velocity, $<c>$ and *(iii)* the root mean square velocity $<c^2>^{1/2}$.

The **most probable velocity** is defined as the velocity possessed by maximum number of molecules of a gas at a given temperature.

The **average velocity** is given by the arithmetic mean of different velocities possessed by the molecules of the gas at a given temperature. If $c_1, c_2, c_3 \ldots\ldots c_n$ are the individual velocities of the gas molecules and n is their total number, then, average velocity is given by

$$\frac{c_1 + c_2 + c_3 + \cdots\cdots c_n}{\quad} \quad (36)$$

If, however, $c_1, c_2, c_3 \ldots\ldots$ are the velocities possessed by *groups* of $n_1, n_2, n_3 \ldots\ldots$ molecules of the gas, respectively, then, average velocity is given by

$$<c> = \frac{n_1c_1 + n_2c_2 + n_3c_3 + \cdots\cdots}{n_1 + n_2 + n_3 + \cdots\cdots} \quad ...(37)$$

The root mean square velocity is defined as the square root of the mean of the squares of different velocities possessed by molecules of a gas at a given temperature. Evidently, the root mean square velocity would be given by

$$<c^2>^{1/2} = \left[\frac{c_1^2 + c_2^2 + c_3^2 + \cdots\cdots c_n^2}{n}\right]^{1/2} \quad ...(38)$$

where $c_1, c_2, c_3 \ldots\ldots c_n$ are the individual velocities of n molecules of the gas. Alternatively,

$$<c^2>^{1/2} = \left[\frac{n_1c_1^2 + n_2c_2^2 + n_3c_3^2 + \cdots\cdots}{n_1 + n_2 + n_3 + \cdots\cdots}\right]^{1/2} \quad ...(39)$$

where $c_1, c_2, c_3, \ldots\ldots$ are velocities possessed by groups of $n_1, n_2, n_3 \ldots\ldots$ molecules, respectively.

With the help of the Maxwell equation (Eq. 29), it is possible to derive mathematical expressions for the three types of velocities, *viz.*, the most probable velocity, c_p ; the average velocity, $<c>$ and the root mean square velocity, $<c^2>^{1/2}$. These expressions are as follows :

$$c_p = (2kT/m)^{1/2} = (2RT/M)^{1/2} \quad ...(40)$$

$$<c> = (8kT/\pi m)^{1/2} = (8RT/\pi M)^{1/2} \quad ...(41)$$

$$<c^2>^{1/2} = (3kT/m)^{1/2} = (3RT/M)^{1/2} \quad ...(42)$$

It is found that

$$<c^2>^{1/2} : <c> : c_p = 1{\cdot}00 : 0{\cdot}92 : 0{\cdot}82$$

Derivation of Expressions for c_p, $<c>$ and $<c^2>^{1/2}$

1. Expression for c_p. Differentiating Eq. 29 with respect to c (using dN/N for $p(c)dc$) and setting the result equal to zero, as required for a maximum, we have

$$\frac{d}{dc}\left(\frac{dN}{N}\right) = \left(\frac{m}{2\pi kT}\right)^{3/2} \exp(-mc^2/2kT)\left[8\pi c + 4\pi c^2\left(-\frac{mc}{kT}\right)\right] = 0 \quad ...(43)$$

The factor $(m/2\pi kT)^{3/2}$ is a constant, different from zero. Also, the factor $\exp(-mc^2/2kT)$ is not equal to zero. Hence, the third factor, *viz.*,

$$8\pi c + 4\pi\varepsilon^2\ (-mc/kT) = 0 \quad ...(44)$$

$$\therefore \quad c \equiv c_p = (2kT/m)^{1/2} = (2RT/M)^{1/2} \quad ...(45)$$

2. Expression for $<c>$. The average velocity is given by the expression

$$<c> = \int_0^\infty cp(c)dc \quad ...(46)$$

Substituting the value of $p(c)dc$ from Eq. 29, we have

$$<c> = 4\pi\left(\frac{m}{2\pi kT}\right)^{3/2}\int_0^\infty c^3 \exp\left(-\frac{mc^2}{2kT}\right)dc \quad ...(47)$$

Let $\quad mc^2/2kT = x^2$ so that $c^2 = 2kTx^2/m$ ...(48)

Differentiating both sides, we have

$$dc = 2kT\,xdx/mc \quad ...(49)$$

Also from Eq. 48, $\quad c = (2kTx^2/m)^{1/2} = (2kT/m)^{1/2}\,x$ ...(50)

Substituting the above value of c in Eq. 49, we have

$$dc = \frac{2kTx\,dx}{m(2kT/m)^{1/2}x} = \left(\frac{2kT}{m}\right)^{1/2} dx \qquad ...(51)$$

From Eq. 50, $\quad c^3 = (2kT/m)^{3/2}x^3 \qquad ...(52)$

Hence, the expression

$$\int_0^\infty c^3 \exp\left(-\frac{mc^2}{2kT}\right) dc = \int_0^\infty \left(\frac{2kT}{m}\right)^{3/2} x^3 e^{-x^2} \left(\frac{2kT}{m}\right)^{1/2} dx \qquad ...(53)$$

$$= \left(\frac{2kT}{m}\right)^2 \int_0^\infty x^3 e^{-x^2} dx = \left(\frac{2kT}{m}\right)^2 \left(\frac{1}{2}\right) \quad \left(\int_0^\infty x^3 e^{-x^2} dx = \frac{1}{2}\right) \qquad ...(54)$$

Thus, from Eqs. 47 and 54,

$$<c> = 4\pi\left(\frac{m}{2\pi kT}\right)^{3/2}\left(\frac{2kT}{m}\right)^2\left(\frac{1}{2}\right) = (8kT/\pi m)^{1/2} = (8RT/\pi M)^{1/2} \qquad ...(55)$$

3. Expression for $<c^2>^{1/2}$. The root mean square velocity is defined as

$$<c^2>^{1/2} = \left\{\int_0^\infty c^2 p(c)dx\right\}^{1/2} \qquad ...(56)$$

From Eq. 29, the expression

$$\int_0^\infty c^2 p(c)dc = 4\pi\left(\frac{m}{2\pi kT}\right)^{3/2} \int_0^\infty c^4 \exp\left(-\frac{mc^2}{2kT}\right) dc \qquad ...(57)$$

Let $\quad mc^2/(2kT) = x^2$ so that $c^4 = \left(\frac{2kT}{m}\right)^2 x^4 \qquad ...(58)$

From Eq. 58, $\quad c = \left(\frac{2kT}{m}\right)^{1/2} x$ so that $dc = \left(\frac{2kT}{m}\right)^{1/2} dx \qquad ...(59)$

From Eqs. 57, 58 and 59, it follows that

$$\int_0^\infty c^2 p(c)dc = 4\pi\left(\frac{m}{2\pi kT}\right)^{3/2}\left(\frac{2kT}{m}\right)^2\left(\frac{2kT}{m}\right)^{1/2}\int_0^\infty x^4 e^{-x^2} dx \qquad ...(60)$$

From the tables of definite integrals, we know that

$$\int_0^\infty x^4 e^{-x^2} dx = (3/8)\pi^{1/2} \qquad ...(61)$$

From the above equations, we have

$$\left\{\int_0^\infty c^2 p(c)dc\right\}^{1/2} = <c^2>^{1/2} = \left(\frac{3kT}{m}\right)^{1/2}$$

$$= \left(\frac{3RT}{M}\right)^{1/2} \qquad ...(62)$$

The molecular distribution of the three types of velocities is shown in Fig. 3

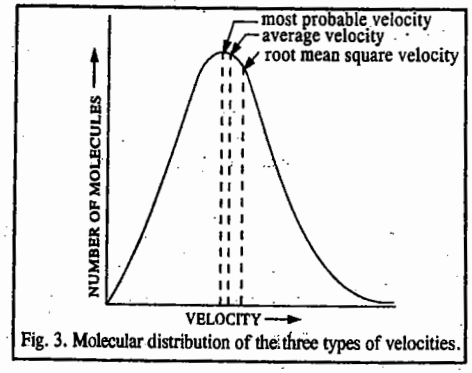

Fig. 3. Molecular distribution of the three types of velocities.

Example 3. For hydrogen gas, calculate *(a)* the root mean square velocity $<c^2>^{1/2}$ *(b)* the average velocity $<c>$ and *(c)* the most probable velocity c_p, at 0°C.

Solution : The molar mass M of H_2 = 2·016 g mol^{-1} = 2·016×10^{-3} kg mol^{-1}

(a) From Eq. 42,

$$<c^2>^{1/2} = \left(\frac{3RT}{M}\right)^{1/2} = \left(\frac{(3)(8\cdot314\ \text{J K}^{-1}\ \text{mol}^{-1})(273\cdot15\ \text{K})}{2\cdot016\times10^{-3}\ \text{kg mol}^{-1}}\right)^{1/2}$$

Recalling that J = kg m^2 s^{-2}, we find that $<c>^{1/2}$ = **1·84×10^3 m s^{-1}**

(b) From Eq. 41, $<c> = \left(\frac{8RT}{\pi M}\right)^{1/2} = \left(\frac{(8)(8\cdot314\ \text{J K}^{-1}\ \text{mol}^{-1})(273\cdot15\ \text{K})}{(3\cdot1416)(2\cdot016\times10^{-3}\ \text{kg mol}^{-1})}\right)^{1/2}$

= **1·69×10^3 m s^{-1}**

(c) From Eq. 40, $c_p = \left(\frac{2RT}{M}\right)^{1/2} = \left(\frac{(2)(8\cdot314\ \text{J K}^{-1}\ \text{mol}^{-1})(273\cdot15\ \text{K})}{2\cdot016\times10^{-3}\ \text{kg mol}^{-1}}\right)^{1/2}$

= **1·50×10^3 m s^{-1}**

The average velocities of some common gaseous molecules are given in Table 1.

TABLE 1

Average Velocities (m s^{-1}) of Some Common Gaseous Molecules at 0°C

Gas	$<c>$	Gas	$<c>$	Gas	$<c>$
Hydrogen	1692·0	Oxygen	425·2	Methane	600·6
Deuterium	1196·0	Chlorine	285·6	Ammonia	582·7
Helium	1204·0	Mercury vapour	170·0	Carbon dioxide	362·5
Nitrogen	454·2	Argon	380·8	Carbon monoxide	454·5

Example 4. Calculate the temperatures at which the root mean square velocity, the average velocity and the most probable velocity of oxygen gas are all equal to 1,500 m s^{-1}.

Solution : Let the respective temperatures be T_1, T_2 and T_3.

$$<c^2>^{1/2} = (3RT_1/M)^{1/2} = 1\cdot5\times10^3\ \text{m s}^{-1}$$

$$\therefore \quad T_1 = \frac{(1\cdot5\times10^3\ \text{m s}^{-1})^2(32\times10^3\ \text{kg mol}^{-1})}{3\times8\cdot314\ \text{J K}^{-1}\ \text{mol}^{-1}} = 2886\ \text{K} \qquad [M = 32\ \text{g mol}^{-1}]$$

$$<c> = (8RT_2/\pi M)^{1/2} = 1\cdot5\times10^3\ \text{m s}^{-1}$$

$$\therefore \quad T_2 = \frac{(1\cdot5\times10^{-3}\ \text{m s}^{-1})^2(32\times10^{-3}\ \text{kg mol}^{-1})(3\cdot1416)}{8\times8\cdot314\ \text{J K}^{-1}\ \text{mol}^{-1}} = 3399\ \text{K}$$

(iii) $\quad c_p = (2RT_3/M)^{1/2} = 1\cdot5\times10^3\ \text{m s}^{-1}$

$$\therefore \quad T_3 = \frac{(1\cdot5\times10^3\ \text{m s}^{-1})^2(32\times10^{-3}\ \text{kg mol}^{-1})}{2\times8\cdot314\ \text{J K}^{-1}\ \text{mol}^{-1}} = 4330\ \text{K}$$

Example 5. Calculate the temperature at which the average velocity of oxygen equals that of hydrogen at 20 K

Solution : $\quad <c> = (8RT/\pi M)^{1/2}$, *i.e.*, $<c> \propto (T/M)^{1/2}$

Let $<c>_1$ and $<c>_2$ be the average velocities of O_2 and H_2, respectively.

$$\frac{<c>_1}{<c>_2} = \left(\frac{T_1/M_1}{T_2/M_2}\right)^{1/2} = 1 \quad \text{so that} \quad T_1/M_1 = T_2/M_2$$

or $\quad T_1/32\ \text{g mol}^{-1} = T_2/2\ \text{g mol}^{-1}$

$$\therefore \quad T_1 = (32/2)T_2 = 16\times20\ \text{K} = 320\ \text{K}$$

Example 6. Calculate the root mean square velocity of nitrogen at 27°C and 70 cm pressure. Density of Hg=13·6 g cm^{-3}.

Solution : Volume V_2 at 27°C and 70 cm pressure is given by the relation $P_2V_2/T_2 = P_1V_1/T_1$:

$$\frac{70\text{ cm} \times V_2}{300\text{ K}} = \frac{76\text{ cm} \times 0{\cdot}0224\text{ m}^3\text{ mol}^{-1}}{273\text{ K}}$$

$$\therefore \quad V_2 = 0{\cdot}026725\text{ m}^3\text{ mol}^{-1}$$

Pressure, $P = (70/76) \times 101{,}325\text{ N m}^{-2}$

$$< c^2 >^{1/2} = \left(\frac{3RT}{M}\right)^{1/2} = \left(\frac{3PV}{M}\right)^{1/2} \qquad \text{(Eq. 42)}$$

$$= \left(\frac{(3)\,(70/76) \times 101{,}325\text{ N m}^{-2})\,(0{\cdot}026725\text{ m}^3\text{ mol}^{-1})}{28 \times 10^{-3}\text{ kg mol}^{-1}}\right)^{1/2}$$

$$= \mathbf{517\text{ m s}^{-1}}$$

(Newton, N = kg m s^{-2})

Expansivity and Compressibility. Gases expand on heating and are compressed on applying pressure. The variation of volume V with temperature T, keeping pressure P constant, is called the **coefficient of thermal expansion** or simply **expansivity**, α, of the gas. Thus,

$$\alpha = \frac{1}{V}\left(\frac{\partial V}{\partial T}\right)_P \qquad \ldots(63)$$

The variation of V with P, keeping T constant, is called the **coefficient of isothermal compressibility** or simply **compressibility**, β, of the gas. Thus,

$$\beta = -\frac{1}{V}\left(\frac{\partial V}{\partial P}\right)_T \qquad \ldots(64)$$

The volume of a gas decreases as pressure increases so that the quantity $(\partial V/\partial P)_T$ is negative. Hence, a minus sign is included in the definition so as to make β positive. Note that α has the dimensions of T^{-1} and β those of P^{-1}.

Example 7. Show that for an ideal gas, $\alpha = 1/T$ and $\beta = 1/P$.

Solution : For n moles of an ideal gas, $PV = nRT$

or $$V = nRT/P \qquad \ldots(i)$$

Differentiating Eq. *(i)* with respect to T at constant P, we have

$$(\partial V/\partial P)_P = -nR/P = V/T$$

$$\therefore \quad \alpha = 1/V\,(\partial V/\partial T)_P = (1/V)(V/T) = 1/T$$

Again, differentiating Eq. *(i)* with respect to P at constant T, we have

$$(\partial V/\partial P)_T = -nRT/P^2 = (nRT/P)\,(-1/P) = -(V/P)$$

$$\therefore \quad \beta = -\frac{1}{V}\left(\frac{\partial V}{\partial P}\right)_T = \left(-\frac{1}{V}\right)\left(-\frac{V}{P}\right) = \frac{1}{P}$$

Thus, $$\alpha = 1/T \quad \text{and} \quad \beta = 1/P$$

Example 8. Writing $V = f(P, T, n)$, taking its differential and using Boyle's law, Charles' law and other relations, derive the ideal gas equation.

Solution : $$V = f(P, T, n) \qquad \ldots(i)$$

i.e., volume of a gas is a function of its pressure, temperature and number of moles. As we shall see in thermodynamics, the volume is a state function so that its total differential can be written as

$$dV = (\partial V/\partial P)_{T,n}\,dP + (\partial V/\partial T)_{P,n}\,dT + (\partial V/\partial n)_{T,P}\,dn \qquad \ldots(ii)$$

From Boyle's law, at constant T and n,

$$PV = K \text{ so that } V = K/P$$

Differentiating with respect to P, at constant T and n, we have

$$(\partial V/\partial P)_{T,n} = -K/P^2 = -PV/P^2 = -V/P \qquad \ldots(iii)$$

Similarly, from Charles' law, at constant P and n, $V = KT$ so that

$$(\partial V/\partial T)_{P,n} = K' = V/T \qquad \ldots(iv)$$

Again, since at constant P and T, $V \propto n$, we can write

$$V = K''n$$

$$\therefore \quad (\partial V/\partial n)_{P,T} = K'' = V/n \qquad \ldots(v)$$

Substituting Eqs. *(iii)*, *(iv)* and *(v)* in Eq. *(ii)*, we have

$$dV = -V\,dP/P + V\,dT/T + V\,dn/n$$

or $$dV/V = -dP/P + dT/T + dn/n \qquad \ldots(vi)$$

Integrating, we get $\int \frac{dV}{V} = -\int \frac{dP}{P} + \int \frac{dT}{T} + \int \frac{dn}{n}$

Setting the constant of integration $= \ln R$, where R is the gas constant, we have

$$\ln V = -\ln P + \ln T + \ln n + \ln R$$

$$\ln V + \ln P = \ln n + \ln R + \ln T$$

$$\ln (PV) = \ln (nRT)$$

or $$PV = nRT \text{ which is the ideal gas equation.}$$

Collision Parameters

Collision Diameter. The kinetic theory of gases treats molecules as point masses. When two such molecules approach each other, a point is reached at which the mutual repulsion between the molecules (resulting from electronic and nuclear replusions) becomes so strong that it causes reversal of the direction of their motion. *The distance between the centres of the two molecules at the point of their closest approach is known as* **collision diameter.** It is denoted by d, as shown in Fig. 4. Evidently, a gaseous molecule can be regarded as a rigid (or hard) sphere of radius d. The volume $(4/3)\pi d^3$ is known as the effective volume of the molecule.

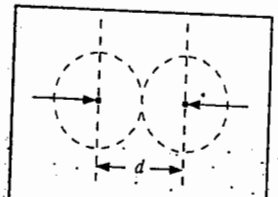

Fig. 4. Collision of two molecules. Concept of collision diameter.

It can be easily seen that if the distance between the centres of two molecules is less than d, there would be a collision between them. Thus, collision is an event in which the centres of two identical molecules come within a distance d from each other.

Collision Cross-section. The model of gaseous molecules as hard, non-interacting spheres of diameter d can satisfactorily account for various gaseous properties such as the transport properties (viscosity, diffusion and thermal conductivity), the mean free path and the number of collisions the molecules undergo. It can be easily visualised that when two molecules collide, the effective area of the target is πd^2. The quantity πd^2 is called the **collision cross-section** σ of the molecule because it is the cross-sectional area of an imaginary sphere surrounding the molecule into which the centre of another molecule cannot penetrate.

Collision Number. It can be shown on kinetic considerations that in a gas, the number of molecules with which a *single molecule* will collide per unit time is given by $\sqrt{2}\pi d^2 < c > \rho$ where $< c >$ is the average velocity of the molecules and ρ is the number density, *i.e.*, the number of molecules per unit volume of the gas. This expression, evidently, gives the number of collisions suffered by a single molecule per unit time per unit volume of the gas. This is known as the **collision number**. Thus,

$$Z_1 = \sqrt{2}\,\pi d^2 < c > \rho \qquad \ldots(65)$$

The total number of molecules colliding per unit time per unit volume of the gas is, therefore, given by $\sqrt{2}\pi d^2 < c > \rho^2$. Since each collision involves two molecules, the number of collisions of

like molecules occurring per unit time per unit volume of the gas is given by

$$Z_{11} = \tfrac{1}{2}(\sqrt{2}\,\pi d^2 < c > \rho^2) = \frac{1}{\sqrt{2}}(\pi d^2 < c > \rho^2) \qquad ...(66)$$

Collision Frequency. The number Z_{11} in Eq. 66 gives the collision frequency of the gas. Thus, **collision frequency** is the number of molecular collisions occurring per unit time per unit volume of the gas.

It readily follows that the number of collisions of molecules of type 1 with those of type 2, would be given by

$$Z_{12} = \frac{1}{\sqrt{2}}(\pi d_{av}^2 < c > \rho_1\rho_2) \quad (d_{av} = (d_1+d_2)/2) \qquad ...(67)$$

where ρ_1 and ρ_2 are the *number densities* of molecules of type 1 and 2, respectively. The number density ρ is equal to P/kT, as shown below :

For an ideal gas, $PV = nRT = nN_Ak$

$$\therefore \qquad P = nN_Ak T/V = NkT/V \qquad ...(68)$$

where $N(=nN_A)$ is the total number of molecules in n moles of the gas. Since ρ is the number of molecules per unit volume, hence $\rho = N/V$. Thus, $P = \rho kT$.

$$\therefore \qquad \rho = P/kT \qquad ...(69)$$

Eqs. 65 and 66 may thus be written as

$$Z_1 = \sqrt{2}\pi d^2 < c > P/kT \qquad ...(70)$$

and

$$Z_{11} = \frac{\pi d^2 < c > P^2}{\sqrt{2}(kT)^2} \qquad ...(71)$$

It may be noted that while units of Z_1 are s^{-1}, those of Z_{11} are $s^{-1}\ m^{-3}$.

Mean Free Path. A very important quantity in kinetic theory of gases is the **mean free path**, λ, defined as the mean distance travelled by a gas molecule between two successive collisions. Evidently,

$$\lambda = \frac{<c>}{Z_1} = \frac{<c>}{\sqrt{2}\pi d^2 <c> P/kT} = \frac{kT}{\sqrt{2}\pi d^2 P} \qquad ...(72)$$

From Eq. 72, we see that $\lambda \propto 1/P$, *i.e., the mean free path of a gas molecule is inversely proportional to pressure.* This fact is of tremendous importance in vacuum systems. It should be borne in mind that at 1 atm pressure, λ is very small compared with the macroscopic dimensions (such as 1 cm) of the container which implies that the molecules collide with one another far more frequently than they collide with the walls of the container and that a molecule moves a distance of several molecular diameters before colliding with another molecule.

In a good vacuum where the pressure is of the order of 10^{-3} atm, a simple calculation shows that λ is very large compared with the dimensions of the container. Thus, in a good vacuum the gas molecules collide far more frequently with the walls of the container than with one another. Under such conditions, the gas is called a **Knudsen gas.**

Example 9. For oxygen gas at 25°C, calculate *(a)* the mean free path at 1 atm pressure *(b)* the mean free path at 10^{-3} mm Hg pressure *(c)* the number of collisions per second per molecule *(d)* the number of collisions per cubic metre per second and *(e)* the number of moles of collisions per dm^3 per second. In parts *(c)*, *(d)* and *(e)*, the pressure is 1 atm. The collision diameter of oxygen molecule is 361 picometre.

Solution : *(a)* 1 atm $= 1{\cdot}01325\times10^5\ N\ m^{-2}$ $\qquad T = 25°C = 298\ K$

$$d = 361\ pm = 361\times10^{-12}\ m = 3{\cdot}61\times10^{-10}\ m$$

From Eq. 72, $$\lambda = \frac{kT}{\sqrt{2}\pi d^2 P} = \frac{(1{\cdot}38\times10^{-23}\,J\,K^{-1})(298\,K)}{(1{\cdot}4142)(3{\cdot}1416)(3{\cdot}61\times10^{-10}\,m)^2(1{\cdot}01325\times10^5\,N\,m^{-2})}$$

$$= 7{\cdot}02\times10^{-8}\ m = 70{\cdot}2\ nm \qquad [J = kg\ m^2\ s^{-2} = N\ m]$$

(b) $$P = 10^{-3}\ mm\ Hg = \frac{(10^{-3}\,mm\,Hg)(1{\cdot}01325\times10^5\,N\,m^{-2}\,atm^{-1})}{760\,mm\,Hg\,atm^{-1}} = 0{\cdot}1333\ N\ m^{-2}$$

$$\therefore \qquad \lambda = \frac{(1{\cdot}38\times10^{-23}\,J\,K^{-1})(298\,K)}{(1{\cdot}4142)(3{\cdot}1416)(3{\cdot}61\times10^{-10}\,m)^2(0{\cdot}1333\,N\,m^{-2})} = 5{\cdot}3\times10^{-2}\ m$$

(c) From Eq. 41, $$<c> = \left(\frac{8RT}{\pi M}\right)^{1/2} = \left[\frac{(8)(8{\cdot}314\,J\,K^{-1}\,mol^{-1})(298\,K)}{(3{\cdot}1416)(32\times10^{-3}\,kg\,mol^{-1})}\right]^{1/2} = 444{\cdot}0\ m\ s^{-1}$$

From Eq. 70, $$Z_1 = \sqrt{2}\pi d^2 <c> P/kT$$

$$= \frac{(1{\cdot}4142)(3{\cdot}1416)(3{\cdot}61\times10^{-10}\,m)^2(444{\cdot}0\,m\,s^{-1})(1{\cdot}01325\times10^5\,N\,m^{-2})}{(1{\cdot}38\times10^{-23}\,J\,K^{-1})(298\,K)}$$

$$= 6{\cdot}32\times10^9\ s^{-1}$$

(d) From Eq. 71, $$Z_{11} = \frac{\pi d^2 <c> P^2}{\sqrt{2}\,(kT)^2} \qquad [\because \rho = P/kT]$$

$$= \frac{(3{\cdot}1416)(3{\cdot}61\times10^{-10}\,m)^2(444{\cdot}0\,m\,s^{-1})(1{\cdot}01325\times10^5\,N\,m^{-2})^2}{(1{\cdot}4142)(1{\cdot}38\times10^{-23}\,J\,K^{-1})^2(298\,K)^2}$$

$$= 7{\cdot}77\times10^{34}\ m^{-3}\ s^{-1}$$

(e) $N_A = 6{\cdot}022\times10^{23}\ mol^{-1}$ and $1\ dm^3 = 10^{-3}\ m^3$

$$\therefore \qquad Z_{11} = \frac{(7{\cdot}77\times10^{34}\,m^{-3}\,s^{-1})(10^{-3}\,m^3\,dm^{-3})}{6{\cdot}022\times10^{23}\,mol^{-1}} = 1{\cdot}29\times10^8\ mol\ dm^{-3}\ s^{-1}$$

Some properties of gas molecules derived from the kinetic theory of gases are given in Table 2.

TABLE 2

Gas Properties at 25°C and 1 atm Pressure

Gas	Collision Diameter d (m)	Mean Free Path λ (m)	Collision Frequency Z_1 (s^{-1})	Collision Frequency Z_{11} ($m^{-3}\ s^{-1}$)
He	$2{\cdot}18\times10^{-10}$	$19{\cdot}0\times10^{-8}$	$6{\cdot}6\times10^9$	$8{\cdot}1\times10^{34}$
H_2	2·73	12·3	14·4	17·7
Ar	3·96	5·8	6·9	8·5
N_2	3·74	6·5	7·3	9·0
O_2	3·57	7·1	6·1	7·5
CO_2	4·56	4·4	8·6	10·6

TRANSPORT PROPERTIES

There is a particularly simple group of processes, called the **transport processes**, in which some physical quantity such as mass or energy or momentum or electrical charge is transported from one region of a system to another. Consider a metal bar connecting two heat reservoirs at different temperatures. Heat flows through the bar from the high-temperature reservoir to the low-temperature reservoir; the heat flow is the manifestation of the transport of energy through the bar. The energy flow is easily measurable. Another example is the transport of electrical charge through a conductor by the application of an electrical potential difference between the ends of the conductor. Mass is transported in the flow of a fluid through a pipe as a result of the pressure difference between the ends of the pipe. Diffusion is the mass transport that occurs in a mixture if a concentration gradient is present. The viscosity of a fluid, its resistance to flow, is determined by the transport of momentum in a direction perpendicular to the direction of the flow.

In all cases, the **flow**, *viz.*, the amount of physical **quantity** transported in unit time through a unit area perpendicular to the direction of flow, is *proportional to the negative gradient* of some other physical property such as temperature, pressure or electrical potential. Choosing the z-axis as the direction of flow, the general flow or transport is given by

$$J_z = L\left(-\frac{\partial Y}{\partial z}\right) \qquad ...(73)$$

where J_z is the flow (also called **flux**), *i.e.*, the amount of quantity transported per square meter per second, L is the proportionality constant (called the **phenomenological coefficient**) and $(-\partial Y/\partial z)$ is the negative gradient of Y in the direction of flow (also called the **generalized force**). Y may be any of the quantities such as temperature, electrical potential, pressure and so on. Since flow occurs in a particular direction, it is a vector quantity; Eq. 73 describes the z-component of the vector. For the cases mentioned above, we have the following equations for flow in the z-direction :

Heat flow	$J_z = -\kappa_T \frac{\partial T}{\partial z}$	(Fourier's law)	...(74)
Electrical current	$J_z = -\kappa \frac{\partial \phi}{\partial z}$	(Ohm's law) (ϕ is potential difference)	...(75)
Fluid flow	$J_z = -f \frac{\partial P}{\partial z}$	(Poiseuille's law)	...(76)
Diffusion	$J_z = -D \frac{\partial \rho}{\partial z}$	(Fick's law)	...(77)

In the above equations, κ_T is the thermal conductivity coefficient, κ is the electrical conductivity, f is a frictional coefficient related to viscosity, D is the diffusion coefficient and ρ is the *number density, i.e.*, the number of molecules per m^3.

Consider the flow of heat from one end of a metal bar to the other. If the hot end is at $z=0$ and the cold end at Z, then in the steady state, the temperature as a function of z appears as shown in Fig. 5. The value of $\partial T/\partial z$ is negative so that $(-\partial T/\partial z)$ is positive. The heat flow is in the positive direction (from the hot to the cold end).

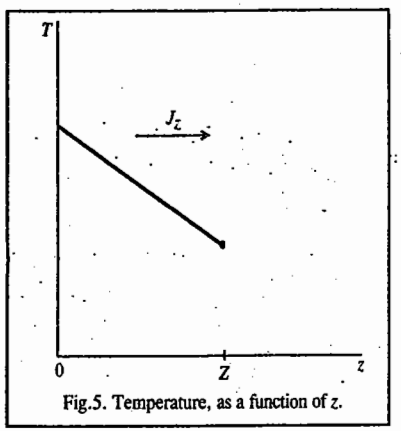

Fig.5. Temperature, as a function of z.

If we define $(X_T)_z = -\partial T/\partial z$ ...(78)

as the 'generalized force' that is driving the heat flow, we can write Eq. 74 as

$$J_z = \kappa_T (X_T)_z \text{ (Fourier's law)} \qquad ...(79)$$

and can say that the flow has the same sign as the force. Thus, any of the transport laws, given by Eqs. 74, 75, 76 and 77 can be written in the form

$$J = LX \qquad ...(80)$$

Eq. 80 shows that the flux of any quantity is proportional to the force that drives the flux. This proportionality between the flux (the flow) and the force is called a linear law. The force is always the *negative gradient* of an intensive quantity. Fundamental contributions to these laws, which have been experimentally verified though they were initially proposed as empirical laws, have been made by L. Onsager.

It can be shown that for any transport

$$j = \rho \bar{c} q \qquad ...(81)$$

where j is the rate of flow, ρ is the number density, $\bar{c}$ is the mean speed of the molecules of the

physical quantity and q is the amount of the physical quantity possessed by each carrier. Eq. 81 is the **general equation for transport phenomena.**

We shall now discuss the three important transport phenomena, *viz.*, thermal conductivity, viscosity and diffusion in gases.

1. Thermal Conductivity of a Gas. Consider a vessel containing a gas. Let us consider two large metal plates parallel to the xy-plane and separated by a distance Z, at temperatures T_1 and T_2, the hotter plate (T_2) being the upper one. After some time a steady state will be established in which there is a downward flow of heat at constant rate. This flow of heat results from the fact that the molecules at the upper levels have a greater thermal energy than those at the lower levels; the molecules moving downwards carry more energy than those moving upwards.

In order to calculate the energy flow in unit time through 1 m^2 parallel to the xy-plane, we imagine a large number of horizontal layers in the gas, each successive layer at a slightly higher temperature than the one below it. The change in temperature with height is given by

$$\frac{\partial T}{\partial z} = \frac{\Delta T}{\Delta z} = \frac{T_2 - T_1}{Z - 0} \qquad ...(82)$$

if the lower plate lies at the position $z = 0$ and the upper one at $z = Z$. The temperature gradient, $\partial T/\partial z$, is constant so that at any height z the temperature is given by

$$T = T_1 + \left(\frac{\partial T}{\partial z}\right) z \qquad ...(83)$$

If the gas is monoatomic with an average thermal energy $\bar{\varepsilon} = 3/2\ kT$, then the average energy of the molecules at the height z is given by

$$\bar{\varepsilon} = \frac{3}{2}kT = \frac{3}{2}k\left[T_1 + \left(\frac{\partial T}{\partial z}\right)z\right] \qquad ...(84)$$

To calculate the heat flow, we consider an area 1 m^2 in a horizontal plane at the height z (Fig. 6).

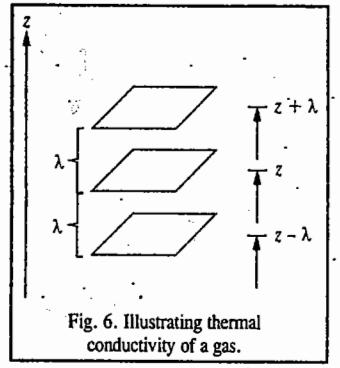

Fig. 6. Illustrating thermal conductivity of a gas.

The energy carried by a molecule as it passes through the plane depends on the temperature of the layer of gas at which the molecule had its last opportunity to adjust its energy. This last adjustment occurred during the last collision with another molecule. Suppose that, on an average, the molecules have travelled a distance λ (the mean free path) since their last collision. If the surface of interest lies at a height z, the molecules going down made their last collision at a height $z+\lambda$, while those going up made their last collision at a height $z - \lambda$ (Fig. 6). The molecules carry an amount of energy appropriate to the height where the last collision occurred. The downward flow of energy is given by Eqs. 81 and 84, as

$$\varepsilon\downarrow = \frac{1}{6}\rho(\bar{c})_{z+\lambda}\frac{3}{2}k\left[T_1 + \left(\frac{\partial T}{\partial z}\right)(z+\lambda)\right] \qquad ...(85)$$

while the upward flow is given by

$$\varepsilon\uparrow = \frac{1}{6}\rho(\bar{c})_{z-\lambda}\frac{3}{2}k\left[T_1 + \left(\frac{\partial T}{\partial z}\right)(z-\lambda)\right] \qquad ...(86)$$

The factor 1/6 appears since, on an average, only 1/6 of the molecules are going down and only 1/6 going up. The net flow upward is denoted by J_ε and is given by

$$J_\varepsilon = \varepsilon\uparrow - \varepsilon\downarrow \qquad ...(87)$$

Now if the gas is not to have net motion through the surface we require that the number of molecules

going up in unit time must equal the number going down, so that

$$\frac{1}{6}\rho(\bar{c})_{z+\lambda} = \frac{1}{6}\rho(\bar{c})_{z-\lambda} \qquad ...(88)$$

which means that $\rho\bar{c}$ has the same value at every height. Substituting for $\varepsilon\downarrow$ and $\varepsilon\uparrow$ from Eqs. 85 and 86 into Eq. 87 and using Eq. 88, we obtain

$$J_\varepsilon = \frac{1}{6}\rho\bar{c}\frac{3}{2}k\left(\frac{\partial T}{\partial z}\right)[(z-\lambda)-(z+\lambda)] = -\frac{1}{2}\rho\bar{c}k\lambda\left(\frac{\partial T}{\partial z}\right) \qquad ...(89)$$

Comparing this equation with the empirical Fourier's law (Eq. 74), we find that

$$\kappa_T = \frac{1}{2}\rho\bar{c}k\lambda$$

$$= \frac{1}{3}\left(\frac{\rho}{N_A}\right)C_{v,m}\bar{c}\lambda \qquad ...(90)$$

since the molar heat capacity $C_{v,m}=(3/2)R=(3/2)kN_A$ or $k=2C_{v,m}/3N_A$. The factor (ρ/N_A) is the concentration in mol m^{-3}. From the kinetic theory of gases, we know that $\bar{c} = (8kT/\pi m)^{1/2}$. The mean free path, λ, is given by

$$\lambda = \frac{1}{\sqrt{2}\sigma\rho} \qquad ...(91)$$

where σ is the collision cross-section ($\sigma=\pi d^2$, where d is the collision diameter of the gaseous molecules, assumed as hard spheres). Hence, from Eqs. 90 and 91, the thermal conductivity of a gas is given by

$$\kappa_T = \frac{\bar{c}C_{v,m}}{3\sqrt{2}\sigma N_A} \qquad ...(92)$$

We see from Eq. 92 that the thermal conductivity is *independent of pressure*. This has been confirmed experimentally. Again, if $C_{v,m}$ is independent of temperature, then everything on the right of Eq. 92 is constant except $\bar{c}$, which is proportional to $T^{1/2}$. Therefore, κ_T should increase as $T^{1/2}$. This, too, has been confirmed experimentally.

Note that Eq. 90 can also be rewritten as

$$\kappa_T = \left(\frac{1}{3}\right)\lambda\bar{c}C_{v,m}[A] \qquad ...(93)$$

because $\rho = N/V$ so that $\rho/N_A = n/V$ where the number of moles $n = N/N_A$ and n/V can be considered as the molar concentration [A] of the gas A.

Example 10. Calculate the thermal conductivity of air at room temperature. Assume that the molar mass of air is 29 g mol^{-1} and the collision cross-section of $O_2(g)$ and $N_2(g)$, which air consists of, is 0·42 nm^2. Since air is a mixture of diatomic gases, its constant volume molar heat capacity is (5/2)R.

Solution : $\kappa_T = (1/3)\lambda\bar{c}C_{v,m}[A]$ [Eq. 93]

It can be easily shown that $[A]=P/RT$. Also, $\lambda = kT/\sqrt{2}\,\sigma P$; $\bar{c} = (8kT/\pi m)^{1/2} = (8RT/\pi M)^{1/2}$, $C_{v,m}=(5/2)R$. Substituting these expressions, we have

$$\kappa_T = \frac{1}{3}\times\frac{kT}{\sqrt{2}\sigma P}\times\left(\frac{8RT}{\pi M}\right)^{1/2}\times\frac{5}{2}R\times\frac{P}{RT} = \frac{5}{3\sqrt{\pi}\sigma}\frac{k}{}\left(\frac{RT}{M}\right)^{1/2}$$

Substituting the given data, we get

$$\kappa_T = \frac{5}{3\sqrt{\pi}}\times\frac{1{\cdot}38\times10^{-23}\,JK^{-1}}{0{\cdot}42\times10^{-18}\,m^2}\times\left(\frac{(8{\cdot}314\,JK^{-1}mol^{-1})(298\,K)}{29\times10^{-3}\,kg\,mol^{-1}}\right)^{1/2}$$

$$= 9{\cdot}0\times10^{-3}\ J\ K^{-1}\ m^{-1}\ s^{-1}$$

Example 11. For hard sphere polyatomic gaseous molecules of water, the thermal conductivity is given by

$$\kappa_T = \frac{5}{16}\left(\frac{kT}{\pi m}\right)^{1/2}\frac{C_{v,m}+(9/4)R}{N_A d^2}$$

Predict κ_T for water vapour at 298 K, assuming that $C_{v,m}$ = 25·26 JK^{-1} mol^{-1} and the collision diameter, d = 0·50 nm.

Solution : Note that here m is the mass of one molecule given by M/N_A, where M is the molar mass.

Substituting the given data,

$$\kappa_T = \frac{5}{16}\left(\frac{(1{\cdot}38\times10^{-23}\,JK^{-1})(298K)[1kg\,m^2s^{-2})(1J)]}{\pi(18{\cdot}02\times10^{-3}\,kg\,mol^{-1})/(6{\cdot}022\times10^{23}\,mol^{-1})}\right)^{1/2}$$

$$\times\frac{\left(25{\cdot}26\,JK^{-1}mol^{-1}+\frac{9}{4}(8{\cdot}314\,JK^{-1}mol^{-1}\right)}{(6{\cdot}022\times10^{23}\,mol^{-1})(5{\cdot}0\times10^{-10}\,m)^2} \qquad (J = kg\ m^2\ s^{-2})$$

$$= 0{\cdot}019\ J\ K^{-1}\ m^{-1}\ s^{-1}$$

This value agrees favourably with the experimental value of 0·018 J K^{-1} m^{-1} s^{-1}.

2. Viscosity. The formula for the coefficient of viscosity of a gas can be derived in a way similar to that used for heat conduction. We imagine two very large parallel flat plates, one lying in the xy-plane, the other at a distance Z above the xy-plane. We keep the lower plate stationary and pull the upper plate in $+x$ direction with a velocity U. The viscosity of the gas exerts a drag on the moving plate. To keep the plate in uniform motion, a force must be applied to balance the viscous drag. If we look at the situation in another way, we find that if the upper plate moves with a velocity U, the viscous force will tend to set the lower plate in motion. A force must be applied to the lower plate to keep it in place.

Again we suppose that the gas between the plates is made up of a series of horizontal layers. The layer next to the lower plate is immobile. As we move upwards, each successive layer has a slightly larger component of velocity in the x-direction, the topmost layer at the height Z having the velocity U. This type of flow, in which there is a regular gradation of velocity in passing from one layer to the next, is called **laminar flow.** The layer at the height z has a velocity in the x-direction given by u_z :

$$u_z = \frac{\partial u}{\partial z}z \qquad ...(94)$$

At $z=Z$, $u=U$ so that

$$\frac{\partial u}{\partial z} = \frac{U}{Z} \qquad ...(95)$$

If we observe a layer at height z, we see that molecules enter this layer from the neighbouring layers. The molecules from the upper layers will bring extra momentum x to this layer while those which come from below are deficient in momentum. There is, therefore, a net downward flow of momentum x through the layer. Now we shall calculate the rate of this flow through 1 m^2 of the layer at height z (Fig. 7).

The number of molecules passing downwards through 1 m^2 s^{-1} is (1/6) $\rho\bar{c}$ and as many come upwards as come downwards. The molecules that pass downwards through the layer at z carry momentum x appropriate to

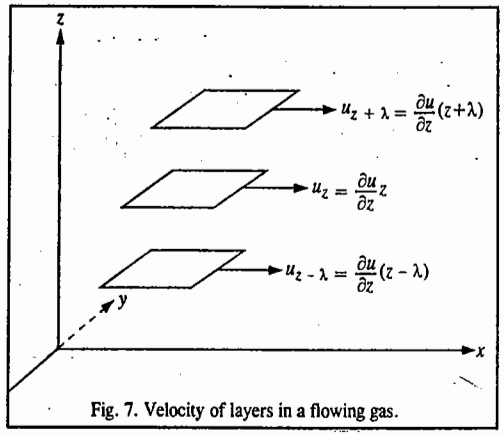

Fig. 7. Velocity of layers in a flowing gas.

the layer in which they made their last collision *viz*,, the layer at height $z + \lambda$. The momentum x is given by

$$mu_{z+\lambda} = m\left(\frac{\partial u}{\partial z}\right)(z+\lambda) \qquad ...(96)$$

Hence, the momentum coming down through 1 m^2 s^{-1} is given by

$$(mu)\downarrow = \frac{1}{6}\rho\bar{c}m\left(\frac{\partial u}{\partial z}\right)(z+\lambda) \qquad ...(97)$$

Similarly, the momentum coming up is given by

$$(mu)\uparrow = \frac{1}{6}\rho\bar{c}m\left(\frac{\partial u}{\partial z}\right)(z-\lambda) \qquad ...(98)$$

since the molecules coming up adjust their momentum in the layer at $z-\lambda$. The net downward flow of momentum x is given by

$$(mu)\downarrow - (mu)\uparrow = \frac{1}{3}\rho\bar{c}m\lambda\left(\frac{\partial u}{\partial z}\right) \qquad ...(99)$$

Since this quantity is independent of z, it must also be equal to the net momentum x transferred in one second to 1 m^2 of the lower plate. Since the momentum transfered per unit time is the force, the force acting in the x-direction on 1 m^2 of the lower plate is given by

$$f_x = \frac{1}{3}\rho\bar{c}m\lambda\left(\frac{\partial u}{\partial z}\right) \qquad ...(100)$$

To hold this plate stationary, we must apply an equal and opposite force f_{-x} such that $f_x + f_{-x} = 0$. The coefficient of viscosity, η, is defined as

$$f_{-x} = -\eta\left(\frac{\partial u}{\partial z}\right) \qquad ...(101)$$

The coefficient of viscosity is the force that must be applied to hold the lower plate stationary if the velocity gradient $\partial u/\partial z$ is unity and the plate has unit area. Comparing Eqs. 99 and 100, we have

$$\eta = \frac{1}{3}\rho\bar{c}m\lambda, \qquad ...(102)$$

If the mass density of the gas is ρ_{mass}, then $\rho_{mass} = \rho m$ and

$$\eta = \frac{1}{3}\rho_{masss}\bar{c}\lambda \qquad ...(103)$$

The numerical factor 1/3 is not quite correct since the flow of gas produces a non-equilibrium situation. For elastic spheres, the factor should be 1/2. The unit of the viscosity coefficient is N s m^{-2} = 1 Pascal second (Pa s) = 1 kg m^{-1} s^{-1}.

Eq. 102 can be further simplified as

$$\eta = \frac{1}{3}\lambda\bar{c}\rho m = \frac{1}{3}\lambda\bar{c}\left(\frac{N}{V}\right)m = \frac{1}{3}\lambda\bar{c}\left(\frac{nN_A}{V}\right)\left(\frac{M}{N_A}\right)$$

[$\because$ number of moles $n = N/N_A$ and $m = M/N_A$ where M is the molar mass]

Thus,

$$\eta = \frac{1}{3}\lambda\bar{c}M[A] \qquad ...(104)$$

where [A] (the molar concentration of the gas A) = n/V.

Note that Eq. 104 is only approximate.

Like thermal conductivity, the viscosity of a gas is also independent of pressure. The physical reason is the same : At higher pressure, more molecules are available to transport momentum but they carry it less far on account of the shorter mean free path. The pressure-independence of both η

and κ_T was one of the great initial triumphs of the kinetic theory of gases. Again, an unexpected result is that, because $\bar{c} \propto T^{1/2}$, η is proportional to $T^{1/2}$. That is, the viscosity of a gas *increases* with increase in temperature (unlike the viscosity of a liquid which *decreases* with increase in temperature). This conclusion can be easily explained when we remember that at high temperatures the molecules travel more quickly, so the flux of momentum is greater.

Comparison of Eqs. 102 and 90 shows that since $M = N_A m$,

$$\frac{\kappa_T}{\eta} = \frac{C_{v,m}}{M} \qquad ...(105)$$

This ratio is heat capacity per unit mass. More accurate theory, as well as experiment, show that for monoatomic gases (such as He, Ne, Ar, etc.),

$$\frac{\kappa_T}{\eta} = 2{\cdot}5\frac{C_{v,m}}{M} \qquad ...(106)$$

Determination of collision diameter from the measurement of the coefficient of viscosity. Since $\bar{c} = (8kT/\pi m)^{1/2}$ and $\lambda = 1/\sqrt{2}\sigma\rho$ where σ is the collision cross-section ($\sigma = \pi d^2$, where d is the collision diameter), we see that when these values are substituted in Eq. 104, we find that

$$\eta = \frac{2(mkT)^{1/2}}{3\pi^{3/2}d^2} = \frac{2(MRT)^{1/2}}{3\pi^{3/2}N_A d^2} \qquad ...(107)$$

which expresses η in terms of M, T and the quantity $N_A d^2$. Knowing N_A, then the collision diameter, can be calculated from the measured values of η.

Alternatively, if another expression involving N_A and d is available, the values of both N_A and d can be calculated. For instance, for a gas obeying the van der Waals equation of state, we know that the van der Waals constant b is given by

$$b = \frac{2}{3}\pi N_A d^2 \qquad ...(108)$$

Eliminating N_A from Eqs. 107 and 108 and solving for d, we get

$$d = \frac{9}{4}\eta b\left(\frac{\pi}{MRT}\right)^{1/2} \qquad ...(109)$$

Using this result in Eq. 107, we obtain

$$N_A = \left(\frac{32}{243\pi b^2}\right)\left(\frac{MRT}{\pi\eta^2}\right)^{3/2} \qquad ...(110)$$

It was from Eqs. 109 and 110 that the first concrete estimates of Avogadro's number (N_A) and the collision diameter (d) were obtained. Table 3 shows the values of d, calculated from η.

TABLE 3

Collision Diameter from η Measurements at 20°C

Gas	η(μPa s)	d(pm)
Ar	22·17	297
NH_3	9·82	361
CH_4	10·87	338
CO_2	14·80	373
C_2H_4	10·08	404

Example 12. The coefficient of viscosity of CO_2 is 14·80 μPa s at 20°C. Calculate its collision diameter.

Solution : From Eq. 107, $\eta = \dfrac{2(MRT)^{1/2}}{3\pi^{3/2}N_A d^2}$ so that $d^2 = \dfrac{2(MRT)^{1/2}}{3\pi^{3/2}N_A\eta}$

Thus,
$$d^2 = \frac{2[(44{\cdot}01\times10^{-3}\,\text{kg mol}^{-1})(8{\cdot}314\,\text{J K}^{-1}\text{mol}^{-1})(293{\cdot}15\,\text{K})]^{1/2}}{3(3{\cdot}1416)^{3/2}(6{\cdot}022\times10^{23}\,\text{mol}^{-1})(14{\cdot}80\times10^{-6}\,\text{Pa s})}$$

Since Pa s = kg m^{-1} s^{-1}, hence

$$d^2 = 13{\cdot}91\times10^{-20}\ \text{m}^2 \qquad [\text{J} = \text{kg m}^2\,\text{s}^{-2}]$$

Hence,
$$d = 3{\cdot}730\times10^{-10}\ \text{m} = \mathbf{373{\cdot}0\ pm} \qquad [\text{pm} = 10^{-12}\ \text{m}]$$

Example 13. For gaseous molecules that can be considered to be rigid hard spheres, the coefficient of viscosity is given by the equation

$$\eta = \frac{5\bar{c}\,m}{32\sqrt{2}d^2}$$

Using the value of the collision diameter, $d = 0{\cdot}353$ nm for O_2 at 1·0 bar and 25°C, calculate η. Repeat the calculation at a pressure of 10·0 bar.

Solution : (Note that the given equation for η is slightly different from Eq. 107).

$$d = 0{\cdot}353 \text{ nm} = 0{\cdot}353\times10^{-9} \text{ m} = 3{\cdot}53\times10^{-10} \text{ m}$$

$$\bar{c} = (8\ kT/\pi m)^{1/2} = (8\ RT/\pi M)^{1/2}$$

$$= \left(\frac{8(8{\cdot}314\,\text{J K}^{-1}\text{mol}^{-1})(298\,\text{K})[\text{kg m}^2\,\text{s}^{-2}/(\text{J})]}{\pi(32{\cdot}00\times10^{-3}\,\text{kg mol}^{-1})}\right)^{12} \qquad [\text{J} = \text{kg m}^2\,\text{s}^{-2}]$$

$$= 444 \text{ m s}^{-1}$$

Hence, substituting in the given equation,

$$\eta = \frac{5(444\,\text{m s}^{-1})(32{\cdot}00\times10^{-3}\,\text{kg mol}^{-1})/(6{\cdot}022\times10^{23}\,\text{mol}^{-1})}{32(\sqrt{2})(3{\cdot}53\times10^{-10}\text{m})^2}$$

$$= 2{\cdot}09\times10^{-5} \text{ kg m}^{-1}\,\text{s}^{-1} = 2{\cdot}09\times10^{-5} \text{ Pa s} \qquad [\text{Pa s} = \text{kg m}^{-1}\,\text{s}^{-1}]$$

$$= 20{\cdot}9 \text{ μPa s}$$

Since η of a gas is independent of pressure, $\eta = 2{\cdot}09\times10^{-5}$ Pas at both 1·0 bar and 10·0 bar.

Example 14. The coefficient of viscosity of gaseous argon at 25°C is $2{\cdot}10\times10^{-5}$ Pa s. Express the value in units of N s m^{-2}, kg m^{-1} s^{-1} and poise, P ($P=10^{-1}$ kg m^{-1} s^{-1}).

Solution : Recall that Pa = N m^{-2} and N = kg m s^{-2}. Hence, making the necessary conversions,

$$\eta = (2{\cdot}10\times10^{-5} \text{ Pa s})\ (\text{N m}^{-2})/\text{Pa} = 2{\cdot}10\times10^{-5} \text{ N s m}^{-2}$$

Again,
$$(2{\cdot}10\times10^{-5} \text{ N s m}^{-2})\ \text{kg m s}^{-2}/\text{N} = 2{\cdot}10\times10^{-5} \text{ kg m}^{-1}\,\text{s}^{-1}$$

and
$$(2{\cdot}10\times10^{-5} \text{ kg m}^{-1}\,\text{s}^{-1})/(10^{-1} \text{ kg m}^{-1}\,\text{s}^{-1}/\text{P}) = 2{\cdot}10\times10^{-4} \text{ P}$$

3. Diffusion. If the concentration is not uniform in a mixture of gases, the gases diffuse into one another until the composition is uniform. The derivation of the diffusion coefficient in such a situation is lengthy and rather complicated since each gas has a different value for mean speed, $\bar{c}$ and mean free path, λ. To simplify matters we treat the case of a single gas so that there is only one value of $\bar{c}$ and λ. The result obtained is very nearly correct for the diffusion of one isotope into another. Let us suppose that some of the molecules of the gas are painted red; the gas is confined in a vertical tube and the number density (*i.e.*, number of molecules per m^3), ρ_r, of red molecules is greater at one end than at the other. Then, the number density, ρ, of unpainted molecules must also vary from one end to the other if the total pressure is to be uniform throughout the tube. For each species we write for the number density at height z, as

$$\rho = \rho_0 + \frac{\partial\rho}{\partial z}z\,;\quad \rho_r = \rho_{r_0} + \frac{\partial\rho_r}{\partial z}z$$

where ρ_0 and ρ_{r_0} are the number densities at $z = 0$.

Consider a horizontal area of 1 m^2 at height z. The number of red molecules passing downwards through this area per second is given by

$$\rho_r\downarrow = \tfrac{1}{6}\bar{c}(\rho_r)_{z+\lambda} = \tfrac{1}{6}\bar{c}\left[\rho_{r_0} + \frac{\partial\rho_r}{\partial z}(z+\lambda)\right] \qquad ...(111)$$

since the molecules originate in the layer at $z+\lambda$. Similarly, the number coming up from below is given by

$$\rho_r\uparrow = \tfrac{1}{6}\bar{c}(\rho_r)_{z-\lambda} = \tfrac{1}{6}\bar{c}\left[\rho_{r_0} + \frac{\partial\rho_r}{\partial z}(z-\lambda)\right] \qquad ...(112)$$

The net flow upwards is thus given by

$$\rho_r\uparrow - \rho_r\downarrow = -(1/3)\bar{c}\lambda\frac{\partial\rho_r}{\partial z} \qquad ...(113)$$

By the law of diffusion (Eq. 77), the upward flow is given by $-D_r(\partial\rho_r/\rho z)$. D_r is the diffusion coefficient for the red molecules.

Thus, we have from Eqs. 77 and 113,

$$D_r = (1/3)\bar{c}\lambda \qquad ...(114)$$

However, the red molecules differ from the others only by a coat of paint so that

$$D = (1/3)\bar{c}\lambda \qquad ...(115)$$

Since $\bar{c}$ is inversely proportional to $M^{1/2}$, we can understand **Graham's law** which states that the rate of diffusion of a gas is inversely proportional to the square root of the molar mass.

Since the mean free path, λ, is inversely proportional to the pressure ($\lambda = kT/\sqrt{2}\,\sigma P$), the diffusion coefficient decreases with increase in pressure. The molecules have to fight their way through the swarm of other molecules by making collisions. At high pressures, they make many more collisions and their progress in any given direction is slowed.

Summary of Transport Properties in a Gas. Kinetic theory interprets the phenomenological laws of transport on the basis of a single mechanism and expresses the values of κ_T, η and D in terms of the mean free path (λ), number density (ρ) and the mean speed ($\bar{c}$) of the gas molecules. The equations are :

$$\kappa_T = (1/3)\lambda\bar{c}\,(\rho/N_A)\,C_{v,m} \qquad \text{(Eq. 90)}$$

$$\eta = (1/3)\lambda\bar{c}\rho m \qquad \text{(Eq. 102)}$$

$$D = (1/3)\lambda\bar{c} \qquad \text{(Eq. 115)}$$

Since all of these depend on λ, they are sometimes called **free path phenomena.**

Example 15. How does the mean free path in a sample of a gas vary with temperature in a constant volume container ?

Solution : $$\lambda = \frac{kT}{\sqrt{2}\sigma P} = \frac{kTV}{n(\sqrt{2})\sigma RT} = \frac{V}{n(\sqrt{2})\sigma N_A} \qquad [P = nRT/V;\ k = R/N_A]$$

Thus, at constant V, λ is independent of T.

Example 16. At what pressure does the mean free path of argon (g) at 25°C become comparable to the size of a 1·0 litre vessel that contains it ? Assume that $\sigma = 0{\cdot}36$ nm^2

Solution : $\lambda = \frac{kT}{\sqrt{2}\sigma\text{H}}$. Thus, $P = \frac{kT}{\sqrt{2}\sigma\lambda}$

Now, $$\lambda \approx (1000 \text{ cm}^3)^{1/3} = 10 \text{ cm} = 0{\cdot}10 \text{ m}$$

$$\therefore\quad P = \frac{(1{\cdot}38\times10^{-23}\,\text{J K}^{-1})(298\,\text{K})}{\sqrt{2}\,(0{\cdot}36\times10^{-18}\,\text{m}^2)(0{\cdot}10\,\text{m})} = 0{\cdot}081 \text{ N m}^{-2} = 0{\cdot}081 \text{ Pa}$$

$$= \frac{0{\cdot}081 \text{ Pa}}{1{\cdot}01325\times10^5 \text{ Pa / atm}} = 8{\cdot}0\times10^{-7} \text{ atm} = 6{\cdot}1\times10^{-4} \text{ Torr} \qquad (1 \text{ atm} = 760 \text{ Torr})$$

Example 17. At what pressure does the mean free path of argon at 25°C become comparable to the diameter of the atoms themselves ? Given $\sigma = 0{\cdot}36$ nm^2.

Solution. $$\lambda = \frac{kT}{\sqrt{2}\sigma P}\text{; thus, } P = \frac{kT}{\sqrt{2}\sigma\lambda}$$

$$\sigma = \pi d^2,\quad d = (\sigma/\pi)^{1/2} = \left(\frac{0{\cdot}36\text{nm}^2}{\pi}\right)^{1/2} = 0{\cdot}34\text{nm}$$

$$\therefore\quad \lambda \approx d = 0{\cdot}34 \text{ nm}$$

$$P = \frac{(1{\cdot}38\times10^{-23}\,\text{J K}^{-1})(298\,\text{K})}{\sqrt{2}\,(0{\cdot}36\times10^{-18}\,\text{m}^2)(0{\cdot}34\times10^{-9}\,\text{m})} = 2{\cdot}4\times10^7 \text{ N m}^{-2}$$

$$= 2{\cdot}4\times10^7 \text{ Pa} = \frac{2{\cdot}4\times10^7 \text{ Pa}}{1{\cdot}01325\times10^5 \text{ Pa / atm}} \approx 240 \text{ atm} \qquad [\text{J} = \text{N m};\ \text{Pa} = \text{N m}^{-2}]$$

This pressure is comparable to the pressure in a compressed gas cylinder in which argon gas is normally stored.

Role of argon in an incandescent lamps. Langmuir made an important application of the concept of the mean free path and diffusion in the construction of an incandescent lamp. When electric current is passed through an ordinary lamp, it heats the tungsten filament white hot. The filament gets oxidized and there occurs an immediate burn out. This can be prevented by evacuating the bulb. However, if the pressure becomes too low, the mean free path of the tungsten atoms becomes large compared with the size of the bulb, with the result that the tungsten atoms which 'boil off' from the filament directly hit the glass wall without colliding with a gas molecule. The tungsten atoms condense on the glass wall thereby blackening the bulb. The un-interrupted loss of tungsten atoms from the filament weakens the filament which soon breaks. Langmuir suggested the introduction of argon gas into the bulb under a pressure of a few centimetres. This reduces λ to a value less than the diameter of the filament. Thus, a tungsten atom that has 'boiled off' travels only a short distance before hitting a gas molecule. As a result of this collision, the tungsten atom is reflected back on to the filament. The tungsten atoms leave the region of the filament by slow diffusion through the argon gas. Thus, we see how the presence of argon in the bulbs lengthens considerably the life of the bulb.

Degrees of Freedom of a Gaseous Molecule

The motion of atoms and molecules is generally described in terms of the degrees of freedom they possess. The **degrees of freedom** *of a molecule are defined as the independent number of parameters required to describe the state of the molecule completely.* When a gaseous molecule is heated, the energy supplied to it may bring about three kinds of motion in it. These are : the translationl motion, the rotational motion and the vibrational motion. This is expressed by saying that the molecule possesses translational, rotational and vibrational degrees of freedom.

Translation Degrees of Freedom. Atoms possess only translational degrees of freedom. If we consider an atom as a *mass point*, then the mass point requires three coordinates (such as x, y, z in the Cartesian coordinates system) to specify its position. The atom has thus *three translational degrees of freedom* in the x, y and z directions. If the atom is moving with a velocity c, then

$$c^2 = c_x^2 + c_y^2 + c_z^2 \qquad ...(116)$$

where c_x, c_y and c_z are the components of velocity c in the three directions. Multiplying Eq. 116 by $m/2$, where m is the mass of the atom, we have

$$\tfrac{1}{2}mc^2 = \tfrac{1}{2}mc_x^2 + \tfrac{1}{2}mc_y^2 + \tfrac{1}{2}mc_z^2 \qquad ...(117)$$

or Kinetic energy, $\varepsilon_k = \varepsilon_{k,x} + \varepsilon_{k,y} + \varepsilon_{k,z}$ ...(118)

Thus, the kinetic energy ε_k, too, can be resolved into three components along the three Cartesian axes.

It may be noted that the rotational motion of an atom about an axis perpendicular to it and passing through its centre contributes negligible energy compared with its translational motion.

As in the case of atoms, three coordinates are needed to specify the centre of gravity of a molecule. Thus, the centre of gravity of any molecule has three translational degrees of freedom.

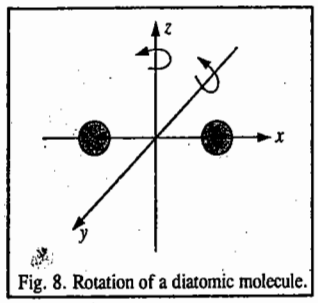

Fig. 8. Rotation of a diatomic molecule.

Rotational Degrees of Freedom. A diatomic molecule lying along the X-axis can undergo rotation about the mutually perpendicular Y-axis and Z-axis passing through its centre of gravity, as shown in Fig. 8. This is expressed by saying that a diatomic molecule has *two rotational degrees of freedom.*

If I is the moment of inertia of the molecule and ω is its angular velocity, then the rotational energy is given by

$$E_{rot} = I\omega^2 \qquad ...(119)$$

It may be noted that the moment of inertia of the molecule and hence its rotational energy along the x-axis is negligible.

All *linear* molecules, such as CO_2 and C_2H_2, have two rotational degrees of freedom because their rotational motion is similar to that of a diatomic molecule.

However, *non-linear* molecules, such as H_2O, H_2S, CH_4, C_6H_6, etc., can undergo rotation about the three Cartesian axes so that they have *three rotational degrees of freedom.* The rotational motion of H_2O molecule is shown in Fig. 9.

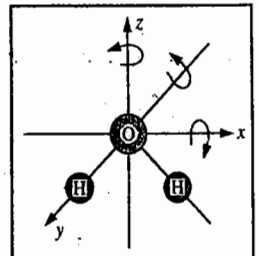

Fig. 9. Rotation of triatomic non-linear H_2O molecule.

Vibrational Degrees of Freedom. As already mentioned, atoms possess only translational degrees of freedom.

In a diatomic molecule, the masses m_1 and m_2 vibrate back and forth relative to their centre of mass in opposite directions, as shown in Fig. 10. The two masses reach the extremes of their respective motions at the same time. The diatomic molecule has only *one vibrational degree of freedom, i.e.,* it has only one frequency, called the fundamental vibrational frequency. During vibrational motion, the bond of the molecule behaves like a spring and the molecule exhibits a simple harmonic motion provided the displacement of the nuclei from the equilibrium configuration is not too much. At the two extremes of motion which correspond to extension and compression of the chemical bond between the two atoms, the potential energy is maximum. On the other hand, when the atoms are in their equilibrium position, the kinetic energy is maximum. Thus, during vibration, there is a constant interchange of kinetic and potential energy.

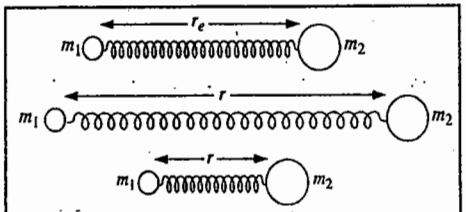

Fig. 10. Vibration of a diatomic molecule.

A polyatomic molecule containing n atoms or nuclei, has $3n$ degrees of freedom since each atom requires 3 degrees of freedom in the x, y and z directions to specify its position. If we subtract the translational and rotational degrees of freedom from the total $3n$ degrees of freedom, we find that we are left with $3n - 6$ *internal degrees of freedom* for a non-linear molecule and $3n - 5$ *internal degrees of freedom* for a linear molecule. The $3n - 6$ internal degrees of freedom of a non-linear molecule correspond to its $3n - 6$ *normal modes of vibration.* Similarly, the $3n - 5$ normal degrees of freedom of a linear molecule correspond to its $3n - 5$ normal modes of vibration. A **normal mode of vibration** *is defined as the molecular motion in which all the atoms in the molecule vibrate with the same frequency and all the atoms pass through their equilibrium positions simultaneously.* The relative vibrational amplitudes of individual atoms may be different in magnitude and direction but the centre of gravity of the molecule does not change.

Modes of vibration may result in the stretching and bending of the molecular bonds. The stretching may be *symmetric* or *asymmetric* while the bending may be *in plane* or *out of plane*. These modes are observed in the infrared region (6500–4,000 cm^{-1}) of the electromagnetic spectrum.

The various modes of vibration of H_2O and CO_2 molecules are shown in Fig. 11

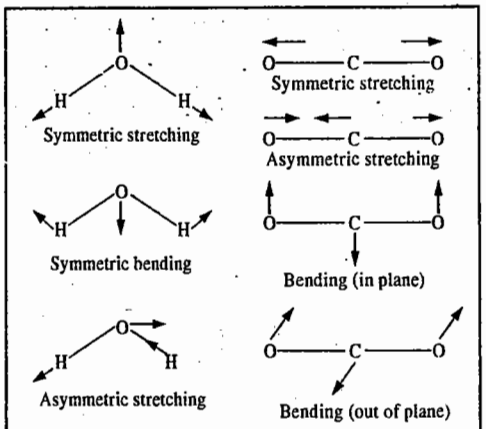

Fig. 11. Various modes of vibration of H_2O and CO_2 molecules.

Example 18. Calculate the various degrees of freedom of the following molecules :

(a) He (b) H_2 (c) HCl (d) H_2O (e) CO_2 (f) C_2H_2 (g) C_6H_6 and (h) a protein molecule containing 44,700 atoms.

Solution : Let N be the number of degrees of freedom and n, the number of atoms in a molecule. Then,

(a) He : $n = 1$; $N_{tr} = 3$ $N_{rot} = 0$ $N_{vib} = 0$

(b) H_2 : $n = 2$; $N_{tr} = 3$ $N_{rot} = 2$ $N_{vib} = 3\times2 - 5 = 1$

(c) HCl : $n = 2$; $N_{tr} = 3$ $N_{rot} = 2$ $N_{vib} = 3\times2 - 5 = 1$

(d) H_2O : It is a non-linear molecule.

$n = 3$; $N_{tr} = 3$ $N_{rot} = 3$ $N_{vib} = 3\times3 - 6 = 3$

(e) CO_2 : It is a linear molecule.

$n = 3$; $N_{tr} = 3$ $N_{rot} = 2$ $N_{vib} = 3\times3 - 5 = 4$

(f) HC≡CH : It is a linear molecule.

$n = 4$; $N_{tr} = 3$ $N_{rot} = 2$ $N_{vib} = 3\times4 - 5 = 7$

(g) C_6H_6 : It is non-linear molecule.

$n = 12$; $N_{tr} = 3$ $N_{rot} = 3$ $N_{vib} = 3\times12 - 6 = 30$

(h) Protein molecule : It is a macromolecule.

$n = 44700$; $N_{tr} = 3$ $N_{rot} = 31$ $N_{vib} = 3\times44700 - 6 = 134,100$

(We can neglet 6 in comparison with 134,100)

The translational, rotational and vibrational degrees of freedom can be written in the shortened notation as follows :

(a) He : (3,0,0) (b) H_2 : (3,2,1) (c) HCl : (3,2,1) (d) H_2O : (3,3,3)

(e) CO_2 : (3,2,4) (f) C_2H_2 : (3,2,7) (g) C_6H_6 : (3,3,30), etc.

It should be remembered that the rotational degrees of freedom are associated with substances in both the gaseous and liquid states. However, in the *solid state*, the molecules possess only *vibrational degrees of freedom*. The translational and rotational motions in solids are converted into vibrational motion where the atoms in the lattice vibrate to and fro about their equilibrium positions.

Principle of Equipartition of Energy

From the kinetic theory of gases we know that the average translational kinetic energy of a molecule of an ideal gas is given by

$$\varepsilon = \tfrac{3}{2}kT \qquad ...(120)$$

According to the **law of equipartition of energy**, *the total energy of a molecule is divided equally amongst the various degrees of freedom of the molecule.*

The distribution of kinetic energy along the x, y and z directions is given by

$$\varepsilon = \varepsilon_x + \varepsilon_y + \varepsilon_z \qquad ...(121)$$

Since the motion of gas molecules is random and the motion along the three Cartesian axes is equally probable, hence from Eqs. 120 and 121,

$$\varepsilon_x = \varepsilon_y = \varepsilon_z = 1/3\text{rd of } \varepsilon = \tfrac{1}{2}kT \qquad ...(122)$$

Eq. 122 shows that each component of kinetic motion contributes equally to the total kinetic energy and that *the kinetic energy for each degree of freedom* is $\frac{1}{2}kT$ *per molecule* or $\frac{1}{2}RT$ *per mole.*

Following similar lines of arguments, it can be shown that *each rotational degree of freedom* also contributes $\frac{1}{2}kT$ per molecule or $\frac{1}{2}RT$ per mole to the total energy.

As regards the *vibrational motion,* the two atoms oscillate against each other, as shown in Fig. 10. The molecule, therefore, possesses *both* potential and kinetic energy, as already discussed. This means that the energy of vibration involves *two degrees of freedom.* The *vibrational motion* in a molecule is, thus, associated with energy = $2\times\frac{1}{2}kT = kT$ per molecule or RT per mole.

Thus, if a gaseous species has n_1 translational degrees of freedom, n_2 rotational degrees of freedom and n_3 vibrational degrees of freedom, then the total energy of the species is given by $n_1(kT/2) + n_2(kT/2) + n_3(kT)$.

Example 19. Using the principle of equipartition of energy, estimate the energy of (a) H_2 (b) H_2O and (c) CO_2 at room temperature, assuming that all the degrees of freedom are excited and contribute towards the energy of the molecules.

Solution : Ordinarily, at room temperature only translational and rotational degrees of freedom are excited and hence they alone contribute to the energy of the molecule. Here, however, we shall assume that vibrational degrees of freedom, too, are excited. According to the principle of equipartition of energy, each translational and rotational degree of freedom contributes $1/2\ kT$ and each vibrational degree of freedom contributes $2\times1/2kT = kT$ to the total energy.

(a) H_2 (3, 2, 1) : $E = 3(\frac{1}{2}kT) + 2(\frac{1}{2}kT) + 1(kT) = (7/2)kT$ per molecule or $(7/2)RT$ per mole

(b) H_2O (3, 3, 3) : $E = 3(\frac{1}{2}kT) + 3(\frac{1}{2}kT) + 3(kT) = 6kT$ per molecule or $6RT$ per mole

(c) CO_2 (3, 2, 4) : $E = 3(\frac{1}{2}kT) + 2(\frac{1}{2}kT) + 4(kT) = (13/2)kT$ per molecule or $(13/2)RT$ per mole

Contributions to Heat Capacity of an Ideal Gas. According to the **Born–Oppenheimer approximation**, the total energy of a molecule is given by

$$E_{total} = E_{tr} + E_{rot} + E_{vib} + E_{el} \qquad ...(123)$$

where E_{tr} is the translational energy, E_{rot} is the rotational energy, E_{vib} is the vibrational energy and E_{el} is the electronic energy. The translational energy is not quantized while the remaining three energies are quantized. E_{el} does not make any contribution towards heat capacity.

According to the *principle of equipartition of energy* discussed above, the kinetic energy of a single particle is equal to $\frac{1}{2}kT$. Since a particle can exhibit only translational motion (along a straight line), its translational energy is equal to its total energy. According to Clausius, the translational energy of a point-particle is distributed among three independent components of motion, say, the motion along the x, y and z axes of a Cartesian coordinates system. This is expressed by saying that the point-particle has *three translational degrees of freedom*, each degree of freedom contributing $\frac{1}{2}kT$ to the translational energy. Hence, the total translational energy of the point-particle (*i.e.*, the atom) is $\frac{3}{2}kT$. The energy per mole is evidently $\frac{3}{2}RT$.

As mentioned above, an n-atomic molecule (*i.e.*, a molecule containing n atoms) has 3n degrees of freedom. Since there are 3 translational degrees of freedom, therefore, the remaining 3n - 3 degrees of freedom are associated with rotational and vibrational motion.

As discussed earlier, a linear polyatomic molecule has only two rotational degrees of freedom while a non-linear polyatomic molecule has three rotational degrees of freedom. Hence, a linear molecule has 3n - 5 vibrational degrees of freedom and a non-linear molecule has 3n - 6 vibrational degrees of freedom.

Since heat capacity C_v is defined as $(\partial U/\partial T)_v$, hence, the total heat capacity is given by

$$C_{v,total} = C_{v,tr} + C_{v,rot} + C_{v,vib} \qquad ...(124)$$

(we neglect the electronic contribution to heat capacity at ordinary temperatures).

According to the principle of equipartition of energy, each translational and each rotational degree of freedom contributes $\frac{1}{2}R$ to C_v while each vibrational degree of freedom contributes $2\times\frac{1}{2}R=R$ to C_v. Here, an approximation is made that at room temperature, the contribution to C_v from vibrational motion is only 20%. The vibrational contribution becomes more prominent at high temperature.

Example 20. Estimate C_v for the following gases at room temperature : *(a)* Helium *(b)* HCl and *(c)* CO_2.

Solution : *(a)* **He :** Helium consists of atoms only. Atoms have only translational motion and the number of translational degrees of freedom = 3. Thus,

$$C_v = 3(R/2) = \frac{3}{2} \times 8{\cdot}314 \text{ J K}^{-1} \text{ mol}^{-1} = \mathbf{12{\cdot}471 \text{ J K}^{-1} \text{ mol}^{-1}}$$

(b) **HCl :** HCl is a linear diatomic molecule. Number of atoms, n=2 so that 3n=6

Number of translational degrees of freedom = 3

Number of rotational degrees of freedom = 2

$\therefore$ Number of vibrational degrees of freedom = 6 - (3 + 2) = 1

Hence, at room temperature, assuming 20% vibrational contribution,

$$C_v = 3(R/2) + 2(R/2) + 0{\cdot}20 \times 1\,(R) = 3(R/2) + (R) + 0{\cdot}20R$$
$$= 2{\cdot}7\,R = 2{\cdot}7 \times 8{\cdot}314 \text{ J K}^{-1} \text{ mol}^{-1} = \mathbf{22{\cdot}45 \text{ J K}^{-1} \text{ mol}^{-1}}$$

(c) **CO_2 :** CO_2 is a linear triatomic molecule. $\therefore$ n=3 ; 3n=9

Number of translational degrees of freedom = 3

Number of rotational degrees of freedom = 2

$\therefore$ Number of vibrational degrees of freedom = 9 - (3 + 2) = 4

$$C_v = 3(R/2) + 2(R/2) + 0{\cdot}20 \times 4(R) = 3{\cdot}3\,R = \mathbf{27{\cdot}44 \text{ J K}^{-1} \text{ mol}^{-1}}$$

Example 21. For ozone, $\gamma = 1{\cdot}17$ (where γ is C_p/C_v). Assuming that it is an ideal gas and the vibrational contribution is full (not just 20%), estimate its C_v and confirm whether the molecule is linear or non-linear.

Solution : $\gamma = C_p/C_v = 1{\cdot}15$. Also for an ideal gas, $C_p - C_v = R$

Suppose the molecule is non-linear. Then,

$$C_v = C_{v,tr} + C_{v,rot} + C_{v,vib} = 3(R/2) + 3(R/2) + 3(R) = 6R$$
$$C_p = C_v + R = 7R \text{ so that } \gamma = 7/6 = 1{\cdot}167$$

Suppose now that the molecule is linear. Then,

$$C_v = (3R/2) + 2(R/2) + 4R = (13/2)R$$
$$C_p = C_v + R = 15/2\,R \text{ so that } \gamma = 1{\cdot}154$$

Since the former value agrees with the given value, the ozone molecule is non-linear.

Example 22. Estimate γ at room temperature for *(a)* helium and *(b)* CH_4 gas, assuming that they are ideal gases.

Solution : *(a)* **Helium :** $C_v = C_{v,tr} = 3(R/2)$

For an ideal gas, $C_p - C_v = R \quad \therefore C_p = 5R/2$

$$\therefore \quad \gamma = C_p/C_v = \frac{5R/2}{3R/2} = \frac{5}{3} = 1{\cdot}66$$

(b) **CH_4 :** Assuming full vibrational contribution,

$$C_v = C_{v,tr} + C_{v,rot} + C_{v,vib} = 3(R/2) + 3(R/2) + 9(R) = 12R$$
$$\therefore \quad C_p = R + C_v = R + 12R = 13R \text{ so that } \gamma = 13/12 = 1{\cdot}02$$

Note. It is customary to neglect the vibrational contribution to C_v at ordinary temperatures. The vibrational degrees of freedom are excited at extremely high temperatures. The temperature above which vibrational degrees of freedom contribute to C_v is called the **characteristic vibrational temperature** of a molecule.

Table 4 lists the calculated and experimental values of the constant volume molar heat capacities of some common gases.

We see that the agreement is excellent for mono-atomic gases. However, considerable discrepancies are noticed for diatomic and polyatomic molecules.

TABLE 4

Calculated and Experimental Values of Molar Heat Capacities of Gases at 298 K

Gas	C_v (J K^{-1} mol^{-1}) (calculated)	C_v (J K^{-1} mol^{-1}) (experimental)
He	12·47	12·47
Ne	12·47	12·47
Ar	12·47	12·47
H_2	29·10	20·50
N_2	29·10	20·50
O_2	29·10	21·05
CO_2	54·06	28·82
H_2O	49·87	25·23
SO_2	49·87	31·51

Example 23. The speed of sound in a gas is given by $c_s = (\gamma\, RT/M)^{1/2}$ where $\gamma = C_p/C_v$ *(i)* Show that this relation can be written as $c_s = (\gamma\, P/\rho)^{1/2}$ where P is the pressure and ρ is the density *(ii)* Calculate the speed of sound in helium at room temperature.

Solution : *(i)* For an ideal gas, $PV = nRT = (m/M)RT$ where m is the mass of the gas. Hence,

$$P = mRT/MV = \rho RT/M \qquad (\because \text{density, } \rho = m/V)$$

or $$RT/M = P/\rho$$

$\therefore$ $$c_s = (\gamma\, RT/M)^{1/2} = (\gamma P/\rho)$$

(ii) For helium, $\gamma = C_p/C_v = 5/3$ and $M = 4{\cdot}0 \text{ g mol}^{-1} = 4{\cdot}0 \times 10^{-3} \text{ kg mol}^{-1}$

$\therefore$
$$c_s = \left[\frac{\gamma RT}{M}\right]^{1/2} = \left\{\frac{5 \times (8{\cdot}314 \text{ J K}^{-1} \text{ mol}^{-1})(298 \text{ K})}{3 \times 4{\cdot}0 \times 10^{-3} \text{kg mol}^{-1}}\right\}^{1/2}$$
$$= (1{\cdot}03 \times 10^6 \text{ m}^{-1} \text{ s}^{-2})^{1/2} = \mathbf{1{\cdot}02 \text{ km s}^{-1}} \qquad [\because \text{J} = \text{kg m}^2 \text{ s}^{-1}]$$

Barometric Formula

It is found that as we go higher up the sea level, the pressure of the atmosphere decreases. The variation of pressure with altitude is given by the so called barometric formula.

The pressure difference, $-dP$, between altitude x and altitude $x+dx$ is equal to the weight (*not mass*) per unit area of a layer of gas of thickness dx and is given by

$$-dP = \rho g dx \qquad \ldots(125)$$

where ρ is the density of the gas and g is the acceleration due to gravity. We know that density of an ideal gas is given by $\rho = PM/RT$ where M is its molar mass. Hence,

$$-dP = (PMg/RT)\,dx \qquad \ldots(126)$$

or $$dP/P = -(Mg/RT)\,dx \qquad \ldots(127)$$

Integrating, $$\ln (P/P_0) = -Mgx/RT \qquad \ldots(128)$$

Taking antilog, $$P = P_0 \exp(-Mgx/RT) \qquad \ldots(129)$$

This is the barometric formula.

Example 24. Calculate the atmospheric pressure at Shimla whose height above the sea level is 2250 m if the pressure at the ground level is 1 atm and temperature is 25°C, assuming that there exist no complications such as turbulence or temperature gradients (M = 29 g mol^{-1}).

Solution : From the barometric formula (Eq. 129),

$$\ln \frac{P_0}{P} = \frac{Mgx}{RT} \qquad \ldots(i)$$

Substituting the given data in Eq. *(i)*, we have

$\therefore$
$$\log\left(\frac{1}{P}\right) = \frac{(29 \times 10^{-3} \text{ kg mol}^{-1})(9{\cdot}81 \text{ m s}^{-2})(2250 \text{ m})}{2{\cdot}303 \times (8{\cdot}314 \text{ J K}^{-1} \text{ mol}^{-1})(298 \text{ K})} = 0{\cdot}1121 \qquad (\text{J} = \text{kg m}^2 \text{ s}^{-2})$$

$$\log P = -0{\cdot}1121 = \bar{1}{\cdot}8879$$

Taking antilog, $$P = \mathbf{0{\cdot}7725 \text{ atm}}$$

We conclude this chapter by offering a few remarks on Robert Boyle (1627-1691), the British chemist. He gave an entirely new approach to experimental science. Historians of chemistry say that he made no outstanding discoveries (he merely confirmed and publicized 'Boyle's law'). As K.J. Laidler wrote, "Boyle's great contribution was to transform chemistry from a subject in which there was much mysticism and charlatanism into an effective branch of natural philosophy, based firmly on experimental evidence. If Boyle was not the father of chemistry, as he has often been called, a good case be made for regarding him as the first physical chemist."

I. Review Questions

1. Starting from the basic postulates of the kinetic theory of gases, derive the kinetic gas equation. Calculate the value of the ideal gas constant.
2. Using the kinetic gas equation $PV = \frac{1}{3}mNc^2$, derive Boyle's law, Charles' Law, Graham's law of diffusion, Dalton's law of partial pressures, Avogadro's law and the ideal (perfect) gas equation.
3. Define average velocity, most probable velocity and root mean square velocity. Derive mathematical expressions for the three types of molecular velocities.
4. Using the expression for the Maxwell distribution of velocities, draw this distribution at three different temperatures and comment on the shapes of the distribution curves.
5. Explain the terms collision diameter, collision cross-section, collision number, collision frequency and mean free path. Show that the mean free path of a gas molecule increases by decrease in pressure.
6. Define the coefficient of viscosity of a fluid. Show that the viscosity of a gas is independent of pressure. How is this parameter used for calculating the mean free path and collision diameter in a gas ?
7. Discuss with the help of suitable illustrations translational, rotational and vibrational degrees of freedom of diatomic and triatomic gaseous molecules.
8. State the principle of equipartition of energy. Discuss the application of this principle in estimating *(i)* the total energy of a given gaseous molecule and *(ii)* the heat capacity of an ideal gas at room temperature.
9. Derive the Barometric formula for the variation of atmospheric pressure with altitude.

II. Problems

1. Calculate the kinetic energy of an ideal gas per molecule and per mole at 27°C. **[Ans. $6{\cdot}21\times10^{-21}$ J ; $3{\cdot}74\times10^{3}$ J]**
2. Calculate the kinetic energy of *(i)* a molecule of hydrogen at 0°C *(ii)* one gram of oxygen at 47°C. **[Ans. *(i)* $5{\cdot}678\times10^{-7}$ J *(ii)* $1{\cdot}24\times10^{2}$ J]**
3. Calculate the number of moles of N_2 contained in 20 dm^3 of the gas at 25°C and a pressure of 700 mm Hg. **[Ans. 0·753 mole]**
4. Calculate the density of CO_2 gas at 0°C and 1 atm pressure. **[Ans. 1·96 kg m^{-3}]**
5. Calculate the approximate molar mass of a gas if 560 ml weigh 1·80 g at N.T.P. **[Ans. 72·0 g mol^{-1}]**
6. Calculate the volume of CO_2 at 25°C and 765 torr required to produce 100 g of $Ca(HCO_3)_2$ by its reaction with $Ca(OH)_2$. **[Ans. 31·79 dm^3]**
7. A 10·0 dm^3 cylinder of O_2 gas at 4·00 atm pressure and 17°C developed a leak. When the leak was repaired, the gas which remained in the cylinder was found to register a pressure of 2·5 atm at 17°C. How many moles of the gas escaped ? **[Ans. 0·630 mole]**
8. At what temperature will the root mean square velocity of SO_2 be the same as that of O_2 at 27°C ? **[Ans. 327°C]**
9. Calculate the mean free path of O_2 molecules at 25°C and a pressure of 10^{-3} mm Hg, given that the collision diameter is 361 pm. **[Ans. 53 mm]**
10. The coefficient of viscosity of oxygen gas is 208 micropoise. Calculate the mean free path and collision diameter of oxygen molecules at N.T.P. **[Ans. $7{\cdot}17\times10^{-8}$ m ; $3{\cdot}57\times10^{-10}$ m]**
11. Determine the possible numbers of vibrational modes of CH_4, C_2H_6, C_6H_6 and SO_2 molecules. **[Ans. 9, 18, 30, 3]**
12. Estimate C_v for the following gases at room temperature, applying the principle of equipartition of energy : (1) Neon (2) Argon (3) Hydrogen bromide (4) Hydrogen sulphide. **[Ans. (1) 12·27 J K^{-1} mol^{-1} (2) Same as for neon (3) 22·45 J K^{-1} mol^{-1} (4) 49·88 J K^{-1} mol^{-1}]**

CHAPTER 10

THE GASEOUS STATE–II REAL GASES

Deviations of Real Gases from Ideal Behaviour. As already discussed in the last chapter, the equation of state $PV=nRT$, derived from the postulates of the kinetic theory, is valid for an ideal gas only. Real gases obey this equation only approximately and that too under conditions of low pressure and high temperature. The higher the pressure and the lower the temperature, the greater are the deviations from the ideal behaviour. In general, the most easily liquefiable and highly soluble gases show larger deviations. Thus, gases like carbon dioxide, sulphur dioxide and ammonia show much larger deviations than hydrogen, oxygen, nitrogen, etc.

The deviations from ideal behaviour are best represented in terms of the compressibility factor (also called the compression factor), Z, which is defined as

$$Z = \frac{PV}{(PV)_{ideal}} = \frac{PV}{nRT} = \frac{PV_m}{RT} \qquad ...(1)$$

where V_m ($= V/n$) is the molar volume, *i.e.*, the volume occupied by one mole of the gas.

For an ideal gas, $Z=1$ under all conditions of temperature and pressure. The deviation of Z from unity is, thus, a measure of the imperfection of the gas under consideration.

The graphs plotted for the compressibility factors determined for a number of gases over a range of pressures at a constant temperature (0°C) are shown in Fig. 1.

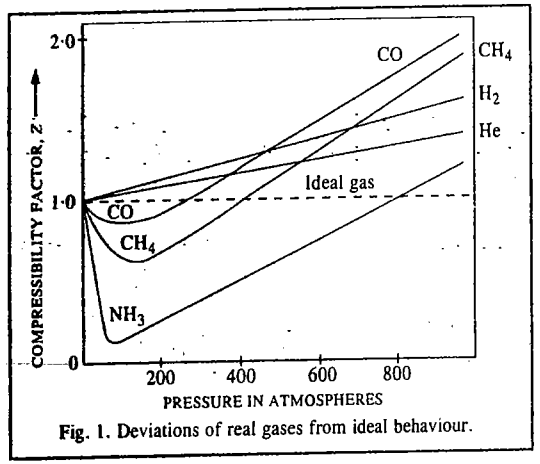

Fig. 1. Deviations of real gases from ideal behaviour.

At extremely low pressures, all the gases are known to have Z close to unity which means that the gases behave almost ideally. At very high pressures, all the gases have Z more than unity indicating that the gases are less compressible than an ideal gas. This is due to the fact that at high pressures, the molecular repulsive forces are dominant.

As can be seen from Fig. 1, at moderately low pressures, carbon monoxide, methane and ammonia are more compressible than an ideal gas, *i.e.*, PV is less than $(PV)_{ideal}$ so that $Z < 1$. This is due to the fact that at low pressures, the long range attractive forces are dominant and favour compression. The compressibility factor Z goes on decreasing with increase in pressure, passes through a minimum at a certain stage and then begins to increase with increase in pressure. The gases now become less compressible than an ideal gas, *i.e.*, PV is more than $(PV)_{ideal}$ so that $Z > 1$. It is evident from the figure that while carbon monoxide and methane exhibit marked deviations from ideal behaviour only at high pressures, ammonia shows large deviation even at low pressures.

Hydrogen and helium at 0°C, however, are seen to be less compressible than the ideal gas *at all pressures, i.e.*, $Z > 1$. However, if the temperature is sufficiently low (*e.g.*, below –48°C for hydrogen and below –242°C for helium), these gases also give the same type of Z—P plots as are shown by ammonia, carbon monoxide and methane at 0°C. On the other hand, if the temperature is sufficiently high, the Z—P plots of ammonia, carbon monoxide and methane will be similar to those of hydrogen and helium at 0°C, *i.e.*, the value of Z will increase continuously with increase in pressure.

Effect of Temperature on Deviations from Ideal Behaviour. The Z—P plots of nitrogen at different temperatures varying between –70° and 50°C, are shown in Fig. 2.

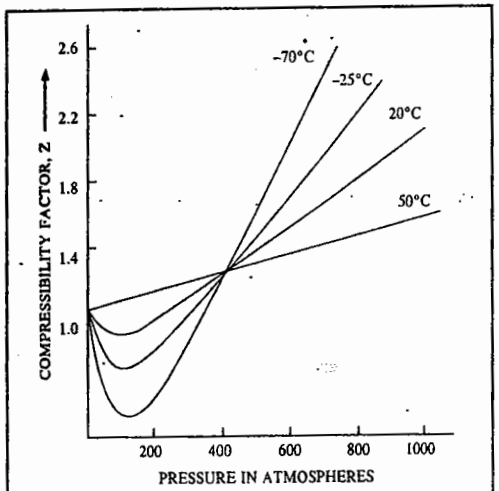

Fig. 2. Effect of temperature on deviation of nitrogen from ideal behaviour.

It is seen that as the temperature is raised, the dip in the curve becomes smaller and smaller. At 50°C, the curve seems to remain almost horizontal for an appreciable range of pressure varying between 0 and about 100 atmospheres, showing thereby that the compressibility factor Z becomes almost equal to unity under these conditions. In other words, the product PV remains constant and thus *Boyle's law is obeyed within this range of pressure at* 50°C. This temperature is called the **Boyle point** or **Boyle temperature.** Below this temperature, the value of Z at first decreases, approaches a minimum and then increases as the pressure is increased continuously. Above 50°C, the value of Z shows a continuous rise with increase in pressure.

The Boyle temperature is different for different gases. The Boyle temperature for helium is –250·4°C. Thus, at –250·4°C, helium obeys Boyle's law for an appreciable range of pressure. However, at any temperature below –250·4°C, the plot of Z *vs* P first shows a fall and then a rise as pressure is increased continuously. At a temperature above –250·4°C, however, Z shows a continuous rise with increase in pressure (see Z—P plot for helium in Fig. 1).

Explanation of the Deviations. In order to explain deviations from ideal behaviour, it is necessary to modify the kinetic theory of gases. The following two postulates of the kinetic theory do not appear to hold good under all conditions. Let us examine them more critically.

Postulate No. 1. *The volume occupied by the molecules themselves is negligibly small as compared to the total volume occupied by the gas.* This postulate can be justified only under ordinary conditions of temperature and pressure. It can be shown by calculations that in some of the common gases, the volume occupied by the molecules themselves, under ordinary conditions, is only 0·014 per cent of the total volume of the gas. This is a negligible fraction indeed. But, if the pressure becomes too high (say, 100 atmospheres or more), the total volume of the gas will decrease appreciably whereas the volume of the molecules will remain almost the same because the molecules are *incompressible.* Hence, under conditions of high pressure, the volume occupied by the gas molecules will no longer be negligible in comparison with the total volume of the gas.

The same thing happens when the temperature is lowered to a large exent. The total volume of the gas decreases considerably, no doubt, but the volume occupied by the molecules themselves remains practically the same. In this case, too, *the volume occupied by the molecules will no longer be negligible.* The postulate No. 1, therefore, is not valid at high pressures and low temperatures.

Postulate No. 2. *The forces of attraction between gas molecules are negligible.* This assumption is valid at low pressures or at high temperatures because under these conditions the molecules lie far apart from one another. But at high pressures or at low temperatures, the volume is small and molecules lie closer to one another. The intermolecular forces of attraction, therefore, are appreciable and *cannot be ignored.* Hence, the postulate No. 2 also does not hold under conditions of high pressure and low temperature.

It is necessary, therefore, to apply suitable corrections to the ideal gas equation so as to make it applicable to real gases.

EQUATIONS OF STATE FOR REAL (IMPERFECT) GASES

A number of equations of state have been suggested to describe the P–V–T relationship in real gases. The earliest and the best known equation is that of van der Waals.

van der Waals Equation of State

In 1873, van der Waals proposed his famous equation of state for a real, *i.e.*, imperfect gas. He modified the ideal gas equation by suggesting that the gas molecules were not mass points but behave like rigid spheres having a certain diameter and that there exist *intermolecular forces of attraction between them.* The two correction terms introduced by van der Waals are described below.

1. Correction due to volume of gas molecules. The ideal gas equation $PV=nRT$ is derived on the assumption that the gas molecules are mass points, *i.e.*, they do not have finite volume. van der Waals abandoned this assumption and suggested that a correction term nb should be subtracted from the total volume V in order to get the *ideal volume which is compressible.* In order to understand the meaning of the correction term nb, let us consider two gas molecules as unpenetrable and incompressible spheres, each of which has a diameter d, as shown in Fig. 3. It is evident that the centres of the two spheres cannot approach each other more closely than the distance d. For this pair of molecules, therefore, a sphere of radius d, and hence of volume $\frac{4}{3}\pi d^3$, constitutes what is known as the **excluded volume.** The excluded volume per molecule is thus half the above volume, *i.e.*, equal to $\frac{2}{3}\pi d^3$. The *actual volume* of one gas molecule of radius r is $\frac{4}{3}\pi r^3 = \frac{4}{3}\pi(d/2)^3 = \frac{1}{6}\pi d^3$.

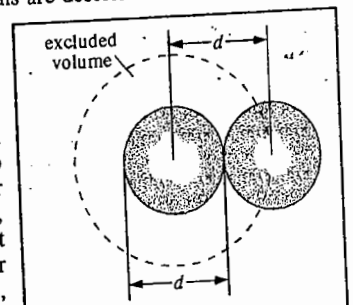

Fig. 3. Illustration of excluded volume.

$\therefore$ Excluded volume *per molecule* $= \frac{2}{3}\pi d^3 = 4\times\frac{1}{6}\pi d^3 = 4$ times the actual volume of the gas molecule

The excluded volume *per mole* of the gas would be $N_A\times 4\times\frac{4}{3}\pi r^3 = b$, where N_A is the Avogadro's number. The compressible volume per mole of the gas would thus be $V - b$. If volume V of the gas contains n moles, then the excluded volume would be nb. Hence the *ideal volume which is compressible* would be $V - nb$. The volume b per mole is also known as co-volume.

2. Correction due to intermolecular forces of attraction. In the derivation of the ideal gas equation, it was assumed that there are no intermolecular forces of attraction. Actually it is not so. In order to take into account the effect of intermolecular forces of attraction, let us consider a molecule lying somewhere in the midst of the vessel, as shown at the point C (Fig. 4). As can be seen, it is being attracted uniformly on all sides by the neighbouring molecules. These forces neutralize one another and there is no resultant attractive force on the molecule. However, as the molecule approaches the wall of the vessel, as shown at W, it experiences attractive forces from the bulk of the molecules behind it. Hence, *it will strike the wall with a lower velocity and will exert a lower pressure than it would have done if there was no force of attraction.* It is, therefore, necessary to

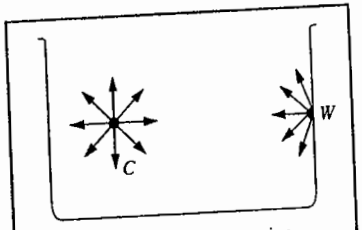

Fig. 4. Molecular attraction.

add a certain correction factor, p, to the pressure of the gas in order to get the *ideal pressure*. The correct pressure, therefore, should be $P + p$.

Calculation of the correction factor, p. The force of attraction exerted on a single molecule which is about to strike the wall evidently depends upon the *number of molecules per unit volume in the bulk of the gas, i.e.,* it depends directly upon the *density* of the gas. Further, the number of molecules striking the wall at any given instant also depends directly upon the *density* of the gas. Thus, the total inward attractive pull on the molecules which accounts for p is proportional to the square of the density (ρ) of the gas, *i.e.,*

$$p \propto \rho^2 \qquad ...(2)$$

But, density is inversely proportional to volume and if V is the volume occupied by *one mole* of a gas, the value of p for *one mole* of a gas will be inversely proportional to the square of volume. Hence,

$$p \propto 1/V^2 = a/V^2 \qquad ...(3)$$

where a is a constant depending upon the nature of the gas. The pressure correction factor p is also called the **internal pressure** of the gas.

The kinetic gas equation for *one mole* of a real gas, therefore, takes the form

$$(P + a/V_m^2)(V_m - b) = RT \qquad ...(4)$$

This is known as the **van der Waals equation.** The constants a and b are known as the **van der Waals constants.** These are characteristic of each gas.

Eq. 4 is valid for one mole of a gas only. If there are n moles of a gas occupying volume V, then, as illustrated above, the *excluded volume* will be given by nb and the compressible volume, will be $V - nb$. The pressure correction factor p for n moles, in the light of Eq. 2, will be proportional to $n^2\rho^2$, *i.e.,*

$$p \propto n^2\rho^2 \propto n^2 \times 1/V^2 = an^2/V^2 \qquad ...(5)$$

Hence, the van der Waals equation for n moles of a real gas becomes

$$(P + n^2a/V^2)(V - nb) = nRT \qquad ...(6)$$

Eq. 6 is more accurate than the ideal gas equation $PV=nRT$ for expressing the P–V–T behaviour of real gases.

The Dutch physicist J.D. van der Waals (1837 - 1923) was awarded the 1910 Physics Nobel Prize for his work on the equation of state for real gases.

The units for the van der Waals constants a and b depend upon the units in which P and V are expressed. It is evident from Eq. 5 that the constant a is expressed by the factor pV^2/n^2, *i.e.,* pressure $\times$ (volume)^2/mol^2. If pressure is expressed in atm and volume in dm^3, the value of a will be in dm^6 atm mol^{-2}. As regards b, it is incompressible volume per mole of a gas. Hence, it must have the same units as volume per mole, *e.g.,* dm^3 mol^{-1}.

The van der Waals constants for some common gases are given in Table 1.

TABLE 1

The van der Waals Constants for Some Common Gases

Gas	a (dm^6 atm mol^{-2})	b (dm^3 mol^{-1})	Gas	a (dm^6 atm mol^{-2})	b (dm^3 mol^{-1})
Ammonia	4·17	0·0371	Hydrogen chloride	3·67	0·0408
Argon	1·35	0·0322	Hydrogen bromide	4·45	0·0443
Carbon dioxide	3·59	0·0427	Methane	2·25	0·0428
Carbon monoxide	1·49	0·0399	Neon	0·21	0·0171
Chlorine	6·49	0·0562	Nitric oxide	1·34	0·0279
Ethane	5·49	0·0638	Nitrogen	1·39	0·0319
Ethylene	4·47	0·0571	Oxygen	1·36	0·0318
Helium	0·034	0·0237	Sulphur dioxide	6·71	0·0564
Hydrogen	0·246	0·0266	Nitrogen dioxide	5·28	0·0442

The constant a is a *measure of the van der Waals forces of cohesion* existing between the molecules of a given gas. The greater the value of a, the greater is the strength of the van der Waals forces. The values of a for hydrogen and helium are very small, being 0·024 and 0·246, respectively, indicating that the cohesive forces (van der Waals forces) in these gases are very weak. The values of a for ammonia, carbon dioxide, chlorine and sulphur dioxide are very high being 4·17, 3·59, 6·49 and 6·71, respectively. This shows that the van der Waals forces in these gases are very strong. The greater the value of a, the greater is the ease with which a gas can be liquefied.

Example 1. Calculate the pressure exerted by one mole of carbon dioxide gas in a 1·32 dm^3 vessel at 48°C using *(a)* the ideal gas equation and *(b)* the van der Waals equation. The van der Waals constants are : a=3·59 dm^6 atm mol^{-2} and b=0·0427 dm^3 mol^{-1}.

Solution : *(a)* For an ideal gas, $PV=nRT$, so that

$$P = \frac{nRT}{V} = \frac{(1\text{ mol})(0{\cdot}08206\text{ dm}^3\text{ atm K}^{-1}\text{ mol}^{-1})(321\text{ K})}{1{\cdot}32\text{ dm}^3} = \mathbf{19{\cdot}95\text{ atm}}$$

(b) For a van der Waals gas, from Eq. 6,

$$P = \frac{nRT}{V - nb} - \frac{n^2a}{V^2}$$

$$= \frac{(1\text{ mol})(0{\cdot}08206\text{ dm}^3\text{ atm K}^{-1}\text{ mol}^{-1})(321\text{ K})}{(1{\cdot}32\text{ dm}^3) - (1\text{ mol})(0{\cdot}0427\text{ dm}^3\text{ mol}^{-1})} - \frac{(1\text{ mol})^2(3{\cdot}59\text{ dm}^6\text{ atm mol}^{-2})}{(1{\cdot}32\text{ dm}^3)^2}$$

$$= 20{\cdot}62\text{ atm} - 2{\cdot}06\text{ atm} = \mathbf{18{\cdot}56\text{ atm}}$$

The experimental value of the pressure is 16·40 atm. Evidently, the van der Waals equation gives a better agreement with experiment than the ideal gas equation.

Discussion of the van der Waals Equation. We are now in a position to discuss the departure of real gases from ideal behaviour at different pressures and temperatures as depicted in Fig. 1.

1. When the pressure is not too high. When the pressure is not very high, the volume V_m will be sufficiently large and b may be ignored in comparison. The van der Waals equation for one mole of a gas, *viz.,*

$$(P + a/V_m^2)(V_m - b) = RT \qquad ...(7)$$

may then be written as $(P + a/V_m^2)V_m = RT$

or $$PV_m + a/V_m = RT \qquad ...(8)$$

or $$PV_m = RT - a/V_m \qquad ...(9)$$

Thus, the product PV_m is less than RT by an amount equal to a/V_m. As pressure increases, V_m decreases, a/V_m increases and, therefore, PV_m becomes smaller and smaller. This explains the dip in the isotherms of most of the gases, as shown in Fig. 1 for carbon monoxide, methane and ammonia.

2. When the pressure is too high. When the pressure is considerably high, the volume V_m will be quite small. Now it may not be possible to ignore b. But, as P is quite high, the pressure correction factor a/V_m^2 may become negligible in comparison with P in Eq. 7, which, therefore, reduces to

$$P(V_m - b) = RT \qquad ...(10)$$

or $$PV_m = RT + Pb \qquad ...(11)$$

Thus, PV_m is now greater than RT by an amount equal to Pb. As the pressure increases, the product Pb increases and, therefore, PV_m increases. This explains why the value of PV_m, after reaching a minimum, increases with further increase of pressure (Fig. 1).

It is evident from the above discussion that at ordinary temperatures, while the effect of the term a/V_m^2 is predominant at low pressures, that of Pb is predominant at high pressures. At some intermediate range of pressure, therefore, the two effects balance each other. In this range of pressure,

the gas shows the ideal behaviour. This explains the existence of a small horizontal portion in the isotherms of gases like carbon monoxide and methane, as shown in Fig. 1.

3. When the temperature is high. If, at a given pressure, the temperature is considerably high, the volume will become sufficiently large to make the value of a/V_m^2 negligibly small. At high temperature, b may also be negligible in comparison to V_m which is now sufficiently large. Under these conditions, the van der Waals equation approaches the ideal gas equation $PV_m=RT$. This explains why the deviations become less at high temperatures (Fig. 2).

4. Exceptional behaviour of hydrogen and helium. Since both hydrogen and helium have comparatively small masses, the attractive forces between their molecules are too small. This is indicated by very small values of the van der Waals constant a for these gases. As a result, the correction term a/V_m^2 due to the attraction factor remains negligible at ordinary temperatures. Thus,

$$PV_m = RT + Pb \qquad ...(12)$$

This explains why there is a continuous increase in PV_m with increase of pressure in the case of these two gases at ordinary temperatures (Fig. 1).

As can be seen from the above discussion, the van der Waals equation explains fairly satisfactorily the behaviour of real gases.

The Boyle Temperature. As already mentioned, the temperature at which a real gas obeys Boyle's law is known as the **Boyle temperature, T_B.** It is given by the expression

$$T_B = a/bR \qquad ...(13)$$

where a and b are the van der Waals constants. (Refer to Example 3 for the derivation of this expression).

Example 2. Calculate the Boyle temperature T_B for CO_2 gas, assuming it to be a van der Waals gas.

Solution : From Table 1, the van der Waals constants for CO_2 are

$$a = 3{\cdot}59 \text{ dm}^6 \text{ atm mol}^{-2} \quad \text{and} \quad b = 0{\cdot}0427 \text{ dm}^3 \text{ mol}^{-1}$$

$$T_B = \frac{a}{bR} = \frac{3{\cdot}59 \text{ dm}^6 \text{ atm mol}^{-2}}{(0{\cdot}0427 \text{ dm}^3 \text{ mol}^{-1})(0{\cdot}08206 \text{ dm}^3 \text{ atm K}^{-1} \text{ mol}^{-1})} = 1026 \text{ K}$$

Other Equations of State. Several other equations have been proposed from time to time to account for the *P-V-T* behaviour of real gases. A 'good' equation of state should be able to express the *P-V-T* behaviour under moderate ranges of pressure and temperature. Other criteria of a workable equation of state are its simplicity of form and the use of only a few adjustable constants or parameters. However, to represent the behaviour of gases to a sufficient degree of accuracy, the number of such parameters has to be at least more than two. A brief description of some of the equations of state, other than the van der Waals equation, is given below. In all these equations, the quantity of the gas is *one mole*.

Dieterici Equation. Dieterici introduced an exponential factor to account for the effect of molecular attraction on the pressure. He suggested the following relationship to account for the behaviour of real gases :

$$P\, e^{a/RTV_m}\, (V_m - b) = RT \qquad ...(14)$$

or

$$P\,(V_m - b) = RT\, e^{a/RTV_m} \qquad ...(15)$$

This equation agrees with the van der Waals equation at moderate pressures but differs appreciably at high pressures and gives more satisfactory agreement with the experimental data.

Berthelot Equation. Berthelot proposed the following empirical equation to explain the behaviour of real gases :

$$\{P + a/(TV_m^2)\}(V_m - b) = RT \qquad ...(16)$$

This equation is virtually the same as the van der Waals equation except that the correction term for intermolecular attraction is a/TV_m^2 instead of a/V_m^2.

The Berthelot equation has been found to be more accurate than the van der Waals equation for determining molar masses of gases.

Clausius Equation. Clausius, accounting for the variation of the van der Waals constant a with temperature, proposed the following equation :

$$\left(P + \frac{a}{T(V_m + c)^2}\right)(V_m - b) = RT \qquad ...(17)$$

where c is a new constant.

This equation is fairly satisfactory to explain the *P–V–T* relationship in some but not in all gases.

Redlich–Kwong Equation. This is a comparatively simple equation involving only two constants. In this equation also, the constant a is temperature-dependent. The equation may be written as

$$\left[P + \frac{a}{V_m(V_m + b)T^{1/2}}\right](V_m - b) = RT \qquad ...(18)$$

It has been shown that the above equation is the best two-parameter equation of state for real gases. Because of its simplicity and accuracy, it is being frequently used for expressing the *P–V–T* behaviour of gases.

The characteristic constants used in the Dieterici and the Redlich-Kwong equations for some common gases are listed in Table 2.

TABLE 2

Characteristic Constants of Dieterici and Redlich-Kwong Equations for Some Common Gases

Gas	Dieterici Equation		Redlich–Kwong Equation	
	a (dm^6 atm mol^{-2})	b (dm^3 mol^{-1})	a (dm^6 atm mol^{-2})	b (dm^3 mol^{-1})
Helium	0·045	0·0260	0·08	0.0170
Hydrogen	0·316	0·0289	1·44	0·0185
Neon	0·279	0·0191	1·47	0·0122
Argon	1·730	0·0350	16·80	0·0220
Nitrogen	1·730	0·0418	15·35	0·0268
Oxygen	1·748	0·0345	17·16	0·0221
Carbon monoxide	1·864	0·0427	16·98	0·0274
Carbon dioxide	4·620	0·0463	63·71	0·0296
Ammonia	5·390	0·0405	85·82	0·0259
Chlorine	8·340	0·0609	134·50	0·0390

It is important to keep in mind that the constants a and b are not strictly constant for a given gas. They vary somewhat with temperature and pressure. Further, the constant a appearing in the two equations is different dimensionally.

A feature common to all the equations of state described above is that regardless of the number of parameters occurring in them, they reduce to the ideal gas equation under conditions of low pressure. Thus, for all the above equations :

$$\lim_{P \to 0} (PV_m/RT) = 1 \qquad ...(19)$$

Virial Equation of State. The most general equation of state for real gases is the **virial equation,** proposed by **Kammerlingh-Onnes.** He expressed the product PV_m as a power series in $1/V_m$, as shown below :

$$PV_m = RT\left(1+\frac{B_2(T)}{V_m}+\frac{B_3(T)}{V_m^2}+\frac{B_4(T)}{V_m^3}+\cdots\cdots\right) \qquad \ldots(20)$$

where $B_2(T)$, $B_3(T)$, $B_4(T)$, etc., are the temperature-dependent second, third, fourth, etc., **virial coefficients,** respectively.

The various virial coefficients can be determined from the P–V–T data for real gases. It is possible to calculate them from a knowledge of intermolecular potential energy. Unfortunately, however, this potential energy is not accurately known and hence the calculation of higher virial coefficients is a formidable problem in theoretical chemistry. The first virial coefficient is, evidently, equal to RT.

The virial equation can also be expressed as a power series in pressure, as shown below :

$$PV_m = RT\{1 + A_2(T)P + A_3(T)P^2 + A_4(T)P^3 + \cdots\cdots\} \qquad \ldots(21)$$

where $A_2(T)$, $A_3(T)$, $A_4(T)$, etc., are new temperature-dependent virial coefficients. At low pressures, only the first virial coefficient (which is equal to RT) is important. It is always *positive.* It increases with increase in temperature. The second virial coefficient is *negative* at low temperatures, becomes zero at a particular temperature and then becomes increasingly positive as the temperature is raised continuously.

The temperature at which the second virial coefficient vanishes is known as the **Boyle temperature.** At this temperature while second virial coefficient disappears, the third, fourth and higher virial coefficients become insignificant so that PV_m becomes almost equal to RT. This implies that at the Boyle temperature, the gas behaves ideally over an appreciable range of pressure.

The physical significance of the virial coefficients is that the first coefficient neglects all molecular collisions, the second coefficient accounts for only bimolecular (binary) collisions and the third coefficient accounts for trimolecular (ternary) collisions, and so on.

Example 3. Show that for a van der Waals gas, the Boyle temperature $T_B = a/Rb$.

Solution : The Bolye temperature is the temperature at which the gas obeys Boyle's law, *i.e.*, the value of PV remains constant for an appreciable range of pressure from zero pressure. Mathematically, the Boyle temperature may be defined as the temperature at which $\underset{P\to 0}{\text{Limit}}[\partial(PV)/\partial P]_T = 0$.

The van der Waals equation for n moles of the gas may be written as

$$P = \frac{nRT}{V-nb} - \frac{n^2a}{V^2}$$

Multiplying throughout by V, we get

$$PV = \frac{nRTV}{V-nb} - \frac{n^2a}{V} \qquad \text{(Note this step)}$$

$$\therefore \quad \left[\frac{\partial(PV)}{\partial P}\right]_T = \left[\frac{nRT}{V-nb} - \frac{nRTV}{(V-nb)^2} + \frac{n^2a}{V^2}\right]\left(\frac{\partial V}{\partial P}\right)_T = 0 \text{ (at the Boyle temperature)}$$

Since $(\partial V/\partial P)_T$ is always negative (*i.e.*, it is not equal to zero), hence the expression in square brackets on the right hand side is equal to zero. Thus,

$$\frac{nRT}{V-nb} - \frac{nRTV}{(V-nb)^2} + \frac{n^2a}{V^2} = 0$$

$$\text{or } nRTV^2(V-nb) - nRTV^3 + n^2a(V-nb)^2 = 0$$

$$\text{or} \qquad n^2a(V-nb)^2 = -nRT[V^2(V-nb) - V^3]$$

$$\therefore \qquad RT = \frac{a}{b}\left(\frac{V-nb}{V}\right)^2 = \frac{a}{b}\left[1-\frac{nb}{V}\right]^2$$

Since at the Boyle temperature, $T = T_B$,

$$\therefore \qquad T_B = \frac{a}{Rb}\left[1-\frac{nb}{V}\right]^2$$

Since, when $P \to 0$, the volume V will be infinitely large so that $nb/V \to 0$, hence $T_B = a/Rb$

Intermolecular Forces

It is now fully established that forces of attraction exist between polar as well as nonpolar molecules. These intermolecular forces are known as **cohesive forces** or **van der Waals forces.** These forces originate from two types of interactions, *viz.*, 1. Dipole-Dipole Interaction and 2. Induced dipole - Induced dipole Interaction.

1. Dipole–Dipole Interaction. In the case of polar molecules which, though neutral, have permanent dipoles, the van der Waals forces are mainly due to electrical interaction between the dipoles known as dipole-dipole interaction. For instance, gases such as ammonia, sulphur dioxide, hydrogen fluoride, hydrogen chloride, etc., have permanent dipoles as a result of which there is appreciable dipole-dipole interaction between the molecules of these gases. The magnitude of this type of interaction depends upon the dipole moment of the molecule concerned. The greater the dipole moment, the greater is the dipole-dipole interaction. Because of the attractive interaction, these gases can be easily liquefied.

The average interaction energy of the two molecules with permanent dipole moments μ_1 and μ_2 is given by the expression

$$\text{Interaction energy, } \phi(r) = -2C/r^6 \qquad \ldots(22)$$

where $C = \frac{2}{3kT}\left[\frac{\mu_1\mu_2}{4\pi\varepsilon_0}\right]^2 r$ is their separation, k is Boltzmann constant and $4\pi\varepsilon_0$ is the permittivity factor of the medium.

2. Induced dipole–Induced dipole Interaction. London Forces or Dispersion Forces. As we know, the van der Waals forces exist even in nonpolar molecules such as O_2 and N_2 and also in nonpolar monoatomic molecules such as He, Ne, Ar, etc. This attraction is evident from the condensation of these gases into liquids at sufficiently high pressures and low temperatures. This could not be understood for several years.

In 1930, F. London provided a satisfactory explanation for the existence of forces of attraction between nonpolar molecules based on quantum mechanics. According to this view, electrons of a neutral molecule keep on oscillating with respect to the nuclei of the atoms. As a result of this, at a given instant, positive charge may be concentrated in one region and negative charge in another region of the same molecule. Thus, a nonpolar molecule may become momentarily self-polarised. This polarised molecule may induce a dipole moment in a neighbouring molecule with antiparallel orientation, as shown in Fig. 5.

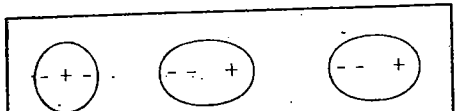

Fig. 5. Origin of cohesive forces in nonpolar molecules.

The electrostatic forces of attraction between induced dipoles and the original dipoles (due to electron oscillation) are known as the **London forces.** These forces are also called **dispersion forces** because the well known phenomenon of dispersion of light is also connected with these dipoles. The van der Waals attraction in nonpolar molecules is thus exclusively due to the London forces.

The average interaction energy in this case is given by

$$\text{Interaction energy, } \phi(r) = -C/r^6 \qquad \ldots(23)$$

where $C = \frac{3}{2}\alpha_1\alpha_2 \frac{(IE)_1(IE)_2}{(IE)_1 + (IE)_2}$. In this expression, $(IE)_1$ and $(IE)_2$ are the ionization energies of the two molecules. Other parameters have the same significance as mentioned above.

Nature of the van der Waals Interactions. Though the van der Waals constants a and b take into consideration the effect of attractive interactions in gaseous molecules, there is need for inquiring into the exact nature of these interactions. Since molecules are composed of positively charged nuclei and negatively charged electrons, whenever any two molecules come closer, interactions occur between the charge clouds of the nuclei and the electrons of the two molecules. At relatively large intermolecular distances, the attractive forces originating from attraction between electrons and atomic nuclei operate between the two molecules. At very small distances, however, the molecules strongly repel each other, the repulsion arising from the interaction between the similarly charged electron clouds. Thus, we expect the intermolecular potential energy to be composed of the long range *attractive term* and the short range *repulsive term*. One of the most widely used intermolecular potentials is the **Lennard-Jones (6–12) potential** given by

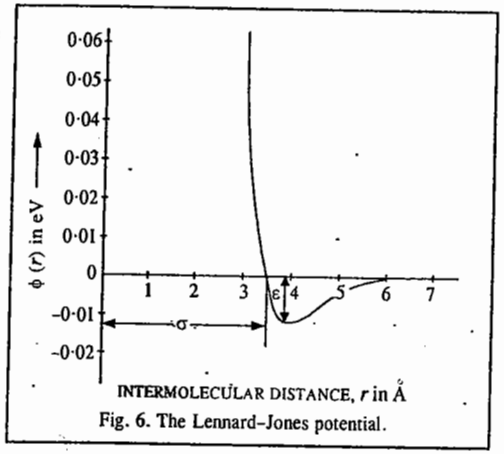

Fig. 6. The Lennard-Jones potential.

$$\phi(r) = 4\varepsilon\,[(\sigma/r)^{12} - (\sigma/r)^6] \qquad \ldots(24)$$

It is sketched in Fig. 6. Here, ε is the depth of the minimum in the potential energy curve, *i.e.*, ε is the *maximum* energy of attraction and σ is the intermolecular distance at which $\phi(r)=0$. For values of $r > \sigma$, the term $1/r^6$ predominates while for $r < \sigma$, the term $1/r^{12}$ predominates. The parameter σ is approximately equal to the sum of the average radii of the two molecules.

To understand the significance of ε, let us find the minimum of the Lennard-Jones potential by differentiating it and setting the derivative equal to zero :

$$d[\phi(r)]/dr = 4\varepsilon\,(-12\sigma^{12}r^{-13} + 6\sigma^6 r^{-7}) = 0, \text{ whence}$$

$$2\sigma^6 = r_m^6 \qquad \text{or} \qquad r_m = (2)^{1/6}\,\sigma = 1{\cdot}122\,\sigma$$

where r_m is the intermolecular distance corresponding to the *minimum* of the potential energy curve. At this distance, the forces of attraction and repulsion just balance each other. Substituting r by r_m in Eq. 24, we see that, at the potential energy minimum,

$$\phi(r_m) = 4\varepsilon\left[\frac{\sigma^{12}}{4\sigma^{12}} - \frac{\sigma^6}{2\sigma^6}\right] = 4\varepsilon\left(\frac{1}{4} - \frac{1}{2}\right) = -\varepsilon \qquad \ldots(25)$$

Second Virial Coefficient and Molecular Diameter. The second virial coefficient of the virial equation of state can be evaluated in terms of the volume of the gaseous molecule which permits easy determination of the molecular diameter of the gas. This is illustrated below.

Example 4. The second virial coefficient of an imperfect (non-ideal) gas is given by

$$B_2(T) = -2\pi N_A \int_0^\infty [e^{-\phi(r)/kT} - 1]r^2 dr$$

where $\phi(r)$ is the intermolecular potential for two molecules separated by the distance r. Evaluate it for a hard-sphere potential and illustrate how the diameter of a molecule can be calculated with its help.

Solution : If the two molecules are approximated as hard spheres or as hard billiard balls, the simplest hard-sphere potential (Fig. 7) is given by

$$\phi(r) = \begin{cases} 0, & r > d \\ \infty, & r < d \end{cases}$$

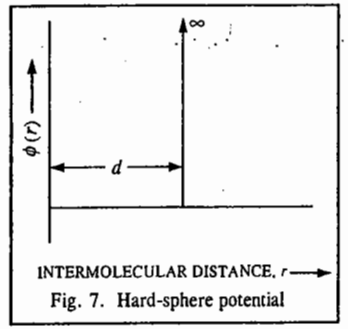

Fig. 7. Hard-sphere potential

where d is the sum of the radii of the molecules. Substituting this potential in the given expression, we have

$$B_2(T) = -2\pi N_A \int_0^d [e^{-\infty} - 1]r^2 dr - 2\pi N_A \int_d^\infty [e^0 - 1]r^2 dr$$

$$= -2\pi N_A \int_0^d -r^2 dr$$

[Since $e^0 = 1$, hence the second integral term vanishes]

$$= 2\pi N_A d^3/3 = 4N_A V_{\text{molecule}}$$

since the volume of one molecule is given by $V_{\text{molecule}} = (4/3)\pi(d/2)^3$.

Thus, knowing the second virial coefficient of the gas, its diameter d can be easily calculated.

CRITICAL PHENOMENA

Critical Constants of a Gas. The most characteristic property of gases is that their molecules lie far apart from one another and are in continuous rapid motion. Each molecule, therefore, leads almost an independent existence. This is particularly so when temperature is high and pressure is low. However, as the temperature of a gas is lowered, the kinetic energy of the molecules decreases. The volume occupied by the gas also decreases. At a sufficiently low temperature, some of the slow moving molecules cannot resist the force of attraction and they come closer and closer and ultimately the gas changes into the liquid state. Thus, liquefaction of gases results from decrease of temperature.

Increase of pressure has also the effect of bringing the gaseous molecules closer and closer to one another (due to decrease in volume). This is an additional helpful factor in converting a gas into liquid. Thus, *increase of pressure* and *decrease of temperature* both tend to cause liquefaction of gases. For instance, sulphur dioxide can be liquefied at -8°C if the pressure is 1 atm. But it can be liquefied even at a higher temperature of 20°C if the pressure is increased to 3·24 atm.

The effect of temperature, however, is more important than that of the pressure because for each gas there is a certain temperature above which it cannot be liquefied, no matter how high a pressure may be applied. This temperature is known as the *critical temperature*. Thus, the **critical temperature** *of a gas may be defined as that temperature above which it cannot be liquefied howsoever high the pressure may be.* For instance, the critical temperature of carbon dioxide is 31·1°C. This means that it is not possible to liquefy carbon dioxide above 31·1°C by any means.

At the critical temperature, a certain pressure is needed to liquefy the gas. This pressure is called the **critical pressure.** For instance, at 31·1°C, carbon dioxide can be liquefied under a pressure of 72·9 atm. Thus, the critical pressure of the gas is 72·9 atm.

The critical temperature of oxygen is -118°C and that of hydrogen is -240°C. These gases, therefore, cannot be liquefied at ordinary temperatures. Their critical pressures are 50·1 and 12·8 atm, respectively.

The volume occupied by *one mole* of a gas at its critical temperature and critical pressure is known as the **critical volume.** For example, critical volumes of carbon dioxide, oxygen and hydrogen are 94·0, 78·2 and 65·5 ml per mole, respectively.

The *P–V* Isotherms of Carbon Dioxide. The importance of critical temperature of a gas was first discovered by T. Andrews in his experiments on pressure-volume relationships (isotherms) of carbon dioxide gas at a series of temperatures. The isotherms of carbon dioxide determined by him at different temperatures are shown in Fig. 8. Consider first the isotherm at the lowest temperature, *viz.*, 13·1°C. The point *A* represents carbon dioxide in the gaseous state occupying a certain volume under a certain pressure. On increasing the pressure, its volume diminishes as is indicated by the curve *AB*. At *B*, which represents a pressure of 49·8 atm, liquefaction of the gas commences and thereafter a rapid decrease in volume takes place at the same pressure, as more and more of the gas is converted into the liquid state. At *C*, the gas has been completely liquefied. Now, as the liquid is only slightly compressible, further increase of pressure produces only a very small decrease in volume. This is shown by a steep line *CD* which is almost vertical.

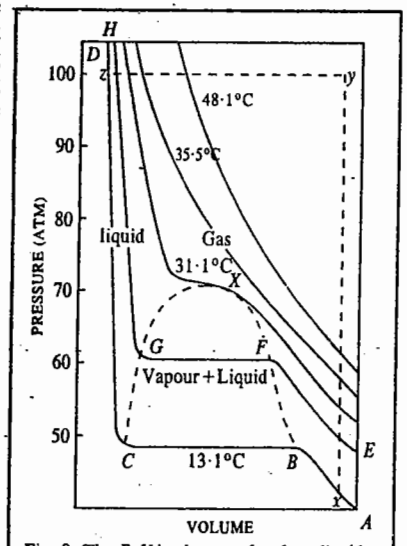

Fig. 8. The *P–V* isotherms of carbon dioxide.

Thus, along the curve *AB*, carbon dioxide exists as gas; along *BC*, it exists partly as gas and partly as liquid while along *CD*, it exists entirely as liquid. It may also be noted that a considerable decrease of volume (represented by *BC*) takes place when the gas changes into the liquid state at a constant pressure.

The isotherm *EFGH* at 21·5°C shows a similar behaviour except that now the liquefaction commences at a higher pressure and the horizontal portion *FG*, representing decrease in volume, becomes smaller. At still higher temperatures, the horizontal portion of the curve becomes shorter and shorter until at 31·1°C *it reduces just to a point* (represented by *X*). At this temperature, therefore, the gas passes into liquid state *imperceptibly*. Above 31·1°C, the isotherm is continuous. There is no evidence of liquefaction at all. Andrews concluded that if the temperature of carbon dioxide is above 31·1°C, it cannot be liquefied, no matter how high the pressure may be. He called 31·1°C as the **critical temperature** of carbon dioxide. Since then, other gases have been found to behave similarly. There is no fundamental difference between the so called 'permanent' gases such as hydrogen, oxygen, nitrogen, etc., and 'temporary' gases such as carbon dioxide, chlorine, hydrochloric acid, ammonia, etc. The difference lies in the fact that while the so-called 'permanent' gases have very low critical temperatures much below the ordinary range of temperature, the so called 'temporary' gases have critical temperatures well within the range of ordinary temperatures.

Continuity of State. A careful examination of the isotherms plotted in Fig. 8 shows that it is possible to convert liquid carbon dioxide into gas and vice-versa, *without any 'discontinuity'*, that is, without having, at any time, more than one phase present. On joining the ends of the horizontal portions of the various isotherms, a boundary curve *CGXFB*, represented by the dotted line, is obtained. At the top lies the critical point *X* (31·1°C). Within the area of the boundary curve, both liquid and gaseous states can coexist but outside this area, either liquid or gaseous state alone can exist. Suppose, a certain volume of carbon dioxide, represented by a point *x* on the 13·1°C isotherm *ABCD* is heated *at constant volume* to a temperature at which the pressure increases to a point *y*, lying above the critical pressure of the gas. Let the gas be now cooled at the *same pressure*. The temperature and volume both will decrease along *yz*. At *z*, the temperature is 21·5°C and carbon dioxide exists as liquid. During this transition from gas to liquid, *there has never been more than one phase present at any time.* As the temperature is decreased from *y* to *z*, the volume of the gas decreases *gradually* till the molecules are close enough for the van der Waals forces of attraction to cause their condensation into the liquid state. The process of transition from gaseous state to liquid state (or vice-versa), therefore, is regarded as **continuous.**

van der Waals Equation and Critical State. For one mole of a gas, the van der Waals equation

$$(P + a/(V_m)^2)(V_m - b) = RT \qquad ...(26)$$

may be written as

$$PV_m - Pb + \frac{a}{V_m} - \frac{ab}{(V_m)^2} - RT = 0 \qquad ...(27)$$

Multiplying by $(V_m)^2$ and dividing by P and rearranging in decreasing powers of V_m, it may be written as

$$(V_m)^3 - \left(b + \frac{RT}{P}\right)(V_m)^2 + \frac{a}{P}V_m - \frac{ab}{P} = 0 \qquad ...(28)$$

This is a cubic equation in the variable V_m and, therefore, for any single set of the values of P and T, there should be *three* values of V_m, all of which may be real or only one may be real and the other two imaginary. If, at a constant temperature, the values of V are plotted against P, then, according to Eq. 28, a curve similar to that marked I in Fig.9, should be obtained. It will be seen readily that, *for a certain pressure, there are three values of V marked as L, N and Q.* As the temperature increases, the isotherm moves up. When it is in position II, the three values of V get closer to one another. At a certain temperature (isotherm III), the three values of V become identical as shown by the point *X*. At a still higher temperature (isotherm IV), there is only one real value of V corresponding to a given pressure. Thus, below the critical temperature of a gas, the isotherm indicates three values of V for a given pressure, in accordance with the above equation.

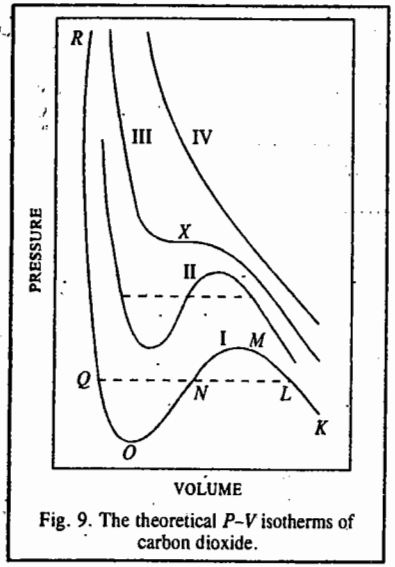

Fig. 9. The theoretical *P–V* isotherms of carbon dioxide.

It may be pointed out that the isotherms plotted in Fig. 9 are based on theoretical calculations of V corresponding to different values of P obtained by using the van der Waals equation. The isotherms for carbon dioxide, obtained by Andrews *experimentally*, were in close resemblance with these curves, with the difference that the wavelike portion *LMNOQ* (Fig. 9) was replaced by a horizontal line (*cf.* experimental isotherms of carbon dioxide represented in Fig. 8). Since then more careful experiments have shown that small portions corresponding to curves *LM* and *OQ* can be realized in practice also. These represent super-saturated vapour and superheated liquid, respectively.

As the temperature is raised, the loops become smaller and smaller, as already stated. At the critical point *X*, all the three values of V become identical. Since the temperature is now critical, this value of V represents the *critical volume* of the gas, that is,

$$V_m = V_{m.c.} \text{ or } (V_m - V_{m,c})^3 = 0 \qquad ...(29)$$

Expanding and writing in decreasing powers of V_m, we have

$$V_m^3 - 3V_{m,c}(V_m)^2 + 3(V_{m,c})^2V_m - (V_{m,c})^3 = 0 \qquad ...(30)$$

Eq. 30 must be identical with the van der Waals equation at critical temperature and pressure, which for 1 mole of the gas may be written as

$$(V_m)^3 - \left(b + \frac{RT_c}{P_c}\right)(V_m)^2 + \frac{a}{P_c}V_m - \frac{ab}{P_c} = 0 \qquad ...(31)$$

Hence, the coefficients of equal powers of V_m in Eqs. 30 and 31 must be equal to one another. Thus,

$$3V_{m,c} = b + RT_c/P_c \qquad ...(32)$$

$$3(V_{m,c})^2 = a/P_c \quad ...(33)$$

$$(V_{m,c})^3 = ab/P_c \quad ...(34)$$

From Eqs. 32, 33 and 34, the critical constants T_c, P_c and $V_{m,c}$ of a gas can be calculated in terms of the van der Waals constants a and b, as shown below.

Dividing Eq. 34 by Eq. 33, we have

$$V_{m,c} = 3b \quad ...(35)$$

Substituting this value in Eq. 33, we get

$$P_c = a/27b^2 \quad ...(36)$$

Inserting these values of $V_{m,c}$ and P_c in Eq. 32, we have

$$T_c = 8a/27Rb \quad ...(37)$$

Thus, knowing the critical constants of a gas, it is possible to calculate the van der Waals constants and *vice versa*.

Critical Compressibility Factor. The critical compressibility factor, Z_c, of a van der Waals gas is given by

$$Z_c = \frac{P_c V_{m,c}}{RT_c} = \frac{(a/27b^2)(3b)}{R[8a/27Rb]} = 0{\cdot}375 \quad ...(38)$$

Thus, we can test whether a gas behaves as a van der Waals gas by seeing whether its critical compressibility factor is equal to 0·375.

The critical constants of some common gases are given in Table 3. We see that although Z_c is less than 0·375, the discrepancy is rather small.

TABLE 3
Critical Constants of Gases

Gas	P_c (atm)	$V_{m,c}$ (dm^3 mol^{-1})	T_c (K)	Z_c
He	2·26	$57{\cdot}9\times10^{-3}$	5·2	0·307
Ne	26·9	$41{\cdot}7\times10^{-3}$	44·4	0·308
Ar	48·1	$75{\cdot}2\times10^{-3}$	150·7	0·292
Xe	58·0	$119{\cdot}0\times10^{-3}$	289·7	0·290
H_2	12·8	$65{\cdot}5\times10^{-3}$	33·0	0·309
O_2	50·1	$78{\cdot}2\times10^{-3}$	154·8	0·308
N_2	33·5	$90{\cdot}1\times10^{-3}$	126·2	0·291
CO_2	72·8	$94{\cdot}0\times10^{-3}$	304·2	0·274
NH_3	111·5	$72{\cdot}5\times10^{-3}$	405·0	0·243
CH_4	54·6	$98{\cdot}7\times10^{-3}$	190·6	0·288
C_2H_6	48·2	$148{\cdot}0\times10^{-3}$	305·4	0·284
C_2H_6	50·5	$127{\cdot}4\times10^{-3}$	282·4	0·278
C_6H_6	48·4	$254{\cdot}1\times10^{-3}$	562·3	0·266

Example 5.. Calculate the critical temperature of a van der Waals gas for which P_c is 100 atm and b is 50 cm^3 mol^{-1}.

Solution : From Eq. 36, $a = P_c\, 27\, b^2$

From Eq. 37, $T_c = \frac{8a}{27Rb} = \frac{(8)(P_c 27b^2)}{27Rb} = \frac{8P_c b}{R} = \frac{(8)(100\text{ atm})(0{\cdot}050\text{ dm}^3\text{ mol}^{-1})}{0{\cdot}08206\text{ dm}^3\text{ atm K}^{-1}\text{ mol}^{-1}} = 487{\cdot}2$ K

Example 6. The van der Waals constants of a gas are : a=0·751 dm^6 atm mol^{-2} and b=0·0226 dm^3 mol^{-1}. Calculate its critical constants.

Solution : $V_{m,c} = 3b = 3(0{\cdot}0226\text{ dm}^3\text{ mol}^{-1}) = 0{\cdot}0678$ dm^3 mol^{-1}

$$P_c = \frac{a}{27b^2} = \frac{(0{\cdot}751\text{ dm}^6\text{ atm mol}^{-2})}{27(0{\cdot}0226\text{ dm}^3\text{ mol}^{-1})^2} = 54{\cdot}5\text{ atm}$$

$$T_c = \frac{8a}{27Rb} = \frac{8(0{\cdot}751\text{ dm}^6\text{ atm mol}^{-2})}{27(0{\cdot}08206\text{ dm}^3\text{ atm K}^{-1}\text{ mol}^{-1})(0{\cdot}0226\text{ dm}^3\text{ mol}^{-1})} = 120\text{ K}$$

Example 7. A certain gas has the following values of its critical constants : P_c=45·6 atm, $V_{m,c}$=0·0987 dm^3 mol^{-1} and T_c=190·6 K. Calculate the van der Waals constants of this gas. Also, estimate the radius of the gas molecules assuming that they are spherical.

Solution :

$$b = \frac{V_{m,c}}{3} = \frac{0{\cdot}0987\text{ dm}^3\text{ mol}^{-1}}{3} = 0{\cdot}0329\text{ dm}^3\text{ mol}^{-1}$$

$$a = 3\,P_c\,(V_{m,c})^2 = 3(45{\cdot}6\text{ atm})(0{\cdot}0987\text{ dm}^3\text{ mol}^{-1})^2 = 1{\cdot}333\text{ dm}^6\text{ atm mol}^{-2}$$

The critical volume of one molecule ($v_{m,c}$) is, evidently, b/N_A where N_A is the Avogadro's number.

$$v_{m,c} = \frac{0{\cdot}0329\text{ dm}^3\text{ mol}^{-1}}{N_A} = \frac{0{\cdot}0329\times10^{-3}\text{ m}^3\text{ mol}^{-1}}{6{\cdot}022\times10^{23}\text{ mol}^{-1}} = 5{\cdot}46\times10^{-29}\text{ m}^3$$

The volume of a sphere $= (4/3)\pi r^3$ where r is its radius, so that $4/3\pi r^3 = 5{\cdot}46\times10^{-29}$ m^3

$$r = \left(\frac{3\times5{\cdot}46\times10^{-29}\text{ m}^3}{4\pi}\right)^{1/3} = 2{\cdot}35\times10^{-10}\text{ m}$$

$$= 235\text{ pm}$$

It may be of interest to know that normal boiling point T_b of a liquid is approximately two-thirds of its critical temperature T_c when both are expressed on Kelvin scale, *i.e.*,

$$T_b/T_c \approx \tfrac{2}{3} \quad ...(39)$$

Example 8. Estimate the critical temperature of *n*-hexane if its boiling point is 68·9°C.

Solution : From Eq. 39, $T_b = \frac{2}{3}T_c$

$$\therefore \quad T_c = \tfrac{3}{2}T_b = 3/2(68{\cdot}9 + 273)\text{ K}$$

$$= 512{\cdot}85\text{ K} = 239{\cdot}85°\text{C} \quad \text{(Experimental value is 234·7°C)}$$

It can also be shown that for a van der Waals gas, the Boyle temperature, $T_B = (27/8)T_c$.

Law (Principle) of Corresponding States

In 1881, van der Waals showed that if the pressure, volume and temperature of a gas are expressed in terms of its critical pressure, critical volume and critical temperature, we can obtain an important generalization called the principle of corresponding states.

Let $P/P_c = P_r$, $V_m/V_{m,c} = V_r$ and $T/T_c = T_r$ where P_r, V_r and T_r are called the *reduced pressure*, the *reduced volume* and the *reduced temperature*, respectively. Substituting in van der Waals equation for one mole of a gas, *viz.*,

$$(P + a/(V_m)^2)(V_m - b) = RT, \text{ we have}$$

$$\left(P_r P_c + \frac{a}{(V_r)^2(V_{m,c})^2}\right)(V_r V_{m,c} - b) = RT_r T_c \quad ...(40)$$

Substituting for P_c, $V_{m,c}$ and T_c from Eqs. 35, 36 and 37, we have

$$\left(\frac{aP_r}{27b^2} + \frac{a}{9(V_r)^2 b^2}\right)(3V_r b - b) = RT_r\left(\frac{8a}{27Rb}\right)$$

or $$(P_r + 3/V_r^2)\,(3V_r - 1) = 8T_r \qquad ...(41)$$

Eq. 41 involves neither R nor the van der Waals constants a and b. Hence, it is a general equation applicable to all substances. It follows from this equation that if *two or more substances have the same reduced temperature and the same reduced pressure, they would have the same reduced volume.* This statement is known as the **principle of corresponding states.**

Two or more substances having the same reduced temperature and the same reduced pressure and thus having the same reduced volume are said to be **in corresponding states.**

Example 9. Calculate the pressure exerted by one mole of CO_2 gas at 40°C, confined to a volume of 0·107 dm^3, using the law of corresponding states, given that the critical constants of the gas are $V_{m,c}$=0·0957 dm^3, T_c=304 K and P_c=73·0 atm.

Solution : From Eq. 41, $P_r = \dfrac{8T_r}{3V_r - 1} - \dfrac{3}{V_r^2} = \dfrac{8(T/T_c)}{3(V_m/V_{m,c}) - 1} - \dfrac{3}{(V_m/V_{m,c})^2}$

$$= \frac{8(313/304)}{3(0{\cdot}107/0{\cdot}0957) - 1} - \frac{3}{(0{\cdot}107/0{\cdot}0957)^2}$$

$$= \frac{(8)(1{\cdot}03)}{3 \times 1{\cdot}18 - 1} - \frac{3}{(1{\cdot}1)^2} = 3{\cdot}51 - 2{\cdot}40 = 1{\cdot}11$$

$$\therefore \quad P = P_r P_c = 1{\cdot}11 \times 73{\cdot}0 \text{ atm} = \mathbf{81{\cdot}03 \text{ atm}}$$

Example 10. Calculate the temperature and pressure that one mole of *(a)* ammonia and *(b)* helium will have in states corresponding to 1 mole of H_2 at 25°C and 1 atm pressure. For relevant data, use Table 3.

Solution : From Table 3, the critical constants of the given gases are

H_2 : T_c = 33·0 K P_c = 12·8 atm

He : T_c = 5·2 K P_c = 2·26 atm

NH_3 : T_c = 405·0 K P_c = 111·5 atm

For H_2 at 298 K and 1 atm pressure, the reduced parameters are

$$T_r = T/T_c = 298 \text{ K}/33{\cdot}0 \text{ K} = 9{\cdot}030$$

$$P_r = P/P_c = 1 \text{ atm}/12{\cdot}77 \text{ atm} = 0{\cdot}078$$

Ammonia and helium will be in their corresponding states when their reduced temperatures and reduced pressures are the same as those of H_2. Thus,

(a) For NH_3 : $T = T_r T_c = 9{\cdot}030 \times 405 \text{ K} = \mathbf{3657{\cdot}15 \text{ K}}$

$P = P_r P_c = 0{\cdot}078 \times 111{\cdot}5 \text{ atm} = \mathbf{8{\cdot}697 \text{ atm}}$

(b) For He : $T = T_r T_c = 9{\cdot}030 \times 5{\cdot}2 \text{ K} = \mathbf{46{\cdot}956 \text{ K}}$

$P = P_r P_c = 0{\cdot}078 \times 2{\cdot}26 \text{ atm} = \mathbf{0{\cdot}176 \text{ atm}}$

Example 13. Calculate the reduced pressure, reduced volume and reduced temperature of one mole of methane gas confined to a volume of 5 dm^3 under a pressure of 5 atm. Also calculate the temperature of the gas. The critical constants of methane are $V_{m,c}$ = 0·0988 dm^3 mol^{-1}, P_c = 54·6 atm, T_c=190·2 K.

Solution : $P_r = P/P_c = 5 \text{ atm}/54{\cdot}6 \text{ atm} = \mathbf{0{\cdot}1096}$

$V_r = V/V_{m,c} = 5 \text{ dm}^3 \text{ mol}^{-1}/0{\cdot}0988 \text{ dm}^3 \text{ mol}^{-1} = \mathbf{50{\cdot}607}$

From Eq. 41, $T_r = \dfrac{(P_r + 3/V_r^2)(3V_r - 1)}{8} = \dfrac{[0{\cdot}1096 + 3/(50{\cdot}607)^2][3 \times 50{\cdot}607 - 1]}{8} = \mathbf{2{\cdot}089}$

$\therefore \quad T = T_r T_c = (2{\cdot}089 \times 190{\cdot}2) \text{ K} = \mathbf{397{\cdot}3 \text{ K}}$

Molar Mass and Density of a Real Gas

We know that for a real gas, the PV versus P plot is not linear. Hence, ρ/P, *i.e.*, m/PV, is not independent of P. In order to calculate the density ρ and the molar mass M, we must obtain the value of ρ/P at P=0.

At low pressures, the van der Waals equation can be written as

$$P(V - nb) = nRT$$

or $$PV = n(RT + Pb) = (m/M)\,(RT + Pb)$$

$$\therefore \quad P = (m/V)\left[\frac{RT}{M} + \frac{Pb}{M}\right] = \rho\left[\frac{RT + Pb}{M}\right]$$

$$\therefore \quad \frac{\rho}{P} = \frac{M}{RT + Pb} = \frac{M/RT}{1 + Pb/RT}$$

Since $\dfrac{1}{1 + Pb/RT} = (1 + Pb/RT)^{-1} = 1 - Pb/RT$ when pressures are low, hence

$$\frac{\rho}{P} = \frac{M}{RT}\left(1 - \frac{Pb}{RT}\right) = \frac{M}{RT} - \frac{Mb}{(RT)^2}P$$

From this equation, we see that a plot of ρ/P verus P would be a straight line with slope = $Mb/(RT)^2$ and intercept = M/RT. The molar mass, M, is obtained from the intercept since as $P \to 0$, the gas behaves ideally and M is independent of P.

LIQUEFACTION OF GASES

As has already been explained, it is necessary to cool a gas below its critical temperature before it can be liquefied. In the case of a gas like ammonia, chlorine, sulphur dioxide or carbon dioxide, which has a fairly high critical temperature (Table 3), the application of a suitable pressure alone is sufficient to cause liquefaction. Gases such as hydrogen, oxygen, nitrogen and helium which have very low critical temperatures (Table 3) could not be liquefied by this simple technique. As the significance of critical temperature was not properly understood at that time, these gases were regarded as 'permanent'. But, now it is known that these gases can also be liquefied *if they are first cooled below their respective critical temperatures and then compressed.*

Two principles are usually applied in cooling gases below their critical temperatures.

1. Joule–Thomson Effect. The British physicists James P. Joule (1818-1889) and William Thomson (1824-1907), later honoured as Lord Kelvin, observed that when a gas under high pressure is made to expand into a region of low pressure, it suffers a fall in temperature. This phenomenon is known as the **Joule–Thomson effect** (see Chapter 13).

The Joule–Thomson effect offers further support to the view that attractive forces do exist between gas molecules. As the gas expands, the molecules fall apart from one another. Therefore, work has to be done in order to overcome the cohesive or attractive forces which tend to hold the molecules together. Thus work is done by the system at the expense of the kinetic energy of the gaseous molecules. Consequently, the kinetic energy decreases and since this is proportional to temperature, cooling results. It may be noted that in this case no external work has been done by the gas in expansion.

Experiment has shown that gases become cooler during the Joule–Thomson expansion only if they are below a certain temperature known as the **inversion temperature, T_i.** The inversion temperature is characteristic of each gas. It is related to the van der Waals constants a and b of the gas concerned by the following expression :

$$T_i = 2a/Rb \qquad ...(42)$$

At the inversion temperature, there is no Joule-Thomson effect. Thus, if a gas under pressure passes through a porous plug and expands adiabatically into a region of very low pressure at the inversion temperature, there is neither fall nor rise in temperature. If, however, the expansion takes place *above* the inversion temperature, there is a small *rise* of temperature and if it takes place *below* the inversion temperature there is a small fall of temperature.

In most gases, the inversion temperature lies within the range of ordinary temperatures, Hence, they get cooled in the Joule-Thomson expansion. Hydrogen and helium, however, have very low inversion temperatures. Thus, at ordinary temperatures, these gases get warmed up instead of getting cooled in the Joule-Thomson expansion. But if these gases are first cooled to their respective inversion temperatures, then these gases also get cooled on expansion in accordance with the Joule-Thomson effect.

2. Adiabatic Expansion Involving Mechanical Work. When a gas is made to expand against a pressure, as in an engine, it does some external work also at the expense of its kinetic energy which decreases. Hence, there is a fall of temperature. This principle, combined with Joule-Thomson effect, has been used in **Claude's process** for the liquefaction of air. George Claude (1870-1960) was a French engineer.

Production of Low Temperatures by Adiabatic Demagnetization of a Paramagnetic Substance. Very low temperatures in the vicinity of absolute zero have been obtained by *(i)* the Joule-Thomson expansion of hydrogen *(ii)* using liquid helium and *(iii) making use of the magnetic properties of paramagnetic substances* such as the salts of the rare earths. The paramagnetism of these substances is due to the presence of odd (unpaired) electrons. The method of adiabatic demagnetization of a paramagnetic substance, first suggested in 1926 by P. Debye and, independently in 1927 by W.F. Giauque, is based on the fact that the temperature of a thermally isolated paramagnetic substance drops when it is demagnetized. This can be best understood by considering the following equation for a magnetic system :

$$dS = \frac{C_B dT}{T} + \varepsilon_0 V \left(\frac{\partial M}{\partial T}\right)_B dB \qquad ...(43)$$

where M is the extent of magnetization in the presence of an external magnetic field B ; V is the volume, ε_0 is the permeability and C_B is the heat capacity of the system at constant magnetic field B.

The extent of magnetization of a paramagnetic substance at constant magnetic field B always decreases with increase in temperature T so that the partial derivative $(\partial M/\partial T)_B$ is always negative. Hence, when the substance is demagnetized reversibly and adiabatically (so that dB is negative and $(dS=0)$, we get

$$\frac{dT}{T} = -\frac{\varepsilon_0 V}{C_B}\left(\frac{\partial M}{\partial T}\right) dB \qquad ...(44)$$

or

$$\left(\frac{\partial T}{\partial B}\right)_S = -\frac{\varepsilon_0 TV}{C_B}\left(\frac{\partial M}{\partial T}\right)_B \qquad ...(45)$$

Eq. 45, which forms the basis of the principle of adiabatic demagnetization, gives the rate of change of temperature with magnetic field upon reversible adiabatic demagnetization. We see from Eq. 44 that dT/T is negative so that dT is also negative. Thus, a paramagnetic substance cools down upon adiabatic demagnetization.

The temperature-entropy (T—S) curve for a paramagnetic salt, such as gadolinium sulphate octahydrate, is shown in Fig. 10.

In the unmagnetized state (when $B=0$), the spins of the unpaired electrons of the paramagnetic material are oriented in a random manner in all directions. Thus, there is a disorder. When, however, the substance is magnetized, the spins and hence the magnetic moments associated with them, tend to align themselves with the magnetic field thereby reducing disorder. In other words, the unmagnetized substance has greater entropy than the magnetized substance at a given temperature. This is apparent from Fig. 10.

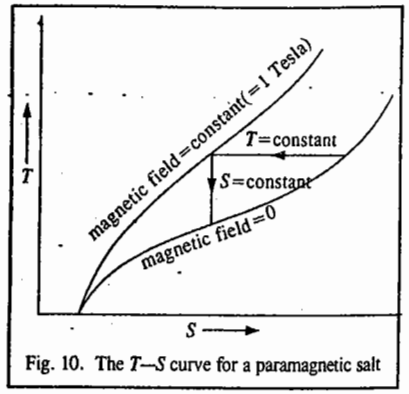

Fig. 10. The T—S curve for a paramagnetic salt

In the first stage of the process, the paramagnetic substance kept in contact with a liquid helium bath at 1 K, is *isothermally magnetized.* Under isothermal conditions (T=constant, $dT=0$), Eq. 43 reduces to

$$TdS = \varepsilon_0 TV(\partial M/\partial T)_B dB \qquad ...(46)$$

Since dB is positive and $(\partial M/\partial T)_B$ is always negative, an increase in B results in an overflow of heat and hence a *decrease* in entropy. This is shown by the T=constant line on the $T-S$ curve of Fig. 10.

In the second stage, the substance is removed and *adiabatically demagnetized.* As mentioned earlier, it cools. This is shown by the S=constant line on the $T-S$ curve. The extent of cooling depends upon the strength of the applied magnetic field, the intensity of magnetization and the heat capacity of the paramagnetic salt.

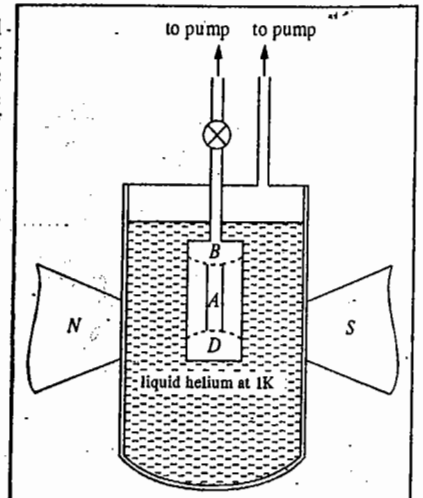

Fig. 11. Experimental set-up for adiabatic demagnetization of a paramagnetic salt.

The experimental set-up for adiabatic demagnetization is shown in Fig. 11. The paramagnetic substance A is suspended inside a cryostat which is cooled by liquid helium boiling under reduced pressure. During the first isothermal stage, the space D contains helium gas; this space allows heat exchange between the substance and liquid helium. During the second stage, the space D is evacuated to establish adiabatic conditions. The cycle of isothermal magnetization, followed by adiabatic demagnetization, is repeated to obtain milli degree temperatures.

Even in the absence of external field B, which is of the order of 1-4 tesla, there is a local magnetic field (or residual field) B_0 present in the paramagnetic substance which arises primarily from magnetic interactions between the dipoles. B_0 is very small as compared with B, its magnitude being of the order of 0·01 tesla. If T_1 is the initial temperature, then the final temperature T_2 is given by the formula

$$T_2/T_1 = B_0/B \qquad ...(47)$$

Suppose $T_1 = 1$ K, $B_0 = 10^{-2}$ tesla and $B = 1$ tesla, then $T_2 \approx 10^{-2}$ K.

We might mention here that the process of adiabatic demagnetization can also be applied to the magnetic moments of *nuclei*. The application of adiabatic demagnetization to nuclear magnetic moments has allowed a temperature of 10^{-6} K to be reached. However, we must remember that *it is not possible to attain absolute zero of temperature by means of a succession of adiabatic cooling processes.* This can be seen from the $T-S$ curve of Fig. 10.

The American chemist W.F. Giauque (1895–1982) was awarded the 1949 Chemistry Nobel Prize for his contributions to the magnetic behaviour of substances at extremely low temperatures.

I. Review Questions

1. Derive the van der Waals equation for describing the *P-V-T* relationship in real gases. Illustrate how this equation satisfactorily explains the departure of real gases from ideal behaviour at different pressures and temperatures.
2. Define excluded volume. Show that excluded volume, designated as b, is four times the actual volume of the gas molecules.
3. Define Boyle temperature. Derive an expression for the Boyle temperature of a van der Waals gas.
4. Write the virial equation of state of a real gas as a power series in *(i)* $1/V_m$ and *(ii)* pressure. Comment briefly.
5. What are van der Waals forces? Discuss them briefly. Using the concept of Lennard-Jones (6 - 12) potential, bring out the exact nature of van der Waals interactions.
6. Derive the expressions for the critical pressure, critical temperature and critical volume of a van der Waals gas.
7. State the principle of corresponding states. Derive an expression interconnecting P_r, V_r and T_r for a van der Waals.
8. Describe the two common methods for producing low temperatures. How have they been used in the liquefaction of gases?
9. Define inversion temperature. How is it related to van der Waals constants ?
10. Discuss production of low temperatures by adiabatic demagnetisation of a paramagnetic substance. Describe briefly the experimental set-up used in the process.

II. Problems

1. Using van der Waals equation, calculate the pressure exerted by one mole of carbon dioxide when it occupies a volume of 0·05 dm^3 at 100°C, given that a=3·59 dm^6 atm mol^{-2} and b=0·0427 dm^3 mol^{-1}. **[Ans. 2041 atm]**
2. Calculate the temperature at which 10 moles of CO_2 (assuming that it is a van der Waals gas) occupies a volume of 5·0 dm^3 under a pressure of 50·0 atm. Given : a=3·59 dm^6 atm mol^{-2}, b=0·4367 dm^3 mol^{-1}. **[Ans. 359 K]**
3. Calculate the pressure of 0·60 mole of NH_3 gas in a 3·00 dm^3 vessel at 25°C *(a)* using the ideal gas equation *(b)* using the van der Waals equation. The van der Waals constants are a = 4·17 dm^6 atm mol^{-2}, b = 0·0371 dm^3 mol^{-1}. **[Ans. *(a)* 4·9 atm *(b)* 4·8 atm]**
4. Calculate the Boyle temperature for oxygen assuming that it is a van der Waals gas. Given : a=1·36 dm^6 atm mol^{-2}, b=0·0318 dm^3 mol. **[Ans. 521·17 K]**
5. Assuming that C_2H_6 behaves as a Dieterici gas, calculate the pressure exerted by 10 moles of the gas confined to a volume of 4·86 dm^3 at 300 K. Given : a=6·97 dm^6 atm mol^{-2}, b=0·0694 dm^3 mol^{-1}. **[Ans. 33 atm]**
6. Calculate the critical constants of C_2H_2 gas using the van der Waals constants a=4·390 dm^6 atm mol^{-2}, b=0·05136 dm^3 mol^{-1}. **[Ans. V_c=0·1541 dm^3 mol^{-1} ; P_c=61·638 atm ; T_c=308·48 K]**
7. Calculate the reduced pressure, reduced volume and reduced temperature of one mole of carbon dioxide gas confined to a volume of 5 dm^3 under a pressure of 5 atm. Also calculate the temperature of the gas. The critical constants of carbon dioxide are $V_{m,c}$=0·094 dm^3 mol^{-1}, P_c=72·8 atm, T_c=304·2 K. **[Ans. P_r=0·069 ; V_r=53·19 ; T_r=1·387 ; T=421·9 K]**
8. The van der Waals constants a and b for a gas are respectively, 0·045 dm^6 atm mol^{-2} and 0·026 dm^3 mol^{-1}. Calculate the inversion temperature of the gas. **[Ans. 42·18 K]**

CHAPTER 11

THE LIQUID STATE

Gaseous, Liquid and Solid States. Of the three states of matter, the solid state in crystalline form exhibits a complete ordered arrangement of molecules, atoms or ions as the case may be and the gaseous state at high temperature and low pressure exhibits complete disorder or randomness. The liquid state lies in between these two extremes of order and disorder. The two-dimensional representation of the three states of matter is shown in Fig. 1.

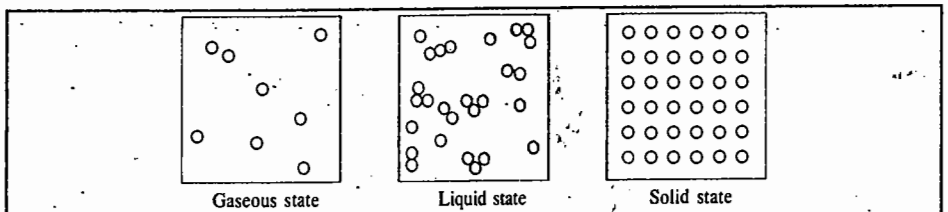

Fig. 1. Two-dimensional arrangement of molecules in gases, liquids and crystalline solids.

In solids, there is close packing of molecules or atoms or ions. This arrangement exists to some extent in the liquid state. In gases, there is no such arrangement of close packing of molecules or atoms considered as spheres.

The definite and ordered arrangement of the constituents of a solid extends over a large distance. This is termed as long range order. The liquids exhibit only a short range order while gases show no order at all.

A liquid may be regarded as a condensed gas or a molten solid. In a solid, the molecules are rigidly fixed and, therefore, it has a definite shape and a definite volume. In a gas, on the other hand, the molecules have random motion and, therefore, it has neither a definite shape nor a definite volume. In a liquid, the molecules are not as rigidly fixed as in solids. They have some freedom of motion which, however, is much more restricted than that in gases. A liquid, therefore, has a definite volume although not a definite shape. It is much less compressible and far denser than a gas.

Since the molecules in a liquid are not far apart from one another, the intermolecular forces are fairly strong. As we shall see shortly, characteristic properties of liquids arise from the nature and the magnitude of these intermolecular forces.

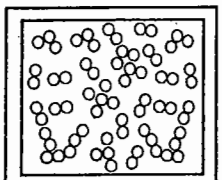

Fig. 2. The liquid as a random congregation of molecules and holes.

Vacancy Theory of Liquids. A liquid is generally less dense than the corresponding solid implying thereby that the intermolecular space in a liquid is more than that in a solid. In 1961, Ering and Ree proposed a simple theory that the intermolecular space in a liquid is not randomly distributed but contains molecular-sized 'holes' or vacancies. The liquid is considered as a random congregation of molecules and these holes, as shown in Fig. 2.

It is assumed that the molecules surrounding a given hole can easily jump into it and are thus 'gas-like' whereas those in immediate contact with the hole are 'solid-like'. If V_l and V_s are the respective molar volumes of the liquid and the solid, then,

$$\frac{\text{Number of holes}}{\text{Number of molecules}} = \frac{V_l - V_s}{V_s} \qquad ...(1)$$

The probability that a hole confers gas-like properties on its neighbouring molecules is proportional to the fraction of the neighbouring positions occupied by the molecules. For a random distribution of holes, this ratio is given by V_s/V_l. Hence,

$$x_g = \left(\frac{V_l - V_s}{V_s}\right)\left(\frac{V_s}{V_l}\right) = \frac{V_l - V_s}{V_l} \qquad ...(2)$$

and

$$x_s = V_s/V_l \qquad ...(3)$$

where x_g and x_s are the mole fractions of the gas-like and the solid-like molecules, respectively. Based on these ideas, Ering and Ree calculated the melting point, boiling point, critical constants and some typical thermodynamic properties of argon. The agreement of theory with experiment was found to be quite satisfactory.

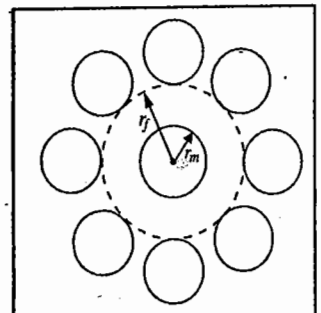

Fig. 3. The free volume in a liquid.

Free Volume in a Liquid. In contrast to a gas, in which under ordinary pressure the molecules move over considerable distances before colliding with one another, in a liquid the molecules move over an infinitesimally small distance before colliding with one another. This is due to the fact that each molecule in a liquid is tightly surrounded by almost 10 to 12 neighbours forming a sort of spherical cage which can be approximated to a spherical box of radius r_f which is only slightly bigger than the enclosed molecule of radius r_m (Fig. 3). It is evident that the centre of the caged molecule can move about in a very small volume. This volume for a mole of molecules is known as free volume.

It can be shown thermodynamically that the magnitude of the free volume is approximately 0·37 cm^3. The free volume per molecule is thus equal to 0·61 $Å^3$. Equating this to the volume of a sphere of radius r_f, we have

$$(4/3)\pi r_f^3 = 0{\cdot}61\ Å^3 \quad \text{whence} \quad r_f = 0{\cdot}54\ Å$$

The radius r_f represents the average distance traversed by a molecule between collisions with the walls of the spherical cage. If we assume that the average speed of the molecules of the liquid is $\approx 3\times10^4$ cm s^{-1}, then the molecule would make about $5{\cdot}6\times10^{12}$ collisions per second with the spherical cage.

Physical Properties of Liquids

The most important physical properties of liquids are :

1. Vapour Pressure 2. Surface Tension 3. Viscosity and 4. Refraction.

VAPOUR PRESSURE

While deriving kinetic gas equation it was assumed that, at a particular temperature, the gaseous molecules have a particular velocity known as the root mean square velocity. This is so in the case of liquid molecules as well. Only a few liquid molecules have lower or higher velocities, *i.e.*, lower or higher kinetic energies. The energy distribution of molecules in a liquid is shown in Fig. 4.

It is evident from the figure that the number of molecules with high kinetic energies, as shown by the shaded area *ABCD* below the dotted curve, is small. This number, however, increases with

rise in temperature, as shown by the shaded area *FBCE* below the bold line curve. The molecules with higher energies are of importance in determining the tendency of a liquid to escape as vapour into a free space if available.

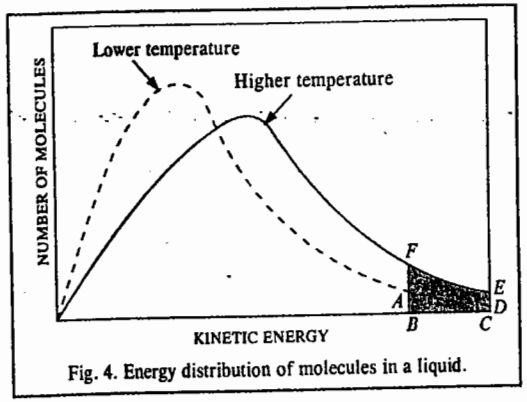

Fig. 4. Energy distribution of molecules in a liquid.

In order to understand this, imagine a liquid contained in an evacuated vessel connected to a manometer so that any pressure that is developed in the free space above the liquid can be measured. The entire system is placed in a thermostat maintained at a constant temperature.

Consider a molecule somewhere in the body of the liquid. It is being attracted by the molecules surrounding it. Since the attractive forces act equally in all directions, the net effect is zero and, therefore, the translatory motion of the molecule is not affected at all.

Now, consider a similar molecule near the surface of the liquid. In this case, the attractive forces operate more strongly in the downward direction because there are many more molecules below than in the space above it. This unbalanced attractive force tends to pull the molecule downwards towards the main bulk of the liquid. Thus, the tendency of the molecule, as a result of its translational energy, to pass into the free space above the surface of the liquid, is being prevented by the inward molecular attraction. However, if this molecule is the one associated with a higher kinetic energy corresponding to the shaded portion *ABCD* of the graph (Fig. 4) at a given temperature, it will be able to break through the forces of molecular attraction and escape into the free space as vapour. Thus, the molecules of a liquid with energy higher than the average energy have a greater tendency to pass into the vapour state. Since the fraction of such molecules increases with rise in temperature (*cf.* shaded portion *FBCE* in Fig. 4), it follows that a liquid has a greater tendency to pass into vapour state with rise in temperature. The escape of liquid molecules into vapour state constitutes a **change of phase.**

Let us suppose that in this phase-change process, all the molecules with high kinetic energies represented by the shaded portion of the graph in Fig. 4 escape from the liquid into the vapour phase. The average kinetic energy of the remaining molecules in the liquid phase will, evidently, go down. Hence, the temperature of the liquid shall fall. We conclude, therefore, that a liquid on evaporation cools itself.

Some of the escaping molecules may return to the body of the liquid, *i.e.*, may change back into liquid state. Ultimately, equilibrium is established at each temperature so that the number of molecules leaving the surface in a given time is equal to the number of molecules returning to it. This is called **phase equilibrium.**

The vapour molecules confined in the space above the liquid strike against the walls of the vessel and thus register a pressure on the manometer attached to the vessel. This pressure at the time when phase equilibrium has been established is found to be constant at a given temperature and is known as vapour pressure. Thus, **vapour pressure** *of a liquid at a given temperature is defined as the pressure of the vapour in equilibrium with the liquid at that temperature.*

The vapour pressure measures the ease with which a liquid can be converted into vapour, *i.e.*, it is a measure of the volatility of the liquid. Stated in other terms, *it is a measure of the escaping tendency of molecules from the surface of the liquid.*

As the temperature rises, the number of molecules escaping from the liquid surface increases and there is increase in the number of vapour molecules in the space above the liquid when phase equilibrium is attained. Hence, vapour pressure of a liquid increases with rise in temperature.

Heat of Vaporisation. The molecules in a liquid are much closer to one another than those in a gas. Intermolecular forces of attraction, therefore, are much stronger in liquids than in gases. When a liquid changes into vapour state, these intermolecular forces have to be overcome. Hence, a certain amount of energy has to be supplied to the liquid in the form of heat. The quantity of heat which has to be supplied to one mole of a liquid at its boiling point so as to change it into vapour state at the same temperature, is known as the **molar heat of vaporisation**, ΔH_{vap}, of the liquid at that temperature.

The molar heat of vaporisation of water at 100°C is 40·67 kJ. The same amount of heat is evolved when one mole of steam condenses into liquid water at 100°C.

The molar heats of vaporisation of some liquids together with their boiling points are given in Table 1.

TABLE 1

Molar Heats of Vaporisation and Normal Boiling Points of Liquids

Liquid	Molar heat of vaporisation ΔH_{vap} (kJ mol^{-1})	Boiling point T_b (K)	$\Delta H_{vap}/T_b$ (J mol^{-1} K^{-1})
Water	40·67	373	109·0
Ethyl alcohol	39·54	351	112·8
Acetic acid	24·31	391	62·2
Benzene	31·38	353	88·9
Carbon tetrachloride	29·96	350	85·6
Ether	25·64	307·6	83·3
Hydrogen fluoride	25·23	377	66·9

As can be seen, the molar heat of vaporisation of water is much higher than that of ether, benzene or carbon tetrachloride. This indicates that intermolecular forces of attraction operating in water are much stronger than those operating in most of the organic liquids.

The values of $\Delta H_{vap}/T_b$ for the various liquids are also included in Table 1 in an appropriate column.

The molar heat of vaporisation of a liquid expressed in joules divided by the normal boiling point of the liquid on the absolute scale is approximately equal to 88. This is known as **Trouton's rule** and may be expressed as

$$\Delta H_{vap}/T_b \approx 88 \text{ J mol}^{-1} \text{ K}^{-1} \quad \ldots(4)$$

Eq. 4 is only approximate as the values of $\Delta H_{vap}/T_b$ are seen to vary over a wide range, *viz.*, from about 60 to about 110 J mol^{-1} K^{-1} (Table 1). The deviations from Trouton's rule, thus, occur in both directions. The quantity $\Delta H_{vap}/T_b$ is also called **entropy of vaporisation**, ΔS_{vap}. Trouton's rule is useful for estimating the heat of vaporisation of a liquid if its boiling point is known.

Example 1. The boiling point of *n*-heptane is 36°C. Estimate its molar heat of vaporisation assuming that it obeys Trouton's rule.

Solution : From Trouton's rule,

$$\Delta H_{vap}/T_b = 88 \text{ J mol}^{-1} \text{ K}^{-1}$$

$$\Delta H_{vap} = (88 \text{ J mol}^{-1} \text{ K}^{-1})(309 \text{ K}) = 27192 \text{ J mol}^{-1} = 27{\cdot}192 \text{ kJ mol}^{-1}$$

SURFACE TENSION

Surface Tension. The existence of strong intermolecular forces of attraction in liquids gives rise to another important property known as **surface tension**. The phenomenon of surface tension may be explained by reference to Fig. 5.

Consider a molecule P somewhere in the body of the liquid. This is attracted equally in all directions by other molecules which surround it as shown and, therefore, cancel the effect of one another.

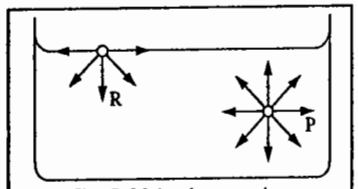

Fig. 5. Molecular attraction.

Consider, next, a molecule R at the surface of the liquid. The downward attractive forces are greater than the upward forces because there are more molecules of the liquid below than in the air above the surface. These unbalanced attractive forces acting downward tend to draw the surface molecules into the body of the liquid and, therefore, tend to reduce the surface to a minimum.

It is well known that *forces of attraction tend to decrease the energy of a system*. In the present case, the attractive forces are more predominant in the bulk of the liquid than at the surface. Therefore, the molecules in the bulk of the liquid are associated with lower energy than those at the surface. In other words, the molecules at the surface possess greater energy than those in the bulk. It is the extra energy of surface molecules which gives rise to their tendency to move into the bulk of the liquid, *i.e.*, the molecules tend to move from a state of higher energy to a state of lower energy. As a consequence of this transfer, the number of molecules at the surface becomes less than that in the bulk. The distance between any two molecules at the surface, therefore, becomes greater than that in the bulk. Consequently, the surface molecules tend to move closer to one another in order to acquire a normal distance between them as before. It is for this reason that drops of a liquid or bubbles of a gas are spherical in shape. A sphere has minimum surface for a given volume. As a result of the tendency to contract, surface of a liquid behaves as if it were in a state of tension. *The force that tends to contract the surface of a liquid is known as surface tension.*

Mathematically, **surface tension** is defined as the force in newtons acting at right angles to the surface of a liquid along 1 metre length of the surface. It is generally represented by the symbol γ.

Surface tensions of some common liquids are given in Table 2.

TABLE 2

Surface Tensions of Some Common Liquids in Nm^{-1} at 20°C

Liquid	Surface tension	Liquid	Surface tension
Water	0·0728	Chloroform	0·0271
Nitrobenzene	0·0418	Carbon tetrachloride	0·0268
Carbon disulphide	0·0335	Methyl alcohol	0·0226
Benzene	0·0289	Acetone	0·0237
Toluene	0·0284	Ethyl alcohol	0·0223
Acetic acid	0·0276	Ethyl ether	0·0170

As can be seen, for most liquids, surface tension at room temperature varies between 0·027 and 0·042 Nm^{-1}. For water, however, γ is 0·072 Nm^{-1} at 20°C. This high value is obviously due to strong intermolecular forces which exist in water *as a result of extensive hydrogen bonding*.

Surface Energy. The effect of surface tension is to reduce the area of the surface to a minimum. If we wish to increase the area of the surface of a liquid, we have to work *against* the force of surface tension. The work that is required to be done in order to extend the area of the surface of a liquid by one m^2, is called **surface energy** of the liquid.

Consider a soap film stretched over a wire-frame (Fig. 6) one end of which is movable. It is observed experimentally that force acts on the moveable membrane in a direction opposite to the arrow shown in the figure.

If the force per unit length is denoted by γ, then the work required to extend the movable membrane by a distance dx is given by the expression

$$\text{work} = \gamma \, 2l dx \quad \ldots(5)$$

Eq. 5 can be written as

$$\text{work} = \gamma \, dA \quad \ldots(6)$$

where dA $(=2l dx)$ is the change in area.

It may be noted that while in Eq. 5, γ is force per unit length, in Eq. 6, γ is work or energy per

unit area. Thus, surface of a liquid can be treated mathematically using either the concept of surface tension or the concept of surface energy. The term surface tension implies that a state of tension exists between the surface molecules whereas the term surface energy implies that work is required to bring molecules from the bulk to the surface of the liquid.

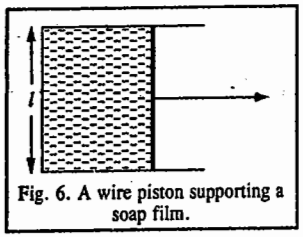

Fig. 6. A wire piston supporting a soap film.

While surface tension has units of force per unit length, *i.e.*, $N\,m^{-1}$, surface energy has units of work (energy) per unit area, *i.e.*, $J\,m^{-2}$.

The dimensions of surface energy, *viz.*, $J\,m^{-2}$ may also be put as $(N\,m)(m^{-2}) = N\,m^{-1}$, which are also the dimensions of surface tension. Thus, *surface tension is equal to surface energy numerically as well as dimensionally.*

Effect of Temperature on Surface Tension. According to the kinetic theory, molecular kinetic energy is proportional to absolute temperature. The rise in temperature of a liquid, therefore, is accompanied by *increase* in energy of its molecules. Since intermolecular forces decrease with increase in the energy of molecules, the intermolecular forces of attraction *decrease* with rise in temperature. Hence, *surface tension of a liquid decreases with rise in temperature.* At critical temperature, since the surface of separation between a liquid and its vapour disappears, the surface tension falls to zero.

Eotvos found that surface tension varies linearly with temperature. He suggested the following expression for the variation of surface tension with temperature :

$$\gamma\,(M/\rho)^{2/3} = a - kt \qquad \ldots(7)$$

where M is molar mass, ρ is density and γ is surface tension of the liquid at the temperature t ; a and k are constants.

At the critical temperature (*i.e.*, when $t = t_c$), the surface tension is zero. Substituting these values in Eq. 7, we may write

$$0 = a - kt_c \quad \text{or} \quad a = kt_c \qquad \ldots(8)$$

The Eotvos equation, therefore, may be written as

$$\gamma\,(M/\rho)^{2/3} = k(t_c - t) \qquad \ldots(9)$$

This equation has been found to be satisfactory in giving variation of surface tension with temperature in the case of a number of liquids over a wide range of temperature.

Since surface tension vanishes roughly 6° above the critical temperature rather than at the critical temperature, Ramsay and Shields proposed the following equation for the temperature-dependence of surface tension :

$$\gamma\,(M/\rho)^{2/3} = k(t_c - t - 6) \qquad \ldots(10)$$

Some Effects of Surface Tension. Some important effects of surface tension may now be considered.

1. The effect of surface tension is to *reduce the area of the surface to a minimum.* Hence, drops of a liquid or bubbles of a gas are spherical in shape, as stated before, A sphere has minimum surface area for a given volume.

2. The rise of a liquid in a capillary tube (*e.g.*, rise of oil in the wick of a lamp, rise of underground water on to the surface of earth, rise of water or sap in plants) is a well known phenomenon. This can be explained in terms of surface tension as shown below.

Consider a capillary tube lowered in a liquid that *wets its surface* (*e.g.*, water). The contact angle between the glass and the liquid is now zero. The liquid will rise almost instantaneously upto a certain height depending upon its surface tension and density. The column of the liquid in the capillary is, evidently, being supported by some force acting along the surface of the water. This is the force of surface tension.

Suppose, a liquid of density ρ, rises in a capillary tube of radius r, through a height h, as shown in Fig. 7.

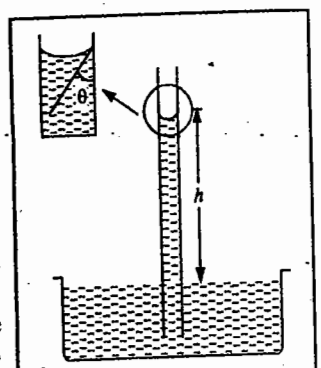

Fig. 7. Capillary rise in a liquid.

Let γ be the force of surface tension.

Then, the total force due to surface tension, raising the liquid column upward

$= \gamma \times$ inside circumference of the capillary

$= 2\pi r\gamma$

Force of gravity pulling the liquid downward = weight of the liquid column.

Weight of the liquid in the column $= V\rho g$ where V is the volume of the liquid in the tube. Since $V = \pi r^2 h$, hence, for equilibrium,

$$2\pi r\gamma = \pi r^2 h\rho g \quad \text{or} \quad \gamma = rh\rho g/2 \qquad \ldots(11)$$

For measuring surface tension, we have to measure the height (h) through which the liquid rises and the radius of the capillary tube both in centimetres. The height is measured by a cathetometer and the radius of the capillary tube by a travelling microscope.

It is assumed in the above derivation that the contact angle θ between the glass and the liquid is zero, that is, wetting is perfect. If this is not so, the vertical component of the upward force would be $2\pi r\gamma\cos\theta$ and hence

$$\gamma = \frac{r\,h\,\rho g}{2}\cos\theta \qquad \ldots(12)$$

As is well known, when a capillary is dipped in mercury, mercury does not rise in it. On the contrary, the upper level of mercury in the capillary is lower than the surface of the free liquid (Fig. 8). We can account for this phenomenon by assigning a value of 180° to the angle of contact θ between mercury and glass. Since $\cos 180° = -1$, hence according to Eq. 12, h would be negative.

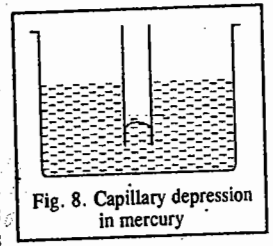
Fig. 8. Capillary depression in mercury

The rise or fall of a liquid in a capillary can be better understood by invoking the concepts of cohesion and adhesion. **Cohesion** means intermolecular attraction between like molecules in the liquid whereas **adhesion** means attraction between the liquid and the walls of the capillary. When adhesion is greater than cohesion, the liquid is said to wet the wall. This is what happens in the case of water and many other liquids. If cohesion is greater than adhesion, the liquid does not wet the wall. This is what happens in the case of mercury. Thus, when a drop of mercury or of water is put on a clean surface, the mercury drop becomes a truncated sphere since cohesion is greater than adhesion while the water drop spreads on the glass surface since adhesion is greater than cohesion.

Capillary-rise phenomenon is partially responsible for the rise of water in plants and soils. The other phenomenon responsible for the rise of water is **osmosis**, which we shall discuss later in this book.

Example 2. Calculate the height to which water will rise in a glass capillary if the radius of the tube is 0·02 cm. The surface tension of water is 0·0728 $N\,m^{-1}$.

Solution : Following Eq. 11,

$$h = \frac{2\gamma}{r\rho g} = \frac{2(0{\cdot}0728\ N\,m^{-1})}{(0{\cdot}02\times10^{-2}\ m)(10^3\ kg\,m^{-3})(9{\cdot}81\ m\,s^{-2})} = 7{\cdot}42\times10^{-2}\ m \qquad (N = kg\ m\ s^{-2})$$

Example 3. A plant has capillaries of radius 0·003 mm. The density of sap in the plant is 1·20 g cm^{-3} and its surface tension is 0·065 $N\,m^{-1}$. Assuming that surface tension alone is responsible for the rise of sap to the top of the plant, calculate how high this plant can grow.

Solution : The height upto which a wetting liquid of density ρ and surface tension γ can rise in a capillary tube of radius r is given by $h = 2\gamma / r\rho g$. Obviously, the height of the plant would also be equal to h.

$$\text{Thus, the height of plant, } h = \frac{2(0{\cdot}065\ \text{N m}^{-1})}{(0{\cdot}003\times10^{-3}\ \text{m})(1{\cdot}2\times10^{3}\ \text{kg m}^{-3})(9{\cdot}81\ \text{m s}^{-2})} = 3{\cdot}681\ \text{m} \qquad (\text{N} = \text{kg m s}^{-2})$$

Example 4. The surface tension of water at 20°C is 0·0728 N m^{-1}. Calculate the minimum amount of work needed to increase the surface area of water from 2·0 to 5·0 cm^2 at this temperature.

Solution : If w is the minimum work required to stretch the surface area by an amount A, then

$$w = \gamma A = (0{\cdot}0728\ \text{N m}^{-1})(3{\cdot}0\times10^{-4}\ \text{m}^2) = 218{\cdot}4\times10^{-5}\ \text{J}$$

Example 5. Consider two liquids A and B such that A has half the surface tension and twice the density of B. If liquid A rises to a height of 2·0 cm in a capillary, what will be the height to which liquid B will rise in the same capillary ?

Solution : It follows from Eq. 11 that

$$\frac{h_A}{h_B} = \frac{\gamma_A/\rho_A}{\gamma_B/\rho_B} = \frac{\gamma_A\rho_B}{\gamma_B\rho_A} = \left(\frac{1}{2}\right)\left(\frac{1}{2}\right) = \frac{1}{4}$$

$$\therefore \quad h_B = 4h_A = 4\times0{\cdot}02\ \text{m} = 0{\cdot}08\ \text{m}$$

Thus, the height to which liquid B would rise = **0·08 m**

Example 6. The surface tension of water is 0·0728 N m^{-1}. Calculate the energy required to disperse one spherical drop of radius 3·0 mm into spherical drops of radius 3·0×10^{-3} mm.

Solution : The surface area of the spherical drop of radius 3·0 mm $= 4\pi r_1^2$

$$= 4\pi(3{\cdot}0\times10^{-3}\ \text{m})^2 = 1{\cdot}13\times10^{-4}\ \text{m}^2$$

The surface area of the spherical drop of radius $3{\cdot}0\times10^{-3}$ mm $= 4\pi r_2^2$

$$= 4\pi(3{\cdot}0\times10^{-6}\ \text{m})^2 = 1{\cdot}13\times10^{-10}\ \text{m}^2$$

The number of drops of radius 3×10^{-3} mm that can be formed from one drop of radius 3 mm

$$= \frac{\text{Volume of bigger drop}}{\text{Volume of smaller drop}} = \frac{(4/3)\pi(3{\cdot}0\ \text{mm})^3}{(4/3)\pi(3{\cdot}0\times10^{-3}\ \text{mm})^3} = 1{\cdot}0\times10^{9}$$

The total surface area of all the small drops

$$= (1{\cdot}13\times10^{-10}\ \text{m}^2)(1{\cdot}0\times10^{9}) = 1{\cdot}13\times10^{-1}\ \text{m}^2$$

$$\text{Increase in surface area} = (1{\cdot}13\times10^{-1}\ \text{m}^2) - (1{\cdot}13\times10^{-4}\ \text{m}^2) = 1{\cdot}13\times10^{-4}\times999\ \text{m}^2$$

$$\therefore \text{ Work done in dispersion} = \text{surface tension} \times \text{increase in surface area}$$

$$= (0{\cdot}0728\ \text{N m}^{-1})(1{\cdot}13\times999\times10^{-4}\ \text{m}^2) = 8{\cdot}2\times10^{-3}\ \text{J} \qquad (\text{N m} = \text{J})$$

3. One of the most interesting consequences of surface tension is the fact that the vapour pressure of a liquid is greater when it is in the form of small droplets than when it has a plane surface. According to the **Kelvin equation**, the vapour pressure P for a very small droplet of radius r is given by the relation

$$\ln (P/P_0) = 2\gamma M/(r\rho RT) \qquad ...(13)$$

where P_0 is the vapour pressure of the bulk sample of the liquid, ρ is its density and R is the gas constant. The conclusions of this equation have been verified experimentally.

Excess Pressure in a Drop. Since the surface tension tends to decrease the surface area, the pressure P_1 inside a spherical drop is greater than the pressure P_2 of the surrounding liquid. The greater the surface tension, the greater is the pressure difference ΔP. If the radius of the bubble is increased by a small amount dr, then the increase in surface area, $dA = 4\pi(r+dr)^2 - 4\pi r^2 = 8\pi r dr$ and the increase in volume $dV = (4/3)\pi(r+dr)^3 - (4/3)\pi r^3 = 4\pi r^2 dr$. The net work done in increasing the surface area is given by

$$w = \gamma\, dA = 8\pi\gamma\, rdr \qquad ...(14)$$

Since the work done by the gas (air) inside the bubble is $P_1 dV$ while that done on the liquid outside the bubble is $P_2 dV$, the net work required to generate the additional surface area is given by

$$w = (P_1 - P_2)dV = \Delta P dV = \Delta P(4\pi r^2 dr) \qquad ...(15)$$

From Eqs. 14 and 15, $8\pi\gamma\, rdr = \Delta P(4\pi r^2 dr)$ or $\Delta P = 2\gamma / r$ ...(16)

Eq. 16 is known as the **Laplace equation.**

It is a special case of the general equation, called the **Young–Laplace equation,** *viz.*,

$$\Delta P = P_1 - P_2 = \gamma\,(1/r_1 + 1/r_2) \qquad ...(17)$$

where r_1 and r_2 are the maximum and the minimum radii of curvature at a point in the surface and P_1 and P_2 are the pressures on the concave and the convex sides of the surface, respectively. For a spherical body, $r_1 = r_2$ so that Eq. 17 reduces to Eq. 16.

From Eq. 16, we see that ΔP is inversely proportional to the radius r of the bubble or the droplet and would evidently become very large for very small droplets. For instance, the excess pressure in a bubble (or droplet) of radius 0·0001 cm in water at 20°C is given by

$$\Delta P = \frac{2\times0{\cdot}0728\ \text{N m}^{-1}}{(1\times10^{-6}\ \text{m})(101325\ \text{N m}^{-2}\ \text{atm}^{-1})} = 1{\cdot}44\ \text{atm}$$

where we have used the conversion factor 1 atm = 101325 N m^{-2}.

In the case of soap bubbles, the pressure difference between the two phases on the two sides of the soap film is *twice* the value obtained from the Laplace equation. This is because the two surfaces of the liquid film are parallel and also so close that their radii of curvature are almost equal.

When a liquid free from dust particles is heated in a container, small gas bubbles are formed for which ΔP is very large. As the bubble size increases, the pressure required to overcome the surface tension decreases and hence the bubble expands rapidly. This leads to bumping or violent heating in superheated liquids.

Interfacial Tension. Suppose, two immiscible liquids are present one above the other in a vessel. Then, the force acting per unit length along the interface is called **interfacial tension.** This is less than the surface tension of the liquid with a higher value. The reason is that the unbalanced forces acting along the surface of each liquid are partly compensated by the force of mutual attraction between the molecules of the two liquids.

Surface tension and interfacial tension involve the same type of force. When one speaks of surface tension of a liquid, it is understood that the force is acting along the surface of separation between the liquid and its vapour. When one speaks of interfacial tension, it is understood that the force is acting along the surface of separation of two immiscible liquids in contact with each other.

Surface Active Agents. A number of substances are known which, when added to water, lower its surface tension. These substances are called **surface active agents** or **surfactants.** Thus, liquids like methanol, ethanol, acetone and acetic acid when added to water, lower its surface tension, Similarly, soaps when mixed with water lower its surface tension. There are a host of other substances such as salts of higher sulphonic acids and higher amines which behave in this manner. They are all surface active materials. These substances act as **detergents.**

Let us explain the action of soap as a detergent. Most of the dirt or dust sticks on to grease or oily materials which somehow gather on cloth. As grease is not readily wetted by water, it is difficult to clean the garment by water alone. The addition of soap lowers the interfacial tension between water and grease so as to facilitate the mixing of the two. The soap molecules get oriented at the interface between water and oil (or grease) in such a way that their polar end (–COONa) is dipping in water and the hydrocarbon chain (R–) in the oil. This helps in bringing the two liquid

phases in more intimate contact with each other. In other words, *the presence of soap causes emulsification of grease in water*. The mechanical action, such as rubbing, releases the dirt. For emulsions and emulsifiers, see Chapter 30 on the Colloidal State.

Detergents are also added to medicinal emulsions, tooth pastes, mouth washes and toilet creams in order to enable them to spread evenly thereby increasing the efficiency of the antiseptic action.

VISCOSITY

The flow is a characteristic property of liquids. Consider a liquid flowing through a narrow glass tube (Fig. 9a). The flow of the liquid molecules can be analysed in terms of *molecular laminar layers* arranged one over another. A laminar layer has negligible thickness. The layer immediately in contact with the surface of the inner wall of the tube is *stationary*. However, the velocity of the successive layers increases as we move away from the surface. As a result, a velocity gradient is set up along the z-axis. If the distance between the two layers is r and the slow-moving layer moves with a velocity v, then the faster-moving layer moves with a velocity $v+r(dv/dz)$ (Fig. 9b).

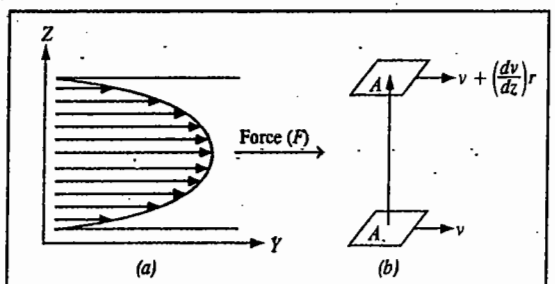

Fig. 9. The velocity profile during flow of a liquid in a glass tube.

When a molecule moves from the faster layer to the slower layer, it transports momentum to the latter thereby speeding it up. Conversely, when a molecule moves from the slower layer to the faster layer, it retards the latter. In this way, there arises a frictional force or drag between the two layers which gives rise to viscosity which may thus be defined as the resistance that one part of a liquid flowing with one velocity offers to another part of the liquid flowing with a different velocity. In simple words, viscosity *may be defined as the force of friction between two layers of a liquid moving past one another with different velocities*.

If we want to maintain the velocity gradient, we must apply an external force along the y-axis. This force is proportional to the area and the velocity gradient, that is,

$$F \propto A(dv/dz) = -\eta A(dv/dz) \qquad ...(18)$$

where the constant of proportionality η is called the **coefficient of viscosity**. The minus sign shows that the viscous force on the faster layer is in the opposite direction to its motion.

Eq. 18 is Newton's law of viscosity. It is experimentally obeyed by several liquids provided their rate of flow is not very high. The fluid flow to which this equation applies is called **laminar** (or streamlined) **flow**. The equation does not apply to turbulent flow. Liquids which do not obey Eq. 18 are called **non-Newtonian liquids**. For Newtonian liquids, η is independent of dv/dz whereas for non-Newtonian liquids, η changes as dv/dz changes.

Units of Viscosity. If F is measured in newtons, dz in metres, A in square metres and dv in metres sec^{-1}, then, we get the coefficient of viscosity in units of kg m^{-1} s^{-1}, as illustrated below :

$$\eta = \frac{Fdz}{Adv} = \frac{\text{kg m s}^{-2}\ \text{m}}{\text{m}^2\ \text{m s}^{-1}} = \text{kg m}^{-1}\ \text{s}^{-1}$$

It can be easily shown that 1 poise = 10^{-1} kg m^{-1} s^{-1}

Common units of viscosity are centipoise and millipoise.

Viscosities of some common liquids, at 20°C, are given in Table 3.

TABLE 3
Coefficients of Viscosity in Centipoises (20°C)

Liquid	η	Liquid	η
Water	1·008	Benzene	0·647
Chloroform	0·563	Acetone	0·329
Ethyl alcohol	1·216	Acetic acid	1·229
Methyl alcohol	0·593	Nitrobenzene	2·010
Ethyl ether	0·233	Carbon tetrachloride	0·968

Polyhydric alcohols like glycerol have high viscosities because of the formation of a network of hydrogen bonds between the molecules. The network which extends throughout the liquid makes the flow difficult.

The *reciprocal of viscosity* is called **fluidity** and is denoted by ϕ. Thus, $\phi = 1/\eta$.

Effect of Temperature on Viscosity. The 'Hole' Theory. The viscosity of a liquid generally decreases with rise in temperature. The decrease is appreciable, being about 2 per cent per degree rise of temperature in many cases. This has been explained in terms of the **'hole theory'** of liquids discussed earlier. According to this theory, there are *vacancies* or *'holes'* in a liquid. The liquid molecules keep on moving continuously into these vacancies. As a consequence, the vacancies also keep on moving around as otherwise the liquid will not be able to flow. This process, however, requires energy. A liquid molecule, therefore, needs some activation energy to move into a 'hole'. As the activation energy becomes increasingly available at increasing temperatures, a liquid can flow more easily at higher temperatures. The coefficient of viscosity, thus, falls appreciably with rise in temperature.

The relationship between coefficient of viscosity of a liquid and temperature is expressed mathematically as

$$\eta = Ae^{E_a/RT} \qquad ...(19)$$

where A and E_a are constants for a given liquid. Most of the experimental data fit in this equation very well. E_a is called the activation energy for viscous flow.

In contrast to liquids, η increases with increasing temperature in the case of gases. This suggests that the mechanism of flow is different for gases (Chapter 9) than for liquids. The concept of momentum transfer between two layers which is so successfully applicable to gases is less justified (and probably not even applicable) in the case of liquids.

Effect of Pressure. The viscosity of liquids, however, increases with increase in pressure. This is attributed to decrease in the number of 'holes' as the pressure is increased. Consequently, it becomes more difficult for liquid molecules to move around and thus it becomes more difficult for them to flow.

Reynolds Number. The flow of a fluid through a pipe of radius r has been associated with a number called **Reynolds number, N_R**, defined as

$$N_R = 2R\bar{v}\rho/\eta \qquad ...(20)$$

where $\bar{v}$ is the average bulk velocity of the fluid, ρ is the density and η is the coefficient of viscosity. If N_R is greater than 4000, the flow is **turbulent** and if it is less than 2100, the flow is **laminar**. In a laminar flow, a velocity profile given by

$$\bar{v} = \frac{\Delta P(R^2 - r^2)}{4\eta l} \qquad ...(21)$$

is observed in a pipe where ΔP is the pressure drop over a length l and r is the distance from the axis of the pipe of radius R.

The volume of liquid flowing in time t through a pipe of radius R is given by the **Poisseuille equation**

$$V = \frac{\pi R^4(\Delta P)t}{8\eta l} \qquad ...(22)$$

Example 7. Consider the flow of water through a horizontal pipe with $R = 2{\cdot}5$ cm and $\bar{v} = 3$ cm s^{-1}. If $\eta = 1{\cdot}008$ cP at 20°C and $\rho = 0{\cdot}9994$ g cm^{-3}, calculate the Reynolds number.

Solution : From Eq. 20, $N_R = 2R\bar{v}\rho/\eta$

$$= \frac{2(2{\cdot}5\times10^{-2}\text{ m})(3\times10^{-2}\text{ m s}^{-1})(0{\cdot}9994\times10^{-3}\times10^{6}\text{ kg m}^{-3})}{(1{\cdot}008\times10^{-2}\text{ Poise})(10^{-1}\text{ kg m}^{-1}\text{ s}^{-1}\text{ Poise}^{-1})} = 1487$$

Since N_R is less then 2100, the flow is **laminar.**

REFRACTION

Refractive Index or Index of Refraction. When a ray of light passes from one medium to another, it suffers *refraction*, that is, *a change of direction.* If it passes from a less dense to a more dense medium, as from air to water, it is refracted towards the normal so that the angle of refraction r is less than the angle of incidence i. The refractive index n_r of the second medium with respect to the first is then given by the relation

$$n_r = \sin i/\sin r \qquad ...(23)$$

The refractive index of a medium may also be defined as the ratio of the velocity of light in vacuum to that in the medium. Refractive indices can be measured easily with a high degree of accuracy.

The values depend upon the temperature as well as the wave length of light used. Generally, the D-line of sodium is used for standard measurements. The symbol $^{20}n_{r,D}$ indicates that the refractive index has been determined at 20°C using D-line of sodium as the source of light.

Instruments used for measuring refractive indices are known as refractometers. The refractive index of a liquid varies with the temperature. The magnitude of variation, however, is not as large as in the case of surface tension and viscosity.

Specific Refraction. The term specific refraction *(R)*, introduced by Lorenz and Lorentz, may be defined as

$$R = \frac{(n_r^2 - 1)}{\rho(n_r^2 + 2)} \qquad ...(24)$$

where ρ is the density and n_r, as usual, is the refractive index of the liquid. The advantage of this term is that it is independent of temperature. The variation in n_r with change in temperature is compensated by the variation in ρ, the density of the liquid.

Molar Refraction. The product of molar mass (M) of the liquid and specific refraction (R) is called *molar refraction* (R_m). Thus,

$$R_m = \frac{M(n_r^2 - 1)}{\rho(n_r^2 + 2)} \qquad ...(25)$$

Molar refraction of a solid is determined by dissolving it first in a suitable solvent so as to get a solution of a known concentration. The refractive index and the density of the solution are then determined experimentally. The molar refraction of the solution, $R_{m,sol}$, is given by

$$R_{m,sol.} = \frac{n_r^2 - 1}{n_r^2 + 2}\left[\frac{x_1M' + x_2M''}{\rho}\right] \qquad ...(26)$$

where M' and M'' are the molar masses of the solvent and the solute, respectively and x_1 and x_2 are their respective mole fractions, while n_r and ρ are the refractive index and density, respectively, of the solution. Since all the quantities on the right-hand side of Eq. 26 are known, $R_{m,sol.}$ can be evaluated.

The molar refraction of the solution $R_{m,sol.}$ is related to molar refractions $R_{1,m}$ and $R_{2,m}$ of the solvent and the solute, respectively, by the following equation :

$$R_{m,sol.} = x_1R_{1,m} + x_2R_{2,m} \qquad ...(27)$$

From Eq. 27, the molar refraction of the solid solute, $R_{2,m}$ can be easily calculated.

Optical Activity. The term optical activity refers to the rotation of the plane of plarized light when it passes through a substance or solution. A substance which rotates the plane of polarized light to the right (or clockwise) is called **dextro-rotatory** and the substance which rotates the plane of polarized light to the left (or anticlockwise) is called **laevo-rotatory.** Both dextrorotatory and laevorotatory substances are said to be optically active. The rotation of the plane polarized light is measured with a polarimeter that consists of a source of light, a linear polarizer (such as a Nichol prism), the sample and an analyzer (another linear polarizer). The rotation of the plane of polarization by the sample is measured by rotating the analyzer. The magnitude of the angle of rotation α is directly proportional to the length l of the sample and the concentration c of the optically active substance. It is convenient to define a term **specific rotation,** $[\alpha]_\lambda$, by

$$[\alpha]_\lambda^{20^\circ} = \frac{100\alpha}{cl} \qquad ...(28)$$

where l is the path length (in decimeters) and c is the percent concentration. The specific rotation varies with the wave length λ, temperature and solvent.

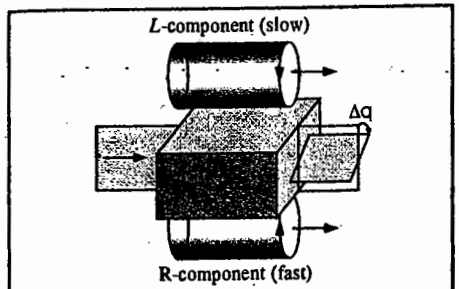

Fig. 10. Linearly polarized light viewed as the superposition of two counter-rotating circularly polarized components.

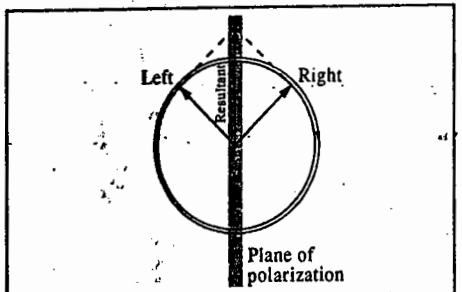

Fig. 11. The superposition as viewed by an observer facing the on-coming beam.

The concept of refractive index is closely related to optical activity. The angle of optical rotation is proportional to the difference between the refractive indices for left and right circularly polarized light (Fig. 10). We shall prove it as follows : Before entering the medium, the beam is plane polarized at an angle $\theta = 0$. This plane polarized light may be regarded as a superposition of two oppositely rotating circularly polarized components (Fig. 11).

On entering the medium, one component propagates faster than the other if their refractive indices are different. If the sample is of path length l, then the difference in the times of passage is given by

$$\Delta t = \frac{l}{c_R} - \frac{l}{c_L} \qquad ...(29)$$

where c_R and c_L are the speeds of the two components (right circularly polarized and the left circularly polarized components). In terms of the refractive indices, this difference is given by

$$\Delta t = (n_R - n_L)\,l/c \qquad ...(30)$$

The phase difference between the two components when they emerge from the sample is thus

$$\Delta\theta = c\,\Delta t = \frac{2\pi}{\lambda} = (n_R - n_L)\,2\pi l/\lambda \qquad ...(31)$$

where λ is the wave length of light (here $\Delta\theta$ is the angle of rotation which we have designated as α in the preceding discussion). The rotating electric vectors (of the electromagnetic radiation) have a different phase when they leave the sample from their initial value. Hence, their superposition gives rise to a plane polarized light rotated through an angle $\Delta\theta$ ($\equiv\alpha$) relative to the plane of the incoming beam. Thus, we see that the angle of optical rotation is proportional to the difference in refractive indices, $n_R - n_L$.

Fig. 12 gives the variation of refractive index (dispersion curve) and the variation of the absorption coefficient (absorption curve) for an optically active substance measured with left and right circularly polarized light. The difference in the refractive indices (Δn) for the two components is referred to as the ORD (optical rotatory dispersion) curve and the difference in the absorption ($\Delta\varepsilon$) is called the CD (circular dichroism) curve. In other words, the plot of Δn *versus* λ is called the ORD curve and the plot of $\Delta\varepsilon$ *versus* λ is called the CD curve. The analysis of ORD and CD curves may be used to determine the structure, configuration and conformations of optically active *d*-metal complexes and

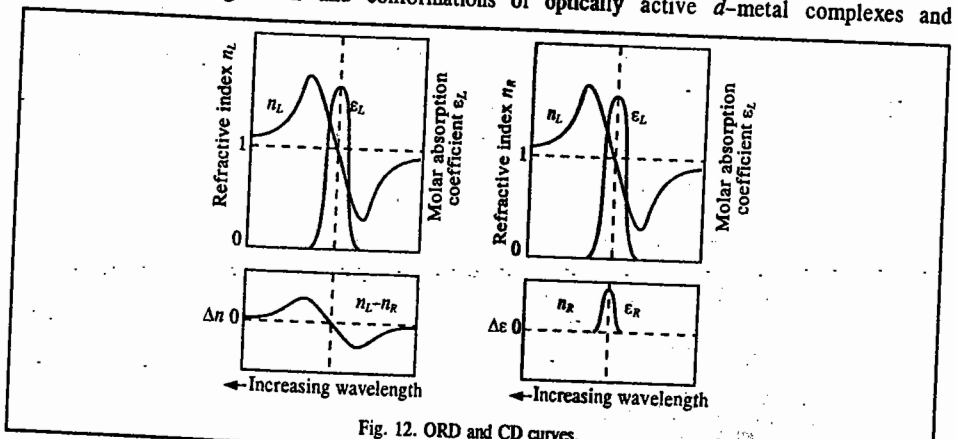

Fig. 12. ORD and CD curves.

other optically active molecules such as proteins, synthetic polypeptides and steroids. We may finally mention that chiral molecules have non-superimposable mirror images and hence are optically active. To be more precise, if we invoke symmetry arguments, then we can say that a molecule possessing any improper rotation axis (S_n), a mirror plane or a centre of symmetry, cannot be optically active.

Structure of Liquids. The structure of simple liquids such as liquid metals and simple monatomic liquefied gases like argon can be deduced from diffraction methods like X-ray diffraction, electron diffraction and neutron diffraction. These methods indicate the existence of **short-range order** and **long-range disorder** in the liquid state. While the short-range order assigns a certain structure, the long-range disorder gives rise to the fluidity of the liquid. The electron diffraction and the neutron diffraction methods are particularly useful for investigating monatomic liquids. The liquid diffraction patterns characteristically show one or two nicely formed small-range diffraction maxima that correspond to the short-range order. They also show rather diffuse diffraction rings corresponding to the farther removed molecules.

The theory of the liquid state is an extremely difficult problem of theoretical chemistry. However, some progress has been made in the **computer simulation of liquids**. The so-called **radial distribution function** characterizes the average structure of a liquid, or more precisely, the average distribution of its molecules relative to one another. For a completely uniform distribution of molecules, the number $N(r)$ of them lying within a spherical shell of radius r and thickness dr is give by

$$N(r) = 4\pi r^2 \rho\, dr \qquad \ldots(32)$$

where ρ is the number density of the species. The radial distribution function $g(r)$ measures the variation with r in the probability of observing one species at a distance r from another and is defined by

$$g(r) = N(r)/(4\pi r^2 \rho)dr \qquad \ldots(33)$$

More explicitly, consider a system of n atoms and take any one of them as an origin. For a sequence of values of r, count the number $N(r)$ of other atoms whose centres lie within spherical shells of volume $4\pi r^2 dr$. This procedure is repeated with each of the other $(n-1)$ atoms as centre and finally the results for each value of r are averaged. In this way one obtains a radial distribution function $g(r)dr$ as a function of the parameter r.

The molar internal energy U_m for a simple liquid consists of the kinetic energy (which is $\frac{3}{2}RT$) and the potential energy {(given by the Lennard-Jones (6-12) potential energy, $V(r)$} and may be written as

$$U_m = \tfrac{3}{2}RT + (4\pi\rho N_A/2)\int_0^\infty r^2 V(r)\, g(r) dr \qquad \ldots(34)$$

The factor $\frac{1}{2}$ arises because each pair of interactions in $V(r)$ must be included only once. The radial distribution function $g(r)$ can be obtained from diffraction studies with X-rays or neutrons, or by computer simulation techniques. The radial distribution function for liquid argon at 85 K, calculated using neutron scattering method, is shown in Fig. 13.

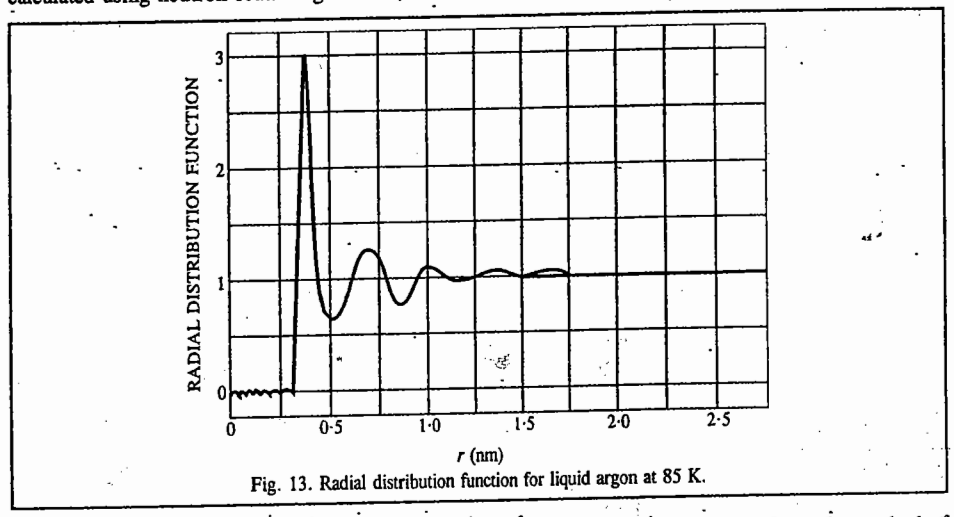

Fig. 13. Radial distribution function for liquid argon at 85 K.

Let us briefly comment on the equation of state for a simple liquid obtained from the method of statistical mechanics :

$$PV = NkT - (\rho N/6)\int_0^\infty g(r)\{r[dV(r)/dr]\}dr \qquad \ldots(35)$$

Recalling that an ideal gas equation is $PV = NkT$, we can appreciate how enormously complicated is the equation of state even for a simple liquid.

In Eq. 35, the second term on the right-hand side corresponds to the **configurational energy** and N is the number of molecules in the volume V ; ρ is, of course, the number density N/V ; the term $\{r[dV(r)/dr]\}$ is known as the **virial**. Eq. 35 has been investigated by computer simulation techniques.

Two methods that have received most attention are the **Monte Carlo (MC)** method and the **Molecular Dynamics (MD)** (time-dependent) method. They lead to the determination of $g(r)$.

In the Monte Carlo method for liquid structure, a model is set up in which an elementary cubic unit cell containing an initial configuration of approximately 10^3 atoms is repeated by side-by-side stacking in three dimensions so that the macroscopic liquid is generated by lattice-type translations of the cubic cell. Fig. 14 shows a projection of a configuration of atoms in a Monte Carlo simulation of a monatomic liquid. The positions of the atoms in any one cubic cell are random ; the other cells are formed by equal translations in three dimensions. After sufficient simulation time, an equilibrium arrangement is obtained. As one molecule, say B_2, moves out of its cell, B_3 moves in from an adjacent cell so as to preserve a constant number density.

Molecular dynamics method treats the evolution with time of systems of particles that interact through conservative forces operating under the laws of classical Newtonian mechanics. This method tracks the motion of molecules in condensed phases by solving the Newtonian equations of motion. Since solids are well represented by other theories, most applications of molecular dynamics have been to liquids, particularly in elucidating transport and equilibrium parameters. In applying molecular dynamics to a simulated liquid system, a set of initial coordinates is generated, usually from a face-centered Bravais lattice, at the required density.

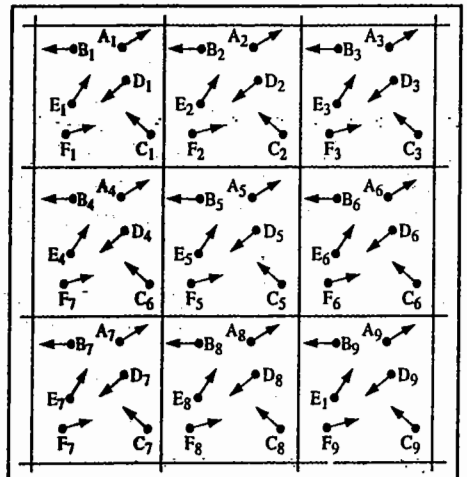

Fig. 14. Monte Carlo simulation of a monatomic liquid.

Many MD calculations have been carried out with the hard-sphere potential energy function, $V(r)$:

$$V(r) = \begin{cases} 0, & r > \sigma \\ \infty, & r \leq \sigma \end{cases} \qquad \ldots(36)$$

The hard-sphere potential energy is infinite when the separation of the two molecules, treated as hard spheres, is less than or equal to a certain value σ and is zero for greater separations. This potential is computationally simple and also shows that the structure of simple liquids is almost independent of their chemical nature and may be approximated by the interaction of rigid spheres.

We may mention in passing and in conclusion that the **so-called BBGKY hierarchy of equations** (abbreviated after the names of the five scientists who independently proposed them, *viz.*, Bogoliubov, Born, Green, Kirkwood and Yvon, during 1930–1945) have been used to derive the Boltzmann transport equation for gases and to study the transport phenomena. They involve a very advanced treatment of the subject. The extension of these methods to the liquid state is a formidable problem in statistical mechanics.

I. Review Questions

1. Define the term vapour pressure of a liquid. With the help of energy distribution of molecules in a liquid, explain why the vapour pressure of a liquid increases with increase in temperature and why a liquid cools down on evaporation.
2. State and explain Trouton's law.
3. Define the terms surface tension and surface energy. Show that surface tension is equal to surface energy numerically as well as dimensionally. Derive an expression for the determination of surface tension by the capillary rise method.
4. Discuss carefully the development of excess pressure in a liquid drop due to surface tension.
5. Explain the term viscosity of a liquid. What are Newtonian and non-Newtonian liquids. Discuss the effect of temperature on the viscosity of a liquid.

   "While the viscosity of a gas increases with increase in temperature, that of a liquid decreases with increase in temperature". How would you account for it.
6. Define the terms refractive index, specific refraction and molar refraction.
7. What is optical activity ? Write short notes on ORD and CD.
8. Briefly discuss the role of the radial distribution function in determining the structure of the liquid state.
9. Briefly discuss the Monte Carlo and the molecular dynamics methods for determining the structure of the liquid state.

II. Problems

1. Using Trouton's rule, estimate the vapour pressure of cyclohexane if its normal boiling point is 81·4°C. **[Ans. 103 torr]**
2. How far will a liquid of density 850 kg m^{-3} and surface tension 0·055 N m^{-1} rise in a glass capillary of 1·40 mm inside diameter ? **[Ans. 19 mm]**
3. The boiling point of an organic liquid is 54°C. Estimate the molar heat of vaporisation of the liquid assuming that it obeys Trouton's rule. **[Ans. 28·776 kJ mol^{-1}]**
4. A liquid rises to 1 cm in a glass capillary of radius r. How much will it rise if the cross-sectional area of the tube is *(a)* halved *(b)* doubled ? **[Ans. *(a)* 1·414 cm *(b)* 0·707 cm]**
5. How far will the mercury level be depressed when a glass capillary with 0·40 mm radius is placed in a dish of mercury ? Given that the surface tension of liquid mercury is 0·90 N m and its density is $13·6\times10^3$ kg m^{-3}. **[Ans. 18·3 mm]**
6. At 20°C, the densities of H_2O and $CHCl_3$ are 998·2 kg m^{-3} and 1595 kg m^{-3}, respectively and the surface tension of $CHCl_3$ is $27·4\times10^{-3}$ N m^{-1}. If the rise of H_2O and $CHCl_3$ in a glass capillary of a certain diameter is 9·9 cm and 2·33 cm, respectively, calculate the surface tension of H_2O. Also, calculate the radius of the tube. **[Ans. $72·86\times10^{-3}$ N m^{-1} ; 0·1505 mm]**
7. What is the excess pressure, in atm, due to surface tension in a drop of aniline 0·001 mm. in diameter at 25°C, given that its surface tension is 42·79 dynes cm ? **[Ans. 1·678 atm]**
8. Consider the flow of a liquid through a horizontal pipe of radius 2 cm with an average velocity of 5 cm s^{-1}. If η=1·23 cP at 25°C and ρ=0·913 g cm^{-3}, calculate the Reynolds number of the liquid. **[Ans. 1484]**
9. The refractive index of CCl_4 at 20°C is 1·4573. If its density at the given temperature is 1·595 g cm^{-3}, calculate the molar refraction. **[Ans. 26·51]**
10. To what height will water rise in a capillary of diameter 0·50 mm at 25°C if the surface tension of water is 71·97 dynes cm^{-1} ? **[Ans. 5·89 cm]**
11. Calculate the surface tension of a liquid which rises to a height of 1 cm in a capillary tube of radius 0·50 mm. The density of the liquid is 1·5 gm cm^{-3}. **[Ans. 36·7 dynes cm^{-1}]**
12. Calcualte the depression of mercury in a capillary tube of radius 0·5 mm if the surface tension of mercury is 460 dynes cm^{-1}. The density of mercury is 13·55 g cm^{-3}. **[Ans. 1·38 cm]**
13. What is the excess pressure, in atm, due to surface tension in a drop of benzene with a radius of 1×10^{-4} cm at 20°C, given that its surface tension is 28·86 dynes cm^{-1} ? **[Ans. 0·57 atm]**
14. The surface tension (γ) and the vapour pressure (P) of very small droplets of a liquid are related by the expression

$$\ln (P/P_0) = 2\gamma M/\rho r RT$$

where P_0 is the normal vapour pressure of the liquid of density ρ and r is the radius of the droplet. Using this equation calculate the vapour pressure of a water bubble of radius 10^{-8} m at 20°C if the vapour pressure of water at this temperature is 23·76 torr. The surface tension is $72·75\times10^{-3}$ N m^{-1} and density is 998·2 kgm^{-3}. **[Ans. P = 26·46 torr]**

CHAPTER 12

LIQUID CRYSTALS : THE MESOMORPHIC STATE

Liquid Crystals. Mesomorphic State. There are certain solids which when heated undergo two sharp phase transformations one after the other. They first fuse sharply yielding turbid liquids and then again equally sharply at a higher temperature yielding clear liquids. These changes are exactly reversed on cooling at the same temperatures. The turbid or transluscent liquids, however, show **anisotropy** (*i.e.*, they have different physical properties in different directions). The anisotropy is observed particularly in their optical behaviour. Thus, they exhibit double refraction and give *interference patterns* in polarised light. True liquids, on the contrary, are **isotropic** (*i.e.*, they have same properties in all directions). Since anisotropic properties like double refraction are associated with crystalline state, the turbid liquids are called **liquid crystals.** This term, however, is not satisfactory since the substances in this state do not have properties of crystalline state. Actually, they are more like liquids in having properties like mobility, surface tension, viscosity, etc. Amongst other names that have been suggested are crystalline liquids and anisotropic liquids, but these are also not satisfactory. The term **mesomorphic state** (meaning intermediate form, in Greek) probably fits best. However, the older term liquid crystals continues to be used even in the present day literature.

Substances showing the above behaviour are usually some long chain organic molecules either terminating in groups such as –OR, –COOR or having groups like –C=N–, –N=NO–, –C=C–, in the middle. Cholesteryl benzoate, $C_6H_5COOC_{27}H_{45}$, was amongst the first solids discovered, in 1888, to have this peculiar property. It fuses sharply at 145°C to give a turbid liquid which on further heating changes suddenly into clear liquid at 178°C. The above changes are reversed on cooling. The clear liquid when cooled first changes into turbid state at 178°C and then into solid state at 145°C.

A few years later, *p*-azoxy anisole and *p*-azoxy phenetole were found to show similar behaviour. Since then, hundreds of compounds capable of showing mesomorphic behaviour have been known. The 1991 Physics Nobel Prize was awarded to the French physicist P.G. de Gennes (1932-) for his contributions to the physics of liquid crystals and polymers.

Obviously, an essential requirement for mesomorphism to occur is that the molecule must be anisotropic in shape, like a *rod* or a *disc*. Industrial lubricants exist, more or less, in liquid crystalline, *i.e.*, mesomorphic state. The proteins and fats also exist or get changed into this state before digestion and are thus easily assimilated into the body. This state is believed to play an important role in nutritional and other processes. Depending upon the detailed molecular structure, the system may pass through one or more mesophases before it is transformed into the isotropic liquid. Transformation into the intermediate states may be brought about either by **thermotropic mesomorphism** (*i.e.*, by thermal processes) or by **lyotropic mesomorphism** (*i.e.*, by the intervention of the solvent).

The first temperature at which solid changes into turbid liquid is known as **transition point** and the second temperature at which turbid liquid changes into clear liquid is known as **melting point.** For *p*-cholesteryl benzoate, for instance, the changes may be represented as

$$\underset{\text{Solid}}{A} \overset{145^\circ C}{\rightleftharpoons} \underset{\text{Liquid crystal}}{A} \overset{178^\circ C}{\rightleftharpoons} \underset{\text{Liquid}}{A}$$

Here A is *p*-cholesteryl benzoate.

The substances showing liquid crystal character are highly stable and do not decompose on heating.

A few examples of compounds showing this behaviour are given in Table 1 together with their transition temperatures and melting points.

TABLE 1

Some Typical Substances Showing Liquid Crystal Character

Substance	Transition Point (°C)	Melting Point (°C)
Anisaldazine $CH_3OC_6H_4CH : NN : CHC_6H_4OCH_3$	165	180
p-Azoxyanisole $CH_3OC_6H_4NONC_6H_4OCH_3$	116	135
p-Azoxyphenetole $C_2H_5OC_6H_4NONC_6H_4OC_2H_5$	137	167
Diethylbenzidine $C_2H_5NHC_6H_4C_6H_4NHC_2H_5$	115	120
Mercury di-(*p*-ethoxybenzal-aminophenyl) $Hg(C_6H_4N : CHC_6H_4OC_2H_5)_2$	204	272
p-Methoxy cinnamic acid $CH_3OC_6H_4CH : CHCOOH$	170	186

There are, evidently, 4 phases or 4 states of matter to be considered. Besides solid, liquid and gaseous states, the fourth state is the **mesomorphic state.**

Vapour Pressure–Temperature Diagrams

The phase changes involved in the conversion of an ordinary solid into liquid and vapour state is usually represented as

$$\text{Solid} \rightleftharpoons \text{Liquid} \rightleftharpoons \text{Vapour}$$

The corresponding changes involved in the case of a solid showing mesomorphic behaviour may be represented as

$$\text{Solid} \rightleftharpoons \underset{\text{(Mesomorphic state)}}{\text{Liquid crystal}} \rightleftharpoons \text{Liquid} \rightleftharpoons \text{Vapour}$$

Such phase transformations are usually represented by pressure–temperature curves, as shown in Fig. 1 for an ordinary substance and in Fig. 2 for a substance capable of undergoing a mesomorphic change.

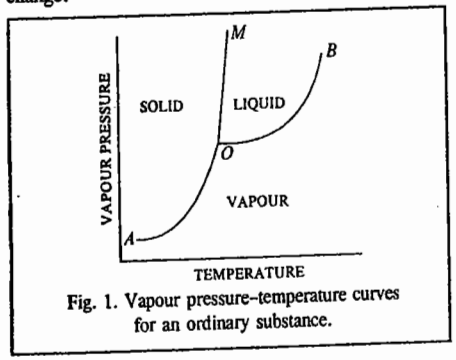

Fig. 1. Vapour pressure–temperature curves for an ordinary substance.

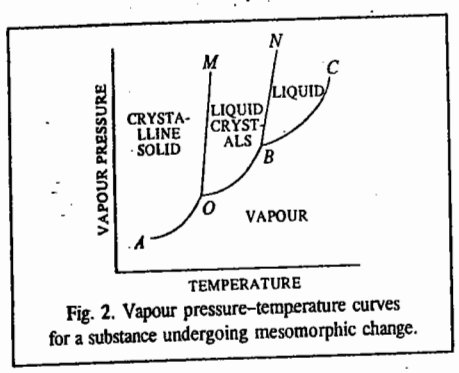

Fig. 2. Vapour pressure–temperature curves for a substance undergoing mesomorphic change.

In Fig. 1, *AO* is the vapour pressure curve of the substance in the solid (crystal) state while *OB* is that of the same substance in the liquid state. Thus, along *AO*, the solid (crystal) phase is in equilibrium with the vapour phase, while along *OB*, the liquid phase is in equilibrium with the vapour phase. At *O*, all the three phases, solid (crystal), liquid and vapour phases coexist in equilibrium with one another. *O* is, therefore, called a **triple point.** It is also the melting point of the solid, or which is the same thing as the freezing point of the liquid. *OM* traces the effect of varying pressure on the melting point (freezing point) of the substance. The areas in which solid, liquid or vapour phases exist singly, are marked as such in the figure.

In Fig. 2, *AO* is the vapour pressure curve of the solid crystal. *OB* is the vapour pressure cuve of the anisotropic liquid (*i.e.*, liquid crystal) and *BC* is that of the isotropic liquid. *O* is the transition point at which the solid crystal is converted into liquid crystal and *B* is the melting point at which the liquid crystal changes into clear liquid. *O* and *B* are two triple points. At *O*, the three phases, namely, *solid crystal, liquid crystal* and *vapour* coexist in equilibrium with one another. At *B*, the three phases, namely, *liquid crystal, liquid* and *vapour* coexist in equilibrium with one another. *OM* shows the effect of pressure on the transition temperature and *BN* that of pressure on the melting point of the substance. The areas within which solid crystal (crystalline solid), liquid crystal, liquid and vapour phases exist singly are marked as such in the figure.

Thermography. The phase changes observed on heating a solid showing mesomorphic behaviour are sometimes represented in the form of a temperature-time graph, as shown in Fig. 3. This is known as **thermography.** On heating a solid, its temperature starts rising (curve *AB*). This continues till the solid starts changing into the liquid crystals (point *B*). The temperature now remains constant as long as both the phases, *viz.*, solid and liquid crystals are present (curve *BC*). When the solid completely changes into liquid crystals, the temperature again starts rising (curve *CD*) and this continues till the liquid crystals start changing into the liquid (point *D*). The temperature again becomes constant and remains so as long as liquid crystals and the liquid are present together (curve *DE*). When the liquid crystals completely change into the liquid, the temperature again starts rising (curve *EF*) and this continues till the liquid starts changing into the vapour (point *E*). The temperature again becomes constant and remains so as long as the liquid and the vapour are present together (curve *FG*). The temperature would again begin to rise when vapour alone are present.

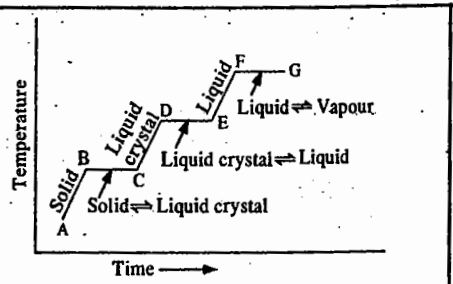

Fig. 3. Thermographic behaviour of a solid showing mesomorphism.

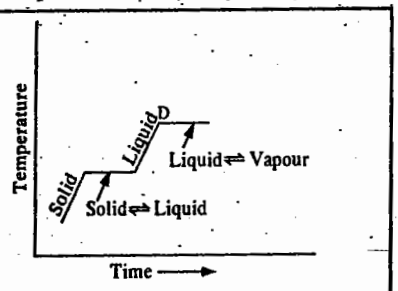

Fig. 4. Thermographic behaviour of an ordinary solid.

The thermographic behaviour of an ordinary solid is also shown for the sake of comparison (Fig. 4).

In recent years thermography has found extensive use in medical applications. It has helped in the detection and diagnosis of tumours and breast cancers and orthopaedic disorders such as back pain and arthritis. The diagnosis is based on the principle that heat changes produced in the affected skin are different from those in the healthy skin. The liquid crystals are pressed against the healthier part as well as the diseased part to be examined and colour photographs are taken of the resulting colour patterns and compared with each other.

LCDs and the Seven Segment Cell. In the electronic industry, the smectic and nematic types of liquid crystals have been used in thin light weight display devices such as digital watches and pocket

calculators; these are called **liquid crystal displays (LCDs).**

The LCDs work on the following principle : A thin film of a liquid crystal, not more than one-thousandth of an inch thick, is placed between two sheets of glass, one of which is coated on one side with a thin layer of an electrically conductive material such as tin oxide. When no current passes through the conductive coating, the molecules are uniformly oriented so that the light can pass through the cell (Fig. 5a). When the electric current is applied, the molecular alignment changes (since the liquid crystal molecules are polar) and the cell appears to be opaque or dark. Thus, a number or a letter is displayed in black against a silvery background. Since LCDs require a very small amount of current, the electronic watches and calculators can run for several years with the help of a small battery.

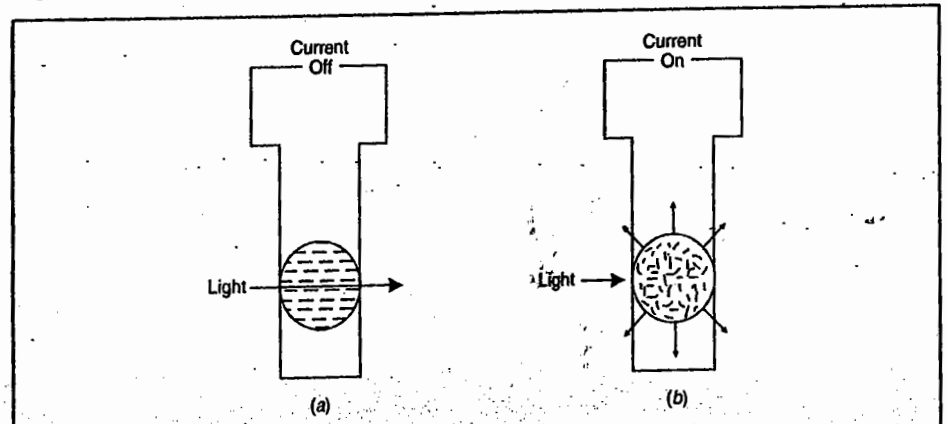

Fig. 5. Principle of working of a liquid crystal cell (*a*) Light passes through nematic liquid crystal when no electric current is passed (*b*) Light is scattered when molecules are disordered due to passing of electric current.

The LCD watches and calculators are generally composed of several 7-segment sections. Each 7-segment section can display one number. The combination of these sections (shown in Fig. 6) displays the numbers. A segment means an active area in the display or image area.

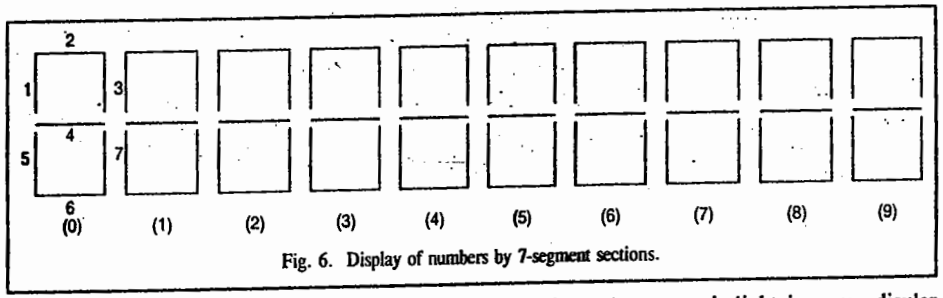

Fig. 6. Display of numbers by 7-segment sections.

The complete display panel is composed of two polarizers that transmit light in perpendicular directions, a mirrored surface and a layer of liquid crystal material between two glass plates (Fig. 7 *a*). In the absence of the applied voltage, the liquid crystal molecules in all the segments are precisely aligned (Fig. 7*a*) so that the entire panel appears silvery because light passes through both the polarizers and finally gets reflected from the mirror. However, when voltage is applied to the segment of a display, the precise alignment of liquid crystal molecules is lost (Fig. 7*b*). As a result, the light from the first polarizer fails to get rotated through the required angle of 90° to align with the second polarizer. The second polarizer thus blocks the passage of light. Since no light gets

reflected from the mirror, the panel appears dark.

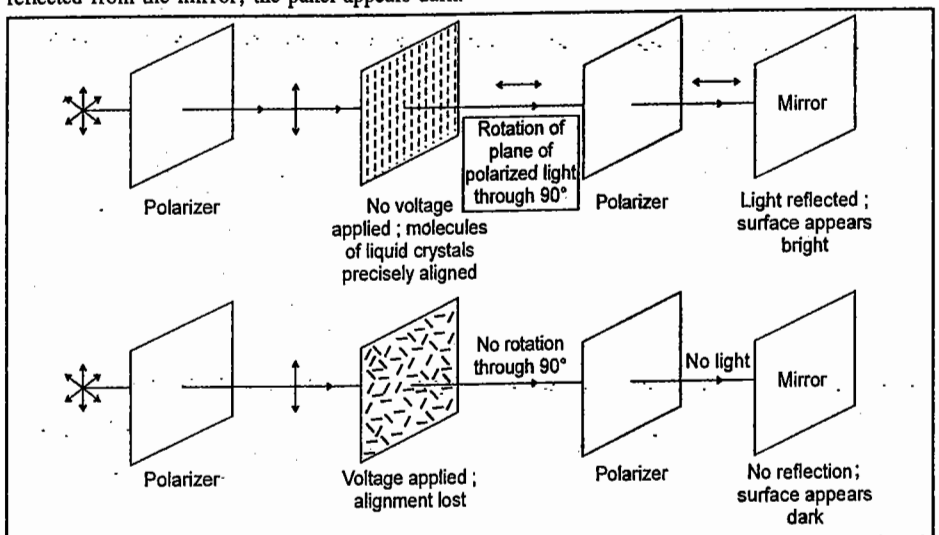

Fig. 7. (*a*) All liquid crystal molecules are precisely aligned in the absence of the applied voltage and light passes through both the polarizers and is reflected back form the mirror. (*b*) Alignment of the liquid molecules is lost when a voltage is applied to a segment in the panel. The segment then appears black against a silvery background.

Classification of Thermotropic Liquid Crystals

Further studies have shown that liquid crystals, *i.e.*, substances showing mesomorphic state, can be classified into two categories : smectic (*soap-like*, in Greek) liquid crystals and nematic (*thread-like*, in Greek) liquid crystals. Some substances are capable of existing in both forms. A few modifications of these forms are also known.

Smectic Liquid Crystals. The smectic liquid crystals do *not* flow as normal liquids. They have limited mobility. They flow in layers as if different planes or sheets are gliding over one another. The distribution of velocity in different layers is different from that found in a true liquid. To put it in other words, the flow of smectic liquid crystals is non-Newtonian while that of a true liquid is Newtonian. The concept of viscosity is, therefore, not applicable to the liquid crystals of this type. When spread over a clean glass surface, they form a series of *terraces* or *strata*, as shown in Fig. 8. The edges of these terraces often show a series of fine lines even in ordinary light, though more so in polarised light.

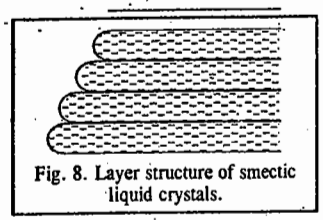

Fig. 8. Layer structure of smectic liquid crystals.

The existence of the layers suggests that the crystal lattice still exists though in somewhat distorted form. However, the spacing of the layers is different from that observed in the solid state.

Smectic liquid crystals also give X-ray diffraction patterns like solid crystals but it is in one direction only. Thus, smectic phase has a complex internal structure. When viewed in polarized light, smectic phases appear to have fan-like appearance. They are always uniaxial and are not affected by a magnetic field.

A few examples of compounds yielding smectic phases when heated at the transition temperatures are given in Table 2.

TABLE 2

Some Compounds giving Smectic Type of Liquid Crystals

Compound	Transition Point (°C)	Melting Point (°C)
Ethyl *p*-azoxy benzoate	114	121
Ethyl *p*-azoxy cinnamate	140	249
n-Octyl-*p*-azoxy cinnamate	94	175

Nematic Liquid Crystals. Nematic type of liquid crystals show near normal flow behaviour of liquids. They flow more readily than the smectic liquid crystals. Their flow is also Newtonian and the concept of viscosity is applicable to their flow. Their viscosity, however, is rather low as compared to that of liquids. Thus, nematic phases have liquid-like character and yet being turbid and anisotropic, they are unlike true liquids. This type is, therefore, regarded less truly anisotropic than the smectic type.

In polarised light, substances in nematic phase appear to have *thread-like structures*. They are uniaxial like smectic substances but unlike the latter, they are affected by a strong magnetic field. Thus, when viewed in the direction of the lines of force of a magnetic field, the turbid liquid appears quite clear. If the magnetic field is cut off, the liquid appears turbid again. Some of the compounds yielding nematic phases are given in Table 3.

TABLE 3

Some Compounds giving Nematic Type of Liquid Cystals

Compound	Transition Point (°C)	Melting Point (°C)
p-Azoxy anisole	116	135
p-Azoxy phenetole	137	167
p-Methoxy cinnamic acid	170	186
Anisaldazine	165	180
Dibenzal benzidine	234	260

Compounds Exhibiting both Smectic and Nematic Characters. Certain substances, notably the higher cholesteryl esters from the caprylate to the myristate, show, on heating, three phase transformations instead of the usual two. They melt sharply at a certain temperature to give smectic type of liquid crystals in the first instance. Then they change sharply at a higher temperature to give nematic type of liquid crystals which, in turn, melt sharply at a still higher temperature to give a clear liquid. Thus, there are three temperatures to be reckoned with : two transition temperatures and one true melting point. These temperatures for the myristate are 72°C, 78°C and 83°C, respectively. Some substances which show more than one smectic phase, are also known. For example, ethyl anisal-*p*-amino cinnamate passes through two smectic phases and one nematic phase before melting into the true liquid state. It, thus, undergoes the following changes :

$$\text{Solid Crystal} \underset{}{\overset{83°C}{\rightleftharpoons}} \text{Smectic Phase I} \overset{91°C}{\rightleftharpoons} \text{Smectic Phase II}$$

$$\overset{118°C}{\rightleftharpoons} \text{Nematic Phase} \overset{139°C}{\rightleftharpoons} \text{Liquid Phase}$$

The compound, evidently, exhibits three transition temperatures and one true melting point.

Cholesteric Liquid Crystals. Certain optically active compounds show many characteristics of nematic behaviour but at the same time they show strong colour effects in polarised light. This indicates that they have a *layer structure* like smectic liquid crystals. But they differ from smectic liquid crystals in having much thicker layers which are of the order of 500 to 5000 molecules thick. Such liquid crystals having some nematic and some smectic characters are called cholesteric liquid crystals. The first substance in which this type of mesomorphism was detected was cholesteryl benzoate. Its transition point is 145°C and melting point 178°C. The *l*-cholesteryl esters from formate to myristate are amongst other examples of compounds which form cholesteric type of liquid crystals.

Further, it has been found that solutions of some polypeptides in organic solvents, for example, poly-γ-benzyl-L-glutamate (PBLG) in dioxane or chloroform spontaneously adopt the cholesteric mesophase above a certain concentration. The same behaviour is shown by poly-γ-benzyl-D-glutamate (PBDG). In fact, the unique optical properties of the cholesteric phase, observed by Reinitzer and Lehmann, had culminated in the discovery of the liquid crystalline state.

Cholesteric mesophase displays a characteristic Lehmann rotation phenomenon. Lehmann had

found that droplets of the material, when heated from below, seemed to be rotating violently. However, from optical studies he concluded that the cholesteric mesophase also shows a highly non-Newtonian flow properties compared with the nematic phase.

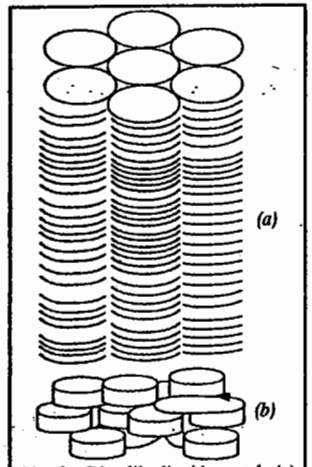

Fig. 9. Disc-like liquid crystals (*a*) Columnar phase (*b*) Nematic phase.

Disc-Shaped Liquid Crystals. In recent years, a number of discotic or disc-shaped liquid crystals have also been prepared which exist in more than one mesophase. They can be classified into two categories : *columnar* and *nematic*. The columnar phase consists of discs stacked one on top of the other aperiodically giving rise to liquid-like columns which form a two-dimensional lattice (Fig.9*a*). Several shapes of the columnar phase (such as hexagonal, tetragonal, tilted) exist. The nematic discotic phase consists of an orientationally ordered arrangement of discs without any long range translational order (Fig. 9*b*). Unlike the nematic rod-like phase, this mesophase is optically inactive.

Polymer Liquid Crystals. This is yet another class of liquid crystals reported recently. The basic monomer units of a polymer liquid crystal are low molar mass mesogens, rod-like or disc-like, which are attached to the polymer backbone in the main chain itself (Fig. 10*a*) or as side groups (Fig. 10*b*). If the repeating unit is rod-shaped, mesophases akin to the nematic, cholesteric and smectic types of rod-like molecules are found to exist.

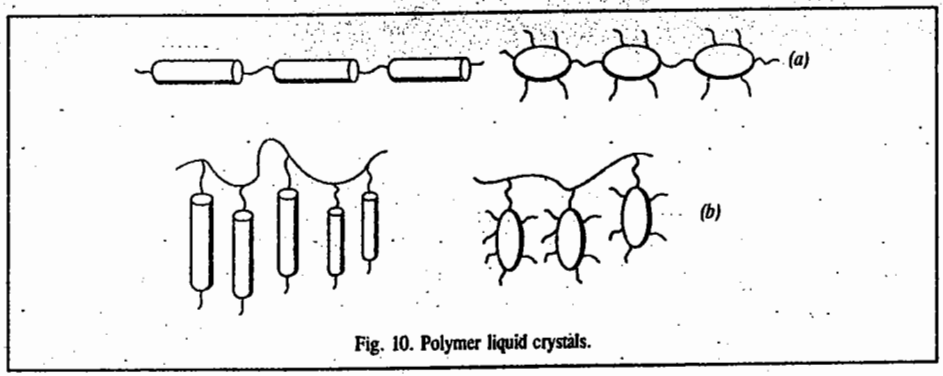

Fig. 10. Polymer liquid crystals.

Polymorphism in Thermotropic Liquid Crystals

Data on several mesogenic compounds with their transition temperatures and latent heats have recently been obtained. The following examples show the rich polymorphism shown by thermotropic liquid crystals. The figures given in kJ are the latent heats.

1. 4, 4′-Dimethoxyazoxy benzene (*p*-azoxyanisole) $CH_3O-C_6H_4-\overset{O}{\overset{\uparrow}{N}}=N-C_6H_4-OCH_3$:

$$\text{Solid} \underset{}{\overset{118{\cdot}2^\circ C,\ 29{\cdot}57\ kJ}{\rightleftharpoons}} \text{Nematic} \underset{}{\overset{135{\cdot}3^\circ C,\ 0{\cdot}57\ kJ}{\rightleftharpoons}} \text{Isotropic}$$

2. 4′-*n*-Pentyl-4-cyanobiphenyl $n\text{-}C_5H_{11}-C_6H_4-C_6H_4-CN$:

$$\text{Solid} \overset{225{\cdot}2^\circ C,\ 17{\cdot}2\ kJ}{\rightleftharpoons} \text{Nematic} \overset{35^\circ C,\ 0{\cdot}8\ kJ}{\rightleftharpoons} \text{Isotropic}$$

3. 4′-*n*-Octyl-4-cyanobiphenyl $n\text{-}C_8H_{17}-C_6H_4-C_6H_4-CN$:

$$\text{Solid} \overset{24^\circ C,\ 25{\cdot}3\ kJ}{\rightleftharpoons} \text{Smectic} \overset{34^\circ C,\ 0{\cdot}13\ kJ}{\rightleftharpoons} \text{Nematic} \overset{42{\cdot}6^\circ C,\ 0{\cdot}97\ kJ}{\rightleftharpoons} \text{Isotropic}$$

4. N-(4-*n*-Pentyloxy benzylidene-4′-*n*-hexylaniline) $C_5H_{11}O-C_6H_4-CH=N-C_6H_4-C_6H_{13}$:

$$\text{Solid} \overset{36^\circ C,\ 15{\cdot}2\ kJ}{\rightleftharpoons} \text{Smectic A} \overset{38{\cdot}4^\circ C,\ 0{\cdot}39\ kJ}{\rightleftharpoons} \text{Smectic B} \overset{42{\cdot}4^\circ C,\ 0{\cdot}15\ kJ}{\rightleftharpoons} \text{Smectic C}$$

$$\text{Isotropic} \overset{72{\cdot}8^\circ C,\ 0{\cdot}66\ kJ}{\rightleftharpoons} \text{Nematic} \overset{60{\cdot}3^\circ C,\ 0{\cdot}42\ kJ}{\rightleftharpoons} \text{Smectic E} \overset{51{\cdot}8^\circ C,\approx 0{\cdot}15\ kJ}{\rightleftharpoons} \text{Smectic D}$$

$$\text{Smectic C} \overset{50^\circ C}{\underset{25 kJ}{\rightleftharpoons}} \text{Smectic D}$$

All the transitions listed in the above examples are **enantiotropic**, *i.e.*, they take place reversibly on heating and cooling, though the reversal to the solid phase is generally accompanied by supercooling. The nematogenic compounds 1 and 2 are of special interest : the first has a permanent dipole moment inclined at an angle of about 60° with respect to the molecular axis, the second has a strong longitudinal dipole moment. These two compounds emphasize the major role played by molecular shape in determining the mesomorphic behaviour.

Melting of Nematic Crystals. When a solid is heated, its transformation to the nematic phase results in the break down of the positional order of the molecules but not of the orientational order. The mesophase is fluid and anisotropic as a result of the ease with which the molecules slide over one another while still preserving their parallelism. As heating continues, the degree of orientational order in the liquid crystal drops further. However, thermodynamic properties such as heat capacity, isobaric expansivity and isothermal compressibility increase rapidly as the temperature approaches the **nematic isotropic point** at which there is complete breakdown of the long orientational order.

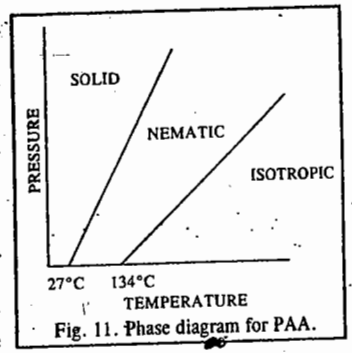

Fig. 11. Phase diagram for PAA.

Pressure-induced Mesomorphism. A very important quantity in the theory of liquid crystals is the so-called **order parameter.** If the molecules are aligned in a perfectly parallel arrangement, the order parameter is equal to unity and if the arrangement is random, the order parameter is zero. The phase diagram for *p*-azoxyanisole (PAA) is shown in Fig. 11.

As the pressure is raised, both the solid $\rightleftharpoons$ nematic and nematic $\rightleftharpoons$ isotropic transition temperatures increase. The slope dT/dP for the latter is greater than that of the former. The phase diagram for *p*-ethoxy benzoic acid (Fig. 12) is very interesting. At atmospheric pressure, it does not form a liquid crystal. However, as the pressure is raised, it exhibits mesophases—initially a nematic phase and at higher pressures a

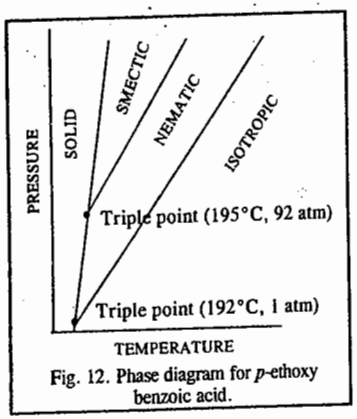

Fig. 12. Phase diagram for *p*-ethoxy benzoic acid.

smectic phase. These transitions have been detected by differential thermal analysis (DTA) and the mesophases have been identified by microscopic observations using a high pressure optical cell. The phase diagram shows the existence of two triple points : solid–nematic–isotropic and solid–smectic–nematic.

Molecular Arrangements in Various States of Liquid Crystals

In smectic state, the molecules are arranged in nearly parallel layers, as represented in Fig. 13*a*. The layers are held at regular distances from one another but the molecules within each layer are not regularly spaced. The anisotropic properties, such as double refraction, can thus be readily understood.

In nematic state, the arrangement of the molecules is still parallel but now there are no layers. The arrangement is irregular and the molecules now have greater freedom of motion, as shown in Fig. 13*b*. This arrangement would still lead to difference in properties in different directions, *i.e.*, it would lead to anisotropic character.

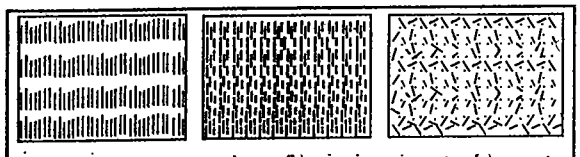

Fig. 13. Molecular arrangements in various states of liquid crystals.

In the case of a normal liquid, the arrangement of molecules is haphazard. The molecules move completely at random and, consequently, there is no scope for double refraction or any anisotropy. The material is now fully isotropic like a true liquid.

It is known that most of the industrial lubricants exist, more or less, in the mesomorphic, *i.e.*, liquid crystal state. In fact, it is believed that their functioning as lubricants is almost entirely due to their existence in this state. The proteins and fats, which are important constituents of food, also exist or get changed into this state before digestion and are, therefore, easily assimilated in the body. This state is believed to play an important role in nutritional and other processes. S. Chandrasekhar, a physicist at the Indian Institute of Science, Bangalore, has made important contributions to the physics of liquid crystals.

In recent years, the nematic and smectic types of liquid crystals have been widely adopted for liquid crystal display devices (LCDs), as already discussed. They operate through their interaction with natural light either in transmission or reflection. They consume very little power.

For more details refer to the following books :

Colling, P.J., *Liquid Crystals : Nature's Delicate Phase of Matter*, Wiley, 1991.

Stegemeyer (ed.), *Liquid Crystals*, Steimkopff, Darmstadt, 1994.

Demus, D. (ed.), *Handbook of Liquid Crystals*, Wiley-VCH, Weinheim, 1999.

Gray, G.W. (ed.), *Physical Properties of Liquid Crystals*, Wiley-VCH, Weinheim, 1998.

Gray, G.W., and J.W. Goodby, *Smectic Liquid Crystals*, Leonhard Hill Glasgow, 1984.

Review Questions

1. What are liquid crystals ? List their characteristics.
2. Draw and discuss the vapour pressure–temperature diagrams of true liquids and liquid crystals.
3. Describe the structures and main characteristics of 1. Smectic liquid crystals 2. Nematic liquid crystals 3. Cholesteric liquid crystals 4. Disc-shaped liquid crystals and 5. Polymer liquid crystals.
4. Give a brief account of the molecular arrangements which exist in various states of liquid crystals. How would you account for the turbidity observed in liquid crystals ?

CHAPTER 13

THE FIRST LAW OF THERMODYNAMICS

The word 'thermodynamics' implies *flow of heat*. The subject, however, is much more comprehensive. *It deals with energy changes accompanying all types of physical and chemical processes.*

Thermodynamics is based on two generalisations, called the First and the Second law of thermodynamics. These are based on human experience. There is no formal proof for these laws. All that one can say is that nothing contrary to these laws has been known to happen whenever we consider the behaviour of matter in bulk. Scientists are of the view that nothing contrary to these laws will ever be known. The laws of thermodynamics are not at all concerned with the atomic or molecular structure of matter.

Importance of Thermodynamics. Thermodynamics is a fundamental subject of great importance in physical chemistry. Most of the important generalisations of physical chemistry, including van't Hoff law of dilute solutions, Raoult's law of vapour pressure lowering, distribution law, law of chemical equilibrium, the phase rule and the laws of thermochemistry, can be deduced from the laws of thermodynamics.

Thermodynamics also helps to lay down the criteria for predicting feasibility or spontaneity of a process, including a chemical reaction, under a given set of conditions. In other words, it helps to predict whether a given process or a chemical reaction is feasible under the given conditions of temperature, pressure and concentration. It also helps us to determine the extent to which a process, including a chemical reaction, can proceed before attainment of equilibrium.

Limitations of Thermodynamics. The laws of thermodynamics apply only to matter in bulk and not to individual atoms or molecules. In other words, the laws of thermodynamics apply to behaviour of assemblages of a vast number of molecules and not to individual molecules.

Thermodynamics can only predict whether a given process, including a chemical reaction, is feasible under a given set of conditions ; it does not tell anything about the rate at which a given process may proceed. For example, thermodynamics predicts that hydrogen and oxygen gases would react at ordinary temperature to yield liquid water. But it does not tell whether the reaction will be fast or slow. We know only from experiment that in the absence of a catalyst, the reaction is extremely slow.

Some Basic Terms used in Thermodynamics. A few terms used frequently in thermodynamics are described below :

System. A system may be defined as any specified portion of matter under study which is separated from the rest of the universe with a bounding surface. A system may consist of one or more susbstances.

Surroundings. The rest of the universe which might be in a position to exchange energy and matter with the system is called the **surroundings.** In simple cases, surroundings generally imply air, or a water-bath in which a system under examination is immersed.

Isolated system. A system which can exchange neither energy nor matter with its surroundings is called an isolated system.

Closed System. A system which can exchange energy but not matter is called a closed system.

Open System. A system which can exchange matter as well as energy with its surroundings is said to be an open system.

Macroscopic Properties. The properties associated with a macroscopic system (*i.e.*, consisting of large number of particles) are called macroscopic properties. They are pressure, volume, temperature, composition, density, viscosity, surface tension, refractive index, etc.

Homogeneous and Heterogeneous Systems. A system is said to be **homogeneous** when it is completely uniform throughout, as for example, a pure solid or a liquid or a solution or a mixture of gases. In other words, a homogeneous system consists of only one phase.

A **phase** is defined as a homogeneous and physically distinct part of a system which is bounded by a surface and is mechanically separable from other parts of the system.

A system is said to be **heterogeneous** when it is not uniform throughout. In other words, a heterogeneous system is one which consists of two or more phases. Thus, a system consisting of two or more immiscible liquids, or a solid in contact with a liquid in which it does not dissolve, is a heterogeneous system. A liquid in contact with its vapour is also a heterogeneous system because it consists of two phases.

State of a System. When macroscopic properties of a system have definite values, the system is said to be in definite state. Whenever there is a change in any one of the macroscopic properties, the system is said to change into a different state. Thus, the state of a system is fixed by its macroscopic properties.

State Variables. Since the state of a system changes with change in any of the macroscopic properties, these properties are called state variables. It also follows that when a system changes from one state (called initial state) to another state (called final state), there is invariably a change in one or more of the macroscopic properties.

Pressure, temperature, volume, mass and composition are the most important state variables. In actual practice, it is not necessary to specify all the state variables because some of them are interdependent. In the case of a single gas, composition is not one of the variables because it remains always 100 per cent. Further, if the gas is ideal and one mole of the gas is under examination, it obeys the equation $PV=RT$, where R is the gas constant. Evidently, if only two of the three variables (P, V and T) are known, the third can easily be calculated. The two variables, generally specified, are temperature and pressure. These are called *independent variables*. The third variable, generally volume, is said to be a *dependent variable*, as its value depends upon the values of P and T. Thus, the thermodynamic state of a system consisting of a single *gaseous* substance may be completely defined by specifying any two of the three variables, *viz.*, temperature, pressure and volume.

Thermodynamic Equilibrium. A system in which the macroscopic properties do not undergo any change with time is said to be in thermodynamic equilibrium. Suppose a system is heterogeneous, *i.e.*, it consists of more than one phase. Then, if it is in equilibrium, the macroscopic properties in the various phases remain unaltered with time.

The thermodynamic equilibrium implies the existence of three kinds of equilibria in the system : *(i)* thermal equilibrium *(ii)* mechanical equilibrium and *(iii)* chemical equilibrium.

A system is said to be in **thermal equilibrium** if there is no flow of heat from one portion of the system to another. This is possible if the temperature remains the same throughout in all parts of the system.

A system is said to be in **mechanical equilibrium** if no mechanical work is done by one part of the system on another part of the system. This is possible if the pressure remains the same throughout in all parts of the system.

A system is said to be in **chemical equilibrium** if the composition of the various phases in the system remains the same throughout.

Extensive and Intensive Properties. An **extensive property** of a system is that which depends upon the amount of the substance or substances present in the system. The examples are mass, volume and energy.

An intensive property of a system is that which is independent of the amount of the substance present in the system. The examples are temperature, pressure, density, viscosity, refractive index, surface tension and specific heat.

In the light of the above definitions, extensive properties of a single (pure) substance will depend upon the number of moles (n) of the substance present and also on any two of the three variables P, V and T (called independent variables). If n is kept constant, the extensive properties of the system will depend only on the two independent variables.

If a system under examination is a mixture of two or more gases, the extensive properties will vary with the number of moles, n_A, n_B, n_C, etc., of the constituents A, B, C, etc., present in the system and also with the two independent variables. The intensive properties in such cases will depend upon the concentration of the various species, besides the two independent variables.

Thermodynamic Processes. The operation by which a system changes from one state to another is called a **process**. Whenever a system changes from one state to another it is accompanied by change in energy. In the case of open systems, there may be change of matter as well.

The following types of processes are known :

Isothermal process. A process is said to be isothermal if the temperature of the system remains constant during each stage of the process.

Adiabatic process. A process is said to be adiabatic if no heat enters or leaves the system during any step of the process.

Isobaric process. A process is said to be isobaric if the pressure of the system remains constant during each step of the process.

Reversible and Irreversible Processes. A process carried out infinitesimally slowly so that the driving force is only infinitesimally greater than the opposing force, is called a **reversible process.**

Any process which does not take place in the above manner, *i.e.*, a process which does not take place infinitesimally slowly, is said to be an **irreversible process.**

A reversible process cannot be realised in practice because it would require infinite time for its completion. Hence, almost all processes occurring in nature or laboratory are irreversible. A reversible process, therefore, remains imaginary and theoretical. Nevertheless, this concept is highly useful since it leads to some definite conclusions, as will be explained a little later in this chapter.

The following example may be given to illustrate the difference between reversible and irreversible processes.

Consider a cylinder provided with an air-tight, 'weightless' and frictionless piston, containing in it a certain quantity of a gas, as shown in Fig. 1. Let the pressure P on the piston be exactly equal to the pressure of the gas within. The piston will neither move downward nor upward and, consequently, there will be no change in the volume of the gas (Fig. 1*a*). Now, suppose the pressure on the piston is decreased by an infinitesimally small amount dP. The pressure on the piston, being $P - dP$, is now infinitesimally

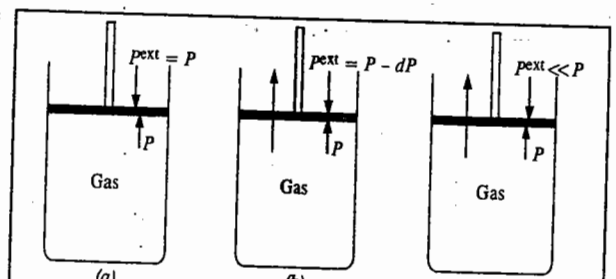

Fig. 1. Reversible and irreversible expansion of a gas.

smaller than the pressure of the gas P within the cylinder (Fig. 1*b*). Hence, the piston will move up and the gas will expand by an infinitesimally small amount. If the pressure on the piston is kept infinitesimally smaller than the pressure of the gas itself, the expansion of the gas will continue infinitesimally slowly, *i.e.*, in a thermodynamically reversible manner. If, however, the pressure on the piston (external pressure), is made much smaller than the pressure of the gas within the cylinder, then the gas will expand rapidly, pushing the piston upward suddenly (Fig. 1*c*). The expansion of the gas, in this case, is said to take place irreversibly.

Nature of Work and Heat. As is well known, whenever a system changes from one state to another, it is accompanied by change in energy. The change in energy may appear in the form of heat, work, light, etc.

The unit of energy is joule. It is defined as the work done when a resistance of 1 newton is moved through a distance of 1 metre. Thus, J = N m.

The British physicist James P. Joule (1818-1889) showed in 1850 that there is a definite relationship between mechanical work done W and heat produced H, *i.e.*,

$$W \propto H \quad \text{or} \quad W = JH$$

J is known as the **joule mechanical equivalent of heat.** Its numerical value is taken as 4·184 joules. Thus, with the expenditure of 4·184 joules of mechanical energy, 1 calorie of heat is produced. Thus, 1 calorie ≡ 4·184 joules. Heat is now invariably expressed in joules.

Energy manifests itself not only in the form of mechanical work (as in Joule's experiments) but also as heat energy, electrical energy and chemical energy. Whatever be the form, energy is composed of two factors : *(i)* an intensity factor and *(ii)* a capacity factor. The product of these two factors gives the energy.

Heat energy, for example, is measured by the product of temperature (*intensity factor*) and the heat capacity (*capacity factor*) of the system concerned. The product gives the energy of the system. If a substance of mass m kg and specific heat s kJ per kg, is heated through $t°$, the heat energy involved is given by *mst* kJ.

When a current flows in an electric circuit for a given interval of time, **electrical energy** produced is obtained by the product of the potential difference V causing the current to flow (*intensity factor*) and the quantity of electricity Q that flows for that interval of time (*capacity factor*). If V is measured in volts and Q in coulombs, the product of the two expresses the electrical energy (or work) in volt coulombs, *viz.*, joules.

When a body of mass m kg is moved through a height of h m, the work done against gravity is obtained by multiplying the intensity factor (mg newtons) with the capacity factor (h metres). The work performed is mgh joules. This work gets stored in the body as potential energy and is released when the body falls back to its original position.

THE FIRST LAW OF THERMODYNAMICS

The **first law of thermodynamics** states that energy can neither be created nor destroyed, although it can be transformed from one form to another. This is also known as the **law of conservation of energy.** Thus, whenever energy in one form disappears, an equal amount of energy in some other form must appear. The law is based on the cumulative experience of ages that *it is impossible to construct a* **perpetual motion machine,** *i.e., a machine which can produce energy without expenditure of energy.*

The equivalence of heat and mechanical work, established by Joule experimentally, also follows as a consequence of the First law. Suppose there is no such equivalence. Then, it may be possible at first to convert a certain amount of heat, say, x joules, into a certain amount of mechanical work and then, in the reverse process, to transform the same amount of mechanical work into heat, producing y joules of heat, where $y > x$. Then, the original state will have been restored but heat energy, equivalent to $y - x$ joules, will have been created. By repeating the above cycle, *energy can be continuously created* and in this way a perpetual motion machine can be fabricated. This is denied by human experience, as already stated. Hence, *there must be exact equivalence of heat and mechanical work.*

It is now known that energy can be produced by the destruction of mass, the two quantities being related by the expression $E = mc^2$ (Eistein equation) where E is the energy produced by the destruction of mass m and c is the velocity of light. *The* modified law, therefore, states that *the total mass and energy of an isolated system remains unchanged.*

It is to be kept in mind that in the entire ensuing discussion, *by the term* **system** *we shall mean an* **ideal gas.**

Internal Energy, U

Every substance is associated with a definite amount of energy which depends upon its chemical nature as well as upon its temperature, pressure and volume. This energy is known as **internal energy**. The exact magnitude of this energy is not known because the chemical nature includes such indeterminant factors as the translational, rotational and vibrational movements of the molecules, the manner in which the molecules are put together, the nature of the individual atoms, the arrangement and number of electrons, the energy possessed by the nucleus, etc. But, one thing is certain that the internal energy of a substance or a system is a definite quantity and it is a function only of the state (*i.e.*, chemical nature, composition, temperature, pressure and volume) of the system at the given moment, irrespective of the manner in which that state has been brought about. It is true that the actual value of internal energy cannot be determined but, fortunately, in thermodynamics the absolute value is not of any significance. It is the change in internal energy accompanying a chemical or a physical process that is of interest and this is a measurable quantity.

Internal Energy and the First Law. Suppose, a system is subjected to change of pressure and volume. Let the initial state be represented by A and the final state by B (Fig. 2) and let U_A and U_B represent energies associated with the system in its states A and B, respectively. These will be definite quantities as explained above. Then, the change in internal energy, ΔU, which is given by

$$\Delta U = U_B - U_A,$$

must also be a definite quantity, *irrespective of the path or the manner in which the change is brought about.* If it were not so, it would again be possible to construct a perpetual motion machine. Suppose, for example, that the system changes from state A to state B by following path I and is accompanied by change of energy equal to ΔU. Now suppose that the same change of state is brought about by another path, say, path II, and the change of energy is $\Delta U'$. Suppose, $\Delta U > \Delta U'$. Then, by a coupling of these two processes :

$A \longrightarrow B$ (by path I) and

$B \longrightarrow A$ (by path II),

as shown in Fig. 2, the system would return to its initial state and at the same time a surplus of energy equal to $\Delta U - \Delta U'$ would become available. By repeating the same cycle over and over again, energy would be generated continuously and a perpetual motion machine would be possible. This is contrary to the First law. Hence, $\Delta U' = \Delta U$. Thus, the energy change accompanying a process is a function only of the initial and the final states of the system and is independent of the path or the manner by which the change is brought about.

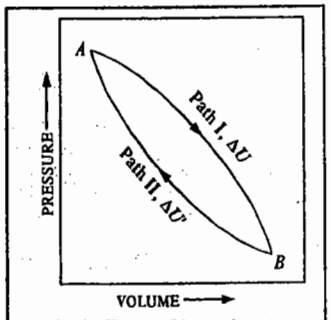

Fig. 2. Change of internal energy.

Energy changes in relation to work and heat changes. Let U_A be the energy of a system in its state A and U_B be the energy in its state B. Suppose the system while undergoing change from state A to state B *absorbs* heat q from the surroundings and also *performs* some work (mechanical or electrical), equal to w. The absorption of heat by the system tends to raise the energy of the system. The performance of work by the system, on the other hand, tends to lower the energy of the system because performance of work requires expenditure of energy. Hence, the change of internal energy, ΔU, accompanying the above process will be given by

$$\Delta U = U_B - U_A = q - w \qquad \ldots(1)$$

In general, if in a given process, the quantity of heat transferred from the surroundings to the system is q and the work done in the process is w, then the change in internal energy, ΔU, is given by

$$\Delta U = q + w \qquad \ldots(2)$$

Eq. 2 is the mathematical statement of the First law of thermodynamics.

If work is done by the surroundings on the system (as during the compression of a gas), w is taken as positive so that $\Delta U = q + w$ (Eq. 2). If, however, work is done by the system on the surroundings (as during the expansion of a gas), w is taken as negative so that $\Delta U = q - w$ (Eq.1).

Example 1. Calculate w and ΔU for the conversion of one mole of water at 100°C to steam at 1 atm pressure. Heat of vaporisation of water at 100°C is 40670 J mol^{-1}.

Solution : Heat required to convert 1 mole of water at 100°C to steam, q = 40670 J (given)

Calculation of w : P = 1 atm = 101,325 N m^{-2}

V_1 = Volume of 1 mole of liquid water at 1 atm pressure = 18 ml = 18×10^{-6} m^3

V_2 = Volume of 1 mole of steam at 100°C at 1 atm pressure

$= (22{\cdot}4 \text{ dm}^3 \times 373)/273 = 30{\cdot}60 \text{ dm}^3 = 0{\cdot}0306 \text{ m}^3$

$\therefore \quad w = P(V_2 - V_1) = 101{,}325 \text{ N m}^{-2} (0{\cdot}0306 \text{ m}^3 - 18 \times 10^{-6} \text{ m}^3)$

$= 101{,}325 \text{ N m}^{-2} \times 0{\cdot}0306 \text{ m}^3 = 3100 \text{ J mol}^{-1}$ (Neglected)

Since conversion of water to steam is accompanied by increase in volume, *work is done by the system on the surroundings*. Hence, w is *negative*, by convention. Thus, $w = -3100$ J mol^{-1}.

Calculation of ΔU : According to the First law equation,

$$\Delta U = q + w = 40670 \text{ J} + (-3100 \text{ J}) = 37570 \text{ J mol}^{-1}$$

State Functions, Exact and Inexact Differentials. The state function is a property of a thermodynamic system which has a definite value for a particular state of the system. It is independent of the manner in which the state is reached. The change in the state function accompanying the change in the state of the system depends only on the initial and the final states of the system and not on the path by which the change is brought about. Pressure, temperature, volume and energy are state functions. On the other hand, *work (w) is not a state function* because the work done in a given change of state depends upon the manner in which the change is brought about. For instance, the work in changing the volume of a gas by one cubic metre would be 100, 10 or 1 joule according as the external pressure is 100, 10 or 1 newton per square metre. The work done would be zero if the gas expands in vacuum. Since in the First law equation ($\Delta U = q + w$), ΔU is a definite quantity, hence, if w is not a state function, q also is not a state function. Mathematically, this is expressed by saying that while the differential of energy, *dU, is an exact differential,* the differentials of heat and work, *viz.*, dq and dw, respectively, are *inexact differentials*. Exact differentials can be integrated between the appropriate limits. This cannot be done in the case of inexact differentials, Thus,

$$\int_{U_1}^{U_2} dU = U_2 - U_1$$

But,

$$\int_{q_1}^{q_2} dq \neq q_2 - q_1 \quad \text{and} \quad \int_{w_1}^{w_2} dw \neq w_2 - w_1$$

Euler Reciprocal Relation. Let z be a state function of two independent variables x and y of the system, *i.e.*, $z = f(x, y)$. Since z is a state function, hence differential of z is *an exact differential* and can be written as

$$dz = (\partial z/\partial x)_y \, dx + (\partial z/\partial y)_x \, dy \qquad \ldots(3)$$

$$= M(x, y)\, dx + N(x, y)\, dy \qquad \ldots(4)$$

where $M(x, y) = (\partial z/\partial x)_y$ and $N(x, y) = (\partial z/\partial y)_x$.

Taking mixed second derivatives, we have

$$(\partial M/\partial y)_x = \partial^2 z/dydx \quad \text{and} \quad (\partial N/\partial x)_y = \partial^2 z/\partial x \partial y$$

Since $\partial^2 z/\partial y \partial x = \partial^2 z/\partial x \partial y$,

Hence, $(\partial M/\partial y)_x = (\partial N/\partial x)_y \qquad \ldots(5)$

Eq. 5 is called the **Euler reciprocal** (or **reciprocity**) **relation.** This is applicable to state functions only.

Since z is a state function, the finite change, Δz, as the system passes from initial state A to final state B, is given by $\Delta z = z_B - z_A$.

Also, $\oint dz = 0$ where cyclic integral $\oint$ means that the system is in the same state at the end of its path as it was at the beginning, *i.e.*, it has traversed a closed path. Thus, dz is an exact differential.

Example 2. Verify whether $dz = (5lx^2y + 47y^4)\, dx + (17x^3 + 188xy^3)\, dy$ is an exact differential or not.

Solution : Here $M(x, y) = 5lx^2y + 47y^4$ and $N(x, y) = 17x^3 + 188xy^3$

Hence, $(\partial M/\partial y)_x = 5lx^2 + 188y^3$ and $(\partial N/\partial x)_y = 51x^2 + 188y^3$

Thus, $(\partial M/\partial y)_x = (\partial N/\partial x)_y$

Hence, dz **is an exact differential.**

Example 3. Writing V as a function of T and P, show that for an ideal gas, dV is an exact differential.

Solution : $V = f(T, P)$

$$\therefore \quad dV = (\partial V/\partial T)_P \, dT + (\partial V/\partial P)_T \, dP \qquad \ldots(i)$$

For an ideal gas, $PV = RT$ so that $V = RT/P$. Hence,

$$(\partial V/\partial T)_P = R/P \quad \text{and} \quad (\partial V/\partial P)_T = -RT/P^2 \qquad \ldots(ii)$$

Substituting Eq. *(ii)* in Eq. *(i)*, we get

$$dV = (R/P)\, dT - (RT/P^2)\, dP \qquad \ldots(iii)$$

According to the Euler reciprocal relation, dV would be an exact differential if

$$\left[\frac{\partial(R/P)}{\partial P}\right]_T = -\left[\frac{\partial(RT/P^2)}{\partial T}\right]_P$$

or if $-R/P^2 = -R/P^2$ *which is true.*

Example 4. Show that for an ideal gas, the work differential dw is not an exact differential.

Solution : As we know, the work differential is given by

$$dw = PdV \qquad \ldots(i)$$

Since volume V is a state function [$V = f(T, P)$], hence dV is an exact differential.

$$\therefore \quad dV = (\partial V/\partial T)_P \, dT + (\partial V/\partial P)_T \, dP \qquad \ldots(ii)$$

For an ideal gas, $PV = RT$ so that $V = RT/P$. Hence,

$$(\partial V/\partial T)_P = R/P \quad \text{and} \quad (\partial V/\partial P)_T = -RT/P^2 \qquad \ldots(iii)$$

Substituting Eqs. *(ii)* and *(iii)* in Eq. *(i)*, we get

$$dw = PdV = RdT - (RT/P)dP = RdT - VdP \qquad \ldots(iv)$$

Applying the Euler reciprocal relation to Eq. *(iv)*, we have

$$\therefore \quad (\partial R/\partial P)_T = -(\partial V/\partial T)_P \qquad ...(v)$$

Since R is the gas constant, hence $(\partial R/\partial P)_T = 0$

Accordingly, from Eq. *v*, $(\partial V/\partial T)_P = 0$

But this is not true because there is always a change in volume with temperature at **constant pressure**. This leads to the conclusion that ***dw* is not an exact differential.**

The Cyclic Rule. From Eq. 3 we see that if the change occurs at constant z, then $dz=0$ so that

$$0 = (\partial z/\partial x)_y\, dx + (\partial z/\partial y)_x\, dy$$

Hence, $$(\partial x/\partial y)_z = -(\partial z/\partial y)_x/(\partial z/\partial x)_y$$

or $$(\partial z/\partial x)_y\,(\partial x/\partial y)_z\,(\partial y/\partial z)_x = -1 \qquad ...(6)$$

Eq. 6 is called the **cyclic rule.** This is applicable only in the case of state functions.

Example 5. Verify the cyclic rule for one mole of an ideal gas.

Solution : For one mole of an ideal gas, $PV = RT$.

Differentiating this equation, we have

$$PdV + VdP = RdT \qquad ...(i)$$

Again, at constant T, $dT=0$ so that $(\partial P/\partial V)_T = -P/V$ ...(ii)

At constant P, $dP=0$ so that $(\partial V/\partial T)_P = R/P$ ...(iii)

At constant V, $dV=0$ so that $(\partial T/\partial P)_V = V/R$ ...(iv)

Hence, from Eqs. *(ii)*, *(iii)* and *(iv)*,

$$(\partial P/V)_T\,(\partial V/\partial T)_P\,(\partial T/\partial P)_V = -(P/V)\,(R/P)\,(V/R) = -1 \quad \textit{which is the cyclic rule.}$$

Example 6. Using the cyclic rule, show that the thermal coefficients α and β are related as $\alpha = \beta\gamma P$ where γ is the pressure coefficient.

Solution : By definition, $\alpha = \frac{1}{V}\left(\frac{\partial V}{\partial T}\right)_P$; $\beta = -\frac{1}{V}\left(\frac{\partial V}{\partial P}\right)_T$ and $\gamma = \frac{1}{P}\left(\frac{\partial P}{\partial T}\right)_V$

Hence, $$\left(\frac{\partial V}{\partial T}\right)_P = \alpha V\,; \quad \left(\frac{\partial P}{\partial V}\right)_T = -\frac{1}{\beta V} \quad \text{and} \quad \left(\frac{\partial T}{\partial P}\right)_V = \frac{1}{\gamma P} \qquad ...(i)$$

From the cyclic rule, $(\partial V/\partial T)_P\,(\partial T/\partial P)_V\,(\partial P/\partial V)_T = -1$ ...(ii)

Substituting Eq. *(i)* in Eq. *(ii)*, we have

$$(\alpha V)\,(1/\gamma P)(-1/\beta V) = -1 \qquad ...(iii)$$

or $$\alpha/\beta\gamma P = 1$$

or $$\alpha = \beta\gamma P$$

Example 7. Show that for a gaseous substance, $(\partial P/\partial T)_V = \alpha/\beta$.

Solution : From the cyclic rule, *viz.*, $(\partial P/\partial T)_V\,(\partial T/\partial V)_P\,(\partial V/\partial P)_T = -1$, we have

$$(\partial P/\partial T)_V = -\frac{1}{(\partial T/\partial V)_P(\partial V/\partial P)_T} = -\frac{(\partial V/\partial T)_P}{(\partial V/\partial P)_T}$$

Multiplying the numerator and the denominator on the R.H.S. by $1/V$, we obtain

$$\left(\frac{\partial P}{\partial T}\right)_V = -\frac{(1/V)(\partial V/\partial T)_P}{(1/V)(\partial V/\partial P)_T} = \frac{\alpha}{\beta}$$

Example 8. Show that for a van der Waals gas, $(\alpha/\beta) = R/(V - b)$.

Solution : We have shown above that $\alpha/\beta = (\partial P/\partial T)_V$

For a van der Waals gas, $(P + a/V^2)(V - b) = RT$

or $$P = \frac{RT}{V - b} - \frac{\alpha}{V^2}$$

$$\therefore \quad \left(\frac{\partial P}{\partial T}\right)_V = \frac{R}{V - b} = \frac{\alpha}{\beta}$$

Example 9. Show that $(\partial\alpha/\partial P)_T = -(\partial\beta/\partial T)_P$.

Solution : Let $$V = f(T, P)$$

$$\therefore \quad dV = (\partial V/\partial T)\,dT + (\partial V/\partial P)_T\,dP \qquad ...(i)$$

Since, by definition, $\alpha = \frac{1}{V}\left(\frac{\partial V}{\partial T}\right)_P$, hence $\left(\frac{\partial V}{\partial T}\right)_P = \alpha V$ ...(ii)

Also, since $\beta = -\frac{1}{V}\left(\frac{\partial V}{\partial P}\right)_T$, hence $\left(\frac{\partial V}{\partial P}\right)_T = -\beta V$ ...(iii)

Substituting Eqs. *(ii)* and *(iii)* in Eq. *(i)*, we have

$$dV = \alpha V dT - \beta V dP \quad \text{or} \quad dV/V = \alpha\, dT - \beta\, dP$$

or $$d \ln V = \alpha\, dT - \beta\, dP$$

Since V and hence $\ln V$ is a state function, therefore, using the Euler reciprocal relation, we get

$$(\partial\alpha/\partial P)_T = -(\partial\beta/\partial T)_P$$

Enthalpy

Suppose the change of state of a system is brought about *at constant pressure.* In that case, there will be change of volume. Let the volume increase from V_A to V_B, at constant pressure P. Then, the work done (w) by the system will be given by

$$w = -P(V_B - V_A) \qquad ...(7)$$

Substituting in Eq. 2, we have

$$\Delta U = q - P(V_B - V_A) \quad \text{or} \quad U_B - U_A = q - P(V_B - V_A)$$

or $$(U_B + PV_B) - (U_A + PV_A) = q \qquad ...(8)$$

The quantity $U+PV$ is known as the **enthalpy** of the system and is denoted by H. It represents the **total energy** stored in the system. Thus,

$$H = U + PV \qquad ...(9)$$

Since, U is a definite quantity and P and V are also definite quantities which define the state of a system, hence H is also a definite quantity depending upon the state of the system.

From Eqs. 9 and 8, we have

$$H_B - H_A = \Delta H = q \qquad ...(10)$$

Since H_B and H_A are definite quantities, it is evident that ΔH, like ΔU, is a definite quantity depending only on the initial and final states of a system. Obviously, ΔH represents increase in the enthalpy of a system when it changes from state A to state B.

Since ΔH is a definite quantity, the heat absorbed (q) under the conditions of the experiment, *i.e.*, at constant pressure, is also a definite quantity.

Further, it follows from Eq. 8 that

$$(U_B - U_A) + P(V_B - V_A) = q$$

Incorporating the above value of q in Eq. 10. we have

$$\Delta H = (U_B - U_A) + P(V_B - V_A) \quad \text{or} \quad \Delta H = \Delta U + P\Delta V \qquad ...(11)$$

where ΔV is the *increase* in volume undergone by the system.

Enthalpy of Vaporisation. When a liquid evaporates, it *absorbs* some heat from the surroundings. Thus, evaporation of a liquid is accompanied by *increase* in enthalpy. The increase for the evaporation of one mole of water at 25°C is 40·70 kJ. We may express this result in the form of a

thermochemical equation :

$$H_2O(l) \longrightarrow H_2O(g) ; \qquad \Delta H_{vap} = +40{\cdot}70 \text{ kJ mol}^{-1}$$

When vapours condense to liquid state, they *give out* (*evolve*) heat. Thus, condensation of vapours is accompanied by *decrease* in enthalpy. The value for the condensation of one mole of water vapour at 25°C is also 40·70 kJ. Therefore; we may write

$$H_2O(g) \longrightarrow H_2O(l) ; \qquad \Delta H = -40{\cdot}70 \text{ kJ mol}^{-1}$$

The change in enthalpy (ΔH) when a liquid changes into vapour state or when vapours change into liquid state, is known as **enthalpy of vaporisation.** This has a positive sign in the former case and a negative sign in the latter case.

Enthalpy of Fusion. When a solid melts and changes into liquid state, it *absorbs* heat. On the contrary, when a liquid freezes and changes into solid state, it *gives out* heat. In the first case, enthalpy of the system *increases*. In the latter case, the enthalpy of the system *decreases*. The change in enthalpy for this type of phase-transformation is known as **enthalpy of fusion.**

The enthalpy of fusion for 1 mole of water at 0°C is 6·02 kJ. We may express this result in the following way :

$$H_2O(s) \longrightarrow H_2O(l) ; \qquad \Delta H_{fus} = +6{\cdot}02 \text{ kJ mol}^{-1}$$
$$H_2O(l) \longrightarrow H_2O(s) ; \qquad \Delta H = -6{\cdot}02 \text{ kJ mol}^{-1}$$

Heat Capacity

Heat capacity of a system, between any two temperatures, is defined as the quantity of heat (q) required to raise the temperature of the system from the lower to the higher temperature divided by the temperature difference.

If the mass of the system is one gram, the heat capacity is called the **specific heat** of the system. If, however, the mass of the system is one mole, as is generally the case in physical chemistry, then the heat capacity is termed as **molar heat capacity**. It is usually denoted by C. Thus, the molar heat capacity of a system between temperatures T_1 and T_2 will be expressed as

$$C = q/(T_2 - T_1) \qquad ...(12)$$

Since the heat capacity varies with temperature, hence the true molar heat capacity is defined by the differential equation

$$C = dq/dT \qquad ...(13)$$

The molar heat capacity of a gaseous system, determined at constant volume, is different from that determined at constant pressure. In the former case, no external work is done *by* the system or *on* the system (*i.e.*, $w=0$) since there is no change in volume. Hence, from the First law equation (Eq. 2),

$$q = \Delta U$$
$$C_V = (q/T_2 - T_1)_V = \Delta U/(T_2 - T_1)_V$$

or
$$C_V = (\partial U/\partial T)_V \qquad ...(14)$$

At constant pressure, however, there is change of volume and some work is done. Suppose, the volume *increases* by ΔV and the work done is w. Then, from the First law equation (Eq. 2),

$$q = \Delta U - w \quad \text{and} \quad C_P = \left(\frac{q}{T_2 - T_1}\right)_P \qquad ...(15)$$

Increase in volume means that the work is done *by the system* on the surroundings so that w, by convention, is *negative*. Hence, $w = -P\Delta V$.

$$\therefore \quad q = \Delta U - (-P\Delta V) = \Delta U + P\Delta V \qquad ...(16)$$

$$C_P = \left(\frac{\Delta U + P\Delta V}{T_2 - T_1}\right)_P = \left(\frac{\Delta H}{T_2 - T_1}\right)_P \qquad ...(17)$$

or
$$C_P = (\partial H/\partial T)_P \qquad ...(18)$$

Thus, while the molar heat capacity of a gaseous system of mass one mole at constant volume is defined as the increase in internal energy of the system per degree rise of temperature, that at constant pressure is defined as the increase in enthalpy of the system per degree rise of temperature.

Relation between C_P and C_V in Gaseous Systems. When a gas is heated at constant volume, no external work is done by the gas. In other words, all the heat supplied to the gas is used in increasing its internal energy. Thus, if the temperature of one mole of gas is raised through 1°C (say from T to $T+1$), the increase in its internal energy itself gives the molar heat capacity at constant volume. However, when a gas is heated *at constant pressure*, there will be increase in its volume, that is, the gas will expand and do some external work. Therefore, some extra heat (in addition to the heat required by it to increase the internal energy of its molecules) must be supplied to the gas to enable it to perform this external work. Hence, the molar heat capacity of a gas at constant pressure must be greater than that at constant volume, *i.e.*, $C_P > C_V$. Thus, $C_P - C_V$ = work done by one mole of the gas in expansion when heated through 1°C at constant pressure.

As we know, the work done by the gas in expansion at constant pressure is numerically given by $w = P\Delta V$.

For one mole of an ideal gas, $PV = RT$ ...(19)

When the temperature is raised by 1°C from T to $T+1$ so that the volume is $V+\Delta V$, then

$$P(V+\Delta V) = R(T+1) \qquad ...(20)$$

Subtracting Eq. 19 from Eq. 20, we have

$$P\Delta V = R \qquad ...(21)$$

Thus, the work done by one mole of an ideal gas in expansion at constant pressure when heated through 1°C is equal to R. Hence,

$$C_P - C_V = R \qquad ...(22)$$

Thus, the difference between the molar heat capacity of a gas at constant pressure (C_P) and at constant volume (C_V) is equal to the gas constant R.

EXPANSION OF AN IDEAL GAS AND CHANGES IN THERMODYNAMIC PROPERTIES

With the help of the First law of thermodynamics it is possible to calculate changes in thermodynamic properties such as q, w, ΔU and ΔH when an ideal gas undergoes expansion. The expansion may be isothermal or adiabatic and the process of expansion may be carried out reversibly or irreversibly.

A. Isothermal Expansion

Calculation of ΔU. In an isothermal process, the temperature of the system remains constant throughout the process of expansion. Since for an ideal gas, the internal energy U depends only on temperature, it follows that at constant temperature (isothermal process), the internal energy of the gas remains constant. This means that $\Delta U = 0$.

Calculation of ΔH. According to Eq. 9.

$$H = U + PV$$
$$\therefore \quad \Delta H = \Delta(U + PV) = \Delta U + \Delta PV = \Delta U + \Delta nRT \qquad ...(23)$$

Since for an isothermal process, ΔT as well as ΔU are equal to zero, hence, $\Delta H=0$.

Calculation of q and w. According to the First law of thermodynamics, $\Delta U=q+w$. Since, for an isothermal process, $\Delta U = 0$, hence $-w = q$. This shows that in an isothermal expansion, the work is done at the expense of the heat absorbed. The magnitude of w (or q) depends upon the manner in which the process of expansion is carried out, *i.e.*, whether it is carried out *reversibly* or *irreversibly*.

Work done in Reversible Isothermal Expansion. Consider a gas enclosed in a cylinder fitted with a 'weightless' and frictionless piston, as shown earlier in Fig. 1. The cylinder is not insulated. It is supposed to be in thermal equilibrium with the surroundings so that the temperature of the gas remains constant all along. The external pressure P on the piston is equal to the pressure of the gas within the cylinder, as shown earlier in (Fig. 1*a*). If the external pressure is lowered by an infinitesimal amount dP, *i.e.*, it falls from P to $P-dP$ (Fig. 1*b*), the gas will expand by an infinitesimal volume dV, *i.e.*, the volume changes from V to $V+dV$. As a result of expansion, the pressure of the gas within the cylinder falls to $P-dP$, *i.e.*, it becomes again equal to the external pressure. The piston then comes to rest.

If the external pressure is lowered again second time by the same infinitesimal amount dP, the gas will undergo the second infinitesimal expansion dV before the pressure again equals the new external pressure. The piston again comes to rest. The process is continued such that the external pressure is lowered by successive small amounts and, as a result, the gas undergoes a series of small successive increments of volume dV at a time.

It may be noted that since the system is in thermal equilibrium with the surroundings, the infinitesimally small cooling produced as a result of infinitesimally small expansion of the gas at each step, is offset by the heat absorbed from the surroundings and the temperature remains constant throughout the operation.

Since during expansion, pressure decreases and volume increases, these two parameters are assigned *opposite signs*. The work done by the gas in an infinitesimal expansion is thus given by

$$dw = -(P - dP)dV = -PdV \qquad ...(24)$$

ignoring the product $dPdV$, as both the quantities are infinitesimal.

The total work w done *by the gas* in expansion, say, from original volume V_1 to final value V_2, will be the sum of the series of the terms *PdV in which the pressure keeps on decreasing gradually*. The result may be expressed mathematically as

$$w = -\int_{V_1}^{V_2} PdV \qquad ...(25)$$

where V_1 is the volume of the gas in the initial state *and* V_2 in the final state.

The above integral can be evaluated by substituting $P=RT/V$ for one mole of an ideal gas. Thus,

$$w = -RT\int_{V_1}^{V_2}\frac{dV}{V} = -RT\ln\frac{V_2}{V_1} \qquad ...(26)$$

Since in an ideal gas, $P_1V_1=P_2V_2$, at constant temperature, the above equation may also be written as

$$w = -RT\ln(P_1/P_2) \qquad ...(27)$$

For n moles, the above expressions may be written as

$$w = -nRT\ln(V_2/V_1) = -nRT\ln(P_1/P_2) \qquad ...(28)$$

Since during expansion, V_2 is more than V_1 and P_2 is less than P_1, hence, from Eq. 28, the work w comes out to be *negative* in conformity with the convention used in this regard.

Work done in Reversible Isothermal Compression. Now suppose the gas undergoes isothermal reversible compression from volume V_2 to V_1. The external pressure will now be made infinitesimally higher than P, the pressure of the gas inside the cylinder. Let the external pressure be $P+dP$. There will be an infinitesimal contraction in volume, say dV, of the gas. Since during compression of a gas, the *pressure increases* and the *volume decreases*, hence these two parameters are assigned *opposite*

signs as before. Thus, the work done by the surroundings on the system for this infinitesimal step is given by

$$dw = -(P + dP)dV = -PdV \qquad ...(29)$$

ignoring the quantity $dPdV$, as before.

If compression is carried out reversibly in a series of steps from the initial volume V_2 to final volume V_1, the work done (w') by the surroundings on the gas will be given by

$$w' = -\int_{V_2}^{V_1} PdV \qquad ...(30)$$

Assuming the gas to be ideal, P, as before, may be substituted by RT/V in the above equation so that

$$w' = -RT\int_{V_2}^{V_1}\frac{dV}{V} = -RT\ln(V_1/V_2) \qquad ...(31)$$

$$= -RT\ln(P_2/P_1) \qquad ...(32)$$

For n moles of the gas, the above expressions may be written as

$$w' = -nRT\ln(V_1/V_2) = -nRT\ln(P_2/P_1) \qquad ...(33)$$

Since during compression, the initial volume V_2 is more than the final volume V_1 and also since the initial pressure P_2 is less than the final pressure P_1, hence, according to Eq. 33, the work done w' comes out to be *positive*, as was chosen as a convention in this regard.

Maximum Work. As discussed above, the work done by a gas during expansion is given by the product $P^{ext}\Delta V$ where ΔV is the increase in volume. If the external pressure P^{ext} is only infinitesimally smaller than the pressure P of the gas (Fig. 1*b*) then, expansion is said to take place *reversibly*. If, however, the external pressure is much smaller than the gas pressure (Fig. 1*c*), the expansion will take place rapidly, *i.e.*, *irreversibly* and the work done *for the same amount of expansion* will be much smaller since P^{ext} is now much smaller than before. Taking an extreme case, if the external pressure is zero (*i.e.*, the gas expands in vacuum), the work done will be zero. Hence, it follows that when a gas expands *freely*, *i.e.*, *when it expands against vacuum* such that $P^{ext}=0$, *no work is done by the gas*.

It is evident from the above discussion that the magnitude of work done by a system on expansion depends upon the magnitude of the opposing (external) pressure. The closer is the opposing pressure to the pressure of the gaseous system in the cylinder, the greater is the work performed by the system on expansion. In other words, maximum work is obtained when the two opposing pressures differ only by an infinitesimal amount from each other. This condition, evidently, is demanded for a thermodynamically reversible process, as discussed earlier. Hence, the condition for maximum work coincides with that for thermodynamic reversibility.

Work done in Irreversible Isothermal Expansion. We come across two types of irreversible isothermal expressions, *viz.*, expansion against zero pressure, *i.e.*, in vacuum (called *free expansion*) and expansion against a particular constant external pressure whose magnitude is less than the pressure of the gas, *i.e.*, $P^{ext} < P$ (called *intermediate expansion*).

Free Expansion. Since in free expansion, the external pressure is zero, therefore,

$$w = -\int dw = -\int P^{ext}dV = 0 \qquad ...(34)$$

Intermediate Expansion. Suppose the volume of the gas increases from V_1 to V_2 against a constant external pressure, P^{ext}. The work done is then given by

$$w = -\int_{V_1}^{V_2} P^{ext}dV = -P^{ext}(V_2 - V_1) \qquad ...(35)$$

Since P^{ext} is less than P, the work done during intermediate isothermal expansion is numerically less than the work done during reversible isothermal expansion in which P^{ext} is almost equal to P.

B. Adiabatic Expansion

In adiabatic expansion, by definition, no heat is allowed to enter or leave the system. Hence, $q=0$. Thus, according to Eq. 2,

$$\Delta U = 0 + w \quad \text{or} \quad w = \Delta U \qquad ...(36)$$

In expansion, work is done *by the system* on the surroundings, hence w is negative. Accordingly, ΔU is *negative, i.e.*, there is decrease in the internal energy of the system and consequently, *the temperature of the system falls*. Evidently, the work in this case is done at the expense of the internal energy of the gas.

If there is compression, w will be positive and hence ΔU would be positive, *i.e.*, there would be increase in internal energy and consequently an increase in temperature. Evidently, in this case work is done by the surroundings on the system and this work is stored in the system in the form of an increase in internal energy.

Calculation of ΔU. As discussed earlier, the molar heat capacity at constant volume of an ideal gas is given by

$$C_V = (\partial U/\partial T)_V \qquad ...(37)$$

Accordingly, $dU = C_V\,dT$ and, for a finite change,

$$\Delta U = C_V \Delta T \qquad ...(38)$$

Calculation of ΔH. According to Eq. 9,

$$H = U + PV$$

$$\therefore \quad \Delta H = \Delta U + \Delta(PV) = \Delta U + R\Delta T \text{ for one mole of the gas,}$$

Substituting the value of ΔU from Eq. 38, we get

$$\Delta H = C_V \Delta T + R\Delta T = (C_V + R)\Delta T \qquad ...(39)$$

$$= C_P \Delta T \qquad ...(40)$$

Calculation of w. Since in an adiabatic process, $q=0$, hence according to the First law equation, $\Delta U = q + w$, the work done in this case is given by the expression

$$w = \Delta U = C_V \Delta T \qquad ...(41)$$

It is evident from the above equations that the magnitude of ΔU, ΔH and w would depend upon the magnitude of ΔT. Since the final temperature and hence the value of ΔT varies with the nature of the process, whether reversible or irreversible, the magnitude of the thermodynamic properties would also vary with the nature of the process.

Final Temperatures in Reversible and Irreversible Adiabatic Expansions

Reversible Adiabatic Expansion. The final temperature in a reversible adiabatic expansion can be calculated from the expressions which relate the initial and final temperatures to the respective volumes or pressures.

Relation between Temperature and Volume. Let P be the external pressure against which expansion is taking place and ΔV be the increase in volume. Then, the external work done *by the system* is equal to $-P\Delta V$. Hence, according to the First law equation,

$$\Delta U = -P\Delta V \qquad ...(42)$$

If ΔT is the fall in temperature, then, since $\Delta U = C_V \Delta T$

$$C_V \Delta T = -PdV \qquad ...(43)$$

For infinitesimally small quantities, as in reversible expansion,

$$C_V dT = -PdV = -RT\,dV/V \qquad \text{(for 1 mole of the gas)}$$

or $$C_V dT/T = -R\,dV/V$$

or $$C_V d(\ln T) = -R\,d(\ln V) \qquad ...(44)$$

Integrating Eq. 44 between temperatures T_1 and T_2 when the corresponding volumes are V_1 and V_2, we have

$$C_V \ln (T_2/T_1) = -R \ln (V_2/V_1) = R \ln (V_1/V_2)$$

or $$\ln (T_2/T_1) = (R/C_V) \ln (V_1/V_2) \qquad ...(45)$$

Knowing that $C_P - C_V = R$ and putting $C_P/C_V = \gamma$, we get

$$\ln (T_2/T_1) = (\gamma - 1) \ln (V_1/V_2) = \ln (V_1/V_2)^{\gamma - 1}$$

$$\therefore \quad T_2/T_1 = (V_1/V_2)^{\gamma-1}$$

or $$T_1/T_2 = (V_2/V_1)^{\gamma-1} \quad \text{(Note that } \gamma > 1) \qquad ...(46)$$

Thus, since $V_2 > V_1$, $T_2 < T_1$. Hence, a gas cools during reversible adiabatic expansion.

Relation between Temperature and Pressure. Since $P_1V_1 = RT_1$ and $P_2V_2 = RT_2$, it follows from Eq. 46 that

$$P_1V_1^{\gamma} = P_2V_2^{\gamma} \qquad ...(47)$$

and $$(T_1/T_2)^{\gamma} = (P_2/P_1)^{1-\gamma} \qquad ...(48)$$

Thus, knowing γ, V_1, V_2 (or P_1, P_2) and the initial temperature T_1, the final temperature T_2 can be readily evaluated with the help of Eq. 46 or 48.

Irreversible Adiabatic Expansion. In this category, we shall consider two cases, *viz.*, the free expansion and the intermediate expansion.

Free Expansion. Since in a free expansion, the external pressure is zero, the work done w is also zero. Accordingly, ΔU which is equal to w, is also zero. Since in an ideal gas, the internal energy is a function of temperature, therefore, if ΔU is zero, ΔT is also zero. It follows, therefore, that ΔH, which is equal to $\Delta U + nR\Delta T$, is also zero. Thus, in a free adiabatic expansion $\Delta T=0$; $w=0$ and $\Delta H=0$.

Intermediate Expansion. Suppose the volume of the gas increases from V_1 to V_2 against a constant pressure P^{Ext} of the gas. The work done in this case would be given by

$$w = -P^{Ext}(V_2 - V_1) \qquad ...(49)$$

Further, from the First law equation (*viz.*, $\Delta U = q + w$), in adiabatic expansion,

$$w = \Delta U = C_V (T_2 - T_1) \qquad ...(50)$$

From Eqs. 49 and 50,

$$P^{Ext}(V_2 - V_1) = -C_V (T_2 - T_1)$$

or $$C_V(T_2 - T_1) = P^{Ext}(V_1 - V_2) = P^{Ext}(RT_1/P_1 - RT_2/P_2)$$

$$= R P^{Ext}(T_1P_2 - T_2P_1)/P_1P_2 \qquad ...(51)$$

Thus, knowing C_V, T_1, P_1, P_2 and P^{Ext}, we can readily calculate T_2, the final temperature of the gas.

Example 10. One mole of an ideal gas expands against a constant external pressure of 1 atm from a volume of 10 dm^3 to a volume of 30 dm^3. Calculate the work done by the gas in joules.

Solution : From Eq. 25, $w = -\int_{V_1}^{V_2} PdV = -P(V_2 - V_1) = -(1 \text{ atm})(30 \text{ dm}^3 - 10 \text{ dm}^3) = -20 \text{ dm}^3 \text{ atm}$

We have to get the result in joules. Recall that

$$R = 8{\cdot}314 \text{ J K}^{-1} \text{ mol}^{-1} = 0{\cdot}08206 \text{ dm}^3 \text{ atm K}^{-1} \text{ mol}^{-1}$$

$$\therefore \quad 1 \text{ atm} = \frac{8{\cdot}314 \text{ J K}^{-1} \text{ mol}^{-1}}{0{\cdot}08206 \text{ dm}^3 \text{ K}^{-1} \text{ mol}^{-1}}$$

$$\therefore \quad w = -20 \text{ dm}^3 \text{ atm} = -20 \text{ dm}^3 \times \frac{8{\cdot}314 \text{ J K}^{-1} \text{ mol}^{-1}}{0{\cdot}08206 \text{ dm}^3 \text{ K}^{-1} \text{ mol}^{-1}} = -2026 \text{ J}$$

Example 11. A gas expands isothermally against a constant external pressure of 1 atm from a volume of 10 dm^3 to a volume of 20 dm^3. In this process it absorbs 800 J of thermal energy from its surroundings. Calculate ΔU for the process in joules.

Solution : From Eq. 25, $w = -\int_{V_1}^{V_2} P dV = -P(V_2 - V_1) = -$ (1 atm)(20 dm^3 – 10 dm^3) = – 10 dm^3 atm

$$= -10 \text{ dm}^3 \times \frac{8{\cdot}314 \text{ J K}^{-1} \text{ mol}^{-1}}{0{\cdot}08206 \text{ dm}^3 \text{ K}^{-1} \text{ mol}^{-1}} = \mathbf{-1013 \text{ J}}$$

From the First law of thermodynamics,

$$\Delta U = q + w = 800 \text{ J} + (-1013 \text{ J}) = \mathbf{-213 \text{ J}}$$

Example 12. Six moles of an ideal gas expand isothermally and reversibly from a volume of 1 dm^3 to a volume of 10 dm^3 at 27°C. What is the maximum work done ? Express the result in joules.

Solution : Work done in this case is given by

$$w = -nRT \ln (V_2/V_1) \qquad \text{(Eq. 28)}$$

$$= -(6 \text{ mol})(0{\cdot}08206 \text{ dm}^3 \text{ atm K}^{-1} \text{ mol}^{-1})(300 \text{ K}) \ln (10 \text{ dm}^3/1 \text{ dm}^3)$$

$$= \mathbf{-340{\cdot}17 \text{ dm}^3 \text{ atm}} = -340{\cdot}17 \text{ dm}^3 \frac{8{\cdot}314 \text{ J K}^{-1} \text{ mol}^{-1}}{0{\cdot}08206 \text{ dm}^3 \text{ K}^{-1} \text{ mol}^{-1}} = \mathbf{-34464{\cdot}8 \text{ J}}$$

Example 13. 10 moles of an ideal gas expand isothermally and reversibly from a pressure of 10 atm to 2 atm at 300 K. What is the largest mass which can be lifted through a height of 1 metre in this expansion ?

Solution : Work done in this case is given by

$$w = -nRT \ln (P_1/P_2) \qquad \text{(Eq. 28)}$$

$$= -10 \text{ mol}(8{\cdot}314 \text{ J K}^{-1} \text{ mol}^{-1})(300 \text{ K}) \ln (10 \text{ atm}/2 \text{ atm}) = -40{\cdot}15 \times 10^3 \text{ J}$$

Let M be the mass which can be lifted through a height of 1m.

Work done in lifting the mass $= Mgh = M \times 9{\cdot}81 \text{ m s}^{-2} \times 1 \text{ m}$

$\therefore \quad M \times 9{\cdot}81 \times 1 \text{ m}^2 \text{ s}^{-2} = 40{\cdot}15 \times 10^3 \text{ J} \qquad (\text{J} = \text{kg m}^2 \text{ s}^{-2})$

$\therefore \quad M = 409{\cdot}28 \text{ kg}$

Example 14. A certain volume of dry air at N.T.P. is expanded reversibly to three times its volume (*a*) isothermally (*b*) adiabatically. Calculate the final pressure and temperature in each case, assuming ideal behaviour. (C_P/C_V for air is 1·4).

Solution : Let V_1 be the volume of dry air at N.T.P.

***a.* Isothermal expansion :**

Final Temperature : During isothermal expansion, there is no change of temperature. Hence, final temperature will be the same as the initial temperature.

Final Pressure : Since $P_1V_1 = P_2V_2$

$$\therefore \quad P_2 = P_1V_1/V_2 = 1 \times V_1/3V_1 = \mathbf{0{\cdot}333 \text{ atm}}$$

***b.* Adiabatic expansion :**

Final Temperature : Under adiabatic conditions,

$$T_1/T_2 = [V_2/V_1]^{\gamma-1}$$

$$273/T_2 = [3V_1/V_1]^{1{\cdot}4-1} = (3)^{0{\cdot}4}$$

Taking logs and solving, we get

$$\therefore \quad T_2 = 176 \text{ K} = -97°\text{C}$$

Final Pressure : Under adiabatic conditions,

$$P_1V_1^{\gamma} = P_2V_2^{\gamma} \quad \text{or} \quad P_1/P_2 = [V_2/V_1]^{\gamma}$$

$$1/P_2 = [3V_1/V_1]^{1{\cdot}4} = [3]^{1{\cdot}4}$$

Taking logs and solving, we get

$$\text{or} \quad P_2 = 1/[3]^{1{\cdot}4} = \mathbf{0{\cdot}217 \text{ atm}}$$

Example 15. A given mass of a gas at 0°C is compressed reversibly and adiabatically to a pressure 20 times the initial value. Calculate the final temperature of the gas. γ for the gas = 1·42.

Solution : $[T_1/T_2]^{\gamma} = [P_2/P_1]^{1-\gamma}$

$$(273/T_2)^{1{\cdot}42} = (20P_1/P_1) = (20)^{-0{\cdot}42}$$

Taking logs and solving, we get

$$T_2 = \mathbf{662{\cdot}2 \text{ K} = 389{\cdot}2°\text{C}}$$

Example 16. One mole of an ideal mono-atomic gas at 27°C expands reversibly and adiabatically from a volume of 10 dm^3 to volume of 20 dm^3. Calculate *(i)* q *(ii)* ΔU *(iii)* w and *(iv)* ΔH. Assume that $C_V = 3/2\ R$.

Solution : *(i)* Since the process is adiabatic, $q = 0$.

(ii) **Calculation of ΔU :** From Eq. 45,

$$(C_V/R) \ln (T_2/T_1) = \ln (V_1/V_2)$$

Since $C_V = 3/2R$ (given), hence $C_V/R = 3/2$

$$\therefore \quad (3/2) \ln (T_2/300) = \ln (10 \text{ dm}^3/20 \text{ dm}^3)$$

Hence, $T_2 = 189 \text{ K}$

$$C_V = (\partial U/\partial T)_V \quad \text{or} \quad dU = C_V dT$$

For a finite change involving n moles,

$$\Delta U = nC_V \Delta T = nC_V(T_2 - T_1) = n\ (3/2)R(189 - 300)$$

$$= (1 \text{ mol})(3/2)(8{\cdot}314 \text{ J K}^{-1} \text{ mol}^{-1})(-111 \text{ K}) = \mathbf{-1384 \text{ J}}$$

(iii) **Calculation of w :** Since for an adiabatic process, $q = 0$, hence, $\Delta U = w$

$$\therefore \quad w = \mathbf{-1384 \text{ J}}$$

(iv) **Calculation of ΔH :** Since, $H = U + PV$

$$\therefore \quad \Delta H = \Delta U + \Delta(PV) = \Delta U + (P_2V_2 - P_1V_1)$$

Note that since the temperature in adiabatic process does not remain constant, we cannot put $P_2V_2 = P_1V_1$.

For n moles of an ideal gas,

$$P_2V_2 = nRT_2 \quad \text{and} \quad P_1V_1 = nRT_1$$

$$\therefore \quad P_2V_2 - P_1V_1 = nR(T_2 - T_1) = (1 \text{ mol})(8{\cdot}314 \text{ J K}^{-1} \text{ mol}^{-1})(189 - 300) \text{ K} = \mathbf{-923 \text{ J}}$$

Hence, $\Delta H = \Delta U + (P_2V_2 - P_1V_1) = -1384 \text{ J} - 923 \text{ J} = \mathbf{-2307 \text{ J}}$

Note : We can also calculate ΔH as follows :

Since $C_P = (\partial H/\partial T)_p$ hence, $dH = C_P \Delta T$

$\therefore$ For a finite change involving n moles of the gas,

$$\Delta H = nC_p \Delta T = nC_p\ (T_2 - T_1)$$

Since for an ideal gas, $C_P - C_V = R$

$$\therefore \quad C_P = C_V + R = 3/2R + R = 5/2R$$

Hence, $\Delta H = (1 \text{ mol})(5/2) \times (8{\cdot}314 \text{ J K}^{-1} \text{ mol}^{-1})(189 - 300) \text{ K} = \mathbf{-2307 \text{ J}}$

Example 17. One mole of an ideal gas (mono-atomic) at 27°C expands adiabatically against a constant external pressure of 1 atm from a volume of 10 dm^3 to a volume of 20 dm^3. Calculate *(i)* q *(ii)* w *(iii)* ΔU and *(iv)* ΔH for this process. Also calculate the final temperature of the gas. Assume that $C_V = 3/2R$.

Solution : *(i)* Since the process is adiabatic, $q = 0$

(ii) $w = -P(V_2 - V_1) = -$ (1 atm)(20 – 10) dm^3 = – 10 dm^3 atm = **– 1013 J** (Example 11)

(iii) Since $\Delta U = q + w$ and $q = 0$ hence, $\Delta U = w = \mathbf{-1013 \text{ J}}$

(iv) $C_V = (\partial U/\partial T)_V$ and $C_P = (\partial H/\partial T)_P$; hence, $dU = C_V dT$ and $dH = C_P dT$

For a finite change, $\Delta U = C_V \Delta T$ and $\Delta H = C_P \Delta T$

$$\therefore \quad \frac{\Delta H}{\Delta U} = \frac{C_P}{C_V} = \frac{(C_V + R)}{C_V} = \frac{5/2R}{3/2R} = 5/3$$

$$\therefore \quad \Delta H = 5/3\ \Delta U = 5/3(-1013 \text{ J}) = \mathbf{-1688 \text{ J}}$$

To evaluate the final temperature T_2, we proceed as follows :

$$\Delta U = nC_V \Delta T = nC_V(T_2 - T_1)$$

$$\text{or} \quad -1013 \text{ J} = (1 \text{ mol})(3/2 \times 8{\cdot}314 \text{ J K}^{-1} \text{ mol}^{-1})(T_2 - 300) \text{ K}$$

$$\therefore \quad T_2 = \mathbf{291{\cdot}8 \text{ K}}$$

Example 18. Show that in an isothermal expansion of an ideal gas *(a)* $\Delta U = 0$ and *(b)* $\Delta H = 0$.

Solution : *(a)* We know that for one mole of an ideal gas, $C_V = (\partial U/\partial T)_V$, hence, $dU = C_V dT$

For a finite change, $\Delta U = C_V \Delta T$

For an isothermal process, T is constant so that $\Delta T = 0$. Hence, $\Delta U = 0$.

(b) We know that $\Delta H = \Delta U + \Delta(PV)$

Since for an ideal gas, $PV = RT$

$\therefore \quad \Delta H = \Delta U + \Delta(RT) = \Delta U + R\Delta T = R\Delta T \qquad (\because \Delta U = 0)$

Since T is constant, $\Delta T = 0$. Hence, $\Delta H = 0$.

Example 19. Calculate q, w, ΔU and ΔH for the reversible isothermal expansion of one mole of an ideal gas at 27°C from a volume of 10 dm³ to a volume of 20 dm³.

Solution : $T = 27°C = 27 + 273 = 300$ K

Since the process is isothermal,

$\Delta U = \Delta H = 0$ (Example 18)

$w = -nRT \ln (V_2/V_1)$ (Eq. 31)

$= -$ (1 mol)(8·314 J K^{-1} mol^{-1})(300 K) ln (20 dm³/10 dm³) $= -$ **1729 J**

From the First law, $\Delta U = q + w$

Since $\Delta U = 0$, $q = -w =$ **1729 J**

Example 20. Calculate q, w, ΔU and ΔH for the isothermal expansion of one mole of an ideal gas at 27°C from a volume of 10 dm³ to a volume of 20 dm³, against a constant external pressure of 1 atm.

Solution : Since the process is isothermal, $\Delta U = \Delta H = 0$ (Examples 18 and 19)

But, in this case, $w = P(V_2 - V_1) = -$ (1 atm)(20 dm³ − 10 dm³)

$= -$ **10 dm³ atm** $= -$ **1013 J** (Example 11)

Since $\Delta U = q + w$ and $\Delta U = 0$, hence $q = -w =$ **1013 J**

Example 21. Calculate the final volume of one mole of an ideal gas initially at 0°C and 1 atm pressure if it absorbs 1000 cal of heat during a reversible isothermal expansion.

Solution : The gas is under the conditions of S.T.P. so that $V_1 = 22{\cdot}4$ dm³. V_2 is to be determined.

Since the expansion is reversible and isothermal, $\Delta U = 0$ so that

$q = -w = 1000$ cal $= 1000 \times 4{\cdot}184$ J

Since $w = -nRT \ln (V_2/V_1)$

$\therefore \quad nRT \ln V_2/V_1 = -w = 1000 \times 4{\cdot}184$ J

(1 mol)(8·314 J K^{-1} mol^{-1})(273 K) ln (V_2/22·4 dm³) $= 1000 \times 4{\cdot}1804$ J

$V_2 =$ **121·25 dm³**

Comparison of Isothermal and Adiabatic Expansions

Let us consider isothermal and adiabatic expansions of an ideal gas from initial volume V_i and pressure P_i to a common final volume V_f. If P_{iso} and P_{adia} are the final pressures, then

$P_iV_i = P_{iso}V_f$ for isothermal expansion

and $P_iV_i^\gamma = P_{adia}(V_f)^\gamma$ for adiabatic expansion.

Accordingly, $V_f/V_i = P_i/P_{iso}$ ...(52)

and $V_f/V_i = P_i/P_{adia}$

Since for expansion $V_f > V_i$ and also for all gases $\gamma > 1$, hence

$(V_f/V_i)^\gamma > (V_f/V_i)$ ...(53)

$\therefore \quad P_i/P_{adia} > P_i/P_{iso}$ or $P_{adia} < P_{iso}$ ...(54)

The above conclusion receives support from the argument that since in adiabatic expansion, there is a fall of temperature, hence, according to the Charles law ($P \propto T$ at constant V), there is a corresponding fall of pressure so that $P_{adia} < P_{iso}$.

The two expansions are shown in Fig. 3*a*. Since in a P-V diagram, the work done is given by the area under the PV curve, the work done in isothermal expansion (shown by the area $ABCD$) is greater than the work done in adiabatic expansion (shown by the area $AECD$).

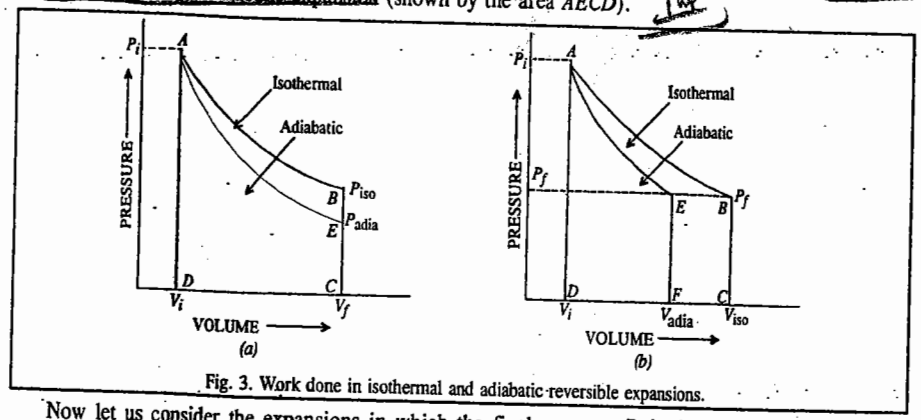

Fig. 3. Work done in isothermal and adiabatic reversible expansions.

Now let us consider the expansions in which the final pressure P_f is the same in both cases. If V_{iso} and V_{adia} are the final volumes in isothermal and adiabatic expansions, respectively, then

$P_iV_i = P_fV_{iso}$ for isothermal expansion

and $P_iV_i^\gamma = P_f(V_{adia})^\gamma$ for adiabatic expansion

Accordingly, $P_i/P_f = V_{iso}/V_i$ and $P_i/P_f = (V_{adia}/V_i)^\gamma$ ...(55)

From Eq. 55, $V_{iso}/V_i = (V_{adia}/V_i)^\gamma$ ...(56)

or $\ln (V_{iso}/V_i) = \gamma \ln (V_{adia}/V_i)$ ...(57)

Since $\gamma > 1$, it follows that

$V_{adia}/V_i < V_{iso}/V_i$ or $V_{adia} < V_{iso}$ ...(58)

This conclusion also receives support from the argument that since in adiabatic expansion, there is a fall of temperature, hence according to the Charles law ($V \propto T$ at constant P), there is a corresponding decrease in volume so that $V_{adia} < V_{iso}$.

The two expansions are shown in Fig. 3*b*. As expected, the work done in isothermal expansion, shown by area $ABCD$ is greater than the work done in adiabatic expansion shown by area $AEFD$.

Reversible Isothermal Expansion of a Real Gas

We shall now derive expressions for w, ΔU, ΔH and q for the reversible isothermal expansion of a real gas obeying the van der Waals equation of state.

Work of expansion, w. As discussed earlier, the work done in the expansion of a gas is given by $-dw = PdV$.

$\therefore \quad -w = \int_{V_1}^{V_2} PdV$ ...(59)

For the van der Waals gas,

$$\left(P + \frac{an^2}{V^2}\right)(V - nb) = nRT \quad \text{so that} \quad P = \frac{nRT}{V - nb} - \frac{an^2}{V^2} \qquad ...(60)$$

Hence,

$$-w = \int_{V_1}^{V_2}\left(\frac{nRT}{V-nb} - \frac{an^2}{V^2}\right)dV = \int_{V_1}^{V_2}\frac{nRT}{V-nb}dV - \int_{V_1}^{V_2}\frac{an^2}{V^2}dV$$

$$= nRT\ln\left(\frac{V_2 - nb}{V_1 - nb}\right) + an^2\left[\frac{1}{V_2} - \frac{1}{V_1}\right] \qquad ...(61)$$

Internal Energy Change, ΔU. For a van der Waals gas, the term $\alpha n^2/V^2$ is the internal pressure of the gas (Eq. 5, Chapter 9). Further, the quantity $(\partial U/\partial V)_T$ is also called the **internal** pressure of the gas. Thus,

$$(\partial U/\partial V)_T = an^2/V^2$$

$$\therefore \quad dU = an^2(dV/V^2) \text{ (at constant temperature)} \qquad ...(62)$$

Integrating between suitable limits,

$$\int dU = U_2 - U_1 = \Delta U = \int_{V_1}^{V_2} an^2 \frac{dV}{V^2} = -an^2\left(\frac{1}{V_2} - \frac{1}{V_1}\right) \qquad ...(63)$$

Enthalpy Change, ΔH. As described earlier, $H = U + PV$.

The enthalpy of the gas in the initial state

$$H_1 = U_1 + P_1V_1 \qquad ...(64)$$

The enthalpy of the gas in the final state

$$H_2 = U_2 + P_2V_2 \qquad ...(65)$$

$\therefore$ The enthalpy change

$$\Delta H = H_2 - H_1 = (U_2 + P_2V_2) - (U_1 + P_1V_1)$$
$$= (U_2 - U_1) + (P_2V_2 - P_1V_1) = \Delta U + (P_2V_2 - P_1V_1) \qquad ...(66)$$

For the van der Waals gas, $P = \dfrac{nRT}{V - nb} - \dfrac{an^2}{V^2}$ ..(67)

Multiplying both sides of this equation by V, we get

$$PV = \frac{nRTV}{V - nb} - \frac{an^2}{V} \qquad ...(68)$$

Substituting the expressions for P_2V_2 and P_1V_1 as obtained from Eq. 68 into Eq. 66, we obtain

$$\Delta H = \Delta U + nRT\left[\frac{V_2}{V_2 - nb} - \frac{V_1}{V_1 - nb}\right] + an^2\left[\frac{1}{V_1} - \frac{1}{V_2}\right] \qquad ...(69)$$

Now,
$$\frac{V_2}{V_2 - nb} - \frac{V_1}{V_1 - nb} = \frac{V_2(V_1 - nb) - V_1(V_2 - nb)}{(V_2 - nb)(V_1 - nb)}$$
$$= \frac{nb(V_1 - V_2)}{(V_2 - nb)(V_1 - nb)} = \frac{nb}{V_2 - nb} - \frac{nb}{V_1 - nb} \qquad ...(70)$$

Substituting Eq. 70 into Eq. 69, we have

$$\Delta H = \Delta U + nRT\left[\frac{nb}{V_2 - nb} - \frac{nb}{V_1 - nb}\right] + an^2\left[\frac{1}{V_1} - \frac{1}{V_2}\right] \qquad ...(71)$$

Substituting for ΔU from Eq. 63, we have

$$\Delta H = n^2bRT\left[\frac{1}{V_2 - nb} - \frac{1}{V_1 - nb}\right] - 2an^2\left[\frac{1}{V_2} - \frac{1}{V_1}\right]$$

Heat Change, q. From the First law we know that $\Delta U = q + w$ or $q = \Delta U - w$.
Substituting the expressions for w and ΔU from Eqs. 61 and 63, we obtain

$$q = nRT \ln\left(\frac{V_2 - nb}{V_1 - nb}\right) \qquad ...(72)$$

Comparison of Work of Expansion of an Ideal Gas and a van der Waals Gas. We know that for an ideal gas,

$$w_{ideal} = nRT \ln (V_2/V_1). \qquad \text{(Eq. 28)}$$

and for a van der Waals gas, from Eq. 61, *numerically*

$$w_{vdw} = nRT \ln\left(\frac{V_2 - nb}{V_1 - nb}\right) + an^2\left[\frac{1}{V_2} - \frac{1}{V_1}\right] \qquad ...(73)$$

If $V \gg nb$, then Eq. 73 reduces to

$$w_{vdw} = nRT \ln\left(\frac{V_2}{V_1}\right) + an^2\left[\frac{1}{V_2} - \frac{1}{V_1}\right] \qquad ...(74)$$

Hence,

$$\therefore \quad w_{ideal} - w_{vdw} = -an^2\left[\frac{1}{V_2} - \frac{1}{V_1}\right] = \frac{an^2(V_2 - V_1)}{V_1V_2} \qquad ...(75)$$

Since for the expansion of a gas, $V_2 > V_1$, it is evident from Eq. 75 that numerically, the work in the reversible isothermal expansion of an ideal gas is greater than that for a van der Waals gas. This result can also be explained physically. An ideal gas has no intermolecular forces whereas a real (van der Waals) gas has considerable intermolecular forces. Thus, in an ideal gas, the heat supplied is fully utilized in doing the work of expansion whereas in a real gas, a part of the heat supplied is used in overcoming the intermolecular forces of attraction between the molecules and the balance amount of heat is utilized in doing the work of expansion. Consequently, the work done in the expansion of an ideal gas is *numerically* greater than the work done in the expansion of a real gas.

Joule-Thomson Effect

If the stream of a gas at high pressure is allowed to expand by passing through a porous plug into vacuum or a region of low pressure, *under adiabatic conditions*, it gets cooled appreciably. Hydrogen and helium are exceptions as they get warmed up under similar circumstances. But, at very low temperatures, these gases also show the usual behaviour. The temperature below which a gas becomes cooler on expansion is known as the **inversion temperature**. Thus, –48°C is the inversion temperature of hydrogen and –242°C is the inversion temperature of helium. The phenomenon of change of temperature produced when a gas is made to expand adiabatically from a region of high pressure to a region of extremely low pressure is known as the **Joule-Thomson effect.** The Joule-Thomson expriment was performed in the 1850s by the two brilliant British physicists J.P. Joule (1818-1889) and William Thomson (1824-1907), later remembered as Lord Kelvin.

The cooling effect is due to decrease in the kinetic energy of the gaseous molecules since a part of this energy is used up in overcoming the van der Waals force of attraction existing between the molecules during expansion. The Joule-Thomson effect is very small when a gas approaches ideal behaviour. It has been concluded, therefore, that the Joule-Thomson effect is zero in an ideal gas. Hence, according to this view, when an ideal gas expands in vacuum, there is neither absorption nor evolution of heat, *i.e.*, q=0. This is quite reasonable since, in an ideal gas, the van der Waals forces are negligible and there is no expenditure of energy in overcoming these forces during expansion.

Further, when an ideal gas expands in vacuum, it does no work because the pressure against which it expands is zero. In other words, w=0. It follows from the general equation of the First law that ΔU=0. Thus, when an ideal gas undergoes expansion under adiabatic conditions in vacuum, no change takes place in its internal energy. In other words, the internal energy of a given quantity of an ideal gas at a constant temperature is independent of its volume, *i.e.*, $(\partial U/\partial V)_T = 0$.

An ideal gas may, therefore, be defined thermodynamically by the following two equations :

(i) PV = constant, at constant temperature

(ii) $(\partial U/\partial V)_T = 0$

The quantity $(\partial U/\partial V)_T$ is called the internal pressure, as already mentioned. Thus, internal pressure of an ideal gas is zero.

Joule-Thomson Coefficient (μ_{JT}). The experimental technique used by Joule and Thomson for deriving the mathematical relation between the fall of pressure of a gas on expansion and the resulting lowering of temperature is illustrated schematically in Fig. 4.

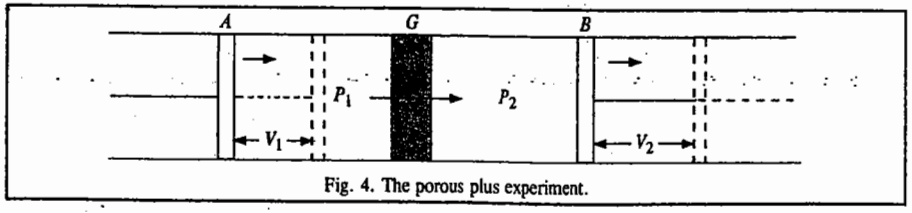

Fig. 4. The porous plus experiment.

A tube made of a non-conducting material is fitted with a porous plug G in the middle and two pistons A and B on the sides, as shown. The tube is thoroughly insulated to ensure adiabatic conditions. A volume V_1 of the gas enclosed between the piston A and the porous plug G at a pressure P_1 is forced *slowly* through the porous plug by moving the piston A inwards and is allowed to expand to a volume V_2 at a lower pressure P_2 by moving the pisten B outward, as shown.

$\therefore$ Work done on the system at the piston $A = + P_1V_1$

Work done by the system at the piston $B = - P_2V_2$

$\therefore$ Net work done by the system $= - P_2V_2 + P_1V_1$

Since the expansion of the gas has taken place adiabatically, the system is not in a position to absorb heat from the surroundings. The system, therefore, performs work at the expense of its internal energy. Consequently, the internal energy of the system changes, say, from U_1 to U_2.

$\therefore \quad - P_2V_2 + P_1V_1 = U_2 - U_1$

or $\quad U_2 + P_2V_2 = U_1 + P_1V_1$

or $\quad H_2 = H_1 \quad \text{or} \quad \Delta H = 0.$

Thus, the Joule-Thomson expansion of a real gas occurs not with constant internal energy but with constant enthalpy. This is, therefore, called an **isenthalpic process.**

Since H is a state function, dH is a complete differential. Taking H as a function of P and T,

$$dH = (\partial H/\partial P)_T\, dP + (\partial H/\partial T)_P\, dT \qquad ...(76)$$

But $\quad (\partial H/\partial T)_P = C_P$

$\therefore \quad dH = (\partial H/\partial P)_T\, dP + C_P\, dT$

Since for adiabatic expansion, $dH=0$, hence $(\partial H/\partial P)_T\, dP + C_P\, dT = 0$

or $$\frac{dT}{dP} = -\frac{(\partial H/\partial P)_T}{C_P} \qquad ...(77)$$

i.e., $$(\partial T/\partial P)_H = -(\partial H/\partial P)_T/C_P \qquad ...(78)$$

The quantity $(\partial T/\partial P)_H$ is called **Joule-Thomson coefficient** and is denoted as μ_{JT}

Assuming μ_{JT} to be constant over a small pressure range, Eq. 78 may be written as

$$\Delta T = -\frac{(\partial H/\partial P)_T}{C_P}\Delta P \qquad ...(79)$$

where ΔT is the fall of temperature produced as a result of the fall of pressure ΔP.

Joule and Thomson verified Eq. 79 experimentally by accurately measuring the fall of temperature (ΔT) accompanying the expansion of a number of real gases. In every case, ΔT was found to be proportional to the difference of pressure ΔP on the two sides of the porous plug, as demanded by Eq. 79.

Joule-Thomson Coefficient in an Ideal Gas. Since $H=U+PV$, Eq.78 may be written as

$$\left(\frac{\partial T}{\partial P}\right)_H = \mu_{JT} = -\frac{1}{C_P}\left(\frac{\partial (U+PV)}{\partial P}\right)_T$$

$$= -\frac{1}{C_P}\left[\left(\frac{\partial U}{\partial P}\right)_T + \left(\frac{\partial (PV)}{\partial P}\right)_T\right]$$

$$= -\frac{1}{C_P}\left[\left(\frac{\partial U}{\partial V}\times\frac{\partial V}{\partial P}\right)_T + \left(\frac{\partial (PV)}{\partial P}\right)_T\right] \qquad ...(80)$$

Since for an ideal gas, $(\partial U/\partial V)_T$ is zero,

$$\therefore \quad (\partial U/\partial V)_T(\partial V/\partial P)_T = 0 \qquad ...(81)$$

Also, since for an ideal gas, PV is constant at constant temperature, $\left(\frac{\partial (PV)}{\partial P}\right)_T = 0$. Hence, Eq. 80 reduces to $\mu_{JT}=0$. The Joule-Thomson coefficient for an ideal gas is thus zero.

Joule-Thomson Coefficient in a Real Gas. For real gases, $(\partial U/\partial V)_T$ is positive. This may be explained as follows.

Suppose a *real* gas expands in vacuum thus doing no external work. However, some work will definitely be done in separating the gas molecules against the forces of cohesion (the van der Waals forces) which exist between the molecules of a *real* gas. This work is stored in the gas in the form of potential energy. In other words, the potential energy of the gas increases. If no heat is gained from outside, the kinetic energy of the gas decreases by an equivalent amount and there would be a fall of temperature of the gas. But, in the present case, temperature is kept constant, evidently, by the absorption of heat from outside. Hence, the kinetic energy remains the same. Thus, during isothermal expansion of a real gas there is net increase in the energy of the gas (in the form of its potential energy). Hence, $(\partial U/\partial V)_T$ is positive. But the factor $(\partial V/\partial P)_T$ in Eq. 80 is negative because the volume of a gas invariably decreases as the pressure increases at constant temperature. Hence, the factor $[(\partial U/\partial V)_T(\partial V/\partial P)_T]$ *is* negative.

The plots of Z *vs* P represented in Fig. 1, Chapter 9, for some of the real gases show that at ordinary temperatures and when the pressure is not very high, the value of PV decreases as the pressure increases (except for H_2 and He), *i.e.*, $(\partial (PV)/\partial P)_T$ is negative, Thus, at ordinary temperatures and at low and moderate pressures, both the terms within the brackets of Eq. 80 are negative. Since the heat capacity is always positive, it follows that the Joule-Thomson coefficient, $(\partial T/\partial P)_H$ is positive for real gases at ordinary temperatures and at low and moderate pressures. Thus, if ΔP is negative, *i.e.*, there is a fall in pressure, then ΔT is also negative, *i.e.*, there is a fall in temperature. In other words, the temperature of a gas falls as a result of its throttled expansion.

Referring again to Fig. 1, it is evident that when the pressures are very high, the value of PV for all gases increases as the pressure increases *i.e.*, $(\partial (PV)/\partial P)_T$ becomes positive. The factor $[(\partial U/\partial V)_T(\partial V/\partial P)_T]$, which is negative as shown above, remains almost constant. Thus, of the two factors within the brackets of Eq. 80, one remains negative and practically constant but the other factor becomes positive and its magnitude increases with increase in pressure. Hence, as the pressure increases, the magnitude of Joule-Thomson coefficient goes on decreasing and becomes zero when the two factors become equal in magnitude. With continued increase in pressure, the magnitude of the positive term exceeds that of the negative term. Joule-Thomson coefficient in that case becomes *negative*. Therefore, if ΔP is negative, *i.e.*, there is fall in pressure, ΔT is positive, *i.e.*, there is increase in temperature. Under such conditions, the throttled expansion of a real gas is accompanied by increase in temperature.

Calculation of the Joule-Thomson Coefficient and the Inversion Temperature. The Joule-Thomson coefficient can be easily calculated with the help of the van der Waals equation. Since, both a and b are small, the term ab/V^2 in the van der Waals equation can be neglected provided the

pressure is not too high. The van der Waals equation may then be written in the form

$$PV = RT - a/V + bP \quad ...(82)$$

Replacing V by RT/P (the approximation used may be noted), we have

$$PV = RT - aP/RT + bP \quad ...(83)$$

or
$$V = RT/P - a/RT + b \quad ...(84)$$

Differentiating with respect to temperature at constant pressure, we get

$$(\partial V/\partial T)_P = R/P + a/RT^2 \quad ...(85)$$

Rearranging Eq. 83, we have

$$RT = P(V - b) + aP/RT \quad ...(86)$$

Dividing both sides by PT,

$$\frac{R}{P} = \frac{V - b}{T} + \frac{a}{RT^2} \quad ...(87)$$

Substituting the value of R/P from Eq. 87 in Eq. 85, we have

$$\left(\frac{\partial V}{\partial T}\right)_P = \frac{V}{T} - \frac{b}{T} + \frac{2a}{RT^2} \quad ...(88)$$

$$\therefore \quad T\left(\frac{\partial V}{\partial T}\right)_P - V = \frac{2a}{RT} - b \quad ...(89)$$

Using the well known thermodynamic relation

$$V = T\left(\frac{\partial V}{\partial T}\right)_P + \left(\frac{\partial H}{\partial P}\right)_P, \quad ...(90)$$

Eq. 89 may be written as

$$-\left(\frac{\partial H}{\partial P}\right)_T = \frac{2a}{RT} - b \quad ...(91)$$

From Eqs. 78 and 91 we have

$$\left(\frac{\partial T}{\partial P}\right)_H = \frac{1}{C_P}\left[\frac{2a}{RT} - b\right] \quad ...(92)$$

It is evident from Eq. 92 that Joule–Thomson coefficient is positive as long as $2a/RT$ is greater than b. It becomes zero if $2a/RT$ is equal to b and negative if $2a/RT$ is less than b. Since a, b and R are constants, it is evident that the magnitude and sign of the Joule–Thomson coefficient depends only upon the temperature at which the gas is allowed to expand.

The temperature at which the Joule–Thomson coefficient changes sign is known as the **inversion temperature**. At this temperature. $\mu_{J.T.}$ is zero so that

$$2a/RT_i = b \quad \text{or} \quad T_i = 2a/Rb \quad ...(93)$$

where T_i represents the inversion temperature. Thus, the inversion temperature depends upon the van der Waals constants a and b of the gas.

Example 22. The van der Waals constants a and b for hydrogen, are $0{\cdot}246\ dm^6\ atm\ mol^{-2}$ and $2{\cdot}67\times10^{-2}\ dm^3\ mol^{-1}$, respectively. Calculate the inversion temperature of hydrogen.

Solution :
$$T_i = 2a/Rb = \frac{2(0{\cdot}246\ dm^6\ atm\ mol^{-2})}{(0{\cdot}08206\ dm^3\ atm\ K^{-1}\ mol^{-1})(0{\cdot}0267\ dm^3\ mol^{-1})}$$
$$= 224{\cdot}72\ K = -48{\cdot}28°C$$

It is amply clear from the above discussion that the sign and magnitude of Joule–Thomson coefficient of a gas depends upon the conditions of temperature and pressure.

Zeroeth Law of Thermodynamics. This law was formulated after the enunciation of the First law of thermodynamics. But, since this law was considered to be of primary importance, it was called zeroeth law. The law states as follows :

If body A is in equilibrium with body C and body B is also in equilibrium with body C, then bodies A and B are in equilibrium with each other.

The common use of thermometer in comparing temperatures of any two or more systems is based on this principle. The thermometer may be likened to the body C in the above statement. While comparing temperatures of two bodies, say, A and B, it is allowed to come into equilibrium first with the body A and then with the body B, by placing it in contact with each other, turn by turn. The temperatures as read from the thermometer give *comparative ideas of degrees of hotness* of the two bodies A and B with which it had been allowed to come to equilibrium, one by one. Since thermometer is only a *very small body*, there is only an insignificant exchange of energy with large bodies B and C. Hence, the energies of bodies B and C remain unchanged during measurement of the temperature.

Temperature measurement by a thermometer rests on determination of some property of a fluid which changes with the degree of hotness. This property in a mercury thermometer involves change in length of the mercury column and in an air thermometer it involves change in volume (V) and pressure (P) of air (or gas) enclosed within.

Consider a fluid system B in a state defined by volume V_B and pressure P_B. Let it be in equilibrium with another fluid system A in a state defined by volume V_A and pressure P_A. The values of V_A and P_A are determined experimentally. There may be several values of V_A and P_A at which there may be an equilibrium with the system B, at constant temperature, say, θ_1. These values may be plotted against each other to get an isotherm, as shown in Fig.5. According to Zeroeth law, this isotherm is independent of the nature of the system B because the same values will be obtained by substituting B by any other system in equilibrium with A at the same temperature. The latter procedure is considered to be more accurate. If the temperature of B, still in equilibrium with A, is changed, say, from θ_1 to θ_2, then another set of values of V_A and P_A at temperature θ_2 will be observed and a new isotherm (Fig. 5.) will be obtained and so on. Three isotherms ($P_A - V_A$ graphs) obtained at three temperatures, θ_1, θ_2 and θ_3 are shown in the figure. Several such isotherms at various other temperatures can also be built. All systems, having the same temperature, will follow the same graph when brought into thermal contact with the body A or even with one another. In this way, the unknown temperature of a system at any time can be obtained by comparing its P–V isotherm determined experimentally with those plotted in Fig. 5.

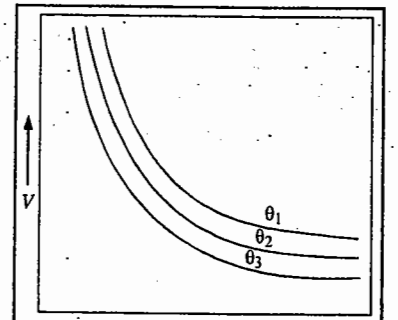

Fig. 5. Isothermals of a fluid obtained at different temperatures.

Absolute Temperature Scale. It may be worthwhile at this stage to define the true zero or natural zero of the temperature scale. Several temperature scales have been known but they are all *arbitrarily* based on freezing and boiling points of water or on some other transition temperatures. But a true scale is based on the observation that $PV - P$ graphs of all real gases when extrapolated

to zero pressure give the same value of PV at a given temperature. This value is denoted by $(PV)_0$, in general and by $(PV_m)_0$, if one mole of a gas is involved.

The values of $(PV_m)_0$ vary linearly with the temperature on the centigrade scale, as shown in Fig. 6. The variation is represented by the equation

$$(PV_m)_0 = a + bt \qquad ...(94)$$

where t is the centigrade temperature measured by a mercury thermometer and a and b are constants. The values of $(PV_m)_0$ at 0°C and 100°C have been found to be 22·4136 and 30·6192 dm^3 atm, respectively.

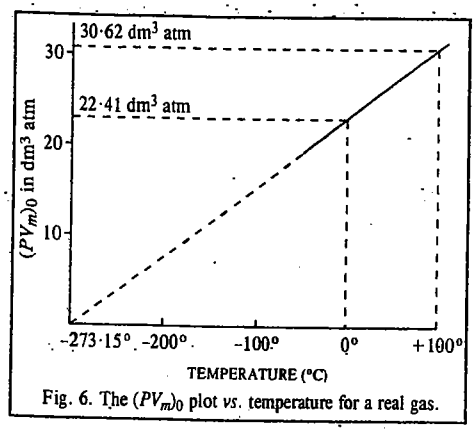

Fig. 6. The $(PV_m)_0$ plot *vs.* temperature for a real gas.

Substituting these values in Eq. 94, we have

$$22{\cdot}4136 \text{ dm}^3 \text{ atm} = a + 0 \qquad ...(95)$$

and $$30{\cdot}6192 \text{ dm}^3 \text{ atm} = a + 100b \qquad ...(96)$$

Hence, $$b = 0{\cdot}082056 \text{ dm}^3 \text{ atm} \qquad ...(97)$$

Substituting the values of a and b in Eq. 94, it is possible to calculate the temperature at which $(PV_m)_0 = 0$. Thus,

$$0 = 22{\cdot}4136 \text{ dm}^3 \text{ atm} + (0{\cdot}082056 \text{ dm}^3 \text{ atm})\, t$$

$$\therefore \quad t = -273{\cdot}15°\text{C}$$

The temperature -273·15° is the **natural** or **true zero**. It is defined *as the temperature at which the limiting value of PV_m, i.e., the product PV_m at pressures approaching zero, is zero itself.* This zero defines an **absolute temperature scale** which is known as the **Kelvin scale**. Thus, -273·15°C = 0 K or 0°C=273·15 K. The temperature t on the absolute scale is denoted by T. Thus, the boiling point of water on this scale is given by $T = 273{\cdot}15+100=373{\cdot}15$ K. We conclude this chapter with the insightful remarks of Schrödinger :

...[temperature] turns out to be a much more fundamental quantity than energy ; so much so, that the physicist is gratified to be given, in every particular case, energy as a function of it, rather than vice versa, which would be quite unnatural.

I. Review Questions

1. Define mathematically the first law of thermodynamics. Comment on the statement "while U is a definite property, q and w are not definite properties".
2. Derive the relation between ΔU and ΔH for an ideal gas.
3. Show that for one mole of an ideal gas $C_p - C_v = R$
4. Derive expressions for the work done in reversible isothermal expansion and reversible isothermal compression of an ideal gas.
5. Distinguish between isothermal and adiabatic processes. Derive the relation between temperature and volume and that between temperature and pressure in reversible adiabatic expansion of an ideal gas.
6. Derive an expression for the Joule-Thomson coefficient of a van der Waals gas.
7. Define the Joule-Thomson coefficient. Show that it is zero for an ideal gas and has a positive value for a real gas.

8. Define Inversion temperature. Show that for a van der Waals gas, the inversion temperature is given by $T_i = 2a/Rb$.
9. State and explain the zeroth law of thermodynamics.

II. Problems

1. In a certain process, 675 J of heat is absorbed by a system while 290 J of work is done on the system. What is the change in internal energy for the process ? **[Ans. 965 J]**
2. In a certain process, 600 J of work is done on a system which gives off 250 J of heat. Calculate the internal energy change for the process. **[Ans. 350 J]**
3. Calculate the internal energy change for the process in which 1·0 kJ of heat is added to 1·2 dm^3 of oxygen gas in a cylinder at a constant pressure of 1·0 atm and the volume changes to 1·5 dm^3. **[Ans. 0·993 kJ]**
4. Calculate ΔU and ΔH when 10·0 dm^3 of helium at N.T.P. is heated in a cylinder to 100°C assuming that the gas behaves ideally. $C_V = 3/2\ R$. **[Ans. 559·8 J ; 933·4 J]**
5. Calculate ΔU and ΔH when 0·42 mole of xenon gas, assumed ideal, is expanded from 27°C, to 127°C, assuming that $C_v = 12{\cdot}47$ J K^{-1} mol^{-1}. **[Ans. 523·7 J ; 873·4 J]**
6. One mole of nitrogen gas contained in a cylinder at 300 K is allowed to expand isothermally against an external pressure of 5 atm from a volume of 1·0 dm^3 to a volume of 3·0 dm^3. Assuming ideality, calculate q, w, ΔU and ΔH. **[Ans. $q=w=1013$ J, $\Delta U=\Delta H=0$]**
7. 3 moles of helium gas at 1 atm are compressed reversibly and isothermally at 400 K to 5 atm pressure. Calculate q, w, ΔU and ΔH. **[Ans. $q=w=1{\cdot}61\times10^4$ J, $\Delta U=\Delta H=0$]**
8. Calculate q, w, ΔU and ΔH for the reversible adiabatic compression of 0·2 mole of an ideal gas from a volume of 1 dm^3 to a volume of 0·25 dm^3. **[Ans. 0, - 98·8 J, 98·8 J ; 138 J]**
9. In a certain process, 6,000 J of heat is added to the system while the system does work equivalent to 9,000 J by expanding against the surrounding atmosphere. Calculate the internal energy change for the system. **[Ans. - 3,000 J]**
10. One mole of benzene is converted reversibly into vapour at the boiling point (80·2°C) by heating it. The vapour undergoes expansion against 1 atm pressure. Assuming that the vapour behaves ideally, calculate ΔH, w and ΔU for the process. The heat of vaporization of benzene is 396 J g^{-1}.

[Ans. ΔH = 30·180 kJ mol^{-1} ; w = 2·936 kJ mol ; ΔU = 2·787 kJ mol^{-1}]

CHAPTER 14

THERMOCHEMISTRY

Chemical reactions are almost invariably accompanied by energy changes which, ordinarily, appear in the form of evolution or absorption of heat. The branch of chemistry which deals with energy changes involved in chemical reactions is called **thermochemistry**. Thermochemistry, in fact, applies the First law of thermodynamics to chemical reactions. The energy change that occurs in a chemical reaction is largely due to change of bond energy, *i.e.*, it results from the breaking of bonds in reactants and formation of new bonds in products.

Change of Internal Energy in a Chemical Reaction. Let us consider a chemical reaction taking place at constant temperature and at constant volume. In such a case, $w=0$ and hence from the equation of the First law (*viz.*, $\Delta U = q + w$),

$$\Delta U = q_V \qquad ...(1)$$

where q_V is the heat exchanged at constant volume.

Suppose U_R is the internal energy of the reactants and U_P that of the products, then,

$$\Delta U = U_P - U_R \qquad ...(2)$$

We may represent this conclusion schematically as below :

Reactants (U_R)

$\downarrow \Delta U = U_P - U_R = q_v$ = Heat of reaction at constant volume

Products (U_P)

Change Enthalpy in a Chemical Reaction. Let q_p be the heat exchanged in the chemical reaction taking place at *constant pressure*. The heat exchanged at constant pressure is termed as the **enthalpy change.** Thus,

$$\Delta H = q_p \qquad ...(3)$$

In general, if H_R is the enthalpy of the reactants and H_P that of the products, then

$$\Delta H = H_P - H_R = q_p \qquad ...(4)$$

This statement is schematically represented as follows :

Reactants (H_R)

$\downarrow \Delta H = H_P - H_R = q_p$ = Enthalpy of reaction

Products (H_P)

Exothermic and Endothermic Reactions. Reactions that give out heat, *i.e.*, which are accompanied by evolution of heat, are called **exothermic reactions.** In such reactions $H_P < H_R$ so that ΔH is negative. On the other hand, reactions that take in heat, *i.e.*, which are accompanied by absorption of heat, are called **endothermic reactions.** In these reactions, $H_P > H_R$ so that ΔH is positive.

The energy level diagram for exothermic and endothermic reactions is shown in Fig. 1.

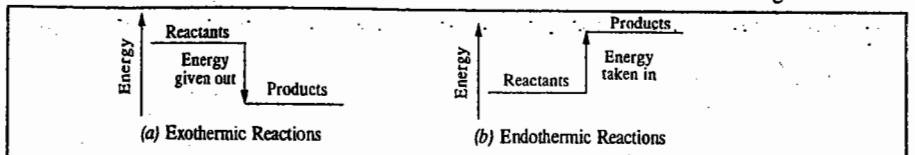

Fig. 1. Energy level diagram for exothermic and endothermic reactions.

Example 1. In an exothermic reaction, how do the strengths of the bonds in the reactants compare with the strengths of the bonds in the products ?

Answer : The bonds in the products are stronger than those in the reactants. The stronger the bonds, the greater is the energy released.

Example 2. In an endothermic reaction, how do the strengths of the bonds in the reactants compare with those of their counterparts in the products ?

Answer : The bonds in the products are weaker than those in the reactants.

Example 3. The two examples of endothermic reactions are the dissolution of $NaHCO_3(s)$ in water and the production of $NH_3(g)$ from the reaction between $Ba(OH)_2(s)$ and $NH_4SCN(s)$. Draw the energy level diagrams for these reactions.

Solution : See Fig. 2.

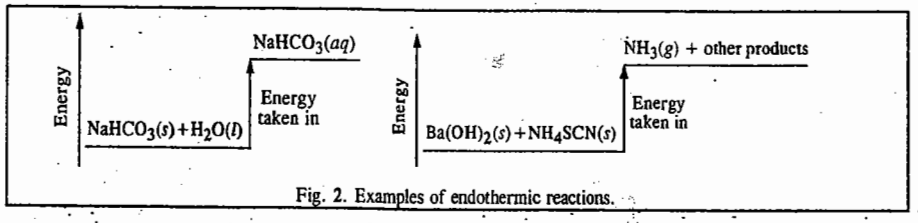

Fig. 2. Examples of endothermic reactions.

Example 4. Draw an energy level diagram for burning of petrol in air.

Solution : See Fig. 3.

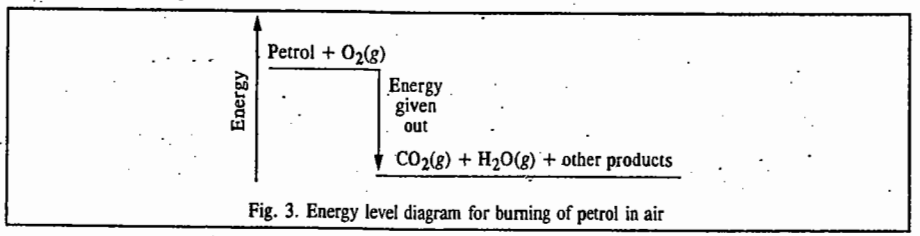

Fig. 3. Energy level diagram for burning of petrol in air

Example 5. A student makes the following comment on an endothermic reaction : *"If the heat is taken in during the reaction, the temperature should go up, not down."* How will you convince him ?

Answer : The reaction being endothermic, the energy taken in is being consumed to break the bonds in reactants so that it does not have a chance to appear as heat and raise the temperature.

Relation between Enthalpy of Reaction at Constant Volume and at Constant Pressure. The quantities ΔH and ΔU are related to each other by the expression

$$\Delta H = \Delta U + P\Delta V \qquad ...(5)$$

where ΔV is the change in volume that takes place in a given reaction.

Since, $q_V = \Delta U$ (vide Eq. 1) and $q_p = \Delta H$ (vide Eq. 3), we may write the above relationship also as

$$q_p = q_V + P\Delta V \qquad ...(6)$$

This relationship can be simplified further as follows :

For n moles of an ideal gas,

$$PV = nRT \qquad ...(7)$$

Let n_1 and n_2 represent the number of moles of *gaseous* reactants and *gaseous* products, respectively. Suppose n_2 is greater than n_1. Then the increase in the number of gaseous moles $= n_2 - n_1 = \Delta n_g$. The corresponding increase in volume (ΔV) will be given by $(V/n)\Delta n_g$. Hence,

$$P\Delta V = P(V/n)\,\Delta n_g = RT \times \Delta n_g \qquad (\because PV = nRT)$$

Thus,
$$P\Delta V = \Delta n_g \times RT \qquad ...(8)$$

Substituting in Eq. 6, we have

$$q_p = q_V + \Delta n_g RT \qquad ...(9)$$

In this equation, Δn_g, is the difference between the number of moles of the gaseous products and the gaseous reactants.

Let us take a few examples. In the reaction involving the dissociation of ammonia into nitrogen and hydrogen,

$$\underset{2\text{ moles}}{2NH_3(g)} \longrightarrow \underset{1\text{ mole}}{N_2(g)} + \underset{3\text{ moles}}{3H_2(g)}$$

$$\Delta n_g = 4 - 2 = 2$$

$$\therefore \quad q_p = q_V + 2RT$$

In the reaction involving combination of hydrogen and oxygen,

$$\underset{2\text{ moles}}{2H_2(g)} + \underset{1\text{ mole}}{O_2(g)} \longrightarrow \underset{2\text{ moles}}{2H_2O(g)}$$

$$\Delta n = 2 - 3 = -1$$

$$\therefore \quad q_p = q_V - RT$$

Example 6. Establish the relationship between q_p and q_v in the Haber synthesis of ammonia, assuming that the gaseous reactants and products are ideal.

Solution : $N_2(g) + 3H_2(g) \longrightarrow 2NH_3(g)$

Here $\Delta n_g = 2 - (1 + 3) = -2$

Hence, $q_p = q_V + \Delta n_g RT = q_v - 2RT$

Example 7. Establish the relationship between q_p and q_v in the synthesis of $H_2O(g)$ from the elements, assuming ideality.

Solution : $2H_2(g) + O_2(g) \longrightarrow 2H_2O(g)$

$$\Delta n_g = 2 - (2 + 1) = -1$$

$$\therefore \quad q_p = q_V + \Delta n_g RT = q_V - RT$$

Example 8. One mole of naphthalene was burnt in oxygen gas at constant volume to give carbon dioxide gas and liquid water at 25°C. The heat evolved was found to be 5138·8 kJ. Calculate the enthalpy of the reaction. $R = 8{\cdot}314\ J\ K^{-1}\ mol^{-1}$.

Solution : The thermochemical equation for the reaction may be written as

$$C_{10}H_8(s) + 12O_2(g) \longrightarrow 10CO_2(g) + 4H_2O(l) \; ; \qquad q_V = -5138{\cdot}8\ kJ$$

The number of moles of *gaseous* reactants, $n_1 = 12$

The number of moles of *gaseous* products, $n_2 = 10$

Hence, $\Delta n_g = n_2 - n_1 = 10 - 12 = -2$

Substituting the various values in Eq. 9, we have

$$q_p = -5138{\cdot}8\ kJ - 2\ mol \times 8{\cdot}314 \times 10^{-3}\ kJ\ K^{-1}\ mol^{-1} \times 298\ K = -5143{\cdot}8\ kJ$$

Standard Enthalpies of Reactions. Enthalpies of reactions determined at 25°C and one atm pressure (101·325 kPa) are denoted by $\Delta H°$ and are known as standard enthalpies of reactions. Examples include the following :

$$\tfrac{1}{2}N_2(g) + \tfrac{3}{2}H_2(g) \longrightarrow NH_3(g) \; ; \qquad \Delta H° = -46{\cdot}0\ kJ\ mol^{-1}$$

$$\tfrac{1}{2}H_2(g) + \tfrac{1}{2}Cl_2(g) \longrightarrow HCl(g) \; ; \qquad \Delta H° = -92{\cdot}3\ kJ\ mol^{-1}$$

$$Zn(s) + Cu^{2+}(aq) \longrightarrow Zn^{2+}(aq) + Cu(s) \; ; \qquad \Delta H° = -210\ kJ\ mol^{-1}$$

$$Mg(s) + \tfrac{1}{2}O_2(g) \longrightarrow MgO(s) \; ; \qquad \Delta H° = -601{\cdot}7\ kJ\ mol^{-1}$$

Standard Enthalpy of Combustion. This is defined as the enthalpy change (ΔH) accompanying complete combustion of one mole of the substance at 25°C and 1 atm pressure. Thus,

Combustion of Methane :

$$CH_4(g) + 2O_2(g) \longrightarrow CO_2(g) + 2H_2O(l) \; ; \qquad \Delta H°_{comb} = -890{\cdot}3\ kJ\ mol^{-1}$$

Combustion of Hydrogen :

$$H_2(g) + \tfrac{1}{2}O_2(g) \longrightarrow H_2O(l) \; ; \qquad \Delta H°_{comb} = -285{\cdot}29\ kJ\ mol^{-1}$$

Standard Enthalpy of Neutralization. Enthalpy of neutralisation of one mole of a base such as NaOH and KOH by an acid such as HCl, H_2SO_4 and HNO_3 in dilute solutions at 25°C and 1 atm pressure is called the standard enthalpy of neutralization of the base by the acid. Thus,

$$NaOH(aq) + HCl(aq) \longrightarrow NaCl\,(aq) + H_2O(l) \; ; \qquad \Delta H = -57{\cdot}3\ kJ\ mol^{-1}$$

$$KOH(aq) + \tfrac{1}{2}H_2SO_4(aq) \longrightarrow KHSO_4\,(aq) + H_2O(l) \; ; \qquad \Delta H = -57{\cdot}4\ kJ\ mol^{-1}$$

Similarly, the enthalpy change accompanying the neutralisation of 1 mole of an acid by a base in dilute solutions at 25°C and 1 atm pressure is known as the standard enthalpy of neutralisation of the acid by the base.

The neutalisation of hydrochloric acid by sodium hydroxide in dilute solutions when the acid, alkali and the salt formed are completely dissociated, may be represented as :

$$H^+ + Cl^- + Na^+ + OH^- \longrightarrow Na^+ + Cl^- + H_2O(l)$$

or
$$H^+ + OH^- \longrightarrow H_2O(l)$$

Considering neutralisation of strong acids by strong bases, it will be seen that in every case, the neutralisation reaction is the same as it simply involves the combination of H^+ ions and OH^- ions to form unionised H_2O. It is expected, therefore, that the enthalpy of neutralization of every strong acid by a strong base and vice versa should be identical. That this is actually so, is evident from the data given in Table 1.

TABLE 1

Standard Enthalpies of Neutralisation of Strong Acids by Strong Bases (kJ mol^{-1})

Acid	Alkali	Enthalpies of neutralisation
HCl	NaOH	−57·32
HNO_3	NaOH	−57·28
HCl	KOH	−57·45
HCl	LiOH	−57·38

If, however, the acid or alkali is weak, the enthalpy of neutralisation is different because the reaction now involves dissociation of the weak acid or the weak alkali as well. The neutralisation of acetic acid by sodium hydroxide, for example, involves the dissociation of the acid as well as the usual neutralisation of H^+ and OH^- ions, as represented below :

$$(i) \quad CH_3COOH\,(aq) \rightleftharpoons CH_3COO^-(aq) + H^+(aq)$$

$$(ii) \quad H^+(aq) + OH^-(aq) \longrightarrow H_2O(l)$$

As H^+ ions are neutralised by OH^- ions furnished by the completely dissociated sodium hydroxide, more H^+ ions are formed by the dissociation of acetic acid to re-establish the equilibrium. Thus, both the reactions proceed side by side till acetic acid is completely neutralised.

The enthalpy of neutralisation of acetic acid by sodium hydroxide has been found to be $-55{\cdot}23$ kJ mol^{-1}. Since the average value for the combination of H^+ and OH^- ions is taken as $-57{\cdot}32$ kJ mol^{-1}, the standard enthalpy of dissociation of acetic acid may be taken as $+ 2{\cdot}09$ kJ mol^{-1}.

The enthalpy of neutralisation of hydrochloric acid by ammonium hydroxide at 25°C is $- 51{\cdot}34$ kJ mol^{-1}. Therefore, the standard enthalpy of dissociation of ammonium hydroxide is taken as $+ 5{\cdot}98$ kJ mol^{-1}.

Standard enthalpies of neutralisation of a few weak acids with sodium hydroxide are given in Table 2. The enthalpies of dissociation obtained from these values are included in the last column.

TABLE 2

Standard Enthalpies of Neutralisation of Weak Acids with Sodium Hydroxide

Acid	Enthalpy of Neutralisation (kJ mol^{-1})	Enthalpy of Dissociation (kJ mol^{-1})
Acetic acid	− 55·23	+ 2·09
Formic acid	− 56·06	+ 1·26
Hydrocyanic acid	− 12·13	+ 45·19
Hydrogen sulphide	− 15·90	+ 41·42

Enthalpy of Solution. It is well known that when a solute is dissolved in a solvent, heat is either absorbed or evolved. Thus dissolution of a solute in a solvent is accompanied by enthalpy change (ΔH) of the system. If the heat is absorbed from the solution, *i.e.*, the solution is cooler, ΔH is given a positive sign. If heat is evolved and given to the solution, *i.e.*, the solution is warmer, ΔH is given a negative sign, as usual.

The amount of heat evolved or absorbed when 1 mole of a solute is dissolved in a sufficient amount of the solvent is called the **enthalpy of solution** of the solute.

The enthalpy change per mole of a solute dissolved varies with the concentration of the solution. It is necessary, therefore, to express the enthalpy change with reference to the concentration of the solution. For this purpose, a term **integral enthalpy of solution** is often used. It is defined as the enthalpy change when one mole of a solute is dissolved in a solvent to give a solution of a specified concentration. If, for example, one mole of potassium chloride is dissolved in 200 moles of water, heat absorbed, *viz.*, 18·58 kJ, is the integral heat of solution of potassium chloride at this concentration. This is expressed by a thermochemical equation as :

$$KCl(s) + 200\ H_2O(l) \longrightarrow KCl\ (200\ H_2O)\ ; \qquad \Delta H = +18{\cdot}58\ kJ$$

Similarly, when one mole of gaseous hydrogen chloride is dissolved in 50 moles of water, heat evolved is 72·2 kJ. Thus, integral enthalpy of solution of gaseous hydrogen chloride per mole when dissolved in 50 moles of water is 72·0 kJ and ΔH has a negative sign. The thermochemical equation is written as :

$$HCl\ (g) + 50\ H_2O\ (l) \longrightarrow HCl\ (50\ H_2O)\ ; \qquad \Delta H = -72{\cdot}0\ kJ$$

The integral enthalpies of solution of a few solutes dissolved in specified moles of water are given in Table 3.

TABLE 3

Integral Enthalpies of Solution in Water at 25°C

Substance	H_2O moles	Enthalpy of Solution kJ mol^{-1}	Substance	H_2O moles	Enthalpy of Solution kJ mol^{-1}
KCl	200	+ 18·6	HCl	200	− 72·9
NaCl	200	+ 5·3	HBr	200	− 83·3
KNO_3	200	+ 35·4	HNO_3	200	− 31·2
Na_2SO_4	400	+ 23·1	NH_3	200	− 35·3
$Na_2SO_4.10H_2O$	390	+ 79·1	$CaCl_2$	400	− 78·6
NH_4NO_3	200	+ 26·5	$CaCl_2.6H_2O$	394	+ 18·8
K_2SO_4	400	+ 27·4	$CuSO_4$	800	− 65·5
KOH	200	− 55·6	$CuSO_4.5H_2O$	795	+11·7

It is evident from the above Table that when gases (*e.g.*, HCl, HBr and NH_3) are dissolved in water, ΔH has a negative value, *i.e.*, the dissolution is accompanied by evolution of heat. The dissolution of hydrated salts (*e.g.*, $Na_2SO_4.10H_2O$, $CuSO_4.5H_2O$) as well as salts which do not form hydrates (*e.g.*, KNO_3, NaCl) is accompanied by increase in the enthalpy of the system (ΔH has a positive value), *i.e.*, the dissolution is accompanied by absorption of heat. However, when an anhydrous salt which is capable of forming hydrates (*e.g.*, $CaCl_2$, $CuSO_4$) is dissolved, ΔH has a negative value, *i.e.*, the dissolution is accompanied by evolution of heat. The difference in the behaviour of hydrated and anhydrous salts is due to the heat evolved in the formation of hydrates. This heat is known as the **enthalpy of hydration** of the salt.

By measuring integral enthalpy of solution of a salt in its hydrated as well as anhydrous state, it is possible to calculate the enthalpy of hydration of the salt. Suppose, it is required to calculate the enthalpy of hydration of $CuSO_4$ to form $CuSO_4.5H_2O$. Taking the data from Table 3, we have :

$$CuSO_4\ (anhydrous) + 800\ H_2O\ (l) \longrightarrow CuSO_4\ (800\ H_2O)\ ; \qquad \Delta H = -66{\cdot}5\ kJ$$

$$CuSO_4.5H_2O + 795\ H_2O\ (l) \longrightarrow CuSO_4\ (800\ H_2O)\ ; \qquad \Delta H = +11{\cdot}7\ kJ$$

By subtracting, we have

$$CuSO_4 + 5H_2O\ (l) \longrightarrow CuSO_4.5H_2O\ ; \qquad \Delta H = -78{\cdot}2\ kJ.$$

Thus, heat evolved when 1 mole of solid anhydrous copper sulphate combines with water to form solid pentahydrate is 78·2 kJ. Thus, the enthalpy of hydration of $CuSO_4$ to form $CuSO_4.5H_2O$ is 78·2 kJ.

When a solution is so dilute that further dilution causes no noticeable heat change, it is said to be at infinite dilution. The thermochemical equations for solutions of infinite dilutions are written as :

$$KCl\ (s) + aq \longrightarrow KCl\ (aq)\ ; \qquad \Delta H = -19{\cdot}7\ kJ$$

$$HCl\ (g) + aq \longrightarrow HCl\ (aq)\ ; \qquad \Delta H = -75{\cdot}4\ kJ$$

Differential Enthalpy of Solution. Another term, frequently used in processes of dissolution, is the differential enthalpy of solution. It is defined as the enthalpy change produced when 1 mole of a solute is dissolved in a large volume of solution of a specified concentration.

To illustrate, consider a solution containing one mole of potassium chloride dissolved in 10 moles of water. Now if we take a large volume of this solution, say, 200 litres and dissolve one mole more of potassium chloride in it, the heat change produced will be called the differential enthalpy of solution of potassium chloride when the solution is already at the given concentration.

Standard Enthalpy of Formation. The standard enthalpy of formation, ΔH_f°, is defined as the enthalpy change when one mole of a substance is formed from its elements in their standard states.

ΔH_f° may be negative or positive (Table 4).

TABLE 4
Standard Enthalpies of Formation of Some Common Compounds

Reaction	ΔH_f° (kJ mol^{-1}) for the compound formed
$C(s) + O_2(g) \longrightarrow CO_2(g)$	- 393·5
$C(s) + \frac{1}{2}O_2(g) \longrightarrow CO(g)$	- 110·5
$H_2(g) + \frac{1}{2}O_2(g) \longrightarrow H_2O(l)$	- 285·9
$H_2(g) + \frac{1}{2}O_2(g) \longrightarrow H_2O(g)$	- 241·9
$\frac{1}{2}H_2(g) + \frac{1}{2}F_2(g) \longrightarrow HF(g)$	- 271·1
$C(s) + 2H_2(g) \longrightarrow CH_4(g)$	- 74·9
$2C(s) + 3H_2(g) \longrightarrow C_2H_6(g)$	- 89·2
$2C(s) + 2H_2(g) \longrightarrow C_2H_4(g)$	+52·3
$2C(s) + H_2(g) \longrightarrow C_2H_2(g)$	+226·8
$6C(s) + 3H_2(g) \longrightarrow C_6H_6(l)$	+49·0
$8C(s) + 4H_2(g) \longrightarrow C_8H_8(l)$	- 224·4
$Si(s) + O_2(g) \longrightarrow SiO_2(s)$	- 910·0
$S(s) + O_2(g) \longrightarrow SO_2(g)$	- 297·5
$Na(s) + \frac{1}{2}Cl_2(g) \longrightarrow NaCl(s)$	- 411·0
$Ca(s) + \frac{1}{2}O_2(g) \longrightarrow CaO(s)$	- 635·5
$1/2N_2(g) + \frac{3}{2}H_2(g) \longrightarrow NH_3(g)$	- 46·0
$N_2(g) + 2H_2(g) \longrightarrow N_2H_4(l)$	+50·6
$C(s) + 2H_2(g) + 1/2\ O(g) \longrightarrow CH_3OH(l)$	- 238·9
$2C(s) + 3H_2(g) + 1/2\ O_2(g) \longrightarrow C_2H_5OH(l)$	- 277·7
$10C(s) + 4H_2(g) \longrightarrow C_{10}H_8(s)$	+60·2

Determination of Enthalpies of Reactions. Enthalpies of reactions at 25°C can be determined if ΔH_f° values of reactants and products involved in the reactions are known since

$$\Delta H^\circ = \Sigma \Delta H_f^\circ \text{(products)} - \Sigma \Delta H_f^\circ \text{(reactants)}$$

By convention, ΔH_f° values for elements in their standard states are taken as zero.

Example 9. The enthalpy of combustion of glucose $C_6H_{12}O_6(s)$ is - 2816 kJ mol^{-1} at 25°C. Calculate $\Delta H_f^\circ(C_6H_{12}O_6)$. The ΔH_f° values for $CO_2(g)$ and $H_2O(l)$ are - 393·5 and - 285·9 kJ mol^{-1}, respectively.

Solution : $C_6H_{12}O_6(s) + 6O_2(g) \longrightarrow 6CO_2(g) + 6H_2O(l)$; ΔH° = -2816 kJ

Since, $\Delta H = \Sigma \Delta H_f^\circ$ (products) - $\Sigma \Delta H_f^\circ$ (reactants), we find that

$$-2816 \text{ kJ} = 6(-393{\cdot}5 \text{ kJ mol}^{-1}) + 6(-285{\cdot}9 \text{ kJ mol}^{-1}) - \Delta H_f^\circ(C_6H_{12}O_6) - 6\Delta H_f^\circ(O_2)$$

which, on simplification and recalling that $\Delta H_f^\circ(O_2) = 0$, gives $\Delta H_f^\circ(C_6H_{12}O_6) = -1260{\cdot}4$ kJ mol^{-1}

Example 10. Using the ΔH_f° values given in Table 4, calculate the enthalpy of combustion of methane at 25°C and 1 atm pressure.

Solution : The combustion of methane is represented as :

$$CH_4(g) + 2O_2(g) \longrightarrow CO_2(g) + 2H_2O(l) \ ; \ \Delta H = ?$$

$$\therefore \quad \Delta H^\circ = \Delta H_f^\circ(CO_2) + 2\Delta H_f^\circ(H_2O) - \Delta H_f^\circ(CH_4) - 0$$
$$= (-393{\cdot}5 \text{ kJ mol}^{-1}) + 2(-285{\cdot}9 \text{ kJ mol}^{-1}) - (-74{\cdot}8 \text{ kJ mol}^{-1})$$
$$= -890{\cdot}5 \text{ kJ mol}^{-1}$$

Thus, enthalpy of combustion of methane at 25°C and 1 atm pressure = - 890·5 kJ mol^{-1}

Example 11. Calculate ΔH for each of the following reactions :

(a) $BaCO_3(s) + 2HCl(aq) \longrightarrow BaCl_2(aq) + CO_2(g) + H_2O(l)$

(b) $AgNO_3(aq) + NaCl(aq) \longrightarrow NaNO_3(aq) + AgCl(s)$

(c) $HNO_3(aq) + NaOH(aq) \longrightarrow NaNO_3(aq) + H_2O(l)$

Given : $\Delta H_f^\circ(BaCO_3(s)) = -1216{\cdot}7$ kJ mol^{-1}, $\Delta H_f^\circ(Ba^{2+}(aq)) = -538{\cdot}3$ kJ mol^{-1}

$\Delta H_f^\circ(Ag^+(aq)) = -105{\cdot}9$ kJ mol^{-1}, $\Delta H_f^\circ(OH^-(aq)) = -230{\cdot}0$ kJ mol^{-1}

$\Delta H_f^\circ(H^+(aq)) = 0$, by convention.

Solution : $\Delta H = \Sigma \Delta H_f^\circ$ (products) - $\Sigma \Delta H_f^\circ$ (reactants)

It is best to use the ionic equations here. Thus,

(a) $BaCO_3(s) + 2H^+(aq) \longrightarrow Ba^{2+}(aq) + CO_2(g) + H_2O(l)$:

$$\Delta H = [\Delta H_f^\circ(Ba^{2+}(aq)) + \Delta H_f^\circ(CO_2) + \Delta H_f^\circ(H_2O)] - [\Delta H_f^\circ(BaCO_3(s)) + 2\Delta H_f^\circ(H^+(aq))]$$
$$= [(-538{\cdot}3) + (-393{\cdot}5) + (-285{\cdot}9) - [-1216{\cdot}7 + 0]] = -1217{\cdot}7 + 1216{\cdot}7 = -1{\cdot}0 \text{ kJ}$$

(b) $Ag^+(aq) + Cl^-(aq) \longrightarrow AgCl(s)$:

$$\Delta H = [\Delta H_f^\circ(AgCl(s))] - [\Delta H_f^\circ(Ag^+(aq)) + \Delta H_f^\circ(Cl^-(aq))]$$
$$= [(-127{\cdot}0)] - (-105{\cdot}9) + (-167{\cdot}5)] = 146{\cdot}4 \text{ kJ}$$

(c) $H^+(aq) + OH^-(aq) \longrightarrow H_2O(l)$:

$$\Delta H = [\Delta H_f^\circ(H_2O)] - [\Delta H_f^\circ(H^+(aq)) - \Delta H_f^\circ(OH^-(aq))] = [(-285{\cdot}9)] - [0 + (-230{\cdot}0)]$$
$$= -55{\cdot}8 \text{ kJ}$$

Example 12. The heat evolved on dissolving $CuSO_4(s)$ in water is 86·6 kJ mol^{-1}. If $\Delta H_f^\circ(Cu^{2+})$ is 64·4 kJ mol^{-1}, what is $\Delta H_f^\circ(SO_4^{2-})$? $\Delta H_f^\circ(CuSO_4(s)) = -770{\cdot}0$ kJ mol^{-1}

Solution : $CuSO_4(s) \longrightarrow Cu^{2+}(aq) + SO_4^{2-}(aq)$

$$\Delta H = \Delta H_f^\circ(Cu^{2+}) + \Delta H_f^\circ(SO_4^{2-}) - \Delta H_f^\circ(CuSO_4(s))$$

On rearranging and using the given data, we find that

$$\Delta H_f^\circ(SO_4^{2-}) = -747{\cdot}8 \text{ kJ}$$

Example 13. In a bomb calorimeter, cyanamide was subjected to combustion at constant volume and the heat evolved was found to be 742·7 kJ at 25°C. Calculate q_p for the reaction.

Solution : $NH_2CN(s) + 3/2O_2(g) \longrightarrow N_2(g) + CO_2(g) + H_2O(l)$

$$\Delta n_g = 1 + 1 - 3/2 = 1/2$$

$$q_p = q_v + \Delta n_g RT = -742{\cdot}7 \text{ kJ} + (0{\cdot}5 \text{ mol})(8{\cdot}314 \text{ J K}^{-1}\text{mol}^{-1})(298\text{K})/1000 \text{ J kJ}^{-1}$$
$$= [-742{\cdot}7 \text{ kJ} + 1{\cdot}240 \text{ kJ}] = -741{\cdot}5 \text{ kJ}$$

Example 14. Calculate the enthalpy change for the transition graphite $\rightleftharpoons$ diamond from the ΔH_{comb}° values of - 393·5 kJ mol^{-1} and - 395·4 kJ mol^{-1} for graphite and diamond, respectively.

Solution : $C(s, \textit{graphite}) + O_2(g) \longrightarrow CO_2(g)$; $\Delta H_{comb}^\circ = -393{\cdot}5$ kJ mol^{-1}

$C(s, \textit{diamond}) + O_2(g) \longrightarrow CO_2(g)$; $\Delta H_{comb}^\circ = -395{\cdot}4$ kJ mol^{-1}

Subtracting the second reaction from the first,

$C(s, \textit{graphite}) \longrightarrow C(s, \textit{diamond})$; $\Delta H_{tr}^\circ = +1{\cdot}9$ kJ mol^{-1}

Example 15. Calculate the enthalpy of formation of OH^- ions at 25°C from the following thermochemical data :

$$H_2O(l) \longrightarrow H^+(aq) + OH^-(aq) ; \qquad \Delta H^\circ = 57{\cdot}3 \text{ kJ}$$

$$H_2(g) + \tfrac{1}{2}O_2(g) \longrightarrow H_2O(l) ; \qquad \Delta H^\circ = -285{\cdot}9 \text{ kJ}$$

Solution : Adding the above two equations, we get

$$H_2(g) + 1/2O_2(g) \longrightarrow H^+(aq) + OH^-(aq) \qquad \Delta H^\circ = -228{\cdot}6 \text{ kJ}$$

$\therefore \Delta H^\circ = -228{\cdot}6 \text{ kJ} = 0 + \Delta H_f^\circ(OH^-(aq)) - (0 + 0)$, since, by convention, $\Delta H_f^\circ[H^+(aq)] = 0$,

$\therefore \quad \Delta H_f^\circ[OH^-(aq)] = -228{\cdot}6 \text{ kJ}$

The standard enthalpies of formation of a few ions at 25°C are given in Table 5.

TABLE 5

Standard Enthalpies of Formation of Ions in Aqueous Solutions

Cation	ΔH_f° (kJ mol^{-1})	Anion	ΔH_f° (kJ mol^{-1})
H^+	0	OH^-	- 229·9
Li^+	- 278·5	Cl^-	- 167·5
Na^+	- 329·7	Br^-	- 121·5
K^+	- 251·2	I^-	- 56·0
Cu^{2+}	+ 64·4	SO_4^{2-}	- 907·5
Mg^{2+}	- 461·9	NO_3^-	- 206·6
Zn^{2+}	- 154·0	PO_4^{3-}	- 1284·0

Variation of Enthalpy of a Reaction with Temperature : The Kirchhoff Equation

The enthalpy of any process, whether physical or chemical, varies with temperature. The exact influence of temperature can be worked out as follows.

The enthalpy of the reaction

$$aA + bB \longrightarrow cC + dD$$

is given by $\Delta H = \Sigma H_{products} - \Sigma H_{reactants} = (cH_C + dH_D) - (aH_A + bH_B)$ ...(10)

Differentiating with respect to temperature, keeping pressure constant, we have

$$\left[\frac{\partial(\Delta H)}{\partial T}\right]_P = c\left(\frac{\partial H_C}{\partial T}\right)_P + d\left(\frac{\partial H_D}{\partial T}\right)_P - a\left(\frac{\partial H_A}{\partial T}\right)_P - b\left(\frac{\partial H_B}{\partial T}\right)_P$$

$$= cC_{P,C} + dC_{P,D} - aC_{P,A} - bC_{P,B} = \Delta C_P \qquad (\because C_P = (\partial H/\partial T)_P) \quad ...(11)$$

where ΔC_P = Sum of heat capacities of products - Sum of heat capacities of reactants

Eq. 11 is called the **Kirchhoff equation.** It states that *the variation of ΔH of a reaction with temperature at constant pressure is equal to ΔC_P of the system.* We can write it as

$$[\partial(\Delta H)/\partial T]_P = \Delta C_P \quad \text{or} \quad d(\Delta H) = \Delta C_P\, dT \qquad ...(12)$$

Analogously, the temperature-dependence of enthalpy of reaction at constant volume is given by

$$[\partial(\Delta U)/\partial T]_v = \Delta C_v \quad \text{or} \quad d(\Delta U) = \Delta C_v\, dT \qquad ...(13)$$

If the temperature range of interest is small, Eqs. 12 and 13 can be easily integrated by assuming that the heat capacities are independent of temperature. Accordingly,

$$\int_{T_1}^{T_2} d(\Delta H) = \int_{T_1}^{T_2} \Delta C_P dT = \Delta C_P \int_{T_1}^{T_2} dT \quad \text{or} \quad \Delta H_2 - \Delta H_1 = \Delta C_P(T_2 - T_1) \qquad ...(14)$$

$$\int_{T_1}^{T_2} d(\Delta U) = \int_{T_1}^{T_2} \Delta C_v dT = \Delta C_v \int_{T_1}^{T_2} dT \quad \text{or} \quad \Delta U_2 - \Delta U_1 = \Delta C_v(T_2 - T_1) \qquad ...(15)$$

If, however, the temperature range is not small, *i.e.*, if it is desired to determine the enthalpy of reaction at a far higher temperature than the initial temperature, then the constancy of heat capacities is no longer a valid assumption and we must express the heat capacities as a function of temperature before carrying out the integration. It is convenient to express the heat capacity as a power series in T, *viz.*,

$$C_P = \alpha + \beta T + \gamma T^2 \qquad ...(16)$$

where α, β and γ are constants for a given species. Hence,

$$\Delta C_P = [(c\alpha_C + d\alpha_D) - (a\alpha_A + b\alpha_B)] + [(c\beta_C + d\beta_D) - (a\beta_A + b\beta_B)]T + \cdots\cdots$$

$$= \Delta\alpha + \Delta\beta T + \Delta\gamma T^2 + \cdots\cdots \qquad ...(17)$$

Substituting Eq. 17 in Eq. 12 and integrating between T_1 and T_2, we have

$$\int_{T_1}^{T_2} d(\Delta H) = \int_{T_1}^{T_2} (\Delta\alpha + \Delta\beta T + \Delta\gamma T^2) dT$$

or $$\Delta H_2 - \Delta H_1 = \Delta\alpha(T_2 - T_1) + (1/2)\Delta\beta(T_2^2 - T_1^2) + 1/3\Delta\gamma(T_2^3 - T_1^3) \qquad ...(18)$$

Eq. 18 is the **integrated Kirchhoff equation.**

Example 16. The enthalpy of reaction (ΔH) for the formation of ammonia according to the reaction : $N_2 + 3H_2 = 2NH_3$ at 27°C was found to be -91·94 kJ. What will be the enthalpy of reaction (ΔH) at 50°C ? The molar heat capacities at constant pressure and at 27°C for nitrogen, hydrogen and ammonia are 28·45, 28·32 and 37·07 joules, respectively.

Solution : According to the Kirchhoff equation, $d(\Delta H) = \Delta C_P\, dT$ or $\Delta H_2 - \Delta H_1/(T_2 - T_1) = \Delta C_P$

In the present case, $\Delta H_1 = -91{\cdot}94$ kJ ; $T_1 = 27 + 273 = 300$ K and $T_2 = 50 + 273 = 323$ K

ΔC_P = Heat capacities of products *minus* heat capacities of reactants

$= 2\times37{\cdot}07 \text{ J K}^{-1} - (28{\cdot}45 \text{ J K}^{-1} + 3\times28{\cdot}32 \text{ J K}^{-1})$

$= -39{\cdot}28 \text{ J K}^{-1} = -39{\cdot}28\times10^{-3} \text{ kJ K}^{-1}$

Assuming that the heat capacities do not change with temperature, ΔH_2, at 50°C, will be given is

$\Delta H_2 = \Delta H_1 + (T_2 - T_1)\Delta C_P$

$= -91{\cdot}94 \text{ kJ} + (323 \text{ K} - 300 \text{ K})(-39{\cdot}28\times10^{-3} \text{ kJ K}^{-1}) = -92{\cdot}85 \text{ kJ}$

Example 17. Calculate the enthalpy change at 125°C for the reaction

$$N_2(g) + 3H_2(g) \longrightarrow 2NH_3(g) ; \qquad \Delta H_{298} = -92{\cdot}41 \text{ kJ}$$

The molar heat capacities (in J K^{-1} mol^{-1}) for the various gases involved in the reaction vary with temperature as follows :

$$C_p(N_2) = 27{\cdot}26 + 5{\cdot}23\times10^{-3}\,T - 4{\cdot}18\times10^{-9}\,T^2$$

$$C_p(H_2) = 29{\cdot}02 - 8{\cdot}35\times10^{-4}\,T + 20{\cdot}80\times10^{-7}\,T^2$$

$$C_p(NH_3) = 25{\cdot}86 + 32{\cdot}94\times10^{-2}\,T - 30{\cdot}42\times10^{-7}\,T^2$$

Solution : We know that $\Delta H_2 - \Delta H_1 = \int_{T_1}^{T_2} \Delta C_p dT$

It is only when ΔC_p is independent of temperature that it can be taken outside the integral sign, giving the result $\Delta H_2 - \Delta H_1 = \Delta C_p(T_2 - T_1)$. In the present case, ΔC_p is *not* independent of temperature. Let us first calculate ΔC_p.

$$\Delta C_p = 2C_p(NH_3) - [C_p(N_2) + 3C_p(H_2)]$$

Substituting the given data, the value of ΔC_p is given by

$$\Delta C_p = -62{\cdot}60 + 63{\cdot}14\times10^{-3}T - 123{\cdot}20\times10^{-7}T^2$$

Hence, $$\Delta H_2 - \Delta H_1 = \int_{T_1}^{T_2} [-62{\cdot}60 + 63{\cdot}14\times10^{-3}\,T - 123{\cdot}20\times10^{-7}\,T^2]\,dT$$

or $$\Delta H_{398} - \Delta H_{298} = \left[-62{\cdot}60 + 63{\cdot}14 \times 10^{-3} T^2/2 - 123{\cdot}20 \times 10^{-7} T^3/3\right]_{298}^{398}$$

Simplifying and putting $\Delta H_{298} = -92{\cdot}41$ kJ, we obtain $\Delta H_{398} = -96{\cdot}50$ kJ

Example 18. For the hypothetical reaction : $2B(g) \longrightarrow B_2(g)$, ΔC_P (in joules) $= 6{\cdot}0 + 2{\cdot}0 \times 10^{-3} T$ and $\Delta H^\circ_{298} = -20{\cdot}0$ kJ mol^{-1}. Estimate the temperature at which $\Delta H^\circ = 0$ for this reaction.

Solution : Using the Kirchhoff equation, $\Delta H_2 = \Delta H_1 + \int_{T_1}^{T_2} (\Delta C_p) dT$

or $$0 = -20{,}000 - \int_{298}^{T} (6{\cdot}0 + 2{\cdot}0 \times 10^{-3} T)\, dT$$

or $$20{,}000 = [(6{\cdot}0)(T - 298)] + [(1{\cdot}0 \times 10^{-3})(T^2 - (298)^2] = 6T - 1788 + 1 \times 10^{-3} T^2 - 88{\cdot}8$$

or $$10^{-3} T^2 + 6T - 1{,}876{\cdot}8 = 0$$

This is a quadratic equation in T which, when solved, gives two roots — one positive and the other negative. The negative root has no physical significance. The positive root gives $T = 2557$ K.

Flame and Explosion Temperatures

The combustion of a gaseous fuel in air takes place so suddenly that the heat produced during combustion does not get any opportunity to be dissipated to the surroundings. The combustion process is, therefore, practically equivalent to an adiabatic process. The entire amount of heat produced thus goes to heat the gases produced during combustion as also the unreacted nitrogen. The maximum temperature attained by the flame-zone (containing the resultant gases) due to the heat liberated by the combustion of the fuel under adiabatic conditions *at constant pressure* is known as the **flame temperature.** If, on the other hand, the combustion is carried out under adiabatic conditions at *constant volume*, the maximum temperature attained is called **explosion temperature.**

For an isobaric (constant pressure) adiabatic process, the flame temperature can be calculated using the Kirchhoff equation, *viz.*,

$$d(\Delta H)/dT = \Delta C_P \quad \text{or} \quad d(\Delta H) = \Delta C_P\, dT \qquad ...(19)$$

Integration of Eq. 19 yields

$$\int d(\Delta H) = \Delta C_P \int_{T_i}^{T_f} dT \quad \text{or} \quad \Delta H = \Delta C_p\, (T_f - T_i) \qquad ..(20)$$

Here we have assumed that over the given temperature range, ΔC_p remains constant so that it can be taken outside the integral sign. Hence, knowing ΔH, ΔC_p and the initial temperature T_i, the final temperature T_f (which in this case is the flame temperature) can be calculated.

We must comment on ΔC_p here. The flame temperature would obviously depend upon the composition and the heat capacities of only the *resultant gases*. In the flames produced by combustion of fuels in air, there is present in gaseous products unreacted nitrogen which is also heated up along with the gaseous products to the flame temperature. Since air contains about 20% by volume of O_2 and 80% by volume of N_2, the combustion reaction involving 1 mole of O_2 is associated with 4 moles of unreacted N_2 in the products. Thus, the combustion of H_2 gas in air can be schematically represented as

$$2H_2(g) + O_2(g) + 4N_2(g) \longrightarrow 2H_2O(g) + 4N_2(g)$$

Hence, ΔC_p is considered as equal to the sum of the C_ps of the *products* plus the C_p of four moles of unreacted N_2 per mole of O_2 used during combustion. Therefore,

$$\Delta C_P = \Sigma C_{P,\,\text{products}} + 4C_{P,\,N_2}$$

Accordingly, for determining flame temperature, ΔC_P in Eq. 19 is replaced by ΣC_p where ΣC_p is the summation of the heat capacities of products of combustion and the unreacted nitrogen.

Example 19. In a Bunsen burner, CH_4 gas is premixed with sufficient air to allow complete combustion and at the flame temperature water is converted into steam. Using the following thermochemical data :

$$CH_4(g) + 2O_2(g) \longrightarrow CO_2(g) + 2H_2O(l)\ ; \qquad \Delta H^\circ_{298} = -890{\cdot}3 \text{ kJ}$$

$$H_2O(l) \longrightarrow H_2O(g)\ ; \qquad \Delta H^\circ_{298} = +40{\cdot}7 \text{ kJ}$$

calculate the flame temperature. Assume that the gaseous products behave ideally. $\Sigma C_P = 41{\cdot}8$ J K^{-1} mol^{-1} and the initial temperature = 25°C.

Solution : From the given thermochemical reactions, we have, at the flame temperature (when water is in *gaseous* state) :

$$CH_4(g) + 2O_2(g) \longrightarrow CO_2(g) + 2H_2O(g)\ ; \qquad \Delta H^\circ_{298} = -890{\cdot}3 + 2(40{\cdot}7) = -802{\cdot}3 \text{ kJ}$$

ΔC_P of the gaseous products (CO_2, H_2O and N_2) $= 41{\cdot}8$ J K^{-1} mol^{-1}

Since for every mole of O_2 reacted, 4 moles of unreacted N_2 remain, hence total number of moles of gaseous products $= 1 + 2 + (4 \times 2) = 11$. Thus, flame temperature, T_f, is attained if 802·3 kJ of heat liberated above is completely utilized to heat (at constant pressure) 1 mole of CO_2, 2 moles of steam and 8 moles of unreacted N_2 (*i.e.*, a total of 11 moles). Using Kirchhoff equation,

$$(11 \text{ mol}) \times (41{\cdot}8 \text{ J K}^{-1} \text{ mol}^{-1})\ (T_f - T_i) = 802{\cdot}3 \text{ kJ}$$

$$T_f - T_i = 802{\cdot}3 \times 10^3 \text{ J}/459{\cdot}6 \text{ J K}^{-1} = 1746 \text{ K}$$

Since $T_i = 25°C = 298$ K, $T_f = (1746 + 298)$ K $= 2{,}043$ K (The experimental value is 1820 K)

It should be noted that if ΔH°_{298} is the enthalpy of the reaction at 298 K and T_f is the final temperature, then the heat required to raise the temperature of the products from 298 K to T_f must be equal in magnitude but opposite in sign to ΔH°_{298}, *i.e.*, $\Delta H_{\text{heating}} = -\Delta H^\circ_{298}$ so that the sum $\Delta H^\circ_{298} + \Delta H_{\text{heating}} = 0$ because, for the adiabatic process, $\Delta H = 0$.

The calculation of explosion temperature is similar to that of the flame temperature except that ΔH is replaced by ΔU. The pressure required for the reacting system at the explosion temperature is called the **explosion pressure.**

Example 20. H_2 gas is mixed with air at 25°C under a pressure of one atmosphere and exploded in a closed vessel. The enthalpy of the reaction $H_2(g) + 1/2\ O_2(g) \longrightarrow H_2O(g)$ at constant volume, $\Delta U_{298} = -240{\cdot}6$ kJ and C_ps for H_2O vapour and N_2 in the temperature range 298 K and 3,200 K are 39·1 J K^{-1} and 26·4 J K^{-1}, respectively. Calculate the explosion temperature under adiabatic conditions.

Solution. For a constant volume process under adiabatic conditions,

$$\Delta U = \Delta U_{\text{heating}} + \Delta U_{298} = 0$$

Hence, $$\Delta U_{\text{heating}} = -\Delta U_{298} = -\int_{298}^{T_f} \Sigma n C_v dT = -240{\cdot}60 \text{ kJ} \qquad ...(i)$$

Since 2 moles of unreacted N_2 are associated with 1/2 mole of O_2, we have

$$\Sigma n C_v = C_v(H_2O,\, g) + 2C_v(N_2,\, g) = (39{\cdot}1 + 2 \times 26{\cdot}4) \text{ J K}^{-1} = 91{\cdot}9 \text{ J K}^{-1}$$

Hence, from Eq. *(i)*, on integrating, we have

$$91{\cdot}9 \text{ J K}^{-1} (T_f - 298) = 240{,}600 \text{ J}$$

$$T_f - 298 = 240{,}600 \text{ J}/91{\cdot}9 \text{ J K}^{-1} = 2618 \text{ K}$$

$$T_f = (2618 + 298) \text{ K} = 2916 \text{ K}$$

Hess's Law of Constant Heat Summation

This law states that the amount of heat evolved or absorbed in a process, including a chemical change, is the same whether the process takes place in one or several steps.

Suppose in a process, the system changes from state A to state B in *one step* and the heat exchanged in this change is q. Now suppose the system changes from state A to state B in *three steps* involving a change from A to C, C to D and finally from D to B. If q_1, q_2 and q_3 are the heats

exchanged in the first, second and third step, respectively, then, according to Hess's law,

$$q_1 + q_2 + q_3 = q \qquad ...(20)$$

This generalisation means, in effect, that the enthalpy of reaction depends only on the initial reactants and final products and not at all on the intermediate products that may be formed.

Applications of Hess's Law. 1. Calculation of enthalpies of reactions. Hess's law makes it possible to calculate enthalpies of many reactions which cannot be determined experimentally. For example, it is extremely difficult to measure the heat evolved when carbon burns in oxygen to form carbon monoxide

$$C(s) + \tfrac{1}{2}O_2(g) \longrightarrow CO(g)\,; \qquad \Delta H = ?$$

Hess's law, starts that the heat *evolved* in the combustion of 1 mole of carbon is the same, *viz.*, 393·5 kJ (*i.e.*, $\Delta H = -393{\cdot}5$ kJ), whether the reaction takes place in a single step as

$$C(s) + O_2(g) \longrightarrow CO_2(g)\,; \qquad \Delta H = -393{\cdot}5 \text{ kJ}$$

or in two steps as

$$C(s) + \tfrac{1}{2}O_2(g) \longrightarrow CO(g)\,; \qquad \Delta H = x \text{ kJ (say)}$$

$$CO(g) + \tfrac{1}{2}O_2(g) \longrightarrow CO_2(g)\,; \qquad \Delta H = y \text{ kJ(say)}$$

Although x, the heat change involved in the combustion of carbon to carbon monoxide cannot be determined easily, y, the heat change involved in the combustion of carbon monoxide to give carbon dioxide can be measured and has been found to be –282·0 kJ. According to Hess's law

$$x + y = -393{\cdot}5 \text{ kJ}$$

or

$$x = -393{\cdot}5 - y = -393{\cdot}5 - (-282{\cdot}0) = -111{\cdot}5 \text{ kJ}$$

Thus, ΔH for the combustion of carbon to give carbon monoxide is – 111·5 kJ.

2. Determination of enthalpies of slow reactions. Hess's law is extremely useful in determining enthalpies of those reactions which take place extremely slowly. For example, the transformation of rhombic sulphur into monoclinic sulphur is so slow that direct measurement of enthalpy is not possible. But the enthalpies of combustion of rhombic sulphur and monoclinic sulphur are known to be – 297·5 and – 300·0 kJ mol^{-1}, respectively, *i.e.*,

(i) $S(rhombic) + O_2(g) \longrightarrow SO_2(g)\,;$ $\Delta H = -297{\cdot}5$ kJ

(ii) $S(monoclinic) + O_2(g) \longrightarrow SO_2(g)\,;$ $\Delta H = -300{\cdot}0$ kJ

Subtracting *(i)* from *(ii)* and transposing, we get

$$S(monoclinic) \longrightarrow S(rhombic)\,; \qquad \Delta H = -2{\cdot}5 \text{ kJ}$$

or

$$S(rhombic) \longrightarrow S(monoclinic)\,; \qquad \Delta H = +2{\cdot}5 \text{ kJ}$$

Thus, transformation of one mole of rhombic sulphur into monoclinic sulphur is accompanied by absorption of 2·5 kJ of heat.

3. Calculation of enthalpies of formation. The enthalpies of formation of compounds can be calculated by the application of Hess's law when it is not possible to determine these experimentally.

For example, it is impossible to determine experimentally the enthalpy of formation of benzene from its elements : carbon and hydrogen. However, it can be calculated from the enthalpy of combustion of benzene and the enthalpies of formation of water and carbon dioxide. The solution is

carried out in two steps :

Step 1. The thermochemical equations for the known values are written as

(i) $C_6H_6(l) + \frac{15}{2}O_2(g) \longrightarrow 6CO_2(g) + 3H_2O(l)\,;$ $\Delta H = -3267{\cdot}7$ kJ

(ii) $C(s) + O_2(g) \longrightarrow CO_2(g)\,;$ $\Delta H = -393{\cdot}5$ kJ

(iii) $H_2(g) + \frac{1}{2}O_2(g) \longrightarrow H_2O(l)\,;$ $\Delta H = -285{\cdot}9$ kJ

Step 2. Equation *(ii)* is multiplied by 6 and equation *(iii)* is multiplied by 3 :

(iv) $6C(s) + 6O_2(g) \longrightarrow 6CO_2(g)\,;$ $\Delta H = -2361{\cdot}0$ kJ

(v) $3H_2(g) + \frac{3}{2}O_2(g) \longrightarrow 3H_2O(l)\,;$ $\Delta H = -857{\cdot}7$ kJ

Adding *(iv)* and *(v)* and subtracting *(i)*, we get

$$6C(s) + 3H_2(g) \longrightarrow C_6H_6(l) \qquad \Delta H = +49{\cdot}0 \text{ kJ}$$

Thus, the enthalpy of formation of benzene is **+ 49·0 kJ.**

Measuring the Enthalpy of Combustion.

Calorimetry is the study of heat transfer during physical and chemical processes. A **calorimeter** is a device for measuring energy transferred as heat. The most common device for measuring D*U* is the **adiabatic bomb calorimeter,** shown in Figs. 5 and 6. The inner vessel or the 'bomb' (Fig. 6) and its cover are made of strong steel coated inside with gold or platinum or some other non-oxidisable material. The cover can be fitted tightly to the vessel by means of a metal lid screwed down on a lead washer. A weighed amount of the substance is taken in a platinum cup *C* which is supported on a rod *R*.

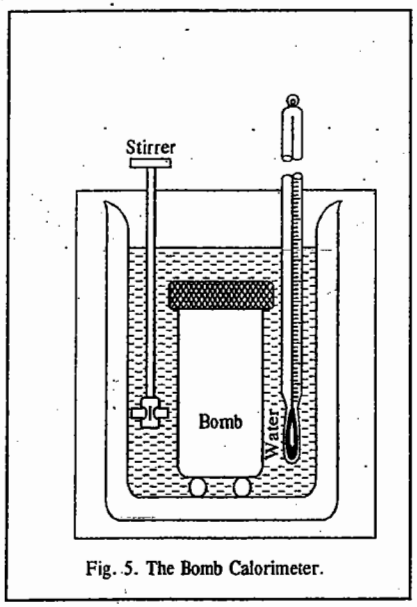

Fig. 5. The Bomb Calorimeter.

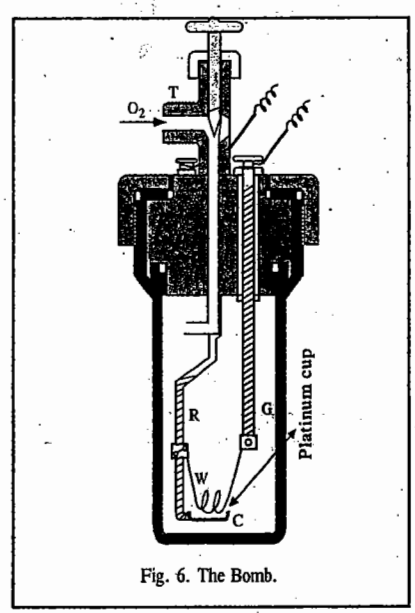

Fig. 6. The Bomb.

A thin platinum wire W is connected between the rods R and G, as shown. This serves to initiate the combustion when heated electrically. The bomb is tightly closed and oxygen introduced through the inlet tube T until a pressure of about 20—25 atmospheres is attained. The bomb is then lowered in water placed in a double jacketed and polished metallic calorimeter so as to minimise error due to radiation. The arrangement ensures that there is no net loss of heat from the calorimeter to the surroundings (the bath) and hence that the process is adiabatic. A mechanical stirrer is provided as shown (Fig. 5). When the temperature of the water has become steady, the substance is ignited by passing electric current through the platinum wire W. The rise of temperature of the water in the calorimeter is noted after every minute by means of a Beckmann thermometer graduated to read up to a hundredth of a degree. The final temperature when corrected for the radiation error in the usual way, *minus* the initial temperature, gives the rise of temperature. The heat capacity of the calorimeter system, called the **calorimeter constant**, C, is obtained by burning a known mass of a substance of known enthalpy of combustion. For this purpose, usually benzoic acid of high grade purity is taken. Its q_v which has been very carefully measured is taken as $-3226{\cdot}7$ kJ mol^{-1}. Suppose the thermal capacity of the calorimeter system including water is C and θ is the change in temperature produced by burning a quantity m of the given substance of molar mass M. Then, the constant volume heat of combustion, q_v of the substance is given by $C\times\theta\times M/m$. The enthalpy of combustion q_p is then obtained with the help of the equation $q_p = q_v + \Delta n_g RT$.

Example 21. 0·50 g of benzoic acid was subjected to combustion in a bomb calorimeter when the temperature of the calorimeter system (including water) was found to rise by 0·55°C. Calculate the enthalpy of combustion of benzoic acid. The ΔT calorimeter constant was found to be 23·85 kJ K^{-1}.

Solution : $q_v = C\times\theta\times M/m$

$= 23{\cdot}85$ kJ K$^{-1}\times 0{\cdot}55$ K$\times 122$ g mol$^{-1}/0{\cdot}50$ g $= 3200{\cdot}7$ kJ mol^{-1} $= -\,3200{\cdot}7$ kJ mol^{-1}

(Heat of combustion has always a negative sign)

$$C_6H_5COOH(s) + \tfrac{15}{2}O_2(g) \longrightarrow 7CO_2(g) + 3H_2O(l)$$

We know that $q_p = q_v + \Delta n_g RT$; $\Delta n = 7 - 7{\cdot}5 = -0{\cdot}5$

$q_p = -\,3200{\cdot}7$ kJ mol^{-1} $+ (-0{\cdot}5)\,(8{\cdot}314\times10^{-3}$ kJ K^{-1} mol^{-1}) (298 K) $= -\,3201{\cdot}9$ kJ mol^{-1}

Example 22. Explain why the following statement, made by a student doing an experiment on bomb calorimeter, is wrong :

"$\Delta H = \Delta U + P\Delta V$. Since in the experiment, $\Delta V=0$, hence, $\Delta H=\Delta U$."

Explanation : The error is due to the fact that the student has applied the equation $\Delta H=\Delta U+P\Delta V$, which holds at constant pressure, to a process which occurs at constant volume.

We know that $H = U + PV$

$\therefore \quad \Delta H = \Delta U + \Delta(PV) = \Delta U + P\Delta V + V\Delta P$

For a constant pressure process, $\Delta P = 0$ so that $\Delta H = \Delta U + P\Delta V$

However, for a constant volume process, $\Delta V = 0$ so that $\Delta H = \Delta U + V\Delta P$

We may mention here that a calorimeter for studying processes at constant pressure, called an **isobaric calorimeter** is also available commercially. A simple example is a thermally insulated vessel, open to the atmosphere; the heat released in the reaction is monitored by measuring the change in temperature of the contents. For a combustion reaction, an adiabatic flame calorimeter can be used to measure ΔT when a given amont of substance burns in oxygen.

Bond Energies

Bond energy for any particular type of bond in a compound may be defined as the average amount of energy required to dissociate (*i.e.*, break) one mole of bonds of that type present in the compound. Bond energy is also called the **enthalpy of formation of the bond.**

It has been found by experiment that isomeric compounds have the same value for enthalpy of formation. Also, in any homologous series, the increase in enthalpy of formation for each CH_2 group is almost constant. This shows that enthalpy of formation of a bond of a particular type is largely an **additive property.**

In order to calculate bond energies (*i.e.*, enthalpies of formation of bonds) of different types of bonds, it is necessary, in the first instance, to know the enthalpies of dissociation of molecules of common elements into atoms. These have been obtained spectroscopically and are given below for hydrogen, oxygen, nitrogen and carbon :

(i) $H_2(g) \longrightarrow 2H(g)$; $\Delta H = 435{\cdot}1$ kJ

(ii) $O_2(g) \longrightarrow 2O(g)$; $\Delta H = 489{\cdot}5$ kJ

(iii) $N_2(g) \longrightarrow 2N(g)$; $\Delta H = 937{\cdot}4$ kJ

(iv) $C(s) \longrightarrow C(g)$; $\Delta H = 719{\cdot}6$ kJ

Suppose, it is required to calculate enthalpy of formation of C—H bond in methane. We should know the enthalpy of formation of methane. This has been calculated from the enthalpy of combustion of methane to be $-74{\cdot}9$ kJ. Thus,

(v) $C(s) + 2H_2(g) \longrightarrow CH_4(g)$; $\Delta H = -74{\cdot}9$ kJ

Multiplying equation *(i)* by 2, we have

(vi) $2H_2(g) \longrightarrow 4H(g)$; $\Delta H = 870{\cdot}2$ kJ

Adding equations *(iv)* and *(vi)* and subtracting from equation *(v)*, we have

$C(g) + 4H(g) \longrightarrow CH_4(g)$; $\Delta H = -\,1664{\cdot}7$ kJ

It follows from above that 1664·7 kJ of energy is required to break four moles of C—H bonds in methane. Therefore, the average bond energy per mole of C—H bonds is $1664{\cdot}7/4 = 416{\cdot}2$ kJ. This is also the **enthalpy of formation** of the C—H bond.

The enthalpy of formation of ethane is known to be $-89{\cdot}2$ kJ, *i.e.*,

(vii) $2C(s) + 3H_2(g) \longrightarrow C_2H_6(g)$; $\Delta H = -\,89{\cdot}2$ kJ

Multiplying equation *(iv)* by 2 and equation *(i)* by 3, we have

(viii) $2C(s) \longrightarrow 2C(g)$; $\Delta H = 1439{\cdot}2$ kJ

(ix) $3H_2(g) \longrightarrow 6H(g)$; $\Delta H = 1305{\cdot}3$ kJ

Adding equations *(viii)* and *(ix)* and subtracting from equation *(vii)*, we have

$2C(g) + 6H(g) \longrightarrow C_2H_6(g)$; $\Delta H = -\,2833{\cdot}7$ kJ

This means that the enthalpy of formation of six moles of C—H bonds and one mole of C—C bonds is 2833·7 kJ. The enthalpy of formation of six moles of C—H bonds is $6\times416{\cdot}2 = 2497{\cdot}2$ kJ. Therefore, the enthalpy of formation of C—C bond is $2833{\cdot}7 - 2497{\cdot}2 = 336{\cdot}5$ kJ per mole of bonds. The average value of enthalpy of formation of C—C bond is taken as 347·3 kJ.

Similarly, the enthalpy of formation of other bonds, such as C—O, C=O and C—OH, can be obtained by knowing the enthalpies of formation of ethers, ketones and alcohols, respectively. Some of the results are given in Table 6. It is to be remembered that each value pertains to one mole

(*i.e.*, Avogadro's number) of bonds of the particular type. Also, these values are considered to be *approximate* since additivity of bond energies has not been established finally.

TABLE 6
Enthalpies of Formation of Bonds, *viz.*, Bond Energies at 25°C

Bond	Enthalpy of formation (kJ mol^{-1})	Bond	Enthalpy of formation (kJ mol^{-1})
H—H	435·1	C—Cl	330·5
H—F	564·8	C—Br	276·1
H—Cl	430·9	C—S	259·4
H—Br	368·2	C=S	477·0
O—O	138·1	C—N	292·9
O=O	493·7	C=N	615·0
O—H	464·4	C≡N	878·6
C—H	416·2	N—N	159·0
C—O	351·4	N=N	418·4
C=O	711·3	N≡N	945·6
C—C	347·3	N—H	389·1
C=C	615·0	F—F	154·8
C≡C	811·7	Cl—Cl	242·7
C—F	439·3	Br—Br	192·5

Applications of Bond Energies. 1. Determination of enthalpies of reactions. The bond energies can be used for determining enthalpies of reactions. This may be illustrated by the following example.

Suppose we want to determine the enthalpy of the reaction

$$H_2C{=}CH_2(g) + H_2(g) \longrightarrow H_3C{-}CH_3(g)\,; \qquad \Delta H = ?$$

In this reaction, the four C—H bonds of C_2H_4 remain unaffected. A double bond breaks in ethylene and an H—H bond breaks in H_2. In turn, one C—C bond and two C—H bonds are formed in C_2H_6. Thus,

$$\Delta H = -\Delta H_{C\text{-}C} - 2\Delta H_{C\text{-}H} + \Delta H_{C=C} + \Delta H_{H\text{-}H}$$

Substituting the bond energies from Table 6, we get

$$\Delta H = -(347{\cdot}3 + 832{\cdot}4) + (615{\cdot}0 + 435{\cdot}1) = \mathbf{-129{\cdot}6\ kJ}$$

The above value is quite close to the experimental value of −133 kJ.

2. Determination of enthalpies of formation of compounds. The bond energies can also be used for determination of enthalpies of formation of compounds. As an example, we may consider the formation of acetone :

$$3C(g) + 6H(g) + O(g) \longrightarrow$$

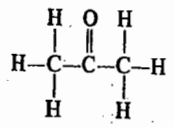

The formation of acetone, evidently, involves

1. Breaking of three H—H bonds to give six atoms of H, breaking of half O—O bond to give one atom of O and sublimation of three atoms of C(*s*) to give three atoms of C(*g*).
2. Formation of two C—C bonds, six C—H bonds and one C=O bond.

The enthalpy of formation of acetone is thus given by

$$\Delta H_f = [3(\Delta H_{H\text{-}H}) + 1/2(\Delta H_{O\text{-}O}) + 3(\Delta H_{C(s)\to C(g)})] - [2(\Delta H_{C\text{-}C}) + 6(\Delta H_{C\text{-}H}) + \Delta H_{C=O}]$$

Incorporating the data given in Table 6, we have

$$\Delta H_f = [3(435{\cdot}1) + 1/2(138{\cdot}1) + 3(719{\cdot}6)] - [2\times347{\cdot}3 + 6\times416{\cdot}2 + 711{\cdot}3]$$
$$= \mathbf{-369{\cdot}95\ kJ\ mol^{-1}}$$

3. Determination of resonance energy. Generally, there is a good agreement between the enthalpies of formation as calculated from bond energies and those determined experimentally. However, if a compound exhibits resonance, there is a considerable difference between the two values. This difference gives a measure of the resonance energy of the compound. As an example, we may consider the dissociation of benzene.:

$$C_6H_6(g) \longrightarrow 6C(g) + 6H(g)$$

Assuming that benzene ring consists of three single and three double bonds.(Kekule's structure), the calculated dissociation energy comes out to be 5384·1 kJ, as illustrated below :

$$\Delta H_d = 3(\Delta H_{C-C}) + 3(\Delta H_{C=C}) + 6(\Delta H_{C-H})$$
$$= 3\times347{\cdot}3 + 3\times615{\cdot}0 + 6\times416{\cdot}2 = \mathbf{5384{\cdot}1\ kJ\ mol^{-1}}$$

The experimental value is known to be 5535·1 kJ mol^{-1}. Evidently, the actual energy required for the dissociation of benzene is 151 kJ more than the calculated value. This clearly shows that the actual structure of benzene is more stable than the Kekule structure by 151 kJ. The actual structure is now known to be a resonance hybrid of the two Kekule structures and may be represented as

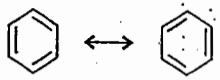

The difference of 151 kJ gives the resonance energy of benzene.

I. Review Questions

1. Derive the relation between ΔH and ΔU for a thermodynamic system.
2. Derive the relation between enthalpy of reaction at constant volume and at constant pressure for an ideal gas.
3. Define the terms $\Delta H_{comb.}$, $\Delta H_{neut.}$, $\Delta H_{soln.}$ and ΔH_f°.
4. Derive Kirchhoff's equation relating the variation of enthalpy of a reaction with temperature. Write down the integrated form of the equation.
5. Define the terms : Flame and explosion temperatures. How are these temperatures determined ?
6. State and explain Hess's law of constant heat summation. Discuss the applications of this law.
7. Define bond energy. Discuss the applications of bond energies.
8. How would you determine the following from bond energies :
   (i) Enthalpies of reactions *(ii)* Enthalpies of formation of compounds and *(iii)* Resonance energy.

II. Problems

1. The $\Delta H°$ for the reaction $C_2H_5OH(l) + 3O_2(g) \longrightarrow 2CO_2(g) + 3H_2O(l)$ is -1,366·5 kJ. Calculate $\Delta U°$.
[Ans. -1,364 kJ]

2. The enthalpy of formation of ethane at 25°C is -84·68 kJ. Calculate the heat of formation at constant volume at this temperature.
[Ans. - 79·70 kJ]

3. The heat of combustion of C_2H_4 at 17°C and at constant volume is -1389·9 kJ. What is the enthalpy of combustion ?
[Ans. - 1394·7 kJ]

4. The enthalpies of combustion of CH_4 and C_2H_6 are - 890·3 and - 1,559·7 kJ mol^{-1}, respectively. Which of the two has greater efficiency as fuel per gram ?
[Ans. CH_4]

5. Calculate ΔH_f for methane, *i.e.*, ΔH for the reaction C(graphite) + $2H_2(g) \longrightarrow CH_4(g)$ from the following data :

$CH_4(g) + 2O_2(g) \longrightarrow CO_2(g) + 2H_2O(l)$; $\Delta H = -890·3$ kJ

$H_2(g) + 1/2\ O_2(g) \longrightarrow H_2O(l)$; $\Delta H = -285·9$ kJ

$C(graphite) + O_2(g) \longrightarrow CO_2(g)$; $\Delta H = -393·5$ kJ

[Ans. - 75·56 kJ mol^{-1}]

6. The enthalpy of neutralization of NH_4OH with HCl is - 51·46 kJ mol^{-1}. Calculate the enthalpy of ionization of NH_4OH. Assume that the enthalpy of neutralization of a strong acid with a strong base is - 57·35 kJ mol^{-1}.
[Ans. 5·89 kJ mol^{-1}]

7. $\Delta H°_{neutr}$ for CH_3COOH with NaOH is - 51·63 kJ mol^{-1}. Calculate ΔH_{ioniz} of CH_3COOH. Assume that the enthalpy of neutralization of a strong acid with a strong base is -57·35 kJ mol^{-1}. **[Ans. 5·72 kJ mol^{-1}]**

8. When H_2 gas is burnt in O_2 gas, 240·5 kJ heat is liberated per mole of the explosion products at 27°C. Calculate the maximum temperature of explosion. Given $C_v(H_2O, g) = 24·15\ J\ K^{-1}$ and the reaction involved is $H_2(g) + 1/2\ O_2(g) \longrightarrow H_2O(g)$; $\Delta U_{300} = -240·5$ kJ. **[Ans. Approx 10^4 K]**

9. 2 gram of $C_6H_6(g)$ was burnt in excess of oxygen in a bomb calorimeter according to the reaction :

$$C_6H_6(g) + 7·5O_2(g) \longrightarrow 6CO_2(g) + 3H_2O(l)$$

If the temperature rise is 42·1°C and the heat capacity of the system is 2·0 kJ K^{-1}, calculate the enthalpy of combustion of benzene at 25°C.
[Ans. - 3920 kJ mol^{-1}]

10. Calculate $\Delta H°$ for the reaction $CH_2=CH_2(g) + 3O_2(g) \longrightarrow 2CO_2(g) + 2H_2O(l)$ at 25°C. Given the following bond energies :

Bond	C—H	O=O	C=O	O—H	C=C
Bond energy (kJ (mol^{-1})	416·2	493·7	711·3	464·4	615·0

[Ans. - 941·9 kJ]

11. For the reaction $CH_4(g) + 2O_2(g) \longrightarrow CO_2(g) + 2H_2O(g)$; $\Delta H° = -802·8$ kJ. Calculate $\Delta H_{C=O}$ from the following bond energy data :
$\Delta H_{C-H} = 416·2$ kJ mol^{-1} ; $\Delta H_{O=O} = 493·7$ kJ mol^{-1} ; $\Delta H_{O-H} = 464·4$ kJ mol^{-1} **[Ans. 798·5 kJ mol^{-1}]**

CHAPTER 15

THE SECOND LAW OF THERMODYNAMICS

Limitations of the First law. Need for the Second law.

The First law of thermodynamics, though exact, has certain limitations, as discussed below.

1. The First law establishes definite relationship between the heat absorbed and the work performed by a system in a given process. But *it puts no restriction on the direction of flow of heat.* According to the first law, for example, it is not impossible to extract heat from ice by cooling it to a low temperature and then use it for warming water. But it is known from experience that such a transfer of heat from a lower to a higher temperature is not possible without expenditure of energy, *i.e.*, without doing some external work. It is known, on the other hand, that heat flows spontaneously, *i.e.*, of its own accord, from a higher to a lower temperature.

2. According to the First law, the energy of an isolated system remains constant during a specified change of state. But it does not tell whether a specified change or a process including a chemical reaction can occur spontaneously, *i.e.*, whether it is feasible.

3. The First law states that energy of one form can be converted into an equivalent amount of energy of another form. But it does not tell that heat energy cannot be completely converted into an equivalent amount of work. There is thus need for another law, *viz.*, the Second law of thermodynamics.

The Second law helps us to determine the direction in which energy can be transferred. It also helps us to predict whether a given process or a chemical reaction can occur spontaneously. It introduces a new concept of entropy. It also helps us to know the equilibrium conditions.

It is known from experience that although various forms of energy can be completely transformed into one another, yet heat is a typical form of energy which cannot be completely transformed into work. The Second law helps us to calculate the maximum fraction of heat that can be converted into work in a given process. Entropy can be thought of as arising from the *dispersal* or *degradation* of the total energy of an isolated system.

Spontaneous or Irreversible Processes

Natural processes are spontaneous and irreversible. A few examples are given below.

1. Water flows downhill spontaneously. We cannot reverse the direction of flow without some external aid.

2. If a bar of metal is hot at one end and cold at the other end, heat flows spontaneously from the hot end to the cold end until the temperature of the rod becomes uniform throughout, *i.e.*, until equilibrium is attained. This process, evidently, cannot be reversed. Our experience does not show that a metal bar having uniform temperature can become hot at one end and cold at the other end spontaneously.

3. The diffusion of a solute from a more concentrated solution to a less concentrated solution when these are brought into contact proceeds spontaneously till the concentration becomes uniformly

the same, *i.e.*, till the equilibrium is attained. This process also cannot be reversed because once the concentration becomes uniform, it is not possible to make spontaneously one part of the solution more concentrated than any other part.

4. Heat flows spontaneously from a hot reservoir to a cold reservoir. For the reverse process, *i.e.*, for the transfer of heat from a cold reservoir to a hot reservoir, as in a refrigerator, energy has to be supplied from outside the system.

5. Electricity flows spontaneously from a point at a higher potential to a point at a lower potential. The direction of flow of current can be reversed only by applying an external field in the opposite direction,

6. A gas expands spontaneously from a region of high pressure to a region of low pressure or in vacuum.

Thus, we see that all natural processes proceed spontaneously and are thermodynamically irreversible in character.

Work can be obtained from spontaneous processes. But since these proceed irreversibly, the work obtained is much less than that obtained from thermodynamically reversible processes in which case the work obtained is maximum.

Cyclic Process. When a system, after completing a series of changes, returns to original state, it is said to have completed a **cycle.** The entire process is known as a **cyclic process.** Since the internal energy of a system depends only upon its state, it follows that in a cyclic process, the net change of internal energy is zero, *i.e.*, $\Delta U=0$. Therefore, according to the First law,

$$\Delta U = 0 = q + w \qquad \text{or} \qquad q = -w$$

If the series of changes in a cycle are conducted at constant temperature, the cycle is said to be an **isothermal cycle.** If the changes are carried out reversibly, the cycle is said to be a **reversible cycle.**

Although the reversible cyclic processes are merely theoretical and imaginary, the concept is highly useful in deriving certain important relationships. The most well known cyclic process is the **Carnot cycle.**

Carnot employed a reversible cycle to demonstrate the maximum convertibility of heat into work. The system consists of one mole of an ideal gas which is subjected to a series of four successive operations, commonly termed as **four strokes,** as given below.

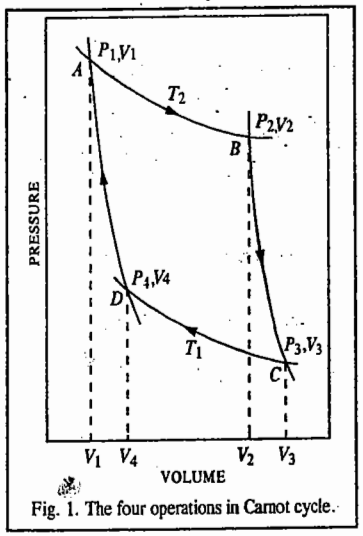

Fig. 1. The four operations in Carnot cycle.

I. Stroke 1. Isothermal Expansion. The gas is allowed to expand reversibly and isothermally at the temperature T_2 so that the volume increases from V_1, represented by the point A, to V_2 represented by the point B (Fig. 1.). Since in the isothermal expansion of an ideal gas $\Delta U=0$, it follows from the First law equation (*viz.*, $\Delta U=q+w$) that $q=-w$, *i.e.*, the heat absorbed is equal to the work done by the system on the surroundings. Let q_2 be the heat absorbed by the system at the temperature T_2 and w_1 be the work done by the system on the surroundings. Then

$$q_2 = -w_1 = RT_2 \ln (V_2/V_1) \qquad ...(1)$$

II. Stroke 2. Adiabatic Expansion. The gas is then allowed to expand reversibly and adiabtically from the volume V_2 to V_3, *i.e.*, from the point B to C.

Since work is done by the system adiabatically, it is not in a position to absorb heat. The temperature of the system, therefore, falls from T_2 to say, T_1. As q is equal to zero in this case, it follows from the First law equation (*viz.*, $\Delta U = q+w$) that $\Delta U=w$. Since the process involves expansion of the gas, therefore, work is done by the system on the surroundings. Hence, by convention, w is negative so that $\Delta U = -w$.

Now, by definition, $C_v = (\partial U/\partial T)_v$ ...(2)

$$\therefore \qquad \Delta U = C_v \Delta T = C_v(T_1 - T_2) = -w \qquad ...(3)$$

(change in temperature, ΔT = final temperature - initial temperature)

or $$-w = C_v(T_1 - T_2) = -C_v(T_2 - T_1) \qquad ...(4)$$

If the work done in this stage is denoted by w_2, then

$$\therefore \qquad -w_2 = -C_v(T_2 - T_1) \qquad ...(5)$$

III. Stroke 3. Isothermal Compression. After this, the gas is subjected to a reversible and isothermal compression at the lower temperature T_1 so that the volume decreases from V_3 to V_4 (*i.e.*, from the point C to D). In this case, evidently, work is done on the system. Hence, heat will be produced and *given up* to the surroundings. Since compression takes place isothermally and reversibly, $\Delta U=0$. Therefore, if q_1 is the heat *given out* to the surroundings at the temperature T_1 and w_3 is the work done on the system in this process, then remembering signs of q and w,

$$-q_1 = w_3 = RT_1 \ln (V_4/V_3) \qquad ...(6)$$

IV. Stroke 4. Adiabatic Compression. Finally, by an adiabatic and reversible compression, the gas is restored to its original volume V_1 and temperature T_2. Thus, the gas is compressed adiabatically from D to A. In this case, work is done on the system. Hence, w is positive. According to the First law, $\Delta U=q+w$. Since in adiabatic process, $q=0$, hence,

$$\Delta U = w = C_v\Delta T = C_v(T_2 - T_1)$$

Let w_4 be the work done in this stage. Then,

$$w_4 = C_v(T_2 - T_1) \qquad ...(7)$$

where $T_2 - T_1$ is the increase in temperature produced by the adiabatic compression.

The net heat absorbed (q) by the ideal gas in the whole cycle is given by

$$q = q_2 + (-q_1) = RT_2 \ln (V_2/V_1) + RT_1 \ln (V_4/V_3)$$
$$= RT_2 \ln (V_2/V_1) - RT_1 \ln (V_3/V_4) \qquad ...(8)$$

In the light of adiabatic expansion of an ideal gas discussed in Chapter 12, the following equations can be written :

$$C_v \ln (T_2/T_1) = R \ln (V_3/V_2) \qquad \text{(For stage II)}$$
$$C_v \ln (T_2/T_1) = R \ln (V_4/V_1) \qquad \text{(For stage IV)}$$

or $$V_3/V_2 = V_4/V_1 \quad \text{or} \quad V_2/V_1 = V_3/V_4 \qquad ...(9)$$

Hence, the net heat absorbed, according to Eq. 8, may be put as

$$q = q_2 - q_1 = R(T_2 - T_1) \ln (V_2/V_1) \qquad ...(10)$$

Similarly, the net work done by the gas is given by

$$w = -w_1 + (-w_2) + w_3 + w_4$$
$$= RT_2 \ln V_2/V_1 - C_v(T_2 - T_1) + RT_1 \ln (V_4/V_3) + C_v(T_2 - T_1)$$
$$= RT_2 \ln (V_2/V_1) - RT_1 \ln (V_3/V_4) \qquad ...(11)$$

Since $$V_2/V_1 = V_3/V_4$$

Hence, $$w = R(T_2 - T_1) \ln (V_2/V_1) \qquad ...(12)$$

It follows from Eqs.10 and 12 that $q=w$. Thus, *the essential condition for a cyclic process that the net work done is equal to the net heat absorbed is fully satisfied.*

The relationship between w, the net work done by the system and q_2, the quantity of heat absorbed at the higher temperature T_2, in Carnot cycle, can be obtained from the following two equations :

$$w = R(T_2 - T_1) \ln (V_2/V_1) \qquad \text{(Eq. 12)}$$

and

$$q_2 = RT_2 \ln (V_2/V_1) \qquad \text{(Eq. 1)}$$

Hence, dividing Eq. 12 by Eq. 1,

$$w = q_2 (T_2 - T_1)/T_2 \qquad (13)$$

Since $(T_2 - T_1)/T_2 < 1$, it follows that $w < q_2$, *i.e.*, work done is less than the heat absorbed. This means that only a part of the heat absorbed by the system at the higher temperature T_2 is transformed into work. The rest of the heat q_1 is given out by the system to the surroundings which is at the lower temperature T_1.

Thus, Kelvin stated the **second law of thermodynamics** as follows :

It is impossible to use a cyclic process to extract heat from a reservoir and to convert it into work without transferring at the same time a certain amount of heat from a hotter to a colder part of the system.

Efficiency of a Heat Engine. *The fraction of the heat absorbed by an engine which it can convert into work gives the* **efficiency** (η) *of the engine.*

From Eq. 13, it is seen that

$$\text{Efficiency, } \eta = w/q_2 = (T_2 - T_1)/T_2 \qquad ...(14)$$

Since $(T_2 - T_1)/T_2$ is invariably less than 1, the efficiency of a heat engine is always less than 1. No heat engine has yet been constructed which has an efficiency equal to unity. Mathematically, however, if $T_1=0$, efficiency=1.

It follows from Eq. 14 that the efficiency depends upon the difference between T_2 and T_1. Thus, the greater the difference between the temperature of the 'source' and the 'sink', the greater is the efficiency. This explains why superheated steam is used in a steam engine.

The net heat absorbed by the system, q, is equal to $q_2 - q_1$ and according to the First law of thermodynamics, this must be equivalent to the net work done by the system. Thus,

$$w = q_2 - q_1$$

Combining this with Eq. 14, we get

$$(q_2 - q_1)/q_2 = (T_2 - T_1)/T_2 \qquad ...(15)$$

Thus,

$$\text{efficiency, } \eta = \frac{q_2 - q_1}{q_2} = \frac{T_2 - T_1}{T_2} \qquad ...(16)$$

Eq. 16 has been arrived at by assuming that the series of changes in the cycle are brought about in a thermodynamically reversible manner so as to obtain maximum possible work. But, in actual practice, it is not possible to carry out the process infinitesimally slowly so that the efficiency is even less than that given by the above equation.

Carnot Theorem. According to Eq. 16, the efficiency of a machine working reversibly depends only on the temperature of the source and the sink. It is independent of the nature of the substance or substances used for operations. The same idea may be expressed by saying that *all periodic machines working reversibly between the same two temperatures have the same efficiency.* This statement is commonly known as the **Carnot theorem,** in honour of S. Carnot (1796-1832), the brilliant French physicist, known for important contributions to thermodynamics.

It may be noted that while the First law states that when one form of energy is transformed into another, the amount of energy that disappears is exactly equivalent to the amount of energy that is produced, it is silent about the extent to which such conversion can take place. The Second law of thermodynamics gives information about this point. It tells us that while all other forms of energy can be *completely* converted into heat, the complete conversion of heat into any other form of energy cannot take place without leaving some lasting change in the system. This has led to the following enunciation of the **Second law of thermodynamics :**

It is impossible to convert heat into work without compensation.

Example 1. Calculate the maximum efficiency of an engine operating between 110°C and 25°C.

Solution : Maximum efficiency of an engine working between temperatures T_2 and T_1 is given by

$$\eta = (T_2 - T_1)/T_2 = (383 \text{ K} - 298 \text{ K})/383 \text{ K} = 0{\cdot}222 = 22{\cdot}2\%$$

Example 2. Heat supplied to a Carnot engine is 1897·8 kJ. How much useful work can be done by the engine which works between 0°C and 100°C ?

Solution :

$$T_2 = 100 + 273 = 373 \text{ K} \; ; \; T_1 = 0 + 273 = 273 \text{ K} \; ; \; q_2 = 1897{\cdot}8 \text{ kJ}$$

$$w = q_2 (T_2 - T_1)/T_2 = 1897{\cdot}8 \text{ kJ} \times (373 \text{ K} - 273 \text{ K})/373 \text{ K} = 508{\cdot}7 \text{ kJ}$$

$\therefore$ Work done by the engine = **508·7 kJ**

An important generalisation. Eq. 16 derived from the Carnot cycle may be rearranged as

$$1 - (q_1/q_2) = 1 - (T_1/T_2)$$

or

$$q_1/T_1 = q_2/T_2 \qquad ...(17)$$

Eq. 17 may also be written, in the general form, as

$$q_{rev}/T = \text{constant} \qquad ...(18)$$

where q_{rev} is the quantity of heat exchanged in a process carried out *reversibly* at a temperature T. This is an important generalisation since the quantity q_{rev}/T, as we shall see presently, represents a definite quantity or state function, *viz.*, the entropy change of the system.

Concept of Entropy

Eq. 17 has been derived by giving positive sign to the heat absorbed (q_2) and negative sign to the heat lost (q_1) by the system. Describing q_1 and q_2 merely as *heats exchanged* (may be evolved or absorbed), Eq.17 may be written as

$$q_1/T_1 + q_2/T_2 = 0 \qquad ...(19)$$

Thus, when the isothermal and adiabatic processes in a Carnot cycle are carried out infinitesimally slowly (*i.e.*, reversibly), the summation of q/T terms is equal to zero.

Any cyclic process, if carried out reversibly, can be shown to consist of a series of Carnot cycles. Consider a cyclic process in which the change from the state A to state B and back to the state A (Fig. 2) is carried out reversibly. The path ABA may be considered to comprise of a number of small Carnot cycles, *i.e.*, of a series of isothermals and adiabatics, as shown in the figure.

The lines slanting horizontally stand for a diabatics and those slanting vertically stand for isothermals of the small

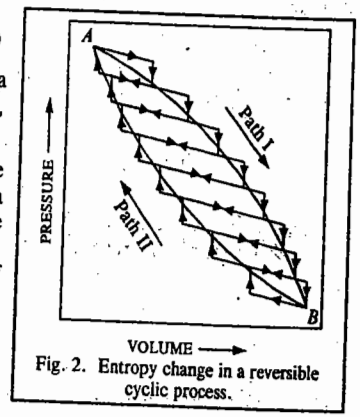

Fig. 2. Entropy change in a reversible cyclic process.

Carnot cycles. If each isothermal and adiabatic change is made extremely minute, *i.e.*, each Carnot cycle is made extremely small by increasing their number, the paths inside the loop cancel one another and the cycle corresponds to the continuous isothermal curve *ABA*. Thus, any reversible cycle can be regarded as being made up of infinite number of small Carnot cycles.

Knowing that for each Carnot cycle, $q_1/T_1 + q_2/T_2 = 0$, it follows that in the case of the reversible cycle *ABA*, comprising of a series of Carnot cycles, the summation term takes the form

$$\Sigma q/T = 0 \qquad ...(20)$$

i.e., the sum of all the q/T terms of the Carnot cycles involved is zero. When the changes are infinitesimal, the above equation may be put as

$$\Sigma dq/T = 0 \qquad ...(21)$$

Since the cycle is performed in two steps, *viz.*, from *A* to *B* and back from *B* to *A*, it follows that

$$\sum \frac{dq}{T} = \int_A^B \frac{dq}{T} + \int_B^A \frac{dq}{T} = 0 \qquad ...(22)$$

The integral $\int_A^B \frac{dq}{T}$ is the summation of all the $\frac{dq}{T}$ terms when the system changes from *A* to *B* along path I and $\int_B^A \frac{dq}{T}$ is the similar summation when the system returns from state *B* to the original state *A* along path II.

From Eq. 22,

$$\int_A^B \frac{dq}{T} = -\int_B^A \frac{dq}{T}$$

or

$$\int_A^B \frac{dq}{T}(\text{path I}) = \int_A^B \frac{dq}{T}(\text{path II}) \qquad ...(23)$$

It follows from above that $\int_A^B \frac{dq}{T}$ *is a definite quantity independent of the path followed for the change and depends only upon the initial and final states of the system.* This quantity, therefore, like ΔU and ΔH, should represent the change in some single-valued function of the states *A* and *B* of the system. This function is called **entropy** and is denoted by the symbol, *S*. If S_A is the entropy in the initial state *A* and S_B is the entropy in the final state *B*, then the change in entropy, ΔS, is given by the equation

$$\Delta S = S_B - S_A = \int_A^B \frac{dq}{T} \qquad ...(24)$$

For each infinitesimally small change,

$$dS = dq/T \qquad ...(25)$$

At constant temperature, for a finite change, dS becomes ΔS and dq becomes q.

$$\therefore \quad \Delta S = q/T \qquad ...(26)$$

It may be emphasised that since entropy is a function of the state only, the change of entropy (ΔS) for the change of state from *A* and *B* will invariably be the same whether the change is reversible or not. However, mathematically, it will be given by the equation

$$\Delta S = \int_A^B \frac{dq}{T} \qquad ...(27)$$

only when the change has been brought about reversibly. This is because the above equation has been derived from Carnot cycle in which all the changes are brought about reversibly.

Thus, the entropy change for a finite change of state of a system at constant temperature is given by

$$\Delta S = q_{rev}/T \qquad ...(28)$$

Unit of entropy. Since entropy change is expressed by a heat term divided by the absolute temperature, entropy is expressed in terms of joules per degree Kelvin ($J\ K^{-1}$). This is known as **entropy unit, e.u.**

Entropy is an extensive property. Its value, therefore, depends upon the amount of the substance involved. It is necessary, therefore, to make a mention of the quantity of the substance taken. This quantity is usually taken as one mole.

Entropy Change in an Isothermal Expansion of an Ideal Gas. In isothermal expansion of an ideal gas carried out *reversibly*, there will be no change in internal energy, *i.e.*, $\Delta U=0$ and hence from the First law equation (*viz.*, $\Delta U=q+w$),

$$q_{rev} = -w \qquad ...(29)$$

In such a case, the work done in the expansion of *n moles* of a gas from volume V_1 to V_2 at constant temperature *T*, is given by

$$-w = nRT \ln (V_2/V_1) \qquad \text{(Eq. 1)}$$

$$\therefore \quad q_{rev} = -w = nRT \ln (V_2/V_1) \qquad ...(30)$$

Hence,

$$\Delta S = q_{rev}/T = 1/T \times nRT \ln V_2/V_1 = nR \ln (V_2/V_1) \qquad ...(31)$$

Example 3. 5 moles of an ideal gas expand reversibly from a volume of 8 dm^3 to 80 dm^3 at a temperature of 27°C. Calculate the change in entropy.

Solution : From Eq. 31, $\Delta S = nR \ln (V_2/V_1)$

$$= (5 \text{ mol})\ (8{\cdot}314\ J\ K^{-1}\ mol^{-1})\ \ln\ (80\ dm^3/8\ dm^3) = 95{\cdot}73\ J\ K^{-1}$$

Entropy Changes in Reversible and Irreversible (Spontaneous) Processes. Consider isothermal expansion of an ideal gas at constant temperature into vacuum. This will, evidently, proceed spontaneously, *i.e.*, irreversibly. Since there is no opposing force, the work done (*w*) by the system will be *zero*. Further, since there is no change in temperature during the process, there will be no change in the internal energy of the system, *i.e.*, $\Delta U=0$. Hence, from the First law equation, $q=0$, *i.e.*, no heat is absorbed or evolved in the process. In other words, no heat is supplied to or removed from the surroundings. The entropy of the surroundings, therefore, remains unchanged.

As has already been stated, entropy of a system is a function only of the state of the system, *i.e.*, its temperature and pressure (or volume) and is independent of the previous history of the system. In the process under consideration, the volume of the gas increases, say, from V_1 to V_2 at constant temperature *T*. Hence, entropy increase of the system, considering that one mole of the gas is involved, would be given by

$$\Delta S = R \ln (V_2/V_1) \qquad \text{(Eq. 31)}$$

The total increase in entropy of the system and its surroundings during the spontaneous process of expansion considered above is, thus, $R \ln(V_2/V_1) + 0 = R \ln V_2/V_1$. Since $V_2 > V_1$, it is obvious that the spontaneous (irreversible) isothermal expansion of a gas is accompanied by an increase in the entropy of the system and its surroundings considered together.

Now consider isothermal expansion of the ideal gas from volume V_1 to V_2 carried out reversibly at the same temperature *T*. The expansion is now carried out infinitesimally slowly, *i.e.*, the pressure on the frictionless piston is so adjusted that it remains always less than that of the gas by an infinitesimally small amount. In this case, the gas does some external work given by $w = -P\Delta V$. Consequently, an equivalent amount of heat (q_{rev}) is absorbed reversibly by the system from the surroundings at temperature *T*. Hence, *increase* in the entropy of the system is q_{rev}/T.

The heat lost reversibly at temperature T by the surroundings is also q_{rev}. Hence, decrease in the entropy of the surroundings is q_{rev}/T. Giving appropriate sign, positive for increase and negative for decrease of entropy, the net entropy change of the system and its surroundings is given by

$$q_{rev}/T - q_{rev}/T = 0 \qquad ...(32)$$

Thus, in the reversible isothermal expansion of a gas, the total entropy change of the system and its surroundings considered together is zero. We may thus conclude that :

A thermodynamically irreversible process is always accompanied by an increase in the entropy of the system and its surroundings taken together while in a thermodynamically reversible process, the entropy of the system and its surroundings taken together remains unaltered. Thus, we can write :

$$(\Delta S_{sys} + \Delta S_{sur}) = 0 \qquad \text{(for reversible process)}$$

$$(\Delta S_{sys} + \Delta S_{sur}) > 0 \qquad \text{(for irreversible process)}$$

Combining the two, we have

$$\Delta S_{sys} + \Delta S_{sur} \geq 0 \qquad ...(33)$$

where 'equal to' sign refers to a reversible process while the 'greater than' sign refers to an irreversible process. Eq. 33. may be stated as follows :

In a reversible process, the entropy of the system and the surroundings taken together remains constant while in an irreversible process, the entropy of the system and the surroundings taken together increases.

This conclusion is of great importance as it helps us to predict whether a given process can take place spontaneously or not, *i.e.*, whether it is thermodynamically feasible or not. We shall discuss this aspect shortly. Since all processes in nature occur spontaneously, *i.e.*, irreversibly, it follows that the entropy of the universe is increasing continuously. This is another statement of the second law. Entropy can infact, be considered as a sort of *degradation* of total energy of an isolated system.

The essentials of the First law and the Second law of thermodynamics were thus summed up by the German physicist Rudolf Clausius (1822-1888) as follows :

The energy of the universe remains constant ; the entropy of the universe tends towards a maximum.

Entropy Changes Accompanying Changes of Phase

a. From Solid Phase to Liquid Phase. Consider a case when a solid changes into liquid state at its fusion point. The process requires *absorption* of heat (heat of fusion).

Consider melting of one mole of a substance reversibly at the fusion point T_{fus}, at constant pressure. Let ΔH_{fus} be the molar heat of fusion. The entropy change of the process, ΔS_{fus}, will then be given by

$$\Delta S_{fus} = \Delta H_{fus}/T_{fus} \qquad ...(34)$$

b. From Liquid Phase to Vapour Phase. Suppose one mole of a substance changes from liquid to vapour state reversibly at its boiling point T_b, under a constant pressure. If ΔH_v is the molar heat of vaporisation, then the entropy change accompanying the process will be given by

$$\Delta S_{vap} = \Delta H_{vap}/T_b \qquad ...(35)$$

Since ΔH_{fus} and ΔH_{vap} are both positive, the processes of fusion and vaporisation are both accompanied by increase of entropy.

If we consider the change of state from vapour to liquid or from liquid to solid, then ΔH_{vap} and ΔH_{fus} will both be negative and hence the process of condensation of vapour or freezing of a liquid would be accompanied by decrease of entropy.

Example 4. Calculate the entropy change in the melting of 1 kg of ice at 0°C. Heat of fusion of ice = 334·72 J g^{-1}.

Solution : From Eq. 34,

$$\Delta S_{fus} = \Delta H_{fus}/T_{fus} = 334{\cdot}72 \text{ J g}^{-1}/273 \text{ K} = 1{\cdot}226 \text{ J K}^{-1} \text{g}^{-1} = 1226 \text{ J K}^{-1} \text{kg}^{-1}$$

Example 5. Calculate the entropy increase in the evaporation of one mole of water at 100°C. Heat of vaporisation of water at 100°C = 2259·4 J g^{-1}.

Solution : From Eq. 35,

$$\Delta S_{vap} = \frac{\Delta H_{vap}}{T_b} = \frac{2259{\cdot}4 \text{ J g}^{-1} \times 18 \text{ g mol}^{-1}}{373 \text{ K}} = 109{\cdot}03 \text{ J K}^{-1} \text{ mol}^{-1}$$

Example 6. Calculate the entropy change accompanying the freezing of one mole of water at 25°C to ice at –10°C; given that the heat of fusion of ice at its fusion point (0°C) is 6·00 kJ mol^{-1}, the heat capacity of ice is 36·82 J K^{-1} mol^{-1} and heat capacity of liquid water is 75·31 J K^{-1} mol^{-1}.

Solution : The irreversible freezing of water at – 10°C can be split into the following three reversible processes :

(i) $H_2O(l)$ at 25°C $\longrightarrow$ $H_2O(l)$ at 0°C ; $\quad \Delta S = \int_{298}^{273} C_{P(l)} \frac{dT}{T}$

(ii) $H_2O(l)$ at 0°C $\longrightarrow$ $H_2O(s)$ at 0°C ; $\quad \Delta S = -\frac{\Delta H_{fus}}{T}$

(iii) $H_2O(s)$ at 0°C $\longrightarrow$ $H_2O(s)$ at – 10°C ; $\quad \Delta S = \int_{273}^{263} C_{P(s)} \frac{dT}{T}$

The total entropy change is the sum of the entropies involved in the three steps indicated above. Thus,

$$\Delta S_{total} = \int_{298}^{273} (75{\cdot}31 \text{ J K}^{-1} \text{ mol}^{-1}) \frac{dT}{T} - \frac{6000 \text{ J mol}^{-1}}{273 \text{ K}} + \int_{273}^{263} 36{\cdot}82 \text{ J K}^{-1} \text{ mol}^{-1} \frac{dT}{T}$$

$$= (75{\cdot}31 \text{ J K}^{-1} \text{ mol}^{-1}) \ln \frac{T_2}{T_1} - \frac{6000 \text{ J mol}^{-1}}{273 \text{ K}} + (36{\cdot}82 \text{ J K}^{-1} \text{ mol}^{-1}) \ln \frac{T_2}{T_1}$$

$$= (75{\cdot}31 \text{ J K}^{-1} \text{ mol}^{-1}) \ln \frac{273 \text{ K}}{298 \text{ K}} - 21{\cdot}98 \text{ K}^{-1} \text{ mol}^{-1} + (36{\cdot}82 \text{ J K}^{-1} \text{ mol}^{-1}) \ln \frac{263 \text{K}}{273 \text{K}}$$

$$= -29{\cdot}96 \text{ J K}^{-1} \text{ mol}^{-1}$$

Example 7. Calculate ΔS when one mole of steam at 100°C is converted into ice at 0°C. Average specific heat of water = $4{\cdot}184 \times 10^3$ J K^{-1} kg^{-1}; heat of vaporisation at boiling point = $2490{\cdot}6 \times 10^3$ J kg^{-1}; heat of fusion at freezing point = $333{\cdot}555 \times 10^3$ J kg^{-1}.

Solution :

$$C_P = (4{\cdot}184 \times 10^3 \text{ J K}^{-1} \text{ kg}^{-1})\ (18{\cdot}0 \times 10^{-3} \text{ kg mol}^{-1}) = 75{\cdot}31 \text{ J K}^{-1} \text{ mol}^{-1}$$

$$\Delta H_{vap} = (2490{\cdot}6 \text{ J} \times 10^3 \text{ J kg}^{-1})\ (18{\cdot}0 \times 10^{-3} \text{ kg mol}^{-1}) = 44831{\cdot}56 \text{ J mol}^{-1}$$

$$\Delta H_{fus} = (333{\cdot}555 \times 10^3 \text{ J kg}^{-1})\ (18{\cdot}0 \times 10^{-3} \text{ kg mol}^{-1}) = 6004{\cdot}00 \text{ J mol}^{-1}$$

The process consists of the following reversible steps :

(i) H_2O (steam, at 100°C) $\longrightarrow$ H_2O (*l*, at 100°C) ; $\Delta S = -\Delta H_{vap}/T_b$

(ii) H_2O (*l*, at 100°C) $\longrightarrow$ H_2O (*l*, at 0°C); $\Delta S = \int_{373}^{273} C_P \frac{dT}{T}$

(iii) H_2O (*l*, at 0°C) $\longrightarrow$ H_2O (*s*, at 0°C) ; $\Delta S = -\Delta H_{fus}/T_{fus}$

The total entropy is the sum of the three contributions. Thus,

$$\Delta S_{total} = -\Delta H_{vap}/T_b + C_p \ln 273 \text{ K}/373 \text{ K} - \Delta H_{fus}/T_{fus}.$$

$$= -\frac{44831{\cdot}56 \text{ J mol}^{-1}}{373 \text{ K}} + (75{\cdot}31 \text{ J K}^{-1} \text{ mol}^{-1}) \ln \frac{273 \text{ K}}{373 \text{ K}} - \frac{6004{\cdot}00 \text{ J mol}^{-1}}{273 \text{ K}}$$

$$= -165{\cdot}73 \text{ J K}^{-1} \text{ mol}^{-1}$$

c. From One Crystalline Form to Another. The change in entropy when one mole of a solid substance undergoes change of state from one crystalline form (say, rhombic form) to another crystalline from (say, monoclinic form) at the transition temperature T, is given by

$$\Delta S_{tr} = \Delta H_{tr}/T \qquad \ldots(36)$$

where ΔH_{tr} is the molar heat of transition of the substance. Molar heat of transition is the amount of heat absorbed or evolved by one mole of a substance when it undergoes change of state from one crystalline form to another at the transition temperature T.

Example 8. Calculate entropy change accompanying change of state of one mole of sulphur from rhombic to monoclinic state. Heat of transition of the process carried out reversibly is 322·17 joules per mole at the transition temperature 95·6°C.

Solution : From Eq. 36, $\Delta S_{tr} = 322{\cdot}17 \text{ J mol}^{-1}/368{\cdot}6 \text{ K} = 0{\cdot}874 \text{ J K}^{-1} \text{ mol}^{-1}$

Calculation of Entropy Change of an Ideal Gas with Change in P, V and T. Since entropy of a system varies with the state of the system, its value for a pure gaseous substance will depend upon any two of the three variables T, P and V. Since T is taken generally as one of the variables, the second variable to be considered may be V or P. Thus, the two variables to be considered are either T and V or T and P.

When T and V are the two variables. The increase in entropy of the gas for an infinitesimally small change is given by the expression

$$dS = dq_{rev}/T \qquad \text{(Eq. 25)}$$

where dq_{rev} is the small amount of heat *absorbed* by the gas (system) *reversibly* from the surroundings at temperature T.

According to the equation of the First law of thermodynamics, *viz.*, $\Delta U = q + w$, we have

$$dq_{rev} = dU - dw \qquad \ldots(37)$$

If the work involved is due to *expansion of the gas*, then, for an infinitesimal increase in volume dV against a pressure P,

$$-dw = PdV \qquad \ldots(38)$$

Substituting the value of dU from $C_V = (\partial U/\partial T)_v$ and $-dw$ from Eq. 38, we have

$$dq_{rev} = C_V\,dT + PdV \qquad \ldots(39)$$

For one mole of an ideal gas,

$$dq_{rev} = C_V\,dT + RT\,dV/V$$

$$\therefore \quad dq_{rev}/T = dS = C_V\,dT/T + R\,dV/V \qquad \ldots(40)$$

For a finite change of state of a system, the entropy change (ΔS) is obtained by integrating the above equation between the limits of the initial state 1 and the final state 2. Assuming C_V to be constant within the temperature range T_1 and T_2, for one mole of the gas we have

$$\Delta S = S_2 - S_1 = C_V \int_{T_1}^{T_2} \frac{dT}{T} + R \int_{V_1}^{V_2} \frac{dV}{V} \qquad \ldots(41)$$

Thus,
$$\Delta S = C_V \ln T_2/T_1 + R \ln V_2/V_1 \qquad \ldots(42)$$

For n moles of the ideal gas, the above equation may be written as

$$\Delta S = nC_V \ln (T_2/T_1) + nR \ln (V_2/V_1) \qquad \ldots(43)$$

It is evident that the entropy change for the change of state of an ideal gas depends upon the initial and final volumes as well as on the initial and final temperatures.

When T and P are the two variables. If P_1 is the pressure of the ideal gas in the initial state and P_2 in the final state, then

$P_1V_1 = RT_1$ for one mole of the gas in the initial state

$P_2V_2 = RT_2$ for one mole of the gas in the final state.

$$\therefore \quad V_2/V_1 = P_1T_2/(P_2T_1) \qquad \ldots(44)$$

Substituting in Eq. 42, for one mole of the gas, we have

$$\Delta S = C_V \ln T_2/T_1 + R \ln T_2/T_1 - R \ln P_2/P_1 \qquad \ldots(45)$$

Remembering that $C_P - C_V = R$

$$\Delta S = C_P \ln T_2/T_1 - R \ln P_2/P_1 \qquad \ldots(46)$$

For n moles of the ideal gas,

$$\Delta S = nC_P \ln (T_2/T_1) - nR \ln (P_2/P_1) \qquad \ldots(47)$$

It is evident from the above equations that the entropy change for the change of state of an ideal gas depends on the initial and final pressure as well as on the initial and final temperature.

Example 9. Calculate the change in entropy accompanying the heating of one mole of helium gas, assumed ideal, from a temperature of 298 K to a temperature of 1000 K at constant pressure. Assume that $C_V = \frac{3}{2}R$.

Solution : Since for an ideal gas, $C_P - C_V = R$, hence, $C_P = C_V + R = \frac{3}{2}R + R = 2{\cdot}5R$

When pressure is constant, Eq. 46 takes the form

$\Delta S = C_P \ln (T_2/T_1) = (2{\cdot}5 \times 8{\cdot}314 \text{ J K}^{-1} \text{ mol}^{-1}) \ln (1000 \text{ K}/298 \text{ K}) = 25{\cdot}17 \text{ J K}^{-1} \text{ mol}^{-1}$

Example 10. One mole of an ideal gas is heated from 100 K to 300 K. Calculate ΔS if (*a*) the volume is kept constant (*b*) the pressure is kept constant Assume that $C_V = 1{\cdot}5R$.

Solution : When volume is kept constant, Eq. 42 reduces to

$\Delta S = C_V \ln (T_2/T_1) = (1{\cdot}5 \times 8{\cdot}314 \text{ J K}^{-1} \text{ mol}^{-1}) \ln (300 \text{ K}/100 \text{ K}) = 13{\cdot}17 \text{ J K}^{-1}$

When pressure is kept constant, Eq. 46 takes the form

$$\Delta S = C_P \ln (T_2/T_1) = (C_V + R) \ln (T_2/T_1) = 2{\cdot}5\,R \ln (T_2/T_1)$$

$$= (2{\cdot}5 \times 8{\cdot}314 \text{ J K}^{-1} \text{ mol}^{-1}) \ln (300 \text{ K}/100 \text{ K}) = 22{\cdot}8 \text{ J K}^{-1} \text{ mol}^{-1}$$

Entropy Changes of an Ideal Gas in Different Processes. We may consider processes of three special kinds. These are :

(1) Isothermal processes (2) Isobaric processes and (3) Isochoric processes.

1. Isothermal Process. In an isothermal process, there is no change in temperature. Hence, from Eqs. 42 and 46,

$$\Delta S_T = R \ln (V_2/V_1) = -R \ln (P_2/P_1) = R \ln (P_1/P_2) \qquad \ldots(48)$$

The subscript T in ΔS_T is used to indicate that the temperature of the ideal gas remains constant during the process. If $V_2 > V_1$, ΔS_T will be positive. This means that isothermal expansion of an ideal gas is accompanied by increase in entropy. Conversely, isothermal compression of an ideal gas is accompanied by decrease in entropy.

2. Isobaric Processes. Isobaric processes are those which proceed at constant pressure. In this case, therefore, $P_1 = P_2$. Hence, Eq. 46 reduces to

$$\Delta S_P = C_P \ln (T_2/T_1) \qquad \ldots(49)$$

The subscript P in ΔS_P indicates that the pressure remains constant during the process. It follows from Eq. 49 that the increase in temperature of an ideal gas at constant pressure is accompanied by increase in entropy of the ideal gas.

3. Isochoric Processes. Isochoric processes are those in which volume of the gas remains constant. Since in this case, $V_1 = V_2$, Eq. 42 reduces to

$$\Delta S_V = C_V \ln (T_2/T_1) \quad ...(50)$$

Thus, increase in temperature of an ideal gas at constant V is accompanied by increase in entropy.

We may mention that an adiabatic process is an **isentropic process** in which entropy remains constant.

Example 11. One mole of an ideal gas expands reversibly from a volume of 10 dm^3 and temperature 298 K to a volume of 20 dm^3 and temperature 250 K. Assuming that $C_V = 3/2\ R$, calculate the entropy change for the process.

Solution : From Eq. 42, $\Delta S = C_v \ln (T_2/T_1) + R \ln (V_2/V_1)$

$= 1{\cdot}5\ (8{\cdot}314\ \text{J K}^{-1}\ \text{mol}^{-1}) \ln (250\ \text{K}/298\ \text{K}) + (8{\cdot}314\ \text{J K}^{-1}\ \text{mol}^{-1}) \ln (20\ \text{dm}^3/10\ \text{dm}^3)$

$= -2{\cdot}19\ \text{J K}^{-1}\ \text{mol}^{-1} + 5{\cdot}76\ \text{J K}^{-1}\ \text{mol}^{-1} = 3{\cdot}57\ \text{J K}^{-1}\ \text{mol}^{-1}$

Example 12. If the gas in the above example expands reversibly and adiabatically, what would be the value of ΔS for the process ?

Solution : Since for a reversible adiabatic process, $q_{rev} = 0$, hence $\Delta S = 0$.

Example 13. One mole of an ideal gas expands reversibly from a temperature of 25°C and pressure of 1 atm to a temperature of 0°C and pressure of 500 mm Hg. Calculate ΔS for the process. Assume that $C_V = 3/2\ R$.

Solution : From Eq. 46, $\Delta S = C_P \ln (T_2/T_1) + R \ln (P_1/P_2)$

For an ideal gas, $C_P - C_V = R$

$\therefore \quad C_P = C_V + R = 3/2\ R + R = 2{\cdot}5\ R = 2{\cdot}5 \times 8{\cdot}314\ \text{J K}^{-1}\ \text{mol}^{-1}$

$\therefore \quad \Delta S = (2{\cdot}5 \times 8{\cdot}314\ \text{J K}^{-1}\ \text{mol}^{-1}) \ln (273\ \text{K}/298\ \text{K}) + (8{\cdot}314\ \text{J K}^{-1}\ \text{mol}^{-1}) \ln 760\ \text{mm Hg}/500\ \text{mm Hg}$

$= -1{\cdot}82\ \text{J K}^{-1}\ \text{mol}^{-1} + 3{\cdot}48\ \text{J K}^{-1}\ \text{mol}^{-1} = \mathbf{1{\cdot}66\ J\ K^{-1}}$

Entropy of a Mixture of Ideal Gases. As mentioned above, for one mole of an ideal gas,

$$dS = C_V\, dT/T + R\, dV/V \quad \text{(Eq. 40)}$$

Integrating Eq. 40, assuming that C_v remains constant for an ideal gas, we have

$$S = C_V \ln T + R \ln V + S_0 \quad ...(51)$$

where S_0 is the integration constant.

Remembering that $C_P - C_V = R$ and $V = RT/P$, we get

$$S = C_P \ln T - R \ln P + R \ln R + S_0 \quad ...(52)$$

$$= C_P \ln T - R \ln P + S_0' \quad ...(53)$$

where S_0' ($= R \ln R + S_0$) is another constant.

Entropy of a system consisting of a mixture of gases would evidently be given by the sum of the individual entropies of the constituents at pressures (or concentrations) existing in the mixture. If n_1, n_2, n_3, etc., are the numbers of moles of the various gases present in the mixture and p_1, p_2, p_3, etc., are their partial pressures, then, the entropy of the mixture is given by

$$S = n_1 (C_P \ln T - R \ln p_1 + S_0') + n_2 (C_P \ln T - R \ln p_2 + S_0') + n_3 (C_P \ln T - R \ln p_3 + S_0') \ldots$$

$$= \Sigma n\ (C_P \ln T - R \ln p + S_0') \quad ...(54)$$

The partial pressure (p) of an ideal gas is given by the expression

$$p = xP \quad ...(55)$$

where x is the mole fraction of that particular gas in the mixture and P is the total pressure.

Substituting p by xP in Eq. 54, we have

$$S = \Sigma n (C_P \ln T - R \ln P - R \ln x + S_0') \quad ...(56)$$

Eq. 56 gives the entropy of a mixture of ideal gases.

Entropy of Mixing. Entropy of mixing is defined as the difference between the entropy of the mixture of gases and the sum of the entropies of the separate gases, each at a pressure P. Thus,

$$\Delta S_{mix} = \Sigma n (C_P \ln T - R \ln P - R \ln x + S_0') - \Sigma n\ (C_P \ln T - R \ln P + S_0') \quad ...(57)$$

$$= -R\ \Sigma n \ln x = -R\ (n_1 \ln x_1 + n_2 \ln x_2 + n_3 \ln x_3 + \cdots) \quad ...(58)$$

$$= -R\ \Sigma n_i \ln x_i \quad ...(59)$$

where n_i and x_i represent the number of moles and the mole fraction, respectively, of each constituent of the mixture.

If n is the total number of moles, then, evidently,

$$n = n_1 + n_2 + n_3 + \cdots \quad ...(60)$$

Dividing both sides by n, we have

$$1 = n_1/n + n_2/n + n_3/n + \cdots = x_1 + x_2 + x_3 + \ldots = \Sigma x_i \quad ...(61)$$

Thus, for a total of 1 mole of the gaseous mixture ($\Sigma n_i = \Sigma x_i$), the entropy of mixing is given by

$$\Delta S_{mix} = -R\ \Sigma x_i \ln x_i \quad ...(62)$$

Since x_i is a fraction, the entropy of mixing is always **positive.**

Example 14. Calculate the entropy of mixing of one mole of oxygen gas and two moles of hydrogen gas, assuming that no chemical reaction occurs and the gas mixture behaves ideally.

Solution : $n = 1$ mole ; $n_2 = 2$ moles

The mole fractions are : $x_1 = 1/(1+2) = 0{\cdot}33$; $x_2 = 1 - 0{\cdot}33 = 0{\cdot}67$

From Eq. 62,

$$\Delta S_{mix} = -R\ \Sigma n_i \ln x_i = -R\ (n_1 \ln x_1 + n_2 \ln x_2)$$

$$= -(8{\cdot}314\ \text{J K}^{-1}\ \text{mol}^{-1})\ [(1\ \text{mol})\ (\ln 0{\cdot}33) + (2{\cdot}0\ \text{mol})\ (\ln 0{\cdot}67)] = \mathbf{15{\cdot}88\ J\ K^{-1}}$$

Example 15. One mole of nitrogen gas is mixed with three moles of oxygen gas at 25°C to form a mixture at the final pressure of 1 atm, the initial pressure of each being also 1 atm. Calculate the molar entropy of mixing.

Solution : In this case, we are interested in calculating ΔS for one mole of the mixture.

The mole fractions are : $x_1 = 1/(1+3) = 0{\cdot}25$; $x_2 = 1 - 0{\cdot}25 = 0{\cdot}75$

From Eq. 62, $\Delta S_{mix} = -R\ \Sigma x_i \ln x_i = -R\ (x_1 \ln x_1 + x_2 \ln x_2)$

$$= -(8{\cdot}314\ \text{J K}^{-1}\ \text{mol}^{-1})\ [0{\cdot}25 \ln 0{\cdot}25 + 0{\cdot}75 \ln 0{\cdot}75] = \mathbf{4{\cdot}676\ J\ K^{-1}\ mol^{-1}}$$

Standard Entropies. Entropy of one mole of a substance in pure state at one atmospheric pressure and 25°C, is termed as **standard entropy** of that substance and is denoted as $S°$. When a reaction involves each reactant and each product in its standard state, the entropy change is said to be standard entropy change. This is denoted by $\Delta S°$. The general equation is then written as

$$\Delta S° = \Sigma S°_{products} - \Sigma S°_{reactants} \quad ...(63)$$

Entropies of various substances at any given temperature and pressure can be calculated by applying the Third law of thermodynamics. Standard entropies of some of the important substances obtained in this manner are recorded in Table 2 of Chapter 15.

Physical Significance of Entropy

1. Entropy as a Measure of the Disorder of the System. It has already been shown that all spontaneous processes, such as flow of heat from a hot end to a cold end of a conductor, flow of electricity from a point at a higher potential to a point at a lower potential, expansion of a gas in vacuum, diffusion of a solute from a concentrated to a dilute solution, are accompanied by increase in the 'disorder' of the system. Spontaneous processes are accompanied by increase in entropy as well as increase in the disorder of the system.

It has also been shown that melting of a solid or evaporation of a liquid is accompanied by increase of entropy. At the same time, it is known that a solid has a definite crystal lattice, *i.e.*, the atoms or ions or molecules in a solid are arranged in a definite order. The order is much less in a liquid and least in a gas. Thus, increase of entropy implies increase in disorder.

Thus, entropy is regarded as a measure of the disorder of a system. The great thermodynamicist Gibbs described entropy as a measure of the "mixed-up-ness" of a system.

2. Entropy as a Measure of Probability. As seen above, all spontaneous processes lead to increase in entropy and also to increase in disorder. A little consideration will show that when a process is spontaneous it means that it is proceeding from a less probable to a more probable state. It appears, therefore, that there is a close relation between entropy S and the thermodynamic probability W of the state of the system both of which increase at the same time. This relationship was expressed by Boltzamm as

$$S = k \ln W + \text{constant} \qquad ...(64)$$

where k is Boltzmann constant, *i.e.*, gas constant per single molecule ($=R/N_A$). Boltzmann defined **thermodynamic probability** of a system as *the ratio of the probability of the actual state to the probability of the state in which there is complete order* for the same energy and volume.

According to Planck, the constant in Eq. 64 is zero. Hence,

$$S = k \ln W \qquad ...(65)$$

Eq. 65 is called the **Boltzmann entropy equation.** A solid at absolute zero temperature is considered to be in a most ordered state. In this case, evidently, W is unity and hence $S_0=0$. The entropy of crystalline solids at absolute zero is, therefore, taken as zero.

Example 16. In the solid state at 0 K, nitric oxide is capable of existing in two orientations, *viz.*, NONO and NOON, which have practically equal probabilities. Calculate the molar entropy of NO at 0 K.

Solution : At 0 K, the probability of orientation of *one molecule* of NO is, evidently, 2. Thus, $W=2$. Hence, from the Boltzmann equation, for *one mole, i.e.*, for Avogadro's number of molecules,

$$S = N_A k \ln 2 = R \ln 2 = (8{\cdot}314 \text{ J K}^{-1} \text{ mol}^{-1}) (\ln 2) = 5{\cdot}74 \text{ K}^{-1} \text{ mol}^{-1}$$

Work and Free Energy Functions

We have seen earlier that the sum total of the entropy change of the system and the surroundings (*viz.*, $\Delta S_{sys} + \Delta S_{sur}$) serves as a criterion of spontaneity or feasibility of a process. If the total entropy change is positive, the process is feasible. If it is *zero*, the system remains in a state of *equilibrium*. However, in order to decide about the feasibility of a process, we shall have to know the entropy change of the system as well as that of the surroundings. This is not always convenient. We, therefore, consider entropy change in terms of other state functions which can be determined more conveniently. Two such functions are the **work function** and the **free energy function** represented by A and G, respectively. These are defined by the equations

$$A = U - TS \qquad ...(66)$$

$$G = H - TS \qquad ...(67)$$

Since, U, H and S depend only upon the state of a system (the temperature is included in the state), it is evident that the functions A and G also depend upon the state of the system only. Let the three functions in Eq. 66. at constant T, be A_1, U_1 and S_1 so that

$$A_1 = U_1 - TS_1 \qquad ...(68)$$

Let an appreciable change take place at the same temperature T so that the three functions in another state of the system become A_2, U_2 and S_2. Then,

$$A_2 = U_2 - TS_2 \qquad ...(69)$$

Subtracting Eq. 68 from Eq. 69, we have

$$A_2 - A_1 = (U_2 - U_1) - T(S_2 - S_1) \quad \text{or} \quad \Delta A = \Delta U - T\Delta S \qquad ...(70)$$

where ΔA is the change in the function A, ΔU is the corresponding change in internal energy and ΔS is the change in entropy of the system.

Suppose the change under reference is brought about reversibly at the constant temperature T and that the heat *absorbed* is equal to q_{rev}.

Since from Eq. 28, $\Delta S = q_{rev}/T$, hence, substituting in Eq. 70, we have

$$\Delta A = \Delta U - q_{rev} \qquad ...(71)$$

From the equation of the First law of thermodynamics, *viz.*, $\Delta U = q + w$, it follows that

$$w_{rev} = \Delta U - q_{rev} \qquad ...(72)$$

If work is done by the system, it is negative so that

$$-w_{rev} = \Delta U - q_{rev} \qquad ...(73)$$

Comparing Eq. 71 with Eq. 73,

$$-\Delta A = w_{rev} \qquad ...(74)$$

Since the process is carried out reversibly, w represents the maximum work. It is thus clear that *decrease in the function A (i.e., $-\Delta A$) gives the maximum work that can be done by the system during the given change.* The function A is, therefore, termed as the **work function.** This is also referred to as **Helmholtz free energy** or **Helmholtz function.**

The German physicist Hermann von Helmholtz (1821-1894) was a versatile scientist who made contributions to optics, thermodynamics, acoustics and physiology.

If G_1, H_1 and S_1 represent the thermodynamic functions in the initial state and G_2, H_2 and S_2 in the final state, the temperature remaining constant at T, we have from Eq. 67,

$$G_2 - G_1 = (H_2 - H_1) - T(S_2 - S_1) \quad \text{or} \quad \Delta G = \Delta H - T\Delta S \qquad ...(75)$$

But, as already shown in Chapter 13, at constant pressure

$$\Delta H = \Delta U + P\Delta V$$

$$\therefore \quad \Delta G = \Delta U + P\Delta V - T\Delta S \qquad ...(76)$$

Comparing with Eq. 70,

$$\Delta G = \Delta A + P\Delta V \qquad ...(77)$$

Since ΔA is equal to $-w$ (Eq. 74), hence

$$\Delta G = -w + P\Delta V \quad \text{or} \quad -\Delta G = w - P\Delta V \qquad ...(78)$$

The quantity $P\Delta V$ is the work done by the gas on expansion against the constant external pressure P. Therefore, $-\Delta G$ gives the maximum work obtainable from a system other than that due to change of volume, at constant temperature and pressure. The work other than that due to change of volume is called the **net work.** Thus,

$$\text{Net work} = w - P\Delta V = -\Delta G \qquad ...(79)$$

Hence, $-\Delta G$ is a measure of the net work that can be obtained from a system at constant temperature and pressure. The quantity G is called the **Gibbs function** or **Gibbs free energy** or merely **free energy**. Thus, $-\Delta G$ is a measure of the decrease in free energy. The net work that it measures may be electrical work or chemical work. This quantity is of great importance in physical chemistry ; it is named in honour of the great American physicist, J.W. Gibbs (1839-1903).

Variation of Free Energy Change with Temperature and Pressure. The variation of free energy change with variation of temperature and pressure may now be considered. According to Eq. 67,

$$G = H - TS$$

Since $H = U + PV$, hence $G = U + PV - TS$ ...(80)

Upon differentiation, $dG = dU + PdV + VdP - TdS - SdT$ ... (81)

The First law equation for an infinitesimal change may be written as

$$dq = dU - dw \quad ...(82)$$

If the work done is only due to expansion, then, $-dw = PdV$

$$\therefore \quad dq = dU + PdV \quad ...(83)$$

For a reversible process,

$$dS = dq/T \quad \text{or} \quad TdS = dq = dU + PdV \quad ...(84)$$

Combining Eqs. 81 and 84, we have

$$dG = VdP - SdT \quad ...(85)$$

This equation gives change of free energy when a system undergoes, reversibly, a change of pressure as well as change of temperature.

If pressure remains constant, *i.e.*, $dP=0$, then, from Eq. 85

$$dG = -SdT \quad \text{or} \quad (\partial G/\partial T)_P = -S \quad ...(86)$$

On the other hand, if temperature remains constant, *i.e.*, $dT=0$, then, from Eq. 85,

$$dG = VdP \quad \text{or} \quad (\partial G/\partial P)_T = V \quad ...(87)$$

Let the free energy of a system be G_1 in the initial state and G_2 in the final state when an appreciable change in pressure has taken place, at constant temperature. Then, integrating Eq. 87, the free energy change, ΔG, is given by

$$\Delta G = G_2 - G_1 = \int_{P_1}^{P_2} VdP \quad ...(88)$$

where P_1 and P_2 are the initial and final pressures, respectively.

If one mole of an ideal gas is under consideration, then $PV = RT$.

$$\therefore \quad \Delta G = RT\int_{P_1}^{P_2}\frac{dP}{P} = RT \ln\frac{P_2}{P_1} = RT \ln\frac{V_1}{V_2} \quad ...(89)$$

where V_1 and V_2 are the initial and final volumes, respectively.

For n moles of the gas,

$$\Delta G = nRT \ln (P_2/P_1) = nRT \ln (V_1/V_2) \quad ...(90)$$

Example 17. Calculate the free energy change (ΔG) which occurs when 1 mole of an ideal gas expands reversibly and isothermally at 37°C from an initial volume of 55 dm^3 to 1000 dm^3.

Solution : Substituting the given data in Eq. 90, we have

$$\Delta G = (8{\cdot}314 \text{ J K}^{-1} \text{ mol}^{-1})\ (310 \text{ K}) \ln (55 \text{ dm}^3/1000 \text{ dm}^3) = -7476{\cdot}8 \text{ J mol}^{-1}$$

The Maxwell Relations. The various expressions connecting internal energy (U), enthalpy (H), Helmholtz free energy (A) and Gibbs free energy (G), with relevant parameters such as entropy,

pressure, temperature and volume, may be put as

(i) $dU = TdS - PdV$

(ii) $dH = TdS + VdP$

(iii) $dA = -SdT - PdV$

(iv) $dG = -SdT + VdP$

If V is constant so that dV is zero, then, Eq. *(i)* yields the result

$$(\partial U/\partial S)_V = T \quad ...(91)$$

If S constant so that dS is zero, then Eq. *(i)* yields the result

$$(\partial U/\partial V)_S = -P \quad ...(92)$$

Differentiating Eq. 91 with respect to V keeping S constant and differentiating Eq. 92 with respect to S keeping V constant, we get

$$\partial^2 U/(\partial S)(\partial V) = (\partial T/\partial V)_S \quad ...(93)$$

and $$\partial^2 U/(\partial V)(\partial S) = -(\partial P/\partial S)_V \quad ...(94)$$

It follows from Eqs. 93 and 94 that

$$(\partial T/\partial V)_S = -(\partial P/\partial S)_V \quad ...(95)$$

Following the same mathematical procedure as above, the following expressions can be easily derived :

$(\partial T/\partial P)_S = (\partial V/\partial S)_P$ from *(ii)* ...(96)

$(\partial S/\partial V)_T = (\partial P/\partial T)_V$ from *(iii)* ...(97)

$(\partial S/\partial P)_T = -(\partial V/\partial T)_P$ from *(iv)* ...(98)

Eqs. 95 to 98 are known as **Maxwell's relations.**

Another set of Maxwell's relationships, which can also be derived from equations *(i)* to *(iv)*, are as follows :

$(\partial U/\partial S)_V = (\partial H/\partial S)_P$ from *(i)* and *(ii)* ...(99)

$(\partial U/\partial V)_S = (\partial A/\partial V)_T$ from *(i)* and *(iii)* ...(100)

$(\partial H/\partial P)_S = (\partial G/\partial P)_T$ from *(ii)* and *(iv)* ...(101)

$(\partial A/\partial T)_V = (\partial G/\partial T)_P$ from *(iii)* and *(iv)* ...(102)

Example 18. Show that $(\partial U/\partial S)_P = T - P(\partial T/\partial P)_S$.

Solution : From the combined form of the First and the Second laws of thermodynamics, we know that in a system undergoing *expansion*,

$$dU = TdS - PdV \quad \text{(Eq. 84)}$$

Dividing by dS, keeping P constant, we have

$$(\partial U/\partial S)_P = T - P(\partial V/\partial S)_P$$

Since $(\partial V/\partial S)_P = (\partial T/\partial P)_S$ [Maxwell's relation, Eq. 96]

$$\therefore \quad (\partial U/\partial S)_P = T - P(\partial T/\partial P)_S$$

Example 19. Using the combined form of the First and the Second laws of thermodynamics and appropriate Maxwell relations, derive the two thermodynamics equations of state.

Solution : $dU = TdS - PdV$ [Eq. 84]

Dividing by dV, keeping T constant, we have

$$(\partial U/\partial V)_T = T(\partial S/\partial V)_T - P$$

Since $(\partial S/\partial V)_T = (\partial P/\partial T)_V$ [Maxwell's relation, Eq. 97]

$\therefore \quad (\partial U/\partial V)_T = T(\partial P/\partial T)_V - P$

This is the **First thermodynamic equation of state.**

Again, $dH = TdS + VdP$

Dividing by dP, keeping T constant, we have

$(\partial H/\partial P)_T = T(\partial S/\partial P)_T + V$

Since, $(\partial S/\partial P)_T = -(\partial V/\partial T)_P$ [Maxwell's relation, Eq. 98]

$\therefore \quad (\partial H/\partial P)_T = V - T(\partial V/\partial T)_P$

This is the **Second thermodynamic equation of state.**

Example 20. Show that for an ideal gas

(*a*) $(\partial U/\partial V)_T = 0$ (*b*) $(\partial H/\partial P)_T = 0$ (*c*) $(\partial U/\partial P)_T = 0$ (*d*) $(\partial H/\partial V)_T = 0$

Solution : (*a*) For an ideal gas, $PV = nRT$ or $P = nRT/V$

$\therefore \quad (\partial P/\partial T)_V = nR/V = P/T$

Substituting this value in the First thermodynamic equation of state (Example 19), we have

$(\partial U/\partial V)_T = T(\partial P/\partial T)_V - P = T(P/T) - P = 0$

(*b*) For an ideal gas, $PV = nRT$ or $V = nRT/P$

$\therefore \quad (\partial V/\partial T)_P = nR/P = V/T$

Substituting this value in the Second thermodynamic equation of state (Example 19), we have

$(\partial H/\partial P)_T = V - T(\partial V/\partial T)_P = V - T(V/T) = 0$

(*c*) Since $H = U + PV$, hence, $U = H - PV = H - nRT$

or $(\partial U/\partial P)_T = (\partial(H - nRT)/\partial P)_T = (\partial H/\partial P)_T - (\partial(nRT)/\partial P)_T = 0 - 0 = 0$

(*d*) Since $H = U + PV = U + nRT$

$\therefore \quad (\partial H/\partial V)_T = (\partial(U+nRT)/\partial V)_T = (\partial U/\partial V)_T + (\partial(nRT)/\partial V)_T = 0 + 0 = 0.$

Example 21. Show that for an ideal gas, $(\partial V/\partial S)_P = nRT/(PC_P)$

Solution : $(\partial V/\partial S)_P = (\partial T/\partial P)_S$ [Maxwell's relation, Eq. 96] ...(*i*)

Also, $(\partial T/\partial P)_S (\partial P/\partial S)_T (\partial S/\partial T)_P = -1$ [The cyclic rule, Chapter 12] ...(*ii*)

$$\left(\frac{\partial T}{\partial P}\right)_S = -\frac{1}{(\partial P/\partial S)_T(\partial S/\partial T)_P} = -\frac{(\partial S/\partial P)_T}{(\partial S/\partial T)_P} \quad ...(iii)$$

We know that $dS = C_P\,dT/T$ so that $(\partial S/\partial T)_P = C_P/T$ ...(*iv*)

Also, $(\partial S/\partial P)_T = -(\partial V/\partial T)_P$ [from Maxwell's relation, Eq. 98]

and $$\left(\frac{\partial T}{\partial P}\right)_S = \frac{(\partial V/\partial T)_P}{C_P/T} \quad ...(v)$$

For an ideal gas, $PV = nRT$ or $V = nRT/P$ so that $(\partial V/\partial T)_P = nR/P$

From Eqs. (*i*), (*v*) and (*vi*),

$(\partial V/\partial S)_P = nRT/(PC_P).$

Example 22. Show that for an ideal gas, the internal pressure $(\partial U/\partial V)_T = 0$.

Solution : $dU = TdS - PdV$ ...(*i*)

Let $S = f(T, V)$, hence, $dS = (\partial S/\partial T)_V\,dT + (\partial S/\partial V)_T\,dV$ ...(*ii*)

Substituting for dS in Eq. (*i*),

$dU = T[(\partial S/\partial T)_V\,dT + (\partial S/\partial V)_T\,dV] - PdV$ ...(*iii*)

Also, since $U = f(T, V)$, hence, $dU = (\partial U/\partial T)_V\,dT + (\partial U/\partial V)_T\,dV$ ...(*iv*)

Equating the coefficients of dV in Eqs. (*iii*) and (*iv*),

$(\partial U/\partial V)_T = T(\partial S/\partial V)_T - P = T(\partial P/\partial T)_V - P$ [$(\partial S/\partial V)_T = (\partial P/\partial T)_V$; Maxwell's relation Eq. 97]

For one mole of an ideal gas,

$PV = RT$ or $P = RT/V$; $\therefore (\partial P/\partial T)_V = R/V$

Hence, $(\partial U/\partial V)_T = T(R/V) - P = P - P = 0$

Criteria for Reversible and Irreversible Processes. We have seen earlier that the net entropy change of a process determines whether the process would proceed irreversibly (*i.e.*, spontaneously) or not. If there is net increase in the entropy of the system and the surroundings taken together, the process would proceed irreversibly, *i.e.*, it would be thermodynamically feasible. If there is no net change in the entropy of the system and the surroundings put together, the process will be reversible, *i.e.*, the system will remain in a state of equilibrium.

We can express the criteria for reversibility and irreversibility in terms of entropy of the system (alone) as well as in terms of other fundamental thermodynamic properties, namely, U, H, A and G.

It was stated earlier that change of entropy for a given change of state is a definite quantity, independent of the fact whether the change is brought about reversibly or irreversibly. But, mathematically, it is given (for a small change) by the equation

$$dS = dq_{rev}/T = (dU + PdV)/T \quad ...(103)$$

only if the change (involving expansion of an ideal gas) is brought about reversibly.

Suppose the small change of state is brought about *irreversibly*. Now the heat absorbed by the system will be *less* ($\because q_{irr} < q_{rev}$). But the entropy change dS will have the same value. Hence, for an *irreversible* process,

$TdS > dq_{rev}$

We may thus write $TdS = dU + PdV$ (For a reversible process)

$TdS > dU + PdV$ (For an irreversible process)

Combining the two, we have

$$TdS \geq dU + PdV \quad ...(104)$$

The 'equal to' sign refers to a reversible process while the 'greater than' sign refers to an irreversible process.

(i) Criterion in Terms of Change of Entropy. If U and V (internal energy and volume) remain constant, then, for an isothermal process (*i.e.*, T is constant),

$$dS \geq 0$$

The 'equal to' sign refers to reversible process while the 'greater than' sign refers to an irreversible process.

(ii) Criterion in Terms of Change of Internal Energy. If S and V (entropy and volume) are kept constant, then, for an isothermal process (*i.e.*, T is constant).

$$dU \leq 0$$

The 'equal to' sign refers to a reversible process while 'less than' sign refers to an irreversible process.

(iii) Criterion in Terms of Change of Enthalpy. If S and P are kept constant, the expression $TdS \geq dU + PdV$ may be written as

$dU + PdV \leq 0$

But $dU + PdV = dH$

$\therefore \quad dH \leq 0$

where the sign 'equal to' refers to a *reversible* process while the sign 'less than' refers to an irreversible process.

(iv) Criterion in Terms of Change of Work Function. Combining Eq. 104, *viz.*, $TdS \geq dU + PdV$ with Eq. 70, *viz.*, $dA = dU - TdS$ for an infinitesimally small change, we have

$dA \leq -PdV$

At constant volume, therefore, $dA \leq 0$

where the sign 'equal to' refers to a reversible process while the sign 'less than' refers to an irreversible process.

(v) Criterion in Terms of Change of Free Energy. Substituting $TdS \geq dU + PdV$ in Eq. 85, we have

$$dG \leq VdP - SdT$$

$\therefore$ At constant temperature and pressure, $dG \leq 0$ ...(105)

where, as usual, the sign 'equal to' refers to a reversible process while the sign 'less than' refers to an irreversible process.

The criterion in terms of free energy change *viz.*, $(\partial G)_{T,P} \leq 0$, is the most useful criterion to decide between reversibility and irreversibility of a process. If free energy change of a process has a negative value, the process is irreversible, *i.e.*, it can take place spontaneously. If, on the other hand, the free energy change of a process is *zero*, then the process is reversible, *i.e.*, a state of equilibrium exists. Lastly, if the free energy change of process is positive, *i.e.*, there is likely to be an increase in the free energy change, then the process will not proceed.

Limitation of the above criteria. Each of the above thermodynamic criteria for determining spontaneity of a process has a limitation. It only helps to *predict* whether a given reaction or a process is thermodynamically feasible or not. It *cannot predict the rate at which a reaction will proceed.* There are other considerations, outside the realm of thermodynamics, which can tell whether the process will take place rapidly or slowly. It is because of this limitation that in the above treatment, we have used the word 'feasible' as synonymous for 'spontaneous' or 'irreversible'. A process may be thermodynamically *feasible*, yet it may not proceed spontaneously under the given experimental conditions. For example, the reaction

$$2H_2(g) + O_2(g) \longrightarrow 2H_2O(l)$$

is thermodynamically *feasible* at room temperature but a mixture of hydrogen and oxygen at room temperature will remain as such almost indefinitely without reacting. The two gases will react only if the reaction is *initiated*, say, by passing an electric spark.

The Gibbs-Helmholtz Equation

Let G_1 represent the free energy of a system in its initial state at temperature T. Suppose the temperature rises to $T+dT$ where dT is infinitesimally small. Let the free energy at the new temperature be G_1+dG_1.

Now suppose that when the system is in its final state, its free energy is given by G_2 at the temperature T and by G_2+dG_2 at the temperature $T+dT$. If the pressure remains constant all along, Eq. 86 is applicable, *i.e.*,

$$dG_1 = -S_1 dT \quad ...(106)$$

and

$$dG_2 = -S_2 dT \quad ...(107)$$

where S_1 and S_2 are the entropies of the system in the initial and final states of the system, respectively.

Subtracting Eq. 106, from Eq. 107, we have

$$d(G_2 - G_1) = -(S_2 - S_1)\, dT$$

$$d(\Delta G) = -\Delta S dT \quad ...(108)$$

As the pressure is constant, therefore,

$$(\partial(\Delta G)/\partial T)_P = -\Delta S \quad ...(109)$$

Also, since from Eq. 75, $-\Delta S = (\Delta G - \Delta H)/T$, hence, Eq. 109 becomes

$$(\Delta G - \Delta H)/T = (\partial(\Delta G)/\partial T)_P \quad ...(110)$$

or

$$\Delta G = \Delta H + T(\partial(\Delta G)/\partial T)_P \quad ...(111)$$

This equation is known as the **Gibbs-Helmholtz equation.** It is applicable to all processes occurring at constant pressure. It has been used for calculating the enthalpy change ΔH for a process or a reaction provided the values of free energy changes at two different temperatures are known.

For a reaction at constant volume, the corresponding equation will be

$$\Delta A = \Delta U + T(\partial(\Delta A)/\partial T)_V \quad ...(112)$$

Example 23. The free energy change (ΔG) accompanying a given process is – 85·77 kJ at 25°C and – 83·68 kJ at 35°C. Calculate the change in enthalpy (ΔH) for the process at 30°C

Solution : ΔG at 25°C = – 85·77 kJ and at 35°C = – 83·68 kJ

$$\therefore \quad \left(\frac{\partial(\Delta G)}{\partial T}\right)_P = \frac{-83{\cdot}68\,\text{kJ} - (-85{\cdot}77\,\text{kJ})}{308\,\text{K} - 298\,\text{K}} = 0{\cdot}209\ \text{kJ K}^{-1}$$

ΔG at 30°C may be taken as the average of the values at 25°C and 35°C,

$$\therefore \quad \Delta G \text{ at } 30°C = -\left(\frac{85{\cdot}77\,\text{kJ} + 83{\cdot}68\,\text{kJ}}{2}\right) = -84{\cdot}725\ \text{kJ}$$

$$-84{\cdot}725\ \text{kJ} = \Delta H + (303\ \text{K})\ (0{\cdot}209\ \text{kJ K}^{-1})$$

Hence,

$$\Delta H = -148{\cdot}05\ \text{kJ}$$

Thermodynamics of Open Systems. Partial Molar Properties

The thermodynamic properties, *U*, *H*, *S*, *A* and *G* are extensive properties because their values change with change in the mass (*i.e.*, the number of moles) of the system. In the derivation of the various thermodynamic equations described earlier, the change of state was considered to be due to change in temperature and pressure only. A tacit assumption was made that the system under consideration was a closed system, *i.e.*, there could be no change in the mass of the system. However, in the case of an **open system** containing two or more components, there can be change in the number of moles of various components as well. In that case, an extensive property, say, *X*, must be a function not only of temperature and pressure but also of the number of moles of the various components present in the system.

Let T and P be the temperature and pressure, respectively, of a system and let $n_1, n_2, n_3 \ldots\ldots n_j$ be the respective numbers of moles of the constituents, 1, 2, 3, $\ldots\ldots j$. Then, in view of what has been said above, the property X must be a function of temperature, pressure and the number of moles of the various constituents, *i.e.*,

$$X = f(T, P, n_1, n_2, n_3, \ldots\ldots n_j) \quad ...(113)$$

where $n_1+n_2+n_3\ldots\ldots+n_i$ = Total number of moles = N (say).

For a small change in temperature, pressure and the number of moles of the components, the change in property dX will be given by the expression

$$dX = (\partial X/\partial T)_{P,N}\, dT + (\partial X/\partial P)_{T,N}\, dP + (\partial X/\partial n_1)_{T,P,n_2\ldots\ldots n_j} dn_1 + (\partial X/\partial n_2)_{T,P,n_1,n_3\ldots n_j} dn_2$$
$$+ (\partial X/\partial n_i)_{T,P,n_1,n_2\ldots\ldots n_{j\neq i}} dn_i \ldots\ldots + (\partial X/\partial n_j)_{T,P,n_1,n_2\ldots\ldots n_{i\neq j}\ldots\ldots} dn_j \quad ...(114)$$

The quantity $(\partial X/\partial n_i)_{T,P,n_1,n_2\ldots\ldots n_{j\neq i}}$ is called the **partial molar property** of the ith component. This is represented as $\overline{X}_i$.

Thus, for the ith component in a system

$$\text{partial molar internal energy} = (\partial U/\partial n_i)_{T,P,n_1,n_2,n_3\ldots\ldots} = \overline{U}_i$$

$$\text{partial molar enthalpy} = (\partial H/\partial n_i)_{T,P,n_1,n_2,n_3\ldots\ldots} = \overline{H}_i$$

$$\text{partial molar entropy} = (\partial S/\partial n_i)_{T,P,n_1,n_2,n_3\ldots\ldots} = \overline{S}_i$$

$$\text{partial molar volume} = (\partial V/\partial n_i)_{T,P,n_1,n_2,n_3\ldots\ldots} = \overline{V}_i$$

A tangent to the curve $\bar{Y}_{total} = f(x_2)$ at any point x_2 has an intercept on the $\bar{Y}_{total}$ axis of $\bar{Y}_1$ (Eq.150) whereas a tangent to the curve $\bar{Y}_{total} = f(x_1)$ at any point x_1 has an intercept on the $\bar{Y}_{total}$ axis of $\bar{Y}_2$ (Eq.151). The slope-intercept method is depicted graphically in Fig. 4.

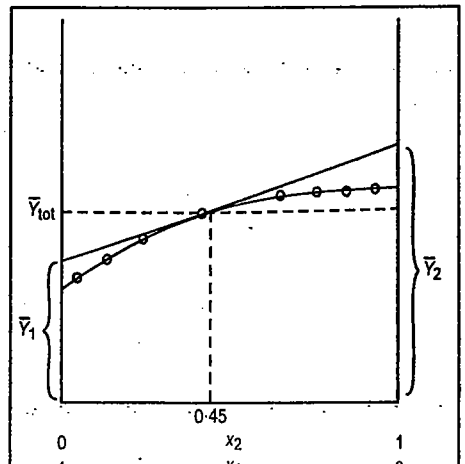

Fig. 4. Slope-intercept method for the determinaiton of partial molar quantities. The tangent to the curve at $x_2 = 0{\cdot}45$ yields as intercepts $\bar{Y}_1$ and $\bar{Y}_2$ at $x = 0{\cdot}45$.

Another useful graphical technique for obtaining partial molar quantities in two-component systems is the following : We define a quantity called the *apparent molar value* of $\bar{Y}$, designated as $^{\phi}Y$, by the expression

$$\phi Y = Y - n_1 \bar{Y}_1 / n_2 \qquad ...(152)$$

where $\bar{Y}_1$ is the molar value of Y for pure component 1 at constant T' and P (we distinguish partial molar quantities from molar quantities by means of a prime on the latter). Thus, $\bar{Y}_i$ and $\bar{Y}_1'$ refer, respectively, to the partial molar value of Y in the solution and the molar value of pure Y for the ith component. From Eq. 152, we obtain

$$Y_2 = \phi_Y + n_2 \left(\frac{\partial \phi Y}{\partial n_2} \right)_{n_1} = \phi_Y + n_2 \frac{d\phi Y}{dn_2} \qquad ...(153)$$

Thus the slope of a plot of ϕY versus n_2 at any particular composition can be inserted into Eq. 153, together with ϕY and n_2 appropriate to that composition, and $\bar{Y}_2$ results. If Y is a thermodynamic coordinate, then, Eq. 152 takes the form

$$\phi \Delta Y = \frac{\Delta Y - n_1 \Delta \bar{Y}_1}{n_2} \qquad ...(154)$$

Fig. 5 shows the reciprocal of the density of ethanol+water solutions versus the mass percent of ethanol. Inspection of Eqs. 150 and 151 shows that, in such a case, the intercepts of a tangent to the curve at a particular mass percent, multiplied by the molar masses of the respective compounds, yields $\bar{V}_1$ and $\bar{V}_2$ at that composition. From Fig 5 at 50·0 mass percent, we find that $\bar{V}_{H_2O} = 0{\cdot}964 \times 18 = 17{\cdot}35$ cm^3 mol^{-1} ; $\bar{V}_{C_2H_5OH} = 1{\cdot}232 \times 46 = 56{\cdot}75$ cm^3 mol^{-1}, compared with the values for the pure compounds *viz.*, $\bar{V}_{H_2O} = 1{\cdot}0029 \times 18 = 18{\cdot}05$ cm^3 mol^{-1} and $\bar{V}_{C_2H_5OH} = 1{\cdot}273 \times 46 = 58{\cdot}56$ cm^3 mol^{-1}.

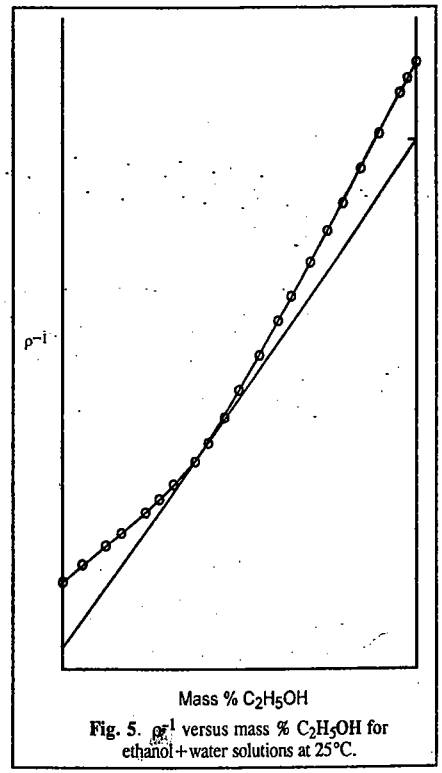

Fig. 5. ρ^{-1} versus mass % C_2H_5OH for ethanol+water solutions at 25°C.

It is worth noting that partial molar volumes can be negative also. A possible physical interpretation of this effect is that if $\bar{V}_i < 0$, then $\Delta V_{mix} < 0$. Hence, molecules of component 1 can be thought of either as entering 'cavities' in the other liquid or the molecules of component 1 cause the partial collapse of an 'open' solution structure to a more compact packing arrangement or possibly, a combination of both of these effects operate simultaneously.

Clapeyron Equation

An important equation for one-component two-phase systems was derived in the nineteenth century by Clapeyron from the Second law of thermodynamics. It is known as the Clapeyron equation. The two phases in equilibrium may be any of the following types :

(i) *Solid and Liquid,* $S \rightleftharpoons L$, at the melting point of the solid.

(ii) *Liquid and Vapour,* $L \rightleftharpoons V$, at the boiling point of the liquid.

(iii) *Solid and Vapour,* $S \rightleftharpoons V$, at the sublimation temperature of the solid.

(iv) *One Crystalline Form and Another Crystalline Form* as, for example, rhombic and monoclinic sulphur, $S_R \rightleftharpoons S_M$, at the transition temperature of the two allotropic forms.

Consider any two phases (say, liquid and vapour) of one and the same substance in equilibrium with each other at a given temperature and pressure. It is possible to transfer any definite amount of the substance from one phase to the other in a thermodynamically reversible manner, *i.e.*, infinitesimally slowly, the system remaining in a state of equilibrium all along. For example, by supplying heat infinitesimally slowly to the system, it is possible to change any desired amount of the substance from the liquid to the vapour phase at the same temperature and pressure. Similarly, by withdrawing heat infinitesimally slowly from the system, it is possible to change any desired amount of the substance from the vapour to the liquid phase without any change in temperature and pressure. Since the system remains in a state of equilibrium, the free energy change of either process will be zero. We may conclude, therefore, that *equal amounts of a given substance must have exactly the same free energy in the two phases at equilibrium with each other.*

Consider, in general, the change of a pure substance from phase A to another phase B in equilibrium with it at a given temperature and pressure. If G_A is the free energy per mole of the substance in the initial phase A and G_B is the free energy per mole in the final phase B, then, since $G_A = G_B$, hence, there will be no free energy change, *i.e.*, $\Delta G = G_B - G_A = 0$.

If the temperature of such a system is raised, say, from T to $T+dT$, the pressure will also have to change, say, from P to $P+dP$, in order to maintain the equilibrium. The relationship between dT and dP can be derived from thermodynamics.

Let the free energy per mole of the substance in phase A at the new temperature and pressure be $G_A + dG_A$ and that in phase B be $G_B + dG_B$. Since the two phases are still in equilibrium, hence,

$$G_A + dG_A = G_B + dG_B \qquad ...(155)$$

According to thermodynamics,

$$dG = VdP - SdT \qquad ...(156)$$

Eq. 152 for phase A may be written as

$$dG_A = V_A\, dP - S_A\, dT \qquad ...(157)$$

and for phase B, as $dG_B = V_B\, dP - S_B\, dT$ ...(158)

Since $G_A = G_B$, hence, from Eq. 151

$$dG_A = dG_B \qquad ...(159)$$

$$\therefore \quad V_A\, dP - S_A\, dT = V_B\, dP - S_B\, dT \qquad ...(160)$$

Chemical Potential

The most important **partial molar property** in physical chemistry is the **partial molar free energy**, designated as **chemical potential** and represented as

$$(\partial G/\partial n_i)_{T,P,n_1 \ldots n_j} = \overline{G}_i = \mu_i \qquad \ldots(115)$$

The chemical potential of a given substance is, evidently, the change in free energy of the system that results on the addition of one mole of that particular substance at a constant temperature and pressure, to such a large quantity of the system that there is no appreciable change in the overall composition of the system.

For an infinitesimal free energy change, we can write

$$dG = (\partial G/\partial T)_{P,N}\, dT + (\partial G/\partial P)_{T,N}\, dP + \mu_1 dn_1 + \mu_2 dn_2 + \cdots\cdots \mu_j dn_j \qquad \ldots(116)$$

where μ_1, $\mu_2 \cdots$ and μ_j are chemical potentials of components 1, 2, $\cdots$ and j, respectively.

If temperature and pressure remain constant, then

$$(dG)_{T,P} = \mu_1 dn_1 + \mu_2 dn_2 + \cdots\cdots \mu_j dn_j \qquad \ldots(117)$$

If a system has a definite composition having n_1, n_2, $\cdots\cdots$ n_j moles of constituents 1, 2, $\cdots\cdots j$, respectively, then, on integrating Eq. 117, we have

$$(G)_{T,P,N} = n_1\mu_1 + n_2\mu_2 + \cdots\cdots n_j\mu_j \qquad \ldots(118)$$

From Eq. 118, **chemical potential** may be defined as the contribution per mole of each particular constituent of the mixture to the total free energy of the system under conditions of constant temperature and pressure. It readily follows that for a total of one mole of a pure substance, $G = \mu$, *i.e.*, free energy is identical with chemical potential.

Gibbs-Duhem Equation. Eq. 118 shows that the free energy of a system, at constant temperature and pressure, can be expressed as a sum of $n\mu$ terms for the individual components of the system.

The total differential of G of Eq. 118 is written as

$$dG = \mu_1 dn_1 + n_1 d\mu_1 + \mu_2 dn_2 + n_2 d\mu_2 \cdots\cdots \mu_j dn_j + n_j d\mu_j$$
$$= (\mu_1 dn_1 + \mu_2 dn_2 + \cdots\cdots \mu_j dn_j) + (n_1 d\mu_1 + n_2 d\mu_2 + \cdots\cdots n_j d\mu_j) \qquad \ldots(119)$$

But, according to Eq. 117, the first term on right hand side of Eq. 119 is equal to dG, at constant temperature and pressure. It follows, therefore, that at constant temperature and pressure, for a system of a definite composition

$$n_1 d\mu_1 + n_2 d\mu_2 + \cdots\cdots n_j d\mu_j = 0 \quad \text{or} \quad \Sigma n_i\, d\mu_i = 0 \qquad \ldots(120)$$

This simple relationship is known as **Gibbs-Duhem equation.**

For a system having only two components (*e.g.*, *a* binary solution), the above equation reduces to

$$n_1 d\mu_1 + n_2 d\mu_2 = 0 \quad \text{or} \quad d\mu_1 = -(n_2/n_1)\, d\mu_2 \qquad \ldots(121)$$

Eq. 121 shows that variation in chemical potential of one component affects the value for the other component as well. Thus, if $d\mu_1$ is positive, *i.e.*, if μ_1 increases, then $d\mu_2$ must be negative, *i.e.*, μ_2 must decrease and *vice versa*.

Some Important Results. In a special case when there is no change in the number of moles of the various constituents of a system, that is, when the system is closed one, then dn_1, dn_2, $\cdots\cdots dn_j$ are all zero. In such a case, Eq. 116 reduces to

$$dG = (\partial G/\partial T)_{P,N}\, dT + (\partial G/\partial P)_{T,N}\, dP \qquad \ldots(122)$$

For a closed system, $dG = VdP - SdT$ (Eq. 85)

Hence, by equating co-efficients of dT and dP in the above two equations, we get

$$(\partial G/\partial T)_{P,N} = -S \qquad \ldots(123)$$

and

$$(\partial G/\partial P)_{T,N} = V \qquad \ldots(124)$$

These results are important as they help us in deriving expressions for the variation of chemical potential with temperature and pressure, as illustrated below.

Variation of chemical potential with temperature. The variation of chemical potential of any constituent i of a system with temperature can be derived by differentiating Eq. 115 with respect to temperature and Eq. 123 with respect to n_i. The results are :

$$\frac{\partial^2 G}{\partial n_i\, \partial T} = \left(\frac{\partial \mu_i}{\partial T}\right)_{P,N} \qquad \ldots(125)$$

$$\frac{\partial^2 G}{\partial T\, \partial n_i} = -\left(\frac{\partial S}{\partial n_i}\right)_{T,P,n_1 \cdots\cdots n_j} = -\overline{S}_i \qquad \ldots(126)$$

where $\overline{S}_i$, by definition, is the partial molar entropy of the component i,

If follows from Eqs. 125 and 126 that

$$(\partial \mu_i/\partial T)_{P,N} = -\overline{S}_i \qquad \ldots(127)$$

Eq. 127 gives the variation of chemical potential (μ_i) of any constituent i of the system with temperature.

Since the entropy of a substance is always positive, hence, according to Eq. 127, the chemical potential would decrease with increase in temperature. This is illustrated in Fig. 3 for a substance in solid, liquid and gaseous states. It is evident that at the melting point (T_m), the chemical potentials of the solid and liquid phases are the same. Similarly, at the boiling point (T_b), the chemical potentials of the liquid and gaseous phases are the same. These observations are extremely useful in the Phase rule studies.

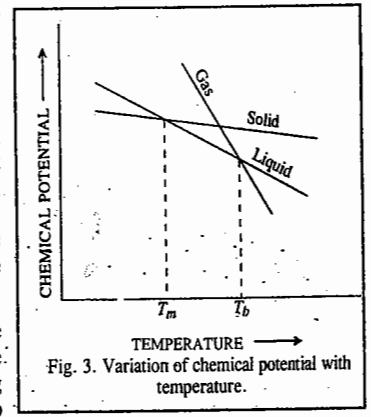

Fig. 3. Variation of chemical potential with temperature.

Variation of chemical potential with pressure. The variation of chemical potential of any constituent i of the gaseous system with pressure may be derived bydifferentiating Eq. 115 with respect to pressure and Eq. 124 with respect to n_i. The results are :

$$\frac{\partial^2 G}{\partial P\, \partial n_i} = \left(\frac{\partial \mu_i}{\partial P}\right)_{T,N} \qquad \ldots(128)$$

and

$$\frac{\partial^2 G}{\partial n_i\, \partial P} = \left(\frac{\partial V}{\partial n_i}\right)_{T,P,n_1 \cdots\cdots n_j} = \overline{V}_i \qquad \ldots(129)$$

where $\overline{V}_i$, by definition, is the partial molar volume of the component i.

If follows from Eqs. 128 and 129 that

$$(\partial \mu_i/\partial P)_{T,N} = \overline{V}_i \qquad \ldots(130)$$

Eq. 130 gives the variation of chemical potential (μ_i) of any constituent of the system with pressure.

Chemical Potential in a System of Ideal Gases. For a system of ideal gases, a further development of Eq. 130 is also possible. In an ideal gas, $PV=nRT$. Consider a system consisting of a number of ideal gases. Let n_1, n_2 $\cdots\cdots$ be the numbers of moles of various constituents present in the

mixture. Then, in the ideal gas equation, n, the total number of moles, may be replaced by $(n_1+n_2+\cdots\cdots)$. Hence,

$$V = nRT/P = (n_1 + n_2 + \cdots\cdots)\, RT/P \qquad \ldots(131)$$

Differentiating Eq. 131 with respect to n_i, at constant temperature and pressure, we have

$$(\partial V/\partial n_i)_{T,P,n_1,n_2\ldots\ldots} = \overline{V}_i = RT/P \qquad \ldots(132)$$

Substituting the value of $\overline{V}_i\,(= RT/P)$ in Eq. 130, we have

$$(\partial \mu_i/\partial P)_{T,N} = RT/P \qquad \ldots(133)$$

For a constant composition of the gas and at a constant temperature, Eq. 133 may also be expressed in the form

$$d\mu_i = (RT/P)\, dP = RT\, d \ln P \qquad \ldots(134)$$

Let p_i be the partial pressure of the constituent i present in the mixture. Since each constituent behaves as an ideal gas, therefore,

$$p_i V = n_i RT \text{ or } p_i = (n_i/n)\, P \qquad \ldots(135)$$

Since n_i and n are constants, therefore, on taking logarithms and then differentiating, we get

$$d \ln p_i = d \ln P \qquad \ldots(136)$$

Substituting in Eq. 134, we have

$$d\mu_i = RT\, d \ln p_i \qquad \ldots(137)$$

Integrating Eq. 137, we get

$$\mu_i = \mu^\circ_{i(p)} + RT \ln p_i \qquad \ldots(138)$$

where $\mu^\circ_{i(p)}$ is the integration constant, the value of which depends upon the nature of the gas and on the temperature.

It is evident from Eq. 138 that the chemical potential of any constituent of a mixture of ideal gases is determined by its partial pressure in the mixture. If the partial pressure of the constituent i is unity, *i.e.*, $p_i = 1$, then

$$\mu_i = \mu^\circ_{i(p)} \qquad \ldots(139)$$

Thus, $\mu^\circ_{i(p)}$ gives the chemical potential of the gaseous constituent i when the partial pressure of the constituent is unity, at a constant temperature.

According to Eq. 135, $p_i = (n_i/V)\, RT \qquad \ldots(140)$

Now n_i/V represents molar concentration, *i.e.*, the number of moles per unit volume of the constituent i in the mixture. If this concentration is represented by c_i, then Eq. 140 gives

$$p_i = c_i RT \qquad \ldots(141)$$

Introducing this value of p_i in Eq. 138, we have

$$\mu_i = \mu^\circ_{i(p)} + RT \ln (c_i\, RT) = \mu^\circ_{i(p)} + \underbrace{RT \ln RT}_{\text{constant}} + RT \ln c_i$$

$$= \mu^\circ_{i(c)} + RT \ln c_i \qquad \ldots(142)$$

where $\mu^\circ_{i(c)}\,(= \mu^\circ_{i(p)} + RT \ln RT)$ is a constant depending upon the nature of the gas and the temperature. If $c_i=1$, then $\mu_i=\mu^\circ_{i(c)}$. Thus, $\mu^\circ_{i(c)}$ represents the chemical potential of the constituent i when the concentration of the constituent in the mixture is unity, at a constant temperature. Lastly, since n_i/n represents the mole fraction (x_i) of the constituent i in the mixture, Eq. 135 may be represented as

$$p_i = x_i P \qquad \ldots(143)$$

Substituting this value of p_i in Eq. 138, at a constant pressure, we have

$$\mu_i = \mu^\circ_{i(p)} + RT \ln (x_i P) = \mu^\circ_{i(p)} + \underbrace{RT \ln P}_{\text{constant}} + RT \ln x_i$$

or $$\mu_i = \mu^\circ_{i(x)} + RT \ln x_i \qquad \ldots(144)$$

where the quantity $\mu^\circ_{i(x)}\,(=\mu^\circ_{i(p)} + RT \ln P)$ is also a constant which depends both on the temperature and the total pressure. If $x_i=1$, $\mu_i=\mu^\circ_{i(x)}$. Thus, $\mu^\circ_{i(x)}$ represents the chemical potential of the constituent i when its mole fraction, at a constant T and P, is unity.

Determination of Partial Molar Quantities. A straightforward, but not precise, method of determining partial molar quantities involves plotting the extensive thermodynamic variable Y at constant T and P versus the number of moles of all components except i, *viz.*, $Y(n_i)$. The slope of the resulting curve at any point is given by $\overline{Y}_i = (\partial Y/\partial n_i)_{T,P,nj\neq i}$ at that particular composition from which $\overline{Y}_i$ can be evaluated. Such a plot is easily obtained for a two-component system by using the molality composition scale which fixes the number of moles of the solvent at $1000/M_1$.

A more precise method for the determination of partial molar quantities is the so-called **slope-intercept method**, which we shall illustrate by taking into consideration the case of a two-component system. In slope-intercept method, we begin by computing the molar value of Y for the solution as a whole, a quantity that we shall designate as $\overline{Y}_{\text{total}}$ where

$$\overline{Y}_{\text{total}} = \overline{Y} \Big/ \sum_i n_i \qquad \ldots(145)$$

For a two-component system, we have

$$\overline{Y} = (n_1 + n_2)\overline{Y}_{\text{total}} \qquad \ldots(146)$$

$$\therefore \quad \overline{Y}_1 = \left(\frac{\partial \overline{Y}}{\partial n_1}\right)_{n_2} = \overline{Y}_{\text{total}} + (n_1 + n_2)\left(\frac{\partial \overline{Y}_{\text{total}}}{\partial n_1}\right)_{n_2} \qquad \ldots(147)$$

where we have omitted T and P as subscripts on the partial derivatives in the interest of simplicity. It is to be understood, however, that the development applies to a system at fixed T and P. Since

$$\left(\frac{\partial \overline{Y}_{\text{total}}}{\partial n_1}\right)_{n_2} = \left(\frac{\partial \overline{Y}_{\text{total}}}{\partial x_2}\right)_{n_2}\left(\frac{\partial x_2}{\partial n_1}\right)_{n_2} \qquad \ldots(148)$$

and mole fraction $x_2 = n_2/(n_1+ n_2)$, we have

$$\left(\frac{x_2}{\partial n_1}\right)_{n_2} = -\frac{x_2}{(n_1 + n_2)} \qquad \ldots(149)$$

Again, since an arbitrary change in x_2 gives rise to a definite change in $\overline{Y}_{\text{total}}$ (for a two-component system), we can write $\left(\partial \overline{Y}_{\text{total}}/\partial x_2\right)_{n_2} = d\overline{Y}_{\text{total}}/dx_2$ and hence,

$$\overline{Y}_{\text{total}} = \overline{Y}_1 + x_2 \frac{d\overline{Y}_{\text{total}}}{dx_2} \qquad \ldots(150)$$

A similar treatment for $\overline{Y}_2$ gives

$$\overline{Y}_{\text{total}} = \overline{Y}_2 + x_1 \frac{d\overline{Y}_{\text{total}}}{dx_1} \qquad \ldots(151)$$

or $$\frac{dP}{dT} = \frac{S_B - S_A}{V_B - V_A} \quad ...(161)$$

It may be noted that since V_A and V_B are the molar volumes of the pure substance in the two phases A and B, respectively, $V_B - V_A$ represents the change in volume when one mole of the substance passes from the initial phase A to the final phase B. It may be represented by ΔV. Similarly, $S_B - S_A$, being the change in entropy for the same process, may be put as ΔS. Hence,

$$dP/dT = \Delta S/\Delta V \quad ...(162)$$

If q is the heat exchanged reversibly per mole of the substance during the phase transformation at temperature T, then the change of entropy (ΔS) in this process is given by $\Delta S = q/T$.

Hence, $$\frac{dP}{dT} = \frac{q}{T\Delta V} \quad ...(163)$$

Thus, $$\frac{dP}{dT} = \frac{q}{T(V_B - V_A)} \quad ...(164)$$

This is the **Clapeyron equation,** named after the French engineer Benoit P. Clapeyron (1799-1864). This equation is useful in the chapter on Phase Equilibria.

This equation, evidently, gives change in pressure dP which must accompany the change in temperature dT or *vice versa,* in the case of a system containing two phases of a pure substance in equilibrium with each other. Suppose the system consists of water in the two phases, *viz.*, liquid and vapour, in equilibrium with each other at the temperature T, *i.e.*,

Water (*liquid*) $\rightleftharpoons$ Water (*vapour*)

Then, q = Molar heat of vaporisation, ΔH_{vap}

V_B = Volume of one mole of water in the vapour state, say, V_g

V_A = Volume of one mole of water in the liquid state, say, V_l

Eq. 164, therefore, takes the form

$$\frac{dP}{dT} = \frac{\Delta H_{vap}}{T(V_g - V_l)} \quad ...(165)$$

If the system consists of water at its freezing point, then, the two phases in equilibrium will be

Water (*Solid*), *i.e.*, ice $\rightleftharpoons$ Water (*liquid*)

Eq. 164 may then be written as

$$\frac{dP}{dT} = \frac{\Delta H_{fus}}{T(V_l - V_s)} \quad ...(166)$$

where ΔH_{fus} is the molar heat of fusion of ice.

Integrated Form of Clapeyron Equation for Liquid $\rightleftharpoons$ Vapour Equilibrium. Clapeyron-Clausuis Equation. The Clapeyron equation (165), as applied to liquid $\rightleftharpoons$ vapour equilibrium, can be easily integrated. The molar volume of a substance in the vapour state is considerably greater than that in the liquid state. In the case of water, for example, the value of V_g at 100°C is $18 \times 1670 = 30060$ ml while that of V_l is only a little more than 18 ml. Thus, $V_g - V_l$ can be taken as V_g without introducing any serious error. The Clapeyron equation (165), therefore, may be written as

$$\frac{dP}{dT} = \frac{\Delta H_{vap}}{TV_g} \quad ...(167)$$

Assuming that the ideal gas law is applicable, *i.e.*, $PV = RT$ (per mole), $V_g = RT/P$. Hence,

$$\frac{dP}{dT} = \frac{\Delta H_{vap}}{T} \times \frac{P}{RT} = P\frac{\Delta H_{vap}}{RT^2} \quad ...(168)$$

or $$\frac{1}{P} \times \frac{dP}{dT} = \frac{\Delta H_{vap}}{RT^2} \quad \text{or} \quad \frac{d(\ln P)}{dT} = \frac{\Delta H_{vap}}{RT^2} \quad ...(169)$$

Assuming that ΔH_v remains constant over a small range of temperature, we have

$$\int d(\ln P) = \frac{\Delta H_{vap}}{R}\int \frac{dT}{T^2} \quad \text{or} \quad P = -\frac{\Delta H_{vap}}{R}\left(\frac{1}{T}\right) + C \quad ...(170)$$

where C is integration constant.

Eq. 170 is, evidently, the equation of a straight line. Hence, the plot of ln P against $1/T$ should yield a straight line with slope $= -\Delta H_{vap}/R$ and intercept $= C$. This enables evaluation of ΔH_{vap}. Eq. 169 can also be integrated between limits of pressures P_1 and P_2 corresponding to temperatures T_1 and T_2. Thus,

$$\int_{P_1}^{P_2} d(\ln p) = \frac{\Delta H_{vap}}{R}\int_{T_1}^{T_2} \frac{dT}{T^2} \quad ...(171)$$

$$\therefore \quad \ln \frac{P_2}{P_1} = -\frac{\Delta H_{vap}}{R}\left[\frac{1}{T}\right]_{T_1}^{T_2} = \frac{\Delta H_{vap}}{R}\left[\frac{1}{T_1} - \frac{1}{T_2}\right] = \frac{\Delta H_{vap}}{R}\left[\frac{T_2 - T_1}{T_1 T_2}\right] \quad ...(172)$$

The integrated form of Clapeyron equation is known as **Clapeyron-Clausius equation.**

Applications of Clapeyron-Clausius Equation for Liquid $\rightleftharpoons$ Vapour Equilibria. Eq. 172 can be used for calculating the molar heat of vapourisation, ΔH_{vap}, of a liquid if we know the vapour pressures at two temperatures. Further, if ΔH_{vap} is known, vapour pressure at a desired temperature can be calculated from the knowledge of a single value of vapour pressure at a given temperature.

1. Calculation of molar heat of vaporisation, ΔH_{vap}.

Example 24. Vapour pressures of water at 95°C and 100°C are 634 and 760 mm, respectively. Calculate the molar heat of vapourisation, ΔH_{vap}, of water between 95°C and 100°C.

Solution : Substituting the given data in Eq. 172, we have

$$\ln \frac{760\,\text{mm}}{634\,\text{mm}} = \left(\frac{\Delta H_{vap}}{8{\cdot}314\,\text{J K}^{-1}\text{mol}^{-1}}\right)\left[\frac{373\,\text{K} - 368\,\text{K}}{(368\,\text{K})(373\,\text{K})}\right]$$

$$\therefore \quad \Delta H_{vap} = 41{,}363\ \text{J mol}^{-1} = 41{\cdot}363\ \text{kJ mol}^{-1}$$

2. Effect of temperature on vapour pressure of a liquid. If vapour pressure of a liquid at one temperature is known, that at another temperature can be calculated.

Example 25. The vapour pressure of water at 100°C is 760 mm. What will be the vapour pressure at 95°C ? The heat of vaporisation of water in this temperature range is 41·27 kJ per mole.

Solution : Substituting the given data in Eq. 172, we have

$$\ln \frac{P_2}{760\,\text{mm}} = \frac{41{\cdot}27 \times 10^3\ \text{J mol}^{-1}}{8{\cdot}314\ \text{J K}^{-1}\ \text{mol}^{-1}}\left[\frac{368\,\text{K} - 373\,\text{K}}{(368\,\text{K})(373\,\text{K})}\right]$$

$$\therefore \quad P_2 = 634{\cdot}3\ \text{mm}$$

3. Effect of pressure on boiling point. If the boiling point of a liquid at one pressure is known, that at another pressure can be calculated.

Example 26. Ether boils at 33·5°C at one atmosphere pressure. At what temperature will it boil at a pressure of 750 mm, given that the heat of vaporisation of ether is 369·86 joules per gram.

Solution : Substituting the given data in Eq. 172, we have

$$\ln \frac{750\,\text{mm}}{760\,\text{mm}} = \frac{(369{\cdot}86\,\text{J g}^{-1})(74\,\text{g mol}^{-1})}{8{\cdot}314\,\text{J K}^{-1}\text{mol}^{-1}}\left[\frac{T_2 - 306{\cdot}5\,\text{K}}{306{\cdot}5\ \text{K}\,(T_2)}\right]$$

$$\therefore \quad T_2 = 305{\cdot}9\ \text{K} = 32{\cdot}9°\text{C}$$

The Clapeyron–Clausius Equation for Solid $\rightleftharpoons$ Vapour Equilibria. The Clapeyron equation for solid $\rightleftharpoons$ vapour equilibrium may be put as

$$\frac{dP}{dT} = \frac{\Delta H_{sub}}{T(V_g - V_s)} \qquad ...(173)$$

where ΔH_{sub} stands for the molar heat of sublimation of the substance. Since the molar volume of a substance in the gaseous state is very much greater than that in the solid state, $V_g - V_s$ can be safely taken as V_g. Eq. 173 can thus be easily integrated, as before, to give the following expression :

$$\ln \frac{P_2}{P_1} = \frac{\Delta H_{sub}}{R}\left[\frac{T_2 - T_1}{T_1 T_2}\right] \qquad ...(174)$$

Eq.174 can be put to the same use for solid $\rightleftharpoons$ vapour equilibria as Eq.172 for liquid $\rightleftharpoons$ vapour equilibria.

Application of Clapeyron-Clausius Equation for Solid $\rightleftharpoons$ Liquid Equilibria. The Clapeyron equation (166) for solid $\rightleftharpoons$ liquid equilibrium cannot be integrated easily since V_s cannot be ignored in comparison with V_l. Also the laws of liquid state are not so simple as those for gaseous state. However, this equation as such can be used for calculating the effect of pressure on the melting point of a solid and also for calculating heats of fusion from vapour pressure data obtained at different temperatures.

Example 27. Calculate the value of *dT/dP* for the ice $\rightleftharpoons$ water system at 0°C. ΔH_{fus} for water is 6007·8 J·mol^{-1} (1 J=9·87×10^{-3} dm^3 atm); molar volume of water=18·00 cm^3 and that of ice 19·63 cm^3).

Solution : From the Clapeyron equation (166),

$$\frac{dP}{dT} = \frac{\Delta H_{fus}}{T(V_l - V_s)}$$

V_l = 18·0 cm^3 mol^{-1} = 0·01800 dm^3 mol^{-1}; V_s = 19·63 cm^3 mol^{-1} = 0·01963 dm^3 mol^{-1}

1 J = 9·87×10^{-3} dm^3 atm

Hence, $$\frac{dT}{dP} = \frac{T(V_l - V_s)}{\Delta H_{fus}}$$

$$= \frac{(273\,\text{K})(0{\cdot}01800\ \text{dm}^3\,\text{mol}^{-1} - 0{\cdot}01963\ \text{dm}^3\,\text{mol}^{-1})}{(6007{\cdot}8\,\text{J mol}^{-1})(9{\cdot}87\times10^{-3}\,\text{dm}^3\,\text{atm J}^{-1})} = -0{\cdot}0075\ \text{K atm}^{-1}$$

Thus, the melting point of ice *decreases* by 0·0075° if pressure is *increased* by 1 atm. It is because of this reason that ice-skating becomes possible. The weight of the skater would exert appreciable pressure on ice due to very small area of the blades of the skates so that if the temperature is not too low, ice would melt. The film of water formed between the skates and ice acts as a lubricant to facilitate movement over ice.

Example 28. The pressure exerted on ice by a skater weighing 330 kg is about 1000 atm. Calculate the depression in freezing point, assuming ΔH_{fus} to remain constant.

Solution : As shown in the last example, the melting point of ice is lowered by 0·0075 K if the pressure is increased by 1 atm. Hence, the depression in freezing point caused by a pressure of 1000 atm would be

$$\Delta T = -(0{\cdot}0075\ \text{K atm}^{-1})\ (1000\ \text{atm}) = -7{\cdot}42\ \text{K}$$

Example 29. At what pressure will ice melt at –1·0°C assuming that ΔH_{fus} is independent of pressure and is equal to 6·0095 kJ mol^{-1} ? Given that the density of water is 0·9998 g cm^{-3} and that of ice is 0·917 g cm^{-3}.

Solution : Density of water = 0·9998 g cm^{-3} = 0·9998×10^{-3} kg m^{-3}

Density of ice = 0·917 g cm^{-3} = 0·917×10^{-3} kg m^{-3}

Molar mass of water = 18·015 g mol^{-1} = 18·015×10^{-3} kg mol^{-1}

$$\frac{dP}{dT} = \frac{\Delta H_{fus}}{T(V_l - V_s)} \qquad \text{(Eq.166)}$$

$$\therefore \quad \int_{P_1}^{P_2} dP = \frac{\Delta H_{fus}}{V_l - V_s}\int_{T_1}^{T_2}\frac{dT}{T}$$

or $$P_2 - P = \frac{\Delta H_{fus}}{V_l - V_s}\ln\frac{T_2}{T_1}$$

T_1 = 0°C = 273 K ; T_2 = – 1°C = 272 K

1 atm = 101,325 N m^{-2} = 101,325 J m^{-3}

$$V_l = \frac{18{\cdot}015\times10^{-3}\,\text{kg mol}^{-1}}{0{\cdot}9998\times10^{3}\,\text{kg m}^{-3}} = 18{\cdot}0186\times10^{-6}\,\text{m}^3\,\text{mol}^{-1}$$

$$V_s = \frac{18{\cdot}015\times10^{-3}\,\text{kg mol}^{-1}}{0{\cdot}917\times10^{3}\,\text{kg m}^{-3}} = 19{\cdot}645\times10^{-6}\,\text{m}^3\,\text{mol}^{-1}$$

$$\Delta H_{fus} = \frac{6009{\cdot}5\,\text{J mol}^{-1}}{101{,}325\,\text{J m}^{-3}\,\text{atm}^{-1}} = 5{\cdot}9309\times10^{-2}\,\text{m}^3\,\text{atm mol}^{-1}$$

$$\ln\frac{T_2}{T_1} = \frac{V_l - V_s}{\Delta H_f}(P_2 - P_1) = \frac{(18{\cdot}0186\times10^{-6} - 19{\cdot}645\times10^{-6})\,\text{m}^3\,\text{mol}^{-1}}{5{\cdot}9309\times10^{-2}\,\text{m}^3\ \text{atm mol}^{-1}}(P_2 - 1)\text{atm}$$

$$\therefore \quad \ln\frac{272\,\text{K}}{273\,\text{K}} = (-2{\cdot}74\times10^{-5})\ (P_2 - 1)\ \text{atm}$$

or $$(P_2 - 1) = \frac{-0{\cdot}00367}{-2{\cdot}74\times10^{-5}} = 133{\cdot}94\ \text{atm}$$

$$\therefore \quad P_2 = 133{\cdot}94\ \text{atm}$$

Example 30. The vapour pressure of ice $\rightleftharpoons$ water system at 0·0075°C is 4·58 mm and at 0°C is 759·80 mm of mercury. Calculate the molar heat of fusion of ice, given that the specific volumes of ice and water at 0°C are 1·0907 cm^3 and 1·0001 cm^3, respectively. Density of mercury at 0°C=13·6 g cm^{-3}.

Solution : $$\frac{dP}{dT} = \frac{\Delta H_{fus}}{T(V_l - V_s)} \qquad \text{(Eq. 166)}$$

$$dP = \frac{75{\cdot}52\,\text{cm Hg}}{76\,\text{cm Hg}}\times101325\,\text{N m}^{-2} = 100685\ \text{N m}^{-2}$$

V_s = 18×1·0907×10^{-6} m^3 mol^{-1}; V_l = 18×1·0001×10^{-6} m^3 mol^{-1} ; T = 273 K, dT = 0·0075 K

Since vapour pressure of ice increases on decreasing the temperature, *dP/dT* will have a *negative sign.* Substituting various values in Eq. 166, we have

$$\Delta H_{fus} = -\frac{(100685\,\text{N m}^{-2})(273\,\text{K})(-18\times0{\cdot}0906\times10^{-6})\ \text{m}^3\,\text{mol}^{-1}}{0{\cdot}0075\ \text{K}} = 5977{\cdot}6\ \text{J mol}^{-1} \qquad (\text{N m} = \text{J})$$

$$= 5{\cdot}978\ \text{kJ mol}^{-1}$$

Fugacity And Activity

Concept of Fugacity. The great American chemist, G.N. Lewis (1875-1946) introduced the concept of fugacity for representing the actual behaviour of real gases which is distinctly different from the behaviour of ideal gases.

Variation of free energy with pressure at constant temperature is given by Eq. 124, *viz.*,

$$(\partial G/\partial P)_T = V \qquad ...(175)$$

This equation is applicable to all gases whether ideal or non-ideal.

If one mole of a gas is under consideration, then V refers to molar volume. For an ideal gas, the above equation may be written as

$$(dG)_T = RT\,dP/P \qquad ...(176)$$

and for n moles as, $$(dG)_T = nRT\,dP/P = nRTd\ (\ln P) \qquad ...(177)$$

Integration of Eq. 177 yields

$$G = G^* + nRT \ln P \quad ...(178)$$

where G^*, the integration constant, is the free energy of n moles of the ideal gas at temperature T when the pressure P is unity.

Eq. 178 gives the free energy of an ideal gas at temperature T and pressure P.

Integration of Eq. 177 between pressures P_1 and P_2, at constant temperature T, yields

$$\Delta G = \int_{P_1}^{P_2} nRT \frac{dP}{P} = nRT \ln \frac{P_2}{P_1} \quad ...(179)$$

The corresponding equation for 1 mole of the gas would be

$$\Delta G = RT \ln (P_2/P_1) \quad ...(180)$$

Eqs. 178 and 180 are not valid for real gases since V is not exactly equal to RT/P.

In order to make these simple equations applicable to real gases, Lewis introduced a new function f, called **fugacity function.** It takes the place of P in Eq. 177 which, for real gases, may be expressed as

$$(dG)_T = nRT\, d\,(\ln f) \quad ...(181)$$

and Eq. 178 may be represented as

$$G = G^* + nRT \ln f \quad ...(182)$$

where G^* is the free energy of n moles of a real gas when its fugacity happens to be 1.

Thus, fugacity is a sort of **'fictitious pressure'** which is used in order to retain for real gases simple forms of equations which are applicable to ideal gases only.

Eq. 182, evidently, gives the **free energy of a real gas** at temperature T and pressure P at which its fugacity can be taken as f.

Eq. 181, on integration between fugacities f_1 and f_2, at constant temperature T, yields

$$\Delta G = nRT \ln (f_2/f_1) \quad ...(183)$$

The corresponding equation for 1 mole of the gas would be

$$\Delta G = RT \ln (f_2/f_1) \quad ...(184)$$

As discussed above, Eqs. 183 and 184 are applicable to real gases.

Example 31. Calculate the free energy change accompanying the compression of 1 mole of a gas at 57°C from 25 to 200 atm. The fugacities of the gas at 57°C may be taken as 23 and 91 atm, respectively, at pressures of 25 and 200 atm.

Solution : We may, in the first instance, calculate ΔG by using Eq. 179, involving pressures. Thus,

$$\Delta G = nRT \ln P_2/P_1 = 1 \text{ mol } (8{\cdot}314 \text{ J K}^{-1} \text{ mol}^{-1}) (330 \text{ K}) \ln \frac{200 \text{ atm}}{25 \text{ atm}} = 5702{\cdot}8 \text{ J}$$

For more accurate value, we should use Eq. 183 involving fugacities. Thus,

$$\Delta G = nRT \ln f_2/f_1 = 1 \text{ mol } (8{\cdot}314 \text{ J K}^{-1} \text{ mol}^{-1}) (330 \text{ K}) \ln \frac{91 \text{ atm}}{23 \text{ atm}} = 3730{\cdot}0 \text{ J}$$

Fugacity at low pressures. The ratio f/P, where P is the actual pressure, approaches unity when P approaches zero since in that case a real gas approximates to ideal behaviour. The fugacity function, therefore, may be defined as

$$\lim_{P \to 0} f/P = 1 \quad ...(185)$$

Evidently, at low pressures, fugacity is equal to pressure. The two terms differ materially only at high pressures.

Determination of Fugacity of a Gas. Eq. 182, for one mole of a gas, may be put as

$$G = G^* + RT \ln f \quad ...(186)$$

Differentiation of Eq. 186 with respect to pressure at constant temperature and constant number of moles of the various constituents, *i.e.*, in a *closed system*, gives

$$\left(\frac{\partial G}{\partial P}\right)_T = RT\left(\frac{\partial (\ln f)}{\partial P}\right) \quad ...(187)$$

Since $(\partial G/\partial P)_T = V$, (Eq. 124)

it follows that

$$\left(\frac{\partial (\ln f)}{\partial P}\right)_T = \frac{V}{RT} \quad ...(188)$$

Thus, at a definite temperature, Eq. 188 may written as

$$RT\, d\,(\ln f) = V dP \quad ...(189)$$

Since one mole of the gas is under consideration, V is the molar volume of the gas.

Knowing that for an ideal gas, $V=RT/P$, the quantity α, *defined as departure from ideal behaviour* at a given temperature, is given by

$$\alpha = RT/P - V \quad ...(190)$$

Multiplying by dP throughout, we get

$$\alpha\, dP = RT\,(dP/P) - V dP \quad ...(191)$$

Combining Eqs. 189 and 190, we have

$$RTd\,(\ln f) = RT\, dP/P - \alpha\, dP$$

or

$$d(\ln f) = d\,(\ln P) - \alpha\, dP/RT \quad ...(192)$$

Integrating Eq. 192 between pressures 0 and P, we have

$$\ln \frac{f}{P} = -\frac{1}{RT} \int_0^P \alpha (dP) \quad ...(193)$$

Now, α, as given by Eq. 190, can be determined experimentally, at different pressures. These values of α are then plotted against corresponding pressures, as shown in Fig. 6. The area under the curve between pressure $P=0$ and any given pressure P, yields the value of the integral $\int_0^P \alpha (dP)$, as illustrated by the shaded portion in Fig. 6. Incorporating this value in Eq. 193, the fugacity f can be evaluated at any given pressure P of the gas.

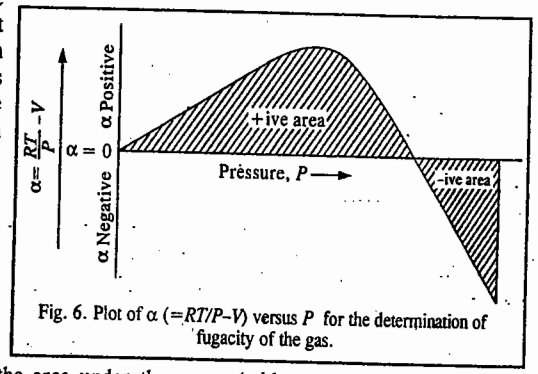

Fig. 6. Plot of α ($=RT/P-V$) versus P for the determination of fugacity of the gas.

Since α, the departure from ideal behaviour, can be both positive as well as negative (recall behaviour of real gases), the area under the curve (with respect to the pressure axis) can be both positive as well as negative. Thus, the fugacity of the gas can be both less than or more than the pressure P.

As is evident from Fig 6, the area and hence the value of $\int_0^P \alpha (dP)$ is positive at low pressures and negative at very high pressures. Hence, in accordance with Eq. 193, fugacity f of the gas would be less than the pressure P at low pressures and more than the pressure P at very high pressures. This is borne out by the data given in Table 1 for nitrogen gas at various pressures at 0°C.

TABLE 1

Fugacities of Nitrogen Gas at Various Pressures at 0°C

Pressure (atm)	Fugacity (atm)
50	48·9
100	96·7
200	194·2
400	424·4
800	1191
1000	1834

It may be recalled that for hydrogen and helium, PV is greater than RT for all pressures at ordinary temperatures. Hence, fugacity in these gases always remains greater than the pressure. This is borne out by the data given in Table 2 for fugacities of hydrogen gas at 0°C.

TABLE 2
Fugacities of Hydrogen Gas at Various Pressures at 0°C

Pressure (atm)	Fugacity (atm)
25	25·4
50	51·5
100	106·1
200	225·8
500	685
1000	1899

Calculation of fugacity at low pressures. It has been found that the experimental value of α at low pressure assumes almost a constant value. Under such conditions, therefore, Eq. 193 becomes

$$\ln f/P = -\alpha P/RT \qquad ...(194)$$

Now, at low pressures, since gases tend to be *ideal*, $f \approx P$.

or $$f/P \approx 1 \qquad ...(195)$$

Making use of the fact that $\ln x$ is approximately equal to $x - 1$ when x approaches unity, we have

$$\ln f/P = f/P - 1$$

Hence,
$$f/P = 1 + \ln f/P \qquad ...(196)$$
$$= 1 - \alpha P/RT \qquad \text{(vide Eq.194)}$$
$$= PV/RT \qquad \text{(vide Eq. 190)}$$

Hence, $$f = P^2V/RT \qquad ...(197)$$

This equation is useful in calculating fugacity at moderately low pressures.

Example 32. For a van der Waals gas, express the fugacity as a function of V, T, R and the van der Waals constants.

Solution : From Eq. 189, for one mole of the gas, $RT\, d \ln f = VdP$ ...(i)

Integrating Eq. *(i)*, $RT \int d \ln f = \int VdP$ ...(ii)

It is advisable to change the variable on the right-hand side of Eq. *(ii)* by resorting to integration by parts. Accordingly,

$$\int VdP = PV - \int VdP \qquad ...(iii)$$

Now, for one mole of the van der Waals gas,

$$P = \frac{RT}{V-b} - \frac{a}{V^2} \qquad \text{(where } V \text{ is the molar volume)} \qquad ...(iv)$$

Hence, from Eqs. *(ii)*, *(iii)* and *(iv)*,

$$RT \ln f = PV - \int \left[\frac{RT}{V-b} - \frac{a}{V^2}\right] dV = RT - RT \ln (V-b) - a/V + C \qquad ...(v)$$

where C is the integration constant.

To evaluate C, we recall that $f \to P$ as $P \to 0$. Also, as $P \to 0$ at constant T, $V \to \infty$ so that $(V - b) \to V$ and $1/V \to 0$. Hence,

$$RT \ln P = RT - RT \ln V + C = RT - RT \ln (RT/P) + C = RT - RT \ln RT + RT \ln P + C$$

$$\therefore \quad C = RT \ln RT - RT \qquad ...(vi)$$

Substituting for C in Eq. *(v)*, we get

$$RT \ln f = PV - RT \ln (V-b) - (a/V) + RT \ln RT - RT$$
$$= PV - RT + RT \ln (RT/V-b) - (a/V) \qquad ...(vii)$$

Rearranging the van der Waals equation after expansion neglecting the term ab/V^2 and later the term a/V^2 as well, we obtain

$$PV - RT = \frac{RTb}{V-b} - \frac{a}{V} \qquad ....(viii)$$

Hence, $$\ln f = b/(V-b) + \ln (RT/(V-b)) - 2a/(RTV) \qquad ...(ix)$$

which is the **required expression for fugacity.**

Fugacity of a Gas in a Gaseous Mixture. Remembering that for one mole of a pure substance, the free energy (G) is identical with chemical potential μ, Eq. 181 for one mole of any gaseous component i of a gaseous mixture may be written as

$$d\mu_i = RT\, d (\ln f_i) \qquad ...(198)$$

and Eq. 182 may be written as

$$\mu_i = \mu_i^* + RT \ln f_i \qquad ...(199)$$

where μ_i^* is the chemical potential of the gaseous component i at its unit fugacity.

Fugacity of a Liquid Component in a Liquid Mixture. Eq. 199 is valid not only for the fugacity of a gas in a gaseous mixture but also for the fugacity of a pure liquid in a liquid mixture. This easily follows from the following discussion.

As is well known, in the case of phase equilibria, the chemical potential of any given component is the same in all phases. Thus, if there are three phases a, b and c, containing a component i, then, at equilibrium,

$$(\mu_i)_a = (\mu_i)_b = (\mu_i)_c$$

Consider, for example, a liquid i in equilibrium with its vapour. The chemical potential of the liquid, $(\mu_i)_l$, is then equal to the chemical potential of its vapour, $(\mu_i)_g$, *i.e.*,

$$(\mu_i)_l = (\mu_i)_g$$

Now, according to Eq. 182, chemical potential of the vapour may be written as

$$(\mu_i)_g = (\mu_i^*)_g + RT \ln f_i \qquad ...(200)$$

where, as before $(\mu_i^*)_g$ is the chemical potential of the vapour when its fugacity is equal to 1. Therefore, chemical potential of a liquid may, evidently, be written as

$$(\mu_i)_l = (\mu_i^*)_l + RT \ln f_i \qquad ...(201)$$

where $(\mu_i^*)_l$ stands for the chemical potential of the liquid when its fugacity is equal to 1.

It follows from the above discussion that fugacity of a pure liquid would be the same as that of its vapour in equilibrium with it, at a given temperature.

Physical significance of fugacity. In order to understand the physical significance of the term fugacity, consider a system consisting of liquid water in contact with its vapour. Water molecules in the liquid phase will have a tendency to escape into the vapour phase by evaporation while those in the vapour phase will have a tendency to escape into the liquid phase by condensation. At equilibrium, the two escaping tendencies will be equal. It is now accepted that each substance in a given state has a tendency to escape from that state. This escaping tendency was termed by Lewis as **fugacity.**

Concept of Activity. It may be pointed out that since the absolute value of free energy or chemical potential is not known, it is not possible to evaluate μ_i^* of a substance. This difficulty has been overcome by referring all free energy or chemical potential measurements for any given substance to a standard reference point. Let μ_i be the chemical potential of a substance i in *pure state* and let f_i be its fugacity. Eq. 199 may then be put as

$$\mu_i = \mu_i^* + RT \ln f_i^\circ \qquad ...(202)$$

Let μ_i be the chemical potential of the same substance in some other state. Then,

$$\mu_i = \mu_i^* + RT \ln f_i \qquad ...(203)$$

The *difference* between chemical potential of a substance in *any state* and that in the *pure state* is given by

$$\mu_i - \mu_i^\circ = RT \ln (f_i/f_i^\circ) \quad \text{or} \quad \mu_i = \mu_i^\circ + RT \ln (f_i/f_i^\circ) \qquad ...(204)$$

We may introduce here a new term, **activity, *a***, and define it as

$$a = f/f^\circ \qquad ...(205)$$

or, for a substance i, as

$$a_i = f_i/f_i^\circ \qquad ...(206)$$

Activity of a substance *in any given state* is thus defined as *the ratio of the fugacity of the substance in that state to the fugacity of the same substance in the pure state.*

Eq. 204, therefore, reduces to

$$\mu_i = \mu_i^\circ + RT \ln a \qquad ...(207)$$

Let a system consisting of one mole of a substance change from a state in which its chemical potential (or free energy, both being identical since we are dealing with one mole of the substance) is μ_1, to another state in which its chemical potential is μ_2. The change in chemical potential, $\Delta\mu$, is then given by

$$\Delta\mu = \mu_2 - \mu_1 = (\mu^\circ + RT \ln a_2) - (\mu^\circ + RT \ln a_1)$$

or

$$\Delta\mu = RT \ln (a_2/a_1) = \Delta G \qquad ...(208)$$

Comparing the above equation with that for an ideal gas, *viz.*,

$$\Delta G = \Delta\mu = RT \ln (P_2/P_1) \qquad \text{(Eq. 180)}$$

we see that for *real gases, activity replaces pressure.* Thus, activity of a gas, like fugacity, *serves as a thermodynamic counterpart of gas pressure.*

Activity Coefficient. For real gases, activity is proportional to pressure, *i.e.*, $a \propto P$ or $a = \gamma P$ where γ is known as the activity coefficient.

Example 33. The activity of 2·5 moles of a substance changes from 0·05 to 0·35. What would be the change in its free energy at 27°C ?

Solution : $\Delta G = RT \ln a_2/a_1$ (Eq. 208)

$\therefore$ For n moles, $\Delta G = nRT \ln a_2/a_1 = (2{\cdot}5 \text{ mol})\ (8{\cdot}314 \text{ J K}^{-1} \text{ mol}^{-1})\ (300 \text{ K})\ \ln \dfrac{0{\cdot}35}{0{\cdot}05} = \mathbf{12133{\cdot}6\ J}$

Reference States or Standard States. It may be emphasised again that there is no means of finding absolute value of free energy (G) or chemical potential (μ) of any substance. It is necessary, therefore, to make such measurements with reference to the value obtained for some convenient though arbitrary reference state called standard state.

The standard state for a gas at any given temperature is defined *as that state in which the fugacity of the gas is equal to unity.* Since $a = f/f^\circ$, it follows that if $f^\circ = 1$, $a = f$. Evidently, the standard state for a gaseous component is such that

$$f_i = a_i = 1 \qquad ...(209)$$

The standard state for a liquid *is the pure state of* the liquid at one atmosphere pressure at any given temperature. In this state of the liquid, $f = f^\circ$ and $a = 1$. The standard state for a liquid component i in a liquid solution is the pure state of the component such that $a_i = 1$.

The standard state for a solid is the pure state of the solid at one atmosphere pressure at any given temperature. In this state, its *activity* $a = 1$.

It is pertinent to conclude this chapter with the remarks of the great philosopher of thermodynamics, P.W. Bridgman. It was noted by Bridgman, a great experimental thermodynamicist, that the laws of thermodynamics convey a stronger sense of their human origins than other laws of science.

> It must be admitted, I think, that the laws of thermodynamics have a different feel from most of the other laws of physics. There is something more palpably verbal about them—they smell more of their human origin. The guiding motif is strange to most of physics : namely, a capitalizing of the universal failure of human beings to construct perpetual motion machines of either the first or the second kind. Why should we expect nature to be interested either positively or negatively in the purposes of human beings, particularly purposes of such unblushingly economic tinge?

I. Review Questions

1. What is a cyclic process ? Describe in detail the Carnot reversible cycle for establishing the maximum convertibility of heat into work.
2. What is meant by efficiency of a heat engine ? Derive an expression for the same.
3. Show that $\Delta S = q_{rev}/T$.
4. Derive an expression for the entropy change accompanying the isothermal expansion of an ideal gas.
5. Show that the entropy of a system and surroundings taken together remains constant in a reversible process while the same increases in an irreversible process.
6. Comment on the statement. "*Entropy of the universe is always increasing.*"
7. Derive expressions for the entropy change accompanying variation of *(i)* temperature and volume *(ii)* temperature and pressure.
8. Derive an expression for the entropy of a mixture of ideal gases.
9. Define the terms Gibbs free energy and Helmholtz free energy. How is each of these terms related to maximum work that can be done by a system during a given change ? Discuss the variation of ΔG with variation in *(i)* temperature and pressure *(ii)* pressure and volume.
10. Derive Gibbs–Helmholtz equation for a process at constant pressure and at constant volume.
11. What is meant by chemical potential ? Derive the Gibbs-Duhem equation.
12. Show that in the case of a mixture of ideal gases, the chemical potential of any constituent is given by the expression :
$$\mu_i = \mu_{i(p)}^\circ + RT \ln p_i \quad \text{or} \quad \mu_i = \mu_{i(c)}^\circ + RT \ln c_i$$
where p_i and c_i represent the partial pressure and concentration, respectively, of the constituent concerned.
13. Derive the Clapeyron equation in the form $dP/dT = \Delta H_v/(TV_g)$.
14. Derive the Clapeyron equations in the integrated form for liquid $\rightleftharpoons$ vapour and solid $\rightleftharpoons$ vapour equilibria.
15. Derive the Clapeyron–Clausius equation.
16. Explain the terms fugacity and activity. How are they related to chemical potential ?
17. Explain clearly why the fugacity of a gas can both be less or more than the pressure. Explain why the fugacity of helium or hydrogen is always more than the pressure.

II. Problems

1. A Carnot engine absorbs 1,000 J of heat from a reservoir at 127°C and rejects 600 J of heat during each cycle. Calculate *(i)* the efficiency of the engine *(ii)* the temperature of the sink and *(iii)* the amount of useful work done during each cycle. **[Ans. *(i)* 40% *(ii)* – 33°C *(iii)* 400 J]**
2. A Carnot engine converts one-sixth of heat input into work. When the temperature of the sink is reduced by 62°C, its efficiency is doubled. Find the temperature of the source and the sink. **[Ans. 372 K, 310 K]**
3. A Carnot engine has the same efficiency *(i)* between 100 K and 500 K and *(ii)* between T K and 900 K. Calculate the temperature T of the sink. **[Ans. 180 K]**

4. Calculate ΔS if one mole of an ideal gas is heated from 27°C to 227°C *(i)* at constant volume and *(ii)* at constant pressure. **[Ans. 8·64 J K^{-1}; 14·4 J K^{-1}]**
5. 10 moles of an ideal gas expand reversibly from a volume of 5 dm^3 to 15 dm^3 at a temperature of 25°C. Calculate the change in entropy of the gas. **[Ans. 91·34 J K^{-1}]**
6. One mole of an ideal gas expands reversibly from a volume of 5 dm^3 and temperature 25°C to a volume of 10 dm^3 and temperature - 23°C. Calculate the entropy change of the process. (C_v=3/2 R) **[Ans. 3·57 J K^{-1} mol^{-1}]**
7. One mole of an ideal gas expands reversibly from a temperature of 298 K and pressure 1 atm to a temperature of 273 K and pressure of 400 mm Hg. Calculate ΔS for the process. C_v=3/2 R. **[Ans. 3·55 J K^{-1} mol^{-1}]**
8. Calculate the entropy change if 2 moles of N_2, 3 moles H_2 and 2 moles of NH_3 are mixed at constant temperature, assuming that no chemical reaction is occurring. **[Ans. 62·80 J K^{-1}]**
9. The free energy change (ΔG) for a given process is -79·8 kJ at 20°C and -77·4 kJ at 30°C. Calculate the change in enthalpy of the process at 25°C. **[Ans. -150·12 kJ]**
10. Calculate the free energy change accompanying the compression of 1 mole of a gas at 25°C from 20 to 200 atm. The fugacities of the gas be taken as 18 and 120 atm, respectively, at pressures of 18 and 200 atm. **[Ans. 4700 J]**
11. Calculate the fugacity of H_2 (g) at 100°C and 300 atm, assuming that it is a van der Waals gas, with a = 0·244 dm^6 atm mol^{-2}, b=0·0266 dm^3 mol^{-1} and V_m=0·119 dm^3 mol^{-1}. **[Ans. 386·6 atm]**
12. Two Carnot engines A and B have their sources at 400 K and 350 K and sinks at 350 K and 300 K, respectively. Which is more efficient and by how much ? **[Ans. B, 1·8%]**
13. Calculate ΔS for the following phase changes :

    (i) H_2O (s, 1 atm, 273 K) ⟶ H_2O (liq, 1 atm, 273 K)

    (ii) H_2O (liq, 1 atm, 273 K) ⟶ H_2O (liq, 1 atm, 373 K)

    (iii) H_2O (liq, 1 atm, 373 K) ⟶ H_2O (vap, 1 atm, 273 K)

    Given : ΔH_f = 406·03 kJ mol^{-1} ; ΔH_{vap} = 40·6 kJ mol^{-1} ; $C_{P,\,liq}$ = 75·3 J K^{-1} mol^{-1}

    [Ans. *(i)* 22·07 J K^{-1} mol^{-1} *(ii)* 23·50 J K^{-1} mol^{-1} *(iii)* 108·9 J K^{-1} mol^{-1}]
14. Calculate ΔS°_{298} for the following reaction : $2SO_2(g) + O_2(g) \longrightarrow 2SO_3(g)$.

    Given : S°_{298} values for SO_2, O_2 and SO_3 are 248·53 J K^{-1}, 205·03 J K^{-1} and 256·23 J K^{-1}, respectively.

    [Ans. - 189·63 J K^{-1}]
15. Calculate ΔS when 4 kJ of heat is transferred from a reservoir at 500 K to a reservoir at 300 K. **[Ans. 5·33 J K^{-1}]**
16. Calculate the zero-point entropy for CO crystal at 0 K. **[Ans. 5·76 J K^{-1} mol^{-1}]**
17. Calculate ΔS° for the reaction

    $2SO_2(g) + O_2(g) \longrightarrow 2SO_3(g)$

    at 500 K. Given that the temperature-dependence of molar heat capacities of the species is as follows :

    $C_p^\circ\,(O_2) = 25{\cdot}72 + 12{\cdot}98\times10^{-3}\,T - 38{\cdot}62\times10^{-7}\,T^2$

    $C_p^\circ\,(SO_2) = 49{\cdot}77 + 4{\cdot}56\times10^{-3}\,T$

    $C_p^\circ\,(SO_3) = 24{\cdot}43 + 98{\cdot}48\times10^{-3}\,T - 405{\cdot}30\times10^{-7}\,T^2$ **[Ans. 200·06 J K^{-1} mol^{-1}]**
18. Calculate ΔA for the process

    2He (g, 27°C, 1 atm) ⟶ 2He (g, 27°C, 5 atm),

    assuming that the process is reversible. **[Ans. 8·029 kJ]**

CHAPTER 16

THE THIRD LAW OF THERMODYNAMICS

First and Second laws of thermodynamics have led to new concepts of energy content and entropy. The Third law, however, does not lead to any new concept. It only places a limitation on the value of the entropy of a crystalline solid. Some scientists hesitate to call it a 'law' at all. All the same, its applications do lead to conclusions which are borne out by experience and hence, in accordance with scientific terminology, it is a law, like the other two laws of thermodynamics.

Nernst Heat Theorem. Before passing on to the Third law of thermodynamics, we may consider briefly the Nernst heat theorem. This is an old generalisation but still has relevance as the forerunner of the Third law of thermodynamics.

From the Gibbs-Helmholtz equation, *viz.*,

$$\Delta G - \Delta H = T\,(\partial(\Delta G)/\partial T)_P \qquad ...(1)$$

where ΔG is the change in free energy and ΔH is the change in enthalpy accompanying any process including a chemical reaction, it is seen that at the absolute zero (*i.e.*, T=0), ΔG=ΔH.

Richards, by measuring EMFs of cells at different temperatures, found that the value of $\partial(\Delta G)/\partial T$ decreases with decrease in temperature and, therefore, concluded that ΔG and ΔH tend to approach each other more and more closely as the temperature is lowered. Nernst, relying on this data, made an important suggestion that *the value of* $\partial(\Delta G)/\partial T$ *approaches zero gradually* as *the temperature is lowered towards the absolute zero.* This is known as the **Nernst heat theorem.** According to this theorem, ΔG and ΔH not only become equal to each other at absolute zero but also approach each other asymptotically, that is, gradually at temperatures close to absolute zero. This is illustrated in Fig. 1. Thus, the approach of ΔG and ΔH towards each other is as represented by the full lines and not as represented by the dotted lines.

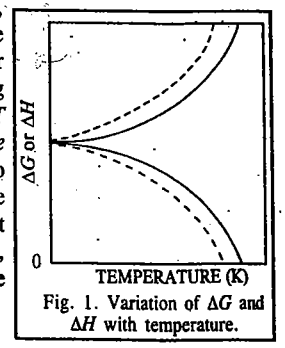

Fig. 1. Variation of ΔG and ΔH with temperature.

Mathematically, the theorem may be expressed as

$$\underset{T\to0}{\text{Lt}}\,[\partial(\Delta G)/\partial T]_P = \underset{T\to0}{\text{Lt}}\,[\partial(\Delta H)/\partial T]_P = 0 \qquad ...(2)$$

where Lt stands for the limiting value.

We also know from the Second law of thermodynamics that

$$(\partial(\Delta G)/\partial T)_P = -\,\Delta S \qquad ...(3)$$

and $$(\partial(\Delta H)/\partial T)_P = \Delta C_P \quad \text{(Kirchhoff equation)} \qquad ...(4)$$

where ΔS is the entropy change of the reaction and ΔC_p is the difference in the heat capacities of the products and the reactants.

It follows from Eqs. 2, 3 and 4 that

$$\lim_{T\to 0} \Delta S = 0 \quad \ldots(5)$$

and

$$\lim_{T\to 0} \Delta C_P = 0 \quad \ldots(6)$$

The significance of these equations is that the entropy change of a reaction tends to approach zero and that the difference between the heat capacities of products and reactants also tends to approach zero as the temperature is lowered towards the absolute zero.

The Nernst theorem holds good only in the case of pure solids.

Third Law of Thermodynamics. According to Eq. 6, ΔC_P tends to approach zero at 0 K. This means that at absolute zero, the heat capacities of products and reactants in solid state are identical. This leads to the suggestion that at absolute zero, all substances have the same heat capacity. The quantum theory, as applied to heat capacities of solids, has shown that heat capacities of solids tend to become zero at 0 K. The Nernst heat theorem may, therefore, be written as

$$\lim_{T\to 0} C_P = 0 \quad \ldots(7)$$

According to Eq. 5, ΔS becomes zero at absolute zero, *i.e.*, the entropy change of a process involving solids becomes zero at 0 K. In other words, the absolute entropies of products and reactants in the solid state are identical. Planck, therefore, suggested that entropies of all pure solids approach zero at 0 K, *i.e.*,

$$\lim_{T\to 0} S = 0 \quad \ldots(8)$$

This statement has led to the following enunciation of the **Third law of thermodynamics :**

At the absolute zero of temperature, the entropy of every substance may become zero and it does become zero in the case of a perfectly crystalline solid.

In a perfect crystal, at absolute zero temperature, there is a state of perfect order, *i.e.*, zero disorder and hence of zero entropy. Walther Nernst (1864–1941), the German chemist, was awarded the 1920 Chemistry Nobel Prize for his work in thermochemistry. He also did pioneering work in electrochemistry.

Determination of Absolute Entropies of Solids, Liquids and Gases. We know that for an infinitesimally small change of state of a substance or a system, the entropy change is given by

$$dS = dq/T \quad \ldots(9)$$

If the change takes place at constant pressure, then

$$(\partial S)_P = (\partial q)_P/T \quad \ldots(10)$$

$$\therefore \quad (\partial S/\partial t)_P = (\partial q/\partial T)_P \times 1/T \quad \ldots(11)$$

By definition,

$$(\partial q/\partial T)_P = C_P \quad \ldots(12)$$

$$\therefore \quad (\partial S/\partial T)_P = C_P \times 1/T \quad \ldots(13)$$

or at constant pressure, $dS = (C_P/T)dT \quad \ldots(14)$

For a perfectly crystalline substance, the absolute entropy $S=0$ at $T=0$. Therefore, we may write

$$\int_{S=0}^{S=S} dS = \int_{T=0}^{T=T} (C_P/T)dT \quad \ldots(15)$$

or

$$S_T = \int_0^T \frac{C_P dT}{T} = \int_0^T C_P \, d(\ln T) \quad \ldots(16)$$

where S_T is the *absolute entropy* of the crystalline solid under examination at the temperature T.

The integral in Eq. 16 can be evaluated by measuring C_p at various temperatures between $T=0$ and the desired temperature T and then plotting C_p against ln T and determining the area under the curve between $T=0$ and the required temperature T. This area gives directly the value of S_T. Since it is not possible to obtain the value of C_P at the absolute zero, heat capacities are measured up to as low a temperature as possible, usually up to 15 K and the value at the absolute zero is obtained by extrapolation. This method, therefore, consists in determining heat capacities of the substance under examination at temperatures varying from approximately 15 K to the required temperature T. A graph of C_P *vs* ln T is then plotted and extrapolated to the absolute zero of temperature, as shown in Fig. 2. The area under the graph gives the required value of S_T, the absolute entropy of the substance at temperature T.

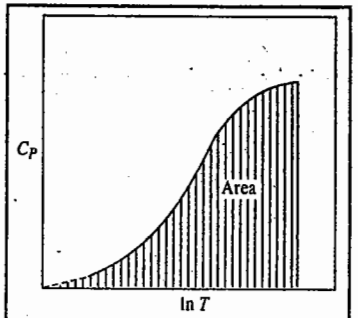

Fig. 2. Determination of absolute entropy.

Eq. 16. is thus written as follows :

$$S_T = \int_0^{T^*} C_P \frac{dT}{T} + \int_{T^*}^{T} C_P \frac{dT}{T} \quad \ldots(17)$$

where $0 < T^* < 15$ K.

The first integral is evaluated with the help of the Debye theory of heat capacities of crystalline substances according to which, at very low temperatures ($0 < T < 15$ K),

$$C_P \approx C_v \approx aT^3 \quad \ldots(18)$$

where a is an empirical constant. Eq. 18 is known as the **Debye T^3 law.**

Accordingly, Eq. 17 may be written as

$$S_T = \int_0^{T^*} aT^3 \frac{dT}{T} + \int_{T^*}^{T} C_P \frac{dT}{T} = \frac{1}{3}a(T^*)^3 + \int_{T^*}^{T} C_P \frac{dT}{T} \quad \ldots(19)$$

The second integral in Eq. 17 is evaluated from experimental measurements of heat capacities. Combining the heat capacity data with the enthalpy data on phase transformations, the absolute entropy of a substance, whether solid, liquid or gas, at temperature T, can be determined, as illustrated below. In every case, the start is made with the substance in the crystalline solid state at the absolute zero when its absolute entropy is taken as zero. Then the total absolute entropy of the substance in the given state and at a given temperature is taken as the sum of all the entropy changes that the substance has to undergo in order to acquire the given state at the given temperature starting from the crystalline solid at absolute zero.

Suppose, it is required to determine absolute entropy of a gas at 25°C under atmospheric pressure. This would be equal to the sum of the entropy changes involved in the following processes each of which is brought about reversibly. It is assumed for general discussion that the substance in solid state exists in two allotropic forms α and β.

1. Heating the crystalline solid from absolute zero to temperature T^*, where $0 < T^* < 15$ K and evaluating the entropy change with the aid of the Debye's theory. Let the entropy change be ΔS_1. Then,

$$\Delta S_1 = \int_0^{T^*} aT^3 \frac{dT}{T} = \frac{1}{3}a(T^*)^3 \quad \ldots(20)$$

2. Heating the crystalline solid from T^* to T_{tr}, where T_{tr} is the transition temperature at which the crystalline solid changes from allotropic form α to allotropic form β. The entropy change in this

process is given by

$$\Delta S_2 = \int_{T_r}^{T_{fus}} C_{P,s}(\alpha) dT \quad \text{...(21)}$$

where $C_{P,s}(\alpha)$ is the heat capacity of the solid in allotropic form α. ΔS_2 is evaluated by the integration of heat capacity data graphically, as described above.

3. Transition of the solid from allotropic form α to allotropic form β at the transition temperature T_{tr}. The entropy change in this process is given by

$$\Delta S_3 = \Delta H_{tr}/T_{tr} \quad \text{...(22)}$$

where ΔH_{tr} is the molar enthalpy of transition.

4. Heating the solid in allotropic form β up to its fusion point, T_{fus}. The entropy change in this process is given by

$$\Delta S_4 = \int_{T_{tr}}^{T_{fus}} C_{P,s}(\beta) dT \quad \text{...(23)}$$

where $C_{P,s}$ (β) is the heat capacity of the solid in allotropic form β.

5. Changing the solid in allotropic form β into the liquid state at the fusion temperature T_{fus}. The entropy change of this process (entropy of fusion) is given by

$$\Delta S_5 = \Delta H_{fus}/T_{fus} \quad \text{...(24)}$$

where ΔH_{fus} is the molar enthalpy of fusion of the substance.

6. Heating the liquid from its freezing point (T_{fus}) to its boiling point (T_b). The entropy change involved in this case is given by

$$\Delta S_6 = \int_{T_{fus}}^{T_b} C_{P,l}\, d\ln T \quad \text{...(25)}$$

where $C_{P,l}$ is the heat capacity of the substance in the liquid state. This can be evaluated by plotting $C_{P,l}$ *vs* ln T between temperatures T_{fus} and T_b and noting the area below the graph, as described before.

7. Changing the liquid into the gaseous state at the temperature T_b. The entropy change involved here, ΔS_7, is the molar entropy of vaporisation and is given by

$$\Delta S_7 = \Delta H_{vap}/T_b \quad \text{...(26)}$$

where ΔH_{vap} is the enthalpy of vaporisation per mole of the substance.

8. Heating the gas from T_b to the required temperature, *i.e.*, 25°C (298·15 K). The entropy change involved in this process is given by

$$\Delta S_8 = \int_{T_b}^{298\cdot15} C_{P,g}\, d\ln T \quad \text{...(27)}$$

where $C_{P,g}$ is the heat capacity of the substance in the gaseous state at constant pressure. ΔS_8 is evaluated by ploting $C_{P,g}$ *vs* ln T between temperatures T_b and 298·15 K and noting the area below the curve.

The absolute entropy of the gas at 298·15 K (25°C), S_T, is equal to the sum of all the entropy changes listed above. Thus,

$$S_T = \Delta S_1 + \Delta S_2 + \Delta S_3 + \Delta S_4 + \Delta S_5 + \Delta S_6 + \Delta S_7 + \Delta S_8$$

Table 1 gives the absolute entropy of HCl at 25°C determined by the procedure outlined above.

TABLE 1
Determination of Absolute Entropy of HCl at 25°C

Contribution	J K^{-1} mol^{-1}
1. Extrapolation from 0 to 15 K [using the Debye T^3 law]	1·3
2. $\int C_P\, d\ln T$ for solid α from 15 to 98·36 K	29·5
3. Transition, solid α ⟶ solid β, 1190/98·36	12·1
4. $\int C_P\, d\ln T$ for solid β from 98·36 to 158·91 K	21·1
5. Fusion, 1992/158·91	12·6
6. $\int C_P\, d\ln T$ for liquid from 158·91 to 188·07 K	9·9
7. Vaporization, 16150/188·07	85·9
8. $\int C_P\, d\ln T$ from 188·07 to 298·15 K	13·5
	$\therefore S^\circ_{298\cdot15} = 185\cdot9$

Absolute entropies of some of the elements and compounds in their standard states at 25°C, calculated from the Third law of thermodynamics, are given in Table 2.

TABLE 2
Standard Absolute Entropies (S°) of Elements and Compounds at 25°C

Substance	Absolute entropy (J K^{-1} mol^{-1})	Substance	Absolute entropy (J K^{-1} mol^{-1})
Hydrogen (*g*)	130·60	Mercury (*l*)	77·40
Nitrogen (*g*)	191·62	Mercury (*g*)	174·83
Oxygen (*g*)	205·01	Mercuric chloride (*s*)	144·76
Hydrogen chloride (*g*)	186·22	Mercurous chloride (*s*)	98·32
Hydrogen bromide (*g*)	199·15	Cuprous iodide (*s*)	6·65
Hydrogen iodide (*g*)	206·27	Lead bromide (*s*)	161·50
Carbon (diamond)	2·43	Silver bromide (*s*)	96·11
Carbon (graphite)	5·69	Silver chloride (*s*)	107·15
Water (*l*)	70·29	Silver iodide (*s*)	115·57
Water (*g*)	188·74	Silver oxide (*s*)	121·75
Ammonia (*g*)	192·46	Ferric oxide (*s*)	89·95
Carbon monoxide (*g*)	197·90	Cupric oxide (*s*)	43·55
Carbon dioxide (*g*)	213·80	Magnesium oxide (*s*)	27·00
Nitric oxide (*g*)	210·45	Mercuric oxide (*s*)	71·46
Sulphur dioxide (*g*)	247·86	Sodium chloride (*s*)	72·38
Sodium (*s*)	51·04	Potassium chloride (*s*)	82·62
Magnesium (*s*)	32·51	Potassium bromide (*s*)	93·72
Sulphur (rhombic)	31·88	Methane (*g*)	186·14
Sulphur (monoclinic)	32·55	Ethane (*g*)	229·49
Chlorine (*g*)	222·96	Ethylene (*g*)	185·35
Bromine (*g*)	245·34	Acetylene (*g*)	201·10
Bromine (*l*)	153·97	Methanol (*l*)	126·69
Aluminium (*s*)	28·32	Ethanol (*l*)	160·66
Iron (*s*)	27·15	Benzene (*l*)	172·79
Copper (*s*)	83·34	Phenol (*l*)	142·24
Silver (*s*)	42·67	Acetone (*l*)	200·03
Iodine (*s*)	116·73	Acetic acid (*l*)	159·82
Iodine (*g*)	260·62	Methyl chloride (*g*)	234·05
Zinc (*s*)	41·00	Methyl chloride (*l*)	245·22
Lead (*s*)	64·85	Ether (*l*)	85·27

Example 1. Show that the entropy of any substance at low temperatures ($0 < T < 20$ K), where Debye's relation for heat capacities of crystals is valid, is one-third of the molar heat capacity.

Solution : At low temperatures ($0 < T < 20$ K),

$$C_P \approx aT^3 \qquad \text{[Debye } T^3 \text{ law]}$$

According to Eq. 14, $dS = (C_p/T)\,dT$

$$\therefore \quad \int_0^T dS = \int_0^T (C_p/T)dT$$

or $$S_T - S_0 = \int_0^T \frac{aT^3}{T}dT = a\int_0^T T^2 dT = \frac{a}{3}T^3$$

or $$S_T = aT^3/3 \qquad [\because S_0 = 0]$$

Evidently, $S_T = C_P/3$. Hence, **proved.**

Example 2. C_v for uranium metal is 3·04 J K^{-1} mol^{-1} at 20 K. Calculate the absolute entropy of the metal at 20 K.

Solution : At low temperatures ($0 < T < 20$ K), $C_P = C_v = aT^3$ [Debye's T^3 law]

$$\therefore \quad a = C_v/T^3 = 3{\cdot}04 \text{ J K}^{-1} \text{ mol}^{-1}/(20 \text{ K})^3 = 38{\cdot}03\times10^{-5} \text{ J K}^{-4} \text{ mol}^{-1}$$

Hence, $$C_P = aT^3 = (38{\cdot}03\times10^{-5} \text{ J mol}^{-1} \text{ K}^{-4})\,T^3$$

From Eq. 14, $$dS = (C_p/T)dT = 38{\cdot}03\times10^{-5} \text{ J mol}^{-1} \text{ K}^{-4}\,T^2\,dT$$

or $$S_{20} - S_0 = aT^3/3 = 38{\cdot}03\times10^{-5} \text{ J K}^{-4} \text{ mol}^{-1} (20 \text{ K})^3/3$$

or $$S_{20} = 1{\cdot}01 \text{ J K}^{-1} \text{ mol}^{-1} \quad [\because S_0 = 0]$$

Example 3. The heat capacity, C_P (in J K^{-1} mol^{-1}) of a substance is given by the following equations :

$$C_P(s) = 16{\cdot}74\times10^{-5}\,T^3 \quad (0 < T < 50 \text{ K})$$

$$C_P(s) = 20{\cdot}92 \quad (50 < T < 150 \text{ K})$$

$$C_P(l) = 25{\cdot}10 \quad (150 < T < 400 \text{ K})$$

At the melting point (150 K), $\Delta H_f = 1255{\cdot}2$ J mol^{-1}. Calculate the absolute entropy of the substance in the liquid state at 300 K.

Solution :

$$\Delta S_1 = \int_0^{50} \frac{C_{P,S}}{T}dT = \int_0^{50} \frac{16{\cdot}74\times10^{-5}\,T^3}{T}dT \qquad \text{(The Debye } T^3 \text{ law)}$$

$$= \left[\frac{16{\cdot}74\times10^{-5}\,T^3}{3}\right]_0^{50} = 5{\cdot}58\times10^{-5}\times(50)^3 = 6{\cdot}97 \text{ J K}^{-1} \text{ mol}^{-1}$$

$$\Delta S_2 = \int_{50}^{150} \frac{C_{P,S}}{T}dT = 20{\cdot}92 \text{ J K}^{-1} \text{ mol}^{-1} \ln\left(\frac{150}{50}\right)$$

$$= 20{\cdot}92 \text{ J K}^{-1} \text{ mol}^{-1}\times1{\cdot}09861 = 22{\cdot}98 \text{ J K}^{-1} \text{ mol}^{-1}$$

$$\Delta S_3 = \Delta S_f = 1255{\cdot}2 \text{ J mol}^{-1}/150 \text{ K} = 8{\cdot}37 \text{ J K}^{-1} \text{ mol}^{-1}$$

$$\Delta S_4 = \int_{150}^{300} \frac{C_{P,l}}{T}dT = 25{\cdot}10 \text{ J K}^{-1} \text{ mol}^{-1} \ln\left(\frac{300}{150}\right)$$

$$= 25{\cdot}10 \text{ J K}^{-1} \text{ mol}^{-1}\times0{\cdot}6931 = 17{\cdot}40 \text{ J K}^{-1} \text{ mol}^{-1}$$

Hence, $$\Delta S = S_T - S_0 = \Delta S_1 + \Delta S_2 + \Delta S_3 + \Delta S_4$$

$$\therefore \quad S_T = 6{\cdot}97 + 22{\cdot}98 + 8{\cdot}37 + 17{\cdot}40 = 55{\cdot}73 \text{ J K}^{-1} \text{ mol}^{-1} \qquad (\because S_0 = 0)$$

Experimental Verification of the Third Law of Thermodynamics

The heat capacity and enthalpy data on substances that exist in two different crystalline forms may serve to verify the Third law of thermodynamics. For reversible isothermal transition, $\alpha \rightarrow \beta$, we can write

$$\Delta S = S_\beta - S_\alpha = \Delta H_{tr}/T_{tr} \qquad ...(28)$$

where ΔH_{tr} and T_{tr} are the experimentally determined enthalpy of transition and the temperature of transition, respectively.

$$\Delta S = S_0(\beta) + \int_0^{T_{tr}} \frac{C_{P,S}(\beta)}{T}dT - S_0(\alpha) - \int_0^{T_{tr}} \frac{C_{P,S}(\alpha)}{T}dT = \Delta H_{tr}/T_{tr} \qquad ...(29)$$

If an experiment proves that

$$\int_0^{T_{tr}} \frac{C_{P,S}(\beta)}{T}dT - \int_0^{T_{tr}} \frac{C_{P,S}(\alpha)}{T}dT = \frac{\Delta H_{tr}}{T_{tr}} \qquad ...(30)$$

then it will also prove that $S_0(\beta) = S_0(\alpha)$.

Thus, both the crystalline modifications α and β would have equal entropies at 0 K, in accordance with Third law of thermodynamics.

Experiments carried out on systems such as sulphur, tin and phosphine have demonstrated the validity of the Third law.

The following results have been obtained on phosphine :

$$\Delta S_{tr} = \frac{\Delta H_{tr}}{T_{tr}} = \frac{185{\cdot}7 \text{ J mol}^{-1}}{49{\cdot}43 \text{ K}} = 15{\cdot}73 \text{ J K}^{-1} \text{ mol}^{-1} \qquad ...(31)$$

In respect of phosphine, the difference of the two integrals in Eq. 30 is experimentally found to be 15·69 J K^{-1} mol^{-1}, *i.e.*,

$$\int_0^{T_{tr}} \frac{C_{P,S}(\beta)}{T}dT - \int_0^{T_{tr}} \frac{C_{P,S}(\alpha)}{T}dT = 15{\cdot}69 \text{ J K}^{-1} \text{ mol}^{-1} \qquad ...(32)$$

A comparison of the two results shows that, within the limits of experimental error, the Third law is valid for phosphine.

Entropies of Real Gases

From one of the Maxwell relations

$$\left(\frac{\partial S}{\partial P}\right)_T = -\left(\frac{\partial V}{\partial T}\right)_P \text{ or } dS = -\left(\frac{\partial V}{\partial T}\right)_P dP \qquad ...(33)$$

Integrating between pressures P_1 and P_2 at constant T, we get

$$\int_1^2 dS = -\int_{P_1}^{P_2}\left(\frac{\partial V}{\partial T}\right)_P dP \qquad ...(34)$$

A real gas behaves ideally at low pressures. Let this pressure be P. Let $(S_r)_1$ be the entropy of the real gas at 1 atm pressure and $(S_r)_P$ be the entropy at pressure P, the temperature remaining constant. Then, Eq. 34 becomes

$$(S_r)_1 - (S_r)_P = -\int_P^1 \left(\frac{\partial V}{\partial T}\right)_P dP \qquad ...(35)$$

For an ideal gas, $(\partial V/\partial T)_P = R/P$. If $(S_i)_1$ and $(S_i)_P$ are the entropies of an ideal gas at 1 atm and P atm, respectively, then, Eq. 35 can be written as

$$(S_i)_P - (S_i)_1 = \int_P^1 (R/P)dP \qquad ...(36)$$

We can equate $(S_r)_P$ with $(S_i)_P$ because at the low pressure P, the real gas behaves ideally.

Adding Eqs. 35 and 36, we get

$$(S_i)_1 - (S_r)_1 = S^\circ - S = \int_P^1 \left[\left(\frac{\partial V}{\partial T}\right)_P - \frac{R}{P}\right]dP \qquad ...(37)$$

where S° is the standard entropy and S is the entropy of real gas both determined at 1 atm. We have to determine S°. Here S is given by

$$S = \frac{1}{3}a(T^*)^3 + \int_{T^*}^{T_f} \frac{C_{P,S}}{T}dT + \frac{\Delta H_{fus}}{T_{fus}} + \int_{T_f}^{T_b} \frac{C_{P,l}}{T}dT + \frac{\Delta H_v}{T_b} + \int_{T_b}^{T} \frac{C_{P,g}}{T}dT \qquad ...(38)$$

Though the integrals in Eq. 38 can be evaluated graphically, it is more convenient to do so with the use of Berthelot's equation of state, *viz.*,

$$\left(P + \frac{a}{TV^2}\right)(V - b) = RT \qquad ...(39)$$

which is more appropriate to use than the van der Waals equation of state.

Multiplying and rearranging, we get

$$PV = RT + Pb - \frac{a}{TV} + \frac{ab}{TV^2} \qquad ...(40)$$

The term ab/TV^2 in the above equation is negligible as compared to other terms since the Berthelot constants a and b are small.

$$PV = RT + Pb - a/TV = \left[1 + \frac{Pb}{RT} - \frac{aP}{R^2T^2}\right] \qquad (\because V \approx RT/P) \quad ...(41)$$

For Berthelot's equation of state, the constants a, b and R can be written in terms of the critical constants. Accordingly,

$$a = (16/3)\, P_c V_c^2 T_c\,; \quad b = V_c/4\,; \quad R = (32/9)\, P_c V_c/T_c \qquad ...(42)$$

Hence, Eq. 41 becomes

$$PV = RT\left[1 + \frac{9}{128}\frac{PT_c}{P_cT}\left(1 - \frac{T_c^2}{6T^2}\right)\right] \qquad ...(43)$$

Dividing by P, we have

$$V = \frac{RT}{P} + \frac{9}{128}\frac{RT_c}{P_c} - \frac{27}{64}\frac{RT_c^3}{P_cT^2} \qquad ...(44)$$

$$\therefore \quad \left(\frac{\partial V}{\partial T}\right)_P = \frac{R}{P} + \frac{27}{32}\frac{RT_c^3}{P_cT^3} \qquad ...(45)$$

Substituting for $(\partial V/\partial T)_P$ in Eq. 37, we get

$$S^\circ = S + \frac{27}{32}\frac{RT_c^3}{P_cT^3}\int_P^1 dP = S + \frac{27}{32}\frac{RT_c^3}{P_cT^3}(1 - P) = S + \frac{27}{32}\frac{RT_c^3}{P_cT^3} \qquad (\because P << 1) \quad ...(46)$$

As mentioned earlier, S is given by Eq. 38. In Eq. 46, the second term is the correction term that should be added to S to give S°, the standard entropy for a real gas.

Entropy Changes in Chemical Reactions

We can calculate ΔS° for a chemical reaction from the tabulated standard entropy values for the reactants and products at 298 K. This is one of the most important applications of the Third law of thermodynamics. For a reaction

$$aA + bB + \cdots\cdots \longrightarrow lL + mM + \cdots\cdots$$

occurring in the standard state, the standard entropy change, ΔS°, is given by

$$\Delta S^\circ = \left[lS_L^\circ + mS_M^\circ + \cdots\cdots\right] - \left[aS_A^\circ + bS_B^\circ + \cdots\cdots\right]$$
$$= \sum S^\circ_{products} - \sum S^\circ_{reactants} \qquad ...(47)$$

where S°s are the molar standard entropies of the species involved and a, b, l, m, etc., are the stoichiometric coefficients.

From the tabulated values of S°, ΔS° for the reaction at 298 K can be calculated. The ΔS° value at any other temperature can be calculated by the Kirchhoff-type equation, *viz.*,

$$\left[\frac{d(\Delta S^\circ)}{dT}\right]_p = \sum\left(\frac{\partial S^\circ_{products}}{\partial T}\right)_P - \sum\left(\frac{\partial S^\circ_{reactants}}{\partial T}\right)_P \qquad ...(48)$$

Since $(\partial S/\partial T)_P = C_P/T$, we have

$$\left[\frac{d(\Delta S^\circ)}{dT}\right]_p = \sum(C_P/T)_{products} - \sum(C_P/T)_{reactants}$$

Rearranging and integrating between 298 K and T K, we have ...(49)

$$\int_{298}^{T} d(\Delta S^\circ) = \int_{298}^{T} (\Delta C_P/T)dT = \int_{298}^{T} \Delta C_P\, d\ln T$$

or
$$\Delta S_T^\circ = \Delta S_{298}^\circ + \int_{298}^{T} \Delta C_P\, d\ln T \qquad ...(50)$$

Eq. 50 is applicable to chemical reactions involving solids, liquids or gases.

Example 4. Calculate the standard entropy change for the reaction

$$C(s) + H_2O(l) \longrightarrow CO(g) + H_2(g)$$

Solution : From Table 2, the total standard entropy of products

= 197·90 J K^{-1} mol^{-1} for CO + 130·60 J K^{-1} mol^{-1} for H_2 = 328·50 J K^{-1}

From the same table, the total standard entropy of reactants

= 5·69 J K^{-1} mol^{-1} for C (*s*) + 70·29 J K^{-1} mol^{-1} for H_2O (*l*) = 75·98 J K^{-1}

The standard entropy change (ΔS°) for the reaction is given by

$$\Delta S^\circ = \Sigma S^\circ_{products} - \Sigma S^\circ_{Reactants} = 328{\cdot}50 - 75{\cdot}98 = 252{\cdot}52 \text{ J K}^{-1}$$

Example 5. Calculate the standard entropy change for the reaction

$$N_2(g) + O_2(g) \longrightarrow 2NO(g)$$

Solution : The standard entropy change (ΔS°) for the reaction is given by

$$\Delta S^\circ = \Sigma S^\circ_{products} - \Sigma S^\circ_{reactants}$$
$$= (2 \text{ mol} \times 210{\cdot}45 \text{ J K}^{-1} \text{ mol}^{-1}) - (1 \text{ mol} \times 191{\cdot}62 \text{ J K}^{-1} \text{ mol}^{-1} + 1 \text{ mol} \times 205{\cdot}01 \text{ J K}^{-1} \text{ mol}^{-1})$$
$$= 24{\cdot}27 \text{ J K}^{-1}$$

Example 6. Calculate the entropy change accompanying the conversion of 1 mole of ice at 273·1 K and 1 atm pressure into steam at 373·1 K and 1 atm pressure, given that at 273·1 K, the molar heat of fusion of ice, ΔH_{fus}, is 6·00 kJ mol^{-1} and at 373·1 K, the molar heat of vaporization of water, ΔH_{vap}, is 40·60 kJ mol^{-1}. Also assume that the molar heat capacity, C_P, in the temperature range 373·1—273·1 K remains constant at 75·2 J K^{-1} mol^{-1}.

Solution : The total entropy change ΔS is given by the relation

$$\Delta S = \Delta S_1 + \Delta S_2 + \Delta S_3$$

where ΔS_1 is the entropy change due to fusion of ice, ΔS_2 is the entropy change for heating 1 mole of water from 273·1 K to 373·1 K and ΔS_2 is the entropy change due to conversion of water at 373·1 K into steam. Thus,

$$\Delta S_1 = \Delta H_{fus}/T_{fus} = 6000 \text{ J mol}^{-1}/273{\cdot}1 \text{ K} = 22{\cdot}0 \text{ J K}^{-1} \text{ mol}^{-1}$$

$$\Delta S_2 = \int_{T_1}^{T_2} \frac{C_P}{T} dT = \int_{273{\cdot}1}^{373{\cdot}1} \frac{75{\cdot}2 \text{ J K}^{-1} \text{ mol}^{-1}}{T} dT$$

$$= 75{\cdot}2 \text{ J K}^{-1} \text{ mol}^{-1} \times 2{\cdot}303 \log (373{\cdot}1 \text{ K}/273{\cdot}1 \text{ K}) = 23{\cdot}5 \text{ J K}^{-1} \text{ mol}^{-1}$$

$$\Delta S_2 = \Delta H_{vap}/T_{vap} = 40600 \text{ J mol}^{-1}/373{\cdot}1 \text{ K} = 108{\cdot}8 \text{ J K}^{-1} \text{ mol}^{-1}$$

Adding, we get $\Delta S = 22{\cdot}0 + 23{\cdot}5 + 108{\cdot}8 = 154{\cdot}3 \text{ J K}^{-1} \text{ mol}^{-1}$

Derivation of the Boltzmann Entropy Equation. The Boltzmann entropy equation, *viz.*, $S = k \ln W$, is probably the most famous equation in statistical thermodynamics. Its derivation is intuitively simple and appealing. Before we derive it, we must distinguish between two kinds of probabilities, *viz.*, mathematical probability and thermodynamic probability.

Mathematical probability is the ratio of the number of cases favourable to the occurrence of an event to the total number of equally probable cases. This probability always lies between 0 and 1. On the other hand, **thermodynamic probability** is the number of microstates corresponding to a given macrostate when we are dealing with the distribution of molecules amongst an extremely large number of energy levels. This probability, W, is a very large number, tending to be infinite.

Boltzmann suggested that entropy can be related to the thermodynamic probability W as

$$S = f(W) \qquad ...(51)$$

Consider two systems A and B whose entropies and microstates are S_A, S_B, W_A and W_B, respectively. When the two systems are combined,

$$S = S_A + S_B \qquad ...(52)$$

By definition, the probability of a thermodynamic state is proportional to the number of microstates required to achieve it. Mathematically, we know that the total probability is the *product* of the probabilities of the independent events. This is also true of the microstates. Hence,

$$W = W_A . W_B \qquad ...(53)$$

and $$S_A + S_B = f(W_A W_B) \qquad ...(54)$$

This relationship suggests that entropies are additive and probabilities are multiplicative. This can be true only if S is a logarithmic function of W, *i.e.*,

$$S = k \ln W \qquad ...(55)$$

which is the Boltzmann entropy equation. Eq. 55 gives the quantitative definition of entropy as disorder.

Residual Entropy. Entropies calculated using the Third law are called thermal entropies. However, the statistical entropies, calculated by the method of statistical mechanics (for instance, by using the Boltzmann entropy equation at 0 K, *viz.*, $S = k \ln W$) are more rigorous. It is found that the thermal entropies are somewhat smaller than the statistical entropies, the deviation ranging from 3·1 to 4·8 J K^{-1} mol^{-1}. We thus conclude that entropies of substance (such as H_2, D_2, CO, NO, N_2O, H_2O, etc.) are not zero at 0 K, as the Third law formulates, but are finite. These entropies are called **residual entropies.** The existence of residual entropy in a crystal at 0 K is presumably due to the alternative

arrangements of molecules in the solid. Such arrangements are shown in Fig. 3 for CO and N_2O :

CO	CO	CO	CO	CO	CO	OC	OC
CO	CO	CO	CO	CO	OC	OC	CO
NNO	NNO	NNO	NNO	NNO	NNO	ONN	ONN
NNO	NNO	NNO	NNO	NNO	ONN	ONN	NNO
(a)				*(b)*			

Fig. 3. Alternative molecular arrangements *(a)* Perfect crystal *(b)* Actual crystal

Since both the arrangements are equally likely, from the Boltzmann entropy equation (55),

$S = k \ln W$, with $W = 2^{N_A}$ (where N_A is Avogadro's number), we find that

$$S = k \ln 2^{N_A} = N_A k \ln 2 = R \ln 2 = (8{\cdot}314 \text{ J K}^{-1} \text{ mol}^{-1})\ 0{\cdot}693 = 5{\cdot}76 \text{ J K}^{-1} \text{ mol}^{-1}$$

Since the residual entropies are found experimentally to be less than this value, it is evident that the two alternative orientations of the CO and N_2O molecules in the solid state at 0 K are not completely random. For H_2 and D_2, too, the thermal entropies at 0 K are less than the corresponding **statistical entropies.** The calculation of the statistical entropy assumes that there exists an equilibrium between ortho H_2 and para H_2 at all temperatures. The ΔS_{mix} of ortho H_2 and para H_2 is found to be 18·37 J K^{-1} mol^{-1} in the vicinity of 0 K. When this value is added to the thermal entropy (calculated from heat capacity measurements), the agreement with the statistical entropy is very good.

Ludwig Boltzmann (1844-1906), the great German mathematical physicist, made outstanding contributions to the kinetic theory of gases, statistical mechanics, and the atomic nature of matter. However, his work on the atomic theory was criticized by several eminent scientists (among them W. Ostwald), and he suffered from severe depression. He committed suicide in 1906 by drowning. It was a tragic loss to physics. After his death his work on atomic theory was corroborated. On his tombstone is inscribed his famous equation : $S = k \ln W$.

I. Review Questions

1. Explain the Nernst heat theorem. How does it lead to the enunciation of the Third law of thermodynamics ?
2. State and explain the Third law of thermodynamics. How can it be verified experimentally ?
3. Explain how the absolute entropy of a substance is determined with the help of the Third law of thermodynamics.

II. Problems

1. Calculate the entropy of SO_2 (*g*) at 400 K from the following data on contribution to entropy :
   (a) 0 to 15 K (using Debye's law) = 1·255 J K^{-1} mol^{-1}
   (b) 15 K to 197·64 K, solid = 84·182 J K^{-1} mol^{-1}
   (c) 197·64 K to 263·08 K, liquid = 24·937 J K^{-1} mol^{-1}
   (d) ΔH_f and ΔH_{vap} are 7·402 kJ mol^{-1} and 24·937 kJ mol^{-1}, respectively.
   (e) The melting point is 197·64 K and the boiling point is 263·08 K.
   (f) The temperature-dependence of C_p of SO_2 (*g*) is given by
   $$C_p = 49{\cdot}769 + 4{\cdot}56 \times 10^{-3} T$$
   [Ans. 264·09 J K^{-1} mol^{-1}]
2. Calculate with the help of entropy values given in Table 2,
   (i) the standard entropy change for the reaction $Pb(s) + Br_2(l) \longrightarrow PbBr_2(s)$
   (ii) the standard entropy change for the formation of methyl alcohol. [Ans. *(i)* – 57·32 J K^{-1} *(ii)* – 242·7 J K^{-1} mol^{-1}]

CHAPTER 17

CHEMICAL EQUILIBRIA

Spontaneous Reactions. By a spontaneous reaction, we mean a reaction which proceeds by itself or when properly initiated, if necessary. For example, hydrogen and oxygen react spontaneously at the room temperature by passing an electric spark through the mixture. The reaction is exothermic.

$$H_2(g) + \tfrac{1}{2}O_2(g) \longrightarrow H_2O(l)\ ; \qquad \Delta H = -286{\cdot}2\ \text{kJ}$$

Carbon (graphite), when initiated by ignition, undergoes almost complete combustion to give carbon dioxide. This reaction is also exothermic.

$$C(s) + O_2(g) \longrightarrow CO_2(g)\ ; \qquad \Delta H = -393{\cdot}5\ \text{kJ}$$

Nitric oxide and oxygen combine readily to produce nitrogen dioxide. This is also an exothermic reaction.

$$NO(g) + \tfrac{1}{2}O_2(g) \longrightarrow NO_2(g)\ ; \qquad \Delta H = -56{\cdot}52\ \text{kJ}$$

This reaction requires no initiation.

A mixture of methane and oxygen, when initiated by ignition, reacts spontaneously to produce carbon dioxide and water, at the room temperature. The reaction is exothermic.

$$CH_4(g) + 2O_2(g) \longrightarrow CO_2(g) + 2H_2O(l)\ ; \qquad \Delta H = -890{\cdot}3\ \text{kJ}$$

Free Energy of a Spontaneous Reaction. While discussing the criteria for reversible and irreversible reactions in Chapter 14, it was concluded that if the free energy change of a chemical reaction is *negative*, the reaction can take place spontaneously, *i.e.*, it is feasible. If the free energy change is zero, the reaction is in a state of equilibrium and if the free energy change is positive, the reaction would not proceed. By definition, $G = H - TS$ so that, at constant temperature,

$$\Delta G = \Delta H - T\Delta S \qquad \ldots(1)$$

There are, evidently, two factors which contribute to the value of ΔG. These are the energy factor, ΔH and the entropy factor, $T\Delta S$. Neither ΔH nor $T\Delta S$ alone can determine the spontaneity of a reaction. The spontaneity would be decided by the overall value of the two factors; *i.e.*, by the value of ΔG. For a reaction to be spontaneous, ΔG must have a negative value, as already stated. For this, ΔH should be negative and $T\Delta S$ should be positive. Thus, negative sign of ΔH and positive sign of $T\Delta S$, both tend to increase the feasibility of a reaction. When both factors are favourable, *i.e.*, ΔH is negative and $T\Delta S$ is positive, then, evidently, their substitution in Eq. 1 will result in a large negative value of ΔG. The reaction would, therefore, be highly feasible.

Now suppose the energy factor is favourable, *i.e.*, ΔH is negative, but the entropy factor is not favourable, *i.e.*, $T\Delta S$ is also negative. In such a case, the feasibility of the reaction will be determined by the factor which predominates. If the energy factor predominates, *i.e.*, the numerical value of ΔH is more than that of $T\Delta S$, the reaction would be feasible. The value of ΔG would again be negative. If, however, the entropy factor predominates, *i.e.*, the numerical value of $T\Delta S$ is greater than that of ΔH, the reaction would not be feasible. The value of ΔG would now be positive.

Let us consider another case in which the energy factor does not favour the reaction (*i.e.*, ΔH has a positive value) but the entropy factor favours the reaction, *i.e.*, $T\Delta S$ is positive. The reaction will occur if the entropy factor predominates, *i.e.*, $T\Delta S$ is numerically greater than ΔH. In such a case, again, ΔG will

be negative and the reaction would be feasible. If, however, the entropy factor does not predominate, *i.e.*, $T\Delta S$ is numerically less than ΔH, then in that case ΔG will be positive and the reaction would not occur.

If neither factor predominates, *i.e.*, both the opposing factors are exactly equal (*viz.*, ΔH is numerically equal to $T\Delta S$), then ΔG will be zero. Under these circumstances, the reaction will be in a state of equilibrium, *i.e.*, no net reaction would occur in any direction.

Role of Temperature. Temperature, being a multiplying parameter for entropy factor ($T\Delta S$) of a system, plays an important role in controlling the spontaneity of a reaction as shown below.

a. At high temperature, the entropy factor predominates. In the case of an endothermic reaction, ΔH is always positive. Thus, the energy factor does not favour the reaction. But if the reaction in accompanied by even a small increase of entropy, the high temperature will increase the entropy factor $T\Delta S$ to a large extent. Hence, ΔG ($= \Delta H - T\Delta S$) may become negative at a sufficiently high temperature. This explains why endothermic reactions become feasible at increasing temperatures.

b. At low temperatures, energy factor predominates. In the case of an exothermic reaction, ΔH is always negative. Thus, the energy factor always tends to favour the reaction. If such a reaction takes place at a low temperature, then even if it is accompanied by *decrease of entropy*, the opposing factor $T\Delta S$ may remain very small and, therefore, the value of ΔG ($= \Delta H - T\Delta S$) may still have a sufficiently large negative value. This explains why exothermic reactions are feasible even at low temperatures.

To sum up, for a reaction to be spontaneous, ΔG should be negative.

Standard Free Energy Change, $\Delta G°$. The standard free energy change of a reaction is defined as the free energy change of a reaction when the reactants and products are in their standard states (25°C, 1 atm pressure). Eq. 1 may thus be written as

$$\Delta G° = \Delta H° - T\Delta S° \qquad \ldots(2)$$

where $\Delta H°$ is the standard enthalpy change of the reaction and $\Delta S°$ is the standard entropy change of the reaction at the temperature T. The standard enthalpy changes of reactions can be calculated from the data given in Table 4 (Chapter 14). The standard entropy changes can be calculated with the help of the standard absolute entropies of elements and compounds given in Table 2 (Chapter 16). It is thus possible to calculate $\Delta G°$ of a reaction.

Example 1. Calculate the standard free energy change ($\Delta G°$) of the reaction :

$CO(g) + 1/2\ O_2(g) \longrightarrow CO_2(g)$; $\Delta H° = -282{\cdot}84$ kJ. Is the reaction feasible at standard state ?

Solution : $\Delta G° = \Delta H° - T\Delta S°$

$\Delta H° = -282{\cdot}84\ \text{kJ} = -282840\ \text{J}$

$\Delta S° = S°_{\text{Products}} - S°_{\text{Reactants}}$

Reference to Table 2 (Chapter 15) shows that standard entropy of $CO_2(g)$ is 213·80 J K^{-1} mol^{-1} while the values for $CO(g)$ and $O_2(g)$ are 197·90 and 205·01 J K^{-1} mol^{-1}, respectively.

$$\Delta S° = S°_{[CO_2]} - \left\{S°_{[CO]} + \tfrac{1}{2}S°_{[O_2]}\right\} = 213{\cdot}8 - (197{\cdot}9 + 102{\cdot}5) = -86{\cdot}6\ \text{J K}^{-1}$$

Hence, $\Delta G° = -282840\ \text{J} - [(298\ \text{K})(-86{\cdot}6\ \text{J K}^{-1})] = -257033{\cdot}2\ \text{J} = -257{\cdot}03\ \text{kJ}$

Since $\Delta G°$ has a *negative value*, the reaction at standard state is **feasible.**

Example 2. Calculate the standard free energy change ($\Delta G°$) of the following reaction and say whether it is feasible at standard state or not.

$$1/2\ H_2(g) + 1/2\ I_2(s) \longrightarrow HI(g)\ ; \qquad \Delta H° = 25{\cdot}95\ \text{kJ}$$

Solution : $\Delta G° = H° - T\Delta S°$; $\Delta H° = 25{\cdot}95\ \text{kJ} = 25950\ \text{J}$

The standard entropies of $HI(g)$, $H_2(g)$ and $I_2(s)$ are 206·27, 130·60 and 116·73 J K^{-1} mol^{-1}, respectively (Table 2, Chapter 16).

Hence, $\Delta S° = S°_{[HI(g)]} - \left\{\frac{1}{2}S°_{[H_2(g)]} + \frac{1}{2}S°_{[I_2(s)]}\right\}$

$= 206{\cdot}27 - (65{\cdot}30 + 58{\cdot}36) = 82{\cdot}61\ \text{J K}^{-1}$

$$\therefore \quad \Delta G^\circ = 25950\ \text{J} - (298\ \text{K} \times 82{\cdot}61\ \text{J K}^{-1}) = 1323{\cdot}20\ \text{J} = \mathbf{1{\cdot}323\ J}$$

Since ΔG is *positive*, the reaction is **not feasible** at standard state.

Standard Free Energy of Formation of Compounds, ΔG_f°. Standard free energy of formation of a compound is defined as the energy change expressed in kilojoules per mole involved in the formation of the compound in its standard state (25°C and 1 atm pressure) from its elements in their standard states (25°C and 1 atm pressure). This is denoted by ΔG_f°.

Standard free energies of formation are generally determined from the standard enthalpies of formation and standard entropy changes by using the expression

$$\Delta G_f^\circ = \Delta H_f^\circ - T\Delta S^\circ \qquad \ldots(3)$$

Example 3. Calculate the standard free energy of formation of $H_2O(l)$. The standard enthalpy of formation (ΔH_f°) of $H_2O(l)$ is –286·20 kJ and standard entropies of $H_2(g)$, $O_2(g)$ and $H_2O(l)$ are 130·60, 205·01 and 70·29 J K^{-1} mol^{-1}, respectively.

Solution : The equation for the formation of $H_2O(l)$ at standard state may be written as

$$H_2(g) + 1/2\ O_2(g) \longrightarrow H_2O(l); \qquad \Delta H_f^\circ = -286{\cdot}20\ \text{kJ mol}^{-1}$$

$$\Delta S^\circ = S^\circ_{\text{Products}} - S^\circ_{\text{Reactants}} = 70{\cdot}29\ \text{J K}^{-1}\text{mol}^{-1} - (130{\cdot}60\ \text{J K}^{-1}\text{mol}^{-1} + 102{\cdot}50\ \text{J K}^{-1}\text{mol}^{-1})$$

$$= -162{\cdot}81\ \text{J K}^{-1}\text{mol}^{-1}$$

$$\Delta G_f^\circ = \Delta H_f^\circ - T\Delta S^\circ = -286200\ \text{J mol}^{-1} - [(298\ \text{K})(-162{\cdot}81\ \text{J K}^{-1}\text{mol}^{-1})]$$

$$= -237683\ \text{J} = \mathbf{-237{\cdot}68\ kJ\ mol^{-1}}$$

Example 4. The standard enthalpy of formation (ΔH_f°) of $NH_3(g)$ is – 46·19 kJ mol^{-1}. The standard entropies of $N_2(g)$, $H_2(g)$ and $NH_3(g)$ are 191·62, 130·60 and 192·46 J K^{-1} mol^{-1}, respectively. Calculate the standard free energy of formation of $NH_3(g)$.

Solution : $\Delta H_f^\circ = -46{\cdot}19\ \text{kJ mol}^{-1} = -46190\ \text{J mol}^{-1}$

$$\Delta S^\circ = S^\circ_{\text{Products}} - S^\circ_{\text{Reactants}}$$

$$= 192{\cdot}46\ \text{J K}^{-1}\text{mol}^{-1} - \left(\tfrac{1}{2} \times 191{\cdot}62\ \text{J K}^{-1} + \tfrac{3}{2} \times 130{\cdot}60\ \text{J K}^{-1}\text{mol}^{-1}\right) = -99{\cdot}25\ \text{J K}^{-1}\text{mol}^{-1}$$

$$T\Delta S^\circ = 298\ \text{K} \times (-99{\cdot}25\ \text{J K}^{-1}\text{mol}^{-1}) = -29576{\cdot}5\ \text{J mol}^{-1}$$

$$\Delta G_f^\circ = \Delta H_f^\circ - T\Delta S^\circ = -46190\ \text{J mol}^{-1} - (-29576{\cdot}5\ \text{J mol}^{-1}) = \mathbf{-16613{\cdot}5\ J\ mol^{-1} = -16{\cdot}61\ kJ\ mol^{-1}}$$

Example 5. Calculate ΔG accompanying the vaporisation of one mole of liquid water at 100°C and 76 torr pressure. Will the process be spontaneous ?

Solution : When water vaporises at 100°C and 1 atm (=760 torr) pressure, liquid and vapour are in equilibrium so that $\Delta G = 0$. It is evident, therefore, that vaporisation of water at 100°C but at a reduced pressure of 76 torr is not a process in equilibrium. The latter process, however, can be divided into two reversible steps : vaporisation at 1 atm (=760 torr) for which $\Delta G = 0$, followed by isothermal expansion of vapour to 76 torr. ΔG for the overall process is given by the sum of the ΔG values involved in the two steps. Thus,

$$\Delta G = 0 + RT \ln (P_2/P_1) = (8{\cdot}314\ \text{J K}^{-1}\text{mol}^{-1})(373\ \text{K}) \ln (76\ \text{torr}/760\ \text{torr})$$

$$= -7140{\cdot}59\ \text{J mol}^{-1} = \mathbf{-7{\cdot}14\ kJ\ mol^{-1}}$$

Since ΔG is negative, the process is **spontaneous.**

Example 6. Consider the vaporisation of water at 100°C when liquid water is in equilibrium with water vapour at 1 atm. The heat of vaporisation of water at 100°C is 40·63 kJ mol^{-1}. Suppose now that the volume of the vapour phase is increased so that the pressure becomes 0·90 atm. Determine whether the vaporisation process will be spontaneous or not.

Solution : At 1 atm pressure and 100°C, liquid water is in equilibrium with its vapour and hence, $\Delta G = 0$. Since $\Delta G = \Delta H - T\Delta S$, it follows that

$$\Delta S = (\Delta H - \Delta G)/T = (40{\cdot}63\ \text{kJ mol}^{-1} - 0)/373\ \text{K} = 108{\cdot}93\ \text{J K}^{-1}\text{mol}^{-1}$$

When the pressure of water vapour changes from 1 atm to 0·9 atm,

$$\Delta S = R \ln (P_1/P_2) = (8{\cdot}314\ \text{J K}^{-1}\text{mol}^{-1}) \ln (1{\cdot}0\ \text{atm}/0{\cdot}9\ \text{atm}) = 0{\cdot}876\ \text{J K}^{-1}\text{mol}^{-1}$$

Thus, the increase in entropy accompanying vaporisation of 1 mole of water at 0·9 atm is given by the sum of the ΔS values involved in the two processes so that

$$\therefore \quad \Delta S = 108{\cdot}93\ \text{J K}^{-1}\text{mol}^{-1} + 0{\cdot}876\ \text{J K}^{-1}\text{mol}^{-1} = 109{\cdot}81\ \text{J K}^{-1}\text{mol}^{-1}$$

$$\therefore \quad T\Delta S = (373\ \text{K})(109{\cdot}81\ \text{J K}^{-1}\text{mol}^{-1}) = 40959{\cdot}1\ \text{J mol}^{-1} = 40{\cdot}96\ \text{kJ mol}^{-1}$$

The change in free energy is, therefore, given by

$$\Delta G = \Delta H - T\Delta S = 40{\cdot}63\ \text{kJ} - 40{\cdot}96\ \text{kJ} = -0{\cdot}33\ \text{kJ mol}^{-1}$$

Since ΔG is negative, the vaporisation process at 0·90 atm is spontaneous.

The standard free energies of formation of various compounds calculated in the above manner are given in Table 1. The standard free energies of elements are arbitrarily taken as zero.

TABLE 1

Standard Free Energies of Formation of Compounds at 25°C

Substance	ΔG_f° (kJ mol^{-1})	Substance	ΔG_f° (kJ mol^{-1})	Substance	ΔG_f° (kJ mol^{-1})
$H_2O(g)$	– 228·60	$H_2O(l)$	– 237·20	$CH_4(g)$	– 50·79
$CO(g)$	– 137·27	$CH_3OH(l)$	– 166·23	$C_2H_6(g)$	– 32·88
$CO_2(g)$	– 394·38	$C_2H_5OH(l)$	– 174·76	$C_2H_4(g)$	+ 68·11
$HCl(g)$	– 95·27	$CH_3COOH(l)$	– 392·50	$C_3H_8(g)$	– 23·47
$N_2O(g)$	+104·18	$HCOOH(l)$	– 346·01	$C_2H_2(g)$	+209·20
$NO(g)$	+ 86·61	$C_6H_6(l)$	+124·51	$C_6H_6(g)$	+129·70
$NO_2(g)$	+ 51·92	$NaCl(s)$	– 384·04	$Cu_2O(s)$	– 146·48
$N_2O_5(g)$	+ 97·90	$AgCl(s)$	– 109·70	$PbSO_4(s)$	– 811·27
$NH_3(g)$	– 16·65	$AgBr(s)$	– 95·81	$CaSO_4(s)$	– 1320·55
$H_2S(g)$	– 33·01	$Ag_2O(s)$	– 10·83	$CaCO_3(s)$	– 1128·88
$SO_2(g)$	– 300·36	$HgO(s)$	– 58·32	$BaSO_4(s)$	– 1465·23
$SO_3(g)$	– 357·77	$CuO(s)$	– 127·19	$BaCO_3(s)$	– 1135·53

The advantage of these values is that we can calculate standard free energy change, ΔG°, for any reaction remembering that

$$\Delta G^\circ = \sum \Delta G_f^\circ(\text{products}) - \sum \Delta G_f^\circ(\text{reactants})$$

Suppose it is required to calculate the standard free energy change of the reaction

$$CO(g) + H_2O(g) \longrightarrow CO_2(g) + H_2(g)$$

The standard free energies of formation of $CO(g)$, $H_2O(g)$ and $CO_2(g)$ are –137·27, –228·60 and –394·38 kJ $mole^{-1}$, respectively (Table 1). The value for $H_2(g)$ is taken as zero.

The standard free energy change of the reaction is given by

$$\Delta G^\circ = \{[\Delta G_f^\circ]_{CO_2} - [\Delta G_f^\circ]_{H_2}\} - \{[\Delta G_f^\circ]_{CO} - [\Delta G_f^\circ]_{H_2O}\}$$

$$= \{(-394{\cdot}38\ \text{kJ mole}^{-1}) + (0)\} - \{(-137{\cdot}27\ \text{kJ mole}^{-1}) + (-228{\cdot}60\ \text{kJ mole}^{-1})\} = \mathbf{-28{\cdot}51\ kJ\ mol^{-1}}$$

Example 7. Calculate the standard free energy change of the reaction

$$\mathbf{4NH_3(g) + 5O_2(g) \longrightarrow 4NO(g) + 6H_2O(l)}$$

and say whether this reaction is feasible at 25°C and 1 atm pressure. The standard free energies of formation of $NH_3(g)$, $NO(g)$ and $H_2O(l)$ are – 16·65, 86·61 and – 237·20 kJ $mole^{-1}$, respectively.

Solution : $\Delta G^\circ = [\Delta G_f^\circ]_{\text{Products}} - [\Delta G_f^\circ]_{\text{Reactants}}$

$$= [(4\ \text{mol})(86{\cdot}61\ \text{kJ mol}^{-1} + (6\ \text{mol})(-237{\cdot}2\ \text{kJ mol}^{-1})] - [(4\ \text{mol}\ (-16{\cdot}65\ \text{kJ mol}^{-1}) + 0]$$

$$= \mathbf{-1010{\cdot}02\ kJ}$$

Since ΔG° is *negative*, the reaction at standard state is feasible

Example 8. Calculate ΔG° for the reaction : $C_6H_{12}O_6(s) + 6O_2(g) \longrightarrow 6CO_2(g) + 6H_2O(l)$. The standard free energies of formation of glucose, $CO_2(g)$ and $H_2O(l)$ are – 910·5, – 394·4 and – 237·2 kJ mol^{-1}, respectively.

Solution : $\Delta G^\circ = [\Delta G_f^\circ]_{Products} - [\Delta G_f^\circ]_{Reactants}$

$= [(6 \text{ mol})(-394{\cdot}4 \text{ kJ mol}^{-1}) + (6 \text{ mol})(-237{\cdot}2 \text{ kJ mol}^{-1})] - [(1 \text{ mol})(-910{\cdot}5 \text{ kJ mol}^{-1})] + 0$

$= -2879{\cdot}1 \text{ kJ}$

CHEMICAL EQUILIBRIUM

Our experimental observations tell us that most of the chemical reactions when carried out in closed vessels do not go to completion. Under these conditions, a reaction starts by itself or by initiation, continues for some time at diminishing rates and ultimately *appears to stop*. The reactants may still be present but they do not appear to change into products any more. What happens in such a case is that the products of the reaction start reacting at the same rate as the reactants. In other words, the rate of the back reaction becomes equal to the rate of the forward reaction. Thus, in a given time as much of the products are formed as react back to give the reactants. The composition of the reaction mixture at a given temperature is the same irrespective of the initial state of the system, *i.e.*, irrespective of the fact whether we start with the reactants or the products. The reaction in such conditions is said to be in a state of equilibrium.

The attainment of equilibrium can be recognised by noting constancy of observable properties such as pressure, concentration, density or colour whichever may be suitable in a given case.

The relationship between the quantities of the reacting substances and the products formed can be worked out readily with the help of the law of mass action.

Law of Mass Action. Assuming that the driving force of a chemical reaction determines its reaction rate, the law of mass action may be stated as follows : The rate at which a substance reacts is proportional to its active mass and the rate of a chemical reaction is directly proportional to the product of the active masses of the reacting substances.

Consider a general reversible chemical reaction

$$aA + bB \rightleftharpoons mM + nN$$

According to the law of mass action, assuming that active masses are equivalent to molar concentrations,

the rate of the forward reaction, $r_f \propto [A]^a[B]^b = k_f[A]^a[B]^b$

and the rate of the reverse reaction, $r_r \propto [M]^m[N]^n = k_r[M]^m[N]^n$

where k_f and k_r are proportionality constants and square brackets represent the molar concentrations of the entities enclosed. The constant k_f is known as the rate constant of the forward reaction and the constant k_r is known as the rate constant of the reverse reaction. At equilibrium, the rate of the forward reaction is equal to the rate of the reverse reaction, that is,

$$k_f[A]^a[B]^b = k_r[M]^m[N]^n$$

$$\therefore \quad k_f/k_r = K_{eq} = [M]^m[N]^n/[A]^a[B]^b \qquad ...(4)$$

The constant K_{eq} is called the **equilibrium constant** of the reaction. Eq. 4 represents the **law of chemical equilibrium.**

The equilibrium concentrations in Eq. 4 can be written in terms of activities (a_i), partial pressures (p_i), molar concentrations (c_i) or mole fractions (x_i) of the species involved in the reaction. Consequently, K_{eq} will have different numerical values for a given chemical reaction.

Thermodynamic Derivation of the Law of Chemical Equilibrium. Consider once again the general reversible reaction

$$aA + bB \rightleftharpoons mM + nN$$

where the reactants and the products are assumed to be ideal gases.

We know that chemical potential (*i.e.*, Gibbs free energy) of reactants consisting of a moles of A and b moles of B is given by the expression

$$G_{reactants} = a\mu_A + b\mu_B \qquad ...(5)$$

where μ_A and μ_B are the **chemical potentials** of the species A and B, respectively. Similarly, for the products we have

$$G_{products} = m\mu_M + n\mu_N \qquad ...(6)$$

In each case, pressure and temperature are constant. The free energy of the reaction is equal to the difference between the free energy of the products and that of the reactants, that is,

$$(\Delta G)_{reaction} = G_{products} - G_{reactants}$$

$$= (m\mu_M + n\mu_N) - (a\mu_A + b\mu_B) \qquad ...(7)$$

At equilibrium, the free energy change $\Delta G = 0$ so that Eq. 7 becomes

$$(m\mu_M + n\mu_N) - (a\mu_A + b\mu_B) = 0 \qquad ...(8)$$

The chemical potential of the ith species in the gaseous state is given by

$$\mu_i = \mu_i^\circ + RT \ln p_i \qquad \text{(Chapter 15)} \qquad ...(9)$$

where p_i is the partial pressure of the ith component and μ_i° is its **standard chemical potential** (*i.e.*, when partial pressure of the ith component is unity). From Eqs. 8 and 9, we obtain

$$[m(\mu_M^\circ + RT \ln p_M) + n(\mu_N^\circ + RT \ln p_N)] - [a(\mu_A^\circ + RT \ln p_A) + b(\mu_B^\circ + RT \ln p_B)] = 0 \qquad ...(10)$$

or $$RT \ln (p_M^m p_N^n)/(p_A^a p_B^b) = -[(m\mu_M^\circ + n\mu_N^\circ) - (a\mu_A^\circ + b\mu_B^\circ)]$$

$$= -[G_{products}^\circ - G_{reactants}^\circ] = -(\Delta G^\circ)_{reaction} \qquad ...(11)$$

or $$(p_M^m p_N^n)/(p_A^a p_B^b) = e^{-\Delta G^\circ/RT} \qquad ...(12)$$

Since ΔG° depends only on temperature and R is the gas constant, hence the right hand side of Eq. 12 is a constant at constant temperature. Thus,

$$(p_M^m p_N^n)/(p_A^a p_B^b) = \text{constant} = K_p \qquad ...(13)$$

Eq. 13 is the **law of chemical equilibrium**

If the chemical potentials of various species are expressed in terms of mole fractions (x_i), then

$$\mu_i = \mu_i^\circ + RT \ln x_i \qquad ...(14)$$

From this the following expression analogous to Eq. 13 is obtained :

$$(x_M^m x_N^n)/(x_A^a x_B^b) = K_x \qquad ...(15)$$

If, on the other hand, the chemical potentials are expressed in terms of molar concentrations (c_i), then

$$\mu_i = \mu_i^\circ + RT \ln c_i \qquad ...(16)$$

from which we obtain the following expression :

$$[M]^m[N]^n/[A]^a[B]^b = K_c \qquad ...(17)$$

If the reactants and the products are not ideal gases, then the **thermodynamic equilibrium constant,** K_{th}, is defined as

$$K \equiv K_{th} = (a_M^m a_N^n)/(a_A^a a_B^b) \qquad ...(18)$$

where a_is are the activities. For non-ideal, *i.e.*, real gases,

$$K \equiv K_f = (f_M^m f_N^n)/(f_A^a f_B^b) \qquad ...(19)$$

where f_is are the *fugacities*. For a mixture of real gases, $\gamma_i = f_i/p_i$ or $f_i = \gamma_i p_i$ where γ_is are the activity coefficients. Hence

$$K_f = \frac{\gamma_M^m \gamma_N^n}{\gamma_A^a \gamma_B^b} \times \frac{p_M^m p_N^n}{p_A^a p_B^b} = K_\gamma K_p \qquad ...(20)$$

Van't Hoff Reaction Isotherm. It readily follows from Eqs. 12 and 13 that

$$K_p = e^{-\Delta G^\circ/RT}$$

or

$$\Delta G^\circ = -RT \ln K_p \qquad ...(21)$$

This equation is known as the **van't Hoff reaction isotherm.**

Eq. 21 is very important. It permits calculation of ΔG° of the reaction from the known value of the equilibrium constant K_p and vice-versa.

Example 9. Calculate K_p for the reaction $3/2\ O_2(g) \rightleftharpoons O_3(g)$ at 298 K. ΔG° for the reaction is 163·43 kJ mol^{-1}.

Solution :

$$\Delta G^\circ = -RT \ln K_p$$

$$\therefore \quad \ln K_p = -\frac{\Delta G^\circ}{RT} = -\frac{163{\cdot}43 \times 10^3 \text{ J mol}^{-1}}{(8{\cdot}314 \text{ J K}^{-1} \text{ mol}^{-1})(298 \text{ K})}$$

$$\therefore \quad K_p = 2{\cdot}0 \times 10^{-29}$$

Example 10. The value of K_p for the water gas reaction $CO(g) + H_2O(g) \rightleftharpoons CO_2(g) + H_2(g)$ is $1{\cdot}06 \times 10^5$ at 25°C. Calculate ΔG° for this reaction.

Solution :

$$\Delta G^\circ = -RT \ln K_p = -(8{\cdot}314 \text{ J K}^{-1} \text{ mol}^{-1})(298 \text{ K}) \ln (1{\cdot}06 \times 10^5)$$

$$= -28{,}673{\cdot}6 \text{ J mol}^{-1} = -28{\cdot}674 \text{ kJ mol}^{-1}$$

Distinction between ΔG and ΔG°. We must emphasize the distinction between ΔG and ΔG° for a reaction. ΔG° is the difference in the free energy of products and reactants when all of them are in their standard states. This does not refer to the actual reaction at equilibrium. ΔG, however, refers to the difference in the free energy of products and reactants at the actual measured concentrations (or partial pressures) of the components. When $\Delta G = 0$, the reaction is at equilibrium and the concentrations (or partial pressures) of the components are those which appear in the equilibrium constant expression.

Relations between K_p, K_c and K_x

We shall now proceed to establish the relations between the three equilibrium constants K_p, K_c and K_x.

a. Relation between K_p and K_x. In an ideal gaseous mixture, each component obeys Dalton's law of partial pressures, *i.e.*, $p_i = x_i P$ where P is the total pressure and p_i is the partial pressure of the ith component with mole fraction x_i in the mixture. For the reaction

$$aA + bB \rightleftharpoons mM + nN$$

we have $p_A = x_A P$, $p_B = x_B P$, $p_M = x_M P$, $P_N = x_N P$

$$\therefore \quad K_p = \frac{p_M^m p_N^n}{p_A^a p_B^b} = \left(\frac{x_M^m x_N^n}{x_A^a x_B^b}\right) P^{(m+n)-(a+b)} = K_x (P)^{\Delta n} \qquad ...(22)$$

where $\Delta n = (m + n) - (a + b)$.

b. Relation between K_p and K_c. For an ideal gaseous mixture,

$$p_i V = n_i RT$$

$$\therefore \quad p_i = (n_i/V)RT = c_i RT$$

where $c_i\ (= n_i/V)$ is the molar concentration of the ith component in the mixture of total volume V. Hence,

$$p_A = c_A RT, \quad p_B = c_B RT, \quad p_M = c_M RT, \quad p_N = c_N RT$$

$$\therefore \quad K_p = \frac{p_M^m p_N^n}{p_A^a p_B^b} = \left(\frac{c_M^m c_N^n}{c_A^a c_B^b}\right)(RT)^{(m+n)-(a+b)} = K_c (RT)^{\Delta n} \qquad ...(23)$$

From Eqs. 22 and 23, $K_p = K_x (P)^{\Delta n} = K_c (RT)^{\Delta n}$ ...(24)

If $\Delta n = 0$, $m+n = a+b$ (*i.e.*, the number of moles of products equals the number of moles of reactants), then

$$K_p = K_x = K_c$$

Note : We can also establish a relation between K_p and K_n where n is the total number of moles. Since the mole fraction, x_i, of a component i in a mixture is given by $x_i = n_i/n$, we can write Eq. 22 as

$$K_p = \frac{n_M^m n_N^n}{n_A^a n_B^b}\left(\frac{P}{n}\right)^{\Delta n} = K_n \left(\frac{P}{n}\right)^{\Delta n} \qquad ...(25)$$

For reactions occurring in liquid phase it is convenient to use as standard state the pure liquid components at the temperature and pressure of the system. In that case, $a_i = \gamma_i x_i$ so that

$$K \equiv K_{th} = \frac{x_M^m x_N^n}{x_A^a x_B^b} \times \frac{\gamma_M^m \gamma_N^n}{\gamma_A^a \gamma_B^b} = K_x K_\gamma \qquad ...(26)$$

where γ_i is the activity coefficient of the ith component. K_γ is a complicated function of concentration which is determined experimentally. For nearly ideal solutions, however, $K_\gamma = 1$ so that $K_{th} = K_x$.

Example 11. Calculate K_c and K_x for the reaction $N_2O_4(g) \rightleftharpoons 2NO_2(g)$ for which $K_p = 0{\cdot}157$ atm at 27°C and 1 atm pressure.

Solution : For the reaction, $N_2O_4(g) \rightleftharpoons 2NO_2(g)$,

$$\Delta n = 2 - 1 = 1$$

Since $K_P = K_c (RT)^{\Delta n}$

$$K_c = \frac{K_p}{(RT)^{\Delta n}} = \frac{0{\cdot}157 \text{ atm}}{(0{\cdot}08206 \text{ dm}^3 \text{ atm K}^{-1} \text{ mol}^{-1} \times 300 \text{ K})} = 6{\cdot}38 \times 10^{-3} \text{ mol dm}^{-3}$$

$$K_x = K_p (P)^{-\Delta n} = (0{\cdot}157 \text{ atm})(1 \text{ atm})^{-1} = 0{\cdot}157$$

Example 12. Calculate K_c for the reaction $2SO_3(g) \rightleftharpoons 2SO_2(g) + O_2(g)$ for which $K_p = 3{\cdot}5 \times 10^{-23}$ atm at 27°C.

Solution : For the reaction $2SO_3(g) \rightleftharpoons 2SO_2(g) + O_2(g)$,

$$\Delta n = 2 + 1 - 1 = 1$$

$$\therefore \quad K_c = \frac{K_p}{(RT)^{\Delta n}} = \frac{3{\cdot}5 \times 10^{-23} \text{ atm}}{(0{\cdot}08206 \text{ dm}^3 \text{ atm K}^{-1} \text{ mol}^{-1} \times 300 \text{ K})} = 1{\cdot}42 \times 10^{-26} \text{ mol dm}^{-3}$$

Example 13. Calculate K_p/K_c for the following reactions at 27°C :

(a) $N_2(g) + O_2(g) \rightleftharpoons 2NO(g)$

(b) $N_2(g) + 3H_2(g) \rightleftharpoons 2NH_3(g)$

(c) $NH_4Cl(s) \rightleftharpoons NH_3(g) + HCl(g)$

Solution : The units of K_p/K_c depend upon the type of the reaction involved, as we shall see in this example. Since $K_p = K_c (RT)^{\Delta n}$, hence $K_p/K_c = (RT)^{\Delta n}$

(a) $N_2(g) + O_2(g) \rightleftharpoons 2NO(g)$; $\Delta n = 2 - (1 + 1) = 0$

$$\therefore \quad K_p/K_c = (RT)^0 = 1$$

(b) $N_2(g) + 3H_2(g) \rightleftharpoons 2NH_3(g)$; $\Delta n = 2 - (3 + 1) = -2$

$\therefore$ $K_p/K_c = (RT)^{-2} = (0{\cdot}08206\ dm^3\ atm\ K^{-1}\ mol^{-1} \times 300\ K)^{-2} = 1{\cdot}65 \times 10^{-3}\ mol^2\ dm^{-6}\ atm^{-2}$

(c) $NH_4Cl(s) \rightleftharpoons NH_3(g) + HCl(g)$; $\Delta n = 2$

$\therefore$ $K_p/K_c = (RT)^2 = (0{\cdot}08206\ dm^3\ atm\ K^{-1}\ mol^{-1} \times 300\ K)^2 = 605{\cdot}2\ dm^6\ atm^2\ mol^{-2}$

De Donder's Treatment of Chemical Equilibria

For a general reaction

$$aA + bB \rightleftharpoons mM + nN,$$

the Gibbs free energy, $G = f(T, P, n)$. Hence, the Gibbs free energy change is given by

$$dG = \left(\frac{\partial G}{\partial T}\right)_{P,n} dT + \left(\frac{\partial G}{\partial P}\right)_{T,n} dP + \left(\frac{\partial G}{\partial n_i}\right)_{P,T,n_j} dn$$

$$= -SdT + VdP + \mu_A dn_A + \mu_B dn_B + \mu_M dn_M + \mu_N dn_N \quad ...(27)$$

If the reaction is carried out at constant T and P (so that $dT = 0$, $dP = 0$), we have

$$(dG)_{T,P} = \mu_A dn_A + \mu_B dn_B + \mu_M dn_M + \mu_N dn_N \quad ...(28)$$

where the dn_is are the changes in the numbers of moles of the chemical species involved and μ_is are their chemical potentials.

For a closed system, the reaction stoichiometry requires that a change in the number of moles of one of the reactants or the products must be accompanied by an equivalent change in all other reactants and the products. If, in the balanced equation for the reaction, all the moles of the reactants get converted into products, the **progress of the reaction** is said to be 100%. This is also expressed by saying that one unit of reaction has occurred. Obviously, the progress of the reaction would be less than 100% if all the moles of the reactants do not get converted into products. It is thus convenient to define a variable ξ to express the progress or **advancement of the reaction**. Introduced by de Dondre, ξ is called the **degree of advancement of a chemical reaction.**

If the reaction advances by ξ units, then n_is can be written as

$$n_A = n_A^\circ - a\xi \ ; \quad n_B = n_B^\circ - b\xi \ ; \quad n_M = n_M^\circ + m\xi \ ; \quad n_N = n_N^\circ + n\xi \quad ...(29)$$

where n_i°s are the numbers of moles of the chemical species present before the reaction is advanced by ξ units. The minus sign for the moles of the reactants denotes that the reactants are *consumed* and the plus sign for the moles of the products denotes that the products are *formed.*

Differentiating Eq. 29 and remembering that n_i°s are constant, we obtain

$$dn_A = -a\,d\xi \ ; \quad dn_B = -b\,d\xi \ ; \quad dn_M = m\,d\xi \ ; \quad dn_N = n\,d\xi \quad ...(30)$$

These equations can be written as

$$d\xi = -dn_A/a = -dn_B/b = dn_M/m = dn_N/n \quad ...(31)$$

The quantity $d\xi$ is called **the differential advancement or the increment of the degree of advancement** of the reaction. We see that $d\xi$ is the ratio of the number of moles of the chemical species and its stoichiometric coefficient in the balanced chemical equation.

Substituting the values of dn_A, dn_B, dn_M and dn_N, as given by Eq. 30, in Eq. 28, we get

$$(dG)_{T,P} = [(m\mu_M + n\mu_N) - (a\mu_A + b\mu_B)]d\xi \quad ...(32)$$

$$(\partial G/\partial\xi)_{T,P} = [(m\mu_M + n\mu_N) - (a\mu_A + b\mu_B)] \quad ...(33)$$

The partial derivative $(\partial G/\partial\xi)_{T,P}$ gives the rate of change of the Gibbs free energy with the advancement of the reaction. The expression on the R.H.S. of Eq. 33 is called the **reaction potential.** Evidently,

$$\text{Reaction potential} = \Delta G = (\partial G/\partial\xi)_{T,P}$$

Thus, reaction potential is the rate of change of total Gibbs free energy per unit advancement of the chemical reaction at constant T and P. Note that the reaction potential is identical with the free energy change of a reaction. The *decrease in the reaction potential* is defined as the **chemical affinity**, A_f. Thus,

$$A_f = -(\partial G/\partial\xi)_{T,P} = -\Delta G \quad ...(34)$$

A few comments on A_f are in order. If the derivative $(\partial G/\partial\xi)_{T,P}$ is negative, this means that the free energy of the reaction mixture decreases as the reaction advances in the forward direction. This means that the reaction is spontaneous and the affinity is positive. If the derivative is positive, the reverse reaction is spontaneous and the affinity is negative. If the derivative is zero, the reaction is in equilibrium and the affinity is zero. Thus, at equilibrium.

$$(\partial G/\partial\xi)_{T,P} = 0 \quad ...(35)$$

Eq. 35 is general, being applicable whether the reactants and products are solids, liquids or gases.

Thermodynamic Relations for Chemical Affinity. For any chemical reaction, the Gibbs free energy depends upon T, P and the concentrations of the reacting substances. However, since these concentrations themselves determine the degree of advancement of the reaction, we can write

$$G = f(T, P, \xi)$$

$$\therefore \quad dG = (\partial G/\partial T)_{P,\xi}\,dT + (\partial G/\partial P)_{T,\xi}\,dP + (\partial G/\partial\xi)_{T,P}\,d\xi$$

We know from thermodynamics that

$$(\partial G/\partial T)_{P,\xi} = -S \text{ and } (\partial G/\partial\xi)_{T,\xi} = V \quad ...(36)$$

and from Eq. 34, $(\partial G/\partial\xi)_{T,P} = -A_f = \Delta G$.

Hence, $$dG = -SdT + VdP - A_f d\xi = -SdT + VdP + \Delta G d\xi \quad ...(37)$$

We can now proceed to determine the relation of A_f to other thermodynamic functions.

1. **Work function and Affinity.** We know that

$$G = H - TS = U + PV - TS = A + PV$$

where $A(=U - TS)$ is the work function.

or $$A = G - PV$$

$$\therefore \quad dA = dG - PdV - VdP \quad ...(38)$$

Substituting for dG from Eq. 37,

$$dA = -SdT + VdP + \Delta G d\xi - PdV - VdP$$

$$= -SdT - PdV + \Delta G d\xi = -SdT - PdT - A_f d\xi \quad ...(39)$$

At constant T and V, $dT = 0$, $dV = 0$, so that

$$(\partial A/\partial\xi)_{T,V} = \Delta G = -A_f \quad ...(40)$$

2. **Enthalpy and Affinity.** We know that

$$H = G + TS$$

$$\therefore \quad dH = dG + TdS + SdT$$

$$= -SdT + VdP + \Delta G d\xi + TdS + SdT \quad ...(41)$$

$$= TdS + VdP + \Delta G d\xi = TdS + VdP - A_f d\xi \quad ...(42)$$

At constant S and P, $dS = 0$, $dP = 0$, so that

$$(\partial H/\partial \xi)_{S,P} = \Delta G = -A_f \quad ...(43)]$$

3. Internal Energy and Affinity. As mentioned above,

$$G = H - TS = U + PV - TS$$

$$\therefore \quad U = G + TS - PV$$

$$dU = dG + TdS + SdT - PdV - VdP \quad ...(44)$$

$$= -SdT + VdP + \Delta G d\xi + TdS + SdT - PdV - VdP$$

$$= TdS - PdV + \Delta G d\xi = TdS - PdV - A_f d\xi \quad ...(45)$$

At constant S and V, $dS = 0$, $dV = 0$, so that

$$(\partial U/\partial \xi)_{S,V} = \Delta G = -A_f \quad ...(46)$$

From the above treatment we find that

$$G = f(T,P,\xi)\ ;\ A = f(T,V,\xi)\ ;\ H = f(S,P,\xi)\ ;\ U = f(S,V,\xi) \quad ...(47)$$

Since G, A, H and U are state functions, we can write their total differentials as

$$dG = (\partial G/\partial T)_{P,\xi}\, dT + (\partial G/\partial P)_{T,\xi}\, dP + (\partial G/\partial \xi)_{T,P}\, d\xi \quad ...(48)$$

$$dA = (\partial A/\partial T)_{V,\xi}\, dT + (\partial A/\partial V)_{T,\xi}\, dV + (\partial A/\partial \xi)_{T,V}\, d\xi \quad ...(49)$$

$$dH = (\partial H/\partial S)_{P,\xi}\, dS + (\partial H/\partial P)_{S,\xi}\, dP + (\partial H/\partial \xi)_{S,P}\, d\xi \quad ...(50)$$

$$dU = (\partial U/\partial S)_{V,\xi}\, dS + (\partial U/\partial V)_{S,\xi}\, dV + (\partial U/\partial \xi)_{V,S}\, d\xi \quad ...(51)$$

These quantities are referred to as **thermodynamic potentials** relative to thermodynamic variables T, P ; T, V ; S, P and S, V, respectively.

HOMOGENEOUS EQUILIBRIA

Homogeneous gaseous equilibria are best classified into two categories, *i.e.*, in which the number of product molecules is equal to the number of reactant molecules and in which the number of product molecules does not equal the number of reactant molecules.

To the first category belong the following equilibrium systems :

$$N_2(g) + O_2(g) \rightleftharpoons 2NO(g)$$

$$H_2(g) + I_2(g) \rightleftharpoons 2HI(g)$$

$$H_2(g) + CO_2(g) \rightleftharpoons H_2O(g) + CO(g)$$

To the second category belong the following equilibrium systems :

$$SO_2Cl_2(g) \rightleftharpoons SO_2(g) + Cl_2(g)$$

$$COCl_2(g) \rightleftharpoons CO(g) + Cl_2(g)$$

$$2CO_2(g) \rightleftharpoons 2CO(g) + O_2(g)$$

$$2SO_2(g) + O_2(g) \rightleftharpoons 2SO_3(g)$$

$$N_2O_4(g) \rightleftharpoons 2NO_2(g)$$

$$3/2\ H_2(g) + 1/2\ N_2(g) \rightleftharpoons NH_3(g)$$

$$PCl_5(g) \rightleftharpoons PCl_3(g) + Cl_2(g)$$

We shall now consider some homogeneous gaseous equilibria having zero, positive and negative values of Δn where

Δn = Number of moles of gaseous products – Number of moles of gaseous reactants

Case I. When $\Delta n_g = 0$. For the reaction

$$A(g) + B(g) \rightleftharpoons C(g) + D(g)$$

$$K_p = (p_C \times p_D)/(p_A \times p_B) \quad ...(52)$$

If the value of K_p and the initial amounts (number of moles) of A and B are known, the number of moles of various species at equilibrium can be calculated as follows :

	A	+	B	$\rightleftharpoons$	C	+	D
Number of moles at $t=0$:	a		b		0		0
Number of moles at equilibrium :	$a-x$		$b-x$		x		x

Total number of moles at equilibrium $= a - x + b - x + x + x = a + b$

Partial pressures : $\left(\frac{a-x}{a+b}\right)P \quad \left(\frac{b-x}{a+b}\right)P \quad \left(\frac{x}{a+b}\right)P \quad \left(\frac{x}{a+b}\right)P$

$$\therefore \quad K_p = \frac{\left[\left(\frac{x}{(a+b)}\right)P\right]^2}{\left(\frac{a-x}{a+b}\right)P\left(\frac{b-x}{a+b}\right)P} = \frac{x^2}{(a-x)(b-x)} \quad ...(53)$$

The solution of quadratic equation (53) will give two values of x, one of which will determine the equilibrium composition of the homogeneous reaction mixture and the other may be negative or otherwise unreasonable and hence has to be ignored.

From Eq. 53, we arrive at the following conclusions :

1. Since $\Delta n_g = 0$, hence $K_p = K_c = K_x$ (Eq. 24)

2. Suppose we are given a set of equilibrium partial pressures. Then the value of K_p remains unaltered if each of the partial pressures is multiplied by the same factor. In other words, the relative amounts of the various species present at equilibrium are independent of the total pressure or total volume of the system.

3. K_p is independent of the units in which the partial pressures of the various species are expressed.

4. The addition of an inert gas to the reaction mixture does not alter the relative amounts of the species and hence does not alter the value of the equilibrium constant.

5. If an extra amount of A, B, C or D is added to the equilibrium reaction mixture, the relative amounts of the various species will be altered without changing the value of K_p. Suppose n moles of gas A are introduced at equilibrium. The system will readjust its equilibrium. If x' is the amount of A consumed at equilibrium, then the amounts (number of moles) of the various species at equilibrium will be as follows :

A(g)	+	B(g)	$\rightleftharpoons$	C(g)	+	D(g)
$a + n - x'$		$b - x'$		x'		x'

$$\therefore \quad K_p = \frac{x'^2}{(a + n - x')(b - x')} \quad ...(54)$$

The denominator in Eq. 54 is now greater than in Eq. 53 so that x' will be greater than x in order that the value of K_p remains the same. Therefore, more of C and D will be formed. On the other hand, if C or D is introduced at equilibrium, the value of x' will decrease.

The effect of temperature on the equilibrium will depend upon whether the reaction is exothermic or endothermic. If the reaction is exothermic, the equilibrium will shift to the left, *i.e.*, lesser amounts of products will be formed. If the reaction is endothermic, the equilibrium will shift to the right, *i.e.*, larger amounts of products will be formed.

Case II. When Δn is positive. Consider the reaction

$$A(g) \rightleftharpoons B(g) + C(g)$$

$$K_P = p_B \times p_C / p_A \qquad ...(55)$$

If the value of K_p and the initial amount of A are known, the amounts (number of moles) of the various species at equilibrium can be calculated as follows :

	A	⇌	B	+	C
Number of moles at $t=0$:	a		0		0
Number of moles at equilibrium :	$a-x$		x		x

Total number of moles at equilibrium $= a - x + x + x = a + x$

Partial pressures : $\left(\frac{a-x}{a+x}\right)P \qquad \left(\frac{x}{a+x}\right)P \qquad \left(\frac{x}{a+x}\right)P$

$$\therefore \quad K_p = \frac{\left[\left(\frac{x}{a+x}\right)P\right]^2}{\left(\frac{a-x}{a+x}\right)P} = \frac{x^2P}{(a-x)(a+x)} = \frac{x^2P}{a^2-x^2} \qquad ...(56)$$

We conclude from Eq. 56 that

1. At a given temperature, the composition of the equilibrium mixture depends on P. Since K_p should be independent of P, it follows that if P increases, x should decrease, *i.e.*, lesser amount of A will dissociate.

2. K_p will have the units of pressure.

3. We also conclude that since $\Delta n_g \neq 0$, $K_p \neq K_c \neq K_x$

We can also write the equilibrium constants of such reactions in terms of the degree of dissociation. The degree of dissociation, α, gives the fraction of the reactant dissociated. If, for instance, we have 1 mole of A in the beginning, then, at equilibrium, an amount α will be dissociated. Thus,

	A(g)	⇌	B(g)	+	C(g)
Number of moles at $t=0$:	1		0		0
Number of moles at equilibrium :	$1-\alpha$		α		α

If, on the other hand, we have a moles of A in the beginning and α is the degree of dissociation, then

	A(g)	⇌	B(g)	+	C(g)
Number of moles at $t=0$	a		0		0
Number of moles at equilibrium :	$a(1-\alpha)$		$a\alpha$		$a\alpha$

$\therefore$ Total number of moles at equilibrium $= a(1-\alpha) + a\alpha + a\alpha = a(1+\alpha)$

$$\therefore \quad K_p = \frac{p_B \times p_C}{p_A} = \frac{\left\{\frac{a\alpha P}{a(1+\alpha)}\right\}\left\{\frac{a\alpha P}{a(1+\alpha)}\right\}}{\left\{\frac{a(1-\alpha)P}{a(1+\alpha)}\right\}} = \frac{\alpha^2 P}{1-\alpha^2} \qquad ...(57)$$

Knowing K_p and P, α can be obtained from Eq. 57.

Example 14. The reaction $AB_2(g) \rightleftharpoons A(g) + 2B(g)$ is studied in a 10-litre flask. Initially there is 0·40 mole of AB_2. When after the introduction of the catalyst, at 27°C, equilibrium is reached, the pressure of the mixture is 1·2 atm. Calculate the equilibrium constant K_p.

Solution : The equilibrium reaction is $AB_2(g) \rightleftharpoons A(g) + 2B(g)$

Number of moles at equilibrium : $(0{\cdot}40 - x) \qquad x \qquad 2x$

$\therefore$ Total number of moles, $n_{total} = 0{\cdot}40 + 2x$

Assuming that the equilibrium mixture behaves ideally,

$$n_{total} = \frac{PV}{RT} = \frac{(1{\cdot}20 \text{ atm})(10 \text{ dm}^3)}{(0{\cdot}08206 \text{ dm}^3 \text{ atm K}^{-1} \text{ mol}^{-1})(300 \text{ K})} = 0{\cdot}487$$

Thus, $0{\cdot}40 + 2x = 0{\cdot}487$ whence $x = 0{\cdot}0435$; $P = 1{\cdot}2$ atm (given)

$$p_A = \left(\frac{x}{0{\cdot}40+2x}\right)P; \; p_B = \left(\frac{2x}{0{\cdot}40+2x}\right)P; \; p_{AB_2} = \left(\frac{0{\cdot}40-x}{0{\cdot}40+2x}\right)P$$

$$K_p = \frac{p_A \times p_B^2}{p_{AB_2}} = \frac{(x)(2x)^2(1{\cdot}20\text{atm})^2}{(0{\cdot}40-x)(0{\cdot}40+2x)^2}$$

Using $x = 0{\cdot}0435$, we find that $K_P = 5{\cdot}607 \times 10^{-3}$ **atm²**

Dissociation of N_2O_4. N_2O_4 dissociates to give NO_2, as shown below. If we start with one mole of N_2O_4 and if α is the degree of dissociation, then,

$$N_2O_4(g) \rightleftharpoons 2NO_2(g)$$
$$(1-\alpha) \qquad (2\alpha)$$

The equilibrium constant, K_p, is given by $K_p = p^2_{NO_2} / p_{N_2O_4}$

Since α is the degree of dissociation of N_2O_4, hence, at equilibrium, $(1 - \alpha)$ is proportional to the number of moles of undissociated N_2O_4 ; 2α is proportional to the number of moles of NO_2. Thus, $(1 - \alpha) + 2\alpha$ or $1 + \alpha$ is proportional to the total number of moles. Let the total pressure of N_2O_4 and NO_2 be P so that the partial pressures are :

$$p_{N_2O_4} = \frac{1-\alpha}{1+\alpha}P \quad \text{and} \quad p_{NO_2} = \frac{2\alpha}{1+\alpha}P$$

Hence, $$K_p = \frac{\left[\frac{2\alpha}{1+\alpha}P\right]^2}{\left(\frac{1-\alpha}{1+\alpha}P\right)} = \frac{4\alpha^2P^2}{(1+\alpha)^2} \times \frac{1+\alpha}{(1-\alpha)P} = \frac{4\alpha^2P}{1-\alpha^2} \qquad ...(58)$$

Example 15. For the dissociation reaction $N_2O_4(g) \rightleftharpoons 2NO_2(g)$, the equilibrium constant K_p is 0·120 atm at 298 K and a total pressure of 2 atm. Calculate the degree of dissociation of N_2O_4.

Solution : $K_p = 4\alpha^2P/(1 - \alpha^2)$ (Eq. 58)

$K_p = 0{\cdot}120$ atm, $P = 2$ atm

$\therefore \quad 0{\cdot}120 = 4\alpha^2(2)/(1 - \alpha^2) = 8\alpha^2/(1 - \alpha^2)$ or $0{\cdot}120(1 - \alpha^2) = 8\alpha^2$

$\therefore$ **Degree of dissociation, $\alpha = (0{\cdot}120/8{\cdot}12)^{1/2} = 0{\cdot}121$**

Example 16. For the dissociation reaction $N_2O_4(g) \rightleftharpoons 2NO_2(g)$, derive the expression for the degree of dissociation in terms of K_p and total pressure P.

Solution : $K_p = 4\alpha^2P/(1 - \alpha^2)$ (Eq. 58)

$\therefore \quad K_p(1 - \alpha^2) = 4\alpha^2P$ or $(1 - \alpha^2)/\alpha^2 = 4P/K_p$

$\therefore \quad (1/\alpha^2) - 1 = 4P/K_p$ or $1/\alpha^2 = 1 + 4P/K_p = (4P + K_p)/K_p$

$\therefore \quad \alpha^2 = K_p/(K_p + 4P) = 1/(1 + 4P/K_p) = (1 + 4P/K_p)^{-1}$

$\therefore \quad \alpha = (1 + 4P/K_p)^{-1/2}$ **which is the desired expression.**

Example 17. Calculate the degree of dissociation of Br_2 gas into Br atoms if at 1600 K and a total pressure of 0·1 atm, $K_p = 0{\cdot}255$ atm.

Solution : $Br_2(g) \rightleftharpoons 2Br(g)$

$K_p = 4\alpha^2P/(1 - \alpha^2)$ (Eq. 58)

$0{\cdot}255 \text{ atm} = 4\alpha^2(0{\cdot}1 \text{ atm})/(1 - \alpha^2) = 0{\cdot}4\alpha^2/(1 - \alpha^2)$

or $\alpha^2/(1 - \alpha^2) = 0{\cdot}255/0{\cdot}4 = 0{\cdot}64$

which can be solved to yield $\alpha = 0{\cdot}62$. Thus, the degree of dissociation is 0·62.

Dissociation of PCl_5. Gaseous PCl_5 dissociates into PCl_3 and Cl_2 according to the reaction

$$PCl_5(g) \rightleftharpoons PCl_3(g) + Cl_2(g)$$

On the dissociation of 1 mole of PCl_5, there is at equilibrium $(1 - \alpha)$ mole of PCl_5, α mole of PCl_3 and α mole of Cl_2 so that the total number of moles $= (1-\alpha) + \alpha + \alpha = 1 + \alpha$ where α is the degree of dissociation.

If P is the total equilibrium pressure, then the partial pressures of the various constituents are :

$$p_{PCl_5} = \frac{(1-\alpha)P}{1+\alpha}; \quad p_{PCl_3} = \frac{\alpha P}{1+\alpha}; \quad p_{Cl_2} = \frac{\alpha P}{1+\alpha}$$

Hence,

$$K_p = \frac{p_{PCl_3} p_{Cl_2}}{p_{PCl_5}} = \frac{\left(\frac{\alpha P}{1+\alpha}\right)\left(\frac{\alpha P}{1+\alpha}\right)}{\frac{(1-\alpha)P}{1+\alpha}}$$

$$= \frac{\alpha^2 P^2}{(1+\alpha)^2} \times \frac{1+\alpha}{(1-\alpha)P} = \frac{\alpha^2 P}{1-\alpha^2} \qquad ...(59)$$

Since at a given temperature, K_p is constant, it is evident that an increase in P results in a decrease of α and *vice-versa*. If $\alpha \ll 1$, α^2 will be still smaller so that α^2 can be neglected in the denominator of Eq. 59, giving

$$K_p = \alpha^2 P \quad \text{whence} \quad \alpha = (K_p/P)^{1/2} \qquad ...(60)$$

Knowing K_P and the total pressure P, α can be calculated with the help of Eq. 60.

Example 18. The dissociation of PCl_5 was studied at 229°C at a total pressure of 1 atm. The value of K_p was found to be 0·460 atm. Calculate the degree of dissociation of PCl_5. If keeping the temperature constant, the pressure on the system is raised to 10 atm, what will be the degree of dissociation ?

Solution : $K_p = 0{\cdot}460$ atm ; $P = 1$ atm

$K_p = \alpha^2 P/(1 - \alpha^2)$ (Eq. 59)

$\therefore$ $0{\cdot}460 \text{ atm} = \alpha^2(1 \text{ atm})/(1 - \alpha^2)$ or $0{\cdot}460(1 - \alpha^2) = \alpha^2$

$\therefore$ $\alpha = (0{\cdot}460/1{\cdot}460)^{1/2} = \mathbf{0{\cdot}56}$

Again, at $P = 10$ atm,

$0{\cdot}460 \text{ atm} = \alpha^2(10 \text{ atm})/(1 - \alpha^2)$ or $0{\cdot}460(1 - \alpha^2) = 10\alpha^2$

$\therefore$ $\alpha = (0{\cdot}460/10{\cdot}460)^{1/2} = (0{\cdot}044)^{1/2} = \mathbf{0{\cdot}21}$

We see that raising the pressure of the system from 1 atm to 10 atm, lowers the extent of dissociation from 56% to 21%.

Example 19. The extent of dissociation of PCl_5 at a certain temperature is 20% at one atm pressure. Calculate the pressure at which this substance is half-dissociated at the same temperature.

Solution : $K_p = \alpha^2 P/(1 - \alpha^2)$

$P = 1$ atm, $\alpha = 0{\cdot}2$

$\therefore$ $K_p = (0{\cdot}2)^2 (1 \text{ atm}) / (1 - 0{\cdot}04) = 0{\cdot}041$ atm

Let P' be the pressure at which $\alpha = 0{\cdot}5$, then

$K_p = \alpha^2 P'/(1 - \alpha^2)$

$0{\cdot}041 \text{ atm} = (0{\cdot}5)^2 P'/(1 - 0{\cdot}25)$

$P' = \mathbf{0{\cdot}123 \text{ atm}}$

Example 20. 2 moles of PCl_5 are heated at 229°C till equilibrium is reached at a total pressure of 1 atm. Calculate the composition of the equilibrium mixture and the percentage decomposition of PCl_5. $K_p = 0{\cdot}46$ atm.

Solution :

	$PCl_5(g)$	$\rightleftharpoons$	$PCl_3(g)$	+	$Cl_2(g)$
	a				
	$a-x$		x		x

It can be easily shown that for the above reaction at a total pressure of 1 atm,

$K_p = x^2/(a^2 - x^2)$

In the present case, $a = 2$ mole ; $P = 1$ atm ; $K_p = 0{\cdot}46$ atm

$\therefore$ $0{\cdot}46 = x^2/(4 - x^2)$

or $0{\cdot}46(4 - x^2) - x^2 = 0$ or $1{\cdot}84 - 1{\cdot}46x^2 = 0$

This equation, on solving for x, gives $x = 1{\cdot}12$ mole

Hence, at equilibrium, the composition of the equilibrium mixture is as follows :

Amount of $PCl_5 = 2 - 1{\cdot}12 = \mathbf{0{\cdot}88}$ mole

Amount of PCl_3 = amount of $Cl_2 = \mathbf{1{\cdot}12}$ moles

$\therefore$ % age decomposition of $PCl_5 = (1{\cdot}12/2) \times 100 = \mathbf{56}$

Example 21. If in the last example, the pressure of the system is raised to 10 atm at the same temperature, what would be the percentage decomposition of PCl_5 ?

Solution : Even when the pressure is raised from 1 to 10 atm, K_p remains the same, *i.e.*, 0·46 atm.

$K_p = x^2 P/(a^2 - x^2)$

$0{\cdot}46 = 10x^2/(4 - x^2)$

This quadratic equation can be solved for x giving $x = 0{\cdot}42$ mole

$\therefore$ % age decomposition of $PCl_5 = (0{\cdot}42/2) \times 100 = 21$

Example 22. At 30°C, K_p for the dissociation reaction $SO_2Cl_2(g) \rightleftharpoons SO_2(g) + Cl_2(g)$ is $2{\cdot}9 \times 10^{-2}$ atm. If the total pressure is 1 atm, calculate the degree of dissociation of SO_2Cl_2.

Solution : For the given equilibrium, $K_p = \alpha^2 P/(1 - \alpha^2)$

In the present case, $K_p = 2{\cdot}9 \times 10^{-2}$ atm ; $P = 1$ atm

$\therefore$ $2{\cdot}9 \times 10^{-2} \text{ atm} = \alpha^2(1 \text{ atm})/(1 - \alpha^2)$.

Since K_p in this case is very small, α would also be very small so that $\alpha^2 << 1$ and can be neglected in the denominator giving $K_p = \alpha^2 P$

$\therefore$ Degree of dissociation at $P = 1$ atm, $\alpha = (K_p)^{1/2} = (2{\cdot}9 \times 10^{-2})^{1/2} = \mathbf{0{\cdot}17}$

Example 23. At 248°C, the K_p for the reaction $SbCl_5(g) \rightleftharpoons SbCl_3(g) + Cl_2(g)$ is 1·07 atm at a total pressure of 1 atm. Calculate the degree of dissociation of $SbCl_5$.

Solution : $K_p = \alpha^2 P/(1 - \alpha^2)$ (Eq. 59)

Since α is not known, we cannot use the approximation that $\alpha^2 \ll 1$. Instead, we shall have to solve for α by using the above expression as such.

$K_p = 1{\cdot}07$ atm ; $P = 1$ atm

$\therefore$ $1{\cdot}07 \text{ atm} = \alpha^2(1 \text{ atm})/(1 - \alpha^2)$ or $1{\cdot}07(1 - \alpha^2) = \alpha^2$

$\therefore$ Degree of dissociation, $\alpha = (1{\cdot}07/2{\cdot}07)^{1/2} = (0{\cdot}517)^{1/2} = \mathbf{0{\cdot}718}$

Example 24. For the homogeneous gaseous reaction $2AB_2(g) \rightleftharpoons 2AB(g) + B_2(g)$, derive an expression for the degree of dissociation, α, in terms of K_p and total pressure P assuming that $\alpha << 1$.

Solution :

	$2AB_2(g)$	$\rightleftharpoons$	$2AB(g)$	+	$B_2(g)$
No. of moles at equilibrium :	$2(1 - \alpha)$		2α		α

$\therefore$ $n = 2(1-\alpha) + 2\alpha + \alpha = 2 + \alpha$

$\therefore$ $p_{AB_2} = \frac{2(1-\alpha)P}{2+\alpha}; \quad p_{AB} = \frac{2\alpha P}{2+\alpha}; \quad p_{B_2} = \frac{\alpha P}{2+\alpha}$

$\therefore$ $K_p = \frac{p_{AB}^2 p_{B_2}}{p_{AB_2}^2} = \frac{\left(\frac{2\alpha P}{2+\alpha}\right)^2 \left(\frac{\alpha P}{2+\alpha}\right)}{\left(\frac{2(1-\alpha)P}{2+\alpha}\right)^2} = \frac{\alpha^3 P}{(2+\alpha)(1-\alpha)^2}$

Since $\alpha << 1$, it can be neglected in the denominator, giving

$K_p = \alpha^3 P/2$ whence $\alpha = (2K_p/P)^{1/3}$

Example 25. A homogeneous gaseous reaction $AB_2(g) \rightleftharpoons A(g) + 2B(g)$ is carried out in a 10-litre flask at 300 K. The flask initially contains 0·4 mole of AB_2. The total pressure of the reaction mixture, after the attainment of equilibrium, is 1·2 atm. Calculate K_p.

Solution :
$$K_p = \frac{p_A p_B^2}{p_{AB_2}} = \frac{(x_A P)(x_B P)^2}{x_{AB_2} P} = \frac{x_A x_B^2 P^2}{x_{AB_2}}$$

where x_is are the mole fractions and P is the total equilibrium pressure.

Since $x_i = n_i / n_{total}$, we have
$$K_p = \frac{n_A n_B^2 P^2}{n_{AB_2}(n_{total})^2} \qquad ...(i)$$

Let y be the number of moles of A formed at equilibrium. Then

$AB_2(g)$	$\rightleftharpoons$	$A(g)$	+	$2B(g)$
$0·40 - y$		y		$2y$

$$n_{total} = (0·40 - y) + y + 2y = 0·40 + 2y$$

Also, assuming that the mixture behaves ideally,
$$n_{total} = \frac{PV}{RT} = \frac{(1·20 \text{ atm})(10 \text{ dm}^3)}{(0·08206 \text{ dm}^3 \text{ atm K}^{-1} \text{ mol}^{-1})(300 \text{ K})} = 0·487 \text{ mole}$$
$$\therefore \quad 0·487 = 0·40 + 2y \quad \text{whence} \quad y = 0·0435 \text{ mole}$$

Hence, from Eq. *(i)*,
$$K_p = \frac{y(2y)^2(1·20)^2}{(0·40 - y)(0·40 + 2y)^2} = 5·607 \times 10^{-3}$$

Example 26. The homogeneous gaseous reaction $2SO_2 + O_2 \rightleftharpoons 2SO_3$ is carried out in a 2-litre flask at 300 K. The flask initially contains 0·1 mole each of SO_2 and SO_3. The total pressure of the reaction mixture, after the equilibrium has been attained, is 2·78 atm. Calculate *(a)* K_p and *(b)* the mole fraction of O_2 at equilibrium.

Solution : a.
$$K_p = \frac{p_{SO_3}^2}{p_{SO_2}^2 p_{O_2}} = \frac{(x_{SO_3} P)^2}{(x_{SO_2} P)^2 (x_{O_2} P)} = \frac{(x_{SO_3})^2}{(x_{SO_2})^2 x_{O_2} P}$$

where x_is are the mole fractions and P is the total pressure ($x_i = n_i / n_{total}$)

$$\therefore \quad K_p = \frac{(n_{SO_3})^2 n_{total}}{(n_{SO_2})^2 n_{O_2}} \times \frac{1}{P}$$

Since, for the ideal gas mixture, $PV = n_{total} RT$,
$$\therefore \quad K_p = \frac{(n_{SO_3})^2}{(n_{SO_2})^2 n_{O_2}} \left(\frac{V}{RT}\right) \qquad ...(i)$$

Let y be the number of moles of O_2 reacted at equilibrium. Then,

$2SO_2(g)$	+	$O_2(g)$	$\rightleftharpoons$	$2SO_3(g)$
$(0·1 - 2y)$		y		$(0·1 + 2y)$

$$\therefore \quad n_{total} = (0·1 - 2y) + y + (0·1 + 2y) = 0·2 + y$$

Also,
$$n_{total} = \frac{PV}{RT} = \frac{(2·78 \text{ atm})(2 \text{ dm}^3)}{(0·08206 \text{ dm}^3 \text{ atm K}^{-1} \text{ mol}^{-1})(300 \text{ K})} = 0·226 \text{ mole}$$

Thus, $0·226 = 0·2 + y$ whence $y = 0·026$ mol

Substituting in Eq. *(i)*, we have
$$K_p = \frac{(0·1 + 2y)^2}{(0·1 - 2y)^2 y} \left(\frac{V}{RT}\right)$$
$$= \frac{(0·152 \text{ mol})^2 (2 \text{ dm}^3)}{(0·048 \text{ mol})^2 (0·026 \text{ mol})(0·08206) \text{ dm}^3 \text{ atm K}^{-1} \text{ mol}^{-1})(300 \text{ K})} = 31·33$$

b.
$$x_{O_2} = n_{O_2} / n_{total} = 0·026 / 0·226 = 0·115$$

Example 27. Consider the homogeneous gaseous reaction $H_2(g) + I_2(g) \rightleftharpoons 2HI(g)$ carried out in a vessel at a temperature T. When 1 mole of H_2 and 3 moles of I_2 are mixed, a certain amount of HI is formed. When, however, 2 additional moles of H_2 are introduced, the amount of HI formed is double the earlier amount. What is the value of K_p ?

Solution : Since the number of moles of reactants and products is the same, hence
$$K_p = K_c = K_x$$

Suppose in the first case, $n_{HI} = x$ so that $n_{H_2} = 1 - (x/2)$ and $n_{I_2} = 3 - (x/2)$
$$\therefore \quad K_p = x^2 / [1 - x/2)(3 - x/2)] \qquad ...(i)$$

In the second case, $n_{HI} = 2x$ so that $n_{H_2} = 3 - x$ and $n_{I_2} = 3 - x$
$$\therefore \quad K_p = (2x)^2 / (3 - x)^2 \qquad ...(ii)$$

Hence, from Eqs. *(i)* and *(ii)*,
$$\frac{x^2}{\left(1 - \frac{x}{2}\right)\left(3 - \frac{x}{2}\right)} = \frac{(2x)^2}{(3 - x)^2}$$

Neglecting x^2 in the denominator on both sides, cross-multiplying and simplifying, we obtain $x = 3/2$. Hence, from Eq. *(i)* or *(ii)*, $K_p = 4$.

Example 28. At 25°C, for the reaction $Br_2(l) + Cl_2(g) \rightleftharpoons 2BrCl(g)$, $K_p = 2·032$. At the same temperature, the vapour pressure of $Br_2(l)$ is 0·281 atm. Pure BrCl(g) was introduced into a closed container of adjustable volume. The total pressure was kept at 1 atm and the temperature at 25°C. Calculate the fraction of BrCl originally present that has been converted into Br_2 and Cl_2 at equilibrium assuming that the gaseous species behave ideally.

Solution : Since for the reaction $Br_2(l) + Cl_2(g) \rightleftharpoons 2BrCl(g)$, $K_p = 2·032$, therefore, for the reverse reaction, *viz.*, $2BrCl(g) \rightleftharpoons Br_2(l) + Cl_2(g)$, $K_p' = 1/K_p = 1/2·032 = 0·4921$

$$p_{BrCl} + p_{Br_2} + p_{Cl_2} = 1 \text{ atm}$$
$$\therefore \quad p_{BrCl} + p_{Cl_2} = 1 \text{ atm} - p_{Br_2} = (1 - 0·281) \text{ atm} = 0·719 \text{ atm}$$

Let n_0 be the number of moles of BrCl initially present and α be its degree of dissociation. Then, at equilibrium,
$$n_{BrCl} = n_0(1 - \alpha)$$
$$n_{Cl_2} = n_0 \times 1/2 \ (\alpha) \qquad [\because \text{ BrCl} \longrightarrow \tfrac{1}{2} \text{ Cl}_2]$$
$$n_{BrCl} + n_{Cl_2} = n_0 (1 - \alpha/2)$$
$$\therefore \quad p_{BrCl} = \left\{\frac{n_0(1 - \alpha)}{n_0(1 - \alpha/2)}\right\} (0·719 \text{ atm})$$
$$p_{Cl_2} = \left\{\frac{1/2\alpha \times n_0}{n_0(1 - \alpha/2)}\right\} (0·719 \text{ atm})$$
$$\therefore \quad K_p' = \frac{p_{Cl_2}}{(p_{BrCl})^2} = \frac{\alpha/2(1 - \alpha/2)}{(1 - \alpha)^2 \times 0·719} = 0·4921$$

This gives the quadratic equation $0·604\alpha^2 - 1·208\alpha + 0·354 = 0$ whose solution yields $\alpha = 0·357$.

Temperature-Dependence of the Equilibrium Constant : The van't Hoff Equation. From Eq. 21,
$$\Delta G^\circ / T = -R \ln K_p \qquad ...(61)$$

Hence,
$$\left[\frac{\partial(\Delta G^\circ / T)}{\partial T}\right] = -R \frac{d \ln K_p}{dT} \qquad ...(62)$$

From the Gibbs-Helmholtz equation,
$$\left[\frac{\partial(\Delta G^\circ / T)}{\partial T}\right] = -\frac{\Delta H^\circ}{T^2} \qquad ...(63)$$

Hence, from Eqs. 62 and 63

$$\frac{d \ln K_p}{dT} = \frac{\Delta H^\circ}{RT^2} \qquad ...(64)$$

where ΔH° is the standard enthalpy of the reaction. Eq. 64 is known as the **van't Hoff equation.**

Integrated Form of the van't Hoff Equation. The integration of Eq. 64 depends upon the manner in which ΔH° depends upon temperature. If, over a short temperature range, ΔH° is assumed to be temperature-independent, then the integration of Eq. 64 gives

$$\int d \ln K_p = \int \frac{\Delta H^\circ}{RT^2} dT = \frac{\Delta H^\circ}{R} \int \frac{dT}{T^2} \qquad ...(65)$$

or

$$\ln K_p = -\frac{\Delta H^\circ}{RT} + I \qquad ...(66)$$

where I is the constant of integration. According to Eq. 66, a plot of $\ln K_p$ versus $1/T$ gives a straight line with slope $= -\Delta H^\circ/R$. Thus, from the slope, ΔH° can be determined since

$$\Delta H^\circ = -R \times \text{slope} \qquad ...(67)$$

If it is desired to carry out the integration of Eq. 64 between two temperatures T_1 and T_2 when the equilibrium constants are $K_{P,1}$ and $K_{P,2}$ respectively, then, assuming that ΔH° is constant over this temperature range, we obtain

$$\int_{K_{P,1}}^{K_{P,2}} d \ln K_p = \frac{\Delta H^\circ}{R} \int_{T_1}^{T_2} \frac{dT}{T^2} \qquad ...(68)$$

or

$$\ln \frac{K_{P,2}}{K_{P,1}} = \frac{\Delta H^\circ}{R}\left[-\frac{1}{T_2} - \left(-\frac{1}{T_1}\right)\right] = \frac{\Delta H^\circ}{R}\left[\frac{T_2 - T_1}{T_1 T_2}\right] \qquad ...(69)$$

This is the **integrated van't Hoff equation.** From this equation, if ΔH° is known, then knowing the value of $K_{P,1}$ at T_1, the value of $K_{P,2}$ at T_2 can be determined. Also, if $K_{P,1}$ and $K_{P,2}$ at T_1 and T_2, respectively, are known, ΔH° can be calculated.

For accurate calculations, however, the temperature-dependence of ΔH° must be taken into account. If the heat capacities of the reactants and products are known as a function of temperature, an explicit expression for the temperature-dependence of ΔH° can be derived from the Kirchhoff equation, obtaining

$$\Delta H^\circ = \Delta H_0^\circ + \Delta\alpha T + \tfrac{1}{2}\Delta\beta T^2 + \tfrac{1}{3}\Delta\gamma T^3 + \cdots \qquad ...(70)$$

where ΔH_0° is the enthalpy of the reaction at absolute zero and $\Delta\alpha$, $\Delta\beta$, $\Delta\gamma$, etc., are derived from heat capacities of the reactants and the products and their variation with temperature. The van't Hoff equation now becomes

$$\frac{d \ln K_p}{dT} = \frac{\Delta H^\circ}{RT^2} + \frac{\Delta H_0^\circ}{RT^2} + \frac{\Delta\alpha}{RT} + \frac{\Delta\beta}{2R} + \frac{\Delta\gamma T}{3R} + \cdots \qquad ...(71)$$

This expression, upon integration, yields the following equation for K_p as a function of temperature :

$$\ln K_p = -\frac{\Delta H_0^\circ}{RT} + \frac{\Delta\alpha}{R} \ln T + \frac{\Delta\beta}{2R} T + \frac{\Delta\gamma}{6R} T^2 \cdots + I \qquad ...(72)$$

The constant of integration, I, can be easily determined if K_p is known at any temperature either experimentally or from the known value of ΔG°.

Example 29. The equilibrium constant K_p for the reaction $H_2(g) + S(g) \rightleftharpoons H_2S(g)$ is 20·2 atm^{-1} at 945°C and 9·1 atm^{-1} at 1·065°C. Calculate ΔH°.

Solution : According to the integrated van't Hoff equation

$$\ln\left(\frac{K_{P,2}}{K_{P,1}}\right) = \frac{\Delta H^\circ}{R}\left(\frac{T_2 - T_1}{T_1 T_2}\right)$$

or

$$\Delta H^\circ = R \ln\left(\frac{K_{P,2}}{K_{P,1}}\right)\left(\frac{T_1 T_2}{T_2 - T_1}\right) = (8{\cdot}314 \text{ J K}^{-1} \text{ mol}^{-1}) \ln (9{\cdot}21/20{\cdot}2) \left[\frac{(1218\text{ K})(1338\text{ K})}{1338\text{ K} - 1218\text{ K}}\right]$$

$$= -88126{\cdot}3 \text{ J mol}^{-1} = -88{\cdot}126 \text{ kJ mol}^{-1}$$

Example 30. Integrate the van't Hoff equation, $d \ln K_p/dT = \Delta H^\circ/RT^2$ and determine the constant of integration.

Solution : $d \ln K_p/dT = \Delta H^\circ/RT^2$ or $d \ln K_p = (\Delta H^\circ/RT^2)\, dT$

Assuming that ΔH° remains constant over the temperature range, we have

$$\int (d \ln K_p) = \frac{\Delta H^\circ}{R} \int \frac{dT}{T^2} \quad \text{or} \quad \ln K_p = -(\Delta H^\circ/RT) + I$$

where I is the constant of integration.

Since $\Delta G^\circ = -RT \ln K_p$, we have

$$-\Delta G^\circ/RT = \ln K_p = -(\Delta H^\circ/RT) + I$$

or $$\Delta G^\circ = \Delta H^\circ - IRT$$

Also, $$\Delta G^\circ = \Delta H^\circ - T\Delta S^\circ \qquad ...(i)$$

From Eqs. *(i)* and *(ii)*, $I = \Delta S^\circ/R$ ...(ii)

Example 31. The equilibrium constant of a reaction doubles on raising the temperature from 25°C to 35°C. Calculate ΔH° for the reaction.

Solution : According to the integrated van't Hoff equation, $\ln\left(\frac{K_{P,2}}{K_{P,1}}\right) = \frac{\Delta H^\circ}{R}\left(\frac{T_2 - T_1}{T_1 T_2}\right)$

Here $T_1 = 25°C = 298 \text{ K}$; $T_2 = 308 \text{ K}$

$K_{P,2}/K_{P,1} = 2$; $R = 8{\cdot}314 \text{ J K}^{-1} \text{ mol}^{-1}$

$\therefore$ $\Delta H^\circ = R\,[T_1 T_2/(T_2 - T_1)] \ln 2 = 52893{\cdot}5 \text{ J} = 52{\cdot}89 \text{ kJ mol}^{-1}$

Example 32. For the reaction $CO(g) + SO_3(g) \rightleftharpoons CO_2(g) + SO_2(g)$, $\Delta G^\circ = 187{\cdot}1$ kJ mol^{-1} and $\Delta H^\circ = 184{\cdot}7$ kJ mol^{-1} at 25°C. Calculate *(a)* ΔG° at 398 K and *(b)* K_p at 398. Assume that ΔH° remains constant over the temperature interval.

Solution : *(a)* $\left[\frac{\partial(\Delta G^\circ/T)}{\partial T}\right]_P = -\frac{\Delta H^\circ}{T^2}$ (Eq. 63)

$\therefore$ $d(\Delta G^\circ/T) = -(\Delta H^\circ/T^2)dT$

Integrating, we get, $\int_{298}^{398} d\left(\frac{\Delta G^\circ}{T}\right) = -\int_{298}^{398} \frac{\Delta H^\circ}{T^2} dT$

$$\left[\frac{\Delta G^\circ}{T}\right]_{298}^{398} = -\Delta H^\circ\left[-\frac{1}{T}\right]_{298}^{398} = \Delta H^\circ\left[\frac{1}{T}\right]_{298}^{398}$$

$$\frac{\Delta G^\circ_{398}}{398\text{ K}} - \frac{\Delta G^\circ_{298}}{298\text{ K}} = \Delta H^\circ\left[\frac{1}{398\text{ K}} - \frac{1}{298\text{ K}}\right]$$

Substituting the values of ΔG° and ΔH° at 25°C we have

$$\frac{\Delta G^\circ}{398\text{ K}} = \frac{187{\cdot}1 \text{ kJ mol}^{-1}}{298\text{ K}} - (184{\cdot}7 \text{ kJ mol}^{-1})\left(\frac{1}{398\text{ K}} - \frac{1}{298\text{ K}}\right)$$

$$= -0{\cdot}472 \text{ kJ K}^{-1} \text{ mol}^{-1}$$

$$\Delta G^\circ_{398} = (-0{\cdot}472 \text{ kJ K}^{-1} \text{ mol}^{-1})(398 \text{ K}) = -187{\cdot}8 \text{ kJ mol}^{-1}$$

(b) Since $\Delta G^\circ = -RT \ln K_p$

$$K_p = \exp\left(\frac{-\Delta G^\circ}{RT}\right) = 4{\cdot}46\times10^{24}$$

Example 33. The following data were obtained for the temperature-dependence of the equilibrium constant of an inhibitor binding an enzyme. Calculate the values of ΔG°, ΔH° and ΔS° for this process at 25°C.

t(°C)	16·0	21·1	25·0	31·9	37·5
K_c	7·25	5·25	4·17	2·66	2·01(×10⁷)

Solution : Let us rewrite the data in the following form :

T (K)	289	294·1	298	304·9	310·5
$1/T\times100$	3·46	3·40	3·36	3·28	3·22
$K_c/10^7$	7·25	5·25	4·17	2·66	2·01
$\ln K_c$	18·10	17·78	17·55	17·10	16·81

A plot of $\ln K_c$ *versus* $1/T$ will give a straight line whose slope can be determined. This comes out to be $5{\cdot}43\times10^3$. Since slope $= -\Delta H^\circ/R$, hence

$$\Delta H^\circ = -\text{slope}\,(R) = -45{\cdot}1 \text{ kJ mol}^{-1}$$

At 25°C, $K_c = 4{\cdot}17\times10^7$, hence

$$\Delta G^\circ = -RT\ln K_c = -(8{\cdot}314\times10^{-3} \text{ kJ K}^{-1} \text{ mol}^{-1})(298 \text{ K}) \ln 4{\cdot}17\times10^7$$
$$= -43{\cdot}5 \text{ kJ mol}^{-1}$$

Since $\Delta G^\circ = \Delta H^\circ - T\Delta S^\circ$

$$\therefore \quad \Delta S^\circ = (\Delta H^\circ - \Delta G^\circ)/T = (-45{\cdot}1 + 43{\cdot}5) \text{ kJ mol}^{-1}/298 \text{ K} = -5{\cdot}4 \text{ J K}^{-1} \text{ mol}^{-1}$$

Example 34. Show that the van't Hoff equation can also be written as $d\ln K_c/dT = \Delta U^\circ/RT^2$. K_c is the equilibrium constant when the concentrations of the species are expressed in terms of mol dm^{-3} and ΔU° is the standard internal energy change.

Solution : $K_p = K_c(RT)^{\Delta n} \quad \therefore \ln K_p = \ln K_c + \Delta n \ln RT$

Differentiating with respect to T, we get

$$\therefore \quad \ln d(\ln K_p)/dT = d(\ln K_c)/dT + \Delta n/T$$

$$\ln d(\ln K_c)/dT = d(\ln K_p)/dT - \Delta n/T = \Delta H^\circ/RT^2 - \Delta n/T$$
$$= \Delta H^\circ/RT^2 - RT\Delta n/RT^2 = (\Delta H^\circ - \Delta nRT)/RT^2 \qquad \text{(Note this step)}$$

For n moles of an ideal gas, $\Delta U^\circ = \Delta H^\circ - \Delta(PV) = \Delta H^\circ - \Delta nRT$

$$\therefore \quad d(\ln K_c)/dT = \Delta U^\circ/RT^2$$

Pressure-Dependence of Equilibrium Constants. We shall now examine the pressure-dependence of equilibrium constants K_p, K_c and K_x.

1. Pressure-dependence of K_p. According to Eq. 21,

$$\Delta G^\circ = -RT \ln K_p$$

Since ΔG° depends upon temperature alone, hence, K_p also depends on temperature alone and is independent of pressure. Hence,

$$\left(\frac{\partial \ln K_p}{\partial P}\right)_T = -\frac{\partial}{\partial P}\left(\frac{\Delta G^\circ}{RT}\right)_T = 0 \qquad \ldots(73)$$

2. Pressure-dependence of K_c. Since

$$K_p = K_c(RT)^{\Delta n} \qquad \text{(Eq. 23)}$$

or $$K_c = K_p(RT)^{-\Delta n}$$

$$\therefore \quad \ln K_c = \ln K_p - \Delta n \ln RT$$

$$\therefore \quad \left(\frac{d\ln K_c}{dP}\right)_T = \left(\frac{d\ln K_p}{dP}\right)_T - \Delta n\left(\frac{d\ln RT}{dP}\right)_T \qquad \ldots(74)$$

Since both the terms on the R.H.S. of Eq. 74 are equal to zero,

$$(d \ln K_c/dP)_T = 0 \qquad \ldots(75)$$

i.e., K_c is also independent of pressure.

3. Pressure-dependence of K_x.

$$K_p = K_x P^{\Delta n} \qquad \text{(Eq. 24)}$$

or $$K_x = K_p P^{-\Delta n}$$

$$\therefore \quad \ln K_x = \ln K_p - \Delta n \ln P \qquad \ldots(76)$$

$$\therefore \quad \left(\frac{d\ln K_x}{dP}\right)_T = \left(\frac{d\ln K_p}{dP}\right)_T - \Delta n\left(\frac{d\ln P}{dP}\right)_T = (d \ln K_p/dP) - \Delta n/P$$

$$= -\Delta n/P \quad (\because d \ln K_p/dP = 0) \qquad \ldots(77)$$

$$= -\Delta V/RT, \text{ where } \Delta V = \Sigma V_{\text{products}} - \Sigma V_{\text{reactants}} \qquad \ldots(78)$$

From Eq. 78 we draw the following conclusions :

1. When $\Delta n = 0$, *i.e.*, the reaction involves no change in the total number of moles of gaseous species in the system so that $\Delta V = 0$, K_x is independent of pressure. Such reactions are

$$CO_2(g) + H_2(g) \rightleftharpoons CO(g) + H_2O(g)$$

and $$H_2(g) + I_2(g) \rightleftharpoons 2HI(g)$$

2. When $\Delta n \neq 0$, K_x is pressure-dependent, as shown by Eq. 77 or Eq. 78. Two cases arise :

(a) $\Delta n > 0$, *i.e.*, there is an increase in the number of moles so that $\Delta V > 0$. This implies that in Eq. 78, the R.H.S. is negative so that K_x decreases with increasing pressure.

(b) $\Delta n < 0$, *i.e.*, there is a decrease in the number of moles so that $\Delta V < 0$. This means that in Eq. 78, the R.H.S. is positive so that K_x increases with increasing pressure. It is for this reason that the synthesis of ammonia by the Haber process,

$$3H_2(g) + N_2(g) \rightleftharpoons 2NH_3(g); \qquad \Delta n = 2 - (3 + 1) = -2$$

is carried out at high pressure. Fritz Haber (1868–1934), the German chemist, was the recipient of the 1918 Chemistry Nobel Prize for his synthesis of ammonia from the elements.

Example 35. Calculate K_p at 25°C and 325°C for the reaction $NO(g) + 1/2\ O_2(g) \rightleftharpoons NO_2(g)$ if at 25°C, $\Delta H^\circ = -56{\cdot}48$ kJ mol^{-1} and $\Delta G^\circ = -34{\cdot}85$ kJ mol^{-1}.

Solution : Since $\Delta G^\circ = -RT \ln K_p$

$$\ln K_p = -\frac{\Delta G^\circ}{RT} = \frac{34{\cdot}85 \text{ kJ mol}^{-1}}{(8{\cdot}314\times10^{-3} \text{ kJ K}^{-1} \text{ mol}^{-1})(298 \text{ K})}$$

$\therefore$ **At 25°C, $K_p = 1{\cdot}28\times10^5$**

To calculate K_p at 325°C we use the integrated van't Hoff equation, *viz.*,

$$\ln\left(\frac{K_{P,2}}{K_{P,1}}\right) = \frac{\Delta H^\circ}{R}\left(\frac{T_2 - T_1}{T_1T_2}\right)$$

$$\ln K_{P,2} = \ln K_{P,1} + \frac{\Delta H^\circ}{R}\left(\frac{T_2 - T_1}{T_1 T_2}\right)$$

$\Delta H^\circ = -56{\cdot}48$ kJ mol^{-1}, $T_1 = 298$ K, $T_2 = 598$ K. Using these values, we get $K_{P,2}$ at 325°C = 13·9

Note that for the exothermic reaction, K_p at higher temperature is smaller than that at lower temperature. The reverse is true for an endothermic reaction.

Example 36. Diamonds are formed from graphite under very high pressure. Calculate the equilibrium pressure at which graphite is converted into diamond at 25°C, given that the densities of graphite and diamond are, respectively, 2·25 and 3·51 g cm^{-3} and are independent of pressure. ΔG_f° values for graphite and diamond are zero and 2·90 kJ mol^{-1}, respectively.

Solution : This example is an application of the thermodynamic relation

$$[\partial(\Delta G)/\partial P]_T = \Delta V \qquad ...(i)$$

For the reaction, C (graphite) $\rightleftharpoons$ C (diamond),

$$\Delta G^\circ = \Delta G_f^\circ(\text{diamond}) - \Delta G_f^\circ(\text{graphite}) = 2{\cdot}90 \text{ kJ} - 0 = 2{\cdot}90 \text{ kJ mol}^{-1}$$

$$= (2{\cdot}90 \text{ kJ mol}^{-1}) \times \frac{(0{\cdot}08206 \text{ dm}^3 \text{ atm K}^{-1} \text{ mol}^{-1})}{8{\cdot}314 \times 10^{-3} \text{ kJ K}^{-1} \text{ mol}^{-1}} = 28{\cdot}6 \text{ dm}^3 \text{ atm mol}^{-1}$$

(Note the change in units for ΔG°)

The respective volumes of diamond and graphite are obtained from their densities, recalling that the atomic mass of carbon is 12 g mol^{-1}.

$$\therefore \quad \Delta V = V_{\text{diamond}} - V_{\text{graphite}} = \frac{12 \text{ g mol}^{-1}}{3{\cdot}51 \times 10^3 \text{ g dm}^{-3}} - \frac{12 \text{ g mol}^{-1}}{2{\cdot}25 \times 10^3 \text{ g dm}^{-3}}$$

$$= -1{\cdot}91 \times 10^{-3} \text{ dm}^3 \text{ mol}^{-1} \qquad ...(ii)$$

From Eq. *(i)*, $d(\Delta G) = \Delta V/dP$, which on integration, gives

$$\int_1^2 d(\Delta G) = \int_{P_1}^{P_2} \Delta V dP$$

Let $P_1 = 1$ atm and $P_2 = P$ Then,

$$\Delta G_2 - \Delta G_1 = \Delta V(P_2 - P_1) = \Delta V(P - 1)$$

or $\quad 0 - 28{\cdot}6 \text{ dm}^3 \text{ atm mol}^{-1} = -1{\cdot}91 \times 10^{-3} \text{ dm}^3 \text{ mol}^{-1} (P - 1)$

or $$P - 1 = \frac{28{\cdot}6 \text{ dm}^3 \text{ atm mol}^{-1}}{1{\cdot}91 \times 10^{-3} \text{ dm}^3 \text{ mol}^{-1}} = 1{\cdot}497 \times 10^4 \text{ atm}$$

$\therefore$ The equilibrium pressure, $P = 2{\cdot}497 \times 10^4 \approx$ **25,000 atm**

HETEROGENEOUS EQUILIBRIA

A chemical reaction is said to be heterogeneous if the species taking part in it constitute more than one phase. Examples of heterogeneous equilibria are :

1. The dissociation of solid calcium carbonate :

$$CaCO_3(s) \rightleftharpoons CaO(s) + CO_2(g)$$

2. The decomposition of solid ammonium chloride :

$$NH_4Cl(s) \rightleftharpoons NH_3(g) + HCl(g)$$

3. The decomposition of solid NH_4HS :

$$NH_4HS(s) \rightleftharpoons NH_3(g) + H_2S(g)$$

Dissociation of Calcium Carbonate

Consider the dissociation of solid calcium carbonate in a closed vessel :

$$CaCO_3(s) \rightleftharpoons CaO(s) + CO_2(g)$$

If ξ is the extent of the reaction, then

$$d\xi = -dn_{CaCO_3} = dn_{CaO} + dn_{CO_2} \qquad ...(79)$$

and $$dG = (\mu_{CaO} + \mu_{CO_2} - \mu_{CaCO_3})d\xi \qquad ...(80)$$

$\therefore$ $$(\partial G/\partial \xi)_{T,P} = \mu_{CaO} + \mu_{CO_2} - \mu_{CaCO_3} = \Delta G \qquad ...(81)$$

At equilibrium, $$(\partial G/\partial \xi)_{T,P} = 0 \qquad ...(82)$$

$\therefore$ $$\mu_{CaO} + \mu_{CO_2} - \mu_{CaCO_3} = 0 \qquad ...(83)$$

Now, under ordinary conditions, the chemical potentials of solids can be taken as equal to the chemical potentials of pure solids,

i.e., $$\mu_{CaO} = \mu_{CaO}^\circ \quad \text{and} \quad \mu_{CaCO_3} = \mu_{CaCO_3}^\circ$$

Also, $$\mu_{CO_2} = \mu_{CO_2}^\circ + RT \ln p_{CO_2} \qquad ...(84)$$

Hence, at equilibrium,

$$\mu_{CaCO_3} (= \mu_{CaCO_3}^\circ) = \mu_{CaO} + \mu_{CO_2} = \mu_{CaO}^\circ + \mu_{CO_2}^\circ + RT \ln p_{CO_2} \qquad ...(85)$$

or $$RT \ln p_{CO_2} = -[\mu_{CaO}^\circ + \mu_{CO_2}^\circ - \mu_{CaCO_3}^\circ] = -\Delta G^\circ \qquad ...(86)$$

But $$-\Delta G^\circ = RT \ln K_p \qquad \text{(Eq. 21)}$$

Hence, $$K_p = p_{CO_2} \qquad ...(87)$$

We find that whereas ΔG° of a reaction involves ΔG_f° values of the reactants and the products, *the equilibrium constant involves only the partial pressures of the gaseous species.*

Example 37. Calculate the pressure of CO_2 gas at 700 K in the heterogeneous equilibrium reaction $CaCO_3(s) \rightleftharpoons CaO(s) + CO_2(g)$ if ΔG° for this reaction is 130·2 kJ mol^{-1}.

Solution : Here $$K_p = p_{CO_2}$$

Also, $$\Delta G^\circ = -RT \ln K_p$$

$\therefore$ $$\ln K_p = -\frac{\Delta G^\circ}{RT} = -\frac{130{\cdot}2 \times 10^3 \text{ J mol}^{-1}}{(8{\cdot}314 \text{ J K}^{-1} \text{ mol}^{-1})(700 \text{ K})}$$

$\therefore$ $$p_{CO_2} = K_p = 1{\cdot}94 \times 10^{-10} \text{ atm}$$

Example 38. For the reaction $NiO(s) + CO(g) \rightleftharpoons Ni(s) + CO_2(g)$, ΔG°(J mol^{-1}) $= -20{,}700 - 11{\cdot}97\,T$. Calculate the temperature at which the product gases at equilibrium at 1 atm will contain 400 ppm (parts per million) of carbon monoxide.

Solution : For the given reaction, $K_p = p_{CO_2}/p_{CO}$

Since $p_{CO} \ll p_{CO_2}$, hence

$$K_p = \frac{1}{p_{CO}} = \frac{1}{400 \times 10^{-6}} = 2{,}500$$

$$\Delta G^\circ = -RT \ln K_p$$

$\therefore$ $$\ln K_p = -\frac{\Delta G^\circ}{RT} = \frac{20{,}700 + 11{\cdot}97\,T}{RT}$$

This equation when solved for T using $R = 8{\cdot}314$ J K^{-1} mol^{-1}, gives $T = 390$ K

Example 39. Calculate the pressure of oxygen over a sample of NiO(s) at 25°C if ΔG° for the reaction $NiO(s) \rightleftharpoons Ni(s) + 1/2\,O_2(g)$ is 211·7 kJ mol^{-1}.

Solution : $$K_p = (p_{O_2})^{1/2}$$

$$K_p = \exp(-\Delta G^\circ/RT) = \exp\left[-\frac{211{\cdot}7 \times 10^3 \text{ J mol}^{-1}}{(8{\cdot}314 \text{ J K}^{-1} \text{ mol}^{-1})(298 \text{ K})}\right] = 7{\cdot}8 \times 10^{-38}$$

$\therefore$ $$p_{O_2} = K_p^2 = (7{\cdot}8 \times 10^{-38})^2 = 6 \times 10^{-75} \text{ atm}$$

Example 40. Calculate the partial pressure of HCl gas above a sample of $NH_4Cl(s)$ as a result of its decomposition according to the reaction $NH_4Cl(s) \rightleftharpoons NH_3(g) + HCl(g)$. ΔG_f° values of $NH_4Cl(s)$, $NH_3(g)$ and $HCl(g)$ are $-202{\cdot}96$ kJ mol^{-1}, $-16{\cdot}48$ kJ mol^{-1} and $-95{\cdot}30$ kJ mol^{-1}, respectively.

Solution : For the given reaction,

$$\Delta G^\circ = [(-16{\cdot}48) + (-95{\cdot}30) - (-202{\cdot}96)] = 91{\cdot}18 \text{ kJ mol}^{-1}$$

$$\therefore \quad K_p = \exp(-\Delta G^\circ/RT)$$

$$= \exp[-91{\cdot}18 \text{ kJ mol}^{-1}/(8{\cdot}314\times10^{-3} \text{ kJ K}^{-1} \text{ mol}^{-1})(298 \text{ K})] = 1{\cdot}04\times10^{-16}$$

$$a_{NH_4Cl} = 1 \quad \text{and} \quad a_{NH_3} = a_{HCl} = p_{HCl} = p_{NH_3}$$

$$K_p = p_{NH_3} \times p_{HCl} = p_{HCl}^2$$

$$\therefore \quad p_{HCl} = K_p^{1/2} = 1{\cdot}02\times10^{-8} \text{ atm}$$

Example 41. Consider the decomposition of solid NH_4HS in a flask containing $NH_3(g)$ at a pressure of 1·50 atm. What will be the partial pressures of $NH_3(g)$ and $H_2S(g)$ after the equilibrium has been attained ? K_p for the reaction is 0·11.

Solution : $NH_4HS(s) \rightleftharpoons NH_3(g) + H_2S(g)$

Since the flask already contains $NH_3(g)$, the equilibrium pressures of NH_3 and H_2S will not be equal after the attainment of equilibrium. At equilibrium,

$$p_{NH_3} = p_{H_2S} + 1{\cdot}50$$

$$K_p = p_{NH_3} \times p_{H_2S} = (p_{H_2S} + 1{\cdot}50)(p_{H_2S}) = 0{\cdot}11$$

or $(p_{H_2S})^2 + 1{\cdot}50\,p_{H_2S} - 0{\cdot}11 = 0$

This quadratic equation can be solved for p_{H_2S} giving $p_{H_2S} = 0{\cdot}06$ atm or $-1{\cdot}56$ atm. The negative value has no physical meaning so that

$$p_{H_2S} = 0{\cdot}06 \text{ atm}$$

Hence, $p_{NH_3} = (0{\cdot}06 + 1{\cdot}50) = 1{\cdot}56$ atm

Example 42. Explain why it is permissible to omit the concentrations of pure solids and liquids in calculating K_c for a heterogeneous reaction.

Solution : The standard state for a solid or a liquid is the state of the substance in its pure form. The chemical potential is given by $\mu = \mu^\circ + RT \ln a$. When the substance is pure, $\mu = \mu^\circ$ so that the activity $a = 1$. Thus, we replace activity or molar concentration of each pure substance by 1 in the equilibrium condition which is equivalent to omitting it.

Example 43. Consider the heterogeneous equilibria :

$$CaCO_3(s) \rightleftharpoons CaO(s) + CO_2(g); \qquad K_p = 4{\cdot}0\times10^{-2} \text{ atm} \qquad ...(i)$$

$$C(s) + CO_2(g) \rightleftharpoons 2CO(g); \qquad K_p' = 2{\cdot}0 \text{ atm} \qquad ...(ii)$$

Calculate the partial pressure of CO when solid $CaCO_3$ and CaO are mixed and allowed to attain equilibrium at the temperature for which the above two equilibria have been studied.

Solution : For equilibrium *(i)*, $K_p = p_{CO_2}$

For equilibrium *(ii)*, $K_p' = p^2_{CO}/p_{CO_2}$

$$\therefore \quad K_p K_p' = (p_{CO})^2 = 8{\cdot}0\times10^{-2} \text{ atm}^2$$

$$\therefore \quad p_{CO} = \sqrt{8{\cdot}0\times10^{-2} \text{ atm}^2} = 0{\cdot}28 \text{ atm}$$

Example 44. Consider the following data for the two reactions :

(i) $FeO(s) + CO(g) \rightleftharpoons Fe(s) + CO_2(g)$

(ii) $Fe_3O_4(s) + CO(g) \rightleftharpoons 3FeO(s) + CO_2(g)$

t(°C)	600	700	800	900	1000
K_1	0·871	0·678	0·552	0·466	0·403
K_2	1·15	1·77	2·54	3·43	4·42

where K_1, K_2 are the equilibrium constants of the first and the second reaction, respectively. Calculate the temperature at which Fe, FeO, Fe_3O_4, CO and CO_2 could all coexist in equilibrium.

Solution : We see that both for the first and the second reaction,

$$K_1 = K_2 = p_{CO_2}/p_{CO}$$

This being so, there is only one temperature at which both reactions can be in equilibrium simultaneously, *i.e.*, the temperature at which $K_1 = K_2$. If we plot log K_1 *versus* $1/T$ and log K_2 versus $1/T$ *on the same graph*, the point of intersection gives $1/T = 1{\cdot}19\times10^{-3}$ whence $T = 840$ K (*i.e.*, 567°C). This is the desired temperature.

Equilibrium Constants of Reactions Involving Real Gases. Consider a general reaction

$$aA(g) + bB(g) \rightleftharpoons mM(g) + nN(g)$$

in which the reactants and the products are real (non-ideal) gases. De Donder's treatment shows that for the equilibrium to exist in this system,

$$(\partial G/\partial \xi)_{T,P} = \Delta G = (m\mu_M + n\mu_N) - (a\mu_A + b\mu_B) = 0 \qquad ...(88)$$

The chemical potential of a real gas is given by

$$\mu_i = \mu_i^\circ + RT \ln f_i \qquad ...(89)$$

where f_i is the fugacity of the ith component.

Using these two equations, we obtain

$$\Delta G^\circ = -RT \ln \left[\frac{f_M^m f_N^n}{f_A^a f_B^b}\right]_{eqbm} \qquad ...(90)$$

The constant term on the R.H.S. of this equation, involving fugacities, is called K_{therm}, *i.e.*,

$$K_{therm} = \left[\frac{f_M^m f_N^n}{f_A^a f_B^b}\right]_{eqbm} \qquad ...(91)$$

Since fugacity is proportional to pressure, hence $f = \gamma P$ where γ is the fugacity coefficient. Thus, we can write

$$K_{therm} = \frac{(\gamma_M p_M)^m (\gamma_N p_N)^n}{(\gamma_A p_A)^a (\gamma_B p_B)^b} = \frac{\gamma_M^m \gamma_N^n}{\gamma_A^a \gamma_B^b} K_p = K_\gamma K_p \qquad ...(92)$$

where K_p is the partial pressure equilibrium constant and K_γ is the corresponding ratio of the fugacity coefficients for the respective pure gases at the specified total pressure.

For an ideal gas, $\gamma = 1$ so that $K_{therm} = K_p$. As the pressure of the system changes, the fugacity coefficients change so that K_γ changes. Since only K_{therm} is expected to remain constant with change in pressure, K_p will no longer be constant. In fact, K_p will be a non-constant equilibrium constant. We, therefore, conclude that for equilibria involving real gases, K_p cannot give a satisfactory description of the equilibrium.

Example 45. At 450°C and 600 atm pressure, the equilibrium constant for the reaction $N_2(g) + 3H_2(g) \rightleftharpoons 2NH_3(g)$ is $4{\cdot}516\times10^{-5}$. *(a)* Calculate the degree of the conversion of N_2 and H_2 to NH_3 assuming that the system is a mixture of real gases. Fugacity coefficients are $\gamma_{N_2} = 1{\cdot}3238$, $H_2 = 1{\cdot}2874$ and $\gamma_{NH_3} = 0{\cdot}8548$. *(b)* Repeat the calculations assuming that the gases behave ideally.

Solution : *(a)* Let α be the degree of conversion. Then, at equilibrium,

$N_2(g)$	+	$3H_2(g)$	$\rightleftharpoons$	$2NH_3(g)$
$1-\alpha$		$3(1-\alpha)$		2α

$$K_{therm} = \frac{(f_{NH_3})^2}{f_{N_2}(f_{H_2})^3} = \frac{(p_{NH_3})^2}{p_{N_2}(p_{H_2})^3} \times \frac{(\gamma_{NH_3})^2}{\gamma_{N_2}(\gamma_{H_2})^3} = K_p K_\gamma$$

At equilibrium, the total number of moles

$$= (1-\alpha) + 3(1-\alpha) + 2\alpha = 2(2-\alpha)$$

$$\therefore \quad p_{N_2} = \frac{(1-\alpha)P}{2(2-\alpha)}; \; p_{H_2} = \frac{3(1-\alpha)P}{2(2-\alpha)}; \; p_{NH_3} = \frac{2\alpha P}{2(2-\alpha)}$$

where $P = 600$ atm.

$$\therefore \quad 4{\cdot}516\times10^{-5} = \frac{4\alpha^2(600)^2}{4(2-\alpha)^2} \times \frac{2(2-\alpha)}{(1-\alpha)600} \times \frac{8(2-\alpha)^3}{27(1-\alpha)^3(600)^3} \times \frac{(0{\cdot}8548)^2}{(1{\cdot}3238)(1{\cdot}2874)^3}$$

This equation, on rearranging, gives a quadratic equation in α which on solving gives two values of α, *viz.*, 1·56 and 0·43. The first value is not acceptable since the conversion to NH_3 cannot be more than 1 (*i.e.*, more than 100%). Thus, $\alpha = 0{\cdot}43$, *i.e.*, the degree of conversion of N_2 and H_2 to NH_3 is **0·43**.

(b) Assuming ideality, $K_{therm} = K_p$

$$4{\cdot}516\times10^{-5} = \frac{16}{(27)(600)^2} \times \frac{(2-\alpha)^2}{(1-\alpha)^4}$$

This equation can be rearranged to give a quadratic equation in α whose solution gives $\alpha = 0{\cdot}55$.

LE CHATELIER'S PRINCIPLE

There are three main factors which alter the state of equilibrium. These are : concentration, temperature and pressure.

The addition of a catalyst has no effect. The function of a catalyst, is merely to hasten the approach of equilibrium. It does so by speeding up the forward as well as the backward reaction.

Henri Louis Le Chatelier (1850–1936), the French chemist, studied the effect of concentration, temperature and pressure on a large number of chemical equilibria. He summed up his conclusion in the form of a generalisation known as **Le Chatelier's principle**, which states as follows :

If an equilibrium is subjected to a stress, the equilibrium shifts in such a way as to reduce the stress.

Thus, if a system at equilibrium is subjected to a change of concentration, pressure or temperature, the equilibrium shifts in the direction that tends to **undo** the effect of the change. This principle, in fact, follows from the van't Hoff equation for the temperature-dependence of the equilibrium constant.

We shall apply this principle to a few well known equilibria.

Effect of Change of Concentration. Consider the following equilibrium :

$$\underset{\text{Pale yellow}}{Fe^{3+}(aq)} + \underset{\text{Colourless}}{(SCN)^-(aq)} \rightleftharpoons \underset{\text{Dark brown}}{[Fe(SCN)]^{2+}(aq)}$$

Suppose, some ferric salt (say, ferric chloride) is added to this equilibrium. The colour of the solution will darken immediately showing that there is increase in the concentration of the coloured complex ion $[Fe(SCN)]^{2+}$. This change is in accordance with Le Chatelier's principle. Addition of more of Fe^{3+} ions has resulted in increasing the concentration of the complex ferri-sulphocyanide ion. The change imposed on the system was meant to raise the concentration of one of the *reactants* (ferric ions) but it has resulted in raising the concentration of the product. Similarly, if some sulphocyanide salt (*e.g.*, potassium sulphocyanide) is added to the equilibrium, the colour will darken again due to the formation of more of the ferri-sulphocyanide ion. Here again the addition of one of the reactants has led to the formation of more of the product.

Now, suppose a small amount of potassium ferri-sulphocyanide capable of giving the complex ion, $[Fe(SCN)]^{2+}$ is added to the equilibrium. The solution will be seen to become less dark showing that the dark coloured $[Fe(SCN)]^{2+}$ complex ion has been changed into Fe^{3+} and $(SCN)^-$ ions. Thus, increasing the concentration of the product shifts the equilibrium in favour of the reactants.

In general, *in a chemical equilibrium, increasing the concentrations of the reactants results in shifting the equilibrium in favour of the products while increasing the concentrations of the products results in shifting the equilibrium in favour of the reactants.*

Effects of Change of Temperature. A chemical equilibrium actually involves two opposing reactions : one favouring the products and the other favouring the reactants. If one of these is exothermic (*i.e.*, accompanied by evolution of heat), the other must be endothermic (*i.e.*, accompanied by absorption

of heat). This follows from the law of conservation of energy.

Let us consider the equilibrium

$$N_2O_4(g) \rightleftharpoons 2NO_2(g); \qquad \Delta H = +59{\cdot}0 \text{ kJ}$$

In this equilibrium, the reaction favouring the product (NO_2) is seen to be endothermic. Therefore, the opposing reaction favouring the reactant (N_2O_4) must be exothermic. Now suppose the system is heated and its temperature is allowed to rise. According to Le Chatelier's principle, the equilibrium will shift in the direction which tends to undo the effect of heat, *i.e.*, which tends to produce *cooling*. Therefore, the equilibrium will shift in favour of NO_2, *i.e.*, the dissociation of N_2O_4 into NO_2 will increase. If the system is cooled, on the other hand, the equilibrium will shift in the direction which tends to produce heat. Therefore, the equilibrium will shift in the reverse direction, *i.e.*, in favour of N_2O_4. The dissociation of N_2O_4 will decrease.

The combination of nitrogen and hydrogen to give ammonia is represented by the following thermochemical equation :

$$N_2(g) + 3H_2(g) \rightleftharpoons 2NH_3(g); \qquad \Delta H = -92{\cdot}38 \text{ kJ}$$

The forward reaction is exothermic. Therefore, the back reaction must be endothermic. By Le Chatelier's principle, the increase of temperature will favour the back reaction, *i.e.*, the dissociation of ammonia. Therefore, in order to get a better yield of ammonia, the temperature of the equilibrium should be low. But since the reaction rate varies with the temperature, the time taken to reach the equilibrium state becomes very long if the temperature is kept low. Therefore, a temperature close to 500°C, which is neither too high nor too low, is maintained. Although the yield of ammonia at this temperature is not so high as that at a lower temperature, yet it is more economical to get a poorer yield than to wait for a long time in the hope of getting a better one.

Finely divided iron is used as a catalyst to hasten the approach of equilibrium.

Effect of Change of Pressure. If a system in equilibrium consists of gases, then the concentrations of all the components can be altered by changing the pressure. Consider, once again, the dissociation of N_2O_4 into NO_2 :

$$\underset{1 \text{ mole}}{N_2O_4(g)} \rightleftharpoons \underset{2 \text{ moles}}{2NO_2(g)}$$

Suppose the pressure on the system is increased. The volume of the system will decrease proportionately. The total number of moles per unit volume will now be more than before. The change can be counteracted if equilibrium shifts in that direction in which the total number of moles is *decreased*. This can take place by the combination of NO_2 molecules to produce N_2O_4 molecules. Thus, according to Le Chatelier's principle, application of pressure on the above system tends to shift the equilibrium in favour of N_2O_4.

Consider another gaseous reaction involving combination of nitrogen and hydrogen to give ammonia :

$$\underbrace{\underset{1 \text{ mole}}{N_2(g)} + \underset{3 \text{ moles}}{3H_2(g)}}_{4 \text{ moles}} \rightleftharpoons \underset{2 \text{ moles}}{2NH_3}$$

As it is evident from the above equation, the forward reaction is accompanied by a decrease in the number of moles. If the pressure is increased, the volume will decrease and, therefore, the number of moles per unit volume will increase. According to Le Chatelier's principle, therefore, the equilibrium will shift in the direction in which there is decrease in the number of moles, *i.e.*, in favour of the formation of ammonia. Thus, the higher the pressure, the greater would be the yield of ammonia. It is on account of this consideration that a pressure of about 200 atm is maintained in the Haber process for the manufacture of ammonia.

Finally, let us consider the equilibrium

$$\underbrace{\underset{1 \text{ mole}}{CO(g)} + \underset{1 \text{ mole}}{H_2O(g)}}_{2 \text{ moles}} \rightleftharpoons \underbrace{\underset{1 \text{ mole}}{CO_2(g)} + \underset{1 \text{ mole}}{H_2(g)}}_{2 \text{ moles}}$$

The above reaction proceeds in either direction without any change in the number of moles. According to Le Chatelier's principle, therefore, the pressure will have no effect on this equilibrium.

Le Chatelier's Principle and Physical Equilibria. Le Chatelier's principle, as already stated, is applicable to all types of equilibria involving not only chemical but physical changes as well. A few examples of its application to physical equilibria are discussed below.

1. Vapour pressure of a liquid. Consider the equilibrium

$$\text{Liquid} \rightleftharpoons \text{Vapour}$$

It is well known that the change of a liquid into its vapour is accompanied by absorption of heat whereas the conversion of vapour into liquid state is accompanied by evolution of heat. According to Le Chatelier's principle, therefore, addition of heat to such a system will shift the equilibrium towards the right. On raising the temperature of the system, liquid will evaporate. This will raise the vapour pressure of the system. Thus, the vapour pressure of a liquid increases with rise in temperature.

2. Effect of pressure on the boiling point of a liquid. The conversion of liquid into vapour, as represented by the above equilibrium, is accompanied by increase of pressure (vapour pressure). Therefore, if pressure on the system is increased, some of the vapours will change into liquid so as to *lower* the pressure. Thus, the application of pressure on the system tends to condense the vapour into liquid state at a given temperature. In order to counteract it, a higher temperature is needed. This explains the rise of boiling point of a liquid on the application of pressure.

3. Effect of pressure on the freezing point of a liquid (or melting point of a solid). At the melting point, solid and liquid are in equilibrium :

$$\text{Solid} \rightleftharpoons \text{Liquid}$$

Now, when a solid melts, there is usually a change, either increase or decrease of volume. For example, when ice melts, there is decrease in volume, or at constant volume, there is decrease in pressure. Thus, increase of pressure on ice $\rightleftharpoons$ water system at a constant temperature will cause the equilibrium to shift towards the right, *i.e.*, it will cause the ice to melt. Hence, in order to retain ice in equilibrium with water at the higher pressure, it will be necessary to lower the temperature. Thus, the application of pressure will lower the melting point of ice. When sulphur melts, there is increase in volume or at constant volume, there is increase in pressure. Thus, it follows that if the pressure on the system, sulphur (solid) $\rightleftharpoons$ sulphur (liquid) is increased, the melting point is raised.

4. Effect of temperature on solubility. In most cases, when a solute passes into solution, heat is absorbed, *i.e.*, cooling results. Therefore, according to Le Chatelier's principle, when heat is supplied to a saturated solution in contact with the solute, the change will take place in that direction which absorbs heat (*i.e.*, which tends to produce cooling). Therefore, some more of the solute will dissolve. In other words, the solubility of the substance increases with rise in temperature. Dissolution of some salts is accompanied by evolution of heat. Here, the solubility decreases with rise in temperature.

Linear Free Energy Relationships (LFERs) :

Hammett Equation

The equilibrium constants and rates of polar organic reactions are strongly affected by substituents on organic molecules. In 1937, Louis P. Hammett of Columbia University (U.S.A.) suggested that the effects of *meta* and *para* substituents on the ionization constants of benzoic acids could predict the influence of substituents in a variety of reactions. The reason why *meta* and *para* substituents are chosen is that these substituents on aromatic rings are held at fixed distances from the points of reaction. Also, the ionization constants of a large number of substituted benzoic acids are available. Hammett specifically excluded *ortho* substituents from his studies since they might influence the reactions by steric hindrance or by hydrogen bonding or even by their direct participation in the reactions.

1. Substituent Constant, σ. Hammett defined a substituent constant, σ (sigma) as the logarithm of the ratio of the ionization constant of a substituted benzoic acid to that of benzoic acid itself in

water solution at 25°C :

$$\sigma = \log \frac{K_a}{K_{a,0}} \qquad \ldots(93)$$

where K_a is the dissociation constant of substituted benzoic acid and $K_{a,0}$ is the dissociation constant of benzoic acid. From Eq. 93,

$$\sigma = \log K_a - \log K_{a,0} \qquad \ldots(94)$$

$$= pK_{a,0} - pK_a \qquad \ldots(95)$$

Since dissociation constants of meta and para substituted benzoic acids differ from each other, each substituent has two sigma constants : σ_{meta} and σ_{para}. Table 2 lists values of σ_{meta} and σ_{para} for a number of compounds. They represent a measure of the electron-donating and electron-attracting powers of substituents. Strongly electron-attracting groups such as $N{\equiv}N^+$, NO_2 and CF_3 groups, have large positive values—that is, they markedly increase the ionization constants of benzoic acids (by stabilizing negative charges on benzoate anions). On the other hand, strongly electron-donating groups, such as NH_2 and OH groups, have large negative values : they decrease the ionization constants of benzoic acids since the negative charges which these groups contribute to the ring would repel the negative charges on benzoate anions. Hydrogen, of course, has a σ value of 0 (the logarithm of 1).

TABLE 2

Some Hammett Substituents Constants

Substituent	σ_{para}	σ_{meta}	σ^{+**}	σ^{-**}
$N{\equiv}N^+$	1·91	1·76	—	3·43
NO_2	0·78	0·71	0·79	1·27
$C{\equiv}N$	0·66	0·56	0·66	1·00
CF_3	0·54	0·43	0·61	0·65
CO_2H	0·45	0·37	0·42	0·77
$CH{=}O$	0·42	0·35	0·73	1·03
Cl	0·23	0·39	0·15	0·25
Br	0·23	0·37	0·11	0·19
I	0·18	0·35	0·14	0·27
F	0·06	0·34	−0·07	−0·03
CH_3	−0·17	−0·07	−0·31	−0·17
OH	−0·37	0·12	−0·92	−0·37
NH_2	−0·66	−0·16	−1·30	−0·15

**applicable to *para* substituents.

It is interesting to compare the effects of the same susbtituents in meta and para positions. For some susbtituents such as the NH_2 group, the absolute value of σ_{para} is much larger than that of σ_{meta}. This is because the electron-donating ability of the amino group is largely due to resonance effects. An amino group in the para position can directly distribute electrons into the carboxyl group of benzoic acid, thus making it more difficult for the carboxyl group to become a negatively charged carboxylate anion :

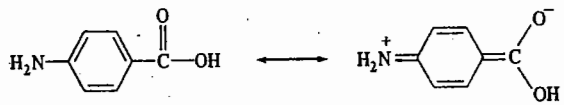

(*i*)

Resonance structures for *p*-minobenzoic acid.

In contrast, there is no direct interaction between a meta amino group and the carboxyl group of benzoic acid.

Most substituents do have somewhat larger effects in para positions than in meta positions even when there is apparently no direct resonance interaction between the substituent and the carboxyl group. An inspection of polarized resonance forms of the benzene rings will show that almost all substituents tend to induce positive or negative charges in para (and ortho) positions of aromatic rings and have smaller effects on meta positions :

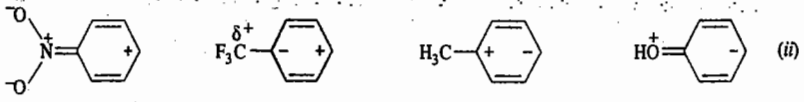

(ii)

Polarized resonance structures of aromatic rings.

For a few substituents, such as **OH and OCH_3** groups, σ_{meta} and σ_{para} have opposite signs, the reason being that electronic effects of substituents are due at least to two different factors : inductive (electronegativity) effects and resonance effects. In alkoxy and hydroxy groups, the two types of electronic effects work in opposite directions. The strongly electronegative oxygen atom has a large electron-attracting inductive effect; it has also a strong electron-donating resonance effect which overpowers the inductive effect when the substituent is in the para position. Thus, the σ_{para} constants for alkoxy and hydroxy groups have large negative values. Halogen atoms also have conflicting inductive and resonance effects. However, halogen atoms are poorer electron donors than oxygen atoms because double bonds to halogens (apart from fluorine) are weak. Thus, σ constants for halogens always have positive signs, but the values are larger for halogens in meta positions than in para positions.

2. Reaction Constant, ρ. The σ constants have been shown to be appropriate measures of the electronic effects of substituents in many reactions of aromatic molecules. This can be demonstrated by Hammett diagrams. In a Hammett diagram the *abscissa* (the *x*-axis) is a scale of σ values for substituents on aromatic rings. The *ordinate* (the *y*-axis) is a scale of the logarithm of the ratios of equilibrium contants for reactions of substituted aromatic compounds to those of similar compounds in which the substituent is a hydrogen atom. For example, Fig. 1 shows a **Hammett plot** for ionization constants of phenylacetic acids. The points fit a straight line which can be reasonably represented by the **Hammett equation**

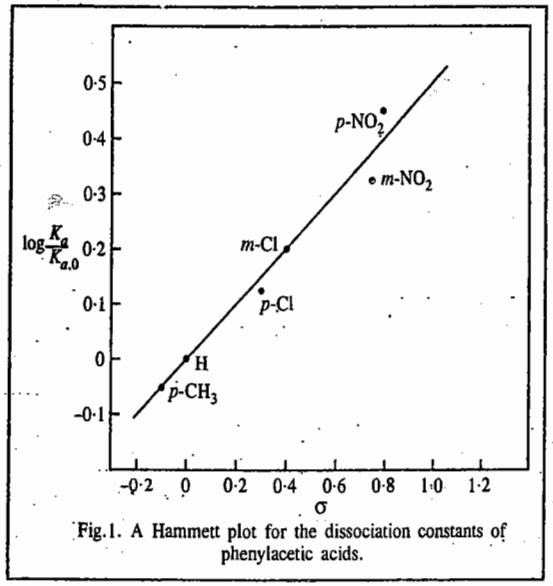

Fig.1. A Hammett plot for the dissociation constants of phenylacetic acids.

$$\log (K_a/K_{a,0}) = \sigma\rho \qquad ...(96)$$

or
$$\log K_a - \log K_{a,0} = \sigma\rho \qquad ...(97)$$

If the equilibrium constants for several cases of a particular reaction of aromatic molecules are known, so that the proportionality constant ρ can be determined, the Hammett equation can be used to estimate the equilibrium constants with different ring substituents with known σ constants.

The slope of the line in a Hammett diagram, ρ, is called the **reaction constant**. The numerical values and signs of ρ differ from reaction to reaction and show how each reaction is affected by the

nature of substituents on the aromatic rings. The value of ρ for the ionization of phenylacetic acids in water at 25°C, for instance, is only about half as large as the value of ρ for the ionization of benzoic acids (which, from the definition of σ, would be exactly 1·00). This is a reasonable result since the substituents in phenylacetic acids are farther from the carboxyl group.

Table 3 shows some Hammett reaction constants.

TABLE 3

Some Hammett Reaction Constants (σ)

Reactions	Solvent	T(°C)	ρ
A. For ionization constants :			
$ArCH_2COH \rightleftharpoons ArCH_2CO^- + H^+$	H_2O	25	0·562
$ArCH_2CH_2COH \rightleftharpoons ArCH_2CH_2CO^- + H^+$	H_2O	25	0·237
B. For rate constants :			
$ArCOC_2H_5 + NaOH \longrightarrow ArCONa + C_2H_5OH$	85% C_2H_5OH	25	2·562
$ArCOC_2H_5 + H_2O \xrightarrow{H^+} ArCOH + C_2H_5OH$	60% CH_3CCH_3	100	0·106
	60% C_2H_5OH	100	0·144
$Ar_2CHCHCl_2 + NaOH \longrightarrow Ar_2C{=}CHCl + NaCl + H_2O$	92·5% C_2H_5OH	20	2·456
$ArCOH + CH_3OH \xrightarrow{H^+} ArCOCH_3 + H_2O$	CH_3OH	25	- 0·577
$ArH + Cl_2 \longrightarrow ArCl + HCl$	CH_3COH	25	- 8·06

A reaction with a positive ρ value is assisted by electron-attracting substituents and adversely affected by electron-donating substituents. The reverse is true for reactions with negative ρ values.

3. Hammett Equation as a Linear Free Energy Relationship. The Hammett equation is a *linear free-energy relationship* (LFER). This can be demonstrated as follows taking into consideration the dissociation constants of substituted and unsubstituted benzoic acids.

For the substituted acid, $\Delta G^\circ = -RT \ln K_a$ ...(98)

For the unsubstituted acid, $\Delta G^\circ_0 = -RT \ln K_{a,0}$ ...(99)

The Hammett equation can be written as

$$\log K_a - \log K_{a,0} = \sigma\rho \qquad ...(100)$$

so that
$$\frac{-\Delta G^\circ}{2{\cdot}303RT} + \frac{\Delta G^\circ_0}{2{\cdot}303RT} = \sigma\rho \qquad ...(101)$$

and
$$-\Delta G^\circ = \sigma\rho\, 2{\cdot}3\, RT - \Delta G^\circ_0 \qquad ...(102)$$

For a given reaction under a given set of conditions, σ, *R*, *T* and ΔG°_0 are all constants so that σ varies linearly with ΔG°.

Just as standard free energy changes of reactions are proportional to logarithms of equilibrium constants, so standard free energies of activation ($\Delta G^{\circ\#}$) are proportional to logarithms of rate constants. In such a case, the analogue of the Hammett equation (96) is :

$$\log (k/k_0) = \sigma\rho \qquad ...(103)$$

where k is the rate constant for the reaction of a meta or para substituted benzene derivative.

Free energy changes may result from changes in enthalpies or entropies or both. Accordingly,

$$\Delta G^\circ = \Delta H^\circ - T\Delta S^\circ$$

and

$$\Delta G^{\circ\#} = \Delta H^{\circ\#} - T\Delta S^{\circ\#} \qquad ...(104)$$

It was initially believed that electronic effects of substituents principally affected enthalpy changes and that th Hammett equation gave linear plots because entropy changes (or changes in entropies of activation) caused by substituents were either small or paralleled enthalpy changes. It has been demonstrated, however, that the actual facts are more complicated. In some cases, substituents exert their influence principally through entropy effects and in others both entropies and enthalpies are affected in ways that seem difficult to predict.

4. Reaction Mechanism and the Hammett Equation. Since the Hammett equation is applicable to reaction rates, it can give important information about the mechanisms of chemical reactions. The signs and magnitudes of the reaction constants, ρ, can be of particular significance.

Consider, for instance, the hydrolysis of benzoyl chloride in water :

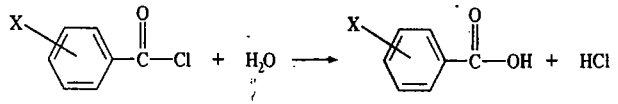

(*i*)

Among the possible mechanisms of this type of reaction are (1) the addition of H_2O to the carbonyl groups to form tetrahedral intermediates in slow, rate-limiting steps, followed by the rapid elimination of chloride ions (or HCl) [Eq.(*ii*)] and (2) the dissociation of the carbon–chlorine bonds in slow, rate-limiting steps, followed by the rapid reaction of water with the resulting carbocations [Eq.(*iii*)].

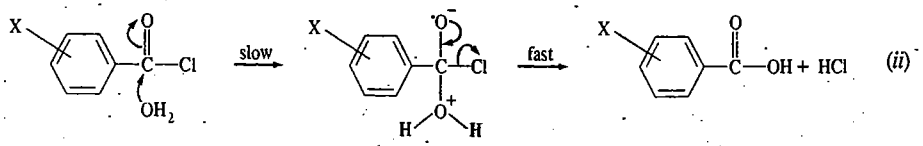

(*ii*)

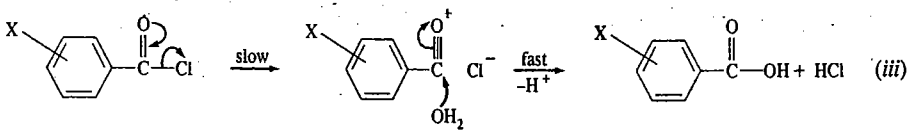

(*iii*)

The dissociation of benzoyl halides to form carbocations would be strongly assisted by electron-donating substituents. On the other hand, the addition of H_2O to the carbonyl groups should be fastest in benzoyl halides with electron-withdrawing substituents. Thus, the fact that a Hammett plot for the rates of aqueous hydrolysis of benzoyl chlorides has a positive value of ρ, is consistent with mechanism (*ii*) and eliminates mechanism (*iii*).

5. σ^+ and σ^- constants. As we have seen, the Hammett sigma (σ) constants for substituents on aromatic rings are a measure of their electronic effects on reaction rates and equilibria. However, the electronic effect of a substituent is a combination of inductive and resonance effects. The fact

that so many reactions of aromatic molecules are correlated by the Hammett equation suggests that the relative importance of inductive and resonance effects is similar in all those reactions. However, it is experimentally found that in some reactions strongly electron-donating groups in para positions accelerate the reaction rates far more than would be predicted by their σ values. Examples of such reactions include S_N1 reactions of *tert*-cumyl chlorides (Eq.*iv*) and electrophilic substitution reactions of aromatic rings (Eq.*v*). In these reactions, direct conjugation may exist between the para substituents and empty (or partially empty) orbitals in the transition states. Modified para substituent constants, σ^+, whose values are derived from the substitution reactions of *tert*-cumyl chloride in 90 per cent aqueous acetone (Eq.*iv*), are generally useful for such reactions. If the use of σ^+ values in a Hammett plot for the rates of a reaction gives a better fit to a straight line than the use of σ values, it provides strong evidence for the existence of a direct resonance interaction between a partially empty orbital and para substituents in the transition states for the reaction. In fact, most reactions that correlate with σ^+ will proceed via the formation of carbocation intermediates.

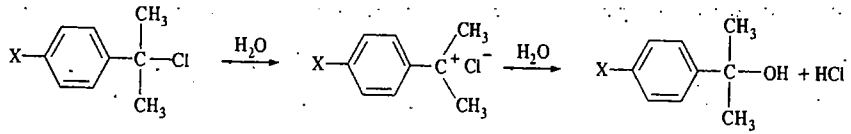

(*iv*)

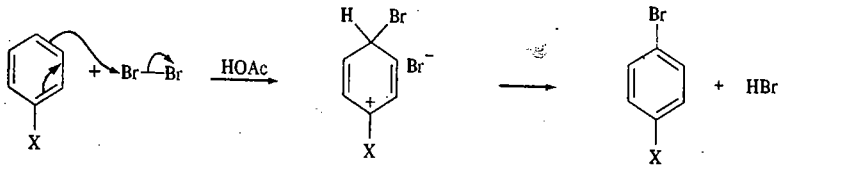

(*v*)

For some reactions, however, negative charges can be directly stabilized by resonance with para substitutents. For these reactions, a modified substituent constant, σ^-, defined as $\log (K_a/K_{a,0})$ for the acid-base reactions of para-substituted phenols or anilinium-salts in water (Eqs. *vii* and *viii*), often provides better plots than standard σ values.

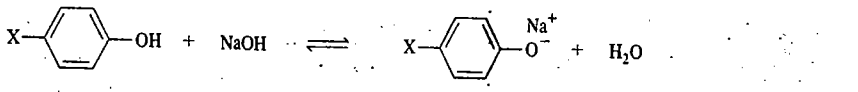

(*vi*)

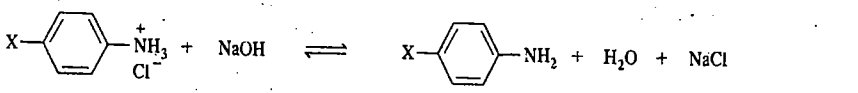

(*vii*)

6. Curved Hammett Plots. For several reactions, Hammett plots yield curved lines even though points for both meta and para substituents fit on to the same line. Frequently, a curved Hammett plot indicates that the reaction has undergone a change in mechanism as the electronic effects of the substituents changed. The observed curve results from the intersection of two straight-line Hammett plots.

The Hammett equation has been used to interpret biological effects of organic molecules and find correlations between LFERs and the effectiveness of synthetic drugs.

Separation of Polar, Resonance and Steric Effects

a. Aliphatic Systems with Fixed Geometry. Researchers have used variations of the Hammett theme to separate the inductive and resonance effects combined in the Hammett σ constants.

J.D. Roberts and W.T. Moreland (1953) measured the pK_as of 4-substituted bicyclo [2,2,2] octane-1-carboxylic acids (1).

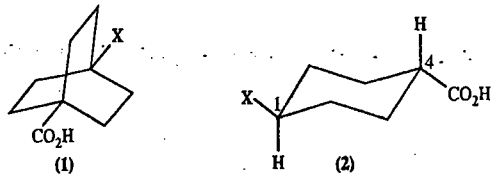

The distance of the substituents from the carboxyl groups and the rigidity of these systems is assumed to eliminate problems with steric effects and that the absence of double bonds would eliminate resonance effects. Thus, value of σ′ in Eq. 105 represents solely the inductive effects of the substituents

$$\log (K_a/K_{a,0}) = \sigma'\rho' \qquad ...(105)$$

To obtain σ′ values, ρ′ was set equal to 1·464. The value of ρ for ionization of benzoic acids in 50% aqueous ethanol solvent was used to measure pK_as of (1). *Trans*-4-substituted cyclohexanecarboxyl acids (2) exist largely in chair conformation, with both large groups in equatorial positions. Their pK_as as well as rates of hydrolysis of their esters, give good correlations with the following equation :

$$\log (K_a/K_{a,0}) = \sigma''\rho'' \quad \text{or} \quad \log (k/k_0) = \sigma''\rho'' \qquad ...(106)$$

Values of σ″ for reactions of (2) parallel those of σ′ for reactions of (1) reasonably well. However, σ″ values are somewhat smaller since substituents at C4 in chair conformation of cyclohexanes are farther from C1 than are substituents in the boat conformation required for cyclohexane rings in (1).

b. Taft Equation. R.W. Taft analyzed the effects of substituents on the rates of reactions of a series of esters, XCO_2R. If R is held constant, the rates of reactions of the esters would depend on the inductive, resonance and steric effects of group X. Also, if a saturated carbon in X were bonded to the carbonyl group, there could be no direct resonance interaction between X and the carbonyl group. Thus, Taft proposed the following equation for the rates of *basic* hydrolysis of esters :

$$\log (k/k_0) = \sigma^*\rho^* + E_s \qquad ...(107)$$

where σ^* and E_s are constants reflecting the inductive and steric effects, respectively, of X. A value of 2·48 was assigned to ρ^* to bring values of σ^* onto a scale comparable to those of Hammett σ values. To obtain values of E_s, Taft found that the rates of *acid* hydrolysis of aromatic esters are not strongly affected by polar effects of substituents. Hence, if changes in X strongly affect the rates of acid-catalysed hydrolysis of ester, the changes are presumably due largely to steric effects. Hence, E_s can be defined by the equation

$$\log (k/k_0) \text{ in acid} = E_s \qquad ...(108)$$

The σ^* and E_s values for various substituents are useful measures of inductive and steric effects, respectively.

BIOCHEMICAL EQUILIBRIA

ATP and its Role in Bioenergetics

Adenosine triphosphate (ATP) (Fig.2) is present in all living cells at concentrations of 10^{-3} to 10^{-2} mol dm^{-3} of cell water. The ATP molecule is composed of three parts: adenine, D-ribose and three phosphate groups in ester linkages. The function of ATP is to store the energy available

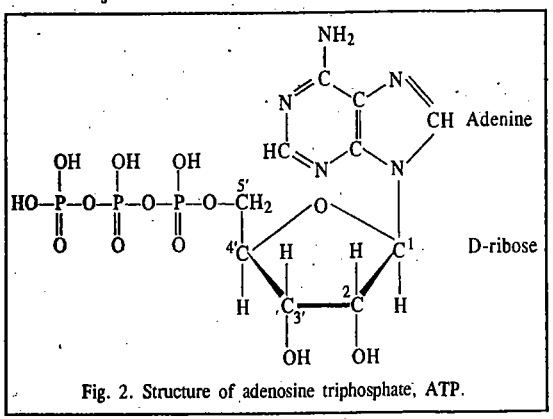

Fig. 2. Structure of adenosine triphosphate, ATP.

when food is metabolized and then to supply it on demand to a wide variety of processes, including muscular contraction, reproduction and vision.

The hydrolysis of ATP to adenosine diphosphate (ADP) and inorganic phosphate (P_i^-) is usually represented by

$$ATP(aq) + H_2O\ (l) \longrightarrow ADP(aq) + P_i^-(aq) + H_3O^+(aq)$$

or, by

$$ATP^{4-}(aq) + H_2O\ (l) \longrightarrow ADP^{3-}(aq) + HPO_4^{2-}\ (aq) + H^+(aq)$$

Under biological standard state conditions, ($[ATP^{4-}] = [ADP^{3-}] = [HPO_4^{2-}] = 1$ mol dm^{-3}, $[H^+] = 10^{-7}$ mol dm^{-3} and $T = 310$ K). The thermodynamic parameters for this reaction are $\Delta G° = -30{\cdot}5$ kJ mol^{-1}, $\Delta H° = -20$ kJ mol^{-1} and $\Delta S° = 34$ J mol^{-1}. We see that this reaction is exergonic (*i.e.*, has negative value of $\Delta G°$) and can drive an endergonic reaction (having a positive value of $\Delta G°$), if suitable enzymes are available.

Now the question arises why the hydrolysis of ATP is thermodynamically favourable. The answer is the following : The *enthalpy change* for the reaction is favourable because (1) electrostatic repulsion between the negative charges in ATP exceeds that in the reaction products (2) the reaction products are resonance-stabilized and (3) the enthalpies of solvation of the products are larger than for ATP. The *entropy change* for the reaction is favourable because of the release of a phosphate group. Note that this implies that the ATP hydrolysis is strongly temperature-dependent. ATP is often referred to as being *energy-rich* containing *high-energy phosphate ester bonds* ; this nomenclature implies that the overall ATP hydrolysis has large negative values of $\Delta G°$ and $\Delta H°$.

We shall now discuss the role of ATP in bioenergetics. ATP is *not* a high-energy compound in comparison with many other biological compounds. The functions of ATP depend on its having a ΔG value for hydrolysis that is *intermediate* in value compared with ΔG values for hydrolysis of other phosphate esters. Thus, ATP and ADP can act as a *donor-acceptor* pair for phosphoryl group transfer. In many cases, the free energy of ATP hydrolysis is used to *support* reactions that would otherwise be thermodynamically unfavourable. This usually occurs via phosphorylation of one of the reactants in an otherwise *unfavourable* reaction.

Example 46. The synthesis of glutamine from glutamate ion and NH_4^+ ion is thermodynamically unfavourable : Glutamate$^-$ + NH_4^+ ⟶ Glutamine ; $\Delta G° = 14{\cdot}2$ kJ mol^{-1}. How could the hydrolysis of ATP be used to render this reaction usable for the synthesis of glutamine ?

Solution : The original reaction is altered by using ATP. The new reaction, which is thermodynamically favourable, consists of two partial reactions linked through a common intermediate via ATP hydrolysis :

$$\text{Glutamate}^- + ATP^{4-} \longrightarrow \text{5-Phosphoglutamate}^{2-} + ADP^{3-}$$

$$\text{5-Phosphoglutamate}^{2-} + NH_4^+ \longrightarrow \text{Glutamine} + \text{Phosphate}^-$$

$\Delta G°$ for this reaction is (− 30·5 + 14·2) kJ mol^{-1}, *i.e.*, − 16·3 kJ mol^{-1}. Hence it is thermodynamically favourable. The enzyme glutamine synthetase catalyzes this reaction in animal cells.

For the ATP hydrolysis reaction, $ATP + H_2O \rightleftharpoons ADP + P_i$, at a specified *p*H, the equilibrium constant expression can be written as

$$K = \frac{[ADP][P_i]}{[ATP]} \qquad ...(109)$$

Here K is called the apparent equilibrium constant. (The concentration of water is omitted because it is constant in dilute solution). K is constant at a given *p*H. Since biological reactions are usually

studied in the neighbourhood of *p*H 7, it is customary to tabulate the value of K at *p*H 7. The corresponding apparent standard reaction Gibbs energy ΔG° is calculated using

$$\Delta G^\circ = -RT \ln K \qquad \ldots(110)$$

Example 47. Given the following reactions :

$$\text{Creatine phosphate} + H_2O \longrightarrow \text{Creatine} + P_i \qquad \Delta G^\circ = -43{\cdot}5 \text{ kJ mol}^{-1}$$

$$\text{ADP} + P_i \longrightarrow \text{ATP} + H_2O \qquad \Delta G^\circ = 39{\cdot}8 \text{ kJ mol}^{-1}$$

Calculate the apparent equilibrium constant, K for the reaction :

$$\text{Creatine phosphate} + \text{ADP} \rightleftharpoons \text{Creatine} + \text{ATP}$$

Solution : We see that for the required reaction,

$$\Delta G^\circ = -43{\cdot}5 + 39{\cdot}8 = -3{\cdot}7 \text{ kJ mol}^{-1}$$

Since $\Delta G^\circ = -RT \ln K$, we have

$$K = \frac{[\text{Cr}][\text{ATP}]}{[\text{CrP}][\text{ADP}]} = 4{\cdot}6 \quad (\text{Cr stands for Creatine})$$

We see in this example that a hydrolysis reaction with a negative Gibbs free energy has been used to drive a phosphorylation reaction with a (smaller) positive Gibbs free energy change. Such reactions are said to be **coupled** and the coupling is provided by the enzyme that catalyzes the phosphate transfer reaction. The mechanism of coupling is as follows :

$$\text{Creatine phosphate} + E \longrightarrow EP + \text{Creatine}$$

$$EP + \text{ADP} \longrightarrow \text{ATP} + E$$

$$\text{Creatine phosphate} + \text{ADP} \longrightarrow \text{Creatine} + \text{ATP} \qquad \Delta G^\circ = -3{\cdot}7 \text{ kJ mol}^{-1}$$

where E is the enzyme and EP is phosphorylated enzyme. The large change in Gibbs free energy for hydrolysis of creatine phosphate is not lost. It is conserved in the enzyme and then in ATP. This is an absolutely essential process for living organisms because this is the way a thermochemically spontaneous reaction can drive a non-spontaneous reaction that synthesizes a needed compound.

Example 48. The negatively charged phosphate groups of ATP provide an effective means of chelating divalent cations such as Mg^{2+}. Given that the following reaction

$$Mg^{2+} + ATP^{4-} \rightleftharpoons MgATP^{2-}$$

has an association equilibrium constant = 10^4 dm^3 mol^{-1}, calculate the proportion of ATP in a cell that is present as Mg^{2+} chelate if the free Mg^{2+} Ion concentration is 2×10^{-2} mol dm^{-3}.

Solution :
$$K = \frac{[MgATP^{2-}]}{[Mg^{2+}][ATP^{4-}]} = 10^4 \text{ dm}^{-3} \text{ mol}^{-1}$$

Hence,
$$\frac{[MgATP^{2-}]}{[ATP^{4-}]} = 2\times10^{-2}$$

Evidently, more than 99 percent of the ATP in a cell is present as the Mg^{2+} chelate. It is thus not surprising that most ATP-utilizing enzymes use $MgATP^{2-}$, rather than ATP^{4-}, as a substrate.

It is pertinent to discuss briefly **anaerobic and aerobic metabolism.** Aerobic metabolism involves a series of reactions in which inhaled oxygen plays a prominent role. Anaerobic metabolism is a metabolism in which inhaled oxygen plays no role. The energy source of anaerobic cells is **glycolysis,**

the partial oxidation of glucose to lactic acid with $\Delta G^\circ = -218$ kJ mol^{-1} and $\Delta H^\circ = -120$ kJ mol^{-1}. The glycolysis is coupled to a reaction in which two ADP molecules are converted into two ATP molecules :

$$\text{Glucose} + 2P_i + 2\text{ADP} \longrightarrow 2\ \text{Lactate}^- + 2\text{ATP} + 2H_2O$$

In this reaction, $\Delta G_r^\circ = -218 \text{ kJ mol}^{-1} - 2(-30 \text{ kJ mol}^{-1}) = -158$ kJ mol^{-1}. Since this reaction is exergonic, it is spontaneous. The metabolism of food is used to 'recharge' ATP.

Metabolism by aerobic respiration is far more efficient. The standard Gibbs free energy of combustion of glucose is -2880 kJ mol^{-1}. This implies that terminating its oxidation at the lactic acid stage is, indeed, a poor use of resources. In aerobic respiration, the oxidation is carried out to completion and an extremely complex set of reactions (the details of which need not concern us here) preserves as much of the energy released as possible. In the overall reaction, 38 ATP molecules are generated for each glucose molecule consumed. Each mole of ATP extracts 30 kJ from the 2880 kJ supplied by 1 mole of glucose. Thus $38 \times 30 = 1140$ kJ of energy is stored for later use.

Each ATP molecule can be used to drive an endergonic reaction for which ΔG° does not exceed +30 kJ mol^{-1}. For instance, the biosynthesis of sucrose ($C_{12}H_{22}O_{11}$) from glucose ($C_6H_{12}O_6$) and fructose ($C_6H_{12}O_6$) can be driven (provided a suitable enzyme system is available) because the reaction is endergonic ($\Delta G^\circ = +23$ kJ mol^{-1}). Taking another example : The biosynthesis of proteins is strongly endergonic, not only on account of the enthalpy change (ΔH) but also on account of the large *decrease* in entropy that occurs when many amino acids are assembled into a precisely determined sequence. For example, the formation of a peptide link is endergonic, with $\Delta G^\circ = +17$ kJ mol^{-1} but the biosynthesis can only occur indirectly and requires the consumption of three ATP molecules for each link. For the biosynthesis of a moderately small protein like myoglobin (Mb), with about 150 peptide links, one requires 450 ATP molecules, *i.e.*, about 12 moles of glucose molecules for 1 mole of protein molecule.

The importance of coupled reactions in biological systems cannot be overemphasized. Vital functions in an organism often depend on reactions which by themselves involve a positive ΔG. These reactions, as we have said earlier, are coupled with the metabolic reactions which have highly negative ΔG. As a trivial example, consider a person whose weight-lifting feat earns him the title of 'Mr. Universe' in the Olympic games. But the lifting of weight is a non-spontaneous event involving an increase in Gibbs free energy. The weight goes up only because that event is coupled with metabolic processes in the body that involve decrease in Gibbs free energy which is sufficient to more than compensate for the increase associated with the lifting of the weight.

Binding of Oxygen by Myoglobin

Myoglobin is an oxygen-storage protein that is found in muscle tissues in many species; its molar mass is 16,000 g mol^{-1} and each molecule contains one heme group, one atom of iron and binds one molecule of oxygen, when it is saturated.

The shape of the binding curve for myoglobin is exactly what is expected for the simple reaction

$$MbO_2 \rightleftharpoons Mb + O_2 \qquad \ldots(111)$$

where Mb represents a molecule of myoglobin. The dissociation constant is given by

$$K = \frac{[Mb](p_{O_2})}{[MbO_2]} \qquad \ldots(112)$$

where p_{O_2} is the partial pressure of oxygen in the gas phase. Conservation of myoglobin requires that

$$[Mb]_0 = [Mb] + [MbO_2] \qquad \ldots(113)$$

where $[Mb]_0$ is the total molar concentration of myoglobin. From Eqs. 112 and 113, we obtain

$$Y = \frac{[MbO_2]}{[Mb]_0} = \frac{p_{O_2}/K}{1+p_{O_2}/K} \qquad ...(114)$$

where Y is the **fractional saturation**. The plot of Y versus p_{O_2} is shown in Fig. 3.

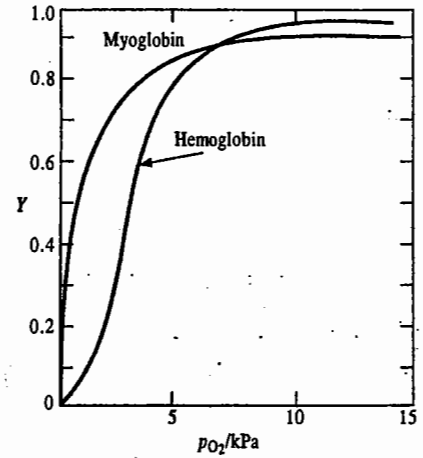

Fig. 3. Fractional saturation Y of myoglobin and hemoglobin with oxygen at pH 7·4 and 38°C.

Binding of Oxygen by Hemoglobin

Hemoglobin is the oxygen transport protein in many species ; it has a molar mass of 64,000 and each molecule contains four heme groups, four atoms of iron and binds four molecules of oxygen when it is saturated. Hemoglobin molecule may be reversibly dissociated into four molecules of molar mass 16,000 g mol^{-1}, each of which contains one heme group and one atom of iron. These smaller molecules are of two types represented by α and β and hemoglobin has the composition $\alpha_2\beta_2$.

The oxygen binding properties of myoglobin and hemoglobin are distinctly different, as shown in Fig. 3. Hemoglobin's S-shaped **(sigmoid) binding curve** is a great advantage for its physiological function because the amount of oxygen bound changes rapidly between the partial pressure of oxygen in the lungs (about 13·3 kPa) and in the tissues (about 2·0 kPa).

The mathematical equation for the fractional saturation, Y, showing the binding of oxygen with hemoglobin, is very complicated compared to that of binding of oxygen with myoglobin. The features of the sigmoid curve can be accounted for by the phenomenon of **co-operativity**. Co-operativity arises when the binding of the first ligand causes changes in the structure of the protein that increase the affinities of the remaining sites. The crystal structure of hemoglobin, obtained from X-ray diffraction, shows that each of its four sub-units has a three-dimensional configuration much like that of myoglobin. When oxygen is bound, groups near the heme group shift slightly and these structural changes affect the configurations of the four sub-units so that the binding properties of the other heme groups are enhanced. A small fraction of hemoglobin exists in the quaternary oxystructure that binds oxygen more strongly. When the first oxygen molecule is bound, it is bound preferentially to this structure ; as more oxygen molecules are bound, the oxystructure is sufficiently stabilized to be the major structure and hence subsequent bonding is strong.

I. Review Questions

1. State the law of mass action and the law of chemical equilibrium. Derive van't Hoff reaction isotherm, *viz.*, $\Delta G^\circ = -RT \ln K_p$.
2. Derive the relation between the equilibrium constants K_p, K_c and K_x. Under what condition $K_p = K_c = K_x$ (p, c and x stand for partial pressure, molar concentration and mole fraction, respectively).
3. State the law of chemical equilibrium. How can it be derived on thermodynamic considerations ?
4. What is meant by degree of advancement of a chemical reaction introduced by de Dondre ? Define the terms reaction potential and thermodynamic potential.
5. Derive van't Hoff equation in the form $d(\ln K_p)/dT = \Delta H^\circ/RT$. Integrate this equation.
6. Show that for the heterogeneous reaction $CaCO_3(s) \rightleftharpoons CaO(s) + CO_2(g)$, the equilibrium constant is given by $K_p = pCO_2$
7. State Le Chatelier's principle. With the help of this principle, work out the conditions which would favour the formation of ammonia and nitric oxide in the following reactions :

$$N_2(g) + 3H_2(g) \rightleftharpoons 2NH_3(g) \; ; \; \Delta H = -92{\cdot}38 \text{ kJ},$$
$$N_2(g) + O_2(g) \rightleftharpoons 2NO(g) \; ; \; \Delta H = 180{\cdot}75 \text{ kJ}$$

8. What are LFERs ?
9. What is the Hammett equation ? Illustrate it graphically.
10. How is the Hammett equation used to determine the reaction mechanism ?
11. Discuss the role of ATP in bioenergetics.
12. Discuss the bonding of oxygen by myoglobin and hemoglobin, and draw the appropriate curves.

II. Problems

1. For the reaction $A(g) + B(s) \rightleftharpoons C(g) + D(g)$; $K_c = 49$ mol dm^{-3} at 127°C. Calculate K_p. **[Ans. $1{\cdot}6\times10^3$ atm]**
2. Calculate K_p, K_c and K_x at 25°C and 1·00 bar total pressure for the reaction $H_2(g) + 1/2\ O_2(g) \rightleftharpoons H_2O(g)$. Given $\Delta G^\circ = -228{\cdot}572$ kJ **[Ans. $1{\cdot}13\times10^{40}$, $5{\cdot}62\times10^{40}$, $1{\cdot}13\times10^{40}$]**
3. Calculate equilibrium constant for the reaction $A + B \rightleftharpoons C + D$ if at equilibrium there are 1·0 mole of A, 2·0 moles of B, 6·0 moles of C and 20·0 moles of D in a one-litre vessel. **[Ans. 60]**
4. The equilibrium constant for the reaction $N_2 + 2O_2 \rightleftharpoons 2NO_2$ is 100. What is the equilibrium constant for the reactions : *(a)* $2NO_2 \rightleftharpoons N_2 + 2O_2$ and *(b)* $NO_2 \rightleftharpoons 1/2\ N_2 + O_2$? **[Ans. *(a)* 0·01 *(b)* 0·10]**
5. Calculate the equilibrium constant for the reaction $A + B \rightleftharpoons 2C$ if 1·0 mole of A, 1·4 moles of B and 0·50 mole of C are placed in a 1·0 dm^3 vessel and allowed to come to equilibrium. The final concentration of C is 0·75 mol dm^{-3}. **[Ans. 0·50]**
6. Calculate the equilibrium constant for the reaction $A + 2B \rightleftharpoons 2C$, if 1·0 mole of A, 2·0 moles of B and 3·0 moles of C are placed in a 1·0 dm^3 vessel and allowed to come to equilibrium. The final concentration of C is 1·4 mol dm^{-3}. **[Ans. $8{\cdot}4\times10^{-2}$]**
7. Calculate the equilibrium constant for the reaction $N_2 + 2O_2 \rightleftharpoons 2NO_2$ if there are present at equilibrium 5·0 moles of N_2 , 7·0 moles of O_2 and 0·10 mole of NO_2 in a 1·5 dm^3 vessel at a certain temperature. **[Ans. $6{\cdot}1\times10^{-5}$]**
8. For the reaction $CaCO_3(s) \rightleftharpoons CaO(s) + CO_2(g)$, $K_p = 1{\cdot}16$ atm at 800°C. If 20·0 g of $CaCO_3$ was placed in a 10·0 dm^3 container and heated to 800°C, what percentage of $CaCO_3$ would remain undecomposed at equilibrium ? **[Ans. 34%]**

9. Calculate the pressure of $CO_2(g)$ over a sample of $CaCO_3(s)$ at 1000 K, given $\Delta G^\circ_{1000} = 22{\cdot}9$ kJ mol^{-1}. [Ans. $6{\cdot}4\times10^{-2}$ bar]

10. When 3·00 moles of A and 1·00 mole of B are mixed in a 1·00 dm^3 vessel to give the reaction $A + B \rightleftharpoons 2C$, the equilibrium contains 0·50 moles of C. Calculate the equilibrium constant of the reaction. [Ans. 0·12]

11. Calculate the equilibrium constant for the reaction $2NO_2(g) \rightleftharpoons N_2O_4(g)$ if initially 1·0 mole of NO_2 and 1·0 mole of N_2O_4 are placed in a 1·0 dm^3 vessel and at equilibrium 0·75 mole of N_2O_4 is present in the vessel. [Ans. 0·33]

12. Calculate the number of moles of Cl_2 produced in the reaction :

$$PCl_5(g) \rightleftharpoons PCl_3(g) + Cl_2(g),$$

when 1·00 mole of PCl_5 is heated at 250°C in a 10·0 dm^3 vessel. $K = 0{\cdot}041$. [Ans. 0·47 mole]

13. Calculate the equilibrium concentration of D after 1·0 mole of A, 2·0 moles of B and 0·50 mole of C are placed in a 1·0 dm^3 flask and allowed to come to equilibrium according to the reaction

$$2A + B \rightleftharpoons C + 2D\ ;\ K = 1{\cdot}5 \times 10^{-3}$$ [Ans. 0·078]

14. Consider the equilibrium $PCl_3(g) + Cl_2(g) \rightleftharpoons PCl_5(g)$. A mixture containing 1 mole of PCl_3 and 2 moles of Cl_2 was allowed to come to equilibrium at 400 K and a total pressure of 1 atm. Calculate the amount of PCl_5 formed at equilibrium. Given $K_p = 2{\cdot}93$ at 400 K. [Ans. 0·63 mole]

15. At 480 K and a total pressure of 1 atm, a mixture of $N_2(g)$ and $H_2(g)$ in the mole ratio of 1 : 3 contains 16% of $NH_3(g)$ at equilibrium. Calculate K_p for the reaction. [Ans. 0·544]

PHASE EQUILIBRIA

The phase rule is an important tool used for the quantitative treatment of systems in equilibrium. It enables us to predict the conditions that must be specified for a system to exhibit equilibrium. J.W. Gibbs enunciated the phase rule in 1876 while investigating heterogeneous equilibria. According to the phase rule, for systems in complete internal equilibrium,

$$F = C - P + 2, \qquad ...(1)$$

where C is the number of *components* ; P is the number of *phases* and F is the number of *degrees of freedom.*

Phase. A phase is defined as any homogeneous and physically distinct part of a system which is bounded by a surface and is mechanically separable from other parts of the system. Examples of various types of phases are :

(i) A gas mixture constitutes a single phase since gases are completely miscible.

(ii) Immiscible liquids constitute different phases. Thus, carbon tetrachloride (CCl_4) and water (H_2O), which do not mix with each other, form two phases.

(iii) Completely miscible liquids such as water and alcohol and benzene and chloroform constitute one-phase systems.

(iv) Consider the decomposition of calcium carbonate into CO_2 and CaO.

$$CaCO_3(s) \rightleftharpoons CaO(s) + CO_2(g)$$

Here there are two solid phases and one gaseous phase. So it is a three-phase system.

Components. The number of components of a system at equilibrium is defined as the smallest number of independently variable constitutents by means of which the composition of each phase can be expressed either directly or in terms of chemical equations. We may consider a few examples :

(i) Water exists in three phases, *viz.*,

$$\text{ice} \rightleftharpoons \text{liquid} \rightleftharpoons \text{vapour}$$

However, the composition of each phase can be expressed in terms of H_2O. Hence, it is a one-component system.

(ii) Sulphur exists in four phases, *viz.*, rhombic sulphur, monoclinic sulphur, liquid and vapour. But since the composition of each phase can be expressed in terms of sulphur only, it is a one-component system.

(iii) Consider an aqueous sucrose solution. The composition of the solution phase can be expressed by specifying the amounts of sugar and water. Hence, it is a two-component system.

In a chemically reactive system, the number of components is given by

$$C = N - m - n - R \qquad ...(2)$$

where N is the number of chemical species, m is the number of independent equilibrium conditions, n is the number of relations between concentrations due to initial conditions and R is the number of independent chemical reactions. We can also write

$$C = N - E \qquad ...(3)$$

where E is the number of independent equations relating the concentrations of the N species. Each independent chemical equilibrium involving the constituents counts as one equation. *The condition that a solution be electrically neutral also counts as one equation if ions are considered as constituents.* All these aspects are illustrated in the following examples.

Example 1. Explain why KCl-NaCl-H_2O system should be regarded as a 3-component system whereas KCl-NaBr-H_2O system should be regarded as a 4-component system.

Solution : We know that the number of components is given by $C = N - E$ where N is the number of species (constituents) and E is the number of *independent* equations relating their concentrations. For the KCl - NaCl - H_2O system, N=3 (*viz.*, KCl, NaCl, H_2O). Since there is no independent equation relating their concentrations, E=0. Hence,

$$C = 3 - 0 = 3$$

For the KCl-NaBr-H_2O system, $N = 5$ (*viz.*, KCl, NaBr, NaCl, KBr, H_2O)

$E = 1$, *viz.*, $KCl + NaBr \rightleftharpoons KBr + NaCl$

$\therefore \quad C = N - E = 5 - 1 = 4$

Example 2. For each of the following systems, determine the number of components :

(a) **$NH_4Cl(s)$, $NH_4^+(aq)$, $Cl^-(aq)$, $H_2O(liq)$, $H_3O^+(aq)$, $H_2O(g)$, $NH_3(g)$, $OH^-(aq)$, $NH_4OH(aq)$**

(b) **$NH_4Cl(s)$, $NH_3(g)$, $HCl(g)$, where the partial pressure of NH_3 is equal to the partial pressure of HCl as is the case when the gaseous mixture is formed by the sublimation of $NH_4Cl(s)$.**

(c) **$NH_4Cl(s)$, $NH_3(g)$, $HCl(g)$, where the partial pressure of NH_3 is not necessarily equal to the partial pressure of HCl.**

(d) **$CH_3COONH_4(s)$, $CH_3COO^-(aq)$, $NH_4^+(aq)$, $H_3O^+(aq)$, $NH_3(g)$, $OH^-(aq)$, $CH_3COOH(aq)$, $H_2O(l)$, $H_2O(g)$, assuming hydrolysis to take place.**

(e) **$NaCl(s)$, $KBr(s)$, $K^+(aq)$, $Na^+(aq)$, $Cl^-(aq)$, $Br^-(aq)$, $H_2O(l)$, $H_2O(g)$.**

(f) **$NaCl(s)$, $KCl(s)$, $Na^+(aq)$, $Cl^-(aq)$, $H_2O(l)$, $H_2O(g)$.**

(g) **$CaCl_2.6H_2O(s)$, $Ca^{2+}(aq)$, $Cl^-(aq)$, $H_2O(l)$, $H_2O(g)$.**

(h) **$CaCO_3(s)$, $CaO(s)$, $CO_2(g)$, when CaO and CO_2 in the system are formed exclusively by the decomposition of $CaCO_3$.**

Solution :

(a) $N = 8$ (*viz.*, NH_4Cl, NH_4^+, Cl^-, H_2O, NH_3, NH_4OH, H_3O^+, OH^-) and $E = 5$, as shown below :

1. Electroneutrality of the solution
2. $NH_4Cl \rightleftharpoons NH_4^+ + Cl^-$
3. $NH_4^+ + H_2O \rightleftharpoons NH_3 + H_3O^+$
4. $NH_3 + H_2O \rightleftharpoons NH_4OH$
5. $2H_2O \rightleftharpoons H_3O^+ + OH^-$

$\therefore \quad C = N - E = 8 - 5 = 3$

(b) $N = 3$ (*viz.*, NH_4Cl, NH_3, HCl)

$E = 2$, as shown below :

1. $NH_4Cl \rightleftharpoons NH_3 + HCl$
2. $p_{NH_3} = p_{HCl}$

$\therefore \quad C = 3 - 2 = 1$

(c) $N = 3$ (*viz.*, NH_4Cl, NH_3, HCl)

$E = 1$, *viz.*, $NH_4Cl(s) \rightleftharpoons NH_3(g) + HCl(g)$

$\therefore \quad C = 3 - 1 = 2$

(d) $N = 8$ (*viz.*, CH_3COONH_4, CH_3COO^-, NH_4^+, H_3O^+, NH_3, OH^-, H_2O, CH_3COOH)

$E = 4$, as shown below :

1. Electroneutrality of the solution.
2. $CH_3COOH + H_2O \rightleftharpoons CH_3COO^- + H_3O^+$

3. $CH_3COO^- + H_2O \rightleftharpoons CH_3COOH + OH^-$
4. $NH_4^+ + H_2O \rightleftharpoons NH_3 + H_3O^+$

$\therefore \quad C = N - E = 8 - 4 = 4$

Note : We have not counted here the equation $2H_2O \rightleftharpoons H_3O^+ + OH^-$ because it can be derived by adding Eqs. 2 and 3.

(e) $N = 9$ (*viz.*, NaCl, KBr, KCl, NaBr, K^+, Na^+, Cl^-, Br^-, H_2O)

$E = 5$, as shown below :

1. Electroneutrality of the solution.
2. $NaCl \rightleftharpoons Na^+ + Cl^-$
3. $KBr \rightleftharpoons K^+ + Br^-$
4. $NaBr \rightleftharpoons Na^+ + Br^-$
5. $NaCl + KBr \rightleftharpoons NaBr + KCl$

$\therefore \quad C = N - E = 9 - 5 = 4$

(f) $N = 6$ (*viz.*, NaCl, KCl, K^+, Na^+, Cl^-, H_2O)

$E = 3$, as shown below :

1. Electroneutrality of the solution.
2. $NaCl \rightleftharpoons Na^+ + Cl^-$
3. $KCl \rightleftharpoons K^+ + Cl^-$

$\therefore \quad C = N - E = 6 - 3 = 3$

(g) $N = 4$ (*viz.*, $CaCl_2.6H_2O$, Ca^{2+}, Cl^-, H_2O)

$E = 2$, as shown below :

1. Electroneutrality of the solution.
2. $CaCl_2.6H_2O \rightleftharpoons Ca^{2+} + 2Cl^- + 6H_2O$

$\therefore \quad C = N - E = 4 - 2 = 2$

(h) $N = 3$(*viz.*, $CaCO_3$, CaO, CO_2)

$E = 1$, *viz.*, $CaCO_3 \rightleftharpoons CaO + CO_2$

$\therefore \quad C = N - E = 3 - 1 = 2$

Degree of Freedom (F). The degree of freedom of a system is defined as the number of independent variables such as temperature, pressure and concentration (or composition) which must be specified in order to define the system completely. Thus, the state of a pure gas can be specified by two variables P and T or P and V, since the third variable can be calculated from the equation of state. This means that a pure gas has two degrees of freedom.

Consider now a one-component system having two phases. The example is furnished by water (liquid) in equilibrium with its vapour. The system will have only one degree of freedom because at a given temperature, the equilibrium vapour pressure of water can have only one fixed value. Thus, if temperature is specified, pressure becomes known automatically and vice-versa. We have to mention only one variable, either temperature or pressure. The system is, therefore, monovariant.

Finally, consider a one-component system having three phases. The example is furnished by ice, liquid water and vapour coexisting at the freezing point of water. This system will have no degree of freedom. The reason is that these three phases can coexist only at one particular temperature under one particular pressure. The mere statement that these three phases coexist defines the system completely.

Thus, if $F = 0$, the system is called invariant; if $F = 1$, univariant (monovariant), if $F = 2$, bivariant and if $F = 3$, trivariant, etc.

We thus conclude that

1. The greater the number of components in a system, the greater is the number of degrees of freedom for a given number of phases.

2. The greater the number of phases, the smaller is the number of degrees of freedom, such as T, P and composition, required to specify the system completely.

3. For a given number of components, the number of phases is maximum when the number of degrees of freedom is zero. Thus, for a one-component system, the maximum number of phases is three and for a two-component system, the maximum number of phases is four.

Conditions for Equilibrium between Phases. The following conditions must be satisfied for the existence of equilibrium between various phases in a multiphase system.

1. Thermal Equilibrium. All the phases must be at the same temperature otherwise there will be flow of heat from one phase to another. Consider two phases α and β at temperatures T_α and T_β, respectively. Let S_α and S_β be the entropies of the two phases and let dq be the heat transferred from phase α to phase β at equilibrium. Then the entropy change of the system is given by

$$dS = dS_\alpha + dS_\beta = 0 \qquad \text{(at equilibrium)} \qquad ...(4)$$

Since $$dS_\alpha = -dq/T \text{ and } dS_\beta = +dq/T \qquad ...(5)$$

$$\therefore \quad (-dq/T_\alpha) + (dq/T_\beta) = 0 \qquad ...(6)$$

$$\therefore \quad T_\alpha = T_\beta$$

2. Mechanical Equilibrium. All the phases must be under the same pressure otherwise the volume of one phase will increase at the expense of another. We can prove it as follows.

Suppose α-phase is expanded into β-phase by the volume change dV. Then the change in the Helmholtz free energy at constant temperature is given by

$$dA = -dA_\alpha + dA_\beta = 0 \qquad \text{(at equilibrium)} \qquad ...(7)$$

But $$dA_\alpha = -P_\alpha dV \text{ and } dA_\beta = -P_\beta dV \qquad \text{(at constant } T\text{)} \qquad ...(8)$$

Since at equilibrium, $dA_\alpha = dA_\beta$, hence $P_\alpha = P_\beta$ ...(9)

3. Chemical Equilibrium. For a system of many phases at equilibrium, the chemical potential of a component i is the same in all the phases. We can prove it as follows.

Consider a closed system of P phases designated as α, β, γ, ···· P containing C components designated as 1, 2, 3, ····C, in equilibrium. It is assumed that each phase is at the same constant temperature and pressure.

The Gibbs free energy of each phase is a function of T, P and the composition of the phase, *i.e.*,

$$\left.\begin{aligned} G_\alpha &= f(T,P,n_i)_\alpha \\ G_\beta &= f(T,P,n_i)_\beta \\ &\cdots\cdots\cdots \\ &\cdots\cdots\cdots \\ G_P &= f(T,P,n_i)_P \end{aligned}\right\} \text{ where } i = 1, 2, 3, \cdots\cdots \qquad ...(10)$$

(The subscript P designates Pth phase)

The Gibbs free energy change for the system is the sum of the Gibbs free energy changes of the various phases. Thus,

$$dG = dG_\alpha + dG_\beta + dG_\gamma + \cdots\cdots\cdots \qquad ...(11)$$

Again, for a multicomponent system, we have

$$dG = -SdT + VdP + \sum_i \mu_i dn_i \qquad ...(12)$$

At constant T and P, $dT = 0$ and $dP = 0$ so that

$$(dG)_{T,P} = \sum_i \mu_i dn_i \qquad ...(13)$$

For an infinitesimal transfer of mass from one phase to another,

$$dG = \sum_{i=1} \mu_{i,\alpha}\, dn_{i,\alpha} + \sum_{i=1} \mu_{i,\beta}\, dn_{i,\beta} + \sum_{i=1} \mu_{i,\gamma}\, dn_{i,\gamma} + \cdots\cdots \qquad ...(14)$$

Also, for a closed system at equilibrium, $dG = 0$.

$$\therefore \quad \sum_i \mu_{i,\alpha}\, dn_{i,\alpha} + \sum_i \mu_{i,\beta}\, dn_{i,\beta} + \sum_i \mu_{i,\gamma}\, dn_{i,\gamma} + \cdots\cdots = 0 \qquad ...(15)$$

Since the system is closed, the total mass of each component at equilibrium is constant. Hence,

$$\left.\begin{aligned} dn_{1,\alpha} + dn_{1,\beta} + dn_{1,\gamma} + \cdots\cdots + dn_{1,P} &= 0 \\ dn_{2,\alpha} + dn_{2,\beta} + dn_{2,\gamma} + \cdots\cdots + dn_{2,P} &= 0 \\ \cdots \quad \cdots \quad \cdots \quad \cdots & \\ dn_{i,\alpha} + dn_{i,\beta} + dn_{i,\gamma} + \cdots\cdots + dn_{i,P} &= 0 \\ \cdots\cdots\cdots\cdots\cdots & \\ dn_{c,\alpha} + dn_{c,\beta} + dn_{c,\gamma} + \cdots\cdots + dn_{c,P} &= 0 \end{aligned}\right\} \qquad ...(16)$$

In order that Eq. 16 remains zero for all variations of n, subject to the restrictions imposed by Eq. 15, we must have the following requirements met with :

$$\left.\begin{aligned} \mu_{1,\alpha} &= \mu_{1,\beta} = \mu_{1,\gamma} = \cdots = \mu_{1,P} \\ \mu_{2,\alpha} &= \mu_{2,\beta} = \mu_{2,\gamma} = \cdots = \mu_{2,P} \\ \cdots \quad \cdots \quad \cdots \quad \cdots & \\ \mu_{c,\alpha} &= \mu_{c,\beta} = \mu_{c,\gamma} = \cdots = \mu_{c,P} \end{aligned}\right\} \qquad ...(17)$$

It follows from the above that for a multiphase system at equilibrium, the chemical potential, μ_i, of a component i is the same in every phase.

Gibbs Phase Rule

The celebrated phase rule, enunciated by J. Willard Gibbs, states that if the equilibrium in a heterogeneous system is not affected by gravity or by electrical and magnetic forces, the number of degrees of freedom, F, of the system is related to the number of components, C and the number of phases, P, existing at equilibrium with one another by the equation

$$F = C - P + 2$$

Derivation of the Phase Rule. Consider a system of C components (C_1, C_2, C_3,..., C_C) distributed between P phases (α, β, γ, δ,···· P), as shown in Fig. 1. Assume that passage of a component from one phase to another does not constitute a chemical reaction. The state of each phase of the system is completely specified by the two variables, temperature and pressure and also by the composition of each phase. In other words, the state of each phase is specified by

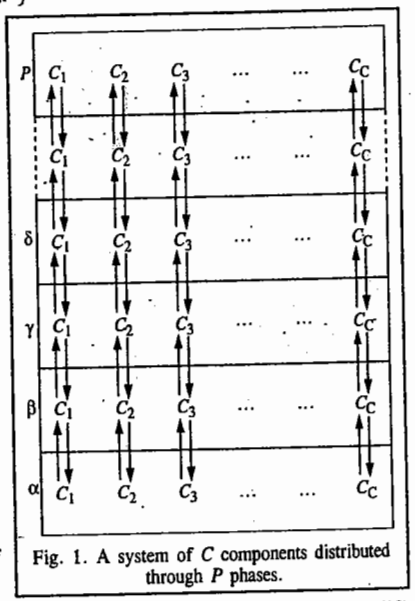

Fig. 1. A system of C components distributed through P phases.

$$T, P, (x_{1,\alpha}, x_{2,\alpha} \cdots\cdots x_{c,\alpha}), (x_{1,\beta}, x_{2,\beta} \cdots\cdots x_{c,\beta}), \cdots\cdots (x_{1,P}, x_{2,P}, \cdots\cdots, x_{c,P}) \qquad ...(18)$$

where x_is are compositions of the component. The total number of variables is thus $CP + 2$. However, in Eq. 18 all the variables are not independent since in each phase, the sum of the mole fractions

must equal unity, *i.e.*,

$$x_{1,\alpha} + x_{2,\alpha} + x_{3,\alpha} + \cdots\cdots = x_{1,\beta} + x_{2,\beta} + x_{3,\beta} + \cdots\cdots, \text{ etc.} = 1$$

In other words, $$\sum_i x_{i;P} = 1 \qquad (i = 1, 2, 3, \cdots\cdots C) \qquad \ldots(19)$$

for all the P phases separately. There are thus P relations of this type.

Again, for complete equilibrium to exist between the phases, the chemical potential of each species must be the same in each phase, *i.e.*,

$$\left.\begin{aligned} \mu_{1,\alpha} &= \mu_{1,\beta} = \mu_{1,\gamma} = \cdots\cdots = \mu_{1,P} \\ \mu_{2,\alpha} &= \mu_{2,\beta} = \mu_{2,\gamma} = \cdots\cdots = \mu_{2,P} \\ &\cdots\quad\cdots\quad\cdots\quad\cdots\quad\cdots \\ \mu_{c,\alpha} &= \mu_{c,\beta} = \mu_{c,\gamma} = \cdots\cdots = \mu_{c,P} \end{aligned}\right\} \quad \text{(cf. Eq. 17)} \qquad \ldots(20)$$

We see that there are $P - 1$ separate equations for each component. Hence, for C components, the number of such equations is $C(P - 1)$.

Also, the equilibrium conditions for the chemical reactions require that the chemical affinity, A_f, for each reaction at equilibrium must be zero, *i.e.*,

$$A_{f,i} = 0 \qquad (i = 1, 2, 3, \cdots\cdots, r') \qquad \ldots(21)$$

This means that there are r' equations of this type.

Hence, total number of restricting conditions is

$$P + C(P - 1) + r' \qquad \ldots(22)$$

The degree of freedom, F, is given by the difference between the number of variables required to specify the state of the system (*i.e.*, $CP + 2$) and the number of restrictions imposed by their interdependence (*i.e.*, Eq. 22). Thus,

$$F = (CP + 2) - (P + CP - C + r') = 2 + (C - r') - P \qquad \ldots(23)$$

Eq. 23 is known as Gibbs Phase rule. If the system is non-reactive, *i.e.*, no reaction takes place in it, then equations of the type $A_f = 0$ will be absent, *i.e.*, $r' = 0$. Hence, the phase rule becomes

$$F = C - P + 2 \qquad \text{(Eq. 1)}$$

Example 3. Determine the number of degrees of freedom in each of the following systems. Suggest the variables that could correspond to these degrees of freedom.

***(a)* Liquid water and water vapour in equilibrium.**

***(b)* Liquid water and water vapour in equilibrium at a pressure of 1 atm.**

Solution : From the Gibbs Phase rule, $F = C - P + 2$

(a) In this case, $C=1$, Hence $F = 1 - 2 + 2 = 1$.

That is, only one variable T or P need to be specified.

(b) Since the pressure is held constant, the degree of freedom reduces by one. Hence, the phase rule equation becomes $F = C - P + 1$.

In this case, $C=1$ and $P=2$.

$$\therefore \qquad F = 1 - 2 + 1 = 0$$

The system under the given conditions is thus **invariant.**

Example 4. Calculate the number of components and the number of the degrees of freedom in : *(a)* an aqueous solution of glucose *(b)* an aqueous solution of acetic acid *(c)* an aqueous solution of sodium chloride *(d)* a mixture of $H_2(g)$, $O_2(g)$ and $H_2O(g)$ *(e)* a mixture of $CaCO_3(s)$, $CaO(s)$ and $CO_2(g)$ *(f)* a mixture of $N_2(g)$, $H_2(g)$ and $NH_3(g)$ *(g)* $Fe(s) + H_2O(g) \rightleftharpoons FeO(s) + H_2(g)$ *(h)* $2KClO_3(s) \rightleftharpoons 2KCl(s) + 3O_2(g)$

Solution : *(a)* In this case, $C=2$ and $P=1$, hence,

$$F = C - P + 2 = 2 - 1 + 2 = 3$$

The choice of variables is T, P and concentration of the solution.

(b) In this case, $C=2$, $P=1$ so that $F=3$

The choice of variables is T, P and concentration of the solution.

(c) In this case, $C=2$. Since $P=1$, hence $F=3$. The choice of variables is T, P and concentration of the solution.

(d) The number of components will depend upon the method used to prepare the system and the final status of the system. Thus, if we are dealing with a mixture of three gases, $C=3$. Since $P=1$, therefore, $F = C-P+2 = 3-1+2 = 4$. This means that T, P and the concentrations of two of the three components must be specified.

If we are dealing with a mixture of gases produced by the decomposition of water vapour $[H_2O(g) \rightleftharpoons H_2(g) + (1/2)O_2(g)]$, then we need to specify only one component because the information regarding the other two can be obtained from the equilibrium constant expression

$$K = \frac{p_{H_2O}}{p_{H_2} \times (p_{O_2})^{1/2}}$$

and the known stoichiometry, *i.e.*, $p_{H_2} = 2p_{O_2}$. Therefore, $C=1$. Since, $P=1$, hence $F = C - P + 2 = 1 - 1 + 2 = 2$. This implies that only T and P need to be specified.

(e) The number of components will depend upon the method used to prepare the system and the final status of the system. Thus, if we are given a mixture of three species, $C=3$. Since $P=3$, hence $F = C - P + 2 = 3 - 3 + 2 = 2$. Thus, we need to specify two variables such as T and P.

If we are dealing with a mixture produced by the decomposition of $CaCO_3$, only two components need to be specified since the third can be calculated from the stoichiometry of the reaction. Thus, $C = 2$ and since $P = 3$, therefore, $F = C - P + 2 = 2 - 3 + 2 = 1$ so that only T or P need to be specified.

(f) This system is analogous to the system considered in *(d)* above. The answer is $C=1$, 2 or 3 so that $F = 2$, 3 or 4.

(g) Here $C = 3$. Since there is an equilibrium, only one gaseous component must be specified along with the two solid phases since the second gaseous component can be calculated from the equilibrium constant expression

$$K = p_{H_2}/p_{H_2O}$$

Here $P = 3$. Hence, $F = C - P + 2 = 3 - 3 + 2 = 2$. This means that T and P define the system. Other possibility is that T and the concentration of one of the gases define the system.

(h) This system is analogous to the system considered in *(e)* above. This answer is $C = 2$ or 3 so that $F = 1$ or 2.

ONE-COMPONENT SYSTEMS

Since the minimum number of phases in any system is 1, it is evident that

$$F = C - P + 2 = 1 - 1 + 2 = 2$$

The one-component system is, thus, bivariant. It can be completely defined by specifying two variables. The two variables are temperature and pressure. The composition or concentration remains invariably 100 per cent because there is only one component.

If a one-component system has two phases in contact with each other,

$$F = C - P + 2 = 1 - 2 + 2 = 1$$

The system is then said to be monovariant. It can be completely defined by specifying only one variable, *viz.*, either temperature or pressure. If temperature is fixed, pressure of the system is fixed automatically and vice-versa. Thus, the system consisting of a liquid in contact with its vapour, *e.g.*,

$$H_2O(l) \rightleftharpoons H_2O(g)$$

is monovariant. If temperature is fixed, the pressure of the vapour is fixed automatically. This is because at each temperature, there can be one and only one vapour pressure.

WATER SYSTEM

Water can exist in three phases, namely, solid, liquid and vapour. Hence, there can be three forms of equilibria, *viz.*,

1. Liquid $\rightleftharpoons$ Vapour 2. Solid $\rightleftharpoons$ Vapour 3. Solid $\rightleftharpoons$ Liquid.

Each equilibrium involves two phases. The phase diagram for the water system is shown in Fig. 2.

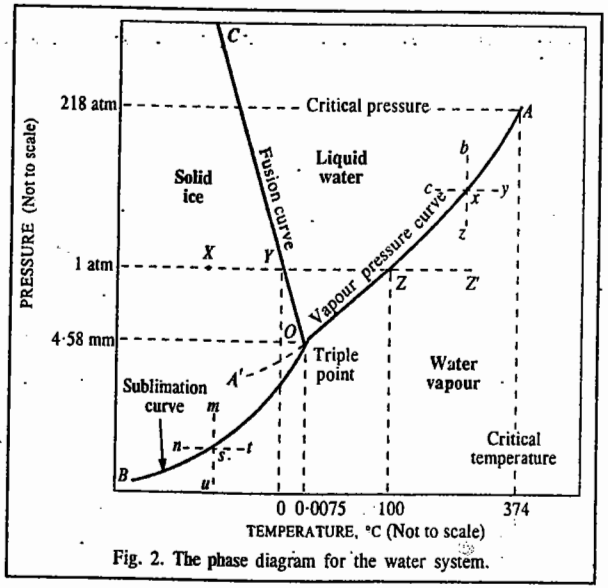

Fig. 2. The phase diagram for the water system.

The curve *OA* represents the equilibrium between liquid water and vapour at different temperatures. It is called the vapour pressure curve of water as it gives the vapour pressure of water at different temperatures. It can be seen that, for any given temperature, there exists one and only one vapour pressure. Similarly, for each vapour pressure, only one temperature can be maintained. Thus, the degree of freedom of the system is one, *i.e.*, the system is univariant :

$$F = C - P + 2 = 1 - 2 + 2 = 1$$

At 100°C, the vapour pressure of water equals the pressure of the atmosphere (1 atm = 760 mm Hg). This is, therefore, the boiling point of water. The curve *OA* extends as far as the critical temperature of water (374°C) since above this temperature liquid water cannot exist.

The variation of vapour pressure with temperature is quantitatively given by Clapeyron equation or Clapeyron-Clausius equation, *viz.*,

$$\frac{dP}{dT} = \frac{\Delta H_{vap}}{T(V_g - V_l)} \quad \text{or} \quad \ln\frac{P_2}{P_1} = \frac{\Delta H_{vap}}{R}\left\{\frac{T_2 - T_1}{T_1 T_2}\right\}$$

Example 5. At 100°C, the specific volumes of water and steam are, respectively, 1 c.c. and 1673 c.c. Calculate the change in vapour pressure of the system by 1°C change in temperature. The molar heat of vaporisation of water in this range may be taken as 40584·8 J mol^{-1}.

Solution :

Molar volume of liquid water, $V_l = 18\ \text{cm}^3\ \text{mol}^{-1} = 18\times10^{-6}\ \text{m}^3\ \text{mol}^{-1}$

Molar volume of steam, $V_g = 18\times1673\ \text{cm}^3\ \text{mol}^{-1} = 30114\times10^{-6}\ \text{m}^3\ \text{mol}^{-1}$

Molar heat of vaporisation, $\Delta H_v = 40584{\cdot}8\ \text{J mol}^{-1}$

According to the Clapeyron equation,

$$\frac{dP}{dT} = \frac{\Delta H_{vap}}{T(V_g - V_l)}$$

In this case, $dT = 1$ K and $T = 273 + 100 = 373$ K

$$\therefore \quad dP = \frac{40584{\cdot}8\ \text{J mol}^{-1}\times1\ \text{K}}{373\ \text{K}(30114-18)\times10^{-6}\ \text{m}^3\ \text{mol}^{-1}}$$

$$= 0{\cdot}00361\times10^6\ \text{N m}^{-2} \qquad (\text{J} = \text{N m})$$

$$= 0{\cdot}03561\ \text{atm} = \mathbf{27{\cdot}08\ mm\ of\ Hg} \qquad (1\ \text{atm} = 101{,}325\ \text{N m}^{-2})$$

Thus, the vapour pressure of water increases by about 27 mm of Hg by 1°C rise in temperature, at 100°C.

Example 6. The vapour pressure of water at 95°C is found to be 634 mm. What would be the vapour pressure at a temperature of 100°C ? The molar heat of vapourisation in this range of temperature may be taken as 40593 J mol^{-1}.

Solution : The Clapeyron-Clausius equation for Liquid $\rightleftharpoons$ Vapour equilibrium is

$$\ln\frac{P_2}{P_1} = \frac{\Delta H_{vap}}{R}\left\{\frac{T_2 - T_1}{T_1 T_2}\right\}$$

In this case, $T_1 = 273 + 95 = 368$ K, $P_1 = 634$ mm ; $T_2 = 273 + 100 = 373$ K, $P_2 = ?$

Thus, $$\ln\frac{P_2}{634\ \text{mm}} = \frac{40593\ \text{J mol}^{-1}}{8{\cdot}314\ \text{J K}^{-1}\ \text{mol}^{-1}}\left[\frac{5\ \text{K}}{368\ \text{K}\times373\ \text{K}}\right]$$

$$\therefore \quad P_2 = \mathbf{759{\cdot}8\ mm}$$

Thus, the vapour pressure of water increases from 634 mm to about 760 mm of Hg when the temperature changes from 95° to 100°C.

The curve *OB* represents the equilibrium between ice and vapour. It is called the vapour pressure curve of ice or sublimation curve of ice. Its lower end *B* extends to absolute zero. Again, as can be seen, for each temperature there can be one and only one pressure and similarly for each pressure, one and only one temperature can be maintained. In other words, the degree of freedom is 1.

The variation of vapour pressure of ice with temperature, is quantitatively given by Clapeyron or Clapeyron-Clausius equation, *viz.*,

$$\frac{dP}{dT} = \frac{\Delta H_{sub}}{T(V_g - V_s)} \quad \text{or} \quad \ln\frac{P_2}{P_1} = \frac{\Delta H_{sub}}{R}\left\{\frac{T_2 - T_1}{T_1 T_2}\right\}$$

Since, along *OA*, the two phases are liquid and vapour and along *OB*, the two phases are solid and vapour, at the point *O*, where the two curves meet, three phases, namely, solid, liquid and vapour, will coexist. Such a point is known as the **triple point**. The temperature and pressure at the triple point of water are 0·0075°C and 4·58 mm of Hg, respectively. According to the phase rule, *O* is an invariant point :

$$F = C - P + 2 = 1 - 3 + 2 = 0$$

The curve *OC* represents the equilibrium between ice and water. It is called the **fusion curve of ice** as it indicates the temperatures and pressures at which the solid (ice) and liquid (water) can coexist in equilibrium. In other words, this curve shows the effect of pressure on the melting point of ice. As can be seen, the line *OC* is inclined towards the pressure axis which indicates that the *melting point of ice is lowered by increase of pressure.* This follows from Clapeyron equation, *viz.*,

$$\frac{dP}{dT} = \frac{\Delta H_{fus}}{T(V_l - V_s)} \quad \text{or} \quad \frac{dT}{dP} = \frac{T(V_l - V_s)}{\Delta H_{fus}}$$

Since density of ice is less than that of water, V_s is greater than V_l. In other words, the expression on the right hand side of the above equation is negative. Hence, dT/dP should also have a negative sign. This means that the increase of pressure must lower and decrease of pressure must raise the freezing point of water. It can be easily shown with the help of the above equation that freezing point of water is lowered by 0·0075°C by 1 atm increase in pressure. Thus, while the freezing point of water at a pressure of 4·58 mm is +0·0075°C, at a higher pressure of 760 mm (*i.e.*, 1 atm) it is reduced to 0°C.

Example 7. The specific volumes of ice and water at 0°C are 1·0907 cm^3 and 1·0001 cm^3, respectively. What would be the change in melting point of ice per atm increase of pressure ? Molar heat of fusion of ice = 6009·9 J mol^{-1}.

Solution :

Molar volume of ice, $V_s = 18 \times 1{\cdot}0907 \times 10^{-6}$ m^3

Molar volume of water, $V_l = 18 \times 1{\cdot}0001 \times 10^{-6}$ m^3

Temperature, $T = 273$ K

Molar heat of fusion of ice, $\Delta H_{fus} = 6009{\cdot}9$ J mol^{-1}

Increase of pressure, $dP = 1$ atm $= 101325$ N m^{-2}; $dT = ?$

$$\frac{dT}{dP} = \frac{T(V_l - V_s)}{\Delta H_{fus}} = \frac{273\,K \times (-0{\cdot}0906) \times 18 \times 10^{-6}\ m^3}{6009{\cdot}9\,J\,mol^{-1}}$$

$$dT = \frac{273\,K \times 18 \times 10^{-6}(-0{\cdot}0906)\,m^3 \times 101325\,N\,m^{-2}}{6009{\cdot}9\,J\,mol^{-1}} = -0{\cdot}0075\ K \qquad (J = N\ m)$$

The negative sign indicates that the melting point of ice (or freezing point of water) *decreases by increase of pressure.* Alternatively, the melting point of ice *increases by decrease of pressure.*

Along the curve *OC*, there are two phases, namely, ice and water. Therefore, according to the Phase rule, the system should be univariant, *i.e.*, the degree of freedom should be 1. This is seen to be actually the case as, for any given pressure, melting point will have one definite value (*i.e.*, solid and liquid phases will coexist in equilibrium at one particular temperature only). The curve *OC* must meet the other two curves at the triple point *O*.

Significance of Areas or Regions Between the Lines. Suppose, the state of equilibrium is represented by a point *x* on the line *OA*. The two phases in contact are liquid and vapour. If the temperature is kept constant and pressure increased, the vapour will be compressed wholly into the liquid phase. This change is represented by the dotted line *xb* in Fig. 2. Similarly, if pressure is kept constant and temperature is decreased, the vapour will change into liquid again. This change is represented by the dotted line *xc*. Thus, the area above the curve *OA* represents exclusively the liquid phase, as shown.

Coming back to the point *x*, if the pressure is maintained constant and the temperature is increased, the liquid will change completely into vapour. The change is represented by the dotted line *xy*. Similarly, if the temperature is kept constant and the pressure is diminished, liquid will again be converted completely into the vapour phase as represented by the dotted line *xz*. Thus, the area or region below the curve *OA* represents the vapour phase only.

Similarly, if a system represented by a point *s* on the solid–vapour equilibrium curve (*OB*) is subjected to increase of temperature at a constant pressure (along *st*) or decrease of pressure at a constant temperature (along *su*), it will change completely into vapour. Thus, any point lying below the curve *OB* also represents the vapour phase only.

Lastly, if the system at *s* is subjected to increase of pressure at constant temperature (along *sm*) or decrease of temperature at constant pressure (along *sn*), the vapour will condense completely into solid phase. Thus, the area lying above the curve *OB* will represent the solid phase exclusively.

It may be noted that if a point representing the state of equilibrium of the system lies within a particular region or area, the number of phases is 1 ; if on a line, the number of phases is 2 and if on a point where the lines meet, the number of phases is 3. Accordingly, the system will be bivariant, univariant and non-variant, respectively.

Metastable Equilibrium. Sometimes it is possible with due care to cool water (or, as a matter of fact, any liquid) below its freezing temperature without the separation of ice. The water is then said to be *supercooled* and can be kept as such almost indefinitely if the presence of ice or any other solid phase is carefully avoided. The vapour pressure curve of liquid water *AO* can, therefore, continue below the point *O*, as shown by the dotted curve *OA'*. The liquid $\rightleftharpoons$ vapour system along the curve

OA' is said to be in metastable equilibrium because as soon as a small particle of ice is brought in contact with the supercooled liquid, the entire liquid solidifies. It will be seen from the phase diagram that the curve *OA'* lies above the curve *OB*. Thus, the metastable system has a higher vapour pressure than the stable one at the same temperature.

Effect of Change of Temperature and Pressure. The significance of the equilibrium diagram can be further understood by following the changes that occur on altering the temperature or pressure of the system. Suppose, it is desired to know the effect of heating ice when it is under a pressure of 1 atm and at a certain temperature represented by the point *X* in the figure. As the system is bivariant, the temperature can have any value at the same pressure. Therefore, heating the ice slowly, at constant pressure, will shift the system along the line *XY*. At *Y* fusion takes place. The liquid phase also appears. The system has now two phases and, therefore, one degree of freedom. Now, the temperature cannot alter without the alteration of pressure. The effect of continued heating will be simply to cause fusion of ice at constant temperature. When fusion is complete, *i.e.*, when ice has changed completely into water, the system again has only one phase and becomes bivariant. The temperature begins to rise along *YZ*. At *Z*, vaporisation begins, *i.e.*, the vapour phase also makes its appearance. The number of phases rises to 2 and the system becomes monovariant. The continued heating will not alter the temperature as the pressure has been kept constant. The only effect will be to convert more and more of the liquid into vapour. When the liquid phase disappears completely, the system will have only one phase (vapour) and will become again bivariant. The temperature of the vapour will rise along the line *ZZ'*.

Triple Point. It will be interesting to note the effect of heating and applying pressure on the system when all the three phases coexist as at the triple point *O*. The effect of heat will be simply to cause more and more of the ice to melt but there will be no rise in temperature or pressure until the whole of the ice has completely changed into liquid. When this happens, the system has only two phases (liquid and vapour). The system changes from non-variant to univariant. Therefore, further addition of heat will cause a rise of temperature. The equilibrium will shift along the curve *OA*.

Now, suppose, pressure is applied to the system at the triple point. There can be no change in pressure or temperature as long as all the three phases are present. The only effect of applying pressure will be to cause condensation of vapour to liquid or solid phase. Ultimately, the vapour phase will disappear and only two phases, solid and liquid, will stay and further application of pressure will cause increase of pressure with change of temperature along the curve *OC*.

CARBON DIOXIDE SYSTEM

The phase diagram for carbon dioxide system is shown in Fig. 3. It has three distinct areas in which carbon dioxide can exist either as solid, liquid or gas.

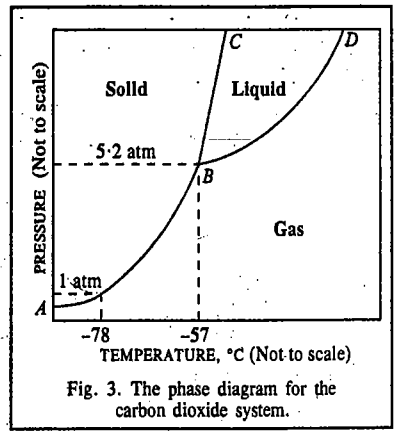

Fig. 3. The phase diagram for the carbon dioxide system.

AB is the sublimation curve along which solid carbon dioxide is in equilibrium with the gas, *BD* is the vaporisation curve along which liquid carbon dioxide is in equilibrium with the gas while *BC* is the fusion curve along which solid and liquid carbon dioxide are in equilibrium with each other.

B is the triple point at which all the three phases of carbon dioxide coexist in equilibrium with one another. The temperature of the system at this point is -57°C while the pressure is 5·2 atm. A slight variation in temperature or pressure at this point may result in the disappearance of one of the two phases. For example, a slight increase in temperature will result in the disappearance of the solid phase and the equilibrium will shift along the curve *BD* while a slight decrease in temperature will result in the

disappearance of the liquid phase and the equilibrium will shift along the curve *BA*. Keeping the temperature constant, if the pressure is increased, the gaseous phase will disappear and the equilibrium will shift along the curve *BC*.

The phase diagram of carbon dioxide resembles that of water (Fig. 2) in showing three distinct areas for solid, liquid and gaseous phases. But it differs essentially from the latter in several respects. In the first place, the fusion curve slopes away from the pressure axis. This indicates that increase of pressure raises the melting point of solid carbon dioxide, *i.e.*, the factor dT/dP of the Clapyron–Clausius equation is positive indicating thereby that $V_l > V_s$, *i.e.*, specific volume of liquid carbon dioxide is greater than that of solid carbon dioxide.

The second point to be noticed is that solid carbon dioxide can exist in equilibrium with its liquid (*i.e.*, it can melt) only at a very high pressure equal to 5·2 atm. This is unlike the water system in which ice and water can exist in equilibrium even at a very low pressure equal to 4·58 mm of Hg (Fig. 2).

The third point of difference is that the vapour pressure of solid carbon dioxide even at extremely low temperature is very high and many times higher than that of ice.

A significant feature of carbon dioxide system is that even at atmospheric pressure (1 atm pressure), carbon dioxide gas can be directly solidified without the appearance of liquid phase merely on cooling to –78°C (Fig. 3). It is for this reason that solid carbon dioxide is commonly known as **dry ice.**

Polymorphism

The existence of a given substance in more than one crystalline forms possessing different physical properties is known as **polymorphism.** This phenomenon occurs in a number of elements and compounds. When it occurs in elements, it is frequently referred to as **allotropy.**

Each polymorphic form constitutes a separate phase. The temperature at which one form changes into another, at a given pressure, is known as the **transition temperature.** For example, rhombic sulphur when heated under a pressure of one atm, changes into monoclinic sulphur at 95·6°C. At the same time, monoclinic sulphur, when cooled under a pressure of one atm, changes into rhombic sulphur at 95·6°C. Thus, 95·6°C is the transition temperature at which one form of sulphur changes reversibly into the other. Polymorphic forms which can undergo reversible transformations into one another at the transition temperature are said to be **enantiotropic** and the phenomenon is known as **enantiotropy.**

In some cases, polymorphic forms do not undergo reversible transformations into one another. For example, diamond can be converted into graphite under suitable conditions of temperature and pressure but the reverse is not possible. Similarly, white phosphorus can be readily transformed into red (or violet) form under suitable conditions but the reverse cannot take place in a direct manner. Such polyphormic forms which cannot be reversibly transformed into one another are said to be **monotropic** and the phenomenon is known as **monotropy.**

SULPHUR SYSTEM

Sulphur exists in two crystalline forms, *rhombic* and *monoclinic*, with 95·6°C as the transition temperature at one atm pressure at which they can be transformed into one another. Below 95·6°C, rhombic is the stable form while above it, monoclinic is the stable variety. At 95·6°C, both forms are in equilibrium with each other. Each form has its own characteristic melting point. Thus, under a pressure of one atm, melting point of rhombic sulphur (S_R) is 114°C while that of monoclinic sulphur (S_M) is 120°C. The liquid form of sulphur (S_L) undergoes notable changes in colour and viscosity when heated and ultimately boils at 444·7°C. Thus, sulphur can exist in four possible phases, two solids (S_R and S_M), one liquid (S_L) and one vapour (S_V) phase. However, all the four phases cannot coexist at the same time since the number of phases coexisting in a one-component system cannot exceed three, as already shown.

The phase diagram of sulphur system is represented in Fig. 4.

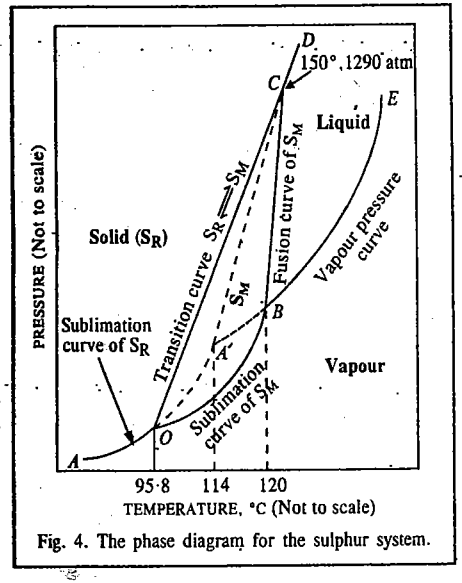

Fig. 4. The phase diagram for the sulphur system.

The curve *AO* is the **sublimation curve of rhombic sulphur** and gives the vapour pressure of rhombic sulphur at different temperatures. The two phases in equilibrium are rhombic sulphur and the vapour. The equilibrium ($S_R \rightleftharpoons S_v$) is monovariant. Therefore, at one temperature, there can be one vapour pressure only.

The point *O* is the transition temperature (95·6°C) at which rhombic sulphur changes into monoclinic sulphur. *O* is thus a triple point at which three phases, two solids and the vapour ($S_R - S_M - S_V$) coexist in equilibrium. This is a non–variant point.

The curve *OB* is the sublimation curve of monoclinic sulphur. It gives vapour pressure of monoclinic sulphur at different temperatures. As the number of phases is 2, the system is monovariant.

The Clapeyron–Clausius equation can be used to study quantitatively the variation of vapour pressure of solid sulphur (S_R or S_M) with temperature.

The point *B* is the melting point (120°C) of monoclinic sulphur. This is another triple point at which three phases, *viz.*, sulphur monoclinic, liquid and vapour ($S_M - S_L - S_V$) are in equilibrium. This is a non–variant point.

The curve *BE* is the vapour pressure curve for liquid sulphur. The two–phase equilibrium ($S_L \rightleftharpoons S_V$) is monovariant.

The variation of vapour pressure of liquid sulphur with temperature can be studied, again, with the help of the Clapeyron–Clausius equation.

The curve *OC* is the transition curve which gives the effect of pressure on the transition temperature of rhombic sulphur into monoclinic sulphur. The equilibrium involved along the curve is $S_R \rightleftharpoons S_M$. Both the phases are solid. The system is monovariant. Since transformation of rhombic into monoclinic sulphur is accompanied by increase of volume, the increase of pressure causes a rise in the transition temperature. This can be predicted with the help of Clapeyron equation which, when applied to $S_R \rightleftharpoons S_M$ equilibrium, may be put as

$$\frac{dP}{dT} = \frac{\Delta H_{trs}}{T(V_B - V_A)}$$

where ΔH_{trs} is the molar heat of transition. Since density of monoclinic sulphur (1·95 g cm^{-3}) is less than that of rhombic sulphur (2·05 g cm^{-3}), V_B is larger than V_A. The right hand side of the above equation is, therefore, positive. Hence, dP/dT should also have a positive sign. This means that increase of pressure raises the transition temperature. The curve *OC*, therefore, slopes away from the pressure axis.

Example 8. Rhombic sulphur changes into monoclinic form at a temperature of 95·6°C at 1 atm pressure. What would be the change in the transition temperature per atm change of pressure ? Given : heat absorbed in the change = 2499·94 J mol^{-1} per mole, density of rhombic sulphur = 2·05 g/c.c. and density of monoclinic sulphur is 1·95 g/c.c.

Solution : The Clapeyron equation for the transition equilibrium may be represented as

$$dT/dP = T(V_B - V_A)/\Delta H_{trs}$$

where V_B = Molar volume of monoclinic sulphur ; V_A = Molar volume of rhombic sulphur and ΔH_{trs} = Molar heat of transition

In this case, $V_B = 32 \text{ g mol}^{-1}/1{\cdot}95 \text{ g cm}^{-3} = 16{\cdot}41 \text{ cm}^3 \text{ mol}^{-1} = 16{\cdot}41\times10^{-6} \text{ m}^3 \text{ mol}^{-1}$

$V_A = 32 \text{ g mol}^{-1}/2{\cdot}05 \text{ g cm}^{-3} = 15{\cdot}61 \text{ cm}^3 \text{ mol}^{-1} = 15{\cdot}61\times10^{-6} \text{ m}^3 \text{ mol}^{-1}$

$\Delta H_{trs} = 2499{\cdot}94 \text{ J mol}^{-1}$

$T = 273 + 95{\cdot}6 = 368{\cdot}6 \text{ K}$; $dP = 1 \text{ atm} = 101325 \text{ N m}^{-2}$

$$dT = \frac{368{\cdot}6 \text{ K}\,(16{\cdot}41 - 15{\cdot}61)\times10^{-6} \text{ m}^3 \text{ mol}^{-1} \times 101325 \text{ N m}^{-2}}{2499{\cdot}94 \text{ J mol}^{-1}} = 0{\cdot}011 \text{ K}\,(J = \text{N m})$$

The curve *BC* is the fusion curve for monoclinic sulphur. This gives the effect of pressure on the melting point of monoclinic sulphur. The two-phase equilibrium ($S_M \rightleftharpoons S_L$) along the curve *BC* is univariant. As the melting of monoclinic sulphur is accompanied by a slight increase of volume, it follows from Clapeyron-Clausius equation that the melting point will rise slightly by the increase of pressure. The curve *BC*, therefore, slopes slightly away from the pressure axis. As the slope of this curve is much less than that of the curve *OC*, the two curves meet at the point *C*. Thus, *C* is another triple point where three phases, *viz.*, rhombic sulphur, monoclinic sulphur and liquid sulphur ($S_R - S_M - S_L$) are in equilibrium and the system is non-variant. At *C*, the temperature is 151°C and the pressure is 1290 atm.

The curve *CD* is the fusion curve for rhombic sulphur. The equilibrium along this curve is $S_R \rightleftharpoons S_L$. As the number of phases is 2, the system is monovariant.

Metastable Equilibria. In addition to the stable equilibria discussed above, there are also some metastable equilibria indicated by the dotted lines in Fig. 4. Since the conversion of one solid into another solid, as that of rhombic sulphur into monoclinic sulphur, at the point *O* (95·6°C) involves molecular rearrangement necessary for bringing about the change in the crystalline form, the process is naturally slow. Therefore, unless heating is done extremely slowly, there is a possibility that the first solid may not change into the second solid at the normal transition point. The first solid, therefore, will exist in metastable equilibrium with its vapour.

This possibility in sulphur system is represented by the dotted line *OA'*. If the temperature of rhombic sulphur is allowed to rise rather quickly at about 95·6°C, it will persist in equilibrium with its vapour phase without changing into monoclinic sulphur for several degrees above the normal transition temperature. Thus, along the dotted curve *OA'* which is the extension of the curve *AO*, the metastable equilibrium, $S_R \rightleftharpoons S_V$ exists. The vapour pressure at each temperature, as can be seen, is higher than the vapour pressure of monoclinic sulphur which is the stable phase in this range.

Similarly, if liquid sulphur is allowed to cool along the curve *EB*, the solid phase (monoclinic sulphur) may not separate out at *B* unless cooling is extremely slow. The line *BA'* in this case represents the metastable equilibrium between liquid sulphur and its vapour (*i.e.*, $S_L \rightleftharpoons S_V$). The point *A'*, therefore, represents the melting point of the metastable rhombic sulphur. This is another triple point where the three phases, $S_R - S_L - S_V$, coexist in metastable equilibrium. The temperature *A'* has been found to be about 114°C.

The curve *A'C*, evidently, gives the effect of pressure on the melting point of metastable rhombic sulphur. In other words, this is the fusion curve of metastable rhombic sulphur along which rhombic sulphur is in metastable equilibrium with the liquid.

Areas. As the curves *AO* and *OC* both involve rhombic sulphur in equilibrium with the vapour phase in one case and solid monoclinic sulphur in the other, it can be shown that the area bounded by these lines towards the left represents conditions for the stable existence of rhombic sulphur alone. Similarly, as the curves *BE* and *BC* both have liquid phase as common, in equilibrium with vapour in the first case and with solid monoclinic sulphur in the second case, the area bounded by these lines represents liquid sulphur as the stable phase. Similarly, as the curves *AO*, *OB* and *BE* have the

vapour phase as common, the area lying below these lines represents only vapour as the stable phase. Lastly, as the lines *OC*, *OB* and *BC* have monoclinic sulphur as the common phase, the triangular area bounded by these lines represents monoclinic sulphur as the stable phase. The existence of this form of sulphur, evidently, is limited on all sides.

SOME TYPICAL SOLVED EXAMPLES FOR ONE-COMPONENT SYSTEMS

Example 9. A lady weighing 50 kg is standing on ice wearing shoes with sole area of 60 cm² per shoe. Calculate the temperature at which the ice will melt under her feet.

Solution : $m = 50 \text{ kg}$; $g = 9{\cdot}80 \text{ m s}^{-2}$

$\therefore$ Weight of the lady $= mg = 50 \text{ kg}\times9{\cdot}80 \text{ m s}^{-2}$

The pressure on ice under the lady's feet $= \dfrac{\text{force}}{\text{area}} = \dfrac{mg}{\text{area}} = \dfrac{mg}{2 \times \text{area of each shoe}}$

$$= \frac{(50 \text{ kg})(9{\cdot}80 \text{ m s}^{-2})}{2\times(60\times10^{-4} \text{ m}^2)} = 4{\cdot}083\times10^4 \text{ N m}^{-2} \qquad (\text{N} = \text{kg m s}^{-2})$$

$$= \frac{4{\cdot}083\times10^4 \text{ N m}^{-2}}{1{\cdot}01325\times10^5 \text{ N m}^{-2}/\text{atm}} = 0{\cdot}403 \text{ atm}$$

We have shown in example 7 that the melting point of ice *decreases* by 0·0075°C if the pressure is increased by 1 atm. Hence, if pressure is increased by 0·403 atm, the melting point of ice will decrease by – 0·003°. Thus, the ice will melt at – **0·003°C** under the lady's feet.

Example 10. The following equations give the vapour pressures of ice and water :

$$\ln P_{\text{vapour}}\ (\text{ice}) = -\,(6140{\cdot}1/T) + 24{\cdot}00 \qquad \ldots(i)$$

$$\ln P_{\text{vapour}}\ (\text{water}) = -\,(5432{\cdot}8/T) + 21{\cdot}41 \qquad \ldots(ii)$$

where *P* is in mm Hg. Calculate *(a)* the temperature and pressure at the triple point of water *(b)* the molar enthalpies of sublimation, vaporization and fusion at the triple point.

Solution : *(a)* Since at the triple point, the vapour pressures of ice and water will be equal, hence from Eqs. *(i)* and *(ii)*,

$$-\,(6140{\cdot}1/T) + 24{\cdot}00 = -\,(5432{\cdot}8/T) + 21{\cdot}41$$

or $-\,(6140{\cdot}1 - 5432{\cdot}8)/T = 21{\cdot}41 - 24{\cdot}00$

$\therefore$ $T = 707{\cdot}3/2{\cdot}59 = \mathbf{273{\cdot}089 \text{ K}}$

The vapour pressure at the triple point can be found by substituting the above value of *T* in either Eq. *(i)* or Eq. *(ii)*. In this way we find that $p = \mathbf{4{\cdot}55 \text{ mm Hg}}$

(b) $\ln P = -\,(\Delta H/RT) + I$ (Clapeyron–Clausius equation)

where ΔH may be ΔH_{vap} or ΔH_{sub} and *I* is the constant of integration.

Comparing this equation with Eqs. *(i)* and *(ii)*, we have

$$-\,\Delta H_{sub}/R = -\,6140{\cdot}1$$

$$-\,\Delta H_{vap}/R = -\,5432{\cdot}8$$

$\therefore$ $\Delta H_{sub} = 6140{\cdot}1\times R = 6140{\cdot}1\times8{\cdot}314 \text{ J K}^{-1} \text{ mol}^{-1} = \mathbf{51{\cdot}05 \text{ kJ mol}^{-1}}$

and $\Delta H_{vap} = 5432{\cdot}8\times R = 5432{\cdot}8\times8{\cdot}314 \text{ J K}^{-1} \text{ mol}^{-1} = \mathbf{45{\cdot}17 \text{ kJ mol}^{-1}}$

At the triple point, $\Delta H_{sub} = \Delta H_{fusion} + \Delta H_{vap}$

$\therefore$ $\Delta H_{fusion} = \Delta H_{sub} - \Delta H_{vap} = 51{\cdot}05 \text{ kJ mol}^{-1} - 45{\cdot}17 \text{ kJ mol}^{-1} = \mathbf{5{\cdot}88 \text{ kJ mol}^{-1}}$

Example 11. As heat is removed from a liquid which tends to supercool, its temperature drops below the freezing point and then rises suddenly to its freezing point. What is the source of heat which causes the temperature to rise ?

Answer. The enthalpy of fusion.

Example 12. As supercooled water freezes spontaneously, its temperature rises to 0°C. What is the source of heat for the process : $H_2O(l)$ (-10°C) $\longrightarrow$ $H_2O(s)$ (0°C) ?

Answer. In this case, $\Delta H=0$. No heat is transferred to or from the system. The heat liberated in the freezing process warms the system to 0°C.

Example 13. ***(a)*** **Distinguish between the triple point and the freezing point of a pure substance.**

(b) **For most pure substances which is apt to be higher : the triple point or the freezing point ?**

Solution : ***(a)*** The triple point is the temperature where solid, liquid and vapour are in equilibrium with one another, with no other substance present. The freezing point is the temperature at which solid and liquid are in equilibrium under 1 atm total pressure. There must be some other substance present to achieve 1 atm pressure.

(b) The freezing point is higher for most substances which have a *positive* slope of the solid-liquid equilibrium line in the phase diagram.

Example 14. For the phase diagram for the water system shown in Fig. 5, answer the following questions :

(a) **What feature represents the equilibrium of solid water (ice) and water vapour ?**

(b) **What phase changes occur when a sample at point *E* is heated at constant pressure until point *F* is reached ?**

(c) **What is the temperature at which the line *BD* intersects the 1 atm line called ?**

Solution : ***(a)*** The line *AB* represents the solid-vapour equilibrium.

(b) When a sample at point *E* is heated, melting and later vaporization occurs until the temperature reaches that represented by the point *F*.

(c) The temperature at which the line *BD* crosses the *P*=1 atm line is called the normal freezing point.

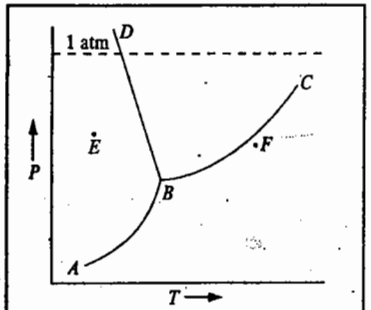

Fig. 5. Schematic phase diagram for the water system.

Example 15. A substance *Z* has its triple point at 18°C and 0·5 atm, its normal melting point is 20°C and its normal boiling point is 300°C. Sketch the schematic phase diagram for *Z*.

Solution : See Fig. 6.

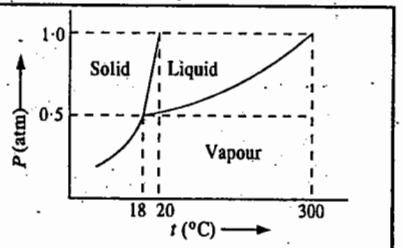

Fig. 6. Phase diagram for a one-component system conforming to the data given in Example 15.

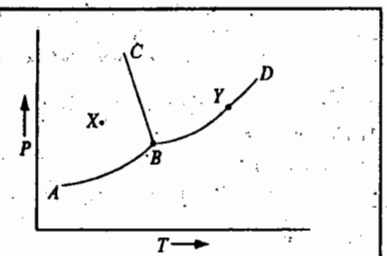

Fig. 7.

Example 16. Consider the phase diagram for a one-component system shown in Fig. 7.

(a) **Calculate the number of degrees of freedom at points *B*, *X* and *Y*.**

(b) **How many phases exist along *AB*, *BC* and *BD* ?**

Solution : ***(a)*** **Degrees of Freedom :**

At ***B***, the number of phases, $P = 3$

$F = C - P + 2 = 1 - 3 + 2 = 0$, *i.e.*, point *B* is **invariant**

At ***X***, $P = 1$ so that $F = C - P + 2 = 1 - 1 + 2 = 2$, *i.e.*, the point is **bivariant.**

At ***Y***, $P = 2$ so that $F = 1$, *i.e.*, the point is **univariant.**

(b) **Number of Phases :** Along *AB*, *BC* or *BD*, two phases coexist, *i.e.*, $P = 2$.

Example 17. Using the following data for the iodine system, draw the phase diagram for the system : Triple point 113°C, 0·12 atm ; Critical point 512°C, 116 atm ; Normal melting point 114°C ; Normal boiling point 184°C. Also ρ (solid) > ρ (liquid).

Solution : The diagram is shown in Fig. 8.

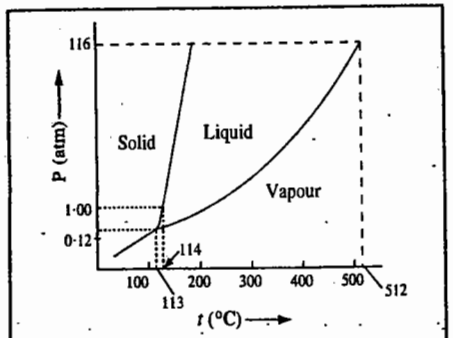

Fig. 8. Phase diagram for the iodine system consistent with data given in Example 17.

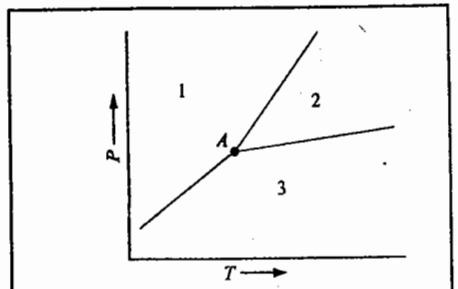

Fig. 9. Phase diagram of a one-component system (Example 18).

Example 18. Consider the phase diagram of a one-component system shown in Fig. 9. Indicate the relative magnitudes of the specific entropies and the molar volumes of phases in the neighbourhood of point *A* which is the 1-2-3 triple point.

Solution : It is evident that region 1 is the *solid phase*, region 2 is the *liquid phase* and region 3 is the *vapour phase*. The entropies and the molar volumes of the vapour phase are the largest. Thus, we have

$S_3 > S_2 > S_1$ and $V_3 > V_2 > V_1$.

Example 19. A substance exists in two solid modifications α and β and also as liquid and vapour. At a pressure of 1 atm, α melts at a lower temperature than β which melts at a higher temperature to form the liquid. Also, α is denser than the liquid but β is less dense than the liquid. Assuming that no metastable equilibria are observed, sketch the pressure-temperature phase diagram showing the significance of each point, line and region. Also, show in the diagram all the triple points that can be observed.

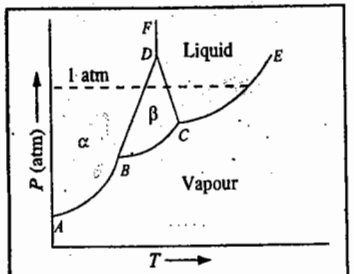

Fig. 10. The partial phase diagram of the substance conforming to the data given in Example 19.

Solution : The required phase diagram is shown in Fig. 10.

Equilibrium Curves :

AB : α $\rightleftharpoons$ vapour ; *BC* : β $\rightleftharpoons$ vapour ; *CE* : liquid $\rightleftharpoons$ vapour ; *BD* : α $\rightleftharpoons$ β ; *CD* : β $\rightleftharpoons$ liquid; *DF* : α $\rightleftharpoons$ liquid.

Triple Points :

B : α $\rightleftharpoons$ β $\rightleftharpoons$ vapour ; *C* : β $\rightleftharpoons$ liquid $\rightleftharpoons$ vapour ; *D* : α $\rightleftharpoons$ β $\rightleftharpoons$ liquid.

Critical Point : *E*

We can determine the signs of the slopes of *BD* and *CD* from the Clapeyron equation, *viz.*,

$$\frac{dP}{dT} = \frac{\Delta H}{T\Delta V} = \frac{H_2 - H_1}{T(V_2 - V_1)}$$

Since higher temperature favours the form with greater enthalpy, hence $H_L > H_\beta > H_\alpha$. From the densities we find that $V_\beta > V_L > V_\alpha$. Thus, for the α $\rightleftharpoons$ β equilibrium, $dP/dT > 0$ and for the β $\rightleftharpoons$ liquid equilibrium, $dP/dT < 0$. Hence, if the slopes of these curves do not change sign, the curves will intersect at the triple point *D*.

LIQUID HELIUM SYSTEM

Helium, so far, is the only pure substance than can exist in two different isotropic liquid phases. There are many organic liquid substances which can exist in two liquid phases ; however, only one of the phases is isotropic, the other is anisotropic (liquid crystals). Helium exists in two liquid forms, *viz.*, liquid He-I and liquid He-II. The phase diagram for liquid helium system is shown in Fig. 11.

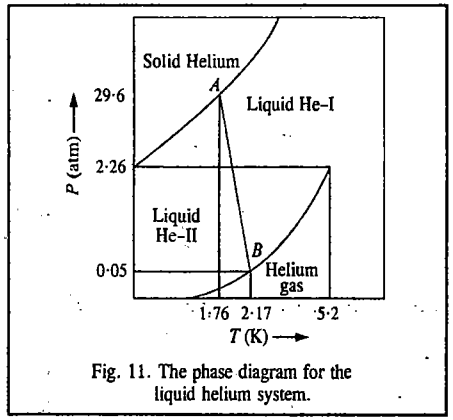

Fig. 11. The phase diagram for the liquid helium system.

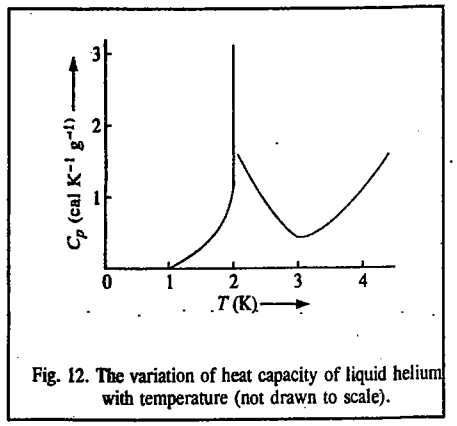

Fig. 12. The variation of heat capacity of liquid helium with temperature (not drawn to scale).

We observe that the liquid helium system does not have any solid-liquid-vapour triple point. There are, however, two triple points A and B showing two equilibria, *viz.*, Solid $\rightleftharpoons$ liquid He-I $\rightleftharpoons$ liquid He-II equilibrium at 1·76 K and 29·6 atm and liquid He-II $\rightleftharpoons$ liquid He-I $\rightleftharpoons$ Vapour equilibrium at 2·17 K and 0·05 atm, respectively. The transition between He-I and He-II in the presence of helium vapour is known as **lambda (λ) transition.** The transition point is called the **lambda point.** The line AB representing the He-I $\rightleftharpoons$ He-II transition is called the **lambda curve.** The name lambda is derived from the fact that the discontinuity in C_p versus T curve (Fig. 12) resembles the Greek letter λ.

Liquid He-II displays unusual properties in the vicinity of 0 K. It is a **superfluid** because it has extremely low viscosity since, by definition, there is practically no internal friction at this temperature. The superfluidity of He-II was discovered by the Russian physicist, P. Kapitza, the 1978 co-winner of the Physics Nobel Prize. The theoretical treatment of superfluidity was given by F. London and L.Tisza. However, it was the remarkable theory proposed by L.D. Landau (1908-1968), the greatest 20th century Russian theoretical physicist, that has satisfactorily explained the superfluidity of liquid helium-II. Landau who had contributed to several areas of theoretical physics, was awarded the 1962 Physics Nobel Prize on his death-bed for his contributions to superfluidity of liquid helium and condensed matter physics. He was also a brilliant teacher.

High-Pressure Phase Diagrams

1. Water System. At high pressure, several modifications of ice are formed (Fig. 13). Ordinary ice is ice-I. The stable high-pressure modifications of ice are designated as ice-II, ice-III, ice-V, ice-VI and ice-VII. When ice-I is compressed, its melting point decreases, reaching -22°C at a pressure of about 2,240 atm. Thereafter, further increase in pressure transforms ice-I into ice-III whose melting point

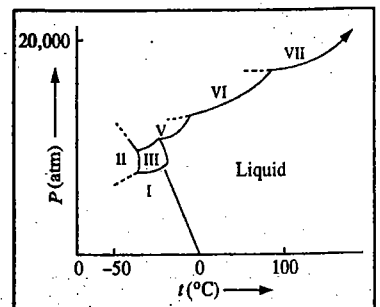

Fig. 13. The high pressure phase diagram (schematic) for the water system.

increases with pressure. In the phase diagram, there are five triple points. Ice-VII, the extreme high-pressure modification, melts to form water at about 100°C under a pressure of 20,000 atm. It is interesting to see *the melting ice to be so hot* ! The existence of ice-IV has not been confirmed.

2. Carbon System. Fig. 14 shows the phase diagram for the carbon system at high pressures. We see from this diagram that it is possible to convert graphite into diamond by compressing it at high temperature. It has been estimated that this conversion can take place at 4,000°C under a pressure of 2×10^6 (*i.e.*, two million) atm. Unfortunately, however, no containers can withstand these extremes of temperature and pressure. In the presence of a catalyst, such as cobalt or tantalum, the transformation can be affected at 2,000°C and 70,000 atm pressure.

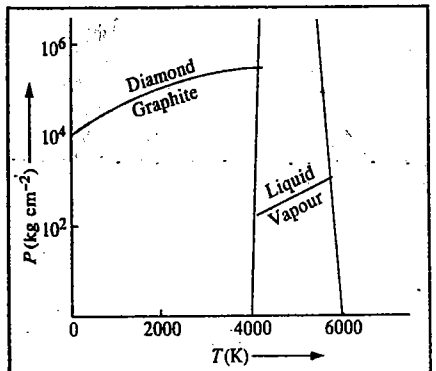

Fig. 14. The high pressure phase diagram for the carbon system.

TWO-COMPONENT SYSTEMS

For a two-component system, the phase rule becomes $F = 4 - P$

Since the minimum number of phases, P, in any system is 1, the maximum number of degrees of freedom, F, is 3. Thus, three variables would be necessary to describe a system. Since three variables are difficult to graph, it is customary to hold one of them say, the pressure, constant on a diagram of temperature plotted versus concentration. This reduces the degree of freedom of the system by one and the phase rule equation is then written as $F' = 3 - P$.

This is known as the **reduced phase rule equation.**

For the two-component solid-liquid equilibria, we come across the following cases : 1. The two components are miscible in the liquid state. 2. The two components are only partially miscible in the liquid state. We shall restrict ourselves to the former case. Under this category, we shall discuss the following cases :

A. The two components are not miscible in the solid state and form a eutectic mixture.

B. The two components form a stable compound with congruent melting point.

C. The two components form a compound with incongruent melting point.

We shall discuss some of these systems in the following pages.

Type A. SIMPLE EUTECTIC SYSTEMS

The general phase diagram of such a system is presented in Fig. 15.

The points A and B represent the melting points of the components A and B. As increasing quantities of B are added to A, the freezing point of A falls along the curve AC. Similarly, as increasing quantities of A are added to B, the freezing point of B falls along the curve BC. Thus, along the curve AC, the solid A is in equilibrium with the solution (liquid) of the component B in A. This is called the freezing point curve of the component A. Similarly, along the curve BC, the solid B is in equilibrium with the

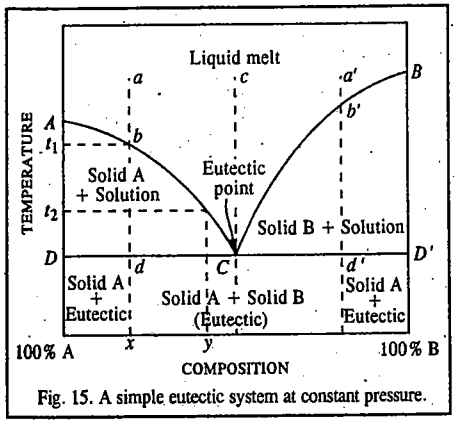

Fig. 15. A simple eutectic system at constant pressure.

solution (liquid) of the component A in B. This represents the freezing point curve of the component *B*. The number of phases along *AC*, as well as along *BC*, is two. Since measurements are made at atmospheric pressure (*i.e.*, at constant pressure), we may apply the reduced phase rule equation. Thus, we have $F' = C-P+1 = 2-2+1 = 1$. Hence, the system is monovariant. The composition varies with temperature along *AC* or *BC*, as the case may be. The two curves intersect at some point *C* where both the solids A and B must be in equilibrium with the liquid phase (*i.e.*, the liquid solution of the two components). The number of phases is 3. Applying the reduced phase rule equation, $F' = 0$. Thus, the system at *C* has no degree of freedom. It is invariant. This means that under a given pressure, the system consisting of two solids and their liquid solution, *i.e.*, A-B-L, can exist only at a definite temperature and that the composition of the liquid (solution) phase also is definite. The point *C*, as can be seen, is the lowest temperature at which liquid can exist in equilibrium with the solids A and B. Since the mixture of A and B of composition corresponding to point *C*, has the lowest melting point, the point *C* is known as the **eutectic point** *(eutectic* means *easy melting)*.

In the area above the lines *AC* and *BC*, the two components are present only as a homogeneous liquid solution. As the system consists of only one phase in this area, it is bivariant. Therefore, in order to define any point in this area, it is necessary to specify the temperature as well as the composition. It is understood that the pressure has been kept constant.

Suppose, a liquid mixture of composition represented by a point *a* is cooled at a constant pressure. The temperature will fall without any change of composition until the point *b* on the freezing point curve *AC* is reached. At this temperature, which corresponds to t_1, the solid A separates out. The system now consists of two phases and is, therefore, monovariant (assuming pressure to be constant). The temperature will fall only with change in composition of the liquid phase. Therefore, as cooling continues, the component A keeps on separating out and the solution becomes relatively richer in B. The temperature and the solution composition both change along the curve *bC*. Thus, at temperature t_1, solid A is in equilibrium with solution of composition *x* and at temperature t_2 it is in equilibrium with solution of composition *y*. It is evident, therefore, that in area *ACD*, solid A is in equilibrium with solutions of varying composition given by the curve *AC* depending upon the temperature.

When the eutectic temperature is reached at *d*, the second solid B also begins to crystallise out. The system now has 3 phases and, therefore, at constant pressure, it becomes invariant. On further cooling the system, solid A and solid B separate out together in a fixed ratio so that the composition of the solution remains constant as indicated by the point *C*. The temperature also remains constant. When the solution phase has been completely solidified and the system consists only of a mixture of solid A and solid B, it becomes monovariant and continued cooling results in fall of temperature below the line *DD'* into the area within which only the two solids coexist, as shown.

Similarly, if the composition of the original liquid is on the right side of the eutectic point, as represented, say, by the point *a'*, similar series of changes will be observed on cooling. In this case, however, on reaching the point *b'* on the freezing point curve *BC*, the solid B will separate out. As cooling continues, B keeps on separating and the solution becomes now richer and richer in A. The temperature and the composition both change along the curve *b'C*. Thus, in the area *BCD'*, solid *B* is in equilibrium with solutions of varying composition. Again, when the eutectic temperature is reached at the point *d'*, A also begins to separate out. The system now becomes invariant. On withdrawing heat further from the system, the temperature remains constant and solid A and solid B continue to separate in the same ratio so that the solution composition also remains constant. Ultimately, the solution phase solidifies completely as before and thereafter the temperature of the system can fall below the line *DD'* into the area of coexistence of two solids A and B.

Consider a special case when the liquid has the same composition as that of the eutectic. This is represented by the point *c*. On cooling, no solid will separate out until the eutectic temperature is reached. At this temperature, both the solids A and B crystallise out simultaneously. The temperature and composition of the solution remain constant until the system gets completely solidified.

Thermal Analysis. Cooling Curves

It can be seen on reference to Fig. 15 that when a liquid mixture (or melt) consisting of A and B is allowed to cool, solid A (or solid B) begins to separate out as soon as the temperature falls to a point on the line *AC* (or *BC*), as the case may be. The number of phases is now two, *viz.*, the liquid mixture and the solid A or B. If cooling is continued thereafter, the given solid continues to deposit with the corresponding fall in temperature till the eutectic temperature (point *C*) is reached. At this point both the solids separate out and the number of phases rises from two to three. The system now becomes invariant and, therefore, the temperature remains constant.

One important point to be remembered in this connection is that the separation of the solid A (or B) from the liquid solution is an exothermic process. The heat evolved in the process is similar to the heat given out when the same substance changes from liquid to solid state at its freezing point. As a result of this, the rate of cooling is diminished as soon as the separation of solid A or B commences to take place. The rate of cooling is, therefore, slower than that before till the eutectic point is reached. After this, temperature remains unchanged.

The above facts can be represented by plotting fall of temperature with time as in Fig. 16. Such a graph is called a **cooling curve.** In the figure, the rate of cooling along *ab* is quite rapid. This is when separation of a solid has not yet commenced. At *b* one of the solids begins to separate. The rate of cooling along *bd*, therefore, slows down. The cooling curve thus shows a distinct break at the point *b*. At *d*, the eutectic point is reached. The temperature, therefore, remains constant along *dd'* until the solidification has taken place completely. With the disappearance of the liquid phase, the system now consisting only of solid phase, becomes univariant and further cooling results in fall of temperature along *d'e*. Thus, there are three breaks in the cooling curve. The first one occurs at the freezing point of the mixture where the solid first commences to form. The second break occurs at the eutectic point and the third one occurs when the mixture gets completely solidified.

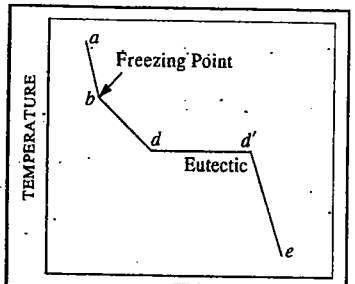

Fig. 16. A cooling curve in a two-component system forming a eutectic.

The above discussion provides a basis for the principle on which the method of **thermal analysis** used in the study of solid-liquid phase equilibria involving metals, is based. In actual practice, a number of mixtures of metals A and B of different compositions lying between 100% A and 100% B are prepared. These are heated above their respective melting points so that there is only one phase (*i.e.*, liquid phase) in every case. Each liquid is then allowed to cool slowly and the temperature is recorded after small intervals of time. In this way several cooling curves are obtained, as shown in Fig. 17. The first break in each curve occurs at the freezing point, that is, at the commencement of

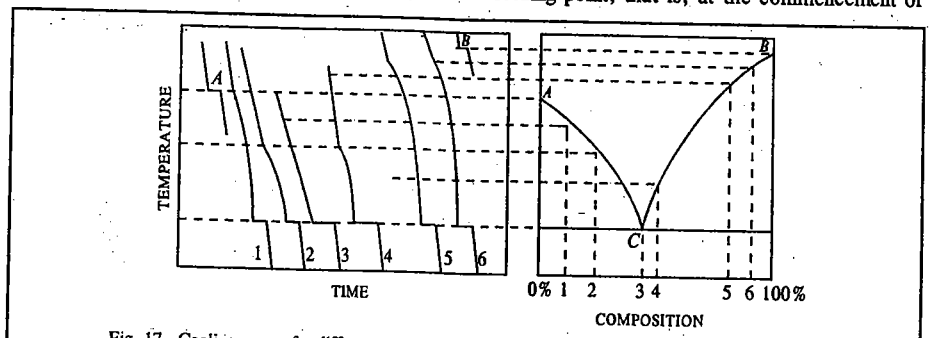

Fig. 17. Cooling curves for different compositions in a two-component system forming a eutectic.

the freezing of the mixture of that particular composition. As the mixtures differ in the compositions, their freezing will commence at different temperatures. The second break occurs at the point at which the temperature remains constant. This gives the eutectic temperature which will be the same in all the mixtures irrespective of their initial compositions. The freezing points of pure A and pure B (*i.e.*, 100% A and 100% B) are also determined in a similar manner. The equilibrium diagram for the system of two metals (A and B) under examination is thus determined. This is illustrated in Fig. 17.

There are many two-component systems which follow the general behaviour as depicted in Fig. 15. They include pairs of metals, metallic alloys, organic compounds and a number of salts and water. Two representative cases, one involving metals and the other involving a salt and water will be discussed here.

LEAD–SILVER SYSTEM

These metals are completely miscible in liquid state and do not give rise to any compound formation. The equilibrium diagram, therefore, is similar to that shown in Fig. 15. The various features are illustrated in Fig. 18.

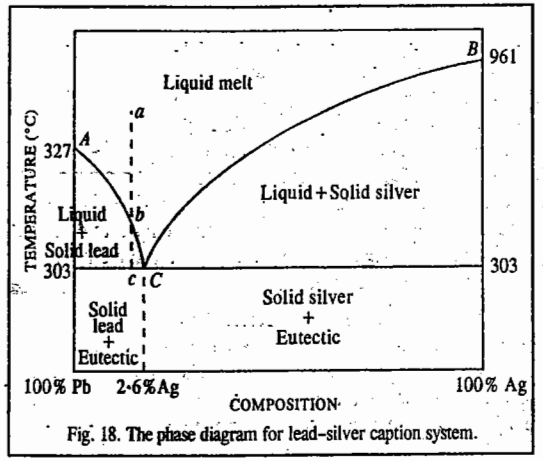

Fig. 18. The phase diagram for lead-silver caption system.

Pure lead melts at 327°C and the addition of silver lowers its melting point along *AC*. Thus, *AC* is the freezing point curve of lead containing varying amounts of silver. Pure silver melts at 961°C and the addition of lead lowers its melting point along *BC*. Thus, *BC* is the freezing point curve of silver. Along *AC*, solid lead and solution (melt) coexist while along *BC*, solid silver and solution (melt) coexist. The system, at constant pressure, is monovariant along *AC* as well as along *BC*.

C is the **eutectic point** where the three phases, solid lead, solid silver and their liquid solution (melt), coexist. It is an invariant point. The temperature of the eutectic is 303°C and the composition of the solution phase is 2·6 per cent silver, as shown in the figure. The phases coexisting in the various areas or regions are also shown in the figure.

The phase diagram of lead—silver system has a special significance in connection with the *desilverisation of lead.* The argentiferous lead consisting of a very small percentage of silver is first heated to a temperature well above its melting point so that the system consists only of the liquid phase represented, say, by the point *a*, in the figure. It is then allowed to cool. The temperature of the melt will fall along the line *ab*. As soon as the point *b* is reached, lead will begin to crystallise out and the solution will contain relatively increasing amounts of silver. Further cooling will shift the system along the line *bC*. Lead continues to separate out and is constantly removed by means of ladels. The melt continues to be richer and richer in silver until the point *C* is reached where the percentage of silver rises to 2·6. Thus, the original argentiferous lead which might have contained 0·1 per cent (or even less) of silver, can now contain up to 2·6 per cent of this metal. The process of raising the relative proportion of silver in the alloy is known as **Pattinson's process.**

BISMUTH–CADMIUM SYSTEM

The fully labelled phase diagram for the bismuth–cadmium system is shown in Fig. 19. The characteristic features of this sytem are similar to those of lead–silver system described above.

Pure bismuth melts at 317°C and the addition of cadmium to molten bismuth lowers its freezing point along the curve *AC* which is the freezing point curve of bismuth containing varying amounts of cadmium. Similarly, addition of bismuth to molten cadmium lowers the freezing point of cadmium along the curve *BC* which is the freezing point curve of cadmium containing varying amounts of bismuth. In the region above the curves *AC* and *CB*, bismuth and cadmium are present in the form of a melt. Since in this region, $P=1$, $F=2$, *i.e.*, the system is bivariant. The two degrees of freedom are the temperature and the composition. Thus in this region, temperature and composition can be varied without changing the number of phases. Along the curve *AC*, bismuth freezes out and along the curve *BC*, cadmium freezes out. Thus, in the area below *AC* and down to the eutectic point there are two phases, *viz.*, bismuth and liquid whose composition is determined by the temperature. Similarly, in the area below *BC* down to the eutectic, the two phases in equilibrium are cadmium and liquid. Since in these regions, $P=2$, $F=1$, *i.e.*, the system is univariant.

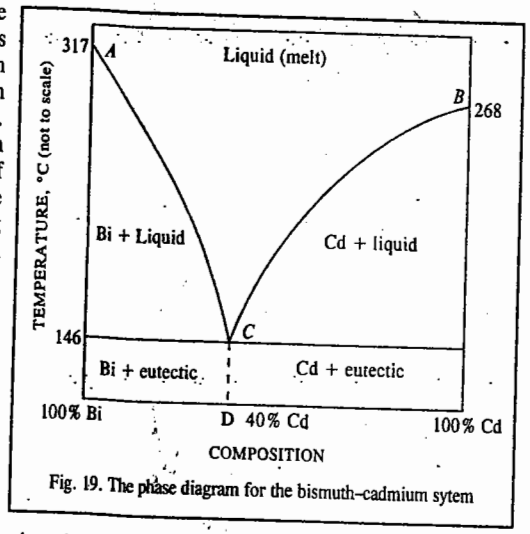

Fig. 19. The phase diagram for the bismuth–cadmium sytem

At the eutectic point *C*, three phases coexist ; these are bismuth, cadmium and liquid. The composition of the eutectic is 40% cadmium. At *C*, $P=3$ so that $F=0$, *i.e.*, the system is invariant. The eutectic temperature is 146°C. The area below the eutectic point is a two-phase region as labelled in the phase diagram. Since in this region $P=2$, $F=1$. Thus, only the temperature need be specified to describe the system completely.

POTASSIUM IODIDE–WATER SYSTEM

The potassium iodide—water system is a typical example of a binary system involving a salt and water which form a eutectic mixture and will be discussed in some details.

One essential feature of a salt—water system is that the melting point of the salt is usually very high, even higher than the critical temperature of water. It is, therefore, not possible to represent melting points of both the components in the equilibrium diagram as has been done in the case of the binary systems involving metals.

The equilibrium diagram of potassium iodide—water system is shown in Fig. 19. Its resemblance with the general diagram for binary systems forming eutectics (Fig. 15) is quite evident. However, the melting point of potassium iodide, as expected, is not realised in practice, as explained above.

A is the melting point of ice (or freezing point of water). At a pressure of 1 atm and in the presence of dissolved air, this temperature is 0°C. As potassium iodide is added, some of it dissolves in the water which was in contact with ice. The number of components rises to two. As the experiments are generally conducted at atmospheric pressure, the vapour pressure of water can be neglected in comparison and hence the vapour phase can be ignored. The system, therefore, may be considered to have two phases, *viz.*, ice and solution. Accordingly, the degree of freedom of the system *at constant*

pressure, will be 1. Thus, corresponding to each temperature, there will be a definite composition of the solution. In other words, if the temperature changes, there will have to be a change in composition (concentration) of the solution and if the composition of the solution changes, there will have to be a corresponding change in temperature.

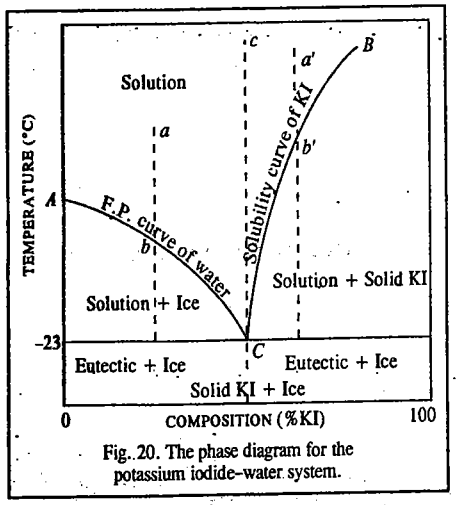

Fig. 20. The phase diagram for the potassium iodide–water system.

If the addition of potassium iodide is continued, there will be a change in the concentration of the solution and there will be a corresponding change in the temperature of the system. This is represented by the curve *AC* which is known as the **freezing point curve of water** (or **fusion curve of ice**). Along this line, the solution (containing potassium iodide in water) is in contact with ice. At the point *C*, the solution becomes saturated and, therefore, potassium iodide also separates out as another solid phase. The system now consists of three phases (solid ice, solid KI and solution) in equilibrium. The point *C*, therefore, is invariant *at a constant pressure*. This is the eutectic point of the system. The temperature at this point is –23°C which is the lowest temperature that can be attained in this system.

If the system at *C* is heated, ice will melt and solid potassium iodide will pass into solution in the same ratio in which it is already present in the solution so that composition of the solution remains unchanged. The temperature of the system does not rise so long as the number of phases is 3. The heat supplied to the system is utilised in bringing about the change of state of ice into water. If heat continues to be supplied to the system and if potassium iodide is present in excess, ultimately ice will disappear. The system will be left with two phases (solid KI and solution) and will become univariant. The temperature will now rise but there will be a corresponding change in composition. The curve *CB* will be traced out. Since solid potassium iodide is in contact with its solution in water along the curve *CB*, this is known as the **solubility curve of potassium iodide**. The steep rise of the curve shows that the solubility of potassium iodide increases slowly with rise of temperature.

It may be noted that along both the curves *AC* and *CB*, the solutions of potassium iodide of varying compositions are in equilibrium with a solid phase, the solid being ice along *AC* and potassium iodide along *CB*. The two curves meet at the eutectic point *C* which has been discussed above. In the area lying above the curves *AC* and *CB*, only solution phase can exist.

The existence of various phases in different regions of the equilibrium diagram is shown in the figure.

If a solution represented by the point *a* is cooled, the temperature will fall along *ab* without any change of composition as the system is bivariant. On reaching *b*, ice will separate out. The system will now become univariant. Therefore, the composition of the solution will change with temperature. Accordingly, on continued cooling, the composition of the solution will move along the freezing point curve *AC* until the eutectic point *C* is reached when potassium iodide will also separate out. The number of phases now rises to 3 and the degree of freedom at constant pressure falls to zero. Ultimately, the whole of the solution will freeze to give the eutectic mixture at a constant temperature. If a solution of composition, say, *a'*, lying on the right of the eutectic point, is cooled, potassium iodide will begin to crystallise out as soon as the point *b'* is reached. The composition will henceforth change with the temperature along *b'C* and more of potassium iodide will continue to separate out until at the eutectic point *C*, ice also begins to deposit. Ultimately, as before, the whole of the solution will freeze to give the eutectic mixture consisting of 52% potassium iodide and 48% ice at a constant temperature.

Finally, consider a solution of composition represented by *c* which lies vertically above the eutectic point. When such a solution is cooled, the temperature will continue to fall along *cC* without any change in composition until the eutectic point *C* is reached when ice and potassium iodide both begin to separate out simultaneously. It will be seen from the above discussion that all solutions on cooling ultimately show an arrest or halt in temperature at the eutectic point. Further, when a solid mixture of the same composition as the eutectic mixture is heated, it melts sharply at the eutectic temperature. Hence, the mixture of potassium iodide and ice deposited at the eutectic point was at one time considered to be a definite compound of the form of a salt hydrate. This was given the name cryohydrate. However, a closer examination showed that physical properties such as density and heat of solution of the eutectic solid were almost exactly equal to the mean values of the two constituents, namely, potassium iodide and ice, indicating that it is a mixture. Further, when the solid was examined under a powerful microscope, both the constituents were seen to lie as separate crystals. There is hardly any doubt, therefore, that the eutectic solid is a mixture and not a compound. The constancy of composition and melting point alone cannot establish a chemical compound.

Freezing Mixtures. The well known observation that the addition of salt to crushed ice produces an appreciable fall in temperature can readily be explained by means of a phase diagram of the kind shown in Fig. 19. Suppose, some salt, such as potassium iodide or sodium chloride, is added to ice in contact with a small amount of water at 0°C (point *A*). As some of the salt will dissolve in the water, there will be three phases, *viz.*, salt, ice and solution in contact with one another. Now three phases can coexist in stable equilibrium only at the eutectic temperature. This temperature, in most cases, is considerably below the normal melting point of ice. Hence, ice will melt and the salt will dissolve in the water thus produced so that the composition varies along the line *AC*. Now, melting of the ice as well as dissolution of the salt are accompanied by absorption of heat. If the system is not in a position to absorb heat from the surroundings, its temperature will fall. This fall, which takes place along the line *AC*, will continue until the eutectic point is reached or until either salt or ice is used up completely. The lowest temperature that can be attained in the presence of excess of a salt and ice depends upon the eutectic temperature of the system.

The eutectic temperatures and eutectic compositions of some of the common systems are given in Table 2.

TABLE 2

Eutectic Temperatures and Eutectic Compositions of Some Common Systems

System	Composition (% salt in the eutectic)	Eutectic Temperature (°C)
NH_4Cl and Ice	20·1	– 16·0
NH_4NO_3 and Ice	43·0	– 18·0
$NaNO_3$ and Ice	33·3	– 18·1
$NaCl.2H_2O$ and Ice	23·0	– 22·0
KI and Ice	52·0	– 23·0
$CaCl_2 \cdot 6H_2O$ and Ice	15·2	– 55·9

Acetone–Dry Ice Freezing Mixture. Another freezing mixture, based on an entirely different principle, is the acetone–dry ice freezing mixture.

Dry ice, *viz.*, solid carbon dioxide, changes directly to the gaseous state under atmospheric pressure. When dry ice is added to acetone contained in a Dewar flask, it sublimes rapidly producing intense cold since the heat required for sublimation is taken from acetone. If sufficient amount of dry ice is added, the temperature of acetone can, theoretically, go down to approaching –95°C, the freezing point of acetone. This exceedingly low temperature can be maintained as long as sufficient amount of dry ice is present in acetone. However, due to radiation factors, etc., the temperature actually attained remains around –60°C which is a sufficiently low temperature indeed.

Type B. SYSTEMS IN WHICH TWO COMPONENTS FORM A STABLE COMPOUND

There are again numerous systems including metals, organic compounds and inorganic salts dissolved in water, which fall under this category. The two components of the system at a certain stage enter

into chemical combination with one another forming stable compounds. Thus, a number of intermetallic compounds when the two components are metals, are formed. Similarly, several double compounds are formed when the two components are organic compounds. In the case of systems involving salt and water, a number of salt hydrates are formed.

Such systems are of two kinds depending upon whether the compound formed has a *congruent* or an *incongruent* melting point.

Class I. Formation of Compounds with Congruent Melting Points. *A compound which melts sharply at a constant temperature into a liquid of the same composition as the solid,* is said to possess a **congruent melting point.** To take a general case, let A and B be the two components and AB a stable solid compound formed by their chemical combination. The phase diagram will be of the type shown in Fig. 21. In this system there are three different solid phases, namely A, B and the compound AB, Accordingly, there will be three fusion or freezing point curves *AC*, *BE* and *CDE*. While along *AC*, the solid A is in equilibrium with the liquid phase and along *BE*, the solid B is in equilibrium with the liquid phase, along the central portion *CDE*, the solid compound AB is in equilibrium with the liquid phase, at different temperatures. The maximum point *D* of the curve is the congruent melting point of the compound because the solid and liquid phases now have the same composition. Evidently, at this temperature, the two-component system has become a one-component system because both solid and liquid phases contain only the compound AB. Therefore, according to the phase rule, *D* is a non-variant point. This represents a definite temperature just like the melting points *A* and *B* of the pure components. The congruent melting point *D* of compound AB has been shown to lie above the melting points of the pure components A and B. But, it is not necessarily so always. There are different types of systems known in which the congruent melting point of the compound formed lies above, below or in-between the melting points of the pure components.

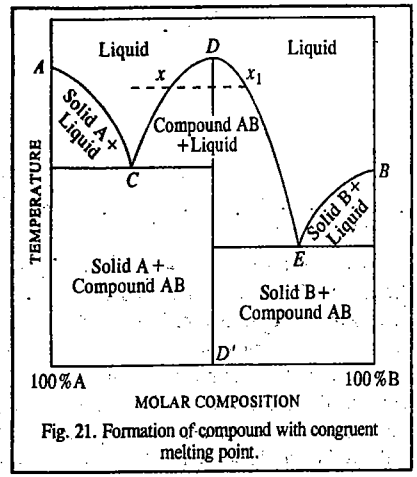

Fig. 21. Formation of compound with congruent melting point.

In the above figure, the compound has been shown to contain equimolar amounts of A and B. This is not necessarily so in every system.

There are two eutectic points in such a system as represented by *C* and *E* in the figure. At *C*, the solids A and AB are in equilibrium with the liquid phase while at *E*, the solids B and AB are in equilibrium with the liquid phase.

It can be seen that at a certain temperature, say, *t*, *the liquid phase can have two compositions, x and x_1 in equilibrium with the same solid* AB. In other words, the compound AB can have two solubilities at the same temperature. This paradox can readily be explained if the diagram is looked upon as made up of two parts with *DD'* as the dividing line. The left half of the diagram shows two-component system : A and AB while the right half shows the two-component system : B and AB. On the left hand side, the curve *DC* represents the usual depression in freezing point of the compound *AB* on the addition of A while on the right hand side, the curve *DE* represents the usual depression in freezing point of the compound *AB* on the addition of B.

The names of the various phases in different areas of the diagram are represented in the figure.

The two component systems which form one or more compounds with congruent melting points

include zinc–magnesium, aluminium–magnesium, mercury–thallium, gold-tin and phenol–aniline systems. Amongst the salt hydrates, $FeCl_3$—H_2O system falls into this category.

Case II. Formation of Compounds with Incongruent Melting Points. In many systems, the compounds formed by the combination of two components, instead of melting congruently, decompose when heated giving a new solid phase and a solution with a composition different from that of the solid phase. Such a compound is said to have an **incongruent melting point.** Its decomposition at this temperature is known as transition reaction or meritectic (or *peritectic*) *reaction* and may be represented by the equation

$$\underset{\text{original solid}}{S_1} \rightleftharpoons \underset{\text{new solid}}{S_2} + \text{solution (or melt)} \qquad \ldots(24)$$

The incongruent melting point is, therefore, also known as **transition temperature** or **meritectic** or **peritectic temperature.**

Since during the peritectic reaction, as represented by the above equation, the number of phases is 3 (two solids and one liquid), the system is invariant (*i.e.*, $F'=0$) as the pressure is fixed. Hence, the temperature as well as the composition of all the phases remain fixed.

The general phase diagram for this type of systems may be represented graphically as in Fig. 22. Let A and B be the two components which combine to form a compound AB_2. The points *A* and *B* represent the respective melting points of the two pure components while *D* represents the incongruent melting point (or transition temperature) of the compound AB_2. Here this compound breaks down to give a new compound. This point lies below *E* which may be taken as the hypothetical congruent melting point of the compound AB_2. *AC* is the fusion curve of *A* along which the solid is in equilibrium with the liquid. *BD* is the fusion curve of *B* along which the solid B is in equilibrium with the liquid. Similarly, *CD* is the fusion curve of the compound AB_2 along which the solid AB_2 is in equilibrium with the liquid.

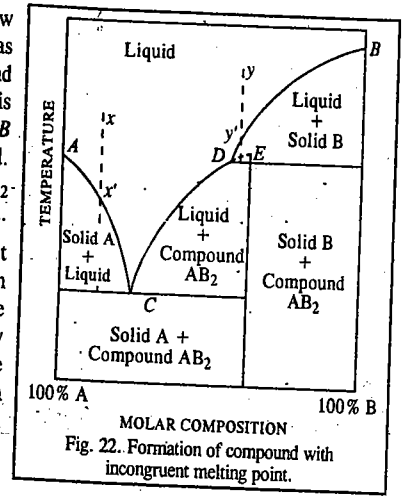

Fig. 22. Formation of compound with incongruent melting point.

On cooling a liquid of composition *x*, A is the first solid to separate out at the point *x'*. Further cooling then proceeds with change of composition along *x'C*. At *C* the compound AB_2 commences to form. Since the system now consists of two solids and one liquid phase (excluding the vapour phase), by applying the reduced phase rule the system at *C* is non-variant. If a liquid of composition *y* is cooled down, the first solid to separate out will be solid *B* at the point *y'*. Further cooling will proceed along *y'D*. At *D*, the meritectic reaction

$$\text{Solid B} + \text{solution} \rightleftharpoons \text{Solid } AB_2$$

takes place and the compound AB_2 separates out. Since the system will now have three phases, it will again become non-variant. The transition of solid B into compound AB_2 will take place at constant temperature till the whole of the solid B disappears. Point *D* is, thus, the peritectic point.

Picric acid–benzene, gold–antimony and sodium–potassium are some examples of two-component systems which give rise to compounds with incongruent melting points. Amongst the salt hydrates, mention may be made of sodium sulphate–water system.

Calculation of Eutectic Point and Eutectic Composition

When a two-component solution is cooled to a low temperature, the component which is present in excess separates out as solid at the freezing point of the solution. The variation of the freezing point with composition is given by the following expressions :

$$d \ln x_A = (\Delta H_{fus,A}/RT^2)\, dT \quad ...(25)$$

$$d \ln x_B = (\Delta H_{fus,B}/RT^2)\, dT \quad ...(26)$$

where the ΔH_{fus}s are the enthalpies of fusion of the two components and x_A and x_B are their mole fractions. Assuming that the components A and B behave ideally and ΔH_{fus} is independent of temperature, we can integrate Eqs. 25 and 26 for the limits $T=T_{fus}$, the melting point and $T=T_e$, the eutectic point, to obtain

$$-\ln (x_A)_e = \frac{\Delta H_{fus,A}}{R}\left(\frac{1}{T_e} - \frac{1}{T_{m,A}}\right) \quad ...(27)$$

and

$$-\ln (x_B)_e = \frac{\Delta H_{fus,B}}{R}\left(\frac{1}{T_e} - \frac{1}{T_{fus,B}}\right) \quad ...(28)$$

Using Eqs. 27 and 28, we can calculate T_e, the eutectic point as well as the eutectic composition, *viz.*, $(x_A)_e$ and $(x_B)_e$.

Example 20. Calculate the eutectic temperature and eutectic composition for a binary solid–liquid system if $\Delta H_{fus,A}$ = 500 cal mol^{-1}, $\Delta H_{fus,B}$ = 1000 cal mol^{-1} and the melting points of pure A and B are 400°C and 600°C, respectively.

Solution : From Eqs. 27 and 28,

$$\ln (x_A)_e = \frac{(500\,\text{cal mol}^{-1})(4{\cdot}184\,\text{J cal}^{-1})}{8{\cdot}314\,\text{J K}^{-1}\,\text{mol}^{-1}}\left(\frac{1}{673\text{K}} - \frac{1}{T_e}\right)$$

$$\ln (x_B)_e = \frac{(1000\,\text{cal mol}^{-1})(4{\cdot}184\,\text{J cal}^{-1})}{8{\cdot}314\,\text{J K}^{-1}\,\text{mol}^{-1}}\left(\frac{1}{873\text{K}} - \frac{1}{T_e}\right)$$

These two equations can be solved simultaneously with $x_A + x_B = 1$ to give $(x_A)_e$ = 0·647, $(x_B)_e$ = 0·352 and T_e = 38°C.

Example 21. For a two-component system, $\Delta H_{fus,A}$ = 500 cal mol^{-1} and $T_{fus,A}$=400°C. If the eutectic temperature is 350°C, calculate the solubility in terms of the fractions of B in A at 350°C.

Solution : According to Eq. 27,

$$\ln (x_A)_e = \frac{\Delta H_{fus,A}}{R}\left(\frac{1}{T_{fus,A}} - \frac{1}{T_e}\right) = \frac{(500\,\text{cal mol}^{-1})(4{\cdot}184\,\text{J cal}^{-1})}{8{\cdot}314\,\text{J K}^{-1}\,\text{mol}^{-1}}\left(\frac{1}{673\text{K}} - \frac{1}{623\text{K}}\right)$$

$\therefore \quad (x_A)_e = 0{\cdot}9333$ and $(x_B)_e = 1 - 0{\cdot}9333 = 0{\cdot}0667$

TYPICAL SOLVED EXAMPLES FOR TWO-COMPONENT SYSTEMS

Example 22. Draw schematic phase diagrams for the following :

***(a)* A temperature-composition phase diagram for a binary system A - B having a single eutectic, a single peritectic (corresponding to the incongruently melting compound AB) and no solid solutions. Label all the areas.**

***(b)* A pressure-composition phase diagram at a given temperature for a binary salt system A - W (where *A* is the anhydrous salt and *W* is water) having compounds A, AW, A.2W, A.4W and A.6W present as solids in equilibrium with vapour. Assume that no liquid phases are formed. Label the lines.**

Solution : The requisite phase diagrams are shown in Fig. 23*(a)* and *(b)*. The diagrams are self-explanatory.

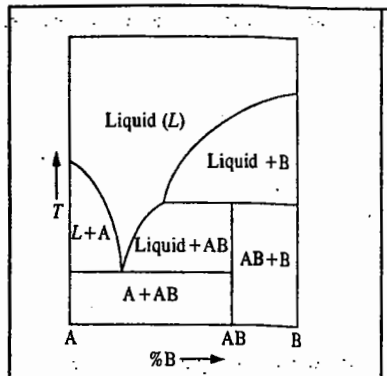

Fig. 23*(a)* Phase diagram for the binary system A–B corresponding to the given data.

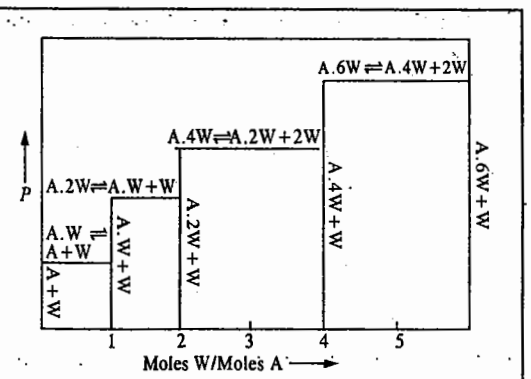

Fig. 23*(b)*. Phase diagram for the binary system A–W corresponding to the given data.

Example 23. Compare the phase diagrams shown in Fig. 24*(a)* and *(b)* below and comment briefly.

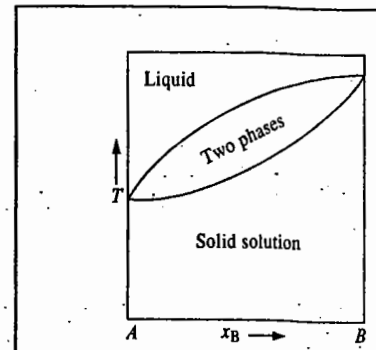

Fig. 24*(a)*

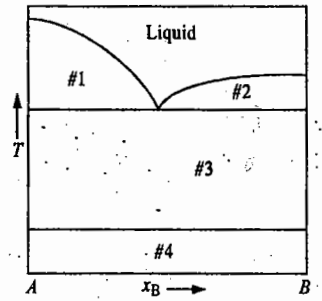

Fig. 24*(b)*

Solution : Fig. 24*(a)* shows complete miscibility of the materials in the solid phase. There are two one-phase areas and one two-phase area. This type of diagram results from the ability of one substance to substitute freely for the other in the crystal lattice because of similarity in the size of molecules (atoms or ions), charge (if any), etc.

Fig. 24*(b)* shows that the two substances are completely immiscible in the solid phase. There are four two-phase areas and one one-phase area. The horizontal 'tie lines' indicate that in area marked #1, the two phases in equilibrium/are solid A and liquid ; in area marked #2, solid B and liquid and in areas marked #3 and #4, solid A and solid B with one of the materials undergoing a phase transition to a second solid.

Example 24. Identify the phases present in the numbered areas of Fig. 25.

Solution : From the figure we see that a *congruently-melting compound is* formed at x_B=0·667 which means that there are two moles of B for every mole of A so that the compound has the empirical formula AB_2. Horizontal 'tie lines' indicate that in area #1, solid A and liquid are in equilibrium; in areas #2 and #4, liquid and solid AB_2; in area #3, solid A and solid AB_2 ; in area #5, solid B and liquid and in area #6, solid B and solid AB_2 are in equilibrium.

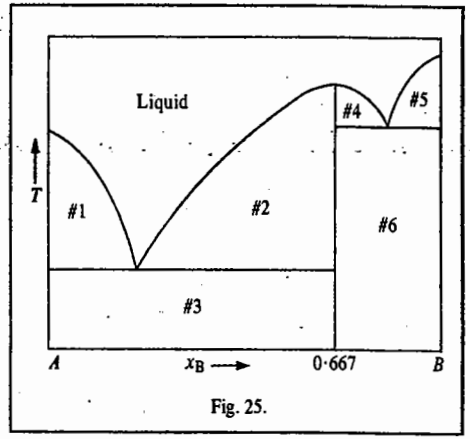

Fig. 25.

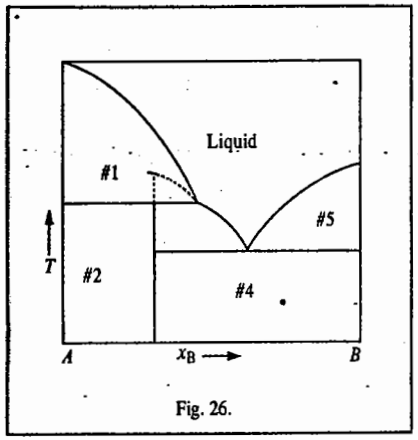

Fig. 26.

Example 25. Identify the phases present in the numbered areas of Fig. 26.

Solution : From the above figure we see that an ***incongruently melting compound*** is formed at $x_B = 0{\cdot}250$ which means that it has an empirical formula of A_3B. **Horizontal 'tie lines'** indicate that in area #1, solid A and liquid are in equilibrium ; in #2, solid A and solid A_3B ; in #3, liquid and solid A_3B ; in #4, solid B and solid A_3B and in #5, solid B and liquid.

THREE-COMPONENT SOLID-LIQUID SYSTEMS

For a three-component system, the phase rule becomes $F=5-P$. For a system having only one phase, the phase diagram must illustrate four variables, which is difficult. Hence, P and T are fixed for a given diagram and triangular graph paper is used to describe the system in terms of the remaining variables—two of the three concentrations. The relative amounts of the three components, usually shown as percentages by mass, can be shown on the triangular plot (Fig. 27). The corners of the triangle labelled A, B and C correspond to the pure components A, B and C, respectively. The side of the triangle opposite the corner labelled A, for instance, implies the absence of A. Thus, the horizontal lines across the triangle show increasing percentage of A from zero at the base to 100% at the apex. Similarly, the percentages of B and C are given by the distances from the other two sides to the remaining two apices. It is possible to read off the composition corresponding to any point from the three composition scales of the diagram. The total composition is always 100 per cent because of the geometrical result that the sum of the three perpendicular distances from any point to the three sides of a triangle is always equal to the height of the triangle.

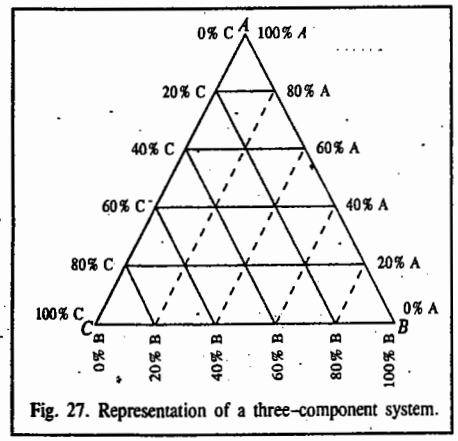

Fig. 27. Representation of a three-component system.

As in the case of two-component systems, the simplest three-component systems are those in which a liquid system breaks down into two phases. The system

CH_3COOH–$CHCl_3$–H_2O

is such a system over a certain temperature range. A two-phase region occurs in systems with relatively low amounts of acetic acid. Fig. 28 shows this system. Here are shown the tie lines through the two-phase regions joining the compositions of the two phases that are in equilibrium. The tie lines, which are experimentally observed, must be specified on the phase diagram in the two-phase regions because they are no longer horizontal as in the two-component diagrams. The tie lines are not used in the three-phase regions. Thus, a total composition corresponding to point a in the two-phase region gives two phases, one of composition b and the other of composition c. A unique point on the two-phase boundary is shown by d. This point, called the **isothermal critical point** or the **plait point,** is similar to the critical solution temperature or consolute temperature in the sense that the compositions of the two phases in equilibrium become equal at this point. Application of the phase rule to a system corresponding to a point in the two-phase region gives $F=3$.

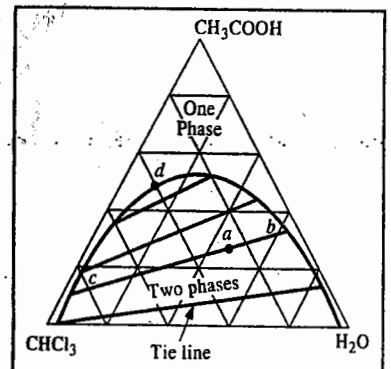

Fig. 28. The three-component system consisting of acetic acid–chloroform–water at 1 atm pressure.

The three degrees of freedom can be accounted for by P, T and one composition variable. We thus find that the composition of both the phases cannot be arbitrarily fixed. If one is fixed, then the tie line from that composition fixes the composition of the second phase.

A system of two salts and water furnishes an example of a three-component system involving solids and liquids. Fig. 29 shows such a system where the two salts show some solubility and also form saturated solutions. Tie lines are drawn to show that the saturated solutions along CD and ED are in equilibrium with the solid salts A and B, respectively. At point D, the solution is in equilibrium with both the salts. If water is removed from the system represented by the point D, the total composition moves towards the base of the triangle. This results in the formation of more solid salts which remain in equilibrium with the decreasing amount but constant concentration of the saturated solution.

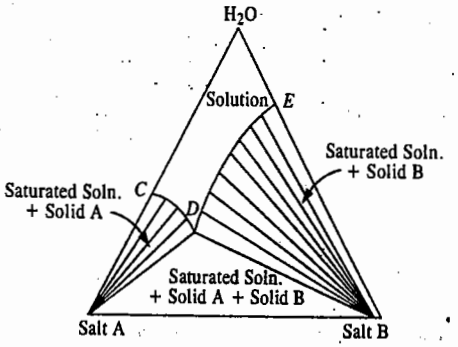

Fig. 29. The phase diagram for a three-component system consisting of two salts and water at a fixed temperature and pressure.

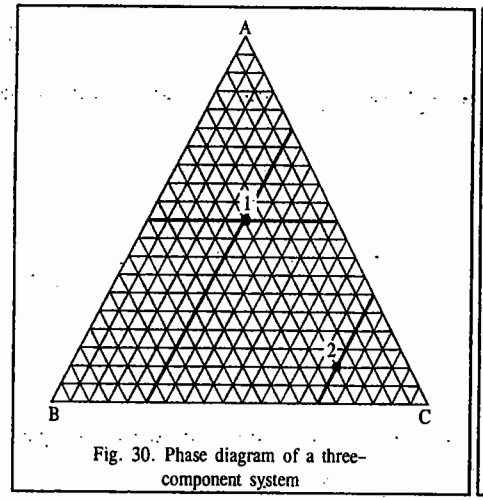

Fig. 30. Phase diagram of a three-component system

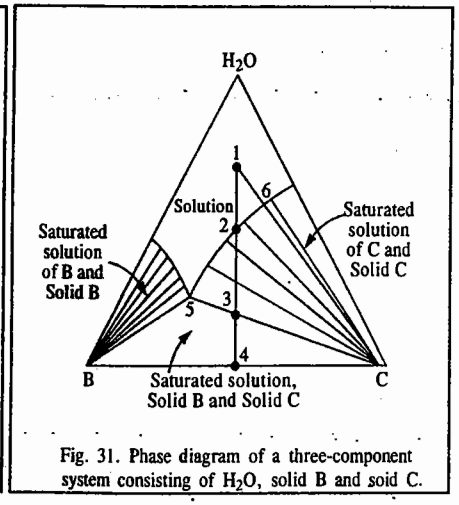

Fig. 31. Phase diagram of a three-component system consisting of H_2O, solid B and soid C.

Example 26. ***(a)*** **Locate the point with x_A=0·50, x_B=x_C=0·25 in Fig. 30.** ***(b)*** **Determine the coordinates of point 2 in Fig. 30.**

Solution : *(a)* Fig. 30. Starting with x_A = 0·50, we find that the point will be located one half the distance between side *BC* and vertex *A*. This is indicated on the graph by a bold horizontal line at x_A = 0·50. Similarly, for x_B, = 0·25, the point will be located on a line one-fourth the distance from side *AC* to vertex *B*. This line is also drawn in bold print. The intersection of these lines (point 1) gives the desired point. We can check that point 1 has x_c=0·25 since the point lies one-fourth the distance from side *AB* to vertex *C*.

(b) Fig. 30. As is evident from the graph, for the point 2, $x_A = 0{\cdot}10$, $x_B = 0{\cdot}70$ and $x_C = 0{\cdot}20$

Example 27. ***(a)*** **Describe the changes that occur in the system shown in Fig. 31 as salt *C* is added to a solution of composition given by point 1.**

(b) **Describe the changes that occur in the system in Fig. 31 as water is evaporated from the composition given by point 1.**

Solution : As pure C is added, the system becomes richer in C and less rich in A and B as indicated by the line drawn from point 1 to vertex *C*. As C is added, it dissolves until sufficient C is present so that the bulk concentration reaches point 6, at which point solid C appears in equilibrium with a solution of concentration given by point 6. Further addition of C only results in a change in the relative amounts of each phase, not the composition.

(b) The following changes occur : we get a solution until point 2 is reached where two phases in equilibrium are solid C and a solution saturated with C. These phases continue until the bulk composition reaches point 3 where three phases in equilibrium are : solid B, solid *C* and a solution saturated with B and C having composition given by point 5. These phases continue till the water is removed giving solid B and solid C, a two-component system, with composition given by point 4.

The Ehrenfest Classification of Phase Transitions

Paul Ehrenfest (1880–1933) devised a scheme for classifying several kinds of phase transitions such as fusion and vaporization and the less common ones like solid–solid, conducting–superconducting and fluid–superfluid transitions. In all these transitions, the behaviour of the chemical potential, μ, a thermodynamic property, plays a prominent role. At the transition point, for the transition from a phase α to another phase β, we find that

$$\left(\frac{\partial \mu_\beta}{\partial P}\right)_T - \left(\frac{\partial \mu_\alpha}{\partial P}\right)_T = V_\beta - V_\alpha = \Delta V_{trs} \qquad \ldots(29)$$

$$\left(\frac{\partial \mu_\beta}{\partial T}\right)_P - \left(\frac{\partial \mu_\alpha}{\partial T}\right)_P = -S_\beta + S_\alpha = -\Delta S_{trs} = -\frac{\Delta H_{trs}}{T} \qquad \ldots(30)$$

Since at the transition, ΔV_{trs} and ΔH_{trs} are non-zero for the processes of melting (fusion) and vaporization, the slopes of μ plotted versus either *P* or *T* are different on either side of the transition (Fig. 32*a*). In other words, the first derivatives of μ with respect to *P* and *T* are discontinuous at the phase transition. A transition is classified as first-order phase transition when $(\partial\mu/\partial T)_P$ is discontinuous at the transition. For a substance, C_p {which is defined as $(\partial H/\partial T)_P$} is the slope of a plot of enthalpy *H* with respect to temperature *T*. At a first-order phase transition, *H* changes by a finite amount for an infinitesimal change in *T*. Hence, at the transition temperature, T_{trs}, the constant pressure heat capacity C_p is infinite, the physical reason being that heating drives the transition rather than raising the temperature.

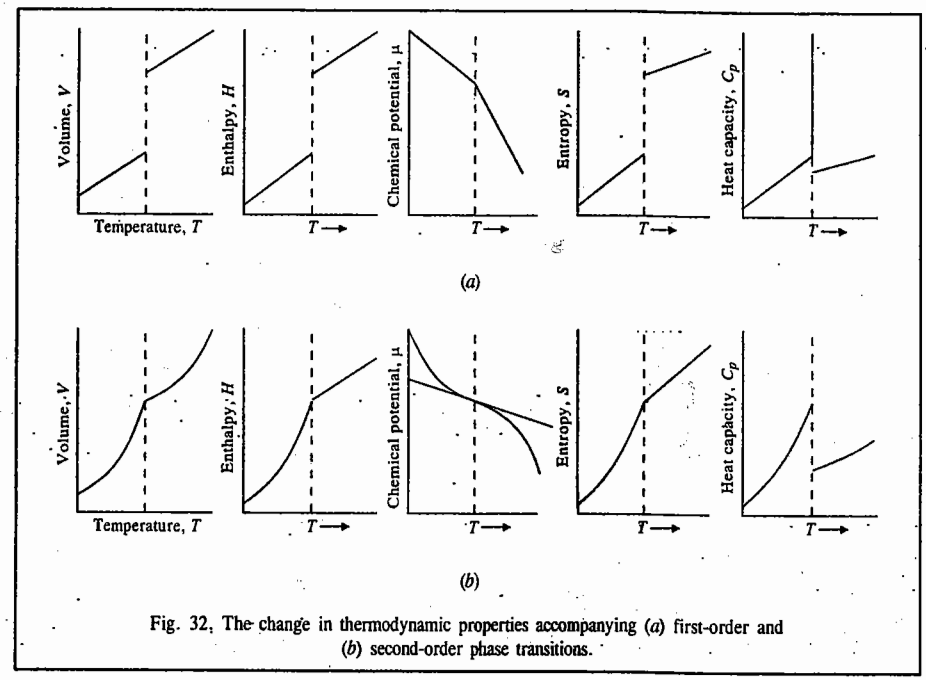

Fig. 32, The change in thermodynamic properties accompanying (*a*) first-order and (*b*) second-order phase transitions.

For a second-order phase transition, $(\partial\mu/\partial T)_P$ is continuous but $(\partial^2\mu/\partial T^2)_P$ (the second-order derivative with respect to temperature) is discontinuous. A continuous slope of μ (a graph with the same slope on either side of the transition) implies that the volume *V* and the entropy *S* (and hence the enthalpy *H*) do not change at the transition (Fig. 32*b*). The heat capacity C_p is discontinuous at the transition but does not become infinite there. An example of a second-order phase transition is the conducting-superconducting transition in metals at extremely low temperatures.

Thus, in first-order or discontinuous transitions, $\Delta H_{trs} \neq 0$ and ΔV_{trs} is also $\neq 0$. In higher order or continuous transitions, $\Delta H_{trs} = 0$ and also $\Delta V_{trs} = 0$. The known higher-order transitions are either second-order transitions or lambda transitions. For a second-order transition, as we said above, $\Delta H_{trs} = 0$ and $\Delta V_{trs} = 0$ and C_p does not become infinite at the transition temperature T_{trs} but does change by a finite amount. The term **λ-transition** (*i.e.*, lambda transition) is a phase transition that is

not first-order (here $\Delta H_{trs} = \Delta V_{trs} = 0$). At the transition temperature (in this case, the lambda point T_λ), C_p shows one of the following two behaviours : either (*a*) C_p goes to infinity as T_λ is approached from the above and from below (Fig. 33*c*) or (*b*) C_p goes to a very large finite value as T_λ is approached from above and below and the slope $\partial C_p/\partial T$ is infinite at T_λ. Fig. 33 shows the C_p versus T curves for the various phase transitions mentioned above.

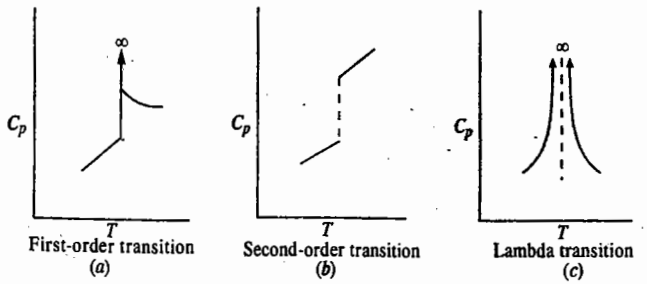

Fig. 33. C_p *versus* T in the region of (*a*) a first-order phase transition ; (*b*) a second-order phase transition ; (*c*) a lambda transition. For some lambda transitions, C_p goes to a very large finite value (rather than ∞) at T_λ.

Examples of lambda transitions include the transition between liquid helium-I and liquid helium-II in ^{4}He ; the transition between ferromagnetism and paramagnetism in metals like Fe or Ni and order–disorder transitions in certain alloys, for example, β-brass (Cu–Zn).

β-brass is a nearly equimolar mixture of Zn and Cu ; for simplicity, let us assume an exactly equimolar mixture. The crystal structure of brass has each atom surrounded by eight nearest neighbours that lie at the corners of a cube. Interatomic forces are such that the lowest-energy arrangement of atoms in the crystal is a completely ordered structure with each Zn atom surrounded by eight Cu atoms and each Cu atom surrounded by eight Zn atoms. (Imagine two interpenetrating cubic arrays of Cu atoms and one of Zn atoms.) Close to 0 K, this is the crystal structure. As the alloy is warmed from temperature T near zero, part of the added energy is used in interchanging Cu and Zn atoms randomly. The degree of disorder increases as T increases. This increase is a cooperative phenomenon in the sense that the greater the disorder, the easier it is to produce further disorder energetically. The rate of change in the degree of disorder with respect to T increases as the lambda point T_λ = 739 K is approached and this rate becomes infinite at T_λ thereby making C_p infinite at T_λ.

At T_λ, all the long-range order in the solid disappears, meaning that an atom located at a site that was originally occupied by a Cu atom at 0 K is now likely to be occupied by a Zn atom or a Cu atom. However, at T_λ, there still remains some short-range order, meaning that it is still somewhat more than 50% probable that a given neighbour of a Cu atom will be a Zn atom. The short-range order finally disappears at a temperature somewhat close to T_λ ; when this happens, the eight atoms that surround a Cu atom will have an average of four Zn atoms and four Cu atoms. At T_λ, the rate of change of both the short-range order and the long-range order with respect to T is infinite.

Another type of second-order transition is associated with a change in symmetry of the crystal structure of a solid. Consider, for instance, the arrangement of atoms in a solid like the one shown in Fig. 34*a* with one unit cell dimension longer than the other two, which are equal. Such a crystal is classified as tetragonal. Now suppose the two shorter dimensions increase more than the long dimension when the temperature is raised. A stage comes when the three dimensions become equal ; at that

point the crystal has cubic symmetry (Fig. 34*b*) and at higher temperature it will expand equally in all the three directions (since there is no longer any distinction between them). In this way, a tetragonal → cubic phase transition occurs ; However, it does not involve a discontinuity in the interaction energy between the atoms or the volume they occupy. The transition is thus not first-order.

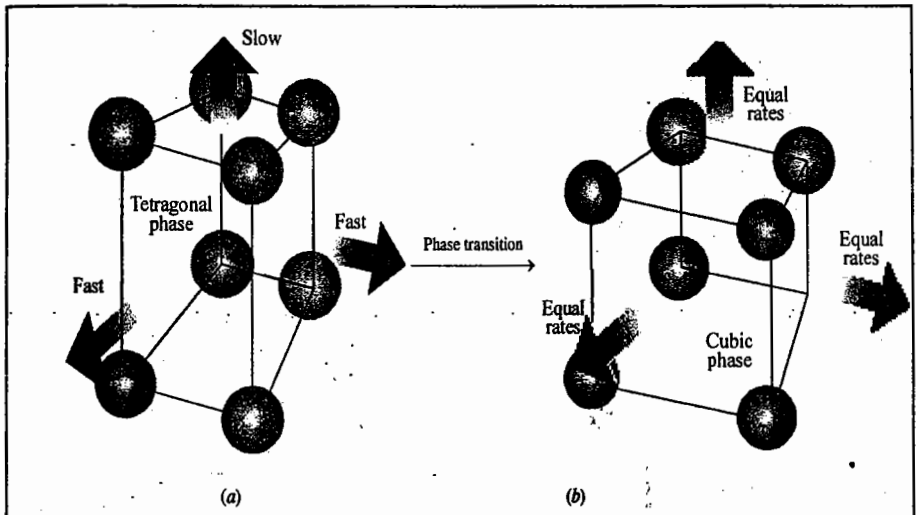

Fig. 34. One version of a second-order phase transition in which (*a*) a tetragonal phase expands more rapidly in two directions than in a third and hence becomes a cubic phase while (*b*) expands uniformly in three directions as the temperature is raised. There is no rearrangement of atoms at the transition temperature and hence does not involve any enthalpy of transition.

I. Review Questions

1. State the phase rule. Explain the various terms involved. Discuss the derivation of the phase rule.
2. Draw schematically the phase diagram for the Water System and apply the Gibbs phase rule to it.
3. Draw and discuss the phase diagram for carbon dioxide system. In what respects does this system differ from the water system.
4. Draw and discuss the phase diagram for the sulphur system.
5. How do you account for the fact that in the phase diagram for a one-component system, the slope of the line representing the solid ⇌ vapour equilibrium is generally more than that of the line representing the liquid ⇌ vapour equilibrium ?
6. Explain how with the help of Clapeyron-Clausius equation, you would predict the following :
   (1) Effect of pressure on the melting point of ice
   (2) Effect of pressure on the melting point of sulphur
   (3) Effect of pressure on the transition temperature of sulphur rhombic.
7. Draw phase diagrams for two-component systems in which the two components form *(i)* a eutectic mixture *(ii)* a stable compound with congruent melting point *(iii)* a compound with incongruent melting point. Apply the phase rule to these diagrams.

8. What is meant by a cooling curve ? Draw and discuss the cooling curves for a two-component system in which the two components are not miscible in solid state and form a eutectic mixture.
9. Draw and discuss the phase diagrams for the following systems.: 1. Lead-Silver 2. Bismuth-Cadmium.
10. Discuss the application of the phase rule to potassium iodide-water system. Explain the formation of freezing mixtures by the addition of suitable salts to ice. Write a note on acetone-dry ice freezing mixture.
11. Draw and discuss the phase diagram for ferric chloride-water system. What changes are observed if a solution of ferric chloride is subjected to isothermal evaporation at 50°C.
12. Discuss the application of the phase rule to solid-gas equilibria taking into consideration the formation of various hydrates of copper sulphate.
13. How are three-component systems studied with the help of the phase rule ? Discuss briefly the system CH_3COOH-$CHCl_3$-H_2O.
14. Draw and discuss the phase diagram for a three-component system consisting of two solids *A* and *B* and water.

II. Problems

1. Prepare a phase diagram for the CO_2 system using the following data : Solid CO_2 (dry ice) sublimes at 1 bar pressure and –78°C. The triple point is at 5·18 bar and 56·6°C. The critical point is at 74 bar and 31·1°C. The density of solid is 1·56 g ml^{-1} and of the liquid 1·11 g ml^{-1}. The enthalpy of fusion is 8·34 kJ mol^{-1}.
2. From the following data : Density of ice at 0°C=0·92 g ml^{-1}, density of water at 0°C=0·9998 g ml^{-1}, density of sulphur rhombic=2·06 g mol^{-1}, density of monoclinic sulphur=1·95 g ml^{-1}, molar heat of fusion of ice =6·02 kJ, molar heat of vaporisation of water =40·6 kJ, molar heat of transition of S_R to S_M =0·322 kJ; Calculate
   (1) Variation of freezing point of water by 1 atm increase in pressure
   (2) Variation of vapour pressure of water by 1°C increase in temperature
   (3) Variation of transistion temperature of S_R to S_M by 1 atm increase of pressure.

   [Ans. 1. 0·0075° 2. 27·08 mm Hg 3. 0·011°]
3. Determine the number of components, number of phases and the degrees of freedom for the following systems :
   (a) $H_2O(s) \rightleftharpoons H_2O(l) \rightleftharpoons H_2O(g)$
   (b) $CaCO_3(s) \rightleftharpoons CaO(s) + CO_2(g)$
   (c) $Na_2SO_4.10H_2O(s) \rightleftharpoons Na_2SO_4(s) + 10H_2O(g)$
   (d) $N_2(g) + O_2(g) \rightleftharpoons 2NO(g)$
   (e) A eutectic mixture in a binary system.
   (f) $PCl_5(g) \rightleftharpoons PCl_3(g) + Cl_2(g)$ when *(i)* $p_{Cl_3} = p_{Cl_2}$ and $p_{PCl_3} \neq p_{Cl_2}$

   [Ans. *(a)* 1, 3, 0 *(b)* 2, 3, 1 *(c)* 2, 3, 1 *(d)* 2, 1, 3 *(e)* 2, 2, 2 *(f)* *(i)* 1, 1, 2 *(ii)* (2, 1, 3]
4. Determine the number of components, number of phases and the degrees of freedom in the following equilibria :
   (a) $N_2O_4(g) \rightleftharpoons 2NO_2(g)$
   (b) $NH_4Cl(s) \rightleftharpoons NH_3(g) + HCl(g)$ when $p_{NH_3} = p_{HCl}$
   (c) $NH_4Cl(s) \rightleftharpoons NH_3(g) + HCl(g)$ when $p_{NH_3} \neq p_{HCl}$
   (d) A liquid at its critical point
   (e) A binary azeotrope **[Ans. *(a)* 1, 1, 2 *(b)* 1, 2, 1 *(c)* 2, 2, 2 *(d)* 1, 2, 0 *(e)* 2, 2, 1]**
5. Two components *A* (melting point 0°C) and *B* (melting point –25°C) form two compounds *X* and *Y* melting congruently. *X* melts at –49·5°C and contains 40 mole percent *B* while *Y* melts at –39°C and contains 60 mole percent *B*. There are three eutectic points at –51·0°C, 28 mole percent *B* ; –63·5°C, 48 mole percent *B* and –49·4 C, 66 mole percent *B*. Construct the phase diagram and determine the formulae of *X* and *Y*. **[Ans. A_3B_2, A_2B_3]**

CHAPTER 19

THE NERNST DISTRIBUTION LAW

Nernst Distribution law. In 1872, Berthelot and Jungfleish found that when solutions of iodine in carbon disulphide, of different concentrations, were shaken with distilled water, the iodine distributed itself between the two solvents in such a way that, at a given temperature, the ratio of its concentrations in the two layers was constant, irrespective of the amount of iodine. In other words,

$$\frac{[I_2]_{CS_2}}{[I]_{H_2O}} = c_1/c_2 = K_D \qquad ...(1)$$

The constant K_D is termed as the **partition coefficient** or **distribution coefficient.**

Nernst, however, showed that the ratio c_1/c_2 is constant only when the solute has the same molecular conditions, *i.e.*, the same molar mass in the two solvents. If a solute partly associates to form double molecules in one solvent but not in the other, the law is valid only if the ratio of concentrations of single molecules in the two phases is taken into consideration.

The distribution of benzoic acid between water and benzene may be taken as a typical example. In water, the acid exists mostly as single molecules, *i.e.*, as C_6H_5COOH. In benzene, however, benzoic acid exists as associated molecules, *i.e.*, as $(C_6H_5COOH)_2$, along with only a small proportion of single molecules. The Nernst distribution law is valid only for concentrations of single molecules in the two phases. Therefore, if total concentration of benzoic acid in benzene is taken, the law will not hold good.

The Nernst distribution law may thus be stated as follows :

When a solute distributes itself between two immiscible solvents in contact with each other, there exists, for similar molecular species, at a given temperature, a constant ratio of distribution between the two solvents irrespective of the total amount of the solute and irrespective of any other molecular species which may be present.

Conditions for the validity of the distribution law. The two essential prerequisites for the validity of the distribution law are :

1. Constant temperature and
2. Existence of similar molecular species in the two phases in contact with each other.

In addition, the following conditions are also necessary :

1. *The solutions are dilute.* The departures usually set in at higher concentrations. Generally speaking, the higher the concentration, the larger is the deviation. In an extreme case, both the solvents may be saturated with respect to the solute. Then, the partition coefficient, K_D, is given by

$$K_D = s_1/s_2 \qquad ...(2)$$

where s_1 and s_2 are the solubilities of the solute in the two solvent layers. The above equation will be strictly valid only if s_1 and s_2 are not large, *i.e.*, if the solute is sparingly soluble in each solvent.

2. The two liquids are mutually immiscible or only very sparingly miscible (*e.g.*, benzene and water) and their mutual miscibility is not altered by the presence of the solute.

Thermodynamic Derivation. Suppose a solute A is present in two immiscible solvents 1 and 2 in contact with each other. Suppose further that its chemical potential in solvent 1 is μ_1 and in solvent 2 is μ_2. When two phases are in equilibrium, their chemical potentials will be equal to one another, *i.e.*,

$$\mu_1 = \mu_2 \qquad ...(3)$$

Since $$\mu = \mu^\circ + RT \ln a, \qquad ...(4)$$

therefore, $$\mu_1 = \mu_1^\circ + RT \ln a_1 \quad \text{for Phase 1} \qquad ...(5)$$

and $$\mu_2 = \mu_2^\circ + RT \ln a_2 \quad \text{for Phase 2} \qquad ...(6)$$

Hence, $$\mu_1^\circ + RT \ln a_1 = \mu_2^\circ + RT \ln a_2$$

or $$RT \ln(a_1/a_2) = \mu_2^\circ - \mu_1^\circ \qquad ...(7)$$

Now, at constant temperature, the standard chemical potentials μ_1° and μ_2° are constant. Since R is also a constant (being the gas constant), it follows that

$$a_1/a_2 = \text{constant (at constant temperature)} \qquad ...(8)$$

Since the solutions are dilute, they behave ideally and hence Henry's law, according to which activity is proportional to mole fraction, is obeyed in each phase.

$$\therefore \quad a_1/a_2 = k_1x_1/k_2x_2 = \text{constant (at constant temperature)} \qquad ...(9)$$

where x_1 and x_2 are the mole fractions of the solute in the two phases and k_1 and k_2 are the Henry's law constants for the solute in the two phases.

$$\therefore \quad x_1/x_2 = \text{constant (at constant temperature)} \qquad ...(10)$$

Further, since the solutions are dilute, the ratio of the mole fractions is almost the same as the ratio of the concentrations. Hence,

$$\because \quad x_1/x_2 = c_1/c_2 = \text{constant (at constant temperature)} \qquad ...(11)$$

Thus, if a substance is present in two phases in contact with each other, then, at equilibrium,

$$\therefore \quad c_1/c_2 = \text{constant (at constant temperature)} = K_D$$

This is the Nernst distribution law.

Let us consider cases in which a solute may associate or dissociate or enter into chemical combination with one of the solvents.

1. Association of the solute in one of the solvents. Let X represent the molecular formula of the solute. Let it remain as such in the first phase marked I (Fig. 1) in which its concentration is c_1. Suppose it is largely associated to give the molecules $(X)_n$ in the second phase marked II. The associated molecules will exist in equilibrium with single molecules as shown. Let c_2 be the total concentration of the solute in this phase.

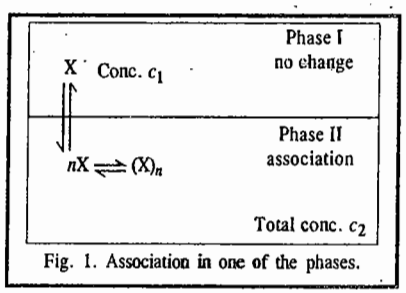

Fig. 1. Association in one of the phases.

Applying the law of chemical equilibrium to the equilibrium between the associated and single molecules, *viz.*, $(X)_n \rightleftharpoons nX$, in the second phase, we have

$$K = [X]^n/[(X)_n] \qquad ...(12)$$

or $$[X] = \sqrt[n]{K \times [(X)_n]} = \text{constant} \times \sqrt[n]{[(X)_n]} \qquad ...(13)$$

If the solute exists largely as associated molecules, which is generally true except at large dilutions, the concentration of the associated molecules, $[(X)_n]$ may be taken as equal to c_2, the total concentration, *i.e.*,

$$[(X)_n] = c_2 \qquad ...(14)$$

From Eqs. 13 and 14, $$[X] = \text{constant} \times \sqrt[n]{c_2} \qquad ...(15)$$

Since the distribution law is valid only for concentrations of similar molecular species in the two phases, hence,

$$c_1/[X] = \text{constant} \qquad ...(16)$$

From Eqs. 15 and 16, $$c_1/\sqrt[n]{c_2} = \text{constant} = K_D \qquad ...(17)$$

Eq. 17 has been checked by studying the distribution of benzoic acid between water and benzene. The acid exists almost entirely as $(C_6H_5COOH)_2$ in benzene but in normal state in water.

Example 1. Experiments in the study of the distribution of phenol between water and chloroform gave the following results :

Concentration in aqueous solutions (c_1)	**0·094**	**0·163**	**0·254**	**0·436**
Concentration in chloroform solution (c_2)	**0·254**	**0·761**	**1·850**	**5·430**

What conclusion can be drawn from these results concerning the molecular condition of phenol in chloroform solution ?

Solution : Phenol in choloroform may be present either as normal molecules or as associated molecules. In the former case, the ratio c_1/c_2 should be constant while in the latter case, the ratio $c/\sqrt[n]{c_2}$ should be constant, n giving the number of molecules of phenol which associate to give a single associated molecule.

The values of c_1/c_2 in the various cases come out to be as follows :

$$c_1/c_2 = \frac{0\cdot094}{0\cdot254} = 0\cdot3701\,;\ \frac{0\cdot163}{0\cdot761} = 0\cdot2142\,;\ \frac{0\cdot254}{1\cdot850} = 0\cdot1373\,;\ \frac{0\cdot436}{5\cdot430} = 0\cdot0803$$

Evidently, the ratio c/c_2 is not constant. Hence, phenol does not exist as single molecules in chloroform.

The values of $c/\sqrt{c_2}$ in the various cases come out to be as follows :

$$\frac{c_1}{\sqrt{c_2}} = \frac{0\cdot094}{\sqrt{0\cdot254}} = 0\cdot1855\ ;\ \frac{0\cdot163}{\sqrt{0\cdot761}} = 0\cdot1868\,;\ \frac{0\cdot254}{\sqrt{1\cdot850}} = 0\cdot1867\,;\ \frac{0\cdot436}{\sqrt{5\cdot430}} = 0\cdot1871$$

A fairly constant value of $c_1/\sqrt{c_2}$ shows that phenol exists as **double molecules in chloroform.**

Example 2. For the distribution of an organic solute between water (c_1) and chloroform (c_2), the following results were obtained :

c_1	**0·0160**	**0·0237**
c_2	**0·338**	**0·753**

Determine the molecular state of the solute in chloroform.

Solution : Let us assume that

$$c_2/c_1 = K_D \qquad \text{(Nernst distribution law)}$$

For the first step, $c_2/c_1 = 0\cdot338/0\cdot160 = 21\cdot1$ and for the second step, $c_2/c_1 = 0\cdot753/0\cdot0237 = 31\cdot8$. The two values are different, hence our assumption is wrong.

Let us now assume that $\sqrt{c_2}/c_1 = K_D$, *i.e.*, the solute exists as a dimer in chloroform. We find that for the first and the second steps, the values of $\sqrt{c_2}/c_1$ are 36·3 and 36·6, respectively. Since the two values are practically the same, hence $\sqrt{c_2}/c_1$ is constant. The solute thus exists as a dimer in chloroform.

2. Dissociation of the solute in one of the solvents. Let X, as before, represent the normal formula of the solute. Suppose, it does not dissociate in the solvent marked I (Fig. 2) but dissociates into A and B in the solvent marked II. Let c_1 be its concentration in the first solvent and c_2, the total concentration in the second solvent. The distribution law is valid only for the ratio of concentrations of similar molecular species in the two solvents.

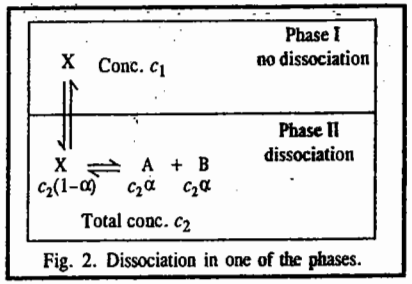

Fig. 2. Dissociation in one of the phases.

Suppose, α is the degree of dissociation of the solute X in phase II. Then, the concentrations of the various species would be as shown below :

$$\underset{c_2(1-\alpha)}{X} \rightleftharpoons \underset{c_2\alpha}{A} + \underset{c_2\alpha}{B}$$

Therefore, according to the distribution law,

$$c_1/[c_2(1-\alpha)] = K_D \qquad ...(18)$$

3. Solute enters into chemical combination with one of the solvents. When the solute enters into chemical combination with one of the solvents, there is no change in the general equation of the Nernst distribution law, as shown below.

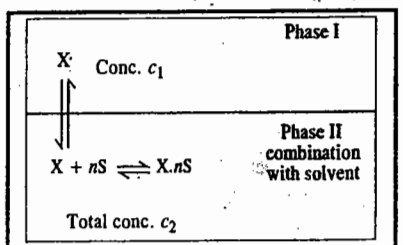

Fig. 3. Combination with the solvent.

Let c_1 be the concentration of the solute X in one of the solvents in which it does not undergo any chemical change (Fig. 3) and c_2 its total concentration in the second solvent with which it enters into chemical combination forming complex molecules, as represented by the equation

$$X + nS \rightleftharpoons X.nS \qquad ...(19)$$

If α is the fraction of the solute that enters into chemical combination with the solvent, then the concentration of the various molecular species would be as follows :

Concentration of uncombined solute molecules $= c_2(1-\alpha)$

Concentration of the complex molecules formed $= c_2\alpha$

Applying the law of chemical equilibrium to the equilibrium represented by Eq. 19, we have

$$K = \frac{c_2\alpha}{c_2(1-\alpha)[\text{solvent}]^n} \qquad ...(20)$$

Since the solvent is in large excess, its concentration may be taken as constant.

$$c_2\alpha/[c_2(1-\alpha)] = \text{constant} \qquad ...(21)$$

Since the distribution law is valid only for concentrations of similar molecular species, *i.e.*, single molecules of *X*, in both the solvents, hence,

$$c_1/[c_2(1-\alpha)] = \text{constant} \qquad ...(22)$$

Dividing Eq. 22 by Eq. 21, we have

$$c_1/c_2\alpha = \text{constant} \qquad ...(23)$$

Now, α, the fraction of the solute that combines with the same solvent, is also constant at a given temperature. Eq. 23 may, therefore, be written as

$$c_1/c_2 = \text{constant} \qquad ...(24)$$

Thus, *the combination of the solute with one of the solvents does not make any change in the fundamental equation of the distribution law except in changing the numerical value of the partition coefficient.*

Applications of Nernst Distribution Law

1. Study of Association of a Solute. As shown above, if a solute associates in one of the solvents in which its concentration is c_2 but not in the other in which its concentration is c_1, then

$$c_1/\sqrt[n]{c_2} = K_D \qquad ...(Eq. 17)$$

n being the number of simple molecules which combine to form one associated molecule. It has thus been possible to show by studying distribution of acetic acid and benzoic acid between water and benzene that these substances exist in benzene as double molecules (or dimers), the value of *n* being 2.

2. Study of Dissociation of a Solute. As has been shown earlier, if a solute undergoes dissociation in one of the solvents in which its concentration is c_2 but not in the other in which its concentration is c_1, then,

$$c_1/[c_2(1-\alpha)] = K_D \qquad (Eq. 18)$$

Thus, if the degree of dissociation (α) of a solute is known at one concentration, its value at any other concentration can be obtained, since K_D is constant.

3. Distribution Indicators. It is a common experience that iodine distributes itself considerably more in carbon disulphide than in water when both the solvents are in contact with each other. Therefore, an extremely dilute solution of iodine in water can be successfully titrated by adding a drop or two of carbon disulphide. The concentration in the carbon disulphide layer becomes large enough to give a distinct violet colour.

4. Study of Complex Ions. The Nernst distribution law has been successfully applied in determining the formula of the complex ions formed between bromine and bromide ion as well as between iodine and iodide ion. The following example will illustrate the method.

On shaking a solution of iodine in carbon disulphide with water, the iodine distributes itself between the two solvents in accordance with the distribution law. Knowing the concentrations of iodine in the two layers, the partition coefficient, K_D, can be determined.

Now, suppose a solution of iodine in carbon disulphide containing *X* moles of iodine per litre is shaken with an aqueous solution of potassium iodide containing *A* moles of potassium iodide per litre (Fig. 4). The total concentration of iodine in the aqueous layer will now be much higher due to formation of the soluble complex KI_3. Let this concentration be *B* moles per litre. Evidently, the concentration of iodine in carbon disulphide layer will fall to $(X - B)$ moles per litre. The concentration of *free iodine* (as I_2) in aqueous solution, according to the Nernst distribution law, should be $= K_D(X - B) = D$ moles per litre (say)

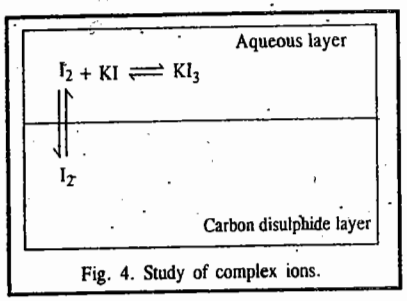

Fig. 4. Study of complex ions.

Suppose the complex ion formed is I_3^-. Then, the following equilibrium will exist in aqueous solution:

$$I^- + I_2 \rightleftharpoons I_3^-$$

Evidently, $B - D$ moles of iodine must have combined with $B - D$ moles of iodide ions (assuming that potassium iodide is completely ionised) to give $B - D$ moles of the complex ion I_3^-.

Therefore, the equilibrium constant will be given by

$$K = [I_3^-]/([I_2]\,[I^-]) \qquad ...(25)$$

The concentrations of the various species in the aqueous layer will be as follows :

$[I_3^-] = B - D$ mol dm^{-3}; $[I_2] = D$ mol dm^{-3} ; $[I^-] = A - (B - D)$ mol dm^{-3}

The results of determinations carried out at 30°C are given in Table 1.

TABLE 1

Study of Complex Ions

A (mol dm^{-3})	B (mol dm^{-3})	D (mol dm^{-3})	K dm^3 mol^{-1}
0·250	0·1111	0·0261	19·72
0·125	0·0686	0·0259	20·04
0·0625	0·0625	0·0257	20·40

The fact that K is reasonably constant, in spite of variations in A and B, shows that the formula of the complex ion is I_3^-.

Example 3. Calculate the dissociation constant of KI_3 from the following data : 37·8 g of iodine were shaken up with one litre of carbon disulphide and one litre of potassium iodide solution in water containing 7·92 g of KI. 35·67 g of iodine were found to be present in carbon disulphide layer. The partition coefficient K_D=410 in favour of carbon disulphide.

Solution : The dissociation of KI_3 is represented as

$$KI_3(aq) \rightleftharpoons KI(aq) + I_2$$

or $$I_3^-(aq) \rightleftharpoons I^-(aq) + I_2$$

$$\therefore \quad K = [I^-][I_2]/[I_3^-]$$

According to the Nernst distribution law,

$$K_D = \frac{[I_2]_{H_2O}}{[I_2]_{CS_2}} = \frac{1}{410}$$

$$\therefore \quad [I_2]_{H_2O} = [I_2]_{CS_2} \times \frac{1}{410}$$

$[I_2]_{CS_2}$ = 35·67 g dm^{-3}/254 g mol^{-1} = 0·1405 mol dm^{-3}

$[I_2]_{H_2O}$ = 0·1405 mol dm^{-3}/410 = 0·000343 mol dm^{-3}

Total free and combined iodine in aqueous layer = (37·8 - 35·67) g dm^{-3}

= 2·13 g dm^{-3} = 2·13 g dm^{-3}/254 g mol^{-1} = 0·008386 mol dm^{-3}

Free iodine in aqueous layer = 0·000343 mol dm^{-3}

Combined iodine in aqueous layer = 0·008386 - 0·000343 = 0·008043 mol dm^{-3}

Since molar concentrations of combined I_2 and I_3^- ion are the same, hence,

Concentration of KI_3 in aqueous layer = 0·008043 mol dm^{-3}

Total concentration of KI in aqueous layer = 7·92 g dm^{-3}/166 g mol^{-1} = 0·04775 mol dm^{-3}

Concentration of free KI or I^- in aqueous layer = (0·04775 - 0·00804) mol dm^{-3} = 0·03971 mol dm^{-3}

Hence, $$K = [I^-][I_2]/[I_3^-] = \frac{(0{\cdot}03971 \text{ mol dm}^{-3})(0{\cdot}000343 \text{ mol dm}^{-3})}{0{\cdot}008043 \text{ mol dm}^{-3}} = \mathbf{0{\cdot}00169 \text{ mol dm}^{-3}}$$

5. Solvent Extraction. The most important application of the distribution law is in the process of extraction, in the laboratory as well as in industry. In the laboratory, for instance, it is frequently used for the removal of a dissolved organic substance from aqueous solution with solvents such as benzene, ether, chloroform, carbon tetrachloride, etc. The advantage is taken of the fact that the partition coefficient of most of the organic compounds is very largely in favour of organic solvents.

The same principle applies in the desilverization of lead by **Parke's process.** The argentiferous lead is melted and heated to 800°C. Molten zinc is then added. Molten lead and molten zinc behave as two immiscible liquids in contact with each other and silver behaves as a solute which is more soluble in zinc than in lead, the partition coefficient being of the order of 300 at 800°C. Silver, therefore, passes readily from the heavier lead layer into the lighter zinc layer which is separated. By repeating the process three or four times, almost the entire amount of silver passes into the zinc layer.

We can derive a general formula which enables the calculation of the amount of the solute that is left **unextracted** after a given number of operations. Let V ml of a solution containing W gram of solute be repeatedly exracted with v ml of another solvent which is immiscible with the first. Let w_1 be the mass of the solute that remains unextracted at the end of the first operation. Then, K_D will be given by

$$\frac{w_1/V}{(W - w_1)/v} = K_D \qquad \ldots(26)$$

or $$w_1 = W\frac{K_D V}{K_D V + v} \qquad \ldots(27)$$

Similarly, at the end of the second extraction, the amount w_2 that remains unextracted is given by

$$w_2 = w_1\frac{K_D V}{K_D V + v} = W\left(\frac{K_D V}{K_D V + v}\right)^2 \qquad \ldots(28)$$

In general, the amount that remains *unextracted* at the end of n operations, w_n, will be given by

$$w_n = W\left(\frac{K_D V}{K_D V + v}\right)^n \qquad \ldots(29)$$

It is evident that in order to make w_n as small as possible, for a given value of K_D, n should be as large as possible. But $n \times v$ is equal to the total volume of the extracting liquid available, *i.e.*, it is constant. Therefore, it is better to keep n large and v small, rather than the reverse. In other words, the efficiency of extraction increases by increasing the *number* of extractions using only a small amount of the extracting solvent each time.

For the same reason, in the washing of precipitates it is more effective to use a small quantity of water at a time and to repeat the process a number of times.

Example 4. The distribution coefficient of iodine between carbon tetrachloride and water is 85 in favour of carbon tetrachloride. Calculate the volume of carbon tetrachloride required for 95% extraction of iodine from 100 ml of aqueous solution in a single stage extraction.

Solution : $[I_2]_{CCl_4}/[I_2]_{H_2O} = 85$

Hence, $[I_2]_{H_2O}/[I_2]_{CCl_4} = 1/85 = K_D$ *(Note this step)*

After the extraction of 95% iodine, 5% still remains *unextracted.*

According to Eq. 29, $$w_n = W\left(\frac{K_D V}{K_D V + v}\right)^n \qquad \ldots(i)$$

In the present case, n=1, w=5, W=100, V=100 ml and K_D=1/85. The volume v is to be determined.

Substituting the various values in Eq. (*i*), we have

$$\frac{5}{100} = \frac{1/85 \times 100}{1/85 \times 100 + v}$$

$$\therefore \quad v = \mathbf{22{\cdot}35 \text{ ml}}$$

Example 5. When 0·83 g of succinic acid was shaken with 100 ml each of water and ether, the water layer was found to contain 0·70 g of the acid. Calculate the quantity of the acid that can be extracted from 1 litre of ether solution containing 1 g of the acid using 100 ml of water (*i*) in two equal instalments and (*ii*) in a single stage extraction.

Solution : $K_D = \frac{c_{ether}}{c_{water}} = \frac{0{\cdot}13}{0{\cdot}70} = 0{\cdot}19$

According to Eq. 29, $w_n = W\left(\frac{K_D V}{K_D V + v}\right)^n$ ...(*i*)

(*i*) **In the first case :** $W = 1$ g ; $V = 1000$ ml ; $v = 100$ ml, $n=2$

$$\therefore \quad w_2 = 1\text{g}\left(\frac{0{\cdot}19 \times 1000\,\text{ml}}{0{\cdot}19 \times 1000\,\text{ml} + 50\,\text{ml}}\right) = 0{\cdot}627\text{g}$$

This is the amount left *unextracted.*

Hence, the amount extracted = 1·0 g − 0·627 g = **0·373 g**

(*ii*) **In the second case :** $W = 1$ g ; $V = 1000$ ml ; $n=1$

$$\therefore \quad w_1 = 1\text{g}\left(\frac{0{\cdot}19 \times 1000\,\text{ml}}{0{\cdot}19 \times 1000\,\text{ml} + 1 \times 100\,\text{ml}}\right) = 0{\cdot}655\text{g}$$

$\therefore$ The amount extracted = 1·0 g − 0·655 g = **0·345 g**

Thus, the amount extracted is greater if the extraction is carried out in two instalments than in one instalment.

Example 6. (*a*) Calculate the minimum volume of benzene required to extract in one step 90 per cent of H_2S present in one litre of 0·1 M aqueous solution.

(*b*) Calculate the total volume of benzene required if the 90 per cent extraction is to be completed in three steps using equal volumes of benzene.

(*c*) How many extractions would be required for completing 90 per cent extraction if 100 ml benzene is used in each step. The partition coefficient of H_2S between water (c_1) and benzene (c_2) defined as $c_1/c_2 = 0{\cdot}17$.

Solution : (*a*) Let v litres be the volume of benzene required. Then, after *one extraction,*

$$c_1 = 0{\cdot}1\text{ M}/10 = 0{\cdot}01\text{ M}; \quad c_2 = 0{\cdot}1 \times 0{\cdot}9 \times 1/v = (0{\cdot}09/v)\text{ M}$$

$$\therefore \quad c_1/c_2 = \frac{0{\cdot}01\text{ M}}{(0{\cdot}09/v)\text{M}} = 0{\cdot}17 \text{ (given)}$$

whence $v =$ **1·53 litres**

(*b*) Let the total volume required for three equal extractions = $3v$ litres

According to Eq. 29, $\frac{w_n}{W} = \left(\frac{K_D V}{K_D V + v}\right)^n$ ...(*i*)

In this case, $w_n = 0{\cdot}01$ mol ; $W=0{\cdot}1$, $V=1$ litre; $K_D=0{\cdot}17$; v is to be determined.

Substituting the various data in Eq. (*i*) and solving for v, we get

$$v = 0{\cdot}196 \text{ litre}$$

Hence, $3v =$ **0·588 litre**

(*c*) Using the expression, $w_n = W\left(\frac{K_D V}{K_D V + v}\right)^n$

with $W=0{\cdot}1$ mol; $w_n=0{\cdot}01$ mol ; $v=0{\cdot}1$ litre ; $v=1$ litre, we find after substituting the data and taking logs of both sides that $n=5$. Thus, the number of extractions required = **5.**

I. Review Questions

1. State the Distribution law. Under what conditions is it valid ? How is the law derived from thermodynamic considerations ?
2. How is the distribution law modified when (*i*) the solute undergoes association in one of the solvents? (*ii*) the solute enters into chemical combination with one of the solvents?
3. How is the Distribution law used in the process of extraction ? Derive the expression which enables calculation of the amount of a solute left unextracted after a given number of extractions.
4. Discuss the practical applications of the Distribution law.

II. Problems

1. The following data were obtained for the distribution of I_2 between CS_2 and H_2O at 25°C :

Conc. of I_2 in H_2O (g dm^{-3})	0·100	0·161	0·314	0·423
Conc. of I_2 in CS_2 (g dm^{-3})	41	66	129	174

Calculate K_D of I_2 between CS_2 and H_2O. **[Ans. Approx 410]**

2. The following data were obtained at 298 K for the distribution of I_2 between H_2O and CCl_4 :

$[I_2]_{H_2O}$ (mol dm^{-3})$\times 10^4$	2·35	4·69	7·03	9·30
$[I_2]_{CCl_4}$ (mol dm^{-3})$\times 10^2$	2·00	4·00	6·00	8·00

Verify that the data obey Nernst distribution law and calculate K_D in favour of CCl_4. **[Ans. 85·5]**

3. The following data were obtained for the distribution of benzoic acid between water and benzene at 25°C :

Conc. (mol dm^{-3}) of acid in water	$1{\cdot}5\times10^{-2}$	$1{\cdot}95\times10^{-2}$	$2{\cdot}89\times10^{-2}$
Conc. (mol dm^{-3}) of acid in benzene	0·242	0·410	0·907

Neglecting the dissociation of the acid in water, predict the molecular state of the acid in benzene. **[Ans. Dimer]**

4. The solubility of a solute is three times as high in ether as in water. Compare the amounts extracted from 100 ml of aqueous solution by (*a*) 100 ml of ether in one step and (*b*) two successive extractions each with 50 ml of ether. **[Ans. (*a*) 75% ; (*b*) 84%]**

5. At 25°C the solubility of methylamine in water is 8·49 times greater than in chloroform. Calculate the percentage of methylamine remaining in 1 litre of chloroform solution if it is extracted (*a*) four times with 200 ml of water (*b*) twice with 400 ml of water. **[Ans. (*a*) 1·89 % (*b*) 5·17%]**

6. To 50 ml of H_2O and 25 ml of CCl_4 were added 4 g of I_2. After the equilibrium was established by thoroughly shaking the two immiscible, it was found that K_D was 86 in favour of CCl_4. Calculate the amount of I_2 present in water layer. **[Ans. 0·395 g]**

7. Benzoic acid dissociates in water and dimerizes in benzene. Given the following data :

Conc. in water (c_1) (mol dm^{-3})	$1{\cdot}758\times10^{-4}$	$11{\cdot}53\times10^{-3}$
Conc. in benzene (c_2) (mol dm^{-3})	$5{\cdot}937\times10^{-3}$	$224{\cdot}8\times10^{-3}$

and the dissociation constant of the acid = $6{\cdot}0\times10^{-5}$ mol dm^{-3}, calculate K_D, the Nernst distribution coefficient. **[Ans. 1·01]**

8. The following data were obtained at 25°C for the distribution of a weak organic acid between water and benzene :

Conc. in water (g/dm^3)	1·50	1·95	2·89
Conc. in benzene (g/dm^3)	14·20	41·20	96·50

Assuming that the acid is not dissociated in water, determine the molecular complexity of the acid in benzene. **[Ans. Dimer]**

CHAPTER 20

IONIC EQUILIBRIA

Chemical equilibria involving dissociation of chemical compounds, both solid and gaseous, and phase equilibria involving various phase transitions such as solid $\rightleftharpoons$ liquid, liquid $\rightleftharpoons$ vapour, solid $\rightleftharpoons$ vapour, one allotropic form $\rightleftharpoons$ another allotropic form, etc., have been discussed in previous chapters. In this chapter, we shall discuss ionic equilibria involving dissociation of weak acids and weak bases in aqueous solutions, dissociation of sparingly soluble salts in aqueous solutions, dissociation of water and hydrolytic dissociation of salts, etc., in some details.

ACIDS AND BASES

Different concepts have been put forth by different investigators to characterise acids and bases. While some of the concepts are quite narrow in their approach, others are fairly comprehensive. Some important concepts of acids and bases are discussed below.

Arrhenius Concept

According to Arrhenius concept, an acid is a substance that dissociates to give hydrogen ions when dissolved in water. Thus, hydrogen chloride gas is an acid because when dissolved in water, it gives hydrogen ions.

$$HCl(g) + \text{water} \rightleftharpoons H^+(aq) + Cl^-(aq)$$

The symbol *aq* indicates that the ions are hydrated, *i.e.*, associated with one or more molecules of water. The dissociation of acetic acid when dissolved in water is represented as

$$CH_3COOH + \text{water} \rightleftharpoons H^+(aq) + CH_3COO^-(aq)$$

Similarly, a base is a substance which dissociates into hydroxyl ions when dissolved in water. The dissociation of a base like calcium hydroxide may be represented by the equation

$$Ca(OH)_2 + \text{water} \rightleftharpoons Ca^{2+}(aq) + 2OH^-(aq)$$

The high dielectric constant of water lowers the force of attraction between the oppositely charged ions and thus causes the dissociation of the electrolyte. The greater the number of H^+ or OH^- ions given by an acid or a base in water, the greater is the strength of the acid or the base.

Although the H^+ ion in aqueous solution is largely hydrated, with H_3O^+ (**hydronium ion**) as its probable structure, it is customary to represent it as $H^+(aq)$ for the sake of convenience.

Since almost all ions are hydrated to more or less extent, therefore, it is customary to put (*aq*) after each ion.

The Swedish chemist S. Arrhenius (1859–1927) was awarded the 1903 Chemistry Nobel Prize for his theory of electrolytic dissociation.

Bronsted-Lowry Concept

In 1923, Lowry and Bronsted suggested a more general definition of acids and bases. According to their concept, an **acid** is defined *as a substance which has a tendency to donate a proton to any other substance* and a **base** *as a substance which has a tendency to accept a proton from any other substance.* In other words, *an* **acid** *is a proton-donor and a* **base** *is a proton-acceptor.*

When an acid loses a proton, *i.e.*, an H^+ ion, the residual part of it has a tendency to regain the proton. Therefore, it behaves as a base. An acid and a base may, therefore, be defined by the general equation

$$\underset{}{\text{Acid}} \rightleftharpoons \underset{\text{(Proton)}}{H^+} + \text{Base} \qquad ...(1)$$

Conjugate Acids and Bases. Consider the dissociation of acetic acid in water which may be represented as

$$\underset{\text{Acid}}{CH_3COOH} + \underset{\text{Base (Solvent)}}{H_2O} \rightleftharpoons \underset{\text{Acid}}{H_3O^+} + \underset{\text{Base}}{CH_3COO^-} \qquad ...(2)$$

It is evident that acetic acid *donates* a proton to water and thus acts as an *acid.* Water *accepts* a proton and, therefore, acts as a *base.* In the reverse reaction, hydronium ion (H_3O^+) *donates* a proton to the acetate ion and, therefore, acts as an *acid.* The acetate ion *accepts* a proton and, therefore, behaves as a *base. Such pairs of substances which can be formed from one another by the gain or loss of a proton are known as* **conjugate acid-base pairs.** Thus, acetic acid is the conjugate acid of acetate ion and acetate ion is the conjugate base of acetic acid. Similarly, water is the conjugate base of hydronium ion and hydronium ion is the conjugate acid of water.

The dissociation of hydrochloric acid in water may be represented as

$$\underset{\text{Acid}}{HCl} + \underset{\text{Base (Solvent)}}{H_2O} \rightleftharpoons \underset{\text{Acid}}{H_3O^+} + \underset{\text{Base}}{Cl^-} \qquad ...(3)$$

Evidently, hydrochloric acid is the conjugate acid of chloride ion and chloride ion is the conjugate base of hydrochloric acid.

The following points emerge out of the above discussion :

1. Firstly, it is evident that a substance is able to show its acidic character only if another substance capable of accepting a proton is present. For example, acetic acid or hydrogen chloride solution in benzene is not acidic because benzene is not in a position to take up protons. But, a solvent like water can take up protons and, therefore, acetic acid or hydrochloric acid can dissociate in water, as shown in the above examples.

2. Secondly, hydrogen ion in aqueous solution does not exist as H^+ ion but as hydrated ion, H_3O^+. It is called **hydronium ion** because of its resemblance with ammonium ion, NH_4^+.

3. Thirdly, not only molecules but even ions may act as acids or bases. Thus, in the above examples, acetate ion (or chloride ion) acts as a base as it can accept a proton to form acetic acid (or hydrochloric acid). In fact, anion of any acid is the conjugate base of the acid.

As will be seen from the dissociation of acetic acid or hydrochloric acid represented above, there is one acid and one base on each side of the equation. Suppose, acetic acid is designated as $Acid_1$, then the acetate ion, its conjugate base, may be designated as $Base_1$. Similarly, if water is referred to as $Base_2$, then the hydronium ion, its conjugate acid, may be designated as $Acid_2$. The dissociation of acetic acid in water may then be represented as

$$Acid_1 + Base_2 \rightleftharpoons Acid_2 + Base_1 \qquad ...(4)$$

$Acid_1$ and $Base_1$ is a *conjugate acid-base pair* and so is $Acid_2$ and $Base_2$.

In general, the dissociation of an acid HA in water may be represented as

$$HA + H_2O \rightleftharpoons H_3O^+ + A^-$$

Just as an acid requires a solvent that can take up a proton (*i.e.*, can act as a base) for its dissociation, similarly, a base requires a solvent that can give up a proton (*i.e.*, that can act as an acid) for its dissociation. Water possesses both basic and acidic properties. Therefore, acids as well as bases

can dissociate in water. Thus, water acts as an acid (a proton-donor) towards ammonia and as a base (a proton-acceptor) towards acetic acid. Such substances are said to be **amphiprotic** or **amphoteric.**

Consider dissociation of ammonia in water which may be represented as

$$\underset{\text{Base}_1}{NH_3} + \underset{\text{Acid}_2}{H_2O} \rightleftharpoons \underset{\text{Acid}_1}{NH_4^+} + \underset{\text{Base}_2}{OH^-}$$

Ammonium ion (NH_4^+) is the conjugate acid (say, $Acid_1$) to the base NH_3 ($Base_1$) and hydroxyl (OH^-) ion is the conjugate base ($Base_2$) to the acid H_2O ($Acid_2$). Thus, this equilibrium also conforms to the usual pattern.

Example 1. Determine the trend in the relative basic strengths of anions in the series : ClO_4^-, ClO_3^-, ClO_2^-.

Solution : ClO_4^-, ClO_3^-, ClO_2^- are, respectively, the conjugate bases of $HClO_4$, $HClO_3$, $HClO_2$. A conjugate acid-base pair stands in complementary relation to each other. The stronger the acid, the weaker is its conjugate base. Since the strength of the acids varies in the order :

$$HClO_4 > HClO_3 > HClO_2,$$

the strength of their conjugate bases varies in the order :

$$ClO_4^- < ClO_3^- < ClO_2^-$$

Let us elucidate it by considering the generalized acid-base reaction

$$HA + B \rightleftharpoons A^- + BH^+$$

wherein HA-A^- and BH^+-B constitute conjugate acid-base pairs. In this reaction, the greater the tendency of HA to react with B, the farther will lie the equilibrium to the right and, the farther the equilibrium lies to the right, the less effective is A^-, the conjugate base of HA, in acting as a base by accepting a proton.

Some common cases of equilibria between acids and bases involving proton transfer are given in Table 1.

TABLE 1

Conjugate Acids and Bases

$Acid_1$	+	$Base_2$	$\rightleftharpoons$	$Acid_2$	+	$Base_1$
HCl	+	H_2O	$\rightleftharpoons$	H_3O^+	+	Cl^-
HNO_3	+	H_2O	$\rightleftharpoons$	H_3O^+	+	NO_3^-
H_2SO_4	+	H_2O	$\rightleftharpoons$	H_3O^+	+	HSO_4^-
H_3PO_4	+	H_2O	$\rightleftharpoons$	H_3O^+	+	$H_2PO_4^-$
HSO_4^-	+	H_2O	$\rightleftharpoons$	H_3O^+	+	SO_4^{2-}
CH_3COOH	+	H_2O	$\rightleftharpoons$	H_3O^+	+	CH_3COO^-
HSO_3^-	+	H_2O	$\rightleftharpoons$	H_3O^+	+	SO_3^{2-}
H_2CO_3	+	H_2O	$\rightleftharpoons$	H_3O^+	+	HCO_3^-
HCN	+	H_2O	$\rightleftharpoons$	H_3O^+	+	CN^-
NH_4^+	+	H_2O	$\rightleftharpoons$	H_3O^+	+	NH_3
HCO_3^-	+	H_2O	$\rightleftharpoons$	H_3O^+	+	CO_3^{2-}
HS^-	+	H_2O	$\rightleftharpoons$	H_3O^+	+	S^{2-}
H_2O	+	H_2O	$\rightleftharpoons$	H_3O^+	+	OH^-

Relative Strengths of Acid-Base Pairs. According to the concept of Lowry and Bronsted, the strength of an acid depends upon its tendency to lose protons and the strength of a base depends upon its tendency to gain protons. If an acid, such as hydrochloric acid, is a strong acid, it will have a strong tendency to donate protons. Thus, the equilibrium,

$$HCl + H_2O \rightleftharpoons H_3O^+ + Cl^-$$

lies very much to the right and the reverse reaction, representing the gain of proton by the chloride ion leading to the reformation of HCl, will take place to a very small extent. Thus, chloride ion is a *weak base.*

If an acid, such as acetic acid, is a *weak acid*, it would have only a weak tendency to lose protons. Thus, the equilibrium

$$CH_3COOH + H_2O \rightleftharpoons H_3O^+ + CH_3COO^-$$

lies mostly towards the left and the reverse reaction, representing the gain of protons by the CH_3COO^- ion leading to the formation of CH_3COOH, will take place to a very large extent. Thus, CH_3COO^- ion is a strong base.

As a general rule, the stronger an acid, the weaker must be its conjugate base and vice versa. If an acid (*e.g.*, HCl) is strong, its conjugate base (Cl^-) is weak. If a base (*e.g.*, CH_3COO^-) is strong, its conjugate acid (CH_3COOH) is weak.

Water is a very weak base because its conjugate acid, hydronium ion (H_3O^+), is a very strong acid. At the same time, water is a very weak acid because its conjugate base, hydroxide ion (OH^-), is a very strong base.

It may be pointed out that while strong acids like HCl, HNO_3, H_2SO_4, etc., being *covalent* compounds, get dissociated only in a solvent like water which can take up protons, strong bases such as NaOH, KOH, $Ba(OH)_2$, etc., being *electrovalent* compounds exist as ions even in the solid state. The basic character of these compounds is exclusively due to the presence of hydroxyl ions which are always there (even without a solvent) and, therefore, no interaction with a solvent is necessary in such cases. They are frequently referred to as *hydroxide bases* to distinguish them from other bases such as C_3COO^-, CO_3^{2-}, S^{2-} and NH_3 which furnish hydroxyl ions only on interaction with a solvent such as water.

Influence of Solvent on Acid Strength. As mentioned before, the term *acid strength* is a relative one. It depends also on the substance which acts as a base. Consider the general equation

$$Acid_1 + Base_2 \rightleftharpoons Acid_2 + Base_1$$

The capacity of the acid to dissociate (*i.e.*, to donate protons) also depends upon the basic strength of acids (*i.e.*, the capacity to accept protons) of the solvent which acts as a base. For the order of the relative strengths of acids given in Table 1, the base (solvent) is water. If some other solvent is used, the order of relative strengths may be quite different. To illustrate this point, three solvents, namely, glacial acetic acid, water and liquid ammonia of increasing basic character may be considered.

Dissociation in acetic acid. Although acetic acid is normally an acid, it is also able, to some extent, to accept a proton and thus to act as a base as well. The dissociation of a strong acid HA in this medium may be represented as

$$\underset{\text{Acid}}{HA} + \underset{\substack{\text{Base}\\(\text{solvent})}}{CH_3COOH} \rightleftharpoons \underset{\text{Acid}}{CH_3COOH_2^+} + \underset{\text{Base}}{A^-}$$

But, the equilibrium cannot lie very much to the right since acetic acid has only very small tendency to accept protons. Therefore, even strong acids are only feebly dissociated in acetic acid.

The degrees of dissociation of a number of acids when dissolved in glacial acetic acid have been determined from conductance measurements (Chapter 22). Taking them as a measure of their relative strengths, some of the common acids have been arranged in the following order of their strengths :

$$HClO_4 > HBr > H_2SO_4 > HCl > HNO_3$$

This is the correct order of decreasing strengths of these acids.

Dissociation in water. Water is a much stronger base, *i.e.*, it has a much greater tendency to accept protons than acetic acid. Therefore, the ionic equilibrium of a strong acid in water, represented as

$$\underset{\text{Acid}}{HA} + \underset{\text{Base (solvent)}}{H_2O} \rightleftharpoons \underset{\text{Acid}}{H_3O^+} + \underset{\text{Base}}{A^-}$$

lies very much to the right. All the five acids mentioned in the above series, therefore, react almost completely with water to form, in every case, hydronium ion, H_3O^+. Therefore, all the strong acids in aqueous solutions appear almost equally strong. Obviously, their relative strengths in aqueous solutions cannot be compared. This phenomenon is called the **levelling effect.**

However, the ionic equilibria in water do not proceed so far in the case of weak acids like formic, acetic, propionic, lactic, tartaric and phosphoric acids. It is, therefore, possible to distinguish between the relative strengths of these acids in aqueous medium.

Dissociation in liquid ammonia. Liquid ammonia has such a strong basic character, *i.e.*, it has such a strong tendency to take up protons, that even a weak acid, like acetic acid, dissociates to a considerable extent and behaves as a strong acid. The ionic equilibrium, represented below, lies very much to the right :

$$\underset{\text{Acid}}{CH_3COOH} + \underset{\text{Base (solvent)}}{NH_3} \rightleftharpoons \underset{\text{Acid}}{NH_4^+} + \underset{\text{Base}}{CH_3COO^-}$$

By conductance measurements it has been found that all acids, which in aqueous solution behave stronger than acetic acid, appear to be of about the same strength when dissolved in liquid ammonia. Thus, such strong acids as hydrochloric and nitric and such weak acids as acetic and propionic, appear to be of almost equal strength when dissolved in liquid ammonia.

Dissociation in hydrogen fluoride. Hydrogen fluoride offers an example on the other extreme. It has strong acidic properties and no basic, *i.e.*, proton-accepting properties at all. Consequently, even the strongest acid is incapable of dissociating as an acid when dissolved in hydrogen fluoride. As a matter of fact, many substances, which are normally acids but have some tendency to accept protons as well under certain conditions, dissociate as bases when dissolved in hydrogen fluoride. Thus, nitric acid dissociates slightly as a base in hydrogen fluoride solution :

$$\underset{\text{Base}}{HNO_3} + \underset{\text{Acid (solvent)}}{HF} \rightleftharpoons \underset{\text{Acid}}{H_2NO_3^+} + \underset{\text{Base}}{F^-}$$

It is thus interesting to note that even a strong acid like HNO_3 behaves as a base (a very weak base though) when dissolved in HF.

Influence of Solvent on Base Strength. The nature of the solvent plays an equally important role in the dissociation and relative strengths of bases as well. If the solvent is a weak acid, such as water, it will be possible to compare the strengths of different bases as they will dissociate to different extents. But if the solvent is even a slightly stronger acid, *e.g.*, acetic acid, it will not be possible to distinguish between the strengths of different bases.

For example, aniline, a very weak base and sodium hydroxide, a very strong base, in water, appear to be equally strong when acetic acid is used as the solvent. Sometimes advantage is taken of this fact in volumetric estimations of those bases which are too weak in aqueous solution to be titrated against acids.

Lewis Concept

In 1923, G.N. Lewis put forth a more general concept of acids and bases. According to him, *an* **acid** *is a species that is capable of accepting a pair of electrons to form a covalent bond and a* **base** *is a species that is capable of donating a pair of electrons to form a covalent bond.*

(i) $\underset{\text{(Acid)}}{BF_3} + \underset{\text{(Base)}}{NH_3} \longrightarrow F_3BNH_3$

(ii) $\underset{\text{(Acid)}}{BF_3} + \underset{\text{(Base)}}{F^-} \longrightarrow BF_4^-$

(iii) $\underset{\text{(Acid)}}{BCl_3} + \underset{\text{(Base)}}{(CH_3)_3N} \longrightarrow (CH_3)_3NBCl_3$

(iv) $\underset{\text{(Acid)}}{Cu^{2+}} + \underset{\text{(Base)}}{4CN^-} \longrightarrow [(Cu(CN)_4]^{2-}$

We see that the Lewis definition does not attribute acidity to any particular element but rather to unique electronic arrangement. Thus, rewriting reaction *(i)*, for instance, as

it is easy to say that NH_3 acts as a base by virtue of its tendency to donate the lone pair of electrons on the N atom to BF_3 which acts as an acid.

Example 2. How does the Lewis acid concept account for the formation of thiosulphate ion from sulphite ion and sulphur ?

Solution : The sulphur atom, S, being electron-deficient, can be considered as a Lewis acid while the SO_3^{2-} ion having an octet structure can be regarded as the Lewis base. Their combination to form $S_2O_3^{2-}$ ion is represented below :

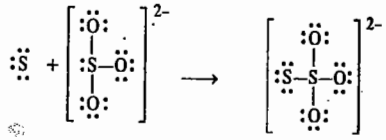

Example 3. Using the Lewis acid-base concept, determine the trend in the acid strengths in the series : *(a)* $HClO_4$, $HClO_3$, $HClO_2$ and *(b)* H_3PO_4, H_3PO_3, H_3PO_2.

Solution : In general, the greater the number of terminal oxygens in the Lewis structure of an oxyacid, the greater is its acidity. The Lewis structures of the given acids are :

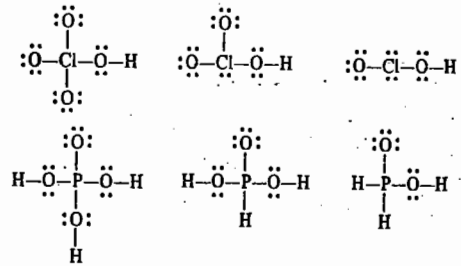

Since oxygen atom is more electronegative than chlorine, each terminal oxygen atom tends to withdraw electrons from the chlorine atom and thereby also from the O—H bond, with the result that the proton acquires a greater tendency to get dissociated. Clearly, if there are more terminal oxygens in the oxyacid, the proton will get dissociated to a greater extent. This accounts for the decreasing acid strength in the series *(a)*, *i.e.*,

$$HClO_4 > HClO_3 > HClO_2$$

In the series *(b)*, on the other hand, an examination of the Lewis structures shows that the number of terminal oxygens is the same (*i.e.*, equal to one) in the three acids. Also, the hydrogens in the three acids are not all bonded to oxygens. The electronegativities of P and H, too, are almost the same. Thus, we do not expect very large differences in the strengths of the three acids.

DISSOCIATION OF WEAK ACIDS AND BASES

Dissociation of a Weak Acid. Consider the dissociation of a weak monobasic acid HA in water, represented by the equation

$$HA + H_2O \rightleftharpoons H_3O^+ + A^-$$

Applying the law of chemical equilibrium, the equilibrium constant K_c is given by the expression

$$K_c = \frac{[H_3O^+][A^-]}{[HA][H_2O]} \qquad ...(5)$$

The square brackets, as usual, represent concentrations in moles per litre of the entities enclosed therein.

Since water is present in large excess in dilute solutions, its concentration may be taken as constant, say, k. Further, since the symbol H_3O^+ simply indicates that hydrogen ion is hydrated, it may be replaced by H^+, for simplicity. The above equation may then be put as

$$K_c = \frac{[H^+][A^-]}{[HA] \times k} \qquad ...(6)$$

assuming that the activity coefficients of the species involved are equal to unity each.

Since the product of the two constants K_c and k is equal to another constant, say, K_a, Eq. 6 may be written as

$$K_a = [H^+][A^-]/[HA] \qquad ...(7)$$

The significance of Eq. 7 is that the product of the concentrations of the hydrogen ion and the anion, irrespective of their source (*i.e.*, whether furnished by the acid itself or by any other substance present in the solution) divided by the concentration of the undissociated acid, is equal to a constant. This constant (K_a) is characteristic of the acid concerned and is known as the **dissociation constant of the acid.** This varies only with temperature, like other equilibrium constants.

If the dissociation of the acid is represented in accordance with Arrhenius concept, *i.e.*, as

$$HA \rightleftharpoons H^- + A^-$$

the same expression as above for the dissociation constant of the acid will be obtained. Therefore, for simplicity, Arrhenius concept may be adopted.

Relative Strengths of Weak Acids. Eq. 7 for the dissociation constant of a weak acid can also be expressed in terms of the degree of dissociation *(α)* and the total molar concentration *(c)* of the acid. Consider, for example, the dissociation of acetic acid, represented below :

	CH_3COOH	$\rightleftharpoons$	H^+	+	CH_3COO^-
Original concs. :	c		0		0
Eqbm. concs. :	$c(1-\alpha)$		$c\alpha$		$c\alpha$

$$K_a = \frac{[H^+][CH_3COO^-]}{[CH_3COOH]} = \frac{c\alpha \times c\alpha}{c(1-\alpha)} = \frac{c\alpha^2}{1-\alpha} \qquad ...(8)$$

Since for weak acids, α is very small, $1-\alpha$ in the denominator may be taken as 1. The above expression, therefore, reduces to

$$K_a = c\alpha^2 \quad \text{or} \quad \alpha = \sqrt{K_a/c} \qquad ...(9)$$

For two weak acids of dissociation constants K_{a_1} and K_{a_2}, at the same concentration c, it follows from Eq. 9 that

$$\alpha_1/\alpha_2 = \sqrt{K_{a_1}/K_{a_2}} \qquad ...(10)$$

where α_1 and α_2 are the respective degrees of dissociation of the two acids.

But, degree of dissociation of an acid is a measure of its capacity to furnish hydrogen ions and hence a measure of its strength.

$$\therefore \quad \frac{\text{Strength of one acid, } HA_1}{\text{Strength of another acid, } HA_2} = \sqrt{\frac{K_{a_1}}{K_{a_2}}} \qquad ...(11)$$

Example 4. The dissociation constants of formic and acetic acids are $1{\cdot}77\times10^{-4}$ and $1{\cdot}75\times10^{-5}$, respectively. Calculate the relative strengths of the two acids.

Solution : According to Eq. 11,

$$\frac{\text{Strength of formic acid}}{\text{Strength of acetic acid}} = \sqrt{\frac{K_a \text{ formic acid}}{K_a \text{ acetic acid}}} = \sqrt{\frac{1{\cdot}77\times10^{-4}}{1{\cdot}75\times10^{-5}}} = 3{\cdot}18$$

Thus, formic acid is **3·18** times stronger than acetic acid.

The dissociation constants of weak acids can be determined by using Eq. 9 since α, the degree of dissociation, can be obtained from conductance measurements, as shown in Chapter 22, by using the expression : $\alpha = \Lambda_m / \Lambda_m^\circ$.

Eq. 9 can also be used for calculating hydrogen ion concentrations of aqueous solutions of acids whose dissociation constants are known. Accordingly,

$$[H^+] = c\alpha = c\sqrt{K_a/c} = \sqrt{cK_a} \qquad ...(12)$$

Example 5. A solution of 0·100 M acetic acid is found to be dissociated to the extent of 1·33 per cent at the room temperature. Calculate the dissociation constant of the acid at this temperature.

Solution : Percentage dissociation of acetic acid = 1·33

$\therefore$ Degree of dissociation of acetic acid, $\alpha = 0{\cdot}0133$

Dissociation constant of acetic acid, $K_a = c\alpha^2/(1-\alpha)$

Since α is very small, hence $K_a = c\alpha^2 = 0{\cdot}1\times(0{\cdot}0133)^2 = 1{\cdot}77\times10^{-5}$

Example 6. A monobasic acid has a dissociation constant equal to $1{\cdot}8\times10^{-5}$ at 25°C. Calculate its degree of dissociation at a concentration of 0·20 M at the same temperature. What will be the concentration of hydrogen ions furnished by it ?

Solution : Assuming that degree of dissociation is very small,

$$\alpha = \sqrt{\frac{K_a}{c}} = \sqrt{\frac{1{\cdot}8\times10^{-5}}{0{\cdot}2}} = 0{\cdot}009486$$

Thus, degree of dissociation of 0·20 M acid = **0·009486**

Further, $[H^+] = \sqrt{cK_a}$ (Eq. 12)

$$= \sqrt{0{\cdot}2\text{M} \times 1{\cdot}8\times10^{-5}} = \mathbf{0{\cdot}001897 \text{ mol dm}^{-3}}$$

Dissociation Constants of Polybasic Acids. Polybasic acids contain two or more hydrogens which can get dissociated. They always dissociate in stages. Consider, for example, the dissociation of carbonic acid :

$$H_2CO_3 + H_2O \rightleftharpoons H_3O^+ + HCO_3^- \qquad \textit{(First stage)}$$

$$HCO_3^- + H_2O \rightleftharpoons H_3O^+ + CO_3^{2-} \qquad \textit{(Second stage)}$$

The equilibrium constants K_{a_1} and K_{a_2}, corresponding to the first and second dissociations, are given by the expressions :

$$K_{a_1} = \frac{[H^+][HCO_3^-]}{[H_2CO_3]} \quad \text{and} \quad K_{a_2} = \frac{[H^+][CO_3^{2-}]}{[HCO_3^-]}$$

K_{a_1} and K_{a_2}, at 25°C are known to be $4{\cdot}5\times10^{-7}$ and $4{\cdot}7\times10^{-11}$, respectively. The second dissociation constant is found to be 1/10000th of the first dissociation constant. K_{a_2} is always smaller than K_{a_1} which shows that second dissociation takes place to a much smaller extent than the first dissociation. Phosphoric acid is a tribasic acid. It dissociates in three stages, as shown below :

$$H_3PO_4 + H_2O \rightleftharpoons H_3O^+ + H_2PO_4^- \quad \text{(First stage)}$$

$$H_2PO_4^- + H_2O \rightleftharpoons H_3O^+ + HPO_4^{2-} \quad \text{(Second stage)}$$

$$HPO_4^{2-} + H_2O \rightleftharpoons H_3O^+ + PO_4^{3-} \quad \text{(Third stage)}$$

The dissociation constants K_{a_1}, K_{a_2} and K_{a_3}, for the three successive stages are $7{\cdot}52\times10^{-3}$, $6{\cdot}23\times10^{-8}$ and $4{\cdot}80\times10^{-13}$, respectively.

The reason for the decrease in the dissociation constant of successive stages is that in the first dissociation, the positively charged proton comes from a neutral molecule while in the second stage of dissociation, the proton is detached from a negatively charged molecule and in the third dissociation, it is detached from a doubly negatively charged molecule.

The dissociation constants of some of the common acids at 25°C are given in Table 2.

TABLE 2

Dissociation Constants of Some Common Acids at 25°C

Acid	Formula	K_{a_1}	K_{a_2}	K_{a_3}
Acetic acid	CH_3COOH	$1{\cdot}75\times10^{-5}$		
Arsenic acid	H_3AsO_4	$5{\cdot}00\times10^{-5}$	$8{\cdot}30\times10^{-8}$	6×10
Benzoic acid	C_6H_5COOH	$6{\cdot}29\times10^{-5}$		
Boric acid	H_3BO_3	$5{\cdot}80\times10^{-10}$		
Carbonic acid	H_2CO_3	$4{\cdot}52\times10^{-7}$	$4{\cdot}69\times10^{-10}$	
Chloracetic acid	$CH_2ClCOOH$	$1{\cdot}38\times10^{-3}$		
Dichloracetic acid	$CHCl_2COOH$	$5{\cdot}00\times10^{-2}$		
Formic acid	$HCOOH$	$1{\cdot}77\times10^{-4}$		
Hydrocyanic acid	HCN	$7{\cdot}20\times10^{-10}$		
Hydrogen sulphide	H_2S	$5{\cdot}70\times10^{-8}$	$1{\cdot}20\times10^{-15}$	
Iodic acid	HIO_3	$1{\cdot}67\times10^{-8}$		
Oxalic acid	$(COOH)_2$	$5{\cdot}02\times10^{-2}$	$5{\cdot}18\times10^{-5}$	
Phosphoric acid	H_3PO_4	$7{\cdot}52\times10^{-3}$	$6{\cdot}23\times10^{-8}$	$4{\cdot}8\times10^{-13}$
Phosphorous acid	H_3PO_3	$1{\cdot}60\times10^{-2}$	$7{\cdot}0\times10^{-7}$	
Propionic acid	C_2H_5COOH	$1{\cdot}34\times10^{-5}$		
Sulphuric acid	H_2SO_4	strong	$1{\cdot}01\times10^{-2}$	
Sulphurous acid	H_2SO_3	$1{\cdot}72\times10^{-2}$	$6{\cdot}24\times10^{-6}$	

Dissociation of a Weak Base. Representing the formula of a weak monoacid base as BOH, its dissociation, in accordance with Arrhenius concept, may by represented by the equation

$$BOH \rightleftharpoons B^+ + OH^-$$

Applying the equilibrium law equation, the dissociation constant, K_b, of the base, will be given by

$$K_b = \frac{[B^+][OH^-]}{[BOH]} \qquad ...(13)$$

assuming that the activity coefficients of various species involved are equal to unity each.

If the initial concentration of the base is c moles per litre and if α is the degree of dissociation, then,

	BOH	$\rightleftharpoons$	B^+	+	OH^-
Original concs. :	c		0		0
Equilibrium concs. :	$c(1-\alpha)$		$c\alpha$		$c\alpha$

$$\therefore \quad K_b = \frac{c\alpha \times c\alpha}{c(1-\alpha)} = \frac{c\alpha^2}{(1-\alpha)} \qquad ...(14)$$

Since, for a weak base, α is very small as compared to 1, Eq. 14, as before, is reduced to

$$K_b = c\alpha^2 \qquad \text{or} \qquad \alpha = \sqrt{K_b/c}$$

$$\therefore \quad [OH^-] = c\alpha = c\sqrt{K_b/c} = \sqrt{cK_b} \qquad ...(15)$$

The dissociation constants of some common weak bases are given in Table 3.

TABLE 3

Dissociation Constants of Some Common Bases at 25°C

Base	Formula	K_b
Ammonia	NH_4OH	$1{\cdot}81\times10^{-5}$
Aniline	$C_6H_5NH_2$	$3{\cdot}83\times10^{-10}$
Dimethyl amine	$(CH_3)_2NH$	$5{\cdot}12\times10^{-4}$
Ethyl amine	$C_2H_5NH_2$	$5{\cdot}60\times10^{-4}$
Hydrazine	NH_2NH_2	$3{\cdot}00\times10^{-6}$
Methyl amine	CH_3NH_2	$4{\cdot}38\times10^{-4}$
Pyridine	C_5H_5N	$1{\cdot}30\times10^{-9}$
Quinoline	C_9N_7N	$6{\cdot}30\times10^{-10}$
Silver hydroxide	$AgOH$	$1{\cdot}10\times10^{-4}$
Trimethyl amine	$(CH_3)_3N$	$5{\cdot}21\times10^{-4}$
Urea	$CO(NH_2)_2$	$1{\cdot}50\times10^{-14}$

Dissociation of Water. Water is dissociated to a very small extent into hydrogen and hydroxyl ions, as represented by the equation

$$H_2O\ (l) \rightleftharpoons H^+(aq) + OH^-\ (aq)$$

More accurately, $$2H_2O\ (l) \rightleftharpoons H_3O^+(aq) + OH^-\ (aq)$$

Applying the law of chemical equilibrium, its dissociation constant, K, is given by

$$K = \frac{[H^+][OH^-]}{[H_2O]} \qquad ...(16)$$

Since dissociation takes place to a very small extent, the concentration of the undissociated water molecules, $[H_2O]$, may be regarded as constant, say k.

$$\therefore \quad K \times k = [H^+][OH^-] \qquad ...(17)$$

The product of the two constants K and k gives another constant which is designated by K_w.

Hence, Eq. 17 is written as

$$K_w = [H^+][OH^-] = 1{\cdot}0 \times 10^{-14}\ \text{mol}^2\ \text{dm}^{-6} \text{ at } 25°C \qquad ...(18)$$

where K_w, the dissociation constant, is called the **ionic product of water.**

Since in pure water, the concentration of hydrogen and hydroxyl ions must be equal to one another, hence

$$[H^+] = [OH^-] = \sqrt{K_w} = \sqrt{1\times10^{-14}\ \text{mol}^2\,\text{dm}^{-6}} = 1\times10^{-7}\ \text{mol dm}^{-3}$$

If a strong acid, like hydrochloric acid, is added to water, the concentration of H^+ ions will become very high and, therefore, the concentration of OH^- ions will correspondingly decrease so that the product of their concentrations remains constant. Similarly, if a strong base, like sodium hydroxide, is added to water, the concentration of OH^- ions will become very large and, therefore, that of H^+ ions will correspondingly become very small.

*p*H Scale

It should be clear from the above discussion that every aqueous solution, whether acidic, alkaline or neutral, contains both H^+ and OH^- ions. The product of their concentrations is always constant, equal to 1×10^{-14} at 25°C. Whether the solution is acidic or alkaline depends upon which of the two ions is present in greater concentration than the other. But, since knowing the concentration of one of these ions, that of the other can be calculated, it is convenient to express acidity or alkalinity of a solution by referring to the concentration of hydrogen ions only. Now, H^+ ion concentration can vary within wide limits, usually from about 1 mole per litre (as in 1 M HCl) to about 10^{-14} mole per litre (as in 1 M NaOH). The *p*H scale was introduced by the Danish biochemist S.P. Sörensen (1868-1939) in 1909. As defined by him, **the *p*H of a solution** is the negative logarithm (to the base 10) of the concentration (in moles per litre) of hydrogen ions which it contains.

Thus, $$pH = -\log [H^+] = -\log [H_3O^+] \qquad ...(19)$$

The *p*H of 1 M HCl solution in which $[H^+] = 1$ mol dm^{-3}, will be zero. In 1M NaOH solution, the $[OH^-] = 1$ mol dm^{-3} and hence $[H^+]$ will be 10^{-14} mol dm^{-3}. The *p*H of 1 M NaOH solution will thus be 14. Obviously, the scale of *p*H would be from 0 to 14.

Example 7. Calculate the *p*H of *(a)* 0·0001 M HCl solution *(b)* 0·04 M HNO_3 solution, assuming complete dissociation in each case.

Solution : *(a)* Concentration of HCl = 0·0001 M

Since HCl is completely dissociated, hence

$$[H^+] = 0{\cdot}0001 \text{ mol dm}^{-3}$$

$$\therefore \quad pH = -\log [H^+] = -\log [0{\cdot}0001] = 4$$

(b) Concentration of HNO_3 = 0·04 M

Since HNO_3 is completely dissociated, hence

$$[H^+] = 0{\cdot}04 \text{ mol dm}^{-3}$$

$$\therefore \quad pH = -\log [H^+] = -\log [0{\cdot}04] = 1{\cdot}398$$

Example 8. Calculate the hydrogen ion concentration in moles per litre of a solution whose *p*H is 5·4.

Solution : *p*H of the solution = 5·4

$$pH = -\log [H^+]$$

or $$\log [H^+] = -5{\cdot}4 = \bar{6}{\cdot}600$$

$$\therefore \quad [H^+] = 3{\cdot}98\times10^{-6} \text{ mol dm}^{-3}$$

Example 9. Calculate the *p*H of an aqueous solution obtained by mixing 50 ml of 0·2 M HCl with 50 ml 0·1 M NaOH.

Solution : Knowing that the product of volume in millilitres and molarity gives the number of millimoles of the acid or the base, we have

Number of millimoles of the acid in the solution = $50\times0{\cdot}2 = 10$

Number of millimoles of the alkali in the solution = $50\times0{\cdot}1 = 5$

Number of millimoles of the acid left in the solution after the addition of alkali = $10 - 5 = 5$

Total volume of the solution = $50+50 = 100$ ml

Thus, we have 5 millimoles of the acid in 100 ml of the solution or 0·05 mole of the acid per litre of the solution.

$\therefore$ Concentration of H^+ ions = 0·05 mol dm^{-3}

$\therefore$ *p*H of the solution = $-\log [H^+] = -\log (0{\cdot}05) = 1{\cdot}30$

Example 10. Calculate the *p*H of an aqueous solution obtained by mixing 25 ml of 0·2 M HCl with 50 ml of 0·25 M NaOH. Take $K_w = 10^{-14}$ mol^2 dm^{-6} at 25°C

Solution : Knowing that the product of volume in millilitres and molarity gives the number of millimoles of the acid or the base, we have

Number of millimoles of the acid in the solution = $25\times0{\cdot}2 = 5$

Number of millimoles of the alkali in the solution = $50\times0{\cdot}25 = 12{\cdot}5$

Number of millimoles of the alkali left in the solution after the addition of the acid = $12{\cdot}5 - 5 = 7{\cdot}5$

Total volume of the solution = $50+25 = 75$ ml

Concentration of OH^- ions $= \dfrac{7{\cdot}5\times1000}{75\times1000} = 0{\cdot}10$ mol dm^{-3}

$$[H^+][OH^-] = 10^{-14} \text{ mol}^2 \text{ dm}^{-6} \text{ at } 25°C$$

$$[OH^-] = 0{\cdot}10 \text{ mol dm}^{-3}$$

$$[H^+] = 10^{-14} \text{ mol}^2 \text{ dm}^{-6}/0{\cdot}10 \text{ mol dm}^{-3} = 10^{-13} \text{ mol dm}^{-3}$$

$$pH = -\log [H^+] = -\log (10^{-13}) = 13$$

Example 11. Calculate the *p*H of 1×10^{-7} M aqueous solution of HCl at 25°C. Take $K_w = 10^{-14}$ mol^2 dm^{-6}.

Solution : The student may be tempted to write down the answer as

$$pH = -\log [H^+] = -\log (10^{-7}) = -(-7) = 7$$

But this value is not acceptable since this is also the *p*H of pure water ! The solution of HCl, howsoever small may be its concentration, must have a *p*H lower than 7. We must, therefore, approach the problem differently.

The dissociation of water may be represented as

	H_2O	$\rightleftharpoons$	H^+	+	OH^-
Concs. if no dissociation :	c		10^{-7} (from HCl)		0
Concs. after dissociation :	$c - x$		$(10^{-7} + x)$		x

where x is the molar amount of H_2O per litre of the solution which dissociates.

If we consider that there is no dissociation of water, then, $[H^+]$ contribution comes only from HCl. If we recognize that a small amount (x mole) of water *does dissociate*, then the $[H^+]$ contribution would be $(10^{-7} + x)$ mol dm^{-3}. Now, at 25°C,

$$K_w = [H^+][OH^-] = 10^{-14} \text{ mol}^2 \text{ dm}^{-6} = (10^{-7} + x) \text{ mol dm}^{-3} \times x \text{ mol dm}^{-3}$$

which reduces to the quadratic equation

$$x^2 + 10^{-7}x - 10^{-14} = 0$$

The roots of this equation are given by

$$x = \frac{-10^{-7} \pm \sqrt{(10^{-7})^2 + 4\times10^{-14}}}{2}$$

Neglecting the negative root which has no physical meaning,

$$x = \frac{-10^{-7} + \sqrt{10^{-14} + 4\times10^{-14}}}{2} = \frac{-10^{-7} + 2{\cdot}24\times10^{-7}}{2} = 0{\cdot}62\times10^{-7} \text{ mol dm}^{-3}$$

$$\therefore \quad [H^+] = 10^{-7} + x = 10^{-7} + 0{\cdot}62\times10^{-7} = 1{\cdot}62\times10^{-7} \text{ mol dm}^{-3}$$

$$\therefore \quad pH = -\log [H^+] = -\log(1{\cdot}62\times10^{-7}) = 6{\cdot}79$$

We conclude that the dissociation of H_2O increases the $[H^+]$ above that due to the acid alone. *Regardless of how dilute the solution, the pH of an acid solution is always less than 7.*

Example 12. Calculate the *p*H of a 2×10^{-5} M aqueous solution of phenol at 25°C. $K_a = 1{\cdot}30\times10^{-10}$, $K_w = 1{\cdot}008\times10^{-14}$.

Solution : The dissociation of phenol may be represented as

$$C_6H_5OH \rightleftharpoons C_6H_5O^- + H^+$$

$$2\times10^{-5} - x \qquad x \qquad x$$

$$K_a = \frac{x^2}{2 \times 10^{-5} - x}$$

Neglecting x in the denominator, we have

$$K_a = x^2/2\times10^{-5} \text{ so that } x = (2\times10^{-5}\times K_a)^{1/2}$$

$$x = [H^+] = (2\times10^{-5}\times K_a)^{1/2} = (2\times10^{-5}\times1{\cdot}30\times10^{-10})^{1/2}$$

$$= 5{\cdot}1\times10^{-8} \text{ mol dm}^{-3}$$

The above answer is obviously incorrect because phenol, even though it is a very weak acid, must have $[H^+]$ greater than 10^{-7}. The error lies in the assumption that $[H^+] = [C_6H_5O^-] = x$. This would normally be true in the absence of any other source of hydrogen ions. To obtain the correct value for $[H^+]$, we make use of the concept of *electroneutrality of the solution, viz.*,

$$[H^+] = [C_6H_5O^-] + [OH^-]$$

$$[H^+][OH^-] = K_w \text{ so that}$$

$$[OH^-] = \frac{K_w}{[H^+]}$$

$$\therefore \quad [C_6H_5O^-] = [H^+] - [OH^-] = \left\{[H^+] - \frac{K_w}{[H^+]}\right\}$$

Since phenol is present either as C_6H_5OH or partly as $C_6H_5O^-$. Hence

$$[C_6H_5OH] + [C_6H_5O^-] = 2\times10^{-5} \text{ mol dm}^{-3}$$

Assuming that $[C_6H_5O^-] << [C_6H_5OH]$,

$$[C_6H_5OH] = 2\times10^{-5} \text{ mol dm}^{-3}$$

$$K_a = \frac{[C_6H_5O^-][H^+]}{[C_6H_5OH]} = \frac{\left\{[H^+] - \frac{K_w}{[H^+]}\right\}[H^+]}{2\times10^{-5}} = 1{\cdot}3\times10^{-10}$$

or $$[H^+]^2 - K_w = 2\times10^{-5}\times K_a = 2\times10^{-5}\times1{\cdot}3\times10^{-10} = 2{\cdot}60\times10^{-15}$$

or $$[H^+]^2 - 1{\cdot}008\times10^{-14} = 2{\cdot}60\times10^{-15}$$

$$\therefore \quad [H^+]^2 = 1{\cdot}268\times10^{-14}$$

or $$[H^+] = 1{\cdot}126\times10^{-7} \text{ mol dm}^{-3}$$

$$\therefore \quad pH = -\log [H^+] = -\log (1{\cdot}126\times10^{-7}) = 6{\cdot}95$$

The value for $[H^+]$, *viz.*, $1{\cdot}126\times10^{-7}$ mol dm^{-3} is acceptable since it is greater than 10^{-7}, as we would expect it to be.

This example shows that in calculating the pH of dilute solution of a very weak acid (or a very weak base), care must be exercised and one must check the validity of the assumption that the given acid or base is the only source of $[H^+]$ or $[OH^-]$.

Some Other Logarithmic Expressions. Just as pH is used to indicate hydrogen ion concentration, pOH is used to indicate hydroxyl ion concentration. Thus,

$$pOH = -\log [OH^-] \qquad ...(20)$$

Ionic product of water, K_w, is also frequently expressed in a similar manner as

$$pK_w = -\log K_w \qquad ...(21)$$

Remembering that $[H^+][OH^-] = K_w$ and taking logs and reversing signs, we have

$$-\log [H^+] - \log [OH^-] = -\log K_w \qquad ...(22)$$

or $$pH + pOH = pK_w \qquad ...(23)$$

This relationship holds good for water as well as for any aqueous solution.

Since K_w at 25°C is about 10^{-14}, pK_w is 14·0. Hence,

$$pH + pOH = 14 \qquad ...(24)$$

In other words, the sum of pH and pOH is equal to 14 in water or in any aqueous solution at 25°C.

We may also represent dissociation constants of acids and bases (K_a and K_b) in the form of the following expressions :

$$pK_a = -\log K_a \qquad ...(25)$$

and $$pK_b = -\log K_b \qquad ...(26)$$

Example 13. Calculate the pH and pOH of 0·03 M aqueous solution of HCl at 25°C.

Solution : HCl, being a strong electrolyte, is completely dissociated in aqueous solution. Hence, the hydrogen ion concentration, $[H^+]$, is equal to the given concentration of HCl in solution :

$$[H^+] = 0{\cdot}03 \text{ M} = 3\times10^{-2} \text{ mol dm}^{-3}$$

$$pH = -\log [H^+] = -\log (3\times10^{-2}) = 1{\cdot}52$$

Since $pH + pOH = 14$ at 25°C,

$$\therefore \quad pOH = 14 - 1{\cdot}52 = 12{\cdot}48$$

Example 14. Calculate the pH and the hydrogen and hydroxyl ion concentrations of a $3{\cdot}2\times10^{-3}$ M solution of $Ba(OH)_2$ in water at 25°C.

Solution : $Ba(OH)_2$ is a strong base which dissociates to furnish two moles of OH^- ions for one mole of the base :

$$Ba(OH)_2 \longrightarrow Ba^{2+} + 2OH^-$$

Hence, $$[OH^-] = 2\times3{\cdot}2\times10^{-3} \text{ M} = 6{\cdot}4\times10^{-3} \text{ mol dm}^{-3}$$

$$pOH = -\log [OH^-] = -\log (6{\cdot}4\times10^{-3}) = -\log 6{\cdot}4 - \log 10^{-3}$$

$$= -0{\cdot}8062 - (-3) = -0{\cdot}8062 + 3 = 2{\cdot}19$$

Since $pH + pOH = 14$ at 25°C

$$\therefore \quad pH = 14 - 2{\cdot}19 = 11{\cdot}81$$

$$[H^+] = \frac{K_w}{[OH^-]} = \frac{1{\cdot}008\times10^{-14} \text{ mol}^2 \text{ dm}^{-6}}{6{\cdot}4\times10^{-3} \text{ mol dm}^{-3}} = 1{\cdot}57\times10^{-12} \text{ mol dm}^{-3}$$

Common Ion Effect. If a salt of a weak acid is added to a solution of the acid itself, the dissociation of the acid is diminished further. For example, the addition of sodium acetate to a solution of acetic acid suppresses the dissociation of acetic acid which is already very small. Consider the equilibrium,

$$CH_3COOH \rightleftharpoons H^+ + CH_3COO^-$$

The addition of one of the products of dissociation (*e.g.*, acetate ions) supplied by the largely dissociated salt (*e.g.*, sodium acetate) pushes the equilibrium to the left. In other words, the dissociation of acetic acid is suppressed. Similarly, the addition of hydrogen ions furnished by the addition of largely dissociated acid such as hydrochloric acid, also suppresses the dissociation of acetic acid.

Likewise the dissociation of a weak base, such as ammonium hydroxide, represented by the equilibrium

$$NH_4OH \rightleftharpoons NH_4^+ + OH^-$$

is suppressed on the addition of a salt like ammonium chloride which supplies ammonium ions. The addition of a strong base like sodium hydroxide which supplies hydroxyl ions, also suppresses the dissociation of ammonium hydroxide.

The suppression of the dissociation of a weak acid or a weak base on the addition of its own ions is called **common ion effect.**

Mixtures of Weak Acids and Salts. The hydrogen ion concentration of a mixture of a weak acid and its highly dissociated salt can be calculated from the simple equilibrium law considerations.

Suppose a monobasic weak acid, say, HA, is dissociated as

$$HA \rightleftharpoons H^+ + A^-$$

The dissociation constant K_a is given by the expression

$$K_a = [H^+][A^-]/[HA]$$

or $$[H^+] = K_a[HA]/[A^-] \quad ...(27)$$

Although the above equation has been derived on the basis of the dissociation of the acid HA alone, it holds good whatever be the source from which H^+ or A^- ions are derived.

Suppose there is a mixture of a weak acid HA and its almost completely dissociated sodium salt NaA. Let c_1 and c_2 represent the molar concentrations of acid and salt, respectively. Since the dissociation of the acid, which is very small by itself, is further suppressed by the presence of A^- ion (common ion effect), while the salt is presumed to be almost entirely dissociated, it follows that the anionic concentration

$$[A^-] = c_2$$

and concentration of undissociated acid, being the same as that of the total acid, is given by

$$[HA] = c_1$$

Hence, Eq. 27 becomes $$[H^+] = K_a c_1/c_2$$

or, in general, $$[H^+] = K_a\,[\text{Acid}]/[\text{Salt}] \quad ...(28)$$

Thus, the hydrogen ion concentration is determined by the dissociation constant of the acid, K_a and the ratio of the concentrations of acid and salt in the mixture. Since K_a is constant, it follows that the hydrogen ion concentration of a weak acid decreases as the ratio [acid]/[salt] in the mixture decreases. This is illustrated in the following table in the case of acetic acid–sodium acetate mixtures.

Ratio [Acid]/[Salt]	16	4	2	1	0·5	0·25	0·062
$[H^+]\times10^5$	28·80	7·21	3·60	1·81	0·91	0·45	0·11

Thus, the hydrogen ion concentration of acetic acid–sodium acetate mixture can be made to decrease from $28{\cdot}8\times10^{-5}$ mole per litre to $0{\cdot}11\times10^{-5}$ mole per litre, simply by adding increasing amounts of sodium acetate.

Example 15. What will be the hydrogen ion concentration of a solution obtained by mixing 500 ml of 0·20 M acetic acid and 500 ml of 0·30 M sodium acetate ? (Dissociation constant of acetic acid = $1{\cdot}75\times10^{-5}$).

Solution : Concentration of acetic acid in the mixture = $500\times0{\cdot}20/1000 = 0{\cdot}10$ mol dm^{-3}

Concentration of sodium acetate = $500\times0{\cdot}30/1000 = 0{\cdot}15$ mol dm^{-3}

$$[H^+] = K_a\,[\text{Acid}]/[\text{Salt}] \quad \text{(Eq. 28)}$$

$$= 1{\cdot}75\times10^{-5} \text{ mol dm}^{-3}\times0{\cdot}10 \text{ mol dm}^{-3}/0{\cdot}15 \text{ mol dm}^{-3} = \mathbf{1{\cdot}17\times10^{-5} \text{ mol dm}^{-3}}$$

BUFFER SOLUTIONS

For many purposes in chemistry, industry and biology, it is necessary to have solutions whose *p*H does not change much even on the addition of appreciable amounts of strong acids or strong alkalies. Such solutions are called buffer solutions.

A* buffer solution *is one which can resist change in its* pH *on the addition of an acid or a base.

Consider a solution of sodium chloride in water. Its *p*H is 7. The addition of even 1 ml of 1 M HCl solution to one litre of sodium chloride solution lowers the *p*H of the solution from 7 to about 3. Similarly, the addition of 1 ml of 1 M NaOH solution to one litre of sodium chloride solution raises the *p*H of the solution from 7 to about 11. Sodium chloride solution, therefore, is *not* a buffer.

The *p*H of an aqueous solution of ammonium acetate is also 7. But the addition of the same amount of acid or alkali, as the one added in the case of sodium chloride solution, does not cause any

appreciable alteration in the *p*H of ammonium acetate solution. Thus, ammonium acetate solution is a buffer as it can resist alterations in its *p*H on the addition of an acid or a base.

Let us see why a solution of ammonium acetate is a buffer while that of sodium chloride is not.

Ammonium acetate, like any other salt, exists almost entirely in the form of its ions, *viz.*, NH_4^+ and CH_3COO^- ions. If an acid is added to this solution, the H^+ ions furnished by the acid combine with acetate ions to form feebly dissociated molecules of acetic acid :

$$CH_3COO^- + H^+ \longrightarrow \underset{\text{Feebly dissociated}}{CH_3COOH}$$

Since most of the H^+ ions added are taken up by acetate ions to form acetic acid which itself is only slightly dissociated, the H^+ ion concentration (and hence the *p*H) of ammonium acetate solution changes only slightly.

Now, suppose a base is added to ammonium acetate solution. The OH^- ions furnished by the base will be taken up by NH_4^+ ions to form feebly dissociated NH_4OH :

$$NH_4^+ + OH^- \longrightarrow \underset{\text{Feebly dissociated}}{NH_4OH}$$

Since most of the OH^- ions added are taken up by NH_4^+ ions to form weakly dissociated NH_4OH, there is very little change in the *p*H of ammonium acetate solution.

Buffer solutions are considered to possess *reserve acidity* as well as *reserve alkalinity*. Thus, ammonium acetate has reserve acidity due to the presence of NH_4^+ ions and reserve alkalinity due to the presence of CH_3COO^- ions.

Now let us see why a solution of sodium chloride is not a buffer. In aqueous solution it is almost entirely dissociated into Na^+ and Cl^- ions. If H^+ ions are added to this solution, the hydrogen ion concentration increases, *i.e.*, the *p*H falls immediately. The reason is that HCl, likely to be formed, is itself almost completely dissociated. If OH^- ions are added to the solution, the hydrogen ion concentration falls, *i.e.*, the *p*H rises. The reason is that NaOH, likely to be formed, is itself almost completely dissociated.

The capacity of a solution to resist alteration in its *p*H, is known as its **buffer capacity.**

Buffer Capacity and Buffer Index. Van Slyke introduced a quantity called **buffer index,** β, as a quantitative measure of the buffer capacity. It is defined as

$$\beta = dB/d(p\text{H})$$

where dB is the increment of a strong base added to a buffer solution and $d(p\text{H})$ is the resulting increment in *p*H. The quantity dB is given in moles per 1000 gram of the solvent. β is always a positive quantity. Addition of a strong acid is equivalent to $-dB$, *i.e.*, a negative increment of base and to $-dp$H (since *p*H decreases on the addition of the acid). Hence, β remains positive.

Most of the important buffer solutions usually consist of mixtures of either weak acids and their salts or weak bases and their salts.

Buffer Mixture of a Weak Acid and its Salt. A very common buffer is prepared by mixing equimolar aqueous solutions of acetic acid and sodium acetate. Acetic acid is very slightly dissociated while sodium acetate, being a salt, is almost completely dissociated. The mixture thus contains CH_3COOH molecules as well as CH_3COO^- and Na^+ ions. Let us consider the buffer action of this mixture.

Suppose a strong acid is added to the above mixture. The H^+ ions added will be taken up immediately by CH_3COO^- ions to form very slightly dissociated CH_3COOH :

$$H^+ + CH_3COO^- \longrightarrow \underset{\text{Feebly dissociated}}{CH_3COOH}$$

Thus, the H^+ ions added are neutralised by the acetate ions present in the mixture. There is very little change in the *p*H of the mixture.

If, on the other hand, a strong base is added, the OH^- ions added are neutralised by the acetic acid present in the mixture :

$$OH^- + CH_3COOH \longrightarrow CH_3COO^- + H_2O$$

Thus, again, there is very little change in the *p*H of the mixture.

It should be clear from the above mechanism of buffer action that reserve acidity of CH_3COOH-CH_3COONa buffer is due to the presence of CH_3COOH and reserve alkalinity is due to the presence of CH_3COO^- ions.

It may be of interest to note that while addition of 1 ml of 1 M HCl to 10 ml of a sodium chloride solution lowers the *p*H from 7·0 to about 1·0, the addition of the same amount of HCl to 10 ml of a buffer containing 1 mole of CH_3COOH and 1 mole of CH_3COONa will lower the *p*H from 4·75 to 4·66 only.

Buffer Mixture of a Weak Base and its Salt. A mixture containing equimolar aqueous solutions of ammonium hydroxide and its almost completely dissociated salt, ammonium chloride, constitutes another good buffer. The mixture contains undissociated NH_4OH as well as NH_4^+ and Cl^- ions. The buffer action of this mixture may now be considered.

If a strong acid is added, the H^+ ions added are neutralised by the base NH_4OH :

$$H^+ + NH_4OH \longrightarrow H_2O + NH_4^+$$

If a strong base is added, the OH^- ions added are neutralised by NH_4^+ ions forming very slightly dissociated NH_4OH.

In this case, evidently, reserve acidity is due to the presence of NH_4^+ ions and reserve alkalinity is due to the presence of NH_4OH.

Calculation of *p*H of Buffer Mixtures

A. Buffer Mixture of a Weak Acid and its Salt. Henderson-Hasselbalch Equation. Consider first a buffer solution containing a weak acid HA and its highly dissociated salt NaA. The hydrogen ion concentration of such a solution is given by the equation

$$[H^+] = K_a\,[\text{Acid}]/[\text{Salt}] \qquad \text{(Eq. 28)}$$

Taking logs and reversing the signs, we have

$$-\log [H^+] = -\log K_a + \log ([\text{Salt}]/[\text{Acid}])$$

or

$$pH = pK_a + \log ([\text{Salt}]/[\text{Acid}]) \qquad \ldots(29)$$

This equation, known as **Henderson-Hasselbalch equation,** enables the calculation of *p*H of a buffer solution made by mixing known quantities of a weak acid and its salt. Alternatively, it enables calculation of the ratio in which acid and salt must be mixed in order to get a buffer solution of a definite *p*H.

Example 16. What would be the *p*H of an aqueous solution obtained by mixing 5 gram of acetic acid and 7·5 gram of sodium acetate and making the volume equal to 500 ml ? Dissociation constant of acetic acid at 25°C is $1{\cdot}75\times10^{-5}$.

Solution : $pH = pK_a + \log ([\text{Salt}]/[\text{Acid}])$ (Eq. 29)

In this case, $pK_a = -\log K_a = -\log (1{\cdot}75\times10^{-5}) = 4{\cdot}76$

$$[\text{Salt}] = \left(\frac{7{\cdot}5}{82}\times\frac{1000}{500}\right) = 0{\cdot}1829 \text{ mol dm}^{-3}$$

$$[\text{Acid}] = \left(\frac{5}{60}\times\frac{1000}{500}\right) = 1{\cdot}666 \text{ mol dm}^{-3}$$

$$pH = 4{\cdot}76 + \log\frac{0{\cdot}1829}{0{\cdot}1666} = 4{\cdot}80$$

Example 17. A buffer solution contains 0·2 mole of acetic acid and 0·25 mole of potassium acetate per litre. Calculate the change in *p*H of the solution if 0·5 ml of 1 M HCl is added to it. The dissociation constant of acetic acid at room temperature is $1{\cdot}75\times10^{-5}$. (The volume change on the addition of HCl may be neglected).

Solution : $pH = pK_a + \log ([\text{Salt}]/[\text{Acid}])$ (Eq. 29)

$pK_a = -\log K_a = -\log 1{\cdot}75\times10^{-5} = 4{\cdot}76$

*p*H of the solution before adding HCl will be given by

$$pH = pK_a + \log\frac{0{\cdot}25}{0{\cdot}20} = 4{\cdot}76 + 0{\cdot}0969 = 4{\cdot}8569$$

Amount of HCl added = 0·5 ml of 1M HCl = 0·5 millimole = 0·0005 mole

Assuming HCl to be completely dissociated, the amount of H^+ ions added will be = 0·0005 mole

The addition of H^+ ion will result in the reaction

$$CH_3COO^- + H^+ \longrightarrow CH_3COOH$$

i.e., the amount of acetic acid will increase and that of the salt will correspondingly decrease by 0·0005 mole.

∴ After adding HCl,

$$[CH_3COOH] = 0{\cdot}20 + 0{\cdot}0005 = 0{\cdot}2005 \text{ mol dm}^{-3}$$

and $$[CH_3COOK] = 0{\cdot}25 - 0{\cdot}0005 = 0{\cdot}2495 \text{ mol dm}^{-3}$$

(The change of volume resulting from the addition of HCl is negligible)

$$pH = pK_a + \log ([\text{Salt}]/[\text{Acid}]) = 4{\cdot}76 + \log\frac{0{\cdot}2495}{0{\cdot}2005} = 4{\cdot}8549$$

∴ Change of *p*H = 4·8569 - 4·8549 = **0·002**

We see that there is only a slight change in the *p*H.

Example 18. Calculate the *p*H before and after the addition of 0·01 mole of NaOH to 1 litre of a buffer solution that is 0·1 M in acetic acid and 0·1 M in sodium acetate. The dissociation constant of acetic acid is $1{\cdot}75\times10^{-5}$.

Solution : Prior to the addition of NaOH,

$$[CH_3COOH] = 0{\cdot}1 \text{ M} ; \qquad [CH_3COO^-] = 0{\cdot}1 \text{ M}$$

Using Eq. 29, $$pH = pK_a + \log\frac{[CH_3COO^-]}{[CH_3COOH]}$$

$$pK_a = -\log K_a = -\log (1{\cdot}75\times10^{-5}) = 4{\cdot}76$$

∴ $$pH = 4{\cdot}76 + \log\frac{0{\cdot}1}{0{\cdot}1} = 4{\cdot}76 + \log 1 = 4{\cdot}76 + 0 = 4{\cdot}76$$

After the addition of 0·01 mole of NaOH, some of the acetic acid is neutralized so that the concentration of the weak acid is diminished while that of the salt (the acetate ion) is increased. Thus, we have

$$[CH_3COOH] = 0{\cdot}1 - 0{\cdot}01 = 0{\cdot}09 \text{ mol dm}^{-3}$$

$$[CH_3COO^-] = 0{\cdot}1 + 0{\cdot}01 = 0{\cdot}11 \text{ mol dm}^{-3}$$

Hence, the *p*H of the buffer is given by

$$pH = 4{\cdot}76 + \log\frac{0{\cdot}11}{0{\cdot}09} = 4{\cdot}76 + 0{\cdot}087 = 4{\cdot}847$$

We see that the *p*H of the buffer solution increases *very slightly*.

B. Buffer Mixture of a Weak Base and its Salt. If a buffer solution consists of a mixture of a weak base and its salt, it can be easily shown that

$$[OH^-] = K_b\,[\text{Base}]/[\text{Salt}]$$

$$\therefore \quad pOH = pK_b + \log([\text{Salt}]/[\text{Base}]) \qquad \ldots(30)$$

Knowing pOH, the pH can easily be calculated from the well known relationship : $p\text{H} + p\text{OH} = pK_w = 14$.

Example 19. A buffer solution contains 0·20 mole of NH_4OH and 0·25 mole of NH_4Cl per litre. Calculate the pH of the solution. Dissociation constant of NH_4OH at the room temperature is $1{\cdot}81\times10^{-5}$.

Solution :

$$pOH = pK_b + \log([\text{Salt}]/[\text{Base}]) \qquad \text{(Eq. 30)}$$

$$pK_b = -\log K_b = -\log(1{\cdot}81\times10^{-5}) = 4{\cdot}7423$$

$$pOH = 4{\cdot}7423 + \log\frac{0{\cdot}25}{0{\cdot}20} = 4{\cdot}839$$

$$p\text{H} = 14 - 4{\cdot}839 = \mathbf{9{\cdot}161}$$

HYDROLYSIS OF SALTS

Water is dissociated to a very small extent into H^+ and OH^- ions :

$$H_2O \rightleftharpoons H^+ + OH^-$$

In pure water, the concentrations of H^+ ions and OH^- ions are equal to each other, *i.e.*,

$$[H^+] = [OH^-]$$

Pure water, therefore, is neutral.

Salts are strong electrolytes. When dissolved in water, they dissociate almost completely into positively charged ions (cations) and negatively charged ions (anions). In some of the salts, the anions of the salt react with H^+ ions furnished by water thereby lowering the concentration of H^+ ions in solution. Since the product of $[H^+]$ and OH^- ions is constant $\{[H^+][OH^-]=K_w\}$, therefore, the concentration of OH^- ions in the solution increases. The solution, therefore, becomes alkaline.

In the case of some other salts, the cations of the salt react with OH^- ions furnished by water thereby lowering the concentration of OH^- ions in solution. Since K_w is constant, the concentration of H^+ ions in the solution increases. The solution, therefore, becomes **acidic.**

The phenomenon of the interaction of anions and cations of the salt with the H^+ and OH^- ions furnished by water yielding acidic or alkaline (or sometimes even neutral) solutions is known as salt **hydrolysis.**

Hydrolysis may also be considered as the reverse of neutralisation. Neutralisation, as we know, involves combination of H^+ and OH^- ions yielding undissociated water, *i.e.*, it involves almost complete disappearance of H^+ and OH^- ions. Hydrolysis, on the other hand, leads to the formation of H^+ or OH^- ions, as discussed above.

For a study of hydrolysis, it is convenient to divide the salts into four categories :

1. Salts of strong acids and strong bases such as potassium chloride and sodium nitrate.
2. Salts of weak acids and strong bases, such as potassium cyanide and sodium acetate.
3. Salts of strong acids and weak bases, such as ammonium chloride and aniline hydrochloride.
4. Salts of weak acids and weak bases, such as ammonium acetate.

1. Salts of Strong Acids and Strong Bases. Salts of strong acids and strong bases *do not hydrolyse.* Consider, for example, potassium chloride. When it is dissolved in water, its ions, K^+ and Cl^-, have no tendency to react with the H^+ and OH^- ions of water. This is because the possible products of such interactions, namely, KOH and HCl, are themselves almost completely dissociated. Consequently,

there is no change in the concentration of H^+ or OH^- ions and the solution continues to remain neutral. Thus, salts of strong acids and strong bases do not undergo hydrolysis.

2. Salts of Weak Acids and Strong Bases. Salts of this category undergo hydrolysis to give alkaline solutions. Consider sodium acetate as an example of this category. When dissolved in water it undergoes almost complete dissociation into Na^+ and CH_3COO^- ions.

$$CH_3COONa \longrightarrow CH_3COO^- + Na^+$$

The acetate ions will take up some of the H^+ ions furnished by the slightly dissociated water to form the feebly dissociated acetic acid :

$$CH_3COO^- + H^+ \longrightarrow CH_3COOH$$

The undissociated water further dissociates so as to maintain the constant value of $K_w = [H^+][OH^-]$. The H^+ ions are again taken up by CH_3COO^- ions. This leads to an increase in the concentration of hydroxyl ions and decrease in the concentration of hydrogen ions. The solution, therefore, becomes alkaline.

Thus, the aqueous solution of the salt of a weak acid and a strong base is alkaline because of hydrolysis.

Hydrolysis Constant. The hydrolytic reaction of sodium acetate may be written as

$$CH_3COO^- + Na^+ + H_2O \rightleftharpoons CH_3COOH + Na^+ + OH^-$$

Since, Na^+ ion is common on both sides of the equation, it may be left out and the equation may be represented as

$$\underset{\text{Unhydrolysed salt}}{CH_3COO^-} + H_2O \rightleftharpoons \underset{\text{Free base}}{OH^-} + \underset{\text{Free acid}}{CH_3COOH}$$

Applying the law of chemical equilibrium and taking the concentration of water as constant (since it is present in large excess), we have

$$K_h = \frac{[OH^-][CH_3COOH]}{[CH_3COO^-]} \qquad \ldots(31)$$

K_h is known as **hydrolysis constant.**

Relation between K_h, K_a and K_w. It should be noted that ultimately when the equilibrium of hydrolytic reaction of CH_3COONa is established, the following two equilibra have also to be satisfied :

$$CH_3COOH \rightleftharpoons CH_3COO^- + H^+$$

$$H_2O \rightleftharpoons H^+ + OH^-$$

Therefore, the following equations should also hold good :

$$K_a = \frac{[H^+][CH_3COO^-]}{[CH_3COOH]} \qquad \ldots(32)$$

where K_a is the dissociation constant of the acid and

$$K_w = [H^+][OH^-] \qquad \ldots(33)$$

Dividing Eq. 33 by Eq. 32, we get

$$\frac{K_w}{K_a} = \frac{[OH^-][CH_3COOH]}{[CH_3COO^-]} = K_h \qquad \text{(from Eq. 31)}$$

Thus,

$$K_h = K_w/K_a \qquad \ldots(34)$$

Evidently, the hydrolysis constant K_h of the salt varies inversely as the dissociation constant K_a of the weak acid. Therefore, the weaker the acid, the greater is the hydrolysis constant of the salt.

Degree of Hydrolysis. Let c moles per litre be the initial concentration of sodium acetate in aqueous solution and let x be the **degree of hydrolysis** which is defined as the fraction of the total salt that has undergone hydrolysis on the attainment of equilibrium. Rewriting the hydrolysis equation as before and putting the equilibrium concentrations of the various species, we have

$$\underset{c(1-x)}{CH_3COO^-} + H_2O \rightleftharpoons \underset{cx}{CH_3COOH} + \underset{cx}{OH^-}$$

$$K_h = \frac{cx \times cx}{c(1-x)} = \frac{cx^2}{1-x}$$

If x is small as compared to unity, $(1 - x)$ in the above equation may be replaced by 1 so that

$$K_h = cx^2 \quad \text{or} \quad x = \sqrt{K_h/c} \qquad ...(35)$$

But, $K_h = K_w/K_a$ (Eq. 34)

$$\therefore \quad x = \sqrt{K_w/(K_a \times c)} \qquad ...(36)$$

By means of Eq. 36 it is possible to calculate the degree of hydrolysis of a salt of a weak acid and a strong base at any concentration c of the salt provided the dissociation constant K_a of the acid is known.

It also follows from Eq. 36 that the weaker the acid (*i.e.*, the smaller the value of K_a), the greater is x, the degree of hydrolysis. Also, since K_w increases rapidly with temperature and K_a changes only slightly, it is evident that the degree of hydrolysis increases considerably with rise of temperature. Lastly, it is seen that the degree of hydrolysis increases when concentration (c) decreases, *i.e.*, when dilution increases.

Example 20. Calculate the degree of hydrolysis of 0·10 M solution of sodium acetate at 25°C. $K_a = 1{\cdot}75 \times 10^{-5}$ and $K_w = 1{\cdot}008 \times 10^{-14}$.

Solution : $$K_h = K_w/K_a = \frac{1{\cdot}008 \times 10^{-14}}{1{\cdot}75 \times 10^{-5}} = 5{\cdot}76 \times 10^{-10}$$

Assuming that the degree of hydrolysis (x) is small,

$$x = \sqrt{K_h/c} = \sqrt{\frac{5{\cdot}75 \times 10^{-10}}{0{\cdot}10}} = 7{\cdot}589 \times 10^{-5}$$

Thus, the degree of hydrolysis $= 7{\cdot}589 \times 10^{-5}$

***p*H of the Hydrolysed Salt Solution.** As shown above, in the hydrolysis of CH_3COONa, $[OH^-] = cx$. Substituting the value of x from Eq. 36, we have

$$[OH^-] = c\left(\frac{K_w}{K_a c}\right)^{\frac{1}{2}} = \left(\frac{K_w c}{K_a}\right)^{\frac{1}{2}}$$

Taking negative logs of both sides, we get

$$pOH = \tfrac{1}{2}\, pK_w - \tfrac{1}{2} \log\, c - \tfrac{1}{2}\, pK_a$$

But $\quad pH + pOH = 14$

$$\therefore \quad pH = 14 - \tfrac{1}{2}\, pK_w + \tfrac{1}{2} \log c + \tfrac{1}{2}\, pK_a \qquad ...(37)$$

Example 21. Calculate the *p*H of 0·01 M aqueous solution of CH_3COONa at 25°C (K_a for $CH_3COOH = 1{\cdot}75 \times 10^{-5}$). $K_w = 1{\cdot}008 \times 10^{-14}$.

Solution :

$$pK_w = -\log K_w = -\log (1{\cdot}008 \times 10^{-14}) = 13{\cdot}997 = 14$$

$$pK_a = -\log K_a = -\log (1{\cdot}75 \times 10^{-5}) = 4{\cdot}76$$

$$\log c = \log (10^{-2}) = -2$$

Substituting in Eq. 37, we have

$$pH = 14 - \tfrac{1}{2}(14{\cdot}0) + \tfrac{1}{2}(-2) + \tfrac{1}{2}(4{\cdot}76) = 8{\cdot}38$$

The *p*H shows that the solution is alkaline, as expected.

3. Salts of Weak Bases and Strong Acids. Consider ammonium chloride as an example of this category of salts. In water, it undergoes almost complete dissociation into NH_4^+ and Cl^- ions. The ammonium ions take up OH^- ions furnished by water to form the feebly dissociated base, ammonium hydroxide (NH_4OH). The undissociated water further dissociates so as to maintain the constant value of K_w. This causes an increase in the concentration of hydrogen ions and a decrease in the concentration of hydroxyl ions. The solution, therefore, becomes *acidic*.

Thus, an aqueous solution of a salt of a weak base and a strong acid is acidic because of hydrolysis.

Hydrolysis Constant. The hydrolytic reaction of ammonium chloride may be represented as

$$NH_4^+ + Cl^- + H_2O \rightleftharpoons NH_4OH + Cl^- + H^+$$

Since Cl^- ion is common on both sides of the equation, it may be left out and the equation may be represented as

$$\underset{\text{Unhydrolysed salt}}{NH_4^+} + H_2O \rightleftharpoons \underset{\text{Free base}}{NH_4OH} + \underset{\text{Free acid}}{H^+}$$

Applying the law of chemical equilibrium, we have

$$K_h = [H^+]\,[NH_4OH]/[NH_4^+] \qquad ...(38)$$

K_h, as already mentioned, is known as hydrolysis constant.

Relation between K_h, K_b and K_w. The following other equilibria also exist in the solution :

$$NH_4OH \rightleftharpoons NH_4^+ + OH^-$$

and $$H_2O \rightleftharpoons H^+ + OH^-$$

Accordingly, the following equations should also hold good :

$$K_b = [NH_4^+][OH^-]/[NH_4OH] \qquad ...(39)$$

where K_b is the dissociation constant of the base and

$$K_w = [H^+][OH^-] \qquad ...(40)$$

Dividing Eq. 40 by Eq. 39, we get

$$K_w/K_b = [H^+][NH_4OH]/[NH_4^+] = K_h \qquad \text{(from Eq. 38)}$$

Thus, $$K_h = K_w/K_b \qquad ...(41)$$

It is evident that the weaker the base, the greater is the hydrolysis constant of the salt.

Degree of Hydrolysis. If c is the initial concentration of the salt in moles per litre and x is the degree of hydrolysis on the attainment of equilibrium, then the concentrations of the various species at equilibrium will be as represented below :

$$\underset{c(1-x)}{NH_4^+} + H_2O \rightleftharpoons \underset{cx}{NH_4OH} + \underset{cx}{H^+}$$

$$K_h = \frac{cx \times cx}{c(1-x)}$$

If, as before, x is too small as compared to unity

$$K_h = cx^2 \qquad ...(42)$$

or $$x = \sqrt{K_h/c} = \sqrt{K_w/(K_b \times c)} \quad \text{(from Eq. 41)} \qquad ...(43)$$

As in the previous case, the degree of hydrolysis of a salt, at a given temperature, is more if the base is weaker, *i.e.*, if K_b is smaller. Also, x increases when concentration decreases, *i.e.*, when dilution increases. Further, since K_w increases much more with temperature than K_b, the degree of hydrolysis at a given concentration increases with rise in temperature.

Example 22. The dissociation constant of NH_4OH at 25°C is $1{\cdot}81\times10^{-5}$. Calculate the degree of hydrolysis of a 0·01 M solution of ammonium chloride. K_w at 25°C = $1{\cdot}008\times10^{-14}$.

Solution : $$K_h = \frac{K_w}{K_b} = \frac{1{\cdot}008 \times 10^{-14}}{1{\cdot}81 \times 10^{-5}} = 5{\cdot}569 \times 10^{-10}$$

Assuming that the degree of hydrolysis x is very small,

$$x = \sqrt{K_h/c} \quad \text{(Eq. 43)}$$

$$= \sqrt{\frac{5{\cdot}569 \times 10^{-10}}{0{\cdot}01}} = 2{\cdot}359\times10^{-6}$$

***p*H of the Hydrolysed Salt Solution.** As shown above, in the hydrolysis of NH_4Cl,

$$[H^+] = cx$$

Substituting the value of x from Eq. 43, we have

$$[H^+] = c\left(\frac{K_w}{K_b c}\right)^{1/2} = \left(\frac{K_w c}{K_b}\right)^{1/2} \qquad ...(44)$$

Taking negative logs of both sides,

$$pH = \tfrac{1}{2}\, pK_w - \tfrac{1}{2} \log c - \tfrac{1}{2}\, pK_b \qquad ...(45)$$

Example 23. What would be the *p*H of 0·01 M solution of NH_4Cl in water at 25°C ? (K_b for $NH_4OH = 1{\cdot}81\times10^{-5}$).

Solution : $pK_w = -\log K_w = -\log 1{\cdot}008\times10^{-14} = 13{\cdot}997 = 14$

$pK_b = -\log K_b = -\log (1{\cdot}81\times10^{-5}) = 4{\cdot}74$

$\log c = \log (10^{-2}) = -2$

Using Eq. 45, $pH = \frac{1}{2}(14{\cdot}0) - \frac{1}{2}(-2) - \frac{1}{2}(4{\cdot}74) = 5{\cdot}63$

The *p*H shows that the solution is acidic, as expected.

4. Salts of Weak Acids and Weak Bases. Salts of this category may be exemplified by ammonium acetate. The NH_4^+ and CH_3COO^- ions furnished by the salt combine with OH^- and H^+ ions of water, respectively, to form feebly dissociated NH_4OH and CH_3COOH. The reaction may be represented as

$$\underset{\text{Unhydrolysed salt}}{CH_3COO^-} + \underset{\text{Unhydrolysed salt}}{NH_4^+} + H_2O \rightleftharpoons \underset{\text{Free acid}}{CH_3COOH} + \underset{\text{Free base}}{NH_4OH}$$

In this case, both H^+ and OH^- ions are removed simultaneously and if they are removed in equivalent amounts, as in the present case, the solution remains **neutral** although hydrolysis of the salt has taken place.

The equilibrium law equation for hydrolysis constant in the present case may be written as

$$K_h = \frac{[CH_3COOH][NH_4OH]}{[CH_3COO^-][NH_4^+]} \qquad ...(46)$$

The following other equilibria also exist in the solution :

$$CH_3COOH \rightleftharpoons CH_3COO^- + H^+$$

$$NH_4OH \rightleftharpoons NH_4^+ + OH^-$$

$$H_2O \rightleftharpoons H^+ + OH^-$$

Accordingly, the following equations should hold good :

$$K_a = \frac{[CH_3COO^-][H^+]}{[CH_3COOH]} \qquad ...(47)$$

$$K_b = \frac{[NH_4^+][OH^-]}{[NH_4OH]} \qquad ...(48)$$

$$K_w = [H^+][OH^-] \qquad ...(49)$$

Dividing Eq. 49 by Eq. 48 as well as by Eq. 47, we have

$$\frac{K_w}{K_a \times K_b} = \frac{[CH_3COOH][NH_4OH]}{[CH_3COO^-][NH_4^+]} = K_h \quad \text{(from Eq. 46)}$$

Thus, in this case, $$K_h = \frac{K_w}{K_a \times K_b} \qquad ...(50)$$

If the initial concentration of the salt is c moles per litre and x is its degree of hydrolysis, then, at the equilibrium point, the concentrations of the various species will be as shown below :

$$\underset{c(1-x)}{CH_3COO^-} + \underset{c(1-x)}{NH_4^+} + H_2O \rightleftharpoons \underset{cx}{CH_3COOH} + \underset{cx}{NH_4OH}$$

$$\therefore \quad K_h = \frac{c^2x^2}{c^2(1-x)^2} = \frac{x^2}{(1-x)^2} \qquad ...(51)$$

Neglecting x as compared to unity, we have

$$K_h = x^2 \qquad ...(52)$$

or $$x = \sqrt{K_h} = \sqrt{\frac{K_w}{K_a \times K_b}} \quad \text{(from Eq. 50)} \qquad ...(53)$$

It is evident from Eq. 53 that the weaker the acid and the base, the greater is the degree of hydrolysis of the salt. It should be noted that in this case *the degree of hydrolysis is independent of the concentration of the solution.* Further, as before, since K_w increases with temperature much more rapidly than either K_a or K_b, the degree of hydrolysis increases with rise of temperature.

Example 24. Calculate the degree of hydrolysis of decimolar solution of ammonium acetate at 25°C. Dissociation constants of acetic acid and ammonium hydroxide are $1{\cdot}75\times10^{-5}$ and $1{\cdot}81\times10^{-5}$, respectively, at 25°C. K_w at 25°C = $1{\cdot}008\times10^{-14}$.

Solution : $$K_h = \frac{K_w}{K_a \times K_b} \quad \text{(Eq. 50)}$$

$$= \frac{1{\cdot}008 \times 10^{-14}}{1{\cdot}75\times10^{-5} \times 1{\cdot}81\times10^{-5}} = 3{\cdot}182\times10^{-5}$$

In the present case, $$K_h = \frac{x^2}{(1-x)^2} \quad \text{(Eq. 51)}$$

or $$3{\cdot}182\times10^{-5} = \frac{x^2}{(1-x)^2}$$

$$\frac{x}{1-x} = \sqrt{3{\cdot}182 \times 10^{-5}}$$

If x is very small, it may be neglected as compared to unity.

$\therefore$ Degree of hydrolysis, $x = \sqrt{3{\cdot}182 \times 10^{-5}} = 5{\cdot}64 \times 10^{-3}$

pH of the Hydrolysed Salt Solution. For the dissociation of a weak acid HA,

$$K_a = \frac{[H^+][A^-]}{[HA]} \qquad ...(54)$$

If the initial concentration of the acid is c and x is the degree of dissociation, then

$$[H^+] = K_a \frac{[HA]}{[A^-]} = K_a \frac{cx}{c(1-x)} = K_a \frac{x}{1-x} \qquad ...(55)$$

From Eq. 51, $x/(1-x) = \sqrt{K_h}$

$$\therefore \quad [H^+] = K_a \sqrt{K_h} = K_a \left(\frac{K_w}{K_a K_b}\right)^{1/2} \quad \text{(from Eq. 50)}$$

$$= \left(\frac{K_w K_a}{K_b}\right)^{1/2} \qquad ...(56)$$

Taking negative logs of both sides,

$$pH = \tfrac{1}{2} pK_w + \tfrac{1}{2} pK_a - \tfrac{1}{2} pK_b \qquad ...(57)$$

From Eq. 57 we see that if K_a and K_b are equal, then $pH = \frac{1}{2} pK_w = 7$, that is, the solution is neutral in spite of the fact that the extent of hydrolysis may be considerable.

Determination of Degree of Hydrolysis. A number of methods for determining degree of hydrolysis are available. Some of these have been discussed below.

1. Indirect Method. The simplest though indirect method makes use of the relationships that exist between degree of hydrolysis of a salt, the ionic product of water and the dissociation constant of the weak acid or weak base from which the salt is obtained. The various equations have been reproduced below :

$$x = \sqrt{\frac{K_w}{K_a \times c}} \quad \text{(for a salt of a weak acid and a strong base)} \qquad \text{(Eq. 36)}$$

$$x = \sqrt{\frac{K_w}{K_b \times c}} \quad \text{(for a salt of a weak base and a strong acid)} \qquad \text{(Eq. 43)}$$

$$x = \sqrt{\frac{K_w}{K_a \times K_b}} \quad \text{(for a salt of a weak acid and a weak base)} \qquad \text{(Eq. 53)}$$

Knowing dissociation constant of acid or base (K_a or K_b) or both, as the case may be, it is a simple matter to calculate the degree of hydrolysis of a given salt at a given concentration. The concentration, however, has no effect if the salt is of a weak acid and a weak base.

Example 25. Calculate the percentage hydrolysis of sodium acetate in 0·1 M solution at 25°C assuming that the salt is completely dissociated. K_a of acetic acid at 25°C = $1{\cdot}75 \times 10^{-5}$. Ionic product of water at 25°C = $1{\cdot}008 \times 10^{-14}$.

Solution : The degree of hydrolysis x of a salt of a weak acid and a strong base is given by

$$x = \sqrt{\frac{K_w}{K_a \times c}} \qquad \text{(Eq. 36)}$$

$$= \sqrt{\frac{1{\cdot}008 \times 10^{-14}}{1{\cdot}75 \times 10^{-5} \times 0{\cdot}1}} = 7{\cdot}589 \times 10^{-5}$$

$\therefore$ Percentage hydrolysis = $7{\cdot}589 \times 10^{-3}$

Example 26. The dissociation constant of aniline as a base at 25°C is $5{\cdot}93 \times 10^{-10}$. The ionic product of water at 25°C is $1{\cdot}008 \times 10^{-14}$. Calculate the percentage hydrolysis of aniline hydrochloride in 0·1 M solution at 25°C.

Solution : The degree of hydrolysis x of the salt of a strong acid and a weak base is given by

$$x = \sqrt{\frac{K_w}{K_b \times c}} \qquad \text{(Eq. 43)}$$

$$x = \sqrt{\frac{1{\cdot}008 \times 10^{-14}}{5{\cdot}93 \times 10^{-10} \times 0{\cdot}1}} = 1{\cdot}30 \times 10^{-2}$$

$\therefore$ Percentage hydrolysis = 1·30

Example 27. The dissociation constants of aniline, acetic acid and water at 25°C are, respectively, $3{\cdot}83 \times 10^{-10}$, $1{\cdot}75 \times 10^{-5}$ and $1{\cdot}008 \times 10^{-14}$. Calculate the percentage hydrolysis of aniline acetate in a decimolar solution.

Solution : The degree of hydrolysis x of a salt of a weak acid and a weak base is given by

$$x = \sqrt{\frac{K_w}{K_a \times K_b}} \qquad \text{(Eq. 53)}$$

$$= \sqrt{\frac{1{\cdot}008 \times 10^{-14}}{1{\cdot}75 \times 10^{-5} \times 3{\cdot}83 \times 10^{-10}}} = 1{\cdot}219$$

But, x cannot be greater than 1. This indicates that the degree of hydrolysis in this case is very large and, therefore, the above formula, which is based on the assumption that x is small, is not applicable

In the present case, therefore, we have to calculate x as follows :

$$K_h = \frac{K_w}{K_a \times K_b} \qquad \text{(Eq. 50)}$$

But $$K_h = \frac{x^2}{(1-x)^2} \qquad \text{(Eq. 51)}$$

i.e., $$\frac{x}{1-x} = \sqrt{\frac{K_w}{K_a \times K_b}} = 1{\cdot}219 \quad \text{or} \quad x = 0{\cdot}5495$$

$\therefore$ Percentage hydrolysis = 54·95

2. Electrical Conductance Method. The electrical conductance of an aqueous solution of a salt of a weak acid or a weak base is due partly to the ions of the unhydrolysed salt and partly to the ions (particularly H^+ or OH^- ions) formed by hydrolysis. Consider, for example, a salt of a weak base and a strong acid, say, ammonium chloride. If x is the degree of hydrolysis, then, for every one mole of the salt, the number of moles of the various species at equilibrium will be as shown in the equation below :

$$\underset{1-x}{NH_4Cl} + H_2O \rightleftharpoons \underset{x}{NH_4OH} + \underset{x}{HCl}$$

Ammonium hydroxide, being a weak base, may be taken as undissociated and to contribute little or nothing towards the total conductance of the solution. The molar conductance of this solution Λ_m, as determined experimentally, will be the sum of the conductance of $1-x$ moles of ammonium chloride and x moles of hydrochloric acid.

$$\Lambda_m = (1-x)\Lambda'_m + x\,\Lambda^\circ_{m(HCl)} \qquad ...(58)$$

where $\Lambda^\circ_{m(HCl)}$ is the molar conductance of hydrochloric acid at infinite dilution and Λ'_m is the molar conductance of the unhydrolysed salt at the given concentration. The value of Λ'_m is obtained

by adding *excess* of the nonconducting or very slightly conducting ammonium hydroxide (base) to the salt solution. This suppresses the hydrolysis of ammonium chloride to such a large extent that the molar conductance of the solution can be taken as Λ_m, *i.e.*, the conductance of the unhydrolysed salt.

From Eq. 58 it follows that

$$x = \frac{\Lambda_m - \Lambda'_m}{\Lambda^\circ_{m(HCl)} - \Lambda'_m} \qquad ...(59)$$

Thus, all that is to be done is to measure the conductance of the salt solution before (Λ_m) and after the addition of excess of ammonia (Λ'_m). Then knowing the value of $\Lambda^\circ_{m(HCl)}$ ($= \lambda^\circ_{H^+} + \lambda^\circ_{Cl^-}$), x can be evaluated.

This is known as **Bredig's method.**

3. From Freezing Point Depression. Freezing point depression, as is well known, is a colligative property depending only upon the *number* of molecules and ions present in the dissolved state. Suppose that the salt under examination is sodium acetate and that one mole of it is dissolved in a given amount of the solvent. Let x be the degree of hydrolysis. Then the number of moles at equilibrium will be as shown below :

$$\underset{1-x}{CH_3COO^-} + \underset{1-x}{Na^+} + H_2O \rightleftharpoons \underset{x}{CH_3COOH} + \underset{x}{Na^+} + \underset{x}{OH^-}$$

Total number of moles $= 1 - x + 1 - x + 3x = 2 + x$

$$\therefore \quad \frac{\text{Observed freezing point depression}}{\text{Calculated freezing point depression}} = \frac{2 + x}{2}$$

Thus, by determining the freezing point depression of a solution of a known concentration experimentally, the degree of hydrolysis x can be easily calculated.

Example 28. 10 gram of ammonium chloride (molar mass=53·5 g mol^{-1}) when dissolved in 1000 gram of water lowered the freezing point by 0·350°C. Calculate the degree of hydrolysis of the salt. The unhydrolysed salt may be taken as completely dissociated. The molal freezing point depression constant K_f of water is 1·86 K kg mol^{-1}.

Solution : We know that the freezing point depression, $\Delta T_f = \dfrac{K_f w_2}{M_2 w_1}$ (Chapter 22)

$$= \frac{(1{\cdot}86\,\text{K kg mol}^{-1})(10 \times 10^{-3}\,\text{kg})}{(53{\cdot}5 \times 10^{-3}\,\text{kg mol}^{-1})(1000 \times 10^{-3}\,\text{kg})} = 0{\cdot}347\,\text{K}$$

Let x be the degree of hydrolysis of ammonium chloride. Then, the number of moles of various species at equilibrium will be as shown below :

$$\underset{1-x}{NH_4^+} + \underset{1-x}{Cl^-} + H_2O \rightleftharpoons \underset{x}{NH_4OH} + \underset{x}{H^+} + \underset{x}{Cl^-}$$

Total number of moles $= 1 - x + 1 - x + 3x = 2 + x$

$$\frac{\text{Observed freezing point depression}}{\text{Calculated freezing point depression}} = \frac{2 + x}{2}$$

$$\frac{0{\cdot}350}{0{\cdot}347} = \frac{2 + x}{2}$$

$$\therefore \quad x = 0{\cdot}017$$

Thus, the degree of hydrolysis of $NH_4Cl = 0{\cdot}017$

4. From Distribution Law. The degree of hydrolysis of a salt can be determined by the application of distribution law, provided the free acid or free base formed during hydrolysis is soluble in an immiscible solvent like benzene. The hydrolysis of aniline hydrochloride may be taken as an example.

The salt on hydrolysis yields free aniline which is soluble in water as well as in benzene and hydrochloric acid which remains soluble only in water. On adding a small amount of benzene, the

free aniline distributes itself between the two solvents, as shown in Fig. 1, in accordance with the distribution law. The concentration of aniline in the benzene layer can be determined experimentally (by evaporating a known amount of the solution or by titrating against an acid) and its concentration in the aqueous layer is calculated knowing the value of its partition coefficient between water and benzene. The amount of free hydrochloric acid must be equal to the *total* amount of free aniline produced and is, therefore, obtained by taking the *total* of aniline in benzene and in aqueous layer. This, divided by the volume of water, gives the concentration of free hydrochloric acid in the aqueous layer. Subtracting this value from the initial concentration of the salt, the concentration of the unhydrolysed salt is obtained.

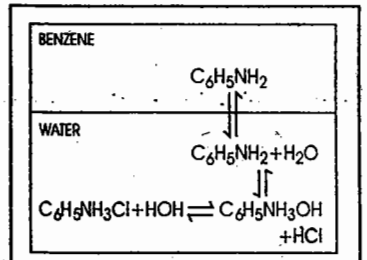

Fig. 1: Hydrolysis of aniline hydrochloride.

The hydrolysis constant K_h is then calculated by the usual equation, *viz.*,

$$K_h = \frac{[\text{Free aniline in aqueous layer}][\text{Free HCl}]}{[\text{Unhydrolysed salt}]}$$

Knowing K_h, the degree of hydrolysis x can be calculated by the relation,

$$x = \sqrt{K_h / c}$$

where c is the initial concentration of the salt in moles per litre.

Acid–Base Indicators

A hydrogen ion (or acid–base) indicator is a substance which changes its colour within limits with variation in *p*H of the solution to which it is added. This gives an easy method of determining *p*H of a solution by simply adding a *suitable* indicator and noting the colour. The *p*H range, over which the colour change occurs, varies considerably from one indicator to another. For example, methyl orange gives full acid colour (red) when added to a solution the *p*H of which is 3 or below and full basic colour (yellow) in a solution whose *p*H is 4·4 or above. In solutions having *p*H between 3 and 4·4, methyl orange gives a colour intermediate between red and yellow. Thus, the *p*H range over which methyl orange can be used as an indicator lies between 3 and 4·4.

Phenolphthalein, another common indicator, gives acid colour (colourless) in a solution of *p*H 8·3 or less and full basic colour (pink) in a solution of *p*H 10 or above. Thus, phenolphthalein can be used to determine *p*H over the range 8·3—10.

Theory of Acid–Base Indicators

Ostwald developed a theory of acid–base indicators which, though incomplete, offers a simple explanation for the colour change with change in *p*H. According to this theory, a hydrogen ion indicator is either a weak organic acid or a base. The undissociated molecule has one colour and the ion furnished by it, on dissociation, has another colour.

Let the indicator be an acid of formula HIn. Then, its dissociation in solution may be represented as

$$\underset{\text{Colour } A}{HIn} \rightleftharpoons H^+ + \underset{\text{Colour } B}{In^-} \qquad ...(60)$$

The undissociated molecule HIn has one colour, say, colour *A*, while the ion In^- has another colour, say, colour *B*.

The equation for the above equilibrium may be written as

$$K_{In} = \frac{[H^+][In^-]}{[HIn]} \qquad ...(61)$$

K_{In} is known as the **indicator constant.**

Since the species In^- and HIn have different colours, the actual colour shown by the indicator will depend upon the hydrogen ion concentration of the solution. Thus, if the solution is acidic, *i.e.*, it contains excess of H^+ ions, the equilibrium in Eq. 60 will shift towards the left. The indicator will, therefore, show predominantly colour *A* (acidic colour).

On the other hand, if the solution is alkaline, *i.e.*, it contains excess of OH^- ions, the H^+ ions furnished by the indicator will be taken up to form undissociated water. Therefore, the equilibrium in Eq. 60 will shift towards the right and there will be larger concentration of the ions In^-. The indicator will, therefore, show predominantly colour *B* (basic colour). Eq. 60, thus, successfully explains the change of colour of an indicator when the solution changes from acidic to alkaline.

Action of Phenolphthalein. Phenolphthalein is a colourless weak acid. It dissolves in water and dissociates to some extent to give colourless hydrogen ions and pink coloured anions. The equilibrium may be represented as :

$$\underset{\text{(Colourless)}}{HPh} \rightleftharpoons \underset{\text{(Colourless)}}{H^+} + \underset{\text{(Pink)}}{Ph^-} \qquad ...(62)$$

The actual state of affairs is not so simple. Phenolphthalein, or any other indicator, first undergoes a reversible tautomeric change into a substance of a different colour which then dissociates almost completely to give the coloured anions or cations, as the case may be. The process in the case of phenolphthalein may be represented as

$$\underset{\text{Colourless}}{HPh} \rightleftharpoons \underset{\text{Coloured tautomeric form}}{HPh^*} \rightleftharpoons \underset{\text{Colourless}}{H^+} + \underset{\text{Pink}}{Ph^-} \qquad ...(63)$$

But, since the concentration of the undissociated molecules of the tautomeric form is usually very small, the simple dissociation equation (Eq. 62) given above is sufficient for most purposes.

If the solution is acidic, the hydrogen ions furnished by the acid suppress the dissociation of phenolphthalein, shifting the equilibrium towards the left (common ion effect). The solution, therefore, remains colourless. In the presence of an alkali, however, the hydroxyl ions combine with the H^+ ions furnished by the indicator to form undissociated water. The equilibrium, therefore, shifts towards the right giving more of the coloured anions. The solution, therefore, turns pink. Thus, the indicator appears colourless in acidic and pink in alkaline solution.

The reason why phenolphthalein is not a suitable indicator for titrating a weak base, like ammonium hydroxide, against a strong acid is that the hydroxyl ions furnished by the weak base at the end point of the titration are too few to shift the equilibrium sufficiently towards the right to raise the *p*H to 8·3 at least and, therefore, pink colour does not appear just at the end point. A sufficient excess of the weak base has to be added to get the end point.

Action of Methyl Orange. Methyl orange is a weak base which, for simplicity, may be represented as MeOH. It dissolves in water and undergoes dissociation to a small extent. The undissociated molecules are yellow while the cations Me^+ are red in colour. The dissociation may be written as

$$\underset{\text{Yellow}}{MeOH} \rightleftharpoons \underset{\text{Red}}{Me^+} + \underset{\text{Colourless}}{OH^-}$$

If the solution is acidic, the hydrogen ions furnished by the acid combine with OH^- ions furnished by the indicator to form undissociated water. This shifts the equilibrium towards the right giving more of the red coloured Me^+ ions. Therefore, in acidic solution, this indicator gives red colour. In the presence of an alkali, the OH^- ions suppress the dissociation of methyl orange. Hence, the solution in alkaline medium remains yellow in colour.

Methyl orange cannot be used as indicator for titrating a weak acid, like acetic acid, against a strong base because the hydrogen ions furnished by the weak acid at the end point are too few to combine with a sufficient number of hydroxyl ions of methyl orange to shift the equilibrium in favour of the red coloured Me^+ ions. A sufficient excess of the weak acid has to be added to get the end point.

Some common indicators together with their useful ranges and extreme colours in acidic and alkaline solutions are given in Table 4.

TABLE 4
Some Useful Indicators

Indicator	*p*H range	Colour in acidic solution	Colour in alkaline solution
Cresol red (acid)	1·2–1·8	Red	Yellow
m-Cresol purple	1·2–1·8	Red	Yellow
Thymol blue (acid)	1·2–2·8	Red	Yellow
Bromophenol blue	3·1–4·6	Yellow	Purple
Methyl orange	3·1–4·5	Red	Yellow
Methyl red	4·2–6·3	Red	Yellow
Bromothymol blue	6·0–7·6	Yellow	Blue
Phenol red	6·4–8·2	Yellow	Red
Cresol red (base)	7·0–8·1	Yellow	Red
Thymol blue (base)	8·1–9·6	Yellow	Blue
Phenophthalein	8·0–9·8	Colourless	Pink
Thymolphthalein	9·3–10·5	Colourless	Blue
Alizarine yellow	10·1–12·1	Yellow	Lilac

Acid–Base Titrations and Use of Indicators. The process of acid–base titrations is accompanied by a change in *p*H. A plot between *p*H of the solution during titration and the amount of acid (or alkali) added from a burette is called a **titration curve.**

Indicators are frequently employed in detecting end points in acid–base titrations. Since, on account of hydrolysis, the *p*H at the end point depends upon the relative strengths of the acid and the base being titrated and since different indicators have different *p*H ranges within which they can be used, the selection of a proper indicator for a given titration is very important. The *p*H changes occurring in some acid–base titrations may be first considered.

Titration of a strong acid against a strong base. The titration of a strong acid with a strong base may be illustrated by the reaction of hydrochloric acid and sodium hydroxide. Suppose, 25 ml of 0·1 M HCl is to be titrated against 0·1 M NaOH. The equivalence or end point will, evidently, occur on the addition of 25 ml of the alkali solution. The *p*H values of the solution at different stages of neutralization are plotted graphically as in Fig. 2 against the increasing amount of the alkali added. It is seen that *p*H changes very slowly at first and rises from 1 to only about 4 when such a large amount as about 24·99 ml of the alkali solution has been added, *i.e.*, when about 99·9 per cent of the acid has been neutralised. Further addition of such a small amount as 0·01 ml of the alkali raises the *p*H by about 3 units to 7. The acid is now completely neutralised. Further addition of such a small amount as 0·01 ml of the sodium hydroxide solution (0·1 M) will amount to adding free hydroxyl ions and the *p*H will jump to a value above 9. Thus, near the end point, the titration curve is almost vertical and there is a rapid change of *p*H from 4 to about 10.

Now an indicator is suitable only if it undergoes a change of colour at the *p*H prevailing near the end point. A reference to Table 4 shows that there are a number of indicators including methyl orange, methyl red, bromothymol blue and phenolphthalein which can undergo colour change within the *p*H range 3 to 10. Thus, while titrating a strong acid with a strong base, any of the above indicators may be used to detect the end point. The *p*H ranges of these indicators are also shown in Fig. 2 for convenience of reference.

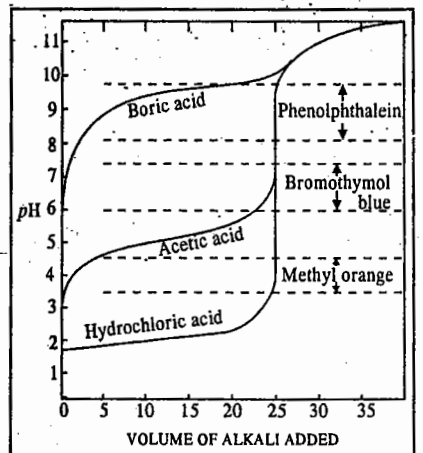

Fig. 2. The *p*H titration curves of different acids with sodium hydroxide. The *p*H ranges of the indicators involved are also shown in the figure.

Titration of a weak acid with strong base. The titration of a weak acid like acetic acid, against a strong base like sodium hydroxide, is included in Fig. 2. It will be seen that the vertical portion now does not begin until beyond *p*H 7 and the end point lies somewhere between *p*H 8 and 10. This is due to the hydrolysis of

sodium acetate. This, being a salt of a weak acid and a strong base, gives excess of free OH^- ions in aqueous solution due to hydrolysis. Hence, phenolphthalein will be a satisfactory indicator but not methyl orange, methyl red or even bromothymol blue. Thymolphthalein (Table 4), though not so common, is another suitable indicator for such titrations.

Fig. 2 also includes a titration curve for the titration of boric acid against sodium hydroxide. This titration curve does not show any sharp rise in *p*H. This is because boric acid is so weak (its dissociation constant being $6{\cdot}0\times10^{-10}$) that its salt sodium borate formed during the reaction gets very largely hydrolysed giving alkaline solution. The *p*H, therefore, goes on rising *continuously* and there is no *sharp rise* at the equivalence point. Hence, there is no abrupt change in the colour of the indicator for the addition of a small amount of sodium hydroxide at the equivalence point. Thus, the acids with dissociation constants less than 10^{-7} cannot be successfully titrated.

Titration of sodium carbonate with hydrochloridc acid. The titration curve obtained on reacting sodium carbonate with hydrochloric acid is shown in Fig. 3. It shows two inflection points. One of these indicates the conversion of sodium carbonate into bicarbonate :

$$Na_2CO_3 + HCl \longrightarrow NaHCO_3 + NaCl$$

This is completed at about *p*H 8·5 and phenolphthalein can be used to detect the end point. The second point of inflection indicates the neutralisation of sodium bicarbonate :

$$NaHCO_3 + HCl \longrightarrow NaCl + CO_2 + H_2O$$

This reaction gets completed at *p*H 4·3. Therefore, methyl orange is a highly suitable indicator in this case while phenolphthalein is not of any use.

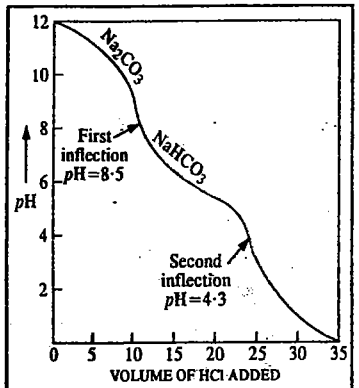

Fig. 3. The *p*H titration curves of sodium carbonate with a strong acid.

Mathematical Treatment of Acid-base Titrations

The *p*H values obtained experimentally at different stages of an acid–base titration can also be calculated mathematically, as illustrated below. (The value of K_w in these calculations is taken as 10^{-14}).

Suppose we are titrating 25 ml of a solution of HCl (0·1 M) against a standard (0·1 M) solution of NaOH and we want to calculate *p*H values of the titration solution after the addition of 20, 24·9, 24·95, 25·00, 25·05, 25·10 and 30 ml of NaOH solution. This is done as follows.

Initial *p*H of the titration solution, *viz.*, 0·1 M HCl $= -\log[H^+] = -\log(0{\cdot}1) = 1{\cdot}0$

Since the product of volume in ml and the concentration in mol dm^{-3} (*i.e.*, molarity) of a solute gives the amount of the solute in millimoles, hence,

Amount of HCl initially present in the titration solution $= 25\times0{\cdot}1 = 2{\cdot}5$ millimoles

The amount of NaOH in 20 ml of 0·1 M solution added during titration

$$= 20\times0{\cdot}1 = 2{\cdot}0 \text{ millimoles}$$

Amount of HCl left in the titration solution on adding 20 ml of NaOH $= 2{\cdot}5 - 2{\cdot}0 = 0{\cdot}5$ millimole

$$\therefore \text{Concentration of HCl or of } H^+ \text{ ions in the solution} = \frac{0{\cdot}5}{1000}\times\frac{1000}{45} \text{ mol dm}^{-3}$$

$$\therefore p\text{H of the titration solution} = -\log[H^+] = -\log\left(\frac{0{\cdot}5}{45}\right) = 1{\cdot}95$$

Proceeding as above, the *p*H of titration solution on the addition of 24·9 and 24·95 ml of NaOH solution comes out to be **3·70** and **4·00**, respectively.

On the addition of 25 ml of NaOH, the acid is completely neutralised giving NaCl. The *p*H of the resulting solution is, therefore, 7.

On adding 25·05 ml of NaOH, the additional volume of NaOH = 0·05 ml

Amount of NaOH in 0·05 ml = 0·005 millimole

$$\therefore \text{Concn. of NaOH or } OH^- \text{ ions} = \frac{0{\cdot}005}{1000}\times\frac{1000}{50{\cdot}05} \text{ mol dm}^{-3}$$

$$[H^+][OH^-] = 10^{-14} \text{ at } 25^\circ C$$

$$\therefore [H^+] = \frac{10^{-14}\times50{\cdot}05}{0{\cdot}005} = 1{\cdot}00\times10^{-10} \text{ mol dm}^{-3}$$

Hence, $$p\text{H} = -\log[H^+] = 10{\cdot}00$$

Proceeding as above, the *p*H values of the titration solution after the addition of 25·10 and 30 ml of NaOH solution come out to be 10·30 and 10·96, respectively.

It is evident from the *p*H values calculated as above that the *p*H increases from 1 to 4 on the addition of 24·95 ml of NaOH. Around the point of equivalence, the *p*H increases from 4 to 7 by the addition of a single drop of NaOH and then from 7 to 10 by the addition of another drop of NaOH. In other words, *around the end point there is a sharp change in* pH *from* 4 *to* 10 *just by the addition of* 2 *drops of NaOH solution.* We shall, thus, select an indicator which undergoes a change in colour in the *p*H range 4 to 10. As can be seen from Table 4, methyl orange as well as phenolphthalein are suitable indicators in this case.

Now suppose that we are titrating 25 ml solution of acetic acid (0·1 M) against 0·1 M solution of NaOH and we want to calculate the *p*H values of the titration solution after the addition of 20, 24·90, 24·95, 25·00, 25·05, 25·10 and 30 ml of NaOH solution. This is now done as follows.

Amount of CH_3COOH present in solution $= 25\times0{\cdot}1 = 2{\cdot}5$ millimoles

Since acetic acid is a weak acid, its H^+ ion concentration is given by the relation $[H^+]=\sqrt{cK_a}$, where c is the molar concentration of the acid and K_a is its dissociation constant.

$\therefore$ The initial concentration of H^+ ion in 0·1 M CH_3COOH solution

$$= \sqrt{0{\cdot}1\times1{\cdot}75\times10^{-5}} = 1{\cdot}32\times10^{-3} \text{ mol dm}^{-3}$$

$$\therefore p\text{H} = -\log[H^+] = -\log(1{\cdot}32\times10^{-3}) = 2{\cdot}88$$

During titration, CH_3COOH gets converted into CH_3COONa. The *p*H of the titration solution would thus depend upon the concentration of CH_3COOH left and of CH_3COONa formed during titration. In a mixture of a weak acid and its salt, the *p*H is given by the relation

$$p\text{H} = pK_a + \log\frac{[\text{Salt}]}{[\text{Acid}]} \qquad \text{(Eq. 29)}$$

With the addition of 20 ml of NaOH solution, the amount of NaOH added to the titration solution $= 20\times0{\cdot}1 = 2{\cdot}0$ millimoles

Amount of CH_3COONa formed = 2·0 millimoles

Since volume of the solution is the same for both CH_3COOH and CH_3COONa, the ratio of their amounts in millimoles can be taken as the ratio of their molar concentrations.

$$\therefore p\text{H of the titration solution} = 4{\cdot}76 + \log\frac{2{\cdot}0}{0{\cdot}5} = 5{\cdot}36$$

(K_a of $CH_3COOH = 1{\cdot}75\times10^{-5}$ $\therefore$ $pK_a = -\log K_a = 4{\cdot}76$)

Proceeding as above, the *p*H of the titration solution on the addition of 24·90 and 24·95 ml of NaOH solution comes out to be 7·16 and 7·46, respectively.

On the addition of 25 ml of NaOH solution, the acetic acid is completely neutralised, the resulting product being CH_3COONa. The amount of CH_3COONa formed would be $25\times0{\cdot}1 = 2{\cdot}5$ millimoles. Since the total volume of the titration solution is 25 + 25 = 50 ml, hence the concentration of $CH_3COONa = \dfrac{2{\cdot}5\times1000}{1000\times50} = 0{\cdot}05$ mol dm^{-3}. Since CH_3COONa is a salt of a strong base and a weak acid, it would get hydrolysed to give an alkaline solution whose *p*H is given by the relation

$$pH = 14 - \tfrac{1}{2}pK_w + \tfrac{1}{2}(\log c) + \tfrac{1}{2}pK_a$$

$$= 14 - \tfrac{1}{2}(14) + \tfrac{1}{2}\log 0{\cdot}05 + \tfrac{1}{2}(4{\cdot}76) = 8{\cdot}73$$

With the addition of 25·05 ml of NaOH, the amount of free NaOH added to the titration solution

$$= 0{\cdot}1\times0{\cdot}05 = 0{\cdot}005 \text{ millimole}$$

$\therefore$ Concentration of OH^- ions due to this addition $= \dfrac{0{\cdot}005}{1000}\times\dfrac{1000}{50{\cdot}05} = 0{\cdot}0001$ mol dm^{-3}

Concentration of OH^- ions due to the hydrolysis of CH_3COONa is given by the expression

$$[OH^-] = \left(\frac{K_w c}{K_a}\right)^{1/2} = \left(\frac{10^{-14}\times0{\cdot}05}{1{\cdot}75\times10^{-5}}\right) \text{ mol dm}^{-3}$$

$= 0{\cdot}534\times10^{-5}$ mol dm^{-3} which is negligible as compared to 0·0001 mol dm^{-3}.

$\therefore$ Total concentration of $[OH^-] = 0{\cdot}0001$ mol dm^{-3}

$$[H^+][OH^-] = 10^{-14} \text{ at } 25°C$$

$\therefore$ $$[H^+] = 10^{-14}/0{\cdot}0001 = 10^{-10} \text{ mol dm}^{-3}$$

$\therefore$ $$pH = 10$$

The *p*H of the titration solution on the addition of 25·10 and 30 ml of NaOH solution would be 10·30 and 10·96, respectively.

The data obtained for the titration of 0·1 M HCl and 0·1 M CH_3COOH solutions against 0·1 M NaOH solution have been summed up in Table 5.

TABLE 5
Titrations of 0·1 M HCl and 0·1 M CH_3COOH solutions against 0·1 M NaOH solution

Volume of NaOH added (ml)	*p*H values in the titration of :	
	HCl solution	CH_3COOH solution
0·00	1·00	2·88
20·00	1·95	5·36
24·90	3·70	7·16
24·95	4·00	7·46
25·00	7·00	8·73
25·05	10·00	10·00
25·10	10·30	10·30
30·00	10·96	10·96

As can be seen, the *p*H in the case of CH_3COOH is higher at each stage upto the end point. This is evidently due to the hydrolysis of CH_3COONa formed during the titration.

If we plot the above data graphically, the *p*H titration curves obtained would be exactly similar to those shown earlier in Fig. 2.

Example 29. 50 ml of a solution of acetic acid (0·1 M) is being titrated against a standard (0·125 M) solution of NaOH. Calculate the *p*H values of the titration solution on the addition of 30, 39·9, 39·95, 40·00, 40·05, 40·10 and 50 ml of NaOH solution. Comment on your result.

Solution : The H^+ ion concentration of a weak acid which is only partially dissociated is given by $[H^+] = \sqrt{cK_a}$

$\therefore$ Initial $[H^+]$ furnished by acetic acid $= (0{\cdot}1\times1{\cdot}75\times10^{-5})^{1/2} = 1{\cdot}32\times10^{-3}$ mol dm^{-3}

$\therefore$ $$pH = -\log(1{\cdot}32\times10^{-3}) = 2{\cdot}88$$

Thus, the initial *p*H of the titration solution is 2·88.

The amount of acetic acid initially present in the titraion solution = $50\times0{\cdot}1 = 5$ millimole. During titration, CH_3COOH gets converted into CH_3COONa. The *p*H of the titration solution would thus depend upon the amount of the acetic acid left and the sodium acetate formed during titration. In the case of a mixture of a weak acid and its salt, the *p*H is given by the well known relation :

$$pH = pK_a + \log [\text{Salt}]/[\text{Acid}]$$

With the addition of 30 ml of NaOH solution, the amount of NaOH added to the titration solution = $30\times0{\cdot}125 = 3{\cdot}75$ millimole.

$\therefore$ Amount of CH_3COONa formed = 3·75 millimoles

Amount of CH_3COOH left behind = 1·25 millimoles

$\therefore$ $$pH \text{ of the titration solution} = pK_a + \log\frac{[\text{Salt}]}{[\text{Acid}]}$$

Since the volume of solution is the same for both the acid and the salt, hence the ratio of their amounts in millimoles can be taken as the ratio of their molar concentrations.

Thus, $$pH = 4{\cdot}76 + \log\frac{3{\cdot}75}{1{\cdot}25} = 5{\cdot}24$$

Proceeding as above, the *p*H of the titration solution, on the addition of 39·9 ml and 39·95 ml of NaOH solution would be **7·34** and **7·46**, respectively. On the addition of 40 ml of NaOH solution, the acetic acid is completely neutralised, the resulting product being CH_3COONa. The amount of CH_3COONa formed would, evidently, be $40\times0{\cdot}125 = 5{\cdot}0$ millimoles. Since the total volume of the titration solution is 50 + 40 = 90 ml, hence the concentration of CH_3COONa would be $\dfrac{5\times1000}{1000\times90} = 5/90$ mol dm^{-3}. Since CH_3COONa is a salt of a strong base and a weak acid, it would get hydrolysed to give an alkaline solution whose *p*H is given by the relation

$$pH = 14 - \tfrac{1}{2}pK_w + \tfrac{1}{2}\log c + \tfrac{1}{2}pK_a$$

$$= 14 - \tfrac{1}{2}(14) + \tfrac{1}{2}\log(5/90) + \tfrac{1}{2}(4{\cdot}76) = 8{\cdot}75$$

With the addition of 40·05 ml of NaOH solution, the amount of free NaOH added to the titration solution $= 0{\cdot}125\times0{\cdot}05 = 0{\cdot}00625$ millimole. Hence, concentration of OH^- ions due to this addition $= \dfrac{0{\cdot}00625}{1000}\times\dfrac{1000}{90{\cdot}05} = 0{\cdot}000069$ mol dm^{-3}. Concentration of OH^- ions due to the hydrolysis of CH_3COONa is given by the expression

$$[OH^-] = \left(\frac{K_w c}{K_a}\right)^{1/2} = \left(\frac{10^{-14}\times(5/90)}{1{\cdot}75\times10^{-5}}\right)^{1/2} = 0{\cdot}563\times10^{-5} \text{ mol dm}^{-3}$$

$\therefore$ Total concentration of OH^- ions in titration solution = 0·0000746 mol dm^{-3}

$$[H^+][OH^-] = 10^{-14} \text{ at } 25°C$$

$\therefore$ $$[H^+] = \frac{10^{-14}}{0{\cdot}0000746} \text{ mol dm}^{-3}$$

$\therefore$ *p*H of titration solution $= -\log[H^+] = 9{\cdot}87$

Proceeding as above, the *p*H of titration solution on the addition of 40·10 and 50 ml of NaOH solution would be **10·16** and **12·10**, respectively.

TABLE 6
Titration of 0·1 M CH_3COOH against 0·125 M NaOH
Volume of CH_3COOH solution = 50 ml
Strength of NaOH solution = 0·125 M

Volume of NaOH solution added (ml)	*p*H of titration solution
0·00	2·88
30·00	5·24
39·00	7·34
39·95	7·46
40·00	8·75
40·05	9·87
40·10	10·16
50·00	12·10

Comments. It is evident from the calculations made as above that the *p*H increases from 2·88 to 7·46 on the addition of 39·95 ml of NaOH solution. Around the end point, the *p*H increases from 7·46 to 8·75 by the addition of a single drop of NaOH and then from 8·75 to 9·87 by the addition of another drop of NaOH. Thus, around the end point, there is considerable increase in *p*H from 7·34 to 9·87 by the addition of just 2 drops of NaOH. An indicator which changes colour in the *p*H range 7·34 to 9·87 would be a suitable indicator in this titration. As can be seen from Table 4, phenolphthalein would be a suitable indicator but not methyl orange.

The data obtained for the titration of 0·1 M CH_3COOH against 0·125 M NaOH have been summed up in Table 6.

SOLUBILITY PRODUCT

Solubility Product. In a saturated solution of a salt, there exists a dynamic equilibrium between the excess of the solute and the ions furnished by that part of the solute which has gone in solution. Consider, for example, the case when a sparingly soluble salt, like silver chloride, is added to water. A very small amount dissolves and the rest of it remains in the solid state. Here the solid silver chloride is in equilibrium with silver and chloride ions furnished by the dissolved silver chloride. This may be represented as

$$AgCl(s,\ satd.\ soln.) \rightleftharpoons Ag^+(aq) + Cl^-(aq)$$

Applying the law of chemical equilibrium, the equilibrium constant would be given by

$$K = \frac{a_{Ag^+} \times a_{Cl^-}}{a_{AgCl}} \qquad ...(64)$$

Since activity of a solid is taken as unity by convention, the above expression may be put as

$$K_{sp} = a_{Ag^+} \times a_{Cl^-} \qquad ...(65)$$

K_{sp} is known as the **solubility product** of silver chloride. It is constant at a given temperature.

Very often, in practice, it is more convenient to use concentration terms instead of activities. The constant is then known as **concentration solubility product**, denoted by K'_{sp}. Thus,

$$K'_{sp} = [Ag^+][Cl^-] \qquad ...(66)$$

where the square brackets, as usual, represent the concentrations of the entities enclosed within. In the case of sparingly soluble salts since the ionic concentrations are very low, activity of each ion is almost equal to its concentration. Hence,

$$K_{sp} = K'_{sp} \qquad ...(67)$$

i.e., solubility product is almost equal to concentration solubility product. Therefore, without introducing any serious error, we may write :

$$K_{sp} = [Ag^+][Cl^-]$$

In the case of silver sulphate, another sparingly soluble salt, the following equilibrium exists :

$$Ag_2SO_4(s,\ satd.\ soln.) \rightleftharpoons 2Ag^+(aq) + SO_4^{2-}(aq)$$

The solubility product will now be given by the expression

$$K_{sp} = [Ag^+]^2[SO_4^{2-}]$$

Similarly, the solubility products in the case of $Al(OH)_3$ and As_2S_3 would be given by the expressions $K_{sp} = [Al^{3+}][OH^-]^3$ and $K_{sp} = [As^{3+}]^2[S^{2-}]^3$, respectively.

Consider, in general, a salt of the type A_xB_y which dissociates as

$$A_xB_y \rightleftharpoons xA^{y+} + yB^{x-}$$

The solubility product of the salt is now given by

$$K_{sp} = [A^{y+}]^x\,[B^{x-}]^y \qquad ...(68)$$

Thus, the solubility product of a sparingly soluble salt forming a saturated solution in water is given by the product of the concentrations of the ions raised to a power equal to the number of times the ions occur in the equation representing the dissociation of the electrolyte.

It may be mentioned in particular that the *solubility product principle can also be applied to saturated solutions of freely soluble salts*. For example, in the case of a saturated solution of sodium chloride in which some solid NaCl is also present, the following equilibrium exists :

$$NaCl(s,\ satd.\ soln.) \rightleftharpoons Na^+(aq) + Cl^-(aq)$$

The true solubility product constant is given by the equation

$$K_{sp} = a_{Na^+} \times a_{Cl^-}$$

and the concentration solubility product is given by the expression

$$K'_{sp} = [Na^+][Cl^-]$$

However, in this case, the activities are considerably less than the concentrations. This is due to high ionic concentrations which enhance interionic effects. K'_{sp} is, therefore, no longer equal to K_{sp}. Apart from this mathematical difference, the solubility product principle is as valid for sparingly soluble as for freely soluble electrolytes.

The solubility products of some of the common sparingly soluble substances are given in Table 7.

TABLE 7

Solubility Products of Some Sparingly Soluble Substances

Substance	K_{sp} at 25°C	Substance	K_{sp} at 25°C	Substance	K_{sp} at 25°C
PbS	$3{\cdot}4\times10^{-28}$	$CaCO_3$	$4{\cdot}8\times10^{-9}$	$Al(OH)_3$	$8{\cdot}5\times10^{-32}$
CdS	$3{\cdot}6\times10^{-28}$	$SrCO_3$	$1{\cdot}1\times10^{-10}$	$Zn(OH)_2$	$1{\cdot}8\times10^{-17}$
CuS	$8{\cdot}5\times10^{-36}$	Ag_2CO_3	$6{\cdot}15\times10^{-12}$	$Mn(OH)_2$	$4{\cdot}0\times10^{-14}$
HgS	$4{\cdot}1\times10^{-53}$	Ag_2S	$1{\cdot}6\times10^{-50}$	$Mg(OH)_2$	$1{\cdot}2\times10^{-11}$
MnS	$1{\cdot}4\times10^{-10}$	$HgBr_2$	$8{\cdot}0\times10^{-18}$	AgCl	$1{\cdot}56\times10^{-10}$
ZnS	$1{\cdot}2\times10^{-28}$	AgBr	$7{\cdot}7\times10^{-13}$	Ag_2CrO_4	$9{\cdot}0\times10^{-12}$
NiS	$1{\cdot}5\times10^{-24}$	PbI_2	$1{\cdot}39\times10^{-8}$	$BaSO_4$	$1{\cdot}08\times10^{-10}$
CoS	$3{\cdot}0\times10^{-25}$	HgI_2	$3{\cdot}2\times10^{-29}$	TlCl	$2{\cdot}0\times10^{-4}$
$Fe(OH)_3$	$1{\cdot}1\times10^{-38}$	AgI	$0{\cdot}94\times10^{-16}$		

Relation between Solubility Product and Molar Solubility of a Sparingly Soluble Salt. For the saturated solution of a sparingly soluble salt AB, the following solubility equilibrium would exist :

$$AB(s,\ satd.\ soln.) \rightleftharpoons A^+(aq) + B^-(aq)$$

If the molar solubility of the salt is s, then

$$[A^+] = s \text{ mol dm}^{-3}$$

$$[B^-] = s \text{ mol dm}^{-3}$$

Hence, $$K_{sp} = [A^+][B^-] = (s \text{ mol dm}^{-3})(s \text{ mol dm}^{-3}) = s^2 \text{ mol}^2 \text{ dm}^{-6}$$

Example 30. The solubility of silver chloride in water at 25°C is 0·00179 g per litre. Calculate its solubility product at 25°C.

Solution : Solubility of silver chloride $= 0{\cdot}00179 \text{ g dm}^{-3} = \dfrac{0{\cdot}00179 \text{ g dm}^{-3}}{143{\cdot}5 \text{ g mol}^{-1}} = 0{\cdot}0000125 \text{ mol dm}^{-3}$

The dissolved salt would be present in the form of ions so that

$$[Ag^+] = [Cl^-] = 0{\cdot}0000125 \text{ mol dm}^{-3}$$

$$K_{sp} = [Ag^+][Cl^-] = (0{\cdot}0000125 \text{ mol dm}^{-3})^2 = 1{\cdot}56\times10^{-10} \text{ mol}^2 \text{ dm}^{-6}$$

Example 31. The solubility product of magnesium hydroxide $Mg(OH)_2$ at 25°C is $1{\cdot}4\times10^{-11}$. Calculate the solubility of magnesium hydroxide in grams per litre ? (Mg=24, O=16, H=1)

Solution : The solubility equilibrium in this case will be

$$Mg(OH)_2(s,\ satd.\ soln.) \rightleftharpoons Mg^{2+}(aq) + 2OH^-(aq)$$

Let the solubility of $Mg(OH)_2$ be s mol dm^{-3}.

$\therefore$ Concentration of $Mg^{2+} = s$ mol dm^{-3}

Now, for each Mg^{2+} ion, two OH^- ions are produced.

$\therefore$ Concentration of OH^- ions $= 2s$ mol dm^{-3}

$$K_{sp} = [Mg^{2+}][OH^-]^2$$

$$\therefore \quad s(2s)^2 = 1{\cdot}2\times10^{-11} \quad \text{or} \quad 4s^3 = 1{\cdot}2\times10^{-11} \quad \text{or} \quad s = 1{\cdot}44\times10^{-4} \text{ mol dm}^{-3}$$

$\therefore$ Solubility of $Mg(OH)_2 = 1{\cdot}44\times10^{-4}$ mol dm^{-3} $= 1{\cdot}44\times10^{-4}$ mol dm$^{-3}\times58$ g mol$^{-1} = 0{\cdot}00835$ g dm^{-3}

Example 32. Calculate the solubility in grams per litre of $Al(OH)_3$ in water at 25°C if $K_{sp}=8{\cdot}5\times10^{-32}$.

Solution : The solubility equilibrium in this case would be written as

$$Al(OH)_3\ (s,\ satd.\ soln.) \rightleftharpoons Al^{3+}(aq) + 3OH^-(aq)$$

If s mol dm^{-3} is the solubility of the salt, then

$$K_{sp} = [Al^{3+}][OH^-]^3 = (s)(3s)^3 = 27\,s^4$$

$\therefore$

$$s = [K_{sp}/27]^{1/4} = [8{\cdot}5\times10^{-32}/27]^{1/4} = 0{\cdot}749\times10^{-8} \text{ mol dm}^{-3}$$

$$= 0{\cdot}749\times10^{-8} \text{ mol dm}^{-3}\times78 \text{ g mol}^{-1} = 5{\cdot}842\times10^{-7} \text{ g dm}^{-3}$$

Applications of Solubility Product Principle

1. Determination of Solubilities of Sparingly Soluble Salts. Suppose, solubility of a sparingly soluble salt, say, silver chloride, is s mole per litre. Since its concentration will be quite small, it may be taken as completely dissociated so that the concentration of both silver and chloride ions will be s mole per litre each.

Therefore, solubility product K_{sp} of silver chloride will be given by

$$K_{sp} = [Ag^+][Cl^-] = s^2$$

Hence, solubility of silver chloride is related to the solubility product by the expression

$$s = \sqrt{K_{sp}}$$

The solubility product of silver chloride at a given temperature is determined by adding silver chloride in a solution of potassium chloride of a known concentration, say, b moles per litre. The concentration of Ag^+ ions in the solution produced by the dissociation of that part of AgCl which dissolves in water is determined by an EMF method. Suppose it is a mole per litre. The concentration of chloride ions in solution will be $(a+b)$ moles per litre due to silver chloride and potassium chloride both. Therefore, solubility product of silver chloride, K_{sp}, is given by

$$K_{sp} = a(a+b)$$

Since, both a and b are known, the solubility product of silver chloride can easily be obtained.

Hence, solubility of silver chloride $= \sqrt{K_{sp}}$ mole per litre

2. Predicting Precipitation Reactions. With the knowledge of solubility product of a sparingly soluble substance, we can predict whether under certain given conditions that substance would be precipitated or not. It may be remembered that a substance gets precipitated when the ionic product, *i.e.*, the product of concentrations of its ions present in a solution, exceeds the solubility product of the substance. We may take an example.

The solubility product of calcium sulphate in water in 25°C is $2{\cdot}4\times10^{-5}$ M^2. A sample of hard water contains 0·01 mole of $CaCl_2$ per litre. It is required to precipitate calcium sulphate by the addition of dilute sulphuric acid. Two solutions of sulphuric acid of concentrations 0·001 M and 0·02 M are given.

Suppose we mix, in the first instance, equal volumes of the hard water and sulphuric acid of lower concentration. Will calcium sulphate be precipitated ?

The solubility equation for calcium sulphate may be written as

$$CaSO_4(s,\ satd.\ soln.) \rightleftharpoons Ca^{2+}(aq) + SO_4^{2-}(aq)$$

$$K_{sp} = [Ca^{2+}][SO_4^{2-}] = 2{\cdot}4\times10^{-5} \text{ M}^2$$

$[Ca^{2+}]$ in water $= 0{\cdot}01$ M

Since volume is doubled on the addition of sulphuric acid solution, hence,

$[Ca^{2+}]$ in the mixture $= 0{\cdot}01/2 = 0{\cdot}005$ M

Concentration of sulphuric acid $= 0{\cdot}001$ M

$\therefore \quad [SO_4^{2-}] = 0{\cdot}001$ M

Since volume is doubled when mixed with equal volume of hard water, hence,

$[SO_4^{2-}]$ in the mixture $= 0{\cdot}001/2 = 0{\cdot}0005$ M

The product of concentrations of ions

$$[Ca^{2+}][SO_4^{2-}] = 0{\cdot}005 \text{ M}\times0{\cdot}0005 \text{ M} = 2{\cdot}5\times10^{-6} \text{ M}^2$$

Evidently, the ionic product is less than the solubility product of $CaSO_4$ which is equal to $2{\cdot}4\times10^{-5}$ M^2. Therefore, precipitation of calcium sulphate will not occur.

Now, suppose we mix equal volumes of hard water and sulphuric acid solution of the higher concentration (0·02 M).

$[Ca^{2+}]$ in the mixture $= 0{\cdot}01/2 = 0{\cdot}005$ M

$[SO_4^{2-}]$ in the mixture $= 0{\cdot}02/2 = 0{\cdot}01$ M

The ionic product $[Ca^{2+}][SO_4^{2-}] = 0{\cdot}005 \text{ M}\times0{\cdot}01 \text{ M} = 5\times10^{-5}$ M^2

The ionic product now exceeds the solubility product of $CaSO_4$. Hence, calcium sulphate will be precipitated.

Example 33. 25 ml of 0·01 $AgNO_3$ solution is mixed with 25 ml of 0·0005 M aqueous NaCl solution. Determine if the precipitate of AgCl will be formed. Given $K_{sp}(AgCl)=1{\cdot}7\times10^{-10}$ M^2.

Solution : Since the volume of the solution *after mixing* is doubled and $AgNO_3$ and NaCl are strong electrolytes which are completely dissociated in solution, we have

$$[Ag^+] = 1/2(0{\cdot}01 \text{ M}) = 5\times10^{-3} \text{ M}$$

$$[Cl^-] = 1/2(0{\cdot}0005 \text{ M}) = 2{\cdot}25\times10^{-4} \text{ M}$$

$$\text{Ionic product} = [Ag^+][Cl^-] = (5\times10^{-3} \text{ M})(2{\cdot}25\times10^{-4} \text{ M}) = 1{\cdot}125\times10^{-6} \text{ M}^2$$

Since ionic product $> K_{sp}$(AgCl), the precipitate of AgCl will be formed.

Example 34. 25 ml of 4×10^{-5} M solution of $Ba(NO_3)_2$ is mixed with 500 ml of 5×10^{-5} M solution of Na_2SO_4. Will a precipitate of $BaSO_4$ be formed ? $K_{sp}(BaSO_4) = 1{\cdot}08\times10^{-10}$ M^2.

Solution : After mixing, the total volume of the solution is 525 ml.

Since $Ba(NO_3)_2$ and Na_2SO_4 are strong electrolytes, they are completely dissociated. Therefore, we have

$$[Ba^{2+}] = 4\times10^{-5} \text{ M}\times(25/525) = 1{\cdot}90\times10^{-6} \text{ M}$$

$$[SO_4^{2-}] = 5\times10^{-5} \text{ M}\times(500/525) = 4{\cdot}76\times10^{-5} \text{ M}$$

$$\text{Ionic product} = [Ba^{2+}][SO_4^{2-}] = [1{\cdot}90\times10^{-6} \text{ M}]\,[4{\cdot}76\times10^{-5} \text{ M}] = 9{\cdot}04\times10^{-11} \text{ M}^2$$

Since ionic product is less then $K_{sp}(BaSO_4)$, the precipitate of $BaSO_4$ will not be formed.

3. Fractional Precipitation. Consider an aqueous solution of KCl and KI to which $AgNO_3$ solution is added. Since K_{sp}(AgI) is less than K_{sp}(AgCl), hence, K_{sp}(AgI) will be exceeded and AgI will be precipitated first :

$$Ag^+(aq) + I^-(aq) \longrightarrow AgI(s) \downarrow \qquad K_{sp} = 0{\cdot}94\times10^{-16}$$

$$Ag^+(aq) + Cl^-(aq) \longrightarrow AgCl(s) \downarrow \qquad K_{sp} = 1{\cdot}56\times10^{-10}$$

$$\frac{[I^-]}{[Cl^-]} = \frac{K_{sp}(AgI)}{K_{sp}(AgCl)} = \frac{0{\cdot}94\times10^{-16}}{1{\cdot}56\times10^{-10}} = 6{\cdot}0\times10^{-7} \approx 10^{-6}$$

Thus, AgI will start precipitating out when $[I^-]$ is approximately one-millionth part of $[Cl^-]$.

AgCl will precipitate only when $[Ag^+]$ is greater than the value given below :

$$[Ag^+] = \frac{K_{sp}(AgCl)}{[Cl^-]} = \frac{1{\cdot}56\times10^{-10}}{[Cl^-]}$$

At that point both AgI and AgCl will start precipitating *simultaneously*.

4. Preferential Precipitation of an Insoluble Salt. Silver chloride is 'insoluble' or sparingly soluble, to be more accurate. So is silver iodide. The question arises as to what would happen if potassium iodide solution is added to silver chloride. Would the reaction

$$\underset{\text{Sparingly soluble}}{AgCl} + KI \rightleftharpoons KCl + \underset{\text{Sparingly soluble}}{AgI}$$

take place towards the right, *i.e.*, would the precipitate of silver chloride change into the precipitate of silver iodide ?

For answer, it is necessary to look to their respective solubility products.

Solubility product of silver chloride

$$K_{sp(AgCl)} = [Ag^+][Cl^-] = 1{\cdot}56\times10^{-10} \qquad \text{(Table 7)}$$

and that of silver iodide,

$$K_{sp(AgI)} = [Ag^+][I^-] = 0{\cdot}94\times10^{-16} \qquad \text{(Table 7)}$$

$$\therefore \quad \frac{[Cl^-]}{[I^-]} = \frac{1{\cdot}56\times10^{-10}}{0{\cdot}94\times10^{-16}} = 1{\cdot}66\times10^{6}$$

This means that at equilibrium, the concentration of Cl^- ions in solution is more than a million times greater than that of I^- ions. In other words, practically nothing of the I^- ions can remain in solution at equilibrium. As the I^- ions can only be removed as AgI, it means that the reaction proceeds virtually to completion towards the right.

As a rule, the compound with the lower solubility product gets precipitated in preference. Silver iodide has lower solubility product than silver chloride. Therefore, the former gets precipitated in preference to the latter.

5. Precipitation of Soluble Salts. ***(a) Purification of common salt.*** The principle of solubility product is also applied in the precipitation of soluble salts in pure state from their saturated solutions. This phenomenon, known as *salting out*, is used in the purification of sodium chloride. This is done by preparing a saturated solution of commercial (impure) sodium chloride in water when the following equilibrium exists :

$$NaCl(s, \textit{said. soln.}) \rightleftharpoons Na^+(aq) + Cl^-(aq)$$

$$K_{sp} = [Na^+][Cl^-]$$

HCl gas is passed through this solution. The $[Cl^-]$, therefore, increases considerably. Hence, the

ionic product exceeds the concentration solubility product of NaCl and, therefore, it precipitates out from the solution in pure state. The soluble impurities remain in solution.

(b) Salting out of soap. The same principle is made use of in the *salting out* of soap which may be considered as sodium salt of stearic acid for simplicity. The following equilibrium exists :

$$C_{17}H_{35}COONa(s, \textit{satd. soln.}) \rightleftharpoons C_{17}H_{35}COO^-(aq) + Na^+(aq)$$

$$K_{sp} = [C_{17}H_{35}COO^-][Na^+]$$

Some sodium chloride is now added. The $[Na^+]$, therefore, increases. Hence, the ionic product exceeds the concentration solubility product of sodium stearate. The soap, therefore, separates out from solution.

6. Inorganic Analysis. The application of solubility product principle to inorganic analysis is of great importance. A few illustrations are given below.

a. Precipitation of sulphides. Hydrogen sulphide is a weak acid. Its small dissociation

$$H_2S \rightleftharpoons 2H^+ + S^{2-}$$

is further suppressed by the addition of dlute hydrochloric acid (common ion effect). Therefore, the concentration of S^{2-} ions which was already small, becomes smaller still. But even then it is larger than that required for the solubility products of sulphides of copper, cadmium, bismuth, arsenic, antimony and tin, to be exceeded. Therefore, these cations get precipitated as sulphides in acidic solution in the Second Group of qualitative analysis.

But, as the solubility products of sulphides of nickel, cobalt, manganese and zinc are comparatively higher, the sulphide ion concentration in the presence of hydrochloric acid is smaller than that required to cause their precipitation. These cations, therefore, do not get precipitated in Group II. Since they require a larger concentration of sulphide ions, a highly ionised sulphide, such as ammonium sulphide, is added (or which is the same thing as passing hydrogen sulphide through ammoniacal solution). By this means, the product $[Zn^{2+}][S^{2-}]$, for example, in solution exceeds the solubility product of zinc sulphide. Therefore, zinc sulphide gets precipitated. Similarly, the sulphides of nickel, cobalt and manganese, which all appear in Group IV of qualitative analysis, get precipitated.

The solubility product of cadmium sulphide is greater than that of the other sulphides of the Second Group. Therefore, the sulphide ion concentration in this case should not be made very low. In other words, excess of hydrochloric acid should be avoided or the solution should be diluted before passing hydrogen sulphide for the detection of Cd^{2+} in the Second Group of qualitative analysis.

b. Precipitation of hydroxides. Advantage is taken of the fact that solubility products of hydroxides of iron, aluminium and chromium are much smaller than those of magnesium, zinc, etc.

Ammonium hydroxide is a weak base. Its ionisation

$$NH_4OH \rightleftharpoons NH_4^+ + OH^-$$

is further suppressed by the addition of largely ionised ammonium chloride (**common ion effect**). But the OH^- ion concentration, although extremely small, is larger than is required to exceed the solubility product of hydroxide of iron, aluminium or chromium. These cations, therefore, get precipitated as hydroxides in Group III of qualitative analysis in the presence of excess of ammonium chloride. But zinc or magnesium cations do not get precipitated (as hydroxides) in the presence of ammonium chloride since their solubility products are much higher.

7. Other Precipitation Reactions. The concept of solubility product also helps in explaining why a moderately weak acid is able to produce a precipitate when added to a solution of a salt of a weak acid but not when added to a solution of a salt of a strong acid. For example, oxalic acid will cause complete precipitation of calcium acetate as calcium oxalate but not that of calcium chloride or

calcium nitrate. The reaction in this case is

$$(CH_3COO)_2Ca + H_2C_2O_4 \longrightarrow CaC_2O_4 + 2CH_3COOH$$

The concentration of oxalate ion ($C_2O_4^{2-}$) is sufficient to make the ionic product $[Ca^{2+}][C_2O_4^{2-}]$ greater than the solubility product of calcium oxalate. The acetic acid that is formed is very slightly ionised and, therefore, it cannot alter the ionisation of oxalic acid which is much stronger than acetic acid. If, however, oxalic acid is added to a solution of calcium chloride, the hydrochloric acid that is formed is largely ionised and the increase in the hydrogen ion concentration will suppress the ionisation of oxalic acid. Therefore, the oxalate ion concentration falls below the value required to exceed the solubility product of calcium oxalate. As a result, the precipitation of calcium oxalate is incomplete.

8. Dissolution of Precipitates of Phosphates, Carbonates, Sulphides, etc., in Acid Solutions. It is well known that the precipitates of salts of weak acids, such as phosphates, carbonates, sulphides, are soluble in dilute hydrochloric or nitric acid but the precipitates of salts of strong acids, such as chlorides and sulphates, are not.

Consider zinc sulphide as a representative of the first category of precipitates. When suspended in water, the following equilibrium exists :

$$ZnS(s,\ satd.\ soln.) \rightleftharpoons Zn^{2+}(aq) + S^{2-}(aq)$$

If a largely dissociated acid such as hydrochloric acid or nitric acid is added, the hydrogen ions combine with sulphide ions to form hydrogen sulphide,

$$2H^+ + S^{2-} \longrightarrow H_2S\uparrow$$

which, being a sparingly soluble gas, will escape into the atmosphere. Therefore, the dynamic equilibrium between solid zinc sulphide and its ions will be disturbed and more of the solid ZnS will pass into solution as Zn^{2+} and S^{2-} ions. The sulphide ions will again be taken up by hydrogen ions to form hydrogen sulphide gas, and so on. In this way the whole of zinc sulphide passes into solution ultimately.

Consider barium sulphate as a representative of the second category of precipitates, *i.e.*, sparingly soluble salts of strong acids. When added to water, the following equilibrium exists :

$$BaSO_4(s,\ satd.\ soln.) \rightleftharpoons Ba^{2+}(aq) + SO_4^{2-}(aq)$$

The added H^+ ions (through the addition of hydrochloric acid or nitric acid) will not be able to remove sulphate ions since sulphuric acid formed is very largely ionised and, therefore, the above equilibrium is not materially disturbed. Consequently, barium sulphate does not dissolve in hydrochloric acid or nitric acid.

Ionic Equilibria Involving Complex Ions

As is well known, AgCl, which is only sparingly soluble in water, dissolves completely in aqueous ammonia solution. The increased solubility is due to the formation of a soluble complex $[Ag(NH_3)_2]Cl$. The various equilibria involved in the dissolution of AgCl in aqueous ammonia solution are as follows :

(i) $$AgCl(s) \rightleftharpoons Ag^+(aq) + Cl^-(aq)$$

$$K_{sp} = [Ag^+][Cl^-]$$

(ii) $$Ag^+ + 2NH_3 \rightleftharpoons [Ag(NH_3)_2]^+$$

(Complex ion)

The equilibrium constant for reaction *(ii)*, designated as **stability constant**, K_{stab}, of the complex ion, is given by

$$K_{stab} = \frac{[Ag(NH_3)_2]^+}{[Ag^+][NH_3]^2}$$

Adding reactions *(i)* and *(ii)*, we have

(iii) $$AgCl(s) + 2NH_3 \rightleftharpoons [Ag(NH_3)_2]^+ + Cl^-$$

The equilibrium constant for the overall reaction *(iii)* is given by

$$K_{eq} = \frac{[Ag(NH_3)_2]^+[Cl^-]}{[NH_3]^2} = \frac{[Ag^+][Cl^-][Ag(NH_3)_2]^+}{[Ag^+][NH_3]^2} = K_{sp}\,K_{stab}$$

The complex ion formed in reaction *(ii)* is highly stable, the stability constant being as high as $1{\cdot}67\times10^7$. The formation of a stable complex ion in reaction *(ii)* upsets equilibrium *(i)* thereby causing it to shift to the right according to Le Chatelier's principle. As a result, AgCl(*s*) dissolves completely on the addition of excess of aqueous ammonia.

Example 35. Calculate the molar solubility of $Zn(OH)_2$ in 1 M ammonia solution at room temperature. $K_{sp}(Zn(OH)_2) = 1{\cdot}8\times10^{-17}$; K_{stab} of $[Zn(NH_3)_4]^{2+} = 1{\cdot}64\times10^{10}$.

Solution : The solubility equilibrium in this case is represented as

(i) $$Zn(OH)_2(s) \rightleftharpoons Zn^{2+}(aq) + 2OH^-(aq)$$

$$K_{sp} = [Zn^{2+}][OH^-]^2 = 1{\cdot}18\times10^{-17}$$

(ii) $$Zn^{2+} + 4NH_3(aq) \rightleftharpoons [Zn(NH_3)_4]^{2+}$$

$$K_{stab} = \frac{[Zn(NH_3)_4]^{2+}}{[Zn^{2+}][NH_3]^4}$$

The overall reaction is obtained by adding reactions *(i)* and *(ii)* :

$$Zn(OH)_2(s) + 4NH_3(aq) \rightleftharpoons [Zn(NH_3)_4]^{2+} + 2OH^-(aq)$$

$$1-4x \qquad\qquad x \qquad\qquad 2x$$

$$K_{eq} = \frac{[Zn(NH_3)_4]^{2+}[OH^-]^2}{[NH_3]^4} = \frac{[Zn^{2+}][OH^-]^2[Zn(NH_3)_4]^{2+}}{[Zn^{2+}][NH_3]^4} = K_{sp}\,K_{stab}$$

If x is the molar solubility of $Zn(OH)_2$ in 1 M NH_3 solution, then, at equilibrium,

$$[NH_3] = 1 - 4x\ ;\quad [OH^-] = 2x \quad \text{and} \quad [Zn(NH_3)_4]^{2+} = x.$$

$$K_{eq} = \frac{x(2x)^2}{(1-4x)^4} = 4x^3 \ (\text{since } 4x \ll 1)$$

$$4x^3 = K_{eq} = K_{sp}\,K_{stab} = (1{\cdot}8\times10^{-17})(1{\cdot}64\times10^{10})$$

$$x = 4{\cdot}19\times10^{-3} \text{ mol dm}^{-3}$$

Example 36. Calculate the solubility of $Mg(OH)_2$ in *(i)* pure water *(ii)* 0·01 M NaOH and *(iii)* 0·01 M $Ba(OH)_2$. Given K_{sp} of $Mg(OH)_2 = 1{\cdot}2\times10^{-11}\ M^3$.

Solution : *(i)* The solubility equilibrium in this case is represented as

$$Mg(OH)_2\ (s,\ satd.\ soln.) \rightleftharpoons Mg^{2+}(aq) + 2OH^-(aq)$$

$$K_{sp} = [Mg^{2+}][OH^-]^2 = s(2s)^2 = 4s^3$$

Hence, the molar solubility s is given by

$$s = (K_{sp}/4)^{1/3} = (1{\cdot}2\times10^{-11}\ M^3/4)^{1/3} = 1{\cdot}442\times10^{-4}\ M$$

(ii) NaOH, being a strong electrolyte, will suppress the dissociation of $Mg(OH)_2$ due to common ion effect, thereby decreasing its solubility.

Let s' be the new molar solubility of $Mg(OH)_2$ in the presence of NaOH. Then

$$[Mg^{2+}] = s'\ ;\ [OH^-] = 0{\cdot}01 + 2s'$$

$$K_{sp}[Mg(OH)_2] = [Mg^{2+}]\,[OH^-]^2 = (s')(0{\cdot}01+2s')^2 = 1{\cdot}2\times10^{-11}$$

Assuming that $2s' << 0{\cdot}1$, it can be neglected giving

$$10^{-4}\,s' = 1{\cdot}2\times10^{-11}$$

$$s' = 1{\cdot}2\times10^{-7}\ \text{M}$$

(iii) Here again $Ba(OH)_2$ is a strong electrolyte. It will suppress the dissociation of $Mg(OH)_2$ due to common ion effect. Let s'' be the molar solubility of $Mg(OH)_2$ in the presence of $Ba(OH)_2$. Then

$$[Mg]^{2+} = s'' ;\ [OH^-] = 0{\cdot}02 + 2s''$$

$$K_{sp}[Mg(OH)_2] = [Mg^{2+}][OH^-]^2 = (s'')(0{\cdot}02 + 2s'')^2 = 1{\cdot}2\times10^{-11}$$

Assuming that $2s'' << 0{\cdot}02$, it can be neglected giving

$$4\times10^{-4}\,s'' = 1{\cdot}2\times10^{-11}$$

$$s'' = \frac{1{\cdot}2\times10^{-11}}{4\times10^{-4}} = 3\times10^{-8}\ \text{M}$$

We see that $s'' < s' < s$.

I. Review Questions

1. Discuss the proton transfer theory of acids and bases. What is meant by a conjugate pair ? Discuss the effect of solvent on the relative strengths of acids and bases.
2. What are Lewis acids and Lewis bases ? Give examples.
3. What do you understand by *p*H of a solution ? What is the range of the *p*H scale and why ?
4. What are buffer solutions ? Explain the terms buffer index and buffer capacity.

   Explain why a solution of a weak acid and its salt behaves as a buffer. Derive the relation between the *p*H of the solution and the relative amounts of the acid and the salt present in it. Explain why a solution containing a strong acid and its salt does not behave as a buffer.
5. Explain clearly why a solution of a weak base and its salt behaves as a buffer. Derive the mathematical relation between the *p*H of the solution and the relative amounts of the base and the salt present in it. Explain why a solution containing a strong base and its salt does not act as a buffer.
6. Discuss in detail the phenomenon of 'hydrolysis of salts'. Illustrate your answer taking examples of the salt of *(i)* a weak acid and strong base *(ii)* a strong acid and a weak base *(iii)* a weak acid and a weak base.
7. What is meant by the terms : degree of hydrolysis and hydrolysis constant ? Describe the various methods used for determining the degree of hydrolysis of a salt.
8. What are acid-base indicators ? Illustrate the mechanism of their action taking suitable examples. What is meant by the useful range of an indicator ?
9. Define the terms solubility and solubility product of a substance. Explain giving at least four examples the use of the concept of solubility product in qualitative analysis.
10. Illustrate the application of the concept of solubility product in the following operations :

    (i) Determination of solubility of sparingly soluble salts *(ii)* Predicting precipitation reactions *(iii)* Purification of common salt *(iv)* Salting out of soap.

II. Problems

1. Calculate the degree of dissociation and the hydrogen ion concentration in 0·001 M aqueous solution of acetic acid at 25°C. Given $K_a = 1{\cdot}85\times10^{-5}$ **[Ans. 12·7% ; $1{\cdot}27\times10^{-4}$ M]**
2. In 0·1M solution, 0·00135 mole of ammonia dissociates. Calculate the dissociation constant of the base. **[Ans. $1{\cdot}84\times10^{-5}$]**

3. *(i)* Calculate the *p*H of $1{\cdot}0\times10^{-3}$ M solution of each of the following :

   (a) HCl *(b)* NaOH *(c)* $Ba(OH)_2$ *(d)* NaCl **[Ans. *(a)* 3·00 *(b)* 11·00 *(c)* 11·30 *(d)* 7]**

   (ii) 500 ml of an aqueous solution of NaOH contains 0·05 mole of NaOH. What is the *p*H of the solution ? **[Ans. 13]**
4. A student reports the *p*H of 1×10^{-7} M solution of HCl at 25°C as 7. Is the answer correct ? If not, what is the correct *p*H of the solution. $K_w = 10^{-14}$. **[Ans. Correct *p*H is 6·79]**
5. What is meant by electroneutrality of a solution ? Based on this principle calculate the *p*H of a 2×10^{-5} M solution of phenol at 25°C. $K_a = 1{\cdot}30\times10^{-10}$ and $K_w = 1{\cdot}008\times10^{-14}$ **[Ans. 6·95]**
6. Calculate $[H_3O^+]$ and *p*H of a buffer solution containing 0·02 M CH_3COONa and 0·05 M CH_3COOH. $K_a = 1{\cdot}80\times10^{-5}$. **[Ans. $[H_3O^+] = 4{\cdot}5\times10^{-5}$ M, *p*H = 4·35]**
7. What would be the *p*H of a solution containing 0·1 mole of NH_4OH and 0·15 mole of NH_4Cl per litre of the solution. $K_b = 1{\cdot}8\times10^{-5}$? **[Ans. 9·08]**
8. Which of the following, when mixed, will give a solution with *p*H greater than 7 :

   (a) 0·1 M HCl + 0·2 M NaCl

   (b) 100 ml of 0·2 M H_2SO_4 + 100 ml of 0·3 M NaOH

   (c) 100 ml of 0·1 M CH_3COOH + 100 ml of 0·1 M KOH

   (d) 50 ml of 0·1 M HCl + 50 ml of 0·1 M CH_3COONa
9. Calculate percent hydrolysis of a 0·01 M solution of KCN. $K_a = 6{\cdot}2\times10^{-10}$ **[Ans. *(c)*]**
10. Calculate the *p*H of 0·10 M NH_4NO_3 solution. Given $K_b = 1{\cdot}80\times10^{-5}$. **[Ans. 4·0%]**
11. Calculate the extent of hydrolysis and the *p*H of 0·01 M CH_3COONH_4. Given $K_a = K_b = 1{\cdot}8\times10^{-5}$. **[Ans. 5·13]**
12. 25 ml of 0·1M solution of HCl is titrated against 0·1M solution of NaOH. Calculate the *p*H of the titration solution after the addition of 5, 10, 15, 20, 24·9, 24·95, 25·00, 25·10, 25 and 30 ml of NaOH solution. Plot the data in the form of a titration curve and suggest a suitable indicator for the titration. **[Ans. 0·56% ; *p*H=7]**
13. 25 ml of 0·1M solution of acetic acid is titrated against 0·1M solution of NaOH. Calculate the *p*H of the titration solution on the addition of 5, 10, 15, 20, 24·90, 24·95, 25·00, 25·10, 25 and 30 ml of NaOH solution. Plot the data in the form of a titration curve and suggest a suitable indicator for the titration.
14. Calculate the solubility products of the following compounds. The solubilities are given in mol dm^{-3} :

    (a) $BaSO_4$, $1{\cdot}05\times10^{-5}$ mol dm^{-3} *(b)* TlBr, $1{\cdot}9\times10^{-3}$ mol dm^{-3} *(c)* $Mg(OH)_2$, $1{\cdot}21\times10^{-4}$ mol dm^{-3} *(d)* $Ag_2C_2O_4$, $1{\cdot}05\times10^{-4}$ mol dm^{-3} *(e)* $La(OH)_3$, $7{\cdot}8\times10^{-4}$ mol dm^{-3}

    [Ans. *(a)* $K_{sp} = 1{\cdot}1\times10^{-10}$ *(b)* $3{\cdot}6\times10^{-6}$ *(c)* $7{\cdot}09\times10^{-12}$) *(d)* $6{\cdot}1\times10^{-22}$ (assuming no hydrolysis of $C_2O_4^{2-}$ ion.) *(e)* $1{\cdot}0\times10^{-11}$].
15. Calculate the *p*H of a solution prepared by mixing 50·0 ml of 0·200 M CH_3COOH and 50·0 ml of 0·100 M NaOH. Given $K_a = 1{\cdot}80\times10^{-5}$. **[Ans. 4·74]**
16. Calculate the *p*H of a solution of 0·10 M acetic acid. Calculate the *p*H after 50·00 ml of this solution is treated with 25·00 ml of 0·10 NaOH. **[Ans. 2·87 ; 4·74]**
17. Calculate the *p*H of a 0·200 M solution of NH_4Cl. Given $K_w = 1{\cdot}008\times10^{-14}$; $K_b = 1{\cdot}80\times10^{-5}$. **[Ans. 4·96]**
18. Calculate $[OH^-]$ of a 0·010 M solution of CH_3COONa. Given $K_a = 1{\cdot}80\times10^{-5}$. **[Ans. $2{\cdot}4\times10^{-6}$ M]**
19. What is the *p*H of a buffer solution that is 0·010 M in HCN and 0·020 M in NaCN ? $K_a = 6{\cdot}2\times10^{-10}$. **[Ans. 5·1]**
20. Calculate $[H^+]$ and $[CH_3COO^-]$ in a solution that is 0·100 M in CH_3COOH and 0·050 M in HCl. $K_a = 1{\cdot}80\times10^{-5}$. **[Ans. $[H^+] \approx 0{\cdot}050$ M, $[CH_3COO^- = 3{\cdot}6\times10^{-5}$ M]**
21. Calculate $[H^+]$, $[CH_3COO^-]$ and $[CN^-]$ in a solution that is 0·100 M in CH_3COOH and 0·200 M in HCN. Given $K_a(CH_3COOH) = 1{\cdot}80\times10^{-5}$; $K_a[HCN] = 6{\cdot}2\times10^{-10}$. **[Ans. $1{\cdot}3\times10^{-3}$; $1{\cdot}3\times10^{-3}$; $9{\cdot}3\times10^{-3}$]**
22. Calculate the *p*H of a solution containing 0·10 M H_3BO_3 and 0·18 M NaH_2BO_3. $K_a = 7{\cdot}3\times10^{-10}$. **[Ans. 9·39]**
23. Calculate the molar solubility of $Fe(OH)_3$ in a solution of *p*H = 8·0. K_{sp} for $Fe(OH)_3 = 1{\cdot}0\times10^{-36}$. **[Ans. $1{\cdot}0\times10^{-12}$ M]**
24. The solubility of $PbSO_4$ in water 0·038 g dm^{-3}. Calculate its K_{sp}. **[Ans. $1{\cdot}6\times10^{-8}$]**

CHAPTER 21

SOLUTIONS OF NON-ELECTROLYTES

Most of the reactions in chemistry and biochemistry are carried out in solution. Hence, the investigation of solutions is a topic of great importance. A **solution** is defined as a homogeneous mixture of two or more substances having uniform properties throughout. Since it is a homogeneous mixture, the solution constitutes a single phase. The substances of which the solution is made are called its *components*. Solutions are generally two-component (or binary) systems consisting of a solute and a solvent. The solute is the component present in smaller proportion that dissolves to form the solution. The solvent, on the other hand, is the component present in larger proportion in which the solute dissolves. The terms solute and solvent do not really signify any essential difference between the two components. For instance, a mixture of ethanol and water may be regarded as a solution of either in the other. A solution may exist in gaseous state, liquid state or solid state. Significant types of solutions are : *1. Solid-in-Liquid Solutions 2. Liquid-in-Liquid Solutions 3. Gas-in-Liquid Solutions.* In the present chapter we shall discuss the last two types of solutions in some details.

SOLUTIONS OF LIQUIDS IN LIQUIDS

We shall discuss only the **binary liquid solutions,** *i.e.,* the solutions containing only two liquids. Both the liquids are supposed to be volatile. In liquid solutions the molecules are very close together. The solubility of a liquid in another liquid is determined by the molecular structure of the solute and the solvent. If the solute molecules exert large intermolecular forces on one another but are not attracted to the solvent molecules, they tend to 'stick' together forming a separate phase from that of the solvent. Similarly, if the solvent molecules, attract one another strongly and show no affinity for the solute molecules, the solvent molecules form a separate phase. For the solute molecules to form a solution with the solvent molecules, the general rule is that *like dissolves like*. Two substances having similar molecular structures and similar intermolecular forces are generally soluble in each other. In general, polar substances dissolve polar substances and nonpolar substances dissolve nonpolar substances.

Concentration Units. The concentrations of solutions are expressed in a number of ways, all of them involving the quantity of the solute and the quantity of solvent or solution.

1. Molarity. The molarity, M_A, of a component A in solution is defined as the number of moles of the component present in one litre (dm^3) of the *solution*. Thus,

$$M_A = \text{Moles of A/Volume of solution} = n_A/V \text{ in litres}$$

2. Molality. The molality, m_A, of a component A in solution is defined as the number of moles of the component present in one kilogram of the *solvent*. Thus,

$$m_A = \text{Moles of A/Mass of solvent} = n_A/\text{kg of solvent}$$

3. Mole Fraction. In a solution containing n_1 moles of component 1, n_2 moles of component 2, n_3 moles of component 3 and so on, the mole fraction, x_i, of the ith component, is defined as

$$x_i = n_i/\Sigma n_i = n_i/(n_1+n_2+n_3+\cdots\cdots)$$

The sum of the mole fractions of the components of a mixture (or a solution) is unity. Thus,

$$\Sigma x_i = 1$$

The less frequently used concentration units are

1. *Mass Percent.* The mass percent of a component A in solution is defined as

$$\text{Mass \% A} = (\text{Mass of A/Total mass}) \times 100$$

2. *Mole Percent.* The mole percent of a component A in solution is defined as

$$\text{Mole \% A} = (\text{Moles of A/Total moles}) \times 100$$

3. *Parts per million.* The concentration of a component A in solution in parts per million (ppm) is defined as

$$(\text{ppm})_A = (\text{Mass of A/Total mass}) \times 10^6$$

In a two-component (binary) solution, it is customary to denote the solvent by subscript 1 and the solute by subscript 2.

Example 1. A solution is prepared by dissolving 43·0 g of naphthalene (M_m=128·0 g mol^{-1}) in 117·0 g of benzene (M_m=78·0 g mol^{-1}). Calculate the mole fractions of the two components of the solution.

Solution : Number of moles, $n = m/M_m$ where m is the mass and M_m is the molar mass.

Thus, $n_2 = 43{\cdot}0 \text{ g}/128 \text{ g mol}^{-1} = 0{\cdot}34 \text{ mol}$

$n_1 = 117{\cdot}0 \text{ g}/78{\cdot}0 \text{ g mol}^{-1} = 1{\cdot}50 \text{ mol}$

$\therefore \quad x_2 = n_2/(n_1+n_2) = 0{\cdot}34 \text{ mol}/(1{\cdot}50 \text{ mol}+0{\cdot}34 \text{ mol}) = \mathbf{0{\cdot}185}$

Since $x_1+x_2 = 1,$

$\therefore \quad x_1 = \mathbf{0{\cdot}815}$

Example 2. Calculate the mole fraction of water in a mixture containing 9·0 g water (M_m=18 g mol^{-1}), 120 g acetic acid (M_m=60 g mol^{-1}) and 115 g ethanol (M_m=46 g mol^{-1}).

Solution :

n_1 (water) = 9·0 g/18 mol^{-1} = 1/2 mol

n_2 (acetic acid) = 120 g/60 g mol^{-1} = 2 mol

n_3 = 115 g/46 g mol^{-1} = 5/2 mol

$n = n_1 + n_2 + n_3$ = 5 mol

Hence, $$x(H_2O) = \left(\frac{1/2 \text{ mol}}{5 \text{ mol}}\right) = \mathbf{0{\cdot}10}$$

Example 3. Concentrated hydrochloric acid contains 37% (by mass) HCl. The density of the solution is 1·18 g/ml. Calculate the molarity and molality of the solution.

Solution : Mass of the solution = 100 g

Since Density ρ = Mass/Volume

$\therefore$ Volume of the solution = mass/density = 100 g/1·18 g ml^{-1} = 85 ml = 85 cm^3 = 0·085 dm^3

n(HCl) = 37 g/36·5 g mol^{-1} = 1·01 mol

$\therefore$ Molarity of HCl = 1·01 mol/0·085 dm^3 = 12·0 mol dm^{-3} = **12·0 M**

Mass of solvent = (100 – 37) = 63 g = 0·063 kg

$\therefore$ Molality of HCl = 1·01 mol/0·063 kg = 16·03 mol kg^{-1} = **16·03 m**

Example 4. The density of 2·0 M solution of acetic acid (M_m=60 g mol^{-1}) in water is 1·02 kg dm^{-3}. Calculate the mole fraction of acetic acid.

Solution : Mass of acetic acid in 2·0 M acetic acid solution = 120 g per dm^3 of the solution.

Mass of solution = volume×density = (1·00 dm^3) (1·02 kg dm^{-3}) = 1·02 kg

$\therefore$ Mass of solvent (water) = 1020 g − 120 g = 900 g

n(acetic acid) = 120 g/60 g mol^{-1} = 2·0 mol

n(water) = 900 g/18 g mol^{-1} = 50·0 mol

$\therefore$ x(acetic acid) = 2·0/(50·0+2·0) = **0·038**

Example 5. Calculate the molality, molarity and mole fraction of ethanol in a solution of total volume 100 ml prepared by adding 50 ml ethanol (density=0·789 g ml^{-1}) to 50 ml water (density=1·00 g ml^{-1}). Also calculate the molality of water in alcohol.

Solution : The numbers of moles of ethanol and of water present in 50 ml of each are calculated as follows :

(0·789 g ml^{-1})(50 ml)/46·0 g mol^{-1} = 0·86 mol C_2H_5OH

(1·0 g ml^{-1})(50 ml)/18·0 g mol^{-1} = 2·8 mol H_2O

$\therefore$ Molality of C_2H_5OH, m = 0·86 mol C_2H_5OH/0·050 kg H_2O = **17 mol kg^{-1}**

Mole fraction of C_2H_5OH, x_1 = 0·86 mol/(0·86 mol+2·8 mol) = **0·23**

Molarity of C_2H_5OH, M = 0·86 mol/0·10 dm^3 = **8·6 mol dm^{-3}**

$$\text{Molality of } H_2O,\ m = \frac{2\cdot8 \text{ mol } H_2O}{(0\cdot050 \text{ dm}^3)(0\cdot789 \text{ kg dm}^{-3})C_2H_5OH} = \mathbf{71 \text{ mol kg}^{-1}}$$

Raoult's Law

The French chemist F. Raoult studied vapour pressures of a number of binary solutions of volatile liquids, such as benzene and toluene, at constant temperature and gave the following generalisation which is known as the **Raoult's law :**

The partial pressure of any volatile component of a solution at any temperature is equal to the vapour pressure of the pure component multiplied by the mole fraction of that component in the solution.

Suppose a binary solution is made of n_A moles of a volatile liquid A and n_B moles of a volatile liquid B. If p_A and p_B are partial pressures of the two liquid components, then, according to the Raoult's law,

$$p_A = x_A p_A^\circ \quad \text{and} \quad p_B = x_B p_B^\circ \qquad \ldots(1)$$

where x_A is the mole fraction of the component A given by $n_A/(n_A+n_B)$, x_B is the mole fraction of the component B given by $n_B/(n_A+n_B)$ and p_A° and p_B° are the vapour pressures of pure components A and B, respectively.

If the vapour behaves like an ideal gas, then, according to Dalton's law of partial pressures, the total vapour pressure P is given by

$$P = p_A + p_B = x_A p_A^\circ + x_B p_B^\circ \qquad \ldots(2)$$

In general, Raoult's law may be expressed as

$$p_i = x_i p_i^\circ \qquad \ldots(3)$$

and the total vapour pressure may be expressed as

$$P = \Sigma p_i \qquad \ldots(4)$$

We know from experiment that Raoult's law is obeyed only approximately for most of the binary solutions. The law is obeyed perfectly only in the case of ideal solutions. This gives us a definition of an ideal solution. *A solution of two or more constituents is said to be* **ideal** *if it obeys Raoult's law exactly at all concentrations and at all temperatures.*

It has been found that liquid pairs which are similar, generally form ideal solutions. This implies that intermolecular or cohesive forces in these solutions are completely uniform, *i.e.*, the magnitude of these forces between molecules A and A, B and B and A and B are of the same magnitude.

The following binary mixtures obey Raoult's law over the entire range of concentration and thus form ideal solutions :

Ethylene bromide and ethylene chloride; *n*-hexane and *n*-heptane; *n*-butyl chloride and *n*-butyl bromide; benzene and toluene and carbon tetrachloride and silicon tetrachloride.

Vapour Pressures of Ideal Solutions. The vapour pressures of an ideal binary solution of two components A and B having different mole fractions are shown in Fig. 1.

It is evident that the graph of the partial pressure of each component against its mole fraction in the solution is a straight line and the total vapour pressure of the solution for any given composition is equal to the sum of the partial vapour pressures of the two constituents.

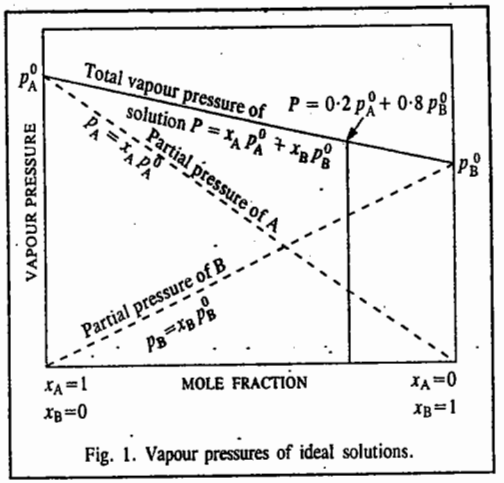

Fig. 1. Vapour pressures of ideal solutions.

The partial vapour pressure of component A is given by $x_A p_A^\circ$ and that of component B is given by $x_B p_B^\circ$. The total vapour pressure of the solution is given by $x_A p_A^\circ + x_B p_B^\circ$. Thus, when the mole fraction of B is, say, 0·80, the total vapour pressure is given by $P = 0{\cdot}2\, p_A^\circ + 0{\cdot}8\, p_B^\circ$ (Fig. 1).

Let us again emphasize that ideality of a solution implies that a molecule of component A will have the same tendency to escape into the vapour phase whether it is surrounded entirely by other molecules of its own type or entirely by molecules of component B or partly by molecules of component A and partly by molecules of component B. Thus, the intermolecular forces between A and A, B and B and between A and B are essentially the same. In other words, it is immaterial for of a molecule as to what type of neighbours it has. The escaping tendency of component A from an ideal solution is the same as that from a pure liquid except that it is proportionally reduced as a result of the lower mole fraction of A molecules in the solution.

Total Vapour Pressure in Terms of Mole Fractions of the Components in Vapour Phase. The total vapour pressure, P, can also be related to the mole fractions x_A and x_B of the two components in the vapour phase. For notational convenience, we shall write

$$x_{A,vap} = y_A \quad \text{and} \quad x_{B,vap} = y_B$$

From the definition of partial pressure,

$$y_A = p_A/P \text{ and } y_B = p_B/P \qquad \ldots(5)$$

where P is the total vapour pressure. Hence, from Eq. 3,

$$x_A p_A^\circ = P y_A \text{ and } x_B p_B^\circ = P y_B \qquad \ldots(6)$$

Eq. 2 may be put in the form, $P = (1 - x_B)p_A^\circ + x_B p_B^\circ = p_A^\circ + x_B(p_B^\circ - p_A^\circ)$ ...(7)

$$\therefore \quad x_B = (P - p_A^\circ)/(p_B^\circ - p_A^\circ) \qquad \ldots(8)$$

Using this value of x_B in Eq. 6, we have

$$P y_B = p_B^\circ(P - p_A^\circ)/(p_B^\circ - p_A^\circ) \qquad \ldots(9)$$

or $$P y_B(p_B^\circ - p_A^\circ) = p_B^\circ P - p_A^\circ p_B^\circ$$

or $$P[y_B(p_B^\circ - p_A^\circ) - p_B^\circ] = -p_A^\circ p_B^\circ \qquad \ldots(10)$$

Hence, $$P = \frac{p_A^\circ p_B^\circ}{p_B^\circ + (p_A^\circ - p_B^\circ)y_B} \quad ...(11)$$

Eq. 11 can be simplified further and put in a better form. Inverting it, we have

$$\frac{1}{P} = \frac{p_B^\circ + (p_A^\circ - p_B^\circ)y_B}{p_A^\circ p_B^\circ} = \frac{p_B^\circ(1 + y_B) - p_A^\circ y_B}{p_A^\circ p_B^\circ} = \frac{p_B^\circ y_A + p_A^\circ y_B}{p_A^\circ p_B^\circ} = \frac{y_A}{p_A^\circ} + \frac{y_B}{p_B^\circ} \quad ...(12)$$

Let us now consider the vapour in equilibrium with the solution. The mole fraction, y_A, of component A in the vapour phase is given by the ratio of its partial pressure to the total pressure, P, of the solution, assuming that the vapour behaves ideally and Dalton's law of partial pressures is applicable to it.

$$y_A = \frac{p_A}{p_A + p_B} = \frac{x_A p_A^\circ}{x_A p_A^\circ + x_B p_B^\circ} = \frac{(1 - x_B)p_A^\circ}{(p_B^\circ - p_A^\circ)x_B + p_A^\circ} \quad ...(13)$$

$$y_B = \frac{p_B}{p_A + p_B} = \frac{x_B p_B^\circ}{(p_B^\circ - p_A^\circ)x_B + p_A^\circ} \quad ...(14)$$

Example 6. The vapour pressures of pure CCl_4 (M_m=154 g mol^{-1}) and $SnCl_4$ (M_m=170 g mol^{-1}) at 25°C are 114·9 and 238·3 torr, respectively. Assuming ideal behaviour, calculate the total vapour pressure of a solution containing 10 g of CCl_4 and 15 g of $SnCl_4$.

Solution : Let x_A be the mole fraction of CCl_4 and x_B that of $SnCl_4$.

$$x_A = \frac{10\text{ g}/(154\text{ g mol}^{-1})}{(10\text{ g}/154\text{ g mol}^{-1}) + (15\text{ g}/170\text{ g mol}^{-1})} = 0{\cdot}424$$

$$x_B = 1 - x_A = 0{\cdot}576$$

According to Raoult's law, the partial pressures are :

$$p_A = x_A p_A^\circ = 0{\cdot}424 \times 114{\cdot}9 \text{ torr} = 48{\cdot}72 \text{ torr}$$

$$p_B = x_B p_B^\circ = 0{\cdot}576 \times 238{\cdot}3 \text{ torr} = 137{\cdot}26 \text{ torr}$$

Total vapour pressure = 48·72 torr + 137·26 torr = **185·98 torr**

Example 7. The vapour pressures of pure benzene and toluene at 40°C are 184·0 torr and 59·0 torr, respectively. Calculate the partial pressures of benzene and toluene, the total vapour pressure of the solution and the mole fraction of benzene in the vapour above the solution that has 0·40 mole fraction of benzene. Assume that the solution is ideal.

Solution : Let us designate benzene by subscript A and toluene by subscript B.

In solution, $x_A = 0{\cdot}40$ and hence $x_B = 0{\cdot}6$ [$\because x_A + x_B = 1$]

$$p_A = x_A p_A^\circ = (0{\cdot}40)\,(184{\cdot}0 \text{ torr}) = 73{\cdot}6 \text{ torr}$$

$$p_B = x_B p_B^\circ = (0{\cdot}60)\,(59{\cdot}0 \text{ torr}) = 35{\cdot}4 \text{ torr}$$

$$P = p_A + p_B = 73{\cdot}6 \text{ torr} + 35{\cdot}4 \text{ torr} = 109{\cdot}0 \text{ torr}$$

$$x_{A,vap} = p_A/P = p_A/(p_A + p_B) = 73{\cdot}6 \text{ torr}/109{\cdot}0 \text{ torr} = 0{\cdot}675$$

Example 8. Liquids A and B form an ideal solution obeying Raoult's law. At 50°C, the total vapour pressure of a solution containing 1 mole of A and 2 moles of B is 300 torr. When 1 more mole of A is added to the solution, the total vapour pressure increases to 400 torr. Calculate the vapour pressures of the pure components.

Solution. In the beginning, $x_A = 1/(1+2) = 1/3$; $x_B = 1 - 1/3 = 2/3$

After the addition of 1 more mole of A to the solution,

$$x_A = 2/(2+2) = 1/2 \text{ ; } \quad x_B = 1/2$$

We now have two simultaneous linear equations :

$$300 = (1/3)p_A^\circ + (2/3)p_B^\circ \text{ and } 400 = (1/2)p_A^\circ + (1/2)p_B^\circ$$

Simplification of the above equations gives

$$900 = p_A^\circ + 2p_B^\circ \text{ and } 800 = p_A^\circ + p_B^\circ$$

Solution of the above equations gives

$$p_A^\circ = 700 \text{ torr ; } p_B^\circ = 100 \text{ torr}$$

Example 9. The vapour pressures of pure liquids A and B (assumed to behave ideally) are 200 torr and 500 torr, respectively, at 27°C. Calculate the mole fractions in the vapour and the liquid phases of a solution of A and B if the total vapour pressure of the solution is 350 torr at 27°C.

Solution : According to Raoult's law,

$$P = p_A + p_B = x_A p_A^\circ + x_B p_B^\circ = x_A(200) + (1 - x_A)(500)$$

$$\therefore \quad 350 = x_A(200) + (1 - x_A)\,(500) = -300\,x_A + 500$$

$$\therefore \quad x_A = 1/2 \text{ and } x_B = 1 - 1/2 = 1/2$$

$$x_{A,vap} = p_A/P = x_A p_A^\circ/P = (1/2)(200)/350 = 1/3{\cdot}5 = 0{\cdot}286$$

$$x_{B,vap} = p_B/P = x_B p_B^\circ/P = (1/2)(500)/350 = 2{\cdot}5/3{\cdot}5 = 0{\cdot}714$$

Notice that the vapour is richer in the more volatile component B.

Example 10. A solution of A and B with 30 mole per cent of A is in equilibrium with its vapour which contains 60 mole per cent of A. Assuming ideality of the solution and the vapour, calculate the ratio of the vapour pressure of pure A to that of pure B.

Solution : In solution, $x_A = 0{\cdot}30$, hence $x_B = 0{\cdot}70$

In the vapour phase, $x_{A,vap} = 0{\cdot}60$ and $x_{B,vap} = 0{\cdot}40$

Using Dalton's law of partial pressures and Raoult's law, we have

$$x_{A,vap} = 0{\cdot}60 = p_A/P = p_A/(p_A + p_B) = 0{\cdot}30\,p_A^\circ/(0{\cdot}30\,p_A^\circ + 0{\cdot}70\,p_B^\circ)$$

$$x_{B,vap} = 0{\cdot}40 = p_B/P = p_B/(p_A + p_B) = 0{\cdot}70\,p_B^\circ/(0{\cdot}30\,p_A^\circ + 0{\cdot}70\,p_B^\circ)$$

$$x_{A,vap}/x_{B,vap} = 0{\cdot}60/0{\cdot}40 = 0{\cdot}30\,p_A^\circ/0{\cdot}70\,p_B^\circ$$

$$\frac{p_A^\circ}{p_B^\circ} = \frac{0{\cdot}60 \times 0{\cdot}70}{0{\cdot}40 \times 0{\cdot}30} = \frac{7}{2} = 3{\cdot}5$$

Example 11. A mixture of two immiscible liquids A and B is distilled under equilibrium conditions at 1 atm pressure. Assuming ideal gas behaviour, calculate the mole fraction of A in the distillate if the vapour pressure of pure B is 425 torr.

Solution : There exists a unique temperature T at which distillation occurs. It is determined implicitly by the equation

$$p_A^\circ(T) + p_B^\circ(T) = 1 \text{ atm}$$

where p_A° and p_B° are the vapour pressures of the pure components A and B at temperature T. Since the liquids are not miscible, Raoult's law is applicable to each phase separately. Thus,

$$p_A = p_A^\circ x_A = p_A^\circ(T); \quad p_B = p_B^\circ x_B = p_B^\circ(T)$$

$$p_A + p_B = P = 1 \text{ atm} = p_A^\circ(T) + p_B^\circ(T)$$

Since $p_B^\circ = 425$ torr, hence $p_A^\circ = 760 - 425 = 335$ torr

$$\therefore \quad x_{A,vap} = p_A/P = 335 \text{ torr}/760 \text{ torr} = 0{\cdot}441$$

Activity of a Component in an Ideal Solution. Consider, once again, a binary solution of components A and B forming an ideal solution. Let x_A and x_B be the mole fractions and a_A and a_B be the activities of the components A and B, respectively. Then, according to Raoult's law, the partial vapour pressure of component A is given by

$$p_A = x_A p_A^\circ \quad \text{or} \quad p_A / p_A^\circ = x_A \qquad \ldots(15)$$

Since vapour pressures of liquid components of a solution at ordinary temperatures are usually low (being very much less than 1 atm), lying well within the range in which the fugacity (f) may be taken as equal to pressure, hence,

$$p_A / p_A^\circ = f_A / f_A^\circ = x_A \qquad \ldots(16)$$

But, as already discussed in Chapter 15, $f_A / f_A^\circ = a_A$ where f_A is the fugacity of component A in the solution, f_A° is the fugacity of pure component A and a_A is the activity of component A in the solution. Hence, $x_A = a_A$ and $x_B = a_B$ where a_B is the activity of component B in the solution.

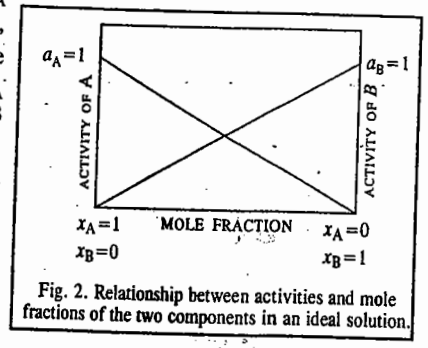

Fig. 2. Relationship between activities and mole fractions of the two components in an ideal solution.

An **ideal solution** is defined *as the one in which the activity of each component is equal to its mole fraction under all conditions of temperature, pressure and concentration.*

If x_i is the mole fraction of a component i, then its activity a_i is given by $a_i = x_i$

The relationship between activities and mole fractions of the components is expressed graphically as in Fig. 2.

Chemical Potentials of Ideal and Non-ideal Solutions

Consider a two-component liquid solution in equilibrium with its vapour assumed ideal. Since for a system in equilibrium the chemical potential of component A is the same in the liquid (l) and the gas (g) phases, we can write

$$\mu_A(l) = \mu_A(g) = \mu_A^\circ(g) + RT \ln p_A \qquad \ldots(17)$$

For pure liquid A,

$$\mu_A^\circ(l) = \mu_A^\circ(g) + RT \ln p_A^\circ \qquad \ldots(18)$$

Alternatively, if we add and subtract $RT \ln p_A^\circ$ on the right-hand side of Eq. 17, we obtain

$$\mu_A(l) = [\mu_A^\circ(g) + RT \ln p_A^\circ] + RT \ln (p_A / p_A^\circ) = \mu_A^\circ(l) + RT \ln (p_A / p_A^\circ) \qquad \ldots(19)$$

Thus, there are two ways of expressing the chemical potential of component A. In Eq. 17, this is done in terms of $\mu_A^\circ(g)$ and p_A while in Eq. 19, this is done in terms of $\mu_A^\circ(l)$ and p_A / p_A°. In the former case, the standard state is the vapour at 1 atm pressure while in the latter case, it is the pure liquid. For component B, we can write equations analogous to Eqs. 17 and 19, *viz.*,

$$\mu_B(l) = \mu_B^\circ(g) + RT \ln p_B \qquad \ldots(20)$$

$$\mu_B(l) = \mu_B^\circ(l) + RT \ln (p_B / p_B^\circ) \qquad \ldots(21)$$

For an ideal solution obeying Raoult's law, $p_A / p_A^\circ = x_A$ and $p_B / p_B = x_B$. Thus, for an ideal

solution, Eqs. 19 and 21 become

$$\mu_A(l) = \mu_A^\circ(l) + RT \ln x_A \qquad \ldots(22)$$

$$\mu_B(l) = \mu_B^\circ(l) + RT \ln x_B \qquad \ldots(23)$$

Again, for an ideal solution, $a_i = x_i$. Accordingly, for an ideal solution, Eqs. 22 and 23 can be written as

$$\mu_A(l) = \mu_A^\circ(l) + RT \ln a_A \qquad \ldots(24)$$

and

$$\mu_B(l) = \mu_B^\circ(l) + RT \ln a_B \qquad \ldots(25)$$

For a non-ideal solution, Raoult's law is expressed as

$$p_i = a_i p_i^\circ \qquad \ldots(26)$$

where a_i is the activity of the ith component.

Defining activity coefficient, γ_i, of a component as $\gamma_i = a_i / x_i$, Eqs. 24 and 25 become

$$\mu_A(l) = \mu_A^\circ(l) + RT \ln x_A + RT \ln \gamma_A \qquad \ldots(27)$$

$$\mu_B(l) = \mu_B^\circ(l) + RT \ln x_B + RT \ln \gamma_B \qquad \ldots(28)$$

Example 12. The partial pressure of bromine over a bromine-carbon tetrachloride solution containing mole fraction of bromine equal to 0·025 is 10·27 torr. If the vapour pressure of pure bromine at the same temperature is 213 torr, what is the activity coefficient of bromine in the given solution ?

Solution : The solution is evidently non-ideal for which Raoult's law is

$$p_i = a_i p_i^\circ \qquad \text{(Eq. 26)}$$

For bromine, designated by subscript A, $p_A = a_A p_A^\circ$

$$\therefore \quad a_A = p_A / p_A^\circ = 10{\cdot}27 \text{ torr}/213 \text{ torr} = 0{\cdot}0482$$

Hence,

$$\gamma_A = a_A / x_A = 0{\cdot}0482/0{\cdot}025 = \mathbf{1{\cdot}93}$$

Example 13. Two miscible liquids A and B form a solution. Assume that the solution is non-ideal but the vapour above it behaves ideally. The vapour pressures of pure A and pure B are 550 torr and 700 torr, respectively at 35°C. If the total pressure above a solution that is 48 mole percent A, is 500 torr and the mole fraction of A in the vapour is 0·45, calculate the activity coefficients of A and B in the solution.

Solution : $x_{A,vap} = 0{\cdot}45$

Since the vapour behaves ideally, hence

$$p_A = x_{A,vap} \times P = 0{\cdot}45 \times 500 \text{ torr} = 225 \text{ torr}$$

$$p_B = P - p_A = 500 \text{ torr} - 225 \text{ torr} = 275 \text{ torr}$$

Since the solution behaves non-ideally, Raoult's law becomes :

$$p_i = a_i p_i^\circ \qquad \text{(Eq. 26)}$$

$$a_A = p_A / p_A^\circ = 225 \text{ torr}/550 \text{ torr} = 0{\cdot}41$$

Hence

$$\gamma_A = a_A / x_A = 0{\cdot}41/0{\cdot}48 = \mathbf{0{\cdot}854}$$

$$a_B = p_B / p_B^\circ = 275 \text{ torr}/700 \text{ torr} = 0{\cdot}393$$

$$\gamma_B = a_B / x_B = 0{\cdot}393/0{\cdot}52 = \mathbf{0{\cdot}768}$$

Gibbs-Duhem-Margules Equation. Let us consider, once again, a binary solution of components A and B in equilibrium with their vapours, at constant temperature and pressure. If n_A and n_B are the numbers of moles of components A and B, respectively, then, according to the well known Gibbs-Duhem equation, (Chapter 15)

$$n_A \, d\mu_A + n_B \, d\mu_B = 0 \qquad \ldots(29)$$

where μ_A and μ_B are the chemical potentials of A and B, respectively. Dividing Eq. 29 by n_A+n_B, we have

$$\frac{n_A}{n_A+n_B}d\mu_A + \frac{n_B}{n_A+n_B}d\mu_B = 0$$

or $$x_A\,d\mu_A + x_B\,d\mu_B = 0 \qquad ...(30)$$

where x_A and x_B are the mole fractions of components A and B.

Thermodynamically, the chemical potential of any constituent of a liquid mixture is represented by the expression

$$\mu_i = \mu_i^\circ + RT\ln f_i \qquad ...(31)$$

where f_i represents the fugacity of the given constituent in the liquid or in the vapour phase in equilibrium and μ_i° is a constant for the substance at constant temperature.

Differentiating Eq. 31 at constant temperature, we have

$$d\mu_i = RTd\ln f_i \qquad ...(32)$$

Inserting this relation in Eq. 30, we get

$$x_A\,RTd\ln f_A + x_B\,RTd\ln f_B = 0 \qquad ...(33)$$

Dividing throughout by dx_A, we get

$$x_A\,RTd\ln f_A/dx_A + x_B\,RTd\ln f_B/dx_A = 0 \qquad ...(34)$$

Since $x_A+x_B = 1$, hence $dx_A = -dx_B$. Therefore, Eq. 34 takes the form

$$\frac{d\ln f_A}{dx_A/x_A} - \frac{d\ln f_B}{dx_B/x_B} = 0 \text{ or } \frac{d\ln f_A}{d\ln x_A} - \frac{d\ln f_B}{d\ln x_B} = 0$$

or $$\frac{d\ln f_A}{d\ln x_A} = \frac{d\ln f_B}{d\ln x_B} \qquad ...(35)$$

This equation is valid whether the vapour phase behaves ideally or non-ideally.

If the vapour behaves as an ideal gas, the fugacity can be replaced by vapour pressure so that Eq. 35 becomes

$$d\ln p_A/d\ln x_A = d\ln p_B/d\ln x_B \qquad ...(36)$$

Eq. 36 is known as the **Gibbs-Duhem-Margules equation.**

This equation relates the composition of the mixture in the liquid phase with the partial vapour pressures in the gas phase.

Ideal Solutions and the Gibbs-Duhem-Margules Equation. For an ideal solution, Raoult's law is applicable, that is, for the component A,

$$p_A = x_A p_A^\circ \qquad ...(Eq. 1)$$

Taking logarithms of both sides and differentiating, we get

$$d\ln p_A = d\ln x_A \text{ or } d\ln p_A/d\ln x_A = 1 \qquad ...(37)$$

Hence, from the Gibbs-Duhem-Margules equation

$$d\ln p_B/d\ln x_B = 1 \qquad ...(38)$$

Integrating Eq. 38, we get, $\ln p_B = \ln x_B + \ln k$

where $\ln k$ is the constant of integration. Taking antilogs, we get

$$p_B = k\,x_B$$

If $x_B = 1$, p_B becomes p_B° so that $k = p_B^\circ$.

$$\therefore \quad p_B = p_B^\circ x_B \qquad ...(39)$$

Eq. 39 is evidently Raoult's law for component B.

Thus, we find that *if in a binary solution, component* A *obeys Raoult's law, then component* B *would also obey Raoult's law.*

Temperature-Dependence of Vapour Pressure of a Solution. For liquid $\rightleftharpoons$ vapour equilibrium in a one-component system, *i.e.*, in the case of a single liquid, the temperature-dependence of the vapour pressure of the liquid is given by the Clapeyron-Clausius equation, *viz.*,

$$\ln\left(\frac{p_2^\circ}{p_1^\circ}\right) = \frac{\Delta H_{vap}^\circ}{R}\left(\frac{1}{T_1}-\frac{1}{T_2}\right) \qquad ...(40)$$

If $T_1 = T_{b,i}$, the boiling point of the liquid i, then $p_i^\circ = 1$ atm so that Eq. 40 becomes

$$p_i^\circ = \exp\left[\frac{\Delta H_{vap,i}^\circ}{R}\left(\frac{1}{T_{b,i}}-\frac{1}{T}\right)\right] \qquad ...(41)$$

For an ideal solution, $p_i = x_i p_i^\circ$. Hence, Eq. 41 becomes

$$p_i = x_i \exp\left[\frac{\Delta H_{vap,i}^\circ}{R}\left(\frac{1}{T_{b,i}}-\frac{1}{T}\right)\right] \qquad ...(42)$$

Thus, for the two components A and B of an ideal solution, the partial pressures are given by

$$p_A = x_A \exp\left[\frac{\Delta H_{vap,A}^\circ}{R}\left(\frac{1}{T_{b,A}}-\frac{1}{T}\right)\right] \text{ and } p_B = x_B \exp\left[\frac{\Delta H_{vap,B}^\circ}{R}\left(\frac{1}{T_{b,B}}-\frac{1}{T}\right)\right] \qquad ...(43)$$

Since the total vapour pressure $P = p_A+p_B$, hence, substitution of Eq. 43 in this expression gives the equation for the dependence of vapour pressure on temperature for the solution of a given composition.

THERMODYNAMICS OF IDEAL SOLUTIONS

Gibbs Free Energy Change of Mixing (ΔG_{mix}) for an Ideal Solution. Suppose a solution is formed by mixing n_A moles of a liquid A and n_B moles of a liquid B, *i.e.*,

$$n_A A + n_B B \longrightarrow \text{Solution}$$

According to thermodynamics, the free energy (G) of the solution at a given temperature and pressure is given by

$$G = n_A\bar{G}_A + n_B\bar{G}_B \qquad ...(44)$$

where $\bar{G}_A$ and $\bar{G}_B$ are the partial molar free energies (*i.e.*, chemical potentials) of the constituents A and B, respectively.

If G_A° and G_B° are free energies per mole of the pure constituents A and B, respectively, then, change in free energy of the system on mixing, called the free energy change of mixing, ΔG_{mix}, is given by the expression

ΔG_{mix} = (Free energy of solution) - {Sum of free energies of the pure constituents}

$$= G - (n_A G_A^\circ + n_B G_B^\circ) \qquad ...(45)$$

Substituting the value of G from Eq. 44, we have

$$\Delta G_{mix} = (n_A \bar{G}_A + n_B \bar{G}_B) - (n_A G_A^\circ + n_B G_B^\circ) = n_A(\bar{G}_A - G_A^\circ) + n_B(\bar{G}_B - G_B^\circ) \quad ...(46)$$

The quantities $(\bar{G}_A - G_A^\circ)$ and $(\bar{G}_B - G_B^\circ)$, evidently, represent changes in partial molar free energies of components A and B, respectively, as a result *of* mixing.

The chemical potential μ_i of a component i in a given state is given by the well known thermodynamic equation

$$\mu_i = \mu_i^\circ + RT \ln a_i \quad ...(47)$$

where T is the temperature and a is the activity of the component in the given state and μ_i° is the chemical potential of the same substance in its standard state (*i.e.*, unit activity). Since chemical potential refers to the same quantity as the partial molar free energy, the above equation for the constituents A and B, may be written as

$$\bar{G}_A = G_A^\circ + RT \ln a_A$$

or $$\bar{G}_A - G_A^\circ = RT \ln a_A \quad ...(48)$$

and $$\bar{G}_B = G_B^\circ + RT \ln a_B$$

or $$\bar{G}_B - G_B^\circ = RT \ln a_B \quad ...(49)$$

Introducing Eqs. 48 and 49 in Eq. 46, we have

$$\Delta G_{mix} = n_A RT \ln a_A + n_B RT \ln a_B \quad ...(50)$$

If the solution is ideal, the activity of each component should be equal to its mole fraction, *i.e.*, $a_A = x_A$ and $a_B = x_B$. Hence, free energy of mixing of an ideal solution may be expressed as

$$\Delta G_{mix} = n_A RT \ln x_A + x_B RT \ln x_B \quad ...(51)$$

If there are more than two components of the solution, the above equation becomes :

$$\Delta G_{mix} = n_A RT \ln x_A + n_B RT \ln x_B + n_c RT \ln x_c + \ldots = RT \Sigma n_i \ln x_i \quad ...(52)$$

Dividing both sides of Eq. 51 by $n_A + n_B$, we get

$$\frac{\Delta G_{mix}}{n_A + n_B} = \frac{n_A}{n_A + n_B} RT \ln x_A + \frac{n_B}{n_A + n_B} RT \ln x_B = x_A RT \ln x_A + x_B RT \ln x_B \quad ...(53)$$

If the total amount of the two components is one mole, *i.e.*, $n_A + n_B = 1$, then Eq. 53, takes the form

$$\Delta G_{mix} = RT (x_A \ln x_A + x_B \ln x_B) \quad ...(54)$$

If there are more than two components of the solution, then

$$\Delta G_{mix} = RT (x_A \ln x_A + x_B \ln x_B + x_C \ln x_C + \ldots) = RT \Sigma x_i \ln x_i \quad ...(55)$$

Since x_i, the mole fraction, is always less than unity, ΔG_{mix} is always a *negative quantity*.

Volume Change and Enthalpy Change of Mixing for an Ideal Solution. Before considering these changes, we may recall the following thermodynamics equations :

$$\left(\frac{\partial(\Delta G)}{\partial T}\right)_P = -\Delta S \quad ...(56)$$

$$\left(\frac{\partial(\Delta G)}{\partial P}\right)_T = -\Delta V \quad ...(57)$$

For free energy of mixing, we may write the above expressions as

$$\left[\frac{\partial(\Delta G_{mix})}{\partial T}\right]_P = \Delta S_{mix} \quad ...(58)$$

$$\left[\frac{\partial(\Delta G_{mix})}{\partial P}\right]_T = \Delta V_{mix} \quad ...(59)$$

Referring now to Eq. 52 for free energy change of mixing for an ideal binary solution, we find that the expression on the right hand side is independent of pressure as it contains no pressure term. Hence, differentiation of Eq. 52 with respect to pressure, at a constant temperature, yields

$$\left[\frac{\partial(\Delta G_{mix})}{\partial P}\right]_T = 0 \quad ...(60)$$

Combining Eqs. 59 and 60, we have

$$\Delta V_{mix} = 0 \quad ...(61)$$

Thus, if two pure liquid constituents are mixed together in any proportion to give an ideal solution, there is no change in volume.

For a binary solution, Eq. 51 may also be written as

$$\Delta G_{mix}/T = n_A R \ln x_A + n_B R \ln x_B \quad ...(62)$$

Since the expression on the right hand side of the above equation is independent of temperature as it contains no temperature term, differentiation of Eq. 62 with respect to temperature yields

$$\left[\frac{\partial(\Delta G_{mix}/T)}{\partial T}\right]_P = 0 \quad ...(63)$$

An alternative expression by differentiating $\Delta G_{mix}/T$ with respect to temperature, at constant pressure, can also be obtained. Thus,

$$\left[\frac{\partial(\Delta G_{mix}/T)}{\partial T}\right]_P = \frac{T\left\{\frac{\partial(\Delta G_{mix})}{\partial T}\right\}_P - \Delta G_{mix}}{T^2} \quad ...(64)$$

Applying the well known Gibbs–Helmholtz equation, *viz.*,

$$\Delta G - \Delta H = T\left\{\frac{\partial(\Delta G)}{\partial T}\right\}_P \quad ...(65)$$

we may write Eq. 64 as

$$\left\{\frac{\partial(\Delta G_{mix}/T)}{\partial T}\right\}_P = \frac{\Delta G_{mix} - \Delta H_{mix} - \Delta G_{mix}}{T^2} = -\Delta H_{mix}/T^2 \quad ...(66)$$

Combining Eqs. 63 and 66, we have

$$-\Delta H_{mix}/T^2 = 0 \quad i.e., \quad \Delta H_{mix} = 0 \quad ...(67)$$

Thus, if two pure liquids are mixed together in any proportion to give an ideal solution, there is no change in enthalpy.

Entropy Change of Mixing for an Ideal Solution. Finally, let us consider entropy change of mixing in the case of an ideal solution. The well known equation

$$\Delta G = \Delta H - T\Delta S$$

may be written as $$\Delta G_{mix} = \Delta H_{mix} - T\Delta S_{mix}$$

Since for an ideal solution, $\Delta H_{mix} = 0$, we have

$$\Delta G_{mix} = -T\Delta S_{mix} \quad ...(68)$$

According to Eq. 51, $G_{mix} = n_A RT \ln x_A + n_B RT \ln x_B$

Hence, from Eq. 68, $\Delta S_{mix} = -[n_A R \ln x_A + n_B R \ln x_B]$ ...(69)

If there are more than two components of the solution, then

$$\Delta S_{mix} = -[n_A R \ln x_A + n_B R \ln x_B + n_c R \ln x_c \ldots.]$$
$$= -R \Sigma n_i \ln x_i \quad ...(70)$$

Since x_i is always less than unity, ΔS_{mix} is a positive quantity.

Example 14. One mole of component A and two moles of component B are mixed at 27°C to form an ideal binary solution. Calculate ΔV_{mix}, ΔH_{mix}, ΔG_{mix} and ΔS_{mix}. Assume that $R = 8{\cdot}314$ J K^{-1} mol^{-1}.

Solution : For an ideal binary solution, $\Delta V_{mix} = \Delta H_{mix} = 0$.

$T = 27°C = 300$ K ; $n_A = 4$ moles; $n_B = 2$ moles

The mole fractions are given by $x_A = 1/(1+2) = 0{\cdot}334$ and $x_B = 1 - 0{\cdot}334 = 0{\cdot}666$

$$\Delta G_{mix} = RT \Sigma n_i \ln x_i = RT (n_A \ln x_A + n_B \ln x_B)$$
$$= 8{\cdot}314 \text{ J K}^{-1} \text{ mol}^{-1} \times 300 \text{ K } (0{\cdot}334 \text{ mol ln } 0{\cdot}334 + 0{\cdot}666 \text{ mol ln } 0{\cdot}66).$$
$$= -1585{\cdot}38 \text{ J}$$

$$\Delta S_{mix} = -R\Sigma n_i \ln x_i = -R (n_A \ln x_A + n_B \ln x_B) = 5{\cdot}28 \text{ J K}^{-1}$$

Alternatively, $\Delta S_{mix} = -\Delta G_{mix}/T = -(-1585{\cdot}38 \text{ J})/300 \text{ K} = 5{\cdot}28 \text{ J K}^{-1}$

Example 15. Show that for an ideal solution containing two components A and B, the Gibbs free energy of mixing is minimum when the mole fractions of the two components are the same, *i.e.*, equal to 1/2 each.

Solution : According to Eq. 54,

$$\Delta G_{mix}/RT = x_A \ln x_A + x_B \ln x_B$$

Since $x_A + x_B = 1$, hence $x_B = 1 - x_A$

$$\therefore \quad \Delta G_{mix}/RT = x_A \ln x_A + (1-x_A) \ln (1 - x_A)$$

For ΔG_{mix} to be *minimum* at a given temperature and pressure,

$$\left(\frac{\partial(\Delta G_{mix})}{\partial x_A}\right)_{T,P} = 0$$

Thus, $$\frac{\partial}{\partial x_A}(x_A \ln x_A + (1 - x_A) \ln (1-x_A) = 0$$

or $x_A (1/x_A) + \ln x_A + (1 - x_A) \times 1/(1 - x_A) (-1) \ln (1 - x_A) (-1) = 0$

or $1 + \ln x_A - 1 - \ln (1 - x_A) = 0$

or $\ln x_A/(1 - x_A) = 0$ or $x_A/(1 - x_A) = 1$

or $x_A = 1/2$ so that $x_B = 1/2$

Thus, $x_A = x_B = 1/2$

Example 16. Show that for an ideal solution containing three components A, B and C, the Gibbs free energy of mixing is a minimum when the mole fractions of these components are the same, *i.e.*, equal to 1/3 each.

Solution : According to Eq. 55,

$$\Delta G_{mix}/RT = x_A \ln x_A + x_B \ln x_B + x_C \ln x_C \quad ...(1)$$

Since $x_A + x_B + x_C = 1$, hence $x_C = 1 - x_A - x_B$

$$\therefore \quad \Delta G_{mix}/RT = x_A \ln x_A + x_B \ln x_B + (1-x_A-x_B) \ln (1-x_A-x_B) \quad ...(2)$$

For ΔG_{mix} to be minimum at a given temperature and pressure,

$$\left[\frac{\partial(\Delta G_{mix})}{\partial x_A}\right]_{T,P,x_B} = \left[\frac{\partial(\Delta G_{mix})}{\partial x_A}\right]_{T,P,x_C} = 0 \quad ...(3)$$

Differentiating Eq. 2 with respect to x_A at constant T, P and x_B, we get

$$\left[\frac{\partial(\Delta G_{mix})}{\partial x_A}\right]_{P,T,x_B} = x_A (1/x_A) \ln x_A + 0 + (1 - x_A - x_B)\left[\frac{1}{1 - x_A - x_B}\right] \times (-1) + \ln(1 - x_A - x_B)(-1)$$

Thus, $1 + \ln x_A - 1 - \ln (1 - x_A - x_B) = 0$

or $$\ln\left(\frac{x_A}{1 - x_A - x_B}\right) = 0 \text{ or } \ln (x_A/x_C) = 0 \text{ whence } x_A/x_C = 1, \textit{ i.e., } x_A = x_C \quad ...(4)$$

Again, since $x_B = 1 - x_A - x_C$, hence,

$$\Delta G_{mix}/RT = x_A \ln x_A + (1 - x_A - x_C) \ln (1 - x_A - x_C) + x_C \ln x_C \quad ...(5)$$

For ΔG_{mix} to be minimum at a given temperature and pressure,

$$\left[\frac{\partial(\Delta G_{mix})}{\partial x_A}\right]_{T,P,x_c} = 0$$

Differentiating Eq. 5, with respect to x_A at constant T, P and x_C we get

$$\left[\frac{\partial(\Delta G_{mix})}{\partial x_A}\right]_{T,P,x_c} = x_A (1/x_A) + \ln x_A + (1 - x_A - x_C)\left[\frac{1}{1 - x_A - x_C}\right](-1) + \ln (1 - x_A - x_C)(-1) + 0$$

Thus, $1 + \ln x_A - 1 - \ln (1 - x_A - x_C) = 0$

or $$\ln \frac{x_A}{1 - x_A - x_C} = 0 \quad \text{whence} \quad \frac{x_A}{1 - x_A - x_C} = 1$$

Thus, $x_A/x_B = 1$ so that $x_A = x_B$

From Eqs. 4 and 6, $x_A = x_B = x_C = 1/3$ ...(6)

Vapour Pressures of Real or Non-ideal Solutions

As discussed earlier, the vapour pressure of a solution is given by Raoult's law. Very few solutions, however, obey Raoult's law over the entire range of composition. Most of them show appreciable deviations (positive or negative) from the ideal behaviour in their vapour pressures. The deviations from Raoult's law arise from the non-ideality of either the vapour phase or the solution. Such solutions, which are called real or non-ideal solutions, may be divided into three types.

Type I. The solutions of Type I show **small positive deviations** from ideal behaviour, the vapour pressure of each component being only slightly greater than that predicted by Raoult's law. The total vapour pressure in such cases remains always within the vapour pressures of the pure components. This behaviour is shown in Fig. 3. It is seen that the total pressure as well as the partial pressure of each component show a small positive deviation from Raoult's law. Nevertheless, the total pressure remains within the pressures of the pure components A and B. The example is furnished by cyclohexane–carbon tetrachloride system.

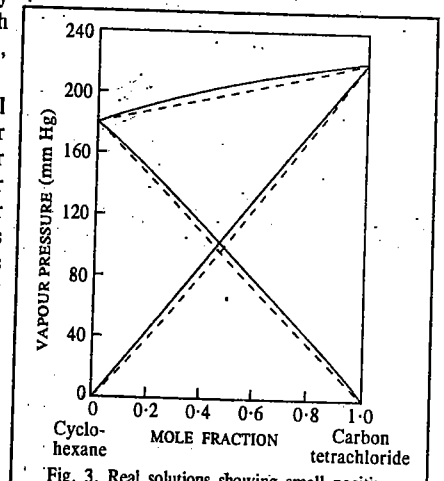

Fig. 3. Real solutions showing small positive deviations from ideal behaviour. The dotted lines represent ideal behaviour.

Type II. The solutions of Type II show **large positive deviations** from ideal behaviour, the vapour pressure of each component being considerably greater than that predicted by Raoult's law. The total vapour

pressure curve rises to a **maximum** which is above the vapour pressure of each of the pure components. This behaviour is shown in Fig. 4. The examples are : acetaldehyde—carbon disulphide, water—propyl alcohol and ethyl alcohol–chloroform mixtures.

Positive deviations occur when the interaction between unlike molecules is weaker than the interaction between like molecules. The solutions of this type are characterised by positive enthalpy of mixing, ΔH_{mix} and positive volume of mixing, ΔV_{mix}.

Type III. The solutions of Type III show **large negative deviations** from ideal behaviour and the vapour pressure of each component is considerably less than that predicted by Raoult's law. The total vapour pressure curve dips to a **minimum,** *i.e.*, for a certain composition, the total vapour pressure of the mixture is below the vapour pressure of either of the pure components. This behaviour is shown in Fig. 5. The examples of liquid pairs showing this type of behaviour are : acetone—chloroform, water—sulphuric acid and water—nitric acid.

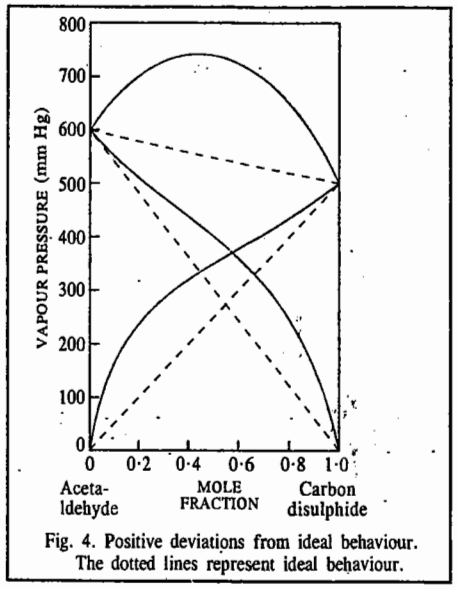

Fig. 4. Positive deviations from ideal behaviour. The dotted lines represent ideal behaviour.

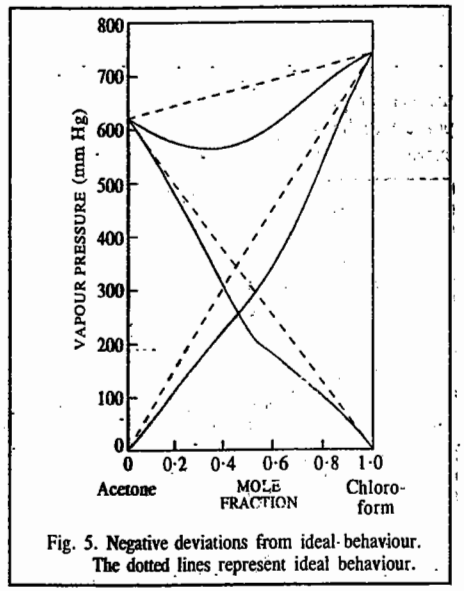

Fig. 5. Negative deviations from ideal behaviour. The dotted lines represent ideal behaviour.

Negative deviations occur when the interaction between unlike molecules is stronger than the interaction between like molecules. The solutions of this type are characterised by negative enthalpy of mixing and negative volume of mixing.

Thus, *if one component in a binary mixture shows negative deviation, the other component would also show negative deviation.*

Vapour Pressure—Composition and Boiling Point—Composition Curves of Completely Miscible Binary Solutions

Consider a binary mixture consisting of two liquid components A and B which are completely miscible with each other. On heating under constant pressure, say, under atmospheric pressure, it will start boiling at a temperature at which its total vapour pressure becomes equal to the atmospheric pressure. If P represents atmospheric pressure, then the condition for boiling is that $P = p_A + p_B$ where p_A and p_B represent the partial pressures of the two components A and B. Since solutions of different compositions have different vapour pressures, it follows that they will boil at different temperatures. Evidently, a solution of higher vapour pressure will boil at a lower temperature and solution of higher vapour pressure will boil at a lower temperature and *vice-versa*. This makes it

possible to draw boiling temperature-composition graphs from the corresponding vapour pressure—composition diagrams, as shown in Fig. 6.

There are three types of mixtures :

Type I. Here the vapour pressure changes continuously with composition of the mixture [Fig. 6*(i)*].

Type II. Here the vapour pressure shows a maximum in its vapour pressure—composition curve [Fig. 6*(ii)*].

Type III. Here the vapour pressure shows a minimum in its vapour pressure—composition curve [Fig. 6*(iii)*].

Since in Type I, the vapour pressure of pure A is the lowest and that of pure B is the highest, it follows that the boiling point of A will be the highest and that of B the lowest. Further, since the vapour pressures of the mixtures of A and B lie in between the two extreme values, their boiling points also lie in between, as shown in Fig. 6*(iv)*. It is also evident that since, at a given temperature, the vapour phase will be richer in the more volatile component B, the composition of the vapour phase will be always richer in B than that of the liquid phase. Therefore, the vapour composition curve will lie above the liquid composition curve [Fig. 6*(iv)*].

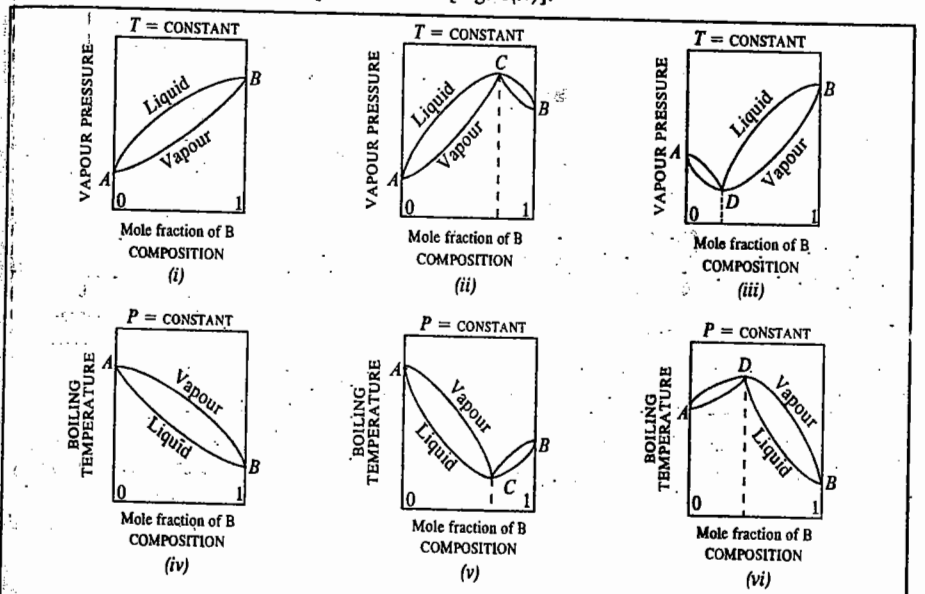

Fig. 6. Vapour pressure—Composition and Boiling point—Composition curves of completely miscible binary solutions.

Since in Type II, the vapour pressure curve shows a maximum for a certain composition, say, C, as shown in Fig. 6*(ii)*, the solution of that composition will boil at the lowest temperature. This will give rise to a minimum in the boiling point curve [Fig. 6*(v)*].

Since in Type III, the vapour pressure curve shows a minimum for a certain composition, say, D [Fig. 6*(iii)*], the solution of that composition will boil at the highest temperature. Consequently, the boiling point curve will show a maximum, as represented in Fig. 6*(vi)*. In all boiling point curves, the vapour pressure—composition curve will lie above the liquid–composition curve.

Fractional Distillation of Binary Liquid Solutions

Since the boiling point curves of the three types of solutions are different, the behaviour of these solutions on distillation at a constant pressure is also different.

Solutions of Type I. The boiling temperature—composition curves for liquid and vapour phases in the case of a binary solution of this type are represented on a comparatively magnified scale in Fig. 7. Suppose, a solution of composition X is heated. The boiling will commence when the temperature T is reached. At this temperature, evidently, the vapour coming off will have composition X_1. Since X_1 is richer in the composition of the residual liquid will become richer in A. Let it be represented by the point Y. This liquid, having a different composition, cannot boil at T but will require a higher temperature, say, T_1. The vapour coming off now will again be richer in B, as represented by the point X_2. Consequently, the composition of the residual liquid will be further enriched in the liquid A. The temperature of this liquid will again have to be raised before it can boil. Thus, if the process is continued, the boiling point of the solution will go on rising from T towards T_A, the boiling point of the pure liquid A. The composition of the residual liquid also becomes richer in A so that ultimately only liquid A remains in the liquid phase.

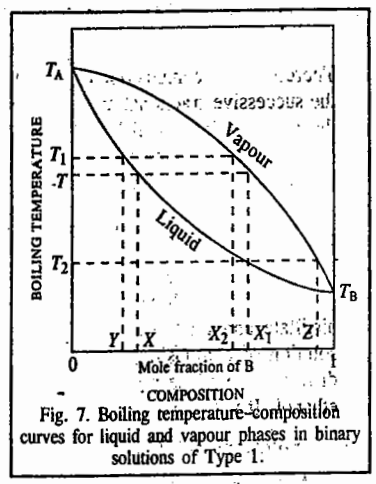

Fig. 7. Boiling temperature–composition curves for liquid and vapour phases in binary solutions of Type I.

Now, as regards the vapour phase, it has already been mentioned that the vapours coming off from the original solution at its boiling point T have the composition represented by the point X_1. If these vapours are condensed and the liquid distilled again, the new boiling point will be T_2 and the composition of the vapours now distilling over will be given by Z. Evidently, the distillate is now richer in B than before. If this process of condensing the vapours and redistilling the liquid obtained is continued, the distillate obtained ultimately will be composed almost entirely of the component B. Thus, by carrying out fractional distillation of a solution of Type I, in the manner explained above, it is possible ultimately to isolate both the pure constituents from each other.

The process of separating mixtures by repeated distillation and condensation, as described above, is extremely tedious. However, this separation can be achieved in one operation by using suitable fractionating columns.

Solutions of Type II. The boiling temperature—composition curves of the liquid and vapour phases in this case meet at the minimum point C (Fig. 8). In other words, the liquid and vapour phases at this point have the same composition. Therefore, the liquid mixture represented by the point C will boil at a constant temperature t and will distil over completely without change of composition. Such a mixture which, like a pure chemical compound, boils at a constant temperature and distils over completely at the same temperature without change in composition, is called **constant boiling mixture** or **azeotropic mixture.**

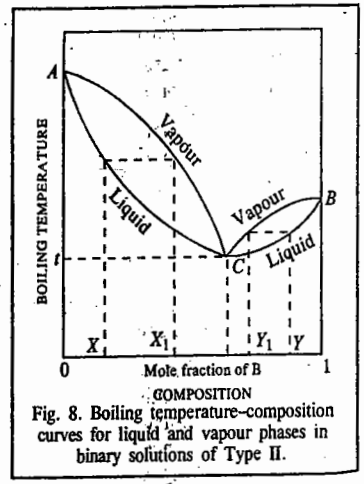

Fig. 8. Boiling temperature–composition curves for liquid and vapour phases in binary solutions of Type II.

Consider the distillation of a mixture of composition represented by X. The first fraction collected will have the composition shown by X_1. Evidently, it will be richer in the constant boiling mixture. The composition of the residual liquid, therefore, will shift towards A. As the distillation proceeds,

the composition of the distillate changes towards C and that of the residual solution towards A. Ultimately by repeated fractional distillation, the mixture of the minimum boiling point of composition C will be obtained as distillate and the pure liquid A will be left as residue in the distillation flask. It will never be possible to have pure B.

If, on the other hand, a mixture of composition indicated by Y is distilled, the composition of the first fraction will be as represented by Y_1. Evidently, it will be richer in the constant boiling mixture. Therefore, the composition of the residual liquid will become richer in B. As the distillation proceeds, the successive fractional distillates will become increasingly rich in the constant boiling mixture while the residual liquid will become increasingly rich in the pure component B. Ultimately, by repeated fractional distillation, the constant boiling mixture will be obtained as the distillate and the pure liquid B as the residue in the distillation flask. It will never be possible to have pure A in this case.

In the water–ethanol system, the constant boiling mixture corresponding to the point C has a composition of 95·6 percent of ethanol by mass. It boils at 78·13°C under a pressure of one atmosphere. If any solution of composition between pure water and 95·6 per cent ethanol (*i.e.*, between A and C) is distilled, it will be possible to separate it into a mixture containing 95·6 per cent ethanol as distillate and pure water as residue. Pure ethanol will not be recovered. On the other hand, if a solution of composition between pure ethanol and 95·6 per cent ethanol (*i.e.*, between B and C) is distilled, it will be possible to separate it into a mixture containing 95·6 per cent ethanol and pure ethanol. It will not be possible to recover pure water.

Solutions of Type III. The boiling temperature—composition curves for the liquid and vapour phases in the case of solutions of this type are given in Fig. 9. The constant boiling mixture in this case has the maximum boiling point, *i.e.*, it is the *least volatile*. The vapour phase for any mixture lying between A and D will, therefore, be richer in A and for any mixture lying between B and D, the vapour phase will be richer in B than is the constant boiling mixture D, as shown.

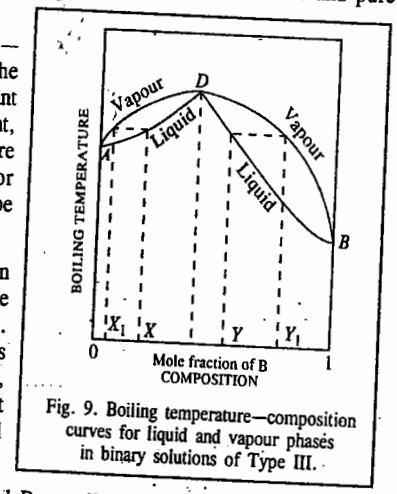

Fig. 9. Boiling temperature—composition curves for liquid and vapour phases in binary solutions of Type III.

Consider the distillation of a mixture of composition represented by X. The first fraction obtained will have composition indicated by X_1. Evidently, it is richer in A. The composition of the residual liquid, therefore, shifts towards the constant boiling mixture D. As the distillation proceeds, the composition of the distillate changes towards A and that of the residue towards D. Ultimately, a distillate of pure A and a residue of constant boiling mixture D will be obtained.

Similarly, a mixture of composition lying between B and D, say Y, will give at first a fraction of composition Y_1 which is richer in B. The residue becomes richer in constant boiling mixture D. Ultimately, a distillate of pure B and a residue of constant boiling mixture D will be obtained on repeated distillation.

It is evident, therefore, that any binary solution of Type III, on complete fractional distillation, can be separated into a residue of composition D and a distillate of either A or B depending upon whether the initial composition lies between A and D or between B and D. It is never possible to separate a mixture completely into the pure components A and B.

Mixtures of acetone and chloroform, water and hydrogen chloride and water and nitric acid are some examples of this type. Pure water boils at 100°C and pure hydrogen chloride at −85°C, while their azeotropic mixture (constant boiling mixture) containing 20·24 per cent of hydrogen chloride boils at 108·5°C under a pressure of one atmosphere. If a solution containing less than 20·24 per cent of HCl (*i.e.*, lying between A and D) is distilled, water will pass over as the distillate and the

residue ultimately left behined in the flask will consist of 20·24 per cent solution of hydrogen chloride in water. It will not be possible to recover pure hydrogen chloride. If a solution containing more than 20·24 per cent of hydrogen chloride (*i.e.*, lying between *B* and *D*) is distilled, pure hydrogen chloride will escape and the residue ultimately will contain a mixture of the same constant composition, *viz.*, 20·24 per cent of hydrogen chloride.

The Lever Rule and Fractional Distillation

Consider a two-component temperature-composition diagram (Fig. 10) of two components A and B where we have assumed that B is more volatile than A, *i.e.*, the boiling point of pure B, T_B°, is less than that of pure A, T_A°. In this system, the composition of the liquid and vapour phases can be determined with the help of **Lever rule**. We proceed as follows : Take any point, say *a* in the two-phase liquid-vapour ($L + V$) region. Draw a horizontal line called the **tie line** passing through *a* and let it meet the liquid $\rightleftharpoons$ (liquid + vapour) equilibrium curve at *l* and vapour $\rightleftharpoons$ (liquid + vapour) equilibrium curve at *v*. Then the ratio of the amount (number of moles) of liquid phase to vapour phase is given by

$$\frac{n_{\text{liquid}}}{n_{\text{vapour}}} = \frac{\text{length } av}{\text{length } al}$$

This is called the Lever rule.

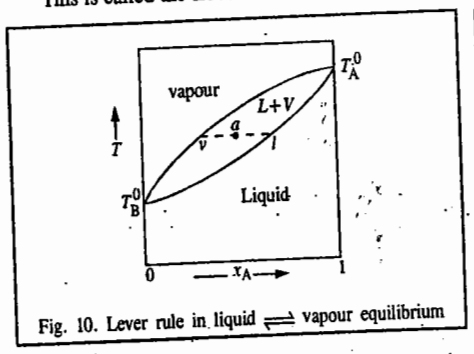

Fig. 10. Lever rule in liquid $\rightleftharpoons$ vapour equilibrium

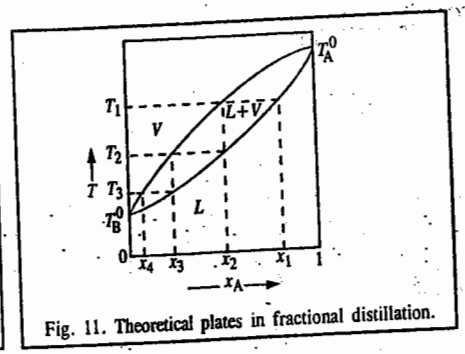

Fig. 11. Theoretical plates in fractional distillation.

We can use this rule to illustrate the principle of fractional distillation of the two liquids (Fig. 11). If liquid of composition x_1 is heated to temperature T_1, the vapour of composition x_2 is obtained which is richer in B. On cooling the vapour to temperature T_2, the liquid phase of composition x_2 is obtained. When the vapour is further cooled to temperature T_3, the liquid phase richer in B is obtained. Proceeding in this way, when the vapour at temperature T_3 is further cooled, we can obtain pure liquid B when the curve meets the point representing the boiling point (T_B°) of pure B.

It is customary to define the **theoretical plate** as a simple distillation step in which an equilibrium between the solution and the vapour is established and the vapour is condensed to liquid of different composition. As shown in Fig. 11, four theoretical plates are sufficient to obtain pure liquid B.

Distillation of Immiscible Liquids

In the case of immiscible liquids, the addition of one liquid to the other does not alter the properties of either liquid. Each liquid, therefore, exerts its own vapour pressure independent of the presence of the other. Hence, the total vapour pressure (P) above the mixture containing two immiscible liquids in any proportion will be the sum of the vapour pressures of the pure liquids at that temperature. Thus, $P = p_A^\circ + p_B^\circ$ where p_A° and p_B° are the vapour pressures of the pure liquids A and B, respectively, at the prevailing temperature.

Since the boiling point of any system is the temperature at which its total vapour pressure becomes equal to the prevailing pressure, the mixture will boil at the temperature at which

$$p_A^\circ + p_B^\circ = \text{atmospheric pressure}$$

Evidently, this temperature will be lower than the normal boiling point of either of the liquids, alone. In other words, *any mixture of two immiscible liquids will boil at a temperature lower than that at which any pure constituent of the mixture boils*. Again, since the total vapour pressure is constant and independent of the amounts of the components, it follows that the boiling point of the mixture will remain constant as long as the two liquids are present together.

The relative proportions of the two liquids in the distillate can be calculated remembering that the number of moles of each component present in the vapour phase is proportional to its vapour pressure. If n_A and n_B are the number of moles of the components A and B in the vapour phase at the boiling point, then

$$n_A/n_B = p_A^\circ / p_B^\circ \qquad \ldots(71)$$

If w_A and w_B represent the actual masses of the two components in the distillate and M_A and M_B are their respective molar masses, then Eq. 71 may be written as

$$\frac{w_A}{w_B} = \frac{n_A M_A}{n_B M_B} = \frac{p_A^\circ M_A}{p_A^\circ M_B} \qquad \ldots(72)$$

Thus, the masses of the liquids in the distillate will be in the ratio of their vapour pressures and molar masses.

The above principle is made use of in the process of **steam distillation.** It is used in the purification of organic compounds which have high boiling points. The compounds must be immsicible or nearly so in water. A common example is that of aniline. Its normal boiling point is 180°C. But it can be made to boil and distil over at a much lower temperature by passing steam through it. The apparatus is shown in Fig. 12. The steam is generated in a metal can. The solution to be distilled is

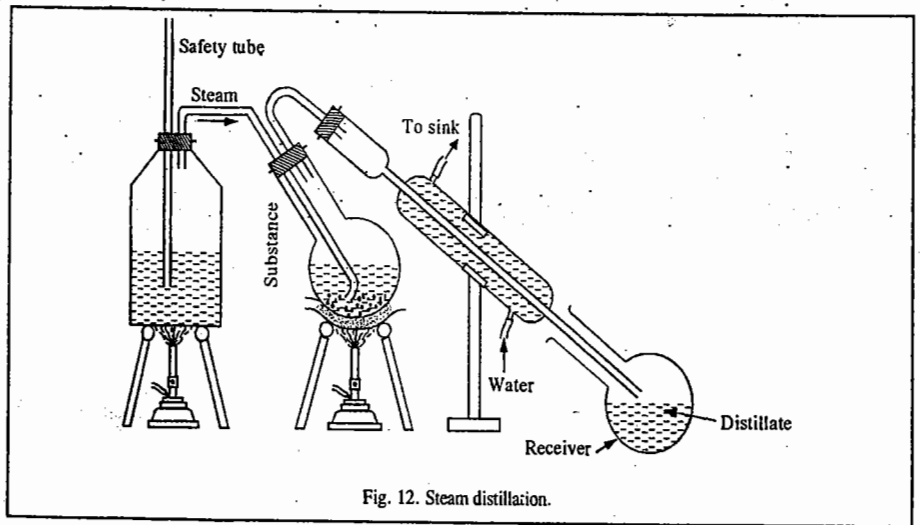

Fig. 12. Steam distillation.

placed in the round-bottomed flask, clamped at an angle so as to prevent the solution from being splashed into the condenser. The tube carrying the steam from the can dips below the liquid in the flask. The distillation flask is kept heated gently on a sand bath in order to avoid too much condensation of water into it. The vapours of the organic compound mixed with steam pass over and are condensed

in the receiver, as shown. The boiling in this manner takes place at about 98·5°C which is lower than the boiling point of either water or aniline.

The vapour pressures of water and aniline at 98·5°C are 717 torr and 43 torr, respectively. As the molar masses of the liquids are 18 and 93 g mol^{-1}, respectively, the relative masses of the two liquids in the distillate will be given by

$$\frac{\text{Mass of water}}{\text{Mass of aniline}} = \frac{18\text{ g mol}^{-1} \times 717\text{ torr}}{93\text{ g mol}^{-1} \times 43\text{ torr}} = 3{\cdot}23$$

It will be seen that although the partial vapour pressure of aniline at the boiling temperature is only 43 torr out of a total of 760 torr (*i.e.*, less than 6 per cent of the total), its relative proportion by mass in the distillate is about 30 per cent. Evidently, its higher molar mass, relative to that of water, compensates to some extent for the lower vapour pressure.

Example 17. When an immiscible liquid A was steam-distilled with water it gave a distillate 200 ml of which contained 57·2 ml of A. The boiling point for distillation was found to be 98·2°C at a pressure of 758 torr. At this temperature the vapour pressure of water was 712 torr. If the density of the liquid is 1·83 g ml^{-1}, what is the molar mass of liquid A ?

Solution : $p_A^\circ = (758\text{ torr} - 712\text{ torr}) = 46\text{ torr}$; $p^\circ_{water} = 712\text{ torr}$

Mass of A in the distillate (w_A) = 57·2 ml × 1·83 g ml^{-1} = 104·7 g

Mass of water in the distillate (w_B) = (200 ml − 57·2 ml) × 1·0 g ml^{-1} = 142·8 g

$$w_A/w_B = p_A^\circ M_A/(p_B^\circ M_B) \qquad \text{[subscript B stands for } H_2O\text{]}$$

$$\therefore \quad M_A = \frac{w_A p_B^\circ M_B}{w_B p_A^\circ} = \frac{(104{\cdot}7\text{g})(712\text{ torr})(18\text{ g mol}^{-1})}{(142{\cdot}8\text{ g})(146\text{ torr})} = 204\text{ g mol}^{-1}$$

Example 18. An immiscible mixture of water and quinoline boils at 98·9°C under a pressure of 740 torr. The distillate contains 77·9 g of quinoline and 1 kg of water. At the given boiling point, the vapour pressure of quinoline is 7·96 torr. Calculate the molar mass of quinoline ?

Solution : Let subscripts A and B stand for H_2O and quinoline, respectively.

$$p_B^\circ = 7{\cdot}96\text{ torr}; \quad p_A^\circ = (740\text{ torr} - 7{\cdot}96\text{ torr}) = 732{\cdot}04\text{ torr}$$

$$w_B = 77{\cdot}9\text{ g}; \quad w_A = 1{,}000\text{ g}$$

Since $$\frac{w_A}{w_B} = \frac{p_A^\circ M_A}{p_B^\circ M_B} \qquad \text{(Eq. 72)}$$

$$M_B = \frac{w_A p_A^\circ M_A}{w_A p_B^\circ} = \frac{(77{\cdot}9\text{g})(732{\cdot}04\text{ torr})(18\text{ g mol}^{-1})}{(1{,}000\text{ g})(7{\cdot}96\text{ torr})} = 129\text{ g mol}^{-1}$$

SOLUBILITY OF PARTIALLY MISCIBLE LIQUIDS

Four types of partially miscible liquid—liquid systems have been observed. These are :

1. Those in which the partial miscibility increases on increasing the temperature. Examples include phenol–water, aniline–water, aniline–hexane, CH_3OH–CS_2 and cyclohexane–methanol systems. At and above a certain temperature, the liquids become completely miscible.

2. Those in which partial miscibility increases on lowering the temperature. Examples include $(C_2H_5)_2NH$–H_2O, and $(C_2H_5)_3N$–H_2O systems. At and below a certain temperature, the two liquids become completely miscible.

3. Those in which partial miscibility increases on both raising as well as lowering the temperature in certain ranges. Examples are H_2O–nicotine and H_2O–β-picoline systems. These liquid pairs show complete miscibility both above and below certain temperatures.

4. Those in which complete miscibility temperature cannot be obtained. A common example is ether–water system.

The temperature above (or below) which a pair of partially miscible liquids becomes miscible in all proportions, is called **critical solution temperature** (CST) or **consolute temperature** for the pair. Some liquid pairs attain complete miscibility above *a* certain temperature in which case they are said to have the **upper critical solution temperature** (UCST) while some liquid pairs show complete miscibility below a certain temperature when they are said to have **lower critical solution temperature** (LCST). On the other hand, some liquid pairs show both UCST and LCST. All partially miscible liquid pairs have, in general, an upper or a lower CST. However, the upper CST cannot be realized if one or both the components boil out before it is reached and the lower CST may not be observed if one or both the components freeze out before it is reached. Thus, under atmospheric conditions none of the CSTs is observed for ether–water system.

The critical solution temperatures for a few partially miscible systems are given in Table 1.

TABLE 1

Critical Solution Temperatures (°C) in Case of Some Partially Miscible Liquid Pairs

Components		UCST	LCST
A	B		
Water	Phenol	68·1	....
Cyclohexane	Methanol	49·0	....
Methanol	CS_2	49·5	....
Aniline	Hexane	59·6	....
Water	$(C_2H_5)_2NH$	....	43·0
Water	$(C_2H_5)_3N$	....	18·5
Water	Nicotine	208·0	60·8
Water	β-picoline	153·0	49·1
Glycerine	*m*-toluidine	120·0	7·1

The two phases having dissimilar composition in equilibrium with each other at a given temperature constitute a pair of **conjugate phases.** The composition points of the conjugate phases are joined by **tie lines.** Any composition-temperature coordinates placing a point in the area of parallel miscibility represent a system of two liquid phases and a vapour phase. We can determine the mass ratio of the liquid phases by locating the overall composition point on the tie line for the specified temperature.

Thus, from Fig. 13, which shows the boiling point–mole fraction diagram for a mixture of partially miscible liquids with an upper CST, we see that

$$\frac{\text{Mass of phase } a}{\text{Mass of phase } b} = \frac{bc}{ac}$$

The above proportionality is called the **lever rule,** as mentioned above.

It may be mentioned here that the presence of another substance dissolved in one or both phases has a marked effect on the CST as well as the liquid phase composition at the CST. A substance soluble in only one of the original liquids raises the upper CST and lowers the lower CST. However, a substance soluble in both the original liquids tends to lower the upper CST and raise the lower CST. As a matter of fact, substances, taken in sufficiently large amounts, may convert *partial* miscibility of a liquid pair into *complete* miscibility.

Small amounts of impurities may produce large changes in the CST. This observation forms the basis of the **Crismer test** which can detect and measure minute quantities of impurities. It is found that the change in the CST value is a linear function of the concentrations of the impurities. Thus, one per

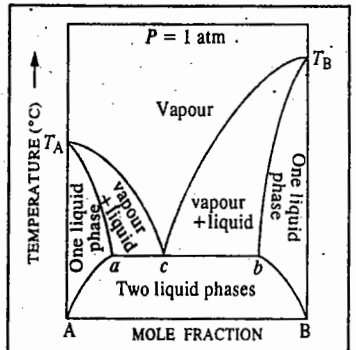

Fig. 13. The Boiling point—composition diagram for a mixture of partially miscible liquids with an upper CST.

cent of NaCl present in water *raises* its upper CST with phenol (in which NaCl is insoluble) by 12°C. Traces of water in alcohols can be estimated by measuring their CSTs with cyclohexane. Sodium oleate is soluble in both phenol and water. Addition of 0·98 % sodium oleate to the phenol–water system, *lowers* the CST by 43·7°C.

A few representative binary systems of partially miscible liquids are described below.

Phenol–Water System. Phenol and water are only partially miscible at ordinary temperatures. Therefore, on shaking these two liquids with each other, two saturated solutions of different compositions, one of phenol in water and the other of water in phenol, are obtained. As already mentioned, such solutions of different compositions coexisting with one another are termed **conjugate solutions.** The mutual solubility of phenol and water increases with rise in temperature and, therefore, the concentration of phenol in water as well as that of water in phenol goes on increasing with rise of temperature and ultimately at a certain temperature the two conjugate solutions change into one homogeneous solution. The consolute temperature for phenol–water system is found to be 68·1°C. The composition of the solution then is 36·10 per cent phenol and 63·90 per cent water. Above the consolute temperature, the two liquids become miscible with each other in all proportions.

The variation of mutual solubility of water and phenol with temperature is represented graphically in Fig. 14.

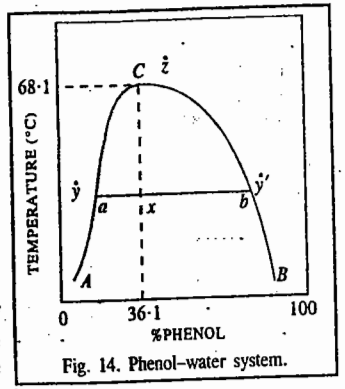

Fig. 14. Phenol–water system.

At any fixed temperature, such as 30°C, the composition of each layer is fixed as indicated by the points *a* and *b* ; *a* giving the composition of aqueous layer and *b* that of the phenol layer. The line joining them is known as **tie line,** as already mentioned.

When the temperature and composition of a mixture of water and phenol is represented by a point, say, *x*, within the curve *ACB*, the system consists of two layers (conjugate solutions) of compositions represented by the points *a* and *b*. If the temperature and composition are represented by a point on the left of curve *AC* or on the right of the curve *CB*, say as at *y* or *y′*, the mixture will consist only of one solution. At *y* it will be an unsaturated solution of phenol in water and at *y′* it will be an unsaturated solution of water in phenol. Further addition of phenol at *y* or of water at *y′* will ultimately result in the separation of the two phases. Lastly, if the temperature and composition are represented by a point, say, *z*, above the curves *ACB*, the system will consist again of one homogeneous solution but, now, since this point lies above the consolute temperature at which the two liquids are miscible in all proportions, further addition of phenol to water or of water to phenol will not lead to formation of two layers. The composition of such a solution thus can have any value.

Aniline–Hexane System. The behaviour of aniline–hexane system is similar to that of phenol–water system. The consolute temperature in this case is 59·6°C. The composition of the solution is then 52 per cent aniline and 48 per cent hexane.

Some other pairs of liquids which are partially miscible at ordinary temperatures and become completely miscible on raising the temperature are : water and aniline, aniline and benzene, carbon disulphide and methyl alcohol, etc. The consolute temperatures of these three systems are 167°C, 59·6°C and 40·5°C, respectively.

Triethylamine–Water System. Triethylamine and water constitute a system in which the mutual solubility increases with decrease in temperature. *i.e.*, it has a **lower consolute temperature.** The mutual solubilities of the two liquids are plotted graphically in Fig. 15. The consolute temperature is 18·5°C. Above this temperature, the liquids give rise to two distinct layers but below this temperature,

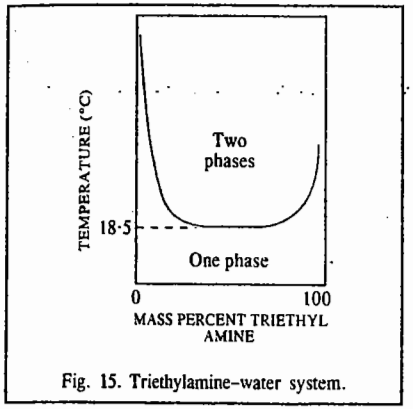

Fig. 15. Triethylamine–water system.

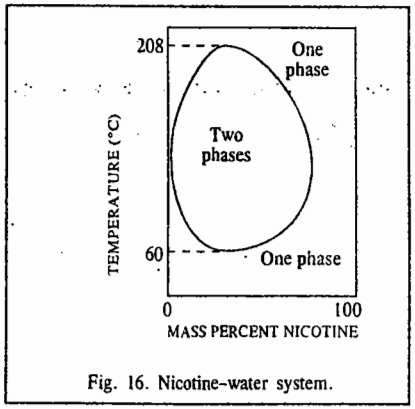

Fig. 16. Nicotine–water system.

Nicotine–Water System. Nicotine and water show an upper as well as a lower consolute temperature. In other words, these liquids are completely miscible above a certain critical temperature (upper consolute temperature) and again below a certain critical temperature (lower consolute temperature). Between these two limiting temperatures, they are partially miscible. The solubilities of these liquids in one another at different temperatures are shown graphically in Fig. 16. Evidently, the upper consolute temperature is 208·0°C and the lower consolute temperature is 60·8°C. Between these two temperatures, mixtures of water and nicotine separate into two liquid layers.

SOLUTIONS OF GASES IN LIQUIDS

Most of the gases are soluble in water as well as in some other liquids to a more or less extent. The solubility is generally expressed in terms of **absorption coefficient (a),** introduced by Bunsen. This is defined as the volume of gas reduced to N.T.P. dissolved by unit volume of solvent at the temperature of the experiment and under a pressure of 1 atmosphere of the gas.

The absorption coefficients of a few gases at 20°C in three common solvents are given in Table 2.

TABLE 2

Absorption Coefficients of Gases at 20°C

Solvent	Hydrogen	Nitrogen	Oxygen	Carbon dioxide
Water	0·017	0·015	0·028	0·88
Ethanol	0·080	0·130	0·130	3·00
Benzene	0·060	0·104	0·165	.....

Factors Influencing the Solubility of a Gas. The solubility of a gas in a liquid depends upon

1. The nature of the gas and the nature of the solvent.
2. The temperature of the gas–liquid system.
3. The pressure of the gas.

1. Nature of Gas and Nature of Solvent. The solubility of a gas in a given solvent varies considerably with the nature of the gas. Generally speaking, the gases which are easily liquefied are more soluble in common solvents. Thus, carbon dioxide is more soluble than hydrogen or oxygen in water or in any other solvent. The gases which are capable of forming ions in aqueous solution, are much more soluble in water than in other solvents. This is illustrated by the fact that gases like hydrochloric acid and ammonia are highly soluble in water but not in benzene in which they are not capable of forming ions.

2. Effect of Temperature. It has been found that under a constant pressure, the solubility of a gas diminishes with rise in temperature.

3. Effect of Pressure. Henry's Law. Although solubilities of solids in liquids are almost independent of pressure, those of gases in liquids vary considerably with pressure. William Henry, in 1805, found that the solubility of a gas at a given temperature increases directly as the pressure. This conclusion forms the basis of what is known as **Henry's law,** which may be stated as below :

The mass of a gas dissolved per unit volume of a solvent is proportional to the pressure of the gas in equilibrium with the solution at constant temperature.

If m is the mass of a gas dissolved *per unit volume* of a solvent and P is the pressure of the gas in equilibrium with the solution, then, at constant temperature,

$$m \propto P \quad \text{or} \quad m = kP \qquad \ldots(73)$$

where k is the proportionality constant.

If Henry's law is valid, then the graph obtained by plotting solubility of a gas against the equilibrium pressure of the gas at a constant temperature should be a straight line.

It has been found that most gases obey Henry's law, provided 1. the pressure is not too high 2. the temperature is not too low and 3. the gas is not highly soluble and does not dissociate or enter into chemical combination with the solvent.

Thus, the law is valid for the solubility of hydrochloric acid and ammonia in benzene in which both the gases are sparingly soluble but not in water in which these are highly soluble and also in which hydrochloric acid dissociates ($HCl+H_2O \longrightarrow H_3O^+ + Cl^-$) and ammonia enters into chemical combination ($NH_3+H_2O \longrightarrow NH_4OH \rightleftharpoons NH_4^+ + OH^-$).

When a mixture of a number of gases is brought in contact with a solvent, each constituent dissolves in proportion to its own partial pressure, Henry's law applying to each gas independent of the presence of the other gases.

The fact that the solubility of a gas is proportional to its partial pressure, is made use of in removing a dissolved gas merely by bubbling an indifferent gas through the solution. Thus, ammonia can be removed from aqueous solution by bubbling nitrogen which itself is insoluble. As the partial pressure of ammonia in nitrogen bubbles is almost zero, the solubility of ammonia decreases almost to zero and, as a consequence, the gas is carried away along with the nitrogen bubbles.

Henry's law is also alternatively stated as follows : *The pressure of a gas over a solution in which the gas is dissolved is proportional to the mole fraction of the gas dissolved in solution.* Thus, $p_2 = kx_2$ where the subscript 2 refers to the gaseous solute and x_2 is its mole fraction. The constant k is known as the **Henry's law constant.** The value of k can be obtained by plotting p_2/x_2 versus x_2 and extrapolating to $x_2 = 0$.

The Henry's law constants for some common gases are given in Table 3.

TABLE 3

The Henry's Law Constants (in torr) for Gases at 25°C

Gas	Solvents	
	Water	Benzene
H_2	$5{\cdot}34\times10^7$	$2{\cdot}75\times10^6$
N_2	$6{\cdot}51\times10^7$	$1{\cdot}79\times10^6$
O_2	$3{\cdot}30\times10^7$	.....
CO_2	$1{\cdot}25\times10^6$	$8{\cdot}57\times10^4$
CH_4	$31{\cdot}4\times10^6$	$4{\cdot}27\times10^5$

Example 19. The Henry's law constant for $H_2(g)$ in water is $5{\cdot}34\times10^7$ torr. Calculate the solubility of this gas in water at 25°C if its partial pressure over the solution is 760 torr. Assume that the density of the solution is the same as the density of the solvent.

Solution : $x_2 = n_2/(n_1+n_2) \approx n_2/n_1$ (assuming that the number of moles of H_2, n_2, is negligible in comparison with the number of moles, n_1, of the solvent).

The number of moles in one dm^3 of water,

$$n_1 = 1000 \text{ g}/18 \text{ g mol}^{-1} = 55{\cdot}5 \text{ mol so that } x_2 = n_2/55{\cdot}5 \text{ mol}$$

$$p_2 = k\,x_2 \qquad \text{[Henry's law]}$$

$$k = 5{\cdot}34\times10^7 \text{ torr} = \frac{p_2}{x_2} = \frac{760 \text{ torr}}{n_2/(55{\cdot}5 \text{ mol})} = \frac{760 \text{ torr} \times 55{\cdot}5 \text{ mol}}{n_2}$$

$$\therefore \quad n_2 = (760 \text{ torr} \times 55{\cdot}5 \text{ mol})/(5{\cdot}34\times10^7 \text{ torr}) = 8\times10^{-4}$$

Thus, the solubility of H_2 gas in water is 8×10^{-4} **mol** dm^{-3}.

Example 20. Using the Henry's law constants for O_2 and N_2 from Table 3, calculate the ratio of mole fractions of O_2 to N_2 dissolved in water at 25°C.

Solution : $p_2 = kx_2$ [Henry's law]

$$k_{N_2} = 6{\cdot}51\times10^7 \text{ torr} ; \quad k_{O_2} = 3{\cdot}30\times10^7 \text{ torr}$$

$$p_{O_2} = k_{O_2}x_{O_2} \quad \text{and} \quad p_{N_2} = k_{N_2}x_{N_2}$$

By definition, partial pressure = Mole fraction×Total pressure, *i.e.*, $p_i = x_iP$

Hence, $p_{O_2} = y_{O_2}P$ and $p_{N_2} = y_{N_2}P$

where the ys are the mole-fractions of the gases in the *vapour phase* and P is the total pressure. Thus,

$$\frac{y_{O_2}P}{y_{N_2}P} = \frac{k_{O_2}x_{O_2}}{(k_{N_2}x_{N_2})}$$

$$\frac{x_{O_2}}{x_{N_2}} = \frac{k_{N_2}y_{O_2}}{(k_{O_2}y_{N_2})}$$

We know that in the atmosphere, the two gases are present in the ratio of 0·21/0·79 = 0·27.

Hence, $$\frac{x_{O_2}}{x_{N_2}} = \frac{6{\cdot}51\times10^7 \text{ torr} \times 0{\cdot}21}{3{\cdot}30\times10^7 \text{ torr} \times 0{\cdot}79} = 0{\cdot}52$$

Notice that the ratio (0·52) of the two gases in water is greater than that in air (*i.e.*, 0·27). Thus, by using fractional solubility we can completely separate O_2 from N_2 in the air.

Henry's Law and Raoult's Law. In Eq. 73, m represents the mass of a gas dissolved per unit volume. This quantity, therefore, can be taken as the concentration of gas molecules in the solution phase. Since Henry's law is applicable only if the gas is not largely soluble, the solution, even though saturated, may be very dilute. The concentration, therefore, can also be expressed as proportional to the mole fraction of the dissolved substance. The Henry's law, therefore, may also be expressed as

$$x_2 = k'p_2 \text{ or } p_2 = x_2/k' \qquad \ldots(74)$$

where x_2 is the mole fraction of the gas (solute) in the solution which is in contact with the gas above having pressure equal to p_2 and k' is a new proportionality constant which is related to constant k of Eq. 73. Henry's law is now more frequently represented by Eq. 74.

We may recall that Raoult's law holds good in ideal solutions for solvent as well as solute if both are volatile. In the above example, we can regard p_2 as the vapour pressure of the volatile solute (gas) when it is present to the extent of mole fraction x_2 in the solution. Applying Raoult's law, we have

$$p_2 = x_2p_2^\circ \qquad \ldots(75)$$

where p_2° is the vapour pressure of the pure solute (dissolved gas in the present case) at the temperature of the solution.

Eqs. 74 and 75 are quite similar. In fact, both become identical if k' is equal to $1/p_2^\circ$. In that case, *Raoult's law may be taken as a special case of Henry's law.* Under these conditions, all

solutions which obey Raoult's law must also obey Henry's law.

This condition (*i.e.*, $k'=1/p_2^\circ$), however, is approached only in a few cases representing ideal solutions of gases in liquids.

In several cases of solutions of gases in liquids, it can be shown that if Henry's law applies to the solute, Raoult's law applies to the solvent. To show this we may make use of Gibbs–Duhem–Margules equation, according to which

$$\frac{d(\log p_1)}{d(\log x_1)} - \frac{d(\log p_2)}{d(\log x_2)} = 0 \qquad \text{(Eq. 36)} \qquad \ldots(76)$$

where x_1 and x_2 are the mole fractions and p_1 and p_2 are the vapour pressures of the solvent and solute, respectively,

Let us assume that the solute obeys Henry's law. Then,

$$x_2 = k'p_2$$

Taking logs, $$\log x_2 = \log k' + \log p_2 \qquad \ldots(77)$$

Differentiating Eq. 77, we get

$$d(\log x_2) = 0 + d(\log p_2) \qquad \ldots(78)$$

or $$d(\log p_2)/d(\log x_2) = 1 \qquad \ldots(79)$$

Hence, from Eqs. 76 and 79, it follows that

$$d(\log p_1)/d(\log x_1) = 1 \qquad \ldots(80)$$

Integrating Eq. 80 and taking antilogs, we have

$$p_1 = kx_1 \qquad \ldots(81)$$

If $x_1=1$, *i.e.*, if we have the *pure solvent*, p_1 will become p_1°, the vapour pressure of the pure solvent. Hence, the value of the constant k in Eq. 81 is equal to p_1°. Eq. 81 may, therefore, be written as

$$p_1 = x_1 p_1^\circ \qquad \ldots(82)$$

Eq. 82 is the expression of Raoult's law for the solvent. Thus, we see that *if in any solution, the solute obeys Henry's law within a certain range of concentration, the solvent obeys Raoult's law over the same range of concentration.*

I. Review Questions

1. State and explain Raoult's law for vapour pressure of binary solutions of volatile liquids.
2. Derive Gibbs–Duhem–Margules equation. Show that if in a binary solution, component *A* obeys Raoult's law, then component *B* would also obey Raoult's law.
3. Derive an expression for Gibbs free energy change of mixing (ΔG_{mix}) for an ideal solution. Show that for an ideal solution *(i)* the volume of mixing (ΔV_{mix}) is zero *(ii)* the enthalpy of mixing (ΔH_{mix}) is zero. *(iii)* the entropy change of mixing (ΔS_{mix}) is always positive.
4. Discuss the variation of vapour pressure of completely miscible liquid pairs with composition.
5. Discuss in detail the principle of distillation at constant pressure. Which type of binary solutions can be completely separated into their constituents and why ?

6. Discuss the vapour pressure properties of two immiscible liquids. How are these facts utilised in determining molar mass of a liquid by steam distillation ?
7. Explain the terms consolute temperature, upper consolute temperature, lower consolute temperature, conjugate solutions and tie line as applied to solubilities of partially miscible liquids. Discuss the variation of mutual miscibility of 1. Phenol-water 2. Aniline-Hexane 3. Nicotine-water and 4. Triethylamine-water with variation of temperature.
8. State and explain Raoult's law and Henry's law. Show that if in any solution, the solvent obeys Raoult's law, the solute obey Henry's law.

II. Problems

1. A solution containing 20·0% ethanol by mass in water has a density of 0·966 kg dm^{-3}. Calculate *(i)* the mole fraction *(ii)* molality and *(iii)* molarity of ethanol in this solution.
(Ans. *(i)* 0·891 *(ii)* 5·43 mol kg^{-1} *(iii)* 4·19 mol dm^{-3})
2. Calculate the molarity of an aqueous solution of HCl if it contains 37% by mass of HCl. The density of the solution is 1·19 kg dm^{-3}. (Ans. 12·1 M)
3. The vapour pressures of pure volatile liquids *A* and *B* are 300 and 800 torr, respectively at 75°C. Calculate the composition of the ideal mixture if it boils at 75°C. Also, calculate the composition of the vapour phase.
(Ans. $x_A=0·80$; $x_B=0·20$; $x_{A,vap}=0·0316$; $x_{B,vap}=0·968$)
4. The vapour pressures of pure volatile liquids *A* and *B* are 860 and 350 torr, respectively, at 80°C. Assuming that they form ideal solutions at all compositions, calculate the composition of the solution such that it boils at 80°C. Also calculate the composition of the vapour phase. (Ans. $x_A=0·804$; $x_{B,vap}=0·91$)
5. Assuming that benzene and toluene form ideal solution, calculate ΔH_{mix}, ΔG_{mix} and ΔS_{mix} at 25°C for the addition of 1·00 mole of C_6H_6 to an infinitely large sample of solution with $x_{(C_6H_6)}=0·35$. The vapour pressure of C_6H_6 at 25°C is 0·153 bar. (Ans. $\Delta H_{mix}=0$; $\Delta G_{mix}=-7·3$ kJ ; $\Delta S_{mix}=24$ J K^{-1})
6. Calculate ΔH_{mix}, ΔV_{mix}, ΔG_{mix}, and ΔS_{mix} of a solution made at 27°C by mixing 0·6 mole of *A* with 0·4 mole of *B*, assuming that the solution is ideal. (Ans. $\Delta V_{mix}=0$; $\Delta H_{mix}=0$; $\Delta G_{mix}=-1·678$ kJ, $\Delta S_{mix}=5·636$ JK^{-1})
7. A mixture of quinoline and water boils at 98·9°C under a pressure of 740 torr. The distillate contains $7·79\times10^{-2}$ kg of quinoline and 1 kg of water. If the vapour pressure of quinoline at 98·9°C is 7·96 torr; calculate the molar mass of quinoline. (Ans. 129 g mol^{-1})
8. A mixture of aniline and water boils at 98°C under 1 atm pressure. The vapour pressure of aniline at this temperature is 42 torr. If the mass ratio of aniline to water in the distillate is 13%, calculate the molar mass of aniline. (Ans. 93 g mol^{-1})
9. Chlorobenzene (M_m=112 g mol^{-1}) is steam distilled at 734 torr and 90°C. The vapour pressure of chlorobenzene at this temperature is 208 torr. Calculate the mass of steam required to distil 0·5 kg of chlorobenzene. (Ans. 0·203 kg)
10. Calculate the solubility of oxygen gas (at 0·20 atm) in one litre of water at 20°C if at this temperature the Henry's law constant for O_2 is $4·58\times10^4$ atm. (Ans. $7·71\times10^{-6}$ kg)
11. Calculate the solubility of CH_4 in water at 25°C if the partial pressure of CH_4 over H_2O is 760 mm Hg. Given the Henry's law constant of CH_4 in water is $3·14\times10^6$ mm Hg. (Ans. $1·34\times10^{-2}$ mol)
12. 40 g of volatile liquid *A* and 70 g of volatile liquid *B* are mixed. Assuming that they form an ideal solution, calculate the composition of the vapour. Given p_A°=200 torr, p_B°=700 torr, M_A = 56 g mol^{-1} ; M_B = 90 g mol^{-1}.
(Ans. $x_{A,vap}=0·208$, $x_{B,vap}=0·792$)
13. Calculate the relative proportion of N_2 and O_2 in water if air contains 80% N_2 and 20% O_2. Henry law constants are $k_{N_2}=6·51\times10^7$ mm Hg ; $k_{O_2}=3·30\times10^7$ mm Hg. Assume that the air pressure over water is 1 atm.
(Ans. $x_{N_2}=9·34\times10^{-6}$; $x_{O_2}=4·61\times10^{-6}$. Thus, the relative proportion is 2 : 1)
14. Calculate ΔH_{mix}, ΔS_{mix} and ΔG_{mix} of one mole of toluene and two moles of benzene at 25°C, assuming ideality.
(Ans. $\Delta H_{mix}=0$; $\Delta G_{mix}=-4·730$ kJ ; $\Delta S_{mix}=15·8$ J K^{-1})
15. A mixture of naphthalene and water boils at 98°C under a pressure of 733 torr. The vapour pressure of water at 98°C is 707 torr, calculate the mass percent of naphthalene in the distillate. (Ans. 20·7%)

CHAPTER 22

COLLIGATIVE PROPERTIES OF DILUTE SOLUTIONS

Colligative Properties. Colligative properties are those *which depend entirely upon the number of particles of the solute dissolved in a known volume of a given solvent and not at all upon the nature (i.e., chemical composition or constitution) of the solute.* These properties, in fact, depend upon the nature of the *solvent*. The colligative properties can thus be rightly regarded as the properties of the solvent in a given solution. In the present discussion, the solute is invariably taken as *non-volatile*. The various colligative properties are :

1. Lowering of Vapour Pressure
2. Osmotic Pressure
3. Elevation of Boiling Point
4. Depression of Freezing Point

The colligative properties are essentially the properties of only dilute solutions which are supposed to behave as ideal solutions.

VAPOUR PRESSURE LOWERING

The addition of a *nonvolatile* solute to a solvent at a given temperature and pressure, results in the lowering of the vapour pressure of the solvent. At the same time, the chemical potential of the solvent is also decreased. At equilibrium, any change in the chemical potential of the solvent vapour is equal to the change in the chemical potential of the liquid solvent in solution, *i.e.*, $d\mu_1^v = d\mu_1^l$.

The chemical potential of the solvent in solution phase depends upon T, P and its mole fraction but in vapour phase it depends only on T and P. Thus,

$$\mu_1^l = f(T, P, x_1) \quad \text{and} \quad \mu_1^v = f(T, P) \qquad \ldots(1)$$

$$\therefore \quad (d\mu_1)^l = (\partial\mu_1/\partial T)^l_{P,x_1}\,dT + (\partial\mu_1/\partial P)^l_{T,x_1}\,dP + (\partial\mu_1/\partial x_1)^l_{T,P}\,dx_1 \qquad \ldots(2)$$

But $$(\partial\mu_1/\partial T)^l_{P,x_1} = -\bar{S}_1 \qquad \text{(Eq. 127, Chapter 15)} \qquad \ldots(3)$$

and $$(\partial\mu_1/\partial P)^l_{T,x_1} = \bar{V}_1 \qquad \text{(Eq. 130, Chapter 15)} \qquad \ldots(4)$$

where $\bar{V}$ and $\bar{S}$ are partial molar volume and partial molar entropy, respectively.

Hence, $$(d\mu_1)^l = -\bar{S}_1^l\,dT + \bar{V}_1^l\,dP + (\partial\mu_1/\partial x_1)^l_{T,P}\,dx_1 \qquad \ldots(5)$$

For an ideal solution, $\mu_1^l = \mu_1^\circ + RT \ln x_1$ (Eq. 144, Chapter 15) $\qquad \ldots(6)$

Hence, $$(\partial\mu_1/\partial x_1)^l_{T,P} = RT/x_1 \qquad \ldots(7)$$

At constant T and P (assumed to be 1 atm), we obtain from Eqs. 5 and 7,

$$(d\mu_1)^l = RT dx_1/x_1 \qquad \ldots(8)$$

Since at a given temperature, the chemical potential of vapour is affected by a change in pressure, we have

$$(d\mu_1)^v = (\partial\mu_1/\partial P)_{T,x_1}\,dP = \bar{V}_1\,dP \qquad \text{(Eq. 4)} \qquad \ldots(9)$$

Since for an infinitely dilute binary solution, $\bar{V} = V$ (see foot note), hence,

$$(d\mu_1)^v = V_1\,dP \qquad \ldots(10)$$

Assuming that the vapour behaves as an ideal gas, $V_1 = RT/P_1$ so that Eq. 10 becomes

$$(d\mu_1)^v = (RT/P_1)dP \qquad \ldots(11)$$

Since at equilibrium, $(d\mu_1)^v = (d\mu_1)^l$, hence from Eqs. 8 and 11, we get

$$(RT/P_1)dP = (RT/x_1)dx_1 \qquad \ldots(12)$$

Since for a binary mixture $x_1 + x_2 = 1$, hence

$$dx_1 + dx_2 = 0, \text{ i.e., } dx_1 = -dx_2 \qquad \ldots(13)$$

(The subscript 1 refers to solvent and the subscript 2 to solute.)

Hence, Eq. 12 becomes

$$(RT/P_1)dP = -[RT/(1-x_2)]dx_2 \qquad \ldots(14)$$

or $$dP/P_1 = -dx_2/(1-x_2) \qquad \ldots(15)$$

Integrating Eq. 15 between the limits $x_2=0$, $P_1=p_1^\circ$ (*i.e.*, the vapour pressure of the pure solvent) and $x_2=x_2$, $P_1=p_1$ (the vapour pressure of the solution), we have

$$\int_{p_1^\circ}^{p_1} \frac{dP}{P_1} = -\int_{x_2=0}^{x_2=x_2} \frac{dx_2}{1-x_2} \qquad \ldots(16)$$

or $$\ln(p_1/p_1^\circ) = \ln(1-x_2)$$

or $$p_1/p_1^\circ = 1 - x_2 = x_1 \qquad \ldots(17)$$

or $$p_1 = x_1 p_1^\circ \qquad \ldots(18)$$

which is **Raoult's law.**

Eq. 18 can be written alternatively as

$$((p_1^\circ - p_1)/p_1^\circ) = x_2 \qquad \ldots(19)$$

where $(p_1^\circ - p_1)$ is the vapour pressure lowering and $((p_1^\circ - p_1)/p_1^\circ)$ is the **relative vapour pressure lowering.** From Eq. 19 we see that the relative vapour pressure lowering is proportional to the mole fraction of the non-volatile solute in solution. *It is independent of the nature of the solute.* The relative vapour pressure lowering is, therefore, a colligative property.

The mole fraction $$x_2 = n_2/(n_1 + n_2) \qquad \ldots(20)$$

For a dilute solution, the number of moles of the solute (n_2) can be neglected as compared to the number of moles of the solvent (n_1). Hence,

$$x_2 = \frac{n_2}{n_1} = \frac{w_2/M_2}{w_1/M_1} = \frac{w_2 M_1}{w_1 M_2} \qquad \ldots(21)$$

where w_2 is the amount of the solute dissolved in w_1 amount of the solvent, M_1 is the molar mass of the solvent and M_2 is the molar mass of the solute. Eq. 19 may, therefore, be written as

$$\frac{p_1^\circ - p_1}{p_1^\circ} = x_2 = \frac{w_2 M_1}{w_1 M_2} \qquad \ldots(22)$$

---

* As shown in Chapter 15, partial molar property $\bar{X} = (\partial X/\partial n)_{T,P,n_1,n_2,\ldots}$ or $dX = d\bar{n}_i\bar{X}_i$ or $\int dX = \int d\bar{n}_i\bar{X}_i$ or $X = \Sigma n_i\bar{X}_i = n_1\bar{X}_1 + n_2\bar{X}_2 + n_3\bar{X}_3 \ldots = n_1\bar{X}_1 + n_2\bar{X}_2$ for a binary solution. For an infinitely dilute binary solution, $n_2=0$ so that $X = n_1\bar{X}_1$. Thus, for an infinitely dilute solution containing one mole of component 1 (*i.e.*, $n_1=1$), $\bar{X}_1 = X$, *i.e.*, $\bar{V}_1 = V$, $\bar{S}_1 = S$, $\bar{H}_1 = H$, $\bar{G}_1 = G$, etc.

Example 1. 0·5 g of a nonvolatile solute of molar mass 60 g mol^{-1} is dissolved in 100 g of ethyl acetate at 20°C. What would be the vapour pressure of this solution at 20°C ? The vapour pressure of ethyl acetate at 20°C is 72·8 torr.

Solution : According to Eq. 22, $\frac{p_1^\circ - p_1}{p_1^\circ} = \frac{w_2 M_1}{w_1 M_2}$

Substituting the various values in this equation, we have

$$\frac{72{\cdot}8 \text{ torr} - p_1}{72{\cdot}8 \text{ torr}} = \frac{0{\cdot}5 \text{ g} \times 78 \text{ g mol}^{-1}}{100 \text{ g} \times 60 \text{ g mol}^{-1}}$$

$$\therefore \quad p_1 = 72{\cdot}3 \text{ torr}$$

Determination of Molar Mass of a Solute from Vapour Pressure Lowering. Eq. 22 can be employed for determining the molar mass of a solute. This is illustrated in the following solved examples.

Example 2. 1·20 g of a nonvolatile organic substance was dissolved in 100 g of acetone at 20°C. The vapour pressure of the solution was found to be 182·5 torr. Calculate the molar mass of the substance (vapour pressure of acetone at 20°C is 185·0 torr.)

Solution : From Eq. 22, $\frac{p_1^\circ - p_1}{p_1^\circ} = \frac{w_2 M_1}{w_1 M_2}$

Substituting the various values, we have

$$\frac{(185{\cdot}0 - 182{\cdot}5) \text{ torr}}{185{\cdot}0 \text{ torr}} = \frac{(1{\cdot}20 \text{ g})(58 \text{ g mol}^{-1})}{(100 \text{ g})(M_2)}$$

$$\therefore \quad M_2 = 51{\cdot}51 \text{ g mol}^{-1}$$

Example 3. 0·50 g of a nonvolatile organic substance was dissolved in 100 ml of carbon tetrachloride at 30°C. The vapour pressure of the solution was found to be 141·9 torr. Calculate the molar mass of the substance. Vapour pressure of carbon tetrachloride at 30°C is 143·0 torr and its density is 1·58 g ml^{-1}.

Solution : From Eq. 22, $\frac{p_1^\circ - p_1}{p_1^\circ} = \frac{w_2 M_1}{w_1 M_2}$

In the present case, $w_1 = 1{\cdot}58 \text{ g ml}^{-1} \times 100 \text{ ml} = 158 \text{ g}$, $w_2 = 0{\cdot}5 \text{ g}$, $M_1 = 154 \text{ g mol}^{-1}$

Substituting the various values, we have

$$\frac{143{\cdot}0 \text{ torr} - 141{\cdot}9 \text{ torr}}{143{\cdot}0 \text{ torr}} = \frac{0{\cdot}5 \text{ g} \times 154 \text{ g mol}^{-1}}{158 \text{ g} \times M_2}$$

$$\therefore \quad M_2 = 63{\cdot}3 \text{ g mol}^{-1}$$

Vapour Pressure Lowering in Terms of Molality of the Solution. If m moles of the solute are dissolved in 1000 grams of the solvent, *i.e.*, $w_2/M_2 = m$ and $w_1 = 1000$ grams, then Eq. 22 takes the form

$$(p_1^\circ - p_1)/p_1^\circ = x_2 = mM_1/1000 \text{ g} \qquad \ldots(23)$$

where m is the molality of the solution.

Example 4. What would be the vapour pressure of 0·5 molal solution of a nonvolatile solute in benzene at 30°C ? The vapour pressure of pure benzene at 30°C is 119·6 torr.

Solution : According to Eq. 23, $(p_1^\circ - p_1)/p_1^\circ = m M_1 /1000 \text{ g}$

In the present case, $m = 0{\cdot}5 \text{ mol}$, $M_1 = 78 \text{ g mol}^{-1}$, $p_1^\circ = 119{\cdot}6 \text{ torr}$

Substituting the various values in Eq. 23, we have

$$\frac{119{\cdot}6 \text{ torr} - p_1}{119{\cdot}6 \text{ torr}} = \frac{0{\cdot}5 \text{ mol} \times 78 \text{ g mol}^{-1}}{1000 \text{ g}}$$

$$\therefore \quad p_1 = 114{\cdot}94 \text{ torr}$$

Example 5. Calculate the mass of the solute of molar mass 342 g mol^{-1} that should be dissolved in 150 gram of water to reduce its vapour pressure to 22·8 torr. The vapour pressure of pure water at 25°C = 23·75 torr.

Solution : According to Eq. 22, $\frac{p_1^\circ - p_1}{p_1^\circ} = \frac{w_2 M_1}{w_1 M_2}$

Substituting the various values in Eq. 22, we have

$$\frac{23{\cdot}75 \text{ torr} - 22{\cdot}8 \text{ torr}}{23{\cdot}75 \text{ torr}} = \frac{w_2 \times 18 \text{ g mol}^{-1}}{150 \text{ g} \times 342 \text{ g mol}^{-1}}$$

$$\therefore \quad w_2 = 114 \text{ g}$$

OSMOSIS AND OSMOTIC PRESSURE

There is a natural tendency of solutes in a solution to diffuse from a higher concentration to a lower concentration so as to bring about a uniform distribution throughout. Thus, if a concentrated solution of copper sulphate is placed at the bottom of a beaker and a layer of water, or that of a dilute solution of copper sulphate, is carefully poured over it, there will be distinct or well defined boundary between the two layers. After sometime, however, the boundary will become indistinct and ultimately disappear when there will be only one homogeneous solution of uniform concentration. This is due to the movement of the solute particles upward from the more concentrated to the less concentrated solution. This phenomenon of the movement of particles of a solute from a more concentrated to a less concentrated solution so as to bring about ultimately a uniform concentration throughout the bulk, is known as **diffusion.**

Let us now consider a solution which is separated from the pure solvent by a **semipermeable membrane (SPM),** *i.e.*, a membrane which allows free passage to solvent molecules but not to the solute molecules (Fig. 1).

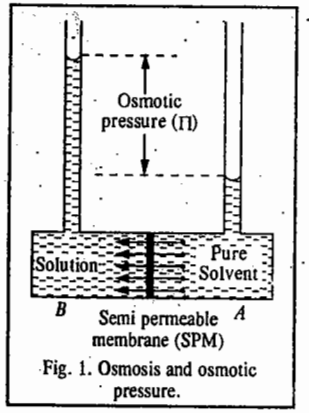

Fig. 1. Osmosis and osmotic pressure.

Since the vapour pressure and the chemical potential of the pure solvent are greater than those of the solvent in the solution, the solvent molecules from chamber A flow through the SPM towards the solution chamber B until the chemical potential of the solvent in the two chambers becomes equal. This process is known as **osmosis** and the extra pressure developed on the solution side as a result of the solvent flow is called **osmotic pressure.** This is usually represented by Π. It is possible to prevent the flow of the solvent through the SPM by applying sufficient pressure to the solution. Thus, osmotic pressure can also be defined as the pressure necessary to stop osmosis.

Derivation of Expression for Calculating Osmotic Pressure. We shall now derive an expression for the calculation of osmotic pressure. For this, refer again to Fig. 1. Before osmosis

$$\mu_1^A > \mu_1^B \qquad \ldots(24)$$

i.e., the chemical potential of the solvent in the solvent chamber A is greater than its chemical potential in the solution chamber B. When osmosis takes place, the pressure on the solution side increases and at equilibrium, the chemical potential of the solvent in the two chambers becomes equal, *i.e.*,

$$\mu_1^A = \mu_1^B \qquad \ldots(25)$$

At equilibrium, the pressure on the solvent is P and that on the solution is $P+\Pi$. Hence,

$$\mu_1^A(T,P) = \mu_1^B(T,P+\Pi) \quad \ldots(26)$$

The chemical potential of the solvent in a solution is a function of temperature, pressure and composition (*i.e.* its mole fraction) so that we can write

$$\mu_1 = f(T,P,x_1) \quad \ldots(27)$$

Hence, $$d\mu_1 = (\partial\mu_1/\partial T)_{P,x_1}dT + (\partial\mu_1/\partial P)_{T,x_1}dP + (\partial\mu_1/\partial x_1)_{T,P}dx_1 \quad \ldots(28)$$

At constant T, $dT = 0$, so that $(\partial\mu_1/\partial T)_{P,x_1}dT = 0$.

Also, $\mu_1 = \mu_1^\circ + RT\ln x_1$ (Eq.6)

so that $$(\partial\mu_1/\partial x_1)_{T,P} = RT/x_1 \quad \ldots(29)$$

Further, $(\partial\mu_1/\partial P)_{T,x_1} = \bar{V}$ (Eq. 4)

$= V_1^\circ$ for an infinitely dilute binary solution $\quad \ldots(30)$

where V_1° is the molar volume of the solvent.

Substituting the various quantities as given by Eqs. 29 and 30 in Eq. 28, we get, at constant temperature,

$$d\mu_1 = V_1^\circ dP + RT\,d\ln x_1 \quad \ldots(31)$$

Integrating Eq. 31 between the limits $P = P$, $x_1 = 1$ and $P = P+\Pi$, $x_1 = x_1$, we get

$$\int_P^{P+\Pi} d\mu_1 = V_1^\circ \int_P^{P+\Pi} dP + RT\int_{x_1=1}^{x_1=x_1} d\ln x_1 \quad \ldots(32)$$

or $$\mu_1(T,P+\Pi) - \mu_1(T,P) = V_1^\circ(P+\Pi-P) + RT\ln x_1 \quad \ldots(33)$$

At equilibrium, the chemical potential of the solvent on the solvent side is equal to the chemical potential of the solvent on the solution side, so that

$$\mu_1(T,P+\Pi) = \mu_1(T,P) \quad \ldots(34)$$

Hence, Eq. 33 becomes

$$RT\ln x_1 = -V_1^\circ\Pi \quad \ldots(35)$$

For a dilute solution, $x_2 << 1$, so that

$$\ln x_1 = \ln(1-x_2) = -x_2 \quad \ldots(36)$$

and, by definition, $x_2 = n_2/(n_1+n_2) = n_2/n_1$ for a dilute solution. $\quad \ldots(37)$

Hence, Eq. 35 becomes

$$\Pi V_1^\circ = x_2RT = (n_2/n_1)RT \quad \ldots(38)$$

or $$n_1\Pi V_1^\circ = n_2RT \quad \ldots(39)$$

Since for a dilute solution, the total volume V is given by

$$V = n_1V_1^\circ + n_2V_2^\circ \approx n_1V_1^\circ \quad \ldots(40)$$

we may write Eq. 39 as $\Pi V = n_2RT$ $\quad \ldots(41)$

or $$\Pi = (n_2/V)RT = c_2RT \quad \ldots(42)$$

where c_2 ($= n_2/V$) is the molar concentration of the solute in the solution.

Eq. 42 is the well known **van't Hoff equation** for the osmotic pressure of a dilute solution. J.H. van't Hoff (1852–1911), the Dutch chemist, was the first recipient of the Chemistry Nobel Prize, awarded in 1901, for his discovery of the laws of chemical dynamics and the laws of osmotic pressure of solutions.

Since osmotic pressure depends only on the molar concentration of the solute and is independent of the nature of the solute, it is, by definition, a colligative property.

The vant't Hoff equation (42) can also be expressed as

$$\Pi = \frac{w_2}{M_2V}RT$$

or $$M_2 = \frac{w_2RT}{\Pi V} \quad \ldots(43)$$

Determination of Molar Mass from Osmotic Pressure Measurement. Eqs. 42 and 43 can be employed for determining the molar mass of a non-volatile solute from the measurement of the osmotic pressure of its dilute solution (supposed to be ideal) in a given solvent. This is illustrated in the following solved examples.

Example 6. Calculate the molar mass of a nonvolatile solute if, at 25°C, its solution containing 1·6 g per dm^3 has an osmotic pressure of 83 torr. Given : $R = 0{\cdot}0821\ dm^3\ atm\ K^{-1}\ mol^{-1}$.

Solution : According to Eq. 43, the molar mass of the solute is given by,

$$M_2 = (w_2RT)/\Pi V$$

Substituting the various values, we have

$$M_2 = \frac{1{\cdot}6\ g \times 0{\cdot}0821\ dm^3\ atm\ K^{-1}mol^{-1} \times 298\ K}{(83/760)\ atm \times 1\ dm^3} = \mathbf{358{\cdot}6\ g\ mol^{-1}}$$

Isotonic Solutions. Solutions which have the same osmotic pressure at the same temperature are said to be isotonic. When two solutions having the same osmotic pressure are put into communication with each other through a semipermeable membrane, there will, evidently, be no transference of solvent from one solution to the other. According to the van't Hoff theory, it is evident that isotonic solutions must have the same molar concentration.

Example 7. A solution containing 8·6 g per dm^3 of urea (molar mass = 60 g mol^{-1}) was found to be isotonic with a 5 per cent solution of an organic nonvolatile solute. Calculate the molar mass of the latter.

Solution : According to the van't Hoff theory, isotonic solutions have the same osmotic pressure at the same temperature and the same molar concentration.

Molar concentration of urea solution = $8{\cdot}6\ g\ dm^{-3}/60\ g\ mol^{-1}$

Let M_2 be the molar mass of the unknown solute.

$\therefore$ Molar concentration of unknown solution = $50\ g\ dm^{-3}/M_2$

Since both the solutions are isotonic, hence, their molar concentrations are equal. Thus,

$$50\ g\ dm^{-3}/M_2 = 8{\cdot}6\ g\ dm^{-3}/60\ g\ mol^{-1}$$

$$M_2 = \mathbf{348{\cdot}8\ g\ mol^{-1}}$$

Example 8. At 37°C, the osmotic pressure of blood is 7·65 atm. How much glucose (M_2=180 g mol^{-1}) should be used per litre for an intravenous injection that is to have the same osmotic pressure as blood.

Solution : $\Pi = c_2RT = (n_2/V)RT$ (Eq. 42)

$$\therefore \quad n_2 = \frac{\Pi V}{RT} = \frac{(7{\cdot}65\ atm)(1{\cdot}00\ dm^3)}{(0{\cdot}0821\ dm^3\ atm\ K^{-1}\ mol^{-1})\ (310\ K)} = 0{\cdot}301\ mol$$

n_2 = mass of the solute/molar mass of the solute = w_2/M_2

$$\therefore \quad w_2 = n_2M_2 = (0{\cdot}301\ mol)\ (180\ g\ mol^{-1}) = \mathbf{54{\cdot}18\ g}$$

If, however, the solution is not dilute, then a virial expansion of the type shown below is used for determining the molar mass :

$$\Pi = (RT/M_2)c_2' + B(c_2')^2 \qquad ...(44)$$

where $c_2'(=w_2/V)$ is the concentration of the solute in grams per unit volume of the solution.

or $$\Pi/c_2' = RT/M_2 + Bc_2' \qquad ...(45)$$

where the second virial coefficient B depends upon the binary solute–solvent interaction in a non-ideal solution. For an ideal dilute solution $B=1$.

According to Eq. 45, a plot of Π/c_2' *versus* c_2' gives a straight line (Fig. 2) which when extrapolated to zero concentration ($c_2' = 0$) gives an intercept equal to RT/M_2 and slope equal to B. Thus,

$$\underset{c_2' \to 0}{\text{Lt}}(\Pi/c_2') = RT/M_2 \qquad ...(46)$$

From the intercept, the molar mass of the solute (M_2) can be calculated.

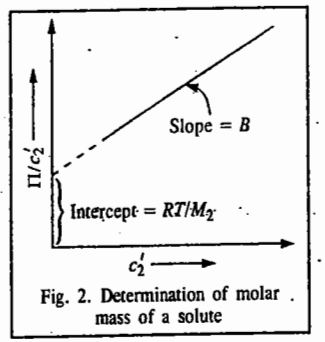

Fig. 2. Determination of molar mass of a solute

Relation between Osmotic Pressure and Vapour Pressure Lowering of an Ideal Solution. It is possible to apply thermodynamics to derive a relationship between osmotic pressure and vapour pressure lowering of an ideal solution. The transfer of solvent to a solution through semipermeable membrane occurs because, at any constant temperature and atmospheric pressure, chemical potential of the pure solvent $\mu°$, is greater than that of the solution, μ. In order to bring about equilibrium between the solvent and the solution, *i.e.*, in order to prevent the flow of the solvent into the solution, it is necessary to apply some additional pressure on the solution. The additional pressure applied is equal to the osmotic pressure (Π) of the solution. Thus, the total external pressure on the solution side of the semipermeable membrane has to be increased from 1 atm to $(1+\Pi)$ atm while the external pressure on the pure solvent side remains 1 atm. The chemical potential on the solution side will also increase from μ to, say $\mu+\Delta\mu$. Since the system is in osmotic equilibrium (*i.e.*, there is no transference of liquid from one side to the other of the membrane), hence,

$$\mu° = \mu + \Delta\mu \quad \text{or} \quad \mu - \mu° = -\Delta\mu \qquad ...(47)$$

The variation of chemical potential with temperature is given by the well known thermodynamic equation

$$\mu = \mu° + RT \ln a \qquad \text{(Chapter 15)} \qquad ...(48)$$

where a is the activity of the solvent in the solution.

Combining Eqs. 47 and 48, we have

$$\therefore \quad -\Delta\mu = RT \ln a \qquad ...(49)$$

If the solution is ideal, we may take $a = p/p°$

$$\therefore \quad -\Delta\mu = RT \ln (p/p°) \qquad ...(50)$$

where $p°$ is the vapour pressure of the pure solvent while p is the vapour pressure of the solvent in the solution at the same temperature.

We also know from thermodynamics that at constant temperature

$$dG = Vdp \qquad ...(51)$$

For partial molar quantities, Eq. 51 may be written as

$$\overline{\quad} = \overline{\quad}\,' \qquad (52)$$

Since partial molar free energy ($\overline{G}$) is the same as chemical potential (μ), we may write

$$d\mu = \overline{V}\, dp \qquad ...(53)$$

where $\overline{V}$ is the partial molar volume of the solvent in the solution.

Integrating Eq. 53 between the limits μ of the solution at 1 atm pressure and μ' of the solvent at $(1+\Pi)$ atm pressure, we get

$$\int_{\mu}^{\mu'} d\mu = \int_{1}^{1+\Pi} \overline{V}\, dp \qquad ...(54)$$

Assuming $\overline{V}$ to be independent of pressure, we have

$$\mu' - \mu = \Delta\mu = \overline{V}\,(1 + \Pi - 1) = \overline{V}\Pi \qquad ...(55)$$

Substituting Eq. 55 into Eq. 50, yields

$$\Pi = \frac{RT}{\overline{V}} \ln (p°/p) \qquad ...(56)$$

This is the desired relation between osmotic pressure and lowering of vapour pressure.

If the solution is infinitely dilute, $\overline{V}$ may be taken as $V°$ (see foot note given earlier), the molar volume of the pure solvent. Eq. 58 may, therefore, be written as

$$\Pi = \frac{RT}{V°} \ln (p°/p) \qquad ...(57)$$

Theories of Semipermeability. A number of theories have been proposed to explain the action of semipermeable membrane. However, none of them appears to be completely satisfactory.

1. Sieve theory. The earlier investigators were of the view that the semipermeable membrane acts as a kind of sieve with pores small enough to allow the water molecules to pass but to retain the larger molecules of the solute. This view was soon discarded as it was found that the membrane did not allow even those molecules of the solute to pass through it which were smaller than the molecules of the solvent.

2. Solubility theory. Another mechanism that was put forward some years later, explains semipermeability by supposing that the solvent is soluble in the membrane whereas the solute is not. The theory may be explained by reference to the following experiment.

An inverted thistle funnel, the lower end of which is closed by an animal membrane thoroughly soaked in water, is filled with a mixture of ether and benzene. The thistle funnel is then immersed in a beaker containing moist ether. The ether is seen to rise in the tube. Thus, the animal membrane when wetted with water behaves as a semipermeable membrane as it permits the passage of ether molecules through it into the tube but not that of benzene molecules in the opposite direction. This may be explained on the basis of the solubility of ether in water with which the membrane was thoroughly wetted earlier. Benzene is almost insoluble in water and, therefore, its passage is prevented.

3. Adsorption theory. According to the adsorption theory, the water (solvent) molecules are attracted and adsorbed on the surface of the membrane. The adsorbed layer maintains a continuous connection between the solvent molecules on both sides of the semipermeable membrane. The molecules of the solvent, therefore, can pass through the membrane easily while those of the solute, which are not adsorbed on the membrane, cannot pass.

4. Capillary theory. According to the capillary theory, which has received sufficient support, the semipermeable membrane consists of fine capillary tubes of such small pores as neither the solvent nor the solute can pass through. However, *vapours can.* Now, as already shown, the vapour pressure of a solution is lower than that of the pure solvent at the same temperature. Therefore, when pure solvent is placed on one side of the membrane and solution on the other, the solvent, on account of its higher vapour pressure, distils through the capillary pores from the solvent side towards the solution side. This gives rise to osmosis.

Some Effects of Osmosis and Semipermeability. 1. The so-called silicate gardens or chemical gardens are produced by dropping small crystals of various inorganic salts such as copper sulphate, nickel sulphate, alum, etc., into a 5 per cent (somewhat viscous) solution of sodium silicate. The metal ions diffusing out of a crystal form precipitate of a metal silicate which acts as a semipermeable membrane round the crystal. Osmosis now sets in causing the flow of water from the weaker sodium silicate solution to the stronger salt solution. The membrane, therefore, bursts at its weaker points to liberate more metal ions which make new membranes. The process continues resulting in the formation of strangely shaped growths around the crystal. The growths produced around various crystals look like a garden.

2. Many animal and vegetable cells contain solutions of salts and sugars (cell saps) enclosed in membranes which are almost completely semipermeable. If such a cell is placed in water or in a solution, the osmotic pressure of which is less than that of the cell sap within, water will tend to enter the cell which will swell. But, if the cell is placed in a solution of higher osmotic pressure, water will pass out from the cell through the membrane and the cell will shrink. The phenomenon of shrinkage of a cell is called **plasmolysis.** It may be illustrated by taking two hen eggs of about the same size. After dissolving away their outer shells by placing them in dilute hydrochloric acid, one egg is placed in distilled water and the other in a saturated solution of sodium chloride which has an osmotic pressure greater than that of the material in the egg. In the first case, water will enter into the egg through the membrane while in the second case, water will come out of the egg through the membrane. In the first case the egg will swell while in the second case it will shrink, that is, it will show plasmolysis.

3. By placing plant or animal cells into solutions of gradually increasing concentration (*i.e.*, increasing osmotic pressure), it is possible to determine the concentration at which plasmolysis just does not occur or where it is just detectable. The solution, then, has the same osmotic pressure as the cell solution and is said to be isotonic with it. This procedure is often used in measuring osmotic pressures of cell saps. The results, however, are only approximate since the cell membrane is not completely semipermeable.

It has been observed that red blood corpuscles are isotonic with a 0·91 per cent solution of sodium chloride.

4. Plants largely get water from the soil by osmosis. The cells at the tips of the roots contain tiny growths, called root-hairs, which are in contact with the soil. As the osmotic pressure inside the cells is higher, water flows into the cells by osmosis.

5. It is a common experience that an excessive dose of ammonium sulphate or any other chemical fertilizer, causes serious damage to plants. This is due to the fact that the osmotic pressure of the fertilizer solution becomes higher than that of the cell sap. This causes the outflow of water from the plant cells into the soil. The plant, therefore, tends to 'wilt' or dry up.

Reverse Osmosis

Consider, once again, a solution separated from the pure solvent by a semipermeable membrane. If the pressure applied on the solution is more than the osmotic pressure, *the solvent will start flowing from the solution towards the pure solvent.* This phenomenon is known as

reverse osmosis (Fig. 3*a*).

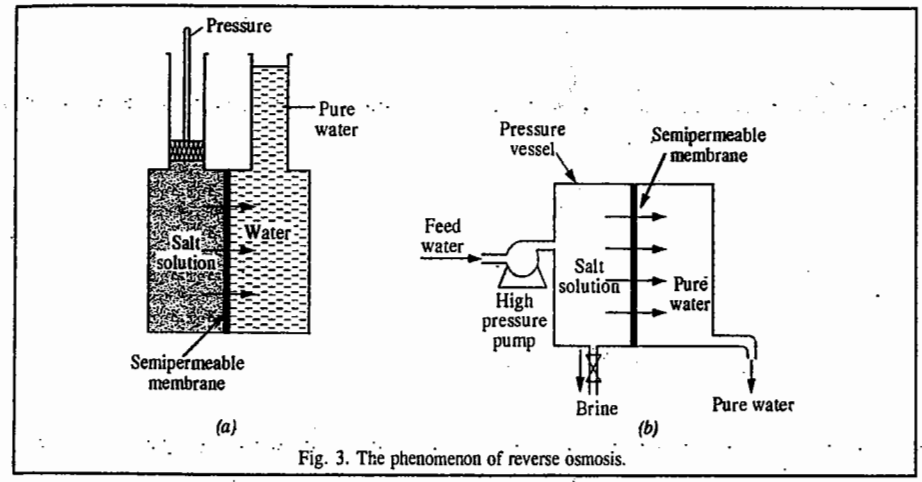

Fig. 3. The phenomenon of reverse osmosis.

Reverse osmosis (RO) technique is now being extensively employed for getting drinking water from the sea water, particularly in Gulf countries. Several other countries are following suit.

A simple schematic of an RO system is shown in Fig. 3(*b*). The sea water is pumped into a pressure vessel fitted with a suitable semipermeable membrane (SPM). Under the influence of high pressure, water from the sea water passes out through the semipermeable membrane as shown.

The rate of flow of water Q_w through the SPM is given by

$$Q_w = (\Delta P - \Delta\Pi)\, K_w\, A/\delta \qquad \ldots(58)$$

where ΔP = hydraulic pressure differential across the membrane, $\Delta\Pi$ = osmotic pressure differential across the membrane, K_w = membrane permeability coefficient for water, A = membrane area and δ = membrane thickness.

Depending upon the salt concentrations, the osmotic pressures of sea waters generally vary from about 4000 to 5500 kPa (Pa = Pascal = 0·009 atm). For RO, the applied pressure should be about 1400 kPa more than the osmotic pressure. This implies that for the purification of sea water by RO, the pressure applied should vary from about 5400 to 6900 kPa. This is quite a high pressure indeed and, for quite sometime, it was a problem to have commercial semipermeable membranes which could withstand such a high pressure.

These days, however, the problem of the availability of such SPMs has been completely solved. SPMs for RO were first obtained in late 1950s from cellulose acetate. But their use in RO was impractical since, being dense, they permitted very low flow rates. A few years later, techniques were developed for the fabrication of cellulose acetate membranes with *asymmetric density*. By using proper composition of casting solution and proper conditions of casting and quenching, it has now been possible to prepare cellulose acetate membranes with thin (0·1–1·0 μm) surfaces (termed as 'skins' of the membranes) supported by porous cellu-lose structures, as shown in Fig. 4.

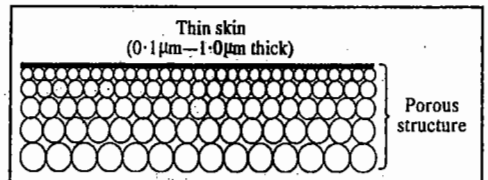

Fig. 4. A cellulose acetate membrane with asymmetric density.

These membranes permit high water flow rates since the rate-determining factor for water transport is only the thickness of the skin of the membrane which is evidently very small.

Cellulose acetate membranes, however, have two major limitations. Firstly, they are susceptible to degradation from biological attack. To avoid this problem, the feed water is properly chlorinated before use. Secondly, cellulose acetate hydrolyses back to cellulose under acidic and more so under basic conditions. To minimise hydrolysis, the *p*H of the system is controlled and kept in the range of 4·5 to 7·5.

As a further development, SPMs have now been obtained from an aromatic polyamide ('aramid'). When operated in the *p*H range of 4–11, the aramid membranes not only resist hydrolysis but also become immune to biological attack. These membranes, however, get degraded by chlorine. The feed water, therefore, must be dechlorinated before use.

Another polyamide membrane has recently been introduced into the market in a thin-film composite form. The membrane is formed *in situ* by an interfacial polymerisation technique. It has a thickness of 250–500Å. This membrane, like the aramid membrane, is resistant to hydrolysis and is not prone to biological attack. It is, of course, highly sensitive to chlorine degradation.

Extensive reasearch is going on for the development of new membranes which would have no limitations. It would not be surprising if all the membranes currently in use become obsolete very soon making room for newer membranes which are far superior in every respect.

It should, nevertheless, be clearly understood that none of the membranes prepared so far is perfectly semipermeable. In fact, a perfectly semipermeable membrane may be a non-reality in future also. They invariably allow the passage of salts also to varying extents. The rate of flow of salts through the membrane is given by

$$Q_s = \Delta c K_s A/\delta \qquad ...(59)$$

where Q_s = flow rate of salts through the membrane, K_s = membrane permeability coefficient for the salts, Δc = salt concentration differential across the membrane and δ = thickness of the membrane.

Evidently, the rate of flow of salts is proportional to concentration differential and is independent of the applied pressure. Thus, an increase in operating pressure would increase the flow of water without changing the flow of salts.

A properly designed RO plant reduces the salt content of sea water from 35,000 to 42,000 mg per litre to about 500 to 725 mg per litre. A part of the product water obtained as above is further purified using an additional RO plant when the salt content reduces to about 100 mg per litre. The product water from the second plant is blended with that obtained from the first plant in such a way that the salt content remains invariably below 500 mg per litre. This water is amply suitable to be used as municipal water.

Sea water purification through RO is highly economical since the energy consumption is very low. This is because the process involves no phase change. Energy consumption for sea water purification ranges between 35 and 40 kWh per 1000 gallons of product water which can be still further reduced to 25–30 kWh per 1000 gallons affixing energy recovery equipment on the feed water stream.

RO, in conjunction with ion-exchangers, is now extensively used by the power industry to produce high-pressure boiler feed water and by the electronic industry to produce ultrapure water for manufacturing electronic components. Small RO plants are set up for sea water purification to supply water to offshore drilling rigs, farms, hospitals, hotels, motels, laboratories, etc. In Gulf countries, municipal water is exclusively obtained through RO, using the sea water as the feed water. In several states of the U.S.A., the lake waters are purified by RO. The development of this technique has been revolutionary indeed !

BOILING POINT ELEVATION

The boiling point, T_b, of a liquid is the temperature at which its vapour pressure is equal to the atmsopheric pressure. When a nonvolatile solute is added to a liquid, the vapour pressure of the liquid is decreased. Hence, it must be heated to a higher temperature in order that its vapour pressure becomes equal to that of the atmospheric pressure. This means that the addition of a non-volatile solute to a liquid raises (elevates) its boiling point.

Consider a solution of a non-volatile solute in a volatile solvent. At a given temperature and pressure, the liquid phase and the vapour phase of the solvent are in equilibrium under which condition the chemical potential of the solvent (component 1) in the liquid phase is equal to that in the vapour phase, *i.e.*, $\mu_1^l = \mu_1^v$.

The same equality would hold at any other temperature, say, at the boiling point of the pure solvent as also at the boiling point of the solution although the numerical values of chemical potentials at higher temperatures would be different.

This implies that the change in the chemical potentials of the liquid and vapour phases with change in temperature will be equal at equilibrium, *i.e.*, $d\mu_1^l = d\mu_1^v$

The chemical potential of the solvent in a solution would evidently depend upon T, P and composition (*i.e.*, its mole fraction) whereas its chemical potential in the vapour phase would depend only on T and P. Thus,

$$\mu_1^l = f(T,P,x_1) \text{ and } \mu_1^v = f(T,P) \qquad ...(60)$$

$$\therefore \quad d\mu_1^l = (\partial\mu_1^l/\partial T)_{P,x_1}dT + (\partial\mu_1^l/\partial P)_{T,x_1}dP + (\partial\mu_1^l/\partial x_1)_{T,P}dx_1 \qquad ...(61)$$

$$= -\bar{S}_1^l dT + \bar{V}_1^l dP + (\partial\mu_1^l/dx_1)_{T,P}dx_1 \qquad ...(62)$$

$$\text{Also,} \quad d\mu_1^v = (\partial\mu_1^v/\partial T)_P dT + (\partial\mu_1^v/\partial P)_T dP = \bar{S}_1^v dT + \bar{V}_1^v dP \qquad ...(63)$$

Since at equilibrium, $d\mu_1^l = d\mu_1^v$, hence, from Eqs. 62 and 63,

$$-\bar{S}_1^l dT + \bar{V}_1^l dP + \left(\partial\mu_1^l/\partial x_1\right)_{T,P}dx_1 = -\bar{S}_1^v dT + \bar{V}_1^v dP \qquad ...(64)$$

$$\text{or} \quad \left(\bar{S}_1^v - \bar{S}_1^l\right)dT + \left(\bar{V}_1^l - \bar{V}_1^v\right)dP = -(\partial\mu_1^l/\partial x_1)_{T,P}dx_1 \qquad ...(65)$$

In general, the pressure is kept constant so that $dP = 0$. Hence, Eq. 65 reduces to

$$\left(\bar{S}_1^v - \bar{S}_1^l\right)dT = -\left(\frac{\partial\mu_1^l}{dx_1}\right)_{T,P}dx_1 \quad \text{or} \quad \Delta\bar{S}_v dT = -\left(\frac{\partial\mu_1^l}{\partial x_1}\right)_{T,P}dx_1 \qquad ...(66)$$

where $\Delta\bar{S}_v\left(=\bar{S}_1^v - \bar{S}_1^l\right)$ is the partial molar entropy of vaporisation of the solvent.

In an ideal solution, $\mu_1 = \mu_1^\circ + RT \ln x_1$ so that $(\partial\mu_1/\partial x_1)_{T,P} = RT/x_1$ ...(67)

From Eqs. 66 and 67,

$$\Delta\bar{S}_v dT = -(RT/x_1)dx_1 = -RT\, d\ln x_1 \qquad ...(68)$$

$$\text{But} \quad \Delta\bar{S}_v = \Delta\bar{H}_{vap}/T \qquad ...(69)$$

where $\Delta\bar{H}_{vap}$ is the partial molar enthalpy of vaporisation of the solvent.

$$\text{Hence,} \quad d\ln x_1 = -(\Delta\bar{H}_{vap}/RT^2)dT \qquad ...(70)$$

Assuming that $\Delta\bar{H}_{vap}$ remains independent of temperature in the given temperature range, Eq.70 can be integrated. At $x_1=1$, $T=T_b$ (the boiling point of the pure solvent) and at $x_1=x_1$, $T=T$ (the

boiling point of the solution). Hence,

$$\int_1^{x_1} d \ln x_1 = -\frac{\Delta\bar{H}_{vap}}{R}\int_{T_b}^{T}\frac{dT}{T^2}$$

or
$$\ln x_1 = -\frac{\Delta\bar{H}_{vap}}{R}\left[\frac{1}{T}-\frac{1}{T_b}\right] = -\frac{\Delta\bar{H}_{vap}}{R}\times\frac{\Delta T_b}{T T_b} \quad ...(71)$$

where $\Delta T_b = T - T_b$ = **elevation in boiling point.**

Now, for dilute solutions, $T \approx T_b$ and $\ln x_1 = \ln (1 - x_2) \approx - x_2$ where x_2 is small. Using these approximations, Eq. 71 reduces to

$$x_2 = (\Delta\bar{H}_{vap}/RT_b^2)\Delta T_b \quad ...(72)$$

$$\therefore \quad \Delta T_b = RT_b^2 x_2 / \Delta\bar{H}_{vap} \quad ...(73)$$

For an infinitely dilute binary solution, $\Delta\bar{H} = \Delta H$ (see foot note given earlier).

$$\therefore \quad \Delta T_b = (RT_b^2 / \Delta H_{vap})x_2 \quad ...(74)$$

where ΔH_{vap} is the molar heat of vaporization of the solvent.

Eq. 74 gives the relationship between the amount (mole fraction) of the solute and the elevation in boiling point of the solution.

The mole fraction

$$x_2 = \frac{n_2}{(n_1 + n_2)} = \frac{n_2}{n_1} = \frac{w_2}{M_2}\times\frac{M_1}{w_1} \text{ for a dilute solution.} \quad ...(75)$$

If m moles of the solute are dissolved in 1 kg of the solvent, *i.e.*, $w_2/M_2 = m$ and $w_1 = 1$kg, then

$$x_2 = mM_1/1 \text{ kg} \quad ...(76)$$

where m is the *molality* of the solution.

Hence, Eq. 74 may be written as

$$\Delta T_b = RT_b^2 M_1 m / \Delta H_{vap} \quad ...(77)$$

For a given solvent, the factor $RT_b^2 M_1 / \Delta H_{vap}$ is constant. It is denoted by K_b and is called molal boiling point elevation constant of the solvent. Thus,

$$K_b = RT_b^2 M_1 / \Delta H_{vap} \quad ...(78)$$

Eq. 77, therefore, simplifies to $\Delta T_b = K_b m$ ...(79)

If molality $m = 1$, *i.e.*, 1 mole of the solute is dissolved in 1 kg of the solvent, then, $K_b = \Delta T_b$. Thus, **molal boiling point elevation constant** or **ebullioscopic constant** of a solvent is defined as the elevation in boiling point of the solution which may theoretically be produced when 1 mole of the solute is dissolved in 1 kg of the solvent.

According to Eq. 79, the elevation in boiling point depends only on the molality of the solute and is independent of the nature of the solute. It is, therefore, a colligative property.

The molal boiling point elevation constants or ebullioscopic constants of some solvents are given in Table 1.

TABLE 1
Ebullioscopic Constants of Some Solvents

Solvent	K_b (K kg mol^{-1})
Water	0·52
Acetone	1·72
Carbon tetrachloride	5·00
Ethyl alcohol	1·20
Methyl alcohol	0·80
Benzene	2·67
Chloroform	3·88
Ethyl ether	2·11

The units of K_b, *viz.*, K kg mol^{-1}, follow directly from Eq. 78. Incorporating the units of various parameters in this equation, the units of K_b come out to be (J K^{-1} mol^{-1}) (K^2) (kg mol^{-1})/(J mol^{-1}), *i.e.*, K kg mol^{-1}.

Example 9. Find the molal boiling point elevation constant of water which evaporates at 100°C with the absorption of 40669·2 J per mole (R = 8·314 J K^{-1} mol^{-1}).

Solution : According to Eq. 78, the molal boiling point elevation constant is given by

$$K_b = \frac{RT_b^2 M_1}{\Delta H_{vap}} = \frac{(8{\cdot}314 \text{ J K}^{-1}\text{mol}^{-1})(373 \text{ K})^2 (0{\cdot}0180 \text{ kg mol}^{-1})}{(40669{\cdot}2 \text{ J mol}^{-1})}$$

$$= 0{\cdot}512 \text{ K kg mol}^{-1}$$

Determination of Molar Mass from Boiling Point Elevation. According to Eq.79; $\Delta T_b = K_b m$. If w_2 kg of the solute of molar mass M_2 is dissolved in w_1 kg of the solvent, then the number of moles of the solute dissolved in 1 kg of the solvent (which gives the molality m of the solution) would be given by $(w_2/M_2)\times 1/w_1$). Eq. 79 then becomes

$$\Delta T_b = K_b \times \frac{w_2}{M_2 w_1} \quad ...(80)$$

$$\therefore \quad M_2 = \frac{K_b w_2}{w_1 \Delta T_b} \quad ...(81)$$

Knowing the elevation in the boiling point of the solution and the molal boiling point elevation constant of the solvent, the molar mass of the solute can be easily calculated.

Example 10. A solution containing 2·44 g of a solute dissolved in 75 g of water boiled at 100·413°C. Calculate the molar mass of the solute (K_b for water = 0·52 K kg mol^{-1}).

Solution : From Eq. 81,

$$M_2 = \frac{K_b w_2}{w_1 \Delta T_b} = \frac{(0{\cdot}52 \text{ K kg mol}^{-1})(2{\cdot}44 \times 10^{-3} \text{ kg})}{(75 \times 10^{-3} \text{ kg})(0{\cdot}413 \text{ K})} = 0{\cdot}04096 \text{ kg mol}^{-1}$$

$$= 40{\cdot}96 \text{ g mol}^{-1}$$

Example 11. A 5 per cent aqueous solution by mass of a nonvolatile solute boils at 100·15°C. Calculate the molar mass of the solute. K_b = 0·52 K kg mol^{-1}.

Solution : ΔT_b = 373·15 K − 373 K = 0·15 K

$\therefore$ From Eq. 79, $m = \Delta T_b / K_b$ = 0·15 K/0·52 K kg mol^{-1} = 0·288 mol kg^{-1}

The solution contains 5% by mass of the solute, *i.e.*, 1000 g of the solution contains 50 g of the solute.

$\therefore$ Mass of solvent, w_1 = 950 g = 0·950 kg

$$\text{Molality, } m = \frac{w_2}{M_2}\times\frac{1}{w_1}$$

Incorporating various values in the above equation, we have

$$0{\cdot}288 \text{ mol kg}^{-1} = \frac{50\times10^{-3}\text{kg}}{M_2}\times\frac{1\text{kg}}{0{\cdot}950\text{kg}}$$

$$\therefore \quad M_2 = \frac{50 \times 10^{-3} \text{ kg}}{0{\cdot}288 \text{ mol kg}^{-1} \times 0{\cdot}950 \text{ kg}} = 0{\cdot}1827 \text{ kg mol}^{-1} = \mathbf{182{\cdot}7 \text{ g mol}^{-1}}$$

Example 12. The heat of vaporisation of water at 100°C is 40·585 kJ mol^{-1}. At what temperature will a solution containing 5·60 g of glucose per 1000 g of water boil ?

Solution : $K_b = \frac{R T_b^2 M_1}{\Delta H_{vap}}$ (Eq.78)

$$= \frac{(8{\cdot}314\ \text{J K}^{-1}\text{mol}^{-1})(373\ \text{K})^2 \times 0{\cdot}0180\ \text{kg mol}^{-1}}{40585\ \text{J mol}^{-1}} = 0{\cdot}513\ \text{K kg mol}^{-1}$$

$$M_2(\text{glucose}) = 180\ \text{g mol}^{-1} = 0{\cdot}180\ \text{kg mol}^{-1}$$

$$\therefore \quad \Delta T_b = \frac{K_b w_2}{w_1 M_2} = \frac{(0{\cdot}513\ \text{K kg mol}^{-1})(5{\cdot}6 \times 10^{-3}\ \text{kg})}{(1\ \text{kg})(18 \times 10^{-3}\ \text{kg mol}^{-1})} = \mathbf{0{\cdot}16\ K}$$

$\therefore$ Boiling point of solution = 373 K + 0·16 K = 373·16 K = **100·16°C**

Example 13. A solution containing 6 g of a solute dissolved in 250 ml of water gave an osmotic pressure of 4·5 atm at 27°C. Calculate the boiling point of the solution. The molal boiling point elevation constant for water is 0·52 K kg mol^{-1}.

Solution : First the molar mass of the solute M_2 will be calculated from the osmotic pressure.

$$c = 6\ \text{g per } 250\ \text{ml} = 24\ \text{g dm}^{-3} = (24 \times 10^{-3}\ \text{kg}/M_2)\ \text{mol dm}^{-3}$$

From the van't Hoff equation, *viz.*, $\Pi = cRT$, we have

$$4{\cdot}5\ \text{atm} = [(24 \times 10^{-3}\ \text{kg}/M_2)\ \text{mol dm}^{-3}]\ (0{\cdot}0821\ \text{dm}^3\ \text{atm K}^{-1}\text{mol}^{-1})\ (300\ \text{K})$$

$$\therefore \quad M_2 = 131{\cdot}34 \times 10^{-3}\ \text{kg mol}^{-1}$$

Further, $$\Delta T_b = \frac{K_b w_2}{w_1 M_2} = \frac{(0{\cdot}52\ \text{K kg mol}^{-1})(6 \times 10^{-3}\ \text{kg})}{(250 \times 10^{-3}\ \text{kg})(131{\cdot}34 \times 10^{-3}\ \text{kg mol}^{-1})} = 0{\cdot}095\ \text{K}$$

$\therefore$ Boiling point of the solution = 373 K + 0·095 K = 375·095 K = **100·095°C**

FREEZING POINT DEPRESSION

Consider the freezing of a pure liquid. At the freezing point of the liquid, there exists an equilibrium between the solid and liquid so that the vapour pressures of the solid phase and the liquid phase are equal and so are their chemical potentials and escaping tendencies.* Now when a non-volatile solute is added to the liquid, the escaping tendency of solvent molecules from liquid to solid phase diminishes whereas the reverse escaping tendency from solid to liquid phase remains unaffected. The solid solvent, therefore, begins to dissolve. In order to prevent this and restore equilibrium, we must favour the formation of the solid phase. This is done by lowering the temperature. Thus, at a certain lower temperature, the two escaping tendencies again become equal and equilibrium is established.

The chemical potential of the solid solvent (component 1) must be equal to the chemical potential of the liquid at the new concentration, *i.e.*,

$$\mu_1^s = \mu_1^l = (\mu_1^\circ)^l + RT \ln x_1^l \qquad \ldots(82)$$

where $(\mu_1^\circ)^l$ is the chemical potential of the pure liquid 1 and x_1^l is its mole fraction in the solution. With the addition of the solute, x_1^l and hence ln x_1^l decreases.

Thus, for a small change in temperature and composition, at equilibrium, we have

$$d\mu_1^s = d\mu_1^l \qquad \ldots(83)$$

Since $\mu_1^s = f(T,P)$ and $\mu_1^l = f(T,P,x_1)$

hence, $$d\mu_1^s = (\partial\mu_1^s/\partial T)_P dT + (\partial\mu_1^s/\partial P)_T dP \qquad \ldots(84)$$

At constant, P, $dP = 0$ so that

$$d\mu_1^s = \left(\frac{\partial\mu_1^s}{\partial T}\right) dT = -\bar{S}_1^s dP \qquad \ldots(85)$$

* According to Lewis, the chemical potential of a substance in a given state is a measure of the escaping tendency of the substance from that state.

Similarly, $$d\mu_1^l = (\partial\mu_1^l/\partial T)_{P,x_1} dT + (\partial\mu_1^l/\partial P)_{T,x_1} dP + (\partial\mu_1^l/\partial x_1)_{T,P} dx_1 \qquad \ldots(86)$$

$$= -\bar{S}_1^l dT + (\partial\mu_1^l/\partial x_1)_{T,P} dx_1 \quad \text{at constant } P \qquad \ldots(87)$$

For an infinitely dilute binary solution, $\bar{S}_1 = S$ (see foot note given earlier). Hence, Eq. 87 may be written as

$$d\mu_1^l = -S_1^l dT + (\partial\mu_1^l/\partial x_1)_{T,P} dx_1 \text{ at constant } P \qquad \ldots(88)$$

For an ideal solution,

$$d\mu_1^l = -S_1^l dT + RT\, d \ln x_1^l \qquad \ldots(89)$$

At equilibrium, $\mu_1^l = \mu_1^s$ so that $d\mu_1^l = d\mu_1^s$. $\qquad \ldots(90)$

Hence, from Eqs. 89 and 90,

$$-S_1^s dT = -S_1^l dT + RT\, d \ln x_1^l \qquad \ldots(91)$$

or $$(S_1^l - S_1^s) dT = RT\, d \ln x_1^l \quad \text{or} \quad \Delta S_{fus} dT = RT\, d \ln x_1^l \qquad \ldots(92)$$

where $\Delta S_{fus}[= S_1^l - S_1^s]$ is the molar entropy of fusion.

Since $\Delta S_{fus} = \Delta H_{fus}/T$, Eq. 92 takes the form

$$\therefore \quad d \ln x_1^l = (\Delta H_{fus}/RT)\, dT \qquad \ldots(93)$$

where ΔH_{fus} is the molar enthalpy of fusion.

Assuming that molar enthalpy of fusion remains constant over the temperature range, Eq. 93 can be integrated as follows :

At $x_1 = 0$, $T = T_0$, the freezing point of the pure solvent and at $x_1 = x_1$, $T = T_{fus}$, the freezing point of the solution. Thus,

$$\int_1^{x_1} d \ln x_1^l = \frac{\Delta H_{fus}}{R} \int_{T_0}^{T_f} \frac{dT}{T^2} \qquad \ldots(94)$$

or $$\ln x_1^l = -\frac{\Delta H_{fus}}{R}\left[\frac{1}{T_{fus}} - \frac{1}{T_0}\right] = -\frac{\Delta H_{fus}}{R}\left[\frac{\Delta T_{fus}}{T_0 T_{fus}}\right] \qquad \ldots(95)$$

where ΔT_{fus} $(= T_0 - T_{fus})$ is the **depression in freezing point** of the solution.

For a dilute solution, $T_0 = T_{fus}$ and ln x_1 = ln $(1 - x_2) = -x_2$ where x_2 is small. Using these approximations, Eq. 95 can be written as

$$x_2 = \frac{\Delta H_{fus}}{R}\left[\frac{\Delta T_{fus}}{T_0^2}\right] \qquad \ldots(96)$$

Eq. 96 gives the relationship between the amount (mole fraction) of the solute and the depression in freezing point of the solution.

The mole fraction, $$x_2 = \frac{n_2}{n_1 + n_2} = \frac{n_2}{n_1} = \frac{w_2}{M_2} \times \frac{M_1}{w_1} \text{ for a dilute solution} \qquad \ldots(97)$$

If m moles of a solute are dissolved in 1 kg of the solvent, *i.e.*, $w_2/M_2 = m$ and $w_1 = 1$ kg, then

$$x_2 = mM_1/1\ \text{kg} \qquad \ldots(98)$$

where m is the molality of the solution. Hence, Eq. 96 takes the form

$$\Delta T_{fus} = RT_0^2 m M_1 / \Delta H_{fus} \quad ...(99)$$

For a given solvent, the factor $RT_0^2 M_1 / \Delta H_{fus}$ is constant. It is denoted by K_f and is called the molal freezing point depression constant of the solvent. Thus,

$$K_f = RT_0^2 M_1 / \Delta H_{fus} \quad ...(100)$$

Eq. 99, therefore, reduces to

$$\Delta T_{fus} = K_f m \quad ...(101)$$

If molality $m = 1$, *i.e.*, 1 mole of the solute is dissolved in 1 kg of the solvent, then

$$K_f = \Delta T_{fus} \quad ...(102)$$

Thus, **molal freezing point depression constant** or **cryoscopic constant of a solvent** is defined as the depression in freezing point of the solution which may theoretically be produced when 1 mole of the solute is dissolved in 1 kg of the solvent.

According to Eq. 101, the depression in freezing point depends only on the molality of the solution and is independent of the nature of the solute. It is, therefore, a colligative property.

The K_f values of some common solvents are given in Table 2. According to Eq. 100, the units of K_f would be

$$\frac{(\text{J K}^{-1}\text{mol}^{-1})\text{K}^2\,\text{kg mol}^{-1}}{\text{J mol}^{-1}} = \text{K kg mol}^{-1}$$

TABLE 2

Cryoscopic Constants of Some Solvents

Solvent	K_f (K kg mol^{-1})
Water	1·86
Acetic acid	3·90
Benzene	5·12
Phenol	7·27
Naphthalene	6·90
Bromoform	14·40
Cyclohexane	20·00
Camphor	37·70

Example 14. Calculate the molal freezing point depression constant of water. The molar heat of fusion of ice at 0°C is 6024·6 J.

Solution : From Eq. 100, $K_f = \dfrac{RT_0^2 M_1}{\Delta H_{fus}}$

$$= \frac{(8{\cdot}314\ \text{J K}^{-1}\ \text{mol}^{-1})(273\text{K})^2(0{\cdot}0180\ \text{kg mol}^{-1})}{(6024{\cdot}6\ \text{J mol}^{-1})}$$

$$= 1{\cdot}85\ \text{K kg mol}^{-1}$$

Determination of Molar Mass from Freezing Point Depression. According to Eq.01, $\Delta T_{fus} = K_f m$. If w_2 kg of the solute of molar mass M_2 is dissolved in w_1 kg of the solvent, then the number of moles of the solute dissolved in 1 kg of the solvent (which gives the molality m of the solution) would be given by $(w_2/M_2)\times(1/w_1)$.

Hence, Eq. 101 takes the form

$$\Delta T_{fus} = K_f \frac{w_2}{M_2 w_1} \quad ...(103)$$

or

$$M_2 = \frac{K_f w_2}{w_1 \times \Delta T_{fus}} \quad ...(104)$$

Thus, knowing the depression in freezing point of the solution and the molal freezing point depression constant of the solvent, the molar mass of the solute can be easily calculated.

Example 15. An aqueous solution containing 0·25 g of a solute dissolved in 20 g of water froze at – 0·42°C. Calculate the molar mass of the solute. Enthalpy of fusion of ice at 0°C is 6024·6 J mol^{-1}.

Solution : $K_f = \dfrac{RT_0^2 M_1}{\Delta H_{fus}} = \dfrac{(8{\cdot}314\ \text{J K}^{-1}\ \text{mol}^{-1})(273\ \text{K})^2(0{\cdot}0180\ \text{kg mol}^{-1})}{6024{\cdot}6\ \text{J mol}^{-1}} = 1{\cdot}84\ \text{K kg mol}^{-1}$

$$M_2 = \frac{K_f w_2}{w_1 \times \Delta T_{fus}} = \frac{(1{\cdot}84\ \text{K kg mol}^{-1})(0{\cdot}25\times10^{-3}\ \text{kg})}{(20\times10^{-3}\text{kg})(0{\cdot}42\ \text{K})}$$

$$= 54{\cdot}76\times10^{-3}\ \text{kg mol}^{-1} = 54{\cdot}76\ \text{g mol}^{-1}$$

Example 16. An aqueous solution of a non-volatile solute boils at 100·17°C. At what temperature would it freeze ? For water, K_b = 0·52 K kg mol^{-1} and K_f = 1·86 K kg mol^{-1}.

Solution : $\Delta T_b = 373{\cdot}17\ \text{K} - 373\ \text{K} = 0{\cdot}17\ \text{K}$

According to Eq. 79, $\Delta T_b = K_b m$

$$\therefore \quad m = \frac{\Delta T_b}{K_b} = \frac{0{\cdot}17\,\text{K}}{0{\cdot}52\,\text{K kg mol}^{-1}} = 0{\cdot}327\ \text{mol kg}^{-1}$$

According to Eq. 101, $\Delta T_{fus} = K_f m = 1{\cdot}86\ \text{K kg mol}^{-1}\times0{\cdot}327\ \text{mol kg}^{-1} = 0{\cdot}61\ \text{K} = T_0 - T_f$

Hence, freezing point, $T_{fus} = 273\ \text{K} - 0{\cdot}61\ \text{K} = 272{\cdot}39\ \text{K} = -0{\cdot}61°\text{C}$

Example 17. A certain solution of benzoic acid in benzene boils at 82·6°C and freezes at 3·1°C. What information about the number of particles and the structure of benzoic acid at the two temperatures can be deduced from the above data ? The boiling point and freezing point of pure benzene are 80·1°C and 5·5°C, respectively. K_f = 5·12 K kg mol^{-1} ; K_b = 2·57 K kg mol^{-1}.

Solution : From freezing point data, the molality of the solution

$$m = \frac{\Delta T_{fus}}{K_f} = \frac{278\,\text{K} - 276{\cdot}1\,\text{K}}{5{\cdot}12\,\text{K kg mol}^{-1}} = 0{\cdot}468\ \text{mol kg}^{-1}$$

From boiling point data, the molality of the solution

$$m = \frac{\Delta T_b}{K_b} = \frac{355{\cdot}6\,\text{K} - 353{\cdot}1\,\text{K}}{2{\cdot}57\,\text{K kg mol}^{-1}} = 0{\cdot}972\ \text{mol kg}^{-1}$$

As can be seen, the molality of the solution at the freezing point is half of its molality at the boiling point. This means that the number of moles (and hence the number of particles) of benzoic acid at the freezing point is half of that at the boiling point. This is attributed to the fact that, at low temperature, benzoic acid exists as dimers, the structure of the dimer being

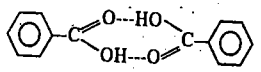

At high temperature, the dimers break up into monomers, thus, doubling the number of particles.

Example 18. At 25°C, the osmotic pressure of human blood due to the presence of various solutes in the blood is 7·65 atm. Assuming that molarity equals molality, calculate the freezing point of blood. K_f =1·86 K kg mol^{-1}.

Solution : According to the van't Hoff equation, $\Pi = cRT$

$$\therefore \quad c = \frac{\Pi}{RT} = \frac{7{\cdot}65\,\text{atm}}{(0{\cdot}0821\,\text{dm}^3\,\text{atm K}^{-1}\,\text{mol}^{-1})(298\,\text{K})} = 0{\cdot}313\ \text{mol dm}^{-3}$$

i.e., the concentration of various solutes present in blood = 0·313 mol dm^{-3}.

In the present case, as given, molality of solution = molarity of solution

$$\therefore \quad m = c = 0{\cdot}313\ \text{mol kg}^{-1}$$

$$\Delta T_{fus} = K_f m = 1{\cdot}86 \text{ K kg mol}^{-1} \times 0{\cdot}313 \text{ mol kg}^{-1} = 0{\cdot}582 \text{ K} = T_0 - T_f$$

or $$T_{fus} = T_0 - \Delta T_f$$

$\therefore$ Freezing point of blood, $T_{fus} = 273 \text{ K} - 0{\cdot}582 \text{ K} = 272{\cdot}418 \text{ K} = -0{\cdot}582°\text{C}$

Abnormal Results and the vant't Hoff Factor

Since colligative properties depend upon the number of particles (molecules or ions) of the solute, in some cases where the solute associates or dissociates in solution, abnormal results are obtained.

1. Association. There are many organic solutes which in non-aqueous solutions undergo association, that is, two or more molecules of the solute associate to form a bigger molecule. Thus, the number of effective molecules or particles decreases and, consequently, the osmotic pressure, the elevation of boiling point or the depression of freezing point is less than that calculated on the basis of single molecules. Two such examples are : acetic acid in benzene and chloroacetic acid in napthalene. The molar masses of solutes in such cases will be higher than the true molar masses as indicated by their formulae. Thus, the molar mass of acetic acid, CH_3COOH, in benzene, as determined from freezing point depression, is 118 instead of 60. It appears, therefore, that the molecules of acetic acid exist largely as $(CH_3COOH)_2$ when dissolved in benzene.

2. Dissociation. Inorganic acids, bases and salts in aqueous solutions undergo dissociation, that is, the molecules break down into positively and negatively charged ions. For instance, sodium chloride in aqueous solution exists almost entirely as Na^+ and Cl^- ions. In such cases, the number of effective particles increases and, therefore, osmotic pressure, elevation of boiling point and depression of freezing point are much higher than those calculated on the basis of undissociated single molecules.

The van't Hoff Factor. In order to account for all abnormal cases, van't Hoff introduced a factor i, known as the van't Hoff factor which is defined as

$$i = \frac{\text{Observed osmotic effect}}{\text{Normal osmotic effect}} \qquad ...(105)$$

The osmotic effect implies osmotic pressure, vapour pressure lowering, boiling point elevation and freezing point depression, as the case may be.

Since these properties vary inversely as the molar masses of the solutes, it follows that

$$i = \frac{\text{Normal molar mass}}{\text{Observed molar mass}} \qquad ...(106)$$

Degree of Association. By degree of association is meant the fraction of the total number of molecules which combine to form bigger molecules.

Consider one mole of a solute dissolved in a given volume of a solvent. Suppose, n simple molecules combine to form an associated molecule, *i.e.*, $nA \rightleftharpoons (A)_n$.

Let α be the degree of association. Then,

The number of unassociated moles $= 1 - \alpha$

The number of associated moles $= \alpha/n$

$\therefore$ The number of effective moles $= 1 - \alpha + \alpha/n$

Since osmotic effect is proportional to the number of moles, therefore, the van't Hoff factor i is given by

$$i = \frac{\text{Observed osmotic effect}}{\text{Calculated osmotic effect}} = \frac{1 - \alpha + (\alpha/n)}{1} \qquad ...(107)$$

Also vide Eq. 106, $$i = \frac{\text{Normal molar mass}}{\text{Observed molar mass}} = \frac{1 - \alpha + (\alpha/n)}{1} \qquad ...(108)$$

Thus, knowing n, *i.e.*, the number of simple molecules which combine to give one associated molecule and the observed osmotic effect or observed molar mass, the degree of association as well as the van't Hoff factor can be easily calculated.

Example 19. Acetic acid (CH_3COOH) associates in benzene to form double molecules. 1·65 g of acetic acid when dissolved in 100 g of benzene raised the boiling point by 0·36°C. Calculate the van't Hoff factor and the degree of association of acetic acid in benzene ($K_b = 2{\cdot}57$ K kg mol^{-1}).

Solution : Normal molar mass of acetic acid $= 60$ g mol^{-1}

$$\text{Observed molar mass of acetic acid, } M_2 = \frac{K_b w_2}{w_1 \Delta T_b}$$

$$= \frac{(2{\cdot}57 \text{ K kg mol}^{-1})\ (1{\cdot}65 \times 10^{-3} \text{ kg})}{(100 \times 10^{-3} \text{ kg}).(0{\cdot}36 \text{ K})} = 0{\cdot}1178 \text{ kg mol}^{-1} = 117{\cdot}8 \text{ g mol}^{-1}$$

$$i = \frac{\text{Normal molar mass}}{\text{Observed molar mass}} = \frac{60 \text{ g mol}^{-1}}{117{\cdot}8 \text{ g mol}^{-1}} = 0{\cdot}508$$

Since acetic acid associates to form double molecules, hence,

No. of moles before association} $\longrightarrow$ 1 0

$$2CH_3COOH \rightleftharpoons (CH_3COOH)_2$$

No. of moles after association $\longrightarrow$ $1 - \alpha$ $\alpha/2$

where α is the degree of association.

The number of unassociated moles $= 1 - \alpha$; the number of associated moles $= \alpha/2$

$\therefore$ The number of effective moles $= 1 - \alpha + \alpha/2$

Hence, vide Eq. 108, $$= \frac{\text{Normal molar mass}}{\text{Observed molar mass}} = \frac{1 - \alpha + \alpha/2}{1}$$

$$\frac{60 \text{ g mol}^{-1}}{117{\cdot}8 \text{ mol}^{-1}} = 1 - \alpha + \alpha/2$$

$$\therefore \quad \alpha = 0{\cdot}983$$

Degree of Dissociation. By degree of dissociation is meant the fraction of the total number of molecules which dissociate, that is, break into simpler molecules or ions. Consider one mole of a uni-univalent electrolyte like potassium chloride dissolved in a given volume of water. Let, α be its degree of dissociation.

Then the number of moles of KCl left undissociated will be $1-\alpha$. At the same time, α moles of K^+ ions and α moles of Cl^- ions will be produced, as shown below :

$$\underset{1-\alpha}{KCl} \rightleftharpoons \underset{\alpha}{K^+} + \underset{\alpha}{Cl^-}$$

Thus, the total number of moles after dissociation $= 1 - \alpha + \alpha + \alpha = 1 + \alpha$

Hence, $$\frac{\text{Observed osmotic effect}}{\text{Normal osmotic effect}} = \frac{1+\alpha}{1} \qquad ...(109)$$

Since, as already mentioned, osmotic effect implies osmotic pressure, vapour pressure lowering, boiling point elevation or freezing point depression and since these properties vary inversely as the molar mass of the solute, it follows that

$$M_{normal}/M_{observed} = (1 + \alpha)/1 \qquad ...(110)$$

Knowing the observed molar mass, the degree of dissociation α can be easily calculated.

Example 20. A 0·5 per cent aqueous solution of potassium chloride was found to freeze at – 0·24°C. Calculate the van't Hoff factor and the degree of dissociation of the solute at this concentration (K_f = 1·86 K kg mol^{-1}).

Solution : M_{normal} of potassium chloride = 74·5 g mol^{-1}

$$M_{observed} = \frac{K_f w_2}{w_1 \Delta T} = \frac{(1{\cdot}86 \text{ K kg mol}^{-1})(0{\cdot}5 \times 10^{-3} \text{ kg})}{(100 \times 10^{-3} \text{ kg})(0{\cdot}24 \text{ K})}$$

$$= 0{\cdot}03875 \text{ kg mol} = 38{\cdot}75 \text{ g mol}^{-1}$$

$$\text{van't Hoff factor, } i = M_{normal}/M_{observed} = \frac{74{\cdot}5 \text{ g mol}^{-1}}{38{\cdot}75 \text{ g mol}^{-1}} = 1{\cdot}92$$

Let α be the degree of dissociation of KCl. Then,

$$\underset{1-\alpha}{KCl} = \underset{\alpha}{K^+} + \underset{\alpha}{Cl^-}$$

The total number of moles after dissociation = 1 – α + α + α = 1 + α

$$\frac{\text{Normal molar mass}}{\text{Observed molar mass}} = \frac{1+\alpha}{1}$$

$$\frac{74{\cdot}5 \text{ g mol}^{-1}}{38{\cdot}75 \text{ g mol}^{-1}} = 1 + \alpha$$

Degree of dissociation, α = **0·923**

Example 21. The freezing point depression of a 1/200 molal solution of sodium sulphate (Na_2SO_4) in water was found to be 0·0265°C. Calculate the degree of dissociation of the salt at this concentration (K_f for water is 1·86 K kg mol^{-1}).

Solution : Normal molar mass of sodium sulphate = 142 g mol^{-1}

Molality of the solution = (1/200) mol kg^{-1}

= (142/200) g kg^{-1} = 0·71 g of solute per kg of solvent

Thus, $w_2 = 0{\cdot}71 \text{ g} = 0{\cdot}71 \times 10^{-3}$ kg and $w_1 = 1$ kg

$$\therefore \quad M_{obs} = \frac{(1{\cdot}86 \text{ K kg mol}^{-1})(0{\cdot}71 \times 10^{-3} \text{ kg})}{0{\cdot}0265 \text{ K} \times 1 \text{ kg}} = 0{\cdot}04983 \text{ kg mol}^{-1} = 49{\cdot}83 \text{ g mol}^{-1}$$

Let α be the degree of dissociation of Na_2SO_4. Then,

$$\underset{1-\alpha}{Na_2SO_4} \rightleftharpoons \underset{2\alpha}{2Na^+} + \underset{\alpha}{SO_4^{2-}}$$

$$\left.\begin{matrix}\text{The total number of moles}\\ \text{after dissociation}\end{matrix}\right\} = 1 - \alpha + 2\alpha + \alpha = 2\alpha$$

$$\frac{\text{Normal molar mass}}{\text{Observed molar mass}} = \frac{1+2\alpha}{1}$$

$$\frac{142 \text{ g mol}^{-1}}{49{\cdot}83 \text{ g mol}^{-1}} = 1 + 2\alpha$$

$$\therefore \quad \text{Degree of dissociation, } \alpha = \mathbf{0{\cdot}925}$$

Example 22. The complex compound $K_4[Fe(CN)_6]$ is 45% dissociated in 0·1 M aqueous solution of the complex at 27°C. What would be the osmotic pressure of the solution ?

Solution : If the complex $K_4[Fe(CN)_6]$ had not been dissociated, its **normal osmotic pressure** would have been given by the van't Hoff equation, *viz.*,

$$\Pi = cRT = (0{\cdot}1 \text{ mol dm}^{-3})(0{\cdot}08206 \text{ dm}^3 \text{ atm K}^{-1} \text{ mol}^{-1})(300 \text{ K}) = 2{\cdot}462 \text{ atm}$$

The complex, however, is dissociated in aqueous solution. If α is the degree of dissociation, then, the dissociation reaction may be represented as

$$\underset{1-\alpha}{K_4[Fe(CN)_6]} \rightleftharpoons \underset{4\alpha}{4K^+} + \underset{\alpha}{[Fe(CN)_6]^{4-}}$$

Number of moles after dissociation = 1 – α + 4α + α = 1 + 4α

Number of moles without dissociation = 1

Since osmotic pressure is directly proportional to the number of moles, hence

$$\Pi_{observed}/\Pi_{normal} = (1 + 4\alpha)/1$$

Since $\alpha = 0{\cdot}45$, hence,

$$\Pi_{observed} = 2{\cdot}462 \times (1 + 4 \times 0{\cdot}45)/1 = \mathbf{6{\cdot}894 \text{ atm}}$$

I. Review Questions

1. State and derive Raoult's law for vapour pressure lowering. How is it used for determining the molar mass of a nonvolatile compound ?
2. Explain the terms osmosis and osmotic pressure. Derive the van't Hoff equation for the osmotic pressure of a dilute solution. How is it used for determining molar mass of a solute ?
3. How are osmotic pressure measurements used for determining molar mass of a nonvolatile solute ? Define isotonic solutions.
4. Explain reverse osmosis. Discuss the various types of semipermeable membranes used for the process. What is the potential of this process for making sea water fit for drinking ?
5. Derive the relation between the boiling point elevation of a solution and the mole fraction of the dissolved solute. How is the expression used for determining molar mass of a nonvolatile solute ?
6. What is molal freezing point constant of a solvent ? Derive the relation between the freezing point depression of a solution and the mole fraction of the dissolved solute. How is this expression utilised for determining molar mass of a nonvolatile solute ?
7. Explain the conditions under which abnormal molar masses of solutes are obtained from the measurement of colligative properties of their solutions.
8. Show that the van't Hoff factor i and degree of association α of an electrolyte X in a solution are related by the expression $\alpha = (i - 1)/(1/n - 1)$.
9. Explain how the degree of dissociation of an electrolyte may be determined from the measurement of colligative properties of an aqueous solution of the electrolyte.
10. Show graphically how the molar mass of a non-volatile solute can be determined from osmotic pressure measurements.

II. Problems

1. When 2 g of a nonvolatile hydrocarbon were dissolved in 100 g of benzene, the vapour pressure of benzene at 20°C was lowered from 74·66 torr to 74·01 torr. Calculate the molar mass of the hydrocarbon. If the hydrocarbon contains 94·4% C, what is the molecular formula ? **[Ans. 179 g mol^{-1} ; $C_{14}H_{10}$]**
2. At 25°C the vapour pressure of pure water is 23·756 torr. Calculate the vapour pressure lowering and the vapour pressure of a solution containing 5·0 g of $C_{12}H_{22}O_{11}$ in 100·0 g of H_2O. **[Ans. 0·0622 torr ; 23·694 torr]**
3. Calculate the amount of sucrose (M=342 g mol^{-1}) that must be dissolved in 175 g of water at 40°C to lower the vapour pressure to 53·95 torr. The vapour pressure of pure water at this temperature is 55·32 torr. **[Ans. 84·5 g]**

4. Calculate the osmotic pressure of an aqueous solution containing 20 g of glucose per litre of the solution at 25°C. **[Ans. 2·718 atm]**

5. Calculate the osmotic pressure of an aqueous solution containing 1 g each of glucose and sucrose per litre at 27°C. **[Ans. 2·17 atm]**

6. A 5·13% of solution of sucrose is isotonic with a 0·9% solution of an unknown nonvolatile solute. Calculate the molar mass of the solute. **[Ans. 60 g mol^{-1}]**

7. The average osmotic pressure of human blood is 7·8 bar at 37°C. What is the concentration of an aqueous NaCl solution that could be used in the blood stream ? Assume ideal behaviour. **[Ans. 0·15 mol dm^{-3}]**

8. Calculate K_b for benzene, given that its normal boiling point is 80·15°C and ΔH_{vap} = 30·775 kJ mol^{-1} **[Ans. 2·63 K kg mol^{-1}]**

9. A solution of $3{\cdot}0\times10^{-4}$ kg of camphor ($C_{10}H_{16}O$) in $25{\cdot}3\times10^{-3}$ kg of chloroform boils at 61·3°C. If the boiling point of chloroform is 61·0°C, calculate K_b and ΔH_{vap} of chloroform. **[Ans. 3·83 K kg mol^{-1} ; 14·5 kJ mol^{-1}]**

10. A solution containing 2·5 g of a solute in 100 g of water, boiled at 100·25°C. Calculate the molar mass of the solute. K_b for water = 0·52 K kg mol^{-1} **[Ans. 52 g mol^{-1}]**

11. Calculate the molal freezing point depression constant of water if the enthalpy of fusion at the freezing point (0°C) is 333·86 J g^{-1}. **[Ans. 1·856 K kg mol^{-1}]**

12. 4 g of a nonvolatile solute were dissolved in 250 g of water. The depression in freezing point was found to be 0·087 K. Calculate the molar mass of the solute. For water K_f = 1·86 K kg mol^{-1}. **[Ans. 344·70 g mol^{-1}]**

13. A solution of 10 g of NaCl in 1 kg of water freezes at - 0·604°C. Calculate the degree of dissociation of NaCl in water. K_f = 1·86 K kg mol^{-1}. **[Ans. 91%]**

14. A solution of 0·3 g of benzoic acid in 20 g of benzene freezes at 0·317°C below the freezing point of the solvent. Calculate *(i)* the degree of association of benzoic acid assuming that the acid exists as a dimer in benzene and *(ii)* the apparent molar mass of the acid. K_f = 5·12 K kg mol^{-1} **[Ans. *(i)* 98·8% *(ii)* 241 g mol^{-1}]**

15. At 27°C, 10 g of a nonvolatile solute in 100 g of benzene lowers the vapour pressure of benzene by 8·8 torr. If the vapour pressure of pure benzene at 27°C is 121·8 torr, calculate the molar mass of the solute. **[Ans. 101 g mol^{-1}]**

16. Calculate the total vapour pressure lowering at 25°C for a solution containing 0·010 mole of sucrose and 0·015 mole of urea dissolved in 100 g of water. At 25°C, $P^{\circ}_{H_2O}$ = 23·756 torr. **[Ans. 0·11 torr]**

17. What mass of a solute having molar mass of 345 g mol^{-1} is needed to decrease the vapour pressure of 100 gram of water at 25°C by 1·00 torr ? At 25°C, $P^{\circ}_{H_2O}$ = 23·756 torr. **[Ans. 84·2 g]**

18. Calculate the osmotic pressure of an aqueous solution containing 1 g each of glucose and sucrose per litre at 27°C. **[Ans. 2·17 atm]**

19. For toluene, the boiling point elevation constant is 3·32 K mol^{-1}. Calculate the enthalphy of vaporization of toluene. The normal boiling point of toluene is 110·7°C. **[Ans. 33·9 kJ mol^{-1}]**

20. Calculate the molality of an aqueous solution that has a boiling point elevation of 1·00 K. For water, K_b = 0·52 K kg mol^{-1} **[Ans. 1·95 mol kg^{-1}]**

21. When 2·1035 g of a nonvolatile solute is dissolved in 70 g of the water, the boiling point is increased by 0·23°C. Calculate the molar mass of the solute. K_b = 0·52 K kg mol^{-1} **[Ans. 66·6 g mol^{-1}]**

22. 1·51 g of NaCl was dissolved in 500 g of water and the elevation in boiling point was observed to be 0·0514°C. Calculate the van't Hoff factor. K_b for water = 0·52 K kg mol^{-1} **[Ans. 0·937]**

23. The freezing point depression of a 0·001 molal aqueous solution of $K_x[Fe(CN)_6]$ is $7{\cdot}10\times10^{-3}$ K. Determine x. K_f = 1·86 K kg mol^{-1}.

24. When 36·0 g of a nonvolatile solute having the empirical formula CH_2O is dissolved in 1·20 kg of water, the solution freezes at - 0·93°C. What is the molecular formula of the compound ? **[Ans. $C_2H_4O_2$]**

CHAPTER 23

ELECTROCHEMISTRY—I. ELECTROLYTIC CONDUCTANCE AND TRANSFERENCE

Electrolytic Conductance. It is now well known that flow of electricity through solutions of electrolytes is due to the migration of ions when potential difference is applied between the two electrodes. The cations which are positively charged move towards the negatively charged electrode, known as **cathode** while the anions which are negatively charged move towards the positively charged electrode, called the **anode.** The ease with which electricity flows through a solution is called the **conductance** (G) of the solution. It is defined as the reciprocal of the resistance (R) of the solution, *i.e.*, $G = 1/R$.

It is expressed in the unit called reciprocal ohm (ohm^{-1} or Ω^{-1}). In SI system, the unit of conductance is Siemen, S.

Specific Conductance. The resistance of any conductor varies directly as its length (l) and inversely as its cross-sectional area (a), *i.e.*, $R \propto l/a$ or $R=\rho(l/a)$ where ρ is a constant depending upon the nature of the material and is called specific resistance of the material. If l=1 m and a=1 m^2, then $\rho=R$. Thus, **specific resistance** is defined as the resistance of a specimen 1 m in length and 1 m^2 cross-section. In other words, it is the resistance of one metre cube of the material.

The reciprocal of specific resistance, *i.e.*, $1/\rho$, is called **specific conductance.** This may be defined as the conductance of one metre cube of a material. It is generally denoted by κ. Thus, $\kappa = 1/\rho = (l/a)(1/R) = (l/a)\times$(conductance).

Since conductance is measured in S, length in m and area in m^2, hence $\kappa = S\times\dfrac{m}{m^2} = S\,m^{-1}$. Thus, the units of specific conductance are S m^{-1}.

Equivalent Conductance. Specific conductance, although a suitable property for characterising metallic conductance, is not so for characterising electrolytic conductance where the value, amongst other things, depends upon the concentration of the solution of the electrolyte as well. While measuring conductances of electrolytes in solutions, another quantity of much greater significance, known as **equivalent conductance,** is frequently used. It is defined as the conducting power of all the ions produced by one gram equivalent of an electrolyte in a given solution. It is denoted by Λ.

Relation Between Specific Conductance and Equivalent Conductance. In order to work out the relationship between specific conductance and equivalent conductance, imagine 1 m^3 of a solution of an electrolyte placed between two large electrodes 1 m apart. The cross-sectional area of the solution will be 1 m^2. The conductance of the solution will evidently be its specific conductance because we are having one metre cube of the solution. Further, suppose that 1 m^3 of the solution contains 1 gram equivalent of the electrolyte dissolved in it. Then, according to the definition given above, the conductance of the solution will be equal to the equivalent conductance, Λ. Thus, in this case,

Conductance (G) = Specific conductance (κ) = Equivalent conductance (Λ)

Suppose the solution is now diluted to 1000 cubic metres. We will be having now 1000 metre cubes of the solution. The conductance of the resulting solution, therefore, will be 1000 times its specific conductance. But even now, as the solution contains only 1 gram equivalent of the electrolyte between

the electrodes, the conductance measured will be the equivalent conductance. Thus, in this case,

$$\Lambda = 1000 \times \kappa$$

If the solution is further diluted to say, 5000 cubic metres, there will be 5000 meter cubes of the solution and hence the equivalent conductance of the resulting solution will be 5000 times its specific conductance. In general,

$$\Lambda = \kappa \times \phi \qquad ...(2)$$

where ϕ is the volume of the solution in cubic metres containing 1 gram equivalent of the electrolyte.

Since the units of specific conductance are S m^{-1} and the units of volume are m^3, hence the units of equivalent conductance are :

$$S\ m^{-1} \times m^3 = S\ m^2$$

Molar Conductance. It is customary to express electrolytic conductance in terms of molar conductance, which is defined as the conducting power of all the ions produced by one mole of the electrolyte in a given solution. It is denoted by Λ_m.

Let us consider a solution containing c moles of an electrolyte in one cubic metre of the solution. The volume of the solution containing 1 mole of the electrolyte would be $1/c$ cubic metre.

$$\Lambda_m = \text{conductance of 1 } m^3 \text{ of the solution} \times \text{volume of the solution in } m^3 \text{ containing 1 mole of the electrolyte}$$

$$= \text{specific conductance} \times 1/c$$

$$= \kappa/c \qquad ...(3)$$

Since units of κ are S m^{-1} and those of c are mol m^{-3}, hence the units of Λ_m are S m^2 mol^{-1}.

Cell Constant. The specific conductance, as already mentioned, is the conductance of one metre cube of the solution. Therefore, the conductance measured by using a conductivity cell (the one which is most commonly used is shown in Fig. 1) will be the specific conductance only if the electrodes are exactly 1 m^2 in area and 1 m apart. This is not usually the case. The conductance obtained will, therefore, have to be multiplied by a certain factor in order to get the specific conductance. This factor is called the **cell constant,** K_{cell}. Since $\kappa = (l/a) \times$ conductance, hence, the conductance measured in a cell has to be multiplied by a factor l/a in order to get the specific conductance. Evidently, the factor l/a is the cell constant; l is the distance in m between the electrodes and a is the cross-sectional area of the electrodes in m^2. Obviously, the unit of cell constant is m^{-1}.

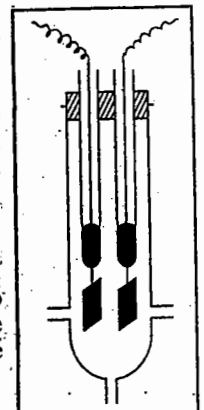

Fig. 1. A conductivity cell.

Example 1. Specific conductance of a decimolar solution of potassium chloride at 18°C is 1·12 S m^{-1}. The resistance of a conductivity cell containing the solution at 18°C was found to be 55 ohm. What is the cell constant ?

Solution : $R = 55\ \Omega$; $G = (1/55)$ S ; $\kappa = 1{\cdot}12$ S m^{-1}.

$$\therefore \quad K_{cell} = \kappa/G = 1{\cdot}12\ S\ m^{-1}/(1/55)\ S = 61{\cdot}6\ m^{-1}$$

Example 2. The resistance of 0·01 M solution of an electrolyte was found to be 210 ohm at 25°C. Calculate the molar conductance of the solution at 25°C. Cell constant = 0·88 cm^{-1}.

Solution : $R = 210\ \Omega$; $G = (1/210)$ S ; $K_{cell} = 0{\cdot}88\ cm^{-1} = 88\ m^{-1}$

$$\kappa = \text{cell constant} \times \text{conductance} = 88\ m^{-1} \times (1/210)\ S$$

$$= 0{\cdot}419\ S\ m^{-1}$$

Concentration of the solution, $c = 0{\cdot}01$ mol $dm^{-3} = 10$ mol m^{-3}

$$\therefore \quad \Lambda_m = \kappa/c = 0{\cdot}419\ S\ m^{-1}/10\ mol\ m^{-3} = 0{\cdot}0419\ S\ m^2\ mol^{-1}$$

Example 3. The resistance of 0·5 M solution of an electrolyte in a cell was found to be 45 Ω. Calculate the molar conductance of the solution if the electrodes in the cell are 2·2 cm apart and have an area of 3·8 cm^2.

Solution : $R = 45\ \Omega$; $\therefore$ $G = (1/45)$ S

$$K_{cell} = l/a = 2{\cdot}2\ cm/3{\cdot}8\ cm^2 = 0{\cdot}5789\ cm^{-1} = 57{\cdot}89\ m^{-1}$$

$$\kappa = 57{\cdot}89\ m^{-1} \times (1/45)\ S = 1{\cdot}286\ S\ m^{-1}$$

$$c = 0{\cdot}5\ mol\ dm^{-3} = 500\ mol\ m^{-3}$$

$$\Lambda_m = \kappa/c = 1{\cdot}286\ S\ m^{-1}/500\ mol\ m^{-3} = 25{\cdot}72 \times 10^{-4}\ S\ m^2\ mol^{-1}$$

Example 4. The specific conductance of water is $7{\cdot}6 \times 10^{-2}$ S m^{-1} and the specific conductance of 0·1 M aqueous solution of KCl is 1·1639 S m^{-1}. A cell has a resistance of 33·20 Ω when filled with 0·1 M KCl solution and 300 Ω when filled with 0·1 M acetic acid solution. Calculate the molar conductance of acetic acid.

Solution : $\kappa = K_{cell}/R$, *i.e.*, $\kappa \propto 1/R$. Thus, we have

$$\frac{\kappa(CH_3COOH)}{\kappa(KCl)} = \frac{R(KCl)}{R(CH_3COOH)}$$

Now, $R(KCl) = 33{\cdot}20\ \Omega$; $R(CH_3COOH) = 300\ \Omega$; $\kappa(KCl) = 1{\cdot}1639$ S m^{-1}

$$\therefore \quad \kappa(CH_3COOH) = \frac{(33{\cdot}20\ \Omega) \times (1{\cdot}1639\ S\ m^{-1})}{300\ \Omega} = 0{\cdot}129\ S\ m^{-1}$$

It should be noted that $\kappa(CH_3COOH)$ contains a contribution of $7{\cdot}6 \times 10^{-2}$ S m^{-1} due to water.

Hence, specific conductance due to $CH_3COOH = 0{\cdot}129\ S\ m^{-1} - 7{\cdot}6 \times 10^{-2}\ S\ m^{-1} = 5{\cdot}3 \times 10^{-2}\ S\ m^{-1}$

$$\therefore \quad \Lambda_m(CH_3COOH) = \frac{\kappa}{c} = \frac{5{\cdot}3 \times 10^{-2}\ S\ m^{-1}}{0{\cdot}1 \times 10^3\ mol\ m^{-3}} = 5{\cdot}3 \times 10^{-4}\ S\ m^2\ mol^{-1}$$

Variation of Molar Conductance with Dilution. Molar conductance of an electrolyte increases with increase in dilution. This was attributed to increase in the degree of dissociation of the electrolyte. We define **degree of dissociation** as the fraction of the total electrolyte in solution which exists in the form of its ions. In other words, on dilution the same amount of electrolyte is capable of furnishing a larger number of ions. It any be pointed out, however, that increase in the number of ions on dilution is much less than increase in the volume of the solution. Therefore, the number of ions per unit volume (*e.g.*, per c.c.) actually decreases. Hence, the specific conductance decreases although the molar conductance increases on progressive dilution.

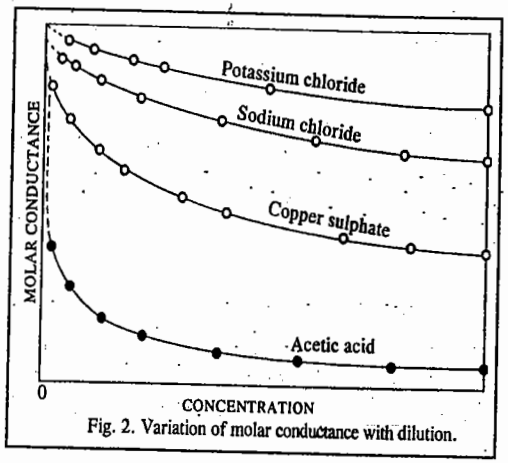

Fig. 2. Variation of molar conductance with dilution.

The variation of molar conductance with dilution in some common electrolytes is shown in Fig. 2. As can be seen, in strong electrolytes there is a tendency for molar conductance to approach a certain limiting value when the concentration approaches zero. The molar conductance at this point is known as **molar conductance at zero concentration** or **at infinite dilution.** It is denoted by Λ_m°.

It may be made clear that by infinite dilution is meant a solution so dilute that it has maximum or limiting molar conductance which does not increase on further dilution. This value, in the case of strong electrolytes, is obtained by extrapolating the molar conductance graph to zero concentration. In the case of weak electrolytes, however, there is no indication that a limiting value can be attained

even when the concentration approaches zero (cf. graph for acetic acid). It is not safe, therefore, to obtain the limiting value by extrapolation in the case of weak electrolytes. There is an indirect method for obtaining molar conductance at infinite dilution for weak electrolytes which is based on Kohlraush's law. This will be discussed a little later in this chapter.

Assuming that increase in molar conductance on dilution is due only to increase in the degree of dissociation of the electrolyte, it is evident that when limiting value of molar conductance is approached, the degree of dissociation is unity. Therefore, at any other concentration, when the molar conductance is, say, Λ_m, the degree of dissociation (α) will be given by

$$\alpha = \Lambda_m/\Lambda_m^\circ \qquad ...(4)$$

Example 5. The specific conductance of 0·01 M solution of acetic acid was found to be 0·0163 S m^{-1} at 25°C. Calculate the degree of dissociation of the acid. Molar conductance of acetic acid at infinite dilution is 390·7×10^{-4} S m^2 mol^{-1} at 25°C.

Solution :

$$\kappa = 0{\cdot}0163 \text{ S m}^{-1};\quad c = 0{\cdot}01 \text{ mol dm}^{-3} = 10 \text{ mol m}^{-3}$$

$$\Lambda_m = \frac{\kappa}{c} = \frac{0{\cdot}0163 \text{ S m}^{-1}}{10 \text{ mol m}^{-3}} = 16{\cdot}3 \times 10^{-4} \text{ S m}^2 \text{ mol}^{-1}$$

$$\Lambda_m^\circ = 390{\cdot}7\times10^{-4} \text{ S m}^2 \text{ mol}^{-1} \text{ (given)}$$

$$\alpha = \frac{\Lambda_m}{\Lambda_m^\circ} = \frac{16{\cdot}3\times10^{-4}\text{ S m}^2\text{ mol}^{-1}}{390{\cdot}7\times10^{-4}\text{ S m}^2\text{ mol}^{-1}} = 0{\cdot}0472$$

Ionic Mobility. Although, at infinite dilution, all electrolytes are completely dissociated, their molar conductances differ vastly from one another. This has been attributed to differences in the speeds of the ions. For example, the molar conductance at infinite dilution of hydrochloric acid is more than three times as high as that of sodium chloride. Since chloride ion is common, it follows that the speed of hydrogen ion is more than three times the speed of sodium ion.

Since the speed of an ion varies with the potential applied, it is better to use the term **ionic mobility** which is defined as the distance travelled by an ion per second under a potential gradient of 1 volt per metre. Potential gradient is given by the potential difference applied at the electrodes divided by the distance between the electrodes.

Example 6. A potential of 12·0 volts was applied to two electrodes placed 20 cm apart. A dilute solution of ammonium chloride was placed between the electrodes when NH_4^+ ion was found to cover a distance of 1·60 cm in one hour. What is the mobility of NH_4^+ ion ?

Solution :

Distance travelled by NH_4^+ ion in 1 hour $= 1{\cdot}60\times10^{-2}$ m

$\therefore$ Distance travelled by NH_4^+ ion per second $= \dfrac{1{\cdot}60\times10^{-2}}{3600}$ m

$$\text{Potential gradient} = 12/20 \text{ V cm}^{-1} = \frac{12\times100}{20} \text{ V m}^{-1}$$

$$\therefore \text{ Mobility of } NH_4^+ \text{ ions} = \frac{\text{Speed}}{\text{Potential gradient}} = \frac{(1{\cdot}60\times10^{-2}/3600) \text{ m s}^{-1}}{(12\times100/20)\text{ V m}^{-1}} = 7{\cdot}41\times10^{-8} \text{ m}^2 \text{ V}^{-1} \text{ s}^{-1}$$

As can be seen, the ionic mobility is extremely small as compared to the speed of gaseous molecules which is about 10^2 m s^{-1}. The low mobility of ions is due to the fact that there are frequent collisions between the ions and the solvent molecules since the mean free path of molecules in liquids is very small.

Lithium and sodium ions have comparatively lower ionic mobilities. This is due to the hydration of ions as a result of higher charge density around these ions because of their smaller radii. The higher charge density causes these ions to be more highly hydrated by ion–dipole interactions than the larger ions. Since a hydrated ion has to drag along a shell of water as it moves through the solution, its mobility is naturally less than that of an unhydrated ion.

The ionic mobility of H^+ ion is found to be five to ten times that of other ions, except OH^- ion. The hydrogen ion, because of its small size and, therefore, high charge density, is heavily hydrated. Experimental evidence suggests that H^+ ion in aqueous solution is hydrated to form $H_9O_4^+$ ion, *i.e.*, a trihydrate of hydronium ion, *viz.*, $H_3O^+.3H_2O$, having the following structure :

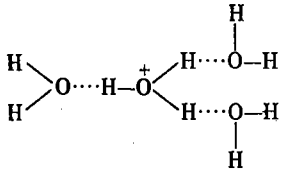

This structure, because of its large size and shape, should predict the mobility of H^+ ion to be low rather than high. The high mobility of H^+ ions in hydroxylic solvents such as H_2O can be explained by **Grotthus type mechanism** in which a proton moves rapidly from H_3O^+ to a hydrogen-bonded water molecule and is transferred further along a series of hydrogen-bonded water molecules by a rearrangement of hydrogen bonds, as illustrated in Fig. 3. This accounts for the high mobility of H^+ ions in water.

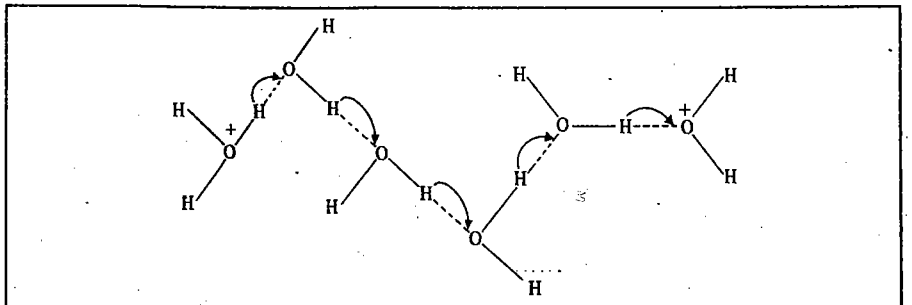

Fig. 3. Grotthus-type mechanism for the high mobility of H^+ ions.

The above model also explains as to why H^+ ions move about 50 times more rapidly through ice than through liquid water. Ice has a tetrahedral structure with each oxygen atom surrounded by four oxygen atoms at a distance of 276 pm. Each hydrogen atom lies on the line joining the centres of the oxygen atoms. Thus, when the water molecules are oriented properly, as in case of ice, the hydrogen ions can move very rapidly through its tetrahedral structure.

It may be mentioned that ionic mobilities increase with increase in temperature, the temperature coefficients being very nearly the same for all ions in a given solvent. Thus, ionic mobilities increase by about 2% per degree in the vicinity of 25°C.

DISCHARGE OF IONS ON ELECTROLYSIS. HITTORF'S THEORETICAL DEVICE

It looks surprising at first sight that although most of the ions differ largely in their mobilities, yet their equal numbers are known to be discharged, on electrolysis, at the appropriate electrodes. Hittorf explained this anomaly by means of a theoretical device represented in Fig. 4. *V* is the vessel containing the solution of an electrolyte giving equal number of positive and negative ions of

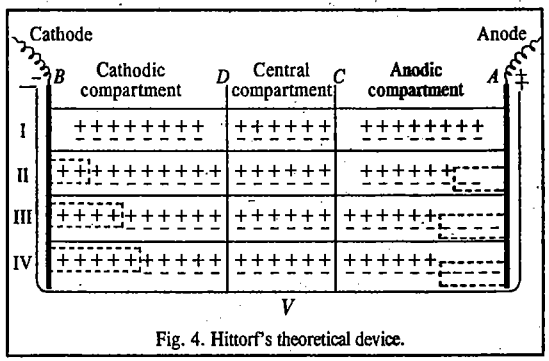

Fig. 4. Hittorf's theoretical device.

the *same* valency. The two metal electrodes *A* and *B* represent the anode and cathode, respectively. The vessel is supposed to be divided into three compartments by putting imaginary partitions at *C* and *D* which are permeable to ions. The three imaginary chambers, *AC*, *CD* and *DB* are termed anodic, central and cathodic compartments, respectively.

Before electrolysis, the position of the solution is represented as at I in the figure. There are, say, 8 pairs of positive and negative ions in the anodic and cathodic compartments and 6 pairs in the central compartment.

Now, suppose that on applying potential, only cations are capable of moving and that in a given time, two of the cations move towards the cathode. The condition will then be as represented in the figure at II. There will be two unpaired cations in the cathodic compartment. There will also be two unpaired anions left in the anodic compartment. As unpaired ions always get discharged at the respective electrodes (by the gain or loss of electrons as the case may be), two cations will be discharged at the cathode and two anions would be discharged at the anode. Thus, the same number of cations and anions will be discharged at the cathode and the anode, respectively, even though only cations were able to move.

Now, suppose that both cations and anions can move and that both have the same speed. Thus, if two cations move towards the cathode, two anions will move towards the anode in the same time. The state of affairs will now be represented as at III. Now four cations and four anions, *i.e.*, the same number, will be discharged at the respective electrodes.

Finally, suppose that cations and anions move with different speed so that if in a given time two cations move towards the cathode, three anions move towards the anode. In this case, too, the same number, *i.e.*, five unpaired cations and five unpaired anions will be discharged at the respective electrodes, as shown at IV. In the above illustration, the concentration of the central compartment has remained constant. This condition is realised in practice provided the current strength is small and there are no temperature variations.

Transport Number. From the above discussion of the Hittorf's theoretical device, it is also evident that the number of ions discharged at each electrode depends upon the sum of the speeds or mobilities of the two ions. For instance, in the first case (Fig. 4, II) when only two cations could move in a given time, the number of ions discharged at each electrode was also two. In the last case, when two cations and three anions moved in a given time, the number of ions discharged at each electrode was equal to five.

Since according to Faraday's first law of electrolysis, the number of ions discharged at an electrode is proportional to the total quantity of electricity passed through the solution, hence it follows that

$$\left.\begin{matrix}\text{Total quantity of electricity that}\\ \text{passes through the solution}\end{matrix}\right\} \propto \text{sum of the mobilities of the ions}$$

$$\left.\begin{matrix}\text{The quantity of electricity}\\ \text{carried by a particular ions}\end{matrix}\right\} \propto \text{the mobility of that particular ion}$$

The fraction of the total current carried by each ion is called its **transport number.** Thus, if u_+ is the mobility of cation and u_- that of the anion, then

$$\text{Transport number of the cation, } t_+ = \frac{\text{Current carried by the cation}}{\text{Total current}} = \frac{u_+}{u_+ + u_-} \qquad \ldots(5)$$

$$\text{Similarly, transport number of the anion, } t_- = u_-/(u_+ + u_-) \qquad \ldots(6)$$

Further, since $t_+ + t_- = 1$, it follows that if the transport number of one of the ions is known, that of the other can be easily calculated.

By means of the Hittorf's theoretical device described above, it is also possible to show that

$$\frac{\text{Mobility of cation}}{\text{Mobility of anion}} = \frac{\text{Fall of concentration round anode}}{\text{Fall of concentration round cathode}}$$

For example, in the last case considered above (Fig. 4, IV), two cations moved towards the cathode while three anions moved towards the anode in the same time. Thus, mobility of cations/mobility of anions is 2/3. As can be seen from the figure, the concentration round anode has fallen by two (from 8 to 6 ions) while that round cathode has fallen by three (8 to 5 ions). Thus, the fall of concentration round anode/fall of concentration round cathode is also 2/3.

Determination of Transport Number. 1. Hittorf's Method. This method is based on concentration changes observed in the vicinity of the electrodes. As mentioned above,

$$\frac{\text{Mobility of cation } (u_+)}{\text{Mobility of anion } (u_-)} = \frac{\text{Fall of concentration round anode}}{\text{Fall of concentration round cathode}}$$

and transport number of cation, $t_+ = u_+/(u_+ + u_-)$. (Eq. 5)

It follows, therefore, that

$$t_+ = \frac{\text{Fall of concentration round anode}}{\text{Fall of concentration round anode + Fall of concentration round cathode}}$$

$$= \frac{\text{Fall of concentration round anode}}{\text{Total fall of concentration}} \qquad \ldots(7)$$

If concentrations are measured in terms of gram equivalents, then

$$t_+ = \frac{\text{Number of gram equivalents lost from the anodic compartment}}{\text{Total number of gram equilvalents lost from both the compartments}}$$

But, total number of gram equivalents lost from both the compartments is equal to the number of gram equivalents deposited on each electrode. This can be shown by referring to Hittorf's theoretical device once again. It will be seen that in each case considered, the total number of ions lost from the anodic and the cathodic compartments put together is invariably equal to the number of ions discharged or deposited on each electrode.

$$\therefore \quad t_+ = \frac{\text{Number of gram equivalents lost from the anodic compartment}}{\text{Number of gram equivalents deposited on each electrode}}$$

Since, according to Faraday's second law, the number of gram equivalents deposited on each electrode must be equal to the number of gram equivalents of copper deposited in a copper coulometer by the same quantity of electricity, it is more convenient to include a copper coulometer in series with the experimental solution and to find out the mass of the copper deposited on the cathode. Then,

$$t_+ = \frac{\text{Number of gram equivalents lost from the anodic compartment}}{\text{Number of gram equivalents of copper deposited in the coulometer}}$$

Also, since $t_+ + t_- = 1$, $t_- = 1 - t_+$

Example 6. A decinormal solution of silver nitrate was elecrolysed between platinum electrodes. After passing a small current for two hours, a fall of concentration of 0·0005124 gram equivalent occurred in the anodic solution. The mass of copper deposited in a copper coulometer placed in series was found to be 0·03879 gram. Calculate the transport numbers of silver and nitrate ions in silver nitrate. (Equivalent mass of copper = 31·8).

Solution : Fall of concentration round the anode = 0·0005124 g equivalent

Mass of copper deposited in the copper coulometer = 0·03879 g

$\therefore$ Gram equivalent of copper deposited in the coulometer $= \frac{0{\cdot}03879}{31{\cdot}8} = 0{\cdot}0012190$

Transport number of Ag^+ ion, t_+, is given by

$$t_+ = \frac{\text{Gram equiv of silver ions lost from the anode}}{\text{Gram equiv of copper deposited in the coulometer}} = \frac{0{\cdot}0005124}{0{\cdot}0012190} = \mathbf{0{\cdot}4203}$$

$\therefore$ Transport number of NO_3^- ion, $t_- = 1 - t_+ = 1 - 0{\cdot}4203 = \mathbf{0{\cdot}5797}$

Example 7. A solution of silver nitrate was electrolysed between silver electrodes. Before electrolysis, 10 gram of the solution contained 0·01788 gram of silver nitrate. After the experiment, 20·09 gram of the anodic solution contained 0·06227 gram of silver nitrate. At the same time, 0·009479 gram of copper was deposited in the copper coulometer placed in series. Calculate the transport number of silver and nitrate ions. (Ag = 108, Cu = 63·6).

Solution :

(*i*) *After Electrolysis* :

20·09 g of the anodic solution contained 0·06227 g of $AgNO_3$.

$\therefore$ Mass of water in the solution = 20·09 − 0·06227 = 20·02773 g

Thus, 20·02773 g of water is associated with 0·06227 g of $AgNO_3$

$$= \frac{0{\cdot}06227}{170} = 0{\cdot}0003663 \text{ gram equiv of } AgNO_3 \text{ or of } Ag^+ \text{ ions}$$

(*ii*) *Before Electrolysis* :

10·00 g of the solution contained 0·01788 g of $AgNO_3$.

$\therefore$ Mass of water in the solution = 10·00 − 0·01788 = 9·98212 g

Thus, 9·98212 g of water is associated with 0·01788 g of $AgNO_3$.

$\therefore$ 20·02773 g of water will be associated with

$$\frac{0{\cdot}01788 \times 20{\cdot}20773}{9{\cdot}98212} = 0{\cdot}03588 \text{ g of } AgNO_3$$

$$= \frac{0{\cdot}03588}{170} = 0{\cdot}0002111 \text{ gram equiv of } AgNO_3 \text{ or of } Ag^+ \text{ ions}$$

(*iii*) Increase in concentration of Ag^+ ions in the anodic solution

$$= 0{\cdot}0003663 - 0{\cdot}0002111 = 0{\cdot}0001552 \text{ gram equiv}$$

(*iv*) Mass of copper deposited in the copper coulometer

$$= 0{\cdot}009479 \text{ g} = 0{\cdot}009479/31{\cdot}8 = 0{\cdot}0002981 \text{ gram equiv}$$

(*v*) If no Ag^+ ions had migrated from the anode, the increase in concentration of Ag^+ ions in the anodic solution should have been 0·0002981 gram equiv because gram equiv of copper deposited in the copper coulometer is equal to the gram equiv of silver dissolved from the anode of the cell by the action of nitrate ions.

But actual increase in the concentration of Ag^+ ions in the anodic solution = 0·0001552 gram equiv

(*iv*) $\therefore$ Fall of concentration of Ag^+ ions round the anode

$$= 0{\cdot}0002981 - 0{\cdot}0001552 = 0{\cdot}0001429 \text{ gram equiv}$$

(*vii*) Transport number of Ag^+ ion,

$$t_+ = \frac{\text{Gram equiv of } Ag^+ \text{ ions lost from the anodic chamber}}{\text{Gram equiv of copper deposited in the coulometer}} = \frac{0{\cdot}0001429}{0{\cdot}0002981} = \mathbf{0{\cdot}4794}$$

Transport number of NO_3^- ion, $t_- = 1 - 0{\cdot}4794 = \mathbf{0{\cdot}5206}$

It may be emphasised that transport number of an ion does not depend upon the mobility of that ion alone. It also depends upon the mobility of the other ion with which it is associated because, by definition,

$$t_+ = u_+/(u_+ + u_-) \qquad \text{(Eq. 5)}$$

and

$$t_- = u_-/(u_+ + u_-) \qquad \text{(Eq. 6)}$$

For example, the transport number of chloride ion in sodium chloride is 0·604 whereas in hydrochloric acid it is 0·166. The reason is that the mobility of hydrogen ion is much greater than that of sodium ion. Therefore, the denominator $(u_+ + u_-)$ in Eq. 6 in the case of hydrochloric acid is much greater than that in the case of sodium chloride while the numerator, u_-, *i.e.*, the mobility of the chloride ion, is the same in each case.

2. Moving Boundary Method. The moving boundary method rests on the direct observation of migration of ions in an electric field. The principle may be explained with reference to determination of transport number of H^+ ions in hydrochloric acid. The conductivity cell, in this method, consists of a vertical tube of uniform bore filled with cadmium chloride and hydrochloric acid, as shown in Fig. 5.

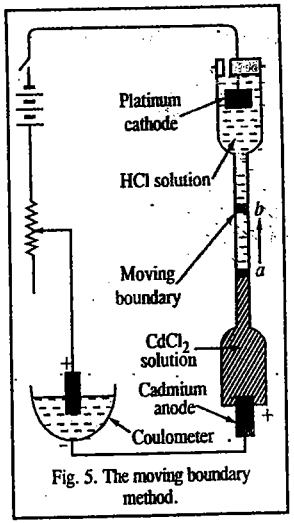

Fig. 5. The moving boundary method.

Hydrochloric acid is the *principal electrolyte* while cadmium chloride serves as the *indicator electrolyte* to enable formation of a boundary. The concentrations of the solutions are so adjusted that hydrochloric acid solution is lighter than the cadmium chloride solution and, therefore, floats over the cadmium chloride solution. A sharp boundary appears between the two solutions. The selection of the indicator electrolyte has to be made carefully. Its cation should not move faster than the cation whose transport number is to be determined and it should have the same anion as the principal electrolyte. Cadmium chloride fulfils both these requirements. The mobility of cadmium ion is less than that of hydrogen ion and it has a common anion with hydrochloric acid.

The *anode* at the bottom is of cadmium metal while the *cathode* at the top is a platinum foil. When a small current is passed through the conductivity cell, the chloride ions move towards the anode while hydrogen ions followed by cadmium ions move towards the cathode. The boundary separating the two solutions moves upwards as indicated by an arrow in the figure.

If the boundary moves through a distance l cm (say, from aa' to bb') then the volume of the liquid that has moved up is lA cm^3 where A is the cross-sectional area of the tube in cm^2. Let the concentration of the acid be c gram equivalents per litre. Then the number of gram equivalents of H^+ ions carried towards the cathode $= lAc/1000$. Since each gram equivalent carries one faraday of electricity, the electricity carried by H^+ ions $= lAc/1000$ faradays.

Suppose the total quantity of electricity that flows in the same time, as measured in a coulometer, is equal to Q faradays. Then,

$$\text{transport number of } H^+ \text{ ions} = \frac{lAc}{1000Q}$$

Example 8. Calculate the transport numbers of H^+ ions and Cl^- ions from the following data obtained by the moving boundary method using cadmium chloride as the indicator electrolyte :

Concentration of HCl solution	**= 0·100 N**
Mass of silver deposited in the coulometer	**= 0·1209 g**
Movement of boundary	**= 7·50 cm**
Cross-section of the tube	**= 1·24 cm^2**

Solution : Transport number of H^+ ions $= lAc/(1000Q)$

$l = 7{\cdot}50$ cm, $A = 1{\cdot}24$ cm^2, $c = 0{\cdot}1$ gram equiv dm^{-3}

Mass of silver deposited in the coulometer = 0·1209 g

We may first calculate Q, the quantity of electricity that flows in the circuit.

$$Q = \frac{0{\cdot}1209}{108} F$$

$\therefore$ Transport number of H^+ ion $= \dfrac{lAc}{1000Q} = \dfrac{7{\cdot}5 \times 1{\cdot}24 \times 0{\cdot}1 \times 108}{1000 \times 0{\cdot}1209} = \mathbf{0{\cdot}8308}$

Transport number of Cl^- ion $= 1 - 0{\cdot}8308 = \mathbf{0{\cdot}1692}$

Kohlrausch's Law

The molar conductances at infinite dilution of some pairs of electrolytes having the same cation or the same anion are given in Table 1.

TABLE 1
Molar Conductances at Infinite Dilution at 18°C

Pairs of electrolytes with the same anions	$\Lambda_m^\circ/10^{-4}$ (S m^2 mol^{-1})	Difference/10^{-4} (S m^2 mol^{-1})	Pairs of electrolytes with the same cations	$\Lambda_m^\circ/10^{-4}$ (S m^2 mol^{-1})	Difference/10^{-4} (S m^2 mol^{-1})
KF	129·21	23·42	KCl	149·86	20·62
NaF	105·79		KF	129·21	
KCl	149·86	23·41	NaCl	126·45	20·66
NaCl	186·45		NaF	105·79	
KNO_3	144·96	23·41	KNO_3	144·96	27·40
$NaNO_3$	121·55		KIO_3	117·56	
KIO_3	117·56	23·41	$NaNO_3$	121·55	27·40
$NaIO_3$	94·15		$NaIO_3$	94·15	

It is evident that the replacement of potassium ion by sodium ion in any of the electrolytes always produces the same difference ($23{\cdot}4\times10^{-4}$ S m^2 mol^{-1}) in molar conductance at infinite dilution, irrespective of the nature of the anion. Similarly, the replacement of chloride ion by fluoride ion or the replacement of nitrate ion by iodate ion produces the same difference in molar conductance at infinite dilution, irrespective of the nature of the cation. In other words, the difference in the conductances of any two cations appears to be about the same, irrespective of the nature of the anion with which they are associated. Similarly, the difference in the molar conductances at infinite dilution of any two anions is always about the same irrespective of the nature of the cation with which they are associated. This led Kohlrausch to state that

At infinite dilution, when dissociation is complete, each ion makes a definite contribution towards molar conductance of the electrolyte irrespective of the nature of the other ion with which it is associated and that the molar conductance at infinite dilution for any electrolyte is given by the sum of the contributions of the two ions. This is known as **Kohlrausch's law**. Thus,

$$\Lambda_m^\circ = \lambda_+^\circ + \lambda_-^\circ \qquad ...(8)$$

where λ_+° is the contribution of the cation and λ_-° is the contribution of the anion towards the molar conductance at infinite dilution. These contributions are called **molar ionic conductances at infinite dilution.** Thus, λ_+° is the molar ionic conductance of cation and λ_-° is the molar ionic conductance of anion, at infinite dilution.

Calculation of Molar Ionic Conductances. By combining Kohlrausch's law with the results of transport number measurements, it has been possible to calculate the molar ionic conductances at infinite dilution. For this purpose, Eq. 5 may be written as

$$t_+^\circ = u_+^\circ/(u_+^\circ + u_-^\circ) \qquad ...(9)$$

where t_+°, u_-° and u_+° represent, respectively, the transport number of the cation, the mobility of the anion and the mobility of the cation, at infinite dilution. Since $\lambda^\circ \propto u^\circ$, hence

$$\therefore \quad t_+^\circ = \lambda_+^\circ/(\lambda_+^\circ + \lambda_-^\circ) \qquad ...(10)$$

But $\lambda_+^\circ + \lambda_-^\circ = \Lambda_m^\circ$ (Kohlraush's law)

$$\therefore \quad t_+^\circ = \lambda_+^\circ/\Lambda_m^\circ \qquad ...(11)$$

Knowing* t_+° and Λ_m°, λ_+° can be easily calculated.

It readily follows that $t_-^\circ = \lambda_-^\circ/\Lambda_m^\circ$ ...(12)

Suppose it is required to determine molar ionic conductance of an anion like CH_3COO^-. The transport number of this ion at infinite dilution in sodium acetate is determined first ; it is 0·44. The molar conductance of sodium acetate at infinite dilution, determined by extrapolation, is $90{\cdot}9\times10^{-4}$ S m^2 mol^{-1}. Therefore,

$$0{\cdot}44 = \frac{\lambda_-^\circ}{90{\cdot}9\times10^{-4}\ \text{S m}^2\ \text{mol}^{-1}}$$

Hence, $\lambda_-^\circ = 0{\cdot}44\times90{\cdot}9\times10^{-4} = 39{\cdot}996\times10^{-4}$ S m^2 mol^{-1}

Molar ionic conductances of some ions at infinite dilution are given in Table 2.

TABLE 2
Molar Ionic Conductances at Infinite Dilution at 25°C

Cation	$\lambda_+^\circ/10^{-4}$ (S m^2 mol^{-1})	Anion	$\lambda_-^\circ/10^{-4}$ (S m^2 mol^{-1})
H^+	349·83	Cl^-	76·34
Na^+	50·11	Br^-	78·40
K^+	73·52	I^-	76·80
Li^+	38·70	OH^-	198·50
NH_4^+	73·40	NO_3^-	71·44
Ag^+	61·92	HCO_3^-	44·50
Ba^{2+}	127·30	SO_4^{2-}	159·60
Ca^{2+}	104·00	CH_3COO^-	40·89

Example 9. For the strong electrolytes NaOH, NaCl and $BaCl_2$, the molar ionic conductances at infinite dilution are $248{\cdot}1\times10^{-4}$, $126{\cdot}5\times10^{-4}$ and $280{\cdot}0\times10^{-4}$ S m^2 mol^{-1}, respectively. Calculate Λ_m° for $Ba(OH)_2$.

Solution : $BaCl_2 + 2NaOH \longrightarrow Ba(OH)_2 + 2NaCl$

Thus, according to Kohlrausch's law of independent migration of ions,

$$\Lambda^\circ_{mBa(OH)_2} = \Lambda^\circ_{mBaCl_2} + 2\Lambda^\circ_{mNaOH} - 2\Lambda^\circ_{mNaCl}$$

$$= (280 + 2\times248{\cdot}1 - 2\times126{\cdot}5)\times10^{-4}\ \text{S m}^2\ \text{mol}^{-1}$$

$$= \mathbf{523{\cdot}2\times10^{-4}\ S\ m^2\ mol^{-1}}$$

Example 10. The molar ionic conductance at infinite dilution of lithium halide (LiX) is found to be $89{\cdot}2\times10^{-4}$ S m^2 mol^{-1}. What would be the molar ionic conductance of the halide ion if the molar ionic conductance of Li^+ ion is $38{\cdot}70\times10^{-4}$ S m^2 mol^{-1} ?

Solution : According to Kohlrausch's law

$$\Lambda_m^\circ = \lambda_+^\circ + \lambda_-^\circ$$

$$\lambda_-^\circ = \Lambda_m^\circ - \lambda_+^\circ = (89{\cdot}20 - 38{\cdot}70)\times10^{-4} = \mathbf{50{\cdot}5\times10^{-4}\ S\ m^2\ mol^{-1}}$$

* t_+°, which refers to transport number of cation at zero concentration (infinite dilution), is obtained by determining transport numbers at various decreasing concentrations and then extrapolating to zero concentration.

Example 11. The molar conductances at infinite dilution for sodium acetate and hydrogen chloride at 30°C are $91{\cdot}0\times10^{-4}$ and $426{\cdot}16\times10^{-4}$ S m^2 mol^{-1}, respectively. Also for H^+ ion in HCl, t_+ is 0·821 and for CH_3COO^- ion in CH_3COONa, t_- is 0·556. Assuming that $t_\pm = t_\pm^\circ$, calculate Λ_m° for CH_3COOH.

Solution : We know that, $\lambda_+^\circ = t_+^\circ(\Lambda_m^\circ)$ and $\lambda_-^\circ = t_-^\circ(\Lambda_m^\circ)$ (Eqs. 11 and 12)

Assuming that $t_+^\circ = t_+$ and $t_-^\circ = t_-$, from the data on HCl, we have

$$\lambda_+^\circ = 0{\cdot}821\times426{\cdot}16\times10^{-4} = 349{\cdot}88\times10^{-4} \text{ S m}^2 \text{ mol}^{-1}$$

From the data on CH_3COONa,

$$\lambda_-^\circ = 0{\cdot}556\times91{\cdot}0\times10^{-4} = 50{\cdot}60\times10^{-4} \text{ S m}^2 \text{ mol}^{-1}$$

Hence, for CH_3COOH, $\Lambda_m^\circ = \lambda_+^\circ + \lambda_-^\circ = (349{\cdot}88 + 50{\cdot}60)\times10^{-4}$ S m^2 mol^{-1}

$$= 400{\cdot}48\times10^{-4} \text{ S m}^2 \text{ mol}^{-1}$$

Example 12. At 25°C, the degree of dissociation (α) of pure water is $1{\cdot}90\times10^{-9}$. Calculate the molar conductance (Λ_m°) and specific conductance (κ) of water at this temperature. The molar ionic conductances of H^+ and OH^- ions are $349{\cdot}83\times10^{-4}$ and $198{\cdot}50\times10^{-4}$ S m^2 mol^{-1}, respectively.

Solution : From Kohlarusch's law,

$$\Lambda_{mH_2O}^\circ = \Lambda_{H^+}^\circ + \lambda_{OH^-}^\circ = (349{\cdot}83 + 198{\cdot}50)\times10^{-4} \text{ S m}^2 \text{ mol}^{-1} = 548{\cdot}33\times10^{-4} \text{ S m}^2 \text{ mol}^{-1}$$

The degree of dissociation of a weak electrolyte is given by $\alpha = \Lambda_m/\Lambda_m^\circ$ (Eq. 4)

$$\therefore \quad \Lambda_m = \alpha\Lambda_m^\circ = (1{\cdot}90\times10^{-9})(548{\cdot}33\times10^{-4} \text{ S m}^2 \text{ mol}^{-1}) = 1{\cdot}401\times10^{-10} \text{ S m}^2 \text{ mol}^{-1}$$

Further, $\Lambda_m = \kappa/c$ (Eq. 3)

In this case, $c = 1000 \text{ g dm}^{-3}/18 \text{ g mol}^{-1} = 55{\cdot}56 \text{ mol dm}^{-3} = 55{\cdot}56\times10^3 \text{ mol m}^{-3}$

$$\therefore \quad \kappa = c\Lambda_m = (55{\cdot}56\times10^3 \text{ mol m}^{-3})(1{\cdot}041\times10^{-10} \text{ S m}^2 \text{ mol}^{-1}) = 5{\cdot}78\times10^{-6} \text{ S m}^{-1}$$

Relation between Molar Ionic Conductance and Ionic Mobility. As described earlier, **ionic mobility** is defined as the speed of the ion per unit potential gradient. The limiting value of ionic mobility, u°, can be related to molar ionic conductance, λ°, as follows :

The equivalent conductance of a solution containing c gram equiv of an electrolyte per litre is given by

$$\Lambda = 1000\,\kappa/c \qquad \ldots(13)$$

Consider a cube of 1 cm edge containing the above solution. Then, by definition, κ is also the actual conductance of the solution in 1 cm cube so that its resistance is $1/\kappa$ ohm. If a potential of 1 volt is applied across the cube, then according to the Ohm law,

$$\text{current strength, } i = E/R = 1/R = \kappa \qquad \ldots(14)$$

From Eqs. 13 and 14,

$$i = \Lambda c/1000 \text{ amperes} \qquad \ldots(15)$$

Let u_+ and u_- cm s^{-1} be the mobilities of the cations and anions, respectively. Accordingly, the distance covered by the corresponding ions under the given potential gradient would be u_+ and u_- cm. Since the cube has a cross-section of 1 cm^2, all the cations in a volume of u_+ c.c. and all the anions in a volume of u_- c.c. would migrate in opposite directions in one second. Assuming that the electrolyte is completely dissociated (the solution being supposed to be dilute), the solution would contain, $c/1000$ gram equiv of each ion per c.c. Since, according to Faraday's law, each gram equiv carries one faraday, *i.e.*, F coulombs of electricity, the total quantity of electricity carried by the ions would be $F(u_+ + u_-)c/1000$ coulombs per second. In other words, the current strength is given by

$$i = F(u_+ + u_-)\,c/1000 \text{ amperes} \qquad \ldots(16)$$

From Eqs. 15 and 16,

$$F(u_+ + u_-) = \Lambda = \lambda_+ + \lambda_-$$

or $$F(u_+^\circ + u_-^\circ) = \lambda_+^\circ + \lambda_-^\circ \text{ for an infinitely dilute solution} \qquad \ldots(17)$$

or $$u_+^\circ + u_-^\circ = \frac{\lambda_+^\circ}{F} + \frac{\lambda_-^\circ}{F}$$

Thus, for either ion, $u^\circ = \lambda^\circ/F$ ...(18)

where u° and λ° are the ionic mobility and the molar ionic conductance, respectively, at infinite dilution.

Ionic mobilities of some common ions calculated from the above considerations are given in Table 3.

TABLE 3

Ionic Mobilities (u) at 25°C in Water at Infinite Dilution

Ions	$u/10^{-8}$ (m^2 V^{-1} s^{-1})	Ions	$u/10^{-8}$ (m^2 V^{-1} s^{-1})	Ions	$u/10^{-8}$ (m^2 V^{-1} s^{-1})
H^+	36·25	Mg^{2+}	5·50	NO_3^-	7·41
Li^+	4·01	Ca^{2+}	6·17	CH_3COO^-	4·24
Na^+	5·19	OH^-	20·64	SO_4^{2-}	8·29
K^+	7·61	F^-	5·74	CO_3^{2-}	7·18
NH_4^+	7·62	Cl^-	7·91		

Example 13. The molar ionic conductance at infinite dilution of silver ions is $61{\cdot}92\times10^{-4}$ S m^2 mol^{-1} at 25° C. Calculate the ionic mobility of silver ions at 25°C at infinite dilution.

Solution : $\lambda_+^\circ = 61{\cdot}92\times10^{-4}$ S m^2 mol^{-1}

$u_+^\circ = \lambda_+^\circ/F$ ..... (Eq. 18)

$$\therefore \quad u_+^\circ = \frac{61{\cdot}92\times10^{-4} \text{ S m}^2 \text{ mol}^{-1}}{96485 \text{ C mol}^{-1}}$$

$$= 6{\cdot}417\times10^{-8} \text{ m}^2 \text{ V}^{-1} \text{ s}^{-1} \qquad (\because \text{ C} = \text{A s} = \text{V S s})$$

Example 14. A dilute solution of potassium chloride was placed between two platinum electrodes 10·0 cm apart, across which a potential of 6·0 volts was applied. How far would the K^+ ion move in 2 hours at 25°C ? Molar ionic conductance of K^+ ion at infinite dilution at 25°C is known to be $73{\cdot}52\times10^{-4}$ S m^2 mol^{-1}

Solution : Molar ionic conductance of K^+ ion at infinite dilution $= 73{\cdot}52\times10^{-4}$ S m^2 s^{-1}

$u_+^\circ = \lambda_+^\circ/F$ (Eq. 18)

$$u_+^\circ = \frac{73{\cdot}52\times10^{-4} \text{ S m}^2 \text{ mol}^{-1}}{96493 \text{ C mol}^{-1}}$$

$$= 7{\cdot}619\times10^{-4} \text{ m}^2 \text{ V}^{-1} \text{ s}^{-1} \qquad (\because \text{ C} = \text{V S s})$$

Potential gradient in this case = 6·0 volts/10 cm = 0·6 volt cm^{-1} = $0{\cdot}6\times10^2$ volt m^{-1}

$\therefore$ Speed of K^+ ion = $7{\cdot}619\times10^{-8}$ m^2 s^{-1} volt^{-1} × $0{\cdot}6\times10^2$ volt m^{-1} = $7{\cdot}619\times10^{-8}\times0{\cdot}6\times10^2$ m s^{-1}

$\therefore$ Distance moved by K^+ ion in 2 hours = $7{\cdot}619\times10^{-8}\times0{\cdot}6\times10^2$ m s^{-1} (2×60×60 s) = $3{\cdot}291\times10^{-2}$ m

Example 15. Calculate the molar conductance at infinite dilution of an aqueous solution of NaCl at room temperature, given that the mobilities of Na^+ and Cl^- ions at this temperature are $4{\cdot}26\times10^{-8}$ and $6{\cdot}80\times10^{-8}$ m^2 V^{-1} s^{-1}, respectively.

Solution : According to Eq. 18,

$$\lambda_+^\circ = Fu_+^\circ$$

$$= (96493 \text{ C mol}^{-1})(4{\cdot}26\times10^{-8} \text{ m}^2 \text{ V}^{-1} \text{ s}^{-1}) = 41{\cdot}10\times10^{-4} \text{ S m}^2 \text{ mol}^{-1}$$

$$\lambda^\circ_- = (96493\ \text{C mol}^{-1})\ (6{\cdot}80\times10^{-8}\ \text{m}^2\ \text{V}^{-1}\ \text{s}^{-1}) = 65{\cdot}61\times10^{-4}\ \text{S m}^2\ \text{mol}^{-1}$$

$$\Lambda^\circ_m = \lambda^\circ_{Na^+} + \lambda^\circ_{Cl^-} = (41{\cdot}10 + 65{\cdot}61)\times10^{-4}\ \text{S m}^2\ \text{mol}^{-1}$$

$$= 106{\cdot}71\times10^{-4}\ \text{S m}^2\ \text{mol}^{-1}$$

Example 16. A conductivity cell, when filled with an aqueous solution of 0·02 M KCl at 25°C, had a resistance of 250 ohm. Its resistance, when filled with 6×10^{-5} M NH_4OH solution was 10^5 ohm. The specific conductance of 0·02 M KCl was 0·277 S m^{-1}. The molar ionic conductances at infinite dilution of NH_4^+ and OH^- ions are $73{\cdot}4\times10^{-4}$ and $198{\cdot}0\times10^{-4}$ S m^2 mol^{-1}, respectively. Calculate the degree of dissociation of 6×10^{-5} M NH_4OH solution.

Solution : Since specific conductance κ = cell constant/R, hence

$$\text{cell constant} = \kappa R = (0{\cdot}277\ \text{S m}^{-1})\ (250\ \Omega) = 69{\cdot}2\ \text{m}^{-1} \qquad (\text{S} = \Omega^{-1})$$

For NH_4OH solution, $c = 6\times10^{-5}$ M $= 6\times10^{-5}$ mol $dm^{-3} = 6\times10^{-2}$ mol m^{-3}

$$\therefore \quad \Lambda_m = \frac{\kappa}{c} = \frac{\text{cell constant}}{cR} = \frac{69{\cdot}2\ \text{m}^{-1}}{(6\times10^{-2}\text{mol m}^{-3})(10^5\Omega)}$$

$$= 115\times10^{-4}\ \text{S m}^2\ \text{mol}^{-1}$$

According to Kohlrauch's law,

$$\Lambda^\circ_m = \lambda^\circ_+ + \lambda^\circ_- = (73{\cdot}4 + 198{\cdot}0)\times10^{-4}\ \text{S m}^2\ \text{mol}^{-1}$$

$$= 271{\cdot}4\times10^{-4}\ \text{S m}^2\ \text{mol}^{-1}$$

$$\alpha = \frac{\Lambda_m}{\Lambda^\circ_m} = \frac{115\times10^{-4}\ \text{S m}^2\ \text{mol}^{-1}}{271{\cdot}4\times10^{-4}\ \text{S m}^2\ \text{mol}^{-1}} = \mathbf{0{\cdot}424}$$

Direct Determination of Ionic Mobility. Ionic mobility can be measured directly by a technique based on the movement of a visible boundary between two electrolytic solutions. Suppose it is required to determine the mobility of K^+ ions. Then KCl may be one of the electrolytes called the principal electrolyte. The second electrolyte, called the indicator electrolyte, should have the same anion (*i.e.*, Cl^- ion in the present case) and its cation should have mobility lower than that of K^+ ion. For KCl as the principal electrolyte, $CdCl_2$ is a suitable indicator electrolyte.

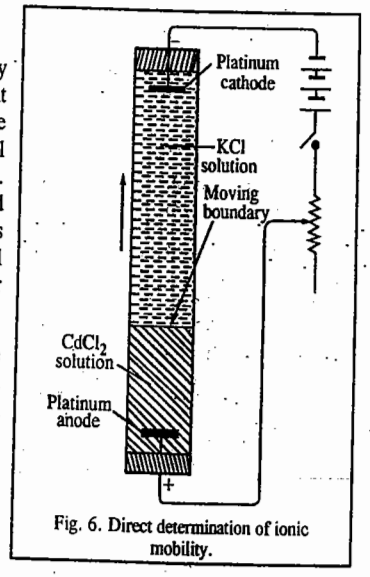

Fig. 6. Direct determination of ionic mobility.

The method of determination may be explained with reference to Fig. 6. A decimolar solution of potassium chloride is held over a solution of similar concentration of cadmium chloride, in a tube of uniform bore. The *anode* is placed at the lower end and the *cathode* at the upper end of the tube, as shown. Both the electrodes are made of platinum. When a small current flows through the cell, the K^+ ions followed closely by Cd^{2+} ions, move upward. As there will be no gap in between, the boundary will continue to remain sharp. The rate of movement of the boundary will be determined by the velocity of K^+ ions.

Suppose the boundary moves through a distance of x metre in t seconds when the fall of potential in the electric field is, say, z volts per metre. Then,

$$\text{the mobility of the } K^+ \text{ ion} = \frac{\text{Speed of ion}}{\text{Potential gradient}} = \frac{(x/t)\ \text{m s}^{-1}}{z\ \text{V m}^{-1}} = (x/tz)\ \text{m}^2\ \text{s}^{-1}\ \text{V}^{-1} \qquad ...(19)$$

Example 17. A moving boundary experiment was carried out with 0·01 M solution of KCl (κ = 1·29 S m^{-1}), using $CdCl_2$ as the indicator electrolyte. A current of 5·21 mA was passed through the tube of 0·230 cm^2 cross-sectional area. It was observed that the boundary moved through 4·16 cm in one hour. Calculate the mobility of the K^+ ion.

Solution : We shall first calculate the potential gradient (V) in volts per metre. Thus,

$$\text{Potential gradient} = \frac{\text{Current in amperes}}{\text{Area of cross-section} \times \kappa} = \frac{5{\cdot}21\times10^{-3}\text{A}}{(0{\cdot}230\times10^{-4}\ \text{m}^2)(1{\cdot}29\,\text{S m}^{-1})} = 175{\cdot}59\,\text{V m}^{-1}$$

($\because$ S = ohm^{-1} and V = ampere×ohm)

From Eq. 19,

$$\text{Mobility of } K^+ \text{ ion} = \frac{\text{Distance moved by the boundary}}{\text{Time} \times \text{Potential gradient}} = \frac{4{\cdot}16\times10^{-2}\ \text{m}}{(60\times60)\text{s}\times175{\cdot}59\ \text{V m}^{-1}}$$

$$= \mathbf{6{\cdot}58\times10^{-8}\ m^2\ V^{-1}\ s^{-1}}$$

Applications of Kohlrausch's Law

1. Calculation of Molar Conductance at Infinite Dilution for Weak Electrolytes. Molar conductances of strong electrolytes at infinite dilution can be obtained graphically by extrapolation, as discussed earlier. This method is not applicable for weak electrolytes because extrapolation is not possible in such cases. The application of Kohlrausch's law enables indirect evaluation in such cases. For instance, the molar conductance of acetic acid at infinite dilution can be obtained from the knowledge of molar conductances at infinite dilution of hydrochloric acid, sodium acetate and sodium chloride (all of which are strong electrolytes), as illustrated below :

$$\lambda^\circ_{CH_3COO^-} + \lambda^\circ_{H^+} = \lambda^\circ_{H^+} + \lambda^\circ_{Cl^-} + \lambda^\circ_{CH_3COO^-} + \lambda^\circ_{Na^+} - \left(\lambda^\circ_{Na^+} + \lambda^\circ_{Cl^-}\right)$$

i.e., $$\Lambda^\circ_{mCH_3COOH} = \Lambda^\circ_{mHCl} + \Lambda^\circ_{mCH_3COONa} - \Lambda^\circ_{mNaCl}$$

Similarly, $$\Lambda^\circ_{mNH_4OH} = \Lambda^\circ_{mNH_4Cl} + \Lambda^\circ_{mNaOH} - \Lambda^\circ_{mNaCl}$$

The molar conductance at infinite dilution of a sparingly soluble substance, like silver chloride, can also be obtained from similar considerations. Thus,

$$\Lambda^\circ_{mAgCl} = \Lambda^\circ_{mNH_4Cl} + \Lambda^\circ_{mAgNO_3} - \Lambda^\circ_{mNH_4NO_3}$$

Example 18. The molar conductances of sodium acetate, hydrochloric acid and sodium chloride at infinite dilution are $91{\cdot}0\times10^{-4}$, $426{\cdot}16\times10^{-4}$ and $126{\cdot}45\times10^{-4}$ S m^2 mol^{-1}, respectively, at 25°C. Calculate the molar conductance at infinite dilution for acetic acid.

Solution : $\Lambda^\circ_{mCH_3COONa} = \lambda^\circ_{CH_3COO^-} + \lambda^\circ_{Na^+} = 91{\cdot}0\times10^{-4}\ \text{S m}^2\ \text{mol}^{-1}$

$\Lambda^\circ_{mHCl} = \lambda^\circ_{H^+} + \lambda^\circ_{Cl^-} = 426{\cdot}16\times10^{-4}\ \text{S m}^2\ \text{mol}^{-1}$

$\Lambda^\circ_{mNaCl} = \lambda^\circ_{Na^+} + \lambda^\circ_{Cl^-} = 126{\cdot}45\times10^{-4}\ \text{S m}^2\ \text{mol}^{-1}$

$$\lambda^\circ_{CH_3COO^-} + \lambda^\circ_{H^+} = \lambda^\circ_{CH_3COO^-} + \lambda^\circ_{Na^+} + \lambda^\circ_{H^+} + \lambda^\circ_{Cl^-} - \lambda^\circ_{Na^+} - \lambda^\circ_{Cl^-}$$

or $$\Lambda^\circ_{mCH_3COOH} = \Lambda^\circ_{mCH_3COONa} + \Lambda^\circ_{mHCl} - \Lambda^\circ_{mNaCl}$$

$$= (91{\cdot}00 + 426{\cdot}16 - 126{\cdot}45)\times10^{-4} = \mathbf{390{\cdot}71\times10^{-4}\ S\ m^2\ mol^{-1}}$$

2. Determination of Transport Numbers. As discussed above, the transport numbers of ions are related to their molar conductances, as follows :

$$t^\circ_\pm = \lambda^\circ_\pm / \Lambda^\circ_m = \frac{\lambda^\circ_\pm}{\lambda^\circ_+ + \lambda^\circ_-} \qquad ...(20)$$

Further, molar conductances of ions are related to their mobilities as follows :

$$\lambda^\circ_\pm = Fu^\circ_\pm \qquad \text{(Eq. 18)} \qquad \ldots(21)$$

Eqs. 20 and 21 may thus be combined to give

$$t^\circ_\pm = \frac{\lambda^\circ_\pm}{\lambda^\circ_+ + \lambda^\circ_-} = \frac{u^\circ_\pm}{u^\circ_+ + u^\circ_-} \qquad \ldots(22)$$

Thus, if molar conductances of ions or their mobilities at infinite dilution are known, the transport numbers of ions at infinite dilution can be easily calculated.

Example 19. Calculate the transport numbers of Li^+ and Br^- ions when a current flows through an infinitely dilute aqueous solution of LiBr at 25°C, given the ionic mobilities of Li^+ and Br^- ions at infinite dilution are $4{\cdot}01\times10^{-8}$ and $8{\cdot}09\times10^{-8}$ $m^2\ V^{-1}\ s^{-1}$, respectively.

Solution : In this case, $u^\circ_+ = 4{\cdot}01\times10^{-8}\ m^2\ V^{-1}\ s^{-1}$ and $u^\circ_- = 8{\cdot}09\times10^{-8}\ m^2\ V^{-1}\ s^{-1}$

From Eq. 22,
$$t^\circ_+ = \frac{u^\circ_+}{u^\circ_+ + u^\circ_-} = \frac{4{\cdot}01\times10^{-8}\ m^2\ V^{-1}\ s^{-1}}{(4{\cdot}01+8{\cdot}09)\times10^{-8}\ m^2\ V^{-1}\ s^{-1}} = 0{\cdot}331$$

Since
$$t^\circ_+ + t^\circ_- = 1$$

$$\therefore \quad t^\circ_- = 1 - 0{\cdot}331 = 0{\cdot}669$$

Example 20. Molar ionic conductances at infinite dilution of Na^+ and Cl^- ions are $50{\cdot}11\times10^{-4}$ and $76{\cdot}34\times10^{-4}$ S m^2 mol^{-1}, respectively. Calculate the transport numbers of Na^+ and Cl^- ions.

Solution : According to Eq. 20,

$$t^\circ_+ = \frac{\lambda^\circ_+}{\lambda^\circ_+ + \lambda^\circ_-} = \frac{50{\cdot}11\times10^{-4}\ S\ m^2\ mol^{-1}}{(50{\cdot}11+76{\cdot}34)\times10^{-4}\ S\ m^2\ mol^{-1}}$$

$$= \frac{50{\cdot}11\times10^{-4}\ S\ m^2\ mol^{-1}}{126{\cdot}45\ S\ m^2\ mol^{-1}} = 0{\cdot}396$$

$$t^\circ_- = \frac{\lambda^\circ_-}{\lambda^\circ_+ + \lambda^\circ_-} = \frac{76{\cdot}34\times10^{-4}\ S\ m^2\ mol^{-1}}{(50{\cdot}11+76{\cdot}34)\times10^{-4}\ S\ m^2\ mol^{-1}} = 0{\cdot}604$$

As can be seen, $t^\circ_+ + t^\circ_- = 0{\cdot}396 + 0{\cdot}604 = 1$

Diffusion and Ionic Mobility. Electrical conductance is a consequence of the motion of ions in an applied electric field. If the electric field is absent, the ions and the solvent molecules in solution move in a random manner as a result of thermal energy. If there exists a *concentration gradient* for a given electrolyte at constant temperature and pressure, then there is a tendency for the diffusion of the electrolyte from a region of higher concentration to a region of lower concentration so as to reach an equilibrium condition wherein the concentration gradient is smoothed out. **Diffusion** is thus a process which involves the migration of a component in solution down a gradient of its own concentration, *i.e.*, from a region of higher to a region of lower concentration.

An ion in a solution possesses a **diffusion coefficient, D,** which measures the mobility of the ion due to its thermal energy, kT. Ionic mobility, u, of the ion, on the other hand, measures the mobility of the ion due to the kinetic energy imparted to it by the applied electric field. The parameters D and u are related by the Nernst–Einstein equation, *viz.*,

$$D = ukT/ez \qquad \ldots(23)$$

where e is the electronic charge and z is the charge number of the ion.

Example 21. Calculate ionic mobility of Na^+ ion in 0·1 M aqueous solution of NaCl at 25°C if the diffusion coefficient of Na^+ ion is $1{\cdot}30\times10^{-9}$ $m^2\ s^{-1}$.

Solution : $D = ukT/ez$ [Eq. 23]

$$\therefore \quad u_+ = \frac{Dez}{kT} = \frac{(1{\cdot}30\times10^{-9}\ m^2\ s^{-1})(1{\cdot}602\times10^{-29}\ C)(1)}{(1{\cdot}38\times10^{-23}\ J\ K^{-1})(298\ K)}$$

$$= 5{\cdot}06\times10^{-8}\ m^2\ V^{-1}\ s^{-1} \qquad (J = \text{volt coulomb} = V\,C)$$

The calculated value compares very favourably with the experimental value of $5{\cdot}19\times10^{-8}$ $m^2\ V^{-1}\ s^{-1}$.

Molar Ionic Conductance and Viscosity. Consider a single ion immersed in a liquid and subjected to an electric field, E. As the ion moves through the liquid, *its motion is retarded by the viscosity of the liquid.* The frictional force, f, acting on a spherical ion of radius r, moving with a velocity v, is given by Stokes's law, *viz.*,

$$f = 6\pi\eta rv \qquad \ldots(24)$$

where η is the coefficient of viscosity of the liquid.

This force is balanced by the electrical force acting on the ion, *viz.*, zeE. Hence,

$$6\pi\eta rv = zeE \qquad \ldots(25)$$

where z is the charge number of the ion and e is the electronic charge.

Hence, the mobility, $u_\pm$, of the ion is given by

$$u_\pm = v/E = ze/6\pi\eta r \qquad \ldots(26)$$

Combining this equation with the expression giving the relation between the limiting ionic mobility and the molar ionic conductance at infinite dilution, *viz.*, $\lambda^\circ_\pm = z\,u^\circ_\pm F$, we have

$$\lambda^\circ_\pm = \frac{z^2eF}{6\pi\eta_0 r} \qquad \ldots(27)$$

where η_0 is the viscosity of the pure solvent.

The only quantity on the right-hand side of Eq. 27 that depends on the medium is η_0. Thus, for a given ion in different solvents, we expect that

$$\lambda^\circ_\pm\eta_0 = \text{constant} \qquad \ldots(28)$$

This is called **Walden's rule.** As is evident, the larger the viscosity of the medium, the lesser would be the mobility and hence the lesser would be the conductance of the ion, as expected. Walden's rule holds only for large ions such as tetramethyammonium ion, $(CH_3)_4N^+$ and the picrate ion, $C_6H_2(NO_2)_3O^-$.

The reason why smaller ions do not satisfactorily obey Walden's rule is that they are solvated. A solvated ion also carries along the solvent molecules as it moves, with the result that the *effective radius* of the ion is larger than the crystallographic radius and is different in each solvent. In the case of larger ions, since the electric field due to the ion itself is small, the amount of the solvent held to the ion is small, *i.e.*, larger ions are less solvated than the smaller ions so that for larger ions the effective radius is nearly the same in different solvents. This is the reason why larger ions satisfy Walden's rule more accurately than do the smaller ions.

Temperature-Dependence of Ionic Conductance. The molar ionic conductances increase considerably with increase in temperature. For ions other than H^+ and OH^-, this increase can be accounted for by recalling that $\lambda_\pm$ is inversely proportional to the coefficient of viscocity η of the medium (Eq. 27). Since η decreases with increase in temperature, therefore, $\lambda_\pm$ increases with increase in temperature. For ions other than H^+ and OH^-, the temperature coefficient is about 2% per degree in aqueous

solutions in the temperature range of 0 to 100°C. For H^+ and OH^- ions, the temperature coefficient is about 14% and 16%, respectively. This is primarily due to differences in the mechanisms of their conductance.

Applications of Conductance Measurements

There are a number of direct applications of conductance measurements in chemistry. Some of the more important ones are discussed below.

1. Determination of degree of dissociation of weak electrolytes. The degree of dissociation of a weak electrolyte at any dilution can be calculated by the relationship

$$\alpha = \Lambda_m / \Lambda_m^\circ \qquad \text{(Eq. 4)}$$

Example 22. The molar conductance of 0·01 M solution of acetic acid was found to be $16{\cdot}30\times10^{-4}$ S m² mol⁻¹ at 25°C. The molar ionic conductances of hydrogen and acetate ions at infinite dilution are $349{\cdot}8\times10^{-4}$ and $40{\cdot}9\times10^{-4}$ S m² mol⁻¹, respectively, at the same temperature. What percentage of acetic acid is dissociated at this concentration ?

Solution : $\Lambda^\circ_{mCH_3COOH} = \lambda^\circ_{CH_3COO^-} + \lambda^\circ_{H^+} = (40{\cdot}9 + 349{\cdot}8)\times10^{-4} = 390{\cdot}7\times10^{-4}\,S\,m^2\,mol^{-1}$

$$\alpha = \frac{\Lambda_m}{\Lambda_m^\circ} = \frac{16{\cdot}30\times10^{-4}\,S\,m^2\,mol^{-1}}{390{\cdot}7\times10^{-4}\,S\,m^2 mol^{-1}} = 0{\cdot}04172$$

Thus, 0·01 M acetic acid is **4·172 per cent** dissociated.

2. Determination of ionic product of water (K_w). Water is known to be slightly dissociated as

$$H_2O \rightleftharpoons H^+ + OH^-$$

The product of the concentrations of hydrogen and hydroxyl ions expressed in mol dm^{-3}, is known as **ionic product of water** (K_w), *i.e.*,

$$[H^+][OH^-] = K_w$$

K_w is constant at a given temperature. Its numerical value can be determined experimentally by conductance measurements. The specific conductance of the purest water at 25°C is found to be $5{\cdot}54\times10^{-6}$ S m^{-1}. The conductance of one cubic metre of water, therefore, will be $5{\cdot}54\times10^{-6}$ S m$^{-1}\times1$ m^3 = $5{\cdot}54\times10^{-6}$ S m². The molar conductance of water if it is completely ionised to give one mole of H^+ ions and one mole of OH^- ions, is obtained by adding up molar ionic conductances of hydrogen and hydroxyl ions which are $349{\cdot}8\times10^{-4}$ and $198{\cdot}5\times10^{-4}$ S m² mol⁻¹, respectively, at 25°C. Thus, molar conductance of water should be $(349{\cdot}8+198{\cdot}5)\times10^{-4}$ S m² mol^{-1} = $548{\cdot}3\times10^{-4}$ S m² mol^{-1} when it can give one mole of hydrogen ions and one mole of hydroxyl ions in solution. It follows, therefore, that when the molar conductance of one cubic metre of water is $5{\cdot}54\times10^{-6}$ S m², the amount of hydrogen ions per cubic metre will be

$$\frac{5{\cdot}54\times10^{-6}\,S\,m^2}{548{\cdot}3\times10^{-4}\,S\,m^2\,mol^{-1}} = 1{\cdot}01\times10^{-4}\,mol^{-1}$$

The number of moles of hydroxyl ions will also be the same. Thus,

$$[H^+] = 1{\cdot}01\times10^{-4}\,mol\,m^{-3} = 1{\cdot}01\times10^{-7}\,mol\,dm^{-3}$$

$$[OH^-] = 1{\cdot}01\times10^{-4}\,mol\,m^{-3} = 1{\cdot}01\times10^{-7}\,mol\,dm^{-3}$$

$$\therefore\quad K_w = [H^+][OH^-] = 1{\cdot}01\times10^{-7}\,mol\,dm^{-3}\times1{\cdot}01\times10^{-7}\,mol\,dm^{-3}$$

$$= 1{\cdot}02\times10^{-14}\,mol^2\,dm^{-6} \approx 10^{-14}\,mol^2\,dm^{-6}\ \text{at 25°C}$$

Example 23. At 25°C the specific conductance of carefully distilled water is $58{\cdot}0\times10^{-7}$ S m^{-1} and the λ°_m values for H^+ and OH^- ions are $349{\cdot}8\times10^{-4}$ and $198{\cdot}5\times10^{-4}$ S m² mol^{-1}, respectively. Assuming that Λ_m differs very little from Λ°_m, calculate the ionic product of water at 25°C.

Solution : $H_2O \rightleftharpoons H^+ + OH^-$

$$K_w = [H^+][OH^-] = (c)\,(c) = c^2 \qquad \ldots(i)$$

where c is the concentration of each of the ionic speices.

From Kohlraush's law, $\Lambda^\circ_m = \lambda^\circ_{H^+} + \lambda^\circ_{OH^-} = (349{\cdot}8 + 198{\cdot}5)\times10^{-4}$ S m² mol^{-1}

$$= 548{\cdot}3\times10^{-4}\ S\ m^2\ mol^{-1} \approx \Lambda_m\ \text{(Given)}$$

Since $\Lambda_m = \kappa/c$ (Eq. 3)

$$\therefore\quad c = \kappa/\Lambda_m = \frac{58{\cdot}0\times10^{-7}\,S\,m^{-1}}{548{\cdot}5\times10^{-4}\,S\,m^2\,mol^{-1}} = 1{\cdot}06\times10^{-4}\,mol\,m^{-3}$$

$$= 1{\cdot}06\times10^{-7}\,mol\,dm^{-3}$$

Hence, from Eq. *(i)*, $K_w = c^2 = (1{\cdot}06\times10^{-7}\,mol\,dm^{-3})^2 = 1{\cdot}12\times10^{-14}\,mol^2\,dm^{-6}$

3. Determination of solubilities and solubility products of sparingly soluble salts. There are a number of salts, such as silver chloride, barium sulphate, lead sulphate, etc., which are so sparingly soluble in water that their solubilties cannot be determined by any chemical method. These are generally regarded as insoluble. However, it is possible to determine even such extremely small solubilities by conductance measurements.

Suppose it is required to find out the solubility of silver chloride in water, say, at 25°C. The salt is repeatedly washed with conductivity water to remove any soluble impurities. It is then suspended in conductivity water, warmed and cooled to 25°C. A very minute quantity of salt will pass in solution and the rest will settle down. The conductance of the solution is determined in the usual way by placing the conductivity cell in a thermostat maintained at 25°C. The conductance of water used in the preparation of the solution is also determined. The difference between the two multiplied by the cell constant gives the specific conductance of the solution due to the dissolved salt. Let this value be z S m^{-1}.

Suppose the solubility of silver chloride is x mole per cubic metre.

$\therefore$ Concentration of AgCl in the aqueous solution, $c = x$ mol m^{-3}

Hence, the molar conductance of the solution will be given by

$$\Lambda_m = \kappa/c = z\ S\ m^{-1}/x$$

As the solubility of silver chloride is extremely low, the minute quantity that is dissolved can be regarded as present at infinite dilution and, therefore, the determined molar conductance can be taken as the molar conductance at infinite dilution.

Now at 25°C, $\Lambda^\circ_{mAgCl} = \lambda^\circ_{Ag^+} + \lambda^\circ_{Cl^-} = (61{\cdot}92+76{\cdot}34)\times10^{-4}$

$$= 138{\cdot}26\times10^{-4}\ S\ m^2\ mol^{-1}$$

$$\therefore\quad z\ S\ m^{-1}/x = 138{\cdot}26\times10^{-4}\ S\ m^2\ mol^{-1}$$

or $$x = \frac{z\,S\,m^{-1}}{138{\cdot}26\times10^{-4}\,S\,m^2\,mol^{-1}} = \frac{z}{138{\cdot}26\times10^{-4}}\,mol\,m^{-3}$$

Thus, the solubility of silver chloride in water at 25°C, is $\dfrac{z}{138{\cdot}26\times10^{-4}}$ mol m^{-3}.

or $\frac{z}{138{\cdot}26\times10^{-7}}$ mol dm^{-3} or $\frac{z}{138{\cdot}26\times10^{-7}}$ mol dm$^{-3}\times143{\cdot}5$ g mol^{-1}

$$= \frac{z\times143{\cdot}5}{138{\cdot}26\times10^{-7}} \text{ g dm}^{-3}$$

Example 24. The specific conductance of a saturated solution of silver chloride at 25°C after subtracting the specific conductance of water is $2{\cdot}28\times10^{-4}$ S m^{-1}. Calculate the solubility of silver chloride in grams per dm^3 at this temperature. $\Lambda^\circ_{mAgCl}=138{\cdot}3\times10^{-4}$ S m^2 mol^{-1} and $M_{(AgCl)}=143{\cdot}5$ g mol^{-1}

Solution : $\kappa = 2{\cdot}28\times10^{-4}$ S m^{-1}

Let the solubility of AgCl be x mol m^{-3}

$\therefore \quad \Lambda_m = \kappa/c = 2{\cdot}28\times10^{-4}$ S m$^{-1}/x$

$2{\cdot}28\times10^{-4}$ S m$^{-1}/x = 138{\cdot}3\times10^{-4}$ S m^2 mol^{-1}

$$x = \frac{2{\cdot}28\times10^{-4}\text{ S m}^{-1}}{138{\cdot}3\times10^{-4}\text{ S m}^2\text{ mol}^{-1}} = 1{\cdot}648\times10^{-2}\text{ mol m}^{-3} = 1{\cdot}648\times10^{-5}\text{ mol dm}^{-3}$$

$$= 143{\cdot}5\text{ g mol}^{-1}\times1{\cdot}648\times10^{-5}\text{ mol dm}^{-3} = 2{\cdot}365\times10^{-3}\text{ g dm}^{-3}$$

Example 25. At 25°C, the specific conductance of a saturated solution of AgCl is $2{\cdot}68\times10^{-4}$ S m^{-1} and that of water with which the solution was made is $0{\cdot}86\times10^{-4}$ S m^{-1}. If molar conductances at infinite dilution of $AgNO_3$, HNO_3 and HCl are, respectively, $133{\cdot}0\times10^{-4}$, $421{\cdot}0\times10^{-4}$ and $426{\cdot}0\times10^{-4}$ S m^2 mol^{-1}, calculate the solubility of AgCl in grams per dm^3 in water at the given temperature.

Solution : $\kappa_{solution} = \kappa_{AgCl} + \kappa_{water}$

$\therefore \quad \kappa_{AgCl} = \kappa_{solution} - \kappa_{water} = (2{\cdot}68 - 0{\cdot}86)\times10^{-4}$ S m^{-1} $= 1{\cdot}82\times10^{-4}$ S m^{-1}

Since AgCl is formed according to the reaction

$$AgNO_3 + HCl \longrightarrow AgCl + HNO_3$$

hence, using Kohlrauch's law,

$$\Lambda^\circ_{mAgCl} = \Lambda^\circ_{mAgNO_3} + \Lambda^\circ_{mHCl} - \Lambda^\circ_{mHNO_3} = (133{\cdot}0 + 426{\cdot}0 - 421{\cdot}0)\times10^{-4}\text{ S m}^2\text{ mol}^{-1}$$

$$= 138{\cdot}0\times10^{-4}\text{ S m}^2\text{ mol}^{-1}$$

$\Lambda_m = \kappa/c$ and for the saturated solution of the sparingly soluble salt, $\Lambda_m = \Lambda^\circ_m$

$$\therefore \quad c = \frac{\kappa}{\Lambda^\circ_m} = \frac{1{\cdot}82\times10^{-4}\text{ S m}^{-1}}{138{\cdot}0\times10^{-4}\text{ S m}^2\text{mol}^{-1}} = 1{\cdot}32\times10^{-2}\text{ mol m}^{-3}$$

$$= 1{\cdot}32\times10^{-5}\text{ mol dm}^{-3}$$

$\therefore$ Solubility of AgCl $= (1{\cdot}32\times10^{-5}$ mol dm$^{-3})$ $(143{\cdot}5$ g mol$^{-1}) = 1{\cdot}89\times10^{-3}$ g dm^{-3}

Example 26. Calculate the solubility product of the sparingly soluble salt CaF_2 from the following data : The molar ionic conductances (at infinite dilution) of Ca^{2+} and F^- ions are 104×10^{-4} and 48×10^{-4} S m^2 mol^{-1}, respectively. The specific conductance of the saturated solution of CaF_2 at room temperature is $4{\cdot}25\times10^{-3}$ S m^{-1} and the specific conductance of water used for preparing the solution is 2×10^{-4} S m^{-1}.

Solution : Let c mol dm^{-3} be the solubility of CaF_2. Accordingly, the solubility equilibrium may be written as

$$CaF_2\,(s) \rightleftharpoons \underset{c}{Ca^{2+}(aq)} + \underset{2c}{2F^-(aq)}$$

Then, at equilibrium, the solubility product of CaF_2 is given by

$$K_{sp} = [Ca^{2+}]\,[F^-]^2 = (c)\,(2c)^2 = 4c^3 \qquad \ldots(i)$$

Specific conductance due to CaF_2 alone

$$= \kappa\text{ (soln)} - \kappa\text{ (water)} = (4{\cdot}25\times10^{-3} - 2{\cdot}0\times10^{-4})\text{ S m}^{-1} = 4{\cdot}05\times10^{-3}\text{ S m}^{-1}$$

$$\Lambda^\circ_{m(CaF_2)} = \lambda^\circ_{(Ca^{2+})} + 2\lambda^\circ_{(F^-)} = (104 + 2\times48)\times10^{-4}\text{ S m}^2\text{ mol}^{-1} = 200\times10^{-4}\text{ S m}^2\text{ mol}^{-1}$$

For saturated solution of sparingly soluble salt, $\Lambda_m \approx \Lambda^\circ_m$. Also, $\Lambda_m = \kappa/c$

$$\therefore \quad c = \frac{k}{\Lambda_m} = \frac{4{\cdot}05\times10^{-3}\text{ S m}^{-1}}{200\times10^{-4}\text{ S m}^2\text{ mol}^{-1}} = 2{\cdot}025\times10^{-1}\text{ mol m}^{-3} = 2{\cdot}025\times10^{-4}\text{ mol dm}^{-3}$$

Hence, from Eq. (i), $K_{sp} = 4c^3 = 4(2{\cdot}025\times10^{-4}$ mol dm$^{-3})^3 = 3{\cdot}32\times10^{-11}$ mol^3 dm^{-9}

4. Conductometric Titrations. Conductance measurements are frequently employed to find the end points of acid–alkali and other titrations. The principle involved is that *electrical conductance depends upon the number and mobility of ions.*

Consider, in the first instance, the titration of a strong acid, like hydrochloric acid, with a strong base, like sodium hydroxide. The acid is taken in the conductivity vessel and the alkali in the burette. The conductance of hydrochloric acid is due to the presence of hydrogen and chloride ions. As alkali is added gradually, the hydrogen ions are replaced by slow moving sodium ions, as represented below :

$$H^+(aq) + Cl^-(aq) + [Na^+(aq) + OH^-(aq)] \longrightarrow \underset{\text{(unionised)}}{Na^+(aq) + Cl^-(aq) + H_2O(l)}$$

Hence, on continued addition of sodium hydroxide, the conductance will go on decreasing until the acid has been completely neutralized. Any subsequent addition of alkali will result in introducing fast moving hydroxyl ions. The conductance, therefore, after reaching a certain minimum value, will begin to increase. On plotting the conductance against the volume of alkali added, the points will lie on two straight lines AB and CD (Fig. 7). The point of intersection X of these two lines gives the volume of alkali required for the neutralization.

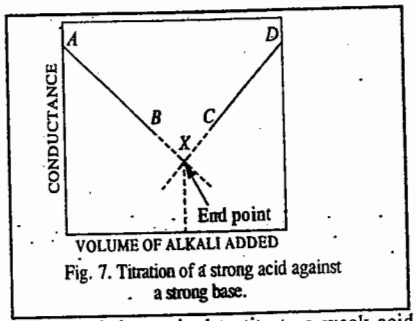

Fig. 7. Titration of a strong acid against a strong base.

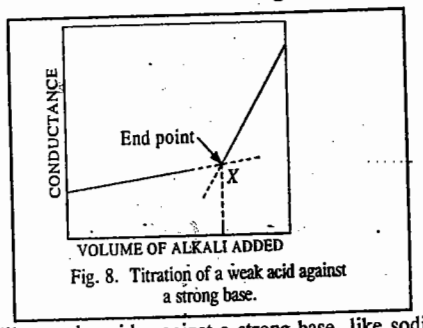

Fig. 8. Titration of a weak acid against a strong base.

Suppose, it is required to titrate a weak acid like acetic acid, against a strong base, like sodium hydroxide. The conductance of the acid will be low on account of its poor dissociation. On adding the base, highly ionised sodium acetate is formed and hence the conductance begins to increase.

$$CH_3COOH(aq) + [Na^+(aq) + OH^-(aq)] \longrightarrow \underset{\text{(unionised)}}{CH_3COO^-(aq) + Na^+(aq) + H_2O(l)}$$

When the acid is completely neutralized, further addition of the base introduces excess of fast moving hydroxyl ions. The conductance of the solution, therefore, begins to increase even more sharply than before. On plotting the conductance against the volume of the alkali added, the two lines obtained will be as shown in Fig. 8. The point of intersection X gives the end point.

When a mixture of a strong and a weak acid is to be titrated against a strong base, a combination of curves shown in Figs. 7 and 8 is obtained. Suppose a mixture of HCl and CH_3COOH is to be titrated against NaOH. Hydrochloric acid, being a much stronger acid, will get titrated first. The titration of acetic acid will commence only after hydrochloric acid has been completely neutralized. Hence, a combination of curves as mentioned above is obtained. This is represented in Fig. 9. While the point B corresponds to the neutralisation of HCl, the point C corresponds to the neutralisation of CH_3COOH.

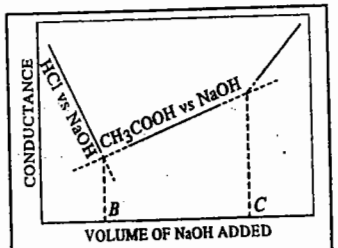

Fig. 9. Titration of a mixture of HCl and CH_3COOH against NaOH.

Finally, suppose it is required to titrate a strong acid like hydrochloric acid, against a weak base, like ammonium hydroxide. The conductance will fall at first due to the replacement of fast moving H^+ ions by slow moving NH_4^+ ions.

$$H^+(aq) + Cl^-(aq) + [NH_4OH] \longrightarrow NH_4^+(aq) + Cl^-(aq) + H_2O(l)$$

After neutralisation of the acid, further addition of weakly ionised ammonium hydroxide will not cause any appreciable change in the conductance. The curves obtained will be as shown in Fig. 10.

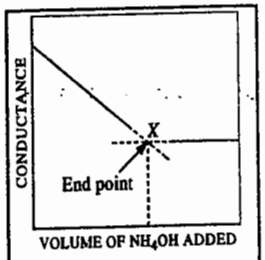

Fig. 10. Titration of a strong acid against a weak base.

5. Precipitation Titrations. The titration of silver nitrate against potassium chloride can also be carried out by this method. The reaction involved may be represented as

$$Ag^+(aq) + NO_3^-(aq) + [K^+(aq) + Cl^-(aq)] \longrightarrow K^+(aq) + NO_3^-(aq) + AgCl(s)$$

Since the mobility of potassium ion is nearly the same as that of silver ion which it replaces, the conductance will remain more or less constant and will begin to increase only after the end point. The curves obtained will be as shown in Fig. 11.

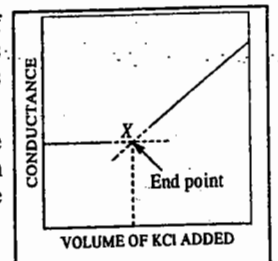

Fig. 11. Titration of silver nitrate against potassium chloride.

In order to get accurate results, the change of volume during the titration should be as small as possible. For this purpose the titration solution in the burette is usually five to ten times stronger than the solution taken in the conductivity vessel.

Conductometric titrations have several advantages. Coloured solutions, which cannot be titrated by ordinary volumetric methods with the help of indicators, can be successfully titrated conductometrically. The method can also be employed in the case of very dilute solutions and also for weak acids and bases. Further, no special care is necessary near the end point as it is determined graphically.

Ostwald's Dilution Law

As is well known, according to Arrhenius theory of electrolytic dissociation, the molecules of an electrolyte in aqueous solution undergo spontaneous dissociation into positive and negative ions and that there is a dynamic equilibrium between ions and the unionised molecules. Ostwald, therefore, applied the law of chemical equilibrium to such systems.

Consider an electrolyte AB, c moles of which are dissolved per dm^3 of an aqueous solution. Let α be its degree of dissociation, *i.e.*, the fraction of total concentration of the electrolyte which exists in dissociated state. Then,

		AB	$\rightleftharpoons$	A^+	+	B^-
Initial concs.	$\longrightarrow$	c		0		0
Equilibrium concs.	$\longrightarrow$	$c(1-\alpha)$		$c\alpha$		$c\alpha$

The equilibrium constant is given by the equation

$$K = \frac{c\alpha \times c\alpha}{c(1-\alpha)} = \frac{c\alpha^2}{1-\alpha} \qquad ...(29)$$

Eq. 29 is the mathematical representation of **Ostwald's dilution law.** The equilibrium constant K is called the **dissociation constant of the electrolyte.**

The degree of dissociation α at different concentrations was determined by conductance measurements using Eq. 4, *viz.*, $\alpha = \Lambda_m / \Lambda_m^\circ$. The law was found to hold good in the case of weak electrolytes, such as acetic acid and ammonium hydroxide.

However, the law failed completely when it was applied to strong electrolytes, such as hydrochloric acid, sodium hydroxide or potassium chloride. The values of K obtained for potassium chloride, for example, varied from 2·350 to 0·015 as the concentration varied from 1·00 M to 0·0001 M. The German chemist, W. Ostwald (1847–1931) was awarded the 1909 Chemistry Nobel Prize for his work on catalysis, chemical equilibria and rates of reactions.

Example 27. At 25°C, the specific conductance of 0·01 M aqueous solution of acetic acid is $1{\cdot}63\times10^{-2}$ S m^{-1} and the molar conductance at infinite dilution is $390{\cdot}7\times10^{-4}$ S m^2 mol^{-1}. Calculate the degree of dissociation and the dissociation constant of the acid.

Solution : $\kappa = 1{\cdot}63\times10^{-2}$ S m^{-1} ; $c = 0{\cdot}01$ mol dm^{-3} $= 0{\cdot}01\times10^3$ mol m^{-3}

$$\therefore \quad \Lambda_m = \frac{\kappa}{c} = \frac{1{\cdot}63\times10^{-2}\ \text{S m}^{-1}}{0{\cdot}01\times10^3\ \text{mol m}^{-3}} = 16{\cdot}3\times10^{-4}\ \text{S m}^2\ \text{mol}^{-1}$$

The degree of dissociation is given by

$$\alpha = \Lambda_m/\Lambda_m^\circ = \frac{16{\cdot}3\times10^{-4}\ \text{S m}^2\ \text{mol}^{-1}}{390{\cdot}7\times10^{-4}\ \text{S m}^2\ \text{mol}^{-1}} = 0{\cdot}0417$$

Using the Ostwald dilution law (Eq. 29), we have

$$K = \frac{c\alpha^2}{1-\alpha} = \frac{(0{\cdot}01\ \text{mol dm}^{-3})(0{\cdot}0417)^2}{1-0{\cdot}417} = 1{\cdot}82\times10^{-5}\ \text{mol dm}^{-3}$$

Example 28. The molar conductances at infinite dilution of HCl, NaCl and NaZ (sodium crotonate) are 425×10^{-4}, 125×10^{-4} and 80×10^{-4} S m^2 mol^{-1}, respectively. The specific conductance of 0·001 M aqueous solution of crotonic acid (HZ) is $3{\cdot}8\times10^{-3}$ S m^{-1}. Calculate the degree of dissociation and the dissociation constant of the acid.

Solution : Crotonic acid is formed as follows :

$$HCl + NaZ \longrightarrow NaCl + \underset{\text{(crotonic acid)}}{HZ}$$

where Z stands for crotonate ion.

Crotonic acid is a weak organic acid and HCl, NaZ and NaCl are strong electrolytes. Hence, using Kohlraush's law of independent migration of ions,

$$\Lambda_{mHZ}^\circ = \Lambda_{mHCl}^\circ + \Lambda_{mNaZ}^\circ - \Lambda_{mNaCl}^\circ$$
$$= (425 + 80 - 125)\times10^{-4}\ \text{S m}^2\ \text{mol}^{-1} = 380\times10^{-4}\ \text{S m}^2\ \text{mol}^{-1}$$

Also, at the given concentration of crotonic acid,

$$\Lambda_m = \frac{\kappa}{c} = \frac{3{\cdot}8\times10^{-3}\ \text{S m}^{-1}}{0{\cdot}001\times10^3\ \text{mol m}^{-3}} = 38{\cdot}0\times10^{-4}\ \text{S m}^2\ \text{mol}^{-1}$$

$$\alpha = \frac{\Lambda_m}{\Lambda_m^\circ} = \frac{38{\cdot}0\times10^{-4}\ \text{S m}^2\ \text{mol}^{-1}}{380\times10^{-4}\ \text{S m}^2\ \text{mol}^{-1}} = 0{\cdot}10$$

Using the Ostwald's dilution law (Eq. 29),

$$K_a = \frac{c\alpha^2}{1-\alpha} = \frac{(1{\cdot}0\times10^{-3}\ \text{mol dm}^{-3})(0{\cdot}10)^2}{1-0{\cdot}10} = 1{\cdot}11\times10^{-5}\ \text{mol dm}^{-3}$$

As mentioned above, Ostwald's dilution law, based on Arrhenius theory of electrolytic dissociation, does not hold good for strong electrolytes. This shows that Arrhenius theory is applicable only in the case of weak electrolytes. The situation in case of strong electrolytes is altogether different.

Situation in the Case of Strong Electrolytes. X-ray analysis of crystals of ionic solids, such as NaF, NaCl, KCl, Na_2SO_4 and NaOH, which are strong electrolytes, has revealed that the crystal lattice in these substances consists exclusively of ions. There are no molecules. Hence, in such cases the question of equilibrium between unionised molecules and their ions, as assumed in Arrhenius theory, does not arise at all.

As is now well recognised, the formation of ions takes place right at the moment of the formation of these compounds by the transference of electrons from one atom to another. Compounds formed in

this manner are called electrovalent compounds. For example, in the formation of sodium fluoride, there is transference of one electron from a sodium atom to a fluorine atom. As a result, the sodium atom acquires positive charge and fluorine atom acquires negative charge. This explains the formation of ions. The crystal of sodium fluoride, therefore, consists entirely of sodium ions and fluoride ions. The ions are held in position by electrostatic forces and are not free to move. When the crystals are melted, the ions acquire freedom of motion and are able to conduct electricity. This explains conductivity of fused salts.

According to Coulomb's law, the electrostatic forces vary inversely as the dielectric constant of the medium. Therefore, when crystals are dissolved in water, the dielectric constant of which is about 80 times greater than that of air, the electrostatic forces of attraction between the ions are considerably weakened. As a result of this, the ions begin to move more freely and conduct electricity more strongly.

Debye-Hückel Theory of Strong Electrolytes

Peter Debye and E. Hückel, in 1923, put forward their well known theory of strong electrolytes. Broadly speaking, according to this theory, strong electrolytes which exist as ions even in the solid state must be completely ionised in solution at all concentrations. If the solvent has a high dielectric constant (*e.g.*, water), the electrostatic forces, as already mentioned, will be small. Further, if the solution is very dilute, the distance between the ions will be large. Therefore, the electrostatic forces which vary inversely as the square of the distance between the ions, will be weakened all the more. Under these conditions, the forces of attraction between the oppositely charged ions, *i.e.*, interionic forces, will become very small and, therefore, the ions will lie far apart from one another. If, on the other hand, the solvent has a low dielectric constant (*e.g.*, ethanol) or if the solution is of a high concentration even when water is used as the solvent, the interionic forces will be appreciable. Under these conditions, some of the ions will not separate out completely from one another and will remain in pairs, such as A^+B^-, known as **ionic doublets.** This state of affairs is expressed by the statement that *the electrolyte is completely ionised but not completely dissociated.*

As the solution is diluted, its molar conductance increases. Arrhenius attributed this increase to increase in the degree of ionisation and used it as a method of calculating the degree of ionisation of an electrolyte by the equation

$$\alpha = \Lambda_m / \Lambda_m^\circ \qquad \text{(Eq. 4)}$$

But, according to the modern theory of strong electrolytes, the degree of ionization of strong electrolytes is unity even at moderate concentrations. Therefore, the above relationship is not correct in the case of strong electrolytes. Debye and Hückel suggested that increase in molar conductance with dilution in the case of strong electrolytes is due to increase in the mobilities of ions due to weaker interionic attraction rather than to increase in the degree of ionisation which remains unity all along. Similarly, decrease in molar conductance with increase in concentration is not due to fall in the degree of ionization but to fall in the mobilities of ions due to greater **interionic effect.**

To understand the interionic effect, consider a very dilute solution of sodium chloride. The ions will be so far apart in this case that the forces of attraction between Na^+ and Cl^- ions will be almost negligible. The ions would act independently of each other. Their mobility or conductance will be maximum and they will make full contribution towards conductance as well as towards colligative properties. Now suppose the concentration is increased. The ions now come closer to one another, comparatively speaking, and the interionic forces of attraction are no longer negligible. In other words, the ionic mobility falls due to mutual attraction of oppositely charged ions. Their contribution towards electrical conductance decreases correspondingly.

As the concentration is increased further, the oppositely charged ions come closer all the more. The interionic forces, therefore, become still more appreciable and the ionic mobility falls further.

Thus, according to this theory, *in the case of strong electrolytes, interionic attraction and not partial dissociation is the cause of decrease of conductance with increase in concentration.*

Debye and Hückel derived an equation which enabled them to calculate the magnitude of the interionic effects. The fundamental idea underlying the calculations is that each ion is surrounded by ions of opposite charge giving rise to an ionic atmosphere. The formation of the ionic atmosphere is explained as follows : Two opposing factors control the state of affairs in solutions of electrolytes : (1) the coulombic interaction which tends to arrange the ions in an ordered and organised structure and (2) the thermal collisions between the ions and solvent molecules which tend to prevent the existence of an organised structure in solution. At higher temperature, the structure is still less organised because of increased thermal collisions. As a result of the above two opposing factors, a situation arises when the negative ions end up as the nearest neighbours of a given central positive ion and vice versa. Thus, a cation is surrounded by more anions than cations. This gives rise to the ionic atmosphere where the central ion is surrounded by a group of ions of opposite charge.

For example, in Fig. 12(*a*), the central ion is positively charged and is surrounded by an atmosphere of negatively charged ions. When an electric field is applied, the ions are set in motion. The central ion moves in one direction and the atmosphere in the opposite direction. Thus, a central positive ion tends to move towards the cathode on the right while its negative ionic atmosphere tends to move towards the anode on the left, as represented in Fig. 12(*b*). The symmetry of the atmosphere about the ion is thus destroyed and the atmosphere becomes distorted. In other words, whereas the force of attraction exerted by the atmosphere on the central ion, before the passage of electricity, is uniform in all directions and, therefore, cancels out, it becomes greater behind the ion than in front, on the passage of electricity, as shown in Fig. 12(*b*). Consequently, the ion experiences a retarding force, a force which tends to drag it backward. The movement of the ion, therefore, is slowed down. The drag on the central ion is known as **the asymmetry effect** because it arises from a lack of symmetry in the atmosphere of a moving ion. Similarly, we conceive of a negative central ion being surrounded by an atmosphere of positively charged ions.

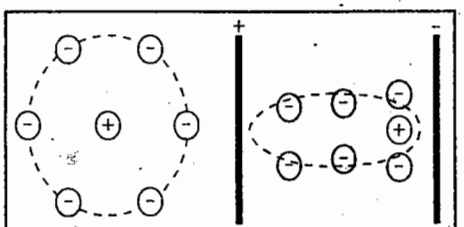

(*a*) Symmetric ionic atmosphere (*b*) Asymmetric ionic atmosphere

Fig. 12. Symmetric and asymmetric ionic atmospheres.

Another factor that slows down the motion of the ions at higher concentrations arises from the tendency of the ionic atmosphere associated with molecules of water of hydration to move in a direction opposite to that in which the central ion is moving. Thus, a positive ion, for example, which migrates towards the cathode has to make its way through the medium (water) which, itself, is moving with the negative ionic atmosphere towards the positive electrode. Similarly, a negative ion has to move towards the anode through the medium (water) associated with positive ionic atmosphere which is moving towards the negative electrode. These counter currents slow down the ions in the same way as counter currents in a stream slow down a swimmer. This effect is known as **electrophoretic effect.**

The third factor which affects the mobility of ions is the **viscous effect.** It arises from the viscous drag of the solvent on the movement of ions. The ion tends to move in the direction of the applied electric field. This electrical force is opposed by the frictional viscous drag exerted by the solvent. For an ion with a given charge, size and shape, the greater the viscosity of the solvent, the greater is the viscous drag and hence the smaller is the ionic mobility and the conductance.

In 1926, Debye, Hückel and Onsager worked out mathematically the magnitudes of asymmetry and electrophoretic effects in terms of such factors as valency of the ion, ionic concentration and dielectric constant and viscosity of the medium. For uni-univalent electrolytes, such as KCl, which

furnish two univalent ions, the following equation was derived :

$$\Lambda_m = \Lambda_m^\circ - \left\{ \frac{82{\cdot}4}{(\varepsilon_r T)^{1/2}\eta} + \frac{8{\cdot}20\times10^5}{(\varepsilon_r T)^{1/2}} \Lambda_m^\circ \right\} \sqrt{c} \qquad ...(30)$$

where ε_r and η are the dielectric constant and coefficient of viscosity of the medium, respectively, at the absolute temperature T and c is the concentration of the solution in moles per litre.

Eq. 30 is known as the **Debye-Hückel-Onsager equation.**

It accounts for the difference between Λ_m and Λ_m°. As is evident, Λ_m is less than Λ_m°. This is partly due to electrophoretic effect and partly due to asymmetry effect. The first term in the bracket gives a measure of the electrophoretic effect while the second term gives a measure of the asymmetry effect. The sum of these two effects multiplied with the square root of the concentration gives the decrease of molar conductance Λ_m from its limiting value Λ_m°.

For a given solvent and at a given temperature, the above equation may be expressed as

$$\Lambda_m = \Lambda_m^\circ - (A + B\Lambda_m^\circ)\sqrt{c} \qquad ...(31)$$

where A and B are the Debye–Hückel constants.

The values of A and B for water at 25°C come out to be 60·2 and 0·229, respectively. Hence,

$$\Lambda_m = \Lambda_m^\circ - (60{\cdot}2 + 0{\cdot}229\Lambda_m^\circ)\sqrt{c} \qquad ...(32)$$

If the equation is correct, then by plotting molar conductances (Λ_m) against the square roots of the concentrations ($\sqrt{c}$), a straight line of slope equal to ($60{\cdot}2 + 0{\cdot}229\Lambda_m^\circ$), should be obtained (Fig. 13). This has been checked in the case of a number of uni–univalent electrolytes and found to be true up to concentrations of the order of 0·02 M. At higher concentrations slight deviations are noticed which increase with further increase in concentration. These are attributed to certain approximations assumed in the derivation of the equation which are not valid when concentration is high.

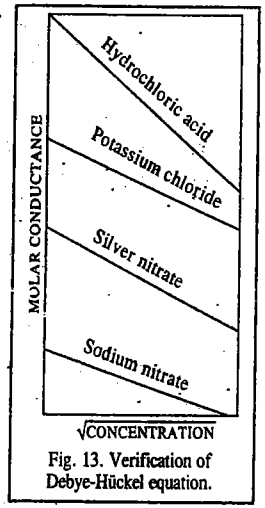

Fig. 13. Verification of Debye-Hückel equation.

If a solution is at infinite dilution, *i.e.*, if c is almost zero, then the second term on the right hand side of the equation becomes negligible and Λ_m approaches Λ_m°, as expected.

Debye-Falkenhagen Effect. Conductance Under High A.C. Frequencies. Debye and Falkenhagen examined the conductance behaviour of a solution of a strong electrolyte by applying alternating currents of different frequencies. They predicted that if the frequency of alternating current is high so that the time of oscillation is small in comparison with the relaxation time of the ionic atmosphere, the asymmetry effect will be virtually absent. In other words, the ionic atmosphere around the central ion will remain symmetric. The retarding effect due to asymmetry may, therefore, be entirely absent and the conductance may be higher. The conductance of a solution, therefore, should vary with the frequency of the alternating current used. The higher the frequency, the higher the conductance, evidently. This effect, also known as **dispersion of conductance,** has been verified experimentally. The conductance remains independent of the frequency of alternating current upto 10 cycles per second. But with further increase in frequency, the conductance starts increasing towards a certain limiting value indicating complete absence of asymmetry effect.

Wien Effect. Conductance Under High Potential Gradient. Speed of an ion in an electric field varies with the applied potential gradient. Thus, under a potential gradient of about 20,000 volt per cm, an ion may have a speed of about 100 cm per sec. The ion, therefore, should pass several times through the thickness of the ionic atmosphere during the time of relaxation. The moving ion, therefore, will be almost free from the effect of the oppositely charged ionic atmosphere. The ion will be moving so fast that there will be no time for the ionic atmosphere to be built up. The asymmetry and electrophoretic effects, under these circumstances, may be negligibly small or even absent. Thus, the conductance of a strong electrolyte in aqueous solution increases to a certain limiting value with increase in potential gradient applied. This observation had been verified experimentally by Wien much before the development of the theory of strong electrolytes and is known as the **Wien effect.**

ACTIVITY COEFFICIENTS OF ELECTROYLTES

Activity Coefficient. Consider the dissociation of a uni–univalent electrolyte represented as

$$MA \rightleftharpoons M^+ + A^-$$

Applying the law of chemical equilibrium, we have

$$K = \frac{(a_{M^+})(a_{A^-})}{a_{MA}} \qquad ...(33)$$

The activity is related to concentration expressed in terms of molality, *i.e.*, in terms of moles per kg of the solvent, by the expression

$$a = \gamma m \qquad ...(34)$$

where γ is called the **activity coefficient.** Thus,

$$K = \frac{(\gamma_{M^+} m_{M^+})(\gamma_{A^-} m_{A^-})}{\gamma_{MA} m_{MA}} = \left(\frac{\gamma_{M^+}\gamma_{A^-}}{\gamma_{MA}}\right)\left(\frac{m_{M^+} m_{A^-}}{m_{MA}}\right) \qquad ...(35)$$

Mean Ionic Activity Coefficient. It is not possible to have only one kind of ions in a solution. If there are anions; there have to be cations as well so that the total positive charge is equal to the total negative charge in a solution which is, evidently, neutral. The question of determining activities or activity coefficients of individual ions, therefore, does not arise. New terms such as **mean ionic activity** and **mean ionic activity coefficient,** therefore, need to be introduced.

Consider ionization of a uni–univalent electrolyte MA :

$$MA \rightleftharpoons M^+ + A^-$$

The activity of the cation may be denoted by a_+ and that of the anion by a_-. Both the quantities are indeterminable since it is not possible to have ions exclusively of one charge present in a solution. Hence, mean ionic activity of the electrolyte has to be taken into consideration. The activity and the mean ionic activity of the electrolyte (solute), denoted by a and $a_\pm$, respectively, are defined by the expression

$$a = (a_+)(a_-) = (a_\pm)^2 \qquad ...(36)$$

For any other electrolyte of the type M_xA_y which ionises as

$$M_xA_y \rightleftharpoons xM^+ + yA^-$$

the activity and mean ionic activity will be given by

$$a = (a_+)^x (a_-)^y = (a_\pm)^{x+y} \qquad ...(37)$$

For the sake of simplicity, the charge on each cation is represented by a single plus sign and that on each anion by a single minus sign.

If m is the initial concentration of the electrolyte M_xA_y in terms of moles per 1000 gram of the solvent, the concentration of M^+ and A^- ions would be xm and ym moles per 1000 gram of the solvent, respectively. Knowing that activity is related to molal concentration (molality) by the expression, $a = \gamma m$, Eq. 37 may be written as

$$a = (x\gamma_+ m)^x (y\gamma_- m)^y \quad ...(38)$$

$$= x^x y^x \gamma_+^x \gamma_-^y m^{x+y} = x^x y^y (\gamma_\pm m)^{x+y} \quad ...(39)$$

where $\gamma_\pm$ is the **mean molal ionic activity coefficient** or simply mean activity coefficient of the electrolyte. It is, evidently, defined as

$$(\gamma_\pm)^{x+y} = (\gamma_+)^x (\gamma_-)^y \quad ...(40)$$

Thus, if a is determined experimentally, it is possible to calculate the mean activity coefficient by applying Eq. 40. The values of x and y depend on the nature of the electrolyte. In the case of uni-univalent electrolytes, like KCl, $x=1$ and $y=1$. Eq. 39 may, therefore, be written as

$$a = (\gamma_\pm m)^2 \quad ...(41)$$

For a uni-bivalent electrolyte, like K_2SO_4, $x=2$ and $y=1$. Eq. 39, therefore, takes the form

$$a = 2^2 \times 1^1 (\gamma_\pm m)^{2+1} \quad ...(42)$$

$$= 4\gamma_\pm^3 m^3 \quad ...(43)$$

Eq. 43 will also be valid for electrolytes like $BaCl_2$, $Zn(NO_3)_2$, etc.

The activity coefficient of each electrolyte at infinite dilution is taken as unity.

Mean activity ionic coefficients of various electrolytes at different concentrations (molalities) can be calculated from Eq. 40. The values of activities (a) are usually determined by E.M.F., freezing point depression and vapour pressure lowering methods. Without going into details of these, some of the results obtained at different molalities are given in Table 4.

TABLE 4

Mean Ionic Activity Coefficients ($\gamma_\pm$) of Electrolytes in Aqueous Solutions at 25°C

Molality	HCl	KCl	NaCl	$CaCl_2$	$ZnCl_2$	H_2SO_4	$ZnSO_4$	KOH
0·001	0·996	0·966	0·966	0·888	0·831	.....	0·734	0·989
0·005	0·930	0·927	0·928	0·789	0·767	0·643	0·477	0·954
0·01	0·906	0·902	0·903	0·732	0·708	0·545	0·387	0·920
0·05	0·833	0·816	0·821	0·584	0·556	0·341	0·202	0·822
0·10	0·798	0·770	0·778	0·524	0·502	0·266	0·148	0·789
0·50	0·769	0·652	0·679	0·510	0·376	0·155	0·063	0·750
1·00	0·811	0·607	0·656	0·752	0·325	0·131	0·044	0·760
2·00	1·010	0·577	0·655	1·554	.....	0·125	0·035	....
3·00	1·310	0·572	0·719	3·384	.....	0·142	0·041	1·062

It is seen that at lower concentrations, the mean ionic activity coefficient is close to unity, *i.e.*, the departure from ideal behaviour is small. But as concentration increases, the activity coefficient falls much below unity and approaches a certain minimum value indicating much larger departures from the ideal behaviour. As concentration rises further, the mean ionic activity coefficient starts increasing and in some cases even exceeds unity, *i.e.*, activity becomes greater than concentration

(molality). This behaviour is shown more clearly in Fig. 14. in which mean activity coefficients of some of the electrolytes have been plotted against square roots of molalities.

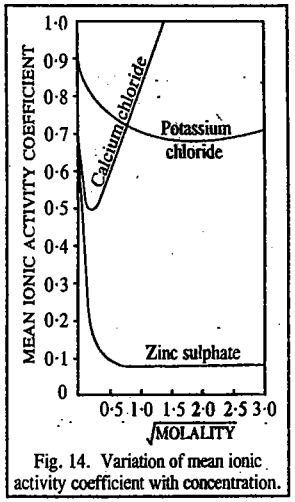

Fig. 14. Variation of mean ionic activity coefficient with concentration.

Reference to Table 4 also shows that the electrolytes of the same valency (*e.g.*, NaCl and KCl) have almost equal values of mean activity coefficient at the same concentration particularly when the concentration is not too high.

Ionic Strength. The ionic strengh I of a solution is a measure of the electrical intensity due to the presence of ions in the solution. It is given by half of the sum of all the terms obtained by multiplying the molality of each ion by the square of its valency. Mathematically, we have

$$I = \tfrac{1}{2}(m_1z_1^2 + m_2z_2^2 + m_3z_3^2 + ...) \quad ...(44)$$

where m_1, m_2, m_3,..... are molalities and z_1, z_2, z_3,.....are the valencies of the various ions present in the solution.

For a single electrolyte, as, for example, potassium chloride or zinc sulphate, Eq. 44 contains only two terms, one for the cation and the other for the anion. Hence,

$$I = \tfrac{1}{2}(m_+z_+^2 + m_-z_-^2) \quad ...(45)$$

where m_+ and m_- are the molalities and z_+ and z_- are the valencies of the cation and the anion, respectively. The ionic strength of a solution which is 0·1 molal in NaCl and 0·01 molal in calcium chloride, assuming complete ionization, may be calculated as under :

Molality of Na^+ ion, $m_1 = 0{\cdot}1$; Molality of Ca^{2+} ion, $m_2 = 0{\cdot}01$

Total molality of Cl^- ion, $m_3 = 0{\cdot}1 + 0{\cdot}02 = 0{\cdot}12$

Accordingly, $I = \tfrac{1}{2}(0{\cdot}1 \times 1^2 + 0{\cdot}01 \times 2^2 + 0{\cdot}12 \times 1^2) = \mathbf{0{\cdot}13}$

Example 30. Calculate the ionic strength of (*i*) 0·15 molal KCl solution (*ii*) 0·25 molal K_2SO_4 solution (*iii*) 0·2 molal $BaCl_2$ solution and (*iv*) a solution which is 0·1 molal in KCl and 0·2 molal in K_2SO_4.

Solution : (*i*) In 0·15 molal KCl solution, the molality of each ion = 0·15. Hence,

$$m_+ = 0{\cdot}15, \quad m_- = 0{\cdot}15 \quad \text{and} \quad z_+ = 1, \quad z_- = 1$$

$$\therefore \quad I = \tfrac{1}{2}(0{\cdot}15 \times 1^2 + 0{\cdot}15 \times 1^2) = \mathbf{0{\cdot}15}$$

(*ii*) Since K_2SO_4 produces two K^+ ions and one SO_4^{2-} ion, hence the molalities of the ions in this case would be as follows :

$$m_+ = 2{\times}0{\cdot}25 = 0{\cdot}50, \quad m_- = 0{\cdot}25 \; ; \quad z_+ = 1 \; ; \quad z_- = 2$$

Hence, $I = \tfrac{1}{2}(\mathbf{0{\cdot}5} \times 1^2 + 0{\cdot}25 \times 2^2) = \mathbf{0{\cdot}75}$

(*iii*) For 0·2 molal $BaCl_2$ solution,

$$m_+ = 0{\cdot}2, \quad m_- = 2{\times}0{\cdot}2 = 0{\cdot}4 \; ; \quad z_+ = 2, \quad z_- = 1$$

$$\therefore \quad I = \tfrac{1}{2}(0{\cdot}2 \times 2^2 + 0{\cdot}4 \times 1^2) = \mathbf{0{\cdot}6}$$

(*iv*) In a solution which is 0·1 molal in KCl and 0·2 molal in K_2SO_4, the total molality of K^+ ions,

$$m_1 = 0{\cdot}1 + 2{\times}0{\cdot}2 = 0{\cdot}5$$

Molality of Cl^- ions, $m_2 = 0{\cdot}1$ and molality of SO_4^{2-} ions, $m_3 = 0{\cdot}2$

Also in this case, $z_1 = 1, \quad z_2 = 1, \quad z_3 = 2$

Hence, $I = \tfrac{1}{2}(0{\cdot}5 \times 1^2 + 0{\cdot}1 \times 1^2 + 0{\cdot}2 \times 2^2) = \mathbf{0{\cdot}7}$

Debye-Hückel Theory of Mean Ionic Activity Coefficients.** Debye-Hückel derived a mathematical expression to account for the deviation of mean activity coefficients from unity fairly satisfactorily at least in the case of dilute solutions.

Consider a uni-univalent electrolyte. From electrostatics it is known that there exists an average potential ψ at a distance r from a given ion. The potential energy of an ion under this potential is $e\psi$ where e is the electronic charge. According to the Boltzmann distribution law, the probability that a given positive ion is in a region of potential ψ around a particular ion having the same charge is given by

$$n_+ = n\, e^{-e\psi/kT} \qquad ...(46)$$

where n is the number of molecules per unit volume (per cubic centimetre). Likewise, for a negative ion,

$$n_- = n\, e^{e\psi/kT} \qquad ...(47)$$

Hence, the net charge density, ρ, is given by

$$\rho = (n_+ - n_-)\, e = ne\,(e^{-e\psi/kT} - e^{e\psi/kT}) \qquad ...(48)$$

In a medium of dielectric constant ε_r, the well known Poisson equation in electrostatics is written as

$$\nabla^2\psi = -4\pi\rho/\varepsilon_r \qquad ...(49)$$

where ∇^2 is the Laplacian operator. In terms of the spherical polar co-ordinates, the Poisson equation is expressed as

$$\nabla^2\psi = \frac{1}{r^2} \times \frac{d}{dr}\left[r^2 \frac{d\psi}{dr}\right] = -\frac{4\pi\rho}{\varepsilon_r} \qquad ...(50)$$

Substituting for charge density from Eq. 48, we obtain the **Poisson-Boltzmann equation,** *viz.*,

$$\nabla^2\psi = -\frac{4\pi ne}{\varepsilon_r}(e^{-e\psi/kT} - e^{e\psi/kT}) \qquad ...(51)$$

If ψ is not large, then exponentials can be expanded to give

$$e^{e\psi/kT} = 1 + \frac{e\psi}{kT} + \text{higher powers of } e\psi/kT \qquad ...(52)$$

$$e^{-e\psi/kT} = 1 - \frac{e\psi}{kT} + \text{higher powers of } e\psi/kT \qquad ...(53)$$

Hence, $$\nabla^2\psi = \left[\frac{8\pi ne^2}{\varepsilon_r kT}\right]\psi \qquad ...(54)$$

Defining a quantity κ by

$$\kappa^2 = \frac{4\pi e^2}{\varepsilon_r kT}\sum n_i z_i^2 \qquad ...(55)$$

where z_i is the charge on the ion, we have for a uni-univalent electrolyte

$$\kappa^2 = \frac{8\pi ne^2}{\varepsilon_r kT} \qquad ...(56)$$

Thus, Eq. 54, becomes

$$\nabla^2\psi = \kappa^2\psi \qquad ...(57)$$

The solution of Eq. 57 further leads to the following expression :

$$\psi(r) = \frac{ze}{\varepsilon_r r} - \frac{ze\kappa}{\varepsilon_r} \qquad ...(58)$$

In Eq. 58, the first term on the right-hand side is the potential due to the charge on the ion itself while the second term can be thought of as the potential due to charge $-ze$ at a distance $1/\kappa$. The

** An advanced treatment of the Debye-Hückel theory of activity coefficients has been given in Chapter 25.

quantity $1/\kappa$, which has the dimensions of length, is known as the **effective radius of the ionic atmosphere** or the **Debye length.**

The free energy associated with the additional potential arising from the ionic atmosphere is equal to the reversible electrical work, w_{el}, required to form the ionic atmosphere. This is obtained by integrating the second term in Eq. 59 from zero charge to full charge ze :

$$w_{el} = \int_0^{ze}\left(-\frac{ze\kappa}{\varepsilon_r}\right)d(ze) \qquad ...(59)$$

$$= -\frac{\kappa}{2\varepsilon_r}(ze)^2 \qquad ...(60)$$

For dilute solutions, w_{el} can also be written as

$$w_{el} = kT \ln \gamma_i = -\frac{z_i^2 e^2 \kappa}{2\varepsilon_r} \qquad ...(61)$$

where γ_i is the **activity coefficient** of the ith ion.

Thus, $$\ln \gamma_i = -\frac{z_i^2 e^2 \kappa}{2\varepsilon_r kT} \qquad ...(62)$$

Since the mean ionic activity coefficient, $\gamma_\pm$, is defined as

$$\gamma_\pm^{\nu} = \gamma_+^{\nu_+}\,\gamma_-^{\nu_-} \qquad ...(63)$$

where ν_+ is the number of positive ions, ν_- is the number of negative ions and $\nu = \nu_+ + \nu_-$.

Hence, $$\ln \gamma_\pm = \frac{\nu_+}{\nu}\ln\gamma_+ + \frac{\nu_-}{\nu}\ln\gamma_- \qquad ...(64)$$

Also, $$\nu_+ z_+ = \nu_- z_- \qquad ...(65)$$

Hence, from Eqs., 62, 63 and 65

$$\ln \gamma_\pm = -|z_+ z_-|\frac{e^2\kappa}{2\varepsilon_r kT} \qquad ...(66)$$

Using the definition of ionic strength, I, as

$$I = \frac{1}{2}\sum c_i z_i^2 \qquad ...(67)$$

and remembering that $n_i = c_i N_A/1000$, where N_A is the Avogadro's number and $c_i = m_i\rho_0$ (ρ_0 being the density of the solvent), we obtain

$$\kappa^2 = \frac{8\pi N_A^2 e^2 \rho_0 I}{1000\varepsilon_r RT} \qquad ...(68)$$

or $$\kappa = \left(\frac{8\pi N_A^2 e^2 \rho_0 I}{1000\varepsilon_r RT}\right)^{1/2} \qquad ...(69)$$

and substituting for κ in Eq. 66, setting $\rho_0 = 1$ g ml^{-1} for water and changing from ln to log, we have

$$\log \gamma_\pm = -A|z_+ z_-|I^{1/2} \qquad ...(70)$$

where the constant A is given by the expression

$$A = \frac{N_A^2 e^3}{2{\cdot}303\varepsilon_r RT}\left(\frac{2\pi}{1000\varepsilon_r RT}\right)^{1/2} = \left(\frac{\pi N_A}{500}\right)^{1/2}\frac{e^3}{2{\cdot}303k^{3/2}(\varepsilon_r T)^{3/2}} \qquad ...(71)$$

Substituting the values of N_A, k and charge e, we get

$$A = 1{\cdot}8246\times10^6/(\varepsilon_r T)^{3/2} \qquad ...(72)$$

At 25°C, the dielectric constant ε_r for water is 78·54 so that the Debye–Hückel constant A becomes equal to 0·509. Thus,

$$\log \gamma_{\pm} = -0{\cdot}509|z_+ z_-|I^{1/2} \qquad ...(73)$$

Eq. 73 is the famous **Debye–Hückel limiting law (DHLL)** relating the mean ionic activity coefficient to the ionic strength of the solution. The negative value for log in this equation implies that mean activity coefficient is less than unity. That is actually so in the case of *dilute* solutions of electrolytes. The limiting law equation is valid for dilute solutions only because at higher concentrations the value even exceeds unity in some cases, as shown in Table 4.

It may be emphasised that according to Debye–Hückel limiting law equation, if z_+ and z_- are the same, the activity coefficients should vary only with the ionic strength of the solution and not at all with the nature of the electrolyte. This can be checked by working with several electrolytes of the same valency type. They should have equal activity coefficients at the same ionic strength. This has been found to be approximately so in the case of dilute solutions.

Eq. 73 can also be checked by plotting $-\log \gamma_{\pm}$ against $\sqrt{I}$. If the equation is valid, the plots for all electrolytes should give straight lines passing through the origin. Not only that; the slopes of the lines should depend on z_+z_-. For uni-univalent electrolytes, the slope should be 0·509, for uni-bivalent and bi-univalent electrolytes, the slope should be 2×0·509 and for uni-trivalent or tri-univalent electrolytes, the slope should be 3×0·509, and so on. This has been found to be approximately so in the case of very dilute aqueous solutions, as is shown in Fig. 15.

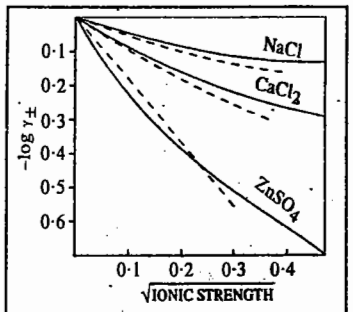

Fig. 15. Experimental verification of the limiting law equation.

The dotted lines show the behaviour to be expected from the limiting law equation. It is evident that the equation becomes more and more valid as the ionic strength decreases, *i.e.*, the solution becomes more and more dilute.

Example 31. Calculate the mean ionic activity coefficient $\gamma_{\pm}$ of (*i*) NaCl at a molality of 0·01 (*ii*) Na_2SO_4 at a molality of 0·001 in aqueous solution at 25°C.

Solution : (*i*) Mean Ionic Activity Coefficient of 0·01 Molal NaCl :

The ionic strength (I) of 0·01 molal solution of NaCl is given by

$$I = \tfrac{1}{2}(m_+z_+^2 + m_-z_-^2) = \tfrac{1}{2}(0{\cdot}01\times1^2 + 0{\cdot}01\times1^2) = 0{\cdot}01$$

(For a uni-univalent electrolyte, the ionic strength is, evidently, equal to its molality)

The mean activity coefficient ($\gamma_{\pm}$) is given by the equation

$$\log \gamma_{\pm} = -A z_+ z_- \sqrt{I} \qquad \text{(Eq. 70)}$$

For water at 25°C, the constant $A = 0{\cdot}509$.

$$\therefore \quad \log \gamma_{\pm} = -0{\cdot}509 \times 1 \times 1 \times \sqrt{0{\cdot}01} = -0{\cdot}0509$$

or $$\gamma_{\pm} = 0{\cdot}889$$

***(ii)* Mean Ionic Activity Coefficient of 0·001 Molal Na_2SO_4 :**

The ionic strength (I) of 0·001 molal Na_2SO_4 solution is given by

$$I = \tfrac{1}{2}(m_+z_+^2 + m_-z_-^2) = \tfrac{1}{2}(0{\cdot}002\times1^2 + 0{\cdot}001\times2^2) = 0{\cdot}003$$

$$\log \gamma_{\pm} = -A z_+ z_- \sqrt{I} = -0{\cdot}509 \times 1 \times 2 \times \sqrt{0{\cdot}003} = -0{\cdot}0558$$

$$\therefore \quad \gamma_{\pm} = 0{\cdot}879$$

Some empirical corrections for Debye–Hückel equation have been suggested to make it applicable also to solutions which are not so dilute. One corrected form is

$$\log \gamma_{\pm} = -Az_+z_-\sqrt{I} + CI \qquad ...(74)$$

where C is an empirical constant which can be evaluated from the experimental data. Its value has been found to depend upon the nature, *i.e.*, valency type of the electrolyte. The results have been found to be in satisfactory agreement with experimental values upto one molar concentration in the case of uni–univalent electrolytes.

Eq. 74 also explains why the activity coefficients, after touching a minimum, start rising again with increase in ionic strength. As can be seen, there are two expressions of opposite sign on the right hand side of Eq. 74. Each term is a function of the ionic strength. It appears that at very low ionic strengths, the negative term predominates and hence log $\gamma_{\pm}$ is negative, *i.e.*, $\gamma_{\pm}$ is less than unity. As concentration increases, the second term becomes increasingly important. The activity coefficient, therefore, starts increasing with increasing ionic strength and may even exceed unity in some cases.

It has not been easy to understand how activity can exceed concentration in cases in which γ is > 1 ($\because \gamma = a/c$). It has been suggested that at relatively higher ionic concentrations, the interaction between ions and solvent dipoles is so large that some of the solvent molecules get *isolated* from the bulk of the solution. The effective concentration of the electrolyte in the solution, therefore, increases.

I. Review Questions

1. Explain the terms conductance, specific conductance, equivalent conductance and molar conductance as applied to solutions of electrolytes. In which units are these quantities expressed ? How is specific conductance related to equivalent conductance and molar conductance ?
2. Define cell constant. How is it determined ?
3. Explain the term ionic mobility. The H^+ion, because of its heavy hydration and consequent large size and shape, should have a low mobility but actually its mobility is very high. How would you account for it ? Why does H^+ ion move about 50 times more rapidly in ice than in liquid water ?
4. Describe Hittorf's theoretical device to show that although most of the ions differ largely in their mobilities, their equivalent amounts are discharged, on electrolysis, at the appropriate electrodes.
5. Define the transport number of an ion. How is it determined ?
6. State and explain Kohlrausch's law. Illustrate how this law is used for calculation of molar ionic conductances at infinite dilution of weak electrolytes ?
7. Define the term : ionic mobility. Derive the relation between ionic mobility and molar ionic conductance. How is ionic mobility determined experimentally ?
8. Explain the term diffusion as applied to an electrolyte. Derive the relation between mobility and diffusion coefficient of an ion.
9. Derive the relation between ionic mobility, viscosity and radius of an ion. What is Walden's rule ?
10. What is the principle underlying conductometric titrations ? Discuss the titration curves obtained in the titration of :
    (*i*) A strong acid with a strong base (*ii*) A strong acid with a weak base (*iii*) A mixture of HCl and CH_3COOH with sodium bydroxide (*iv*) silver nitrate against potassium chloride.
11. Illustrate how the solubility of a sparingly soluble salt can be determined with the help of conductance measurements.
12. Derive Ostwald's dilution law for weak electrolytes.
13. Give an account of the Debye–Hückel theory of strong electrolytes. Explain clearly what is meant by asymmetry effect and electrophoretic effect.
14. Explain the terms activity coefficient and mean ionic activity coefficient. Discuss in detail the Debye–Hückel theory of mean ionic activity coefficients.
15. Discuss the Debye-Hückel theory of mean ionic activity coefficients. Derive the Debye-Hückel limiting law. How can it be verified ?

II. Problems

1. Calculate the cell constant of a conductance cell if the dimensions of the electrodes are 0·95 cm and 1·015 cm and the two electrodes are separated by 0·45 cm. **[Ans. 0·467 cm^{-1}]**
2. Calculate the specific conductance and molar conductance of a 0·0075 M aqueous solution of KCl. Given : the conductance is $1·49\times10^{-3}$ S and the cell constant is 1·05 cm^{-1}. **[Ans. 0·1565 S m^{-1}, 0·021 S m^2 mol^{-1}]**
3. A solution of silver nitrate containing 0·00739 gm of $AgNO_3$ per gram of water was electrolysed between silver electrodes. During the experiment, 0·078 gm of silver was deposited in a silver coulometer placed in series. At the end of the experiment, the anodic solution contained 23·14 gm H_2O and 0·236 gm of $AgNO_3$. What are the transport numbers of Ag^+ and NO_3^- ions ? **[Ans. Ag : 0·464 : NO_3^-, 0·536]**
4. Calculate Λ_m° for KCl solution if molar ionic conductances at infinite dilution are $7·352\times10^{-3}$ S m^2 mol^{-1} for K^+ and $7·634\times10^{-3}$ S m^2 mol^{-1} for Cl^-. **[Ans. $1·4986\times10^{-2}$ S m^2 mol^{-1}]**
5. Calculate Λ_m° for $CH_2ClCOOH$, given that the $\Lambda_m^\circ/10^{-2}$ S m^{-2} mol^{-1} values are 4·261 for HCl, 1·4986 for KCl and 1·132 for $CH_2ClCOOK$. **[Ans. 3·8944 S m^2 mol^{-1}]**
6. In experimental determination of ionic mobility of K^+ ion, the boundary moved 38·7 mm in 20 min when a steady current of 1·82 mA was passed. The strength of the solution of KCl used was 0·02 M; specific conductance of the solution κ = 0·278 S m^{-1} and the tube had a bore (*i.e.*, diameter) equal to 4·146 mm. Calculate the electric field and the mobility of the K^+ ion. **[Ans. 483·3 V m^{-1} ; $6·673\times10^{-8}$ m^2 V^{-1} s^{-1}]**
7. Given : $\lambda_0(Ca^{2+})=1·04\times10^{-2}$ S m^2 mol^{-1} and $\lambda_0(Cl^-)=7·634\times10^{-3}$ S m^2 mol^{-1}. Calculate the diffusion coefficient of each ion at 25°C. **[Ans. $7·922\times10^{-10}$ m^2 s^{-1}, $2·033\times10^{-9}$ m^2 s^{-1}]**
8. At 25°C, the specific conductance of distilled water is $58·0\times10^{-7}$ S m^{-1} and that of saturated solution of AgCl at 25°C is $2·338\times10^{-4}$ S m^2. Calculate the solubility of AgCl in gram per dm^3 at this temperature. **[Ans. $2·365\times10^{-3}$ g dm^{-3}]**
9. At 25°C, the molar conductance of a 0·01 M aqueous solution of acetic acid is $16·32\times10^{-4}$ S m^2 mol^{-1} and the molar conductance at infinite dilution is $390·72\times10^{-4}$ S m^2 mol^{-1}. Calculate the degree of dissociation and the dissociation constant of the acid. **[Ans. 0·0418, $1·823\times10^{-5}$ mol dm^{-3}]**
10. What is meant by ionic strength of a solution ? Calculate the ionic strength of a solution prepared by mixing 50 ml of 0·2 M KNO_3, 20 ml of 0·15 M K_2SO_4 and 30 ml of 0·05 M $Cu(NO_3)_2$. **[Ans. I = 0·205 M]**
11. Calculate *(a)* the activity coefficients of Cu^{2+} and NO_3^- ions in $2·0\times10^{-3}$ M aqueous solution of $Cu(NO_3)_2$. Using these values calculate *(b)* the mean ionic activity coefficient *(c)* the mean ionic concentration and *(d)* the mean ionic acitivity. **[Ans. *(a)* 0·6950, 0·9133 *(b)* 0·8341 *(c)* $3·17\times10^{-3}$ M *(d)* $2·64\times10^{-3}$]**
12. A 0·2% solution of NaOH was electrolyzed using platinum electrodes in the Hittorf cell by passing a 120 mA current for 30 minutes. After electrolysis, 25·64 g cathode solution was found to contain 0·0560 g of NaOH. Calculate the transport numbers of Na^+ and OH^-. **[Ans. 0·21 and 0·79]**
13. For $K^+(aq)$, λ° = $7·352\times10^{-3}$ S m^{-2} mol^{-1}. Determine the speed of the ion under the influence of an electric field strength of 1·52 V cm^{-1}. **[Ans. $1·16\times10^{-5}$ m s^{-1}]**
14. Calculate the ionic mobilities of K^+ and OH^- ions at infinite dilution. Given $\lambda^\circ(K^+)=73·50\times10^{-4}$ S m^2 mol^{-1} and $\lambda^\circ(OH)$ = $197·6\times10^{-4}$ S m^2 mol^{-1}. **[Ans. $7·62\times10^{-8}$ m^2 V^{-1} s^{-1}, $2·05\times10^{-7}$ m^2 V^{-1} s^{-1}]**

CHAPTER 24

ELECTROCHEMISTRY–II
EMF OF GALVANIC CELLS

Galvanic Cells. A galvanic cell is a device in which *the free energy of a physical or chemical process is converted into electrical energy*. Such a cell, usually, consists of two electrodes immersed in one or more suitable electrolytes. When the electrodes are connected externally as well as internally if required, a chemical reaction occurs in the cell involving *oxidation* at one electrode and *reduction* at the other electrode. According to the latest convention, the electrode at which oxidation occurs is called the **anode** while the electrode at which reduction occurs is called the **cathode.**

Consider, for instance, a copper rod dipping in a solution of copper sulphate and a zinc rod dipping in a solution of zinc sulphate, as in the **Daniell cell.** The two metal rods are connected through an ammeter and the two solutions are connected through a salt bridge, *i.e.*, an inverted U–shaped glass tube filled with a solution of potassium chloride. As soon as the circuit is closed, current starts flowing which is indicated by deflection in the ammeter. The flow of current is accompanied by the following processes :

The zinc metal passes into the solution as Zn^{2+} ions liberating two electrons ($Zn \longrightarrow Zn^{2+} + 2e^-$). The process involves *oxidation*. The liberated electrons move into the ammeter and then enter the copper rod. Cu^{2+} ions extract two electrons each from the copper rod and are discharged as copper metal on the copper electrode ($Cu^{2+}+2e^- \longrightarrow Cu$). The process involves *reduction*. The overall chemical reaction taking place in the cell, usually called the **cell reaction,** is, thus,

$$Zn(s) + Cu^{2+}(aq) \longrightarrow Zn^{2+}(aq) + Cu(s)$$

Since in the present case electrons are generated at the zinc electrode and consumed at the copper electrode, the flow of electrons, that is, the flow of electricity, in the cell is from the zinc electrode to the copper electrode.

The SO_4^{2-} ions left unpaired due to the reduction of Cu^{2+} ions to metallic copper migrate through the salt bridge to the other segment of the cell where they serve as partners for the Zn^{2+} ions produced by the oxidation of zinc. Thus while electrons move from the zinc rod to the copper rod in the outside circuit, the SO_4^{2-} ions move from the solution surrounding the copper rod to the solution surrounding the zinc rod through the salt bridge. This completes the electrical circuit of the cell.

With the passage of time, the concentration of Zn^{2+} ions increases and that of Cu^{2+} decreases. This pushes the cell reaction in the backward direction. Ultimately, a state of equilibrium is reached and the cell stops producing electricity.

For thermodynamic treatment of galvanic cells it is essential that these cells operate in a thermodynamically reversible manner. A cell is said to work reversibly in the thermodynamic sense when it is generating infinitesimally small current so that the cell reaction always remains virtually in a state of equilibrium.

In order to find out if a given cell is reversible or not, it is connected to an external source of EMF acting in the opposite direction. The cell will be reversible if it satisfies the following conditions :

1. If the opposing EMF is exactly equal to that of the cell itself, no current is given out by the cell and no chemical reaction takes place in the cell.

2. If the opposing EMF is infinitesimally smaller than that of the cell itself, an extremely small current is given out by the cell and a correspondingly small amount of the chemical reaction takes place in the cell.

3. If the opposing EMF is infinitesimally greater than that of the cell itself, an extremely small current flows through the cell in the oposite direction and a small amount of the chemical reaction also takes place in reverse direction.

We emphasize here that a **galvanic cell** is an electrochemical cell that produces electricity as a result of the spontaneous reaction occurring inside it. On the other hand, an **electrolytic cell** is an electrochemical cell in which a non-spontaneous reaction is driven by an external source of current. In this chapter we shall deal with galvanic cells.

A reversible galvanic cell consists of two reversible electrodes, one of which acts as the cathode and the other as the anode. Each electrode along with the electrolytic reagent associated with it is called the **half-cell** and the reaction that occurs in the half-cell is called the **half-cell reaction.**

Reversible Electrodes

1. Metal–Metal Ion Electrodes. An electrode of this type consists of a metal rod dipping in a solution containing its own ions, as, for example, zinc rod dipping in zinc sulphate solution or a copper rod dipping in copper sulphate solution, as in the Daniell cell.

If the metal is univalent, the electrode reaction may be represented as

$$M^+(aq) + e^- \rightleftharpoons M(s)$$

If the metal rod behaves as positive electrode (*i.e.*, the reaction at the electrode involves reduction), the equilibrium will shift towards the right. The concentration of M^+ ions in solution will, therefore, decrease.

If, on the other hand, the metal rod behaves as negative electrode (*i.e.*, the electrode reaction involves oxidation), the above equilibrium will shift towards the left. The concentration of the M^+ ions in solution will, therefore, increase.

The electrode is thus reversible with respect to M^+ ions.

If the metal is bivalent, the above equilibrium may be represented as

$$M^{2+}(aq) + 2e^- \rightleftharpoons M(s)$$

In general, if the valency of the metal is z, the equilibrium is represented as

$$M^{z+}(aq) + ze^- \rightleftharpoons M(s)$$

The electrode, in general, is represented as

$$M(s),\ M^{z+}(aq)$$

2. Gas Electrodes. a. Hydrogen Electrode. Hydrogen gas bubbling in a 1M solution of an acid (say, hydrochloric acid) forms an electrode of this type. The equilibrium in this case is represented as

$$H^+(aq) + e^- \rightleftharpoons \tfrac{1}{2}H_2(g)$$

The electrode is reversible with respect to hydrogen ion.

Since hydrogen gas is nonconducting, platinum or some other metal which is not attacked by the acid and easily comes into equilibrium with hydrogen, is used for making electrical contact in the circuit (Fig. 1) The electrode is represented as Pt ; $H_2(g)$, H^+. It is called **standard hydrogen electrode (SHE).**

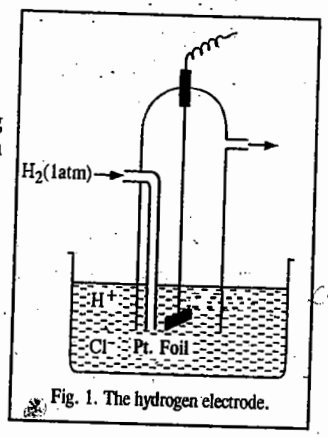

Fig. 1. The hydrogen electrode.

b. Chlorine Electrode. In this electrode, chlorine gas at a given pressure is bubbled into a solution of hydrochloric acid. The electrode is represented as

$$Pt,\ Cl_2(g),\ Cl^-(aq)$$

and the electrode reaction is written as

$$\tfrac{1}{2}Cl_2(g) + e^- \rightleftharpoons Cl^-(aq)$$

The electrode is evidently reversible with respect to chloride ion.

c. Oxygen Electrode. In this electrode, oxygen gas at a given pressure is bubbled through a solution containing hydroxyl, OH^-, ions. The electrode reaction is written as

$$O_2(g) + 2H_2O + 4e^- \rightleftharpoons 4OH^-(aq)$$

But, since equilibrium between oxygen gas and hydroxyl ions in solution cannot be established *quickly*, oxygen electrode does not behave as a truly reversible electrode.

3. Metal–Insoluble Metal Salt Electrodes. These electrodes consist of a metal and a sparingly soluble salt of the same metal dipping in a solution of a soluble salt having the *same anion*. An important electrode of this type is the calomel electrode.

Calomel Electrode. Calomel electrode consists of mercury, solid mercurous chloride and a solution of potassium chloride. The electrode is represented as Hg, $Hg_2Cl_2(s)$; KCl (solution).

It can be easily set up in the laboratory as follows : Mercury of high grade purity is placed at the bottom of a glass tube having a side tube on each side (Fig. 2.) Mercury is covered by a paste of mercurous chloride (calomel), as shown. A solution of potassium chloride is introduced above the paste through the side tube shown on the right. The concentration of the solution is either decinormal, normal or else the solution is fully saturated. The solution also fills the side tube ending in a jet on the left. A platinum wire sealed into a glass tube serves to make electrical contact of the electrode with the circuit.

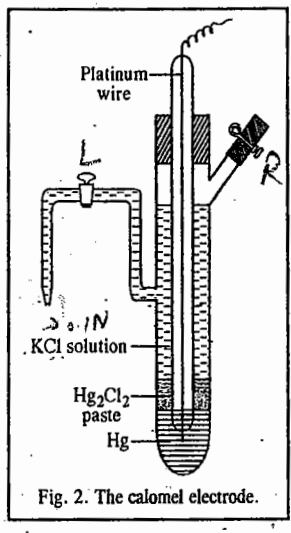

Fig. 2. The calomel electrode.

If the electrode reaction involves *reduction*, the Hg_2^{2+} ions furnished by the sparingly soluble mercurous chloride would be discharged at the electrode. Hence, more and more of calomel would pass into solution. The result is *an increase in the concentration of chloride ions*. The reactions may be represented as follows :

$$Hg_2^{2+}(aq) + 2e^- \rightleftharpoons 2Hg(l)$$

$$Hg_2Cl_2(s) \rightleftharpoons Hg_2^{2+}(aq) + 2Cl^-(aq)$$

If, on the other hand, the electrode reaction involves *oxidation*, it would liberate electrons and send Hg_2^{2+} ions into solution. The Hg_2^{2+} ions would combine with Cl^- ions (furnished by KCl) forming sparingly soluble Hg_2Cl_2. The result is *a fall in the concentration of chloride ions* in the solution. The reactions may be represented as follows :

$$2Hg(l) \rightleftharpoons Hg_2^{2+}(aq) + 2e^-$$

$$Hg_2^{2+}(aq) + 2Cl^-(aq) \rightleftharpoons Hg_2Cl_2(s)$$

Thus, in the case of the calomel electrode, the electrode reaction may be represented as

$$Hg_2Cl_2(s) + 2e^- \rightleftharpoons 2Hg(l) + 2Cl^-(aq)$$

The electrode, therefore, is reversible with respect to chloride ion.

Another common electrode of this type is the **silver–silver chloride electrode** which consists of a silver wire coated with a layer of silver chloride. This is inserted in a solution of KCl or HCl of a known concentration. The electrode is schematically represented as

$$Ag, AgCl(s) ; Cl^-(aq)$$

The electrode is reversible with respect to Cl^- ion.

4. Oxidation-Reduction Electrodes. The term oxidation-reduction electrode is used for those electrodes in which the potential is developed due to the presence of ions of the same substance in two different valence (*i.e.*, oxidation) states. Such an electrode is set up by inserting an unattackable metal (*e.g.*, platinum) in an appropriate solution. Thus, when a platinum wire is inserted in a solution containing Fe^{2+} and Fe^{3+} ions, it is found that the wire acquires a potential. The same thing happens when a platinum wire is inserted in a solution containing Sn^{2+} and Sn^{4+} ions or Ce^{3+} and Ce^{4+} ions. *The potential at the electrode arises from the tendency of the ions in one oxidation state to change into the other more stable oxidation state.*

The electrode reactions may be represented as follows :

$$Fe^{3+}(aq) + e^- \rightleftharpoons Fe^{2+}(aq)$$

$$Sn^{4+}(aq) + 2e^- \rightleftharpoons Sn^{2+}(aq)$$

$$Ce^{4+}(aq) + e^- \rightleftharpoons Ce^{3+}(aq)$$

The function of the platinum wire is to 'pick up' the electrons and to provide electrical contact to the electrode.

Another important but a slightly different type of oxidation-reduction electrode is the so called **quinhydrone electrode** which consists of a platinum wire placed in a solution containing hydroquinone(QH_2) and quinone(Q) in equimolar amounts. The electrode reaction in this case is represented as follows :

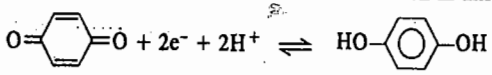

Quinone Hydroquinone

This electrode, which may be represented as Pt, Q, QH_2 ; $H^+(aq)$, is evidently reversible with respect to H^+ ions.

Single Electrode Potential

As mentioned earlier, each galvanic cell is made up of two electrodes. At one electrode oxidation takes place, *i.e.*, electrons are evolved. At the other electrode reduction takes place, *i.e.*, electrons are taken up.

The tendency of an electrode to lose or gain electrons when it is in contact with its own ions in solution, is called **electrode potential.** Since the tendency to gain electrons means also the tendency to get reduced, this tendency is called **reduction potential.** Similarly, the tendency to lose electrons means the tendency to get oxidised. Hence, this tendency is called **oxidation potential.** Needless to mention that oxidation potential is the reverse of reduction potential. Thus, if the reduction potential of an electrode under given conditions is 1·5 volts, then its oxidation potential is taken as −1·5 volts and *vice-versa*.

It is not possible to determine experimentally the potential of a single electrode (*i.e.*, of a half-cell). It is only the difference of potentials between two electrodes that we can measure by combining them to give a complete cell. By arbitrarily fixing potential of one electrode as zero (just as the freezing point of water at atmospheric pressure is arbitrarily fixed as zero on the temperature scale), it is possible to assign numerical values to potentials of the various other electrodes. Accordingly, the potential of a reversible hydrogen electrode in which the gas at one atmospheric pressure is

bubbled through a solution of hydrogen ions of unit activity (or, to be approximate, 1 M concentration) has been fixed as zero. This electrode is known as **standard hydrogen electrode (SHE)** and is represented as

$$Pt ; H_2(g) \text{ (1 atm)}, H^+(aq) \ (c=1 \text{ M})$$

All other single electrode potentials measured with respect to standard hydrogen electrode are referred to as potentials on the hydrogen scale.

If it is required to find the electrode potential of, say, zinc electrode dipping in a solution of zinc sulphate (*i.e.*, Zn, Zn^{2+} electrode), all that is needed is to combine it with the standard hydrogen electrode so as to have a complete cell represented as :

$$Zn, Zn^{2+} \text{ solution} \mid H^+(aq)(c=1 \text{ M}), H_2(g) \text{ (1 atm)} ; Pt$$

The EMF of the cell, determined potentiometrically, is then equal to the potential of the zinc electrode (on the hydrogen scale) since potential of the standard hydrogen electrode is taken as zero.

In this case, reduction occurs at the hydrogen electrode and oxidation takes place at the zinc electrode, as shown below :

Hydrogen electrode : $2H^+(aq) + 2e^- \rightleftharpoons H_2(g)$

Zinc electrode : $Zn(s) \rightleftharpoons Zn^{2+}(aq) + 2e^-$

∴ The *net reaction* is

$$Zn(s) + 2H^+(aq) \rightleftharpoons Zn^{2+}(aq) + H_2(g) \text{ (1 atm)}$$

It may be mentioned, however, that it is not convenient to use the standard hydrogen electrode as the reference electrode. This is because it is difficult to maintain the activity of H^+ ions in the solution at unity and to keep the pressure of the gas uniformly at one atmosphere. A far better reference electrode is the calomel electrode which has been described above. It can be set up conveniently and can be used for long without any subsequent attention. The potential of the calomel electrode, on the hydrogen scale, has been measured carefully by connecting it to a standard hydrogen electrode. The potential of the electrode depends upon the concentration of KCl solution. The values for 0·1 M KCl, 1·0 M KCl and a saturated solution of KCl are 0·3335 volt, 0·2810 volt and 0·2422 volt, respectively, at 25°C. The calomel electrode with saturated KCl solution is most commonly used and is referred to as **saturated calomel electrode (SCE).**

Sign of Electrode Potential. According to the latest convention adopted by IUPAC (International Union of Pure and Applied Chemistry), the electrode potential is given a *positive sign* if the electrode reaction involves *reduction* (*i.e.*, taking up of electrons from the electrode) when connected to the standard hydrogen electrode and a *negative sign* if the electrode reaction involves *oxidation* (*i.e.*, liberation of electrons) when connected to the standard hydrogen electrode whose potential is taken arbitrarily as zero.

Thus, when copper electrode (copper rod dipping in a solution of a copper salt) is connected with a standard hydrogen electrode, *reduction* takes place at the copper electrode. The electrode reactions are as follows :

Copper electrode : $Cu^{2+}(aq) + 2e^- \rightleftharpoons Cu(s)$ (Reduction)

Hydrogen electrode : $H_2(g) \rightleftharpoons 2H^+(aq) + 2e^-$ (Oxidation)

Hence, according to the above convention, the potential of copper electrode is taken as *positive*. Thus, $E_{(Cu^{2+},Cu)}$ is positive.

However, if zinc electrode is connected with the standard hydrogen electrode, *oxidation* takes place at the zinc electrode. The electrode reactions are as follows :

Zinc electrode : $Zn(s) \rightleftharpoons Zn^{2+} + 2e^-(aq)$ (Oxidation)

Hydrogen electrode : $2H^+(aq) + 2e^- \rightleftharpoons H_2(g)$ (Reduction)

Hence, the potential of the zinc electrode is taken as *negative*. Thus, $E_{(Zn^{2+},Zn)}$ is negative.

THERMODYNAMICS OF REVERSIBLE ELECTRODES AND REVERSIBLE CELLS

Electrical Energy in a Galvanic Cell. The electrical energy produced by a galvanic cell is given by the product of its electromotive force and the quantity of electricity which passes. If EMF is measured in volts and quantity of electricity in coulombs, the electrical energy is obtained in volt coulombs or joules (volt coulomb=joule). For example, in the Daniell cell, the EMF is 1·10 volts. The cell reaction involves liberation as well as taking up of 2 electrons, *i.e.*, deposition of 2 moles of copper (or dissolution of 2 moles of zinc). Therefore, the quantity of electricity produced, is 2 faradays, *i.e.*, 2×96,485 coulombs (faraday, F = 96485 C mol^{-1}). Hence, the electrical energy generated in the cell for the complete cell reaction = 2 mol × 96485 C mol^{-1} × 1·10 V = 212,267 volt coulombs, *i.e.*, joules.

Electrical Energy and Free Energy Change of the Cell Reaction. Till about the middle of the nineteenth century it was generally believed that electrical energy of a reversible cell originated from the *decrease in the enthalpy* ($-\Delta H$) of the cell reaction. This view received support from the fact that the enthalpy of the reaction

$$Zn(s) + Cu^{2+}(aq) \rightleftharpoons Zn^{2+}(aq) + Cu(s)$$

taking place in the Daniell cell is about 210,000 joules which is very close to the electrical energy of the cell, *viz.*, 212,300 joules, as calculated above. However, towards the close of the century, it was pointed out by Gibbs, and independently by Helmholtz, that the electrical energy of a reversible cell originates from the free energy decrease ($-\Delta G$) of the reaction occurring in the cell.

Suppose in a particular cell reaction, n is the number of electrons liberated at one electrode (or taken up at the other electrode). Then, evidently, n faradays (nF) of electricity will be generated in the complete cell reaction. If, for the sake of simplicity, the EMF of the cell, *viz.*, E_{cell}, is denoted by E, then,

Electrical energy produced by the cell $= nFE$

Hence,
$$-\Delta G = nFE \qquad ...(1)$$

Example 1. For the Daniel cell involving the cell reaction

$$Zn(s) + Cu^{2+}(aq) \rightleftharpoons Zn^{2+}(aq) + Cu(s),$$

the standard free energies of formation of Zn(*s*), Cu(*s*), $Cu^{2+}(aq)$ and $Zn^{2+}(aq)$ are 0, 0, 64·4 kJ mol^{-1} and −154·0 kJ mol^{-1}, respectively. Calculate the standard EMF of the cell.

Solution. We know that

$$\Delta G^\circ = \Delta G_f^\circ(\text{Products}) - \Delta G_f^\circ(\text{Reactants})$$

$$= (-154{\cdot}0 + 0) - (0 + 64{\cdot}4\ \text{kJ}) = -218{\cdot}4\ \text{kJ}$$

From Eq.1, $-\Delta G^\circ = nFE^\circ$

Since the reaction involves a 2-electron change, n=2

$$E^\circ = -\frac{\Delta G^\circ}{nF} = -\frac{-218{\cdot}4\text{kJ mol}^{-1}}{2\times 96485\ \text{C mol}^{-1}} = \frac{218400\ \text{V C mol}^{-1}}{2\times 96485\ \text{C mol}^{-1}}$$

$$= 1{\cdot}13\ \text{V} \qquad (\text{J} = \text{V C})$$

Relation between Electrical Energy and Enthalpy of a Cell Reaction. According to the well known Gibbs-Helmholtz equation, decrease in free energy, $-\Delta G$, of the cell reaction at constant pressure, would be given by the expression

$$-\Delta G = -\Delta H + T\left(\frac{\partial(\Delta G)}{\partial T}\right)_P \qquad ...(2)$$

where $-\Delta H$ is the decrease in the enthalpy of the cell reaction at constant pressure.

Substituting the value of $-\Delta G$ from Eq. 1 in Eq. 2, we get

$$nFE = -\Delta H - T\left(\frac{\partial(-nFE)}{\partial T}\right)_P = -\Delta H + TnF\left(\frac{\partial E}{\partial T}\right)_P \qquad ...(3)$$

since n and F are constants.

Evidently, whether the electrical energy, *viz.*, nFE, is equal to or greater or less than the enthalpy of the cell reaction (*i.e.*, ΔH), depends upon the sign of $(\partial E/\partial T)_P$, *i.e.*, ***upon the sign of the temperature coefficient of EMF of the cell.*** If it is zero, the electrical energy will be equal to the enthalpy of the cell reaction. If it is positive, *i.e.*, if the EMF of the cell increases with rise in temperature, the electrical energy will be greater than the enthalpy of the cell reaction. The additional energy will be supplied to the cell by the surroudings and if that is not possible, the temperature of the cell will fall during its working. If $(\partial E/\partial T)_P$ is negative, the electrical energy will be smaller than the enthalpy of the reaction. The difference between the two values will be given out as heat to the surroundings and if that is not possible, the temperature of the cell will rise during its operation. In the case of the Daniell cell, $(\partial E/\partial T)_P$ is very small. Therefore, electrical energy is very close to the enthalpy of the cell reaction.

It follows from Eq. 3 that

$$E = -\Delta H/nF + T(\partial E/\partial T)_P \qquad ...(4)$$

Determination of ΔH, ΔG and ΔS of a Cell Reaction. With the help of Eqs. 1 and 4, it is possible to determine various thermodynamic quantities such as enthalpy change (ΔH), free energy change (ΔG) and entropy change (ΔS) accompanying the cell reaction, by measuring the EMF of the cell and its temperature coefficient. This is illustrated below.

Example 2. The EMF of the cell $Cd,CdCl_2.2{\cdot}5H_2O(saturated)\ ||\ AgCl(s), Ag$ in which the cell reaction is

$$Cd(s) + 2AgCl(s) + aq \rightleftharpoons CdCl_2{\cdot}5/2\,H_2O\ (sat.) + 2Ag(s)$$

is 0·6753 V at 25°C and 0·6915 V at 0°C. Calculate the free energy change (ΔG), enthalpy change (ΔH) and entropy change (ΔS) of the cell reaction at 25°C.

Solution : 1. Free Energy Change (ΔG) :

The cell reaction, requires 2 faradays of electricity for its completion since n=2.

Free energy change is given by the relation $-\Delta G = nFE$

$$\therefore \quad \Delta G = -2\ \text{mol}\times 96{,}485\ \text{C mol}^{-1}\times 0{\cdot}6753\ \text{V} \qquad (\text{J} = \text{V C})$$

$$= -130{,}332{\cdot}9\ \text{J} = -130{\cdot}33\ \text{kJ}$$

2. Enthalpy Change (ΔH) :

The EMF of the cell is given by

$$E = -\frac{\Delta H}{2F} + T\left(\frac{\partial E}{\partial T}\right)_P \qquad (\text{Eq. 4})$$

In this case, EMF decreases with increase in temperature, *i.e.*, $(\partial E/\partial T)_P$ is negative. Thus,

$$\left(\frac{\partial E}{\partial T}\right)_P = -\left(\frac{0{\cdot}6915\ \text{V} - 0{\cdot}6753\ \text{V}}{25\ \text{K}}\right) = -0{\cdot}00065\ \text{V K}^{-1} \text{ at atmospheric pressure}$$

$$\therefore \quad 0{\cdot}6753\ \text{V} = \frac{\Delta H}{2\text{mol}\times 96{,}485\ \text{C mol}^{-1}} + 298\ \text{K}\ (-0{\cdot}00065\ \text{V K}^{-1}) \qquad (\text{J} = \text{V C})$$

$$\therefore \quad \Delta H = -167717\ \text{joules} = -167{\cdot}72\ \text{kJ}$$

3. Entropy Change (ΔS) :

The entropy change is related to enthalpy change and free energy change by the well known thermodynamic expression, $\Delta G = \Delta H - T\Delta S$.

$$\therefore \quad -\Delta S = \frac{\Delta G - \Delta H}{T} = \frac{-130{\cdot}33\ \text{kJ} - (-167{\cdot}72\ \text{kJ})}{298\ \text{K}} = 0{\cdot}1238\ \text{kJ K}^{-1} = 123{\cdot}8\ \text{J K}^{-1}$$

Determination of $\Delta G°$, $\Delta S°$ and $\Delta H°$ of a Cell Reaction. The EMF and its temperature-dependence help us in determining various thermodynamic quantities in standard state such as standard free energy change, $\Delta G°$; standard entropy change, $\Delta S°$ and standard enthalpy change, $\Delta H°$ of a cell reaction.

From Eq. 1, the standard free energy change of a cell reaction is given by

$$\Delta G° = - nFE° \qquad ...(5)$$

where $E°$ is the standard EMF, *i.e.*, the EMF obtained when the concentration of each constituent of the cell reaction is 1 M.

Differentiating Eq. 5 with respect to temperature at constant pressure, we have

$$[\partial(\Delta G°)/\partial T]_P = - nF(\partial E°/\partial T)_P \qquad ...(6)$$

Since $$[\partial(\Delta G°)/\partial T)_P = - \Delta S°, \qquad ...(7)$$

hence, from Eqs. 6 and 7,

$$\Delta S° = nF(\partial E°/\partial T)_P \qquad ...(8)$$

$$\Delta H° = \Delta G° + T\Delta S° \qquad ...(9)$$

$$= - nFE° + nFT(\partial E°/\partial T)_P \qquad ...(10)$$

Thus, by measuring the standard EMF of a cell at a series of temperatures, we can calculate the thermodynamic quantities $\Delta G°$, $\Delta S°$ and $\Delta H°$ for the cell reaction. As a matter of fact, since the EMF measurements can be carried out with good accuracy, the determination of thermodynamic quantites by this method is more accurate than their determination from calorimetry or from equilibrium constant determination.

Example 3. The E.M.F. of the Standard Weston cell written as

$$Cd(Hg),\ CdSO_4.8/3\,H_2O(s)\ ||\ CdSO_4(sat.),\ Hg_2SO_4(s),\ Hg$$

in which the cell reaction is

$$Cd(Hg) + Hg_2SO_4(s) + 8/3\ H_2O(l) \rightleftharpoons CdSO_4.8/3H_2O(s) + 2Hg(l)$$

is 1·0185 V at 25°C. Calculate $\Delta G°$, $\Delta S°$ and $\Delta H°$ for the cell reaction if $(\partial E°/\partial T)_P$ for the cell is $5·00\times10^{-5}$ V K^{-1}. F = 96485 C mol^{-1}.

Solution : 1. Standard Free Energy Change, $\Delta G°$:

The value of n, *i.e.*, the number of electrons involved in the cell reaction is evidently 2. Thus, 2 faradays of electricity would be generated in the complete cell reaction.

$$\therefore \quad \Delta G° = - nFE° \qquad \text{(Eq. 5)}$$

$$= - 2(96485\ C\ mol^{-1})\ (1·0183\ V) = - 196501·3\ joule = \mathbf{- 196·501\ kJ}$$

2. Standard Entropy Change, $\Delta S°$:

$$\Delta S° = nF(\partial E°/\partial T)_P \qquad \text{(Eq. 8)}$$

$$= 2\times96485\ C\times(5·00\times10^{-5}\ V\ K^{-1}) = \mathbf{9·65\ J\ K^{-1}}$$

3. Standard Enthalpy Change, $\Delta H°$:

$$\Delta H° = \Delta G° + T\Delta S° \qquad \text{(Eq. 9)}$$

$$= - 196501\ J + (298\ K)(9·65\ J\ K^{-1}) = - 193625\ J = \mathbf{- 193·6\ kJ}$$

Electromotive force and Equilibrium Constant of a Cell Reaction. Suppose the reaction occurring in a reversible cell is represented by the general equation

$$aA + bB \rightleftharpoons cC + dD$$

The decrease in free energy, $-\Delta G$, accompanying the process is given by the well known thermodynamic equation

$$-\Delta G = - \Delta G° - RT \ln Q \qquad ...(11)$$

where $-\Delta G°$ is the decrease in free energy accompanying the same process when all the reactants and products are in ***their standard states of unit activity*** and Q stands for the reaction quotient of the activities of the products and the reactants at any given stage of the reaction, that is,

$$Q = (a_C)^c\,(a_D)^d/(a_A)^a(a_B)^b$$

If E is the EMF of the cell in volts and the cell reaction involves the passage of n faradays, *i.e.*, nF coulombs, the electrical energy produced by the cell is nFE volt coulombs *i.e.*, joules.

$$\therefore \quad nFE = - \Delta G° - RT \ln Q \qquad ...(12)$$

We know that $$-\Delta G° = RT \ln K \qquad \text{(van't Hoff reaction isotherm)} \qquad ...(13)$$

where K is the equilibrium constant of the cell reaction.

Substituting in Eq. 12, we get

$$nFE = RT \ln K - RT \ln Q \qquad ...(14)$$

Substituting the expression for Q, we have

$$nFE = RT \ln K - RT \ln \frac{(a_C)^c(a_D)^d}{(a_A)^a(a_B)^b} \qquad ...(15)$$

Replacing activities by concentrations as an approximation and changing ln to $\log_{10}$, we have

$$E = \frac{2·303RT}{nF} \log K - \frac{2·303RT}{nF} \log \frac{[C]^c[D]^d}{[A]^a[B]^b} \qquad ...(16)$$

At 25°C, $$\frac{2·303RT}{F} = \frac{2·303\times8·314\ J\ K^{-1}\ mol^{-1}\times298\ K}{96485\ C\ mol^{-1}}$$

$$= 0·0591\ volt \qquad \text{(joule = volt coulomb)} \qquad ...(17)$$

$$\therefore \quad E = \frac{0·0591}{n} \log K - \frac{0·0591}{n} \log \frac{[C]^c[D]^d}{[A]^a[B]^b} \qquad ...(18)$$

Knowing the EMF of the cell and the concentrations of reactants and products of the cell reaction, we can calculate the equilibrium constant of the cell reaction.

Example 4. Calculate the equilibrium constant of the cell reaction $2Ag^+ + Zn \rightleftharpoons 2Ag + Zn^{2+}$ occurring in the zinc-silver cell at 25°C when $[Zn^{2+}]$ = 0·10 M and $[Ag^+]$ = 10 M. The EMF of the cell is found to be 1·62 V.

Solution : According to Eq. 18, at 25°C

$$E = \frac{0·0591\,V}{n} \log K - \frac{0·0591\,V}{n} \log \frac{[Ag]^2[Zn^{2+}]}{[Ag^+]^2[Zn]}$$

$$1·62\,V = \frac{0·0591\,V}{2} \log K - \frac{0·0591\,V}{2} \log \frac{[Zn^{2+}]}{[Ag^+]^2}$$

(∵ concentrations of solids are taken as unity)

$$= \frac{0·0591\,V}{2} \log K - \frac{0·0591\,V}{2} \log \frac{0·10}{10·0} \quad \text{whence } \log K = 52·91$$

Hence, $K = 8·128\times10^{52}$

Standard EMF and Equilibrium Constant. If the standard EMF ($E°$) of a particular cell is known, the equilibrium constant of the cell reaction can be calculated straightaway by making use of the relation

$$-\Delta G° = RT \ln K = nFE° \text{ whence } \ln K = \frac{nFE°}{RT}$$

or
$$\log K = \frac{nFE°}{2{\cdot}303RT} \qquad ...(19)$$

Example 5. The standard EMF of the Daniell cell involving the cell reaction

$Zn(s) + Cu^{2+}(aq) \rightleftharpoons Zn^{2+}(aq) + Cu(s)$, is 1·10 volts. Calculate the equilibrium constant of the cell reaction at 25°C.

Solution :
$$\log K = nFE°/(2{\cdot}303RT) \qquad \text{(Eq.19)}$$

$$= \frac{2 \times 96500 \text{ C mol}^{-1} \times 1{\cdot}10 \text{ V}}{2{\cdot}303 \times 8{\cdot}314 \text{ J K}^{-1} \text{ mol}^{-1} \times 298 \text{ K}} = 37{\cdot}20 \qquad (\text{J} = \text{V C})$$

$$\therefore \quad K = 1{\cdot}585 \times 10^{37}$$

Effect of Concentration of Electrolyte on Cell Potential. As discussed above,

$$-\Delta G = -\Delta G° - RT \ln Q \qquad \text{(Eq. 11)}$$

In this equation, $-\Delta G = nFE$ and $-\Delta G° = nFE°$ where $E°$ is the **standard EMF** of the cell, *i.e.*, the EMF when the activity, or to be approximate, concentration, of each of the reactants and products of the cell reaction is unity.

$$\therefore \quad nFE = nFE° - RT \ln Q$$

or
$$E = E° - \frac{RT}{nF} \ln Q$$

where Q is the reaction quotient of the cell reaction. Thus,

$$E = E° - \frac{RT}{nF} \ln \frac{(a_C)^c (a_D)^d}{(a_A)^a (a_B)^b} \qquad ...(20)$$

$$= E° - \frac{0{\cdot}0591}{n} \log \frac{[C]^c [D]^d}{[A]^a [B]^b} \text{ at } 25°C \qquad ...(21)$$

This equation gives the effect of the concentrations of reactants and products involved in the cell reaction on the EMF of the cell.

Effect of Electrolyte Concentration on Electrode Potential : Nernst Equation

Consider an electrode consisting of a metal in contact with a solution of its own cations. As an example, we may consider a zinc rod in contact with a solution of zinc sulphate furnishing Zn^{2+} ions. The following equilibrium will be established considering that the reaction from left to right involves reduction :

$$Zn^{2+}(aq) + 2e^- \rightleftharpoons Zn(s)$$

The decrease in free energy accompanying the electrode reaction in accordance with Eqs.15 and 19 is given by

$$nFE_{el} = nFE°_{el} - RT \ln (a_{Zn}/a_{Zn^{2+}})$$

$$E_{el} = E°_{el} - \frac{RT}{2F} \ln \frac{a_{Zn}}{a_{Zn^{2+}}} = E°_{el} + \frac{RT}{2F} \ln \frac{a_{Zn^{2+}}}{a_{Zn}}$$

$$= E°_{el} - \frac{RT}{2F} \ln a_{Zn^{2+}} \qquad (\because \text{ for solids, } a = 1) \qquad ...(22)$$

$$= E°_{el} - \frac{RT}{2F} \ln [Zn^{2+}] \text{ as an approximation.} \qquad ...(23)$$

where E_{el} is the electrode potential of zinc electrode under the operating conditions and $E°_{el}$ is the **standard electrode potential** of zinc electrode, *i.e.*, the potential developed on the zinc rod when it is in contact with a solution of Zn^{2+} ions of unit activity (or to be approximate, unit molar concentration).

Consider the half-cell reaction

$$Ag^+(aq) + e^- \rightleftharpoons Ag(s),$$

the electrode potential of which is given by

$$E_{el} = E°_{el} - \frac{RT}{F} \ln \frac{1}{[Ag^+]} \qquad \{\because [Ag(s)] \text{ is taken as unity}\}$$

$$= E°_{el} + \frac{RT}{F} \ln [Ag^+] \qquad ...(24)$$

Hence, the general expression for the electrode potential of a metal M in contact with M^{n+} ions, involving the electrode reaction

$$M^{n+}(aq) + ne^- \rightleftharpoons M(s),$$

may be written as

$$E_{el} = E°_{el} - \frac{RT}{nF} \ln \frac{1}{[M^{n+}]} \qquad \{\because [M] \text{ is taken as unity}\}$$

$$= E°_{el} + \frac{RT}{nF} \ln [M^{n+}] \qquad ...(25)$$

$$= E°_{el} + \frac{0{\cdot}0591}{n} \log [M^{n+}] \text{ at } 25°C \qquad ...(26)$$

Eq. 26, which gives the effect of the concentration of M^{n+} ion on the potential of M^{n+},M electrode, is known as the **Nernst equation.**

In the case of hydrogen electrode, the equilibrium is represented as

$$H^+(aq) + e^- \rightleftharpoons \tfrac{1}{2} H_2(g)$$
$$\text{1 atm}$$

Hence,
$$E_{el} = E°_{el} - \frac{RT}{F} \ln \frac{1}{[H^+]}$$

($\because$ activity of H_2 gas at 1 atm pressure is taken as unity)

$$= E°_{el} + \frac{RT}{F} \ln [H^+] = \frac{RT}{F} \ln [H^+] \qquad ...(27)$$

because $E°_{el}$ for hydrogen electrode is arbitrarily taken as zero.

In the case of Fe^{3+}, Fe^{2+} electrode, the equilibrium is represented as

$$Fe^{3+}(aq) + e^- \rightleftharpoons Fe^{2+}(aq)$$

Hence,
$$E_{el} = E°_{el} - \frac{RT}{F} \ln \frac{[Fe^{2+}]}{[Fe^{3+}]} = E°_{el} + \frac{RT}{F} \ln \frac{[Fe^{3+}]}{[Fe^{2+}]} \qquad ...(28)$$

It follows from the above discussion that if we write the electrode reaction, in general, as

$$\text{Oxidised state} + ne^- \rightleftharpoons \text{Reduced state},$$

the potential of the electrode is given by

$$E_{el} = E^\circ_{el} - \frac{RT}{F} \ln \frac{[\text{Reduced state}]}{[\text{Oxidised state}]} = E^\circ_{el} + \frac{RT}{F} \ln \frac{[\text{Oxidised state}]}{[\text{Reduced state}]} \quad \ldots(29)$$

In the case of a chlorine electrode, in which chlorine gas is bubbled at a pressure of 1 atmosphere through a solution containing Cl^- ions, the equilibrium is represented as

$$\underset{(1\text{ atm})}{\tfrac{1}{2}Cl_2(g)} + e^- \rightleftharpoons Cl^-(aq)$$

The potential of the electrode is given by

$$E_{el} = E^\circ_{el} - \frac{RT}{F} \ln \frac{[Cl^-]}{[Cl_2]} = E^\circ_{el} - \frac{RT}{F} \ln [Cl^-] \quad \ldots(30)$$

(since activity of chlorine gas at 1 atm pressure is taken as unity)

For the calomel electrode, the electrode reaction is

$$Hg_2Cl_2(s) + 2e^- \rightleftharpoons 2Hg(l) + 2Cl^-(aq)$$

The potential of the calomel electrode is given by

$$E_{el} = E^\circ_{el} - \frac{RT}{2F} \ln \frac{[Cl^-]^2[Hg]^2}{[Hg_2Cl_2]}$$

$$= E^\circ_{el} - \frac{RT}{2F} \ln [Cl^-]^2 = E^\circ_{el} - \frac{RT}{F} \ln [Cl^-] \quad \ldots(31)$$

{[(Hg(*l*)] and $[Hg_2Cl_2(s)]$ is also taken as unity each}

Example 6. A zinc rod is placed in 0·1 M solution of zinc sulphate at 25°C. Assuming that the salt is dissociated to the extent of 95 per cent at this dilution, calculate the potential of the electrode at this temperature. $E^\circ_{(Zn^{2+},Zn)} = -0.76$ V.

Solution : Concentration of zinc sulphate solution = 0·1 M ; dissociation = 95%

$$\therefore \quad [Zn^{2+}] = 0.1 \times 95/100 = 0.095 \text{ M}$$

The electrode reaction in this case is

$$Zn^{2+}(aq) + 2e^- \rightleftharpoons Zn(s) \qquad (i.e.,\ n = 2)$$

According to the Nernst equation, the potential of the electorde is given by

$$E_{el} = E^\circ_{el} - \frac{RT}{nF} \ln \frac{1}{[Zn^{2+}]} = E^\circ_{el} + \frac{RT}{nF} \ln [Zn^{2+}]$$

$$= E^\circ_{el} + \frac{0.0591}{n} \log [Zn^{2+}]$$

Substituting the various values in the above equation, we have

$$E_{el} = -0.76 + \frac{0.0591}{2} \log 0.095 = -0.79 \text{ V}$$

Standard Electrode Potentials : Electrochemical Series

As discussed above, the potential of an electrode, at a given temperature, depends upon the concentration of the ions in the surrounding solution. If the concentration of the ions is unity and the temperature is 25°C, the potential of the electrode is termed as the standard electrode potential.

The standard electrode potentials of a number of electrodes are given in Table 1. These values are said to be on hydrogen scale since in these determinations the potential of the standard hydrogen electrode, used as the reference electrode, has been taken as zero. The values of standard electrode potentials arranged in the decreasing order as in Table 1, constitute what is called the **electrochemical series.**

TABLE 1

Electrochemical Series : Standard Electrode Potentials at 25°C

Electrode	Electrode Reaction	E°_{el} (volts)
$F_2(g);2F^-$	$F_2 + 2e^- \rightleftharpoons 2F^-$	+2·87
Co^{3+},Co^{2+}; Pt	$Co^{3+} + e^- \rightleftharpoons Co^{2+}$	+1·82
Ce^{4+},Ce^{3+}; Pt	$Ce^{4+} + e^- \rightleftharpoons Ce^{3+}$	+1·61
Mn^{2+},MnO_4^-; Pt	$MnO_4^- + 8H^+ + 5e^- \rightleftharpoons Mn^{2+} + 4H_2O$	+1·51
Au^{3+}, Au	$Au^{3+} + 3e^- \rightleftharpoons Au$	+1·50
$Cl_2(g), 2Cl^-$; Pt	$Cl_2(g, 1\text{ atm}) + 2e^- \rightleftharpoons 2Cl^-$	+1·36
Cr^{3+}, $Cr_2O_7^{2-}$	$Cr_2O_7^{2-} + 14H^+ + 6e^- \rightleftharpoons 2Cr^{3+} + 7H_2O$	+1·33
Tl^{3+}, Tl^+	$Tl^{3+} + 2e^- \rightleftharpoons Tl^+$	+1·25
$Br_2(l), 2Br^-$; Pt	$Br_2(l) + 2e^- \rightleftharpoons 2Br^-$	+1·06
Hg^{2+}, Hg_2^{2+}; Pt	$2Hg^{2+} + 2e^- \rightleftharpoons Hg_2^{2+}$	+0·92
Ag^+; Ag	$Ag^+ + e^- \rightleftharpoons Ag$	+0·80
Fe^{3+}, Fe^{2+}; Pt	$Fe^{3+} + e^- \rightleftharpoons Fe^{2+}$	+0·77
$Hg_2SO_4(s), SO_4^{2-}$; Hg	$Hg_2SO_4(s) + e^- \rightleftharpoons 2Hg + SO_4^{2-}$	+0·61
$I_2(s)$; $2I^-$; Pt	$I_2(s) + 2e^- \rightleftharpoons 2I^-$	+0·53
Cu^+, Cu	$Cu^+ + e^- \rightleftharpoons Cu$	+0·52
Cu^{2+}, Cu	$Cu^{2+} + 2e^- \rightleftharpoons Cu$	+0·34
$Hg_2Cl_2(s), Cl^-$; Hg	$Hg_2Cl_2(s) + 2e^- \rightleftharpoons 2Hg + 2Cl^-$	+0·28
$AgCl(s), Cl^-$; Ag	$AgCl(s) + e^- \rightleftharpoons Ag(s) + Cl^-$	+0·22
Sn^{4+}, Sn^{2+}; Pt	$Sn^{4+} + 2e^- \rightleftharpoons Sn^{2+}$	+0·15
Cu^{2+}, Cu^+	$Cu^{2+} + e^- \rightleftharpoons Cu^+$	+0·15
$Hg_2Br_2(s), Br^-$; Hg	$Hg_2Br_2(s) + 2e^- \rightleftharpoons 2Hg + 2Br^-$	+0·13
$AgBr(s), Br^-$; Ag	$AgBr(s) + e^- \rightleftharpoons Ag(s) + Br^-$	+0·07
$2H^+, H_2(g)$; Pt	$2H^+ + 2e^- \rightleftharpoons H_2(g, 1\text{ atm})$	0·00
Pb^{2+}, Pb	$Pb^{2+} + 2e^- \rightleftharpoons Pb$	−0·13
Sn^{2+}, Sn	$Sn^{2+} + 2e^- \rightleftharpoons Sn$	−0·15
$AgI(s), I^-$; Ag	$AgI(s) + e^- \rightleftharpoons Ag(s) + I^-$	−0·15
Ni^{2+}, Ni	$Ni^{2+} + 2e^- \rightleftharpoons Ni$	−0·24
Co^{2+}, Co	$Co^{2+} + 2e^- \rightleftharpoons Co$	−0·27
Tl^+,Tl	$Tl^+ + e^- \rightleftharpoons Tl$	−0·34
Cd^{2+}, Cd	$Cd^{2+} + 2e^- \rightleftharpoons Cd$	−0·40
Fe^{2+},Fe	$Fe^{2+} + 2e^- \rightleftharpoons Fe$	−0·44
Cr^{3+}, Cr	$Cr^{3+} + 3e^- \rightleftharpoons Cr$	−0·74
Zn^{2+},Zn	$Zn^{2+} + 2e^- \rightleftharpoons Zn$	−0·76
Mn^{2+}, Mn	$Mn^{2+} + 2e^- \rightleftharpoons Mn$	−1·18
Al^{3+}, Al	$Al^{3+} + 3e^- \rightleftharpoons Al$	−1·66
Mg^{2+}, Mg	$Mg^{2+} + 2e^- \rightleftharpoons Mg$	−2·52
Na^+, Na	$Na^+ + e^- \rightleftharpoons Na$	−2·71
Ca^{2+}, Ca	$Ca^{2+} + 2e^- \rightleftharpoons Ca$	−2·87
Ba^{2+}, Ba	$Ba^{2+} + 2e^- \rightleftharpoons Ba$	−2·90
K^+, K	$K^+ + e^- \rightleftharpoons K$	−2·92
Li^+, Li	$Li^+ + e^- \rightleftharpoons Li$	−3·04

The magnitude of E°_{el} is a measure of the tendency of the half-cell reaction to occur in the forward direction (which is the direction of reduction). The higher its positive value, the greater is the tendency of the oxidized form to get reduced by accepting electrons. And, conversely, the greater the negative value, the greater is the tendency of the reduced form to get oxidized by donating electrons.

Electromotive Force of Galvanic Cells

Table 1 includes a large variety of electrodes (half-cells) along with their electrode (half-cell) reactions and the standard electrode potentials. Any two suitable half-cells can be combined to form a **galvanic cell.** The EMF of the cell and the feasible cell reaction can be easily determined with the help of the information given in this Table. For this purpose, the following rules have been suggested :

1. *Representation of the Cell.* The electrode on the right is written in the order : ion, electrode (*e.g.*, Cu^{2+},Cu) and the electrode on the left is written in the order : electrode, ion (*e.g.*, Zn, Zn^{2+}). In the galvanic cell formed by the combination of the two electrodes, *oxidation* occurs at the left hand electrode and *reduction* at the right hand electrode so that the electric current (electrons) in the external circuit flows from the L.H.E. to the R.H.E.

2. *Determination of the Cell Potential and the Cell Reaction.* According to the latest convention, both the half-cell reactions are written as **reduction reactions** alongwith their standard electrode potentials in the form of chemical equations and after balancing the number of electrons, if necessary, the half-cell reaction equation with a lower electrode potential is subtracted from the one with a higher electrode potential. The resultant gives the cell potential as well as the feasible cell reaction.

The two half-cell reactions in the Daniel cell are thus witten as

(i) $Cu^{2+}(aq) + 2e^- \rightleftharpoons Cu(s)$; $E^\circ_{el} = +0{\cdot}34$ V

(ii) $Zn^{2+}(aq) + 2e^- \rightleftharpoons Zn(s)$; $E^\circ_{el} = -0{\cdot}76$ V

Subtracting Eq. *(ii)* from Eq. *(i)*, we get

$Cu^{2+}(aq) + Zn(s) \rightleftharpoons Cu(s) + Zn^{2+}(aq)$ as the feasible cell reaction and $0{\cdot}34 - (-0{\cdot}76) = 1{\cdot}10$ V as the cell potential.

Example 7. Write the cell reaction and calculate E° for the cell .

$$Zn, Zn^{2+}\ (1\ M)\ |\ Fe^{2+}(1\ M), Fe^{3+}(1M)\ ;\ Pt$$

Solution : Writing both the half-cell reactions as reduction reactions and balancing the number of electrons involved, we get

(i) $2Fe^{3+}(aq) + 2e^- \rightleftharpoons 2Fe^{2+}(aq)$; $E^\circ_{el} = +0{\cdot}77$ V

(ii) $Zn^{2+}(aq) + 2e^- \rightleftharpoons Zn(s)$; $E^\circ_{el} = -0{\cdot}76$ V

Substracting Eq. *(ii)* from Eq. *(i)*, we get

$Zn(s) + 2Fe^{3+}(aq) \rightleftharpoons 2Fe^{2+}(aq) + Zn^{2+}(aq)$ as the **cell reaction** and $E^\circ = 0{\cdot}77 - (-0{\cdot}76) = 1{\cdot}53$ V as the **cell potential.**

It should be noted that the E°_{el} values remain unchanged when the number of electrons in the two half-cell reaction equations are balanced.

Example 8. Given the following half-cell reactions :

$Zn^{2+}(aq) + 2e^- \rightleftharpoons Zn(s)$; $E^\circ_{el} = -0{\cdot}76$ V

$CuI(s) + e^- \rightleftharpoons Cu(s) + I^-(aq)$; $E^\circ_{el} = +0{\cdot}17$ V

calculate the standard potential, E°, of the cell

$$Zn, Zn^{2+}(1\ M)\ |\ I^-(1M), CuI\ ;\ Cu$$

Solution : *(i)* $2CuI(s) + 2e^- \rightleftharpoons 2Cu(s) + 2I^-(aq)$; $E^\circ_{el} = -0{\cdot}17$ V

(ii) $Zn^{2+}(aq) + 2e^- \rightleftharpoons Zn(s)$; $E^\circ_{el} = -0{\cdot}76$ V

Substracting Eq. *(ii)* from Eq. *(i)*, we get

$Zn(s) + 2CuI(s) \rightleftharpoons Zn^{2+}(aq) + 2Cu(s) + 2I^-(aq)$ as the cell reaction

and $E^\circ = -0{\cdot}17 - (-0{\cdot}76) = +0{\cdot}59$ V as the **standard cell potential.**

Example 9. With the help of the electrochemical series, show which substance can be used for oxidizing fluorides to fluorine ?

Solution : From the values of standard potentials given in Table 1, we see that the reduction half-cell reaction involving reduction of fluorine to fluoride ion

$F_2 + 2e^- \rightleftharpoons 2F^-$; $E^\circ_{el} = 2{\cdot}87$ V

has the highest positive potential. The reverse reaction, *viz.*, oxidation of F^- ion to fluorine will thus have the highest negative potential, *i.e.*, the F^- ion will have the highest negative tendency to get oxidised. This implies that **fluorides cannot be oxidized chemically by any substance listed in Table 1.** They can be oxidized only electrolytically.

Example 10. Calculate the EMF of the following electrochemical cell at 25°C :

$$Cu, Cu^{2+}(c=0{\cdot}1\ M)\ |\ H^+\ (c=0{\cdot}01\ M), H_2\ (1\ atm)\ ;\ Pt.$$

Solution : The half-cell reactions are :

(i) $2H^+ + 2e^- \rightleftharpoons H_2(g)$; $E^\circ_{el} = 0 + 0{\cdot}0591 \log [H^+] = -0{\cdot}118$ V (from Nernst equation)

(ii) $Cu^{2+}(aq) + 2e^- \rightleftharpoons Cu(s)$; $E^\circ_{el} = 0{\cdot}34 + \frac{0{\cdot}0591}{2} \log [Cu^{2+}] = +0{\cdot}31$ V

Substracting Eq. *(i)* from Eq. *(ii)*, we get

$Cu^{2+}(aq) + H_2(g) \rightleftharpoons Cu(s) + 2H^+(aq)$ as the cell reaction and

$E^\circ = 0{\cdot}31 - (-0{\cdot}118) = 0{\cdot}428$ V as the **cell potential.**

Example 11. Consider the electrochemical cell, Fe, Fe^{2+} (0·1 M) | Cd^{2+} (0·001 M), Cd. *(a)* Write the cell reaction *(b)* Calculate the EMF of the cell *(c)* Calculate the equilibrium constant of the cell reaction.

Solution : *(a)* The half-cell reactions are :

(i) $Cd^{2+}(aq) + 2e^- \rightleftharpoons Cd(s)$; $E_{el} = -0{\cdot}40 + \frac{0{\cdot}0591}{2} \log [Cd^{2+}] = -0{\cdot}488$ V (Nernst equation)

(ii) $Fe^{2+}(aq) + 2e^- \rightleftharpoons Fe(s)$; $E_{el} = -0{\cdot}44 + \frac{0{\cdot}0591}{2} \log [Fe^{2+}] = -0{\cdot}469$ V (Nernst equation)

Substracting Eq. *(i)* from Eq. *(ii)*, we get

$F^{2+}(aq) + Cd(s) \rightleftharpoons Fe(s) + Cd^{2+}(aq)$ as the **cell reaction**

and $E^\circ = -0{\cdot}469 - (-0{\cdot}488) = +0{\cdot}0191$ V as the **cell potential.**

From Eq. 19,

$$\log K = \frac{nFE^\circ}{2{\cdot}303RT} = \frac{2E^\circ}{0{\cdot}0591} (\text{at } 25°C) = \frac{2(0{\cdot}019)}{0{\cdot}0591} = 0{\cdot}643$$

$\therefore$ Equilibrium constant, $K = 4{\cdot}39$

Example 12. Set up the electrochemical cell for the cell reaction : $H_2(g) + Cl_2(g) \rightleftharpoons 2HCl\ (aq)$ and calculate the equilibrium constant of the reaction.

Solution : The electrode reactions along with the standard electrode potentials, as given in Table 1, are as follows :

(i) $2H^+(aq) + 2e^- \rightleftharpoons H_2(g)$ $E^\circ_{el} = 0{\cdot}00$ V

(ii) $Cl_2(g) + 2e^- \rightleftharpoons 2Cl^-\ (aq)$ $E^\circ_{el} = +1{\cdot}36$ V

From the standard electrode potentials we see that the reduction of Cl_2 is more spontaneous than that of H_2. Hence, the latter will be taken as the R.H.E. The cell is, therefore, represented as

$$Pt\ ;\ H_2(g),\ H^+(aq)\ |\ Cl^-(aq),\ Cl_2(g)\ ;\ Pt$$

Substracting Eq. *(i)* from Eq. *(ii)*, we get

$$H_2(g) + Cl_2(g) \rightleftharpoons 2H^+(aq) + 2Cl^-(aq)$$ as the cell reaction

and $E^\circ = 1{\cdot}36 - 0 = +1{\cdot}36$ V as the cell potential.

From Eq. 19, at 25°C,

$$\log K = \frac{2E^\circ}{0{\cdot}0591} = \frac{1{\cdot}36}{0{\cdot}02955} = 46{\cdot}02$$

$$\therefore \quad \text{Equilibrium constant, } K = 1{\cdot}047\times10^{46}$$

Such a high value of K implies that the reaction, as written, is highly *spontaneous*, H_2 and Cl_2 reacting quantitatively to yield HCl(*aq*).

Example 13. Set up the electrochemical cell for the reaction

$$2Fe^{3+}(aq) + Sn^{2+}(aq) \rightleftharpoons 2Fe^{2+}(aq) + Sn^{4+}(aq)$$

and calculate the equilibrium constant for the reaction.

Solution. The electrode reactions along with the standard electrode potentials, as given in Table 1, are as follows :

(i) $2Fe^{3+} + 2e^- \rightleftharpoons 2Fe^{2+}(aq)$; $E^\circ_{el} = +0{\cdot}77$

(ii) $Sn^{4+} + 2e^- \rightleftharpoons Sn^{2+}(aq)$; $E^\circ_{el} = +0{\cdot}15$

From the standard electrode potentials we see that the reduction of Fe^{3+} is more spontaneous than that of Sn^{4+} ions. Hence, the former will be taken as the R.H.E. The electrochemical cell is, therefore, represented as

$$Pt\ ;\ Sn^{2+},\ Sn^{4+},\ |\ Fe^{3+},\ Fe^{2+}\ ;\ Pt$$

Substracting Eq. *(ii)* from Eq. *(i)*, we get

$$2Fe^{3+}(aq) + Sn^{2+}(aq) \rightleftharpoons 2Fe^{2+}(aq) + Sn^{4+}(aq)$$ as the cell reaction

and $E^\circ = 0{\cdot}77 - 0{\cdot}15 = 0{\cdot}62$ V as the cell potential.

According to Eq. 19, at 25°C,

$$\log K = \frac{2E^\circ}{0{\cdot}0591} = \frac{2\times0{\cdot}62}{0{\cdot}0591} = 20{\cdot}98$$

$$\therefore \quad K = 9{\cdot}55\times10^{20}$$

The very high value of K suggests that the reaction, as written, is *highly spontaneous*, the stannous ion reducing the ferric ion quantitatively.

Example 14. With the help of the data given in Table 1, find out whether zinc and silver would react with dilute sulphuric acid or not.

Solution : The reaction of zinc with dilute sulphuric acid may be represented as

$$Zn + H_2SO_4 \rightleftharpoons ZnSO_4 + H_2(g)$$

or $$Zn(s) + 2H^+(aq) \rightleftharpoons Zn^{2+}(aq) + H_2(g)$$

The above reaction may be split up into two reduction half-cell reactions, as represented below :

(i) $Zn^{2+}(aq) + 2e^- \rightleftharpoons Zn(s)$; $E^\circ_{el} = -0{\cdot}76$ V

(ii) $2H^+(aq) + 2e^- \rightleftharpoons H_2(g)$ $E^\circ_{el} = 0$

Subtracting Eq. *(ii)* from Eq. *(i)*, we get

$$Zn(s) + 2H^+(aq) \rightleftharpoons Zn^{2+}(aq) + H_2(g)\ ;\quad E^\circ = 0{\cdot}76\ V$$

Since E° is positive, $\Delta G^\circ(= -nFE^\circ)$ is *negative*. Hence, the reaction of zinc with sulphuric acid is feasible, *i.e.*, **Zn will react with H_2SO_4.**

Now let us consider the reaction of silver with dilute sulphuric acid :

$$2Ag + H_2SO_4 \rightleftharpoons Ag_2SO_4 + H_2(g)$$

or $$2Ag(s) + 2H^+(aq) \rightleftharpoons 2Ag^+(aq) + H_2(g)$$

The above reaction may be split up into two reduction half-cell reactions as shown below :

(i) $2Ag^+(aq) + 2e^- \rightleftharpoons 2Ag(s)$; $E^\circ_{el} = 0{\cdot}80$ V

(ii) $2H^+(aq) + 2e^- \rightleftharpoons H_2(g)$; $E^\circ_{el} = 0$

Subtracting Eq. *(ii)* from Eq. *(i)* and rearranging, we get

$$Ag(s) + 2H^+(aq) \rightleftharpoons 2Ag^+(aq) + H_2(g)\ ;\quad E^\circ = -0{\cdot}80\ V$$

Since E° is negative, the value of ΔG° $(= -nFE^\circ)$ is positive. Hence, the reaction of silver with sulphuric acid is not feasible, *i.e.*, Ag will not react with H_2SO_4.

A little reflection will show that any metal lying below the hydrogen electrode in Table 1 will reduce H^+ ions to give H_2 gas while any metal lying above the hydrogen electrode will not be able to reduce H^+ ions to give H_2 gas. In other words only those metals which lie below the hydrogen electrode in Table 1 will react with H_2SO_4 or HCl to give hydrogen gas.

Example 15. Using the data given for the standard electrode potentials, determine whether on mixing H_2O_2 with Fe^{2+}, the oxidation of Fe^{2+} to Fe^{3+} would be spontaneous or not.

Solution : The reaction involving the oxidation of Fe^{2+} to Fe^{3+} with H_2O_2 may be represented as follows :

(i) $Fe^{2+}(aq) \rightleftharpoons 2Fe^{3+}(aq) + 2e^-$; $E^\circ_l = -0{\cdot}77$ V

(ii) $H_2O_2 + 2H^+(aq) + 2e^- \rightleftharpoons 2H_2O$; $E^\circ_l = 1{\cdot}77$ V

Adding Eqs. *(i)* and *(ii)*, we get

$$H_2O_2 + 2H^+(aq) + 2Fe^{2+}(aq) \rightleftharpoons 2H_2O + 2Fe^{3+}(aq)\ ;\quad E^\circ = +1{\cdot}00\ V$$

Since E° for the oxidation reaction is positive, ΔG° will be negative. Hence the oxidation of Fe^{2+} to Fe^{3+} by H_2O_2 will be spontaneous.

Example 16. Calculate the equilibrium constant of the disproportionation reaction $2Cu^+(aq) \rightleftharpoons Cu^{2+}(aq) + Cu$. The standard electrode potentials are given in Table 1.

Solution : The reduction half-cell reactions are :

(i) $2Cu^+(aq) + 2e^- \rightleftharpoons 2Cu(s)$; $E^\circ_{el} = 0{\cdot}52$ V

(ii) $Cu^{2+}(aq) + 2e^- \rightleftharpoons Cu(s)$; $E^\circ_{el} = 0{\cdot}34$ V

Substracting Eq. *(ii)* from Eq. *(i)*, we get

$$2Cu^+(aq) \rightleftharpoons Cu^{2+}(aq) + Cu(s)$$ as the cell reaction

and $E^\circ = 0{\cdot}52 - 0{\cdot}34 = 0{\cdot}18$ V as the cell potential.

From Eq. 19, at 25°C, $$\log K = \frac{2E^\circ}{0{\cdot}0591} = \frac{2\times0{\cdot}18}{0{\cdot}0591} = 6{\cdot}09$$

whence $$K = 1{\cdot}23\times10^6$$

The large value of K suggests that Cu^+ ion is unstable and readily disproportionates into Cu^{2+} ion and Cu(*s*) in solution.

Example 17. Calculate the stability constant of the complex $[Zn(NH_3)_4]^{2+}$ formed in the reaction $Zn^{2+} + 4NH_3 \rightleftharpoons [Zn(NH_3)_4]^{2+}$.

Solution : The electrode reactions and the standard electrode potentials are as follows :

(i) $2Zn^{2+}(aq) + 2e^- \rightleftharpoons 2Zn(s)$; $E_1^\circ = 0{\cdot}76$ V

ii) $[Zn(NH_3)_4]^{2+} + 2e^- \rightleftharpoons Zn(s) + 4NH_3$; $E_2^\circ = -1{\cdot}03$ V

Substracting Eq. *(ii)* from Eq. *(i)*, we get

$$Zn^{2+} + 4NH_3 \rightleftharpoons [Zn(NH_3)]_4^{2+}, \text{ as the cell reaction}$$

and $E^\circ = -0{\cdot}76 - (-1{\cdot}03) = 0{\cdot}27$ V as the cell potential.

From Eq. 19, at 25°C, $\log K = \dfrac{2E^\circ}{0{\cdot}0591} = \dfrac{2 \times 0{\cdot}27}{0{\cdot}0591} = 9{\cdot}14$

$$\therefore \quad K = 1{\cdot}38 \times 10^9$$

The large value of the stability constant shows that the complex is very stable.

Activity and Mean Ionic Activity of an Electrolyte

In a number of cases discussed above, references have been made to activities of individual ions. But it should be clearly understood that there is no method by which activities of individual ionic species can be determined experimentally. The reason is that it is not possible to have a solution containing only one kind of ions. By experiment, therefore, the quantity that is determined is activity a or mean ionic activity $a_\pm$ of the electrolyte concerned.

Consider a uni-univalent electrolyte, like HCl, in aqueous solution. Let a_+ and a_- be the hypothetical activities of H^+ and Cl^- ions, respectively, in a solution of a given concentration. The activity a of the electrolyte is defined by the expression

$$a = a_+ a_- \qquad ...(32)$$

while mean ionic activity $a_\pm$ of the electrolyte is defined by the expression

$$a_\pm = \sqrt{a_+ a_-} \qquad ...(33)$$

Thus, while the activity of an electrolyte is given by the product of activities of component ions, the mean ionic activity of the electrolyte is given by *the geometric mean of activities of component ions.*

Squaring Eq. 33, we have

$$(a_\pm)^2 = a_+ a_- \qquad ...(34)$$

Combining Eqs. 32 and 34, we get

$$a = a_+ a_- = (a_\pm)^2 \qquad ...(35)$$

Mean Ionic Activity Coefficients of Electrolytes. Consider an electrolyte M_xA_y ionising as

$$M_xA_y \rightleftharpoons xM^+ + yA^-$$

For the sake of simplicity, the charge on each cation is represented by a single plus and that on each anion by a single minus sign. Accordingly, the activity of the electrolyte in this case would be given by

$$a = (a_+)^x (a_-)^y \qquad ...(36)$$

$$= (a_\pm)^{x+y} \text{ (by definition)} \qquad ...(37)$$

If m is the concentration of the electrolyte in terms of molality, *i.e.*, number of moles per kg of the solvent, then, molality of the cations, $m_+ = xm$ and molality of the anions, $m_- = ym$.

The activity and molality are known to be related by the expression

$$a = \gamma m \qquad ...(38)$$

where γ is the activity coefficient.

Activity of the electrolyte M_xA_y is, therefore, given by

$$a = (\gamma_+ m_+)^x (\gamma_- m_-)^y \qquad ...(39)$$

$$= (\gamma_+ x m)^x (\gamma_- y m)^y \qquad ...(40)$$

$$= x^x y^y (\gamma_\pm m)^{x+y} \qquad ...(41)$$

where $\gamma_\pm$ is the mean ionic activity coefficient related with γ_+ and γ_- by the expression

$$(\gamma_\pm)^{x+y} = (\gamma_+)^x (\gamma_-)^y \qquad ...(42)$$

For a uni-univalent electrolyte, *e.g.*, HCl or NaCl, $x=1$ and $y=1$. Hence by Eq. 37,

$$a = (a_\pm)^2 \qquad ...(43)$$

and by Eq. 41, $$a = (\gamma_\pm m)^2 \qquad ...(44)$$

The quantity measured by experiment is either activity a or mean ionic activity of the electrolyte $a_\pm$, at a given molality m. Hence, mean activity coefficient $\gamma_\pm$ of the electrolyte at a given concentration (molality) can be easily calculated.

For a uni-bivalent electrolyte, *e.g.*, Na_2SO_4, $x=2$ and $y=1$. Hence, by Eq. 37,

$$a = (a_\pm)^3$$

and by Eq. 41, $$a = 2^2 \times 1(\gamma_\pm m)^3 = 4\gamma_\pm^3 m^3$$

and so on.

The concept of activity and activity coefficients has immense relevance in the discussion of concentration cells.

CONCENTRATION CELLS

In the case of galvanic cells discussed earlier, the electrical energy arises from the chemical reactions which take place in the cells. There is, however, another category of cells in which the EMF arises not due to any chemical reaction but due to transfer of matter from one half-cell to the other because of a difference in the concentrations of the species involved. These are called **concentration cells.**

Cocentration cells are of two types, *viz.*,

1. Electrode-Concentration Cells and 2. Electrolyte-Concentration Cells.

1. Electrode-Concentration Cells. In these cells, two like electrodes at different concentrations are dipping in the same solution. Two hydrogen electrodes at unequal gas pressures immersed in the same solution of hydrogen ions constitute an electrode-concentration cell. This may be represented as follows :

$$Pt\ ;\ H_2(p_1)\ |\ \text{Solution of } H^+ \text{ ions, say, HCl solution}\ |\ H_2(p_2)\ ;\ Pt$$

The reactions occurring are :

R.H.E. : $2H^+ + 2e^- \rightleftharpoons H_2(p_2)$ (Reduction)

L.H.E. : $H_2(p_1) \rightleftharpoons 2H^+ + 2e^-$ (Oxidation)

Overall reaction : $H_2(p_1) \rightleftharpoons H_2(p_2)$

This reaction is evidently independent of the concentration of the electrolyte.

At moderate pressures, H_2 can be considered to be an ideal gas so that the ratio of the activities can be considered to be equal to the ratio of the gas pressures. Hence, the Nernst equation may be written as

$$E = E^\circ - \frac{0{\cdot}0591}{2} \log (p_2/p_1) \quad \text{at } 25^\circ C$$

Since, by definition, $E^\circ = 0$, we have

$$E = -0{\cdot}02955 \log (p_2/p_1) = 0{\cdot}02955 \log (p_1/p_2)$$

When $p_2 < p_1$, the EMF is positive so that the whole process is spontaneous, being equivalent to the expansion of H_2 gas.

Another example of the electrode-concentration cell is that of an amalgam with *two different concentrations* of the same metal :

$$Hg\text{–}Pb(c_1),\ PbSO_4(soln.),\ Hg\text{–}Pb(c_2)$$

The electrode reactions are :

R.H.E. : $Pb^{2+} + 2e^- \rightleftharpoons Pb(c_2)$ (Reduction)

L.H.E. : $Pb(c_1) \rightleftharpoons Pb^{2+} + 2e^-$ (Oxidation)

Overall reaction : $Pb(c_1) \rightleftharpoons Pb(c_2)$

The EMF of the cell is given by

$$E = E_R - E_L = \left(E^\circ_{Pb} - \frac{0{\cdot}0591}{2} \log c_2\right) - \left(E^\circ_{Pb} - \frac{0{\cdot}0591}{2} \log c_1\right)$$

$$= \frac{0{\cdot}0591}{2} \log \frac{c_1}{c_2} = 0{\cdot}02955 \log \frac{c_1}{c_2}$$

Here, too, if $c_2 < c_1$, the EMF is positive so that the whole process is spontaneous, *i.e.*, lead will go spontaneously from the higher concentration amalgam to the lower concentration amalgam.

Example 18. Calculate the EMF of the electrode-concentration cell $Hg\text{–}Zn(c_1)$, $Zn^{2+}(aq)$, $Hg\text{–}Zn(c_2)$ at 25°C, if the concentrations of the zinc amalgam are : c_1=2 g of zinc per 100 g of mercury and c_2=1 g of zinc per 100 g of mercury.

Solution : The half-cell reactions in this case are :

R.H.E. : $Zn^{2+} + 2e^- \rightleftharpoons Zn(c_2)$ (Reduction)

L.H.E. : $Zn(c_1) \rightleftharpoons Zn^{2+} + 2e^-$ (Oxidation)

Overall reaction : $Zn(c_1) \rightleftharpoons Zn(c_2)$

$$\therefore \quad E = \frac{0{\cdot}0591}{2} \log \frac{c_2}{c_1} = -0{\cdot}02955 \log \left(\frac{1}{2}\right) = 8{\cdot}8\times10^{-3}\ V$$

Example 19. Calculate the EMF of the electrode-concentration cell : Pt ; $H_2(p_1)$, HCl, $H_2(p_2)$; Pt at 25°C if p_1=600 torr and p_2=400 torr.

Solution : The cell reactions in this case are :

R.H.E. : $2H^+ + 2e^- \rightleftharpoons H_2(p_2)$ (Reduction)

L.H.E. : $H_2(p_1) \rightleftharpoons 2H^+ + 2e^-$ (Oxidation)

Overall reaction : $H_2(p_1) \rightleftharpoons H_2(p_2)$

$$\therefore \quad E = -\frac{0{\cdot}0591}{2} \log \frac{400\ torr}{600\ torr} = -0{\cdot}02955 \log \frac{2}{3} = 5{\cdot}19\times10^{-3}\ V$$

2. Electrolyte-Concentration Cells. In these cells, the two electrodes of the same metal are dipping in solutions of metal ions of different concentrations and hence of different activities. One such cell is represented below :

$$Zn,\ Zn^{2+}(a_+)_1 \parallel Zn^{2+}(a_+)_2,\ Zn$$

In this case, both the electrodes are of the same metal (Zn) and these are in contact with solutions of the same ions (Zn^{2+}). The concentrations and hence activities of the ions are, however, different. Let $(a_+)_1$ and $(a_+)_2$ be the activities of zinc ions in the two electrolytes surrounding the electrodes. The two electrolytes, which are generally $ZnSO_4$ solutions, are separated from each other by a *salt bridge*. This is represented by the double line put in between the two half-cells.

The reactions occurring are :

R.H.E. : $Zn^{2+}(a_+)_2 + 2e^- \rightleftharpoons Zn(s)$ (Reduction)

L.H.E. : $Zn(s) \rightleftharpoons Zn(a_+)_1 + 2e^-$ (Oxidation)

Overall reaction : $Zn^{2+}(a_+)_2 \rightleftharpoons Zn^{2+}(a_+)_1$

The net process thus involves the transfer of 1 mole of Zn^{2+} ions from the solution in which the activity is $(a_+)_2$ to the solution in which the activity is $(a_+)_1$.

According to Nernst equation, the reduction potentials of R.H.E. and L.H.E. are given by

$$E_R = E^\circ_{el} - \frac{RT}{nF} \ln \frac{1}{(a_+)_2} = E^\circ_{el} + \frac{RT}{nF} \ln (a_+)_2 \qquad ...(45)$$

and $$E_L = E^\circ_{el} - \frac{RT}{nF} \ln \frac{1}{(a_+)_1} = E^\circ_{el} + \frac{RT}{nF} \ln (a_+)_1 \qquad ...(46)$$

$$\therefore \quad E_{cell} \equiv E = E_R - E_L = \frac{RT}{nF} \ln \frac{(a_+)_2}{(a_+)_1} \qquad ...(47)$$

For the process to be feasible, EMF should be positive. Hence, $(a_+)_2 > (a_+)_1$.

Substituting activities $(a_+)_1$ and $(a_+)_2$ by molalities m_1 and m_2 (vide Eq. 38), in Eq. 47, we have

$$E_{cell} \equiv E = \frac{RT}{2F} \ln \frac{\gamma_2 m_2}{\gamma_1 m_1} \qquad ...(48)$$

where γ_1 and γ_2 are activity coefficients of the electrolytes in the two solutions.

Consider another similar concentration cell represented by

$$\underset{1\ atm}{Pt,\ H_2(g),\ H^+(a_+)_1} \parallel \underset{1\ atm}{H^+(a_+)_2,\ H_2(g),\ Pt}$$

In this case, both the electrodes are hydrogen gas electrodes which are in contact with hydrogen ions of different activities. The two solutions which are generally solutions of hydrochloric acid, are separated by a salt bridge, as before.

The following processes take place at the two electrodes :

R.H.E. : $H^+(a_+)_2 + e^- \rightleftharpoons 1/2\ H_2(g)$ (Reduction)

L.H.E. : $1/2\ H_2(g) \rightleftharpoons H^+(a_+)_1 + e^-$ (Oxidation)

Overall reaction : $H^+(a_+)_2 \rightleftharpoons H^+(a_+)_1$

The EMF of the cell will be given, as before, by reduction potential of right hand electrode minus reduction potential of left hand electrode. The reduction potentials of the two electrodes and the EMF of the cell are given as follows :

$$E = E_R - E_L = \left(E^\circ_{el} - \frac{RT}{F} \ln \frac{1}{(a_+)_2}\right) - \left(E^\circ_{el} - \frac{RT}{F} \ln \frac{1}{(a_+)_1}\right)$$

$$= \frac{RT}{F} \ln \frac{(a_+)_2}{(a_+)_1} \qquad ...(49)$$

For E to be positive, $(a_+)_2$ should be greater than $(a_+)_1$.

We shall now consider a cell consisting of two cells connected back to back through silver electrodes :

$$Pt\ ;\ H_2,\ HCl(a_1),\ AgCl(s),\ Ag,\ |\ Ag,\ AgCl(s), HCl(a_2),\ H_2\ ;\ Pt$$

The electrode reactions are :

R.H.E. : $Ag + H^+(a_2) + Cl^-(a_2) + e^- \rightleftharpoons 1/2\ H_2(1\ atm) + AgCl(s)$ (Reduction)

L.H.E. : $1/2\ H_2(1atm) + AgCl(s) \rightleftharpoons Ag + H^+(a_1) + Cl^-(a_1) + e^-$ (Oxidation)

Overall reaction : $H^+(a_2) + Cl^-(a_2) \rightleftharpoons H^+(a_1) + Cl^-(a_1)$

Thus, the overall reaction involves no chemical change. It consists only of the transfer of HCl from solution of activity a_2 to solution of activity a_1.

The EMF of the cell is given by

$$E_{cell} \equiv E = E_R - E_L$$

$$= E^\circ_{el} - \frac{RT}{F} \ln \frac{1}{\left(a_{H^+}\right)_2 \left(a_{Cl^-}\right)_2} - \left(E^\circ_{el} - \frac{RT}{F} \ln \frac{1}{\left(a_{H^+}\right)_1 \left(a_{Cl^-}\right)_1}\right)$$

$$= \frac{RT}{F} \ln \frac{\left(a_{H^+}\right)_2 \left(a_{Cl^-}\right)_2}{\left(a_{H^+}\right)_1 \left(a_{Cl^-}\right)_1} = \frac{RT}{F} \ln \frac{(a_\pm)_2^2}{(a_\pm)_1^2}$$

$$= \frac{2RT}{F} \ln \frac{(a_\pm)_2}{(a_\pm)_1} = 0{\cdot}1182 \log \frac{(a_\pm)_2}{(a_\pm)_1} \text{ at } 25°C$$

where $(a_\pm)_1$ and $(a_\pm)_2$ are the mean ionic activities of the HCl solutions in the two cells.

Here, too, we see that when $a_2 > a_1$, E is positive so that the process is spontaneous from right to left and consists in the dilution of HCl from activity a_2 to activity a_1 even though the two solutions are not in contact with each other.

Example 20. Calculate the EMF of the concentration cell consisting of zinc electrodes, one immersed in a solution of 0·01 molality (number of moles dissolved per kg of the solvent) and the other in a solution of 0·1 molality at 25°C. The two solutions are separated by a salt bridge. The mean activity coefficient of the electrolyte may be assumed to be unity.

Soluton. The cell may be represented as

$$Zn,\ Zn^{2+}(m_1{=}0{\cdot}01)\ \|\ Zn^{2+}(m_2{=}0{\cdot}1),\ Zn$$

The EMF of the cell, E, is given by

$$E = \frac{RT}{nF} \ln \frac{(a_+)_2}{(a_+)_1} = \frac{2{\cdot}303\,RT}{2F} \log \frac{\gamma_2 m_2}{\gamma_1 m_1} \qquad \text{(Eq. 48)}$$

$$= \frac{0{\cdot}0591}{2} \log \frac{0{\cdot}10}{0{\cdot}01} \text{ at } 25°C \qquad (\because\ \gamma_1 = \gamma_2 = 1)$$

$$= 0{\cdot}0295\ V$$

Example 21. Find the pontential difference between the hydrogen electrodes in the cell

$$Pt,\ H_2(g),\ HCl,\ AgCl(s),\ Ag\ \|\ Ag,\ AgCl(s),\ HCl,\ H_2(g),\ Pt$$

1 atm $m_1 = 0{\cdot}01$ $m_2 = 0{\cdot}10$ 1 atm

at 25°C. The activity coefficients of 0·01 *m* and 0·10 *m* solutions are 0·95 and 0·85, respectively.

Solution : The potential difference (E) between the two hydrogen electrodes is given by Eq. 49, *viz.*,

$$E = \frac{RT}{nF} \ln \frac{(a_+)_2}{(a_+)_1} = \frac{2{\cdot}303\,RT}{nF} \log \frac{\gamma_2 m_2}{\gamma_1 m_1}$$

$$= \frac{0{\cdot}0591}{1} \log \frac{0{\cdot}10 \times 85}{0{\cdot}01 \times 95} \quad \text{at } 25°C = 0{\cdot}056\ V$$

Types of Electrolyte-Concentration Cells

Electrolyte-concentration cells in which solutions of the same electrolyte of different concentrations are used are of two types. In one of the types, the two electrolytic solutions are not in direct contact with each other and the transference of ions from one solution to the other does not take place directly. These are called **concentration cells without transference.** The two solutions are separated from each other by means of a salt bridge or by some other means to be considered shortly. In the second type, the two solutions are in direct contact with each other. The transference of ions from one solution to the other takes place directly. Such cells are called **concentration cells with transference.** We shall consider here both the types of concentration cells.

Concentration Cells Without Transference. The two concentration cells discussed above in which the two solutions are separated from each other through a salt bridge fall in this category. But, more often some other means are employed to keep the solutions apart and bring about the transference of ions indirectly.

In order to understand the setting up of such a cell, consider a simple electrochemical cell such as

$$Pt,\ H_2(g),\ HCl\ (a_1)\ |\ AgCl(s),\ Ag$$

1 atm

Let the activity of H^+ ions in the solution be $(a_+)_1$ and that of Cl^- ions be $(a_-)_1$. Since reduction takes place at the right hand electrode and oxidation at the left hand electrode, the two half-cell

reactions will be as follows :

Reduction half-cell reaction :

$$AgCl(s) + e^- \rightleftharpoons Cl^-(a_-)_1 + Ag(s) \quad ...(i)$$

Oxidation half-cell reaction :

$$1/2\ H_2(g) \rightleftharpoons H^+(a_+)_1 + e^- \quad ...(ii)$$

The *net reaction* taking place in the cell for one faraday of electricity is obtained by adding equations *(i)* and *(ii)*. Thus,

$$1/2\ H_2(g) + AgCl(s) \rightleftharpoons H^+(a_+)_1 + Cl^-(a_-)_1 + Ag(s) \quad ...(iii)$$

Now consider the same cell with the difference that the activity of HCl solution is now a_2.

$$\underset{1\ atm}{Pt, H_2(g), HCl(a_2)} \mid AgCl(s), Ag$$

The net *cell reaction* for one faraday of electricity will now be as follows :

$$1/2\ H_2(g) + AgCl(s) \rightleftharpoons H^+(a_+)_2 + Cl^-(a_-)_2 + Ag(s) \quad ...(iv)$$

Finally, consider the situation when the two cells are connected to each other in such a way that they send current in *opposite direction*. Thus,

$$\underset{1\ atm}{Pt, H_2(g), HCl(a_1), AgCl(s), Ag} \mid \underset{1\ atm}{Ag, AgCl(s), HCl(a_2), H_2(g), Pt}$$

The overall reaction of the combined cell for the passage of one faraday of electricity will, evidently, be obtained by subtracting equation *(iv)* from equation *(iii)*, *i.e.*,

$$H^+(a_+)_2 + Cl^-(a_-)_2 \rightleftharpoons H^+(a_+)_1 + Cl^-(a_-)_1 \quad ...(51)$$

Thus, for the flow of one faraday of electricity, the overall reaction is the transfer of one mole of each of H^+ and Cl^- ions or one mole of HCl, from a solution of activity a_2 to that of activity a_1.

Hence, EMF of such a cell would be given by

$$E_{w.o.t.} = \frac{RT}{F} \ln \frac{(a_+)_2}{(a_+)_1} + \frac{RT}{F} \ln \frac{(a_-)_2}{(a_-)_1} \quad ...(52)$$

$$= \frac{RT}{F} \ln \frac{(a_\pm)_2^2}{(a_\pm)_1^2} \quad \text{(vide Eq. 37)} \quad ...(53)$$

where $(a_\pm)_1$ and $(a_\pm)_2$ are the mean ionic activities of the electrolyte in the two solutions and the subscript w.o.t. stands for 'without transference'. Applying Eq. 43, we have

$$E_{w.o.t.} = (RT/F) \ln (a_2/a_1) \quad ...(54)$$

where a_1 and a_2 are the activities of hydrochloric acid in the two solutions.

It will be observed that the cell reaction does not involve transfer of electrolyte from one solution to the other directly. It takes place indirectly. The cell is, therefore, a concentration cell without transference.

If the middle electrode, *viz.*, Ag, AgCl(s), is withdrawn, the two solutions of HCl will be in direct contact with each other. The cell will then become a concentration cell with transference. A little reflection shows that a concentration cell with transference in which the two electrodes are

reversible with respect to cations (H^+ ions in the present case) can be converted into a concentration cell without transference by interposing in between another electrode which is reversible with respect to anions (Cl^- ions in the present case).

Another example of a concentration cell without transference, in which the electrodes are reversible with respect to a cation, is given below :

$$Zn, ZnSO_4(a_1), PbSO_4(s), Pb, PbSO_4(s), ZnSO_4(a_2), Zn$$

Concentration cells without transference in which the end electrodes are reversible with respect to an anion and in which an electrode reversible with respect to a cation is inserted in between, are also known. One such cell is as represented below :

$$Ag, AgCl(s), HCl(a_1), H_2(g), HCl(a_2), AgCl(s), Ag$$

The end electrodes are reversible with respect to Cl^- ions while the intermediate electrode is reversible with respect to H^+ ions.

Concentration Cells with Transference. Now consider a concentration cell formed by combining two hydrogen gas electrodes in contact with HCl solutions of different concentrations. The two solutions are in direct contact with each other, as shown :

$$\underset{1\ atm}{Pt, H_2(g), HCl(a_1)} \mid \underset{1\ atm}{HCl(a_2), H_2(g), Pt}$$

$H^+ \longrightarrow$

$\longleftarrow Cl^-$

The reaction on the left involves oxidation and that on the right involves reduction, as usual.

The following changes are involved for the flow of one faraday of electricity :

Left Hand Electrode :

$$\tfrac{1}{2}H_2(g) \rightleftharpoons H^+(a_+)_1 + e^- \quad ...(i)$$

Right Hand Electrode :

$$H^+(a_+)_2 + e^- \rightleftharpoons \tfrac{1}{2}H_2(g) \quad ...(ii)$$

Thus, H^+ ions are generated at the left hand electrode and consumed at the right hand electrode as the current follows. Since the solutions *are in direct contact* with each other, *the ions are free to move from one solution to the other* when current flows through the cell. In the present case, evidently, H^+ ions move from the solution on the left hand side to that on the right hand side. Since anions move in direction opposite to that in which cations move, Cl^- ions migrate from right to left, as shown in the cell above.

Let t_- be the transport number of Cl^- ion and t_+ (= 1 – t_-) that of H^+ ion in HCl. Then, for one faraday of electricity passing through, t_- faraday will be carried by Cl^- ions and t_+ faraday by H^+ ions. According to Faraday's second law, t_- equivalent of Cl^- ions will be transferred from the solution of activity a_2 to the solution of activity a_1. This may be represented as

$$t_- Cl^-(a_-)_2 \rightleftharpoons t_- Cl^-(a_-)_1 \quad ...(iii)$$

At the same time, t_+ equivalent of H^+ ions will be transferred from the solution of activity a_1 to that of activity a_2 which may be represented as

$$t_+ H^+(a_+)_1 \rightleftharpoons t_+ H^+(a_+)_2 \quad ...(iv)$$

The net result for the flow of one faraday of electricity is summed up below :

Left Hand Electrode. The following operations occur at this electrode :

Gain of 1 gram equivalent of H^+ ions by process *(i)*

Loss of t_+ gram equivalent of H^+ ions by process *(iv)*

$\therefore$ Net gain of H^+ ions $= (1 - t_+)$ gram equivalent $= t_-$ gram equivalent

At the same time,

net gain of Cl^- ions $= t_-$ gram equivalent by process *(iii)*

Right Hand Electrode. The following operations occur at this electrode :

Loss of 1 gram equivalent of H^+ ions by process *(ii)*

Gain of t_+ gram equivalent of H^+ ions by process *(iv)*

$\therefore$ Net loss of H^+ ions $= (1 - t_+)$ gram equivalent $= t_-$ gram equivalent

At the same time,

net loss of Cl^- ions $= t_-$ gram equivalent by process *(iii)*

Thus, for every one faraday of electricity, there is net transfer of t_- gram equivalent of H^+ ions and t_- gram equivalent of Cl^- ions from right to left, *i.e.*, from the solution in which activity of HCl is a_2 to that in which activity of HCl is a_1.

These changes are represented as

$$t_- H^+(a_+)_2 \rightleftharpoons t_- H^+(a_+)_1$$

$$t_- Cl^-(a_-)_2 \rightleftharpoons t_- Cl^-(a_-)_1$$

The EMF of concentration cell with transport, on analogy with Eq. 52, therefore, is given by

$$E_{w.t.} = t_- \frac{RT}{F} \ln \frac{(a_+)_2}{(a_+)_1} + t_- \frac{RT}{F} \ln \frac{(a_-)_2}{(a_-)_1} \qquad ...(55)$$

If $(a_\pm)_1$ and $(a_\pm)_2$ are the mean ionic activities of the two hydrochloric acid solutions, it follows by the definition given in Eq. 33 that

$$(a_\pm)_1^2 = (a_+)_1(a_-)_1 \text{ and } (a_\pm)_2^2 = (a_+)_2(a_-)_2$$

Eq. 55, therefore, may be put as

$$E_{w.t.} = t_- \frac{RT}{F} \ln \frac{(a_\pm)_2^2}{(a_\pm)_1^2} \qquad ...(56)$$

Knowing that the activity of a uni-univalent electrolyte is given by $a=(a_\pm)^2$, Eq. 56 may also be written as

$$E_{w.t} = t_- \frac{RT}{F} \ln \frac{a_2}{a_1} \qquad ...(57)$$

where a_2 and a_1, as already stated, are activities of HCl solutions of the right and the left hand electrode, respectively.

Eq. 57 is used for calculating activity of an electrolyte at a given concentration from the experimental value of $E_{w.t.}$ One of the solutions used should be of known activity.

Liquid Junction Potential (L.J.P.)

Eq. 57 derived above for the EMF of a concentration cell with transference *includes the potential at the junction of the two solutions* of HCl as well. Eq. 53 for EMF derived earlier when the two

solutions are not in direct contact with each other *does not include the liquid junction potential.* Eqs. 57 and 53 may be reproduced as

$$E_{w.t.} = 2t_- \frac{RT}{F} \ln \frac{(a_\pm)_2}{(a_\pm)_1} \qquad ...(58)$$

$$E_{w.o.t.} = \frac{RT}{F} \ln \frac{(a_\pm)_2}{(a_\pm)_1} \qquad ...(59)$$

Hence, liquid junction potential E_l is given by

$$E_l = E_{w.t.} - E_{w.o.t.} = (2t_- - 1)\frac{RT}{F} \ln \frac{(a_\pm)_2}{(a_\pm)_1}$$

$$= (t_- + (1 - t_+) - 1] \frac{RT}{F} \ln \frac{(a_\pm)_2}{(a_\pm)_1}$$

$$= (t_- - t_+) \frac{RT}{F} \ln \frac{(a_\pm)_2}{(a_\pm)_1} \qquad ...(60)$$

It is evident from Eq. 60 that the sign as well as the magnitude of L.J.P. depends on *the transference numbers of the anion and cation.* If the transference numbers of the anion and cation of an electrolyte are the same or nearly the same, *i.e.*, $t_- = t_+$, then L.J.P. = 0 or negligibly small. If the transference number of cation is greater than that of anion, *i.e.*, $t_+ > t_-$, then L.J.P. will be negative and if reverse is the case, *i.e.*, $t_- > t_+$, then L.J.P. will be positive and will add to the EMF of the cell.

Potassium chloride and ammonium nitrate are amongst the electrolytes in which transference numbers of cations and anions are nearly the same. The solutions of these electrolytes are, therefore, frequently used as salt bridge because the liquid junction potential is then reduced to a minimum.

Example 22. Calculate the liquid junction potential at 25°C between two solutions of HCl having mean ionic activities of 0·01 and 0·001, respectively. The transference number of H^+ ion (t_+) in HCl may be taken as 0·83.

Solution : In this case, $t_+ = 0{\cdot}83$ so that $t_- = 1 - t_+ = 0{\cdot}17$

$$(a_\pm)_1 = 0{\cdot}01 \; ; \quad (a_\pm)_2 = 0{\cdot}001$$

$$E_l = (t_- - t_+)\frac{RT}{F} \ln \frac{(a_\pm)_2}{(a_\pm)_1} \qquad \text{(Eq. 60)}$$

$$= (0{\cdot}17 - 0{\cdot}83) 0{\cdot}0591 \log \frac{0{\cdot}001}{0{\cdot}01} = 0{\cdot}0039 \text{ V} \quad \text{(at 25°C)}$$

Example 23. Calculate the liquid junction potential associated with the following cell :

Ag(*s*), AgCl(*s*), HCl (m_1=1·0, γ_1 = 0·809) : HCl (m_2=0·05, γ_2=0·830), AgCl(*s*), Ag(*s*),

if the transference number of H^+ is 0·83.

Solution : $t_+ = 0{\cdot}83$ so that $t_- = 1 - 0{\cdot}83 = 0{\cdot}17$. Hence, from Eq. 60,

$$E_l = (t_- - t_+)\frac{RT}{F} \ln \frac{(a_\pm)_2}{(a_\pm)_1} = (t_- - t_+)\frac{RT}{F} \ln \frac{\gamma_2 m_2}{\gamma_1 m_1}$$

$$= (0{\cdot}17 - 0{\cdot}83) \times 0{\cdot}0591 \log \frac{0{\cdot}83 \times 0{\cdot}05}{0{\cdot}809 \times 1{\cdot}0} \text{ at 25°C}$$

$$= 0{\cdot}050 \text{ volt} = 50 \text{ mV}$$

Example 24. The EMF of the concentration cell with transference, *viz.*,

$Pt ; H_2$ (1 atm), HCl ($a_\pm$ = 0·009) : HCl ($a_\pm$ = 0·017), H_2(1 atm) ; Pt,

is 0·028 V at 25°C. The EMF of the corresponding cell without transference is 0·017 V. Calculate the liquid junction potential, E_l and the transference number of the H^+ ion.

Solution : Since the concentration cell with transference includes in it the liquid junction potential while the cell without transference does not, the liquid junction potential would be given by

$$E_L = E_{w.t.} - E_{w.o.t.} = 0{\cdot}028 - 0{\cdot}017 = 0{\cdot}011 \text{ V}$$

Using Eq. 60 and remembering that during the operation of the cell, there is transfer of HCl from a solution of higher activity to one of lower activity, we have

$$E_l = (t_- - t_+)\frac{RT}{F}\ln\frac{(a_\pm)_2}{(a_\pm)_1} = (t_- - t_+)\times 0{\cdot}0591 \log\frac{0{\cdot}009}{0{\cdot}017}$$

$$0{\cdot}011 = (t_1 - t_+)\times(-\,0{\cdot}0167)$$

or $$t_+ - t_- = \frac{0{\cdot}011}{0{\cdot}017} = 0{\cdot}65$$

Since $t_+ + t_- = 1$, hence $t_+ = 0{\cdot}825$

Thus, the transference number of H^+ ion = **0·825**

Fuel Cells

Fuel cells are galvanic cells in which *chemical energy of fuels is directly converted into electrical energy.*

Conventional conversion of chemical energy of fuels into electrical energy is carried out by burning the fuel, using the heat energy to raise steam which is then used for spinning the turbines connected with electric generators. The efficiency of this process, which cannot exceed that of a reversible Carnot engine, varies from 20 to 40 per cent. Fuel cells, on the other hand, convert about 75 per cent of the available chemical energy into electrical energy.

Hydrogen-Oxygen Fuel Cell. A common type of fuel cell is based on the combustion of hydrogen to form water :

$$2H_2(g) + O_2(g) \longrightarrow 2H_2O(l)$$

This is known as hydrogen-oxygen fuel cell. A schematic diagram of the cell is shown in Fig. 3.

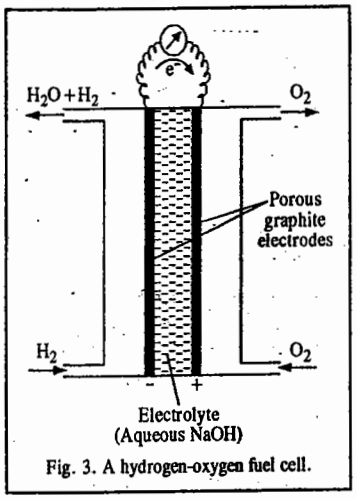

Fig. 3. A hydrogen-oxygen fuel cell.

It consists of two electrodes made of *porous* graphite impregnated with a catalyst (platinum, silver or a metal oxide). The inner sides of the graphite electrodes are in contact with an aqueous solution of KOH or NaOH. Oxygen and hydrogen are continuously fed into the cell, as shown, under a pressure of about 50 atm. The gases diffuse into the electrode pores and so does the electrolyte solution.

The half-cell reactions which occur at the electrodes are as follows :

Oxidation Half-cell Reaction. Hydrogen is oxidised to H^+ ions which are neutralised by the OH^- ions of the electrolyte :

$$H_2 \longrightarrow 2H^+ + 2e^-$$

$$2H^+ + 2OH^- \longrightarrow 2H_2O$$

The net oxidation half-cell reaction is

$$H_2 + 2OH^- \longrightarrow 2H_2O + 2e^-$$

Reduction Half-cell Reaction. Reduction half-cell reaction involves the reduction of oxygen to OH^- ions :

$$O_2(g) + 2H_2O + 4e^- \longrightarrow 4OH^-$$

The **overall fuel cell reaction** is thus given by

$$2H_2(g) + O_2(g) \longrightarrow 2H_2O$$

The EMF of the cell is found to be 1 volt.

The water produced vaporises off since the cell is operated at temperature above 100°C. This can be condensed and used.

In place of KOH or NaOH, **phosphoric acid** can also be used as an electrolyte. This cell is operated at about 200°C. At this temperature, phosphoric acid polymerises to pyrophosphoric acid which has considerably higher ionic conductivity than the parent acid. Pt–Co–Cr alloy is used as the catalyst.

Hydrocarbon-Oxygen Fuel Cells. Fuel cells based on the combustion of hydrocarbons such as CH_4, C_2H_6, C_3H_8, etc., in the presence of catalysts, have also been operated. The half-cell reactions with propane as the fuel are as follows :

Oxidation Half-cell Reaction :

$$C_3H_8 + 6H_2O \longrightarrow 3CO_2 + 20H^+ + 20e^-$$

$$H^+ + OH^- \longrightarrow H_2O] \times 20$$

The net oxidation half-cell reaction is

$$C_3H_8 + 20OH^- \longrightarrow 3CO_2 + 14H_2O + 20e^-$$

Reduction Half-cell Reaction :

$$O_2 + 2H_2O + 4e^- \longrightarrow 4OH^-] \times 5$$

Overall fuel cell reaction :

$$C_3H_8 + 5O_2 \longrightarrow 3CO_2 + 4H_2O$$

The catalyst in this case is essentially platinum. This makes the fuel cell operation highly expensive.

Coal-fired Fuel Cells. In these cells, coal is gassified by raising the temperature to above 650°C to give a mixture of H_2 and CO which serve as the fuel for the cell. Molten sodium carbonate is used as an electrolyte. An alloy of Pt with other non-noble metals such as Cr, V and Ti acts as the catalyst. The reactions which occur in the cell are as follows :

Coal gassification :

$$C + H_2O \xrightarrow{O_2} CO + H_2$$

Anode reaction :

$$H_2 + CO_3^{2-} \longrightarrow CO_2 + H_2O + 2e^-$$

$$CO + CO_3^{2-} \longrightarrow 2CO_2 + 2e^-$$

Overall anode reaction :

$$H_2 + CO + 2CO_3^{2-} \longrightarrow 3CO_2 + H_2O + 4e^-$$

Cathode reaction :

$$4e^- + 2CO_2 + O_2 \longrightarrow 2CO_3^{2-}$$

Overall fuel cell reaction :

$$CO + H_2 + O_2 \longrightarrow CO_2 + H_2O$$

The efficiency of the coal-fired fuel cells is greater than 55%.

In coal-fired fuel cells, **solid electrolytes** have also been used in place of molten alkali carbonate. In one of the cells of this type, ZrO_2 stabilised by Y_2O_3 is used as the solid electrolyte which exhibits adequate ionic conductivity at the temperatures of operation (*viz.*, 1000°C and above). In the case of fuel cells using solid electrolytes, the cathode material is porous strontium-doped $LaMnO_3$ and the anode is Ni or ZrO_2. The efficiency of this type of cells is at least 33% which is greater than that obtained in thermal power plants.

Hydrogen-Oxygen Fuel Cells in Manned Space Flights. The hydrogen-oxygen fuel cells are playing important role in some of the manned space flights. The electrolyte used in these cells is an ion-exchange material and not a solution of KOH or NaOH. The ion-exchange material which is used in the form of a membrane *allows easy passage of protons.*

The graphite electrode on one side of the membrane is impregnated with Pt metal catalyst. This electrode acts as the cathode. This is in contact with H_2.

H_2 fuel ionises on the metal-catalyst and the protons produced by the electricity-producing reaction, *viz.*, $H_2(g) \longrightarrow 2H^+ + 2e^-$, pass through the thin (0·1 mm thick) membrane since it allows free proton mobility, as mentioned above and reach the other graphite electrode which is also impregnated with platinum catalyst . This acts as the anode. This electrode is in contact with O_2. Here the following reaction occurs :

$$O_2(g) + 4H^+(aq) + 4e^- \longrightarrow 2H_2O\ (l)$$

The protons required for this reaction are those which come through the membrane from the ionisation of H_2 on the other side of the membrane as stated above.

It may be mentioned that this type of fuel cell is slated for development as part of the electrochemical engine to be used in automobiles in place of the too heay lead-acid batteries that are being used at present in vehicular transportation. The electrochemical engine will have a far greater efficiency than the internal combustion engine. The main advantage would be the elimination of hazardous air polltants such as CO, NO_x, SO_2, etc., which are inherently associated with the internal combustion engine.

Recently, a **zinc-air fuel cell (ZAFC)**, in which zinc metal is used in place of hydrogen gas, has been developed in the U.S.A. as a source of power in automobiles. In this cell, the OH^- ions produced by the reduction of oxygen of the air ($O_2(g) + 2H_2O + 4e^- \longrightarrow 4OH^-$), brought about in the presence of a catalyst, travel through the liquid electrolyte (NaOH or KOH) and reach the zinc anode (comprising of a perforated pack of zinc pellets) where they react to form zinc oxide ($Zn + 2OH^- \longrightarrow ZnO + H_2O + 2e^-$). These oxidation-reduction reactions generate electricity, the overall fuel cell reaction being $2Zn + O_2 \longrightarrow 2ZnO$.

The zinc oxide produced dissolves in the electrolyte. The spent electrolyte is pumped out and subjected to a special treatment for the regeneration of zinc in the form of zinc pellets. The regenerated electrolyte and the zinc pellets are used again.

Fuel cells are associated with a number of advantages. Their efficiency is very high. About 75 per cent of chemical energy can be converted into electrical energy. The individual cells can be stacked and connected in series to generate higher voltages. They are also very light.

However, there are a number of engineering porblems which shall have to be solved before fuel cells become practical sources of electrical energy. Once it is done, fuel cell technology would bring revolution in the area of energy production.

Applications of EMF Measurements

The EMF measurements find a number of useful applications. Some of these are given below.

1. Determination of Activity Coefficients of Electrolytes. Suppose we want to determine the activity coefficient of hydrochloric acid. Consider a cell without liquid junction containing HCl. The two electrodes are so chosen that one is reversible with respect to the cation of the electrolyte (in this case, the H^+ ion) and the other is reversible with respect to the anion (*i.e.*, the Cl^- ion). Evidently, the first electrode is the hydrogen electrode and the other can be the silver-silver chloride electrode. Accordingly, the cell arrangement is as follows :

$$Pt\ ;\ H_2(g)\ (1\ atm)\ |\ HCl\ (m)\ |\ AgCl(s),\ Ag(s)$$

where m is the molality of HCl solution.

The cell reaction is

$$1/2\ H_2(g) + AgCl(s) \rightleftharpoons Ag(s) + H^+(m) + Cl^-(m)$$

According to Eq. 20, the EMF of the cell at 25°C is given by

$$E = E^\circ - 0{\cdot}0591 \log \frac{a_{H^+} a_{Cl^-}}{\left(a_{H_2}\right)^{1/2}} \qquad ...(61)$$

$$= E^\circ - 0{\cdot}0591 \log a_{H^+} a_{Cl^-} \qquad ...(62)$$

because activity of each of Ag(*s*), AgCl(*s*) and $H_2(g)$ at 1 atm pressure is taken as unity.

As already discussed,

$$a_{H^+} a_{Cl^-} = (a_\pm)^2 = (\gamma_\pm m)^2 = \gamma_\pm^2 m^2 \qquad \text{(Eqs. 43 and 44)}$$

where $\gamma_\pm$ and m are the mean ionic activity coefficient and the molality of HCl, respectively. Substituting in Eq. 62, we get

$$E = E^\circ - 0{\cdot}0591 \log \gamma_\pm^2 m^2 \qquad ...(63)$$

$$= E^\circ - 0{\cdot}1182 \log \gamma_\pm - 0{\cdot}1182 \log m \qquad ...(64)$$

Rearranging,

$$E + 0{\cdot}1182 \log m = E^\circ - 0{\cdot}1182 \log \gamma_\pm \qquad ...(65)$$

The two unknowns E° and $\gamma_\pm$ in Eq. 65 can be determined by measuring the EMFs of the cell over various concentrations of HCl, including dilute concentrations. At infinite dlution, $m=0$ and $\gamma_\pm=1$ so that $\log \gamma_\pm=0$. Thus, a plot of $E+0{\cdot}1182 \log m$ versus m, extrapolated to $m=0$ gives E° as the y-intercept. Knowing the value of E°, the mean ionic activity coefficient $\gamma_\pm$ of HCl at any other concentration can be determined from the EMF data of the cell at that concentration.

Alternatively, we can use the Debye-Hückel limiting law (DHLL) equation, *viz.*,

$$\log \gamma_\pm = -0{\cdot}509\ |z_+ z_-|\ I^{1/2} \qquad ...(66)$$

to substitute for the $\log \gamma_\pm$ term in Eq. 65, giving

$$E + 0{\cdot}1182 \log m = E^\circ + 0{\cdot}0602\ I^{1/2} \qquad ...(67)$$

Thus, a plot of $E + 0{\cdot}1182 \log m$ versus $I^{1/2}$ will give a straight line at low concentrations where the limiting law is valid. The extrapolation of this plot to $I^{1/2}=0$ gives E° as the y-intercept of the line.

In practice, however, an extension of the DHLL is needed to make a satisfactory linear extrapolation. For a uni-univalent electrolyte in dilute aqueous solution at 25°C, an empirical extension of Eq. 66 is

$$\log \gamma_\pm = -0{\cdot}509\ m^{1/2} + bm \qquad ...(68)$$

where b is an empirical constant.

Substituting this equation in Eq. 65 and rearranging the terms, we obtain

$$E + 0{\cdot}1182 \log m - 0{\cdot}0602\, m^{1/2} = E' = E^\circ - (0{\cdot}1182\, b)m \qquad ...(69)$$

This equation shows that the left hand side (which we have designated as E'), when plotted against m, will give a straight line whose intercept at $m=0$, is E° (Fig. 4).

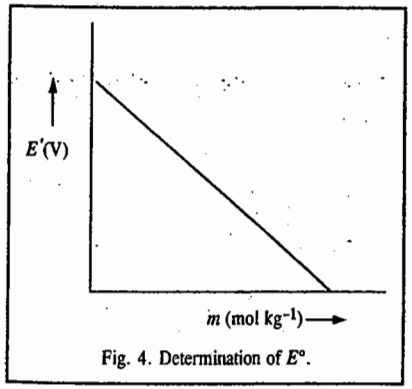

Fig. 4. Determination of E°.

Example 25. Consider the following cell :

$Ag(s), Ag^+(a=0{\cdot}001\ m)$ || $Ag^+(c=0{\cdot}1\ m,\ a$ unknown$), Ag(s)$ Its EMF at 25°C is + 1·11V. *(a)* Write the cell reaction and *(b)* Calculate the activity coefficient of the Ag^+ ion in 0·1 *m* solution.

Solution : *(a)* The cell reaction is

$$Ag^+ (c=0{\cdot}1\ m,\ a=\text{say},\ x) \rightleftharpoons Ag^+(a=0{\cdot}001\ m)$$

It is a concentration cell with *no net reaction*. Hence,

$$E = -\,0{\cdot}0591 \log (0{\cdot}001/x)$$

$$\log \frac{0{\cdot}001}{x} = -\frac{1{\cdot}11\,V}{0{\cdot}0591\,V} = -\,1{\cdot}878$$

$$\log x = \log 0{\cdot}001 + 1{\cdot}878 = -\,1{\cdot}122 = \bar{2}{\cdot}878$$

Taking antilogs, $x=0{\cdot}076$. Thus, $a = 0{\cdot}076$. Hence, the activity coefficient

$$\gamma = a/c = 0{\cdot}076/0{\cdot}1 = 0{\cdot}76$$

Example 26. EMF of the cell $Cd(s), CdCl_2(m=0{\cdot}02)$ | $AgCl(s), Ag(s)$ is found to be 0·780 V at 25°C. Using the standard potentials, *viz.*, $E^\circ_{Cd^{2+},Cd} = -\,0{\cdot}403$ V and $E^\circ_{AgCl,Cl^-} = +\,0{\cdot}222$ V, calculate the mean ionic activity coefficient of $CdCl_2$ at this temperature.

Solution : The half-cell reactions are :

(i) R.H.E. : $2AgCl\,(s) + 2e^- \rightleftharpoons 2Ag(s) + 2Cl^-$; $\quad E_l^\circ = +\,0{\cdot}222$ V

(ii) L.H.E. : $2Cd(s) \rightleftharpoons Cd^{2+}(aq) + 2e^-$; $\quad E_l^\circ = -\,0{\cdot}403$ V

Hence, adding Eqs. *(i)* and *(ii)*, we get

$$Cd(s) + 2AgCl(s) \rightleftharpoons Cd^{2+}(aq) + 2Ag(s) + 2Cl^-(aq),$$

$$E^\circ = E_R^\circ - E_L^\circ = 0{\cdot}222 - (-\,0{\cdot}403) = 0{\cdot}625\ V$$

$CdCl_2$ ionises in solution as $CdCl_2(aq) \rightleftharpoons Cd^{2+}(aq) + 2Cl^-(aq)$

Thus, the number of ions produced on ionization of $CdCl_2 = 3$ with $x=1$ and $y=2$. Hence,

$$a_{CdCl_2} = (a_\pm)^{x+y} = (a_+)^x\,(a_-)^y \ ;\ a_+ = \gamma_+ m_+ = \gamma_+ mx = \gamma_+ m \qquad (\because\ x = 1)$$

$$a_- = \gamma_- m_- = \gamma_- my = 2\gamma_- m \qquad (\because\ y = 2)$$

$$\therefore\quad a_{CdCl_2} = (a_\pm)^3 = (\gamma_+ m)\,(2\gamma_- m)^2 = 4(\gamma_+ \gamma_-^2)\, m^3 = 4(\gamma_\pm)^3 m^3$$

The EMF of the cell is given by $E = E^\circ - \dfrac{0{\cdot}0591}{2} \log a_+ a_-^2 = E^\circ - \dfrac{0{\cdot}0591}{2} \log (a_\pm)^3$ at 25°C

or $\quad 0{\cdot}780 = 0{\cdot}625 - 0{\cdot}0295 \log [4(\gamma_\pm)^3 m^3]$

$$\log 4(\gamma_\pm)^3 m^3 = -\frac{0{\cdot}780 - 0{\cdot}625}{0{\cdot}0295} = -\,5{\cdot}2546 = \bar{6}{\cdot}754$$

Taking antilogs, $\quad 4(\gamma_\pm)^3 m^3 = 5{\cdot}57 \times 10^{-6}$

$$\therefore\quad \gamma_\pm = \left(\frac{5{\cdot}57 \times 10^{-6}}{4m^3}\right)^{1/3} = \left(\frac{5{\cdot}57 \times 10^{-6}}{4(0{\cdot}02)^3}\right)^{1/3} = 0{\cdot}558$$

Example 27. Calculate the EMF of the following cell at 25°C :

$$Cd(s), CdCl_2(m=0{\cdot}005,\ \gamma_\pm=0{\cdot}817) \mid AgCl(s), Ag(s)$$

using the data given in the last example.

Solution : As shown in the last example, $E^\circ = 0{\cdot}625$ V

Also, $\quad a_{CdCl_2} = (a_\pm)^3 = 4(\gamma_\pm)^3 m^3$

The EMF of the cell is given by

$$E = E^\circ - \frac{0{\cdot}0591}{2} \log (a_+ a_-^2) = E^\circ - \frac{0{\cdot}0591}{2} \log (a_\pm)^3$$

$$= E^\circ - 0{\cdot}0295 \log [4\gamma_\pm)^3 m^3]$$

$$= 0{\cdot}625 - 0{\cdot}0295 \log [4(0{\cdot}817)^3 (0{\cdot}005)^3] = 0{\cdot}819\ V$$

2. Determination of Transport Numbers. As has been shown earlier, the EMF of a concentration cell *with transference*, represented by $E_{w.t.}$, in which the end electrodes are reversible with respect to cation, is given by Eq. 57, *viz.*,

$$E_{w.t.} = t_-(RT/F) \ln (a_2/a_1) \qquad ...(i)$$

The EMF of the same cell with the same solutions but *without transference*, denoted by $E_{w.o.t.}$, is given by Eq. 54, *viz.*,

$$E_{w.o.t.} = (RT/F) \ln (a_2/a_1) \qquad ...(ii)$$

Dividing *(i)* by *(ii)*, we have

$$t_- = E_{w.t.}/E_{w.o.t.} \qquad ...(61)$$

Thus, the ratio of the EMFs of the two concentration cells, one with transference and the other without transference, gives the *transference number of the anion*, if the end electrodes are reversible with respect to the *cation*.

If the end electrodes are reversible with respect to the *anion*, then the ratio of the two EMFs will give the transference number of the *cation* of the electrolyte.

3. Determination of Valency of Ions in Doubtful Cases. The valency of mercurous ion was in doubt for a considerable time. It was finally established by determining the EMF of a concentration cell of the type given below :

Mercury, Mercurous nitrate solution (c_1) || Mercurous nitrate solution (c_2), Mercury

The salt bridge represented by the two vertical lines connecting the two solutions contains saturated solution of ammonium nitrate.

The EMF of the cell, E, assuming the activity coefficients to be equal to unity, is given by the expression

$$E = (RT/nF) \ln (c_2/c_1)$$

where n is the valency of mercurous ion and c_2 is greater than c_1. Thus,

$$E = \frac{0{\cdot}0591}{n} \log \frac{c_2}{c_1} \quad \text{(at 25°C)}$$

It was found that when c_2/c_1 was 10, the EMF was 0·0295 volt. Therefore, the valency of mercurous ion is 2 and it should be represented as Hg_2^{2+}.

4. Determination of the Solubility Product Constants. The solubility product constant of a sparingly soluble salt is a kind of equilibrium constant. Consider the salt MX in equilibrium with its ions in a *saturated solution.*

$$MX(s) \rightleftharpoons M^+(aq) + X^-(aq)$$

The solubility product of the salt is given by $K_{sp} = a_{M^+} \times a_{X^-} = [M^+][X^-]$, assuming an ideal solution so that activities equal concentrations. The above reaction is the cell reaction for the following cell :

$$M, M^+X^- \text{ (}satd.\text{ soln.)} \mid MX(s), M$$

The half-cell reactions are :

R.H.E. : $MX(s) + e^- \rightleftharpoons M + X^-$

L.H.E. : $M \rightleftharpoons M^+(aq) + e^-$

Overall reaction : $MX(s) \rightleftharpoons M^+(aq) + X^-(aq)$; $\quad E^\circ = E_R^\circ - E_L^\circ$

The values of E_R° and E_L° are taken from Table 1.

Knowing the value of E° for the cell under consideration and using the relations : $\Delta G^\circ = nFE^\circ$ and $-\Delta G^\circ = 2{\cdot}303\ RT \log K_{sp}$, we get

$$\log K_{sp} = \frac{nFE^\circ}{2{\cdot}303\,RT}$$

i.e., $$E^\circ = \frac{2{\cdot}303\,RT}{nF} \log K_{sp} = \frac{0{\cdot}0591}{n} \log K_{sp} \text{ at } 25°C$$

Thus, K_{sp} can be calculated from the known value of E°.

Example 28. Calculate the solubility product of AgBr in water at 25°C from the cell :

Ag, Ag^+Br^- (*satd. soln*) | AgBr(*s*), Ag.

The standard potentials are $E^\circ_{AgBr,Ag} = 0{\cdot}07$ V ; $E^\circ_{Ag^+,Ag} = 0{\cdot}80$ V

Solution : The electrode reactions are :

R.H.E. : $AgBr(s) + e^- \rightleftharpoons Ag(s) + Br^-(aq)$; $\quad E_R^\circ = 0{\cdot}07$ V

L.H.E. : $Ag(s) \rightleftharpoons Ag^+(aq) + e^-$; $\quad E_L^\circ = 0{\cdot}80$ V

Hence, for the overall reaction $AgBr(s) \rightleftharpoons Ag^+(aq) + Br^-(aq)$,

$$E^\circ = E_R^\circ - E_L^\circ = -0{\cdot}73 \text{ V}$$

$$= \frac{0{\cdot}0591}{1} \log \{[Ag^+][Br^-]\}_{eqbm} = 0{\cdot}0591 \log K_{sp}$$

$$\therefore \quad \log K_{sp} = \frac{E^\circ}{0{\cdot}0591} = -\frac{0{\cdot}73}{0{\cdot}0591} \quad \text{whence } K_{sp} = 4{\cdot}81 \times 10^{-11}$$

Example 29. The EMF of the cell :

Ag, AgCl in 0·1 M KCl || Sat. NH_4NO_3 || 0·1 M $AgNO_3$, Ag

is 0·45 volt at 25°C. Calculate *(i)* the solubility product and *(ii)* the solubility of AgCl. 0·1 M KCl is 85% dissociated and 0·1 M $AgNO_3$ is 82% dissociated.

Solution : Since at 25°C, 0·1 M $AgNO_3$ is 82 per cent dissociated, hence, the Ag^+ ion concentration (c_2) on the $AgNO_3$ side = $0{\cdot}1 \times 82/100 = 0{\cdot}082$ mol dm^{-3}.

Let c_1 be the concentration of Ag^+ ions on the AgCl side due to the solubility of AgCl. Then, assuming that activity coefficients are each equal to unity, the EMF of the cell is given by

$$E = \frac{0{\cdot}0591}{n} \log \frac{c_2}{c_1} \text{ (at 25°C)}$$

Substituting the value of E=0·45 V, n=1 and c_2=0·082 mol dm^{-3}, we get

$$0{\cdot}45 \text{ V} = 0{\cdot}0591 \text{ V} \log \frac{0{\cdot}082 \text{ mol dm}^{-3}}{c_1}$$

Hence, $$c_1 = 2{\cdot}008 \times 10^{-9} \text{ mol dm}^{-3}$$

Since at 25°C, 0·1 M KCl is 85 per cent dissociated, hence the Cl^- ion concentration is given by

$$[Cl^-] = \frac{0{\cdot}1 \times 85}{100} = 0{\cdot}085 \text{ mol dm}^{-3}$$

$$\therefore \quad K_{sp} \text{ of AgCl} = [Ag^+][Cl^-] = 2{\cdot}008 \times 10^{-9} \text{ mol dm}^{-3} \times 0{\cdot}085 \text{ mol dm}^{-3}$$

$$= \mathbf{1{\cdot}7068 \times 10^{-10}\ mol^2\ dm^{-6}}$$

$$\therefore \quad \text{Solubility of AgCl} = \sqrt{\text{Solubility product of AgCl}}$$

$$= \sqrt{1{\cdot}7068 \times 10^{-10} \text{ mol}^2 \text{ dm}^{-6}} = 1{\cdot}308 \times 10^{-5} \text{ mol dm}^{-3}$$

$$= 1{\cdot}308 \times 10^{-5} \text{ mol dm}^{-3} \times 143{\cdot}5 \text{ g mol}^{-1} = 1{\cdot}875 \times 10^{-3} \text{ g dm}^{-3}$$

5. Determination of *p*H. a. By using hydrogen electrode. The potential of a hydrogen electrode in contact with a solution of H^+ ions involving the reaction

$$H^+ + e^- \rightleftharpoons 1/2\ H_2 \text{ (1 atm)}$$

is given by Nernst equation, *viz.*,

$$E_{el} = E^\circ_{el} + 2{\cdot}303(RT/F) \log [H^+] \quad \ldots(70)$$

By convention, $= E^\circ_{(el)}$, *i.e.*, the standard electrode potential of hydrogen electrode, is zero.

$$\therefore \quad E_{el} = \frac{2{\cdot}303\,RT}{F} \log [H^+] = -0{\cdot}0591\ pH \quad \text{(at 25°C)} \quad \ldots(71)$$

Thus, the potential of a hydrogen electrode depends upon the *p*H of the solution with which it is in contact. This can be determined by combining the hydrogen electrode with a reference electrode, say, calomel electrode. The complete cell is represented as

$$Pt, H_2 \text{ (1 atm)}, H^+(c = \text{unknown}) \mid\mid KCl \text{ (sat. soln.)}, Hg_2Cl_2(s), Hg.$$

The EMF of the cell is determined potentiometrically. This is given by

$$E = E_R - E_L = 0{\cdot}2422 - (-0{\cdot}0591\ pH)$$

or $$0{\cdot}0591\ pH = E - 0{\cdot}2422$$

or $$pH = \frac{E - 0{\cdot}2422}{0{\cdot}0591}$$

b. By using quinhydrone electrode. The quinone-hydroquinone system involves the following equilibrium :

$$\underset{\text{Quinone (Q)}}{C_6H_4O_2} + 2H^+ + 2e^- \rightleftharpoons \underset{\text{Hydroquinone (QH}_2\text{)}}{C_6H_6O_2}$$

For the reduction reaction given above, the potential developed on a platinum electrode immersed in this system is given by the Nernst equation as

$$E_{el} = E^\circ_{el} - \frac{2{\cdot}303RT}{2F}\log\frac{[QH_2]}{[Q][H^+]^2} \qquad ...(73)$$

$$= E^\circ_{el} + \frac{2{\cdot}303RT}{2F}\log\frac{[Q][H^+]^2}{[QH_2]} \qquad ...(74)$$

$$= E^\circ_{el} + \frac{2{\cdot}303RT}{2F}\log\frac{[Q]}{[QH_2]} + \frac{2{\cdot}303RT}{F}\log H^+ \qquad ...(75)$$

Instead of taking quinone and hydroquinone, a small amount of *quinhydrone*, which is an equilimolar compound of quinone (Q) and hydroquinone $[QH]_2$, is taken. Since hydroquinone (QH_2) is a weak acid, its ionisation is very small particularly if the *p*H of the solution is less than 7. Therefore, the concentration of hydroquinone $[QH_2]$ is the same as that of quinone [Q], *i.e.*, the quantity $[Q]/[QH_2]$ is unity. The middle term in Eq. 75, therefore, reduces to zero. Hence,

$$E_{el} = E^\circ_{el} + \frac{2{\cdot}303RT}{2F}[H^+] = E^\circ_{el} + 0{\cdot}0591\log[H^+] \text{ at } 25°C$$

$$= E^\circ_{el} - 0{\cdot}0591\,pH \qquad ...(76)$$

The standard electrode potential of the quinhydrone electrode, $E^\circ_{el} = +0{\cdot}06996$ V

$$\therefore \quad E^\circ_{el} = +0{\cdot}6996 - 0{\cdot}0591\,pH \qquad ...(77)$$

Thus, the potential of the quinhydrone electrode, just as that of the hydrogen electrode, depends upon the *p*H of the solution with which it is in contact, *i.e.*, the quinhydrone electrode behaves as a reversible hydrogen electrode. Consequently, this electrode can be used for measuring *p*H values of solutions.

This electrode is preferred to the hydrogen electrode as it can be set up easily by merely adding a pinch of quinhydrone to the solution under examination and inserting a clean platinum electrode for making electrical connection. The electrode gives accurate results even in the presence of oxidising ions which usually interfere with the working of the hydrogen electrode.

The quinhydrone electrode is combined with a saturated calomel electrode to form a cell. The combination may be represented as

$$Hg, Hg_2Cl_2\,(s), KCl\ (\text{sat. soln.}) \parallel H^+(\text{unknown conc.})\ Q, QH_2; Pt$$

The EMF of the above cell is given by

$$E = E_R - E_L = (0{\cdot}6996 - 0{\cdot}591\,pH) - 0{\cdot}2422 \text{ at } 25°C$$

or $$0{\cdot}0591\,pH = 0{\cdot}6996 - 0{\cdot}2422 - E$$

$$\therefore \quad pH = \frac{0{\cdot}6996 - 0{\cdot}2422 - E}{0{\cdot}0591} \qquad ...(78)$$

Limitation of quinhydrone electrode. The quinhydrone electrode cannot be used for solutions of *p*H more than 8. In more alkaline solutions, hydroquinone ionises appreciably as an acid and also gets oxidised partly by atmospheric oxygen. This alters the normal equilibrium between quinone and hydroquinone which forms the basis of the above equation.

Example 30. While determining the *p*H of a solution, the quinhydrone electrode, H^+, Q, QH_2 was used in conjunction with a saturated calomel electrode, as represented below :

$$Hg, Hg_2Cl_2\,(s)\ ;\ KCl\ (\text{sat. soln.}) \parallel H^+(\text{unknown}); Q, QH_2, Pt$$

The EMF of the cell was found to be 0·26 volt at 25°C. Calculate the *p*H of the solution at this temperature. $E_{\text{calomel}} = +0{\cdot}24$ volt at 25°C and $E^\circ_{(H^+, Q, QH_2)} = +0{\cdot}70$ V.

Solution : The EMF of the cell is given by

$$E = E_R - E_L$$

$$\therefore \quad 0{\cdot}26 = 0{\cdot}70 - 0{\cdot}0591\,pH - 0{\cdot}24 \qquad \text{(at 25°C)}$$

$$\therefore \quad pH = \frac{0{\cdot}70 - 0{\cdot}24 - 0{\cdot}26}{0{\cdot}0591} = 3{\cdot}37$$

c. By using glass electrode. It has been found by experiment that difference of potential exists at the interface between glass and a solution containing hydrogen ions. The magnitude of this difference of potential for a given variety of glass varies with the concentration of the hydrogen ions and, at 25°C, is given by the equation

$$E_G = E^\circ_G + 0{\cdot}0591\log[H^+] \qquad ...(79)$$

$$= E^\circ_G - 0{\cdot}0591\,pH \qquad ...(80)$$

where E°_G is a constant for the given glass electrode. The electrode reaction is assumed to involve the reduction of H^+ ions. The glass electrode, thus, functions in the same manner as a reversible hydrogen electrode.

The glass electrode is made of a special glass of relatively low melting point and high electrical conductivity. It is blown in the form of a bulb which is then sealed to the bottom of a glass tube (Fig. 5). A solution of 0·1 molar hydrochloric acid, which furnishes a constant hydrogen ion concentration, is placed inside the bulb and a Ag,AgCl electrode or simply a platinum wire is inserted to make electrical contact as shown. The reference electrode employed is usually the calomel electrode. The schematic arrangement of the cell thus formed may be represented as

$$Pt, 0{\cdot}1\ M\ HCl \mid \text{glass} \mid \text{Experimental soln.} \mid KCl\ (\text{salt. soln.})\ Hg_2Cl_2(s), Hg.$$

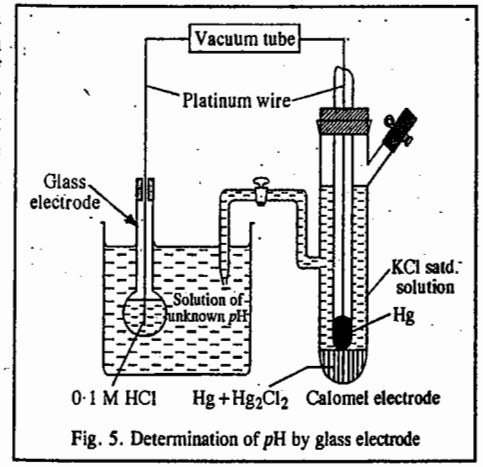

Fig. 5. Determination of *p*H by glass electrode

The EMF of such a cell can be determined conveniently by means of a potentiometer. Since the potential of the calomel electrode is known, that of the glass electrode can be easily calculated and the *p*H of the experimental solution is evaluated. The value of E°_G is first obtained by working with solutions of known *p*H.

The pH of the solution is given by

$$pH = \frac{E^\circ_G - 0{\cdot}2422 - E}{0{\cdot}0591} \quad \text{at } 25°C \qquad ...(81)$$

The glass electrode has a number of advantages over other electrodes. It can be used even in strong oxidising solutions which interfere even with quinhydrone electrode. It can also be used in the presence of metallic ions, poisons, etc. It is simple to operate and is, therefore, extensively used in chemical, industrial, agricultural and biological laboratories.

Potentiometric Tirations. As discussed earlier, the potential of an electrode depends upon the concentration of the ion to which it is reversible in accordance with Nernst equation. In a titration, there is change in ionic concentration which can be followed by measuring the potential of a suitable electrode. The potentiometric titrations are, thus, those titrations which involve the measurement of electrode potentials with the addition of the titrant.

The potentiometric titrations generally fall into the following three categories :

1. Acid-Base Titrations
2. Oxidation-Reduction (Redox) Titrations
3. Precipitation Titrations

There are a number of advantages of potentiometric titrations over the ordinary titrations involving the use of indicators. Potentiometric titrations can be carried out in coloured solutions while indicators cannot be used in such cases. Also, in ordinary titrations, one must have a prior information about the relative strengths of acids and bases before a proper indicator is selected. However, no such information is required in the case of potentiometric titrations.

Acid-Base Titrations. Suppose we want to titrate a solution of HCl against NaOH. Any electrode whose potential depends upon H^+ ion concentration (*e.g.*, hydrogen electrode, quinhydrone electrode, glass electrode) is placed in the HCl solution. It is connected to a reference electrode (*e.g.*, calomel electrode, Ag,AgCl electrode) to form a galvanic cell. If hydrogen electrode is used as the H^+ indicating electrode and a saturated calomel electrode is used as the reference electrode, then the galvanic cell may by represented as

$$Pt, H_2(1 \text{ atm}), H^+(c=\text{unknown}) \;||\; \text{KCl sat. soln} ; Hg_2Cl_2(s), Hg$$

The EMF of the cell is measured potentiometrically. It is given by

$$E \equiv E = E_R - E_L = E_{\text{calomel}} - E_{\text{hydrogen}}$$
$$= 0{\cdot}2422 - 0{\cdot}0591 \log H^+ = 0{\cdot}2422 + 0{\cdot}0591\, pH \qquad ...(82)$$

Suppose 100 ml of 0·1 M HCl is to be titrated against 1 M NaOH (the titrant). The concentration of the titrant is usually 5 to 10 times higher than that of the solution to be titrated so that the volume change is as small as possible.

As the titration proceeds, the H^+ ion concentration goes on decreasing, *i.e.*, pH of the solution goes on increasing, hence, according to Eq. 82, the EMF of the cell goes on increasing. It is evident that the EMF of the cell would increase by 0·0591 volt for every ten-fold decrease in the concentration of H^+ ions or one unit increase in the pH of the solution.

Assuming, for the sake of simplicity of calculations, that there is no change in volume during the titration, it is evident that the addition of first 9 ml of NaOH solution will give a change of 0·0591 volt. However, the addition of next 0·90 ml will produce the same change and the addition of next 0·09 ml will also produce the same change and so on. Thus, the EMF of the cell changes slowly at first but more and more rapidly as the end point approaches.

After the end point, further addition of NaOH produces very little change in the H^+ ion concentration and hence there is very little change in the EMF of the cell.

A plot of E against the volume of NaOH added is shown in Fig. 7*(a)*. As can be seen, the EMF of the cell initially rises gradually and thereafter more rapidly near the equivalence point. Beyond the equilvalence point, the EMF of the cell again increases slightly on adding more of NaOH.

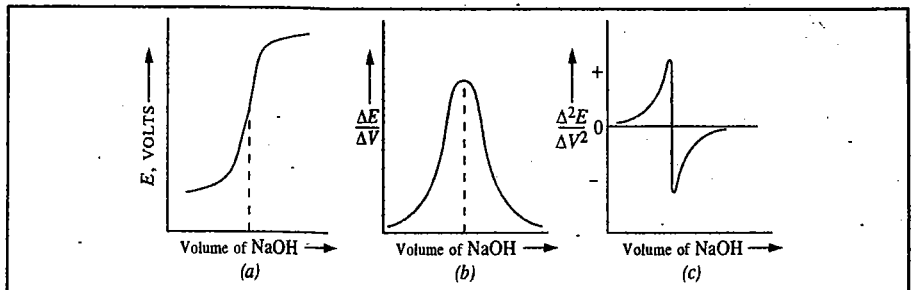

Fig. 7*(a)*. Potentiometric curve obtained in acid-base titration. Fig. 7 *(b)* and *(c)* determination of end point in acid-base titration.

Once the titration curve is obtained, the analyst has to determine, by inspection, where the curve is steepest. He may draw a vertical line through the steep portion of the curve and find the intersection of this line with the volume axis. There occurs some uncertainty in this procedure and this will be reflected in the ultimate volume reading. For a reaction that goes to completion, the titration curve is so steep near the equilvalence point that the uncertainty is small. However, for a reaction with small equilibrium constant, the precision with which the equilvalence point may be determined becomes poorer.

Fig. 7*(b)* shows a plot of the slope of the titration curve, that is, the change in the EMF with change in volume ($\Delta E/\Delta V$) against the volume of the titrant. The resulting curve rises to a maximum at the equivalence point. The volume at the equilvalence point is determined by drawing a vertical line from the peak to the volume axis. Of course, there is some uncertainty in locating exactly the peak. The more complete the reaction, the sharper the peak and hence the more accurate is the location of the equilvalence point.

Fig. 7*(c)* shows a plot of the change in the slope of a titration curve ($\Delta^2E/\Delta V^2$) against the volume of the titrant. At the point where the slope $\Delta E/\Delta V$ is a maximum, the derivative of the slope is zero. The equivalence point is located by drawing a vertical line from the point at which $\Delta^2E/\Delta V^2$ is zero on the volume axis. The steeper the portion of the curve joining the maximum and minimum value of $\Delta^2E/\Delta V^2$, the more complete is the titration reaction.

Example 31. 25 ml of a solution of HCl (0·1 M) is being titrated potentiometrically against a standard (0·1 M) solution of NaOH using a hydrogen electrode as the indicator electrode and saturated calomel electrode (SCE) as the reference electrode. What would be the EMF of the cell initially and after the addition of 20, 24·9, 24·95, 25·00 25·05, 25·10 and 30·00 ml of NaOH solution ? Comment on the data obtained.

Solution : The galvanic cell formed in this case may be represented as follows :

$$Pt, H_2(1 \text{ atm}), H^+ (c=\text{unknown}) \;||\; \text{KCl sat. soln.}, Hg_2Cl_2\,(s), Hg$$

The EMF of the cell would be given

$$E = E_{SCE} - E_{\text{hydrogen}} = 0{\cdot}2422 - 0{\cdot}0591 \log H^+$$
$$= 0{\cdot}2422 + 0{\cdot}0591\, pH \text{ at } 25°C \qquad \text{(Eq. 82)}$$

Initial pH of the titration solution, *viz.*, 0·1 M HCl = $-\log [H^+] = -\log (0{\cdot}1) = 1$ so that $E = 0{\cdot}3013$ V.

Since the product of volume of the solution in ml and the concentration in mol dm^{-3} of a solute gives the amount of the solute in millimoles, hence

Amount of HCl initially present in the titration solution = $25 \times 0{\cdot}1 = 2{\cdot}5$ millimoles

The amount of NaOH in 20 ml of 0·1 M solution added during titration = $20 \times 0{\cdot}1 = 2{\cdot}0$ millimoles

Amount of HCl left in the titration solution on adding 20 ml of NaOH } = 2·5 - 2·0 = 0·5 millimole

Total volume of titration solution = 25 + 20 = 45 ml

$\therefore$ Concn. of HCl or of H^+ ions in the solution $= \frac{0{\cdot}5 \times 1000}{1000 \times 45}$ mol dm^{-3}

$\therefore$ pH of the titration solution = - log $[H]^+$ = - log (0·5/45) = 1·95

The corresponding value of E is 0·2422 + 0·0591×1·95 = 0·3574 V

Proceeding as above, the pH values of the titrand on the addition of 24·90 and 24·95 ml of NaOH solution come out to 3·70 and 4·00, respectively and the corresponding values of E are 0·4609 and 0·4786 V, respectively.

On the addition of 25 ml of NaOH, the acid is completely neutralised giving NaCl. The pH of the resulting solution is, therefore, 7 and E = 0·6560 V

On adding 25·05 ml of NaOH, the excess volume of NaOH = 0·05 ml

Amount of NaOH in 0·05 ml solution = 0·05×0·1 = 0·005 millimole

$\therefore$ Concn. of NaOH or OH^- ions $= \frac{0{\cdot}005}{1000} \times \frac{1000}{50{\cdot}05}$ mol dm^{-3}

Since $[H^+]\,[OH^-] = 10^{-14}$ at 25°C,

$\therefore$ $[H^+] = \frac{10^{-14} \times 50{\cdot}05}{0{\cdot}005}$ mol dm^{-3} and hence pH = 10·0

The corresponding E value is 0·8332 V

Proceeding as above, the pH values of the titrand after the addition of 25·10 and 30·00 ml of NaOH solution would be 10·30 and 10·96, respectively and the corresponding E values are 0·8510 and 0·890 V, respectively.

The titration data obtained as above are summed up in Table 2.

TABLE 2

Potentiometric Titration of 0·1 M HCl Solution against 0·1 M NaOH Solution, at 25°C

Volume of NaOH solution added (ml)	EMF of the cell, E (volt)	Change in EMF (volt)
0·00	0·3013	0·0561
20·00	0·3574	0·1035
24·90	0·4609	0·0177
24·95	0·4786	0·1774
25·00	6560	0·1772
25·05	0·8332	0·0178
25·10	0·8510	0·0390
30·00	0·8900	

The EMF of the cell first increases only gradually and that too by small amounts at various steps of the titration. Thus, the EMF increases only from 0·3013 to 0·4786 V, *i.e.*, by 0·1773 V, by the addition of as large a volume as 24·95 ml of NaOH. Around the end point, however, the same change in EMF is brought about by the addition of just a single drop of the titrant. As can be seen, the EMF around the end point increases sharply from 0·4786 to 0·8332 V by the addition of just two drops of NaOH. After the end point, there is again a small change in EMF.

If the above data are plotted graphically, the titration curve obtained would be exactly similar to the one shown earlier in Fig. 7*(a)*.

2. Redox Titrations. Like acid-base titrations, the redox titrations are also carried out potentiometrically. In this case, the electrode reversible with respect to H^+ ions is replaced by an inert metal, such as platinum wire, immersed in a solution containing both the oxidised and the reduced forms of the same species. The electrode acts as an oxidation-reduction electrode.

Let us consider the redox reaction

$$Fe^{2+}(aq) + Ce^{4+}(aq) \rightleftharpoons Fe^{3+}(aq) + Ce^{3+}(aq)$$

involving the oxidation of Fe^{2+} ions by Ce^{4+} ions being carried out potentiometrically. Prior to the addition of Ce^{4+} ions, the solution contains only the Fe^{2+} ions. On adding a small amount of Ce^{4+} ions to the solution, a small amount of Fe^{2+} ions is oxidised to Fe^{3+} ions. With the presence of both the Fe^{2+} and Fe^{3+} ions, the electrode behaves as an oxidation-reduction electrode whose potential, according to the Nernst equation, is given by

$$E_{el} = E^\circ_{el} + \frac{RT}{F} \ln \frac{[Fe^{3+}]}{[Fe^{2+}]} \qquad \text{(Eq. 28)}$$

$$= E^\circ_{el} + 0{\cdot}0591 \log \frac{[Fe^{3+}]}{[Fe^{2+}]}, \text{ at } 25°C \qquad ...(83)$$

Evidently, the electrode potential is controlled by the ratio $[Fe^{3+}]/[Fe^{2+}]$. For instance, if the ratio is equal to 0·01, the electrode potential would be given by

$$E_{el} = E^\circ_{el} + 0{\cdot}0591 \log (0{\cdot}01) = E° - 0{\cdot}1182$$

With further addition of Ce^{4+} ions, the ratio $[Fe^{3+}]/[Fe^{2+}]$ changes, thereby changing the value of E_{el}. For every ten-fold change in the ratio of $[Fe^{3+}]/Fe^{2+}$, the potential of the electrode would change by 0·1182 V, evidently.

At the equivalence point, $[Fe^{2+}] = [Ce^{4+}]$ and $[Fe^{3+}] = Ce^{3+}]$ so that the electrode potential at the equilvalence point, E_{eq}, is given by

$$E_{eq} = E^\circ_1 + 0{\cdot}0591 \log \frac{[Fe^{3+}]}{[Fe^{2+}]} = E^\circ_2 + 0{\cdot}0591 \log \frac{[Ce^{4+}]}{[Ce^{3+}]} \qquad ...(84)$$

The above equations may be rewritten as

$$E_{eq} = E^\circ_1 + 0{\cdot}0591 \log [Fe^{3+}]/[Fe^{2+}] \qquad ...(85)$$

and $$E_{eq} = E^\circ_2 + 0{\cdot}0591 \log [Ce^{4+}]/[Ce^{3+}] \qquad ...(86)$$

Adding and simplifying, keeping in mind that at the equivalence point,

$[Fe^{2+}] = [Ce^{4+}]$ and $[Fe^{3+}] = [Ce^{3+}]$, we get

$$E_{eq} = (E^\circ_1 + E^\circ_2)/2 \qquad ...(87)$$

The numerical values of E°_1 and E°_2 are 0·77 V and 1·61 V, respectively, according to the equations :

$Fe^{3+}(aq) + e^- \rightleftharpoons Fe^{2+}(aq)$; $E^\circ_1 = 0{\cdot}77$ V

$Ce^{4+}(aq) + e^- \rightleftharpoons Ce^{3+}(aq)$; $E^\circ_2 = 1{\cdot}61$ V

Beyond the equivalence point, $[Fe^{3+}] \approx 0$ as a result of which the electrode potential thereafter is controlled only by the $[Ce^{4+}]/[Ce^{3+}]$ ratio.

For potentiometric measurements, the oxidation-reduction electrode (*viz.*, Pt ; Fe^{3+}, Fe^{2+}) is combined with a reference electrode, *e.g.*, a saturated calomel electrode, to form a galvanic cell which is represented as

$$Hg, Hg_2Cl_2\ (s), KCl\ (sat.\ soln.)\ ||\ Fe^{2+}, Fe^{3+}; Pt$$

in accordance with the positions of these electrodes in the electrochemical series (Table 1).

Before the equilvalence point, the EMF of the cell would be given by

$$E = E_R - E_L = E^\circ_{el} = 0{\cdot}0591 \log \{[Fe^{3+}]/[Fe^{2+}]\} - E_{calomel}$$
$$= 0{\cdot}77 + 0{\cdot}0591 \log \{[Fe^{3+}]/[Fe^{2+}]\} - 0{\cdot}24 \quad \ldots (88)$$

and *after the equilvalence point,* the EMF of the cell is given by

$$E = 1{\cdot}61 + 0{\cdot}0591 \log \{[Ce^{4+}]/[Ce^{3+}]\} - 0{\cdot}24$$

At tne equivalence point, as already discussed, the EMF of the cell is given by

$$E = \frac{0{\cdot}77 + 1{\cdot}61}{2} - 0{\cdot}24 \quad \ldots (89)$$

The EMF of the cell is measured potentiometrically at each stage of titration and the EMF data thus obtained are processed for the equivalence point. The redox titration curve is exactly similar to the acid–base titration curve shown earlier in Fig. 7(*a*).

Example 32. Calculate the potential at 25°C of a cell consisting of saturated calomel electrode (SCE) and a platinum-wire indicator electrode dipping in a titration vessel that initially contains 25·00 ml of 0·01 M Fe^{2+}, after the addition of 5·00, 12·50, 20·00, 24·00, 25·00, 26·00 30·00 and 50·00 ml of 0·01 M Ce^{4+} solution. The SCE is attached to the negative terminal of the voltmeter.

Solution : The half-cell reactions in this case are :

$$Fe^{2+} \rightleftharpoons Fe^{3+} + e^- ; \qquad E^\circ_{el} = 0{\cdot}77\ V$$
$$Ce^{4+} + e^- \rightleftharpoons Ce^{3+} ; \qquad E^\circ_{el} = 1{\cdot}61\ V$$

The overall reaction in the titration flask is the redox reaction

$$Fe^{2+} + Ce^{4+} \rightleftharpoons Fe^{3+} + Ce^{3+}$$

Before the equilvalence point, the cell potential is controlled by the concentrations of Fe^{2+} and Fe^{3+} ions present in solution and after the equivalence point the cell potential is controlled by the concentrations of Ce^{3+} and Ce^{4+} ions.

Thus, **before the equilvalence point,** the cell potential is given by

$$E = E_1 - E_{SCE}, \quad \text{where } E_{SCE} = 0{\cdot}24\ V$$
$$= E^\circ_1 - 0{\cdot}0591 \log \{[Fe^{2+}]/[Fe^{3+}]\} - E_{SCE}$$
$$= 0{\cdot}77 - 0{\cdot}0591 \log \{[Fe^{2+}]/[Fe^{3+}]\} - E_{SCE}$$
$$= 0{\cdot}53 - 0{\cdot}0591 \log \{[Fe^{2+}]/[Fe^{3+}]\}$$

During titration, the Fe^{2+} ions present in the titrand are oxidised to Fe^{3+} ions by the titrant. The concentrations of Fe^{3+} and Fe^{2+} ions which prevail after the addition of various of amounts of Ce^{4+} solution of known molarity and the resulting cell potentials can be calculated as shown below :

After the addition of 5·00 ml of Ce^{4+} solution, we have

$$[Fe^{3+}] = \frac{5{\cdot}00\ ml \times 0{\cdot}01\ millimol/ml}{(25{\cdot}00 + 5{\cdot}00)\ ml} = 1{\cdot}67 \times 10^{-3}\ M$$

$$[Fe^{2+}] = \frac{(25{\cdot}00\ ml \times 0{\cdot}10\ millimol/ml^{-1}) - (5{\cdot}00\ ml \times 0{\cdot}01\ millimol/ml^{-1})}{(25{\cdot}00 + 5{\cdot}00)\ ml}$$

$$= 6{\cdot}67 \times 10^{-3}\ M$$

Hence, using these values of $[Fe^{3+}]$ and $[Fe^{2+}]$, $E = 0{\cdot}491$ V

Similarly, after the addition of 12·50, 20·00 and 24·00 ml of the titrant (Ce^{4+} solution), the concentrations and

the cell potentials would be as follows :

12·50 ml :
$$[Fe^{3+}] = \frac{12{\cdot}50 \times 0{\cdot}0100}{25{\cdot}00 + 12{\cdot}50} = 3{\cdot}33 \times 10^{-3}\ M$$
$$[Fe^{2+}] = \frac{25{\cdot}00 \times 0{\cdot}010 - 12{\cdot}50 \times 0{\cdot}0100}{25{\cdot}00 + 12{\cdot}50} = 3{\cdot}33 \times 10^{-3}\ M$$
$$E = 0{\cdot}53\ V \quad (\because \text{the logarithmic term} = 0)$$

20·00 ml : $[Fe^{3+}] = 4{\cdot}44 \times 10^{-3}$ M ; $[Fe^{2+}] = 1{\cdot}11 \times 10^{-3}$ M ; $E = 0{\cdot}56$ V

24·00 ml : $[Fe^{3+}] = 4{\cdot}90 \times 10^{-3}$ M ; $[Fe^{2+}] = 2{\cdot}04 \times 10^{-3}$ M ; $E = 0{\cdot}61$ V

The **equivalence point** of the titration is reached when 25·0 ml of the titrant is added. At the equivalence point we must use both half-cell reactions to calculate the potential :

$$E = 0{\cdot}77 - 0{\cdot}0591 \log \{[Fe^{2+}]/[Fe^{3+}]\}$$

and
$$E = 1{\cdot}61 - 0{\cdot}0591 \log \{[Ce^{3+}]/[Ce^{4+}]\}$$

Adding, we obtain,
$$2E = 2{\cdot}38 - 0{\cdot}0591 \log \{[Fe^{2+}]/[Ce^{3+}]/[Fe^{3+}]\ [Ce^{4+}]\}$$

At the equivalence point it is evident from the balanced chemical equation that

$$[Fe^{3+}] = [Ce^{3+}] \text{ and } [Fe^{2+}] = [Ce^{4+}]$$

Using these substitutions, we obtain

$$2E = 2{\cdot}38\ V \quad (\because \text{the logarithmic term} = 0)$$
$$\therefore \quad E_{eq} = 1{\cdot}19\ V \text{ and } E = E_{eq} - E_{SCE} = 1{\cdot}19 - 0{\cdot}24 = 0{\cdot}95\ V$$

After the equivalence point, we use the following equation to calculate the cell potential :

$$E = E_2 - E_{SCE} = E^\circ_2 - 0{\cdot}0591 \log \{[Ce^{3+}]/[Ce^{4+}]\} - E_{SCE}$$
$$= 1{\cdot}61 - 0{\cdot}0591 \log \{[Ce^{3+}]/[Ce^{4+}]\} - E_{SCE}$$
$$= 1{\cdot}37 - 0{\cdot}0591 \log \{[Ce^{3+}]/[Ce^{4+}]\}$$

After the addition of 26·00, 30·00 and 50·00 ml of titrant, the concentrations and cell potentials are as follows :

26·00 ml : $[Ce^{4+}] = \frac{(26{\cdot}00 - 25{\cdot}00)(0{\cdot}01)}{25{\cdot}00 + 26{\cdot}00} = 1{\cdot}96 \times 10^{-4}\ M$

$$[Ce^{3+}] = \frac{(25{\cdot}00)(0{\cdot}01)}{25{\cdot}00 + 26{\cdot}00} = 4{\cdot}90 \times 10^{-3}\ M$$
$$E = 1{\cdot}37 - 0{\cdot}0591 \log (4{\cdot}90 \times 10^{-3})(1{\cdot}96 \times 10^{-4}) = 1{\cdot}29\ V$$

30·00 ml : $[Ce^{4+}] = 9{\cdot}09 \times 10^{-4}$ M ;
$[Ce^{3+}] = 4{\cdot}55 \times 10^{-3}$ M
$E = 1{\cdot}33$ V

50·00 ml : $[Ce^{4+}] = 3{\cdot}33 \times 10^{-3}$ M
$[Ce^{3+}] = 3{\cdot}33 \times 10^{-3}$ M
$E = 1{\cdot}37$ V ($\because$ the logarithmic term = 0)

The results of the calculations are plotted as a titration curve shown in Fig. 8.

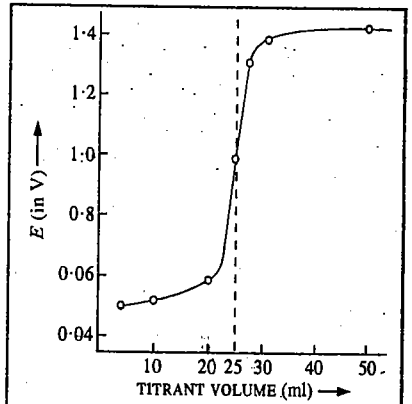

Fig. 8. The calculated potentiometric titration curve for the titration of 25·00 ml of 0·01 M Fe^{2+} with 0·01 M Ce^{4+}. The equilvalence point and the end point are located at titrant volume of 25·00 ml.

Note : The end point of a titration is usually considered to correspond to the inflection point. The equilvalence point in the curve corresponds to the inflection point only for titrations in which the molar quantities of *titrand* and *titrant* at the equilvalence point are equal (when the coefficients for titrand and titrant in the balanced chemical equations are identical) and for titrations in which the titrand is not significantly diluted by the addition of the titrant during the titration.

Example 33. Calculate the potential of the indicator electrode at 25°C relative to SCE at the equivalence point of the titration of 25·00 ml of 0·010 M Fe^{2+} with 0·010 M $Cr_2O_7^{2-}$ in a solution that is buffered at pH 3·50.

Solution : The half-cell reactions in this case are :

$$Fe^{2+} \rightleftharpoons Fe^{3+} + e^- ; \qquad E^\circ_{el} = 0{\cdot}77\ V$$

$$Cr_2O_7^{2-} + 14H^+ + 6e^- \rightleftharpoons 2Cr^{3+} + 7H_2O ; \qquad E^\circ_{el} = 1{\cdot}33\ V$$

The overall reaction is :

$$6Fe^{2+} + Cr_2O_7^{2-} + 14H^+ \rightleftharpoons 6Fe^{3+} + 2Cr^{3+} + 7H_2O ;$$

The potential of the indicator electrode, relative to the standard hydrogen electrode, is given by

$$E_{el} = 0{\cdot}77 - 0{\cdot}0591 \log \{[Fe^{2+}]/Fe^{3+}]\} \qquad ...(i)$$

as well as by

$$E_{el} = 1{\cdot}33 - \frac{0{\cdot}0591}{6} \log \{[Cr^{3+}]^2/[Cr_2O_7^{2-}][H^+]^{14}\} \qquad ...(ii)$$

We must combine these two equations in such a manner as to eliminate the concentrations of the reactants that cannot be calculated at the equivalence point.

In this titration, neither $[Fe^{2+}]$ nor $[Cr_2O_7^{2-}]$ can be calculated at the equivalence point without prior knowledge of the equilibrium constant for the reaction. Hence, multiplying equation *(ii)* by 6 and then adding with Eq. *(i)*, we obtain

$$7\,E_{el} = 8{\cdot}75 - 0{\cdot}0591 \log \frac{[Fe^{2+}][Cr^{3+}]^2}{[Fe^{3+}][Cr_2O_7^{2-}][H^+]^{14}} \qquad ...(iii)$$

At the equivalence point, $[Fe^{2+}] = 6[Cr_2O_7^{2-}]$. Hence, Eq. *(iii)* simplifies to

$$7E_{el} = 8{\cdot}75 - 0{\cdot}0591 \log \frac{6[Cr_2O_7^{2-}][Cr^{3+}]^2}{[Fe^{3+}][Cr_2O_7^{2-}][H^+]^{14}}$$

$$= 8{\cdot}75 - 0{\cdot}0591 \log \frac{6[Cr^{3+}]^2}{[Fe^{3+}][H^+]^{14}} \qquad ...(iv)$$

Let x be the volume of $Cr_2O_7^{2-}$ solution added at the point of equivalence. Since at the equivalence point,

$$[Fe^{2+}] = 6[Cr_2O_7^{2-}], \text{ hence}$$

$$x = 4{\cdot}16 \approx 4{\cdot}2 \text{ ml}$$

$$\therefore \quad [Fe^{3+}] = \frac{0{\cdot}010 \text{ millimol/ml}^{-1} \times 25{\cdot}0 \text{ ml}}{25{\cdot}0 \times 4{\cdot}2 \text{ ml}} = 8{\cdot}6 \times 10^{-3} \text{ M}$$

At the equivalence point, $[Cr^{3+}] = [Fe^{3+}] \times 2/6 = 2{\cdot}9 \times 10^{-3}$ M

Since $pH = 3{\cdot}50$, hence $[H^+] = 3{\cdot}2 \times 10^{-4}$ M

Substituting these values in Eq. *(iv)* and simplifying, we obtain $E_{el} = 0{\cdot}855$ V

Hence, the potential of the indicator electrode relative to SCE = 0·855 − 0·242 = **0·613 V**

Precipitation Titrations. Suppose we want to standardise a solution of silver nitrate by titrating against a standard solution of potassium chloride. The silver electrode is used as the indicator electrode in this case.

The potential of the half-cell, Ag^+,Ag, is measured by connecting it with the calomel electrode, as usual. The solution is titrated against a standard solution of potassium chloride the strength of which is about 10 times higher. As the reaction proceeds, the Ag^+ ions get gradually precipitated as silver chloride.

$$Ag^+ + NO_3^- + (K^+ + Cl^-) \rightleftharpoons AgCl\downarrow + K^+ + NO_3^-$$

The concentration of Ag^+ ions goes on decreasing and hence the potential of the Ag^+, Ag

electrode, given by the Nernst equation, *viz.*,

$$E_{el} = E^\circ_{el} + 0{\cdot}0591 \log [Ag^+] \qquad \text{(at 25°C)} \qquad ...(90)$$

goes on decreasing continuously on the progressive addition of KCl solution. The electrode potential will change slowly at first but more and more rapidly as the end point approaches. At the end point, the concentration of Ag^+ ions is very small as this is now only on account of slight solubility of AgCl. Hence, the change in electrode potential is maximum at the end point. If the addition of KCl is continued further, the concentration of Ag^+ ions remains almost unaffected except for very small decrease on account of the common ion effect. The addition of KCl beyond the end point, therefore, causes only a small change in the electrode potential.

The potentiometric titration curve obtained in this case is exactly similar to the one obtained in the case of acid–base titration described earlier.

Oxidation–Reduction Indicators

There are a few organic compounds which can exist in oxidised form (say, O) as well as reduced form (say, R). The interconversion of such compounds from one form to the other may be represented as

$$O + nH^+ + ne^- \rightleftharpoons R$$

Applying Nernst equation to the above equilibrium, we have

$$E_{(O,R)} = E^\circ_{(O,R)} - \frac{RT}{nF} \ln \frac{[R]}{[O][H^+]^n}$$

$$= E^\circ_{(O,R)} + \frac{RT}{nF} \ln \frac{[O]}{[R]} + \frac{RT}{nF} \ln [H^+] \qquad ...(91)$$

where $E^\circ_{(O,R)}$ is the standard potential of the redox system involved in this case.

One important feature of these compounds is that their oxidised and reduced forms have different colours. If the hydrogen ion concentration is kept constant, it is evident from Eq. 91 that the ratio of $O : R$ and hence the ratio of the two colours will enable evaluation of the redox potential, $E_{(O,R)}$.

Another important feature of these substances is that when added in small amounts to excess of a solution containing any other redox system (say, $Fe^{3+} + e^- \rightleftharpoons Fe^{2+}$), they spontaneously adjust themselves to the same potential as that of the latter. Hence, the potential of any redox system can be easily obtained by noting the colour shade developed visually or by means of a colorimeter on adding a small amount of a substance of this class. Such compounds are known as **oxidation–reduction indicators** since they enable evaluation of redox potential of a system without setting up potentiometric technique.

However, a particular indicator can be used successfully only if the potentials to be measured are about 0·03 volt on either side of its $E^\circ_{(O,R)}$ value. Fortunately, there are several indicators having different values of $E^\circ_{(O,R)}$. Thus, redox potentials can be measured by using them.

Oxidation-Reduction Indicators in Volumetric Analysis. The main application of these indicators lies, however, in *detecting end points* in volumetric titrations involving oxidation–reduction systems. Since potential of a system changes rapidly at the end point, as already explained, the colour of a suitable indicator that is added to the solution *also changes rapidly at the end point* which can, therefore, be detected easily. There is no need to carry out titration potentiometrically. It has been found, however, that in order to get a sharp change in colour at the end point, the indicator used should be such that its standard potential $E^\circ_{(O,R)}$ lies in between the standard potentials of the oxidation-reduction systems being titrated against each other.

To take an example, diphenylamine can be used as a redox indicator for locating the end point in titrating ferrous ions against dichromate ions. This process actually involves titration of ferrous–ferric

ions system against dichromate-chromic ions system. The $E^{\circ}_{(O,R)}$ value of the indicator is about 0·75 volt while the standard potential for ferric-ferrous ions system is about 0·78 volt and that of chromic-dichromate ions system is about 1·3 volt. Evidently, the standard potential of the indicator does not lie in between the standard potentials of the two reacting systems and hence the end point will not be very sharp. Some phosphoric acid or a fluoride is, therefore, added to the test solution before commencing the titration. These substances form complexes with ferric ions and this results in varying the standard potential of the ferric-ferrous system to about 0·5 volt. Now, evidently, the standard potential of the indicator lies in between the standard potentials of the two systems being titrated against each other.

We conclude this chapter by adding that electrochemical science is highly indebted to the pioneering researches of the two great 18th century Italian scientists Luigi Galvani (1737-1798) and Alessandro Volta (1745-1827), and the 19th century British scientist Michael Faraday (1791-1867) who has been called the greatest experimental physicist of all time.

I. Review Questions

1. *(i)* Write the half-cell reactions and the overall cell reactions for the following cells :
   (a) Pt ; Hg, Hg_2Cl_2, Cl^- | H^+ , H_2 (*g*); Pt
   (b) Pt; H_2 (1 atm), HCl (a=1) | AgCl ; Ag
   (c) Pt; QH_2, Q, H^+ | Cl^-, AgCl; Ag

   (ii) Write the half-cell reactions for electrochemical cells involving the following cell reactions :

   (a) $Zn(s) + 2AgCl(s) \rightleftharpoons 2Ag(s) + ZnCl_2$

   (b) $Cl_2 + 2Fe^{2+} \rightleftharpoons 2Fe^{3+} + 2Cl^-$

   (c) $H_2(g) + Cu^{2+} \rightleftharpoons Cu(s) + 2H^+$

2. What is meant by Electrochemical Series ? Using the data given in the series explain why
   (i) Cu(I) sulphate does not exist in solution.
   (ii) Neither Cu^+ nor Co^{3+} is stable in aqueous solution.
   (iii) Zinc reacts with H_2SO_4 to give H_2 but silver does not.
3. Derive expressions for the EMFs of concentration cells *(i)* with transference, *(ii)* without transference.
4. What are Fuel cells ? Describe the functioning of *(i)* Hydrogen-Oxygen fuel cell *(ii)* Hydrocarbon-Oxygen fuel cell. *(iii)* Coal-fired fuel cells. *(iv)* Zinc-air fuel cell. What type of H_2-O_2 fuel cells are used in manned space flights ?
5. Describe briefly various types of electrodes which can be used for determining *p*H of a solution.
6. What is meant by activity coefficient of an electrolyte ? How would you determine the mean ionic activity coefficient of HCl in a given solution of the acid.
7. Discuss the principle underlying potentiometric titrations. How would you carry out potentiometric titration of a solution of HCl against a standard solution of NaOH.
8. 20 ml of 0·1 M HCl solution is being titrated against 0·1 M solution of NaOH using a hydrogen electrode as the indicator electrode and a saturated calomel electrode as the reference electrode. What would be the EMF of the cell initially and after the addition of 5·0, 10·0, 19·9, 19·95, 20·0, 20·05, 20·10 and 25 ml of NaOH solution. Plot the data in the form of a potentiometric titration curve and comment on the result.
9. What are redox titrations ? Illustrate giving a suitable example how these titrations are carried out potentiometrically.

   A titration vessel contains 25 ml of 0·01 M Fe^{2+}. A platinum wire as indicator electrode and a SCE as reference electrode are dipped in the Fe^{2+} ion solution. Calculate the potential of the cell at 25°C after the addition of 5, 12·5, 20, 24, 25, 26, 30 and 50 ml of 0·01 M Ce^{4+} solution. SCE is attached to the negative terminal of the voltmeter. Plot the data in the form of a potentiometric titration curve and comment on the result.

II. Problems

1. EMF of the cell Sn, $SnCl_2$ (0·5 M) | AgCl, Ag is 0·430V at 25°C and 0·448 at 0°C. Calculate the free energy change (ΔG), enthalpy change (ΔH) and entropy change (ΔS) of the cell reaction at 25°C. **[Ans. – 82·99 kJ, – 124·30 kJ, – 138·6 J]**
2. Calculate the potential of an electrode consisting of zinc metal in zinc sulphate solution in which $[Zn^{2+}]$ = 0·01 M, for the reaction $Zn^{2+}(aq) + 2e^- \rightleftharpoons Zn(s)$. E° = – 0·76 V. **[Ans. 0·822 V]**
3. Calculate the EMF of the following cell :

   Pt; H_2 (0·50 atm), H^+ (0·10 M) || MnO_4^- (0·10 M), Mn^{2+} (0·10 M), H^+ (0·10 M); Pt **[Ans. 1·45V]**
4. Calculate the EMF of the following cell :

   Pt; Co^{2+} (2·0 M), Co^{3+} (0·010 M) || Cr^{3+} (0·50 M), $Cr_2O_7^{2-}$ (4·0 M), H^+(1·5 M); Pt **[Ans. – 0·49 V]**
5. Using the standard electrode potential data given in Electrochemical Series, determine the equilibrium constants of the following reactions :

   (i) $Sn^{2+}(aq) + Cl_2(g) \rightleftharpoons Sn^{4+}(aq) + 2Cl^-(aq)$

   (ii) $Fe^{3+}(aq) + Sn^{2+}(aq) \rightleftharpoons 2Fe^{2+}(aq) + Sn^{4+}(aq)$

   (iii) $Zn(s) + Fe^{2+}(aq) \rightleftharpoons Zn^{2+}(aq) + Fe(s)$

   [Ans. *(i)* $1{\cdot}2\times10^{-41}$ *(ii)* $9{\cdot}58\times10^{20}$ *(iii)* $8{\cdot}89\times10^{11}$**]**
6. For the concentration cell Pb; $PbSO_4$ (*s*), H_2SO_4 (m=1·0) | H_2SO_4 (m=0·1), $PbSO_4$; Pb
   (a) Calculate the EMF of the cell without transference of ions.
   (b) Calculate the EMF of the cell with transference; given t_{H^+} = 0·831. **[Ans.** *(a)* **0·0295 V** *(b)* **0·025 V]**
7. For the concentration cell Hg (*l*), $Hg_2Cl_2(s)$, KCl (0·06 *m*) | KCl (0·025 *m*), $Hg_2Cl_2(g)$, Hg(*l*)
   (a) Calculate the EMF of the cell
   (b) Calculate the EMF of the cell when transference of both ions takes place. Given t_{K^+} = 0·49.

   [Ans. *(a)* **0·045 V** *(b)* $7{\cdot}73\times10^{-3}$ **V]**
8. For the electrochemical cell Cd, $CdCl_2{\cdot}5/2H_2O(aq)$ | AgCl(*s*), Ag, the EMF at 0°C and 25°C is 0·6915 V and 0·6753 V, respectively. The cell reaction is $Cd(s) + 2AgCl(s) + aq \rightleftharpoons CdCl_2{\cdot}2{\cdot}5H_2O$ (sat.) + 2Ag(*s*). Calculate ΔG°, ΔS° and ΔH° at 25°C. **[Ans.** ΔG° = – 130·3 kJ ; ΔS = – 125·4 J K^{-1} ; ΔH° = – 167·6 kJ**]**
9. Calculate the stability constant, K_s of the formation of complex ion, $[PdI_4]^{2-}$ from Pd^{2+} and I^- at 27°C. Given :

   $[PdI_4]^{2-} + 2e^- \rightleftharpoons Pd(s) + 4I^-$; E° = 0·18 V

   $Pd^{2+} + 2e^- \rightleftharpoons Pd(s)$; E° = 0·92 V

   [Ans. $1{\cdot}1\times10^{25}$**]**
10. Calculate the stability constant, K_s, of the formation of $[Cu(NH_3)_4]^{2+}$ at 25°C. Given :

    $Cu^{2+} + 2e^- \rightleftharpoons Cu(s)$; E° = + 0·34 V

    $[Cu(NH_3)_4]^{2+} + 2e^- \rightleftharpoons Cu(s) + 4NH_3(g)$; E° = – 0·12 V

    [Ans. $2{\cdot}92\times10^{15}$**]**
11. For the concentration cell

    Pt ; H_2(1 atm), $H^+(a_{H^+} = x)$ || H^+ (a_{H^+} = 0·1) (1 atm) ; Pt,

    E° at 298 K is 0·118 V. Calculate the *p*H of the unknown solution. **[Ans. 3·0]**
12. Calculate the solubility product of $Fe(OH)_3$ at 25°C. Given

    $Fe(OH)_3 + 3e^- \rightleftharpoons Fe + 3OH^-$; E° = – 0·77 V

    $Fe^{3+} + 3e^- \rightleftharpoons Fe$ E° = – 0·36 V

    [Ans. $1{\cdot}82\times10^{-37}$**]**

CHAPTER 25

ELECTROCHEMISTRY–III. ADVANCED TOPICS

(DEBYE-HÜCKEL THEORY, ELECTRIFIED INTERFACES, ELECTROCATALYSIS, BIOELECTROCHEMISTRY, KINETICS OF ELECTRODE REACTIONS AND POLAROGRAPHY)

I. DEBYE-HÜCKEL THEORY OF ACTIVITY COEFFICIENTS OF STRONG ELECTROLYTES

The Debye-Hückel theory of activity coefficients of strong electrolytes has already been discussed at an introductory level in Chapter 23, We shall give here a detailed account of the theory, emphasizing salient features. Three assumptions are made in the discussion of this theory. Three are : 1. The solution is a dielectric continuum of dielectric constant (relative permittivity) ε_r .2.The ions are hard spheres of diameter *a*. 3.The concentration is relatively low (at higher concentrations the validity of the Debye-Hückel theory is approximate). Consider a charge density ρ in a volume element dv at a distance r from an arbitrarily selected central ion and assume that the mean electrostatic potential is $\psi(r)$. The charge density ρ in volume element dv is related to the electrical potential $\psi(r)$ by the **Poisson equation**, *viz.*,

$$\nabla^2 \psi(r) = -4\pi\rho/\varepsilon_r \qquad ...(1)$$

where ∇^2 is the Laplacian operator.

The mean distribution of positively and negatively charged ions around the central ion is spherically symmetrical provided no additional forces are acting on the ions. The distribution simply represents the time-averaged effects of the mutual interaction and thermal motion of the ions. In terms of the spherical polar coordinates, the Poisson equation is expressed as

$$\nabla^2 \psi(r) = \frac{1}{r^2} \times \frac{d}{dr}\left[r^2 \frac{d\psi(r)}{dr} \right] = -\frac{4\pi\rho}{\varepsilon_r} \qquad ...(2)$$

The charge density in the volume element is equal to the excess charge in the volume element which is equal to the sum of each ion density n_i times the charge $z_i e$ on the ion (n_i is the average number of *i* ions per unit volume). Thus,

$$\rho = \sum_i n_i z_i e \qquad ...(3)$$

where e is the electronic charge. For the central ion, the following equation is satisfied from the electroneutrality condition of the solution :

$$\int_{r_0}^{\infty} 4\pi r^2 \rho \, dr = -ze \qquad ...(4)$$

where ze is the charge on the central ion and r_0 is the distance of closest approach between the central ion and the surrounding ions. The ion density n_i in Eq. 3 is related to the electrical potential by the Boltzmann expression, *viz.*,

$$n_i = n_i^0 \exp(-z_i e \, \psi(r)/kT) \qquad ...(5)$$

where n_i^0 is the average bulk density of *i*th ion at the point where $\psi(r)=0$. This is the first Debye-Hückel approximation. The charge density $\rho(r)$, which is a function of r of the volume element

may thus be written as,

$$\rho(r) = \sum_i n_i^0 z_i e \exp(-z_i e \, \psi(r)/kT) \qquad ...(6)$$

Since, as stated above, there is no additional force applied to the system, therefore, the kinetic energy of ions due to their thermal motion is expected to be much greater than their electrostatic energy, *i.e.*, $z_i e \, \psi(r)/kT \ll 1$ (otherwise complete dissociation of a strong electrolyte would not occur in a dilute solution). This is the second Debye-Hückel approximation which is justified when the solution is dilute. Thus, the exponential in Eq. 6 can be expressed in the form of linear Taylor series and the **Poisson-Boltzmann equation** finally becomes :

$$\frac{1}{r^2} \times \frac{d}{dr}\left[r^2 \frac{d\psi(r)}{dr} \right] = \kappa^2 \psi(r) \qquad ...(7)$$

where

$$\kappa^2 = \frac{4\pi e^2}{\varepsilon kT} \times \sum_i n_i^0 z_i^2 \qquad ...(8)$$

and where the electroneutrality condition of the solution, *viz.*,

$$\sum_i n_i^0 z_i e = 0 \qquad ...(9)$$

is employed.

The symbol kappa (κ) is an important parameter concerning the distribution of ions around the central ion. The value of κ^2 is proportional to ionic strength and becomes zero as the solution approaches an infinite dilution. The linearized Poisson-Boltzmann equation can be solved by the variable transform. The substitution $y(r) = r\,\psi(r)$ reduces Eq. 7 to the following form :

$$d^2y(r)/dr^2 = \kappa^2 y(r) \qquad ...(10)$$

This differential equation has the solution :

$$y(r) = A \exp(-\kappa r) + B \exp(\kappa r) \qquad ...(11a)$$

or

$$\psi(r) = A \exp(-\kappa r)/r + B \exp(\kappa r)/r \qquad ...(11b)$$

where A and B are the integration constants determined from the physical conditions. Since $\psi(r) \to 0$ as $r \to \infty$, we have $B = 0$.

Our next problem is to determine the constant A. This can be done by using Eqs. 4 and 6. Similar to the derivation of Eq. 7, the following equation is derived from Eq. 6 :

$$\rho(r) = -\frac{A\kappa^2\varepsilon_r}{4\pi} \times [\exp(-\kappa r)/r] \qquad ...(12)$$

where $\psi(r) = A \exp(-\kappa r)/r$ is used for $\psi(r)$ in Eq. 6. Substituting $\rho(r)$ from Eq.12 into Eq. 4, we have

$$A\kappa^2\varepsilon_r \int_{r_0}^{\infty} r \exp(-\kappa r)\, dr = ze \qquad ...(13)$$

Integrating Eq. 13 by parts, we get

$$A = ze \exp(\kappa r_0)/[\varepsilon_r(1+\kappa r)] \qquad ...(14)$$

Finally, we obtain the following equation for the electrical potential $\psi(r)$ around a central ion whose charge is $z_j e$:

$$\psi(r) = z_j e \exp[(-\kappa(r-a)]/[\varepsilon_r(1+\kappa r)] \qquad ...(15)$$

Here we have used a in place of r_o (the distance of closest approach of ions); a is the sum of the effective radii of ions in solution and is the same for all pairs of ions (a rather bold assumption). Eq. 15 is the **Debye-Hückel equation** for a dilute electrolyte solution and is the fundamental equation for evaluating the activity coefficients of ionic species in solution.

From the derivation of Eq. 15 it is clear that the electrical potential $\psi(r)$ is the sum of the contributions from the central ion and the surrounding ions ; these contributions are additive. Thus,

$$\psi(r) = \psi'(r) + \psi''(r) \qquad ...(16)$$

where $\psi'(r)$ is the contribution of the central ion to the electrical potential and $\psi''(r)$ is the contribution of all the surrounding ions (**the ion atmosphere**). The electrical potential $\psi'(r)$ in the same dielectric continuum is given by

$$\psi'(r) = z_j e/\varepsilon_r \qquad ...(17)$$

Hence, the electrical potential $\psi''(r)$ becomes

$$\psi''(r) = (z_j e/\varepsilon_r) \times \{\exp[-\kappa(r-a)]/(1+\kappa a) - 1\} \qquad ...(18)$$

This equation is applicable over a range $r > a$. On the other hand, no other ions enter the spherical region $r < a$ and, therefore, the electrical potential $\psi''(a)$ remains constant within the sphere. The substitution $r = a$ in Eq. 18 yields

$$\psi''(a) = -z_j e\,\kappa/\varepsilon_r\,(1+\kappa a) = -(z_j e/\varepsilon_r) \times [1/(a+1/\kappa)] \qquad ...(19)$$

This is the electrical potential imposed on the central ion by all of the surrounding ions when the charge of the central ion is $z_j e$. The central ion then comes to occupy the centre of the spherically constant potential due to the ion atmosphere which results, in turn, from the electrical potential of the central ion. It is evident from Eq. 19 that the surrounding ions are distributed over a spherical surface at a distance $(a+1/\kappa)$ from the centre of the sphere so that their total charge is equal and opposite to the charge on the central ion. The parameter $1/\kappa$, called the **radius of the ion sphere**, represents the distance of the ion atmosphere from the central ion at closest approach (Fig. 1). Therefore, the free energy change, ΔG, of the central ion due to electrical interaction with the surrounding ion atmosphere is given by

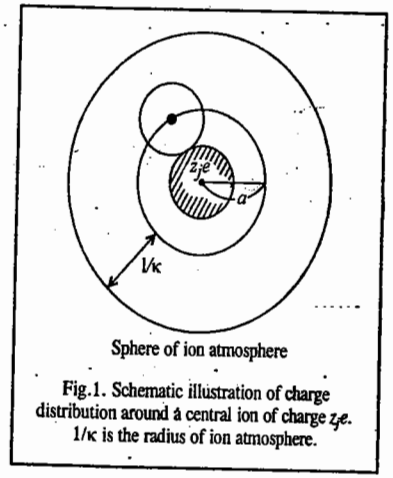

Fig.1. Schematic illustration of charge distribution around a central ion of charge $z_j e$. $1/\kappa$ is the radius of ion atmosphere.

$$\Delta G = \int_0^{z_j e} \psi''(a)\,d\rho = -\int_0^{z_j e} \frac{\kappa z_j e}{\varepsilon_r (1+\kappa a)}\,d(z_j e)$$

$$= -\kappa z_j^2 e^2/[2\varepsilon_r(1+\kappa a)] \qquad ...(20)$$

where ρ is the charge density in the electrical field $\psi''(a)$. This ΔG is also the excess energy of ideal mixing and contributes to the activity coefficient γ_j of an ion with charge $z_j e$. The activity coefficient γ_j is given by

$$kT \ln \gamma_j = -\kappa z_j^2 e^2/[2\varepsilon_r(1+\kappa a)] \qquad ...(21)$$

Also, κ is related to the ionic strength I as

$$\kappa = \left[\frac{8\pi N_A e^2 I}{1000\,\varepsilon kT}\right]^{1/2} \qquad ...(22)$$

because from Eq. 8, $n_i^0 = cN_A/1000$ where c is the molar concentration and N_A is the Avogadro's number.

The ionic strenth is given by

$$I = \frac{1}{2}\sum_i c_i z_i^2 \qquad ...(23)$$

Eq. 21 gives the expression for an individual activity coefficient but it cannot be determined experimentally obviously because we cannot have a solution containing only one kind of ions. What we really determine experimentally is the **mean ionic activity coefficient**, $\gamma_\pm$, which is given by

$$\ln \gamma_\pm = -(|z_+ z_-|\, e^2/2\varepsilon_r kT) \times [\kappa/(1+\kappa a)] \qquad ...(24)$$

for an electrolyte that dissociates in solution to produce ν_+ cations of valency z_+ and ν_- anions of valency z_-, where the following equations are applicable :

$$\nu_+ \ln \gamma_+ + \nu_- \ln \gamma_- = (\nu_+ + \nu_-) \ln \gamma_\pm \qquad ...(25)$$

$$\nu_+ z_+ + \nu_- z_- = 0 \qquad ...(26)$$

Finally, we can express the mean ionic activity coefficient in aqueous solution in terms of the ionic strength I as

$$\log \gamma_\pm = -0{\cdot}512\,|z_+ z_-|\, I^{1/2}/(1 + 0{\cdot}329 \times 10^8\, a\, I^{1/2}) \qquad ...(27)$$

where $\varepsilon = 78{\cdot}3$ at 298·15 K and a is the length in centimeters.

Determination of Activities of Solutes from Activities of Solvent

A characteristic of ionic solutions is that the vapour pressure due to the dissolved electrolyte itself is effectively zero. The vapour pressure of the solvent in the solution, therefore, falls with increasing concentration of the electrolyte in the solution. Thus, the vapour pressure of the solvent in the solution will be less than the vapour pressure of the pure solvent because the non-volatile ions block out part of the surface from which solvent molecules can evaporate. The solvent activity is given by

$$a_1 = p_1/p_1^0 \qquad ...(28)$$

where p_1^0 is the vapour pressure of the *pure solvent* and p_1 is the vapour pressure of the solvent in the solution. From Raoult's law,

$$p_1 = x_1 p_1^0 \qquad ...(29)$$

where x_1 is the mole fraction of the solvent. The non-ideal behaviour of the solvent is taken into account by the relation

$$a_1 = f_1 x_1 \qquad ...(30)$$

where a_1 is the activity and f_1 is the fugacity of the solvent. As $x_1 \to 1$, $f_1 \to 1$. Thus, the standard state is the pure solvent. Now, according to the Gibbs-Duhem equation,

$$\sum_i n_i d\mu_i = 0 \qquad ...(31)$$

Thus, for a two-component system (solvent and electrolyte),

$$n_1 d\mu_1 + n_2 d\mu_2 = 0 \qquad ...(32)$$

where subscript 1 represents the solvent and subscript 2 represents the electrolyte. Recalling that $\mu_i = \mu_i^0 + RT \ln a_i$, we can write

$$d \ln a_2 = -(n_1/n_2)\, d \ln a_1 \qquad ...(33)$$

or

$$\ln\left(\frac{a_2}{c_2}\right) = -\int_1^{a_1} \frac{n_1}{n_2}\, d \ln a_1 \qquad ...(34)$$

Thus, if a number of values of the vapour pressure of the solvent p_1 are measured at a corresponding number of solute concentrations, x_2 (to which there are matching solvent concentrations x_1), one can plot the ln a_1 values against the (n_1/n_2) ratios. Then the area under the plot will give ln a_2, the a_2 being the solute activity corresponding to the limit of the integral at a_1 (a_1 is the measured activity of the solvent for a solution containing a solute, the activity of which is a_2).

The left-hand side of Eq. 34 results from $\int_{a_2 \to 0}^{a_2} d \ln a_2$; $a_2 \to 0$ is simply c_2 because when the solute concentration of the solute (hence also activity) tends to zero, its activity becomes equal to its concentration.

The vapour pressure method for measuring the activity of electrolytes has the advantage that the actual experiments to be done are simple. The method can be applied conveniently to high concentrations; the difficulty arises at low concentrations when the difference between the vapour pressure of the solution and that of the solvent becomes limitingly small.

Dependence of Electrolyte Activity on the Hydration Number. For convenience, we assume that the interionic interaction is switched off. Thus, we have to take into account two kinds of work :

1. The work done = $RT \ln (c_1/c_2)$ when there is a change in the concentration of the free solvent water caused by introducing ions of a certain concentration into the solution. It is easy to calculate the work done in this case. Before the addition of ions, the concentration of the water is unaffected by anything; it is the concentration of pure water and its activity, the activity of a pure substance, can be regarded as unity. After the ions are added, let the activity of water be a_w. Then the work done when the activity of water changes from 1 to a_w is $RT \ln (a_w/1)$. We are, however, interested in knowing the change of activity in the *electrolyte* by this change of activity of water. Let the number of moles of water in the primary sheath per litre of solution for both ions of the imagined 1:1 electrolyte be n_h (for 1 molar solution, this is the hydration number). Then if there are n moles of the electrolyte in the water, the change in the free energy due to the transfer of the water to the ion's sheaths is $-(n_h/n)RT \ln a_w$ per mole of the electrolyte.

2. We now come to the second kind of work. Using the ideal solution (no interactions), the equation for the work done will be $RT \ln (c_1/c_2)$.

The free energy change due to change in concentrations of the ions is $RT \ln (x_1/x_2)$ where x_1 is the mole fraction after the removal of water from free to solvated state and x_2 is the mole fraction before the removal of water from free to solvated state; x is the mole fraction of the electrolyte in the solution. Before the water is removed,

$$x_{\text{before}} = n/(n_w + n) \qquad \ldots(35)$$

where n is the number of moles of electrolyte present in n_w moles of water.

After the water is removed to the sheaths,

$$x_{\text{after}} = n/(n_w - n_h + n) \qquad \ldots(36)$$

The change in free energy is given by

$$\Delta G = RT \ln [(n_w + n)/(n_w + n - n_h)] \qquad \ldots(37)$$

Hence, the total free energy change in the solution, calculated per mole of the electrolyte present, is given by

$$\Delta G_{\text{total}} = -\frac{n_h}{n} RT \ln a_w + RT \ln \frac{n_w + n}{n_w + n - n_h} \qquad \ldots(38)$$

We shall now switch back to the coulombic interactions. Assuming that the expression for the work done in building up an ionic atmosphere is still valid in the region of relatively high concentrations in which the effect of change of concentration is occurring, we have

$$RT \ln \gamma_{\pm} = -\frac{A\sqrt{c}}{1 + Ba\sqrt{c}} - 2 \cdot 303\, RT \frac{n_h}{n} \log a_w + 2 \cdot 303\, RT \log \frac{n_w + n}{n_w + n - n_h} \qquad \ldots(39)$$

where $\gamma_{\pm}$ is the mean ionic activity coefficient of the electrolyte.

If we examine the ion-solvent terms in Eq. 39, we see that since $a_w \leq 1$ and, in general, $n_h > n$ (more than one molecule of hydration of water per ion), both the terms are positive. Hence, we conclude that the Debye-Hückel treatment, which ignores the withdrawal of solvent from solution, gives values of activity coefficients that are smaller than those when these effects are taken into account. As the electrolyte concentration increases, a_w decreases and n_h increases; hence both ion-solvent terms (the second and third terms in Eq. 39) increase the value of $\log \gamma_{\pm}$. Again, the numerical evaluation shows that the above ion-solvent term can equal and become larger than the Debye-Hückel coulombic term $(\sqrt{c})$. This means that the $\log \gamma_{\pm}$ versus $I^{1/2}$ curve can pass through a minimum and then start rising, which is precisely what was observed in 1948 in the research work of R.A. Robinson and R.H. Stokes. It may be mentioned that n_h and a_w can be determined experimentally. Thus, Eq. 39 gives the quantitative statement of the influence of hydration number on activity coefficients of strong electrolytes in aqueous solution.

Bjerrum's Theory of Ion Association in Electrolyte Solutions

In the Debye-Hückel theory of strong interactions, we did not consider the possibility that some negative ions in the cloud would get sufficiently close to the central positive ion in the course of their quasi-random solution movements so that their thermal translational energy would not be sufficient for them to continue their independent movements in the solution. The Danish physicist, N. Bjerrum suggested that a pair of oppositely charged ions may get trapped in each others coulombic field resulting in the formation of an ion pair. The ions of the pair together form an ionic dipole in which the net charge is zero. Within the ionic cloud, the locations of such uncharged pairs are completely random, since, being uncharged, they are not acted upon by the coulombic field of the central ion. Furthermore, on an average, a certain fraction of the ions in the electrolytic solution will get stuck together in the form of ion pairs.

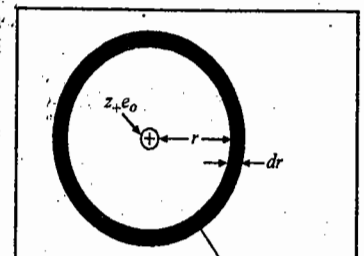

Fig. 2. The probability $P(r)$ of finding an ion of charge z_-e_0 in a dr-thick spherical shell of radius r around a reference ion of charge z_+e_0.

Let us consider a spherical shell of thickness dr and radius r from a reference positive ion (Fig. 2). The probability $P(r)dr$ that a negative ion is in the spherical shell is proportional, first, to the ratio of the volume $4\pi r^2 dr$ of the shell to the total volume V of the solution; second, to the total number N_- of the negative ions present and third, to the Boltzmann factor $\exp(-U/kT)$, where U is the potential energy of a negative ion at a distance r from a cation, *i.e.*,

$$P(r)dr = 4\pi r^2 dr\, (N_-/V) \exp(-U/kT) \qquad \ldots(40)$$

Since (N_-/V) is the concentration n_- of negative ions in the solution and

$$U = -z_- z_+ e^2/\varepsilon_r r \qquad \ldots(41)$$

we see that

$$P(r)dr = (4\pi n_-)\, r^2 \exp(z_- z_+ e^2/\varepsilon_r r\, kT)dr \qquad \ldots(42)$$

Representing the expression $z_- z_+ e^2/\varepsilon_r kT$ by λ, we have $\ldots(43)$

$$P(r)dr = (4\pi n_-) \exp(\lambda/r) r^2 dr \qquad \ldots(44)$$

A similar expression is valid for the probability of finding a positive ion in a dr-thick shell at a radius r from a reference negative ion. Hence, we may write for the probability of finding an i type of

ion in a *dr*-thick spherical shell of radius r from a reference ion k of opposite charge

$$P(r)dr = (4\pi n_i) \exp(\lambda/r) r^2 dr \text{ where } \lambda = z_i z_k e^2/\varepsilon_r kT \quad ...(45)$$

Fig. 3 shows the variation of the probability of finding an ion of one type of charge near an ion of opposite charge. For small values of r, the function $P(r)$ is dominated by $\exp(\lambda/r)$ rather than by r^2 and under these conditions $P(r)$ *increases with decreasing* r. For large values of r, $\exp(\lambda/r) \to 1$ and $P(r)$ *increases with increasing* r because the volume of the spherical shell, $4\pi r^2 dr$, increases as r^2. It follows from these conditions that $P(r)$ goes through a minimum for a particular critical value of r, as shown in Fig. 3.

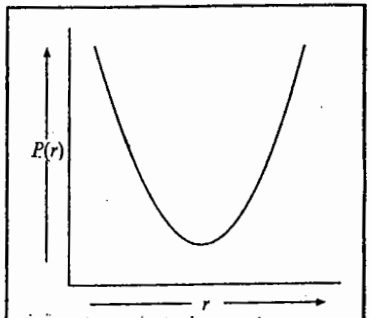

Fig. 3. The probability $P(r)$ of finding an ion of one type of charge as a function of distance.

We shall now consider the fraction of ion pairs in the Bjerrum theory. For two oppositely charged ions to stick together to form an ion pair, it is necessary that they should be close enough for the coulombic attractive energy to overcome the thermal energy that scatters them apart. Suppose that this 'close enough' distance is q. Then an ion pair will be formed when the distance r between a positive and a negative ion becomes less than q. Thus, the probability of ion-pair formation is given by the integral of $P(r)$ between a lower limit of a, the distance of closest approach of ions and an upper limit of q. In other words, the probability of ion-pair formation is the fraction θ of ions that get associated into ion pairs. Thus,

$$\theta = \int_a^q P(r)\, dr = \int_a^q 4\pi n_i \exp(\lambda/r)\, r^2 dr \quad ...(46)$$

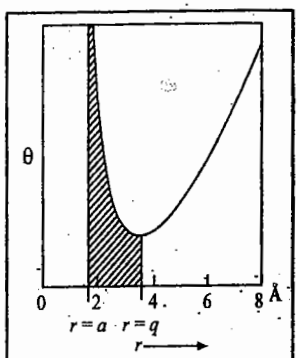

Fig.4. Graphical representation of the integral in Eq.46 between the limits a and q.

We see from Fig. 4 that the integral in Eq. 46 is the area under the curve between the limits $r=a$ and $r=q$. It is obvious that as r increases past the minimum, the integral becomes greater than unity. Since, however, θ is a fraction, it means that the integral diverges.

Bjerrum arbitrarily cut off the integral at the value $r=q$ corresponding to the minimum of $P(r)$ versus r curve. The minimum probability can be shown to occur at

$$q = \frac{z_+ z_- e^2}{2\varepsilon_r kT} = \frac{\lambda}{2} \quad ...(47)$$

Bjerrum suggested that it is only the short-range coulombic interactions that lead to ion-pair formation. When, however, a pair of oppositely charged ions are situated at a distance $r > q$, it is more appropriate to consider them free ions. Bjerrum thus concluded that ion-pair formation occurs when an ion of one type of charge (*e.g.*, a negative ion) enters a sphere of radius q around a reference ion of the opposite charge (*e.g.*, a positive ion). It is, however, the size of the ion that defines the distance of closest approach of a pair of ions. Therefore, according to the Bjerrum hypothesis, if $a < q$, then ion-pair formation can occur; if $a > q$, the ions remain free (Fig. 5).

We shall now derive the Bjerrum expression for the **ion-association constant**, K_A. The ions that get associated are those that get sufficiently close to an ion of opposite sign so that the energy of coulombic attraction is greater than the thermal energy of the pair. Consider an equilibrium between free ions (the positive M^+ ions and the negative A^- ions) and the associated ion-pairs (symbolized as IP) :

$$M^+ + A^- \rightleftharpoons IP \quad ...(48)$$

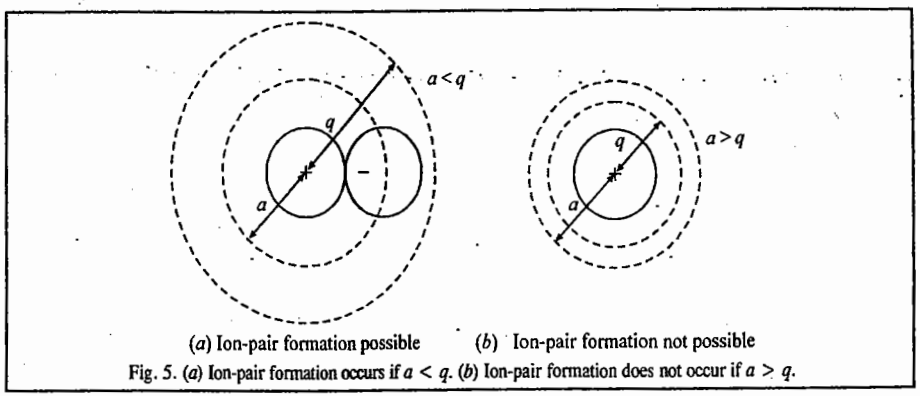

(*a*) Ion-pair formation possible (*b*) Ion-pair formation not possible

Fig. 5. (*a*) Ion-pair formation occurs if $a < q$. (*b*) Ion-pair formation does not occur if $a > q$.

The ion–pair association constant, K_A, is given by

$$K_A = \frac{a_{IP}}{a_{M^+}\, a_{A^-}} \quad ...(49)$$

where *a*s are the activities of the species. From Eq. 49 we see that K_A is the reciprocal of the ion–pair dissociation constant. Since θ is a fraction of ions in the form of ion–pairs, θc is the concentration of the ion-pairs and $(1-\theta)c$ is the concentration of free ions. If the activity coefficients of the positive and negative free ions are γ_+ and γ_-, respectively and the activity coefficient of the ion-pairs is γ_{IP}, then we can write

$$K_A = \frac{\theta c \gamma_{IP}}{(1-\theta) c\gamma_+ (1-\theta) c\gamma_-} = \frac{\theta}{(1-\theta)^2} \frac{1}{c} \frac{\gamma_{IP}}{\gamma_+ \gamma_-} \quad ...(50)$$

$$= \frac{\theta}{(1-\theta)^2} \frac{1}{c} \frac{\gamma_{IP}}{\gamma_\pm^2} \quad ...(51)$$

where $\gamma_\pm$ is the mean ionic activity coefficient. Next, we assume that the ion-pair activity coefficient γ_{IP} is unity because deviations of activity coefficients from unity are ascribed in the Debye-Hückel theory to electrostatic interactions. But, ion pairs are not involved in such interactions owing to their overall zero charge and hence they behave ideally like uncharged particles, *i.e.*, $\gamma_{IP}=1$. Again, in very dilute solutions, the ions rarely come close enough together (*i.e.*, to within a distance q) to form ion-pairs and one can consider $\theta \ll 1$ or $1 - \theta = 1$. Also, activity coefficients tend to unity, *i.e.*, γ_i or $\gamma_\pm \to 1$. Hence, at very large dilution, Eq. 51 becomes

$$K_A \approx \theta/c \quad ...(52)$$

It can be shown that

$$\theta = 4\pi n_i \left(\frac{z_+ z_- e^2}{\varepsilon_r kT}\right)^3 \int_2^b e^y y^{-4}\, dy \quad ...(53)$$

where $b = \frac{\lambda}{a} = \frac{z_+ z_- e^2}{\varepsilon_r k\, Ta} = \frac{2q}{a}$ and the variable $y = \frac{\lambda}{r} = \frac{2q}{r}$.

Substituting the above value of θ in Eq. 52, we get

$$K_A = \frac{4\pi n_i}{c} \left(\frac{z_+ z_i e^2}{\varepsilon_r kT}\right)^3 \int_2^b e^y y^{-4}\, dy \quad ...(54)$$

However, $n_i = cN_A/1000$ ...(55)

so that $$K_A = \frac{4\pi N_A}{1000}\left(\frac{z_+z_-e^2}{\varepsilon kT}\right)^3 \int_2^b e^y y^{-4} dy$$ ...(56)

The higher the value of K_A, the more extensive is the ion-pair formation (Table 1).

TABLE 1

Ion-Association Constants, K_A, for Some Electrolyte Solutions

Salt	Solvent	Temperature (K)	ε_r	K_A
KBr	Acetic acid	303	6·20	$9·09 \times 10^6$
KBr	Ammonia	239	22	$5·29 \times 10^2$
KI	Acetone	298	20·70	$1·25 \times 10^2$
KI	Pyridine	298	12·0	$4·76 \times 10^3$

From Eq. 56 we see that the factors that increase K_A are : 1. Low dielectric constant ε, 2. Small ionic radii which lead to a small value of a and hence to a large value of the upper limit b of the integral in Eq. 56 and 3. Large z_+ and z_-. We thus find that in aqueous media, ion association in pairs rarely occurs for 1:1-valent electrolytes but can be important for 2:2-valent electrolytes. In non-aqueous solutions, most of which have dielectric constants less than that of water ($\varepsilon_r = 80$), ion association is extremely important.

We can consider how the activity coefficients of electrolytes depend on the extent of association. Ion pairs have no relevance in the Debye-Hückel theory since they carry no net charge and, therefore, cannot be eligible for membership in the ion cloud. However, the extent of ion-pair formation does decide the value of the concentration of the ions to be used in the ionic-cloud model. By removing a fraction θ of the total number of ions, only a fraction $1-\theta$ of the ions remains for the Debye-Hückel treatment which interests itself only in the free charges. Thus, the Debye-Hückel expression for the activity coefficients is valid for the free ions, with two important modifications : 1. Instead of there being a concentration c of ions, the concentration to be reckomed with is only $(1-\theta)c$; the remainder θc is not taken into account owing to association. 2. The distance of closest approach of free ions is q and not a. These modifications yield

$$\log \gamma_\pm = -\frac{A(z_+z_-)[(1-\theta)c]^{1/2}}{1+Bq[(1-\theta)c]^{1/2}}$$ ...(57)

The calculated mean activity coefficient $\gamma_\pm$ is related to the measured mean activity coefficient of the electrolyte $(\gamma_\pm)_{obs}$ by the relation

$$(\gamma_\pm)_{obs} = (1-\theta)\gamma_\pm$$ ...(58)

or $$\log(\gamma_\pm)_{obs} = \log\gamma_\pm + \log(1-\theta)$$

$$= -\frac{A(z_+z_-)[(1-\theta)c]^{1/2}}{1+Bq[(1-\theta)c]^{1/2}} + \log(1-\theta)$$ ...(59)

Eq. 59 gives the dependence of the activity coefficients on the extent of ion association.

We may in conclusion comment on how ion pairs may lead to triple ions and clusters of ions. The coulombic forces given by $z_+z_-e^2/\varepsilon_r r^2$ are large when the dielectric constant is small. Thus, as already mentioned, in non-aqueous solutions of small dielectric constant, ion pair formation is favoured. When the electrostatic forces are sufficiently large, the ion-pair 'dipoles' may attract ions and *triple ions* may be formed. Thus,

$$M^+ + (A^-M^+)_{ion\ pair} = [M^+A^-M^+]_{triple\ ion}$$ ...(60a)

or $$A^- + (M^+A^-)_{ion\ pair} = [A^-M^+A^-]_{triple\ ion}$$ ...(60b)

We see that charged triple ions are formed from uncharged ion pairs. These charged triple ions play a role in determining activity coefficients; their formation occurs when $\varepsilon < 15$. When ε falls to about 10, still larger clusters of four, five or even more ions may be formed. There is experimental evidence for their formation.

Determination of Interfacial Tension of Mecury as a Function of Potential Across the Interface. We shall briefly describe the experimental method for the determination of interfacial tension of mercury as a function of the potential difference across the interface. The interfacial tension can be related to the surface excess of various species in solution. A great advantage of metal mercury is that the mercury-solution interface approaches closest to the ideal polarizable interface over a range of 2V. This means that this interface responds exactly to all the changes in the potential difference of an external source when it is coupled to a non-polarizable interface and there are no complications of charges leaking through the double layer (charge-transfer reactions).

Fig. 6 shows the electrochemical system that can be used to measure the surface tension of the mercury-solution interface. Its essential parts are : (1) A mercury—solution polarizable interface (2) A non-polarizable interface (3) An external source of variable potential difference V and (4) An arrangement to measure the surface terision of the mercury in contact with the solution.

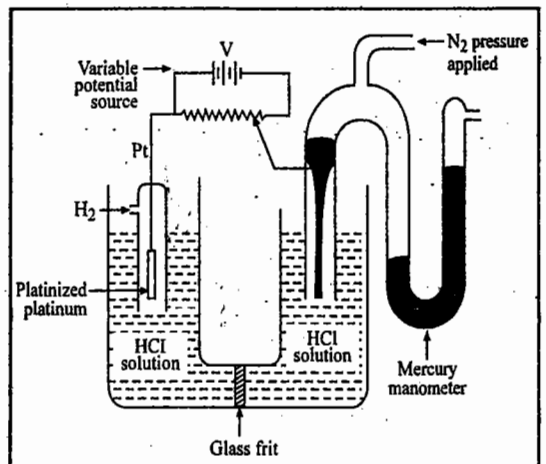

Fig. 6. Apparatus for the measurement of surface tension of mercury as a function of cell potential V.

Since the system consists of a polarizable interface coupled to a non-polarizable interface, changes in the potential of the external source are almost equal to the changes of potential only at the polarizable interface. Hence, the system can be used to produce predetermined $\Delta\phi$ changes at the mercury-solution interface. Since measurement of surface tension of the mercury-solution interface is conveniently possible and since it is related to the surface excess, we can measure this quantity for a given species in the interface. In other words, the system permits what are called **electrocapillary measurements**, *i.e.*, the measurements of surface tension of the metal (in contact with the solution) as a function of the electrical potential difference across the interface.

The surface tension is measured by using a fine capillary and adjusting the height of a mercury column so that the mercury in the capillary is stationary. This is the simplest version of a capillary electrometer. Under the conditions of mechanical equilibrium, the surface tension γ is obtained from the expression

$$\gamma = \frac{1}{2}h\rho gr$$ ...(61)

where r is the radius of the capillary, ρ the density of mercury, g the acceleration due to gravity and h the height to which mercury rises or falls in the capillary. The experimental set up can be made sophisticated by using controlled gas pressure to force the mercury in the capillary to desired distances from the tip by using advanced optical systems in recording the height of the mercury column and by using a sensing device for measuring the gas pressure and the applied potential.

We shall comment briefly on the electrocapillary curves. The interfacial tension depends on the forces arising from the particles present in the interface region. If the arrangement of these particles (*i.e.*, the composition of the interface) is altered by varying, for example, the potential difference across

the interface, then the forces at the interface should change, thereby causing a change in the interfacial tension. Thus, the surface tension γ of the metal-solution interface is expected to vary with the external potential difference, V.

The γ versus V curves obtained experimentally by electrocapillary measurements depict the variation of surface tension γ with potential difference V across the cell. A typical electrocapillary curve is almost a parabola (Fig. 7). The potential at which the surface tension is a maximum is known as the potential of the **electrocapillary maximum** (ecm).

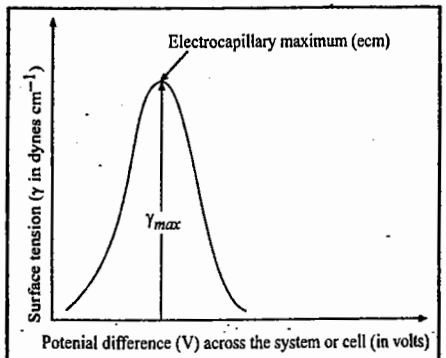

Fig.7. A typical γ *vs* V electrocapillary curve.

The measurements also show that the surface tension varies with the composition of the electrolyte. As the solution is diluted, the maximum of surface tension rises. The surface tension is related to the surface excess of the species in the interface; the surface excess, in turn, represents in some way the structure of the interface. Therefore, the electrocapillary curves give important information about the double layer at the electrode-electrolyte interface.

II. ELECTRIFIED INTERFACES

A. Quantitative Thermodynamic Treatment of Electrified Interfaces

The system of interest is an electrode-electrolyte interface. If the system is a closed one (*i.e.*, no matter enters or leaves it), the combined statement of the First and the Second laws of thermodynamics is

$$dU = TdS - PdV \qquad ...(62)$$

For an open system, this statement becomes

$$dU = TdS - PdV - \sum_i \mu_i dn_i \qquad ...(63)$$

where the last term represents the work done by the system in expelling dn_i moles of species i and μ_i is the chemical potential of the species i. For the electrode-electrolyte interface M - S (M stands for metal and S for solution), in addition to the work of volume expansion (the second term in Eq. 63), we have the work, γdA, required to increase the area A of the interface, where γ is the interfacial tension. Finally, we have to take into account the work involved in connecting the metallic phase to an external source of electricity thereby altering the charge on the metal by an amount dq_M. The electrical work involved in transferring the charge dq_M is given by ${}^{M}\Delta^{S}\phi\, dq_M$. In this expression M is the metal and $\Delta\phi$ is the potential difference between the metal M and the electrolyte interface (S). Introducing all the work terms in Eq. 63, we get

$$dU = TdS - PdV - \gamma dA - {}^{M}\Delta^{S}\phi\, dq_M - \sum_i \mu_i dn_i \qquad ...(64)$$

Each term on the R.H.S. of Eq. 64 is a product of an intensive factor (one that does not depend on the amount of matter present in the system) and an extensive factor (one that does depend on the amount of matter in the system). Thus,

$$dU = \Sigma \text{ intensive factor} \times \text{extensive factor} \qquad (65)$$

Keeping the intensive factors (T, P, γ, $\Delta\phi$, μ) constant, let the extensive factors be increased from their differential values to their absolute values for the system concerned, *viz.*, S, V, A, q_M, n_i. Thus, we have for the internal energy of the system

$$U = TS - PV - \gamma A - {}^{M}\Delta^{S}\phi\, q_M - \sum_i \mu_i n_i \qquad ...(66)$$

Differentiation of this equation gives

$$dU = (TdS - PdV - \gamma dA - {}^{M}\Delta^{S}\phi\, dq_M - \sum_i \mu_i dn_i + [SdT - VdP - Ad\gamma - q_M d({}^{M}\Delta^{S}\phi) - \sum_i n_i d\mu_i] \qquad ...(67)$$

Since Eqs. 64 and 67 are equal to each other, we have

$$0 = SdT - VdP - Ad\gamma - q_M d({}^{M}\Delta^{S}\phi) - \sum_i n_i d\mu_i \qquad ...(68)$$

At constant T and P, Eq. 68 becomes

$$0 = -Ad\gamma - q_M d({}^{M}\Delta^{S}\phi) - \sum_i n_i d\mu_i \qquad ...(69)$$

or,
$$d\gamma = -\frac{q_M}{A} d({}^{M}\Delta^{S}\phi) - \sum_i \frac{n_i}{A} d\mu_i \qquad ...(70)$$

From Eq. 70 we see that changes in surface tension have been related to changes in the absolute potential differences across an electrode-electrolyte interface and to changes in the chemical potential of all the species, *i.e.*, to changes in solution composition. Next, we define surface excess by recalling that

$$n_i/A = \Gamma_i + n_i^0/A \qquad ...(71)$$

whence
$$(n_i/A)\, d\mu_i = \Gamma_i d\mu_i + (n_i^0/A)\, d\mu_i \qquad ...(72)$$

or
$$\sum_i (n_i/A)\, d\mu_i = \sum_i \Gamma_i d\mu_i + \sum_i (n_i^0/A)\, d\mu_i \qquad ...(73)$$

From the Gibbs-Duhem equation, we know that

$$\sum_i n_i^0 d\mu_i = 0 \qquad ...(74)$$

Substituting this relation in Eq. 73, we have

$$\sum_i (n_i/A)\, d\mu_i = \sum_i \Gamma_i d\mu_i \qquad ...(75)$$

Substituting this expression in Eq. 70 gives

$$d\gamma = -q_M\, d({}^{M}\Delta^{S}\phi) - \sum_i \Gamma_i d\mu_i \qquad ...(76)$$

Eq. 76 contains the quantity $d({}^{M}\Delta^{S}\phi)$ which is the change in the inner (or galvanic) potential difference across the interface under study. Though the absolute value of ${}^{M}\Delta^{S}\phi$ cannot be determined, a change in ${}^{M}\Delta^{S}\phi$, *i.e.*, $d({}^{M}\Delta^{S}\phi)$, can be measured. For this measurement, we have to set up an electrochemical cell in which hte polarizable M - S interface, designated as M_1 - S interface, is linked to a non-polarizable interface, designated as M_2- S interface.

$$V = {}^{M_1}\Delta^{S}\phi + {}^{S}\Delta^{M_2}\phi + {}^{M_2}\Delta^{M_1}\phi \qquad ...(77)$$

since the sum of the potential drops around a circuit must be zero. The inner potential difference ${}^{M_2}\Delta^{M_1}\phi$ does not depend upon the potential V applied from the external source or upon the solution composition. Hence, differentiation of Eq. 77 yields

$$-d({}^{M_1}\Delta^{S}\phi) = -dV + d({}^{S}\Delta^{M_2}\phi) \qquad ...(78)$$

Substituting this expression in Eq. 76, we find that

$$d\gamma = -q_M dV + q_M d({}^{S}\Delta^{M_2}\phi) - \sum_i \Gamma_i d\mu_i \qquad ...(79)$$

We now introduce the non-polarizable characteristics of the second interface M_2-S which is a

necesseary part of the cell and the measuring set up. There is equilibrium at this interface so that

$$d({}^{S}\Delta^{M_2}\phi) = -(1/z_j F)\, d\mu_j \qquad ...(80)$$

where j is the particular species involved in the leakage of charge across the non-polarizable interface. Thus, for example, for the hydrogen electrode (with $z_+ = 1$), we have

$$d({}^{S}\Delta^{M_2}\phi) = -(1/F)\, d\mu_H \qquad ...(81)$$

If we use a calomel electrode in which Cl^- ions can be considered as leaking across the interface, then (with $z_- = 1$),

$$d({}^{S}\Delta^{M_2}\phi) = +(1/F)\, d\mu_{Cl^-} \qquad ...(82)$$

Substitution of Eq. 80 in Eq. 79 gives

$$d\gamma = -q_M\, dV - (q_M/z_j F)\, d\mu_j - \sum_i \Gamma_i d\mu_i \qquad ...(83)$$

Eq. 83 is the fundamental equation for the thermodynamic treatment of polarizable interfaces. It relates interfacial tension γ, with surface excess Γ_i, applied potential difference V, charge density q_M and solution composition. It shows that interfacial tension varies with the applied potential and the solution composition.

In order to obtain experimentally an electrocapillary curve, a solution of a fixed composition is taken, *i.e.*, $d\mu_i$ for all the species is zero. Thus, the conditions for the determination of the electrocapillary curve correspond to

$$\sum_i \Gamma_i d\mu_i = 0 \quad \text{and} \quad d\mu_j = 0 \qquad ...(84)$$

Thus, it follows from Eq. 83 that

$$(\partial\gamma/\partial V)_{\text{const. comp}} = -q_M \qquad ...(85)$$

This equation is known as the **Lippmann equation.** The slope of the electrocapillary curve at any cell potential V is equal to the charge density on the electrode (Fig. 8).

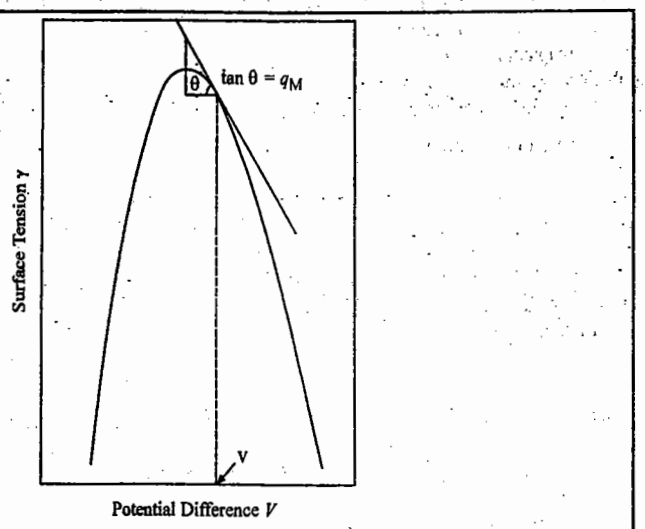

Fig. 8. The charge density on the electrode at a particular value of the potential difference V is given by the slope of the electrocapillary curve at that potential. The curve shown is for mercury in contact with 1·0 MHCl.

Electrical Capacitance of the Interface. We next differentiate the γ versus V electrocapillary curve at various values of the cell potential and plot the values of the slope (electrode charge) as a function of electrode potential (Fig. 9*a*). If the electrocapillary curve were a perfect parabola, then the charge (strictly excess charge density) on the electrode would vary linearly with the cell potential (Fig. 9*b*). An electrified interface can be considered as a system capable of storing charge, since it is a region where charges are accumulated or depleted relative to the bulk of the electrolyte. We know, however, that it is an electric capacitor that has this characteristic property of storing charge. Hence, we can speak of the capacitance of an electrified interface in a manner similar to that of a capacitor. This capacitance is given by

$$K = q/V \qquad ...(86)$$

i.e., it is the total charge required to raise the potential difference across the condenser by one volt. This is the *integral capacitance* which is generally used for electrical capacitors where the capacity is constant and independent of the potential. This need not necessarily be true of electrified interfaces so that it is convenient to define a **differential capacitance** C as

$$C = \left(\frac{\partial q_M}{\partial V}\right)_{\text{const.comp}} = -\left(\frac{\partial^2\gamma}{\partial V^2}\right)_{\text{const.comp}} \qquad ...(87)$$

This equation shows that the slope of the curve of the electrode charge versus cell potential gives the *differential capacity* (capacitance) of the double layer. For an ideal parabolic γ versus V curve, which yields a linear q versus V curve, we obtain a constant capacitance (Fig. 9*c*).

We see from the q_M versus V curve (Fig. 9*b*) that the charge on an electrode starts off with one sign and then changes this sign after passing through a zero-charge value. The potential difference across the system (or cell) at which the charge on the electrode is zero is the potential of zero charge, denoted by the symbol $E_{q=0}$ or E_{pzc} if this potential is measured on the hydrogen scale. Since q_M is given by the slope of the curve, the *pzc* is defined by

$$q_M = -(\partial\gamma/\partial V)_{\text{const. comp}} = 0 \qquad ...(88)$$

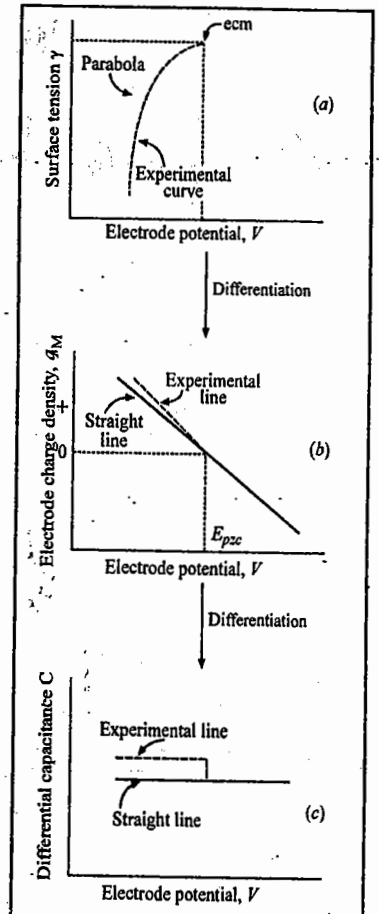

Fig. 9. When the electrocapillary curve is a perfect parabola, the electrode charge density varies linearly with potential difference. A further differentiation gives capacitance that is potential independent. However, experimental electrocapillary curves are not perfect parabolas.

Hence, the *pzc* is the potential at which the electrocapillary maximum (ecm) occurs (Fig. 9*a*). With liquid metals, the *pzc* can be conveniently determined from electrocapillary measurements. From the γ versus V curve, the q_M versus V curve can be obtained and thereby the value of E_{pzc} determined.

Determination of the Surface Excess

Eq. 83 describes how surface tension changes with both potential and composition. For determining surface excess Γ_i, we must eliminate one variable, the potential, in this equation. For this purpose, the

electrocapillary curves obtained for various salt concentrations are plotted in a diagram and a perpendicular erected to the cell potential axis. This will contain points relating γ to concentration when, in Eq. 79, $dV=0$. We must, however, remember that this equation contains the term $d({}^{S}\Delta^{M2}\phi)$, *i.e.*, changes in the potential difference across the reference electrode-solution interface produced by changes in solution composition via Eq. 80. Thus, the potential V read on the potentiometer refers, for every concentration in which the γ versus V relation is determined, to a reference electrode consisting of metal immersed in a solution of the *same* concentration as that surrounding the test electrode. It is this value of V (obtained *not* with a standard reference electrode, but with a reference electrode whose potential varies with the concentration of the ions that leak charge across the interface) that should be kept constant.

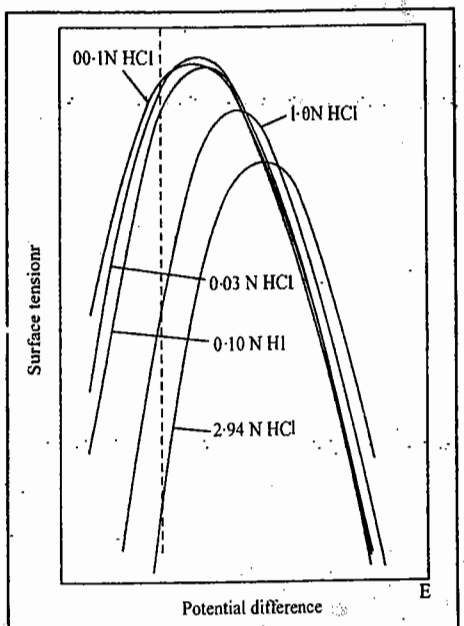

Fig. 10. Electrocapillary curves obtained in solutions of different electrolyte (HCl) concentrations.

It is customary to denote these potential values referred *not* to the standard electrode but to one reversible to ions of given (varying) concentrations, as V_+ or V_- indicating at the same time whether the electrode is one at which cations or anions leak, respectively. A perpendicular erected on the axis of the cell potential V_+ or V_- (Fig.10) intersects the electrocapillary curves at points for which the condition $dV=0$ in Eq. 83 is satisfied so that

$$d\gamma = -\frac{q_M}{z_j F} d\mu_j - \sum_i \Gamma_i \, d\mu_i \qquad ...(89)$$

Eq. 89 describes changes in surface tension with composition at any particular cell potential V_+ or V_-.

We now consider a polarizable interface consisting of a metal electrode in contact with a 1:1-valent electrolyte (*i.e.*, $z_+=1$ and $z_-=-1$). We should remember that in order to apply electrocapillary thermodynamics to a polarizable interface M_1-S, the interface should be assembled in a cell along with a non-polarizable interface. Let the non-polarizable interface be the one at which the negative ions interchange charge with the metal surface, *i.e.*, $z_j = -1$. Hence, Eq. 89 for the polarizable interface becomes

$$d\gamma = +(q_M/F)\, d\mu_- - \Gamma_+ d\mu_+ - \Gamma_- d\mu_- \qquad ...(90)$$

We shall transform this expression so that it contains the concentration of the electrolyte used in the cell. We first note that the chemical potential μ of the electrolyte is the sum of the chemical potentials of the ions, *i.e.*,

$$\mu = \mu_+ + \mu_- \qquad ...(91)$$

or

$$d\mu = d\mu_+ + d\mu_- \qquad ...(92)$$

Using Eq. 92 we substitute for $d\mu_+$ in Eq. 90, obtaining

$$d\gamma = (q_M/F)\, d\mu_- - \Gamma_+ d\mu + \Gamma_+ d\mu_- - \Gamma_- d\mu_-$$

$$= -\Gamma_+ d\mu + \left(\frac{q_M + F\Gamma_+ - F\Gamma_-}{F}\right) d\mu_- \qquad ...(93)$$

Next, we remember that there is electroneutrality across the interface, *i.e.*, the charge on the metal is always equal and opposite to the total charge on the solution side of the interface. Before the double layer is formed, the metal is uncharged and in the solution, the charge per unit area of a lamina due to positive and negative ions is zero, *i.e.*,

$$F\left(\frac{n_+^0}{A}\right) - F\left(\frac{n_-^0}{A}\right) = 0 \qquad ...(94)$$

After the double layer is formed, the electroneutrality condition requires that

$$F\left(\frac{n_+}{A}\right) - F\left(\frac{n_-}{A}\right) + q_M = 0 \qquad ...(95)$$

Subtracting Eq. 94 from Eq. 95, we get

$$q_M + F\left(\frac{n_+ - n_+^0}{A}\right) - F\left(\frac{n_- - n_-^0}{A}\right) = 0 \qquad ...(96)$$

However, from the definition of surface excess (Eq. 71),

$$\Gamma_+ = (n_+ - n_+^0)/A \quad \text{and} \quad \Gamma_- = (n_- - n_-^0)/A \qquad ...(97)$$

Hence, according to the electroneutrality condition,

$$q_M + F\Gamma_+ - F\Gamma_- = 0 \qquad ...(98)$$

Substituting this condition in Eq. 93, we find that, for a polarizable interface built in a cell with a non-polarizable interface that leaks negative ions, the second term is zero so that

$$d\gamma = -\Gamma_+ d\mu \qquad ...(99)$$

or

$$\left(\frac{\partial \gamma}{\partial \mu}\right)_{\text{const } V_-} = -\Gamma_+ \qquad ...(100)$$

Now,

$$\mu = (\mu_+ + \mu_-) = (\mu_+^0 + \mu_-^0) + RT\,(\ln a_+ + \ln a_-) \qquad ...(101)$$

$$= (\mu_+^0 + \mu_-^0) + RT\,(\ln a_+ a_-) \qquad ...(102)$$

Instead of a_+a_-, we can use mean ionic activity, $a_\pm$, defined as follows :

$$a_\pm^2 = a_+ a_- \qquad ...(103)$$

Hence, from Eqs. 102 and 103,

$$\mu = (\mu_+^0 + \mu_-^0) + 2RT \ln a_\pm \qquad ...(104)$$

or,

$$d\mu = 2RT\, d \ln a_\pm \qquad ...(105)$$

Thus, substituting Eq. 105 into Eq. 100,

$$\left(\frac{\partial \gamma}{2RT\,\partial \ln a_{\pm}}\right)_{\text{const. V}_-} = -\Gamma_+ \qquad \ldots(106)$$

Eq. 106 shows that the slope of the surface tension versus ln $a_{\pm}$ curve at constant potential yields the surface excess. The activity of the electrolyte $a_{\pm}$ is obtained by taking the bulk concentration and multiplying it by the mean activity coefficient at that concentration.

It should be noted that the surface excess of the positive ion is determined by choosing a non-polarizable interface that leaks negative ions. Following a similar argument, we can show that the non-polarizable interface that leaks positive ions enables the determination of the surface excess of negative ions. Thus, in a study of the Hg–HCl polarizable interface, the surface excess Γ_- of the Cl^- ions may be obtained by coupling the Hg–HCl interface with a hydrogen reference electrode that leaks H^+ ions.

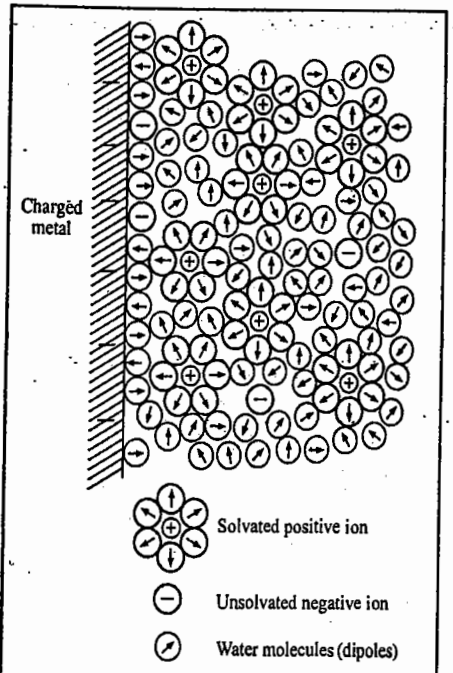

Fig. 11. A schematic representation of the structure of an electrified interface. The smaller positive ions tend to be solvated while the larger negative ions are usually unsolvated.

B. Structures of Electrified Interfaces

We shall now consider the metal–solution interface (Fig. 11). The metal is made up of a lattice of positive ions and free electrons. When the metal is charged with an excess-charge density, there is either an excess (q_M is negative) or a deficit (q_M is positive) of free electrons at the metal surface. The particles of the solution respond to the excess-charge density q_M on the metal surface. The first row is primarily occupied by the water dipoles (Fig. 11) which are preferentially oriented by q_M. This is the *hydration sheath* of the electrode.

The net orientation of the water dipoles varies with the charge on the metal. The second row consists largely of solvated ions the locus of whose centres is called the outer Helmholtz plane (OHP) (Fig. 12). On top of the first-row water (the primary water layer) and in between the solvated ions are other water molecules—a kind of secondary hydration sheath, weakly bound to the electrode.

We have given above a brief description of the metal–solution interface; it merely gives a qualitative description of how ions or molecules in solution are arranged. However, in order to understand the structure of electrified interfaces, we need to propose

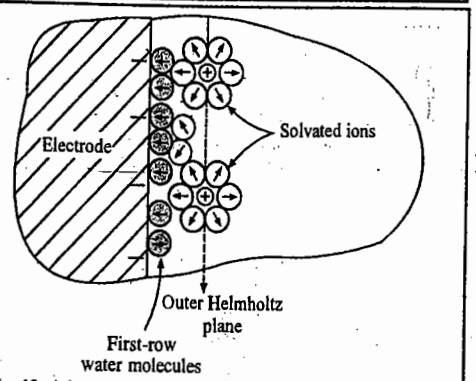

Fig. 12. A layer of solvated ions on the layer of first-row water molecules. The locus of the centres of these solvated ions defines the outer Helmholtz plane (OHP).

mathematical models which explain the experimental findings. We shall consider three such models.

1. Helmholtz–Perrin Model. In this model, proposed by Helmholtz and Perrin, it is suggested that the charge on the metal draws out from the random distribution of ions in solution a counter-layer of a charge of opposite sign. Thus, the electrified interface consists of two sheets of charge, one on the electrode and the other in solution (Fig. 13*a*). Hence, we make use of the term *double layer*, which behaves like a parallel plate condenser (Fig. 13*b*), since the charge densities on the two sheets are equal in magnitude but opposite in sign. The potential drop between these two layers of charge is linear (Fig. 13*c*).

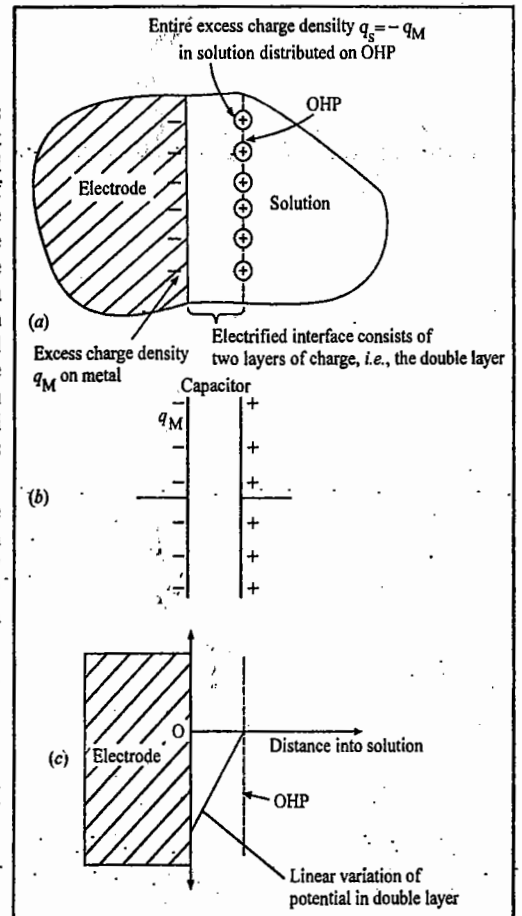

Fig. 13. The Helmholtz–Perrin parallel plate model. (*a*) A layer of ions on the OHP constitutes the entire excess charge in the solution, q_S. (*b*) The electrical equivalent of such a double layer is a parallel plate condenser. (*c*) The corresponding variation of potential is a linear one.

Since we have invoked an equivalence between an electrified interface and a condenser, we can use the electrostatic theory of capacitors for the double layers. We know that the potential difference V across a condenser of unit area is given by

$$V = (d/\varepsilon_r \varepsilon_0)\, q_M \qquad \ldots(107)$$

or $$dV = (d/\varepsilon_r \varepsilon_0)\, dq_M \qquad \ldots(108)$$

where d is the distance between the plates, ε_r is the dielectric constant of the material between the plates and ε_0 is the permittivity of free space.

From Eqs. 85 and 108,

$$\int d\gamma = -\frac{d}{\varepsilon_r \varepsilon_0} \int q_M\, dq_M \qquad \ldots(109)$$

Integration of Eq. 109 gives

$$\gamma + \text{constant} = -\frac{d}{\varepsilon_r \varepsilon_0}\,\frac{q_M^2}{2} \qquad \ldots(110)$$

To evaluate the constant, we apply the known condition that at $q_M = 0$, $\gamma = \gamma_{max}$. Hence, constant $= -\gamma_{max}$. Therefore,

$$\gamma = \gamma_{max} - \frac{d}{\varepsilon_r \varepsilon_0}\,\frac{q_M^2}{2} \qquad \ldots(111)$$

Substituting the value of q_M from Eq. 107, we get

$$\gamma = \gamma_{max} - \frac{\varepsilon_r \varepsilon_0}{d}\,\frac{V^2}{2} \qquad \ldots(112)$$

This is the equation of a parabola symmetrical about γ_{max}, *i.e.*, about the electrocapillary maximum.

Rearranging Eq. 108 in the form of the definition of differential capacity (Eq. 87), we have

$$C = \frac{dq}{dV} = \frac{\varepsilon_r \varepsilon_0}{d} \qquad ...(113)$$

Thus, if ε_r and d are assumed to be constant, the parallel plate model predicts a constant capacity which does not change with potential. We conclude that the Helmholtz Perrin model is quite satisfactory for electrocapillary curves that are perfect parabolas. Since, however, experimental electrocapillary curves are asymmetric, not perfect parabolas, the electrified interface does not behave like a simple electrical double layer.

2. Gouy-Chapman Diffuse Charge Model of the Double Layer. We saw above that the Helmholtz-Perrin model fixes the solution charges onto a sheet parallel to the metal. Gouy and Chapman liberated the ions from a sheet parallel to the electrode. However, once the ions are free, they get exposed to thermal buffeting from the solution particles. Both, the electric force arising from the charge on the electrode and the thermal jostling, influence the behaviour of ions in the vicinity of the electrode. Thus, in the Gouy—Chapman model, the excess charge density on the OHP is not equivalent to that on the metal, but is less (Fig. 14*a*). A few solvated ions leave the second row and randomly walk in solution. The excess charge density in the solution decreases with distance from the electrode; the electrode processes a kind of ionic atmosphere.

Near the metal, its charge attracts the solvated ions to the second row. Further out, the influence of thermal motion is comparable to the forces from the electrode. Sufficiently far into the solution, the net charge density vanishes because positive and negative ions are equally likely to be found in any region—thermal motion reigns supreme.

Since the electrode has an ionic cloud, the Gouy—Chapman model appears to resemble the theory of interionic interactions in solution. In the latter, the 'central ion' is arbitrarily chosen as the source of the electric field. Here, on the other hand, the discussion involves ion-electrode interactions with the electrode as the source of the field. Thus, the theory of ion-ion interactions is similar to the theory of ion-electrode interactions. There are, however, differences in the geometry encountered in the two situations—differences which affect the mathematical treatment. Thus, whereas the central ion produces a spherically symmetrical field, the electrode behaves like an infinite plane and its field has a planar symmetry.

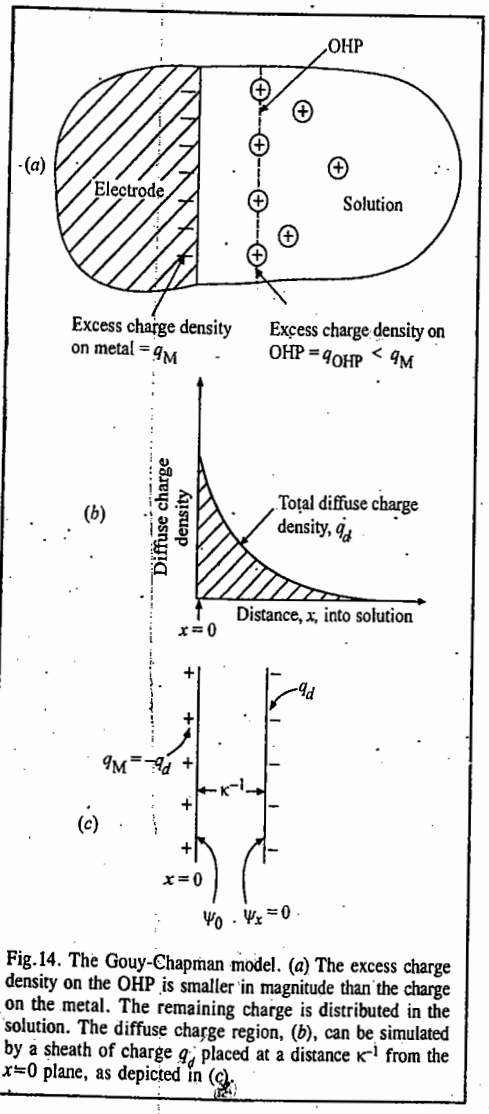

Fig.14. The Gouy-Chapman model. (*a*) The excess charge density on the OHP is smaller in magnitude than the charge on the metal. The remaining charge is distributed in the solution. The diffuse charge region, (*b*), can be simulated by a sheath of charge q_d placed at a distance κ^{-1} from the x=0 plane, as depicted in (*c*).

Otherwise, the theory of the diffuse double layer is analogous to that of the long range ion—ion interactions. Thus, the corresponding electric field (or potential gradient) at a distance x from the electrode, according to the Gouy-Chapman diffuse charge model, is given by the following expression :

$$\frac{d\psi}{dx} = -\left(\frac{8kTc_0}{\varepsilon_r \varepsilon_0}\right)^{1/2} \sinh \frac{ze\psi_x}{2kT} \qquad ...(114)$$

where c_0 is the concentration of the ith species in the bulk of the solution and ψ_x is the outer potential difference between a point x from the electrode and the bulk of the solution. Eq. 114 relates the electric field and the electric potential at a distance x from the electrode.

According to Gauss's law of electrostatics, the charge contained within a closed volume (Gaussian box) is equal to $\varepsilon_r \varepsilon_0$ times the area of the closed surface (taken here as unity) times the component of the field normal to the surface of the enclosed volume. Thus,

$$q = \varepsilon_r \varepsilon_0 (d\psi/dx) \qquad ...(115)$$

However, in order to determine the total diffuse charge density, q_d, the Gaussian box should extend from a place very close to the electrode, *e.g.*, $x = 0$ to a place deep inside the solution, $x \to \infty$, where $\psi_x = 0$ and $d\psi_x/dx = 0$. Therefore, with these conditions the total diffuse charge density scattered in the solution under the combined influence of thermal and electrical forces, q_d is given, according to Eqs. 109 and 115, by the expression

$$q_d = -2(2\varepsilon_r \varepsilon_0 c_0 kT)^{1/2} \sinh \frac{ze\psi_0}{2kT} \qquad ...(116)$$

where ψ_0 is the potential at x=0 relative to the bulk of the solution where the potential is taken as zero.

We are also interested in knowing the variation of potential with distance; this can be obtained by integrating Eq. 114. Assuming that $\sinh (ze\psi_x/2kT) \approx (ze\psi_x)/2kT$, we have

$$\ln \psi_x = -\left(\frac{2c_0 z^2 e^2}{\varepsilon_r \varepsilon_0 kT}\right)^{1/2} x + \text{constant} \qquad ...(117)$$

The quantity inside the brackets is the familiar κ^2 of the Debye—Hückel theory. The integration constant in Eq. 117 can be evaluated from the boundary condition that at $x \to 0$, $\psi_x \to \psi_0$. Hence,

$$\psi_x = \psi_0 \exp(-\kappa x) \qquad ...(118)$$

This expression shows that the potential decays exponentially as the distance x from the electrode increases (Fig. 14*b*). Also, as the solution concentration c_0 increases, κ increases and ψ_x falls more and more sharply. In Eq. 118, the κ used is the same as used in the Debye-Hückel theory. Does this variable have the same meaning in both the Debye-Hückel theory and the Gouy-Chapman model ? In the ionic cloud model, the cloud on the central ion is simulated by placing the entire charge of the cloud, $-ze$, at the distance κ^{-1} from the central ion. Given the similarity between the two systems, we can use similar reasoning for the electrode and its diffuse charge. Thus, the diffuse charge of the electrode can be simulated by placing the total charge q_d at a distance κ^{-1} from the electrode. We, in fact, encounter a parallel plate condenser situation, *i.e.*, a charge of $-q_d = q_M$ at x=0 plate and the diffuse charge q_d at the $x = \kappa^{-1}$ plate (Fig. 14*c*).

We next proceed to determine the third quantity, *viz.*, the differential capacity. This can be done by differentiating Eq. 116 with respect to potential V. However, in Eq. 116, the variable is ψ_0, *i.e.*, potential at $x = 0$. We, therefore, seek to relate V to ψ_0. At x=0, $V = \psi_0 - \psi_{bulk}$, so that $dV = d\psi_0$ since ψ_{bulk}=0. Also, ψ_0 can be replaced by ψ_M since the ions are considered as point-charge ions. Thus, with $dq_M = -dq_S = -dq_d$, the differential capacity becomes

$$C = \left(\frac{\partial q_M}{\partial V}\right)_{\text{const.comp}} = -\left(\frac{\partial q_d}{\partial \psi_M}\right)_{\text{const.comp}} = \left(\frac{2\varepsilon_r \varepsilon_0 z^2 e^2 c_0}{kT}\right) \cosh\left(\frac{ze\psi_M}{2kT}\right) \qquad ...(119)$$

The cosh function gives inverted parabolas. Hence, the differential capacity of an electrified interface, according to the Gouy-Chapman diffuse charge model, should not be a constant : it should show an inverted parabola dependence on the potential across the interface. This is found to be so experimentally.

One of the reasons why this model fails is that it neglects ion-ion interactions which are important at high concentrations. A second, and very serious, error is the assumption of point-charge ions. Also doubtful is the constancy of the dielectric constant in the region between the electrode and the bulk of the solution. Nevertheless, the Gouy-Chapman model gives a better picture of the double layer.

3. Stern Model. This model which attempts a synthesis of the Helmholtz-Perrin and the Gouy-Chapman models, eliminates the point charge approximation of the diffuse layer theory. The Stern theory divides the solution charge into two contributions (Fig. 15*a*) part of the charge q_S on the solution is immobilized close to the electrode in the OHP (the Helmholtz-Perrin charge, q_H). The remainder is diffusely spread out in the solution (the Gouy-Chapman charge, q_G). Thus,

$$q_S = q_H + q_G \qquad ...(120)$$

As a result of separation of charges, there occur drops in potential. Thus, the Stern model suggests two potential drops, *viz.*,

$$\phi_M - \phi_{bulk} = (\phi_M - \phi_H) + (\phi_H - \phi_{bulk}) \qquad ...(121)$$

where ϕ_M and ϕ_H are the inner potentials at the metal and the Helmholtz planes, respectively and ϕ_{bulk} is the potential in the bulk of the solution.

The Stern synthesis of the two models implies a synthesis of the potential-distance relations characteristic of these two models (Fig. 16*b*) : a *linear* variation in the region from $x=0$ to the position of the OHP according to the Helmholtz-Perrin model, and an *exponential* potential drop in the region from OHP to the bulk of the solution according to the Gouy-Chapman model (Fig. 14).

Another implication is that the separation of charges and potential regions produces a separation of differential capacities. Differentiating the potential difference across the interface (Eq. 121) with respect to the charge on the metal, q_M, we have

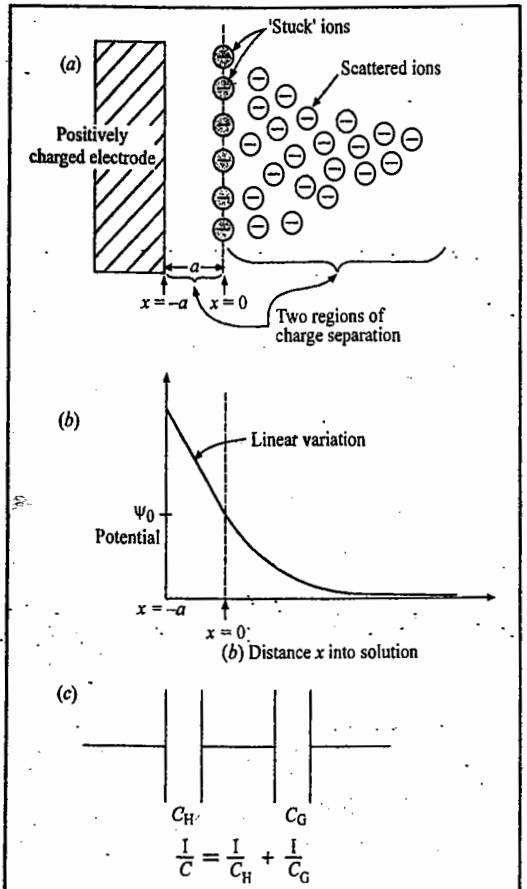

Fig.15. The Stern model. (*a*) A layer of ions stuck to the electrode and the remainder scattered in cloud fashion. (*b*) The potential variation according to this model. (*c*) The corresponding total differential capacity C is given by the Helmholtz and Gouy capacities in series.

$$\frac{\partial(\phi_M - \phi_{bulk})}{\partial q_M} = \frac{\partial(\phi_M - \phi_H)}{\partial q_M} + \frac{\partial(\phi_H - \phi_{bulk})}{\partial q_M} \qquad ...(122)$$

We can replace ∂q_M with ∂q_d (in the denominator of the last term) because the total charge on the electrode is equal to the total diffuse charge. Thus,

$$\frac{\partial(\phi_M - \phi_{bulk})}{\partial q_M} = \frac{\partial(\phi_M - \phi_H)}{\partial q_M} + \frac{\partial(\phi_H - \phi_{bulk})}{\partial q_d} \qquad ...(123)$$

Each term in this equation represents the reciprocal of a differential capacity (Eq. 87). Hence, Eq. 123 can be written as

$$\frac{1}{C} = \frac{1}{C_H} + \frac{1}{C_G} \qquad ...(124)$$

where C is the total capacity of the interface, C_H is the Helmholtz-Perrin capacity and C_G is the Gouy-Chapman or diffuse-charge capacity. This result is formally identical to the expression for the total capacity of two capacitors in series (Fig. 16*c*). Thus, we conclude that an electrified interface has a total differential capacity which is given by the Helmholtz and Gouy capacities in series.

The three double layer models and their characteristic features are summed up in Table 2.

TABLE 2

Various Models of the Double Layer and Their Characteristic Features

Model	Relevant Equations	Schematic	General Remarks
Helmholtz-Perrin parallel plate model	$q_M = -q_S = -q_{OHP}$ $C = \frac{\varepsilon_r \varepsilon_0}{d}$	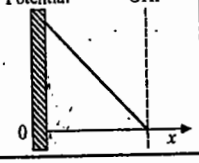	The model predicts constant differential capacities. Ions are arranged in a layer (OHP) close to the electrode
Gouy-Chapman diffuse charge model	$q_M = -q_d = -2(2\varepsilon_r\varepsilon_0 C_0 kT)^{1/2} \sinh \frac{ze_0\psi_0}{2kT}$ $C = \left(\frac{2\varepsilon_r\varepsilon_0 z^2 e^2 C_0}{kT}\right)^{1/2} \cosh \frac{ze_0\psi_M}{2kT}$ $\psi_x = \psi_0 e^{-kx}$	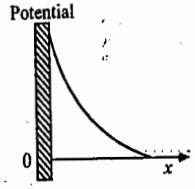	The model predicts that differential capacities have the shape of inverted parabolas. Ions are considered as point charges. Ion-ion interactions are not considered. The dielectric constant is taken as a constant.
Stern combination of parallel plate and diffuse charge model	$q_M = -q_S = -[q_H + q_G]$ $\frac{1}{C} = \frac{1}{C_H} + \frac{1}{C_G}$	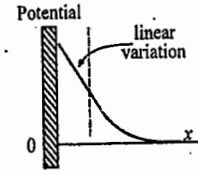	Ions are under the combined influence of the ordering electrical and the disordering thermal forces. The model agrees with the experiment only for ions nonspecifically adsorbed on the electrode.

We shall consider two extreme cases. Let us see what happens when the concentration c_0 of ions in solution is very large. Eqs. 113 and 119 show that while C_G increases with increasing c_0, C_H remains constant. Thus, as c_0 increases, $1/C_G \ll 1/C_H$ and for all practical purposes, $C \approx C_H$. That is, in concentrated solutions, the capacity of the interface is effectively equal to the capacity of the Helmholtz region, *i.e.*, of the Helmholtz-Perrin parallel plate model. This implies that most of the solution charge is squeezed onto the Helmholtz plane or confined in a region very close to this plane. In other words, only a small charge is scattered diffusely into the solution in the Gouy-Chapman model.

At the other extreme, *i.e.*, when c_0 is low $(1/C_G) \gg (1/C_H)$ and thus, $C \approx C_G$. This implies that the electrified interface assumes Gouy-Chapman-like structure, with the solution charge scattered under the combined influence of electrical and thermal forces. Thus, we can say that under certain experimental conditions, the Stern model is successful, particularly for ions (such as Na^+ and F^-) which do not interact with the electrode. However, for ions such as Cl^-, Br^-, I^- or PO_4^{3-} which may get *adsorbed* on the electrode, this model is not successful.

C. Structure of Semiconductor Interfaces

In our previous treatment of the metal—electrolyte interface, consideration of the metal was restricted to the statement that the charge density q_M was confined close to the surface of the metal and on to a narrow region—a few angstroms—extending into the solution. Thereafter, we turned our attention to the solution side of the interface, *i.e.*, towards the ionic double layer and we wanted to know how the excess charges are arranged as a function of distance from the metal, how the potential decays and how the electrolyte concentration alters the picture, etc. In a semiconductor–electrolyte interface, the view point will be reversed. The situation in the solution will be considered to be understood and the focus will be on the distribution of excess charge inside the electrode, *i.e.*, the **electronic double layer.**

Let us consider a concentrated electrolyte solution and assume that the entire Gouy—Chapman diffuse charge is located on the OHP. Let us also suppose that there is no contact adsorption so that the IHP is unpopulated. This means that we are considering a single layer of charge on the solution side of the interface. The situation inside the electrode depends upon whether the electrode is a metal or a semiconductor. The most important difference between a metal and a semiconductor is the order of magnitude of conductivity. Metals have conductivities of the order of 10^6 ohm^{-1} cm^{-1} and semiconductors, about 10^2—10^9 ohm^{-1} cm^{-1}. These significant differences in conductivity reflect predominantly the concentration of free charge carriers. In crystalline solids, the atomic nuclei are relatively fixed and the charge carriers that drift in response to electric fields are electrons. Before we try to find out what determines the concentration of mobile electrons, we shall outline the band picture of an intrinsic semiconductor.

In an intrinsic semiconductor (Fig. 16), there is an energy gap separating the valence band from the upper band. But this energy gap, in contrast to that in the case of insulators, is not much more than the thermal energy of the electrons and, therefore, is small enough for electrons in the valence band to be excited into the upper conduction band.

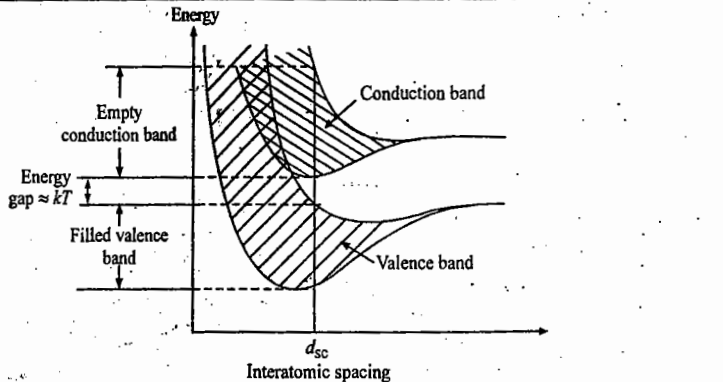

Fig. 16. The band picture of a semiconductor with an interatomic spacing of d_{SC}, showing the small energy gap between the valence and conduction bands.

The energy required for the excitation of electrons into the upper band may come from the thermal motion of electrons or from light incident on the material. Once they enter the upper band, these electrons find several unoccupied energy states into which they can move. Hence, the conduction-band electrons conduct electricity. This is the mechanism of conduction of an intrinsic semiconductor. When an electron is excited across the energy gap E_g to the conduction band in an intrinsic semiconductor, an unoccupied energy state, or hole, is left behind in the normally full valence band. Another electron in the valence band can jump into this vacant state (Fig. 17) but this leads to a vacant state in the place where the jumping electron was. Thus, the motion of electrons into unoccupied energy states, or holes, in the valence band is equivalent to the movement of the vacant states, or holes, in the opposite direction. Since an electric field moves the holes in an opposite direction to electrons, the holes may be treated as if they were positively charged (Fig. 18).

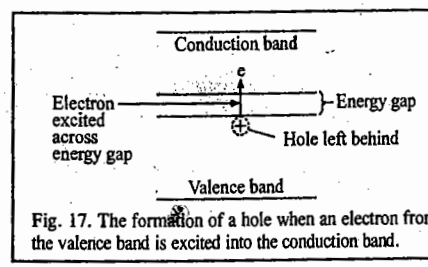

Fig. 17. The formation of a hole when an electron from the valence band is excited into the conduction band.

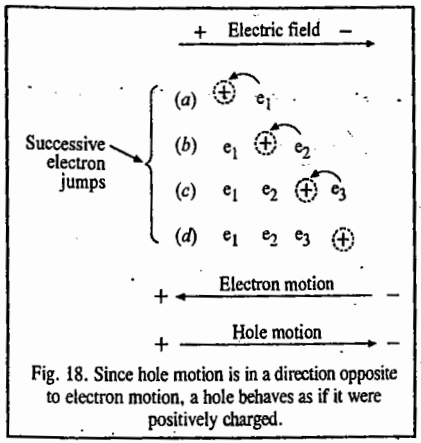

Fig. 18. Since hole motion is in a direction opposite to electron motion, a hole behaves as if it were positively charged.

A semiconductor is analogous to an electrolyte solution and we shall pursue this analogy here. The removal of a valence electron by excitation to move into the conduction band implies the cleavage of a bond in the lattice (since the valence band electrons bind the atoms together). Hence, the creation of an electron–hole pair may be treated as an ionization reaction :

$$\text{Lattice} \rightleftharpoons e + h \qquad \ldots(125)$$

(where e stands for electron and h for hole). We thus see that there is a parallel between the ionization of the lattice of an intrinsic semiconductor and the ionization of water :

$$H_2O \rightleftharpoons OH^- + H^+ \qquad \ldots(126)$$

Just as $$K_w = c_{H^+} \times c_{OH^-} \qquad \ldots(127)$$

at a constant temperature, similarly, for an intrinsic semiconductor

$$K_{SC} = np \qquad \ldots(128)$$

where n stands for the electron concentration and p stands for the hole concentration; K_{SC} is a constant characteristic of the intrinsic semiconductor; it depends upon the energy gap E_g between the valence band and the conduction band. Again, just as in pure water, the concentrations of hydroxyl and hydrogen ions are equal, so the electron and hole concentrations are equal in an intrinsic semiconductor. Hence,

$$n = p = \sqrt{K_{SC}} \qquad \ldots(129)$$

In an intrinsic semiconductor, the density of charge carriers at room temperature is in the range of 10^{13} to 10^{16} compared with about 10^{22} in a metal. It is this relatively low concentration of charge carriers in intrinsic semiconductors that is responsible for the most important differences between semiconductor electrodes and metal electrodes.

Diffuse Charge Region Inside an Intrinsic Semiconductor : Garrett-Brattain Space Charge. Here we are concerned with the following problem : Given a layer on the OHP of the electrolyte, what is the distribution of electrons and holes inside an intrinsic semiconductor as a function of the distance from the interface ? This problem was tackled by Garrett and Brattain by invoking its formal similarity to the problem of a diffuse charge in solution. Inside the electrolyte, the positive and negative ions are charge carriers; inside the intrinsic semiconductor, the electrons and holes are charge carriers. Again, in the bulk of the electrolyte solution, the excess-charge density in any volume element is zero because the numbers per unit volume of positive and negative charges are exactly equal. Similarly, deep inside the intrinsic semiconductor, the excess-charge density is zero because of the equality of the density of electrons n^0 and of the holes p^0. Hence, for the semiconductor bulk

$$n^0 = p^0 \qquad \ldots(130)$$

and $$\rho_{bulk} = ep^0 - en^0 = 0 \qquad \ldots(131)$$

Just as the charged electrode exerts an electric field on the positive and negative ions in solution, similarly the sheet of charge on the OHP of the electrolyte exerts an electric field on the holes and the electrons in the intrinsic semiconductor with the result that in the vicinity of the surface, electrons and holes are not present in equal numbers. Also, just as the Poisson equation in combination with the Boltzmann distribution is used to determine the charge density ρ_x on any electrolyte lamina (parallel to the electrode) as a function of distance x, similarly, the Poisson equation for an intrinsic semiconductor is written as

$$\rho_x = -\varepsilon_r \varepsilon_0 (d^2\psi_x/dx^2) \qquad ...(132)$$

The Boltzmann distribution is

$$\rho_x = e(p_x - n_x) = e[p^0 \exp(-e\psi_x/kT) - n^0 \exp(e\psi_x/kT)] \qquad ...(133)$$

where ψ_x is the potential of the semiconductor at a distance x from the electrode surface ($\psi_{x\to\infty}$ is taken as zero). From Eq. 130, we have

$$\rho_x = -en^0 [\exp(e\psi_x/kT) - \exp(-e\psi_x/kT)] = -2en^0 \sinh(e\psi_x/kT) \qquad ...(134)$$

Equating these two expressions for ρ_x, we obtain the Poisson–Boltzmann equation :

$$\frac{d^2\psi_x}{dx^2} = \frac{2en^0}{\varepsilon_r\varepsilon_0}\sinh(e\psi_x/kT) \qquad ...(135)$$

Eq. 135, the differential equation for the space variation of the potential inside the semiconductor, can be identified with that for the space variation of potential inside the electrolyte in the Gouy–Chapman theory of the diffuse double layer. Hence, we can borrow the result of this theory, *viz.*,

$$\frac{d\psi_x}{dx} = -\left(\frac{8kTn^0}{\varepsilon_r\varepsilon_0}\right)^{1/2} \sinh\frac{e\psi_x}{2kT} \qquad ...(136)$$

Also,
$$q_{sc} = (2\varepsilon_r\varepsilon_0 n^0 kT)^{1/2} \sinh\frac{e\psi_s}{2kT} \qquad ...(137)$$

where q_{sc} is the total space charge and ψ_s is the potential at the surface of the semiconductor. Linearizing the hyperbolic sine function, we have

$$\sinh\frac{e\psi_x}{2kT} \approx \frac{e\psi_x}{2kT} \qquad ...(138)$$

and solving the differential equation

$$\frac{d\psi_x}{dx} = -\left(\frac{2n^0e^2}{\varepsilon_r\varepsilon_0 kT}\right)^{1/2} \psi_x = -\kappa\psi_x, \qquad ...(139)$$

we obtain
$$\psi_x = \psi_s \exp(-\kappa x) \qquad ...(140)$$

We find that the potential due to the space charge inside the semiconductor decays exponentially (Fig. 19). This potential decay suggests the existence of an electric field inside the semiconductor and that the excess-charge density decays slowly to zero as if there were an electronic cloud analogous to the ionic cloud adjacent to an electrode in solution. We see that the potential due to the atmosphere of holes and electrons is determined by the same parameter

$$\kappa = \left(\frac{2n^0e^2}{\varepsilon_r\varepsilon_0 kT}\right)^{1/2} \qquad ...(141)$$

as that which occurs in the Debye–Hückel ionic cloud and the Gouy–Chapman diffuse-charge treatment. The parameter κ^{-1} is a measure of the thickness of the Garrett–Brattain space charge inside

a semiconductor. Its value decreases as the bulk concentration of charge carriers increases. This means that as the carrier concentration increases, the thickness of the space charge region decreases. This is one way of looking at the metal ; because of high concentration of charge carriers, the space charge is all squeezed onto the surface. The situation is analogous to the diffuse charge in solution which gets compressed on the OHP when the electrolyte concentration is sufficiently high.

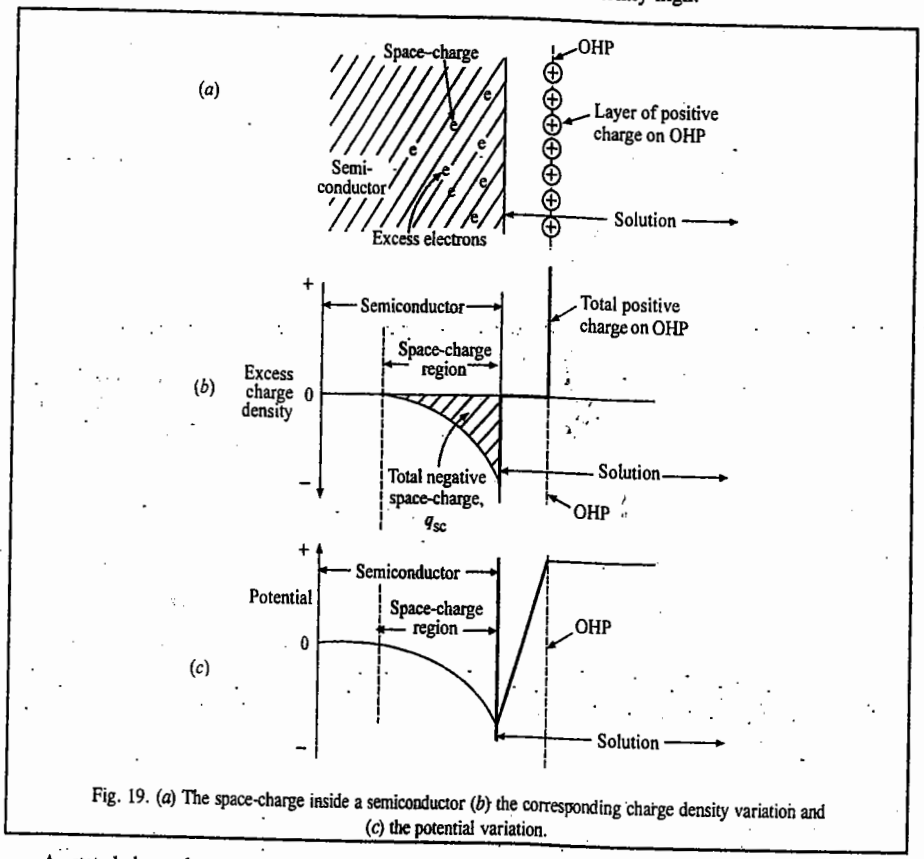

Fig. 19. (*a*) The space-charge inside a semiconductor (*b*) the corresponding charge density variation and (*c*) the potential variation.

As stated above, because of the existence of a layer of charge in the solution, there is a space charge potential drop inside the semiconductor. An electron in this space charge region will interact with the field and its energy will either increase or decrease compared with the value in the absence of the field. This implies that the enery bands near the surface of an intrinsic semiconductor are disturbed by the existence of an electric field. The electron energies are given by the sum of the energies due to the intrinsic-band structure and that due to the deviation of the inner potential from its zero value in the bulk.

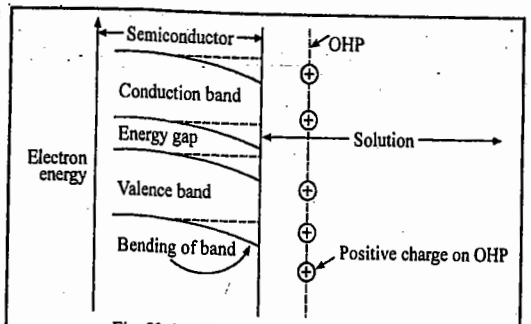

Fig. 20. The bending of bands near the surface of a semiconductor.

Thus, near the surface, there is a bending of the bands up and down, depending upon the sign of the ionic charge populating the OHP (Fig. 20).

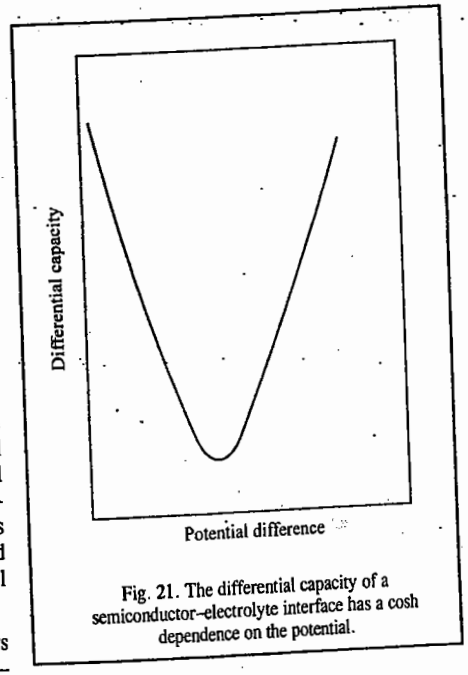

Fig. 21. The differential capacity of a semiconductor–electrolyte interface has a cosh dependence on the potential.

We shall now consider the differential capacity due to the space charge. In the experimental measurements of capacitance carried out on a semiconductor–electrolyte interface, we should bear in mind that the space-charge region inside the semiconductor has the ability to store charge. We can easily calculate the contribution of this region to the differential capacity of the interface. Differentiating Eq. 137 for q_{sc} by the potential drop ψ_s inside the semiconductor, we get

$$C_{sc} = \frac{dq_{sc}}{d\psi_s} = 2(\varepsilon_r \varepsilon_0 n^0 kT) \cosh \frac{e\psi_s}{kT} \quad ...(142)$$

Thus, we expect that C_{sc}, the differential capacity of a semiconductor–electrolyte interface due to the space charge inside an intrinsic semiconductor, will vary in a hyperbolic manner with the potential (Fig. 21). We see that the values of the space-charge capacities are low compared with the capacities of the region between the semiconductor surface and the OHP plane, *i.e.*, the Helmholtz–Perrin parallel plate region.

The observed capacity is given by two capacitors in series–the space charge C_{sc} and the Helmholtz–Perrin C_{HP} capacitors. Thus,

$$\frac{1}{C_{obs}} = \frac{1}{C_{sc}} + \frac{1}{C_{HP}} \quad ...(143)$$

Since $C_{HP} \gg C_{sc}$, we have

$$\frac{1}{C_{obs}} \approx \frac{1}{C_{sc}} \quad ...(144)$$

When the electrolyte solution is dilute, a diffuse-charge region will also appear in the solution. There will be three potential drops : one inside the semiconductor, the Garrett—Brattain drop $\Delta\phi_{sc}$; a linear Helmholtz—Perrin drop $\Delta\phi_{HP}$ and, finally, the Gouy–Chapman drop, $\Delta\phi_{GC}$ in the solution. The total $\Delta\phi$ across the interface is given by

$$\Delta\phi = \Delta\phi_{sc} + \Delta\phi_{HP} + \Delta\phi_{GC} \quad ...(145)$$

and the total differential capacity by

$$\frac{1}{C} = \frac{1}{C_{sc}} + \frac{1}{C_{HP}} + \frac{1}{C_{GC}} \quad ...(146)$$

We thus see that there are three capacitors in series at a semiconductor–electrolyte interface rather than two capacitors as at a metal–solution interface. What is experimentally observed depends upon the electron concentration in the semiconductor (how low it is) and the ionic concentration in the electrolyte solution.

III. ELECTROCATALYSIS

Electrocatalysis is similar to heterogeneous catalysis. It may be recalled that heterogeneous catalysis involves surfaces of metal and/or their oxides. The surfaces may be prepared in several ways, *i.e.*, may be roughened or they may be in the form of powders to enable them to have greater surface areas. In fact, all electrodes on whose sites reactions involving adsorbed intermediates occur, can be regarded as catalysts, though, of course, only those on which electrochemical rates are relatively rapid are thought of as catalysts. The electrocatalytic reactions are potential-dependent in rate, like all other electrode reactions. In considering chemical (thermal) and electrochemical (electrical) catalysis, we should pay attention to the reference potential at which a comparison of electrocatalysts is made.

An electrode catalyst can be rationally chosen only if we know what the rate-determining step (rds) is in the electrode reaction. Then the key factor is to choose a material that increases the rate of the rds. Also, the heterogeneity of the surface is vital. It is evident that a surface containing a greater number of defects, kinks, ledges and holes is likely to be a good catalyst if the rds is such that strong bonding to the radical is helpful.

Mechanism of Electrocatalysis. Let us consider the electrocatalysis of the evolution of oxygen from alkaline solutions on perovskites, described by the general formula RTO_3 where R is a rare earth element such as lanthanum and T is a transition element such as nickel, cobalt, iron, managanese and chromium. The perovskite lattice is shown in Fig. 22. The figure shows the active surface of the perovskite. From the empirical formula of perovskites RTO_3, it is not obvious how the OH^- ions in an alkaline solution would be able to get discharged on an oxide surface. It would appear that O, which might be on the surface facing the OH^-, diffuses in from the solution and evidently no bonding would occur. However, the slice through the crystal exposing the surface (Fig. 22) shows that the transition metal ion, with its multiple valencies and strong bonding power is indeed on the surface. Thus, OH^- discharges on the transition metal ion of the perovskite and not on the Os.

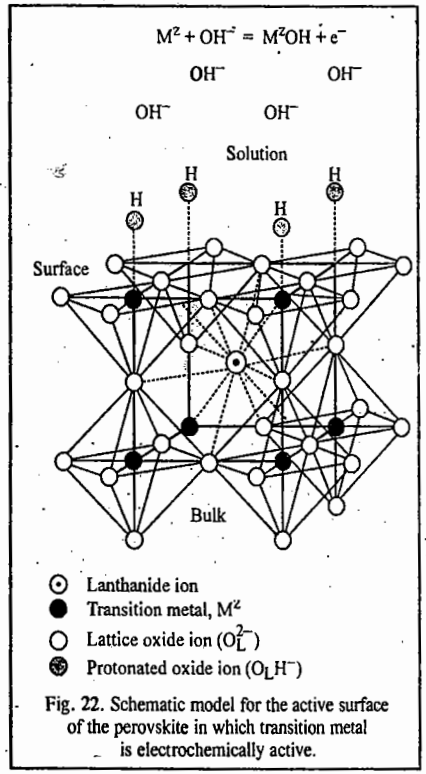

Fig. 22. Schematic model for the active surface of the perovskite in which transition metal is electrochemically active.

We are interested in the relation between the rate of reaction (here measured uniformly for all the perovskites studied at an overpotential of 0·3V) and the strength of the OH bond to be linked to the transition metal ion. From Fig. 23 we see that the stronger the bond strength, the slower the reaction. This information suggests that the reaction mechanism must involve a *desorption* of OH in the rate determining step (rds). The more difficult it becomes (stronger bonding), the more difficult it is for the reaction to occur.

Any proposed mechanism for the reaction must involve desorption of OH formed in the first step. The second and rate-determining step in the series going to O_2 is thus likely to be

$$M^{z+}\text{–}OH_{ads} + OH^- \xrightarrow{rds} M^{z+} \longrightarrow H_2O_2 + e^-$$

The remaining steps leading to the evolution of O_2 will be beyond the rds and hence will not be of primary influence on the electrocatalysis process. These are probably

$$H_2O_2 + OH^- \rightleftharpoons (HO_2^-)_{phys\ ads} + H_2O$$

$$H_2O_2 + (HO_2^-)_{phys} \rightleftharpoons H_2O + OH^- + O_2$$

Some factors are of paramount importance here. An important factor is the availability of electrons in the oxide which for a metal would not be a factor for there are always plenty. *Pure* perovskites are non-conductors and before they can be used as electrodes, it is necessary to add to them other substances that increase their conductance. BaO is one such substance. This process is analogous to the addition of doping agents to semiconductors. It is also necessary to know the effect of the OH^- adsorbed on the resulting electron density created by the addition of BaO. The entropy of activation can also affect the reaction rate. The catalysis is largely due to M-OH bonding.

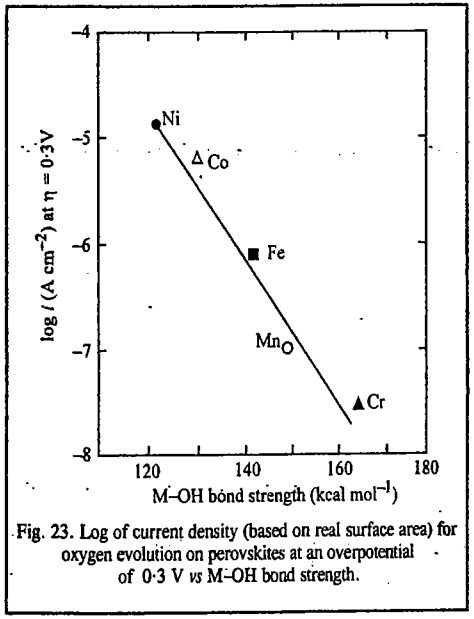

Fig. 23. Log of current density (based on real surface area) for oxygen evolution on perovskites at an overpotential of 0·3 V *vs* M–OH bond strength.

Volcanoes

A commonly encountered phenomenon in electrocatalysis is the so called volcano. It is found that for a given reaction carried out on a variety of catalysts, the rates on each catalyst pass through a maximum. In a volcano we plot the rate on a catalyst as a function of some property of the catalyst, *e.g.*, its heat of sublimation (which would be proportional to its metal–metal bond strength) or the actual bond strength of the bond formed between catalyst material and an adsorbed radical taking part in the rds (Fig. 24).

We can explain the occurrence of volcanoes in electrocatalysis as follows : Consider a series of differing electrode surfaces, on each of which the same reaction occurs. Imagine the electrocatalysts as having a bonding power to some atom in the reactants. Thus, for instance, in the case of the oxidation of methanol, the relevant bond may be the M-C bond where M represents the series of catalysts arranged in sequence so that they bind to C to an increasing degree. Now, at the beginning of this imaginary series of catalysts when the bonding power is minimal, the degree of coverage of a unit area of the electrode, θ, with an adsorbed reactant will also be small so that the rate at which final product (CO_2 if we begin with methanol) is produced will be very low. As the bonding power of catalyst to the relevant reactant in the rds increases in the series of catalysts, θ will also increase and so will the rate of production per unit area. This increase will continue as we move through the series of catalysts, always with increasing bonding power. Hence, θ keeps on increasing in the steady state. However, as θ increases, the free surface available for adsorption decreases. This can be taken care of in the rate expression with a $(1 - \theta)$ term. Thus, the reaction rate is proportional to both θ and $(1 - \theta)$:

$$\text{Rate} \propto \theta(1-\theta) \qquad \ldots(147)$$

The maximum rate is given by

$$d[\text{Rate}]/d\theta = 0, \textit{ i.e.}, \text{ at } \theta = 1/2 \qquad \ldots(148)$$

This argument leads us to conclude that as the adsorption bond of catalyst to a radical increases and θ also increases with it, there will occur a value of the bonding strength of the substrate to the radical formed during the oxidation of methanol, for which the value of θ will be so large that more than half of the electrode surface will be covered. The reaction rate will then begin to decrease with a further increase in θ. Finally, when $\theta \to 1$, nearly all of the surface will be covered with the entities participating in the reaction. Because of the strong M—C bond, the desorption of the products will also be difficult, with the result that the reaction rate will become very slow, just as it was when the M-C bond strength was very small. Qualitatively, then, as the bonding power of the catalyst increases, the reaction rate will increase, pass through a maximum and then decrease. This accounts for the formation of volcanoes in electrocatalysis.

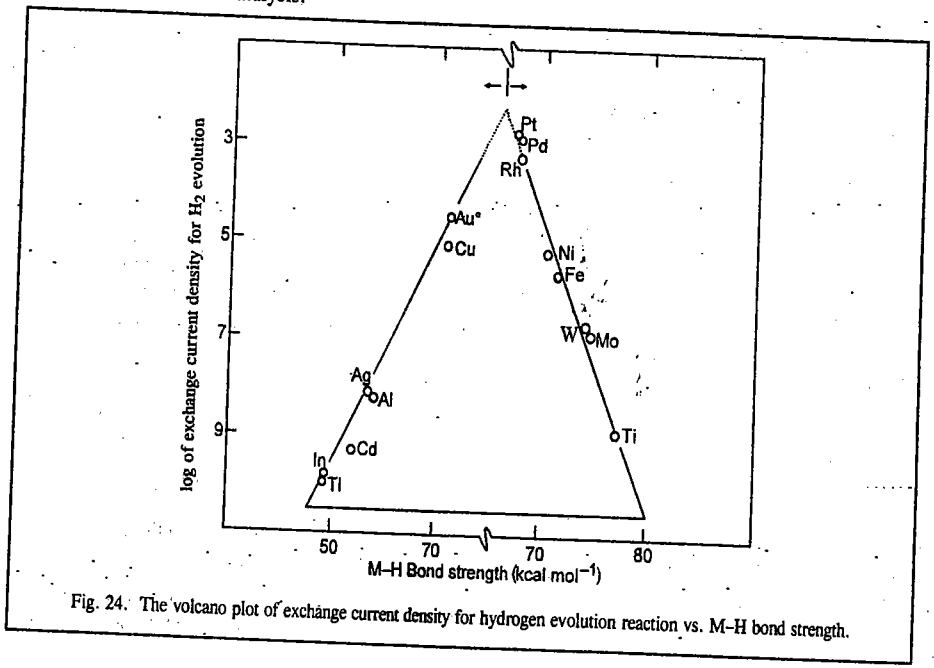

Fig. 24. The volcano plot of exchange current density for hydrogen evolution reaction vs. M–H bond strength.

IV. KINETICS OF ELECTRODE REACTIONS

A reaction occurring at an electrode surface involves the following steps in succession :

1. Diffusion of the reactants to the electrode.
2. Adsorption of reactants on the electrode.
3. Transfer of electrons to or from the adsorbed reactant species.
4. Desorption of products from the electrode.
5. Diffusion of products away from the surface of the electrode.

In an electrode reaction, the charged species, *viz.*, ions and electrons, are enabled to surmount the activation energy barrier by the energy of the electric field. Since electrochemical reactions are investigated at temperatures $T > 0$, there is both thermal and electrical contribution to activation energy.

For each ionic species at equilibrium. the rate of electron transfer in the cathodic direction is exactly balanced by the rate of electron transfer in the anodic direction so that the *current density*

(current per unit area)

$$i_c = i_a = i_o \qquad ...(149)$$

The current density i_o at equilibrium is called the *exchange current density*. The rate r of a chemical reaction at the surface of an electrode is given by

$$r = i/z F \qquad ...(150)$$

where z is the charge on the ionic species and F is the faraday, 96458 C mol^{-1}. We see that in an electrochemical reaction, $r \propto i$.

It may be mentioned that while the rate of the chemical reaction at the electrode is expressed in units of mol m^{-2} s^{-1}, the rate of the charge transfer at the electrode is expressed in units of A m^{-2}.

For a given electrochemical reaction, the electrodes are said to be nonpolarizable if they have high exchange current density and polarizable if they have a low exchange current density. Application of potential difference across a nonpolarizable electrode results in an increased flow of charge between the electrode and solution, though the potential difference across the electrical double layer does not change. Thus, charge moves rapidly to and from the electrode with the result that no charge density is built up in the surface layers. The calomel electrode furnishes an example of a nonpolarizable electrode.

If the applied potential difference across a polarizable electrode is increased, there is little flow of charge into the solution. The charges remain in the electrical double layer and increase the potential difference across it. The dropping mercury electrode is an example of a polarizable electrode.

When an electrochemical cell operates under *non-equilibrium* conditions, $i_c \neq i_a$ and there is *net* current density $i = i_a - i_c$. In such a case the potential difference between the cell terminals departs from the equilibrium value $\Delta\phi = E$, the cell EMF. If the cell is converting chemical free energy into electrical energy, $\Delta\phi < E$. If, on the other hand, the cell is using an external source of energy to cause the chemical reaction, $\Delta\phi > E$. The actual value of $\Delta\phi$ depends upon the current density i at the electrodes. It is customary to define the **quantity overpotential** η of the cell as

$$\Delta\phi - \Delta\phi_{eq} = \eta \qquad ...(151)$$

The value of η is largely determined by the potential difference (iR) required to overcome the resistance R in the electrolyte and the leads. The corresponding electrical energy is dissipated as heat.

Kinetics of an Electrode Reaction. Consider the electrode reaction

$$M^{z+}(aq) + ze \longrightarrow M(s)$$

which occurs when the reactant ion M^{z+} is in the vicinity of an electrode surface so that the electrons are transferred from the electrode to the ion.

According to Eyring activated complex theory (ACT), the rate constant k_2 of the chemical reaction is given by

$$k_2 = B \exp(-\Delta G^{\neq}/RT) \qquad ...(152)$$

where $\Delta G^{\neq}$ is the Gibbs free energy of activation and B is some constant. Fig. 25 shows the reaction paths along the free energy surfaces between the reactants and the products. The "reaction coordinate" is normal to the electrode surface. The electrochemical reaction involving electron transfer occurs in a region near the electrode that coincides with the region of the electrical double layer. It may be mentioned that the

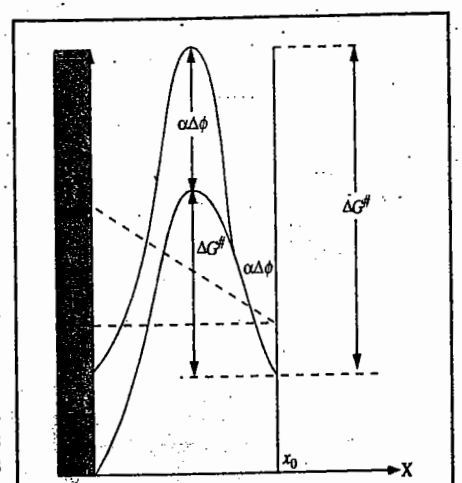

Fig. 25. Gibbs free energy curves for the electrode reaction $M^{z+} + ze \longrightarrow M(s)$ in the vicinity of the electrode surface showing the lowering of $\Delta G^{\#}$ by the electric potential.

double layer has very high electric field of the order of 10^9 $V m^{-1}$, assuming that a potential difference of one volt exists across a typical double layer of thickness 1 nm. Such fantastically high electric field can literally tear the ions from the solid metal surface, dragging them into the solution. Assuming the Helmholtz model of the double layer, the potential varies linearly with x (Fig. 25). The position of the outer Helmholtz plane is at x_0 where the reactant molecule can be located.

We shall consider a reaction at the electrode in which a particular species is reduced by the transfer of a single electron in a rate-determining step. Let [Ox] and [Red] be the concentrations of the oxidized and reduced forms of the species, respectively, outside the double layer. Clearly, the net current at the electrode is the difference of the currents resulting from the reduction of Ox and oxidation of Red. The rates of these processes are k_c[Ox] and k_a[Red], respectively. In a reduction process, the magnitude of charge transferred per mole of reaction events is $F = eN_A$ where F is the Faraday constant. Hence, the *cathodic current density* i_c, arising from the reduction is given by

$$i_c = F k_c [Ox] \qquad ... (153)$$

An opposing *anodic current density* i_a, arising from oxidation is given by

$$i_a = F k_a [Red] \qquad ...(154)$$

where the k_is are the corresponding rate constants. Hence, the net *current density* at the electrode is given by

$$i = i_a - i_c = F k_a [Red] - F k_c [Ox] \qquad ...(155)$$

$$= F B_a [Red] \exp(-\Delta G_a^{\neq}/RT) - F B_c [Ox] \exp(-\Delta G_c^{\neq}/RT) \qquad ...(156)$$

where we have made use of Eq. 152 and assumed that Gibbs free energy of activation is different for the cathodic and anodic processes. When $i_a > i_c$ so that $i > 0$, the current is anodic and when $i_c > i_a$ so that $i < 0$, the current is cathodic.

Let us consider a reduction reaction. As an electron is transferred from one electrode to another, the electrical work done is $e\Delta\phi$, where e is the electronic charge and $\Delta\phi$ is the potential difference between the electrodes. Hence, the Gibbs free energy of activation is changed from $\Delta G^{\neq}$ to $\Delta G^{\neq} + F\Delta\phi$, if the transition state corresponds to Ox being very close to the electrode. Thus, if $\Delta\phi > 0$, more work has to be done to bring Ox to its transition state, with the result that Gibbs free energy of activation is increased. On the other hand, if the transition state corresponds to Ox being *far from the electrode.* (*i.e.*, close to the outer plane of the double layer), then $\Delta G^{\neq}$ is independent of $\Delta\phi$. In practice, however, the situation is midway between the two extremes. Hence, we can write the Gibbs free energy of activation for reduction as $\Delta G^{\neq} + \alpha F\Delta\phi$, where α, called the **transfer coefficient** or symmetry factor, lies between 0 and 1, *i.e.*, $0 < \alpha < 1$.

Let us next consider the oxidation of Red. Here Red discards an electron to the electrode with the result that the extra work needed for reaching the transition state is zero if this state lies close to the electrode. If that state lies away from the electrode (*i.e.*, close to the outer plane of the double layer), the work needed is $-F\Delta\phi$, so that $\Delta G^{\neq}$ changes to $\Delta G^{\neq} - (1 - \alpha) F\Delta\phi$. Substituting for the two Gibbs free energies of activation in Eq. 166, we obtain the following expression for the current density :

$$i = \{FB_a [Red] \exp(-\Delta G_a^{\neq}/RT)\} e^{(1-\alpha) F\Delta\phi/RT} - \{FB_c [OX] \exp(-\Delta G_c^{\neq}/RT)\} e^{-\alpha F\Delta\phi/RT} \qquad ...(157)$$

$$= i_a - i_c \qquad ...(158)$$

At equilibrium, $\Delta\phi = \Delta\phi_{eq}$ and the net current is zero and the equilibrium current densities are equal. Thus, if the potential difference differs from its equilibrium value by the overpotential η, so that

$$\eta = \Delta\phi - \Delta\phi_{eq}, \qquad ...(159)$$

the two current densities are :

$$i_a = \{FB_a[Red] \exp(-\Delta G_a^{\neq}/RT)\} e^{(1-\alpha)F\Delta\phi_{eq}/RT} e^{(1-\alpha)\eta F/RT}$$

$$= i_{a,e} e^{(1-\alpha)\eta F/RT} \qquad ...(160)$$

$$i_c = \{FB_c\,[\mathrm{Ox}] \exp(-\Delta G_c^{\neq}/RT)\}\, e^{-\alpha F \Delta\phi_{eq}/RT}\, e^{-\alpha\eta F/RT}$$

$$= i_{a,e}\, e^{-\alpha\eta F/RT} \qquad ...(161)$$

Since the two equilibrium current densities, $i_{a,e}$ and $i_{c,e}$ are equal, we can drop the subscripts and designate each of them as i_o, the *exchange current density* and write

$$i = i_0 \{e^{(1-\alpha)\eta F/RT} - e^{-\alpha\eta F/RT}\} \qquad ...(162)$$

Eq. 162 is the well known **Butler-Volmer equation.**

Let us examine the exponentials in Eq. 162. When the overpotential η is very small so that $\eta F/RT \ll 1$, we can use the series expansion

$$e^x = 1 + x + \frac{x^2}{2!} + \ldots..$$

to obtain

$$i = i_0 \{[1 + (1-\alpha)\eta F/RT + \cdots] - [1 - (\alpha\eta F/RT) + \cdots]\} \qquad ...(163)$$

$$= i_0\, \eta F/RT \qquad ...(164)$$

From Eq. 164 we see that the *current density is proportional to the overpotential.* It is evident from Eq. 164, that

$$\eta = (RT/F)(i/i_0) \qquad ...(165)$$

When η is small and positive, the current is anodic ($i > 0$ when $\eta > 0$) and when η is small and negative, the current is cathodic ($i < 0$ when $\eta < 0$).

When the overpotential is large and positive (which is the case of an electrode being an anode in electrolysis), the second exponential in Eq. 172 is much smaller than the first and may be neglected, giving

$$i = i_0\, e^{(1-\alpha)\eta F/RT} \qquad ...(166)$$

Hence, taking logs of both sides

$$\ln i = \ln i_0 + (1-\alpha)\eta F/RT \qquad ...(167)$$

When the overpotential is large but negative (corresponding to the cathode in electrolysis), the first exponential in Eq. 162 is much smaller than the second and may be neglected and we have

$$i = -\,i_0\, e^{-\alpha\eta F/RT} \qquad ...(168)$$

so that $\ln(-i) = \ln i_0 - \alpha\eta F/RT$ ...(169)

Eqs. 167 and 169 are called the **Tafel equations.**

Fig. 26 shows the plot of the current density i versus the overpotential η in accordance with the Butler-Volmer equation. We consider two cases labelled *A* and *B*. In the case *A* there are high exchange current densities i_0 at both electrodes. (The individual electrode curves are lebelled A' and A''). In this case even a small overpotential will produce appreciable flow through

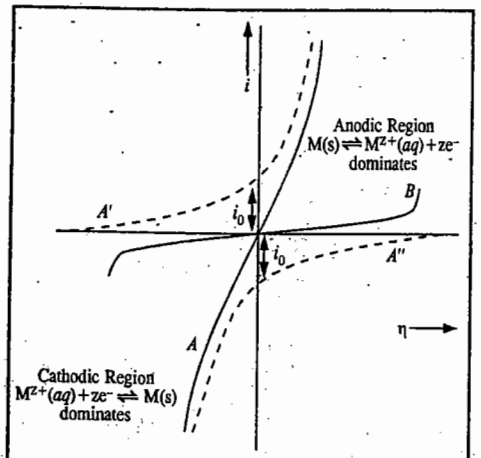

Fig. 26. Variation of current density with overpotential in accordance with the Butler-Volmer equation.

the cell. The other case *B* corresponds to very low exchange current density i_0. In this case, a large value of overpotential is required to cause appreciable current flow through the cell. Thus, we see that it is the exchange current density i_0 which, according to the Butler-Volmer equation, determines the activation overpotential. The shape of the current density *versus* overpotential curves is evidently determined by the value of the transfer coefficient α which can be determined by fitting the experimental curve into the Butler-Volmer equation.

The transfer coefficient can also be determined from the **Tafel plot**, which is the plot of the logarithm of the current density against the overpotential (Fig. 27). The linear portions of the curves in Fig. 27 agree with the Tafel equation. From the slope and the intercept of the Tafel plot, α and i_0 can be determined.

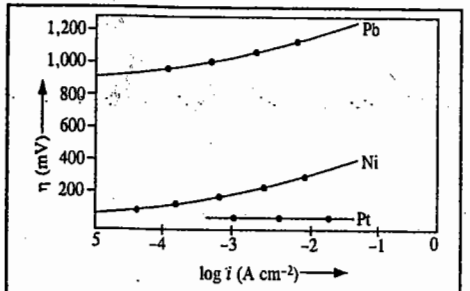

Fig.27. Variation of overpotential for the discharge of H^+ ion on the various metals with current density

Example 1. At 25°C the exchange current density of a Pt | $H_2(g)$ | $H^+(aq)$ electrode is 0·79 mA cm^{-2}. Calculate the current flowing through a standard eletrode of area 5·0 cm^2 when the overpotential is +5·0 mV.

Solution : From Eq. 165,

$$\eta = \frac{RT}{F}(i/i_0) \text{ so that}$$

$$i = i_0 \eta F/RT = \frac{(0{\cdot}79\,\mathrm{mA\,cm^{-2}})(5{\cdot}0\,\mathrm{mV})(96{,}485\,\mathrm{C\,mol^{-1}})}{(8{\cdot}314\,\mathrm{J\,K^{-1}})(298\mathrm{K})}$$

$$= 0{\cdot}15\ \mathrm{mA\ cm^{-2}}$$

Current, $I = iA = (0{\cdot}15\ \mathrm{mA\ cm^{-2}})(5{\cdot}0\ \mathrm{cm^2}) = 0{\cdot}75\ \mathrm{mA}$

Example 2. The following data were obtained on the anodic current through a platinum electrode of area 2·0 cm^2 in contact with an Fe^{3+}/Fe^{2+} aqueous solution at 25°C.

η (mV)	50	100	150	200	250
i_a (mA)	8·8	25·0	58·0	131	299

Calculate the exchange current density and the transfer coefficient for the electrode process using the Tafel plot.

Solution : Here the anodic process involves the oxidation reaction $Fe^{2+} \longrightarrow Fe^{3+} + e^-$.

Let us draw up the following Table :

η (mV)	50	100	150	200	250
i_a (mA cm^{-2})	4·4	12·5	29·0	65·5	149·5
ln i_a (mA cm^{-2})	1·48	2·53	3·37	4·18	5·01

The reader can plot ln i_a versus η (Tafel plot). The intercept at $\eta = 0$ gives ln i_0 and the slope is $(1-\alpha)\,F/RT$. The high overpotential region gives a straight line with intercept = 0·92 and slope = 0·0163. Since ln i (mA cm^{-2}) = 0·92, we have $i_0 = 2{\cdot}5$ mA cm^{-2}. From the slope, $(1-\alpha)\,F/RT = 0{\cdot}0163$ mV, whence $\alpha = 0{\cdot}58$.

Example 3. At 25°C the exchange current density for the reaction $H^+(aq) + e^- \longrightarrow \frac{1}{2}H_2(g)$ on the nickel surface is $1{\cdot}00\times10^{-2}$ mA cm^{-2}. Calculate the current density required to attain an overpotential of 100 mV, using (*a*) the Butler-Volmer equation (*b*) the Tafel equation. Assume that the transfer coefficient, $\alpha = 0{\cdot}50$.

Solution : Here $\eta \approx 100$ mV : $a = 0{\cdot}50$; $i_0 = 1{\cdot}00\times10^{-2}$ mA cm^{-2}

(*a*) $i = i_0\,[e^{(1-\alpha)\eta F/RT} - e^{-\alpha\eta F/RT}]$ (Butler-Volmer Equation)

Substituting the given data and then evaluating the two exponentials, we find that

$$i = 6{\cdot}85\times10^{-2} \text{ mA cm}^{-2}$$

(*b*) Using the Tafel equation we find that

$$i = 6{\cdot}99\times10^{-2} \text{ mA cm}^{-2}$$

Diffusion Overpotential

Most of the electrode reactions in solution are diffusion-controlled. The diffusion-controlled surface reactions were first investigated by W. Nernst in 1904. Consider a steady-state diffusion towards a stationary plane electrode immersed in a solution. Assume that the solution is vigorously stirred so that a very thin layer of thickness of the order of 0·01mm, adjacent to the electrode surface functions as a diffusion layer called the **Nernst diffusion layer.** In the Nernst model, the concentration of the ion being discharged at the electrode is constant in the bulk of the solution. It declines rapidly and evenly through the Nernst diffusion layer (Fig. 28).

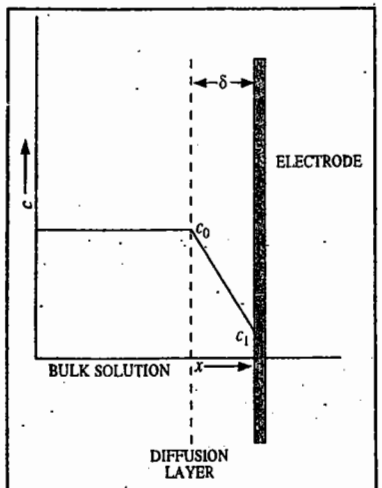

Fig. 28. Steady-state diffusion of the ions in the Nernst diffusion layer.

Let us consider the discharge of Cu^{2+} ions and deposition of copper on the cathode. With the removal of Cu^{2+} ions from the solution at the electrode, a layer of electrolyte solution of thickness δ is formed in which the concentration of Cu^{2+} ions is depleted. The rate of diffusion of Cu^{2+} across the layer is equal to the rate of deposition of Cu on the cathode. According to Fick's first law of diffusion, the amount of Cu deposited on the electrode is given by

$$-\frac{dn}{dt} = DA(dc/dx) = DA(c_0 - c_1)/\delta \qquad ...(170)$$

where A is the area of the electrode and c_0 and c_1 are the concentrations of Cu^{2+} ions in the bulk electrolyte solution and the electrode surface, respectively and D is the diffusion coefficient of Cu^{2+} ion

The diffusion current to the cathode is given by

$$i_d = -nF(dn/dt) = nFDA(c_0 - c_1)/\delta \qquad ...(171)$$

where n is the number of Faradays transferred in the reduction reaction

$$Cu^{2+}(aq) + 2e^- \rightleftharpoons Cu(s)$$

Here $n=2$. As a result of the difference in the activity of Cu^{2+} ion across the double layer there occurs a potential difference, called the **diffusion overpotential,** η_D, which can be calculated from the expression analogous to that of a concentration cell, *viz.*,

$$\eta_D = \frac{RT}{nF} \ln (a_1/a_0) \qquad ...(172)$$

Since $\gamma = a/c$, where γ is the activity coefficient, we find from Eq. 172 that

$$\eta_D = \frac{RT}{nF} \ln (\gamma_1 c_1/\gamma_0 c_0) \qquad ...(173)$$

Rearranging, we obtain

$$c_1 = c_0(\gamma_0/\gamma_1) \exp\left(\frac{nF\eta_D}{RT}\right) \qquad ...(174)$$

From Eqs. 171 and 174, $$\eta_D = \frac{RT}{nF} \ln\left[\frac{\gamma_1}{\gamma_0}\left(1 - \frac{\delta i_d}{Ac_0 DnF}\right)\right] \qquad ...(175)$$

The limiting value of i_d corresponds to the discharge of each ion striking the electrode so that $c_1 = 0$ and from Eq. 171 we obtain

$$i_{max} = nFDAc_0/\delta \qquad ...(176)$$

Assume that $\delta \approx 10^{-2}$ cm and $D \approx 10^{-5}$ cm^2 s^{-1}. Then from Eq. 176, i_{max} is about $10^2 c_0 A$ cm^{-2} when c_0 is in mol cm^{-3}. If we further assume that $\gamma_1/\gamma_0 \approx 1$, we obtain from Eqs. 175 and 176,

$$\eta_D = \frac{RT}{nF} \ln (1 - i_d/i_{max}) \qquad ...(177)$$

V. IRREVERSIBLE ELECTRODE PROCESSES

In Chapter 24, we dealt with reversible EMFs, the measurements of which are made under conditions when practically no current flows through the cell. Practical applications of electrochemistry, however, involve appreciable current flow. The electrode processes studied under these conditions are called **irreversible electrode processes,** the most important of which are :

1. Overvoltage and 2. Polarography

Both the processes are discussed below in some details.

OVERVOLTAGE

It is a common experience that in electrolysis, the potential at which metal ions start depositing at appreciable rates on the cathode is generally close to the reversible electrode potential of the same metal. For example, the reversible electrode potential of zinc in contact with 1 M solution of Zn^{2+} ions is – 0·76 volt. It is known from experiment that the potential at which Zn^{2+} ions deposit on zinc rod used as cathode is also close to or only slightly higher (*i.e.*, more negative) than – 0·76 volt. However, in some cases, particularly in the case of evolution of gases, say, hydrogen at cathode or oxygen at anode, the potential required is much higher than the reversible potential of hydrogen or oxygen electrode in the same solution. *The difference between the potential of the electrode when gas evolution is actually observed and the theoretical (i.e., reversible) value for the same evolution is called the* **overvoltage.**

TABLE 3

Hydrogen and Oxygen Bubble Overvoltages

Electrode	Hydrogen overvoltage (volt)	Oxygen overvoltage (volt)
Platinised platinum	0·00	0·25
Iron	0·08	0·24
Smooth platinum	0·09	0·43
Nickel	0·22	0·06
Cadmium	0·48	0·43
Lead	0·64	0·32
Zinc	0·70	....
Mercury	0·80	....

This overvoltage is sometimes referred to as the **bubble overvoltage** as it is observed just at the point at which gas bubbles begin to appear. The values for hydrogen overvoltage, using different metals as the cathode at low current density are given in Table 3.

It is evident that the value varies largely with the nature of the metal. The occurrence of overvoltage indicates that some step involved in the process of evolution of hydrogen at the cathode is slow.

The evolution of oxygen at a metal anode also involves overvoltage. The values for bubble overvoltage of oxygen using different metals as anode at low current density are also given in Table 3.

Applications of Overvoltage. 1. Electrodeposition of Metals in Aqueous Solutions. Consider electrolysis of a solution which is molar with respect to zinc sulphate as well as sulphuric acid. The reversible standard electrode potentials ($E°$) of hydrogen and zinc are ± 0·00 and – 0·76 volt, respectively. Evidently, hydrogen alone should be liberated at the cathode. The deposition of zinc on the

cathode should commence only after all the H^+ ions have been reduced to hydrogen gas. But, in actual practice, it has been found that zinc starts depositing along with liberation of hydrogen in spite of a large difference in their reversible potentials. The reason lies in the high overvoltage for hydrogen evolution at a zinc cathode, the value for which is about 0·7 volt. In other words, this value is very close to the reversible potential of zinc. This explains almost simultaneous evolution of hydrogen and deposition of zinc. Hence, metals such as iron can be electroplated by zinc in acidic solution. If there were no hydrogen overvoltage, it would not have been possible to do so. Hydrogen alone would have been evolved. Thus, in the absence of high overvoltage of hydrogen, zinc-plating would not have been possible at all.

Let us consider the electrolysis of a neutral solution (*p*H 7) of a cadmium salt. The reversible electrode potential of hydrogen at *p*H 7 comes out to be – 0·41 V. If there were no hydrogen overvoltage, hydrogen and cadmium would have been produced together during electrolysis since $E°$ for Cd is –0·40 V. However, since the overvoltage of hydrogen over cadmium at the operational current density of 1 milliampere cm^{-2} is about 0·99 volt, no hydrogen will be evolved unless a potential of about one volt is applied. As a result of this, during electrolysis at about 0·9 volt, only cadmium is deposited.

2. Corrosion of Metals. Consider the dissolution of lead in hydrochloric acid. The standard electrode potential ($E°$) of lead is – 0·13 volt. It should, therefore, dissolve readily in dilute hydrochloric acid, evolving hydrogen. Zinc ($E° = -0·76$ volt) should do so even much more readily. However, in actual practice, neither lead nor pure zinc dissolves in hydrochloric acid and no evolution of hydrogen occurs. This is because of hydrogen overvoltage. The bubble overvoltage of hydrogen over lead is 0·64 volt and that over zinc is 0·70 volt.

However, if *pure* zinc is connected to a piece of copper and both are dipped in a dilute acid solution (as in a simple voltaic cell), the dissolution of zinc takes place very readily and hydrogen is evolved at the copper electrode. In this case, while zinc electrode dissolves to produce Zn^{2+} ions, the hydrogen ions are discharged and evolved as hydrogen gas at the copper electrode, the bubble overvoltage of hydrogen over copper being only 0·2 volt. Similar effect is observed if zinc contains copper or any other metal having low hydrogen overvoltage as an *impurity*. In such a case zinc dissolves producing Zn^{2+} ions while hydrogen is liberated on the copper part (or any impurity part) of the zinc rod itself. *This results in corrosion or dissolution of zinc.* The same thing can happen to any other base metal (iron, lead, etc.) if it contains a metal with low hydrogen overvoltage as an impurity.

In the presence of oxygen or air or an oxidising agent (depolariser), there may be no evolution of hydrogen gas as it may get oxidised as soon as formed. There is thus no evolution of the gas. Therefore, even if a base metal (like zinc, lead, iron, etc.) contains a metal with high hydrogen overvoltage, it will dissolve in acid solution readily in the presence of air or oxygen. This is the reason why iron present in 'tin plate' gets readily corroded in air. But in the absence of oxygen or air it does not dissolve at all because of high hydrogen overvoltage over tin.

It is also a well known laboratory experience that pure lead and pure zinc which, ordinarily, do not dissolve in acid solutions, do so if air is bubbled through the acid solution.

Inhibition of Corrosion. Several techniques can be employed for inhibiting corrosion. Coating the surface with an impermeable layer (such as a paint) helps to prevent the access of damp air. If, however, the paint becomes porous, this protection fails disastrously because then oxygen has access to the exposed metal and corrosion continues beneath the paint work. **Galvanizing,** *i.e.*, the coating of iron with zinc, is another form of surface coating. Since $E°_{(Fe^{2+}, Fe)}$ is –0·44 V while $E°_{Zn^{2+}, Zn}$ is –0·76 V, the corrosion of zinc is favoured thermodynamically and iron survives. The zinc survives because it is protected by a layer of hydrated oxide. The oxides are inert kinetically because they adhere to the metal surface forming an imperetrable layer over a fairly wide range. This kinetic protection, called **passivation**, can be interpreted as a method of decreasing the exchange currents by sealing the surface.

Another method of protection involves changing the electrical potential of the metal to be protected by pumping in electrons that can be used to satisfy the demands of oxygen reduction without involving the oxidation of the metal. Thus, in **cathodic protection,** the metal to be protected is connected to a metal with a more negative standard potential (such as magnesium, $E_{Mg^{2+}, Mg}$ –2·36 V). The maganesium acts as a **sacrificial anode,** supplying its own electrons to the iron and becoming oxidized to Mg^{2+} in the process, thereby eliminating the need for iron to transfer its own electrons.

POLAROGRAPHY

Polarography is based on the electrolysis of a minute fraction of a solution by using a cell that consists of a 'polarizable' microelectrode (*i.e.*, an electrode whose potential changes from its reversible value) such as a dropping mercury electrode and a 'non-polarizable' current-carrying electrode (*i.e.*, an electrode whose potential does not change from its reversible value) such as a calomel electrode. The data are obtained by measuring the current as a function of the applied voltage. The current-voltage curve is called a **polarogram.** The polarographic technique was developed in 1922 by the Czech chemist, Jaroslav Heyrovsky (1890-1967). He was awarded the Chemistry Nobel Prize in 1959 for the development of polarographic methods of analysis.

In polarography, the rate-determining step in the discharge of ions is essentially **diffusion.** The technique explicitly depends upon *concentration polarization* produced at the microelectrode.

Concentration Polarization. Let us consider a metal rod M dipping in its ions M^+ of, say, molar concentration. The electrode M^+, M will develop a certain potential depending upon the tendency of the metal to change into ions and the concentration of the ions in solution , in accordance with the Nernst equation. Suppose, the metal is made the cathode and the potential applied is slightly greater than the reversible potential of the electrode M^+, M. The metal ions will begin to be discharged ($M^+ + e^- \longrightarrow M$) and there will be a fall in the concentration of ions in the vicinity of the metal electrode. If the fall in concentration is not made good by instantaneous migration of the M^+ ions from the bulk of the solution to the cathode surface, there will be a fall in concentration of the ions in the immediate vicinity of the metal rod. The potential of the electrode M^+, M will, thus, decrease in accordance with the Nernst equation

$$E_{(M^+, M)} = E^0_{(M^+, M)} + \frac{RT}{nF} \ln [M^+] \qquad \ldots(178)$$

Similarly, if the metal M is made the anode and the potential is *slightly* more than the reversible potential of the electrode M^+, M, the metal will begin to dissolve giving M^+ ions ($M \longrightarrow M^+ + e^-$). If these ions do not migrate or diffuse away from the anode towards the bulk of the solution as fast as they are produced, there will be an increase in the concentration of the M^+ ions in the vicinity of the metal rod. As a result, the potential of the electrode M^+, M would increase.

This phenomenon of the departure of the electrode potential (increase or decrease) from the reversible value as a result of the change of concentration in the vicinity of the electrode, is known as **concentration polarization.** It is evident from the above discussion that concentration polarisation arises out of the slow diffusion of the ions *towards* or *away* from the electrode. There will be no concentration polarisation if the change in concentration of the ions around the electrode is compensated *instantaneously* by quick migration of the ions away from or towards the electrode, as the case may be.

The evidence for the existence of concentration polarisation at an electrode is furnished by the fact that its magnitude decreases by agitating the solution or by raising the temperature. Both these factors tend to increase the migration of the ions.

Let us suppose that the metal rod M is made sufficiently cathodic to enable the M^+ ions to get discharged when they come in contact with the rod.

As already mentioned, owing to slow diffusion there will be a fall of concentration of ions in the immediate vicinity of the electrode resulting from the depletion of the ions. Consequently, a concentration gradient will be set up between the electrode and the bulk of the solution. The concentration will be minimum at the electrode surface and will gradually increase in passing from the

electrode to the electrolyte till at a certain distance, it becomes equal to the bulk concentration. This is represented by the curve *PQR* in Fig. 29 where *P* represents the concentration *(c)* at the electrode surface and *R* represents the bulk concentration (c^0). For the sake of convenience, the gradient *PQR* may be considered as mathematically equivalent to the linear gradient *PS*. The distance from *Y* to *S* is known as the **diffusion layer.**

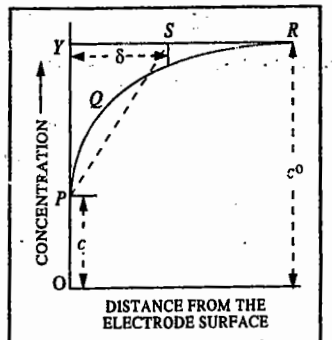

Fig. 29. Concentration gradient due to slow diffusion of ions.

Now, according to Fick's first law of diffusion, the rate of diffusion dc/dt of an ion across the layer *YS*, is given by the expression

$$\frac{dc}{dt} = \frac{AD}{\delta}(c^0 - c) \qquad ...(179)$$

where *A* is the exposed area of the electrode surface, *D* is the diffusion coefficient of the ionic species, δ is the thickness of the diffusion layer, *c* is the ionic concentration at the electrode surface and c^0 is the bulk concentration. On the attainment of equilibrium, the rate of discharge of the ions by the current becomes equal to the rate of diffusion of the ions towards the electrode. Since one faraday of electricity is associated with the discharge of 1 gram equivalent of an ion, it is evident that *nF* coulombs will be associated with the discharge of 1 mole of the ion, where *n* is the valency of the ion. The value of *n* also gives the number of moles of electrons involved in the discharge of the ion (*e.g.*, $n=2$ for the discharge of Zn^{2+} ion). If *i* is the current and *A* is area, then, the rate of discharge of ions = i/nF.

$$\therefore \quad \frac{i}{nF} = \frac{DA}{\delta}(c^0 - c) \qquad ...(180)$$

In the derivation of Eq. 180 it is assumed that the ionic species which is being discharged is brought to the electrode surface only by diffusion. In actual practice, the cationic species may also be carried by *convection* as well as by the normal process of electrolytic *transference*. If the solution is kept unstirred, convection is eliminated. But, the transference will be there. If t_+ is the transport number of the cation being discharged, the rate at which the cations are brought to the electrode surface due to transference, will be equal to $t_+ i/nF$. Hence, Eq. 180 is modified as

$$\frac{i}{nF} = \frac{DA}{\delta}(c^0 - c) + \frac{t_+ i}{nF} \qquad ...(181)$$

or
$$\frac{i}{nF} - \frac{t_+ i}{nF} = \frac{DA}{\delta}(c^0 - c) \qquad ...(182)$$

$$\therefore \quad i = \frac{DnFA}{(1-t_+)\delta}(c^0 - c) \qquad ...(183)$$

$$= \frac{DnFA}{t\delta}(c^0 - c) \qquad ...(184)$$

where *t*, written in place of $(1 - t_+)$, represents the sum of the transport numbers of all ions *other than the ion which is being discharged*. If the electrolysis is carried out in the presence of an excess of an *indifferent electrolyte* whose ions are not discharged at the applied potential, then almost the entire amount of current will be carried by the ions of the indifferent electrolyte. Such electrolytes are known as **supporting electrolytes.** In the presence of a supporting electrolyte, the value of *t* in Eq. 184, evidently, becomes almost unity. Hence,

$$i = \frac{DnFA}{\delta}(c^0 - c) \qquad ...(185)$$

$$= k\,(c^0 - c) \qquad ...(186)$$

where *k* is written for the factor $DnFA/\delta$, for the sake of brevity.

$$\therefore \quad c = c^0 - i/k \qquad ...(187)$$

Since the concentration of the key ion (*i.e.*, the ion which is being discharged), in the immediate vicinity of the electrode is *c*, the actual reversible potential of the electrode will be given by the Nernst equation, *viz.*,

$$E = E^0 + \frac{RT}{nF}\ln c \qquad ...(188)$$

When no current flows, the concentration of the key ion in contact with the electrode is the same as the bulk concentration. The reversible potential of the electrode will then be given by

$$E' = E^0 + \frac{RT}{nF}\ln c^0 \qquad ...(189)$$

Evidently, the numerical value of the concentration polarisation is equal to $E' - E$. Thus,

$$E' - E = \Delta E = \frac{RT}{nF}\ln\frac{c^0}{c} \qquad ...(190)$$

Substituting the value of *c* from Eq. 187, in Eq. 190, we get

$$\Delta E = \frac{RT}{nF}\ln\frac{kc^0}{kc^0 - i} \qquad ...(191)$$

It can be shown that, when *i* is small, ΔE is small and it is approximately proportional to *i*. As the current is increased and as it approaches the value of kc^0, ΔE begins to increase very rapidly and ultimately when *i* becomes equal to kc^0, ΔE should theoretically increase to infinity. This behaviour is illustrated in Fig. 30. In actual practice, however, ΔE does not increase to infinity. It increases only to a finite value until the discharge of another cation, *e.g.*, hydrogen ion or the cation of the supporting electrolyte, takes place.

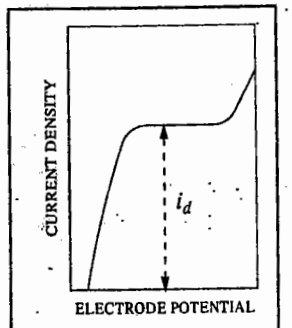

Fig. 30. Variation of concentration polarization with current density.

The current at which the rapid increase of potential takes place is known as the **limiting current density** (i_d) because it represents the limiting rate at which the particular ionic species can be discharged under the given experimental conditions. The value of limiting current is thus given by

$$i_d = \frac{DnF}{\delta}c^0 \qquad ...(192)$$

The electrolysis current obtained as above is commonly referred to as the **diffusion current** because the ions which are discharged at the electrode to produce the current are brought to the electrode by the process of diffusion only.

It follows from Eqs. 185 and 192 that the electrolysis current *i* approaches the limiting value i_d when $c=0$, *i.e.*, when the concentration of the key ions at the electrode surface is zero. This, in effect, means that the magnitude of the current density is such that all the key ions which migrate to the electrode surface get discharged instantaneously. Since under such conditions, the concentration at the electrode surface is zero, the concentration gradient becomes equal to the bulk concentration. Since, now the concentration gradient is maximum and also constant (as long as c^0 is constant), therefore, the rate of diffusion also becomes maximum and constant. Hence, the diffusion current also becomes maximum and constant. It is frequently known as the **limiting diffusion current.**

The current i, given by Eq. 198, is the diffusion current, i_d, *i.e.*, we can write

$$i_d = nFAD^{1/2}c^0/(\pi t)^{1/2} \quad ...(199)$$

The DME is a spherical electrode of expanding radius and surface area. Its surface area changes with the age of the drop. Ilkovic assumed linear diffusion for the current for DME. He calculated the surface area of the electrode-electrolyte boundary, A_t, at time t, as follows :

$$\text{Drop volume at time } t = \tfrac{4}{3}\pi r_t^3 \quad ...(200)$$

$$\text{Drop mass at time } t = \text{volume} \times \text{density} = \tfrac{4}{3}\pi r_t^3 \rho \quad ...(201)$$

where ρ is the density of mercury and r_t is the drop radius at time t.

If m is the mass rate of flow of mercury, then the drop mass at time t is equal to mt. Hence,

$$\tfrac{4}{3}\pi r_t^3 \rho = mt \quad \text{or} \quad r_t = \left(3mt/(4\pi\rho)\right)^{1/3} \quad ...(202)$$

$$A_t = 4\pi r_t^2 = 4\pi\left(3mt/(4\pi\rho)\right)^{2/3}$$

$$= 4\pi\left(3/4\pi\rho\right)^{2/3} m^{2/3}\, t^{2/3} \quad ...(203)$$

$$= 0{\cdot}8515\, m^{2/3}\, t^{2/3} \quad ...(204)$$

Substituting this value of area in Eq. 199, we get

$$i_d = nFD^{1/2}\frac{c^0}{(\pi t)^{1/2}} \times 0{\cdot}8515\, m^{2/3}\, t^{2/3} \quad ...(205)$$

As the mercury drop grows, the linear diffusion process is disturbed. The electrode surface moves into a region where there has yet been no depletion of ions due to electrolysis. This results in larger concentration at the electrode surface than that stipulated for a stationary electrode surface. To take into account this effect, Ilkovic introduced a correction of $(7/3)^{1/2}$ for the current thereby changing Eq. 205 to

$$i_d = (7/3)^{1/2}\,(0{\cdot}8515)\, n\, \mathrm{F}\, D^{1/2}\, m^{2/3}\, t^{2/3}\, c^0/(\pi t)^{1/2} \quad ...(206)$$

This equation, on simplification, taking $F = 96{,}485$ C mol^{-1}, becomes

$$i_d \text{ (in microamperes)} = 708\, n\, m^{2/3}\, t^{1/6}\, c^0\, D^{1/2} \quad ...(207)$$

where m is in units of milligram per second; c^0 is in milliomoles dm^{-3}; t is in seconds, D is in cm^2 s^{-1}.

If t is the drop time for DME, Eq. 207 gives the maximum value of the diffusion current for the DME for a particular applied potential.

Thus, $$i_d \text{ (maximum)} = 708\, n\, m^{2/3}\, t^{1/6}\, D^{1/2}\, c^0 \quad ...(208)$$

The average value of i_d during the life of a drop is estimated to be 6/7th of its maximum value at the time of drop fall, that is

$$i_d \text{ (average)} = 607\, n\, m^{2/3}\, t^{1/6}\, D^{1/2}\, c^0 \quad ...(209)$$

Both the forms of Ilkovic equation (*viz.*, Eqs. 208 and 209) show that i_d is directly proportional to the bulk concentration $c°$ of the ions reducible at the DME. Thus,

$$i_d = k\, c^0 \quad ...(210)$$

Half-Wave Potential. The half-wave potential, $E_{1/2}$, is *characteristic of the electroactive material.* Consider the reversible and rapid half-cell reaction at the microelectrode

$$\mathrm{Ox} + ne \longrightarrow \mathrm{Red}$$

where Ox is the substance being reduced and Red stands for the product. The constituents of the thin layer in the film surrounding the microelectrode are in *instantaneous equilibrium* with the electrode surface. Hence, the electrode potential is given by the Nernst equation. Accordingly,

$$E_{\text{cathode}} = E^0 - \frac{0{\cdot}0591}{n}\log\frac{[\mathrm{Red}]_0}{[\mathrm{Ox}]_0} \quad ...(211)$$

where the zero subscripts denote that the concentrations apply only to the film surrounding the DME which acts as cathode. The applied potential is given by

$$E_{\text{applied}} = E_{\text{cathode}} + E_{\text{anode}} \quad ...(212)$$

The anode is the saturated calomel electrode (SCE). Hence, we can write

$$E_{\text{applied}} = E^0 - \frac{0{\cdot}0591}{n}\log\frac{[\mathrm{Red}]_0}{[\mathrm{Ox}]_0} + E_{\text{SCE}} \quad ...(213)$$

$$E_{\text{applied}} - E_{\text{SCE}} = E^0 - \frac{0{\cdot}0591}{n}\log\frac{[\mathrm{Red}]_0}{[\mathrm{Ox}]_0} \quad ...(214)$$

Suppose in the beginning, the solution at the electrode surface consists only of the oxidized form. When the applied voltage is sufficiently large to reduce some of the oxidant, the oxidant concentration at the electrode surface starts decreasing. Some ions move towards the surface of the microelectrode from the bulk of the solution building up a concentration gradient. Thus, at the applied voltage, the observed current is given by

$$i = K([\mathrm{Ox}] - [\mathrm{Ox}]_0) \quad ...(215)$$

where K stands for the capillary characteristics and other constants of the Ilkovic equation. At the diffusion current plateau, the concentration of the oxidant at the electrode surface is virtually zero so that the diffusion current is given by

$$i_d = K\,[\mathrm{Ox}] \quad ...(216)$$

Subtracting Eq. 216 from Eq. 215, we get

$$[\mathrm{Ox}]_0 = (i_d - i)/K \quad ...(217)$$

Again, the concentration of the product Red at the electrode surface, provided it is soluble, is also given by

$$i = K'\,[\mathrm{Red}]_0 \quad ...(218)$$

where K' is another constant analogous to K.

or $$[\mathrm{Red}]_0 = i/K' \quad ...(219)$$

Substituting Eqs. 217 and 218 into Eq. 214, we obtain

$$E_{\text{applied}} - E_{\text{SCE}} = E^0 - \frac{0{\cdot}0591}{n}\log\left[\frac{i}{i_d - i} \times \frac{K}{K'}\right]$$

Rewriting, $$E_{\text{applied}} = E_{\text{SCE}} + E^0 - \frac{0{\cdot}0591}{n}\log\frac{K}{K'} - \frac{0{\cdot}0591}{n}\log\frac{i}{i_d - i} \quad ...(220)$$

By definition, when $i = i_d/2$, $E_{\text{applied}} = E_{1/2}$. ...(221)

Here, $n = 2$; $c = 5\times10^{-4}$ M or 0·5 millimoles dm^{-3}, mass of Hg = 0·0750 g/20 drops = 3·75 mg/drop; $i_d = 4{\cdot}0$ μA. Thus,

$$m = (3{\cdot}75 \text{ mg/drop})\ (24/60 \text{ drop s}^{-1}) = 1{\cdot}5 \text{ mg s}^{-1}$$

$$t = 60/24 \text{ drops} = 2{\cdot}5 \text{ s drop}^{-1}$$

Substituting the data in the Ilkovic equation, *viz*, $i_d = 607\ n\ m^{2/3}\ t^{1/6}\ D^{1/2}\ c^0$, we have

$$4{\cdot}0 = 607\times2\times D^{1/2}\times(1{\cdot}5)^{2/3}\times(2{\cdot}5)^{1/6}\times(0{\cdot}5)$$

$$\therefore \quad D = \left[\frac{4.0}{607\times2(1.5)^{2/3}\times(2.5)^{1/6}\times(0.5)}\right]^2 = 1{\cdot}9\times10^{-5} \text{ cm}^2 \text{ s}^{-1}$$

4. Determination of the Stability Constant of a Metal-Ion Complex. Consider the reduction of a metal ion at the DME :

$$Ox + ne \rightleftharpoons Red \qquad ...(224)$$

The Nernst equation corresponding to this electrode reaction is

$$E = E^0 - \frac{0{\cdot}0591}{n}\log\frac{[Red]}{[Ox]} \qquad ...(225)$$

Suppose a complexing agent X forms a complex with the metal ion :

$$Ox + pX \rightleftharpoons OxX_p \qquad ...(226)$$

The stability constant of this complex is given by

$$K = \frac{[OxX_p]}{[Ox][X]^p} \qquad ...(227)$$

$$\therefore \quad [Ox] = \frac{[OxX_p]}{K[X]^p} \qquad ...(228)$$

Substituting in Eq. 225, we get

$$E = E^0 - \frac{0{\cdot}0591}{n}\log\frac{K[Red][X]^p}{[OxX_p]} \qquad ...(229)$$

At the half-wave potential, one-half of the oxidized form reaching the DME is reduced to the corresponding reduced form. Thus, when [Ox] = [Red], we have, for the *simple* metal ion,

$$(E_{1/2})_s = E_1 \qquad ...(230)$$

Similarly, for the reduction of the metal-ion complex,

$$(E_{1/2})_c = E_1 - \frac{0{\cdot}0591}{n}\log K[X]^p \qquad ...(231)$$

From Eqs. 230 and 231,

$$(E_{1/2})_s - (E_{1/2})_c = \frac{0{\cdot}0591}{n}\log K[X]^p \qquad ...(232)$$

or

$$(E_{1/2})_s - (E_{1/2})_c = \frac{0{\cdot}0591}{n}\log K + \frac{0{\cdot}0591\log[X]_p}{n} \qquad ...(233)$$

First the $E_{1/2}$ for the simple metal ion is determined. Then the half-wave potentials of a series of solutions containing a known concentration of the metal ion and several known concentrations of the complexing agent are determined. From these data, the stability constant K of the complex is easily obtained.

AMPEROMETRIC TITRATIONS

As discussed above, if, in a polarographic measurement, we go on increasing the potential applied across the indicator electrode, a stage is reached when the electrolysis current reaches a limiting values. This is known as the limiting diffusion current. In this situation, the key ions get discharged at the indicator electrode as fast as they migrate to the electrode from the bulk of the solution with the result that the concentration of the key ions at the surface of the electrode becomes practically zero. The concentration gradient, c^*-c, which is responsible for the migration of the ions, becomes equal to c^* since $c=0$. In other words, the magnitude of the limiting diffusion current arising out of the discharge of the key ions would depend only on the bulk concentration c^* of the key ions. *If the bulk concentration decreases, the limiting diffusion current obtained at a constant potential also decreases proportionately.* This fact is made use of in *amperometric titrations* in which voltage applied across the indicator electrode and reference electrode is kept constant and the current passing through the cell containing a reducible species measured after suitable additions of the appropriate reagent.

For illustration, we may consider the precipitation of reducible Pb^{2+} ions by the addition of a non-reducible species, say, SO_4^{2-} ions. In the first place, a polarogram of the solution of Pb^{2+} ions is obtained and from the current-voltage curve, the potential falling well within the limiting current region is noted. The cell comprising of an indicator electrode (a rotating platinum electrode) and a reference electrode (a saturated calomel electrode) is exposed to the potential noted as above *which is kept constant.* A known volume of the lead salt solution is taken in the cell and a standard solution of sulphate ions (say, K_2SO_4) is added to the cell, about 1 ml at a time and after each addition, the current passing through the cell is recorded. Since by the addition of SO_4^{2-} ions the Pb^{2+} ions are removed from the solution as insoluble $PbSO_4$, the concentration of Pb^{2+} ions, goes on decreasing. With decrease in the concentration of Pb^{2+} ions, the diffusion current also goes on decreasing and ultimately when the Pb^{2+} ions are completely removed from the solution, the diffusion current becomes zero. The only current which now flows through the cell is the residual current which is characteristic of the supporting electrolyte used.

The successive values of diffusion current are then plotted against volumes of the titrant added when we get a curve as shown in Fig. 34. The intersection of the extrapolated branches of the curves gives the end point of the titration.

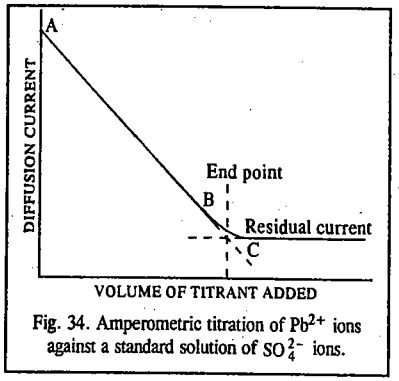

Fig. 34. Amperometric titration of Pb^{2+} ions against a standard solution of SO_4^{2-} ions.

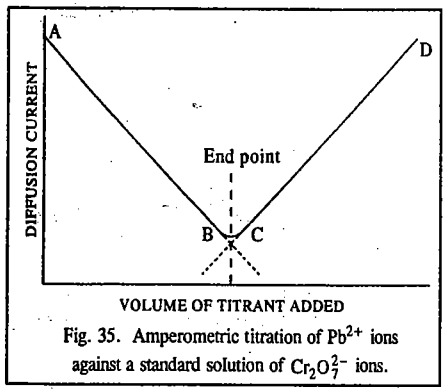

Fig. 35. Amperometric titration of Pb^{2+} ions against a standard solution of $Cr_2O_7^{2-}$ ions.

Polarographic Cell Assembly

A diagrammatic sketch of the polarographic cell assembly is shown in Fig. 31. It consists of a dropping mercury electrode (DME), a saturated calomel electrode (SCE) and the solution to be electrolysed.

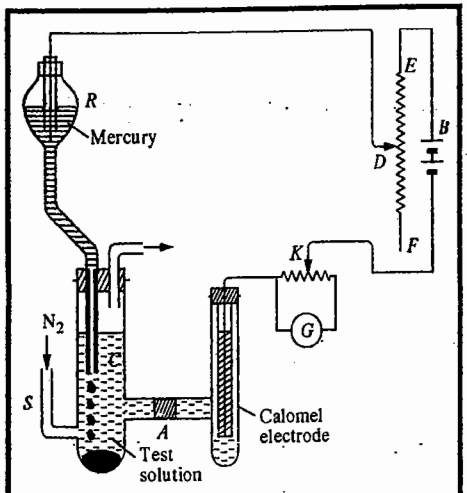

Fig. 31. The dropping mercury electrode assembly for polarographic measurements.

The test solution containing about 10^{-3}M to 10^{-4}M concentration of the reducible species and about 1M concentration of the suitable supporting electrolyte is taken in the cell and is deaerated by passing pure nitrogen or hydrogen through the side tube *S*. This is essential otherwise the dissolved oxygen begins to be reduced at the dropping mercury electrode thus interfering with the work of analysis. Pure mercury from the reservoir *R* is allowed to fall through the test solution at the end of the capillary tube *C*, at a rate of 20 to 30 drops per minute. Each drop which is held at the end of the capillary tube for 2–3 seconds acts as the cathode. When one drop falls, the second takes its place, and so on. There is, thus, a continuous renewal of the mercury drops. A calomel electrode which forms a part of the cell through a cintered glass frit *A* as shown, serves as the anode. The calomel anode and mercury cathode are joined, respectively, to the positive and negative poles of a battery *B*. The applied voltage can be easily varied by moving the sliding contact *D* along the potentiometer wire *EF*. The current strength is measured by means of a sensitive galvanometer or microammeter *G*, across the terminals of which is connected a shunt *K*. This makes provision for varying the sensitivity of the instrument. The potential of the cathode is easily determined by subtracting from the applied EMF the potential of the calomel electrode.

If the test solution contains a single electroactive species, the current-voltage curve, which is commonly known as a **polarogram**, will be of the shape as shown in Fig. 31. The limiting current, which is given by the height of the wave, corresponds to the concentration of the electroactive species. The potential at the centre of the rising part of the wave, referred to as the **half-wave potential**, is *characteristic of the species being discharged* and is independent of its concentration. The half-wave potential, designated as $E_{1/2}$ is thus used to identify the particular species.

Advantages of Using DME. There are a number of advantages of using dropping mercury electrode (DME) as the microelectrode in polarography. Some of these advantages are as follows :

1. Its surface area is reproducible with any given capillary.

2. It furnishes ideal conditions for obtaining a completely diffusion controlled limiting current.

3. The current falls when the drop falls. Hence, an oscillation is observed. However, the oscillation is so uniform that it is easy to observe the average current. The average current becomes reproducible soon after the applied voltage is changed. In contrast, a stationary solid microelectrode requires several minutes before steady current can be obtained. This difference in behaviour arises from the fact that whereas the diffusion layer in the DME is very thin, that in the case of the stationary solid microelectrode is thick. As a result, in the latter case a decrease in current is observed; the current becomes steady only after a stable diffusion layer is formed. No doubt, current variations occur with the DME, too, but the current becomes steady very soon since the mercury drop is re-formed quickly.

4. Since the electrode surface is constantly renewed, the surface poisoning effects are minimized.

5. Mercury forms amalgam with many metals thereby lowering their reduction potentials and decreasing their tendency to redissolve.

6. Since the overvoltage of hydrogen gas on mercury is very high, the DME is useful for polarographic reduction of a large number of ions in acidic solution.

A serious limitation of DME is that metallic mercury gets electro-oxidized easily. It can, therefore, be employed for the analysis of only those substances which can undrego any type of electro-reduction or an easy electro-oxidation.

Ilkovic Equation

In 1934, D. Ilkovic derived the following equation, known as the *Ilkovic equation*, for describing the diffusion current density produced in the polarographic cell :

$$i_d = 607\, n\, D^{1/2}\, m^{2/3}\, t^{1/2}\, c^0 \qquad ...(193)$$

where i_d is the average diffusion current (in microamperes) flowing during the lifetime of the drop; n is the number of electrons involved in the electrode reaction ; D is the diffusion coefficient of the electroactive species in units of $cm^2\ s^{-1}$, m is the mass rate of flow of mercury through the capillary in milligrams per second; t is the drop time in seconds and c is the bulk concentration of the electroactive material in millimoles per litre. It is customary to write the Ilkovic equation as comprising of two parts. *viz.*, $nD^{1/2}c^0$, determined by the properties of the solution and the quantity $m^{2/3}t^{1/6}$, known as *capillary constant*, determined by the characteristics of the capillary. The quantities m and t depend upon the DME and the pressure exerted on the capillary orifice due to the height of the mercury column attached to the electrode.

The diffusion coefficient which is a measure of the rate at which a given species diffuses through a unit concentration gradient, is highly temperature-dependent, changing by about 2·5 percent per degree. Hence, for accurate work, temperature in the polarographic cell must be controlled to ± 0·5°C.

Derivation of the Ilkovic Equation from Fick's Laws of Diffusion. The diffusion current in polarography can be related to the concentration of the reducible ions using the two Fick's laws of diffusion. According to Fick's first law of diffusion, the number of moles of a substance that diffuse across a plane of unit area per unit time (dN/Adt) is proportional to the concentration gradient (dc/dx) in the diffusion field, *i.e.*,

$$dN/Adt = D\,(dc/dx) \qquad ...(194)$$

where dN is the number of moles of the diffusible ions that diffuse across a cross-sectional plane of area A cm^2 in the time interval dt.

According to Fick's second law, the rate of change of concentration with time, dc/dt, as a result of diffusion of the substance across the plane, is proportional to the differential of the concentration gradient, *i.e.*,

$$dc/dt = D(\partial^2 c/\partial x^2) \qquad ...(195)$$

In both these laws, the proportionality constant, D, is the diffusion coefficient of the diffusible ion.

The flow of current i, across a plane during electrolysis, is given by

$$i = \left(\frac{dN}{Adt}\right) A \times n \times F = nF\,AD\frac{dc}{dx} \qquad ...(196)$$

It is found theoretically that for *linear diffusion* to a flat electrode surface,

$$\partial c/\partial x = c^0/(D\pi t)^{1/2} \qquad ...(197)$$

where c^0 is the concentration of the ionic species in the bulk of the solution and t is the time elapsed since the onset of electrolysis. Substituting for dc/dx in Eq. 196, we get

$$i = nFAD^{1/2}c^0/(\pi t)^{1/2} \qquad ...(198)$$

The current i, given by Eq. 198, is the diffusion current, i_d, *i.e.*, we can write

$$i_d = nFAD^{1/2}c^0/(\pi t)^{1/2} \quad ...(199)$$

The DME is a spherical electrode of expanding radius and surface area. Its surface area changes with the age of the drop. Ilkovic assumed linear diffusion for the current for DME. He calculated the surface area of the electrode-electrolyte boundary, A_t, at time t, as follows :

$$\text{Drop volume at time } t = \tfrac{4}{3}\pi r_t^3 \quad ...(200)$$

$$\text{Drop mass at time } t = \text{volume} \times \text{density} = \tfrac{4}{3}\pi r_t^3 \rho \quad ...(201)$$

where ρ is the density of mercury and r_t is the drop radius at time t.

If m is the mass rate of flow of mercury, then the drop mass at time t is equal to mt. Hence,

$$\tfrac{4}{3}\pi r_t^3 \rho = mt \quad \text{or} \quad r_t = \left(3mt/(4\pi\rho)\right)^{1/3} \quad ...(202)$$

$$A_t = 4\pi r_t^2 = 4\pi\left(3mt/(4\pi\rho)\right)^{2/3}$$

$$= 4\pi\left(3/4\pi\rho\right)^{2/3} m^{2/3}\, t^{2/3} \quad ...(203)$$

$$= 0{\cdot}8515\, m^{2/3}\, t^{2/3} \quad ...(204)$$

Substituting this value of area in Eq. 199, we get

$$i_d = nFD^{1/2}\frac{c^0}{(\pi t)^{1/2}} \times 0{\cdot}8515\, m^{2/3}\, t^{2/3} \quad ...(205)$$

As the mercury drop grows, the linear diffusion process is disturbed. The electrode surface moves into a region where there has yet been no depletion of ions due to electrolysis. This results in larger concentration at the electrode surface than that stipulated for a stationary electrode surface. To take into account this effect, Ilkovic introduced a correction of $(7/3)^{1/2}$ for the current thereby changing Eq. 205 to

$$i_d = (7/3)^{1/2}\,(0{\cdot}8515)\, n\, \mathrm{F}\, D^{1/2}\, m^{2/3}\, t^{2/3}\, c^0/(\pi t)^{1/2} \quad ...(206)$$

This equation, on simplification, taking $F = 96{,}485$ C mol^{-1}, becomes

$$i_d \text{ (in microamperes)} = 708\, n\, m^{2/3}\, t^{1/6}\, c^0\, D^{1/2} \quad ...(207)$$

where m is in units of milligram per second; c^0 is in milliomoles dm^{-3}; t is in seconds, D is in cm^2 s^{-1}.

If t is the drop time for DME, Eq. 207 gives the maximum value of the diffusion current for the DME for a particular applied potential.

Thus, $$i_d \text{ (maximum)} = 708\, n\, m^{2/3}\, t^{1/6}\, D^{1/2}\, c^0 \quad ...(208)$$

The average value of i_d during the life of a drop is estimated to be 6/7th of its maximum value at the time of drop fall, that is

$$i_d \text{ (average)} = 607\, n\, m^{2/3}\, t^{1/6}\, D^{1/2}\, c^0 \quad ...(209)$$

Both the forms of Ilkovic equation (*viz.*, Eqs. 208 and 209) show that i_d is directly proportional to the bulk concentration $c°$ of the ions reducible at the DME. Thus,

$$i_d = k\, c^0 \quad ...(210)$$

Half-Wave Potential. The half-wave potential, $E_{1/2}$, is *characteristic of the electroactive material.* Consider the reversible and rapid half-cell reaction at the microelectrode

$$\mathrm{Ox} + ne \longrightarrow \mathrm{Red}$$

where Ox is the substance being reduced and Red stands for the product. The constituents of the thin layer in the film surrounding the microelectrode are in *instantaneous equilibrium* with the electrode surface. Hence, the electrode potential is given by the Nernst equation. Accordingly,

$$E_{\text{cathode}} = E^0 - \frac{0{\cdot}0591}{n}\log\frac{[\mathrm{Red}]_0}{[\mathrm{Ox}]_0} \quad ...(211)$$

where the zero subscripts denote that the concentrations apply only to the film surrounding the DME which acts as cathode. The applied potential is given by

$$E_{\text{applied}} = E_{\text{cathode}} + E_{\text{anode}} \quad ...(212)$$

The anode is the saturated calomel electrode (SCE). Hence, we can write

$$E_{\text{applied}} = E^0 - \frac{0{\cdot}0591}{n}\log\frac{[\mathrm{Red}]_0}{[\mathrm{Ox}]_0} + E_{\text{SCE}} \quad ...(213)$$

$$E_{\text{applied}} - E_{\text{SCE}} = E^0 - \frac{0{\cdot}0591}{n}\log\frac{[\mathrm{Red}]_0}{[\mathrm{Ox}]_0} \quad ...(214)$$

Suppose in the beginning, the solution at the electrode surface consists only of the oxidized form. When the applied voltage is sufficiently large to reduce some of the oxidant, the oxidant concentration at the electrode surface starts decreasing. Some ions move towards the surface of the microelectrode from the bulk of the solution building up a concentration gradient. Thus, at the applied voltage, the observed current is given by

$$i = K([\mathrm{Ox}] - [\mathrm{Ox}]_0) \quad ...(215)$$

where K stands for the capillary characteristics and other constants of the Ilkovic equation. At the diffusion current plateau, the concentration of the oxidant at the electrode surface is virtually zero so that the diffusion current is given by

$$i_d = K\,[\mathrm{Ox}] \quad ...(216)$$

Subtracting Eq. 216 from Eq. 215, we get

$$[\mathrm{Ox}]_0 = (i_d - i)/K \quad ...(217)$$

Again, the concentration of the product Red at the electrode surface, provided it is soluble, is also given by

$$i = K'\,[\mathrm{Red}]_0 \quad ...(218)$$

where K' is another constant analogous to K.

or $$[\mathrm{Red}]_0 = i/K' \quad ...(219)$$

Substituting Eqs. 217 and 218 into Eq. 214, we obtain

$$E_{\text{applied}} - E_{\text{SCE}} = E^0 - \frac{0{\cdot}0591}{n}\log\left[\frac{i}{i_d - i} \times \frac{K}{K'}\right]$$

Rewriting, $$E_{\text{applied}} = E_{\text{SCE}} + E^0 - \frac{0{\cdot}0591}{n}\log\frac{K}{K'} - \frac{0{\cdot}0591}{n}\log\frac{i}{i_d - i} \quad ...(220)$$

By definition, when $i = i_d/2$, $E_{\text{applied}} = E_{1/2}$. ...(221)

Substituting in Eq. 220, we get

$$E_{1/2} = E_{SCE} + E^0 - \frac{0{\cdot}0591}{n} \log \frac{K}{K'} \quad ...(222)$$

We see from Eq. 222 that the half-wave potential is a constant which depends on the standard potential of the redox system and is independent of the concentration of the electroactive substance. Substituting Eq. 222 in Eq. 220, we obtain

$$E_{applied} = E_{1/2} - \frac{0{\cdot}0591}{n} \log \frac{i}{i_d - i} \quad ...(223)$$

Eq. 223 is the equation of the **polarographic wave.** A plot of $E_{applied}$ versus log $i/(i_d - i)$ gives a straight line with slope equal to $-0{\cdot}0591/n$ (Fig. 32). From the slope, the value of n, *viz.*, the number of electrons gained by the reductant, can be determined. From the plot, $E_{1/2}$ can also be determined. It is the potential at which the term log $i/(i_d - i) = 0$, *i.e.*, when $i = i_d/2$.

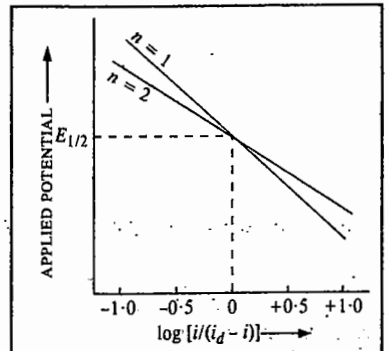

Fig. 32. Graphical representation of equation for the polarographic wave. Determination of $E_{1/2}$.

By means of the polarographic technique, concentrations in the range of 10^{-2} to 10^{-4} M, and sometimes as low as 10^{-6} M, can be determined. The polarographic method is seldom used for qualitative identification of substances because several substances give the same value of half-wave potentials and hence are not easily distinguishable from one another.

Applications of Polarography. Polarography has very wide applications some of which are discussed below.

1. Estimation of Inorganic and Organic Substances. Polarographic technique has been successfully applied for estimating a large variety of electroactive materials, both inorganic and organic, using the dropping mercury electrode. Since, hydrogen overvoltage on mercury is very high, the discharge of H^+ ions does not take place even upto a potential of about 2·3 V (cathodic). If the molecules or ions undergo reduction at the DME, the polarographic waves are called *cathodic waves* and if they undergo oxidation, the waves are called *anodic waves*. From the magnitude of the limiting diffusion current obtained from the polarographic wave for the reduction/oxidation of a given species, the concentration of the species can be easily determined since limiting diffusion current is directly proportional to the concentration of the electroactive species. Thus, almost all metallic cations such as Cu^{2+}, Cd^{2+}, Hg^{2+}, Pb^{2+}, etc. ; a large number of anions such as iodate, bromate, dichromate, vanadate, nitrate, etc.; several neutral molecules such as oxygen, nitric oxide, sulphur dioxide, cyanogen, hydrazine, etc., can be estimated polarographically. Atmospheric oxygen dissolved in an aqueous solution shows two distinct *cathodic waves* called oxygen waves, the first resulting from its reduction to hydrogen peroxide,

$$O_2 + 2H^+ + 2e^- \longrightarrow H_2O_2$$

and the second resulting from the reduction of H_2O_2 to H_2O

$$H_2O_2 + 2H^+ + 2e^- \longrightarrow 2H_2O$$

Both the oxygen waves have almost the same height. In fact, determination of oxygen in gaseous mixtures, biological fluids and water is a very important application of polarography.

However, the presence of dissolved oxygen seriously interferes with the routine polarographic analysis involving reduction of other electroactive species. This is the reason why the solution in polarographic cell is first deaerated for a few minutes by passing an inert gas such as nitrogen through it.

Several organic compounds such as aldehydes, ketones, carboxylic acids, nitro, nitroso and diazo compounds; compounds containing conjugated double-bond systems, etc., are easily reduced at the DME. However, organic electrode reactions are comparatively slow and more complex than inorganic electrode reactions. Hence, the interpretation of the polarographic data is more difficult. Despite this difficulty, organic polarography has been successfully employed in identifying the slow step in a complex reaction. This is done by taking polarograms at a number of *p*H values which helps in isolating the various steps in a multi-electron complex organic electrode reaction. After isolating the various steps in a mechanism, the number of electrons involved in each step is calculated and the nature of the reduction postulated.

There are several organic compounds in which the functional groups do not undergo electro-reduction. These include aromatic amino and phenolic compounds, ethers, diketones, thio compounds and a large number of pharmaceuticals and drugs such as purines, phenothiazines, sulpha drugs, antibiotics, local anaesthetics, etc. These compounds undergo electro-oxidation at potentials that are more anodic than the oxidation potential of mercury. Hence, DME cannot be used as an indicator electrode for carrying out anodic oxidation of these compounds. We have to make use of solid micro-electrodes, both metallic and non-metallic, for the estimation of these compounds. Common amongst these are platinum and graphite electrodes.

2. Analysis of Mixtures. In a multicomponent solution, *i.e.*, a solution containing several ions, the polarographic wave is a synthesis of the waves corresponding to various individual species. The composition of such a mixture can be determined if the half-wave potentials of the various ionic species are sufficiently different. As the applied EMF is gradually increased, the most easily reducible cation deposits first at the DME. With the continued increase of the applied EMF, the current increases and consequently the concentration of the ion being discharged at the cathode gets more and more depleted in the vicinity of the cathode. When the diffusion current plateau is reached, the current-voltage curve becomes flat and remains so until the applied EMF rises to a value at which the next most easily reducible cation is discharged at the cathode (DME). At this stage the second ion begins to be discharged, though the first ion may still be present in appreciable amounts in the bulk of the solution. The current rises again with further increase in the applied EMF and attains a new steady value corresponding to the diffusion current plateau. This process is continued with increasing applied EMF until all the reducible ions in the mixture have been discharged.

A polarographic wave obtained when a number of reducible ionic species are present in the solution is shown in Fig. 33.

From this polarographic wave, the $E_{1/2}$ and i_d for each ion can be determined. Since i_d is proportional to the ionic concentration in the bulk, the concentration of the various ions in the solution can be determined easily.

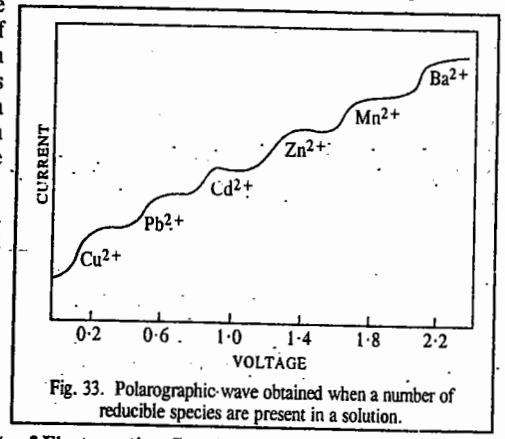

Fig. 33. Polarographic wave obtained when a number of reducible species are present in a solution.

3. Determination of Diffusion Coefficients of Electroactive Species. Polarography places at our disposal a fairly reliable method for determining diffusion coefficients of electroactive species. The method, which involves the use of the Ilkovic equation, is illustrated in the following example.

Example 4. A 5×10^{-4} M solution of $BaCl_2$ in 0·1 M $(CH_3)_4NCl$ was found to give the half-wave potential of −1·94 V versus SCE and the average diffusion current of 4·0 microamperes (μA). The dropping rate was 24 drops per minute ; the mass of 20 drops collected was 0·0750 g. Calculate the diffusion coefficient of Ba^{2+} ion.

Solution : The reaction at the DME is

$$Ba^{2+} + 2e^- \longrightarrow Ba$$

Here, $n = 2$; $c = 5\times10^{-4}$ M or 0·5 millimoles dm^{-3}, mass of Hg = 0·0750 g/20 drops = 3·75 mg/drop; $i_d = 4{\cdot}0$ μA. Thus,

$$m = (3{\cdot}75 \text{ mg/drop})\ (24/60 \text{ drop s}^{-1}) = 1{\cdot}5 \text{ mg s}^{-1}$$

$$t = 60/24 \text{ drops} = 2{\cdot}5 \text{ s drop}^{-1}$$

Substituting the data in the Ilkovic equation, *viz*, $i_d = 607\ n\ m^{2/3}\ t^{1/6}\ D^{1/2}\ c^0$, we have

$$4{\cdot}0 = 607\times2\times D^{1/2}\times(1{\cdot}5)^{2/3}\times(2{\cdot}5)^{1/6}\times(0{\cdot}5)$$

$$\therefore \quad D = \left[\frac{4.0}{607\times2(1.5)^{2/3}\times(2.5)^{1/6}\times(0.5)}\right]^2 = 1{\cdot}9\times10^{-5} \text{ cm}^2 \text{ s}^{-1}$$

4. Determination of the Stability Constant of a Metal-Ion Complex. Consider the reduction of a metal ion at the DME :

$$Ox + ne \rightleftharpoons Red \qquad ...(224)$$

The Nernst equation corresponding to this electrode reaction is

$$E = E^0 - \frac{0{\cdot}0591}{n}\log\frac{[Red]}{[Ox]} \qquad ...(225)$$

Suppose a complexing agent X forms a complex with the metal ion :

$$Ox + pX \rightleftharpoons OxX_p \qquad ...(226)$$

The stability constant of this complex is given by

$$K = \frac{[OxX_p]}{[Ox][X]^p} \qquad ...(227)$$

$$\therefore \quad [Ox] = \frac{[OxX_p]}{K[X]^p} \qquad ...(228)$$

Substituting in Eq. 225, we get

$$E = E^0 - \frac{0{\cdot}0591}{n}\log\frac{K[Red][X]^p}{[OxX_p]} \qquad ...(229)$$

At the half-wave potential, one-half of the oxidized form reaching the DME is reduced to the corresponding reduced form. Thus, when [Ox] = [Red], we have, for the *simple* metal ion,

$$(E_{1/2})_s = E_1 \qquad ...(230)$$

Similarly, for the reduction of the metal-ion complex,

$$(E_{1/2})_c = E_1 - \frac{0{\cdot}0591}{n}\log K[X]^p \qquad ...(231)$$

From Eqs. 230 and 231,

$$(E_{1/2})_s - (E_{1/2})_c = \frac{0{\cdot}0591}{n}\log K[X]^p \qquad ...(232)$$

or

$$(E_{1/2})_s - (E_{1/2})_c = \frac{0{\cdot}0591}{n}\log K + \frac{0{\cdot}0591\log[X]_p}{n} \qquad ...(233)$$

First the $E_{1/2}$ for the simple metal ion is determined. Then the half-wave potentials of a series of solutions containing a known concentration of the metal ion and several known concentrations of the complexing agent are determined. From these data, the stability constant K of the complex is easily obtained.

AMPEROMETRIC TITRATIONS

As discussed above, if, in a polarographic measurement, we go on increasing the potential applied across the indicator electrode, a stage is reached when the electrolysis current reaches a limiting values. This is known as the limiting diffusion current. In this situation, the key ions get discharged at the indicator electrode as fast as they migrate to the electrode from the bulk of the solution with the result that the concentration of the key ions at the surface of the electrode becomes practically zero. The concentration gradient, c^*-c, which is responsible for the migration of the ions, becomes equal to c^* since $c=0$. In other words, the magnitude of the limiting diffusion current arising out of the discharge of the key ions would depend only on the bulk concentration c^* of the key ions. *If the bulk concentration decreases, the limiting diffusion current obtained at a constant potential also decreases proportionately.* This fact is made use of in *amperometric titrations* in which voltage applied across the indicator electrode and reference electrode is kept constant and the current passing through the cell containing a reducible species measured after suitable additions of the appropriate reagent.

For illustration, we may consider the precipitation of reducible Pb^{2+} ions by the addition of a non-reducible species, say, SO_4^{2-} ions. In the first place, a polarogram of the solution of Pb^{2+} ions is obtained and from the current-voltage curve, the potential falling well within the limiting current region is noted. The cell comprising of an indicator electrode (a rotating platinum electrode) and a reference electrode (a saturated calomel electrode) is exposed to the potential noted as above *which is kept constant.* A known volume of the lead salt solution is taken in the cell and a standard solution of sulphate ions (say, K_2SO_4) is added to the cell, about 1 ml at a time and after each addition, the current passing through the cell is recorded. Since by the addition of SO_4^{2-} ions the Pb^{2+} ions are removed from the solution as insoluble $PbSO_4$, the concentration of Pb^{2+} ions, goes on decreasing. With decrease in the concentration of Pb^{2+} ions, the diffusion current also goes on decreasing and ultimately when the Pb^{2+} ions are completely removed from the solution, the diffusion current becomes zero. The only current which now flows through the cell is the residual current which is characteristic of the supporting electrolyte used.

The successive values of diffusion current are then plotted against volumes of the titrant added when we get a curve as shown in Fig. 34. The intersection of the extrapolated branches of the curves gives the end point of the titration.

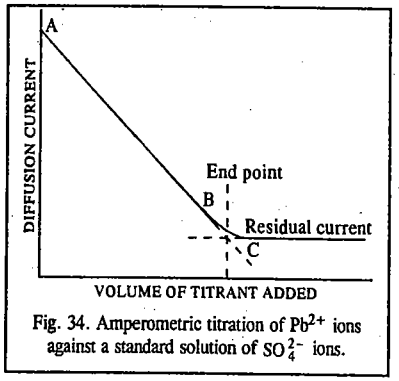

Fig. 34. Amperometric titration of Pb^{2+} ions against a standard solution of SO_4^{2-} ions.

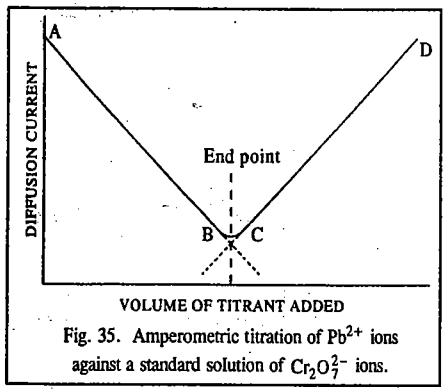

Fig. 35. Amperometric titration of Pb^{2+} ions against a standard solution of $Cr_2O_7^{2-}$ ions.

We may now consider a case in which both the reactant and the titrant produce diffusion current. The titration of Pb^{2+} ions with dichromate ions, carried out at electrode potential of –0·80 vs SCE, is a typical example.

The titration curve obtained in this case is shown in Fig. 35.

The branch *AB* of the curve depicts the decrease in diffusion current due to the removal of Pb^{2+} ions while the branch *CD* depicts the increase in diffusion current due to continuous increase in the concentration of the dichromate ions added which also undergo reduction at the applied potential and give rise to diffusion current.

Finally, let us consider the case in which the original material does not react electrolytically but the titrant does. The titration of Pb^{2+} ions with dichromate ions performed at zero electrode potential *vs* SCE in an acetate buffer of *p*H 4·2 is a typical example. Under the specific values of potential and *p*H mentioned as above, dichromate ions are readily reduced but not the lead ions. The titration curve obtained in this case is shown in Fig. 36.

Since Pb^{2+} ions are not reduced, the initial part of the titration curve is a horizontal line. The curve starts rising after the end point due to the reduction of dichromate ions. With increase in the concentration of dichromate ions added, the diffusion current goes on increasing, as shown.

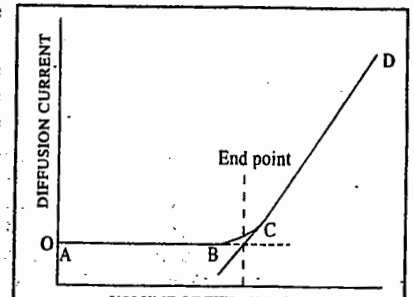

Fig. 36. Amperometric titration of Pb^{2+} ions at zero electrode potential in acetate buffer of *p*H 4·2, against a standard solution of $Cr_2O_7^{2-}$ ions.

VI. BIOELECTROCHEMISTRY

Traditional electrochemistry consists in the study of ionic solutions and electrodes where ions and electrons combine and separate. It is now well known that some specific electrochemical events take place in living cells as well. The nervous system, for instance, is based on the flow of electric currents and nerves can be thought of as the wires that run between the enzymes, the electrodes of the body. Bodies, like electrochemical cells, are full of membranes. In the brain, too, the electrical oscillations have been shown not only to signal mental activity but also to be connected with consciousness itself. They too have an electrochemical origin.

Biochemistry basically deals with the study of the electrochemical character of biological cells. It has been shown with the help of electron microscope that biological cells have honeycomb-like complicated structures the description of which is given in books on Biology. Each cell contains a liquid which comprises of a variety of species, prominently salts of alkali metals such as NaCl and KCl. The cells are enclosed in sorts of bags called **membranes**. The essential constituents of biological membranes are phospholipids and proteins. These are semiconducting in nature.

Bios and Reymond put forth the concept that a biological cell surface could be considered as though it were an electrode. Obvously, the surface of a biological membrane which encloses the cell can also be considered as an electrode. Thus, a biological membrane in contact with solutions of electrolytes of varying concentrations constitutes what may be called a **biological electrochemical cell**. The **membrane potentials** of these cells which, in fact, are concentration cells with or without transference; would be given by the Nerst equations, viz.,

$$E_{w.o.t} = (RT/F) \ln (c_2/c_1) \qquad ...(234)$$

$$E_{w.t.} = (t_+ - t_-)\,(RT/F) \ln (c_2/c_1) \qquad ...(235)$$

where t_+ and t_- represent the transport numbers of the cations and anions, respectively. If we take the difference in concentrations of the potential-determining species (2 and 1) as 10 times and $t_+ - t_- = 0{\cdot}15$,

then, according to Eqs. 234 and 235, the potential differences would be 57 and 9 mV, respectively. These values correspond to the normal range of the measured values of potential across the membranes.

In order to measure membrane potential, one places an electrode (*e.g.*, a calomel electrode if the solution contains Cl^- ions) on either side of the membrane which usually has a hole about 1mm in diameter in a Teflon sheet. Since the potential of the calomel electrode is accurately known and varies with Cl^- ion concentration according to the Nernst equation, the difference in potential arising from the two different Cl^- ion concentrations on each side of the membrane is easily known and can be subtracted from the total potential differences registered between the two electrodes to give the value due to the membrane. The membrane potentials thus obtained lie within values of tens to hundreds of millivolts.

It was, however, realised that differences in ionic concentrations around the membranes alone do not completely determine the membrane potentials in living cells. There were a number of objections to this concept of membrane potentials. Jahn, in 1962, proposed a radically different theory of membrane potentials. Instead of seeing this potential as being caused by the concentration gradients, he imagined these potentials as *results of two bioelectrode redox reactions* : a redox reaction occurring on the α side and another on the β side of a membrane. Jahn pictured the membrane as a bioelectrode in which each side of the membrane is a site of differing (but coupled) redox reactions, the membrane itself acting almost like the membrane in a fuel cell. Thus, it appears that potential differences across biological membranes arise both from fluxes of ions across the membrane and interfacial electron transfer.

In Jahn's model we are speaking of two coupled reactions joined by an ionic pathway connecting two hypothetical electrode reactions and occurring at the two surfaces, respectively, of what are regarded as semiconducting materials on which electrons are accepted and rejected (Fig. 37). This situation is reminiscent of a corrosion couple in the theory of corrosion. Thus, the reasoning underlying a corrosion couple can be applied to the comings and goings of the Na^+, K^+ and Cl^- ions which would determine the potential of the membrane. Koryta formulated this theory by writing electrode kinetic equations similar to those that lie behind the Butler-Volmer equation. Thus, we can write the sum of the fluxes for positive charges as equal to the sum of the fluxes for negative charges :

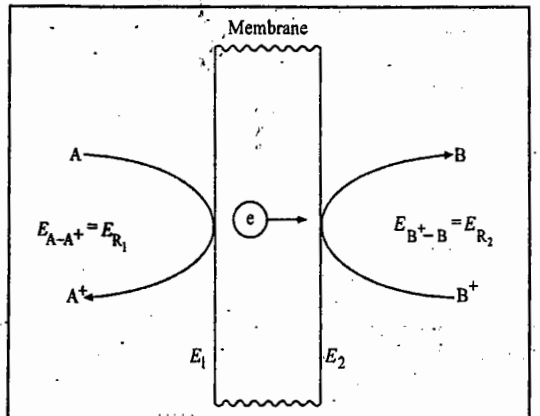

Fig. 37. Schematic diagram showing the oxidation and reduction reactions occurring at a membrane solution interface on sides 1 and 2 of the membrane.

$$J_{Na^+} + J_{K^+} = J_{Cl^-} \qquad ...(236)$$

Based on the above arguments, Koryta (1991) derived the following equation for membrane potential:

$$\Delta\phi = \frac{RT}{F} \ln \frac{k^0_{K^+} c_{K^+} + k^0_{Na^+} c_{Na^+} + k^0_{Cl^-} c_{Cl^-}}{k^0_{K^+} c_{K^+} + k^0_{Na^+} c_{Na^+} + k^0_{Cl^-} c_{Cl^-}} \qquad ...(237)$$

Electrochemical Mechanisms of the Nervous System

Mammals are wired machines, the brain telegraphs the muscles what to do. However, several unsolved problems concerning the passage of information still remain. That the signals pass *electrically* is clear enough. But they do not pass as electrons pass through a metallic conductor, since there are no

metallic conductors in the nervous system of mammals and the rate of passage of electricity is 10^8 times slower than that of electrons through a wire. Electrical activities are an integral part of the activity of the brain. However, tens of millivolts are needed to trigger passage of a pulse through the nervous system. In 1902, Bernstein drew attention to the importance of the ratios of the concentrations of Na^+ and K^+ ions in intra and extracellular fluids of the nerve axon and related them via a Nernst-type equation to the electrical potential measured across it. Axon is the longest part of the length of the nerve through which message is transferred to the particular muscle. Thus, the theoretical approach to the passage of electricity through nerves acquired electrochemical basis.

Fundamental experimental work on the current-potential relation across the membrane of the nerve sheath during the triggering of a nerve impulse had been done by Hodgkin and Huxley in 1952. They had also given a phenomenological theory of the variation of potential across the membrane containing the intracellular fluid when the passage of a current through the nerve was triggered. The 1963 Nobel Prize in Physiology/Medicine was jointly awarded to J.C. Eccles, A.L. Hodgkin and A.F. Huxley for their discoveries concerning the ionic mechanisms involved in excitation and inhibition in the peripheral and central portions of the nerve cell membrane. The Hodgkin–Huxley (H–H) theory of the nervous system is an example of bioelectrochemistry to be compared in status with the best known work in electrochemistry—the Debye-Hückel theory of interionic interactions in ionic solutions.

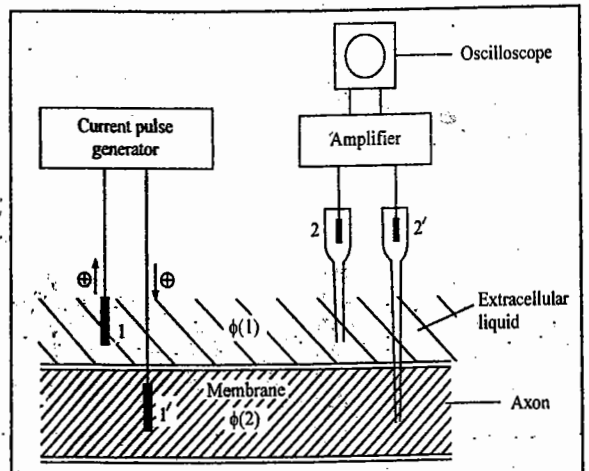

Fig. 38. Unit for potential transient measurement during excitation of a squid axon by current pulses from electrodes 1 and 1′ ; 2 and 2′ are micropipettes.

The Hodgkin-Huxley work concentrated upon the potential difference generated across the wall of the axon, which they regarded as a partly permeable membrane. Their apparatus is shown schematically in Fig. 38. This equipment allows current pulses to be sent across any section of the wall of an axon that is regarded as a membrane. When these current pulses cross the membrane, the potential difference between the solutions inside and outside of the membrane changes significantly. It is this change in potential (and the development of the spike potential) that is to be emphasized here because the movement of the spike potential along the axon is regarded as an essential act in the transmission of information in the nervous system.

Initially, the membrane (the wall of the axon) is at rest, *i.e.*, it is in its natural undisturbed state. In this state, the solution on the *inside* of the axon is at a potential of about -70 mV. The K^+ ion concentration is larger on the inside and smaller on the outside, while the concentration of Na^+ ion is smaller on the inside and larger on the outside. Thus, the phenomena that Hodgkin and Huxley observed pertained to the behaviour

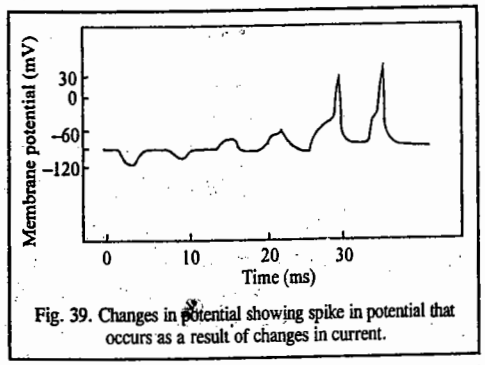

Fig. 39. Changes in potential showing spike in potential that occurs as a result of changes in current.

of potential difference between the two solutions, respectively, in contact with the outside and inside of the axon. Because they could not conceive why the unexpected changes in potential should arise *in* the solution (they neglected the possibility of changes at the interfaces), Hodgkin and Huxley supposed that the changes originated across the membrane. The changes in the current applied across the membrane and the resultant potential changes are shown in Fig. 39.

When several small negative current pulses are passed across the membrane (Fig. 40), the potential changes. It becomes more negative than the negative rest potential ; it becomes hyperpolarized. Then, when the direction of the current pulse changes to positive, the potential becomes less negative, *i.e.*, more positive. However, when the current increases sufficiently in the positive direction, there occurs a threshold value at which the potential changes abnormally; it increases to a greater degree than expected. This larger than expected potential peak is called the *spike potential* (or *action potential*). It is this spike potential triggered into existence in the H–H experiments by the passage of a sufficiently high positive current across the membrane wall, which then takes off *along* the axon until it reaches the relevant muscle. The movement of the spike potential is the way the message is delivered. The current–time plot at constant potential (Fig. 40) greatly resembles a potentiostatic transient at a metal–solution interface.

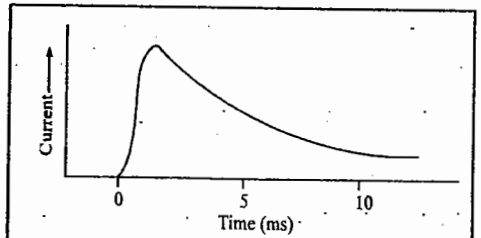

Fig. 40.Time dependence of membrane current.

The expression for membrane potential could be written as follows :

$$E = \frac{RT}{F} \ln \frac{P_i\, c_{in} + P_{j,in} + \ldots..}{P_i\, c_{i,out} + P_j c_{j,out} + \ldots..} \qquad \ldots(238)$$

In Eq. 238, the permeability coefficients P were varied by H–H so that the value of E could fit their observed values. Thus, Ps could change with current which passed across the membrane and also with time. With changes in Ps, there occurs a transfer of K^+ ions from inside to outside and Na^+ ions from outside to inside the membrane. By adjusting the P values to fit their observations, H–H could duplicate any results they found. They also asserted that the various movements of Na^+ and K^+ ions between the inner and outer fluids in contact with the membranes corresponded to the permeation changes occurring therein. Eq. 238 was experimentally tested by Jahn in 1962.

I. Review Questions

1. Outline the mathematical steps in the Debye-Hückel theory of determining the activity coefficients of strong electrolytes in solution.
2. How are solute activities determined from the solvent activities ?
3. Discuss the Bjerrum theory of ion association in electrolytic solutions.
4. Discuss the thermodynamic treatment of electrified interfaces leading to the derivation of the Lippmann equation.
5. Discuss the structure of electrified interfaces with reference to (*i*) the Helmholtz-Perrin model (*ii*) The Gouy-Chapman model and (*iii*) The Stern model.
6. Discuss the Garrett-Brattain space charge model of semi conductor interfaces.
7. Write a short note on electrocatalysis.
8. Discuss the Hodgkin-Huxley theory of membrane potentials in bioelectrochemistry.
9. Outline the electrochemical mechanism of the nervous system.

10. Derive the Butler-Volmer equation in the kinetics of the electrode reactions.
11. What is overvoltage ? Discuss the important applications of this phenomenon.
12. What is meant by corrosion of metals? How does it occur and how can it be inhibited ?
13. Derive the Ilkovic equation for the diffusion current in a polarographic cell.
14. Discuss the mathematics of the polarographic wave obtained in the case of a dropping mercury electrode in polarography.

II. Problems

1. The data below refer in control with a Fe^{3+}, Fe^{2+} aqueous solution at 298 K. Calculate the exchange current density and the transfer coefficient for the electrode process :

η (mV)	-50	-100	-150	-200	-250	-300
i_c (mA)	-0.3	-1.5	-6.4	-27.6	-118.6	-510

(Ans. $\alpha = 0.75, j_0 = 0.040$ mA cm^{-2})

2. The transfer coefficient of a certain electrode in contact with M^{3+} and M^{4+} in aqueous solvents at 25°C is 0·39. The current density is found to be 55·0 mA an^{-2} when the overvoltage is 125 mV. What is the overvoltage required for a current density of 75 mA cm^{-2} ? **(Ans. 138 mV)**
3. Determine the exchange current density from the information given in problem 14. **(Ans. 2·8 mA cm^{-2})**
4. A typical exchange current density, that for H^+ discharge of plantinum, is 0·79 mA cm^{-2} at 25° C. What is this current density at an electrode when its overpotential is (*a*) 10mV, (*b*) 100mV, (*c*) -5·0 V? Take $\alpha = 0{\cdot}5$.

(Ans. (*a*) 0·31A cm^{-2}, (*b*) 5·41mA cm^{-2}, (*c*) 8.3A cm^{-2})

CHAPTER 26

STATISTICAL THERMODYNAMICS

Statistical thermodynamics or statistical mechanics provides a link between quantum mechanics (or wave mechanics) and classical thermodynamics. Classical thermodynamics deals with *macroscopic* properties of matter and describes the behaviour of large number of molecules in terms of properties such as pressure, volume, temperature, composition, etc. Quantum mechanics, on the other hand, deals almost exclusively with matter at the microscopic level. It tells us that each microscopic system can be described by a wave function. However, it does not indicate which wave function of a molecule will represent the state of the system at a given instant. Neither classical thermodynamics nor quantum mechanics is able to calculate the macroscopic properties of matter from the microscopic structures of individual molecules.

Since any observed equilibrium property of matter must be some kind of an average of a large number of molecules, it is evident that we must use statistical methods to determine this property. *The discipline which deals with the computation of the macroscopic properties of matter from the data on the microscopic properties of individual atoms (or molecules)* is called **statistical mechanics** or **statistical thermodynamics.**

Fundamental contributions to the subject were made by J.C. Maxwell, L. Boltzmann and J. Willard Gibbs and several other scientists such as M. Planck, A. Einstein, S.N. Bose, E. Fermi, P.A.M. Dirac, R.C. Tolman, R.H. Fowler, E.A. Guggenheim, M. Born, P. Debye, L. Onsager, L.D. Landau, N. Bogoliubov, J.G. Kirkwood, I. Prigogine, A. Khinchin, N. Wiener, J.E. Mayer, K.G. Wilson, A. Sommerfeld and R. Kubo. The 1983 Physics Nobel Laureate, S. Chandrasekhar (1910-1995) was the first to apply quantum statistics to stellar dynamics—in particular, to white dwarfs.

Statistical mechanics can be applied easily to simple ideal systems such as monoatomic and diatomic gases. For application to interacting systems such as liquids (where strong intermolecular forces exist), the details of the intermolecular potential energy, which is not always known accurately, have also to be taken into account. That is why statistical mechanics of liquids is a difficult but fascinating subject. Gases under high pressures, too, are difficult to treat statistically since they deviate strongly from ideality. In recent years statistical methods have been applied successfully to simple liquids and dense gases. Progress in this area has been made possible by the application of both the advanced mathematical methods and high-speed computers which can numerically solve the otherwise highly intractable differential and integro-differential equations involved in advanced theoretical treatments.

Types of Statistics. Different physical situations encountered in nature are described by three types of statistics, *viz.*, the *Maxwell-Boltzmann* (or M-B) *statistics, the Bose-Einstein* (or B-E) *statistics and the Fermi-Dirac* (*or* F-D) *statistics.* The M-B statistics, developed long before the advent of quantum mechanics, is also called **classical statistics** whereas the Bose-Einstein statistics and the Fermi-Dirac statistics are collectively called **quantum statistics.** The characteristics of the three types of statistics are summed up as follows :

1. In **M-B statistics,** the particles are assumed to be *distinguishable* and any number of particles may occupy the same energy level. Particles obeying M-B statistics are called **boltzons** or **maxwellons.**

2. In **B-E statistics,** the particles are *indistinguishable* and any number of particles may occupy a given energy level. This statistics is obeyed by particles having integral spin, such as hydrogen (H_2) deuterium (D_2), nitrogen (N_2), helium-4 (^4He) and photons. Particles obeying B-E statistics are called **bosons.**

3. In **F-D statistics,** the particles are *indistinguishable* but only one particle may occupy a given energy level. This statistics is obeyed by particles having half-integral spin, *e.g.*, the protons, electrons, helium-3 (^3He) and nitric oxide (NO). Particles obeying F-D statistics are called **fermions.**

We will mention here, without proof, another equivalent definition of fermions and bosons. **Fermions** are those species whose wave functions are *antisymmetric* with respect to the exchange of particles whereas **bosons** are those species whose wave functions are *symmetric* with respect to the exchange of particles. These ideas on quantum statistics are discussed in Chapter 27.

The three types of statistics are described here.

1. Maxwell-Boltzmann Statistics. Consider a system of N *distinguishable* particles occupying energy levels ε_0, ε_1, ε_2, etc. The total number of arrangements for placing n_0 particles in the ground state energy level ε_0, n_1 particles in the first excited state energy level ε_1, n_2 particles in the second excited state energy level ε_2, and so on, is known as the **thermodynamic probability, W,** of the given macrostate. It is, in general, a very large number. Our problem is to determine W, *i.e.*, to determine how many *microstates* correspond to a given *macrostate.* It can be shown that W is given by

$$W = \frac{N!}{n_1!\, n_2!\, n_3! \cdots n_j!} = \frac{N!}{\Pi n_i!} \qquad \ldots(1)$$

where $N = \Sigma n_i$.

In Eq. 1, N is the total number of particles and the summation is over all the energy levels. It is possible to realize a given energy level in more than one way, *i.e.*, more than one quantum state has the same energy. When this happens, the energy level is said to be **degenerate,** Let g_i be the **degeneracy** (or **multiplicity**) of the energy level ε_i. This means that if there is one particle in the ith energy level, there are g_i ways of distributing it. For two particles in the ith energy level, there are g_i^2 possible distributions. Thus, for n_i particles in the ith energy level, there are $g_i^{n_i}$ possible distributions. Hence, the thermodynamic probability for the system of N particles is given by

$$W = N! \prod_i \frac{g_i^{n_i}}{n_i!} \times \text{constant} \qquad \ldots(2)$$

It is well known that the entropy S and probability W of a given state of a system are related by the Boltzmann equation, the most famous equation in statistical mechanics, *viz.*,

$$S = k \ln W \qquad \ldots(3)$$

The probability must be a maximum for an equilibrium state so that at equilibrium

$$S = k \ln W_{max} \qquad \ldots(4)$$

We are thus interested in finding a distribution that will make W a maximum. It is more convenient, however, to maximize the logarithm of W. It is known from calculus that at the maximum, the derivative of a function vanishes. Hence, at equilibrium,

$$d \ln W = \frac{\partial \ln W}{\partial n_1} dn_1 + \frac{\partial \ln W}{\partial n_2} dn_2 + \cdots \frac{\partial \ln W}{\partial n_3} dn_3 + \cdots$$

$$= \sum_i \frac{\partial \ln W}{\partial n_i} dn_i = 0 \qquad \ldots(5)$$

If we confine our investigation to a *closed system of independent particles,* it would meet the following two requirements :

(i) The total number of particles is *constant, i.e.,*

$$N = \sum_i n_i = \text{constant} \qquad \ldots(6)$$

(ii) The total energy, U, of the system is *constant, i.e.,*

$$U = \Sigma n_i \varepsilon_i = \text{constant} \qquad \ldots(7)$$

The constancy of the total number of particles implies that

$$dN = \Sigma dn_i = 0 \qquad \ldots(8)$$

and the constancy of the total energy implies that

$$dU = \Sigma \varepsilon_i\, dn_i = 0 \qquad \ldots(9)$$

From Eq. 2, taking logarithms of both sides, we get

$$\ln W = \ln N! + \sum_i n_i \ln g_i - \sum_i \ln n_i! + \text{constant} \qquad \ldots(10)$$

Here we invoke the **Stirling approximation** according to which, for large x,

$$\ln x! = x \ln x - x \qquad \ldots(11)$$

Using this approximation for $\ln n_i!$, Eq. 10 becomes

$$\ln W = \ln N! + \sum_i n_i \ln g_i - \sum_i n_i \ln n_i + \sum_i n_i + \text{constant}$$

$$= (N \ln N - N) + \sum_i n_i \ln g_i - \sum_i n_i \ln n_i + N + \text{constant}$$

$$= N \ln N + \sum_i n_i \ln g_i - \sum_i n_i \ln n_i + \text{constant} \qquad \ldots(12)$$

Differentiating and bearing in mind that N and g_i are constants, we get

$$d \ln W = \sum_i \ln g_i\, dn_i - \sum_i \ln n_i\, dn_i - \Sigma n_i\, d \ln n_i \qquad \ldots(13)$$

Now, $$\sum_i n_i d \ln n_i = \sum_i n_i \frac{dn_i}{n_i} = \sum_i dn_i = 0 \qquad \ldots(14)$$

Hence, at equilibrium,

$$d \ln W = \Sigma \ln g_i\, dn_i - \Sigma \ln n_i\, dn_i = 0 \qquad \ldots(15)$$

Eq. 15 gives *the change in* ln W *which results when the number of particles in each energy level is varied.*

If our system is *open,* then n_i would vary without restriction and the variations would be *independent* of one another. It would then be possible to solve Eq. 15 by setting each of the coefficients of the dn_i terms in Eq. 15 equal to zero. However, our system is not open but closed and since N is constant, the values of dn_i are not independent of one another, as is seen from Eq. 14. Again, the energy of the system is constant, too. How, then, can we solve Eq. 15 subject to the constraints of Eqs. 6 and 7 ?

The desired solution is obtained by applying the method of **Lagrange's undetermined multipliers.** Rewriting Eq. 15, we have

$$\sum_i \ln \frac{g_i}{n_i} dn_i = 0 \qquad \ldots(16)$$

Multiplying Eqs. 8 and 9 by the arbitrary constants α and β (known as Lagrange's undetermined multipliers) and subtracting from Eq. 16, we get

$$\sum_i \left[\ln \frac{g_i}{n_i} - \alpha - \beta \varepsilon_i \right] dn_i = 0 \qquad \ldots(17)$$

We can now select values of α and β in such a manner that one of the terms in the summation (say, $i=1$) is zero, the value of dn_i being immaterial. The remaining dn_i terms then become independent of one another since dn_i can be obtained from these dn_i terms (Eq. 8). We are now in a position to set each of the coefficients of dn_i in Eq. 17 equal to zero. Thus,

$$\ln (g_i/n_i) - \alpha - \beta\varepsilon_i = 0 \quad \text{or} \quad \ln g_i/n_i = \alpha + \beta\varepsilon_i \quad \text{or} \quad \ln n_i = \ln g_i - \alpha - \beta\varepsilon_i$$

$$\text{or} \qquad n_i = g_i e^{-\alpha-\beta\varepsilon_i} \qquad \ldots(18)$$

Eq. 18 which is one form of the **Boltzmann distribution law, gives the most probable distribution for a macrostate,** *i.e.*, it gives the occupation numbers of the molecular energy levels for the most probable distribution in terms of the energies ε_i, the degeneracy g_i and the undetermined multiplies α and β.

2. Bose-Einstein Statistics. Consider a system of N *indistinguishable* particles such that n_i particles are in the ith energy level with degeneracy g_i. The n_i particles have to be distributed among g_i states. For the sake of simplicity, imagine that the ith energy level has $g_i - 1$ partitions which are sufficient to separate the energy level into g_i intervals. Now the possible number of distributions of n_i particles among the g_i states may be determined by permuting the array of partitions and particles. The total number of permutations of n_i particles and $(g_i - 1)$ partitions is $(n_i+g_i-1)!$. However, *the partitions and the particles are indistinguishable.* This implies that interchanging two partitions does not alter an arrangement ; also interchanging two particles does not alter an arrangement. Hence, we must divide $(n_i+g_i-1)!$ by the number of permutations of the $g_i - 1$ partitions, *viz.*, $(g_i - 1)!$ and the number of permutations of n_i particles, *viz.*, $n_i !$ to obtain the number of possible arrangements of the n_i particles in the energy level ε_i. Thus,

$$\text{The number of arrangements} = \frac{(n_i + g_i - 1)!}{n_i!(g_i - 1)!} \qquad \ldots(19)$$

As in the case of Maxwell-Boltzmann statistics, we assume that in the present case also the total number of particles is constant and the total energy of the system is also constant, *i.e.*,

$$N = \sum_i n_i = \text{constant} \qquad \text{(Eq. 6)}$$

$$U = \Sigma\, n_i\, \varepsilon_i = \text{constant} \qquad \text{(Eq. 7)}$$

Thus, the thermodynamic probability W for the system of N particles (*i.e.*, the number of ways of distributing N particles among the various energy levels) is given by

$$W = \prod_i \frac{(n_i + g_i - 1)!}{n_i!\,(g_i - 1)!} \times \text{constant} \qquad \ldots(20)$$

Taking logarithms of both sides of Eq. 20, we get

$$\ln W = \sum_i [\ln (n_i + g_i - 1)! - \ln n_i! - \ln (g_i - 1)!] + \text{constant} \qquad \ldots(21)$$

Here, too, since n_i and g_i are very large numbers, we can invoke Stirling's approximation, *viz.*, $\ln x ! = x \ln x - x$, to obtain

$$\ln W = \sum_i [(n_i + g_i) \ln (n_i + g_i) - n_i \ln n_i - g_i \ln g_i] + \text{constant} \qquad \ldots(22)$$

where we have set $n_i+g_i-1 = n_i+g_i$ and $g_i-1=g_i$. Since, n_i is very large, it can be treated as a *continuous variable.* Differentiation of Eq. 22 with respect to n_i and setting the differential equal to zero gives for the most probable thermodynamic state of the system,

$$\delta \ln W = \Sigma [\ln n_i - \ln (n_i+g_i)]\, \delta n_i = 0 \text{ or } \sum_i \left[\ln \frac{n_i}{(n_i + g_i)}\right] \delta n_i = 0 \qquad \ldots(23)$$

$$\text{From Eqs. 6 and 7,} \quad \delta N = \sum_i \delta n_i = 0 \qquad \ldots(24)$$

$$\delta U = \sum_i \varepsilon_i\, dn_i = 0 \qquad \ldots(25)$$

Applying the method of Lagrange's undetermined multipliers to Eqs. 23, 24 and 25, we get

$$\sum_i \left[\ln \frac{n_i}{(n_i + g_i)} + \alpha + \beta\varepsilon_i\right] \delta n_i = 0 \qquad \ldots(26)$$

Since the variations δn_i are independent of one another, hence

$$\ln \frac{n_i}{(n_i + g_i)} + \alpha + \beta\varepsilon_i = 0 \qquad \ldots(27)$$

$$\text{whence} \qquad \ln\left[\frac{g_i}{n_i} + 1\right] = \alpha + \beta\varepsilon_i \quad \text{or} \quad \frac{g_i}{n_i} + 1 = e^{\alpha} + \beta\varepsilon_i \qquad \ldots(28)$$

$$\therefore \qquad n_i = g_i/[\exp (\alpha + \beta\varepsilon_i) - 1] \qquad \ldots(29)$$

Eq. 29 *is the expression for the most probable distribution of N particles among the various energy levels according to the Bose-Einstein statistics.*

3. Fermi-Dirac Statistics. Consider that the n_i particles are distributed among the g_i states $(n_i < g_i)$ where g_i , as before, is the degeneracy of the ith energy level. Imagine that the particles are *distinguishable.* This implies that the first particle may be placed in any one of the g_i states and for each one of these choices, the second particle may be placed in any one of the remaining $g_i - 1$ states, and so on. Thus, the number of arrangements is given by the expression $g_i !/(g_i - n_i)!$.

Since, however, the particles are *indistinguishable,* the above expression has to be divided by the possible number of permutations of n_i particles, *viz.*, $n_i !$. Hence, the number of arrangements of n_i particles in the ith energy level is given by the expression $g_i !/(n_i ! (g_i - n_i) !)$.

Thus, the thermodynamic probability W for the system of N particles (*i.e.*, the number of ways of distributing N particles among the various energy levels) is given by

$$W = \prod_i \frac{g_i !}{n_i !\,(g_i - n_i)!} \times \text{constant} \qquad \ldots(30)$$

Taking logarithms of both sides of Eq. 30, we have

$$\ln W = \sum_i [\ln g_i ! - \ln n_i ! - \ln (g_i - n_i)!] + \text{constant} \qquad \ldots(31)$$

Assuming that n_i, g_i and $g_i - n_i$ are very large, we can apply Stirling's approximation, obtaining

$$\ln W = \sum_i [(n_i - g_i) \ln (g_i - n_i) - n_i \ln n_i + g_i \ln g_i] + \text{constant} \qquad \ldots(32)$$

Thus, for the most probable state,

$$\delta \ln W = \sum_i [\ln n_i - \ln (g_i - n_i)] \delta n_i = 0 \quad \text{or} \quad \sum_i [\ln n_i /(g_i - n_i)]\, \delta n_i = 0 \qquad \ldots(33)$$

$$\text{Since} \qquad N = \sum_i n_i = \text{constant} \quad \text{and} \quad U = \sum_i n_i \varepsilon_i = \text{constant},$$

$$\text{hence,} \qquad \delta N = \sum_i \delta n_i \quad \text{and} \quad \delta U = \sum_i \varepsilon_i dn_i = 0 \qquad \ldots(34)$$

Applying Lagrange's method of undetermined multipliers, we obtain

$$\sum_i [\ln n_i /(g_i - n_i) + \alpha + \beta\varepsilon_i]\, \delta n_i = 0 \qquad \ldots(35)$$

Since the variations δn_i are independent of one another, hence.

$$\ln n_i /(g_i - n_i) + \alpha + \beta\varepsilon_i = 0 \quad \text{or} \quad \ln [(g_i /n_i) - 1] = \alpha + \beta\varepsilon_i \quad \text{or} \quad (g_i/n_i) - 1 = e^{\alpha+\beta\varepsilon_i} \qquad \ldots(36)$$

$$\therefore \quad n_i = g_i/[\exp(\alpha + \beta\varepsilon_i) + 1] \qquad \ldots(37)$$

Eq. 37 is *the expression for the most probable distribution of N particles among the energy levels according to the Fermi-Dirac statistics.*

Evaluation of Lagrange's Undetermined Multipliers. We now proceed to determine α and β. Since $N = \sum_i n_i$, hence from Eq. 18,

$$\sum_i g_i e^{-\alpha-\beta\varepsilon_i} = N \quad \text{or} \quad e^{-\alpha} = N/\sum_i g_i e^{-\beta\varepsilon_i} \qquad \ldots(38)$$

Defining a quantity q, called the **molecular partition function,** as

$$q = \sum_i g_i e^{-\beta\varepsilon_i} \qquad \ldots(39)$$

we obtain $$e^{-\alpha} = N/q \qquad \ldots(40)$$

Accordingly, the Boltzmann distribution law equation (*viz.*, Eq. 18), becomes

$$n_i = N g_i e^{-\beta\varepsilon_i}/q \qquad \ldots(41)$$

The partition function, q, is a quantity of immense importance in statistical thermodynamics. We shall see presently that by evaluating the partition function for a system we can calculate the value of any thermodynamic function for that system.

However, before we proceed with the task of evaluating the partition function, let us determine the constant β. Taking logs of Eq. 2 and applying Stirling's approximation to $\ln N!$ and $\ln n_i!$, we have

$$\ln W = \ln N! + \Sigma(n_i \ln g_i - \ln n_i!) \qquad \ldots(42)$$

$$= N \ln N - N + \sum_i (n_i \ln g_i - n_i \ln n_i + n_i) = N \ln N + \sum_i n_i \ln g_i - \sum_i n_i \ln n_i \qquad \ldots(43)$$

Taking logs of Eq. 41, we have

$$\ln n_i = \ln N - \ln q + \ln g_i - \beta\varepsilon_i \qquad \ldots(44)$$

Substituting in Eq. 43, we get

$$\ln W = N \ln N + \sum_i n_i \ln g_i \sum_l n_i (\ln N - \ln q + \ln g_i - \beta\varepsilon_i)$$

$$= N \ln N + \sum_i n_i \ln g_i - N \ln N + N \ln q - \sum_l n_i \ln g_i + \beta \sum_l n_i \varepsilon_i \qquad \ldots(45)$$

$$= N \ln q + \beta U$$

Substituting this result into the Boltzmann equation (*viz.*, Eq. 3), we have

$$S = k \ln W = N k \ln q + k\beta U \qquad \ldots(46)$$

From the combined statement of the First and the Second laws of thermodynamics, we know that for a simple system,

$$dU = TdS - PdV \qquad \ldots(47)$$

At constant volume (V = constant ; $dV = 0$), $dU = TdS$ $\qquad \ldots(48)$

$$\therefore \quad (\partial S/\partial U)_V = 1/T \qquad \ldots(49)$$

Differentiating Eq. 46 with respect to U at constant V, we get

$$\left(\frac{\partial S}{\partial U}\right)_V = \frac{Nk}{q}\left(\frac{\partial q}{\partial U}\right)_V + k\beta + kU\left(\frac{\partial \beta}{\partial U}\right)_V = \frac{Nk}{q}\frac{dq}{d\beta}\left(\frac{\partial \beta}{\partial U}\right)_V + k\beta + kU\left(\frac{\partial \beta}{\partial U}\right)_V \qquad \ldots(50)$$

Also, from Eq. 39, $$dq/d\beta = -Uq/N \qquad \ldots(51)$$

Substitution of Eq. 51 in Eq. 50 results in cancellation of the first and the last terms, giving

$$(\partial S/dU)_V = k\beta \qquad \ldots(52)$$

Comparing Eqs. 49 and 52, we find that

$$\beta = 1/kT \qquad \ldots(53)$$

Hence, from Eq. 39, the molecular partition function q becomes

$$q = \sum_i g_i e^{-\varepsilon_i/kT} \qquad \ldots(54)$$

and the Maxwell-Boltzmann distribution equation (Eq. 41) becomes

$$n_i = (N g_i e^{-\varepsilon_i/kT})/q \qquad \ldots(55)$$

From Eq. 55 we can easily obtain the ratio of the populations, *i.e.*, the number of particles in any two energy levels ε_i and ε_j. Thus,

$$\frac{n_i}{n_j} = \frac{g_i}{g_j} e^{-(\varepsilon_i - \varepsilon_j)/kT} \qquad \ldots(56)$$

Example 1. A system of N particles has, among others, two energy levels with $g_1 = 2$, $g_2 = 3$, $U_1 = 41{\cdot}84$ kJ mol^{-1} and $U_2 = 58{\cdot}58$ kJ mol^{-1}. Calculate the ratio of the number of particles in the two energy states at 1000 K.

Solution : From Eq. 56,

$$\frac{n_2}{n_1} = \frac{g_2}{g_1}\exp\left[-\frac{\varepsilon_2 - \varepsilon_1}{kT}\right] = \frac{g_2}{g_1}\exp\left[\frac{U_2 - U_1}{RT}\right]$$

$$= \frac{3}{2}\exp\left[-\frac{(58580 - 41840)\text{ J mol}^{-1}}{(8{\cdot}314\text{ J K}^{-1}\text{ mol}^{-1})(1000\text{ K})}\right] = 0{\cdot}201$$

Example 2. Using the Stirling approximation, calculate $\ln N_A!$ where N_A is Avogadro's number.

Solution : $N_A = 6{\cdot}022 \times 10^{23}$

Using Stirling's approximation,

$$\ln N_A! = N_A \ln N_A - N_A = (6{\cdot}022\times10^{23}) \ln (6{\cdot}022\times10^{23}) - (6{\cdot}022\times10^{23}) = 3{\cdot}238\times10^{25}$$

The formulas for the Bose-Einstein statistics and the Fermi-Dirac statistics, both of which are applicable to *indistinguishable* particles, can be derived in an analogous manner.

The results for the three types of statistics are summarized in Table 1.

TABLE 1

Results for the Three Types of Statistics

Statistics	Thermodynamic Probability	Number of particles in the ith state
Maxwell-Boltzmann	$W_{MB} = N! \prod_i \frac{g_i^{n_i}}{n_i!}$	$n_i = \frac{g_i}{e^{\alpha+\beta\varepsilon_i}}$
Bose-Einstein	$W_{BE} = \prod_i \frac{(n_i + g_i - 1)!}{n_i!(g_i - 1)!}$	$n_i = \frac{g_i}{e^{\alpha+\beta\varepsilon_i} - 1}$
Fermi-Dirac	$W_{FD} = \prod_i \frac{g_i!}{n_i!(g_i - n_i)!}$	$n_i = \frac{g_i}{e^{\alpha+\beta\varepsilon_i} + 1}$

The constant β in all the three types of statistics is equal to $1/kT$. The constant α has to be determined for each type of statistics.

Effect of Temperature. Figs. 1, 2 and 3 show the number of particles per energy level plotted against energy ε for various temperatures for the three types of statistics.

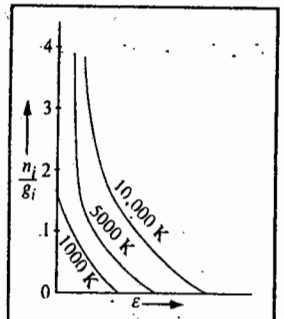

Fig. 1. Plots of number of particles per energy level *versus* energy at different temperatures in cases of Maxwell-Boltzmann statistics.

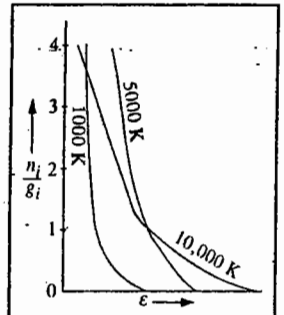

Fig. 2. Plots of number of particles per energy level *versus* energy at different temperatures in cases of Bose-Einstein statistics.

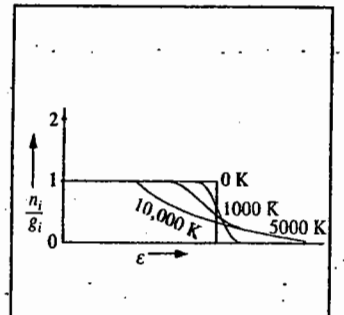

Fig. 3. Plots of number of particles per energy level *versus* energy at different temperatures in cases of Fermi-Dirac statistics.

It may be mentioned that under certain conditions, the Bose-Einstein and the Fermi-Dirac statistics yield results which are virtually identical with those obtained from the Maxwell-Boltzmann statistics. This happens when *g_i/n_i is very large compared with unity* so that

$$(g_i/n_i) + 1 \approx (g_i/n_i) - 1 \approx g_i/n_i \qquad ...(57)$$

In general, if temperature is not too low or the pressure is not too high, the number of available eigenstates g_i is large compared with the number of particles n_i, so that $g_i/n_i >> 1$. Thus, for conditions under which the normal gases exist, the classical (*i.e.*, Maxwell-Boltzmann) statistics is adequate to describe their actual behaviour.

PARTITION FUNCTIONS

Molecular Partition Functions for an Ideal Gas

The molecular energy levels needed for the evaluation of the molecular partition functions are obtained from the solution of the Schrödinger equation. According to the *Born-Oppenheimer approximation,* the total energy of a molecule is composed of contributions from the translational, rotational, vibrational and electronic modes of motion. Thus,

$$\varepsilon = \varepsilon_{tr} + \varepsilon_{rot} + \varepsilon_{vib} + \varepsilon_{el} \qquad ...(58)$$

This equation holds good if there is no coupling between the different modes of motion. It is only for the simplest atoms that expressions for the electronic energy, ε_{el}, can be explicitly obtained. For molecules it is generally not possible to do so. Again, the shapes of the molecules often change when they are electronically excited. Hence, the concept of an electronic energy level (and hence of the *electronic partition function*) has limited usefulness. We will, therefore, not include the electronic energy in Eq. 58 and instead will write

$$\varepsilon = \varepsilon_{tr} + \varepsilon_{rot} + \varepsilon_{vib} \qquad ...(59)$$

According to the laws of conservation of momentum, angular momentum and energy, there cannot be any interaction between the translational motion of a body and the internal motions (rotational and vibrational motions) when the motion is taking place in a field-free environment. However, there is always some coupling between the rotational and vibrational modes of motion (and even between the different vibrational modes themselves). In the present discussion we will neglect such couplings and assume that Eq. 59 holds.

Using Eqs. 39 and 59, the molecular partition function can be written as

$$q = \sum_i \sum_j \sum_k g \exp\left[\frac{\varepsilon_{i,tr} + \varepsilon_{j,rot} + \varepsilon_{k,vib}}{kT}\right]$$

$$= \sum_i g_i \exp\left[-\frac{\varepsilon_{i,tr}}{kT}\right] \times \sum_j g_j \exp\left[-\frac{\varepsilon_{j,rot}}{kT}\right] \times \sum_k g_k \exp\left[-\frac{\varepsilon_{k,vib}}{kT}\right] \qquad ...(60)$$

or $$q = q_{tr} \times q_{rot} \times q_{vib} \qquad ...(61)$$

Thus, the **molecular partition function** of a molecule is the product of the translational, rotational and vibrational partition functions. This is known as the multiplication theorem for the partition functions.

If, however, for the sake of completeness, we do want to include the electronic contribution also, then the molecular partition function is given by

$$q = q_{tr} \times q_{rot} \times q_{vib} \times q_{elec} \qquad ...(62)$$

Translational Partition Function. For a particle of mass m, moving in an infinite three-dimensional box of sides a, b and c, assuming that the potential is zero within the box, the energy levels obtained by the solution of the Schrödinger equation are given by the expression

$$\varepsilon_{n_x,n_y,n_z} \equiv \varepsilon_{tr} = \frac{h^2}{8m}\left[\frac{n_x^2}{a^2} + \frac{n_y^2}{b^2} + \frac{n_z^2}{c^2}\right] \qquad ...(63)$$

where each of the quantum numbers n_x, n_y, n_z vary from one to infinity. Using Eqs. 39 and 63, the translational partition function, neglecting degeneracy, is given by

$$q_{tr} = \sum_{n_x}\sum_{n_y}\sum_{n_z} \exp\left[-\frac{h^2}{8mkT}\left(\frac{n_x^2}{a^2} + \frac{n_y^2}{b^2} + \frac{n_z^2}{c^2}\right)\right] \qquad ...(64)$$

where the triple summation is taken over all integral values of n_x, n_y and n_z from one to infinity. The motion of the particle in the three x, y and z directions being independent, we can replace the triple summation as a product of three summations. Thus,

$$q_{tr} = \sum_{n_x=1}^{\infty} \exp\left[-\frac{n_x^2h^2}{8ma^2kT}\right] \times \sum_{n_y=1}^{\infty} \exp\left[-\frac{n_y^2h^2}{8mb^2kT}\right] \times \sum_{n_z=1}^{\infty} \exp\left[-\frac{n_z^2h^2}{8mc^2kT}\right] \qquad ...(65)$$

It is well known that the spacing between the energy levels of a particle in a three-dimensional box is very small compared with the thermal energy, kT. Hence, we can replace the summation by integration. Accordingly,

$$q_{tr} = \int_0^{\infty} \exp\left[-\frac{n_x^2h^2}{8ma^2kT}\right] dn_x \times \int_0^{\infty} \exp\left[-\frac{n_y^2h^2}{8mb^2kT}\right] dn_y \times \int_0^{\infty} \exp\left[-\frac{n_z^2h^2}{8mc^2kT}\right] dn_z \qquad ...(66)$$

From calculus, it is known that the standard integral

$$\int_0^{\infty} e^{-ax^2} dx = \frac{1}{2}\left(\frac{\pi}{a}\right)^{1/2} \qquad ...(67)$$

Using this result, the three integrals in Eq. 66 which are identical except for the constants a, b and c, can be calculated, giving

$$q_{tr} = \frac{a}{h}(2\pi mkT)^{1/2} \times \frac{b}{h}(2\pi mkT)^{1/2} \times \frac{c}{h}(2\pi mkT)^{1/2}$$

$$= \left(\frac{2\pi mkT}{h^2}\right)^{3/2} \times abc = \left(\frac{2\pi mkT}{h^2}\right)^{3/2} \times V \qquad ...(68)$$

where V (= abc) is the volume of the box in which the molecule moves. Eq. 68 can also be written as

$$q_{tr} = q_{tr}^{\circ} \times V \qquad ...(69)$$

where q°_{tr} is the *partition function per unit volume*. From Eq. 68 we see that the translational partition function depends upon temperature and volume.

If M is the mass per mole then $m = M/N_A$ where N_A is Avogadro's number. Also, $k = R/N_A$. Hence,

$$q_{tr} = \frac{(2\pi MRT)^{3/2} \times V_m}{h^2 N_A^2} \qquad ...(70)$$

where V_m is the volume per mole.

Sometimes we are interested in calculating the quantity q_{tr}/N_A. For a gas at 1 atm pressure (101·325 kN m^{-2}), the volume per mole, *viz.*, $V_m = (8{\cdot}206\times10^{-5})T$ m^3. Hence, Eq. 70 takes the form

$$q^\circ_{tr}/N_A = 0{\cdot}02559\, M^{3/2} T^{5/2} \qquad ...(71)$$

where q°_{tr} is the translational partition function per unit volume evaluated for the gas at 1 atm pressure. Thus, for H_2 at 27°C and 1 atm pressure, we have

$$q^\circ_{tr}/N_A \approx 10^5 \qquad ...(72)$$

Using the Boltzmann distribution, the number of molecules in any translational state i is given by

$$n_{i,tr} = (Ne^{-\varepsilon_{i,tr}/kT})/q_{tr} \qquad ...(73)$$

where N is the total number of molecules.

Since the factor $\varepsilon_{i,tr}/kT$ is a positive number, $n_{i,tr}$ cannot be greater than N/q_{tr}. It follows from Eq. 72 that $N/q_{tr} \approx 10^{-5}$

The above result implies that though the number of molecules (N) is very large, the number of available quantum states (or energy levels), *i.e.*, q_{tr}, is even larger so that the probability of any one quantum state being occupied by a given molecule is very small.

The quantity $h/(2\pi mkT)^{1/2}$ in Eq. 68, is called the **thermal de Broglie wave length** and is represented by the symbol Λ. Thus, $q_{tr} = V/\Lambda^3$.

Example 3. Calculate the translational partition function for benzene (molar mass=78·0 g mol^{-1}) in a volume of 1 m^3 at 25°C.

Solution : We shall use Eq. 68, taking care that m is the mass of a molecule obtained by dividing the molar mass by Avogadro's number. It should be converted into kg by further dividing by 1000 since the volume is given in SI units. Thus,

$$q_{tr} = \left[\frac{(2)(3{\cdot}1416)(78{\cdot}0\times10^{-3}\,\text{kg mol}^{-1})(1{\cdot}38\times10^{-23}\,\text{J K}^{-1})(298\,\text{K})}{(6{\cdot}626\times10^{-34}\,\text{J s})^2(6{\cdot}022\times10^{23}\,\text{mol}^{-1})}\right]^{3/2} \times 1{\cdot}00\ \text{m}^3$$

$$= 6{\cdot}66\times10^{32} \qquad (\text{J} = \text{kg m}^2\,\text{s}^{-2})$$

Notice that the partition function is always dimensionless (*i.e.*, it has no units). It is a pure number and is approximately equal to the number of quantum states having energies below the thermal energy available to the molecule in the given volume.

Example 4. Calculate the translational partition function for hydrogen atom at 3000 K confined to move in a box of volume of 2·494×10^5 cm^3. Also determine the thermal de Broglie wave length.

Solution :

$$V = 2{\cdot}494\times10^5\ \text{cm}^3 = \frac{2{\cdot}494\times10^5\,\text{cm}^3}{10^6\,\text{cm}^3/\text{m}^3} = 0{\cdot}2494\ \text{m}^3$$

From Eq. 68, the translational partition function is given by

$$q_{tr} = \left[\frac{(2)(3{\cdot}1416)(1{\cdot}0080\times10^{-3}\,\text{kg mol}^{-1})(1{\cdot}38\times10^{-23}\,\text{J K}^{-1})(3000\,\text{K})}{(6{\cdot}022\times10^{23}\,\text{mol}^{-1})(6{\cdot}626\times10^{-34}\,\text{J s})^2}\right]^{3/2} \times (0{\cdot}2494\,\text{m}^3)$$

$$= 7{\cdot}586\times10^{30} \quad (\text{J} = \text{kg m}^2\,\text{s}^{-2})$$

The thermal de Broglie wave length is given by

$$\Lambda = \left(\frac{V}{q_{tr}}\right)^{1/3} = \left(\frac{0{\cdot}2494\,\text{m}^3}{7{\cdot}586\times10^{30}}\right)^{1/3} = 3{\cdot}20\times10^{-11}\ \text{m}$$

Rotational Partition Function. The simplest system that undergoes rotational motion is a diatomic molecule. The rotational energy levels of a rigid diatomic rotor (*i.e.*, a rotor whose internuclear distance remains fixed during rotation), obtained by solving the Schrödinger wave equation, are

$$\varepsilon_J = \frac{J(J+1)h^2}{8\pi^2 I} \qquad ...(74)$$

where the rotational quantum number J has the values 0, 1, 2, 3,·····, and I is the moment of inertia of the molecule about an axis perpendicular to the internuclear axis.

The degeneracy g_J of rotational energy levels is equal to $(2J + 1)$. Thus, using Eqs. 39 and 74, the **rotational partition function** of a rigid diatomic rotor is given by

$$q_{rot} = \sum_{J=0}^{\infty}(2J+1)\exp\left[-\frac{J(J+1)h^2}{8\pi^2 IkT}\right] = \sum_{J=0}^{\infty}(2J+1)\exp[-J(J+1)C] \qquad ...(75)$$

where $C = h^2/8\pi^2 IkT$.

When $kT \gg h^2/8\pi^2 I$, the spacing between the neighbouring rotational energy levels is much larger than that between the translational energy levels. Still it is found that for practically all diatomics (exceptions are the hydrogen isotopes at low temperatures), $h^2/8\pi^2 IkT$ is small so that the successive rotational energy levels are closer to one another. It is thus possible to replace the summation in Eq. 75 by integration. Accordingly,

$$q_{rot} = \int_0^\infty (2J+1)\exp[-J(J+1)C]\,dJ \qquad ...(76)$$

Let $x = J^2 + J$. Therefore, $dx = (2J + 1)\,dJ$.

$$\therefore \quad q_{rot} = \int_0^\infty e^{-Cx}dx = -\frac{1}{C}\left[e^{-\infty} - e^0\right] = \frac{1}{C} \qquad ...(77)$$

Substituting for C, we have

$$q_{rot} = (8\pi^2 IkT)/h^2 \qquad ...(78)$$

The quantity $h^2/(8\pi^2 Ik)$ in Eq. 78 has the dimensions of temperature and is called **characteristic rotational temperature** which can be written as

$$\Theta_{rot} = T/q_{rot} \qquad ...(79)$$

From Eq. 74 we see that the value of Θ_{rot}/T gives an idea as to how close the energy levels are to kT. The assumption of the replacement of summation by integration used in evaluating q_{rot} is valid when Θ_{rot} is far less than T.

Eq. 78 can be applied to rotational degrees of freedom in which identical configurations occur only after a rotation of 2π. If the molecule has elements of symmetry such that identical configurations occur after a rotation of $2\pi/\sigma$ where σ is the symmetry number, then the rotational partition function is given by

$$q_{rot} = \frac{8\pi^2 IkT}{\sigma h^2} = \frac{T}{(\sigma\Theta_{rot})} \qquad ...(80)$$

The symmetry number ensures the avoidance of too many identical configurations being taken into account. For homonuclear diatomic molecules such as H_2, O_2, N_2, etc., $\sigma = 2$, whereas for heteronuclear diatomic molecules such as CO, NO, HD, HCl, etc., $\sigma = 1$.

We can also write Eq. 80 as

$$q_{rot} = kT/(\sigma hcB) \qquad ...(81)$$

where B is the **rotational constant** of the diatomic rotor defined as

$$B = h/(8\pi^2 Ic) \qquad ...(82)$$

Characteristic rotational temperatures and rotational partition functions for some molecules are given in Table 2.

TABLE 2

Θ_{rot} and q_{rot} for Some Common Molecules

Molecule	Θ_{rot} (K)	q_{rot}	
		At 300 K	At 1,000 K
H_2	85·38	1·76	5·86
HD	64·27	4·67	15·56
D_2	43·03	3·49	11·62
N_2	2·863	52·41	174·70
O_2	2·069	72·51	241·70
CO	2·766	108·50	316·51
$^{35}Cl_2$	0·3495	429·30	1,431

Example 5. Calculate the characteristic rotational temperature and the rotational partition function for H_2 gas at 2727°C given that the moment of inertia of hydrogen gas molecule at this temperature is $4·6033 \times 10^{-48}$ kg m^2.

Solution : $T = 2727°C = 3000$ K ; $\sigma = 2$

From Eqs. 78 and 79, the characteristic rotational temperature is given by

$$\Theta_{rot} = \frac{h^2}{8\pi^2 Ik} = \frac{(6·626 \times 10^{-34}\ \text{J s})^2}{(8\pi^2)(4·6033 \times 10^{-48}\ \text{kg m}^2)(1·38 \times 10^{-23}\ \text{J K}^{-1})} = 87·49\ \text{K}$$

From Eq. 80, the rotational partion function is given by

$$q_{rot} = \frac{T}{\sigma\Theta_{rot}} = \frac{3{,}000\ \text{K}}{2(87·49\ \text{K})} = 17·144$$

Example 6. The rotational constant of gaseous HCl, determined from microwave spectroscopy, is $10·59$ cm^{-1}. Calculate the rotational partition function of HCl at *(a)* 100 K and *(b)* 500 K.

Solution : $B = 10·59$ cm^{-1} ; $\sigma = 1$

(a) From Eq. 81,

$$q_{rot} = \frac{kT}{\sigma hcB} = \frac{(1·38 \times 10^{-23}\ \text{J K}^{-1})(100\ \text{K})}{(1)(6·626 \times 10^{-34}\ \text{J s})(3 \times 10^{10}\ \text{cm s}^{-1})(10·59\ \text{cm}^{-1})} = 6·56$$

(b) Similarly, q_{rot} at 500 K = **32·8**

Vibrational Partition Function. For a diatomic molecule vibrating as a simple harmonic oscillator (S.H.O.), the vibrational energy levels, obtained by the solution of the Schrödinger wave equation, are given by

$$E_{vib} = (v + 1/2)hv \qquad ...(83)$$

where v is the vibrational frequency and v is the vibrational quantum number which has the values $v = 0, 1, 2, 3, \cdots$

The energy levels are non-degenerate, *i.e.*, the degeneracy, g, is unity. Using Eqs. 39 and 83, the vibrational partition function of the diatomic molecule is given by

$$q_{vib} = \sum_{v=0}^{\infty} \exp\left[-\frac{(v + 1/2)hv}{kT}\right] = e^{-hv/2kT} \sum_{v=0}^{\infty} \exp\,[-vhv/kT] \qquad ...(84)$$

In the case of a simple harmonic oxcillator, the spacing between the neighbouring energy levels (which are equally spaced by an amount hv) is very large compared with the translational or the rotational energy levels. In other words, $hv >> kT$. Hence, the summation cannot be replaced by integration. The summation can, however, be carried out as follows :

Let $x = hv/kT$. Then,

$$\sum_{v=0}^{\infty} \exp[-vhv/kT] = \sum_{v=0}^{\infty} e^{-vx} = 1 + e^{-x} + e^{-2x} + e^{-3x} + \cdots \qquad ...(85)$$

$$= \frac{1}{1 - e^{-x}} = \frac{1}{1 - e^{-hv/kT}} \qquad ...(86)$$

Hence, from, Eq. 84

$$q_{vib} = \frac{e^{-hv/2kT}}{1 - e^{-hv/kT}} \qquad ...(87)$$

If we define Θ_{vib}, the **characteristic vibrational temperature**, of the oscillator as

$$\Theta_{vib} = hv/k \qquad ...(88)$$

then, the vibrational partition function is given by

$$q_{vib} = \frac{e^{-\Theta_{vib}/2T}}{1 - e^{-\Theta_{vib}/T}} \qquad ...(89)$$

According to Heisenberg's uncertainty principle, the oscillator cannot have a total energy of zero because this would imply that both the position and the momentum of the oscillator can be precisely determined. Thus, as seen from Eq. 83, even in the ground vibrational state (v=0), the osciallator possesses an energy ($hv/2$), called the **zero-point energy**, above the classical energy zero. Sometimes it is convenient to measure the energies of the various quantum states from the ground state rather than from the classical energy zero. Hence, the energy level expression (Eq. 83) for the S.H.O. is modified to

$$\varepsilon_{vib} = vhv \ (v = 0, 1, 2, 3, \ldots.) \qquad ...(90)$$

Hence the new vibrational partition function is given by

$$q'_{vib} = \sum_{v=0}^{\infty} \exp\,[-vhv/kT] = 1 + x + x^2 + x^3 + \cdots \qquad ...(91)$$

where $x = \exp(-hv/kT)$

For $x < 1$, $1 + x + x^2 + x^3 + \cdots = 1/(1 - x)$

Since $\exp(-hv/kT) < 1$, we have

$$q'_{vib} = \frac{1}{1 - e^{-hv/kT}} = \frac{1}{1 - e^{-\Theta_{vib}/T}} \qquad ...(92)$$

If the temperature is very high or very low, Eq. 89 can assume a simpler form, as illustrated below.

Case (i). T is very low so that $\Theta_{vib}/T >> 1$. Then, $\exp(-\Theta_{vib}/T)$ is negligible compared with unity in the denominator of Eq. 89 and we obtain

$$q_{vib} = e^{-\Theta_{vib}/2T} \quad \text{(at low temperatures)} \qquad ...(93)$$

Case (ii). T is very high so that $\Theta_{vib}/T << 1$. Then, the exponential in the denominator can be expanded as a series, retaining only the first two terms :

$$e^{-\Theta_{vib}/T} = 1 - \Theta_{vib}/T + \cdots \qquad ...(94)$$

Hence, $q_{vib} = \dfrac{T}{\Theta_{vib}} e^{-\Theta_{vib}/2T}$

(at high temperatures) ...(95)

The value of v, and hence Θ_{vib}, is obtained from the vibrational (infrared) spectrum of a molecule. Some results are shown in Table 3.

TABLE 3

Characteristic Vibrational Temperatures and Vibrational Partition Functions for Some Common Molecules

Molecule	Θ_{vib} (K)	q_{vib}	
		At 300 K	At 1000 K
H_2	5,987	1·000	1·002
HD	5,226	1·000	1·005
D_2	4,307	1·000	1·014
N_2	3,352	1·000	1·036
O_2	2,239	1·000	1·019
Cl_2	798	1·075	1·816

Example 7. For H_2 gas at 3,000 K, calculate the characteristic vibrational temperature Θ_{vib} and the vibrational partition function q'_{vib} given that the fundamental vibrational frequency of H_2 molecule, obtained from its Raman spectrum, is 4,405·3 cm^{-1}.

Solution : $T = 3{,}000$ K and $\bar{\nu} = 4405{\cdot}3$ cm^{-1}

$\nu = c/\lambda = c\bar{\nu}$ where $1/\lambda = \bar{\nu}$ and c is the velocity of light.

The characteristic vibrational temperature is given by

$$\Theta_{vib} = \frac{h\nu}{k} = \frac{hc\bar{\nu}}{k} = \frac{(6{\cdot}626\times10^{-34}\ \text{J s})(3\times10^{8}\ \text{m s}^{-1})(4{,}405{\cdot}3\ \text{cm}^{-1})(10^{2}\ \text{cm m}^{-1})}{1{\cdot}38\times10^{-23}\ \text{J K}^{-1}}$$

$$= \mathbf{6{,}338{\cdot}3\ K}$$

From Eq. 92 $$q'_{vib} = \frac{1}{1-e^{-\Theta_{vib}/T}} = \frac{1}{1-\exp[-6{,}338{\cdot}3\ \text{K}/3{,}000\ \text{K}]}$$

$$= \frac{1}{1-e^{-2{\cdot}1128}} = \frac{1}{1-0{\cdot}1210} = \frac{1}{0{\cdot}879} = \mathbf{1{\cdot}137}$$

Table 4 presents the typical values of the various partition functions of a diatomic molecule :

TABLE 4

Various Partition Functions of a Diatomic Molecule

Motion	Partition function	Order of Magnitude
Translational, q_{tr}	$= \dfrac{(2\pi mkT)^{3/2}\times V}{h^2}$	$10^{24} - 10^{25}\ V$
Rotational, q_{rot}	$8\pi^2 IkT/(h^2)$	$10 - 10^2$
Vibrational, q'_{vib}	$\dfrac{1}{[1-\exp(-h\nu/kT)]}$	$1 - 10$

Electronic Partition Function. Though it is possible, in principle, to solve the Schrödinger equation for the electronic states and energies of a molecule, it is more convenient to obtain this information from the spectroscopic data. For most of the molecules, the excited electronic energy levels lie so far above the ground state compared with kT (a typical excited state value being greater than 2eV $\approx 3\times10^{-19}$ J) that all the molecules may be considered to be in the ground state at ordinary temperatures. Thus, contriubtions to the electronic partition function arising from excited electronic states may be neglected. The electronic partition function is given by

$$q_{el} = \sum_i g_{el,i}\, e^{-\varepsilon_i/kT} = g_0 e^0 + g_1 e^{-\varepsilon_1/kT} + g_2 e^{-\varepsilon_2/kT} + \cdots\cdots \quad \ldots(96)$$

$$= g_0 \quad \ldots(97)$$

since the second, third and subsequent terms are considered negligible.

Thus, the electronic partition function is simply the degeneracy, g_0, of the ground electronic state. In the **Russell–Saunders coupling scheme**, the degeneracy of an atomic electronic level is given by

$$g_0 = 2J + 1 \quad \ldots(98)$$

where J is the total angular momentum quantum number. The degeneracies of the electronic ground states of atoms are given in Table 5.

TABLE 5

Ground State Electronic Degeneracies

Atom	H	He	Na	Ca	Cl	Pb
Term symbol : $^{2S+1}L_J$	$^2S_{1/2}$	$^1S_0$	$^2S_{1/2}$	$^1S_0$	$^2P_{3/2}$	$^3P_0$
$g_0 = 2J + 1$	2	1	2	1	4	1

The term symbol $^{2S+1}L_J$ is a short-hand notation for all the angular momenta of an atom, *viz.*, the spin angular momentum S, the orbital angular momentum L and the total angular momentum J. Mathematically,

$$S = \Sigma s_i \ ; \ L = \Sigma l_i \ \text{ and } \ J = L + S \quad \text{(for atoms with } Z \le 30\text{)}$$

where s_i and l_i are, respectively, the spins and the orbital angular momenta of individual electrons in the atom.

The ground electronic states of *free atoms* are generally degenerate. For hydrogen atom with electronic configuration $1s^1$, spin $S = 1/2$ and $L = 0$ so that $J = L + S = 1/2$ and $g_0 = 2\times1/2 + 1 = 2$. For helium atom with electronic configuration $1s^2$, $S = 1/2 - 1/2 = 0$ and $L = 0$ so that $J = 0$ and hence $g_0 = 1$. Thus, for H atom, $q_{el} = 2$ and for He atom, $q_{el} = 1$. Similarly, the ground state of chlorine atom, Cl, has a degeneracy of 4 so that $q_{el} = 4$. The alkali metal atoms having one electron in their outermost orbital, like the H atom, have $q_{el} = 2$.

The ground electronic states of most *molecules* and *stable ions* are invariably non-degenerate, *i.e.*, are singlets, so that $g_0 = 1$ and hence, $q_{el} = 1$. A very important exception is the oxygen molecule, O_2, having a triply degenerate ground state, *i.e.*, $g_{el} = 3$ so that $q_{el}=3$. For NO molecule, $g_0 = 2$ so that $q_{el} = 2$.

For atoms like chlorine and molecules like NO and O_2, the difference between the ground state energy level and the first excited state energy level is small. Hence, the contribution of the excited state must be taken into account in calculating the electronic partition function.

Example 8. The first excited state of chlorine atom, $^2P_{1/2}$, lies at 0·11 eV above the ground state, $^2P_{3/2}$. Calculate the electronic partition function of Cl atom at 1,000 K.

Solution : For the ground state, $g_0 = 2(3/2) + 1 = 4$

For the first excited state, $g = 2(1/2) + 1 = 2$

Hence, at 1,000 K, $q_{el} = g_0\, e^{-\varepsilon_0/kT} + g_1 e^{-\varepsilon_1/kT}$

$$= 4e^0 + 2\exp\left[-\frac{(0{\cdot}11\ \text{eV})(1{\cdot}602\times10^{19}\ \text{J/eV}}{1{\cdot}38\times10^{-23}\ \text{J K}^{-1}\times1{,}000\ \text{K}}\right]$$

$$= 4 + 2(0{\cdot}28) = \mathbf{4{\cdot}56}$$

Example 9. The energies of the first three energy levels of fluorine atom, determined from spectroscopy, are as follows :

Energy Level	Energy, cm^{-1}
$^2P_{3/2}$	0·0
$^2P_{1/2}$	404·0
$^2D_{5/2}$	102,406·5

Calculate *(i)* the electronic partition function and *(ii)* the fractions of fluorine atoms in the three energy levels at 1,000 K.

Solution : *(i)* According to Eq. 98, the degeneracies of the three energy levels are

$$g_0 = 2\times\tfrac{3}{2} + 1 = 4\ ; \ g_1 = 2\times\tfrac{1}{2} + 1 = 2\ ; \ g_2 = 2\times\tfrac{5}{2} + 1 = 6$$

From Eq. 96, $$q_{el} = g_0 e^{-\varepsilon_0/kT} + g_1 e^{-\varepsilon_1/kT} + g_2 e^{-\varepsilon_2/kT}$$

We must first convert the energies in cm^{-1} to energies in joules by multiplying by hc. Thus,

$$q_{el} = 4e^{-(0)(hc)/kT} + 2e^{-(404{\cdot}0)hc/kT} + 6e^{-(102{,}406{\cdot}5)hc/kT}$$

Substituting for k, h, c and T and simplifying, we get

$$q_{el} = 4e^0 + 2e^{-0{\cdot}5813} + 6e^{-147{\cdot}4} = \mathbf{5{\cdot}118}$$

(ii) From Boltzmann distribution,

$$n_i = N g_i e^{-\varepsilon_i/kT}/q \quad \text{(Eq. 41)}$$

Hence, for ground state (i=0),

$$\frac{n_0}{N} = \frac{g_0 e^{-\varepsilon_0/kT}}{q_{el}} = \frac{4 \times 1}{5{\cdot}118} = 0{\cdot}72$$

Similarly, for the first excited state (i = 1),

$$\frac{n_1}{N} = \frac{g_1 e^{-\varepsilon_1/kT}}{q_{el}} = \frac{2 \times e^{-0{\cdot}5813}}{5{\cdot}118} = 0{\cdot}218$$

and for the second excited state (i=2),

$$\frac{n_2}{N} = \frac{g_2 e^{-\varepsilon_2/kT}}{q_{el}} = \frac{6 \times e^{-147{\cdot}4}}{5{\cdot}118} = 0$$

Notice that at the given temperature, the fractions of molecules at the successive energy levels go on decreasing. The second excited state is empty even at 1,000 K.

Example 10. Consider the molecules of a gas which have two quantum states of energies 0 and ε and degeneracies g_1 and g_2, respectively. Calculate the contribution of these quantum states to the molar heat capacity of the gas at constant volume.

Solution : From Boltzmann distribution we know that the relative population of the two quantum states is given by

$$\frac{n_2}{n_1} = \frac{g_2}{g_1} e^{-(\varepsilon_2 - \varepsilon_1)/kT} = \frac{g_2}{g_1} e^{-\varepsilon/kT}$$

For one mole of the gas, $n_1 + n_2 = N_A$. Hence,

$$\frac{N_A - n_1}{n_1} = \frac{g_2}{g_1} e^{-\varepsilon/kT}$$

or

$$n_1 = \frac{N_A}{1 + \frac{g_2}{g_1} e^{-\varepsilon/kT}}$$

$$n_2 = N_A - n_1 = \frac{\left(N_A \frac{g_2}{g_1} e^{-\varepsilon/kT}\right)}{\left(1 + \frac{g_2}{g_1} e^{-\varepsilon/kT}\right)}$$

$\therefore$ The molar internal energy of the gas is given by

$$U = n_1\varepsilon_1 + n_2\varepsilon_2 = \frac{\left(N_A \varepsilon \frac{g_2}{g_1} e^{-\varepsilon/kT}\right)}{\left(1 + \frac{g_2}{g_1} e^{-\varepsilon/kT}\right)}$$

Hence,

$$C_V = \left(\frac{\partial U}{\partial T}\right)_V = \frac{\partial}{\partial T}\left[\frac{\left(N_A \varepsilon \frac{g_2}{g_1} e^{-\varepsilon/kT}\right)}{\left(1 + \frac{g_2}{g_1} e^{-\varepsilon/kT}\right)}\right]_V$$

$$= \frac{\left(N_A \varepsilon^2 \frac{g_1}{g_2} e^{-\varepsilon/kT}\right)}{(g_1 - e^{-\varepsilon/kT} + g_2)^2} \qquad \left[\text{Differential of } \frac{U}{V} = \frac{VdU - UdV}{V^2}\right]$$

Nuclear Partition Function. At terrestrial temperatures, the value of nuclear energy ε_{nucl} for excited states is very large so that the terms involving exp ($-\varepsilon_{nucl}/kT$) are negligible. We, therefore, need to consider only the ground state term. Thus,

$$q_{nucl} = g_{nucl(0)} e^{0/kT} = g_{nucl(0)} \qquad ...(99)$$

where subscript zero designates the ground state ; $g_{nucl(0)}$ represents the degeneracy of the ground nuclear state. For most calculations, q_{nucl} cancels out, except in the case of homonuclear molecules such as H_2 and D_2. It is known from quantum mechanics that homonuclear diatomics can be considered as mixtures of two species called *ortho* and *para molecules*. Their nuclear spin wave functions have different symmetry properties. For instance, it is found that for *ortho* molecules.

$$g^{ortho}_{nucl\,(0)} = (I+1)(2I+1) \qquad ...(100)$$

and for *para* molecules

$$g^{para}_{nucl\,(0)} = I(2I+1)$$

where I is the **nuclear spin quantum number** which can be determined from the hyperfine structure of atomic spectra and also from the variation in intensity in the microwave (rotational) spectra of molecules.

For hydrogen atom, I=1/2 so that for hydrogen molecule,

$$g^{ortho}_{nucl\,(0)} = 3 \; ; \; g^{para}_{nucl\,(0)} = 1$$

For the deuterium atom, I = 1 so that for deuterium molecule,

$$g^{ortho}_{nucl(0)} = 6 \; ; \; g^{para}_{nucl\,(0)} = 3$$

Thermodynamic Properties in Terms of the Partition Function

We can use the Boltzmann distribution law and the related partition functions to calculate the macroscopic (thermodynamic) properties such as internal energy, enthalpy, entropy, free energy, etc., of matter. The partition functions are, therefore, of great importance in statistical thermodynamics.

Internal Energy, U. The internal energy, U, of a system consisting of N independent particles (atoms or molecules) is equal to the sum of the energies of individual particles. Thus,

$$U = \sum_i N_i \varepsilon_i = N\bar{\varepsilon} \qquad ...(101)$$

where $\bar{\varepsilon}$ is the *average energy* of the particles defined by

$$\bar{\varepsilon} = (\sum_i N_i\varepsilon_i)/\sum_i N_i = (\sum_i \varepsilon_i e^{-\beta\varepsilon_i})/\sum_i e^{-\beta\varepsilon_i} = (\sum_i \varepsilon_i e^{-\beta\varepsilon_i})/q \qquad ...(102)$$

Now,

$$\left(\frac{\partial q}{\partial \beta}\right)_V = \frac{\partial[\Sigma e^{-\beta\varepsilon_i}]}{\partial\beta} = -\sum_i \varepsilon_i e^{-\beta\varepsilon_i} \qquad ...(103)$$

where the differentiation is carried out at *constant volume* since the energies ε_i depend upon the volume. Hence,

$$\bar{\varepsilon} = \frac{1}{q}\left(\frac{\partial q}{\partial \beta}\right)_V = -\left(\frac{\partial \ln q}{\partial \beta}\right)_V \qquad ...(104)$$

Therefore, from Eqs. 101 and 104 for a system containing N particles,

$$U = -N\left(\frac{\partial \ln q}{\partial \beta}\right)_V \qquad ...(105)$$

Since $\beta = 1/kT$ and $Nk = nR$ (where n is the number of moles), we have

$$U = -nR\left(\frac{\partial \ln q}{\partial(1/T)}\right)_V$$

or
$$U = nRT^2\left(\frac{\partial \ln q}{\partial T}\right)_V \quad \ldots(106)$$

Molar Heat Capacity, C_V. For one mole of a system ($n = 1$), differentiation of U with respect to T at constant V, yields the molar heat capacity C_V. Hence,

$$C_V = \left(\frac{\partial U}{\partial T}\right)_V = R\frac{\partial}{\partial T}\left[T^2\left(\frac{\partial \ln q}{\partial T}\right)_V\right] = \frac{R}{T^2}\left[\frac{\partial^2 \ln q}{\partial(1/T)^2}\right]_V \quad \ldots(107)$$

Entropy, S. If the particles are considered *indistinguishable*, then the thermodynamic probability for the system, given by Eq. 2, must be divided by $N!$ to yield the new thermodynamic probability of the Boltzmann distribution as

$$W = \prod_i g^{n_i}/n_i! \quad \ldots(108)$$

Using the Boltzmann equation for entropy, *viz.*,

$$S = k \ln W \quad \ldots(109)$$

we have
$$S = k(\sum_i n_i \ln g_i - \sum_i \ln n_i!) \quad \ldots(110)$$

Using the Stirling approximation, *viz.*,

$$\ln n_i ! = n_i \ln n_i - n_i \quad \ldots(111)$$

we obtain
$$S = k \sum_i n_i \ln (g_i/n_i) + kN \quad \ldots(112)$$

From Eq. 55, $\ln (g_i/n_i) = \ln (q/N) + \varepsilon_i/kT$ ...(113)

Substituting in Eq. 112, we have

$$S = k\sum_i n_i \ln\frac{q}{N} + k\sum_i \frac{n_i\varepsilon_i}{kT} + kN = kN\ln\frac{q}{N} + \frac{U}{T} + kN \quad \ldots(114)$$

For n moles of the system, $kN = nR$. Also, using the expression for U given by Eq. 106, we have

$$S = nR\left[\ln\frac{q}{N} + T\left(\frac{\partial \ln q}{\partial T}\right)_V + 1\right] \quad \ldots(115)$$

Helmholtz Function or Work Function, A.

$$A = U - TS \quad \ldots(116)$$

Hence, after substituting for U from Eq. 106 and for S from Eq. 114, we have

$$A = nRT^2\left(\frac{\partial \ln q}{\partial T}\right)_V - nRT\left[\ln\frac{q}{N} + \left(\frac{\partial \ln q}{\partial T}\right)_V + 1\right]$$

$$= -nRT(\ln q/N + 1) \quad \ldots(117)$$

Since $nR = Nk$, we can write Eq. 117 as

$$A = -kT[\ln q^N - (N \ln N - N)] = -kT \ln (q^N/N!) \quad \ldots(118)$$

or
$$A = -kT \ln Q \quad \ldots(119)$$

where Q is the **molar partition function**, *i.e.*, the partition function for one mole, *viz.*, for Avogadro's number of particles and q is the **molecular partition function**, *viz.*, the partition function for a single molecule.

Pressure, P. By definition, pressure is given by

$$P = -(\partial A/\partial V)_T \quad \ldots(120)$$

Differentiating Eq. 118 with respect to V at constant T, we have

$$(\partial A/\partial V)_T = -nRT(\partial \ln q)/(\partial V)_T \quad \ldots(121)$$

$$\therefore \quad P = -nRT(\partial \ln q)/(\partial V)_T \quad \ldots(122)$$

Gibbs Function, G. The Gibbs free energy is defined as

$$G = H - TS = (U + PV) - TS = A + PV \quad \ldots(123)$$

Substituting Eq. 117 for A and Eq. 122 for P, we obtain

$$G = -nRT\left[\ln\frac{q}{N} + 1 - V\left(\frac{\partial \ln q}{\partial V}\right)_T\right] \quad \ldots(124)$$

Enthalpy, H. Enthalpy is defined as $H = U + PV$.

Substituting Eq. 106 for U and Eq. 122 for P, we have

$$H = -nRT^2\left(\frac{\partial \ln q}{\partial T}\right)_V + nRTV\left(\frac{\partial \ln q}{\partial V}\right)_T$$

$$= nRT\left[\left(\frac{\partial \ln q}{\partial \ln T}\right)_V + \left(\frac{\partial \ln q}{\partial \ln V}\right)_T\right] \quad \ldots(125)$$

Thermodynamic Properties of an Ideal Monatomic Gas

A monatomic gas, such as helium, neon, argon, etc., has only translational and electronic degrees of freedom. Hence, from Eq. 62, molecular partition function is given by

$$q = q_{tr}\, q_{el} \quad \ldots(126)$$

However, as we have shown in Eq. 97,

$$q_{el} = g_0$$

where g_0 is the degeneracy of the electronic ground state. Hence,

$$q = g_0\, q_{tr} \quad \ldots(127)$$

Using Eq. 68 for q_{tr}, $q = g_0 (2\pi mkT/h^2)^{3/2} V$ ...(128)

Taking $g_0 = 1$ for most atomic systems,

$$q = (2\pi mkT/h^2)^{3/2} V \quad \ldots(129)$$

According to Eq. 106, $U = nRT^2\left(\frac{\partial \ln q}{\partial T}\right)_V = nRT^2\left(\frac{3}{2T}\right) = \frac{3}{2}nRT$ ...(130)

The molar heat capacity is given by

$$C_V = (\partial U/T)_V = \tfrac{3}{2}R \quad \ldots(131)$$

Entropy is obtained by substituting Eq. 129 in Eq. 115. Accordingly,

$$S = nR\left[\tfrac{5}{2} - \ln (Nh^3) + \tfrac{3}{2}\ln (2\pi mk) + \tfrac{3}{2}\ln T + \ln V\right] \quad \ldots(132)$$

For one mole of an ideal gas,

$$V = RT/P\ ;\ \ln V = \ln R + \ln T - \ln P = \ln N_A + \ln k + \ln T - \ln P$$

Substituting in Eq. 132 and simplifying, we get

$$S = nR\left[\tfrac{5}{2} + \tfrac{5}{2}\ln T - \ln P + \tfrac{5}{2}\ln k + \tfrac{3}{2}\ln 2\pi m - 3\ln h\right] \qquad ...(133)$$

Eq. 133 can be rewritten as

$$S = nR\ln\left(\frac{e^{5/2}kT}{P\Lambda^3}\right),\ \Lambda = h/(2\pi mkT)^{1/2} \qquad ...(134)$$

Eq. 134 is known as the **Sackur-Tetrode** equation.

From Eq. 122, the pressure is given by

$$P = nRT\left(\frac{\partial \ln q}{\partial V}\right)_T = nRT\left(\frac{1}{V}\right) = \frac{nRT}{V} \qquad \text{or} \qquad PV = nRT \qquad ...(135)$$

which is the **equation of state** for n moles of an ideal gas.

Substituting Eqs. 130 and 135, in the relation $H = U + PV$, the **enthalpy** is given by

$$H = \tfrac{3}{2}nRT + (nRT/V)\,V = \tfrac{3}{2}nRT + nRT = \tfrac{5}{2}nRT \qquad ...(136)$$

From Eq. 117, 129, 135, we have

$$A = -nRT\left[1 - \ln h^2 + \tfrac{3}{2}\ln 2\pi m + \tfrac{5}{2}\ln k + \tfrac{5}{2}\ln T - \ln P\right] \qquad ...(137)$$

From Eqs. 137 and 123, the **Gibbs free energy** for an ideal gas is given by

$$G = -nRT\ln(q/N) \qquad ...(138)$$

This is further simplified to give

$$G = -nRT\left[-\ln h^2 + \tfrac{3}{2}\ln 2\pi m + \tfrac{5}{2}\ln k + \tfrac{5}{2}\ln T - \ln P\right] \qquad ...(139)$$

Example 11. Calculate the constant volume heat capacity of an ideal monatomic gas.

Solution : From Eq. 131, $C_V = \frac{3}{2}R = \frac{3}{2}(8{\cdot}314\ J\ K^{-1}\ mol^{-1}) = 12{\cdot}47\ J\ K^{-1}\ mol^{-1}$

Thermodynamic Properties of an Ideal Diatomic Gas

An ideal diatomic gas has translational, rotational, vibrational and electronic energies. Hence, its molecular partition function is given by

$$q = q_{tr}\,q_{rot}\,q_{vib}\,q_{el} \qquad ...(140)$$

The translational and electronic contributions to q have been discussed above while considering the thermodynamic properties of an ideal monoatomic gas. We will, therefore, concern ourselves with the rotational and vibrational contributions to thermodynamic properties. For convenience, we will consider one mole of the gas.

From Eq. 80, $q_{rot} = T/\sigma\Theta_{rot}$

Hence, $$U_{rot} = RT^2\left(\frac{\partial \ln q_{rot}}{\partial T}\right)_V = RT^2\left(\frac{\partial \ln T}{\partial T}\right)_V = RT \qquad ...(141)$$

The rotational contribution to molar heat capacity at constant volume is given by

$$C_{V,rot} = (\partial U_{rot}/\partial T)_V = R \qquad ...(142)$$

Fig. 4 shows the rotational contribution to molar energy and molar heat capacity as functions of temperature. For $T << \Theta_{rot}$, the rotational contribution to energy (Fig. 4*a*) is very small. The energy required to excite molecules rotationally comes from collisions between the gas molecules. Since at low temperature, collisions between molecules produce very little kinetic energy, it is impossible for collisions to furnish a whole quantum of rotational energy, with the result that most of the molecules remain rotationally unexcited. This is expressed by saying that rotational energy is *frozen out*.

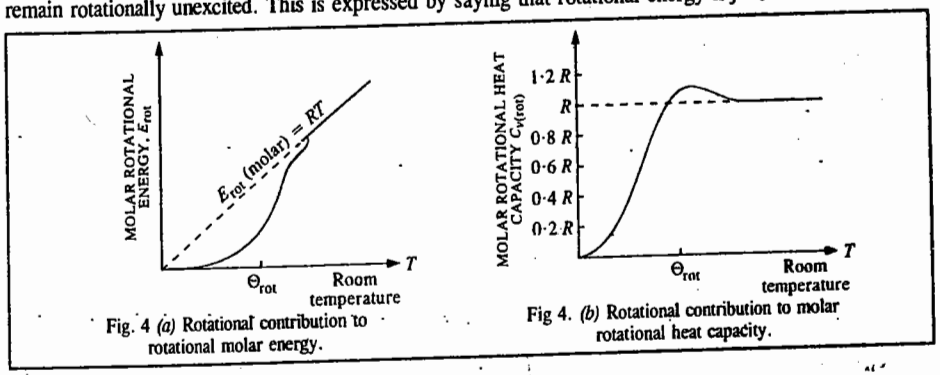

Fig. 4 *(a)* Rotational contribution to rotational molar energy.

Fig 4. *(b)* Rotational contribution to molar rotational heat capacity.

Let us now calculate the vibrational contribution to thermodynamic properties.

$$U_{vib} = RT^2\left(\frac{\partial \ln q_{vib}}{\partial T}\right)_V \qquad \text{(Eq. 106)}$$

$$= \frac{RT^2}{q_{vib}}\left(\frac{\partial q_{vib}}{\partial u}\right)_V \times \frac{du}{dT} \quad \text{where } u = \Theta_{vib}/T \qquad ...(143)$$

From Eq. 92, $q_{vib} = 1/(1 - e^{-u})$

Thus, $$U_{vib} = RT^2\,\frac{e^{-u}}{1-e^{-u}} \times \frac{\Theta_{vib}}{T^2} = R\Theta_{vib}\left(\frac{1}{e^u - 1}\right) = RT\,\frac{(\Theta_{vib}/T)}{e^{vib/T} - 1} \qquad ...(144)$$

Hence, $$C_{V,vib} = \left(\frac{\partial U_{vib}}{\partial T}\right)_V = R\left(\frac{\Theta_{vib}}{T}\right)^2 \times \frac{e^{\Theta_{vib}/T}}{(e^{\Theta_{vib}/T} - 1)^2} = \frac{Ru^2e^u}{(e^u - 1)^2} \qquad ...(145)$$

Fig. 5 shows the vibrational contributions to molar vibrational energy and molar vibrational heat capacity of a diatomic gas, plotted as a function of temperature. Notice that the vibrational modes 'thaw out' over a relatively much greater temperature range than the rotational modes.

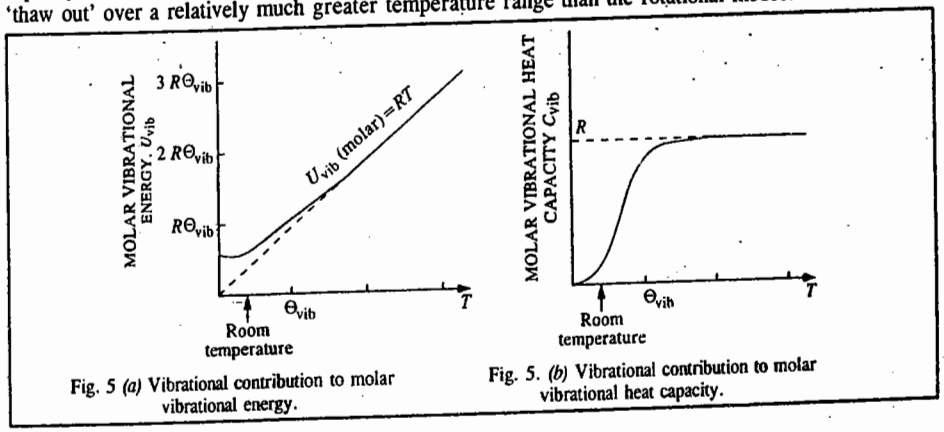

Fig. 5 *(a)* Vibrational contribution to molar vibrational energy.

Fig. 5. *(b)* Vibrational contribution to molar vibrational heat capacity.

Let us calculate the limiting values of the right hand side of Eq. 145 :

Let $$r = -\frac{u}{e^u - 1} e^{u/2} \quad ...(146)$$

so that $$C_{V,\text{vib}} = Rr^2 \quad ...(147)$$

Hence, $$r = \frac{u}{e^{u/2} - e^{-u/2}} = \frac{u}{\left[1 + \frac{u}{2} + \frac{1}{2!}\left(\frac{u}{2}\right)^2 + \cdots\right] - \left[1 - \frac{u}{2} + \frac{1}{2!}\left(\frac{u}{2}\right)^2 - \cdots\right]}$$

$$= \frac{u}{\left[\frac{u}{2} + \frac{1}{3!}\left(\frac{u}{2}\right)^3 + \cdots\right]} = \frac{1}{1 + \frac{u^2}{24} + \cdots} \quad ...(148)$$

As $u \to 0$, $r \approx 1$ and when $u \to \infty$, $r \approx 0$. Thus, we see that if $T >> \Theta_{\text{vib}}$ (*i.e.*, u is small), Eq. 147 simplifies to $C_{V,\text{vib}} \approx R$.

Also, if $T >> \Theta_{\text{vib}}$ (*i.e.*, u is large), then $C_{V,\text{vib}} >> 0$. Thus, at a temperature far below the characteristic vibrational temperature, the vibrational contribution to C_V is negligible.

Adding the translational contribution and vibrational contribution to the molar heat capacity of an ideal diatomic gas, we have

$$C_{V,\text{vib}} = \begin{cases} \frac{5}{2}R \; (T << \Theta_{\text{vib}}) \\ \qquad\qquad\qquad\qquad \text{(For intermediate temperatures)} \\ \frac{7}{2}R \; (T >> \Theta_{\text{vib}}) \\ \qquad\qquad\qquad\qquad \cdots\cdots \\ R\left[\frac{5}{2} + 2\frac{e^u}{(e^u - 1)^2}\right] \end{cases}$$

Rotational Partition Function of Homonuclear Diatomic Molecules and Nuclear Spin

We usually ignore the contribution of nuclear spin to the partition function because it is not excited at room temperature. However, for homonuclear diatomic molecules (such as H_2, N_2, D_2, etc.) its inclusion can lead to quantum states with different statistical weights (degeneracies) even in the ground state of the molecule.

Before proceeding further, we shall make an important digression here. The total wave function ψ_T of any molecule (including diatomics) can be written as

$$\psi_T = \psi_{\text{internal}}\, \psi_t = \psi_e\, \psi_v\, \psi_r\, \psi_n\, \psi_t \quad ...(149)$$

In Eq. 149, ψ_e specifies the electronic state; the product $\psi_e\psi_v$ specifies a vibrational level because vibrational levels are associated with some particular electronic state. Similarly, a rotational level is specified only when the product $\psi_e\psi_v\psi_r$ is given. We refer to ψ_v and ψ_r as the vibrational and rotational eigenfunctions, respectively. ψ_v depends only on the magnitude of the internuclear distance and thus, remains unchanged by reflection at the origin. ψ_e depends on a set of coordinates rigidly attached to the nucleus; it is unchanged if the nuclei rotate. If we ignore the nuclear spin, then for symmetry considerations, it is enough to examine the expression

$$\psi = \psi_e\, \psi_r \quad ...(150)$$

For a heteronuclear diatomic rotator, the ψ_r are the spherical harmonics Y_{JM} whose parity is $(-1)^J$. This implies that, under a reflection in the origin, ψ_r changes sign only for odd J. If ψ_e of the ground state is even and remains unchanged, then the ψ is symmetric for J even and antisymmetric for J odd.

However, for homonuclear diatomics, the interchange of nuclei can change the sign of ψ, with the result that each rotational level is charaterized by two symmetry labels—plus or minus with respect to a reflection in the origin of all particles symmetric or antisymmetric w.r.t. an interchange of nuclei. Hence, from quantum mechanical indistinguishability of like particles, we conclude that *symmetric linear molecules can have either even (0, 2, 4, ...) values or odd (1, 3, 5, ...) values of J but not both.* Hence, for a homonuclear diatomic molecule, the allowed energy levels will yield a summation term just half as big as if the atoms were different. Here, then, we must divide the sum over all states by the symmetry number $\sigma=2$. This is the reason for the origin of the symmetry number and we have already seen that the rotational partition function for a diatomic molecule is given by $q_r = T/\sigma\theta_r$, where $\sigma=2$ for a symmetric linear (homonuclear) rotor and $\sigma=1$ for an antisymmetric linear (heteronuclear) rotor.

After this brief digression, let us return to our subject and consider the contribution of nuclear spin to the partition function since its inclusion (in the case of homonuclear diatomics) leads to quantam states with different statistical weights (degeneracies) even in the ground state of the molecule at room temperature. As we have remarked above, each rotational level $\psi_R = \psi_e\, \psi_v\, \psi_r$ is either symmetric or antisymmetric w.r.t. interchange of nuclei. The ψ_R is a function of coordinates. Including the effect of the nuclear spin,

$$\psi_{RN} = \psi_R\, \chi_N \quad ...(151)$$

where the nuclear spin wave function χ_N is not a function of coordinates. The ψ_{RN} is really the product of the wave function for the independent rotational and spin modes of energy storage. It is known that nuclei are either bosons or fermions depending on whether the nuclear spin, I, is integral or half-integral, respectively. Also, for bosons, χ_N is symmetric since the interchange of the two nuclei does not change the sign of the molecular wave function. For fermions, on the other hand, the sign changes. Thus, we can write schematically :

I	Statistics	ψ_{RN}
Integral	BE	Symmetric
Half-integral	FD	Antisymmetric

If $I = 0$, as in O_2, the nuclei are bosons and hence $\psi_{RN} = \psi_R$ is symmetric. The antisymmetric levels are thus not occupied. If, however, $I = 1/2$, as in H_2, the nuclei (protons) are bosons and hence ψ_{RN} is antisymmetric. In H_2 molecule, for the two protons 1 and 2, the total nuclear spin is $I = I_1 + I_2 = 0, 1$. On the basis of the symmetry conditions, we obtain two spin wave functions χ_N :

$$\chi_N^a(I=0, I_z=0) = (1/\sqrt{2})(\uparrow\downarrow - \uparrow\downarrow) \quad ...(152)$$

$$\left.\begin{aligned} \chi_N^s(1,1) &= \uparrow\uparrow \\ \chi_N^s(1,0) &= (1/\sqrt{2})(\uparrow\downarrow + \downarrow\uparrow) \\ \chi_N^s(1,-1) &= \downarrow\downarrow \end{aligned}\right\} \quad ...(153)$$

where ($\uparrow$) denotes spin up, ($\downarrow$) denotes spin down and the superscript denotes symmetric (s) or antisymmetric (a) property of the two nuclear spins. For H_2 we have finally the combinations shown schematically below :

ψ_{RN}	I	χ_N	ψ_R	Spin degeneracy $(2I+1)$	Statistical weight
a	0	a	s (even J)	1	$1(2J+1)$
a	1	s	a (odd J)	3	$3(2J+1)$

(Recall that the degeneracy of the rotational energy levels is $2J+1$).

Thus, for H_2 we find that the symmetric rotational levels ψ_R have a statistical weight of $(2J+1)$ whereas the antisymmetric ones have a statistical weight of $3(2J+1)$.

If, as in the case of D_2 or N_2, the nuclear spin $I=1$, the nuclei are bosons and ψ_{RN} is symmetric. The Russell-Saunders type coupling of the two spins gives $I = 0, 1, 2$ with χ_N symmetric for I=0, antisymmetric for $I=1$, and symmetric for $I=2$. For the molecules the allowed combinations are shown schematically below :

ψ_{RN}	I	χ_N	ψ_R	Spin degeneracy $(2I+1)$	Statistical weight
s	0	s	s	1	$1(2J+1)$
s	1	a	a	3	$3(2J+1)$
s	2	s	s	5	$5(2J+1)$

Thus, we find that the symmetric rotational levels ψ_R have a statistical weight of $6(2J+1)$ whereas the antisymmetric ones have a statistical weight of $3(2J+1)$

Statistical Thermodynamics of Ortho and Para Hydrogen

From the above discussion we conclude that two types of H_2 molecules are possible—the *ortho hydrogen* molecules with $I=1$ (parallel spins) occupy odd-J rotational levels with $J=1, 3, 5 \ldots$, whereas the *para hydrogen* molecules with $I=0$ (antiparallel spins) occupy even J rotational levels with $J = 0, 2, 4, \ldots$. Because each quantum state has equal a priori probability, there exist three times as many odd rotational states (ortho) as even (para), due to the different statistical weights. After the establishment of thermal equilibrium between nuclear spin orientation, we have the following expressions for the rotational partition function, q_{rot} :

$$q_{rot,\,equil} = 3q_{rot,\,ortho} + q_{rot,\,para} \qquad \ldots(154)$$

$$q_{rot,\,ortho} = \sum_{J=1,3,5\ldots}^{\infty} (2J+1)\exp[-J(J+1)\theta]$$

$$= 3e^{-2\theta} + 7e^{-12\theta} + \ldots \qquad \ldots(155)$$

$$q_{rot,\,para} = \sum_{J=0,2,4\ldots}^{\infty} (2J+1)\exp[-J(J+1)\theta] = 1 + 5\,e^{-6\theta} + \ldots \qquad \ldots(156)$$

where $\theta=\Theta_{rot}/T$; Θ_{rot} is the characteristic rotational temperature defined elsewhere in this chapter. For H_2 molecule, Θ_{rot} = 85 K.

The relative Boltzmann population, according to MB statistics, gives

$$\frac{N_i}{N} = \frac{g_i \exp(-\beta\varepsilon_i)}{\sum_i g_i \exp(-\beta\varepsilon_i)} = \frac{(2J+1)\exp(-J(J+1)\theta}{q_{rot}} \qquad \ldots(157)$$

Thus, at equilibrium, the ratio of the number of ortho H_2 molecules to para H_2 molecules is given by

$$\frac{N_{ortho}}{N_{para}} = \frac{3q_{rot,\,ortho}}{q_{rot,\,para}} \qquad \ldots(158)$$

Fig. 6 shows percentage of para-H_2 in the equilibrium mixture ($N = N_{para} + N_{ortho}$).

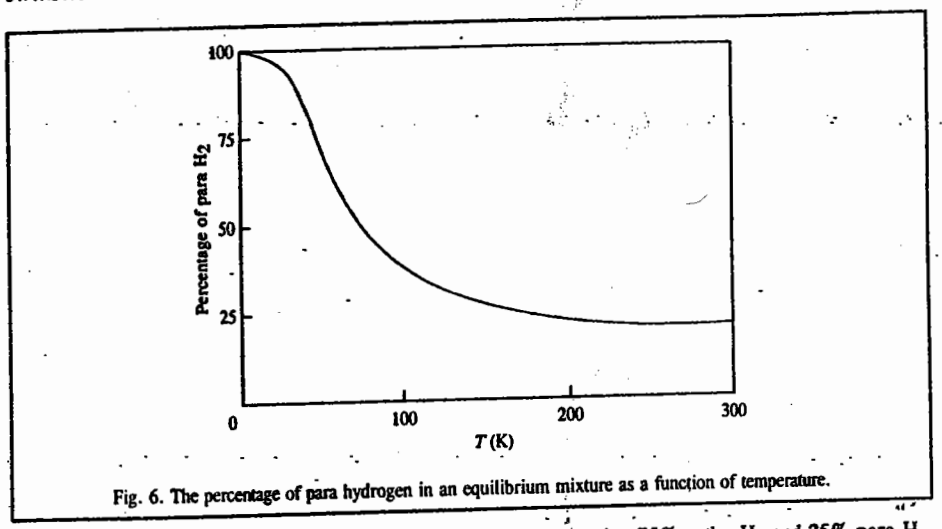

Fig. 6. The percentage of para hydrogen in an equilibrium mixture as a function of temperature.

At room temperature (298 K), the equilibrium mixture contains 75% ortho H_2 and 25% para H_2. As the temperature is decreased, we expect the ortho state (higher energy as odd $J>0$) to be converted into the para state (ground state, $J=0$) (Fig. 6). It should be noted that the expression for the rotational partition function at equilibrium (Eq. 154) will hold even as $T \to 0$ where the H_2 gas is entirely para. The experimental rotational heat capacity curve (Fig. 7, curve *B*), according to this prescription, is found to disagree with experimental data. This anomaly can be explained by the fact that thermal equilibrium is established very slowly. As a matter of fact, it might take about three years for the equilibrium to be established !

Consider next the case of complete inhibition of ortho—para conversion. We must then regard the ortho and para molecules as quite distinct so that the sum in Eq. 154 should be replaced by a product:

$$q_{rot} = [q_{rot,\,ortho}]^{3/4}\,[q_{rot,\,para}]^{1/4} \qquad \ldots(159)$$

Using Eqs. 155, 156 and 159, we have for the rotational heat capacity,

$$C_{V,rot}\,(ortho) = Nk\frac{\partial}{\partial T}\left[-\frac{\partial \ln q_{rot,\,ortho}}{\partial(1/T)}\right] \qquad \ldots(160)$$

$$= Nk\frac{\partial}{\partial T}\left\{-\frac{\partial}{\partial(1/T)}\ln\left[3e^{-2\theta}\left(1+\frac{7}{3}e^{-10\theta}+\cdots\right)\right]\right\}$$

$$= \frac{700}{3}Nk\theta^2\,e^{-10\theta} + \cdots \qquad (161)$$

$$C_{V,rot}\,(para) = 180\,Nk\,\theta^2\,e^{-6\theta} + \cdots \qquad \ldots(162)$$

Hence, $$C_{V,rot} = \frac{3}{4}C_{V,rot}\,(ortho) + \frac{1}{4}C_{V,rot}\,(para),\ \theta = 85/T \qquad \ldots(163)$$

Eq. 163 is in agreement with experiment (Fig. 7, curve *C*). The curve *A* (Fig. 7) has been observed by producing pure para H_2 using a catalyst.

The explanation of the rotational heat capacity of H_2 was one of the great triumphs of post-quantum statistical mechanics. In principle, such nuclear effects should be observable in other homonuclear diatomics. However, the characteristic rotational temperatures for all the other molecules are so small that these molecules reach the "high temperature limit" while still in the solid state. H_2 is somewhat unusual in that its characteristic rotational temperature is so much greater than its boiling point.

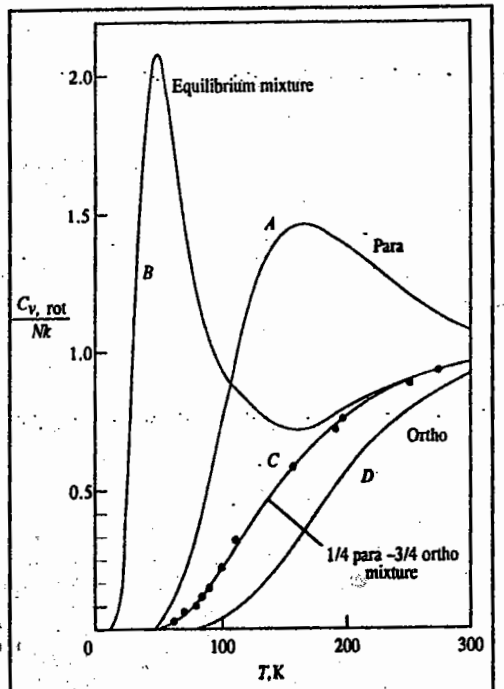

Fig. 7. The rotational and nuclear contributions to the molar heat capacity for ortho hydrogen, para hydrogen, an equilibrium mixture of ortho and para hydrogen, a metastable 75 percent ortho and 25 percent para mixture and the experimental data.

Application of BE Statistics to Black body Radiation (*i.e.*, Ideal Photon Gas)

Electromagnetic radiation in thermal equilibrium is called black body radiation. Max Planck, the father of old quantum theory, proposed in 1900 that the radiation is emitted or absorbed in quanta (packets) of energy $\varepsilon = h\nu$, where ν is the radiation frequency. Einstein, in 1905, proposed that radiation also travels as quanta of energy called photons (having spin 1). The photons do not interact with one another and hence form an ideal, Bose–Einstein (BE) gas. For radiation in a material medium, the interaction between radiation and matter must be very small for the gas to be considered an ideal BE gas. This condition is satisfied for gases at all frequencies, except near the absorption lines of the medium. Since there is no interaction between the photons, the presence of the material medium is necessary to enable thermal equilibrium to be set up. The thermal equilibrium is brought about by the absorption and the emission of photons by the matter present. Thus, the number of photons N is not a fixed quantity and has to be determined from the condition of thermal equilibrium. In thermal equilibrium, the Helmholtz free energy A is minimum for a given T and V; thus, the necessary condition is

$$(\partial A/\partial N)_{V,T} = 0 \qquad ...(164)$$

Since $$\mu = (\partial A/\partial N)_{V,T}, \qquad ...(165)$$

we find that the chemical potential, μ, of the ideal photon gas is zero, *i.e.*,

$$\mu = 0 \qquad ...(166)$$

Now, for a photon (travelling with the speed of light, c), the momentum $p = h/\lambda = h\nu/c$ so that $dp = h d\nu/c$ and the number of states for photons with momenta between p and $p+dp$ is

$$g(p)dp = \frac{4\pi p^2 dp}{h^3/V} = \frac{4\pi V}{c^3}\nu^2 d\nu \qquad ...(167)$$

where V is the volume of the enclosure for the black body radiation. As there are two independent directions of polarization,

$$g(\nu)d\nu = \frac{8\pi V}{c^3}\nu^2 d\nu \qquad ...(168)$$

for the total number of states lying in the frequency range $d\nu$ at ν. Then, the BE distribution for photons is

$$dn = \frac{g(\nu)\,d\nu}{\exp(\alpha+\beta\varepsilon)-1} = \frac{8\pi V}{c^3}\frac{\nu^2 d\nu}{\exp(\alpha+\beta\varepsilon)-1} \qquad ...(169)$$

where $\varepsilon = h\nu$. The energy density $u d\nu = (dn/V)\varepsilon$ in the specified energy range is

$$u d\nu = \frac{8\pi h\nu^3}{c^3}\frac{d\nu}{\exp(\alpha+\beta\varepsilon)-1} \qquad ...(170)$$

This is the celebrated Planck radiation formula if we put for photons

$$\alpha = 0,\ \beta = 1/kT \qquad ...(171)$$

The requirement $\alpha=0$ (or $\mu=0$) simply means dropping the condition $\delta N = \Sigma\delta n = 0$, for the fixed number of particles. Thus, as mentioned above, photons differ from other bosons in that their number is not conserved. Thus, for photons, the energy density is given by

$$u d\nu = \frac{8\pi h\nu^3}{c^3}\frac{d\nu}{\exp(h\nu/kT)-1} \qquad \textbf{(Planck's law)} \ ...(172)$$

This derivation of Planck's radiation law was given by the great Indian physicist S.N. Bose (1894–1974) in 1924. (Bose derived this result in purely quantum terms, without referring to classical oscillators as Planck had done. Einstein later applied Bose's technique to a collection of particles, the resulting treatment being known as Bose–Einstein (BE) statistics.)

For $$h\nu \ll kT,\ \exp(h\nu/kT) - 1 \simeq h\nu/kT, \qquad ...(173)$$

$$u d\nu = (8\pi kT/c^3)\,\nu^2 d\nu \qquad \textbf{(Rayleigh-Jeans law)} \ ...(174)$$

For $$h\nu \gg kT,\ \exp(h\nu/kT) - 1 \simeq \exp(h\nu/kT)$$

$$u d\nu = (8\pi h\nu^3/c^3)\exp(-h\nu/kT)d\nu \qquad \textbf{(Wien's law)} \ ...(175)$$

The total energy density is given by

$$\frac{U}{V} = \int_0^\infty u(\nu,t)\,d\nu = \frac{8\pi h}{c^3}\int_0^\infty \frac{\nu^3 d\nu}{\exp(h\nu/kT)-1}$$

$$= \frac{8\pi h}{c^3}\left(\frac{kT}{h}\right)^4 \int_0^\infty \frac{x^3 dx}{e^x - 1} = bT^4,\ b = \frac{8\pi^5 k^4}{15c^3h^3} \qquad ...(176)$$

where $x = h\nu/kT$ and the integral is given by

$$\Gamma(4)\Sigma\pi^4 = 6\zeta(4) = \frac{\pi^4}{15} \qquad ...(177)$$

where Γ is the **gamma function** and ζ is the **Riemann zeta function**, defined by the great German mathematician Bernhard Riemann (1826–1866). (The gamma function $\Gamma(n)$ and the Riemann zeta function $\xi(n)$ are the standard functions of mathematical physics, defined in books on mathematics.)

Eq. 176 is called the **Stefan–Boltzmann law.**

With no restraint on n_i, the photon partition function is given by

$$Q_{ph}(T,V) = \sum_{n_1=0}^{\infty}\sum_{n_2=0}^{\infty}...\exp[-\beta(n_1\varepsilon_1 + n_2\varepsilon_2 + ...)] \quad ...(178)$$

$$= \prod_{i=0}^{\infty}\left[\sum_{n_i=0}^{\infty}...\exp(-\beta\varepsilon_i n_i)\right] = \prod_{i=0}^{\infty}\frac{1}{1-\exp(-\beta\varepsilon_i)} \quad ...(179)$$

so that

$$\ln Q_{ph}(T,V) = \sum_i \ln[1-\exp(-\beta\varepsilon_i)] = -\int \ln[1-\exp(-\beta h\nu)]\, g(\nu)\, d\nu \quad ...(180)$$

The Helmholtz free energy (work function) is given by

$$A(V,T) = -kT \ln Q_{ph}(V,T)$$

$$= \frac{8\pi VkT}{c^3}\int_0^{\infty} v^2 dv \ln[1-\exp(-\beta h\nu)]$$

$$= \frac{8\pi VkT}{c^3\beta^3h^3}\int_0^{\infty} x^2\, dx \ln[1-e^{-x}] = -\frac{1}{3}bVT^4 \quad ...(181)$$

where $x = \beta h\nu$, b is given by Eq. 176 and the integral is equal to

$$\frac{1}{3}\int_0^{\infty} d(x^3)\ln(1-e^{-x}) = \left[\frac{1}{3}x^3\ln(1-e^{-x})\right]_0^{\infty} - \frac{1}{3}\int_0^{\infty}\frac{x^3dx}{e^x-1} = -\frac{\pi^4}{45} \quad ...(182)$$

Note that Q can be interpreted as the grand partition function for an ideal Bose gas with $\mu=0$. From Eq. 181 we can evaluate the thermodynamic quantities of the ideal photon gas :

$$S = -(\partial A/\partial T)_V = (4/3)bVT^3 \quad ...(183)$$

$$P = -(\partial A/\partial V)_T = (1/3)\, bT^4 \quad ...(184)$$

$$U \equiv E = A + TS = bVT^4 \quad ...(185)$$

From Eqs. 184 and 185, we see that the radiation pressure is one-third of the energy density (U/V) :

$$P = \frac{1}{3}\left(\frac{U}{V}\right) = \frac{u}{3} \text{ where } u = U/V \quad ...(186)$$

The heat capacity of the radiation is given by

$$C_V = \left(\frac{\partial E}{\partial T}\right)_V = 4bVT^3 \quad ...(187)$$

$$= \frac{16\sigma}{c}VT^3 \quad ...(188)$$

where σ is the **Stefan-Boltzmann constant** defined as

$$\sigma = \frac{\pi^2k^4}{60c^2\hbar^3} = 5{\cdot}67 \times 10^{-8} \text{ W m}^{-2} \text{ K}^{-4}$$

Quantum Statistics : Ideal Bose-Einstein Gas

a. Bose-Einstein Distribution. We have shown earlier (Eq. 29) that for an ideal BE gas of N molecules in a volume V, the most probable number of particles with energy ε_i is given by

$$\bar{n}_i(\varepsilon_i) = \frac{g_i}{\exp(\alpha+\beta\varepsilon_i)-1} = \frac{g_i}{\exp[(\varepsilon_i-\mu)/kT-1} \quad ...(189)$$

where $\beta = 1/kT$, $\alpha = -\beta\mu$, and g_i is the degeneracy of the ith level. The parameter α (or μ) is determined as a function of N and T for the condition

$$N = \sum_{\substack{i=0\\ \text{levels}}}^{\infty} n_i = \frac{g_i}{\exp[\beta(\varepsilon_0-\mu)]-1} + \frac{g_i}{\exp[\beta(\varepsilon_i-\mu)]} + \cdots = \bar{n}_0 + \bar{n}_1 + \cdots \quad ...(190)$$

where the sum is over the energy levels since we have included the degeneracy g_i in Eq. 189. Equivalently, we can replace g_i by 1 in Eq. 189 and then the sum is over quantum states in Eq. 190. Since the number of particles in a level cannot be negative, we must have $\bar{n}_i \geq 0$. Thus, for a boson gas at all temperatures $(\varepsilon_i - \mu)$ must be greater than zero for all ε_i, *i.e.*,

$$\exp(-\beta\mu) = \exp(-\mu/kT) \geq 1 \text{ or } \mu \leq 0 \quad ...(191)$$

Replacing g_i by the density of states, $g(\varepsilon)d\varepsilon = \frac{2\pi V}{h^3}(2m)^{3/2}\varepsilon^{1/2}d\varepsilon$ ...(192)

(which is a standard result whose derivation we omit here), the sum can be replaced by an integral in Eq. 190, giving

$$N = \int_0^{\infty}\frac{g(\varepsilon)\,d\varepsilon}{e^{-\beta\mu}e^{\beta\varepsilon}-1} = \frac{2\pi V}{h^3}(2m)^{3/2}\int_0^{\infty}\frac{\varepsilon^{1/2}d\varepsilon}{\frac{1}{z'}e^{\beta\mu}-1}$$

$$= \frac{V}{\lambda^3}F_{3/2}(z') = Vn_QF_{3/2}(z') \quad ...(193)$$

where z' [$= \exp(\beta\mu)$] is the absolute activity, or fugacity, for a gas and $n_Q = 1/\lambda^3$ = quantum concentration (*i.e.*, concentration associated with one atom in a cube of side λ). Thus,

$$e^{\beta\mu} \equiv z' \leq 1, \quad \lambda = h/(2\pi mkT)^{1/2} \quad ...(194)$$

Introducing a dimension parameter $x = \beta\varepsilon = \varepsilon/kT$,

$$F_{3/2}(z') = \frac{2}{\pi^{1/2}}\int_0^{\infty}\frac{x^{1/2}dx}{1/z'e^x-1} = \frac{2}{\pi^{1/2}}\int_0^{\infty}dx\,x^{1/2}z'e^{-x}(1+z'e^{-x}+z'^2e^{-2x}+\cdots)$$

$$= z' + \frac{z'^2}{2^{3/2}} + \frac{z'^3}{3^{3/2}} = \sum_{n=1}^{\infty}\frac{z'^n}{n^{3/2}} \quad ...(195)$$

The $F_{3/2}(z')$ is a special case of the general class of functions defined as

$$F_s(z') = \sum_{n=1}^{\infty} \frac{z'^n}{n^s} \quad \text{[see Fig. 8]} \qquad \ldots(196)$$

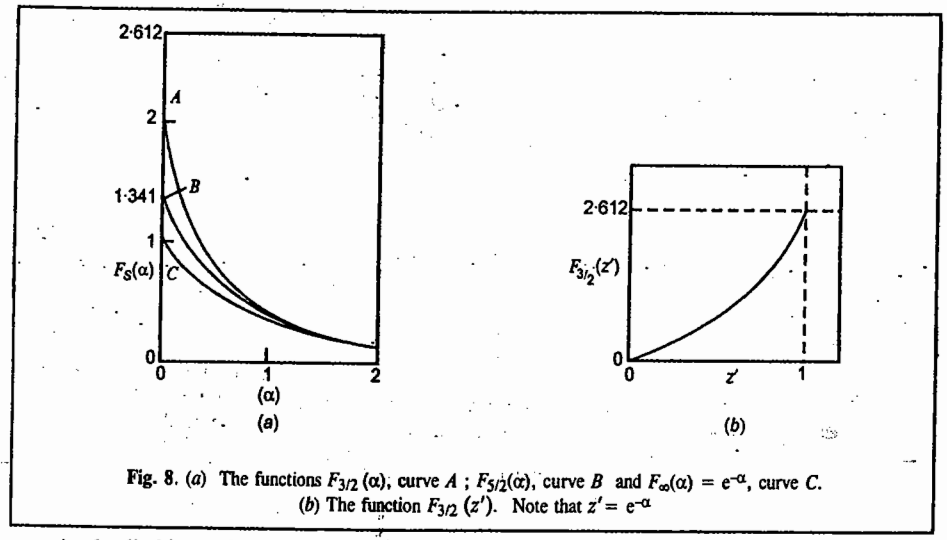

Fig. 8. (*a*) The functions $F_{3/2}(\alpha)$, curve *A* ; $F_{5/2}(\alpha)$, curve *B* and $F_\infty(\alpha) = e^{-\alpha}$, curve *C*. (*b*) The function $F_{3/2}(z')$. Note that $z' = e^{-\alpha}$

At the limiting value of $z'=1$ (or $\mu=0$) the derivative of $F_{3/2}(z'=1)$ diverges but the series (Eq. 195) converges :

$$F_{3/2}(z'=1) = \sum_{n=1}^{\infty} \frac{1}{n^{3/2}} = 1 + \frac{1}{2^{3/2}} + \frac{1}{3^{3/2}} + \cdots = \zeta\left(^3/_2\right) = 2{\cdot}612 \qquad \ldots(197)$$

where ζ is the **Riemann zeta function.** This is the *maximum* possible value of $F_{3/2}(z')$ due to Eq. 191.

We can define a minimum temperature T_0, called the **critical temperature**, at which z' has the maximum value=1, by

$$N = \frac{V}{\lambda_0^3}(2{\cdot}612) = V\left(\frac{2\pi mkT_0}{h^2}\right)^{3/2}(2{\cdot}612) \qquad \ldots(198)$$

so that

$$T_0 = \frac{h^2}{2\pi mk}\left(\frac{\rho}{2{\cdot}612}\right)^{2/3}, \qquad (\rho = N/V) \qquad \ldots(199)$$

For one mole of a gas, $N=N_A$, the Avogadro's number. Hence,

$$T_0 = (115/MV_m^{2/3})\ \text{K} \qquad \ldots(200)$$

where M is the molar mass and V_m is the molar volume in $cm^3\ mol^{-1}$.

b. Bose-Einstein Condensation. It is found that Eq. 193 has no solution for $T < T_0$. This difficulty does not occur in the original sum (Eq. 190). Thus, we conclude that it must come from improperly changing the sum (Eq. 190) into the integral (Eq. 193). For low temperatures $T < T_0$, it

introduces serious error. As discussed below, large contributions coming from the first few terms in Eq. 190 are left out.

For small z' {or large exp $(-\beta\mu)$}, the terms with the lowest ε_i do not contribute much to the sum so that little error occurs when the sum is replaced by the integral. However, when $z' \to 1$ (or exp $(-\beta\mu)$ is small), the first few terms in Eq. 190 become important so that we cannot replace the sum with an integral. For $\varepsilon_1 > \varepsilon_0$, we find that at sufficiently low temperatures,

$$\bar{n}_1 = \frac{1}{\exp[\beta(\varepsilon_1 - \mu)] - 1} \ll \frac{1}{\exp[\beta(\varepsilon_0 - \mu)] - 1} = \bar{n}_0 \qquad \ldots(201)$$

As a matter of fact, for $T \to 0$, the first term $\bar{n}_0$ approaches N, the total number of particles. Thus,

$$\underset{T\to 0}{\text{Lt}}\ \bar{n}_0 = N \underset{T\to 0}{\simeq} \frac{1}{\exp[\beta(\varepsilon_0 - \mu)] - 1} \simeq \frac{kT}{\varepsilon_0 - \mu} \qquad (\bar{n}_0 \text{ large}) \qquad \ldots(202)$$

This is possible because for the BE case (which is defined by a symmetric wave function), there is no restriction on the occupation number. When the temperatures are so low, μ is very close to ε_0. As μ is closer to ε_0 than to the first excited level, most of the particles tend to occupy ε_0 (*Bose-Einstein condensation*) for $T \to 0$. Thus, the BE condensation can be accounted for by the behavior of the chemical potential μ of a boson gas at low temperatures. The BE condensation is a special case of the BE distribution (statistics) (Eq. 189), arising from the minus sign of unity in the denominator.

For $T \to 0$, the sum for $N - \bar{n}_0$ can be approximated by an integral without serious error, as shown below :

$$N - \bar{n}_0 = \sum_{i=1}^{\infty} \bar{n}_i \approx \frac{2\pi V}{h^3}(2m)^{3/2} \int_0^{\infty} \frac{\varepsilon^{1/2}\,d\varepsilon}{\frac{1}{z'}e^{\beta\varepsilon} - 1} = \frac{V}{\lambda^3} F_{3/2}(z') \qquad \ldots(203)$$

Eliminating V using Eq. 198, Eq. 203 can be written as

$$N = \bar{n}_0 + N\left(\frac{T}{T_0}\right)^{3/2} \frac{F_{3/2}(z')}{2{\cdot}612} \qquad \ldots(204)$$

We shall consider two cases of this result :

Case (i) : $T < T_0$. Without any loss of generality, let us take $\varepsilon_0=0$ and $g_0=1$. Then, Eq. 202 gives

$$\bar{n}_0 = \frac{1}{e^{-\beta\mu} - 1} \approx -\frac{kT}{\mu} \qquad (\text{large } \bar{n}_0) \qquad \ldots(205)$$

For low temperatures, $\mu \to 0$ so that

$$\mu \to 0\ ;\ z' \to 1 \qquad \text{(quantum region)} \qquad \ldots(206)$$

Hence, for energy states above ε_0, we can neglect μ (or put $z'=1$) and write Eq. 204 as

$$\bar{n}_0 \equiv N_0 = N - N' = N\,[1 - (T/T_0)^{3/2}] \qquad \ldots(207)$$

where N' is the number of particles in the excited state. Thus,

$$N' = N\,(T/T_0)^{3/2} \qquad \ldots(208)$$

A plot of N_0/N as a function of T/T_0 is shown in Fig.9(*a*). At the condensation temperature T_0, we have $N(T_0) = N$.

As the temperature is decreased below T_0, more and more particles begin to occupy the ground state ε_0. The BE gas is then said to be **degenerate** and is in the quantum region characterised by $\mu \to 0$. For this reason, the temperature T_0 is also called the **degeneracy temperature.**

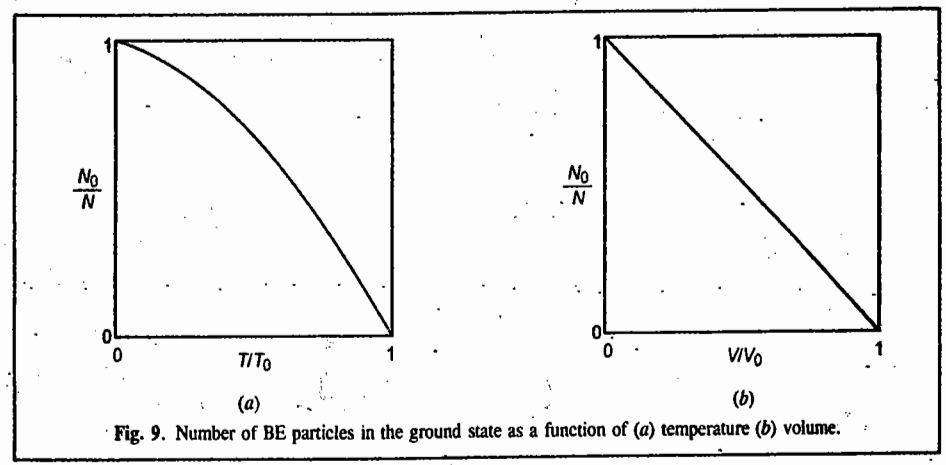

Fig. 9. Number of BE particles in the ground state as a function of (*a*) temperature (*b*) volume.

As an alternative to defining critical temperature T_0 (Eq. 198), we can define the **critical volume** V_0 such that at temperature T,

$$N = \frac{V_0}{\lambda^3} F_{3/2}(1) = V_0 \left(\frac{2\pi mkT}{h^2}\right)^{3/2} (2{\cdot}612) = V_0 n_Q (2{\cdot}612) \qquad ...(209)$$

Eliminating T by using Eq. 209, we can write Eq. 204 as

$$N = \bar{n}_0 + N \frac{V}{V_0} \frac{F_{3/2}(z')}{2{\cdot}612} \approx N_0 + N \frac{V}{V_0} \qquad ...(210)$$

Hence, $$N_0 = N(1 - V/V_0), \qquad (V < V_0) \qquad ...(211)$$

This result is shown in Fig. 9(*b*). Below T_0 (or V_0), we have BE condensation. Eq. 198 can thus be written as

$$\lambda_0^3 = 2{\cdot}612/\rho \qquad ...(212)$$

At T_0, the thermal de Broglie wave length λ_0 is of the order of the average interparticle distance. Thus, the wave functions overlap and the quantum effects become important.

Case (ii) : $T > T_0$. For $T > T_0$, we have $z' < 1$ (classical region). In Eq. 204, the first term $\bar{n}_0$ on the right becomes negligible and the second term increases as $T^{3/2}$ when the BE gas is heated above T_0. Thus, Eq. 193 reduces to $N = (V/\lambda^3) F_{3/2}(z')$ and Eq. 195 reduces to

$$F_{3/2}(z') = \left(\frac{T_0}{T}\right)^{3/2} F_{3/2}(1) = \left(\frac{T_0}{T}\right)^{3/2} (2{\cdot}612) = \left(\frac{\lambda}{\lambda_0}\right)^3 (2{\cdot}612) \qquad T > T_0$$

...(213)

For $T \gg 0$, the ground state is almost empty and most of the particles are in the states with $\varepsilon > 0$. We can approximate the BE distribution (statistics) by the MB distribution (statistics). In fact, for $z' \ll 1$, $F_{3/2}(z') \cong z'$ from Eq. 195 and Eq. 213 becomes

$$z' = \left(\frac{\lambda}{\lambda_0}\right)^{3/2} (2{\cdot}612 = \rho\lambda^3 = e^{-\alpha} \qquad \text{(Classical limit)}$$

(It may be recalled that for the MB gas, the molecular partition function q is given by $e^{-\alpha} = N/q = N/(V/\lambda^3) = \rho\lambda^3$; q can also be written as $n_Q V = n_Q/n$ where $n_Q = 1/\lambda^3$ is the quantum concentration and $n = 1/V$ is the concentration. The ideal BE gas distribution functions for $T < T_0$ and $T > T_0$ are shown in Fig. 10. The BE condensation has been called the **fifth state of matter** (the fourth state being plasma, the fully ionized gaseous state in the interior of stars).

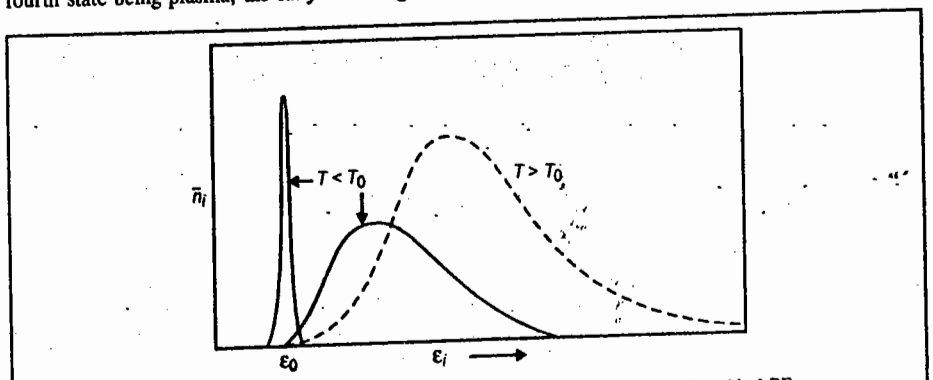

Fig. 10. Schematic diagram of the distribution function for the particles of an ideal BE gas.

c. Thermodynamic Properties of an Ideal BE Gas

(*i*) Energy U : From Eqs. 189 and 192,

$$U = \sum_i \varepsilon_i \bar{n}_i = \int_0^\infty \varepsilon dn = \int_0^\infty \frac{\varepsilon g(\varepsilon) d\varepsilon}{e^{\beta(\varepsilon-\mu)} - 1} = \frac{V}{h^3} 2\pi (2m)^{3/2} \int_0^\infty \frac{\varepsilon^{3/2} d\varepsilon}{e^{\beta(\varepsilon-\mu)} - 1}$$

$$= \frac{VkT}{\lambda^3} \frac{2}{\pi^{1/2}} \int_0^\infty x^{3/2} \left(\frac{1}{z'} e^x - 1\right)^{-1} dx = \frac{3}{2} kT \frac{V}{\lambda^3} F_{5/2}(z') \qquad ...(214)$$

where $x = \beta\varepsilon$ and $F_{5/2}(z') = \dfrac{1}{(3/4)\pi^{1/2}} \displaystyle\int_0^\infty x^{3/2} \left(\frac{1}{z'} e^x - 1\right)^{-1} dx$

$$= \frac{1}{(3/4)\pi^{1/2}} \int_0^\infty x^{3/2} z' e^{-x} \left(1 + z' e^{-x} + z'^2 e^{-2x} + \cdots\right) dx$$

$$= z' + \frac{z'^2}{2^{5/2}} + \frac{z'^3}{3^{5/2}} + \cdots = e^{-\alpha} + \frac{e^{-2\alpha}}{2^{5/2}} = F_{5/2}(\alpha) \qquad ...(215)$$

A plot of $F_{5/2}(\alpha)$ is given in Fig. 8(*a*). We note that

$$F_{3/2}(z') = z'\frac{\partial}{\partial z'}F_{5/2}(z')$$

We now distinguish two cases, *viz.*, U_- for $T<T_0$ (degenerate gas) and U_+ for $T>T_0$ (nondegenerate gas).

For $T < T_0$, $z'=1$ so that from Eqs. 198 and 214,

$$U_- = \frac{3}{2}kT\frac{V}{\lambda^3}F_{5/2}(z'=1) = \frac{3}{2}kT\frac{N\lambda_0^3}{F_{3/2}(z'=1)\lambda^3}F_{5/2}(z'=1)$$

$$= \frac{3}{2}NkT\left(\frac{T}{T_0}\right)^{3/2}(0{\cdot}51) = NkT\left(\frac{T}{T_0}\right)(0{\cdot}77) \qquad ...(216)$$

where we have used $F_{5/2}(z'=1)/F_{3/2}(z'=1)=\zeta\left({}^5/_2\right)/\zeta\left({}^3/_2\right)=1{\cdot}341/2.612 = 0{\cdot}5134$ and $\lambda_0^3/\lambda^3 = (T/T_0)^{3/2}$

For $T > T_0$, $z' \ll 1$ so that we can omit the first term in Eq. 216 and write

$$N = \frac{V}{\lambda^3}F_{3/2}(z'), \qquad T > T_0 \qquad ...(217)$$

From Eqs. 216 and 217,

$$U_+ = \frac{3}{2}kT\frac{V}{\lambda^3}F_{5/2}(z') = \frac{3}{2}NkT\frac{F_{5/2}(z')}{F_{3/2}(z')}$$

$$= \frac{3}{2}NkT\left[1-2^{-5/3}F_{3/2}(z')-2(3^{-5/2}-2^{-4})F_{3/2}^2(z')-\cdots\right]$$

$$= \frac{3}{2}NkT\left[1-0{\cdot}177F_{3/2}(z')-0{\cdot}003F_{3/2}^2(z')-\cdots\right]$$

$$= \frac{3}{2}NkT\left[1-0{\cdot}462(T_0/T)^{3/2}-0{\cdot}023(T_0/T)^3-\cdots\right] \qquad ...(218)$$

where, in the last step, we have used Eq. 213. Values of $F_{5/2}(z')/F_{3/2}(z')$ are given in standard books.

(*ii*) Heat Capacity, C_V. Recalling that $C_V = (\partial U/\partial T)_V$, we have

$$C_{V-} = \left(\frac{15}{4}\right)0{\cdot}51Nk\left(\frac{T}{T_0}\right)^{3/2} = 1{\cdot}926Nk\left(\frac{T}{T_0}\right)^{3/2} \qquad ...(219)$$

$$C_{V+} = \frac{3}{2}Nk\left[1+0{\cdot}231\left(\frac{T_0}{T}\right)^{3/2}+0{\cdot}045\left(\frac{T_0}{T}\right)^3+\cdots\right] \qquad ...(220)$$

These heat capacity values are plotted in Fig. 11.

For $T = T_0$,

$$C_{V-} = C_{V+} = 0{\cdot}51(15/4)\,Nk = 1{\cdot}926\,Nk$$

We see that C_V varies as $T^{3/2}$ near absolute zero. At $T=T_0$, $C_{V-}=C_{V+}$ but their slopes are different. This means that the heat capacity is continuous at $T=T_0$ but a graph of C_V/Nk against T/T_0 will show a kink (cusp) at $T=T_0$ (as shown in Fig. 11). This suggests that the BE condensation is a third-order phase transition. However, the discontinuity of entropy (see below) implies a latent heat which would, in turn, imply a first-order phase transition !

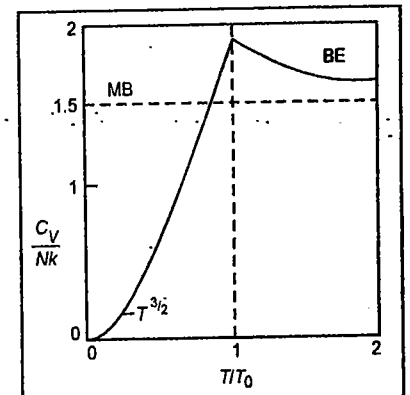

Fig. 11. Heat capacity of an ideal BE gas.

***(iii)* Entropy, S.** Realling that $(\partial S/\partial T)_V = C_V/T$, we have

$$S_-(T) = \int_0^T\frac{C_{V-}}{T}dT = \frac{2}{3}C_{V-} = \left(\frac{2}{3}\right)1{\cdot}926Nk\left(\frac{T}{T_0}\right)^{3/2} \qquad ...(221)$$

$$S_+(T) = S(T_0) + \int_{T_0}^T\frac{C_{V+}}{T}dT$$

$$= S(T_0) + \frac{3}{2}Nk\left[\ln\left(\frac{T}{T_0}\right)+\frac{2}{3}(0{\cdot}231)\left(1-\frac{T_0}{T}\right)^{3/2}+\cdots\right] \qquad ...(222)$$

We see that the entropy shows a sudden drop for $T < T_0$. We know that, $S=0$ as $T=0$, in accordance with the Third law of thermodynamics. This means that for the condensed phase (which exists at $T=0$), the entropy is zero, that is, all the particles are in one state.

***(iv)* Pressure, P.** Recalling that for all ideal gases (MB, BE or FD gases), the pressure is given by $P=(2/3)(U/V)$, using $V/V_0 = (T/T_0)^{3/2}$, we have

$$P_- = \frac{2}{3}\frac{U_-}{V} = (0{\cdot}51)\frac{NkT^{5/2}}{VT_0^{3/2}} = \frac{0{\cdot}51\,NkT}{V_0} \qquad ...(223)$$

$$P_+ = \frac{2}{3}\frac{U_+}{V} = \frac{NkT}{V}\left[1-0{\cdot}462\left(\frac{V_0}{V}\right)-\cdots\right] \qquad ...(224)$$

We see from Eq. 223 that P_- is independent of V and is a function of T only, as for a condensing gas (Fig. 12). In this region, further reduction in volume simply condenses more particles in the ground state.

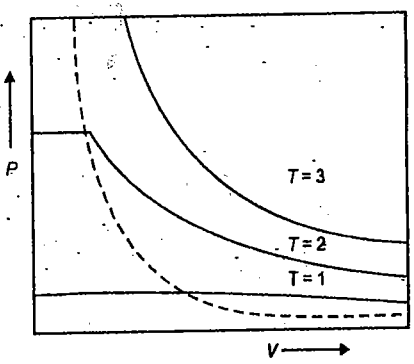

Fig. 12. Isotherms of an ideal BE gas. The region below the dotted curve corresponds to the degenerate state.

Quantum Statistics : Ideal Fermi-Dirac Gas

a. Fermi-Dirac Distribution. We have shown that for an ideal FD gas of N molecules in a volume V, the most probable number of particles with energy E is given by

$$\bar{n}_i(\varepsilon_i) = \frac{g_i}{\exp(\alpha+\beta\varepsilon_i)+1} = \frac{g_i}{\exp[(\varepsilon_i-\mu)/kT]+1} \qquad ...(225)$$

where $\beta = 1/kT$, $\alpha = -\beta\mu$, and g_i is the degeneracy of the ith level. The parameter α (or μ) is determined as a function of N and T by the condition :

$$N = \sum_{\substack{i=0 \\ \text{levels}}}^{\infty} n_i = \sum_i \frac{g_i}{\exp[\beta(\varepsilon_i - \mu)] + 1} \qquad \ldots(226)$$

where the sum is over energy levels since we have included g_i in Eq. 225. Because of the presence of the term $+1$ in the dominator of Eq. 225, α need not be restricted to $\alpha \geq 0$ as in the BE case. For the FD gas α can be positive or negative. It is more convenient to work with the chemical potential $\mu(T)$, since μ approaches μ_0 (a finite value) at $T=0$ whereas α becomes negatively infinite. The finite value μ_0 at $T=0$ follows from the Pauli exclusion principle. The fermions in the gas occupy all possible quantum states with energies between zero and **Fermi energy** $\varepsilon_F(T=0) \equiv \mu_0$ whose value depends on the number of fermions in the gas. The states with energy greater than μ_0 are empty at absolute zero. The **Fermi level** is defined by $\mu(T)$ for $T > 0$.

As in the BE case, we can approximate the sum by an integral. Here in the FD case, due to the Pauli principle, there is no danger that a considerable fraction of the gas particles will be in the ground state. Introducing the Fermi-Dirac distribution (Fig. 13),

$$f(\varepsilon) = \frac{1}{\exp[(\varepsilon - \mu)/kT + 1]} \qquad \ldots(227)$$

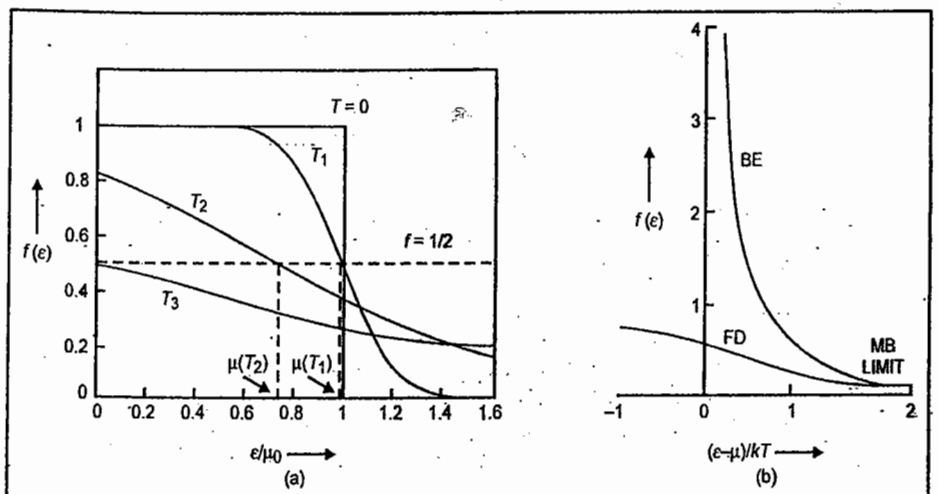

Fig. 13 (a) FD distribution function for a gas in three dimensions. At the Fermi level, the value of f is 1/2. As $k = 8{\cdot}62 \times 10^{-5}$ eV K^{-1}, for $\mu/kT \simeq 1$, we have $\mu(T) \simeq 1$ eV for $T \simeq 10^4$ K. For a metal, μ_0 might correspond to 5×10^4 K as here.
(b) Comparison of Fermi-Dirac and Bose-Einstein distribution functions. For $(\varepsilon - \mu) \gg kT$, we get the classical limit.

Eq. 226 becomes

$$N = \int_0^\infty f(\varepsilon)\, g(\varepsilon)\, d\varepsilon$$

where

$$g(\varepsilon)\, d\varepsilon = g_s \left(\frac{2\pi V}{h^3}\right)(2m)^{3/2} \varepsilon^{1/2} d\varepsilon \qquad \ldots(228)$$

In Eq. 228, $g_s = 2s+1$ is the spin degeneracy which arises from $(2s+1)$ different spin orientations possible for the same energy, ε. For electrons, $s = \frac{1}{2}$ so that $g_s = 2$. In general, μ is determined from N,

$$N = g_s \left(\frac{2\pi V}{h^3}\right)(2m)^{3/2} \int_0^\infty \frac{\varepsilon^{1/2} d\varepsilon}{\exp[(\varepsilon - \mu/kT)] + 1}$$

$$= g_s \frac{V}{\lambda^3} \frac{2}{\pi^{1/2}} \int_0^\infty \frac{x^{1/2} dx}{\frac{1}{z'} e^x + 1} = g_s \frac{V}{\lambda^3} G_{3/2}(z') \qquad \ldots(229)$$

where $x = \varepsilon/kT$, $z' = \exp(\beta\mu) = \exp(\mu/kT)$ is the absolute activity (or fugacity for a gas) and

$$G_{3/2}(z') = \frac{2}{\pi^{1/2}} \int_0^\infty dx\, x^{1/2} \left(\frac{1}{z'} e^x + 1\right)^{-1} \qquad \ldots(230)$$

$$\text{For small } z', \quad G_{3/2}(z') = z' - \frac{z'^2}{2^{3/2}} + \frac{z'^3}{3^{3/2}} - \ldots = \sum_{n=1}^{\infty} \frac{(-1)^{n+1} z'^n}{n^{3/2}} \qquad \ldots(231)$$

If can be easily verified that $G_{3/2}(z')$ is a monotonically increasing function of z'. The value of ε_F is determined by noting that at $T=0$, $f(\varepsilon)$ is 1 for $\varepsilon < \varepsilon_F(0)$ and 0 for $\varepsilon > \varepsilon_F(0)$.

$$N = \int_0^{\varepsilon_F(0)} g(\varepsilon)\, d\varepsilon = g_s \left(\frac{2\pi V}{h^3}\right)(2m)^{3/2} \int_0^{\varepsilon_F(0)} \varepsilon^{1/2} d\varepsilon$$

$$= g_s \left(\frac{2\pi V}{h^3}\right)(2m)^{3/2} \frac{2}{3} [\varepsilon_F(0)]^{3/2} \qquad \ldots(232)$$

or equivalently, with $\varepsilon = p^2/2m$,

$$N = \frac{4\pi g_s V}{h^3} \int_0^{p_F} p^2 dp = \left(\frac{4\pi g_s V}{3h^3}\right) p_F^3 \qquad \ldots(233)$$

where p_F is the value of the momentum corresponding to the largest energy value and is called the **Fermi momentum.** This gives

$$p_F = h \left(\frac{3}{4\pi g_s} \frac{N}{V}\right)^{1/3}$$

Thus,

$$E_F(0) = \frac{h^2}{2m} \left(\frac{3}{4\pi g_s} \frac{N}{V}\right)^{2/3} = \mu_0 = \frac{p_F^2}{2m} \qquad \ldots(234)$$

With the degeneracy $g_s = 2$ and the density of gas $\rho = (Nm/V)$ kgm^{-3}, $\varepsilon_F(0) = 0{\cdot}625 \times 10^{-17}\, \rho^{2/3}$ J or $39\rho^{2/3}$ eV for electrons.

The Fermi energy $\varepsilon_F(0)$ represents the energy of the highest level occupied at 0 K for electrons—which are fermions—in a metal. For conduction electrons in metals, $\rho \approx 0{\cdot}1$ kg m^{-3}. Thus, we see that a Fermi gas possesses an appreciable energy at 0 K while both MB and BE statistics predict a zero value in the energy.

The reason why this is so is that the occupation number for each quantum state is 0 or 1 only for the FD distribution (statistics). As the temperature increases above 0 K, the distribution near $\varepsilon_F(0)$ rounds off (Fig. 13). Defining a temperature called the **Fermi temperature,** by

$$T_F = \varepsilon_F(0)/k \quad (= 4{\cdot}52\times10^5\ \rho^{2/3}\ \text{K for electrons}) ; \qquad ...(235)$$

for $T \ll T_F$ or $kT_F \ll \varepsilon_F(0)$, the distribution is called **degenerate.** For $T \gg T_F$, the distribution is said to be nondegenerate and we obtain the classical limit. The parameter $\alpha = -\mu(T)/kT$ is ***negative*** in the former case and *positive* in the latter case. It implies that $\mu > 0$ at low temperatures and $\mu < 0$ at high temperatures (Fig. 13).

Example 12. What is the significance of Fermi energy ? Comment briefly.

Solution : Consider a system of fermions (spin 1/2 particles such as electrons) at $T = 0$K and investigate the occupancy of states whose energies are less than the Fermi energy ε_F and greater than ε_F. We find that

$$T = 0, \quad \varepsilon < \varepsilon_F \qquad f_{FD}(\varepsilon) = \frac{1}{e^{(\varepsilon-\varepsilon_F)/kT}+1} = \frac{1}{e^{-\infty}+1} = \frac{1}{0+1} = 1$$

$$T = 0, \quad \varepsilon > \varepsilon_F \qquad f_{FD}(\varepsilon) = \frac{1}{e^{(\varepsilon-\varepsilon_F)/kT}+1} = \frac{1}{e^{\infty}+1} = 0$$

Thus, at absolute zero all energy states upto ε_F are occupied, and none above. If a system contains N fermions, we can calculate its Fermi energy ε_F by filling up its energy states with the N particles in order of increasing energy starting with $\varepsilon = 0$. The highest state to be occupied will then have energy $\varepsilon = \varepsilon_F$. Thus, Fermi energy $\varepsilon_F(0)$ represents the energy of the highest level occupied at 0K by fermions.

Example 13. Calculate the Fermi energy of Cu(s) assuming that each copper atom contributes one free electron to the electron gas in copper metal. (This is a reasonable assumption since a Cu atom has a single 4s electron outside closed inner shells.) The density of copper is $8{\cdot}94 \times 10^3$ kg/m^3 and its atomic mass is 63·5 u.

Solution : The electron density N/V in copper is equal to the number of copper atoms per unit volume.

Since $\quad u = 1{\cdot}6605\times10^{-27}$ kg,

$$\frac{N}{V} = \frac{\text{atoms}}{\text{m}^3} = \frac{\text{mass/m}^3}{\text{mass/atom}} = \frac{8{\cdot}94\times10^3\ \text{kg/m}^3}{(63{\cdot}5\,\text{u})(1{\cdot}6605\times10^{-27}\,\text{kg/u})}$$

$$= 8{\cdot}48\times10^{28}\ \text{atoms/m}^3 = 8{\cdot}48\times10^{28}\ \text{electrons/m}^3$$

Hence, Fermi energy (from Eq. 234) is given by

$$\varepsilon_F = \frac{h^2}{2m_e}\left(\frac{3N}{8\pi V}\right)^{2/3} = \frac{(6{\cdot}626\times10^{-34}\,\text{J s})^2}{(2)(9{\cdot}11\times10^{-31}\,\text{kg/electron})}\left[\frac{(3)(8{\cdot}48\times10^{28}\,\text{electrons/m}^3)}{8\pi}\right]^{2/3}$$

$$= 1{\cdot}13\times10^{-18}\ \text{J} = 7{\cdot}04\ \text{eV}. \quad [1\ \text{eV} = 1{\cdot}602\times10^{-19}\ \text{J}]$$

Comment : At absolute zero, $T = 0$K, there would be electrons with energies of upto 7·04 eV in copper (corresponding to speeds of upto $1{\cdot}6\times10^5$ ms^{-1}). By contrast, *all* the molecules in an ideal gas at 0K would have zero energy. The electron gas in a metal is said to be **degenerate.**

Example 14. How many photons are present in 1·00 cm^3 of radiation in thermal equilibrium at 1000K ? What is the mean (average) energy ?

Solution : (*a*) The number of photons per unit volume is given by

$$\frac{N}{V} = \int_0^\infty n(\nu)d\nu \qquad ...(i)$$

where $n(\nu)d\nu$ is the number of photons per unit volume with frequencies between ν and $\nu+d\nu$. Since such photons

have energies of $h\nu$,

$$n(\nu)d\nu = \frac{u(\nu)d\nu}{h\nu} \qquad ...(ii)$$

with $u(\nu)d\nu$ being the energy density given by Planck's radiation formula

$$u(\nu)d\nu = \frac{8\pi h}{c^3}\frac{\nu^3 d\nu}{e^{h\nu/kT}-1} \qquad ...(iii)$$

Hence the total number of photons in the volume V is given by

$$N = V\int_0^\infty \frac{u(\nu)d\nu}{h\nu} = \frac{8\pi V}{c^3}\int_0^\infty \frac{\nu^2 d\nu}{e^{h\nu/kT}-1} \qquad ...(iv)$$

If $h\nu/kT = x$, then $\nu = kTx/h$, and $d\nu = (kT/h)dx$ so that

$$N = 8\pi V\left(\frac{kT}{hc}\right)^3\int_0^\infty \frac{x^2 dx}{e^x-1} \qquad ...(v)$$

The definite integral in Eq. (*v*) is a standard one equal to 2·404. Inserting the numerical values of the other quantities, with $V = 1{\cdot}00$ cm^3 $= 1{\cdot}00\times10^{-6}$ m^3, we find that

$$N = 2{\cdot}03\times10^{10}\ \text{photons}$$

(*b*) The mean energy $\bar{\varepsilon}$ of the photons is equal to the total energy per unit volume divided by the number of photons per unit volume :

$$\bar{\varepsilon} = \frac{\int_0^\infty u(\nu)d\nu}{n(\nu)d\nu} = \frac{aT^4}{N/V} \qquad ...(vi)$$

Since $a = 4\sigma/c$ (where σ is Stefan's constant and $N = (2{\cdot}405)[8\pi V(kT/hc)^3]$,

$$\bar{\varepsilon} = \frac{\sigma c^2 h^3 T}{(2{\cdot}405)(2\pi k^3)} = 3{\cdot}73\times10^{-20}\ \text{J} = 0{\cdot}233\ \text{eV} \qquad [1\text{eV} = 1{\cdot}602\times10^{-19}\text{J}]$$

Example 15. Radiation from the Big Bang has been Doppler-shifted to longer wave lengths by the expansion of the universe and today has a spectrum corresponding to that of a blackbody at 2·7 K. Calculate the wave length at which the energy density of this radiation is a maximum. In what region of the spectrum is this radiation ?

Solution : $\lambda_{max}T = \dfrac{hc}{4{\cdot}965k} = 2{\cdot}898\times10^{-3}$ mK [Wien's displacement law]

Hence, $\lambda_{max}T = \dfrac{2{\cdot}898\times10^{-3}\,\text{mK}}{T} = \dfrac{2{\cdot}898\times10^{-3}\,\text{mK}}{2{\cdot}7\text{K}} = 1{\cdot}1\times10^{-3}$ m $= 1{\cdot}1$ mm

This wave length is in the microwave region. This radiation was first detected by American physicists A. Penzias and R.W. Wilson in 1964 who were awarded the 1978 Physics Nobel Prize for this discovery in support of the Big Bang theory of the Universe.

b. Thermodynamic Properties of an Ideal FD Gas. Expressions for these properties can be derived under the following three cases : (*i*) $T = 0$, the gas is *completely degenerate* (*ii*) $T \ll T_F$, low temperatures, the gas is ***degenerate*** and (*iii*) intermediate temperatures, the gas is ***slightly degenerate.***

For a completely degenerate gas, $T=0$ K, we have

$$dn = \begin{cases} g_s\left(\frac{2\pi V}{h^3}\right)(2m)^{3/2}\varepsilon^{1/2}\,d\varepsilon, & 0 \le \varepsilon, \le \varepsilon_F(0) \\ 0 & \varepsilon > \varepsilon_F(0) \end{cases} \quad \ldots(236)$$

The internal energy is given by

$$U_0 = \int_0^{\mu_0} \varepsilon\, dn = g_s\left(\frac{2\pi V}{h^3}\right)(2m)^{3/2}\int_0^{\mu_0}\varepsilon^{3/2}\,d\varepsilon$$

$$= \frac{3}{5}N\mu_0 = \frac{3}{5}N\varepsilon_F(0) \quad \ldots(237)$$

Other thermodynamic functions are :

$$S_0 = 0 \quad \ldots(238)$$

$$= U_0 - S_0T - \mu_0 N = -\frac{2}{5}N\mu_0 \quad \ldots(239)$$

$$P = \frac{2}{3}\left(\frac{U}{V}\right) = \frac{2}{5}\left(\frac{N}{V}\right)\mu_0 = \frac{1}{5}\frac{h^2}{m}\left(\frac{3}{4\pi g_s}\right)^{2/3}\left(\frac{N}{V}\right)^{5/2} \quad \ldots(240)$$

$$= 2{\cdot}71\times10^7\rho \text{ atm for electrons.}$$

We thus see that even at 0 K, a fermion gas exerts a pressure. If the electrons in a metal were neutral they would exert a pressure of about 10^6 atm. The coulomb attraction to metal ions counterbalances the pressure. We emphasize again that the chemical potential μ is positive (though small) at $T=0$ K and decreases as temperature increases and is negative at high temperatures.

For a completely degenerate extreme relativistic electron gas (at high densities, *i.e.*, for a very compressed gas), the energy of the electron gas increases and the energy becomes comparable with mc^2, the relativistic case arises), we have

$$E = cp \quad \ldots(241)$$

and Eqs. 236 and 237 still holding, the Fermi energy is given by

$$\varepsilon_F = cp_F = c\,h\left(\frac{3}{4\pi g_s}\frac{N}{V}\right)^{1/3} \quad \ldots(242)$$

The total energy of the gas is given by

$$U = \frac{4\pi g_s cV}{h^3}\int_0^{p_F} p^3dp = \frac{\pi g_s}{h^3}cp_F^4V = \frac{3}{4}chN\left(\frac{3}{4\pi g_s}\frac{N}{V}\right)^{1/3} \quad \ldots(243)$$

The pressure of the gas is obtained by using the relation $P=-(\partial U/\partial V)_S$ (which is obtained from the relation $dU = TdS - PdV$). Thus,

$$P = \frac{1}{4}ch\left(\frac{3}{4\pi g_s}\right)^{1/3}\left(\frac{N}{V}\right)^{4/3} = \frac{1}{3}\frac{U}{V}\ ;\ g_s = 2 \text{ for the electron gas} \quad \ldots(244)$$

We see that while for a non-relativistic gas, $PV=(2/3)U$, for an extreme relativistic gas $PV=(1/3)U$.

For a degenerate case, $T \ll T_F$, *i.e.*, at low temperatures, the mathematical treatment becomes complicated. We shall merely quote the results here. For the FD electron gas,

$$U = U_0\left[1+\frac{5\pi^2}{12}\left(\frac{kT}{\mu_0}\right)^2-\cdots\right] \quad \ldots(245)$$

The heat capacity is given by

$$C_V = \left(\frac{\partial U}{\partial T}\right)_V = \frac{4\pi g_s V}{3h^3}(2m\mu_0)^{3/2}\frac{k^2T}{\mu_0} = \frac{\pi^2}{2}\frac{Nk^2T}{\mu_0} = \frac{\pi^2}{2}Nk\frac{T}{T_F} \quad \ldots(246)$$

This remarkable result was derived by Sommerfeld in 1928. Thus, C_V is proportional to the temperature at low temperatures and is much smaller than the classical value $(3/2)Nk$, which is the value H.A. Lorentz had suggested in 1905 on the assumption that electron gas in metals obeyed MB statistics. Notice that the classical value is temperature-independent at room temperature. Fig. 14 compares the heat capacity of a gas according to the three statistics.

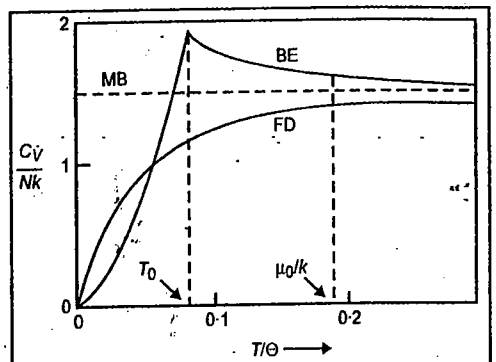

Fig. 14. Comparison of heat capacity of a gas according to the three statistics, $\Theta=(h^2/mk)(\bar{N}/gV)^{2/3}$

The total heat capacity of a metal is the sum of the contributions due to the electronic part (obtained above) and the contribution due to the phonons (the quanta of lattice vibrations) at low temperatures, as given by the Debye T^3- law :

$$C_{V,\text{lattice}} = \frac{12}{5}\pi^4Nk(T/\Theta_D)^3 \quad \ldots(247)$$

where Θ_D is the Debye temperature. Hence, the heat capacity of a metal at low temperatures can be written as

$$C_V = C_{V,\text{elec}} + C_{V,\text{lattice}} = \gamma T + \alpha T^3 \quad \ldots(248)$$

where γ and α are constants. Thus,

$$C_V/T = \gamma + \alpha T^2 \quad \ldots(249)$$

The relation (Eq. 249) is shown graphically (Fig. 15) for copper metal.

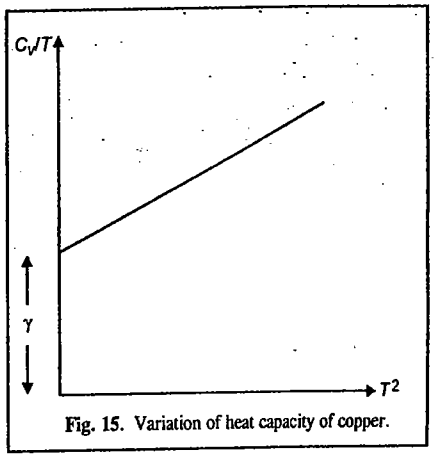

Fig. 15. Variation of heat capacity of copper.

The observed value of γ was found to be higher than the calculated value from Eq. 249, the reason being that electrons become heavy when moving in a periodic lattice.

The equation of state of the fermion gas is

$$P = \frac{2}{3}\frac{U}{V} = \frac{2}{5}\frac{N}{V}\mu_0\left[1+\frac{5\pi^2}{12}\left(\frac{kT}{\mu_0}\right)^2+\cdots\right] \quad \ldots(250)$$

Further applications of FD statistics occur in thermionic emission and photoelectric emission, Pauli spin paramagnetism of conduction electrons in metals, Landau diamagnetism resulting from quantization of electron orbits in a magnetic field, the equation of state at high densities, white dwarf stars (wherein occurs the term **Chandrasekhar limit**, for which the great Indian-American astrophysicist S.Chandrasekhar (1910-1995) won the 1983 Physics Nobel Prize, sharing it with the American astrophysicist W. Fowler), neutron stars, semiconductor statistics and superconductivity. These topics are discussed in advanced books on statistical mechanics.

Molar (or Canonical) Partition Function of a System

So far we have limited our discussion to the molecular partition function, *i.e.*, the partition function of a single molecule. We shall now derive expression for the molar partition function of a system in terms of the molecular partition function. Thermodynamic properties can be discussed in terms of both the molecular and the molar partition functions.

For a system containing N independent non-interacting particles, the total energy, E_i, of the system is given by

$$E_i = \varepsilon_1(1) + \varepsilon_2(2) + \varepsilon_3(3) + \cdots + \varepsilon_N(N) \qquad \ldots(251)$$

where particle 1 has energy ε_1, particle 2 has energy ε_2, and so on. The particles being indentical, they all have the same energy levels. Thus, each different manner of assigning the molecules among these energy levels gives rise to a new allowable energy level of the system. Hence, the partition function of the system is given by

$$Q = \sum_i e^{-E_i/kT} \qquad \ldots(252)$$

where, for convenience, we have omitted the degeneracy. From Eqs. 251 and 252,

$$Q = \sum_i \exp\ [-\{\varepsilon_i(1) + \varepsilon_i(2) + \varepsilon_i(3) + \cdots + \varepsilon_i(N)\}]/kT$$

$$= \sum_i \exp\ [-\varepsilon_i(1)]/kT \times \exp\ [-\varepsilon_i(2)]/kT \ldots \times \exp\ [-\varepsilon_i(N)]/kT \qquad \ldots(253)$$

Since all the particles have the same energy levels, hence

$$Q = [\Sigma \exp\ (-\varepsilon_i/kT)]^N = q^N \qquad \ldots(254)$$

Thus, Q is the **canonical** or **molar partition function** of the system while q is the **molecular partition function.**

Such a behaviour is characteristic of an ideal crystal where the different oscillators (vibrating particles) occupy different positions at different locations in the crystal lattice and an interchange of two oscillators in the lattice creates a new quantum state.

However, in the case of an ideal gas where each particle moves independently of the other throughout the whole system, an interchange of coordinates between particles does not create a new quantum state. Thus, the particles of an ideal gas lose their distinguishability. The result is that quantum states in the gaseous phase that differ merely by the interchange of two particles are *indistinguishable* and should be counted only once. Now if each energy level contains only one particle (which is a good approximation for a gas at moderate and low pressures where the number of available energy levels is much larger than the number of particles), then the number of permutations of particles among themselves is N !. Thus, the canonical partition function for a gas becomes

$$Q = q^N/N! \qquad \ldots(255)$$

Since $q = q_{tr}\, q_{rot}\, q_{vib}\, q_{el}$,

we have $$Q = \frac{1}{N!}(q_{tr}\, q_{rot}\, q_{vib}\, q_{el})^N = Q_{tr}\, Q_{rot}\, Q_{vib} Q_{elec} \qquad \ldots(256)$$

where $Q_{tr} = q_{tr}^N/N!$; $Q_{rot} = q_{rot}^N$; $Q_{vib} = q_{vib}^N$; $Q_{el} = q_{el}^N$.

Partition Function for a Real Gas

Real gases and liquids are difficult to treat statistically because of the presence of considerable intermolecular interactions. Without going into details, we shall merely state that the molar (canonical) partition function of a real gas *factorises* into a part arising from the kinetic energy which is the same as for a perfect (ideal) gas and a factor called the *configurational integral*, Z, which depends upon the intermolecular potential energy. Thus, we can write for a real gas containing N particles in a container of volume V,

$$Q = Z/\Lambda^{3N} \qquad \ldots(257)$$

where $\Lambda = h/(2\pi mkT)^{1/2}$.

For a perfect gas, $Z = V^N/N!$

However, in this case, Q is the partition function for a collection of N non-interacting particles. For a real gas, Z is related to the total potential energy V_N of interaction of all the particles as :

$$Z = \frac{1}{N!}\int \exp(-V_N/kT)\, dr_1 dr_2 \cdots dr_N \qquad \ldots(258)$$

For interactions between pairs of particles, the configurational integral simplifies to

$$Z_2 = \frac{1}{2}\int \exp(-V_2/kT)\, dr_1 dr_2 \qquad \ldots(259)$$

Statistical mechanics of real gases has been treated in the next chapter.

Equilibrium Constant of an Ideal Gas Reaction in terms of Partition Functions.

For an ideal gas, $G = A + PV = A + RT$

Since $A = -RT \ln (q/N_A) - RT$ (from Eq. 117)

$\therefore$ $G = -RT \ln (q/N_A)$ ...(260)

Hence, the standard molar Gibbs free energy is given by

$$G^0 = -RT \ln (q^0/N_A) \qquad \ldots(261)$$

where q^0 is the molecular partition function for a gas at standard pressure which may be represented as

$$q^0 = q_{tr}^0\, q_{rot}^0\, q_{vib}^0\, q_{el}^0\, q_{nucl}^0 \qquad \ldots(262)$$

Here q_0 is the *zero-point energy term defined as*

$$q_0 = e^{-\varepsilon_0/kT} \qquad \ldots(263)$$

and $$q_{tr}^0 = (2\pi mkT/h^2)^{3/2} \times V^0 \qquad \ldots(264)$$

where V^0 is the molar volume at pressure P^0.

If we represent a *new* partition function q' as

$$q' = q_{tr}^0\, q_{rot}^0\, q_{vib}^0\, q_{el}^0\, q_{nucl}^0 \qquad \ldots(265)$$

we obtain $$q^0 = q_0 q' = q' e^{-\varepsilon_0/kT} \qquad \ldots(266)$$

Let us consider a homogeneous gasous reaction

$$aA + bB \rightleftharpoons cC + dD$$

In order to calculate the equilibrium constant of this reaction, we have to calculate the partition

functions of the reactant and product species relative to the same zero energy. For the reaction $A \rightleftharpoons B$, the energy levels for A and B molecules are shown in Fig. 16. (Similar diagram can be constructed for the reaction under consideration).

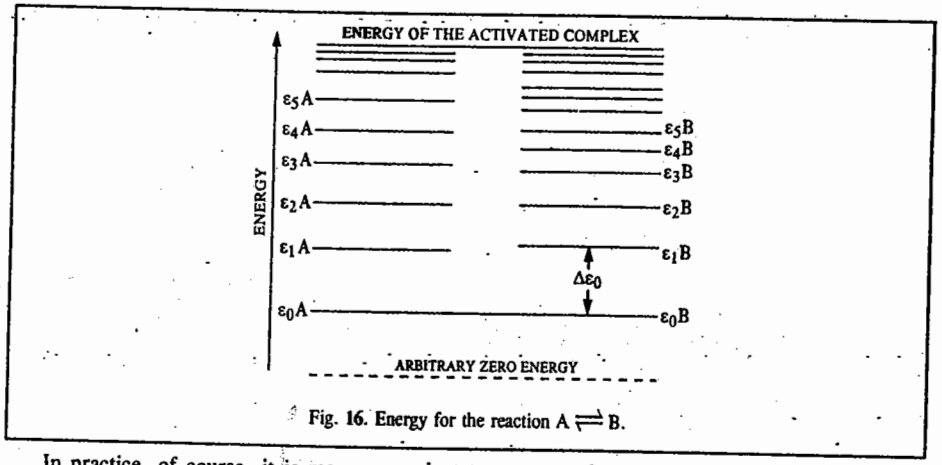

Fig. 16. Energy for the reaction $A \rightleftharpoons B$.

In practice, of course, it is more convenient to compute the partition function of each species relative to its own ground energy level, setting the energy of each ground level to zero. Thus, relative to arbitrary zero, the lowest energy levels of A, B, C and D are ε_{0A}, ε_{0B}, ε_{0C} and ε_{0D}, respectively.

The standard Gibbs free energy change for the reaction is given by

$$\Delta G^0 = (cG_C^0 + dG_D^0) - (aG_A^0 + bG_B^0) \qquad ...(267)$$

Using Eqs. 267 and 261,

$$\Delta G^0 = -RT\left[\left\{c \ln \frac{q_C'}{N_A} + d \ln \frac{q_D'}{N_A}\right\} - \left\{a \ln \frac{q_A'}{N_A} + b \ln \frac{q_B'}{N_A}\right\} - \frac{c\varepsilon_{0C} + d\varepsilon_{0D} - a\varepsilon_{0A} - b\varepsilon_{0B}}{kT}\right]$$

$$= -RT\left[(c \ln q_C' + d \ln q_D') - (a \ln q_A' + b \ln q_B') + \ln\left(\frac{1}{N_A}\right)^{\Delta\nu} - \frac{\Delta\varepsilon_0}{kT}\right] \qquad ...(268)$$

where $\Delta\nu$ is the change in the number of molecules represented in the stoichiometric equation, *i.e.*,

$$\Delta\nu = (c + d) - (a + b) \qquad ...(269)$$

and

$$\Delta\varepsilon_0 = (c\varepsilon_{0C} + d\varepsilon_{0D}) - (a\varepsilon_{0A} + b\varepsilon_{0B}) \qquad ...(270)$$

Hence,

$$\Delta G^0 = -RT\left[\ln\left\{\frac{(q_C')^c (q_D')^d}{(q_A')^a (q_B')^b}\left(\frac{1}{N_A}\right)^{\Delta\nu}\right\} - \frac{\Delta\varepsilon_0}{kT}\right] \qquad ...(271)$$

Since from the van't Hoff isotherm,

$$\Delta G^0 = -RT \ln K_p \qquad ...(272)$$

where K_p is the equilibrium constant of the reaction in terms of partial pressures, we obtain

$$K_p = \frac{(q_C')^c (q_D')^d}{(q_A')^a (q_B')^b}\left(\frac{1}{N_A}\right)^{\Delta\nu} e^{-\Delta\varepsilon_0/kT} \qquad ...(273)$$

We can also express K_p in terms of the change in molar zero-point energy, ΔE_0. Since

$$E_0 = N_A\varepsilon_0 \qquad ...(274)$$

we have

$$K_p = \frac{(q_C')^c (q_D')^d}{(q_A')^a (q_B')^b}\left(\frac{1}{N_A}\right)^{\Delta\nu} e^{-\Delta E_0/RT} \qquad ...(275)$$

We shall apply Eq. 275 to two specific cases of chemical interest :

Case 1. Dissociation of Diatomic Molecules. Consider the following dissociation reaction :

$$A_2(g) \rightleftharpoons 2A(g),$$

for which, using Eq. 275,

$$K_p = \frac{(q_A')^2}{q_{A_2}'}\left(\frac{1}{N_A}\right) e^{-\Delta E_0/RT} \qquad ...(276)$$

The nuclear factors in q_A' and q_{A_2}' cancel and

$$\frac{(q_A')^2}{q_{A_2}'} = \frac{(q_{tr,A}^0)^2}{q_{tr,A_2}^0}\left(\frac{1}{q_{rot,A_2}}\right)\left(\frac{1}{q_{vib,A_2}}\right)\left(\frac{q_{elec,A}'}{q_{elec,A_2}'}\right)^2 \qquad ...(277)$$

It the mass of atom A is m, then the mass of molecule A_2 is $2m$ so that the ratio of the translational factors is

$$\frac{(q_{tr,A}^0)^2}{q_{tr,A_2}^0} = \frac{[(2\pi mkT/h^2)^{3/2} \times V^0]^2}{(4\pi mkT/h^2)^{3/2} \times V^0} = \left(\frac{\pi mkT}{h^2}\right)^{3/2} \times VH^0 \qquad ...(278)$$

The moment of inertia of A_2 is given by

$$I = \tfrac{1}{2}mr^2 \qquad ...(279)$$

and the symmetry number σ is 2. Hence,

$$\frac{1}{q_{rot,A_2}} = \frac{2h^2}{8\pi^2 IkT} = \frac{h^2}{2\pi^2 mr^2 kT} \qquad ...(280)$$

Again, for A_2,

$$1/(q_{vib,A_2}) = 1 - e^{-h\nu/kT} \qquad ...(281)$$

If we further assume that $q_{el} = q_{el(0)}$, then

$$K_p = \frac{1}{2}\left(\frac{mkT}{\pi}\right)^{1/2} \frac{1}{hr^2}(1 - e^{-h\nu/kT})\left(\frac{q_{el(0),A}^2}{q_{el(0),A_2}}\right)\left(\frac{V_0}{N_A}\right) e^{-\Delta E_0/RT} \qquad ...(282)$$

For the dissociation of H_2, $H_2(g) \rightleftharpoons 2H(g)$, the interatomic distance $r = 74$ pm ; the dissociation energy, ΔE_0, obtained spectroscopically is 432·2 kJ mol^{-1} ; $g_{el(0)H} = 2$; $g_{el(0)H_2} = 1$. Since $\Theta_{vib} \approx 6{,}000$ K for H_2, $q_{vib} \approx 1$ if $T \leq 3{,}000$ K. Using these values, Eq. 282 can be further

simplified to obtain an expression for K_p as a function of T. The results are shown in Table 6.

TABLE 6

K_p for the Reaction, $H_2(g) \rightleftharpoons 2H(g)$				
T(K)	1,000	2,000	2,500	3,000
K_p	$1{\cdot}4\times10^{-18}$	$3{\cdot}9\times10^{-7}$	$1{\cdot}9\times10^{-4}$	$7{\cdot}9\times10^{-3}$

Case 2. Isotopic Exchange Equilibria. Let us now consider the gaseous equilibrium

$$A_2 + B_2 \rightleftharpoons 2AB$$

where A and B are two isotopes. The equilibrium constant for this reaction is

$$K_p = \frac{(q'_{AB})^2}{q'_{A_2} q'_{B_2}} e^{-\Delta\varepsilon_0/kT} \qquad ...(283)$$

We can evaluate the q' terms appearing in Eq. 283 in the usual way. Let us, for simplicity, consider the case when

$$\Theta_{rot} < T \leq \Theta_{vib} \qquad ...(284)$$

so that $q'_{vib} = 1$. Since the two isotopes A and B have the same nuclear charge, the molecules involved in the exchange reaction, *viz.*, A_2, B_2 and AB have, to a first approximation, the same charge distributions and electronic energies and hence the same internuclear distances and vibrational force constants. The nuclear and electronic factors in the q' terms cancel so that

$$\frac{(q'_{AB})^2}{q'_{A_2} q'_{B_2}} = \left(\frac{(q^0_{tr,AB})^2}{q^0_{tr,A_2}\, q^0_{tr,B_2}}\right)\left(\frac{(q_{rot,AB})^2}{q_{rot,A_2}\, q_{rot,B_2}}\right) \qquad ...(285)$$

Since $q^0_{tr} = \left(\frac{2\pi mkT}{h^2}\right)^{3/2} V^0$, (Eq. 68)

hence, the translational factor becomes

$$\frac{(m_A+m_B)^3}{(2m_A)^{3/2}(2m_B)^{3/2}} = \frac{1}{8}\frac{(m_A+m_B)^3}{(m_A m_B)^{3/2}} \qquad ...(286)$$

Since from Eq. 80, $q_{rot} = 8\pi^2 IkT/\sigma h^2$ with $\sigma_{A_2} = \sigma_{B_2} = 2$ and $\sigma_{AB} = 1$, hence the rotational factor becomes

$$\frac{4I^2_{(AB)}}{I_{A_2} I_{B_2}} = \frac{16 m_A m_B}{(m_A + m_B)^2} \qquad ...(287)$$

where we have made use of the fact that $I = \mu r^2$

Let us now consider the exponential term in Eq. 283. Since the reactants and the products have the same electronic energy, the only contributions to $\Delta\varepsilon_0$ arise from the zero-point vibrational energy terms (*i.e.*, $\frac{1}{2}h\nu$ per molecule) :

$$\Delta\varepsilon_0 = h/2(2\nu_{AB} - \nu_{A_2} - \nu_{B_2}) \qquad ...(288)$$

It is known from vibrational spectroscopy that the frequency ν and force constant k of a diatomic

molecule are related by

$$\nu = \frac{1}{2\pi}\left(\frac{k}{\mu}\right)^{1/2} \qquad ...(289)$$

where μ, the reduced mass of the molecule, is given by

$$\mu = \frac{m_A m_B}{m_A + m_B} \qquad ...(290)$$

Since the molecules A_2, B_2 and AB have the same force constants, we find that

$$\nu_{AB} = \nu_{A_2}\left(\frac{\mu_{A_2}}{\mu_{AB}}\right)^{1/2} = \nu_{A_2}\left(\frac{m_A + m_B}{2m_B}\right)^{1/2}$$

and

$$\nu_{B_2} = \nu_{A_2}\left(\frac{m_A}{m_B}\right)^{1/2} \qquad ...(291)$$

Hence,

$$\Delta\varepsilon_0 = \frac{\Theta_{vib,A_2}}{2}\left[\sqrt{2}\left(\frac{m_A + m_B}{m_B}\right)^{1/2} - \left(\frac{m_A}{m_B}\right)^{1/2} - 1\right] \qquad ...(292)$$

where Θ_{vib,A_2}, the **characteristic vibrational temperature of A_2**, is given by $\Theta_{vib,A_2} = h\nu_{A_2}/k$

Substituting Eqs. 285 — 292 into Eq. 283, we obtain

$$K_p = \frac{2(m_A + m_B)}{(m_A m_B)^{1/2}} \exp\left[-\frac{\Theta_{vib,A_2}}{2T}\left\{\sqrt{2}\left(\frac{m_A + m_B}{m_B}\right) - \left(\frac{m_A}{m_B}\right)^{1/2}\right\}\right] \qquad ...(293)$$

Let us apply Eq. 293 to the deuterium–hydrogen exchange reaction :

$$D_2 + H_2 \rightleftharpoons 2DH$$

Here $m_A = 2m_H$, $m_B = m_H$, where m_H is the mass of hydrogen atom.

Hence,

$$K_p = 3\sqrt{2}\exp\left[-\frac{\Theta_{vib,D_2}}{2T}(\sqrt{6} - \sqrt{2} - 1)\right]$$

Since $\Theta_{vib,D_2} = 4{,}307$ K

$$\therefore \quad K_p = 4{\cdot}24\, e^{-75/T} \qquad ...(294)$$

The K_p values as a function of T are shown in Table 7. The agreement between the experimental and theoretical values is quite satisfactory.

TABLE 7

K_p for the Reaction $D_2 + H_2 \rightleftharpoons 2DH$				
T(K)	273	298	383	670
K_p (calculated)	3·22	3·30	3·49	3·79
K_p (observed)	3·24	3·28	3·50	3·80

Heat Capacities of Monatomic Crystals

In 1819 the French physicists Dulong and Petit found that, at constant pressure, the molar heat capacity at constant volume of most of the solid elements at room temperature was given by

$$C_V \approx 6 \text{ cal K}^{-1} \text{ mol}^{-1} \quad \ldots(295)$$

In order to account for this value, two theories of heat capacities were developed—the first by Albert Einstein in 1907 and the second (which is a modification of the Einstein theory) by Peter Debye in 1912.

1. The Einstein Theory of Heat Capacities. Einstein made the following assumptions in constructing his theory of heat capacities of monoatomic crystals.

1. The atoms in a crystal lattice undergo small oscillations (vibrations) about their equilibrium configurations. In fact, an ideal crystal can be considered as a system of N non-interacting particles (*i.e.*, atoms).

2. Each atom vibrates independently of the others and has three independent vibrational degrees of freedom. Thus, the crystal may be treated as a system of $3N$ *independent and distinguishable* harmonic oscillators.

3. There are no electronic, translational or rotational modes of motion in a monoatomic crystal.

Using assumptions 2 and 3, the molar vibrational partition function of the crystal can be written as

$$Q_{vib} = (q_{vib})^{3N} \quad \text{(From Eq. 254)} \quad \ldots (296)$$

or
$$\ln Q_{vib} = 3N \ln q_{vib} = -\frac{3}{2}\frac{N\Theta_E}{T} - 3N\ln(1 - e^{-\Theta_E/T}) \quad \ldots(297)$$

where Θ_E is the **characteristic Einstein temperature for vibration.** $\Theta_E = h\nu/k$ where ν is the vibrational frequency of the oscillator. Thus, the internal energy of an ideal Einstein crystal is given by

$$U = kT^2\left(\frac{\partial \ln Q_{vib}}{\partial T}\right)_{V,N} = \frac{3}{2}Nh\nu + \frac{3Nk\Theta_E}{e^{\Theta_E/T} - 1} \quad \ldots(298)$$

or
$$U - U_0 = 3RT\,\frac{\Theta_E/T}{e^{\Theta_E/T} - 1} \quad \ldots(299)$$

where U_0 is the zero-point energy ($= \frac{3}{2}Nh\nu = \frac{3}{2}R\Theta_E$). Hence, the molar heat capacity

$$C_V = 3R\left(\frac{\Theta_E}{T}\right)^2 \frac{e^{\Theta_E/T}}{(e^{\Theta_E/T} - 1)^2} \quad \ldots(300)$$

Experimentally it is found that at temperatures approaching zero, C_V approaches zero and in the limit of high temperatures, C_V approaches the Dulong–Petit value of $3R$ (*i.e.*, ≈ 6 cal K^{-1} mol^{-1}). Einstein's theory predicts these limiting values of C_V quite successfully. Thus, as

$$T \to 0,\ e^{\Theta_E/T} - 1 \approx e^{\Theta_E/T} \text{ so that} \quad \ldots(301)$$

$$\lim_{T\to 0} C_V \approx 3R\,(\Theta_E/T)^2\, e^{\Theta_E/T} \approx 0 \quad \ldots(302)$$

Again, as $T \to \infty$, $e^{\Theta_E/T} \approx 1 + (\Theta_E/T)$ so that

$$\lim_{T\to\infty} C_V \approx 3R\left(\frac{\Theta_E}{T}\right)^2 \frac{e^{\Theta_E/T}}{(1 + \Theta_E/T - 1)^2} \approx 3R \quad \ldots(303)$$

The above results are illustrated in Fig. 17 for a number of metallic and non-metallic crystals.

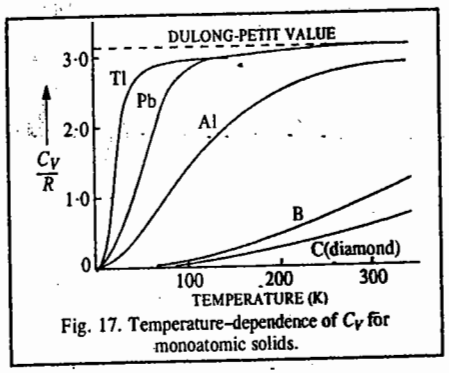

Fig. 17. Temperature-dependence of C_V for monoatomic solids.

Einstein's theory, however, is not successful in predicting the C_V values in the lower and intermediate temperature ranges ; the values predicted by it are lower than those actually observed.

2. Debye Theory of Heat Capacities. Peter Debye avoided the most serious assumption of the Einstein theory, namely, that the vibrations in a crystal lattice are independent. He recognized that the interatomic forces in a crystal are very strong and hence the atoms may not be treated as being independent. Debye assumed that the crystal behaves like a huge molecule wherein the motion of any one atom affects the motion of the neighbouring atoms. The oscillations or normal modes of vibration which characterize the motion of the crystal as a whole, have long wave lengths compared with the lattice spacings. The various vibrational modes are distinguished by their unique frequency. Debye further assumed that the properties of the crystal could be determined from a superposition of contributions due to each possible vibrational mode, rather than by summing the contributions made by individual atoms. Thus, the determination of the crystal properties depends upon determining the possible frequencies for the vibrational modes.

In order to determine the normal vibrational frequencies, Debye assumed them to be equivalent to the fundamental vibrational frequencies which are induced in an elastic solid of fixed boundaries. The oscillations represent acoustic standing waves in the elastic medium. We can also remark that each normal mode of vibration is equivalent to the motion of a hypothetical phonon (the phonon is to acoustics what the photon is to electromagnetic radiation).

The next task is to determine the frequency distribution of the normal modes. In a crystal containing N atoms, the number of degrees of freedom is $3N$. Subtracting the 3 translational degrees of freedom and the 3 rotational degrees of freedom, the number of vibrational degrees of freedom of the crystal is $3N - 6$. Since, however, N is very large, to an approximation, there are $3N$ vibrational degrees of freedom. Therefore, Debye assumed the atomic crystal to have $3N$ normal vibrations, each having a unique frequency.

Assuming a continuous distribution of frequencies, the frequency distribution function is defined by

$$dN = f(\nu)d\nu \quad \ldots(304)$$

where dN is the number of normal modes of vibration in the frequency range from ν to $\nu + d\nu$. It is, thus, required that

$$\int_0^{\nu_D} f(\nu)d\nu = 3N \quad \ldots(305)$$

where ν_D (or ν_{max}) is the maximum possible oscillation frequency. Fig. 18 shows the plots of frequency distribution of normal modes in a crystal for both the Einstein and the Debye theories. The area under either curve between any two values of ν is the number of vibrational quantum states in the crystal with frequency between the two values.

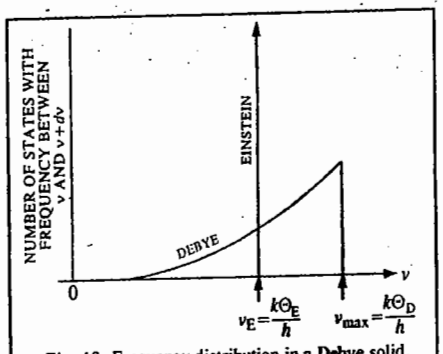

Fig. 18. Frequency distribution in a Debye solid.

The partition function for the system of the Debye oscillators is given by

$$Q = q(\nu_1)^{f(\nu_1)} q(\nu_2)^{f(\nu_2)} \ldots q(\nu_D)^{f(\nu_D)} \quad \ldots(306)$$

or
$$\ln Q = \sum_{i=1}^{\nu_D} f(\nu_i) \ln q(\nu_i) \quad \ldots(307)$$

As a result of the continuity, the summation may be replaced by integration so that

$$\ln Q = \int_0^{\nu_D} f(\nu) \ln q(\nu) d\nu \quad \ldots(308)$$

where $q(\nu)$ is the partition function of the oscillator defined by

$$q(\nu) = q_{vib} = \frac{e^{-\Theta_{vib}/2T}}{1 - e^{-\Theta_{vib}/T}} \quad \ldots(309)$$

Debye used the Rayleigh-Jeans relation for the distribution function, *viz.*,

$$f(\nu)d\nu = c\nu^2 d\nu \quad \ldots(310)$$

where the constant c is determined from the restriction that

$$\int_0^{\nu_D} f(\nu)d\nu = c\int_0^{\nu_D} \nu^2 d\nu = \frac{2}{3}c\nu_D^3 = 3N \quad \ldots(311)$$

Thus,
$$c = 9N/\nu_D^3 \quad \ldots(312)$$

Hence, Eq. 310 is written as

$$f(\nu)d\nu = (9N/\nu_D^3)\,\nu^2 d\nu \quad \ldots(313)$$

Thus, the partition function of the Debye crystal becomes

$$\ln Q = -\frac{9N}{\nu_D^3}\int_0^{\nu_D}\left[\frac{h\nu}{2kT} + \ln(1 - e^{-h\nu/kT})\nu^2 d\nu\right] \quad \ldots(314)$$

which helps us to obtain

$$U = \frac{9NkT}{\nu_D^3}\int_0^{\nu_D}\left[\frac{h\nu/kT}{e^{h\nu/kT} - 1} + \frac{h\nu}{2kT}\right]\nu^2 d\nu \quad \ldots(315)$$

$$= \frac{9Nh\nu_D}{8} + \frac{9NkT}{\nu_D^3}\int_0^{\nu_D}\left[\frac{h\nu/kT}{\exp(h\nu/kT) - 1}\right]\nu^2 d\nu$$

Putting $\Theta = h\nu/k$ and $\Theta_D = h\nu_D/k$, where Θ_D is called the **characteristic Debye temperature** of the crystal, we obtain

$$U = \frac{9R\Theta_D}{8} + 9RT\left(\frac{T}{\Theta_D}\right)^3\int_0^{\Theta_D/T}\left[\frac{(\Theta/T)^3}{e^{\Theta/T} - 1}\right]d\left(\frac{\Theta}{T}\right) \quad \ldots(316)$$

The integral in Eq. 316 can be evaluated numerically. It is convenient to define the **Debye function** as

$$D(x) = \frac{3}{x^3}\int_0^x \frac{z^3 dz}{e^z - 1} \quad \ldots(317)$$

where $x = \Theta_D/T$ and $z = \Theta/T$

(The Debye function is tabulated in standard books on Statistical Thermodynamics.) The energy of the crystal becomes

$$U = 9R\Theta_D/8 + 3RTD(\Theta_D/T) \quad \ldots(318)$$

Differentiating $D(\Theta_D/T)$ and then carrying out the integration by parts, we obtain

$$C_V = 3RD\left(\frac{\Theta_D}{T}\right) + 3RT\frac{\partial}{\partial T}\left[D\left(\frac{\Theta_D}{T}\right)\right] = 3R\left[4D\left(\frac{\Theta_D}{T}\right) - \frac{3(\Theta_D/T)}{e^{\Theta_D/T} - 1}\right] \quad \ldots(319)$$

At high temperatures,

$$e^{\Theta_D/T} - 1 \approx 1 + \Theta_D/T - 1 \approx \Theta_D/T \quad \ldots(320)$$

and
$$\lim_{T\to\infty} D(\Theta_D/T) \approx 1 \quad \ldots(321)$$

Hence,
$$\lim_{T\to\infty} C_V \approx 3R \quad \ldots(322)$$

Al low temperatures,

$$\lim_{T\to 0} D(\Theta_D/T) \approx \frac{\pi^4}{5}(T/\Theta_D)^3 \quad \ldots(323)$$

so that
$$\lim_{T\to 0} C_V \approx 12/5\pi^4 R(T/\Theta_D)^3 = 234R(T/\Theta_D)^3 \quad \ldots(324)$$

The above results are illustrated in Fig. 19 in which C_V/R values are potted against T/Θ.

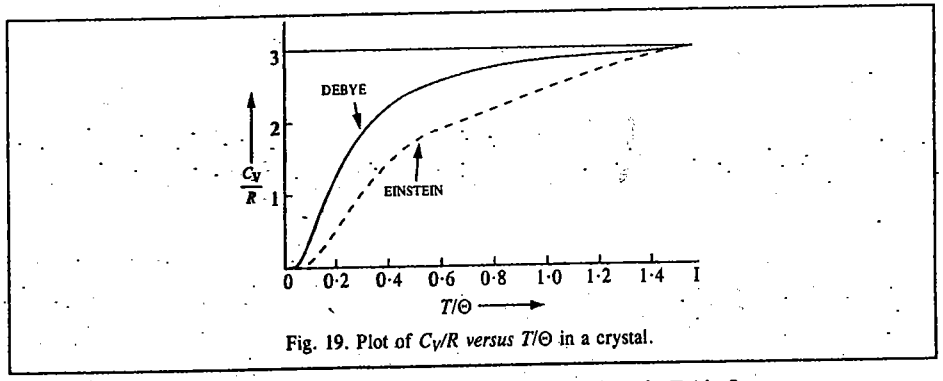

Fig. 19. Plot of C_V/R *versus* T/Θ in a crystal.

The characteristic Debye temperatures for some solids are given in Table 8.

TABLE 8

Debye Temperatures, Θ_D, for Some Common Substances

Subtance	Θ_D (K)	Subtance	Θ_D (K)
Lead	88	Zinc	235
Mercury	97	Sodium chloride	281
Cadmium	168	Copper	315
Sodium	172	Aluminium	398
Potassium bromide	177	Iron	453
Silver	215	Diamond	1,860
Calcium	226		

Since all the quantities on the right side of Eq. 324 except the temperature are constant for a particular crystal, we can write this equation as

$$C_V = aT^3 \qquad ...(325)$$

where $a = 12\pi^4 R / 5\Theta_D^3$.

This is the famous **Debye *T*-cubed law** for the heat capacity of a crystal. It is in excellent agreement with experimental data at temperatures lower than Θ_D, even for crystals which are more complex than those of the elements but the agreement is significantly poor at higher temperatures. The deficiencies of the Debye theory of heat capacity of crystals arise from the fact that it replaces the actual distribution of vibrational frequencies by an oversimplified distribution function which is obtained by ignoring the structure of the crystals.

I. Review Questions

1. Maximizing the thermodynamic probability of a macrostate and invoking Lagrange's undetermined multipliers, derive the expression for Maxwell-Boltzmann statistics.
2. Repeat question No. 1 for Fermi-Dirac statistics.
3. Repeat question No. 1 for Bose-Einstein statistics.
4. Derive an expression for the molecular translational partition function of an ideal gas.
5. Derive an expression for the molecular rotational partition function of an ideal diatomic gas.
6. Derive an expression for the molecular vibrational partition function of an ideal diatomic gas.
7. Show that the internal energy of a system of independent particles is given by $U = nRT^2(\partial \ln q/\partial T)_V$. Hence, show that for an ideal gas $U = \frac{3}{2} nRT$.
8. Using the concept of molecular partition function show that for an ideal monatomic gas, $P = nRT/V$. This is the ideal gas equation.
9. Derive an expression for the equilibrium constant of an ideal gaseous mixture in terms of the partition functions of the reactants and the products.
10. Discuss the salient features of the Einstein theory of the heat capacity of monatomic crystals. How did Debye modify it ? Show the results of the Einstein and the Debye theories on a plot and comment briefly.
11. How is nuclear spin incorporated in the rotational partition function of a diatomic gas and what are its consequences?
12. How do you account for the rotational heat capacity of ortho and para H_2 using the incorporation of the nuclear spin in the rotational partition function ?
13. Discuss the application of BE statistics to the thermodynamics of an ideal photon gas (black body radiation).

II. Problems

1. Calculate the relative Boltzmann population of two energy levels at 25°C if the energy levels are separated by *(a)* 1000 cm^{-1} *(b)* 10 kJ mol^{-1}. **[Ans. *(a)* 0·0080 *(b)* 0·0177]**
2. Calculate the translational partition function for hydrogen atom at 1,000 K and 1 atm. **[Ans. $4{\cdot}94\times10^{29}$]**
3. Calculate the translational partition function for $H_2(g)$ at 1,000 K and 1 atm pressure. **[Ans. $1{\cdot}396\times10^{30}$]**
4. Calculate the translational partition function for argon atom in a cubical box of side 1 cm^3 at 25°C. **[Ans. $2{\cdot}45\times10^{26}$]**
5. Calculate the rotational partition function for the O—H radical at 27°C, given that the bond length (O—H) = 0·971 Å. **[Ans. 11·05]**

6. Calculate the rotational partition function for F_2 at 25°C, given that $I = 32{\cdot}5\times10^{-47}$ kg m^2. **[Ans. 120]**
7. The fundamental vibrational frequency of F_2 is $2{\cdot}676\times10^{13}$ Hz. Calculate the vibrational partition function of F_2 at 25°C. **[Ans. 1·1177]**
8. The vibrational energy levels of iodine vapour occur at the following wave numbers above the zero-point energy level : 213·30 cm^{-1}, 425·39 cm^{-1}, 636·27 cm^{-1}, 845·93 cm^{-1}, 1054·38 cm^{-1}. Calculate the vibrational partition function of iodine at 27°C. **[Ans. 1·5553]**
9. Calculate the relative Boltzmann populations of I_2 molecules in their ground, first excited and second excited vibrational energy levels at 25°C. The vibrational frequency of I_2 is 214·6 cm^{-1}. **[Ans. 0·645, 0·229, 0·081]**
10. For CO, $\Theta_{rot} = 2{\cdot}77$ K, and $\Theta_{vib} = 3{\cdot}084$ K. For one mole of this gas at 25°C and 1 atm pressure, calculate the translational, rotational, vibrational and electronic partition functions. **[Ans. $q_{tr} = 3{\cdot}51\times10^{30}$; $q_{rot} = 108$; $q_{vib} = 1{\cdot}000032$, $q_{el} = 1$]**
11. Calculate, using statistical mechanics, the value of $S°$, $H°$ and $G°$ for $H_2(g)$ at 3,000 K. **[Ans. 162·707 J K^{-1} mol^{-1} ; 62·353 ; – 425·763 kJ mol^{-1}]**
12. At 150 K the C_V for Cu is 19·66 J K^{-1} mol^{-1}. What is the characteristic Einstein temperature, Θ_E for Cu? Estimate C_V for Cu at 50 K using both the Einstein and the Debye theories. **[Ans. Θ_E = 262 K ; 0·87 and 6·23 J K^{-1} mol^{-1}]**
13. For Al, $\Theta_E = 240$ K. Calculate C_V of Al on the Einstein model at *(a)* 50 K and *(b)* 240 K. **[Ans. *(a)* 4·81 J K^{-1} mol^{-1} *(b)* 22·97 J K^{-1} Mol^{-1}]**
14. For I_2 at 10 K, $C_V = 4{\cdot}02$ J K^{-1} mol^{-1}. Calculate *(a)* Θ_D and *(b)* C_V of I_2 at 12 K. **[Ans. *(a)* 78 K ; *(b)* 6·94 J K^{-1} mol^{-1}]**
15. The first excited state of Cl(*g*) atom is 875·4 cm^{-1} higher in energy than the ground state. Both the states are doubly (*i.e.*, two-fold) degenerate. Calculate the electronic partition function at *(a)* 25°C, *(b)* 1000 K. **[Ans. *(a)* 2·029 *(b)* 2·568]**
16. Calculate $S°$ and C_p° for argon (M = 39·948 g mol^{-1}) at 25°C and 1 bar. **[Ans. 154·844, 20·786 J K^{-1} mol^{-1}]**
17. Calculate the statistical mechanical values of C_p°, $S°$, $H°$ and $G°$ for $H_2(g)$ at 3,000 K. **[Ans. 34·907 ; 201·012 J K^{-1} mol^{-1} ; – 337·524 ; – 940·560 kJ mol^{-1}]**
18. Using the Boltzmann equation for entropy, *viz.*, $S = k \ln W$, where W is the number of microstates corresponding to a given macrostate, calculate the residual entropy of crystalline carbon monoxide (CO) molcules at 0 K. **[Ans. 5·76 J K^{-1} mol^{-1}]**
19. Calculate the molar entropy of H atom *(g)* at 1000 K and *(a)* 1 bar *(b)* 1,000 bar. **[Ans. (a) 139·871 J K^{-1} mol^{-1} *(b)* 82·437 J K^{-1} mol^{-1}]**
20. Calculate the temperature at which 10% of the moleculas in a system will be in the first excitd electronic state if this state is 400 kJ mol^{-1} above the ground state. **[Ans. 22,000 K]**
21. For CO, $\Theta_{rot} = 2{\cdot}77$ K, and $\Theta_{vib} = 3{,}084$ K. For one mol of this gas at 25°C and 1 atm pressure calculate the translational, rotational, vibrational, and electronic partition functions. **[Ans. $q_{tr} = 3{\cdot}51\times10^{30}$; $q_{rot} = 108$; $q_{vib} = 1{\cdot}000032$, $q_{el} = 1$]**
22. Calculate the number of ways in which (*a*) two distinguishable balls can be placed in two boxes (*b*) two distinguishable balls can be placed in three boxes. (*c*) What are the answers to (*a*) and (*b*) if the balls are indistinguishable ? **[Ans. (*a*) 4 (*b*) 9 (*c*) 3, 6]**
23. Evaluate 11 ! (*a*) by using Strilling's approximation (*b*) by using the improved approximation in $N! = N \ln N - N + 1/2 \ln 2N$ and (*c*) by actual computation. **[Ans. (*a*) $4{\cdot}77\times10^6$ (*b*) $2{\cdot}24\times10^7$ (*c*) 39916800]**
24. Using the Boltzmann equation for entropy, calculate the *residual* entropy of crystal line CH_3D near 0 K. **[Ans. 11·5 JK^{-1} mol^{-1}]**
25. Using the Sackur-Tetrode equation, calculate the (translational) entropies of the inert gases He, Ne, Ar, Kr, Xe and Rn at 298·15 K at 1 atm pressure (101·32 kPa). **[Ans. 126, 146, 155, 164, 170, 176, J K^{-1} mol^{-1})]**

26. At 150 K the $C_{V,mol}$ for Cu is 4·7 cal K^{-1} mol^{-1}. What is the characteristic Einstein temperature, θ_E for Cu ? Estimate $C_{V,mol}$ for Cu at 50 K using both Einstein and the Debye theories.
[Ans. Θ_E = 262 K; 0·87 and 1·49 cal K^{-1} mol^{-1}]

27. For Al, Θ_E = 240 K. Calculate $C_{V,mol}$ of Al on the Einstein model at (*a*) 50 K and (*b*) 240 K.
[Ans. (*a*) 1·15 cal K^{-1} mol^{-1}, (*b*) 5·49 cal K^{-1} mol^{-1}]

28. For I_2 at 10 K, $C_{V,mol}$ = 0·96 cal K^{-1} mol^{-1}. Calculate (*a*) Θ_D and (*b*) $C_{V,mol}$ of I_2 at 12 K.
[Ans. (*a*) 78 K; (*b*) 1·66 cal K^{-1} mol^{-1}]

29. The first excited state of O_2 is $15·72\times10^{-20}$ J above the ground level. Calculate N_1/N_0 at 25°C and 1500 K. The degeneracies are $g_0 = 3$ and $g_1 = 2$. **[Ans. $1·6 \times 10^{-17}$; $3·3 \times 10^{-4}$]**

30. For $N_2(g)$, Θ_{rot} = 2·88 K and Θ_{vib} = 3374 K. Estimate the temperature at which the rotational and vibrational contributions to C_v have half the classical value, R per mole.
[Ans. 1·24 K and 1280 K, respectively]

31. Calculate, using statistical mechanics, the value of C_p°, S°, H° and G° for H(g) to 3,000 K.
[Ans. 20·786 ; 162·707 JK^{-1} mol^{-1}; 62·353 ; –425·763 kJ mol^{-1}]

CHAPTER 27

CLASSICAL STATISTICAL MECHANICS

We have discussed in the last chapter the basic principles of statistical thermodynamics. We have seen that the partition function plays a central role in statistical thermodynamics analogous to the role the wavefunction plays in quantum mechanics. The expressions developed for the molecular partition functions for translational, rotational, vibrational and electronic motions were then used to express the various thermodynamic quantities in terms of the appropriate partition functions. The thermodynamic quantities were then evaluated for ideal gases.

In this chapter we shall discuss the subject from the classical point of view. Classical statistical mechanics was developed by Gibbs in the 19th century using the concepts of phase space and ensemble of systems. We shall develop expressions for partition functions in three commonly used ensembles and then derive expressions for thermodynamic quantities in terms of these partition functions. We shall also deal with quantal ensembles. The chapter will end with a brief discussion of the theories of the superfluidity of liquid helium and statistical mechanics of imperfect gases.

Classical Statistical Mechanics

Phase Space, Ensemble Theory, Ensembles and Ensemble Average

1. Phase Space. Consider an ideal gas in which, by definition, there are no intermolecular interactions. The ideal (perfect) gas molecule can be represented as a structureless particle; it has three translational degrees of freedom. The instantaneous state of this molecule can be represented by a representative point in a hypothetical six-dimensional phase space where Cartesian coordinates are x_1, x_2, x_3, p_1, p_2, p_3 (where x_i are the position coordinates and p_i are the corresponding momenta). This phase space is called the μ space where μ stands for the molecule. For a system of N identical gas molecules the instantaneous state (Fig. 1*a*) is represented by a set of N points in the μ space, one for each molecule (Fig. 1*b*). It should be borne in mind that it is a symbolic picture of the space because it is not possible to display a six-dimensional space. The total number of translational degrees of freedom is $3N$. Following P. Ehrenfest, we can construct a phase space

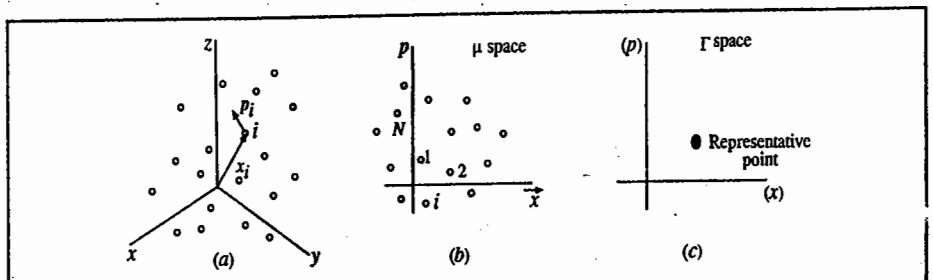

Fig. 1(*a*) A gas containing N molecules (system). (*b*) μ space for the system. (*c*) Γ space and the representative point for the entire system.

for all the molecules, which is $6N$-dimensional; this phase space is called the Γspace where Γ stands for gas. This $6N$-dimensional phase space is spanned by $3N$ coordinate axes and $3N$ momentum axes. The $6N$ coordinates (x_{11}, x_{21}, x_{31}..., x_{1N}, x_{2N}, x_{3N}, p_{11}, p_{21}, p_{31},..., p_{1N}, p_{2N}, p_{3N}) represent the positions and momenta of all the molecules (state of the system) at a given time. In the Γ space, the instantaneous state of the whole system (*e.g.*, a gas of N molecules) is given by a single *representative point (or phase point)* (Fig. 1*c*). The notation [x], [p] stands for the $3N$ coordinate axes and $3N$ momentum axes.

In general, a system is said to possess *f degrees of freedom* if f independent position coordinates and f momentum coordinates are required to fully specify the state of the system. Any set of f generalized coordinates q_1, q_2,..., q_f (Cartesian, polar or some other convenient set) can be used to uniquely determine the configuration of the system. The corresponding generalized momenta are p_1, p_2,..., p_f. The phase space (Γ space) is thus a conceptual Euclidean space having $2f$ rectangular axes [q], [p]. The microscopic state of the whole system is specified by a representative point in this space. If we consider our physical system—say, the ideal gas—composed of N identical particles confined to a space of volume V and having energy E, then we designate its macrostate at equilibrium by (N,V,E). In a typical case, $N \approx 10^{23}$, *i.e.*, a very large number and we define the thermodynamic limit as $N \to \infty$, $V \to \infty$ (such that the ratio N/V, called the particle density, n, stays fixed at a pre-assigned value). The specification of the actual values of the parameters N, V and E defines the macrostate of the system. Since the particles of the system are in motion, with the lapse of time its macrostate changes and the $2f$ coordinates assume different values. As a consequence, the representative point traces a phase line (or phase trajectory) in the accessible phase space (Fig. 2). Each point on the phase line represents one such macrostate. A point in the Γ space is *accessible* if it corresponds to the physical specification of the system under investigation. The system is likely to pass through all the accessible states so that the $2f$ coordinates take on all possible values. This is expressed by saying that they are *randomized*. The phase trajectory tends to fill the accessible phase space.

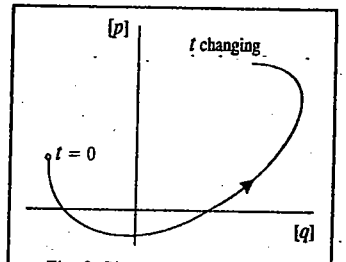

Fig. 2. Phase space and a portion of the phase line.

2. Ensemble. Each phase point on the phase trajectory of a single system develops out of the previous point in time. The great American mathematical physicist, J.W. Gibbs (1839-1903) replaced this time-dependent picture by a static picture in which the *entire phase line exists at one time* (Fig. 3). In Gibbs formulation of classical equilibrium statistical mechanics, each phase point represents a separate system with the same macroscopic properties (N, V, E) as the system of interest but a different microstate. In other words, we imagine a large number M ($M \to \infty$) of

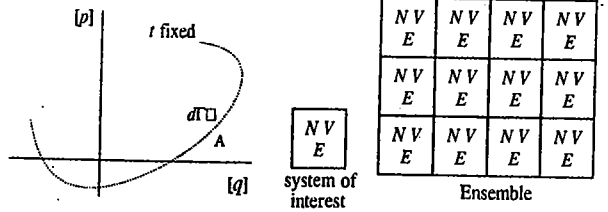

Fig. 3 (*a*) The ensemble (a small portion) at one time, Any region like A will appear to contain a swarm of phase points. (*b*) Schematic 'lattice' representation of an ensemble of M ($M \to \infty$) imaginary systems, at one time, each with the same N,V,E.

systems having a structure similar to the system of interest but suitably *randomized* in the accessible, unobservable microstates. Therefore, instead of taking the time average, following Gibbs we take an average over this artificially constructed group existing simultaneously at one time. *Such a group of replicas or collection of similar, noninteracting, independent, imagined systems is called an* **ensemble** *or* **Gibbsian ensemble** (Fig. 3). There is also a well known hypothesis called **the ergodic hypothesis,** *according to which the time average of some property of a system in equilibrium is the same as the instantaneous ensemble average.* All the systems, or the members, of an ensemble which are replicas of the actual system of interest are called the **elements**. Though it is difficult to prove the ergodic hypothesis, the following conditions must be satisfied by a Gibbsian ensemble :

1. The system of interest is a macroscopic system consisting of a large number, N, of molecules ($N \to \infty$) so that the microscopic variables can be randomized.

2. The number, M, of the imagined elements of the ensemble is large ($M \to \infty$) so that they can truly represent the range of states available to the actual system over a really long period of time ($t \to \infty$). We shall employ the terms system and ensemble in the above sense only.

3. Ensemble Average. We can describe the condition of an ensemble by a density D with which the phase points are distributed in the Γ space; it is called the *distribution function* (or *density distribution or probability density function*). In an ensemble of systems of f degrees of freedom, this function is a function of $2f$ position and momentum coordinates which correspond to the $2f$ axes in phase space. This function can also depend on time t explicitly, the reason being that we are not sure that the distribution, once fixed at any given time, will remain the same at a later time. If it remains the same, then that particular distribution will be one of equilibrium. Thus, we can write

$$D = D(q_1, q_2,..., q_f, p_1, p_2,..., p_f t) \equiv D(q, p, t) \qquad ...(1)$$

Let us now consider a small region A of the Γ space such that the position coordinates lie between q_1 and q_1+dq_1,..., q_f and q_f+dq_f, and the corresponding canonically conjugate momenta lie between p_1 and p_1+dp_1,...p_f and p_f+dp_f (Fig. 3). The hyper volume element of this region is :

$$d\Gamma = dq_1...dq_f\, dp_1...dp_f$$

$$= \prod_{i=1}^{f} dq_i \prod_{i=1}^{f} dp_i \equiv dq\, dp \qquad ...(2)$$

The density function symbolizes the manner in which the members of the ensemble are distributed over all possible microstates at different instants of time. Using the definition of density, the number of systems or elements dM lying in the infinitesimal region at the phase point q_1,..., p_f at the instant t is given by

$$dM = D(q, p; t)\, d\Gamma \qquad ...(3)$$

If M is the total number of elements in phase space, then at time t,

$$M = \int D\, d\Gamma \qquad ...(4)$$

where the integration is over the whole Γ space.

The **ensemble average** of a physical quantity $f(q, p)$, which may be different for systems in different microstates, is given by

$$\langle f \rangle = \frac{\int f(q,p)\, D(q,p;t)\, d\Gamma}{\int D(q,p,t)\, d\Gamma} = \frac{1}{M}\int f(q,p)\, D(q,p;t)\, d\Gamma \qquad ...(5)$$

For a system selected at random from the ensemble, the probability of selecting one whose phase

point lies in the small region at the point $q_1,\ldots, p_f$ is $\rho d\Gamma$ where

$$\rho = \frac{D}{\int D d\Gamma} = \frac{D}{M}\ ; \quad \int \rho\, d\Gamma = 1 \qquad \ldots(6)$$

In terms of $\rho(q, p; t)$, called the *normalized density distribution*,

$$\langle f \rangle = \frac{\int f(q,p)\rho(q,p;t) dq\, dp}{\int \rho(q,p;t)\, dq\, dp} = \int f \rho\, d\Gamma \qquad \ldots(7)$$

The integrations in Eq. 7 extend over the whole of the phase space; however, it is only the populated regions of phase space ($\rho \neq 0$) that really contribute. The ensemble average (Eq. 7) gives the average value of the physical quantity $f(q, p)$ for the actual system of interest. We may note that, in general, the ensemble average $\langle f \rangle$ may itself be a function of time. An ensemble is said to be *stationary* if ρ does not depend explicitly on time, *i.e.*, at all times,

$$\partial\rho/\partial t = 0 \qquad \ldots(8)$$

This equation is called the **Liouville theorem** (We shall not give the proof of this very important theorem here.). Clearly, for such an ensemble, the average value $\langle f \rangle$ of any physical property $f(q, p)$ will be independent of time. Naturally, a stationary ensemble qualifies to represent a system in equilibrium.

4. Postulate of Equal A Priori Probability in Classical Statistical Mechanics. Here we introduce the fundamental postulate of classical statistical mechanics known as the postulate of **equal a priori probability**. *It states that for a macroscopic system in equilibrium, all different microstates corresponding to the macroscopic conditions of the system are equally probable.* The macroscopic state of the system is characterized by the variables N, V, E. A very large number of different microscopic states will satisfy the said macrostate. The postulate states that all of them have equal probability, *i.e.*, no microstate has preference of one over the other. This postulate is the basis of statistical mechanics; it leads to results that agree with experimental observations.

It should be emphasized that in classical mechanism, every point in phase space represents a possible microstate of the system. Hence, we can say that the number of microstates in a given region of phase space is proportional to the hyper volume elements $d\Gamma = dq_1 \ldots dq_f\, dp_1 \ldots dp_f$ of that region. Since, classically, the number of possible microstates form a continuum, the constant of proportionality cannot be fixed. (In quantum mechanics, however, we can imagine the phase space as subdivided into cells of volume h^f each, where h is Planck's constant). The constant of proportionality involves h as a result of the quantal picture (of discrete eigenstates).

5. Statistical Equilibrium. A statistical ensemble is defined by the density distribution function ρ which characterizes it. In general, there are seven constant independent additive integrals of motion in classical mechanics : the energy, the three components of the momentum vector and the three components of the angular momentum vector. Usually, energy is the only constant known. For a large system, the total momentum and angular momentum have zero value or can be reduced to zero by a suitable choice of the coordinate system. We are thus concerned with only those ensembles that are functions of energy and are thus useful in thermodynamics.

Since the energy E is a constant of the motion for a conservative system, we shall take ρ as a function of energy (which, in turn, can be expressed as a function of q and p) :

$$\rho = \rho(E) \qquad \ldots(9)$$

Using the Liouville theorem it can be shown that the ensemble characterized by Eq. 9 is in

statistical equilibrium. Such an ensemble enables us to apply statistical mechanics to thermodynamics, where we are interested in a system for which the total energy $H(q, p) = E$ is conserved :

$$E(q_1,\ldots, p_f) = \text{constant} \qquad \ldots(10)$$

The locus of phase points corresponding to Eq. 10 forms a $(2f - 1)$-dimensional hypersurface, called an *energy surface* or *ergodic surface*, in the Γ-space (Fig. 4*a*). We can have a family of such surfaces constructed in the Γ space (Fig. 4*b*). Each energy surface divides the phase space in two parts, one of lower and the other of higher energy. It is evident that two surfaces of constant energy cannot intersect. The representative point of a conservative system remains always on the same ergodic surface. The ensemble for a conservative system at one time will populate one such ergodic surface. For the stationary ensemble, $(\partial\rho/\partial t)_{q,p} = 0$

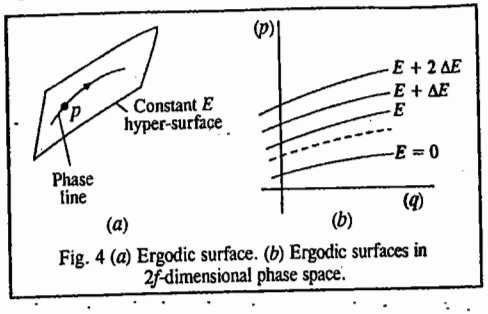

Fig. 4 (*a*) Ergodic surface. (*b*) Ergodic surfaces in $2f$-dimensional phase space.

In practice, three types of ensembles are useful : microcanonical ensemble, canonical ensemble and grand canonical ensemble. **Microcanonical ensemble** represents *isolated* systems so that no exchange of energy or mass (*i.e.*, number of particles) occurs between them. In other words, N, V and E are taken as constants. **Canonical ensemble** represents *closed* isothermal systems which can exchange energy with one another (and with a heat reservoir) but not mass. In this case, N, V and T remain constant. **Grand canonical ensemble** represents open isothermal systems which can exchange both E and N. In this case, μ, V and T remain constant where μ is the chemical potential. Other types of ensembles are possible but are not in general use.

Microcanonical Ensemble. An ensemble defined on the ergodic surface (Eq. 10) satisfies the condition for statistical equilibrium, *viz.*, $(\partial\rho/\partial t)_{q,p} = 0$, for any ρ which is a function of energy alone. A simple choice is

$$\rho = \begin{cases} \text{constant} & \text{for } E = E_0 \\ 0 & \text{otherwise} \end{cases} \qquad \ldots(11)$$

The ensemble characterized by this density distribution is called the **microcanonical ensemble,** shown schematically in Fig. 5*a*.

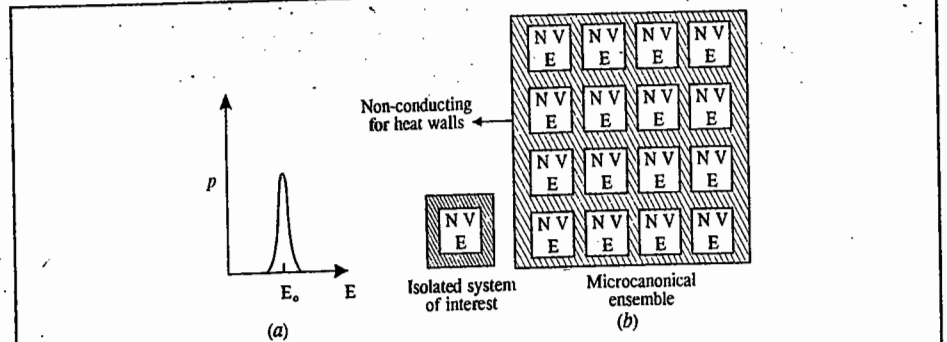

Fig. 5 (*a*) Density distribution for the microcanonical ensemble. (*b*) Schematic lattice representation of the microcanonical ensemble. The shaded walls are non-conducting for heat and impermeable to all molecules.

$$\rho(E) = C \times \delta(E - E_0)\ ;\ C \text{ is a constant} \qquad ...(12)$$

where δ is the **Dirac delta function** with the property

$$f(x') = \int_{-\infty}^{\infty} \delta(x - x')\, f(x)\, dx \qquad ...(13)$$

where $f(x)$ is an arbitrary well behaved function. In particular,

$$\int_{-\infty}^{\infty} \delta(x - x')\, dx = 1 \qquad ...(14)$$

In fact, $\delta(x - x') = 0$ except at $x = x'$

As stated above, the microcanonical ensemble is appropriate for an isolated system (N, V, E constant), because the energy of an isolated system is constant. The microcanonical ensemble is shown schematically in Fig. 5*b*.

It is not possible to specify exactly the energy of a system. We can, however, specify the energy within a narrow range, say, between E and $E+\Delta E$. We can, then, select two neighbouring surfaces, one at E and the other at $E+\Delta E$. The phase point of a conservative system always remains on the same ergodic surface. In the phase space the representative points of the ensemble can lie anywhere within a 'hyper shell' defined by the condition :

$$E \le H(q, p) \le E + \Delta E \qquad \text{(Fig. 6)} \quad ...(15)$$

The microcanonical ensemble can now be defined as

$$\rho(q, p) = \begin{cases} \text{constant} & \text{if } E \le H(q, p) \le E + \Delta E \\ 0 & \text{otherwise} \end{cases} \qquad ...(16)$$

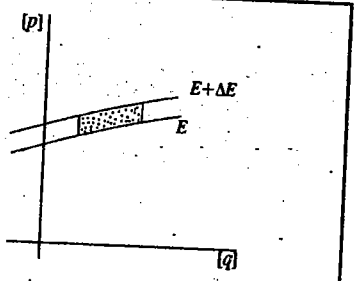

Fig. 6. The microcanonical ensemble representing an isolated system (gas contained in a finite volume) with energy between E and $E+\Delta E$. The shaded region represents the accessible portion of the phase space. It corresponds to a uniform distribution of representative points bounded by the ergodic surfaces of constant energy E and $E+\Delta E$ and the surfaces corresponding to the physical boundary of the container.

Entropy of a Perfect Gas Using the Classical Microcanonical Ensemble

Consider an isolated ideal gas of N identical molecules of mass m in a volume V, the degrees of freedom $f=3N$. The statistical weight $\Delta\Gamma$ [which is actually the number of quantum states $\Omega(N, V, E)$ [(Ω is degeneracy of energy level E system)] for energy less than or equal to E is given by

$$\Delta\Gamma = \frac{1}{h^{3N}} \int_{H<E} dq_1 \ldots dq_{3N} dp_1 \ldots dp_{3N} \qquad ...(17)$$

The integration over the generalized coordinates q_i gives V^N ; the integration over the canonically conjugate momenta p_i is the volume of a $3N$-sphere of radius $p = (2mE)^{1/2}$.

$$E = \frac{1}{2m} \sum_{i=1}^{3N} p_i^2 \qquad ...(18)$$

It is known that the volume of an n-sphere of radius R is given by

$$V_n(R) = \pi^{n/2} \frac{R^n}{(n/2)!} \qquad ...(19)$$

According to the Boltzmann equation, the entropy of a microcanonical ensemble is given by

$$S = k \ln \Omega\,(N, V, E) \equiv k \ln \Delta\Gamma(N, V, E) \qquad ...(20)$$

Using Eqs. 17 and 19,

$$\Delta\Gamma = \frac{V^N}{h^{3N}} \frac{\pi^{3N/2}}{(3N/2)!} (2mE)^{3N/2} \qquad ...(21)$$

Hence, from Eq. 20,

$$S = Nk \ln \left[V \left(\frac{4\pi m E}{3h^2 N} \right)^{3/2} \right] + \frac{3}{2} Nk \qquad ...(22)$$

where we have used the Sterling approximation, $\ln n! = n \ln n - n$. Solving for E, Eq. 22 yields

$$E = \frac{3}{4\pi} \frac{h^2}{m} \frac{N}{V^{2/3}} \exp\left(\frac{2}{3} \frac{S}{Nk} - 1 \right) \qquad ...(23)$$

From the thermodynamic definitions of temperature and pressure, *viz.*, $T = (\partial E/\partial S)_V$ and $P = -(\partial E/\partial V)_S$ and from the definition of the heat capacity, $C_V = (\partial q/\partial T)_V = T(\partial S/\partial T)_V$, we find from Eq. 23 that

$$T = \frac{2}{3} \frac{E}{Nk}\ ;\quad P = \frac{2}{3} \frac{E}{V} = \frac{NkT}{V} \quad \text{and} \quad C_V = \frac{3}{2} Nk \qquad ...(24)$$

These are important results for an ideal gas.

Entropy of Mixing of Ideal Gases and the Gibbs Paradox

Eq. 22 can be rewritten as

$$S = Nk \ln [V(E/N)^{3/2}] + NS_0 \qquad ...(25)$$

where

$$S_0 = \frac{3}{2} k\,(1 + \ln(4\pi m/3h^2) \qquad ...(26)$$

Consider two gases both at the same T, having the number of particles N_1 and N_2, entropy S_1 and S_2 and volume V_1 and V_2. When the gases are mixed, the volume of the mixture will be $V = V_1 + V_2$. Since the process is irreversible, the increase in entropy is given by

$$\Delta S = S_{12} - (S_1 + S_2) > 0 \qquad ...(27)$$

where S_{12} is the entropy of the mixture. Substituting from Eq. 25 and solving, we have

$$\Delta S/k = N_1 \ln (V/V_1) + N_2 \ln (V/V_2) > 0 \qquad ...(28)$$

Since, V is greater than both V_1 and V_2, the left hand side of Eq. 28 is always positive. This agrees with the experimental observation if the two gases are different. Now, any gas can be arrived at by putting any number of imaginary partitions in it and then removing them. Since, the number of partitions can be any digit, the very definition of entropy as a function of the thermodynamic state of the gas loses its meaning. This is known as **Gibbs paradox**. Gibbs resolved this paradox empirically by dividing the right-hand expression of Eq. 22 by a factor N ! to yield, instead of Eq. 25, the following equation :

$$S = Nk \ln [(V/N)\,(E/N)^{3/2}] + NS_0 \qquad ...(29)$$

where S_0 is now given by

$$S_0 = \frac{3}{2} k \left(\frac{5}{3} + \ln \frac{4\pi m}{3h^2} \right) \qquad ...(30)$$

The division by N ! does not affect the equation of state and other thermodynamic functions. The mixing of gases will now yield

$$\frac{\Delta S}{k} = N_1 \ln \frac{V_1 + V_2}{V_1} + N_2 \ln \frac{V_1 + V_2}{V_2} \qquad \text{(for two different gases)} \quad ...(31)$$

and

$$\frac{\Delta S}{k} = (N_1 + N_2) \ln \frac{V_1 + V_2}{N_1 + N_2} - N_1 \ln \frac{V_1}{N_1} - N_2 \ln \frac{V_2}{N_2} \qquad \text{(for the same gas)}$$

...(32)

For a mixture of two different gases, $\Delta S > 0$, since $V(= V_1 + V_2)$ is greater that both V_1 and V_2. However, if the two gases are the same, the specific volume, *i.e.*, volume per particle, is the same so that $\Delta S = 0$. Thus, the paradox is resolved.

The reason for dividing by the factor $N!$ is inherently quantal (quantum mechanical) and has no classical explanation. In quantum statistical mechanics, the identical particles being *indistinguishable*, an interchange of particles does not produce a new quantum state. The N particles have $N!$ permutations among themselves, and hence the counting of states must be divided by the factor $N!$. This is referred to as **correct Boltzmann counting**, and must be appended to calculations based on classical statistical mechanics to arrive at the correct result. In contrast to the quantal picture, in the classical picture the particles are *distinguishable*.

Quantum Statistical Mechanics. In classical mechanics, the state of a particle is described by exact specification of qs and ps. In quantum mechanics, however, as a result of the Heisenberg uncertainty principle, the simultaneous determination of q and p is not possible and the state of the particle is described by the wave function which obeys the Schrödinger wave equation. Also, to every observable quantity there corresponds a linear operator. (Recall the postulates of quantum mechanics.) The possible eigenvalues of the physical quantity $\hat{G}$ are given by the eigenvalue equation :

$$\hat{G}\,\psi(q) = G\,\psi(q) \qquad ...(33)$$

where $\psi(q)$ is the eigenfunction representing the state of the particle and G is its eigenvalue. The expectation value of G is given by :

$$< G > = \int \psi^*(q)\,\hat{G}\,\psi(q)\,dq \equiv < \psi\,|\hat{G}|\,\psi > \qquad ...(34)$$

where the last expression is written in Dirac's **bra and ket notation.** The probability density is given by the Born interpretation of the wave function as

$$P(q) = \psi^*(q)\,\psi(q) = |\psi(q)|^2 \qquad ...(35)$$

The time development of the wave function is given by the time-dependent Schrödinger wave equation

$$i\hbar\frac{\partial\Psi(q,t)}{\partial t} = \hat{H}\Psi(q,t) \qquad ...(36)$$

where $\hat{H}$ the Hamiltonian operator for the N-particle system, is given by

$$\hat{H} = \sum_{n=1}^{3N}(\hat{p}_n^2/2m) + U(\hat{q}_1,\ldots,\hat{q}_{3N}) \qquad ...(37)$$

The time and space parts of the Schrödinger wave equation can be separated to give

$$\Psi_n(q,t) = \psi_n(q)\exp(-i\,E_n\,t/\hbar) \qquad ...(38)$$

and

$$\hat{H}\,\psi_n(q) = E_n\psi_n(q) \qquad ...(39)$$

The fundamental difference between the quantal description and the classical description of matter is that quantum mechanics itself is a statistical theory (dealing with probabilities rather than certainties) and, therefore, quantum statistics investigating an N-particle system with many degrees of freedom will envisage a statistical averaging superimposed on the inherent quantum mechanical averaging. Thus, quantum statistics involves a double averaging process.

We must emphasize that in quantum mechanics, the description of the state of a system by means of the wave function is most complete and exhaustive. If, therefore, the macroscopic conditions of an N-particle system are such that they entirely determine the state of its microparticles, then the state of the particles of the system may be described by a single wave function; the system is then said to

be in a **pure state.** However, in real situations we often encounter the situation in which, from the very beginning, the particles of the system are in different states, described by different wave functions $\psi_1, \psi_2\ldots,\psi_N$ with the corresponding probabilities $P_1, P_2,\ldots, P_N$. The state of such a system is referred to as the **mixed state** and is described by a **statistical matrix** called the **density matrix,** introduced in 1927 by the great Russian physicist L.D. Landau (1908-1968) and, independently, by the brilliant Hungarian-American mathematician John von Neumann (1903-1957), pioneer of game theory and computer science. Note that this description is based on incomplete information about the system. The knowledge of the density matrix enables the calculation of the mean value of any arbitrary physical quantity of the system.

The mean value of an arbitray quantity G is given by

$$< G > = \sum_j P_j < G_j > = \sum_j P_j \int \Psi_j \hat{G}\,\Psi_j\,d\tau \qquad ...(40)$$

We can expand Ψ_j as

$$\Psi_j = \sum_n a_{jn}\,\psi_n \qquad ...(41)$$

where the coefficients a_{jn} are the *probability amplitudes* for the various particles of the system to be in the various states ψ_n. To be practical, $|a_{jn}|^2$ represents the *probability* that a measurement at a given time finds the jth particle of the system to be in the particular state ψ_n. (In the language of the ensemble theory, we shall say that $|a_{jn}|^2$ represents the probability that a measurement at a given time finds the jth system of the ensemble to be in the particular state ψ_n). Clearly, we must have,

$$\sum_n |a_{jn}|^2 = 1 \text{ (for all } j) \qquad ...(42)$$

From Eqs. 40 and 41, we obtain

$$< G > = \sum_j\sum_m\sum_n P_j\,a_{jm}^*\,a_{jn}\int\psi_m^*\,G\psi_n\,d\tau \qquad ...(43)$$

which can be rewritten as

$$< G > = \sum_m\sum_n \rho_{nm}\,G_{mn} \qquad ...(44)$$

where

$$G_{mn} = < \psi_m\,|G|\,\psi_n > \equiv \int\psi_m^*\,\hat{G}\,\psi_n\,d\tau \qquad ...(45)$$

and

$$\rho_{nm} = \sum_j P_j\,a_{jm}^*\,a_{jn} = \frac{1}{N}\sum_{j=1}^{N} a_{jm}^*\,a_{jn} \qquad ...(46)$$

The set of quantities ρ_{nm}, which are generally time-dependent, is the **density matrix** in the energy representation. If the matrix elements ρ_{nm} correspond to an operator $\hat{\rho}$, called the density operator (or statistical operator), then the sum on the right-hand side of Eq. 44 will be the diagonal elements of the matrix of the operator $\hat{\rho}\hat{G}$. In other words, the mean value of $< G >$ will be given by the trace (Tr) of the operator $\hat{\rho}\hat{G}$:

$$< G > = \sum_{m,n}\rho_{nm}\,G_{mn} = \sum_n(\hat{\rho}\hat{G})_{nn} = \mathrm{Tr}(\hat{\rho}\hat{G}) \qquad ...(47)$$

$$= \sum_n\int\psi_n\,\hat{\rho}\hat{G}\,\psi_n\,d\tau \qquad ...(48)$$

(Recall that in matrix algebra, the trace of a matrix is defined as the sum of its diagonal elements.)

Since the trace of a matrix is independent of the choice of the functions which define its matrix elements, we can work with any arbitrary orthonormal set of wave functions :

$$< \psi_n | \psi_m > = \delta_{nm} = \begin{cases} 1, & n = m \\ 0, & n \neq m \end{cases} \quad \ldots(49)$$

where δ_{nm} is the Kronecker delta. Replacing G_{mn} by δ_{nm}, therefore, we have

$$< G > = 1 = \sum_{m,n} \rho_{nm} \delta_{mn} = \sum_{n} \rho_{nn} = \mathrm{Tr}(\hat{\rho}) \quad \ldots(50a)$$

i.e.,
$$\mathrm{Tr}(\hat{\rho}) = 1 \quad \ldots(50b)$$

Since $\rho_n = \rho_{nn}$ is the probability that the system is in the nth state, the probability is always positive, *i.e.*, $\rho_n > 0$. If we now compare Eq. 44 with Eq. 7, we find that integration over q and p in the classical statistical mechanics has been replaced by the double sum over quantum states in quantum statistical mechanics, and Eq. 50(*b*) corresponds to the normalization condition given by Eq. 6. It can be shown that the density matrix satisfies the quantum version of the Liouville theorem :

$$d\hat{\rho}/dt = 0 \quad \ldots(51)$$

Thus, we conclude that *the density matrix plays the same role in quantum statistics as the density distribution function does in classical statistical mechanics.*

We shall conclude this discussion by commenting on the mathematical expressions for the density matrix in the three commonly encountered ensembles. The particular elements of the density matrix are specified when we select the appropriate ensemble. For the microcanonical ensemble, all systems lying within the small energy shell are accorded equal weight and if there are N energy eigen states forming this set, then the density matrix formed with these eigen states is diagonal and has the value $1/N$ (where N is the number of elements of the ensemble) for each of these states whose eigenvalues lie within the energy shell. For a canonical ensemble, which is appropriate to a system in contact with a heat bath (reservoir at constant T), the density matrix is

$$\hat{\rho} = \frac{\exp(-\beta \hat{H})}{\sum \exp(-\beta \hat{H})} \quad \ldots(52)$$

Similarly, for a grand canonical ensemble in which the systems can interchange particles as well as energy with the surroundings, the density matrix is :

$$\hat{\rho} = \frac{\exp(-\beta \hat{H} - \hat{N}\mu)}{\sum \exp(-\beta \hat{H} - \hat{N}\mu)}, \text{ where } \mu \text{ is the chemical potential.} \quad \ldots(53)$$

The denominators in Eqs. 52 and 53 are called the canonical partition function and the grand canonical partition function, respectively, as we shall see later. Incidentally, the density matrix has an important property, *viz.*, that it is **idempotent** : $\hat{\rho} = \hat{\rho}^2$.

Quantal Microcanonical Ensemble. The classical statistical mechanics is useful only as an approximation to quantum statistical mechanics. We use the method of classical statistical mechanics for dealing with a very complex problem where the number of particles is very large ($N \sim 10^{23}$). However, the Heisenberg uncertainty principle forces us to abandon classical mechanics. It says that we cannot simultaneously measure exactly both the position and the conjugate momentum coordinates of a particle, needed for a classical description. Hence, no single microstate of a system can be found from measurement. We have to resort to method based on probabilities and

averages as mentioned already. Hence, as a consequence of the Heisenberg uncertainty principle, the classical phase space cannot be used as such in quantum statistical mechanics.

The microstate of a system is defined, in quantum statistical mechanics, in quantum mechanical sense. Thus, a stationary system of N particles confined to a volume V can be in any one of the quantum states determined by the Schrödinger wave equation

$$\hat{H}_N \psi_i[(q)] = E_i \psi_i[(q)] \quad \ldots(54)$$

where $\hat{H}_N$ is the Hamiltonian operator of the N-particle system, $\psi_i[(q)]$ is the wave function for the entire system in the quantum state i and E_i is the energy of the quantum state i. The set of microstates of quantum statistical mechanics is, thus, a discrete denumerable set $\{i\}$ of quantum states denoted by the quantum number i. If N and V are known, we can always, in principle, solve Eq. 54 and know the allowed quantum states (accessible microstates) i. The system must be in one or another of these states.

It is possible, then, for us to mentally construct an ensemble of the physical systems of interest. Each element of the ensemble can be in one of the discrete quantum states allowed by the system. The probability P_i of finding an element in the state i is determined in such a way as to reflect the initial information (like energy) on the system of interest. The number of different quantum states which have a given energy is called the degeneracy g of the energy level. It is emphasized that the word 'level' will always denote the value of the energy for one or more states. Thus, energy levels can have degeneracies while quantum states do not.

We now consider the basic assumption of quantum statistical mechanics, *viz.*, that the probability P_i of the ith N-particle quantum state being occupied is a function of E_i only :

$$P_i = P_i(E_i) \quad \ldots(55)$$

[Recall the result $\rho = \rho(E)$, Eq. 9]

Also, all quantum states with the same energy (say, $E_i = E_j = E_k = E_l = \cdots = E$) have the same probability ($P_i = P_j = P_k = P_l = \cdots = P(E)$. The probabilities of all degenerate quantum states in one level are equal. We can thus say that in a state of macroscopic equilibrium, all stationary quantum states of equal energy have equal a priori probability. This replaces the familiar hypothesis of equal a priori probability of microstate in the classical phase space.

Since, for an isolated system, the energy E_{system} is constant, the P_i should depend on i such that zero probability is assigned to all states i unless $E_i = E_{\text{system}}$. If Ω is the degeneracy of the energy level E_{system}, then these states are the only ones which are represented in the ensemble; each such state has equal probability.

$$P_i = \text{constant} \equiv a \qquad (E_i = E_{\text{system}}) \quad \ldots(56)$$

$$\sum_{i=1}^{g} P_i = \sum_{i=1}^{g} a = ga = 1, \quad g = \Omega(N, V, E_i) \quad \ldots(57)$$

This defines the microcanonical ensemble with the probability distribution

$$P_i = \begin{cases} 1/\Omega & E_i = E_{\text{system}} \\ 0 & E_i \neq E_{\text{system}} \end{cases} \quad \ldots(58)$$

where $\Omega = \Omega(E_{\text{system}}, N, V)$ and E_{system} is well determined so as to lie between E and $E + \Delta E$. We should regard ΔE as large compared with the Heisenberg uncertainty principle $\delta E \approx h/\delta t$ where δt is the time available for observation and h is Planck's constant. It should be noted that as the energy of a macroscopic system increases, the degeneracies of the different energy levels also increase. Thus, the larger the system energy, the more quantum states are available to the system and the smaller

the probability of any one state being occupied, as it should be (Fig. 7).

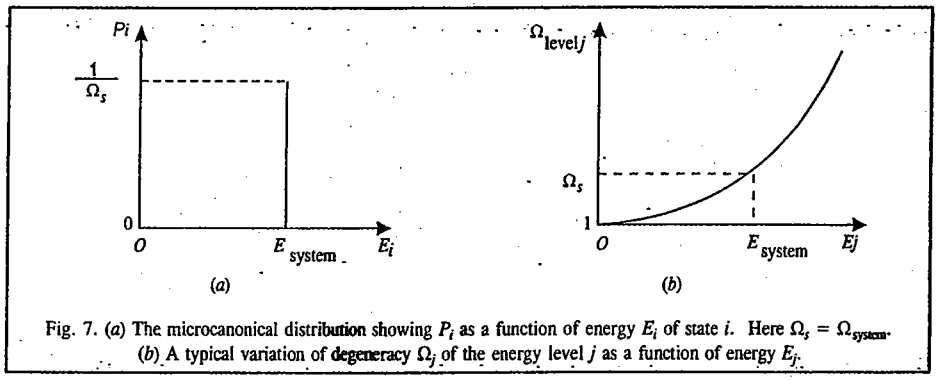

Fig. 7. (*a*) The microcanonical distribution showing P_i as a function of energy E_i of state i. Here $\Omega_s = \Omega_{system}$. (*b*) A typical variation of degeneracy Ω_j of the energy level j as a function of energy E_j.

Quantization of Phase Space and Calculation of the Number of Microstates Ω (*N, V, E*) Accessible to a System

As a consequence of the Heisenberg uncertainty (indeterminacy) principle, $\delta x \delta p_x \approx h$ (where δx is the uncertainty in the position coordinate and δp_x is the uncertainty in the corresponding canonically conjugate momentum coordinate), the classical states in a cell of size h (Planck's constant) per degree of freedom, or h^f per f degrees of freedom, merge into a single quantum state. Within such a cell the states cannot be further differentiated. If we imagine the phase space as divided into cells, each of size h^f, then the set of microstates contained in a volume element $\Delta\Gamma$ corresponds to a set of $\Delta\Gamma/h^f$, *i.e.*,

$$\Omega\ (N,\ V,\ E)\ = \Delta\Gamma/h^f \qquad \ldots(59)$$

in a microcanonical ensemble (*N, V, E*). In other words, Ω (*N, V, E*) is the number of microstates in a macrostate (*N, V, E*) in a microcanonical ensemble. As h is very small ($h = 6{\cdot}626 \times 10^{-34}$ Js), this is a fairly good approximation. Thus, a discrete quantum state occupies a volume equal to h^f in the *cellular* quantal phase space. It was Max Planck who proposed this result of converting continuous classical phase space into a cellular one, while investigating the black body radiation.

To calculate Ω (*N, V, E*), we consider a particle of mass m in an infinite cubical box of width L (volume $V = L^3$). The Schrödinger wave equation for the motion of the particle is

$$\hat{H}_{N=1}\ = \psi_i\ [(q)] = \varepsilon_i \psi_i[(q)] \qquad \ldots(60)$$

where

$$\hat{H}\ = p^2/2m = -(\hbar^2/2m)\nabla^2 \qquad \ldots(61)$$

We know that the eigenfunctions and energy eigenvalues of the particle are given by :

$$\psi_i\ (q)\ \equiv \psi_{n_1\, n_2\, n_3}$$

$$= A\ \sin\left(\frac{n_1 \pi\ x_1}{L}\right)\ \sin\left(\frac{n_2 \pi\ x_2}{L}\right)\ \sin\left(\frac{n_3 \pi\ x^3}{L}\right) \qquad \ldots(62)$$

(where A is the normalization constant);

$$\varepsilon_n\ =\ \varepsilon_{n_1} + \varepsilon_{n_2} + \varepsilon_{n_3}\ =\ \frac{n^2 h^2}{8mL^2}\ ;\ n^2\ =\ n_1^2 + n_2^2 + n_3^2\ ;\quad n_1,\ n_2,\ n_3 = 1,\ 2,\ 3,\ldots \qquad \ldots(63)$$

In the quantum number space, *i.e.*, (n_1, n_2, n_3)-space, each lattice point, whose coordinates are all positive integers, corresponds to a quantum state (an eigenstate), as depicted in Fig. 8. Hence, invoking Bohr's correspondence principle, we can write, for large n,

$$\Omega(\varepsilon_n)\ =\ \frac{1}{8}\left(\frac{4\pi n^3}{3}\right)\ =\ \frac{4\pi}{3}\ \frac{L^3}{h^3}\ (2\mathrm{m}\ \varepsilon_n)^{3/2}\ =\ \frac{\Omega_r(\varepsilon_n)}{h^3} \qquad \ldots(64)$$

because classically the volume in the phase space is given by

$$\Omega_r\ (\varepsilon) = \int_{p^2 \le 2m\,\varepsilon} d^3x\ d^3p\ \ = L^3 \int d^3p\ \ = L^3 \frac{4\pi}{3}\ (2m\,\varepsilon)^{3/2} \qquad \ldots(65)$$

The quantity $\Omega(\varepsilon_n)$ gives the number of microstates or Γ-cells which are accessible to the particle. For an ideal gas containing N particles in a volume V and energy E, this number, now designated as Ω(*N, V, E*), will evidently be extremely large, in fact, of astronomical proportions. The degree of degeneracy grows with n, that is, with energy. If we consider a thin shell of energy ε_n in the accessible phase space, then all quantum cells corresponding to the degeneracy of the energy level ε_n can be imagined to have been included. For an ideal gas in which there are no inter-particle interactions (intermolecular potential energy is zero), each particle behaves quantum mechanically as if it is alone in the box. Each particle then is in one of the accessible single particle quantum states given by Eq. 64.

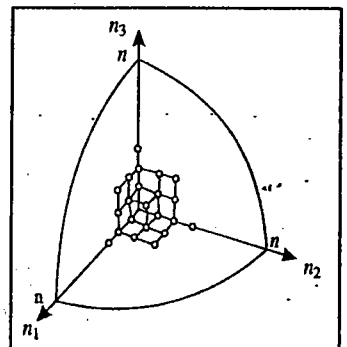

Fig. 8. Lattice points for the combinations of integers n_1, n_2, n_3.

Validity of Classical Limit of Statistical Mechanics

In classical mechanics, as stated earlier, one can specify simultaneously both the generalized coordinates q_i and the canonically conjugate momenta p_i for a particle. However, in quantum mechanics, the Heisenberg uncertainty principle does not allow this exact specification. It is only when $h \to 0$ that the classical description is a reasonable approximation, *i.e.*,

$$\delta q \delta p \gg h \qquad \ldots(66)$$

For a molecule in a gas, the classical description is valid when

$$< r >< p \gg h \qquad \ldots(67)$$

where $< r >$ is the mean interparticle separation and $< p >$ is the mean momentum. Using the de Broglie relationship $p = h/\lambda$, we have

$$< r \gg\ \ < \lambda >\quad \text{(classical limit)} \qquad \ldots(68)$$

Since $< \lambda >$ is a measure of the spread of the molecule in space, it follows that when Eq. 68 holds, the molecular wave functions do not overlap and therefore they are distinguishable by their position.

Consider the gas containing N identical particles in a volume V. The total wave function for the system is given by the product

$$\Psi(1,\ 2,\ldots,\ N)\ =\ \psi_a\ (1)\ \psi_b\ (2) \ldots \psi_z(N) \qquad \ldots(69)$$

where $\psi_a(1)$ is the wave function of particle 1 in state a, $\psi_b(2)$ is the wave function of particle 2 in state b and so on. When Eq. 68 holds, the individual wave functions $\psi_a(1)$, $\psi_b(2)$,... do not overlap

appreciably and an exchange of particles (say, 1 and 2) in Eq. 69 produces a new state :

$$\Psi'(1, 2,...N) = \psi_a(2)\,\psi_b(1)...\psi_3(N) \qquad ...(70)$$

This means that in the familiar classical language, a new microstate results with the result that the phase point is shifted from a cell in the Γ space to another. Thus, $N!$ product wave functions are obtained from $N!$ possible permutations of the particles among the one-particle wave functions. Thus, the particles are **distinguishable** and the classical approximation is valid.

If, on the other hand,

$$< r > \ll <\lambda > \qquad \text{(quantum limit)} \qquad ...(71)$$

then, the one-particle wave functions overlap, with the result that a given particle in a gas cannot be localized. The state of the whole gas is described by a single wave function $\psi(1, 2,..., N)$ which cannot be decomposed meaningfully. Thus, the particles are indistinguishable and we must employ quantum statistics.

We can elucidate Eq. 68 further by considering each particle of the gas to be confined to a tiny cube of side $< r >$, all these cubes filling the volume V. Thus,

$$< r >^3 N = V \quad \text{or} \quad < r > = (V/N)^{1/3} \qquad ...(72)$$

The mean energy of the ideal gas is given by

$$\bar{\varepsilon} \simeq < p >^2 /2m = (3/2)\,kT \text{ so that } <p > \simeq (3mkT)^{1/2}$$

where k is the Boltzmann constant. Hence,

$$< \lambda > \simeq h/(3\,m\,kT)^{1/2} \qquad ...(73)$$

Therefore, the condition (Eq. 68) becomes

$$\left(\frac{V}{N}\right)^{1/3} \gg \frac{h}{(3mkT)^{1/2}} \qquad \text{(classical limit)} \qquad ...(74)$$

We thus see that classical statistics is valid when (*i*) N is small (*ii*) T is large and (*iii*) m is not too small.

The following two examples illustrate the validity of classical and quantum statistics beautifully. First, consider a gas containing N molecules at NTP. Since, the molecular density is 10^{19} molecules/cm^3, the volume available to each molecule is 10^{-19} cm^3. Assuming that the molecular radius $\approx 10^{-8}$ cm, the molecular volume $\approx 10^{-24}$ cm^3. Since, the molecular volume is far less than the volume available to it, we can, in principle, identify each molecule in a gas so that the molecules are localized and **distinguishable** and classical statistics is applicable.

Next, consider the conduction electrons in a metal. Since the density of electrons $\approx 10^{22}$/cm^3, the volume available to each electron is 10^{-22} cm^3. For a 1e*V*-electron, the momentum is $p_x = (2mE))^{1/2} = 0{\cdot}5\times10^{-19}$ erg s cm^{-1} so that the corresponding de Broglie wave length is $\lambda = h/p_x = 1{\cdot}3\times10^{-7}$ cm. Thus, the volume of conduction electrons is $\approx 2\times10^{-21}$ cm^3. Since this volume is far greater than the volume available to the electron (10^{-22} cm^3), the electron wave functions overlap considerably. It is not possible to localize the electrons; they become *indistinguishable*. Hence, quantum statistics must be applied.

System of Identical Particles and Symmetry of Wave Functions

Let us consider, for simplicity, a two-particle system described by the wave function $\Psi(1,2)$. As we have seen, in the quantum region, unlike the classical region, we cannot distinguish between identical particles. This can be stated in a formal manner by the introduction of the permutation operator $\hat{P}_{12}$, which, acting on a state, interchanges all the coordinates of particles 1 and 2 :

$$\hat{P}_{12}\Psi(1,2) = \Psi(2,1) \qquad ...(75)$$

If the particles are indistinguishable, the interchange (Eq. 75) produces no observable effect, even if the wave function changes by a phase factor δ which leaves $\Psi^*\Psi$ unchanged.

$$\hat{P}_{12}\Psi(1,2) = \Psi(2,1) = e^{i}\Psi(1,2) \qquad ...(76)$$

By repeating the interchange, the original wave function must be obtained :

$$(\hat{P}_{12})^2\Psi(1,2) = \hat{P}_{12}\Psi(2,1) = \Psi(1,2) = e^{2i}\Psi(1,2) \qquad ...(77)$$

Thus, $$e^{2i\delta} = 1 \text{ or } e^{i\delta} = \pm 1 \qquad ...(78)$$

so that

$$\Psi(1,2) = \begin{cases} \Psi(2,1) & \text{(symmetric)} \\ -\Psi(2,1) & \text{(antisymmetric)} \end{cases} \qquad ...(79)$$

It is, in fact, a law of nature that the symmetry or antisymmetry under the interchange of two particles is a property of the particles themselves. The important question as to which particles obey Bose-Einstein (BE) Statistics and which Fermi-Dirac (FD) statistics, remained theoretically unsettled until Belifante (1939) and Pauli (1940) discovered the vital connection between spin and statistics. It turns out that those particles whose spin is an integral multiple of $\hbar\,(0, 1\hbar, 2\hbar, ...)$ are described by the symmetric wave function $\Psi^{(S)}$ and obey BE statistics, while those whose spin is half-odd integral multiple of $\hbar\,[(1/2)\hbar, (3/2)\hbar, (5/2)\hbar, ...)$ are described by the antisymmetric wave function, $\Psi^{(A)}$ and obey FD statistics. To date, no third category of particles has been discovered.

It may be recalled that articles obeying BE statistics are called *bosons*. Examples are photon, graviton, π-meson, ^{4}He, etc. Particles obeying FD statistics are called *fermions*. Examples are electron, proton, neutrino, ^{3}He, etc. Classical statistics is Maxwell-Boltzmann (MB) statistics whereas quantum statistics includes BE statistics and FD statistics. The simple product type wave function, applicable to MB statistics, must be properly symmetrized in quantum statistics. For the two-particle system which we are considering here,

$$\Psi(1, 2) = \psi_a(1)\,\psi_b(2) \qquad \text{(MB)} \qquad ...(80)$$

$$\Psi^{(S)}(1, 2) = \left(1/\sqrt{2}\right)[\psi_a(1)\,\psi_b(2) + \psi_a(2)\,\psi_b(1)] = \Psi^{(S)}(2, 1) \quad \text{(BE)} \qquad ...(81)$$

$$\Psi^{(A)}(1, 2) = \left(1/\sqrt{2}\right)[\psi_a(1)\,\psi_b(2) + \psi_a(2)\,\psi_b(1)]$$

$$= \frac{1}{\sqrt{2}}\begin{vmatrix} \psi_a(1) & \psi_a(2) \\ \psi_b(1) & \psi_b(2) \end{vmatrix} = -\Psi^{(A)}(2, 1) \qquad \text{(FD)} \qquad ...(82)$$

Eq. 82 is called the **Slater determinant**. Two fermions cannot be in the same state $a=b$, because in that case $\Psi^A(1,2)$ vanishes. This is also true for a system of N fermions. The slater determinant for N fermions (such as for an N-electron atom) can be written as

$$\Psi^{(A)}(1, 2,...,N) = \frac{1}{\sqrt{N!}}\begin{vmatrix} \psi_a(1) & \psi_a(2) & \cdots & \psi_a(N) \\ \psi_b(1) & \psi_b(2) & \cdots & \psi_b(N) \\ \vdots & \vdots & & \vdots \\ \psi_z(1) & \psi_z(2) & \cdots & \psi_z(N) \end{vmatrix} \qquad ...(83)$$

where $1/\sqrt{N!}$ is the normalization factor. The interchange of two particles involves the interchange of two columns of the Slater determinant resulting in the change in the sign of the determinant. Any attempt to put two fermions in the same state causes the determinant to vanish. Thus, the

requirement of antisymmetry keeps the otherwise non-interacting fermions to stay away from one another. The Pauli exclusion principle states that *no two fermions can be in the same quantum state.* If the discrete quantum states are labelled as $\psi_a, \ldots, \psi_i \ldots$, then for fermions the occupation number n_i in any state is given by

$$n_i = 0, 1 \qquad \text{(all } i\text{, for fermions)} \qquad \ldots(84)$$

For bosons, however, there is no restriction on the occupation numbers. Thus,

$$n_i = 0, 1, 2, 3, 4, \ldots \qquad \text{(all } i\text{, for bosons)} \qquad \ldots(85)$$

We must remember that fermions obey Pauli's exclusion principle whereas bosons do not.

Entropy and Probability

From the definition of the quantal microcanonical ensemble (Eq. 58), the normalization condition requires that

$$\sum_{i=1}^{\Omega} P_i = 1 \qquad \ldots(86)$$

It is customary to call the quantity Ω the **microcanonical partition function**; it represents the number of states of the system between E and $E+\Delta E$. Infact, Ω is proportional to $\Delta\Gamma$ or to $\Delta\Gamma/h^f$ (Eq. 59), and entropy can be defined by the celebrated **Boltzmann equation** as

$$S/k = \ln \Omega = -\Omega\left(\frac{1}{\Omega}\right) \ln\left(\frac{1}{\Omega}\right)$$

or,
$$S = -k\sum_i P_i \ln P_i \qquad \ldots(87)$$

Note that since $0 < P_i < 1$, we have $\ln P_i < 0$ so that the right-hand side is positive. One can interpret $\Delta\Gamma$ as a measure of the imprecision of our knowledge of the state of a system or as a measure of its randomness. In the macrostate of maximum $\Delta\Gamma$, the microstate of the system (in equilibrium) is least well defined. It is, in fact, a macrostate of maximum disorder. Thus, in the state of equilibrium, the entropy attains its maximum value. The general definition of entropy (Eq. 87) reduces to the Boltzmann definition of entropy for an isolated system. We may mention finally that the following definitions of entropy, σ (= S/k, where k is the Boltzmann constant) are equivalent upto additive constants :

$$\sigma = \ln \Delta\Gamma(E), \quad \sigma = \ln g(E), \quad \sigma = \ln \Omega_\Gamma(E), \quad \sigma = \ln \Omega(n_i), \quad \sigma = \ln W \qquad \ldots(88)$$

The last relation is called Boltzmann's definition of entropy.

Canonical Ensemble. The microcanonical ensemble provides a general basis for the formulation of statistical mechanics. It is of fundamental importance because (1) it deals with the simplest system known, that is, an *isolated* system, (2) the postulate of equal a priori probability is strictly applicable in this case and (3) other ensembles can be deduced from the microcanonical ensemble. As we have shown, with its help the basic postulates of statistical mechanics lead to correct thermodynamic relations. However, this ensemble is inconvenient in practice for two reasons : 1. We do not know how to specify the width of the 'ergodic shell' between E and $E + dE$ in any given case. 2. It deals with systems isolated from the rest of the universe, with a given E, that do not occur in the laboratory. In thermodynamics we deal with systems kept in contact with a heat reservoir at a given temperature. The temperature is introduced (in the microcanonical ensemble) in an artificial way. We would thus like to construct an ensemble based on this fact. In a microcanonical ensemble the temperature would differ from element to element.

As we have seen, an ensemble is stationary if $P_i = P_i(E)$. For the microcanonical ensemble we made the simple choice $P_i = P_i(E_i \text{ only}) = \text{constant}$. However, other choices are also possible. Thus, we can replace the constant energy constraint with the constant temperature constraint. Thus, for a system (N,V,T) in a thermal equilibrium with a large heat reservoir (Fig. 9*a*) we can allow the energy to vary from element to element in the representative canonical ensemble (Fig. 9*b*). This is possible because the heat reservoir is such a large source of energy that the exchange of energy with a system in contact does not change it appreciably. We will now show that for such a canonical ensemble (N,V,T), P_i has a suitable functional dependence on E_i and that, in fact, quantum mechanically,

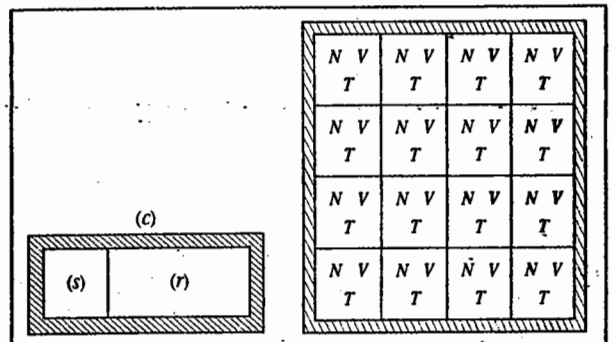

Fig. 9 (*a*) Isolated composite system (*c*) consisting of the system (*s*) and the reservoir (*r*) in thermal contact. (*b*) Canonical ensemble of replicas in thermal contact (exchange of energy across the conducting walls) forming a lattice.

$$P_i = C \exp(-\beta E_i) \qquad \ldots(89)$$

where C is a constant; the factor $\exp(-\beta E_i)$ is called the **Boltzmann factor.**

Classical Canonical Distribution

We consider a closed isothermal system; we assume that the system consists of two subsystems, one smaller part but still macroscopic (our subsystem of interest, denoted by the subscript *s*) and the other remaining, a larger part, called the *reservoir* (denoted by the subscript *r*). The wall separating the subsystem from the reservoir is thermally conducting but impervious to mass transfer, thereby enabling an exchange of energy; the number of particles remains constant, thus, making N,V,T constant. We now apply the microcanonical distribution to the system to write the probability dw assuming that the closed system has a given value of energy E_0, the subsystem of interest has energy E_s and the reservoir has energy E_r.

$$dw = C\,\delta(E_s + E_r - E_0)\, d\Gamma_s\, d\Gamma_r \qquad \ldots(90)$$

where $d\Gamma_S$ and $d\Gamma_r$ are the statistical weights of the subsystem of interest and the reservoir and C is a constant.

We are interested in determining the probability density that the closed system has in a state in which the subsystem of interest is in some particular state with energy $E = E(q, p) = H(q, p)$. The required probability density can be found by replacing $d\Gamma_S$ by unity (only one state around E per unit volume of the phase space) in Eq. 90, putting $E_s = E$ and integrating over $d\Gamma_r$:

$$\rho(q,p) = C\int \delta(E + E_r - E_0)\, d\Gamma_r \qquad \ldots(91)$$

where C is a constant

Using the following result

$$d\Gamma_r = \frac{\Delta\Gamma_r}{\Delta E_r}\, dE_r = \frac{e^{S_r/k}}{\Delta E_r}\, dE_r \qquad \ldots(92)$$

(where $\Delta\Gamma_r$ is the statistical weight corresponding to energy range ΔE_r) in Eq. 91 and carrying out the integration, we have

$$\rho(q, p) = C\left(\frac{e^{S_r/k}}{\Delta E_r}\right)_{E_r = E_0 - E} \qquad \ldots(93)$$

The subsystem of interest is small in comparison with the whole closed system, *i.e.*, $E_0 \gg E_1$ and ΔE_r changes relatively little with small changes in E_r; thus, $(\Delta E_r)_{E_r=E_0-E}$ becomes almost a constant, independent of E, and can be absorbed in the constant, C Treating entropy as a function of energy, making use of the Taylor expansion, retaining only the linear term, we can write

$$S_r(E_0 - E) = S_r(E_0) - E\frac{dS_r(E_0)}{dE_0} \qquad ...(94)$$

Recalling that thermodynamically the temperature is defined as $T = (\partial E/\partial S)_V$, Eq. 94 reduces to

$$S_r(E_0 - E) = S_r(E_0) - E/T \qquad ...(95)$$

The factor exp $[S_r(E_0)/k]$ is constant and can again be absorbed in the constant to yield

$$\rho(q, p) = \frac{C}{h^{3N}} e^{-\beta E(q,p)} = \frac{C}{h^{3N}} e^{-\beta H(q,p)} \qquad ...(96)$$

where $\beta = 1/kT$. (The division by h^{3N} takes into account the quantization of phase space). Eq. 96 is the celebrated classical canonical distribution obtained by J.W. Gibbs in 1901. The constant of proportionality is obtained from the normalization condition :

$$\int \rho(q,p)\, dq\, dp = 1 \qquad ...(97)$$

Canonical Partition Function and Thermodynamic Quantities

The reciprocal of the constant in Eq. 96 is called the **canonical partition function.** For a classical system of N identical particles at temperature T, the canonical partition function $Q_N(V, T)$ is given by

$$Q_N(V, T) = \frac{1}{N!h^{3N}} \int\cdots\int e^{-\beta H(q,p)} \prod_{i=1}^{3N} dq_i \prod_{i=1}^{3N} dp_i \qquad ...(98)$$

the degrees of freedom being $f = 3N$. It is obvious that the partition function is a function of N, V and T. The factor $N!$ is included to take into account '*correct Boltzmann counting*', being a result of the indistinguishability of the particles. The factor h^{3N} is the quantum constant included to take into account the quantization of phase space, *i.e.*, it is included for the reason that the classical distribution can be obtained as a limiting case of quantum distribution when Planck's constant $h \to 0$.

Since, the classical Hamiltonian $H(q,p)$ can be written as a sum of the kinetic energy and potential energy, *i.e.*,

$$H(q, p) = \sum_{i=1}^{3N} (p_i/2m) + U_N(q_1, \ldots, q_{3N}), \qquad ...(99)$$

we can write

$$Q_N(V, T) = \frac{1}{N!h^{3N}} \int\cdots\int \exp[-\beta\{\sum_i (p_i^2/2m) + U_N(q_i)\}] \prod_{i=1}^{3N} dq_i \prod_{i=1}^{3N} dp_i \qquad ...(100)$$

The integration over the momenta can be carried out to yield

$$Q_N(V, T) = \frac{(2\pi m/\beta)^{3N/2}}{N!\,h^{3N}} \int\cdots\int e^{-\beta U_N} \prod_{i=1}^{3N} dq_i \qquad ...(101)$$

$$= \frac{Z_N}{N!\,\lambda^{3N}} \qquad (\beta = 1/kT) \qquad ...(102)$$

where

$$Z_N = \int_V \cdots \int e^{-\beta U_N} \prod_{i=1}^{3N} dq_i \qquad ...(103)$$

and $$\lambda = h/(2\pi mkT)^{1/2} \qquad ...(104)$$

The quantity Z_N is called the **configurational integral** (or configurational partition function) and λ is the *thermal de Broglie wave length* at temperature T. The Gibbs classical canonical distribution (Eq. 96) can be written as

$$\rho(q, p) = \frac{1}{h^{3N}} \frac{e^{-\beta E(q,p)}}{Q_N(V, T)} \qquad ...(105)$$

to yield

$$E = \langle E \rangle = -kT \langle \ln h^{3N} \rho \rangle - kT \ln Q_N(V, T) \qquad ...(106)$$

Recalling that $A = E - TS$, where A is the Helmholtz free energy and S is the entropy, it can be shown that

$$A = -kT \ln Q_N(V, T) \qquad ...(107)$$

Eq. 107 is very important for it serves as a link between a thermodynamic quantity A and a statistical mechanical quantity (the partition function); it, in fact, serves as a basis for the thermodynamic applications of the Gibbs canonical distribution. Other thermodynamic quantities can be derived from this equation and expressed in terms of the canonical partition function :

$$P = -\left(\frac{\partial A}{\partial V}\right)_T = kT\left(\frac{\partial \ln Q_N}{\partial V}\right)_T \qquad ...(108)$$

$$S = -\left(\frac{\partial A}{\partial T}\right)_V = k \ln Q_N + kT\left(\frac{\partial \ln Q_N}{\partial T}\right)_V \qquad ...(109)$$

$$G = A + PV = -kT \ln Q_N + kT\left(\frac{\partial \ln Q_N}{\partial \ln V}\right)_T \qquad ...(110)$$

$$\Omega_g = A - G = -PV = -kT\left(\frac{\partial \ln Q_N}{\partial \ln V}\right)_T \qquad ...(111)$$

where Ω_g is called the **grand potential.**

The internal energy is given by

$$E = -\frac{\partial \ln Q_N}{\partial \beta} \qquad ...(112)$$

Application of the Classical Canonical Distribution to an Ideal Gas

For an ideal (perfect) monatomic gas of N particles each of mass m, the potential energy is zero so that

$$H \equiv E = \frac{1}{2m} \sum_{i=1}^{3N} p_i^2 \qquad ...(113)$$

and the partition function is given by

$$Q_N(V, T) = \frac{1}{N!\,h^{3N}} \int\cdots\int \exp\left[-\sum_i p_i^2/2m\,kT\right] \prod_{i=1}^{3N} dq_i \prod_{i=1}^{3N} dp_i \qquad ...(114)$$

Integration over the generalized coordinates yields V^N :

$$\int \cdots \iint \prod_{i=1}^{3N} dq_i = V^N \qquad \ldots(115)$$

Again, since the kinetic energy of the gas is the sum of the kinetic energies of all the individual particles and that the probabilities of all the particles are independent of each other and can be written as a product of factors, Eq. 114 reduces to

$$Q_N(V, T) = \frac{1}{N!}\left(\frac{V}{h^3}\iiint \exp[-p^2/2m\,kT]\,dp\right)^N$$

$$= \frac{q^N}{N!} \qquad \ldots(116)$$

where

$$q = \frac{V}{h^3}\iiint \exp[-p^2/2mkT]\,dp = V\left(\frac{2\pi mkT}{h^2}\right)^{3/2} \qquad \ldots(117)$$

is called the *single particle partition function.*

Hence, $$Q_N(V, T) = \frac{V^N}{N!}\left(\frac{2\pi mkT}{h^2}\right) = \frac{1}{N!}\left(\frac{V}{\lambda^3}\right)^N \qquad \ldots(118)$$

where $\lambda = h/(2\pi m\,kT)^{1/2}$ is the thermal de Broglie wave length, as already said.

The Helmholtz free energy (work function) A is given by Eq. 107 as

$$A = -NkT \ln\left[\frac{Ve}{N}\left(\frac{2\pi mkT}{h^2}\right)^{3/2}\right] \qquad \ldots(119)$$

From Eq. 108, the expression for pressure becomes

$$P = NkT/V \qquad \ldots(120)$$

which is the equation of state for an ideal gas

From Eq. 109, we obtain for entropy

$$S = Nk \ln \frac{V}{N}\left(\frac{2\pi kT}{h^2}\right)^{3/2} + \frac{5}{2}Nk \qquad \ldots(121)$$

From Eq. 112, the expression for internal energy is

$$E = \left(\frac{3}{2}\right)NkT \qquad \ldots(122)$$

Hence, the molar heat capacity is given by

$$C_V = (\partial E/\partial T)_V = (3/2)Nk \qquad \ldots(123)$$

And finally, the chemical potential is given by

$$\mu = (\partial A/\partial N)_{V,T} = kT \ln (n\lambda^3) \qquad \ldots(124)$$

where n $(= N/V)$ is the *number density.*

The law of Equipartition of Energy. This law states that the energy associated with each degree of freedom of a molecule is $(1/2)kT$. We can write the energy as

$$E = \varepsilon_i + E'(p') \qquad \ldots(125)$$

where ε_i is the energy associated with the momentum coordinate p_i and E' is the energy contributed by all other momenta except p_i. Then, we have the mean energy :

$$<\varepsilon_i> = \frac{\int \varepsilon_i e^{-\beta E} dp}{\int e^{-\beta E} dp} = \frac{\int \varepsilon_i e^{-\beta \varepsilon_i} dp_i}{\int e^{-\beta \varepsilon_i} dp_i}\,\frac{\int e^{-\beta E'} dp'}{\int e^{-\beta E'} dp'} \qquad \ldots(126)$$

where $dp' = dp_1 dp_2 \ldots dp_{i-1}\, dp_{i+1} \ldots dp_{3N}$; and $\beta = 1/kT$

The last factor in Eq. 126 is unity, giving

$$<\varepsilon_i> = -\frac{(\partial/\partial\beta)\int e^{-\beta\varepsilon_i}\,dp_i}{\int e^{-\beta\varepsilon_i}\,dp_i} = -\frac{\partial}{\partial\beta}\ln\left(\int e^{-\beta\varepsilon_i}\,dp_i\right) \qquad \ldots(127)$$

Writing $\varepsilon_i = p_i^2/2m$ and carrying out the integration, we get

$$<\varepsilon_i> = -\frac{\partial}{\partial\beta}\ln\left(\frac{2\pi m}{\beta}\right)^{1/2} = \frac{1}{2\beta} = \frac{1}{2}kT \qquad \ldots(128)$$

which is the law of equipartition of energy.

The above law can also be derived alternatively as follows : Suppose the Hamiltonian of a system of particles is a quadratic function of the generalized coordinates q_is and the canonically conjugate momenta p_is :

$$H = \sum_i (a_i p_i^2 + b_i q_i^2) \qquad \ldots(129)$$

For the particular term $a_i p_i^2$, the mean energy is given by

$$<\varepsilon> = \frac{a_i \int_0^\infty p_i^2 \exp(-a_i p_i^2/kT)dp_i}{a_i \int_0^\infty \exp(-a_i p_i^2/kT)dp_i}$$

$$= \frac{-a_i kT \dfrac{\partial}{\partial a_i}\displaystyle\int_0^\infty \exp(-a_i p_i^2/kT)dp_i}{\displaystyle\int_0^\infty \exp(-a_i p_i^2/kT)dp_i}$$

$$= -a_i kT \frac{\partial}{\partial a_i}[\ln \int_0^\infty \exp(-a_i p_i^2/kT)dp_i]$$

$$= -a_i kT \frac{\partial}{\partial a_i}\left[\ln\left(\frac{\pi kT}{a_i}\right)^{1/2}\right] = \frac{1}{2}kT \qquad \ldots(130)$$

The same result is obtained for the second term $b_i q_i^2$. Thus, each term in H which depends quadratically on a q_i or a p_i contributes a mean energy of $kT/2$ (which is the law of equipartition of energy).

Quantal Canonical Distribution. The derivation of classical canonical distribution from microcanonical distribution remains valid in the quantal (quantum mechanical) case also, the only change being the replacement of integration over phase (Γ) space by a sum over all the states of the system :

$$\frac{1}{N!h^{3N}}\int dq\, dp \longrightarrow \sum_i \qquad ...(131)$$

Consider an isothermic closed system consisting of two subsystems, the smaller but still macroscopic subsystem is the subsystem of interest, denoted by the subscript s, and the larger part, called the *reservoir*, is designated by the subscript r. The probability that with a given value of the energy E_0 of the closed system, the system of interest has energy E_S and the reservoir has energy E_r is given by

$$dP = C\delta(E_s + E_r - E_0)\, d\Gamma_s\, d\Gamma_r \qquad ...(132)$$

where C is a constant and $d\Gamma_s$ and $d\Gamma_r$ refer to the statistical weights of the subsystem of interest and the reservoir, respectively.

Quantum mechanically, the probability P_i that the closed system be in a state in which the system of interest is in a particular state with energy E_i, is obtained by putting $d\Gamma_s=1$, $E_s=E_i$ and integrating over $d\Gamma_r$:

$$P_i = C\int \delta(E_i + E_r - E_0)\, d\Gamma_r \qquad ...(133)$$

Using, as before,

$$d\Gamma_r = \frac{\Delta\Gamma_r}{\Delta E_r}\, dE_r = \frac{e^{S_r/k}}{\Delta E_r}\, dE_r \qquad ...(134)$$

the integration yields

$$P_i = C\left(\frac{e^{S_r/k}}{\Delta E_r}\right)_{E_r=E_0-E_i} \qquad ...(135)$$

Since $E_0 \gg E_i$ and ΔE_r changes relatively little with changes in E_r, $(\Delta E_r)_{E_r=E_0-E_i}$ is constant and is absorbed in the constant C. Using a Taylor expansion of

$$S_r(E_r) \equiv S_r(E_0 - E_i) \qquad ...(136)$$

retaining only the linear term, we obtain

$$S_r(E_0 - E_i) = S_r(E_0) - E_i\frac{dS_r(E_0)}{dE_0} \qquad ...(137)$$

which yields, with the definition of temperature as $T = (\partial E/\partial S)_V$, the following result :

$$S_r(E_0 - E_i) = S_r(E_0) - E_i/T \qquad ...(138)$$

The factor $\exp[S_r(E_0)/k]$ is constant and can be absorbed in the constant in Eq. 135, to give

$$P_i = C\exp(-\beta E_i) \qquad ...(139)$$

$$= C\int \psi_i^*(r_1,...,r_N)e^{-\beta\hat{H}}\psi_i(r_1,...,r_N)\prod_{i=1}^{N} dr_i \qquad ...(140)$$

$$= C < \psi_i | e^{-\beta\hat{H}} | \psi_i > \qquad ...(141)$$

The constant is determined from the normalization condition

$$\sum_i P_i = 1 \qquad ...(142)$$

The reciprocal of the constant is called the partition function $Q_N(V, T)$ and is given by

$$Q_N(V, T) = \sum_i \exp(-\beta E_i) = \sum_i \int \psi_i^* \exp(-\beta\hat{H})\psi_i \prod_{i=1}^{N} dr_i \qquad ...(143)$$

$$\equiv \sum_i < \psi_i | \exp(-\beta\hat{H}) | \psi_i > = \mathrm{Tr}\, \exp(-\beta\hat{H}) \qquad ...(144)$$

where Tr is the *trace* of the matrix (*i.e.*, the sum of the diagonal elements of the matrix).

The sum on the right-hand side is the sum over the states and not on the energy levels. The quantum mechanical anologue of the configurational partition function is written as :

$$Z_N = \int S_N dr_1 ... dr_N \qquad ...(145)$$

where S_N is the Slater sum defined by

$$S_N = N!\, \lambda^{3N} \sum_i \psi_i^*(r_1,...,r_N)\exp(-\beta\hat{H})\, \psi_i(r_1,...,r_N) \qquad ...(146)$$

The classical counterpart of the Slater sum is the **Boltzmann factor** $\exp(-\beta U_N)$.

The thermodynamic quantities can be expressed, as in the classical case, with P_i replacing $\rho(q, p)$:

$$A = < E > - TS = -kT \ln Q_N = -kT \ln \left(\sum_i \exp(-\beta E_i)\right) \qquad ...(147)$$

$$P = -\left(\frac{\partial A}{\partial T}\right)_V = kT\left(\frac{\partial \ln Q_N}{\partial T}\right)_T \qquad ...(148)$$

$$S = -\left(\frac{\partial A}{\partial T}\right)_V = k \ln Q_N + kT\left(\frac{\partial \ln Q_N}{\partial T}\right)_V \qquad ...(149)$$

$$G = A + PV = kT\left[-\ln Q_N + \left(\frac{\partial \ln Q_N}{\partial \ln V}\right)_T\right] \qquad ...(150)$$

$$\Omega_g = -PV = -kT\left(\frac{\partial \ln Q_N}{\partial \ln V}\right)_T \qquad ....(151)$$

Grand Canonical Ensemble. In going from the microcanonical ensemble to the canonical ensemble, we relaxed the condition of constant energy E. This simplified the calculations of thermodynamic quantities where the exchange of energy, resulting in the constancy of temperature, is a common occurrence. We now consider chemical processes where the number of particles varies. In several quantum processes, too, creation and annihilation of particles occurs frequently. Hence, it is imperative that we relax the condition of constancy of total number of particles N as well.

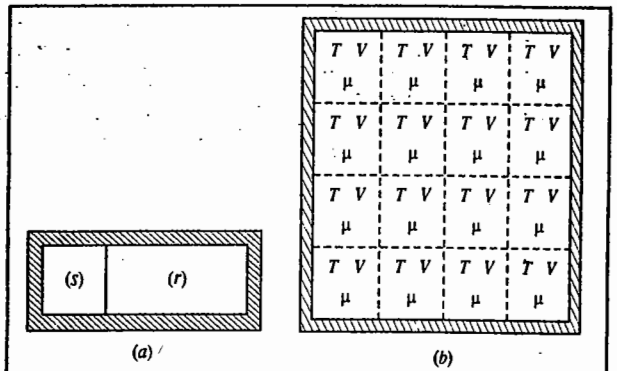

Fig. 10. (*a*) Isolated composite system consisting of the system (*s*) and the reservoir (*r*) in thermal and material contact. (*b*) Grand canonical ensemble of replicas in thermal and material contact forming a lattice.

In a canonical ensemble, the subsystem could exchange energy, but not particles, with the heat reservoir. We now consider the *grand canonical ensemble* in which the subsystem (s) can exchange energy as well as particles with the reservoir (r) (Fig. 10 a). The variable N is replaced by the variable μ, the *chemical potential* per particle. The composite system (c) is again represented by a microcanonical ensemble (Fig. 10 b) because the total energy E_c and the total number of particles are fixed. Thus, the grand canonical ensemble is described by (μ, V, T), *i.e.*, an ensemble where these variables are held constant.

We now apply the microcanonical distribution to the closed system to write the probability dw assuming that the closed system has the given value of energy E_0 and number of particles N_0, the subsystem of interest has the energy $E_{s\,N_s}$ (with N_s particles) and the reservoir has the energy $E_{r\,N_r}$ (with N_r particles) :

$$dw = C\delta\,(E_{s\,N_s} + E_{r\,N_r} - E_0)\,d\Gamma_s\,d\Gamma_r \qquad ...(152)$$

where C is a constant. We want to find the probability that the closed system is in a state in which the subsystem of interest is in some particular state with energy E_N (with N particles) by putting $d\Gamma_s = 1$, $E_{s\,N_s} = E_N$ and integrating over $d\Gamma_r$:

$$\rho(q, p, N) = C\int\delta(E_N + E_{r\,N_r} - E_0)\,d\Gamma_r \qquad ...(153)$$

Using $$d\Gamma_r = \frac{\Delta\Gamma_r}{\Delta E_{r\,N_r}}\,dE_{r\,N_r} \qquad ...(154)$$

and performing the integration, we have

$$\rho(q, p, N) = C\left(\frac{e^{S_r/k}}{\Delta E_{r\,N_r}}\right)_{E_{r\,N_r} = E_0 - E_N} \qquad ...(155)$$

We again assume that $\Delta E_{r\,N_r}$ remains relatively constant as before and is absorbed in the constant. We further assume that the entropy of the reservoir is a function of both its energy equal to $(E_0 - E_N)$ and its number of particles equal to $(N_0 - N_N)$. Applying Taylor expansion in the two variables we have :

$$S_r\,(E_0 - E_N, N_0 - N) = S_r\,(E_0, N_0) - E_N\left(\frac{\partial S_r(E_0)}{\partial E_0}\right)_{V, N_0} - N\left(\frac{\partial S_r(N_0)}{\partial N_0}\right)_{V, E_0} \qquad ...(156)$$

Note that we have retained only the linear term in the expansion.

Substituting the well known expression of the combined statement of the First and Second laws of thermodynamics for an open system, *viz.*,

$dE = TdS - PdV + \mu\,dN$, we obtain

$$S_r(E_0 - E_N, N_0 - N) = S_r\,(E_0, N_0) - \frac{E_N}{T} - \frac{N\mu}{T} \qquad ...(157)$$

The factor $\exp[S_r(E_0, N_0)/k]$ is a constant and is absorbed in the constant C to give

$$\rho(q, p, N) = \frac{C}{h^{3N}}\exp\,[-\beta(E_N - N\mu)];\quad \beta = 1/kT \qquad ...(158)$$

Eq. 158 is the classical grand canonical distribution. The constant is determined from the

normalization condition

$$\sum_{N\geq 0}\int\rho(q, p, N)\,dq^{3N}\,dp^{3N} = 0 \qquad ...(159)$$

Grand Canonical Partition Function and Thermodynamic Quantities

The reciprocal of the constant in Eq. 158 is called the grand canonical partition function $\mathcal{Z}$ and is given by

$$\mathcal{Z} = \sum_{N\geq 0}\frac{e^{\beta N\mu}}{N!\,h^{3N}}\int\ldots\int\exp[-\beta H(q^{3N}, p^{3N})]\,d^{3N}q\,d^{3N}p \qquad ...(160)$$

In terms of the canonical partition function $Q_N\,(V, T)$, we have

$$\mathcal{Z}\,(\mu, V, T) = \sum_{N\geq 0}e^{\beta N\mu}\,Q_N\,(V, T) = \sum_{N\geq 0}\frac{z^N Z_N}{N!} \qquad ...(161)$$

where z, called the fugacity, is defined by

$$z = \exp\,(\beta\mu)/\lambda^3 = z'/\lambda^3 \qquad ...(162)$$

where $z' = \exp(\beta\mu)$ is called the absolute activity and Z_N is the configurational partition function.

From thermodynamics we know that the chemical potential μ is related to the Helmholtz free energy, A, by

$$\mu = (\partial A/\partial N)_{V, T} \qquad ...(163)$$

Thus, we have

$$\mu = A_{N+1} - A_N = kT\ln\,(Q_N/Q_{N+1}) \qquad ...(164)$$

which gives

$$z = \frac{(N+1)!}{N!}\frac{Z_N}{Z_{N+1}} = \frac{z'}{\lambda^3} \qquad ...(165)$$

Also, we have for the entropy S :

$$S = -k < \ln h^{3N}\rho > = -\frac{\mu < N > - < E_N >}{T} + k\ln\mathcal{Z} \qquad ...(166)$$

Since $< N > = N$ and $< E_N > = E_N$, we obtain

$$-kT\ln\mathcal{Z} = E_N - TS - N\mu = A - N\mu = \Omega_g \qquad ...(167)$$

where Ω_g is the grand canonical potential. This gives

$$\rho(q, p, N) = h^{-3N}\exp[-\beta(E_N + N\mu - \Omega_g)] \qquad ...(168)$$

Other thermodynamic quantities can be obtained from the grand canonical potential :

$$S = -\left(\frac{d\Omega_g}{dT}\right) = k\left(\frac{\partial T\ln\mathcal{Z}}{\partial T}\right)_{\mu, V} \qquad ...(169)$$

$$P = (kT/V)\ln\mathcal{Z} \qquad ...(170)$$

$$N = -\left(\frac{\partial\Omega_g}{\partial\mu}\right)_{V, T} = kT\left(\frac{\partial\ln\mathcal{Z}}{\partial\mu}\right)_{V, T} = z\left(\frac{\partial\ln\mathcal{Z}}{\partial z}\right)_{V, T} \qquad ...(171)$$

$$A = N\mu + \Omega_g = NkT\ln\,(\lambda^3 z) - kT\ln\mathcal{Z} \qquad ...(172)$$

$$G = N\mu = NkT\ln\,(\lambda^3 z) \qquad ...(173)$$

Quantal Grand Canonical Distribution

The generalization of the Gibbs distribution to quantal model of systems with variable number of particles can be done in the same manner as in the classical model by considering a subsystem of interest and the reservoir, both parts of the closed isothermic system. The only difference is that we have to take the energy quantum states to vary with the number of particles and denote it by E_{N_i}, the energy in the ith quantum state. The probability P_{N_i} that the subsystem of interest contains N particles and is in the ith state is obtained in the same way and is given by

$$P_{N_i} = C \exp [S_r (E_0 - E_{N_i}, N_0 - N)/k] \quad ...(174)$$

Again, taking the Taylor expansion in two variables and absorbing $\exp[S_r(E_0, N_0)/k]$ in the constant, we obtain

$$P_{N_i} = C \exp [-\beta(E_{N_i} - N\mu)] \quad ...(175)$$

which is the quantal distribution. The constant is again found by normalization condition with integration over q, p being replaced by summation over the states to give the quantal grand canonical partition function

$$\Xi(\mu, V, T) = \sum_{N\geq 0} \sum_i \exp[-\beta(E_{N_i} - N\mu)] \quad ...(176)$$

$$= \sum_{N\geq 0} \exp(\beta N\mu) Q_N(V,T) = \sum_{N\geq 0} \frac{z^N Z_N}{N!} \quad ...(177)$$

where Z_N is now the quantal analogue of the configurational partition function given by Eq. 145.

We have for the entropy of the system

$$S = -k \ln P_{N_i} = -\frac{N\mu - E_{N_i}}{T} + k \ln \Xi \quad ...(178)$$

From this we obtain

$$-kT \ln \Xi = E_{N_i} - TS - N\mu = A - N\mu = \Omega_g \quad ...(179)$$

Hence, Eq. 175 can be rewritten as :

$$P_{N_i} = \exp [-\beta(E_{N_i} - N\mu - \Omega_g)] \quad ...(180)$$

From the grand canonical potential (Eq. 179), we get the other thermodynamic quantities :

$$S = -\left(\frac{\partial \Omega_g}{\partial T}\right)_{\mu,V} = k\left(\frac{\partial (T \ln \Xi)}{\partial T}\right)_{\mu,V} + k \ln \Xi \quad ...(181)$$

$$P = (kT/V) \ln \Xi \quad ...(182)$$

$$N = -\left(\frac{\Omega_g}{\partial \mu}\right)_{V,T} = kT \left(\frac{\partial \ln \Xi}{\partial \mu}\right)_{V,T} = z\left(\frac{\partial \ln \Xi}{\partial z}\right)_{V,T} \quad ...(183)$$

$$A = N\mu + \Omega_g = NkT \ln (\lambda^3 z) - kT \ln \Xi \quad ...(184)$$

$$G = N\mu = NkT \ln (\lambda^3 z) \quad ...(185)$$

These relations are exactly similar to those obtained in the classical grand canonical distribution (Eqs. 169—173)

Fluctuations in Various Ensembles

With the passage of time the properties of a system vary about the mean (average) of the equilibrium values. The same behaviour is applicable to the elements of the ensemble. These fluctuations about the mean value are generally negligible for equilibrium systems ; we shall prove this important result in the following discussion. In fact, the equivalence of the three ensembles depends on the fluctuations being very small. For example, if energy E fluctuations in the systems of a canonical ensemble are small, it is equivalent to a microcanonical ensemble. If the fluctuations in the number of particles in a grand canonical ensemble are small, it is equivalent to a canonical ensemble. Thus, the negligibility of fluctuations estabilishes the equivalence of the three ensembles.

1. Canonical Ensemble. Fluctuations in energy occur because the system is in thermal equilibrium with the reservoir. We shall evaluate the *standard relative deviation of energy* which is a measure of the fluctuations. For a canonical ensemble.

$$Q_N(V, T) = \sum_i \exp(-\beta E_i) = \sum_i \exp(-E_i / kT) \quad ...(186)$$

The mean (or ensemble average) of energy is given by

$$< E > = \Sigma_i P_i E_i = \frac{\sum_i E_i \exp(-E_i / kT)}{\sum_i \exp(-E_i / kT)} = \frac{\Sigma E_i \exp(-E_i / kT)}{Q_N(V,T)} \quad ...(187)$$

Differentiating w.r.t. temperature T, keeping the number of particles N and the volume V constant, we obtain

$$\left(\frac{\partial < E >}{\partial T}\right)_{N,V} Q_N + < E > \left(\frac{\partial Q_N}{\partial T}\right)_{N,V} = \frac{\partial}{\partial T}\left(\sum_i E_i \exp(-E_i / kT)\right)$$

or, $$\left(\frac{\partial < E >}{\partial T}\right)_{N,V} Q_N + \frac{< E >}{kT^2} \sum_i E_i \exp(-E_i / kT) = \frac{1}{kT^2} \sum_i E_i \exp(-E_i / kT) \quad ...(188)$$

The above simplifies to

$$\frac{< E^2 > - < E >^2}{kT^2} = \left(\frac{\partial < E >}{\partial T}\right)_{N,V} \quad ...(189)$$

Since thermodynamically $E \leftrightarrow < E >$ and $(\partial E/\partial T)_V = C_V$, we have

$$\frac{< E^2 > - < E >^2}{< E >^2} = \frac{kT^2 C_V}{E^2} \quad ...(190)$$

Since, $E = O(NkT)$ and $C_V = O(Nk)$ (*i.e.*, E is of the order of NkT and C_V is of the order of Nk), hence

$$\frac{< E^2 > - < E >^2}{< E >^2} = O(1/N) \quad ...(191)$$

Since for one mole, $N = N_A \approx 10^{23}$, the standard relative deviation of energy (fluctuation in energy) is of the order of $1/\sqrt{N}$, *i.e.*, $O(10^{-11})$. Thus, we conclude that the fluctuations in energy are extremely small, *i.e.*, negligible. In other words, the distribution in energy is extremely sharp and the canonical ensemble is practically a microcanonical ensemble.

We shall now calculate fluctuations in pressure. The ensemble average of pressure is given by

$$< P > = \frac{\sum_i P_i \exp(-E_i / kT)}{\sum \exp(-E_i / kT)} = \frac{\sum_i P_i \exp(-E_i / kT)}{Q_N(V,T)} \quad ...(192)$$

(Note the symbol for pressure P_i used here should not be confused with the probability which we have been using earlier.)

$$\text{or} \qquad < P > Q_N = \sum_i -\left(\frac{-\partial E_i}{\partial V}\right)_S \exp(-E_i/kT) \qquad ...(193)$$

where we have used the thermodynamic definition of pressure as $P = -(\partial E/\partial V)_S$

Differentiating w.r.t. V, with N and T constant, we obtain

$$\left(\frac{\partial < P >}{\partial V}\right)_{N,T} Q_N + \frac{< P >}{kT} \sum_i \left(\frac{-\partial E_i}{\partial V}\right)_{N,T} \exp(-E_i/kT)$$

$$= \sum_i \left(\frac{-\partial^2 E_i}{\partial V^2}\right) \exp(-E_i/kT) + \frac{1}{kT} \sum_i \left(\frac{\partial E_i}{\partial V}\right)^2 \exp(-E/kT) \qquad ...(194)$$

$$\text{Hence,} \quad \left(\frac{\partial < P >}{\partial V}\right)_{N,T} + \frac{< P^2 >}{kT} = \frac{< P^2 >}{kT} - \left\langle \frac{\partial^2 E}{\partial V^2} \right\rangle \qquad ...(195)$$

This yields

$$< P^2 > - < P >^2 = kT\left[\left(\frac{\partial < P >}{\partial V}\right)_{N,T} + \left\langle \frac{\partial^2 E}{\partial V^2} \right\rangle\right] \qquad ...(196)$$

Since thermodynamically, $P \leftrightarrow < P >$, we have

$$\frac{< P^2 > - < P >^2}{< P >^2} = \frac{kT}{P^2}\left[\left(\frac{\partial P}{\partial V}\right)_{N,T} - \left\langle \frac{\partial^2 E}{\partial V^2} \right\rangle\right] \qquad ...(197)$$

The first term on the right-hand side is $O(-1/N)$ since $PV=NkT$ and $(\partial P/\partial V)_{N,T} = -P^2/NkT$. The second term can be evaluated using the expression for energy, *viz.*, $\varepsilon = (n^2\pi^2\hbar^2)/2V^{2/3}$ of a particle in a cubic box (of infinite height) of volume V and energy $E = N\varepsilon$ (with potential energy equal to zero inside the box). This gives $< \partial^2 E/\partial V^2 > = (5/3)\,(P^2/N\,kT)$. Thus, we find that the standard relative deviation of pressure is of the order of $N^{-1/2}$ and hence negligible.

2. Grand Canonical Ensemble. By definition,

$$< N > = \frac{\sum_{N,i} \exp[-(E_{N_i} - N\mu)/kT]}{\mathcal{Z}(\mu, V, T)} \qquad ...(198)$$

Differentiating w.r.t. μ, we have

$$\left(\frac{\partial \langle N \rangle}{\partial \mu}\right)_{V,T} = \mathcal{Z} + \frac{< N >}{kT} \sum_{N,i} N \exp[-(E_{N_i} - N\mu)/kT] = \frac{1}{kT} \sum_{N,i} N^2 \exp[-(E_{N_i} - N\mu)/kT] \qquad ...(199)$$

(We should bear in mind that N is not a function of μ but $< N >$ is)

This gives

$$\left(\frac{\partial < N >}{\partial \mu}\right)_{V,T} = \frac{< N^2 > - < N >^2}{kT} \qquad ...(200)$$

From the Gibbs-Duhem equation, $d\mu = (V/N)dP - (S/N)dT$, we have for constant T with $V/N = v$,

$$d\mu = v\,dP \qquad ...(201)$$

$$\text{or} \quad (\partial\mu/\partial v)_T = v(dP/\partial v)_T \qquad ...(202)$$

$$\text{Also,} \quad \frac{d\mu}{dN} = \left(\frac{\partial \mu}{\partial v}\right)\left(\frac{\partial v}{\partial N}\right) = v\left(\frac{\partial P}{\partial v}\right)_T \left(\frac{\partial v}{\partial N}\right)$$

$$= v\left(\frac{\partial P}{\partial v}\right)\left(-\frac{V}{N^2}\right) = -\frac{V^2}{N^2}\frac{dP}{dV} \qquad ...(203)$$

$$\text{Hence,} \quad \left(\frac{\partial N}{\partial \mu}\right)_{V,T} = -\frac{N^2}{V^2}\left(\frac{\partial V}{\partial P}\right)_{N,T} = \frac{N^2}{V}\kappa_T \qquad ...(204)$$

where $\kappa_T = -(1/V)(\partial V/\partial P)_{N,T}$ is isothermal compressibility. Substituting Eq. 204 in Eq. 200, we obtain

$$\frac{< N^2 > - < N >^2}{< N >^2} = \frac{kT}{V}\kappa_T = \frac{< \rho^2 > - < \rho >^2}{< \rho >^2} \qquad ...(205)$$

where ρ ($= N/V$) is the number density.

Now, for an ideal gas,

$$\frac{kT}{V}\kappa_T = -\frac{kT}{V^2}\left(\frac{\partial V}{\partial P}\right)_{N,T} = O\left(\frac{1}{N}\right) \qquad ...(206)$$

Thus, the standard relative deviation of number density is of the order of $N^{-1/2}$. We must, however, remember that the number density fluctuations are very large near the liquid-gas critical point as the isothermal compressibility, κ_T, tends to infinity at this point. In this case, these fluctuations give rise to very large scattering of light, known as **opalescence of light.**

Comparison of Various Ensembles. We have seen that the standard relative fluctuation in a thermodynamic property is $O(N^{-1/2})$ using both the canonical and the grand canonical ensembles; hence, in the formulation of thermodynamics, fluctuations can be neglected. Thus, in principle, all the three ensembles—microcanonical (Fig. 5), canonical (Fig. 9) and grand canonical (Fig. 10)—are applicable in the determination of the thermodynamic properties of a system. The three ensembles are compared in Table 1. As far as thermodynamic calculations are concerned, it is simply a matter of convenience which method is followed; all the ensembles give equivalent results. Usually, the most convenient from the point of view of factorizability of the partition function is the grand canonical ensemble. It is possible to construct other ensembles as the need arises. The relation between the grand canonical ensemble and the canonical ensemble is in some sense similar to the relation between the canonical and microcanonical ensembles. The description of a subsystem by means of the microcanonical distribution ignores fluctuations in its total energy while the canonical distribution takes it into account. However, the latter ignores the fluctuations in the number of particles (that is, it is microcanonical with respect to the number of particles), whereas the grand canonical distribution takes this into account (that is, it is canonical both as regards energy and the number of particles).

TABLE 1

Comparison of Various Ensembles

Ensemble (Macroscopic constraints)	Distribution	Partition function	Thermodynamic function	Contact with surroundings
Microcanonical (N, V, E)	$P(E) = \delta(E - E_0)$	$\Delta\Gamma$ or $\Omega\,(N, V, E)$	$-TS = -kT \ln \Omega$	None
Canonical (N, V, T)	$P_i = C \exp(-\beta E_i)$	$Q_N(V, T) = \int \exp(-\beta E)\, d\Gamma$	$A = E - TS$ $= -kT \ln Q_N$	Thermal
Grand canonical (μ, V, T)	$P_{N_i} =$ $C \exp[-\beta(E_{N_i} - N\mu)]$	$\mathcal{Z}(\mu, V, T) =$ $\sum_N \exp(\beta N\mu) \int \exp(-\beta E)\, d\Gamma(N)$	$\Omega_g = E - TS - N\mu$ $= -kT \ln \mathcal{Z}$	Thermal and material

Liquid Helium. Helium is a remarkable substance. A ^4He atom contains an even number of fermions (2 protons, 2 neutrons and 2 electrons); total spin is zero and hence it obeys BE statistics. The phase diagram for helium is shown in Fig. 11. The normal boiling point of liquid ^4He is 4·2 K. The liquid–gas vapour pressure curve extrapolates to the origin, with no sign of the triple point, *i.e.*, it remains liquid at almost absolute zero. The solid phase of helium comes into being only under an external pressure of 25 atm. There are two isotopes of helium of mass three and four (in atomic units) ^3He and ^4He. At temperatures of the order of 1K or 2K, the de Broglie wave length of helium atoms is comparable to the interatomic distance and hence helium shows quantum properties. While ^4He obeys BE statistics, ^3He with half-integral spin, obeys FD statistics.

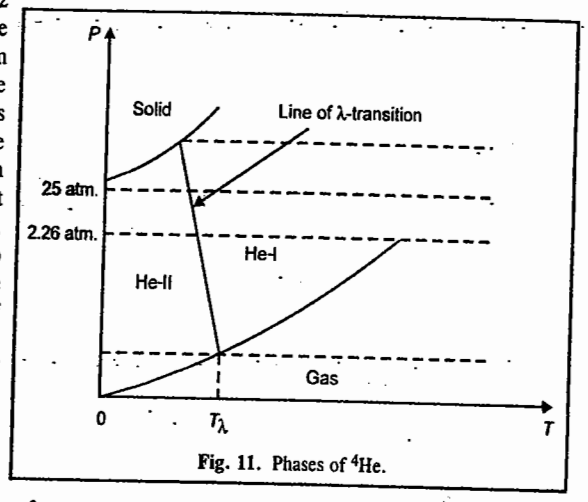

Fig. 11. Phases of ^4He.

As liquid ^4He in contact with its vapour is cooled, it begins to show dramatic change in properties at $T=T_\lambda=2{\cdot}1K$. For $T > T_\lambda$, its behaviour is that of a normal liquid which is called He-I. However, for $T < T_\lambda$, liquid helium begins to show remarkable properties such as zero viscosity (under certain conditions) or **superfluidity.** This phenomenon was discovered by P. Kapitza in 1938. Also, the liquid shows zero entropy. This liquid is called He-II. There is apparently a further phase transition in the liquid phase, called the **Lambda transition,** which divides the liquid state into the phases He-I and He-II (Fig. 11). The transition from He-I to He-II is not accompanied by latent heat. The specific heat along the vapour pressure curve becomes logarithmically infinite as the point of intersection is reached from either side. The shape of the heat capacity curve near the transition point has the shape of the Greek letter lambda. This has given rise to the name lambda transition (λ transition); the corresponding temperature is called **lambda temperature** T_λ. It is a phase transition of the second kind (Fig. 12). We may note that liquid ^3He which obeys FD statistics does not exhibit superfluidity in the above temperature range. (However, in the 1970s it was theoretically predicted that in the ^3He liquid at sufficiently low temperatures around 0·001 K, pairing should occur leading to the formation of bosons and to the occurrence of superfluidity.) It is thus tempting to assume that the λ transition is a BE condensation modified by interparticle interactions. The superfluidity of ^4He at low temperatures is primarily due to (*i*) weak intermolecular forces between atoms and (*ii*) small mass of ^4He. The other noble gases, because of their greater mass, have strong intermolecular interactions

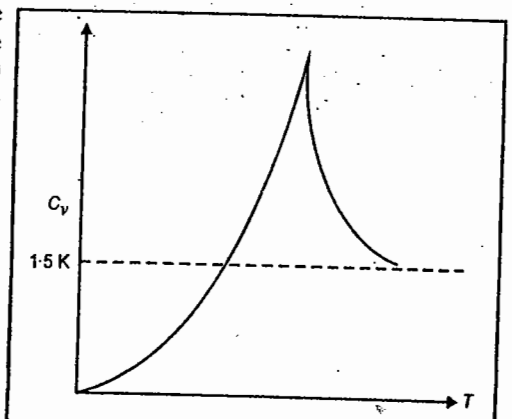

Fig. 12. Heat capacity of liquid He^4 (experimental) along the vapour pressure curve.

and solidify at comparatively higher temperatures. The above reasons suggest a large zero-point motion of He atoms so that the localization of the atoms at well-defined lattice points is not possible. From the pair-potential (Lennard-Jones (6,12-potential) curve of two helium atoms, it is found that depth of the potential well is of the order of 10 K ; the average interparticle distance is of the order of 4·44Å. We thus see that even a small uncertainty of the order of 0·5Å in the localization of atoms gives rise to uncertainty in the energy of the same order as the depth of the potential well, *viz.*,

$$\Delta E \approx (\Delta p)^2/2m = (h/\Delta x)^2/2m \approx 10 \text{ K for } \Delta x \approx 0{\cdot}5 \text{ Å}$$

This energy is enough to allow the atoms to escape from the potential well. Therefore, localization is impossible and ^4He remains a liquid almost down to absolute zero. ^3He, too, remains liquid like ^4He and forms more complex-ordered pairs. It may be mentioned that the connection between BE condensation and the λ-transition remains only a conjecture. The fact that BE condensation does take place in liquid ^4He was shown by Penrose and Onsager using the quantized field formalism, a treatment beyond the scope of this book.

The Two-Fluid Model for Liquid Helium-II : London-Tisza Theory

In 1938, L.Tisza proposed a macroscopic theory of liquid helium, called the two-fluid theory, employing the properties of the degenerate Bose-Einstein (BE) gas. He suggested that at $T < T_\lambda$, He-II consists of *two* independent mutually interpenetrating components, a normal fluid and a superfluid. The total number of particles N is given by

$$N = N_s + N_n \qquad (T < T_\lambda) \qquad ...(207)$$

In Eq. 207, N_s is the number of superfluid particles and N_n is the number of normal fluid particles. Thus, at any point in space, the mass density and mass current density can be written as

$$\rho = \rho_s + \rho_n \qquad ...(208)$$

$$j = \rho_n = \rho_s u_s + \rho_n u_n \qquad ...(209)$$

The superfluid corresponds to the condensed phase of the BE fluid. Thus, ρ_s increases from 0 to ρ as the temperature decreases from 2·18 K (the λ-point) to 0 K. The superfluid as a whole is virtually one quantum state and has zero entropy ($S_s=0$). Also, the superfluid, being a one quantum state, there is no collision of any kind within it so that it has no viscosity ($\eta_s=0$). The normal fluid is the carrier of the whole thermal excitation. Thus, the entropy of liquid He-II is entirely attributed to normal liquid :

$$\rho S = \rho_n S_n \qquad ...(210)$$

where S and S_n refer to entropies per gram. The normal fluid has a viscosity which goes over continuously to the value of liquid He-I at the λ-point :

$$\lim_{T \to T_\lambda} \eta_n(T) = \eta_l(T_\lambda) \qquad ...(211)$$

The two-fluid model explained several experimental observations. For instance, it was found by Keesom and MacWood, using a rotating disc method, that the viscosity of liquid helium below T_λ decreases with decreasing temperature very considerably and continuously and at 1·5 K has a value one-tenth of the value just above T_λ. On the other hand, Kapitza, and (independently) Allen and Meisner, using the capillary flow method, found that the viscosity was immeasurably small below the λ point. The two-fluid theory resolves this contradiction in a very simple manner. In the capillary flow method, the flow is mainly realized by the superfluid, the normal fluid being held back

by its viscosity. However, in the rotating disc method, the rotating disc interacts with the normal fluid only and is not affected by the superfluid. Thus, the two experiments deal with two different fluids and there is no contradiction. The existence of the two fluids and measurement of the ratio ρ_n/ρ was made by the experiments of Andronikashvili in 1946, whose details we shall not describe here. Suffice it to state that when liquid helium was made to oscillate between two discs, only normal fluid moved between them and contributed to the moment of inertia. At each temperature,

$$\frac{\text{Experimental moment of inertia}}{\text{Geometrical moment of inertia}} = \frac{\rho_n}{\rho}$$

It was observed that ρ_n/ρ was unity at T_λ and its value almost disappears below 1 K. Between 1·3 K and 2·18 K, it was observed that

$$\rho_n/\rho = (T/T_\lambda)^{5.6}$$

The two-fluid theory also predicted a notable phenomenon known as the second sound. The first familiar sound is a pressure wave in which the two fluids move in phase (oscillations of ρ_n and ρ_s) with each other. Another type of wave in which the two fluids vibrate with a phase difference of π, a compression wave of entropy accompanied by the periodic fluctuations of temperature, mass density remaining constant, is also possible. This mode of oscillation is excited by local heating of liquid He-II. The temperature gradient produced does not propagate by diffusion (as in heat conduction) but propagates like a wave with a characteristic velocity. This phenomenon is called second sound.

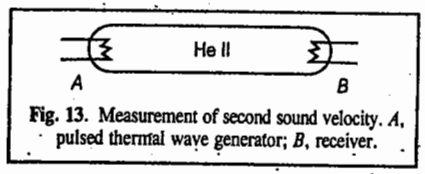

Fig. 13. Measurement of second sound velocity. *A*, pulsed thermal wave generator; *B*, receiver.

Thus, whereas the familiar (first) sound is a pressure wave, the second sound is an entropy wave, predicted by Tisza and first observed by Peshkov using a continuous resonance technique (Fig. 13). Periodic heat produced at *A* was found to travel through He-II and detected at the other end by the thermometer coil at the end *B*.

Tisza pointed out that the two types of interpenetrating fluids, ρ_s and ρ_n, do not resist the motion of each other. Any temperature gradient tends to be smoothed out by a current of normal (warm, $\varepsilon>0$) fluid in the direction of falling temperature and a current of superfluid (cold, $\varepsilon=0$) in the opposite direction (out of phase by 180°) such that the total density remains constant. This process is in agreement with the Le Chatelier principle. As the total density remains constant, we have to imagine a motion of fluid for which the average velocity u is zero. Then there is no net transport of mass across any plane in the liquid and the flow equation reduces to

$$\rho_s u_s + \rho_n u_n = 0 \qquad ...(212)$$

This mode of motion in which the normal fluid and the superfluid oscillate out of phase by π, *i.e.*, 180°, leads to the thermal waves or second sound.

The velocity u_2 of the second sound can be easily calculated. The superfluid component has zero entropy. Hence, the total entropy S per gram of liquid He-II can be written as

$$\rho S = \rho_n S_n \qquad ...(213)$$

For the sake of simplicity, we shall consider the transport of entropy in one direction only. Imagine a parallelopiped of unit cross-section and length Δx inside the liquid with one pair of opposite faces vertical. The amount of entropy entering the volume per second at one face is

$\rho S u_n = \rho_n S_n u_n$ and leaving at the opposite face $= \rho S u_n + \frac{\partial}{\partial x}(\rho S u_n)\frac{\partial}{\partial x}\Delta x$.

Therefore, the net transport of entropy per unit volume per second is $= \frac{\partial}{\partial x}(\rho S u_n)$.

The original entropy within the volume is ρS and the loss in unit time is $-(\partial/\partial t)(\rho S)$. This gives the equation of continuity, *viz.*,

$$-\frac{\partial}{\partial t}(\rho S) = -\frac{\partial}{\partial x}(\rho S u_n) \qquad ...(214)$$

If ρ is constant and u_n is small, we can write

$$-\frac{\partial S}{\partial t} = S\frac{\partial u_n}{\partial x} \qquad ...(215)$$

after neglecting the small term $(\partial S/\partial x)\, u_n$. ...(216)

Let the opposite faces have temperatures T and $T+\Delta T$. Then, the quantity of heat transferred across Δx per second is $q=\rho S u_n T$. By the Second law of thermodynamics, $w/q = \Delta T/T$ where w is the reversible work done in heat transfer. Thus,

$$w = q(\Delta T/T) = \rho S u_n \Delta T \qquad ...(217)$$

This work causes change in kinetic energy $(\partial E/\partial t)\Delta x$, within Δx. There is no mass flow. The kinetic energy is, therefore, expressed as

$$E = \frac{1}{2}\left(\rho_n u_n^2 + \rho_s u_s^2\right) = \frac{1}{2}\rho_n u_n\left[1+\frac{\rho_s}{\rho_n}\left(\frac{u_s}{u_n}\right)^2\right] \qquad ...(218)$$

$$= \frac{1}{2}\rho_n u_n^2\left(1+\rho_n/\rho_s\right) = \frac{1}{2}\frac{\rho\rho_n}{\rho_s}u_n^2 \qquad ...(219)$$

Therefore, $$\left(\frac{\partial E}{\partial t}\right)\Delta x = \frac{\rho\rho_n}{\rho_s}u_n\frac{\partial u_n}{\partial t}\Delta x = -w = -\rho S u_n \Delta T \qquad ...(220)$$

or $$\frac{\rho_n}{\rho_s}\frac{\partial u_n}{\partial t} = -S\frac{\partial T}{\partial x} \qquad ...(221)$$

Using the relations $C_V\, dT = T dS$ and $\partial T/\partial S = T/C_V = (\partial T/\partial x)(\partial x/\partial S)$, we have $\partial T/\partial x = (T/C_V)(\partial S/\partial x)$, so that

$$\frac{\rho_n}{\rho_s}\frac{\partial u_n}{\partial t} = -S\frac{T}{C_V}\frac{\partial S}{\partial x} \qquad ...(222)$$

Eliminating u_n from Eqs. 214 and 222, we get

$$\frac{\partial^2 S}{\partial t^2} = \left(\frac{\rho_s S^2 T}{\rho_n C_V}\right)\frac{\partial^2 S}{\partial x^2} \qquad ...(223)$$

The velocity u_2 of the second sound defined by this equation is given by

$$u_2 = \left(\frac{\rho_s}{\rho_n}\frac{S^2T}{C_V}\right)^{1/2} \qquad ...(224)$$

It follows that Tisza's two-fluid model predicts $u_2 \to 0$ both when $T \to 0$ and when $T \to T_\lambda$ ($\rho_s \to 0$). The prediction for $T \to 0$ turned out to be wrong. In fact, $u_2 \to u_1/3^{1/2} = 137$ m s^{-1} for $T \to 0$, where u_1 is the first sound velocity. This shows that Tisza's idea of associating the condensed particles with super-fluid, as a natural extension of London's theory, is not correct.

Landau Theory of Liquid Helium. The Landau theory proposed a molecular foundation for the two-fluid Tisza–London theory. Landau rejected the Tisza–London approach from the side of gas statistics. He, instead, approached the problem from the solid side (wherein the Bose-Einstein condensation is irrelevant). At 0 K the atoms of the solid body are in the lowest energy state, *i.e.*, the ground state. At higher temperatures, the atoms undergo oscillations around their equilibrium positions; these oscillations are *phonons* which correspond to sound waves in the same way as the photons correspond to light waves. These phonons behave like **quasi-particles** having definite energy and momentum. Landau assumed that the excited state of liquid He-II can be represented by two kinds of elementary excitations—the **phonons** and the **rotons**. The phonons are excitations of the longitudinal sound waves.

The energy of the phonons is a linear function of momentum :

$$\varepsilon_{ph} = u_1 p \qquad \text{(phonon)} \qquad ...(225)$$

where u_1 is the first sound velocity. However, this does not exhaust all the $3N$ degrees of freedom if there are N atoms in the liquid helium-II system. A liquid is not expected to sustain high energy transverse (shear) wave, as a solid can. Therefore, for $1K < T < T_\lambda$, Landau assumed the existence of excitations called *rotons* (quanta of vortex motion) with the energy spectrum. Accordingly,

$$\varepsilon_{rot} = \Delta + p^2/2\mu_r \qquad ...(226)$$

where Δ is the energy gap (minimum energy to excite a roton at rest), p is the linear momentum of the roton and μ_r the effective mass of the roton. Phonons, like photons, obey BE statistics because they have integral spins. Rotons are also assumed to obey BE statistics. However, since the ε_{rot} involves $\Delta > kT$ for $T < T_\lambda$, the aggregate of rotons can be treated, to a good approximation, by an MB gas. Both phonons and rotons behave like quasiparticles that can move about and form the normal fluid He-II. The superfluid has zero entropy. In order to improve the agreement with experiments, Landau proposed the following energy spectrum of the quasi-particles :

$$\varepsilon = \begin{cases} \varepsilon_{ph} = u_1 p & (phonon) \\ \varepsilon_{rot} + \Delta + \dfrac{(p-p_0)^2}{2\mu_r} & (roton) \end{cases} \qquad ...(227)$$

where p_0 is the value of the momentum at which energy has a minimum equal to Δ. The whole energy spectrum of excitations, determined from neutron scattering experiments, gives the following values of the parameters :

$u_1 = 226$ m s^{-1}, $\Delta/k = 8{\cdot}6$ K, $p_0/\hbar = 1{\cdot}91$ Å^{-1}, $\mu_r = 0{\cdot}3m$ where m is the mass of the helium atom.

In Fig. 14, the active portions of the spectrum are shown by solid curves. At low temperatures ($0 < T < T_\lambda$), only the linear part of the spectrum corresponding to phonons becomes active. At above 1K, both phonons and rotons exist. He-II can be regarded as a mixture of two ideal gases—a phonon gas and a roton gas, provided the number of phonons and rotons per unit volume is not large.

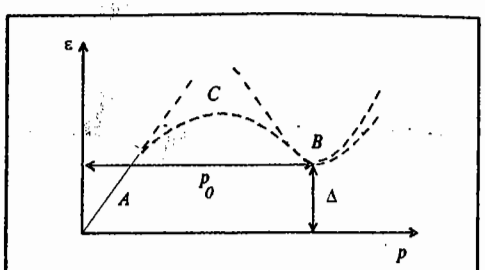

Fig. 14. Dispersion curve (ε *vs* p plot) for liquid ^{4}He showing the two branches (*A*, linear phonon branch and *B*, parabolic roton branch of the Landau spectrum. The ad hoc curve *C* smoothly joins the two distinct branches.

The superfluidity of He-II can be shown to follow from the motion of the elementary excitations. Consider the liquid helium at 0 K (*i.e.*, in the ground state) and the liquid flowing through a capillary with velocity v. If this flow is accompanied by friction, a part of the kinetic energy would be dissipated and converted into thermal energy, thereby heating up the liquid and undergoing transition to excited states. If $\varepsilon(p)$ is the energy of an excitation with momentum p in the frame moving with the liquid, in the fixed frame the energy changes by an amount $= \varepsilon(p) + pv$. The transition to the excited state is possible if

$$\varepsilon(p) + pv < 0 \qquad ...(228)$$

The favourable situation results when the momentum of the created excitation is directed opposite to the velocity. We then have

$$v > \varepsilon(p)/p \qquad ...(229)$$

It is obvious that an excitation can appear if Eq. 229 is satisfied, at least at that point of the spectrum where $\varepsilon(p)/p$ has a minimum value. Thus, the necessary condition for the creation of an excitation is

$$v > \min\,[\varepsilon(p)/p] \qquad (230)$$

or

$$v_{critical} = \min\,[\varepsilon(p)/p] \neq 0 \qquad ...(231)$$

For values of v less than $v_{critical}$, no excitation is created, *i.e.*, the liquid would flow without friction (without dissipation of energy); it will be a superfluid. The criterion given by Eq. 230 is valid at finite temperatures too. The pressure of excitations in the liquid at finite temperatures introduces special features into the flow of the liquid in the capillary. The excitations, reflected against the walls, transfer a part of this momentum to the walls. As a result, that part of the liquid which is carried along by the motion of excitations, behaves like a normal viscous liquid and is slowed down by friction with the walls. Thus, at 0 K, the whole liquid flows frictionless—a superfluid, in fact—whereas at $T \neq 0$ K only a part does so, *i.e.*, the liquid consists of two components, the superfluid and the normal fluid, which satisfy the same equations as in the Tisza theory :

$$\rho = \rho_n + \rho_s \qquad ...(232)$$

and

$$j = \rho v = \rho_s v_s + \rho_n = v_n \qquad ...(233)$$

The ratio $\rho_n/\rho = 1$ at $T = T_\lambda$ and zero at $T = 0$ K.

We shall now consider the thermodynamic properties of liquid He-II. Both phonons and rotons contribute to them. At temperatures below 1K, phonons play a dominant role as a few rotons exist. Rotons are quanta of vortex motion. Above 1K, however, the roton contribution becomes important. At about 1K both phonons and rotons exist. If the number of phonons and rotons per unit volume of liquid He-II is not large, their aggregate can be regarded as a mixture of two ideal gases—a phonon gas and a roton gas. Both phonons and rotons behave like quasi-particles that can move about and form the normal fluid. The superfluid has, strictly speaking, zero entropy.

Phonon Contribution. For the phonon gas obeying BE statistics, we can write the energy as

$$U_{ph} = \frac{4\pi}{h^3}\int_0^\infty \frac{\varepsilon p^2 dp}{\exp(u_1 p/kT)-1} = \frac{4\pi u_1}{h^3}\int_0^\infty \frac{p^3 dp}{\exp(u_1 p/kT)-1}$$

$$= \frac{4\pi}{h^3 u_1^3}(kT)^4 \int_0^\infty \frac{x^3 dx}{e^x - 1} \quad \text{where } x = u_1 p/kT \qquad \ldots(234)$$

Using the integral $F_s(z') = \frac{1}{\Gamma_{(s)}}\int_0^\infty \frac{x^{s-1}\,dx}{(1/z')e^x - 1} = \sum_{k=1}^{\infty}\frac{z'^k}{k^s}$,

the above expression becomes

$$U_{ph} = \frac{4}{15}\frac{\pi^5}{h^3 u_1^3}(kT)^4 = \frac{bT^4}{4} \quad \text{where } b = \frac{16\pi^5 k^4}{15 h^3 u_1^3} \qquad \ldots(235)$$

The heat capacity per unit volume is given by

$$C_{ph} = \left(\frac{\partial U_{ph}}{\partial T}\right)_V = bT^3 \qquad \ldots(236)$$

and the entropy per unit volume is given by

$$S_{ph} = \int \frac{C_{ph}}{T} dT = \frac{bT^3}{3} \qquad \ldots(237)$$

It should be noted that, for phonons, $\mu = 0$. In Landau's theory, phonons play an important role for $T < 1$K where few rotons exist. Unlike the London–Tisza theory, here they contribute to the normal fluid and so lead to the correct prediction of u_2 at low temperatures.

This result is borne out by experiment. In the London–Tisza theory, $u_2 \to 0$ as $T \to 0$.

Roton Contribution. The rotons obey MB statistics. Now,

$$A = -kT \ln Q_N = -kT \ln \frac{q^N}{N!} = -NkT \ln q + NkT \ln N - NkT \qquad \ldots(238)$$

where q, the single particle partition function, is given by

$$q = \frac{4\pi V}{h^3}\int_0^\infty \exp(-\varepsilon/kT)\,p^2 dp = \frac{4\pi V}{h^3}\int_0^\infty \exp\left[-\frac{\Delta + (p-p_0)^2/\mu_r}{kT}\right]p^2 dp \qquad \ldots(239)$$

Substituting $p - p_0 = t$, $dp = dt$ and $p^2 = (p_0 + t)^2 \approx p_0^2$ since $p_0^2/2\mu_r kT \gg 1$, we have

$$q = \frac{4\pi V}{h^3}\exp(-\Delta/kT)\,p_0^2 \int_0^\infty \exp(-t^2/2\mu_r kT)\,dt = \frac{4\pi V}{h^2}p_0^2 \exp(-\Delta/kT)(2\pi\mu_r kT)^{1/2} \qquad \ldots(240)$$

In the above expressions, the lower limit has been extended from $-p_0$ to $-\infty$.

The number of rotons changes with temperature ; this must be determined from the condition that A is a minimum, *i.e.*,

$$(\partial A/\partial N)_V = 0 = -kT \ln q + kT \ln N \qquad \ldots(241)$$

which gives the number of rotons per unit volume :

$$N_{rot} = \frac{q}{V} = \frac{4\pi}{h^3}p_0^2 (2\pi\mu_r kT)^{1/2} \exp(-\Delta/kT) \qquad \ldots(242)$$

The Helmholtz free energy (*i.e.*, work function) per unit volume is given by

$$A_{rot} = -kT N_{rot} = -\frac{4\pi}{h^3}p_0^2 (2\pi\mu_r kT)^{1/2} \exp(-\Delta/kT) \qquad \ldots(243)$$

The entropy per unit volume is given by

$$S_{rot} = -\left(\frac{\partial A_{rot}}{\partial T}\right)_V = k N_{rot}\left(\frac{3}{2} + \frac{\Delta}{kT}\right) \qquad \ldots(244)$$

The heat capacity per unit volume is given by

$$C_{rot} = T\left(\frac{\partial S_{rot}}{\partial T}\right)_V = k N_{rot}\left[\left(\frac{\Delta}{kT}\right)^2 + \frac{\Delta}{kT} + \frac{3}{4}\right] \qquad \ldots(245)$$

Because of the factor $\exp(-\Delta/kT)$, very few rotons are present at low temperatures ($N_{rot} \to 0$ as $T \to 0$).

Adding up the contributions due to the phonon gas and roton gas, we obtain the following expressions for the entropy and heat capacity of liquid helium-II :

$$S = S_{ph} + S_{rot} = \frac{16\pi^5 k^4}{45 h^3 u_1^3}T^3 + k N_{rot}\left(\frac{\Delta}{kT} + \frac{3}{2}\right) \qquad \ldots(246)$$

$$C_V = C_{ph} + C_{rot} = \frac{16\pi^5 k^4}{15 h^3 u_1^3}T^3 + k N_{rot}\left[\left(\frac{\Delta}{kT}\right)^2 + \frac{\Delta}{kT} + \frac{3}{4}\right] \qquad \ldots(247)$$

We shall not discuss in this brief account the quantization of the motion of the liquid which involves difficult mathematics and is of interest to theoretical physicists. Suffice it to mention, in conclusion, that the Landau theory does not explain the existence of T_λ satisfactorily. Also, the Landau theory gives only the linear part and the parabola part of the energy spectrum and not the whole spectrum. The Feynman theory of liquid helium, which we shall not discuss here, throws more light on the nature of elementary excitations. The Feynman curve differs considerably from the Landau curve but the roton part comes out qualitatively. The quantitative agreement is poor but the notable feature of the Feynman theory is that there are no ad hoc adjustable parameters. Further contributions to the subject have been made by N.N. Bogoliubov, D.S. Kothari, B.N. Singh, J.G. Daunt, Z. Mikura, R.B. Dingle, D.D. Osheroff, B.K. Agarwal, and other physicists.

The role of quantum statistics in the London–Tisza and the Landau theories of liquid helium was further investigated by a study of a mixture of a BE gas of ^{4}He atoms and a FD gas of ^{3}He atoms below 2·2 K during 1950—1980. The superfluid phases of ^{3}He were studied by the American physicist A.J. Leggett in the 1970s. In spite of many differences between liquid ^{4}He and liquid ^{3}He, the two-fluid model is applicable to ^{3}He. A.J. Leggett shared the 2003 Physics Nobel Prize with the Russian physicists A.A. Abrikosov and V.L. Ginzburg who were honoured for contributions to superconductivity.

Statistical Mechanics of Imperfect (Non-ideal or Real) Gases : Classical Cluster Expansion

This is a very difficult area of theoretical chemistry. We shall give here a brief account of the treatment, leading to the derivation of the virial equation of state for real gases.

The Hamiltonian for a real gas can be written as :

$$H(q, p) = E(p) + \sum_{i<j} u_{ij}(r_{ij}) \qquad ...(248)$$

where $E(p)$ is the total kinetic energy and u_{ij} is potential energy between particles i and j. It is assumed that u_{ij} depends only upon the interparticle distance $r_{ij}=|r_i-r_j|$ between the pairs of particles i and j. The potential energy term can also be written as

$$\sum_{i<j} u_{ij}(r_{ij}) = \frac{1}{2}\sum_{i\neq j} u_{ij}(r_{ij}) \qquad ...(249)$$

where the factor 1/2 is included to compensate for counting each interaction term twice (once as ij and once as ji). For a perfect (ideal) gas $u_{ij}=0$ so that

$$\phi(r_1,...,r_N) = \sum_{i<j} u_{ij}(r_{ij}) = 0 \qquad ...(250)$$

For a real gas, the classical partition function, neglecting internal degrees of freedom, is

$$Z = \frac{1}{N!h^{3N}}\int \exp[-\beta H(q,p)]\, dq\, dp \qquad ...(251)$$

$$= \left[\frac{V^N}{N!}\int \exp[-\beta E(p)]\frac{dp}{h^{3N}}\right]\left[\frac{1}{V^N}\int \exp[-\beta\phi(q)]dq\right]$$

$$= Z_p Z_\phi \qquad ...(252)$$

where Z_p is the partition function for the perfect gas and

$$Z_\phi = \frac{1}{V^N}\int \exp[-\beta\phi(q)]\, dq_1...,dq_N \qquad ...(253)$$

the **configurational partition function** of the gas. For a perfect gas, $Z_\phi=1$. Using the proximation (Eq. 248) for an imperfect gas,

$$Z_\phi = \frac{1}{V^N}\int \exp\left[-\left(\sum_{i<j}\beta u_{ij}\right)\right]\prod_{i=1}^{N} d^3r_i \qquad ...(254)$$

$$= \frac{1}{V^N}\int\prod_{i<j}\exp(-\beta u_{ij})\prod_{i} d^3r_i \qquad ...(255)$$

Note that in Eq. 255, each coordinate can vary within the entire volume V of the gas.

We now introduce the **Mayer f function** (named after J.E. Mayer), defined by

$$f_{ij} = f_{ij}(r_{ij}) \equiv \exp(-\beta u_{ij}) - 1 \qquad ...(256)$$

which is a measure of the degree of imperfection of the real gas (in the ideal gas limit, $f_{ij}\to 0$). Eq. 255 may be rewritten as

$$Z_\phi = \frac{1}{V^N}\int_{3N}...\int\prod_{i<j}(1+f_{ij})\prod_{i=1}^{N} d^3r_i \qquad ...(257)$$

$$= \frac{1}{V^N}\int d^3r_1...d^3r_N(1+f_{12})(1+f_{13})...(1+f_{N-1,N}) \qquad ...(258)$$

$$= \frac{1}{V^N}\int d^3r_1...d^3r_N\left(1+\sum_{i<j} f_{ij} + \sum_{\substack{i<j\\k<l\\i,j\neq k,l}} f_{ij}f_{kl}+...\right) \qquad ...(259)$$

The complicated integral (259) is reduced to a sum of relatively simple but still multiple integrals. Except for the first two of these integrals, the remaining integrals are extremely difficult to evaluate even approximately. The introduction of the Mayer f function facilitates a more clear exposition of the inter-particle interactions. The general forms of $u(r)$, the intermolecular potential, and $f(r)$ are shown in Fig. 15*a*. We see that f_{ij} is zero except when $r_{ij} \leq 2r_0$ where r_0 is the radius of one molecule. Thus, f_{12} is negligible unless molecules 1 and 2 are close together (binary collision). Similarly, $f_{12}\, f_{23}$ contributes only when molecules 1, 2, 3 are all simultaneously close together (ternary collision) and so on. These terms are shown graphically in Fig. 15*b*; they represent clusters of molecules. The series (Eq. 259) is called a **cluster expansion**. Here we shall consider only the first two terms, 1 and f_{ij}, in the cluster expansion series.

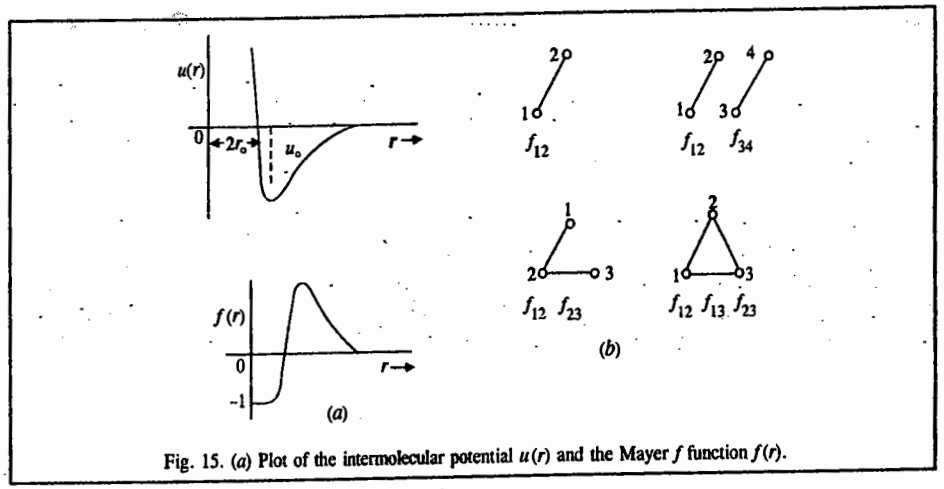

Fig. 15. (*a*) Plot of the intermolecular potential $u(r)$ and the Mayer f function $f(r)$.

If we retain only the first term, 1, neglecting all fs (that is all collision terms), then, Eq. 259 gives $Z_\phi = 1$, $Z = Z_p$ (perfect gas approximation).

We shall now consider the second term, Σf_{ij} in Eq. 259. This sum contains $(1/2)N(N-1)$ terms determined by the number of ways we can choose pairs of molecules. All these terms are equal since they differ only in the labels of integration variables. Hence, the contribution of the second

term can be written as

$$C_2 = V^{-N}\frac{1}{2}N(N-1)\int d^3r_1 \ldots d^3r_n f_{12} \qquad \ldots(260)$$

$$= V^{-N}\frac{1}{2}N(N-1)V^{N-2}\int d^3r_1 d^3r_2[\exp(-\beta u(r_{12}))-1] \qquad \ldots(261)$$

where $u(r_{12})$ is the potential energy of interaction between the particles 1 and 2 as a function of their interparticle separation $r_{12} = |r_1 - r_2|$. If we define the new variables of integration

$$r = r_1 - r_2$$

$$R = 1/2(r_1 + r_2),$$

then, the integration over R yields one more factor V so that

$$C_2 = V^{-1}\frac{1}{2}N^2\int d^3r \exp[-\beta u(r)-1] = \frac{N^2[I_2]}{2V} \qquad \ldots(262)$$

where we have written $\frac{1}{2}N(N-1) \simeq \frac{1}{2}N^2$ for $N \gg 1$.

For Z_ϕ, Eq. 259 can be approximately written as

$$Z_\phi = \left[1 + N\left(\frac{NI_2}{2V}\right) + \ldots\right] \simeq \left(1 + \frac{NI_2}{2V}\right)^N \text{ since } NI_2/2V \ll 1 \qquad \ldots(263)$$

Note that $NI_2/2V \ll 1$ because the cluster integral I_2 is of the order of the volume v_0 of one molecule (the integrand in I_2 differs appreciably from zero only within such a volume and is nearly 1 there).

The deviation from ideality at low densities ($Nv_0 \ll V$) can now be determined from Eq. 263. Using $Z = Z_p Z_\phi$, the Helmholtz free energy is given by

$$A = -kT \ln Z = -kT \ln Z_p - kT \ln Z_\phi \qquad \ldots(264)$$

$$= A_p - kT\,N \ln\left(1 + \frac{NI_2}{2V}\right) \simeq A_p - kT\,\frac{NI_2}{2V} \qquad \ldots(265)$$

A_p is the Helmhaltz free energy in an ideal gas.

The pressure of the gas is given by

$$P = -\left(\frac{\partial A}{\partial V}\right)_{T,N} = \frac{NkT}{V} - kT\,\frac{N^2 I_2}{2V^2} = \frac{NkT}{V}\left(1 - \frac{NI_2}{2V}\right) \qquad \ldots(266)$$

The virial equation of state of a real gas is written as a power series in number density as :

$$P = \frac{NkT}{V}\left[1 + \frac{N}{V}B_2(T) + \left(\frac{N}{V}\right)^2 B_3(T) + \ldots\right] \qquad \ldots(267)$$

or

$$\frac{P}{kT} = \rho + B_2(T)\,\rho^2 + B_3(T)\,\rho^3 + \ldots \qquad \ldots(268)$$

where $\rho(= N/V)$ is the number density and the quantities $B_2(T)$, $B_3(T)$,... are called second, third,... virial coefficients which depend only on the temperature T and on the nature of the particular gas under consideration. The goal of the statistical mechanics of real gases is to derive the expressions for the virial coefficients in terms of interparticle potential energy. The second virial coefficient $B_2(T)$ is related to the cluster integral I_2 as $B_2(T) = -I_2/2$.

Evaluation of the Second Virial Coefficient

We shall evaluate $B_2(T)$ for the following three well known forms of intermolecular potential energy : (*a*) a hard-sphere potential (*b*) a hard-sphere potential followed by a square-well potential, and (*c*) the Lennard-Jones (6,12) potential, named after the great British theoretical chemist, J. E. Lennard-Jones (1894-1954).

a. Hard-Sphere Potential. This potential is defined by

$$u(r) = \begin{cases} \infty, & \text{for } 0 < r < a \\ 0, & \text{for } r > a \end{cases} \qquad \ldots(269)$$

Sketched in Fig. 16, this potential has a steep repulsive part in the region $0 < r < a$ and no attractive part. Substituting this potential in the expression for $B_2(T)$, *viz.* ;

$$B_2(T) = -\frac{1}{2}\int \exp[-\beta u(r)] - 1\,dr \qquad \ldots(270)$$

we have

$$B_2(T) = -\frac{1}{2}\int_0^a (-1)\,4\pi r^2 dr = \frac{2\pi a^3}{3} \qquad \ldots(271)$$

This is four times the volume of a sphere of radius $a/2$ and is temperature-independent.

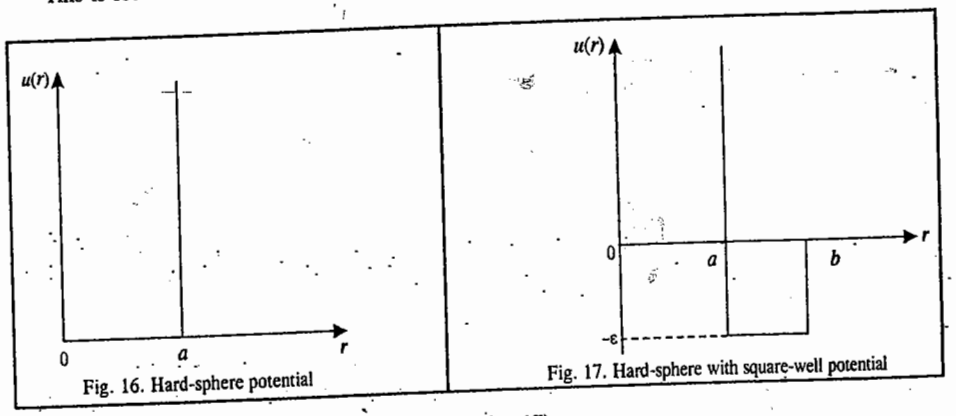

Fig. 16. Hard-sphere potential

Fig. 17. Hard-sphere with square-well potential

b. Hard-sphere with Square-Well Potential (Fig. 17) :

$$u(r) = \begin{cases} \infty & \text{for } 0 < r < a \\ -\varepsilon & \text{for } a < r < b \\ 0 & \text{for } r > b \end{cases} \qquad \ldots(272)$$

This potential has a steep repulsive core in the region $0 < r < a$, followed by an attractive well of constant depth in the region $a < r < b$, and is zero beyond b. Substituting this potential in the expression for $B_2(T)$, we have

$$B_2(T) = -\frac{1}{2}\int_0^a (-1)\,4\pi r^2 dr - \frac{1}{2}\int_0^b \exp(\beta\varepsilon - 1)\,4\pi r^2 dr$$

$$= \frac{2\pi a^3}{3} - \frac{2}{3}\pi(b^3 - a^3)\,[\exp(\beta\varepsilon - 1)] \qquad \ldots(273)$$

The above expression reduces to the hard-sphere result if $b \to a$ or $\varepsilon \to 0$.

c. The Lennard-Jones (6,12) Potential (Fig. 18) :

$$u(r) = 4\varepsilon\,[(\sigma/r)^{12} - (\sigma/r)^6] \qquad ...(274)$$

where ε and σ are called the **Lennard-Jones parameters** whose values vary from gas to gas. Typical values are ε/k = 10·22 K and σ = 2·556 Å.

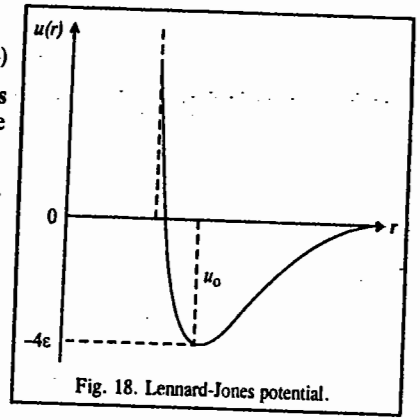

Fig. 18. Lennard-Jones potential.

The minimum in the potential occurs at $r = 2^{1/6}\sigma$. Using this potential, we obtain

$$B_2(I) = -\frac{1}{2}\int_0^\infty [\exp\{-4\beta\varepsilon[(\sigma/r)^{12} - (\sigma/r)^6]\} - 1]\, 4\pi r^2\, dr \qquad ...(275)$$

which, on simplification (using $\beta = 1/kT$), yields :

$$B_2(T) = \frac{2}{3}\pi\sigma^3\,(kT/\varepsilon)^{-1/4}\,[1{\cdot}733 - 2{\cdot}56\,(kT/\varepsilon)^{-1/2} - 8{\cdot}66\,(kT/\varepsilon)^{-1} - 4{\cdot}27(kT/\varepsilon)^{-3/2} + \ldots] \qquad ...(276)$$

Derivation of the van der Waals Equation for a Gas from the Virial Equation

Assume that the gas molecules are hard spheres of radius r_0 and volume $v_0 = (4/3)\pi r_0^3$. Then we can divide the cluster integral I_2 in two parts. In the first part, $0 < r < 2r_0$, the potential energy term is infinite (since two hard spheres are in contact, Fig. 19) so that $\exp[-\beta u(r)] - 1 \simeq -1$. The second term extends from $2r_0$ to ∞. Thus,

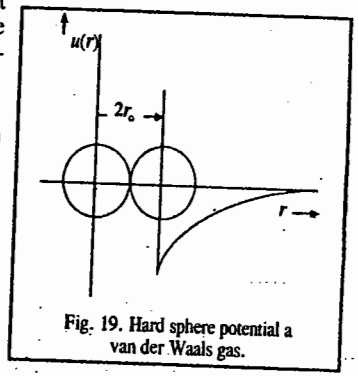

Fig. 19. Hard sphere potential a van der Waals gas.

$$B_2(T) = -\frac{1}{2}I_2 = -\frac{1}{2}\int_0^\infty d^3r[\exp(-\beta u(r)) - 1] \qquad ...(277)$$

$$= -\frac{1}{2}\int_0^{2r_0}(-1)d^3r - \frac{1}{2}\int_{2r_0}^\infty d^3r[\exp(-\beta u(r)) - 1]$$

$$\simeq \frac{1}{2}4\pi\int_0^{2r_0} r^2\,dr + \frac{1}{2}\int_{2r_0}^\infty 4\pi r^2\,dr\,p\,u(r)$$

$$= 2\pi\frac{1}{3}(2r_0)^3 + \frac{2\pi}{kT}\int_{2r_0}^\infty dr\,r^2\,u(r) \equiv b - \frac{a}{kT}; \qquad ...(278)$$

where we have set $\exp(-u(r)/kT) - 1 \simeq -u(r)/kT$ assuming u_0 (Fig. 18) to be numerically far less compared with kT and

$$b = 4v_0 \quad \text{and} \quad a = -2\pi\int_{2r_0}^\infty dr\,r^2 u(r) \qquad ...(279)$$

where a and b are the van der Waals constants

The virial equation of state upto the second virial coefficient (neglecting the higher virial coefficients which become smaller and smaller) is

$$P = \frac{NkT}{V}\left[1 + \frac{N}{V}\left(b - \frac{a}{kT}\right)\right] \text{ where from Eq. 278, } B_2(T) = b - a/kT \qquad ...(280)$$

$$= \frac{NkT}{V}\left[\left(1 + \frac{N}{V}b\right) - \frac{N^2}{V^3}a\right]$$

$$\simeq \frac{NkT}{V}\left[\left(1 - \frac{N}{V}b\right)^{-1} - \frac{N^2}{V^3}a\right] \qquad ...(281)$$

which gives the van der Waals equation for a gas :

$$\left(P + \frac{N^2a}{V^2}\right)(V - Nb) = NkT \qquad ...(282)$$

The correction term a, according to van der Waals, comes from the long-range weak attractive interaction between the gas molecules and the term b from the finite volume v_0 of the molecule.

Concluding remarks. The statistical mechanics of real gases (and by extension, of the liquid state) is a highly mathematical topic. Contributions to the subject were made from 1930s to 1960s by theoretical chemists and physicists such as J.E.Mayer, G.E.Uhlenbeck, B.Kahn, E.Beth, C.N.Yang, T.D.Lee, J.G.Kirkwood, N.N. Bogoliubov and several other scientists. Statistical mechanics at the advanced level has become the formidable **'many-body problem'**, and quantum field theoretical methods have been employed to solve its intricacies. The time-correlation function formalism to study transport processes in nonequilibrium statistical mechanics is another area of research pioneered in the 1950s by Green and Kubo.

In conclusion, it is appropriate to quote the physicist who is not only one of the three founders of quantum mechanics (the other two being Heisenberg and Dirac) but who has also written perceptively on the nature of statistical thermodynamics :

There is, essentially, only one problem in statistical thermodynamics : the distribution of a given amount of energy U over N identical systems. Or perhaps better : to determine the distribution of an assembly of N identical systems over the possible states in which this assembly can find itself, given that the energy of the assembly is a constant U. The idea is that there is weak interaction between them, so weak that the energy of interaction can be disregarded, that one can speak of the "private" energy of every one of them and that the sum of their "private" energies has to equal U. The distinguished role of the energy is, therefore, simply that it is a constant of the motion—the one that always exists, and, in general, the only one.

Erwin Schrödinger,
Statistical Thermodynamics,
Cambridge University Press, 1946.

I. Review Questions

1. Define the following terms :
   Phase space, ensemble, and ensemble average in the Gibbs formulation of classical statistical mechanics.
2. Define classically microcanonical ensemble, the canonical ensemble and the grand canonical ensemble, illustrating them with suitable diagrams.
3. What is the postutate of equal a priori probability in classical statistical mechanics ?
4. Derive the expression for the entropy of a perfect gas using the classical microcanonical ensemble. Why is this ensemble so inconvenient to work with ?

5. What is the Gibbs paradox in the entropy of mixing of ideal gases and how did Gibbs resolve it ?
6. What is the role played by density matrix in quantum statistics ?
7. Discuss briefly the quantal microcanonical ensemble.
8. Why do we feel the need to quantize phase space ? Also derive the expression for the number of microstates accessible to a system such as a particle in an infinite dimensional cubical box.
9. Under what conditon is the classical limit of statistical mechanics valid ?
10. Discuss how the symmetry of wave functions of identical particles leads to the three kinds of statistics—MB, BE and FD.
11. How is entropy related to probabilty ? Briefly discuss.
12. Drive the classical canonical distribution in a canonical ensemble.
13. How can the various thermodynamic quantities be derived from the classical canonical partition function ?
14. Discuss the application of classical canonical distribution to an ideal gas, deriving the results for thermodynamic quantities.
15. Derive the law of equipartition of energy from first principles.
16. Derive the classical grand canonical distribution in a grand canonical ensemble.
17. Derive the expressions for energy fluctuations in a canonical ensemble, and the number density fluctuations in a grand canonical ensemble. Comment briefly and show how the equivalence between the three ensembles is established.
18. Derive the van der Waals equation of state from the virial equation of state.
19. Discuss the Landau theory of liquid helium.
20. What are cluster integrals ? Express the classical partition function in terms of cluster integrals.
21. Derive the cluster expansion of the pressure of a classical gas and hence relate the virial coefficients with the cluster integrals.
22. Evaluate the second virial coefficient for a classical hard-sphere gas, and also the hard-sphere gas followed by an attractive square well potential.

CHEMICAL KINETICS

Chemical kinetics constitutes an important topic in physical chemistry. It concerns itself with *measurement of rates of reactions proceeding under given conditions of temperature, pressure and concentration.* The study of this subject has been highly useful in determining the factors which influence rates of reactions as well as in understanding mechanisms of a number of chemical reactions. The experimental data have led to the development of the modern theories of chemical reactivity of molecules. The studies have also been useful in working out conditions for getting maximum yields of several industrial products.

Thermodynamics predicts that at room temperature hydrogen and oxygen react to form water, all the reactants being essentially converted into the product. But when we actually carry out the experiment we find that the reaction takes place so slowly that unless we are willing to wait indefinitely, practically no water results. On the other hand, experiment shows that N_2O_4 decomposes into NO_2 under atmospheric conditions almost instantaneously even though $-\Delta G°$, which is a measure of the spontaneity of a reaction, is far less for the decomposition of N_2O_4 than that for the reaction between hydrogen and oxygen to form water. These two examples suggest that there is essentially no correlation between thermodynamic instability and the rate of a chemical reaction. In fact, the rate of a reaction depends upon structural and energetic factors which are not uniquely specified by thermodynamic quantities such as the free energy change. Hence, chemical kinetics is a technique complimentary to thermodynamics for studying a given reaction.

Experimental Methods for Studying Kinetics of Reactions. The first stage in studying the rate and mechanism of a chemical reaction is the determination of the overall stoichiometry of the reaction and to identify any side-reaction. The next step involves the determination of the change of the concentrations of the reactant and product species with time. Since the reaction rate depends sharply on temperature (and for an elementary reaction doubles for every 10° rise in temperature), the temperature of the reacting mixture must be kept constant.

Several experimental techniques have been developed to monitor the concentrations of the reactants and the products and their variation with time. The selection of a typical method depends on the nature of the species involved and how rapidly their concentrations change. For reactions that are relatively slow, conductometric, potentiometric, optical methods, polarimetry and spectrophotometry are used.

For reactions in which one or more of the products are gases, the reaction rate involves monitoring pressure, as in the reaction :

$$N_2O_5(g) \longrightarrow 2NO_2(g) + \tfrac{1}{2}O_2(g)$$

The optical method involves monitoring optical activity, as for mutarotation of glucose :

$$\alpha\text{-D-glucose} \rightleftharpoons \beta\text{-D-glucose}$$

studied polarimetrically.

The specific rotation $[\alpha]_D^{20}$ of an optically active substance present in a solution is given by

$$[\alpha]_D^{20} = \frac{\text{Observed rotation (deg)}}{\text{Length (dm)} \times \text{density (g cm}^{-3})}$$

at 20°C in sodium *D* light.

For α-D-glucose, $[\alpha]_D^{20} = +112°$; for β-D-glucose, $[\alpha]_D^{20} = +19°$ and at equilibrium, it is 52·7°. Similarly, the inversion of sucrose to glucose and fructose can also be studied polarimetrically.

Reactions in solution involving ionic species may be studied by monitoring their conductivity. The change in EMF of an electrochemical reaction, as given by the Nernst equation, can be followed potentiometrically. Spectrophotometry, the measurement of the intensity of absorption in a particular spectral region, is widely used to monitor concentration. This technique is particularly useful when one substance in the reaction mixture has a strong characteristic absorption in a conveniently assessible region of the spectrum. Reactions that involve a change in the concentration of H^+ ions may be studied by monitoring the *p*H of the solution with a glass electrode.

Other methods of monitoring the composition include the detection of fluorescence and phosphorescence, mass spectrometry, gas chromatography and magnetic resonance (both NMR, *i.e.*, nuclear magnetic resonance, and EPR, *i.e.*, electron paramagnetic resonance, also called ESR, *i.e.*, electron spin resonance).

In a *real-time analysis*, the composition of the reaction mixture is analyzed while the reaction is in progress by direct spectroscopic observation. In the *quenching method*, the reaction is stopped after being allowed to proceed for a certain time and the composition is analyzed. The entire reaction mixture may be quenched either by sudden cooling or by adding it to a large volume of the solvent. This method is applicable for reactions that are slow enough so that there is very little reaction during the time it takes to quench the reaction mixture.

The *flow method* and the *stopped-flow method* involve mixing the reactants as they flow in a chamber; these have been discussed fully in this chapter. For fast reactions, the techniques of *flash photolysis* and *relaxation*, described in detail in this chapter, are used. Suffice it to mention here that in flash photolysis, the gaseous or liquid sample is exposed to a brief photolytic or photoactivating flash or UV radiation and then the contents of the reaction chamber are monitored spectrophotometrically. Lasers can be used to generate nanosecond, picosecond or femtoseeond flashes. The reaction can be monitored either by emission or absorption spectroscopy. In the relaxation technique, the reaction mixture, initially at equilibrium, is disturbed by rapidly changing the reaction conditions which involve either a sudden increase in temperature (as in a *temperature-jump* method) or a sudden increase in pressure (as in a *pressure-jump* method). The 'relaxation' of the system to equilibrium after the perturbation is monitored spectrophotometrically.

Thanks to the work of A.H. Zewail, the 1999 Chemistry Nobel Laureate, **femtochemistry** has emerged as the most exciting field for investigating extremely fast reactions whose time-scale is of the order of a femtosecond. In a typical pulse-probe experiment, a femtosecond pulse is used to excite a molecule to a dissociative state and then a second femtosecond probe pulse is fired at an interval after the dissociating pulse. The frequency of the probe is set at an absorption of one of the free fragmentation products, so its absorption is a measure of the abundance of the dissociation product.

Femtochemistry is extremely useful for studying biological processes such as the energy-converting processes of photosynthesis and the photostimulated processes of vision in which the primary energy and electron-transfer reactions occur on the femtosecond or picosecond time-scales.

Rates of Reactions. Consider a simple hypothetical reaction of the type

$$A \longrightarrow P$$

The rate of the reaction at any given time will depend upon the concentration of the reactant A at that time. As the reaction progresses, the concentration of A keeps on falling with time. The rate

of the reaction at any given instant is given by the expression

$$r = -dc_A/dt \qquad \ldots(1)$$

where $-dc_A$ is the infinitesimally small *decrease* in the concentration of A in an infinitesimally small interval of time dt, c_A gives the concentration of the reactant A at the given instant and k is a constant called the *rate constant* or *velocity constant* of the reaction.

The concentration of the product P goes on increasing with time. Hence, the rate of the reaction can also be expressed in terms of increase in concentration of the product P, as well. Thus,

$$r = dc_P/dt \qquad \ldots(2)$$

where dc_P is an infinitesimally small *increase* in the concentration of the product P in an infinitesimally small interval of time dt.

From Eqs. 1 and 2, $r = -dc_A/dt = dc_P/dt$ ...(3)

For a reaction of the type $A + B \longrightarrow L + M$,

the reaction rate can be expressed as

$$r = -dc_A/dt = -dc_B/dt = dc_L/dt = dc_M/dt \qquad \ldots(4)$$

Consider a general reaction of the type,

$$aA + bB + cC \longrightarrow lL + mM + pP$$

The rate of such a reaction is expressed in terms of fall in concentration of a reactant per mole or increase in concentration of a product per mole. Accordingly,

$$r = -\frac{1}{a}\frac{dc_A}{dt} = -\frac{1}{b}\frac{dc_B}{dt} = -\frac{1}{c}\frac{dc_C}{dt} = \frac{1}{l}\frac{dc_L}{dt} = \frac{1}{m}\frac{dc_M}{dt} = \frac{1}{p}\frac{dc_P}{dt} \qquad \ldots(5)$$

The Rate Law and the Rate Constant. The rate of the reaction : A ⟶ Products, is experimentally found to be given by

$$r = kc_A \qquad \ldots(\text{Eq. 1})$$

where k is the *rate constant* or the *velocity constant* of the reaction at the given temperature. If concentration of A is unity, *i.e.*, $c_A = 1$, then, evidently, $r = k$. For a general reaction of the type :

$$aA + bB + cC \longrightarrow \text{Products}$$

the rate of the reaction is given by the rate-law expression

$$r = kc_A^a c_B^b c_C^c \qquad \ldots(6)$$

If $c_A = c_B = c_C = 1$, then $k = r$. Thus, the **rate constant** of a reaction, in general, is defined as *the rate of the reaction when the concentration of each reactant is unity*.

The Order of a Reaction. In the study of chemical kinetics, reactions are generally classified in terms of their 'order'. We may define the **order of a reaction** as the sum of the powers to which the concentration (or pressure) terms are raised in the rate-law expression. Thus, a reaction is said to be of the **first order** if its rate is given by the expression of the type : $r = k_1 c_A$; of the **second order** if the rate is given by the expression of the type : $r = k_2 c_A^2$ or $r = k_2 c_A c_B$; of the **third order** if the rate is given by the expression of the type : $r = k_3 c_A^3$ or $r = k_3 c_A^2 c_B$ or $r = k_3 c_A c_B^2$ or $r = k_3 c_A c_B c_C$ and so on. For a **zero-order** reaction, the rate equation is written as $r = k_0$. It is to be noted that the order of a reaction is essentially an experimental quantity. Thus, the order of the general reaction given above may or may not be numerically equal to $a+b+c$.

The concentrations of the various species involved in a reaction such as c_A, c_B, c_L, c_M, etc., can also be expressed as [A], [B], [L], [M], etc.

Example 1. Write the differential rate equations for the following reactions, assuming them to be elementary reactions :

(a) $A + 2B + 3C \longrightarrow$ Products

(b) $A + 3B \longrightarrow 2C + D + 2E$

Solution : (a) Rate, $r = -d[A]/dt = -1/2\ d[B]/dt = -1/3\ d[C]/dt$

(b) Rate, $r = -d[A]/dt = -1/3\ d[B]/dt = 1/2\ d[C]/dt = d[D]/dt = 1/2\ d[E]/dt$

Example 2. The rate of the homogeneous gaseous reaction $2NO(g) + Cl_2(g) \longrightarrow 2NOCl(g)$ is doubled when the chlorine concentration is doubled but increases by a factor of eight when the concentrations of both the reactants are doubled. Determine the overall order of the reaction and the order with respect to NO and Cl_2.

Solution : Rate $= k[NO]^a[Cl_2]^b$ where we have to determine a and b.

If $a=0$ and $b=1$ (overall first-order), then $r = k_1[Cl_2]$

A little reflection will show that this is not at all acceptable.

If $a=1$, $b=1$ (overall second-order), then $r = k_2[NO][Cl_2]$

Doubling the concentration of both the reactants will increase the rate by a factor of 4, which is not given.

If $a=0$, $b=2$ (overall second-order), then $r = k_2[Cl_2]^2$

Doubling the concentration of Cl_2 will increase the rate by a factor of 4 which, too, is not given.

If $a=1$, $b=2$ (overall third-order), then $r = k_3[NO][Cl_2]^2$

Doubling the concentrations of both the reactants will, no doubt, increase the rate by a factor of 8 but doubling the concentration of Cl_2 alone will increase the rate by a factor of 4, which again, is not given. The other alternative for a third-order reaction is $a=2$, $b=1$ so that $r = k_3[NO]^2[Cl_2]$. We immediately see that this rate equation satisfies both the given conditions. Hence, **overall the reaction is of the third order, being of the second order in NO and of the first order in Cl_2.**

Example 3. At 1100 K, the following data were obtained on the homogeneous reaction :

$$2NO(g) + 2H_2(g) \longrightarrow N_2(g) + 2H_2O(g)$$

	[NO] (mol dm^{-3})	[H_2] (mol dm^{-3})	Rate, r (mol dm^{-3} s^{-1})
(1)	$5{\cdot}0\times10^{-3}$	$2{\cdot}5\times10^{-3}$	$3{\cdot}0\times10^{-5}$
(2)	$15{\cdot}0\times10^{-3}$	$2{\cdot}5\times10^{-3}$	$9{\cdot}0\times10^{-5}$
(3)	$15{\cdot}0\times10^{-3}$	$10{\cdot}0\times10^{-3}$	$36{\cdot}0\times10^{-5}$

(i) Calculate the order of the reaction with respect to NO, with respect to H_2 and the overall reaction order (ii) Write the rate law expression for the reaction (iii) Calculate the rate constant of the reaction (iv) What will be the rate of the reaction if $[NO]=[H_2]=8{\cdot}0\times10^{-3}$ mol dm^{-3} ?

Solution : (i) Let the rate law be represented as $r = k[NO]^a[H_2]^b$.

Comparing rows (1) and (2), we see that tripling [NO], keeping [H_2] constant, triples the rate so that $a=1$. Again, comparing rows (2) and (3), we see that increasing [H_2] 4 times, keeping [NO] constant, increases the rate 4 times. Since $a=1$, hence $b=1$. Thus, the reaction is of the first order with respect to both NO and H_2 and overall order$=1+1=2$. *i.e.*, the reaction is of the **second order.**

(ii) $r = k[NO][H_2]$

(iii) Using any set of data,

$$k = \frac{r}{[NO][H_2]} = \frac{3{\cdot}0\times10^{-5}\ \text{mol dm}^{-3}\ \text{s}^{-1}}{(5{\cdot}0\times10^{-3}\ \text{mol dm}^{-3})(2{\cdot}5\times10^{-3}\ \text{mol dm}^{-3})} = 2{\cdot}4\ \text{dm}^3\ \text{mol}^{-1}\ \text{s}^{-1}$$

(iv) $r = k[NO][H_2]$

$= (2{\cdot}4\ \text{dm}^3\ \text{mol}^{-1}\ \text{s}^{-1})(8{\cdot}0\times10^{-3}\ \text{mol dm}^{-3})(8{\cdot}0\times10^{-3}\ \text{mol dm}^{-3}) = 1{\cdot}536\times10^{-4}\ \text{mol dm}^{-3}\ \text{s}^{-1}$

Example 4. Consider the following data on the hypothetical reaction $2A + 2B \longrightarrow C + 3D$ between reactants A and B to give products :

	[A] (mol dm^{-3})	[B] (mol dm^{-3})	Rate, r (mol dm^{-3} s^{-1})
(1)	$6{\cdot}0\times10^{-3}$	$1{\cdot}0\times10^{-3}$	0·012
(2)	$6{\cdot}0\times10^{-3}$	$2{\cdot}0\times10^{-3}$	0·024
(3)	$2{\cdot}0\times10^{-3}$	$1{\cdot}5\times10^{-3}$	0·002
(4)	$4{\cdot}0\times10^{-3}$	$1{\cdot}5\times10^{-3}$	0·008

If the reaction rate is given by $r = [A]^a[B]^b$, then (i) what is the order of the reaction with respect to A ? (ii) What is the order of the reaction with respect to B ? (iii) What is the overall order ? (iv) Write the rate law equation (v) Calculate the rate constant.

Solution : Comparing rows (1) and (2), we see that doubling the concentration of B, keeping [A] constant, doubles the rate ; hence, $b=1$. Comparing rows (3) and (4), we find that doubling [A], keeping [B] constant, increases the rate four-fold. Since $b=1$, therefore, $a=2$. Thus, the reaction is

(i) of the **second order** with respect to A

(ii) of the **first order** with respect to B

(iii) the **overall order** $= 1 + 2 = 3$, *i.e.*, the reaction is of the **third order**

(iv) the rate law expression is $r = k[A]^2[B]$

(v) Using any set of the given data, we obtain

$$k = \frac{r}{[A]^2[B]} = \frac{0{\cdot}012\ \text{mol dm}^{-3}\ \text{s}^{-1}}{(6{\cdot}0\times10^{-3}\ \text{mol dm}^{-3})^2(1{\cdot}0\times10^{-3}\ \text{mol dm}^{-3})} = 3{\cdot}3\times10^5\ \text{dm}^6\ \text{mol}^{-2}\ \text{s}^{-1}$$

Units of Rate Constant. The units of rate constant for a given reaction can be determined by starting with the appropriate rate equation for the reaction, as is shown in the following examples.

Example 5. Staring from the full rate equation, determine the units of the rate constant k for (a) a zero-order reaction (b) a first-order reaction (c) a second-order reaction (d) a third-order reaction and (e) a half-order reaction. Assume that concentrations are expressed in molar units and time in seconds.

Solution : (a) Rate, $r = -d[A]/dt = k_0$

$$\therefore \quad \text{Units of } k_0 = \frac{\text{units of [A]}}{\text{units of } t} = \frac{\text{mol dm}^{-3}}{\text{s}} = \text{mol dm}^{-3}\ \text{s}^{-1}$$

It should be noted that units of $d[A]$, the change in concentration, are the same as those of [A]. Similarly, the units of dt are the same as those of t.

(b) Rate, $r = -d[A]/dt = k_1[A]$ or $k_1 = -\frac{1}{[A]} \times \frac{d[A]}{dt}$

$$\therefore \quad \text{Units of } k_1 = \frac{1}{\text{mol dm}^{-3}} \times \frac{\text{mol dm}^{-3}}{\text{s}} = \text{s}^{-1}$$

(c) (i) Rate, $r = -d[A]/dt = k_2[A]^2$ or $k_2 = -\frac{1}{[A]^2} \times \frac{d[A]}{dt}$

$$\therefore \quad \text{Units of } k_2 = \frac{1}{(\text{mol dm}^{-3})^2} \times \frac{\text{mol dm}^{-3}}{\text{s}} = \text{dm}^3\ \text{mol}^{-1}\ \text{s}^{-1}$$

(ii) Rate, $r = -d[A]/dt = k_2[A][B]$ or $k_2 = -\frac{1}{[A][B]} \times \frac{d[A]}{dt}$

$$\therefore \quad \text{Units of } k_2 = \frac{1}{(\text{mol dm}^{-3})^2} \times \frac{\text{mol dm}^{-3}}{\text{s}} = \text{dm}^3\ \text{mol}^{-2}\ \text{s}^{-1}$$

(d) Rate, $r = -d[A]/dt = k_3[A]^3$ or $k_3 = -\frac{1}{[A]^3} \times \frac{d[A]}{dt}$

$$\therefore \quad \text{Units of } k_3 = \frac{1}{(\text{mol dm}^{-3})^3} \times \frac{\text{mol dm}^{-3}}{\text{s}} = \text{dm}^6\ \text{mol}^{-2}\ \text{s}^{-1}$$

(e) Rate, $r = -d[A]/dt = k_{1/2}[A]^{1/2}$ or $k_{1/2} = -\frac{1}{[A]^{1/2}} \times \frac{d[A]}{dt}$

$$\therefore \quad \text{Units of } k_{1/2} = \frac{1}{(\text{mol dm}^{-3})^{1/2}} \times \frac{\text{mol dm}^{-3}}{\text{s}} = \text{mol}^{1/2}\ \text{dm}^{-3/2}\ \text{s}^{-1}$$

In general, for an ***nth-order reaction***, the units of k_n are $(\text{dm}^3)^{n-1}\ \text{mol}^{1-n}\ \text{s}^{-1}$

Example 6. Write the units of the rate constants for a *(i)* zeroth-order *(ii)* half-order *(iii)* first-order *(iv)* $\frac{3}{2}$-order *(v)* second-order *(vi)* $\frac{5}{2}$-order and *(vii)* third-order reaction.

Solution : The units of the rate constant for the *n*th-order reaction are given by $(\text{dm}^3)^{n-1}\ \text{mol}^{1-n}\ \text{s}^{-1}$.

(i) $n = 0$, the units are $\text{dm}^{-3}\ \text{mol}\ \text{s}^{-1}$

(ii) $n = 1/2$, the units are $(\text{dm}^3)^{-1/2}\ \text{mol}^{1/2}\ \text{s}^{-1}$

(iii) $n = 1$, the units are s^{-1}

(iv) $n = 3/2$, the units are $(\text{dm}^3)^{1/2}\ \text{mol}^{-1/2}\ \text{s}^{-1}$

(v) $n = 2$, the units are $\text{dm}^3\ \text{mol}^{-1}\ \text{s}^{-1}$

(vi) $n = 5/2$, the units are $(\text{dm}^3)^{3/2}\ \text{mol}^{-3/2}\ \text{s}^{-1}$

(vii) $n = 3$, the units are $\text{dm}^6\ \text{mol}^{-2}\ \text{s}^{-1}$

Integration of Rate Expressions

1. Integration of Rate Expression for First-Order Reactions

The differential rate expression for the first-order reaction, $A \longrightarrow P$ is given by

$$r = -dc_A/dt = dc_P/dt = kc_A \qquad \ldots(7)$$

Separating the variables, *i.e.*, bringing concentration terms on one side and the time on the other side, we get

$$-dc_A/c_A = k_1 dt \qquad \ldots(8)$$

Before performing the actual integration, let us first ascertain the limits of integration. Let the initial concentration at initial time $t=0$ be c_0. Subsequently, at any other time, t, the concentration will be c. On integration, we obtain

$$\int_{c_0}^{c} -dc_A/c_A = k_1 \int_0^t dt \qquad \ldots(9)$$

$$\therefore \quad [-\ln c_A]_{c_0}^{c} = k_1[t]_0^t$$

or $$-\ln(c/c_0) = k_1 t$$

or $$c = c_0 e^{-k_1 t} \qquad \ldots(10)$$

From Eq. 10, we can also write

$$k_1 = 1/t \ln c_0/c \qquad \ldots(11)$$

Eq. 11 gives the expression for the first-order rate constant, k_1.

Eq. 11 is usually written in another form. If initial concentration of the reactant is a and x moles of it react in time t, then the concentration of the reactant left behind at time t will be $a-x$. In such a case, $c_0 \propto a$ and $c \propto (a - x)$. Hence, Eq. 11 takes the form

$$k_1 = \frac{1}{t} \ln \frac{a}{a-x} \qquad \ldots(12)$$

Eq. 12 shows that the concentration of reactant in a first-order reaction decreases exponentially with time ; this is shown graphically in Fig. 1. The plot of ln c versus t is shown in Fig. 2.

For a first-order reaction, the concentration of the reactant decreases and that of the product increases exponentially with time, as illustrated in Fig. 3.

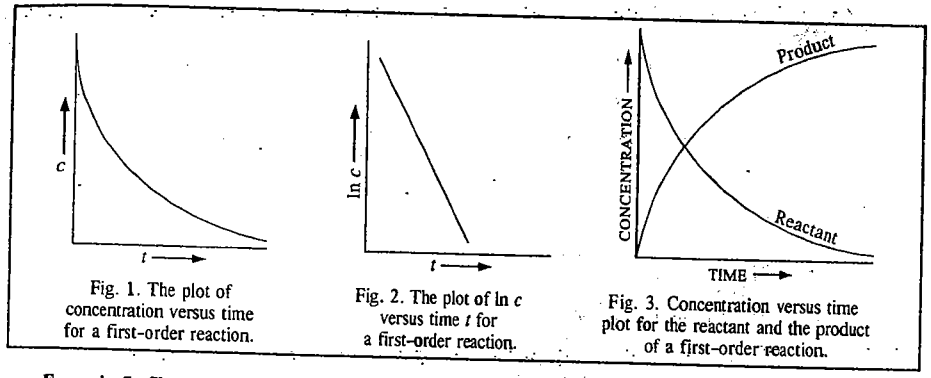

Fig. 1. The plot of concentration versus time for a first-order reaction.

Fig. 2. The plot of ln c versus time t for a first-order reaction.

Fig. 3. Concentration versus time plot for the reactant and the product of a first-order reaction.

Example 7. Show diagrammatically how the rate of a first-order reaction varies with concentration of reactant.

Solution : For a first-order reaction, $r = k_1[A]$

Hence the plot of rate versus [A] is a straight line passing through the origin, as shown in Fig. 4.

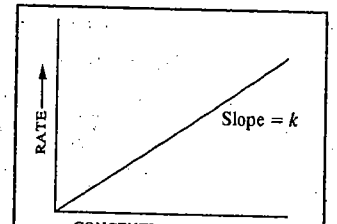

Fig. 4. The plot of rate *versus* reactant concentration for a first-order reaction.

The student should bear in mind that though Eq. 12 is easy to remember and use in simple numerical problems, it has to be expressed in appropriate form in certain decomposition reactions before the rate constants of those reactions can be determined. This is illustrated in various examples given below.

Example 8. Nitrous oxide, N_2O, decomposes into N_2 and O_2, the reactants and the products being all gaseous. If the reaction is first-order, develop expression for the rate constant as a function of time, initial pressure and the total pressure.

Solution : $N_2O(g) \longrightarrow N_2(g) + 1/2\ O_2(g)$

Let the initial pressure of N_2O be P_i. If x is the decrease in pressure after time t, then

$$p_{N_2O} = P_i - x, \quad p_{N_2} = x, \quad p_{O_2} = x/2$$

According to Dalton's law of partial pressures, the total pressure of the system at time t is given by

$$P = p_{N_2O} + p_{N_2} + p_{O_2} = (P_i - x) + x + x/2 = P_i + x/2$$

Hence, $$x = 2(P - P_i)$$

$$p_{N_2O} = P_i - x = P_i - 2(P - P_i) = 3P_i - 2P$$

Evidently, in the first-order rate equation (Eq. 12) applied here, $a \propto P_i$. Hence,

$$k_1 = \frac{1}{t} \ln \frac{P_i}{3P_i - 2P}$$

Example 9. The gas-phase thermal decomposition of one mole of di-tert-butyl peroxide, in a constant volume apparatus, yields two moles of acetone and one mole of ethane. If the reaction obeys first-order kinetics, develop expression for the rate-constant as a function of time, initial pressure and total pressure.

Solution : Stoichiometrically, we have

$$(CH_3)_3C{-}O{-}O{-}C(CH_3)_3 \longrightarrow 2(CH_3)_2C{=}O + C_2H_6$$

Let the initial pressure of the peroxide be P_i. If x is the decrease in pressure after time t, then the pressure of the peroxide at time t is $(P_i - x)$, that of acetone is $2x$ and that of ethane is x. Hence, from Dalton's law of partial pressures, the total pressure is given by

$$P = (P_i - x) + 2x + x = P_i + 2x$$

or $$x = (P - P_i)/2$$

The pressure of peroxide $= P_i - x = P_i - (P - P_i)/2 = (3P_i - P)/2$

Hence, $$k_1 = \frac{1}{t} \ln \frac{a}{a-x} = \frac{1}{t} \ln \frac{P_i}{(3P_i - P)/2} = \frac{1}{t} \ln \frac{2P_i}{(3P_i - P)}$$

Example 10. From the following data for the decomposition of ammonium nitrite in aqueous solution, show that the reaction is of the first order.

Time (minutes)	10	15	20	25	∞
Volume of N_2(c.c.)	6·25	9·00	11·40	13·65	35·05

Solution : For this reaction

$$k_1 = \frac{1}{t} \ln \frac{V_\infty}{V_\infty - V_t}; \quad V_\infty = 35{\cdot}05 = a$$

The values of k_1 at different times are obtained as follows :

Time	$V_\infty - V_t$	$\frac{1}{t} \ln \frac{V_\infty}{V_\infty - V_t} = k_1$
10 min	35·05 − 6·25 = 28·80	$\frac{1}{10} \ln \frac{35{\cdot}05}{28{\cdot}80} = 0{\cdot}01976\ \text{min}^{-1}$
15 min	35·05 − 9·00 = 26·05	$\frac{1}{15} \ln \frac{35{\cdot}05}{26{\cdot}05} = 0{\cdot}01976\ \text{min}^{-1}$
20 min	35·05 − 11·40 = 23·65	$\frac{1}{20} \ln \frac{35{\cdot}05}{23{\cdot}65} = 0{\cdot}01964\ \text{min}^{-1}$
25 min	35·05 − 13·65 = 21·40	$\frac{1}{25} \ln \frac{35{\cdot}05}{21{\cdot}40} = 0{\cdot}01971\ \text{min}^{-1}$

A constant value of k_1 shows that the reaction is of the first order.

Example 11. 5 ml of ethyl acetate was added to a flask containing 100 ml of 0·1 M HCl placed in a thermostat maintained at 30°C. 5 ml of the reaction mixture was withdrawn at different intervals of time and after chilling, titrated against a standard alkali. The following data were obtained :

Time (minutes)	0	75	119	183	∞
ml of alkali used	9·62	12·10	13·10	14·75	21·05

From the above data show that the hydrolysis of ethyl acetate is a first-order reaction.

Solution : The hydrolysis of ethyl acetate will be a first-order reaction if the above data conform to the equation

$$k_1 = \frac{1}{t} \ln \frac{V_\infty - V_0}{V_\infty - V_t}$$

where V_0, V_t and V_∞ represent the volumes of alkali used at the commencement of the reaction, after time t and at the end of the reaction, respectively. Hence

$$V_\infty - V_0 = 21{\cdot}05 - 9{\cdot}62 = 11{\cdot}43$$

The values of k_1 at different times are obtained as follows :

Time	$V_\infty - V_t$	$\frac{1}{t} \ln \frac{V_\infty - V_0}{V_\infty - V_t} = k_1$
75 min	21·05 − 12·10 = 8·95	$\frac{1}{75} \ln \frac{11{\cdot}43}{8{\cdot}95} = 0{\cdot}003259\ \text{min}^{-1}$
119 min	21·05 − 13·10 = 7·95	$\frac{1}{119} \ln \frac{11{\cdot}43}{7{\cdot}95} = 0{\cdot}003264\ \text{min}^{-1}$
183 min	21·05 − 14·75 = 6·30	$\frac{1}{183} \ln \frac{11{\cdot}43}{6{\cdot}30} = 0{\cdot}003254\ \text{min}^{-1}$

A constant value of k_1 shows that the hydrolysis of ethyl acetate is a **first-order** reaction.

Example 12. The optical rotations of sucrose in 0·5 M HCl at 35°C at various time intervals are given below. Show that the reaction is of the first order :

Time (minutes)	0	10	20	30	40	∞
Rotation (degrees)	+32·4	+28·8	+25·5	+22·4	+19·6	−11·1

Solution : The inversion of sucrose will be a first-order reaction if the above data conform to the equation

$$k_1 = \frac{1}{t} \ln \frac{r_0 - r_\infty}{r_t - r_\infty}$$

where r_0, r_t and r_∞ represent optical rotations at the commencement of the reaction, after time t and at the completion of the reaction, respectively.

In this case, $a_0 = r_0 - r_\infty = +32{\cdot}4 - (11{\cdot}1) = +43{\cdot}5$

The value of k_1 at different times are calculated as follows :

Time	r_t	$r_t - r_\infty$	$\frac{1}{t} \ln \frac{r_0 - r_\infty}{r_t - r_\infty} = k_1$
10 min	+28·8	39·9	$\frac{1}{10} \ln \frac{43{\cdot}5}{39{\cdot}9} = 0{\cdot}008625\ \text{min}^{-1}$
20 min	+25·5	36·6	$\frac{1}{20} \ln \frac{43{\cdot}5}{36{\cdot}6} = 0{\cdot}008625\ \text{min}^{-1}$
30 min	+22·4	33·5	$\frac{1}{30} \ln \frac{43{\cdot}5}{33{\cdot}5} = 0{\cdot}008694\ \text{min}^{-1}$
40 min	+19·6	30·7	$\frac{1}{40} \ln \frac{43{\cdot}5}{30{\cdot}7} = 0{\cdot}008717\ \text{min}^{-1}$

The constancy of k_1 indicates that the inversion of sucrose is a **first order** reaction.

Example 13. In a first-order reaction, it takes the reactant 40·5 minutes to be 25% decomposed. Calculate the rate constant of the reaction.

Solution : Since the reactant is 25% decomposed in 40·5 min, the remaining reactant is 75%, *i.e.*, at t=40·5 min, $(a - x) = 0{\cdot}75\ a$.

From Eq. 12, $$k_1 = \frac{1}{t} \ln \frac{a}{a-x} = \frac{1}{40{\cdot}5\ \text{min}} \ln \frac{a}{0{\cdot}75a} = 7{\cdot}11 \times 10^{-3}\ \text{min}^{-1}$$

Example 14. Show that for a first-order reaction, the time required for 99·9% completion of the reaction is 10 times that required for 50% completion.

Solution : From Eq. 12, $$t = \frac{1}{k_1} \ln \frac{a}{a-x}$$

$$\therefore \quad \frac{t(99{\cdot}9\%)}{t(50\%)} = \frac{\frac{1}{k_1} \ln \frac{100}{(100 - 99{\cdot}9)}}{\frac{1}{k_1} \ln \frac{100}{(100 - 50)}} = \frac{3{\cdot}00}{0{\cdot}3010} \approx 10$$

Example 15. During decomposition of N_2O_5 dissolved in carbon tetrachloride, at 35°C, the following results were obtained. Show that the reaction is of the first order.

Time (min)	0	40	80	100	160	240	∞
Volume of oxygen collected at constant pressure (c.c.)	0	15·6	27·6	7·7	45·8	58·3	84·6

Solution : The rate equation for the first-order reaction is

$$k_1 = \frac{1}{t} \ln \frac{a}{a-x}$$

The initial concentration of N_2O_5 in the solution = 84·6 - 0 = 84·6, *i.e.*, a = 84·6

The values of $(a - x)$ at different intervals of time are :

Time (min), t	40	80	120	160	240
$a - x$	69·0	57·0	46·9	36·8	26·3

Incorporating the values of t, a and $(a - x)$ in Eq. 12, the values of k_1 at different time intervals come out to be as follows :

Time (min)	40	80	120	160	240
k_1 per min	$5·03\times10^{-3}$	$4·94\times10^{-3}$	$4·92\times10^{-3}$	$5·02\times10^{-3}$	$4·87\times10^{-3}$

Since k_1 is fairly constant, the reaction is of the first order.

Example 16. The following data are obtained for the hydrolysis of benzene diazonium chloride :

$$C_6H_5N{=}N{-}Cl + H_2O \longrightarrow C_6H_5OH + HCl + N_2(g) :$$

Time (min)	0	2	8	16	24	50	∞
Pressure (p) of N_2 at constant volume (arbitrary units)	0	1·6	6·2	11·2	15·5	24·4	34·0

Assuming first-order kinetics, calculate the rate constant.

Solution : In this case, evidently, $a \propto (p_\infty - p_0) \propto 34·0$ and $(a - x) \propto (p_\infty - p_t)$

Time (min), t	2	8	16	24	50
$(a - x)$	32·4	27·8	22·8	18·5	9·6

$$k_1 = \frac{1}{t} \ln \frac{a}{a-x}$$

Incorporating the various values of t, a and $a - x$, in Eq. 12, we get the following values of k_1 at different intervals of time :

Time (min)	2	8	16	24	50
k_1 per min	$2·41\times10^{-2}$	$2·52\times10^{-2}$	$2·50\times10^{-2}$	$2·53\times10^{-2}$	$2·53\times10^{-2}$

The average value of rate constant thus comes out to be $2·498\times10^{-2}$ min^{-1}.

2. Integration of Rate Expressions for Second-Order Reactions.

The differential rate expressions for the second-order reactions are as follows :

Case I. When the Reactants are Different. Consider a second-order reaction

$$A + B \longrightarrow P$$

where the initial concentration of A is a mol dm^{-3} and that of B is b mol dm^{-3}. After time t, x mol dm^{-3} of A and x mol dm^{-3} of B react to form x mol dm^{-3} of the product. Thus, the reactant concentrations at time t are $(a - x)$ and $(b - x)$, respectively. The differential rate expression for the second-order reaction is, evidently,

$$r = -d[A]/dt = -d[B]/dt = d[P]/dt = k_2[A][B]$$

This can be written as $r = dx/dt = k_2(a - x)(b - x)$ ...(13)

where k_2 is the second-order rate constant. Separating the variables, we have

$$dx/(a - x)(b - x) = k_2 dt \quad ...(14)$$

Resolving into partial fractions (assuming that $a > b$), we have

$$\frac{1}{(a-x)(b-x)} = \frac{1}{a-b}\left[\frac{1}{b-x} - \frac{1}{a-x}\right] \quad ...(15)$$

Using this result, we can integrate Eq. 14 as follows :

$$\int \frac{dx}{(a-x)(b-x)} = \frac{1}{a-b}\left[\int \frac{dx}{b-x} - \int \frac{dx}{a-x}\right] = k_2 \int dt \quad ...(16)$$

We have taken the factor $1/(a - b)$ outside the integral sign because this quantity is a constant. Carrying out the integration, we have

$$\frac{1}{a-b}\left[-\ln(b-x) - \{-\ln(a-x)\}\right] = k_2 t + C$$

or
$$\frac{1}{a-b} \ln \left[\frac{a-x}{b-x}\right] = k_2 t + C \quad ...(17)$$

where C is the constant of integration. To determine C, we recall that at $t=0$, $x=0$. Hence, from Eq. 17,

$$C = \frac{1}{a-b} \ln \left(\frac{a}{b}\right) \quad ...(18)$$

Substituting this value of C in Eq. 17, we have

$$\frac{1}{a-b} \ln \left(\frac{a-x}{b-x}\right) = k_2 t + \frac{1}{a-b} \ln \left(\frac{a}{b}\right)$$

Rearranging and solving for k_2, we get

$$k_2 = \frac{1}{(a-b)t}\left[\ln\left(\frac{a-x}{b-x}\right) - \ln\left(\frac{a}{b}\right)\right] = \frac{1}{(a-b)t} \ln \frac{b(a-x)}{a(b-x)} \quad ...(19)$$

Eq. 19 is the required integrated expression for the rate constant of a second-order reaction. Here we have assumed that $a > b$. If we had assumed that $b > a$, then the reader can easily verify that

$$k_2 = \frac{1}{(b-a)t} \ln \frac{a(b-x)}{b(a-x)} \quad ...(20)$$

It can be easily seen that neither Eq. 19 nor Eq. 20 is applicable when the concentrations of both the reactants are the same, *i.e.*, when $a=b$.

If we write Eq. 19 in the form

$$\frac{1}{a-b} \ln \frac{b(a-x)}{a(b-x)} = k_2 t \quad ...(21)$$

we see that it is the equation of a straight line passing through the origin (*viz.*, $y=mx$), where

$$y \equiv \frac{1}{a-b} \ln \frac{b(a-x)}{a(b-x)} \; ; \; m \equiv k_2 \; ; \; x \equiv t$$

The plot of the left-hand side of Eq. 21 versus t gives a straight line (Fig. 5) whose slope is equal to the rate constant, k_2.

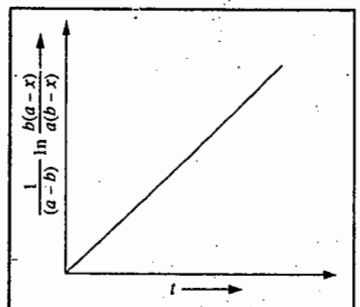

Fig. 5. Evaluation of rate constant for a second-order reaction.

Case II. When Both the Reactants are the Same. This, in effect, means that two molecules of the same reactant are involved in the chemical reaction. The second-order reaction in this case would be represented as

$$2A \longrightarrow P$$

and the rate of the reaction would be expressed as

$$r = dx/dt = k_2(a - x)^2 \qquad ...(22)$$

where, as before, a is the initial concentration of A, x is the concentration of the product formed after time t and $(a - x)$ is the concentration of A remaining at time t.

Separating the variables and integrating, we have

$$\int \frac{dx}{(a-x)^2} = k_2 dt \qquad ...(23)$$

$$\left[-\frac{1}{a-x}\right](-1) = k_2 t + C \quad \text{or} \quad \frac{1}{a-x} = k_2 t + C \qquad ...(24)$$

We know that at $t=0$, $x=0$ so that $C=1/a$. Hence,

$$\frac{1}{a-x} = k_2 t + \frac{1}{a}$$

Transposing and solving for k_2, we get

$$k_2 = \frac{1}{t}\left[\frac{1}{a-x} - \frac{1}{a}\right] = \frac{1}{t}\left[\frac{x}{a(a-x)}\right] \qquad ...(25)$$

which is the required integrated expression for the rate constant of a second-order reaction in which two molecules of the same reactant are involved in the reaction.

The classic example of the above type of the second-order reaction is the gaseous decomposition of hydrogen iodide.

$$2HI(g) \longrightarrow H_2(g) + I_2(g)$$

The rate expression for this reaction is

$$r = -d[HI]/dt = k_2[HI]^2$$

The plot of r versus reactant concentration is shown in Fig. 6.

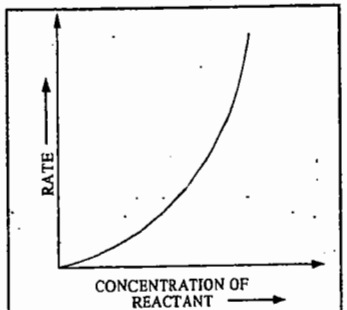

Fig. 6. The plot of *r versus* concentration for a second-order reaction.

The rate constants of second-order reactions in which the two reactants, although different, have the same initial concentration, are also determined with the help of Eq. 25.

Example 17. The following results were obtained for the saponification of ethyl acetate ($CH_3COOC_2H_5$ + NaOH $\longrightarrow$ CH_3COOH + C_2H_5OH) using equal concentrations of ester and alkali :

t (minutes)	**0**	**4·89**	**10·07**	**23·66**	**∞**
ml of acid used	**47·65**	**38·92**	**32·62**	**22·58**	**11·84**

Show that the reaction is of the second order.

Solution : The equation for the second order reactions, using equivalent concentrations of the reactants, is

$$k_2 = \frac{1}{t}\left[\frac{x}{a(a-x)}\right] \qquad \text{(Eq. 25)}$$

In the saponification of ethyl acetate, the volume of the acid used corresponds to the amount of unused sodium hydroxide. Therefore, the volume of acid used at zero time, *i.e.*, at the commencement of the reaction, corresponds to the initial concentration a and the volume used after time t corresponds to $(a - x)$ at that time.

In the present case, a = 47·65.

The value of k_2 is calculated as follows :

t	$a-x$	x	$\frac{1}{t}\left[\frac{a}{a(a-x)}\right] = k_2$(dm^3 mol^{-1} min^{-1})
4·89	38·92	8·73	$\frac{1}{4\cdot89} \times \frac{8\cdot73}{47\cdot65 \times 38\cdot92} = 0\cdot000962$
10·07	32·62	15·03	$\frac{1}{10\cdot07} \times \frac{15\cdot03}{47\cdot65 \times 38\cdot62} = 0\cdot000960$
23·66	22·58	25·07	$\frac{1}{23\cdot66} \times \frac{25\cdot07}{47\cdot65 \times 22\cdot58} = 0\cdot000983$

A fairly constant value of k_2 indicates that the reaction is of the second order.

Example 18. For the second-order reaction A + 3B $\longrightarrow$ P, where P stands for the product, the differential rate equation is $dx/dt = k_2(a - x)(b - 3x)$. Integrate this rate equation.

Solution : $dx/dt = k_2(a - x)(b - 3x)$ ...(*i*)

where a and b are the initial molar concentrations of A and B, respectively and x is the concentration of the product formed at time t so that the concentrations of A and B at time t are $(a - x)$ and $(b - 3x)$, respectively. Separating the variables in Eq. *(i)* and integrating, we get

$$\int \frac{dx}{(a-x)(b-3x)} = k_2 \int dt \qquad ...(ii)$$

Resolving into partial fractions, we get

$$\frac{1}{(a-x)(b-3x)} = \frac{1}{(3a-b)}\left[\frac{3}{b-3x} - \frac{1}{a-x}\right] \qquad ...(iii)$$

Hence, Eq. *(ii)* becomes

$$\int \frac{dx}{(a-x)(b-3x)} = \frac{1}{(3a-b)}\left[\int \frac{3dx}{b-3x} - \int \frac{dx}{(a-x)}\right] = k_2 t + C \qquad ...(iv)$$

where C is the constant of integration.

or $$\frac{1}{(3a-b)}\left[\frac{3}{-3}\ln(b-3x) - (-\ln(a-x)\right] = k_2 t + C \qquad ...(v)$$

or $$\frac{1}{(3a-b)}\left[\ln\left(\frac{a-x}{b-3x}\right)\right] = k_2 t + C \qquad ...(vi)$$

Since at $t=0$, $x=0$, we have from Eq. *(v)*,

$$\frac{1}{(3a-b)}\ln\left(\frac{a}{b}\right) = C$$

Substituting for C in Eq. *(vi)*, we obtain

$$\frac{1}{(3a-b)}\ln\left[\frac{a-x}{b-3x}\right] = k_2 t + \frac{1}{(3a-b)}\ln\left(\frac{a}{b}\right)$$

or $$\frac{1}{(3a-b)}\left[\ln\left(\frac{a-x}{(b-3x)}\right) - \ln\left(\frac{a}{b}\right)\right] = k_2 t \quad \text{or} \quad \frac{1}{(3a-b)}\ln\left[\frac{(a-x)/(b-3x)}{a/b}\right] = k_2 t$$

or $$\frac{1}{(3a-b)}\ln\left[\frac{b(a-x)}{a(b-3x)}\right] = k_2 t \qquad ...(vi)$$

This is the desired integrated rate equation.

3. Integration of Rate Expression for Third-Order Reactions

Let us consider a third-order reaction of the type

$$3A \longrightarrow P$$

Let a be the initial concentration of A and x the amount of A that has reacted at time t so that the amount of A remaining at time t is $a - x$. The differential rate equation is

$$r = \frac{dx}{dt} = k_3(a - x)^3 \qquad ...(26)$$

where k_3 is the third-order rate constant. Separating the variables and integrating, we get

$$\int \frac{dx}{(a-x)^3} = \int k_3 dt = k_3 \int dt$$

or $$\frac{1}{2(a-x)^2} = k_3 t + C \qquad ...(27)$$

To determine the integration constant, C, we know that at $t=0$, $x=0$ so that $C = 1/2\ a^2$.

Substituting in Eq. 27, transposing and solving for k_3, we get

$$k_3 = \frac{1}{2t}\left[\frac{1}{(a-x)^2} - \frac{1}{a^2}\right] = \frac{1}{2t}\left[\frac{x(2a-x)}{a^2(a-x)^2}\right] \qquad ...(28)$$

Example 19. For the third-order reaction $2A+B \longrightarrow P$, the differential rate equation is $dx/dt = k_3(a-2x)^2(b-x)$. Integrate this rate equation.

Solution : $$dx/dt = k_3(a-2x)^2(b-x) \qquad ...(i)$$

where a and b are the initial molar concentrations of A and B, respectively and x is the concentration of the product formed at time t so that at time t, the concentrations of A and B are $(a-2x)$ and $(a-x)$, respectively. Separating the variables in Eq. *(i)* and integrating, we get

$$\int \frac{dx}{(a-2x)^2(b-x)} = k_3 \int dt = k_3 t + C \qquad ...(ii)$$

where C is the constant of integration,

Resolving into partial fractions, we have

$$\frac{1}{(a-2x)^2(b-x)} = -\frac{2}{(2b-a)^2(a-2x)} + \frac{2}{(2b-a)(a-2x)^2} + \frac{1}{(2b-a)^2(b-x)} \qquad ...(iii)$$

Carrying out the integration of Eq. *(iii)*, making use of the above partial fractions, we obtain

$$\int \frac{dx}{(a-2x)^2(b-x)} = -\frac{2}{(2b-a)^2}\int \frac{dx}{a-2x} + \frac{2}{(2b-a)}\int \frac{dx}{(a-2x)^2} + \frac{1}{(2b-a)^2}\int \frac{dx}{b-x}$$

$$= -\frac{2}{(2b-a)^2}\left[-\frac{1}{2}\right]\ln(a-2x) - \frac{1}{(2b-a)^2}\ln(b-x) + \frac{2}{(2b-a)}\left[\frac{1}{a-2x}\right]\left[\frac{1}{2}\right]$$

$$= \frac{1}{(2b-a)^2}\ln(a-2x) - \frac{1}{(2b-a)^2}\ln(b-x) + \frac{1}{(2b-a)}\left[\frac{1}{a-2x}\right]$$

$$= \frac{1}{(2b-a)^2}\ln\left[\frac{a-2x}{b-x}\right] + \frac{1}{(2b-a)(a-2x)} = k_3 t + C \qquad ...(iv)$$

At $t=0$, $x=0$, so that from Eq. *(iv)*,

$$C = \frac{1}{(2b-a)^2}\ln(a/b) + \frac{1}{(2b-a)a} \qquad ...(v)$$

Substituting for C in Eq. *(iv)* and transposing, we have

$$\frac{1}{(2b-a)^2}\left\{\ln\left[\frac{(a-2x)/(b-x)}{a/b}\right] + (2b-a)\left[\frac{a-(a-2x)}{a(a-x)}\right]\right\} = k_3 t \qquad ...(vi)$$

or $$\frac{1}{(2b-a)^2}\left[\ln\frac{b(a-2x)}{a(b-x)} + \frac{(2b-a)(2x)}{a(a-2x)}\right] = k_3 t \qquad ...(vii)$$

This is the **desired integrated rate equation.**

4. Integration of Rate Expression for Zero-Order Reactions. Examples are known of reactions in which the reaction rate is not affected by changes in concentrations of one or more reactants. These are called zero-order reactions. In such reactions, the rate may be determined by some other limiting factor such as the amount of catalyst used in a catalytic reaction or the intensity of light absorbed in a photochemical reaction. Mathematically, for a zero-order reaction $A \longrightarrow P$,

$$r = -d[A]/dt = k_0 \qquad ...(29)$$

where k_0 is the rate-constant. Rearranging,

$$-d[A] = k_0 dt \qquad ...(30)$$

If at $t=0$, the initial concentration is $[A]_0$ and the concentration at $t=t$, is $[A]$, then, integration yields

$$-\int_{[A]_0}^{[A]} d[A] = k_0 \int_{t=0}^{t=t} dt$$

so that $$k_0 t = [A]_0 - [A]$$

or $$k_0 = 1/t\ ([A]_0 - [A]) \qquad ...(31)$$

Eq. 31 is the integrated rate equation for a zero-order reaction.

Half-Life Time of a Reaction

In order to characterize the rate at which a chemical reaction may proceed, it is customary to introduce a convenient parameter called the **half-life time** of the reaction. It is defined as *the time required for the reaction to be half completed* and is denoted by the symbol, $t_{1/2}$. It can be related to the corresponding rate constant.

1. $t_{1/2}$ for a First-Order Reaction. It follows from Eq. 12 that at $x=a/2$, $t=t_{1/2}$. Hence,

$$k_1 = \frac{1}{t_{1/2}}\ln\frac{a}{a-(a/2)} = \frac{1}{t_{1/2}}\ln 2 = \frac{0{\cdot}693}{t_{1/2}}$$

Thus, $$t_{1/2} = 0{\cdot}693/k_1 \qquad ...(32)$$

Example 20. The rate constant for a first-order reaction is $1{\cdot}54\times10^{-3}\ s^{-1}$. Calculate its half-life time.

Solution : Substituting the data directly in Eq. 32, we have

$$t_{1/2} = \frac{0{\cdot}693}{k_1} = \frac{0{\cdot}693}{1{\cdot}54\times10^{-3}\,s^{-1}} = 450\ s$$

Example 21. The half-life of the homogeneous gaseous reaction $SO_2Cl_2 \longrightarrow SO_2 + Cl_2$, which obeys first-order kinetics, is 8·0 minutes. How long will it take for the concentration of SO_2Cl_2 to be reduced to 1% of the initial value ?

Solution : From Eq. 32, by rearranging, we get

$$k_1 = \frac{0{\cdot}693}{t_{1/2}} = \frac{0{\cdot}693}{8{\cdot}0\ min} = 0{\cdot}087\ min^{-1}$$

For a first-order reaction, $k_1 = \frac{1}{t}\ln\frac{a}{a-x}$

or $$t = \frac{1}{k_1}\ln\frac{a}{a-x} = \frac{1}{0{\cdot}087\ min^{-1}}\ln\left(\frac{100}{1}\right) = 52{\cdot}93\ min$$

Example 22. In an enzyme solution, sucrose undergoes fermentation. If 0·10 M solution of sucrose is reduced to 0·05 M in 10 hours and to 0·025 M in 20 hours, what is the order of the reaction and what is the rate constant?

Solution : Since on doubling the time from 10 hours to 20 hours, fractional reduction of sucrose concentration is also doubled, the reaction must be of the first order.

Since for a first-order reaction, $t_{1/2} = 0{\cdot}693/k_1$, hence

$$k_1 = \frac{0{\cdot}693}{t_{1/2}} = \frac{0{\cdot}693}{10\times60\times60\,s} = 1{\cdot}9\times10^{-5}\ s^{-1}$$

Example 23. The inactivation of a viral preparation in a chemical bath is found to be a first-order reaction. *(a)* Calculate the rate constant for the viral inactivation if in the beginning 1·5% of the virus is inactivated per minute. *(b)* Also calculate the time required for 50% inactivation.

Solution : *(a)* The rate law for a first-order reaction is

$$-d[A]/dt = k_1[A] \quad \text{or} \quad k_1 = \frac{1}{[A]} \times \frac{d[A]}{dt}$$

For a finite, though small change, we can write

$$k_1 = -\frac{1}{[A]} \times \frac{\Delta[A]}{\Delta t}$$

Since in the beginning, [A] is not changing appreciably, we have

$$\Delta[A]/[A] = 1{\cdot}5\% \text{ (per minute)}$$

or $$k_1 = 0{\cdot}015/60 \text{ s} = \mathbf{2{\cdot}5\times10^{-4}\ s^{-1}}$$

(b) Since [A] changes appreciably during the reaction, the time for 50% inactivation, *i.e.*, $t_{1/2}$, is given by

$$t_{1/2} = \frac{0{\cdot}693}{k_1} = \frac{0{\cdot}693}{2{\cdot}5\times10^{-4}\,s^{-1}} = 2{\cdot}77\times10^3\,s = \mathbf{46{\cdot}17\ min}$$

$$\therefore \quad k_1 = \frac{1}{t}\ln\left[\frac{a}{a-x}\right] = \frac{1}{t}\ln\left[\frac{100}{100-80}\right] = \frac{1}{t}\ln 5$$

or $$t = \frac{\ln 5}{k_1} = \frac{1{\cdot}61}{2{\cdot}5\times10^{-4}\,s^{-1}} = 6{\cdot}44\times10^{-3}\ s = \mathbf{10{\cdot}7\ min}$$

Example 24. The radioactive decay of elements such as thorium and radon emitting alpha particles follows first-order kinetics. Calculate the number of alpha particles emitted per second by one gram of pure ThO_2 if the half-life of Th^{232} is $1{\cdot}39\times10^{10}$ years. The molar mass of ThO_2 is 264 g mol^{-1}.

Solution : $t_{1/2} = 0{\cdot}693/\lambda$

$$k_1 \equiv \lambda = \frac{0{\cdot}693}{t_{1/2}} = \frac{0{\cdot}693}{1{\cdot}39\times10^{10}\,yr} = \frac{0{\cdot}693}{(1{\cdot}39\times10^{10}\times365\times24\times3600)\,s} = 1{\cdot}58\times10^{-18}\ s^{-1}$$

The number of ^{232}Th atoms in 1 g of ThO_2,

$$N = 6{\cdot}022\times10^{23}\ mol^{-1}\times\frac{1\,g}{264\,g\,mol^{-1}} = 2{\cdot}28\times10^{21}$$

$$-dN/dt = \lambda N = (1{\cdot}58\times10^{-18}\ s^{-1})(2{\cdot}28\times10^{21}) = \mathbf{3{\cdot}60\times10^3\ s^{-1}}$$

This is the number of thorium nuclei disintegrating per second by the emission of alpha particles. Thus, the number of alpha particles emitted per second by 1 g of ThO_2 is $3{\cdot}60\times10^3$ or **3,600.**

2. $t_{1/2}$ for a Second-Order Reaction. From Eq. 25, we see that at $x=a/2$, $t=t_{1/2}$. Hence,

$$k_2 = \frac{1}{t_{1/2}}\left[\frac{a/2}{a(a-a/2)}\right] = \frac{1}{t_{1/2}} \times \frac{a/2}{a(a/2)} = \frac{1}{a\,t_{1/2}}$$

Thus, $$t_{1/2} = 1/(k_2 a) \qquad ...(33)$$

From Eq. 33, we find that $t_{1/2}$ of a second-order reaction is inversely proportional to the initial concentration of the reactant and, thus, it does not remain constant as the reaction proceeds.

Example 25. The rate constant for a second-order reaction is $3{\cdot}33\times10^{-2}$ $dm^3\ mol^{-1}\ s^{-1}$. If the initial concentration of the reactant is 0·05 mol dm^{-3}, calculate its half-life.

Solution : Substituting in Eq. 33, we have

$$t_{1/2} = \frac{1}{(3{\cdot}33\times10^{-2}\ dm^3\ mol^{-1}\ s^{-1})(5\times10^{-2}\ mol\ dm^{-3})} = 600\ s = \mathbf{10\ min}$$

Example 26. Derive an expression for the half-life of an *n*th-order reaction where $n \geq 2$.

Solution : An *n*th-order reaction may be represented as

$$nA \longrightarrow \text{Products}$$

The differential rate equation is

$$-d[A]/dt = k_n[A]^n \qquad ...(i)$$

where k_n is the *n*th-order rate constant.

Separating the variables and integrating, we obtain

$$\int -\frac{d[A]}{[A]^n} = k_n \int dt \qquad ...(ii)$$

or $$t = \frac{1}{k_n(n-1)[A]^{n-1}} + C \qquad ...(iii)$$

where C is the constant of integration which we have to determine.

Let $[A] = a$ and $[A]_0 = a_0$, the initial concentration. Then, Eq. *(iii)* can be written as

$$t = \frac{1}{k_n(n-1)a^{n-1}} + C \qquad ...(iv)$$

At $t=0$, $a=a_0$, so that $$C = \frac{1}{k_n(n-1)a_0^{n-1}} \qquad ...(v)$$

Substituting for C in Eq. *(iv)*, we get

$$t = \frac{1}{k_n(n-1)}\left[\frac{1}{a^{n-1}} - \frac{1}{a_0^{n-1}}\right] \qquad ...(vi)$$

When $t=t_{1/2}$, $a=a_0/2$ so that from Eq. *(vi)*,

$$t_{1/2} = \frac{1}{k_n(n-1)}\left[\frac{1}{(a_0/2)^{n-1}} - \frac{1}{a_0^{n-1}}\right] \qquad ...(vii)$$

or $$t_{1/2} = \frac{2^{n-1}-1}{k_n(n-1)a_0^{n-1}} \qquad ...(viii)$$

which is the desired expression. This expression shows that for an nth-order reaction, $t_{1/2} \propto (1/a_0)^{n-1}$ where $n \geq 2$.

Example 27. Show that the ratio $t_{1/2}/t_{3/4}$ for an *n*th-order reaction is a function of *n* alone.

Solution : Here $t_{1/2}$ is the half-life and $t_{3/4}$ is the three-quarter life (*i.e.*, time required for the reactant concentration to drop to 3/4 of its initial value). As shown in the last example, for the *n*th-order reaction, $nA \longrightarrow$ Products,

$$k_n t = \frac{1}{(n-1)}\left[\frac{1}{a^{n-1}} - \frac{1}{a_0^{n-1}}\right] \qquad \text{(Eq. } (vi) \text{ above)}$$

When $t=t_{1/2}$, $a=a_0/2$, so that

$$k_n t_{1/2} = \frac{1}{n-1}\left[\left(\frac{2}{a_0}\right)^{n-1} - \left(\frac{1}{a_0}\right)^{n-1}\right] = \frac{1}{n-1}\left(\frac{1}{a_0}\right)^{n-1}(2^{n-1}-1) \qquad ...(i)$$

Again, when $t=t_{3/4}$, $a=3a_0/4$, so that

$$k_n t_{3/4} = \frac{1}{n-1}\left[\left(\frac{4}{3a_0}\right)^{n-1} - \left(\frac{1}{a_0}\right)^{n-1}\right] = \frac{1}{n-1}\left(\frac{1}{a_0}\right)^{n-1}\left[\left(\frac{4}{3}\right)^{n-1} - 1\right] \qquad ...(ii)$$

Hence, from Eqs. *(i)* and *(ii)*,

$$\frac{t_{1/2}}{t_{3/4}} = \frac{2^{n-1}-1}{(4/3)^{n-1}-1} \qquad ...(iii)$$

From Eq. *(iii)* we see that **$t_{1/2}/t_{3/4}$ is a function of *n* alone.** This result can, in fact, be used for determining the order of a reaction.

3. $t_{1/2}$ for an nth-Order Reaction. In general, for an nth-order reaction, $nA \longrightarrow$ Products,

$$r = d[A]/dt = k_n[A]^n,$$

It has been shown in Example 26, that

$$t_{1/2} = \frac{2^{n-1} - 1}{k_n(n-1)a_0^{n-1}} \qquad ...(34)$$

where a_0 is the initial concentration of A and k_n is the nth-order rate constant. From Eq. 34 we see that

$$t_{1/2} \propto 1/a_0^{n-1} \qquad ...(35)$$

It is easy to see from Eq. 35 that for a first-order reaction ($n=1$), $t_{1/2}$ is independent of a_0, for a second-order reaction ($n=2$), $t_{1/2} \propto 1/a_0$, for a third-order reaction ($n=3$), $t_{1/2} \propto 1/(a_0)^2$, and so on.

Example 28. The $t_{1/2}$ of a reaction is halved as the initial concentration of the reacant is doubled. What is the order of the reaction ?

Solution : From Eq. 35, $t_{1/2} \propto 1/a_0^{n-1}$

In the present case, $\frac{1}{2}t_{1/2} = \frac{1}{(2a_0)^{n-1}}$

Hence, $\frac{t_{1/2}}{\frac{1}{2}t_{1/2}} = \frac{1/(a_0^{n-1})}{1/(2a_0)^{n-1}}$

or $2 = 2^{n-1}$ or $2^1 = 2^{n-1}$ so that

$n-1 = 1$ or $n = 2$

The reaction is of the second order.

Example 29. The $t_{1/2}$ of a reaction is doubled as the initial concentration of the reactant is doubled. What is the order of the reaction ?

Solution : Proceeding as in the last example,

$$\frac{t_{1/2}}{2t_{1/2}} = \frac{1/(a_0^{n-1})}{1/(2a_0)^{n-1}}$$

or $\frac{1}{2} = 2^{n-1}$ or $2^{-1} = 2^{n-1}$ or $n-1 = -1$ so that $n=0$

The reaction is of the zero order.

Example 30. The following data were obtained for the decomposition of a compound at 580°C :

a_0 (mol dm^{-3})	0·50	1·10	2·48
$t_{1/2}$ (s)	4280	885	174

Determine the order of the reaction and the rate constant.

Solution : From the tabulated data we see that the half-life, $t_{1/2}$, is not independent of the initial concentration, a_0. Hence, the reaction is not of the first order.

We know that for an nth-order reaction ($n \geq 2$),

$$t_{1/2} = \frac{2^{n-1} - 1}{k_n(n-1)a_0^{n-1}} \qquad \text{(Eq. 34)}$$

Taking logs, $\ln t_{1/2} = \ln\frac{2^{n-1} - 1}{k_n(n-1)} - (n-1)\ln a_0$

This is the equation of a straight line with slope $= -(n-1) = 1-n$.

From the given data, we obtain another data tabulated below :

$\ln t_{1/2}$	8·362	6·785	5·160
$\ln a_0$	−0·693	0·095	0·908

The reader can verify that the plot of $\ln t_{1/2}$ versus $\ln a_0$ gives a straight line with slope $= -1·99 = 1-n$ so that $n = 2·99$ which, rounded off to the next nearest digit, gives $n=3$. Thus, the given reaction is of the **third order.**

Now, for a third-order reaction,

$$t_{1/2} = \frac{3}{2k_3a_0^2} \quad \text{or} \quad k_3 = \frac{3}{2t_{1/2}a_0^2}$$

For one set of the given data, *i.e.*, for $a_0 = 0·5$ mol dm^{-3} and $t_{1/2} = 4{,}280$ s

$$k_3 = \frac{3}{2(4{,}280\text{ s})(0·50\text{ mol dm}^{-3})^2} = 1·40\times10^{-3}\text{ dm}^6\text{ mol}^{-2}\text{ s}^{-1}$$

METHODS FOR DETERMINING THE ORDER OF A REACTION

The order of a reaction is never known before hand, though majority of reactions are of the first or of the second order. The following methods are commonly used for determining the order of a reaction.

1. The Use of Differential Rate Expressions. According to this method, which was devised by van't Hoff, the rate of an nth-order reaction is given by

$$r = k_n c^n \qquad ...(36)$$

Taking logs, we have

$$\ln r = \ln k_n + n \ln c . \qquad ...(37)$$

Thus, if the double-logarithmic plot of rate versus concentration gives a straight line, then the slope gives the value of n and the intercept gives $\ln k_n$ (Fig. 7).

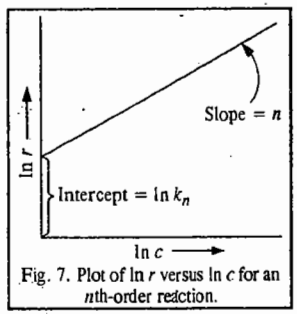

Fig. 7. Plot of $\ln r$ versus $\ln c$ for an nth-order reaction.

Also, if r_1 and r_2 are the rates at two different reactant concentrations c_1 and c_2, then

$$\frac{r_1}{r_2} = \frac{-dc_1/dt}{-dc_2/dt} = \frac{k_n c_1^n}{k_n c_2^n} = \left(\frac{c_1}{c_2}\right)^n$$

Taking logs, $\ln\frac{r_1}{r_2} = n\ln\frac{c_1}{c_2}$ whence $n = \frac{\ln(r_1/r_2)}{\ln(c_1/c_2)}$ ...(38)

2. The Use of Integral Rate Expressions. We have already demonstrated this method in solving problems for reactions of various orders. This method can be used either analytically or graphically. In the analytical method, we assume a certain order for the reaction and calculate the rate constants from the given data. The constancy of the k-values obtained suggests that the assumed order is correct. If the k-values obtained are not constant, we assume a different order for the reaction and again calculate the k-values using the new rate expression and see if k is constant.

In the graphical method, if the plot of $\ln c$ versus t is a straight line, the reaction is of the first order. Similarly, the integrated expression for the second-order reaction can be utilized graphically to ascertain if the reaction is of the second order, and so on.

3. The Half-life Method. We have shown above that, provided all reactants are present in the same molar concentrations, the half-life, $t_{1/2}$, of an nth-order reaction is given by Eq. 35.

If two experiments are carried out at different initial molar concentrations, then

$$\frac{(t_{1/2})_1}{(t_{1/2})_2} = \left(\frac{a_2}{a_1}\right)^{n-1} \quad \text{or} \quad \ln\frac{(t_{1/2})_1}{(t_{1/2})_2} = (n-1)\ln\frac{a_2}{a_1}$$

or $$n = 1 + \frac{\ln(t_{1/2})_1/\ln(t_{1/2})_2}{\ln(a_2/a_1)} \qquad ...(39)$$

This method was suggested by Ostwald. The determination of half-lives of a reaction at two different initial concentrations leads to the determination of n.

4. Isolation Method. Sometimes the kinetics of a reaction are studied in successive experiments by keeping the concentrations of all but one reactant in large excess so that the result gives the order with respect to the reactant whose concentration is changing significantly. Thus, the synthesis of HI from H_2 and I_2 is pseudo first-order with respect to H_2 in the presence of large excess of I_2 and also pseudo first order with respect to I_2 in the presence of large excess of H_2. Hence, overall it is a second order reaction.

Molecularity of a Reaction

The molecularity of a reaction should not be confused with its order. **Molecularity of a reaction** is defined as the number of molecules involved in the step leading to the chemical reaction. If only one molecule is involved, the reaction is said to be unimolecular. The example is the dissociation of nitrogen pentoxide :

$$N_2O_5(g) \longrightarrow N_2O_4(g) + (1/2)O_2(g)$$

If *two* molecules are involved, the reaction is said to be bimolecular.

$$2HI(g) \longrightarrow H_2(g) + I_2(g)$$

Similarly, if three molecules are involved, the reaction is said to be trimolecular. The example is the oxidation of nitric oxide :

$$2NO(g) + O_2(g) \longrightarrow 2NO_2(g)$$

Order and Molecularity of Simple Reactions. From a study of the kinetics of a number of *simple reactions*, we conclude that their order is the same as their molecularity. Thus, the order of the reaction involving the decomposition of nitrogen pentoxide is 1, that of the reaction involving the dissociation of hydrogen iodide is 2 and that of the reaction involving combination of nitric oxide and oxygen is 3.

But, this is not always the case. In several reactions, the order is different from molecularity. This is particularly so when one of the reactants is present in large excess. The examples are hydrolysis of ethyl acetate and inversion of cane sugar in aqueous solutions :

$$CH_3COOC_2H_5 + H_2O \xrightarrow{H^+} CH_3COOH + C_2H_5OH$$

(large excess)

$$\underset{\text{Sucrose}}{C_{12}H_{22}O_{11}} + \underset{\text{(large excess)}}{H_2O} \xrightarrow{H^+} \underset{\text{Glucose}}{C_6H_{12}C_6} + \underset{\text{Fructose}}{C_6H_{12}O_6}$$

The molecularity of each reaction is 2. The order of each reaction, however, is 1 since we know from experiment that the rate of the reaction varies directly as the concentration of ethyl acetate in the first case and that of sucrose in the second case. The reason is that water is present in such a large excess that its concentration (*i.e.*, the number of moles per litre) remains almost constant in the course of the reaction in each case. The rate of the reaction, therefore, varies only with the concentration of the ester in the first case and that of sucrose in the second case. Such reactions are known as **pseudo-monomolecular reactions.**

How, during the hydrolysis of ethyl acetate, the concentration of water remains almost constant, will be clear from the following discussion.

Suppose a decimolar solution of ethyl acetate undergoes complete hydrolysis. Evidently, 0·1 mole of the ester reacts with 0·1 mole of water to give 0·1 mole of acetic acid and 0·1 mole of ethanol. The concentrations of various species before and after hydrolysis will thus be as shown below :

Concentrations before hydrolysis		0·1 mol dm^{-3}		1000 g dm^{-3}/18 g mol^{-1} = 55·5 mol dm^{-3}		0	0
	$CH_3COOC_2H_5$	+	H_2O	$\longrightarrow$	CH_3COOH	+	C_2H_5OH
Concentrations after hydrolysis	0		55·4 mol dm^{-3}		0·1 mol dm^{-3}		0·1 mol dm^{-3}

As is evident, on the completion of the reaction, the concentration of the ester falls from 0·1 mol dm^{-3} to zero while the concentration of water falls from 55·5 mol dm^{-3} to 55·4 mol dm^{-3}. This is obviously a negligible change in comparison. In other words, the concentration of water practically remains constant.

Order and Molecularity of Complex Reactions. Many reactions are known to occur in two or more steps. Such reactions, from the point of view of chemical kinetics, are often termed as **complex reactions.** *Each step of the reaction, however, is a simple reaction, i.e., an elementary reaction.* Each elementary reaction has its own molecularity depending upon the number of molecules of the reactant or reactants taking part in that reaction. Consider a hypothetical reaction

$$3A + 2B \longrightarrow P + Q$$

taking place in four steps as shown below :

1.	A + B	$\longrightarrow$	C + D
2.	A + C	$\longrightarrow$	E
3.	A + D	$\longrightarrow$	F
4.	E + F + B	$\longrightarrow$	P + Q
	3A + 2B	$\longrightarrow$	P + Q

Each step represents an elementary reaction. The rates of the various elementary reactions generally differ from one another. Let the first elementary reaction be the slowest. The rate of the overall reaction, evidently, cannot be faster than the rate of the slowest reaction.

The rate of reaction (1), which is supposed to be the slowest, is given by

$$r = -dc_A/dt = -dc_B/dt = k[A][B]$$

This is also the rate of the overall reaction. The order of the slowest reaction and, therefore, the order of the overall reaction will be 2.

The molecularity of the slowest reaction, *i.e.*, the first elementary reaction, is also 2. The molecularity of the succeeding reactions is 2, 2 and 3, respectively.

The **order of a complex reaction** is given by the order of the slowest step in the sequence of various steps involved in that reaction. The **molecularity of a complex reaction** as such, however, has no significance. Each step (elementary reaction) involved in the complex reaction has its own value. This is given by the number of molecules of the reactant or reactants taking part in that particular step of the overall reaction. The molecularity of the slowest step is the same as the order of the overall reaction.

Mechanisms of Complex Reactions

Most of the elementary reactions are classified as unimolecular and bimolecular. This classification is generally possible for gaseous reactions only. Complex reactions proceed in a number of steps, each step having its own molecularity.

After the reaction has been found to be complex, we naturally want to know what is its mechanism? To find answer to this question the kineticist obtains kinetic data on it and then suggests a mechanism for the rate law which is consistent with the kinetic data.

In dealing with the progress and mechanism of a chemical reaction we speak of such concepts as the '*reaction coordinate*' and the '*activated complex*'. We shall deal with these concepts in detail a little later in this chapter when we discuss the theories of reaction rates. Suffice it to remark here that the reaction coordinate, though it cannot be explicitly defined, is a function of all the coordinates in space of all species taking part in a reaction. It is a measure of the progress of a given reaction along the path of minimum potential energy at any instant, beginning with the reactant molecules and terminating in the product molecules. At a point where the reaction coordinate has the maximum potential energy is located the activated complex. At this point, the reactants have maximum energy of mutual repulsion.

Two approximations are generally used for elucidating the mechanism of a complex reaction. These are : 1. *The Equilibrium Approximation* and 2. *The Steady State Approximation.* We shall deal with both of them briefly.

1. The Equilibrium Approximation. Consider a reaction in which reactant R gives rise to product P through the formation of a series of consecutive intermediates I_1, I_2, I_3, ..., I_n, as follows:

$$R \xrightarrow{k_0} I_1 \xrightarrow{k_1} I_2 \xrightarrow{k_2} I_3 \xrightarrow{k_3} \cdots\cdots\cdots \xrightarrow{k_{n-1}} I_n \xrightarrow{k_n} P$$

The whole reaction sequence may be described in terms of a single reaction coordinate composing the coordinates of the individual steps, as illustrated in Fig. 8. The intermediates are supposed to be stable, occupying points on the energy valley.

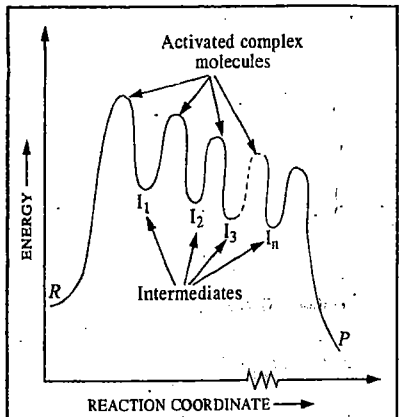

Fig. 8. Energy *versus* reaction coordinate profile for a complex reaction.

In order to derive the rate equation for the reaction, we assume that a rate-determining step exists. *This rate-determining step is the slowest in a sequence of steps.* It is further assumed that all the steps preceding the rate-determining step are in equilibrium, that is,

$$R \underset{}{\overset{K_0}{\rightleftharpoons}} I_1 \overset{K_1}{\rightleftharpoons} I_2 \overset{K_2}{\rightleftharpoons} \cdots \overset{K_{n-1}}{\rightleftharpoons} I_n \overset{K_n}{\rightleftharpoons} P$$

where the K_is are the various equilibrium constants.

2. The Steady State Approximation. In a case where the reactions are investigated under such conditions that the slowest rate-determining step does not exist, one assumes the *steady state approximation* (*s.s.a*) for the transient, *i.e.*, short-lived, intermediate. In such a mechanism, as shown below

$$R \xrightarrow{k_0} I_1 \xrightarrow{k_1} I_2 \xrightarrow{k_2} I_3 \xrightarrow{k_3} \cdots\cdots \xrightarrow{k_{n-1}} I_n \xrightarrow{k_n} P,$$

the rate of formation of an intermediate is equal to the rate of its decomposition so that

$$\frac{d[I_1]}{dt} = \frac{d[I_2]}{dt} \cdots\cdots = \frac{d[I_n]}{dt} = 0$$

Collisions and Encounters. In reactions occurring in liquids and solids, a molecule A in a condensed medium is surrounded by a 'cage' of other molecules, usually the solvent molecules. It continually bumps into the molecules which constitute the walls of the cage. This is known as the **cage effect** or **Franck–Rabinovich effect.** We express it by saying that the molecule A is undergoing diffusion (jumping) from one solvent cage to another where it may encounter another molecule B and react with it. Thus, while we speak of collisions between molecules in gaseous phase, we speak of 'encounters' between molecules in condensed phases. We, therefore, replace the word 'collision' by the term 'encounter' for reactions in liquids and solids. Because of the cage effect, there is no clear distinction between uni, bi and tri-molecular reactions in condensed phases.

Investigation of the mechanism of chemical reactions is an area of research which is both fascinating and frustrating. There is no last word about a reaction mechanism. In the words of the eminent kineticist, K.J. Laidler, "If evidence points towards a particular mechanism, it is always possible to devise a more complicated mechanism that is equally consistent with the facts. In view of this, one must accept the simplest mechanism that is consistent with all of the evidence that is available at a given time."

Example 31. The gaseous decomposition of ozone, $2O_3 \longrightarrow 3O_2$, obeys the rate law, $r = -d[O_3]/dt = k[O_3]^2/[O_2]$. Show that the following mechanism is consistent with the above rate law :

$$O_3 \underset{}{\overset{K}{\rightleftharpoons}} O_2 + O \qquad \text{(fast equilibrium)}$$

$$O + O_3 \xrightarrow{k_1} 2O_2 \qquad \text{(slow)}$$

Solution : From the slow rate-determining step,

$$r = -d[O_3]/dt = k_1[O][O_3]$$

From the fast equilibrium step,

$$K = [O_2][O]/[O_3] \quad \text{or} \quad [O] = K[O_3]/[O_2] \qquad \ldots(i)$$

Substituting for [O] in the expression for r, we have

$$r = k_1K[O_3]^2/[O_2] = k[O_3]^2/[O_2]$$

where $k = k_1K$.

Thus, the given mechanism is consistent with the rate law.

Example 32. For the thermal decomposition of ozone to oxygen, the following mechanism has been suggested:

Step 1. $O_3 \underset{k_{-1}}{\overset{k_1}{\rightleftharpoons}} O_2 + O$; **Step 2.** $O_3 + O \xrightarrow{k_2} 2O_2$

Use steady state approximation (s.s.a.) and other suitable approximation to account for the observed rate-law, *viz.*, $r = -k[O_3]^2/[O_2]$

Solution : Ozone decomposes in steps 1 and 2 and is formed in the reverse of step 1. Hence,

$$r = d[O_3]/dt = -k_1[O_3] + k_{-1}[O_2][O] - k_2[O_3][O]$$

Using *s.s.a.* for the O atom which is the transient (short-lived) intermediate, we have

$$d[O]/dt = k_1[O_3] - k_{-1}[O_2][O] - k_2[O_3][O] = 0$$

$$\therefore \quad k_1[O_3] = \{k_{-1}[O_2] + k_2[O_3]\}[O]$$

or

$$[O] = \frac{k_1[O_3]}{k_{-1}[O_2] + k_2[O_3]}$$

Substituting for [O] in the rate expression, we have

$$r = -k_1[O] + \frac{k_1k_{-1}[O_2][O_3]}{k_{-1}[O_2] + k_2[O_3]} - \frac{k_1k_2[O_3]^2}{k_{-1}[O_2] + k_2[O_3]}$$

$$= \frac{-k_1k_{-1}[O_2][O_3] - k_1k_2[O_3]^2 + k_1k_{-1}[O_2][O_3] - k_1k_2[O_3]^2}{k_{-1}[O_2] + k_2[O_3]}$$

The first and the third terms in the numerator of this equation cancel and the second and fourth terms are added algebraically giving

$$r = -\frac{2k_1k_2[O_3]^2}{k_{-1}[O_2] + k_2[O_3]} \qquad \ldots(ii)$$

If we make a further approximation that in the above equation $k_{-1}[O_2] >> k_2[O_3]$, then, the second term in the denominator is dropped to give

$$r = -\frac{2k_1k_2[O_3]^2}{k_{-1}[O_2]} = -k\frac{[O_3]^2}{[O_2]}$$

which agrees with the observed rate law where $k = 2k_1k_2/k_{-1}$.

Example 33. The rate law for the decomposition of gaseous N_2O_5, $N_2O_5 \longrightarrow 2NO_2 + 1/2O_2$ is observed to be $r = -d[N_2O_5]/dt = k[N_2O_5]$. A reaction mechanism which has been suggested to be consistent with this rate law is

$$N_2O_5 \underset{}{\overset{K}{\rightleftharpoons}} NO_2 + NO_3 \qquad \text{(fast equilibrium)}$$

$$NO_2 + NO_3 \xrightarrow{k_1} NO_2 + NO + O_2 \qquad \text{(slow)}$$

$$NO + NO_3 \xrightarrow{k_2} 2NO_2 \qquad \text{(fast)}$$

(a) Show that the mechanism is consistent with the observed rate law.

(b) If $k = 5\times10^{-4}$ s^{-1}, calculate the time required for the N_2O_5 concentration to be reduced to 10% of its original value.

Solution : (a) Since the slow step is the rate-determining step, hence

$$r = k_1[NO_2][NO_3] \qquad ...(i)$$

However, from the fast equilibrium step,

$$K = [NO_2][NO_3]/[N_2O_5] \quad \text{or} \quad [NO_2][NO_3] = K[N_2O_5] \qquad ...(ii)$$

Substituting in Eq.(*i*), we have

$$r = k_1K[N_2O_5] = k[N_2O_5] \quad \text{where } k = k_1K.$$

This shows that the mechanism is **consistent** with the observed rate law.

(*b*) From the equation for the first-order reaction,

$$t = \frac{1}{k}\ln\frac{a}{a-x} = \frac{1}{5\times10^{-4}\,s^{-1}}\ln\left(\frac{100}{100-90}\right) = \frac{1}{5\times10^{-4}\,s^{-1}}\ln 10 = 4{\cdot}6\times10^{3}\text{ s}$$

Example 34. Suggest a probable mechanism for the following oxidation-reduction reaction in aqueous solution : $Hg_2^{2+} + Tl^{3+} \longrightarrow 2Hg^{2+} + Tl^{+}$, which is consistent with the rate law $r = k[Hg_2^{2+}][Tl^{3+}]/[Hg^{2+}]$

Solution : A probable mechanism is as follows :

(*i*) $Hg_2^{2+} \underset{k'}{\overset{K}{\rightleftharpoons}} Hg^{2+} + Hg$ (fast equilibrium)

(*ii*) $Hg + Tl^{3+} \xrightarrow{k'} Hg^{2+} + Tl^{+}$ (slow)

From Eq. (*ii*), $r = k'[Hg][Tl^{3+}]$

From Eq. (*i*), $K = [Hg^{2+}][Hg]/[Hg_2^{2+}]$ or $[Hg] = K[Hg_2^{2+}]/[Hg^{2+}]$

Hence, substituting in rate equation, we have

$$r = k'K[Hg_2^{2+}]/[Tl^{3+}]/[Hg^{2+}]$$

which satisfies the observed rate law with $k = k'K$.

The reader will notice a puzzling thing in the given rate law. It predicts that at the start of the reaction when $[Hg^{2+}]=0$, $r=\infty$, which is absurd. However, it is to be remembered that the rate law does not hold in the beginning but only after the equilibrium has been established.

Effect of Temperature on Reaction Rates

It is a common experience that increase of temperature has a marked effect on the rate of a chemical reaction. The ratio of the rate constants of a reaction at two temperatures differing by 10°C is known as the **temperature coefficient** of the reaction. The temperatures usually selected for this purpose are 25° and 35°C. Thus,

$$\textbf{Temperature coefficient} = \frac{\text{Rate constant at 35° C}}{\text{Rate constant at 25° C}} = \frac{k_{35}}{k_{25}} \qquad ...(40)$$

The value of the temperature coefficient for most of the reactions is close to 2 and in some cases it approaches even 3.

Why such a small rise of temperature speeds up a reaction to such a large extent can be explained on the basis of the **collision theory.** According to this theory, for chemical reactions to occur, there *must* be collisions between the reactant molecules. However, most of the collisions taking place between the molecules are *ineffective*. The important postulate of the collision theory is that *only those collisions result in chemical reaction in which the colliding molecules are associated with a certain minimum energy called the* **threshold energy**.

Arrhenius used the Maxwell's distribution of molecular energies to explain the temperature-dependence of reaction rates.

As the temperature increases from T_1 to T_2, the energy distribution undergoes a change (Fig. 9). There is a general shift in the distribution of energies as shown in the figure. Now there are more molecules on the high side of kinetic energy. The number of molecules whose energies are equal to or greater than the threshold energy E at temperature T_1 is represented by the shaded area *efcd* and at temperature T_2 by the shaded area *abcd*. As can be seen, the shaded area *abcd* is nearly *twice* the shaded area *efcd*. This means that the number of molecules having energy equal to or greater than the threshold energy (whose collisions result in chemical reaction) becomes nearly double even with a small increase of temperature from T_1 to T_2. Consequently, the rate of reaction which depends upon the number of effective collisions, becomes almost double with a small increase of temperature.

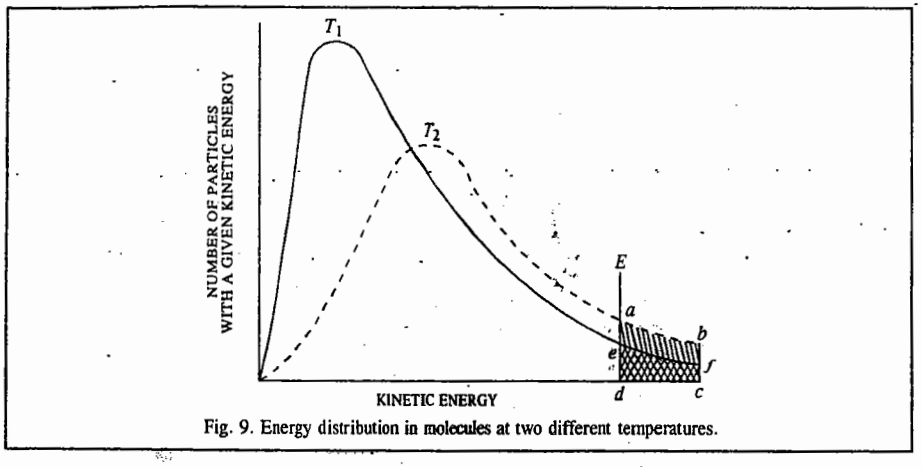

Fig. 9. Energy distribution in molecules at two different temperatures.

As discussed above, there is a certain minimum energy (threshold energy) which the colliding molecules must acquire before they are capable of reacting. Most of the molecules, however, have much less kinetic energy than the threshold energy. The excess energy that the reactant molecules having energy less than the threshold energy must acquire in order to react to yield products is known as **activation energy**. Thus,

Activation Energy = Threshold energy - Energy actually possessed by molecules

It follows from the above discussion that there is an **energy barrier** placed between reactants *and products* (Fig. 10). This barrier has to be crossed before reactants can yield products. This barrier determines the magnitude of threshold energy which reactant molecules must acquire before they can yield products.

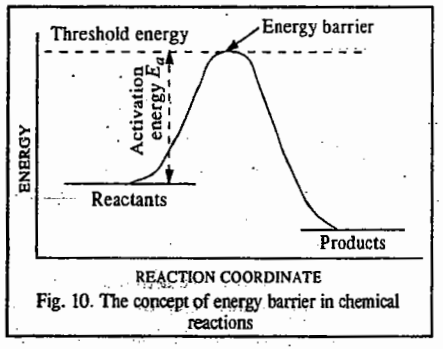

Fig. 10. The concept of energy barrier in chemical reactions

Effect of a Catalyst. A catalyst is a substance that *can increase the rate of a reaction but which itself remains unchanged in amount and chemical composition at the end of the reaction*. When a catalyst is added, a new reaction path with a lower energy barrier is provided (cf. dotted curve in Fig. 11). Since the energy barrier is reduced in magnitude, a larger number of molecules of the reactants can get over it. This increases the rate of the reaction.

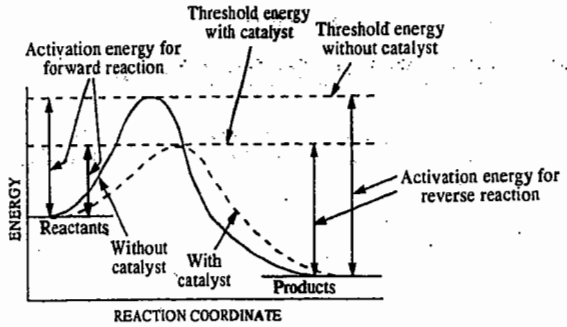

Fig. 11. Effect of catalyst on the rate of reaction.

A catalyst does not alter the position of equilibrium in a reversible reaction. It simply hastens the approach of the equilibrium by speeding up both the forward and the backward reactions.

Arrhenius Equation. Arrehenius proposed the following empirical equation for calculating the energy of activation of a reaction having rate constant k at temperature T :

$$k = A\,e^{-E_a/RT} \qquad ...(41)$$

where E_a is called the **Arrhenius activation energy** and A is called the **Arrhenius pre-exponential factor.** Since the exponential factor in Eq. 41 is dimensionless, the pre-exponential factor A has the same units as the rate constant k. The units of k for a first-order reaction are s^{-1}, which is the unit of frequency. Hence, A is also called the **frequency factor.** E_a and A are called the **Arrhenius parameters.**

Taking logs of Eq. 41, we have

$$\ln k = -E_a/(RT) + \ln A \qquad ...(42)$$

From Eq. 42, it is evident that a plot of $\ln k$ versus the reciprocal of absolute temperature ($1/T$) gives a straight line with slope $= -E_a/R$ and intercept $= \ln A$.

Differentiating Eq. 42 with respect to temperature, we

$$d \ln k/dT = E_a/RT^2 \qquad ...(43)$$

Integrating Eq. 43 between temperatures T_1 and T_2 when the corresponding rate constants are k_1 and k_2, respectively and assuming that E_a is constant over this temperature range, we obtain

$$\ln \frac{k_2}{k_1} = \frac{E_a}{R}\left[\frac{T_2 - T_1}{T_1T_2}\right] \qquad ...(44)$$

This is the **integrated Arrhenius equation.** Thus, knowing the rate constants at two different temperatures, the energy of activation E_a can be readily determined.

Example 35. Calculate the activation energy of a reaction whose rate constant is tripled by a 10°C rise in temperature in the vicinity of 27°C.

Solution : The given temperature is 27°C=300 K. In the vicinity of this temperature, the two temperatures, are, evidently, 295 and 305 K.

Eq 43 can be written as, $k = A\,e^{-E_a/RT}$

$$\frac{k_{305}}{k_{295}} = \frac{e^{-E_a/RT_{305}}}{e^{-E_a/RT_{295}}} = 3$$

Taking logs, $\ln 3 = -\frac{E_a}{R}\left[\frac{1}{305} - \frac{1}{295}\right] = \frac{E_a}{R}\left[\frac{10}{305 \times 295}\right]$

$$E_a = \frac{(\ln 3)(8{\cdot}314\ \text{J K}^{-1}\ \text{mol}^{-1})(305\ \text{K})(295\ \text{K})}{10\ \text{K}} = 82182\ \text{J mol}^{-1} = \mathbf{82{\cdot}18\ kJ\ mol^{-1}}$$

Example 36. The activation energy of a non-catalysed reaction at 37°C is 83·68 kJ mol^{-1} and the activation energy of the same reaction catalysed by an enzyme is 25·10 kJ mol^{-1}. Calculate the ratio of the rate constants of the enzyme-catalysed and the non-catalysed reactions.

Solution : According to the Arrhenius equation, $k = A\,e^{-E_a/RT}$

Let k_e and k_n be the rate constants of the enzyme-catalysed and non-catalysed reactions, respectively. Assuming that the Arrhenius pre-exponential factor A is the same in both cases, we have

$$\frac{k_e}{k_n} = \frac{e^{-E_a/RT}\,(\text{enzyme-catalysed})}{e^{-E_a/RT}\,(\text{non-catalysed})} = \exp\left(\frac{83{\cdot}68\ \text{kJ mol}^{-1} - 25{\cdot}10\ \text{kJ mol}^{-1}}{RT}\right)$$

$$= \exp\left[\frac{58{\cdot}58\ \text{kJ mol}^{-1}}{8{\cdot}314 \times 10^{-3}\ \text{kJ K}^{-1}\text{mol}^{-1} \times 310\ \text{K}}\right] = e^{22{\cdot}728}$$

or $\ln \frac{k_e}{k_n} = 22{\cdot}728$ and hence $\frac{k_e}{k_n} = \mathbf{10^{10}}$

Thus, the enzyme-catalysed reaction is about **10 billion times faster** than the non-catalysed reaction.

Example 37. The rate constant of a second-order reaction is 5·70×10^{-5} dm^3 mol^{-1} s^{-1} at 25°C and 1·64×10^{-4} dm^3 mol^{-1} s^{-1} at 40°C. Calculate the activation energy and the Arrhenius pre-exponential factor.

Solution : Substituting the given data in Eq. 44, we have

$$\ln \frac{k_2}{k_1} = \frac{E_a}{R}\left[\frac{T_2 - T_1}{T_1T_2}\right] \quad \text{or} \quad E_a = R(\ln k_2/k_1)\left[\frac{T_1T_2}{T_2 - T_1}\right]$$

$$E_a = (8{\cdot}314\ \text{J K}^{-1}\ \text{mol}^{-1})\left[\ln \frac{1{\cdot}64 \times 10^{-4}\ \text{dm}^3\ \text{mol}^{-1}\ \text{s}^{-1}}{5{\cdot}70 \times 10^{-5}\ \text{dm}^3\ \text{mol}^{-1}\ \text{s}^{-1}}\right] \times \left[\frac{298\ \text{K} \times 313\ \text{K}}{313\ \text{K} - 298\ \text{K}}\right]$$

$$= 54478\ \text{J mol}^{-1} = \mathbf{54{\cdot}48\ kJ\ mol^{-1}}$$

To calculate the Arrhenius pre-exponential factor A, we incorporate one of the given data in Arrhenius equation, *viz.*, $k = A\,e^{-E_a/RT}$. Thus,

$$\ln k = \ln A - E_a/RT \quad \text{or} \quad \ln A = \ln k + E_a/RT$$

At $T = 298$ K, $k = 5{\cdot}7 \times 10^{-5}$ dm^3 mol^{-1} s^{-1}

$$\therefore \quad \ln A = \ln (5{\cdot}7 \times 10^{-5}\ \text{dm}^3\ \text{mol}^{-1}\ \text{s}^{-1}) + \frac{54478\ \text{J mol}^{-1}}{(8{\cdot}314\ \text{J K}^{-1}\ \text{mol}^{-1})(298\ \text{K})}$$

$$\therefore \quad A = \mathbf{2{\cdot}01 \times 10^5\ dm^3\ mol^{-1}\ s^{-1}}$$

Note that the units of A are the same as those of the rate constant.

Example 38. Can the activation energy of a reaction be zero or negative ?

Solution : From the Arrhenius relation $k = A\,e^{-E_a/RT}$, we see that if E_a is zero, then, $k=A$, *i.e., every collision between molecules leads to the chemical reaction which is not true.* Hence, E_a **cannot be zero.** If, on the other hand, E_a is negative, then the exponential factor can be written as e^x where $x = E_a/RT$.

If $x \ll 1$, then

$$e^x = 1 + x + \frac{x^2}{2!} + \frac{x^3}{3!} + \cdots = 1 + x \text{ (neglecting higher powers of } x) = 1 + E_a/RT$$

Hence, $k = A(1 + E_a/RT)$, *i.e.*, $k > A$, which is absurd.

Hence, E_a **cannot be negative either.**

THEORIES OF REACTION RATES

There are two important theories of reaction rates. These are the collision theory developed by Arrhenius and van't Hoff and the modern transition state theory, also called the activated complex theory developed by Eyring, Polanyi and Evans in 1935.

Collision Theory of Bimolecular Gaseous Reactions

This is the earliest theory of reaction rates. Since reaction between two species takes place only when they are in contact, it is reasonable to suppose that the reactant species must collide before they react. Since our knowledge of molecular collisions is more complete for the gaseous phase than for the liquid phase (in the latter case we speak of encounters rather than collisions), we will restrict our discussion to bimolecular reactions in the gaseous phase.

From the kinetic theory of gases, the number of bimolecular collisions per second per cm^{-3} among molecules of one species is given by

$$Z = 2n^2 d^2 (8\pi kT/\mu)^{1/2} \qquad ...(45)$$

For a reaction involving two different gases A and B, the rate of bimolecular collisions between unlike molecules is given by

$$Z_{AB} = n_A n_B (d_{av})^2 (8\pi kT/\mu)^{1/2} \qquad ...(46)$$

where n_A and n_B are numbers of A and B molecules, respectively, d_{av} is the average collision diameter defined as $(d_A+d_B)/2$ and μ is the reduced mass defined as $\mu = (m_A m_B)/(m_A+m_B)$. The collision number Z_{AB} is given, in terms of molar masses M_A and M_B of the two gases, by the expression

$$Z_{AB} = n_A n_B (d_{av})^2 \left[\frac{(M_A+M_B)8\pi RT}{M_A M_B}\right]^{1/2} \qquad ...(47)$$

Let us calculate Z_{AB} for the reaction between H_2 and I_2 at 700 K and 1 atm pressure, the quantities of the two gases being 1 mole each. Accordingly, $n_{H_2} = n_{I_2} \approx 10^{19}$ molecules cm^{-3} ; $d_{H_2} = 2{\cdot}2$ Å, $d_{I_2} = 4{\cdot}6$ Å so that $d_{av} = 3{\cdot}4$ Å. Hence, according to Eq. 47,

$$Z_{AB} = (10^{19})^2 (3{\cdot}4\times10^{-8})^2 \left[\frac{(2+254)8\times3{\cdot}14\times8{\cdot}314\times10^7\times700}{2\times254}\right]^{1/2}$$

$$= 10^{38}\times1{\cdot}16\times10^{-15}\times8{\cdot}58\times10^5 \approx 10^{29} \text{ collisions } s^{-1} \text{ } cm^{-3}$$

Since there are approximately 10^{29} collisions s^{-1} for 10^{19} molecules of each species, each molecule makes about 10^{10} collisions s^{-1} with the molecules of the other species. If each collision were to lead to a chemical reaction, then the whole reaction would have been completed in about 10^{-10} s. However, this predicted rate of the reaction is in complete disagreement with the experimental rate. Hence, we conclude that all collisions do not result in chemical reaction.

In order for a reaction to occur, the energy of collision must equal or exceed the threshold energy. The effective energy is, of course, not the total kinetic energy of the two colliding molecules but is, instead, the kinetic energy corresponding to the component of the relative velocity of the two molecules along the line of their centres at the moment of collision. It is this energy with which the two molecules are pressed together.

The detailed analysis of the dynamics of bimolecular collisions leads to the result that the number of collisions s^{-1} cm^{-3} between molecules A and B, when the relative kinetic energy E along the line of centres is greater than the threshold energy is given by

$$Z'_{AB} = Z_{AB}\, e^{-E/RT} \qquad ...(48)$$

Assuming that Z'_{AB} gives the rate of relative collisions between A and B, we can write

$$-dn_A/dt = Z'_{AB}$$

$$= n_A n_B (d_{av})^2 \left[\frac{(M_A+M_B)8\pi RT}{M_A M_B}\right]^{1/2} e^{-E/RT} \text{ molecules } cm^{-3}\, s^{-1} \qquad ...(49)$$

Let us now proceed to obtain the theoretical expression for the rate constant. If the concentration is expressed in mol dm^{-3}, then

$$[A] = 10^3\, n_A/N_A \quad \text{and} \quad [B] = 10^3\, n_B/N_A \qquad ...(50)$$

where N_A is Avogadro's number. Hence, the rate law expression

$$-d[A]/dt = k_2[A][B]$$

can be written as

$$-\frac{10^3\, dn_A}{N_A dt} = k_2 \frac{10^6}{(N_A)^2} n_A n_B \qquad ...(51)$$

Hence,

$$k_2 = -\frac{N_A}{10^3 n_A n_B} \times \frac{dn_A}{dt} \qquad ...(52)$$

Using Eq. 49 for $-dn_A/dt$, we have

$$k_2 = \frac{N_A (d_{av})^2}{10^3}\left[\frac{(M_A+M_B)8\pi RT}{M_A M_B}\right]^{1/2} e^{-E/RT} \qquad ...(53)$$

Comparing Eq. 53 with the Arrhenius equation $k_2 = A\, e^{-E_a/RT}$, we find that the Arrhenius pre-exponential factor is given by

$$A = \frac{N_A (d_{av})^2}{10^3}\left[\frac{(M_A+M_B)8\pi RT}{M_A M_B}\right]^{1/2} \qquad ...(54)$$

The activation energy E_a in the Arrhenius equation is thus identified with the relative kinetic energy E along the line of centres of the two colliding molecules which is required to cause a reaction between them.

Let us calculate A and k_2 for the H_2—I_2 reaction at 700 K. E_a has been found to be 167·4 kJ mol^{-1}. Substituting the various values in Eq. 54, A comes out to be $= 6{\cdot}0\times10^{11}$ dm^3 $mol^{-1}\,s^{-1}$. Hence, from Arrhenius equation (Eq. 41),

$$k_2 = 6{\cdot}0\times10^{11} \text{ dm}^3 \text{ mol}^{-1} \text{ s}^{-1} \exp(-167400 \text{ J mol}^{-1}/8{\cdot}314 \text{ J K}^{-1} \text{ mol}^{-1} \times 700 \text{ K}) = 0{\cdot}22 \text{ dm}^3 \text{ mol}^{-1} \text{ s}^{-1}$$

which compares favourably with the experimental value of 0·064 dm^3 mol^{-1} s^{-1}, keeping in view the uncertainty in the values of the activation energy and the average collision diameter.

The collision theory is applicable to simple gaseous reactions. For reactions between complicated molecules, the observed rate is found to be much smaller than the theoretically predicted rate, sometimes by a factor of 10^5 for reactions involving fairly complicated molecules. The discrepancy is explained by the fact that the colliding molecule is treated as a hard sphere having no internal energy. Again, the spherical model ignores the dependence of the effectiveness of a collision on the relative orientation of the colliding molecules. Also, the activation energy has been treated as though it were related entirely to translational motion, ignoring the effect of rotational and vibrational motion. For these reasons the collision theory is applicable only to reactions between very simple gaseous molecules.

The collision theory can be generalized by introducing the so-called steric factor, p, into the equation for the bimolecular rate constant in order to take account of the orientational requirement. Accordingly,

$$k_2 = p\, A\, e^{-E_a/RT} \qquad ...(55)$$

The steric factor is supposed to be equal to the fraction of molecular collisions in which the molecules A and B possess the relative orientations necessary for the reaction. However, the steric factor cannot be reliably calculated. Perhaps its introduction oversimplifies the actual situation.

Using collision theory, the Arrhenius pre-exponential factor for *unlike* molecules including the steric fator p is given by

$$A = (2{\cdot}753\times10^{29})\, p(d_{av})^2 \left[\frac{T(M_A + M_B)}{M_A M_B}\right]^{1/2} \qquad ...(56)$$

and for *like* molecules it is given by

$$A = (3{\cdot}893\times10^{29})\, p\, d_{av}^2 \left(\frac{T}{M}\right)^{1/2} \qquad ...(57)$$

In these equations, the molar mass is in units of g mol^{-1} and the units of A are dm^3 mol^{-1} s^{-1}.

Example 39. Consider a bimolecular gaseous reaction between like molecules with collision diameter = 200 pm, molar mass = 100 g mol^{-1} and the steric factor = 1·00. Calculate the Arrhenius pre-exponential factor at *(a)* 100 °C and *(b)* 200 °C. Also calculate the exponential factor at the two temperatures and comment on your results. E_a = 150 kJ mol^{-1}.

Solution : $d = 200 \text{ pm} = 2\times10^{-10} \text{ m}$; $p = 1{\cdot}00$

(a) For a bimolecular reaction between like molecules, the **pre-exponential factor**, is given by

$$A = (3{\cdot}893\times10^{29})\, p\, d^2(T/M)^{1/2} \text{ dm}^3 \text{ mol}^{-1} \text{ s}^{-1} \qquad \text{(Eq. 57)}$$

At 100 °C, $A = (3{\cdot}893\times10^{29})(1{\cdot}00)(2\times10^{-10})^2(373/100)^{1/2} = 3{\cdot}01\times10^{10}$ dm^3 mol^{-1} s^{-1}

(b) At 200 °C, $A = (3{\cdot}893\times10^{29})(1{\cdot}00)(2\times10^{-10})(473/100)^{1/2} = 3{\cdot}39\times10^{10}$ dm^3 mol^{-1} s^{-1}

We see that the magnitude of A increases by about 12%.

Let us now calculate the **exponential factor**, $e^{-E_a/RT}$

(a) At 100 °C : $e^{-E_a/RT} = \exp\left[\dfrac{-150{,}000 \text{ J mol}^{-1}}{(8{\cdot}314 \text{ J K}^{-1} \text{ mol}^{-1})(373 \text{ K})}\right] = 9{\cdot}92\times10^{-22}$

(b) At 200 °C : $e^{-E_a/RT} = 2{\cdot}73\times10^{-17}$

We see that the exponential factor increases from $9{\cdot}92\times10^{-22}$ to $2{\cdot}73\times10^{-17}$, a factor of $2{\cdot}75\times10^{4}$. Thus, we conclude that the temperature-dependence of the exponential factor is many orders of magnitude larger than that of the pre-exponential factor.

Example 40. In the temperature range of 250 K to 450 K, the pre-exponential factor, A, for the reaction $Cl(g) + H_2(g) \longrightarrow HCl(g) + H(g)$ is found to be equal to $1{\cdot}20\times10^{10}$ dm^3 mol^{-1} s^{-1}. If $M(Cl) = 35{\cdot}453$ g mol^{-1}, $M(H_2) = 2{\cdot}016$ g mol^{-1}, $d(Cl) = 200$ pm and $d(H_2) = 150$ pm, determine the value of the steric factor, p.

Solution : $d_{av} = (200 + 150)/2 = 175 \text{ pm} = 1{\cdot}75\times10^{-10}$ m ; average temperature = 350 K

According to Eq. 56, for a bimolecular reaction between *unlike* molecules, Arrhenius pre-exponential factor

$$A = (2{\cdot}753\times10^{29})\, p\, (d_{av})^2 \left[\frac{T(M_A + M_B)}{M_A M_B}\right]^{1/2} \text{ dm}^3 \text{ mol}^{-1} \text{s}^{-1}$$

$$= (2{\cdot}753\times10^{29})\, p\, (1{\cdot}75\times10^{-10})^2 \left[\frac{350(35{\cdot}453 + 2{\cdot}016)}{35{\cdot}453\times2{\cdot}016}\right]^{1/2} = 1{\cdot}142\times10^{11}\, p \text{ dm}^3 \text{ mol}^{-1} \text{ s}^{-1}$$

$$\therefore \quad \text{Steric factor, } p = \frac{1{\cdot}20\times10^{10}}{1{\cdot}142\times10^{11}} = 0{\cdot}11$$

Example 41. The rate constant for the second-order decomposition of N_2O follows the following equation : $k = (5{\cdot}00\times10^{11} \text{ dm}^3 \text{ mol}^{-1} \text{ s}^{-1}) \exp(-29{,}000 \text{ K}/T)$. Calculate the activation energy of the reaction.

Solution : Comparing the given equation with the Arrhenius equation, *viz.*, $k = A \exp(-E_a/RT)$, we find that

$$E_a/RT = 29{,}000 \text{ K}/T$$

$$\therefore \quad \text{Activation Energy, } E_a = (29{,}000 \text{ K})(8{\cdot}314 \text{ J K}^{-1} \text{ mol}^{-1}) = 241{\cdot}1 \text{ kJ mol}^{-1}$$

Example 42. The rate constant for the first-order decomposition of ethylene oxide into CH_4 and CO follows the equation : $\log k$ (in s^{-1}) = 14·34 − (1·25×10^4 K)/T. Calculate *(a)* the activation energy of the reaction *(b)* the rate constant at 700 K and *(c)* the frequency factor, A.

Solution : $k = Ae^{-E_a/RT}$ [Arrhenius equation]

or $\log k = \log A - E_a/(2{\cdot}303\, RT)$ ...*(i)*

Also, $\log k = 14{\cdot}34 - 1{\cdot}25\times10^4 \text{ K}/T$ (given) ...*(ii)*

(a) From Eqs. *(i)* and *(ii)*,

$$E_a/2{\cdot}303\, RT = 1{\cdot}25\times10^4 \text{ K}/T$$

$\therefore$ Activation energy, $E_a = (1{\cdot}25\times10^4 \text{ K})(2{\cdot}303)(8{\cdot}314 \text{ J K}^{-1} \text{ mol}^{-1}) = 23{\cdot}93\times10^4 \text{ J mol}^{-1}$

$= 239{\cdot}3 \text{ kJ mol}^{-1}$

(b) At T = 700 K : $\log k = 14{\cdot}34 - (1{\cdot}25\times10^4 \text{ K}/700 \text{ K}) = -3{\cdot}52 = \bar{4}{\cdot}48$

$\therefore$ Rate constant, $k = 3{\cdot}02\times10^{-4} \text{ s}^{-1}$

(c) It is evident from Eqs. *(i)* and *(ii)* that

$$\log A = 14{\cdot}34$$

$\therefore$ Frequency factor, $A = 2{\cdot}168\times10^{14} \text{ s}^{-1}$

Example 43. Derive a relation between half-life ($t_{1/2}$) and temperature for an nth-order reaction where $n > 2$.

Solution : $k = Ae^{-E_a/RT}$ [Arrhenius equation] ...*(i)*

$\therefore \quad \ln k = \ln A - E_a/(RT)$ ...*(ii)*

Also, for nth-order reaction

$$t_{1/2} = \frac{2^{n-1} - 1}{k_n (n-1) a_0^{n-1}} \qquad \text{(Eq. 34)}$$

$$\ln t_{1/2} = \ln \frac{2^{n-1} - 1}{(n-1) a_0^{n-1}} - \ln k_n \qquad ...(iii)$$

Substituting the value of $\ln k$ from Eq. *(ii)*, we have

$$\ln t_{1/2} = \ln \frac{2^{n-1} - 1}{(n-1) a_0^{n-1}} - \ln A + \frac{E_a}{RT} = \ln A' + E_a/RT \qquad ...(iv)$$

where $A' = \dfrac{2^{n-1} - 1}{(n-1) a_0^{n-1} A}$.

From Eq. *(iv)* we see that $t_{1/2}$ *decreases* with an increase in temperature, as expected. A plot of $\ln t_{1/2}$ vs $1/T$ gives a straight line with slope equal to E_a.

Activated Complex Theory (ACT) of Bimolecular Reactions

As a result of the development of quantum mechanics, another theoretical approach to chemical reaction rates has been developed which gives a deeper understanding of the reaction process. It is known as the **absolute reaction rate theory (ARRT)** or the **transition state theory (TST)** or, more commonly, as the **activated complex theory (ACT),** developed by Eyring, Polanyi and Evans in 1935. According to ACT, the bimolecular reaction between two molecules A_2 and B_2 progresses through the formation of the so-called activated complex which then decomposes to yield the product AB, as illustrated below :

$$A_2 + B_2 \rightleftharpoons (A_2B_2)^{\#} \longrightarrow 2AB$$

or

$$\begin{array}{ccc} A-A & & A\cdots A \\ + & \rightleftharpoons & \vdots\ \ \vdots \\ B-B & & B\cdots B \\ \text{Reactants} & & \text{Activated complex} \end{array} \longrightarrow \begin{array}{c} A\quad A \\ |\quad + \quad | \\ B\quad B \\ \text{Product} \end{array}$$

Though somewhat ill-defined, the activated complex can be treated as a distinct chemical species in equilibrium with the reactants which then decompose into products. It is amenable to thermodynamic treatment, like any ordinary molecule. It is, however, a special molecule in which one vibrational degree of freedom has been converted to a translational degree of freedom along the reaction coordinate. The reaction coordinate shown as the abscissa in Fig. 12 could be the bond length which changes in going from the reactants to the products. In other words, the reaction coordinate is a measure of the progress of a reaction. It must be remembered that the activated complex is not merely an intermediate in the process of breaking or forming of chemical bonds. It is unstable because it is situated at the maximum of the potential energy barrier separating the products from the reactants. The difference between the energy of the activated complex and the energy of the reactants is the activation energy, E_a.

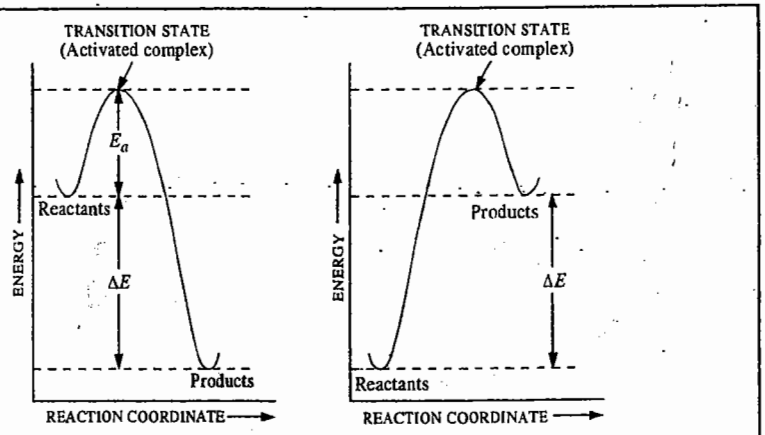

(a) Exothermic reaction (b) Endothermic reaction

Fig. 12. The profile of energy versus reaction coordinate in ACT in the case of an exothermic and an endothermic reaction.

For the thermodynamic formulation of the activated complex theory, consider a simple bimolecular reaction,

$$A + B \underset{}{\overset{K^{\#}}{\rightleftharpoons}} (AB)^{\#} \xrightarrow{k_2} \text{Products} \qquad ...(58)$$

where $(AB)^{\#}$ is the activated complex and $K^{\#}$ is the equilibrium constant between the reactants and activated complex. As said above, in $(AB)^{\#}$ one of the vibrational degrees of freedom has become a translational degree of freedom. From classical mechanics, the energy of vibration is given by RT/N_A (or k_BT where k_B is the Boltzmann constant) whereas from quantum mechanics, it is given by $h\nu$ so that $h\nu = RT/N_A$ or $\nu = RT/N_Ah = k_BT/h$. The vibrational frequency ν is the rate at which the activated complex molecules move across the energy barrier. Thus, the rate constant k_2 can be identified with ν.

The reaction rate is given by

$$-d[A]/dt = \kappa k_2[(AB)^{\#}] = \kappa(k_BT/h)[(AB)^{\#}] \qquad ...(59)$$

where the factor κ, called the *transmission coefficient*, is a measure of the probability that a molecule, once it passes over the barrier, will keep on going ahead and not return. The value of κ is taken to be unity ; it is thus omitted from the rate expression. The concentration of the activated complex, $[(AB)^{\#}]$, can be obtained by writing the equilibrium expression

$$K^{\#} = [(AB)^{\#}]/[A][B]$$

whence $$[(AB)^{\#}] = K^{\#}[A][B] \qquad ...(60)$$

Substituting in Eq. 59, we obtain

$$-d[A]/dt = (k_BT/h)\,K^{\#}[A][B] \qquad ...(61)$$

Thus, the rate constant k_2 may be expressed as

$$k_2 = (k_BT/h)\,K^{\#} \qquad ...(62)$$

The equilibrium constant $K^{\#}$ can be expressed in terms of $(\Delta G°)^{\#}$, called the standard Gibbs free energy of activation. Since for the activated complex, we can write

$$(\Delta G°)^{\#} = -RT \ln K^{\#} \quad \text{and} \quad (\Delta G°)^{\#} = (\Delta H°)^{\#} - T(\Delta S°)^{\#}, \qquad ...(63)$$

we obtain $$K^{\#} = e^{-(\Delta G°)^{\#}/RT} = e^{(\Delta S°)^{\#}/R} e^{-(\Delta H°)^{\#}/RT} \qquad ...(64)$$

Hence, substituting in Eq. 62, we get

$$k_2 = (k_BT/h)\, e^{(\Delta S°)^{\#}/R} e^{-(\Delta H°)^{\#}/RT} \qquad ...(65)$$

Eq. 65 is the well known **Eyring equation.** Here $(\Delta S°)^{\#}$ is the standard entropy of activation and $(\Delta H°)^{\#}$ is the standard enthalpy of activation. Although the application of the activated complex theory (ACT) to reactions in solution is quite complicated because of the participation of the solvent in the activated complex, fortunately, the Eyring equation holds for reactions in solution, too. The American chemist Henry Eyring (1901-1981) was a brilliant kineticist ; however, he was not awarded the Nobel Prize in chemistry.

Taking logs of both sides of Eq. 65 and differentiating with respect to T, we obtain

$$d \ln k_2/dT = (\Delta H°)^{\#}/RT^2 + 1/T = \{(\Delta H°)^{\#} + RT\}/RT^2 \qquad ...(66)$$

Also, from the Arrhenius equation,

$$d \ln k_2/dT = E_a/RT^2 \qquad ...(67)$$

Comparing Eqs. 66 and 67, we obtain

$$E_a = (\Delta H°)^{\#} + RT \quad \text{or} \quad (\Delta H°)^{\#} = E_a - RT \qquad ...(68)$$

Comparing Eq. 65 with Eq. 55, we have

$$pA\, e^{-E_a/RT} = \frac{k_BT}{h}\, e^{(\Delta S°)^{\#}/R} e^{-(\Delta H°)^{\#}/RT} \qquad ...(69)$$

If $(\Delta H°)^{\#} \approx E_a$, we can equate the exponential factors in Eq. 69, obtaining

$$pA = (k_BT/h)\, e^{(\Delta S°)^{\#}/RT} \qquad ...(70)$$

For a first-order gaseous reaction, $p=1$ and $A=10^{10}$ s^{-1}. Also, at room temperature, $k_BT/h=10^{13}$ s^{-1}. Hence,

$$e^{(\Delta S°)^{\#}/R} = 10^{10}\ s^{-1}/10^{13}\ s^{-1} = 10^{-3}$$

$$\therefore \quad (\Delta S°)^{\#} = -57{\cdot}4\ J\ K^{-1}\ mol^{-1}$$

If $p < 1$ (as in the case of complex molecules), $(\Delta S°)^{\#}$ is lower than this value. Qualitatively, a negative value of entropy of activation corresponds to an increase in molecular order and a loss of excited degrees of freedom in the activated complex relative to the reactant molecules. A large negative value of $(\Delta S°)^{\#}$ corresponds to a highly ordered activated complex and this implies a small value of the steric factor. Finally, it may be remarked that for reactions involving simple molecules, the collision theory and ACT give identical results.

The first direct experimental evidence for the existence of the activated complex was obtained in 1989 by Ahmed Zewail (1946—) using femtosecond laser spectroscopy. A. Zewail, the Egyptian-American chemist, was awarded the 1999 Chemistry Nobel Prize for his contributions to molecular reaction dynamics using femtosecond laser techniques.

The pre-exponential factors for some simple bimolecular gaseous reactions are given in Table 2.

TABLE 2

Pre-exponential Factors for Simple Bimolecular Gaseous Reactions Calculated by ACT, Compared with Experimental Values

Reaction	A_{cal} ($cm^3\ mol^{-1}\ s^{-1}$)	A_{expt} ($cm^3\ mol^{-1}\ s^{-1}$)
$H + H_2 \longrightarrow H_2 + H$	75×10^{13}	$5{\cdot}4\times10^{13}$
$Br + H_2 \longrightarrow HBr + H$	1×10^{14}	3×10^{13}
$H + CH_4 \longrightarrow H_2 + CH_3$	2×10^{13}	1×10^{13}
$CH_3 + H_2 \longrightarrow CH_4 + H$	1×10^{12}	2×10^{12}

The pre-exponential factors obtained from collision theory are in the range of 10^{13}-10^{15} $cm^3\ mol^{-1}\ s^{-1}$. The agreement between the ACT and the collision theory is quite satisfactory. However, for reactions involving complex molecules, the collision theory fails while ACT still gives meaningful results. The ACT, when developed to its most sophisticated form, does permit a detailed treatment of reaction rates. However, this has not been realized so far because of formidable computational difficulties.

Example 44. Show that for a gaseous bimolecular reaction A(g) + B(g) $\longrightarrow$ $(AB)^{\#}$ $\longrightarrow$ Products, $E_a = \Delta H_m^{\#} + 2RT$ where the subscript m stands for molar.

Solution :

$$k_2 = Ae^{-E_a/RT} \quad \text{[Arrhenius equation]} \qquad ...(i)$$

$$\ln k_2 = \ln A - E_a/RT$$

$$d \ln k_2/dT = E_a/RT^2 \quad [\because \ln A = \text{constant}] \qquad ...(ii)$$

Also, from the activated complex theory (ACT), we know that

$$k_2 = (k_BT/h)\ K^{\#} \quad \text{(Eq. 62)} \qquad ...(iii)$$

$$\therefore \quad \ln k_2 = \ln (k_BT/h) + \ln K^{\#} \qquad ...(iv)$$

$$d \ln k_2/dT = 1/T + d \ln K^{\#}/dT \qquad ...(v)$$

Also, at constant volume,

$$d \ln K^{\#}/dT = \Delta E_m^{\#}/RT^2 \qquad ...(vi)$$

$$\therefore \quad \frac{d \ln k_2}{dT} = \frac{1}{T} + \frac{\Delta E_m^{\#}}{RT^2} = \frac{RT + \Delta E_m^{\#}}{RT^2} \qquad ...(vii)$$

Hence, from Eqs. *(ii)* and *(vii)*,

$$E_a = \Delta E_m^{\#} + RT \qquad ...(viii)$$

Again, since $H = E + PV$, hence

$$\Delta H_m^{\#} = \Delta E_m^{\#} + \Delta PV_m^{\#} \qquad ...(ix)$$

For an ideal bimolecular reaction,

$$\Delta PV_m^{\#} = \Delta n_g RT \qquad ...(x)$$

In the present case, $\Delta n_g = -1$ so that $\Delta PV_m^{\#} = -RT$ $\qquad ...(xi)$

Hence, from Eqs. *(viii)*, *(ix)*, *(x)* and *(xi)*, $E_a = \Delta H_m^{\#} + 2RT$

Example 45. For the first-order isomerization of an organic compound at 130°C, the activation energy is 108·4 kJ mol^{-1} and the rate constant is $9{\cdot}12\times10^{-4}$ s^{-1}. Calculate the standard entropy of activation for this reaction.

Solution : $E_a = 108{,}400\ J\ mol^{-1}$; $T = 403\ K$

$$(\Delta H^{\circ})^{\#} = E_a - RT = 08{,}400\ J\ mol^{-1} - (8{\cdot}314\ J\ K^{-1}\ mol^{-1} \times 403\ K) = -105{,}049\ J\ mol^{-1}$$

$$k_1 = 9{\cdot}12\times10^{-4}\ s^{-1} \quad \text{(given)}$$

From Eyring equation, we obtain

$$e^{(\Delta S^{\circ})^{\#}/R} = (h/k_BT)(k_1)\ e^{(\Delta H^{\circ})^{\#}/RT}$$

Substituting the given data and the values of constants, we get

$$e^{(\Delta S^{\circ})^{\#}/R} = \frac{(6{\cdot}626\times10^{-34}\ J\ s)(9{\cdot}12\times10^{-4}\ s^{-1})\ \ e^{105{\cdot}049/(8{\cdot}314)(403)}}{(1{\cdot}38\times10^{-23}\ J\ K^{-1})(403\ K)}$$

The units on the R.H.S. of this equation cancel out giving a dimensionless quantity $e^{(\Delta S^{\circ})^{\#}/R}$ from which $(\Delta S^{\circ})^{\#}$ is found to be $-45{\cdot}2\ J\ K^{-1}\ mol^{-1}$.

Statistical Mechanical Derivation of the Rate Constant of a Gaseous Bimolecular Reaction using ACT

We shall focus our attention on what happens at the top of the potential energy barrier (Fig.13) for the reaction

$$A + B \longrightarrow C$$

The rate of this elementary gaseous reaction is given by

$$r = k\,[A][B] \qquad ...(71)$$

According to activated complex theory ACT), the reaction proceeds through an activated complex $C^{\#}$ that produces C at a rate of $k^{\#}[C^{\#}]$. $C^{\#}$ is not an intermediate compound in the reaction; it is a structure that is in the process of change in the direction of the products. The rate of reaction can be expressed as

$$rk[A][B] = k^{\#}[C^{\#}] \qquad ...(72)$$

The rate constant is given by

$$k = \frac{k^{\#}[C^{\#}]}{[A][B]} \qquad ...(73)$$

Since the ACT assumes that there is rapid equilibrium in the reaction $A + B \rightleftharpoons C^{\#}$, we can represent Eq. 73 as

$$\frac{K_c}{c^0} = \frac{[C^{\#}]}{[A][B]} \qquad ...(74)$$

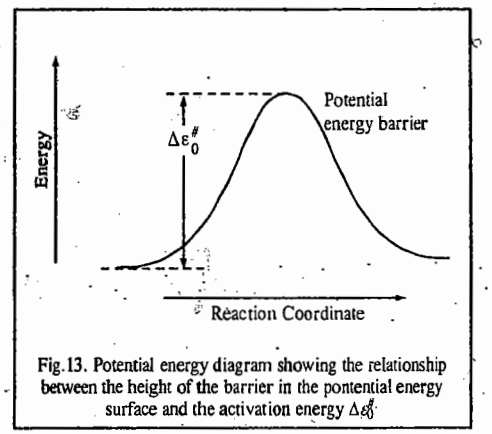

Fig.13. Potential energy diagram showing the relationship between the height of the barrier in the pontential energy surface and the activation energy $\Delta\varepsilon_0^{\#}$

Here the standard state concentration c^0 is required because the equilibrium constant K_c is dimensionless. Thus, Eq. 73 can be written as

$$k = \frac{k^{\#}K_c}{c^0} \qquad ...(75)$$

Eq. 75 shows that if we can derive expressions for $k^{\#}$ and K_c theoretically, we can calculate k. In order to derive the expression for K_c theoretically from statistical mechanics, we must first make a purely thermodynamic adjustment from a dimensionless K_p (obtained from statistical mechanics) to a dimensionless K_c needed for Eq. 75 :

$$K_c = (c^0RT/p^{\circ})^{-\sum_i \nu_i} K_p \qquad ...(76)$$

where p^0 is the standard pressure. For the reaction under consideration, $\sum_i \nu_i = -1$ (where ν_i is the stoichiometric coefficient of the reacting species i). Thus, this adjustment is given by

$$K_c = (c^0 RT/p^0)K_p \qquad ...(77)$$

Both the equilibrium constants K_c and K_p are dimensionless. Substituting Eq. 77 in Eq. 75, we get

$$k = k^{\#}(RT/p^0)K_p \qquad ...(78)$$

It is easy to calculate $k^{\#}$ because $C^{\#}$ is going through the transition state and becoming C. $C^{\#}$ may have vibrations perpendicular to the reaction coordinate and they may have normal frequencies because their potential energy functions have the usual Hooke's law-type parabolic shape. However, the motion of $C^{\#}$ in the direction of the reaction coordinate has an inverted potential energy curve since the transition state is at the saddle point at which the potential energy is a maximum. Hence, this motion represents advancement along the reaction coordinate through the transition state. Therefore, the reaction rate is proportional to the inverse time (or frequency ν) at the transition state. Replacing $k^{\#}$ with ν, we obtain

$$k = \nu(RT/p^0)K_p \qquad ...(79)$$

It is customary to include the **transmission coefficient** κ in this equation to allow for the possibility that some of the activated complex may return to reactants instead of going on to the product C. However, it is difficult to calculate the transmission coefficient and we assume that its value is unity so that the rate constant k, calculated from the ACT, is a maximum value for the reaction.

We now proceed to calculate K_p. From statistical thermodynamics we know that for the reaction under consideration,

$$K_p = (k_B T/p^0)^{-1} \frac{q(C^{\#})/V}{[q(A)/V][q(B)/V]} \exp(-\Delta\varepsilon_0^{\#}/k_B T) \qquad ...(80)$$

where the change in energy at absolute zero is $\Delta\varepsilon_0^{\#} = \varepsilon_0(C^{\#}) - \varepsilon_0(A) - \varepsilon_0(B)$. In writing Eq. 80 we have assumed that $A + B \rightleftharpoons C^{\#}$ is an ordinary reaction, but this is not the case because the activated complex $C^{\#}$ is falling apart. The partition function for the motion of $C^{\#}$ along the reaction coordinate can be written as if the motion is a vibration with frequency ν :

$$q_{vib} = \frac{1}{1 - \exp(-h\nu/k_B T)} \qquad ...(81)$$

This frequency is lower than the frequencies of the other vibrations because the potential energy curve is relatively flat near the transition state. Since $h\nu/k_B T$ is small, $e^{-x} = 1-x$, so the denominator of Eq. 81 is close to $h\nu/k_B T$. Thus,

$$q_{vib} = k_B T/h\nu \qquad ...(82)$$

Therefore, we write the partition function for $C^{\#}$ as $(k_B T/h\nu)q'(C^{\#})$. Substituting this result in Eq. 80 and then substituting Eq. 80 in Eq. 79, we obtain

$$k = \left(\frac{k_B T}{h}\right)\left(\frac{RT}{p^0}\right)\left(\frac{k_B T}{p^0}\right)^{-1} \frac{q'(C^{\#})/V}{[q(A)/V][q(B)/V]} \exp(-\Delta\varepsilon_0^{\#}/k_B T) \qquad ...(83)$$

Notice that the frequency ν of passage over the potential energy barrier has cancelled. The last three terms in Eq. 83 represent the equilibrium constant $K^{\#}$ for the formation of the activated complex from the reactants, omitting the partition function for the vibration along the reaction coordinate. Thus, Eq. 83 can be written as

$$k = \left(\frac{k_B T}{h}\right)\left(\frac{RT}{p^0}\right) K^{\#} \qquad ...(84)$$

where

$$K^{\#} = \left(\frac{k_B T}{p^0}\right)^{-1} \frac{q'(C^{\#})/V}{[q(A)/V][q(B)/V]} \exp(-\Delta\varepsilon_0^{\#}/k_B T) \qquad ...(85)$$

Eq. 85 has been derived for a bimolecular reaction ; it can be generalized to

$$k = \left(\frac{k_B T}{h}\right)\left(\frac{RT}{p^0}\right)^{m-1} K^{\#} \qquad ...(86)$$

where m is the order of the reaction.

For a unimolecular reaction, the translational partition functions for the activated complex and the reactant cancel. Hence, the unimolecular rate constant is given by

$$k = \left(\frac{k_B T}{h}\right) \frac{q'_{int}(C^{\#})}{q_{int}(A)} \exp(-\Delta\varepsilon_0^{\#}/k_B T) \qquad ...(87)$$

where the subscript int indicates that only the internal coordinates are involved. This yields a rate constant in s^{-1}, as it must. This is the rate constant in the high-pressure limit where there are enough collisions to maintain the Boltzmann distribution of A^*. However, in the falloff region, the rate of formation of the vibrationally excited A^* molecules is too slow to maintain the Boltzmann distribution. To calculate the rate constant in the falloff region we have to use the RRKM theory discussed later in this chapter.

Example 46. Using the ACT result, calculate the pre-exponential factor for the gaseous reaction

$$H + H_2 \longrightarrow H_2 + H$$

at 500 K. Assume that the activated complex is linear with the nuclei separated by $0{\cdot}94\times10^{-10}$ m. You may ignore the vibrational partition functions because their values are so close to unity.

Solution.

$$k = \left(\frac{k_B T}{h}\right)\left(\frac{RT}{p^0}\right)^{m-1} K^{\#} \qquad \text{(Eq. 86)} \qquad ...(i)$$

where m is the order of the reaction. Here for the second-order (bimolecular) reaction, $m=2$. The Arrhenius pre-exponential factor is given by

$$A = \left(\frac{RT}{h}\right) \frac{q'^{\#}}{(q_H/V)(q_{H_2}/V)} \qquad ...(ii)$$

where $q'^{\#} = q_{tr}^{\#} q_{int}^{\#}$; $q_H = q_{tr,H}\, q_{int,H}$ and $q_{H_2} = q_{tr,H_2} q_{int,H_2}$

Since $q_{tr}^{\#}/V$ and $q_{tr,H_2}/V$ cancel, hence

$$A = \left(\frac{RT}{h}\right) \frac{q_{int}^{\#}/V}{(q_{tr,H}/V)\, q_{int,H}\, q_{int,H_2}} \qquad ...(iii)$$

The internal partition function $q_{int}^{\#}$ for the transition state is the rotational partition function for a symmetrical and linear arrangement of three hydrogen atoms. Since the central hydrogen atom is on the axis of rotation, it does not contribute to the moment of inertia, I. Accordingly,

$$I = \mu r^2 = \frac{(m_1 m_2) r^2}{m_1 + m_2} = \frac{(1{\cdot}0078\times10^{-3}\ \text{kg mol}^{-1})^2\,(1{\cdot}88\times10^{-10}\ \text{m})^2}{(2{\cdot}0156\times10^{-3}\ \text{kg mol}^{-1})\,(6{\cdot}022\times10^{23}\ \text{mol}^{-1})}$$

$$= 2{\cdot}96 \times 10^{-47}\ \text{kg m}^2 \qquad \text{(Here } r \text{ is the internuclear distance)}$$

The internal partition function for the transition state is thus given by

$$q_{int}^{\#} = \frac{8\pi^2 I k_B T}{2h^2} = \frac{8\pi^2 (2{\cdot}96\times10^{-47}\ \text{kg m}^2)\,(1{\cdot}381\times10^{-23}\ \text{JK}^{-1})\,(500\ \text{K})}{2\,(6{\cdot}626\times10^{-34}\ \text{Js})^2} = 18.4$$

The translational partition function for the relative motion of the reactants is given by

$$\frac{q_{tr}}{V} = \frac{(2\pi\mu k_B T)^{3/2}}{h^3}$$ where μ is the reduced mass of a hydrogen atom and a hydrogen molecule.

$$= \frac{[2\pi(1{\cdot}116\times10^{-27}\text{ kg})(1{\cdot}381\times10^{-23}\text{ JK}^{-1})(500\text{ K})]^{3/2}}{(6{\cdot}626\times10^{-34}\text{ Js})^3} = 1{\cdot}157\times10^{30}\text{ m}^{-3}$$

Using the formula $q_{rot} = 8\pi^2 I k_B T/\sigma h^2$, where σ, the symmetry number, is equal to 2, we can calculate the q_{rot,H_2} for H_2 at 500 K. It is found to be $=2{\cdot}86$.

Thus, the pre-exponential factor

$$A = \frac{(8{\cdot}3145\text{ JK}^{-1}\text{ mol}^{-1})(500\text{ K})(18{\cdot}4)}{(6{\cdot}626\times10^{-34}\text{ Js})(1{\cdot}157\times10^{30}\text{ m}^{-3})(2{\cdot}86)} = 3{\cdot}49\times10^{7}\text{ m}^3\text{ mol}^{-1}\text{ s}^{-1}$$

$$= (3{\cdot}49\times10^{7}\text{ m}^3\text{ mol}^{-1}\text{ s}^{-1})(100\text{ cm m}^{-1})^3 = 3{\cdot}49\times10^{13}\text{ cm}^3\text{ mol}^{-1}\text{ s}^{-1}$$

Theories of Unimolecular Gaseous Reactions

It is easy to understand a bimolecular reaction on the basis of collision theory. Thus, when two molecules A and B collide, their relative kinetic energy exceeds the *threshold energy* with the result that the collision results in the breaking of bonds and the formation of new bonds. But how can one account for a unimolecular reaction ? If we assume that in such a reaction ($A \longrightarrow P$), the molecule A acquires the necessary activation energy by colliding with another molecule, then the reaction should obey second-order kinetics and not the first-order kinetics which is actually observed in several unimolecular gaseous reactions. A number of theories of unimolecular gaseous reactions have been put forth. These are Lindemann theory, Hinshelwood theory, Rice-Ramps-Kassel (RRK) theory, N.B. Slaters theory and the most important of them all, the Marcus extension of RRK theory, known as RRKM theory. These theories (excepting Slaters theory) have been discussed below.

1. Lindemann Theory. According to this theory, a unimolecular reaction $A \longrightarrow P$ proceeds via the following mechanism :

$$A + A \underset{k_{-1}}{\overset{k_1}{\rightleftharpoons}} A^* + A$$

$$A^* \xrightarrow{k_2} P$$

Here A^* is the energized A molecule which has acquired sufficient vibrational energy to enable it to isomerize or decompose. In other words, the vibrational energy of A exceeds the threshold energy for the overall reaction $A \longrightarrow$ Products. It must be borne in mind that A^* is simply a molecule in a high vibrational energy level and not an activated complex. In the first step, the energized molecule A^* is produced by collision with another molecule A. What actually happens is that the kinetic energy of the second molecule is transferred into the vibrational energy of the first. In fact, the second molecule need not be of the same species ; it could be a product molecule or a foreign molecule present in the system which, however, does not appear in the overall stoichiometric reaction $A \longrightarrow P$. The rate constant for the energization step is k_1. After the production of A^*, it can either be de-energized back to A (in the reverse step, with rate constant k_{-1}) by collision in which case its vibrational energy is transferred to the kinetic energy of an A molecule or be decomposed or isomerized to products (in the step with rate constant k_2) in which case the excess vibrational energy is used to break the appropriate chemical bonds.

In the Lindemann mechanism, *a time lag exists* between the energization of A to A^* and the decomposition (or isomerization) of A^* to products. During this time lag, A^* can be de-energized back to A. According to the steady state approximation (s.s.a), whenever a reactive (*i.e.*, short-lived) species is produced as an intermediate in a chemical reaction, its rate of formation is equal to its rate of decomposition. Here, the energized species A^* is short-lived. Its rate of formation $=k_1[A]^2$

and its rate of decomposition $=k_{-1}[A][A^*]+k_2[A^*]$. Thus,

$$d[A^*]/dt = k_1[A]^2 - k_{-1}[A][A^*] - k_2[A^*] = 0 \quad \ldots(88)$$

so that $$[A^*] = \frac{k_1[A]^2}{k_{-1}[A] + k_2} \quad \ldots(89)$$

The rate of the reaction is given by

$$r = -d[A]/dt = k_2[A^*] \quad \ldots(90)$$

Substituting Eq. 89 in Eq. 90,

$$r = \frac{k_1 k_2[A]^2}{k_{-1}[A] + k_2} \quad \ldots(91)$$

The rate law given by Eq. 91 has no definite order. We can, however, consider two limiting cases, depending upon which of the two terms in the denominator of Eq. 99 is greater. If $k_{-1}[A] \gg k_2$, then the k_2 term in the denominator can be neglected giving

$$r = (k_1 k_2/k_{-1})[A] \quad \ldots(92)$$

which is the rate equation for a first-order reaction. In a gaseous reaction, this is the high-pressure limit because at very high pressures, [A] is very large so that $k_1[A] \gg k_2$.

If $k_2 \gg k_{-1}[A]$, then the $k_{-1}[A]$ term in the denominator can be neglected giving

$$r = k_1[A]^2 \quad \ldots(93)$$

which is the rate equation for a second-order reaction. This is the low pressure limit. The experimental rate is defined as

$$r = k_{uni}[A] \quad \ldots(94)$$

where k_{uni} is the unimolecular rate constant. Comparing Eqs. 91 and 94, we have

$$k_{uni} \equiv k^1 = \frac{k_1 k_2[A]}{k_{-1}[A] + k_2} = \frac{k_1 k_2}{k_{-1} + k_2/[A]} \quad \ldots(95)$$

Example 47. Consider the following Lindemann mechanism for the unimolecular decomposition of a molecule A in the presence of a species M (which may be any molecule such as an inert gas like helium or even A itself) :

$$A + M \xrightarrow{k_1} A^* + M \quad \text{(activation)}$$

$$A^* + M \xrightarrow{k_{-1}} A + M \quad \text{(deactivation)}$$

$$A^* \xrightarrow{k_2} P \quad \text{(decomposition reaction)}$$

Using the steady state approximation (s.s.a.), derive the rate law for the formation of the product.

Solution : $$r = -d[A]/dt = +d[P]/dt = k_2[A^*] \quad \ldots(i)$$

Applying *s.s.a.* to the transient species A^*,

$$k_1[A][M] - k_{-1}[A^*][M] - k_2[A^*] = 0 \quad \text{or} \quad k_1[A][M] = (k_{-1}[M] + k_2)[A^*]$$

$$[A^*] = \frac{k_1[A][M]}{k_{-1}[M] + k_2}$$

Substituting this expression in Eq. *(i)*, we obtain

$$r = k_1 k_2 \frac{[M][A]}{k_{-1}[M] + k_2}$$

Example 48. Consider the following Lindemann mechanism for the unimolecular decomposition of a molecule A in the presence of an inert gas molecule M :

$$A + A \underset{k_{-1}}{\overset{k_1}{\rightleftharpoons}} A^* + A$$

$$A + M \underset{k_{-2}}{\overset{k_2}{\rightleftharpoons}} A^* + M$$

$$A^* \xrightarrow{k_3} P$$

Applying the steady state approximation to A^*, derive the rate law for the formation of the product.

Solution : The rate of formation of product is given by $r = k_3[A^*]$ ...(i)

Applying *s.s.a* to A^*,

$$k_1[A]^2 - k_{-1}[A^*][A] + k_2[A][M] - k_{-2}[A^*][M] - k_3[A^*] = 0$$

or $$k_1[A]^2 + k_2[A][M] = [A^*]\{k_{-1}[A] + k_{-2}[M] + k_3\}$$

or $$[A^*] = \frac{k_1[A]^2 + k_2[A][M]}{k_{-1}[A] + k_{-2}[M] + k_3}$$

Substituting this expression in Eq. *(i)*, we get

$$r = k_3[A^*] = \frac{k_3(k_1[A]^2 + k_2[A][M])}{k_{-1}[A] + k_{-2}[M] + k_3}$$

Limitations of Lindemann Theory. Eq. 95 can also be written as

$$k^1 = \frac{k_2(k_1/k_{-1})}{1 + (k_2/k_{-1})[A]} \quad ...(96)$$

According to Eq. 96, the plot of the first-order rate constant k^1 versus [A] is a hyperbola (Fig. 14). The rate constant k^1 is a constant in the higher concentration range but falls off at lower concentrations. It can be shown that $k^1 = k^1_\infty/2$ when $k_{-1}[A] = k_2$ and we write the concentration at which this is true as $[A]_{1/2}$.

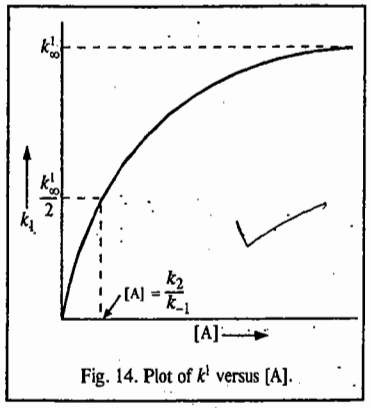

Fig. 14. Plot of k^1 versus [A].

Thus, $$[A]_{1/2} = \frac{k_2}{k_{-1}} = \frac{k^1_\infty}{k_1} \quad ...(97)$$

Application of this relationship to experimental data raises some difficulties. The value of k^1_∞ is an experimental quantity; it was thought that, using the simple collision theory, it could be written as $z_1 \exp(-E_1/RT)$, where z_1 is the collision frequency factor and E_1 is the activation energy. Experimentally, however, it was found that the values of $[A]_{1/2}$ were always smaller than those estimated in this way. Thus, the error must lie in the estimation of k_1 rather than k^1_∞ (which is an experimental quantity). Thus, we should modify k_1 so that it is larger than $z_1 \exp(-E_1/kT)$.

Another difficulty with the Lindemann mechanism becomes evident when experimental results are plotted in another way. Rewriting Eq. 95 as

$$\frac{1}{k^1} = \frac{k_{-1}}{k_1 k_2} + \frac{1}{k_1[A]} \quad ...(98)$$

and plotting $1/k^1$ *versus* $1/[A]$ should give a straight line. However, deviations from linearity have been found (Fig. 15).

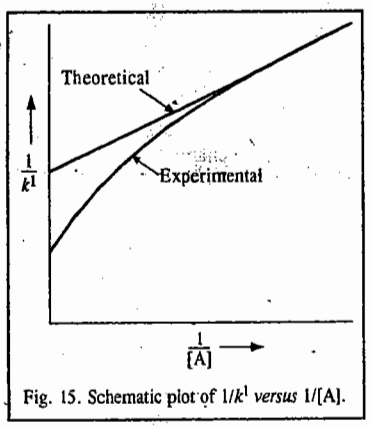

Fig. 15. Schematic plot of $1/k^1$ *versus* $1/[A]$.

2. Hinshelwood Theory. The first difficulty with the Lindemann treatment that the first-order rates are maintained down to lower concentrations than the theory appeared to permit, was overcome by Hinshelwood's suggestion that the expression $z_1 \exp(-E/RT)$ applied only if the energy is distributed among two degrees of freedom. However, for some unimolecular reactions, the number of degrees of freedom, s, is very large. The activation energy is distributed initially among these degrees of freedom ; this distribution can be affected in many ways. Once the energy is in the molecule, distributed in any way among s vibrational degrees of freedom, the molecule is in a position eventually to react. After a number of vibrations of the energized molecule A^* — which may be a very large number — the energy may find its way into the appropriate degrees of freedom so that A^* can immediately pass into the products. Hinshelwood derived the following formula for the fraction of molecules having energy in excess of ε^*:

$$f^* = \frac{1}{(s-1)!}\left(\frac{\varepsilon^*_0}{kT}\right)^{s-1} \exp(-\varepsilon^*_0/kT) \quad ...(99)$$

where s is the number of degrees of freedom. He then expressed the rate constant k_1 as

$$k_1 = z_1 \frac{1}{(s-1)!}\left(\frac{\varepsilon^*_0}{kT}\right)^{s-1} \exp\left(-\frac{\varepsilon^*_0}{kT}\right) \quad ...(100)$$

instead of simply as $z_1 \exp(-\varepsilon^*_0/kT)$. Thus, an additional factor $\frac{1}{(s-1)!}\left(\frac{\varepsilon^*_0}{kT}\right)^{s-1}$ has appeared and if s is sufficiently large, this may be greater than unity by many powers of 10. Eq. 99 can give much higher rates of activation and, therefore, much higher k_1/k_{-1} values than those given by the simple collision theory. It can be shown that the experimental activation energy per molecule ε_a is related to ε^*_0 as

$$\varepsilon^*_0 = \varepsilon_a + \left(s - \frac{3}{2}\right)kT$$

Thus, if $\varepsilon_a = 170$ kJ mol^{-1} and $s = 12$, then Eq. 99 gives a value of k_1/k_{-1} that is larger by more than 10^6 than that given by the older theory.

Objections to Hinshelwood Theory. 1. The number s of the degrees of freedom required to give agreement with experiment on the basis of the Hinshelwood theory is about one-half of the total number of vibrational modes. There is no satisfactory explanation for this.

2. According to the Hinshelwood theory,

$$k^1_\infty = \frac{k_1 k_2}{k_{-1}} = k_2 \frac{1}{(s-1)!}\left(\frac{\varepsilon^*_0}{kT}\right)^{s-1} \exp\left(-\frac{\varepsilon^*_0}{kT}\right) \quad ...(101)$$

Thus, one would expect a strong temperature-dependence of the pre-exponential factor, especially for large values of s. No experimental evidence exists for this.

3. The Hinshelwood treatment cannot account for the lack of linearity found experimentally for the plot of $1/k^1$ versus $1/[A]$.

3. RRK (Rice–Rampsberger–Kassel) Theory. With a slight modification of the Lindemann theory, the mechanism of unimolecular reactions can, following the Hinshelwood suggestion, be written as

$$A + M \underset{k_{-1}}{\overset{k_1}{\rightleftharpoons}} A^* + M$$

$$A^* \longrightarrow A^{\#} \longrightarrow \text{products}$$

where M is any molecule, including another A, that can transfer energy to A when a collision occurs; A^* is the energized molecule and $A^{\#}$ is the activated molecule. To become an activated molecule, the molecule A must acquire at least the energy ε_0^*. The energy scheme for the Lindemann, Hinshelwood and RRK, theory is shown in Fig. 16. Hinshelwood's modification allowed A to acquire an amount of energy ε_0^* at an enhanced rate but regarded the rate at which A^* becomes $A^{\#}$ to be independent of that energy. In the subsequent theoretical treatment, the rate constant k_2 was not treated as a constant but was considered to be larger the greater the value of ε^*. Eq. 104 can now be written in the more general form :

$$k^1 = \frac{k_2(k_1/k_{-1})}{1 + k_2/k_{-1}[M]} \qquad \ldots(102)$$

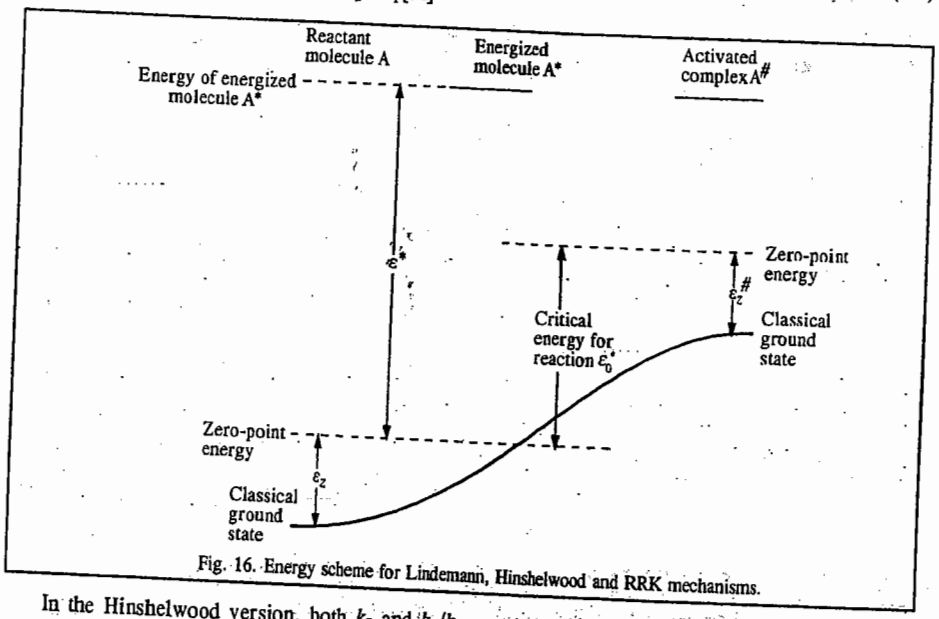

Fig. 16. Energy scheme for Lindemann, Hinshelwood and RRK mechanisms.

In the Hinshelwood version, both k_2 and k_1/k_{-1} are treated as independent of ε^*, the amount of energy in the energized molecule. Hinshelwood's result involves the critical energy ε_0^*, rather than ε^*. After the derivation of the Hinshelwood formula (in 1927), O.K. Rice and H.C. Rampsberger, and independently L.S. Kassel, proposed theories (in 1928) wherein both k_2 and k_1/k_{-1} were treated as dependent on ε^*. These theories are referred to jointly as the RRK theory. In this theory, k_2 is replaced by $k_2(\varepsilon^*)$ and k_1/k_{-1} by $f(\varepsilon^*)$, which is a distribution function, so that Eq. 102 is

written as

$$dk^1 = \frac{k_2(\varepsilon^*)f(\varepsilon^*)}{1 + k_2(\varepsilon^*)/k_{-1}[M]}\, d\varepsilon^* \qquad \ldots(103)$$

Here dk^1 is a microcanonical rate constant which relates to energized molecules having energy between ε^* and $\varepsilon^*+d\varepsilon^*$. To obtain the ordinary rate constant k^1, this expression must be integrated from ε_0^* — the minimum energy that may lead to reaction— to infinity :

$$k^1 = \int_{\varepsilon^*}^{\infty} \frac{k_2(\varepsilon^*)f(\varepsilon^*)}{1 + k_2(\varepsilon^*)/k_{-1}\,[M]}\, d\varepsilon^* \qquad \ldots(104)$$

In the RRK formatism, a molecule is regarded as a system of loosely coupled oscillators. In the energized molecule A^*, the energy ε^* is distributed among the normal modes of vibration. Because the normal modes are coupled loosely, the energy can flow between them and after a sufficient number of vibrations, the critical amount of energy ε_0^* may be in a particular normal mode and reaction can occur. Thus, for example, energy in an energized ethane molecule, $C_2H_6^*$, may pass into a normal vibrational mode which corresponds to an extension of the C—C bond and if the energy is sufficiently large, the bond will break leading to the formation of two $\cdot CH_3$ radicals. In the RRK theory, the oscillators are all assumed to have the same vibrational frequency.

An important feature of the RRK theory is that the energized molecules A^* have random lifetimes, which means that the energy is distributed randomly among the various normal modes so that the process $A^* \longrightarrow A^{\#}$ depends entirely on statistical factors. Another important feature of the theory is that the collisions that produce A^* molecules and also those that deactivate them are strong collisions. This means that during collisions large amounts of energy ($>> kT$) are transferred. This implies that activation more often occurs in a single collision than as a result of successive collisions. When an energized molecule A^* undergoes a collision it is assumed that it inevitably gets de-energized.

According to the RRK theory, the dependence of k_2 on ε^* is as follows : The statistical weight of a system of s degrees of vibrational freedom containing j quanta of vibrational energy is equal to the number of ways in which J objects can be divided among s boxes each of which can contain any number of objects. The number of such ways is given by

$$w = \frac{(j + s - 1)!}{j!(s - 1)!} \qquad \ldots(105)$$

The statistical weight for states in which s oscillators have j quanta among them, and one particular one has m quanta, is similarly given by

$$w' = \frac{(j - m + s - 1)!}{(j - m)!(s - 1)!} \qquad \ldots(106)$$

The probability that a particular oscillator has m quanta and all s oscillators have j quanta is given by the ratio

$$r = \frac{w'}{w} = \frac{(j - m + s - 1)!\, j!}{(j - m)!(j + s - 1)!} \qquad \ldots(107)$$

Applying the Stirling approximation ($n ! = n^n/e^n$), the terms in e^n cancel out, giving

$$r = \frac{(j - m + s - 1)^{j-m+s-1}\, j^j}{(j - m)^{j-m}(j + s - 1)^{j+s-1}} \qquad \ldots(108)$$

If $j - m >> s - 1$, this reduces to

$$r = \frac{(j - m)^{j-m+s-1}\, j^j}{(j - m)^{j-m}\, j^{j+s-1}} = \left(\frac{j - m}{j}\right)^{s-1} \qquad \ldots(109)$$

The total number of quanta j may be taken as proportional to ε^*, the total energy of the molecule, while m is proportional to ε_0^*, the minimum energy that a molecule must have for decomposition to take place. Eq.109, thus, becomes

$$r = \left(\frac{\varepsilon^* - \varepsilon_0^*}{\varepsilon^*}\right)^{s-1} \qquad ...(110)$$

The rate at which the energy ε_0^* passes into this particular oscillator is proportional to this quantity so that

$$k_2 = k^{\#}\left(\frac{\varepsilon^* - \varepsilon_0^*}{\varepsilon^*}\right)^{s-1} \qquad ...(111)$$

We next turn our attention to the distribution function $f(\varepsilon^*)$ which, according to the RRK theory, is given by

$$f(\varepsilon^*) = \frac{1}{(s-1)!}\left(\frac{\varepsilon^*}{kT}\right)^{s-1}\frac{1}{kT}\exp(-\varepsilon^*/kT) \qquad ...(112)$$

It is assumed here that the energy ε^* is distributed among s normal modes of vibration.

Substituting Eqs. 111 and 112 into Eq. 104, we obtain

$$k^1 = \int_{\varepsilon_0^*}^{\infty}\left[\frac{k^{\#}\left(\frac{\varepsilon^* - \varepsilon_0^*}{\varepsilon^*}\right)^{s-1}\frac{1}{(s-1)!}\left(\frac{\varepsilon^*}{kT}\right)^{s-1}\frac{1}{kT}\exp(-\varepsilon^*/kT)}{1 + \frac{k^{\#}}{k_{-1}[M]}\left(\frac{\varepsilon^* - \varepsilon_0^*}{\varepsilon^*}\right)^{s-1}}d\varepsilon^*\right] \qquad ...(113)$$

This equation may be reduced using the following substitutions : $x = (\varepsilon^* - \varepsilon_0^*)/kT$; $b = \varepsilon_0^*/kT$. Changing $d\varepsilon^*/kT$ to dx and thereby the limits of integration, we obtain

$$k^1 = \int_0^{\infty}\frac{1/[(s-1)!]e^{-(x+b)}k^{\#}x^{s-1}dx}{1 + (k^{\#}/k_{-1}[M])[x(x+b)]^{s-1}} \qquad ...(114)$$

$$= \frac{k^{\#}e^{-b}}{(s-1)!}\int_0^{\infty}\frac{x^{s-1}e^{-x}dx}{1 + (k^{\#}/k_{-1}[M])[x(x+b)]^{s-1}} \qquad ...(115)$$

or

$$k^1 = \frac{k^{\#}\exp(-\varepsilon_0^*/kT)}{(s-1)!}\int_0^{\infty}\frac{x^{s-1}e^{-x}dx}{1 + (k^{\#}/k_{-1}[M])[x/(x+b)]^{s-1}} \qquad ...(116)$$

When [M] is very large, that is, at the high pressure first-order limit, this expression reduces approximately to

$$k_{\infty}^1 = k^{\#}\exp(-\varepsilon_0^*/kT) \qquad ...(117)$$

For given values of [M], ε_0^* and s, the integral in Eq. 116 can be evaluated numerically. Eq. 116 generally gives a reasonable agreement with experiment if s is taken to be about one-half of the total number of normal vibrational modes in the molecule.

Limitations of RRK Theory. 1. This is one unsatisfactory feature of the theory ; it is impossible to predict what value of s should be taken for a given reaction. In this expression, the rate constant $k^{\#}$ corresponds to the free passage of the system through the dividing surface. When ε^* is sufficiently large, the energized molecule is essentially an activated molecule and, therefore, can pass immediately to the final state. The variation of k_2 with $\varepsilon^*/\varepsilon_0^*$, given by Eq. 111, is shown in Fig. 17.

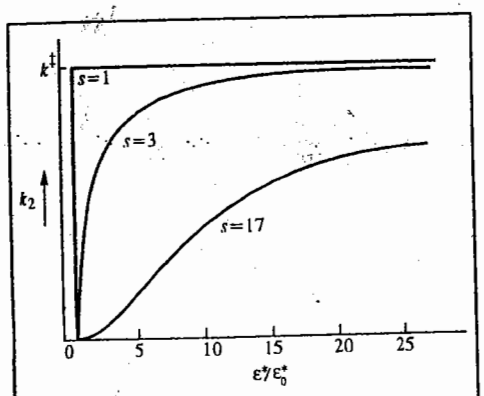

Fig. 17. Variation of k_2 with $\varepsilon^*/\varepsilon_0^*$ for different values of s.

2. The significance of $k^{\#}$ in RRK theory is also rather unsatisfactory. If there were a complete redistribution of energy among the normal modes on every vibration, the theory would predict that the pre-exponential factor for the reaction in its high pressure limit (Eq. 117) would be the average of the various normal-mode frequencies. It would, therefore, predict a pre-exponential factor of about 10^{13} s^{-1} for all unimolecular reactions. This is true for some reactions, but for many the values are very much greater than this. The RRK theory provides no explanation for such high values. According to Laidler and Steel (1961), the interpretation is provided by CTST (conventional transition state theory), which gives the following expression for $k^{\#}$:

$$k^{\#} = (kT/h)\,(q^{\#}/q_r) \qquad ...(118)$$

where $q^{\#}$ is the partition function for the activated complexes and q_r for the reactants. If it is reasonably assumed that the activated complexes have much looser structures than the reactants, $q^{\#} >> q_r$ and the large pre-exponential factors are accounted for.

4. RRKM (Rice-Rampsberger-Kassel-Marcus) Theory

During 1951-52, R.A. Marcus extended the RRK theory to bring it in line with the ACT

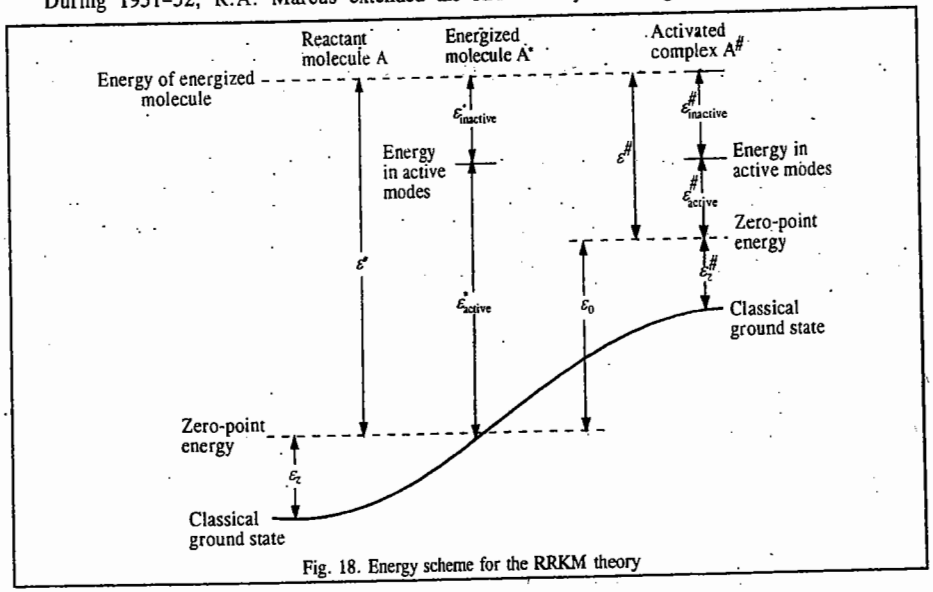

Fig. 18. Energy scheme for the RRKM theory

(activated complex). In the RRKM theory, the individual vibrational frequencies of the energized species and activated complexes are considered explicitly : account is taken of the way the various normal mode vibrations and rotations contribute to reaction, and allowance is made for zero-point energies. Fig. 18 shows the energy scheme for the RRKM theory.

The total energy contained in the energized molecule is classified as either active or inactive. The inactive energy is the energy that remains in the same quantum state during the course of the reaction and, therefore, cannot contribute to the breaking of bonds. The zero-point energy is inactive, as is the energy of overall translation and rotation, since this energy is preserved as such when the activated molecule $A^{\#}$ is formed. Vibrational energy and the energy of internal rotations are active. In the RRKM theory, the distribution function $\int(\varepsilon^*)d\varepsilon^*$ is calculated using quantum statistics and is given by

$$f(\varepsilon^*)d\varepsilon^* = \frac{\rho(\varepsilon^*)\exp(-\varepsilon^*/kT)d\varepsilon^*}{\int_0^\infty \rho(\varepsilon^*)\exp(-\varepsilon^*/kT)d\varepsilon^*} \qquad (119)$$

where $\rho(\varepsilon^*)$ is the density of states (DOS) having energy between ε^* and $\varepsilon^* + d\varepsilon^*$. The DOS is defined as the number of states per unit energy range. The denominator in Eq. 127 is the partition function relating to the active energy contributions.

According to the RRKM theory, the rate constant $k_2(\varepsilon^*)$ is given by

$$k_2(\varepsilon^*) = \frac{l^{\#}\Sigma P(\varepsilon^{\#}_{\text{active}})}{h\rho(\varepsilon^*)F_r} \qquad (120)$$

where $l^{\#}$ is the statistical factor and $\Sigma P(\varepsilon^{\#}_{\text{active}})$ is the number of vibration-rotation quantum states for the activated molecule corresponding to all energies upto and including $\varepsilon^{\#}_{\text{active}}$. The factor F_r is introduced to correct for the fact that the rotations may not be the same in the activated molecule as in the energized molecule.

A noteworthy feature of the RRKM theory is that it leads to the same expression for the limiting high-pressure unimolecular (first-order) rate constant as is given by the actviated complex theory, *viz.*,

$$k^1_\infty = \left(\frac{kT}{h}\right)\frac{q^{\#}}{q_i}\exp(-\varepsilon^*_0/kT) \qquad ...(121)$$

where $q^{\#}$ and q_i are the partition functions for the activated and initial states. Thus, the theory can explain the abnormally high pre-exponential factors that are sometimes observed. In order to use the RRKM theory for detailed calculations, we must decide on models for the energized and activated molecules. Vibrational frequencies for the various normal modes must be estimated and decisions made as to which energies are active and which are inactive. Numerical methods are used to calculate the rate constants k^1 at various concentrations. Reactions which have been successfully investigated include the isomerization of cyclopropane, the isomerization of cyclobutane and the dissociation of cyclobutane into two ethylene molecules. The isomerization of cyclopropane to propylene was the first unimolecular gaseous reaction investigated in the 1920s.

A major difficulty in applying the RRKM theory is that the vibrational frequencies of the activated complexes usually cannot be estimated very reliably and there is evidence for the non-RRKM behaviour.

In conclusion, we must remark that none of the theories of unimolecular reactions we have described so far addresses the possibility of *nonstatistical* energy distribution in the original A molecule or of non-statistical reaction dynamics. Much recent work is directed towards finding the

extent to which non-statistical behaviour exists. A key factor affecting the energy distribution is the mode of excitation of A. Thus, we have concentrated on excitation by collisions, that is, *thermal excitation*, which it seems should produce a statistical energy distribution. However, there are methods such as chemical and photochemical excitation wherein there is evidence for nonstatistical energy distributions.

One potential method for obtaining information about unimolecular reactions with non-thermal activation is the use of molecular beams. In such studies, it has been found that the translational energy distribution of reaction fragments is nonstatistical, contrary to the predictions of (say) the RRKM theory ; this implies that not all degrees of freedom participate in the fragmentation of the complex.

The reaction dynamics of molecules with many degrees of freedom is far from understood and is an area of intensive research. The issues we must analyze to construct a complete theory of unimolecular reactions are the process of acquisition of sufficient energy by a molecule for the breaking of a bond or bond rearrangement, the process of energy transfer within the molecule and the elementary chemical reaction steps. The last two processes compete with each other. The occurrence of chemical reaction requires the concentration of energy, say, within the bond that is to be broken, whereas energy transfer within the molecule tends to distribute the available energy among many, possibly all available degrees of freedom. There may occur the so-called bottlenecks to *intramolecular energy transfer* which restrict that transfer. These topics, including chaos in molecular dynamics, are being investigated by theorists and mathematical physicists.

Kinetics of Complex Reactions

The study of chemical kinetics becomes highly complicated due to the occurrence of *complex reactions* which involve more than one step. Important among such reactions are the following categories :

1. *Opposing or Reversible Reactions*
2. *Consecutive Reactions*
3. *Chain Reactions*.

We shall discuss here the kinetics of these three types of reactions briefly.

1. Kinetics of Opposing or Reversible Reactions. The kinetics of such reactions are usually studied in the initial stages of the process when the products are at too low a concentration to set up the opposing reaction at a noticeable rate. However, when the opposing reaction also takes place at a comparable rate, the problem becomes complicated and the rate constant obtained is not quite reliable.

Consider the simplest case of an opposing reaction in which the forward as well as the reverse reactions are both first-order :

$$A \underset{k_{-1}}{\overset{k_1}{\rightleftharpoons}} B$$

where k_1 and k_{-1} are the rate constants of the forward and the reverse reactions, respectively. Let a be the initial concentration of the reactant A. (It is assumed that initially the concentration of B=0). Then, after time t, the concentration of A will be $(a-x)$ and that of the product B will be x. The rate of the forward reaction is equal to $k_1(a-x)$ while that of the reverse reaction is $k_{-1}x$. Hence, the net rate of the formation of B is given by

$$dx/dt = k_1(a-x) - k_{-1}x \qquad ...(122)$$

If x_e is the concentration of B at equilibrium when the net rate is zero, then

$$k_1(a-x_e) - k_{-1}x_e = 0 \quad \text{or} \quad k_1(a-x_e) = k_{-1}x_e \qquad ...(123)$$

or $$k_{-1} = k_1(a - x_e)/x_e \quad ...(124)$$

Substituting for k_{-1} in Eq. 122, we have

$$dx/dt = k_1(a - x) - k_1\left(\frac{a - x_e}{x_e}\right)x = k_1\frac{(x_e - x)a}{x_e} \quad ...(125)$$

Separating the variables, we have

$$\frac{dx}{x_e - x} = \frac{a}{x_e}k_1 a\, t \quad ....(126)$$

Integrating, we get

$$-\ln(x_e - x) = \frac{a}{x_e}(k_1 t + I) \quad ...(127)$$

where I is the constant of integration.

or $$-\frac{x_e}{a}\ln(x_e - x) = k_1 t + I \quad ...(128)$$

At $t=0$, $x=0$, so that $$I = -\frac{x_e}{a}\ln x_e \quad ...(129)$$

Hence, substituting for I in Eq. 128, we have

$$-\frac{x_e}{a}[\ln(x_e - x)] = k_1 t - \frac{x_e}{a}\ln x_e$$

or $$k_1 t = \frac{x_e}{a}\ln\left(\frac{x_e}{x_e - x}\right) \quad \text{or} \quad k_1 = \frac{x_e}{at}\ln\left(\frac{x_e}{x_e - x}\right) \quad ...(130)$$

Eq. 130 gives k_1 in terms of easily measurable quantities.

From Eq. 124, we have

$$(1 + k_{-1}) = k_1\frac{a}{x_e} = \frac{1}{t}\ln\left(\frac{x_e}{x_e - x}\right) \quad ...(131)$$

Thus, from a knowledge of k_1, a and x_e, the rate constant k_{-1} for the reverse reaction can be calculated.

Let us now suppose that initially a small amount of B, say b moles, is present. Then, the net rate of formation of B is given by

$$dx/dt = k_1(a - x) - k_{-1}(b + x) \quad ...(132)$$

Since at equilibrium, $dx/dt = 0$, hence

$$k_1(a - x_e) = k_{-1}(b + x_e) \quad ...(133)$$

or $$k_{-1} = k_1(a - x_e)/(b + x_e) \quad ...(134)$$

Substituting for k_1 in Eq. 132, we get

$$\frac{dx}{dt} = k_1(a - x) - k_1\frac{(a - x_e)(b + x_e)}{b + x_e} = k_1\left(\frac{a + b}{b + x_e}\right)(x_e - x) \quad ...(135)$$

Separating the variables,

$$\left(\frac{b + x_e}{a + b}\right)\left(\frac{dx}{x_e - x}\right) = k_1 dt \quad ...(136)$$

Integration yields

$$(b + x_e)/(a + b)\,[-\ln(x_e - x)] = k_1 t + I \quad ...(137)$$

Since at $t=0$, $x=0$, we have

$$I = \left(\frac{b + x_e}{a + b}\right)(-\ln x_e) \quad ...(138)$$

Substituting for I in Eq. 137, we have

$$k_1 = \frac{b + x_e}{t(a + b)}\ln\left(\frac{x_e}{x_e - x}\right) \quad ..(139)$$

From Eq. 134, $$x_e = \frac{k_1 a - k_{-1}b}{k_1 + k_{-1}} \quad ...(140)$$

Substituting for x_e in Eq. 139, we have

$$(k_1 + k_{-1}) = \frac{1}{t}\ln\left(\frac{x_e}{x_e - x}\right) \quad ...(141)$$

Notice that Eq. 141 is similar to Eq. 131 which is obtained when no B was present initially.

2. Kinetics of Consecutive Reactions. Reactions which take place in two or more steps, one after the other, are called consecutive reactions. Their characteristic features are illustrated in the following example,

Example 49. Consider two consecutive first-order reactions : $A \xrightarrow{k_1} B \xrightarrow{k_2} C$. Assuming that $k_1 \neq k_2$ and at time $t=0$ only A is present and [B]=[C]=0, show that as the reaction proceeds, [B] reaches a maximum and falls off thereafter. Derive expressions for t_{max} (*i.e.*, the time when [B] is a maximum) in terms of the rate constants k_1 and k_2 and for $[B_{max}]$, *i.e.*, the maximum concentration of B. Also, plot the concentrations of A, B and C as a function of time.

Solution : To simplify notation, we write

Concentrations at time t :

$$[A] = a\,; \qquad [B] = b\,; \qquad [C] = c \quad ...(i)$$

Initial concentrations :

$$[A] = a_0\,; \qquad [B] = b_0\,; \qquad [C] = c_0 \quad ...(ii)$$

$$d[A]/dt = \dot{a}\,; \qquad d[B]/dt = \dot{b}\,; \qquad d[C]/dt = \dot{c} \quad ...(iii)$$

With this notation, the rate equations are

$$\dot{a} = -k_1 a\,; \quad \dot{b} = k_1 a - k_2 b\,; \quad \dot{c} = k_2 b \quad ...(iv)$$

The condition for mass conservation requires that

$$a_0 = a + b + c \qquad (a_0 \text{ is the initial concentration at } t = 0) \quad ...(v)$$

$$\therefore \quad a = a_0 - b - c \quad ...(vi)$$

Hence, $$\dot{b} = k_1(a_0 - b - c) - k_2 b \quad ...(vii)$$

Since $\dot{a}_0 = 0$, hence $\ddot{b} = k_1(-\dot{b} - \dot{c}) - k_2\dot{b} = k_1(-\dot{b} - k_2 b) - k_2\dot{b}$ ...(viii)

which can be rearranged to yield

$$\ddot{b} + (k_1 + k_2)\dot{b} + k_1 k_2 b = 0 \quad ...(x)$$

The general solution of this equation is

$$b = C_1\exp(m_1 t) + C_2\exp(m_2 t) \quad ...(x)$$

where C_1 and C_2 are constants and m_1, m_2 are the two roots of the equation, $m^2 + (k + k_2)m + k_1 k_2 = 0$ ...(xi)

This quadratic equation can be easily solved to give

$$m_1 = -k_1 \quad \text{and} \quad m_2 = -k_2 \quad ...(xii)$$

Substituting Eq. *(xii)* into Eq. *(x)*, we get

$$b = C_1\exp(-k_1 t) + C_2\exp(-k_2 t) \quad ...(xiii)$$

Since at $t = 0$, $b = 0$, hence from Eq. *(x)*

$$C_1 + C_2 = 0 \quad \text{or} \quad C_1 = -C_2 \qquad \ldots(xiv)$$

$$\therefore \quad b = C_1[\exp(-k_1t) - \exp(-k_2t)] \qquad \ldots(xv)$$

We now evaluate C_1 : $\quad \dot{b} = C_1[-k_1 \exp(-k_1t) + k_2 \exp(-k_2t)] \qquad \ldots(xvi)$

$$\text{At} \quad t = 0, \ \dot{b} = C_1(-k_1 + k_2) \qquad \ldots(xvii)$$

Also from equation *(vii)*, at $t = 0$, $b = c = 0$, so that

$$\dot{b} = k_1a_0 \qquad \ldots(xviii)$$

Hence, from Eqs. *(xvii)* and *(xviii)*,

$$C_1 = k_1a_0/(k_2 - k_1) \qquad \ldots(xix)$$

Substituting for C_1 in Eq. *(xv)*, we have

$$b = \frac{k_1a_0}{(k_2 - k_1)}[\exp(-k_1t) - \exp(-k_2t)] \qquad \ldots(xx)$$

Again, since $\dot{a} = -k_1a$ (Eq. *(iv)*]

$$\therefore \quad a = a_0 \exp(-k_1t) \qquad \ldots(xxi)$$

To calculate the value of c, we use the mass conservation requirement, *viz.*, $a_0 = a + b + c$,

$$\therefore \quad c = a_0 - a - b = a_0\left[1 - \frac{k_2\exp(-k_1t) - k_1\exp(-k_2t)}{k_2 - k_1}\right] \qquad \ldots(xxii)$$

Maximum Value of [B] : For a maximum value of b, *i.e.*, b_{max}, $\dot{b} = db/dt = 0$ and $\ddot{b} = d^2b/dt^2 < 0$. Hence, from Eq. *(xx)*, after putting $\dot{b} = 0$, we have

$$k_1 \exp(-k_1t_{max}) = k_2 \exp(-k_2t_{max}) \qquad \ldots(xxiii)$$

or $\quad k_1/k_2 = \exp[(k_1 - k_2)t_{max}] \qquad \ldots(xxiv)$

Taking logs, $\quad \ln(k_1/k_2) = (k_1 - k_2)t_{max}$

$$t_{max} = \frac{\ln(k_1/k_2)}{k_1 - k_2} \qquad \ldots(xxv)$$

Again, from Eq. *(ix)*, $\ddot{b} + (k_1 + k_2)\dot{b} + k_1k_2b = 0$

or $\quad \ddot{b} = -k_1k_2b = \text{a negative quantity}$

$$(\because \dot{b} = 0) \qquad \ldots(xxvi)$$

Thus, we see that at $t = t_{max}$, b reaches a maximum ; it does not have a minimum or a point of inflection.

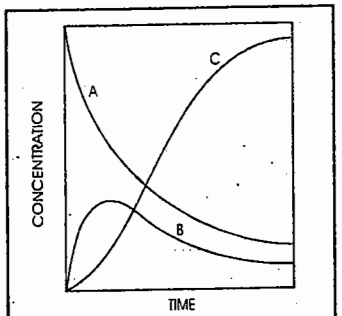

Fig. 19. Concentration-time graph in a consecutive reaction :

$$A \xrightarrow{k_1} B \xrightarrow{k_2} C, \text{ when } k_1 \neq k_2$$

Substituting Eq. *(xxv)* into Eq. *(xx)*, we get

$$b_{max} = \frac{k_1a_0}{k_2 - k_1}\left\{\exp\left[-\frac{k_1\ln(k_1/k_2)}{k_1 - k_2}\right] - \exp\left[-\frac{k_2\ln(k_1/k_2)}{k_1 - k_2}\right]\right\} \qquad \ldots(xxvii)$$

which, on simplification, yields

$$b_{max} = a_0(k_2/k_1)^{k_2/(k_1-k_2)} \qquad \ldots(xxviii)$$

The time-dependence of a, b and c is shown in Fig. 19. The curve for [B] clearly shows that [B] reaches a maximum and falls off thereafter.

3. Kinetics of Chain Reactions. Chain reactions are a specific class of reactions in which highly reactive (transient, *i.e.*, short-lived) species (atoms or free radicals) are produced as intermediates which carry out the reaction at a rapid rate for a long time. These reactions were first studied in 1934 by Frank O. Rice (1890–1989) and Karl F. Herzfeld (1892–1978) and are referred to as Rice–

Herzfeld chain reactions. The steady state approximation has proved highly useful in accounting for their rate laws.

Such reactions include gas-phase pyrolysis (*i.e.*, high temperature decomposition) of hydrocarbons, aldehydes, several other carbonyl compounds, polymerizations and reactions of hydrogen with halogens and oxygen.

A typical chain reaction is that between H_2 and Br_2 to form HBr [$H_2(g) + Br_2(g) \longrightarrow 2HBr(g)$] for which a five-step mechanism has been proposed :

(1)	$Br_2 \xrightarrow{k_1} 2Br$	(Chain initiation)
(2)	$Br + H_2 \xrightarrow{k_2} HBr + H$	(Chain propagation)
(3)	$H + Br_2 \xrightarrow{k_3} HBr + Br$	(Chain propagation)
(4)	$H + HBr \xrightarrow{k_4} H_2 + Br$	(Chain retardation)
(5)	$2Br \xrightarrow{k_5} Br_2$	(Chain termination)

Here k_is ($i = 1, 2, \ldots, 5$) are the rate constants for the different steps.

In this chain reaction, the reactive intermediate is consumed, the reactants are converted to products and the intermediate is regenerated. The regeneration of the intermediate allows the cycle to be repeated over and over again. Let us discuss the various steps briefly.

Step 1. Chain initiation. Bromine molecule acquires energy as a result of collision (with another bromine molecule or sometimes with a foreign molecule which may be present as an impurity) to dissociate into two Br atoms. This is a chain-initiation step since it produces the chain-carrying reactive (transient, short-lived) Br atoms.

Steps 2, 3. Chain propagation. Steps (2) and (3) are chain propagation steps. Here the chain consumes Br, converting H_2 and Br_2 into HBr and regenerating Br.

Step 4. Chain retardation (or *Chain inhibition*). In this step, the chain is inhibited by the destruction of product, HBr, thereby decreasing the rate of its formation.

Step 5. Chain termination. This step removes Br atoms, converting them back to Br_2 molecule. This step is the reverse of the chain-initiation step.

The reactive species H and Br, which are responsible for propagating the chain, are called *chain carriers*.

The rate law for the formation of HBr from H_2 and Br_2 in the temperature range 500 – 1500 K is found to be given by

$$r = d[HBr]/dt = k_2'[Br_2]^{1/2}$$

This rate law was accounted for by Rice and Herzfeld by using steady state approximation for [H] and [Br], according to which

$$d[H]/dt = d[Br]/dt = 0$$

Example 50. Using the Rice-Herzfeld mechanism for the reaction $H_2 + Br_2 \longrightarrow 2HBr$, given above and employing steady state approximation for [H] and [Br], derive the rate law expression for the formation of HBr.

Solution : In writing the rate expression for any species we should bear in mind that the sign is positive if given species is formed in a certain step and negative if it is consumed in the step. Consider $d[HBr]/dt$. HBr is formed in steps (2) and (3) and consumed in step (4). Thus,

$$d[HBr]/dt = k_2[Br][H_2] + k_3[H][Br_2] - k_4[H][HBr] \qquad \ldots(i)$$

Similarly, $\quad d[H]/dt = k_2[Br][H_2] - k_3[H][Br_2] - k_4[H][HBr] = 0$ (according to *s.s.a.*) $\qquad \ldots(ii)$

$$d[Br]/dt = 2k_1[Br_2] - k_2[Br][H_2] + k_3[H][Br_2] + k_4[H][HBr] - 2k_5[Br]^2 \quad ...(iii)$$
$$= 0 \text{ (according to } s.s.a.\text{)}$$

Adding Eqs. *(ii)* and *(iii)*, we get

$$2k_1[Br_2] - 2k_5[Br]^2 = 0 \text{ whence } [Br] = (k_1/k_5)^{1/2}[Br_2]^{1/2} \quad ...(iv)$$

From Eq. *(ii)*, $$[H] = \frac{k_2[Br][H_2]}{k_2[Br_2] + k_4[HBr]} \quad ...(v)$$

Substituting Eq. *(iv)* into Eq. *(v)*, we have

$$[H] = k_2\left(\frac{k_1}{k_5}\right)^{1/2}\frac{[Br_2]^{1/2}[H_2]}{k_3[Br_2] + k_4[HBr]} \quad ...(vi)$$

Substituting Eqs. *(iv)* and *(vi)* into Eq. *(i)*, we get

$$\frac{d[HBr]}{dt} = k_2\left(\frac{k_1}{k_2}\right)^{1/2}[Br_2]^{1/2}[H_2] + k_2k_3\left(\frac{k_1}{k_5}\right)^{1/2}\frac{[Br_2]^{1/2}[H]}{k_3[Br_2] + k_4[HBr]} - k_4k_2\left(\frac{k_1}{k_5}\right)^{1/2}\frac{[Br_2]^{1/2}[H_2][HBr]}{k_3[Br_2] + k_4[HBr]}$$

$$= \frac{2k_2(k_1/k_5)^{1/2}[Br_2]^{3/2}[H_2]}{k_3[Br_2] + k_4[HBr]} + \frac{k_4k_2(k_1/k_5)^{1/2}[Br_2]^{1/2}[H_2][HBr]}{k_3[Br_2] + k_4[HBr]} - \frac{k_4k_2(k_1/k_5)^{1/2}[Br_2]^{1/2}[H_2][HBr]}{k_3[Br_2] + k_4[HBr]} \quad ...(vii)$$

The last two terms in the above equation cancel out, giving

$$\frac{d[HBr]}{dt} = \frac{2k_2(k_1/k_5)^{1/2}[Br_2]^{3/2}[H_2]}{k_3[Br_2] + k_4[HBr]} \quad ...(viii)$$

Dividing the numerator and the denominator by $[Br_2]$, we get

$$\frac{d[HBr]}{dt} = \frac{2k_2(k_1/k_5)^{1/2}[Br_2]^{1/2}[H_2]}{k_3 + k_4\frac{[HBr]}{[Br_2]}} = \frac{2k_2(k_1/k_5)^{1/2}[Br_2]^{1/2}[H_2]}{1 + \left(\frac{k_4}{k_3}\right)\frac{[HBr]}{[Br_2]}} \quad ...(ix)$$

If in Eq. *(ix)*, the term $\left(\frac{k_4}{k_3}\right)\frac{[HBr]}{[Br_2]} < 1$, then it can be neglected in the denominator so that the rate law becomes

$$r = \frac{d[HBr]}{dt} = k[H_2][Br_2]^{1/2} \quad ...(x)$$

where $k = 2k\left(\frac{k_1}{k_5}\right)^{1/2}$ is the observed rate constant.

We see from Eq. *(x)* that the reaction is pseudo 3/2-order. This is experimentally observed.

Note : We can reach the above conclusion by proceeding after Eq. *(vii)* as follows :

In the initial stages, $[HBr] = 0$ so that Eq. *(vii)* becomes

$$\frac{d[HBr]}{dt} = 2\left(\frac{k_2}{k_3}\right)\left(\frac{k_1}{k_5}\right)^{1/2}[H_2][Br_2]^{1/2} = k'[H_2][Br_2]^{1/2}$$

where k' is the effective rate constant given by $k' = 2(k_2/k_3)(k_1/k_5)^{1/2}$.

Example 51. The following Rice-Herzfeld mechanism has been proposed for the gas phase pyrolysis of methane, CH_4 :

$$CH_4 \xrightarrow{k_1} \cdot CH_3 + H\cdot$$
$$\square\cdot CH_3 + CH_4 \xrightarrow{k_2} C_2H_6 + H\cdot$$
$$H\cdot + CH_4 \xrightarrow{k_3} \cdot CH_3 + H_2$$
$$H + \cdot CH_3 + M \xrightarrow{k_4} CH_4 + M$$

In the last reaction, M is a molecule (CH_4 or C_2H_6) which can carry away the energy of recombination of $\cdot CH_3$ and $H\cdot$. Assuming the steady state approximation (*s.s.a.*) for $[H\cdot]$ and $[\cdot CH_3]$, derive the rate law for the formation of C_2H_6.

Solution : $$\frac{d[C_2H_6]}{dt} = k_2[\cdot CH_3][CH_4] \quad ...(i)$$

Also, $$\frac{d[\cdot CH_3]}{dt} = k_1[CH_4] - k_2[\cdot CH_3][CH_4] + k_3[H\cdot][CH_4] = 0 \text{ (according to } s.s.a\text{)} \quad ...(ii)$$

Similarly, $$\frac{d[\cdot H]}{dt} = k_1[CH_4] + k_2[\cdot CH_3][CH_4] - k_3[H\cdot[CH_4] - k_4[H\cdot][\cdot CH_3][M]$$
$$= 0 \text{ (according to } s.s.a.\text{)}$$

Adding Eqs. *(ii)* and *(iii)*, ...(iii)

$$2(k_1[CH_4] - k_4[H\cdot][\cdot CH_3][M] = 0 \quad \text{or} \quad k_1[CH_4] - k_4[\cdot H][\cdot CH_3][M] = 0 \quad ...(iv)$$

Substracting Eq. *(iii)* from Eq. *(ii)*,

$$-2k_2[\cdot CH_3][CH_4] + 2k_3[\cdot H][CH_4] = 0$$

$$\therefore \quad k_3[H\cdot] = k_2[\cdot CH_3] \quad \text{or} \quad [\cdot CH_3] = (k_3/k_2)H\cdot \quad ...(v)$$

From Eq. *(iv)* ...(vi)

$$k_4[\cdot H][\cdot CH_3]][M] = [k_1CH_4]$$

Rewriting Eq. *(v)* as ...(vii)

$$(k_3/k_2)[\cdot H] = [\cdot CH_3] \quad \text{(Note this step)}$$

and dividing Eq. *(vi)* by Eq. *(vii)* to eliminate $[\cdot H]$, we get ...(viii)

$$\frac{k_2k_4[\cdot CH_3[M]}{k_3} = \frac{k_1[CH_4]}{[\cdot CH_3]} \quad ...(ix)$$

$$[\cdot CH_3] = \left(\frac{k_2k_3[CH_4]}{k_2k_4[M]}\right)^{1/2} \quad ...(x)$$

Substituting Eq. *(x)* into Eq. *(i)*, we get

$$\frac{d[C_2H_6]}{dt} = k_2\left(\frac{k_1k_3[CH_4]}{k_2k_4[M]}\right)^{1/2}[CH_4] = \left(\frac{k_1k_2k_3[CH_4]^3}{k_4[M]}\right)^{1/2}$$

which is the **required rate law.**

Kinetics of Branched Chain Reactions. Consider a general gaseous chain reaction in which A is the *reactant*, R is a reactive *chain carrier*, P is the *product* and α is the number of chain carriers produced by one carrier in the propagation step. Then, we can write

$$A \xrightarrow{k_1} R \qquad \textit{(Chain initiation)}$$
$$R + A \xrightarrow{k_2} \cdot P + \alpha R \qquad \textit{(Chain propagation)}$$
$$R \xrightarrow{k_3} \text{destruction} \qquad \textit{(Chain termination)}$$

The chain carrier may be destroyed by either collision against the walls of the vessel or with other molecules. The rate of formation of chain carrier is given by

$$d[R]/dt = k_1[A] - k_2[R][A] + \alpha k_2[R][A] - k_3[R] \quad ...(142)$$

Assuming steady state approximation for the chain carrier, *i.e.*, $d[R]/dt = 0$, we have

$$[R] = \frac{k_1[A]}{k_2[A](1 - \alpha) + k_3} \quad ...(143)$$

The constant k_3 may be considered as equal to the sum of two terms, k_w for the wall reaction

and k_g for the gas-phase reaction, so that Eq. 143 becomes

$$[R] = \frac{k_1[A]}{k_2[A](1-\alpha) + k_w + k_g} \quad ...(144)$$

Consider the following cases of Eq. 144 :

Case 1. When $\alpha=1$, *i.e.*, each propagation sequence of the reaction results in the formation of a product molecule with the regeneration of only *one* chain carrier. Such chain reactions are called **non-branched** or **stationary chain reactions.** In these reactions, the radical concentration is proportional to the ratio of its rate of formation to the rate of its decomposition. Examples of such reactions include pyrolysis of several organic compounds.

Case 2. When $\alpha > 1$, *i.e.*, more than one chain carriers are produced in the propagation sequence of the reaction. Such chains are called **branched chains** or **non-stationary chains.** The theory of branched chain reactions was proposed independently by the Soviet chemist, N.N. Semenov (1896–1986) and the British chemist, C.N. Hinshelwood (1897–1967). They shared the 1956 Chemistry Nobel Prize for their researches into the mechanism of chemical reactions. Semenov was the only 20th century Rnssian Nobel Laureate in Chemistry.

In a situation when $\alpha >> 1$, *i.e.*, a very large number of chain carriers are produced in the propagation sequence, the carrier concentration [R], becomes almost infinite. As a result, the rate of reaction also becomes almost infinite resulting in *explosion*. When [R] tends to infinity, the denominator of Eq. 144 tends to zero which implies that

$$k_2[A](1-\alpha) = -(k_w + k_g) \quad ...(145)$$

Such explosions are called **isothermal explosions.** We see that the transition from a relatively slow rate to a very rapid explosion depends upon the relative magnitudes of (k_w+k_g) and $k_2[A](1-\alpha)$.

The rate constant k_w, which determines the rate of destruction of the chain carriers on the walls, depends on the diffusion of the carriers to the walls and is fast at low pressures. When the pressure falls to a stage that chain carriers are destroyed on the walls at the same rate at which they are produced, no explosion occurs (under these conditions k_g is unimportant). This gives a lower explosion limit which depends upon the size and material of the reaction vessel. With increase in pressure, the diffusion of the chain carriers to the walls decreases so that k_w also decreases. Under these conditions the destruction of the chain carriers due to collisions in the gas phase increases. Accordingly, k_g increases so that the term $[k_w+k_g+k_2[A](1-\alpha)]$ is still positive. If, however, the pressure is further increased, a stage is reached when the term (k_w+k_g) counterbalances $k_2[A](1-\alpha)$ leading to an explosion. This is called the **first explosion limit.** With a further increase in pressure, the chain ending process in the gas phase predominates (diffusion to the walls being negligible) and the term $k_w+k_g+k_2[A](1-\alpha)$ steadily increases thereby giving a **second explosion limit.** Above this pressure, the reaction proceeds at a finite rate. The variation of reaction rate with pressure in the case of H_2—O_2 reaction is shown in Fig. 20.

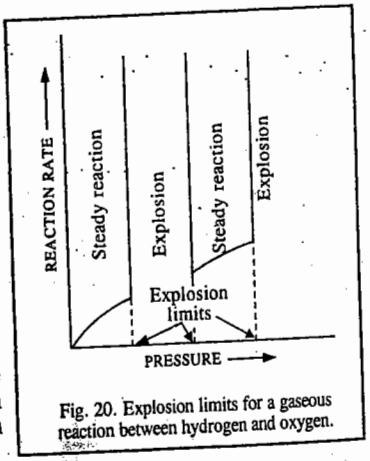

Fig. 20. Explosion limits for a gaseous reaction between hydrogen and oxygen.

Kinetics of Reactions in Solution

The collision theory of bimolecular reactions discussed eariler applies to gas phase reactions. It is not expected to apply to reactions in solution since the solvent would hinder the collisions. And yet, surprisingly, there are certain reactions for which the rate constant and the activation energy

are almost the same when the reactions are studied in a solvent as when they are investigated in the gas phase. We conclude, therefore, that the Arrhenius factors for these cases are nearly the same.

How can we account for this ? The answer probably lies in the fact that, as already pointed out, in solution the word *collision* is replaced by the word *encounter*. When the two molecules collide with each other in solution they are hindered from separating after an unreactive collision (encounter) since they are surrounded by a cage of solvent molecules. Thus, they make many collisions before separating. These collisions (encounters) compensate for the relatively slow diffusion of the reactant molecules towards each other in the liquid phase.

Diffusion-Controlled Reactions in Solution. Diffusion-controlled reactions in solution are generally very fast, requiring very small, nearly zero, activation energy. Examples of diffusion-controlled reactions are the electron-transfer, the proton-transfer and atom-recombination reactions in organic solvents. For a reaction taking place extremely rapidly in solution, the rate of chemical interaction is often greater than the rate with which the reacting molecules approach each other by diffusing through the liquid. In such a case, the experimentally measured rate is not the rate of interaction between the molecules but is, instead, the rate of diffusion. Such reactions are called **diffusion-controlled reactions.**

The theory of diffusion-controlled reactions was developed by Peter Debye, who made use of the ideas of the Polish physicist, M. Smoluchowski. In 1917, Smoluchowski had developed a theory of the growth of the colloidal particles and their diffusion towards the surface.

Let us consider two uncharged reactant molecules A and B having radii r_A and r_B and diffusion coefficients D_A and D_B, respectively. If n_A and n_B are the numbers of A and B molecules per cm^3, then the number of encounters ν per cubic centimetre per second between A and B is given by

$$\nu = 4\pi (D_A + D_B)(r_A + r_B) n_A n_B \text{ cm}^{-3} \text{ s}^{-1} \quad ...(146)$$

Eq. 146 also gives the reaction rate in terms of molecules cm^{-3} s^{-1} if each encounter leads to chemical reaction.

To obtain the rate in mol cm^{-3} s^{-1} we divide ν by N_A, the Avogadro's number. Then, evidently,

$$\nu/N_A = k_D(n_A/N_A)(n_B/N_A) \text{ mol cm}^{-3} \text{ s}^{-1} \quad ...(147)$$

where k_D is the diffusion-controlled rate constant (in cm^3 mol^{-1} s^{-1}) and n_A/N_A and n_B/N_A are the molar concentrations (mol cm^{-3}) of A and B, respeetively. From Eq. 147,

$$\nu = k_D n_A n_B / N_A \quad ...(148)$$

Hence, from Eqs. 146 and 148

$$k_D = 4\pi N_A(D_A + D_B)(r_A + r_B) \text{ cm}^3 \text{ mol}^{-1} \text{ s}^{-1} \quad ...(149)$$

The diffusion coefficient of a spherical molecule in a liquid is related to the coefficient of viscosity η of the liquid and the radius r of the molecule by the Stokes' equation, *viz.*, $D=k_BT/6\pi\eta r$. Thus, for the molecules A and B,

$$D_A = k_BT/6\pi\eta r_A ; \qquad D_B = k_BT/6\pi\eta r_B \quad ...(150)$$

where k_B is Boltzmann constant$=R/N_A$.

Substituting Eq. 150 into Eq. 149, we have

$$k_D = \frac{2RT}{3\eta} \times \frac{(r_A + r_B)^2}{r_A r_B} \text{ cm}^3 \text{ mol}^{-1} \text{ s}^{-1}$$

where R $(= N_A k_B)$ is the ideal gas constant. If we assume that $r_A=r_B$, then

$$k_D = (8RT/3\eta) \text{ cm}^3 \text{ mol}^{-1} \text{ s}^{-1} \quad ...(151)$$

Eq. 151 is the well-known **Debye-Smoluchowski equation** for the rate constant of a diffusion-

controlled reaction. It may be noted that in this equation the radii of the molecules have been cancelled out. Thus, the bimolecular rate constant of a diffusion-controlled reaction is independent of the size of the molecules. Also, we see that k_D is inversely proportional to the coefficient of viscosity of the solvent.

Note : Had we used SI units in this derivation, we would have obtained the expression $k_D = (8RT/3\eta)$ m^3 mol^{-1} s^{-1}.

Example 52. Estimate the diffusion-controlled rate constant for the combination of molecules A and B in water at 25°C. The coefficient of viscosity of water at this temperature is 1 cP (centipoise).

Solution : $\eta = 1$ cP $= 10^{-2}$ P $= 10^{-3}$ kg m^{-1} s^{-1}

From Eq. 151, $$k_D = \frac{8RT}{3\eta} = \frac{8 \times (8{\cdot}314 \text{ J K}^{-1} \text{ mol}^{-1})(298 \text{ K})}{3 \times 10^{-3} \text{ kg m}^{-1} \text{ s}^{-1}}$$

$$= 7 \times 10^6 \text{ m}^3 \text{ mol}^{-1} \text{ s}^{-1} = \mathbf{7 \times 10^9 \text{ dm}^3 \text{ mol}^{-1} \text{ s}^{-1}}$$

Thus, we see that the diffusion-controlled reactions between neutral molecules in water have the rate constant of the order of 7×10^9 dm^3 mol^{-1} s^{-1}. The rate constant greater than this value should not be observed, a fact that is borne out by experiment. Of course, if the reactant species are oppositely charged, *e.g.*, H^+ and OH^- ions, then, the rate constant is about $1{\cdot}3 \times 10^{11}$ dm^3 mol^{-1} s^{-1}. This is due to the enhancement of diffusion as a result of electrostatic attraction between the two ions.

When the two reacting molecules are the same, *i.e.*, A=B, the Debye-Smoluchowski equation (Eq. 151) in SI units reduces to

$$k_D = (4RT/3\eta) \text{ m}^3 \text{ mol}^{-1} \text{ s}^{-1} \qquad \ldots(152)$$

Example 53. Estimate the diffusion-controlled rate constant for the recombination of iodine atoms in *n*-hexane solution at 25°C, given that η for hexane is 0·325 cP.

Solution : $\eta = 0{\cdot}325$ cP $= 0{\cdot}325 \times 10^{-2}$ P $= 3{\cdot}25 \times 10^{-3}$ P $= 3{\cdot}25 \times 10^{-4}$ kg m^{-1} s^{-1}

$$k_D = \frac{4RT}{3\eta} = \frac{(4)(8{\cdot}314 \text{ J K}^{-1} \text{ mol}^{-1})(298 \text{ K})}{(3)(3{\cdot}25 \times 10^{-4} \text{ kg m}^{-1} \text{ s}^{-1})}$$

$$= 1{\cdot}01 \times 10^7 \text{ m}^3 \text{ mol}^{-1} \text{ s}^{-1} = \mathbf{1{\cdot}01 \times 10^{10} \text{ dm}^3 \text{ mol}^{-1} \text{ s}^{-1}}$$

Influence of Ionic Strength on the Rates of Ionic Reactions. The Salt Effects

Ionic strength of a solution can considerably affect the rates of reactions, particularly the enzyme reactions. Consider a general reaction involving ions in solution, *viz.*,

$$A^{zA} + B^{zB} \rightleftharpoons [X^{\#}]^{(z_A + z_B)} \longrightarrow \text{Products}$$

where z_A and z_B are the charges on the reactants A and B and the charge on the activated complex is equal to $z_A + z_B$. Since the rate of the reaction is proportional to the concentration of the activated complex $X^{\#}$, hence

$$r = k' [X^{\#}] \qquad \ldots(153)$$

The equilibrium between the activated complex and the reactants is written as

$$K^{\#} = \frac{a^{\#}}{a_A a_B} = \frac{[X^{\#}]}{[A][B]} \frac{\gamma^{\#}}{\gamma_A \gamma_B} \qquad \ldots(154)$$

where as are the activities and γs are the activity coefficients of the species involved.

Rearranging Eq. 154 to obtain $[X^{\#}]$ and substituting in Eq. 153, we obtain

$$r = k'K^{\#}[A][B]\frac{\gamma_A \gamma_B}{\gamma^{\#}} = k_0[A][B]\frac{\gamma_A \gamma_B}{\gamma^{\#}} \qquad \ldots(155)$$

where $k_0 = k'K^{\#}$. For a second-order reaction, $r = k$ [A][B] so that $k = r/$[A][B]. Hence,

$$k = \frac{r}{[A][B]} = \frac{k_0[A][B]}{[A][B]}\left(\frac{\gamma_A \gamma_B}{\gamma^{\#}}\right) = k_0 \frac{\gamma_A \gamma_B}{\gamma^{\#}} \qquad \ldots(156)$$

Taking logs, $$\ln k = k_0 + \ln \gamma_A \gamma_B / \gamma^{\#} \qquad \ldots(157)$$

From the Debye-Huckel limiting law for electrolyte solutions, we know that

$$\ln \gamma_i = -A z_i^2 \sqrt{I} \qquad \ldots(158)$$

where A is a constant and I is the ionic strength of the solution defined by

$$I = (1/2)\Sigma m_i z_i^2 \qquad \ldots(159)$$

where m_is are molalities and z_is are valencies of the various species.

Substituting Eqs. 156 and 157 into Eq. 155, we obtain

$$\ln k = \ln k_0 + \ln \gamma_A + \ln \gamma_B - \ln \gamma^{\#} = \ln k_0 - A[z_A^2 + z_B^2 - (z_A + z_B)^2] I^{1/2}$$

$$= \ln k_0 + 2A z_A z_B I^{1/2} \qquad \ldots(160)$$

For aqueous solutions as 25°C, the constant $A = 0{\cdot}51$ so that

$$\ln k = \ln k_0 + 1{\cdot}02 z_A z_B I^{1/2} \qquad \ldots(161)$$

or $$\ln (k/k_0) = 1{\cdot}02 z_A z_B I^{1/2} \qquad \ldots(162)$$

which is the equation of a straight line. A plot of ln (k/k_0) versus $I^{1/2}$ gives a straight line with slope $= 1{\cdot}02 z_A z_B$ (Fig. 21).

The reactions represented in the figure are:

1. $[Co(NH_3)_5Br]^{2+} + Hg^{2+}$ $(z_A z_B = 4)$
2. $S_2O_3^{2-} + I^-$ $(z_A z_B = 2)$
3. $[Co(OC_2H_5)N{:}NO_2]^+ + OH^-$ $(z_A z_B = 1)$
4. $CH_3COOC_2H_5 + OH^-$ $(z_A z_B = 0)$
5. $H^+ + Br^- + H_2O_2$ $(z_A z_B = -1)$
6. $[Co(NH_3)_5Br]^{2+} + OH^-$ $(z_A z_B = -2)$
7. $Fe^{2+} + [Co(C_2O_4)_3]^{3-}$ $(z_A z_B = -6)$

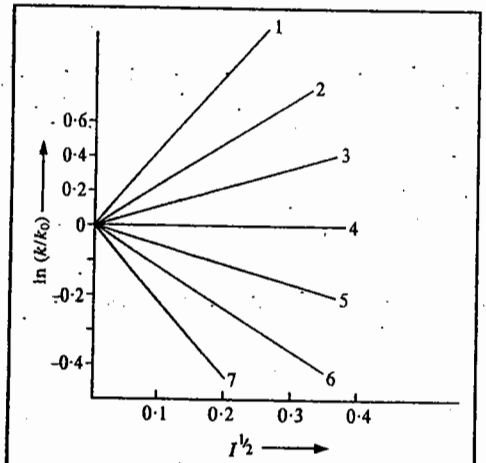

Fig. 21. Effect of ionic strength on the rate constant of a reaction. The product $z_A z_B$ gives the slope of the line.

We see that if one of the reactants is a neutral molecule, the product $z_A z_B = 0$ and the rate constant will be independent of the ionic strength. This is true for the base-catalyzed hydrolysis of ethyl acetate.

The salt effects were first investigated by the Danish chemists J.N. Brönsted (1879–1947) and N. Bjerrum (1879–1958) in 1922 and 1924, respectively.

Influence of Solvent on the Rates of Ionic Reactions

Ionic reactions in solution are affected by electrostatic interactions.

Let us consider an ionic reaction involving two ions A and B of radius r_A and r_B and charge z_Ae and z_Be in solution. Suppose that the two ions are initially at infinite distance apart but they touch each other when they form the activated complex (Fig. 22).

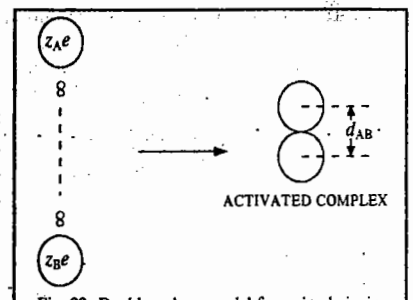

Fig. 22. Double-sphere model for a simple ionic reaction.

The work done in bringing the two ions together from infinity to a distance d_{AB} is given by

$$w = z_Az_B e^2/(\varepsilon_r d_{AB}) \qquad ...(163)$$

where ε_r is the dielectric constant of the solvent. This work is equal to the electrostatic contribution to the Gibbs free energy increase in going from the initial to the transition state. If the signs of charges on the ions are the same, this work is positive; if they are different, it is negative. There is also a molar non-electrostatic term, $\Delta G^{\#}_{n.e.s.}$. The free energy of activation *per molecule* may thus be written as

$$\frac{\Delta G^{\#}}{N_A} = \frac{\Delta G^{\#}_{n.e.s.}}{N_A} + \frac{z_Az_Be^2}{\varepsilon_r d_{AB}} \qquad ...(164)$$

From the activated complex theory, the rate constant is given by

$$k = (k_BT/h) \exp(-\Delta G^{\#}/RT) \qquad ...(165)$$

Substitution of Eq. 164 in Eq. 165 gives

$$k = \left(\frac{k_BT}{h}\right) \exp\left(\frac{-\Delta G^{\#}_{n.e.s.}}{RT}\right) \exp\left(-\frac{z_Az_BN_Ae^2}{\varepsilon_r RTd_{AB}}\right) \qquad ...(166)$$

Taking logs,

$$\ln k = \ln(k_BT/h)\left(\frac{-\Delta G^{\#}_{n.e.s.}}{RT}\right) - \frac{z_Az_BN_Ae^2}{\varepsilon_r RTd_{AB}}$$

$$= \ln k_0 - \frac{z_Az_BN_Ae^2}{\varepsilon_r RTd_{AB}} \qquad ...(167)$$

Eq. 167 is the equation of a straight line. It shows that the logarithm of the rate constant of an ionic reaction varies inversely with the dielectric constant of the solvent at a given temperature (Fig. 23). Several ionic reactions obey this plot over a limited range. The measurement of the slope, which equals $N_Az_Az_Be^2/RTd_{AB}$, can lead to the estimation of d_{AB}.

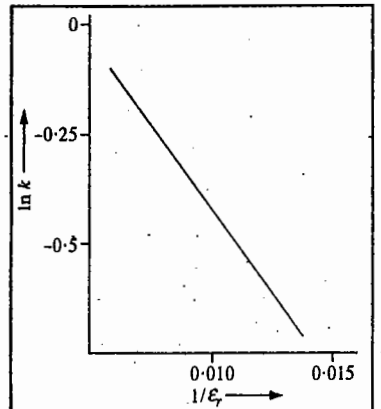

Fig. 23. A plot of log k *versus* the reciprocal of the dielectric constant for a typical ionic reaction.

Reactions in Flow Systems

The rate equations for reactions of various orders developed so far apply to *static systems, i.e.*, systems in which reactants are introduced in a reaction vessel and their concentration changes are followed as the reaction proceeds. In some cases, however, it is desirable to study the kinetics of reactions in flow systems in which the reaction mixture is flowing through a reaction vessel known as a reactor. Kinetic measurements in flow systems are generally useful when the reactants are at extremely low pressures or concentrations. Flow systems are also used for studying kinetics of fast reactions.

Types of Flow Systems. Flow systems are of two types. In the first type, *there is no stirring in the reactor* and the flow through it is often called the **plug flow**. In the second type, *there is stirring which is vigorous enough to cause complete mixing in the reactor*. This is called **stirred flow.** Intermediate situations, though possible, are difficult to analyze.

Plug Flow. Fig. 24 shows the schematic representation of the plug flow.

The reaction mixture is passed through the reactor at a volumetric flow rate (units: $m^3\ s^{-1}$) equal to u.

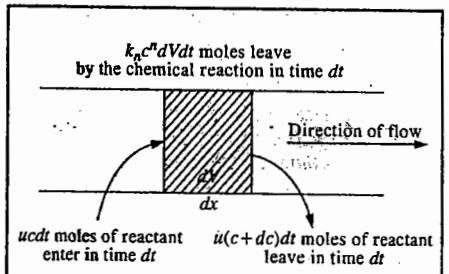

Fig. 24. Schematic representation of the process occurring in plug flow through a reaction vessel.

Let us consider an element of volume dV in the reactor. Assume that the reaction rate depends upon the concentration c of a single reactant. We know that for an nth-order reaction, the rate of consumption of the reactant is given by $r = k_nc^n$. Hence, the rate of consumption of the reactant in volume $dV = k_nc^ndV$.

After the system has been operating for a sufficient time, a steady state is reached, *i.e.*, there occurs no further change in the concentration of the reactant with time in the volume element dV.

Three processes contribute to the steady state. These are :

1. The reactant molecules enter the slab (shown by slanting lines) through the left face, the amount entering in time dt being $ucdt$.

2. The molecules leave the slab by the right face, the amount leaving in time dt being $u(c+dc)\,dt$.

3. Molecules disappear by chemical reaction. For an nth-order reaction, the amount consumed in time dt is k_nc^ndVdt.

We can obtain the steady-state equation by equating the rate of entry of reactant into the slab (by process 1) to the sum of the rates of its removal (by processes 2 and 3) :

$$ucdt = u(c+dc)dt + k_nc^ndVdt \text{ or } -dc/c^n = dV\,k_n/u \qquad ...(168)$$

The above equation needs to be integrated over the volume V_0 of the reactor. At the entrance to the reactor $V=0$ and $c=c_i$ (the initial concentration) while at the exit $V=V_0$ and $c=c_f$ (the final concentration of the reactant). Hence,

$$-\int_{c_i}^{c_f} \frac{dc}{c^n} = \frac{k^n}{u}\int_0^{V_0} dV \qquad ...(169)$$

For a first-order reaction ($n=1$), integration of Eq. 168 yields

$$-\ln(c_f/c_i) = k_1V_0/u \text{ or } c_f = c_i \exp(-k_1V_0/u) \qquad ...(170)$$

Comparing this equation with that for a static first-order reaction, *viz.*, $c_f = c_i \exp(-k_1t)$, we see that the two are equivalent if V_0/u is replaced by t. The quantity V_0/u is called the contact time for the reaction. The **contact time** *is the average time that a molecule takes to pass through the reactor.* Eq. 170 may be tested by varying V_0/u (by changing either the volume of the reactor or the flow rate), just as time is varied in a static system. Reactions that are too rapid for convenient investigation in a static system may be studied in a flow system, the contact time being reduced by using a high flow rate and a small volume.

For an nth-order reaction ($n > 1$), integration of Eq. 168 yields

$$\frac{n}{n-1}\left[\frac{1}{c_f^{n-1}}\right] = \frac{k_nV_0}{u} \qquad ...(171)$$

This equation can be compared with the equation for the rate constant of a static nth-order reaction with $V_0/u=t$.

We have assumed above that there is no volume change during the course of the reaction ; any such change will cause the volumetric flow rate to vary. The consideration of volume change, however, complicates the integration of the rate equation, the discussion of which is beyond the scope of the present book.

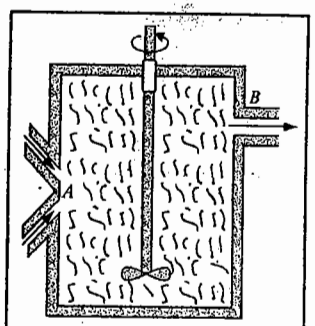

Fig. 25. A stirred-flow reaction.

In a **stirred-flow reactor** (shown in Fig. 20), the reactants enter the vessel at A. The concentrations are maintained constant within the reactor by stirring at a high speed (about 3000 rpm). The mixing occurs within a second or so. In this case it is not necessary to consider a thin slab; instead, we consider the reactor as a whole. After a steady state is reached, the product mixture is withdrawn at B. The rate of flow of reactants into the reactor is uc_i and the rate of flow out is uc_f. The difference between these gives the rate of reaction in the reactor which is rV where r is the rate per unit volume. Thus,

$$uc_i - uc_f = rV \qquad \text{or} \qquad r = u\,(c_i - c_f)V \qquad \ldots(172)$$

By measuring c_i and c_f at a given flow rate, the reaction rate can be calculated. The order of the reaction and the rate constant can then be determined by working at different initial concentrations and flow rates.

The stirred-flow reactor finds application in the study of transient reaction intermediates, the concentrations of which in a static system might quickly reach a maximum and then fall to zero. It is interesting to note that there is an analogy between a living cell and a continuous stirred-flow reactor. The theoretical principles of kinetics are the same in each case. Though there is no obvious 'internal stirrer' in the case of a cell, the process of diffusion of molecules across the cell can maintain the 'well-stirred' conditions. Again, though there are no inlets and outlets in a cell as are in the case of a reactor, the entire cell wall adequately serves these functions.

Example 54. An equimolar mixture of NO and Cl_2 in an inert carrier gas is passed through a tubular furnace whose radius is 0·01 m and length 0·30 m, at 973°C and 1 atm pressure, at a rate of 0·01 m^3 s^{-1}. The reaction is second-order with rate constant $k_2=8{\cdot}0\times10^5$ dm^3 mol^{-1} s^{-1}. If Cl_2 constitutes 1·0% of the gas stream at the entry to the furnace, calculate the percentage of Cl_2 in the gas stream at the exit (1 atm = 101 × 10^3 Nm^{-2}).

Solution : P = 1 atm = 101×10^3 $N\,m^{-2}$. There is no stirring in the reactor and, therefore, this is a *plug flow*.

For the given second-order reaction, $r = dx/dt = k_2(a-x)^2$ and the integrated rate law is

$$k_2 = \frac{1}{t}\frac{x}{a(a-x)} \qquad \ldots(i)$$

The contact time, t, is given by

$$t = V/u = \pi\cdot(0{\cdot}01\text{ m})^2\,(0{\cdot}30\text{ m})/0{\cdot}01\text{ m}^3\text{ s}^{-1} = 9{\cdot}4\times10^{-3}\text{ s}$$

Assuming that the gas mixture behaves ideally, $PV = nRT$.

The initial concentration of the reactants is

$$a = \frac{n}{V} = \frac{P}{RT} = \frac{(10^{-2})(101\times10^3\,\text{N m}^{-2})}{(8{\cdot}314\,\text{J K}^{-1}\,\text{mol}^{-1})(1200\,\text{K})} = 0{\cdot}10\text{ mol m}^{-3} = 1{\cdot}0\times10^{-4}\text{ mol dm}^{-3}$$

From Eq. *(i)*, $k_2t = x/a(a-x)$

$$(8{\cdot}0\times10^5\text{ dm}^3\text{ mol}^{-1}\text{ s}^{-1})\,(9{\cdot}4\times10^{-3}\text{ s}) = \frac{x}{1{\cdot}0\times10^{-4}(1{\cdot}0\times10^{-4}-x)}$$

which, on solving, gives $x = 0{\cdot}43\times10^{-4}$ **mol dm^{-3}**. Hence, the amount of Cl_2 in the carrier gas leaving the exit is 0·43%.

Kinetics of Fast Ractions

Reactions that take place in times shorter than the time required to mix the reactants cannot be investigated by conventional methods. Such reactions are termed fast reactions. Powerful experimental techniques for studying the kinetics of fast reactions have been developed by the German chemist Manfred Eigen since 1950.

Eigen and his coworkers used **relaxation methods** to investigate fast reactions in solution. In these methods, the reacting system in equilibrium is subjected to a sudden variation in some physical parameter on which the equilibrium constant of the reaction depends. The system changes to new state of chemical equilibrium. The rate of this change, called *relaxation,* is then investigated. Relaxation studies are carried out with such parameters as temperature, pressure and electric field.

Fig. 26 shows the apparatus for the **'temperature jump' method.** A high-voltage power supply charges a capacitor C. When a certain voltage is reached, the spark gap G breaks down, discharging the capacitor and sending a strong current through the cell containing the reactive system at equilibrium in a conducting aqueous solution. As the current passes, the temperature of the system rises by about 10°C in a few microseconds. In the ensuing time interval the concentration of the reacting species adjusts to the new equilibrium value appropriate to the temperature jump. As a result, the intensity of the light beam leaving the cell and entering the detector (the photomultiplier tube, *PM*) is changed. The output of the photomultiplier tube is displayed on the vertical axis of the oscilloscope. In this way the curve showing the variation of concentration *versus* time is displayed on the oscilloscope screen.

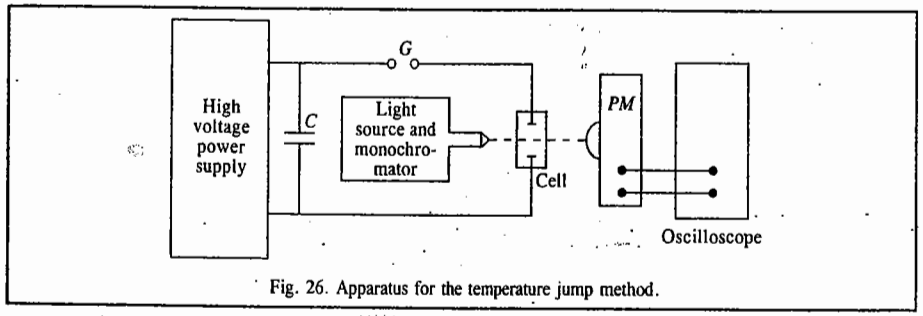

Fig. 26. Apparatus for the temperature jump method.

We shall now derive expressions for the rate constants of fast reactions. If the displacement from equilibrium is very small, the rate of relaxation, *i.e.*, restoration of equilibrium, always follows first-order kinetics. Consider a reversible first-order reaction :

$$\text{A} \underset{k_{-1}}{\overset{k_1}{\rightleftharpoons}} \text{B}$$

Let a be the total concentration of (A+B) and x the concentration of B at any instant. Then

$$r \equiv dx/dt = k_1(a-x) - k_{-1}\,x \qquad \ldots(173)$$

If x_e is the equilibrium concentration, then

$$\Delta x = x - x_e \qquad \text{or} \qquad x = \Delta x + x_e \qquad \ldots(174)$$

Since $d(\Delta x)/dt = dx/dt$, we have

$$d(\Delta x)/dt = k_1(a - x_e - \Delta x) - k_{-1}\,(x_e + \Delta x) \qquad \ldots(175)$$

At equilibrium, $dx/dt=0$ and $x=x_e$. Hence, from Eq. 173,

$$k_1(a - x_e) = k_{-1}\,x_e \qquad \ldots(176)$$

Substituting in Eq. 175, we have

$$d(\Delta x)/dt = -(k_1 + k_{-1})\,\Delta x = -k_r\,\Delta x \qquad ...(177)$$

where $k_r = (k_1 + k_{-1})$ is the **relaxation rate constant.**

Eq. 177 can be integrated to give

$$\Delta x = \Delta x_0 \exp(-k_r t) \qquad ...(178)$$

The reciprocal of k_r, *viz.*, $(k_1 + k_{-1})^{-1}$ is called the **relaxation time,** τ, *i.e.*,

$$\tau = 1/(k_1 + k_{-1}) = 1/k_r \qquad ...(179)$$

Let us now consider a somewhat more complicated case involving a first-order forward reaction with a second-order reverse reaction :

$$A \underset{k_{-1}}{\overset{k_1}{\rightleftharpoons}} B + C$$

Let a be the total concentration and x the concentration of B which is equal to the concentration of C. Then, the rate law is given by

$$r \equiv dx/dt = k_1 (a - x) - k_{-2}\,x^2 \qquad ...(180)$$

Now $\Delta x = x - x_e$, where x_e is, as before, the equilibrium concentration.

Hence,
$$d(\Delta x)/dt = k_1(a - x_e - \Delta x) - k_{-2}(x_e + \Delta x)^2$$
$$= k_1(a - x_e) - k_1\Delta x - k_{-2}\,x_e^2 - 2k_{-2}\,x_e\,\Delta x - k_{-2}(\Delta x)^2 \qquad ...(181)$$

At equilibrium, $(dx)/dt = 0$; hence from Eq. 181,

$$k_1(a - x_e) = k_{-2}x_e^2 \qquad ...(182)$$

Substituting in Eq. 182 and simplifying, we get

$$d(\Delta x)/dt = -k_1\Delta x - 2k_{-2}\,x_e\,\Delta x - k_{-2}(\Delta x)^2 \qquad ...(183)$$

Assuming that Δx is very small, $(\Delta x)^2$ can be neglected, giving

$$d(\Delta x)/dt = -(k_1 + 2k_{-2}\,x_e)\,\Delta x = -k_r\,\Delta x \qquad ...(184)$$

where $k_r = (k_1 + 2k_{-2}x_e)$ is the **relaxation rate constant.**

Eq. 184 can be integrated to give

$$\Delta x = \Delta x_0 \exp(-k_r t) \qquad ...(185)$$

The relaxation time τ in this case is given by

$$\tau = (k_1 + 2k_{-2}\,x_e)^{-1} \qquad ...(186)$$

Example 55. The relaxation time for the fast reaction $A \underset{k_{-1}}{\overset{k_1}{\rightleftharpoons}} B$ **is 10** μs **(*i.e.*, microseconds) and the equilibrium constant is** $1{\cdot}0\times10^{-3}$**. Calculate the rate constants for the forward and the reverse reactions.**

Solution : From Eq. 179,

$$\tau = 1/(k_1 + k_{-1}) = 10\times10^{-6}\ s = 10^{-5}\ s \qquad ...(i)$$
$$K = k_1/k_{-1} = 1{\cdot}0\times10^{-3}$$
$$\therefore \quad k_1 = 1{\cdot}0\times10^{-3}\,k_{-1} \qquad ...(ii)$$

Since $k_{-1} \ll k_1$, it can be neglected in comparison with k_1 in Eq. *(i)* so that

$$1/k_1 = 10^{-5}\ s \quad \text{or} \quad k_1 = 10^5\ s^{-1}$$
$$k_{-1} = 10^5\ s^{-1}/10^{-3} = 10^8\ s^{-1}$$

Example 56. Calculate the rate constants involved in the dissociation of NH_4OH**, *viz.*,** $NH_4OH \underset{k_{-1}}{\overset{k_1}{\rightleftharpoons}} NH_4^+ + OH^-$ **from the following data : *A* 0·01 molar solution of** NH_4OH **is subjected to a sudden temperature jump terminating at 25°C, at which temperature, the equilibrium constant is** $1{\cdot}8\times10^{-5}$ **mol dm**$^{-3}$**. The observed relaxatiou time is 0·109** μs **and** $x_e = 4{\cdot}1\times10^{-4}$ **mol dm**$^{-3}$**.**

Solution : $\tau = 0{\cdot}109\ \mu s = 1{\cdot}09\times10^{-7}\ s$; $\quad k_r = 1/\tau = 9{\cdot}2\times10^9\ s^{-1}$

For the given reaction which is first-order forward and second-order reverse, we have

$k_r = k_1 + 2k - 2x_e$ which can be simplified to

$k_r = k_1[1 + 2\,(k_{-2}/k_1)\,x_e] = k_1(1 + 2x_e/K)$

where the equilibrium constant $K = k_1/k_{-2}$

$$k_1 = k_r/(1 + 2x_e/K) = \frac{9{\cdot}2\times10^6\ s^{-1}}{1 + (2\times4{\cdot}1\times10^{-4}\,\text{mol dm}^{-3}/1{\cdot}8\times10^{-5}\,\text{mol dm}^{-3})} = 2\times10^5\ s^{-1}$$

$$k_{-2} = k_1/K = 2\times10^5\ s^{-1}/1{\cdot}8\times10^{-5}\ \text{mol dm}^{-3} = 1{\cdot}1\times10^{10}\ \text{dm}^3\ \text{mol}^{-1}\ s^{-1}$$

Example 57. For the dissociation of water, $H_2O \underset{k_{-1}}{\overset{k_1}{\rightleftharpoons}} H^+ + OH^-$**, the relaxation time obtained from the temperature jump method is 40** μs**, at 25°C, at which temperature,** $K_w = [H^+][OH^-] = 1{\cdot}0\times10^{-14}$ **(mol dm**$^{-3}$**)**^{2}**. Calculate the rate constants** k_1 **and** k_{-2}**.**

Solution : $\tau = 40\ \mu s = 40\times10^{-6}\ s = 4{\cdot}0\times10^{-5}\ s$

$\therefore \quad k_r = 1/\tau = 2{\cdot}5\times10^4\ s^{-1}$

Since $K_w = [H^+][OH^-] = x_e^2 = 1{\cdot}0\times10^{-14}\ (\text{mol dm}^{-3})^2$

$\therefore \quad x_e = 1{\cdot}0\times10^{-7}\ \text{mol dm}^{-3}$

For water, $K = \dfrac{K_w}{[H_2O]} = \dfrac{1{\cdot}0\times10^{-14}(\text{mol dm}^{-3})^2}{55{\cdot}5\,\text{mol dm}^{-3}} = 1{\cdot}8\times10^{-16}\ \text{mol dm}^{-3} = k_1/k_{-2}$

Proceeding as in the last example,

$$k_1 = \frac{k_r}{(1 + 2x_e)/K} = \frac{2{\cdot}5\times10^4\ s^{-1}}{1 + (2\times10^{-9}\ \text{mol dm}^{-3}/1{\cdot}8\times10^{-16}\ \text{mol dm}^{-3})} = 2{\cdot}5\times10^{-4}\ s^{-1}$$

$$\therefore \quad k_{-1} = \frac{k_1}{K} = \frac{2{\cdot}5\times10^{-5}s^{-1}}{1{\cdot}8\times10^{-16}\text{mol dm}^{-3}} = 1{\cdot}4\times10^{11}\ \text{dm}^3\ \text{mol}^{-1}\ s^{-1}$$

Flow Methods for Fast Reactions. The **stopped-flow method** is the most popular flow method. The schematic diagram of its experimental set up is shown in Fig. 27. Syringes *A* and *B* contain the separate reactants; these syringes are fitted with suitable valves. The solution is forced into the mixing chamber *M* by means of the common drive mechanism *D*, consisting of an air-driven piston. The solution then enters the stopping syringe *C*, whose plunger comes to rest against the fixed stop *S*. This triggers the recording device, usually an oscilloscope. The reaction is observed in the stationary solution at point *P* at a distance *d* from the mixing chamber. The method of detection utilizes the ultraviolet/visible spectrophotometry.

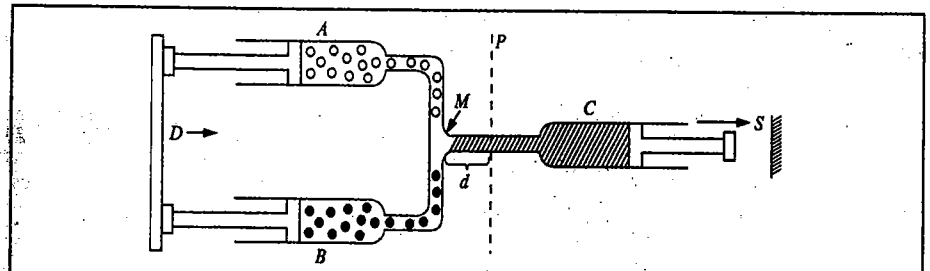

Fig. 27. Schematic diagram of a stopped-flow apparatus.

Kinetic data are obtained by measuring the values of an appropriate physical property as determined at various times after mixing with the help of a suitable technique.

The **continuous-flow** and **quenched-flow methods** are also used though they are less popular. In the former methods, measurements are made at different distances down the flow tube (*i.e.*, at varying distances d in Fig. 27). The stopping syringe is not used. The principle of this procedure utilizes the fact that measurements along the flow stream amount in effect to determinations at different times. With a known and constant flow rate, the time corresponding to each reading is known. The measurement can be made by positioning several detectors along the tube or moving a single detector to different positions. There is a slight improvement in time resolution in the continous-flow method as compared with the stopped-flow methods.

Since, however, the continuous-flow method uses large quantities of solutions, it is less commonly used. In the quenched-flow procedure, samples of the reaction mixture are rapidly mixed with a quenching mixture, following which the analytical determination can be made at leisure. The timing of different samples can be varied by using different flow rates or different distances along the flow stream. This method is best applicable to the study of exchange reactions which occur too rapidly for the usual sampling techniques.

Pulse Methods. Fast reactions are also studied using the so-called **pulse methods.** Short pulses of electromagnetic radiation using light, ultraviolet radiations, X-rays or charged particles (usually electrons) initiate the reaction by producing very high concentrations of excited state molecules. It may be mentioned that in a *conventional photochemical reaction*, excited state molecules are obtained in such low concentrations that they cannot be studied directly. If a powerful flash of visible or UV radiation is used, the method is called *flash photolysis*. If, on the other hand, charged particles (electrons) from a generator are used, the method is referred to as *pulse radiolysis*.

Flash photolysis. This method was pioneered by R.G.W. Norrish and G. Porter in 1949. The apparatus for flash photolysis studies is shown schematically in Fig. 28. The sample is subjected to a very powerful flash having energy of the order of 10^5 J and a duration of 10 μs (*i.e.*, microseconds). The flash is so intense that in some cases almost all the molecules of the sample are excited and as a result most of the molecules are dissociated into free radicals. Powers of the order of 50 megawatt may be obtained for a few microseconds. In recent years, high power pulsed laser light sources have been used in flash photolysis. The concentration of the intermediates produced by flash photolysis is followed as a function of time by absorption photometry.

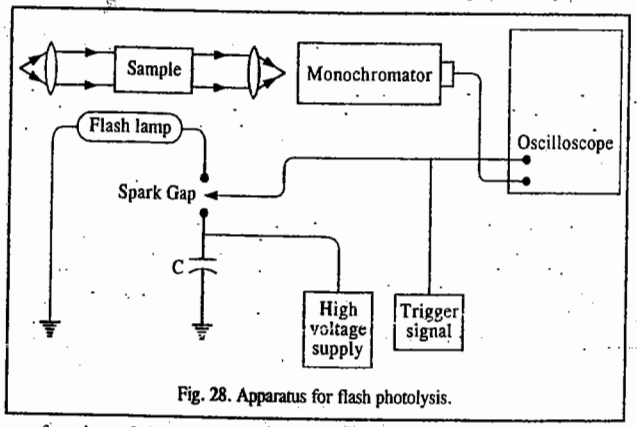

Fig. 28. Apparatus for flash photolysis.

As shown in Fig. 28, a condenser of high microfarad capacity is charged to 10,000 volt by a high voltage supply. By means of a trigger signal, a spark is produced in the spark gap which permits rapid passage of current through the flash lamp. The condenser discharges in a few microseconds. The lasers can produce a flash of the duration of a few nanoseconds. Soon after the capacitor discharges, the flash lamp is automatically triggered off. The rate of the disappearance of excited molecules or free radicals is followed by the rate of increase in the monochromatic transmitted light as measured with an oscilloscope and photomultiplier. The spectrometer is so set that the light

passing through the illuminated cell is of the wave length that is absorbed by the excited molecule or free radical. This technique is called **kinetic spectroscopy.**

Eigen, Norrish and Porter shared the 1967 Chemistry Nobel Prize for contributions to fast reaction kinetics "by disturbing the equilibrium by means of very short pulses of energy."

Flash photolysis has been used for determining the absorption spectra of free radicals such as $\cdot NH_2$, $\cdot CH_3$ and $\cdot ClO$, whose concentration may be as small as 10^{-6} M.

Pulse Radiolysis. Pulse radiolysis can be used for generating transient species by direct ionizing radiation. If a beam of high-energy electrons impinges on water, a number of stable and unstable species are produced. They arise from the energy transferred to water molecule by the electron beam. It is customary to express the yield of each species by a G-value, which represents the number of species formed per 100 eV of energy absorbed by water. The species formed in the pulse radiolysis of water, with the G-value shown as the coefficient of each species, are given by the equation

$$4{\cdot}0\ H_2O \longrightarrow 2{\cdot}6\ e^-(aq) + 2{\cdot}6\ HO\cdot + 0{\cdot}6\ H\cdot + 2{\cdot}6\ H^+ + 0{\cdot}4\ H_2 + 0{\cdot}7\ H_2O_2 \quad ...(i)$$

The first three are highly reactive entities. The hydrated electron and the hydrogen atom are strong reducing agents and the hydroxyl radical HO· is a very powerful oxidizing agent. In the absence of suitable scavengers, the species rapidly decay by reactions of the following types :

$$e^-(aq) + H_3O^+ \longrightarrow H\cdot + H_2O\ ;\quad k = 2{\cdot}2\times10^{10}\ dm^3\ mol^{-1}\ s^{-1} \quad ...(ii)$$

$$e^-(aq) + 2H_2O \longrightarrow H_2 + 2OH^-;\quad k = 5{\cdot}5\times10^{9}\ dm^3\ mol^{-1}\ s^{-1} \quad ...(iii)$$

$$e^-(aq) + HO\cdot \longrightarrow OH^-\ ;\quad k = 3{\cdot}0\times10^{10}\ dm^3\ mol^{-1}\ s^{-1} \quad ...(iv)$$

$$e^-(aq) + H\cdot + H_2O \longrightarrow H_2 + OH^-\ ;\quad k = 2{\cdot}3\times10^{10}\ dm^3\ mol^{-1}\ s^{-1} \quad ...(v)$$

$$HO\cdot + HO\cdot \longrightarrow H_2O_2\ ;\quad k = 1{\cdot}0\times10^{10}\ dm^3\ mol^{-1}\ s^{-1} \quad ...(vi)$$

Owing to these and several other reactions, selective methodologies have been developed to permit study of each of $e^-(aq)$, HO· and H·, separately. For instance, if it is desired to study only $e^-(aq)$ or use exclusively hydrated electrons to generate other species, one must work in neutral or basic solution to avoid destruction of $e^-(aq)$ by H_3O^+ [reaction *(ii)*]. The HO· and H· are often removed by scavenging reactions such as those with formate ion or *t*-butyl alcohol :

$$HO\cdot\ (\text{or } H\cdot) + HCOO^- \longrightarrow H_2O\ (\text{or } H_2) + CO_2^- \quad ...(vii)$$

$$HO\cdot\ (\text{or } H\cdot) + (CH_3)_3COH \longrightarrow H_2O\cdot\ (\text{or } H_2) + \cdot CH_2C(CH_3)_2OH \quad ...(viii)$$

The hydrogen atoms in alkaline solution are converted into hydrated electrons.

$$H\cdot + OH^- \longrightarrow e^-(aq) + H_2O\ ;\quad k = 2{\cdot}0\times10^{7}\ dm^3\ mol^{-1}\ s^{-1}$$

Molecular Reaction Dynamics

Both the collision theory and the activated complex theory rely on statistical treatment of the reacting systems to give information about the average behaviour of an assemblage of molecules. This subject constitutes what is known as **macroscopic kinetics.** The disadvantage of macroscopic kinetics is that the reactant molecules are present in a range of energy states and convey only an indirect information about the individual molecular events that occur during a chemical reaction. In recent years, another branch called **molecular reaction dynamics** or **microscopic kinetics** has gained importance, thanks to the pioneering work of D.R. Herschbach, Y.T. Lee and J.C. Polanyi. These chemists shared the 1986 Chemistry Nobel Prize for studying reaction dynamics which deals with the intermolecular and intramolecular motions that occur in the elementary act of chemical change and with the quantum states of the reactant and product molecules. It must be emphasized that molecular reaction dynamics does not supersede macroscopic kinetics. It simply aims at gaining a detailed picture of the elementary chemical act.

The experimental technique of studying molecular reaction dynamics includes the **molecular**

beam method in which the reaction dynamics is investigated by utilizing a mono-energetic beam of atoms or molecules.

In a molecular beam investigation of a bimolecular reaction, narrow beams of atoms or molecules are made to cross one another. The directions and speeds of the product molecules and of the unreacted species are determined by movable detectors. Experimental results are analyzed to yield detailed information about the distribution of energy and angular momentum among the reaction products, the dependence of overall kinetics on the states of the reactant molecules, the quantum states of the product molecules and other features of the elementary reaction event.

The schematic apparatus used in a molecular beam experiment is shown in Fig. 29. The two essential features of this apparatus are :

1. Devices for producing extremely narrow beams of reactants with provisions for controlling the speeds of the molecules and their rotational, vibrational and electronic states.

2. Movable devices for the detection of the reaction products at various positions.

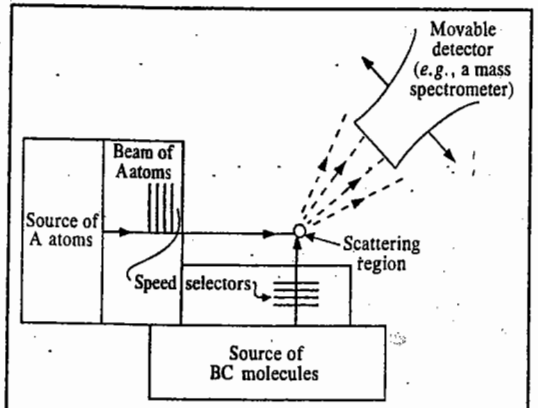

Fig. 29. Schematic diagram for a molecular beam apparatus for investigating the reaction $A + BC \longrightarrow AB + C$.

In the molecular beam experiments performed in the 1930s, the beams were produced by taking the reactants in a small vessel with a very small opening allowing the atoms or molecules to effuse into an evacuated vessel. A rectangular slit served as the orifice and a second small slit, placed close to it, made the molecules travel in the required direction. However, these early molecular beam experiments suffered from the fact that the beams produced had a very low intensity and also there was a thermal spread of molecular velocities.

In the modern molecular beam experiments, the earlier disadvantages have been overcome by using supersonic nozzle sources which can produce beam intensities greater by about three orders of magnitude. Fig. 30 shows the schematic diagram of a typical nozzle beam source. The gas is taken in an oven at a pressure that is several orders of magnitude greater than that used for effusive flow. The molecules emerging through the slit form a slightly divergent beam at supersonic velocities. Part of the beam is allowed to pass through a specially designed skimmer which selects only the core of the beam. The beam passes through some evacuated vessels and finally enters the main scattering chamber through a slit. The molecular beams thus produced have a much narrower range of molecular speeds than the effusive beams and have also greater intensity. The translational kinetic energy of the molecules can be varied by varying the oven temperature. A technique known as *seeding* is used for

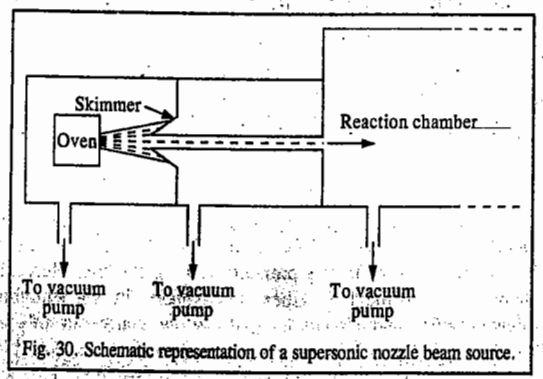

Fig. 30. Schematic representation of a supersonic nozzle beam source.

increasing the energy range of heavy molecules. This technique consists in mixing the heavy molecules with an excess of a gas which emerges from the oven at much higher velocities and sweeps the heavier molecules along with it. The heavier molecules tend to travel along the centre of the beam whereas the lighter molecules are scattered towards the edges of the beam and are studied using appropriate techniques.

As a result of the collisions of molecules in the crossed molecular beams, the following three processes may occur :

(a) Elastic scattering which involves no energy transfer among different degrees of freedom.

(b) Inelastic scattering which involves energy transfer among different degrees of freedom but in which no chemical reaction occurs.

(c) Reactive scattering in which a chemical change occurs. The chemists are primarily interested in reactive scattering.

In the earlier molecular beam work, the scattered beams were studied by using differential surface ionization detectors. This technique was based on the fact that the alkali metal atoms and their salts could be easily ionized when they came in contact with a heated wire of appropriate work function. This technique was, however, limited to the reactions of alkali metals only.

In recent work, mass spectrometers have been used for analysing the scattered beams. The velocities of the scattered beams in all types of reactions are measured by a time-of-flight mass spectrometer. A chopper is inserted in the front of the mass spectrometer and is rotated at high speed. After the product molecules manage to pass the chopper the time required by them to reach the detector depends upon their translational velocities. Thus, the distribution of speeds in the scattered beams can be determined.

Potential Energy Surfaces

Consider one of the simplest reactions, *viz.*, $D + H_2 \longrightarrow DH + H$. We need three spatial coordinates to describe the configuration of this reacting system at any point along the reaction path (Fig. 31). These coordinates are : the internuclear distance r_1 between H and H; the distance r_2 of D from the midpoint of the H—H bond and the angle θ between the H—H bond and the vector from the midpoint of the bond to D.

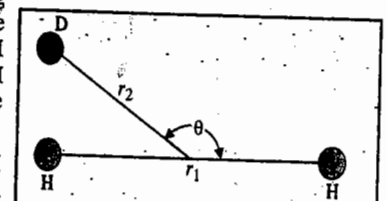

Fig. 31. Coordinates required to describe the relative positions of the atoms in the reaction $D + H_2 \longrightarrow DH + H$.

It is evident that one particular approach of D to H—H is energetically more favourable than any other. This is, in fact, the path in which D approaches H—H along the line of centres of the three-body system, *i.e.*, the angle θ is either 0° or 180°. The reason for this is that when D approaches H—H along the $\theta = 0°$ direction, the D atom 'feels' appreciable repulsion from any one of the H atoms whereas in an approach from any other direction, the D atom is under the influence of repulsive field from *both* the H atoms.

Now, as the D atom approaches H—H along the line of centres of the atoms, the potential energy depends only on two coordinates, *viz.*, the distances D—H and H—H. If one distance is plotted against the *X*-axis and the other along the *Y*-axis in a plane, the potential energy can be plotted along the *Z*-axis normal to the plane. In this way the potential energy $V(x, y)$ of the reacting system can be visualized as a *surface in three dimensions*.

It was R. Marcelin (1885-1914) who, in 1915, had suggested the idea of representing a chemical reaction by such a potential energy surface. However, the first potential energy surface was actually computed in 1931 by H. Eyring and M. Polanyi (1891-1976). Since the computational techniques at that time were not perfect, these researchers were not able to perform a purely theoretical calculation and had to rely on a semi-empirical approach based on spectroscopic data. However,

more accurate calculations performed later showed that the potential energy surface constructed by Eyring and Polanyi by a combination of calculation and intuition was essentially correct. This surface is shown in Fig. 32 in the form of a three-dimensional model.

We can easily trace the path of the reaction over this surface. It is the path from the reactant side to the product side that follows the contour of minimal potential energy. If we consider the interconversion of translational and vibrational energy, then the reaction path resembles that of bobsled sliding on its run. The path traverses a deep valley ($D+H_2$), rises over a hump to a saddle point at the activated complex (D—H—H) and then passes down the other side of the pass into another valley (DH+H). The reaction path is called the reaction coordinate. Fig. 28 shows a contour map of the region of the saddle point. The elevation of the saddle point is 38 kJ which is the activation energy of the reaction. This occurs at the configuration of the activated complex where $r_1=r_2=93$ pm. This distance is considerably greater than the normal interatomic distance (174 pm) in H_2.

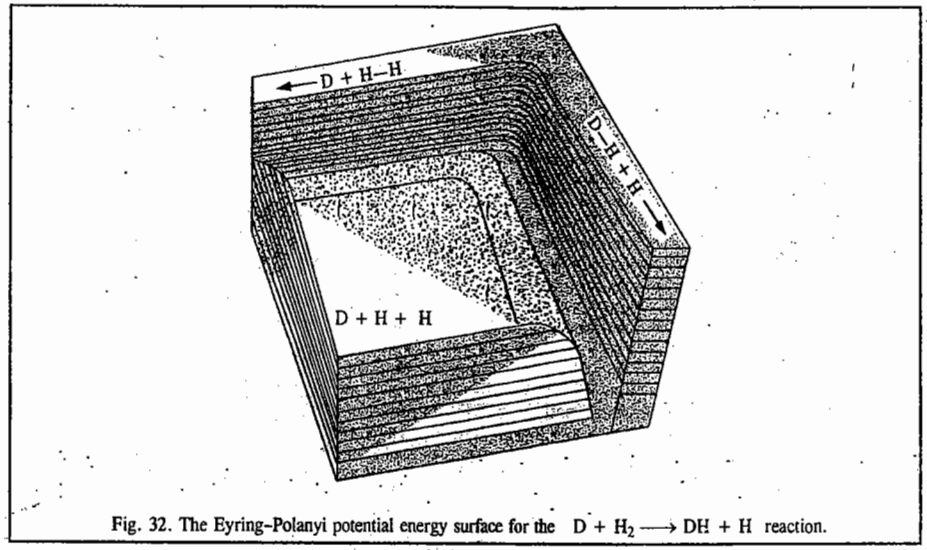

Fig. 32. The Eyring-Polanyi potential energy surface for the $D + H_2 \longrightarrow DH + H$ reaction.

The potential energy surface gives a map of a chemical reaction from beginning to end. In any reaction, there is always a particular configuration at the saddle point. In many respects, the activated complex which results from this configuration of atoms is like an ordinary molecule except that it is not an equilibrium configuration. Thus, we can imagine a reaction to take place in two stages, *viz.*, the formation of the activated complex from the reactants and the decomposition of the activated complex into products. These stages are not sharply defined in any way and from a dynamic point of view the reaction proceeds smoothly and continuously. However, we can designate a transition state as the highest region of potential energy surface along the reaction path.

Though kinetic theory gives us useful information about molecular collisions, it does not deal with changes that take place at the molecular level when reactants are converted into products. When two molecules are very close to each other, they cannot be considered separately because their wave functions overlap. Thus, from the time the reactant molecules are close to each other until the products are well separated, the system is a kind of supermolecule. This supermolecule is different from an ordinary molecule because it is in the process of change, but it is a molecule in the sense that its energy and electron distribution can be calculated for each nuclear configuration by using quantum mechanics. According to the Born-Oppenheimer approximation, the electrons move much more rapidly than the nuclei so the molecular electronic energy and wave functions can be calculated

for a given nuclear configuration by using the electronic Schrödinger wave equation. This procedure has been used to calculate the electronic potential energy function so that the Schrödinger wave equation may yield the molecular vibrational energy levels.

For a reaction involving N nuclei, there are $3N$ nuclear coordinates, three translational coordinates of the centre of mass and two or three rotational coordinates (about the centre of mass) that do not affect the potential energy. Thus, potential energy is a function of $3N-5$ coordinates if the nuclei are constrained to a straight line and $3N-6$ coordinates in general. For the simplest type of reaction

$$A + BC \longrightarrow AB + C \quad ...(187)$$

where A, B and C are atoms, three coordinates are required. It is not possible to plot the potential energy as a function of three coordinates, but if the angle θ of approach of A to BC is fixed, the potential energy can be plotted as a function of r_{AB} and r_{BC}, where r is the intermolecular distance. Such a plot is shown in Fig. 33. If r_{AB} is rather large, as shown on the left face of the diagram, the potential energy is essentially that of the BC molecule. Similarly, the right face gives the potential energy of the AB molecule. Initially, the r_{AB} distance is very large. As A approaches BC, the lowest energy path is given by the dashed line from reactants R to products P. This dashed line gives the minimum energy path which is sometimes referred to as the **reaction coordinate**. We will shortly see that the configuration of the system does not actually move along the reaction coordinate in the reaction but the reaction coordinate does help us visualize the surface. The highest point along the reaction coordinate is a saddle point. At the **saddle point**, the potential energy is a maximum along the reaction coordinate but it is a minimum in the direction perpendicular to the reaction coordinate. The reaction system at this point is said to be in the **transition state**. In Fig.33, D is a high plateau giving the potential energy of three atoms well separated from each other.

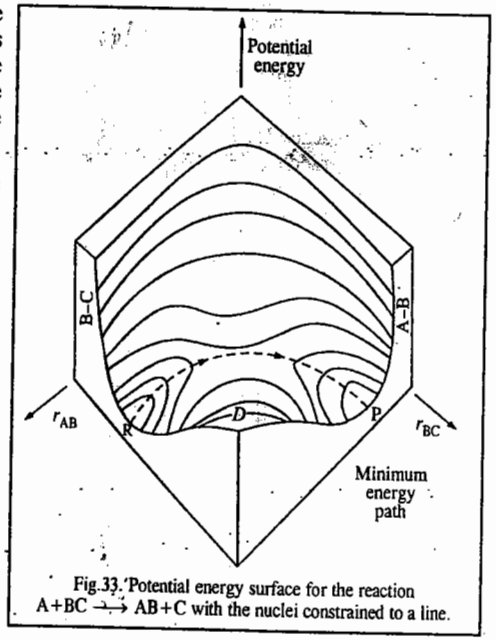

Fig.33. Potential energy surface for the reaction $A+BC \longrightarrow AB+C$ with the nuclei constrained to a line.

As a simple example, let us consider what happens when A approaches a non-vibrating BC molecule along the internuclear axis. The point representing the configuration of the system moves along the minimum energy path, the dashed line in Fig.33. As r_{AB} decreases, the kinetic energy is converted into potential energy as the point representing the system of three nuclei moves up the valley from the left. If there is initially enough kinetic energy for the system to go over the saddle point, AB and C are formed and gain energy as the system goes down the valley to the right. If the kinetic energy is too low, the system returns down the valley to the left. This is expressed by saying that the reactants bounce off each other. Fig. 33 applies only when the nuclei are constrained to a line. The potential energy surface will be different if there is a different angle θ of approach. It is very difficult to calculate quantum mechanically an accurate potential energy surface for reaction of type (1). In fact, surfaces have been calculated only for a few reactions.

The reaction of a hydrogen atom with a hydrogen molecule

$$H_A + H_BH_C \longrightarrow H_AH_B + H_C \quad ...(188)$$

has been extensively studied. The potential energy surface for this reaction for $\theta = 180°$ is described by means of the contour diagram in Fig. 34. This surface has been calculated by M. Karplus and R.N. Porter using *ab initio* methods with configuration interaction (*CI*). The error at any point on the surface is less than 0·03 eV (2·9 kJ mol^{-1}).

As H_A approaches H_BH_C, along the minimum energy path, the potential energy of the system increases until the saddle point is reached at ✚. At this point $r_{AB} = r_{BC} = 93$ pm and the potential enegy of the system is 0·37 eV (42 kJ mol^{-1}), the highest along the dashed line. Since the saddle point is 0·37 eV higher than the potential of H_A and H_BH_C at an infinite distance, this energy must be supplied from relative kinetic energy or vibrational energy in order for the reaction to occur. In the upper right-hand corner of Fig. 34, there is a high plateau with energy of 432 kJ mol^{-1}. This is the energy of three hydrogen atoms infinitely far apart with respect to separated reactants or products.

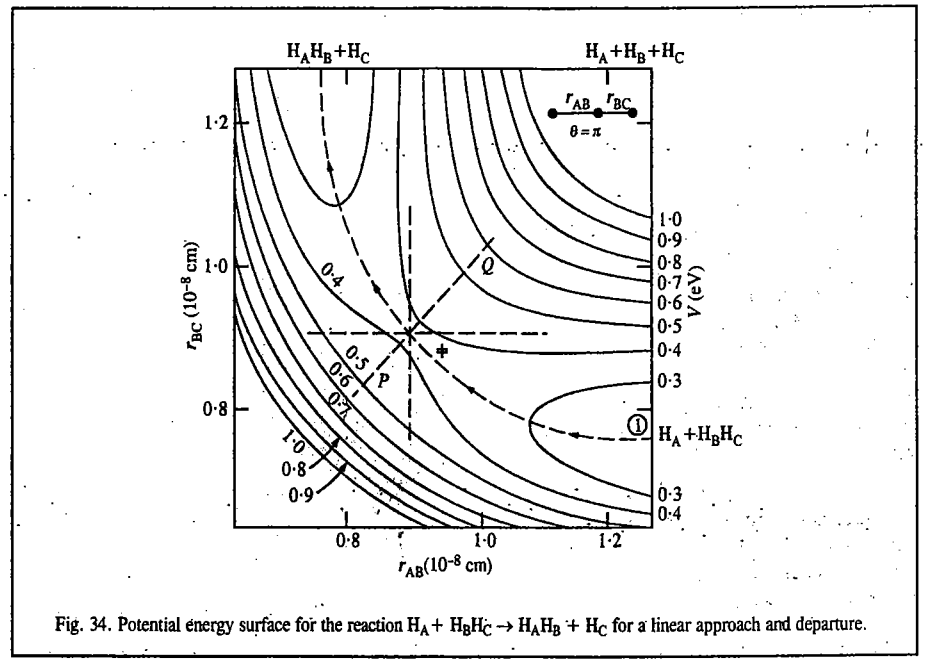

Fig. 34. Potential energy surface for the reaction $H_A + H_BH_C \rightarrow H_AH_B + H_C$ for a linear approach and departure.

Theoretical Calculation of the Rate Constant

Once the potential energy curve has been obtained for various approach angles θ, the probability of a reaction to occur for certain initial conditions (relative kinetic energy, vibrational energy and θ) can, in principle, be calculated using TDSE (time-dependent Schrödinger equation). However, this kind of calculation involves formidable difficulties and theorists have, instead, used the classical mechanical approach. We know that the force on a particular nucleus is given by the negative gradient of the potential energy. Thus, for example, the x-component of the force on nucleus i is given by

$$F_{x,i} = -\partial V/\partial x_i \qquad ...(189)$$

where V is the potential energy and x_i is the x-coordinate of the nucleus. At each instant, the system is represented by a point on the surface and Newton's law of motion $F = ma$ is integrated numerically to obtain the coordinates of the system as a function of time. Calculations can also be performed

when H_BH_C initially has vibrational motion and this is treated classically, as an approximation. Rotational motion is unimportant in these calculations. These trajectory calculations yield a reaction probability of 0 for certain initial conditions and 1 for others. Fig. 35 shows the results of two calculations of this type for collinear collisions. In Fig. 35(*a*), the H_BH_C molecule is vibrating and H_A approaches with a certain initial velocity, but the reaction does not occur. It may be noted that in this non-reactive, inelastic collision, translational energy is converted to vibrational energy in H_BH_C molecule. In Fig. 35(*b*), the reaction does occur.

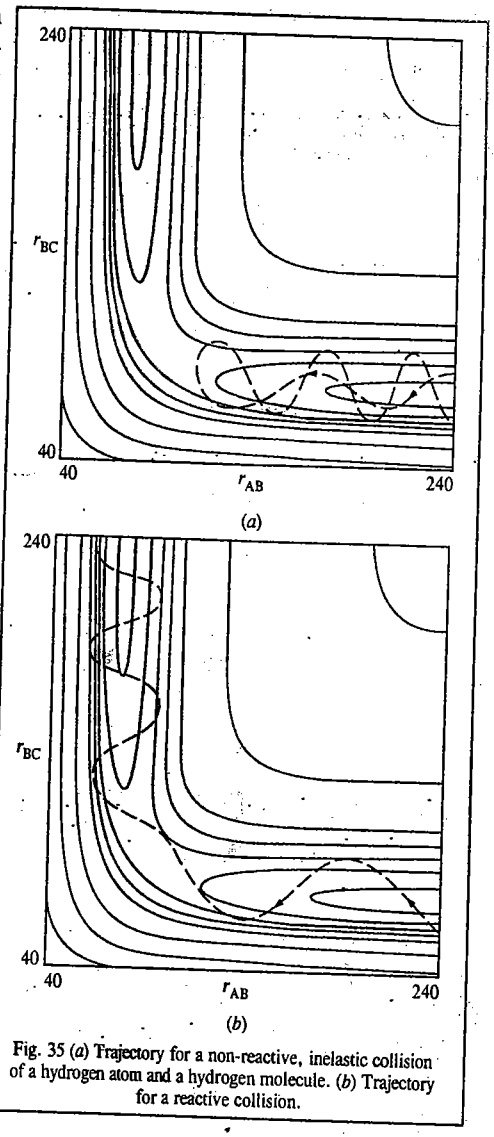

Fig. 35 (*a*) Trajectory for a non-reactive, inelastic collision of a hydrogen atom and a hydrogen molecule. (*b*) Trajectory for a reactive collision.

In order to carry out rate constant calculations in this way, it is necessary to perform a very large number of trajectory calculations with initial states chosen to give a satisfactorily representative sample of possible initial states at the chosen temperature. The initial conditions can be chosen by a **Monte Carlo procedure** to ensure that the distribution of each initial parameter approaches the correct distribution as the number of calculated trajectories increases. The relative kinetic energies of H_A and H_BH_C are given by the Boltzmann equation. All angles θ of approach must be included, though most reactive collisions for reaction (2) occur at angles close to 180°.

To see how a rate constant can be evaluated from a series of trajectory calculations, we need to consider the reaction probability $P(b)$, often referred to as the **opacity function**, and the way it is used to calculate a **reaction cross-section** $\sigma(v)$. The reaction probability $P(b)$ is defined as the fraction of the total number of trajectories at a selected reactant relative velocity and the **impact parameter** b that result in reaction. Fig. 36 shows the reaction probability $P(b)$ for the H + H_2 reaction for a relative velocity of $1{\cdot}17 \times 10^6$ cm s^{-1} as a function of the impact parameter b. The reaction probability is greatest for $b = 0$, decreasing to zero at some finite value of b.

The reaction cross-section $\sigma(v)$ is given by

$$\sigma(v) = \int_0^{b_{max}} 2\pi b\, P(b) ab \qquad ...(190)$$

For a chemical reaction taking place in bulk, molecules collide at all possible relative velocities and so the rate constant $k(T)$ at temperature T is made up of a sum of terms for all possible relative velocities, each term being weighted by the fraction f_i of collisions with that relative velocity :

$$k(T) = f_1 k(v_1) + f_2 k(v_2) + \ldots.$$
$$= f_1 \sigma(v_1) v_1 + f_2 \sigma(v_2) v_2 + \ldots. \quad \ldots(191)$$

or $$k(T) = \int_0^\infty f(v,T) v \sigma(v) dv \quad \ldots(192)$$

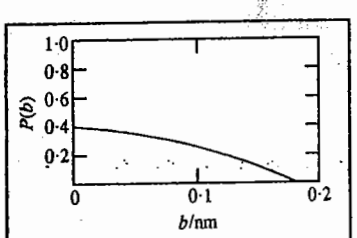

Fig.36. Reaction probability $P(b)$ for the reaction $H + H_2$ for a relative velocity of $1{\cdot}17 \times 10^6$ cm s^{-1} as a function of impact parameter b.

where $f(v,T)$ is the Maxwell-Boltzmann distribution for relative velocity v at temperature T. In 1965, M. Karplus, R.N. Porter and R.D. Sharma calculated a very large number of trajectories for the $H+H_2$ reaction and found that their results could be expressed by the following (Arrhenius type) equation :

$$k(T) = (4{\cdot}3 \times 10^{13} \text{ cm}^3 \text{ mol}^{-1} \text{ s}^{-1}) \exp\left[-\frac{31{,}000 \text{ J mol}^{-1}}{(8{\cdot}3145 \text{ J K}^{-1} \text{ mol}^{-1}) T}\right] \quad \ldots(193)$$

This result agrees very well with the experimental results obtained for the reaction

$$D + H_2 \longrightarrow DH + H \quad \ldots(194)$$

or $$H + \text{para-}H_2 \longrightarrow \text{ortho-}H_2 + H \quad \ldots(195)$$

and with the value calculated using the activated complex theory (ACT) over the same temperature range :

$$k(T) = (7{\cdot}4 \times 10^{13} \text{ cm}^3 \text{ mol}^{-1} \text{ s}^{-1}) \exp\left[-\frac{34{,}440 \text{ J mol}^{-1}}{(8{\cdot}3145 \text{ J K}^{-1} \text{ mol}^{-1}) T}\right] \quad \ldots(196)$$

The general conclusion is that classical calculations, performed on a number of simple reactions, provide an adequate description of the collision dynamics of these reactions. Of course, at low temperatures, quantum mechanical tunnelling (*i.e.*, penetration into classically forbidden regions) may become important.

A few potential energy surfaces are shown in Fig. 37. The potential energy diagram is symmetrical for the reaction $H_A + H_BH_C \rightarrow H_AH_B + H_C$. However, this is not generally true. The shape of the potential energy surface determines whether translational motion or vibrational motion will be most effective in causing the reaction. It may be noted that the reaction begins at the right-hand side of each diagram in Fig. 37 and proceeds from right to left. It is customary to distinguish between potential energy surfaces with early barriers and late barriers. Fig. 37(*a*) shows a potential energy surface with an **early barrier** and a reactant with sufficient translational energy to cross the saddle point into the trough for products. The energy released as the system passes down the saddle point results in vibrational energy for the products. Fig. 37(*b*) shows a potential energy surface with an early barrier and a reactant with vibrational energy. Even though the total energy may be the same as in (*a*), the reactant may be reflected back from the barrier. We thus conclude that an early barrier favours a reactant with translational energy and produces vibrationally excited products. Fig. 37(*c*) shows a potential energy surface with a **late barrier** and a reactant with vibrational energy. The molecule may bounce off of the wall of the valley it is in and across the saddle point into the reactant valley where it does not have much vibrational energy. Fig. 37(*d*) shows

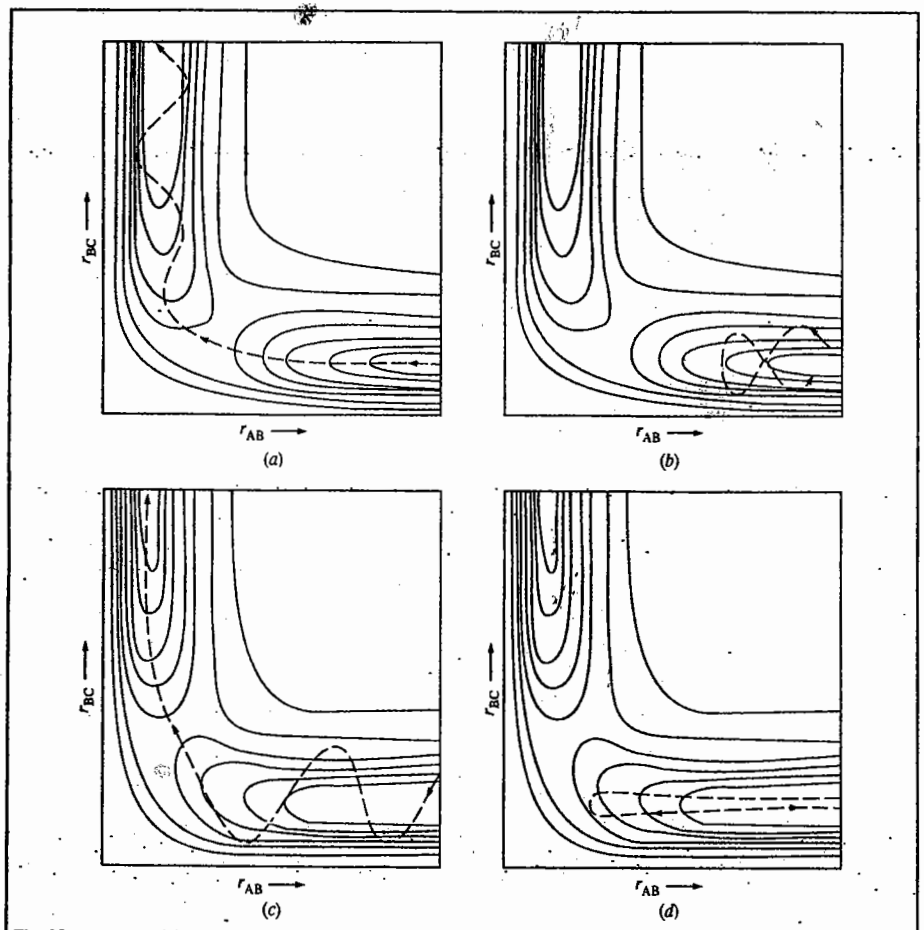

Fig. 37 (*a*) A potential energy surface with an early barrier and a reactant with sufficient translational energy to cross the saddle point. (*b*) A potential energy surface with an early barrier and a vibrationally excited reactant. (*c*) A potential energy surface with a late barrier and a vibrationally excited reactant. (*d*) A potential energy surface with a late barrier and a reactant that has sufficient translational energy to reach the saddle point, but does not.

that if the reactant does not have vibrational energy, it may bounce back into the reactant valley. Thus, a late barrier favours a reactant with vibrational energy and produces a product with less vibrational energy. Also, a potential energy surface that has an early barrier in one direction has a late barrier in the other direction.

Electron Transfer Reactions : The Marcus Theory

There are several kinds of electron transfer reactions. The field of electron transfer (*ET*) processes has grown exponentially in the closing decades of the 20th century. An example is the transfer of an electron from the reduced form of a reactant A, A(red), to the oxidized form of a reactant B, B(ox), in solution :

$$A(red) + B(ox) \longrightarrow A(ox) + B(red)$$

Electron transfers occur in inorganic systems and organic systems, in reactions that occur in solution and those which occur across interfaces in complex biological systems.

Let us consider the simplest of all electron transfers, a self-exchange reaction :

$$MnO_4^{2-} + MnO_4^- \longrightarrow MnO_4^- + MnO_4^{2-} \quad ...(197)$$

in aqueous solution. Experimentially, the rates of such reactions are measured for a wide variety of central metal atoms and of ligands (here, Mn and O, respectively), by labelling one of the metal atoms in a particular valence state with a radioactive atom as a tracer and following its appearance in the other valence state.

According to R.A. Marcus (1923 –), who was awarded the 1992 Chemistry Nobel Prize for his contributions to the theory of electron transfer reactions, the central idea underlying his *ET* theory is two-fold and can be illustrated using reaction (1). When the electron jumps from the MnO_4^{2-} to the MnO_4^-, it does so rapidly that the atoms in the reactants and in the solvent molecules do not have time to move in that brief instant, since the atoms are much heavier than the electron, *i.e.*, the transfer should obey the Franck-Condon principle. This constraint has major consequences. It may be recalled that the solvent dipolar molecules are partially oriented, on an average, towards the ions and much more so towards the more highly charged ions. Thus, each of the newly formed ions in reaction (Eq. 197) suddenly finds itself in a wrong solvent environment. If the electron transfer occurs this way, the total energy of the system would suddenly increase. However, if such a transfer occurs in the absence of absorption of light, this mechanism would violate the law of energy conservation. Accordingly, for a thermal electron transfer to proceed, an appropriate redistribution of the orientations of the solvent molecules in the vicinity of each ion needs to occur prior to the electron transfer. With a suitable fluctuation, both the Frank-Condon principle and energy conservation can be satisfied simultaneously whereas the latter would be violated in the absence of this fluctuation.

Marcus in his formulation of the *ET* theory (in 1956), devised a way for finding the needed redistribution, using it to describe the transition state and calculate the reaction rate. Initially, he used a dielectric continuum model for the solvent and set up an expression for the free energy G of such a dielectric continuum undergoing fluctuations (non-equilibrium dielectric polarization). This G was obtained by finding a reversible path for forming such a non-equilibrium state of the solvent, with an arbitrary dielectric polarization function $\boldsymbol{P}(r)$ at each point r in the system and calculating the reversible work to form that state. To find the $\boldsymbol{P}(r)$ characterizing the transition state of the reaction, G was minimized subject to the constraint that the transition state was an ensamble of configurations of the system that satisfied the Franck-Condon principle and the energy conservation upon electron transfer. In this way, an expression for the rate constant of the reaction was obtained.

Mathematics of Electron Transfer. Consider electron transfer from a donor species D (which is MnO_4^{2-} in reaction 1) to an acceptor species A (which is MnO_4^-) in solution. First D and A must diffuse through the solution and collide to form a complex DA in which the donor and the acceptor are separated by a distance r which is the distance between the edges of each species. Assuming that D, A and DA exist in a pre-equilibrium :

$$D + A \rightleftharpoons DA; \quad K_1 = \frac{[DA]}{[D][A]}, \quad ...(198)$$

the electron transfer occurs in DA to yield D^+A^- :

$$DA \longrightarrow D^+A^-; \quad \text{rate} = k_{et}[DA] \quad ...(199)$$

The D^+A^- complex then breaks apart and the ions diffuse through the solution :

$$D^+A^- \rightleftharpoons D^+ + A^-; \quad K_2 = \frac{[D^+][A^-]}{[D^+A^-]} \quad ...(200)$$

Marcus treated the electron transfer process $DA \longrightarrow D^+A^-$. as follows :

From ACT (activated complex theory), we know that

$$k_{et} = \kappa\nu\exp(-\Delta G^{\#}/RT) \quad ...(201)$$

where κ is the transmission coefficient, ν is the vibrational frequency with which the activated complex approaches the transition state and $\Delta G^{\#}$ is the Gibbs energy of activation. We are now interested in the theoretical expressions for $\kappa\nu$ and $\Delta G^{\#}$. There are two central concepts in the Marcus treatment of electron transfer reactions :

1. Electrons are transferred by tunnelling through a potential energy barrier, the height of which is partly determined by the ionization energies of the DA and D^+A^- complexes ; electron tunnelling influences the magnitude of $\kappa\nu$. Recall that tunnelling is a purely quantum mechanical phenomenon ; its best known examples are in semiconductors and superconductors.

2. The complex DA and the solvent molecules surrounding it undergo structural rearrangements prior to electron transfer. The energy associated with these rearrangements and the standard reaction Gibbs energy, ΔG_r°, are used to determine $\Delta G^{\#}$. We have discussed above how Marcus proceeded to determine the free energy G. Marcus showed that

$$\Delta G^{\#} = \frac{(\Delta G_r^\circ + \lambda)^2}{4\lambda} \quad ...(202)$$

In Eq. 202, ΔG_r° is the standard reaction Gibbs energy for the electron transfer process $DA \longrightarrow D^+A^-$ and λ is the reorganization energy, *i.e.*, the energy associated with molecular rearrangements that must take place so that DA can assume the equilibrium geometry D^+A^-. These molecular rearrangements include the relative orientation of the D and A molecules in DA and the relative orientation of the solvent molecules surrounding DA.

Dynamics of Electron Tunnelling in the Marcus Theory. We have already mentioned about the role of the Franck-Condon principle in electron transfer processes. Here the electron migrates from one energy surface, representing the dependence of the energy of DA on its geometry, to another representing the energy of D^+A^-. We can represent the potential energy (and the Gibbs energy) surfaces of the two complexes (the reactant complex, DA and the product complex, D^+A^-) by parabolas characteristic of simple harmonic oscillators (S.H.Os), with the displacement coordinate corresponding to the changing geometries (Fig. 38). This coordinate represents a collective mode of donor, acceptor and solvent. Since, according to the Franck-Condon principle, the nuclei do not have time to move when the system passes from the reactant to the product surface as a result of the transfer of an electron, the electron transfer can occur only after thermal fluctuations bring the geometry of DA to q^* (Fig. 38), the value of the nuclear coordinate at which the two parabolas intersect.

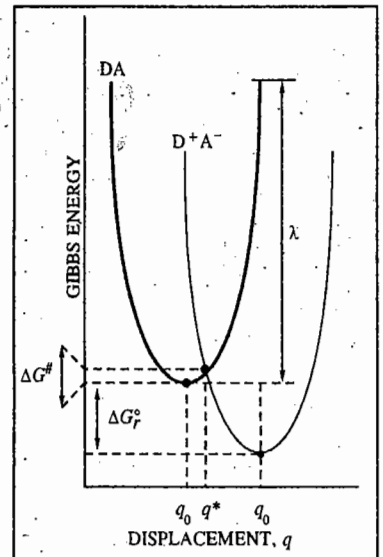

Fig. 38. The Gibbs energy surfaces of the complexes DA and D^+A^- involved in an ET process

The factor $\kappa\nu$ in Eq. 201 is a measure of the probability that the system will convert from reactants (DA) to products (D^+A^-) at q^* by electron transfer within the thermally excited DA complex. In order to understand this process, we shall consider the effect which the rearrangement of

nuclear coordinates has on electronic energy levels of DA and D^+A^- for a given distance r between D and A (Fig. 39). Initially, the electron to be transferred occupies the HOMO (highest occupied molecular orbital) of D, and the overall energy of DA is lower than that of D^+A^- (Fig. 39*a*). As the nuclei rearrange to a configuration represented by q^* in Fig. 39*b*, the highest occupied electronic level of DA and the lowest unoccupied electronic level of D^+A^- become degenerate and electron transfer becomes energetically feasible (Fig. 39*b*). Over reasonably short distance r, the main mechanism of electron transfer is tunnelling through the potential energy barrier depicted in Fig. 39. The height of the barrier increases with increase in the ionization energies of DA and D^+A^- complexes. After an electron moves from the HOMO of D to the LUMO of A, the system relaxes to the configuration represented by q_0^P in Fig. 39. As shown in Fig. 39*c*, now the energy of D^+A^- is lower than that of A, indicating the thermodynamic tendency of A to remain reduced and for D to remain oxidized. The rate of the electron tunnelling from an energy level described by the wave function ψ_D to a level described by the wave function ψ_A is (as in the case of electronic transitions in electronic spectra) proportional to the square of the matrix element $< \psi_A | \hat{H}_{DA} | \psi_D >$ where $\hat{H}_{DA}$ is the Hamiltonian that describes the coupling of the electronic wave functions. In cases where the coupling is weak, it is found that

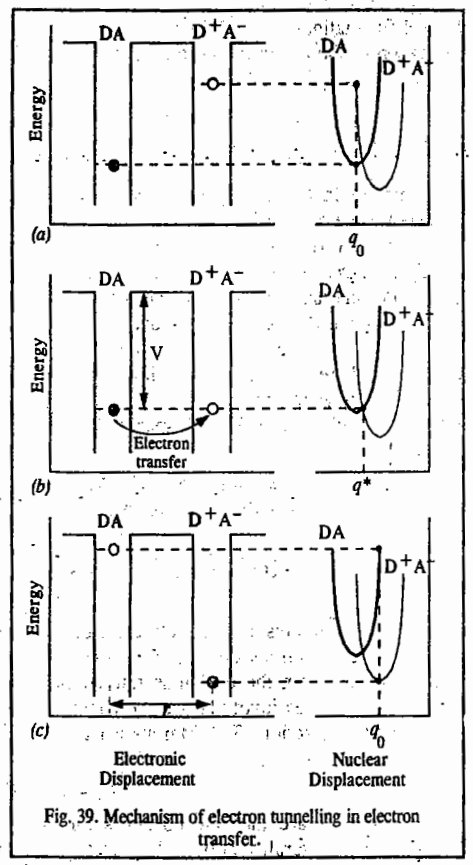

Fig. 39. Mechanism of electron tunnelling in electron transfer.

$$|< \psi_A | \hat{H}_{DA} | \psi_D >|^2 = |< \psi_A | \hat{H}^\circ_{DA} | \psi_D >|^2 \, e^{-\alpha r} \qquad ...(203)$$

where r is the edge-to-edge distance between D and A, α is a parameter that measures the sensitivity of the electronic coupling matrix element to distance, and $< \psi_A | \hat{H}^\circ_{DA} | \psi_D >$ is the value of the electronic coupling matrix element when D and A are in contact ($r=0$). The exponential dependence on distance in Eq. 203 is essentially the same as the exponential decrease in transmission probability through a potential energy barrier that one encounters in tunnelling through barriers generally.

The rate constant for electron transfer, k_{et}, turns out to be given by the following equation :

$$k_{et} = \frac{2|< \psi_A | \hat{H}_{DA} | \psi_D >|^2}{h} \left(\frac{\pi^3}{4\lambda RT} \right)^{1/2} \exp(-\Delta G^\# / RT) \qquad ...(204)$$

where $\Delta G^\#$ is given by Eq. 202.

We are not interested in the detailed discussion of Eq. 204. Suffice it to state that it is applicable only to processes with weak electronic coupling between donor and acceptor. Also, the term $(\pi^3/4\lambda RT)^{1/2} \exp(-\Delta G^\#/RT)$ should be used only at high temperatures. At low temperatures,

thermal fluctuations alone cannot bring the reactants to the transition state and ACT, which forms the foundation of the electron transfer discussed here, fails to account for any electron transfer.

From Eqs. 202 and 204, we have

$$\ln k_{et} = -\frac{1}{4\lambda}\left(\frac{\Delta G_r^\circ}{RT}\right)^2 - \frac{1}{2}\left(\frac{\Delta G_r^\circ}{RT}\right) + \text{constant} \qquad ...(205)$$

and a plot of $\ln k_{et}$ or ($\log k_{et}$) versus ΔG_r° (or $-\Delta G_r^\circ$) is predicted to be shaped like a downward parabola. Eq. 205 implies that the rate constant for electron transfer increases as ΔG_r° decreases but only upto $-\Delta G_r^\circ = \lambda$, the reorganization energy. Beyond that, the reaction enters the inverted parabola region in which the rate constant decreases as the reaction becomes more exergonic (ΔG_r° becomes more negative). The inverted region has been observed in a series of compounds in which the electron donor and acceptor are linked covalently to a molecular spacer of known and fixed size (Fig. 40)

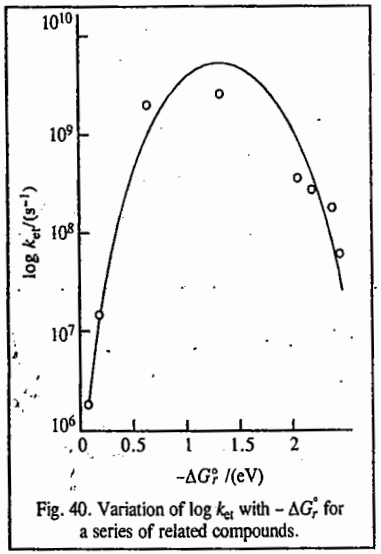

Fig. 40. Variation of log k_{et} with $-\Delta G_r^\circ$ for a series of related compounds.

The Marcus Cross Relation. The Marcus theory has successfully explained the mechanism of the outer-sphere exchange reactions such as the following :

$$[Fe(OH_2)_6]^{2+} + [Fe^*(OH_2)_6]^{3+} \longrightarrow [Fe(OH_2)_6]^{3+} + [Fe^*(OH_2)_6]^{2+}$$

where the * indicates a radioactive isotope of iron that acts as a tracer. Marcus derived an equation for an outer-sphere reaction from the exchange rate constants for each of the redox couples involved and the equilibrium constant for the overall reaction. The Marcus equation for the rate constant is

$$k^2 = f\, k_1 k_2 K \qquad ...(206)$$

where k_1 and k_2 are the rate constants for the two exchange reactions and K is the equilibrium constant for the overall reaction. The factor f is a complex parameter composed of the rate constants and the encounter rate ; it may be taken as near unity for approximate calculations. The idea of the weighted average of the two rates of self exchange is emphasized by the name **Marcus cross relation.**

Example 58. Using the Marcus cross relation, calculate the rate constant at 0°C for the outer-sphere reduction of $[Co(bipy)_3]^{3+}$ by $[Co(terpy)_2]^{2+}$.

Solution: The required exchange reactions are

$$[Co(bipy)_3]^{2+} + [Co^*(bipy)_3]^{3+} \xrightarrow{k_1} [Co(bipy)_3]^{3+} + [Co^*(bipy)_2]^{2+}$$

$$[Co(terpy)_2]^{2+} + [Co^*(terpy)_2]^{3+} \xrightarrow{k_2} [Co(terpy)_2]^{3+} + [Co^*(terpy)_2]^{2+}$$

where $k_1 = 9{\cdot}0$ dm^3 mol^{-1} s^{-1}, $k_2 = 48$ dm^3 mol^{-1}s^{-1} and $K = 3{\cdot}57$, all at 0°C. Setting $f=1$ and using the Marcus cross relation and substituting the given data, we get

$$k^2 = f\, k_1 k_2\, K \qquad \text{[Eq. 206]}$$

$$\therefore \quad k = (f\, k_1 k_2\, K)^{1/2}$$

$$= [(9{\cdot}0 \text{ dm}^3 \text{ mol}^{-1}\text{s}^{-1})\,(48 \text{ dm}^3 \text{ mol}^{-1}\text{s}^{-1})\,(3{\cdot}57)]^{1/2}$$

$$= \mathbf{39 \text{ dm}^3 \text{ mol}^{-1} \text{ s}^{-1}}$$

I. Review Questions

1. What is meant by the terms rate constant and order of a reaction ?
2. Integrate the rate expression for a first-order reaction.
3. Integrate rate expressions for second-order and zero-order reactions. Derive expressions for half-life time of a first-order, second-order, third-order and nth order reaction.
4. State and explain the term : temperature coefficient of a reaction. What is meant by the energy of activation ? Explain how energy of activation is determined with the help of the Arrhenius equation.
5. Discuss the collision theory of bimolecular reactions.
6. Discuss the activated complex theory (ACT) of bimolecular reactions. Explain how this theory helps in evaluating standard enthalpy of activation and standard entropy of activation. Show that for reactions involving simple molecules, the collision theory and ACT give identical results.
7. Discuss statistical mechanical derivation of the rate constant of a gaseous bimolecular reaction.
8. Describe the Lindemann theory of unimolecular reactions.
9. What are the shortcomings of the Lindemann theory ? How are they overcome in Hinshelwood theory ?
10. What are the shortcomings of the Hinshelhood theory ? How are they overcome by RRK theory of unimolecualr reaction ?
11. Discuss in detail the RRKM theory of unimolecular reactions. What are the salient features of this theory ?
12. Discuss the kinetics of *(i)* reversible reactions and *(ii)* consecutive reactions.
13. Discuss the kinetics of branched chain reactions.
14. Discuss the kinetics of diffusion controlled reactions in solution.
15. Illustrate the influence of ionic strength and the nature of the solvent on the rates of ionic reactions.
16. Discuss the kinetics of reactions taking place in flow systems involving *(i)* plug flow, *(ii)* stirred flow.
17. Illustrate the technique used in studying kinetics of fast reactions. What is meant by the term relaxation time ?
18. Describe the stopped flow method, pulse methods and flash photolysis for studying kinetics of fast reactions.
19. Describe the molecular beam method for studying molecular reaction dynamics.
20. Discuss the statistical mechanical treatment of the rate constant of a gaseous bimolecular reaction.
21. Using appropriate diagrams discuss the role of potential energy surfaces in reaction kinetics.
22. What are electron transfer reactions ? Discuss the Marcus theory of electron transfer reactions.

II. Problems

1. Identify the reaction order from each of the following expressions :

   (a) $k = 5{\cdot}6\times10^{-4}$ mol dm^{-3} s^{-1} *(b)* $k = 4{\cdot}5\times10^{-3}$ dm^3 mol^{-1} s^{-1}
   (c) $k = 3{\cdot}2\times10^{-3}$ s^{-1} *(d)* $k = 1{\cdot}6\times10^{-2}$ dm^6 mol^{-2} s^{-2}
   (e) $k = 4{\cdot}0\times10^{-6}$ atm^{-1} s^{-1} **[Ans. *(a)* zero *(b)* second *(c)* first *(d)* third *(e)* second]**

2. The following data was obtained for the vapour phase decomposition of ethylene oxide into methane and carbon monoxide at 414·5°C.

t, min	0	5	7	9	12	18
p, mm Hg	116·51	122·56	125·72	128·74	133·23	141·37

   Show that the reaction is first-order and calculate the rate constant. **[Ans. 0·0123 min^{-1}]**

3. Azomethane $(CH_3)_2N_2$ decomposes with first-order kinetics according to the equation

$$(CH_3)_2N_2(g) \longrightarrow N_2(g) + C_2H_6(g).$$

   The following data were obtained for the decomposition in a 200 ml flask at 300°C.

t, min	0	15	30	48	95
Total pressure, torr	36·2	42·4	46·5	53·1	59·3

   Calculate the rate constant and the half-life for this reaction. **[Ans. $1{\cdot}30\times10^{-2}$ min^{-1} ; 53·3 min]**

4. In the fermentation of sugar in an enzymation solution that is initially 0·12 M, the concentration of sugar is reduced to 0·06 M in 10 hours and 0·03 M in 20 hours. What is the order of the reaction and what is the rate constant ? **[Ans. First-order ; $k = 1{\cdot}9\times10^{-5}$ s^{-1}]**

5. The reaction between triethylamine and methyl iodine $((C_2H_5)_3N + CH_3I \longrightarrow [C_2H_5)_3NCH_3]^+I^-)$ was studied kinetically in nitrobenzene as solvent. The data obtained were as follows :

t(s)	1200	1800	2400	3600	5400
x (mol dm^{-3})	0·00876	0·01066	0·01208	0·01392	0·01538

   where x is the concentration of $(C_2H_5)_3N$ or CH_3I that has reacted at time t. The initial concentration of both the reactants was 0·0198 mol dm^{-3}. Assuming that the reaction is second-order, calculate the rate constant for the first and the last set of data. **[Ans. 0·0334 dm^3 mol^{-1} s^{-1}, 0·0325 dm^3 mol^{-1} s^{-1}]**

6. The rate constant for a second-order reaction is $8{\cdot}00\times10^{-5}$ M^{-1} min^{-1}. How long will it take for a 1·0 M solution to be reduced to 0·5 M in the reactant ? How long will it take from that point until the solution is 0·25 M in reactant ? **[Ans. $1{\cdot}25\times10^4$ min ; $2{\cdot}50\times10^4$ min]**

7. The rate constant for the first-order decomposition of ethylene oxide into CH_4 and CO is described by $\ln k\,(\text{in s}^{-1}) = 14{\cdot}34 - (1{\cdot}25\times10^4\ \text{K})/T$. Calculate *(a)* the activation energy and *(b)* the rate constant at 670 K. **[Ans. *(a)* 239 kJ mol^{-1} *(b)* $4{\cdot}8\times10^{-5}$ s^{-1}]**

8. Derive the relationship between the relaxation time τ and k_1 & k_2 for the fast reaction

$$A + B \underset{k_1}{\overset{k_2}{\rightleftharpoons}} C$$

   [Ans. $1/\tau = k_2 + k_1([A]+[B])$]

9. The reaction $2NO(g) + Cl_2(g) \longrightarrow 2NOCl(g)$ was studied at 10°C and the following data were obtained :

	Initial concentrations (mol dm^{-3})		Initial rate of formation of
	NO	Cl_2	NOCl, mol dm^{-3} min^{-1}
1	0·10	0·10	0·18
2	0·10	0·20	0·36
3	0·10	0·20	1·44

   What is the order of reaction with respect to Cl_2, with respect to NO and the overall reaction order ? **[Ans. First order, second order, third order]**

10. From the data given in Problem 11, determine the rate constant at 10°C. **[Ans. 180 dm^3 mol^{-1} min^{-1}]**

11. Express the rate constant k in units of dm^3 mol^{-1} s^{-1} if $k = 4{\cdot}45\times10^{-4}$ atm^{-1} s^{-1} for an ideal gas reaction. **[Ans. $1{\cdot}00\times10^{-2}$ dm^{-3} mol^{-1} s^{-1}]**

12. For the hypothetical reaction, $2A + B \longrightarrow$ products, the following data have been obtained :

Expt. No.	$[A]_0$ (mol dm^{-3})	$[B]_0$ (mol dm^{-3})	*Initial Rate* (mol dm^{-3} s^{-1})
1	0·10	0·20	$3{\cdot}0\times10^2$
2	0·30	0·40	$3{\cdot}6\times10^3$
3	0·30	0·80	$1{\cdot}44\times10^4$

   Determine the rate law expression, the order of the reaction with respect to A and B, the overall order and the rateconstant.
   [Ans. $r = k[A][B]^2$; first-order in B, third-order overall; rate constant = $7{\cdot}5\times10^4$ dm^{-1} mol^{-1} s^{-1}]

13. The gaseous decomposition of N_2O into N_2 and O_2 in the presence of gaseous argon follows second-order kinetics with $k = 5{\cdot}0\times10^{11}$ dm^3 mol^{-1} s^{-1} exp (−29,000 K/T). Calculate the activation energy of the reaction. **[Ans. 241 kJ mol^{-1}]**

14. For a first-order radioactive decay of a nucleus, find the amount of time, expressed in units of $t_{1/2}$, at which $[A]/[A]_0 = 0{\cdot}125$. **[Ans. 3]**

15. The acid-catalyzed reaction of acetic acid with ethanol,

$$CH_3COOH + C_2H_5OH \xrightarrow{H^+} CH_3COOC_2H_5 + H_2O$$

   follows the rate law $-d[CH_3COOH]/dt = k[H^+][CH_3COOH][C_2H_5OH]$
   If $[CH_3COOH]_0 = [C_2H_5OH]_0 = 0{\cdot}2$ M, $pH = 3$ and $t_{1/2} = 50$ min, calculate the apparent rate constant and the true rate constant. **[Ans. $k_{app} = 0{\cdot}1$ M^{-1} min^{-1} ; $k = 1{\cdot}0\times10^2$ M^{-2} min^{-1}]**

16. The following mechanism has been suggested for the reaction

$$2NO + Br_2 \longrightarrow 2NOBr$$

   (i) $NO + Br_2 \longrightarrow NOBr_2$ *(fast)*
   (ii) $NOBr_2 + NO \longrightarrow 2NOBr$ *(slow)* **[Ans. Rate = $k[NO]^2[Br_2]$]**

   Determine the rate law consistent with the mechanism where the constant k is equal to the product of two other constants.

17. The rate law expression for the reaction $2NO + O_2 \longrightarrow 2NO_2$ is Rate = $k[NO][O_2]$. Suggest a possible mechanism consistent with this law. **[Ans. $NO + O_2 \longrightarrow NO_2$ *(slow)*, $NO_3 + NO \longrightarrow 2NO_2$ *(fast)*]**

CHAPTER 29

PHOTOCHEMISTRY

Photochemistry deals with the study of chemical reactions which are caused by the absorption of light radiations (photons). Only the absorbed radiation can cause a chemical change. The light radiations of the visible and ultraviolet regions lying between 800 nm and 200 nm wave lengths bring about such reactions. The related photons should be of sufficient energy (given by $h\nu$) to raise the atom or the molecule from the ground electronic state to an excited electronic state which essentially involves the promotion of an electron from a bonding molecular orbital (BMO) to an antibonding molecular orbital (ABMO). In the excited state, the atom or the molecule is more likely to undergo a chemical reaction than in the ground state.

In ordinary thermal reactions, the activation energy results from the random intermolecular collisions. In photochemical reactions, on the other hand, activation energy is acquired by the absorption of photons of light associated with a particular amount of energy. By using monochromatic light of a particular wave length in the visible or ultraviolet region, it is possible to excite a particular atom or a molecule in a reaction mixture instantaneously to an excited state. Thus, in a photochemical reaction only a single selected species (atom or molecule) can be promoted to an excited state independent of the other species present in the reaction system. In contrast, thermal reactions do not permit such selectivity. Thermal excitation increases, in a random manner, the translational, rotational and vibrational energies of all the molecules resulting in the excitation of all the molecules to almost the same extent. For example, exposure of a mixture of hydrogen and bromine to radiations of wave lengths between 450 nm and 550 nm, results in excitation of only the bromine molecules whereas exposure to thermal radiations (heat) would cause excitation of both the bromine and the hydrogen molecules.

Photochemistry has emerged as one of the most powerful tools in research. The synthesis of complex molecules such as proteins and nucleic acids occurs through photochemical reactions between simple gaseous molecules such as CO_2, NH_3 and methane. Formation of vitamin D, formation of ozone from oxygen in the earth's stratosphere, formation of smog and unfortunate development of skin cancer are important examples of photochemical reactions. A new field of research, called photobiology, has emerged recently. It deals with photochemistry of biological reactions and has helped a great deal in partly understanding the mechanism of **photosynthesis** and other complex biological phenomena. The day we succeed in fully establishing the exact mechanism of photosynthesis, the world's food problem would be solved considerably. Organic compounds such as vitamin D_2, cubanes (antiviral agents), caprolactam (a monomer for nylon) and several insecticides and cleaning solvents have also been synthesised photochemically. Photochromic materials which have the peculiar property of changing colour when exposed to radiations of suitable wave lengths, have also been prepared photochemically. These substances reverse their absorption characteristics on withdrawing the incident radiations. Spiropyrans belong to the class of photochromic materials. They are used in photochromic sun glasses. They have also been used in the production of information-storage and self-developing, self-erasing films in digital computers.

The phenomena of fluorescence and phosphorescence find useful applications in the development of X-ray and television screens, fluorescent tube lights, optical brightners in white dress materials, luminescent dials for watches, microanalytical reagents for tracing the course of rivers through caves and so on. The development of laser technology is a recent marvellous application of photochemistry and photophysics.

The impact of photochemistry on medicine is felt in the **photodynamic therapy (PDT)**. Here laser radiation, which is usually delivered to diseased tissue through a fibre optic cable, is absorbed by a drug which in its first excited triplet state, photosensitizes the formation of an excited singlet state of O_2. The singlet oxygen molecules are very reactive and destroy cellular components, and it is believed that cell membranes are the primary cellular targets. The resulting photochemical cycle leads to the shrinkage (and sometimes the total destruction) of the diseased tissue.

Finally, photochemistry is finding increasing application in solving the energy crisis. Scientists are looking for ways and means for conversion and storage of solar energy. One of the ways of achieving solar energy conversion is by manufacturing solar batteries which operate on the principle of photovoltaic effect. For countries lying between the tropic of Cancer and the tropic of Capricorn, solar energy can provide an excellent source of energy. It has been estimated that in these regions, the daily incident energy per square kilometre is equivalent to the energy produced from about 3000 tonnes of coal. If and when the solar energy is harnessed, the world's energy crisis would be solved to a large extent.

Consequences of Light Absorption : The Jablonski Diagram

According to the Grotthus-Draper law of photochemistry, also called the principle of photochemical activation, only that light which is absorbed by a system can bring about a photochemical change. However, it is not essential that the light which is absorbed must bring about a photochemical change. The absorption of light may result in a number of other phenomena as well. For instance, the light absorbed may cause only a decrease in the intensity of the incident radiation. This event is governed by the Beer-Lambert law. Secondly, the light absorbed may be re-emitted almost instantaneously in one or more steps. This phenomenon is known as **fluorescence**. The emission in fluorescence ceases with the removal of the source of light. Sometimes the light absorbed is given out slowly and even long after the removal of the source of light. This phenomenon is known as **phosphorescence**. The phenomena of fluorescence and phosphorescence are best explained with the help of the **Jablonski diagram.**

In order to understand this diagram, we need to define some terminology. Most molecules have an *even* number of electrons and thus in the ground state, all the electrons are *spin paired*. The quantity $2S+1$, where S is the total electron spin, is known as the **spin multiplicity** of a state. When the spins are paired ($\uparrow\downarrow$), as shown in Fig. 1*(a)*, the upward orientation of the electron spin is cancelled by the downward orientation so that $S=0$. This is illustrated below :

$$s_1 = \tfrac{1}{2}\ ;\ s_2 = -\tfrac{1}{2} \text{ so that } S = s_1 + s_2 = \tfrac{1}{2} - \tfrac{1}{2} = 0$$

Hence, $2S+1=1$. Thus, the spin multiplicity of the molecule is 1. We express it by saying that the molecule is in the **singlet ground state.**

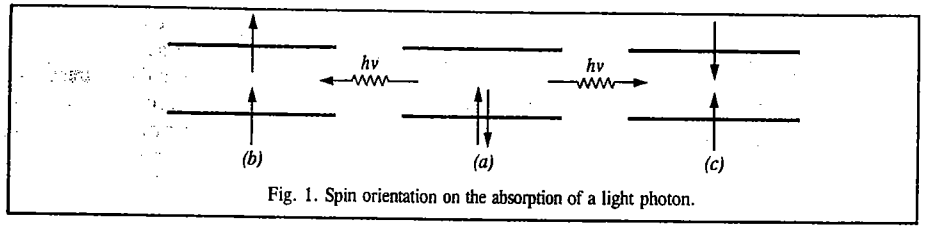

Fig. 1. Spin orientation on the absorption of a light photon.

When by the absorption of a photon of a suitable energy *hν*, one of the paired electrons goes to a higher energy level (excited state), the spin orientations of the two single electrons may be either parallel ↑↑, as shown in Fig. 1*(b)* or antiparallel ↑↓, as shown in Fig. 1*(c)*. If the spins are parallel, then

$$S = s_1 + s_2 = \tfrac{1}{2} + \tfrac{1}{2} = 1 \text{ so that } 2S+1 = 3$$

Thus, the spin multiplicity of the molecule is 3. This is expressed by saying that the molecule is in the **triplet excited state.**

If, however, the spins are antiparallel, then

$$S = s_1 + s_2 = \tfrac{1}{2} - \tfrac{1}{2} = 0 \text{ so that } 2S+1 = 1$$

Thus, the spin multiplicity of the molecule is 1. This is expressed by saying that the molecule is in the *singlet excited state*, as already mentioned.

Since the electron can jump to any of the higher electronic states depending upon the energy of the photon absorbed, we get a series of singlet excited states, S_n where n = 1, 2, 3, 4..... and a series of triplet excited states, T_n where n = 1, 2, 3, 4,..... Thus, S_1, S_2, S_3, etc., are known as the first singlet excited state, second singlet excited state, third singlet excited state, etc. Similarly, T_1, T_2, T_3, etc., are called the first triplet excited state, second triplet excited state, third triplet excited state, etc. (The symbol S in S_n should not be confused with S used for denoting the total spin).

It has been shown quantum mechanically that a singlet excited state has higher energy than the corresponding triplet excited state. Accordingly, the energy sequence is as follows :

$$E_{S_1} > E_{T_1}; \quad E_{S_2} > E_{T_2}; \quad E_{S_3} > E_{T_3} \text{ and so on.}$$

On absorption of light photon, the electron of the absorbing molecule may jump from S_0 to S_1, S_2 or S_3 singlet excited state depending upon the energy of the light photon absorbed, as shown in Jablonski diagram (Fig. 2). For each singlet excited state (S_1, S_2, S_3, etc.), there is a corresponding triplet excited state (T_1, T_2, T_3, etc.) The molecule, whether in singlet or triplet excited state, is said to be activated. Thus,

$$A_0 + h\nu \longrightarrow A^*$$

where A_0 is the molecule in the ground state and A* is the molecule in the excited state.

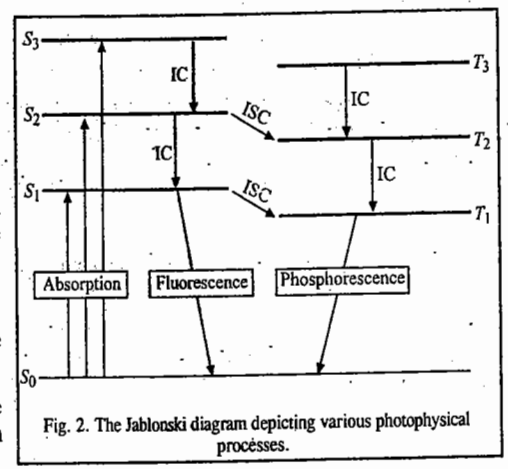

Fig. 2. The Jablonski diagram depicting various photophysical processes.

The activated molecule returns to the ground state by dissipating its energy through the following types of processes :

1. Non-radiative Transitions. These transitions involve the return of the activated molecule from the higher excited states (S_3, S_2, or T_3, T_2) to the first excited state (S_1 or T_1). These transitions do not involve the emission of any radiations and are thus referred to as *non-radiative* or *radiationless* transitions. The energy of the activated molecule is dissipated in the form of heat through molecular collisions. The process is called **internal conversion (IC)** and occurs in less than about 10^{-11} second.

The molecule may also lose energy by another process called **intersystem crossing (ISC).** This process involves transitions between states of different spins, *i.e.*, different multiplicity, as, for example, from S_2 to T_2 or S_1 to T_1. These transitions are also non-radiative or radiationless. Spectroscopically, such transitions are forbidden. However, they do occur though at relatively slow rates.

2. Radiative Transitions. These transitions involve the return of the activated molecule from the singlet excited state S_1 and triplet excited state T_1 to the ground state S_0. Such transitions are accompanied by the emission of radiation. Spectroscopically, the transition from S_1 to S_0 state is an 'allowed' transition and occurs in about 10^{-8} second. The emission of radiation in this transition is called **fluorescence.**

The transition from the triplet excited state T_1 to the ground state S_0 is rather slow since it is a 'forbidden' transition. The emission of radiation in this transition is called **phosphorescence.** The life times of phosphorescence are much longer being of the order of 10^{-3} sec or greater, since the transition involves spin inversion which needs time for its occurrence.

Both fluorescent and phosphorescent radiations are of shorter frequencies than the exciting light. This is obviously because some part of the light energy absorbed by the molecules is dissipated in the form of heat during non-radiative transitions.

3. Chemical Reactions. The activated molecule may also lose energy by undergoing chemical reaction. Since the molecule in singlet excited state returns quickly to the ground state, it gets no chance to react chemically. The molecule in a triplet excited state, however, returns to the ground state comparatively slowly, as explained above. This provides ample opportunity to the activated molecule to undergo chemical reaction. Thus, *the molecule which undergoes chemical reaction is the one which is previously in a triplet excited state.*

Light Absorption by Solutions

The absorption of light in the visible and near ultraviolet regions by a solution is governed by a photophysical law, known as the Beer-Lambert law.

Beer-Lambert Law. When a beam of monochromatic radiation of a suitable frequency passes through a solution, it is absorbed by the solution. As a result, the intensity of the light when it finally emerges from the solution, is considerably reduced. If I_0 is the intensity of the incident beam and I_t is the intensity of the transmitted beam, then the intensity of the light absorbed, I_a, is given by

$$I_a = I_0 - I_t \qquad \ldots(1)$$

The intensity of the beam is defined as the energy falling on unit area perpendicular to the beam per unit time. It is proportional to the number of photons incident on unit area in unit time.

The probability that the photons of a beam of intensity I will be absorbed by the sample is directly proportional to the concentration and the thickness of the absorbing solution. Mathematically, we express it by writing

$$dI/I = -\alpha c dx \qquad \ldots(2)$$

where dI is the change in intensity produced by the absorption of radiation on passing through a thickness dx of the solution of concentration c and α is the proportionality constant. The minus sign is introduced because there is reduction in intensity. Integration of Eq. 2 between the limits $I=I_0$ at $x=0$ and $I=I$ at $x=b$ gives

$$\int_{I_0}^{I} \frac{dI}{I} = -\alpha c \int_0^b dx \qquad \ldots(3)$$

or

$$\ln (I/I_0) = 2{\cdot}303 \log (I/I_0) = -\alpha bc \qquad \ldots(4)$$

According to Eq. 4, *the intensity of a beam of monochromatic radiation decreases exponentially with increase in the thickness x and the concentration c of the absorbing medium.* This is **Beer-Lambert law.**

Putting $\alpha/2{\cdot}303 = \varepsilon$ and defining $\log (I_0/I)$ as the **absorbance,** A, of the solution, we get

$$A = \log (I_0/I) = \varepsilon bc \qquad \ldots(5)$$

In Eq. 5, ε is called the absorption coefficient or extinction coefficient of the absorbing medium. It is characteristic of the solute and depends upon the nature of the solvent, temperature and the wave length of the radiation employed. If the concentration c is expressed in mol dm^{-3} and the path length b in cm, then ε (expressed as $dm^3\ mol^{-1}\ cm^{-1}$) is referred to as **molar absorption coefficient** (formerly, and still widely, called the **molar extinction coefficient).**

The **transmittance,** T, is defined as

$$T = I/I_0 \qquad \ldots(6)$$

Evidently, absorbance A and transmittance T are related as

$$A = -\log T$$

or $$T = 10^{-A} = 10^{-\varepsilon bc} \qquad \ldots(7)$$

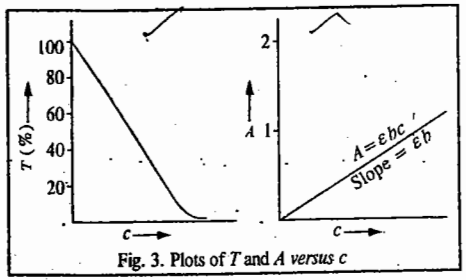

Fig. 3. Plots of T and A *versus* c

The plots of T and A versus c are shown in Fig. 3. As can be seen, the plot of A versus c is a straight line passing through the origin. Hence, this plot is more convenient to interpret than the plot of T versus c. The modern spectrophotometers are, therefore, calibrated to read absorbance although it is the transmitted light which is actually measured by the instrument.

Limitations of the Beer-Lambert Law. 1. The Beer-Lambert law is not obeyed if the radiation used is not monochromatic.

2. The law governs the absorption behaviour of dilute solutions only. At high solute concentrations, the ions of a solute, if it is an electrolyte, are close enough to disturb the charge distribution of their neighbours. The interionic interaction can drastically alter the ability of the solute to absorb a given wave length of the incident radiation. Thus, the relationship between A and c is no longer linear. Hence, at higher concentrations there are distinct deviations from linearity, as shown in Fig. 4.

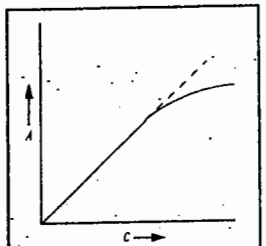

Fig. 4. Deviations from the Beer-Lambert law.

At higher concentrations, the refractive index (n) of the solution also changes. It has been found that in the Beer-Lambert law, it is the quantity $[n/(n+2)^2]\varepsilon$, rather than ε, which remains constant. Hence, severe deviations from the Beer-Lambert law will be observed when the factor $n/(n+2)^2$ changes with change in concentration.

The temperature of the system should not be allowed to vary to a large extent. This is because the increase in temperature has a bathochromic effect on ions in solution, *i.e.*, the absorption bands shift towards longer wave length.

Example 1. A monochromatic radiation is incident on a solution of 0·05 molar concentration of an absorbing substance. The intensity of the radiation is reduced to one-fourth of the initial value after passing through 10 cm length of the solution. Calculate the molar extinction coefficient of the substance.

Solution. According to the Beer-Lambert law,

$$\log I/I_0 = \varepsilon bc \qquad \text{(Eq. 5)}$$

In this case, $I/I_0 = 0{\cdot}25 = 25\%$, *i.e.*, $I_0/I = 100/25$

$\therefore$ $\log (100/25) = \varepsilon \times 10\ cm \times 0{\cdot}05\ mol\ dm^{-3}$

$\therefore$ $\varepsilon = 1{\cdot}204\ dm^3\ mol^{-1}\ cm^{-1}$

Example 2. A substance when dissolved in water at 10^{-3} M concentration absorbs 10 per cent of an incident radiation in a path of 1 cm length. What should be the concentration of the solution in order to absorb 90 per cent of the same radiation ?

Solution : $A = \log (I_0/I) = \varepsilon bc$ (Eq. 5)

In the first case, $A = 10\%$ so that $T = I/I_0 = 90\%$

$b = 1$ cm, $c_1 = 10^{-3}$ mol dm^{-3}

$\therefore$ $\log (100/90) = \varepsilon bc_1 \qquad \ldots(i)$

In the second case, $A = 90\%$ so that $T = I/I_0 = 10\%$, $b = 1$ cm

Let c_2 be the concentration in the second case.

$\therefore$ $\log (100/10) = \varepsilon bc_2 \qquad \ldots(ii)$

From Eqs *(i)* and *(ii)*,

$$\frac{\log (100/90)}{\log 10} = \frac{c_1}{c_2} = \frac{0{\cdot}001\ mol\ dm^{-3}}{c_2}$$

$\therefore$ $c_2 = 0{\cdot}0218\ mol\ dm^{-3}$

Example 3. In a Beer-Lambert law cell, the aqueous solution of a substance of known concentration absorbs 10 per cent of the incident light. What fraction of the incident light will be absorbed by the same solution in a cell five times as long ?

Solution :

In the first case, $A_1 = \log (I_0/I)_1 = \varepsilon b_1 c$

In the second case, $A_2 = \log (I_0/I)_2 = \varepsilon(5b_1)c$

$\therefore$ $A_2/A_1 = 5$

or $A_2 = 5A_1 = 5 \log (I_0/I)_1 = 5 \log (100/90) = 5\ (2{\cdot}00 - 1{\cdot}9542) = 0{\cdot}2290$

i.e., $A_2 = \log (I_0/I)_2 = 0{\cdot}2290$

Taking antilogs, $(I_0/I)_2 = 1{\cdot}694$

$\therefore$ $T = (I/I_0)_2 = 1/1{\cdot}694 = 0{\cdot}59$

Hence, the fraction of light absorbed $= 1 - 0{\cdot}59 = \mathbf{0{\cdot}41}$

It may be pointed out that absorbances are additive in nature. Thus, in a solution containing n independently absorbing species, the total absorbance is given by

$$A = A_1 + A_2 + A_3 + \cdots\cdots A_n$$

$$= (\varepsilon_1 c_1 + \varepsilon_2 c_2 + \varepsilon_3 c_3 + \cdots\cdots \varepsilon_n c_n) b = \log (I_0/I) \qquad \ldots(8)$$

where c_1, c_2, ... c_n are the concentrations of the species and ε_1, ε_2, ... ε_n are their respective absorption coefficients.

Example 4. In an absorption cell, the transmittance of 0·1 M solution of a substance X is 80% and that of 0·1 M solution of another substance Y is 60% at a given wave length. What is the transmittance of a solution that is simultaneously 0·1 M in X and 0·1 M in Y ?

Solution : Since absorbances are additive, hence

$$A = A_1 + A_2 = \log (I_0/I)_1 + \log (I_0/I)_2$$

$$= \log (100/80) + \log (100/60) = 0{\cdot}0969 + 0{\cdot}2219 = 0{\cdot}3188$$

$$A = \log (I_0/I) = 0{\cdot}3188$$

$$\therefore \quad I_0/I = 2{\cdot}084$$

$$T = I/I_0 = 1/2{\cdot}084 = 0{\cdot}48, \textit{ i.e.,} \ 48\%$$

The absorption of radiation by molecules at specific wave lengths is frequently used for quantitative analysis owing to the applicability of Eq. 5. The sensitivity of spectrometric analysis is dictated by the magnitude of the extinction coefficient ε and the minimum absorbance A that can be measured.

Example 5. The molar extinction coefficient of phenanthroline complex of iron (II) is 12,00 $dm^3\ mol^{-1}\ cm^{-1}$ and the minimum detectable absorbance is 0·01. Calculate the minimum concentration of the complex that can be detected in a Lambert-Beer law cell of path length 1·00 cm.

Solution :

$$A = \varepsilon bc$$

$$c = \frac{A}{b\varepsilon} = \frac{0{\cdot}01}{(1{\cdot}00\ \text{cm})\,(12,00\ \text{dm}^3\ \text{mol}^{-1}\ \text{cm}^{-1})}$$

$$= 8{\cdot}33\times10^{-6}\ \text{mol dm}^{-3} = 8{\cdot}33\times10^{-6}\ \text{M}$$

Laws of Photochemistry

The Lambert-Beer law for absorption of light has been discussed above. There are two other laws of photochemistry, *viz.*, 1. The Grotthus-Draper Law and 2. The Stark-Einstein Law.

1. Grotthus-Draper Law. This law was enunciated by the two scientists in the 19th century. They found that all the light that was incident on a simple was not effective in bringing about a chemical change. According to the Grotthus-Draper law (also called the **principle of photochemical activation),** only that light which is absorbed by a system can bring about a photochemical change.

2. Stark-Einstein law of Photochemical Equivalence. This law (also called the **principle of quantum activation)** was enunciated by Stark in 1908 and, independently, by Einstein in 1912. The two scientists applied the concept of energy quantum to photochemical reactions. According to this law, one molecule is activated by the absorption of one quantum of radiation in the primary (or first) step of a photochemical reaction. The law, however, does not imply that one molecule must react for each photon absorbed.

Suppose ν is the frequency of the radiation absorbed. Then the corresponding quantum of energy absorbed per molecule will be $h\nu$. The energy E absorbed per mole of the reacting substance is, therefore, given by

$$E = N_A h\nu = N_A hc/\lambda \qquad \ldots(9)$$

where c is the velocity of light and λ its wave length.

The quantity E, *i.e.*, the energy absorbed per mole of the reacting substance is called one **einstein.** It is evident that its numerical value varies inversely as the wave length of the light absorbed ; the shorter the wave length, the greater is the energy absorbed.

Quantum Yield

The quantum yield of a photochemical process is defined as

$$\phi = \frac{\text{Number of molecules that react}}{\text{Number of quanta of radiation absorbed}} = \frac{\text{Number of moles that react}}{\text{Number of einsteins of radiation absorbed}} \qquad \ldots(10)$$

The quantum yield for product formation is similarly defined as

$$\phi = \frac{\text{Number of molecules of product formed}}{\text{Number of quanta of radiation absorbed}} = \frac{\text{Number of moles of product formed}}{\text{Number of einsteins of radiation absorbed}} \qquad \ldots(11)$$

$$= \frac{\text{Rate of process}}{\text{Intensity of light absorbed}} = \frac{v}{I_{abs}}$$

If the law is correct, the quantum yield should be *unity*. This, however, is very rare. The quantum yields may be as high 10^6 or as low as 10^{-2} for several photochemical reactions. The reasons for these divergences would be discussed shortly.

Experimental Determination of Quantum Yields. In order to find out quantum yields of photochemical reactions, two types of determinations are needed. These are :

1. Determination of the number of moles of the light-absorbing substance that react in a given time and

2. Determination of the number of einsteins of light of required wave length that are absorbed by the same substance in the same time.

1. Determination of number of moles reacting. The number of moles reacting in a given time can be determined by the usual analytical techniques used in chemical kinetics. The reaction cell is usually made of glass unless violet or ultraviolet radiation is to be used. In that case the cell is made of quartz. The incident radiation is made to fall at right angles to it in the form of a parallel beam. The design of the cell varies with the nature of the reaction depending upon the fact whether it involves gases or liquids or both. The extent of photochemical reaction depends upon the intensity of the light used irrespective of its wave length. It has been calculated that one candle power of light falling on one square centimetre of surface per second corresponds to 2×10^{14} quanta. This shows that if the law is strictly valid, 2×10^{14} molecules or $3{\cdot}32\times10^{-10}$ moles of the light-absorbing substance would react per square centimetre of surface in one second. This is a very small quantity indeed. It is necessary to use light of high intensity. It may be remembered that energy of light radiation falling per square centimetre of surface is given by the product of the intensity of light and the time of exposure of the surface.

In all photochemical experiments, it is desirable to work with light of a single wave length, *i.e.*, a monochromatic light, as far as possible. This is usually done by employing discharge tubes which give atomic line spectra. A common source of light used for this purpose is the mercury vapour lamp. Iron and carbon arcs and, in some cases, metal filament lamps (*e.g.*, tungsten lamp) are also used as light sources. The spectrum given out by these sources consists only of a few sharp lines out of which the line of a desired wave length can be isolated by means of suitable filters. For very accurate work, a special device called monochromator is used. It acts like a spectrometer in which the wave length of light within a narrow range can be determined and isolated. It consists, essentially, of a suitable source of light and a prism which is ordinarily of glass or of quartz if the monochromatic light to be used is in the violet or ultraviolet region. The light of the required wave length is isolated and made to fall on the reaction cell.

If polychromatic light is used, some other reactions may also take place simultaneously.

2. Determination of the number of einsteins of light absorbed. The energy of monochromatic radiation (in terms of the number of einsteins absorbed) is determined accurately by employing a thermopile which consists of a number of thermocouples joined in series. One set of junctions of the thermocouples is blackened so as to absorb all the radiation that falls on it. The other set is protected from radiation and maintained at a constant temperature. The heat radiation associated with

light while falling on one set of junctions of the thermocouples generates thermoelectric current in the circuit. The EMF set up due to thermoelectric effect is measured from which the energy of the incident radiation can be easily calculated.

The measurements are made before and after passing the light through the cell. The difference gives the energy of the radiation absorbed by the reacting substance.

The energy of radiation can also be measured, though not so accurately, by employing an **actinometer.** In this device, a standard photochemical reaction is employed to estimate the energy of the radiation absorbed. One of the actinometers, which is in common use, is the **uranyl oxalate actinometer.** It consists of a dilute solution of oxalic acid mixed with uranyl sulphate. The latter serves to sensitise the decomposition of oxalic acid on exposure to violet or ultraviolet light whose wave length falls in the range of 250 nm to 435 nm. The extent of decomposition of oxalic acid is determined at the conclusion of the experiment by titration against potassium permanganate. The assumption made is that the amount of decomposition is propotional to the product of the intensity of light of a given wave length and the time of exposure. The apparatus is first standardised with respect to radiations of different wave lengths. It is possible, therefore, to evaluate the amount of energy of light radiation of a given wave length absorbed in the photochemical reaction. The measurements are made before and after passing the light through the reacting cell.

Example 6. Radiation of wave length 2500 Å was passed through a cell containing 10 ml of a solution which was 0·05 molar in oxalic acid and 0·01 molar in uranyl sulphate. After absorption of 80 joules of radiation energy, the concentration of oxalic acid was reduced to 0·04 molar. Calculate the quantum yield for the pohotochemical decomposition of oxalic acid at the given wave length.

Solution : The energy of einstein associated with radiation of wave length 2500 Å is given by

$$E = \frac{N_A hc}{\lambda} = \frac{6{\cdot}022\times10^{23}\ \text{mol}^{-1}\times6{\cdot}626\times10^{-34}\ \text{J s}\times3\times10^{8}\ \text{m s}^{-1}}{2500\times10^{-10}\ \text{m}} = \frac{11{\cdot}97\times10^{8}}{2500}\ \text{J}$$

$\therefore$ Number of einsteins corresponding to 80 J of radiation energy absorbed

$$= \frac{80\ \text{J}\times2500}{11{\cdot}97\times10^{8}\ \text{J}} = 0{\cdot}000167$$

$$\text{Decrease in the concentration of oxalic acid} = 0{\cdot}05 - 0{\cdot}04 = 0{\cdot}01\ \text{mol dm}^{-3}$$

$$\text{Quantity of oxalic acid decomposed in 10 ml of the solution} = \frac{0{\cdot}01\times10}{1000} = 0{\cdot}0001\ \text{mole}$$

$$\phi = \frac{\text{Number of moles decomposed}}{\text{Number of einsteins absorbed}} = \frac{0{\cdot}0001}{0{\cdot}000167} = 0{\cdot}60$$

Example 7. Photobromination of cinnamic acid to dibromocinnamic acid was carried out in blue light of wave length 440 nm at 35°C using light intensity of $1{\cdot}5\times10^{-3}$ J per second. An exposure of 20 minutes produced a decrease of 0·075 millimole of bromine. The solution absorbed 80 percent of the light passing through it. Calculate the quantum yield of the reaction.

Solution :

$$\text{Energy associated with a quantum of light of wave length 440 nm} = \frac{hc}{\lambda} = \frac{6{\cdot}626\times10^{-34}\ \text{J s}\times3\times10^{8}\ \text{m s}^{-1}}{440\times10^{-9}\ \text{m}} = 4{\cdot}51\times10^{-19}\ \text{J}$$

$$\text{Intensity of light} = 1{\cdot}5\times10^{-3}\ \text{J s}^{-1}$$

$$\text{Radiation energy absorbed in 20 minutes with 80\% absorption} = 1{\cdot}5\times10^{-3}\ \text{J s}^{-1}\times1200\ \text{s}\times\frac{80}{100}\times = 1{\cdot}44\ \text{J}$$

$$\text{Number of quanta absorbed} = \frac{1{\cdot}44\ \text{J}}{4{\cdot}51\times10^{-19}\ \text{J}} = 3{\cdot}19\times10^{18}$$

Amount of bromine that has reacted = 0·075 millimole = 0·075/1000 mole

$$\text{Number of molecules of bromine that react} = (0{\cdot}075/1000)\ \text{mol}\times6{\cdot}022\times10^{23}\ \text{mol}^{-1} = 45{\cdot}15\times10^{18}$$

$$\phi = \frac{\text{Number of molecules that react}}{\text{Number of quanta of radiation absorbed}} = \frac{45{\cdot}15\times10^{18}}{3{\cdot}19\times10^{18}} = 14{\cdot}15$$

Example 8. Calculate the number of moles of HCl(*g*) produced by the absorption of one joule of radiant energy of wave length 480 nm in the reaction $H_2(g) + Cl_2(g) \longrightarrow 2HCl(g)$ if the quantum yield of the photochemical reaction is $1{\cdot}0\times10^{6}$.

Solution : The energy of einstein associated with radiation of wave length 480 nm is given by

$$E = \frac{N_A hc}{\lambda} = \frac{(6{\cdot}022\times10^{23}\ \text{mol}^{-1})(6{\cdot}626\times10^{-34}\ \text{J s})(3\times10^{8}\ \text{m s}^{-1})}{480\times10^{-9}\ \text{m}} = 2{\cdot}492\times10^{5}\ \text{J}$$

$$\text{Number of einsteins corresponding to one joule of radiant energy absorbed} = \frac{1\ \text{J}}{2{\cdot}492\times10^{5}\ \text{J}} = 0{\cdot}40\times10^{-5}$$

$$\phi = 1\times10^{6}\ \text{(given)}$$

$$\text{Number of moles of HCl}(g)\text{ produced} = 1\times10^{6}\times0{\cdot}40\times10^{-5} = 4{\cdot}0$$

The quantum yields of some important photochemical reactions together with the effective wave lengths are given in Table 1.

TABLE 1

Effective Wave Lengths and Quantum Yields of Photochemical Reactions

Reaction	Effective Wave length (nm)	Quantum Yield (ϕ)
$2NH_3 \longrightarrow N_2 + 3H_2$	210	0·2
$2HI \longrightarrow H_2 + I_2$	207 - 282	2
$2HBr \longrightarrow H_2 + Br_2$	207 - 253	2
$H_2 + Cl_2 \longrightarrow 2HCl$	400	$10^4 - 10^6$
$CO + Cl_2 \longrightarrow COCl_2$	400 - 436	10^3
$SO_2 + Cl_2 \longrightarrow SO_2Cl_2$	420	1
$2NO_2 \longrightarrow 2NO + O_2$	405	0·7
$H_2S \longrightarrow H_2 + S$	208	1
$3O_2 \longrightarrow 2O_3$	170 -190	3
CH_3COCH_3 (vapour) $\longrightarrow CO + C_2H_6$	300	0·3
Maleic acid $\longrightarrow$ Fumaric acid	200 - 280	0·04
$2Fe^{2+} + I_2 \longrightarrow 2Fe^{3+} + 2I^-$	579	1
$2H_2O_2 \longrightarrow 2H_2O + O$	310	>7
$H_2 + Br_2 \longrightarrow 2HBr$	510	0·01

The various photochemical reactions can be divided into three categories :

1. Those in which the quantum yield is a small integer such as 1, 2 or 3. Examples are : Combination of SO_2 and Cl_2, dissociation of HI or HBr, ozonisation of O_2, etc.

2. The quantum yield is less than 1. Examples are dissociation of NH_3 and NO_2.

3. The quantum yield is extremely high. Examples are : Combination of hydrogen and chlorine and of carbon monoxide and chlorine.

M. Bodenstein (1871–1942) proposed that photochemical reactions involve two distinct processes :

1. Primary process in which light quantum $h\nu$ is absorbed by a molecule A resulting in the formation of an excited molecule A*. Thus,

$$A + h\nu \longrightarrow A^*$$

The molecule which absorbs light may get dissociated yielding excited state atoms or free radicals. The primary process may also involve loss of vibrational energy of excited molecules by collision with other molecules as well as by fluorescence and phosphorescence.

2. Secondary process in which the excited atoms, or free radicals produced in the primary stage react further giving rise to higher quantum yields. Sometimes, the atoms or free radicals initiate a series of chain reactions, as for example, in the combination of H_2 and Cl_2 to give HCl, when the resulting quantum yields are of the order of 10^6 or more. If the secondary reaction is exothermic, the heat of the reaction may activate other molecules thereby causing them to react. This is another reason for higher quantum yields. The reasons for low quantum yields are :

1. Excited molecules may get deactivated before they form products.

2. Collisions of excited molecules with non-excited molecules may cause the former to lose energy.

3. The primary photochemical process may get reversed.

4. The dissociated fragments may recombine to form the original molecule.

The law of photochemical equivalence can be applied only to **primary processes** in which each molecule capable of entering into chemical reaction absorbs one quantum of radiation. The secondary processes take place of themselves quite independent of the light radiation.

The sum of primary quantum yields ϕ_i for all photophysical and photochemical events i must be equal to 1, regardless of reactions involving the excited state. Thus,

$$\sum_i \phi_i = 1 \qquad \ldots(12)$$

It follows that for an excited state that decays to the ground state only via the photophysical processes described in the Jablonski diagram, we can write

$$\phi_F + \phi_{IC} + \phi_{ISC} + \phi_P = 1 \qquad \ldots(13)$$

where ϕ_F, ϕ_{IC}, ϕ_{ISC} and ϕ_P are the quantum yields of fluorescence, internal conversion, intersystem crossing and phosphorescence, respectively.

The quantum yield is also affected by the intensity of light. For instance, when radiation from a highly intense source, such as the laser, falls on a molecule, the latter can absorb even two photons simultaneously. For such biphotonic and multiphotonic effects, the Stark–Einstein law needs to be modified.

Example 9. A sample of gaseous HI was irradiated by light of wave length 253·7 nm when 307 J of energy was found to decompose $1{\cdot}30\times10^{-3}$ mole of HI. Calculate the quantum yield for the dissociation of HI.

Solution : The energy of quantum of radiation of wave length 253·7 nm,

$$E = \frac{hc}{\lambda} = \frac{(6{\cdot}626\times10^{-34}\ \text{J s})(3\times10^{8}\ \text{m s}^{-1})}{253{\cdot}7\times10^{-9}\ \text{m}} = 7{\cdot}835\times10^{-19}\ \text{J}$$

$$\text{Number of quanta of radiation absorbed by HI} = \frac{307\ \text{J}}{7{\cdot}835\times10^{-19}\ \text{J}} = 3{\cdot}92\times10^{20}$$

$$\text{Number of molecules of HI decomposed} = 1{\cdot}30\times10^{-3}\ \text{mol}\times6{\cdot}022\times10^{23}\ \text{mol}^{-1} = 7{\cdot}83\times10^{20}$$

$$\phi = \frac{\text{Number of molecules that react}}{\text{Number of quanta of radiation absorbed}} = \frac{7{\cdot}83\times10^{20}}{3{\cdot}92\times10^{20}}$$

$$= 1{\cdot}997 = 2{\cdot}00$$

Example 10. For the photochemical formation of ethylene from di-*n*-propylketone using a radiation of wave length 313 nm, the quantum yield is 0·21. Calculate the number of moles of ethylene formed when the sample is irradiated with 50 watt of this radiation assuming that all the radiation is absorbed by the sample.

Solution : The energy of quantum of radiation of wave length 313 nm is given by

$$E = \frac{hc}{\lambda} = \frac{(6{\cdot}626\times10^{-34}\ \text{J s})(3\times10^{8}\ \text{m s}^{-1})}{313\times10^{-9}\ \text{m}} = 6{\cdot}35\times10^{-19}\ \text{J}$$

Recalling that 1 watt = 1 J s^{-1}, the number of quanta emitted by 50 watt of radiation

$$= 50\ \text{J}/6{\cdot}35\times10^{-19}\ \text{J} = 7{\cdot}87\times10^{19}$$

The quantum yield for product formation is given by

$$\phi = \frac{\text{Number of ethylene molecules formed}}{\text{Number of quanta of radiation absorbed}}$$

$$0{\cdot}21 = \frac{\text{Number of ethylene molecules formed}}{7{\cdot}87\times10^{19}}$$

$$\text{Number of molecules of ethylene formed} = 7{\cdot}87\times10^{19}\times0{\cdot}21 = 1{\cdot}65\times10^{19}$$

$$\text{Amount of ethylene formed} = \frac{1{\cdot}65\times10^{19}\ \text{molecules}}{6{\cdot}022\times10^{23}\ \text{molecules mol}^{-1}} = 2{\cdot}74\times10^{-5}\ \text{mol}$$

Photochemical Reactions. There is a large variety of reactions which can occur by the absorption of photons of suitable energy. The photon energies lie mostly in the visible and ultraviolet regions. A few photochemical reactions are as follows :

1. Photochemical Decomposition of Hydrogen Halides :

$$2HI \xrightarrow{h\nu} H_2 + I_2$$

$$2HBr \xrightarrow{h\nu} H_2 + Br_2$$

2. Photochemical Decomposition of Ammonia :

$$2NH_3 \xrightarrow{h\nu} N_2 + 3H_2$$

3. Photochemical Decomposition of Acetone :

$$CH_3COCH_3 \xrightarrow{h\nu} C_2H_6 + CO$$

4. Photochemical Combination of Hydrogen and Halogens to form Hydrogen Halides :

$$H_2 + X_2 \xrightarrow{h\nu} 2HX$$

5. Isomerization of Maleic acid to Fumaric acid :

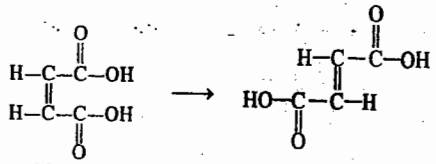

Maleic acid (*cis* isomer) Fumaric acid (*trans* isomer)

6. Dimerization of anthracene in benzene solution in the absence of oxygen :

$$2CH_{14}H_{10} \xrightarrow{h\nu} C_{28}H_{20}$$

7. Cleavage Reactions when the double bonds are suitably placed as, for example, in the following reaction :

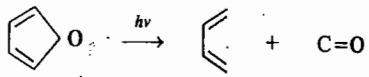

Photochemical Rate Law

Consider the photochemical decomposition reaction brought about by the absorption of a quantum of energy $h\nu$:

$$A \xrightarrow{h\nu} \text{Products}$$

If a beam of intensity I_0 is incident on the reaction cell of width b and cross-sectional area S, then the number of einsteins absorbed per second is $S(I_0 - I)$ where I is the intensity of transmitted radiation. The intensity of radiation is expressed in einsteins $cm^{-2}\ s^{-1}$.

According to the Beer–Lambert law,

$$\ln I/I_0 = -\alpha b[A] \quad \text{(Eq. 4)} \qquad ...(14)$$

or

$$I = I_0\, e^{-\alpha b[A]} \qquad ...(15)$$

Number of einsteins absorbed per second $= S(I_0 - I)$

Substituting the value of I from Eq. 15, we have

$$S(I_0 - I) = SI_0(1 - e^{-\alpha b[A]})$$

$$= SI_0(\alpha b[A] \qquad (\because e^{-x} = 1 - x \text{ when } x \text{ is very small})$$

Thus, the number of einsteins absorbed per second $= SI_0\alpha b[A]$

Hence, the quantum yield, $\phi = \dfrac{\text{Number of moles of A decomposed per second}}{\text{Number of einsteins absorbed per second}}$

$$= \frac{\text{Number of moles of A decomposed per second}}{SI_0\alpha b[A]} \qquad ...(16)$$

Since Sb is the volume of the reaction cell, hence the number of moles of A decomposed per second divided by the cell volume gives the concentration of A in moles per unit volume. Hence,

$$\phi = \frac{\text{Change in [A] per second}}{I_0\alpha[A]} = \frac{-d[A]/dt}{I_0\alpha[A]} \qquad ...(17)$$

$$\therefore \quad -\frac{d[A]}{dt} = \phi I_0\alpha[A] \qquad ...(18)$$

This is the **photochemical rate law.** Evidently, the photochemical decomposition of A is first-order in A.

The rate laws for a number of photochemical reactions have been derived using the well known steady state approximation *(s.s.a.)* for transient species. The rate laws and the kinetics of a few important photochemical reactions have been discussed below.

KINETICS OF PHOTOCHEMICAL REACTIONS

1. Kinetics of the Hydrogen–Chlorine Reaction :

$$H_2(g) + Cl_2(g) \xrightarrow{k_1} 2HCl\ (g)$$

The following mechanism has been suggested for this reaction :

(i) $Cl_2 + h\nu \xrightarrow{k_1} 2Cl$

(ii) $Cl + H_2 \xrightarrow{k_2} HCl + H$

(iii) $H + Cl_2 \xrightarrow{k_3} HCl + Cl$

(iv) Cl (at the walls) $\xrightarrow{k_4} \frac{1}{2}Cl_2$

Let us derive the rate law for the formation of HCl.

According to the mechanism given above,

$$r = d[HCl]/dt = k_2[Cl][H_2] + k_3[H][Cl_2] \qquad ...(19)$$

Applying *s.s.a.* to [Cl], we have

$$d[Cl]/dt = k_1I_a - k_2[Cl][H_2] + k_3[H][Cl_2] - k_4[Cl] = 0 \qquad ...(20)$$

where I_a is the intensity of absorbed radiation.

Applying *s.s.a.* to [H], we have

$$d[H]/dt = k_2[Cl][H_2] - k_3[H][Cl_2] = 0 \qquad ...(21)$$

Adding Eqs. 20 and 21,

$$k_1I_a - k_4[Cl] = 0 \text{ so that}$$

$$[Cl] = k_1I_a/k_4 \qquad ...(22)$$

Substituting in Eq. 21 and simplifying, we have

$$[H] = \frac{k_1k_2I_a[H_2]}{k_3k_4[Cl_2]} \qquad ...(23)$$

Substituting Eqs. 22 and 23 in Eq. 19, we get

$$r = \frac{k_1k_2I_a[H_2]}{k_4} + \frac{k_1k_2I_a[H_2]}{k_4} = \frac{2k_1k_2I_a[H_2]}{k_4}$$
$$= 2(k_1k_2/k_4)I_a[H_2] = kI_a[H_2] \quad ...(24)$$

where $k = 2(k_1k_2/k_4)$.

We see that *the rate is directly proportional to the intensity I_a of the absorbed radiation.* The rate law given by Eq. 24 agrees with the observed rate law.

The quantum yield for this reaction varies between 10^4 - 10^6.

2. Kinetics of the Hydrogen-Bromine Reaction

$$H_2(g) + Br_2(g) \xrightarrow{h\nu} 2HBr(g)$$

The mechanism of this reaction is the same as that of the thermal reaction discussed in Chapter 26, the only difference being that the first step in the photochemical reaction is the decomposition of Br_2 into Br atoms by the absorption of a quantum of energy $h\nu$. Thus,

(i) $Br_2 + h\nu \xrightarrow{k_1} 2Br$

(ii) $Br + H_2 \xrightarrow{k_2} HBr + H$

(iii) $H + Br_2 \xrightarrow{k_3} HBr + Br$

(iv) $H + HBr \xrightarrow{k_4} H_2 + Br$

(v) $2Br \xrightarrow{k_5} Br_2$

The rate of formation of HBr is given by

$$r = \frac{d[HBr]}{dt} = k_2[Br][H_2] + k_3[H][Br_2] - k_4[H][HBr] \quad ...(25)$$

Applying steady state approximation to [Br], we have

$$d[Br]/dt = k_1I_a - k_2[Br][H_2] + k_3[H][Br_2] + k_4[H][HBr] - k_5[Br]^2 = 0 \quad ...(26)$$

Applying *s.s.a.* to [H], we have

$$d[H]/dt = k_2[Br][H_2] - k_3[H][Br_2] - k_4[H][HBr] = 0 \quad ...(27)$$

Adding Eqs. 26 and 27,

$k_1I_a - k_5[Br]^2 = 0$ whence

$$[Br] = \left(\frac{k_1I_a}{k_5}\right)^{1/2} \quad ...(28)$$

From Eq. 27, $$[H] = \frac{k_2[H_2][Br]}{k_3[Br_2] + k_4[HBr]} \quad ...(29)$$

Substituting Eq. 28 into Eq. 29, we have

$$[H] = \frac{k_2(k_1I_a/k_5)^{1/2}[H_2]}{k_3[Br_2] + k_4[HBr]} \quad ...(30)$$

Sustituting Eqs. 28 and 30 into Eq. 25 and simplifying, we get

$$r = \frac{d[HBr]}{dt} = \frac{2k_2(k_1/k_5)^{1/2}I_a^{1/2}[H_2]}{1 + \frac{k_4[HBr]}{k_3[Br_2]}} \quad ...(31)$$

We see that the *rate varies as the square root of the intensity I_a of the absorbed radiation.* The rate law given by Eq. 31 agrees with the observed rate law. The quantum yield for this reaction is 0·01.

The reader might be puzzled by the fact that the quantum yield of the hydrogen-chlorine reaction is so high whereas that of hydrogen-bromine reaction is so low, even though both are chain reactions. This is explained by the fact that whereas reaction *(ii)* in the mechanism for the former reaction is exothermic and hence takes place spontaneously, reaction *(ii)* in the mechanism for the latter reaction is endothermic and takes place extremely slowly at ordinary temperatures. The quantum yield in each case depends upon the number of times the reaction steps *(ii)* and *(iii)* are repeated before the chain is terminated in the final step.

3. Kinetics of Decomposition of HI

$$2HI \xrightarrow{h\nu} H_2 + I_2$$

The following mechanism has been suggested for the photochemical decomposition of HI :

(i) $HI + h\nu \xrightarrow{k_1} H + I$

(ii) $H + HI \xrightarrow{k_2} H_2 + I$

(iii) $I + I \xrightarrow{k_3} I_2$

The rate law for the decomposition of HI is given by

$$-d[HI]/dt = k_1I_a + k_2[H][HI] \quad ...(32)$$

Applying steady state approximation to [H], we have

$$d[H]/dt = k_1I_a - k_2[H][HI] = 0$$

$$\therefore \quad k_2[H][HI] = k_1I_a \quad ...(33)$$

Substituting Eq. 33 in Eq. 32, we obtain

$$-d[HI]/dt = 2k_1I_a \quad ...(34)$$

The quantum yield of the reaction is given by

$$\phi = \frac{\text{Rate of disappearance of HI}}{\text{Rate of absorption of light}} = \frac{-d[HI]/dt}{k_1I_a}$$
$$= \frac{2k_1I_a}{k_1I_a} = 2$$

In this case ϕ decreases as the reaction proceeds. This is due to the fact that as iodine accumulates, the thermal reaction

$$H + I_2 \xrightarrow{k_4} HI + I$$

becomes significant.

If this reaction is also included in the mechanism, then the steady state approximation for [H] gives

$$d[H]/dt = k_1 I_a - k_2[H][HI] - k_4[H][I_2] = 0 \quad ...(35)$$

$$\therefore \quad [H] = \frac{k_1 I_a}{k_2[HI] + k_4[I_2]} \quad ...(36)$$

Substituting for [H] from Eq. 36 in Eq. 32, we obtain

$$-\frac{d[HI]}{dt} = k_1 I_a + k_2[HI]\frac{k_1 I_a}{k_2[HI] + k_4[I_2]}$$

$$= k_1 I_a \left(1 + \frac{1}{1 + \{k_4[I_2]/k_2[HI]\}}\right) \quad ...(37)$$

$$\therefore \quad -\frac{d[HI]/dt}{I_a} = k_1 + \frac{k_1}{1 + \{k_4[I_2]/k_2[HI]\}} \quad ...(38)$$

As the reaction proceeds, $[I_2]$ increases and hence the quantum yield decreases.

4. Kinetics of the Anthracene Reaction

Anthracene in benzene solution dimerizes and simultaneously fluoresces when irradiated with light of a certain frequency ν. The frequency of radiation emitted in fluorescence is ν' where $\nu' < \nu$. The following two mechanisms have been proposed for the reaction (A stands for anthracene molecule) :

Mechanism 1 :

$$A + h\nu \xrightarrow{k_1} A^* \quad \text{(excitation)}$$

$$A^* + A \xrightarrow{k_2} A_2 \quad \text{(dimerization)}$$

$$A^* \xrightarrow{k_3} A + h\nu' \quad \text{(fluorescence)}$$

Mechanism 2 :

$$A + h\nu \xrightarrow{k_1} A^* \quad \text{(excitation)}$$

$$A^* + A \underset{k_{-2}}{\overset{k_2}{\rightleftarrows}} A_2$$

$$A^* \xrightarrow{k_3} A + h\nu' \quad \text{(fluorescence)}$$

Let us derive the rate law for the formation of the dimer from the two mechanisms and calculate the quantum yield.

Using mechanism 1 and applying *s.s.a.* to A*, *viz.*, the anthracene molecule in the excited state, we get

$$d[A^*]/dt = k_1 I_a - k_2[A^*][A] - k_3[A^*] = 0 \quad ...(39)$$

where I_a is the intensity of light absorbed. Hence,

$$[A^*] = \frac{k_1 I_a}{k_2[A] + k_3} \quad ...(40)$$

The rate of formation of the dimer A_2 is given by

$$r = \frac{d[A_2]}{dt} = k_2[A^*][A] \quad ...(41)$$

Substituting Eq. 40 into Eq. 41, we have

$$r = \frac{k_1 k_2 I_a[A]}{k_2[A] + k_3} \quad ...(42)$$

The quantum yield for the formation of the dimer is given by

$$\phi(A_2) = \frac{\text{Number of moles of } A_2 \text{ formed}}{\text{Number of einsteins absorbed}} = \frac{d[A_2]/dt}{I_a}$$

$$= \frac{k_1 k_2[A]}{k_2[A] + k_3} \quad \text{(using Eqs. 41 and 42)} \quad ...(43)$$

We find that $\phi(A_2)$ *is independent of the intensity of the light absorbed.*

Eq. 43 can also be written as

$$\phi(A_2) = \frac{k_1[A]}{[A] + (k_3/k_2)} \quad ...(44)$$

If anthracene concentration, [A], is very low, *i.e.*, $[A] << (k_3/k_2)$, it can be neglected in the denominator, giving

$$\phi(A_2) = (k_1 k_2/k_3)[A] \quad ...(45)$$

Thus, $\phi(A_2)$ *increases with increase in the concentration* [A] *of the monomer.*

When $[A] >> (k_3/k_2)$,

$$\phi(A_2) = k_1 \quad ...(46)$$

i.e., the quantum yield is independent of [A].

Using the second mechanism, it can be shown that

$$\phi(A_2) = \frac{k_1 k_2[A] - k_{-2}k_3[A_2]I_a^{-1}}{k_2[A] + k_3} \quad ...(47)$$

i.e., the quantum yield depends upon the intensity of light absorbed.

Thus, while according to the first mechanism the quantum yield is independent of the intensity of light absorbed, according to the second mechanism it depends upon the intensity of the light absorbed. Experimental evidence is in favour of the former observation showing thereby that the anthracene reaction follows the first mechanism.

Eqs. 45 and 46 have also been shown to be true experimentally. This observation further supports the first mechanism for the anthracene reaction.

Ozone Layer in the Stratosphere

The formation of the ozone layer in the stratosphere is an example of a photochemical stationary state. The ozone thus formed is important because it absorbs ultraviolet radiation that would otherwise cause damage to life at the surface of the earth. The following is the proposed simplified mechanism

for the formation and destruction of ozone in the stratosphere :

$$O_2 \xrightarrow[J_{O_2}]{h\nu} 2O \qquad ...(48)$$

$$O + O_2 \xrightarrow{k_2} O_3 \qquad ...(49)$$

$$O_3 \xrightarrow[J_{O_3}]{h\nu} O_2 + O \qquad ...(50)$$

$$O_3 + O \xrightarrow{k_4} 2O_2 \qquad ...(51)$$

where the Js are photodissociation coefficients defined below. The photolysis reaction in the first step occurs at wave lengths less than 242 nm. Ozone is formed as shown in the reaction in step 2. The protective role of ozone is due to the third step in which radiation from the sun in the 190 to 300 nm range dissociates the ozone. The fourth step is a slow reaction. The recombination of oxygen atoms to form O_2 is very slow in the stratosphere and can be neglected. If the absorption of solar radiation in the first and third steps is steady, the concentration of ozone rises to a steady level.

The rate of change of ozone concentration is given by

$$\frac{d[O_3]}{dt} = k_2 [O] [O_2] - J_{O_3}[O_3] - k_4[O][O_3] \qquad ...(52)$$

where J_{O_3} is the **photodissociation coefficient** for ozone. This coefficient is the probability of dissociation of a molecule per second by light absorption. It can be calculated from the relation

$$J = \int_0^\infty \phi_{\bar{\nu}} I_{\bar{\nu}} \sigma_{\bar{\nu}} \, d\bar{\nu} \qquad ...(53)$$

where $\phi_{\bar{\nu}}$ is the quantum yield of dissociation of the molecule at wave number $\bar{\nu}$, $I_{\bar{\nu}}$ is the intensity of sunlight per unit area per unit time per unit wave number and $\sigma_{\bar{\nu}}$ is the absorption cross-section of the molecule at wave number $\bar{\nu}$. Thus, $I_{\bar{\nu}}$ has units of $m^{-1} s^{-1}$ and J has units of s^{-1}.

Since oxygen atoms are present at very low concentration, the rate of change in their concentration is assumed to be zero in the steady state :

$$\frac{d[O]}{dt} = 2J_{O_2}[O_2] - k_2[O][O_2] + J_{O_3}[O_3] - k_4[O][O_3] = 0 \qquad ...(54)$$

Adding Eqs. 52 and 54, we obtain

$$d[O_3]/dt = 2J_{O_2}[O_2] - 2k_4[O][O_3] \qquad ...(55)$$

Experimentally it is known that

$$J_{O_3}[O_3] \gg J_{O_2}[O_2] \text{ and}$$

$$k_2 [O] [O_2] \gg k_4 [O] [O_3]$$

Hence, Eq. 54 becomes

$$J_{O_3}[O_3] = k_2 [O] [O_2] \qquad ...(56)$$

Substituting this for [O] in Eq. 55, we get

$$\frac{d[O_3]}{dt} = 2J_{O_2}[O_2] - \frac{2k_4 J_{O_3}[O_3]^2}{k_2[O_2]} \qquad ...(57)$$

Hence, the steady-state concentration of O_3 is given by

$$[O_3]_{ss} = [O_2](k_2 J_{O_2} / k_4 J_{O_3})^{1/2} \qquad ...(58)$$

Since J_{O_2} increases with altitude and $[O_2]$ decreases with altitude, there is a maximum steady-state concentration in the stratosphere at an altitude of about 20 km.

In the 1960s it was found that nitrogen oxides can catalyse reaction (51) :

$$NO + O_3 \longrightarrow NO_2 + O_2$$
$$NO_2 + O \longrightarrow NO + O_2$$
$$O_3 + O \longrightarrow 2O_2 \qquad ...(59)$$

Also, in the mid-1970s it was discovered that chlorine atoms resulting from the photolysis of chlorofluorocarbons, also called **freons**, ($CFCl_3 + h\nu \longrightarrow CFCl_2 + Cl$ and $CF_2Cl_2 + h\nu \longrightarrow CF_2Cl + Cl$) in the stratosphere at the level of the ozone layer also catalyze the decomposition of O_3 :

$$Cl + O_3 \longrightarrow ClO + O_2$$
$$ClO + O \longrightarrow Cl + O_2$$
$$O_3 + O \longrightarrow 2O_2 \qquad ...(60)$$

Elimination of ozone from the stratosphere results in unrestricted passage of ultraviolet radiation from the sun to the earth. Excess of ultraviolet radiation causes skin cancer. The destruction of ozone by chlorine atoms in the stratosphere, creating an ozone hole, has thus become a serious topic of discussion. The American chemists Paul Crutzen, Mario J. Molina and F. Sherwood Rowland were awarded the 1995 Chemistry Nobel Prize for their work in atmospheric chemistry, concerning the formation and decomposition of ozone.

Energy Transfer in Photochemical Reactions. Photosensitization and Quenching

Some chemical reactions take place not by the absorption of light by one of the reactants but by a third substance which transfers the absorbed energy to the reactants. This third substance which itself does not undergo any change is called the **photosensitizer** and the process is known as **photosensitization.** Among the photosensitizers in common use are the atomic sensitizers such as mercury, cadmium and zinc and the molecular photosensitizers such as benzophenone and sulphur dioxide.

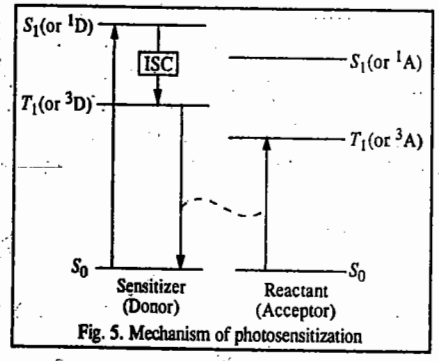

Fig. 5. Mechanism of photosensitization

Consider a general donor-acceptor system in which only the donor D, *i.e.*, the *sensitizer*, absorbs the incident photon and the triplet state of the donor is higher in energy than the triplet state of the acceptor A, *i.e.*, the reactant (Fig. 5). Absorption of the photon produces the singlet excited state of the donor, ^{1}D which, via intersystem crossing (ISC), gives the triplet excited state of the donor, ^{3}D. This triplet excited state then collides with the acceptor producing the triplet excited state of the acceptor, ^{3}A and the ground state of the donor. If ^{3}A gives the desired products, the mechanism is called photosensitization. If, however, the products of interest result from ^{3}D, then A is called the *quencher* and the process is known as **quenching.**

The reactions depicting photosensitisation and quenching may be represented as follows :

$$D + h\nu \longrightarrow {}^1D$$

$${}^1D \xrightarrow{ISC} {}^3D$$

$${}^3D + A \longrightarrow D + {}^3A$$

$${}^3A \longrightarrow \text{Products} \qquad \text{(photosensitization)}$$

$${}^3D \longrightarrow \text{Products} \qquad \text{(quenching)}$$

It must be emphasized that *the triplet excited state of the sensitizer must be higher in energy than the triplet excited state of the reactant* so that the energy available is enough to raise the reactant molecule to its triplet excited state. The dotted line in Fig. 5 links the transition in which the sensitizer loses energy with that in which the reactant gains energy. Photosensitization was discovered by Franck and Cario in 1922. The German physicists James Franck (1882-1964) and Gustav Hertz (1887-1975) were awarded the 1925 Physics Nobel prize for their research on the atom-electron collisions. A few examples of photosensitized reactions are given below.

1. Photosynthesis in Plants. The most important photochemical reaction and the most outstanding example of photosensitization is the photosynthesis of carbohydrates in plants from CO_2 and H_2O in which chlorophyll, the green colouring matter of plants, acts as a photosensitizer. Neither CO_2 nor H_2O absorbs any radiation in the visible region but chlorophyll does. It absorbs visible light of almost any wave length in the range of 400 - 700 nm. The energy of the light absorbed by chlorophyll is transferred to CO_2 and H_2O molecules which then react to form the carbohydrate $(CH_2O)_n$:

$$CO_2 + H_2O + \text{light} \longrightarrow \frac{1}{n}(CH_2O)_n + O_2$$

In the absence of light, the $\Delta G°$ for this reaction is +2878 kJ. Since this is a very large positive value, the equilibrium lies too far to the left. In the presence of light absorbed by chlorophyll, $\Delta G°$ becomes negative thereby causing the reaction to proceed to the right. Chlorophyll contains an extensively conjugated system of alternately single and double bonds which helps the molecule to absorb visible radiation. Photosynthesis requires eight photons per molecule of CO_2 consumed. The efficiency of conversion of light of 600 nm into chemical energy in this process is about 30%.

Photosynthesis, according to M. Calvin, proceeds through two main stages : 'light reactions' and 'dark reactions'. The first stage involves light reactions taking place on the absorption of light and being complete within 10^{-12} to 10^{-8} s. The second stage consisting of dark reactions - so called because they occur in the absence of light - is the rate-determining step for the overall reaction. Once mechanism of photosynthesis in plants is fully understood, the food problem of the world would be solved to a large extent. The American chemist Melvin Calvin was awarded the 1961 Chemistry Nobel Prize for his research on the carbon dioxide assimilation in plants.

2. Dissociation of H_2 Molecule. Irradiation of a mixture of hydrogen gas and mercury vapour with light of wave length 253·7 nm brings about dissociation of hydrogen molecule into hydrogen atoms :

$$Hg + h\nu \longrightarrow Hg^*$$

$$Hg^* + H_2 \longrightarrow H_2^* + Hg \quad \text{[Here mercury acts as the photosensitizer]}$$

$$H_2^* \longrightarrow 2H$$

3. Dissociation of Ethylene. Irradiation of a mixture of ethylene and mercury vapour with light of wave length 253·7 nm brings about the following reactions :

$$Hg + h\nu \longrightarrow Hg^*$$

$$Hg^* + C_2H_4 \longrightarrow C_2H_4^* + Hg$$

$$C_2H_4^* \longrightarrow C_2H_2 + H_2$$

4. Decomposition of Diazomethane (CH_2N_2). Diazomethane undergoes decomposition when exposed to radiation of 320 nm wave length in the presence of benzophenone which acts as a photosensitizer.

$$Bz \xrightarrow{h\nu} Bz^*$$

$$Bz^* + CH_2N_2 \longrightarrow Bz + CH_2N_2^*$$

$$CH_2N_2^* \longrightarrow CH_2 + N_2$$

5. Isomerization of Butene-2. The *cis* butene-2 undergoes isomerization to yield *trans* butene-2 when exposed to radiation of 253·7 nm wave length in the presence of sulphur dioxide.

$$SO_2 \xrightarrow{h\nu} SO_2^*$$

$$SO_2^* + \textit{cis}\text{ Butene-2} \longrightarrow SO_2 + \textit{cis}\text{ Butene-2}^*$$

$$\textit{cis}\text{ Butene-2}^* \longrightarrow \textit{trans}\text{ Butene-2}$$

Quenching of Fluorescence

Fluorescence may be quenched (*i.e.*, stopped) when the excited state species undergoes collision with a normal molecule before it has the chance to fluoresce. The quenching of fluorescence occurs because of the energy transfer from the excited state species to the molecule with which it collides. Quenching may also occur when the molecule changes from the singlet excited state to the triplet excited state. This phenomenon is called **internal quenching.** Quenching may also result from the presence of an externally added species which takes up energy from the excited state molecule. This phenomenon is called **external quenching.** If Q is the quencher, we may then write :

$$A + h\nu \longrightarrow A^* \qquad \text{(activation)}$$

$$A^* \xrightarrow{k_1} A + h\nu \qquad \text{(fluorescence)}$$

$$A^* \xrightarrow{k_2} A \qquad \text{(internal quenching)}$$

$$A^* + Q \xrightarrow{k_3} A + Q'$$

Applying *s.s.a.* to A*, we have

$$I_a = k_1[A^*] + k_2[A^*] + k_3[A^*][Q]$$

where I_a is the intensity of light absorbed.

If I_f is the intensity of fluorescence, the quantum yield for fluorescence is given by

$$\phi_f \equiv \phi_Q = \frac{I_f}{I_a} = \frac{k_1[A^*]}{k_1[A^*] + k_2[A^*] + k_3[A^*][Q]} = \frac{k_1}{k_1 + k_2 + k_3[Q]}$$

In the absence of quenching, *i.e.*, when [Q] = 0, we have

$$\phi_0 = \frac{k_1}{k_1 + k_2}$$

Hence, the ratio of the two quantum yields

$$\frac{\phi_0}{\phi_Q} = \frac{k_1 + k_2 + k_3[Q]}{k_1 + k_2} = 1 + \frac{k_3}{k_1 + k_2[Q]}$$

$$= 1 + k_3\tau\,[Q] = 1 + K_{SV}\,[Q] \qquad \ldots(61)$$

where $K_{SV} = k_3\tau$ and $\tau = 1/(k_1 + k_2)$

Eq. 61 is known as the **Stern-Volmer equation** in which K_{SV} is called the **Stern-Volmer constant** and τ is lifetime of A^* in the absence of external quenching. From the Stern-Volmer equation we see that ϕ_0/ϕ_Q depends linearly on [Q]. The slope of the line gives $k_3\tau$ from which τ can be determined.

When pure chlorophyll solution is irradiated, there results fluorescence. Addition of an external quencher such as oxygen or quinone quenches the fluorescence. The quenching is also brought about by the electron-transfer enzyme systems which are present in the living plants.

Chemiluminescence

Chemiluminescence is defined as the production of light by a chemical reaction and is thus the reverse of a photochemical reaction. In order for a reaction to be chemiluminescent it must furnish sufficient energy to raise at least one of the reactants or intermediates to an electronically excited state so that as it returns to the ground state, it emits energy in the form of radiation. Some chemiluminescent reactions are :

1. The glow of phosphorus and its oxide.
2. Oxidation-reduction reactions of hydrazine.
3. 'Cold light' emission by glowworms. This is an example of bioluminescent reaction involving the oxidation of luciferon—a protein, by atmospheric oxygen in the catalytic presence of an enzyme called luciferase.
4. Reaction between alkaline solutions of H_2O_2 and either Cl_2 or hypochlorite ion which produces a red glow at a number of wave lengths. One of the glows has been identified as resulting from the excitation of the oxygen produced in the reaction.
5. Electron-transfer reactions.
6. Interaction between the aromatic anions Ar^- and cations Ar^+ generated during electrolysis of large polycylic hydrocarbons :

$$Ar^- + Ar^+ \longrightarrow {}^1Ar^* + Ar$$
$$^1Ar^* \longrightarrow Ar + h\nu$$

This is illustrated in Fig. 6.

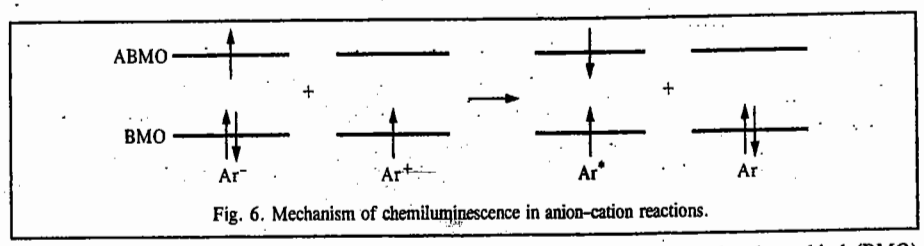

Fig. 6. Mechanism of chemiluminescence in anion-cation reactions.

The aromatic anion, Ar^-, contains two paired electrons in the bonding molecular orbital (BMO) and one unpaired electron in the antibonding molecular orbital (ABMO). The ABMO of the aromatic cation Ar^+ is empty. When the electron is transferred from the ABMO of the anion to the ABMO of the cation in such a way that the singlet excited state $^1Ar^*$ is formed, the excited state can be deactivated by the emission of photon of energy $h\nu$.

7. The luminescence observed at night in the ocean is probably due to the decay of the luminous jelly-fish.

Rates of Intramolecular Photophysical Processes and Intermolecular Energy Transfer

Consider the electronic excitation of a molecule and the dissipation of excitation energy by internal conversion (IC), intersystem crossing (ISC), fluorescence (F) or phosphorescence (P), as shown in the Jablonski diagram (Fig. 7).

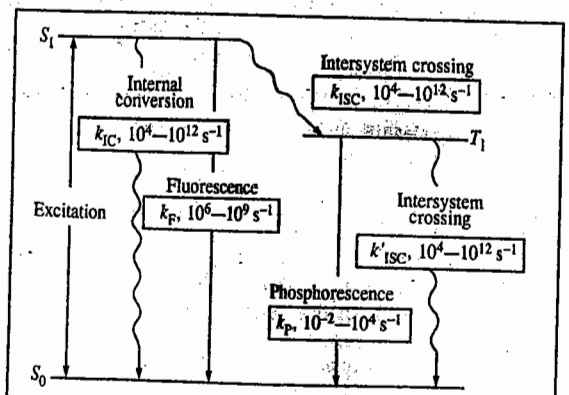

Fig. 7. First-order rate constants for the various intramolecular processes. The wavy lines represent radiationless transitions.

Each of these processes is characterized by the average lifetime of an excited molecule before it undergoes the process. Since we are interested in comparing the rates of these photophysical processes with the rates of chemical reactions, we shall emphasize here the rate constant k which is reciprocal of the lifetime T. Fig. 7 summarizes the approximate first-order rate constants for the various intramolecular processes involved. We assume, for the sake of simplicity, that the absorbing molecule, usually in the singlet ground state S_0, is excited to the first singlet excited state S_1. Upon illumination with radiation of constant intensity, the molecule attains a steady state wherein the rates of formation of intermediates are equal to the rates of their disappearance. The steady-state concentration of S_1 is related to the intensity of light absorbed I_a (expressed in moles of photons absorbed per unit volume per unit time) by the equation

$$I_a = k_{IC}[S_1] + k_F[S_1] + k_{ISC}[S_1] \qquad ...(62)$$

whence

$$[S_1] = \frac{I_a}{k_{IC} + k_F + k_{ISC}} \qquad ...(63)$$

The steady-state rate equation for the first triplet state T_1 (assuming that T_1 is populated by ISC from S_1) is given by

$$k_{ISC}[S_1] = k'_{ISC}[T_1] + k_P[T_1] \qquad ...(64)$$

whence

$$[T_1] = \frac{k_{ISC}[S_1]}{k'_{ISC} + k_P} \qquad ...(65)$$

Substituting for $[S_1]$ from Eq. 63, yields

$$[T_1] = \frac{k_{ISC} I_a}{(k'_{ISC} + k_P)(k_{ISC} + k_F + k_{ISC})} \qquad ...(66)$$

The radiative lifetime τ_0 is approximately inversely proportional to molar absorptivity ε, that is,

$$\tau_0 \approx (10^{-4}\ dm^3\ mol^{-1}\ cm^{-1}\ s)/\varepsilon \qquad ...(67)$$

This means that the states that are populated readily are also depopulated readily. A strongly absorbing compound with $\varepsilon = 10^5\ dm^3\ mol^{-1}\ cm^{-1}$ is expected to have a natural radiative lifetime of about 10^{-9} s, whereas a weakly absorbing compound with $\varepsilon = 10^{-2}\ dm^3\ mol^{-1}\ cm^{-1}$ would have a natural radiative lifetime of about 10^{-2} s. The observed lifetime of an excited singlet state τ_S is less than the radiative lifetime τ_0 because there are other deactivation processes involved. From Fig. 7, the rate of decay of

S_1 is given by

$$-\frac{d[S_1]}{dt} = (k_{IC} + k_F + k_{ISC})[S_1] \quad ...(68)$$

so that the singlet lifetime is given by

$$\tau_S = 1/(k_{IC} + k_F + k_{ISC}) \quad ...(69)$$

This follows from the fact that the relaxation time τ for a first-order process is equal to the reciprocal of the first-order rate constant : $\tau = 1/k$, so that in the first-order reaction A $\longrightarrow$ products, the equation $[A] = [A]_0 \exp(-kt)$ can be written as $[A] = [A]_0 \exp(-t/\tau)$.] The singlet lifetime τ_S may be experimentally determined by observing the decay of intensity of fluorescence after a short ($\ll \tau_S$) pulse of excitation because the intensity of fluorescence is proportional to the excited state concentration. Thus, for the benzene molecule in solvent hexane, at 25°C, the fluorescence lifetimes are τ_S=26 ns, τ_0=370 ns and the quantum yield of fluorescence $\phi_F = 0{\cdot}070$.

The quantum yield of fluorescence ϕ_F is equal to the ratio of fluorescence $k_F[S_1]$ to the total rate of deactivation of the S_1 state which is given by $(k_{IC} + k_F + k_{ISC})[S_1]$. Thus,

$$\phi_F = k_F/(k_{IC} + k_F + k_{ISC}) = \tau_S k_F = \tau_S/\tau_0 \quad ...(70)$$

Note that this is the value of ϕ_F in the absence of any quenching or chemical reaction. From Eq. 70 we see that the singlet lifetime is given by

$$\tau_S = \tau_0 \phi_F \quad ...(71)$$

Thus, measurement of τ_S and ϕ_F enables calculation of the radiative lifetime τ_0. Also,

$$\phi_{IC} = k_{IC}/(k_{IC} + k_F + k_{ISC}) \quad ...(72)$$

$$\phi_{ISC} = k_{ISC}/(k_{IC} + k_F + k_{ISC}) \quad ...(73)$$

where ϕ_{IC} and ϕ_{ISC} are, respectively, the quantum yield for internal conversion and the quantum yield for intersystem crossing. Referring again to Fig. 7, we see that if the rate constant k_{ISC} for the intersystem crossing S_1 to T_1 is fast enough, T_1 will be present at an appreciable concentration. As a consequence, the triplet state molecules may have long lifetimes compared with singlet state molecules and may, therefore, have greater probability of undergoing a chemical reaction. From Fig.7, the phosphorescence lifetime of the first triplet state T_1 is given by

$$\tau_{T_1} = 1/(k_P + k'_{ISC}) \quad ...(74)$$

and the quantum yield for phosphorescence is given by

$$\phi_P = \frac{\text{Rate of phosphorescence emission}}{\text{Rate of absorption of radiation}} = \frac{k_P[T_1]}{I_a} \quad ...(75)$$

$$= \frac{k_P\, k_{ISC}}{(k'_{ISC} + k_P)(k_{IC} + k_F + k_{ISC})} = k_P\, k_{ISC}\, \tau_{ISC}\, \tau_{T_1} \quad ...(76)$$

where the second form has been obtained by substituting the expression for the steady-state value of $[T_1]$ given in Eq. 65.

Excited state molecules may undergo several different types of reactions. When the chemical reaction of an excited molecule with another molecule is accompanied by the deactivation of an excited molecule, the excited state is said to be quenched. Quenching of an excited molecule (donor D) with a second molecule (acceptor A) may result in the electronic excitation of A with concomitant deactivation of D. This quenching process is called **intermolecular energy transfer.** It is important to note that since minute

traces of impurities (quenchers) can rapidly deactivate excited molecules, substances and solvents used in photochemical investigations must be carefully purified. Thus, for instance, molecular oxygen reacts rapidly with excited molecules ($k \approx 10^9$ dm^3 mol^{-1} s^{-1}) ; it is, therefore, important to deoxygenate the solutions under study.

The quenching of phosphorescence provides a means of determining the rate constant for the reaction of the triplet state molecules and the quencher Q. The steady-state concentration of molecules in triplet state in the absence of a quencher is given by Eq. 65. In the presence of a quencher this equation becomes

$$[T_1] = \frac{k_{ISC}[S_1]}{k_P + k'_{ISC} + k_Q[Q]} \quad ...(77)$$

because of the additional pathway for reaction of the triplet state molecules with the quencher. The quantum yield for phosphorescence in the absence of a quencher is given by Eq. 76 and will be represented by ϕ_P^0. If the steady-state concentration of T_1 in the presence of a quencher is given by Eq. 77, the ratio of the quantum yields in the absence and presence of the quencher is given by

$$\frac{\phi_P^0}{\phi_P} = \frac{k_P + k'_{ISC} + k_Q[Q]}{k_P + k'_{ISC}} = 1 + k_Q \tau_{T_1}[Q] \quad ...(78)$$

where τ_{T_1}, the phosphorescence lifetime, is defined by Eq. 74. Since the ratio of the intensity I_P^0 of phosphorescence in the absence of quencher to the intensity I_P of phosphorescence in the presence of quencher is proportional to the ratio of the corresponding quantum yields, Eq. 78 may be written as

$$\frac{I_P^0}{I_P} = 1 + k_Q \tau_{T_1}[Q] \quad ...(79)$$

Eq. 79 is called the **Stern-Volmer equation.**

Electronic Spectra and Photochemistry

Since due to intermolecular collisions, the fine structure is wiped out in the electronic spectrum of a sample in solution, the electronic band is generally broad containing many unresolved lines. The band has usually a Gaussian profile, as shown in Fig. 8 where a plot of molar extinction coefficient *versus* frequency (in cm^{-1}) is given. The band intensity cannot be as accurately measured by the maximum absorption (as represented by the maximum value of the extinction coefficient ε_{max}) as by the integral over the entire band. The **integrated absorption coefficient, *A*,** of the band is defined by

$$A = \int_{\text{band}} \varepsilon \, d\bar{\nu}$$

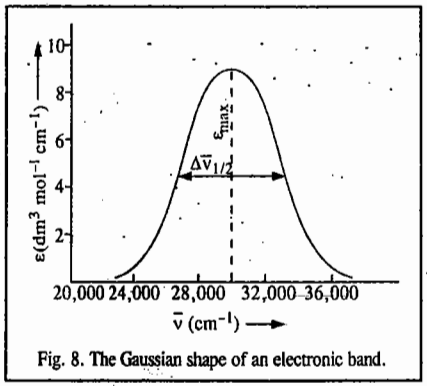

Fig. 8. The Gaussian shape of an electronic band.

A has the units of dm^3 mol^{-1} cm^{-2}. For a Gaussian absorption band,

$$A = \int_{\text{band}} \varepsilon \, d\bar{\nu} = 1{\cdot}06\ \varepsilon_{max}\, \Delta\bar{\nu}_{1/2} \quad ...(80)$$

where $\Delta\bar{\nu}_{1/2}$ is the band-width at half the maximum of the extinction coefficient.

Extensively conjugated systems like organic dyes have very intense and sharp electronic bands with $\varepsilon_{max}=10^4$ to 10^5 dm^3 mol^{-1} cm^{-1} and $\Delta\bar{\nu}_{1/2}$ of the order of 1,000 – 5,000 cm^{-1}. For weak absorption bands, on the other hand, $\varepsilon_{max}=10$ dm^3 mol^{-1} cm^{-1} and $\Delta\bar{\nu}_{1/2}$ is of the order of 100 cm^{-1}. Extremely weak (forbidden) bands have ε_{max} of the order of 10^{-3} to 10^{-4} dm^3 mol^{-1} cm^{-1}.

Example 11. The maximum value of the extinction coefficient of an electronic band in solution is 40,000 dm^3 mol^{-1} cm^{-1} and the width at half maximum is 5,000 cm^{-1}. Assuming that the band has a Gaussian shape, calculate the integrated absorption coefficient of the band.

Solution : $\varepsilon_{max} = 45{,}000$ dm^3 mol^{-1} cm^{-1} ; $\Delta\bar{\nu}_{1/2} = 5{,}000$ cm^{-1}

$$A = \int_{\text{band}} \varepsilon\bar{\nu} = 1{\cdot}06\varepsilon_{max}\Delta\bar{\nu}_{1/2}$$

$$= 1{\cdot}06\ (40{,}000\ \text{dm}^3\ \text{mol}^{-1}\ \text{cm}^{-1})\ (5{,}000\ \text{cm}^{-1})$$

$$= \mathbf{2{\cdot}12\times18^8\ dm^3\ mol^{-1}\ cm^{-2}}$$

The oscillator strength, f, of a spectral transition is defined as *the ratio of the experimental intensity to the theoretical intensity of the band.* It is related to the integrated absorption coefficient, A, by the equation

$$f = (6{\cdot}259\times10^{-19}\ \text{mol s m}^{-2})\times A \qquad ...(81)$$

The allowed electronic transitions which show strongest absorptions have oscillator strengths nearly equal to unity. For weak allowed transitions, $f = 10^{-4}$. Forbidden transitions are much weaker. For instance, for spin–forbidden transitions, f lies in the range 10^{-6} – 10^{-11}.

It may be noted that for a single electron undergoing more than one transition, the sum of all the oscillator strengths for all transitions from one energy level to other energy levels is unity, that is,

$$\sum_i f_i = 1 \qquad ...(82)$$

The oscillator strength is a dimensionless quantity.

Example 12. Calculate the oscillator strength of the electronic band in Example 11. Is the spectral transition allowed or forbidden ?

Solution : $A = 1{\cdot}471\times10^{19}$ dm^3 mol^{-1} cm^{-1} s^{-1} (Example 11)

According to Eq. 81, $f = (6{\cdot}259\times10^{-19}\ \text{mol s m}^{-2})\ (1{\cdot}471\times10^{19}\ \text{dm}^3\ \text{mol}^{-1}\ \text{cm}^{-1}\ \text{s}^{-1}) = \mathbf{0{\cdot}9207 \approx 1}$

Since $f=1$, the electronic transition is **allowed.**

We can also calculate the oscillator strength for a Gaussian electronic band from the formula

$$f = 4{\cdot}60\times10^{-9}\ \varepsilon_{max}\ \Delta\bar{\nu}_{1/2} \qquad ...(83)$$

Geometry of the Excited States

The excited states have become one of the most active areas of photochemical research in recent years. However, not much is known about them. The short life times of these states preclude application of ordinary structural methods to them. The excited states have often different equilibrium geometries than the ground states. For instance, acetylene, which is linear in the ground state S_0, has a bent geometry in the first singlet excited state S_1 :

(linear S_0) (bent S_1)

Again, formaldehyde, which is planar in its ground state S_0, distorts to a pyramidal structure in the first singlet excited state S_1 :

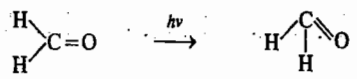

(S_0) (S_1)

μ=2·3 D μ=1·5 D

The dipole moments of formaldehyde in the S_0 and S_1 states are also quite different, thus, indicating significantly different electron distribution.

Life time of an Excited State. The life times of excited states are generally very short, ranging from a few picoseconds (10^{-12} s) to a few microseconds (10^{-6} s). It is possible to determine the life time of a state by measuring the natural line–width of the spectral line originating from the transition between the excited state and the ground state.

Example 13. Calculate the life time of an excited state if the natural width of the spectral line arising from the transition between this state and the ground state is 0·053 cm^{-1}.

Solution : $\Delta E\times\Delta t \approx h/4\pi$ (Heisenberg's uncertainty principle)

where ΔE is the uncertainty in the energy of the excited state and Δt is the uncertainty in its life time. Since $E = h\nu$, $\Delta E=h\Delta\nu$. Hence,

$$h\Delta\nu\times\Delta t \approx h/4\pi \quad \text{or} \quad \Delta\nu\times\Delta t \approx 1/4\pi$$

or $$\Delta t \approx 1/(4\pi\Delta\nu)$$

Since $\nu = c\bar{\nu}$, $\Delta\nu = c\Delta\bar{\nu}$. Again we can set $\Delta t=\tau$, where τ is the life time of the excited state. Thus,

$$\tau = \frac{1}{4\pi c\Delta\bar{\nu}} = \frac{1}{(4\pi)(3\times10^{10}\ \text{cm s}^{-1})(0{\cdot}053\ \text{cm}^{-1})}$$

$$= \mathbf{5\times10^{-11}\ s = 50\ ps} \quad [\because 1\ \text{ps} = 10^{-12}\ \text{s}]$$

The investigation of life times of excited states has gained importance in photochemistry. The occurrence of relatively long-lived high-energy species such as the triplet excited states that lead to phosphorescence provides means for the occurrence of photochemical reactions.

THE LASER AND THE MASER

The theory of the laser and the maser was developed by the American physicist Charles Townes and the Soviet physicists N.G. Basov and A.M. Prokhorov. Townes, Basov and Prokhorov shared the 1964 Nobel Prize for Physics. Other internationally famous scientists who contributed significantly to the laser research are T.H. Maiman, Ali Javan and C.K.N. Patel. C.K.N. Patel, the India-born American scientist, did important research on lasers at the Bell Telephone Laboratories in the U.S.A. in the 1960s.

To understand the basic principles underlying the laser, one has to go back to Einstein's quantum theory of interaction of radiation with matter, proposed in 1917. Consider a quantum system (an atom or a molecule) having two non-degenerate states n and m such that $E_m > E_n$ (Fig. 9). When exposed to electromagnetic radiation, it can undergo transition from state n to state m. Clearly, the probability of transition from state n to state m is proportional to the number N_n of molecules in state n and to the radiation density $\rho(\nu_{nm})$ where ν_{nm} is the frequency of the radiation. Hence, the rate of absorption from n to m is given by $B_{n\to m}N_n\rho(\nu_{nm})$ where the proportionality constant $B_{n\to m}$ is

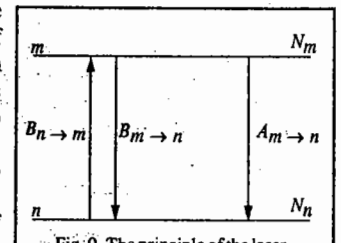

Fig. 9. The principle of the laser

known as the Einstein transition probability for absorption. Similarly, the rate of stimulated emission from m to n, caused by the perturbing radiation is given by $B_{m\to n} N_m \rho(\nu_{nm})$

In addition to the **stimulated emission** of radiation, there is the so-called **spontaneous emission**, its rate being given by $A_{m\to n} N_m$, where the proportionality constant $A_{m\to n}$ is known as the Einstein transition probability for spontaneous emission. The spontaneous emission probability does not depend upon the presence or absence of radiation.

Maser

Maser is an acronym for microwave amplification for stimulated emission of radiation. When the matter and radiation have attained equilibrium in a cavity at temperature T, the number of $n \to m$ transitions equals the number of $m \to n$ transitions. Thus,

$$B_{n\to m} N_n \rho(\nu_{nm}) = N_m [A_{m\to n} + B_{m\to n} \rho(\nu_{nm})] \quad ...(84)$$

whence

$$\frac{N_m}{N_n} = \frac{B_{n\to m} \rho(\nu_{nm})}{A_{m\to n} + B_{m\to n} \rho(\nu_{nm})} \quad ...(85)$$

At equilibrium, the ratio N_m/N_n is given by the Boltzmann distribution law, *viz.*,

$$N_m/N_n = \exp[-(E_m - E_n)/kT] = \exp(-h\nu_{nm}/kT) \quad ...(86)$$

Also, from the Planck distribution law,

$$\rho(\nu_{nm}) = \frac{8\pi h\nu_{nm}^3}{c^3(e^{h\nu_{nm}/kT} - 1)} \quad ...(87)$$

From Eqs. 85, and 86,

$$\rho(\nu_{nm}) = \frac{A_{m\to n}}{B_{n\to m} e^{h\nu_{nm}/kT} - B_{m\to n}} \quad ...(88)$$

If Eq. 88 is to be consistent with Eq. 87, we require that

$$B_{n\to m} = B_{m\to n} \quad ...(89)$$

$$\therefore \quad A_{m\to n}/B_{m\to n} = 8\pi h\nu_{nm}^3/c^3 \quad ...(90)$$

Also, from Eqs. 85, 86 and 89,

$$\frac{N_n}{N_m} = \frac{A_{m\to n} + B_{m\to n}\rho(\nu_{nm})}{B_{m\to n}\rho(\nu_{nm})} = \frac{A_{m\to n}}{B_{m\to n}\rho(\nu_{nm})} + 1$$

$$= e^{h\nu_{nm}/kT} \quad ...(91)$$

Hence,

$$\frac{A_{m\to n}}{B_{m\to n}\rho(\nu_{nm})} + 1 = e^{h\nu_{nm}/kT} \quad ...(92)$$

From Eq. 92 we see that when $h\nu \gg kT$, 1 is negligible as compared with $\exp(h\nu_{nm}/kT)$ so that $A_{m\to n} \gg B_{m\to n}\rho(\nu_{nm})$. Thus, in visible and ultraviolet regions, which are regions of high frequency, spontaneous emission has far greater probability than induced emission which is negligible. However, when $h\nu \ll kT$, the exponential can be expanded as a power series, retaining only the first two terms:

$$\frac{A_{m\to n}}{B_{m\to n}\rho(\nu_{nm})} = 1 + \frac{h\nu_{nm}}{kT} + \ldots - 1 \approx \frac{h\nu_{nm}}{kT} \ll 1 \quad ...(93)$$

i.e., $A_{m\to n} \ll B_{m\to n}\rho(\nu_{nm})$. This condition obtains in the microwave region. The **maser devices** are constructed using this condition.

Laser

Laser is an acronym for 'light amplification by stimulated emission of radiation'. Thus, in a laser action we are interested in increasing the probability of stimulated emission which is given by $B_{m\to n}N_m\rho(\nu_{nm})$. The way to do it when $B_{m\to n}$ is small is to somehow increase N_m, *i.e.*, increase the population of the excited state over that of the ground state. In other words, we must bring about what is known as **population inversion**. The population inversion can be achieved through **optical pumping** by electrical discharges or by a chemical reaction that produces molecules in the excited state. Once the population inversion has been achieved, the impinging photon has a greater likelihood of encountering an excited state molecule rather than the one in the unexcited state. As a consequence, *photon emission rather than photon absorption is stimulated.* Thus, the emitted photon beam has greater intensity than the incident intensity. This is called the ***laser action.***

The laser action can be best understood by considering Fig. 10. Here the ground state molecule absorbs a photon and is raised to the excited state [Fig. 10(*a*)]. In Fig. 10(*b*), the excited state molecule undergoes spontaneous emission of a photon, reverting to the ground state. In Fig. 10(*c*), the impinging photon encounters a molecule that is already in the excited state; it stimulates the molecule to revert to the ground state by emitting a second photon. Here laser action has been achieved.

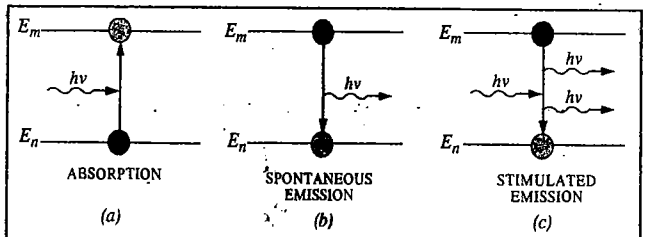

Fig. 10. Elucidation of the laser action.

Three types of energies can be delivered to an absorbing system to bring about population inversion. These are radiation energy, collision energy and chemical energy. Population inversion can occur in systems which have three or four energy levels (Fig. 11*a*). In a *three level system,* irradiation of the system at the correct frequency populates energy level 3, the process being called optical pumping, as already mentioned. *If the system then rapidly decays to energy level 2, a population inversion is said to occur between energy levels 2 and 1* (Fig. 11*a*). Population inversion occurs better in systems having four energy levels (Fig. 11*b*). If such a system is raised to energy level 3 by pumping and there is fast decay to energy level 2, a population inversion occurs between energy levels 2 and 1.

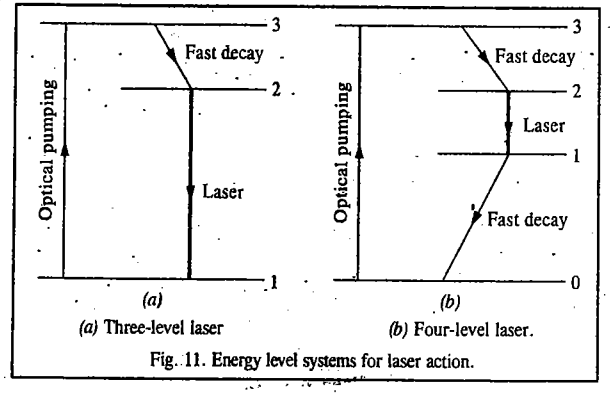

Fig. 11. Energy level systems for laser action.

For a *four-level-laser* to give continuous wave (*cw*) operation, the $1 \to 0$ transition should be very fast so that there can be a steady state pumping from energy level 0 to energy level 3.

Very high intensity of radiation can be obtained by placing mirrors at each end of a cavity containing the medium of interest. The mirrors are placed in such a manner that they form a resonant cavity for the frequency $\nu = (E_2-E_1)/h$, that is, the cavity is exactly an integral number of half wave lengths in length. The electromagnetic radiation is reflected back and forth between the mirrors and is amplified on each passage through the medium by stimulated emission of radiation from energy level 2 to energy level 1. The energy required for the population inversion may be supplied by an electric discharge or by a chemical reaction as already mentioned. The laser beam is **highly directional** since it propagates along the cavity direction. Because of its directional property, it is extremely bright, *i.e.*, the power per unit area per unit solid angle is very high. Another characteristic feature of the laser radiation is that it is **monochromatic**.

The laser radiation is **coherent** in the sense that the electromagnetic waves are all in step. In *spatial coherence*, the waves are in step across the cross-section of the beam emerging from the cavity. In *temporal coherence,* the waves remain in step along the beam. The latter is expressed in terms of a **coherence length**, l_C, the distance over which the waves remain coherent and is related to the range of wave lengths $\Delta\lambda$ present in the medium as

$$l_C = \lambda^2/(2\Delta\lambda) \qquad ...(94)$$

For a perfectly monochromatic beam, with strictly one wave length, $\Delta\lambda = 0$ and the waves would remain in step for an infinite distance. However, when many waves are present, the waves get out of step in a short distance and the coherence length is small. As an example, a typical light bulb gives out light with coherence length of only about 400 nm; a He—Ne laser with $\Delta\lambda \approx 2$ pm has a coherence length of about 10 cm. We may mention here that the laser beam can also be polarized, with its electric vector in a particular plane (or in some other state of polarization), by including a polarizing filter into the cavity.

We next consider two important features of lasers, *viz.*, the **Q-switching** and the **mode locking**. A laser can generate radiation for as long as the population inversion is maintained; it can operate continuously when heat is easily dissipated, since then the population of the upper level can be replenished by pumping. If, however, overheating occurs, the laser can be operated only in *pulses* (of microsecond or millisecond duration) so that the medium gets a chance to cool or the lower state discards its population.

It is, in fact, desirable to have pulses of radiation rather than a continuous output, with considerable power concentrated into a brief pulse. Such pulses can be achieved by **Q-switching**, the modification of the characteristics of the resonant cavity. The name comes from the 'Q-factor' used as a measure of the quality of a resonance cavity in microwave engineering. The aim of Q-switching is to achieve a heathly population inversion in the absence of the resonant cavity, then to plunge the population-inverted medium into a cavity and hence to obtain a sudden pulse of radiation. This is illustrated in Fig. 12.

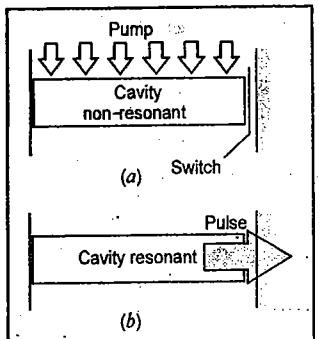

Fig 12. The principle of Q-switching. The excited state is populated while the cavity is non-resonant. Then the resonance characteristics are suddenly restored and the stimulated emission emerges as a giant pulse.

To achieve Q-switching, we use a **Pockels cell** (named after a lady scientist, Anne Pockels), which is an electro-optical devise based on the ability of some crystals, such as those of potassium dihydrogen phosphate (KH_2PO_4), to convert plane polarized light to a circularly polarized light when an electrical potential difference is applied. If a Pockels cell is made part of a laser cavity, it brings about a change in polarization so that the light polarized in one plane after reflection gets polarized in the perpendicular plane. The result is that the reflected light does not stimulate more emission. If, however, the cell is suddenly turned off, the polarization effect is extinguished and all the energy stored in the cavity emerges as an intense pulse of stimulated emission.

The technique of **mode locking** results in the production of pulses of picosecond duration and less. A laser radiates at a number of different frequencies, depending upon the precise details of the resonance characteristics of the cavity and in particular on the number of half wave lengths of radiation that can be trapped within the mirrors (the cavity modes). The resonant modes differ in frequency by multiples of $L/2$ where L is the length of the cavity. Normally, these modes have random phases relative to each other. However, it is possible to lock their phases together. Then the interference occurs giving a series of sharp peaks and the energy of the laser is obtained in short bursts (Fig. 13)

The sharpness of the peaks depends on the range of modes superimposed; the wider the range, the narrower the pulses. Thus, for instance, in a laser with a cavity of length 30 cm, the peaks are separated by 2 ns; if 1000 modes contribute, the width of the pulses is 4 ps.

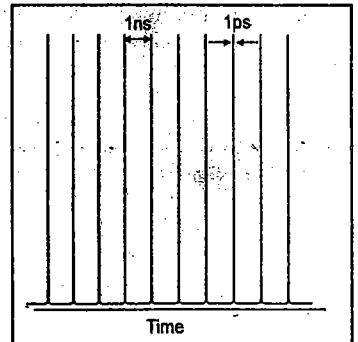

Fig. 13. The output of a mode-locked laser consists of a stream of very narrow pulses separated by an interval equal to the time it takes for light to make a round trip inside the cavity

Application of Lasers in Chemistry

1. Multiphoton Spectroscopy. In an incident laser beam, the photon density is so high that more than one photon can be absorbed by a single molecule giving rise to **multiphoton process**, with the result that states inaccessible by conventional one-photon spectroscopy become observable because the overall transition occurs with no change in parity. Thus, for example, in one-photon spectroscopy, only $g \leftrightarrow u$ transitions are observable. In two-photon spectroscopy, however, the otherwise forbidden transistions $g \rightarrow g$ and $u \rightarrow u$ become observable.

2. Raman Spectroscopy. The advent of lasers has revolutionized Raman spectroscopy. With an intense laser source, the intensity of the scattered radiation (Stokes and anti-Stokes lines constituting the Raman spectrum) is increased and hence the sensitivity of Raman spectroscopy is also dramatically increased. The laser radiation, being monochromatic, also makes possible the observance of scattered light that differs by only fractions of wave numbers from the incident radiation. Such a high degree of resolution is particularly important for observing the rotational Raman lines since the rotational transitions are of the order of a few wave numbers. Also, the techniques of Fourier-transform Raman spectroscopy and resonance Raman spectroscopy can be investigated. Lasers can also be used in **stimulated Raman spectroscopy**. In this form of spectroscopy, the Stokes and anti-Stokes radiations in the forward direction are powerful enough to undergo more scattering thereby giving up or acquiring more quanta of energy from the molecules in the sample. This multiple scattering results in the emission of lines of frequency $\nu_i \pm 2\nu_M$, $\nu_i \pm \nu_M$, and so on, where ν_i is the frequency of the incident radiation and ν_M the frequency of molecular excitation.

3. Precision Specified Transitions. The monochromatic laser radiation allows us to excite specific states with very high precision. A consequence of state specificity for photochemistry is that the illumination of a sample may be photochemically precise and hence efficient in stimulating a reaction because its frequency can be tuned exactly to an absorption. A related phenomenon is the study of state-to-state reaction dynamics in which a specific state of a reactant molecule is excited and we monitor not only the rate at which it forms products but also the states in which they are produced.

4. Time-resolved Spectroscopy. In this branch of spectroscopy, laser pulses are used to obtain the absorption, emission or Raman spectrum of reactants, intermediates, products and even transition states of reactants. It is also possible to study energy transfer, molecular rotations, vibrations and conversion from one mode of motion to another.

5. Single-molecule Spectroscopy. In the 1990s, a new technique was developed which involves new experimental probes of very small specimens. It is becoming possible, using the spectroscopy of single molecules, to understand biochemical processes such as enzymatic catalysis, folding and the insertion of DNA into the nucleus of a cell. Also, the techniques that can probe the structure, dynamics and reactivity of single molecules will be required to explore the frontier areas of research on nanometer-sized molecules. Though still a relatively new technique, single-molecule spectroscopy has already been used to address important problems in chemistry and biology. Two such techniques whose details we shall not consider here but where lasers are finding wide use are the ***near-field optical microscopy*** and the ***far-field confocal microscopy.*** These techniques are based on fluorescence microscopy with laser excitation.

6. Isotope Separation. The laser isotope separation is possible because of highly precise state-selectivity of lasers. Isotope separation is possible because two *isotopomers* (species that differ only in their isotopic composition) have slightly different energy levels and have slightly different absorption frequencies. One uses the process of ***photoionization***, the ejection of an electron by the absorption of electromagnetic radiation. Direct photoionization by the absorption of a single photon does not distinguish between isotopomers because the upper level belongs to a *continuum*. To distinguish isotopomers we must deal with *discrete states*. At least two absorption processes are required. In the first step, a photon excites an atom to a higher state; in the second step another photon brings about the ionization of the excited atom (Fig. 15). The energy separation between the two states involved in the first step depends on the nuclear mass. Hence, if the laser radiation is tuned to the appropriate frequency, only one of the isotopomers will undergo excitation and hence will be available for photoionization in the second step. We shall consider the photoionization of uranium vapour, in which the incident laser is tuned to excite ^{235}U but not ^{238}U. The ^{235}U atoms in the atomic beam are ionized in the two-step process; they are then attracted to a negatively charged electrode and may be collected. This procedure is being used in the latest uranium separation plants.

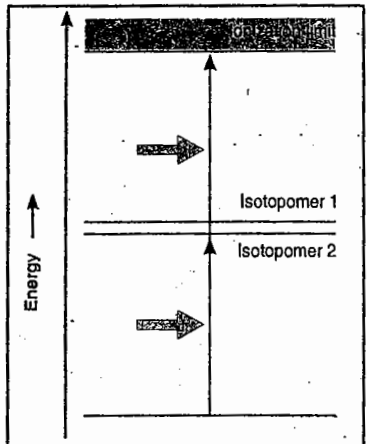

Fig. 15. In one method of isotope separation, one photon excites an isotopomer to an excited state, and then a second photon achieves photoionization. The success of the first step depends on the nuclear mass.

Practical Lasers. It is customary to classify lasers as gas lasers, solid state lasers, chemical lasers, dye lasers and semiconductor lasers, etc. In the case of **gas lasers,** pumping is caused by passing an electric current. The ions and electrons produced are accelerated. The electrons, colliding with the gas molecules, excite the molecules of the gas. The first gas laser produced was the helium–neon laser. It is generally used at 0·633 μm, though it can oscillate at any of the following wave lengths : $\lambda_1 = 3{\cdot}39$ μm, $\lambda_2 = 0{\cdot}633$ μm and $\lambda_3 = 1{\cdot}15$ μm. While the pumping process occurs between the helium energy levels, the laser action occurs between the neon energy levels. A commonly used **solid state laser** is made of $Y_3Al_2O_{15}$ (*i.e.*, yttrium aluminium garnet abbreviated as YAG) in which some of the Y^{3+} ions are replaced by Nd^{3+} ions. It is pumped with a xenon-filled flash lamp. Lasers can also be produced from organic dyes. The **dye lasers** have the advantage that they are *tunable* over a range of about 30 nm. Thus, with a series of dye lasers the entire visible and near ultraviolet ranges may be covered continuously.

The so-called **excimer lasers** have also been prepared. This is a peculiar type of laser in which the lower state does not exist. *An excimer is a combination of two atoms that survives only in an excited state* and which dissociates as soon as the excitation energy has been discarded. An example of an excimer is a mixture of xenon, chlorine and neon (which acts as a buffer gas). The passage of an electric discharge through the mixture produces excited Cl atoms which attach to the Xe atoms

giving the excimer XeCl*. This excimer survives for about 10 ns during which time it can participate in laser action at 308 nm (in the UV region). As soon as XeCl* discards a photon, the atoms separate because the molecular potential energy curve of the ground state is ***dissociative*** and the ground state of the excimer cannot become populated. Another example of an excimer laser is KrF* which produces laser action at 249 nm.

Lasers may also be produced by causing transitions between the rotation–vibration energy levels of a molecule. The well known CO_2 **laser** (which contains small amounts of N_2 and He) utilizes transitions between the vibrational energy levels of the CO_2 molecule. It is one of the most powerful and efficient lasers. It can be operated at 1 MW continuously. It may be mentioned that optical pumping method was also applied by the French physicist Alfred Kastler (1902-1984) to study hertzian resonances in atoms. Kastler was awarded the 1966 Physics Nobel Prize for this work.

Uses in Industries. Since lasers have high peak power, coherence and high degree of monochromaticity, they find many uses in industry. Lasers with peak intensities of the order of 5×10^{14} watt cm^{-2} have been prepared. This value corresponds to the fluctuating electronic fields of the order of 3×10^8 V cm^{-1} and fluctuating magnetic fields of the order of 100 T.

Example 14. Calculate the power output of a laser in which a 2·0 J pulse can be delivered in 1·0 ns.
Solution : The power P is the energy per unit time. Thus,

$$P = \frac{2{\cdot}0\ \text{J}}{1 \times 10^{-9}\ \text{s}} = 2{\cdot}0 \times 10^9\ \text{J s}^{-1} = 2{\cdot}0 \times 10^9\ \text{W} = \mathbf{2{\cdot}0\ GW} \quad (\text{Watt, W} = \text{J s}^{-1})$$

Q-switched lasers produce nanosecond pulses which are fast enough to study extremely fast reactions. Even femtosecond pulses ($1\text{fs} = 10^{-15}$s) have recently been generated. Femtosecond chemistry studies extremely fast dynamical rate processes such as intermolecular energy transfers.

Femtosecond Transition-State Spectroscopy

After the breakthrough in molecular reaction dynamics brought about by the 1986 Chemistry Nobel Laureates Herschbach, Lee and Polanyi, Ahmed H. Zewail pioneered femtosecond revolution in chemical kinetics using laser pulses. He was awarded the 1999 Chemistry Nobel Prize for his work. We shall briefly discuss his work here. In a chemical reaction a molecule remains in the transition state for about 10 fs (femtoseconds) ; however, the processes that occur in so short a time can be investigated by modern laser spectroscopic techniques. It is, for instance, found that irradiation of molecular iodine by an ultrashort laser pulse, called the *pump pulse*, can produce a coherent (*i.e.*, in-phase) superposition of vibrational states. From this observation we find how the wave functions for the coherent superposition interfere constructively and destructively to give a resultant **wavepacket** that has a large amplitude only in the limited part of the classical region at a given time. After the pump pulse, this wave packet oscillates back and forward in the parabolic potential energy well much like a classical particle. Under some conditions, however, the particle may oscillate back and forth a number of times, finally dissociating to form iodine atoms immediately. Since it is not possible to observe this phenomenon with a single molecule, we must bear in mind that all the iodine molecules in the sample have very nearly the same internuclear distance before the pulse because in the ground state, the highest probability density is at this distance. Therefore, the wave packets are launched from the same internuclear distance for the entire sample of molecules. Thus, a single-molecule trajectory is observed.

Probe pulses are then used to study the details of what happens. These probe pulses can be used to follow the particle-like oscillations and the decreases in intensity of the wave packet signal that indicate chemical reaction. Since the experimenter can alter the wave length distribution in the probe pulse, the formation of product atoms or molecules can also be studied on a femtosecond scale.

The range of applications of transition-state time domain spectroscopy has enlarged in recent years. In some cases, the vibrational and rotational motions are discernible in the observed signal as a function of time. It has become possible to view bond breaking or formation in real time and investigate molecular dynamics in the region of the transition state. For an exciting account of the subject, the reader is referred to Zewail's article, "Femtochemistry : Reaction Dynamics with Atomic Resolution", reprinted in *Physical Chemistry* by Berry, Rice and Ross, 2nd edn., Wiley, 2000.

A few relevant references are :

Polanyi, J.C., and A.H. Zewail, "Direct Observation of the Transition State", *Accounts of Chemical Research* **28**, 119 (1995).

Zewail, A.H., "Laser Femtochemistry", *Science* **242**, 1645 (1998).

Zewail, A.H., "The Birth of Molecules", *Scientific American* **263**, 76 (1990).

Zewail, A.H., "Femtochemistry : Recent Progress in Studies of Dynamics and Control of Reactions and Their Transition States", *Journal of Physical Chemistry, Centennial Issue* **100**, 12701 (1996).

I. Review Questions

1. Draw and discuss the Jablonski diagram for depicting various photophysical processes.
2. State and derive Lambert-Beer law for light absorption by solutions.
3. State and explain the term 'quantum yield'. How do you account for the fact that the quantum yield of the photochemical reaction $H_2(g) + Br_2(g) \longrightarrow 2HBr(g)$ is low (=0·01) while that of the reaction $H_2(g) + Cl_2(g) \longrightarrow 2HCl(g)$ is very large ($=10^5$) ?
4. Discuss the kinetics of the following photochemical reaction : $H_2(g) + Cl_2(g) \xrightarrow{h\nu} 2HCl(g)$
5. Discuss the mechanism of photosensitization and quenching using suitable examples.
6. What is chemiluminescence ? Discuss its mechanism in anion-cation reactions.
7. Explain laser action with reference to a three-level laser and a four level laser.
8. Write a short note on femtosecond transition state spectroscopy.
9. Discuss the kinetics of the ozone layer depletion in the stratoshere.

II. Problems

1. A 0·005 M aqueous solution of a certain substance absorbs 15% of the incident light in a Lambert-Beer law cell of path length 2 cm. Calculate the concentration required for 90% absorption of the incident light. **[Ans. 0·0708 M]**
2. Calculate the energy of an einstein of radiation of wave length 253·7 nm. **[Ans. 471·9 kJ]**
3. A system absorbs $2{\cdot}0\times10^{16}$ quanta of radiation per second. When it is irradiated for 15 minutes it is found that $3{\cdot}0\times10^{-4}$ mole of the reactant has reacted. What is the quantum yield of the reaction ? **[Ans. 10·03]**
4. For the photochemical reaction $H_2(g) + Cl_2(g) \xrightarrow{h\nu} HCl(g)$; the quantum yield is $1{\cdot}0\times10^5$ at a wave length of 600 m. Calculate the number of moles of HCl (g) produced per joule of radiant energy absorbed. **[Ans. 0·501 mol]**
5. The following mechanism has been proposed for the photodecomposition of H_2O_2 in the presence of carbon monoxide :

$$H_2O_2 + h\nu \longrightarrow 2HO$$
$$OH + CO \xrightarrow{k_1} CO_2H$$
$$CO_2H + H_2O_2 \xrightarrow{k_2} CO_2 + H_2O + OH$$
$$2CO_2H \xrightarrow{k_3} \text{Products.}$$

Using the steady state approximation for OH and CO_2H, show that the rate law for the reaction is given by

$$d[H_2O_2]/dt = -\phi I_a = \frac{k_2(2\phi I_a)^{1/2}}{k_3^{1/2}}[H_2O_2]$$

where I_a in the intensity of absorbed radiation and ϕ is the quantum yield.

CHAPTER 30

CATALYSIS

It is, indeed, fascinating that certain reactions which do not proceed to completion even when carried out for indefinite periods of time, get completed within a matter of a few minutes when a small quantity of a foreign substance is added. This foreign substance is known as the catalyst. A catalyst is defined as a substance which increases the rate of the reaction without undergoing any change and can be recovered as such at the completion of the reaction. The phenomenon of increase in the rate of a reaction with the help of a catalyst is known as **catalysis.**

As discussed in Chapter 26, a catalyst provides for the reaction another path that has a lower energy of activation E_a. A better explanation is offered by the activated complex theory on the basis of the decrease in Gibbs free energy of activation. According to the activated complex theory of reaction rates, $k_f = (k_BT/h)\exp(-\Delta G_f^\circ)^\#/RT)$ where k_f is the rate constant for the forward reaction, k_B is Boltzmann constant and $(\Delta G_f^\circ)^\#$ is the standard Gibbs free energy of activation. In the presence of the catalyst we can write

$$k_f' = (k_BT/h)\exp(-\Delta G_f^\circ)^{\#'}/RT) \quad ...(1)$$

where prime (') denotes a catalyzed reaction. Since $(\Delta G_f^\circ)^{\#'}$ is less than $(\Delta G_f^\circ)^\#$, k_f' is greater than k_f. As is evident from Fig. 1, the Gibbs free energy of activation is lowered in the presence of the catalyst.

It can easily visualised that the Gibbs free energy of activation for the backward reaction is also lowered in the presence of the catalyst without changing the overall free energy change of the reaction. This implies that a catalyst changes the rates of both the forward and the backward reactions.

Since ΔG° is not changed, the equilibrium constant K remains unchanged in the presence of the catalyst ($-\Delta G^\circ = RT \ln K$). It follows that a catalyst helps in attaining the equilibrium position rapidly but does not help in changing the relative proportions of reactants and products at equilibrium.

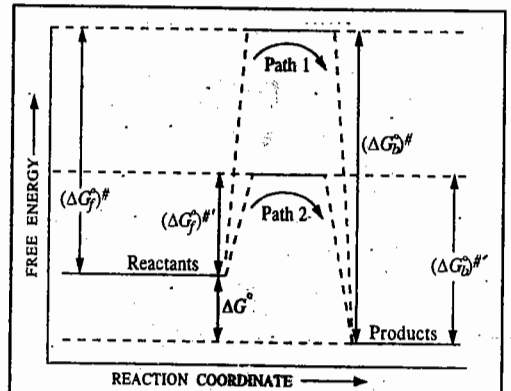

Fig. 1. Lowering of Gibbs free energy of activation $(\Delta G^\circ)^\#$ of a reaction by a catalyst. Path 1 is without catalyst; path 2 is with catalyst.

For the forward and the backward reactions in the presence of the catalyst, we can write

$$k_f' = (k_BT/h)\exp(-(\Delta G_f^\circ)^{\#'}/RT) \quad ...(2)$$
$$k_b' = (k_BT/h)\exp(-\Delta(G_b^\circ)^{\#'}/RT) \quad ...(3)$$

Hence, $$K_{eq} = \frac{k_f'}{k_b'} = \frac{(k_BT/h)\exp(-\Delta G_f^\circ)^{\#'}/RT)}{(k_BT/h)\exp(-(\Delta G_b^\circ)^{\#'}/RT)} \quad ...(4)$$

$$= \exp[-(\Delta G_f^\circ)^{\#'}/RT - (-(\Delta G_b^\circ)^{\#'}/RT] = \exp(-\Delta G^\circ/RT) \quad ...(5)$$

where $\Delta G^\circ = (\Delta G_b^\circ)^{\#'} - (\Delta G_f^\circ)^{\#'}$ (Fig. 1). Since ΔG° has the same value in the presence or absence of a catalyst, K_{eq} remains the same.

General Characteristics of Catalytic Reactions

The following characteristics are generally common to most of the catalytic reactions.

1. The catalyst remains unchanged in amount and chemical composition at the end of the reaction.

2. Only a small quantity of the catalyst is generally needed. However, in some homogeneous catalytic reactions, the rate of the reaction is proportional to the concentration of the catalyst. For example, the rate of inversion of cane sugar catalyzed by hydrogen ions varies with the concentration of the hydrogen ions present in the solution. In certain heterogeneous reactions, the rate increases with increase in the area of the catalytic surface. This explains why the efficiency of a solid catalyst increases when it is present in a finely divided state or deposited on some inactive material such as asbestos (cf. platinised asbestos).

3. The catalyst does not alter the position of equilibrium in a reversible reaction. Bodenstein was able to show that although the use of a catalyst hastened the approach of equilibrium in the decomposition of hydrogen iodide, it did not alter the concentrations of the reactants or the products. This has been found to be true in the case of several other reversible reactions as well.

4. The catalyst does not initiate the reaction. The reaction is already occurring, though extremely slowly, in the absence of the catalyst. The function of the catalyst seems to be only to speed up the reaction considerably. The reaction in the presence of a catalyst takes place through some alternative path which requires much lower energy of activation. Hence, it is speeded up.

5. The catalyst is generally specific in its action. Manganese dioxide, for example, can catalyze the decomposition of potassium chlorate but not that of potassium perchlorate or potassium nitrate. Thus, manganese dioxide is specific in its action. Enzymes have also specific catalytic action.

6. The catalyst cannot alter the nature of the products of the reaction. The combination of nitrogen and hydrogen, for example, under suitable conditions, results invariably in the formation of ammonia whether a catalyst is added or not. Similarly, potassium chlorate on decomposition gives potassium chloride and oxygen whether manganese dioxide is added or not.

7. A catalyst is poisoned by certain substances. It has been found that impurities of any type, even if present in small amounts, inhibit or retard the rate of catalyzed reactions to a large extent. These impurities are, therefore, called **catalytic poisons.** For example, the rate of combination of sulphur dioxide and oxygen (in the Contact process) is slowed down considerably if some arsenic compounds are present even in traces.

Types of Catalysis. Catalysis is classified into two broad types :

1. **Homogeneous catalysis** in which the reactants and the catalyst form a single phase and

2. **Heterogeneous catalysis** in which the reactants form one phase but the catalyst forms a different phase, usually solid.

Homogeneous Catalysis

There are several examples of homogeneous Catalysis amongst which the acid–base catalysis and enzyme catalysis are the most important.

ACID–BASE CATALYSIS

Acid–base catalysis includes reactions in solution which are catalyzed by acids or bases or both. A reaction which is catalyzed by H^+ (or H_3O^+) ions but not by other Bronsted acids (proton donors)

is said to be *specifically proton-catalyzed.* Examples are solvolysis of esters, inversion of sugars and keto–enol transformation. On the other hand, a reaction that is catalyzed by any Bronsted acid, is an example of *general acid catalysis.* Similarly, a reaction catalyzed only by OH^- ions is said to be *specifically base-catalyzed* while a reaction catalyzed by any Bronsted base is an example of *general base catalysis.* The solvent water may act as a Bronsted acid or a Bronsted base. There are also reactions such as the mutarotation of glucose which require the presence of both a proton-donor and a proton-acceptor. This is also an example of *acid–base catalysis.*

Kinetics of Acid–Base Catalysed Reactions. If the rate of disappearance of a substrate S is first-order with respect to S, then, $-d[S]/dt = k[S]$. However, in a buffer solution, the first-order rate constant k for a reaction may depend linearly on $[H^+]$, $[OH^-]$, [HA] and $[A^-]$, where HA is the weak acid in the buffer and A^- is the corresponding conjugate base. Thus, we can write

$$k = k_0 + k_{H^+}[H^+] + k_{OH^-}[OH^-] + k_{HA}[HA] + k_{A^-}[A^-] \quad ...(6)$$

Here k_0 is the first-order rate constant for the uncatalyzed reaction and k_{H^+}, k_{OH^-}, k_{HA} and k_{A^-} are the catalytic coefficients. These coefficients may be evaluated experimentally using different concentrations of these species. The reaction is said to be subjected to *specific hydrogen ion catalysis* if only the $k_{H^+}[H^+]$ term is important. If, however, the term $k_{HA}[HA]$ is important, then the reaction is said to be subjected to *general acid catalysis.* Similarly, if only the term $k_{OH^-}[OH^-]$ is important, the reaction is said to be subjected to *specific hydroxyl ion catalysis* and, if the term $k_{A^-}[A^-]$ is important, the reaction is said to be subjected to *general base catalysis.*

We are interested in knowing how the various terms in Eq. 6 arise. This will be illustrated by considering two types of catalytic mechanisms.

1. First mechanism. Here we assume that a proton is transferred from an acid AH^+ to the substrate S. The acid form of the substrate then reacts with a water molecule to form the product P :

$$S + AH^+ \underset{k_{-1}}{\overset{k_1}{\rightleftharpoons}} SH^+ + A$$

$$SH^+ + H_2O \xrightarrow{k_2} P + H_3O^+$$

Applying steady state approximation (*s.s.a.*) for $[SH^+]$, we have

$$d[SH^+]/dt = 0 = k_1[S][AH^+] - k_{-1}[A][SH^+] - k_2[SH^+] \quad ...(7)$$

Since we work with very dilute solutions, the concentration of H_2O remains almost constant so that in Eq. 7, the last term on the right hand side is written as $k_2[SH^+]$ rather than $k_2[SH^+][H_2O]$.

Solving for $[SH^+]$, we find that

$$[SH^+] = \frac{k_1[S][AH^+]}{k_{-1}[A] + k_2} \quad ....(8)$$

Making use of Eq. 3, the rate of formation of the product is given by

$$\frac{d[P]}{dt} = k_2[SH^+] = \frac{k_1k_2[S][AH^+]}{k_{-1}[A] + k_2} \quad ...(9)$$

If $k_2 \gg k_{-1}[A]$, then $d[P]/dt = k_1[S][AH^+]$ ...(10)

Thus, we may say that the reaction is *general acid-catalyzed.*

If, however, $k_2 \ll k_{-1}[A]$, then

$$\frac{d[P]}{dt} = \frac{k_1k_2[S][AH^+]}{k_{-1}[A]} = \left(\frac{k_1k_2}{k_{-1}K}\right)[S][H^+] \quad ...(11)$$

where $K = [A][H^+]/[AH^+]$. In this case we say that the reaction is *specifically hydrogen ion-catalyzed.*

2. Second mechanism. Here we assume that in the second step, the acid form of the substance reacts with a base A instead of a water molecule :

$$S + AH^+ \underset{k_{-1}}{\overset{k_1}{\rightleftharpoons}} SH^+ + A$$

$$SH^+ + A \xrightarrow{k_2} P + AH^+$$

Applying steady state approximation for $[SH^+]$, as before, we have

$$\frac{d[SH^+]}{dt} = 0 = k_1[S][AH^+] - k_{-1}[SH^+][A] - k_2[SH^+][A] \quad ...(12)$$

$$\therefore \quad [SH^+] = \frac{k_1[S][AH^+]}{[k_{-1} + k_2][A]} \quad ...(13)$$

Making use of Eq. 13, the rate of formation of the product is given by

$$\frac{d[P]}{dt} = k_2[SH^+][A] = \frac{k_1k_2[S][AH^+]}{k_{-1} + k_2} \quad ...(14)$$

This is an example of *general acid catalysis*.

Example 1. In the acid hydrolysis reaction $A + H_2O + H^+ \longrightarrow$ Products where $[H^+]=0{\cdot}1$ mol dm^{-3} and H_2O is present in large excess, the apparent rate constant (*i.e.*, the pseudo first-order rate constant) is $1{\cdot}5\times10^{-5}$ s^{-1}. Calculate the true rate constant.

Solution : $r = -d[A]/dt = k[A][H_2O][H^+]$

Since $[H^+]$ is essentially constant (because the catalyst is regenerated) and $[H_2O] \gg [A]$, hence

$$r = k_{app}[A] \quad \text{where} \quad k_{app} = k[H_2O][H^+]$$

$$\therefore \quad k = k_{app}/([H_2O][H^+])$$

Since $[H^+] = 0{\cdot}1$ mol dm^{-3} and $[H_2O] = 1000$ g dm^{-3}/18 g mol^{-1}
$= 55{\cdot}6$ mol dm^{-3}, hence,

$$k = 2{\cdot}70\times10^{-6} \text{ dm}^6 \text{ mol}^{-2} \text{ s}^{-1}$$

ENZYME CATALYSIS

A very important type of homogeneous catalysis includes reactions catalyzed by certain complex organic substances known as **enzymes**. Enzymes are proteins with high relative molar mass of the order of 10,000 or even more and are derived from living organisms. Each enzyme can catalyze a specific reaction. For instance, the enzyme diastase produced in the germinated barley seeds converts starch into maltose sugar.

Mechanism and Kinctics of Enzyme-catalyzed Reactions. In 1913, biochemists L. Michaelis and Miss Maud Menten proposed a mechanism for the kinetics of enzyme-catalyzed reactions which envisages the following steps :

Step 1. Formation of the Enzyme-Substrate Complex :

$$E + S \underset{k_{-1}}{\overset{k_1}{\rightleftharpoons}} ES \quad \text{(complex)} \qquad \text{(fast)}$$

Step 2. Decomposition of the Complex :

$$ES \xrightarrow{k_2} P + E \qquad \text{(slow)}$$

where E is the (free) enzyme ; S is the substrate (*i.e.*, the reactant); ES is the enzyme-substrate complex and P is the product. In the overall reaction $S \longrightarrow P$, the enzyme is consumed in step 1 and regenerated in step 2.

The problem can be handled using either the equilibrium approximation or the steady state approximation. Experiment shows, however, that true equilibrium is not achieved in the fast step because the subsequent slow reaction is constantly removing the intermediate enzyme-substrate complex, ES. Generally, the enzyme concentration is far less than the substrate concentration, *i.e.*, $[E] \ll [S]$, so that $[ES] \ll [S]$. Hence, we can use the steady state approximation for the intermediate, ES.

According to the slow rate-determining step, the rate of the reaction is given by

$$r = -[dS]/dt = +d[P]/dt = k_2[ES] \quad ...(15)$$

Using steady state approximation for ES, we have

$$d[ES]/dt = k_1[E][S] - k_{-1}[ES] - k_2[ES] = 0 \quad ...(16)$$

Now, [E] cannot be measured experimentally. The equilibrium between the free and the bound enzyme is given by the **enzyme conservation equation**, *viz.*,

$$[E]_0 = [E] + [ES] \quad ...(17)$$

where $[E]_0$ is the total enzyme concentration (which can be measured) ; [E] is the free enzyme concentration and [ES] is the bound (or reacted) enzyme concentration. Thus,

$$[E] = [E]_0 - [ES] \quad ...(18)$$

Substituting for [E] in Eq. 16,

$$d[ES]/dt = k_1\{[E]_0 - [ES]\}[S] - k_{-1}[ES] - k_2[ES] = 0 \quad ...(19)$$

Collecting terms and simplifying,

$$k_1[E]_0[S] = \{k_{-1} + k_2 + k_1[S]\}[ES] \quad ...(20)$$

$$[ES] = \frac{k_1[E]_0[S]}{k_{-1} + k_2 + k_1[S]} \quad ...(21)$$

Substituting for [ES] in Eq. 15,

$$r = \frac{k_1k_2[E]_0[S]}{k_{-1} + k_2 + k_1[S]} \quad ...(22)$$

Dividing the numerator and the denominator by k_1,

$$r = \frac{k_2[E]_0[S]}{(k_{-1} + k_2)/k_1 + [S]} = \frac{k_2[E]_0[S]}{K_m + [S]} \quad ...(23)$$

where the new constant K_m, called the **Michaelis constant**, is given by

$$K_m = (k_{-1} + k_2)/k_1 \quad ...(24)$$

Note that K_m is not an equilibrium constant.

Eq. 23 is known as the **Michaelis-Menten equation.**

Further simplification of Eq. 23 can be made. When all the enzyme has reacted with the substrate at high concentration, the reaction will be going at maximum rate. No free enzyme will remain so that $[E]_0=[ES]$. Hence, from Eq. 15,

$$r_{max} = V_{max} = k_2[E]_0 \quad ...(25)$$

where V_{max} is the maximum rate, using the notation of enzymology.

The Michaelis-Menten equation can now be written as

$$r = V_{max}[S]/(K_m + [S]) \quad ...(26)$$

Two cases arise :

(*a*) $K_m \gg [S]$ so that [S] can be neglected in the denominator of Eq. 26, giving

$$r = V_{max}[S]/K_m = k'[S] \quad \text{(first-order reaction)} \quad ...(27)$$

(*b*) [S] >> K_m so that K_m can be neglected in the denominator, giving

$$r = V_{max} = \text{constant} \qquad \text{(zero-order reaction)} \qquad ...(28)$$

These two cases are shown diagrammatically in Fig. 2.

Again, $$if K_m = [S],\ r = \tfrac{1}{2} V_{max} \qquad ...(29)$$

Thus, **Michaelis constant** is equal to that concentration of S at which the rate of formation of product is half the maximum rate obtained at high concentration of S.

The constant k_2 in Eq. 25 is called the **turnover number** of the enzyme. The turnover number is the number of molecules converted in unit time by one molecule of enzyme. Typical values of k_2 are 100 to 1,000 per second though they may be as large as 10^5 to 10^6 per second.

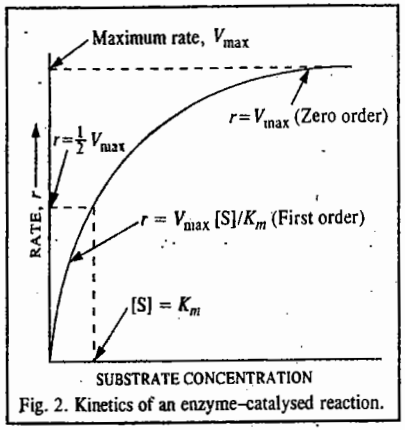

Fig. 2. Kinetics of an enzyme-catalysed reaction.

We would like to know the physical reason why the reaction rate of an enzyme-catalyzed reaction changes from first-order to zero-order as the substrate concentration is increased. The answer is that each *enzyme molecule has one or more 'active sites' at which the substrate must be bound in order that the catalytic action may occur.* At low substrate concentration, most of these active sites remain unoccupied at any time. As the substrate concentration is increased, the number of active sites which are occupied increases and hence the reaction rate also increases. However, at very high substrate concentration, virtually all the active sites are occupied at any time so that further increase in substrate concentration cannot further increase the formation of enzyme-substrate complex.

It is rather difficult to determine V_{max} (and hence K_m) directly from the plot of r against [S]. It is, however, possible to rearrange Eq. 26 so as to permit some alternative plots for easy determination of V_{max}. Two of the best known methods which make use of the re-arranged equations are as follows.

1. The Lineweaver-Burk method. This method uses the rearranged equation

$$1/r = K_m/([S]\ V_{max}) + 1/V_{max} \qquad ...(30)$$

A plot of $1/r$ against $1/[S]$ gives a straight line whose intercepts on the x-axis and y-axis are $(-1/K_m)$ and $1/V_{max}$, respectively and whose slope is (K_m/V_{max}), as shown in Fig. 3.

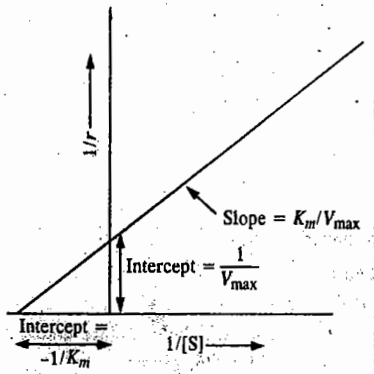

Fig. 3. The Lineweaver-Burk method of plotting enzyme kinetic data.

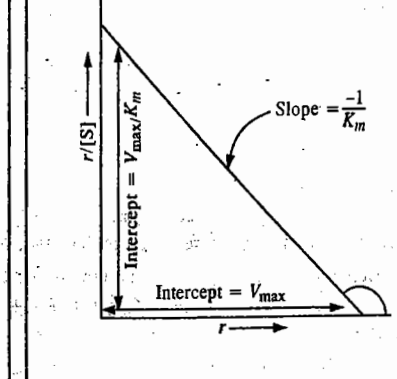

Fig. 4. Eadie-Hofstee method of plotting enzyme kinetic data.

2. The Eadie-Hofstee method. This method uses the rearranged equation

$$r/[S] = V_{max}/K_m - r/K_m \qquad ...(31)$$

A plot of $r/[S]$ against r gives a straight line with slope equal to $-1/K_m$ and an intercept on the y-axis equal to V_{max}/K_m, as shown in Fig. 4. From the graph, both K_m and V_{max} can be determined.

Example 2. Consider the following mechanism for an enzyme catalysis :

$$E + S \underset{k_{-1}}{\overset{k_1}{\rightleftharpoons}} ES \underset{k_{-2}}{\overset{k_2}{\rightleftharpoons}} E + P$$

where E stands for enzyme, S for substrate, ES for enzyme-substrate complex and P for product. Applying steady state approximation for [ES], derive the rate law for the formation of the product during the initial stages.

Solution : Applying steady state approximation to [ES], we have

$$d[ES]/dt = k_1[E][S] - k_{-1}[ES] - k_2[ES] + k_{-2}[E][P] = 0 \qquad ...(i)$$

Conservation of mass and the restriction that [S] >> $[E]_0$ require that

$$[E]_0 = [E] + [ES] \qquad ...(ii)$$

and

$$[S]_0 = [S] + [P] \qquad ...(iii)$$

Eq. (*ii*) may be written as $$[E] = [E]_0 - [ES] \qquad ...(iv)$$

Substituting for [E] in Eq. (*i*), we have

$$d[ES]/dt = k_1([E]_0 - [ES])[S] - k_{-1}[ES] - k_2[ES] + k_{-2}([E]_0 - [ES])[P] = 0$$

or $$[ES]\ (k_1[S] + k_{-1} + k_2 + k_{-2}[P]) = k_1[E]_0[S] + k_{-2}[E]_0[P]$$

$$\therefore \quad [ES] = \frac{k_1[E]_0[S] + k_{-2}[E]_0[P]}{k_1[S] + k_{-2}[P] + k_{-1} + k_2} \qquad ...(v)$$

The rate of formation of the product in the initial stages is given by

$$r = -d[S]/dt = d[P]/dt = k_2[ES] - k_{-2}[E][P]$$

$$= k_2[ES] \qquad (\because [P] = 0) \qquad ...(vi)$$

Substituting for [ES] from Eq. (*v*) into Eq. (*vi*),

$$r = \frac{k_2k_1[E]_0[S] + k_2k_{-2}[E]_0[P]}{k_1[S] + k_{-2}[P] + k_{-1} + k_2}$$

During the initial stages of the reaction we can put [P] = 0, so that

$$r = \frac{k_2k_1[E]_0[S]}{k_1[S] + k_{-1} + k_2} = \frac{V_{max}[S]}{[S] + K_m}$$

where $V_{max} = k_2[E_0]$ and $K_m = (k_{-1} + k_2)/k_1$

(*i*) If K_m >> [S], $r = V_{max}.[S]/K_m = k'[S]$, *i.e.*, the reaction is **first-order** with respect to *S*.

(*ii*) If K_m << [S], $r = V_{max}$ = constant, *i.e.*, the reaction is **zero-order** with respect to *S*.

Example 3. For an enzyme-substrate system obeying the simple Michaelis-Menten mechanism, the rate of product formation when the substrate concentration is very large, has the limiting value 0·02 mol dm^{-3}. At a substrate concentration of 250 mg dm^{-3}, the rate is half this value. Calculate k_1/k_{-1} assuming that $k_2 >> k_{-1}$.

Solution : $$r = \frac{k_2[E]_0[S]}{K_m + [S]} \qquad \text{[Eq. 23]}$$

For [S] >> K_m, $r \equiv V_{max} = k_2[E]_0$

When r is half of this maximum value, then, by definition,

$$[S] = K_m = (k_{-1} + k_2)/k_1 = k_{-1}/k_1 \qquad \text{(assuming that } k_2 << k_{-1})$$

$$\therefore \quad k_1/k_{-1} = 1/[S] = 1/(250 \text{ mg dm}^{-3}) = \mathbf{0{\cdot}004\ dm^3\ mg^{-1}}$$

Example 4. When both the substrate *S* and the inhibitor *I* compete for the enzyme site *E*, the phenomenon is called competitive inhibition. The following mechanism has been proposed for the competitive inhibition of an enzyme-catalyzed reaction :

$$(a)\quad E + S \underset{k_{-1}}{\overset{k_1}{\rightleftharpoons}} ES$$

$$(b)\quad E + I \rightleftharpoons EI$$

$$(c)\quad ES \xrightarrow{k_2} E + P$$

where ES is the enzyme–substrate complex, EI is the enzyme–inhibitor complex and P is the product. It is assumed that step (*b*) is an equilibrium reaction involving the dissociation constant K_{EI} for the enzyme–inhibitor complex. Applying steady state approximation to [ES], derive an expression for the rate of product formation.

Solution : Applying steady state approximation to [ES],

$$d[ES]/dt = k_1 [E] [S] - (k_{-1} [ES] + k_2 [ES]) = 0, \text{ we get} \quad ...(i)$$

$$[ES] = \frac{k_1[S][E]}{k_{-1} + k_2} = \frac{[E][S]}{K_m} \quad ...(ii)$$

where $K_m = (k_{-1} + k_2)/k_1$ is the Michaelis constant.

The rate of formation of the product is given by

$$r = k_2[ES] = k_2[E][S]/K_m \quad ...(iii)$$

Also, in the present case, the total enzyme concentration is given by

$$[E]_0 = [E] + [ES] + [EI] \quad ...(iv)$$

From the equilibrium reaction (*b*), $K_{EI} = [E][I]/[EI]$. ...(*v*)

or $$[EI] = [E][I]/K_{EI} \quad ...(vi)$$

Substituting Eqs. (*ii*) and (*vi*) in Eq. (*iv*), we get

$$[E]_0 = [E] + [E] [S]/K_m + [E][I]/K_{EI}$$

$$= [E](1 + [S]/K_m + [I]/K_{EI}) = [E] \frac{[S] + K_m(1 + [I]/K_{EI})}{K_m}$$

$$[E] = \frac{K_m[E]_0}{[S] + K_m(1 + [I]/K_{EI})} \quad ...(vii)$$

Substituting Eq. (*vii*) in Eq. (*iii*), we have

$$r = \frac{k_2[E]_0[S]}{[S] + K_m(1 + [I]/K_{EI})} = \frac{V_{max}[S]}{[S] + K_m(1 + [I]/K_{EI})} \quad ...(viii)$$

where $V_{max} = k_2[E]_0$.

Notice that the maximum rate, V_{max}, is the same as in the absence of inhibitor. However, the rate at any given concentration is reduced. From Eq. (*viii*) we see that when the substrate concentration is very large, the inhibitor is unable to compete successfully for the binding site on the enzyme; hence the rate will not be affected by the inhibitor.

Eq. (*viii*) can be recast into the Lineweaver–Burk form :

$$\frac{1}{r} = \frac{K_m}{V_{max}}(1+[I]/K_{EI})\frac{1}{[S]} + \frac{1}{V_{max}} \quad ...(ix)$$

The plot of $1/r$ versus $1/[S]$ gives a straight line whose slope is a linear function of the inhibitor concentration [I].

Effect of Temperature on Enzyme Catalysis. Like chemical catalysts, the enzyme catalysts also decrease the activation energy of a reaction at a given temperature. In fact, the decrease of activation energy by an enzyme catalyst is far greater than that by a non-enzyme catalyst. Hence, while the rate of a reaction generally increases with an increase in temperature, this condition would be highly unfavourable for a living cell. Enzymes are, in fact, very sensitive to high temperatures. Because of the

proteinous nature of an enzyme, increase in temperature results in *denaturation* of the enzyme protein which leads to a decrease in effective concentration of the enzyme and hence a decrease in reaction rate. Upto about 45°C, the reaction rates of enzyme-catalyzed reactions increase with temperature. At temperatures greater than 45°C, thermal denaturation of the enzyme becomes increasingly significant. At about 55°C, rapid denaturation completely destroys the catalytic function of the enzyme protein. The effect of temperature on the rates of enzyme-catalyzed reactions is illustrated in Fig. 5.

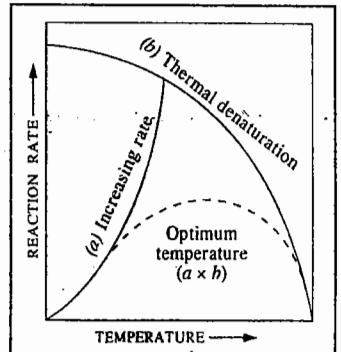

Fig. 5. Temperature-dependence of the rate of an enzyme-catalyzed reaction. (*a*) represents the increase in rate with increase in temperature. (*b*) represents the decrease in rate as a result of thermal denaturation of the enzyme ; the dashed-line curve shows the combination of (*a*) and (*b*).

Heterogeneous Catalysis : Surface Reactions

Reactions between gaseous reactants are catalyzed by solid state catalysts. Solid state catalysts are used in many large scale processes in chemical industries. The heterogeneous catalysis in which the catalyst is in a different phase (usually the solid phase) than the gaseous reactants has emerged as one of the most important tools in industrial research.

Important advances in the field of surface catalysis were made by I. Langmuir (1881-1957), C.N. Hindshelwood (1897-1967), E.K. Rideal (1890-1974) and H.S. Taylor (1890-1974).

According to the **Langmuir–Hinshelwood mechanism,** a gaseous reaction taking place on the surface of a solid catalyst, *i.e.*, a surface reaction, involves the following elementary steps :

1. Diffusion of reactants to surface.
2. Adsorption of reactants at the surface.
3. Chemical reaction at the surface.
4. Desorption of products from the surface.
5. Diffusion of products from the surface.

These steps are consecutive. If any of them has a slower rate constant than the others, it will become the rate-determining step. Steps 1 and 5 are usually very fast. Also, steps 2 and 4 are generally faster than step 3 though they may sometimes be slower. It is generally believed that the kinetics of surface reactions can be treated successfully on the basis of the following assumptions :

1. The rate-determining step is the chemical reaction occurring at the surface, *i.e.*, the reaction involving the molecules adsorbed on the surface, *i.e.*, step 3 given above.

2. Chemisorption plays an important role in heterogeneous catalysis. In chemisorption, chemical bonds are formed between the adsorbate and the surface resulting in the formation of a monolayer (Langmuir adsorption).

3. The reaction rate per unit surface area is proportional to θ, the fraction of the surface covered. The value of θ is given by the Langmuir adsorption isotherm.

The reason for heterogeneous catalytic activity is the same as for homogeneous catalysis, *i.e.*, the catalyst increases the rate of the reaction by lowering the activation energy of the rate-determining step. Therefore, although it does not disturb the thermodynamically determined equilibrium composition of the reaction system, it increases the rate at which the equilibrium is attained.

Kinetics of Surface Reactions. Study of kinetics of gaseous reactions on solid surfaces has become one of the most important areas of research in chemistry.

1. Unimolecular Surface Reactions. A unimolecular surface reaction may involve a reaction between a molecule A of the reactant and a vacant site S on the surface. The mechanism may be

represented schematically as follows :

$$A + S \xrightarrow{k_1} AS \quad \text{(adsorption)}$$

$$AS \xrightarrow{k_{-1}} A + S \quad \text{(desorption)}$$

$$AS \xrightarrow{k_2} \text{Products} \quad \text{(decomposition)}$$

If r is the rate of the reaction, then according to the Langmuir-Hinshelwood hypothesis, r is proportional to the fraction θ of the surface covered. Thus,

$$r = k_2\theta \qquad ...(32)$$

Assuming steady state approximation for the concentration of AS, we have

$$r = \frac{d[AS]}{dt} = k_1[A][S] - k_{-1}[AS] - k_2[AS] = 0 \qquad ...(33)$$

If C_s is the total concentration of *active* sites on the surface, then the concentration [S] of the vacant sites on the surface is equal to the product of C_s and $(1-\theta)$, the fraction of sites remaining uncovered. Thus,

$$[S] = C_s(1-\theta) \qquad ...(34)$$

From Eq. 33, $$[AS] = \frac{k_1[A][S]}{k_{-1} + k_2} \qquad ...(35)$$

Also, the concentration of AS on the surface, *viz.*, [AS], is given by

$$[AS] = C_s\theta \qquad ...(36)$$

From Eqs. 34, 35 and 36, we get

$$C_s\theta = \frac{k_1[A]C_s(1-\theta)}{k_{-1} + k_2} \qquad ...(37)$$

or $$\frac{1-\theta}{\theta} = \frac{k_{-1} + k_2}{k_1[A]} \quad \text{or} \quad \frac{1}{\theta} - 1 = \frac{k_{-1} + k_2}{k_1[A]} \qquad ...(38)$$

or $$\frac{1}{\theta} = \frac{k_{-1} + k_2}{k_1[A]} + 1 = \frac{k_1[A] + k_{-1} + k_2}{k_1[A]} \qquad ...(39)$$

$$\therefore \quad \theta = \frac{k_1[A]}{k_1[A] + k_{-1} + k_2} \qquad ...(40)$$

Substituting this value of θ in Eq. 32, we get

$$r = \frac{k_1k_2[A]}{k_1[A] + k_{-1} + k_2} \qquad ...(41)$$

Eq. 41 may be rewritten in the form

$$\frac{1}{r} = \frac{1}{k_2} + \frac{k_{-1} + k_2}{k_1k_2[A]} \qquad ...(42)$$

According to Eq. 42, a plot of $1/r$ versus $1/[A]$ would give a straight line with intercept equal to $1/k_2$ and slope equal to $(k_{-1}+k_2)/k_1k_2$.

For gaseous adsorbates, the concentration is conveniently expressed in terms of the partial pressure. Thus, Eqs. 41 and 42 can be written as follows :

$$r = \frac{k_1k_2p_A}{k_1p_A + k_{-1} + k_2} \qquad ...(43)$$

or $$\frac{1}{r} = \frac{1}{k_2} + \frac{k_{-1} + k_2}{k_1k_2p_A} \qquad ...(44)$$

Let us consider the limiting cases of Eq. 41.

Case 1. If the rate of decomposition is very large in comparison with the rate of adsorption and desorption, *i.e.*, $k_2 >> (k_1[A]+k_{-1})$, then Eq. 41 reduces to

$$r = k_1[A] \qquad ...(45)$$

i.e., the reaction is of the first order with respect to A.

Case 2. If the rate of decomposition is very small compared with the rate of adsorption and desorption, *i.e.*, $k_2 << (k_1[A]+k_{-1})$, then Eq. 41 becomes

$$r = \frac{k_1k_2[A]}{k_1[A] + k_{-1}} = \frac{k_2K[A]}{k_1[A] + 1} = \frac{k_2K'p_A}{K'p_A + 1} \qquad ...(46)$$

where K or K' $(= k_1/k_{-1})$ is the **adsorption equilibrium constant.**

Now, two situations arise depending upon the pressure :

At low pressure when the reactant is slightly adsorbed, $\theta \to 0$ and $K'p_A << 1$ so that

$$r = k_2K'p_A = kp_A \qquad ...(47)$$

i.e., the reaction is of the first order with respect to A. Here, $k = k_2K'$. Thus,

$$r = -dp_A/dt = kp_A$$

or $$p_A = p_A^\circ \exp(-kt) \qquad ...(48)$$

This means that the partial pressure of the gas decreases exponentially with time.

At high pressure when the reactant is strongly adsorbed, $\theta \to 1$ and $K'p_A >> 1$ so that

$$r = k_2 \qquad ...(49)$$

i.e., the *reaction is of the zero order with respect to* A. Thus, we can write

$$r = -dp_A/dt = k_2, \quad i.e., \text{ constant}$$

which can be integrated to give :

$$p_A = p_A^\circ - k_2t \qquad ...(50)$$

This means that the partial pressure of the gas decreases linearly with time.

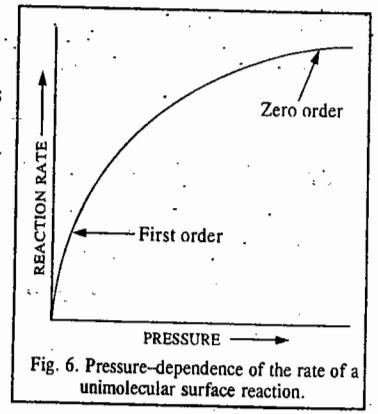

Fig. 6. Pressure-dependence of the rate of a unimolecular surface reaction.

The pressure-dependence of the rate of a unimolecular surface reaction is shown schematically in Fig. 6.

Some typical unimolecular surface reactions are the decomposition of N_2O on gold, of NH_3 on molybdenum and of HI on platinum.

Example 5. Using Langmuir adsorption theory, account for the experimental observation that the decomposition of phosphine, PH_3, on tungsten follows first-order kinetics at low pressures and zeroth-order kinetics at high pressures.

Solution : From Eq. 46, the rate of the reaction is given by

$$r = \frac{k_2K'p_A}{K'p_A + 1} \quad \text{where} \quad K' = k_1/k_{-1}$$

At low pressures, $K'p_A << 1$, so that $K'p_A$ can be neglected in the denominator, giving $r = k_2K'p_A$, *i.e.*, $r \propto p_A$. This is a **first-order reaction**. At high pressures, $K'p_A >> 1$ so that 1 can be neglected in the denominator, giving $r = k_2$, *i.e.*, constant, independent of the pressure of A, p_A. This is a **zero-order reaction.**

2. Bimolecular Surface Reactions. A bimolecular surface reaction may involve a reaction between two molecules A and B on a surface. The Langmuir-Hinshelwood mechanism assumes that the two molecules are adsorbed on neighbouring sites on the surface of the catalyst. This mechanism may be represented schematically as follows :

$$A + S \underset{k_{-1}}{\overset{k_1}{\rightleftharpoons}} AS$$

$$B + S \underset{k_{-2}}{\overset{k_2}{\rightleftharpoons}} BS$$

$$AS + BS \xrightarrow{k_3} S + \text{Products}$$

where S is a vacant site on the surface.

The rate of the reaction is given by

$$r = k_3\,[AS][BS] = k_3\,\theta_A\theta_B \qquad ...(51)$$

where θ_A and θ_B are the fractions of the surface sites covered by A and B, respectively. Assuming steady state approximation for [AS] and [BS], we have

$$d[AS]/dt = k_1[A][S] - k_{-1}[AS] - k_3[AS][BS] = 0 \qquad ...(52)$$

$$d[BS]/dt = k_2[B][S] - k_{-2}[BS] - k_3[AS][BS] = 0 \qquad ...(53)$$

where [S] is the concentration of the vacant sites on the surface. The *fraction* of the vacant sites, θ_V, is given by

$$\theta_V = 1 - (\theta_A + \theta_B) \qquad ...(54)$$

If C_S is the total concentration of the sites on the surface, then,

$$[S] = C_S\,(1 - \theta_A - \theta_B) = C_S\theta_V \qquad ...(55)$$

Also, $$[AS] = C_S\theta_A \quad \text{and} \quad [BS] = C_S\theta_B \qquad ...(56)$$

Using these expressions, Eqs. 52 and 53 become

$$k_1[A]\,C_S\,\theta_V - k_{-1}C_S\,\theta_A - k_3C_S^2\,\theta_A\,\theta_B = 0 \qquad ...(57)$$

$$k_2[B]\,C_S\,\theta_V - k_{-2}C_S\theta_B - k_3C_S^2\,\theta_A\,\theta_B = 0 \qquad ...(58)$$

Eqs. 57 and 58 can be solved to yield θ_A and θ_B.

Consider, however, a case when k_3 is very small so that Eqs. 52 and 53 become

$$k_1[A]\,\theta_V - k_{-1}\,\theta_A = 0 \qquad ...(59)$$

$$k_2[B]\,\theta_V - k_{-2}\,\theta_B = 0 \qquad ...(60)$$

(The common factor C_S cancels out).

Rearranging Eqs. 57 and 58, we have

$$\theta_A = (k_1/k_{-1})[A]\theta_V = K_1[A]\theta_V \qquad ...(61)$$

$$\theta_B = (k_2/k_{-2})[B]\theta_V = K_2[B]\theta_V \qquad ...(62)$$

where $K_1 = k_1/k_{-1}$ and $K_2 = k_2/k_{-2}$.

Substituting for θ_A and θ_B in Eq. 54, we get

$$\theta_V = 1 - K_1[A]\theta_V - K_2[B]\theta_V \qquad ...(63)$$

which can be rearranged to give

$$\theta_V = 1/(K_1[A] + K_2[B] + 1) \qquad ...(64)$$

Substituting for θ_V in Eqs. 61 and 62, we obtain

$$\theta_A = K_1[A]/(K_1[A] + K_2[B] + 1) \qquad ...(65)$$

$$\theta_B = K_2[B]/(K_1[A] + K_2[B] + 1) \qquad ...(66)$$

Substituting for θ_A and θ_B in Eq. 51, the rate of the reaction becomes,

$$r = \frac{k_3K_1K_2[A][B]}{(1 + K_1[A] + K_2[B])^2} \qquad ...(67)$$

Expressing concentrations in terms of partial pressures and taking proportionality constant as unity for the sake of convenience of discussion,

$$r = \frac{k_3K_1K_2p_Ap_B}{(1 + K_1p_A + K_2p_B)^2} = \frac{K'p_Ap_B}{(1 + K_1p_A + K_2p_B)^2} \qquad ...(68)$$

where $K' = k_3\,K_1\,K_2$.

Let us consider the following three cases :

Case 1. When A and B are both weakly adsorbed. In this case, $K_1p_A \ll 1$ and $K_2p_B \ll 1$, so that Eq. 68 becomes

$$r = K'p_A\,p_B \qquad ...(69)$$

i.e., the reaction is of the *first order with respect to A, of the first order with respect to B* and *overall of the second order.*

The reaction between NO and O_2 on glass surface belongs to this category.

Case 2. When A is adsorbed more strongly than B. In this case, $K_1p_A \gg K_2p_B$, so that Eq. 68 becomes

$$r = K'p_A\,p_B/(1 + K_1\,p_A)^2 \qquad ...(70)$$

i.e. the reaction is of the *first order with respect to* B, the weakly adsorbed component. The reaction between CO_2 and H_2 on platinum belongs to this category.

Case 3. When one reactant is very strongly adsorbed. Let A be the very strongly adsorbed component. Then, $K_1\,p_A \gg K_2\,p_B$ and $K_1\,p_A \gg 1$. Eq. 68, therefore, becomes

$$r = K'p_Ap_B/K_1^2\,p_A^2 = K_3(p_B/p_A) \qquad ...(71)$$

where $K_3 = K'/K_1^2 = (k_3K_2/K_1)$

Evidently, the rate is inversely proportional to the concentration of the *very strongly* adsorbed component. This is expressed by saying that the reaction is *inhibited* by such a component. The reaction between H_2 and O_2 on platinum belongs to this category.

***p*H-Dependence of Rate Constants of Catalyzed Reactions.** Consider a specific acid-catalyzed reaction $S + H^+ \longrightarrow P + H^+$ where S is the substrate and P is the product. The rate of decomposition of the reactant is given by

$$-d[S]/dt = k_{H^+}[S]\,[H^+] \qquad ...(72)$$

Since H^+ ions are not consumed in the reaction, their concentration remains the same. Thus, the reaction obeys pseudo first-order kinetics so that at constant *p*H,

$$-d[S]/dt = k_{app}\,[S] \qquad ...(73)$$

where k_{app} is the 'apparent' (or observed or pseudo first-order) rate constant.

From Eqs. 72 and 73, we have

$$k_{app} = k_{H^+}[H^+]$$

or $$\log k_{app} = \log k_{H^+} + \log H^+ = \log k_{H^+} - pH \qquad ...(74)$$

The variation of k_{app} with pH and of log k_{app} with pH for a specific acid-catalyzed reaction is shown in Fig. 7.

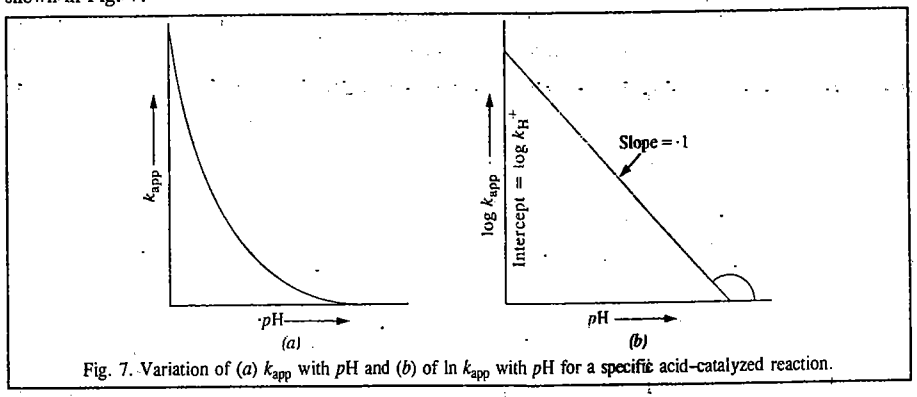

Fig. 7. Variation of (*a*) k_{app} with pH and (*b*) of ln k_{app} with pH for a specific acid-catalyzed reaction.

Hydrolysis of acetals is a specific acid-catalyzed reaction.

Consider now a specific base-catalyzed reaction :

$$S + OH^- \longrightarrow P + OH^-$$

The rate of decomposition of the reactant is given by

$$-d[S]/dt = k_{OH^-}[S][OH^-] \qquad ...(75)$$

Since OH^- ions are not consumed in the reaction, hence $[OH^-]$ is constant, we have

$$K_{app} = k_{OH^-}[OH^-] \qquad ...(76)$$

We know that with increasing pH, $[OH^-]$ increases. Also, the ionic product of water is given by

$$K_w = [H^+][OH^-] \simeq 10^{-14} \quad (\text{at } 25°C)$$

$$\therefore \quad [OH^-] = K_w/[H^+] \qquad ...(77)$$

Substituting Eq. 77 into Eq. 76, we have

$$k_{app} = (k_{OH^-})\,(K_w/[H^+]) \qquad ...(78)$$

$$\therefore \quad \log k_{app} = \log k_{OH^-} + \log K_w + \log (1/[H^+]) = \log k_{OH^-} - 14 + pH \qquad ...(79)$$

The variation of k_{app} with pH and of log k_{app} with pH for a specific base-catalyzed reaction is shown in Fig. 8.

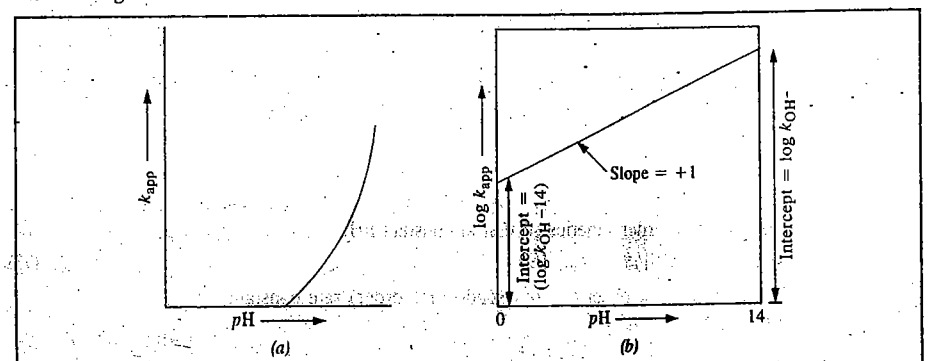

Fig. 8. Variation of (*a*) k_{app} with pH and (*b*) of log k_{app} with pH for a specific base-catalyzed reaction.

The hydrolysis of esters and amides are specific base-catalyzed reactions.

Now for a reaction such as the hydrolysis of an ester RCOOR′ which is a classic example of specific acid-base catalysis, the rate of the reaction is given by

$$r = \{k_H + [H^+] + k_{OH^-}[OH^-]\}\,[RCOOR'] \qquad ...(80)$$

In this rate law, the concentration of water does not appear since it remains constant throughout the reaction. As a consequence of the relation $K_w = [H^+][OH^-]$, the rate constant k ($= k_{H^+}[H^+] + k_{OH^-}[OH^-]$) has a minimum value at a pH that depends on K_w, k_{H^+} and k_{OH^-}. The pH-dependence of log k for this reaction is shown in Fig. 9.

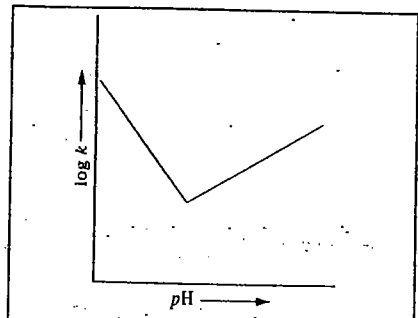

Fig. 9. The variation of log k with pH for a reaction catalyzed by both H^+ and OH^- ions.

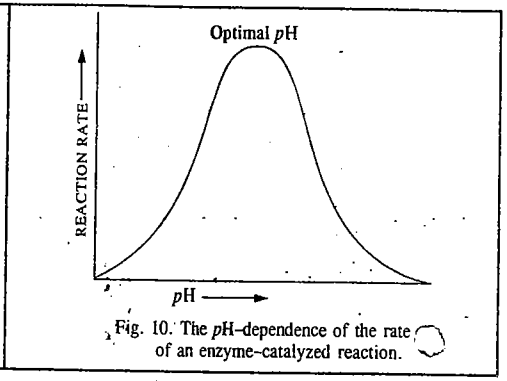

Fig. 10. The pH-dependence of the rate of an enzyme-catalyzed reaction.

The pH-dependence of enzyme kinetics is of paramount importance. Since enzymes are proteins, the pH changes profoundly affect the ionic character of the amino acid and carboxylic acid groups of the protein, thereby affecting the catalytic site and conformation of the enzyme. Also, pH changes can cause considerable *denaturation* (*i.e.*, unfolding of the enzyme), leading to the inactivation of the enzyme protein. Again, since substances (such as adenosine triphosphate (ATP) and amino acids) are ionic in character, the active site of an enzyme may require particular ionic species for optimum activity.

The activity of an enzyme, and hence the reaction rate, generally passes through a maximum at a particular pH (usually 7). A bell-shaped curve is thus obtained (Fig. 10). It has a relatively small plateau and sharply decreasing rates on either side. The plateau is called the **optimal pH point.** The maximum in the enzyme activity versus pH curve is interpreted by assuming that there are three forms of the enzyme in equilibrium :

$$EH_2 \rightleftharpoons EH \rightleftharpoons E,$$

of which only EH can combine with the substrate to yield an intermediate, EHS, which later forms products; the other intermediates EH_2S and ES do not form products. Since [EH] passes through a maximum at a particular pH, the enzyme activity, too, shows a maximum.

AUTOCATALYSIS AND OSCILLATORY REACTIONS

One of the hottest areas of research in kinetics has emerged in the 1970s and 1980s based on *autocatalysis* and *oscillations* which are non-linear in nature. We shall briefly deal with such reactions. One of the best known reactions is the so-called **B-Z reaction** or the **Belousov-Zhabotinski** reaction, named after the two Russian chemists. Consider the reaction

$$A \longrightarrow P$$

where P is the product. If the rate law is given by

$$r = k[A][P]$$

then the product P is said to catalyse the reaction. In the B–Z reaction, described in steps (*a*) and (*b*) below,

(*a*) $BrO_3^- + HBrO_2 + H_3O^+ \longrightarrow 2BrO_2 + 2H_2O$

(*b*) $2BrO_2 + 2Ce(III) + 2H_3O^+ \longrightarrow 2HBrO_2 + 2Ce(IV) + 2H_2O$

the two steps furnish the example of autocatalysis. The product $HBrO_2$ is a reactant in step (*a*).

In autocatalysis, several intermediates cause oscillations which are not ordinary sinusoidal oscillations but a superposition of such oscillations, leading to complexity of the reaction mechanism.

Long before the B–Z reaction was discovered, the so-called **Lotka-Volterra mechanism** was suggested to understand the nature of oscillatory reactions in biochemical systems. This mechanism involves the following steps :

(*a*) $A + X \longrightarrow 2X$; $d[A]/dt = -k_a[A][X]$

(*b*) $X + Y \longrightarrow 2Y$; $d[X]/dt = -k_b[X][Y]$

(*c*) $Y \longrightarrow B$; $d[B]/dt = k_c[Y]$

Steps (*a*) and (*b*) are autocatalytic. The concentration of A is held constant by supplying it to the reaction vessel, as required. B is normally removed from the reaction vessel and plays no part in the reaction once it is produced. Thus, the concentrations of the intermediates [X] and [Y] are left as variables. It is the interplay of [X] and [Y] which causes oscillatory behaviour. A steady state condition is maintained by the flow of *A* into a **continuously stirred tank reactor** (CSTR). This steady state should not be confused with the steady state approximation used in the kinetics of chain reactions. The Lotka–Volterra equations are solved numerically on the computer and the results are displayed in two ways. One way is to plot [X] and [Y] versus time (Fig. 11).

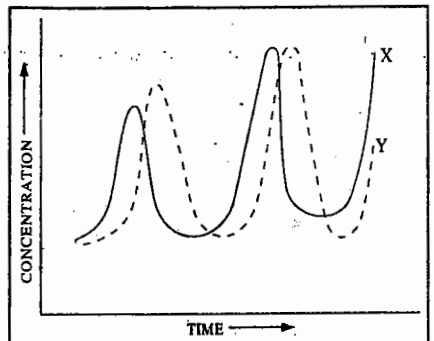

Fig. 11. The periodic variation of the concentrations of the intermediates X and Y as a function of time in a Lotka–Volterra mechanism.

The other way is to plot [Y] versus [X]. The second manner of plotting the data gives a better picture since this kind of diagrammatic representation gives a series of *closed curves* (Fig. 12.).

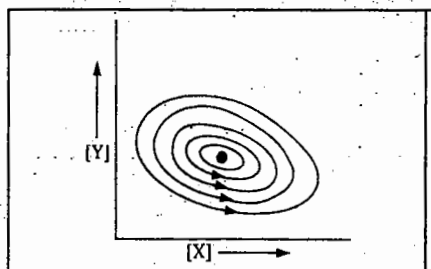

Fig. 12. Plot of [Y] versus [X], showing closed curves in a Lotka–Volterra mechanism.

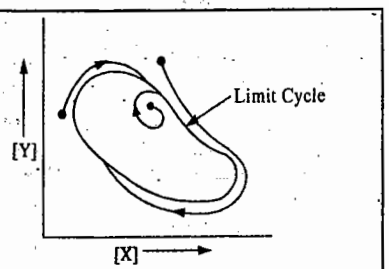

Fig. 13. The limit cycle in an oscillatory reaction.

We can explain the periodic variation of the concentration of intermediates as follows. It is possible that at some stage of the reaction, only a little X is present However, reaction (*a*) furnishes more of X and the production of X autocatalyses the production of even more X. However, as X is formed, reaction (*b*) starts. Initially this reaction is slow because [Y] is small but autocatalysis increases the production of [Y] tremendously. However, now X is also removed so that reaction (*a*) slows and less X is produced. Since less X is available, so reaction (*b*) slows. As less Y becomes available to remove X, X gets a chance to surge forward again, and this process continues.

We shall now consider two most studied oscillatory reactions, characteristically called the brussellator and the oregonator.

a. The Brussellator. It consists of the following sets of reactions :

(*a*) $A \longrightarrow X$; $d[X]/dt = k_a[A]$

(*b*) $2X + Y \longrightarrow 3Y$; $d[Y]/dt = k_b[X]^2[Y]$

(*c*) $B + X \longrightarrow Y + C$; $d[Y]/dt = k_c[B][X]$

(*d*) $X \longrightarrow D$; $-d[X]/dt = k_d[X]$

This osciliator was extensively studied by Ilya Prigogine and his coworkers in Brussels (Belgium). Since reactants A and B are maintained at constant concentration, we are left with the two concentration variables X and Y, which can be calculated by solving the rate equations numerically. This result is shown in Fig. 13. We notice that regardless of the values of initial concentrations of X and Y, the system settles down into the same periodic variation of the concentration, migrating to common trajectory called the **limit cycle.** The period of the limit cycle depends upon the values of the rate constant k_a, k_b, k_c and k_d. This limit cycle is an example of what mathematicians call an **attractor** since it appears to attract to itself trajectories in its vicinity. In chemical terms, the equilibrium state is an attractor but in systems that are away from equilibrium, the limit cycle may act as an attractor.

b. The Oregonator. The mechanism of the B–Z reaction mentioned above, which takes place in a mixture of potassium bromate, malonic acid and cerium (IV) salt in an acidic solution, was elucidated by the American chemists, R.M. Noyes and his coworkers in the University of Oregon (U.S.A.). Hence the name *oregonator,* for this highly complex mechanism which involves 18 elementary steps and 21 different chemical species. The following sequence of steps has been suggested for the oregonator, where A stands for $HBrO_2$, B for Br^- and Z for Ce^{4+} :

(*a*) $A + Y \longrightarrow X$

(*b*) $X + Y \longrightarrow C$

(*c*) $B + X \longrightarrow 2X + Z$

(*d*) $2X \longrightarrow D$

(*e*) $Z \longrightarrow Y$

(In the oregonator, A, B, C, D are held constant.)

The oscillations arise in a manner similar to the brussellator ; they can be accounted for by the autocatalysis in the third step and the sequence of reactions in the other steps.

The following three conditions should be fulfilled by oscillatory reactions :

(*a*) The reactions must be far from equilibrium.

(*b*) The reactions must involve autocatalytic steps.

(*c*) The system must exist in two steady states, *i.e.,* it must have **bistability.**

Let us illustrate the concept of bistability by considering a reaction involving two intermediates X and Y. Suppose the concentration of Y is at some high value in a reactor (Fig. 14*a*) and the addition of X decreases the concentration of Y, as shown by the upper line. Again, if X is at some high value, then the addition of Y might result in a slow increase of Y as shown by lower line. It is possible that at each stage a concentration may be reached at which the concentration will jump from one curve

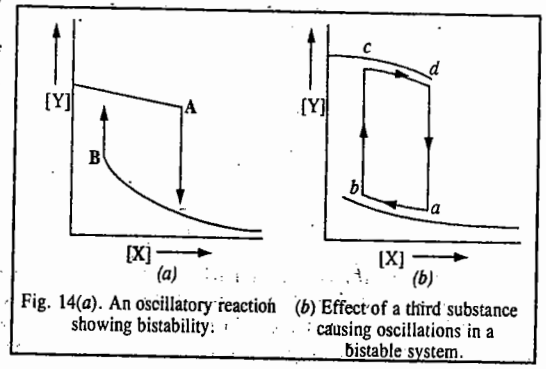

Fig. 14(*a*). An oscillatory reaction showing bistability. (*b*) Effect of a third substance causing oscillations in a bistable system.

to the other curve. We see that *the two curves represent the two stable states of a bistable system.* (We can, in fact, liken bi-stability of a chemical reaction to supercooling wherein a liquid may be cooled below the freezing point without solidifying). It may be emphasized that the two states are not in equilibrium states in the thermodynamic sense. They are in *steady states* which are far away from the equilibrium. The concentrations of X and Y are maintained as a result of the reactants continuously flowing into and of the products flowing out of the reactor.)

The presence of third intermediate Z, capable of reacting with both X and Y, causes dramatic change. Suppose that in the absence of Z, the flows of the reacting species correspond to the stable state *c* on the upper curve (Fig. 14*b*). When, however, Z reacts with Y to produce X, Y decreases and X increases so that the state of the system moves ..vards the right along the curve until a sudden transition occurs to the lower curve. Therefore, Z reacts with X producing Y, with the result that the state of the system moves towards the left along the lower curve until another sudden transition occurs to the upper curve when the process starts again. The result is a periodic surge and depletion of concentration of Y, arising out of a sudden leaping from one stable state to another in the bistability occurring in an oscillatory reaction (Fig. 15).

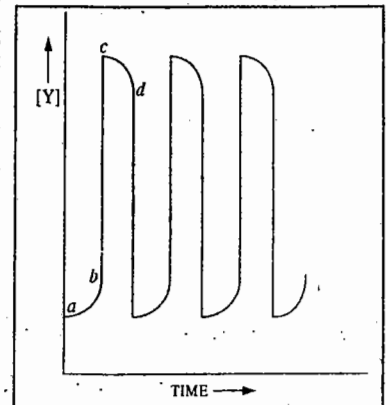

Fig. 15. Periodic surge and depletion of concentration in a bi-stable system.

Considerable research is going on to discover oscillatory reactions of industrial importance. The rhythm of the heartbeat is maintained by oscillatory reactions.

I. Review Questions

1. Illustrate the lowering of Gibbs free energy of activation of a reaction by a catalyst. Discuss carefully the general characteristics of catalytic reactions.
2. Discuss the kinetics of an acid–base catalyzed reaction.
3. Discuss the mechanism and kinetics of enzyme–catalyzed reactions.
4. The following mechanism has been proposed for enzyme catalysis :

$$E + S \underset{k_{-1}}{\overset{k_1}{\longrightarrow}} ES, \quad ES \xrightarrow{k_2} P + E \quad \cdots\cdots$$

Using steady state approximation for [ES], show that the reaction rate is given by

$$r = k_2[E]_0[S]/(K_m + [S])$$

where the symbols have their usual meanings. Discuss the rate when $K_m >> [S]$ and $K_m >> [S]$.

5. Consider the following mechanism for an enzyme–catalyzed reaction :

$$E + S \underset{k_{-1}}{\overset{k_1}{\longrightarrow}} ES; \quad ES \xrightarrow{k_2} EP; \quad EP \xrightarrow{k_3} E + P$$

where the symbols have their usual meanings and EP represents the complex formed between the enzyme and the product. Using steady state approximation, show that

$$r = \frac{k_2[E]_0[S]}{(k_{-1} + k_2)/k_1 + (1 + k_2/k_3)[S]}$$

6. Discuss the kinetics of (*i*) unimolecular surface reactions (*ii*) bimolecular surface reactions.
7. Discuss the pH-dependence of rate constants of catalyzed reactions.
8. What are oscillatory reactions ? Discuss in detail their mechanism.

CHAPTER 31

THE SOLID STATE

Solids are characterised by incompressibility, rigidity and mechanical strength. This indicates that the molecules, atoms or ions that make up a solid are closely packed. They are held together by strong cohesive forces and cannot move at random. Thus, in solids we have well ordered molecular, atomic or ionic arrangement.

Some solids, like sodium chloride, sulphur and sugar, besides being incompressible and rigid, have also characteristic geometrical forms. Such substances are said to be crystalline solids. The X-ray diffraction studies reveal that their ultimate particles (*viz.*, molecules, atoms or ions) are arranged in a definite pattern throughout the entire three-dimensional network of a crystal. This definite and ordered arrangement of molecules, atoms or ions (as the case may be) extends over a large distance. This is termed as **long range order.** There is another category of solids such as glass, rubber and plastics, which possess properties of incompressibility and rigidity to a certain extent but they do not have definite geometrical forms. Such substances are called **amorphous solids.**

Difference between Crystalline and Amorphous Solids. Crystalline and amorphous solids differ from one another in the following respects.

1. Characteristic Geometry. A crystalline solid has a definite and regular geometry due to definite and orderly arrangement of molecules or atoms or ions in three-dimensional space. An amorphous solid, on the other hand, does not have any pattern of arrangement of molecules or atoms and, therefore, does not have any definite geometrical shape. It has been found that even if some orderly arrangement of molecules or atoms exits in a few amorphous solids, it does not extend more than a few Angstrom units. Thus, unlike crystalline solids, amorphous solids do not have a long range order.

2. Melting Points. Consider a molecular solid which is being heated. With increase in temperature its molecular vibrations increase and ultimately become so great that molecules break away from their fixed positions. They now begin to move more freely and have rotational motion as well. The solid now changes into liquid state. The temperature at which this occurs is known as the **melting point.**

A crystalline substance has a sharp melting point, *i.e.*, it changes abruptly into liquid state. An amorphous substance, on the contrary, does not have a sharp melting point. For example, if glass is heated gradually, it softens and starts to flow without undergoing a definite and abrupt change. The amorphous solids are, therefore, regarded as 'liquids at all temperatures'. There is some justification for this view because it is known from X-ray examination that amorphous substances do not have well ordered molecular or atomic arrangements. Strictly speaking, solid state refers only to crystalline state, *i.e.*, only a crystalline material can be considered to be a true solid.

3. Isotropy and Anisotropy. Amorphous substances differ from crystalline solids and resemble liquids in another important respect. Their properties such as electrical conductivity, thermal conductivity, mechanical strength and refractive index are the same in all directions. Amorphous substances are, therefore, said to be **isotropic.** Liquids and gases are also isotropic. Crystalline

solids, on the other hand, are anisotropic, *i.e.*, their physical properties are different in different directions. For example, the velocity of light passing through a crystal varies with the direction in which it is measured. Thus, a ray of light entering such a crystal may split up into two components each following a different velocity. This phenomenon is known as **double refraction.** Thus, anisotropy itself is a strong evidence for the existence of ordered molecular or atomic or ionic arrangement in such materials. This can be shown on reference to Fig. 1 in which a simple two-dimensional arrangement of only two different kinds of atoms is depicted. If the properties are measured along the direction indicated by the slanting line CD, they will be different from those measured in the direction indicated by the vertical line AB. The reason is that while in the first case, each row is made up of alternate types of atoms, in the second case, each row is made up of one type of atoms only. In amorphous solids, atoms or molecules are arranged at random and in a disorderly manner and, therefore, all directions are identical and all properties are alike in all directions.

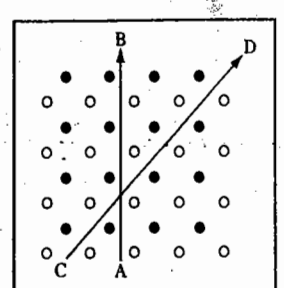

Fig. 1. Anisotropic behaviour of crystals.

Size and Shape of Crystals. Several naturally occurring solids have definite crystalline shapes which can be recognised easily. There are many other solid materials which occur as powders or agglomerates of fine particles and appear to be amorphous. But when an individual particle is examined under a microscope, it is also seen to have a definite crystalline shape. Such solids, in which the crystals are so small that they can be recognised only under a powerful microscope, are said to be **microcrystalline.** The size of a crystal depends on the rate at which it is formed : the slower the rate, the bigger the crystal. This is because time is needed by the atoms or ions or molecules to find their proper positions in the crystal structure. Thus, large transparent crystals of sodium chloride, silver nitrate, lithium chloride, etc., can be prepared by melting these salts and allowing them to cool very slowly at a uniform rate. It is for this reason that crystals of most of the minerals formed by geological processes in nature are often very large.

Interfacial Angles. Crystals are bound by plane faces. The angle between any two faces is called an **interfacial angle.** Although the size of the faces or even shapes of the crystals of one and the same substance may vary widely with conditions of formation, etc., yet the interfacial angles between any two corresponding faces of the crystal remain invariably the same throughout. This is illustrated in Fig. 2. Although the external shape is different yet the interfacial angles are the same. The measurement of interfacial angles in crystals is, therefore, important in the study of crystals. The subject is known as crystallography.

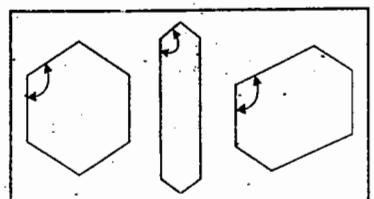
Fig. 2. Interfacial angles in a crystal.

SYMMETRY IN CRYSTAL SYSTEMS

Besides the interfacial angles, another important property of crystals is their symmetry. There are various types of symmetry, only three of which will be described here. These are : *(i)* Plane of Symmetry *(ii)* Axis of Symmetry and *(iii)* Centre of Symmetry.

Plane of Symmetry. When an imaginary plane can divide a crystal into two parts such that one is the exact mirror image of the other, the crystal is said to have a **plane of symmetry.**

Axis of Symmetry. An **axis of symmetry** is a line about which the crystal may be rotated such that it presents the same or similar appearance more than once during the complete revolution.

For example, in the case of a cube, an axis passing perpendicularly through the centre is such

that when the cube is rotated it presents similar appearance in three rotations of 90° each and the same appearance after the fourth rotation. Such an axis is called a **four-fold** or a **tetrad axis** (Fig. 3*a*). If the same or similar appearance is repeated after an angle of 180°, the axis is called a **two-fold** or a **diad axis** (Fig. 3*b*). In the same way, if the same or similar appearance is repeated after an angle of 120°, the axis is called a **three-fold** or **triad axis** (Fig. 3*c*). If the same or similar appearance is repeated after an angle of 60°, as in the case of a hexagonal crystal, the axis is called a **six-fold** or **hexad axis** (Fig. 3*d*). In general, if the same or similar appearance of a crystal is repeated on rotation through an angle of 360°/n, around an imaginary axis, the axis is called an **n-fold axis.** A crystal can have only 2-fold, 3-fold, 4-fold and 6-fold axes of rotation. The angle through which the crystal will have to be rotated to get the same or similar appearance, evidently, will be 180°, 120°, 90° and 60°, respectively.

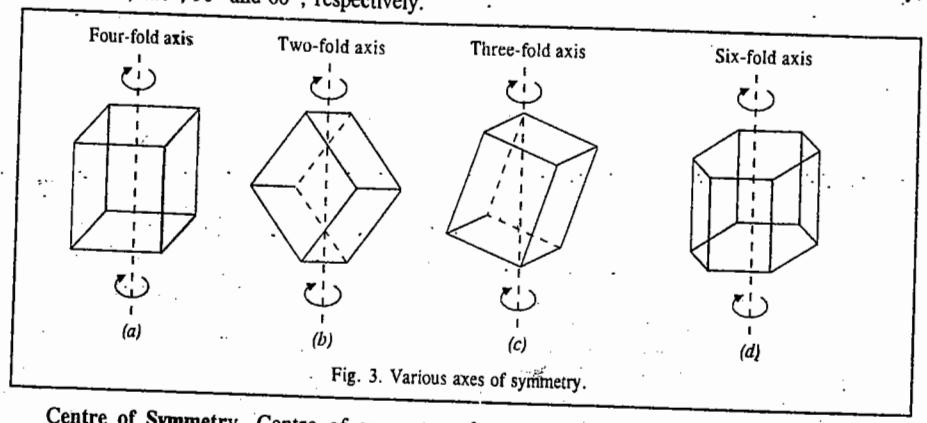

Fig. 3. Various axes of symmetry.

Centre of Symmetry. Centre of symmetry of a crystal is such a point that any line drawn through it intersects the surface of the crystal at equal distances in both directions.

It may be pointed out that a crystal may have any number of planes or axes of symmetry but it has only one centre of symmetry.

Elements of Symmetry of a Crystal. As mentioned above, there are different types of symmetries which are possible in a crystal. A crystal may have different numbers of each type of symmetry. The total number of **planes, axes** and **centre** of symmetries possessed by a crystal is termed as **elements of symmetry** of the crystal. To explain this term further, we may consider the elements of symmetry possessed by a **cubic crystal,** such as NaCl crystal. A cubic crystal possesses **a total of 23 elements of symmetry,** as will be clear from the discussion given below. These elements of symmetry are :

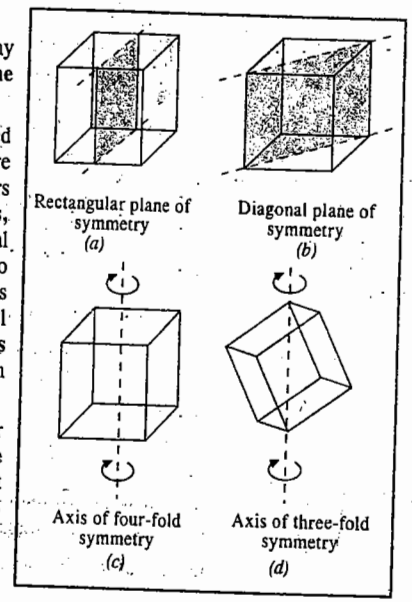

a. Rectangular planes of symmetry. One rectangular plane of symmetry is shown in Fig. 4*a*. There will be two more such planes, each of which will be at right angles to the plane shown in the figure. Thus, there are 3 rectangular planes of symmetry in all.

b. Diagonal planes of symmetry. One plane passing

diagonally through the cube is shown in Fig. 4*b*. There can be a total of 6 such planes passing diagonally through the cube, as a little reflection will show.

c. Axes of four-fold symmetry. One of the four-fold axes is shown in Fig. 4*c*. Evidently, there can be a total of 3 such four-fold axes at right angles to one another.

d. Axes of three-fold symmetry. One such axis passing through opposite corners is shown in Fig. 4*d*. There can be a total of 4 such three-fold axes.

e. Axes of two-fold symmetry. One such axis emerging from opposite edges is shown in Fig. 4*e*. There are, evidently, 6 such axes of two-fold symmetry.

f. Centre of symmetry. There is only one centre of symmetry lying at the centre of the cube (Fig. 4*f*).

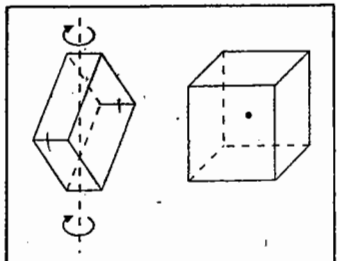

Axis of two-fold symmetry (*e*) Centre of symmetry (*f*)

Fig. 4. Various elements of symmetry in a cubic crystal.

Thus, the number of symmetry elements of various types in a cubic crystal are :

Planes of symmetry = 3 + 6 = 9 elements

Axes of symmetry = 3 + 4 + 6 = 13 elements

Centre of symmetry = 1

Total number of symmetry elements = 23

Point Groups and Space Groups

It can be shown from geometrical considerations that, theoretically, there can be 32 different combinations of elements of symmetry of a crystal. These are called 32 point groups or 32 crystal systems. Some of the systems, however, have been grouped together so that we have only seven different categories, known as the seven basic crystal systems. These are cubic, orthorhombic, tetragonal, monoclinic, triclinic, hexagonal and rhombohedral or trigonal.

These systems together with the maximum numbers of planes of symmetry and axes of symmetry and their examples are given in Table 1.

TABLE 1

Crystal Systems and their Maximum Symmetry Elements

Sr.	System	Maximum Symmetry Elements	Examples
1.	Cubic or Regular	Nine planes of symmetry Thirteen axes of symmetry	NaCl, KCl, CaF_2, ZnS, Cu_2O. Diamond, Alums, Pb, Ag, Au.
2.	Orthorhombic	Three planes of symmetry Three axes of symmetry	KNO_3, K_2SO_4, $BaSO_4$ Mg_2SiO_4, Rhombic sulphur
3.	Tetragonal	Five planes of symmetry Five axes of symmetry	SnO_2, TiO_2, $ZrSiO_4$, KH_2PO_4 $PbWO_4$, Sn
4.	Monoclinic	One plane of symmetry One axis of symmetry	$Na_2SO_4.10H_2O$, $Na_2B_4O_7.10H_2O$, $CaSO_4.2H_2O$, Monoclinic sulphur
5.	Triclinic	No plane of symmetry No axis of symmetry	$CuSO_4.5H_2O$, $K_2Cr_2O_7$, H_3BO_3
6.	Hexagonal	Seven planes of symmetry Seven axes of symmetry	ZnO, CdS, HgS, Graphite Ice, PbI_2, Beryl, Mg, Zn, Cd
7.	Rhombohedral or Trigonal	Seven planes of symmetry Seven axes of symmetry	$NaNO_3$, ICl, Calcite, Magnesite Quartz, As, Sb, Bi

The 32 point groups can further produce 230 space groups, as discussed in Chapter 3 on Group theory.

Space Lattice and Unit Cell. A space lattice is an array of points showing how molecules, atoms or ions are arranged at different sites in three-dimensional space. An array of points in a three-dimensional space lattice is shown in Fig. 5. Each point represents a molecule, an atom or an ion or a group of any of these constituents.

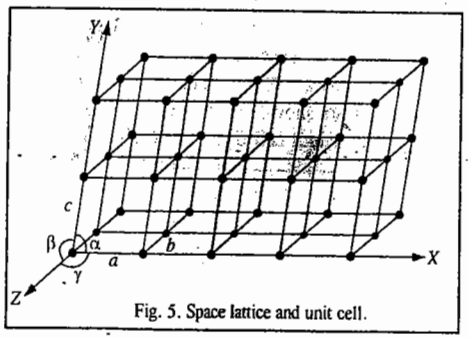

Fig. 5. Space lattice and unit cell.

The lattice points can be broken up into a number of unit cells. This is done by connecting the points by a regular network of lines, as shown in the figure. A **unit cell** *is the smallest repeating unit in space lattice which when repeated over and over again results in a crystal of the given substance.* Thus, space lattice of a crystal has been likened to a wall paper on which a single pattern is continuously repeated. Just as a pattern on the wall paper is repeated again and again, similarly, a unit cell (representing a definite pattern) is repeated again and again to build up a crystal. The only difference is that while wall paper is in two dimensions, space lattice of a crystal is in three dimensions. The unit cell, in fact, is the smallest sample that represents the picture of the entire crystal. The crystal may be considered to consist of infinite number of unit cells. Each unit cell in a three-dimensional space has, evidently, three vectors, *a*, *b* and *c*, as shown in Fig. 5.

It may be noted that these are the *points* and *not the lines* which constitute the space lattice. The lines joining the points are drawn simply to represent three axes by means of which the relative positions of the points can be described. For example, in Fig. 5, three imaginary axes, *OX*, *OY* and *OZ*, which may be used to represent the unit cell, have been shown. In order to describe a unit cell, we should know the distances *a*, *b* and *c* which give the lengths of the edges of the unit cell and the angles α, β and γ, which give the angles between the three imaginary axes, as shown. Knowing the unit cell dimensions, the theoretical density ρ of a crystal can be calculated from the relation

$$\rho = nM/(N_A V) \qquad ...(1)$$

where n is the number of molecules or atoms or ions in the unit cell ; M is the molar mass of the substance and V is the volume of the unit cell.

Bravais Lattices

The French crystallographer Auguste Bravais in 1848 showed from geometrical considerations that there can be only 14 different ways in which similar points can be arranged in a three-dimensional space. Thus, the total number of space lattices belonging to all the seven basic crystal systems put together is only 14, as given in column 2 of Table 2.

The crystals belonging to the cubic system have three kinds of Bravais lattices depending upon the shape of the unit cell. These are :

1. The **simple** or **primitive cubic lattice (P)** in which there are points only at the corners of each unit cell (Fig. 6*a*).

2. The **face-centred cubic lattice (F)** in which there are points at the corners as well as at the centre of each of the six faces of the cube (Fig. 6*b*).

3. The **body-centred cubic lattice (I)** in which there are points

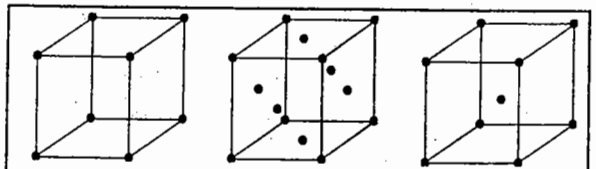

Fig. 6(*a*) Simple or primitive cubic lattice (P) Fig. 6(*b*) Face-centred cubic lattice (F) Fig. 6(*c*). Body-centred cubic lattice (I)

at the corners as well as in the body centre of each cube (Fig. 6*c*).

The Bravais space lattices associated with various crystal systems are shown in Figs. 7*a*, 7*b*, 7*c* and 7*d*. The parameters of unit cell, *i.e.*, the cell dimensions *a*, *b*, *c* and the interfacial angles α, β and γ are also shown in each case. The actual lattice in a crystal of a given kind consists of a repetition of a unit cell of that kind all over in three-dimensional space.

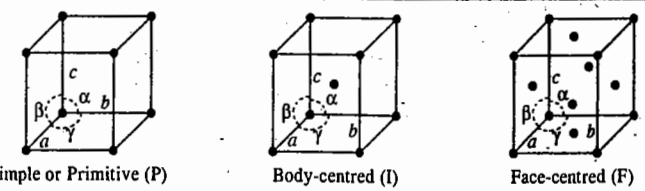

Fig. 7*a*. Cubic Space Lattices

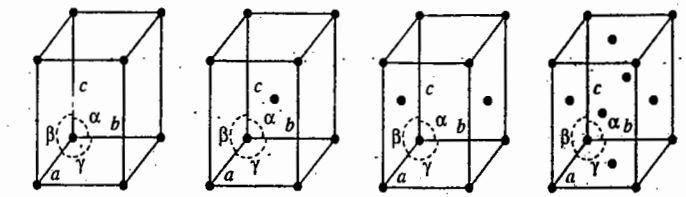

Fig. 7*b*. Orthorhombic Space Lattices

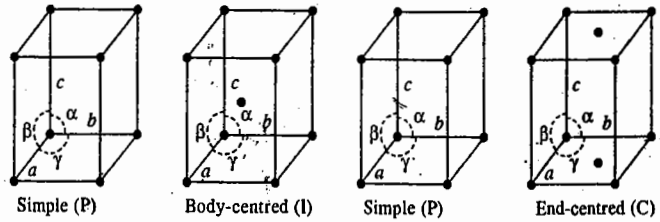

Fig. 7*c*. Tetragonal and Monoclinic Space Lattices

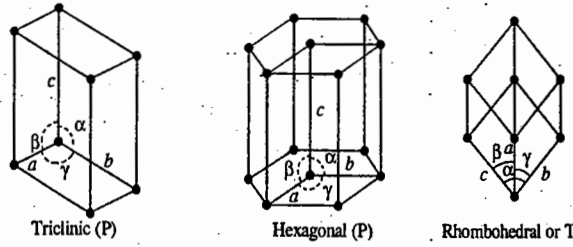

Fig. 7*d*. Triclinic, Hexagonal and Rhombohedral Space Lattices

Seven Crystal Systems. The crystallographers have been able to divide 32 point groups and 14 space lattices into seven crystal systems. Some detailed descriptions of these seven crystal systems are given in Table 2.

TABLE 2
Seven Crystal Systems

Crystal System	Bravais Lattices	Minimum symmetry Elements	Parameters of Unit Cell	
			Cell Dimensions	Interfacial Angles
1. Cubic	Primitive, Face-centred, Body-centred = 3	Four 3-fold axes : Three 4-fold axes	$a=b=c$	$\alpha=\beta=\gamma=90°$
2. Orthorhombic	Primitive, Face-centred, Body-centred, End-centred = 4	Three mutually perpendicular 2-fold axes	$a\neq b\neq c$	$\alpha=\beta=\gamma=90°$
3. Tetragonal	Primitive, Body-centred = 2	One 4-fold axis	$a=b\neq c$	$\alpha=\beta=\gamma=90°$
4. Monoclinic	Primitive, End-centred = 2	One 2-fold axis	$a\neq b\neq c$	$=\gamma=90°, \beta\neq 90°$
5. Triclinic	Primitive = 1	One 1-fold axis	$a\neq b\neq c$	$\alpha\neq\beta\neq\gamma\neq 90°$
6. Hexagonal	Primitive = 1	One 6-fold axis	$a=b\neq c$	$\alpha=\beta=90°, \gamma=120°$
7. Rhombohedral or Trigonal	Primitive = 1	One 3-fold axis	$a=b=c$	$\alpha=\gamma=\beta\neq 90°$

The first column gives the name of the crystal system. The second column gives the number and types of space lattices present in the given crystal system. The third column contains information with regard to minimum symmetry elements of each system. These are the absolutely essential symmetry requirements of a given crystal system. A crystal belonging to that system may have more symmetry elements but it cannot have less. The unit cell parameters, *viz.*, the cell dimensions *a*, *b* and *c* and the interfacial angles α, β and γ between the three imaginary axes are given in the last column.

Example 1. A metallic element exists as a cubic lattice. Each edge of the unit cell is 2·88 Å. The density of the metal is 7·20 g cm^{-3}. How many unit cells there will be in 100 g of the metal ?

Solution : Volume of the unit cell $= (2\cdot88\ \text{Å})^3 = 23\cdot9\times10^{-30}\ \text{m}^3$

$$\text{Volume of 100 g of the metal} = \frac{m}{\rho} = \frac{0{\cdot}1\ \text{kg}}{7\cdot20\times10^3\ \text{kg m}^{-3}} = 13\cdot9\times10^{-6}\ \text{m}^3$$

$$\text{Number of unit cells in this volume} = \frac{13\cdot9\times10^{-6}\ \text{m}^3}{23\cdot9\times10^{-30}\ \text{m}^3} = 5\cdot82\times10^{23}$$

Example 2. Iron (II) oxide, FeO, crystal has a cubic structure and each edge of the unit cell is 5·0 Å. Taking density of the oxide as 4·0 g cm^{-3}, calculate the number of Fe^{2+} and O^{2-} ions present in each unit cell.

Solution : Volume of the unit cell $= (5\times10^{-10}\ \text{m})^3 = 1\cdot25\times10^{-28}\ \text{m}^3$

Density of FeO $= 4\cdot0\times10^3\ \text{kg cm}^{-3}$

$\therefore$ Mass of the unit cell $= 1\cdot25\times10^{-28}\ \text{m}^3\times4\cdot0\times10^3\ \text{kg m}^{-3} = 5\cdot0\times10^{-25}\ \text{kg}$

$$\text{Mass of one molecule of FeO} = \frac{\text{Molar mass}}{\text{Avogadro's number}} = \frac{72\times10^3\ \text{kg mol}^{-1}}{6\cdot022\times10^{23}\ \text{mol}^{-1}}$$

$$= 1\cdot195\times10^{-25}\ \text{kg}$$

$$\therefore\ \text{Number of FeO molecules per unit cell} = \frac{5\cdot0\times10^{-25}\ \text{kg}}{1\cdot195\times10^{-25}\ \text{kg}} = 4\cdot19 \approx 4$$

Thus, there are **four Fe^{2+} ions and four O^{2-} ions** in each unit cell.

Example 3. Calculate the number of atoms contained within *(i)* a primitive cubic unit cell *(ii)* a body-centred cubic (b.c.c.) unit cell *(iii)* a face-centred cubic (f.c.c.) unit cell and *(iv)* the unit cell for the diamond lattice.

Solution : *(i)* The primitive cubic unit cell consists of one atom at each of the 8 corners. Each atom is thus

shared by 8 unit cells. Hence, $n = 8\times(1/8) = 1$.

(ii) The b.c.c. unit cell consists of 8 atoms at the 8 corners and one atom at the centre. At each corner only 1/8th of the atom is within the unit cell. Thus, the contribution of the 8 corners is $8\times(1/8)=1$ while that of the body-centred atom is 1. Hence, $n = 1+1 = 2$.

(iii) The 8 atoms at the corners contribute $8\times(1/8) = 1$. There is one atom at each of the 6 faces, which is shared by 2 unit cells each. Therefore, the contribution of 6 face-centred atoms $= 6\times(1/2) = 3$. Hence, $n = 1+3 = 4$.

(iv) If we consider the unit cell of a diamond lattice, we find that there are 8 atoms on the 8 corners, each shared by 8 unit cells. Also, there are 6 atoms on the faces, each shared by 2 unit cells. In addition, there are 4 atoms inside the unit cell. Hence, $n = 8\times(1/8) + 6\times(1/2) + 4 = 8$.

Example 4. Calculate the coordination number (C.N.) of an atom in *(i)* a primitive cubic unit cell *(ii)* a body-centred cubic unit cell and *(iii)* a face-centred cubic unit cell.

Solution : *(i)* A little consideration shows that in a primitive cubic unit cell, each atom has 6 equally-spaced nearest neighbour atoms. Thus, C.N. = 6.

(ii) Considering the atom at the centre of the unit cell, we find that it is surrounded by 8 nearest neighbour atoms situated at the corners of the cube. Thus, C.N. = 8.

(iii) C.N. for a face-centred atom in an f.c.c. unit cell is, evidently, equal to **12.**

Example 5. At room temperature, pollonium crystallizes in primitive cubic unit cell. If $a = 3{\cdot}36$ Å, calculate the theoretical density of pollonium. Molar mass M of pollonium = 209 g mol^{-1}.

Solution : A primitive cubic unit cell contains atoms only at the 8 corners with each corner contributing 1/8th of an atom. Hence, $n = 8\times(1/8) = 1$.

$$\text{Volume, } V = a^3 = (3{\cdot}36\ \text{Å})^3 = (3{\cdot}36\times10^{-10}\ \text{m})^3$$

$$\text{From Eq. 1, } \rho = \frac{nM}{N_A V} = \frac{(1)(209\times10^{-3}\ \text{kg mol}^{-1})}{(6{\cdot}022\times10^{23}\ \text{mol}^{-1})(3{\cdot}36\times10^{-10}\ \text{m})^3} = 9{\cdot}15\times10^3\ \text{kg m}^{-3}$$

Example 6. At room temperature, sodium crystallizes in a body-centred cubic cell with a = 4·24 Å. Calculate the theoretical density of sodium. Molar mass M of sodium = 23·0 g mol^{-1}.

Solution : As shown in Example 3, the value of n for a b.c.c. unit cell is 2.

$$\text{Volume, } V = (4{\cdot}24\ \text{Å})^3 = (4{\cdot}24\times10^{-10}\ \text{m})^3$$

$$\text{From Eq. 1, } \rho = \frac{nM}{N_A V} = \frac{2\times(23{\cdot}0\times10^{-3}\ \text{kg mol}^{-1})}{(6{\cdot}022\times10^{23}\ \text{mol}^{-1})(4{\cdot}24\times10^{-10}\ \text{m})^3} = 1{\cdot}00\times10^3\ \text{kg m}^{-3}$$

Example 7. Lithium borohydride, $LiBH_4$, crystallizes in an orthorhombic system with 4 molecules per unit cell. The unit cell dimensions are : $a = 6{\cdot}81$ Å, $b = 4{\cdot}43$ Å and $c = 7{\cdot}17$ Å. If the molar mass M of $LiBH_4$ is 21·76 g mol^{-1}, calculate the density of the crystal.

Solution :
$$\rho = \left(\frac{nM}{N_A V}\right) = \frac{4\times(21{\cdot}76\times10^{-3}\ \text{kg mol}^{-1})}{(6{\cdot}022\times10^{23}\ \text{mol}^{-1})(6{\cdot}81\times4{\cdot}43\times7{\cdot}17\times10^{-30}\ \text{m}^3)} = 0{\cdot}668\times10^3\ \text{kg m}^{-3}$$

Example 8. An organic compound crystallises in an orthorhombic system with two molecules per unit cell. The unit cell dimensions are 12·05, 15·05 and 2·69 Å. If the density of the crystal is 1·419 g cm^{-3}, calculate the molar mass of the organic compound.

Solution : From Eq. 1, $M = \rho N_A V/n$

$$= \frac{(1{\cdot}419\times10^3\ \text{kg m}^{-3})(6{\cdot}022\times10^{23}\ \text{mol}^{-1})(12{\cdot}05\times15{\cdot}05\times2{\cdot}69\times10^{-30}\ \text{m}^3)}{2} = 0{\cdot}209\ \text{kg mol}^{-1}$$

Example 9. Iron (α-Fe) crystallises in a b.c.c. system with $a = 2{\cdot}861$ Å. Molar mass M of iron is 55·85 g mol^{-1}. Calculate the density of iron.

Solution : From Eq. 1, $\rho = \frac{nM}{N_A V} = \frac{2\times(55{\cdot}85\times10^{-3}\ \text{kg mol}^{-1})}{(6{\cdot}022\times10^{23}\ \text{mol}^{-1})(2{\cdot}861\times10^{-10}\ \text{cm})^3} = 7{\cdot}92\times10^3\ \text{kg m}^{-3}$

Lattice Energy of an Ionic Crystal. It is defined as the amount of energy released when cations and anions in their gaseous state are brought together from infinite separation to form a crystal.

$$M^+(g) + X^-(g) \xrightarrow{-U} MX(s)\ ;\ U = \text{lattice energy}$$

The theoretical treatment of ionic lattice energy was given by M. Born and A. Lande'. This treatment has been discussed below.

Consider the potential energy of an ion pair, M^+,X^- in a crystal separated by a distance r. The coulombic electrostatic energy of attraction is given by

$$U_{att}(r) = \frac{z_+ z_- e^2}{4\pi\varepsilon_0 r} \qquad ...(2)$$

Since z_- is negative, the electrostatic energy is negative (with respect to energy at infinite separation) and becomes increasingly so as the interionic distance decreases, as shown by the dotted line in Fig. 8. Note that the charge on the cation is z_+e and that on the anion is z_-e.

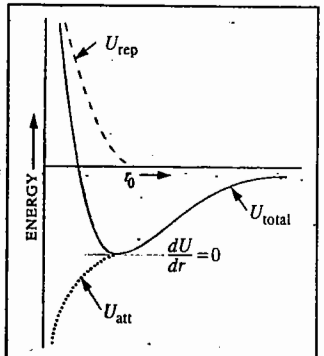

Fig. 8. Energy curves for an ion pair in an ionic solid.

In a crystal lattice there are more interactions between the ions than the simple one in an isolated ion pair. Thus, in NaCl lattice, each sodium ion experiences attraction to the six nearest chloride ions, repulsions by the next twelve nearest sodium ions, attractions to the next eight chloride ions and repulsions by the next six sodium ions and so on. The summation of all these geometrical interactions is known as the **Madelung constant**, M. The energy of attraction in an ion pair in a crystal is thus given by

$$U_{att}(r) = \frac{M z_+ z_- e^2}{4\pi\varepsilon_0 r} \qquad ...(3)$$

The value of Madelung constant depends only on the geometry of the lattice and is independent of ionic radius and charge. Thus, the value of Madelung constant in NaCl lattice is given by

$$M = 6 - \frac{12}{\sqrt{2}} + \frac{8}{\sqrt{3}} - \frac{6}{\sqrt{4}} + \ldots. \qquad ...(4)$$

A stable lattice can result only if there is also repulsion energy to balance the attractive coulombic energy. The attractive energy becomes infinite at infinitesimally small distances. However, ions are not point charges but consist of electron charge-clouds which repel each other at very close distances. This repulsion is shown by the broken line in Fig. 8. It is negligible at large distances but increases very rapidly as the ions approach each other closely. According to Born, the repulsive energy is given by

$$U_{rep}(r) = B/r^n \qquad ...(5)$$

where B is a constant. Experimentally, the Born exponent n can be determined from the compressibility data because the latter measure the resistance which the ions exhibit when forced to approach each other very closely.

Thus, for a crystal lattice consisting of Avogadro's number of ions, the total energy is given by

$$U_{total}(r) = U_{att}(r) + U_{rep}(r) = \frac{M N_A z_+ z_- e^2}{4\pi\varepsilon_0 r} + \frac{N_A B}{r^n} \qquad ...(6)$$

The total energy is shown by the solid line in Fig. 8. At the minimum in the curve, corresponding to the equilibrium lattice configuration, $(r = r_0)$

$$\left(\frac{dU}{dr}\right)_{r=r_0} = 0 = -\frac{M N_A z_+ z_- e^2}{4\pi\varepsilon_0 r_0^2} - n\frac{N_A B}{r_0^{n+1}} \qquad ...(7)$$

In this lattice configuration, the attractive forces between the ions balance the repulsive forces. Let U_0 represent the energy at the equilibrium distance r_0. From Eq. 7,

$$B = -\frac{Mz_+z_-e^2r_0^{n-1}}{4\pi\varepsilon_0 n} \qquad ...(8)$$

and

$$U_0 = \frac{MN_A z_+z_-e^2}{4\pi\varepsilon_0 r_0} - \frac{MN_A z_+z_-e^2}{4\pi\varepsilon_0 r_0 n} \qquad ...(9)$$

$$= \frac{MN_A z_+z_-e^2}{4\pi\varepsilon_0 r_0}\left(1 - \frac{1}{n}\right) \qquad ...(10)$$

This is the **Born–Lande' equation** for the lattice energy of an ionic crystal. The Born exponent n depends upon the type of the ion involved. Larger ions having relatively higher electron densities have larger values of n.

Example 10. Calculate the lattice energy of NaCl crystal from the following data :

$$M = 1{\cdot}7476 \; ; \; r_0 = 2{\cdot}814 \text{ Å} \; ; \; n = 8$$

Solution : Substituting the given data and the values of the other constants in Eq. 10, we have

$$U_0 = \frac{(1{\cdot}7476)(6{\cdot}022\times10^{23}\text{ mol}^{-1})(1)(-1)(1{\cdot}602\times10^{-19}\text{ C})^2}{4(3{\cdot}1416)(8{\cdot}854\times10^{-12}\text{ C}^2\text{ N}^{-1}\text{ m}^{-2})(2{\cdot}814\times10^{-10}\text{ m})}\left(1 - \frac{1}{8}\right)$$

$$= -775 \text{ kJ mol}^{-1} \text{ (Experimental value } = -770 \text{ kJ mol}^{-1})$$

We see that the agreement of Born–Lande equation with experiment is satisfactory.

Substitution of the various constants in Eq. 10 gives the following equation :

$$U_0 = 1{\cdot}39\times10^5\left(\frac{z_+z_-M}{r_0\,(\text{pm})}\right)\left(1 - \frac{1}{n}\right)\text{ kJ mol}^{-1} \qquad ...(11)$$

Experimentally, the lattice enthalpy of an ionic compound can be determined by using the **Born–Haber cycle** which can be represented diagrammatically as shown below :

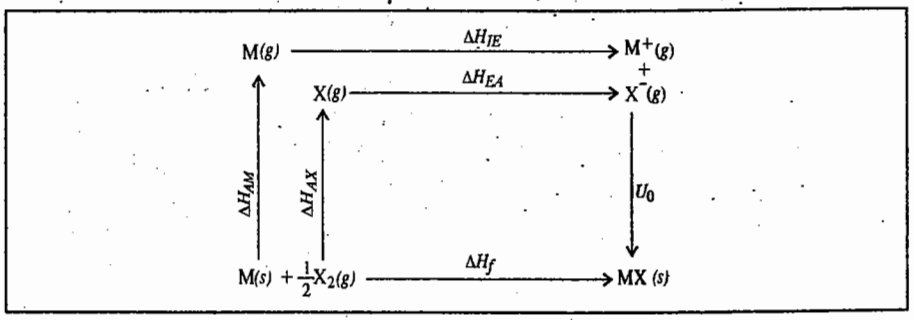

We find that

$$\Delta H_f = \Delta H_{AM} + \Delta H_{AX} + \Delta H_{IE} + \Delta H_{EA} + U_0$$

Here the terms ΔH_{AM} and ΔH_{AX} are the enthalpies of atomization of the metal and the non-metal, respectively ; ΔH_{IE} and ΔH_{EA} are the ionization energy of the metal and electron affinity of the non-metal, respectively.

Law of Rational Indices. This law states that the intercepts of any face of a crystal along the crystallographic axes are either equal to the unit intercepts (a, b, c) or some simple whole number multiples of them, *e.g.*, na, n'b, n''c, etc., where n, n', n'', etc., are simple whole numbers.

Let *OX*, *OY* and *OZ* represent the three crystallographic axes and let *ABC* be a unit plane (Fig. 9). The unit intercepts will then be *a*, *b* and *c*. According to the above law, the intercepts of any face such as *KLM*, on the same three axes will be simple whole number multiples of *a*, *b* and *c*, respectively. As can be seen from the figure, the simple multiples in this case are 2, 2 and 3.

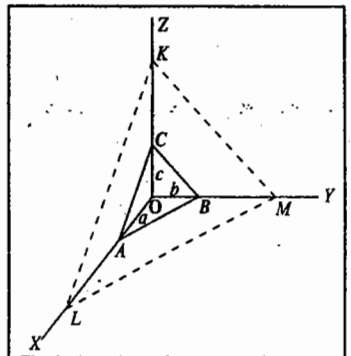

Fig. 9. Crystallographic axes and the law of rational indices.

Miller Indices. Miller indices are a set of integers (*h*, *k*, *l*) which are used to describe a given plane in a crystal. The miller indices of a face of a crystal are inversely proportional to the intercepts of that face on the various axes. The procedure for determining the Miller indices for a plane is as follows :

1. Prepare a three-column table with the unit cell axes at the tops of the columns.
2. Enter in each column the intercept (expressed as a multiple of *a*, *b* or *c*) of the plane with these axes.
3. Invert all numbers.
4. Clear fractions to obtain *h*, *k* and *l*.

Example 11. Calculate the Miller indices of crystal planes which cut through the crystal axes at *(i)* (2*a*, 3*b*, *c*) *(ii)* (*a*, *b*, *c*) *(iii)* (6*a*, 3*b*, 3*c*) and *(iv)* (2*a*, – 3*b*, – 3*c*).

Solution : Following the procedure given above, we prepare the table as follows :

(i)	*a*	*b*	*c*		*(ii)*	*a*	*b*	*c*	
	2	3	1	intercepts		1	1	1	intercepts
	1/2	1/3	1	reciprocals		1	1	1	reciprocals
	3	2	6	clear fractions		1	1	1	clear fractions

Hence, **the Miller Indices are (326).** Hence, **the Miller indices are (111).**

(iii)	*a*	*b*	*c*		*(iv)*	*a*	*b*	*c*	
	6	3	3	intercepts		2	– 3	– 3	intercepts
	1/6	1/3	1/3	reciprocals		1/2	–1/3	–1/3	reciprocals
	1	2	2	clear fractions		3	– 2	– 2	clear fractions

Hence, **the Miller indices are (122).** Hence, **the Miller indices are $(3\bar{2}\bar{2})$**

Note. The negative sign in the Miller indices is indicated by placing a bar on the integer. The Miller indices are enclosed within parentheses.

Interplanar Spacing in a Crystal System. It can be shown that in a crystal, the interplanar distance d_{hkl} is given by

$$1/(d_{hkl})^2 = (h/a)^2 + (k/b)^2 + (l/c)^2 \qquad ...(12)$$

where *h*, *k*, *l* are the Miller indices of the planes and *a*, *b*, *c* are the dimensions of the cell.

For a *cubic system*, $a = b = c$ so that from Eq. 12,

$$d_{hkl} = a/[h^2 + k^2 + l^2]^{1/2} \qquad ...(13)$$

For a *tetragonal system*, $a = b \neq c$ so that

$$1/(d_{hkl})^2 = (h^2 + k^2)/a^2 + l^2/c^2 \qquad ...(14)$$

For an *orthorhombic system*, $a \neq b \neq c$ so that

$$1/(d_{hkl})^2 = h^2/a^2 + k^2/b^2 + l^2/c^2 \qquad ...(15)$$

Example 12. The parameters of an orthorhombic unit cell are a=50 pm, b=100 pm, c=150 pm. Determine the spacing between the (123) planes.

Solution : For an orthorhombic unit cell, the interplanar distance, d_{hkl}, is given by

$$1/(d_{hkl})^2 = (h^2/a^2) + (k^2/b^2) + (l^2/c^2) \qquad ...(\text{Eq. } 15)$$

$$1/(d_{hkl})^2 = 1/(d_{123})^2 = (1/50 \text{ pm})^2 + (2/100 \text{ pm})^2 + (3/150 \text{ pm})^2 = 3(1/50 \text{ pm})^2$$

$$1/d_{123} = \sqrt{3}/50\text{pm} \text{ so that } d_{123} = 50\text{pm}/\sqrt{3} = \mathbf{29\ pm}$$

Example 13. The density of Li metal is 0·53 g cm^{-3} and the separation of the (100) planes of the metal is 350 pm. Determine whether the lattice is f.c.c. or b.c.c. M(Li)=6·941 g mol^{-1}.

Solution : Density, $\rho = 0{\cdot}53 \text{ g cm}^{-3} = 530 \text{ kg m}^{-3}$

For the cubic system, $d_{hkl} = a/[h^2 + k^2 + l^2]^{1/2}$

$$\therefore \quad d_{100} = \frac{a}{\sqrt{1^2+0^2+0^2}} = 350 \text{ pm} = 350\times10^{-12} \text{ m}$$

We know from Eq. 1, that

$$\rho = nM/(N_A V) = nM/(N_A a^3) \qquad (\because V = a^3)$$

$$\therefore \quad n = \frac{\rho N_A a^3}{M} = \frac{(530\,\text{kg m}^{-3})(6{\cdot}022\times10^{23}\,\text{mol}^{-1})(350\times10^{-12}\text{m})^3}{6{\cdot}941\times10^{-3}\,\text{kg mol}^{-1}} = 1{\cdot}97 \approx 2$$

As shown in Example 3, for an f.c.c. lattice, n=4 and for a b.c.c. lattice, n=2. Hence, lithium has a *b.c.c. lattice.*

X-RAY DIFFRACTION

The German physicist M. von Laue (1879–1960), in 1913, suggested the possibility of diffraction of X-rays by crystals. The reason for this suggestion was that the wave length of X-rays was of about the same order as the interatomic distances in a crystal. von Laue was awarded the 1914 Physics Nobel Prize for his discovery of diffraction of X-rays by crystals. In fact, W.H. Bragg succeeded in diffracting X-rays from sodium chloride crystal. This observation has proved to be highly useful in determining structures and dimensions of crystals as well as in the study of a number of properties of X-ray themselves.

The Bragg Equation. Bragg pointed out that unlike reflection of ordinary light, the reflection of X-rays can take place only at certain angles which are determined by the wave length of the X-rays and the distance between the planes in the crystal. The fundamental equation which gives a simple relation between the wave length of the X-rays, the interplanar distance in the crystal and the angle of reflection, is known as the Bragg equation.

Derivation of the Bragg Equation. Consider Fig. 10. The horizontal lines in this figure represent parallel planes in the crystal structure separated from one another by the distance d. Suppose a beam of X-rays falls on the crystal at glancing angle θ, as shown. Some of these rays will be reflected from the upper plane at the same angle θ while some others will

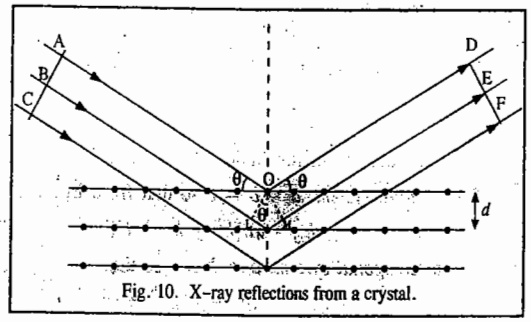

Fig. 10. X-ray reflections from a crystal.

be absorbed and get reflected from the successive layers, as shown. Let the planes ABC and DEF be drawn perpendicular to the incident and reflected beams, respectively. The waves reflected by different layer planes will be in phase with one another (i.e., will coincide with one another in the plane DEF) only if the difference in the path lengths of the waves reflected from the successive planes is equal to an integral number of wave lengths. Drawing OL and OM perpendicular to the incident and reflected beams, it will be seen that the difference in the path lengths (say, δ) of the waves reflected from the first two planes is given by

$$\delta = LN + NM \qquad ...(16)$$

This should be equal to a whole number multiple of wave length λ, *i.e.*,

$$LN + NM = n\lambda \qquad ...(17)$$

Since the triangles OLN and OMN are congruent, hence LN = NM.

$$\therefore \quad 2LN = n\lambda \text{ or } 2d\sin\theta = n\lambda \qquad ...(18)$$

This is the Bragg equation. Knowing θ, n and λ, d can be calculated.

For a given set of lattice planes, d has a fixed value. Therefore, the possibility of getting maximum reflection (*i.e.*, the possibility of getting reflected waves in phase with one another) depends upon θ. If θ is increased gradually, a number of positions will be found at which the reflections will be maximum. At these positions, n will have values equal to 1, 2, 3, 4, 5, etc. Generally, in experiments on X-ray reflections, n is set as equal to 1. If λ is known, it is possible to determine d, the distance between atomic planes in the crystal by determining θ experimentally. On the other hand, if d is known, λ can be evaluated.

Experimental Methods. The X-ray diffraction techniques used in the study of crystals are of two types known as the rotating crystal technique and the powder technique. Both the techniques make use of the X-ray diffractometer, the setting of which for the former technique is shown in Fig. 11.

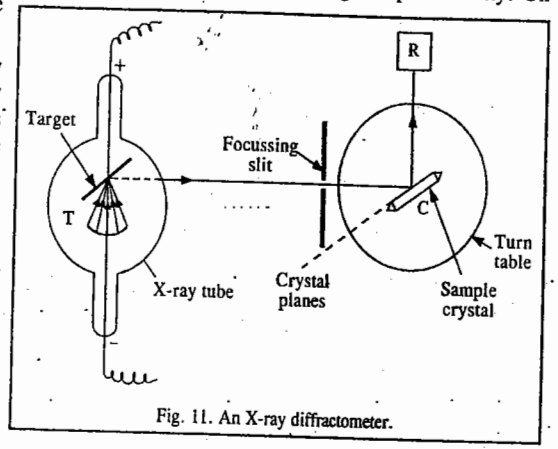

Fig. 11. An X-ray diffractometer.

X-rays generated in the tube T are passed through a slit so as to obtain a narrow beam which is then allowed to strike a single crystal C mounted on the turn-table. The crystal is rotated gradually by means of the turn-table so as to increase the glancing angle at which the X-rays are incident at the exposed face of the crystal. The intensities of the reflected rays are measured on a recording device R, such as a photographic plate or an ionisation chamber. The angles for which reflections are maximum give the value of θ. The process is carried out for each plane of the crystal. The lowest angle at which the maximum reflection occurs corresponds to n=1. This is called the first order reflection. The next higher angle at which the maximum reflection occurs again, corresponds to n=2. This is the second order reflection, and so on.

The values of θ for the first order reflection from the three faces of sodium chloride crystal are found to be 5·9°, 8·4° and 5·2°, respectively. Applying the Bragg equation and knowing that n and λ are the same in each case, the distance d between successive planes in the three faces will be in the ratio of

$$1/\sin 5{\cdot}9° : 1/\sin 8{\cdot}4° : 1/\sin 5{\cdot}2° = 9{\cdot}61 : 6{\cdot}84 : 11{\cdot}04 = 1{\cdot}00 : 0{\cdot}70 : 1{\cdot}14$$

This ratio is very close to that expected to exist between spacings along the three planes of a face-centred cube. Thus, *sodium chloride has face-centred cubic structure.*

Powder Method : The Debye-Scherrer Method. The powder method is more widely used particularly for crystals with simple structures. The powder, in fact, consists of many small crystals which are oriented in all possible directions. As a result of this, X-rays are scattered from all sets of planes (*e.g.*, 100, 110, etc.). The scattered rays are detected by using an X-ray-sensitive film. The principle of the method is illustrated in Fig. 12. The substance to be examined is finely powdered and is kept in the form of a cylinder inside a thin glass tube. A narrow beam of X-rays is allowed to fall on the powder. The diffracted X-rays strike a strip of photographic film arranged in the form of a circular arc, as shown in the figure.

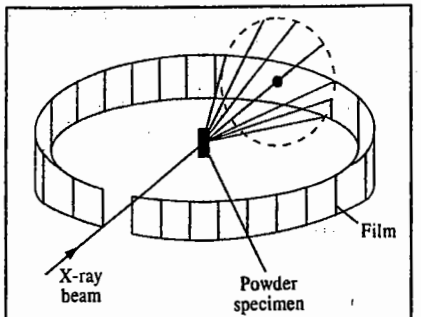

Fig. 12. The powder method for X-ray diffraction.

In this method, no rotation is necessary since the powder sample already contains microcrystals arranged in all possible orientations. Hence, a large number of them will have their lattice planes in correct positions for maximum X-ray reflection to occur. As a result of this we get lighted areas in the form of arcs of lines at different distances from the incident beam, as shown. These distances can be converted into scattering angles to be used in the Bragg equation for different planes of the crystal.

The British physicists W.H. Bragg (1862–1942) and his son W.L. Bragg (1890–1971) shared the 1915 Physics Nobel Prize for the analysis of crystal structure with X-rays. W.L. Bragg became at 25 the youngest Nobel Laureate in history. The Bragg equation is named after both the father and the son.

Example 14. KNO_3 crystallizes in orthorhombic system with the unit cell dimensions a=542 pm, b=917 pm and c=645 pm. Calculate the diffraction angles for first order X-ray reflections from (100), (010) and (111) planes using radiation with wave length=154·1 pm.

Solution : $2d_{hkl} \sin\theta = n\lambda$

For an orthorhombic system, we have

$$1/(d_{hkl})^2 = (h/a)^2 + (k/b)^2 + (l/c)^2 \qquad \text{...(Eq. 15)}$$

$$\therefore \quad 1/(d_{100})^2 = (1/542\ \text{pm})^2 + (0/917\ \text{pm})^2 + (0/645\ \text{pm})^2 = (1/542\ \text{pm})^2$$

$$\therefore \quad d_{100} = a = 542\ \text{pm}$$

Similarly, $d_{010} = b = 917$ pm and $d_{111} = c = 378$ pm

For first order reflection, $n = 1$. Also $\lambda = 154{\cdot}1$ pm

$$\therefore \quad \sin\theta_{100} = \frac{\lambda}{2d_{100}} = \frac{154{\cdot}1\ \text{pm}}{2 \times 542\ \text{pm}} = 0{\cdot}142 \qquad \text{whence} \quad \theta_{100} = 8°10'$$

$$\sin\theta_{010} = \frac{\lambda}{2d_{010}} = \frac{154{\cdot}1\ \text{pm}}{2 \times 917\ \text{pm}} = 0{\cdot}084 \qquad \text{whence} \quad \theta_{010} = 4°\ 49'$$

$$\sin\theta_{111} = \frac{\lambda}{2d_{111}} = \frac{154{\cdot}1\ \text{pm}}{2 \times 378\ \text{pm}} = 0{\cdot}204 \qquad \text{whence} \quad \theta_{111} = 11°\ 46'$$

Example 15. $HgCl_2$ crystallizes in orthorhombic system. Using radiation with λ=154 pm, the (100), (010) and (001) reflections (first order) from $HgCl_2$ in an X-ray diffractometer occur at 7° 25′, 3° 28′ and 10° 23′, respectively. If the density of the crystal is 5·42 g cm^{-3}, calculate the dimensions of the unit cell and the number of $HgCl_2$ molecules in the unit cell. $M(HgCl_2)$=271·5 g mol^{-1}.

Solution : **Dimensions of the unit cell :** For first order reflections, n=1. Hence,

$$2\,d_{hkl} \sin\theta_{hkl} = \lambda \quad \text{so that} \quad d_{hkl} = \lambda/2 \sin\theta_{hkl}$$

For the orthorhombic system,

$$1/(d_{hkl})^2 = (h/a)^2 + (k/b)^2 + (l/c)^2$$

$$1/(d_{100})^2 = (1/a)^2 + (0/b)^2 + (0/c)^2 = 1/a^2$$

$$\therefore \quad d_{100} = a = \lambda/2\sin\theta_{100} = 154\ \text{pm}/2\sin(7°\ 25') = \mathbf{597\ pm}$$

Similarly, $d_{010} = b = 154\ \text{pm}/2 \sin 3°\ 28' = \mathbf{1270\ pm}$

$d_{001} = c = 154\ \text{pm}/2 \sin 10°13' = \mathbf{434\ pm}$

Number of molecules in unit cell : The volume of the unit cell,

$$V = abc = 597 \times 1270 \times 434\ \text{pm}^3 = 3{\cdot}29 \times 10^{-28}\ \text{m}^3$$

$$\therefore \quad \rho = \frac{nM}{VN_A} = \frac{(n)(271{\cdot}5\,\text{g mol}^{-1})}{(3{\cdot}29 \times 10^{-28}\,\text{m}^3)(6{\cdot}022 \times 10^{23}\,\text{mol}^{-1})}$$

$$= 1{\cdot}37\ n \times 10^6\ \text{g m}^{-3} = 1{\cdot}37\ n \times 10^3\ \text{kg m}^{-3}$$

ρ (given) = 5·42 g cm^{-3} = 5420 kg m^{-3}

$$\therefore \quad n = 5420\ \text{kg m}^{-3}/1{\cdot}37 \times 10^3\ \text{kg m}^{-3} = 3{\cdot}97 \approx 4$$

Since n=4, hence there are **4 molecules of $HgCl_2$ per unit cell.**

Example 16. Calculate the angle at which (*a*) first order reflection and (*b*) second order reflection will occur in an X-ray spectrometer when X-rays of wave length 1·54 Å are diffracted by the atoms of a crystal, given that the interplanar distance is 4·04 Å.

Solution : *(a)* For first order reflection (n=1), the Bragg equation is $2d \sin\theta = \lambda$

$$\therefore \quad \theta = \sin^{-1}(\lambda/2d) = \sin^{-1}(1{\cdot}54\ \text{Å}/8{\cdot}08\ \text{Å}) = \sin^{-1}(0{\cdot}191) = \mathbf{10°\ 59'}$$

(b) For second order reflection (n = 2), the Bragg equation is $2d \sin\theta = 2\lambda$

$$\therefore \quad \theta = \sin^{-1}(\lambda/d) = \sin^{-1}(1{\cdot}54/4{\cdot}04) = \sin^{-1}(0{\cdot}381) = \mathbf{22°\ 24'}$$

Example 17. The density of LiF is 2·601 g cm^{-3}. The (111) first order reflection in the X-ray diffraction from LiF occurs at 8°44′ when X-rays of wave length 70·8 pm are used. If there are four LiF molecules per unit cell, calculate Avogadro's number. LiF crystallizes in the cubic system. Li=6·939, F=18·998.

Solution : $2d_{hkl} \sin\theta_{hkl} = n\lambda$; n=1 for first order reflection

$$\therefore \quad d_{111} = \frac{\lambda}{2\sin\theta_{111}} = \frac{70{\cdot}8\,\text{pm}}{2\sin(8°44')} = 233\ \text{pm}$$

Also, for the cubic system,

$$d_{hkl} = a/[h^2 + k^2 + l^2]^{1/2}$$

$$\therefore \quad d_{111} = a/[1^2 + 1^2 + 1^2]^{1/2} = a/\sqrt{3} \quad \text{so that} \quad a = \sqrt{3}\ d_{111}$$

Thus, $a = \sqrt{3} \times 233\ \text{pm} = 40{\cdot}356\ \text{pm} = 403{\cdot}56 \times 10^{-12}\ \text{m}$

Density, $\rho = M/V = 2{\cdot}601\ \text{g cm}^{-3}$ (given) = 2,601 kg m^{-3}

Since there are four LiF molecules in the unit cell, hence,

$$M = 4\ (25{\cdot}937\ \text{g mol}^{-1}) = 103{\cdot}748\ \text{g mol}^{-1} = 103{\cdot}748 \times 10^{-3}\ \text{kg mol}^{-1}$$

$$V = N_A a^3 = M/\rho$$

$$\therefore \quad N_A = \frac{M}{\rho\, a^3} = \frac{103{\cdot}748 \times 10^{-3}\,\text{kg mol}^{-1}}{(2{,}601\,\text{kg m}^{-3})(403{\cdot}56 \times 10^{-12}\,\text{m})^3} = \mathbf{6{\cdot}49 \times 10^{23}\ mol^{-1}}$$

This value compares very well with the accepted value of $6{\cdot}022 \times 10^{23}$ mol^{-1}.

X-Ray Diffraction Patterns of a Cubic System

It is of particular importance to discuss the X-ray diffraction patterns of a cubic system. We know that for a cubic system, the interplanar distance d_{hkl} is given by

$$d_{hkl} = a/(h^2 + k^2 + l^2)^{1/2} \quad ...(19)$$

Combining this result with the Bragg equation, *viz.*, $\lambda = 2d_{hkl} \sin \theta_{hkl}$, we get

$$\lambda = \frac{2a \sin \theta_{hkl}}{(h^2 + k^2 + l^2)^{1/2}} \quad ...(20)$$

$$\therefore \quad \sin^2 \theta_{hkl} = (\lambda^2/4a^2)\,(h^2 + k^2 + l^2) = K(h^2 + k^2 + l^2) \quad ...(21)$$

where $K=\lambda^2/4a^2$. K has a constant value for a given cubic crystal and a given wave length λ.

We can use Eq. 21 for predicting the diffraction patterns of the three types of lattices of the cubic system, as illustrated below.

1. Primitive Cubic Lattice. Using Eqs. 19 and 21 and integral values (0, 1, 2,...) for the Miller indices h, k, and l, we construct Table 3. It may be noted that since the integer 7 cannot be written in the form $h^2+k^2+l^2$, hence, $\sin^2 \theta$ cannot be equal to $7K$. The diffraction lines will be observed at angles shown in Table 3. The diffraction pattern for a primitive cubic lattice will thus consist of a set of equally spaced six lines followed by an extinction (*i.e.*, a gap) and then another series of six lines.

TABLE 3

Interplanar distances and angles ($\sin^2 \theta_{hkl}$ values) for which diffraction lines are observed for a primitive cubic lattice

hkl	100	110	111	200	210	211	220	300 221	310	311	222	320
d_{hkl}	a	$\frac{a}{\sqrt{2}}$	$\frac{a}{\sqrt{3}}$	$\frac{a}{\sqrt{4}}$	$\frac{a}{\sqrt{5}}$	$\frac{a}{\sqrt{6}}$	$\frac{a}{\sqrt{8}}$	$\frac{a}{\sqrt{9}}$	$\frac{a}{\sqrt{10}}$	$\frac{a}{\sqrt{11}}$	$\frac{a}{\sqrt{12}}$	$\frac{a}{\sqrt{13}}$
$\sin^2 \theta_{hkl}$	K	$2K$	$3K$	$4K$	$5K$	$6K$	$8K$	$9K$	$10K$	$11K$	$12K$	$13K$

2. Body-Centered Cubic Lattice. Using Eqs. 19 and 20 and integral values (0, 1, 2,....) for h, k and l, we construct Table 4. We see that all diffraction lines for which $(h+k+l)$ is an odd integer, are absent. We observe lines at angles shown in Table 4.

TABLE 4

Interplanar distances and angles ($\sin^2 \theta_{hkl}$ values) for which diffraction lines are observed for a body-centred cubic lattice

hkl	100	110	111	200	210	211	220	300 221	310	311	222	320
d_{hkl}		$\frac{a}{\sqrt{2}}$		$\frac{a}{\sqrt{4}}$		$\frac{a}{\sqrt{6}}$	$\frac{a}{\sqrt{8}}$		$\frac{a}{\sqrt{10}}$		$\frac{a}{\sqrt{12}}$	
$\sin^2 \theta_{hkl}$		$2K$		$4K$		$6K$	$8K$		$10K$		$12K$	

3. Face-Centred Cubic Lattice. Proceeding as above, we construct Table 5. We see that the diffraction lines are observed only from those planes for which the values of h, k and l are either all odd or all even. We observe diffraction lines at angles shown in Table 5.

TABLE 5

Interplanar distances and angles ($\sin^2 \theta_{hkl}$ values) for which diffraction lines are observed for a face-centred cubic lattice

hkl	100	110	111	200	210	211	220	300 221	310	311	222
d_{hkl}			$\frac{a}{\sqrt{3}}$	$\frac{a}{\sqrt{4}}$			$\frac{a}{\sqrt{8}}$			$\frac{a}{\sqrt{11}}$	$\frac{a}{\sqrt{12}}$
$\sin^2 \theta_{hkl}$			$3K$	$4K$			$8K$			$11K$	$12K$

The X-ray diffraction patterns for the three types of cubic lattices are collectively shown in Fig. 13.

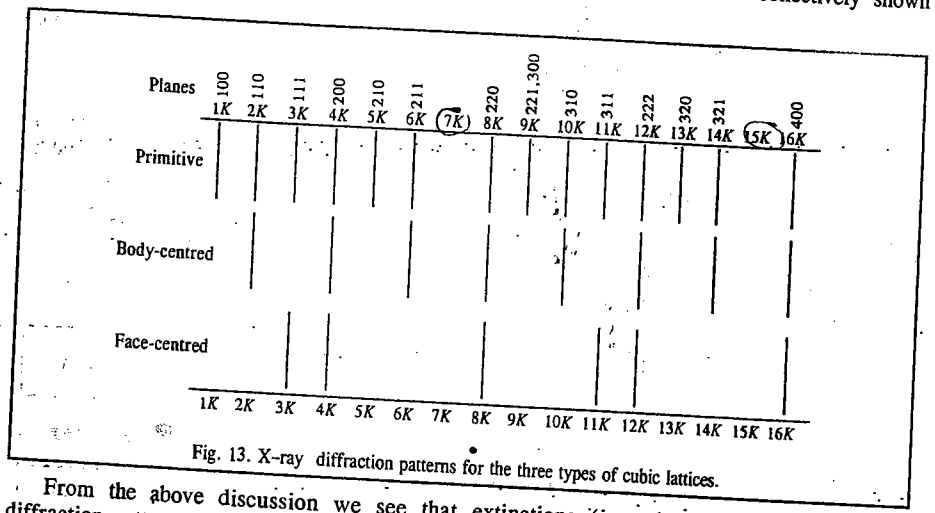

Fig. 13. X-ray diffraction patterns for the three types of cubic lattices.

From the above discussion we see that extinctions (*i.e.*, missing reflections) in the diffraction patterns can help in distinguishing between the three types of cubic lattices. In the X-ray diffraction studies, the crystallographer searches for the missing reflections. It should be noted that whereas the spacing between the lines of a primitive cubic system is equal to K (with a gap after the 6th, 14th and 22nd, etc., lines) the spacing between lines of a body-centred cubic system is equal to $2K$. Thus, the number of lines obtained in the diffraction pattern can help in distinguishing between these two systems. After the identification of the diffraction pattern, it is possible to assign each line with the correct values of the Miller indices h, k and l. From the measurement of any one of these lines, we can determine the value of a, the length of the edge of the cube, by using the equation

$$a = (\lambda/2 \sin \theta_{hkl})\,(h^2 + k^2 + l^2)^{1/2} \quad ...(22)$$

If the lines are indexed correctly, the same value of a is obtained from all the values of $\sin \theta_{hkl}$.

X-ray Diffraction Pattern for Tungsten Crystal. The X-ray diffraction pattern for tungsten crystal is shown in Fig. 14.

We notice that there is variation in intensity of the diffracted X-ray beam for different sets of hkl planes. This is presumably due to the variation of density of atoms in these

planes. The planes having high atomic density give rise to a better X-ray diffraction thereby producing a more intense diffracted beam.

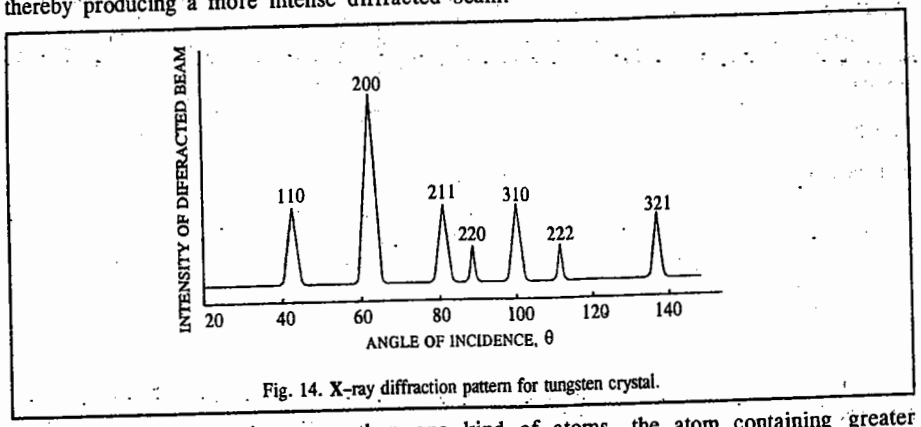

Fig. 14. X-ray diffraction pattern for tungsten crystal.

If the crystal contains more than one kind of atoms, the atom containing greater number of electrons scatters the X-rays to a greater extent. It is found that the *scattering power of an atom is directly proportional to the number of electrons* in the atom. Thus, when the unit cell of a crystal contains hydrogen atoms and other heavier atoms, the scattering effect of hydrogen atoms is overshadowed by that of the other atoms which contain larger number of electrons. Hence, *the positions of hydrogen atoms in the unit cell of a crystal cannot be determined from the X-ray diffraction pattern.* Their positions can be determined by *neutron diffraction.* We shall discuss this aspect a little later in this chapter.

Example 18. The X-ray diffraction pattern of silver, known to crystallize in the cubic system, was obtained using X-rays with wave length 154·1 pm. The first six lines occurred at the following angles : 19·08°, 22·17°, 32·26°, 38·74°, 40·82° and 49·00°. *(a)* Determine the type of the cubic system, *(b)* Calculate the length of the edge of the cube, *(c)* Calculate the interplanar distance of the plane (111).

Solution : *(a)* From Eq. 21, $\sin^2\theta_{hkl} = K(h^2 + k^2 + l^2)$ where $K = \lambda^2/4a^2$,

We construct the following table with $K = 0{\cdot}0356$:

θ	19·08°	22·17°	32·26°	38·74°	40·82°	49·00°
sin θ	0·3268	0·3773	0·5338	0·6257	0·6536	0·7547
$\sin^2\theta$	0·1067	0·1424	0·2848	0·3915	0·4272	0·5696
	3K	4K	8K	11K	12K	16K

Comparing this pattern with that given in Fig. 13, we see that silver crystallizes in face-centred cubic system.

(b) From Eq. 22, $a = \dfrac{\lambda}{2\sin\theta_{hkl}}(h^2 + k^2 + l^2)^{1/2}$

The reflection at 19·08° is due to the (111) plane.

$$\therefore \quad a = \frac{154{\cdot}1\text{ pm}}{2\times 0{\cdot}3268}(1^2 + 1^2 + 1^2)^{1/2} = 408{\cdot}6\text{ pm}$$

(c) From Eq. 13, $d_{hkl} = a/(h^2 + k^2 + l^2)^{1/2}$

$$d_{111} = 408{\cdot}6\text{ pm}/(1^2 + 1^2 + 1^2)^{1/2} = 408{\cdot}6\text{ pm}/\sqrt{3} = 235{\cdot}9\text{ pm}$$

Example 19. AgCl has a face-centred cubic unit cell whereas CsCl has a body-centred unit cell. Determine which of the following Miller indices are permitted in the X-ray diffraction pattern of *(a)* AgCl and *(b)* CsCl : 100, 010, 001, 200, 020, 002, 110, 101, 011, 120, 102, 012, 210, 201, 021, 220, 202, 022, 111, 222, 221, 212, 122, 211, 121, 112.

Solution : *(a)* AgCl has a f.c.c. unit cell. So, the only allowed reflections are those in which all indices are even or all are odd, giving Miller indices 200, 020, 002, 220, 202, 022, 111 and 222. Since $a=b=c$, 200=020=002 and 220=202=022 so that only four peaks will be observed corresponding to 200, 220, 111 and 222.

(b) CsCl has a b.c.c. unit cell. So, the only allowed reflections are those in which $h+k+l=$ even, giving 200=020=002 ; 110=101=011 ; 220=202=022 and 211=121=112.

Fourier Synthesis of Electron Density in a Crystal

Since X-rays are scattered by the electrons in a crystal, the ultimate goal of X-ray crystallography is to determine the electron density $\rho(xyz)$ as a function of the coordinates x, y, z. Since the number of electrons and the size of the atomic orbitals both vary from atom to atom, different atoms have different scattering efficiencies. The ***scattering factor f*** of an atom is defined as

$$f = 4\pi\int_0^\infty \rho(r)\frac{\sin kr}{kr}r^2dr \qquad ...(23)$$

where $\rho(r)$ is the spherically symmetric electron density (number of electrons per unit volume) of the atom and $k = (4\pi/\lambda)\sin\theta$ where λ is the wave length of the X-rays and θ is the scattering angle. Since the wave length of the X-rays used for recording the X-ray diffraction pattern is of the size of an atom, the scattered waves from different regions of an atom interfere constructively. The integral in Eq. 23 takes this interference into account through the factor $(\sin kr)/kr$. Before proceeding further we shall prove an important result that the scattering factor of an atom in the direction $\theta \to 0$ is equal to the number of electrons (N_e) in the atom, *i.e.*,

$$\lim_{\theta\to 0} f = N_e \qquad ...(24)$$

Here $\theta \to 0$ implies that the X-rays pass straight through the atom. If $\theta = 0$, then $k = 0$ and the term $(\sin kr)/kr$ in Eq. 23 is indeterminate. Hence, to evaluate the integrand, we evaluate the $\lim_{kr\to 0}(\sin kr)/kr$.

We know from the result of the power series that

$$\lim_{\theta\to 0}\frac{\sin\theta}{\theta} = \lim_{\theta\to 0}\frac{\theta - \frac{\theta^3}{3!} + \frac{\theta^5}{5!} - \cdots}{\theta} \qquad ...(25)$$

$$\approx 1 - \frac{\theta^3}{3!} + \frac{\theta^4}{4!} - \cdots \approx 1 \qquad ...(26)$$

Hence, $\lim_{kr\to 0}(\sin kr)/kr = 1$ so that

$$f = 4\pi\int_0^\infty \rho(r)r^2dr = N_e \qquad ...(27)$$

since the integrand is the product of the electron density and the spherical volume element $4\pi r^2dr$, which upon integration yields the total number of electrons in the atom.

Let us now return to the electron density $\rho(xyz)$ which is so defined that $\rho(xyz)dxdydz$ is the number of electrons in the volume element $dxdydz$. Since the electron density is a periodic function, it can be expanded by a Fourier series :

$$\rho(xyz) = \frac{1}{V}\sum_{h=-\infty}^{\infty}\sum_{k=-\infty}^{\infty}\sum_{l=-\infty}^{\infty}F(hkl)\exp\left[-2\pi i\left(\frac{hx}{a} + \frac{ky}{b} + \frac{lz}{c}\right)\right] \qquad ...(28)$$

where V is the volume of the unit cell ; x, y, z are the coordinates of a point in the unit cell ; a, b, c are the unit cell dimensions ; (hkl) are the Miller indices and $F(hkl)$ are the Fourier coefficients which are also referred to as the **structure factors**. Each structure factor is associated with a particular reflection from the (hkl) planes. Though the triple summation in Eq. 28 is over all the values ($-\infty$ to $+\infty$) of h, k, l, in practice all the terms need not be included in the summation although the more the terms included, the higher is the resolution of $\rho(xyz)$. The structure factors contain all the information about all the atoms in a unit cell. The structure factor $F(hkl)$ is defined as

$$F(hkl) = \sum_j f_j \exp\left[2\pi i\left(\frac{hx_j}{a} + \frac{ky_j}{b} + \frac{lz_j}{c}\right)\right] \qquad ...(29)$$

where f_j is the scattering factor of the jth atom in the unit cell and the summation is over all the atoms in the unit cell. To account for the above expression for $F(hkl)$, we recall that when the Bragg law is satisfied for a given reflection, the amplitude of the wavelet scattered from an atom in one unit cell of the crystal is in phase with the amplitudes of the scattered wavelets from the corresponding atoms in the millions of the other unit cells of the crystal. However, the wavelet scatterred by one atom may, in general, not be in phase with the wavelet scattered by another atom within the same unit cell with the result that the intensity $I(hkl)$ of reflection will depend upon the extent to which amplitudes of the wavelets reflected from different atoms (denoted by f_j) are in phase with one another. It is known that

$$I(hkl) \propto |F(hkl)|^2 \qquad ...(30)$$

i.e., the intensities of the X-ray diffraction patterns from the (hkl) planes of the crystal are proportional to the square of the modulus (absolute value) of $F(hkl)$. $I(hkl)$ can be determined from the densities of spots on the photographic film. From the values of $I(hkl)$, $|F(hkl)|^2$ can be determined. But the crystallographer needs $F(hkl)$ rather than $|F(hkl)|^2$ to calculate $\rho(xyz)$ with the help of Eq. 28. Since $F(hkl)$ is a complex number, we can write

$$F(hkl) = A(hkl) + iB(hkl) \qquad ...(31)$$

Hence,
$$|F(hkl)|^2 = [A(hkl) + iB(hkl)]\,[A(hkl) - iB(hkl)]$$
$$= [A(hkl)]^2 - [B(hkl)]^2 \qquad ...(32)$$

Since the values of $A(hkl)$ and $B(hkl)$ are not obtained directly, indirect methods are employed to determine these quantities for the evaluation of $F(hkl)$. For a centrosymmetric crystal, $F(hkl)$ is of the form

$$F(hkl) = \pm f_{heavy} \pm f_{light} \qquad ...(33)$$

where f_{heavy} are the scattering factors of the heavy atoms and f_{light} are the scattering factors of the light atoms. The f_{light} are much smaller than f_{heavy} and their phases are almost random if the atoms are distributed throughout the unit cell. Thus, the heavy atoms dominate scattering since their scattering factors are of the order of their atomic numbers. Since the net result of f_{light} changes $F(hkl)$ only slightly, it follows that $F(hkl)$ will have the same sign as that calculated from the location of the heavy atoms. This phase is then combined with the observed $|F(hkl)|$ obtained from the observed value of $I(hkl)$ to perform the Fourier synthesis of the entire electron density in the unit cell thereby enabling the location of both the heavy and the light atoms. This is how the **phase problem** in crystallography is solved.

Patterson Synthesis. This technique is employed for determining relative orientations of pairs of atoms in a given crystal structure. The technique makes use of the Patterson equation, *viz.*,

$$P(\vec{r}) = \frac{1}{V}\sum_{h=-\infty}^{\infty}\sum_{k=-\infty}^{\infty}\sum_{l=-\infty}^{\infty}|F(hkl)|^2 \exp\left[-2\pi i\left(\frac{hx}{a} + \frac{ky}{b} + \frac{lz}{c}\right)\right] \qquad ...(34)$$

The values of $|F(hkl)|^2$ can be obtained without ambiguity from the value of $I(hkl)$. The Patterson equation is manifested in the form of a map of *vector separation* between the atoms in the unit cell. Thus, if (x_A, y_A, z_A) and (x_B, y_B, z_B) are, respectively, the coordinates of atoms A and B in the unit cell, then there would occur a peak at $(x_A-x_B, y_A-y_B, z_A-z_B)$ and also at $(x_B-x_A, y_B-y_A, z_B-z_A)$ since there is a vector from B to A as well as a vector from A to B. The height of the peak in the map is proportional to the product Z_AZ_B where Z_is are the atomic numbers. Thus, the relative orientation of each pair of atoms in the original structure can be obtained from the Patterson map. This technique was used extensively by the British crystallographer Dorothy Hodgkin (1910–1994) during 1940–1960 to determine the structures of important biochemical substances. She was awarded the 1964 Chemistry Nobel Prize for her work.

More advanced techniques, known as direct methods, were developed in the 1950s by the American crystallographers H. Hauptman and J. Karle for the determination of crystal structures. The discussion of these methods is, however, beyond the scope of the present volume. Hauptman and Karle were awarded the 1985 Chemistry Nobel Prize for their contributions.

Example 20. Calculate the structure factor $F(hkl)$ values for the three types of cubic lattices, *viz.*, the primitive cubic (P), body centred cubic (I) and face-centred cubic (F) and therefrom determine which reflections would be absent from the diffraction pattern. The fractional coordinates (x_j, y_j, z_j) of the atoms in the three types of lattices are :

P : (0, 0, 0) ; I : (0, 0, 0) and (1/2, 1/2, 1/2) and F : (0, 0, 0), (1/2, (1/2, 0), (1/2, 0, 1/2) and (0, 1/2, 1/2)

Solution : This example illustrates the use of the structure factors to distinguish between the three types of cubic lattices.

For the primitive cubic (P) lattice,

$$F(h\ k\ l) = \sum_j f_j \exp\left[2\pi i\left(\frac{hx_j}{a} + \frac{ky_j}{b} + \frac{lz_j}{c}\right)\right]$$
$$= \sum_j f_j \qquad \text{(since } x_j, y_j, z_j \text{ are zero and } e^0=1\text{)}$$

Thus, $F(hkl)$ has the same value for all h, k and l. Hence there would be reflections in the diffraction pattern for all integral values of h, k and l.

For the body-centred cubic (I) lattice,

$$F(h, k, l) = f \exp[2\pi i\,(0 + 0 + 0)] + f \exp[2\pi i\,(h/2 + k/2 + l/2)]$$
$$= f\,[1 + \exp i\pi\,(h+k+l)]$$

Recalling that $e^{i\theta} = \cos\theta + i \sin\theta$ (Euler's relation) with $\theta=\pi$, we have

$$e^{i\pi} = \cos\pi + i \sin\pi = -1$$

Thus, $F(h, k, l) = f\,[1 + (-1)^{h+k+l}]$

If $(h+k+l)$ is even, $F(h,k,l) = 2f$ and if $(h+k+l)$ is odd, $F(hkl) = 0$. Thus, in the X-ray diffraction pattern, reflections such as (110), (200), (211), (310), etc., will be present and reflections such as (100), (111), (210), (300), etc., will be absent.

For the face-centred cubic (F) lattice,

$$F(hkl) = f \exp[2\pi i\,(0+0+0)] + f \exp[2\pi i\,(h/2+k/2+0)] + f \exp[2\pi i\,(h/2+0+h/2)] + f \exp[2\pi i(0 + k/2 + l/2)]$$
$$= f\,[1 + \exp(i\pi\,(h+k)) + \exp(i\pi\,(h+l) + \exp(i\pi\,(k+l)]$$
$$= f\,[1 + (-1)^{h+k} + (-1)^{h+l} + (-1)^{k+l}]$$

If h, k, l are all even or all odd, $F(hkl) = 4f$ and these reflections will be present. If one is even and the other two are odd, or the reverse, then these reflections will be absent.

ELECTRON DIFFRACTION

The wave-particle duality of matter was proposed by the French physicist Louis de Broglie in 1924. According to de Broglie's hypothesis, the wave length λ of electrons moving with velocity v is given by $\lambda=h/(m_eV)$, where m_e is the mass of the electron. Electrons can be accelerated to precisely controlled energies by applying a known potential difference. When accelerated through 10 keV, they acquire a wave length of 12 pm which makes them suitable for molecular diffraction investigations. Electron diffraction studies generally utilize electrons with energies of the order of 40 keV. Since electrons are charged, they are scattered strongly by their interaction with electrons and nuclei of atoms of the sample. Hence, they cannot be used for studying the interiors of solid samples. They can, however, be used *for* studying molecules in the gaseous state held on surfaces and in thin films. The most important application involves the study of electron diffraction by substances in their vapour state at low pressures (of the order of 10^{-5} torr). The strong interaction of electrons with molecules of the sample plus a very great effect on the photographic plate combine to require a very short exposure of the order of tenths of a second.

Whereas the diffraction of X-rays by a crystal depends upon the spacing between the layers, *the diffraction of electrons by gaseous molecules depends upon the distances between the atoms in a molecule.* Since the gaseous molecules are randomly oriented relative to the electron beam, the diffraction pattern, like that of an X-ray powder photograph, consists of concentric rings. There is an appreciable amount of background scatter of the electron beam with the result that diffraction bands are only poorly resolved. New experimental techniques have, however, greatly improved the resolution of the bands.

It is possible to calculate the electron scattering from a pair of nuclei separated by a distance R_{ij} and oriented at a definite angle to the incident beam. The overall diffraction pattern is then calculated by allowing for all possible orientations of this pair of atoms. This procedure amounts to integration over all possible orientations. The final expression obtained for the diffraction intensity is

$$I_{ij}(\theta) = 2f_if_j\{(1 + \sin sR_{ij})/sR_{ij}\} \quad \ldots(35)$$

where $s = -(4\pi/\lambda)\sin(\theta/2)$, λ is the wave length of electron beam and θ is the scattering angle. The quantities f_i and f_j are the scattering factors of the ith and jth atoms. They determine the scattering power of the atoms. If a molecule consists of a number of atoms, the total intensity is given by the Wierl equation, *viz.*,

$$I(s) \propto \sum_{i,j} f_if_j \frac{\sin sR_{ij}}{sR_{ij}} \quad \ldots(36)$$

where the summation is over all the atoms i and j of the molecule. The electron diffraction pattern can be interpreted in terms of the distances between all possible pairs of atoms in the molecule (not simply those bonded together). The Wierl equation does not, unfortunately, allow the direct calculation of the internuclear distances R_{ij} from the measurements of $I(s)$ at various values of s.

The electron diffraction studies are useful for evaluating the bond lengths and bond angles in relatively simple gaseous molecules. As the number of atoms in the molecules increases, one soon reaches the situation where the number of pieces of information available (*viz.*, the spacings of the resolved diffraction rings) is not great enough to evaluate all of the necessary structural parameters. The number of electron diffraction rings observed is usually much less than the number of X-ray diffraction spots observed in the X-ray crystal study. This shows that difficulties lie in the path of structure determination by electron diffraction. In spite of these difficulties, however, many molecular structures have been determined by this method. The accuracy of bond length and bond angles obtained from electron diffraction studies is comparable to that obtained from X-ray diffraction studies for simple molecules.

NEUTRON DIFFRACTION

As dissussed above, diffraction patterns can be obtained by means of electron beams when they are scattered by molecules. Because of their negative charge and hence low penetrating power, the electron beams are generally used for the investigation of surfaces and thin films. Neutrons, on the other hand, have a high penetrating power and are particularly useful for structural studies of solids. Neutron diffraction by crystals was demonstrated as early as in 1936 but the method did not become important until the advent of nuclear piles. Fast neutrons produced in a nuclear pile are slowed down by collisions with a moderator (D_2O or graphite) to produce thermal neutrons, *i.e.*, neutrons for which the range of kinetic energies is determined by the temperature of the surroundings.

The wave length of a neutron beam is related to the neutron mass and velocity by de Broglie relation $\lambda=h/p=h/m_nv$, where m_n is the neutron mass and v its velocity. The spectrum of the neutron beam emerging from a nuclear pile is continuous, the wave lengths covering several Angstroms. A monochromatic beam which is used for neutron crystallography, is obtained by reflection at a flat crystal surface. Wide beams, with cross-sectional areas of a few square centimetres, are used in order to obtain a sufficiently high counting rate in the detector. The large size and high cost of neutron spectrometers combined with the need for a nuclear pile have made neutron diffraction a less popular method in crystallography.

Whereas X-rays are scattered by the orbital electrons, the neutrons are scattered by atomic nuclei. The atomic nuclei contribute nothing to X-ray scattering. Neutron diffraction is caused by two additional factors : (1) *nuclear scattering* due to the interaction of neutrons with the atomic nuclei and (2) *magnetic scattering* due to the interaction of the magnetic moments of neutrons with permanent magnetic moments of atoms or ions. The X-ray scattering power increases fairly regularly with the atomic number but there is no regular trend for neutron scattering. The neutron scattering power does not vary greatly while the X-ray scattering power increases from hydrogen atom to the heavy elements by about three orders of magnitude. In uranium hydride, X-ray diffraction has been used to locate the uranium coordinates and neutron diffraction to locate the hydrogen coordinates.

The differences between neutron and X-ray scattering offer great advantages and equally great disadvantages to neutron crystallography. The major advantage is that light elements such as H or D, which cannot be located by X-ray diffraction, can be located by neutron diffraction because they are comparable in neutron scattering power to heavy elements. The great disadvantage is that the background scatter is likely to be much more serious because different isotopes of the same element, which would be expected to be randomly distributed among the sites for that element, might differ greatly in their scattering power.

Neutrons which possess magnetic moment by virtue of having a spin of 1/2, interact with nuclei which have magnetic moments to produce further background scattering for substances for which the nuclear spins are randomly oriented. The spin-disorder scattering is so great for hydrogen in comparison with the ordered scattering that deuterated compounds are often used for neutron diffraction studies. Paramagnetic substances also contribute to the general background scattering because of the interaction of the magnetic moments of neutrons with the randomly oriented orbital magnetic moments of the electrons. The magnetic moments of neighbouring atoms are oriented in the *same direction in ferromagnetic substances* whereas the magnetic moments of neighbouring atoms are oriented *in opposite directions in antiferromagnetic substances*. Neutron diffraction thus offers a tool for the investigation of the magnetically ordered lattices. Neutron diffraction is reserved for special applications for which it can yield information not obtainable from X-ray diffraction studies. The Canadian physicist B.N. Brockhouse and the American physicist C.G. Shull were awarded the 1994 Physics Nobel Prize for the development of neutron spectroscopy and neutron diffraction techniques.

TYPES OF CRYSTALS

It is convenient to classify solid crystals into the following four types :

1. Molecular crystals in which the units occupying the lattice points are molecules.
2. Covalent crystals in which the units are atoms.
3. Ionic crystals in which the units are positively and negatively charged ions.
4. Metallic crystals in which the units are positive metallic ions surrounded by a 'sea' of electrons.

The main characteristics of the various types of crystals are summed up in Table 6.

TABLE 6
Characteristics of Various Types of Crystals

Characteristics	Molecular crystals	Covalent crystals	Ionic crystals	Metallic crystals
Units that occupy lattice points	Molecules	Atoms	Positive and negative ions	Positive ions in a 'sea' of electrons
Binding force	*(i)* van der Waals *(ii)* Dipole-dipole	Shared electrons	Electrostatic attraction	Electrical attraction between +ive ions and – ive electrons
Physical properties	Very soft Low melting points Good insulators	Very hard Very high melting points Non-conductors	Quite hard and brittle Fairly high melting points Semi-conductors due to crystal imperfections	Hard or soft Moderate to high melting points Good conductors
Examples	NH_3, H_2O, CO_2	Diamond, carborundum, quartz	NaCl, KNO_3 Na_2SO_4	Na,Cu, Fe

Some further description of these crystals is given below.

Molecular Crystals

The lattice points in molecular crystals consist of specific molecules which do not carry any charge. The forces binding the molecules together are of two types : ***(i) Dipole-dipole forces (ii) The van der Waals forces.*** Dipole-dipole forces occur in solids which consist of polar molecules. Thus, in the case of water molecules (in ice or even in liquid state), the negative end of one molecule attracts the positive end of a neighbouring molecule, as shown in Fig. 15.

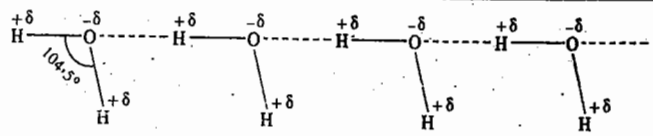

Fig. 15. Dipole-dipole forces of attraction between water molecules.

The van der Waals forces are more general and occur in all kinds of molecular crystals. Both types of molecular forces mentioned above are much weaker than the coulombic forces of attraction between oppositely charged ions existing in ionic crystals. The binding energy in molecular crystals, therefore, is considerably less than in ionic crystals. Accordingly, the heat of vaporisation, *i.e.*, the energy required to separate molecules from one another in a molecular crystal is very low in comparison to the value for ionic or covalent crystals. The molecular crystals are, therefore, more volatile and have lower melting and boiling points.

On account of weak forces binding the molecules together, molecular crystals are usually soft, easily compressible and can be easily distorted. Since no ions or charged particles are present, molecular crystals are bad conductors of electricity in solid, liquid as well as in dissolved state.

Covalent Crystals

The lattice in covalent crystals consists of atoms linked together by a continuous system of covalent bonds. Diamond furnishes a good example of this type. Its structure is represented in Fig. 16.

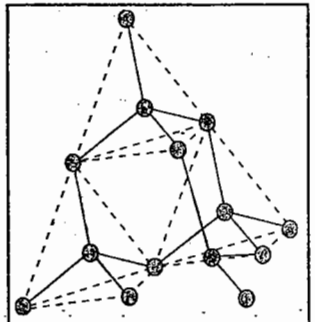

Fig. 16. Structure of diamond.

Each carbon atom is covalently bonded by sharing of electrons to four other atoms involving sp^3 hybrid orbitals. Thus each carbon atom is surrounded by four others at the four corners of a regular tetrahedron. This gives rise to a rigid three-dimensional network. This is the reason why diamond is the hardest substance known, with a high density and melting point. The entire crystal is regarded as one large carbon molecule and is called a *macromolecule.*

In some crystals belonging to this type, the continuous network of covalent bonds is two-dimensional. Graphite offers a very good example. Its structure is represented in Fig. 17. Each carbon atom is covalently bonded to three others involving sp^2 hybrid orbitals instead of four as in diamond. Thus, all atoms in a single plane are linked to give flat hexagons as in benzene, naphthalene, anthracene, etc. The hexagons are held together in sheet-like structures, parallel to one another. The C—C covalent bond distance is 1·42 Å. The distance between the sheets or layers, however, is comparatively large being about 3·35 Å. This rules out the possibility of covalent bonding between the layers. Such crystals in which the various sheets of atoms are separated from one another by a distance larger than the maximum permissible for the formation of chemical bond are said to have **layer lattices.**

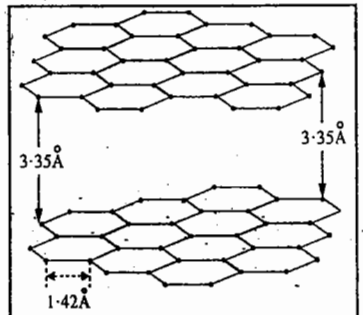

Fig. 17. Structure of graphite.

Since a chemical bond is not possible between carbon atoms in different layers, the fourth valency remains unsatisfied, *i.e.*, some electrons remain free or unpaired. This permits the passage of electricity through graphite making it a good conductor of electricity.

As the cohesive forces between different layers or sheets are relatively feeble, rupture between the various layers can occur easily. Such substances, therefore, are soft. They are used as lubricants because one plane of atoms can readily slip over another.

Ionic Crystals

In ionic crystals, the units occupying lattice points are positive and negative ions. In sodium chloride, for example, the units are Na^+ ions and Cl^- ions. Each ion of a given sign in held by coulombic forces of attraction to all ions of opposite sign. These forces are very strong and, therefore, the amount of energy required to separate ions from one another is very high. Accordingly,

the ionic crystals have the following characteristics :

1. The heats of vaporisation of ionic crystals are high.
2. The vapour pressures of ionic crystals at ordinary temperatures are very low.
3. The melting and boiling points of ionic crystals are very high.
4. Ionic crystals are hard and brittle.
5. Ionic crystals are insulators in the solid state. The reason is that ions are entrapped in fixed places in the crystal lattice and cannot move when electric field is applied. However, when melted, they become good conductors of electricity. This is due to the fact that in the molten state, the well-ordered arrangement of ions in the crystals is destroyed and the ions are in a position to move about in the liquid medium when an electric field is applied.
6. Ionic crystals are soluble in water and also in other polar solvents. They are insoluble or very slightly soluble in non-polar solvents such as benzene and carbon tetrachloride.
7. Ionic solids are good conductors when dissolved in water. The ions held by coulombic forces fall away from one another when dissolved in water or in any other solvent having high dielectric constant. This is in accordance with the Coulomb's law that forces of attraction between oppositely charged particles vary inversely as the dielectric constant.

Characteristic Structures of Ionic Crystals. The ionic model treats a crystal as an assembly of oppositely charged spheres that interact primarily through coulombic forces. If the thermo-dynamic properties of the crystal calculated on the basis of the ionic model agree with experiment, the crystal may be taken as ionic. We shall briefly discuss the characteristic structures which are prototypes of a wide range of ionic crystals

1. The Rock Salt (NaCl) Structure. This structure is based on an f.c.c. array of bulky anions in which the cations occupy all the octahedral holes (Fig. 18). Alternatively, it can also be treated as a structure in which anions occupy all the octahedral holes in an f.c.c. array of cations. It is evident from the diagram that each ion is surrounded by an octahedron of six counter ions. Thus, the coordination number (C.N.) of each type of ion is 6 and the structure is referred to as (6 : 6) coordination. In this notation, the first number in the parenthesis is the coordination number of the cation and the second number is the coordination number of the anion.

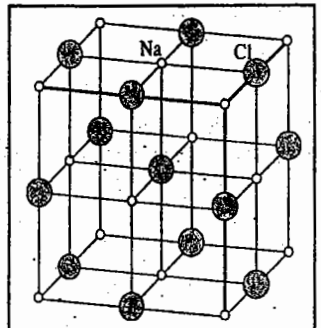

Fig. 18. The rock salt structure.

In order to determine the number of ions of each type in a unit cell, the following rules should be borne in mind :

(*i*) An ion in the body of a unit cell belongs entirely to that unit cell and counts as 1.

(*ii*) An ion in a face is shared by two unit cells and contributes 1/2 to the unit cell in question.

(*iii*) An ion on an edge is shared by four unit cells and thus contributes 1/4.

(*iv*) An ion at a vertex is shared by eight unit cells that share the vertex and so contributes 1/8.

Applying the above rules to the rock salt (NaCl) structure, we find that there are four Na^+ ions and four Cl^- ion so that each unit cell contains four NaCl formula units.

The structure of KCl crystal is similar to that of NaCl crystal.

2. The Cesium Chloride Structure. This structure (Fig. 19) has a cubic unit cell with each vertex occupied by an anion having a cation at the centre of the unit cell (or vice versa). The coordination number for both types of ions is 8 and the structure is referred to as (8 : 8) coordination.

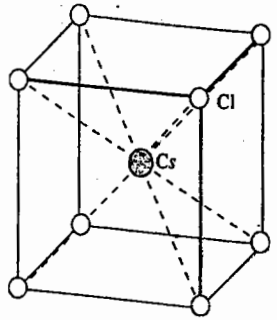

Fig. 19. The cesium chloride structure.

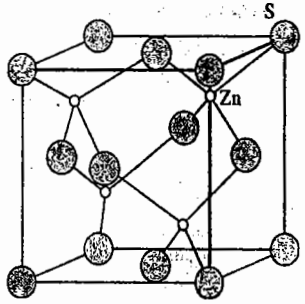

Fig. 20. The sphalerite (zinc blende) structure.

3. The Zinc Blende (Sphalerite) Structure. This structure (Fig. 20), deriving its name from the mineral form of ZnS, is based on an expanded f.c.c. anionic lattice where cations occupy one type of tetrahedral holes. Each anion is surrounded by four neighbours. Thus the structure has (4 : 4) coordination.

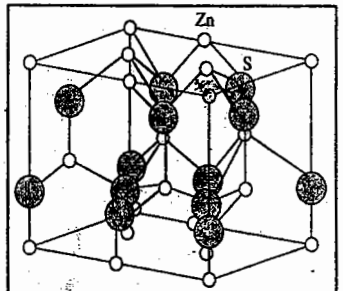

Fig. 21. The wurtzite structure.

4. The Wurtzite Structure. This structure (Fig. 21) differs from the zinc blende structure in being derived from an expanded hexagonally close packed array of anions rather than an f.c.c. array. However, as in the zinc blende structure, the cations occupy one type of tetrahedral holes. The structure, thus, has a (4 : 4) coordination.

5. The Fluorite Structure. This structure (Fig. 22) takes its name from CaF_2. In this structure, the cations occupy half the cubic holes of a primitive cubic array of anions. Alternatively, the anions occupy both types of tetrahedral holes in an expanded f.c.c. lattice of cations. (In the **antifluorite structure**, an example of which is K_2O, the roles of the cations and anions are reversed). In the fluorite structure, the coordination number is 8 for the cations (eight fluoride ions forming a cube about each calcium ion) and 4 for the anions (four Ca^{2+} ions tetrahedrally arranged about each F^- ion). Thus, the fluorite structure has (8 : 4) coordination.

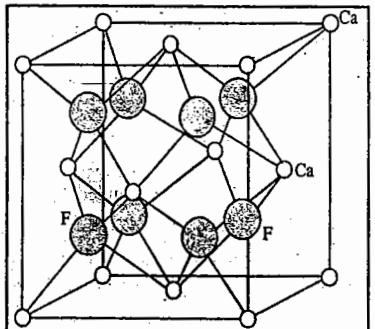

Fig. 22. The fluorite structure.

6. The Rutile Structure. This structure (Fig. 23) takes its name from rutile, the mineral form of titanium (IV) oxide, TiO_2. The coordination numbers are 6 for the cations (six oxide anions arranged approximately octahedrally about the Ti^{4+} ions) and 3 for the anion (three Ti^{4+} ions arranged trigonally about the oxide ions). The rutile structure has, thus, (6 : 3) coordination.

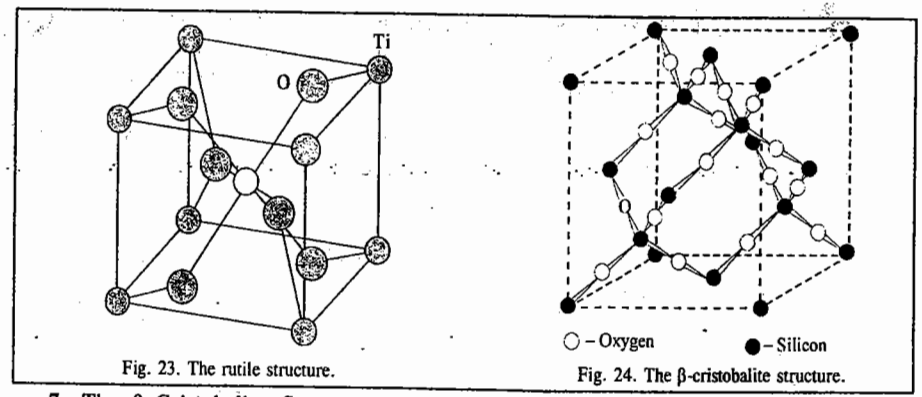

Fig. 23. The rutile structure.

Fig. 24. The β-cristobalite structure.

7. The β-Cristobalite Structure. SiO_2 crystallizes in several forms, one of which is β-cristobalite (Fig. 24) which is related to the zinc blende structure. It has silicon atoms in place of zinc and sulphur atoms with oxygen atoms lying in between the silicon atoms.

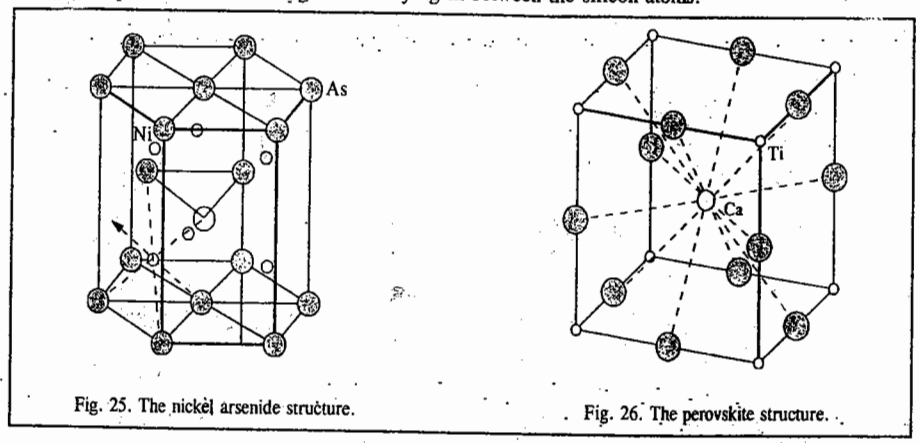

Fig. 25. The nickel arsenide structure.

Fig. 26. The perovskite structure.

In addition to the above mentioned seven types of structures of ionic solids, we have three more structures. These are the **nickel arsenide structure** (Fig. 25), the **perovskite structure** (Fig. 26) and the **spinel structure** (Fig. 27). The *nickel arsenide structure* is based on an expanded, distorted *hcp* anionic array with cations occupying the octahedral holes. The *perovskite structure*, the prototype of which is the mineral calcium titanate, $CaTiO_3$, is cubic with Ca atoms surrounded by 12 oxygen atoms and the titanium atoms surrounded by 6 oxygen atoms. The *spinel structure*, typified by $MgAl_2O_4$, consists of an f.c.c. array of O^{2-} ions in which Mg^{2+} cations occupy one-eighth of the tetrahedral holes and Al^{3+} cations occupy the octahedral holes.

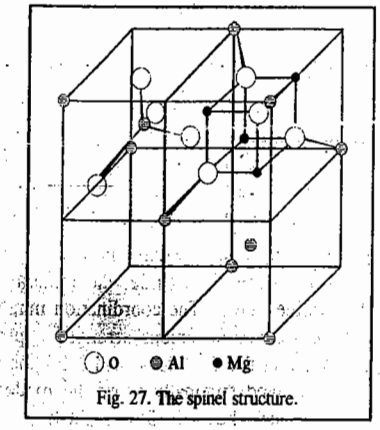

Fig. 27. The spinel structure.

METALLIC CRYSTALS

Metals are characterised by high electrical and thermal conductivity, bright lustre, malleability, ductility and high tenstile strength. It has been observed that metals, generally, have *low* ionisation energies because the valency electrons (*i.e.*, the electrons in the outermost shell) can be taken out relatively easily. This implies that valency electrons in metals are weakly bound to the kernel (by kernel, we mean the nucleus and electrons other than those in the outermost shell).

Consider the case of lithium. It has one valency electron, the electronic configuration being $1s^2\ 2s^1$. The X-ray examination of a crystal of lithium shows that each lithium atom is surrounded by eight other lithium atoms. It is not possible for one lithium atom to get bonded to eight other atoms through covalent bonds, *i.e.*, electron pair bonds, as it contains only one valency electron. But it has other valency orbitals (*viz.*, $2s$, $2p_x$, $2p_y$, $2p_z$) available. Hence, besides its own valency electron, the valency electrons of the neighbouring atoms can also come quite close to its nucleus. In other words, there can be complete freedom of movement of electrons in the vacant valency orbitals around the nucleus of each lithium atom. The valency electrons of metallic atoms, thus, are not localized at each atom. They do not belong to one atom in particular. They are mobile and move about from one kernel to another in the crystal. They are, in effect, a common property of all the atoms present in a metallic crystal.

Electron Sea Model. To account for the nature of bonding in metals, H.A. Lorentz proposed a model known as **'electron sea' model.** According to this model, a metal behaves as if it is an assemblage of positive ions (kernels) immersed in a 'sea' of mobile electrons (Fig. 28). Thus, each electron belongs to a number of positive ions and each positive ion belongs to a number of electrons. The force that binds a metal atom to a number of electrons within its sphere of influence is known as a **metallic bond.**

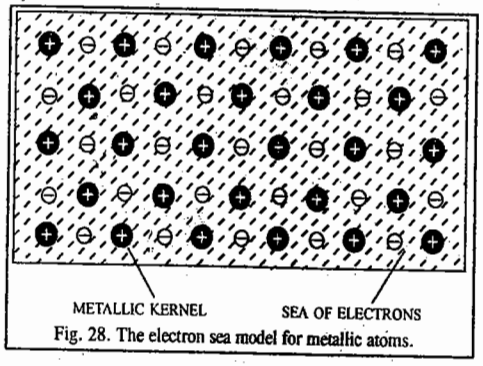

Fig. 28. The electron sea model for metallic atoms.

Explanation of Metallic Properties. All the metallic properties such as electrical and thermal conductivity, bright lustre, malleability, ductility, elasticity, etc., can be explained satisfactorily on the basis of the metallic structure described above.

1. The high electrical conductivity of metals, for example, is due to the presence of the mobile valency electrons. They move readily in an electric field and thus conduct electricity throughout the metal from one end to the other.

2. The high thermal conductivity is also due to the presence of these mobile electrons. If one part of a metal is heated, the electrons in that part acquire a large amount of kinetic energy. Being free, these electrons move rapidly through the crystal and convey heat (*i.e.*, conduct heat) to other parts of the metal.

3. The bright metallic lustre can also be explained as due to the presence of these highly mobile electrons. As a beam of light comprising of electromagnetic waves falls on the surface of a metal, the electric field associated with light waves sets the electrons present on the surface of the metal into to and fro oscillations. Since a moving charge always emits electromagnetic energy, hence, oscillating electrons emit electromagnetic energy in the form of light. Thus, when light falls on a metal surface, it appears as if light is being reflected. The surface, therefore, emits the typical metallic lustre.

4. The model of free valency electrons can also explain the softness, malleability and ductility

associated with metals. The metallic bond holding the positive ions (say, M^+) and the valency electrons is *non-directional*, as already mentioned. In other words, the force of attraction between the M^+ ions and the valency electrons is uniform in all directions. There are no localized bonds. Also the bonds holding the crystal lattice in metals are not rigid as in covalent solids such as ice. The result is that M^+ ions can be easily moved from one lattice site to another. In terms of the crystal, nothing has been changed. The environment of each metal ion remains the same as before since delocalized electrons are available everywhere.

The nearest neighbours can thus be changed easily and new metal bonds can be formed readily. This explains why metals are malleable, *i.e.*, they can be flattened out into thin sheets when hammered. A crystal of ice, on the other hand, is hard. It is neither malleable nor ductile. It is brittle, *i.e.*, it breaks into small pieces when hammered. This is obviously due to the fact that atoms in water molecules (oxygen and hydrogen) are covalently bonded to each other. Covalent bond is rigid and highly directional.

The ease with which the metal ions can be moved from one lattice site to another is also responsible for the fact that the metals are *ductile, i.e.*, they can be drawn into wires by very little expenditure of energy. This also explains why metals like sodium and potassium are soft and can easily be cut with a knife.

5. Metals have high tensile strength, *i.e.*, they can resist stretching without breaking. This is due to the existence of strong electrostatic attraction between the positively charged metal ions and the 'sea' of negative electrons surrounding them. Substances which have covalent bonds, do not possess high tensile strength. This is due to the absence of electrostatic forces of attraction in the crystal, there being no oppositely charged units in the lattice.

6. Metals possess elasticity. Elasticity is a property by virtue of which a substance can resist a deforming force or a property by virtue of which a substance can recover its original form soon after the removal of the deforming force. The elasticity of metals is also due to the ease with which metal ions can move from one lattice site to another.

7. The delocalized electron model can also explain the well known observation that only a small force is needed to bend a straight copper wire sharply. However, straightening out of a bent wire is not so easy. It requires much more force to do so. Not only that ; a small kink always remains. The reason is that the formation of a sharp bend amounts to separation of some of the metal ions from their adjacent electrons and also from their nearest ion neighbours. The previous pattern of ions and electrons is disturbed and a new pattern is set up in the crystal giving rise to new planes and new edges. It is not so easy to restore the previous pattern because the new planes and edges formed during the bending do not ordinarily fit together to restore the original pattern once again.

The electron sea model, however, cannot explain vast variations in properties of certain metals. For example, while mercury melts at such a low temperature as - 39°C, tungsten melts at such a high temperature as 3300°C. While metals, in general, are good conductors of electricity, copper is more than 50 times better conductor than bismuth. Similarly, while metals like sodium and potassium are so soft that they can be cut easily with a knife, osmium is so hard that it can scratch even glass.

Free Electron Model. The free electron model gives a deeper insight into the cause of high electrical conductivity of metals than the electron sea model. In this model each valence electron of the metal is treated as particle in a three-dimensional box of the size of the metal crystal. As discussed in Chapter 1, the energy levels of an electron in an atom are given by the expression

$$E_n = n^2h^2/8m_e a^2 \qquad (n = 1, 2, 3\ldots) \qquad \ldots(37)$$

where m_e is the mass of the electron and a is the width of the box of infinite height. For each eigenstate, there are two states of the electron corresponding to the two values of the electron spin.

It can be shown that the density of states (DOS) function, $g(\varepsilon)$, is given by

$$g(\varepsilon) = C\varepsilon^{1/2} \qquad \ldots(38)$$

where C is a constant. The number of one-electron states with energy between ε and $\varepsilon+d\varepsilon$ is given by $g(\varepsilon)d\varepsilon$. The DOS function, $g(\varepsilon)$, is plotted as a function of energy ε in Fig. 19(*a*). As electrons are added at 0 K, the energy levels are filled up to some maximum energy called the Fermi energy, ε_F, determined by the number of electrons. This is indicated by the cross hatching in Fig. 29. The Fermi energy is, in fact, the electrochemical potential of the electrons and determines their tendency to move at an interface. The same information can be obtained by plotting $g(\varepsilon)/\varepsilon^{1/2}$ versus ε as shown in Fig. 29(*b*).

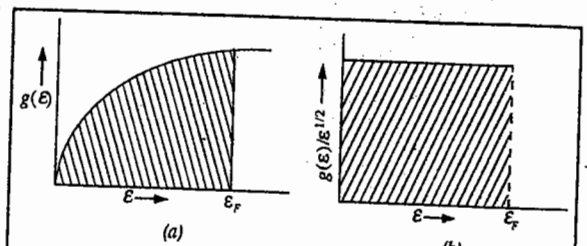

Fig. 29. *(a)* DOS function for a free electron gas as a function of energy *(b)* $g(\varepsilon)/\varepsilon^{1/2}$ versus energy for a free electron gas. The cross-hatching indicates the energy levels occupied at 0 K.

Free electrons having spin equal to $\frac{1}{2}$ obey Fermi-Dirac statistics and are called fermions (Chapter 25). Only one fermion occupies each energy state of the system. At a temperature above 0 K, the number of occupied states with energy range ε to $\varepsilon+d\varepsilon$ is given by

$$d(N/V) = f(\varepsilon, T)g(\varepsilon)d\varepsilon \qquad \ldots(39)$$

where $f(\varepsilon, T)$ is the Fermi-Dirac distribution function. The function $f(\varepsilon, T)$ is related with ε and T as follows :

$$f(\varepsilon, T) = \frac{1}{\exp[(\varepsilon - \mu)/k_BT)] + 1} \qquad \ldots(40)$$

where μ is a constant.

When $\varepsilon = \mu$, $f(\varepsilon, T) = 1/2$. Thus, the quantity μ is equal to energy at which $f(\varepsilon, T)$ has half its maximum value. At 0 K, $f(\varepsilon, 0) = 1$ for energies ε less than the Fermi energy, ε_F and $f(\varepsilon, 0) = 0$ for energies ε greater than ε_F. As $T \to 0$, $\mu \to \varepsilon_F$. Thus, it is a good approximation to take $\mu \approx \varepsilon_F$ at any other temperature as well provided $\varepsilon_F >> k_BT$.

Using this approximation and combining Eq. 39 with Eq. 40, we obtain

$$d(N/V) = \frac{C\varepsilon^{1/2}d\varepsilon}{\exp[(\varepsilon - \varepsilon_F/k_BT) + 1} \qquad \ldots(41)$$

Fig. 30 shows distribution of electron energies at temperatures T_1 and T_2 where $0 < T_1 < T_2$. At room temperature, the distribution of electron energies differs only slightly from that at 0 K for ε_F = 5eV. A small fraction of electrons have energies greater than ε_F ; they leave behind holes in the lattice when they are excited. *The holes and the excited electrons both contribute to electrical conductivity*, σ. This is how the free electron model of metals accounts for high electrical conductivity of metals. It predicts an infinite

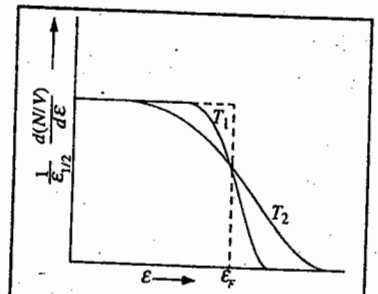

Fig. 30. Distribution of electron energies in a metal at 0 K (dotted line) and two higher temperatures $T_2 > T_1$.

value of σ because the excited electrons can, in principle, be excited to infinite velocities. However, in a metal crystal, the scattering of electrons from the vibrating atoms produces friction which restricts the mobility of the electrons. Electrical conductivity σ is given by

$$\sigma = neu \qquad ...(42)$$

where n is the number of electrons per unit volume, e is the electronic charge and u is the electron mobility.

The free electron model of metals discussed above is only a special case of the more general model, *viz.*, the band model of metals. The Fermi energy is mathematically given by the expression,

$$\varepsilon_F = h^2/8m_e\,(3N/\pi V)^{2/3} \qquad ...(43)$$

where N is the number of valence electrons per mole of the metal and V is the molar volume of the metal. At temperature above 0 K, the electronic kinetic energy per mole is given by

$$\varepsilon = \frac{3}{5}N\varepsilon_F\left[1 + \frac{5\pi^2}{12}\left(\frac{kT}{\varepsilon_F}\right)^2 + \ldots\ldots\ldots\right] \qquad ...(44)$$

The electronic contribution to thermal energy is given by

$$\varepsilon_{thermal} = \varepsilon_T - \varepsilon_0 = \pi^2 N(kT)^2/4\varepsilon_F \qquad ...(45)$$

where ε_T is the internal energy of the metal at some temperature T and ε_0 is the internal energy of the metal at 0 K.

We may mention here that deeper insight into the metallic state has been provided by L. Pauling, N.F. Mott, P.W. Anderson and A.H. Cottrell. The great Indian chemist C.N.R. Rao, who has contributed to several areas of structural chemistry, is another pioneer here. Mott and Anderson have given new theoretical insights on metals. Mott is best known for the metal-insulator transition and A.H. Cottrell is one of the founding fathers of modern metallurgy.

Example 21. Calculate the Fermi energy of sodium metal, given that the density (ρ) of the metal is 0·97 g cm^{-3} and the atomic mass is 23 g mol^{-1}.

Solution : $\rho = 0{\cdot}97 \text{ g cm}^{-3} = 0{\cdot}97\times10^3 \text{ kg m}^{-3}$

The molar volume V of Na metal is given by

$$V = \frac{M}{\rho} = \frac{23\times10^{-3}\text{ kg mol}^{-1}}{0{\cdot}97\times10^3\text{ kg m}^{-3}} = 2{\cdot}37\times10^{-5}\text{ m}^3\text{ mol}^{-1}$$

Since one atom of Na contains one valence electron, therefore, the number of valence electrons per mole of the metal is N=6·022×10^{23}. Thus,

$$\varepsilon_F = \frac{h^2}{8m_e}\left(\frac{3N}{\pi V}\right)^{2/3} \qquad \text{(Eq. 43)}$$

$$= \frac{(6{\cdot}626\times10^{-34}\text{ J s})^2}{8(9{\cdot}107\times10^{-31}\text{ kg})}\left[\frac{3(6{\cdot}022\times10^{23}\text{ mol}^{-1})}{\pi(2{\cdot}37\times10^{-5}\text{ m}^3\text{ mol}^{-1})}\right]^{\frac{2}{3}} = \mathbf{5{\cdot}04\times10^{19}\text{ J}} \quad (\text{J} = \text{kg m}^2\text{ s}^{-2})$$

Example 22. Calculate the electronic contribution to the thermal energy at 25°C in sodium metal, given that the Fermi energy of Na is 5·04×10^{-19} J.

Solution : $E_{thermal} = \dfrac{\pi^2 N(kT)^2}{4\varepsilon_F}$ (Eq. 45)

$$= \frac{\pi^2(6{\cdot}022\times10^{23}\text{ mol}^{-1})(1{\cdot}38\times10^{-23}\text{ JK}^{-1})^2(298\text{ K})^2}{4(5{\cdot}04\times10^{-19}\text{ J})} = \mathbf{49{\cdot}9\text{ J mol}^{-1}}$$

Notice that the electronic contribution to thermal energy in Na metal at room temperature is far greater than the Fermi energy of the metal.

Example 23. Calculate the fermi energy of silver metal, given that the atomic mass of silver is 107·868 g mol^{-1}, the density of the metal is 10·5 g cm^{-3}.

Solution : $\rho = 10{\cdot}5 \text{ g cm}^{-3} = 10{\cdot}5\times10^3 \text{ kg m}^{-3}$

$$\therefore \quad V = \frac{M}{\rho} = \frac{107{\cdot}868\times10^{-3}\text{ kg mol}^{-1}}{10{\cdot}5\times10^3\text{ kg m}^{-3}} = 1{\cdot}03\times10^{-5}\text{ m}^3\text{ mol}^{-1}$$

Since one atom of Ag contains one valence electron, therefore, the number of valence electrons per mole of the metal is N=6·022×10^{23}. Thus,

$$\varepsilon_F = \frac{h^2}{8m_e}\left(\frac{3N}{\pi V}\right)^{2/3} = \frac{(6{\cdot}626\times10^{-34}\text{ J s})^2}{8(9{\cdot}107\times10^{-31}\text{ kg})}\left[\frac{3(6{\cdot}022\times10^{23}\text{ mol}^{-1})}{\pi(1{\cdot}03\times10^{-5})\text{m}^3\text{ mol}^{-1}}\right]^{2/3} = \mathbf{8{\cdot}80\times10^{-19}\text{ J}}$$

Band Theory of Solids. The band theory of solids aims at explaining vast differences in the conductivity of metals which the wave mechanical free electron theory failed to do. This theory was first formulated by F. Bloch (of NMR fame, best known for the Bloch equations in NMR), begins with the Schrödinger wave equation and incorporates the *periodic* potential energy $V(x)$ of a lattice of atoms. The equation thus obtained, called the **Bloch equation**, is written as

$$-\frac{\hbar^2}{2m_e}\frac{d^2\psi}{dx^2} + V(x) = E\psi \qquad ...(46)$$

Since the potential energy is periodic, $V(x) = V(x+na)$ where a is the repeat distance along the x direction in the lattice and n is an integer. Bloch gave the solution of Eq. 46 as

$$\psi_k(x) = u_k(x)\exp(ikx) \qquad ...(47)$$

where $u_k(x)$ is an eigenfunction with the periodicity a of the lattice. A one-electron wave function of the form (47) is called a **Bloch function** and can be decomposed into a sum of *travelling waves*. Bloch functions can be assembled into *localized wave packets* to represent electrons that propagate freely through the periodic potential field of the ion cores. The dependence of the energy on k is quadratic ($E_k = \hbar^2k^2/2m_e$), as in the free-electron theory. However, for $k = \pm n\pi/a$, discontinuities appear in energy that lead to a band structure (Fig. 31).

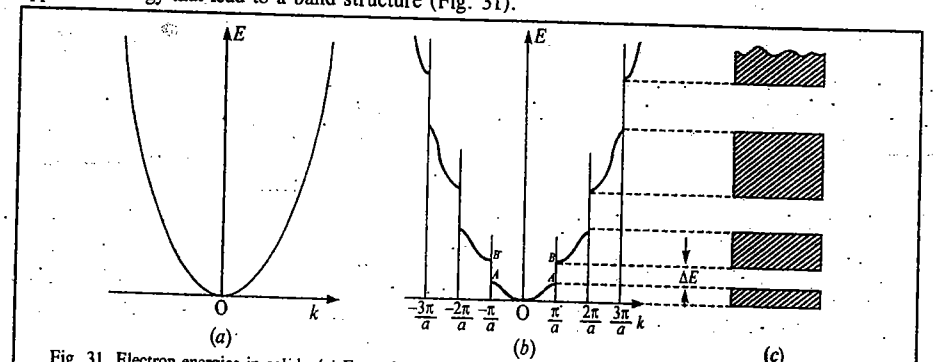

Fig. 31. Electron energies in solids *(a)* Free-electron theory showing the quadratic dependence of E on k ($k\hbar$ is the quasi-momentum of the electron). *(b)* Energy bands showing gaps ΔE at values of k for which the Bragg equation holds. The positions A and B correspond to waves ψ_1 (cos ($\pi x/a$)) and ψ_2 (sin ($\pi x/a$)), respectively ; the values of k ($\pm n\pi/a$) define the boundaries of the one-dimensional Brillouin zones. *(c)* Structure of quasi-continuous energy bands separated by gaps ΔE_i (i = 1, 2, ...).

The space in which k is measured is generally called ***k*-space.** It is the reciprocal space of X-ray crystallography but whereas crystallography is concerned with the (weighted) reciprocal lattice points, *k*-space is the *entire* space under investigation. As expected, k has the dimensions of reciprocal length. Each energy state specified by k or by n_x, n_y and n_z, can accommodate two electrons with spins ±1/2 and can be regarded as a point in *k*-space. [For a cubic crystal, $k = i(k_x + k_y + k_z) = i(\pi/a)(n_x + n_y + n_z)$].

The surface of constant energy E_F in k-space is called the **Fermi surface** ; it separates filled orbitals from unfilled orbitals.

For most values of k, the electrons behave very much like free electrons. However, at values of equal to $\pm n\pi/a$, the condition for Bragg reflection of electron waves in one dimension is realized : $k = \pm n\pi/a$ is equivalent to the Bragg equation $2a \sin\theta = n\lambda$ where $k = 2\pi/\lambda$ and $\sin\theta = 1$. The first order reflection at $k = \pm n\pi/a$ arises because waves reflected from adjacent atoms interfere constructively, the phase difference being 2π. The region lying between $\pm \pi/a$ is called the first **Brillouin zone** (Fig. 32). The energy is quasi-continuous within a zone because the energy levels are very closely spaced in a solid but discontinuous at the zone boundaries. As k increases towards $n\pi/a$, the eigenfunctions (6) contain increasing amounts of Bragg-reflected wave. At $k = \pi/a$, for example, the wave $\exp(i\pi x/a)$ reflects as $\exp(-i\pi x/a)$ and the resulting combinations are *standing waves* ψ_1 and ψ_2 of the forms $\cos(\pi x/a)$ and $\sin(\pi x/a)$, respectively. Brillouin zones are not normally encountered in X-ray crystal structure analysis but they are essential to an analysis of electron energy levels in solids.

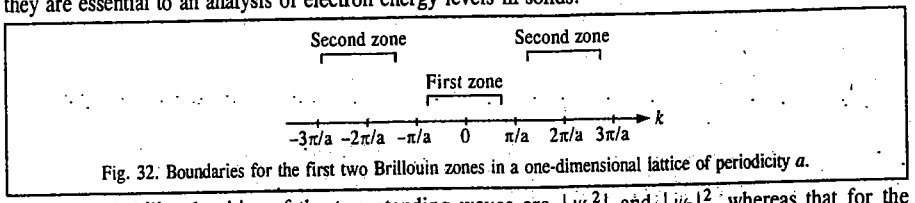

Fig. 32. Boundaries for the first two Brillouin zones in a one-dimensional lattice of periodicity a.

The probability densities of the two standing waves are $|\psi_1^2|$ and $|\psi_2|^2$, whereas that for the *travelling wave* is $\exp(i2kx)$.

Fig. 33. Illustrates a one-dimensional periodic potential field and the wave probability functions described above. The travelling wave distributes charge uniformly along the x-axis ; ψ_1 has its peaks at na and ψ_2 has its peaks at $(n+1/2)a$. The potential energies of the two distributions follow the order $|\psi_1|^2 < \exp(i2kx) < |\psi_2|^2$. Hence, an energy gap ΔE arises and the waves ψ_1 and ψ_2 correspond to the points A and B in Fig. 31. The combination of the waves $\exp(\pm ikx)$ at $k = \pm n\pi/a$, *i.e.*, at the boundaries of the Brillouin zones leads to an energy gap ΔE of $2V_k$ where V_k is the potential energy function at the position in k-space corresponding to k. This result may be compared with the bonding/antibonding situation in MOT (molecular orbital theory) which also depends on a core potential energy.

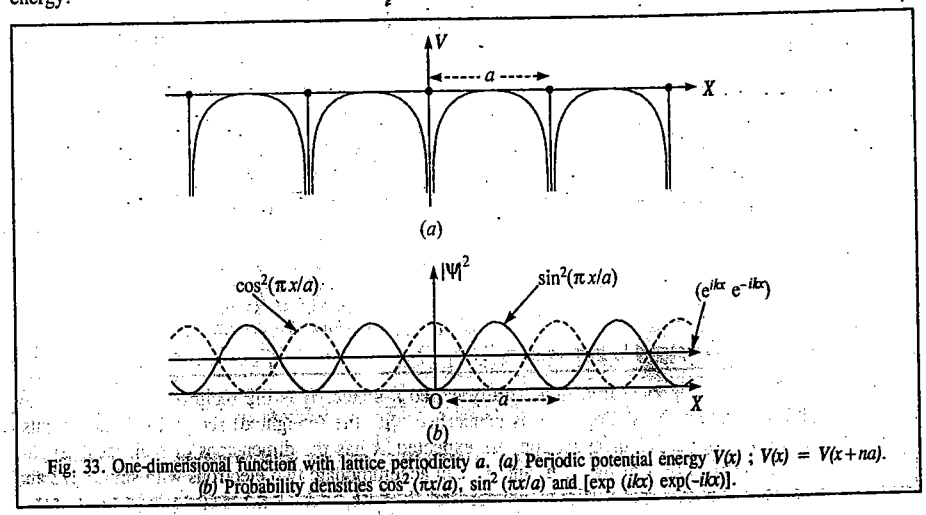

Fig. 33. One-dimensional function with lattice periodicity a. *(a)* Periodic potential energy $V(x)$; $V(x) = V(x+na)$. *(b)* Probability densities $\cos^2(\pi x/a)$, $\sin^2(\pi x/a)$ and $[\exp(ikx)\exp(-ikx)]$.

Brillouin zones may be extended to two and three dimensions. The zone boundaries are determined by the regions in k-space where the Bragg equation is satisfied : they are governed by crystal structure rather than by chemical composition.

The first Brillouin zone is the smallest volume in k-space that is entirely enclosed by planes that are normal to and bisect the shortest reciprocal lattice vectors drawn from the origin of k-space. The Brillouin zones correspond to Wigner-Seitz cells in k-space. The **Wigner-Seitz cell** for the lattice based on a conventional primitive cubic unit cell is, itself, a cube ; for the lattice based on the conventional face-centered cubic unit cell, it is a rhombic dodecahedron.

A Wigner-Seitz cell is obtained by joining a point of the Bravais lattice to all the nearest lattice points and then bisecting these lines with perpendicular planes. (The same construction is encountered with Voronoi polyhedra). The intersections of these planes contain the Wigner-Seitz cell. The planes of larger areas are those which are closer to the origin point ; beyond a certain distance, lattice points will not contribute to a Wigner-Seitz cell because the bisecting planes lie outside the confines of the smallest polyhedron. Wigner-Seitz cells are unit cells in the sense that they stack to fill space completely.

Energy Band Theory of Conductors, Semiconductors and Insulators

The basic difference between conductors, semiconductors and insulators lies in the number of *free electrons* present in the material. This difference can be best understood on the basis of the band theory of solids. We know that the energy levels of electrons in an atom are quantized. When an array of several atoms is considered, as is the case in a metallic solid where the atoms occupy the lattice sites, the energy levels of electrons form a series which can be grouped into **bands**, as shown in Fig. 34.

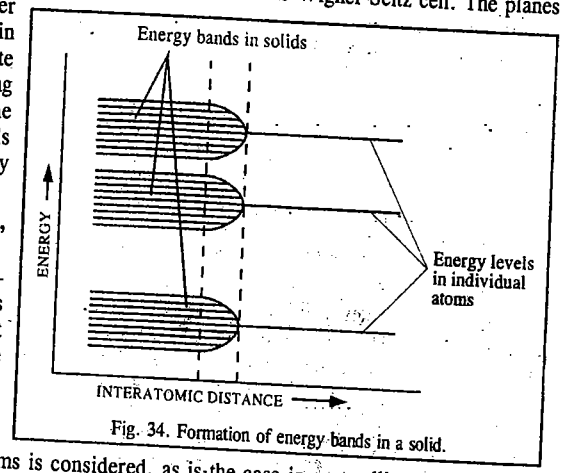

Fig. 34. Formation of energy bands in a solid.

The difference of energy between the energy levels within a band is very small compared with the **energy gap** between the bands. The energy band diagrams of a conductor, an insulator and a semi-conductor are given in Fig. 35.

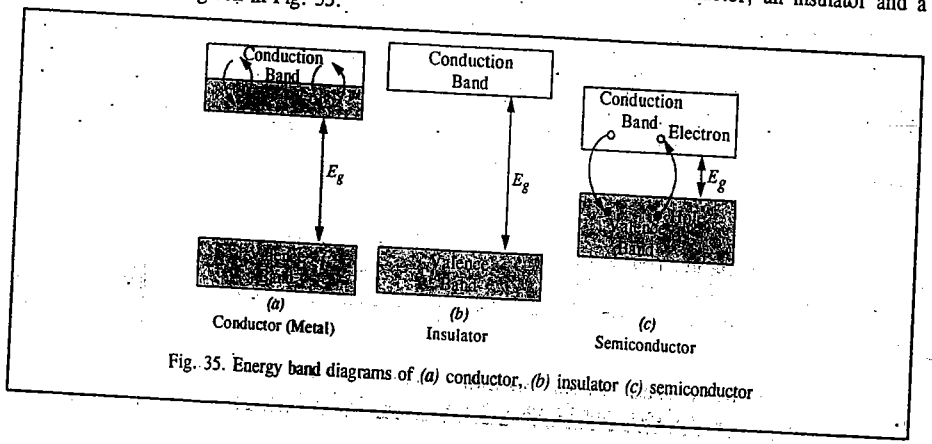

Fig. 35. Energy band diagrams of *(a)* conductor, *(b)* insulator *(c)* semiconductor

Conductors. In a conductor (such as a metal), the valence band (V.B.) is full of electrons while the conduction band (C.B.) is only partly filled. Only a small amount of energy suffices to allow electrons to move within the conduction band, some rising to a higher energy level and others returning to a lower energy level. This movement of electrons within the C.B. constitutes electrical conduction. In some metallic conductors, the V.B. and the C.B. actually overlap resulting in a partly filled top band. The diference in energy between the V.B. and the C.B. is called the energy gap, E_g.

Insulators. In an insulator, the V.B. is full and the E_g is very large. Thus, it will take a great deal of energy to make an electron jump the energy gap and to cause the insulator to break down. The break-down does not occur even at very high temperatures or under very large electric fields. Rubber is an example of an insulator.

Semiconductors. We shall deal with the so-called **intrinsic semiconductor** which is a semiconductor in 'its own right', *i.e.*, no impurity has been added to it. The best known intrinsic semiconductors are silicon and germanium. In an intrinsic semiconductor, the V.B. is full and the C.B. is empty at very low temperatures. The E_g between the two bands is, however, so small that electrons can jump across it by the addition of a small amount of thermal energy (k_B/T) alone, *i.e.*, only heating the material results in electrical conduction. The electrical conductivity increases with increase in temperature since more and more electrons are liberated with increase in temperature. The smaller the value of E_g, the better the semiconductor. Thus, germanium (E_g=0·67 eV) is a better conductor than silicon (E_g=1·14 eV). As an electron jumps from the V.B. to the C.B., it leaves behind a **hole** in the V.B. The hole is positively charged and since an electron can jump into the hole from another part of V.B., it is as if the hole was moving ! Conduction can occur either by the negative electrons moving within the C.B. or by positive holes moving within the V.B.

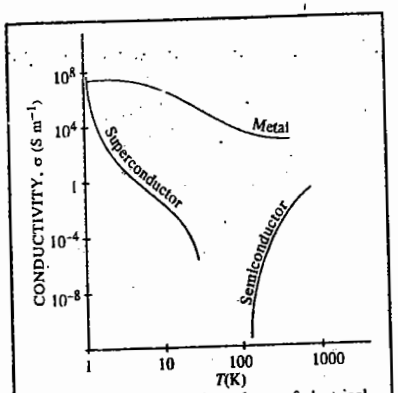

Fig. 36. Temperature-dependence of electrical conductivity of a metal, a semiconductor and a superconductor.

A semiconductor at room temperature generally has much lower conductivity than a metallic conductor because only very few electrons and holes can act as charge carriers. The temperature-dependence of electrical conductivity, σ, for a metallic conductor, a semiconductor and a superconductor is shown in Fig. 36. A super conductor is one which has zero or very little electrical resistance.

As can be seen, a **metallic conductor** is a substance with electrical conductivity that decreases with increasing temperature, a **semiconductor** is a substance with an electrical conductivity that increases with increasing temperature and a **superconductor** is a substance that has zero electrical resistance below a certain temperature called critical temperature.

The conductivity of a semiconductor follows the Arrhenius type temperature-dependence with activation energy, E_a, approximately equal to half of the energy gap, E_g. Thus,

$$\sigma = \sigma_0 \exp(-E_a/kT) = \sigma_0 \exp(-E_g/2kT)$$

The E_g and σ values for the elements of Group IV are given in Table 8.

TABLE 8
Electrical Conductivities and Energy Gaps for the Elements of Group IV

Element	E_g (eV)	σ (S m^{-1})
C (diamond)	6·0	$< 10^{-4}$
Si	1·14	$1·5\times10^{-3}$
Ge	0·67	2
Sn (gray)	0·08	> 100

Extrinsic Semiconductors

It is possible to increase the charge carriers if atoms with more electrons than the parent element can be introduced by the process known as **doping**. Extremely low concentrations of the dopant (about one atom per 10^9 atoms of the host material) are needed. Pure silicon (Si) and germanium (Ge) can be made more conducting in a controlled manner by adding dopant impurities which act as charge carriers. Si or Ge are first made extremely pure by zone refining. Then some arsenic (As) atoms with five valence electrons are added to the Ge crystal. An extremely small number of Ge atoms are randomly replaced by As atoms. Only four of the five outer electrons on each As atom are required to form bonds in the lattice. The fifth electron on As atom is not bonded. At low temperatures, the fifth electron is localized on the As atom. However, at normal temperatures, some of these fifth electrons on As are excited into the conduction band where they act as charge carriers. This produces what is known as **extrinsic conduction.** Since the current is carried by excess electrons, this is known as ***n*-type semiconduction.** The magnitude of semiconductivity in an extrinsic semiconductor is far greater than that in an intrinsic pure semiconductor.

If the donor As atoms are far apart from one another, their electrons are localised and the **donor band** will be narrow (Fig. 37*a*). The filled dopant band lies near (just below) the empty conduction band of the lattice.

Alternatively, a crystal of pure Si or Ge is doped with atoms of an element which has three valence electrons per atom, such as gallium (Ga) or indium (In). Each gallium atom has three outer electrons to form three bonds in the lattice, these electrons cannot form four bonds in the lattice to complete the covalent structure. One bond is incomplete and the site which remains unoccupied because of the missing electron is called a **positive hole.** More formally, the dopant atoms form a very narrow empty **acceptor band** that lies above the full silicon valence band (Fig. 37*b*). At T=0 K, the acceptor band is empty but at $T > 0$ K, it can accept thermally excited electrons from the Si valence band. This forms new positive holes in the Si valence band. The holes appear to move in a direction opposite to the motion of electrons. The positive holes 'hop' through the band. Since the charge carriers are now the positive holes, this type of conduction is known as ***p*-type conduction.** In principle, any of the Group V elements (such as P, As, Sb, Bi) can be used to make *n*-type semiconductors but, because of its low melting point, As is most commonly used. Similarly, any of the Group III elements (such as B, Al, Ga and In) can be used to make *p*-type semiconductors, though indium (In) is most commonly used because of its low melting point. A minute amount of donor impurity can produce a dramatic change in the conductivity of a semicondcutor. For example, 1 part of a donor impurity per 10^9 parts of germanium increases its conductivity by a factor of 10^3.

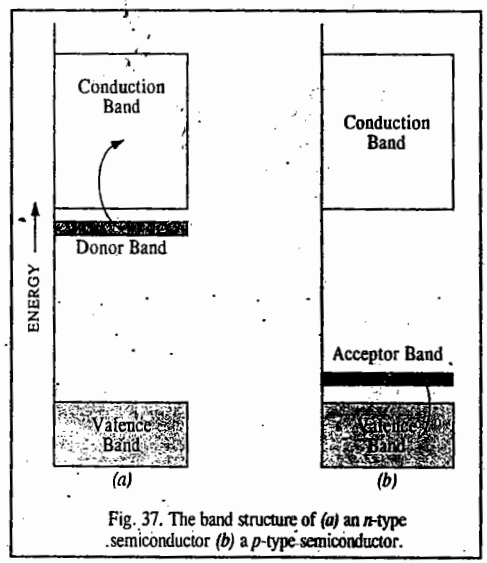

Fig. 37. The band structure of *(a)* an *n*-type semiconductor *(b)* a *p*-type semiconductor.

The combination of ***n*** and *p*-type semi-conductors (known as ***n*–*p* junction**), finds interesting applications in the manufacture of **transistors**. This device can conduct electric current more easily in one particular direction than in the reverse direction and, therefore, can be used as a **rectifier** for

changing alternating current into direct current. The device is schematically represented in Fig. 38.

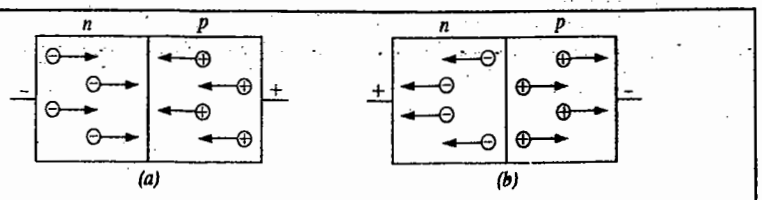

Fig. 38. Semiconductor acting as rectifier.

The material on the left side of each junction is *n*-type conductor obtained by doping germanium with, say, arsenic. The minus signs represent extra electrons. The material on the right side of the junction is *p*-type conductor obtained by doping germanium with, say, indium. The positive signs represent 'positive holes' arising from the deficiency of electrons at the indium impurity centres. When an external voltage is applied in such a way as to cause motion of electrons (*n*-current) from left to right and motion of positive holes (*p*-current) from right to left (Fig. 35*a*), current is readily conducted. If direction of voltage is reversed so that there is separation of electrons and positive holes as shown in Fig. 35(*b*), there is cancellation of *n* and *p*-currents and hence the conduction stops. Thus, the *n*–*p* junction permits the current from an out side source to flow in one direction only.

Superconductivity

Superconductivity or superconduction is of two types, *viz.*, low temperature superconductivity (LTSC) and high temperature superconductivity (HTSC). An ideal superconductor is supposed to have zero or very little electrical resistance.

Low Temperature Superconductivity (LTSC). LTSC was first discovered in 1911 by the Dutch physicist H. Kamerlingh-Onnes who was awarded the 1913 Physics Nobel Prize for his contributions to low temperature physics which led to the production of liquid helium. He found that down to 4·15 K, the resistance of mercury decreased with decrease in temperature as is the case with most metals. However, at critical temperature T_c=4·15 K, the resistance fell sharply close to zero. Thus, at or below the critical temperature, mercury became a **superconductor.** At very low temperatures, many metals, alloys and certain compounds become superconductors, the critical temperatures for superconductivity lying between 0·1 K and 10 K. Since a superconductor has almost zero resistance, it can carry an electric current without losing energy and, in principle, the current can flow for ever. Superconductors also exhibit what is called **Meissner effect :** it states that a superconductor does not allow the magnetic field to pass through it. In other words, it behaves like a perfectly **diamagnetic substance.** The Meissner effect gives rise to **levitation;** levitation occurs when objects float in air. This can be achieved by the mutual repulsion between a permanent magnet and a superconductor. A superconductor is diamagnetic because it expels all internal magnetic fields arising from unpaired electrons. The key to understanding LTSC was provided by the celebrated **BCS theory** proposed in 1957 by the American physicists J. Bardeen, L. Cooper and J. Schreifer who were awarded the 1972 Physics Nobel Prize. The central role in the BCS theory of LTSC is played by the **Cooper pair.** L. Cooper explained how two electrons could interact in a superconductor forming a *'bound state'* despite their coulombic repulsion. The Cooper pair of electrons exist on account of the indirect interaction of the two electrons via the nuclei of the atoms in the lattice. The lattice is slightly *deformed* as an electron moves through it, with the positive ions in the path of the electrons being displaced towards it. The deformation produces a region of increased positive charge. Another electron passing through this polarized region will be attracted by the greater concentration of the positive charge there. If the attraction is stronger than the repulsion between the electrons, the electrons are effectively coupled together into a Cooper pair with the deformed lattice as the intermediary.

A Cooper pair undergoes less scattering than an individual electron as it travels through the lattice because the distortion caused by one electron can attract back the other electron should it be scattered out of its path in a collision. Since the Cooper pair is stable against scattering, it can carry charge freely through the solid thereby giving rise to superconduction. The BCS theory, which is a mathematical *tour de force*, shows that the two electrons of the Cooper pair must be moving in opposite directions and their correlations may persist over lengths as large as 10^{-6} m. The binding energy of the Cooper pair is of the order of 10^{-3} eV. That is why superconductivity is a low-temperature phenomenon. When $h\nu >>$ binding energy, strong absorption occurs as the Cooper pairs break down. The binding energy at 0 K, $E_g(0)$, is given by

$$E_g(0) = 3{\cdot}53\ kT_c \qquad \ldots(48)$$

Eq. 48 shows good agreement with the observed values of E_g and T_c. At $T > 0$ K, only a few of the Cooper pairs break down. The resulting individual electrons interact with the remaining Cooper pairs and reduce E_g. Finally, at T_c, E_g disappears ; there are no more Cooper pairs and the material ceases to be a superconductor.

It may be mentioned that since the electrons in a Cooper pair have opposite spins, the pair has resultant zero spin. Thus, the electron pairs in a superconductor are bosons (unlike individual electrons with spin $\frac{1}{2}$ which are fermions) and any number of them can exist in the same quantum state at the same time. Also, the current in a superconductor involves the entire system of Cooper pairs acting as a unit.

We may mention here that the American physicist John Bardeen (1908-1991) was the only physicist to win two Nobel Prizes in physics. He had shared the first Nobel Prize in 1956 with Walter Brattain (1902-1987) and William Shockley (1910-1989) for their researches on semiconductors and their discovery of the transistor effect.

High Temperature Superconductivity (HTSC). Because of the very low temperatures at which most materials become superconducting which implies that T_c is very low, LTSC has not found widespread use. The highest value of T_c known until 1986 was about 23 K. In that year, G. Bednorz and A. Muller (who were working for IBM in Zurich; Switzerland) discovered a cuprate, *viz.*, a mixed oxide Ba–La–Cu–O system, which had a T_c of about 35 K. Bednorz and Muller were awarded the 1987 Physics Nobel Prize for the discovery of HTSC. Another high T_c superconductor $YBa_2Cu_3O_{7-x}$ ($x \lesssim 0{\cdot}1$) was discovered in 1987 by Chinese-American physicists, Wu, Chu and their coworkers, the T_c being 93 K. This temperature is significant because it allows liquid nitrogen (boiling point 77 K) to be used as a coolant rather than the more expensive liquid helium. This superconductor, called yttrium-barium-cuprate, is the 1–2–3 system because of the ratio of the metals present. The non-stoichiometry appears to be necessary for HTSC. It appears that copper is necessary for superconductivity since efforts to replace it by other elements have not borne fruit. This cuprate has the **perovskite structure.** This comprises of three cubic perovskite units stacked one on top of the other giving an elongated (tetragonal) unit cell.

Cu Ba O_3
Cu Y O_3
Cu Ba O_3

The upper and the lower cubes have a Ba^{2+} ion at the body-centred position and the smaller Cu^{2+} ion at each corner. The middle cube is similar but has a Y^{3+} ion at the body centre. A perovskite structure has the formula ABO_3 and the stoichiometry of this compound would be $YBa_2Cu_3O_9$. Since the formula actually found is $YBa_2Cu_3O_{7-x}$, there is evidently a massive oxygen deficiency ; about 25% of oxygen sites in the crystal are vacant.

The LTSC of metals and alloys has been explained by the BCS theory. However, there is at present no satisfactory theory of HTSC. Nevertheless, the following features may be borne in mind :

1. Many warm superconductors contain copper which is known to exist in three oxidation states, (+I), (+II) and (+III). Also Cu(II) forms many tetragonally distorted complexes.

2. The high T_c superconductors are related to the perovskite structure.

3. The oxygen deficiency is very important. Neutron diffraction studies reveal that the vacancies left by the missing O atoms are well ordered. Since Cu is normally octahedrally surrounded by six O atoms, when an O vacancy occurs, the two Cu atoms may interact directly with each other. Interactions such as Cu^{II}–Cu^{III} or Cu^{I}–Cu^{II} may occur by the transfer of an electron between the two Cu atoms. Similarly, HTSC of $YBa_2Cu_3O_{7-x}$ is believed to occur by the ready transfer of electron between Cu(I), Cu(II) and Cu(III).

The preparation of warm superconductors is an art involving grinding, heating, annealing or slow cooling, etc. The '1-2-3' superconductor (yttrium barium cuprate) can be prepared by the *p*H–adjusted precipitation and high-temperature decomposition of the carbonates :

$$2Y^{3+} + 3HCO_3^- \xrightarrow{-H^+} Y_2(CO_3)_3\downarrow$$

$$Ba^{2+} + HCO_3^- \xrightarrow{-H^+} BaCO_3\downarrow$$

$$Cu^{2+} + HCO_3^- \xrightarrow{-H^+} CuCO_3\downarrow$$

$$Y_2(CO_3)_3 + 4BaCO_3 + 6CuCO_3 \xrightarrow{950°C} 2YBa_2Cu_3O_{7-x} + 13CO_2\uparrow$$

IMPERFECTIONS IN A CRYSTAL

The discovery of imperfections in an otherwise ideally perfect crystal is one of the most fascinating aspects of solid state science. An ideally perfect crystal is one which has the same unit cell and contains the same lattice points throughout the crystal. The term **imperfection** or **defect** is generally used to describe any deviation of the ideally perfect crystal from the periodic arrangement of its constitutents. Two types of defects are generally observed in crystals. These are : 1. Point Defects 2. Line Defects.

Point Defects

If the deviation occurs because of missing atoms, displaced atoms or extra atoms, the imperfection is named as a **point defect.** Such defects can be the result of imperfect packing during the original crystallisation or they may arise from thermal vibrations of atoms at elevated temperatures because with increase in thermal energy there is increased probability of individual atoms jumping out of their positions of lowest energy. The most common point defects are the Schottky defect and the Frenkel defect. Comparatively less common point defects are the *metal excess defect* and the *metal deficiency defects*. All these defects have been discussed below in some details.

Schottky Defects. These defects arise if some of the lattice points in a crystal are unoccupied. The points which are unoccupied are called *lattice vacancies*. The existence of two vacancies, one due to a missing Na^+ ion and the other due to a missing Cl^- ion in a crystal of NaCl, is shown in Fig. 39. The crystal, as a whole, remains netural because the number of missing positive and negative ions is the same.

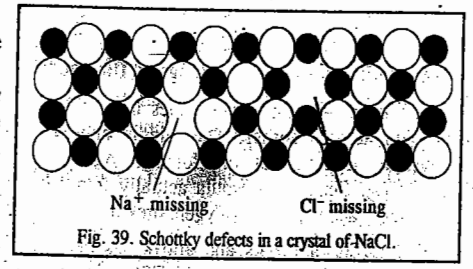

Fig. 39. Schottky defects in a crystal of NaCl.

Schottky defects appear generally in ionic crystals in which the positive and the negative ions do not differ much in size. Sodium chloride and cesium chloride furnish good examples of ionic crystals in which Schottky defects occur.

Because of Schottky defects, the crystal is in a position to conduct electricity to a small extent by an ionic mechanism. It happens as follows : As an electric field is applied, a nearby ion moves from its lattice site to occupy a vacancy. This results in creating a new vacancy and another nearby ion moves into it, and so on. This process continues resulting in the migration of the vacancy and thereby of the ion from one end to the other end of the crystal. In this way, electricity gets conducted across the whole of the crystal.

The existence of vacancies also enables easy movement of atoms or ions in the crystal changing places with one another. *This accounts for the phenomenon of diffusion in solids.*

Number of Schottky defects. Consider an ionic crystal containing N ions in which n Schottky defects are produced by the removal of n cations and n anions from the interior of the crystal. The different ways in which each kind of ion can be removed is given by

$$\frac{N(N-1)(N-2)\ldots(N-n+1)}{n!} = \frac{N!}{(N-n)\,n!} \qquad \ldots(49)$$

The different ways in which n Schottky defects can be produced is obtained by squaring the expression in Eq. 44 because the number of cation and anion vacancies is equal. Creation of defects in a crystal means creation of disorder. Since entropy is a measure of the disorder of the system, with the creation of defects there is increase in the entropy of the crystal. The entropy S is related to thermodynamic probability W by the Boltzmann equation, *viz.*, $S = k \ln W$, where k is the Boltzmann constant. In the present case, evidently,

$$W = \left(\frac{N!}{(N-n)!\,n!}\right)^2 \qquad \ldots(50)$$

The increase in entropy causes a change in the Helmholtz free energy. If ε is the enrgy required to create a Schottky defect, then $n\varepsilon$ would be the energy required to create n Schottky defects. Let this energy be designated as E. The Helmholtz free energy is given by $A = E - TS$.

$$\Delta A = \Delta E - T\Delta S = \Delta E - T(S - S_0) = E - TS \qquad \text{(Entropy at 0 K = 0)}$$

$$= E - T\,(k \ln W) = E - kT \ln \left(\frac{N!}{(N-n)!\,n!}\right)^2 \qquad \ldots(51)$$

Using the Stirling approximation, *viz.*, $\ln x! = x \ln x - x$, for evaluating factorial terms, we find that

$$\ln \left(\frac{N!}{(N-n)!\,n!}\right)^2 = 2\,[\ln N! - \ln (N-n)! - \ln n\,!]$$

$$= 2\,[N \ln N - N - (N-n) \ln (N-n) + (N-n) - n \ln n + n]$$

$$= 2\,[N \ln N - (N-n) \ln (N-n) - n \ln n] \qquad \ldots(52)$$

Hence, $$\Delta A = E - 2kT\,[N \ln N - (N-n) \ln (N-n) - n \ln n] \qquad \ldots(53)$$

At equilibrium, at a given temperature, $(\partial(\Delta A)/\partial n)_T = 0$. Also, since N is constant, $\partial N/\partial n)_T = 0$. Hence, from Eq. 52,

$$\left(\frac{\partial(\Delta A)}{\partial n}\right)_T = E - 2\,kT \ln \frac{N-n}{n} = 0 \qquad \ldots(54)$$

$$\therefore \quad E = 2\,kT \ln [(N-n)/n] \qquad \ldots(55)$$

or $$(N-n)/n = \exp(E/2kT) \qquad \ldots(56)$$

Since the number of Schottky defects, n, is much smaller than the number of ions, N, in a crystal, *i.e.*, $n << N$, hence $N - n = N$. Eq. 55, may thus be written as

$$n = N \exp(-E/2kT) \qquad ...(57)$$

Eq. 56 gives the number of Schottky defects in a crystal.

We may consider a specific example. In NaCl crystal, E is known to be approximately 2eV. Accordingly, the number of Schottky defects present in the NaCl crystal at room temperature comes out to be 10^6 per cm^3. Since the number of the Na^+ and Cl^- ions is approximately 10^{22} per cm^3, we find that, on an average, there is one Schottky defect for 10^{16} ions. Thus, the application of the Stirling approximation in the above derivation is perfectly justified.

Frenkel Defects. These defects arise when *an ion occupies an interstitial position between the lattice points*. This is shown in Fig. 40 for the crystal of AgBr.

Ag^+	Br^-	Ag^+	Br^-	Ag^+	Br^-	Ag^+	Br^-	Ag^+
Br^-	Ag^+	Br^-	Ag^+	Br^-	Ag^+	Br^-	Ag^+	Br^-
Ag^+	Br^-	●	Ag^+	Br^-	Ag^+	Br^-	Ag^+	Br^-	Ag^+
Br^-	Ag^+	Br^-	Ag^+	Br^-	Ag^+	Br^-	Ag^+	Br^-

Fig. 40. Frenkel defects in a crystal of AgBr.

As can be seen, one of the Ag^+ ions occupies a position in the interstitial space rather than its own appropriate site in the lattice. A vacancy is thus created in the lattice as shown. It may be noted again that the crystal remains neutral since the number of positive ions is the same as the number of negative ions. The presence of Ag^+ ions in the interstitial space of AgBr crystal is responsible for the formation of a photographic image on exposure of AgBr crystals (*i.e.*, photographic plate) to light.

ZnS is another crystal in which Frenkel defects appear. Zn^{2+} ions are entrapped in the interstitial space leaving vacancies in the lattice.

Frenkel defects appear in crystals in which the negative ions are much larger than the positive ions. Like Schottky defects, the Frenkel defects are also responsible for the conduction of electricity in crystals and also for the phenomenon of diffusion in solids.

Number of Frenkel defects. Consider an ionic crystal having N ions and N_i interstitial spaces in its structure. The number of ways in which n Frenkel defects can be formed is given by

$$n = \frac{N!}{(N-n)!n!} \times \frac{N_i!}{(N_i - n)n!} \qquad ...(58)$$

Let the energy required to displace an ion from its proper position to an interstitial position be ε. Then the energy required to produce n Frenkel defects would be $n\varepsilon$. Let this energy be designated by E.

Proceeding as before, using the Boltzmann entropy equation, *viz.*, $S = k \ln W$, the Helmholtz free energy equation, *viz.*, $\Delta A = E - T\Delta S$ and the Stirling approximation for evaluating factorial terms, we arrive at the conclusion that

$$n = (NN_i)^{1/2} \exp(-E/2kT) \qquad ...(59)$$

Eq. 57 gives the number of Frenkel defects in a crystal.

It is evident from Eqs. 57 and 58 that the number of Schottky and Frenkel defects would increase exponentially with increase in temperature. It has been observed by X-ray diffraction of NaCl that while at room temperature there is only one Schottky defect for 10^{15} lattice sites, the number increases to 10^6 at 500°C and to 10^{11} at 800°C for the same number of lattice sites.

Example 24. Estimate the mole fractions of Schottky and Frenkel defects in a NaCl crystal at 1000 K. The energies of formation of these defects are 2eV and 3eV, respectively. 1eV = 1·602 × 10^{-19} J ; k = 1·38 × 10^{-23} J K^{-1}.

Solution :

Schottky Defects : According to Eq. 52, the mole fraction of Schottky defects is given by

$$n/N = \exp(-E/2kT)$$

$$= \exp\left[\frac{-(2\text{eV})(1{\cdot}602 \times 10^{-10}\,\text{J(eV)}^{-1}}{2(1{\cdot}38 \times 10^{-23}\,\text{J K}^{-1})(1000\,\text{K})}\right] = \exp(-11{\cdot}6) = 9{\cdot}17 \times 10^{-6}$$

Frenkel Defects. According to the structure of the unit cell of NaCl crystal, the number of interstitial spaces is twice the number of Na^+ ions present in the unit cell, that is, $N_i = 2N$. The Frenkel defects are formed only by the migration of the smaller Na^+ ion. According to Eq. 54,

$$n = (NN_i)^{1/2} \exp(-E/2kT)$$

Since $N_i = 2N$, hence

$$n/N = 2^{1/2} \exp(-E/2kT) = 2^{1/2} \exp\left[\frac{-(3\text{eV})(1{\cdot}602 \times 10^{-19}\,\text{J(eV)}^{-1}}{(2 \times 1{\cdot}38 \times 10^{-23}\,(\text{J K}^{-1})(1000\,\text{K}))}\right] = 3{\cdot}82 \times 10^{-8}$$

Metal Excess Defects. The Colour Centres. It has been observed that if a crystal of NaCl is heated in sodium vapour, it acquires a yellow colour. This yellow colour is due to the formation of a non-stoichiometric compound of sodium chloride in which there is a slight excess of sodium ions. What happens in this case is that some sodium metal gets doped into the sodium chloride crystal each atom of which gets ionised into Na^+ and e^- due to crystal energy. This electron occupies a site that would otherwise be filled by a chloride ion, as illustrated in Fig. 41.

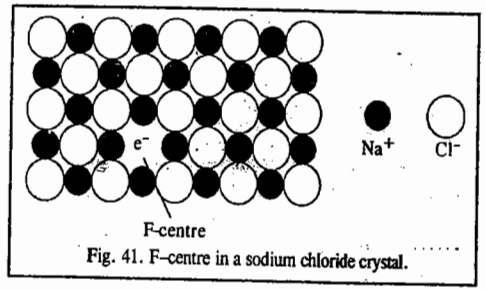

Fig. 41. F-centre in a sodium chloride crystal.

There is evidently an excess of Na^+ ions although the crystal as a whole is neutral. A little reflection would show that there are six Na^+ sites adjacent to the vacant site occupied by the electron. The extra electron is thus shared between all the six Na^+ ions which implies that this electron is *not localised* at the vacant Cl^- site. On the other hand, this electron is similar to the delocalised π electrons present in molecules containing conjugate double bonds. Light is absorbed when this delocalised electron makes an easy transition from its ground state to an excited state. As a result, the non-stoichiometric form of sodium chloride *appears coloured*. Because of this, the sites occupied by the extra electrons are known as **colour centres**. These are also called **F-centres**. This name comes from the German word Farbe meaning *colour*. The non-stoichiometric sodium chloride may be represented by the formula $Na_{(1+\delta)}Cl$ where δ is the excess sodium metal doped in the crystal because of its exposure to sodium vapour.

Another common example of metal excess defects is the formation of *magenta coloured* non-stoichiometric compound of potassium chloride by exposing the crystals of KCl to K metal vapour. The coloured compound contains an excess of K^+ ions, the vacant Cl^- sites being filled by electrons obtained by the ionization of the excess K metal doped into the crystal.

Metal Deficiency Defects. In certain cases, one of the positive ions is missing from its lattice site and the extra negative charge is balanced by some nearby metal ion acquiring two charges instead of one. There is, evidently, *a deficiency of the metal ions* although the crystal as a whole is neutral. This type of defect is generally found amongst the compounds of transition metals which can

exhibit variable valency. Crystals of FeO, FeS and NiO show this type of defects. The existence of metal deficiency defects in the crystal of FeO is illustrated in Fig. 42.

Fe^{2+}	O^{2-}	Fe^{2+}	O^{2-}	Fe^{2+}	O^{2-}	Fe^{2+}	O^{2-}	Fe^{2+}	O^{2-}
O^{2-}	Fe^{2+}	O^{2-}	Fe^{2+}	O^{2-}	Fe^{2+}	O^{2-}	Fe^{2+}	O^{2-}	Fe^{2+}
Fe^{2+}	O^{2-}	Fe^{2+}	O^{2-}	Fe^{2+}	O^{2-}	●	O^{2-}	Fe^{2+}	O^{2-}
O^{2-}	Fe^{2+}	O^{2-}	Fe^{2+}	O^{2-}	Fe^{3+}	O^{2-}	Fe^{3+}	O^{2-}	Fe^{2+}
Fe^{2+}	O^{2-}	Fe^{2+}	O^{2-}	Fe^{2+}	O^{2-}	Fe^{2+}	O^{2-}	Fe^{2+}	O^{2-}

Fig. 42. Metal Deficiency defects in a crystal of FeO.

It is evident from the above discussion that all types of point defects result in the creation of vacancies or 'holes' in the lattices of crystals. The presence of holes lowers the density as well as the lattice energy or the stability of the crystals. The presence of too many holes may cause a partial collapse of the lattice.

Line Defects : Dislocations

In addition to the point defects discussed above, another kind of imperfection occurs when the periodicity of the atomic lattice array is interrupted along certain directions in a crystal. Such interruptions occur along rows of a crystal structure and are called **line defects.** The most common type of line defect within a crystal is a **dislocation.** The presence of dislocations results in easy deformation of a crystal under the influence of a shear stress. The common types of dislocations are the *edge dislocations* and the *screw dislocations*. These are described below.

Edge Dislocations. Edge dislocations arise when there is a slight mismatch in the orientation of adjacent parts of the growing crystal resulting in the introduction of an extra row of atoms. The edge of the atomic plane terminates within the crystal instead of passing all the way through. Under the impact of the shear, the dislocation moves across the crystal in such a way that the top half of the crystal is displaced one lattice distance with respect to the lower half. The motion of an edge dislocation under shear is illustrated in Fig. 43.

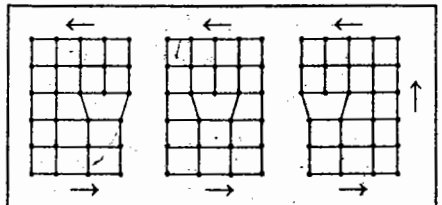

Fig. 43. Motion of an edge dislocation.

Near the edge dislocation, the atoms are pushed together above the edge and pulled apart below the edge. In this way, the impurity atoms with larger diameters than the parent atoms tend to concentrate below the edge and the impurity atoms with smaller diameters tend to concentrate above the edge. As a result of the binding of the impurity at the dislocation, it is more difficult to move a dislocation in an impure material. This is the reason why alloys require greater shear force for permanent deformation than do the pure metals.

Screw Dislocations. The formation of a screw dislocation can be visualised by cutting a rubber stopper parallel to its axis and then pushing on one end so that a jog is created on the other end. If initially the stopper contained atoms at regular lattice points, deformation would convert the parallel planes of atoms normal to the axis into a kind of spiral ramp. Such a displacement of the atoms constitutes what is known as screw dislocation (Fig. 44). A screw dislocation helps in easy crystal growth because

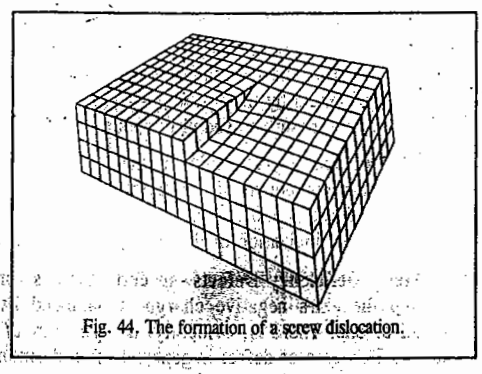

Fig. 44. The formation of a screw dislocation.

atoms can be added at the step. Screw dislocations result in easy deformation of crystal in the same way as is done by edge dislocations. In practice, real dislocations are mixtures of edge dislocations and screw dislocations. Dislocations provide for preferred sites within a crystal for chemical reactions and physical changes (such as phase transformation, precipitation or etching). The point of emergence of a dislocation at the surface of a crystal is a site of enhanced chemical reactivity. The number of dislocations per unit area can be measured by counting the etch pits which are formed at the surface. The number of etch pits formed ranges from 10^5 m^{-2} in the best silver crystal to 10^{15} m^{-2} in a severely deformed crystal.

Imperfections due to Transient Atomic Displacement. The vibrations of a crystal, like those of an S.H.O., have three normal modes of vibration which correspond to one longitudinal mode and two mutually perpendicular transverse modes. When a transition takes place from a higher vibrational to a lower vibrational state, a quantum of thermal energy is emitted. In analogy with a *photon* of radiation energy, the quantum of thermal energy is termed as **phonon.** Absorption of phonons by a crystal can produce atomic displacement leading to imperfections. Unlike point defects and line defects, phonons produce atomic displacements that are time-dependent and hence transient, *i.e.*, short-lived. As the phonons flow through a solid, they collide with atoms and also with one another and are scattered. Energy and momentum are conserved in the scattering process. In addition to phonon-atom and phonon-phonon interactions, there can also be phonon-electron interactions in the crystal. If in a phonon-electron interaction, the electron is raised to an excited state, this would result in the formation of 'holes' in the empty energy state. The excited electron may interact with the hole to form what is called an **exciton**. Thus, all kinds of fascinating phenomena can occur in the crystal lattice as a result of such dynamic interactions. No wonder that solid state physics is, next to elementary particle physics, the most exciting area of scientific research.

The spectacular applications of solid state science have been in materials science, nanotechnology and computers. The 2007 physics Nobel Prize was awarded to the German physicist Peter Gruenberg and the French physicist Albert Fert for their independent discovery of **Giant Magnetoresistance** (GMR). The GMR effect has revolutionized techniques for retrieving data from hard disks in computers, making it possible to miniaturize hard disks radically. Also, another triumph for research in the solid state is the 2009 Physics Nobel Prize for achievements that have helped lay the foundation for the Information Technology (IT) revolution and modern network societies. Charles K. Kao was honoured for achievements concerning the transmission of light in fibres for optical communicaiton and Willard S. Boyle and George E. Smith were honoured for the invention of an imaging semiconductor circuit—the **charge-coupled device (CCD) sensor.**

Quasicrystals

Researchers discovered in 1984 that a rapidly cooled alloy of composition $Al_{86}Mn_{14}$ gave a pattern of discrete spots by electron diffraction that showed the **icosahedral symmetry** $m\bar{5}m$. It follows that, although the structure is not based on a translation unit cell, it has to possess a high degree of three-dimensional regularity in order to exhibit Bragg reflection. Such materials are termed quasicrystals. Fig. 45. shows an icosahedron ; the vertical direction is one of the six $\bar{5}$ axes. An icosahedron may be formed by allowing 20 regular tetrahedra to share a common apex, the central dot in Fig. 45, each tetrahedron distorting slightly in the process.

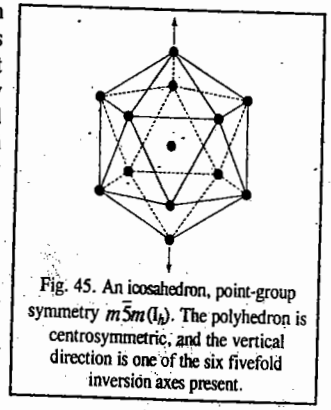

Fig. 45. An icosahedron, point-group symmetry $m\bar{5}m(I_h)$. The polyhedron is centrosymmetric, and the vertical direction is one of the six fivefold inversion axes present.

Other species of icosahedral symmetry are known. For example, the turnip yellow mosaic virus has crystals of point group 532(I). In this case, the inherent icosahedral strain is relieved by incorporating water molecules into the structure. Molecules are known that show five-fold symmetry, as in the metal

biscyclopentadienyls $(C_5H_5)M$. For M=Fe, with the cyclopentadienyl rings staggered (Fig. 46), the point group symmetry is $\bar{5}m(D_{5d})$ whereas for M = Ru, with the rings in the eclipsed position, the symmetry is $\overline{10}m2(D_{5h})$.

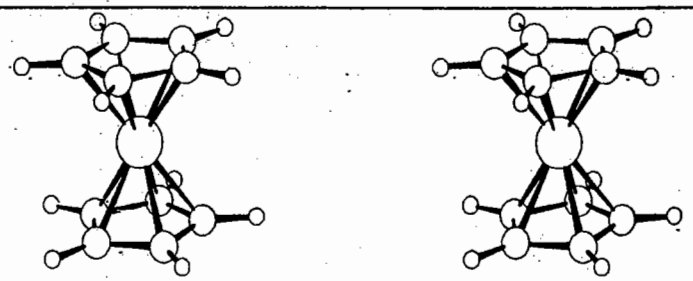

Fig. 46. Stereoview of the molecular structure of biscyclopentadienyl iron, showing the centrosymmetric point-group symmetry $\bar{5}m$ for the molecules ; the two rings are in the staggered position.

A quasicrystal may be considered as a three-dimensional generalization of the two-dimensional Penrose tiling pattern (Fig. 47) which consists of rhombi of angles 144° and 108°; the former occurs

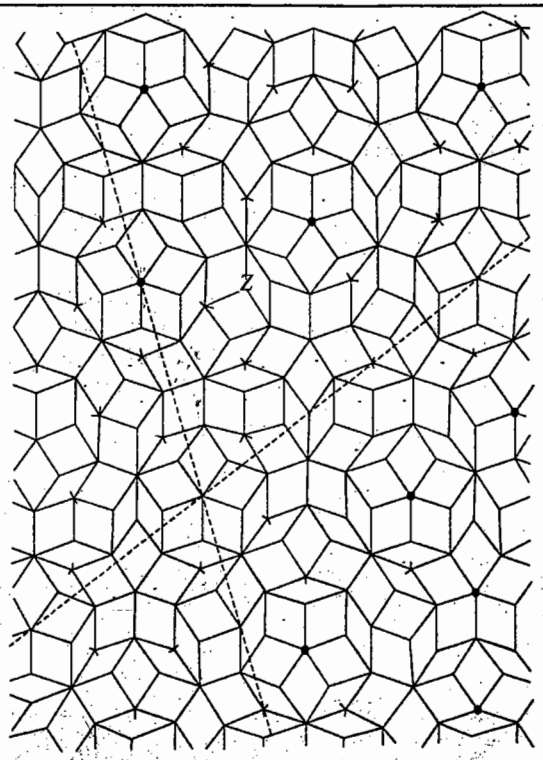

Fig. 47. Two-dimensional Penrose tiling pattern ; the rhombi have angles of 144° and 108°. The similar orientations of the decagons are highlighted by dashed lines at 72° to each other, such lines permeating the whole pattern. It is this type of regularity in three dimensions that enables a quasicrystal to develop Bragg reflections.

$(1+\sqrt{5})/2$ times more frequently than the latter ; this number is referred to as the *golden mean* τ. A pentagon of unit side has a diagonal of 2 cos $(\pi/5)$ or τ, the same value occurs for the distance from the vertex of a regular decagon of unit length sides to its centre. If three rectangular cards with sides in the ratio τ:1 are slotted centrally such that they can be interlinked to form three mutually perpendicular planes, the corners of the card become the vertices of an icosahedron. The value of τ is :.. (1·618033989).

Although there is no pure translational symmetry in the tiling pattern, the regular decagons are similarly oriented and lines can be drawn through the corners (atom positions) at 72° (360°/5). In three dimensions, two different rhombohedral cells (compressed cubes) can be packed together to give an icosahedral structure.

For several aspects of the solid state, refer to :

C.N.R. Rao, *Solid State Chemistry : Selected Papers of C.N.R. Rao*,(ed., S.K. Joshi and R.A. Mashelkar), World Scientific, Singapore, 1995.

I. Review Questions

1. Derive the Bragg equation in X-ray crystallography.
2. Discuss how you would use the systematic absences of reflection in the diffraction pattern to distinguish between the three types of cubic Bravais lattices.
3. Derive Born-Lande' equation for the lattice energy of an ionic solid.
4. Discuss the Fourier synthesis of electron density in a crystal.
5. Describe the Patterson synthesis for determining the relative orientations of pairs of atoms in a crystal.
6. Describe in details the free electron model of metallic structure. Explain how this model accounts for high conductivity of metals. Explain the term Fermi energy.
7. What are extrinsic semiconductors ? Discuss briefly giving diagrams.
8. What are *n*-type and *p*-type semiconductors ? Explain the fabrication of transistors.
9. What is superconductivity ? How would you explain superconductivity of metals.
10. Discuss briefly the following types of defects : *(i)* Schottky defects *(ii)* Frenkel defects *(iii)* Metal excess defects *(iv)* Metal deficiency defects *(v)* Line defects.
11. What are Schottky defects ? Derive an expression for the number of Schottky defects in a crystal.
12. What are Frenkel defects ? Derive an expression for the number of Frenkel defects in a crystal.
13. What are colour centres ? How do they arise ?
14. What are the common types of dislocations ?

II. Problems

1. NaCl has a f.c.c. structure. How many Na^+ and Cl^- ions are there in the unit cell ? **[Ans. Na^+=4, Cl^-=4]**
2. CsCl has a b.c.c. structure. How many Cs^+ and Cl^- ions are there in the unit cell ? **[Ans. Cs^+=1, Cl^-=1]**
3. NaCl crystallises in a face-centred cubic lattice. Calculate the number of unit cells in 1·0 g of the crystal. What is the number along each edge of the crystal ? **[Ans. $2{\cdot}57\times10^{21}$ unit cells, $1{\cdot}37\times10^{7}$]**
4. Insulin forms crystals of orthorhombic type with unit cell dimensions of 13·0 nm×7·48 nm×3·09 nm. If the density of the crystal is $1{\cdot}315\times10^{3}$ kg m^{-3} and there are six insulin molecules per unit cell, what is the molar mass of insulin ? **[Ans. 39·7 kg mol^{-1}]**

5. Copper crystallizes in a f.c.c. lattice with the edge length, a=360 pm. If the density of Cu is $8{\cdot}94\times10^3$ kg m^{-3}, calculate the Avogadro's number. (Molar mass of copper = 63·54 g mol^{-1}). [Ans. $6{\cdot}095\times10^{23}$ mol^{-1}]

6. Calculate the lattice energy of cesium iodide which crystallizes in the cesium chloride structure and has an interionic distance of 395 pm. The Madelung constant and the Born exponent for CsI are 1·76 and 12, respectively. [Ans. – 564·8 kJ mol^{-1}]

7. The only metal that crystallizes in a primitive cubic lattice is polonium which has a unit cell side of 334·5 pm. What are the perpendicular distances between planes with Miller indices (110), (111), (210) and (211) ? [Ans: 236·5, 193·1, 149·5 and 136·6 pm]

8. Calculate the interplanar spacing (d_{hkl}) for a cubic system between the following sets of planes : *(a)* 110 *(b)* 111 *(c)* 222. Assume that a is the edge length of the unit cell. [Ans. *(a)* $d_{110}=a/\sqrt{2}$ *(b)* $d_{111}=a/\sqrt{3}$ *(c)* $d_{222}=a/2\sqrt{3}$]

9. Calculate the angles at which first, second, and third order reflections are obtained from planes 500 pm apart, using X-rays of wave length 100 pm. [Ans. 5·74°, 11·54°, 17·46°]

10. X-rays of wave length 154 pm are diffraction by the 200 plane of AgCl crystal. At what angle would the maximum reflection occur ? Given : a = 555 pm. [Ans. θ = 16·1°]

11. A powder pattern of MgO, known to crystallize in the cubic system, shows diffraction lines at sin θ values of 0·1461, 0·1690, 0·2801, 0·2801, 0·2935 and 0·3697. Determine the lattice type of MgO. [Ans. f.c.c.]

12. NaCl has a face-centred cubic lattice ? What is the coordination number of *(a)* the sodium, and *(b)* the ion ? *(c)* What are the individual lattice structures of sodium and ions in NaCl ? *(d)* What is the number of Na^+ and Cl^- ions in the unit cell of NaCl ? [Ans. *(a)* 6 *(b)* 6 *(c)* f.c.c., *(d)* Na^+=4, Cl=4]

13. A compound alloy of gold and copper crystallizes in a cubic lattice in which gold atoms occupy the lattice points at the corners of a cube and the copper atoms occupy the centres of each of the cube faces. What is the formula of the compound ? [Ans. $AuCu_3$]

14. Ag crystallizes in a cubic lattice. The density is $10{\cdot}7\times10^3$ kg m^{-3}. If the edge length of the unit cell is 406 pm, determine the type of the latice. [Ans. f.c.c.]

15. Calculate the interplanar spacing (d_{hkl}) for a cubic system between the following sets of planes :*(a)* 110 *(b)* 111 *(c)* 222. Assume that a is the edge length of the unit cell. [Ans. *(a)* $d_{110} = a/\sqrt{2}$ *(b)* $d_{111}=a/\sqrt{2}$ *(c)* $d_{222} = a/2\sqrt{3}$]

16. The density of NaCl at 25°C is $2{\cdot}163\times10^3$ kg m^{-3}. When X-rays from a palladium target having a wave length of 58·1 pm are used, the 200 reflection of NaCl occurs at an angle of 5·91°. Calculate the number of Na^+ and Cl^- ions in the unit cell. [Ans. n = 3·999 ≈ 4]

CHAPTER 32

THE COLLOIDAL STATE

The Colloidal Systems. A colloidal dispersion has traditionally been defined as a suspension of small particles in a continuous medium. Because of their ability to scatter light and their very low osmotic pressure, these particles were recognized to be much larger than simple small molecules such as water, alcohol or benzene and simple salts like NaCl. It was assumed that they were aggregates of many small molecules, held together in a kind of amorphous state quite different from the usual crystalline state of these substances. Today we recognize that many of these "aggregates" are in fact single molecules that have a very high molar mass. The size limits are difficult to specify but if the dispersed particles are between 1 μm and 1 nm, we may say that the system is a colloidal dispersion.

There are two classical subdivisions of colloidal systems : (1) *lyophilic* or *solvent-loving* colloids (also called *gels*) and (2) *lyophobic* or *solvent-fearing* colloids (also called *sols*).

The **lyophilic colloids** are invariably polymeric molecules so that the colloidal solution consists of a dispersion of single molecules. The stability of the lyophilic colloid is a consequence of the strong, favourable solvent–solute interactions. Typical lyophilic systems would be proteins (especially gelatin) or starch in water, rubber in benzene and cellulose nitrate or cellulose acetate in acetone. The process of dissolution may be rather slow. The first additions of solvent are slowly absorbed by the solid which swells as a result (this stage is called *imbibition*). Further addition of solvent together with mechanical kneading (as in the case of rubber) slowly distributes the solvent and solute uniformly. In the case of ordinary gelatin, the dissolution process is aided considerably by raising the temperature. As the solution cools, the long and twisted protein molecules get entangled in a network with r uch open space between the molecules. The presence of the protein induces some structure in the water which is physically trapped in the interstices of the network. The result is a gel. The addition of gross amounts of salts to a hydrophilic gel will ultimately precipitate the protein. However, this is a consequence of competition between the protein and the salt for the solvent, water. Lithium salts are particularly effective because of the large amount of water than can be bound by the lithium ion. The charge of the ion is not a primary determinant of its effectiveness as a precipitant.

The **lyophobic colloids** are invariably substances that are highly insoluble in the dispersion medium. The lyophobic colloids are usually aggregates of small molecules (or in cases where a molecule is not defined, such as AgI, they consist of a large number of units of the formula).

Preparation of Lyophobic Colloidal Solutions

The primary consideration in the preparation of colloidal solutions is that the dispersed particles should be within the size range of 1 mμ–200 mμ. The lyophilic sols can be readily prepared since colloidal materials such as starch, gelatin, acacia, etc., when added to water swell up and spontaneously break into particulates of matter of colloidal range. The lyophobic sols, however, require special techniques for their preparation. The methods consist either in 1. *Breaking down the coarser aggregates into particles of colloidal size* or 2. *Grouping molecules into larger aggregates of colloidal size*. The methods belonging to these two categories are known as **dispersion** and **condensation** methods, respectively.

A. Dispersion Methods. 1. Mechanical Dispersion. The most obvious method of dispersion

consists in breaking down the coarser solid particles by mechanical grinding. This is done in the so-called 'colloid mill' which generally consists of two metal discs held at a very small distance apart from one another which are capable of revolving at a high speed (of the order of 7000 rpm) in opposite direction. The material to be ground is fed in between the two discs in the form of a wet slurry. The particles get broken to colloidal dimensions by the operating shearing force. However, it is doubtful if this method produces particles uniformly of colloidal dimensions.

Some sols can alternatively be prepared by mechanical dispersion in a high intensity ultrasonic generators operating at a frequency of 20 kHz (not audible to human ear) and above. This technique is effective only if the substance being dispersed is of low mechanical strength such as sulphur, graphite, resins and gypsum. Ultrasonic vibrations are usually obtained by piezoelectric oscillations which convert electric vibrations of high frequency into mechanical vibrations. Ultrasonic waves of vibrations of 1 MHz frequency are obtained from quartz oscillators whereas those having vibrations of 50 kHz frequency are obtained from magnetostriction oscillators whose working component is a ferromagnetic rod. Ultrasonic vibrations cause local, rapidly alternating contractions and expansions of the solid substance resulting in the formation of minute cavities which disappear immediately under the action of external pressure thereby destroying the solid and converting it into a colloidal dispersion.

2. Electrical Dispersion. In this method an arc is struck between two electrodes of a metal like platinum, gold, silver or copper, in water containing traces of an alkali, when the metal passes into colloidal solution of a reasonable, though not high concentration (Fig. 1). It is believed that in this method, introduced by G. Bredig in 1898, the metal first changes into vapours (molecular state) on account of the heat of the spark and the vapours then condense in water to give aggregates of colloidal range. The function of the alkali will be explained shortly in this chapter.

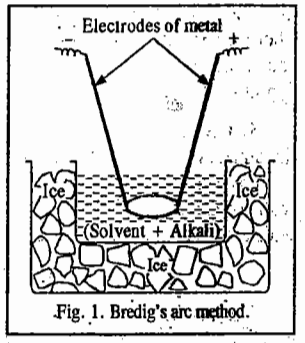

Fig. 1. Bredig's arc method.

T. Svedberg devised a method to obtain organosols of metals and non-metals. In Svedberg's method, the electrodes are usually of iron or aluminium and alternating current (instead of the direct current used in Bredig method) is employed. The material to be dispersed is taken in the form of granules and pasted on the electrodes (immersed in the organic medium) through which the electric arc is passed. Electroputtering occurs as the electric spark gets through the granules of the material pasted on the electrode. Electroputtering technique is used for obtaining organosols of several metals and non-metals.

Organosols of metals are used (*i*) in the hydrogenation and reduction of organic compounds, (*ii*) as catalysts for combustion of liquid fuels in rockets, (*iii*) as fillers of plastics, glues, anticorrosive lacquers and paints and (*iv*) in medicine.

3. Peptization. Certain freshly formed precipitates, such as silver chloride, ferric hydroxide, aluminium hydroxide, can be converted into colloidal solutions by the addition of a small amount of a suitable electrolyte. An electrolyte having an ion in common with the material to be dispersed is required for sol formation. The peptization action is due to the preferential adsorption of one of the ions of the electrolyte by the particles of the material. As would be illustrated a little later in this chapter, as a result of the preferential adsorption of the ion which is more closely related chemically to the precipitate, the particles acquire a positive or a negative charge depending upon the charge on the ion adsorbed. Because of the presence of the same type of charge, the particles of the precipitate are pushed apart. The precipitate thus gets dispersed resulting in the formation of a stable sol. Thus, ferric hydroxide sol is obtained when a small quantity of ferric chloride solution is added. The peptization action is due to the preferential adsorption of Fe^{3+} ions. Similarly, an aluminium hydroxide sol is obtained when dilute hydrochloric acid is added to freshly precipitated aluminium hydroxide. The ion preferentially adsorbed, *viz.*, the Al^{3+} ion, is generated by the action of hydrochloric acid on $Al(OH)_3$.

B. Condensation Methods. Colloidal systems can be obtained by various chemical reactions such as double decomposition, oxidation, reduction, hydrolysis, etc. It should be noted that colloidal systems are not always formed in reactions capable of producing sols ; they are formed under specific conditions, as for example, at definite concentrations of the initial substances, at a definite temperature and a definite order of their mixing, etc.

1. Double Decomposition. A sol of arsenious sulphide is prepared by passing H_2S gas through a dilute solution of arsenious oxide and removing the excess H_2S by boiling.

$$As_2O_3 + 3H_2S \longrightarrow As_2S_3 + 3H_2O$$

2. Oxidation. A colloidal sulphur sol is obtained by the oxidation of an aqueous solution of hydrogen sulphide with air or sulphur dioxide.

$$2H_2S + O_2 \longrightarrow 2S + 2H_2O$$

$$2H_2S + SO_2 \longrightarrow 3S + 2H_2O$$

During the oxidation of H_2S to S, complex oxidation reactions occur simultaneously resulting in the formation of polythionic acids. These acids readily get associated with the colloidal particles of sulphur to form bigger colloidal particles called miscelles which are thermodynamically more stable than the constituent species. In other words, polythionic acids act as *stabilizers* for the sulphur sol. There is experimental evidence that pentathionic acid, $H_2S_5O_6$, formed during the oxidation reaction acts as the stabilizing electrolyte, converting the sulphur colloidal particle into a *miscelle* having the formula : $(m[S]nS_5O_6^{-2}.2(n-x)H^+)2xH^+$.

3. Reduction. Sols of metals such as silver, copper, gold and platinum are obtained by reducing the aqueous solutions of their salts by non-electrolytes such as formaldehyde, tannin, phenyl hydrazine, carbon monoxide and phosphorus. Zsigmondy prepared the gold hydrosol by reducing potassium aurate with formaldehyde. In this reaction, chloroauric acid, $H[AuCl_4].4H_2O$, first formed, is made to react with potassium carbonate in an aqueous solution to yield potassium aurate :

$$2H[AlCl_4] + 5K_2CO_3 \longrightarrow 2KAuO_2 + 5CO_2 + 8KCl + H_2O$$

The resulting solution is heated and a dilute solution of formaldehyde is added dropwise when reduction occurs according to the reaction :

$$2KAuO_2 + 2CH_2O + K_2CO_3 \xrightarrow{\Delta} 2Au\ (sol) + 3HCOOK + KHCO_3 + H_2O$$

Potassium aurate, $KAuO_2$, acts as the stabilizer of the red gold sol obtained. The miscelle of the gold sol is represented by the formula :

$$(m[Au]nAuO_2^-.(n-x)K^+)xK^+$$

4. Hydrolysis. Colloidal sols of heavy metals are obtained by the hydrolysis of the solutions of their salts. Thus, when a small amount of ferric chloride is added to boiling water, a red-brown sol of ferric hydroxide is obtained :

$$FeCl_3 + 3H_2O \xrightarrow{\Delta} Fe(OH)_3 + 3HCl$$

Boiling promotes the reaction because HCl formed is removed along with water vapours from the system.

In this reaction, iron oxychloride, FeOCl, formed as a result of incomplete hydrolysis of $FeCl_3$, is believed to act as the stabilizer :

$$FeCl_3 + H_2O \longrightarrow FeOCl + 2HCl$$

The stabilizer can also be $FeCl_3$ or HCl. The stabilising action of $FeCl_3$ is evidently due to the Fe^{3+} ions which it yields in solution. Evidence in favour of HCl comes from the fact that the surface

of ferric hydroxide sol has a number of hydroxyl groups which are capable of adsorbing the hydrogen ions provided by HCl. Thus, the structure of the $Fe(OH)_3$ sol can be expressed by any of the following formulae depending upon which substance acts as a stabilizer :

1. $(m[Fe(OH)_3]\ n FeO^+.(n-x)Cl^-)\ xCl^-$
2. $(m[Fe(OH)_3]\ n Fe^{3+}.3(n-x)Cl^-)\ 3xCl^-$
3. $(m[Fe(OH)_3]\ n H^+.(n-x)Cl^-)\ xCl^-$

5. Exchange of Solvents. Sols can also be obtained by exchange of solvents. For instance, when a concentrated solution of sulphur in alcohol is poured in a large amount of boiling water, the alcohol evaporates leaving behind sulphur particles which form nuclei that rapidly grow into a colloidal sol.

Purification of Colloidal Solutions. The presence of impurities, particularly the electrolytes, renders the sols unstable. The cause of this instability will be discussed shortly in this chapter. These impurities must be eliminated by suitable means. Two simple methods are generally employed.

1. Dialysis. It has already been stated that while particles in true solution can easily diffuse through parchment and other fine membranes, the colloidal particles, being much larger, cannot do so readily. If a mixture, containing colloidal particles as well as particles in true solution, is placed in a parchment bag which is then held in a wider vessel containing pure water, the substances in true solution pass out while the colloids remain in the bag. The distilled water in the wider vessel is renewed frequently.

The process of separating substances in colloidal state from those present in true solution with the help of fine membranes, is known as **dialysis** and the membrane used for the purpose is known as **dialyser.**

Ordinarily, the process of dialysis is quite slow but it can be quickened by applying an electric field if the substance in true solution is an electrolyte. The process is then called **electrodialysis.** The mixture is placed between two dialysing membranes while pure water is contained in a compartment on each side. There is one electrode in each compartment by means of which the required voltage is applied. The ions of the electrolyte migrate out to the oppositely charged electrodes while the colloidal particles are held back.

2. Ultra-filtration. The separation of solutes from colloidal systems can also be carried out by the process known as **ultra-filtration.** Ordinarily, filter papers have pores larger than 1 μ (*i.e.*, 1000 mμ) so that the colloidal particles which are less than 200 mμ can readily pass through along with the ions or molecules in solution. But the pores can be made smaller by soaking the filter papers in a solution of gelatin or collodion and subsequently hardening them by soaking in formaldehyde. The pores thus become very small and the colloidal particles may be retained on the treated filter paper. The treated filters are known as **ultra-filters.** This process of separating colloids from solutes is known as ultra-filtration. A series of graded ultra-filters can be prepared by soaking filter papers in solutions of collodion of different concentrations. The pores even in the finest ultra-filters will be large enough to permit the passage of ions or molecules in true solution but these will be small enough to withhold the colloidal particles. By using a series of graded ultra-filters, it may be possible to separate colloidal particles of different sizes from one another. The process is very slow and sometimes a small pressure is needed to drive the solute particles through the filters.

General Properties of Colloidal Systems

1. Heterogeneous Character. As already stated, colloidal systems, unlike true solutions, are heterogeneous in character. They consist of two phases : the dispersed phase and dispersion medium.

2. Diffusibility. The colloidal particles constituting the dispersed phase do not readily diffuse through parchment or other fine membranes. In fact, it was this property which led Thomas Graham to lay the foundation of colloid science, as already mentioned.

3. Filterability. The colloidal particles readily pass through ordinary filter papers along with any dissolved material. This is because even the finest filter paper has pores bigger than the colloidal dimensions.

4. Visibility. It is not possible to see colloidal particles even with the help of a most powerful microscope. A gold sol, for instance, appears to be as clear as a true solution of gold chloride in water. The reason of the invisibility of colloidal particles has already been discussed.

Attempts have been made in recent times to use ultraviolet rays or cathode rays for seeing the colloidal particles. But, these rays make no impression on the retina of the eye. However, the images formed by them can be photographed. The **electron microscope,** for instance, makes use of a beam of cathode rays and by combination of special types of lenses, images of colloidal particles can be obtained on photographic plates.

5. Colligative Properties. The magnitude of osmotic pressure, lowering of vapour pressure, depression in freezing point and elevation in boiling point, depend upon the number of solute particles present in a given mass of the solvent. Now, colloidal particles are not simple molecules. These are physical aggregations of molecules. In arsenic sulphide sol, for instance, each particle is composed of about 1000 molecules. Thus, for a given mass of arsenic sulphide, the number of particles in the sol will be only $\frac{1}{1000}$th of the number present in true solution. Hence, all colloidal dispersions (unlike true solutions) give very low osmotic pressure and show very small freezing point depression or boiling point elevation.

6. Optical Properties. It was observed by Tyndall, in 1869, that when a beam of light is passed through a true solution, it cannot be seen unless the eye is placed directly in its path. However, when the same beam of light is passed through a colloidal dispersion, it becomes visible as a bright streak. This phenomenon is known as the **Tyndall effect** and the illuminated path (streak of light) is known as **Tyndall cone** (Fig. 2). This phenomenon is due to the scattering of light from the surface of colloidal particles. In a true solution, there are no particles of sufficiently large diameter to scatter light and hence the beam is invisible.

The visibility of dust particles in a semi-darkened room when a sun beam enters or when light is thrown from a light projector, are familiar examples of Tyndall effect. The dust particles are large enough to scatter light and thus render the path of light visible.

The intensity of the scattered light depends on the difference between the refractive indices of the dispersed phase and the dispersion medium. In lyophobic sols, this difference is appreciable and, therefore, the Tyndall effect is quite well-defined. In lyophilic sols, the particles are largely solvated. This lowers the difference in the refractive indices of the two phases and hence the Tyndall effect is much weaker. Thus, in the sols of freshly prepared silicic acid, blood serum, albumins, etc., there is little or no Tyndall effect.

The Tyndall effect has been used by Zsigmondy and Siedentopf in devising the **ultra-microscope.** A strong beam of light from an arc lamp or any other source is condensed by a system of lenses and passed through the colloidal solution. The scattered beam (Tyndall beam) is viewed through a microscope placed at right angles to the beam (Fig. 2). In this way, the colloidal

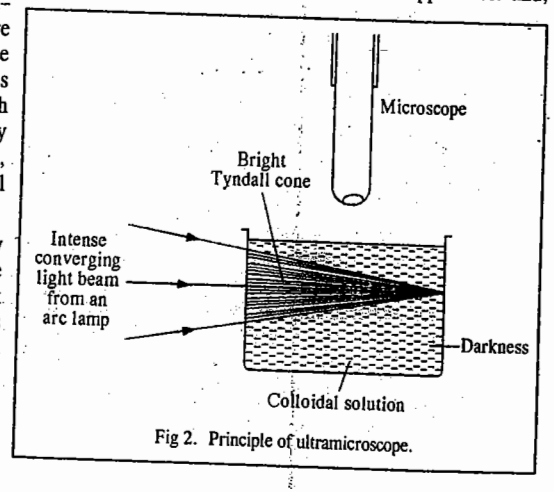

Fig 2. Principle of ultramicroscope.

particles which are too small to be seen under an ordinary microscope, can be detected as spots of light moving irregularly. It may be emphasised that we do not see the actual particles ; they are too small to be visible. We see only the light scattered by them. Our eye pictures various spots of light as round or spherical particles.

7. The Brownian Movement. Robert Brown, an English botanist, in 1827, observed that pollen grains in aqueous suspensions were in constant motion. Later on when ultra-microscope was invented, it was found that particles of lyophobic sols were also in a state of ceaseless erratic and random motion similar to pollen grains. This kinetic activity of particles suspended in a liquid is called **Brownian movement.** The Brownian movement is due to the bombardment of colloidal particles by molecules of dispersion medium which are in constant motion like molecules in a gas. As a result, the colloidal particles acquire almost the same amount of kinetic energy as possessed by the molecules of the dispersion medium. But, since the colloidal particles are considerably heavier than molecules of the dispersion medium, their movement is considerably slower than that of the molecules of the medium.

The Brownian movement is not observed in ordinary suspensions because the mass of each particle in this case is so large that the bombardment by molecules of the dispersion medium produces little effect on them. Brownian movement offers a visible proof of the random kinetic motion of molecules in a liquid.

Properties of Hydrophobic Colloidal Systems

I. Electrical Properties

Charge on Colloidal Particles. The most important property of hydrophobic colloidal dispersions is that the particles carry electric charge. All the particles in a given hydrophobic colloidal system carry the same charge and the dispersion medium has an opposite and equal charge, the system as a whole being electrically neutral. The presence of similar charges on colloidal particles is largely responsible in giving stability to colloidal systems because the mutual forces of repulsion between similarly charged particles prevent them from coalescing and coagulating or aggregating when they come closer to one another. Metallic hydroxides, some metals (such as bismuth, lead, iron), methyl violet and methylene blue, are *electropositive colloids* while metallic sulphides, prussian blue, many metals (such as silver, gold, platinum), silicic acid, tannic acid and mastic are *electronegative colloids.*

The Origin of Charge on Colloidal Particles. The origin of charge on colloidal particles has not been completely understood. However, it has been observed that sols are invariably associated with minute quantities of electrolytes and that if the latter are completely removed by persistent dialysis, the sols become unstable. It is believed, therefore, that *the charge on the colloidal particles is due to* **preferential adsorption** *of either positive or negative ions on their surface.* If the particles have a preference to adsorb positive ions, they acquire a positive charge and if they prefer to adsorb negative ions, they acquire a negative charge. According to this view, positive charge on ferric hydroxide sol prepared by hydrolysis of ferric chloride is largely due to preferential adsorption *of* Fe^{3+} ions on the surface of particles of ferric hydroxide. The ferric ions come from ionisation of ferric chloride which is always present in traces in the sol.

Similarly, the negative charge on arsenic sulphide sol is due to preferential adsorption of sulphide ions on the surface of arsenic sulphide particles. The sulphide ions are furnished by ionisation of hydrogen sulphide which is present in traces. Likewise, the negative charge on metal sols prepared by the Bredig's arc method is due to adsorption of hydroxyl ions furnished by traces of the alkali added. It should be remembered that *the ion which is more nearly related chemically to the colloidal particle is preferentially adsorbed by it.* Thus, in ferric hydroxide sol, *ferric* and not chloride ion is preferred. Similarly, in arsenic sulphide sol, *sulphide* and not hydrogen ion is preferred.

An interesting case is furnished by stannic oxide sol. If a freshly formed precipitate of stannic oxide is *peptised* by a small amount of hydrochloric acid, the sol carries a positive charge but if peptised by a small amount of sodium hydroxide, the sol carries a negative charge. In the former case, a small amount

of stannic chloride, $SnCl_4$, is formed and the positively charged Sn^{4+} ion is preferred and the sol is positively charged. In the latter case, a small amount of sodium stannate, Na_2SnO_3, is formed and now the negatively charged SnO_3^{2-} ion is preferred and accordingly the sol is negatively charged. The chloride and sodium ions, known as counter ions, are directed towards the liquid phase.

Another interesting case is furnished by the formation of positively as well as negatively charged sols of silver iodide. If a dilute solution of silver nitrate is added to a slight excess of a dilute solution of sodium iodide, a negatively charged sol of silver iodide is formed. This is due to the adsorption of iodide ions. The structure of the sol particle is represented as in Fig. 3(*a*). But, if a dilute solution of sodium iodide is added to a slight excess of dilute solution of silver nitrate, a positively charged sol of silver iodide is formed due to the adsorption of silver ions. The structure of the sol particle is now represented as in Fig. 3(*b*). However, if silver nitrate and sodium iodide are mixed in equivalent amounts, there is precipitation of silver iodide and no sol is formed. It may be mentioned once again that the ions preferred by colloidal particles are those which are common to them. Thus, in the above example, in the first case, silver iodide prefers iodide ion and not sodium ion. In the second case, it prefers silver ion and not nitrate ion. The counter ion, in each case, is directed towards the liquid phase.

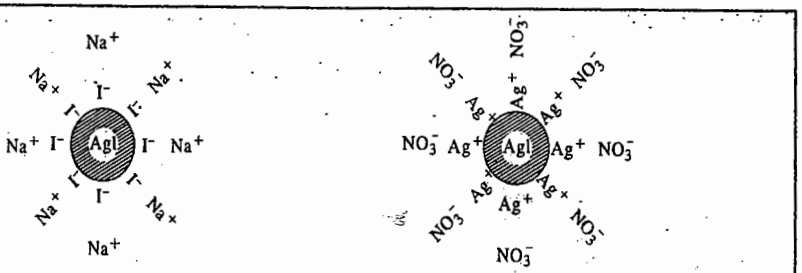

Fig. 3(*a*). Negatively charged sol of AgI

Fig. 3(*b*). Positively charged sol of AgI

Thus, on the surface of a colloidal particle there is an electrical double layer of opposite charges. The aspect has been discussed in adequate details in the next section.

Another possible way in which colloidal particles may acquire charge is by direct ionisation of the material constituting the particles. This phenomenon is observed mostly in the case of acidic and basic dyestuffs. An acidic dyestuff, for example, ionises yielding hydrogen ions in solution and thereby leaving an equivalent amount of negative charge on the particles. The structure of the colloidal particles of the dye may be represented as shown in Fig. 4(*a*).

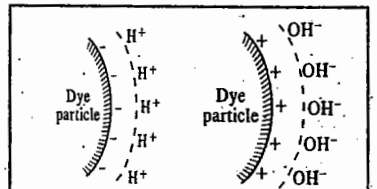

(*a*) An acidic dyestuff (*b*) A basic dyestuff

Fig. 4. Origin of charge in dyestuffs from ionisation of surface groups.

A basic dyestuff, on the other hand, ionises yielding hydroxyl ions in solution and thereby leaving an equivalent amount of positive charge on the particles. The structure of the colloidal dye particles in this case may be represented as shown in Fig. 4(*b*).

The Electrical Double Layer. Central to the understanding of the electrical properties of colloids is the concept of **electrical double layer.** Consider once again the formation of silver iodide sol from the double decomposition reaction

$$AgNO_3\ (aq) + NaI\ (aq) \longrightarrow AgI\ (s) \downarrow + NaNO_3\ (aq)$$

Let us suppose that the electrolyte used in excess is sodium iodide. This would result in preferential adsorption of I^- ions giving a negatively charged sol of silver iodide, as illustrated above (Fig. 3*a*).

The ions preferentially **adsorbed on the surface of** a particle of a colloidal system are called *potential-determining ions.*

The negatively charged surface of AgI particle attracts the positive ions (Na^+) and repels the negative ions (NO_3^-). As a result, the positive Na^+ ions tend to form a compact layer in the vicinity of the potential-determining I^- **ion layer.** This is called the **Stern layer** (Fig. 5). The ions present in the Stern layer are called the **counter ions.**

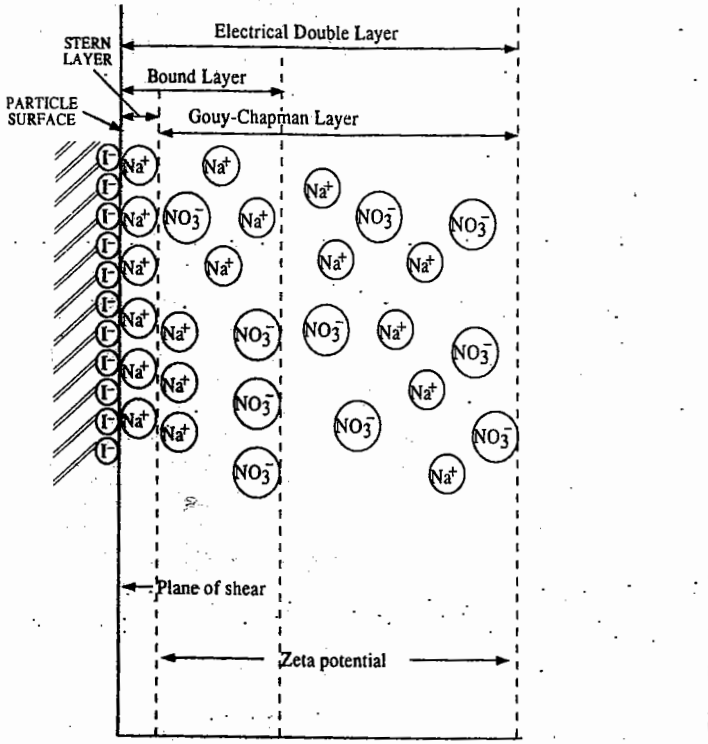

Fig. 5. The electrical double layer in colloidal systems.

The influence of the surface charge decreases with distance and so does the number of ions with the result that at a certain distance from the surface of the particle, the concentration of Na^+ ions equals the concentration of NO_3^- ions and a state of electroneutrality prevails (Fig. 5). It must be borne in mind that the system as a whole is electrically neutral even though there exist regions of unequal distribution of anions and cations. The diffuse layer between the Stern layer and the electrically neutral part of the system is referred to as the **Gouy-Chapman layer.**

The presence of charge gives rise to potential at the surface of the particle. This potential drops to zero at some distance away from the surface depending upon the concentration of the counter ions in the bulk phase. The region in which the influence of the charge is appreciable is known as the

electrical double layer. The double layer consists of two parts : the Stern layer, the thickness of which is of the order of ionic dimensions and the Gouy-Chapman diffuse layer, the thickness of which is given by

$$r_D = \left(\frac{\varepsilon_r RT}{2\rho F^2 I}\right)^{1/2} \qquad ...(1)$$

where ρ, ε_r and I are, respectively, the density, the dielectric constant and the ionic strength of the solution. F is the Faraday constant. The value of r_D is of the order of 1–100 nm. It decreases as the ionic strength of the solution increases; more rapidly for counter ions of high valency.

A very important quantity reckoned with in the present context is the so-called **zeta potential** (ζ) defined as the difference in potential between the surface of the tightly bound layer (called the **plane of shear**) and the electroneutral region of the solution. The zeta potential is located at the shear plane. It determines the stability of colloidal systems.

DLVO Theory of the Stability of Lyophobic Colloids

This theory, involving the concept of zeta potential, was developed by the Russian scientists D. Derjaguin and L.D. Landau, and independently, by the Dutch scientists E. Verwey and J.T.G. Overbeek. According to this theory, there is a balance between the repulsive interactions between the charges of the electrical double layers on neighbouring particles and the attractive van der Waals interactions between the molecules in the particles. The repulsive potential energy of the double layer on particles, each of radius a, is given by

$$V_{rep} = \frac{Aa^2\zeta^2}{R} e^{-s/r} \; ; \; a \ll r_D \qquad ...(2)$$

where A is a constant, ζ is the **zeta potential,** R is the separation of the centres, s is the separation of the surfaces of the two particles ($s = R - 2a$ for spherical particles of radius a) and r_D is the thickness of the electrical double layer. Eq. 2 holds for a *thick* double layer ($a \ll r_D$). For a *thin* double layer ($a \gg r_D$),

$$V_{rep} = \frac{Aa\zeta^2}{2} \ln(1 + e^{-s/r_D}) \; ; \quad a \gg r_D \qquad ...(3)$$

The potential arising from the attractive interaction is given by

$$V_{att} = -B/s \qquad ...(4)$$

where B is another constant.

Treating the electrical double layer as a simple electrical condenser, the zeta potential ζ is given by the expression,

$$\zeta = 4\pi\eta u/\varepsilon_r \qquad ...(5)$$

where η are ε_r are the viscosity and the dielectric constant, respectively, of the dispersion medium and u is the mobility of the colloidal particles.

For water as the dispersion medium, ζ is found to lie between 0·03 and 0·06 V. The value of ζ decreases when an ion of opposite charge to that of the colloidal particle is adsorbed. This reduces the mutual repulsion between the similarly charged colloidal particles. As a result, the colloidal particles easily come closer to one another to coalesce and form bigger aggregates which lie outside the colloidal range. This phenomenon of changing colloidal state to a suspended state is known as **coagulation, flocculation or precipitation** of colloidal solutions.

In the case of lyophobic colloids, the stability is due to the electrical charge present on the colloidal particles whereas the stability of the lyophilic colloids depends upon both the electrical

charge and solvation. In order to cause precipitation of the dispersed particles, it is necessary that they coalesce into large aggregates. Since in a lyophobic sol, the charge on all the colloidal particles is of the same sign, the repulsive forces prevent the particles from approaching sufficiently close to one another and to coalesce and coagulate. The magnitude of the repulsive forces depends upon the magnitude of the surface charge and the thickness of the electrical double layer. These factors also determine the value of the zeta potential which actually governs the stability of the colloidal system. If ζ is small, the resultant potential energy is negative so that the van der Waals attraction predominates over the electrostatic repulsion and the sol coagulates rapidly.

On the other hand, in the case of lyophilic sols, solvation plays a very important role. Since the colloidal particles are enclosed in a solvent 'cage', the cage serves as a barrier preventing the particles from coalescing to form aggregates. Thus, whereas in the case of lyophobic sols, removal of electrical charge may easily bring about coagulation, in the case of lyophilic colloids, the charge removal may not necessarily result in coagulation though it may decrease the stability of the sol.

When a lyophilic colloid is added to a lyophobic colloid, the latter is rendered less sensitive to the precipitating action of an electrolyte. This is expressed by saying that the *lyophilic colloid protects a lyophobic colloid* from precipitation by the action of electrolytes. That is why substances such as gum acacia, gelatin, tragacanth, etc., are known as **protective colloids.** They probably function by getting adsorbed on the solid surface in the form of loops wherein water gets trapped. These loops prevent the approach of particles to cause coagulation.

Zsigmondy gave quantitative treatment of the stabilizing action of the protective colloids. He introduced a quantity called the gold number of a protective colloid. The **gold number** is defined as the largest number of milligrams of a protective colloid which, when added to 10 ml of a special standard gold sol, just fails to prevent the colour change from red to blue upon the addition of one ml of 10 percent sodium chloride solution. It must be emphasized that the protective action of a lyophilic sol depends upon several factors such as sol dispersity, the molar mass of the lyophilic sol, the *p*H of the solution at which the experiment is carried out, and so on.

It is customary to use sols other than gold sols to determine the protective action of a high molar mass colloid. Thus, silver, sulphur, prussian blue, etc., sols have been used and the corresponding 'numbers' determined accordingly (Table 1)

TABLE 1

Protective Action of High Molar Mass Lyophilic Colloids on Some Hydrophobic Sols

Protective Colloids	Numbers					
	Gold	Silver	Sulphur	Iron oxide	Rubin	Prussian blue
Gelatin	0·01	0·035	0·00012	5	2·5	0·05
Dextrin	20	100	0·125	20	.....	250
Saponin	115	35	0·015	11·5	.....	2·5
Potato starch	20	.....	.....	.....	20	.....
Haemoglobin	0·03–0·07	.....	.....	.....	0·8	....
Egg albumin	2·5	1·5	0·025	15	2·0	25
Gum arabic	0·5	1·25	0·125	20	.....	5

Coagulation of Colloidal Sols. The stability of the colloidal state rests on the existence of charge on the particles. If this charge is destroyed or reduced, the sol is precipitated. The following methods generally bring about coagulation.

1. By the Action of Electrolytes. If traces of electrolytes are essential for the stability of sols, the presence of large amounts of electrolytes cause their coagulation. This due to the fact that colloidal

particles take up ions carrying charge opposite to that present on them as a result of which the charge is neutralized or reduced to a certain critical value so that the zeta potential falls below 0·02 V. This results in the reduction of the repulsion between the colloidal particles to such an extent that the sol gets precipitated or coagulated or flocculated. Based on the experiments carried out on coagulation, **Hardy and Schulze** formulated the following **rules :**

1. Coagulation is brought about by ions having opposite charge to that of the sol. Accordingly, negative ions cause coagulation of the positively charged sols and positive ions cause coagulation of negatively charged sols. Thus, $Fe(OH)_3$ sol, which is positively charged, is coagulated by negative ions such as Cl^-, NO_3^-, SO_4^{2-}, etc. Similarly, As_2S_3 sol, which is negatively charged, is coagulated by positive ions such as Na^+, Mg^{2+}, Ba^{2+}, etc.

2. The efficacy of an ion to cause coagulation depends upon its valency. Thus, the efficacy of $Al^{3+} >> Mg^{2+} > Na^+$ and that of $[Fe(CN)_6]^{4-} >>> PO_4^{3-} >> SO_4^{2-} > Cl^-$.

Quantitatively, the efficacy varies directly as the square of the valency of the ion. Thus a Mg^{2+} ion is 4 times more effective and an Al^{3+} ion is 9 times more effective than a Na^+ ion in flocculating a negatively charged sol.

3. The minimum concentration of an electrolyte required to cause coagulation or flocculation of a sol is called its **flocculation value.** This is usually expressed in terms of millimoles per litre of the electrolyte. The flocculation values of a few electrolytes for arsenic sulphide and ferric hydroxide sols are given in Table 2.

TABLE 2

Flocculation Values of Different Electrolytes

Arsenic Sulphide Sol			Ferric Hydroxide Sol		
Electrolyte	Cation Valency	Flocc. Value (millimoles per litre)	Electrolyte	Anion Valency	Flocc. Value (millimoles per litre)
NaCl	1	52	HCl	1	132
KCl	1	52	KBr	1	138
HCl	1	30	KNO_3	1	132
K_2SO_4	1	64	$KBrO_3$	1	31
$MgSO_4$	2	0·72	K_2CrO_4	2	0·315
$CaCl_2$	2	0·69	K_2SO_4	2	0·210
$ZnCl_2$	2	0·68	$K_2C_2O_4$	2	0·238
$AlCl_3$	3	0·093	$K_3[Fe(CN)_6]$	3	0·096

We find significant departures from the Hardy–Sehulze rules in this Table. For example, the flocculation value of HCl for As_2S_3 sol and that of $KBrO_3$ for $Fe(OH)_3$ sol are relatively low. This can be attributed to strong adsorption of H^+ ions in the first case and that of BrO_3^- ions in the second case.

Even more striking departures are known. For instance, the flocculation values of potassium citrate, potassium acetate and potassium formate for arsenic sulphide sol are known to be 270, 115 and 85 millimoles per litre. Since potassium ion which is effective in the present case is common, one would have expected the flocculation value of each electrolyte to be about the *same.* The marked discrepancy in the flocculation values shows that the ion carrying the same *charge* as the colloidal particles is also effective in some way in determining the flocculation value of an electrolyte. It has been established by experiment that citrate, acetate and formate ions in the above electrolytes are also adsorbed to different extents on the surface of arsenic sulphide particles thus raising the negative zeta potential of the particles to different extents. Hence, different concentrations of potassium ions

are needed to bring about neutralisation or reduction of the negative charge on the arsenic sulphide sol particles in order to cause their flocculation.

Generally, hydrophobic sols are coagulated by electrolytes at 0·0001—0·1 M concentrations. The coagulation is *irreversible* so that the removal of the coagulating electrolyte does not allow the coagulum to be redispersed. Lyophilic sols, on the other hand, are not easily coagulated. They require much higher concentrations (usually of the order of 1M) of the electrolyte for precipitation. The coagulation of lyophilic sols by the addition of electrolytes is not due to the neutralization of charge on the particles. The electrolyte binds part of the water thereby getting hydrated. As a result, the polymer molecules in the hydrophilic sol get dehydrated. The dehydration leads to coagulation.

Various ions are arranged in increasing order of their efficacy for coagulating a lyophobic sol in the form of a series, as shown below :

$$Mg^{2+} > Ca^{2+} > Ba^{2+} > Na^{2+} > K^{+}$$

$$SO_4^{2-} > Cl^{-} > NO_3^{-} > ClO_3^{-} > I^{-}$$

This series is known as **lyotropic series** or **Hofmeister series.**

2. By the Mutual Action of Sols. When two sols carrying opposite charges are mixed together in suitable proportions, mutual precipitation occurs. For example, when negatively charged arsenic sulphide sol is added to positively charged ferric hydroxide sol in suitable proportions, precipitation of both the sols takes place simultaneously.

3. By Presistent Dialysis. It has been reported earlier that traces of electrolytes are invariably associated with colloidal systems and that this is essential for their stability. If the sols are subjected to prolonged dialysis, these traces of electrolytes also pass out through the dialyser and the colloids become unstable.

4. Coagulation by Mechanical Means. Violent stirring of a sol may coagulate it. Also, sols may coagulate due to the vibratory action caused by ultrasound. Vibratory coagulation is used in technological processes relating to the manufacture of pastes and other similar materials.

II. Electrokinetic Properties

Since the solid particles and the liquid medium carry opposite charges, it is obvious that when an electric field is applied, the particles and the liquid will migrate in opposite directions. When experiments are so arranged that the particles can move but not the medium, we have the phenomenon of **electrophoresis.** If, on the other hand, the experiments are designed in such a way that the medium can move but not the particles, we come across the phenomenon of **electro-osmosis.** Both these phenomena are discussed below.

Electrophoresis. The electrophoretic effect can be studied by the simple apparatus shown in Fig. 6. It consists of a U-tube provided with a stop-cock through which it is connected to a funnel-shaped reservoir. A small amount of water is first placed in the U-tube and a reasonable quantity of the sol is taken in the reservoir. The stop-cock is then slightly opened and the reservoir gradually raised so as to introduce the sol into the U-tube gently. The water is displaced upwards producing a sharp boundary in each arm. A voltage of 50 to 200 volts is then applied by means of the platinum electrodes which are immersed in water layer only. The movement of the particles can readily be followed by observing

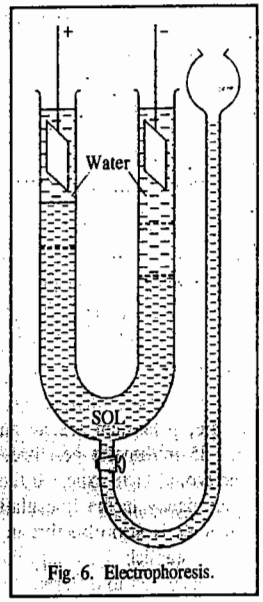

Fig. 6. Electrophoresis.

the position of the boundary by means of naked eye or a lens or a cathetometer. When the particles are *negatively charged* (as in the case of arsenic sulphide sol), the boundary on the negative electrode side is seen to move down and that on the positive electrode side to move up, showing that *the particles move towards the positive electrode.* Thus, by noting the direction of motion of the particles in the electric field, it is possible to determine the *sign of the charge* carried by the particles. It is also possible by this technique to determine the rate at which colloidal particles migrate in an electric field. This rate is expressed in terms of electrophoretic mobility of colloidal particles.

The **electrophoretic mobility** of colloidal particles is defined as the distance travelled by them in one second under a potential gradient of one volt per centimetre. It has been found that the electrophoretic mobilities of colloidal particles are of the same order as those of ions under similar conditions, that is, of the order of $(10 - 60) \times 10^{-5}$ cm/sec/volt/cm.

Since different colloidal materials have different mobilities, it is possible to separate them from one another from their mixtures. This method has been used for the fractionation of proteins, polysaccharides, nucleic acids and other complex substances.

Electro-osmosis. When electrophoresis of dispersed particles in a colloidal system is prevented by some suitable means, it is observed that *the dispersion medium itself begins to move in an electric field.* This phenomenon is known as **electro-osmosis.**

A simple apparatus for studying electro-osmosis is shown in Fig. 7. The colloidal system is placed in the central compartment A which is separated from the compartments B and C filled with water, by the dialysing membranes M and M'. The water in the compartments B and C also extends to the side tubes T and T', as shown. The membranes prevent the movement of the colloidal particles. Therefore, when a potential difference is applied across the electrodes held close to the membranes in the compartments B and C, as shown, the water begins to move. If the particles carry positive charge, the water will carry negative charge. Therefore, it would start moving towards the anode and hence the level of water in the side tube T would be seen to rise. If, on the other hand, the particles carry negative charge, the water, which now carries positive charge, will start moving towards the cathode and the level of water in the side tube T' would start rising.

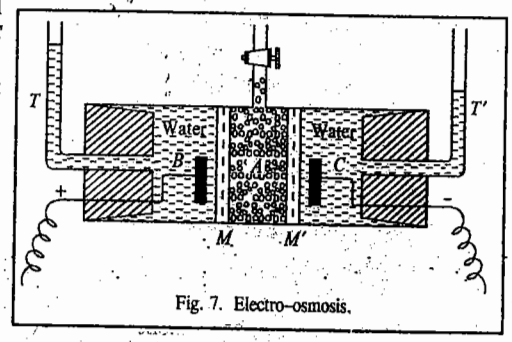

Fig. 7. Electro-osmosis.

Determination of Size of Colloidal Particles. There are a number of methods for the determination of size of colloidal particles. Some of these are given below.

1. By Using Ultrafilters. An approximate idea about the size of particles in a colloidal system can be obtained by the use of ultrafilters. These are prepared by impregnating filter papers with collodion or gelatin which are subsequently hardened by immersing in formaldehyde. The pores can be made small enough to retain particles of colloidal dimensions. The size of the pores depends upon the particular filter paper employed and the concentration of the colloidion or gelatin solution used for impregnating it. It is thus possible to obtain a series of graded ultrafilters by means of which a colloidal solution may be separated into fractions containing particles of different sizes. An approximate estimate of the size of particles can be obtained from a knowledge of the dimensions of the pores of the ultrafilters. The latter parameter is determined from the pressure required to force air or water through the pores. The results obtained by this method are only approximate because pore size is by

no means the only factor which determines whether a given particle will pass through an ultrafilter or not.

2. From Brownian Movement. Colloidal particles suspended in a liquid medium are subjected to Brownian movement. They also tend to settle down due to gravitation. Under the influence of both these effects, the particles distribute themselves in a vertical column in accordance with the equation

$$(RT/N_A) \ln (n_1/n_2) = (4/3)\pi r^3/(h_2 - h_1)(\rho - \rho') \quad ...(6)$$

Since the number of particles n_1 and n_2 at two depths h_1 and h_2 of the vertical column can be counted with the help of an ultra-microscope and densities of the particles and of the liquid medium, ρ and ρ', can be determined by the usual methods, the radius of the particles, r, can be easily calculated. Brownian motion of colloidal systems was investigated by the French physicist Jean Perrin (1870–1942) to determine the Avogadro's number. Perrin was awarded the 1926 Physics Nobel prize for his work on the discontinuous structure of matter and especially for his discovery of the sedimentation equilibrium.

3. From Scattering of Light. Zsigmondy used the ultra-microscope for determining the size of the particles of colloidal dimensions. As already mentioned, each spot of light viewed in ultra-microscope corresponds to a particle. The number of particles in a given volume of a solution, therefore, can be counted. The observation is repeated several times and an average is taken. The length and breadth of the field of vision are measured with the help of an eye-piece micrometer. The depth is determined by rotating the slit through 90°. From these dimensions, the exact volume of the solution containing the observed number of particles can be obtained. From this, the number of particles n, contained per unit volume of the solution can be determined.

Next, a known volume of the colloidal solution is evaporated to dryness. From the mass of the residue, the mass of colloidal particles per unit volume can easily be obtained. Let this be m. Now two assumptions are made. Firstly, the particles are spherical. Secondly, the density ρ of the colloidal particles is the same as that of the material in the bulk state. The volume of colloidal phase is m/ρ and, therefore,

$$m/\rho = (4/3)\pi r^3 \times n \quad \text{or} \quad r = (3m/4\pi\rho n)^{1/3} \quad ...(7)$$

Richard Zsigmondy (1865–1929), the German chemist, was the recipient of the 1925 Chemistry Nobel Prize for demonstration of the heterogeneous nature of colloidal solutions.

SURFACTANTS (SURFACE-ACTIVE AGENTS)

Surface-active agents or surfactants, derive their name from their behaviour at surfaces and interfaces. They are positively adsorbed at interfaces between two phases and the adsorption of surfactant lowers the interfacial tension between the two phases. Because of their ability to lower interfacial tension, surfactants are used as emulsifiers, detergents, dispersing agents, foaming agents, wetting agents, penetrating agents, and so forth. The surfactants are frequently referred to as **amphiphiles.** Many types of substances act as surfactants but they all share the property of **amphipathy.** The molecule is composed of a non-polar hydrophobic portion and a polar hydrophilic portion and is, therefore, partly hydrophilic and partly hydrophobic. The property to partly have both these characters is known as amphipathy. Surfactants may be referred to as either *amphiphilic* or *amphipathic*; the terms are synonymous. The polar, hydrophilic part of the molecule is called the *hydrophilic* or *lipophobic group* and the non-polar, hydrophobic part is called the *hydrophobic* or *lipophilic group*. Often the hydrophilic part of the molecule is simply called the *head* and the hydrophobic part (usually including an elongated alkyl substituent) is called the *tail*. The presence of a hydrophilic group makes surfactants somewhat soluble in aqueous media. This is central to the physicochemical properties of aqueous surfactant solutions.

Surfactants can be classified on the basis of the charge carried by the polar head group as *anionic, cationic, non-ionic* or *amphoteric*. Tables 3 to 6 show the chemical structures of typical examples of these classes.

TABLE 3

Chemical Structures of Hydrophilic Groups for Anionic Amphiphiles

Chemical Structure [a]	Name
$R\text{-}(COO^-)_nM^{n+}$	Carboxylate
$R\text{-}COO^-M^{2+}$ SO_3^-	Sulphocarboxylate
$R\text{-}COO^-M^{(n+1)+}$ OPO_3H_{3-n}	Phosphonocarboxylate
$R\text{-}OSO_3^-M^+$	Sulphate
$R\text{-}(OCH_2CH_2)_n\text{-}OSO_3^-M^+$	Polyoxyethylene sulfate
$R\text{-}SO_3^-M^+$	Sulphonate
$R\text{-}(OCH_2CH_2)_n\text{-}SO_3^-M^+$	Polyoxyethylene sulfonate
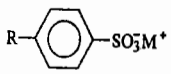	Benzene sulphonate
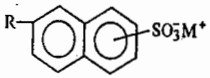	Naphthalene sulphonate
$R\text{-}OPO_3H_{3-n}M^{n+}$	Phosphate

[a] R stands for long hydrophobic tail.

TABLE 4

Chemical Structures of Hydrophilic Groups for Cationic Amphiphiles

Chemical structure *	Name	Chemical structure *	Name
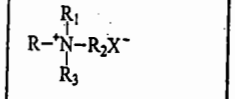	Ammonium	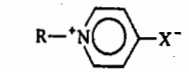	Pyridinium
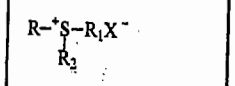	Sulphonium	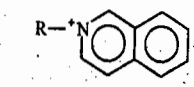	Quinolinium
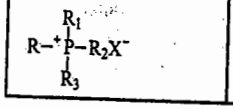	Phosphonium		

* R stands for long hydrophobic tail; R_1, R_2 and R_3 stand for hydrogen or a short alkyl chain.

TABLE 5

Chemical Structure of Hydrophilic Groups for Non-ionic Amphiphiles

Chemical structure *	Name	Chemical structure *	Name
$R-(OCH_2CH_2)_n-OH$	Polyoxyethylene alcohol	$R-(OCH_2CH_2CH_2)_n-OH$	Polyoxypropylene alcohol
$R-COO-(CH_2CH_2O)_n-R_1$	Polyoxyethylene ester	$R-(CH_2CH_2O)_n$	Crown ether
$R-\underset{\underset{O}{\downarrow}}{S}-R_1$	Sulphoxide	$R-\underset{\underset{O}{\downarrow}}{S}-(CH_2)_n-OH$	Sulphinyl alkanol
$R-S-(CH_2CH_2O)_n$	Polyoxypropylene thioether	$R-\overset{R_1}{\underset{R_2}{N}}\rightarrow O$	Amine oxide
$R-(CH_2CH_2NH)_n$	Azacrown	$R-\overset{R_1}{\underset{R_2}{P}}\rightarrow O$	Phosphine oxide

* R stands for long hydrophobic tail; R_1 and R_2 stand for a short alkyl chainS.

TABLE 6

Chemical Structure of Hydrophilic Groups for Amphoteric Amphiphiles (Zwitter Ions)

Chemical structure *	Name	Chemical structure *	Name
$R-\underset{\underset{COO^-}{|}}{\overset{R_1}{\overset{|}{CH}}}-{}^+\underset{R_3}{\overset{|}{N}}-R_2$	C betaine	$R-{}^+\underset{CH_2COO^-}{\overset{CH_2COOH}{\overset{|}{\underset{|}{N}}}}-CH_2COOH$	Triglycine
$R-{}^+\underset{R_2}{\overset{R_1}{\overset{|}{\underset{|}{N}}}}-CH_2COO^-$	N betaine		

* R stands for long hydrophobic tail; R_1, R_2 and R_3 stand for short alkyl chains.

Hydrophile–Lipophile Balance (HLB)

This term, first suggested by Clayton, refers to the balance in size and strength between the hydrophilic and hydrophobic parts of a surfactant molecule. Griffin later developed the concept of the HLB for emulsifiers on the basis of their aqueous solubility. The **HLB value** is an empirical number assigned to non-ionic surfactants on the basis of a wide variety of experiments carried out on surfactants. The HLB values range from 1 to 40, the low numbers generally indicating solubility in oil and the high numbers indicating solubility in water. Nevertheless, emulsifiers with the same HLB value may differ in solubility. An emulsifier has two different actions : it promotes the formation of an emulsion and it determines whether an *oil/water* (O/W) or a *water/oil* (W/O) emulsion will be formed. The second action is closely connected with the HLB value.

On the basis of systematic experiments, Griffin found that the HLB values of mixtures of two or more emulsifiers are additive : the HLB value of a mixture is equal to the sum of the HLB values of the constituents multiplied by their mass fractions in the mixture x_i^m :

$$\text{HLB} = \sum_i x_i^m (\text{HLB})_i \qquad ...(8)$$

Griffin also listed several estimated HLB values for emulsifiers which had been determined and correlated by an extensive series of emulsifier blending tests (Table 5). Using these values and Eq. 9, we can determine an HLB value for any surfactant by blending it with a surfactant of known HLB value.

For most polyhydric alcohols, fatty acid and esters, approximate HLB values may be obtained using the following equation :

$$\text{HLB} = 20\,(1 - S/A) \qquad ...(9)$$

where S is the saponification number of the ester and A is the acid number of the acid. This equation can be written as

$$\text{HLB} = 20\,(1 - M_h/M_m) \qquad ...(10)$$

where M_h is the mass of the hydrophobic group and M_m is the molar mass of the emulsifier.

HLB values for the various types of emulsifiers are shown below in parenthesis :

(*a*) Anionic : (*i*) Tea oleate (12); (*ii*) Sodium oleate (18).

(*b*) Cationic : (*i*) Atlas G-251 (25–35).

(*c*) Non-ionic : (*i*) Oleic acid (~1); (*ii*) Span 85 (1·8); (*iii*) Span 80 (4·3); (*iv*) Span 60 (4·7); (*v*) Tween 20 (16·7).

Davies suggested assigning an **HLB contribution group number** to each functional group in a molecule after studying the relative coalescence rates of stabilized oil droplets in water and water droplets in oil. The **Davies equation** which is applicable to ionic as well as non-ionic surfactants is

$$\text{HLB} = \Sigma\,(\text{hydrophilic group number}) - \Sigma\,(\text{hydrophobic group number}) + 7 \qquad ...(11)$$

Table 7 lists the HLB group numbers of some common functional groups.

TABLE 7

HLB Group Numbers for Various Hydrophilic and Hydrophobic Groups

Hydrophilic	Group number	Hydrophobic	Group number
$-SO_4Na$	38·7	$=CH-$	0·475
$-CO_2Na$	19·1	$-CH_2-$	0·475
$-SO_3Na$	11·0	$-CH_3$	0·475
N (tertiary amine)	9·4		
Ester (free)	2·4	$-CF_2-$	0·870
$-CO_2H$	2·1		
-OH (free)	1·9		
-O-	1·3		

MICELLE FORMATION

An important property of amphiphilic molecules is their capacity to aggregate in solutions. The aggregation process depends on the amphiphilic species and the condition of the system in which they are dissolved. The abrupt change in many physicochemical properties seen in aqueous solutions of amphiphilic molecules or surfactants with long hydrophobic chains when a specific concentration is exceeded is attributed to the formation of **oriented colloidal aggregates**. The narrow concentration range over which these changes occur is called the **critical micelle concentration (CMC)** and the molecular aggregates that are formed above the CMC are known as **micelles**. The difference between micellar colloids and other colloids is that micellar colloids are in dynamic equilibrium with monomers in the solution. Micellar colloids represent dynamic association–dissociation equilibria. However, the theoretical treatment of micelles depends on whether the micelle is regarded as a chemical species or as a separate phase. The **mass action model**, which has been used ever since the discovery of micelles, takes the former point of view whereas the **phase separation model** regards micelles as a separate

phase. To apply the mass action model strictly, one must know every association constant over the whole stepwise association from monomer to micelle, a requirement almost impossible to meet experimentally. Therefore, this model has the disadvantage that either monodispersity of the micelle aggregation number must be employed or numerical values of each association constant have to be assumed. The phase separation model, on the other hand, is based on the assumption that the activity of a surfactant molecule and/or the surface tension of a surfactant solution remain constant over the CMC. In practice, however, neither quantity remains constant; so this model is also not strictly correct.

The variety of the theories on micelle formation results from the versatile properties of micelles. Thus, although a micelle may not have such a large aggregation number that it can be regarded as a phase in the usual sense, it will still have properties similar to those of a phase. At the same time, each micelle contains too many aggregated monomer molecules to be regarded as a chemical species, even a bulky chemical species.

It is thus instructive to consider the micellar solution system from the viewponit of the phase rule. Fig. 8 illustrates the changes in solubility and CMC of sodium tetradecyl sulphonate with temperature. If the micelle is regarded as a phase, three phases (intermicellar bulk phase, surfactant solid phase and micellar phase) coexist along the solubility curve above T_k, called the Krafft point and Gibbs's phase rule $F = C - P + 2$ (where F, C and P are the number of degrees of freedom, number of components and the number of phases, respectively) gives only one degree of freedom since the number of components is two (solvent water and surfactant). In other words, according to this model, the solubility cannot change with temperature at constant pressure because the solubility is determined only by the pressure. On the other hand, if the mass action model is applied to micelle formation, the solubility problem can be solved in a way consistent with the phase rule. In addition, increase in the solubility observed above the point of micellization can be elucidated by the following semiquantitative discussion. Let us consider a simple association equilibrium between surfactant monomers (S) and micelles (M_n) of aggregation number n :

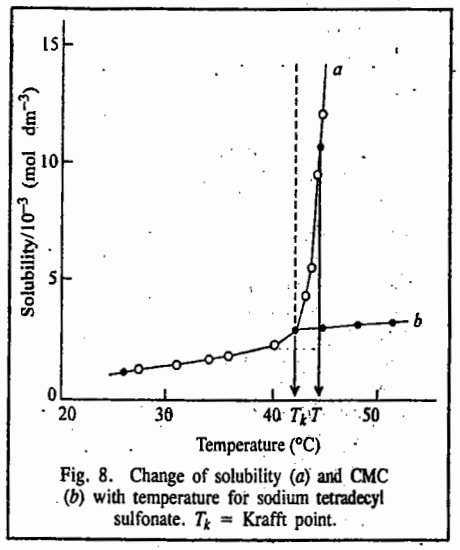

Fig. 8. Change of solubility (a) and CMC (b) with temperature for sodium tetradecyl sulfonate. T_k = Krafft point.

$$nS \rightleftharpoons M_n \quad (K_n)$$

The micellization constant K_n is, therefore, written as

$$K_n = [M_n] / [S]^n \qquad ...(12)$$

The equivalent concentration of surfactant (C_t) used for micelles then becomes :

$$C_t - [S] = nK_n [S]^n \qquad ...(13)$$

The ratio of the equivalent concentration at T to that at T_k is given by

$$\frac{\{C_t(T) - [S(T)]\}}{\{C_t(T_k) - [S(T_k)]\}} = \frac{[S(T)]}{[S(T_k)]^n} \qquad ...(14)$$

where K_n is assumed constant because of the very small temperature range. The heat of dissolution obtained from the solubility change with temperature is about 100 kJ mol^{-1} for many ionic surfactants.

Hence the solubility change with temperature may be expressed roughly as :

$$\frac{[S(T_k + \Delta T)]}{[S(T_k)]} = 1 + 0{\cdot}13 \times \Delta T \qquad ...(15)$$

For $\Delta T = 0{\cdot}2°C$, the above ratios become 2·8 and 13·8 for $n=50$ and $n=100$, respectively.

It is evident that a small temperature increase brings about a large increase in solubility and that the micelle aggregation number n has a strong influence (Fig. 9). As is clear from the above discussion, the abrupt increase in the total solubility above T_k is due not to an increase in the solubility of the monomeric surfactant but rather to an increasing number of micelles. In addition, the treatment of micelles as a separate phase has turned out to be incorrect whereas the mass action model is consistent not only with the phase rule but also with the solubility increase.

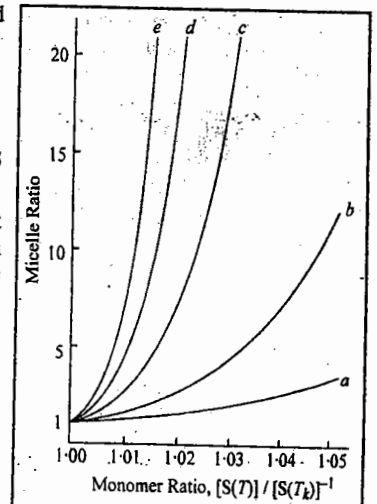

Fig. 9. Solubility increase above the micelle temperature range depending on the aggregation number of micelle (n). (a) n = 25; (b) n = 50; (c) n = 100; (d) n = 150; (e) n = 200.

Shape and Structure of Micelles

Ever since McBain proposed the presence of molecular aggregates in soap solutions on the basis of the unusual changes in electrical conductivity observed with changing soap concentration, the structure of micelles has been a matter of discussion. Hartley proposed that micelles are spherical with the charged groups situated at the micellar surface (Fig. 10c) whereas McBain suggested that lamellar (Fig. 10a) and spherical forms coexist. X-ray studies by Harkins suggested the sandwich or lamellar model. Later, Debye and Anacker proposed that micelles are rod-shaped rather than spherical or disc-like (Fig. 10b). The cross-section of such a rod would be circular with the polar heads of the micelle lying on the periphery and the hydrocarbon tails filling the interior. The ends of the rod would almost certainly have to be rounded and polar. In 1956, Hartley's spherical micelle model was established by Reich from the viewpoint of entropy, and the spherical form is now generally accepted as approximating the actual structure (Fig. 10c). The formation of micelles by ionic surfactants is ascribed to a balance between hydrocarbon chain attraction and ionic repulsion. The net charge on micelles is less than the degree of micellar aggregation, indicating that a large fraction of counter ions remains associated with the micelle; these counter ions form the Stern layer (*cf.* Fig. 5) at the micellar surface. For non-ionic surfactants, however, the hydrocarbon chain attraction is opposed by the requirements of hydrophilic groups for hydration and space. Therefore, the micellar structure is determined by an equilibrium between the repulsive forces among hydrophilic groups and the short-range

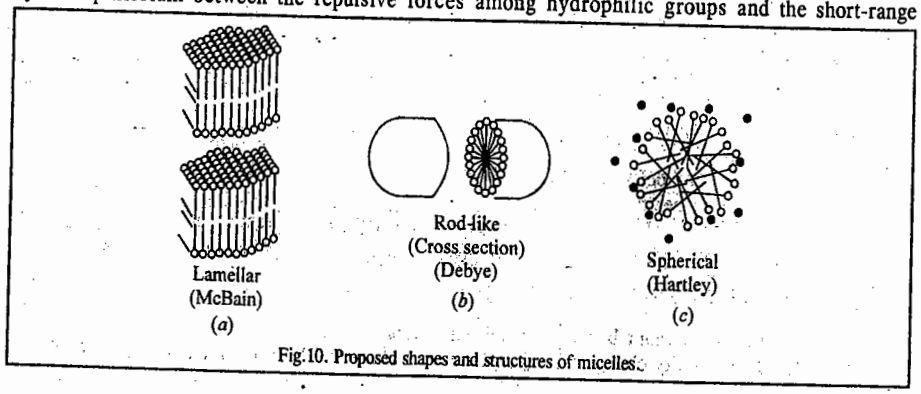

Fig. 10. Proposed shapes and structures of micelles.

attractive forces among hydrophobic groups. In other words, the chemical structure of a given surfactant determines the size and shape of its micelles.

The shape and structure of micelles have been elucidated with the help of techniques such as NMR, ESR, neutron scattering, etc. Neutron scattering experiments on sodium dodecyl sulphate and other ionic micelles support the basic Hartley model of a spherical micelle. However, as the ion concentration is increased, the shape of ionic micelles changes in the sequence : spherical ⟶ cylindricalhexagonal ⟶ lamellar (Fig. 11). For non-ionic micelles, on the other hand, the shape seems to change from spherical directly to lamellar with increasing concentration.

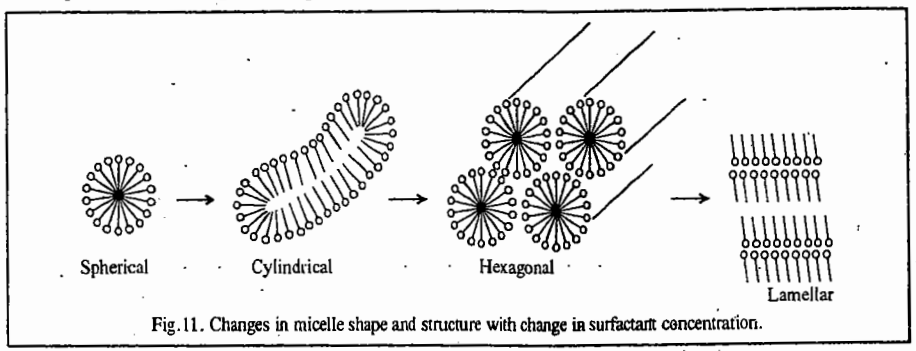

Fig.11. Changes in micelle shape and structure with change in surfactant concentration.

The shape of the micelle produced in aqueous media is of importance in determining various properties of the surfactant solution, such as its viscosity and its capacity to solubilize water-insoluble materials. The major types of micelles appear to be (1) relatively small, spherical structures (aggregation number < 100), (2) elongated cylindrical, rodlike micelles with hemispherical ends (prolate ellipsoids), (3) large, flat lamellar micelles (disc-like extended oblate spheroids) and (4) vesicles — more or less spherical structures consisting of lamellar micelles arranged in one or more concentric spheres.

In aqueous media, the surfactant molecules are oriented, in all these structures, with their polar heads toward the aqueous phase and their hydrophobic groups away from it. In vesicles, there will also be an aqueous phase in the interior of the structure. In ionic micelles, the interfacial region between the aqueous solution and the miscelle contains the ionic head groups and the Stern layer portion of the electrical double layer contains more than half of the counter ions associated with the micelle and water. The remaining counter ions are contained in the Gouy-Chapman portion of the double layer that extends further into the aqueous phase. For polyoxyethylenated non-ionics, the structure is essentially the same except that the outer region contains no counter ions but includes coils of hydrated polyoxyethlene chains. The interior region of the micelle, containing the hydrophobic groups, is of the radius approximately equal to the length of the fully extended hydrophobic chain. The aqueous phase is believed to penetrate into the micelle beyond the hydrophobic head group and the first few methylene groups of the hydrophobic chain adjacent to the hydrophobic head are often concentrated in the hydration sphere. It is, therefore, useful to divide the interior region into an outer core that may be penetrated by water and an inner core from which water is excluded. In non-polar media, the structure of the micelle is similar but reversed, with the hydrophilic heads comprising the interior region surrounded by an outer region containing the hydrophobic groups and non-polar solvent. Dipole–dipole interactions hold the hydrophilic heads together in the core. Changes in temperature, concentration of surfactant, additives in the liquid phase and structural groups in the surfactant may all cause change in the size, shape and aggregation number of the micelle, with the structure varying from spherical through rod or disc-like to lamellar in shape.

Micellar Aggregation Numbers

Micellar aggregation numbers have classically been determined by light-scattering and from sedimentation rates in the ultracentrifuge. Currently, NMR, Small Angle Neutron Scattering (SANS) and freezing point and vapour pressure methods are being used. A convenient method using fluorescent

probes has also been used to calculate aggregation numbers of several different types of surfactants. Micelle aggregation numbers range from less than 100 for ionic surfactants to several hundred for non-ionic surfactants.

From geometric considerations, the aggregation numbers of micelles in aqueous media should increase rapidly with increase in the length of the hydrophobic group l_c of the surfactant molecule and decrease with increase in the cross-sectional area of the hydrophilic group a_0 or the volume of the hydrophobic group V_h. For example, in a spherical micelle in aqueous media, the surface area, $n \times a_0 = 4\pi (l_c+\Delta)^2$ or $n = 4\pi (l_c+\Delta)^2/a_0$, where Δ is the added length of the radius of the sphere due to the hydrophilic group. Similarly, the volume of the hydrophobic core $n \times V_h = (4/3)\pi(l_c)^3$ or $n = (4/3)\pi(l_c)^3/V_h$.

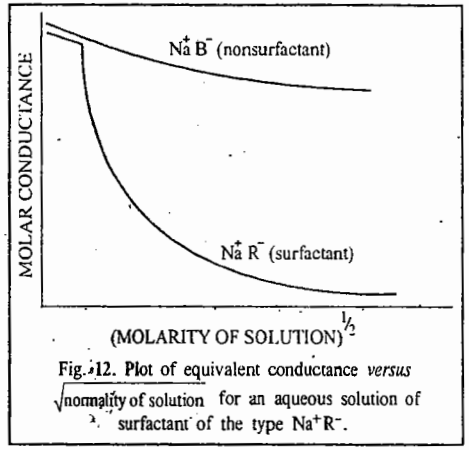

Fig.12. Plot of equivalent conductance *versus* √normality of solution for an aqueous solution of surfactant of the type Na^+R^-.

Critical Micelle Concentration (CMC)

When molar conductance of an anionic surfactant of the type Na^+R^- in water is plotted against the square root of the molarity of the solution, the curve obtained, instead of being the smoothly decreasing curve characteristic of ionic electrolytes of this type, has a sharp break in it, at low concentrations (Fig.12). This sharp break in the curve accompanied by reduction in the conductance of the solution, indicating a sharp increase in the mass per unit charge of the material in solution, is interpreted as evidence for the formation of micelles at that point. The concentration at which this phenomenon occurs is called the critical micelle concentration (CMC). Similar breaks in almost every measurable physical property that depends on size or number of particles in solution are shown by all types of surfactants—non-ionic, anionic, cationic and zwitter ionics in aqueous media. Changes in some physical properties in the neighbourhood of the CMC are shown in Figure. 13.

We can determine the value of the CMC by using any of these physical properties, but most commonly the breaks in the molar conductance, surface tension, light scattering or refractive index versus concentration curves have been used for this purpose. Critical micelle concentrations have also very frequently been determined from the change in the spectral characteristics of some dyestuff added to the surfactant solution when the CMC of the latter is reached. However, this method is open to the serious objection that the presence of the dyestuff may affect the value of the CMC.

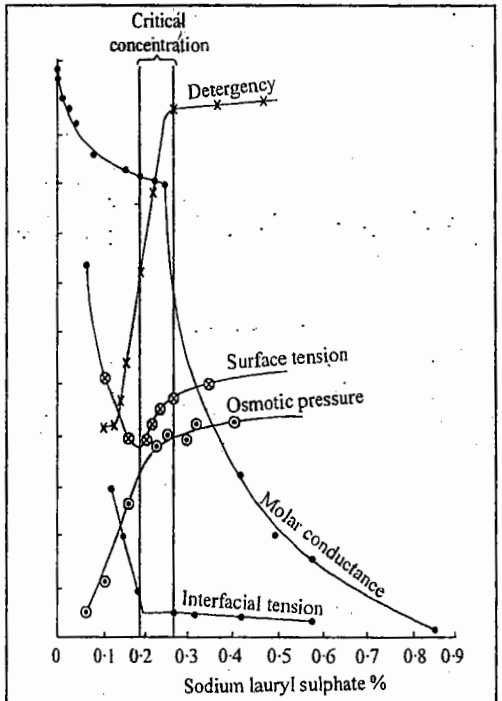

Fig.13. Changes in some physical properties of an aqueous solution of sodium lauryl sulphate in the neighbourhood of the critical micelle concentration.

Factors Affecting Critical Micelle Concentration in Aqueous Media

Several factors such as the structure of the surfactant, concentration of electrolyte, addition of organics, presence of a second liquid phase and temperature affect the CMC in aqueous media. These are discussed below.

1. Structure of the Surfactant

Role of the Hydrophobic Group. In aqueous medium, the CMC decreases as the number of carbon atoms in the hydrophobic group increases to about 16 and a general rule for ionic surfactants is that the CMC is halved by the addition of one methylene group to a straight-chain hydrophobic group attached to a single terminal hydrophilic group. For non-ionics and zwitter ionics, the decrease with increase in the hydrophobic group is somewhat larger, an increase by two methylene units decreasing the CMC to about one-tenth its previous value (compared to one-quarter in ionics). A phenyl group that is part of a hydrophobic group with terminal hydrophilic group is equivalent to about three and a half methylene groups. When the number of carbon atoms in a straight-chain hydrophobic group exceeds 16, however, the CMC no longer decreases so rapidly with increase in the length of the chain and when the chain exceeds 18 carbons it may remain substantially unchanged with further increase in the chain length. This may be due to the coiling of these long chains in water.

When the hydrophobic group is branched, the carbon atoms on the branches appear to have about one-half the effect of carbon atoms on a straight chain. When carbon–carbon double bonds are present in the hydrophobic chain, the CMC is generally higher than that of the corresponding saturated compound, with the cis isomer generally having a higher CMC than the trans isomer. This may be the result of a steric factor in micelle formation. Surfactants with either bulky hydrophobic or bulky hydrophilic groups have larger CMC values than those with similar but less bulky groups.

Role of the hydrophilic group. In aqueous medium, ionic surfactants have much higher CMCs than non-ionic surfactants containing equivalent hydrophobic groups. The 12-carbon straight chain ionics have CMCs of approximately 1×10^{-2} M, whereas non-ionics with the same hydrophobic group have CMCs of approximately 1×10^{-4} M. Zwitter ionics appear to have slightly smaller CMCs than ionics with the same number of carbon atoms in the hydrophobic groups. As expected, surfactants containing more than one hydrophilic group in the molecule show larger CMCs than those with one hydrophilic group and the equivalent hydrophobic group.

Role of the degree of binding of the counter ion to the micelle. The critical micelle concentration in aqueous solution reflects the degree of binding of the counter ion to the micelle. Increased binding of the counter ion, in aqueous systems, causes a decrease in the CMC of the surfactant. It may, however, be mentioned that CMC is not a measure of the degree of binding of the counter ion to the miscelle, when different types of surfactants are compared. The degree of binding of the counter ion to the micelle also depends on the surface charge density of the micelle. The greater the surface charge density, *i.e.*, the smaller the surface area per head group, the greater is the degree of binding of the counter ion.

For homologous straight chain ionic surfactants (soaps, alkane sulphonates, alkyl sulphates, alkylammonium chlorides) in aqueous medium, a relation between the CMC and the number of carbon atoms N in the hydrophobic chain is found to be given by

$$\log \text{CMC} = A - BN \qquad \ldots(16)$$

where A is a constant for a particular ionic head at the given temperature and B is a constant $\approx 0{\cdot}3$ (= log 2) at 35°C.

2. Concentration of Electrolyte

It is found experimentally that for the first two classes of surfactants, the effect of the concentration of electrolyte is given by

$$\log \text{CMC} = -a \log c_i + b$$

where a and b are constants for a given ionic head at a particular temperature and c_i is the molar concentration of the counter ion. The decrease in the CMC in these cases is due mainly to the decrease in the thickness of the ionic atmosphere sorrounding the ionic head groups in the presence of the additional electrolyte and the consequent decreased electrical repulsion between them in the micelle. For non-ionics and zwitter ionics the above relation does not hold.

3. Addition of Organic Materials

Small amounts of organic materials may produce marked changes in the CMC in aqueous media. A knowledge of the effects of organic materials on the CMC of surfactants is, therefore, of great importance, both for theoretical and practical purposes. To understand the effects produced, it is necessary to distinguish between two classes of organic materials that markedly affect the critical micelle concentrations of aqueous solutions surfactants : Class I materials that affect the CMC by being incorporated in the micelle and Class II materials that change the CMC by modifying solvent micelle or solvent surfactant interactions.

Class I Materials. Materials in Class I are generally polar organic compounds such as alcohols and amides. They affect the CMC at much lower liquid phase concentrations than those in Class II. Water-soluble compounds in this class may operate as members of Class I at low bulk phase concentrations and as members of Class II at high bulk phase concentrations. Members of Class I reduce the CMC. Shorter-chain members of this class are probably adsorbed mainly in the outer portion of the micelle close to the water-micelle 'interface'. The longer-chain members are probably adsorbed mainly in the outer portion of the core, between the surfactant molecules. Adsorption of the additives in this manner decreases the work required for micellization in the case of ionic surfactants by decreasing the mutual repulsion of the ionic heads in the micelle.

Class II Materials. Members of Class II change the CMC but at bulk phase concentration which are usually considerably higher than those at which Class I members are effective. The members of this class change the CMC by modifying the interaction of water with the surfactant molecule or with the micelle, by modifying the structure of the water, its dielectric constant or its solubility parameter (cohesive energy density). Members of this class include urea, formamide, *N*-methylacetamide, guanidinium salts, short-chain alcohols, water-soluble esters, dioxane, ethylene glycol and other polyhydric alcohols such as fructose and xylose.

Urea, formamide and guanidinium salts are believed to increase the CMC of surfactants in aqueous solution because of their tendency to distort the structure of water. This may increase the degree of hydration of the hydrophilic group and since hydration of the hydrophilic group opposes micellization, this causes an increase in the CMC.

4. The Presence of Second Liquid Phase

The CMC of a surfactant in aqueous phase is changed very little by the presence of a second liquid phase in which the surfactant does not dissolve appreciably and which, in turn, either does not dissolve appreciably in the aqueous phase or is solubilized only in the inner core of the micelles (*e.g.*, saturated aliphatic hydrocarbons). When the hydrocarbon is a short-chain unsaturated hydrocarbon or an aromatic hydrocarbon, the CMC is significantly less than that in air, with the more polar hydrocarbon causing a larger decrease. This is presumably because some of the second liquid phase adsorbs on the outer portion of the surfactant micelle and acts as a Class I material.

5. Temperature

The effect of temperature on the CMC of surfactants in aqueous medium is complex, the value first decreases with increase in temperature to a certain minimum and then increases with further increase in temperature. Temperature increase causes decreased hydration of the hydrophilic group which favours micellization. However, temperature increase also produces distortion in the structure of water surrounding the hydrophobic group, an effect that disfavours micellization. The relative

magnitude of these two opposing effects, therefore, determines whether the CMC increases or decreases over a particular temperature range.

Thermodynamic Approach to CMC. Several equations relating the CMC to its various determining factors have been derived from theoretical considerations by Hobbs, Shinoda and Molyneux. These equations are based on the fact that for non-ionics, the CMC is related to the free energy change ΔG_{mic} associated with the aggregation of the individual surfactant molecules to form micelles by the expression

$$\Delta G_{mic} = 2{\cdot}303RT \log x_{CMC} \quad ...(17)$$

Here x_{CMC} is the mole fraction of the surfactant in the liquid phase at the CMC. In aqueous solutions where the CMC is generally $< 10^{-1}$ M, $x_{CMC} = CMC/c$ and

$$\Delta G_{mic} = 2{\cdot}303RT (\log CMC - \log c) \quad ...(18)$$

or

$$\log CMC = \frac{\Delta G_{mic}}{2{\cdot}303RT} + \log c \quad ...(19)$$

where c is the molar concentration of water (55·6 mol dm^{-3} at 25°C).

ΔG_{mic} can be broken into contributions from the component parts of the surfactant molecule, $CH_3(CH_2)_mW$, where W is the hydrophilic group, as follows :

$$\Delta G_{mic} = \Delta G_{mic}(CH_3) + m\Delta G_{mic}(CH_2) + \Delta G_{mic}(-W) \quad ...(20)$$

Studies on the solubility of alkanes in water indicate that $\Delta G_{mic}(CH_3)$ does not change with increase in the length of the alkyl chain and can be represented by $\Delta G_{mic}(CH_3) = \Delta G_{mic}(CH_2) + k$ where k is a constant. Thus,

$$\log CMC = \frac{\Delta G_{mic}(-W) + k}{2{\cdot}303RT} + \log c + \left[\frac{\Delta G_{mic}(CH_2)}{2{\cdot}303RT}\right] N \quad ...(21)$$

where $N (= m+1)$ is the total number of carbon atoms in the hydrophobic group.

Assuming that the contribution of the hydrophilic head group ΔG (-W) and the fraction of counter ions bound to the micelle, α, do not change with increase in the length of the hydrophobic group for any homologous series of surfactants, the relation between CMC and the number of carbon atoms in the hydrophobic group can be written in the form

$$\log CMC = A - BN \quad ...(Eq. 16)$$

where

$$A = \frac{\Delta G_{mic}(-W) + k}{2{\cdot}303RT} + \log c \quad ...(22)$$

and

$$B = \frac{-\Delta G_{mic}(CH_2)}{2{\cdot}303RT} \quad ...(23)$$

Thus, A and B are constants which reflect the free energy changes involved in transferring the hydrophilic group and a methylene unit of the hydrophobic group, respectively, from an aqueous environment to the micelle. This accounts for both the forms of the empirical relations between the CMC and the number of carbon atoms in the hydrophobic group (Eqs. 16 and 19) and the relatively small variation of B in different homologous series of ionic surfactants.

We also see from Eqs. 16 and 23 that the free energy change $\Delta G(CH_2)$ involved in the transfer of a methylene unit of the hydrophobic group from an aqueous environment to the interior of the micelle is negative, thus, favouring micellization which accounts for the fact that the CMC decreases with increase in the length of the hydrophobic group. From Eq. 22, we can see that the free energy

change involved in the transfer of the hydrophilic group from an aqueous environment to the exterior of the micelle is positive and, therefore, opposes micellization.

Thermodynamics of Micellization

We find from the previous discussion that a clear understanding of the process of micellization is necessary for rational explanation of the effects of structural and environmental factors on the value of the CMC and for predicting the effects on it of new structural and environmental variations. The determination of thermodynamic parameters of micellization, *viz.*, ΔG^0_{mic}, ΔH^0_{mic} and ΔS^0_{mic} has played an important role in developing such an understanding.

The standard free energy of micellization ΔG^0_{mic} may be calculated by choosing a hypothetical state at unit mole fraction x, for the standard initial state of the non-micellar surfactant species but with the individual ions or molecules behaving as at infinite dilution and for the standard final state, the micelle itself. For non-ionic surfactants, the standard free energy of micellization is given by

$$\Delta G^0_{mic} = RT \ln x_{CMC} \quad ...(24)$$

When CMC is 10^{-2} M or less, this can be approximated as

$$\Delta G^0_{mic} = 2{\cdot}303\ RT \log (CMC/c) \quad ...(25)$$

where the CMC is expressed in molar units and c is the number of moles of water per litre of water at temperature T. For ionic surfactants of 1:1 electrolyte type AB, where A is the surfactant ion and B the counter ion,

$$\Delta G^0_{mic} = 2{\cdot}303\ RT [\log CMC/c + \log \gamma_A + K_g(\log c_B/c + \log \gamma_B)] \quad ...(26)$$

where the activity coefficients γ_A and γ_B can be evaluated by the Debye-Hückel limiting law (DHLL). Often, the activity coefficients are neglected and the expression is used in the form

$$\Delta G^0_{mic} = 2{\cdot}303\ RT [\log(CMC/c) + K_g(\log c_B/c)] \quad ...(27)$$

where c_B is the total molar concentration of the counter ion.

K_g can be evaluated by determining the value of CMC in aqueous solutions containing different amounts of 1:1 electrolyte, MB. From Eq. 27,

$$\log (CMC/c) = -K_g \log (c_B/c) + \Delta G^0_{mic}/2{\cdot}303RT \quad ...(28)$$

If we assume that ΔG^0_{mic} does not change significantly with change in the concentration c_B of the counter ion, then K_g can be evaluated from the negative slope of the log-log plot of (CMC/c) versus (c_B/c).

Since

$$\Delta G^0_{mic} = \Delta H^0_{mic} - T\Delta S^0_{mic} \quad ...(29)$$

$$\therefore \quad d(\Delta G^0_{mic})/dT = -\Delta S^0_{mic} \quad ...(30)$$

if ΔH^0_{mic} is constant over the temperature range investigated.

Alternatively,

$$T^2\, d(\Delta G^0_{mic}/T)/dT = -\Delta H^0_{mic} \quad ...(31)$$

if ΔS^0_{mic} is constant over the temperature range investigated.

Values of ΔH_{mic} can also be determined calorimetrically. The data available (mainly for aqueous systems) indicate that the negative values of ΔG^0_{mic} are due mainly to the large positive values of ΔS^0_{mic}, ΔH^0_{mic} is often positive and, even when negative, is much smaller than the value of $T\Delta S^0_{mic}$. Therefore, the micellization process is governed primarily by the entropy gain associated with it and

the driving force for the process is the tendency of the lyophobic group of the surfactant to transfer from the solvent environment to the interior of the micelle.

The large entropy increase on micellization in aqueous medium has been explained in two ways : 1. Change in the structure of the water molecules surrounding the hydrocarbon chains in aqueous medium resulting in an increase in the entropy of the system when the hydrocarbon chains are removed from the aqueous medium to the interior of the micelle—'hydrophobic bonding'. 2. Increased freedom of the hydrophobic chain in the non-polar interior of the micelle compared to the aqueous environment. Any structural or environmental factors that may affect solvent–lyophobic group interactions or interactions between the lyophobic groups in the interior of the micelle will, therefore, affect ΔG^0_{mic} and consequently the value of the CMC.

SOLUBILIZATION

A very important property of surfactants that is directly related to micelle formation is **solubilization**. Solubilization plays a very important role in industrial and biological processes. McBain and Hutchinson defined **solubilization** as 'a particular mode of bringing into solution substances that are otherwise insoluble in a given medium, involving the previous presence of a colloidal solution whose particles take up and incorporate within or upon themselves the otherwise insoluble meterial.' This definition is too narrow. A broad definition of solubilization is as follows : **"Solubilization** is the preparation of a thermodynamically stable isotropic solution of a substance normally insoluble or very slightly soluble in a given solvent by the introduction of an additional amphiphilic component or components."

In other words, solubilization may be defined as spontaneous dissolving of a substance (solid, liquid or gas) by reversible interaction with the micelles of a surfactant in a solvent to form a thermodynamically stable isotropic solution. Fig. 14 shown a plot of amount of material solubilized as a function of the concentration of the surfactant in the bulk phase.

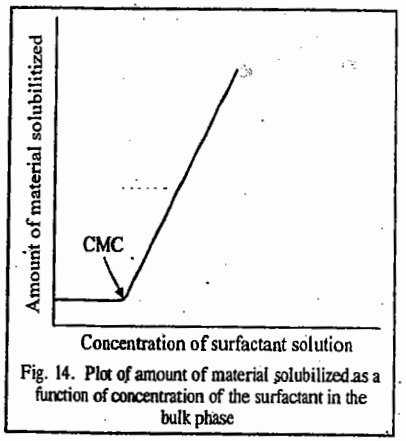

Fig. 14. Plot of amount of material solubilized as a function of concentration of the surfactant in the bulk phase

Several applications, for example, the dissolution of drugs in aqueous solutions and their transport through the body, the preparation of agricultural chemical solutions and the recovery of oil, etc., depend upon solubilization by suitable surfactants. Also, studies of the physical chemistry of bile acids and bile salts, on the one hand and their physiological function as solubilizers, on the other hand, make it clear that the behaviour of bile salts *in vitro* and their function *in vivo* are closely related. Solubilization in aqueous media is of major practical importance in areas such as detergency where solubilization is believed to be one of the major mechanisms involved in (1) the removal of oily soil; (2) in micellar catalysis of organic reactions; (3) in emulsion polymerization where it appears to be an important factor in the initiation step; (4) in the separation of materials for manufacturing or analytical purposes; (5) in the formulation of products containing water-insoluble ingredients where it can replace the use of organic solvents or co-solvents and (6) in enhanced oil recovery where solubilization produces ultra low interfacial tension required for mobilization of the oil. Solubilization in non-equeous media is of major importance in dry cleaning. The solubilization of materials in biological systems sheds light on the mechanisms of interaction of drugs and other pharmaceutical materials with lipid bilayers and membranes.

Solubilization is distinguished from emulsification (the dispersion of one liquid phase in another) by the fact that in solubilization, the solubilized material (the solubilizate) is in the same phase as the solubilizing solution and the system is consequently thermodynamically stable.

Location of Solubilizates in Micelles

The position of solubilizates in micelles as well as in living membranes, provides very important information concerning the physico-chemical properties and physiological functions of both the solubilizate and the micelle or the membrane. This property can be investigated using probe molecules, the molecular spectrum of which indicates the surrounding conditions. The absorption spectrum of a molecule depends on the dielectric constant (relative permittivity) of the medium surrounding the molecule. The dielectric constant of a micelle ranges from 2 for the liquid hydrocarbons in the inner core to 80 for the water of the outer micellar surface. The following generally accepted rules for solubilizate position are derived from several works : (1) Non-polar aliphatic hydrocarbons locate in an inner hydrophobic micellar core. (2) Semipolar and polar compounds such as alcohols, acids and amines locate at the so-called palisade layer of the micelle with the polar group at the micellar surface and the non-polar hydrocarbon groups in the micellar core. (3) Aromatic hydrocarbons such as benzene, toluene, and naphthalene sit in the micellar core and at the micellar surface.

Research work done in the 1980s on micelle formation and solubilization has treated micelles as a separate phase. With regard to solubilization, in particular, an increased pressure within the micelle, in accordance with Laplace's law, is generally invoked to explain a diminished transfer of free energy per methylene group from the aqueous medium into the micellar interior compared with the free energy transfer from an aqueous medium into the bulk liquid hydrocarbon. The decreased free energy transfer per methylene group associated with micelle formation has also been attributed to partial crystallization of the alkyl chain in the interior of the micelle, caused by the same Laplace–induced pressure increase. An interfacial tension exists at the boundary between two bulk phases. Therefore, a pressure increase can occur only when micelles are in a separate phase. If interfacial tension exists within the micelle, a difference would be observed in the association constant (K_1) between solubilizate (R) and a vacant micelle (M), depending on whether the solubilization site lies inside or outside the plane of interfacial tension :

$$M + R \overset{K_1}{\rightleftharpoons} MR$$

This differance might be seen by using solubilization molecules with hydrophobic alkyl chains of varying lengths as probes, since the alkyl chain is believed to be located partly inside and partly outside the micellar plane of tension. Fig. 15 shows the change in the solubilization constant observed in 4-n-alkylbenzoic acid and dodecyl-sulphonic acid micelles when alkyl chains of varying lengths are used. The alkyl chains of the solubilizates range in length from C_0 to C_8 where the C_8 chain is almost as long as the surfactant molecule. Therefore, if a plane of tension is located inside the micelle, the alkyl chains

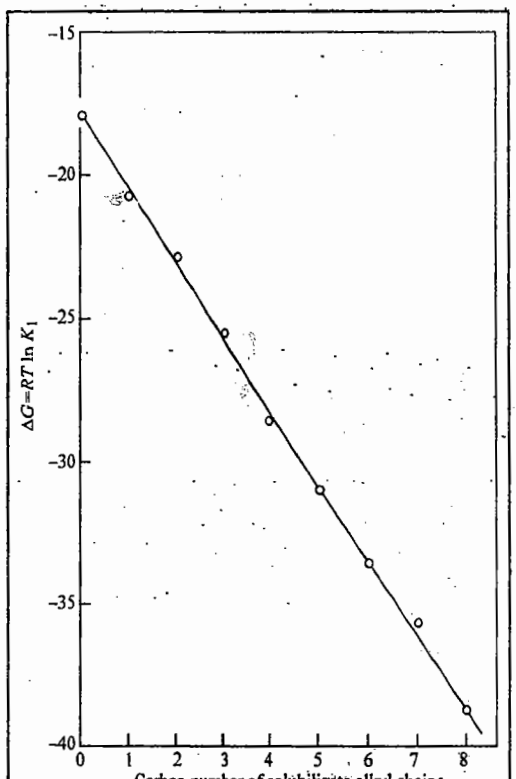

Fig. 15. Standard free energy change for the association constant between solubilizate and micelles plotted against carbon number of the solubilizate alkyl chain. The solubilizate is 4-*n*-alkylbenzoic acid and the micelle is made of dodecylsulphonic aicd.

long enough to penetrate the micelle core would encounter an increased Laplace pressure and the plot in Fig. 15 should become less steep above a certain carbon number. The experimental data did not show this effect indicating that probably there is no plane of interfacial tension in the micelle.

The Phase Rule of Solubilization

Research on solubilization has used the phase-separation model of the micelle. Accordingly, solubilization has been treated as partitioning of solubilizate molecules between a micellar phase and the intermicellar bulk phase. Some published work has also been based on the mass-action approach. Here we shall examine solublization in terms of the Gibbs phase rule.

If the micelles are regarded as a separate phase, then adding an excess solubilizate means there are three phases (the third is the intermicellar bulk phase). The total number of components is three (solvent, surfactant and solubilizate). Thus, the presence of three phases makes the system bivariant. This would mean that surfactant concentration would be constant at constant temperature and pressure. But, in practice, the maximum additive concentration (MAC) changes with total surfactant concentration. Even if we assume that the increase in the MAC with surfactant concentration above the CMC is due to an increase in the total micellar phase, the concentration of solubilizate in the micellar phase should still remain constant because the concentration is an intensive property of the system and is, therefore, homogeneous throughout the micellar phase.

If, on the other hand, the micelles are regarded as a separate phase and the system does not contain an excess solubilizate phase, there are three degrees of freedom. The surfactant concentration is then a unique variable that determines every intensive property of the system at constant temperature and pressure. In other words, the solubilizate monomer concentration in the intermicellar bulk phase (and, therefore, also in the micellar phase) is set automatically by the surfactant concentration, irrespective of the total solubilizate concentration in the system. This is not only totally incorrect in theory but is contrary to the experimental evidence that the concentration of solubilizates is determined only by the amount added to the system.

MICELLAR CATALYSIS

Micelles in aqueous media have either a polar region or a region of high charge density, accompanied by an electrostatic potential of upto a few hundred millivolts at the micellar surface and a non-polar hydrophobic region in the micelle core. The kinetics of micellar reactions are governed by electrostatic and hydrophobic interactions between micelles and reactants, transition state complexes and products. If any of the reaction species interacts with micelles, then the presence of micelles will affect the reaction rate. Micelle-catalyzed reactions are somewhat similar to enzyme-catalyzed reactions. The proper choice of surfactant brings about a rate increase of upto 1000-fold. The diameter of micelles is 30–50 Å, similar in size to globular enzymes. Micelle-catalyzed reactions can be treated in a manner analogous to the reaction scheme for enzymatic catalysis.

However, the analogy between the high reactivity of an enzyme-substrate complex and the reactivity of substrates bound to micelles is not entirely satisfactory. In a substrate-enzyme complex the reactants are fixed in position, whereas reactants incorporated into a micelle are free to move about in the micellar region. Furthermore, reactants distribute into micelles according to their solubilities and not according to the stoichiometry of the reaction. The solubilization of reactants and their distribution among micelles play the most important role in micelle-catalyzed reactions. In addition, the rate enhancement generally increases with increasing hydrophobicity of reactants and amphiphiles, which is not always the case for enzymatic reactions. These differences are mainly due to the fact that micelles do not maintain a definite configuration but are in dynamic association–dissociation equilibrium with monomeric surfactants in the bulk phase, changing their size and shape at rates involving milliseconds and microseconds.

The incorporation of reagents into micelles often alters the CMC of the surfactant. Therefore, the CMC must be determined for each reaction system in order to correctly interpret the results.

The effect of micelles on organic reactions can be attributed to both electrostatic and hydrophobic interactions. Electrostatic interaction may affect the rate of a reaction either by its effect on the transition state of the reaction or by its effect on the concentration of reactant in the vicinity of the reaction site. Thus, a cationic micelle with its multiplicity of positively charged hydrophilic heads may catalyze the reaction between a nucleophilic anion and a neutral substrate by delocalizing the negative charge developing in the transition state of this reaction, thereby decreasing the energy of activation of the reaction. It may also catalyze the reaction by increasing the concentration of nucleophilic anion at the micelle–water interface close to the reactive site of the substrate. For catalysis to occur, it is necessary (1) that the substrate be solubilized by the micelle and (2) that the *locus of solubilization* be such that the reactive site of the substrate is accessible to the attacking reagent. It is here that hydrophobic interactions become important because they determine the extent and the locus of solubilization in the micelle.

In the simplest case, where we assume that the surfactant does not complex with (*i.e.*, solubilize) the substrate S, except when the former is in the form of micelles M and that complexing between the substrate and the micelle is in a 1:1 stoichiometric ratio, we can symbolize the formation of a reaction product P as

$$\begin{array}{ccc} M + S & \overset{K}{\rightleftharpoons} & MS \\ \downarrow k_0 & & \downarrow k_m \\ P & & P \end{array}$$

where k_0 is the rate constant for the reaction of the substrate in the bulk phase and k_m is the rate constant for the reaction of the substrate in the micelle. The overall rate constant for the reaction k_p is then given by the expression

$$k_p = k_0[f_0] + k_m[f_m] \qquad ...(32)$$

where f_0 is the fraction of the uncomplexed substrate and f_m is the fraction of the complexed substrate. The equilibrium constant K for the interaction between substrate and micelle, usually called the **binding constant**, is then given by the relation

$$K = \frac{[f_m]}{[M][f_0]} \qquad ...(33)$$

from which

$$k_p = k_0[f_0] + k_m K[M][f_0] = (k_0 + k_m K[M])f_0 \qquad ...(34)$$

Since $f_0 + f_m = 1$,

$$K = \frac{[f_m]}{[M][f_0]} = \frac{[1 - f_0]}{[M][f_0]} \qquad ...(35)$$

and

$$f_0 = \frac{1}{1 + K[M]} \qquad ...(36)$$

Hence,

$$k_p = \frac{k_0 + k_m K[M]}{1 + K[M]} \qquad ...(37)$$

If we assume that [M] is given by the expression

$$[M] = \frac{(c - CMC)}{N} \qquad ...(38)$$

where c is the total concentration of surfactant and N is the aggregation number in its micelles, then the expression for the overall rate constant becomes

$$\frac{1}{k_0 - k_p} = \frac{1}{k_0 - k_m} + \left(\frac{1}{k_0 - k_m}\right)\left[\frac{N}{K(c - CMC)}\right] \qquad ...(39)$$

Since the overall rate constant for the reaction k_p and the rate constant for the reaction in the absence of micelles k_0 are readily obtained from kinetic data, a plot of $1/(k_0 - k_p)$ versus $[1/c - \text{CMC})]$, which should be a straight line with slope $= N/K(k_0-k_m)$ and intercept $= 1/(k_0 - k_m)$, allows the calculation of k_m, the rate constant for the substrate complexed with the micelles and K, the binding constant of the substrate to the micelle.

Since surfactant concentrations are usually below 10^{-1} M , there will generally be little enhancement of the rate of reaction in the presence of micelles unless the product k_mK is 10^2 or more. Since the binding constant K depends on the extent of hydrophobic bonding between surfactant and substrate, it can be expected that K will increase with increase in the chain length of both the surfactant and the substrate. However, if the length of the hydrophobic group of the substrate is too long, it may be solubilized so deeply in the micelle that access to its reactive site by a reagent in an aqueous solution phase is hindered. In that case, solubilization will inhibit, rather than catalyze, the reaction.

EMULSIFICATION BY SURFACTANTS

Emulsification—the formation of emulsions from two immiscible liquid phases—is probably the most versatile property of surface-active agents for practical applications. Paints, polishes, pesticides, metal cutting oils, margarine, ice cream, cosmetics, metal cleaners and textile processing oils are all emulsions and are used in emulsified form. An **emulsion** *is a significantly stable suspension of particles of a liquid of certain size in another immiscible liquid.* The term *significantly stable* means relative to the intended use and may range from a few minutes to a few years. At the present time, investigators in this field distinguish between three different types of emulsions based upon the size of the dispersed particles : (1) **macroemulsions**, the most well known type, opaque emulsions with particles > 400 nm, easily visible under a microscope ; (2) **microemulsions**, transparent dispersions with particles < 100 nm in size that have been intensively studied during the 1970s because of their use in enhanced oil recovery; (3) **miniemulsions**, a type that is blue-white with particle sizes between the first two types (100-400 nm). Recently, **multiple emulsions** in which the dispersed particles are themselves emulsions, have been the subject of considerable investigation.

Two immiscible, pure liquids cannot form an emulsion. For a suspension of one liquid in another to be stable enough to be classified as an emulsion, a third component must be present to *stabilize the system.* The third component is called the **emulsifying agent (or emulsifier)** and it is usually a surface-active agent, although not necessarily of the type that is usually considered a surface-active agent (finely divided solids, for example, may act as emulsifying agents).

Macroemulsions and microemulsions have been discussed below in some details.

Macroemulsions

Macroemulsions are of two types based on the nature of the dispersed phase: oil-in-water (*O/W*) and water-in-oil (*W/O*). The oil-in-water type emulsion is a dispersion of a water-immiscible liquid or solution, always called the 'oil' (*O*), regardless of its nature in an aqueous phase (*W*). The oil is, in this case, the 'discontinuous' (inner) phase; the aqueous phase is the 'continuous' (outer) phase. The water-in-oil type emulsion is a dispersion of water or an aqueous solution (*W*) in a water-immiscible liquid (*O*). The type of emulsion formed by water and oil depends primarily on the nature of the emulsifying agent and to a minor extent, on the process used in preparing the emulsion and the relative proportions of oil and water present. In general, *O/W* emulsions are produced by emulsifying agents that are more soluble in water than in the oil phase whereas *W/O* emulsions are produced by emulsifying agents that are more soluble in the oil than in water. This is known as the **Bancroft rule**. *O/W* and *W/O* emulsions are not in thermodynamic equilibrium with each other; one type is usually inherently more stable than the other for a particular emulsifying agent at a given concentration under a given set of conditions. However, the one type of emulsion can be converted to the other by changing conditions. This is called **inversion of the emulsion**.

These two types of macroemulsions are easily distinguished : 1. A macroemulsion can readily be diluted with more of the outer phase but not as easily with the inner phase. Consequently while *O/W* emulsions disperse readily in water, *W/O* emulsions do not. But they do disperse readily in oil. This method works best on dilute emulsions. 2. *O/W* emulsions have electrical conductivities similar to that of the water phase; *W/O* emulsions do not conduct current significantly. 3. *W/O* emulsions will be coloured by oil-soluble dyes whereas *O/W* emulsions show the colour faintly, if at all, but will be coloured by water-soluble dyes. 4. If the two phases have different refractive indices, microscopic examination of the droplets will determine their nature. A droplet, on focusing upward, will appear brighter if its refractive index is greater than that of the continuous phase and darker if its refractive index is less than that of the continuous phase. This clearly identifies the substance in the droplet if one knows the relative refractive indices of the two phases. 5. In filter paper tests, a drop of an *O/W* emulsion produces an immediate wide, moist area; a drop of *W/O* emulsion does not. If the filter paper is first impregnated with a 20% cobaltous chloride solution and dried before the test, the area around the drop immediately turns pink if the emulsion is *O/W* and remains blue (shows no colour change) if it is *W/O*.

There are a number of similarities between macroemulsions and foams : 1. They both consist of a dispersion of an immiscible state of matter in a liquid phase. Foams are dispersions of a gas in a liquid; emulsions are dispersions of a liquid in a second immiscible liquid. 2. The interfacial tension γ_l at the relevant interface is always greater than zero and since there is a marked increase in interfacial area ΔA during the process (of emulsification or foaming), the minimum work involved is the product of the interfacial tension and the increase in interfacial area ($w_{min} = \Delta A \times \gamma_l$). (3) The system will spontaneously revert to two bulk phases unless there is an interfacial film present that produces steric and/or electrical barriers to coalescence of the dispersed phase.

On the other hand, there are a number of significant differences between macroemulsions and foams: 1. The surfactants in the interfacial film of a foam cannot dissolve in the dispersed (gas) phase, while in a macroemulsion the solubility of the surfactants in the liquid being dispersed is a major factor determining the stability of the emulsion. 2. In macroemulsions, both *O* and *W* can serve as the continuous phase, *i.e.*, both *O/W* and *W/O* emulsions are commonly encountered while in foams, only the liquid acts as the continuous phase.

Formation of Macroemulsions. In the formation of macroemulsions, one of the two immiscible liquids is broken up into particles that are dispersed in the second liquid. Since the interfacial tension between two immiscible pure liquids is always greater than zero, the dispersion of the inner liquid, which produces a tremendous increase in the area of the interface between them, results in a correspondingly large increase in the interfacial free energy of the system. The emulsion produced is consequently highly unstable thermodynamically, relative to the two bulk phases separated by a minimum surface area. It is for this reason that two immiscible liquids when pure, cannot form an emulsion. The function of the emulsifying agent is to stabilize this basically unstable system for a sufficient time so that it can perform some function. The emulsifying agent does this job by getting adsorbed at the liquid–liquid interface as an oriented interfacial film. The oriented film performs two functions : (1) It reduces the interfacial tension between the two liquids and hence reduces the thermodynamic instability of the system which results from the increase in the interfacial area between the two phases. (2) It decreases the rate of coalescence of the dispersed liquid particles by forming mechanical, steric and/or electrical barriers around them. The steric and electrical barriers inhibit the close approach of one particle to another. The mechanical barrier increases the resistance of the dispersed particles to mechanical shock and prevents them from coalescing when they do collide. In the formation of macroemulsions, the reduction of interfacial tension reduces the amount of mechanical work required to break the inner phase into dispersed particles.

Factors Determining Stability of Emulsions. The term **stability**, when applied to emulsions used for practical applications, usually refers to the resistance of emulsions to the coalescence of

their dispersed droplets. The rate of coalescence of the droplets in an emulsion is stated to be the only quantitative measure of emulsion stability. It can be measured by counting the number of droplets per unit volume of the emulsion as a function of time in a haemocytometer cell under a microscope. The rate at which the droplets of a macroemulsion coalesce to form larger droplets and eventually 'break' the emulsion, has been found to depend on the following factors :

1. Physical nature of the interfacial film. The droplets of dispersed liquid in an emulsion are in constant motion and, therefore, there are frequent collisions between them, If, on collision, the interfacial film surrounding the two colliding droplets in a macroemulsion ruptures, the two droplets will coalesce to form a larger one, since this results in a decrease in the free energy of the system. If this process continues, the dispersed phase will separate from the emulsion, and it will 'break'. The mechanical strength of the interfacial film is, therefore, one of the prime factors determining macroemulsion stability. Liquid-crystal formation can also stabilize the emulsion. By accumulating at the interface surrounding the dispersed particles, liquid crystals surround the particles with a high viscosity region that resists the coalescence of individual droplets.

2. Existence of an electrical or steric barrier to coalescence of the dispersed droplets. The presence of a charge on the dispersed droplets constitutes an electrical barrier to the close approach of two particles to each other. This is believed to be a significant factor only in *O/W* emulsions. In *O/W* emulsions, the source of the charge on the dispersed droplets is the adsorbed layer of surfactant with its hydrophilic end oriented toward the water phase. In emulsions stabilized by ionic surfactants, the sign of the charge on the dispersed droplets is always that of the amphipathic ion. In emulsions stabilized by non-ionic surfactants, the charge on the dispersed phase may arise either from adsorption of ions from the aqueous phase or from frictional contact between droplets and the aqueous phase. In the latter case, the phase with the higher dielectric constant is charged positively. In *W/O* emulsions, there is very little charge, if any, on the dispersed particles and experimental data indicate no correlation between stability and any charge present.

3. Viscosity of the continuous phase. An increase in the viscosity η of the continuous phase reduces the diffusion coeffient D of the droplets, since for spherical droplets of radius a,

$$D = \frac{kT}{6\pi\eta a} \qquad \ldots(38)$$

As the diffusion coefficient is reduced, the frequency of collision of the droplets and their rate of coalescence are reduced. The viscosity of the external phase is increased as the number of suspended particles increases. This is one of the reasons that many emulsions are more stable in concentrated form than when diluted. The viscosity of the external phase in emulsions is often increased by the addition of special ingredients for this purpose, such as natural and synthetic 'thickening' agents.

4. Size distribution of droplets. A factor influencing the rate of coalescence of the droplets is the size distribution. The smaller the *range* of sizes, the more stable the emulsion. Since larger particles have less interfacial surface per unit volume than smaller droplets in macroemulsions, they are thermodynamically more stable than the smaller droplets and tend to grow at the expense of the smaller ones.

5. Phase volume ratio. As the volume of the dispersed phase in a macroemulsion increases, the interfacial film expands further and further to surround the droplets of dispersed material and the basic instability of the system increases. As the volume of the dispersed phase increases beyond that of the continuous phase, the type of emulsion (*O/W*) or (*W/O*) becomes basically more and more unstable relative to the other type of emulsion, since the area of the interface that is now enclosing the dispersed phase is larger than that which would be needed to enclose the continuous phase. It often happens, therefore, that the emulsion inverts as more and more of the dispersed phase is added, unless the emulsifying agent is so unbalanced as to be capable of forming only one type of emulsion.

6. Temperature. A change in temperature causes changes in the interfacial tension between the two phases, in the nature and viscosity of the interfacial film, in the relative solubility of the emulsifying agent in the two phases, in the vapour pressures and viscosities of the liquid phases and in the thermal agitation of the dispersed particles. Therefore, temperature changes usually cause considerable changes in the stability of emulsions; they may invert the emulsion or cause it to break. Emulsifying agents are usually most effective when near the point of minimum solubility in the solvent in which they are dissolved since at that point they are most surface active.

Inversion of Macroemulsions

Macroemulsions may be changed from *W/O* or *O/W* and vice versa by varying the emulsification conditions. Thus : 1. The addition of water to the oil plus emulsifier produces *W/O* emulsion whereas the addition of oil to the same emulsifier plus water produces an *O/W* emulsion. 2. If the emulsifier is rendered more oil-soluble, it tends to produce a *W/O* emulsion and if it is rendered more water-soluble it tends to produce an *O/W* emulsion. 3. Increasing the ratio of oil to water tends to produce a *W/O* emulsion and vice versa. 4. As the temperature of an *O/W* emulsion stabilized with a polyoxyethylenated non-ionic surfactant is increased, the surfactant becomes more hydrophobic and the emulsion may invert to *W/O*.

Microemulsions

Although microemulsions have been produced commercially since the 1930s, their importance has become significant only since the 1970s, mainly as a result of the intense interest generated in them by laboratory and field tests that showed that they could increase the recovery of petroleum from reservoir rock. This is due to the ultra low interfacial tensions attained at the microemulsion–petroleum interface, a pre-requisite for the displacement of the residual petroleum in the capillaries of the rock. There has also been considerable recent interest in microemulsions of fluorocarbons as a result of the exceptionally high solubility of oxygen in these systems and their consequent use as oxygen carriers in cases of circulatory disfunction.

Microemulsions are transparent dispersions containing two immiscible liquids with particles of 10–100 nm diameter that are generally obtained upon mixing the ingredients *gently*. Macroemulsions, on the other hand, need intense agitation for their formation. Like macroemulsions, the microemulsions may be oil-in-water (*O/W*) or water-in-oil (*W/O*) type. Certain aspects of microemulsions remain controversial, such as the nature of the interface between the dispersed particles, the nature of the continuous phase and whether they contain one type of dispersed particles or micelles or more.

Whether one considers a microemulsion to be a solution of micelles, swollen by solubilized second liquid, in one liquid or a dispersion of tiny droplets of one liquid in a second liquid, the interfacial tension of the microemulsion against both these liquids must be close to zero. In the first case, the system is one-phase and, therefore, has no interface against either liquid as long as the micelles are capable of solubilizing more of the second liquid. In the second case, the interfacial area is so large that an exceedingly low interfacial tension must be present to permit formation of the microemulsion with so little work. In addition, the interfacial region must be highly flexible, either to permit the large curvature required to surround exceedingly small particles or to allow the easy transition from oil-continuous to water-continuous structure that is characteristic of microemulsions.

It is generally accepted that the clear, fluid (surfactant) phase between a non-polar phase (*O*) and an aqueous phase (*W*) in a three-phase system is a microemulsion. If the concentration of surfactant is increased, the middle phase incorporates both the *O* and *W* phases into a single (microemulsion) phase.

Microemulsions are generally prepared with more than one surfactant or with a mixture of a surfactant and a co-surfactant (*e.g.*, a polar compound of intermediate chain length). The combination is usually required to provide the proper balance between hydrophilic and lipophilic properties for the required oil and water phases under the conditions of use. This balance can be determined experimentally by mixing the oil and water phases in the desired proportions with appropriate surfactant–cosurfactant

combination. It is advisable to use graduated vessels for this purpose so that the volumes of the phases can be measured. If a three-phase system is finally obtained instead of a one-phase microemulsion, the concentration of surfactant–co-surfactant mixture can be increased until both water and oil phases disappear by solubilization into the surfactant phase.

Theories of Emulsions

The theories to decide the type of emulsion formed can be classified into : Qualitative theories and 2. Quantitative theories.

1. Qualitative Theories. All the theories which attempt to explain the formation of *O/W* and *W/O* emulsions are based on the empirical **Bancroft rule**. It is believed by some researchers that the interfacial region produced by the adsorption and orientation of the surface-active molecules at the liquid–liquid interface can have different interfacial tensions on each of its two sides; that is, the interfacial tension between the hydrophilic ends of the surfactant molecules and the water phase molecules is different from the interfacial tension between the hydrophobic ends of the surfactant and the oil phase molecules. In the formation of emulsion, this interfacial tension would tend to curve so as to shorten the area of that side which has greater interfacial tension thus minimizing the interfacial free energy. A preferentially oil-soluble emulsifying agent would, of course, produce a lower interfacial tension at the oil interface, yielding a *W/O* emulsion; a preferentially water-soluble emulsifying agent would produce a lower interfacial tension at the water interface, yielding an *O/W* emulsion.

According to Schulmann (1954), however, the formation of the two types of emulsions can be explained on the basis of the difference in the contact angles at the oil–water–emulsifier boundary (Fig.16). If, at the contact between oil, water and emulsifier, the oil contact angle (the contact angle, measured in the oil phase) is less than 90°, then the oil surface is concave toward the water producing a *W/O* emulsion. On the other hand, if at the same oil-water-emulsifier contact, the water contact angle is less than 90°, then the water surface is concave toward the oil, producing an *O/W* emulsion.

It may, however, be noted that if the oil contact angle is $< 90°$, then $\gamma_{OE} < \gamma_{WE}$ (*i.e.*, the emulsifier is more hydrophobic than hydrophilic). If the water contact angle is $< 90°$, then $\gamma_{WE} < \gamma_{OE}$ and the emulsifying agent is more hydrophilic than hydrophobic. Thus, emulsifying agents with mainly hydrophilic character produce *O/W* emulsions whereas those with mainly hydrophobic character produce *W/O* emulsions.

2. Quantitative Theory. Davies (1957) developed a quantitative theory relating the type of emulsion formed to the *kinetics of coalescence* of the two types of droplets present : oil droplets and water droplets. According to this theory, the type of emulsion formed when oil and water are agitated together in the presence of an emulsifying agent is due to the relative rates of the two competing processes, *viz.*, coalescence of oil droplets and coalescence of water droplets. Agitation is presumed to break simultaneously both the oil and water phases into droplets, with the emulsifying agent being adsorbed at the interface around these droplets. The phase that becomes the continuous one is that which has the faster rate of coalescence. If the rate of coalescence of the water droplets is much greater than that of the oil droplets, then an *O/W* emulsion is formed. If the rate of coalescence of the oil droplets is much greater than that of the water droplets, then a *W/O* emulsion is formed. When the rates of coalescence of the two phases are similar, then the phase of larger volume becomes the outer phase.

In general, hydrophilic groups in the interfacial film constitute a barrier to the coalescence of oil droplets whereas hydrophobic groups in the interfacial film constitute a barrier to the coalescence of water droplets. Hence, an interfacial film that is predominantly hydrophilic tends to form *O/W* emulsions whereas one that is predominantly hydrophobic tends to produce *W/O* emulsions.

The Selection of Surfactants as Emulsifying Agents (Emulsifiers)

1. The HLB Method. The most frequently used method is known as the HLB (hydrophile-

lipophile balance) method. In this method (Griffin, 1949), a number (between 0 and 40) indicative of emulsification behavior and related to the balance between the hydrophilic and lipophilic (hydrophobic) portions of the molecule has been assigned to many commercial emulsifying agents. In addition; a similar range of numbers has been assigned to various substances that are frequently emulsified, such as oils, lanolin, paraffin wax, xylene, carbon tetrachloride, and so on. These numbers are generally based on the emulsification experience, rather than on structural considerations. Then an emulsifying agent—or better still, a combination of emulsifying agents—is selected whose HLB number is approximately the same as that of the ingredients to be emulsified. As expected from the definition of the HLB value, materials with high HLB values are *O/W* emulsifiers and materials with low HLB value are *W/O* emulsifiers. An HLB value of 3–6 is the recommended range for *W/O* emulsification while an HLB value of 8–18 is recommended for *O/W* emulsification.

It has been pointed out (Shinoda, 1968) that a single surfactant can produce either an *O/W* or a *W/O* emulsion, depending on the temperature at which the emulsion is prepared. At high oil concentrations, it depends on the ratio of surfactant to oil.

2. The PIT Method. An *O/W* emulsion made with a non-ionic surfactant may invert to a *W/O* emulsion when the temperature is raised; a *W/O* emulsion may invert to an *O/W* emulsion when the temperature is lowered. The temperature at which inversion occurs is known as the **phase inversion temperature** or **PIT** and is the temperature at which the hydrophilic and lipophilic tendencies of the surfactant (or surfactant–cosurfactant mixture) 'balance' in that particular system of *O* and *W* phases. For optimum stability, the Japanese pioneers in emulsion science—Shinoda and Saito—have suggested 'emulsification by the PIT method' in which the emulsion is prepared at a temperature 2–4°C below the PIT and then cooled down to the storage temperature (for *O/W* emulsion). This is because an emulsion prepared near the PIT has a very fine average particle size but is not very stable to coalescence. Cooling it down to a temperature considerably below the PIT increases its stability without significantly increasing its average particle size.

GELS

Several lyophilic sols and a few lyophobic sols as well, when coagulated under certain conditions, change into a semi-rigid mass, enclosing the entire amount of the liquid within itself. Such a product is called a gel. The process of tranformation of a sol into a gel is known as **gelation.**

Gel represents a liquid–solid system, *i.e.*, a liquid dispersed in a solid. Amongst lyophilic sols, the examples are : gelatin, agar-agar, gum arabic, mastic and gamboge sols, etc. Amongst lyophobic sols, the examples are : silicic acid, ferric hydroxide, ferric phosphate sols, etc. The sols should be of sufficiently high concentration to facilitate the gelation process. Gels and gelation are very important in medicine and biology because plants and animals are primarily composed of gels. The gelation of macromolecular solutions is of great importance in technology. The formation of a glue layer in pastings, the gelation of pyroxlin and the production of artificial fibres are all gelation processes. Several processes in food and bread-baking industries make use of gelation. Clear raw hide which does not have a hair cover and from which leather is obtained is a gel.

Preparation of Gels. Gels may be prepared by any one of the following methods.

1. Cooling of Sols of Moderate Concentrations. Gels of gelatin and agar-agar, etc., are obtained by cooling their sols of moderate concentrations prepared in hot water. As has been mentioned earlier, the particles of hydrophilic sols are extensively hydrated. When cooled, the hydrated particles agglomerate together to form larger aggregates which ultimately form a semi-solid network entrapping the entire liquid within itself. The product is a semi-rigid gel structure.

2. Double Decomposition. The hydrophobic gels like silicic acid, aluminium hydroxide (commonly known as silica gel and alumina gel) are prepared by this method. By adding hydrochloric acid to an aqueous solution of sodium silicate, highly hydrated silicic acid gets precipitated. This when allowed to stand sets into a gel.

Similarly, by mixing solutions of sodium hydroxide and aluminium chloride of suitable concentration, a highly hydrated precipitate of aluminium hydroxide is obtained. On standing it changes into a gel.

3. Change of Solvents. This method is also used for preparing some of the hydrophobic gels. To take an example, when ethanol is added rapidly to a solution of calcium acetate of fair concentration, the salt separates out to give a colloidal solution. When allowed to stand, it undergoes gelation. The ultimate product is a semi-rigid gel of calcium acetate. The entire liquid is entrapped within.

Elastic and Non-elastic Gels. Gels are divided into two categories depending upon their properties. These are : elastic gels and non-elastic gels. The two varieties are distinguished chiefly by their behaviour on dehydration and rehydration. Elastic gels are reversible. When partially dehydrated, they change into a solid mass which, however, changes back into the original form on simple addition of water followed by slight warming, if necessary. Non-elastic gels, on the contrary, are irreversible. When dehydrated they become glassy or change into a powder which on addition of water and followed by warming does not change back into the original gel.

Gelatin, agar-agar and starch are examples of elastic gels. In these cases, dehydration and rehydration on exposure to water vapour are almost reversible even when the cycle is carried out more than once.

Silica, alumina and ferric oxide gels are examples of non-elastic gels. Thus, if silica gel is dehydrated, addition of water will not reset it into the form of a gel.

There is another point of difference between elastic and non-elastic gels. While elastic gels can imbibe water when placed in it and undergo swelling, non-elastic gels are incapable of doing so. This phenomenon is known as **imbibition** or **swelling.**

Another characteristic property possessed both by elastic and non-elastic gels is to undergo *shrinkage in volume* when allowed to stand. This phenomenon is called **syneresis.** Application of external pressure to a gel enhances syneresis. For amphoteric proteins, maximum syneresis is observed at the isoelectric point since the molecules then have equal number of opposite charges and this favours the shrinkage of the molecular framework of a gel. Syneresis decreases as the *p*H of the medium declines from the isoelectric point because the molecular chains aquire a charge of the same sign. The chains unfold and repel one another.

Some of the gels, particularly gelatin (reversible gel) and silica (irreversible gel), liquefy on shaking, changing into the corresponding sol. The sol on standing reverts back to the gel. This phenomenon of reversible sol—gel transformation is generally referred to as **thixotropy.**

Importance and Application of Colloids

Colloids play a very important role in everyday life as well as in industry, agriculture, medicine and biology. The following discussion, therefore, will be of interest.

1. Foods. Many of our foods are colloidal in nature. For example, milk is an emulsion of fat dispesed in water. It is stabilised by casein which itself is a lyophilic colloid and, being a protein, is a nutrient of great value. Gelatin is added to ice cream as a protective agent so as to preserve its 'smoothness'. Whipped cream, fruit jellies, salad dressings, eggs and a host of other materials used as food, are colloidal in nature.

2. Medicines. A number of medicinal and pharmaceutical preparations are emulsions, *i.e.*, colloidal in nature. It is believed that in this form they can be more effective and are easily assimilated. Colloidal calcium and gold, for instance, are administered by injections to raise the vitality of the human system.

3. Industrial goods. Soap, the index of modern civilization, is a colloidal electrolyte. The same is true of a series of newer detergents and wetting agents that have been produced in recent years. Paints, varnishes, enamels, celluloses, resins, gums, glues and other adhesives; rayon, nylon, terylene,

textiles, leather, paper, etc., are all colloidal in nature. Latex, from which rubber is obtained, is suspension of negatively charged colloidal particles of rubber. Industrial processes such as tanning, dyeing, lubrication, etc., are of colloidal nature. This list is by no means exhaustive and can be extended further.

4. Rubber-plating. The negatively charged particles of rubber (latex) are made to deposit on to wires or handles of various tools (in order to insulate them) by electrophoresis. The article to be rubber-plated is made the anode. The rubber particles migrate in an electric field towards the anode and get deposited on it.

5. Chrome-tanning. The chrome-tanning of leather is brought about by the penetration of positively charged particles of hydrated chromic oxide into the leather. The rate of penetration can be increased by applying an electric field, *i.e.*, by the process of electrophoresis.

6. Cottrell precipitator. Smokes and dusts are a nuisance and create health problems in industrial areas. Actually these are dispersions of electrically charged colloidal particles in air. The removal of these particles from air involves the principle of electrophoresis. The air from a furnace or an industrial plant carrying these particles is passed between metal electrodes maintained at a high difference of potential (about 50,000 volts). The particles are discharged and deposited as precipitates on the oppositely charged electrodes from which they can be scrapped mechanically.

7. Sewage disposal. Sewage water consists of particles of dirt, rubbish, mud, etc., which are of colloidal dimensions and carry electric charge and, therefore, do not settle down easily. On creating an electric field in the sewage tank, these particles migrate to the oppositely charged electrodes, get neutralised and settle down at the bottom. It will be seen that here, too, the electrolphoretic property of colloids has been made use of.

8. Clarification of water. Sometimes slight turbidity is noticed in water. This is due to the presence of negatively charged particles of very fine clay. The addition of potash alum or aluminium sulphate furnishes the trivalent aluminium ions (Al^{3+}) which cause the coagulation of the clay particles, which, therefore, settle down leaving water in clear state.

9. Detergent action of soap. Most of the dirt or dust sticks on to grease or some oily material which somehow gathers on cloth. As grease is not readily wetted by water, it is difficult to clean the garment by water alone. The addition of soap lowers the interfacial tension between water and grease and this causes the emulsification of grease in water. The mechanical action, such as rubbing, etc., releases the dirt.

10. Artifical rain. Clouds consist of charged particles of water dispersed in air. Rain is caused by the aggregation of these minute particles. Some workers have succeeded in causing such aggregation by artifical means such as by throwing electrified sand from aeroplanes.

11. Formation of deltas. The deltas at the mouths of great rivers are formed by the precipitation of the charged clay particles, carried as suspension in the river water, by the action of salts present in sea water.

12. Smoke screens. Smoke screens are used in warfare for the purpose of concealment and camoulfage. Smoke screens generally consist of very fine particles of titanium oxide dispersed in air and are ejected from aeroplanes. As titanium oxide is very heavy, the smoke screen drops down rapidly as a curtain of dazzling whiteness.

It is worth mentioning that since 1950, colloid science has generated a number of important fields such as the study of polymers, semiconductors, liquid crystals, membranes and vesicles. Micellar aggregates have served as an important bridge between microscopic and macroscopic chemical species in the development of new technologies. The importance of colloid science is now fully recognized. It is the basic foundation of almost all fields of solution science.

I. Review Questions

1. Carefully distiniguish between a molecular solution, a colloidal dispersion and a coarse dispersion.
2. Explain the use of (*a*) dialysis (*b*) electro-dialysis and (*c*) ultrafiltration in the purification of colloidal solutions.
3. Discuss the electrical properties of colloidal solutions and explain the action of electrolytes on them.
4. Discuss the origin of charge on colloidal particles. What is meant by electrical double layer ? What is DLVO theory?
5. What are protective colloids ? Explain how a lyophilic colloid can stabilise a lyophobic colloid.
6. Describe various methods for the determination of the size of colloidal particles.
7. What are colloidal miscelles ? Discuss the structure of miscelles in polar and non-polar media.
8. What does HLB stand for ? What is its significance ?
9. Define critical miscelle concentration. Show graphically how the physical properties of solutions of surfactants such as molar conductance, surface tension, osmotic pressure change at the critical miscelle concentration.
10. How is CMC related to free energy change, enthalpy change and entropy change accompanying the process of miscelle formation ?
11. State and explain the Laplace's law. Discuss solubilization from the point of view of the phase rule.
12. Compare and contrast miscellar catalysis from enzyme catalysis.
13. What are emulsions ? Discuss the methods used in finding the type of an emulsion. How are emulsions prepared ?
14. What are gels ? How would you distinguish between elastic and non-elastic gels.

CHAPTER 33

SURFACE CHEMISTRY

ADSORPTION BY SOLIDS

Surface chemistry research is an interdisciplinary area on the frontiers of physical chemistry, chemical physics, materials science and nanoscience. Its impact on industrial processes and technlogy has grown over the years and will continue to grow in future. Residual unbalanced forces exist on the surface of a solid. As a result of these residual forces, the surface of a solid has a tendency to attract and retain molecules of other species with which it is brought into contact. As these molecules remain only at the surface, their concentration is more at the surface than in the bulk of the solid. The phenomenon of higher concentration of any molecular species at the surface than in the bulk of a solid is known as **adsorption.** Solids, when finely divided, have a large surface area and, therefore, show this property to a large extent. The solid that takes up a gas or vapour or a solute from a solution, is called the **adsorbent** while the gas or vapour or the solute, which is held to the surface of the solid, is called **the adsorbate.** Colloids, on account of their extremely small dimensions, possess enormous surface area per unit mass and are, therefore, good adsorbents. The examples are charcoal, silica gel, **alumina gel,** clay, etc.

Adsorption is to be carefully distinguished from **absorption.** The latter term implies that a substance is uniformly distributed throughout the body of a solid or a liquid. Thus, while water vapours are absorbed by anhydrous calcium chloride, these are adsorbed by silica gel. Similarly, while ammonia is absorbed in water, it is adsorbed by charcoal. When a hot crucible is cooled in atmosphere, a film of moisture collects at its surface. This is a case of adsorption of water vapour on the material of the crucible. Charcoal when mixed with a coloured solution of sugar, adsorbs the colouring matter and is used as a decoloriser. McBain suggested the use of the term **sorption** to describe a process in which both absorption and adsorption take place simultaneously.

Adsorption is not necessarily a physical phenomenon always. It may as well be a chemical process involving chemical interaction between the surface atoms of the adsorbent and the atoms of the adsorbate. This type of adsorption is known as **chemisorption.** For example, oxygen is chemisorbed by carbon and hydrogen is chemisorbed by nickel under suitable conditions. In each case, a stable surface compound, frequently referred to as **surface complex,** results.

Chemisorption differs from physical adsorption (or physisorption) in the following respects :

1. Physical adsorption occurs appreciably only at very low temperatures falling below the boiling point of the adsorbate. Chemisorption can occur at all temperatures.

2. The magnitude of chemisorption increases with rise in temperature. This is just as the magnitude of a chemical reaction in a given time increases with rise in temperature. Physisorption, on the other hand, decreases with rise in temperature.

3. The heat evolved in chemisorption is very high, varying generally between 40—400 kJ mol^{-1}, as in many chemical reactions. The heat evolved in physisorption, on the other hand, is quite low, varying generally between 4—40 kJ mol^{-1}.

4. Chemisorption is irreversible as the gas adsorbed cannot be recovered from the adsorbent as such on lowering the pressure of the system at the same temperature. Physisorption is, however, reversible as the gas adsorbed can be recovered from the adsorbent easily on lowering the pressure of the system at the same temperature.

5. Since chemical forces operate within short distances only, chemisorption does not extend beyond a monolayer of gas molecules or atoms on the surface of the solid. Physisorption may extend beyond a monolayer also.

6. In physisorption, the adsorbate molecules are held by comparatively weak **van der Waals** forces. Hence, the activation energy of desorption, in this category, is very low. In chemisorption, the adsorbate molecules are held by comparatively strong valence forces. Hence, the activation energy of desorption is very high.

Applications of Adsorption. Adsorption finds extensive applications. A few examples are given below.

1. A very good method of creating a high vacuum is to connect a bulb of charcoal cooled in liquid air to a vessel which has already been exhausted as far as possible by a vacuum pump. Since the magnitude of adsorption at such low temperatures is quite high, the remaining traces of air, in spite of the low pressure, are adsorbed by the charcoal almost completely.

2. Activated charcoal is used in gas masks in which all toxic gases and vapours are adsorbed by the charcoal while pure air passes through its pores practically unchanged.

3. Silica and alumina gels are used as adsorbents for removing moisture and for controlling humidity of rooms.

4. Animal charcoal is used as a decoloriser in the manufacture of cane-sugar.

5. Soil contains small amounts of colloidal fractions in the form of very fine particles of clay. It can, therefore, always adsorb and retain certain amount of moisture in which nutrients, such as compounds of nitrogen, phosphorus and potassium, can dissolve and pass up to the plant through the roots.

6. Adsorption also plays an important role in heterogeneous catalysis, *e.g.*, the role of finely divided iron in the manufacture of ammonia and that of finely divided nickel in the hydrogenation of oils.

Adsorption of Gases by Solids. Several methods for determining adsorption of gases on solid adsorbents under the given conditions have been devised. In one such method, the gas is contained in a vessel of known volume at a given temperature. The pressure of the gas is measured on a manometer attached to the vessel. The adsorbent is then introduced into the vessel by a suitable device. Adsorption takes place fairly quickly and the pressure of the gas falls. This is noted on the manometer. Knowing the fall of pressure, the quantity of the gas adsorbed by the solid can be calculated, assuming Boyle's law to hold good. It is necessary to apply correction due to the volume of the adsorbent added.

Example 1. A sample of charcoal weighing 6·00 g was brought into contact with a gas contained in a vessel of one litre capacity at 27°C. The pressure of the gas was found to fall from 700 to 400 torr. Calculate the volume of the gas (reduced to STP) that is adsorbed per gram of the adsorbent under the conditions of the experiment. The density of the charcoal sample was 1·5 g cm^{-3}.

Solution : Initial pressure of the gas = 700 torr

Initial volume of the gas = 1 litre

Final pressure of the gas = 400 torr

Let the final volume of the gas be V ml.

$$700 \text{ torr} \times 1000 \text{ ml} = 400 \text{ torr} \times V$$

$$\therefore \quad V = \frac{700 \text{ torr} \times 1000 \text{ ml}}{400 \text{ torr}} = 1750 \text{ ml}$$

But, the volume of the gas in the flask= 1000 ml – the volume of charcoal added

$$= 1000 \text{ ml} - 6{\cdot}00 \text{ g}/1{\cdot}50 \text{ g ml}^{-1} = 996 \text{ ml}$$

Volume of the gas adsorbed by charcoal = 1750 ml – 996 ml = 754 ml

$\therefore$ Volume of the gas adsorbed per gram of charcoal = 754 ml/6 = 125·6 ml

$\therefore$ Volume of the gas at STP adsorbed per gram of charcoal will be given by

$$V_1 = \frac{VPT_1}{TP_1} = \frac{125{\cdot}6 \text{ ml} \times 400 \text{ torr} \times 273}{300 \text{ K} \times 760 \text{ torr}} \times = \mathbf{60{\cdot}15 \text{ ml}}$$

The direct weighing of the sample on a microbalance during the experiment can also lead to the determination of the extent of adsorption.

Since in the adsorption of a gas by a solid sample, the surface of the solid removes the gas molecules, the sample acts as a pump. We can thus monitor the rates of flow of the gas into and out of the system; the difference yields the rate of uptake of the gas by the sample. The extent of adsorption at any instant can be obtained by integrating this rate.

As a result of adsorption, there is decrease in residual forces acting along the surface of the adsorbent. Consequently, there is decrease of surface energy which appears as heat. *Adsorption, therefore, is invariably accompanied by decrease in enthalpy of the system, i.e.,* ΔH of the process is invariably negative. Further, since the adsorbate changes from the more random gaseous (or solution) state to the less random adsorbed state on the surface of a solid, adsorption is also accompanied by *decrease in entropy* of the system, *i.e.,* $T\Delta S$ of the process is also negative. Adsorption is thus accompanied by decrease in enthalpy as well as decrease in entropy of the system. For a spontaneous process, the free energy change given by the expression

$$\Delta G = \Delta H - T\Delta S,$$

should be negative. Since ΔH and ΔS are both negative, it is evident that ΔH should have a sufficiently high negative value so that the net result of the expression on the right hand side of the above equation is negative, *i.e.,* the value of $\Delta H - T\Delta S$ should be negative. This is actually the case. However, we know from experiment that the heat of adsorption per mole of the adsorbate goes on decreasing, *i.e.,* ΔH becomes less and less negative as adsorption proceeds further and further. Ultimately, ΔH becomes equal to $T\Delta S$ and ΔG becomes zero. At this stage, equilibrium is attained.

As illustrated above, adsorption is always accompanied by evolution of heat, *i.e.,* it is an exothermic process. The amount of heat evolved when one mole of a gas or vapour is adsorbed on a solid, is known as the **molar enthalpy of adsorption.** It is of the same order as the molar heat of condensation of the gas but is always greater than the latter.

Factors Influencing Adsorption. The magnitude of adsorption depends upon the following factors:

(*i*) Temperature (*ii*) Pressure (*iii*) Nature of the gas and(*iv*) Nature of the adsorbent.

Effect of temperature and pressure. Since adsorption is invariably accompanied by evolution of heat, therefore, in accordance with Le Chatelier's principle, the magnitude of adsorption should increase with fall in temperature. This actually happens. Further, since adsorption of a gas leads to decrease of pressure, the magnitude of adsorption increases with increase in pressure. Thus, *decrease of temperature and increase of pressure both tend to cause increase in the magnitude of adsorption of a gas on a solid.*

The Freundlich Adsorption Isotherm

The variation of adsorption with pressure at a given constant temperature is generally expressed graphically as in Fig. 1. Each curve is known as **adsorption isotherm** for the particular temperature. The relationship between the magnitude of adsorption and pressure can be expressed mathematically by an empirical equation commonly known as **Freundlich adsorption isotherm,** *viz.,*

$$a = kp^n \qquad \ldots(1)$$

where a is the amount of the gas adsorbed *per unit mass of the adsorbent* at pressure p, and k and n are constants depending upon the nature of the gas and the nature of the adsorbent. The value of n is less than 1 and, therefore, a does not increase as rapidly as p, as is evident from the adsorption isotherms (Fig. 1).

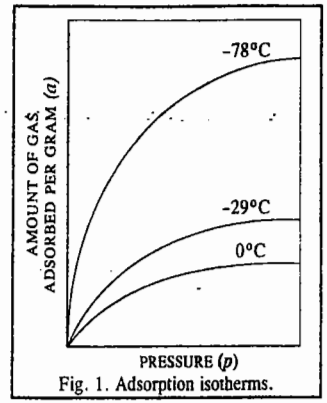

Fig. 1. Adsorption isotherms.

Nature of the gas and nature of the adsorbent. It has been found that the more readily soluble and easily liquefiable gases such as ammonia, hydrochloric acid, chlorine and sulphur dioxide are adsorbed more than the so called 'permanent' gases such as hydrogen, nitrogen and oxygen. The reason is that van der Waals or intermolecular forces which are involved in adsorption are more predominant in the former category than in the latter category of gases.

Since adsorption is a surface phenomenon, it is evident that the greater the surface area per unit mass of the adsorbent, the greater is its capacity for adsorption under the given conditions of temperature and pressure.

Adsorption Isobar and Adsorption Isostere. The effect of temperature on the extent of adsorption, *at a given pressure* of the adsorbate, is also expressed graphically, as shown in Fig. 2.

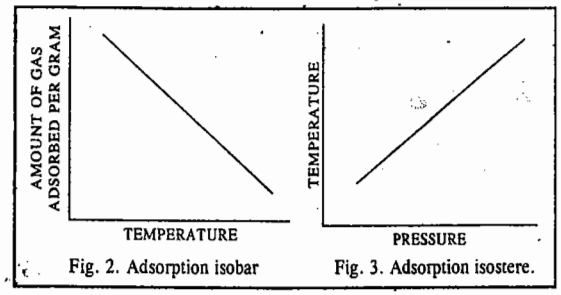

Fig. 2. Adsorption isobar Fig. 3. Adsorption isostere.

The curve showing the effect of temperature on the extent of adsorption at a given pressure is called an **adsorption isobar.** The amount of adsorption, evidently, decreases with rise in temperature. This is in accordance with Le Chatelier's principle, the process of adsorption being exothermic.

Since rise of temperature tends to lower the extent of adsorption, it is evident that in order to get the same amount of adsorption at a higher temperature, we shall have to raise the pressure of the system as well. Hence, a straight line relationship between temperature and pressure is generally obtained. The curve showing the variation of pressure with temperature, for a given amount of adsorption, is called an **isostere** (Fig. 3).

Desorption Activation Energy. Since an adsorbed molecule has a low binding energy, it may easily shake itself off the surface. This implies that such a molecule will remain on the surface for only a very short time before it is *desorbed*. The rate constant for the process of desorption follows an Arrhenius-type relation, *viz.*,

$$k_{\text{desorption}} = Ae^{-E_a/RT} \qquad ...(2)$$

Hence, $1/k_{\text{desorption}}$ may be called the *life time*, τ, of the adsorbate molecule on the surface. Eq. 2 then takes the form

$$\tau = \tau_0 e^{E_a/RT} \qquad ...(3)$$

where $\tau_0 (= 1/A)$ is known as the pre-exponential factor and E_a is the **desorption activation energy** of the adsorbate.

Example 2. Calculate how long a hydrogen atom will remain on the surface of a solid at 298 K if its desorption activation energy is : (a) 15 kJ mol^{-1} (b) 150 kJ mol^{-1}. Assume that $\tau_0 = 10^{-13}$ s.

Solution :

$$\tau = \tau_0 e^{E_a/RT} \qquad \text{[Eq. 3]}$$

(a) $E_a = 15$ kJ mol^{-1}

$$\tau = (10^{-13}\text{ s}) \exp\left(\frac{15 \times 10^3 \text{ J mol}^{-1}}{(8{\cdot}314 \text{ J K}^{-1} \text{ mol}^{-1})(298 \text{ K})}\right)$$

$$= (10^{-13}\text{ s})\ e^{6{\cdot}05} = 4{\cdot}2 \times 10^{-11}\text{ s}$$

(b) $E_a = 150$ kJ mol^{-1}

$$\tau = (10^{-13}\text{ s}) \exp\left(\frac{150 \times 10^3 \text{ J mol}^{-1}}{(8{\cdot}314 \text{ J K}^{-1} \text{ mol}^{-1})(298 \text{ K})}\right)$$

$$= (10^{-13}\text{ s})\ e^{60{\cdot}5} = 1{\cdot}9 \times 10^{13}\text{ s} \approx 600{,}000 \text{ years}$$

Example 3. Calculate how long a hydrogen atom will remain on the surface of a solid at 1000 K if its desorption activation energy is (a) 15 kJ mol^{-1} (b) 150 kJ mol^{-1}. Assume that $\tau_0 = 10^{-13}$ s.

Solution : Proceeding as in the last example, we have

(a)

$$\tau = (10^{-13}\text{ s}) \exp\left(\frac{15 \times 10^3 \text{ J mol}^{-1}}{(8{\cdot}314 \text{ J K}^{-1} \text{ mol}^{-1})(1000 \text{ K})}\right)$$

$$= (10^{-13}\text{ s})\ e^{1{\cdot}81} = 6{\cdot}1 \times 10^{-13}\text{ s}$$

(b) $\tau = (10^{-13}\text{ s})\ e^{18{\cdot}1} = 7{\cdot}3 \times 10^{-6}\text{ s}$

From the above two examples we see that the time for a hydrogen atom to remain on the surface of the adsorbent depends upon the desorption activation energy and the temperature : the greater the desorption activation energy (E_a), the greater the time ; the greater the temperature, the lesser the time.

Taking logs of both sides of Eq. 3,

$$\ln \tau = \ln \tau_0 + E_a/RT \qquad ...(4)$$

Thus, at two different temperatures T_1 and T_2, the above equation may be written as

$$\ln \tau_1 = \ln \tau_0 + E_a/RT_1 \qquad ...(5)$$

$$\ln \tau_2 = \ln \tau_0 + E_a/RT_2 \qquad ...(6)$$

Subtracting Eq. 5 from Eq. 6, we have

$$\ln\left(\frac{\tau_2}{\tau_1}\right) = \frac{E_a}{R}\left(\frac{1}{T_2} - \frac{1}{T_1}\right) \qquad ...(7)$$

which is the integrated Arrhenius-type equation or the integrated van't Hoff-type equation. Thus, knowing the life time τ_1 of an adsorbed species at temperature T_1 and the life time τ_2 at temperature T_2, the activation energy of desorption of the adsorbate can be calculated.

Example 4. The time for which the oxygen atom remains adsorbed on a tungsten surface is 0·36 s at 2550 K and 3·49 s at 2360 K. Calculate the activation energy of desorption of oxygen atom. Also, assuming that the oxygen atom is tightly chemisorbed, calculate the pre-exponential factor τ_0 in the Arrhenius-type expression.

Solution :

$$E_a = \frac{R \ln (\tau_2/\tau_1)(T_1T_2)}{T_1 - T_2} \qquad \text{(Eq. 7)}$$

$$= \frac{(8{\cdot}314 \text{ J K}^{-1} \text{ mol}^{-1}) \ln (3{\cdot}49 \text{ s}/0{\cdot}36 \text{ s})(2550 \text{ K})(2360 \text{ K})}{(2550 - 2360) \text{ K}}$$

$$= 598{\cdot}29 \text{ kJ mol}^{-1}$$

$$\tau = \tau_0 \exp(E_a/RT) \qquad \text{(Eq. 3)}$$

$\therefore$ Pre-expondential factor, $\tau_0 = \tau \exp(-E_a/RT)$

$$= (3{\cdot}49\ \text{s}) \exp\left(\frac{-598{\cdot}28 \times 10^3\ \text{J mol}^{-1}}{(8{\cdot}314\ \text{J K}^{-1}\ \text{mol}^{-1})(2360\ \text{K})}\right) = 1{\cdot}99 \times 10^{-13}\ \text{s}$$

The Langmuir Theory of Adsorption

In 1916 Langmuir proposed his theory of adsorption of a gas on the surface of a solid. He considered the surface of the solid to be made up of elementary *sites* each of which could adsorb one gas molecule. It is assumed that all adsorption sites are equivalent and the ability of the gas molecule to get bound to any one site is independent of whether or not the neighbouring sites are occupied. It is further assumed that a *dynamic equilibrium* exists between the adsorbed molecules and the free molecules. If A is the gas molecule and M is the surface site, then

$$A(g) + M(\text{surface}) \underset{k_d}{\overset{k_a}{\rightleftharpoons}} AM$$

where k_a and k_d are the rate constants for adsorption and desorption, respectively. The rate of adsorption is proportional to the pressure of A, *viz.*, p_A and the number of *vacant sites* on the surface, *viz.*, $N(1-\theta)$ where N is the total number of sites and θ is the fraction of surface sites occupied by the gas molecules, *i.e.*,

$$\theta = \frac{\text{Number of adsorption sites occupied}}{\text{Number of adsorption sites available}}$$

Thus, the rate of adsorption $= k_a p_A N(1-\theta)$ ...(8)

The rate of desorption is proportional to the number of adsorbed molecules, $N\theta$.

Thus, the rate of desorption $= k_d N \theta$ ...(9)

Since at equilibrium, the rate of adsorption is equal to the rate of desorption, we can write from Eqs. 8 and 9,

$$k_a p_A N(1-\theta) = k_d N \theta \qquad ...(10)$$

or $$K p_A (1-\theta) = \theta \qquad ...(11)$$

where $K = k_a/k_d$.

Eq. 11 may, thus, be written as

$$\frac{1-\theta}{\theta} = \frac{1}{Kp_A} \qquad ...(12)$$

or $$\frac{1}{\theta} - 1 = \frac{1}{Kp_A} \qquad ...(13)$$

$$\frac{1}{\theta} = \frac{1}{K p_A} + 1 = \frac{1 + Kp_A}{Kp_A} \qquad ...(14)$$

Hence, $$\theta = \frac{K p_A}{1 + Kp_A} \qquad ...(15)$$

Eq. 15 is called the **Langmuir adsorption isotherm.**

The following assumptions are involved in the derivation of the Langmuir adsorption isotherm : 1. The adsorbed gas behaves ideally in the vapour phase. 2. Only a monolayer is formed by the adsorbed gas. 3. The surface of the solid is homogeneous so that each binding site has the same affinity for the gas molecules. 4. There is no lateral interaction between the adsorbate molecules. 5. The adsorbed gas molecules are localized, *i.e.*, they do not move around on the surface.

The first assumption holds at low pressure; the second assumption breaks down when the pressure of the gas is increased. The third assumption is not strictly true because the real surfaces are quite heterogeneous so that affinity for gas molecules is different at different sites. Crystal imperfections and cracks lead to the creation of different sites on the surface. The fourth and fifth assumptions, too, are not strictly valid.

Now, let us consider Eq. 15. At low pressures, $Kp_A << 1$ so that

$$\theta = Kp_A \qquad ...(16)$$

i.e., the fraction of the surface covered is directly proportional to the partial pressure of the gas molecules. This behaviour corresponds to first-order reaction and is depicted by the initial steep rise of the isotherm (Fig. 4).

At high pressure, $Kp_A >> 1$ so that Eq. 15 reduces to

$$\theta = 1 \qquad ...(17)$$

Thus, at high pressures, the value of θ tends to become unity, *i.e.*, the entire surface gets covered by a monomolecular layer of the gas thereby making the reaction rate independent of the pressure. Thus, the reaction is of the zero order (Fig. 4).

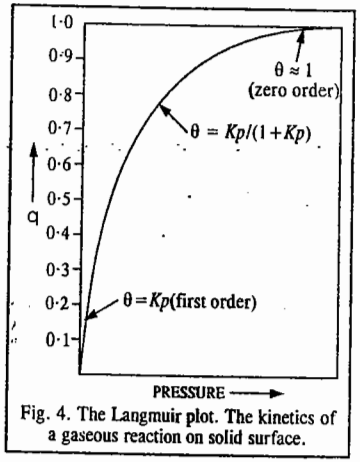

Fig. 4. The Langmuir plot. The kinetics of a gaseous reaction on solid surface.

Combining the results of Eqs. 16 and 17, it is evident that according to this theory, the magnitude of adsorption at a given temperature should first increase in proportion to increase of pressure and finally tend to attain a certain limiting value. This is exactly as indicated by the adsorption isotherms plotted earlier in Fig. 1.

Since at low pressures, adsorption is proportional to pressure, *i.e.*,

$$\theta = K(p_A)^1 \qquad \text{(from Eq. 16)}$$

and, at high pressures, $\theta = 1 = (p_A)^0$ (from Eq. 17).

it follows that, at intermediate pressures, the following expression should hold good :

$$\theta = K(p_A)^n \quad \text{where } n \text{ lies between 0 and 1.} \qquad ...(18)$$

Since, according to Langmuir's theory, only a single layer of molecules is adsorbed on the surface of the adsorbent, the fraction θ gives the amount of the gas adsorbed per unit mass of the adsorbent, that is, $a \propto \theta$ or $a = k_1\theta$ where k_1 is another constant. Thus,

$$a = k_1\theta = k_1 K(p_A)^n = k(p_A)^n \qquad ...(19)$$

Eq. 19 is the same as the Freundlich empirical equation (1). This agreement was taken as a proof for the theory of monomolecular adsorption advanced by Langmuir. Irving Langmuir (1881–1957), the American chemist, was awarded the 1932 Chemistry Nobel Prize for his contributions to surface chemistry. Research in surface science has now acquired tremendous importance and a research journal called *Langmuir* is exclusively devoted to contributions in all areas of surface science.

Example 5. Show that when a diatomic gas adsorbs as atoms on the surface of a solid, the Langmuir adsorption isotherm becomes $\theta = (Kp)^{1/2}/[1+(Kp)^{1/2}]$ where the symbols have their usual meanings.

Solution : Suppose a gas A_2 is in equilibrium with a surface layer on the solid M. The rate of adsorption is proportional to the rate of striking the surface which is proportional to pressure p. The probability that one atom will stick to the surface site is proportional to $N(1-\theta)$ and the probability that the other atom will also stick to the surface site is also proportional to $N(1-\theta)$. Thus, the rate of adsorption is proportional to pressure as well as to $N^2(1-\theta)^2$ and is thus equal to $k_a\, p\, N^2(1-\theta)^2$. Here θ is the fraction of surface covered by the gas.

The rate of desorption is proportional to the rate of encounters of the atoms on the surface and is, thus, proportional to the amount of each. Since this amount is $N\theta$, the rate of desorption is $k_d(N\theta)(N\theta) = k_d N^2\theta^2$. At equilibrium, the rate of adsorption is equal to the rate of desorption. Hence,

$$k_a p N^2(1-\theta)^2 = k_d N^2\theta^2$$

or
$$Kp(1-\theta)^2 = \theta^2 \qquad \text{where} \quad K = k_a/k_d$$

$$\left(\frac{1-\theta}{\theta}\right)^2 = \frac{1}{Kp}$$

$$\frac{1-\theta}{\theta} = \frac{1}{(Kp)^{1/2}}$$

$$\frac{1}{\theta} = \frac{1}{(Kp)^{1/2}} + 1 = \frac{1+(Kp)^{1/2}}{(Kp)^{1/2}}$$

$$\theta = \frac{(Kp)^{1/2}}{1+(Kp)^{1/2}}.$$

Example 6. If v is the volume of a gas (corrected to STP) adsorbed on the surface of a solid, then show that a plot of p/v versus p, where p is the gas pressure in the Langmuir adsorption isotherm, gives a straight line. Also show that for small surface coverages, a plot of ln (θ/p) versus θ gives a straight line.

Solution : Rearranging the Langmuir adsorption isotherm, $\theta = Kp/(1 + Kp)$, we get

$$\frac{1}{\theta} = 1 + \frac{1}{Kp} \qquad \ldots(i)$$

Let $\theta = v/v_{mono}$ where v_{mono} is the volume corresponding to complete coverage, *i.e.*, the volume required for the formation of a monolayer on the surface. Then,

$$\frac{v_{mono}}{v} = 1 + \frac{1}{Kp}$$

Multiplying throughout by p/v_{mono}, we get

$$\frac{p}{v} = \frac{p}{v_{mono}} + \frac{1}{K\, v_{mono}} \qquad \ldots(ii)$$

Thus, a plot of (p/v) versus p will give a straight line with slope equal to $1/v_{mono}$ and intercept equal to $1/Kv_{mono}$. From the measurement of the slope and the intercept, v_{mono} and K can be determined.

Again from Eq. (i), $\theta = Kp(1-\theta)$ so that $\theta/p = K(1-\theta)$. Taking logs, ln (θ/p) = ln K + ln $(1-\theta)$. If $\theta \ll 1$, then, mathematically, ln $(1-\theta) \approx -\theta$ so that ln (θ/p) = ln $K - \theta$. Hence, a plot of ln (θ/p) versus θ should give a straight line with slope equal to -1.

Example 7. The following data were obtained for the adsorption of carbon monoxide gas on 3·022 g of charcoal at 0°C and 1 atm pressure. Verify that the data obey the Langmuir monolayer adsorption isotherm. Also determine the constant K and the volume corresponding to complete surface coverage.

p (torr)	100	200	300	400	500	600
v (cm^3)	10·2	18·6	25·5	31·4	36·9	41·6

Solution : The Langmuir adsorption isotherm should be converted into proper form before using the given data. This has been done in the last example where we have shown that

$$p/v = p/v_{mono} + 1/Kv_{mono}$$

where v_{mono} is the volume corresponding to complete surface coverage.

Thus, we can construct the following table :

p (torr)	100	200	300	400	500	600
p/v_{mono} (torr cm^{-3})	9·80	10·80	11·80	12·70	13·60	14·40

The student can verify that a plot of p/v_{mono} versus p gives a straight line with slope = 0·009 and intercept = 9·0. Thus,

$$1/v_{mono} = 0{\cdot}009 \quad \text{whence} \quad v_{mono} = 111 \text{ cm}^3$$

$$1/Kv_{mono} = 9{\cdot}0 \quad \text{whence} \quad K = \frac{1}{(111\,\text{cm}^3)\times(9{\cdot}0\,\text{torr cm}^{-3})} = 1{\cdot}0\times10^{-3} \text{ torr}$$

Example 8. The mass x of a solute adsorbed per gram of a solid adsorbent is given by the Freundlich adsorption isotherm as $x = kc^n$, where k and n are 0·160 and 0·431, respectively. Calculate the amount of acetic acid (M_m = 60·05 g mol^{-1}) that 1 kg of charcoal would adsorb from a 0·837 M vinegar solution.

Solution : $x = kc^n = (0{\cdot}160)\,(0{\cdot}837)^{0{\cdot}431}$ per gram of charcoal

= (0·148 g acetic acid) (g charcoal)$^{-1}$ = (148 g acetic acid) (kg charcoal)$^{-1}$

$$= \frac{(148\,\text{g acetic acid})\,(\text{kg charcoal})^{-1}}{60{\cdot}05\,\text{g mol}^{-1}} = 2{\cdot}47 \text{ mol acetic acid (kg charcoal)}^{-1}$$

Example 9. Assuming that van't Hoff type equation can be used to determine the temperature-dependence of the amount of gas adsorbed on the surface of a solid, calculate the enthalpy of adsorption, ΔH_{ads}, for N_2 at 1 atm, given that 155 cm^3 of the gas (measured at STP) is adsorbed by 1 g of charcoal at 88 K and 15 cm^3 at 273 K.

Solution :
$$\ln(v_2/v_1) = \frac{-\Delta H_{ads}}{R}\left(\frac{1}{T_2} - \frac{1}{T_1}\right)$$

$$\therefore \quad \Delta H_{ads} = \frac{-R\ln(v_2/v_1)}{\left(\frac{1}{T_2} - \frac{1}{T_1}\right)}$$

Incorporating the given data, we find that $\Delta H_{ads} = -2{\cdot}52$ kJ mol^{-1}

BET Theory of Multilayer Adsorption

The Langmuir theory of adsorption is restricted to the formation of a monomolecular layer of the gas molecules on the solid surface and disregards the possibility that multilayer adsorption may also take place. The theory of adsorption proposed in 1938 by Brunauer, Emmett and Teller (known as the **BET theory**, after the initials of these scientists) assumes that physical adsorption resulting in the formation of multilayers, is the true picture of adsorption. In the BET theory, it is assumed that the solid surface possesses uniform, localized sites and that adsorption at one site does not affect adsorption at neighbouring sites, as was assumed in the Langmuir theory. It is further assumed that molecules can be adsorbed in second, third,..... and nth layers, the surface area available for the nth layer being equal to the coverage of the $(n-1)$th layer. The energy of adsorption in the first layer, E_1, is assumed to be constant and the energy of adsorption in succeeding layers is assumed to be the same as E_L, the energy of liquefacation of the gas. Based on the above assumptions, Brunauer, Emmett and Teller derived the following equation, known after them as the **BET equation :**

$$\frac{p}{v_{total}(p_0 - p)} = \frac{1}{v_{mono}c} + \frac{c-1}{v_{mono}c}\left(\frac{p}{p_0}\right) \qquad \ldots(20)$$

where v_{total} is the volume of the gas adsorbed at the pressure p, v_{mono} is the volume adsorbed when the surface of the solid is covered completely with a monolayer of the adsorbed molecules of the gas and c is a constant depending upon the nature of the gas. Its numerical value is given approximately by the expression $c = \exp(E_1 - E_L)/RT$ in which E_1 is the heat of adsorption in the first layer and E_L is

the heat of liquefacation of the gas. Since c is a constant for a given gas and v_{mono} is a constant for a given gas-solid system, the plot of $p/v_{total}(p_0 - p)$ against p/p_0 should give a straight line. This has been checked in the case of adsorption of a number of gases on various solid adsorbents. The results obtained in the case of adsorption of nitrogen on silica gel at –183°C are shown in Fig. 5. As can be seen, the plot obtained is a good straight line. Fairly satisfactory straight lines are obtained in most cases as long as pressure p does not exceed one-third of the saturation pressure p_0, *i.e.*, the pressure required to condense the gas into the liquid state at the prevailing temperature. At higher pressures, however, deviations set in.

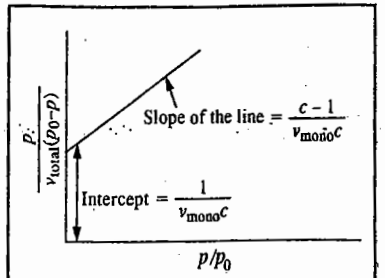

Fig. 5. BET plot for the adsorption of N_2 on silica gel at –183°C.

The slope of the linear plot, evidently, gives the value of $(c-1)/(v_{mono}c)$ while the intercept yields the value of $1/(v_{mono}c)$. Thus, from the slope and the intercept, both v_{mono} and c can be evaluated.

Determination of Surface Area. Knowing v_{mono}, the surface area of the adsorbent can be easily calculated, as shown in the following example: The assumption is that the molecules of the gas adsorbed in the first layer are closely packed on the surface.

Example 10. At 0°C and 1 atm pressure, the volume of nitrogen gas required to cover a sample of silica gel, assuming Langmuir monolayer adsorption, is found to be 130 $cm^3\ g^{-1}$ of the gel. Calculate the surface area per gram of silica gel. Given that the area occupied by a nitrogen molecule is 0·162 $(nm)^2$.

Solution : $v_{mono} = 130\ cm^3\ g^{-1} = 0{\cdot}130\ dm^3\ g^{-1}$; $V_m = 22{\cdot}144\ dm^3\ mol^{-1}$

Number of molecules contained in $v_{mono} = \frac{6{\cdot}022 \times 10^{23}\ mol^{-1}}{22{\cdot}414\ dm^3\ mol^{-1}} \times 0{\cdot}130\ dm^3\ g^{-1} = 3{\cdot}49 \times 10^{22}\ g^{-1}$

Area of cross-section of one molecule $= 0{\cdot}162\ (nm)^2 = 0{\cdot}162 \times 10^{-18}\ m^2$

∴ Area covered by $3{\cdot}49 \times 10^{22}$ molecules, *viz.*,

surface area $= 0{\cdot}162 \times 10^{-18}\ m^2 \times 3{\cdot}49 \times 10^{22}\ g^{-1} = \mathbf{565{\cdot}8\ m^2\ g^{-1}}$

Determination of Area of Cross-Section of a Molecule. The area of cross-section a of the molecule can be determined from the density of the liquefied or solidified adsorbate. Thus, if ρ is the density and M_m is the molar mass of the adsorbate, then the volume v occupied by a single molecule, assuming the adsorbate to be closely packed with no void volume, is obtained as follows :

$$\rho = M_m/V = M/(N_A v)$$

$$v = M_m/(N_A \rho)$$

Assuming the molecule to be spherical with radius r, we have

$$v = (4/3)\pi r^3 = M_m/(N_A \rho) \qquad ...(21)$$

$$r = \left[\frac{3M_m}{4\pi N_A \rho}\right]^{1/3} \qquad ...(22)$$

Hence, $$a = \pi r^2 = \pi\left[\frac{3M_m}{4\pi N_A \rho}\right]^{2/3} \qquad ...(23)$$

Eq. 23 is only approximate for calculating the area of cross-section of a molecule since it does not take into account the nature of packing at the surface of the adsorbent. Also, the presence of void volumes in the crystal lattice has been ignored. The areas of cross-section of some common molecules are given in Table 2.

TABLE 2

Areas of Cross-section of Some Common Molecules

Molecules	Temperature (°C)	Liquid Density (ρ) ($g\ cm^{-3}$)	$a\ (nm)^2$
Ar	– 183	1·374	0·144
N_2	– 196	0·808	0·162
O_2	– 183	1·140	0·141
CO	– 183	0·763	0·168
CO_2	– 57	1·179	0·170
CH_4	– 140	0·392	0·181
NH_3	– 36	0·688	0·129

Derivation of the BET quation. In 1938, Brunauer, Emmett and Teller proposed a model, known as the BET isotherm, for multilayer adsorption. According to them, the first step in adsorption is

$$A(g) + S \rightleftharpoons AS; \quad K_1 = \theta_1/\theta_v p \qquad ...(24)$$

where A is the gaseous adsorbate, S is a vacant site on the surface, AS represents an adsorbed molecule of A or an occupied site on the surface, K_1 is the equilibrium constant, θ_1 is the fraction of the surface sites covered by single molecules, θ_v is the fraction of vacant sites and p is the pressure of the gas.

They further assumed that additional molecules sit on top of one another to form a variety of multilayers. This process was interpreted as a sequence of chemical reactions, each with an appropriate equilibrium constant :

$$A(g) + AS \rightleftharpoons A_2S; \quad K_2 = \theta_2/\theta_1 p$$

$$A(g) + A_2S \rightleftharpoons A_3S; \quad K_3 = \theta_3/\theta_2 p$$

$$A(g) + A_{n-1}S \rightleftharpoons A_nS; \quad K_n = \theta_n/\theta_{n-1} p$$

where the symbol A_nS indicates a surface site that has a stack of n A molecules piled up on it. The θ_i is the fraction of sites on which the stack of A molecules is i layers deep. The interaction between the first A molecule and the surface site is unique, depending on the nature of the particular A molecule and the surface. However, when the second A molecule sits on the first A molecule, the interaction cannot be very different from the interaction of two A molecules in the liquid. The same is true when the third molecule sits on the second. All of these processes except the first can be regarded as being essentially equivalent to liquefaction. Hence, they should have the same equilibrium constant, K. Thus, the BET treatment assumes that

$$K_2 = K_3 = K_4 = \ldots = K_n = K \qquad ...(25)$$

where K is the equilibrium constant for the reaction $A(g) \rightleftharpoons A(liq)$. Obviously,

$$K = 1/p^\circ \qquad ...(26)$$

where p° is the equilibrium vapour pressure of the liquid.

We can use the equilibrium conditions to calculate the values of the various θ_i. We have

$$\theta_2 = \theta_1 Kp, \quad \theta_3 = \theta_2 Kp, \quad \theta_4 = \theta_3 Kp, \ \ldots \qquad ...(27)$$

Combining the first two, we have, $\theta_3 = \theta_1 (Kp)^2$

Repeating the operation, we find that

$$\theta_i = \theta_1 (Kp)^{i-1} \qquad ...(28)$$

The sum of all these fractions must be equal to unity :

$$1 = \theta_v + \sum_{i=1}\theta_i = \theta_v + \sum_i \theta_1 (Kp)^{i-1} \quad ...(29)$$

where we have used Eq. 28 for θ_i. Let $Kp = x$, then Eq. 29 becomes

$$1 = \theta_v + \theta_1(1 + x + x^2 + x^3 + ...)$$

Assuming that the process can go on indefinitely, then $n \to \infty$ and the series is simply the expansion of $1/(1-x) = 1 + x + x^2 + ...$ Thus,

$$1 = \theta_v + \theta_1/(1-x) \quad ...(30)$$

Using the equilibrium condition for the first adsorption, we find that $\theta_v = \theta_1/K_1 p$. Defining a new constant, $c = K_1/K$, we have $\theta_v = \theta_1/(cx)$ and Eq. 30 becomes

$$1 = \theta_1\left(\frac{1}{cx} + \frac{1}{1-x}\right)$$

or
$$\theta_1 = \frac{cx(1-x)}{1 + (c-1)x} \quad ...(31)$$

Let N be the total number of molecules adsorbed per unit mass of adsorbent and c_s be the total number of surface sites per unit mass. Then $c_s\theta_1$ is the number of sites carrying one molecule, $c_s\theta_2$ is the number of sites carrying two molecules, and so on. Accordingly,

$$N = c_s(1\theta_1 + 2\theta_2 + 3\theta_3 + \ldots) = c_s\sum_i i\theta_i \quad ...(32)$$

From Eq. 28, we have $\theta_i = \theta_1 x^{i-1}$ so that

$$N = c_s\theta_1\sum_{i=1} i x^{i-1} = c_s\theta_1 (1 + 2x + 3x^2 + \ldots) \quad ...(33)$$

This series is the derivative of the earlier one. Thus,

$$1 + 2x + 3x^2 + \ldots = \frac{d}{dx}(1 + x + x^2 + x^3 + \ldots) = \frac{d}{dx}\left(\frac{1}{1-x}\right) = \frac{1}{(1-x)^2} \quad ...(34)$$

Using this result, the expression for N becomes

$$N = c_s\theta_1/(1-x)^2 \quad ...(35)$$

If the entire surface is covered with a monolayer, then N_m molecules would be adsorbed so that $N_{mono} = c_s$ and

$$N = N_m\theta_1(1-x)^2 \quad ...(36)$$

Substituting the value of θ_1 from Eq. 31, we have

$$N = \frac{N_m c x}{(1-x)[1 + (c-1)x]} \quad ...(37)$$

The amount adsorbed is usually reported as the volume of the gas adsorbed measured at STP. The volume is, of course, proportional to N so that we have $N/N_{mono} = v/v_{mono}$

or
$$v_{total} = \frac{v_m c x}{(1-x)[1 + (c-1)x]} \quad ...(38)$$

where v_m stands for v_{mono}

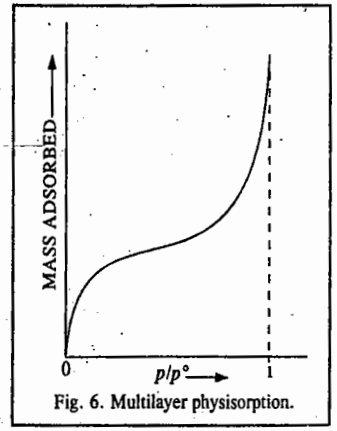

Fig. 6. Multilayer physisorption.

Recalling that $x = Kp$ and that $K = 1/p°$, we obtain the BET isotherm :

$$v_{total} \equiv v = \frac{v_m c p}{(p° - p)[1 + (c-1)(p/p°)]} \quad ...(39)$$

The volume v_{total} is measured as a function of p. From the data we can obtain the value of v_{mono} and c. Note that when $p = p°$, the equation has a *singularity* and $v \to \infty$. This accounts for the steep rise of the isotherm (Fig. 6) as the pressure approaches $p°$.

To obtain the constants c and v_m, we multiply both sides of Eq. 39 by $(p° - p)/p$:

$$\frac{v(p° - p)}{p} = \frac{v_m c}{1 + (c-1)(p/p°)} \quad ...(40)$$

Taking the reciprocal of both sides, we have

$$\frac{p}{v(p° - p)} = \frac{1}{v_m c} + \left(\frac{c-1}{v_m c}\right)\left(\frac{p}{p°}\right) \quad ...(41)$$

This is the well known **BET equation.**

The left-hand side of this equation is experimentally measured. The plot of $p/[v(p°-p)]$ versus p gives a straight line. From the intercept, $(1/v_m c)$ and the slope, $(c-1)/(v_m c p°)$, we can calculate the value of v_m, *i.e.*, v_{mono}.

From the value of v_{mono} at STP, N_{mono} can be calculated :

$$N_{mono} = \frac{N_A v_{mono}}{0{\cdot}022414\,m^3\,mol^{-1}} \quad ...(42)$$

Since N_{mono} is the number of molecules required to cover a unit mass of the adsorbent with a monolayer, then if we know the area, a, covered by a molecule, we can calculate the area of unit mass of material :

$$\text{Area/unit mass} = N_{mono}\, a \quad ...(43)$$

In this way the surface area of a finely divided solid can be determined.

Types of Adsorption Isotherms. A large number of adsorption isotherms of gases on a variety of adsorbents at different temperatures have now been determined. It has been possible to divide them broadly into five different types, as shown in Fig. 7. In each case, p_0 represents the saturation pressure of the gas.

Type I corresponds to mono-molecular adsorption as postulated by Langmuir. The volume of the gas adsorbed approaches a limiting value, just enough to complete a mono-molecular layer even when the gas pressure is rather low. Further increase in pressure hardly produces any

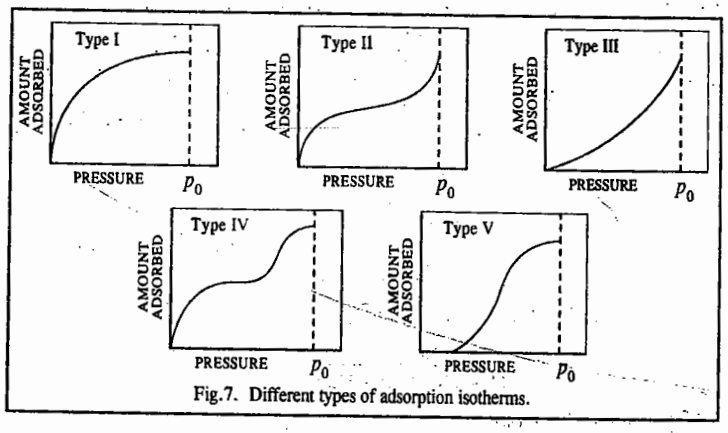

Fig.7. Different types of adsorption isotherms.

further rise in the amount of adsorption. The examples are furnished by adsorption of nitrogen or hydrogen on charcoal at temperatures close to –180°C.

Types II and **III** show large deviations from Langmuir model. The amount of adsorption keeps on rising in each case with increase in pressure. This is attributed to the formation of additional layers of physically adsorbed gas molecules. It is postulated that the gas molecules adsorbed in the first layer may hold by van der Waals forces a second layer of gas molecules which, in turn, may hold a third layer and so on. The examples of Type II isotherms are furnished by adsorption of nitrogen on an iron or a platinum catalyst at –195°C and those of Type III by adsorption of bromine on silica or alumina gel at 80°C.

Types IV and **V** have been observed in those cases in which there is a possibility of condensation of gases in the minute capillary pores of the adsorbent at pressures even below the saturation pressure p_0 of the gas. An example of Type IV is furnished by adsorption of benzene on silica gel at 50°C and that of Type V by adsorption of water vapour on activated carbon at 100°C. It may again be noted that in the case of adsorption isotherms of Types IV and V, there is not only formation of multimolecular adsorbed layers of the gas molecules but also condensation of some of the gas molecules within the narrow capillary pores of the adsorbent. This latter phenomenon is known as **capillary condensation** of the gas.

ADSORPTION FROM SOLUTION

Adsorption of a solute from a solution onto a solid adsorbent is more difficult to treat theoretically than the corresponding adsorption of gases on solids. It appears, however, that in this case, too, like the gas–solid adsorption, a monomolecular layer is formed. The solvating power of the solvent inhibits the formation of a multilayer.

For adsorption from solutions, a commonly used isotherm is the Freundlich adsorption isotherm. If x is the mass of the solute adsorbed on mass m of adsorbent and c is the concentration of the solute in the solution, then the Freundlich adsorption isotherm is expressed as

$$x/m = a = kc^n \qquad ...(44)$$

where k and n are empirical constants. Taking logs,

$$\ln a = \ln k + n \ln c \qquad ...(45)$$

This logarithmic form is convenient to use. If we plot ln a versus ln c, the plot would be a straight line with slope equal to n and intercept equal to ln k.

The Gibbs Adsorption Isotherm for Adsorption From Solutions

The concentration of a solute at the surface of a solution is, in general, markedly different from that in the bulk. If the surface tension of the solute is lower than that of the liquid, it tends to accumulate at the surface of the liquid thereby decreasing the surface tension (or the surface free energy per unit area) of the liquid. A quantitative treatment of the thermodynamics of adsorption of a solute at the surface of a liquid was given in 1878 by J.W. Gibbs (1839-1903), the greatest 19th century American mathematical physicist.

For a system containing two components, the Gibbs free energy can be written as

$$G = n_1\mu_1 + n_2\mu_2 \qquad ...(46)$$

where n_1 and n_2 are the amounts (number of moles) and μ_1 and μ_2 are the chemical potentials (*i.e.*, partial molar Gibbs free energies) of the two components, respectively. Since we are dealing with the adsorption of one of the components on the surface which results in changing the surface free energy, Eq. 46 is modified to

$$G = n_1\mu_1 + n_2\mu_2 + \gamma\sigma \qquad ...(47)$$

where γ is the *surface energy* which is numerically the same as the surface tension and σ is the surface area.

The complete differential of Eq. 47 is written as

$$dG = n_1d\mu_1 + \mu_1dn_1 + n_2d\mu_2 + \mu_2dn_2 + \gamma d\sigma + \sigma d\gamma \qquad ...(48)$$

We see that free energy G now depends upon five independent variables, *viz.*, T, P, n_1, n_2 and σ. Thus,

$$G = f(T, P, n_1, n_2, \sigma) \qquad ...(49)$$

$$\therefore dG = \left(\frac{\partial G}{\partial T}\right)_{P,n_1,n_2,\sigma} dT + \left(\frac{\partial G}{\partial P}\right)_{T,n_1,n_2,\sigma} dP + \left(\frac{\partial G}{\partial n_1}\right)_{T,P,n_2,\sigma} dn_1 + \left(\frac{\partial G}{\partial n_2}\right)_{T,P,n_1,\sigma} dn_2 + \left(\frac{\partial G}{\partial \sigma}\right)_{T,P,n_1,n_2} d\sigma \qquad ...(50)$$

According to thermodynamics, the partial derivatives

$-\left(\frac{\partial G}{\partial T}\right)_{P,n_1,n_2,\sigma}$, $\left(\frac{\partial G}{\partial P}\right)_{T,n_1,n_2,\sigma}$, $\left(\frac{\partial G}{\partial n_1}\right)_{T,P,n_2,\sigma}$, $\left(\frac{\partial G}{\partial n_2}\right)_{T,P,n_1,\sigma}$ and $\left(\frac{\partial G}{\partial \sigma}\right)_{T,P,n_1,n_2}$ in Eq. 50 are, respectively, equal to S, V, μ_1, μ_2 and γ.

Hence, $$dG = -SdT + VdP + \mu_1dn_1 + \mu_2dn_2 + \gamma d\sigma \qquad ...(51)$$

At constant temperature, $dT=0$ and at constant pressure, $dP=0$. Hence, Eq. 51 reduces to

$$(dG)_{T,P} = \mu_1dn_1 + \mu_2dn_2 + \gamma d\sigma \qquad ...(52)$$

From Eqs. 48 and 49,

$$n_1d\mu_1 + n_2d\mu_2 + \sigma d\gamma = 0 \qquad ...(53)$$

The corresponding expression for the bulk of the liquid is

$$n_1^\circ d\mu_1 + n_2^\circ d\mu_2 = 0 \qquad ...(54)$$

where n_1° and n_2° are the amounts (number of moles) of the liquid and the solute, respectively, in the bulk phase.

Since the system is in equilibrium, the chemical potential of each component in the bulk and the surface phase must be the same. The system, on being disturbed, attains a new equilibrium so that the changes in the chemical potentials must be identical in both the phases, *i.e.*, $d\mu_1$ and $d\mu_2$ in Eqs. 53 and 54 must be identical. Elimination of $d\mu_2$ from these equations gives

$$n_1[-(n_2^\circ/n_1^\circ)d\mu_2] + n_2d\mu_2 + \sigma d\gamma = 0 \qquad ...(55)$$

or $$(n_2 - n_1n_2^\circ/n_1^\circ)d\mu_2 + \sigma d\gamma = 0$$

or $$-\frac{d\gamma}{d\mu_2} = \frac{n_2 - (n_1n_2^\circ/n_1^\circ)}{\sigma} \qquad ...(56)$$

The quantity within parenthesis of Eq. 56 gives the amount n_2° of solute 2 associated with the amount n_1° of liquid 1 in the *bulk* phase. On the other hand, n_2 is the amount of the solute associated with the amount n_1 of the liquid at the *surface*. Thus, the numerator on the right hand side of Eq. 56 gives the *excess amount of the solute* present in the surface of the liquid. Evidently, the right hand

side of Eq. 56 gives the **surface excess**, *i.e.*, the excess concentration of the solute per unit area of the surface, designated as Γ_2, *i.e.*, $[n_2 - (n_1 n_2^\circ / n_1^\circ)]/\sigma = \Gamma_2$.

Thus, from Eq. 56,

$$\Gamma_2 = -d\gamma/d\mu_2 \qquad \ldots(57)$$

The chemical potential of solute 2 is given by

$$\mu_2 = \mu_2^*(l) + RT \ln a_2 \qquad \ldots(58)$$

where $\mu_2^*(l)$ is the chemical potential of the pure solute in the liquid phase. Hence,

$$d\mu_2 = RT\, d \ln a_2 \qquad [\because d\mu_2^*(l) = 0] \qquad \ldots(59)$$

Substituting for $d\mu_2$ in Eq. 57, we obtain

$$\Gamma_2 = -\frac{1}{RT}\left(\frac{\partial\gamma}{\partial \ln a_2}\right)_T = -\frac{a_2}{RT}\left(\frac{\partial\gamma}{\partial a_2}\right)_T \qquad \ldots(60)$$

When the solution is very dilute, it behaves ideally so that the activity a_2 of the solute can be replaced by its concentration c_2. Thus,

$$\Gamma_2 = -\frac{1}{RT}\left(\frac{\partial\gamma}{\partial \ln c_2}\right)_T = -\frac{c_2}{RT}\left(\frac{\partial\gamma}{\partial c_2}\right)_T \qquad \ldots(61)$$

Eq. 61 is called the **Gibbs adsorption isotherm.** Knowing the concentration-dependence of γ, Γ_2 can be calculated.

For a solute that lowers the surface tension, the surface excess concentration Γ_2 is *positive* and for a solute that raises the surface tension, Γ_2 is *negative*. Soaps have a higher concentration in the neighbourhood of the surface than in the bulk aqueous phase whereas inorganic salts have lower concentrations in the neighbourhood of the surface than in the bulk aqueous phase.

Solutes are classified as capillary-active or capillary-inactive on the basis of their effect on surface tension. For the aqueous solution—air interface, **capillary-active** solutes are organic acids, alcohols, ethers, esters, amines, ketones, etc., and **capillary-inactive** solutes are inorganic electrolytes, salts of organic acids and bases of lower molar mass and certain nonvolatile compounds such as sugar and glycerol.

The surface tension of water is quite high, *viz.*, 0·072·8 N m^{-1} at room temperature and most of the solutes tend to reduce this value. Therefore, most of the solutes are positively adsorbed from aqueous solutions by adsorbents such as charcoal and silica gel. The surface tension of ethanol (0·0223 N m^{-1}) is considerably lower than that of water. Hence, most of the solutes decrease the surface tension of ethanol to a much smaller magnitude than they do in the case of water. It leads to the conclusion that a given solute would be more readily adsorbed from aqueous solution than from alcoholic solution. This has been fully supported by experiment in majority of cases.

Example 11. The surface tension of dilute solutions of a solute varies linearly with the solute concentration c_2 as $\gamma = \gamma_0 - ac_2$, where γ_0 is the surface tension of the solvent and a is a constant. Show that $\Gamma_2 = (\gamma_0 - \gamma)/RT$.

Solution :

$$\gamma = \gamma_0 - ac_2 \qquad \text{(Given)} \qquad \ldots(i)$$

$$\therefore \quad (d\gamma/dc_2)_T = -a$$

Hence, from Eq. 61, $$\Gamma_2 = -\frac{c_2}{RT}\left(\frac{d\gamma}{dc_2}\right)_T = \frac{ac_2}{RT} \qquad \ldots(ii)$$

From Eq. (*i*), $ac_2 = \gamma_0 - \gamma$

Substituting the value of ac_2 in Eq. (*ii*), we have

$$\Gamma_2 = (\gamma_0 - \gamma)/RT$$

Example 12. An 18°C, the surface tension γ of an aqueous solution of butyric acid is represented by the equation $\gamma = \gamma_0 - 29{\cdot}8 \log (19{\cdot}64\, c_2 + 1)$ where γ_0, the surface tension of water, is 0·073 N m^{-1} and c_2 is the bulk concentration of the solute. Calculate, using the Gibbs adsorption isotherm, the surface excess of butyric acid at concentration c_2 equal to 0·01 mol dm^{-3}.

Solution : $\gamma = \gamma_0 - 29{\cdot}8 \log (19{\cdot}64\, c_2 + 1)$ (Given)

$$\left(\frac{d\gamma}{dc_2}\right)_T = -\frac{29{\cdot}8 \times 19{\cdot}64}{2{\cdot}303 \times (19{\cdot}64 c_2 + 1)} = -\frac{254{\cdot}13}{19{\cdot}64 c_1 + 1}$$

$$\Gamma_2 = -\frac{c_2}{RT}\left(\frac{d\gamma}{dc_2}\right)_T = \frac{254{\cdot}13\, c_2}{(19{\cdot}64 c_2 + 1)RT}$$

At $c_2 = 0{\cdot}01$ mol dm^{-3} $= 0{\cdot}01 \times 10^{-3}$ mol m^{-3},

$$\Gamma_2 = \frac{254{\cdot}13 \times (0{\cdot}01 \times 10^{-3}\,\text{mol m}^{-3})}{(19{\cdot}64 \times 0{\cdot}01 \times 10^{-3}\,\text{mol m}^{-3} + 1)(8{\cdot}314\,\text{J K}^{-1}\,\text{mol}^{-1} \times 291\,\text{K})}$$

$$= 8{\cdot}79 \times 10^{-7}\ \text{mol m}^{-2}$$

Example 13. For a $1{\cdot}0 \times 10^{-4}$ M aqueous solution of *n*-butanoic acid $d\gamma/dc = -0{\cdot}080$ N m^2 mol^{-1}, at 25°C. Using the Gibbs adsorption equation, determine the surface excess of butanoic acid and also calculate the average surface area available to each molecule.

Solution :

$$\Gamma_2 = -\frac{c}{RT}\frac{d\gamma}{dc} \qquad \text{[Gibbs adsorption equation]}$$

$$= -\frac{(1{\cdot}00 \times 10^{-4}\,\text{mol dm}^{-3})(10^3\,\text{dm}^3\,\text{m}^{-3})}{(8{\cdot}314\,\text{J K}^{-1}\,\text{mol}^{-1})(298\,\text{K})}(-0{\cdot}080\,\text{N m}^2\,\text{mol}^{-1})$$

$$= 3{\cdot}2 \times 10^{-6}\ \text{mol m}^{-2}$$

The average surface area available for each molecule

$$= \frac{1}{(3{\cdot}2 \times 10^{-6}\,\text{mol m}^{-2})(6{\cdot}022 \times 10^{23}\,\text{mol}^{-1})} = 5{\cdot}2 \times 10^{-19}\ \text{m}^2$$

Example 14. 0·106 mg of stearic acid (M_m = 284 g mol^{-1}) is found to cover 500 cm^2 of water surface at the point where the surface pressure just begins to rise sharply. Estimate the cross-sectional area, *a*, per stearic acid molecule and thickness, *t*, of the surface film of stearic acid on water. Given : density of stearic acid = 0·85 g cm^{-3}.

Solution :

$$\frac{0{\cdot}106 \times 10^{-3}\,\text{g}}{284\,\text{g mol}^{-1}} \times (6{\cdot}022 \times 10^{23}\,\text{mol}^{-1})\, a = 500\ \text{cm}^2$$

$$\therefore \quad a = 22 \times 10^{-16}\ \text{cm}^2$$

Again, $(500\ \text{cm}^2)\, t = 0{\cdot}106 \times 10^{-3}\ \text{g}/0{\cdot}85\ \text{g cm}^{-3}$

$$\therefore \quad t = 25 \times 10^{-8}\ \text{cm} = 2{\cdot}5\ \text{nm} = 2500\ \text{pm}$$

Insoluble Surface Films on Liquids

The long-chain, water-insoluble compounds like stearic acid, $CH_3(CH_2)_{16}COOH$, lauryl alcohol, $CH_3(CH_2)_{11}OH$ and ethyl palmitate, $CH_3(CH_2)_{14}COOC_2H_5$ spread spontaneously on the water surface giving rise to *surface films*. These films are found to be one molecule thick and are called *spread monolayers*. Both solids and liquids can form spread monolayers but the rate of spreading of liquids is more than that of solids. These surface films can be studied by a surface balance in which a floating

barrier (*float*) separates a clean water surface from a water surface containing the monolayer. The force on the float is measured by a torsion wire attached to it. This is the principle of the **Langmuir film balance.**

The lowering of the surface tension of a solvent by the surface film can be expressed in terms of the **surface film pressure,** π, which is the negative of the change in surface tension :

$$\pi = -\Delta\gamma = \gamma_0 - \gamma \qquad ...(62)$$

where γ_0 is the surface tension of water and γ that of the solution containing the long-chain compound. The surface film is found to behave like an *ideal* two-dimensional gas whose equation of state can be derived easily. We know that at low concentrations, the surface tension of a binary solution becomes a linear function of concentration and is given by

$$\gamma = \gamma_0 - bc_2 \qquad ...(63)$$

Substituting this relation in the Gibbs adsorption isotherm, *viz.*,

$$\Gamma_2 = -\frac{c_2}{RT}\left(\frac{d\gamma}{dc_2}\right)_T \qquad ...(64)$$

we find that, since from Eq. 63, $d\gamma/dc_2 = -b = (\gamma - \gamma_0)/c_2$, hence

$$\Gamma_2 = \frac{c_2}{RT}\left(\frac{\gamma - \gamma_0}{c_2}\right) \qquad ...(65)$$

Using the definition for surface film pressure, π, from Eq. 62,

$$\pi = \Gamma_2 RT \qquad ...(66)$$

Eq. 66 is the two-dimensional analogue of an ideal gas equation.

The surface excess concentration may by written as

$$\Gamma_2 = N/(N_A A) \qquad ...(67)$$

where N is the number of molecules contained in a film of area A. Thus, Eq. 66 may be written as

$$\pi A = (N/N_A)RT = Nk_BT \qquad ...(68)$$

Fig. 8 shows the variation of the surface film pressure with film area. Solid lines show experimental curves for different bulk concentrations.

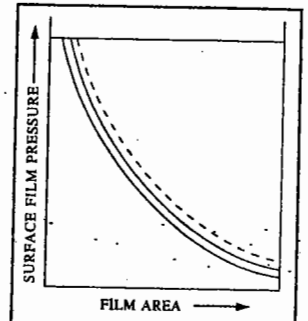

Fig. 8. Graph showing surface film pressure versus film area.

Example 15. In an experiment it was found that 0·106 mg of stearic acid covered 500 cm² of water surface at a point where the surface pressure just begins to rise sharply. Estimate the cross-sectional area of the stearic acid molecule and thickness of the stearic acid film on water. The molar mass of stearic acid is 284 g mol⁻¹ and its density is 0·85 g cm⁻³.

Solution : The number of molecules in the given mass of stearic acid

$$= \frac{(0{\cdot}106\times10^{-3}\,\text{g})(6{\cdot}022\times10^{23}\,\text{mol}^{-1})}{284\,\text{g mol}^{-1}}$$

Let σ be the cross-sectional area of a molecule. Then,

$$\text{area of water surface covered} = \frac{(0{\cdot}106\times10^{-3}\,\text{g})(6{\cdot}022\times10^{23}\,\text{mol}^{-1})(\sigma)}{284\,\text{g mol}^{-1}} = 500\ \text{cm}^2\ \text{(given)}$$

whence we find that $\sigma = 22\times10^{-16}$ **cm²**

If t is the thickness of the surface film, then

$$\text{Volume} = \text{area}\times\text{thickness} = (500\,\text{cm}^2)(t) = \frac{\text{mass}}{\text{density}} = \frac{0{\cdot}106\times10^{-3}\,\text{g}}{0{\cdot}85\ \text{g cm}^{-3}}$$

$\therefore$ Thickness of film, $t = 25\times10^{-8}$ cm = **2·5 nm = 2500 pm**

Example 16. Derive the two-dimensional analogue of the ideal gas law for the surface pressure of the surface film of a fatty acid on water.

Solution : The surface pressure of a surface film on water is given by

$$\pi = \gamma_0 - \gamma \quad \text{(see Eq.62)} \qquad ...(i)$$

where γ_0 is the surface tension of pure water and γ is the surface tension of the film-covered surface. At low concentrations,

$$\gamma = \gamma_0 - bc_2 \quad \text{(see Eq. 63)} \qquad ...(ii)$$

Also,
$$\Gamma_2 = -\frac{c_2}{RT}\left(\frac{d\gamma}{dc_2}\right) \qquad ...(iii)$$

From Eq. (*ii*), $d\gamma/dc_2 = -b$

Using Eq. (*iii*),
$$\Gamma_2 = -\frac{c_2}{RT}\frac{\gamma - \gamma_0}{c_2} = \frac{\gamma_0 - \gamma}{RT} = \pi/RT\ ;$$

or
$$\pi = \Gamma_2 RT \qquad \text{[using Eq. (}i\text{)]}$$

Example 17. An organic fatty acid forms a surface film on water that obeys the two-dimensional ideal gas law. If the surface tension lowering is 10 mN m⁻¹ at 25°C, calculate the surface excess concentration and the surface area per adsorbed molecule.

Solution : Γ_2 is equal to $N/(N_A A)$ where N is the number of molecules contained in a film of area A.

$$\Gamma_2 = \frac{\pi}{RT} = \frac{10\times10^{-3}\ \text{N m}^{-1}}{(8{\cdot}314\ \text{J K}^{-1}\ \text{mol}^{-1})(298\ \text{K})} = 4{\cdot}04\times10^{-6}\ \text{mol m}^{-2}$$

$$\therefore \quad \frac{A}{N} = \frac{1}{\Gamma_2 N_A} = \frac{1}{(4{\cdot}04\times10^{-6}\,\text{mol m}^{-2})(6{\cdot}022\times10^{23}\,\text{mol}^{-1})} = 4{\cdot}11\times10^{-19}\ \text{m}^2 = \mathbf{0{\cdot}411\ (nm)^2}$$

Modern Techniques for Investigating Surfaces

1. Low Energy Electron Diffraction (LEED). When a surface is bombarded with electrons, the electrons may be scattered elastically (*i.e.*, with no loss of energy) or inelastically. The elastically scattered electrons are diffracted if their de Broglie wave length is quite small. Thus, LEED provides a means for studying the atomic geometry of a surface. In the LEED experiment, the electrons are accelerated in an electron gun and strike the surface normally. Some of the electrons are backscattered by the surface. The inelastically scattered electrons are removed by means of the grids in front of the screen while the elastically scattered electrons are accelerated onto the phosphorescent screen for viewing the diffraction pattern. The presence of sharp diffraction spots shows that the surface is ordered on the atomic scale. LEED can also yield information about the structure of an adsorbed layer in chemisorption.

2. Photo Electron Spectroscopy (PES). We have discussed the basic principles of PES in the chapter on Spectroscopy. Suffice it to mention here that the photons with energies in the UV region (the technique is then called UPES) eject electrons from the valence orbitals of an adsorbed molecule or from the valence bands of the solid. UPES experiments are carried out using the He-I radiations (21·22 eV) or the He-II radiations (40·8 eV). The UPES of a molecule physisorbed on a solid is a superposition of the UPES of the valence band of the solid and the gas-phase MOs of the adsorbed molecule. The UPES of the physisorbed molecule is similar to UPES of the corresponding gas molecule because of the weak interaction with the surface. However, in a chemisorbed molecule, chemisorption affects the valence orbitals of the molecule and the valence band of the solid resulting in a complex UPES.

In XPES in which X-ray photons are used for photoelectron spectroscopy, the core electrons are ejected from the metal and from the adsorbed species, the source of X-rays being either the Mg K_α (1253·6 eV) or Al K_α (1486·6 eV). Since the energies of the atomic core levels are characteristic of each element in the Periodic table, XPES is often used to obtain the elemental analysis of the surface.

In Auger Electron Spectroscopy (AES), an electron is ejected by an X-ray photon, as in XPES, but *the emission of secondary electrons is analyzed* rather than the primary electrons. When a core electron is ejected by an X-ray photon, an electron from a higher energy level may jump into the core energy level. The energy liberated in this manner may bring about emission of a second electron called Auger electron (this effect was studied by the French physicist P. Auger). The energies of the Auger electrons are characteristic of the core levels. AES can thus yield information about the bonding of the core electrons of the adsorbed species.

3. Scanning Tunnelling Microscopy (STM). A major breakthrough in experimental physics was achieved in the early 1980s, thanks to the major discovery of scanning tunnelling microscopy (STM) by the German scientists G. Binnig and H. Rohrer (who shared the 1986 Physics Nobel Prize with E. Ruska (1906-1988), the discoverer of the electron microscope). With STM, one can 'see' a single molecule adsorbed on a surface. In a simple, ingeniously designed STM, experiment, a very sharp metal tip is moved over the surface of an electrical conductor at a height of about 500 pm. Since the tip remains close to the surface, the wave functions of the atoms of the tip overlap with those of the surace. **Quantum mechanical tunnelling**, caused by the application of an electric field between the tip and the surface, allows a current to flow through the vacuum gap. The potential of the tip with respect to the surface is held constant and a peizoelectric feedback mechanism regulates the vertical motion of the tip, thereby keeping the tunnelling current constant. This tip traces the surface topography as it is moved over the surface. These traces can be used to produce an image of the surface.

4. EXAFS and SEXAFS. An extension of X-ray absorption and Auger techniques to the investigation of the structure of solids and of the near-surface region gives information about the interatomic distances and angles. The information obtained from X-ray absorption concerns mainly the bulk material whereas the Auger electrons furnish information about the surface and near-surface region. The two techniques are called EXAFS (Extended X-ray Absorption Fine Structure) and SEXAFS (Surface Extended X-ray Absorption Fine Structure), respectively.

EXAFS. In this technique, we think of electrons in terms of their wave properties, rather than as particles. When the absorption of an X-ray photon results in the emission of a core electron, the outgoing photoelectron can be thought of as a *spherical wave* (Fig. 9*a*). Here an X-ray photon

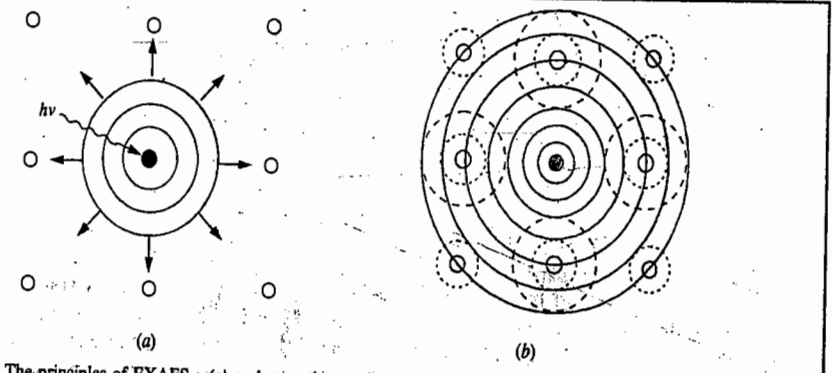

Fig. 9. The principles of EXAFS ; *(a)* a photon ejects an electron as an expanding wave *(b)* the wave reflects from surrounding atoms to cause interference.

displaces an electron from the core levels of the central atom (shown shaded in the figure). The emitted electron behaves as an expanding wave which, when reaches neighbouring atoms, is partially reflected or 'back-scattered' (Fig. 9*b*). The scattered wave interferes with the original electron wave. If it is in phase with the original wave, constructive interference occurs resulting in enhancement of the absorption of X-rays. If, however, it is out of phase, there is a destructive interference and the absorption of X-rays is reduced. The net result is that the detector 'sees' a variation in X-ray absorption close to a transition (the so-called *absorption edge*). Evidently, this variation or oscillation of the signal will depend on the number, nature and distance of the surrounding atoms from which the wave is back-scattered.

Fig. 10*a* shows the oscillations resulting from the bombardment of a palladium foil with X-rays ; this is the EXAFS signal adjacent to the absorption edge. After subtracting the background with the help of a computer and carrying out fourier transform of the data, we obtain the EXAFS of palladium foil showing separation of peaks from which the interatomic distances are obtained (Fig. 10*b*). For palladium, the nearest neighbours are 2·75 Å away, while the next nearest neighbours are at 3·89 Å, etc. Since EXAFS technique requires a high intensity tunable X-ray source such as as a synchrotron, it cannot be used as a routine laboratory tool.

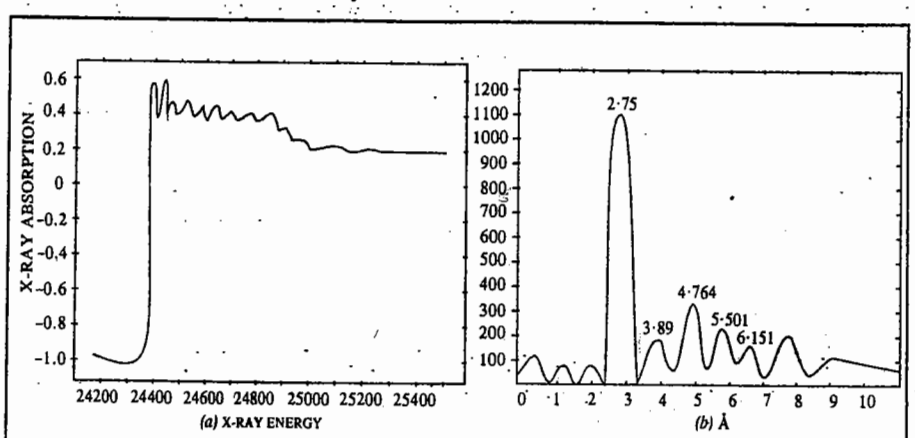

Fig. 10. EXAFS of palladium foil : *(a)* oscillations of the signal adjacent to the absorption edge; *(b)* Fourier-transformed data (after the background subtraction by the computer) showing peaks from which interatomic distances are obtained.

SEXAFS. If, instead of observing the X-ray absorption of the solid sample, the intensity of the Auger electrons is observed, the resulting diffracted waves carry information about the surface and the near-surface region rather than the bulk material, the reason being that electrons cannot travel far through the bulk material and can only be detected if they escape from the surface and near-surface regions. This technique of SEXAFS is closely similar to EXAFS technique. In SEXAFS technique which uses intense X-radiation from a synchrotron, oscillations in X-ray absorbance are observed on the high frequency side of the absorption edge (the start of the X-ray absorption band) of a substance. These oscillations arise from quantum mechanical interference between the wave function of a photoejected electron and parts of wave function of those electrons that are scattered by the neighbouring atoms. Surface chemistry, like quantum mechanics and spectroscopy, is rich in acronyms.

Gerhard Ertl (1934—), the German chemist who was awarded the 2007 Nobel Prize in chemistry, has revolutionized surface chemistry. He provided a detailed description of how chemical reactions take place on surfaces, thereby laying the foundations of modern surface chemistry. Using surface study techniques such as LEED, he has "married together a range of techniques that let scientists measure exactly what happens when gas molecules stick to a solid surface". His research has explained why the ozone layer is thinning and how fuel cells produce energy without pollution.

I. Review Questions

1. How does chemisorption differ from physisorption? Discuss the factors which influence adsorption of a gas on a solid.
2. Discuss briefly Langmuir's unimolecular theory of adsorption. Derive an expression for Langmuir's adsorption isotherm. Show that at normal pressures, Langmuir's unimolecular adsorption isotherm becomes identical with Freundlich adsorption isotherm.
3. Discuss briefly BET theory of multilayer adsorption.
4. Derive thermodynamically the Gibbs adsorption isotherm for the adsorption of a solute on the surface of a liquid.
5. What are surface films on liquids ? Show how the surface film pressure varies with film area.
6. Describe briefly the modern techniques used for studying surfaces.

II. Problems

1. At 0°C and 1 atm pressure, the volume of nitrogen gas required to form a monolayer on a sample of charcoal is 155·5 $cm^3\ g^{-1}$ of charcoal. Calculate the surface area per gram of charcoal. Area of cross-section of N_2 molecule is 0·160 $(nm)^2$. [Ans. 668·4 $m^2\ g^{-1}$]
2. The following data were obtained on the adsorption of acetic acid on charcoal :

{acid} (mol dm^{-3})	0·05	0·10	0·50	1·0	1·5
a (g)	0·01	0·06	0·12	0·16	0·19

Verify that the data obey the Freundlich isotherm, $a = kp^n$ where a is the mass adsorbed per unit mass of charcoal. Determine the constants k and n. [Ans. k = 0·160 ; n = 0·43]

3. The density of liquid methane is $0{\cdot}466\times10^3$ kg m^{-3}. Calculate the approximate cross-sectional area of a methane molecule. [Ans. $14{\cdot}8\times10^{-20}\ m^2$]
4. Calculate the surface excess concentration for a 1·00 M aqueous solution of NH_4NO_3 using the following data at 20°C :

c (mol dm^{-3})	0·50	1·00	2·00	3·00	4·00
$y/10^{-3}$ (N m^{-1})	73·25	73·75	34·65	75·52	76·33

[Ans. $\Gamma_2 = -3{\cdot}6\times10^{-7}$ mol m^{-2}]

5. Calculate the effective thickness of the 1-butanol layer in the system described in Problem 6. [Ans. $2{\cdot}3\times10^{-8}$ m]
6. Calculate how long a hydrogen atom will remain on the surface of a solid at 0°C if its desorption activation energy is : 150 kJ mol^{-1}. Assume that $\tau_0 = 10^{-13}$ s. [Ans. $3{\cdot}98\times10^{17}$ seconds]

CHAPTER 34

MACROMOLECULES

Macromolecules or polymers are very high molar mass compounds consisting of structural units inter connected by covalent bonds. Their molar mass may vary from 5,000 to several millions. The chemistry of these *giant molecules* is known as polymer chemistry or marcromolecular chemistry. Fundamental research in polymer chemistry was done from 1920 to 1950 by the German chemist, Hermann Staudinger (1881–1965) who won the 1953 Chemistry Nobel Prize. Karl Ziegler (1898–1973), Giulio Natta (1903–1979) and Paul J. Flory (1910–1985) also made significant contributions to the subject. Flory was awarded the 1974 Chemistry Nobel Prize. P.G. de Gennes (1932–), the French physicist was awarded the 1991 Physics Nobel Prize for studying polymer liquid crystals and developing the scaling concept in polymer dynamics.

Research in synthetic polymer chemistry has grown at huge pace. Several industries in the U.S.A., the former Soviet Union and Japan have specialized in the synthesis of high molar mass compounds from low molar mass compounds as starting materials. Some industries have specialized in the production of plastics, synthetic rubber, synthetic fibres, lacquers, paints, varnishes, adhesives and insulators. In fact, the plastics industry covers several varieties of synthetic polymers having a wide range of properties. Some of them are superior to even gold and platinum in chemical resistance and retain their mechanical properties even when cooled to −50°C and heated to +500°C. The strength of other polymers equals that of metals approaching even diamond in hardness. Synthetic rubber is superior to natural rubber in many respects. Some varieties act as gas-impermeable and petrol and oil-resistant rubbers; others do not lose their elastic properties at temperatures ranging from −80°C to +300°C. Also, synthetic fibres are far stronger than natural fibres. These can be converted into crease-proof fabrics and excellent artificial furs. A major discovery in the late 1970s was the preparation of conducting organic polymers such as the halogen derivatives of polyacetylene and the one-dimensional polymers, $(SN)_x$, by H. Shirakawa, A. MacDiarmid and A. Heeger. These scientists were awarded the 2000 Chemistry Nobel Prize.

A polymer consists of a large number of simple monomeric structural units which are repeated over and over again to form a giant molecule called a **macromolecule.** The simple unit is called the *repeat unit.* In the polymers ·····A—A—A—A—A—A····· and ·····A—B—A—B—A—B·····, for instance, the repeat units are A and A—B, respectively. The monomeric structural unit of polyethylene is $-CH_2-CH_2-$. For natural rubber, *viz.*,

$$\cdots\!-CH_2-\underset{\displaystyle CH_3}{\overset{\displaystyle |}{C}}=CH-CH_2-CH_2-\underset{\displaystyle CH_3}{\overset{\displaystyle |}{C}}=CH-CH_2-CH_2-\underset{\displaystyle CH_3}{\overset{\displaystyle |}{C}}=CH-CH_2-$$

the repeat unit is $-CH_2-\underset{\displaystyle CH_3}{\overset{\displaystyle |}{C}}=CH-CH_2-$, and so on.

The polymers are formed from monomers by a process analogous to the threading of beads. Some

common examples are given below.

1. Polyethylene. This is obtained by the polymerisation of ethylene.

$$n\ CH_2{=}CH_2 \longrightarrow (-CH_2{-}CH_2-)_n$$

(Ethylene) (Polyethylene)

2. Polystyrene. This is obtained by the polymerisation of styrene.

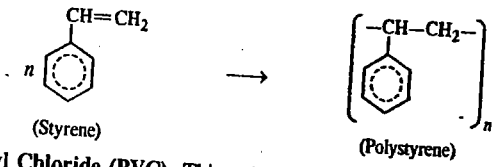

(Styrene) (Polystyrene)

3. Polyvinyl Chloride (PVC). This polymer is prepared from the monomer vinyl chloride which is obtained from the catalytic addition of hydrogen chloride to acetylene.

$$CH{\equiv}CH + HCl \xrightarrow{\text{Catalyst}} CH_2{=}CH{-}Cl$$

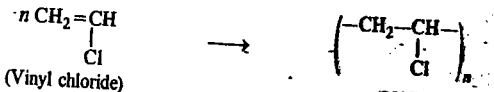

(Vinyl chloride) (PVC)

4. Poly (methyl methacrylate) (PMMA). This is obtained by the polymerization of methyl methacrylate. The monomer is prepared from acetone through the cyanohydrin reaction.

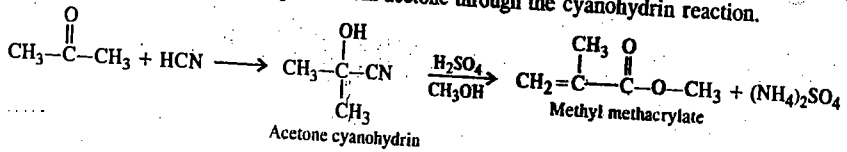

Acetone cyanohydrin Methyl methacrylate

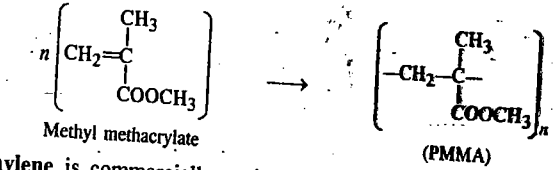

Methyl methacrylate (PMMA)

Polyethylene is commercially available in two grades : low-density polyethylene (LDPE) and high-density polyethylene (HDPE). While HDPE consists of linear unbranched chains, LDPE consists of several short and long branches, as shown in the following structure :

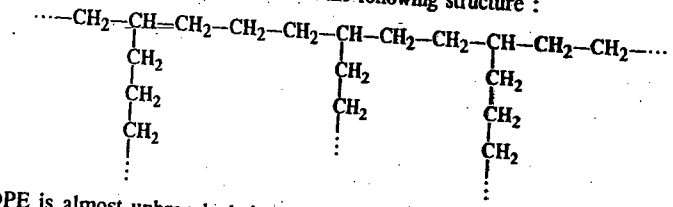

Since HDPE is almost unbranched, its chains can be close-packed in the solid state. Such close packing would not be possible in the case of branched LDPE. This is the reason why the former polymer has higher density than the latter. LDPE is used for the fabrication of king toys, pipes, containers, wires and cable insulation while HDPE is used for making industrial containers. HDPE is stronger and chemically more inert than LDPE.

Polystyrene is used for making bottles and jars, refrigerator linings and also films and frames.

PVC is a tough and rigid material used in making phonograph records. **Plasticised PVC**, obtained by the addition of appreciable amounts of low molar mass materials to PVC to increase its plasticity, finds extensive use in the manufacture of floor tiles, rain coats, hand bags, upholstery, curtains, etc.

The degree of polymerization *represents the number of structural or monomeric units contained in a polymer.* It is generally designated by the symbol, p. The molar mass M of the polymer is related to p by the equation $p=M/m$ where m is the molar mass of monomeric unit. Thus, $M=mp$.

Classification of Polymers. During polymerization, the monomer molecules may combine in a head-to-head (α, α) and tail-to-tail (β, β) arrangement, as shown :

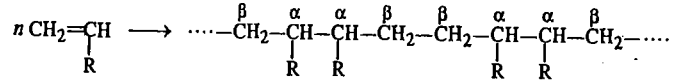

Alternatively, they may combine in a head-to-tail (α, β) arrangement, as shown :

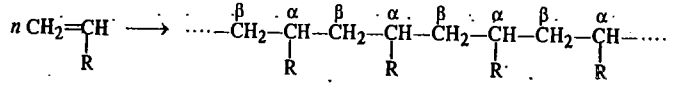

Polymerization may also proceed in a random manner, as shown :

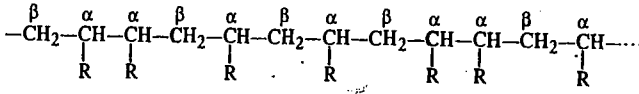

It may be noted that α carbon atoms of the polymer are *asymmetric* since each of them is attached to H, R and molecular chains of different lengths. This results in optical isomerism of the monomer units which may thus have *d*- and *l*-configurations. The spatial arrangement of the substituent R groups depends upon the manner in which the *d*- and *l*-configurations are distributed in the molecular chain.

Polymers in which all the asymmetric carbon atoms have the same (*d*- or *l*-) configuration are called **isotactic polymers.** The plane representation of an isotactic polymer is as shown below :

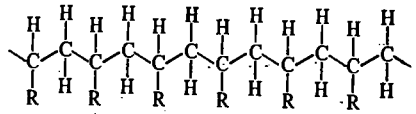

Polymers having random sequences of *d*- and *l*-configurations are known as **atactic polymers.** The plane representation of an atactic polymer is as shown below :

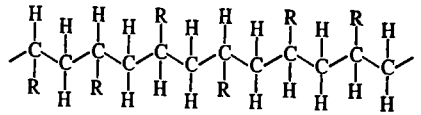

Polymers having regular alternation of *d*- and *l*-configurations in the molecular chains are called **syndiotactic polymers.** In syndiotactic polymers, the substituent groups lie alternately above and below the main chain, as shown below :

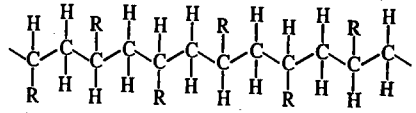

Isotactic and syndiotactic polymers are collectively referred to as **stereoregular polymers.** They are always arranged in a head-to-tail (α, β) arrangement. Karl Ziegler and Giulio Natta, the co-winners of the 1963 Nobel Prize in Chemistry, developed methods for synthesizing polymers with specified stereoisomerism. These scientists discovered that a mixture of $TiCl_4$ and $Al(C_2H_5)_3$ was an excellent heterogeneous catalyst, called **Ziegler-Natta catalyst,** for synthesizing stereoregular polymers.

We have given above examples of polymers having alternate units of the same monomer. There also exist **copolymers** which consist of monomeric units of different composition, arranged at random in the polymeric chain, as shown below :

$$\cdots\text{—A—A—B—A—B—B—A—A—B—A—}\cdots$$

where A and B are the monomeric units of different composition. For instance, A could be $CH_2{=}CHCl$ and B, $CH_2{=}CHCOOCH_3$ (vinyl acetate), etc. If, in a copolymer, the different monomeric units in the polymeric chain are not arranged at random but as alternations of runs of them, as shown, it is called a **block copolymer :**

$$\cdots\text{—A—A—A—A—B—B—B—B—A—A—A—A—}\cdots$$

Proteins, nucleic acids and mixed polysaccharides are well known examples of copolymers. The statistics of polymeric chains have been studied by the American polymer scientist P. Flory and the Russian biophysicist M. Volkenshtein.

Polymers are also classified according to their shapes. Thus, we speak of **linear polymers, branched polymers** and **cross-linked** or **network polymers.** The linear polymers (such as natural rubber, cellulose, amylase and proteins like casein and zein) possess chains of high degree of asymmetry. Branched polymers (such as glycogen and amylopectin) have chains containing several branches. In some branched polymers, known as **graft copolymers,** branches of a different monomeric species can be added, *i.e.*, grafted, on to linear chain of the polymer, as shown :

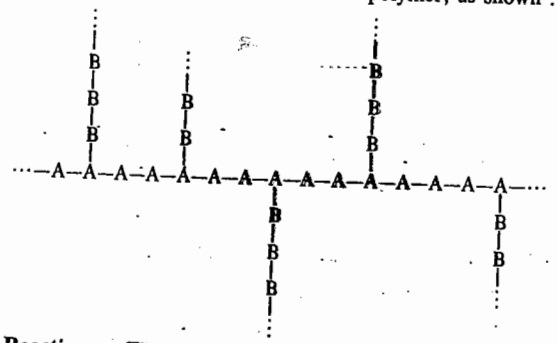

Polymerization Reactions. The polymerization reactions can be classified into *(a) Addition Polymerization* and *(b) Condensation Polymerization.* Whereas the condensation polymerization is generally accompanied by the elimination of a small molecule such as H_2O, the addition polymerization involves no such elimination of small molecules. Consider the addition polymerization of styrene in the presence of a suitable catalyst M :

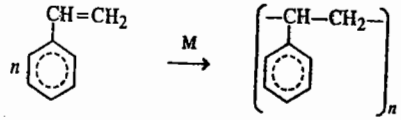

The mechanism of addition polymerization involves the production of a 'growth centre' which may be a free radical, a carbonium ion or a carbanion. The step by step addition of monomeric molecules to a growth centre leads to a polymeric chain in which the length of the growth centre is

increased. The following mechanism is suggested for the free radical polymerization of styrene :

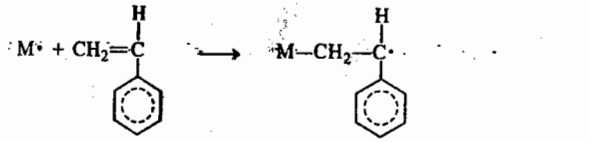

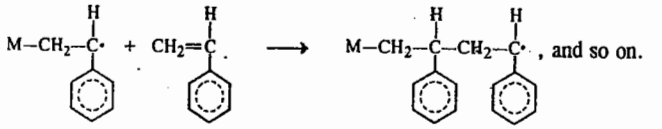

Nylons and polyesters are the products of condensation polymerization. The former are polyamides having 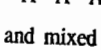 linkage whereas the latter are polyesters having linkage.

Nylon 66, first synthesized by W.H. Carothers in 1934, is obtained by the polymerization of adipic acid and hexamethylene diamine.

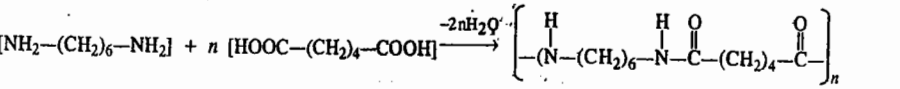

The most common variety of polyester, the so-called **PET** (polyethylene terephthalate), **terylene** or **dacron,** is synthesized by polymerizing ethylene glycol with dimethyl terephthalate :

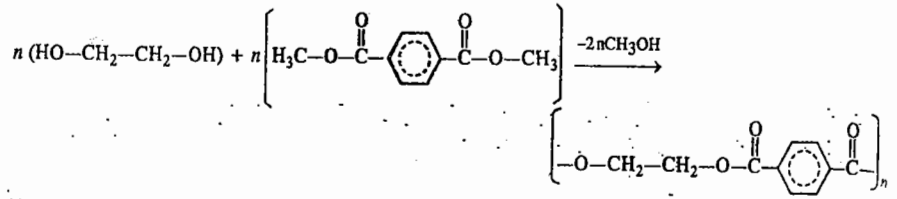

We may mention here that **polymer morphology** is the study of the solid-state structure and behaviour of polymers, their crytallinity and phase transitions.

Molar Masses of Polymers

The molar mass of a polymer increases continuously during the condensation reaction involved depending upon the degree of polymerisation. However, since the polymerisation chains might be broken at different stages, the final product generally contains macromolecules of different masses. It is necessary, therefore, to take an average molar mass in these substances. Two types of molar mass are reckoned with. These are number average molar mass. $\overline{M}_N$ and mass-average molar mass, $\overline{M}_M$. For a sample consisting of N polymer molecules containing n_1 monomer molcules of molar mass M_1, n_2 monomer molecules of molar mass M_2, etc., the **number-average molar mass** is defined as

$$\overline{M}_N = \frac{n_1M_1 + n_2M_2 + n_3M_3 + \cdots}{n_1 + n_2 + n_3 + \cdots} = \sum_i n_iM_i \,/\, \Sigma n_i \qquad \ldots(1)$$

The **mass-average molar mass is defined as**

$$\overline{M}_M = \frac{n_1M_1^2 + n_2M_2^2 + n_3M_3^2 + \cdots}{n_1M_1 + n_2M_2 + n_3M_3 + \cdots} = \sum_i n_iM_i^2 \,/\, \Sigma n_iM_i \qquad \ldots(2)$$

If c denotes the concentration of the polymer solution in grams per unit volume, then, $c_i = \Sigma n_i M_i$ so that

$$\overline{M}_M = \Sigma c_i M_i / \Sigma c_i \quad \ldots(3)$$

We see that the number-average molar mass is simply the arithmetic mean of all the molar masses whereas the mass-average molar mass is the sum of the fractional masses that each molecule in a given sample contributes to the average according to the ratio of its mass to that of the whole sample. In the number-average, each molecule counts equally but in the mass-average, molecules contribute according to their masses.

Owing to the lack of uniformity among the polymer molecules in solution, serious problems were encountered in the early studies of macromolecules. A polymer is, in general, composed of a large number of monomer units. If it is not fractionated or purified carefully, the sample will contain molecules of different chain lengths. The heterogeneity of the polymer sample is called its **polydispersity,** as opposed to a **monodisperse sample** in which all the chains are identical chemically as well as in size. The mass-average molar mass, $\overline{M}_M$ is always larger than the number-average molar mass, $\overline{M}_N$; *unless the sample is monodisperse* in which case $\overline{M}_M = \overline{M}_N$. The ratio $\overline{M}_M / \overline{M}_N$ is called the **polydispersity index (P.D.I.)** of a polymer sample.

Example 1. Equal numbers of molecules with $M_1 = 10{,}000$ and $M_2 = 100{,}000$, are mixed. Calculate $\overline{M}_N$ and $\overline{M}_M$.

Solution : Let $n_1 = n_2 = 10$ (say). Then

$$\overline{M}_N = \frac{n_1M_1 + n_2M_2}{n_1 + n_2} = \frac{10 \times 10{,}000 + 10 \times 100{,}000}{10 + 10}$$

$$= \frac{10^5 + 10^6}{20} = \frac{10^5(1 + 10)}{20} = \frac{11}{2} \times 10^4 = 55{,}000$$

$$\overline{M}_M = \frac{n_1M_1^2 + n_2M_2^2}{n_1M_1 + n_2M_2} = \frac{10 \times (10{,}000)^2 + 10 \times (100{,}000)^2}{10 \times 10{,}000 + 10 \times 100{,}000}$$

$$= \frac{10^9 + 10^{11}}{10^5 + 10^6} = \frac{10^9(1 + 100)}{10^5(1 + 10)} = \left(\frac{101}{11}\right) \times 10^4 = 91{,}818$$

Example 2. Equal masses of polymer molecules with $M_1 = 10{,}000$ and $M_2 = 100{,}000$ are mixed. Calculate $\overline{M}_N$ and $\overline{M}_M$.

Solution : Let $m_1 = m_2 = 200{,}000$ (say)

$$n_1 = \frac{\text{Mass } m_1}{\text{Molar mass } M_1} = \frac{200{,}000}{10{,}000} = 20; \quad n_2 = \frac{\text{Mass } m_2}{\text{Molar mass } M_2} = \frac{200{,}000}{10{,}000} = 2$$

$$\overline{M}_N = \frac{n_1M_1 + n_2M_2}{n_1 + n_2} = \frac{20 \times 10{,}000 + 2 \times 100{,}000}{20 + 2}$$

$$= \frac{10^5 + 10^5}{11} = \frac{2 \times 10^5}{11} = 18{,}182$$

$$\overline{M}_M = \frac{n_1M_1^2 + n_2M_2^2}{n_1M_1 + n_2M_2} = \frac{20 \times (10{,}000)^2 + 2 \times (100{,}000)^2}{20 \times 10{,}000 + 2 \times 10{,}0000}$$

$$= \frac{2 \times 10^9 + 2 \times 10^{10}}{2 \times 10^5 + 2 \times 10^5} = \frac{10^9(1 + 10)}{2 \times 10^5} = \frac{11}{2} \times 10^4 = 55{,}000$$

DETERMINATION OF MOLAR MASSES OF MACROMOLECULES

1. Viscometry

Of all the methods used for the determination of molar masses of macromolecules, the viscosity method, introduced by Staudinger, is the one most commonly employed in research. Accurate measurement of absolute viscosity being difficult, it is convenient to measure **relative viscosity,** η_{rel}, defined as

$$\eta_{rel} = \eta/\eta_0 \quad \ldots(4)$$

where η and η_0 are, respectively, the viscosity of the solution and the viscosity of the solvent. The relative viscosity is related to some other quantities as follows :

$$\eta_{sp} = \eta_{rel} - 1 \quad \ldots(5)$$

$$\eta_{red} = \eta_{sp}/c \quad \ldots(6)$$

$$[\eta] = \lim_{c \to 0}(\eta_{sp}/c) \quad \ldots(7)$$

where η_{sp} **is specific viscosity,** η_{red} **is reduced viscosity and** $[\eta]$ **is intrinsic viscosity** (also called **the viscosity number** or **Staudinger index**). In these equations, c is the concentration of the polymer. Note that none of these quantities has the units of viscosity.

In 1906, Einstein derived the following relation between the viscosity of a dilute suspension of hard spherical molecules and the **volume fraction,** ϕ, of the solute molecules :

$$\eta = \eta_0 (1 + 2{\cdot}5\phi) \quad \ldots(8)$$

Rearrangement of Eq. 8 gives

$$\eta/\eta_0 - 1 = \eta_{sp} = 2{\cdot}5\phi \quad \ldots(9)$$

Hence, from, Eqs. 7 and 9,

$$[\eta] = \lim_{c \to 0}\left(\frac{\eta_{sp}}{c}\right) = \frac{2{\cdot}5\phi}{c} \quad \ldots(10)$$

It is, however, very difficult to measure ϕ, **the volume fraction** of the polymer molecules in **solution.** The plots of η_{sp}/c and $\ln \eta_{red}/c$ versus c give straight lines which conform to the following equations :

Huggin's equation : $\eta_{sp}/c = [\eta] + k'[\eta]^2c$ ....(11)

Kraemer's equation : $\ln \eta_{red}/c = [\eta] - k''[\eta]^2c$ ...(12)

Both these equations are applicable only in dilute solutions. For a large number of polymers, $k' = 0{\cdot}4 \pm 0{\cdot}1$ and $k'' = 0{\cdot}50 \pm 0{\cdot}05$.

Fortunately, Staudinger found, in 1950, that for a series of samples of the same polymer in a given solvent and at a constant temperature, the intrinsic viscosity (or the viscosity number) is related to the molar mass of the polymer by the following equation, known as **Mark-Kuhn-Houwink-Sakurada equation,** formerly called Staudinger equation :

$$[\eta] = K(\overline{M}_{visc})^a \quad \ldots(13)$$

where $\overline{M}_{visc}$ is the viscosity-average molar mass of the polymer and K and a are constants, usually determined by intrinsic viscosity measurements on a series of polymer samples for which the molar mass has been determined by a different method, say, the light-scattering method. The value of the exponent a depends upon the geometry or the shape of the macromolecule. The more elongated a molecule, the more effective are the higher molar mass fractions in reducing the viscosity of the solution. The values of a vary from 0·5 to 1. For polymers behaving as random coils, a is about 0·8 and for globular proteins possessing a compact structure, it is about 0·5. Note that $[\eta]$ has the

dimensions of reciprocal density and hence its units are $cm^3\ g^{-1}$. Typical values of K and a are summarized in Table 1.

TABLE 1

Parameters for the Mark-Kuhn-Houwink-Sakurada Equation

Polymer	Solvent	Temperature (°C)	$K\times10^5$	a
Polystyrene	Benzene	25	10·3	0·74
Polystyrene : Atactic	Toluene	30	11·0	0·72
Isotactic	Toluene	30	10·6	0·73
Polyacrylonitrile	Dimethyl formamide	25	16·6	0·81
Polyisobutylene	Cyclohexane	30	26·0	0·70
	Benzene	25	107·0	0·51
Polyisoprene	Cyclohexane	27	30·0	0·70
Natural rubber	Toluene	25	50·0	0·62
Polyvinyl alcohol	Water	25	20·0	0·76
Polyvinyl chloride	Tetrahydrofuran	20	3·6	0·92
Polyethylene	Decalin	35	62·0	0·70
Polyisobutylene	Benzene	25	107·0	0·50
	Toluene	40	43·0	0·60
	Cyclohexane	30	27·6	0·69
Polymethyl methacrylate	Toluene	25	7·1	0·73

Taking logs of both sides of Eq. 13, we have

$$\ln [\eta] = \ln K + a \ln \overline{M}_{visc} \qquad ...(14)$$

Eq. 14 shows that a log-log plot of $[\eta]$ versus $\overline{M}_{visc}$ gives a straight line with slope equal to a and intercept equal to $\ln K$. Thus, the constants a and K can be easily determined.

Knowing the values of a and K, the viscosity-average molar mass $\overline{M}_{visc}$ can be determined from intrinsic viscosity measurements.

Example 3. The intrinsic viscosity of myosin is 217 $cm^3\ g^{-1}$. Calculate the approximate concentration of myosin in water which would have a relative viscosity of 1·5.

Solution : From Eq. 7, $[\eta] = \lim_{c\to0}(\eta_{sp}/c) \lim_{c\to0}\left(\frac{\eta_{rel}-1}{c}\right) = 217\,cm^3\,g^{-1}$; $\eta_{rel} = 1{\cdot}5$ (given)

$$\frac{1{\cdot}5-1}{c} = 217\ cm^3\,g^{-1}$$

$$\therefore \quad c = \frac{0{\cdot}5}{217\ cm^3\,g^{-1}} = 2{\cdot}3\times10^{-3}\ g\ cm^{-3}$$

Example 4. The intrinsic viscosity of a solution of polyisobutylene at 20°C is 180 cm^3 per gram. If $[\eta]$ is related to the viscosity-average molar mass $\overline{M}_{visc}$ by the expression, $[\eta] = 3{\cdot}60\times10^{-2}(\overline{M}_{visc})^{0{\cdot}64}$, calculate the molar mass of the polymer.

Solution : $[\eta] = 3{\cdot}60\times10^{-2}(\overline{M}_{visc})^{0{\cdot}64}$

or $180\ cm^3\,g^{-1} = 3{\cdot}60\times10^{-2}(\overline{M}_{visc})^{0{\cdot}64}$

$$\therefore \quad (\overline{M}_{visc})^{0{\cdot}64} = \frac{180\ cm^3\,g^{-1}}{3{\cdot}60\times10^{-2}} = 5{\cdot}0\times10^3$$

Taking logs, $0{\cdot}64 \ln \overline{M}_{visc} = \ln (5{\cdot}0\times10^3)$

$$\therefore \quad \overline{M}_{visc} = 6{\cdot}0\times10^5\ g\ mol^{-1}$$

Example 5. The following data were obtained for the intrinsic viscosity of polyisobutylene in CCl_4 solutions at 30°C as a function of the viscosity-average molar mass :

$[\eta]$, $cm^3\ g^{-1}$	$\overline{M}_{visc}$, g mol^{-1}	$[\eta]$, $cm^3\ g^{-1}$	$\overline{M}_{visc}$, g mol^{-1}
430	1,260,000	43	48,000
206	463,000	15·1	10,000
78	110,000	13·8	9,550
73	92,700	11·5	7,080

Verify by a suitable plot that the data fit in the equation $[\eta] = K(\overline{M}_{visc})^a$. Determine the constants K and a.

Solution : Since $[\eta] = K(\overline{M}_{visc})^a$ [Eq. 13]

$$\therefore \quad \ln [\eta] = \ln K + a \ln \overline{M}_{visc}$$

The student can plot $\ln [\eta]$ versus $\ln \overline{M}_{visc}$. It will be found that slope $= a = 0{\cdot}70$ and intercept $= \ln K = -8{\cdot}245$ from where, taking antilogs, $K = 2{\cdot}6\times10^{-4}$.

We shall now comment on the viscosity-average molar mass, $\overline{M}_{visc}$. If the exponent a in Eq. 13 has the value $=1$ and $c\to0$, then the viscosity-average molar mass can be written as

$$\overline{M}_{visc} = [\eta]/K = (\eta_{rel}-1)/Kc \qquad ...(15)$$

The $(\eta_{rel}-1)$ values of the individual fractions can then be added to yield the total $(\eta_{rel}-1)$. Thus,

$$\eta_{rel} - 1 = (\eta_{rel}-1)_1 + (\eta_{rel}-1)_2 + (\eta_{rel}-1)_3 + \cdots\cdots$$

$$= Kc_1M_1 + Kc_2M_2 + Kc_3M_3 + \cdots\cdots$$

Therefore, the viscosity-average molar mass can be written as

$$\overline{M}_{visc} = \frac{K(c_1M_1 + c_2M_2 + c_3M_3 + \cdots)}{K(c_1 + c_2 + c_3 + \cdots)} = \frac{\sum_i c_iM_i}{\sum_i c_i}$$

$$= \overline{M}_M \qquad \text{(vide Eq. 3)} \qquad ...(16)$$

We see that when the constant $a=1$, the viscosity average molar mass yields the mass-average molar mass.

If $a \neq 1$, then, according to Eqs. 13 and 15,

$$(\overline{M}_{visc})^a = (\eta_{rel}-1)/Kc \qquad ...(17)$$

$$= \frac{K(c_1M_1^a + c_2M_2^a + c_3M_3^a + \cdots)}{K(c_1 + c_2 + c_3 + \cdots)} = \frac{\sum_i c_iM_i^a}{\sum_i c_i} \qquad ...(18)$$

Hence, $$\overline{M}_{visc} = \left[\frac{\sum_i c_iM_i^a}{\sum_i c_i}\right]^{1/a} \qquad ...(19)$$

It follows from Eq. 19 also that $\overline{M}_{visc} \longrightarrow \overline{M}_M$ when $a \longrightarrow 1$.

2. Osmometry

Osmotic pressure measurements are used for studying macromolecules because osmotic changes are larger than the changes in boiling point elevation, freezing point depression and vapour pressure lowering. For instance, an order-of-magnitude calculation shows that for an aqueous solution containing 10 g dm^{-3} of a polymer having molar mass 20,000, the boiling point elevation and freezing

point depression are 0·0025°C and 0·00093°C, respectively. Evidently, these values are too low to be measured.

If Π is the osmotic pressure of a solution in which the mole fraction of the solvent is x_1, then, the condition for equilibrium for the chemical potential of the solvent on both sides of the semipermeable membrane gives

$$RT \ln \gamma_1 x_1 + \Pi \bar{V}_1 = 0 \qquad \ldots(20)$$

where γ_1 is the activity coefficient of the solvent and $\bar{V}_1$ is the partial molar volume of the solvent in the solution. For a dilute solution, $x_1 \to 1$ and $\bar{V}_1 \to V_1^\circ$, the molar volume of the pure solvent. If we replace x_1 by $(1-x_2)$, where x_2 is the mole fraction of the solute, then the expansion of the logarithm gives

$$\Pi V_1^\circ = RT\left(x_2 + x_2^2/2 + x_2^3/3 + \cdots\cdots\right) \qquad \ldots(21)$$

For a polymer solution of concentration c, x_2 is given by

$$x_2 = \frac{c/M}{1/V_1^\circ + c/M} \approx \frac{V_1^\circ c}{M} \text{ for a dilute solution.} \qquad \ldots(22)$$

Here M is the molar mass of the polymer.

Substituting Eq. 22 in Eq. 21, we obtain, for an ideal solution,

$$\frac{\Pi}{c} = \frac{RT}{M}\left[1 + \frac{1}{2}\left(\frac{V_1^\circ}{M}\right)c + \frac{1}{3}\left(\frac{V_1^\circ}{M}\right)^2 c^2 + \cdots\cdots\right] \qquad \ldots(23)$$

which is the virial expression of the form

$$\frac{\Pi}{c} = \frac{RT}{M}(1 + A_2 c + A_3 c^2 + \cdots\cdots) \qquad \ldots(24)$$

Eq. 24 is often written in the form

$$\frac{\Pi}{c} = RT\left[\frac{1}{M} + B_2 c + B_3 c^2 + \cdots\cdots\right] \qquad \ldots(25)$$

where B_2, B_3, etc., are the second, third, etc., virial coefficients. Eq. 25 is the **van't Hoff equation** relating the osmotic pressure of a polymer solution with the molar mass of the polymer. The quantity Π/c is called *reduced osmotic pressure*. As can be seen, if the third term is neglected, a graph of Π/c versus c would be a straight line which when extrapolated to $c=0$, gives RT/M as the intercept on the Π/c axis, that is,

$$\lim_{c \to 0} (\Pi/c) = RT/M \qquad \ldots(26)$$

From the intercept, the molar mass M can be easily calculated.

Example 6. The following data were obtained on the osmotic pressure of solutions of γ-globulin in 0·15 M NaCl at 37°C :

c, g/100 ml	19·27	12·53	5·81
Π, mm H_2O	453	253	112

Calculate the molar mass of the polymer.

Solution : 100 ml = 0·1 litre = 0·1 dm^3

$$\frac{\Pi}{c} = \frac{453 \text{ mm } H_2O}{192{\cdot}7 \text{ g dm}^{-3}} = 2{\cdot}35 \text{ mm } H_2O \text{ dm}^3 \text{ g}^{-1}$$

Construct the following table :

c (g dm^{-3})	192·7	125·3	58·1
Π/c (mm H_2O dm^3 g^{-1})	2·35	2·05	1·93

Plot Π/c versus c to obtain a straight line. It will be seen from the plot that

$$\lim_{c \to 0} (\Pi/c) = 1{\cdot}86 \text{ mm } H_2O \text{ dm}^3 \text{ g}^{-1} = RT/M \qquad \text{(Eq. 26)}$$

$$M = \frac{RT}{\lim\limits_{c \to 0}(\Pi/c)} = \frac{RT}{18{\cdot}6 \text{ mm } H_2O \text{ dm}^3 \text{ g}^{-1}}$$

$$\left\{\begin{aligned} R &= 0{\cdot}08206 \text{ dm}^3 \text{ atm K}^{-1} \text{ mol}^{-1}) = 0{\cdot}08206 \times 760 \times 13{\cdot}56 \text{ mm } H_2O \text{ dm}^3 \text{ K}^{-1} \text{ mol}^{-1} \\ &1 \text{ atm} = 760 \text{ mm Hg; } 1 \text{ mm Hg} = 13{\cdot}56 \text{ mm } H_2O \\ &= 845{\cdot}67 \text{ mm } H_2O \text{ dm}^3 \text{ K}^{-1} \text{ mol}^{-1} \end{aligned}\right\}$$

$$\therefore \quad M = \frac{(845{\cdot}67 \text{ mm } H_2O \text{ dm}^3 \text{ K}^{-1} \text{ mol}^{-1})(310\text{K})}{1{\cdot}86 \text{ mm } H_2O \text{ dm}^3 \text{ g}^{-1}} = 1{\cdot}49 \times 10^5 \text{ g mol}^{-1}$$

The osmotic pressure measurement leads to number-average molar mass because osmotic pressure is a colligative property which depends upon the *number* of molecules of the polymer and not on their mass and all molecules whether heavy or light make equal contribution.

This can also be shown mathematically remembering that the osmotic pressure Π consists additively of the partial osmotic pressures Π_1, Π_2, Π_3, ····· for the molecules of different degrees of polymerization, 1, 2, 3, etc. Thus,

$$\Pi = \Pi_1 + \Pi_2 + \Pi_3 + \cdots\cdots = \frac{c_1 RT}{M_1} + \frac{c_2 RT}{M_2} + \frac{c_3 RT}{M_3} + \cdots\cdots \qquad \ldots(27)$$

The same holds for the total concentration : $c = c_1 + c_2 + c_3 + \cdots\cdots$

Thus, the osmotic-average molar mass can be written as

$$\bar{M}_{\text{osmotic}} = \frac{(c_1 + c_2 + c_3 + \cdots\cdots)RT}{\Pi_1 + \Pi_2 + \Pi_3 + \cdots\cdots} \qquad \ldots(28)$$

$$= \frac{(c_1 + c_2 + c_3 + \cdots\cdots)RT}{RT(c_1/M_1 + c_2/M_2 + c_3/M_3 + \cdots\cdots)} \qquad \ldots(29)$$

$$= \frac{\sum\limits_i c_i}{\sum\limits_i c_i / \sum\limits_i M_i} = \bar{M}_N \qquad \ldots(30)$$

Molar Mass of Charged Macromolecules : Donnan Membrane Equilibrium

The molar masses of charged macromolecules (*e.g.*, proteins), determined by osmotic pressure measurements *in electrolytic media* were found to be considerably smaller than those determined by other methods. This was found to be due to an electrical phenomenon, known as **Donnan membrane equilibrium,** *which occurs when a large, non-diffusible, charged ion (e.g., a protein ion), is separated by a semipermeable membrane from a diffusible salt.*

Suppose a solution of a salt Na^+P^- of concentration c_1 (where P^- is a protein particle carrying a negative charge) is separated by a semipermeable membrane from a solution of sodium chloride of concentration c_2 (see the *initial state* shown below). During osmosis, the chloride ions tend to diffuse from a region of higher concentration c_2 on the right to a region of lower concentration c_1 on the left. However, the protein ions P^- cannot pass through the membrane. In order to maintain electrical

neutrality, an equal number of Na^+ ions would pass from right to left across the membrane (see the *equilibrium state* shown below).

Initial State

Na^+	P^-		Na^+	Cl^-
c_1	c_1	⋮	c_2	c_2

Equilibrium State

Na^+	P^-	Cl^-		Na^+	Cl^-
$c_1 + x$	c_1	x	⋮	$c_2 - x$	$c_2 - x$

The osmotic pressure measurement would thus get complicated by the additional number of particles present on the left side, *i.e.*, on the protein side of the membrane. Let x be the concentration change due to the diffusion of NaCl across the membrane. In both the compartments, electrical neutrality must be maintained, *i.e.*, the total concentration of positive ions should be equal to that of the negative ions in each solution.

At equilibrium, the chemical potential of NaCl which is present on both sides of the membrane, must be the same on each side. Accordingly,

$$\mu^\circ + RT \ln (a_{NaCl})_l = \mu^\circ + RT \ln (a_{NaCl})_r \quad \ldots (31)$$

where a_{NaCl} represents the activity of sodium chloride and the subscripts l and r refer to the solutions on the left and the right of the semipermeable membrane. Thus, we have for the left compartment,

$$(a_{NaCl})_l = (a_{Na^+})_l (a_{Cl^-})_l = (\gamma_\pm)_l^2 (Na^+)_l (Cl^-)_l \quad \ldots(32)$$

and for the right compartment,

$$(a_{NaCl})_r = (a_{Na^+})_r (a_{Cl^-})_r = (\gamma_\pm)_r^2 (Na^+)_r (Cl^-)_r \quad \ldots(33)$$

Assuming that the mean ionic activity coefficients in the left and the right compartments are equal, *i.e.*, $(\gamma_\pm)_l = (\gamma_\pm)_r$, which is usually the case since the ionic strengths are equal, we can express the Donnan equilibrium as

$$[Na^+]_l [Cl^-]_l = [Na^+]_r [Cl^-]_r$$

or $$(c_1 + x)\, x = (c_2 - x)(c_2 - x) = (c_2 - x)^2$$

or $$c_1 x + x^2 = c_2^2 + x^2 - 2c_2 x \quad \text{or} \quad x(c_1 + 2c_2) = c_2^2$$

$$\therefore \quad x = c_2^2 / (c_1 + 2c_2) \quad \ldots(34)$$

It is evident from Eq. 34 that the magnitude of x depends on c_2, the concentration of salt, as well as on c_1, the concentration of the protein. This means that the extent of diffusion of sodium chloride, *viz.*, x, is distinctly affected by the presence of the non-diffusible protein ion P^-. If the solution behaves ideally, the osmotic pressure can be calculated with the help of the van't Hoff equation, *viz.*, $\Pi = RTc$; the concentration term c, in the present case, being the *difference* in the molar concentrations on the two sides of the membrane. Thus, at equilibrium,

$$\Pi = RT \{[(c_1 + x) + (c_1 + x)] - [(c_2 - x) + (c_2 - x)]\}$$
$$= 2RT (c_1 - c_2 + 2x) \quad \ldots(35)$$

If the concentration of the salt c_2 is *small* as compared to the concentration of the non-diffusible ion, c_1, the osmotic pressure would be given by $\Pi = 2RT(c_1 + 2x)$. Since this pressure is *higher* than the actual pressure which should have been given by $\Pi = 2RTc_1$, the molar mass determined from osmotic pressure measurement would be *smaller* than the actual value.

If the concentration of the salt c_2 is *large* as compared to the concentration c_1 of the non-diffusible ion, then, according to Eq. 34, $2x$ is equal to c_2. Eq. 35, therefore, takes the form

$$\Pi = 2RTc_1 \quad \ldots(36)$$

This equation does not involve the concentration of the chloride ion. In other words, the effect of Donnan equilibrium on osmotic pressure is practically eliminated by using a high concentration of salt in the solution. This is precisely the condition under which molar masses of such macromolecules should be determined from osmotic pressure measurements.

3. Ultracentrifugation

The rate of sedimentation of suspended particles under the action of gravity is very small. However, it can be increased considerably by applying the ultracentrifugation technique devised by Svedberg. A particle sedimenting in a centrifugal field is subjected to an acceleration given by $\omega^2 x$, where ω is the angular velocity of the centrifuge (given by $2\pi \times$number of revolutions per second) and x is the distance of the particle from the axis of rotation. The rate of sedimentation can, therefore, be increased considerably by increasing the number of revolutions per second.

In some of the ultracentrifuges, the number of revolutions is as high as 1000 per second. If the particle is at a distance of 10 cm from the axis of rotation (*i.e.*, $x = 10$ cm), the acceleration in the centrifugal field would be $\omega^2 x = (2\pi \times 1000)^2 \times 10 = 3.94 \times 10^8$ cm per sec^2. This is nearly 400,000 times greater than the acceleration due to normal gravity which is only 981 cm per sec^2. The rate of sedimentation, therefore, can be raised by 400,000 times the normal rate.

When a polymer solution is placed in the cell of an ultracentrifuge, the polymer molecules tend to distribute themselves during rotation perpendicularly to the axis of rotation throughout the cell in accordance with their individual molar masses. At constant force, the larger molecules move rapidly towards the periphery, the largest molecules being found nearest the periphery, at equilibrium. If a strong beam of light passing parallel to the axis of rotation and perpendicular to the axis of the cell, is used to measure the refractive index, then the concentration of the polymer solution in any given section can be measured. This enables determination of the velocity of the molecular movement towards the periphery, at equilibrium. The ultracentrifugation technique for the determination of molar mass of a polymer may involve *(a) the Sedimentation Velocity Method* or *(b) the Sedimentation Equilibrium Method*. While the first method yields the number-average molar mass, the second method yields the mass-average molar mass.

a. The Sedimentation Velocity Method. Consider a polymer solution being spun in a centrifuge tube under the influence of a very strong gravitational field. The centrifugal force acting on the solute particle of mass m, at a distance r from the centre of rotation, is $m\omega^2 r$, where ω is the angular velocity of the rotor in radians per second. The particle is also subjected to a buoyant force in addition to the centrifugal force so that the resultant force acting on the particle is given by

$$\text{Resultant force} = \text{Centrifugal force} - \text{Buoyant force} = m\omega^2 - m_s\omega^2 r \quad \ldots(37)$$

where m_s is the mass of the displaced solvent. If ρ is the density of the solvent and v, the volume of the solute particle, then $m_s = v\rho$. However, the measurement of v is extremely difficult. Hence, it is customary to define a quantity, $\bar{v}$, *the partial specific volume*, as the increase in volume when one gram of a dry polymer solute is dissolved in a very large volume of the solvent. Then, obviously, the quantity $m\bar{v}$ will represent the increase in volume obtained on adding a solute particle of mass m to the solvent. In other words, $m\bar{v} = v$. Hence, Eq. 37 becomes

$$\text{Resultant force} = m\omega^2 r - m\omega^2 r\bar{v}\rho = m\omega^2 r(1 - \bar{v}\rho) \quad \ldots(38)$$

This resultant force, according to Newton's second law of motion, will cause the solute particle to accelerate. However, the acceleration in this case will not last long since the medium exerts a frictional force on it which is proportional to the sedimentation velocity, dr/dt. Thus,

$$\text{Frictional force} = f(dr/dt) \quad \ldots(39)$$

where f is the *frictional coefficient*. The frictional force acts in the opposite direction to the resultant force. When the steady state is reached, we have, from Eqs. 38 and 39,

$$f(dr/dt) = m\omega^2 r(1 - \bar{v}\rho) \qquad ...(40)$$

Eq. 40 can be rearranged to give a quantity, S, defined as

S = Sedimentation velocity/Centrifugal acceleration,

i.e.,
$$S = \frac{dr/dt}{\omega^2 r} = \frac{m(1 - \bar{v}\rho)}{f} = \frac{(\overline{M}_N / N_A)(1 - \bar{v}\rho)}{f} \qquad ...(41)$$

The quantity S is called the **sedimentation coefficient**; it is the *sedimentation rate for a unit centrifugal acceleration*. For a given molecular species in a given solvent at a given temperature, S is a constant. It is expressed in the unit *svedberg*, named after the Swedish chemist T. Svedberg (1884–1971) who did fundamental work on disperse systems for which he was awarded the Nobel Prize in Chemistry in 1926. One svedberg $= 10^{-13}$ s.

For a spherical polymer particle of radius r, the frictional coefficient, f, is related to the coefficient of viscosity of the solvent, η, by Stokes' equation, *viz.*,

$$f = 6\pi\eta r \qquad ...(42)$$

Hence, from Eqs. 41 and 42,

$$\overline{M}_N = \frac{SN_A f}{1 - \bar{v}\rho} = \frac{6\pi\eta r S N_A}{1 - \bar{v}\rho} \qquad ...(43)$$

Unfortunately, the above relation applies only to *spherical* molecules. For polymers which are shaped like rods, ellipsoids or coils, the Stokes' law does not apply. Hence, f must be determined experimentally. This is usually done by diffusion measurements which are not simple to carry out but which have the advantage that the phenomenon of diffusion is very similar to that of sedimentation so that one can expect the frictional coefficient f determined from diffusion to be identical with the frictional coefficient f which is characteristic for sedimentation. The relationship between the experimentally determined diffusion coefficient D and the frictional coefficient f is given by Stokes–Einstein diffusion equation, *viz.*;

$$D = RT/(N_A f) = kT/f \qquad ...(44)$$

whence
$$f = kT/D \qquad ...(45)$$

Thus, from Eqs. 43 and 45,

$$\overline{M}_N = \frac{SN_A kT}{D(1 - \bar{v}\rho)} = \frac{SRT}{D(1 - \bar{v}\rho)} \qquad ...(46)$$

which is the **Svedberg equation** for the determination of molar mass of a polymer. The sedimentation coefficient S and the diffusion coefficient D must be corrected to the same temperature, usually 20°C, and if both these coefficients are concentration-dependent, their values must be extrapolated to zero concentration.

The Experimental Set-up. The ultracentrifuge is shown schematically in Fig. 1. The measurement of sedimentation velocity in the ultracentrifuge leads to the determination of the sedimentation coefficient. The dilute solution of the polymer contained in a cell is introduced into the rotor of the ultracentrifuge. The cell is fitted with two quartz windows to permit photographing of the

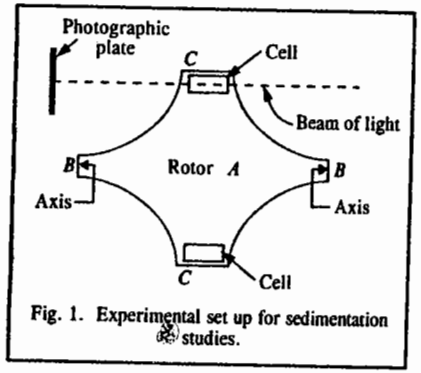

Fig. 1. Experimental set up for sedimentation studies.

solution. As rotation in the centrifuge proceeds, the polymer molecules slowly sediment with constant velocity under the influence of the gravitational force towards the bottom of the cell. Depending upon the homogeneity of the dissolved particles, one observes at the upper edge of the cell an almost sharp boundary against the pure solvent which, as centrifugation continues, moves towards the bottom of the cell. (This process may take several hours). The velocity with which the boundary moves is the sedimentation velocity. It is, however, not possible to obtain a very sharp boundary between the solution and the solvent layer above it because the separation is smeared out through rediffusion of the sedimenting particles and the boundary for the non-homogeneous system is spread out further since the components with low molar mass remain behind during sedimentation while the components with high molar mass sediment more rapidly.

Now, by definition,
$$S = \frac{dr/dt}{\omega^2 r} \quad \text{or} \quad Sdt = \frac{1}{\omega^2}\frac{dr}{r} \qquad ...(47)$$

If the boundary is at a distance r_1 from the axis of the ultracentrifuge at time t_1 and at a distance r_2 from the axis at time t_2, then integration of Eq. 47 yields

$$\int_{t_1}^{t_2} Sdt = \frac{1}{\omega^2}\int_{r_1}^{r_2}\frac{dr}{r} \qquad ...(48)$$

$$S(t_2 - t_1) = \frac{1}{\omega^2}\ln(r_2/r_1) \qquad ...(49)$$

or
$$S = \frac{1}{\omega^2(t_2 - t_1)}\ln(r_2/r_1) \qquad ...(50)$$

The sedimentation coefficient for a given macromolecule is ***independent*** of the angular velocity ω of the rotor, the reason being that as $\omega^2 r$ increases, dr/dt increases, too, so that the ratio of the two remains constant. The sedimentation coefficients for proteins lie in the range of 10^{-13}s to 200×10^{-13} s.

Example 7. A sample of serum globulin is placed in an ultracentrifuge which is operating at 50,000 rotations per minute (rpm). If the sedimentation coefficient of this protein is $7{\cdot}1 \times 10^{-13}$ s, how far will the solution boundary move in 30 minutes at a distance of 6·5 cm from the axis of rotation ?

Solution : Since from Eq. 47, $S = (dr/dt)/\omega^2 r$, hence $dr/dt = S\omega^2 r$

$$\omega = 2\pi\nu = \frac{2(3{\cdot}142)(50{,}000)}{60\text{ s}} = 5237\text{ rad s}^{-1}$$

$$\therefore \quad dr/dt = (7{\cdot}1\times10^{-13}\text{ s})\,(5237\text{ rad s}^{-1})^2\,(6{\cdot}5\text{ cm}) = 1{\cdot}27\times10^{-4}\text{ cm s}^{-1}$$

$$\Delta r = (1{\cdot}27\times10^{-4}\text{ cm s}^{-1})\,(30\times60\text{ s}) = 0{\cdot}229\text{ cm}$$

Example 8. A sample of solution of bovine serum albumin is placed in an ultracentrifuge which is operating at a speed of 45,000 rpm. If the boundary position of the solution moves from an initial r-value of 6·15 cm to a final r-value of 6·83 cm in a time interval of 157 min, calculate the sedimentation coefficient of bovine serum albumin.

Solution : Substituting the given data in Eq. 50, we have

$$S = \frac{\ln\left(\frac{6{\cdot}83\text{ cm}}{6{\cdot}15\text{ cm}}\right)}{\left(2\pi\times\frac{45{,}000\text{ rpm}}{60\text{ s min}^{-1}}\right)^2(157\text{ min}\times60\text{ s min}^{-1})} = 5{\cdot}01\times10^{-13}\text{ s}$$

Physical constants of some common protein molecules are given in Table 2.

TABLE 2

Physical Constants of Some Common Protein Molecules at 20°C

Protein	Svedberg (svedberg=10^{-13} s)	D(cm^2 s^{-1})×10^7	$\bar{v}$ (cm^3 g^{-1})	$\bar{M}_n$ (g mol^{-1})
Insulin (beef)	1·70	15·0	0·72	12,000
Haemolglobin (man)	4·48	6·9	0·75	63,000
Haemoglobin (horse)	4·41	6·3	0·75	68,000
Myoglobin (beef heart)	2·04	11·3	0·74	16,900
Serum albumin (man)	4·67	5·9	0·74	72,000
Serum albumin (horse)	4·46	6·1	0·75	70,000
Serum globulin	7·10	4·0	0·75	167,000
Lysozyme (egg yellow)	1·90	11·2	0·75	16,400
Edestin	12·81	3·2	0·74	381,000
Pepsin (pig)	3·30	9·0	0·75	35,500
Urease	18·61	3·4	0·73	490,000
Tobacco mosaic virus	18·50	0·53	0·72	40,000,000

Example 9. Using data of Table 2, calculate the molar mass of serum globulin at 20°C. The density of water of 20°C is 0·9982 g cm^{-3}.

Solution : $T = 20 + 273{\cdot}15 = 293{\cdot}15$ K $\quad R = 8{\cdot}314$ J K^{-1} mol^{-1}

$S = 7{\cdot}10\times10^{-13}$ s; $\quad D = 4{\cdot}0\times10^{-7}$ cm^2 s^{-1} $= 4{\cdot}0\times10^{-11}$ m^2 s^{-1}

$\bar{v} = 0{\cdot}75$ cm^3 g^{-1}; $\quad \rho = 0{\cdot}9982$ g cm^{-3}

Substituting the above data in Eq. 46, we have

$$\bar{M}_N = \frac{SRT}{D(1-\bar{v}\rho)} = \frac{(7{\cdot}1\times10^{-13}\text{ s})(8{\cdot}314\text{ J K}^{-1}\text{ mol}^{-1})(293{\cdot}15\text{ K})}{(4{\cdot}0\times10^{-11}\text{ m}^2\text{ s}^{-1})\{1-(0{\cdot}75\text{ cm}^3\text{ g}^{-1})(0{\cdot}9982\text{ g cm}^{-3})\}}$$

$$= 167{\cdot}0\text{ J m}^{-2}\text{ s}^2\text{ mol}^{-1} \qquad (\text{J} = \text{kg m}^2\text{ s}^{-2})$$

$$= 167{\cdot}0\text{ kg mol}^{-1} = \mathbf{167{,}000\text{ g mol}^{-1}}$$

b. Sedimentation Equilibrium Method. In the sedimentation equilibrium method, the rotor speed is lower (about 10,000 rpm) than in the sedimentation velocity method where the rotor speed is of the order of 60,000 rpm. When an equilibrium between sedimentation and diffusion is reached, there is no net flow. Now, according to Fick's law of diffusion, the rate of diffusion, *i.e.*, number of solute particles n crossing a vertical plane per second, from higher concentration to lower concentration, is directly proportional to the area of cross-section, A and the concentration gradient, dc/dr, *i.e.*,

$$\text{Rate of diffusion} = \frac{dn}{dt} = -DA\frac{dc}{dr} \qquad ...(51)$$

where D is the diffusion coefficient in units of cm^2 s^{-1}. For solute molecules flowing through unit area ($A=1$),

$$\frac{dn}{dt} = D\frac{dc}{dr} \qquad ...(52)$$

The negative sign in Eq. 52 has been omitted since the concentration gradient increases with increasing value of r. Since, from Nernst-Einstein diffusion equation, $D = kT/f$, hence,

$$\frac{dn}{dt} = \frac{kT}{f}\frac{dc}{dr} = \frac{RT}{N_A f}\frac{dc}{dr} \qquad ...(53)$$

From Eq. 40, the rate of sedimentation of the polymer solution is given by

$$\frac{dr}{dt} = \frac{m\omega^2 r}{f}(1-\bar{v}\rho) \qquad ...(54)$$

or $$c\frac{dr}{dt} = \frac{m\omega^2 rc}{f}(1-\bar{v}\rho) \qquad ...(55)$$

Since, at equilibrium, the diffusion rate is equal to the sedimentation rate, we have from Eqs. 53 and 55,

$$dn/dt = c\,dr/dt \qquad ...(56)$$

or $$\frac{RT}{N_A f}\frac{dc}{dr} = \frac{m\omega^2 rc}{f}(1-\bar{v}\rho) \qquad ...(57)$$

Cancelling f from both sides of Eq. 57, setting $m = \bar{M}_M/N_A$ and separating the variables, we have

$$\frac{dc}{c} = \frac{\bar{M}_M\omega^2 r(1-\bar{v}\rho)}{RT}dr \qquad ...(58)$$

Integrating Eq. 58, $$\int_{c_1}^{c_2}\frac{dc}{c} = \frac{\bar{M}_M\omega^2(1-\bar{v}\rho)}{RT}\int_{r_1}^{r_2} r\,dr \qquad ...(59)$$

or $$\ln\frac{c_2}{c_1} = \frac{\bar{M}_M\omega^2(1-\bar{v}\rho)}{2RT}(r_2^2 - r_1^2) \qquad ...(60)$$

which can be rearranged to give

$$\bar{M}_M = \frac{2RT\ln(c_2/c_1)}{\omega^2(1-\bar{v}\rho)(r_2^2 - r_1^2)} \qquad ...(61)$$

where ω is the angular velocity of the rotor (in radians s^{-1}) ; ρ is the density of the solution; c_1 is the concentration at distance r_1 and c_2 is the concentration at distance r_2 from the axis. The concentration ratio (c_2/c_1) is determined by photometric measurement. From Eq. 61, we see that a plot of ln c versus r^2 should be linear with slope equal to $\bar{M}_M\omega^2(1-\bar{v}\rho)/2RT$. Thus, from the measurement of slope, $\bar{M}_M$ can be calculated. Unlike the sedimentation velocity method, this method does not require prior knowledge of the shape of the macromolecule or its diffusion coefficient. Hence, it is one of the best methods for determination of molar masses of polymers. However, the sedimentation equilibrium method requires a long time (upto several days or weeks) for completion.

4. Light Scattering

When a beam of light is passed through a colloidal solution, it suffers scattering. This phenomenon, called **Tyndall effect**, was observed by Tyndall in 1871. John William Strutt (Lord Rayleigh) gave a theory of the scattering of light by isotropic particles with dimensions less than one-tenth of the wave length of the light. He found that the ratio of the intensity I_θ, scattered at an angle θ from the direction of the transmitted beam, to the the intensity I_0 of the incident unpolarized,

monochromatic light, is given by

$$\frac{I_\theta}{I_0} = \frac{8\pi^4 a\alpha^2}{\lambda^4 r^2}(1+\cos^2\theta) \qquad ...(62)$$

where r is the distance of the observer from the sample, a is the number of scattering particles per unit volume and α is the electrical polarizability of the particle. Notice that in Rayleigh equation, the *scattered intensity is proportional to the inverse fourth power of wave length*. Thus, blue light is scattered much more than the red light. This accounts for the blue colour of the sky when viewed in any direction except towards the sun. The existence of polarizability, α, in Rayleigh equation arises from the fact that the incident light induces vibrating dipoles in the particle which, in turn, act as light sources and radiate light in all directions. The more polarizable a particle, the greater is the magnitude of the vibrating (oscillating) dipoles.

It is customary to use the refractive index n of the scattering particles as a measure of their polarizability. It is known from optics that specific refraction, *i.e.*, refraction per unit volume, is given by

$$\frac{n^2-1}{n^2+2} = \frac{4}{3}\pi a\alpha \qquad ...(63)$$

Assuming that $n \approx 1$ so that $n^2 + 2 \approx 3$, this equation reduces to

$$\alpha = \frac{n^2-1}{4\pi a} \qquad ...(64)$$

In the case of a solution we are interested in knowing the difference between the polarizability α of the solution and the polarizability α_0 of the solvent so that

$$\alpha - \alpha_0 = \frac{n^2 - n_0^2}{4\pi a} \qquad ...(65)$$

where the subscript zero denotes the solvent. For a solution having concentration c, the refractive index can be written as a Taylor's series, *viz.*,

$$n = n_0 + c(dn/dc) + \cdots\cdots \qquad ...(66)$$

where n_0 is the refractive index when the concentration c (in mass per unit volume) is zero.

Squaring both sides of this equation, we get

$$n^2 = n_0^2 + 2n_0 c\frac{dn}{dc} + c^2\left(\frac{dn}{dc}\right)^2 + \cdots\cdots \qquad ...(67)$$

The last term, being small, can be neglected, giving

$$n^2 - n_0^2 = 2n_0 c\frac{dn}{dc} \qquad ...(68)$$

Since the light scattering method yields the mass-average molar mass, hence a may be written as $cN_A/\overline{M}_M$, Combining Eqs. 65 and 68 and assuming that the polarizability of the solvent, α_0, is negligible, we obtain

$$\alpha = \frac{n_0(dn/dc)\overline{M}_M}{2\pi N_A} \qquad ...(69)$$

Squaring both sides of this equation and substituting for α^2 in the Rayleigh equation 62, we obtain

$$\frac{I_\theta}{I_0} = \left(\frac{2\pi^2 n_0^2 (dn/dc)^2}{N_A\lambda^4}\right)\left(\frac{1+\cos^2\theta}{r^2}\right)\overline{M}_M c \qquad ...(70)$$

which may be rewritten as, $R_\theta = K\overline{M}_M c$ ...(71)

where $R_\theta = \left(\frac{I_\theta}{I_0}\right)\left(\frac{r^2}{1+\cos^2\theta}\right)$ ...(72)

and $K = \frac{2\pi^2 n_0^2 (dn/dc)^2}{N_A\lambda^4}$ ...(73)

R_θ is called **Rayleigh ratio** ; it represents the intensity ratio corrected for the geometry of the system. K is called the **optical constant;** it contains the wave length of the light and information about the refractive index. R_θ is independent of the value of θ. Eq. 71 can be used to calculate the molar mass of the polymer. Light-scattering measurements give mass-average molar mass, as already stated. Lord Rayleigh (1842–1919), the versatile British physicist, was awarded the 1904 Physics Nobel Prize for his contributions to mathematical physics and the discovery of argon in the atmosphere.

For non-ideal polymer solutions where there are interactions between the polymer molecules, Einstein and Debye showed independently that if the solute is uniformly distributed throughout the solution, no light is scattered by the solution because light scattered by one particle will interfere destructively with light scattered by the neighbouring particle. Random Brownian motion causes fluctuations in concentration, the extent of fluctuations is inversely proportional to the osmotic pressure developed by the concentration difference. It is found that

$$\frac{Kc}{R_\theta} = \frac{1}{RT}\frac{d\Pi}{dc} \qquad ...(74)$$

where Π is the osmotic pressure. It may be recalled that for an ideal solution, $\Pi = cRT/\overline{M}_M$. For a non-ideal solution,

$$\frac{\Pi}{c} = RT\left(\frac{1}{M_M} + Bc\right) \qquad ...(75)$$

where B is the second virial coefficient.

From Eqs. 73 and 74, $\frac{Kc}{R_\theta} = \frac{1}{M_M} + 2Bc$ ...(76)

A graph of Kc/R_θ *versus* c gives a straight line with slope $= 2B$ and intercept $= 1/\overline{M}_M$. This permits determination of $\overline{M}_M$, the mass-average molar mass of the polymer.

We shall now consider the case *when the dimensions of the macromolecules are no longer small compared with the wave length of light*. If the dimensions of the macromolecules are comparable with the wave length of light, there occurs interference between light scattered from different parts of the same macromolecule. It is customary to define a quantity $P(\theta)$, called the **particle scattering factor,** as the ratio of the intensity of light scattered at an angle θ to the intensity which would be observed if the polymer particle had the same molar mass but had small dimensions compared with the wave length of light. This factor depends upon the shape of the polymer particle which is determined by the so-called **radius of gyration,** R_g (defined later in this chapter). Macromolecules generally behave as *spheres, rods* and *coils* in solution and R_g is different for different shapes. Omitting details, suffice it to mention that $P(\theta)$ is plotted as a function of θ. For low values of θ, the function $P(\theta)$ is independent of the shape of the particles and it is found that

$$P(\theta) \approx 1 - \left(\frac{1}{3}\right)s^2 R_g^2 \qquad ...(77)$$

where $s = (4\pi/\lambda)\sin(\theta/2)$.

From Eq. 77, R_g can be easily determined.

The value of R_g obtained as above is **incorporated in the Zimm equation,** *viz.*,

$$\frac{Kc}{R_\theta} = \frac{1}{M_M}\left[1 + 2Bc + \left(\frac{1}{3}\right)s^2R_g^2\right] \quad ...(78)$$

and the quantity Kc/R_θ is plotted against ($\sin^2 \theta/2 + Kc$). Here K is the **scattering constant** which depends upon the refractive index of the solution; $\sin^2(\theta/2)$ is proportional to s^2. The constant is so chosen as to make the data points spread **conveniently** over the graph. The experimental light-scattering data are plotted over a wide **range** of concentration c and angles θ. Lines are drawn through points at constant angle and extrapolated to zero concentration. Also, lines are drawn through points at constant concentration and extrapolated to zero angle. The two sets of limiting values are then extrapolated to common intercept at zero value of the abscissa from where we get the value of $1/\overline{M}_M$. The by of graphical plot obtained is **called the Zimm plot.** A typical Zimm plot for the light scattering by collagen at 15°C is shown in **Fig. 2.** The molar mass, $\overline{M}_M$, determined from the plot is 310,000 g mol^{-1}.

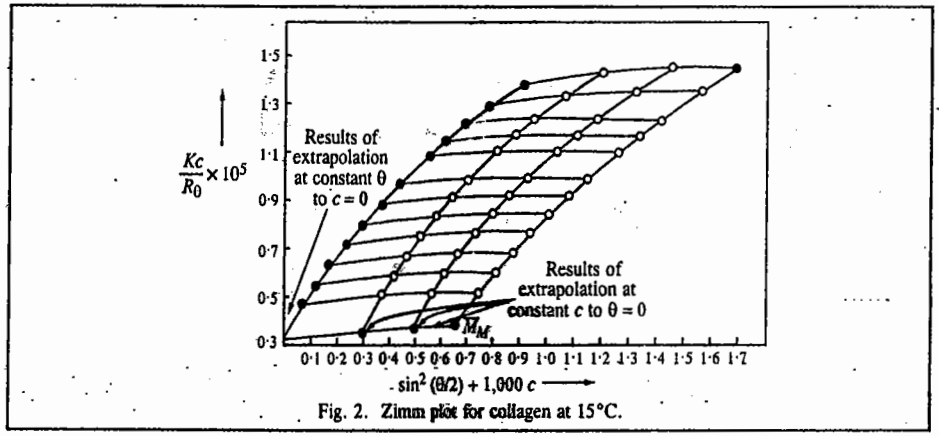

Fig. 2. **Zimm plot for collagen at 15°C.**

It may be mentioned once again that light **scattering** gives mass-average molar mass, the reason being that the intensity of light scattering is greater for larger particles so that the average is weighted more heavily in their favour.

Turbidity. The scattering from polymer solutions can also help in the determination of a quantity called **turbidity** of the solution. The method is similar to that of measuring the absorbance of a solution in a Beer's law cell. The intensity I of the scattered light is measured after it is passed through a dilute solution of the polymer.

Mathematically, $I = I_0 e^{-\tau x}$ ...(79)

where I_0 is the intensity of the incident light, x is the path length and τ is the turbidity.

It can be shown theoretically that the turbidity is given by

$$\tau = (16/3)\pi K\overline{M}_M c \quad ...(80)$$

where K is the *optical constant* defined by Eq. 73 and c is the concentration of the polymer in terms of *mass per unit volume, i.e.,* $c = n\overline{M}_M/V$. (Note that c is *not molar concentration* here). Also, from Eq. 71,

$$R_\theta = K\overline{M}_M c \quad ...(81)$$

Hence, $\tau = (16\pi/3)R_\theta$ ...(82)

Thus, from a measurement of R_θ, we can **calculate** τ, or, conversely, from a measurement of τ, R_θ can be calculated. Since the size of the polymer particle may be comparable to that of the wave length of light, we can use a virial expression of the type :

$$\frac{c}{\tau} = \left(\frac{c}{\tau}\right)_0\left(1 + 2Bc + (3/4)C^2c^2 + ...\right) \quad ...(83)$$

where B, C, are the second and third virial coefficients, respectively. The value of τ is measured as a function of c and c/τ is plotted as a function of c. The intercept at $c=0$ yields, vide Eq. 80, the mass-average molar mass, $\overline{M}_M$:

$$\left(\frac{c}{\tau}\right)_0 = \frac{3}{16\pi K\overline{M}_M} \quad ...(84)$$

The apparatus for turbidity measurements is **available** commercially.

DIFFUSION

The diffusion of particles through a solution is an important phenomenon. The diffusion of a substance across a plane perpendicular to the direction of motion is given by **Fick's first law of diffusion,** *viz.*,

$$J = -D(dc/dx) \quad ...(85)$$

where $J = dm/dt$ is the amount of mass diffusing across a plane of unit area per unit time, D is the diffusion coefficient and dc/dx, the concentration gradient, is the change in concentration (expressed in mass per unit volume) per unit distance, across the plane.

The diffusion of particles through the solution is due to the *decrease* in free energy. The driving force F for diffusion is given by

$$F = -d\mu/dx \quad ...(86)$$

where μ is the chemical potential of the solute.

Since, *per molecule,* $\mu = \mu^0 + (RT/N_A)\ln c$, hence ...(87)

$$F = -\frac{RT}{N_A}\frac{d(\ln c)}{dx} = -\frac{RT}{N_A c}\left(\frac{dc}{dx}\right) \quad ...(88)$$

The diffusion of the solute in the solution is *opposed* by the fricitional drag due to the solvent given by Stokes's equation, *viz.*,

$$F = 6\pi\eta rv = 6\pi\eta r\frac{dx}{dt} \quad ...(89)$$

where v is the velocity of the particle of radius r through the solution, the particle being assumed to be spherical. Since these two forces must be equal, hence

$$6\pi\eta r\left(\frac{dx}{dt}\right) = -\frac{RT}{N_A c}\left(\frac{dc}{dx}\right) \quad ...(90)$$

or $$c\left(\frac{dx}{dt}\right) = -\frac{RT}{6\pi\eta rN_A}\left(\frac{dc}{dx}\right) \quad ...(91)$$

But, $c(dx/dt) = dm/dt$ which means that all the molecules with total mass m at a distance dx from

the boundary and travelling with a velocity dx/dt will cross the boundary in time dt. Hence,

$$\frac{dm}{dt} = -\frac{RT}{6\pi\eta r N_A}\left(\frac{dc}{dx}\right) \quad \ldots(92)$$

Comparing Eq. 92 with Eq. 85, we find that

$$D = \frac{RT}{6\pi\eta r N_A} = \frac{kT}{6\pi\eta r} = \frac{kT}{f} \quad \ldots(93)$$

The quantity f ($= 6\pi\eta r$) is called the **frictional coefficient** of the particle, as already stated (Eq. 42). Eq. 93 shows that the diffusion coefficient of a particle is inversely proportional to its frictional coefficient at a given temperature.

Eq. 93 is known as the **Stokes–Einstein equation.** It offers a good physical interpretation of the diffusion coefficient since it defines D as the ratio of the thermal energy of the solute molecule, kT and the frictional resistance to its diffusion (f). It is, in fact, the ratio of these two opposing quantities that determines how easily the solute molecules would diffuse through a solvent. From measurements of η and D, the radius of the solute particles can be determined. Since, however, the macromolecules are not exactly spherical, the results give only the approximate size of the molecules. Also, solute molecules are solvated and while moving through the solution, will tend to carry along the solvent layer. Nevertheless, when diffusion measurements are coupled with the sedimentation experiments, they give fairly reliable molar masses of the polymers.

Root Mean Square Distance. In experiments on diffusion we are also interested in the distance travelled by a solute molecule from its place of origin in a given time t. The *average distance*, $< x >$, travelled by a diffusing molecule is, of course, zero, since in the case of diffusion occurring in one direction, the molecule moves randomly in an upredictable manner. However, the *root mean square distance*, $< x^2 >^{1/2}$, is not zero. It has been shown that

$$< x^2 >^{1/2} = (2Dt)^{1/2} \quad \ldots(94)$$

Eq. 94 is known as the **Einstein–Smoluchowski equation.**

Example 10. The diffusion coefficient of myoglobin in water at 25°C is $0{\cdot}113\times10^{-9}$ m^2 s^{-1}. If the coefficient of viscosity of water at this temperature is 1 cP (*i.e.*, centipoise), calculate the radius of the myoglobin molecule.

Solution : 1P (*i.e.*, Poise) = 0·1 kg m^{-1} s^{-1}

$$\eta = 1 \text{ cP} = 1\times10^{-2} \text{ P} = 1\times10^{-3} \text{ kg m}^{-1} \text{ s}^{-1}$$

Since from Eq. 93, $D = kT/(6\pi\eta r)$, hence

$$r = \frac{kT}{6\pi\eta D} = \frac{(1{\cdot}38\times10^{-23} \text{ J K}^{-1})(298 \text{ K})}{6(3{\cdot}1416)(1\times10^{-3} \text{ kg m}^{-1} \text{ s}^{-1})(0{\cdot}113\times10^{-9} \text{ m}^2 \text{ s}^{-1})}$$

$$= 19{\cdot}1\times10^{-10} \text{ m} = 1{\cdot}91 \text{ nm} = 1{,}910 \text{ pm} \qquad (\text{J} = \text{kg m}^2 \text{ s}^{-2})$$

Example 11. Calculate the time required for glucose molecule to diffuse through a distance of 10,000 Å. The diffusion coefficient of glucose is $0{\cdot}462\times10^{-9}$ m^2 s^{-1}.

Solution : x = 10,000 Å = (10,000 Å) (1×10^{-10} m/Å) = 1×10^{-6} m

According to the Einstein–Smoluchowski equation (Eq. 94).

$$< x^2 >^{1/2} = (2Dt)^{1/2} \text{ so that } < x^2 > = 2Dt$$

$$\therefore \quad t = \frac{< x^2 >}{2D} = \frac{(1\times10^{-6} \text{m})^2}{2\times(0{\cdot}462\times10^{-9} \text{ m}^2 \text{ s}^{-1})} = 1{\cdot}08\times10^{-9} \text{ s}$$

Example 12. The diffusion coefficient of ribonuclease is $1{\cdot}1\times10^{-6}$ cm^2 s^{-1} at 20° C. Calculate its frictional coefficient.

Solution :

$$D = kT/f \quad \ldots(\text{Eq. } 93)$$

$$\therefore \quad f = \frac{kT}{D} = \frac{(1{\cdot}38\times10^{-23} \text{ J K}^{-1})(293 \text{ K})}{1{\cdot}1\times10^{-10} \text{ m}^2 \text{ s}^{-1}}$$

$$= 3{\cdot}67\times10^{-8} \text{ J m}^{-2} \text{ s} = 3{\cdot}67\times10^{-11} \text{ kg s}^{-1} \qquad (\text{J} = \text{kg m}^2 \text{ s}^{-2})$$

Example 13. The diffusion coefficient of insulin at 25°C is 15×10^{-11} m^2 s^{-1}. If the coefficient of viscosity of water at 25°C is 0·000891 Pa s, estimate the radius of the insulin molecule.

Solution : 1 Poise = 0·1 Pa s = 0·1 kg m^{-1} s^{-1}

$$\eta = 0{\cdot}000891 \text{ Pa s} = 0{\cdot}000891 \text{ kg m}^{-1} \text{ s}^{-1}$$

$$= 0{\cdot}000891 \text{ J m}^{-3} \text{ s} \qquad (\text{J} = \text{kg m}^2 \text{ s}^{-2})$$

From Eq. 93,

$$r = \frac{kT}{6\pi\eta D} = \frac{(1{\cdot}38\times10^{-28} \text{ J K}^{-1})(298 \text{ K})}{6(3{\cdot}1416)(15\times10^{-11} \text{ m}^2 \text{ s}^{-1})(8{\cdot}91\times10^{-4} \text{ J m}^{-3} \text{ s})}$$

$$= 1{\cdot}632\times10^{-9} \text{ m} = 1632 \text{ pm}$$

Example 14. At 25°C, the density of glucose is 1·55 g cm^{-3} ; its diffusion coefficient is $6{\cdot}81\times10^{-6}$ cm^2 s^{-1} and the coefficient of viscosity of water is $8{\cdot}937\times10^{-3}$ Poise. Assuming that the glucose molecule is spherical, estimate its molar mass.

Solution :

$$\rho = 1{\cdot}55 \text{ g cm}^{-3} = 1{\cdot}55\times10^3 \text{ kg m}^{-3}$$

$$D = 6{\cdot}81\times10^{-6} \text{ cm}^2 \text{ s}^{-1} = 6{\cdot}81\times10^{-10} \text{ m}^2 \text{ s}^{-1}$$

$$\eta = 8{\cdot}937\times10^{-3}\text{P} = 8{\cdot}937\times10^{-4} \text{ kg m}^{-1} \text{ s}^{-1}$$

Hence, from the Stokes–Einstein equation (Eq. 93),

$$r = \frac{kT}{6\pi\eta D} = \frac{(1{\cdot}38\times10^{-23} \text{ J K}^{-1})(298\text{K})}{(6\pi)(8{\cdot}937\times10^{-4} \text{ kg m}^{-1} \text{s}^{-1})(6{\cdot}81\times10^{-10} \text{ m}^{-2} \text{ s}^{-1})}$$

$$= 3{\cdot}59\times10^{-10} \text{ J kg}^{-1} \text{ m}^{-1} \text{ s}^2 = 3{\cdot}59\times10^{-10} \text{ m} \qquad (\text{J} = \text{kg m}^2 \text{ s}^{-2})$$

Volume of the glucose molecule is given by

$$V = (4/3)\pi r^3 = (4/3)(\pi)(3{\cdot}59\times10^{-10} \text{ m})^3 = 1{\cdot}94\times10^{-28} \text{ m}^3$$

so that its mass is given by

$$m = V\rho = (1{\cdot}94\times10^{-28} \text{ m}^3)(1{\cdot}55\times10^3 \text{ kg m}^{-3})$$

$$= 3{\cdot}01\times10^{-25} \text{ kg} = 3{\cdot}01\times10^{-22} \text{ g}$$

Hence, the molar mass of glucose is given by

$$M = N_A m = (6{\cdot}022\times10^{23} \text{ mol}^{-1})(3{\cdot}01\times10^{-22} \text{ g}) = 181{\cdot}3 \text{ g mol}^{-1}$$

This compares favourably with the actual value 180·2.

It may be mentioned here that if f is the experimental value of frictional coefficient as obtained from diffusion measurement and f_0 is the frictional coefficient of the particle assuming that it behaves as a perfect Stokes' law sphere, then the ratio f/f_0 is termed the **frictional ratio** of the molecule. If frictional ratio is close to unity, the molecule has a *nearly spherical shape* but if this value is greater than unity, the molecule has a **rod-like shape.** A knowledge of the frictional ratio is very useful in ascertaining the shape of biomolecules.

Example 15. At 20°C, the diffusion coefficient, the molar mass and specific volume of haemoglobin are $6{\cdot}9\times10^{-11}$ m^2 s^{-1}, 64,500 g mol^{-1} and 0·75 cm^3 g^{-1}, respectively. Calculate its frictional ratio and comment on your result. The coefficient of viscosity of water at the given temperature is 1·005 cP.

Solution : Since from Eq. 93, $D = kT/f$

$$\therefore \quad f = \frac{kT}{D} = \frac{(1{\cdot}38\times10^{-23} \text{ J K}^{-1})(293 \text{ K})}{6{\cdot}9\times10^{-11} \text{ m}^2 \text{ s}^{-1}}$$

$= 5{\cdot}86\times10^{-11}$ kg s^{-1} (J = kg m^2 s^{-2})

If we assume that the molecule is spherical, then $f_0=6\pi\eta r_0$. Let us first calculate the radius r_0 of haemoglobin molecule assuming that it is spherical. Since M=64,500 g mol^{-1} and v=0·75 cm^3 g^{-1} =0·75×10^{-6} m^3 g^{-1}, hence

Molar volume, V_m = (64,500 g mol^{-1}) (0·75×10^{-6} m^3 g^{-1}) = 0·048 m^3 mol^{-1}

$$\therefore \quad \text{Volume per molecule,} \quad v_m = \frac{V_m}{N_A} = \frac{0{\cdot}048\,\text{m}^3\,\text{mol}^{-1}}{6{\cdot}022\times10^{23}\,\text{mol}^{-1}} = 7{\cdot}97\times10^{-26}\,\text{m}^3$$

If the molecule is spherical, $v_m = (4/3)\pi r_0^3$

$$\therefore \quad r_0 = \left(\frac{7{\cdot}97\times10^{-26}\,\text{m}^3}{(4/3)\pi}\right)^{1/3} = 2{\cdot}670\times10^{-9}\,\text{m}$$

Hence, $f_0 = 6\pi\eta r_0 = (6)\,(3{\cdot}1416)\,(1{\cdot}005\times10^{-3}$ kg m^{-1} s^{-1}) (2·670×10^{-9} m)

$= 5{\cdot}06\times10^{-11}$ kg s^{-1}

$$\therefore \quad \text{The frictional ratio,} \quad \frac{f}{f_0} = \frac{5{\cdot}86\times10^{-11}\,\text{kg s}^{-1}}{5{\cdot}06\times10^{-11}\,\text{kg s}^{-1}} = 1{\cdot}16$$

Since f/f_0 is close to unity, the haemoglobin molecule **behaves as a sphere** in aqueous solution.

Conformations and Configurations of Macromolecules in Solution. It is convenient to speak of *configurations* and *conformations* of macromolecules in solution. The term **configuration** *implies aspects of structure that can be changed only by breaking bonds and re-forming new ones* while the term **conformation of a polymer chain** refers to the *spatial arrangement of the different parts of the macromolecule*. Thus, whereas the chain —A—B—C— has a configuration different from —A—C—B—, one conformation of a chain can be transformed into another simply by rotating one part of the chain round the bond joining it to another part. It is possible to determine the features of a *randomly coiled polymer chain* in solution.

The simplest model of a randomly coiled polymer chain is **freely-jointed chain** where any bond is free to make any angle with respect to the preceding one (Fig. 3). This model is the exact analogue of the three-dimenstional random walk model in which each bond represents a step taken in a random direction. The **contour length,** R_c, is the length of the macromolecule measured along its backbone from atom to atom (the maximum distance that the random walker could walk). For a polymer of N monomer units each of length l, the contour length $R_c=Nl$. It is known that the probability of the ends of the chain (*i.e.*, the net distance travelled by a random walker) lying in the range R to $R+dR$ is given by $f(R)dR$ where

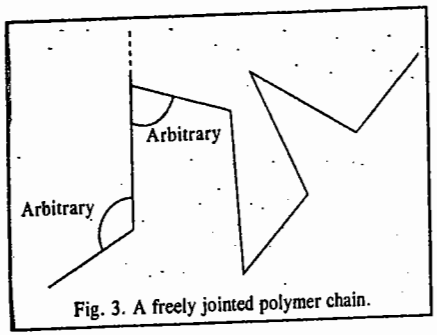

Fig. 3. A freely jointed polymer chain.

$$f(R) = \left(\frac{a}{\pi^{1/2}}\right)^3 4\pi R^2 e^{-a^2R^2}; \quad a^2 = \frac{3}{2Nl^2} \qquad ...(95)$$

where N is the number of bonds (*viz.*, the number of paces) and l is the bond length (*viz.*, the length of each pace).

Using the function defined in Eq. 95 we can calculate three important quantities, *viz.*, the root mean square end-to-end distance of the chain, R_{rms}; the mean end-to-end distance of the chain, $\overline{R}$

and the most probable end-to-end distance, R_{mp}, as illustrated below :

(i) $$R_{rms} = \left(\int_0^\infty R^2 f(R)dR\right)^{1/2} \qquad ...(96)$$

We know that $$\int_0^\infty R^2 f(R)dR = \left(\frac{a}{\sqrt{\pi}}\right)^2 (4\pi)\int_0^\infty R^4 e^{-a^2R^2}dR \qquad ...(97)$$

The integral on the right hand side can be evaluated using the standard integral,

$$\int_0^\infty x^{2n} e^{-ax^2}dx = \frac{(1)(3)(5)\cdots(2n-1)}{2^{n+1}a^n}\left(\frac{\pi}{a}\right)^{1/2} \qquad ...(98)$$

giving $$\int_0^\infty R^4 e^{-a^2R^2}dR = \frac{(1)(3)}{2^3(a^2)^2}\left(\frac{\pi}{a^2}\right)^{1/2} = \frac{3\pi^{1/2}}{8a^5} \qquad ...(99)$$

$$\therefore \quad \int_0^\infty R^2 f(R)dR = \left(\frac{a}{\pi^{1/2}}\right)^3 (4\pi)\frac{3\pi^{1/2}}{8a^5} = \frac{3}{2a^2} = Nl^2 \qquad ...(100)$$

Thus, $$R_{rms} = N^{1/2}l \qquad ...(101)$$

(ii) $$\overline{R} = \int_0^\infty R f(R)dR = \left(\frac{a}{\pi^{1/2}}\right)^3 (4\pi)\int_0^\infty R^3 e^{-a^2R^2}dR \qquad ...(102)$$

Using the standard integral,

$$\int_0^\infty x^3 e^{-ax^2}dx = \frac{1}{2a^2}, \qquad ...(103)$$

we obtain $$\int_0^\infty R^3 e^{-a^2R^2}dR = \frac{1}{2(a^2)^2} = \frac{1}{2a^4} \qquad ...(104)$$

so that $$\overline{R} = \left(\frac{a}{\sqrt{\pi}}\right)^3 (4\pi)\left(\frac{1}{2a^4}\right)$$

$$= \frac{2}{a\pi} = \left(\frac{8}{3\pi}\right)^{1/2} N^{1/2}l \qquad ...(105)$$

(iii) To obtain R_{mp}, we differentiate $f(R)$ with respect to R and set the derivative equal to zero.

$$\frac{df(R)}{dR} = \left(\frac{a}{\pi^{1/2}}\right)^3 (4\pi)(2R - 2a^2R^3)e^{-a^2R^2} = 0 \qquad ...(106)$$

$$R_{mp} = (2/3)^{1/2} N^{1/2} l \qquad ...(107)$$

From Eq. 101 we see that root mean square end-to-end distance for a completely flexible polymer chain molecule is proportional to the square root of the number of bonds, the proportionality factor being the bond length l. However, for actual polymer molecules, R_{rms} is greater. This is due

to the following reasons :

(i) There is a fixed bond angle θ between the bonds forming the backbone of the chain.

(ii) There are restrictions to free rotations about bonds

(iii) Chain segments occupy volume and this volume is excluded to other chain segments.

Example 16. Evaluate R_{rms}, $\overline{R}$ and R_{mp} for a freely jointed randomly coiled polymer chain if the number of bonds is 4,000 and the bond distance is 154 pm.

Solution : $N = 4{,}000$; $l = 154$ pm $= 154\times10^{-12}$ m

$$R_{rms} = N^{1/2}\, l = (4000)^{1/2}\,(154\times10^{-12}\text{ m}) = 9{\cdot}74\times10^{-9}\text{ m} = \mathbf{9{\cdot}74\text{ nm}}$$

$$\overline{R} = \left(\frac{8}{3\pi}\right)^{1/2} N^{1/2} l = \left(\frac{8}{3\pi}\right)^{1/2} (4000)^{1/2}(154\times10^{-12}\text{ m})$$

$$= 8{\cdot}97\times10^{-9}\text{ m} = \mathbf{8{\cdot}97\text{ nm}}$$

$$R_{mp} = \left(\frac{2}{3}\right)^{1/2} N^{1/2} l = \left(\frac{2}{3}\right)^{T/2} (4000)^{1/2}(154\times10^{-12})\text{m} = \mathbf{7{\cdot}95\text{ nm}}$$

Another quantity of interest is the so-called **radius of gyration,** defined as the *average root mean square distance* of the atoms from the centre of mass. It is given by the equation

$$R_g = \frac{1}{N}\left(\frac{1}{2}\sum_{i,j} R_{i,j}^2\right)^{1/2} \qquad ...(108)$$

where R_i is the distance from the centre of mass of each mass element m_i in the polymer molecule. Notice that R_g has the dimensions of length and is roughly the radius of the polymer molecule. If ρ is the density of a spherical polymer molecule of radius a, then, we have

$$R_g = \left(\frac{\int_0^a \rho\times 4\pi R^2 dR}{\int_0^\infty \rho\times 4\pi R^2 dR}\right)^{1/2} = \left[\frac{3a^5}{5a^3}\right]^{1/2} = \left(\frac{3}{5}\right)^{1/2} a = 0{\cdot}775\,a \qquad ...(109)$$

For a linear coil polymer chain, it is found that

$$R_g = \frac{1}{\sqrt{6}} R_{rms} \qquad ...(110)$$

Example 17.—Calculate R_{rms} and R_g for a linear polymeric chain containing 250 monomeric units, each being 45 Å long.

Solution : According to Eq. 101,

$$R_{rms} = N^{1/2}\, l = (250)^{1/2}\times 45\text{ Å} = \mathbf{711{\cdot}5\text{ Å}}$$

According to Eq. 110, $$R_g = \frac{1}{\sqrt{6}} R_{rms} = \frac{711{\cdot}5\text{ Å}}{\sqrt{6}} = \mathbf{290{\cdot}4\text{ Å}}$$

It is pertinent to remark here that a **constrained chain** is a better approximation to a random coil than a *freely jointed chain* considered above. In a constrained chain, the individual bonds are constrained in a random cone of angle θ but the resultant lies in a random direction.

Theoretical calculations show that the values of R_{rms}, $\overline{R}$, etc., obtained above are to be multiplied by a factor $F = (1 - \cos\theta)/(1 + \cos\theta)]^{1/2}$. For tetrahedral bonds, for example, $\theta = 109{\cdot}5°$

so that $\cos\theta = -1/3$ and $F = \sqrt{2}$. Hence,

$$R_{rms} = (2N)^{1/2} l \text{ and } R_g = (N/3)^{1/2} l$$

It may be mentioned that the dissolution of a polymer in a solvent is often a very slow process; this is particularly the case with the highly crosslinked network polymers. As the solvent permeates the polymer network, considerable swelling occurs. In some cases, after the initial swelling, the polymer dissolves in the solvent after a considerable period of time. In polymer solution chemistry, we often speak of **'good solvents'** and **'poor solvents'**. In a good solvent, there is a stronger interaction between the solvent and the polymer than between the solvent and the solvent or between the various segments of the polymer. On the other hand, in a poor solvent, there is stronger interaction between the various segments of the polymer than between the polymer and the solvent. Thus, while in a good solvent, the polymer stretches out, *i.e., uncoils,* in solution, in a poor solvent the polymer *coils* upon itself.

Let us remark in passing that the effectiveness of a solvent can also be measured by the value of the second virial coefficient, B. For an ideal solution of two components 1 and 2 (1 designating the solvent and 2 the solute),

$$B_{ideal} = \overline{V}_1^{\circ}/2(M_2)^2 \qquad ...(111)$$

Assume that $M_2 = 10^4$ g mol^{-1}. Since $\overline{V}_1^{\circ}$ for water is 18 cm^3 mol^{-1}, hence, $B_{ideal} = 9\times10^{-8}$ cm^3 mol g^{-2}. Solvents for which $B > B_{ideal}$ are called **good solvents** for that polymer and solvents for which $B \le 0$ are called **poor solvents.** For good solvents, B lies in the range of 10^{-5} to 10^{-3} which is much larger than the ideal value. The polymer can be precipitated relatively easily from poor solvents.

MISCELLANEOUS SOLVED EXAMPLES

Example 18. A protein sample consists of an equimolar mixture of haemoglobin (M=15·5 kg mol^{-1}), ribonuclease (M = 13·7 kg mol^{-1}) and myoglobin (M = 17·2 kg mol^{-1}). Calculate the number-average and mass-average masses. Which is greater ?

Solution : According to Eq. 1,

$$\overline{M}_N = \frac{[(0{\cdot}333\times15{\cdot}5) + (0{\cdot}333\times13{\cdot}7) + (0{\cdot}333\times17{\cdot}2)]\text{ kg mol}^{-1}}{0{\cdot}333 + 0{\cdot}333 + 0{\cdot}333} = \mathbf{15{\cdot}5\text{ kg mol}^{-1}}$$

$$= \mathbf{15500\text{ g mol}^{-1}}$$

According to Eq. 2,

$$\overline{M}_M = \frac{0{\cdot}333\times(15{\cdot}5)^2 + 0{\cdot}333\times(13{\cdot}7)^2 + 0{\cdot}333\times(17{\cdot}2)^2}{(0{\cdot}333\times15{\cdot}5) + (0{\cdot}333\times13{\cdot}7) + (0{\cdot}333\times17{\cdot}2)} = \mathbf{15{\cdot}6\text{ kg mol}^{-1}}$$

Thus, $\overline{M}_M > \overline{M}_N$.

Example 19. Calculate the intrinsic viscosity of polystyrene in toluene from the following relative viscosity data obtained at 25°C :

c (×10^3 kg m^{-3})	0·002	0·004	0·006	0·008	0·010
η_r	1·102	1·208	1·317	1·430	1·548

Also calculate $\overline{M}_{visc}$ if the Mark-Kuhn-Houwink-Sakurada constants are a=0·69 and K=1·7×10^{-3} m^3 kg^{-1}.

Solution : $[\eta] = K(\overline{M}_{visc})^a$ [Mark-Kuhn-Houwink-Sakurada equation]

where $\overline{M}_{visc}$ is the viscosity-average molar mass of the polymer.

Intrinsic viscosity $[\eta]$ = the intercept of the plot of $(\eta_r - 1)/c$ versus c. It is found that

$$[\eta] = \mathbf{50{\cdot}1\times10^{-3}\text{ m}^3\text{ kg}^{-1}}$$

$$\therefore \quad \overline{M}_{visc} = \left(\frac{\eta}{K}\right)^{1/a} = \left[\frac{50{\cdot}1\times10^{-3}\text{ m}^3\text{ kg}^{-1}}{1{\cdot}7\times10^{-3}\text{ m}^3\text{ kg}^{-1}}\right]^{1/0{\cdot}69} = \mathbf{130\text{ kg mol}^{-1}}$$

Example 20. Calculate the vapour pressure lowering, the boiling point elevation and the osmotic pressure of a 1·0 mass percent solution of polystyrene ($\overline{M}_N$ = 50·0 kg mol^{-1}) in toluene (M = 92·15 g mol^{-1}) at 25° C and comment on your result. At 25°C, for toluene K_b = 3·33 K m^{-1} and the vapour pressure of pure toluene is 3760 Pa.

Solution : The mole fraction x_2 of the polymer is given by

$$x_2 = \frac{1\cdot0\text{g}/(50\cdot0\times10^3\text{ g mol}^{-1})}{1\cdot0\text{g}/(50\cdot0\times10^3\text{ g mol}^{-1}) + 99\cdot0\text{ g}/(92\cdot15\text{ g mol}^{-1})} = 1\cdot86\times10^{-5}$$

Assuming that the concentration c of the polymer ≈ molality m,

$$c = \frac{1\cdot00\text{g}/(50\cdot0\times10^3\text{ g mol}^{-1})}{0\cdot099\text{ kg solvent}} = 2\cdot02\times10^{-4}\text{ m}$$

Hence, vapour pressure lowering is given by

$$\Delta p = x_2 p_1^0 = (1\cdot86\times10^{-5})(3750\text{ Pa}) = 6\cdot99\times10^{-2}\text{ Pa}$$

The boiling point elevation is given by

$$\Delta T = K_b m = (3\cdot33\text{ K } m^{-1})\,(2\cdot02\times10^{-4}\ m) = 6\cdot73\times10^{-4}\text{ K}$$

The osmotic pressure is given by $\Pi = cRT$

$$= (2\cdot02\times10^{-4}\text{ mol dm}^{-3})\,(0\cdot082\text{ dm}^3\text{ atm K}^{-1}\text{ mol}^{-1})\,(298\text{ K})\times(1\cdot01\times10^5\text{ Pa atm}^{-1})$$
$$= 5\cdot00\times10^3\text{ Pa}$$

We notice that the vapour pressure lowering, boiling point elevation (and also freezing point depression) are extremely small for polymer solutions and it would be difficult to measure them experimentally. Osmotic pressures are, however, sufficiently large for experimental measurement.

Example 21. In the ultracentrifugation set-up, the relative displacement (r/r_0) of bovine serum albumin was studied as a function of time as follows :

t (s)	700	3580	4540	5020
r/r_0	1·013	1·068	1·087	1·097

If the angular velocity, ω, of the rotor is 6260 s^{-1}, calculate the sedimentation coefficient, S. Use this value of S and the Svedberg equation to calculate the molar mass of the polymer sample. Given : $\bar{v}$ = 7·34×10^{-3} m^3 kg^{-1}, ρ = 9·93×10^2 kg m^{-3}, D = 6·97×10^{-11} m^2 s^{-1} at 25°C.

Solution : We know that $S = \dfrac{dr/dt}{\omega^2 r}$ [Eq. 41]

In terms of relative displacement, we have $S = \dfrac{d(r/r_0)/dt}{\omega^2(r/r_0)}$

Rearranging we get, $\dfrac{d(r/r_0)}{r/r_0} = \omega^2 S dt$

Integrating the above expression, we get $\ln(r/r_0) = \omega^2 St$ + constant which is the equation of a straight line. It can be verified that the plot of $\ln(r/r_0)$ versus t gives a straight line whose slope $= \omega^2 S = 1\cdot84\times10^{-5}$ s^{-1} whence $S = 4\cdot70\times10^{-13}$ s. Substituting this value of S and the given data in the Svedberg equation, it is found that $\overline{M}_M$ = 61·6 kg mol^{-1}.

Example 22. Calculate the molar mass of haemoglobin from the fact that in an equilibrium ultracentrifuge experiment at 20°C, c_2/c_1 = 9·40, r_1 = 5·5 cm and r_2 = 6·5 cm. The ultracentrifuge rotor is operated at 120 rps. $\bar{v}$ = 0·749 cm^3 g^{-1} and ρ = 0·9982 g cm^{-3}.

Solution : $\overline{M}_M = \dfrac{2RT\ln(c_2/c_1)}{\omega^2(1-\bar{v}\rho)(r_2^2 - r_1^2)}$ [Eq. 61]

$$= \frac{2(8\cdot314\text{ J K}^{-1}\text{ mol}^{-1})(293\text{K})\ln(9\cdot40)}{(2\pi\times120\text{ s}^{-1})^2(1-0\cdot749\times0\cdot9982)[\{(0\cdot065)^2-(0\cdot055)^2\}\text{m}^2]}$$
$$= 63\cdot4\text{ kg mol}^{-1} = 63400\text{ g mol}^{-1}$$

Example 23. Calculate the ratio of the equilibrium concentrations of a polymer with $\overline{M}_M$ = 50·0 kg mol^{-1} at a distance of 5·00 cm compared to a distance of 4·00 cm in an ultracentrifuge operating (at 25°C) at 1·0×10^4 min^{-1}. Given $\bar{v}$ = 8·0×10^{-4} m^3 kg^{-1} and ρ = 1·02×10^3 kg m^{-3}.

Solution : $\overline{M}_M = \dfrac{2RT\ln(c_2/c_1)}{\omega^2(1-\bar{v}\rho)(r_2^2 - r_1^2)}$ (Eq. 61)

$$\therefore \quad \ln\left(\frac{c_2}{c_1}\right) = \frac{\overline{M}_M(1-\bar{v}\rho)(r_2^2 - r_1^2)\omega^2}{2RT}$$

ω = 1·0×10^4 min^{-1}/(60 s min^{-1}) (given)

Substituting the relavant data in the above equation, we find that $\ln(c_2/c_1)$ = 1·83 whence c_2/c_1 = 6·2.

Example 24. Use the following data to calculate the osmotic pressure and the second virial coefficient of the solution of collagen at 25°C :

c (kg m^{-3})	2·4	4·1	5·0	5·5	6·4
Π/cRT (10^{-3} mol kg^{-1})	3·7	4·2	4·2	4·2	4·9

Solution : According to the van't Hoff osmotic virial equation

$$\Pi/cRT = \left[\frac{1}{\overline{M}_N} + B_2 c + B_3 c^2 + \cdots\right]$$

where $\overline{M}_N$ is the number-average molar mass. Thus, a plot of Π/cRT versus c will be a straight line with intercept $= 1/\overline{M}_N$ and slope = B_2. If we plot the data, we find that

$$\overline{M}_N = 1/(3\cdot1\times10^{-3}\text{ mol kg}^{-1}) = 320\text{ kg mol}^{-1}$$
$$B_2 = 2\cdot5\times10^{-4}\text{ mol m}^3\text{ kg}^{-2}$$

Kinetics of Polymerization

We shall briefly deal with the kinetics of addition polymerization and condensation polymerization.

a. Kinetics of Addition Polymerization. Consider the catalytic polymerization of a monomer, M, say, CH_2=CHX (X=halogen). The following stages are involved in this process :

(i) The initiator molecule I yields a free radical R :

$$\text{I} \xrightarrow{k_1} \text{R} \quad \cdots$$

The rate of production of the free radical is given by

$$r = k_1[\text{I}] \qquad \ldots(112)$$

2. The free radical R adds to the double bond of the monomer molecule generating new free radicals :

$$\text{CH}_2\text{=CHX} + \text{R} \xrightarrow{k_2} \text{RCH}_2\text{CHX}$$

$$\text{RCH}_2\text{CHX} + \text{CH}_2\text{=CHX} \longrightarrow \text{R—(CH}_2\text{—CHX)}_2\text{, and so on.}$$

The rate of the disappearance of the monomer M is given by

$$-\frac{d[\text{M}]}{dt} = k_2[\text{R}][\text{M}] \qquad \ldots(113)$$

These chain propagation steps are of the **second order** and very rapid.

3. Chain termination is achieved by the recombination of two free radicals, *viz.*,

$$\text{R—(CH}_2\text{—CHX)}_n + \text{(XCH—CH}_2\text{)—R} \xrightarrow{k_3} \text{R—(CH}_2\text{—CHX)}_n\text{—(XCH—CH}_2\text{)}_n\text{—R}$$

Since the free radicals have a very low concentration, we can reasonably assume that their rate of production is equal to their rate of disappearance (*the steady state approximation*) so that

$$k_1[I] = k_3[R]^2 \qquad ...(114)$$

Hence, $$[R] = (k_1/k_3)^{1/2}\,[I]^{1/2} \qquad ...(115)$$

Substituting for [R] into Eq. 113, we obtain

$$-\frac{d[M]}{dt} = k_2\left(\frac{k_1}{k_3}\right)^{1/2}[I]^{1/2}[M] = k[I]^{1/2}[M] \qquad ...(116)$$

We define the **kinetic chain length**, γ, as the ratio of the overall rate to the rate of the initiation step. It can also be defined as the number of repeating chain units in the polymer chain.

$$\gamma = \frac{-d[M]/dt}{r} = \frac{-d[M]/dt}{k_1[I]} \qquad ...(117)$$

Also the probability p for the addition of another monomer to the growing chain radical is given by

$$p = \frac{k_2[M]}{k_2[M] + k_3[R]} = \frac{1}{1 + \dfrac{(k_1k_3)^{1/2}[I]^{1/2}}{k_2[M]}} \qquad ...(118)$$

In vinyl polymerization, p is of the order of 0·999.

b. Kinetics of Condensation Polymerization. Consider the reaction

$$M_m + M_n \longrightarrow M_{m+n}$$

where m, n are integers greater than one.

The monomer M_1 may be removed by reaction with itself and with any other molecule present. The net rate of disappearance of the monomer is given by

$$-\frac{d[M_1]}{dt} = k\{[M_1]^2 + [M_1][M_2] + \cdots\} = k[M_1]\sum_{n=1}^{\infty}[M_n] \qquad ...(119)$$

The net rate of production of the dimer is given by

$$\frac{d[M_2]}{dt} = \frac{1}{2}k[M_1]^2 - k[M_2]\sum_{n=1}^{\infty}[M_n] \qquad ...(120)$$

The first term on the right hand side of Eq. 120 gives the rate of formation of the dimer from two monomers. We can similarly show that the net rate of formation of n-mers, *i.e.*, polymer containing n monomers, is given by

$$\frac{d[M_n]}{dt} = \frac{1}{2}k\sum_{s=1}^{s=n-1}[M_s][M_{n-s}] - k[M_n]\sum_{n=1}^{\infty}[M_n] \qquad ...(121)$$

Adding these equations, we obtain

$$\frac{d\sum_{n=1}^{\infty}[M_n]}{dt} = -\frac{1}{2}k\left\{\sum_{n=1}^{\infty}[M_n]^2\right\} \qquad ...(122)$$

If $[M_1]_0$ is the total concentration of the monomers in the beginning and $\sum_{n=1}^{\infty}[M_n]$ that of all the molecules at time t, the fraction f of the reaction that has occurred at time t is given by

$$f = \left\{[M_n]_0 - \sum_{n=1}^{\infty}[M_n]\right\}\Big/[M_1]_0 \qquad ...(123)$$

Hence, from Eqs. 122 and 123, we obtain

$$df/dt = \tfrac{1}{2}[M_1]_0k(1-f)^2 \qquad ...(124)$$

Integration yields, $$f = \frac{[M_1]_0kt}{2 + [M_1]_0kt} \qquad ...(125)$$

The concentration of the n-mers is given by

$$[M_n] = [M_1]_0f^{n-1}(1-f)^2 \qquad ...(126)$$

Molar Mass Distribution in Step-Growth (Condensation) Polymerization

Consider a linear polymer that might be produced by the condensation of a hydroxy acid HO—$(CH_2)_n$—COOH to produce a polyester. Let the monomer be represented as AB to symbolize the two functional groups. Then, if we consider a polymer

1 2 3

AB—AB—AB—.....

the bond (—) indicates that the end-group B (a COOH group) is attached through an ester linkage to the end-group A (the OH) on another molecule. Next we ask what is the probability that the polymer contains k units ? Let p be the probability that the end-group B is esterified and let us assume that this probability does not depend on how many AB units are attached to the AB unit of interest. Then the probability of an ester linkage at position 1 is p, the probability of an ester linkage at position 2 is also p. The probability that both linkages are present is given by the product of the independent probabilities or p^2. If there are k units in the polymer, there are k–1 ester linkages and the probability is p^{k-1}. However, the probability that end-group B is not linked is $1 - p$. Thus, if the molecule is to terminate after k–1 links, the probability must be $(1 - p)\,p^{k-1}$. This probability must be equal to N_k/N where N_k is the number of molecules that are k units long and N is the total number of molecules. Then, the mole fraction, x_k of k-mers, is given by

$$x_k = \frac{N_k}{N} = (1-p)p^{k-1} = \frac{(1-p)p^k}{p} \qquad ...(127)$$

The mean value of k is given by

$$\langle k\rangle = \frac{\sum_{k=1}^{\infty}kN_k}{N} \qquad ...(128)$$

Substituting the value of N_k from Eq. 127, Eq. 128 becomes

$$\langle k\rangle = (1-p)\sum_{k=1}^{\infty}kp^{k-1} \qquad ...(129)$$

However, we know that

$$\sum_{k=0}^{\infty} p^k = 1 + p + p^2 + p^3 + \ldots = \frac{1}{1-p} \qquad \ldots(130)$$

Differentiating both sides we get

$$\sum_{k=1}^{\infty} k p^{k-1} = (1-p)^{-2} \qquad \ldots(131)$$

Substituting this result in Eq. 129, we obtain

$$\langle k \rangle = \frac{1}{1-p} \qquad \ldots(132)$$

From Eq. 132 we see that the higher the value of p, the probability of the formation of the link, the smaller is the value of $1 - p$ and hence the greater the value of $\langle k \rangle$. For instance, if $\langle k \rangle = 50$, then $p = 1 - 1/50 = 0{\cdot}98$; if $\langle k \rangle = 100$, then $p = 0{\cdot}99$. It is evident that high degree of polymerization will exist only when the probability of linkage is close to unity (Fig. 4). Even with $p = 0{\cdot}90$, $\langle k \rangle$ is only 10.

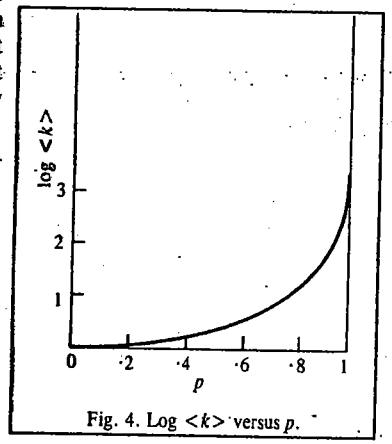

Fig. 4. Log $\langle k \rangle$ versus p.

In order to calculate the total number of monomer units, N_1, present in all the species, we multiply N_k by k. Thus,

$$N_1 = \sum_{k=1}^{\infty} k N_k$$

$$= N \langle k \rangle = \frac{N}{1-p} \qquad \ldots(133)$$

In terms of monomer units present, since $N_k = N p^{k-1}(1-p)$, we have

$$N_k = N_1 p^{k-1}(1-p)^2 \qquad \ldots(134)$$

The molar mass of k-mer is given by

$$M_k = k M_1 + M_e \qquad \ldots(135)$$

where M_1 is the molar mass of the repeating unit and M_e is the excess mass due to the presence of the end groups. When k is large, M_e may be neglected.

The number-average molar mass, $\overline{M}_N$, is defined as

$$\overline{M}_N = \frac{\Sigma N_k M_k}{N} = \frac{\Sigma N_k k M_1 + M_e \Sigma N_k}{N} \qquad \ldots(136)$$

But $\Sigma N_k = N$ and $\Sigma k N_k = \langle k \rangle N$, hence we obtain

$$\overline{M}_N = \langle k \rangle M_1 + M_e = \frac{M_1}{1-p} + M_e \qquad \ldots(137)$$

The total mass of this system is given by

$$\sum_{k=1}^{\infty} \frac{N_k M_k}{N_A} = \frac{N \overline{M}_N}{N_A} = \frac{N_1 (1-p) \overline{M}_N}{N_A} \qquad \ldots(138)$$

so that the *mass fraction* of molecules having k units is given by

$$w_k = \frac{N_k M_k}{\Sigma N_k M_k} = \frac{N_1 p^{k-1}(1-p)^2 (k M_1 + M_e)}{N_1 (1-p) \overline{M}_N} = \frac{p^{k-1}(1-p)^2 (k M_1 + M_e)}{M_1 + (1-p) M_e} \qquad \ldots(139)$$

Neglecting M_e, which is negligible except when $\langle k \rangle$ is very small, we have

$$w_k = k p^{k-1} (1-p)^2 \qquad \ldots(140)$$

Fig. 5 shows the mass fraction distribution as a function of k for several values of p.

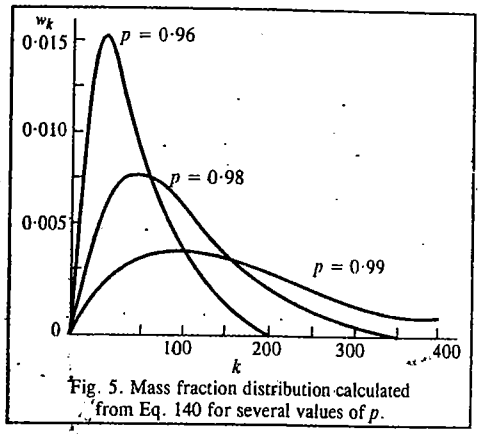

Fig. 5. Mass fraction distribution calculated from Eq. 140 for several values of p.

The mass-average molar mass is defined by

$$\overline{M}_M = \sum_{k=1}^{\infty} w_k M_k \qquad \ldots(141)$$

Using Eq. 140 for w_k, Eq. 135 for M_k and neglecting M_e, we obtain

$$\overline{M}_M = M_1 (1-p)^2 \sum_{k=1}^{\infty} k^2 p^{k-1} \qquad \ldots(142)$$

Eq. 131 can then be written as

$$\Sigma k p^k = p/(1-p)^2 \qquad \ldots(143)$$

Differentiating with respect to p, we get

$$\sum_{k=1}^{\infty} k^2 p^{k-1} = \frac{1+p}{(1-p)^3} \qquad \ldots(144)$$

Substituting this result in the expression for $\overline{M}_M$, we find

$$\overline{M}_M = \frac{(1+p) M_1}{1-p} \qquad \ldots(145)$$

From Eqs. 137 (neglecting M_e) and Eq. 145, we get

$$\frac{\overline{M}_M}{\overline{M}_N} = 1 + p \qquad \ldots(146)$$

Since $p \approx 1$, we conclude that the mass-average molar mass is twice the number-average molar mass.

The molar mass distribution of a polymer can be determined by (1) precipitation (2) gel permeation chromatography and (3) ultracentrifugation. In the precipitation method, we consider a solution of a polymer in a solvent. If a precipitant that decreases polymer's solubility is added, some polymer precipitates out ; the material having the highest molar mass precipitates first. Removal of the precipitated polymer and addition of more precipitant causes another precipitate to be formed. In this way the dissolved polymer is separated into fractions whose molar masses can then be determined. A comparison of the mass fraction *versus* size determined in this manner agrees reasonably well with the hypothesis underlying Eq. 140 : the probability of forming an ester linkage does not depend on how many links have already been formed.

In the method using gel permeation chromatography, a solution of a polymer is forced through a gel that contains a network of pores of various sizes. Smaller molecules diffuse into the network with greater ease than larger molecules. Consequently, the larger molecules pass through the column more quickly than do the smaller ones which become trapped in the network and require more time to become disentangled. This method is considerably more convenient than the classical precipitation method described above.

Electronically Conducting Polymers

Conducting polymers are macromolecules which in the solid state provide pathways for electronic conduction. They provide pathways for electrons (or their counterparts, *positive holes*) to migrate along a polymer chain and jump from chain to chain. This process superficially resembles electronic conduction in metals or metalloid semiconductors. In polymers, the process generally depends on the presence of arrays of 'conjugated', delocalized double bonds, as found in poly(sulphur nitride) or polyacetylene. Doping of such polymers is often required to inject electrons into the delocalized framework or to remove electrons to leave positive holes. Many systems of this type—poly (sulphur nitride), polyacetylene, polyphenylene, poly(phenylene sulphide), polypyrrol, polythiophene, polyaniline, and transition metal-bound polymers—appear to depend as much on the ordered, crystalline nature of the solid state arrangement as on the molecular structure of the polymer. We shall discuss here the following three best-studied conducting polymers.

1. Poly(Sulphur Nitride), $(SN)_x$

This polymer has remarkable properties, including its metallic (gold) appearance and its metal-level electrical conductivity at room temperature. Its conductivity is only slightly lower than that of mercury or of bismuth. The conductivity of $(SN)_x$ is more pronounced along the direction of the polymer chains than at right angles to them. However, when cooled to 0·3K, the material undergoes a change to a superconductor at which there is no resistance to electrical flow (Fig. 6). The superconductivity is anisotropic (*i.e.*, in three dimensions) and probably occurs *between* the chains. The electrical properties can be explained in terms of polymer structure. The packing of chains is illustrated in Fig. 7. Individual chains occupy a *cis-trans* planar conformation, with S—N bond lengths intermediate between those of single and double bonds. This suggests that a delocalized bonding arrangement exists along the chain via delocalized half-filled π-orbitals which would permit the existence of a metallic conduction band. The inter-chain packing is such that electronic transmission could occur via orbital overlaps between S—S, N—N or S—N pairs on adjacent chains. This would produce a system of pockets of

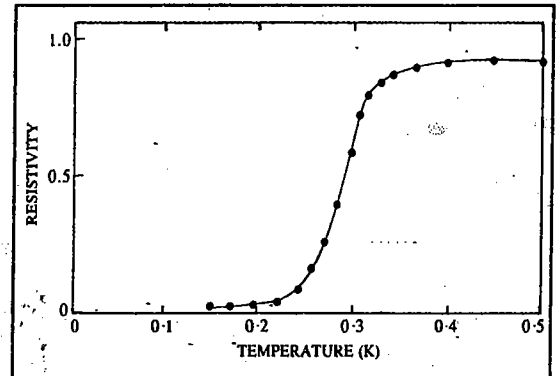

Fig. 6. $(SN)_x$ undergoes a change from a metallic conductor to a superconductor as it is cooled below 0·3 K.

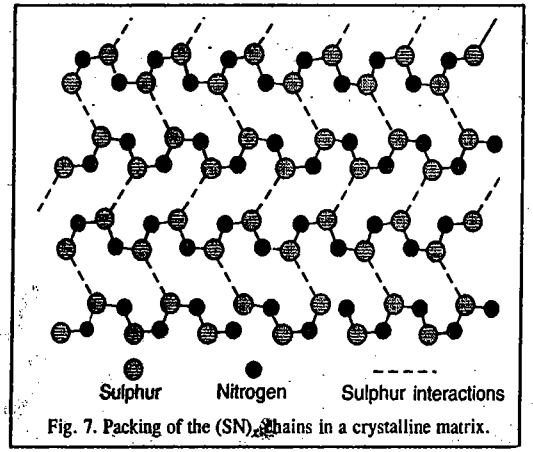

Fig. 7. Packing of the $(SN)_x$ chains in a crystalline matrix.

electrons and holes (as in a semimetal such as bismuth). Of course, the exact reasons for metal-like conductivity and superconductivity of $(SN)_x$ are still a subject for debate and are not very well understood. An alternative explanation for room-temperature conductivity is that the material behaves as a semimetal in which formally filled and unfilled bands overlap in energy and redistribute the electrons into two partially filled bands.

These explanations neglect a complication normally expected for polymers with delocalized skeletal systems — the so called **Peierl's distortion** that would lead to a segregation of skeletal bonds into (shorter) double bonds and (longer) single bonds with a resultant change from metallic properties to those of a medium-band-gap semiconductor. This does not happen with $(SN)_x$ and it is speculated that bonding linkages *between* chains prevent the distortion from occurring. The reasons for the transition to a superconductor at 0·3 K are not understood, though many theoretical viewpoints have been presented.

2. Polyacetylene

Polyacetylene has received more attention than any other electronically conducting polymer. It exists in *cis-trans* planar form and *trans-trans* planar form :

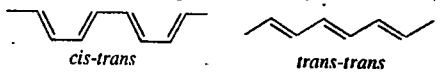

cis-trans *trans-trans*

The most widely used technique for synthesizing this polymer is the **Shirakawa technique**, which involves the polymerization of acetylene in contact with a concentrated Ziegler-Natta catalyst (typically, a 4 : 1 mixture of triethylaluminium and titanium tetra-*n*-butoxide). Under these conditions polyacetylene is formed as a microfibrilar mat, each fibril being about 200 Å in diameter. The polymer is metallic in appearance despite its porous structure. If the polymerization is carried out at –78°C, the polymer exhibits a *cis-trans* planar conformation. If the reaction temperature is 150°C, the polymer is generated as the *trans-trans* form. The formation of the latter conformer is favoured thermodynamically. The conversion of *cis-trans* to *trans-trans* form occurs slowly at ambient temperature or more quickly at 200°C. The polyacetylene produced by this method is about 85% crystalline. The electrical conductivity of pure polymer is quite low ($10^{-9}\ \Omega^{-1}\ cm^{-1}$ for the *cis-trans* form and $10^{-5}\ \Omega^{-1}\ cm^{-1}$ for the *trans-trans* form), both values being near the insulator-semiconductor boundary. However, it was discovered in 1977 that pure polyacetylene can be reduced by alkali metals, radical anions or electrochemically or oxidized by electron acceptors such as AsF_5, SbF_5, iodine and again by electrochemical methods, to give materials with markedly increased conductivities (of the order of $10^6\ \Omega^{-1}\ cm^{-1}$), following doping. Thus, doping has a dramatic effect on the conductivity. How do we account for it ?

The classical structure of polyacetylene is the one in which π-electron delocalization would generate equal bond lengths along the chain (as, for example, in benzene) with a continuous (valence band) molecular orbital providing a pathway for facile electron migration. This would correspond roughly to the structure of a metal and would yield a half-filled valence band. Conductivity along the chain would be high because, as in a metal, unpaired electrons would have ready access to the unoccupied levels of the valence band. However, Peierl's distortion precludes the existence of such a structure. Instead, the system would separate into a sequence of alternating single and double bonds (Fig. 8*b* and *c*). Such a system would no longer be metallic because the energy levels would segregate into a filled valence band and an unfilled conduction band, the two being separated by a significant band gap. Hence, electrical conduction would occur only after thermal or photolytic activation of electrons to give them sufficient energy to jump the gap into the lower levels of the conduction band. This may explain why pure polyacetylene is a near insulator (*cis-trans* form) and only a modest semiconductor (*trans-trans* form) rather than a metal.

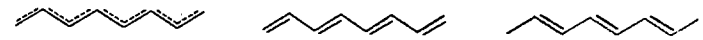

(*a*) delocalized structure (*b*) (*c*)

Fig. 8. Structures of polyacetylene

The effect of the dopants on polyacetylene is explained as follows : It is postulated that an

electron added to polyacetylene by doping goes *not* into the conduction band but into an intermediate electronic state within the band gap. This is illustrated in Fig. 9. The product of reduction is a radical anion, in which the intergap energy states are occupied by two electrons from one π-bond and the other is added by reduction. This state is known as a **polaron.** Addition of a second electron to the same site yields a di-anion, called a **bipolaron** (Fig. 9).

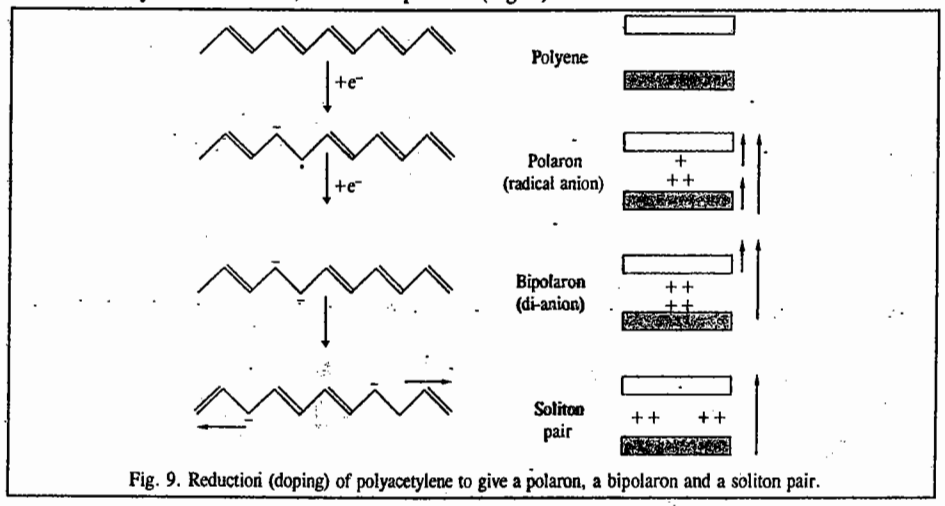

Fig. 9. Reduction (doping) of polyacetylene to give a polaron, a bipolaron and a soliton pair.

The bipolaron contains no unpaired electrons but its energy levels in the band gap would allow facile jumps of electrons into the conduction band. Conduction pathways would thus be generated without the presence of semipermanent free-electron states. Oxidation of polyacetylene would lead to removal of one electron from the valence band and formation of a radical cation—a positive polaron. Further oxidation would generate a **positive bipolaron.**

Polyacetylene exists in two equal-energy resonance states (Fig. 8*a* and *b*). These provide access to an alternative mechanism of conduction via defects known as solitons. Undoped polyacetylene contains approximately one unpaired electron for each 3,000 carbon atoms. This is a larger number that can be accounted for by thermally induced electron transitions from the valence band to the conduction band. It has been proposed that these unpaired electrons are located at defect sites formed at the boundaries in the chain between two types of structures shown as Fig. 8(*b*) and (*c*). A defect of this type might be represented by the following structure :

Such a defect structure is known as a **soliton.** A neutral soliton (free radical) could arise from conformational changes such as the isomerization of *cis-trans* to *trans-trans* polyacetylene. But irrespective of its origin, it should be able to move readily in either direction along the chain as a current carrier. It is calculated that it costs the system only 0·4 eV to create a soliton while it costs 0·7 eV for an electron to jump from the valence band to the conduction band. This is because the energy state for a soliton is in the middle of the band gap.

Solitons can theoretically function as current carriers in doped polyacetylene also. As shown in Fig. 9, a bipolaron could lower its energy by segregating into two solitons at the midgap energy level. Current could then be carried as the charged solitons and the defect sites would move along the chain.

3. Poly(para-phenylene)

Poly(para-phenylene) whose structure is shown below :

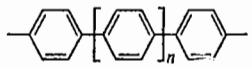

has long been considered a good candidate for electrical conductivity because of its extensively delocalized π-electron structure. However, the development of electroactive polymers of this type has been held up because of their synthesis and fabrication problems. Short-chain polyphenylenes are insoluble in most solvents and have very high melting points. Thus, during a synthesis process, oligomers (low molar mass polymers) precipitate from solution and chain growth is terminated. For this reason, oligomers rather than high polymers have been used for doping and conductivity experiments. The conductivity of undoped oligophenylenes is low (10^{-14} Ω^{-1} cm^{-1}) but doping with AsF_5 raises the conductivity and brings it into the range of 5×10^{2} Ω^{-1} cm^{-1}. Reduction with the usual dopants also raises the conductivity dramatically. It has been proposed that reduction or oxidation generates a radical anion or radical cation (polaron) and that further reduction or oxidation gives a bipolaron (Fig. 10). In contrast to polyacetylene, the conversion of a bipolaron to a soliton pair is considered to be unlikely in polyphenylenes because the quinonoid structure required for the solitons would be less stable than the aromatic form. As with polyacetylene, the polaron and bipolaron states would occupy two energy levels in the band gap. These states would provide easy access to the unfilled levels of the band.

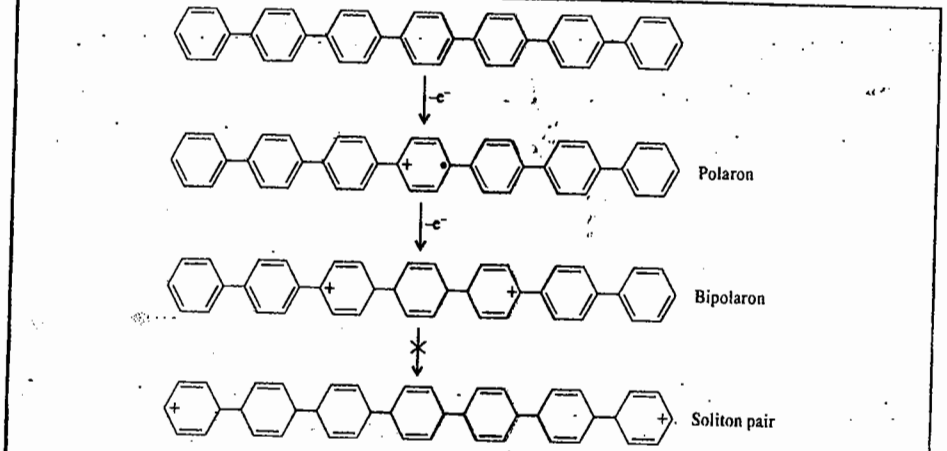

Fig. 10. Oxidative doping of an oligo-*para*-phenylene. Removal of one electron would generate first a radical cation (polaron) and then a bipolaron. The separation of a bipolaron into a soliton pair is unlikely in this system because of the relatively high energy of the quinonoid structure.

Thermodynamics of Polymer Solutions : Flory–Huggins Theory

The theory of polymer solutions, developed independently by Paul Flory and M.L. Huggins, is based on the lattice model. It is assumed that a solvent molecule occupies one site in the lattice and each monomer unit, of which the polymer molecule is composed, also occupies one lattice site so that the *polymer molecule as a whole* occupies many lattice sites, say, of the order of 10^3–10^4. A simplified two-dimensional model of a polymer solution is given in Fig. 11.

It is further assumed that the polymer molecules are completely flexible so that they occupy the available lattice sites in a purely random manner. Let r be the number of sites occupied by a polymer molecule. The following simple result is obtained for Gibbs free energy of mixing, ΔG_{mix}, of n_1

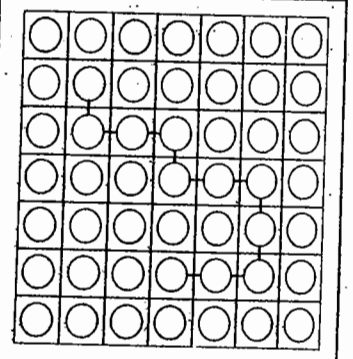

Fig. 11. A simplified two-dimensional model of a polymer solution.

moles of solvent and n_2 moles of solute (polymer) by calculating the number of ways of arranging N_1 molecules of the solvent and N_2 molecules of the polymer having r segments (assuming that $r >> 1$):

$$\Delta G_{mix} = RT\,(n_1 \ln \phi_1 + n_2 \ln \phi_2) \qquad ...(147)$$

where ϕ_1 and ϕ_2 are the *volume fractions* of the solvent and polymer, respectively, defined as

$$\phi_1 = \frac{n_1 \overline{V}_1^\circ}{n_1 \overline{V}_1^\circ + n_2 \overline{V}_2^\circ};\quad \phi_2 = \frac{n_2 \overline{V}_2^\circ}{n_1 \overline{V}_1^\circ + n_2 \overline{V}_2^\circ} \qquad ...(148)$$

Here $\overline{V}_1^\circ$ and $\overline{V}_2^\circ$ are the partial molar volumes of the pure solvent and pure solute (polymer), respectively. Defining a quantity ρ as $\overline{V}_2^\circ / \overline{V}_1^\circ$, the ϕ_is become

$$\phi_1 = n_1/(n_1+n_2\rho) \quad \text{and} \quad \phi_2 = n_2\,\rho/(n_1+n_2\rho) \qquad ...(149)$$

Now, $n_1+n_2 = n$ where n is the total number of moles. Also, $x_1=n_1/n$ and $x_2=n_2/n$ where the x_is are mole fractions. Hence, we can write

$$\phi_1 = (1 - x_2)/[1 + (\rho - 1)\,x_2] \quad \text{and} \quad \phi_2 = x_2\rho/[1 + (\rho - 1)\,x_2] \qquad ...(150)$$

It may be mentioned that for an ideal polymer solution, Eq. 147 is replaced by

$$\Delta G_{mix} = RT\,(n_1 \ln x_1 + n_2 \ln x_2) \qquad ...(151)$$

For any solution we can write

$$\Delta G_{mix} = \sum_i n_i(\mu_i - \mu_i^\circ) \qquad ...(152)$$

where μ_i° is the chemical potential of the pure component, i. Differentiating Eq. 152 with respect to n_j, keeping T, P and all other n_is constant, we obtain

$$[(\partial G_{mix}/\partial n_j)_{T,P,n_i} = \mu_j - \mu_j^\circ + \sum_i n_i[\partial(\mu_i - \mu_i^\circ)/\partial n_j] \qquad ...(153)$$

According to the Gibbs–Duhem equation,

$$\sum_i n_i d\mu_i = 0 \qquad ...(154)$$

so that the summation term on the right hand side of Eq. 153 vanishes, giving

$$[(\partial G_{mix}/\partial n_j)_{T,P,n_i} = \mu_j - \mu_j^\circ = RT \ln a_j \qquad ...(155)$$

It was formerly believed that the polymer solution would behave ideally if the enthalpy of mixing ΔH_{mix} is zero. However, if there are large differences between the molar volumes of the solvent and the polymer solute, the solution would not behave ideally even if ΔH_{mix} is zero.

Differentiating Eq. 147 with respect to n_1, substituting the result in Eq. 155 and dividing by RT we obtain

$$\ln a_1 = \ln \phi_1 + n_1\,\partial(\ln \phi_1)/\partial n_1 + n_2\,\partial(\ln \phi_2)/\partial n_1 \qquad ...(156)$$

Substituting for ϕ_1 and ϕ_2 from Eq. 150 and remembering that $\phi_1 = 1 - \phi_2$, we can show after simplification that

$$\ln a_1 = \ln (1 - \phi_2) + (1 - 1/\rho)\phi_2 \qquad ...(157)$$

Since $\overline{V}_2^\circ >> \overline{V}_1^\circ$, so that $\rho >> 1$ and hence $1/\rho << 1$. Thus, we can write

$$\ln a_1 = \ln (1 - \phi_2) + \phi_2 \qquad ...(158)$$

Taking antilogs,

$$a_1 = (1 - \phi_2)\,e^{\phi_2} \qquad ...(159)$$

Since $a_1 = p_1/p_1^\circ$ where p_1 is the vapour pressure of the solvent over the solution and p_1° is the vapour pressure of the pure solvent,

$$p_1/p_1^\circ = (1 - \phi_2)\,e^{\phi_2} \qquad ...(160)$$

Eq. 160 is the well known **Flory–Huggins equation** for the vapour pressure of a polymer solution. According to Raoult's law,

$$p_1/p_1^\circ = 1 - x_2 \qquad ...(161)$$

From Eq. 150,

$$1 - x_2 = (1 - \phi_2)/[1 - (1 - 1/\rho)\,\phi_2] \qquad ...(162)$$

so that Eq. 161 becomes

$$p_1/p_1^\circ = (1 - \phi_2)/[1 - (1 - 1/\rho)\,\phi_2] \qquad ...(163)$$

which is the Raoult's law for the vapour pressure of a polymer solution giving the dependence of p_1/p_1° on the volume fraction of the solute. The Flory–Huggins equation has been verified for the polystyrene-toluene system at different temperatures. The aggrement with experiment is partially satisfactory.

THE HELIX-RANDOM COIL TRANSITIONS IN POLYPEPTIDES

Proteins and polypeptides are polymers of α-amino acids ($H_2NCHRCO_2H$) that have molar masses greater than about 10,000 g mol^{-1}. About 22 different amino acids occur in natural proteins and they are all of the L-configuration. In proteins and polypeptides, amino acid residues are connected through amide bonds :

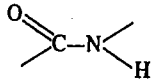

The nuclei of H, N, C and O lie in a plane and the connecting bonds are *trans*. Smaller polymers of amino acids called *oligopeptides* form random coils in solution but proteins have a more or less fixed three-dimensional structure held together by hydrogen bonds, disulphide bonds (—S—S—) between crystine residues and ionic and van der Waals interactions. According to the **Pauling-Corey model**, in the amide group the bond lengths and angles can be considered to be fixed. Only two angles are to be given per each α carbon atom to specify the configuration of the chain. If certain angles, which are not prohibited by steric hindrance, are repeated indefinitely, a helical structure results. A peptide helix is characterized by the number n of amino acid residues per turn of helix and by the distance d traversed parallel to the helix axis per amino acid residue.

The α **helix** is basically important to show the structures of the right-handed and left-handed varieties as presented in Fig. 12. It is primarily the right-handed helix that exists in proteins. The α-helix is held together by hydrogen bonds between a carbonyl oxygen and the N—H of the fourth residue along the chain. This produces an especially stable structure with n=3·6 residues per turn. In the direction of the axis of the helix there is a residue every 0·15 nm.

A number of synthetic polypeptides show structural transitions in solution when there is a change in temperature or pH. A single polypeptide chain can

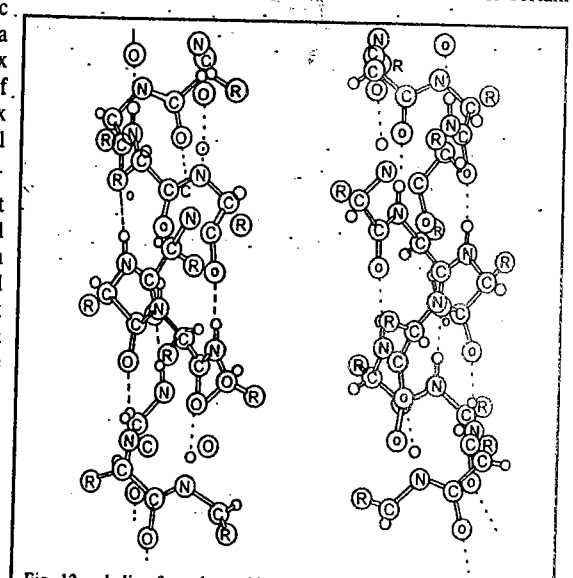

Fig. 12. α helix of a polypeptide. A left-hand helix is shown on the left and a right-hand helix is shown on the right.

exist in three states in solution, as illustrated in Fig. 13.

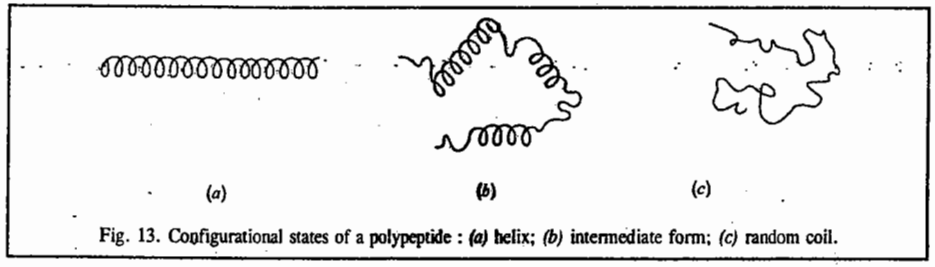

Fig. 13. Configurational states of a polypeptide : *(a)* helix; *(b)* intermediate form; *(c)* random coil.

Polymers generally have the helical form at low temperatures and the random coil form at high temperatures ; that is, the helix is the low-energy form and the random coil is the high-energy form. However, since the energy of a configuration depends on the difference between unit-unit interactions and unit-solvent interactions, the helix is sometimes the high-energy form.

The **helix-coil transition** is sometimes referred to as the 'melting' of the helix. In contrast to the melting of a crystal, melting of a helix generally takes place over a range of temperature. If the angles of a monomer unit are incompatible with the formation of a helix, we say there is a *kink* in the polymer chain. If the probability of occurrence of a kink at one position is strongly coupled to the existence of a kink in a neighbouring position, the helix-coil transition is said to be **cooperative.** If there is a strong interaction, the transition has a strong all-or-none character ; that is, the melting takes place over a narrow range of temperature. On the other hand, if the probability of a kink occurring at a given position is independent of whether there are neighbouring kinks, the helix melts gradually and the transition is said to be **non-cooperative.**

Structure of Proteins

Proteins are naturally occurring polypeptides composed of linked α-amino acids, $NH_2CHRCOOH$, where R is one of about 20 groups; they have molar mass greater than 5,000. These *macromolecules* show greater diversity of physical properties, ranging from water-soluble enzymes to the insoluble keratin of hair and horn. They perform a wide range of biological functions, a few of which are listed below :

1. ***Enzymatic catalysis.*** Enzymes are protein catalysts which can enhance reaction rates by factors upto 10^{12}.

2. ***Transport and storage.*** Many small molecules and ions are transported in the blood and within cells by being bound to carrier proteins. The best example is the oxygen-carrying protein *haemoglobin.* Iron is stored in the various tissues by the protein ferretin.

3. ***Mechanical functions.*** Proteins often fulfil structural roles. The protein collagen provides tensile strength in skin, teeth and bones. The membranes surrounding cells and cell organelles are also partly composed of proteins, having both functional and structural roles.

4. ***Movement.*** Muscle contraction is accompanied by the interaction between two types of protein filaments, actin and myosin. Myosin also processes enzymatic activity of facilitating the conversion of the chemical energy of adenosine triphosphate (ATP) into mechanical energy.

5. ***Protection.*** The antibodies are proteins, aided in mammals by *complement*, a complex set of proteins involved in the destruction of foreign cells.

6. ***Information processing.*** Stimuli external to a cell, such as hormone signals of light intensity, are detected by specific proteins that transfer a signal to the interior of the cell. A well-characterized example is the visual protein rhodopsin, located in the membranes of the retinal cells.

In 1951, Linus Pauling and Robert Corey formulated the rules known after their names — the **Corey-Pauling rules** — to account for the origin of the secondary structures of proteins. The essential feature is the stabilization of structures by hydrogen bonds involving the peptide link ; the latter can act both as a donor of the H atom (the NH part of the link) and as an acceptor (the CO part). The Corey-Pauling rules are as follows :

1. The four atoms of the peptide link lie in a relatively rigid plane. The planarity of the link is due to delocalization of π electrons over the O, C and N atoms and the maintenance of maximum overlap of their *p* orbitals.

2. The N, H and O atoms of a hydrogen bond lie in a straight line (with displacements of H tolerated upto not more than 30° from the N—O vector.)

3. All NH and CO groups are engaged in hydrogen bonding.

Detailed structure of a peptide link is depicted in Fig. 14.

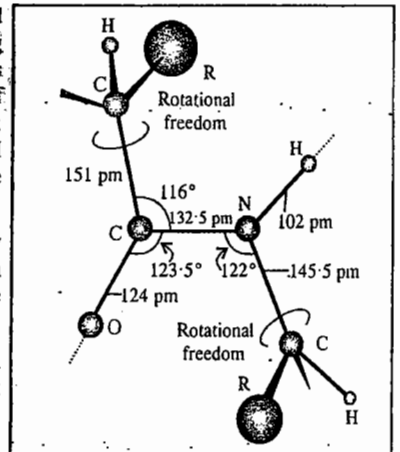

Fig. 14. The dimensions that characterize the peptide link. The C—NH—CO—C atoms define a plane (the C—N bond has partial double-bond character), but there is rotational freedom around the C—CO and N—C bonds.

These rules are satisfied by two structures. One, in which hydrogen bonding between peptide links leads to a helical structure, is the **α-helix.** The other, in which hydrogen bonding between peptide links leads to a planar structure, is the **β-sheet,** also called **β-pleated sheet.**

One could completely describe the three-dimensional structure of a protein by placing it in a Cartesian coordinate system and listing (*x, y, z*) coordinates for each atom in the protein. Indeed, this is how experimentally determined protein structures are stored in the Protein Data Bank at the Brookhaven National Laboratory in the United States of America. However, the structure of a protein can be more precisely described by listing the angles of rotation *(torsion angles)* of each of the bonds in the protein (Fig. 15.). For example, the backbone conformation of an amino acid residue can be specified by listing the torsion angles ϕ (rotation about the N—C_α bond), ψ (rotation around the C_α—C′ bond) and ω (rotation about the N—C′ bond).

The zero position for ϕ is defined with the —N—H group *trans* to the C_α—C′ bond and for ψ with C_α—N bond *trans* to the —C=O bond (Fig. 15) The peptide bond torsion angle (ω) is generally 180°. A full description of the three-dimensional structure of a protein also requires a knowledge of the side-chain χ torsion angles.

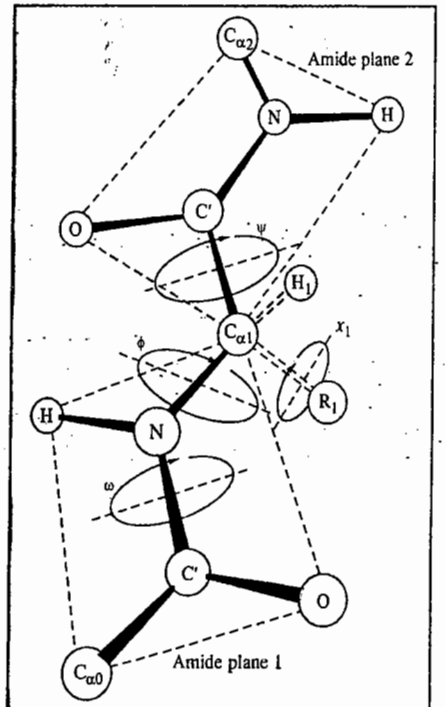

Fig. 15. Definition of protein torsion angles ω, ϕ, ψ, and χ. The conformation shown is obtained when ω, ϕ and ψ are all set to 180°.

A question arises : Why is the peptide group planar ? The answer is as follows :

The C—N bond has a partial double bond character owing to resonance between the two forms as shown :

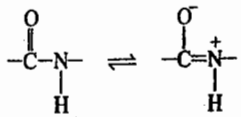

The length of the C—N bond (0·132 nm) is intermediate between that of a C—N single bond (0·149 nm) and a C=N double bond (0·129 nm). The partial double bond character restricts rotation around the C—N bond such that the favoured arrangement for the O, C, N and H atoms is to lie in a plane, with the O and H atoms *trans*. This corresponds to a torsion angle of $\omega = 180°$.

Another question that naturally arises is : Are there any restrictions on the structures that protein molecules can form ? The answer is the following :

Not all combinations of ϕ and ψ are possible, as many lead to clashes between atoms in adjacent residues. For all residues except glycine, the existence of such steric restriction involving side chain atoms reduces drastically the possible conformations. The possible combinations of ϕ and ψ angles that do not lead to clashes can be plotted on a conformation map, also known as the **Ramachandran diagram** or **Ramachandran plot,** named after the brilliant Indian biophysicist G.N. Ramachandran (1922–1998), one of the founders of molecular biophysics, who did considerable pioneering work in this field. The torsional contribution to the potential energy is given by

$$V_{\text{torsion}} = A\,(1 + \cos 3\phi) + B\,(1 + \cos 3\psi) \qquad ...(164)$$

where A and B are constants of the order of 1 kJ mol^{-1}. Only two angles are needed to specify the conformation of a helix; they range from −180° to +180°. Thus, a Ramachandran plot is actually the torsion potential energy contour diagram in which one axis represents ϕ and the other represents ψ. Fig. 16 shows a Ramachandran plot for the allowed conformations of alanylalanine. The double-hatched areas represent conformations (combinations of ϕ and ψ) for which no hindrance exists. The single-hatched axis represents conformations for which some hindrance exists, but which may be possible if the distortion can be compensated for by interactions elsewhere in the protein.

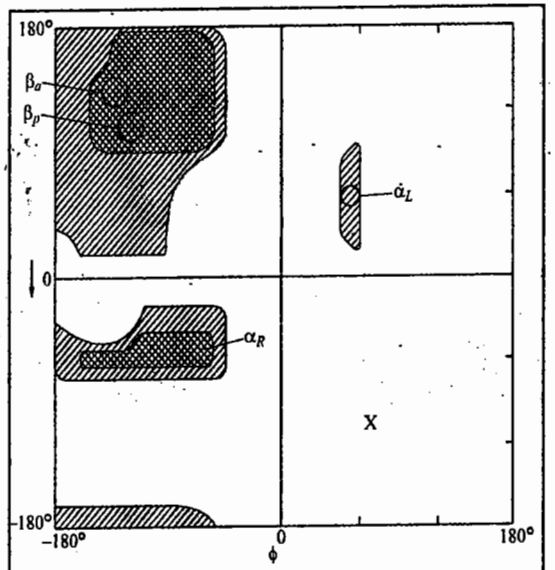

Fig. 16. Ramachandran plot for alanylalanine showing the fully allowed regions (double-hatched) and partially allowed regions (single-hatched) of ϕ and ψ angles (see Fig. 15). The coordinates for the parallel and antiparallel β structures (β_p and β_a, respectively) and for the left-handed and right-handed α helices (α_L and α_R, respectively) are indicated.

A few remarks will explain the **hydrophobic interaction.** The placing of a nonpolar group in water leads to energetically unfavourable ordering of the water molecules about it, *i.e.*, a lowering of the entropy of the solution. Transfer of nonpolar groups from water to a nonpolar environment is thus accompanied by an increase in entropy (of the water molecules) and is spontaneous. The folding of a protein chain into a compact globular conformation removes nonpolar groups from contact with water; the increase in entropy arising from the liberation of water molecules compensates for the decrease in entropy of the folded polypeptide chain. Burial of a methylene ($-CH_2-$) group in the interior of a protein is as energetically favourable (≈ 3 kJ mol^{-1}) as a strong hydrogen bond.

Hydrophobic interactions are such an important driving force in the folding of water-soluble globular proteins that we can formulate the general rule : *hydrophobic residues tend to be buried in the interior of proteins which minimizes their exposure to water.*

Protein Folding. In order to understand the functions of proteins, we need to know something about the *conformation* or the three-dimensional folding pattern that the polypeptide chain adopts. Though many polyamino acids have no well-defined conformation and seem to exist in solution as nearly random coils, most biological proteins adopt a well-defined *folded structure*. Some proteins, such as the keratins of hair and feathers, are *fibrous* and are organized into linear or sheet-like structures with a regular, repeating folding pattern. Others, such as most enzymes, are folded into compact, nearly spherical, *globular* conformations.

The question arises : why do proteins fold ? The answer is the following : The folding of a protein into compact structure is accompanied by a large *decrease in conformational entropy* (disorder) of the protein which is thermodynamically unfavourable. The native folded conformation is maintained by a large number of *weak, noncovalent interactions* that act cooperatively to offset the unfavourable reduction in entropy. The noncovalent interactions include hydrogen bonds and electrostatic, hydrophobic and van der Waals interactions. These interactions ensure that the folded protein is (often just marginally) more stable than the unfolded form. The order of magnitude of these interactions is given in Table 3.

TABLE 3

Types of Noncovalent Interactions involved in Stabilizing Protein Structure

Interaction	Example	Bond Energy (kJ mol^{-1})*
van der Waals	C—H····H—C	0·4 – 2·0
Electrostatic	$-COO^-\cdots H_3N^+-$	0·5 – 15
Hydrogen bond	—N—H····O = C—	2·0 – 7·5
Hydrophobic	Burial of $-CH_2-$	≈ 3

* The bond energy is the energy required to break the interaction.

Protein denaturation. The three-dimensional structure of a protein may be disrupted by changing the temperature adding a denaturant such as urea or changing the *p*H significantly. This phenomenon is known as **denaturation of protein.** Denaturation may involve a large number of steps as a result of which there is transition from the folded to the unfolded state. Sometimes, the changes are reversible and sometimes these are irreversible. Generally, denaturation occurs on increasing the temperature. Some proteins however, show **cold denaturation,** that is, denaturation increases when the temperature is reduced to below 0°C.

α-Helix and the β-Pleated Sheet Structures of Proteins

If the backbone torsion angles of a polypeptide are kept constant from one residue to the next, a regular repeating structure will result. Given the normal van der Waals radii of the atoms, expected bond angles and the planarity of the peptide link, only two regular, repeating structures exist without distortion with maximum hydrogen-bond formation. These are :

1.The α-helix found in α-keratins.

2. The β-pleated sheets (parallel and antiparallel), exemplified by the β-forms of stretched keratin and silk protein.

In the **α-helix**, the polypeptide *backbone* is folded in such a way that the —C=O group of each amino acid residue is hydrogen-bonded to the —N—H group of the *fourth* residue along the chain, *i.e.*, the —C=O group of the first residue is bonded to the —NH— group of the fifth residue, and so on. The backbone of the α-helix winds around the long axis (Fig. 17). The hydrogen bonds are all aligned approximately parallel to this axis and the side chains protrude outward. Each residue is spaced 150 pm from the next along the axis and 3·6 residues are required to make a complete turn of the helix. Although both left and right screw senses are possible, the right-handed screw sense is energetically favoured with *L*-amino acids.

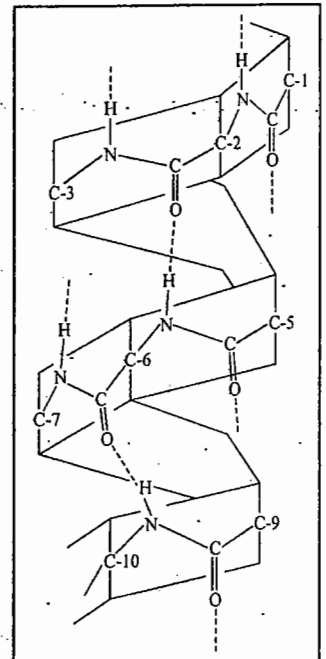

Fig. 17. The right-handed α helix. This diagram shows the peptide groups represented as planar segments, with the α-carbon atom at the junctions of successive planes.

The second major regular repeating structure, *viz.*, the **β-structure** differs from the α-helix in that the polypeptide chains are extended as in Fig. 18*a* and hydrogen bonding occurs *between* polypeptide strands, rather than *within* a single strand, as shown in Fig. 18*c*. Adjacent chains can be aligned in the same direction (*i.e.*, N terminal to C terminal) as in the *parallel* β *sheets* or alternate chains may be aligned in opposite orientations as in the *antiparallel* β *sheets* (Fig. 18 *c*). These structures often form extensive sheets, as shown in Fig. 18 *b*. Sometimes it is possible for several sheets to be stacked upon one another. Because the side chains tend to protrude above and below the sheet in alternating sequence, as shown in Fig. 18*b*, the β sheet structures are favoured by amino acids with relatively small side chains, such as alanine and glycine. Large, bulky side chains lead to steric interference between the various parts of the protein chain.

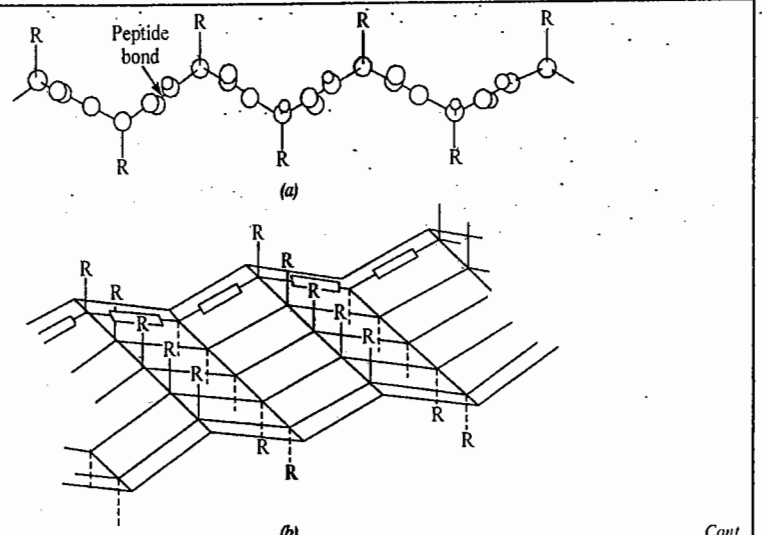

Cont.

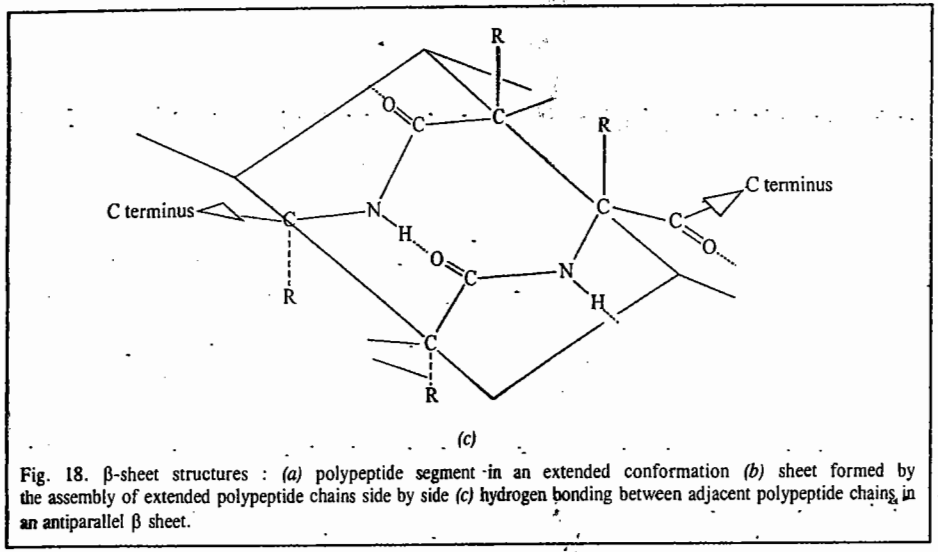

Fig. 18. β-sheet structures : *(a)* polypeptide segment in an extended conformation *(b)* sheet formed by the assembly of extended polypeptide chains side by side *(c)* hydrogen bonding between adjacent polypeptide chains in an antiparallel β sheet.

Hierarchy of Protein Structure. As proposed by the Danish protein chemist, Kai Linderstrom-Lang, it is possible to consider the structure of a protein on several levels :

(a) Primary structure giving the sequence of amino acids.

(b) Secondary structure depicting the regular, repeating folding pattern (such as the α-helix and β-pleated sheet structures), stabilized by hydrogen bonds between peptide groups close together in sequence. The secondary structure elements in a protein are often summarized in the form of a topology diagram (Fig. 19.) which defines, in two dimensions, their extent and relative orientations. These diagrams are often used to show relationships within families of proteins.

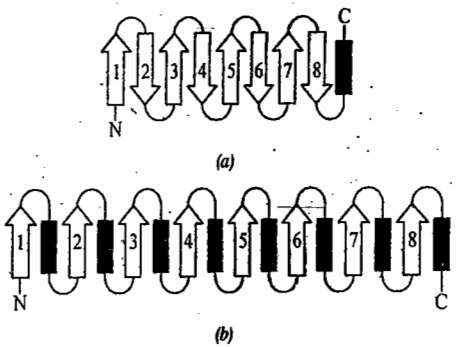

Fig. 19. Topology diagram depicting secondary structure elements in proteins. The arrows represent β strands (numbered from N to C) and the dark boxes represent α helices. Note that both of these proteins form a barrel structure comprised of eight β strands with the first strand hydrogen bonded to last strand in order to 'close' the barrel.

(c) Supersecondary structure showing common repeating patterns of secondary structure that occur in many proteins. One common recurring pattern is the β-α-β motif, which has a segment of β sheet, an intervening α helix and a second segment of β-sheet hydrogen bonded to the first

(Fig. 20). Other motifs include : the β hairpin which comprises two antiparallel β strands connected by a tight reverse turn ; the αα motif comprised of two closely packed antiparallel α helices and β barrels in which extended β sheets wrap around to form a continuous cylinder.

(d) Tertiary structure for a globular protein. The tertiary structure which depicts the way that segments of secondary structure fold together in three dimensions, stabilized by interactions often far apart in the sequence. For those proteins with little or no detectable α helix or β structure, the tertiary structure can be considered as the way the protein folds in three dimensions, stabilized by interactions between distant parts of the sequence.

(e) Domain structure. Domains are a common feature of many globular proteins, particularly where the molar mass is more than 20000 g mol^{-1}.

(f) Quaternary structure. This shows the interaction between different polypeptide chains to produce an *oligomeric* structure, stabilized by noncovalent bonds only.

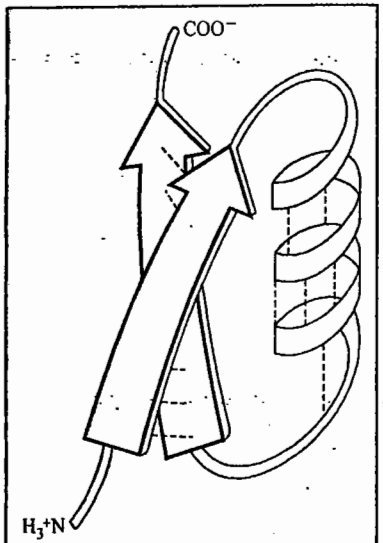

Fig. 20. Diagrammatic representation of the supersecondary β-α-β folding unit of a protein. β regions are represented by the arrows while the α-helical segment is indicated by the coiled structure. Approximate positions of hydrogen bonds are shown with dashed lines.

Experimental Methods for Determination of Protein Structures. There are two methods for determining the structures of proteins. These are : (1) **X-ray crystallography** and (2) **NMR spectroscopy.** The coordinates of the atoms in many proteins and nucleic acid structures are available in the Protein Data Bank, which may be accessed via the *Internet*. The following generalizations or folding rules can be drawn from the known data base of experimentally determined protein structures :

1. Most electrically charged groups are on the surface of the molecule, interacting with water. Exceptions to this rule are often catalytically important residues in enzymes which may well be partially stabilized by specific polar interactions within a hydrophobic portion of the molecule.

2. Most nonpolar (*e.g.*, hydrocarbon) groups are in the interior of the molecule, thus avoiding thermodynamically unfavourable contact with water.

3. Maximal hydrogen bonding occurs within the molecule.

The advantages and limitations of protein crystallography are :

1. The technique is applicable to a wide range of samples which include proteins, enzymes, nucleic acids and viruses and is not limited by the size of the molecules.

2. Not all proteins can be crystallized. This is especially true of intrinsic membrane proteins which need to be solubilized in the presence of detergents.

3. Most protein crystals do not diffract to true atomic resolution. Due to an inherent lack of perfection in protein crystals, the high angle component of the diffraction pattern which contains the fine detail, is lost. NMR studies are performed on proteins in their native solution state. Since the protein molecules are moving around in solution, the NMR technique measures scalar quantities (torsion angles and interproton distances). This is fundamentally different from X-ray crystallography in which the static crystal lattice allows a vector 'image' of the molecule to be obtained.

The advantages and limitations of protein NMR spectroscopy are :

1. The technique is applicable to both proteins and nucleic acids in their native solution state.
2. There is an upper size-limit of 35–40 kDa.
3. The final resolution is not as good as in X-ray crystallography.

Max Perutz and J.C. Kendrew were jointly awarded the 1962 Chemistry Nobel Prize for their studies of the structures of globular proteins. In the same year (1962), the Nobel Prize for Physiology/Medicine was awarded to F.H.C. Crick, J.D. Watson and M. Wilkins for their discoveries concerning the molecular structure of nucleic acids (DNA and RNA). And six years later, the 1968 Nobel Prize for Physiology/Medicine was awarded jointly to the American biochemists R.W. Holley, H.G. Khorana, and M.W. Nirenberg for "their interpretation of the genetic code and its function in protein synthesis".

The 2009 Chemistry Nobel Prize was awarded jointly to Venkatraman Ramakrishnan, Thomas Steitz and Ada Yonath for mapping ribosomes, the protein-producing factories within cells, at the atomic level and for showing how antibiotics bind to ribosomes.

The Structure of Nucleic Acids

The nucleic acids DNA (deoxyribonucleic acid) and RNA (ribonucleic acid) are **polynucleotides**, *i.e.*, they are polymers containing nucleotides (various types) as the repeating subunits. **DNA** is a polynucleotide of the four nucleotides with thymidylic acid (T), deoxyadenylic acid (A), deoxycytidilic acid (C) and deoxyguanilic acid (G). The nucleotides are joined to one another through phosphodiester linkages between the 3′C of one nucleotide and the 5′C of the adjacent one (Fig. 21). This linkage is repeated many times to build up large structures (chains or strands) containing hundreds to millions of nucleotides within a single giant molecule. DNA is the major nucleic acid in the nucleus of cells. It contains the pentose sugar *deoxyribose* as one of its chemical constituents. DNA is now known to be the genetic material. The other type of nucleic acid RNA contains *ribose* instead of deoxyribose. Its main role is in the transmission of the genetic information from DNA into protein. DNA molecules are very large, much larger than proteins. RNA is more comparable to proteins in size. Complete hydrolysis of DNA (or RNA) by acid cleaves it into a mixture of nitrogeneous bases, 2-deoxy-*D*-ribose (or *D*-ribose for RNA), and orthophosphate. There are two general types of nitrogenous bases in both DNA and RNA, *pyrimidines* and *purines*. Pyrimidines are derivatives of the heterocyclic compound *pyrimidine*; and purines are derivatives of the fused-ring compound *purine* :

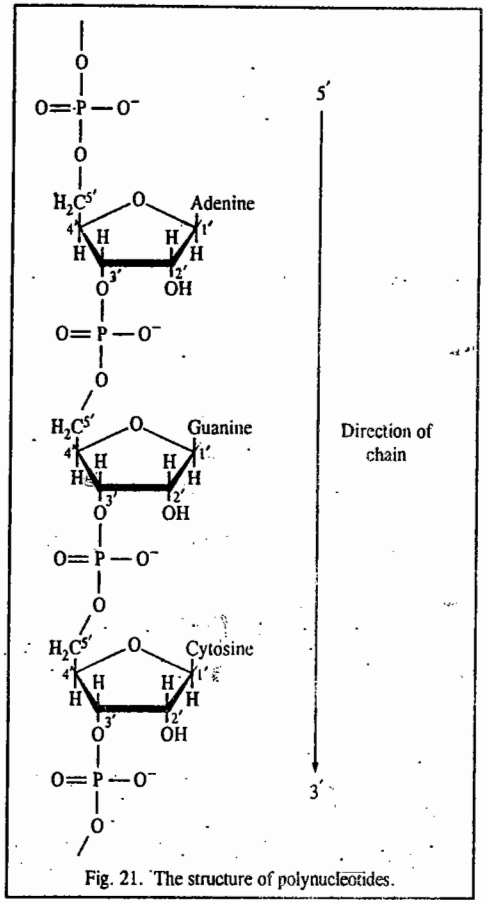

Fig. 21. The structure of polynucleotides.

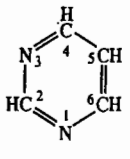
Pyrimidine

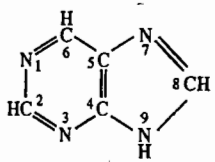
Purine

The numbering of the positions in the rings has been established by IUPAC convention. The major pyrimidines found in DNA are ***thymine*** and ***cytosine*** ; in RNA, they are uracil and cytosine :

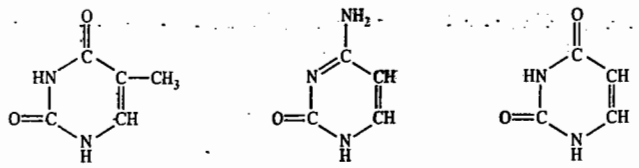

(*a*) Thymine (*b*) Cytosine (*c*) Uracil

The major purines found in both DNA and RNA are *adenine* and *guanine* :

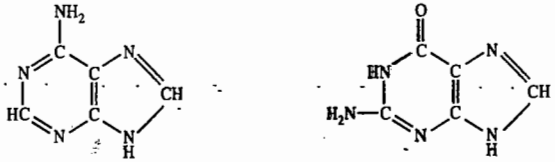

Adenine Guanine

DNA molecules comprise more than 10^8 nucleotides. They contain adenine, thymine, guanine and cytosine as the bases, and the genetic information is encoded within the nucleotide sequence which is precisely defined over the entire length of the molecule. One of the simplest methods for determining the nucleotide sequence of DNA makes use of the enzyme, DNA *polymerase*, which catalyzes the synthesis of DNA.

DNA is a duplex molecule in which two polynucleotide chains (or strands) are linked to one another through specific *base pairing* (Fig. 22). Adenine in one strand is paired to thymine and

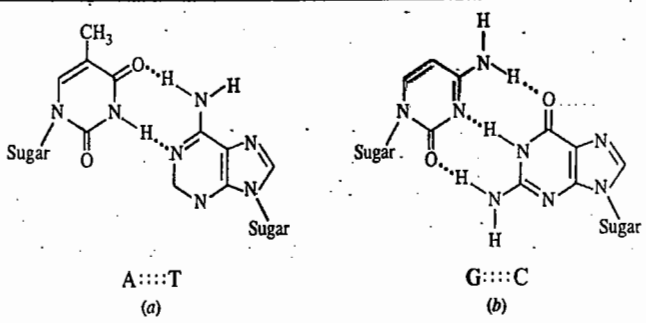

Fig. 22. Base pairing in DNA

guanine is paired to cytosine. The two chains are said to be *complementary*. This was one of the essential features of the **Watson-Crick model** of the structure of DNA. Hydrogen bonds are formed between the opposing bases within a pair. In the structure proposed by Watson and Crick, A····T and G···· C base pairs are roughly planar, with H bonds (dotted lines) as shown in Fig. 22. It may be noted that two H bonds are formed in an A:T pair and three in a G:C pair. The base pairs are stacked on top of one another, the plane of the base pairs being perpendicular to the length of the

duplex. This is shown diagrammatically in the ladder-type structure (Fig. 23).

This model for DNA incorporating base pairing between complementary strands and consistent with X-ray diffraction data was proposed by J. D. Watson and F.H.C. Crick in 1953. Basic to the structure was the twisting of the two strands around one another to give a **right-handed helix** (the **double helix**), and to achieve a structure consistent with the data available at that time. It was necessary to orient the complementary chains in opposite directions (Fig. 24). Direct proof for this *opposite polarity* in chain direction was achieved about ten years later.

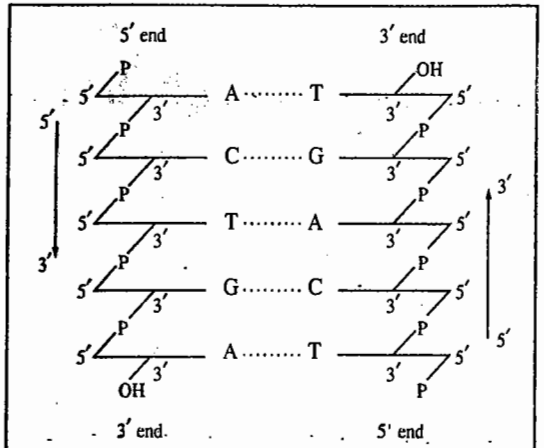

Fig.23. Stacking of base pairs within the DNA duplex. The dotted lines, representing the H bonds between the base pairs, is in a plane perpendicular to the surface of the page.

We are next interested in knowing how the twisting of the two strands to give a helix contributes to the stability of the overall structure of DNA. In fact, one of the most significant effects of twisting into a helix is to bring the stacked pairs very close to one another. The double helix can exist in several forms. In the so-called B form of the helix (Fig. 24), this distance, which is called the rise, is 0·34 nm. Consequently, water is excluded from what is now a hydrophobic core; the charged phosphates are on the surface. The hydrophobic interactions within the core contribute, along with the H bonds between the base pairs, to the overall stability of the helix. It should also be noted that there is one complete twist of the helix every 10 base pairs or 3·4 nm. This distance is referred to as the pitch of the helix. The surface of the helix shows alternating major and minor grooves which follow the twist of the double-stranded molecule along its length. The major groove is now known to accommodate interactions with proteins that recognize and bind to specific nucleotide sequences.

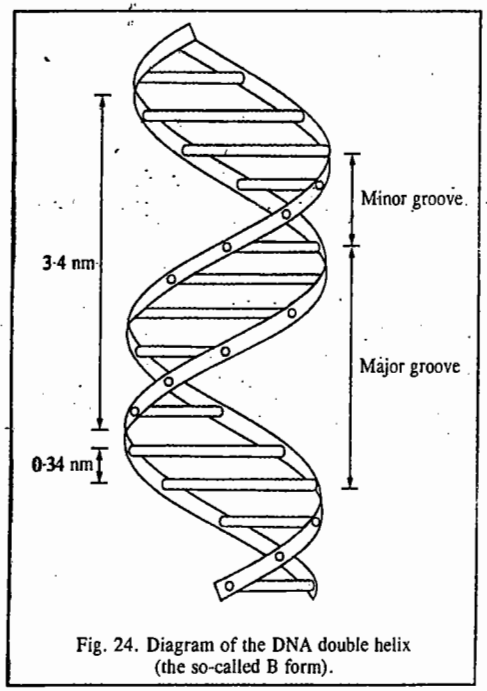

Fig. 24. Diagram of the DNA double helix (the so-called B form).

Supercoiled DNA. Supercoiling represents a twisting of the DNA double helix upon itself. It occurs in circular DNAs and in DNAs that are *topologically constrained* by being complexed to proteins. If a circular DNA molecule in a relaxed conformation (no supercoiling) is broken across both strands and one or more additional right-handed helical turns are inserted before rejoining the ends, the molecule would twist on itself to form a positive supercoil. If, on the other hand, the helix is unwound (given left-handed turns) before rejoining, the result is negative supercoil. These

forms, called topomers, are shown in Fig. 25. Each supercoil depicted here contains a single supertwist. The number of supertwists in a molecule can be very large. Supercoiled DNA is readily converted into its relaxed form by the introduction of a break (or *nick*) between adjacent nucleotides in one of the two strands ; this form is no longer topologically constrained.

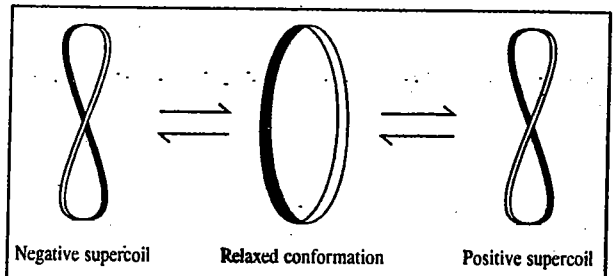

Fig. 25. Depiction of negative and positive supercoils in a supercoiled DNA.

Denaturation of DNA. The double helix is a relatively stiff and elongated molecule. Consequently, a solution of DNA has high viscosity. If such a solution is heated to 95°C, the viscosity of the solution drops markedly, reflecting a collapse of the double-helical structure. This is known as **denaturation** and is accompanied by separation of the duplex into its single strands which are fairly flexible. Denaturation and renaturation provide valuable information on important properties of the DNA obtained from various sources. Denaturation also provides the basis for very precise and sensitive approaches to the identification of specific sequences in both DNA and RNA. This has been of paramount significance for the rapid developments in molecular genetics.

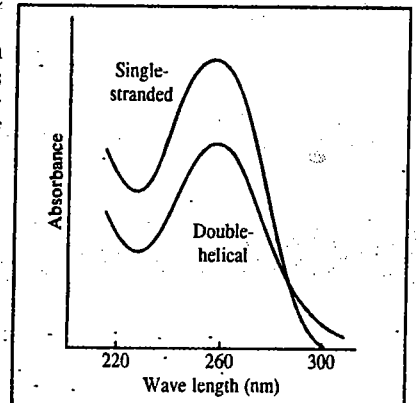

Fig. 26. Absorption spectra of double-helical and single-stranded forms of DNA.

While denaturation can be detected readily through changes in viscosity, a much more convenient way to detect it is by ultraviolet (UV) absorption measurement. The difference in the UV absorption spectra of the native (double-helical) and denatured (single-stranded) forms of DNA is shown in Fig. 26. At the wave length of maximum absorption (260 nm), absorption by single-stranded DNA is approximately 40 per cent higher than that by double-stranded DNA. This is referred to as the **hyperchromic effect** and results from the *unstacking* of the base pairs in the helix.

The DNA helix is stabilized by H bonds between individual base pairs as well as by hydrophobic forces between stacked base pairs. Reagents that reduce the H bonding and decrease the polarity of the surrounding medium, such as formamide, will cause denaturation. Extremes of *p*H, which endow the bases with a charge, are also effective. Thus, DNA at *p*H 10 shows absorption at 260 nm which is 40 per cent higher than that of the native form.

If the temperature of a solution of DNA is increased gradually, the change to the denatured form can be monitored by change in absorbance at 260 nm. Typical results for several types of DNA are shown in Fig. 27.

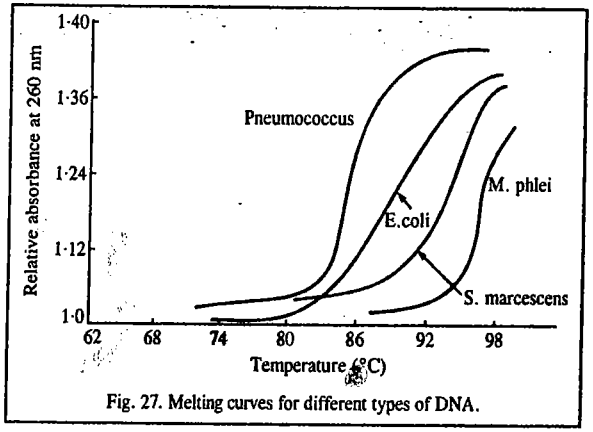

Fig. 27. Melting curves for different types of DNA.

The curves are referred to as melting curves because the region over which the absorbance increases reflects the collapse (or *melting*) of the highly organized, semicrystalline state of double-helical DNA. The temperature at which 50 per cent melting has occurred is called the melting temperature or T_m.

The T_m at neutral *p*H is dependent on the ionic strength of the medium. The curves shown in Fig. 27 are those obtained at an ionic strength of just above 0·15. If the ionic strength is reduced by 90 per cent, all T_m values are lowered by about 20°C. This results from the additional negative charge and consequently greater electrostatic repulsion (which helps disruption of the helix) within the DNA structure at the lower ionic strength.

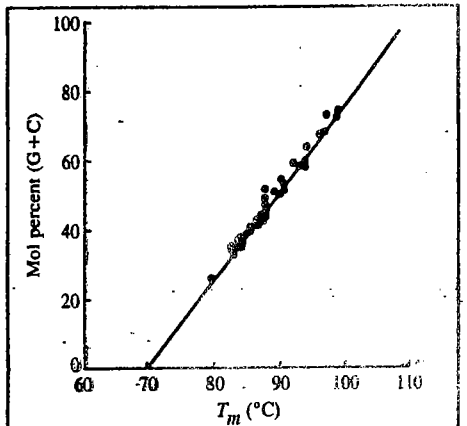

Fig. 28. Melting temperature of DNA as a function of the (G + C) content.

The DNAs from different sources have different T_m values. This is because the DNAs have different amounts of G:C and A:T base pairs and the former confer greater stability on the helix through the presence of three H bonds per base pair than two. Thus, the higher the G+C content, the higher the T_m. The value of T_m under standard conditions can be used, therefore, to obtain an estimate of the (G+C) content of an unknown DNA. This is evident from Fig. 28 which shows a plot of T_m versus (G+C) content of a number of DNAs.

Renaturation of DNA. The complementary strands of DNA, separated by heat, spontaneously reassociate when the temperature is lowered below the T_m. This renaturation is also referred to as annealing. The rate of annealing depends on the concentration of complementary sequences. Viral DNA has a smaller variety of sequences than does bacterial DNA ; this reflects the higher level of genetic complexity in bacteria. Thus, for viral and bacterial DNA fragments of the same average size and at the same molar concentration, there would be a higher concentration of complementary sequences in the former. Viral DNA, therefore, would renaturate faster than bacterial DNA.

The Polymerase Chain Reaction (PCR). In order to obtain sufficient quantities of a *particular* DNA sample to enable determination of its properties, we make use of the **polymerase chain reaction (PCR)** which is, indeed, a type of chain reaction. PCR provides a way to generate a vast number of double-stranded copies of a specific DNA sequence.

The polymerase chain reaction uses : (1) a thermostable DNA polymerase, (2) a DNA template which is to be amplified, (3) two primers, each typically of 20 nucleotides, which anneal to distinct parts on the complementary strands of the target and serve as sites for commencing DNA polymerase reaction, (4) a solution containing deoxynucleoside triphosphates, Mg^{2+} salts and *p*H buffer.

PCR uses DNA polymerase to make complementary copies of DNA corresponding to the region of interest. To direct the enzyme to the correct sequence, PCR relies on primers which anneal to complementary sequences in target single-stranded DNA. DNA polymerase cannot start DNA synthesis *de novo* and can extend the chain only from the annealed primers. An excess of these primers is provided in the reaction mixture to allow sufficient material for generating amplified product. PCR reactions include the cyclical use of high temperatures which can lead to the denaturation of thermolabile enzymes.

Without going into the details of this very important reaction, we mention here that for PCR, there are only three steps involving DNA. These are (1) double-stranded DNA denaturation, (2) DNA annealing and (3) DNA extension. Each step is initially conducted at a different temperature in a programmable machine called a **thermal cycler**. A 'step' in the chain reaction typically takes less

than a few minutes, and all three steps are described collectively as a cycle. Each cycle results in approximately a doubling of the number of target DNA molecules. Typically more than 30 cycles are performed. If each cycle is assumed to give a doubling in target sequence copies, it can be seen that 30 cycles give over a billion ($> 10^9$) double-stranded DNA copies of the specific sequence. Thus, beginning with even just a single molecule of DNA, the PCR can generate 100 billion copies in a single afternoon.

The PCR is the mainstay in forensic science as well, where it may be used to copy DNA for a trace sample of blood or semen or a hair left at the scene of the crime. It is also used in evolutionary biology and anthropology where the DNA of interest may come from a 40,000 year-old wooly mammoth or the tissue of a mummy such as that of an Egyptian pharaoh. It is also used to match families with lost relatives. There is almost no area with biological significance that does not in some way have application for use of the PCR reaction.

Separation of Proteins and Nucleic Acids. We may mention here that amino acids which form the building blocks of polypeptides and proteins, contain amino and carboxylic acid groups that can ionize or protonate, depending on the *p*H. At a certain *p*H, the net charge of an amino acid is zero and it exists as a **zwitterion** that exhibits no **electrophoretic mobility**. This *p*H is called the **isoelecric point (pI)** of the amino acid. Electrophoretic methods are used to separate substances (such as charged colloidal particles or macromolecular ions like those of proteins, nucleic acids and polysacchardes). There are several kinds of electrophoresis.

In **pulsed-field electrophoresis,** the direction of the electric field is periodically reversed for a brief time and this repeated reversal causes very large DNA fragments to migrate at a rate that depends on size. In **isoelectric focusing**, one establishes a *p*H gradient within the gel. Each protein migrates until it reaches its isoelectric point, thereby allowing separation of proteins with different isoelectric points.

In **capillary electrophoresis,** instead of moving through a gel slab, the polyelectrolyte molecules move through narrow (0·01 cm inside diameter) quartz capillaries. The capillaries can be filled with a gel. More commonly, the capillaries are filled with a solution of a polymer (such as polyacrylamide) at high concentration. Interactions between the migrating polyelectrolyte molecules and polymer molecules lead to separation by size. Detection of the migrating molecules is by ultraviolet absorption or by fluorescence. The high resistance of the medium in a capillary reduces the magnitude of the current that flows and reduces the heat that occurs. This allows a higher voltage to be applied than when using a gel slab, thereby speeding up the separation.

Gel electrophoresis, which is used to measure the approximate molar mass of a protein, involves migration of a peptide or protein dissolved in a buffer through a porous polymer gel under the influence of a high voltage electric field. The buffer used (typically about *p*H 9) imparts an overall negative charge to the protein such that the protein migrates towards the positively charged terminal. Migration rate depends on the overall charge and size of the protein as well as the average pore size of the gel. The molar mass of the protein is inferred by comparing the distance travelled through the gel by the protein of interest with the migration distances of proteins with known molar masses used as internal standards.

A recent technique used for the separation of proteins and nucleic acids involves two-dimensional multicapillary HPLC (high-performance liquid chromatography) coupled with mass spectrometry. In this technique called multidimensional protein identification technology, developed by John Yates and coworkers at Scripps Research Institute in U.S.A. a microcapillary HPLC column is used that has been packed first with a strong cation-exchange resin and then a reversed phase (hydrophobic) material. The two packing meterials used in sequence and with different resolving properties represent the two-dimensional aspect of the technique. A protein extract is introduced in the microcapillary column and eluted with *p*H and solvent gradients over a sequence of automated steps. As the separated proteins are eluted from the column, they pass directly into a mass spectrometer.

Mass spectrometric data obtained for each protein represent a signature that allows identification of the protein by comparison with a protein mass spectrometry database. The structures of the identified proteins are determined by X-ray crystallography and NMR.

The 1993 Chemistry Nobel Prize was awarded "for contributions to the developments of methods within DNA-based chemistry." The prize was shared by the American biochemist Kary B. Mullis and the Canadian biochemist Michael Smith. Mullis was honoured "for his invention of the polymerase chain reaction (PCR) method"; and Smith was honoured "for his fundamental contributions to the establishment of oligonucleotide-based, site-directed mutagenesis and its development for protein studies."

I. Review Questions

1. Give the structures of the following types of polymers :
   Isotactic polymers, atactic polymers, syndiotactic polymers, stereoregular polymers, copolymers, block copolymers, linear polymers, branched polymers, crosslinked or network polymers.
2. What is meant by number-average molar mass and weight-average molar mass of a polymer ? What is polydispersity index of a polymer sample ?
3. Describe the viscosity method for the determination of molar masses of macromolecules.
4. Describe the method based on measurements of osmotic pressure of solutions of polymers for the determination of their molar masses.
5. What is Donnan membrane equilibrium ? Discuss the importance of this phenomenon in the determination of molar masses of charged macromolecules such as proteins.
6. Discuss the sedimentation velocity method for the determination of molar mass of polymers.
7. Describe the light scattering method for the determination of molar mass of macromolecules. Draw the Zimm plot.
8. Explain how the measurement of turbidity of a polymer solution can be used for determining the molar mass of the polymer.
9. State and explain Stokes-Einstein equation for the evaluation of diffusion coefficient of a macromolecule. How is this equation utilised for determining the radius of the polymer molecule and the molar mass of the polymer ?
10. What is meant by contour length of a macromolecule ? How is it determined ?
11. Discuss briefly the kinetics of *(i)* addition polymerization and *(ii)* condensation polymerization.
12. What is meant by condensation or step-growth polymerization ? Discuss with the help of suitable diagram, the molar mass distribution in the process of step-growth polymerisation. Show that the weight-average molar mass is generally twice the number-average molar mass.
13. What are electronically conducting polymers ? How are they produced ? Discuss the electrical conductivity of *(i)* poly(sulphur nitride) and polyacetylene.
14. Explain with the help of a suitable diagram the formation of polaron, bipolaron and soliton pair.
15. Discuss the electrical conductivity of poly(paraphenylene), with reference to the formation of polaron and bipolaron. Why is soliton pair not formed in this case ?
16. Derive Flory–Huggins equation for the vapour pressure of a polymer solution.
17. Discuss the helix-random coil transitions which occur in polypeptides.
18. What are proteins ? Describe briefly the functions that are performed by proteins in human body.
19. What are the dimensions which characterise a peptide link in proteins ?
20. State the Corey-Pauling rules for the structures of proteins.
21. Explain what the following symbols stand for in the context of the structure of proteins : ω, ϕ, ψ and χ.
22. What is a Ramachandran plot ? What is its significance ?
23. Describe the α-helix and β-pleated sheet structures of proteins.
24. What information is conveyed by the following visa-vis the structure of proteins :
    (1) Primary structure (2) secondary structure (3) supersecondary structure (4) tertiary structure (5) domain structure (6) quaternary structure.
25. Discuss the advantages and limitations of the following in connection with the determination of structures of proteins:
    (1) crystallography (2) NMR spectroscopy.

II. Problems

1. The following data are given for relative viscosity η_r of solutions of polyvinyl alcohol in water :

η_r	1·409	1·198	1·098
c(g dm^{-3})	10·00	5·00	2·50

Use the Mark–Kuhn–Houwink–Sakurada equation to determine the $\overline{M}_{visc}$ of the polymer. Given : $K = 3{\cdot}8\times10^{-3}$ and $a = 0{\cdot}76$. [Ans. 21 kg mol^{-1}]

2. The following data are given on the aqueous solutions of polyvinyl alcohol :

$\overline{M}_{visc}$ (kg mol^{-1})	10	20	35	50	65	80
[η] (dm^3 g^{-1})	0·0213	0·0394	0·575	0·0740	0·0901	0·1059

Evaluate the Mark–Kuhn–Houwink–Sakurada parameters for this polymer. [Ans. $K = 3{\cdot}9\times10^{-3}$; $a = 0{\cdot}76$]

3. The following sedimentation velocity data at 25°C are given on the enzyme fumarase :

c(g dm^{-3})	0·70	1·60	3·40
S (10^{-12} s)	9·03	8·96	8·87

The diffusion coefficient D, the specific volume $\bar{v}$ and density ρ of the solution are $4{\cdot}05\times10^{-11}$ m^2 s^{-1}, 0·75 cm^3 g^{-1} and 0·993 g cm^{-3}, respectively. Calculate the molar mass of fumarase. [Ans. 213 kg mol^{-1}]

4. Given the following composition-molar mass data for a polydisperse polymer mixture :

mass %	25·0	50·0	25·0
M_i (kg mol^{-1})	1·00	1·20	1·40

Calculate $\overline{M}_n$ and $\overline{M}_w$. [Ans. 1·18 kg mol^{-1} ; 1·20 kg mol^{-1}]

5. Calculate the polydispersity index for the polymer mixture described in Problem 4. [Ans. 1·02]

6. Calculate the R_{rms} for a polymer sample containing tetrahedral bonding. Given $\overline{M}_n = 1{\cdot}00$ kg mol^{-1} and the length of monomer ($\overline{M}_w = 14{\cdot}0$ g mol^{-1}) is 150 pm. [Ans. 1·8 nm]

7. Calculate the contour length (*i.e.*, the length of the extended polymer chain) and the root-mean-square end-to-end distance of a polyethylene molecule with molar mass equal to 280 kg mol^{-1}. Assume that the length of the monomer is 154 pm. [Ans. 1·54 μm, 15·4 nm]

8. Given the following data for the relative viscosity η_r of solutions of polyvinyl alcohol in water :

η_r	1·409	1·198	1·098
c (g dm^{-3})	10·00	5·00	2·50

Calculate [η] for this polymer. [Ans. 0·0386 dm^3 g^{-1}]

9. A solution of a protein was investigated in an ultracentrifugation velocity measurement at 20°C, the rotor speed being 50,000 pm. The boundary receded as follows :

t(s)	0	300	600	900	1200	1500	1800
r (cm)	6·127	6·153	6·179	6·206	6·232	6·258	6·284

Calculate the sedimentation coefficient and the molar mass of the protein. Further data are as follows : $\bar{v} = 0{\cdot}728$ cm^3 g^{-1} ; $D = 7{\cdot}62\times10^{-11}$ m^2 s^{-1} ; $\rho = 0{\cdot}9981$ g cm^{-3}. [Ans. $5{\cdot}14\times10^{-13}$ s ; 60·1 kg mol^{-1}]

10. In a turbidity measurement experiment, the intensity of light passing through a 1·00 cm sample of a solution of polystyrene in methyl ethyl ketone ($c = 12{\cdot}3$ g dm^{-3}) was found to decrease by 2·3 per cent. Calculate the turbidity (τ) of the solution. [Ans. $\tau = 2{\cdot}33$ m^{-1}]

CHAPTER 35

MASS SPECTROMETRY

Mass spectrometry is primarily used (1) to measure the RMM (relative molar mass), M_r, with high precision and thence to deduce the molecular formula of a compound, (2) to detect the site of fragmentation in a molecule which enables the detection of the presence of recognizable groupings in the molecule and (3) to identify an unknown compound by comparing its mass spectrum with the digitalized mass spectra usually available in a university library.

Basic Theory

A high resolution double-focusing mass spectrometer is shown in Fig. 1.

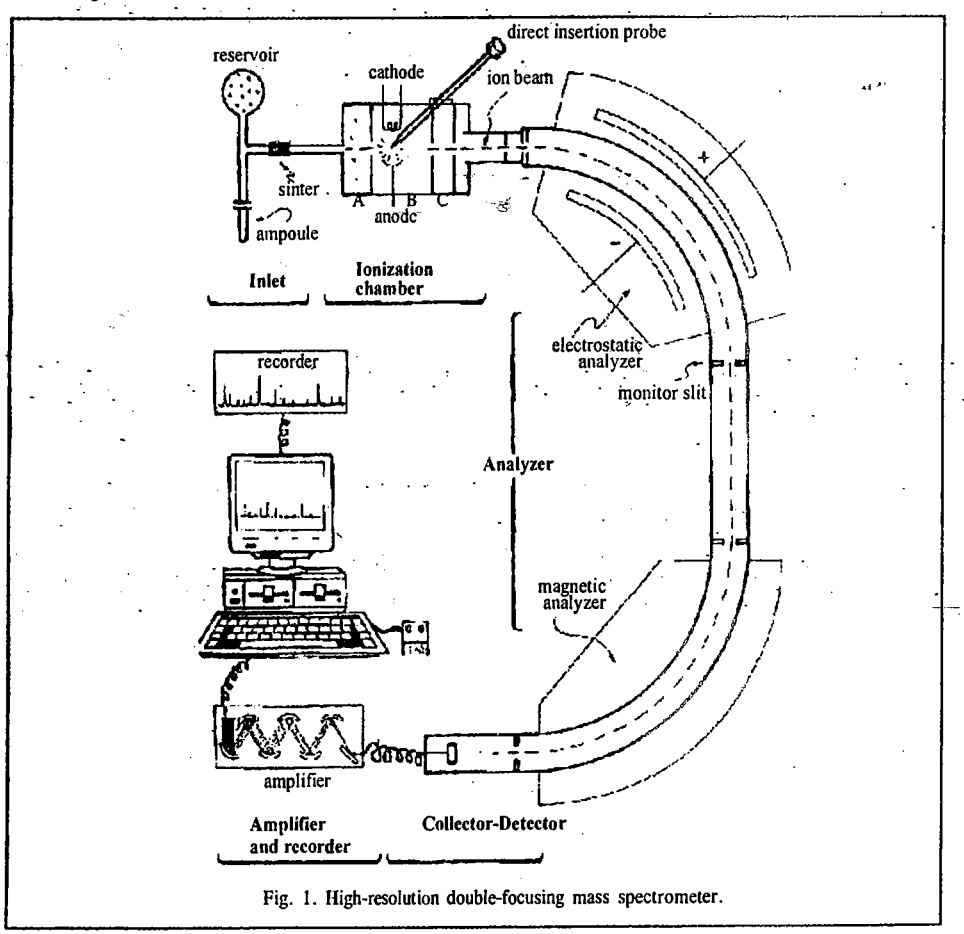

Fig. 1. High-resolution double-focusing mass spectrometer.

Organic or inorganic molecules are bombarded with energetic electrons and thereby converted into highly energetic positively charged ions, called *molecular ions or parent ions*, which can undergo further break up into small ions, called *fragment ions* or *daughter ions*. The loss of an electron from a molecule resulting in the formation of a molecular ion may thus be represented as $M \longrightarrow M^{+\bullet}$. The molecular ion, $M^{+\bullet}$, may decompose to a pair of fragments which could be either a radical plus an ion, or a small molecule plus a radical cation :

$$M^{+\bullet} \longrightarrow m_2^{\bullet} + m_1^{+} \quad \text{or} \quad m_2 + m_1^{+\bullet}$$

All the species—the molecular ions, the fragment ions and the fragment radical ions—are separated by deflection in a variable magnetic field according to their mass to charge ratio. They generate an *ion current* at the collector, the magnitude of which depends on their *relative abundances*. For singly charged ions, the lower the mass, the more easily is the ion deflected in the magnetic field. We may mention here that organic molecules react on electron bombardment in two ways : either an electron is captured by the molecule, giving a radical anion or an electron is ejected from the molecule giving a radical cation :

$$M \xrightarrow{e^-} M^{-\bullet} \quad \text{or} \quad M \xrightarrow{-e^-} M^{+\bullet} + 2e^-$$

The latter mode is far more probable and **positive-ion mass spectrometry** is the result. Most organic molecules form molecular ions ($M^{+\bullet}$) when **bombarded with** electron beam of energy 10–15 eV. However, electron bombardment energies of the order **of 70 eV** are generally employed for it is only at these energies that substantial fragmentation of molecules occurs.

The ions produced in the ionization chamber are separated in the magnetic analyzer on the basis of their m/z values. The kinetic energy, E, of the ion is given by the expression $E = \frac{1}{2}mv^2$, where m is the mass of the ion travelling with velocity v. The molecular ions generated in the ionization chamber are expelled electrostatically by means of a low positive potential on a repeller plate (A) in the chamber. After emerging from the plate, they are accelerated down the ion tube by a very high potential, V (of the order of several thousand volts) **between plates** B and C. When the ion is repelled, its potential energy, zV, is converted into the **kinetic energy**. Thus,

$$zV = \tfrac{1}{2}mv^2 \quad \text{or} \quad v^2 = 2zV/m \qquad ...(1)$$

When the ions are subjected to the magnetic **field, B, of the analyzer**, they execute a circular motion. At equilibrium, the centrifugal force of the ion (mv^2/r) equals the centripetal force (zBv) exerted on it by the magnet, where r is the radius of the circular motion. Thus,

$$mv^2/r = zBv \qquad ...(2)$$

Hence, $$v = zBr/m \qquad ...(3)$$

From Eqs. 1 and 3, $$2zV/m = (zBr/m)^2 \qquad ...(4)$$

so that $$m/z = B^2r^2/2V \qquad ...(5)$$

Since B, V and r can be controlled experimentally, the ratio m/z can be determined. It should be noted that a dipositive ion of mass 54 gives rise to the same m/z as a monopositive ion of mass 27. Under the experimental conditions employed here, most of the ions produced are singly charged species.

When the ions pass through the detector, the signal, after being amplified (if it is of weak intensity) is recorded. The most common amplification system used is the *electron multiplier* which operates in a manner similar to the photomultiper-detector. Two essential features of the recording system in a mass spectrometer are that it must (*a*) **have a very fast** response and be able to scan several hundred peaks per second and (*b*) be able to **record peak** intensities varying by a factor of more than 10^3. The analog signal coming from the detector is first converted to a digital form in an analog-to-digital converter and the digitalized data are stored in computer memory.

In order to obtain the mass spectrum we have to determine the m/z ratio for all fragments produced when a molecule is bombarded by highly energetic electrons, as stated above. To do this, the detector set can be moved and the value of r measured for all particles continuously produced by electron bombardment in the ion source. It is, however, much simpler to vary B and V continuously (Eq. 5). This way all particles eventually travel in a semi-circle of fixed radius r. The signal intensity, which is directly proportional to the number **of ions** striking the detector, can be plotted as a function of B or V, whichever is varied. In practice, however, it is convenient to measure a varying potential so that B is often held constant. If B and r are constant, V is inversely proportional to m/z (Eq. 5) and m/z can be plotted versus the signal intensity, giving the desired mass spectrum.

Fig. 2. shows the mass spectrum of 2-methylpentane (C_6H_{14}). The most abundant ion has m/z value of 43 (corresponding to $C_3H_7^+$), showing that the most favoured point of rupture occurs between C_x and C_y. The most abundant ion (the *base peak*) is arbitrarily assigned an abundance of 100 ; all other intensities are expressed as a percentage of this (*relative abundances*). The small peak at m/z 86 is evidently the molecular ion. The peaks at m/z 15, 29 and 71 correspond to CH_3^+, $C_2H_5^+$ and $C_5H_{11}^+$, respectively, etc. The fragment ions arise from the rupture of the molecular ion, either directly or indirectly.

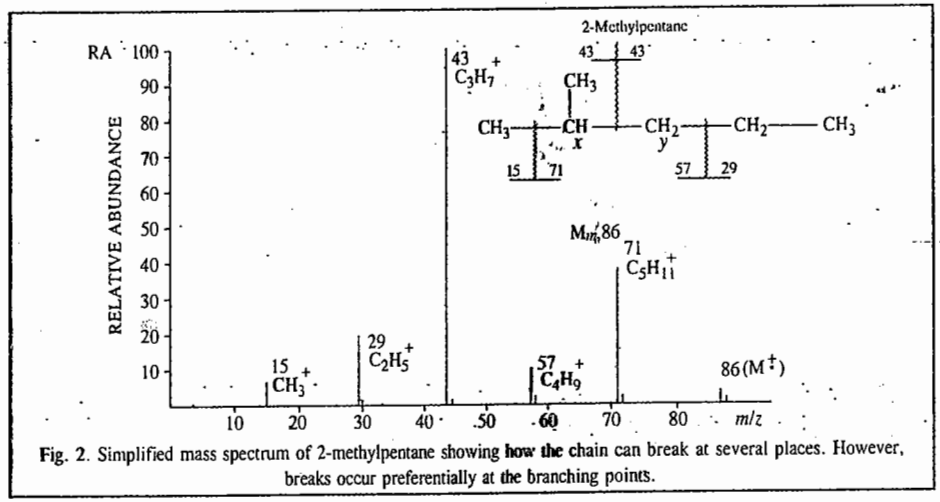

Fig. 2. Simplified mass spectrum of 2-methylpentane showing **how the** chain can break at several places. However, breaks occur preferentially at the branching points.

The mass spectrum of a compound can be obtained on a smaller sample size (of the order of 10^{-12} g) than for any other spectroscopic technique. The principal disadvantage is the destructive nature of the process, which precludes the sample recovery, the difficulty of introducing very small samples into the high vacuum system needed for handling the ionic species involved and the high cost of the instruments. Modern mass spectrometers provide a wide range of options in inlet systems, ion sources, mass analyzers, detectors and signal processors. Batch inlet systems volatilize a sample externally and allow it to leak into the ionization region. The sample must have an appreciable vapour pressure below about 500°C. The molecular ion ($M^{+\bullet}$) in the mass spectrum usually has the highest m/z value, with the exception of a characteristic group of peaks at m/z values of $M^{+\bullet}+1$, $M^{+\bullet}+2$, $M^{+\bullet}+3$,..., etc. The latter are **isotope peaks** which arise from the fact that many of the elements present in organic molecules are not mono-isotopic. Peaks in the mass spectrum are usually sharp and appear at integral mass values (with the exception of those arising from some doubly charged ions). Occasionally, peaks are observed which are broad, spread over several mass units and are of low intensity. These are called **metastable peaks** and give valuable information about the mode of fragmentation.

Most commercial mass spectrometers are equipped with accessories that allow use of several ion

sources interchangeably. Some of these are listed in Table 1.

TABLE 1

Some Common Ion Sources in Mass Spectrometers

Name	Acronym	Type	Ionizing Agent
Electron ionization	EI	Gas phase	Energetic electrons
Field ionization	FI	Gas phase	High-potential electrode
Chemical ionization	CI	Gas phase	Reagent positive ions or electron capture
Fast atom bombardment	FAB	Desorption	Energetic atoms
Field desorption	FD	Desorption	High-potential electrode
Laser desorption	LD	Desorption	Laser beam
Plasma desorption	PD	Desorption	High-energy fission fragments from ^{252}Cf
Secondary ion mass spectrometry	SIMS	Desorption	1 – 20 keV ions
Thermal ion mass spectrometry	TIMS	Desorption	Heat

Electron ionization, EI, uses, as said earlier, a beam of monoenergetic electrons to ionize the gaseous molecule. The desorption types use a sample probe from which energy directly transfers ions or molecules in the condensed phase to ions in the gas phase. Field ionization, FI and field desorption, FD, employ large voltages to produce large electric fields (10^8 V/cm) to ionize molecules. Gaseous samples are used in the former and non-volatile samples on a probe in the latter. In chemical ionization, CI, the sample is bombarded by positive ions produced by electron bombardment of a gaseous atom or molecule (often CH_4) present in the sample in 1000 to 10,000-fold excess. Less fragmentation results with CI than with EI. In fast atom bombardment, FAB, the sample in a condensed state (often a glycerol matrix) is ionized by bombardment with energetic Xe or He atoms.

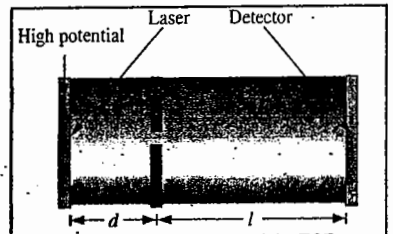

Fig. 3. The diagram of a MALDI-TOF mass spectrometer

Macromolecules present a challenge for molar mass determination using mass spectrometry because it is difficult to produce gaseous ions of large species without fragmentation. However, two new techniques have emerged that circumvent this problem. These are : matrix-assisted Laser desorption/ ionization (MALDI) and electrospray ionization (ESI). We shall briefly discuss here MALDI-TOF mass spectrometry, so called because the MALDI technique is coupled to time-of-flight-(TOF) ion-detector. Fig. 3 shows a schematic view of MALDI-TOF mass spectrometer.

The macromolecule is first embedded in a solid matrix that often consists of an organic compound such as *trans*-3-indoleacrylic acid and inorganic salts such as NaCl or silver trifluoroacetate. A laser beam (usually a pulsed laser, such as N_2 laser) ejects macromolecules and ions from the solid matrix. The ionized macromolecules are accelerated by an electrical potential difference ($\Delta\phi$) over a distance d and then travel through a drift region of length l.

The time, t, required for an ion of mass m and charge number z to reach the detector at the end of the drift region is calculated as follows : The kinetic energy of the ion is given by

$$E_k = \tfrac{1}{2} mv^2 = z\, e\, \Delta\phi\, d \qquad ...(6)$$

where v is the speed of the ion. The drift region, l and the time of flight, t, in the mass spectrometer are both sufficiently short so that we can ignore acceleration and write $v = l/t$. Hence, substitution in Eq. 6 gives

$$\tfrac{1}{2} m(l/t)^2 = z\, e\, \Delta\phi\, d \qquad ...(7)$$

Rearrangement of Eq. 7 gives

$$t = l\, (m/2z\, e\, \Delta\phi\, d)^{1/2} \qquad ...(8)$$

Since d, l and $\Delta\phi$ are fixed for a given experiment, the time of flight, t of the ion is a direct measure of its m/z ratio, which is given by

$$m/z = 2\, e\, \Delta\phi\, d\, (t/l)^2 \qquad ...(9)$$

The mass spectroscopic techniques of MALDI-TOF, ESI and SLD (soft laser desorption), have many areas of application. Sophisticated biochemical analyses, which seemed impossible only a few years ago, are now routinely performed, thanks to these techniques. MS(mass spectrometry)-based analytical methods are relatively cheap and are thus widely used in research laboratories around the world. The ESI and SLD techniques, developed, respectively, by Fenn and Tanaka, are standard techniques for structure analyses of peptides, proteins and carbohydrates. In the pharmaceutical industry, drug development has undergone a radical change because of the new MS techniques. ESI- and SLD-based methods are now used in the rapid diagnosis of diseases such as malaria and ovarian, breast and prostate cancers. The 2002 Chemistry Nobel Prize was jointly awarded to the American chemist J.B. Fenn, the Japanese chemist K. Tanaka and the Swiss chemist, K. Wüthrich "for identification and structure analyses of biological molecules". (Wüthrich used NMR spectroscopy for determining the three-dimensional structure of biological macromolecules.)

Dynamics of Electron–Molecule Collisions in Mass Spectrometry

We shall deal, in some details, with the various processes that occur when energetic electrons bombard a molecule. The excess electron energy can be high enough to break bonds in the molecular ion, leading to its fragmentation. The acceleration potential of the bombarding electron that is just large enough to initiate fragmentation is called the appearance potential of the fragment ion. As the electron bombardment energy becomes high, several bonds can undergo cleavage. Consider a hypothetical molecule BCDE bombarded with an electron. The following processes may occur in sequence :

(*a*) *Ionization* :

$$BCDE + e^- \longrightarrow BCDE^+ + 2e^- \qquad ...(10)$$

(*b*) *Fragmentation of the Positive Ion* :

$$BCDE^+ \longrightarrow B^+ + CDE\cdot \qquad ...(11)$$

$$BCDE^+ \longrightarrow BC^+ + DE\cdot \qquad ...(12)$$

$$BC^+ \longrightarrow B^+ + C\cdot \qquad ...(13)$$

or $$BC^+ \longrightarrow B\cdot + C^+ \qquad ...(14)$$

$$BCDE^+ \longrightarrow DE^+ + BC\cdot \qquad ...(15)$$

$$DE^+ \longrightarrow D^+ + E\cdot \qquad ...(16)$$

or $$DE^+ \longrightarrow D\cdot + E^+ \qquad ...(17)$$

$$BCDE^+ \longrightarrow BE^+ + CD\cdot, \text{ etc.} \qquad ...(18)$$

$$BCDE^+ \longrightarrow CD^+ + BE\cdot, \text{ etc.} \qquad ...(19)$$

(*c*) *Pair Production* :

$$BCDE + e^- \longrightarrow BC^+ + DE^- + e^- \qquad ...(20)$$

(*d*) *Resonance Capture* :

$$BCDE + e^- \longrightarrow BCDE^- \qquad ...(21)$$

It can be easily visualised that only positively charged species can travel to the detector to give rise to peaks in the mass spectrum.

The above mentioned reactions are unimolecular decay processes. Fragment ions are generally formed in vibrationally excited states that have an excess of internal energy. Sometimes, an ion, formed in an excited electronic state on the removal of a low-energy ion, undergoes internal conversion of energy, thereby producing an electronic ground state of the ion that has an excess of vibrational energy. In that case the molecule can dissociate in any of the excited states involved in

the internal conversions associated with radiationaless energy transfer. It is relevant to compare the time scales for some of the processes listed above. The time for a bond vibration is $\sim 10^{-13}$ s ; the maximum lifetime of an excited state ion is $\sim 10^{-8}$ s and the time an ion spends in the mass spectrometer ion chamber is 10^{-5} to 10^{-6} s. We see that there is ample time for the excess electronic energy in an ion to be converted into an excess of vibrational energy in a lower electronically excited state. Thus, molecular ions in the ionization chamber are produced in different energy states which further undergo rapid internal energy conversions to give rise to ions with varying amounts of energy. Thus, all the above processes of fragmentation of the ion $BCDE^+$ are reflected in the mass spectrum.

Factors Influencing Fragmentation. We shall briefly list some factors that involve fragmentation of organic compounds :

a. Functional groups. Some functional groups may direct the course of fragmentation profoundly while other functional groups may have little effect.

b. Thermal decomposition. Thermal decompositions of thermolabile compounds may occur in the ion source leading to difficulty in interpreting mass spectra. For instance, alcohols may undergo dehydration before ionization. If thermal decomposition is suspected, the compound may be ionized in a *cooled* ion source so that electron bombardment of the whole molecule takes place.

c. Bombardment energies. Organic mass spectra are routinely recorded at about 70 eV electron energy. It may be noted that even with these high energies, the molecular ions possess a maximum of about 6 eV energy in excess of their ionization potentials and there is little change in the fragmentation pattern if this 70 eV energy is reduced to about 20 eV. However, the *ion field* (*i.e.*, the efficiency of ionization) is reduced and the spectra are weaker in intensity overall. From about 20 eV down to the ionization potential of the molecule, the mass spectrum becomes progressively simpler since only the most favoured fragmentations are occurring. Thus, recording low-energy spectra is a useful method for bond-energy studies.

d. Relative rates of fragmentation processes. These are also helpful in dictating relative abundances. Thus, in the simple case of A^+ changing either to B^+ and $C^\bullet$ or to $B^\bullet$ and C, the equilibrium abundances of A^+, B^+ and $B^\bullet$ depend on the relative rate constants for the two competing reactions. These rate constants may, in turn, depend on the excitation energy possessed by $A^\bullet$ and will also depend on the heats of formation of ***all*** the products.

Evaluation of Heats of Sublimation of Solids

The mass spectroscopic technique enables the evaluation of the heats of sublimation of solids having high melting points. The principle is based on the fact that the intensity of peaks in the spectrum is directly proportional to the pressure of the sample in the ion source. The sample is placed in a reservoir containing a very small pinhole (a **Knudsen cell**) which is connected to the ion source; the sample enters the source by diffusion through the hole. Enough sample is placed in the thermostated cell ; the solid phase is present in the cell. The change in peak intensity, which is related to the vapour pressure, is followed as a function of temperature. From this the heat of sublimation is calculated. Although a small amount of the sample diffuses into the ion beam, it does not alter the equilibrium in the cell. It has been found that monomers, dimers and trimers are present in the vapour of alkali metal chlorides.

Calculation of Appearance Potentials and Ionization Potentials

As we have stated earlier, when an electron with energy equal to, or greater than, the ionization energy of the molecule, collides with the molecule, a molecular ion is produced. Fig. 4 shows the ***ionization efficiency curve*** which is the curve of relative intensity of a peak (*i.e.*, the number of ion fragments of a particular type) versus the incident electron energy. At electron energies below the ionization energy no ions are produced. As the energy of the electron beam equals the ionization

energy, a peak of very low intensity is obtained because the probability of all the energy of the electron being transferred to the molecule in the electron–molecule collision is very small. However, with increase in electron energy, the probability of the ionization of the molecule increases (since electron energy transfer to the molecule increases), resulting in a more intense peak until a plateau occurs in the curve. The curve shows a tail at lower electron energies because of the variation in the electron energies in the bombarding electron beam. The extrapolation of the curve (shown by a dotted line) yields the ionization energy. When the observed peak is that due to the molecular ion, $e^- + RX \longrightarrow RX^+ + 2e^-$, the extrapolation of the ionization efficiency curve gives the ionization energy of the molecule. When, however, the observed peak is that of the fragment, extrapolation of the ionization efficiency curve yields the **appearance potential** of the fragment. If, for instance, the peak under investigation is that of the fragment R^+ from the molecule R–X, the appearance potential A_{R^+}, is obtained by the extrapolation of the efficiency curve for this peak :

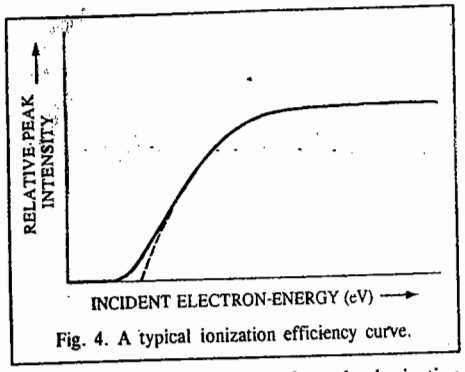

Fig. 4. A typical ionization efficiency curve.

$$A_{R^+} = D_{R\text{-}X} + I_R + E_{kin} + E_e \quad \ldots(22)$$

In Eq. 22, $D_{R\text{-}X}$ is the gas phase dissociation energy of the R–X bond ; I_R is the ionization energy of R ; E_{kin} is the kinetic energy of the particles produced and E_e is the excitation energy of the fragments, *i.e.*, the electronic, vibrational and rotational energy if the fragments are produced in excited states. Since E_{kin} and E_e are generally small, they can be neglected, giving

$$A_{R^+} = D_{R\text{-}X} + I_R \quad \ldots(23)$$

Knowing $D_{R\text{-}X}$, I_R can be calculated from the appearance potential data using Eq. 23. It should be noted that I_R must be less than I_X otherwise X^+ gets dissociated or electronically excited.

Fragmentation Processes

There are two important factors which determine the intensities of the fragment ions in the mass spectrum, *viz.*, the stability of the ion and the energy relationships of the bonds broken and formed in the reactions leading to the ion. Though the experimental conditions in the mass spectrometer (very low pressure, unimolecular reactions) differ greatly from those normally encountered in organic chemistry, the basic ideas of chemistry can be used to rationalise the appearance of the mass spectrum. Thus, the following fragmentations produce stable carbocations :

(*a*)
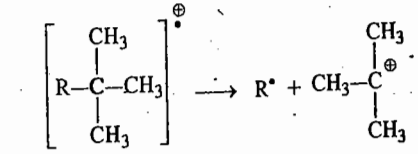

The order of stability of saturated carbocations decreases in the order : tertiary > secondary > primary > methyl. Thus, a stable tertiary carbocation in formed.

(*b*) Formation of a resonance-stabilised allylic carbocation :

$$R{-}CH_2{-}\overset{\oplus}{C}H{-}CH_2 \longrightarrow R^\bullet + \overset{\oplus}{C}H_2{-}CH{=}CH_2 \longleftrightarrow CH_2{=}CH{-}\overset{\oplus}{C}H_2$$

(*c*) Formation of a seven-membered cyclic tropylium ion, $C_7H_7^\oplus$:

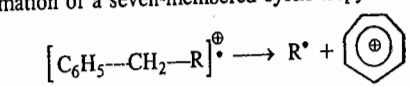

(*d*) The carbocation is stabilised by delocalisation of the lone-pair electrons on the adjacent heteroatom :

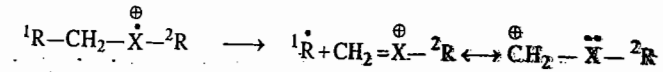

(*e*) Formation of the resonance-stabilised acylium ion :

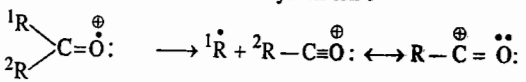

Note that the molecular ion is formed by removal of electron of the lowest ionisation potential from the molecule. The energy required to remove an electron varies in the order

lone-pair < conjugated π < non-conjugated π < σ

A radical ion is thus formed which may fragment in a variety of ways. Simple bond cleavage may occur to give a neutral and an ionic fragment. Alternatively, several rearrangements may occur which are then followed by bond cleavage reactions. We shall give below some examples of fragmentations and rearrangements.

Fragmentation by Movement of One Electron. Bonds are broken by movement of one electron, represented by a fish-hook arrow (↶).

(*a*) *σ-cleavage (sigma cleavage)* :

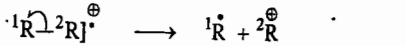

Ionisation results in the removal of a σ-electron and the σ-bond then breaks preferentially to give a stable carbocation with the ejection of the largest possible group as the radical.

(*b*) *α-cleavage (alpha cleavage)* :

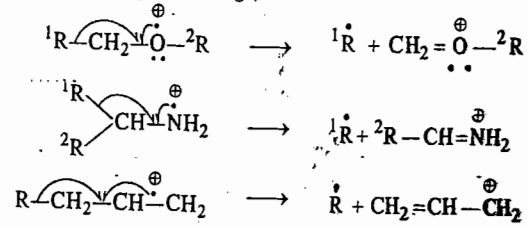

In all these processes an uncharged alkyl radical is lost enabling the residual electron to pair with that associated with the original radical ion to form an even-electron ionic species.

Fragmentation by Movement of an Electron Pair. In this process bonds are broken by movement of an electron pair (two electrons) towards the positive charge represented by a normal 'curly arrow' (↷).

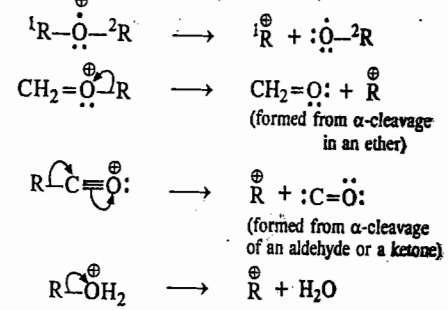

In all of these processes an electron pair is donated to the charge site. The electron pair may come from the bond adjacent to the charge site.

Rearrangements. Rearrangements may yield odd-electron ions which are normally recognized in the spectrum. They are useful aids in the interpretation of the mass spectrum. Since large amounts of energy are normally available in the ion source, rearrangements are extremely common. Several kinds of rearrangements are possible. The most frequently encountered example is the McLafferty rearrangement which involves the transfer of a γ-hydrogen atom in the unsaturated system via a low energy six-membered transition state :

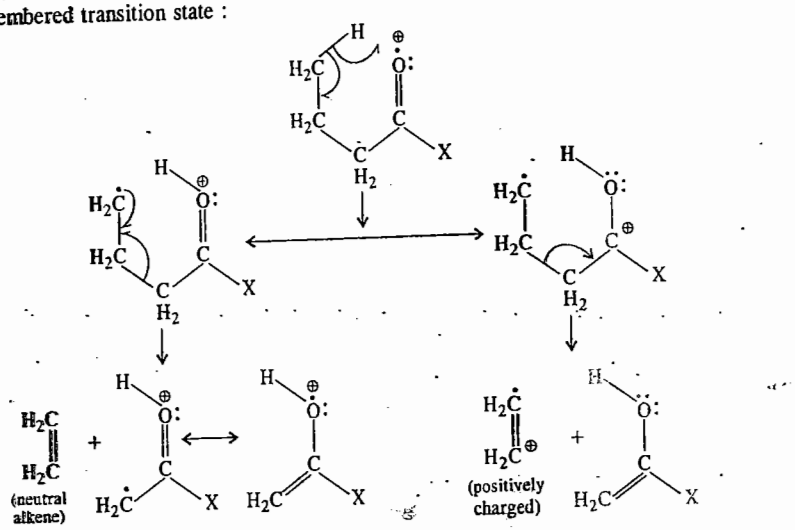

The ionic fragment may be either the alkene or the fragment containing the heteroatom. This is determined by the relative ionisation potentials of the two groups. The arrangement is general for this type of functional grouping and also occurs with oximes, hydrazones, ketimines, carbonates, phosphates, sulphites, alkenes and phenylalkanes.

Even-Even Rule. This rule is a rule-of-thumb interpretation of basic thermodynamic principles. It states that an even-electron species (an ion, as opposed to a radical ion) will not normally fragment to two odd-electron species (*i.e.*, it will not degrade to a radical and a radical ion), since the total energy of this product mixture would be too high :

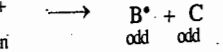

The ion will preferentially degrade to another ion and a neutral molecule :

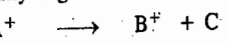

Radical ions, being odd-electron species, can extrude a neutral molecule, leaving a radical ion as coproduct :

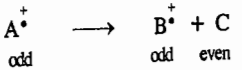

Radical ions can also degrade to a radical and an ion :

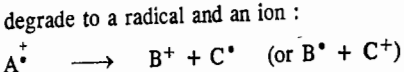

We may mention here *that peaks which arise from metastable ion decomposition* are *normally broad and of low intensity*. They arise from the fragmentation of ions which have already been accelerated out of the ion source but have not yet reached the magnetic field. They are thus displaced

from the position in the spectrum which would correspond to their true mass. The position of the peak due to metastable ion, m^*, is related to the mass of the precursor ion (m_1) and the mass of the product ion (m_2) by the equation :

$$m^* = (m_2)^2/m_1 \qquad \ldots(24)$$

The existence of a metastable ion and its relation to m_1 and m_2 thus confirm that the ion m_2 was, in fact, formed directly from m_1. There are theoretically many possible solutions to this equation but the actual solution is normally obtained by the inspection of the mass spectrum using major peaks, usually of similar intensity, as possible values of m_1 and m_2. For spectrometers which have an exponential mass scan, this is a simple operation since the distances between m^* and m_2 ; and m_2 and m_1 will be identical.

Further Remarks on the Molecular Ion

Though the molecular ion is invariably represented as $M^{+\bullet}$, *i.e.*, a radical cation produced when a neutral molecule loses an electron, we naturally ask : where does the electron come from ? For electron bombardment around their ionizational potentials (≈ 15 eV), one can specify the orbitals which are likely to lose electrons in the case of organic molecules. The HOMOs of aromatic systems and the non-bonding orbitals on oxygen and nitrogen atoms readily lose an electron. The π-orbitals of double and triple bonds are also vulnerable. At the instant of ionization in a Franck-Condon process, before any structural rearrangement can occur, these ionizations can then be represented schematically as follows :

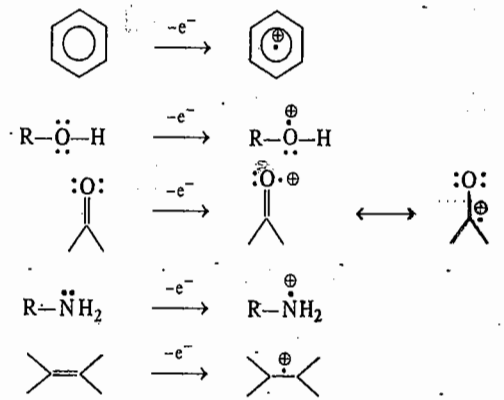

For bombardment of complex molecules around 70 eV, any specificity in the site of electron removal is lost entirely. These arguments apply also to the structures of fragment ions and fragment radical ions. These are frequently written in square brackets, *e.g.*, $[C_5H_5]^{\oplus\bullet}$ or $[C_4H_7]^{\oplus\bullet}$, no attempt being made to speculate on the precise structures.

Recognition of the Molecular Ion. Since the molecular formula is invariably the most important information to be derived from the mass spectrum, it is necessary to be as certain as possible that the molecular ion within the molecular cluster ($M^{+\bullet}$, $M^{+\bullet}+1$, $M^{+\bullet}+2$, etc.) has been correctly identified. We can apply a number of tests which can determine if an ion is not the molecular ion.

The ion must be an odd-electron species since the molecular ion is produced by the loss of one electron from the neutral molecule. The converse is not true since there may be odd-electron ions other than the molecular ion in the spectrum, arising from rearrangement reactions. If the elemental composition of the ion can be determined, the index of hydrogen deficiency (the sum of multiple bonds and ring systems) can be used to determine whether the ion is an odd-electron ion. The index of hydrogen deficiency is the number of pairs of hydrogen atoms which must be removed from the

saturated open-chain formula to give the observed molecular formula. For a molecule $I_yII_nIII_zIV_x$, the index of hydrogen deficiency $= x - y/2 + z/2 + 1$ where

I = any monovalent atom,
II = O, S or any other divalent atom,
III = N, P or any other trivalent atom,
IV = C, Si or any other tetravalent atom.

Thus, for example, thiophene, C_4H_4S, 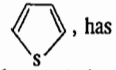 , has an index of hydrogen deficiency $= \left(4 - \frac{4}{2} + 1\right) = 3$.

The index of hydrogen deficiency must be a whole number for an odd-electron ion. For an even-electron ion the value will be non-integral.

The second test that can be applied is the nitrogen rule. If a molecule (or ion) contains an odd number of nitrogen atoms, it will have an odd numerical value of the molar mass, whereas if it contains zero or an even number of nitrogen atoms, it will have an even-numbered molar mass. The rule applies to all compounds containing C, H, O, N, S, halogens, P, B, Si. Thus, for a species with zero or even number of nitrogen atoms, odd-electron ions will have an even mass number and even-electron ions will have an odd mass number.

A third test that an ion is, indeed, the molecular ion, may be obtained from an examination of the fragment ion peaks in the vicinity of the ion. Mass losses ranging between 3 and 15 and between 20 and 26 are highly unlikely. If they are observed, they would suggest that the molecular ion is, in fact, a fragment ion.

Alteration of instrumental conditions may also provide evidence to confirm the recognition of the molecular ion. The use of maximum sensitivity may show up a very weak molecular ion. Alternatively, if the energy of the electron beam is decreased, the intensity of the fragment ions will decrease relative to the molecular ion. This also applies to fragment ions arising from impurities.

Intensity of the Molecular Ion Peak. The lower the energy required for ionization of the molecule and the more stable the molecular ion, the more intense will be the peak in the mass spectrum. Structural features within the molecule have characteristic values of ionisation energy and hence determine the amount of energy required to form the molecular ion. Table 2 gives a general indication of the intensity of molecular ion for several types of compounds. In general, the intensity of the molecular ion peak increases with unsaturation and with the number of rings but decreases with chain-branching. The presence of heteroatoms with easily ionised outer shell electrons, increases the intensity of the molecular ion.

TABLE 2

Intensity of Molecular Ion Peak in the Mass Spectrum

Strong	Medium	Weak or non-existent
Aromatic hydrocarbons	ArBr, ArI	Aliphatic alcohols, amines and nitriles
ArF, ArCl, ArCN, $ArNH_2$	Conjugated alkenes Benzyl and benzoyl compounds	Branched chain compounds
Saturated cyclic compounds	Alkyl halides, ethers, straight chain ketones and aldehydes, acids, ester, amides	Nitro compounds.

Molar Mass Determination by Mass Spectrometry

Determination of molar mass requires methods that will produce the parent ion peak. Fig. 5 shows the spectra of glutamic acid, $HO_2C{-}CH(NH_2)CH_2CH_2CO_2H$, obtained by field ionization (FI) and field desorption (FD) methods. Very little fragmentation occurs with field desorption. Either method is adequate for the molar mass determination. FAB is the most frequently used method for molar mass determination of nonvolatile materials giving the dominant $(M+H)^+$ and $(M-H)^+$ ions for organic materials. With organic materials and organometallic compounds, significant fragment ion

information is obtained providing structural information.

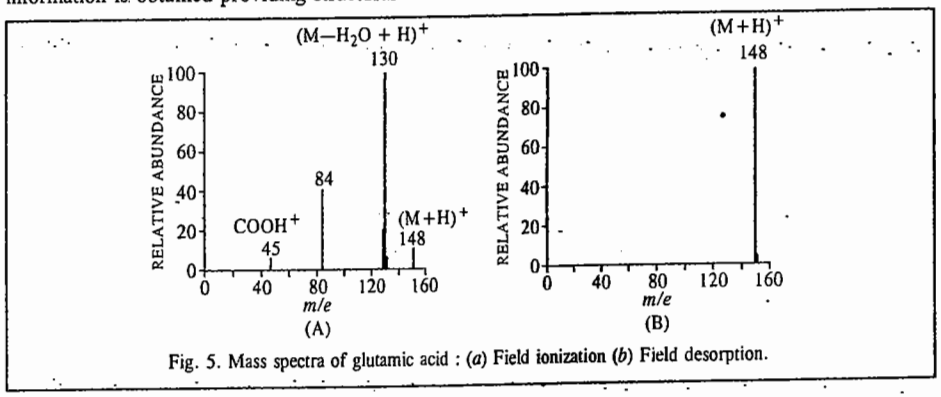

Fig. 5. Mass spectra of glutamic acid : (*a*) Field ionization (*b*) Field desorption.

Fingerprint Application of Mass Spectra. For the fingerprint application, an electron beam of 70 eV is usually employed as it yields reproducible spectra. The accelerating potential here is above the appearance potential of most fragments. Several fragmentation processes can occur (as shown in Eqs.10-20), resulting in a large number of peaks in the spectra of simple compounds. The weak peaks observed are useful for a fingerprint application though they are not generally accounted for in the interpretation of the spectrum. In fact, for a fingerprint application, the more the peaks, the better it is. Accordingly, EI methods are preferred. Spectral-libraries for EI at 70 eV are available in computer form for matching an unknown spectrum to a known one. It is best to make a comparison of the spectrum of the unknown compound with that of a known sample on the same instrument if a decision is to be made on relative intensities.

Concluding Remarks. Mass spectrometry is used for routine sequencing of small peptides. The low volatility of many substances hampers their analysis by MS. The volatility can often be increased by making derivatives of the polar groups of the molecule, *e.g.*, the carboxyl groups can be converted to methyl esters or trimethylsilylesters. Field ionization techniques are also advantageous for this problem.

The combination of mass spectrometry with gas-liquid chromatography (GLC) provides an excellent method for analysis of mixtures. Very small amounts of material are needed. The mass spectrometer may be used as the GLC detector and numerous mass spectra may be accumulated as each component emerges from the spectrum. A partially resolved GLC peak is readily detected by the change in mass spectra of the peak with time.

Problem 1. Use R : S as the typical generalized compound to write ionic equations for the first two steps leading to mass spectral analysis. Identify the steps and each moiety in the equations.

Answer : **Step 1.** $R:S \underset{\text{Parent}}{} + \underset{\substack{\text{High}\\\text{energy}}}{e^-} \longrightarrow R{\cdot}S^+ + 2e^-$ (ionization)

Step 2. $R{\cdot}S^+ \rightarrow \begin{cases} R{\cdot} + S^+ \\ \text{or} \\ S{\cdot} + R^+ \end{cases}$ (fragmentations)

Radicals Cations

Fragmentation can also release a smaller radical cation and a non-radical molecule :

$$R{\cdot}S^+ \longrightarrow R + {\cdot}S^+ \quad \text{or} \quad {\cdot}R^+ + S$$

Problem 2. After ionization and fragmentations occur, what does the mass spectrometer do to provide a mass spectrum ?

Answer : The spectrometer sorts out all the cations (including the radical cations) according to their mass/charge (*m/z* or *m/e*) values and records these values (decreasing from right to left) as line signals along the abscissa. At the same time, the instrument records their relative abundances as signal heights plotted as intensities along the ordinate. The radicals are not detected.

Problem 3. (*a*) Why can the *m/z* values be taken as the molar mass of the cation in most cases ? (*b*) How can the molar mass of a compound be determined by mass spectral analysis ? (*c*) Why is less than 1 mg of the parent compound used in the vapour state for analysis ? (*d*) Why do several signals appear in a typical spectrum ? (*e*) Which fragment cations are the most abundant ? (*f*) How are relative intensities calculated ?

Answer : (*a*) In most cases, the charge on the cation (the value of *z*) is +1, making $m/z = m$.

(*b*) If all the parent (molecular) cations do not fragment (the typical situation), the largest *m/z* value can be assigned as the molar mass of the parent cation and hence the parent itself.

(*c*) A relatively small number of molecules are taken in the vapour state to prevent collisions and reactions between fragments. Combination of fragments might lead to ions with larger masses than the parent cation, making it impossible to determine the molar mass. Fragmentation patterns that are so very useful in structure determination would become confusing.

(*d*) The parent can fragment in several ways and each cationic fragment can further fragment to give smaller cations.

(*e*) The most abundant cations are the most stable ones. Hence, a good understanding of cation stabilities is essential for interpreting fragmentation patterns necessary for structure determination.

(*f*) The most intense peak, called the *base peak*, is arbitrarily assigned a value of 100%. The smaller peak heights are measured and divided by the base peak height to give their relative percentage abundances. Thus, for example, a peak with 2/3 height of the base peak has a relative abundance of 66·7%.

Problem 4. (*a*) Give molecular formulas of hydrocarbon cations with *m/z* values of (*i*) 29 (*ii*) 51 (*iii*) 91.

(*b*) Give a combination of C, H and N to account for *m/z* values of (*i*) 29 (*ii*) 57.

Answer : (*a*) Divide the given values by 12 to get the number of Cs ; the remainder is the mass due to Hs. Molecular formulae are : (*i*) $C_2H_5^+$ (*ii*) $C_4H_3^+$ (*iii*) $C_7H_7^+$.

(*b*) (*i*) If one N is present, subtracting 14 leaves a mass of 15, enough for one C and three Hs. The formula is CH_3N^+. (*ii*) One, two or three Ns can be present giving three cations : $C_3H_7N^+$, $C_2H_5N_2^+$ or $CH_3N_3^+$.

Problem 5. (*a*) Do parent (molecular) ions, RS^+, of hydrocarbons ever have odd *m/z* values ? (*b*) if an RS^+ contains only C, H and O, may its *m/z* value be either odd or even ? (*c*) If an RS^+ contains only C, H and N, may its *m/z* value be either odd or even ? (*d*) Why can an ion, $m/z = 31$, not be $C_2H_7^+$? What might it be ?

Answer : (*a*) No. Hydrocarbons and their parent ions must have an even number of Hs : C_nH_{2n+2}, C_nH_{2n}, C_nH_{2n-2}, C_nH_{2n-6}, etc. Since the atomic mass of C is even (12), the *m/z* values must be even.

(*b*) The presence of O in a formula does not change the ratio of C to H. Since mass of O is even (16), the mass of RS^+ with C, H and O *must be even.*

(*c*) The presence of each N (m=14) requires an additional H ($C_nH_{2n+3}N$, $C_nH_{2n+1}N$, $C_nH_{2n-1}N$). Therefore, if the number of Ns is odd, an odd number of Hs and an odd *m/z* value result. An even number of Ns requires an even number of Hs and an even *m/z* value. These statements apply *only* to parent ions, *not* to fragment ions.

(*d*) The largest number of Hs for two Cs is six (C_2H_6). Some possibilities are CH_3O^+ and CH_5N^+.

Problem 6. Which electron is most likely to be lost in ionization of the following compounds ? Write an electronic structure for RS^+ (*a*) CH_4 (*b*) CH_3CH_3 (*c*) $H_2C{=}CH_2$ (*d*) CH_3Cl (*e*) $H_2C{=}O$.

Answer : Since the electron in the HOMO is most likely to be lost, the decreasing order of ionizability is $n > \pi > \sigma$. When no *n* or π electrons are present, the lost electron most likely comes from the high energy σ bond. The + in each formula below shows the charge and the missing electron.

(*a*) 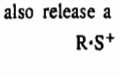 (+ is the charge due to the missing electron)

(*b*) 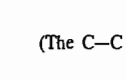 (The C—C bond is weaker than the C—H bond)

(*c*) $H_2C \overset{+}{=} CH_2$ (Electron comes from the π bond)

(*d*) $H_3C : \ddot{Cl}\ddot{:}^{+}$ (An *n* electron is lost)

(*e*) $H_2C = \ddot{O}\ddot{:}^{+}$ (An *n* electron is lost)

Problem 7. Give the structure of a compound $C_{10}H_{12}O$, whose mass spectrum shows *m/z* values of 15, 43, 57, 91, 105 and 148.

Answer : A peak at *m/z* = 15 suggests a CH_3 group. Because 43 – 15 = 28, the mass of C=O, the *m/z* value of 43 may be due to an acetyl, CH_3CO, group in the compound. The highest peak gives the molar mass. Cleaving an acetyl group (*m/z* = 43) from 148 gives 105, which is an observed peak. Next below 105 is 91, a difference of 14 ; this suggests a CH_2 group attached to CH_3CO. So far we have CH_3COCH_2 adding upto 57, leaving 148 – 57 = 91 to be accounted for. This peak is likely to be $[C_7H_7]^+$, whose precursor is the stable benzyl cation, $C_6H_5CH_2^+$. Piecing together all this information, the structure is $CH_3—\overset{\overset{O}{\|}}{C}—CH_2—CH_2—C_6H_5$.

Problem 8. Explain the appearance of *m/z* = 44 in the mass spectrum of $CH_3CH_2CH_2CH{=}O$.

Answer : The value of *m/z* (72) of the molecular ion, minus 44 equals 28, the molar mass of the lost uncharged molecule. High resolution mass spectrometry shows that the lost molecule is $H_2C{=}CH_2$ and the fragment cation is $[H_2C{=}CHOH]^{+\bullet}$. These species arise from the McLafferty rearrangement of the parent cation, as shown below :

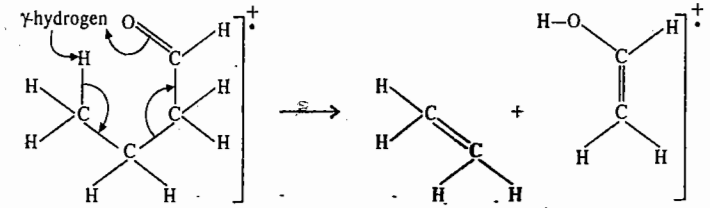

Problem 9. Summarize the kind of information provided by the following spectral techniques : (*a*) UV (*b*) IR (*c*) PMR (*d*) ^{13}C NMR and (*e*) Mass Spectrometry (MS).

Answer : (*a*) Conjugation (*b*) functional groups (*c*) environment of Hs in a molecule and consequently its molecular skeleton including the Hs (*d*) carbon skeleton and (*e*) molar mass of the parent and major structural features from the fragmentation pattern.

Problem 10. Write equations involving the electron-dot formulas for each fragmentation used to explain the following : (*a*) Isobutane, a typical branched-chain alkane, has a lower-intensity RS^+ peak than does *n*-butane, a typical unbranched alkane. (*b*) All primary alcohols, RCH_2CH_2OH, have a prominent fragment cation at *m/z* = 31. (*c*) All $C_6H_5CH_2R$-type hydrocarbons have a prominent fragment cation at *m/z* = 91. (*d*) Alkenes of the type $H_2C{=}CHCH_2R$ have a prominent fragment cation at *m/z* = 41. (*e*) Aldehydes, $RCH{=}O$, show intense peak at *m/z* 29.

Answer : (*a*) The weaker C—C bond cleaves more easily than the stronger C—H bond. Fragmentation of the parent cation of isobutane,

$$(CH_3)_2—\overset{+}{C}\bullet CH_3 \longrightarrow (CH_3)_2\overset{+}{C} + \bullet CH_3$$

gives a 2^0R^+ that is more stable than the 1^0R^+ from n-butane,

$$H_3C\,\overset{H}{\underset{H}{C}}\bullet\overset{+}{\underset{H}{C}}\,CH_3 \longrightarrow H_3C\,\overset{+}{C}\,H + \bullet CH_2CH_3$$

Hence, RS^+ of isobutane undergoes fragmentation more readily than does RS^+ of n-butane, and fewer RS^+ cations of isobutane survive. As a result, isobutane has a lower-intensity RS^+ peak than n-butane.

(*b*) 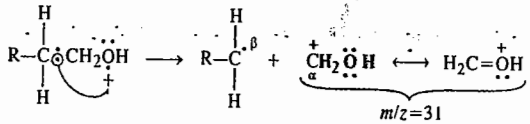

AC^+ next to an O is stabilized by extended π-bonding (resonance). The RS^+ species of alcohols generally undergo cleavage of the bond : $\overset{\alpha}{C}\overset{\beta}{C}—OH$.

(*c*) 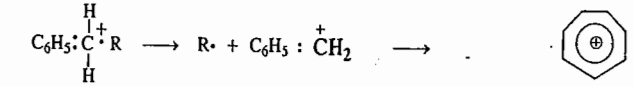

(*d*) 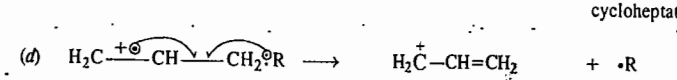

(*e*) 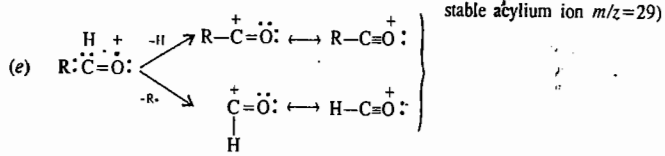

Problem 11. Fig. 6 shows the mass spectrum of nonane. Assign the spectrum to the appropriate compound by analyzing the fragmentation pattern with the aid of equations.

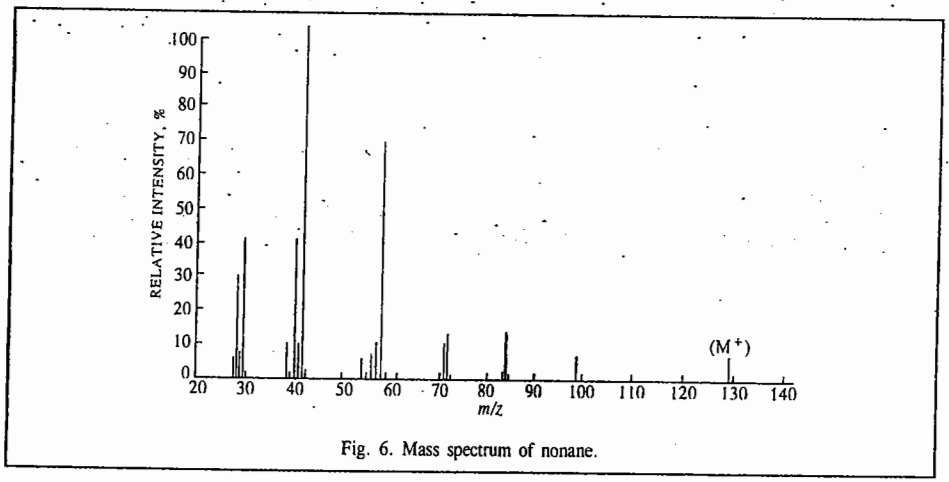

Fig. 6. Mass spectrum of nonane.

Answer : The spectrum in Fig. 6. has a parent peak at *m/z* = 128. The next lower one at *m/z* = 99 indicates a loss of 29 (128 – 99) mass units corresponding to CH_3CH_2. From this point the prominent peaks arise from a sequential loss of CH_2s. This fragmentation pattern is typical for straight chain alkanes.

Problem 12. (*a*) What information can be obtained from the mass spectrum in Fig. 7 about the structure of an aromatic hydrocarbon ? (*b*) What other spectroscopies could help pinpoint the compound ?

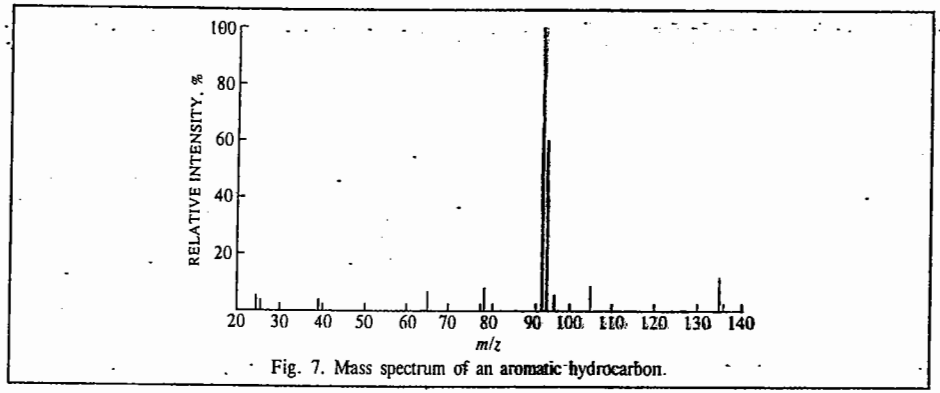

Fig. 7. Mass spectrum of an aromatic hydrocarbon.

Answer. (*a*) Peaks for parent cations of aromatic compounds usually appear in mass spectra. The parent has a molar mass of 134 and a molecular formula of $C_{10}H_{14}$. The base peak at 91 is typically due to $C_6H_5CH_2^+$, indicating that the compound is a monosubstituted benzene with a CH_2 group attached to the ring. Two compounds, $C_6H_5CH_2CH_2CH_2CH_3$ and $C_6H_5CH_2CH(CH_3)_2$, can give this fragment. (*b*) A ^{13}C nmr spectrum would help, as *n*-butylbenzene would give eight signals, and *t*-butylbenzene would give seven signals. A pmr spectrum would show the characteristic septet for 3° H.

For further reading, refer to :

McLafferty F.W., *Interpretation of Mass Spectra*, University Science Books, 1980.

Hill, H.C., *Introduction to Mass Spectrometry*, 2nd edn., London, 1972.

Biemann, K., *Mass Spectrometry : Organic Chemical Applications*, McGraw-Hill, 1962.

Howe, I., D.H. Williams, and R.D. Bowden, *Principles of Organic Mass Spectrometry*, 2nd edn., London, 1982.

McLafferty, F.W., and D.B. Stauffer, *Registry of Mass Spectral Data*, Wiley, 1989.

Davis, R., and M. Frearson, *Mass Spectrometry*, Wiley, 1987.

Christian, G.D., *Analytical Chemistry*, 6th edn., Wiley, 2004.

McMaster, M.C., and C. McMaster, *GC/MS : A Practical User's Guide*, Wiley, 1998.

Hubschmann, H. J., *Handbook of GC/MS*, Wiley, 2001.

I. Review Questions

1. Discuss the basic instrumentation of a high-resolution double-focusing mass spectrometer and derive an expression for the *m/z* in the mass spectrum.
2. Draw schematically the mass spectrum of 2-methylpentane (C_6H_{14}) showing how the chain can break in several places. Discuss briefly the fragmentation pattern observed.
3. Outline briefly the dynamics of electron-molecule collisions in mass spectrometry.
4. Enumerate and discuss the factors which influence fragmentation of organic compounds in mass spectrometry.
5. How are appearance potentials and ionization potentials determined from mass spectrometry ?
6. How is mass spectrometry used to determine the molar mass of a volatile organic compound ?

CHAPTER 36

IRREVERSIBLE THERMODYNAMICS

Classical thermodynamics deals primarily with the study of systems which are in a state of equilibrium. It adequately deals with processes which begin and end with equilibrium states though the intervening states of a given process may be non-equilibrium.

An equilibrium state, in fact, is only an oversimplification of the real state of a system as it can be realized only partially in the man-made systems dealt with in laboratory. Natural processes, on the other hand, are irreversible processes taking place in open systems. As a consequence of several dissipative processes occurring therein, the time-invariant of these irreversible processes is a steady state and not an equilibrium state. The steady state, in fact, is more comprehensive than the equilibrium state, which is merely a limiting case of the former when the 'fluxes' (*viz.*, flow of heat, mass, electricity, etc.) arising from the environment cease to exist. Irreversible thermodynamics is also known as non-equilibrium thermodynamics.

Phenomenological Laws and Onsager's Reciprocal Relations

The irreversible processes involve the transport of one or more of the quantities such as heat, mass, momentum and electric charge. In all these cases, a quantity called the **flux** is transported as a result of a **driving force** which is derived from the gradient of some physical property of the system. Thus, the driving force for a heat flux is the temperature gradient ; that for a mass flux is the concentration gradient and that for an electric current is the potential gradient. In all these cases, the magnitude of the flux (or flow) is directly proportional to the driving force. In general, the transport phenomenon for a one-dimensional system is written as

$$J = LX \qquad ...(1)$$

where J is the **flux** (flow per unit area) of the quantity transported along a given direction ; X is the **driving force** (or the gradient) which causes the flow in that direction and L is the proportionality constant called the **transport coefficient.**

For the various transport (transfer) processes, we can now write the following relations :

1. **Heat Transfer** : $J_Q = -\kappa \dfrac{dT}{dx}$ (Fourier's law) ...(2)
2. **Mass Transfer** : $J_m = -D \dfrac{dc}{dx}$ (Fick's law) ...(3)
3. **Momentum Transfer** : $J_M = -\mu \dfrac{du}{dx}$ (Newton's law) ...(4)
4. **Flow of electricity** : $J_e = -\lambda \dfrac{dE}{dx}$ (Ohm's law) ...(5)

Here the J_is are the corresponding fluxes : J_Q is the heat flux ; J_m, the mass flux ; J_M, the

momentum flux and J_e, the electric flux (*i.e.*, the electric current). The transport coefficients κ, D, μ and λ depend upon the material properties of the system. It should be borne in mind that Eqs. 2, 3, 4 and 5 are not 'laws' in the traditional usage of the term ; they are **phenomenological laws** introduced to define the transport processes.

Phenomenological equations describe in a simple way how the system changes. Ohm's law and Fick's law of diffusion are some familiar examples of phenomenological equations. The phenomenological equations of irreversible thermodynamics are similar to these equations but are more general. Fick's law of diffusion, $dm/dt = D(dc/dx)$, where dm/dt is the rate of change of solute across unit surface area under the influence of the concentration gradient dc/dx and D is the diffusion coefficient, may be adequate in a simple system. Suppose, however, that while one solute diffuses under its own concentration gradient, another solute is also diffusing under its concentration gradient. Can we assume that the movement of the second solute has no influence on that of the first ? Again, suppose that while one solute is diffusing, there also simultaneously exists a *temperature gradient* in the system resulting in a flow of heat. Will the movement of the solute still be described by the equation given above ? The answer to these questions given by theory and also by intuition is no.

We can generalize the equation $dm/dt = D\,(dc/dx)$ for a one dimensional flow as follows :

$$\frac{dm_1}{dt} = D\frac{dc_1}{dx} + E\frac{dc_2}{dx} \qquad ...(6)$$

where the second term incorporates the influence of the gradient of the second solute on the movement of the first solute. Similarly, we can write down another equation for the movement of the second solute :

$$\frac{dm_2}{dt} = F\frac{dc_2}{dx} + G\frac{dc_1}{dx} \qquad ...(7)$$

where D, E, F, G are the corresponding diffusion coefficients. If there are more solutes and thermal gradients, other terms will have to be written.

To simplify notation, we use a single symbol J for dm/dt. Symbols J_1, J_2, ... are used for the rates of movement of different entities (solute, heat, etc.). Again, the multiplicity of coefficients D, E, F, G, ... can be replaced by a single symbol L with appropriate subscripts. Accordingly, D becomes L_{11}, E becomes L_{12}. Here the first subscript refers to the component that moves (and is thus the same as the subscript on the corresponding J) while the second subscript refers to the component whose gradient is being considered. The gradient or driving force is designated by the symbol X. Thus, $X_1 = dc_1/dx$, $X_2 = dc_2/dx$, and so on. This notation is both convenient and easy to remember.

For a given driving force in a system, there is associated with it a *single* irreversible flow which can be described by an appropriate phenomenological relation. Likewise, two simultaneous irreversible flows, provided they are independent of each other, can be described by appropriate phenomenological relations. In practice, however, the simultaneous flows are not independent of each other's gradient. Such flows are known as **coupled flows.** Onsager developed the irreversible thermodynamics (or non-equilibrium thermodynamics) in 1931 for analyzing coupled irreversible flows.

If the gradients X_is are not too great, the fluxes J_is are linear functions of the driving forces. Thus, we can write

$$J_i = L_{i1}X_1 + L_{i2}X_2 + ... + L_{in}X_n \qquad ...(8)$$

where $i = 1, 2, 3, ..., n$.

The relations depicted by Eq. 8 are called **linear phenomenological relations.** The coefficients L_{ii} are called the **primary phenomenological coefficients** while the coefficients L_{ij} are called **Onsager's phenomenological coefficients.** In the Onsager coefficients, the subscript i denotes the flux and the subscript j denotes the driving force.

The solution of Eq. 8 is extremely difficult. Several scientists including Kelvin had attempted its

solution in the 19th century. It was, however, Onsager who finally solved it in 1931. The difficulty in solving this equation lies in the fact that the phenomenological coefficients have to be determined experimentally. The primary coefficients can, of course, be determined easily. The *coupling coefficients* (Onsager's phenomenological coefficients, L_{ij}), however, present severe difficulties for their experimental measurement since they involve the control of many experimental parameters. Onsager theoretically showed that

$$L_{ij} = L_{ji} \qquad ...(9)$$

Eq. 9 gives **Onsager's reciprocal relations** (also called *reciprocity relations*).

Let us dwell further upon the reciprocal relations. Onsager showed that these relations exist for a properly selected pair of flows, called the **conjugate flows.** It is, however, not clear what constitutes a properly selected pair. Suffice it to say that in the case of a one-dimensional conducting rod or wire, if ΔE is the potential difference and ΔT is the temperature difference between the ends, then using ΔE and ΔT as the driving forces, the electric current I ($\equiv J_e$) and the entropy current (or entropy flux) J_s form a pair of conjugate flows, though the electric current and the heat flux J_Q do not do so. The expressions for I and J_s are

$$I = L_{11}\Delta E + L_{12}\Delta T \qquad ...(10)$$

$$J_s = L_{21}\Delta E + L_{22}\Delta T \qquad ...(11)$$

Using the definitions of electrical and thermal conductivities, we can obtain two equations relating the four phenomenological coefficients L_{11}, L_{12}, L_{21} and L_{22} to measurable properties of the system. The fourth expression is furnished by the *Onsager reciprocity relation, viz.*,

$$L_{12} = L_{21} \qquad ...(12)$$

Thus, all the coefficients can be determined. In general,

$$L_{ij} = L_{ji} \qquad ...(13)$$

In simple words this means that the coefficient which expresses the influence of force j on the flux i is the same as the coefficient which expresses the effect of force i on the flux j.

Consider, for instance, Ohm's law, $E = IR$ or $I = E(1/R)$, where E is the potential difference, I the current, R the resistance and $1/R$ the conductance. Comparing this equation with the equation

$$J_i = L_{11}X_1 + L_{12}X_2 + L_{13}X_3 ..... + ... \qquad ...(14)$$

we see that L_{ij} can be regarded as conductance coefficients. Like electrical conductance, their magnitude will depend upon the dimensions and the temperature of the system. If the physical size of the system is doubled, the values of L_s will also be doubled. In biological systems the presence of enzymes will profoundly influence them. It may be remarked here that while Onsager's relations were originally proved only for small deviations from equilibrium, they have also been found applicable to considerable departures from equilibrium. Lars Onsager (1903-1976), the Norwegian-American theoretical chemist, was awarded the 1968 Chemistry Nobel Prize for the discovery of reciprocal relations in irreversible thermodynamics.

Conservation of Mass and Energy in Closed and Open Systems

Consider a closed system ' containing c components ($\gamma = 1, \cdots c$) among which a chemical reaction may take place. In such a system, any variation of masses will result only from the chemical reaction. Thus, the change of mass m_γ of component γ during the time interval dt is given by

$$dm_\gamma = \nu_\gamma M_\gamma d\xi \qquad ...(15)$$

where M_γ is the molar mass of component γ and ν_γ is the stoichiometric coefficient in the chemical reaction. By convention, this stoichiometric coefficient is taken as positive for the product and negative for the reactant ; ξ is the **degree of advancement** or **extent of reaction** introduced by

de Donder. For example, for the reaction,

$$N_2 + 3H_2 \longrightarrow 2NH_3,$$

Eq. 15 gives $$\frac{dm_{N_2}}{-M_{N_2}} = \frac{dm_{H_2}}{-3M_{H_2}} = \frac{dm_{NH_3}}{2M_{NH_3}} = d\xi$$

The total mass of the system is given by $m = \sum_\gamma m_\gamma$. Summing Eq. 15 over γ, the principle of conservation of mass for a closed system is expressed by

$$dm = \left(\sum_\gamma \nu_\gamma M_\gamma\right) d\xi = 0 \qquad ...(16)$$

The equation $$\sum_\gamma \nu_\gamma M_\gamma = 0, \qquad ...(17)$$

is called the **stoichiometric equation** of the chemical reaction.

Instead of the mass of the component it is convenient to use the mole numbers $n_1, n_2, \ldots, n_\gamma$. Thus, we have

$$dn_\gamma = \nu_\gamma \, d\xi \qquad ...(18)$$

Eq. 16 or Eq. 18 introduces ξ. The chemical reaction rate per unit time is defined as

$$v = d\xi/dt \qquad ...(19)$$

It is the ratio between the increment $d\xi$ and the time interval dt. From Eqs. 18 and 19, the increase in the number of moles n_γ will be given by

$$dn_\gamma/dt = \nu_\gamma v \qquad ...(20)$$

Eqs. 16 to 20 can be extended to r simultaneous reactions designated by indices ρ ($\rho = 1, \ldots r$). The total change of mass dm_γ is then equal to the sum of the changes resulting from the various reactions :

$$dm_\gamma = M_\gamma \sum_{\rho=1}^{r} \nu_{\gamma\rho} \, d\xi_\rho \qquad ...(21)$$

where $\nu_{\gamma\rho}$ denotes the stoichiometric coefficient of γ in the ρth reaction. The rate of the ρth reaction is evidently given by

$$v_\rho = d\xi_\rho/dt \qquad ...(22)$$

Let us illustrate the above discussion by considering the following two simultaneous reactions:

$$2C + O_2 \longrightarrow 2CO \qquad (\rho=1)$$

$$C + O_2 \longrightarrow CO_2 \qquad (\rho=2)$$

We have

$$dn_C = -2d\xi_1 - d\xi_2$$

$$dn_{O_2} = -d\xi_1 - d\xi_2$$

$$dn_{CO} = 2\,d\xi_1$$

$$dn_{CO_2} = d\xi_2$$

We next consider an open system. For this system the change in mass dm_γ of component γ is split into two terms :

$$dm_\gamma = d_e m_\gamma + d_i m_\gamma \qquad ...(23)$$

where the first term is due to the mass exchange with the exterior surroundings and the second term is due to the internal changes inside the system.

From Eq. 21, $$dm_\gamma = d_e m_\gamma + M_\gamma \sum_{\rho=1}^{r} \nu_{\gamma\rho} \, d\xi_\rho \qquad ...(24)$$

or $$dn_\gamma = d_e n_\gamma + \sum_{\rho=1}^{r} \nu_{\gamma\rho} \, d\xi_\rho \qquad ...(25)$$

Summing Eq. 23 over γ and taking into consideration the stoichiometric equation (Eq. 17), we find that

$$dm = d_e m \qquad ...(26)$$

This relation expresses the **principle of conservation of mass** in open systems ; it shows that the change in the total mass is equal to the mass exchanged with the exterior (surroundings).

Some thermal energy associated with matter depends on the nature of matter and temperature. For an open system, the application of the principle of conservation of energy requires taking into account the thermal energy transfer which may occur independently of any matter transfer and also because of the matter transfer. Thus, in an open system, the flow of thermal energy transfer, $d\phi$, during the time interval dt consists of the mass-independent energy transfer as well as the mass-dependent energy transfer.

Since $H = U + PV$, we have

$$dH = dU + PdV + VdP \qquad ...(27)$$

Also from the First law of thermodynamics,

$$d\phi = dU + PdV \qquad ...(28)$$

Hence, Eq. 27 can be written as

$$dH = d\phi + VdP \qquad ...(29)$$

We now consider a system consisting of two phases I and II, wherein both matter and energy are exchanged between phases I and II although the entire system is a closed system. Application of Eq. 29 to each phase at constant P yields

$$dH^{I} = d^{I}\phi + V^{I}dP^{I} \quad \text{and} \quad dH^{II} = d^{II}\phi + V^{II}dP^{II}$$

If $P^{I} = P^{II} = P$ and $V = V^{I} + V^{II}$, then the above two equations can be combined to give for the closed system :

$$dH = dH^{I} + dH^{II} = d^{I}\phi + d^{II}\phi + VdP \qquad ...(30)$$

(Though the enthalpy is a state function and hence dH is an exact differential, and the thermal energy is not a state function and hence $d\phi$ an inexact differential, yet for the sake of convenience we have used the same symbol d to show the infinitesimal variations in both these quantities).

Again, since ϕ is not characteristic of the two phases but pertains to them, we have written the variations in ϕ in the two phases as $d^{I}\phi$ and $d^{II}\phi$ rather than as $d\phi^{I}$ and $d\phi^{II}$.) Substituting the expression $dq = dU + PdV$ in Eq. 27, we get

$$dH = dq + VdP \qquad ...(31)$$

Eq. 31 is applicable to the closed system consisting of the two phases. From Eqs. 30 and 31 ; we find that

$$dq = d^{I}\phi + d^{II}\phi \qquad ...(32)$$

Since the system is closed, the term $d^{I}\phi$ can be considered as made up of the energy flow from phase II to phase I and heat flow from the exterior (surroundings) to phase I. Thus, we can write

$$d^{I}\phi = d_e^{I}q + d_i^{I}\phi \quad \text{and} \quad d^{II}\phi = d_e^{II}q + d_i^{II}\phi \qquad ...(33)$$

where e and i are abbreviations for external and internal, respectively.

Eq. 32, therefore, becomes

$$dq = d_e^{\mathrm{I}}q + d_i^{\mathrm{I}}\phi + d_e^{\mathrm{II}}q + d_i^{\mathrm{II}}\phi \qquad ...(34)$$

If dq is the heat exchanged between the entire system and the exterior,

$$dq = d_e^{\mathrm{I}}q + d_e^{\mathrm{II}}q \qquad ...(35)$$

Thus, we see that

$$d_i^{\mathrm{I}}\phi + d_i^{\mathrm{II}}\phi = 0 \qquad ...(36)$$

Considering the heat flow from phase I to phase II,

$$d_i^{\mathrm{I}}q + d_i^{\mathrm{II}}q = 0 \qquad ...(37)$$

Eq. 37 represents the **conservation of energy** for the entire system.

Entropy Production due to Heat Flow. Though energy is conserved as stated in the law of conservation of energy, entropy is not a conserved quantity. Natural or spontaneous processes are accompanied by increase in entropy. We can thus say that entropy is *produced* in such processes. The entropy of a system is an extensive property. If a system consists of several parts, then the total entropy is equal to the sum of the entropies of each part. The change in entropy, dS, can be split into two parts. If we denote the flow of entropy due to interactions with the exterior by d_eS and the contribution due to changes inside the system by d_iS, then we have

$$dS = d_eS + d_iS \qquad ...(38)$$

$d_iS=0$ for a reversible process and $d_iS > 0$ for an irreversible process; it is never negative. We may mention that the splitting of entropy change into two terms d_eS and d_iS permits an easy discussion of the difference between closed and open systems. Evidently, this difference has to appear in the term d_eS which, for open systems, must contain terms due to the exchange of matter.

Consider a closed system consisting of two phases I and II maintained respectively at uniform temperatures T^{I} and T^{II}. According to the Second law of thermodynamics, entropy change is given by the relation

$$dS = dq/T \qquad ...(39)$$

where dq is the heat received from the surroundings and T is the temperature. dS is positive and is an *intensive* property.

Applying Eq. 39 to each phase, we have for the whole system

$$dS = dS^{\mathrm{I}} + dS^{\mathrm{II}} \qquad ...(40)$$

We now split the heat received by each phase into two parts. Accordingly,

$$d^{\mathrm{I}}q = d_e^{\mathrm{I}}q + d_i^{\mathrm{I}}q;\ d^{\mathrm{II}}q = d_e^{\mathrm{II}}q + d_i^{\mathrm{II}}q \qquad ...(41)$$

(Because of the conservation of energy in the system, $d_i^{\mathrm{I}}q + d_i^{\mathrm{II}}q = 0$).

The entropy change for the system of the two phases is given by

$$d^{\mathrm{I}}S = \frac{d^{\mathrm{I}}q}{T^{\mathrm{I}}} = \frac{d_e^{\mathrm{I}}q}{T^{\mathrm{I}}} + \frac{d_i^{\mathrm{I}}q}{T^{\mathrm{I}}} \qquad ...(42a)$$

$$d^{\mathrm{II}}S = \frac{d^{\mathrm{II}}q}{T^{\mathrm{II}}} = \frac{d_e^{\mathrm{II}}q}{T^{\mathrm{II}}} + \frac{d_i^{\mathrm{II}}q}{T^{\mathrm{II}}} \qquad ...(42b)$$

Substituting Eqs. 42*a* and 42*b* into Eq. 40, we have

$$dS = \frac{d_e^{\mathrm{I}}q}{T^{\mathrm{I}}} + \frac{d_e^{\mathrm{II}}q}{T^{\mathrm{II}}} + d_i^{\mathrm{I}}q\left(\frac{1}{T^{\mathrm{I}}} - \frac{1}{T^{\mathrm{II}}}\right) \qquad ...(43)$$

The first two terms in Eq. 43 correspond to d_eS of Eq. 38 and the third term of Eq. 43 gives d_iS, which is the **entropy production** arising from the transfer of heat from phase II to phase I as a result of the temperature difference $(T^{\mathrm{II}} - T^{\mathrm{I}})$. Thus,

$$d_iS = d_i^{\mathrm{I}}q\left(\frac{1}{T^{\mathrm{I}}} - \frac{1}{T^{\mathrm{II}}}\right) \qquad ...(44)$$

From Eq. 44, we see that if $T^{\mathrm{II}} > T^{\mathrm{I}}$, $d_iS > 0$ since $d_i^{\mathrm{I}}q > 0$. Even if $T^{\mathrm{I}} > T^{\mathrm{II}}$, d_iS will still be > 0 though the quantity inside the parentheses in Eq. 44 is < 0, since $d_i^{\mathrm{I}}q$ will also be < 0. The entropy production can only be zero when thermal equilibrium is established, that is, when

$$T^{\mathrm{I}} = T^{\mathrm{II}} \qquad ...(45)$$

From Eq. 44 we can define **entropy production per unit time**, σ, by

$$\sigma = \frac{d_iS}{dt} = \frac{d_i^{\mathrm{I}}q}{dt}\left(\frac{1}{T^{\mathrm{I}}} - \frac{1}{T^{\mathrm{II}}}\right) > 0 \qquad ...(46)$$

Eq. 46 shows that the rate of entropy production, σ, is the product of two terms, *viz.*, the rate of heat transfer $(d_i^{\mathrm{I}}q/dt)$ and a difference of state functions $(1/T^{\mathrm{I}} - 1/T^{\mathrm{II}})$. The latter can be considered as the *macroscopic cause* or the *driving force* for the heat transfer which can be considered as a flux or flow or a consequence of the driving force.

Entropy Production in Chemical Reactions

Let us consider a chemical reaction occurring at constant T and P. Let the surroundings absorb an infinitesimal quantity of enthalpy dH at temperature T. Then $d_eS = dH/T$, where d_eS is the infinitesimal entropy change of the external surroundings. Further, let d_iS be the infinitesimal entropy change arising from the chemical reaction. Then, since $dS = d_eS + d_iS$, we have

$$dS = dH/T + d_iS \qquad ...(47)$$

or

$$-Td_iS = dH - TdS \qquad ...(48)$$

Comparing this result with the thermodynamic relation $dG = dH - TdS$, we find that

$$d_iS = -dG/T \qquad ...(49)$$

Thus, the rate of entropy production is given by

$$\sigma = \frac{d_iS}{dt} = -\frac{1}{T}\left(\frac{dG}{dt}\right) \qquad ...(50)$$

This can be expressed by saying that σ is proportional to the *decrease* in the Gibbs free energy. According to Claussius, the uncompensated heat d_iq, is given by

$$d_iq = TdS - d_eq \qquad ...(51)$$

where dS is the entropy change of the system and d_eq is the heat exchanged with the surroundings. Since $dS = d_eS + d_iS$, hence

$$dS = d_eq/T + d_iq/T \qquad ...(52)$$

or

$$TdS = d_eq + d_iq \qquad ...(53)$$

Treating the chemical reaction as an open system containing c components ($\gamma = 1, \ldots\ldots c$), we have the well known relation

$$dG = -SdT + VdP + \sum_{\gamma}\mu_\gamma\, dn_\gamma \qquad ...(54)$$

where μ_γ is the chemical potential of the γ-th component and n_γ is the number of moles of the γ-th component. At constant T and P, Eq. 54 becomes

$$(dG)_{T,P} = \sum_\gamma \mu_\gamma \, dn_\gamma \qquad ...(55)$$

From Eqs. 50 and 55, $$\sigma = \frac{d_i S}{dt} = -\frac{1}{T}\sum_\gamma \mu_\gamma \frac{dn_\gamma}{dt} \qquad ...(56)$$

Substituting for dn_γ from Eq. 18, we have

$$\frac{d_i S}{dt} = -\frac{1}{T}\frac{d\xi}{dt}\sum_\gamma \nu_\gamma \mu_\gamma \qquad ...(57)$$

Following De Donder, we define the term **affinity**, A, of a chemical reaction as

$$A = -\sum_\gamma \nu_\gamma \mu_\gamma \qquad ...(58)$$

Thus, from Eqs. 57 and 58,

$$d_i S = (A/T)\, d\xi > 0 \qquad ...(59)$$

or $$d_i S/dt = (A/T)\,(d\xi/dt) > 0 \qquad ...(60)$$

The reaction rate, v, is defined in terms of the extent of reaction, ξ, as

$$v = d\xi/dt = \frac{1}{\nu_\gamma}\frac{dn_\gamma}{dt} \qquad ...(61)$$

The molar concentration of the γ-th component is defined as

$$c_\gamma = n_\gamma/V \qquad ...(62)$$

where n_γ is the number of moles of the γ-th component dissolved in volume V.

$$\therefore \quad \frac{dc_\gamma}{dt} = \frac{d}{dt}\frac{n_\gamma}{V} = \frac{1}{V}\frac{dn_\gamma}{dt} - \frac{n_\gamma}{V^2}\frac{dV}{dt} \qquad ...(63)$$

Assuming that the volume remains constant during the reaction, we obtain

$$\frac{dc_\gamma}{dt} = \frac{1}{V}\frac{dn_\gamma}{dt} = \frac{1}{V}\nu_\gamma \frac{d\xi}{dt} = \nu_\gamma / V \qquad ...(64)$$

From Eqs. 60 and 61, we obtain

$$\sigma = \frac{d_i S}{dt} = \frac{1}{T} Av > 0 \quad \text{or} \quad T\sigma = Av > 0 \qquad ...(65)$$

Since T is positive, we see that A and v must have the same sign. Comparing Eqs. 46 and 65 we find that the affinity A plays the role of the driving force $(1/T^{\mathrm{I}} - 1/T^{\mathrm{II}})$ in Eq. 46.

From Eq. 65, we see that the expression for σ is the product of the force (A) and the flow (v).

It is evident from Eq. 65 that when both A and v are positive, the reaction occurs from left to right. If, however, both A and v are negative, the reaction takes place from right to left. If $A=0$, the reaction is in a state of equilibrium. If $v=0$, it does not necessarily follow that A is also zero. If $v=0$ and $A \neq 0$, we have the case of *false equilibrium.*

Eq. 60 can be extended to several reactions occurring simultaneously. Thus, for r reactions ($\rho = 1, \cdots\cdots r$) occurring simultaneously, we get

$$d_i S = \frac{1}{T}\sum_\rho A_\rho d\xi_\rho > 0 \qquad ...(66)$$

where A_ρ is the affinity of the ρ^{th} reaction related to the chemical potentials by

$$A_\rho = -\sum_\gamma \nu_{\gamma\rho}\, \mu_\gamma \qquad ...(67)$$

In the equilibrium state, all affinities are zero, that is

$$A_1 = A_2 = \cdots = A_\rho = 0 \qquad ...(68)$$

The entropy production per unit time is now given by

$$\frac{d_i S}{dt} = \frac{1}{T}\sum_\rho A_\rho \nu_\rho > 0 \qquad ...(69)$$

We see that the entropy production per unit time is the sum of the entropy productions due to the various reactions. It must be emphasized that the entropy production resulting from all the simultaneous reactions is positive. However, it may happen that a system undergoes two simultaneous reactions such that

$$A_1 \nu_1 < 0, \quad A_2 \nu_2 > 0 \qquad ...(70)$$

provided that the sum

$$A_1 \nu_1 + A_2 \nu_2 > 0 \qquad ...(71)$$

Both the reactions are then said to be **coupled reactions.**

If follows from the above discussion that De Donder's definition of chemical affinity is closely related to entropy production.

Example 1. Derive the relationships between the reaction affinity and (*a*) the equilibrium constant (*b*) the Gibbs free energy and (c) the rate of the reaction $H_2(g) + I_2(g) \rightleftharpoons 2HI(g)$, assuming that the system behaves ideally.

Solution. $\quad H_2(g) + I_2(g) \rightleftharpoons 2HI(g)$

(*a*) Since the system behaves ideally, the activities are equal to molar concentrations of the reactant and the product species. Thus, by definition,

$$A = -\sum_\gamma \nu_\gamma \mu_\gamma \qquad ...(i)$$

For a component γ, the chemical potential is given by

$$\mu_\gamma = \mu_\gamma^\circ + RT \ln a_\gamma = \mu_\gamma^\circ + RT \ln c_\gamma \qquad ...(ii)$$

Hence, for the given reaction, we have

$$A = -[2\mu_{HI}^\circ - (\mu_{H_2}^\circ + \mu_{I_2}^\circ) + RT \ln c_{HI}^2/(c_{H_2} c_{I_2})]$$
$$= -\Delta G^\circ + RT \ln Q \qquad ...(iii)$$

Since $\Delta G^\circ = -RT \ln K$, Eq. *iii* can be written as

$$A = RT \ln (K/Q) \qquad ...(iv)$$

where Q is the reaction quotient and K is the equilibrium constant. Eq. *iv* gives the desired relation between A and K.

(*b*) By definition, the chemical potential of γ-th component is given by

$$\mu_\gamma = (\partial G/\partial n_\gamma)_{T,P,n_{\gamma'}} \qquad ...(v)$$

Substituting for μ_γ in Eq. *i*, we obtain

$$A = \sum_\gamma \nu_\gamma \left(\frac{\partial G}{\partial n_\gamma}\right)_{T,P,n_{\gamma'}} \qquad ...(vi)$$

$$\left(\frac{\partial G}{\partial \xi}\right)_{T,P} = \sum_\gamma \nu_\gamma \left(\frac{\partial G}{\partial n_\gamma}\right)_{T,P,n_{\gamma'}} = \sum_\gamma \left(\frac{\partial G}{\partial n_\gamma}\right)_{T,P,n_{\gamma'}} \left(\frac{\partial n_\gamma}{\partial \xi}\right) = -A \qquad ...(vii)$$

(since from Eq. 18, $\partial n_\gamma = \nu_\gamma \partial \xi$)

$$\therefore \quad A = -(\partial G/\partial \xi)_{T,P} \qquad ...(viii)$$

which is the required relation between A and G.

(*c*) The net rate of formation of HI is given by

$$\nu = \nu_f - \nu_r \qquad ...(ix)$$

where ν_f is the rate of the forward reaction and ν_r is the rate of the reverse reaction. Now,

$$\nu_f = k_f c_{H_2} \cdot c_{I_2} ; \nu_r = k_r c_{HI}^2 \text{ so that}$$

$$\nu = k_f c_{H_2} \cdot c_{I_2} \left(1 - k_r \frac{c_{HI}^2}{k_f c_{H_2} c_{I_2}}\right)$$

Since $K = k_f/k_r$, we have

$$\nu = \nu_f (1 - Q/K) \qquad ...(x)$$

As shown in Eq. (*iv*), $A = RT \ln (K/Q) = -RT \ln (Q/K)$

$$\ln (Q/K) = -A/RT \text{ so that}$$

$$Q/K = \exp(-A/RT).$$

Hence, $$\nu = \nu_f [1 - \exp(-A/RT)] \qquad ...(xi)$$

which is the required relation between A and ν.

Entropy Production and Entropy Flow in Open Systems

We consider a system consisting of two phases I and II. Each phase is open so that it can exchange both matter and energy with the other phase. The entire system is, however, closed since it can exchange only energy with the surroundings.

For an open system, we have from thermodynamics,

$$dU = TdS - PdV + \sum_\gamma \mu_\gamma dn_\gamma \qquad ...(72)$$

or $$TdS = dU + PdV - \sum_\gamma \mu_\gamma dn_\gamma \qquad ...(73)$$

The number of components in each phase is c ($\gamma = 1, \cdots c$). Recalling that $dU = dq - PdV$ and $dn_\gamma = \nu_\gamma d\xi$, Eq. 73 becomes

$$dS = \frac{dq}{T} - \frac{1}{T}\sum_\gamma \mu_\gamma \nu_\gamma d\xi \qquad ...(74)$$

Since $A = -\sum_\gamma \nu_\gamma \mu_\gamma$, Eq. 74 becomes

$$dS = \frac{dq}{T} + \frac{A}{T} d\xi \qquad ...(75)$$

Since we are dealing with an open system, we must replace the heat transfer term dq by $d\phi$ which represents the energy flow due to heat transfer and exchange of matter. There is also the probability of the occurrence of a chemical reaction in each phase. We must also take into account the entropy exchange with the surroundings, *i.e.*,

$$d_e S = \frac{d\phi}{T} - \sum_\gamma \frac{\mu_\gamma}{T} d_e n_\gamma \qquad ...(76)$$

Thus, Eq. 75 can be written as

$$dS = \frac{d\phi}{T} - \sum_\gamma \frac{\mu_\gamma}{T} d_e n_\gamma + \frac{A}{T} d\xi \qquad ...(77)$$

For the phases I and II, Eq. 77 is written as

$$dS = \frac{d^I\phi}{T^I} + \frac{d^{II}\phi}{T^{II}} - \sum_\gamma \left(\frac{\mu_\gamma^I}{T^I} - \frac{\mu_\gamma^{II}}{T^{II}}\right) d_e n_\gamma^I + \frac{A^I d\xi^I}{T^I} + \frac{A^{II} d\xi^{II}}{T^{II}} \qquad ...(78)$$

Here A^I and A^{II} are the affinities of reactions occurring in phases I and II, respectively ; $d_e n_\gamma^I$ represents the number of moles of component γ entering phase I from phase II. Similarly, for the energy flow we can write :

$$\frac{d^I\phi}{T^I} = \frac{d_e^I\phi}{T^I} + \frac{d_i^I\phi}{T^I} \qquad ...(79a)$$

and $$\frac{d^{II}\phi}{T^{II}} = \frac{d_e^{II}\phi}{T^{II}} + \frac{d_i^{II}\phi}{T^{II}} \qquad ...(79b)$$

Substituting for $d^I\phi/T^I$ and $d^{II}\phi/T^{II}$ in Eq. 78, we get

$$dS = \frac{d_e^I q}{T^I} + \frac{d_e^{II} q}{T^{II}} + d_i^I\phi\left(\frac{1}{T^I} - \frac{1}{T^{II}}\right) - \sum_\gamma \left(\frac{\mu_\gamma^I}{T^I} - \frac{\mu_\gamma^{II}}{T^{II}}\right) d_e n_\gamma^I + \frac{A^I d\xi^I}{T^I} + \frac{A^{II} d\xi^{II}}{T^{II}} \qquad ...(80)$$

The first two terms in Eq. 80 represent entropy flow $d_e S$ arising from the heat exchange between the closed system and the external surroundings. The third, fourth, fifth and sixth terms represent entropy production, $d_i S$. The third term represents entropy change due to energy exchange between phases I and II ; the fourth term represents entropy change due to the exchange of matter between phases I and II and the last two terms represent the entropy change resulting from chemical reactions taking place in each phase. The rate of entropy production is given by

$$\sigma = \frac{d_i S}{dt} = \frac{d^I\phi}{dt}\left(\frac{1}{T^I} - \frac{1}{T^{II}}\right) - \sum_\gamma \left(\frac{\mu_\gamma^I}{T^I} - \frac{\mu_\gamma^{II}}{T^{II}}\right)\frac{d_e n_\gamma^I}{dt} + \left(\frac{A^I}{T^I}\right)\nu^I + \left(\frac{A^{II}}{T^{II}}\right)\nu^{II} \geq 0 \qquad ...(81)$$

In Eq. 81, the coefficient of each rate (flow) term enclosed in parentheses is the *force* term. We can thus express the rate of entropy production as a sum of the products of generalized forces (affinities) denoted by X_j and the corresponding fluxes (or flows) denoted by J_j. Thus,

$$\sigma = \frac{d_i S}{dt} = \sum_j J_j X_j > 0 \qquad ...(82)$$

Transformation Properties of Fluxes and Forces. For a chemical reaction, the rate of entropy production is given by

$$\sigma = d_i S/dt = JX \qquad \text{(Eq. 82)} \qquad ...(83)$$

In Eq. 83, the flux J, is identified with the rate ν and the generalized force X is identified with the affinity : $X = A/T$.

We consider a consecutive reaction of the type

$$A \longrightarrow B \qquad ...(i)$$

$$B \longrightarrow C \qquad ...(ii)$$

For reaction (*i*), the affinity is given by

$$A_1 = -(\mu_B - \mu_A) = \mu_A - \mu_B \qquad ...(84)$$

Similarly, for reaction (*ii*), the affinity is given by

$$A_2 = -(\mu_C - \mu_B) = \mu_B - \mu_C \qquad ...(85)$$

The change in the number of moles of A per unit time is given by

$$-dn_A/dt = v_1 \quad \text{or} \quad dn_A/dt = -v_1$$

The change in the number of moles of C per unit time is given by

$$dn_C/dt = v_2$$

Hence, the change in the number of moles of B per unit time is given by

$$dn_B/dt = -dn_A/dt - dn_C/dt = v_1 - v_2$$

Hence, from Eq. 65, the rate of entropy production is represented as

$$Td_iS/dt = A_1v_1 + A_2v_2 \qquad ...(86)$$

Consider now the reaction scheme written as

$$A \longrightarrow C \qquad ...(iii)$$

$$B \longrightarrow C \qquad ...(iv)$$

The corresponding affinities for reactions (*iii*) and (*iv*) are

$$A_1' = \mu_A - \mu_C = A_1 + A_2$$

$$A_2' = \mu_B - \mu_C = A_2$$

Hence, $dn_A/dt = -v_1'$; $dn_B/dt = -v_2'$; $dn_C/dt = v_1' + v_2'$

We find that $v_1 = v_1'$ and $v_2 = v_1' + v_2'$

Hence, the corresponding rate of entropy production is expressed as

$$Td_iS/dt = A_1v_1 + A_2v_2 = A_1'v_1' + A_2'v_2' \qquad ...(87)$$

Notice that the new set of equations are such that the entropy production is the same. The transformation properties of the fluxes J_k and the generalized forces X_k are such that we can take a linear combination of the forces to give a new set of forces X_k' and choose a new set of fluxes J_k' such that Eq. 88 holds. Thus,

$$\sum_k J_kX_k = \sum_k J_k'X_k' \qquad ...(88)$$

Principle of Microscopic Reversibility and The Onsager Reciprocal Relations

The principle of microscopic reversibility states that mechanical equations of motion of individual particles of a system of particles are *invariant* with respect to the transformation $t \to -t$ (the **time reversal**). The theory of **fluctuations**, which is an important topic in statistical mechanics, plays an important role here. Details about the fluctuation theory will not be dealt with here.

We consider the value of the fluctuation α_i at a time instant t and of fluctuation α_j after a time interval τ and we form the product of both the quantities. The average value of this product during a sufficiently long lapse of time is given by

$$\overline{\alpha_i(t)\alpha_j(t+\tau)} = \lim_{T\to\infty} \frac{1}{T}\int_0^T \alpha_i(t)\alpha_j(t+\tau)dt \qquad ...(89)$$

According to the well known **ergodic theorem**, the *time-average* (Eq. 89) is equal to the *ensemble-average*. This is another result of the **ensemble theory** in statistical mechanics.

We next consider the average value of the product $\alpha_j(t)\alpha_i(t+\tau)$ in which we consider the fluctuations $\alpha_j(t)$ and $\alpha_i(t+\tau)$, the latter occurring after the time interval τ. The mean value $\overline{\alpha_j(t)\alpha_i(t+\tau)}$ differs from that given by Eq. 89 only by the temporal order of the two fluctuations, or more briefly, by the substitution $t \to -t$. Thus, we can express the microscopic reversibility by the relation

$$\overline{\alpha_i(t)\alpha_j(t+\tau)} = \overline{\alpha_j(t)\alpha_i(t+\tau)} \qquad ...(90)$$

Subtracting the same quantity $\alpha_i(t)\,\alpha_j(t)$ from both sides of Eq. 90, we have

$$\alpha_i(t)\overline{[\alpha_j(t+\tau) - \alpha_j(t)]} = \alpha_j(t)\overline{[\alpha_i(t+\tau) - \alpha_i(t)]} \qquad ...(91)$$

Now as $\tau \to 0$, we have

$$\overline{\alpha_i(t)\dot{\alpha}_j(t)} = \overline{\alpha_j(t)\dot{\alpha}_i(t)} \qquad ...(92)$$

where the time-derivative of $\alpha(t)$ is designated as $\dot{\alpha}(t)$. Assuming that the decay of fluctuation $\dot{\alpha}_i$ follows the ordinary macroscopic phenomenological rate laws, we can write

$$J_i = \dot{\alpha} = \sum_k L_{ik}X_k \qquad ...(93)$$

Introducing Eq. 93 into Eq. 92, we obtain

$$\sum_k L_{jk}\overline{\alpha_i X_k} = \sum_k L_{ik}\overline{\alpha_j X_k} \qquad ...(94)$$

Making use of an important fluctuation theory result, *viz.*,

$$\overline{X_\rho\,\alpha_{\rho'}} = -k\delta_{\rho'\rho} \qquad ...(95)$$

where k is a constant and $\delta_{\rho'\rho}$ is the Kronecker-delta, defined as

$$\delta_{\rho'\rho} = \begin{cases} 1, & \rho' = \rho \\ 0, & \rho' \neq \rho \end{cases}$$

we find from Eqs. 94 and 95 that

$$L_{ji} = L_{ij} \qquad ...(96)$$

These are the celebrated **Onsager reciprocal relations** (Eq. 9). Though they have been proved here for small fluctuations around thermodynamic equilibrium, they are also valid for systems with systematic deviations from equilibrium as long as the relations between fluxes (flows) and forces (affinities) remain linear.

Verification of the Onsager Relations

We shall apply the Onsager theory concepts to a simple reversible reaction and investigate it kinetically and thermodynamically. Let us study the kinetic aspects first. For the reaction

$$A \underset{k_{-1}}{\overset{k_1}{\rightleftharpoons}} B$$

$$-dc_A/dt = k_1c_A - k_{-1}c_B \qquad ...(97a)$$

$$dc_B/dt = k_1c_A - k_{-1}c_B \qquad ...(97b)$$

At equilibrium, the macroscopic reaction rate $J_{ch} = -dc_A/dt = dc_B/dt = 0$. Thus,

$$k_{-1}c_B^e = k_{-1}c_A^e \text{ ; and } K = k_1/k_{-1} = c_B^e/c_B^e \qquad ...(98)$$

Here the superscript e refers to equilibrium and K is the equilibrium constant. Let

$$\alpha_A = c_A - c_A^e \text{ and } \alpha_B = c_B - c_B^e \qquad ...(99)$$

Suppose x moles of A react to give x moles of B when equilibrium is attained. Then, $c_A - x = c_A^e$ and $c_B + x = c_B^e$ so that

$$c_A + c_B = c_A^e + c_B^e \qquad ...(100)$$

From Eqs. 99 and 100, we have

$$\alpha_A + \alpha_B = c_A - c_B - (c_A^e + c_B^e) = 0 \qquad ...(101)$$

If the rate of the chemical reaction v is designated as J_{ch}, Eq. 97 can be written as

$$J_{ch} = k_1(c_A^e + \alpha_A) - k_{-1}(c_B^e + \alpha_B) \quad ...(102)$$

Since $k_1 c_A^e = k_{-1} c_B^e$ and $\alpha_A = -\alpha_B$, we have

$$J_{ch} = \alpha_A (k_1 + k_{-1}) = \alpha_A k_1 (1 + 1/K) \quad ...(103)$$

Let us now study the thermodynamic aspects of the reaction. The affinity (*i.e.*, the generalized force) is given by $A = \mu_A - \mu_B$. Since the flux, *i.e.*, the rate of the chemical reaction is, according to the Onsager theorem, proportional to the generalized force, *i.e.*, the affinity, we have

$$J_{ch} = LA = L(\mu_A - \mu_B) \quad ...(104)$$

We know that for an ideal system at constant T and P, the chemical potential of the species is given by

$$\mu_i = \mu_i^\circ + RT \ln c_i \quad ...(105)$$

Substituting for c from Eq. 99 and writing $c^e + \alpha$ as $c^e(1 + \alpha/c^e)$, we have

$$\mu_A = \mu_A^\circ + RT \ln c_A^e + RT \ln[1 + (\alpha_A/c_A^e)] \quad ...(106a)$$

$$\mu_B = \mu_B^\circ + RT \ln c_B^e + RT \ln[1 + (\alpha_B/c_B^e)] \quad ...(106b)$$

Thus, $A = [\mu_A^\circ + RT \ln c_A^e] + RT \ln(1 + \alpha_A/c_A^e) - [\mu_B^\circ + RT \ln c_B^e] - RT \ln(1 + \alpha_B/c_B^e)$ ...(107)

Since at equilibrium $\mu_A^e = \mu_B^e$, the terms in brackets of Eq. 107 cancel giving

$$A = RT[\ln(1 + \alpha_A/c_A^e) - \ln(1 + \alpha_B/c_B^e)] \quad ...(108)$$

If $(\alpha_i / c_i^e) \ll 1$, then $\ln(1 + \alpha_i/c_i^e \approx \alpha_i/c_i^e)$, so that

$$A = RT[(\alpha_A/c_A^e) - (\alpha_B/c_B^e)] \quad ...(109)$$

$$= RT[(\alpha_A/c_A^e) + (\alpha_A/c_B^e)] \quad (\because \alpha_A = -\alpha_B)$$

$$= RT\alpha_A/[c_A^e(1 + c_A^e/c_B^e)]$$

$$= RT\frac{\alpha_A}{c_A^e}\left(1 + \frac{1}{K}\right) \quad (\because c_B^e/c_A^e = K) \quad ...(110)$$

Substituting for A from Eq. 110 in Eq. 104, we obtain

$$J_{ch} = LA = \frac{LRT\alpha_A}{c_A^e}\left(1 + \frac{1}{K}\right) \quad ...(111)$$

Eq. 111 is derived by assuming that the reaction is close to equilibrium so that $\alpha_i^e / c_i^e \ll 1$. Comparing Eqs. 103 and 111, we find that

$$L = k_1 c_A^e / RT = v_f^e / RT \quad ...(112)$$

where v_f^e is the rate of the forward reaction at equilibrium : $v_f^e = k_1 c_A^e$. Eq. 112 shows that the phenomenological coefficient L depends on the equilibrium concentration of A, c_A^e, at a given temperature.

Electrokinetic Effects. We shall use the Onsager reciprocal relations (Eq. 96) to study a few examples of interference between irreversible processes. These are the elctrokinetic effects. We consider a system consisting of two vessels I and II which communicate by means of a porous wall or a capillary. It is assumed that the temperature and the concentrations are uniform throughout the system and both phases differ only with respect to pressure and electrical potentials. The entropy

production due to the transfer of the constituents from vessel I to vessel II is given by

$$d_i S = \frac{1}{T}\sum_\gamma \tilde{A}_\gamma \, d\xi_\gamma = -\frac{1}{T}\sum_\gamma \tilde{A}_\gamma \, dn_\gamma^I \quad ...(113)$$

where $\tilde{A}_\gamma$ is the electrochemical affinity corresponding to the transfer of the component γ from phase I to phase II. It is defined as

$$\tilde{A}_\gamma = A_\gamma + z_\gamma F(\phi^I - \phi^{II}) = (\mu_\gamma^I + z_\gamma F \phi^I) - (\mu_\gamma^{II} + z_\gamma F \phi^{II}) \quad ...(114)$$

Here z_γ is the charge number (electrovalence) of the ionic component which is being transferred and F is Faraday ($1F = 96{,}485$ C mol^{-1}). For convenience we assume that the system as a whole is closed and the degree of advancement of phase change is given by

$$-dn_\gamma^I = dn_\gamma^{II} = d\xi_\gamma$$

Eq. 114 can be written more simply as

$$\tilde{A}_\gamma = (\mu_\gamma^I - \mu_\gamma^{II}) + z_\gamma F(\phi^I - \phi^{II}) \quad ...(115)$$

$$= \Delta\mu_\gamma + z_\gamma F \, \Delta\phi \quad ...(116)$$

Since the temperature and composition are the same in both the vessels, we have

$$\Delta\mu_\gamma = v_\gamma \Delta P \quad ...(117)$$

where v_γ is the specific molar volume of component γ. We can write Eq. 113 as

$$\frac{d_i S}{dt} = -\frac{1}{T}\sum_\gamma v_\gamma \frac{dn_\gamma^I}{dt}\Delta P - \frac{1}{T}\sum_\gamma z_\gamma F \frac{dn_\gamma^I}{dt}\Delta\phi \quad ...(118)$$

We define the fluxes as $J = -\sum_\gamma v_\gamma \frac{dn_\gamma^I}{dt}$; $I = -\sum_\gamma z_\gamma F \frac{dn_\gamma^I}{dt}$ ...(119)

where I is the electrical current due to the transfer of charges from vessel I to vessel II and J is the resulting flow of matter.

Thus, the entropy production (Eq. 113) becomes

$$\frac{d_i S}{dt} = \frac{J\Delta P}{T} + \frac{I\Delta\phi}{T} \quad ...(120)$$

and the phenomenological equations are given by

$$I = L_{11}\frac{\Delta\phi}{T} + L_{12}\frac{\Delta P}{T} \quad ...(121)$$

$$J = L_{12}\frac{\Delta\phi}{T} + L_{22}\frac{\Delta P}{T} \quad ...(122)$$

where the Onsager relation $L_{12} = L_{21}$ holds good.

In the above discussion we have dealt with two irreversible effects, *viz.*, the transfer of matter under the combined influence of a difference of pressure and flow of electrical current due to the difference of electrical potential. Also, we have a cross effect related by the coefficient $L_{12} = L_{21}$, which is due to the interference of the two irreversible processes.

We shall now define the four elctrokinetic effects, called the **streaming potential** (*SP*), the electro-osmosis (*EO*), the **electro-osmotic pressure** (*EOP*) and the **streaming current** (*SC*), as follows :

$$SP = \left(\frac{\Delta\phi}{\Delta P}\right)_{I=0} = -\frac{L_{12}}{L_{11}} \quad ...(123)$$

$$EO = \left(\frac{J}{I}\right)_{\Delta P=0} = \frac{L_{21}}{L_{11}} \qquad ...(124)$$

$$EOP = \left(\frac{\Delta P}{\Delta \phi}\right)_{J=0} = -\frac{L_{21}}{L_{22}} \qquad ...(125)$$

$$SC = \left(\frac{I}{J}\right)_{\Delta\phi=0} = \frac{L_{12}}{L_{22}} \qquad ...(126)$$

From Eq. 123, SP is defined as the potential difference per unit pressure difference in the state with zero electrical current. From Eq. 124, EO is the flow of matter per unit electrical current in the state with uniform pressure. From Eq. 125, EOP is the pressure difference per unit potential difference when the flow J is zero. From Eq. 126, SC is the electric current flux per unit matter flux when electrical potential difference tends to zero. These four electro kinetic effects can be verified. They are related as follows :

$$\left(\frac{\Delta\phi}{\Delta P}\right)_{I=0} = -\left(\frac{J}{I}\right)_{\Delta P=0}, \quad i.e., \quad SP = -EO \qquad ...(127)$$

$$\left(\frac{\Delta P}{\Delta\phi}\right)_{J=0} = -\left(\frac{I}{J}\right)_{\Delta\phi=0}, \quad i.e., \quad EOP = -SC \qquad ...(128)$$

Eqs. 127 and 128 relate an osmotic effect to a streaming effect. Eq. 127 is known as **Saxen's relation.**

Thermomolecular Pressure Difference (*TPD*) and Thermomechanical (or Mechanocalorific) Effect. We shall next consider a one-component system (fluid) contained in two vessels I and II which are connected by means of a capillary, a small hole, a membrane or a porous wall. If a temperature difference is maintained between the two vessels, a matter flux J_m results. We have already calculated the rate of entropy production for such a system (Eq. 81). Modifying this equation suitably and assuming that no reaction is taking place, we have

$$\frac{d_i S}{dt} = \frac{d^I\phi}{dt}\left(\frac{1}{T^I} - \frac{1}{T^{II}}\right) - \left(\frac{\mu_\gamma^I}{T^I} - \frac{\mu_\gamma^{II}}{T^{II}}\right)\frac{d_e^I n_\gamma}{dt} \qquad ...(129)$$

$$X_{th} = \left(\frac{1}{T^I} - \frac{1}{T^{II}}\right) = \Delta\left(\frac{1}{T}\right) = \frac{T^{II} - T^I}{T^I T^{II}} = -\frac{\Delta T}{T^2} \qquad ...(130)$$

(if ΔT is small $T^I \approx T^{II} \approx T$)

$$X_m = -\frac{(\Delta\mu)_T}{T} = -\frac{v}{T}\Delta P \quad (\because \Delta\mu = vdP + sdT \text{ and } dT = 0) \qquad ...(131)$$

Here v is specific molar volume and s is specific molar entropy.

The thermal energy flux J_{th} and the matter flux J_m are given by

$$J_{th} = d^I\phi/dt \quad \text{and} \quad J_m = \frac{d_e^I n_\gamma}{dt} \qquad ...(132)$$

The entropy production becomes

$$\frac{d_i S}{dt} = -J_{th}\frac{1}{T^2}\Delta T - J_m\frac{v}{T}\Delta P \qquad ...(133)$$

and the phenomenological law now becomes

$$J_{th} = -L_{11}\frac{\Delta T}{T^2} - L_{12}\frac{v\Delta P}{T} \qquad ...(134)$$

$$J_m = -L_{21}\frac{\Delta T}{T^2} - L_{22}\frac{v\Delta P}{T} \qquad ...(135)$$

We have again the Onsager relation

$$L_{12} = L_{21} \qquad ...(136)$$

We shall study two phenomena, *viz.*, thermomolecular pressure difference (*TPD*) and thermomechanical effect. The thermomolecular pressure difference is defined as the difference of pressure which arises between the two phases in the stationary state $J_m=0$ when a temperature difference is maintained. From Eq. 135, this pressure is given by

$$\left(\frac{\Delta P}{\Delta T}\right)_{J_m=0} = -\frac{L_{21}}{L_{22}vT} \qquad ...(137)$$

This cross-phenomenon is due to the interference of the irreversible processes of transport of energy and matter. The *TPD* is called **Knudsen effect** if the system consists of a gas and the vessels are separated by narrow capillaries or small openings. When the same effect occurs in gases or liquids with a membrane separating the two phases, it is called **thermo-osmosis.**

Let us now study the other phenomenon. We deal with the same system defined above. If we maintain a pressure difference between the two vessels and a uniform temperature throughout the system, matter flows from one vessel to the other and an associated energy flow, proportional to the matter flow, is observed. This energy flow can be measured by determining the heat necessary to maintain a uniform temperature in the system. This effect is known as **thermomechanical effect** ; it is expressed in terms of the phenomenological coefficients (Eqs. 134 and 135) as follows :

$$\left(\frac{J_{th}}{J_m}\right)_{\Delta T=0} = \frac{L_{12}}{L_{22}} \qquad \text{(Thermomechanical effect)} \qquad ...(138)$$

The quantity L_{12}/L_{22} is called the **heat of transfer** defined as energy transfer per unit transfer of mass. Thus,

$$q^* = L_{12}/L_{22} \qquad ...(139)$$

From Eqs. 137 and 138, using the Onsager relation (Eq. 136), we obtain the following relationship between *TPD* and the thermomechanical effect :

$$\left(\frac{\Delta P}{\Delta T}\right)_{J_m=0} = -\frac{1}{vT}\left(\frac{J_{th}}{J_m}\right)_{\Delta T=0} \qquad ...(140)$$

Thus, both effects will appear in the same system.

Stationary Non-Equilibrium States

We have earlier dealt with a typical stationary non-equilibrium state in discussing thermomolecular potential difference. In this case the transport of matter J_m is zero; yet the transport of energy between the two phases at different temperatures as well as the entropy production are different from zero. By contrast, the state variables are independent of time, so that we may describe this state as stationary non-equilibrium state or simply as stationary state. There should not be any confusion between such states and equilibrium states which are characterized by zero entropy production. A stationary state arises when the concentrations of the intermediate components no longer vary with time.

Consider a one-component system in which both the temperature gradient (X_{th}) as well as the concentration gradient (X_m) exist. In the vicinity of equilibrium, the entropy production per unit time is given by

$$\frac{d_i S}{dt} = J_{th}X_{th} + J_m X_m > 0 \qquad \text{(Eq. 133)} \qquad ...(141)$$

and the linear phenomenological laws are (Eqs. 134 and 135) :

$$J_{th} = L_{11}X_{th} + L_{12}X_m \qquad ...(142a)$$

$$J_m = L_{21}X_{th} + L_{22}X_m \qquad ...(142b)$$

Here L_{11} and L_{22} are the coefficient of thermal conductivity and diffusion coefficient, respectively. L_{12} represents the coefficient of heat flow associated with a concentration gradient and L_{21} represents

the coefficient of mass flow associated with a temperature gradient. We shall see below that stationary states may be characterized by an **extremum principle** which states that in the stationary state, the entropy production has its minimum value compatible with some auxiliary conditions to be specified in each case. Thus, we shall derive an equation (Eq. 146) which would specify the condition that the entropy production is a minimum for a given value of X_{th}. Using Eqs. 141 and 142 and the Onsager reciprocal relation $L_{12}=L_{21}$, the entropy production becomes

$$\frac{d_iS}{dt} = L_{11}X_{th}^2 + 2L_{12}X_{th}X_m + L_{22}X_m^2 > 0 \qquad ...(143)$$

Taking the derivative of Eq. 141 with respect to X_m at constant X_{th}, we have

$$\frac{\partial}{\partial X_m}\left(\frac{d_iS}{dt}\right) = 2\,(L_{12}X_{th} + L_{22}X_m) = 2J_m \qquad ...(144)$$

In the steady state, $J_m=0$, which means that the rate of entropy production has an extremum in the state. This extremum is a minimum as can be shown by taking the second derivative. Since in the steady state, $(\partial/\partial X_m)\,(d_iS/dt)=0$ (as shown above), we have

$$\frac{\partial^2}{\partial X_m^2}\left(\frac{d_iS}{dt}\right) = \frac{\partial}{\partial X_m}(2J_m) \quad \text{(at constant } X_{th}\text{)}$$

$$= 2\frac{\partial}{\partial X_m}(L_{21}X_{th} + L_{22}X_m) \qquad ...(145)$$

$$= 2L_{22} \qquad ...(146)$$

Since L_{22} is positive, the second derivative is also positive so that the extremum is a minimum. This statement furnishes the mathematical statement of **Prigogine's principle of minimum entropy production** according to which, at the steady state, all the flows corresponding to unrestricted forces vanish. Ilya Prigogine (1917-2003), the Belgian theoretical chemist, was awarded the 1977 Chemistry Nobel Prize for his contributions to non-equilibrium thermodynamics.

The above argument can be generalized to the case of n independent affinities $X_1, \ldots X_n$, of which a certain number k, $X_1, \ldots X_k$, are kept constant. In that case, we have for the stationary state,

$$J_{k+1} \ldots = J_n = 0 \qquad ...(147)$$

These conditions are equivalent to the minimum conditions for entropy production

$$\frac{\partial}{\partial X_j}\left(\frac{d_iS}{dt}\right) = 0 \qquad (j = k+1, \cdots n) \qquad ...(148)$$

Prigogine proved that the time variation of the rate of entropy production, *viz.*, $(d/dt)\,(d_iS/dt)$ can be split up into two terms : (*i*) due to the irreversible processes occurring inside the system and (*ii*) due to the flow of entropy from the system to the surroundings. The irreversible processes occurring inside the system decrease the rate of entropy production until this rate becomes minimum. When the system is in this non-equilibrium steady state, it cannot by itself come out of it despite being a spontaneous irreversible state. If some fluctuations occur which disturb the system from the steady state, the internal changes will occur so as to bring it back to the steady state.

Application of Irreversible Thermodynamics to Biological Systems

Biological systems are open systems which exchange both matter and energy with the environment. The growth of a living organism or cell is characterized by transitions resulting in greater order and thus decrease of entropy from the initial state. Recall that for an isolated system, spontaneous change results in an increase of entropy and hence of disorder. Thus, if we treat a biological system as an isolated system, rather than as an open system, then it appears to violate the basic principles of thermodynamics. The theory of stationary non-equilibrium states leads to a better understanding of the global behavior of living organisms.

The evolution of the living organism upto the stationary state may be considered as taking place under a number of constraints determined by the outside world, constraints such as the concentrations of some substances in the outside world which are transformed inside the living organisms. Regardless of the nature of the constant parameters, the stationary state may be regarded as the state of minimum entropy production per unit time. In a biological system, the main contribution to entropy production, d_iS/dt, arises from the process of metabolism whereby the assimilated food is degraded to simple substances such as CO_2, accompanied by an energy release. As the organism grows, though d_iS/dt is positive, d_eS/dt is negative and greater than d_iS/dt. Thus, their sum dS/dt becomes negative. This reduction in entropy implies a greater order (or organization) in the organism. During the growth of the organism, it is subjected to several fixed constraints, as said above, exerted by the outside world, so that the maturation of the organism is accompanied by a decease in entropy. When the steady state, or the stationary state of the biological system, is reached, $d_iS/dt=d_eS/dt$ so that $dS/dt=0$. In the steady state the system remains stable to external perturbations.

Non-linear Thermodynamics of Irreversible Processes

The irreversible thermodynamics in the linear regime, we may recall, assumes (*a*) linear phenomenological laws (*b*) validity of the Onsager reciprocal relations and (*c*) treating the phenomenological coefficients as constants. However, in the case of chemical reactions, linear phenomenological laws may not be a sufficiently good approximation. Also in the transport processes it becomes necessary to take into account the variation of the phenomenological coefficients (for instance, the variation of the coefficient of thermal conductivity with temperature). Such effects, which may be considered to be non-linear, introduce complications in the general treatment of the thermodynamics of irreversible processes since they destroy the linear phenomenological equations or transform the macroscopic equations of change into non-linear equations. Prigogine and Glansdorff consider the rate of entropy production to be given by

$$\sigma = \frac{d_iS}{dt} = \sum_k J_kX_k \geq 0 \qquad ...(149)$$

and split the time change $d\sigma$ into two parts. One is related to the change of forces and the other to the change of flows. Thus,

$$d\sigma = d_X\sigma + d_J\sigma = \sum_k J_k dX_k + \sum_k X_k dJ_k \qquad ...(150)$$

The following theorems have been proved by Glansdorff and Prigogine :

(*a*) Under the restrictive conditions,

$$d_X\sigma = d_J\sigma = \tfrac{1}{2}d\sigma \qquad ...(151)$$

The contribution of the time change of the forces to the entropy production is equal to that of the time change of flows. In fact,

$$d_X\sigma = \sum_k J_k dX_k = \sum_{kl} L_{kl}X_l dX_k \qquad ...(152)$$

Using the Onsager reciprocal relations and treating the phenomenological coefficients L_{kl} as constants, we have

$$d_X\sigma = \sum_{kl} X_l(L_{kl}dX_k) = \sum_l X_l dJ_l = d_J\sigma \qquad ...(153)$$

(*b*) Since in the thermodynamics of irreversible process the contribution of the time change of forces to the entropy production is negative or zero, we have

$$d_X\sigma \leq 0 \qquad ...(154)$$

This inequality holds whenever the boundary conditions used are time-independent. It is the most general result in the thermodynamics of irreversible process. The discussion of the general proof of

this result, first proved for chemical reactions by Glansdorff and Prigogine, is beyond the scope of the present treatment.

Concluding Remarks. Exciting things are happening in irreversible thermodynamics. Irreversible thermodynamics is the creation of one scientist, Onsager, who has been called the greatest theoretical chemist that ever lived. Prigogine has also made further contributions to the subject (both of them were awarded Nobel Prizes in Chemistry). Irreversibility and non-linear phenomena have attracted a host of mathematical physicists and mathematicians such as Birkhoff, von Neumann, J.F. Nash, Hopf, Einstein, Landau, Kolmogorov, Bogoliubov, Markov, Lyapunov, Poincare, Langevin, Mandelbrot, Sinai, Eddington and S. Chandrasekhar. Terms such as irreversibility, entropy as disorder, entropy as time's arrow, science of complexity, chemical chaos, quantum chaos, fractals, earthquakes as fractals, strange attractors, oscillatory reactions, fluctuations in ensemble theory, fluctuation-dissipation theorem, bifurcations, Hopf bifurcation, Lyapunov exponent, butterfly effect, etc., have enriched this fascinating subject.

It is pertinent to conclude this chapter by three quotations. A.S. Eddington (1882—1944), the great British astronomer, remarked :

"The law that entropy always increases—the Second law of thermodynamics —holds, I think, the supreme position among the laws of Nature. If someone points out to you that your pet theory of the universe is in disagreement with Maxwell's equations—then so much the worse for Maxwell's equations. If it is found to be contradicted by observation—well, these experimentalists do bungle things sometimes. But, if your theory is found to be against the Second law of thermodynamics, I can give you no hope; there is nothing for it but to collapse in deepest humiliation."

The other quotation of great historical interest is that due to Einstein :

"A theory is more impressive the greater the simplicity of its premises is, the more different kinds of things it relates and the more extended its area of applicability. Therefore, the great impression which classical thermodynamics made upon me. It is the only physical theory of universal content concerning which I am convinced that, within the framework of the applicability of its basic concepts, it will never be overthrown."

"I do not know what I may appear to the world; but to myself I seem to have been only like a boy playing on the seashore, and diverting myself in now and then finding a smoother pebble or a prettier shell than ordinary, whilst the great ocean of truth lay all undiscovered before me."

This statement by Isaac Newton shortly before his death in 1727 eloquently reflects the sentiments of all mature scientists from the ancient past to the present.

I. Review Questions

1. List the various transport processes and write their phenomenological equations.
2. Discuss the conservation of mass and energy in closed and open systems.
3. Derive an expression for entropy production due to heat flow.
4. Derive an expression for entropy production in chemical reactions.
5. Derive an expression for entropy production and entropy flow in an open system.
6. Discuss the transformation properties of fluxes and forces in a chemical reaction.
7. Derive the Onsager reciprocal relations from the principle of microscopic reversibility.
8. Verify the Onsager reciprocal relations for a simple reversible reaction.
9. Use Onsager's reciprocal relations to study electrokinetic effects.
10. Define and discuss the four electrokinetic effects SP, EO, EOP and SC.
11. Discuss the system in stationary non-equilibrium states leading to prigogine's principle of minimum entropy production.

GENERAL BIBLIOGRAPHY

(A) Textbooks on Physical Chemistry and Refated Subjects

Alberty, R.A., R.S. Silbey, and M.G. Bawendi, *Physical Chemistry*, 4th edn., Wiley, 2005.
Adamson, A.W., *A Textbook of Physical Chemistry*, Academic Press, 1973.
Atkins, P.W., and J. de Paula, *Physical Chemistry*, 8th edn., Oxford University Press, 2006.
Barrow, G.M., *Physical Chemistry*, 5th edn., McGraw-Hill, 1988.
Berry, R.S., S.A. Rice, and J. Ross, *Physical Chemistry*, 2nd edn., Wiley, 2000.
Castellan, G.W., *Physical Chemistry*, 3rd edn., Addison-Wesley, 1983.
Engel, T., and P. Reid, *Physical Chemistry*, Pearson Education, 2006.
Kuhn, H. and H-D Försterling, *Principles of Physical Chemistry*, Wiley, 2000.
Glasstone, S., *A Textbook of Physical Chemistry*, Macmillan (India) Ltd., New Delhi, 1976.
Eyring, H., D. Henderson, and W. Jost (eds.), *Physical Chemistry : An Advanced Treatise* (a multi-volume series), Academic, 1967–1975.
Jain, D.V.S., and Jauhar S.P., *Physical Chemistry : Principles and Problems*, Tata McGraw-Hill, 1988.
Dogra, S.K., and Dogra S., *Physical Chemistry Through Problems*, Wiley Eastern Ltd., 1984.
Kapoor, K.L., *Physical Chemistry*, Vols. I, II, III, and IV, Macmillan (India) Ltd., New Delhi, 1980-84.
Kundu, N., and Jain, S.K., *Physical Chemistry*, S. Chand and Co., New Delhi, 1984.
Levine, I.N., *Physical Chemistry*, 5th edn., McGraw-Hill, 2002.
McQuarrie, D.A., and J.D. Simon, *Physical Chemistry*, University Science Books, 1996.
Moore, W.J., *Physical Chemistry*, 5th edn., Prentice-Hall, 1972.
Vemulapalli, G.K., *Physical Chemistry*, Prentice-Hall of India, 1993.
Beiser, A., *Concepts of Modern Physics*, 6th edn., McGraw-Hill, 2006.
Lehn, J.M., *Supramolecular Chemistry*, VCH, Weinheim, 1995.
Nicolis, G., and I. Prigogine, *Exploring Complexity*, Freeman, NewYork, 1989.
Hall, Nina (ed.), *The New Chemistry*, Cambridge University Press, 2000.

(B) Textbooks and Monographs

1. **QUANTUM MECHANICS**

Atkins, P.W., and R.S. Friedman, *Molecular Quantum Mechanics*, 4th edn., Oxford, 2005.
Atkins, P.W., *Quanta : A Handbook of Concepts*, Oxford University Press, 1991.
Bohm, A., *Quantum Mechanics : Foundations and Applications*, 3rd edn., Springer, 1994.
Bethe, H.A., and R.H. Jackiw, *Intermediate Quantum Mechanics*, 3rd edn., Benjamin-Cummings, 1985.
Cohen-Tannoudji, C., B. Diu, and F. Laloë, *Quantum Mechanics*, Vols. I & II, Wiley, 1977.
Chandra, A.K., *Introductory Quantum Chemistry*, 4th edn., Tata McGraw-Hill, New Delhi, 1994.
Christofferson, R.E., *Basic Principles and Techniques of Molecular Quantum Mechanics*, Springer 1989.
Engel, T., *Quantum Chemistry and Spectrocopy*, Pearson Education, 2006.
Dykstra, C.E., *Introduction to Quantum Chemistry*, Prentice-Hall, 1994.
Fayer, M.D., *Elements of Quantum Mechanics*, Oxford, 2001.
Fitts, D.D., *Principles of Quantum Mechanics as Applied to Chemistry and Chemical Physics*, Cambridge, 1999.
Griffiths, D.J., *Introduction to Quantum Mechanics*, 2nd edn., Pearson Education, 2005.
Ghatak, A.K., and S. Lokanathan, *Quantum Mechanics*, 5th edn., Macmillan, New Delhi, 2004.
Hehre, W.J., L. Radom, P. Schleyer, and J.A. Pople, *Ab Initio Molecular Orbital Theory*, Wiley, 1986.
Landau, L.D., and E.M. Lifshitz, *Quantum Mechanics*, Pergamon, 1984.
Levine, I.N., *Quantum Chemistry*, 5th edn., Pearson Education, Inc., 2000.
McQuarrie, D.A., *Quantum Chemistry*, 2nd edn., University Science Books, 2008.
Peres, A., *Quantum Theory : Concepts and Methods*, Kluwer-Academic, 1995.
Pilar, F.L., *Elementary Quantum Chemistry*, 2nd edn., McGraw-Hill, 1990.
Pathania, M.S., *Quantum Chemistry and Spectroscopy*, 2nd edn., Vishal Publications, Jalandhar (India), 1984.
Pauling, L., and E. B. Wilson, Jr., *Introduction to Quantum Mechanics*, McGraw-Hill, 1935.
Prasad, R.K., *Quantum Chemistry*, Wiley-Eastern Ltd., New Delhi, 1992.
Peebles, P.J.E., *Quantum Mechanics*, Princeton University Press, 1992.
Agarwal, B.K., and Hari Prakash, *Quantum Mechanics*, Prentice-Hall of India, New Delhi, 1997.
Simons, J., and J. Nichols, *Quantum Mechnics in Chemistry*, Oxford, 1997.
Schwabl, F., *Quantum Mechanics*, Springer-Verlag, Berlin, 1992.
Thankappan, V.K., *Quantum Mechanics*, New Age International, New Delhi, 1997.
Aruldhas, G., *Quantum Mechanics*, Prentice-Hall of India, New Delhi, 2002.
Sakurai, J.J., *Modern Quantum Mechanics*, Pearson Education, 1994.
Salem, L., *The Molecular Orbital Theory of Conjugated Molecules*, Benjamin, 1966.
Schatz, G.C., and M.A. Ratner, *Quantum Mechanics in Chemistry*, Ellis Horwood, 1993.
Simons, J., and J. Nichols, *Quantum Mechanics in Chemistry*, Oxford, 1997.
Szabo, A., and N. Ostlund, *Modern Quantum Chemistry*, McGraw-Hill 1989.
Lowe, J.P., and K.A. Peterson, *Quantum Chemistry*, 2nd edn., Academic Press, 2006.
Merzbacher, E., *Quantum Mechanics*, 3rd edn., Wiley, 1998.

Yarkony, D.R. (ed.), *Electronic Structure Theory*, World Scientific, 1995.

2. SPECTROSCOPY AND PHOTOCHEMISTRY

Banwell, C.N., and E. McCash, *Fundamentals of Molecular Spectroscopy*, 4th ed., McGraw-Hill, 1994.
Barrow, G.M., *Introduction to Molecular Spectroscopy*, McGraw-Hill, 1962.
Sobelman, I.I., *Introduction to the Theory of Atomic Spectra*, Pergamon, 1972.
Chang, R., *Basic Principles of Spectroscopy*, McGraw-Hill, 1971.
McHale, J.L., *Molecular Spectroscopy*, Prentice-Hall, 1999.
Drago, R.S., *Physical Methods for Chemists*, Saunders, 1992.
Lever, A.B.P. *Inorganic Electronic Spectroscopy*, Elsevier, 1984.
Steinfeld, J.I., *Molecules and Radiation*, MIT Press, 1985.
Akitt, J.W., and B.E. Mann, *NMR and Chemistry*, Taylor and Francis, London, 2000.
Friebolin, H., *Basic One-and Two-Dimensional NMR*, Wiley-VCH, 1998.
Levitt, M.H., *Spin Dynamics : Basics of Nuclear Magnetic Resonance*, 2nd edn., Wiley, 2008.
Nelson, J.H., *Nuclear Magnetic Resonance Spectroscopy*, Pearson Education, 2003.
King, G.W., *Spectroscopy and Molecular Structure*, Holt, Rinehart and Winston, 1964.
Ebbsworth, E.A.V., D. Rankin, and S. Cradock, *Structural Methods in Inorganic Chemistry*, ELBS,1991.
Atherton, N.M., *Principles of Electron Paramagnetic Resonance*, Ellis/Horwood, 1993.
Derome, A.E., *Modern NMR Techniques for Chemistry Research*, Pergamon, 1987.
Herzberg, G., *Molecular Spectra and Molecular Structure*, Vols. 1–3, Van Nostrand Reinhold, 1945, 1950, 1967.
Suzuki, H., *Electronic Absorption Spectroscopy and Geometry of Organic Molecules*, Academic, 1967.
Gordy, W., and R.L. Cook, *Microwave Molecular Spectra*, 3rd edn., Wiley-Interscience, 1984.
Ghosh, P.K. *Introduction to Photoelectron Spectroscopy*, Wiley, 1983.
Graybeal, J.D., *Molecular Spectroscopy*, McGraw-Hill, 1988.
Hollas, J.M., *Modern Spectroscopy*, Wiley, 4th edn.,2004.
Jaffe, H., and M. Orchin, *Theory and Applications of Ultraviolet Spectroscopy*, Wiley, 1962.
Levine, I.N., *Molecular Spectroscopy*, Wiley-Interscience, 1975.
Sindhu, P.S., *Molecular Spectroscopy*, Tata McGraw-Hill, 1985.
Kemp, W., *Organic Spectroscopy*, 3rd edition, ELBS, 1991.
Bovey, F.A., *Nuclear Magnetic Resonance Spectroscopy*, Academic, 1989.
Carrington, A., and A.D. McLachlan, *Introduction to Magnetic Resonance*, Harper and Row, 1967.
Slichter, C.P., *Principles of Magnetic Resonance*, Springer, New York, 1990.
Parish, R.V., *NMR, NQR, EPR and Mössbauer Spectroscopy in Inorganic Chemistry*, Ellis Horwood,1990.
Wertz, J.E., and J.R. Bolton, *Electron Spin Resonance*, McGraw-Hill, 1972.
Rohatgi-Mukherjee, K.K., *Fundamentals of Photochemistry*, Wiley-Eastern Ltd., New Delhi, 1978.
Wayne, R.P., *Principles and Applications of Photochemistry*, Oxford University Press, 1988.
Andrews, D.L., and A.A. Demidov (eds.), *An Introduction to Laser Spectroscopy*, Plenum, 1995.

3. SOLID STATE CHEMISTRY AND PHYSICS

Hammond, C., *The Basis of Crystallography and Diffraction*, Oxford, 2001.
Hoffmann, R.A., *Solids and Surfaces : A Chemist's View of Bonding in Extended Structures*, VCH, 1988.
Glusker, J.P., and K.N. Trueblood, *Crystal Structure Analysis*, Oxford University Press, 1985.
Hannay, N.B., *Solid State Chemistry*, Prentice-Hall, 1967.
Kittel, C., *Introduction to Solid State Physics*, 7th edn., Wiley, 1996.
Keer, H.V., *Principles of the Solid State*, Wiley Eastern Ltd., 1993.
Ladd, M.F.C., and R.A. Palmer, *Structure Determination by X-Ray Crystallography*, Plenum, 1994.
Rao, C.N.R., and J. Gopalakrishnan, *New Directions in Solid State Chemistry*, 2nd edn., Cambridge, 1997.
West, A.R., *Solid State Chemistry and Its Applications*, Wiley, 1984.

4. THE GASEOUS STATE

Chapman, S., and T.G. Cowling, *The Mathematical Theory of Non-Uniform Gases*, Cambridge, 1970.
Kauzmann, W., *Kinetic Theory of Gases*, Benjamin, 1966.
Hirschfelder, J.H., C.F. Curtiss, and R.B. Bird, *Molecular Theory of Gases and Liquids*, Wiley, 1954.
Maitland, G.C., M. Rigby, E.B. Smith, and W.A. Wakeham, *Intermolecular Forces*, Clarendon, 1986.

5. THE LIQUID STATE, SOLUTIONS AND PHASE EQUILIBRIA

Gray, G.C., and K.E. Grubbins, *Theory of Molecular Fluids*, Clarendon, 1984.
Hillert, M., *Phase Equilibria, Phase Diagrams and Phase Transformations*, Cambridge, 1998.
Marcus, Y., *Introduction to Liquid State Chemistry*, Wiley, 1977.
Pryde, J.A., *The Liquid State*, Hutchinson, 1966.
Rowlinson, J.S., and F.S. Swinton, *Liquids and Liquid Mixtures*, Butterworths, 1982.

6. CHEMICAL THERMODYNAMICS

Adkins, C.J., *Equilibrium Thermodynamics*, Cambridge University Press, 1983.
Denbigh, K., *The Principles of Chemical Equilibrium*, 4th edn., Cambridge, 1981.
Guggenheim, E.A., *Thermodynamics*, 5th edn., North-Holland, 1967.
Glasstone, S., *Thermodynamics for Chemists*, Van Nostrand, 1967.
Klotz, I.M., and R.M. Rosenberg, *Chemical Thermodynamics*, 3rd edn., Benjamin, 1982.
Kuriacose, J.C., and J. Rajaram, *Thermodynamics and Irreversible Thermodynamics*, S. Nagin and Co., 1986.
Lewis, G.N., and M. Randall, *Thermodynamics* (rev., by K.S. Pitzer and L. Brewer), McGraw-Hill,1961.
McGlashen, M.L., *Chemical Thermodynamics*, Academic Press, 1979.

Pitzer, K.S., *Thermodynamics*, 3rd edn., McGraw-Hill, 1995.
Rastogi, R.P., and R.R. Misra, *An Introduction to Chemical Thermodynamics*, Vikas Publications, 1994.
Rock. P.A., *Chemical Thermodynamics*, Oxford University Press, 1983.
Srivastava, R.C., S.K. Saha, and A.K. Jain, *Thermodynamics : A Core Course*, Prentice-Hall of India, 2007.

7. STATISTICAL THERMODYNAMICS

Agarwal, B.K., and M. Eisner, *Statistical Mechanics*, 2nd edn., New Age International, 1998.
Carter, A.H., *Classical and Statistical Thermodynamics*, Prentice-Hall, 2001.
Chandler, D., *Introduction to Modern Statistical Mechanics*, Oxford University Press, 1987.
Davidson, N., *Statistical Mechanics*, McGraw-Hill, 1962.
Garrod, C., *Statistical Mechanics and Thermodynamics*, Oxford, 1995.
Gopal, E.S.R., *Statistical Mechanics*, Macmillan (India) Ltd., New Delhi, 1974.
Gupta, M.C., *Statistical Thermodynamics*, Wiley-Eastern Ltd., New Delhi, 1990.
Hill, T.L., *Introduction to Statistical Thermodynamics*, Addison-Wesley, 1960.
Huang K., *Statistical Mechanics*, 2nd edn., Wiley, 1987.
Landau, L.D., and E.M. Lifshitz, *Statistical Physics*, Pergamon, 1958.
Lee, J.F., W. Sears, and D. Turcotte, *Statistical Thermodynamics*, Addison-Wesley, 1962.
Ma, S.K., *Statistical Mechanics*, World Scientific, Philadelphia, 1985.
McLelland, B.J., *Statistical Thermodynamics*, Wiley, 1973.
Widom, B., *Statistical Mechanics : A Concise Introduction for Chemists*, Cambridge, 2002.
Tolman, R.C., *Principles of Statistical Mechanics*, Oxford University Press, 1938.
Reif, F., *Fundamentals of Statistical and Thermal Physics*, McGraw–Hill, 1965.
Pathria, R.K., *Statistical Mechanics*, 2nd edn., Elsevier, 1996.
Srivastava, R.K., and J. Ashok, *Statistical Mechanics*, Prentice-Hall of India, 2005.
McQuarrie, D., *Statistical Mechanics*, Harper and Row, 1976.
McQuarrie, D.A., and J.D. Simon, *Molecular Thermodynamics*, University Science Books, Sausalito, 1990.
Fitts, D.D., *Non-Equilibrium Thermodynamics*, McGraw-Hill, 1962.
Wilde, R.E., and S. Singh, *Statistical Mechanics—Fundamentals and Modern Applications*, Wiley, 1998.
de Groot, S.R., and P. Mazur, *Non-Equilibrium Thermodynamics*, North-Holland, 1962.
Prigogine, I., *Introduction to Thermodynamics of Irreversible Processes*, Springfield, 1955.

8. CHEMICAL KINETICS AND CATALYSIS

Bernasconi, C.F., *Relaxation Kinetics*, Academic, 1976.
Connors, K.A., *Chemical Kinetics : The Study of Reactions in Solutions*, VCH, 1990.
Espenson, J.H., *Chemical Kinetics and Reaction Mechanisms*, McGraw-Hill, 1995.
Hammes, G.G., *Thermodynamics and Kinetics for the Biological Sciences*, Wiley, 2000.
Holbrook, K.A., M.J. Pilling, and S.H. Robertson, *Unimolecular Reactions*, 2nd edn., Wiley, 1996.
Houston, P.L., *Chemical Kinetics and Reaction Dynamics*, McGraw-Hill, 2011.
Laidler, K.J., *Chemical Kinetics*, 3rd edn., Harper and Row, 1987.
Levine, R.D., and R.B. Bernstein, *Molecular Reaction Dynamics and Chemical Reactivity*, Oxford, 1989.
Moore, J.W., and R. Pearson, *Chemical Kinetics*, 3rd edn., Wiley, 1983.
Steinfeld, J., J. Francisco, and W. Hase, *Chemical Kinetics and Dynamics*, Prentice-Hall 1989.
Nakamura, A., and M. Tsutsui, *Principles and Applications of Homogenous Catalysis*, Wiley, 1980.
Pilling, M.J., and P.W. Seakins, *Reactions Kinetics*, Oxford, 1996.
Billing, G.D., and K.V. Mikkelsen, *Advanced Molecular Dynamics and Chemical Kinetics*, Wiley, 1997.
Kondratiev, V.N., and E.E. Nikitin, *Gas-Phase Reactions*, Springer-Valley, Berlin, 1981.

9. ELECTROCHEMISTRY

Bockris, J.O.M., and A.K.N. Reddy, *Modern Electrochemistry*, 2nd edn., Plenum, 1998.
Crow, D.R., *Principles and Applications of Electrochemistry*, 4th edn., Chapman and Hall, 1994.
Goodisman, J., Electrochemistry : *Theoritical Foundations*, Wiley, 1987.
Hamman, C.H., W. Wielstich, and A. Hamnett, *Electrochemistry*, Wiley-VCH, 1998.
Rieger, P.H., *Electrochemistry*, 2nd edn., Chapman and Hall, 1983.

10. SURFACE CHEMISTRY AND COLLOID SCIENCE

Adamson, A.W., and A. Gast, *Physical Chemistry of Surfaces*, 5th edn., Wiley, 1997.
Ertl, G., and J. Küppers, *Low Energy Electrons and Surface Chemistry*, 2nd edn., Weinheim VCH, 1985.
Hiemenz., P.C., and R. Rajagopalan, *Principles of Colloid and Surface Chemistry*, Dekker, 1997.
Everett, D.H., *Basic Principles of Colloid Science*, Royal Society of Chemistry, 1988.
Evans, D.F., and H. Wennerström, *The Colloidal Domain : Where Physics, Chemistry, Biology and Technology Meet*, Wiley-VCH, 1999.
Hunter, R.J., *Foundations of Colloid Science*, Vols., I and II, Clarendon, 1987.
Somorjai, G.A., *Introduction to Surface Chemistry and Catalysis*, Wiley, 1994.
Mittal, K.L., and D.O. Shah (ed.), *Surfactants in Solution*, Vol. 11, Plenum, 1992.
Moroi, Y., *Micelles*, Plenum, 1992.
Rosen, M.J., *Surfactants and Interfacial Phenomena*, 2nd edn., Wiley, 1989.
Zangwill, A., *Physics at Surfaces*, Cambridge, 1988.

11. MACROMOLECULES

Alcock, H.R., F.W. Lampe, and J.E. Mark, *Contemporary Polymer Chemistry*, Pearson education, 2003.
Billmeyer, F.W., *Textbook of Polymer Science*, 3rd edn., Wiley, 1984.

Bovey, F.A., and F.W. Winslow, *Macromolecules*, Academic, 1979.
Carraher, Jr., C.E., *Seymour/Carraher's Polymer Chemistry*, Dekker, 2000.
Flory, P.J., *Principles of Polymer Chemistry*, Cornell University Press, 1953.
Hiemenz, P.C., and T.P. Lodge, *Polymer Chemistry*, 2nd edn., CRC Press, Boca Raton, 2007.
Kumar, A., and S.K. Gupta, *Fundamentals of Polymer Science and Engineering*, Tata McGraw-Hill, 1978.
Sperling , L.H., *Physical Polymer Science*, Wiley-Interscience, 1986.
Skotheim, T.A. (ed.), *Handbook of Conducting Polymers*, Vols. I and II, Dekker, 1986.
Van Holde, K.E., W.C. Johnson, and P.S. Ho, *Principles of Physical Biochemistry*, Prentice-Hall, 1998.
Volkenshtein, M.V., *Biophysics*, Mir Publishers, Moscow, 1983.
Prasad, P.N. (ed.), *Frontiers of Polymers and Advanced Materials*, Plenum, 1994.
Ciferri, A. (ed.), *Supramolecular Polymers*, Macel Dekker, 2000.
De Gennes, P.G., *Scaling Concepts in Polymer Physics*,Cornell University Press, 1979.

12. ELECTRIC AND MAGNETIC PROPERTIES

Carlin, R.L., *Magnetochemistry*, Springer, 1986.
Dutta, R.L., and A. Syamal, *Elements of Magnetochemistry*, 2nd edn., Affiliated East West Press, 1993.
Davies, D.W., *Theory of Electric and Magnetic Properties of Molecules*, Wiley, 1967.
Earnshaw, E.A., *Introduction to Magnetochemistry*, Academic, 1968.

13. MOLECULAR SYMMETRY AND GROUP THEORY

Bunker, P.R., and P. Jensen, *Molecular Symmetry and Spectroscopy*, NRC Research Press, Ottawa, 1998.
Cotton, F.A., *Chemical Applications of Group Theory*, 3rd Edn., Wiley, 1990.
Douglas, B.E., and C.A. Hollingsworth, *Symmetry in Bonding and Spectra : An Introduction*, Academic, 1985.
Gopinathan, M.S., and V. Ramakrishnan, *Group Theory in Chemistry*, Vishal Publications, Jalandhar, 1988.
Hargittai, I., and M. Hargittai, *Symmetry Through the Eyes of a Chemist*, VCH, 1987.
Harris, D.C., and M.D. Bertolucci, *Symmetry and Spectroscopy : An Introduction to Vibrational and Electronic Spectroscopy*, Dover, 1989.
Hollas, J.M., *Symmetry in Molecules*, Chapman and Hall, 1972.
Kettle, S.F.A., *Symmetry and Structure*, Wiley, 1985.
Raman, K.V., *Group Theory and its Applciations to Chemistry*, Tata McGraw-Hill, New Delhi, 1990.
Tinkham, M., *Group Theory and Quantum Mechanics*, McGraw-Hill, 1964.
Wigner, E.P., *Group Theory and Its Applications to Quantum Mechanics of Atomic Spectra*, Academic, 1959.

14. MATHEMATICS

Arfken, G., and H.J. Weber, *Mathematical Methods for Physicists*, 5th edn., Academic, 2001.
Ghatak, A.K., I.C. Goyal, and S.J. Chua, *Mathematical Physics*, Macmillan India Ltd., New Delhi, 1995.
Mortimer, R.G., *Mathematics for Physical Chemistry*, Academic 2005.
McQuarrie, D.A., *Mathematical methods for Scientists and Engineers*, University Science Books, 2003.
Boas, Mary, *Mathematical Methods in the Physical Sciences*, 2nd edn., Wiley, 2003.
Hecht, H.G., *Mathematics in Chemistry*, Prentice-Hall, 1990.
Riley, K.F., *Mathematical Methods for the Physical Sciences*, Cambridge, 1974.
Sen, B.K., *Mathematical Techniques of Chemistry & Other Physical Sciences*, Kalyani (India), 1999.
Kreyszig, H., *Advanced Engineering Mathematics*, 8th edn., Wiley, 2000.

15. HISTORY AND PHILOSOPHY OF SCIENCE

(This part of the bibliography is meant for the edification of the discerning lover of science.)
Atkins, P.W., *Galileo's Finger : The Ten Great Ideas of Science*, Oxford, 2003.
Bell, E.T., *Men of Mathematics*, Simon and Schuster, 1937.
Broch, H., *A Fontana History of Chemistry*, Fontana Press, 1992.
Datta, N.C., *The Story of Chemistry*, Universities Press (India) Pvt. Ltd., Hyderabad, 2005.
Chandrasekhar, S., *Truth and Beauty*, Penguin Books, 1991.
Davies, P. (ed.), *The New Physics*, Cambridge, 1989.
Gleick, J., *Genius : Richard Feynman and Modern Physics*, Rupa and Co., Calcutta (India), 1993.
Hawking, S., *A Brief History of Time*, Bantam Books, 1988.
Hoffmann, B., *Strange Story of the Quantum*, Dover. 1959.
Holton, G., *Thematic Origins of Scientific Thought*, Harvard, 1988.
Jammer, M., *Conceptual Development of Quantum Mechanics*, McGraw-Hill, 1966.
Jeans, J., *Physics and Philosophy*, Ann Arbor Paperback, 1958.
Kuhn, T.H., *The Structure of Scientific Revolutions*, 2nd edn., The University of Chicago Press, 1970.
Kanigel, R., *The Man Who Knew Infinity : A Life of Genius S. Ramanujan*, Rupa & Co., Calcutta (India), 1993.
Laidler, K.J., *The World of Physical Chemistry*, Oxford, 1993.
Newman, J.R. (ed.), *The World of Mathematics* (in four volumes), Simon and Schuster, 1956.
Partington, J.R., *History of Chemistry* (four volumes), Macmillan, 1962-70.
Clark, R.W., *Einstein : The Life and Times*, HarperCollins, 2012.
Pais, A., *Subtle is the Lord ... The Science and the Life of Albert Einstein*, Oxford, 1982.
Penrose, R., *The Emperor's New Mind*, Oxford, 1999.
Servos, J.W., *Physical Chemistry from Ostwald to Pauling*, Princeton, 1990.
Spangenburg, R., and D.K. Moser, *On the Shoulders of the Giants : The History of Science, Vols. 1, 2, 3, 4 and 5*, Universities Press (India) Limited, Hyderabad, 2000.
Venkataraman, G., *QED : The Jewel of Physics*, Universities Press (India) Limited, Hyderabad, 1994.

INDEX

Chapter 0 Mathematical Concepts

Chapters 1–36

MODERN PERIODIC TABLE. LONG FORM

s Block Elements | *p* Block Elements | *d* Block Elements | *f* Block Elements

1	2	13/III	14/IV	15/V	16/VI	17/VII	18/0
1 1·0079 H Hydrogen $1s^1$							2 4·0026 He Helium $1s^2$
3 6·941 Li Lithium $2s^1$	4 9·012 Be Beryllium $2s^2$	5 10·811 B Boron $2s^2p^1$	6 12·011 C Carbon $2s^2p^2$	7 14·007 N Nitrogen $2s^2p^3$	8 15·999 O Oxygen $2s^2p^4$	9 18·998 F Fluorine $2s^2p^5$	10 20·179 Ne Neon $2s^2p^6$
11 22·990 Na Sodium $3s^1$	12 24·305 Mg Magnesium $3s^2$	13 26·982 Al Aluminium $3s^2p^1$	14 28·086 Si Silicon $3s^2p^2$	15 30·974 P Phosphorus $3s^2p^3$	16 32·064 S Sulphur $3s^2p^4$	17 35·453 Cl Chlorine $3s^2p^5$	18 39·948 Ar Argon $3s^2p^6$
19 39·098 K Potassium $4s^1$	20 40·078 Ca Calcium $4s^2$	31 69·723 Ga Gallium $3d^{10}4s^2p^1$	32 72·61 Ge Germanium $3d^{10}4s^2p^2$	33 74·922 As Arsenic $3d^{10}4s^2p^3$	34 78·960 Se Selenium $3d^{10}4s^2p^4$	35 79·909 Br Bromine $3d^{10}4s^2p^5$	36 83·801 Kr Krypton $3d^{10}4s^2p^6$
37 85·468 Rb Rubidium $5s^1$	38 87·620 Sr Strontium $5s^2$	49 114·82 In Indium $4d^{10}5s^2p^1$	50 118·69 Sn Tin $4d^{10}5s^2p^2$	51 121·75 Sb Antimony $4d^{10}5s^2p^3$	52 127·60 Te Tellurium $4d^{10}5s^2p^4$	53 126·90 I Iodine $4d^{10}5s^2p^5$	54 131·29 Xe Xenon $4d^{10}5s^2p^6$
55 132·91 Cs Cesium $6s^1$	56 137·33 Ba Barium $6s^2$	81 204·38 Tl Thallium $5d^{10}6s^2p^1$	82 207·19 Pb Lead $5d^{10}6s^2p^2$	83 208·98 Bi Bismuth $5d^{10}6s^2p^3$	84 208·98* Po Polonium $5d^{10}6s^2p^4$	85 209·99* At Astatine $5d^{10}6s^2p^5$	86 222·02* Rn Radon $5d^{10}6s^2p^6$
87 223·02* Fr Francium $7s^1$	88 226·03* Ra Radium $7s^2$						

3	4	5	6	7	8	9	10	11	12
21 44·956 Sc Scandium $3d^14s^2$	22 47·902 Ti Titanium $3d^24s^2$	23 50·942 V Vanadium $3d^34s^2$	24 51·996 Cr Chromium $3d^54s^1$	25 54·938 Mn Manganese $3d^54s^2$	26 55·847 Fe Iron $3d^64s^2$	27 58·93 Co Cobalt $3d^74s^2$	28 58·699 Ni Nickel $3d^84s^2$	29 63·546 Cu Copper $3d^{10}4s^1$	30 65·70 Zn Zinc $3d^{10}4s^2$
39 88·906 Y Yttrium $4d^15s^2$	40 91·224 Zr Zirconium $4d^25s^2$	41 92·906 Nb Niobium $4d^45s^1$	42 95·940 Mo Molybdenum $4d^55s^1$	43 98·906 Tc Technetium $4d^55s^2$	44 101·07 Ru Ruthenium $4d^75s^1$	45 102·9 Rh Rhodium $4d^85s^1$	46 106·42 Pd Palladium $4d^{10}5s^0$	47 107·87 Ag Silver $4d^{10}5s^1$	48 112·41 Cd Cadmium $4d^{10}5s^2$
57 138·91 La Lanthanum $5d^16s^2$	72 178·49 Hf Hafnium $5d^26s^2$	73 180·95 Ta Tantalum $5d^36s^2$	74 183·85 W Tungsten $5d^56s^1$	75 186·20 Re Rhenium $5d^56s^2$	76 190·20 Os Osmium $5d^66s^2$	77 192·2 Ir Iridium $5d^76s^2$	78 195·09 Pt Platinum $5d^86s^2$	79 196·97 Au Gold $5d^{10}6s^1$	80 200·59 Hg Mercury $5d^{10}6s^2$
89 227·03* Ac Actinium $6d^17s^2$	104 261·11* Unq Un-nil-quadium $6d^27s^2$	105 262·114* Unp Un-nil-pentium $6d^37s^2$	106 263·118* Unh Un-nil-hexium $6d^47s^2$	107 262·12* Uns Un-nil-septium $6d^57s^2$	108 .265* Uno Un-nil-octium $6d^67s^2$	109 * Une Un-nil-ennium $6d^77s^2$	110 ** Uun Un-un-nilium $6d^87s^2$	111 ** Uuu Un-un-unium $6d^{10}7s^1$	112 ** Uub Un-un-bium $6d^{10}7s^2$

ATOMIC NUMBER — 1 1·0079 H Hydrogen $1s^1$ — ATOMIC MASS (a.m.u.); OUTER ELECTRONIC CONFIGURATION

Atomic masses are based on 1987 IUPAC Table of Standard Atomic Masses of the Elements.

* Atomic mass of the isotope of the longest half-life.

** Elements beyond atomic number 108 are yet to be discovered.

f Block Elements

	58	59	60	61	62	63	64	65	66	67	68	69	70	71
LANTHANIDES *f* Block Elements	140·12 Ce Cerium $4f^15d^16s^2$	140·91 Pr Praseodymium $4f^25d^16s^2$	144·24 Nd Neodymium $4f^35d^16s^2$	146·92 Pm Promethium $4f^45d^16s^2$	150·5 Sm Samarium $4f^55d^16s^2$	151·97 Eu Europium $4f^65d^06s^2$	157·25 Gd Gadolinium $4f^75d^16s^2$	158·93 Tb Terbium $4f^85d^16s^2$	162·50 Dy Dysprosium $4f^95d^16s^2$	164·93 Ho Holmium $4f^{10}5d^16s^2$	167·26 Er Erbium $4f^{11}5d^16s^2$	168·93 Tm Thullium $4f^{12}5d^16s^2$	173·04 Yb Ytterbium $4f^{13}5d^16s^2$	174·97 Lu Lutetium $4f^{14}5d^16s^2$
ACTINIDES *f* Block Elements	90 232·04* Th Thorium $5f^16d^17s^2$	91 231·04* Pa Protactinium $5f^26d^17s^2$	92 238·03* U Uranium $5f^36d^17s^2$	93 237·05* Np Neptunium $5f^46d^17s^2$	94 242·0* Pu Plutonium $5f^56d^17s^2$	95 243·06* Am Americium $5f^76d^07s^2$	96 247·07* Cm Curium $5f^76d^17s^2$	97 247·07* Bk Berkelium $5f^86d^17s^2$	98 251·08* Cf Californium $5f^96d^17s^2$	99 252·08* Es Einsteinium $5f^{10}6d^17s^2$	100 257·10* Fm Fermium $5f^{11}6d^17s^2$	101 258·10* Unu Un-nil-unium $5f^{12}6d^17s^2$	102 259·10* Unb Un-nil-bium $5f^{13}6d^17s^2$	103 260·11* Unt Un-nil-trium $5f^{14}6d^17s^2$

Elements with atomic numbers beyond 100 have been named according to the IUPAC system. Accordingly, elements mendelevium (Md,101), nobelium (No,102) and lawrencium (Lr,103) are named as un-nil-unium (Unu), un-nil-bium (Unb) and un-nil-trium (Unt), respectively.